EF-G and EF-Tu Structures and Translation Elongation in Bacteria

Poul Nissen and Jens Nyborg
University of Aarhus, Aarhus, Denmark

The elongation cycle is the productive phase of protein biosynthesis. The genetic message in mRNA is a working transcript of a gene on DNA and it is translated one triplet codon at a time during this phase. Thereby, a specific amino acid sequence is synthesized and the final product represents a functional protein of the living cell. The translation is performed on the ribosome, which is a large complex of ribosomal RNA and ribosomal proteins. The ribosome is organized into two subunits, the large 50S subunit and the small 30S subunit. tRNA molecules provide amino acids for the protein biosynthesis and they are activated by the attachment to tRNA by an aminoacyl bond. During the elongation phase the ribosome is assisted by three elongation factors: (1) elongation factor Tu (EF-Tu), which brings to the ribosome amino-acylated tRNAs (aa-tRNAs) for decoding at the 30S subunit, (2) elongation factor G (EF-G), which assists the ribosome in translocating mRNA and tRNAs, and (3) elongation factor Ts (EF-Ts), which reactivates EF-Tu by exchanging its cofactor GDP for GTP. EF-Tu and EF-G are both G proteins that are active when GTP is bound as cofactor and inactive when GDP is bound. There is no nucleotide exchange factor for EF-G. The elongation phase and both EF-Tu and EF-G are surprisingly well preserved during evolution, for all living organisms. The proteins corresponding to EF-Ts are more complex in eukaryotes.

Elongation

The process by which the growing polypeptide on the ribosome is elongated by one amino acid according to the codon on mRNA involves the activities of the three elongation factors: EF-Tu, EF-Ts, and EF-G. EF-Tu in its active complex with GTP interacts with any aa-tRNA and prevents the spontaneous hydrolysis of the ester bond between the amino acid carboxyl acid moiety and the terminal 3′-ribose hydroxyls of the tRNA. EF-Tu in this so-called ternary complex interacts with the ribosome in its decoding activity where the correct match between the codon positioned in the decoding center of the 30S subunit and the anti-codon on tRNA is achieved. A signal is sent through as yet unknown routes to the 50S subunit, which reacts by inducing hydrolysis of GTP on EF-Tu at the GTPase center of the ribosome. EF-Tu in its GDP form undergoes a large conformational change and is released from the ternary complex and from the ribosome. The universal 3′-CCA end of tRNA is then free to swing into the peptidyl transferase center of the 50S subunit, where the formation of a new peptide bond between the growing polypeptide and the incoming amino acid is performed with the help of catalytic residues of the ribosomal RNA. The released EF-Tu:GDP is reactivated to EF-Tu:GTP with the help of the nucleotide exchange factor EF-Ts.

After peptidyl transfer the nascent polypeptide chain is attached to the incoming tRNA, with its anticodon still at the A site of the 30S subunit. It must be shifted to the P site together with the mRNA by exactly one codon. This is performed by EF-G in the translocation stage of elongation, where EF-G pushes the tRNA and the attached codon of the mRNA from the A site into the P site of the 30S subunit. After this the GTP of EF-G is hydrolyzed to GDP at the GTPase center of the ribosome, and EF-G:GDP is released. The high level of GTP in the cell and the relatively low affinity of GDP for EF-G is enough to ensure that EF-G reactivates into EF-G:GTP spontaneously, without the aid of a nucleotide exchange factor.

The ribosome has now completed one elongation cycle, and is left with a tRNA with its attached polypeptide in the P site of both the 50S and 30S subunits, and with the previous tRNA pushed into the E (exit) site. The ribosome exposes the next codon in the A site of the 30S subunit and is ready to receive the next cognate tRNA in its complex with EF-Tu:GTP.

Elongation Factor EF-Tu

EF-Tu has been the focus of structural studies for several decades. The name stems from early characterization of this factor as “translation factor unstable”. The biochemically most stable form is the biologically inactive EF-Tu:GDP, and was therefore the first form to be

structurally investigated. It was shown that EF-Tu consists of ~400 amino acids containing three domains (Figure 1). Domain 1 is a typical nucleotide binding domain with a central β-sheet surrounded by α-helices on both sides. This domain also contains all the consensus sequences now recognized as typical for a GTP-binding protein (G protein). Of these, there is a P-loop GXXXXGK(S/T) and a DXXG sequence motif also found in many ATP-binding proteins, where they are called Walker A and B motifs, respectively. Furthermore, there is a NKXD sequence motif involved in specific recognition of the G base of GTP, and a threonine residue in the so-called switch I region, which is now known to be involved in Mg^{2+} binding, and in the large conformational change of EF-Tu. A similar domain is found in all known G proteins, like the small GTPases (ras P21 or ran) and in the α-subunit of the heterotrimeric G proteins involved in cellular responses to external signals. The domain is therefore often referred to as the G domain. The remaining two domains, domain 2 and domain 3, of EF-Tu are both β-barrel structures and are in all known conformations of EF-Tu kept together as a single structural unit.

The biologically active form, EF-Tu:GTP, has been structurally determined with a nonhydrolyzable GDPNP nucleotide, where the O atom between the β- and γ-phosphate of GTP has been altered to the electronically similar NH group (Figure 1). The presence of the extra γ-phosphate in EF-Tu:GDPNP, when comparing to EF-Tu:GDP, has a dramatic effect on the overall conformation of the EF-Tu molecule. First of all, the γ-phosphate attracts the DXXG sequence motif, such that the peptide bond between the G residue and its preceding P residue is rotated by ~150°, and such that the NH group of this peptide bond makes a hydrogen bond with the γ-phosphate group. Like all G proteins, EF-Tu has switch regions of the G-domain that have significantly different structures in the GDP and GTP forms. The DXPGH motif of EF-Tu is at the beginning of its switch region II. This region in both the GDP and the GTP form includes an α-helix. However, between the two forms the helix is shifted by 4 residues along the sequence, and the position of its axis is therefore rotated by ~45°. As this helix is a major part of the interface towards domain 3 this change results in an overall rotation of the G-domain relative to domains 2 and 3 by ~90°. From biochemical studies, the histidine residue of the DXPGH motif of EF-Tu is known to be involved in the intrinsic GTPase activity of EF-Tu, and is presumably involved in stabilization of the transition state of GTP hydrolysis on the ribosome. Secondly, the presence of the γ-phosphate, and the shift in position of the proline residue of the DXPGH motif alters the conformation of the switch I region of EF-Tu such that its

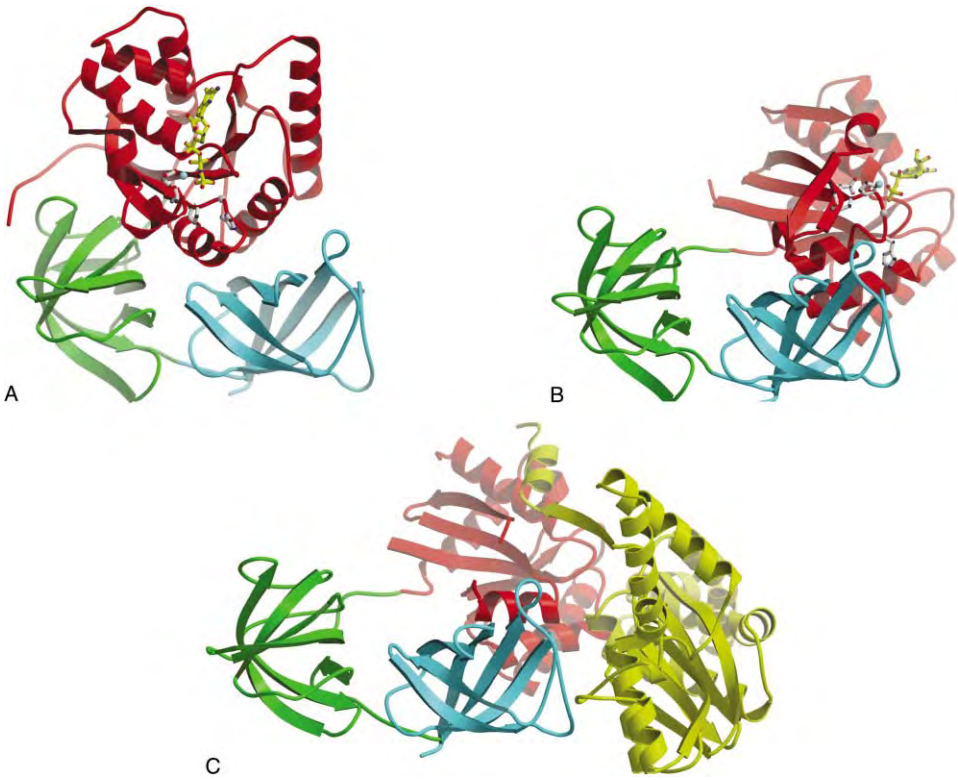

FIGURE 1 Structures of various forms of EF-Tu complexes: (A) EF-Tu:GDP, (B) EF-Tu:GTP, and (C) EF-Tu:EF-Ts. Domains of EF-Tu are colored: domain 1, red with nucleotides in yellow ball-and-stick where present; domain 2, green; domain 3, blue. EF-Ts is in yellow.

T residue becomes a ligand to the Mg^{2+} ion of the GTP form, and part of its secondary structure interchanges between a β-hairpin in the GDP form and an α-helix in the GTP form.

The structure of the complex between EF-Tu and its nucleotide exchange factor EF-Ts is also known. EF-Ts interacts with the G-domain of EF-Tu at the loops responsible for the nucleotide binding, and in many ways it alters the GDP binding pocket. Furthermore, EF-Ts interacts with the tip of domain 3 of EF-Tu in such a way that the G-domain and domain 3 are separated from each other. This separation represents an intermediate in the large conformational change of EF-Tu, and is also part of the catalysis of nucleotide exchange.

Elongation Factor EF-G

The structure of EF-G is known in its GDP-bound and in its nucleotide-free form (Figure 2). EF-G is much larger than EF-Tu and contains ~690 residues organized in five domains. The first domain of EF-G is the G-domain that has many similarities with the G-domain of EF-Tu in structure and in amino acid sequence. Apart from that, it contains an insert of ~90 residues (the G′-domain). The switch I region of EF-G in the GDP form is disordered. Domain 2 of EF-G is also similar to that of EF-Tu although it has a β-hairpin in the cleft between the G-domain and domain 2. The arrangement of the two domains in EF-G:GDP is like that of EF-Tu:GTP. Domains 3–5 have folds containing a small β-sheet with helices on one side only. This fold is very similar to that of some ribosomal proteins. Domain 4 contains an unusual left-handed $\beta-\alpha-\beta$ folding motif. Furthermore, this domain is more elongated and sticks out from the rest of the protein. It is known that the very tip of this domain is functionally important in translocation, as a histidine residue in the eukaryotic factor is modified into the unusual diftamide, and that ADP-ribosylation of this residue by difteria toxin blocks its function on the ribosome.

Despite numerous attempts by several research groups, it has not been possible to determine the structure of the biologically active EF-G:GTP. Studies by cryo-electron microscopy indicate that significant conformational changes occur when EF-G is bound on the ribosome.

The Ternary Complex of EF-Tu

Two structures have been determined of the ternary complex of EF-Tu (Figure 2). The first one was a complex between yeast Phe-tRNA and bacterial EF-Tu:GDPNP, while the second one was of bacterial Cys-tRNA and bacterial EF-Tu:GDPNP. The two are very similar and point to the fact that tRNAs are very similar in all organisms and that therefore the ternary complex is most likely to have the same general structures in all kingdoms of life. The large conformational change of EF-Tu from the GDP to the GTP form creates

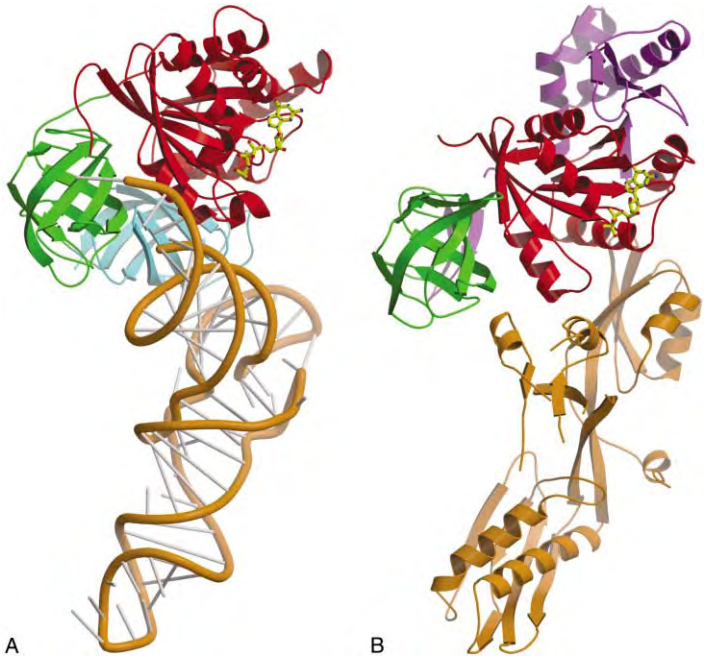

FIGURE 2 Structures of (A) the ternary complex of EF-Tu, and (B) EF-G:GDP. EF-Tu is colored as in Figure 1. The tRNA is in orange, domains 1 and 2 of EF-G are colored as for EF-Tu with an insert in domain 1 in magenta. Domains 3, 4, and 5 of EF-G are in orange.

a preformed binding surface for the tRNA. The structures of both tRNA and EF-Tu:GDPNP in the ternary complex are thus very similar to the structures of the free components. The universally conserved 3′-CCA end of tRNA is bound to a cleft between the G-domain and domain 2 of EF-Tu. This cleft as mentioned above is filled with a β-hairpin in EF-G. The terminal A base is recognized in a deep pocket on the surface of domain 2, while a pocket between the G-domain and domain 2 holds the amino acid attached to tRNA. The aminoacyl bond of the amino acid is recognized by main chain groups of EF-Tu in such a way that the amino group must be deprotonated in the complex. Other contacts involve general features of the tRNA structure.

The Structural Similarity of EF-G and the Ternary Complex

When the structure of the first ternary complex of EF-Tu was determined it was observed that its shape was very similar and points to that of the previously known EF-G:GDP (Figure 2). Domains 3, 4, and 5 of EF-G are thus a structural mimic of the tRNA of the ternary complex. The elongated domain 4 of EF-G directly mimics the anti-codon stem-and-loop of tRNA. There has been much speculation why this should be, and whether this would be a general phenomenon for parts of proteins known to interact with the A site of the ribosome. This does not seem to be the case according to recent results, and the simplest explanation of the mimicry is that the ternary complex has to interact with the ribosome after EF-G:GDP left the ribosome. Possibly, EF-G reshapes the ribosome into a form that is ready to interact with a ternary complex.

Action of Elongation Factors on the Ribosome

Electron microscopy of ribosomal particles in flash-frozen vitreous ice (cryo-EM) has revealed information on how elongation factors interact with the ribosome. The results obtained make use of the fact that some antibiotics interact specifically with the elongation factors on the ribosome. The antibiotic fusidic acid is thus known to interact with EF-G, while the antibiotic kirromycin interacts with the ternary complex of EF-Tu. Both antibiotics block the release of the target proteins on the ribosome after GTP hydrolysis has been induced. The antibiotics are believed to prevent conformational changes in the elongation factors that are needed for their release from the ribosome. The cryo-EM reconstructions of both EF-G and of the ternary complex on the ribosome reveal that they indeed occupy very similar positions and are found to have very similar shapes. The G-domain is seen to be very close to features of the 50S subunit that are very close to the GTPase-activating center of the ribosome. Domain 2 interacts with the 30S subunit such that the G-domain and domain 2 together fill the gap between ribosomal subunits.

The tip of domain 4 of EF-G and the tip of the anti-codon stem-and-loop of tRNA both reach into the decoding center of the 30S subunit. Thus, the similarity in the structures of EF-G:GDP and of the ternary complex of EF-Tu is reflected in their similar interaction with the ribosome.

Antibiotic Action on EF-Tu

A few families of antibiotics are known to interact directly with the function of EF-Tu. These families seem

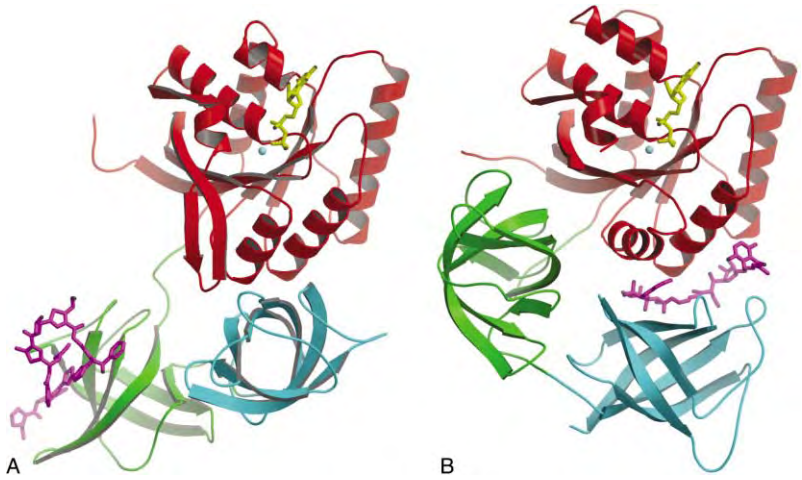

FIGURE 3 Structures of complexes of EF-Tu and antibiotics: (A) GE2770A bound to EF-Tu:GDP, and (B) aurodox bound to EF-Tu:GDP. Antibiotics are shown in magenta.

to fall into two functional groups. One group (examples are GE2270A and pulvomycin) prevents the formation of the ternary complex, while another group (examples kirromycin and enacyloxin IIa) prevents the release of EF-Tu from the ribosome. A structural complex of GE2270A with EF-Tu:GDP has been determined, and reveals that the antibiotic partly occupies the pocket on domain 2, which in the ternary complex accommodates the terminal A base. Furthermore, GE2270A stabilizes EF-Tu in the GDP-bound conformation and prevents the formation of the GTP-bound conformation. This structure thus explains how this group of antibiotics prevents the formation of a ternary complex of EF-Tu.

A structure of EF-Tu:GDP in complex with aurodox (a methylated version of kirromycin) shows the antibiotic in a cleft between the G-domain and domain 3, keeping the two together in a GTP-like form of EF-Tu although the nucleotide bound is GDP. This will explain how kirromycin blocks the release of EF-Tu from tRNA and from the ribosome upon GTP hydrolysis.

These results (Figure 3) may indicate that the conformations trapped by antibiotics are biologically relevant forms, which effectively can be blocked by inhibitors aimed at stopping protein biosynthesis in bacteria.

See Also the Following Articles

G_i Family of Heterotrimeric G Proteins • G_q Family • G_s Family of Heterotrimeric G Proteins • G_{12}/G_{13} Family • Translation Elongation in Bacteria

Glossary

anti-codon A triplet of bases on tRNA that by Watson–Crick base pairing can decode a codon.

codon A triplet of bases on mRNA that codes for one amino acid.

EF-G Translation factor controlled by GTP.

EF-Ts Translation factor (stable).

EF-Tu Translation factor (unstable).

G protein Protein whose action is controlled by GTP and GDP. The protein is active in its GTP-bound form, while hydrolysis of GTP into GDP inactivates the protein.

GDP Guanosine di-phosphate.

GTP Guanosine tri-phosphate.

mRNA Messenger ribonucleic acid containing the triplet codons, each specifying one amino acid.

ribosome Cellular particle that synthesizes proteins with the amino acid sequence given by the sequence of triplet codons of mRNA.

tRNA Transfer ribonucleic acid that carries on its 3′ CCA end an amino acid corresponding to its anti-codon.

Further Reading

Kjeldgaard, M., Nyborg, J., and Clark, B. F. C. (1996). The GTP-binding motif—variations on a theme. *FASEB J.* **10**, 1347–1368.

Krab, I. M., and Parmeggiani, A. (1998). EF-Tu, a GTPase odyssey. *Biochim. Biophys. Acta* **1443**, 1–22.

Merrick, W. C., and Nyborg, J. (2000). The protein biosynthesis elongation cycle. In *Translational Control of Gene Expression* (N. Sonenberg, J. W. B. Hershey and M. B. Mathews, eds.) CSHL Press, New York.

Nissen, P., Kjeldgaard, M., and Nyborg, J. (2000). Macromolecular mimicry. *EMBO J.* **19**, 489–495.

Nyborg, J., Nissen, P., Kjeldgaard, M., Thirup, S., Polekhina, G., Clark, B. F. C., and Reshetnikova, L. (1996). Structure of the ternary complex of EF-Tu: Macromolecular mimicry in translation. *TIBS* **21**, 81–82.

Ramakrishnan, V. (2002). Ribosome structure and the mechanism of translation. *Cell* **108**, 557–572.

Valle, M., Zavia lov, A., Li, W., Stagg, S. M., Sengupta J., Nielsen, R. C., Nissen, P., Harvey, S. C., Ewemberg, M., and Frank, J. (2004). Incorporation of aminoacyl tRNA into the ribosome as seen by cryo-electron microscopy. *Nat. Struct. Biol.* **10**, 899–906.

Biography

Poul Nissen is an Associate Professor at the University of Aarhus, Denmark. His major scientific interest has been the structural investigation of the ternary complex of EF-Tu and of the large 50S ribosomal subunit and the transition state of its peptidyl transferase center. He received his Ph.D. in protein crystallography at the University of Aarhus, and spent his postdoctoral period at Yale University. He is now working on the yeast ribosome and membrane transport proteins. He is an EMBO Young Investigator and a Danish Research Council Ole Rømer Stipendiate.

Jens Nyborg is an Associate Professor at the University of Aarhus, Denmark. His major scientific interests have been the structural investigations of translation factors and of components of the innate immune system. He received his Ph.D. in crystallography on inorganic chemical compounds and spent his postdoctoral period at the Medical Research Councils Laboratory of Molecular Biology in Cambridge, UK. He is a member of the Royal Danish Academy of Sciences and Letters and EMBO.

Eicosanoid Receptors

Richard M. Breyer and Matthew D. Breyer
Vanderbilt University, Nashville, Tennessee, USA

Eicosanoids are the oxygenated metabolites of the 20-carbon polyunsaturated fatty acid arachidonic acid. These compounds are locally acting autacoids and are rapidly metabolized with a half-life of minutes to seconds. Once formed, eicosanoids exert their physiologic effects via interaction with specific receptors. The best characterized of these receptors belong to the superfamily of G protein-coupled receptors, although some eicosanoids are thought to interact with nuclear hormone receptors as well.

Eicosanoid Biosynthesis Pathways

The 5,8,11,14-eicosatrienoic acid, a 20-carbon polyunsaturated fatty acid with the trivial name arachidonic acid, is esterified in the lipid bilayer of cell membranes. Upon its enzymatic release by the action of phospholipase, free arachidonate is rapidly metabolized. Oxygenated metabolites of arachidonic acid are collectively known as the eicosanoids. These compounds are formed by the action of three distinct enzymatic pathways.

The Lipoxygenase (LO) Pathway

This pathway leads to the formation of the monoxygenated compounds such as hydroperoxytetraenoic acids (HPETEs), hydroxytetraenoic acids (HETEs), and trihydoxylated metabolites known as lipoxins via three principal enzymes: 5-LO, 12-LO, and 15-LO. The 5-HPETEs are substrates for the leukotriene synthases that lead to the formation of a series of key inflammatory mediators, the leukotrienes, including the unstable intermediate LTA_4, which is converted to the potent mediator LTB_4 and the cysteinyl leukotrienes LTC_4, LTD_4, and LTE_4. Sequential oxidation of arachidonic acid by the action of both 12-LO and 5-LO or 12-LO and 15-LO leads to the formation of the lipoxins LXA_4 and LXB_4. The lipoxins are structurally related to the leukotrienes, but appear to act through a distinct set of receptors and have very different actions *in vivo*. Finally, the 5-LO metabolite HPETE can be further metabolized to the 5-oxo ETE(5-oxo-6E,8Z,11Z,14Z-eicosatetraenoic acid), for which a unique receptor has recently been cloned.

The Cyclooxygenase (COX) Pathway

Cyclooxygenase metabolism leads to the production of the five principal prostanoids via two distinct isozymes, COX-1 and COX-2. Four of the principal prostaglandins, PGE_2, PGD_2, $PGF_{2\alpha}$, and PGI_2 are analogues of the 20-carbon unnatural fatty acid prostanoic acid, which is distinguished by its five carbon "prostane" ring group comprised of carbons five through eight. The fifth prostanoid, thromboxane, has an inserted ether oxygen and thus has a six-member ring structure and is an analogue of the unnatural fatty acid thrombanoic acid.

The Epoxygenase Pathway

Oxidation of arachidonic acid by the cytochrome P450 pathway leads to the formation of epoxytrienoic acids (EETs). Although physiologic effects have been attributed to these compounds no specific EET receptors have been identified to date.

Eicosanoid Action

As a class, eicosanoids mediate a wide array of physiologic effects including pain, inflammation, and modulation of smooth muscle tone. Many of these effects are receptor-mediated by cell surface G protein-coupled receptors (GPCRs). There is recent evidence that some PG metabolites can activate nuclear hormone receptors of the peroxisome-proliferation-activated receptor family (PPARs). In addition to the enzymatic products of arachidonic acid metabolism, prostanoid-like products resulting from nonenzymatic oxidation have also been described and designated isoprostanes. These products are structurally related to the COX-derived prostanoids, but are the product of non-enzymatically free radical oxidation. Isoprostanes are markers of oxidative stress and evidence suggests that these metabolites can also evoke receptor-mediated physiologic effects.

Receptors of Lipoxygenase Metabolites

The action of lipoxygenase metabolites of arachidonic acid is mediated by a distinct family of GPCRs. Six GPCRs have been identified that bind lipoxygenase metabolites of arachidonic acid: four leukotriene receptors designated BLT_1, BLT_2, $CysLT_1$, and $CysLT_2$ have been described, a lipoxin receptor designated ALX, and the receptor for 5-oxo ETE.

Leukotriene Receptors

The leukotriene receptors fall into two groups of structurally related GPCRs: the chemoattractant-like BLT receptors and the CysLT receptors, which are related to the family of nucleotide-binding receptors. Of the four cloned leukotriene receptors, BLT_1 and BLT_2 receptors have highest affinity for the leukotriene LTB_4 with BLT_1 binding LTB_4 with much higher affinity as compared to BLT_2. The BLT receptors are predominantly expressed in the peripheral blood including leukocytes, granulocytes, macrophages, and eosinophils. The $CysLT_1$ and $CysLT_2$ receptors in contrast each bind the cysteinyl leukotrienes LTC_4 and LTD_4 with high affinity. CysLT receptors are expressed in peripheral blood leukocytes, spleen, and lung as well in a number of other tissues at lower levels. The $CysLT_1$ receptor has been implicated as an important mediator in asthma, and antagonists of this receptor such as monteleukast have been used clinically in the treatment of asthma.

Lipoxin Receptors

The lipoxin A_4 receptor (ALX), is a member of the GPCR family of chemoattractant receptors, as are the BLT receptors discussed above. This receptor was identified as an orphan receptor cDNA sharing significant homology with the fMLP chemoattractant receptor and was designated FMLP-like receptor 1 (FPLR1). Subsequent identification of this receptor as a mediator of LXA_4 action resulted in its designation as the ALX receptor. Activation of this receptor mediates the anti-inflammatory actions of lipoxin LXA_4. Northern blot analysis of ALXR mRNA in mouse tissues demonstrates that the receptor is most highly expressed in neutrophils, lung, and spleen with lower levels detected in the liver and heart. Some actions of lipoxins cannot be accounted for by the ALXR, and the existence of other lipoxin receptors has been postulated, but existence of other lipoxin receptor cDNAs has not been confirmed.

The 5-Oxo-ETE Receptor

The orphan GPCR TG1019 and closely related R527 have been identified as receptors for 5-oxo-ETE. These receptors have no official designation at this time. These receptors have been shown to be highly expressed in the kidney and may mediate the observed hemodynamic effects of 5-oxo-ETE described in this tissue.

Prostaglandin (PG) Receptors

The local action of PGs depends in part, on activation of a family of specific GPCRs, designated EP for E-prostanoid receptors, FP, DP, IP, and TP receptors respectively, for the other prostanoids. The EP receptors are unique in that four receptors, designated EP1 through EP4, have been described for PGE_2 each encoded by a distinct gene. A second class of Prostaglandin D receptor designated chemoattractant receptor-homologous molecule expressed on Th2 cells (CRTH2) has been identified, which has no sequence homology to the remaining PG receptors. This receptor has been unofficially designated "DP2." Each of the other PGs has a single receptor, and taken together there are nine PG GPCRs, each encoded by distinct genes. Alternative mRNA splice variants have been cloned for the EP1, EP3, TP, and FP receptors. In each case, these splice variants generate receptor sequence diversity in the intracellular C-terminal tail of the receptor protein (Figure 1). Functionally, these splice variants appear to modulate the specificity of G protein coupling, as well as regulation of receptor desensitization by encoding alternate phosphorylation sites. Pharmacologically, the PG receptors are distinguished by their ligand-binding selectivity as well as the signal transduction pathway they activate. In general, PG receptors may have significant affinity for more than one prostanoid ligand. Moreover, multiple PG receptors are frequently coexpressed in a single cell type or tissue. COX activation and resulting PG production may lead to complex effects in the target tissue by activation of multiple PG receptor subtypes. Thus, a given PG ligand may elicit multiple, and at times apparently opposing, functional effects on a given target tissue. For example, prostaglandin receptors were initially characterized by their actions on smooth muscle, where they may lead to either smooth muscle contraction or relaxation. The vasodilator effects of PGE_2 have long been recognized in both arterial and venous beds. Smooth muscle relaxation by PGE_2 is, however, not uniformly observed, and PGE_2 is a potent constrictor in other smooth muscle beds, including trachea, gastric fundus, and ileum. Importantly, some structural analogues of PGE_2 are capable of reproducing the dilator effects of PGE_2, but are inactive on tissues where it is a constrictor. Conversely, analogues that reproduce the constrictor effects of PGE_2 may fail to affect tissues where PGE_2 is a dilator. The EP receptor mRNAs exhibit differential

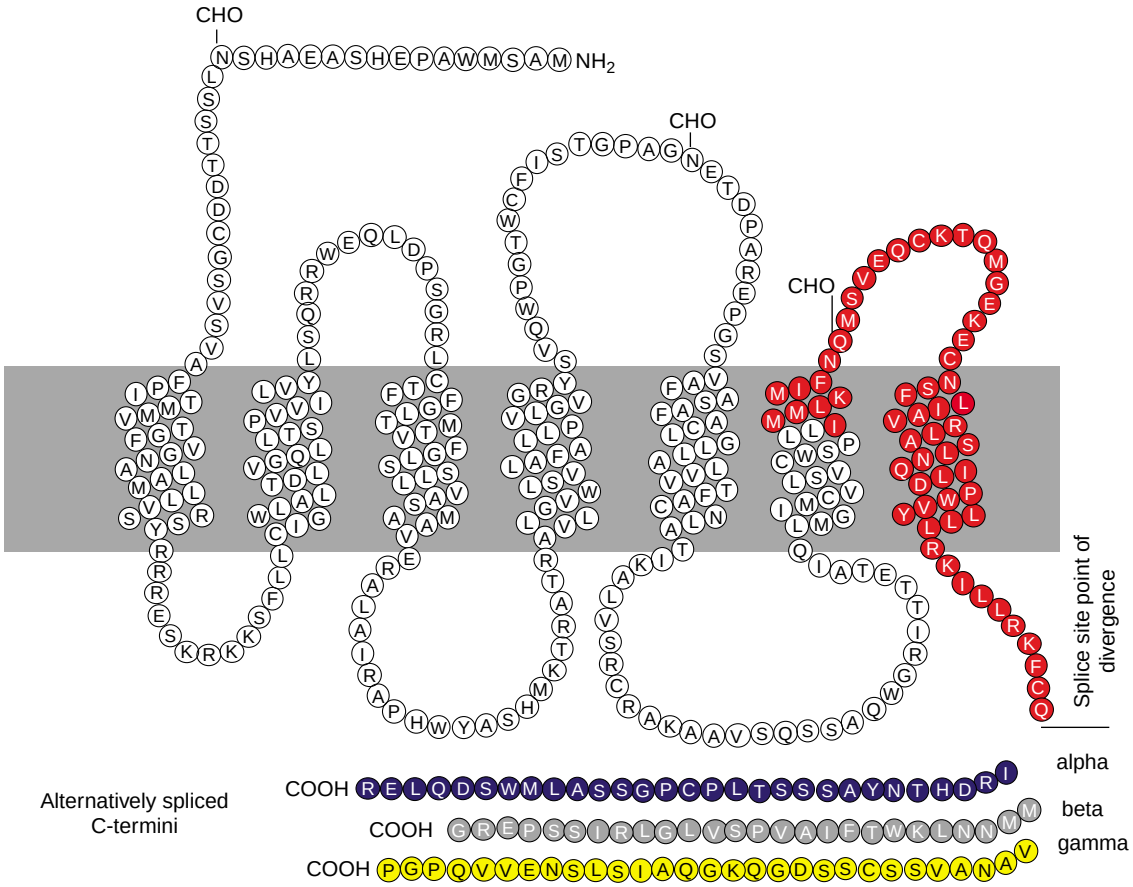

FIGURE 1 EP_3 receptor sequence of three mouse EP_3-receptor splice variants differing only in their intracellular carboxyl termini. The predicted amino acid sequences of each splice variant is represented by the one-letter amino acid code. Exons are color-coded. The common region is comprised of two exons (in white and red circles) which are spliced to three possible C-terminal tails. The carboxyl variable tails are designated alpha (blue), beta (gray), and gamma (yellow), each encoded by distinct exons.

expression in a number of tissues with distinct functional consequences of activating each receptor subtype. Functional antagonism among PGs can also be observed in platelet aggregation, where TXA_2 activation of the TP receptor causes platelet aggregation. Conversely, prostacyclin activates platelet IP receptors which opposes this platelet aggregation. Thus, the balance of PGs synthesized as well as the complement of PG receptors expressed determines the net effect of COX metabolism on platelet function.

PPARs

In addition to the GPCR-mediated effects there is evidence that prostaglandin metabolites are capable of activating some nuclear transcription factors. This action is exemplified by the cyclopentenone prostaglandins of the J-series, e.g., 15-deoxy -Δ12,14-PGJ_2 (15d-PGJ_2) which are derived from PGD_2. 15d-PGJ_2 activates a nuclear hormone receptor designated peroxisome proliferation activated receptor gamma (PPARgamma). There is also evidence that prostacyclin (PGI_2) also activates another member of this family designated PPARdelta. It is unclear whether the PGs represent true endogenous ligands of these receptors, as their affinity is generally in the micromolar range, which is two to three orders of magnitude lower than the nanomolar affinities observed for PGs at the GPCRs; nonetheless, these concentrations could be achieved in the intracellular environment.

See Also the Following Articles

DNA Polymerase δ, Eukaryotic • Peroxisome Proliferator-Activated Receptors • Processivity Clamps in DNA Replication: Clamp Loading • Prostaglandins and Leukotrienes

Glossary

autacoid A class of physiologically active substances that act upon the cell that elaborated this compound or on adjacent cells.

cyclooxygenase (COX) Enzymes that catalyze the oxidation of arachidonic acid. Also known as PGH synthase. COX catalyzes two sequential reactions, a *bis* oygenase, or cycloxygenase, reaction leading to the formation of PGG_2 and a subsequent peroxidase activity at the C15 position leading to the conversion of PGG_2 to PGH_2.

eicosanoid Any of the collections of oxygenated metabolites of the 20-carbon fatty acid, 5,8,11,14-eicosatetranoic acid (arachidonic acid) that are the products of cyclooxygenase, cytochrome P450, lipoxygenase, and nonenzymatic pathways.

GPCRs G protein-coupled receptors. A class of integral membrane protein cell-surface receptors that change conformation upon binding cognate agonists. This conformational change causes the dissociation of heterotrimeric G proteins leading to the initiation of the signal transduction cascade.

leukotriene Monoxygenated metabolites of arachidonic acid formed by the action of the lipoxygenases.

nonsteroidal anti-inflammatory drugs (NSAIDs) A class of drugs that effect their action by inhibiting the activity of cyclooxygenase. They have potent analgesic, antipyretic, and anti-inflammatory properties.

prostanoids Oxygenated metabolites of the 20-carbon essential fatty acid arachidonic acid. They are analogues of the 20-carbon unnatural fatty acids, prostanoic, and thrombanoic acid, produced by the action of cyclooxygenase.

Further Reading

Breyer, R. M., Bagdassarian, C. K., Myers, S. A., and Breyer, M. D. (2001). Prostanoid receptors: subtypes and signaling. *Annu. Rev. Pharmacol. Toxicol.* **41**, 661–690.

Brink, C., Dahlen, S. E., Drazen, J., Evans, J. F., Hay, D. W., Nicosia, S., Serhan, C. N., Shimizu, T., and Yokomizo, T. (2003). International union of pharmacology XXXVII. Nomenclature for leukotriene and lipoxin receptors. *Pharmacol. Rev.* **55**, 195–227.

Forman, B. M., Tontonoz, P., Chen, J., Brun, R. P., Spiegelman, B. M., and Evans, R. M. (1995). 15-Deoxy-delta 12, 14-prostaglandin J2 is a ligand for the adipocyte determination factor PPAR gamma. *Cell* **83**, 803–812.

Hosoi, T., Koguchi, Y., Sugikawa, E., Chikada, A., Ogawa, K., Tsuda, N., Sato, N., Tsunoda, S., Taniguchi, T., and Ohnuk, T. (2002). Identification of a novel eicosanoid receptor coupled to Gi/o. *J. Biol. Chem.* **277**, 31459–31465.

Jones, C. E., Holden, S., Tenaillon, L., Bhatia, U., Seuwen, K., Trantes, P., Turner, J., Kettle, R., Bouhelal, R., Charlton, S., Nirmala, N. R., Jarai, G., and Finun, P. (2003). Expression and characterization of a 5-oxo-6E,8Z,11Z,14Z-eicosatetraenoic acid receptor highly expressed on human eosinophils and neutrophils. *Mol. Pharmacol.* **63**, 471–477.

Morrow, J. D., and Roberts, L. J. (2001). Lipid-derived autacoids. In *Goodman & Gilman's the Pharmacological Basis of Therapeutics* (J. G. Hardman, L. E. Limbird and A. G. Gilman, eds.) 2nd edition. McGraw-Hill, New York.

Biography

Richard M. Breyer is an Associate Professor of Medicine (Nephrology) and Pharmacology at Vanderbilt University. His principal research interests are in prostaglandin receptor structure, function, and pharmacology. He holds a Ph.D. in biochemistry from the Massachusetts Institute of Technology, and received his postdoctoral training at the Pasteur Institute in Paris, France.

Matthew D. Breyer is a VA Merit Awardee and Professor of Medicine (Nephrology) and Molecular Physiology and Biophysics at Vanderbilt University. His principal research interests are in eicosanoid regulation of renal physiology. He holds an M.D. from Harvard University, and received his postdoctoral fellowship training at the University of Texas, Southwestern Medical Center in Dallas, Texas.

Elastin

Judith Ann Foster
Boston University School of Medicine, Boston, Massachusetts, USA

Elastin is a protein that exists as fibers in the extracellular spaces of many connective tissues. Elastin derives its name from its ability to act as an elastic band, i.e., to stretch and recoil with transient force. It is located throughout many tissues and organs of higher vertebrates and plays an important functional role in maintaining pressures associated with liquid and air flow in the cardiovascular and pulmonary systems. Elastogenic cells synthesize and secrete a soluble monomeric form of elastin into the extracellular space. The enzyme, lysyl oxidase, initiates cross-linking of the soluble monomers into insoluble fibers. Extracellular elastin associates closely with other proteins in the matrix including microfibrillar proteins and collagens. Once laid down in the matrix, the insoluble protein is very stable and resistant to degradation. Because of its critical role in the normal development and function of vital organs, impairment of elastin synthesis or proteolytic degradation of the insoluble fibers results in major clinical pathologies.

Composition and Primary Sequence

Elastin, as any protein, possesses a unique amino acid composition and a unique sequence of those amino acid residues along the polypeptide chain.

Amino Acid Composition

The soluble form of elastin, sometimes referred to as tropoelastin, contains a preponderance of uncharged and nonpolar amino acids. The polypeptide chain contains appropriately 850 amino acids and a molecular mass of 65–72 kDa. The actual size varies somewhat among different species. Glycine (33%), alanine (18%), proline (13%), valine (17%), and leucine (5%) residues represent 86% of the total amino acids. Prolyl hydroxylase converts 1–2% of the proline residues to hydroxyproline but it is unclear as to the significance of this cotranslational modification. There are ~36–38 lysine residues per molecule so the overall charge of monomer is basic with an isoelectric point over pH 10. Once lysyl oxidase deaminates the epsilon amino group of most lysine residues in the protein, the resulting semialdehydes undergo a series of aldol condensations and Schiff bases to form the desmosine cross-links. At this stage, the protein is irreversibly insoluble and any success in extracting soluble fragments requires cleavage of peptide bonds.

Amino Acid Sequence

Unlike the classical triple repeat of collagen wherein glycine residues occupy every third position of the triplet, elastin does not contain a uniform repeating structure. Instead, elastin contains two broad sequence motifs that accommodate much subdivision. Most lysine residues segregate together with alanine residues to create pairs of lysines separated by two or three alanine residues. These sequences exist within stretches of uncharged, nonpolar amino acid residues such as glycine, valine, and proline. The latter amino acid residues occur together with other nonpolar, hydrophobic, and polar residues, form tri, tetra, penta, and hexa repeats with not a single consistent motif. The carboxy terminal sequence is unique and highly conserved among different species. It contains the only cysteine residues within the molecule.

Isolation of Elastin

Insoluble Elastin

An early operational definition of elastin was that it represented the protein remaining after one extracted all other connective tissue proteins. Consequently, the insolubility of elastin serves as the basis for all isolation methods. Isolation procedures involve very harsh treatments such as autoclaving, extraction with hot alkali or strong denaturants, and exposure to cyanogen bromide or collagenases. Amino acid analysis of the material remaining insoluble after these treatments confirms the presence and homogeneity of the elastin.

Soluble Elastin

In vivo the conversion of soluble to insoluble elastin occurs rapidly making the isolation of soluble elastin very difficult. In order to isolate quantitative amounts of soluble elastin from a tissue, one must block the

conversion of the soluble to the insoluble form. Inhibition of the cross-linking enzyme, i.e., lysyl oxidase, is the most effective approach for isolating intact elastin monomers. Since lysyl oxidase is a copper-dependent enzyme that is specific for lysine residues it can be inhibited by removing copper or adding a noncompetitive inhibitor. In practice, this involves rendering an animal copper deficient by dietary restriction or by adding β-aminopropionitrile, a lathyrogen, to the diet of young animals. The procedure for isolating soluble elastin is based primarily on its unique solubility in organic solvents.

The Elastin Gene

Gene Structure

The single copy, elastin gene spans ~35–40 kb of DNA but only 7% of the sequences represent exons that are transcribed into the mRNA. The huge amount of intron sequences in the gene (19:1, intron to exon) makes this one of the most disperse genes reported. The short exon sequences (less than 190 bp) encode separate cassettes for the nonpolar and lysine/alanine residues of the protein. Many of the intron sequences encode elastin-like sequences.

Gene Promoter

The elastin gene promoter contains features of a constitutively expressed (housekeeping) gene. It lacks a classic TATA box, is very GC rich (67%), has two CAAT boxes and possesses multiple transcription start sites. There are also several Sp1 sites as well as a cryptic GC box and several consensus AP2 sequences within the proximal promoter. In addition, consensus sequences for glucocorticoid, TPA-inducible, and CRE response elements reside in the distal promoter regions.

Elastin Gene Expression

Elastin mRNAs

Transcription of the elastin gene results in multiple mRNAs. The multiple forms all possess a size in the 24S range arising from alternate splicing of several different exons. All of the transcripts contain ~3.5 kb that includes a large untranslated 3′ region of ~1.0 kb in addition to the polyA tail.

Elastin Protein Isoforms

Translation of multiple mRNA results in different isoforms of soluble elastin that reflect insertion of different exons sequences. Although there is variance in the presence of isoforms dependent on cell type and age, the function of the different variations of soluble elastin is still not clear. There is speculation that different isoforms play a major role in the early phase of elastic fiber assembly by providing interactive sites for specific binding to other components of the extracellular matrix.

Regulation of Elastin Gene Expression

The expression of elastin is high in developing tissues and through early growth to maturity. In the adult animal, elastin synthesis is very low and its reinitiation occurs only in normal injury/repair situations or in some pathological conditions. Many studies have focused on understanding how elastin expression is regulated in development and disease conditions. The results show that expression is regulated at both the transcriptional and posttranscriptional levels.

Transcriptional Regulation

Many studies have shown that elastin expression in developing pulmonary and cardiovascular tissues is controlled primarily at the transcriptional level. These results have been confirmed in transgenic animals carrying the transgene with a reporter driven by the elastin promoter and by *in vitro* tissue transfections of the same reporter gene. In addition, primary cultures of elastogenic cells demonstrate that elastin transcription plays a major role in the action of elastin modulators such as basic fibroblast growth factor and insulin-like growth factor. Putative *cis*-acting elements in the 5′ flanking region of the gene have been broadly defined through transient transfections of various cell types with a series of deletion reporter constructs. Of the *cis*-acting elements identified within the elastin promoter, few have been functionally shown to convey an increase in elastin transcription. In fact, the majority were found to be repressors. These latter observations suggest that a possible route to increase elastogenesis is to block the repressor complex from binding via the disruption of the receptor and/or ligand binding, as well as blocking the resultant signal pathway.

Posttranscriptional Regulation

Studies on the expression of elastin in cultures of elastogenic cells challenged with biologically significant factors show that elastin mRNA stability is important in regulating expression especially in the adult animal.

See Also the Following Articles

Amino Acid Metabolism • Collagens

Glossary

cyanogen bromide A chemical reagent used to cleave peptide bonds adjacent to methionine residues.

desmosine A pyridinium ring alkylated in four positions; serves as a cross-link derived from four lysine residues.

lathyrism A disease caused by ingestion of seeds of *Lathyrus odoratus*, a sweet pea. The active agent is β-aminopropionitrile which inhibits lysyl oxidase.

polyA tail A string of adenine nucleotides added to the 3′ end of most eukaryotic mRNAs.

promoter A DNA sequence that binds RNA polymerase resulting in transcription initiation.

svedberg unit (S) A unit used for the sedimentation coefficient; equivalent to 10–13 s.

Further Reading

Franzblau, C., and Lent, R. W. (1968). Studies on the chemistry of elastin. In *Structure, function, and evolution of proteins* Vol 21, Brookhaven Symposia in Biology, pp. 358–377.

Gallop, P. M., and Paz, M. A. (1975). Posttranslational protein modifications, with special attention to collagen and elastin. *Physiol. Rev.* **55**, 418–487.

Gray, W. R., Sandberg, L. B., and Foster, J. A. (1973). Molecular model for elastin structure and function. *Nature* **246**, 461–466.

Indik, Z., Yeh, H., Ornstein-Goldstein, N., Kucich, U., Abrams, W., Rosenbloom, J. C., and Rosenbloom, J. (1989). Structure of the elastin gene and alternative splicing of elastin mRNA: Implications for human disease. *Am. J. Med. Genet.* **34**, 81–90.

Lansing, *et al.* (1952). *Anat. Rec.* **114**,550–575.

Partridge and Davis (1955). *J. Biochem.* **61**, 21–30.

Perrin, S., and Foster, J. A. (1997). Developmental regulation of elastin gene expression. *Crit. Rev. Eukaryot. Gene Expr.* **7**, 1–10.

Sandberg, L. B., Weissman, N., and Smith, D. W. (1969). The purification and partial characterization of a soluble elastin-like protein from copper-deficient porcine aorta. *Biochemistry* **8**, 2940–2945.

Biography

Dr. Judith Ann Foster is currently a Professor of Biochemistry at Boston University School of Medicine. She has held faculty positions at the Utah University School of Medicine, the University of Georgia and served as the Chairperson of the Biology Department at Syracuse University. She has been studying elastin for the last 30 years. She began her work on characterizing soluble elastin and the regions of cross-link formation and progressed to examining the biosynthesis and expression of elastin in lung and aortic cells. Dr. Foster has spent the last decade studying the regulation of elastin gene transcription.

Endocannabinoids

Daniele Piomelli
University of California, Irvine, California, USA

The endocannabinoids are a family of biologically active lipids that bind to and activate cannabinoid receptors, the G protein-coupled receptors targeted by Δ^9-tetrahydrocannabinol in marijuana. The term encompasses several derivatives of arachidonic acid, which are generated on demand by neurons and other cells in response to physiological or pathological stimuli. The two best-characterized endocannabinoids are anandamide (arachidonoylethanolamide) and 2-arachidonoylglycerol (2-AG). Others are noladin ether (2-arachidonoyl glyceryl ether) and virodhamine (O-arachidonoyl ethanolamine).

Synthesis

Anandamide

Anandamide is produced from the hydrolysis of an N-acylated species of phosphatidylethanolamine (PE), called N-arachidonoyl-PE. This reaction is initiated by activating neurotransmitter receptors and/or by elevating intracellular levels of Ca^{2+} ions and is probably catalyzed by phospholipase D. The anandamide precursor, N-arachidonoyl-PE, is present at low levels in nonstimulated cells, but its formation can be stimulated by Ca^{2+} and occurs simultaneously with that of anandamide. N-arachidonoyl-PE synthesis is catalyzed by membrane-bound N-acyltransferase, which has been partially purified. (See Figures 1 and 2.)

2-Arachidonoylglycerol

In brain neurons, 2-AG formation is probably initiated by the activation of phospholipase C, which cleaves membrane phospholipids (e.g., phosphatidylinositol-4,5-bisphosphate) at the proximal phosphate ester bond, producing 1,2-diacylglycerol. This intermediate is broken down by diacylglycerol lipase to yield 2-AG and free fatty acid. Another pathway of 2-AG release might involve the hydrolytic cleavage of a phospholipid at the *sn*-1 position of the glycerol backbone, catalyzed by phospholipase A_1. This reaction yields a *sn*-2 lysophospholipid, which can be further hydrolyzed to produce 2-AG (Figure 3). Finally, 2-AG might be formed by hormone-sensitive lipase acting on triacylglycerols or by lipid phosphatases acting on lysophosphatidic acid. However, as these enzymes preferentially target lipids enriched in saturated or monounsaturated fatty acids, they are unlikely to play a role in the synthesis of a polyunsaturated species such as 2-AG.

Physiological Regulation of Endocannabinoid Synthesis

Anandamide

Anandamide synthesis is initiated by intracellular Ca^{2+} rises and/or by activation of G protein-coupled receptors. For example, activation of vanilloid receptors elevates intracellular Ca^{2+} levels and stimulates anandamide synthesis in rat sensory neurons in culture. In addition, activation of dopamine D_2-receptors enhances anandamide release in the brain striatum of the rat *in vivo*. The molecular steps involved in these effects have not yet been clarified.

2-Arachidonoylglycerol

2-AG formation is also linked to intracellular Ca^{2+} rises. For example, in freshly dissected slices of rat hippocampus, electrical stimulation of the Schaffer collaterals (a glutamatergic fiber tract that projects from CA3 to CA1 neurons) produces a fourfold increase in 2-AG levels, which is prevented by the Na^+ channel blocker tetrodotoxin or by removing Ca^{2+} from the medium. It is notable that anandamide levels are not changed by the stimulation, suggesting that the syntheses of 2-AG and anandamide can be independently regulated. This idea is supported by the fact that activation of D_2 receptors, a potent stimulus for anandamide release in the rat striatum, has no effect on striatal 2-AG levels.

Deactivation

In the brain and other tissues, anandamide and 2-AG are rapidly eliminated through a two-step process consisting of uptake into cells and enzymatic hydrolysis.

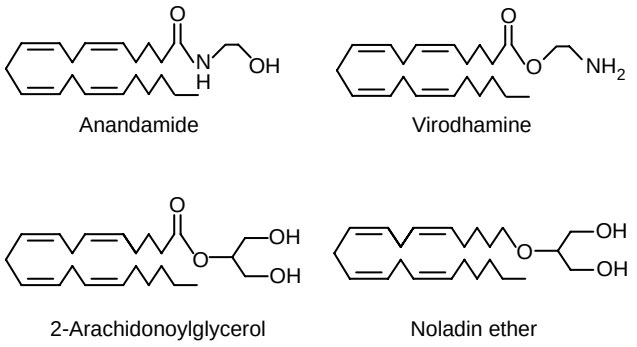

FIGURE 1 Chemical structures of the endocannabinoids anandamide (arachidonoylethanolamide), 2-arachidonoylglycerol (2-AG), noladin ether, and virodhamine.

The two endocannabinoids share a functionally similar transport mechanism, but they follow distinct routes of intracellular degradation.

Transport into Cells

The transport of anandamide and 2-AG into neurons and astrocytes is structurally specific, displays classical saturation kinetics, and is selectively inhibited by compounds such as N-(4-hydroxyphenyl)-arachidonamide (AM404). The putative transporter involved has not yet been identified, but transport has been shown to be Na^+-independent, which is suggestive of a facilitated diffusion mechanism.

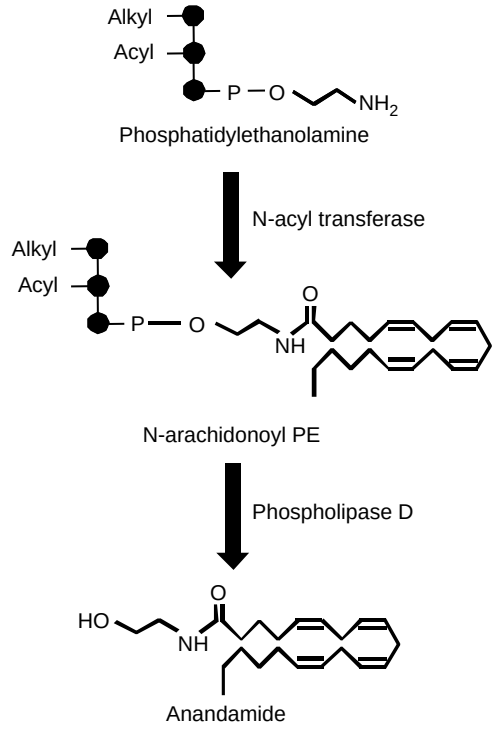

FIGURE 2 Anandamide biosynthesis. PE, phosphatidylethanolamine.

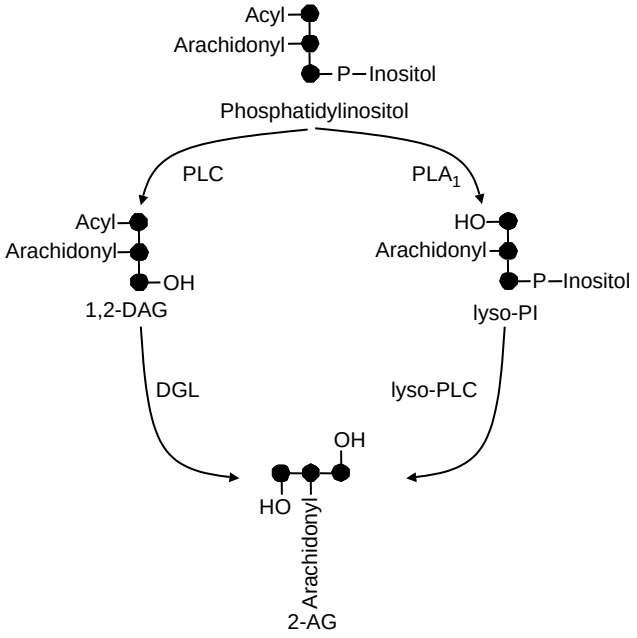

FIGURE 3 2-AG biosynthesis. 1,2,-DAG, 1,2- diacylglycerol; DGL, diacylglycerol lipase; PL, phospholipase.

Intracellular Hydrolysis

Inside cells, anandamide is metabolized by fatty acid amide hydrolase (FAAH), a membrane-bound intracellular serine hydrolase that also cleaves oleoylethanolamide, an endogenous satiety factor, and other lipid amides. Hydrolysis of 2-AG is catalyzed instead by monoglyceride lipase (MGL), a cytosolic serine hydrolase that converts 2- and 1-monoglycerides into fatty acid and glycerol. The contribution of other lipases to 2-AG degradation cannot be excluded at present.

Cannabinoid Receptors

The endocannabinoids regulate the function of multiple organs and tissues of the body. These regulatory effects are primarily mediated by two G protein-coupled receptors: CB_1 and CB_2. CB_1 is highly expressed in the central nervous system, but is also present at lower levels in a variety of peripheral tissues. By contrast, CB_2 is mostly found in immune cells such as lymphocytes. Both subtypes are linked to G_i/G_o proteins and can initiate signaling events typical of these transducing proteins, which include inhibition of adenylyl cyclase activity, opening of K^+ channels, closing of Ca^{2+} channels, and stimulation of protein kinase activities. Nevertheless, CB_1 and CB_2 are structurally different (they have only 44% sequence homology), which has allowed the development of subtype-selective ligands such as the CB_1 antagonist SR141716A (rimonabant) and the CB_2 antagonist SR144528. There is evidence for the

existence of at least two additional cannabinoid-sensitive sites in the brain and vasculature, which remain however uncharacterized.

Functions

In broad terms, the endocannabinoids are considered paracrine mediators, substances that act on cells near their sites of synthesis without entering the bloodstream. For example, they are formed by circulating leukocytes and platelets during hypotensive shock and induce the vascular relaxation that accompanies this phenomenon by activating CB_1 receptors on the surface of smooth muscle cells. Similar paracrine actions occur in the brain, where the endocannabinoids mediate a localized signaling mechanism through which neurons modify the strength of incoming inputs. The endocannabinoids are generated by neuronal depolarization and travel backward across the synapse to regulate the release of neurotransmitters from neighboring axon terminals, a process called retrograde signaling.

See Also the Following Articles

Adenylyl Cyclases • G Protein-Coupled Receptor Kinases and Arrestins • Neurotransmitter Transporters • Phospholipase C

Glossary

arachidonic acid Common name for eicosatetraenoic acid (eicosatetraenoic acid, $20{:}4\Delta^{5,8,11,14}$), an essential fatty acid that serves as metabolic precursor for eicosanoids and endocannabinoids.

axon terminal Specialized structure of a neuron that secretes neurotransmitters.

G proteins Heterotrimeric proteins with GTPase activity that link the occupation of certain cell surface receptors to cellular responses.

neurotransmitter Substance secreted by a neuron at a synapse.

phospholipase A group of enzymes that catalyze the hydrolysis of phospholipids at their glycerol ester (PLA) of phosphodiester (PLC, PLD) bonds.

protein kinase Enzyme that transfers a phosphate group from ATP to a protein.

stereospecific numbering (sn) A convention on how to designate the stereochemistry of glycerol-based lipids. When the glycerol moiety is drawn with the secondary hydroxyl to the left, the carbons are numbered 1,2,3 from top to bottom.

striatum A subcortical brain structure involved in the control of movement, habit learning, and the rewarding properties of drugs of abuse.

synapse Specialized junction between the ending of the presynaptic neuron and the dendrite, cell body, or axon of a postsynaptic neuron.

vanilloid receptor A receptor channel permeable to monovalent cations and activated by heat, acid, and capsaicin, the active ingredient of chili peppers.

Further Reading

Devane, W. A., Hanus, L., Breuer, A., Pertwee, R. G., Stevenson, L. A., Griffin, G., Gibson, D., Mandelbaum, A., Etingers, A. and Mechoulam, R. (1992). Isolation and structure of a brain constituent that binds to the cannabinoid receptor. *Science* **258**, 1946–1949.

Di Marzo, V., Fontana, A., Cadas, H., Schinelli, S., Cimino, G., Schwartz, J. C. and Piomelli, D. (1994). Formation and inactivation of endogenous cannabinoid anandamide in central neurons. *Nature* **372**, 686–691.

Piomelli, D. (2003). The molecular logic of brain endocannabinoid signaling. *Nat. Neurosci. Rev.* **4**, 873–884.

Wagner, J. A., Varga, K. and Kunos, G. (1998). Cardiovascular actions of cannabinoids and their generation during shock. *J. Mol. Med.* **76**, 824–836.

Biography

Daniele Piomelli is a Professor in the Department of Pharmacology at the University of California, Irvine. His principal research interest is in the field of lipid signaling, including the endocannabinoids. He holds a doctorate in pharmacy from the University of Naples (Italy) and a Ph.D. in pharmacology from Columbia University, New York. He served as postdoctoral fellow at the Rockefeller University, New York, and worked at the INSERM, Paris, and at the Neurosciences Institute in La Jolla, California. He is a member of the American College of Neuropsychopharmacology.

Endocytosis

Julie G. Donaldson
National Heart, Lung, and Blood Institute, National Institutes of Health, Bethesda, Maryland, USA

Endocytosis is a process carried out by all eukaryotic cells that involves the invagination of the cell surface membrane and constricted closure to form a vesicle that enters the cell interior. Included in the internalized vesicle are extracellular fluid and plasma membrane proteins and lipids. Endocytosis enables the cell to take up extracellular nutrients, remove activated receptors from the cell surface, and turnover cell surface proteins and lipids. Endocytosis is also used for the removal of extracellular debris such as dead cells and bacteria, and as a cellular port of entry for infectious bacteria and viruses. Endocytosis can be broadly divided into pinocytosis (cell drinking) and phagocytosis (cell eating) (Figure 1). There are several types of pinocytosis. The best-characterized type is that involving endocytosis of vesicles coated on the cytoplasmic surface with a protein called clathrin. Phagocytosis involves ingestion of particles by extension and wrapping of plasma membrane around the particle, bringing it into the cell. After internalization, the endocytosed material meets different fates: degradation, recycling back to the cell surface, or routing to other destinations within the cell.

Clathrin-Mediated Endocytosis

Endocytosis that is associated with clathrin coating enables certain plasma membrane proteins to be concentrated and efficiently internalized (Figure 1A). The transferrin receptor and low-density lipoprotein (LDL) receptor are cell surface proteins that are internalized by this mechanism, carrying iron-loaded transferrin protein and cholesterol-bearing LDL particles bound to these receptors into the cell. The clathrin coat that assembles on these structures forms a distinctive basket-like structure that can be visualized by electron microscopy. The polymerization of the clathrin coat is believed to facilitate changes in membrane curvature, deformation of the surface membrane, and formation of the vesicle. Once the vesicle has separated from the cell surface (fission), the clathrin coat is rapidly shed and then reutilized for additional endocytic events. Clathrin-coated pits cover 2% of the plasma membrane and since they are believed to have a lifetime of ~1 min, ~2% of the cell surface membrane is internalized each minute in the average cell. Clathrin-mediated endocytosis accounts for the bulk of pinocytosis in most cells. Clathrin assembly onto membrane requires the prior binding of a set of cytosolic adaptor proteins onto the plasma membrane.

Adaptor Proteins

The clathrin adaptor protein 2 complex (AP2) is composed of four different cytosolic proteins that bind to specific lipids and proteins at the plasma membrane and to clathrin, thus initiating clathrin assembly at distinct sites along the cell surface. There are three additional AP complex proteins in cells that associate with other cellular membranes such as the Golgi complex where they also facilitate clathrin assembly. One of the subunits of AP2 specifically binds to tyrosine-based, amino acid sorting signals in the cytoplasmic regions of plasma membrane proteins. The transferrin receptor contains such a tyrosine signal that sorts transferrin receptor into forming clathrin-coated PM vesicles enabling the transferrin receptor to be efficiently and rapidly internalized into cells. The ability to concentrate specific surface cargo proteins into clathrin-coated pits is the hallmark of clathrin-mediated endocytosis (Figure 2). There are other amino acid sorting signals that allow for rapid internalization via clathrin endocytosis including paired leucine and/or isoleucine residues. Plasma membrane proteins that contain these sorting sequences are continually brought into cells by clathrin-mediated endocytosis. Some hormone receptors such as the β2-adrenergic receptor lack these sorting sequences and do not appreciably enter clathrin-coated vesicles in the absence of hormonal stimulation. However, when the receptor is activated by a hormone, a special adaptor protein called β-arrestin binds to the receptor, allowing the receptor–arrestin complex to associate with AP2 and be rapidly internalized by the clathrin-dependent pathway.

Dynamin

The final step in endocytosis is membrane fission that allows the vesicle to detach from the cell surface. A GTP-binding protein called dynamin facilitates this process

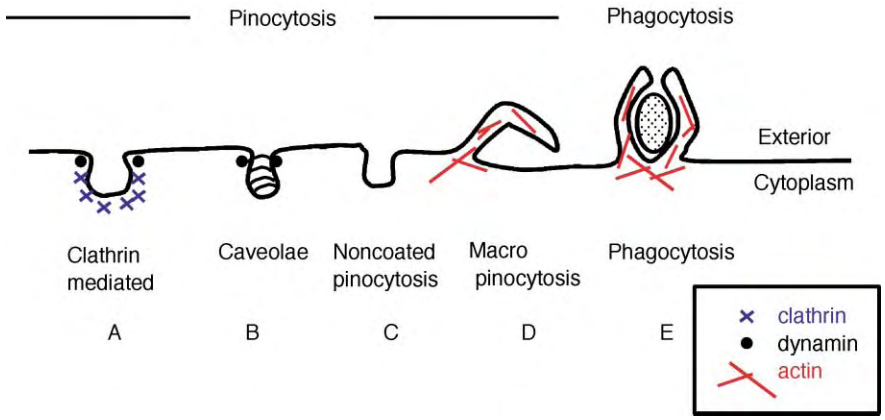

FIGURE 1 Types of endocytosis. Features of the various types of endocytosis (pinocytosis and phagocytosis) are shown. (A) Clathrin-mediated pinocytosis is associated with a cytosolic coat of clathrin (X) and uses dynamin (black spots) for vesicle fission. (B) Caveolae are flask-shaped structures coated with caveolin that also use dynamin for vesicle fission. (C) Non-coated pinocytosis involves invagination of membrane that does not have a recognizable protein coat. (D) Macropinocytosis is associated with cell surface actin-dependent protrusions and forms by fusion of the protruding membrane back onto the cell surface. (E) Phagocytosis is a process that is stimulated by an extracellular particle that induces actin-dependent cell extensions to envelope the particle.

by assembling into ring-like structures and constricting at the necks forming clathrin-coated vesicles. Mutations in dynamin, originally described for *Drosophila melanogaster* mutants, freeze clathrin-forming vesicles at the constricted state and the vesicles are not released. All clathrin-mediated and some other types of endocytosis are dependent upon the function of dynamin. Dynamin also associates with other factors that may facilitate the fission process. Rearrangements in membrane lipids and changes in lipid composition also contribute to the changes in membrane curvature required for vesicle budding and vesicle fission.

Clathrin-Independent Endocytosis

Several other types of pinocytosis have been identified that are not associated with clathrin coats. We know less about the mechanisms of these processes and how they are regulated. Plasma membrane proteins that lack the

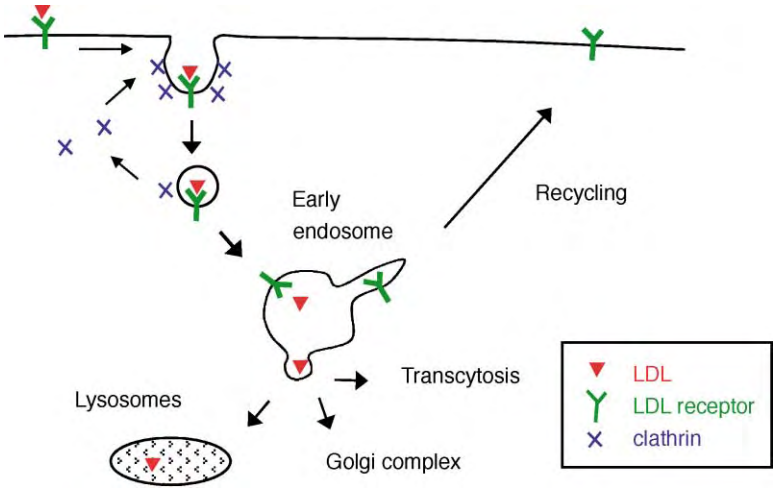

FIGURE 2 Itinerary of internalized cell surface receptors and vesicle contents. Shown here is the pathway followed by internalized LDL bound to the LDL receptor. Cell surface–LDL receptor binds to LDL and is sorted into forming clathrin-coated vesicles at the plasma membrane. After vesicle fission, the clathrin coat is rapidly released from the vesicle so it can assemble again onto the plasma membrane. The vesicle membrane then fuses with the early endosome, a membrane compartment that serves as a sorting station for membrane proteins and lipids. The low pH of the early endosome causes release of LDL from its receptor. The LDL particle and other molecules present in the fluid portion of the early endosome can then be routed to lysosomes for degradation. The LDL receptor enters regions of the early endosome that break off and carry these receptors and membrane back to the plasma membrane. Some membrane proteins leave the early endosome and are transported to other regions of the plasma membrane (transcytosis) or to the Golgi complex.

cytoplasmic amino acid sequences specifying association with AP2 and clathrin, can be endocytosed into cells by these processes.

Caveolae

Some proteins associate with cholesterol and glycosphingolipid-enriched regions of the plasma membrane referred to as membrane raft domains. In many cells, especially in endothelial cells that line blood vessels, these raft domains are present in flask-shaped invaginations of the plasma membrane. These flask-shaped invaginations are called caveolae (caves), and the cytoplasmic coat protein associated with these structures that give them their distinctive shape is called caveolin (Figure 1B). Caveolar endocytosis is dependent upon dynamin and is used as an endocytic mechanism for the transport of materials across endothelial cells. Interestingly, simian virus 40 stimulates caveolar endocytosis and enters many types of cells through this mechanism. Finally, there are cells that lack caveolin and hence caveolae and yet endocytose proteins that associate with membrane raft domains.

Noncoated Endocytosis and Macropinocytosis

Plasma membrane proteins and lipids are also observed in invaginations budding from the membrane that lack any identifiable protein coat (Figures 1C and 1D). This process may or may not require dynamin function depending upon the cell type. Although this process may account for a smaller fraction of cell-surface endocytosis than clathrin-mediated endocytosis, it can be greatly stimulated when cells get activated and form membrane ruffles and protrusive structures. In this case, the membrane ruffle can fuse with the plasma membrane forming a large, macropinosome that internalizes a large amount of surrounding fluid. Dendritic cells of the immune system are very active in macropinocytosis as a means of sampling foreign material in the extracellular fluid. Macropinosome formation is actin dependent. Some bacteria, notably *Salmonella typhi*, stimulate host cells to form membrane ruffles and macropinosomes, and then use these structures as a port of entry into the cells.

Phagocytosis

In lower eukaryotes, such as protozoa, this process of particle ingestion is used for nutrient uptake. However, in mammals phagocytosis is observed in specialized cell types, namely, macrophages and neutrophils that ingest bacteria and dead cells and degrade them. When a macrophage encounters a bacterium that has been coated with antibodies generated by the immune system, cell surface receptors that recognize the Fc portion of the antibodies get activated. This stimulates changes in the macrophage actin cytoskeleton and leads to the extension of membrane around the bacteria, and final closure of the structure through membrane fusion (Figure 1E). Macrophages are also active in phagocytosing senescent-red blood cells and other cells that have undergone programmed cell death. It is believed that macrophages can detect alterations on the cell surface of the senescent cell, such as appearance of a phospholipid on the outer surface that is normally present only on the cytoplasmic side of the plasma membrane. After phagocytosis, the resulting phagosome usually fuses with lysosomes and membrane-bound organelles that contain hydrolytic enzymes that degrade the bacteria. However, some bacteria such as *Mycobacterium tuberculosis*, can actively prevent the fusion of the phagosome with lysosomal membranes, and hence escape degradation.

Fate of Internalized Membrane and Content

After endocytosis, the endocytic vesicle usually fuses with a membrane-bound structure called the early endosome (Figure 2). The early endosome accepts newly endocytosed material and serves as a sorting station that directs incoming proteins and lipids to their final destination. The early endosomal membrane contains a special membrane lipid, phosphatidylinositol 3-phosphate that recruits cytosolic proteins onto these membranes and facilitates the fusion of incoming vesicles with the early endosome. The interior, lumenal environment of the early endosome is moderately acidic (pH 6.5–6.0). The low pH facilitates the sorting process, releasing bound proteins from their receptors and sorting membrane proteins and lipids into different domains. A good example of how low pH serves this function is the itinerary of the transferrin receptor that carries iron-saturated transferrin into the cell. The acidic environment of the early endosome causes the release of iron from transferrin. The iron is then transferred across the membrane into the cytosol, while the transferrin bound to the transferrin receptor is recycled back to the cell surface via membrane carriers that are released from the early endosome. Another example of this sorting of incoming material is the fate of internalized LDL particles bound to the LDL receptor (shown in Figure 2). LDL is released from the receptor in the early endosome and is transferred with other lumenal material to late endosomes and lysosomes. There the LDL is degraded, causing cholesterol

release inside the cell. Meanwhile, the LDL receptor returns to the cell surface to carry out additional rounds of endocytosis. For the transferrin and LDL receptors, endocytosis is a mechanism for delivery of iron and LDL into the cell. By contrast, for signaling receptors, such as those activated by hormones and growth factors, endocytosis is generally used to halt the signaling process by removal of the receptor from the cell surface. An exception to this is the recent observation that the epidermal growth factor (EGF) receptor may require endocytosis for some signaling functions.

Endocytosed membrane proteins can be transported to different locations in the cell (Figure 2). Some membrane proteins are sorted into vesicles that fuse to another region of the plasma membrane, a process called transcytosis. Mucosal immunoglobulins such as IgA are transcytosed across intestinal epithelia via IgA receptors that ferry IgA from the basal (serosal) side to the apical (mucosal) surface of the epithelia. Other proteins leave the early endosome in vesicles that fuse with membranes adjacent to the *trans* side of the Golgi complex.

Regardless of how a membrane is brought into the cell, it must be balanced by addition of membrane back to the plasma membrane. This is accomplished by endosomal-membrane recycling and also through the contribution of newly synthesized membranes from the secretory pathway. The cell has to regulate and coordinate the flux of membrane into and out of the cell to maintain cell surface area and for proper localization of important cell surface receptors.

See Also the Following Articles

Epidermal Growth Factor Receptor Family • Glycoprotein Folding and Processing Reactions • Lipoproteins, HDL/LDL

Glossary

caveolae Flask-shaped invaginations from the plasma membrane that are enriched in cholesterol and glycosphingolipids and are coated with the protein caveolin.

clathrin Cytosolic protein that polymerizes into basket-like coat complex on membranes, facilitating deformation of the plasma membrane to form a vesicle.

dynamin GTP-binding protein that assembles at the necks of forming vesicles and facilitates the fission of membranes to release the vesicle.

phagocytosis Endocytic process involving particle ingestion through extension of cell-surface membranes around particle (typically >250 nm in diameter) and membrane fusion to form phagosome.

pinocytosis Endocytic process involving invaginations of the plasma membrane to generate small (~ 100 nm in diameter) intracellular vesicles.

Further Reading

Alberts, B., Johnson, A., Lewis, J., Raff, M., Roberts, K., and Walter, P. (2002). *Molecular Biology of the Cell*, 4th edition, Garland Science, New York.

Conner, S. D., and Schmid, S. L. (2003). Regulated portals of entry into the cell. *Nature* **422**, 37–44.

Lodish, H., Berk, A., and Zipursky, L. (1999). *Molecular Cell Biology*, 4th edition, W.H. Freeman, New York.

Marsh, M. (ed.) (2001). *Endocytosis*. Oxford University Press, New York.

Slepnev, V. I., and DeCamilli, P. (2000). Accessory factors in clathrin-dependent synaptic vesicle endocytosis. *Nat. Rev. Neurosci.* **1**, 161–172.

Sorkin, A., and von Zastrow, M. (2002). Signal transduction and endocytosis: Close encounters of many kinds. *Nat. Rev. Mol. Cell Biol.* **3**, 600–614.

Biography

Julie G. Donaldson is a Senior Investigator in the Laboratory of Cell Biology in the National Heart, Lung, and Blood Institute at the National Institutes of Health in Bethesda, Maryland. Her research interests are in understanding the mechanisms and regulation of endosomal and secretory membrane traffic in the cell. She holds a Ph.D. from the University of Maryland and was a Postdoctoral Fellow in the National Institute of Child Health and Human Development prior to her current position.

Endoplasmic Reticulum-Associated Protein Degradation

Maurizio Molinari
Institute for Research in Biomedicine, Bellinzona, Switzerland

For proper functioning, a protein has to fold into a characteristic three-dimensional structure and may have to form a multimeric complex. The endoplasmic reticulum (ER) provides an environment optimized for the folding and assembly of proteins that will then be secreted (hormones, antibodies, pancreatic enzymes, etc.), or displayed at the plasma membrane (receptors, channels, etc.), or that reside in intracellular compartments such as the lysosomes and the Golgi. Only native proteins leave the ER to be transported along the secretory pathway to their final destination. A quality control system is in place to prevent forward transport of polypeptides for which folding and assembly have failed. To prevent their accumulation in the lumen of the ER, a series of events regulated by luminal and cytosolic components, and collectively named ER-associated protein degradation (ERAD) ensures that terminally misfolded polypeptides are transferred into the cytosol to be degraded by the 26S proteasome. This article summarizes recent advances in understanding how malfolded glycoproteins are cleared from the ER lumen of mammalian cells.

Protein Synthesis and Folding in the ER

In mammalian cells, secreted proteins are expressed by ribosomes attached at the cytosolic face of the endoplasmic reticulum (ER) at an average synthesis rate of three to five amino acids per second. Nascent chains are translocated into the ER lumen and most of them become N-glycosylated upon addition of pre-assembled, branched oligosaccharides (N-glycans) at asparagines in Asn–Xaa–Ser/Thr sequons. The highly hydrophilic N-glycans preserve the solubility of yet unstructured chains likely to expose hydrophobic, aggregation-prone patches. Moreover, they are the ligands of calnexin and calreticulin, two lectin chaperones that make nascent chains accessible to ERp57. ERp57 is an oxidoreductase that catalyzes the formation of disulfide bonds, a rate-limiting step of the folding process peculiar for proteins expressed in the ER. As thoroughly reviewed by Armando Parodi and Ari Helenius, calnexin, calreticulin and ERp57, together with the sugar-processing enzymes glucosidase I and II and UDP-glucose:glycoprotein glucosyltransferase (GT) compose the calnexin/calreticulin cycle, a chaperone network that assists folding and quality control of glycoproteins.

The kinetics and the efficiency of the folding process are highly variable and depend on the substrate protein considered, and on the cell type where folding occurs. Somewhat surprisingly, the folding of heterologous proteins may be faster and significantly more efficient compared to the maturation of cell-self proteins. So it may take only ten minutes for a viral glycoprotein (e.g., influenza virus hemagglutinin) to complete the folding and oligomerization processes and to leave the ER with an efficiency approaching 100%. On the other hand, it may take several hours before ~20% of the cystic fibrosis channel (CFTR) expressed in the ER lumen becomes native and leaves the compartment. About 80% of the wild-type CFTR is produced just to be degraded, a fate probably shared with a significant fraction of any cellular protein. In some cases, degradation may actually start even before the synthesis of a given polypeptide has been completed. This has no consequences for cell viability and ER-associated protein degradation (ERAD) actually plays an important regulatory role, as shown by Randy Hampton for the HMG-CoA reductase, a rate-limiting enzyme for production of sterols and a variety of essential isoprenoids, whose intracellular level is controlled, at least partially, by regulated degradation.

Folding efficiency may drop substantially, and can be the cause of impaired cell, organ, and/or organism viability when genetic mutations occur that change or delete amino acids in polypeptides (e.g., deletion of phenylalanine at position 508 of the CFTR). If the mutated protein cannot fold properly, it will not fulfill the quality control standard for ER exit and will eventually become a substrate of the ERAD machinery.

Diseases Related to Failure of Protein Folding and Quality Control in the ER

An increasing number of strongly debilitating human diseases has been ascribed to defective protein folding and quality control. Together with cystic fibrosis, one could mention the hereditary lung emphysema and liver failure caused by alpha1-antitrypsin deficiency, diabetes mellitus caused by retention and degradation from the ER of mutant insulin receptors, familial hypercholesterolemia (low-density lipoprotein receptor), osteogenesis imperfecta (type I procollagen), retinitis pigmentosa, and several neurodegenerative diseases. In these so-called "conformational diseases," mutated proteins that do not acquire their native structure are diverted to ERAD. If their disposal is not efficient, they accumulate intra- or extracellularly triggering severe damages to cells and tissues. In some cases, such as the hereditary lung emphysema caused by alpha1-antitrypsin deficiency (alpha1-antitrypsin is the principal blood-borne inhibitor of the destructive neutrophil elastase in the lungs), the lack-of-function phenotype observed at the level of patient's lungs is accompanied by a gain-of-toxic-function phenotype at the level of the patient's liver because the mutated protein accumulates in the ER of hepatocytes.

Degradation of Aberrant Proteins Expressed in the ER: The Mannose Timer

But how are polypeptides recognized as being "non-native," retained in the ER, and targeted for ERAD? The mechanisms, better known for glycoproteins and named GERAD for glycoprotein ERAD by Rick Sifers, are summarized in the following paragraphs.

The quality control machinery of the ER checks the structure and not the function of newly synthesized proteins. Therefore, function-competent proteins can be retained in the ER and destroyed because they are structurally imperfect, as exemplified by the case of the ΔPhe508 CFTR.

The modification of N-glycans can determine the fate of newly synthesized glycoproteins. Glycans are added as preassembled units composed of two N-acetyl-glucosamine, nine mannose, and three glucose residues. Two glucoses are removed in a matter of seconds after addition of the N-glycan to nascent chains. In the minutes following the synthesis of a glycoprotein, the number of glucoses on N-glycans can vary from zero to one in response to the counteracting enzymatic activities of glucosidase II and GT. These modifications control cycles of dissociation from/association with the lectin chaperones, calnexin and calreticulin (as described in Armando Parodi's review). How long newly synthesized proteins are retained in the calnexin/calreticulin cycle depends on their rate of folding. N-glycans of native glycoproteins are inaccessible to GT; they are therefore not re-glucosylated so that mature proteins exit the folding cycle, leave the ER, and are transported along the secretory pathway.

In this model, proteins unable to fold properly persist in the calnexin/calreticulin cycle. To prevent accumulation of aberrant polypeptides in the ER, the terminally misfolded polypeptides have to be released from the calnexin/calreticulin cycle and targeted for degradation. After several unsuccessful folding attempts, N-glycans become substrates of ER-resident mannosidases. Therefore, long retention in the ER as signaled by a reduced number of mannose residues on N-glycans is a clear symptom of a problematic folding. It has originally been proposed by Helenius in 1994 that a timer based on mannose cleavage exists in the ER that decides when it is time to stop folding attempts and to divert unlucky polypeptides for degradation. The timer function that mannosidase activities play during ER quality control is supported by findings which show that cleavage of mannoses from the N-glycans has to take place for GERAD to proceed (as first shown by Green and then elucidated by Sifers, mannosidase inhibitors interfere potently and specifically with GERAD). It is conceivable that GERAD candidates are subjected to folding attempts and remain shielded from the degradation machinery while in the calnexin/calreticulin cycle. Accordingly, the degradation of glycoproteins is usually preceded by a lag phase whose length is determined by the retention of the GERAD candidates in association with the ER lectins.

Distinct ER Chaperone Networks are Involved in the GERAD Process

Involvement of at least two distinct chaperone networks (the calnexin/calreticulin cycle and the BiP/PDI system) has been shown (by the groups of Rick Sifers and Maurizio Molinari) to regulate degradation of GERAD candidates in mammalian cells. Interestingly, misfolded glycoproteins remain in the calnexin/calreticulin cycle when degradation is blocked by mannosidase inhibitors; they are released from the lectin chaperones to remain trapped in the BiP/PDI system, in the lumen of the ER when the proteasome activity is specifically shut down. These data show that the two chaperone networks work sequentially and offer the appealing view that GERAD

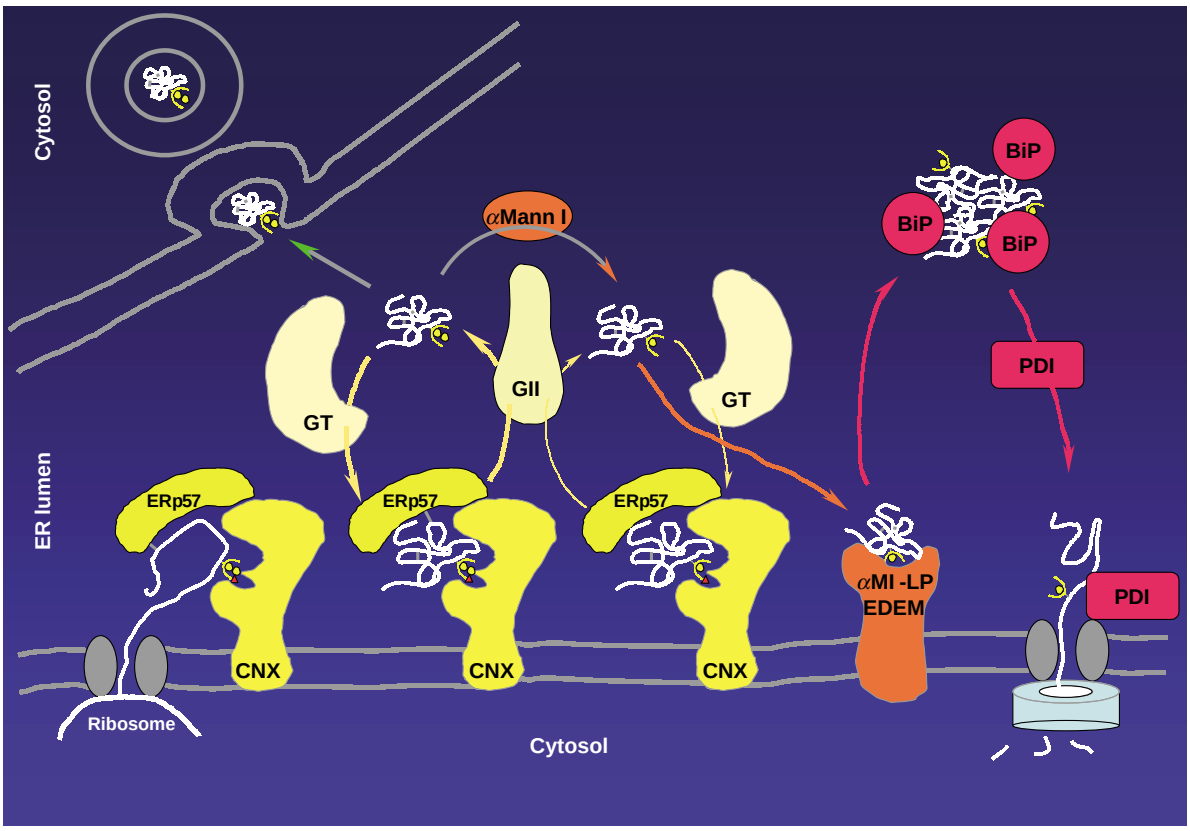

FIGURE 1 The GERAD mechanism can be divided into four steps. First, the GERAD candidate is subjected to folding attempts in the calnexin cycle. Second, the folding-incompetent protein is extracted from the calnexin cycle by the concerted activity of a mannose-trimming enzyme (the ER α-mannosidase I) and a mannose-binding lectin (EDEM). Third, the aberrantly folded polypeptide has to be unfolded (e.g., the wrong disulfide bonds formed during the folding attempts have to be reduced) in order to (fourth) allow dislocation of the GERAD candidate across the ER membrane to be degraded by the proteasome.

candidates are first subjected to folding attempts in the calnexin/calreticulin cycle (lag between synthesis and degradation onset) to be then transferred into the BiP/PDI system that would regulate unfolding and dislocation of the aberrant polypeptide into the cytosol for proteasome-mediated degradation (Figure 1).

A Role for a Mannose-Binding Lectin in GERAD

Mechanistically, the sequential cleavage of mannoses affects the retention of the aberrant protein in the calnexin/calreticulin cycle by decreasing the capacity of glucosidase II and GT to further re- and de-glucosylate the sugar moiety associated with a misfolded chain. Moreover, at least one mannose-binding lectin (EDEM for ER degradation enhancing alpha mannosidase-like protein) is present in the ER lumen and is involved in recognition of aberrant proteins carrying N-glycans with a reduced number of mannose residues, and in deviating them from the folding into the GERAD machinery. The role of EDEM as an acceptor of misfolded glycoproteins released from the calnexin/calreticulin cycle has been recently elucidated by the groups of Kazuhiro Nagata and Maurizio Molinari. It has actually been shown that the intracellular level of EDEM regulates kinetics of the GERAD process by determining the permanence of misfolded proteins in the calnexin cycle. Importantly, as shown by Kazutoshi Mori, the level of EDEM is adapted to the cargo load of the ER, so as to ensure, at any time, optimal disposal of wastes produced during secretory protein synthesis and to prevent processes, which may ultimately lead to cell death through intracellular accumulation of malfolded proteins. Whether EDEM represents the last acceptor of ERAD candidates before their dislocation into the cytosol for proteasome-mediated degradation, or if EDEM regulates the transfer of GERAD candidates from the folding into the unfolding cycles driven by the ER lectins and by the BiP/PDI system, respectively, remains an open question.

See Also the Following Articles

Chaperones, Molecular • Glycoprotein Folding and Processing Reactions • *N*-Linked Glycan Processing

Glucosidases and Mannosidases • Protein Degradation • Protein Folding and Assembly • 26S Proteasome, Structure and Function • Proteoglycans

Glossary

calnexin and calreticulin Calnexin is a nonglycosylated, type I protein of the ER membrane with 573 amino acids. Most of them are in the lumen of the ER and comprise a glucose-binding site for transient association with folding substrates and a P-domain for noncovalent association with the co-chaperone ERp57; 89 residues are cytosolic and contain a RKPRRE ER-retention sequence. Calreticulin is the soluble homologue of calnexin; it has 400 amino acids with a KDEL ER-retrieval sequence.

EDEM *E*R *d*egradation *e*nhancing α-*m*annosidase-like protein is a type II glycoprotein of the ER membrane that shares sequence homology with ER mannosidases. It has, however, no enzymatic activity possibly because it lacks two cysteines conserved in all active mannosidases. The intracellular level of EDEM is increased in response to accumulation in the lumen of the ER of misfolded proteins.

ERAD ER-associated protein degradation (also GERAD for glycoproteins), the processes leading to recognition of misfolded proteins present in the ER lumen and their dislocation into the cytosolic compartment for proteasome-mediated destruction.

quality control The capacity of cells to distinguish and retain in the ER lumen to be eventually targeted for degradation, proteins that have structural defects.

Further Reading

Cabral, C. M., Liu, Y., and Sifers, R. N. (2001). Dissecting glycoprotein quality control in the secretory pathway. *Trends Biochem. Sci.* **26**, 619–624.

Cabral, C., Liu, Y., Moremen, K. W., and Sifers, R. N. (2002). Organizational diversity among distinct glycoprotein ER-associated degradation programs. *Molecul. Biol. Cell* **13**, 2651–2663.

Ellgaard, L., Molinari, M., and Helenius, A. (1999). Setting the standards: Quality control in the secretory pathway. *Science* **286**, 1882–1888.

Hampton, R. Y. (2002). ER-associated degradation in protein quality control and cellular regulation. *Curr. Opin. Cell Biol.* **14**, 476–482.

Helenius, A. (1994). How N-linked oligosaccharides affect glycoprotein folding in the endoplasmic reticulum. *Molecul. Biol. Cell* **5**, 253–265.

Hosokawa, N., Wada, I., Hasegawa, K., Yorihuzi, T., Tremblay, L. O., Herscovics, A., and Nagata, K. (2001). A novel ER {alpha}-mannosidase-like protein accelerates ER-associated degradation. *EMBO Rep.* **2**, 415–422.

Molinari, M., Galli, C., Piccaluga, V., Pieren, M., and Paganetti, P. (2002). Sequential assistance of molecular chaperones and transient formation of covalent complexes during protein degradation from the ER. *J. Cell Biol.* **158**, 247–257.

Molinari, M., Calanca, V., Galli, C., Lucca, P., and Paganetti, P. (2003). Role of EDEM in the release of misfolded glycoproteins from the calnexin cycle. *Science* **299**, 1397–1400.

Oda, Y., Hosokawa, N., Wada, I., and Nagata, K. (2003). EDEM as an acceptor of terminally misfolded glycoproteins released from calnexin. *Science* **299**, 1394–1397.

Parodi, A. J. (2000). Protein glucosylation and its role in protein folding. *Annu. Rev. Biochem.* **69**, 69–93.

Parodi, A. J. (2000). Role of N-oligosaccharide endoplasmic reticulum processing reactions in glycoprotein folding and degradation. *Biochem. J.* **348**, 1–13.

Yoshida, H., Matsui, T., Hosokawa, N., Kaufman, R. J., Nagata, K., and Mori, K. (2003). A time-dependent phase shift in the mammalian unfolded protein response. *Dev. Cell* **4**, 265–271.

Biography

Maurizio Molinari obtained a Ph.D. from the ETH in Zurich, Switzerland, under the guidance of Ernesto Carafoli in 1995. He then performed two postdoctoral training periods in the group of Cesare Montecucco (University of Padua, Italy), and in the group of Ari Helenius (ETH, Zurich). Since October 2000 he has been Group Leader at the Institute for Research in Biomedicine in Bellinzona, Switzerland. His research interests are in the characterization of the mechanisms of folding and degradation of proteins expressed in the endoplasmic reticulum of mammalian cells.

Energy Transduction in Anaerobic Prokaryotes

Gottfried Unden
Johannes-Gutenburg-Universität Mainz, Mainz, Germany

Many prokaryotes (bacteria and archaea) are able to grow in the absence of molecular O_2. In the absence of O_2 metabolic energy can be gained by the catabolic reactions of fermentation, anaerobic respiration, anoxygenic photosynthesis, decarboxylation of dicarboxylic acids, or electrogenic transport of substrate and product molecules. Many of the reactions are unique for prokaryotes. Anaerobic metabolism is essential for many biotopes which are permanently or occasionally anoxic. The bacteria responsible for anaerobic metabolism and mineralization are either strictly anaerobic and restricted to anaerobic biotopes, or facultatively anaerobic, using either aerobic or anaerobic metabolism depending on the O_2 supply. The facultative bacteria switch between aerobic and anaerobic metabolism by using molecular O_2 sensors, which control the expression of aerobic or anaerobic metabolic systems mostly at the transcriptional level.

ADP Phosphorylation Driven by Chemical Coupling or by the Membrane Potential

Synthesis of ATP by fermentation relies on substrate level phosphorylation, whereas the other reactions for anaerobic energy conservation use a membrane potential as the coupling device between energy-supplying and energy-consuming reactions, in particular ADP phosphorylation (Figure 1). Phosphorylation of ADP for generation of ATP requires a free energy ($\Delta G_0'$) of $\sim +50\ \mathrm{kJ\ mol^{-1}}$ under cellular conditions. This amount of free energy has to be supplied in fermentation by one chemical reaction and direct coupling. In the metabolic systems using the membrane or proton potential (Δp) as the coupling device (Figure 1), the energy-supplying reaction on the other hand has to supply only $12-17\ \mathrm{kJ\ mol^{-1}}$ per reaction which is the amount required for translocating 1 H^+ (or Na^+) across the membrane. Three or four H^+ are then used to drive ADP phosphorylation. Therefore, storing the free energy in a membrane potential is favorable for anaerobic catabolic processes which often provide only small amounts of free energy.

The overview will demonstrate, by examples, the functioning of anaerobic metabolism of prokaryotes, in particular fermentation and reactions using a membrane potential for coupling between energy-supplying and energy-consuming reactions.

Fermentation

Typical habitats for fermentation are sediments in freshwater, sewage fermenters, or the digestive tract of vertebrates and insects. Fermentation means growth in the absence of external electron acceptors or light. ADP is phosphorylated under these conditions by substrate level phosphorylation, or direct chemical coupling, without involvement of membranes or membrane potential. Most common substrates for fermentative metabolism are sugars and amino acids. The substrates are first degraded in an oxidative part of metabolism yielding pyruvate or related compounds plus NAD(P)H. For oxidation of the sugars, most bacteria use the glycolytic (Embden–Meyerhof–Parnas, EMP) pathway to pyruvate (glucose + $2NAD^+$ + 2ADP + 2 $P_i \rightarrow$ 2pyruvate + 2NADH + $2H^+$ + 2ATP). Some bacteria use the phosphoketolase (modified pentose-phosphate) pathway (glucose + $3NAD(P)^+$ + ADP + P_i + HSCoA → pyruvate + acetyl-CoA + 3NADH + $3H^+$ + 1ATP) for pyruvate formation, whereas the Entner–Doudoroff (or 2-keto-3-deoxy-6-P-gluconate, KDPG) pathway (glucose + $2NAD(P)^+$ + ADP + $P_i \rightarrow$ 2pyruvate + 2NAD(P)H + $2H^+$ + 1ATP) is found only rarely in anaerobic bacteria.

In simple fermentations pyruvate is used as the electron acceptor for reoxidation of the NAD(P)H formed in sugar oxidation, yielding lactate or ethanol as the fermentation products. In more complicated fermentation reactions (mixed acid fermentation, butyrate fermentation, and others), pyruvate is further oxidized yielding acetate and additional ATP. In these

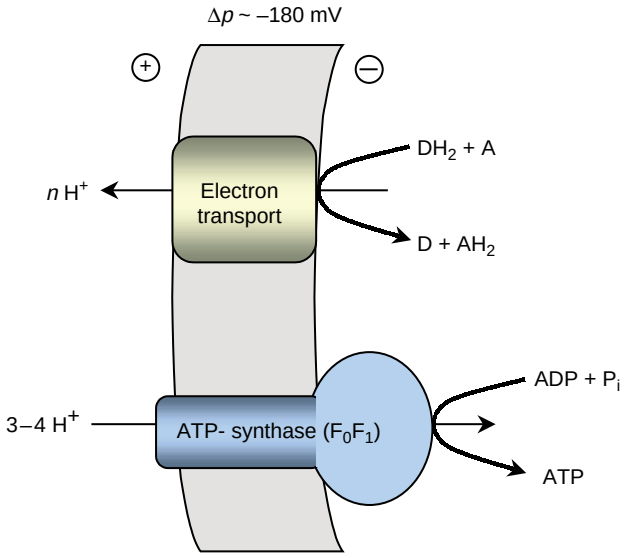

FIGURE 1 Generation of a proton potential (Δp) by translocation of protons across a cytoplasmic membrane by anaerobic respiration and coupling to ADP phosphorylation by ATP synthase. DH_2, electron donor; A, electron acceptor.

pathways butyrate or ethanol (plus acetate) can be obtained as fermentation products among others.

Typical fermentation products derived from sugars and amino acids are carboxylic acids (formate, acetate, propionate, butyrate, and lactate), alcohols (ethanol, 2-propanol, *n*-butanol, and 2,3-butandiol), but also polyols (glycerol, erythritol, and mannitol), CO_2, and H_2 (Table I). The well-known fermentation reactions of this type are homo- and heterofermentative lactic acid, propionic acid, butyric acid, mixed acid, or ethanolic fermentations which are named according to the major or characteristic products (Table I). The ATP yields of the fermentation reactions are generally in the range of 1–3 ATP mol^{-1} of hexose (compared to up to 38 ATP mol^{-1} glucose in aerobic metabolism).

The most important primary or energy-conserving reactions in fermentation are the oxidation of aldehyde to carbonates (thioester formation by glyceroaldehyde-3-phosphate dehydrogenase), the oxidative decarboxylation of α-ketoacids (thioester formation by pyruvate-ferredoxin oxidoreductase), and phosphoroklastic cleavage of ketuloses (acetyl-phosphate formation by phosphoketolase) which are all located in the oxidative part of fermentative metabolism. Reductive desamination of amino acids (acetyl-phosphate formation by glycine reductase) is an example for an energy-conserving reaction in the reductive branch of Stickland fermentation. The energy-rich products obtained from these reactions are then used finally for the phosphorylation of ADP yielding ATP.

Organic matter (polysaccharides, proteins, fats, and monomers derived thereof) can be mineralized in the absence of electron acceptors to methane and CO_2 by interaction of fermenting and methanogenic prokaryotes. The primary fermenters degrade sugars and amino acids to propionate, butyrate, succinate, lactate, acetate, alcohols, CO_2, H_2, and NH_3. H_2, CO_2, and acetate are converted by homoacetogenic and methanogenic prokaryotes to methane and CO_2. Alcohols and fatty acids (short chain fatty acids such as propionate, up to C_{18}), on the other hand, are degraded by secondary fermenters to methane and CO_2. The secondary fermenters are synthrophic bacteria which convert alcohols, fatty acids, and aromatic compounds such as benzoate to H_2, CO_2, and acetate. Secondary fermentation is an endergonic process under standard conditions (e.g., butyrate + $2H_2O \rightarrow$ 2acetate + $H^+ + 2H_2$; $\Delta G_0' = +48.2$ kJ mol^{-1} butyrate) and becomes only exergonic in the presence of syntrophic prokaryotes which consume H_2 to keep it at very low levels. By this the reaction becomes exergonic under environmental conditions ($\Delta G_{env} = -18$ kJ mol^{-1} butyrate) enabling growth of the bacteria. Acetate, H_2, and CO_2 are metabolized by methonogenic archaea and the homoacetogenic bacteria finally to methane and CO_2. In this way fatty acids, alcohols, and aromatic compounds are mineralized yielding CO_2 and methane as the final products.

TABLE I

Fermentation Products of Sugars (Primary Fermentations)

Fermentation (pathway for sugar degradation)	Products per mol glucose (ATP yield per glucose)	Bacterium or microorganism
Lactic acid, homof ermentative (EMP)	2 lactate (+2ATP)	*Lactobacillus lactis*
Lactic acid, heterof ermentative (PK)	1 lactate + 1 ethanol + $1CO_2$ (+1ATP)	*Leuconostoc*
Propionic acid (EMP)	2 propionate (+2–3ATP)	*Propionibacterium*
Butyric acid (EMP)	1 butyrate + $2CO_2$ + $2H_2$ (+3ATP)	*Clostridium butyricum*
Mix acid (EMP)	1 acetate + 1 ethanol + 2 formate (+3ATP)	*Escherichia coli*
Ethanolic (ED)	2 ethanol + $2CO_2$ (+1ATP)	*Zymomonas mobilis*
Ethanolic (EMP)	2 ethanol + $2CO_2$ (+2ATP)	*Saccharomyces cerevisiae* (yeast)

EMP, Embden–Meyerhof–Parnas pathway (glycolysis); PK, phosphoketolase pathway; ED, Entner–Doudoroff pathway.

Fermentation reactions are used on a large scale for preparation of food and beverages. The fermentation reactions and products improve food (nutritional) quality, taste, and durability. For this purpose mainly primary fermentation reactions such as ethanol (beverages), lactic acid (dairy products, vegetables, sour dough), propionic acid fermentation (cheese), and others are used. Solvent production (ethanol, propanol, butanol, and acetone) by Clostridia also depend on type I fermentations. Biotechnological processes for microbiological production of amino acids, citrate, and others, on the other hand, rely on an overflow metabolism of central pathway and anabolic reactions.

Electron Transport Phosphorylation in Anaerobic Respiration

Anaerobic respiration is able to generate an electrochemical proton potential ($\Delta p \sim -0.18$ V) over the membrane which is driven by the oxidation of an electron donor by an (mostly externally added) electron acceptor. The free energy of the redox reaction is converted to and conserved in a proton potential (Figure 1). The proton potential then drives phosphorylation of ADP and formation of ATP by ATP synthase. The Δp generating respiratory chain and the Δp consuming ATP synthase are thus coupled only by the Δp. The free energy of the redox reaction of the respiratory chain under standard conditions and pH 7 is directly related to the difference in the redox potentials of the electron donors and acceptors ($\Delta E_0'$), the Faraday constant ($F = 96.5 \times 10^3$ J mol^{-1} V^{-1}) and the number of participating electrons (n):

$$\Delta G_0' = -nF\Delta E_0'$$

Figure 2 gives a selection of important electron donors and acceptors used by prokaryotes in anaerobic respiration and the corresponding midpoint potentials. The $\Delta E_0'$ value sets the maximal (theoretical) amount of electrons (H^+/e ratio) which can be translocated across the membrane for the given Δp value (-0.18 V):

$$(H^+/e)_{max} = \Delta E_0'/\Delta p$$

The actual H^+/e ratio generally is lower than the calculated value due to lower coupling efficiency, and since some electron transport enzymes lack coupling mechanisms for H^+ translocation. From the above equations it follows that the minimal amount of free energy required for translocation of 1 H^+ across membranes ($\Delta p = -180$ mV) amounts to -17.4 kJ mol^{-1}. Thus free energy as low as $\Delta G_0' = -17$ kJ mol^{-1} can be conserved in a membrane potential by anaerobic respiration (or other Δp generating reactions) compared to $\Delta G_0'$ value of ~ -50 kJ mol^{-1} required in substrate level phosphorylation. Therefore storage of free energy in a membrane potential allows use of energy-supplying reaction with low $\Delta G_0'$ values, since 3–4 translocated H^+ or Na^+ ions are equivalent to phosphorylation of one ADP. This coupling mechanism is of particular significance for reactions of anaerobic metabolism which are only weakly exergonic.

In anaerobic respiration a large number of different electron acceptors can be used, including S^0, CO_2, sulfate, fumarate, nitrate, tetrachlorethen, and Fe^{3+} (Figure 2). The free energy, and thus the ATP yields, are distinctly lower than in aerobic respiration due to the more negative redox potentials (and thus $\Delta E_0'$ values) of the electron acceptors. Most of the anaerobic respiratory systems are composed of two enzymes, a dehydrogenase and a terminal reductase. The enzymes are linked by diffusible low molecular redox mediators (quinones). In anaerobic respiration menaquinone (MK, a lipophilic naphtoquinone derivative with $E_0' = -80$ mV) replaces ubiquinone (Q, a lipophilic benzoquinone derivative with $E_0' = +110$ mV) from aerobic respiratory chains. Figure 3 gives a schematic presentation on the topology and arrangement of enzymes in fumarate and nitrate respiration with formate as the electron donor. The biochemistry and energetics of the enzymes have been studied in detail, and the structures of the enzymes have been solved by X-ray cristallography. Each of the enzymes is anchored in the membrane with a hydrophobic anchor protein, which contains the active site for the lipophilic quinone. The second active site for the hydrophilic substrates formate, fumarate, or nitrate, is located in the cytoplasmic or periplasmic protrusions of the enzymes.

In formate:fumarate reductase respiration the enzymes catalyze the following reactions:

Formate dehydrogenase :

$$\text{Formate} + \text{MK} + 2H^+_{in} \rightarrow CO_2 + \text{MKH}_2 + 2H^+_{ex}$$

Fumarate reductase :

$$\text{Fumarate} + \text{MKH}_2 + 2H^+_{in} \rightarrow \text{succinate} + \text{MK} + 2H^+_{in}$$

Formate : fumarate reduction :

$$\text{Formate} + \text{fumarate} + 2H^+_{in} \rightarrow \text{Succinate} + CO_2 + 2H^+_{ex}$$

The overall reaction of formate : fumarate respiration results in the release of $2H^+$ at the periplasmic, and consumption of $2H^+$ at the cytoplasmic side of the membrane resulting in a H^+/2e ratio of 2, which is due to the action of formate dehydrogenase. The enzyme has the

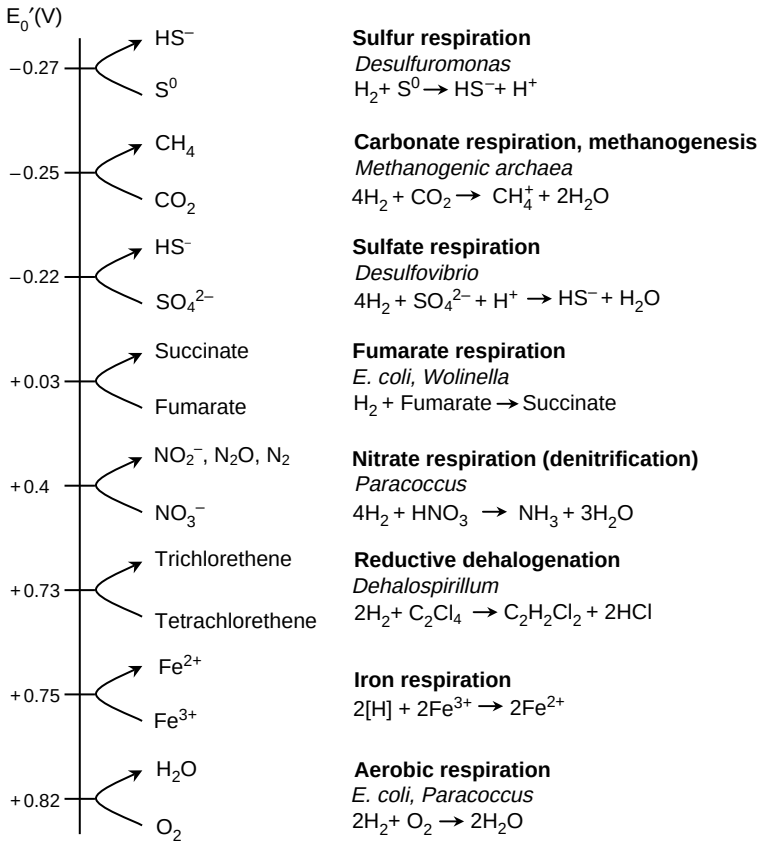

FIGURE 2 Important electron acceptors of anaerobic respiration by prokaryotes. The scheme gives the redox potentials of the redox pairs, the type of respiration, the metabolic balance using H_2 as the electron donor and examples for prokaryotes catalyzing the reaction. The free energy of the reaction can be calculated from $\Delta G_0' = -nF\Delta E_0'$, and is for example for fumarate respiration (H_2 + fumarate → succinate) $\Delta G_0' = -87$ kJ mol^{-1}.

active sites for formate oxidation and menaquinone reduction on opposite sides of the membrane, and translocates $2e^-$ from the formate to the quinone site, resulting in an overall translocation of two charges across the membrane (without actual translocation of H^+) and generation of Δp. Many anaerobic respiratory enzymes generate Δp in the same way. This mechanism of Δp generation has to be distinguished from proton-pumping redox enzymes, such as cytochrome *c* oxidase, which transfer protons across the membrane in a reaction, which is driven by a redox reaction (proton pump).

In fumarate reductase the protons are released (menaquinol site) and consumed (fumarate site) finally on the same (cytoplasmic) side of the membrane. The reaction therefore is not electrogenic and does not contribute to the formation of Δp, and fumarate reductase functions only as an electron sink. The overall $H^+/2e^-$ ratio of formate fumarate reduction is 2 (2 from formate dehydrogenase, 0 from fumarate reductase). These findings are in agreement with the energetics of the overall formate fumarate reduction, and of the partial reactions. The big difference in the redox potentials of the electron donor formate and of the electron acceptor menaquinone of formate:menaquinone reductase ($\Delta E_0' = -340$ mV) allows generation of a proton potential (max. H^+/e^- ratio ≤ 1.9). For fumarate reductase $\Delta E_0'$ is much lower ($\Delta E_0' = -110$ mV) which is not sufficient for generation of a proton potential in agreement with the scheme of Figure 3. In the same way other terminal reductases such as nitrite reductase from *Wolinella succinogenes* function as electron acceptors without contributing directly to Δp production.

Formate–nitrate respiration is catalyzed by an electron transport chain consisting of formate dehydrogenase and nitrate reductase:

Formate dehydrogenase:

$$\text{Formate} + \text{MK} + 2\text{H}^+_{\text{in}} \rightarrow \text{CO}_2 + \text{MKH}_2 + 2\text{H}^+_{\text{ex}}$$

Nitrate reductase:

$$\text{Nitrate} + \text{MKH}_2 + 2\text{H}^+_{\text{in}} \rightarrow \text{Nitrite} + \text{MK} + \text{H}_2\text{O} + 2\text{H}^+_{\text{ex}}$$

Formate:nitrate reduction:

$$\text{Formate} + \text{nitrate} + 4\text{H}^+_{\text{in}} \rightarrow \text{nitrite} + \text{CO}_2 + 4\text{H}^+_{\text{ex}}$$

For quinol:nitrate reduction with nitrate ($E_0' = +430$ mV) as the electron acceptor, $\Delta E_0'$ amounts to -510 mV with

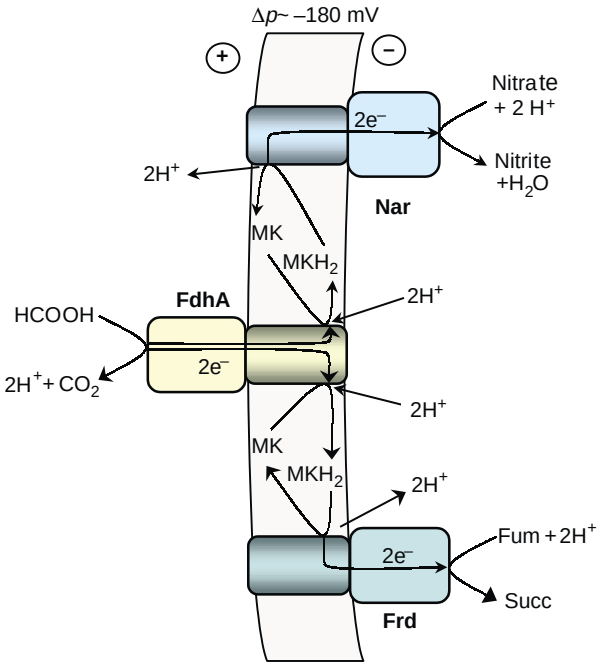

FIGURE 3 Formate–fumarate and formate–nitrate respiration. The figure shows topology and reactions of formate dehydrogenase (formate:quinol reductase), fumarate reductase (quinol:fumarate reductase) and nitrate reductase (quinol:nitrate reductase). Note the topology of the active sites for formate, fumarate, nitrate, and the quinones, the release and consumption of H^+ at the active sites, and transmembrane transfer of electrons in formate dehydrogenase and nitrate reductase. Frd, fumarate reductase; Nar, Nitrate reductase; Fdh, formate dehydrogenase. Examples of this type of fumarate respiration are found in *E. coli* and *Wolinella* of the nitrate respiration in *E. coli*.

menaquinol, or to -350 mV with ubiquinol as the electron donor, which allows conservation of the redox energy in a proton potential (Figure 3). Accordingly, the enzyme functions as a redox half-loop very similar to (but mirror-inverted) formate dehydrogenase, resulting in the translocation of two positive charges across the membrane (inside to outside).

A similar organization is found for many anaerobic respiratory chains, which are composed of one respiratory dehydrogenase and terminal reductase each, and which are linked by the quinones. In this way a large number of different respiratory dehydrogenases and terminal reductases can be linked to each other in branched respiratory chains.

Decarboxylation of Dicarboxylic Acids

Some anaerobic bacteria grow at the expense of decarboxylation of dicarboxylic acids such as oxaloacetate or succinate. The free energy of this reaction amounts to ~ -20 kJ mol^{-1} and is used for translocation of one Na^+ across the membrane by a membraneous decarboxylase as the energy-conserving reaction. The sodium motive force generated in this way can be used to drive secondary substrate transport, flagella, motility, or for phosphorylation of ADP if the bacteria contain an Na^+ potential-driven ATP synthase. The Na^+-dependent ATP synthase is very similar in function and composition to H^+-translocating F_1F_0-ATP synthase. In this way 3–4 decarboxylation reactions are required for phosphorylation of one ADP. *Propionigenium modestum* grows by conversion of succinate to propionate, including decarboxylation of methylmalony-CoA by a membraneous decarboxylase (Figure 4). Succinate is converted to methylmalonyl-CoA which is then decarboxylated in a reaction coupled to Na^+ translocation. The enzyme in addition consumes one H^+ from the periplasmic side of the membrane for the formation of propionyl-CoA + CO_2. Thus, the free energy of decarboxylation is used for generating an electrochemical Na^+ potential. The decarboxylation represents an intramolecular redox reaction producing an oxidized (CO_2) and a reduced (propionate) product. The reaction, however, does not comprise electron transport and depends only on the membraneous decarboxylase for generation

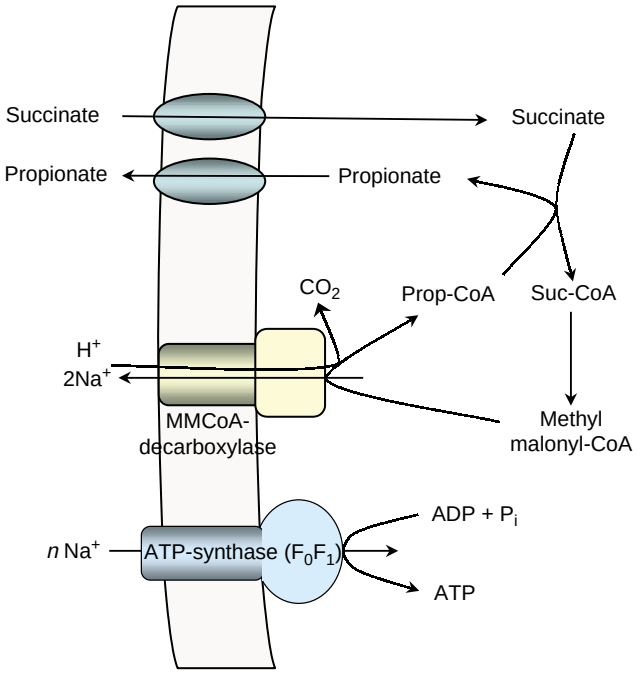

FIGURE 4 Anaerobic growth on succinate by *P. modestum* (succinate + $H_2O \rightarrow$ propionate + CO_2; $\Delta G_0' = -21$ kJ mol^{-1}) and generation of an Na^+ potential by decarboxylation. The membraneous methylmalony-CoA decarboxylase couples decarboxylation to translocation of $2Na^+$ ions over the membrane. H^+ for the decaroxylation reaction is derived from the outside.

of the electrochemical potential. In *Klebsiella*, an enterobacterium closely related to *Escherichia coli*, a membraneous Na^+ translocating decarboxylase of this type (oxaloacetate decarboxylase) is part of citrate fermentation and decarboxylates oxaloacetate yielding pyruvate which can be further converted to acetate + formate. In citrate fermentation ATP is formed in addition by substrate level phosphorylation, or a H^+ potential is generated in respiratory pathways. Therefore, the ATP synthase of *Klebsiella* is H^+ dependent, and the Na^+ potential is used mainly for secondary substrate transport.

Generation of a H^+-Potential by Transport of Charged Substrate and Product Molecules

Some bacteria use the (electrogenic) transport of substrate and product molecules for the generation of a proton potential. *Oxalobacter formigenes* and lactic acid bacteria like *Lactococcus lactis* or *Oenococcus oeni* are able to generate a proton potential by decarboxylation of the dicarboxylic acids oxalate or malate. The decarboxylation is catalyzed by cytoplasmic enzymes, and the free energy of the reaction is not directly stored in a membrane potential as in the membraneous decarboxylases. In *Oxalobacter* oxalate^{2-} is taken up by an electrogenic antiport with formate, the end product of the pathway (Figure 5). Decarboxylation of activated oxalate (oxalyl-CoA) produces CO_2 and consumes one H^+. The antiport of the dianionic oxalate against the monoanionic formate generates an electrical gradient (outside positive), and consumption of $1H^+$ by the decarboxylation generates a ΔpH (alkaline inside). The resulting proton potential is then used to drive ADP phosphorylation by a H^+-ATP synthase.

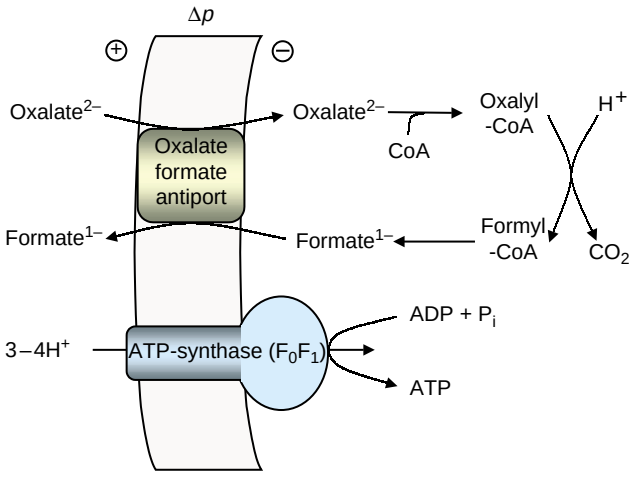

FIGURE 5 Anaerobic growth on oxalate by *Oxalobacter formigenes* (oxalate → formate + CO_2; $\Delta G_0' = -27$ kJ mol^{-1}) and generation of a H^+ potential by electrogenic oxalate^{2-}/formate^{1-} antiport and decarboxylation of oxalate by a cytoplasmic (H^+ consuming) decarboxylase.

Decarboxylation of malate by lactic acid bacteria (malolactic fermentation: malate^{2-} + H^+ → lactate$^-$ + CO_2) uses a similar mechanism of energy conservation. In *Lactococcus lactis* malate^{2-} is taken up and converted by a cytoplasmic decarboxylase to lactate$^-$ + CO_2, consuming H^+ as a cosubstrate. Malate^{2-} and lactate$^-$ are transported by an electrogenic antiporter generating an electrical potential (outside positive), and H^+ consumption in the cytoplasm during decarboxylation generates a ΔpH value (inside alkaline). The proton potential can be used for driving ADP synthesis by a membraneous ATP synthase.

Anoxygenic Photosynthetic Prokaryotes

Anoxygenic photosynthetic bacteria use only one photosystem for converting light energy into an electrochemical proton potential which is then used for driving ADP phosphorylation. Anoxygenic photosynthetic bacteria are found in three different phylogenetic groups which contain different photosynthetic systems: the purple bacteria, the green phototrophic bacteria with the subgroups of green sulfur bacteria (Chlorobiaceae) and *Chloroflexus*, and the gram-positive Heliobacteria. The three groups show differences in the type of photosynthetic reaction center, photosynthetic electron transfer and the electron donors used, pigments, and the pathway for CO_2 fixation. In anoxygenic photosynthesis, light is used to raise electrons to a more electronegative redox potential and to feed the electrons into a cyclic electron transport to generate a proton potential. The cyclic electron transport systems contain only one reaction center in contrast to oxygenic photosynthesis in cyanobacteria, green algae, or plants. The archaeon *Halobacterium salinarum*, on the other hand, contains a proton pump which is directly driven by light to translocate protons over the membrane without involvement of a photosynthetic electron transport. In contrast to the photosynthetic bacteria using chlorophyll containing proteins for photosynthesis and energy conversion, *Halobacterium* contains bacteriorhodopsin with retinal as a chromophor for light absorption and conversion to an electrochemical proton potential.

See Also the Following Articles

Chemiosmotic Theory • Energy Transduction in Anaerobic Prokaryotes • Pentose Phosphate (Hexose Mono Phosphate) Pathway • Pentose Phosphate Pathway, History of • Photosynthesis • Propionyl CoA–Succinyl CoA Pathway • Respiratory Chain and ATP Synthase

Glossary

ATP synthase (F_0F_1-ATPase) Enzyme in mitochondria and bacteria for the phosphorylation of ADP which is driven by the proton potential over the membrane.

chemiosmotic hypothesis Mechanisms for the coupling of the endergonic ATP synthesis by ATP synthase to the exergonic electron transport via a proton potential over the membrane.

prokaryotes Microorganisms, mostly unicellular, in which the chromosome is organized in a nucleoid (rather than a nucleus) which is not separated from the cytoplasm by a membrane. Bacteria and Archaea, two of the three major domains of living organisms, are prokaryotes.

Further Reading

Lengeler, J. W., Drews, G., and Schlegel, H. G. (1999). *Biology of the Prokaryotes.* Thieme, Stuttgart and Blackwell Science, Oxford.

Madigan, M. T., Martinko, J. M., and Parker, J. (2000). *Brock Biology of Microorganisms*, 9th edition, Prentice-Hall, Upper Saddle River, NJ.

Mitchell, P. (1961). Coupling of phosphorylation to electron and hydrogen transfer by a chemi-osmotic type of mechanism. *Naturwissenschaften* **191**, 144–148.

Unden, G., and Bongaerts, J. (1997). Alternative respiratory pathways of *Escherichia coli*: Energetics and transcriptional regulation in response to electron acceptors. *Biochim. Biophys. Acta* **1320**, 217–234.

Biography

Dr. Gottfried Unden is a professor for microbiology at the department for Microbiology and Wine Research at the Johannes Gutenberg-University, Mainz, Germany. His principal research interest is in facultatively anaerobic bacterial metabolism, function of bacterial sensors for environmental stimuli, and bacterial fermentation reactions in wine.

Enzyme Inhibitors

Vern L. Schramm
Albert Einstein College of Medicine, Yeshiva University, Bronx, New York, USA

Enzymes catalyze the chemical reactions necessary for life. They typically increase chemical reaction rates by factors of 10^{10}–10^{15}. The first step to initiate catalysis is binding the reactant molecules into the catalytic sites to form the Michaelis complex. In most enzymes, a conformational change occurs to enclose the reactants tightly in the enzyme and to make contacts between reactants and the enzyme that will achieve the transition state and subsequently form products. The enzyme then relaxes to open the catalytic site and release products. Enzyme inhibitors prevent enzymes from their catalytic function by interfering with any step in this catalytic cycle. Four common types of enzyme inhibitors are given as follows:

1. catalytic site inhibitors that compete with the substrate for formation of the Michaelis complex, traditionally called competitive inhibitors;

2. inhibitors that alter formation of the Michaelis complex and full expression of catalytic potential are called noncompetitive inhibitors;

3. covalent inhibitors that form a Michaelis complex followed by a chemical reaction with the enzyme to form a stable and inactive complex, often called mechanism-based inhibitors or "suicide inhibitors"; and

4. transition-state analogue inhibitors that resemble the unstable reactant complex at the transition state of the reaction.

Reversible Catalytic-Site Inhibitors

Reactant and Product Analogues

Molecules with shape and charge similar to the substrate or products may bind to the catalytic site similar to the normal reactants. When they are bound, substrate cannot bind and the enzyme is prevented from catalyzing the reaction. The relative affinity of these competing molecules for the catalytic site and their abundance relative to substrate will determine if they prevent substrate binding (Figures 1 and 2). Thus, if reactants and inhibitors bind with equal affinity, at equal concentrations, the enzyme catalytic site will be equally occupied with reactants and inhibitor resulting in 50% inhibition. This relationship is described in quantitative terms by the competition between an inhibitor (I) and a reactant (A) for a simple enzyme with one reactant by the equation: $v = (k_{cat})(A)/(K_m + A(1 + I/K_i))$, where v is the enzymatic reaction rate, k_{cat} is the maximum catalytic rate of the enzyme, K_m is related to the binding affinity between enzyme and substrate, defined as the concentration of substrate to achieve 50% of k_{cat} in the absence of inhibitor, and K_i is the dissociation constant for the enzyme–inhibitor complex, defined by the equation: $K_i = (E)(I)/(EI)$, and A and I are reactant and inhibitor concentrations. Diagrams of substrate and product inhibition illustrate the mutually exclusive or "competitive" inhibition relative to the catalytic site (Figure 2). Complete graphical and mathematical analyses of enzyme inhibition cases are available.

Bisubstrate Mimics

Many enzymatic reactions combine two different molecules at the catalytic site to transfer a chemical group between them. An example is the enzyme adenylate kinase that transfers the terminal phosphoryl group of ATP to AMP to generate two molecules of ADP (Figure 3). The catalytic site must accommodate ATP and AMP at the same time in preparation for group transfer. The bisubstrate mimic for the adenylate kinase reaction is chemically similar to ATP combined with AMP to make a bisubstrate molecule called AP_5A (Figure 3). Such molecules compete for both substrate sites, since they prevent either substrate from binding by competition for the same sites. Bisubstrate mimics can bind tightly to the enzyme since connected molecules bind with affinity equal to the product of the affinity of the individual molecules. For example, if individual dissociation constants (K_i values) for ATP and AMP are both 10^{-4} M, the dissociation constant for the bisubstrate mimic would be expected to be related to the product of these constants or $10^{-4} \times 10^{-4}$ M $= 10^{-8}$ M.

Transition-State Analogues

A special class of competitive inhibitors resembles the reactant molecule at the very point where it

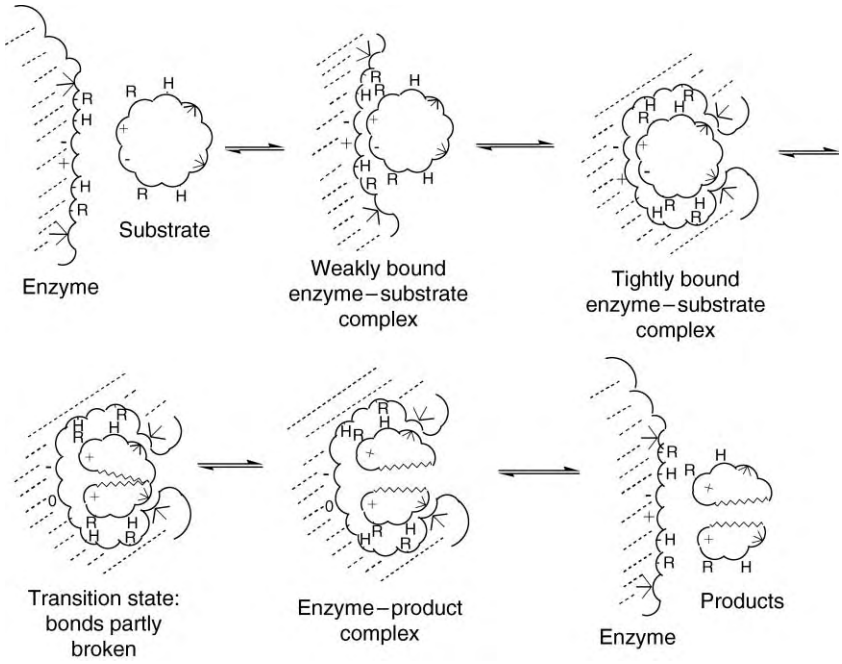

FIGURE 1 A schematic for the steps in enzyme-catalyzed reactions. In the first step diffusion causes collision between the substrate and an open catalytic site. The weakly bound enzyme–substrate complex causes the protein to close to form the tightly bound enzyme–substrate complex. Hydrogen bonds (H–R), ionic bonds (+ −), and hydrophobic interactions (><) in this closed complex at the transition state are shown. Following bond changes, the enzyme–product complex relaxes to release product and regenerate the original form of the enzyme to repeat the cycle.

crosses the chemical energy equivalence point of bond breaking/bond making called the transition state. These inhibitor molecules must be chemically stable, but have close similarity to the unstable transition state. Based on the theory of transition-state stabilization for enzyme-catalyzed reactions, the perfectly designed transition-state analogue is capable of binding to the enzyme by the factor: K_i for transition state inhibitor $= K_m$/catalytic rate enhancement. Since enzymatic catalytic rate enhancements are typically 10^{10}–10^{15}, perfectly designed transition-state inhibitors can bind 10^{10}–10^{15} times better than substrate. These incredibly large affinities have been rarely achieved. It is impossible to match the nonequilibrium bond lengths and partial charges present at the precise moment of the transition state with chemically stable molecules. However, incorporation of even modest similarities between the actual transition-state and transition-state analogues can achieve binding affinities 10^5–10^7 times that of reactants, and this improvement is adequate to achieve inhibition of the targeted enzymes in biological systems.

Enzymatic Transition States

This point of the chemical reaction is often the most energetic point in the reaction cycle, and therefore the rarest and the most difficult to detect. The exact shape and charge of the substrate molecule at the moment of the transition state is of great interest, since chemically stable molecules that resemble the substrate molecule at the transition state bind extremely tightly to the enzyme, as discussed above. This concept was proposed early in the history of biochemistry by Linus Pauling, and was formalized several decades later by Richard Wolfenden. An example of the substrate, enzyme-stabilized transition state and a transition analogue for purine nucleosidase phosphorylase is shown (Figure 4). These inhibitors commonly bind to the catalytic sites of enzymes millions of times more tightly than the substrates. Many of the antibiotics isolated in nature have been found to be transition-state analogues. Recently, molecules designed to be transition-state analogues are being tested in medical applications such as anticancer agents. Transition-state inhibitors compete at the catalytic site and cause the enzyme to fold into its tightly binding mode and keep it closed for long times, preventing catalysis (see Figure 1).

Design of Transition-State Analogues

Both the shape and charge of reactant molecules change as they reach the transition state (see Figure 1). The structure of the transition state can be experimentally measured by using kinetic isotope effects, combined with computational chemistry to locate the enzymatic

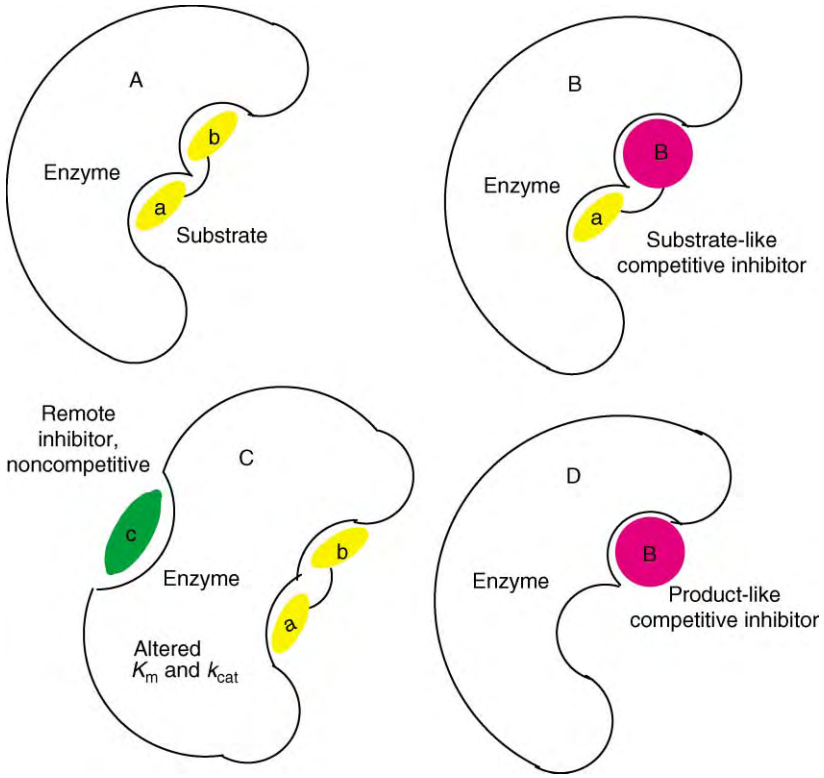

FIGURE 2 Enzyme A is a normal Michaelis complex with substrate a–b at the catalytic site (yellow). The bond to be broken by the enzyme connects a and b. The substrate-like competitive inhibitor (pink, enzyme B) has a difference in the B part of the bound molecule and is not a substrate but competes directly for a–b at the catalytic site. Since this is a competition, large amounts of a–b will displace a–B. A noncompetitive inhibitor binds to influence catalysis but does not directly compete for the catalytic site. There are many variants of noncompetitive inhibition and binding at a remote site to change features of the catalytic site is one example (green in enzyme C). Competitive inhibitors can also be product-like as shown in enzyme D (pink).

transition state. The electron distribution at the van der Waals surface of a molecule is called its molecular electrostatic potential surface. This can be described for substrate and transition states for enzyme reactions provided the transition-state structure is known, and can also be established for proposed inhibitor molecules. Electrostatic matches to the transition state make powerful inhibitors by capturing some of the transition-state energy usually applied to catalysis (Figure 4).

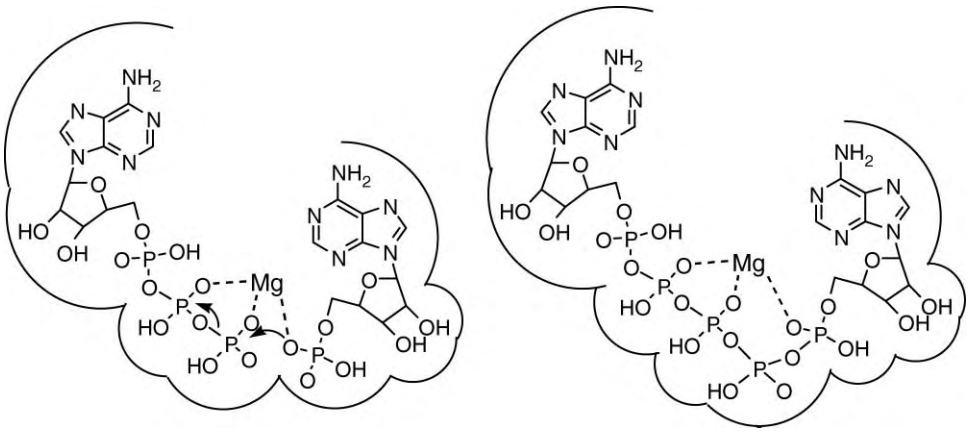

FIGURE 3 The Michaelis complex for adenylate kinase (ATP + AMP → 2ADP) is shown on the left with the arrows indicating electron flow for the phosphoryl group transfer. The inhibited complex with adenosyl–pentaphosphate–adenosine (A–P5–A) is on the right. The bisubstrate inhibitor competes for both ATP- and AMP-binding sites. Ionic charges are omitted for clarity and the ribosyl groups are all β-D-ribose in stereochemistry.

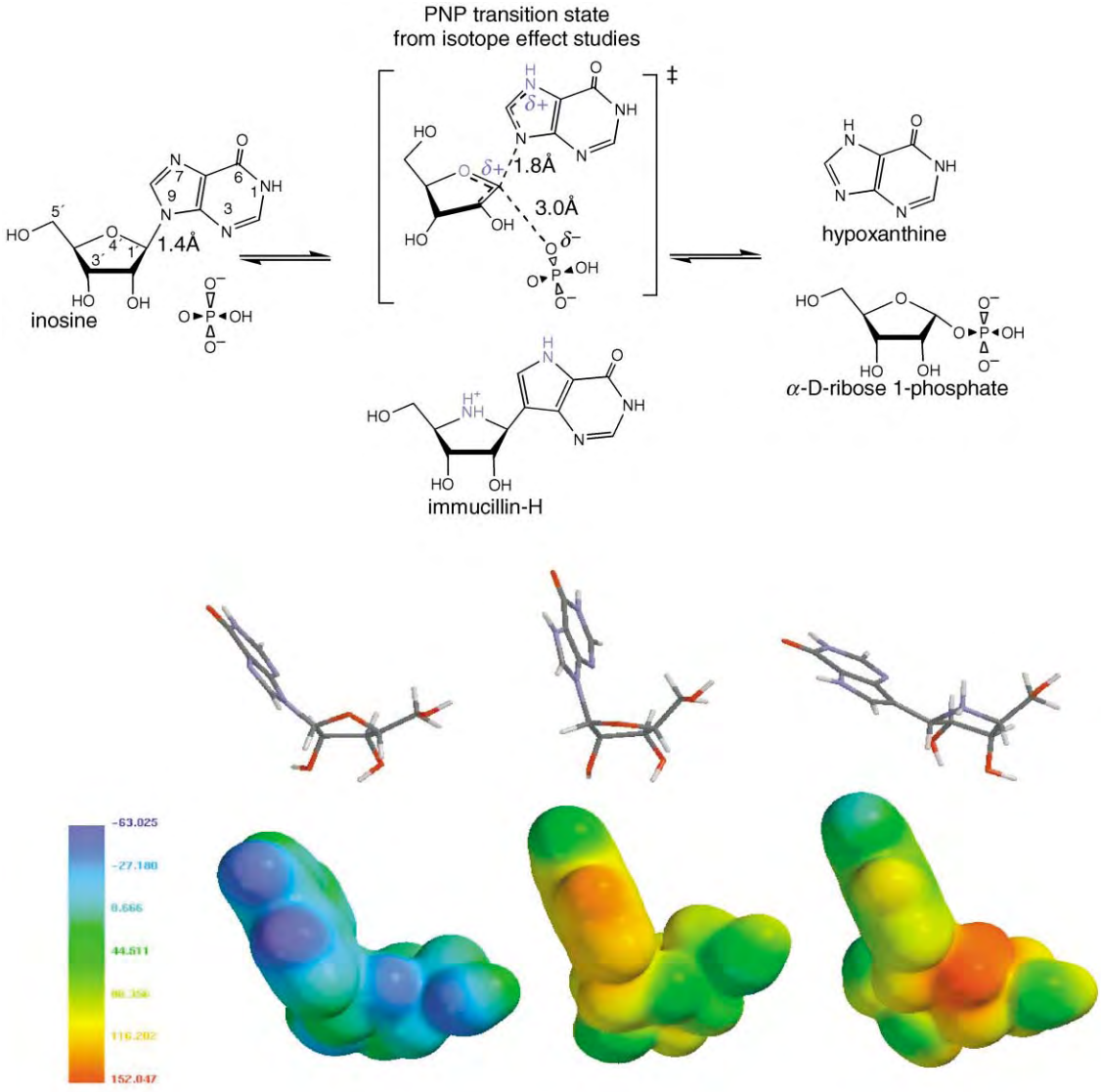

FIGURE 4 The reaction catalyzed by bovine purine nucleoside phosphorylase (PNP), transition-state structure, and a transition-state analogue inhibitor (immucillin-H). Novel features of the transition state are protonation at N7 and the partial positive charge on the ribosyl group. Both are represented in the inhibitor, shown in blue. Immucillin-H binds approximately 1 million times more tightly to PNP than does the substrate inosine. Shown below are the electronic van der Waals surfaces of inosine (left), transition state (middle), and Immucillin-H (right). Note the electrostatic similarity between transition state and Immucillin-H. Reproduced with permission of Elsevier Ltd., from Vern, L. Schramn. Development of transition state analogues of purine nucleoside phosphorylase as anti-T-cell agents. (2002) *Biochem. Biophys. Acta* **1587**, 107–117.

Natural Product Transition-State Analogues

Many antibiotics isolated from natural sources are transition-state inhibitors. One example is an antibiotic formed in the culture medium of *Streptomyces antibioticus* that is apparently made as an agent of microbial warfare between species of soil organisms. R-Coformycin binds to the catalytic sites of adenine nucleoside and nucleotide deaminases millions of times tighter than the reactant molecules. The transition-state structure for deaminase enzymes has been solved and the similarity of transition-state analogue and transition state is greater than either to the substrate (Figure 5).

Noncatalytic Site Inhibitors

Noncatalytic site inhibitors include all inhibitors binding at sites other than the catalytic site. These inhibitor molecules can cause several different types of enzymatic inhibition, both competitive inhibition and noncompetitive inhibition. The reason for this diversity arises by inhibitor binding distant to the catalytic site but, in so doing, changing the enzyme conformation to prevent proper function of the enzyme either in binding its substrate or in formation of the products.

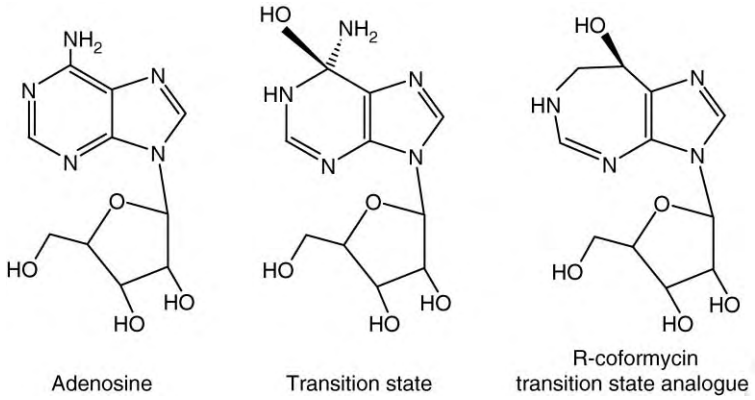

FIGURE 5 Reactant (adenosine), transition state, and transition-state analogue inhibitor for adenosine deaminase. R-Coformycin is a natural product transition state analogue inhibitor that binds 10 million times tighter to adenosine deaminase than does adenosine.

Prevent Catalytic-Site Binding

An inhibitor may bind remote from the catalytic site to change the protein conformation to cause mutual exclusion between reactant binding at the catalytic site and inhibitor binding at the remote site. For this interaction, kinetic analysis of the type shown above will be kinetically indistinguishable from competitive inhibition. The surfaces of proteins contain highly irregular and charged surfaces that interact with specific molecules. Current practice of testing libraries of diverse chemical compounds against a specific enzyme to find any type of interaction that can cause inhibition often discovers this class of inhibitor.

Prevent Subunit Formation

Most enzymes have multiple protein subunits that must interact to provide a functional catalytic unit. An example is the ribonucleotide diphosphate reductase required to form deoxynucleotides for the biological production of DNA. During cellular protein synthesis of these enzymes, the protein subunits are formed separately and must then combine to make the functional catalyst. In the cell, these subunits are thought to separate and recombine many times, providing an opportunity to insert an inhibitory molecule in the protein interface between subunits. Selection of such molecules from chemical libraries or designing them from known protein–protein interfaces prevents formation of the active enzyme molecule in the cell. Inhibitors of this type have been designed for ribonucleotide diphosphate reductase and show promise in this new area of specific inhibitor design.

Prevent Conformational Change for Catalysis

A related inhibitor type is one binding remote from the catalytic site to prevent an enzymatic conformational change that is required for catalysis. Most enzymes require protein motion to close the catalytic site prior to formation of the transition state. These loop or domain motions involve physical motion of segments of the proteins, often over relatively large distances. A consequence of the motion is to position amino acid residues in the catalytic site where they are required for catalysis. An inhibitor that binds outside the catalytic site and prevents this protein motion required for catalysis will provide complete loss of enzyme function without blocking access of reactants to the catalytic site. As knowledge of the protein surfaces becomes more complete, it will be increasingly possible to design molecules that act in these novel inhibitory roles.

Mechanism-Based Inhibitors

Mechanism-based enzymatic inhibitors are designed to be stable molecules that resemble the substrate. They bind at the catalytic site of the target enzyme and are converted by the enzyme to a chemically reactive form that covalently reacts with the catalytic site of the enzyme. This covalent intermediate of enzyme inhibitor differs from normal catalytic intermediates by its chemical stability and long lifetime. Trapping the enzyme in a stable covalent complex blocks the catalytic site from normal interaction and provides long-term inhibition of the enzyme. Mechanism-based inhibitors are in broad use in biology, and our example of this chemical inhibitor logic is in the pathway of polyamines (Figure 6).

Polyamine Synthesis

The polycationic polyamines are essential counterions for DNA replication in dividing cells. The first step in

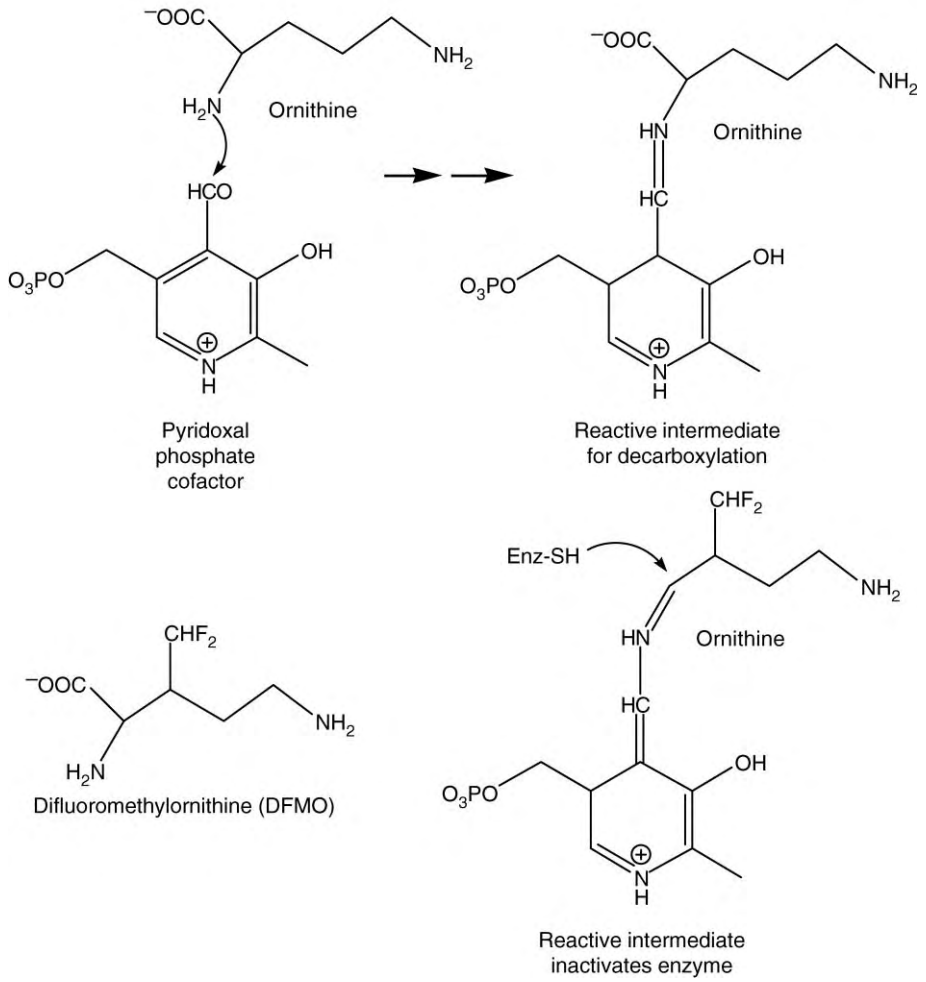

FIGURE 6 Covalent suicide inhibition of ornithine decarboxylase by DFMO. In the normal reaction, the enzymatic cofactor, pyridoxal phosphate, forms a Schiff base favoring decarboxylation of ornithine. With DMFO, the same steps occur but decarboxylation generates a reactive difluoro-conjugated imine. A nearby cysteine nucleophile reacts to form a stable, inactive enzyme.

polyamine synthesis is catalyzed by ornithine decarboxylase which uses a transient covalent intermediate to the enzymatic cofactor pyridoxal phosphate. Difloromethylornithine (DFMO) is decarboxylated in similar fashion to orinithine, but the reaction creates a highly reactive intermediate that reacts with a nearby group on the enzyme to form a stable covalent intermediate, resulting in an inactive ornithine decarboxylase. It therefore stops polyamine biosynthesis. It has been used as an anticancer agent and an antibiotic against *Trypanosoma* species that cause sleeping sickness. Specificity is provided by the binding of DFMO only to the target enzyme and long biological action is provided by the stable covalent interaction with the enzyme. These are features of most mechanism-based enzyme inhibitors. Care is needed that chemical reactivity causing enzymatic inactivation is revealed only to the target enzyme.

Other Mechanism-Based Inhibitors

Many of the common antimetabolites are mechanism-based inhibitors. Thus, certain insecticides form covalent interactions with the catalytic site of enzymes involved in insect neurotransmission. Deprenyl is a drug used to treat Parkinson's disease and mental depression by increasing brain dopamine levels. It functions by suicide inhibition at the catalytic site of monamine oxidase, the enzyme that degrades dopamine.

Conclusion

The intricate steps in enzymatic action can be disrupted in numerous ways, each causing inhibition of catalytic steps. Enzymes have evolved to function in the presence of the complex mixture of normal cellular components, but inhibitors can be designed to specifically target a

single enzyme of the thousands that function in coordination in a normal cell.

See Also the Following Articles

Enzyme Kinetics • Enzyme Reaction Mechanisms: Stereochemistry • Substrate Binding, Catalysis, and Product Release

Glossary

biological efficency The ability of an enzyme inhibitor to achieve significant inhibition at the physiological conditions of substrates and cofactors.

catalytic site A cavity on the enzymatic surface that binds substrates and causes them to be converted to product by increasing the probability that they will achieve the transition state.

inhibitor design Selection or synthesis of stable molecules intended to disrupt catalytic function of a specific enzyme.

mechanism-based inhibitor A molecule resembling a substrate that is chemically activated by the action of the enzyme to form a stable covalent link with the enzyme – also known as suicide substrates or suicide inhibitors.

substrate analogue A molecule with shape and charge features similar to a substrate of the enzyme that binds at the catalytic site and prevents substrate binding.

transition-state analogue A chemically stable molecule with shape and electrostatic features that mimic those of the transition state and that inhibit at the catalytic site by converting energy of catalysis to energy of binding.

Further Reading

Abeles, R. H., and Alston, T. A. (1990). Enzyme inhibition by fluoro compounds. *J. Biol. Chem.* **265**, 16705–16708.

Cleland, W. W. (1970). Steady state enzyme kinetics. In *The Enzymes*, 3rd edition, Vol. 2, (P. S. Boyer, ed.) Academic Press, New York pp. 1–65.

Northrop, D. B. (1999). Rethinking fundamentals of enzyme action. *Adv. Enzymol. Relat. Areas Mol. Biol.* **73**, 25–55.

Schramm, V. L. (1998). Enzymatic transition states and transition state analog design. *Ann. Rev. Biochem.* **67**, 693–720.

Schramm, V. L. (2003). Enzymatic transition state poise and transition state analogues. *Acc. Chem. Res.* **36**, 588–596.

Wolfenden, R. (1976). Transition state analog inhibitors and enzyme catalysis. *Ann. Rev. Biophys. Bioeng.* **5**, 271–306.

Biography

Vern Schramm received his Ph.D. at the Australian National University, John Curtain School of Medical Research in 1968. In the Department of Biochemistry at the Temple University School of Medicine (1971), he began to apply isotope effects to the study of enzymatic transition states. At the Albert Einstein College of Medicine in 1987, he began a systematic program of solving enzymatic transition states by kinetic isotope effects. Enzymatic transition-state information is then applied to the design of transition-state analogue inhibitors. The inhibitors are applied to biomedical problems.

Enzyme Kinetics

Irwin H. Segel
University of California, Davis, California, USA

Enzymes are protein catalysts that accelerate the rates at which reactions approach equilibrium. *Enzyme kinetics* is the branch of biochemistry that deals with a quantitative description of this process, mainly, how experimental variables affect reaction rates. The variables that are studied include the concentrations of the enzyme, substrates (reactants), products, inhibitors, activators, the pH, temperature, and ionic strength. A complete kinetic analysis (together with complementary studies of equilibrium ligand binding, isotope exchange, covalent modification of amino acid side chains, etc.) can disclose most of the functional characteristics of a particular enzyme. These include (1) the specificities and affinities of the ligand subsites, (2) the order in which substrates bind and products leave, (3) the enzyme species that are intermediates in the overall reaction, (4) the magnitudes of component rate constants, (5) the possible identities of active-site residues, (6) the mode of action of an inhibitory drug, and (7) how the enzyme might be regulated *in vivo*. Enzyme kinetics combined with related approaches can show how the functional properties of a mutant or "engineered" enzyme compare to those of its wild-type parent. Many of the equations of enzyme kinetics are also applicable to other saturable biological processes, e.g., membrane transport and receptor–ligand interactions.

Unireactant Enzymes and the Michaelis–Menten Equation

By the mid- to late 1800s, most of the laws governing the effect of reactant concentrations on the rates of chemical reactions were known. But enzyme-dependent reactions did not always follow these simple rate laws. In 1902, Victor Henri proposed the first useful equation for an enzyme-dependent reaction. Henri's equation took into account the known properties of enzymes, including that (1) an enzyme was highly specific for a particular substrate (or class of substrates), (2) substrates often protected an enzyme from inactivation by heat, and (3) a plot of initial velocity versus substrate concentration was hyperbolic. (These properties all pointed to the participation of an enzyme–substrate complex.) Subsequent workers, including Michaelis and Menten (1913), Van Slyke and Cullen (1914), and Briggs and Haldane (1925) confirmed and/or extended Henri's equation, which is derived below.

The Rapid Equilibrium Assumption

The following assumptions and procedures led Henri and others to the relationship between substrate concentration and reaction rate, which is now known as the Michaelis–Menten equation:

1. The overall reaction occurs in two steps, as shown below:

$$\mathrm{E} + \mathrm{S} \underset{k_{-1}}{\overset{k_1}{\rightleftharpoons}} \mathrm{ES} \xrightarrow{k_2} \mathrm{E} + \mathrm{P}. \qquad (1)$$

This sequence recognizes that the enzyme is not consumed in the reaction, but rather, is a recycling catalyst. The first step is the rapid equilibration of the free enzyme, E, and the free substrate, S, to form an ES complex. This is followed by the unidirectional, rate-limiting decomposition of ES to E + P. The rapid equilibrium between E, S, and ES is maintained throughout the course of the reaction. (This condition requires that $k_{-1} >> k_2$.) The equilibrium is described by the dissociation constant, K_s of the ES complex:

$$K_s = [E][S]/[ES] = k_{-1}/k_1. \qquad (2)$$

Equation (2) allows the concentration of the ES complex to be expressed in terms of the concentration of free E, free S, and K_s:

$$[ES] = [S][E]/K_s. \qquad (3)$$

2. At any time, the total enzyme, $[E]_t$ is present as either free E or as the ES complex. Thus, the mass balance (conservation) equation is

$$[E]_t = [E] + [ES]. \qquad (4)$$

The total substrate is also distributed between the free and complexed species:

$$[S]_t = [S] + [ES]. \qquad (5)$$

However, for most enzyme-dependent reactions that are studied *in vitro*, the enzyme is present at a very low (catalytic) level (i.e., $[E]_t << [S]_t$), so that the

maximum $[ES]$ that can form will be much smaller than the $[S]_t$ added. Consequently, it can be assumed that the free S concentration is essentially identical to the total added S (i.e., $[S] \approx [S]_t$). This assumption is not valid for many enzymes inside the cells, where $[E]_t$ may be in the same range as $[S]_t$.

3. The instantaneous or "initial" rate, $\mathrm{d}[P]/\mathrm{d}t$ or $-\mathrm{d}[S]/\mathrm{d}t$ (usually indicated as "v" for "velocity"), is proportional to the concentration of the ES complex:

$$v = k_2[ES]. \tag{6}$$

4. It is assumed that the accumulating product has no effect on the reaction. That is, the P concentration remains close to zero throughout the course of the reaction, or P has no affinity for the enzyme.

5. The final velocity equation is obtained by dividing eqn. (6) by eqn. (4) and substituting for $[ES]$ from eqn. (3):

$$\frac{v}{[E]_t} = \frac{k_2[ES]}{[E] + [ES]} \quad \text{or} \quad v = \frac{k_2[E]_t \dfrac{[S][E]}{K_S}}{[E] + \dfrac{[S][E]}{K_S}} \tag{7}$$

$k_2[E]_t$ is defined as V_{max} because when all the enzyme is in the ES form, the observed velocity will be maximal. This substitution and canceling $[E]$ in eqn. (7) yields the final Michaelis–Menten equation:

$$v = \frac{V_{max} \dfrac{[S]}{K_s}}{1 + \dfrac{[S]}{K_s}} = \frac{V_{max}[S]}{K_s + [S]}. \tag{8}$$

The Steady-State Assumption

By the 1920s, researchers realized that the rapid equilibrium assumption was too restrictive and would not be valid for enzymes where the ES complex proceeds on to E + P much faster than it dissociates back to E + S. In such cases, E, S, and ES would not attain equilibrium. In 1925, Briggs and Haldane offered a more general method for deriving velocity equations that did not require a rapid equilibrium assumption. Their *steady-state* approach recognized that under most assay conditions, $[E]$ and $[ES]$ would attain certain levels very quickly after mixing E and S, but that the concentrations of these enzyme species would change very little thereafter. In other words, for the duration of the assay, the rate at which ES is formed (from E + S) remains identical to the rate at which it decomposes (back to E + S, plus forward to E + P). Similarly, the rate at which E is produced from ES equals the rate at which E is used to form ES. Scheme (1) is still applicable, but now rate constants for individual steps must be taken into account. Applying the steady-state assumption we can write

$$\mathrm{d}[ES]/\mathrm{d}t = 0 \quad \text{or} \quad k_1[E][S] = (k_{-1} + k_2)[ES] \tag{9}$$

and

$$\mathrm{d}[E]/\mathrm{d}t = 0 \quad \text{or} \quad (k_{-1} + k_2)[ES] = k_1[E][S]. \tag{10}$$

Solving either equation for $[ES]$ yields

$$[ES] = k_1[E][S]/(k_{-1} + k_2) \quad \text{or} \quad [ES] = [S][E]/K_m \tag{11}$$

where in the latter expression, the three rate constants are combined into a single kinetic constant, K_m, as shown below:

$$K_m = (k_{-1} + k_2)/k_1. \tag{12}$$

The initial velocity, v, at any $[S]$ still equals $k_2[ES]$. So, proceeding as described earlier, but substituting for $[ES]$ from eqn. (11), we obtain

$$v = \frac{V_{max}[S]}{K_m + [S]}. \tag{13}$$

Thus, the velocity equation is the same as that derived for rapid equilibrium conditions, except that the constant in the denominator (now called a Michaelis constant) is more complex than a simple dissociation constant. The Briggs–Haldane approach is more general than the rapid-equilibrium approach because it makes no assumptions about the relative magnitudes of the various rate constants. If $k_2 \ll k_{-1}$, K_m reduces to k_{-1}/k_1, which is equivalent to the simpler K_s.

Equation (13) is valid throughout the experimental [S] range provided that the rate of P formation is measured before [S] changes appreciably. (In practice, substrate use should be restricted to less than 5% (or at most 10%) of $[S]_t$.) When $[S] \ll K_m$, eqn. (13) reduces to $v = V_{max}[S]/K_m = k[S]$, i.e., the reaction is *first order* with respect to $[S]$ with a rate constant equivalent to V_{max}/K_m. When $[S] >> K_m$, v is essentially constant at V_{max} and independent of $[S]$. (The reaction is *zero order* with respect to $[S]$.)

A More Realistic Unireactant Reaction Sequence

Equation (1) contains the minimum number of steps that must be considered in the description of a uni–uni (one substrate, one product) reaction. A more realistic scheme takes into account the conversion of enzyme-bound S to enzyme-bound P (before P is released) and the reversibility of each step as shown below:

$$\mathrm{E} + \mathrm{S} \underset{k_{-1}}{\overset{k_1}{\rightleftharpoons}} \mathrm{ES} \underset{k_{-2}}{\overset{k_2}{\rightleftharpoons}} \mathrm{EP} \underset{k_{-3}}{\overset{k_3}{\rightleftharpoons}} \mathrm{P} + \mathrm{E}. \tag{14}$$

A steady-state treatment of the above reaction sequence once again yields the familiar Michaelis–Menten equation when $[P] = 0$, except that now

$$K_m = \frac{k_{-1}k_3 + k_{-1}k_{-2} + k_2k_3}{k_1(k_2 + k_{-2} + k_3)} \tag{15}$$

and

$$V_{max} = \frac{k_2k_3[E]_t}{k_2 + k_{-2} + k_3}. \tag{16}$$

So, in the absence of other information, the rate constant compositions of the two kinetic constants, K_m and V_{max}, are not usually known. But regardless of its makeup, K_m is a valuable characteristic because it is equivalent to the substrate concentration that yields half-maximal velocity. V_{max} is not a true constant because it depends on the enzyme concentration. However, $V_{max}/[E]_t$, expressed as moles of S converted to P per second per mole of enzyme active site (which reduces to per second, or s^{-1}) is the *catalytic rate constant* (or *turnover number*) of the enzyme, k_{cat}. The ratio k_{cat}/K_m has been used to compare the action of an enzyme on a series of related substrates. The higher the value of this *specificity constant*, the better the substrate. If an enzyme is evolutionarily perfected so that the catalytic and product release rate constants are very much larger than any of the reverse first-order rate constants, the ratio k_{cat}/K_m reduces to k_1, the second-order rate constant for the interaction of E and S to form ES. In aqueous solution, this constant has a maximum, diffusion-limited value of $\sim 10^9\ M^{-1}\ s^{-1}$. Many enzymes have k_{cat}/K_m values that approach this maximum.

Reversible Reactions

In the presence of both the substrate and product, the net steady-state velocity is given by the difference between the forward and reverse rates of any step, e.g.,

$$v = k_2[ES] - k_{-2}[EP] \tag{17}$$

or

$$\frac{v}{[E]_t} = \frac{k_2[ES] - k_{-2}[EP]}{[E] + [ES] + [EP]}. \tag{18}$$

After substituting for $[ES]$ and $[EP]$ and grouping rate constants into kinetic constants, the equation is

$$v = \frac{V_{max,f}\dfrac{[S]}{K_{mS}} - V_{max,r}\dfrac{[P]}{K_{mP}}}{1 + \dfrac{[S]}{K_{mS}} + \dfrac{[P]}{K_{mP}}} \tag{19}$$

where $V_{max,f}$ and $V_{max,r}$ are the forward and reverse maximal velocities, respectively; K_{mS} and K_{mP} are the Michaelis constants of S and P, respectively. Equation (19) can also be written as

$$v = \frac{V_{max,f}[S]}{K_{mS}\left(1 + \dfrac{[P]}{K_{mP}}\right) + [S]} - \frac{V_{max,r}[P]}{K_{mP}\left(1 + \dfrac{[S]}{K_{mS}}\right) + [P]} \tag{20}$$

which shows that in this unireactant process, P acts as a competitive inhibitor of the forward reaction and S acts as a competitive inhibitor of the reverse reaction. (In reactions catalyzed by multireactant enzymes, individual products might be competitive, uncompetitive, or noncompetitive with respect to different substrates.)

The Velocity Curve and its Linear Forms

Figure 1 shows the typical hyperbolic dependence of the velocity of an enzyme-catalyzed reaction on the substrate concentration. The kinetic constants, K_m and V_{max}, can be obtained by fitting the v versus $[S]$ data directly to the Michaelis–Menten equation using an appropriate computer application. Alternatively, K_m and V_{max} can be obtained by plotting the data in a linear form such as $1/v$

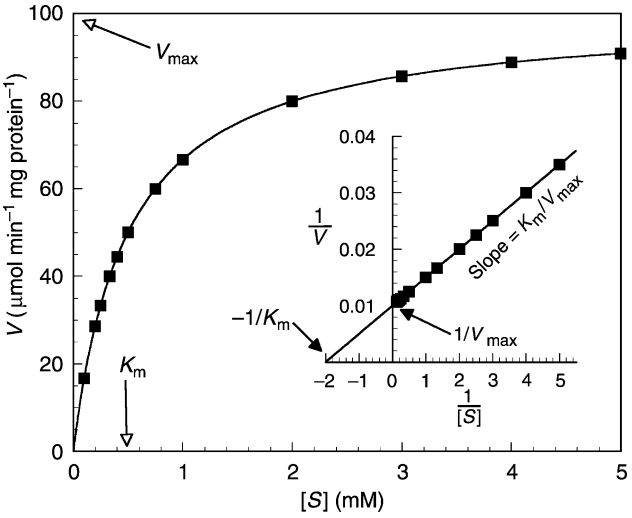

FIGURE 1 Theoretical plot of initial velocity versus substrate concentration in the absence of the product for an enzyme with a K_m of 0.5 mM and a V_{max} of 100 μmol min^{-1} mg^{-1} protein. The $[S]$ at which v is 50% of V_{max} (i.e., $[S]_{0.5}$) is equivalent to K_m. The curvature of the plot is the same for all enzymes obeying Henri–Michaelis–Menten kinetics, regardless of the absolute values of the kinetic constants. For example, the ratio of substrate concentration that yields 90% of V_{max} ($[S]_{0.9}$) to that yielding 10% of V_{max} ($[S]_{0.1}$) is always 81. Similarly, the $[S]_{0.75}/[S]_{0.5}$ ratio is always 3. Note that V_{max} is difficult to determine visually. But a computer-assisted fit to $v = Vmax^*[S]/(Km + [S])$ will return both V_{max} and K_m. (Inset) Double-reciprocal plot of the data. A wide range of substrate concentrations is needed to construct both the primary plot and the double-reciprocal plot because $[S]$ values that are evenly spaced on one plot do not space evenly on the other.

versus $1/[S]$ (usually called the Lineweaver–Burk or double-reciprocal plot), $v/[S]$ versus v (usually called the Scatchard plot), v versus $v/[S]$, or $[S]/v$ versus $[S]$. The most popular of these is the double-reciprocal plot, which is based on the linear transformation of the Michaelis–Menten equation shown below.

$$\frac{1}{v} = \frac{K_m}{V_{max}}\frac{1}{[S]} + \frac{1}{V_{max}}. \quad (21)$$

A major advantage of a linear plot is that data obtained at several different fixed concentrations of a second ligand (e.g., a cosubstrate, product, inhibitor, or activator) can be displayed simultaneously and the resulting slope and intercept characteristics used to diagnose the kinetic mechanism or the mode of inhibition or activation.

Multireactant Enzymes

Common Mechanisms

Most enzymes catalyze reactions between two or more substrates to yield two or more products. The substrates bind to the enzyme either in a random manner or in a compulsory order. Similarly, product release is random in some cases, and ordered in others. Mechanisms in which catalysis occurs only after two (or more) substrates are brought together on the enzyme are called "sequential." Some enzymes catalyze the formation and release of a product before all the substrates have bound. For example, an enzyme might capture a substrate, A, and retain part of that molecule (sometimes as a covalent adduct with the enzyme) releasing the rest of the molecule as product P. Only then does substrate B bind and combine with the part of A that was left on the enzyme to form product Q, which then leaves. This type of substituted enzyme or "ping-pong" mechanism is common for transaminases; the amino group of substrate A is left temporarily on the enzyme. A reaction catalyzed by a terreactant (three-substrate) enzyme might proceed by a combination of sequential and ping-pong steps. The order of addition of substrates and release of products is called the *kinetic mechanism*. Four bireactant examples are shown in Figure 2.

Velocity Equations for Some Bireactant Mechanisms

In some cases, different kinetic mechanisms are described by different velocity equations. (See standard enzyme kinetics texts for the procedures used to derive these equations.) Consequently, it is sometimes possible to distinguish between mechanisms from the characteristics of the double-reciprocal plots. For example, the velocity equation for an ordered bireactant mechanism under steady-state conditions in the absence of products is

$$v = \frac{V_{max}[A][B]}{K_{ia}K_{mB} + K_{mB}[A] + K_{mA}[B] + [A][B]} \quad (22)$$

where K_{mA} and K_{mB} are the Michaelis constants of the two substrates and K_{ia} is the simple dissociation constant of the EA complex. (Velocity equations for multireactant mechanisms often contain both types of constants.) When $[A]$ is varied at different fixed concentrations of B, the velocity dependence can be written in the form of the Michaelis–Menten equation:

$$v = \frac{V_{max}[A]}{K_{mA}\left(1 + \frac{K_{ia}K_{mB}}{K_{mA}[B]}\right) + [A]\left(1 + \frac{K_{mB}}{[B]}\right)}. \quad (23)$$

Or, in double reciprocal form:

$$\frac{1}{v} = \frac{K_{mA}}{V_{max}}\left(1 + \frac{K_{ia}K_{mB}}{K_{mA}[B]}\right)\frac{1}{[A]} + \frac{1}{V_{max}}\left(1 + \frac{K_{mB}}{[B]}\right). \quad (24)$$

When $[B]$ is varied at different fixed concentrations of A, the equations are

$$v = \frac{V_{max}[B]}{K_{mB}\left(1 + \frac{K_{ia}}{[A]}\right) + [B]\left(1 + \frac{K_{mA}}{[A]}\right)} \quad (25)$$

and

$$\frac{1}{v} = \frac{K_{mB}}{V_{max}}\left(1 + \frac{K_{ia}}{[A]}\right)\frac{1}{[B]} + \frac{1}{V_{max}}\left(1 + \frac{K_{mA}}{[A]}\right). \quad (26)$$

At a fixed concentration of one substrate, e.g., A, the velocity dependence on the concentration of substrate B can also be described by a simplified form of eqn. (25):

$$v = \frac{V_{max,app}[B]}{K_{mB,app} + [B]} \quad (27)$$

where the *apparent constants* are related to the true or limiting constants as shown below.

$$V_{max,app} = \frac{V_{max}}{\left(1 + \frac{K_{mA}}{[A]}\right)} \quad \text{and} \quad K_{mB,app} = \frac{\left(1 + \frac{K_{ia}}{[A]}\right)}{\left(1 + \frac{K_{mA}}{[A]}\right)}. \quad (28)$$

In other words, the experimentally determined "K_m" and "V_{max}" depend on the concentration of the co-substrate and will not equal the limiting values unless that concentration is infinitely high ("saturating"). In practice, the limiting kinetic constants are obtained from appropriate replots of the slopes and $1/v$-axis intercepts

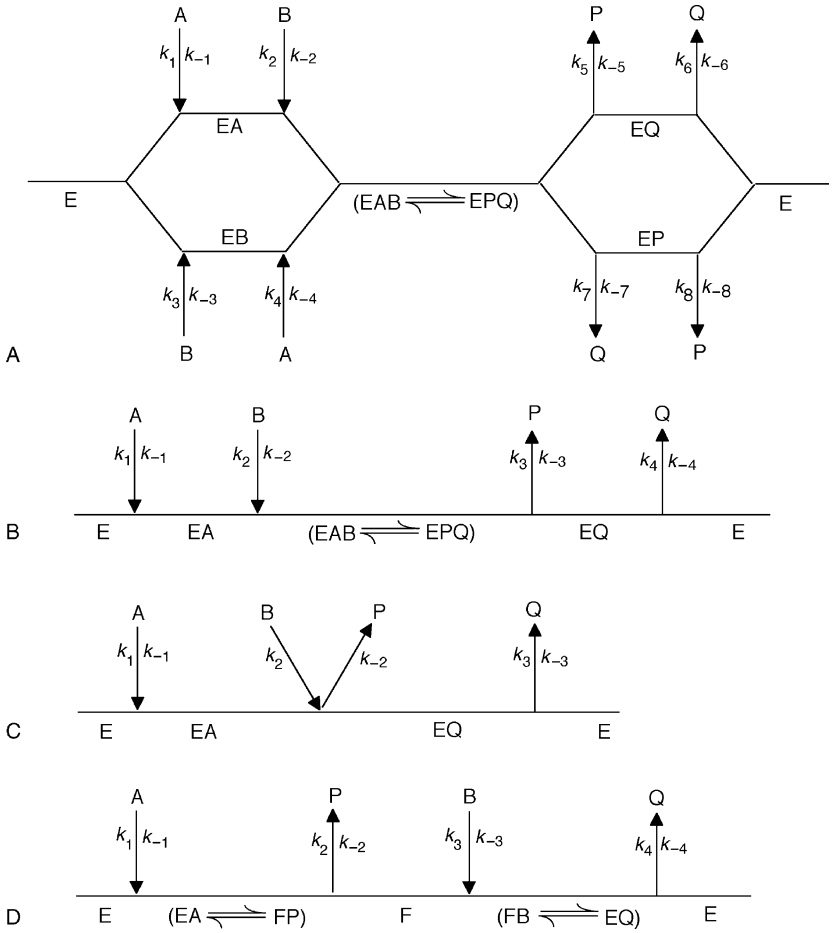

FIGURE 2 Four common kinetic mechanisms for bireactant enzymes shown in the Cleland shorthand notation. Substrates are indicated above a horizontal line as A, B, C, etc., in the order in which they add to the enzyme. Products are indicated as P, Q, R, etc., in the order in which they dissociate from the enzyme. Arrows are shown pointing in a single direction, but all the reactions are reversible. Rate constants for each reversible reaction are shown alongside of the arrows. For computer-based derivations of the velocity equation, it is usually more convenient to indicate all rate constants with positive subscripts (odd numbers for the forward steps; even numbers for the reverse direction). The various enzyme species present in the mechanism are placed below the horizontal line (in sequence of their formation). Species that are interconverted by a unimolecular step are usually grouped together within parentheses. (A) Random mechanism, (B) ordered mechanism, and (C) Theorell–Chance mechanism. The last is a limiting case of an ordered mechanism in which the EAB + EPQ central complex does not account for a significant fraction of the total enzyme in the steady state. (D) Ping-pong mechanism where stable enzyme form F may be a covalent adduct of E with the part of substrate A left behind.

of the double-reciprocal plots. (The former is a replot of $K_{m,app}/V_{max,app}$; the latter is a replot of $1/V_{max,app}$.) For example, the replots for the family of $1/v$ versus $1/[B]$ plots at different fixed $[A]$ are described by the following linear equations:

$$\text{int} = \frac{K_{mA}}{V_{max}}\frac{1}{[A]} + \frac{1}{V_{max}} \tag{29}$$

$$\text{slope} = \frac{K_{mB}K_{ia}}{V_{max}}\frac{1}{[A]} + \frac{K_{mB}}{V_{max}}. \tag{30}$$

V_{max}, K_{mA}, K_{mB}, and K_{ia} can be determined from the intercepts of the replots.

The equations for the substituted enzyme (ping-pong) bireactant mechanism in the absence of products is

$$v = \frac{V_{max}[A][B]}{K_{mB}[A] + K_{mA}[B] + [A][B]}. \tag{31}$$

When $[A]$ is varied at different $[B]$, the Michaelis–Menten and double reciprocal equations are

$$v = \frac{V_{max}[A]}{K_{mA} + \left(1 + \dfrac{K_{mB}}{[B]}\right)} \tag{32}$$

and

$$\frac{1}{v} = \frac{K_{mA}}{V_{max}}\frac{1}{[A]} + \frac{1}{V_{max}}\left(1 + \frac{K_{mB}}{[B]}\right). \qquad (33)$$

The equations for varied $[B]$ at different $[A]$ are symmetrical to those shown for varied $[A]$. Figure 3 shows the families of $1/v$ versus $1/[A]$ plots for an ordered and a ping-pong mechanism. In both mechanisms different fixed $[B]$ values affect the vertical-axis intercepts. In the ordered mechanism, changing $[B]$ also affects the slopes of the $1/v$ versus $1/[A]$ plots. But in the ping-pong mechanism, changing the fixed $[B]$ has no effect on the slopes. (Note that eqns. (24) and (33) predict these effects.) The absence of a slope effect is often sufficient to identify the ping-pong mechanism. But the presence of both slope and intercept effects (as shown in Figure 3A) is not sufficient to diagnose the mechanism as ordered because in the absence of products, a steady-state ordered, a Theorell–Chance, and a rapid-equilibrium random mechanism all have the same velocity equation. Consequently, the double-reciprocal plot patterns of the three different mechanisms are the same. Additional measurements are needed to distinguish between these mechanisms. Product inhibition studies can be informative. For example, in a steady-state ordered mechanism, one of the products (P, the first to dissociate from the enzyme) is noncompetitive with respect to both substrates, but in a Theorell–Chance and random mechanism, each product is competitive with at least one substrate. Dead-end inhibition studies may also be useful. For example,

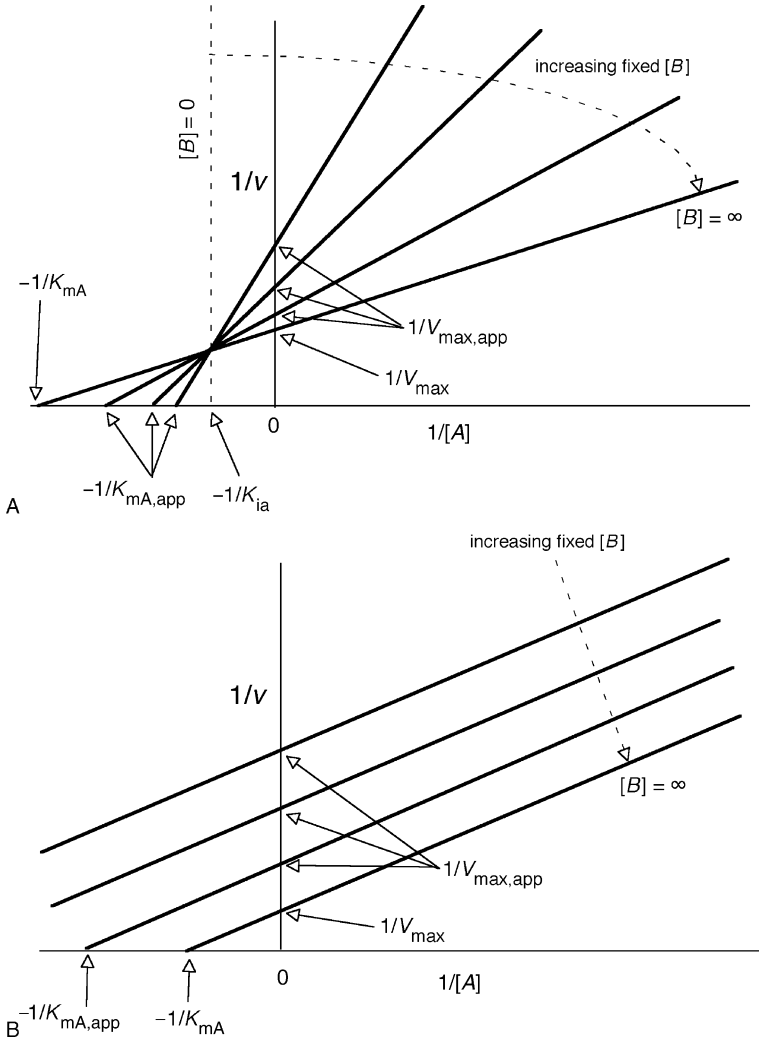

FIGURE 3 Double-reciprocal plots of $1/v$ versus $1/[A]$ at different fixed concentrations of B. A is called the varied substrate; B is called the changing fixed substrate. (A) A sequential mechanism. The plots could be for a steady-state ordered, Theorell–Chance, or a rapid-equilibrium random mechanism. (B) Ping-pong mechanism. For the above mechanisms, the plots of $1/v$ versus $1/[B]$ at different fixed $[A]$ have the same appearance as for varied $1/[A]$. The limiting kinetic constants, K_{mA}, K_{mB}, K_{ia}, V_{max}, etc., are obtained by replotting the slopes and/or $1/v$-axis intercepts of the double-reciprocal plots against the reciprocal of the changing fixed substrate concentration.

a nonreactive analogue that is competitive with B will be uncompetitive with A in the ordered and Theorell–Chance mechanisms, but noncompetitive with A in the random mechanism. (This assumes that the inhibitor forms an EAI complex in the Theorell–Chance mechanism and mimics substrate B completely in the random mechanism by binding to both E and EA.)

Cleland's Slope and Intercept Rules

W. W. Cleland has presented a series of rules for predicting the effect of changing the fixed concentration of a co-substrate or product on the slopes and vertical-axis intercepts of $1/v$ versus 1/[varied substrate] plots. The slope and intercept effects are predicted separately and then combined to deduce the appearance of the double-reciprocal plot family. Conversely, the slope and intercept patterns can help to diagnose the kinetic mechanism. The rules are as follows.

Intercept Effect

A changing fixed substrate or product will cause an intercept effect if it and the varied substrate combine with different enzyme forms. Exceptions: an intercept effect will not be seen for a changing fixed ligand that adds to the enzyme before the varied substrate under rapid-equilibrium conditions, or in a Theorell–Chance "hit-and-run" sequence between a substrate and the immediately released product (B and P in Figure 2C).

Slope Effect

A changing fixed substrate or product will cause a slope effect if it and the varied substrate combine with the same enzyme form, or with different forms that are "reversibly connected" in the upstream or downstream direction. Two enzyme forms will not be reversibly connected if either (1) a product release step occurs between them and that product is at zero concentration in the assay solution, or (2) a substrate addition step occurs between the two enzyme forms and that substrate is present at a saturating concentration. Both the upstream and downstream directions must be blocked to eliminate reversibility.

A product will have no effect on slopes or intercepts if the steady-state level of the enzyme form with which it combines is zero because of saturation with a competitive substrate.

Similar rules predict the slope and intercept effects produced by dead-end inhibitors.

See Also the Following Articles

Allosteric Regulation • Enzyme Inhibitors

Glossary

catalytic rate constant (k_{cat}) Moles of substrate converted to product per second per mole of enzyme active site; also called active-site turnover number.

kinetic mechanism The order in which substrates add and products are released in an enzyme-catalyzed reaction.

maximal velocity (V_{max}) Maximum reaction rate (v observed at saturating substrate concentrations) for a given concentration of enzyme: $V_{max} = k_{cat}[E]_t$.

Michaelis constant (K_m) Kinetic constant equivalent to the concentration of the varied substrate that yields half-maximal velocity when all other substrates are saturating.

rapid equilibrium Condition where the ligands and enzyme species present are at chemical equilibrium.

steady state Condition where the rate of formation of an intermediate is equal to the rate of its utilization.

Further Reading

Cleland, W. W. (1963). The kinetics of enzyme-catalyzed reactions with two or more substrates or products. *Biochim. Biophys. Acta* **67**, 104–137, 173–187, 188–196.

Cornish-Bowden, A. (1995). *Fundementals of Enzyme Kinetics*. Portland Press, London.

Fromm, H. J. (1975). *Initial Rate Enzyme Kinetics*. Springer, Berlin.

Gutfreund, H. (1995). *Kinetics for the Life Sciences*. Cambridge University Press, Cambridge.

Kuby, S. A. (1991). *A Study of Enzymes, Vol 1: Enzyme Catalysis, Kinetics, and Substrate Binding*. CRC Press, Boca Raton, FL.

Purich, D. L., and Allison, R. D. (2000). *Handbook of Biochemical Kinetics*. Academic Press, San Diego, CA.

Segel, I. H. (1976). *Biochemical Calculations*. 2nd edition, Ch. 4, Wiley, New York.

Segel, I. H. (1993). *Enzyme Kinetics: Behavior and Analysis of Rapid Equilibrium and Steady State Enzyme Systems*. Wiley Classics Library, Wiley-Interscience, New York.

Biography

Irwin H. Segel is a Professor in the Section of Molecular and Cellular Biology at the University of California, Davis. His major research interests are in the structure–function relationships of the inorganic sulfate activating enzymes, ATP sulfurylase and APS kinase. He received his Ph.D. from the University of Wisconsin and did postdoctoral research at the Centre National de la Recherche Scientifique in Marseille. He is a Fellow of the American Association for the Advancement of Science.

Enzyme Reaction Mechanisms: Stereochemistry

Ming-Daw Tsai, Li Zhao and Brandon J. Lamarche
The Ohio State University, Columbus, Ohio, USA

Stereochemistry **is the facet of chemistry concerned with the three-dimensional properties of molecules. The history of stereochemistry began in 1815 when Jean-Baptiste Biot discovered that some molecules are capable of rotating the plane of polarized light. Louis Pasteur suggested in 1850 that this phenomenon could be attributed to the stereochemical properties of molecules. In the subsequent 150 years it has come to be understood that stereochemistry is all-important in biology, where a molecule's structure and function are inextricably related. Though synthetic chemists are increasingly adept at controlling the stereochemistry of chemical reactions, enzymes – nature's catalysts – remain the paradigm for stereochemical control. Stereochemical analysis of enzymatic reactions can therefore yield information about the mechanism of enzyme action. That is the focus of this entry.**

Explanation of Stereochemical Terms

Figure 1 uses chemical structures to illustrate key stereochemical terms. *Stereomers* (or stereo isomers) are molecules that have the same molecular formula and the same order of attachment of atoms, but they differ in the way their atoms are oriented in space. Any molecule that cannot be superimposed on its mirror image is said to be *chiral*. Though chirality can result from a number of molecular properties, it is usually due to the presence of one or more carbon or phosphorus atoms, called chiral centers, which are surrounded by four unique substituents. Chiral molecules are classified as either *enantiomers* (stereoisomers that are mirror images of each other) or *diastereomers* (stereoisomers that are not mirror images of each other).

Configuration specifies how substituents are oriented around a chiral center and is determined by the *R*–*S* notation system, where *R* and *S* refer to the Latin terms *rectus* (right) and *sinister* (left). To assign *R*/*S* configuration, a priority rating is given to each substituent at a chiral center using the following rules: Priority is first assigned on the basis of atomic number with highest priority given to the atom with the highest atomic number. When identical atoms are directly attached to the chiral center, the next atoms on the substituent are compared, until a difference is noted. Once priority has been established, the molecule is oriented so that the lowest priority substituent is pointing away from the viewer. The direction of rotation observed when moving from the highest to lowest priority will now be either clockwise or counterclockwise and the configuration is designated *R* or *S*, respectively.

An atom that is attached to two unique substituents and two identical substituents is said to be prochiral. The two identical groups at a prochiral center can be designated as pro-*R* and pro-*S* following a prochirality rule. As shown in Figure 1C, the pro-*R* hydrogen (H_R) is the one that leads to R configuration if it is given a higher priority than the other hydrogen atom. When a chiral center or prochiral center is phosphorus instead of carbon, a subscript p is added (i.e., R_P, S_P, pro-R_P, pro-S_P).

Stereoselectivity, Stereospecificity, and Stereochemical Course of Enzymatic Reactions

If exposed to a racemic mixture of substrates, most enzymes utilize one enantiomer or diastereomer preferentially. In reactions where chemistry is occurring at a prochiral center, an enzyme is also likely to act on just one of the two available enantiotopic or diastereotopic groups. The enzyme is said to be *stereoselective* in both cases.

Enzymatic reactions are almost always *stereospecific*, which means that they convert one stereoisomer of substrate to one stereoisomer of product. For substitution reactions, *stereochemical course* refers to the change (or lack thereof) in configuration at the reaction center in a stereospecific reaction. While *retention* means the new group occupies the same position as the

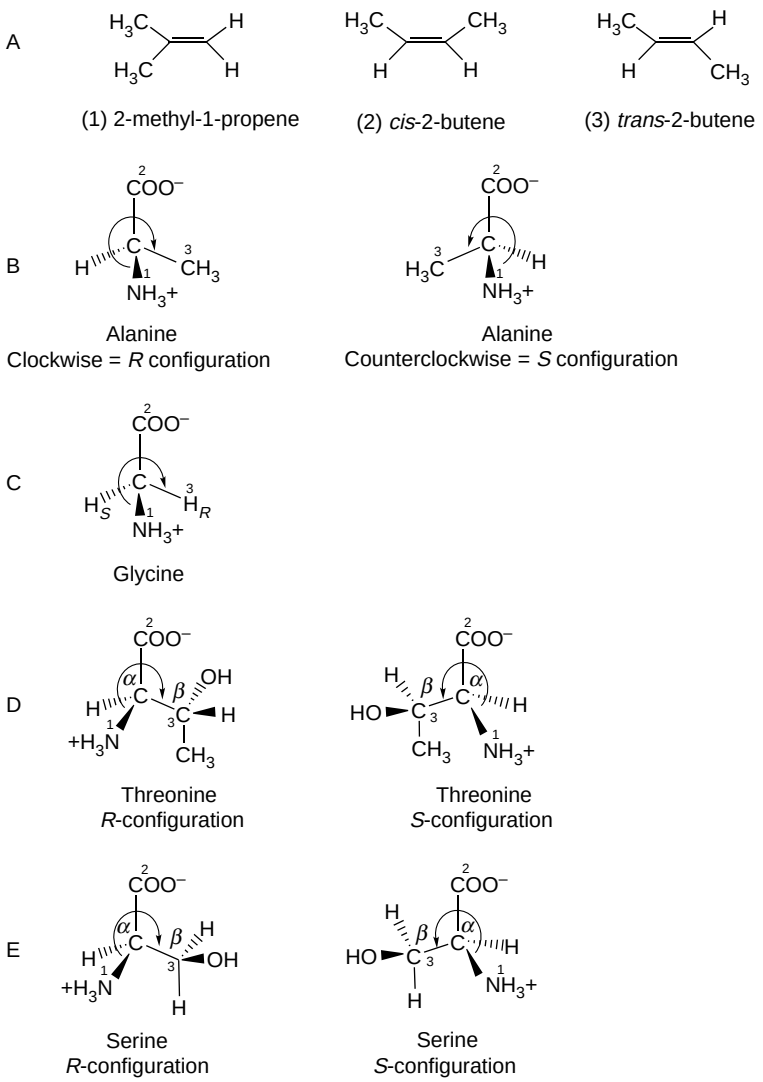

FIGURE 1 Demonstration of stereochemical terms using structures. (A) Though molecules 1, 2, and 3 have the same molecular formula, only 2 and 3 are stereoisomers. Molecule 1 has a different pattern of bonding (i.e., a different linkage of atoms) and is therefore a structural isomer of molecules 2 and 3. (B) Alanine stereoisomers are *enantiomers* since they are mirror images of each other. Note that the different configuration of substituents about the central carbon makes it impossible to superimpose the two isomers. (C) Glycine is *achiral* and therefore does not have stereoisomers. However, the central carbon is a prochiral center since it can be converted to a chiral center by replacing one of the two hydrogens with a different group. The two hydrogens are said to be *enantiotopic* since the separate replacement of each hydrogen results in a pair of enantiomers. (D) The two stereoisomers of threonine shown are diastereomers, i.e., stereo isomers that are not complete mirror images of each other. Note that this pair of molecules results by altering the configuration at C_α while leaving the configuration at the C_β unmodified. (E) Serine contains a chiral center at C_α and a prochiral center at C_β. Unlike glycine, the two hydrogen atoms at the prochiral center of serine are *diastereotopic* groups since the separate replacement of each hydrogen results in a pair of diastereomers.

displaced group, *inversion* means it occupies the opposite position. If the reaction is non-stereospecific, it leads to racemization, with both isomers being formed at a ratio close to 1:1. Note that an *R*-substrate does not necessarily give an *S*-product in an inversion reaction, since the priority of the substituents at the reaction center can be altered on going from substrate to product. Also note that there is a steric course (inversion or retention) even when the displacement occurs at a prochiral center or a pro-prochiral center (a methyl group or phosphoryl group). The three hydrogen atoms of a methyl group and the three oxygen atoms of a phosphoryl group are homotopic and cannot be differentiated from one another by an enzyme. In these cases, there is no issue of stereoselectivity, only steric cause. Experimentally, pro-prochiral centers can be made chiral via isotope substitution, which in turn allows elucidation of the steric course of the reaction as illustrated in Figures 2B and 2C.

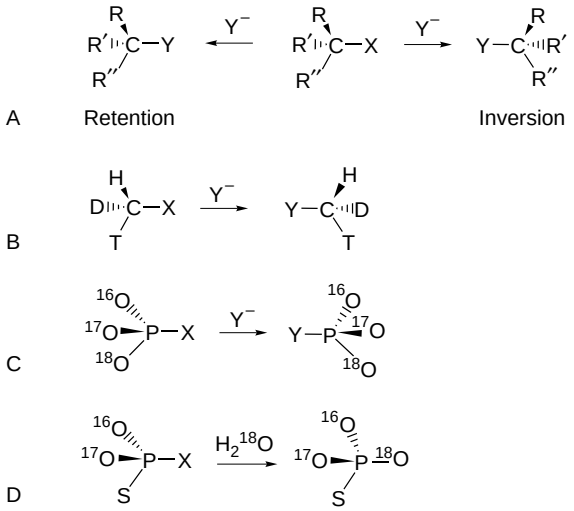

FIGURE 2 Illustration of possible steric courses of enzymatic reactions and application of isotope substitutions to elucidate the steric course. Steric courses shown in B, C, and D are inversion, inversion, and retention, respectively.

In addition to the use of oxygen isotopes, an oxygen atom at a prochiral or pro-prochiral center can also be replaced by a sulfur atom. These phosphorothioate analogs have found broad applications in the study of diverse biological systems. The stereochemical course of phosphatases, which convert a phosphomonoester to inorganic phosphate, have been deciphered in this manner, as illustrated in Figure 2D.

Key steps in conducting stereochemical experiments are the synthesis of isomers of chiral substrates and/or substrate analogs and the analysis of a compound's stereochemical configuration before and after being processed by an enzyme. Since different substrate analogs are required for each enzyme studied, and since isotopes are frequently used, these studies are particularly challenging.

Pioneering Study: Alcohol Dehydrogenase (ADH)

Yeast alcohol dehydrogenase (ADH) catalyzes the reversible transfer of a hydrogen atom between a molecule of ethanol and a molecule of the coenzyme nicotinamide-adenine dinucleotide (NAD^+). By use of deuterated ethanol or coenzyme, ADH was shown to abstract the pro-*R* hydrogen of ethanol and adding it to the *re* face of NAD^+, as illustrated in Figure 3.

Analysis of Steric Course to Probe an Enzymatic Reaction Pathway

In nonenzymatic reactions, a bimolecular S_N2 reaction leads to inversion of configuration of the chiral carbon, while a unimolecular S_N1 reaction generates a planar carbonium ion that reacts randomly at each face to generate a racemic product. In enzymatic reactions, however, the steric course is usually an inversion for both types of mechanisms, since the carbonium ion is not free to rotate within the active site. Thus, an inversion of steric course can be used to conclude that the reaction involves an odd number of displacements (most likely single displacement), whereas retention can be used to conclude that the reaction involves an even number of displacements (most likely two displacements involving an E–S intermediate).

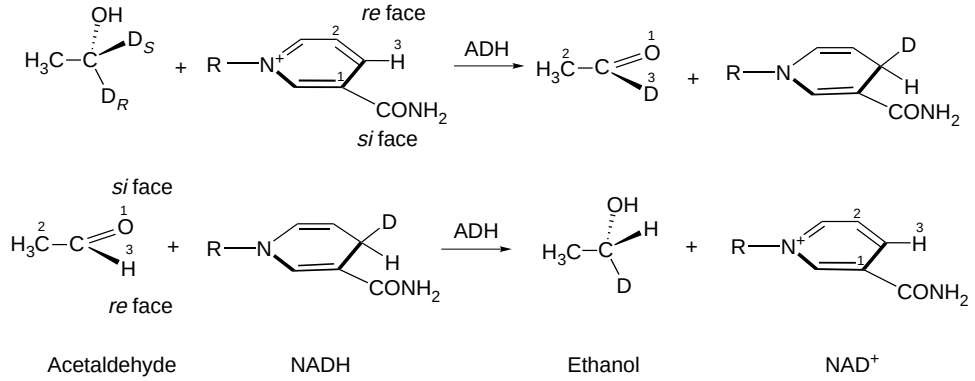

FIGURE 3 Stereochemistry involved in the reaction catalyzed by yeast alcohol dehydrogenase (ADH). In the forward reaction, the pro-*R* hydrogen of ethanol is transferred to the *re* face of NAD^+ to give NADH and acetaldehyde. In the reverse reaction, the pro-*R* hydrogen of NADH is transferred to the *re* face of acetaldehyde. The numbers 1, 2, and 3 designate the priorities of the substituents at the sp^2 carbon. The *re* and *si* faces of NADH are diastereotopic faces (since "R" includes stereocenters) whereas those of acetaldehyde are enantiotopic faces.

Phosphoryl transfer reactions are described by different terminology, where dissociative and associative mechanisms generally correspond to S_N1 and S_N2, respectively. The associative mechanism can be executed via in-line or adjacent mechanisms. In the adjacent mechanism, the nucleophile enters on the same side as the leaving group, generating a pentavalent intermediate with trigonal bipyramidal geometry. However, for the reaction to proceed, both the nucleophile and the leaving group must occupy apical positions. Therefore, pseudorotation – rearrangement of substituents about the reaction center such that the leaving group shifts from an equatorial to an axial position – must occur before the leaving group can be expelled. Except when the adjacent mechanism appears likely, the steric course of the reaction is also used to obtain information about the number of phosphoryl transfers.

Information about an enzyme's steric course is very useful for elucidating the reaction pathway as illustrated by the following example: mammalian phosphatidylinositol-specific lipase C (mPI-PLC) catalyzes the simultaneous formation of 1,2-cyclic phosphate (IcP) and inositol phosphate (IP) from phosphatidylinositol (DPPI). Two reaction schemes, sequential and parallel, can account for this behavior (Figure 4). Examination of the steric course of the mPI-PLC catalyzed reaction, where inversion of configuration at the phosphate center of IcP and retention of configuration at the phosphate center of IP were found, led to the conclusion that the reaction pathway is sequential.

Stereoselectivity Can Probe Metal–Nucleotide or Enzyme–Substrate Interactions at the Transition State

Enzymes catalyze reactions by stabilizing the transition state. Knowledge of enzyme substrate interactions at the transition state is therefore requisite for understanding the mechanism of enzyme action. Though structures of enzyme–substrate complexes are useful, they can only provide information about ground state interactions. Since enzymatic stereoselectivity is a consequence of steric and electronic constraints within the enzyme active site at the transition state, stereochemical studies can provide information about catalytic interactions that is often unattainable via structural work alone.

Since there are numerous points of contact between an enzyme and its substrate throughout a reaction pathway, stereoselectivity alone is often not sufficient for providing information about a particular enzyme–substrate interaction. However, this difficulty is circumvented by employing substrate analogs in conjunction with stereochemical analysis. For example, most enzymes that utilize ATP prefer one isomer of ATPαS or ATPβS over the other. Such R_P/S_P (or S_P/R_P) stereoselectivity can be caused by phosphate–metal-ion interactions, phosphate–enzyme interactions, or both types of interactions. A reversal (or a dramatic change) of stereoselectivity in the presence of an

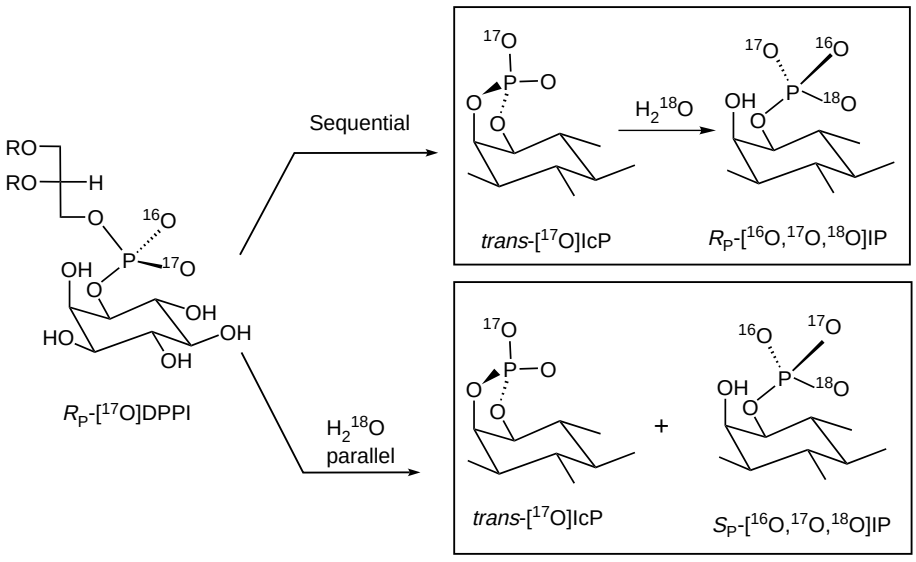

FIGURE 4 Proposed sequential and parallel mechanisms for the formation of IcP and IP catalyzed by mPI-PLC. In the sequential mechanism, intramolecular attack by the axial ring hydroxyl forms the cyclic intermediate (IcP), which is then broken down by hydrolysis ($H_2^{18}O$) to give R_P-[^{16}O, ^{17}O, ^{18}O] IP. In the parallel mechanism, intramolecular attack by the axial ring hydroxyl and direct water ($H_2^{18}O$) attack gives S_P-[^{16}O, ^{17}O, ^{18}O] IP, respectively.

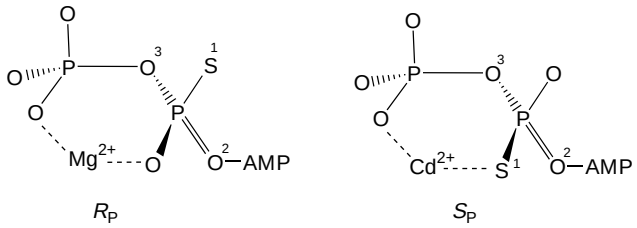

FIGURE 5 Metal–nucleotide interactions showing that substitution of Mg^{2+} by Cd^{2+} leads to a change in the stereoselectivity of AK from R_P-ATPβS to S_P-ATPβS.

"unnatural" metal ion or upon mutating an active site residue provides strong evidence that the metal ion or mutated residue interacts with that particular phosphate moiety. Studies of adenylate kinase (AK) described below further illustrate this point.

AK catalyzes the reversible phosphoryl transfer reactions: $Mg^{2+} \cdot ATP + AMP \leftrightarrow Mg^{2+} \cdot ADP + ADP$. Of the R_P and S_P isomers of ATPβS shown in Figure 5, AK prefers the S_P isomer by a factor of 9 in the presence of Mg^{2+}. However, this stereoselectivity is reversed (R_P isomer is preferred by a factor of 10) when Mg^{2+} is substituted by Cd^{2+}. Since Cd^{2+} preferentially coordinates sulfur over oxygen, which is opposite to the ligand preference of Mg^{2+}, the switch of stereospecificity upon Cd^{2+} substitution is strong evidence for direct coordination of the metal ion by the pro-*S* oxygen of the

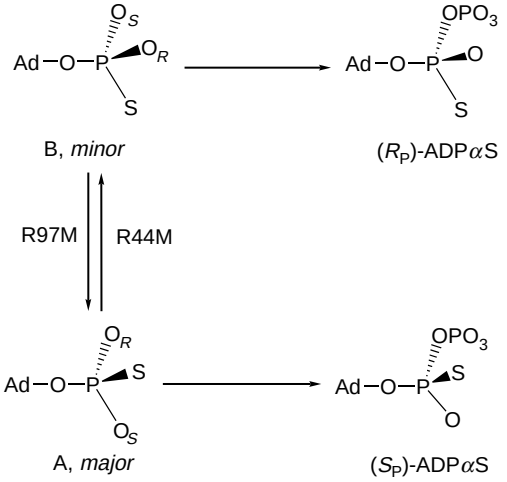

FIGURE 6 Enhancement and reversal of adenylate kinase stereoselectivity by site-directed mutagenesis (Ad, adenosine). In the reaction catalyzed by WT protein, phosphate is preferentially attached to the pro-*R* oxygen of AMPS. The R97M and R44M mutations enhance and reverse this stereoselctivity, respectively. This provides strong evidence that R97 and R44 interact with the phosphate moiety of AMP at the transition state. A and B represent two "conformers" of AMPS when bound to the active site of the enzyme.

β-phosphate of ATP. Additional mechanistic information for AK was derived using active site mutants. Wild type AK catalyzes the stereoselective conversion of AMPS to S_P-ADPαS. Such stereoselectivity could be achieved by restricting orientation of the P–S and P–O bonds at the active site as shown in Figure 6. Experimental results demonstrated that the stereoselectivity of this reaction is further enhanced by the R97M mutant, but is completely reversed in the reaction catalyzed by the R44M mutant. These results indicate that the conformational equilibrium of the AMPS substrate in the active site is perturbed in both mutants, suggesting that the Arg97 and Arg44 residues interact with the phosphate moiety of AMPS.

See Also the Following Articles

Carbohydrate Chains: Enzymatic and Chemical Synthesis • Enzyme Inhibitors • Substrate Binding, Catalysis, and Product Release

Glossary

enzyme-catalyzed reaction Usually stereospecific; many of them are also stereoselective. The stereochemical property of an enzymatic reaction is useful in elucidating its reaction mechanism.

stereoselectivity The ability of an enzyme to choose from two or more possible stereoisomers as a preferred substrate, to choose from two enantiotopic groups or from two diastereotopic groups, or to produce one stereoisomer as a preferred product when more than one stereoisomeric products are possible.

stereospecificity The ability of an enzyme to convert a particular stereoisomeric substrate to a specific stereoisomeric product. For a substitution reaction, the stereochemical course of a stereospecific reaction can be retention or inversion.

Further Reading

Bruzik, K. S., and Tsai, M.-D. (1991). Phospholipase stereospecificity at phosphorus. *Methods Enzymol.* **197**, 258–269.

Fersht, A. (1998). *Structure and Mechanism in Protein Science: A Guide to Enzyme Catalysis and Protein Folding*. Freeman, New York.

Floss, H. G., and Tsai, M.-D. (1979). Chiral methyl groups. *Adv. Enzymol.* **50**, 243–302.

Knowles, J. R. (1980). Enzyme-catalyzed phosphoryl transfer reactions. *Ann. Rev. Biochem.* **49**, 877–919.

Tomasselli, A. G., and Noda, L. H. (1983). Baker's yeast adenylate kinase. Evidence of conformational change from intrinsic fluorescence and difference spectra. Determination of the structure of enzyme-bound metal-nucleotide by use of phosphorothioate analogues of ATP. *Eur. J. Biochem.* **132**, 109–115.

Tsai, M.-D. (1982). Use of $^{31}P(^{18}O)$, $^{31}P(^{17}O)$, and ^{17}O NMR methods to study enzyme mechanisms involving phosphorus. *Methods Enzymol.* **87**, 235–279.

Tsai, M.-D., Jiang, R. T., Dahnke, T., and Shi, Z. (1995). Manipulating phosphorus stereospecificity of adenylate kinase by site-directed mutagenesis. *Methods Enzymol.* **249**, 425–443.

Biography

Ming-Daw Tsai is a Professor in the Departments of Chemistry and Biochemistry at The Ohio State University. Dr. Tsai's overall research interest lies at the interface between chemistry and biology, in particular, the structure–function relationship of enzymes and proteins. He holds a Ph.D. in Medicinal Chemistry from Purdue University.

Li Zhao holds a Ph.D. in Chemistry from The Ohio State University. Her research focus has been the catalytic mechanism of Phosphatidylinositol-specific lipase C.

Brandon J. Lamarche earned a B.Sc. in Chemistry from Westmont College. In 1999 he started doctoral work in the Department of Chemistry at The Ohio State University. His research interests involve the enzymology of DNA repair.

Epidermal Growth Factor Receptor Family

Denis Tvorogov and Graham Carpenter
Vanderbilt University School of Medicine, Nashville, Tennessee, USA

The physiological state of a single cell in a multicellular organism is generally determined by different extracellular signals presented to the cell. Many of these extracellular signals transduce their cellular response by recognizing and activating a receptor with intrinsic tyrosine kinase activity. Among these is the epidermal growth factor receptor family, also known as the ErbB family of receptors.

Receptors and Ligands

The ErbB family is comprised of four receptor tyrosine kinases: ErbB-1 (also known as an epidermal growth factor [EGF] receptor), ErbB-2, ErbB-3, and ErbB-4. These receptors are thought to mediate signal for cell proliferation, differentiation, migration, or apoptosis. Deregulated expression or mutational activation of ErbB receptors, especially ErbB-1 and ErbB-2, has been found in numerous types of human cancer.

Eleven different EGF-like growth factors, which directly activate ErbB receptors, have been identified: EGF, transforming growth factor alpha (TGF-α), amphiregulin, heparin-binding-EGF (HB-EGF), epiregulin, betacellulin, epigen, and the neuregulins (NRG-1, NRG-2, NRG-3, NRG-4) also known as heregulins. ErbB receptors are subgrouped by their ligand-binding properties. ErbB-1 recognizes EGF, TGF-α, amphiregulin, HB-EGF, epiregulin, epigen, and betacellulin. ErbB-3 binds NRG-1 and NRG-2. ErbB-4 binds NRG-1–4, betacellulin, epiregulin, and HB-EGF (Figure 1). As yet no ligand has been identified for ErbB-2, but significant data suggest that ErbB-2 serves as a coreceptor for all other ErbBs. The binding of a ligand with an ErbB receptor induces the formation of homodimers and heterodimers, particularly with ErbB-2. Dimerization is a mechanism to provoke receptor autophosphorylation and thereby stimulate the intrinsic tyrosine kinase activity of the receptors.

The Structure of ErbB Receptors

The domain structure of the ErbB receptors consists of an extracellular ligand-binding domain, a single transmembrane (TM) domain, and an intracellular region (Figure 1). The extracellular domains of all ErbB receptors are highly glycosylated and are subdivided into four subdomains, termed I, II, III, and IV. Domains II and IV are cysteine-rich regions, and are highly conserved among the ErbBs. Domains I and III cooperate to form a growth factor-binding site as demonstrated by the crystal structure of the extracellular region of the ErbB-1 receptor with EGF and TGF-α. These data further indicate that growth factor binding induces conformational changes in subdomain II, which leads to dimerization through a direct receptor:receptor interaction.

The TM domain of each ErbB receptor contains 20–25 amino acid residues forming five loops of α-helical structure, and probably plays a passive role in signal transduction. This conclusion is based on experiments with ErbB-1 receptors containing a mutated TM region. Different forms of the ErbB-1 receptor with extended or shortened TM regions were able to bind EGF and dimerize. Alterations generated within the TM domain did not prevent receptor autophosphorylation.

The intracellular domain of ErbB receptors contains a tyrosine kinase domain and autophosphorylation sites (Figure 1). The tyrosine kinase domain is highly conserved among all four ErbB receptors; however, the ErbB-3 has a defective tyrosine kinase domain due to several residue changes. ErbB-3, therefore, must dimerize with a kinase competent receptor (ErbB-2 is preferred) to form a signaling competent complex.

Binding of ligand to an ErbB receptor provokes autophosphorylation of multiple tyrosine residues within the carboxy-terminal domain. Together with adjacent residues each phosphotyrosine residue serves as a receptor docking site for proteins involved in

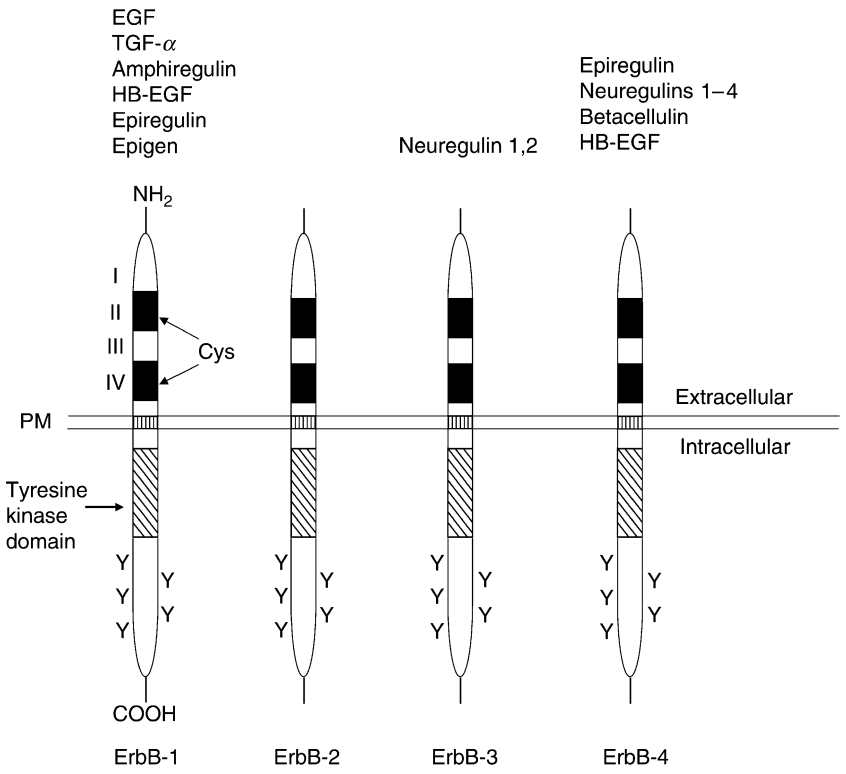

FIGURE 1 Structure of ErbB receptors. Each receptor contains an extracellular region bearing with cysteine-rich domains (Cys, filled), a single TM domain (vertical hatched), and a cytoplasmic region consisting of a tyrosine kinase domain (diagonal hatched) and tyrosine residues (Y) on the C-terminal domain which can be phosphorylated by the tyrosine kinase domain. The ErbB-3 receptor has a deficient tyrosine kinase domain (diagonal hatched with a cross). The ligands which bind to these receptors are listed above each receptor.

downstream signaling events (Figure 2). The association between tyrosine phosphorylated sequences and each signaling protein is facilitated by the presence of either an Src homology 2 (SH2) or a phosphotyrosine binding (PTB) domain in the signaling protein. The specificity of the interaction of any given ErbB receptor with an SH2 or PTB domain-containing protein is determined by the exact amino acid sequences surrounding the phosphorylated tyrosine residue, as well as sequences within each SH2 or PTB domain. Generally, receptor docking of these proteins is a prerequisite for tyrosine phosphorylation of these signaling proteins by the receptor and the activation of signal transduction pathways that cooperate to produce cellular responses.

ErbB-1	ErbB-2	ErbB-3	ErbB-4
Shc	Shc	Shc	Shc
Cb1			
Grb2	Grb2		
PLCγ1			
Shp1			
		p85	p85
		Grb7	
STAT	STAT	STAT	STAT

FIGURE 2 Subsets of signaling proteins activated by each ErbB receptor.

ErbB Receptor Substrates

ErbB receptors are involved in the initiation of a variety of cell responses, such as proliferation, differentiation, or cell locomotion, which require changes in gene expression, intracellular Ca^{2+} level, protein and lipid phosphorylation, and other intracellular conditions. Therefore, every activated ErbB receptor interacts with a battery of proteins involved in different signal intracellular pathways. Different ErbB receptors associate with overlapping subsets of intracellular proteins to activate subsets of the same downstream signaling pathways (Figure 2). The list of signaling partners for each ErbB receptor is not entirely determined and most data have been obtained from experiments with the ErbB-1 (or EGF) receptor. Proteins that interact with activated ErbB receptors can be categorized according to

their signaling properties: enzymes participating in phosphatidylinositol metabolism, such as phospholipase Cγ1 and the regulatory subunit of phosphatidylinositol 3-kinase; protein kinases, such as Src; phosphatases, such as Shp1 and Shp2; adaptor proteins, such as Cbl, Shc, Grb2, Nck; and transcription factors, such as STATs. As shown in Figure 2. the signaling pathways activated by the four ErbB receptors frequently overlap. How signaling pathways are actually integrated to provoke a cellular response, such as proliferation, is unknown.

Receptor-Mediated Endocytosis

A second consequence of ligand binding to ErbB receptors is an initiation of rapid receptor-mediated endocytosis (Figure 3). During this process ligand–receptor complexes cluster in cell-surface clathrin-coated pits, which subsequently become intracellular clathrin-coated endosomes. The clathrin coat is then removed to produce early endosomes and this compartment matures to form multivesicular bodies. There are two fates for internalized receptor. First, receptors may undergo recycling, from early endosomes or from multivesicular bodies, to the plasma membrane. Multivesicular bodies become late endosomes and then primary lysosomes where receptor and ligand degradation occurs. Hence, a receptor may be degraded or recycled following the endocytic pathway. Under most circumstances the degradation route is kinetically favored.

Interestingly, only ErbB-1 receptors have been shown to be rapidly internalized following ligand binding. Other ErbB receptors are endocytosis impaired or demonstrate only a very slow endocytotic rate. Experiments with chimeric receptors containing the ErbB-1 extracellular domain and different ErbB-2, ErbB-3, ErbB-4 cytoplasmic regions show extremely low rates of internalization. These data suggest that the structure of the ErbB cytoplasmic domains determines whether or not a given ErbB receptor will be rapidly internalized by clathrin-coated pits. It also has been shown that ErbB-1 tyrosine kinase activity is necessary for ligand-dependent receptor trafficking into clathrin-coated pits and subsequent internalization.

There are two different points of view regarding the significance of endocytosis for growth factor receptor signal transduction. One view is that endocytosis serves as a desensitization mechanism by removing the receptors from the plasma membrane and degrading the activated receptors in the lysosome. Indeed, introduction of a truncated form of EGF receptor that retains kinase activity is internalization defective and leads to enhanced mitogenic responses and cellular transformation after treatment with EGF. A second viewpoint is that positive signaling occurs during endocytosis. It has been shown that EGF receptors in endosomes retain bound EGF, are authophosphorylated, and are able to activate some intracellular signaling pathways. This suggests that receptor-mediated endocytosis may serve as a mechanism for spatial redistribution of activated EGF receptors and transduction of signals.

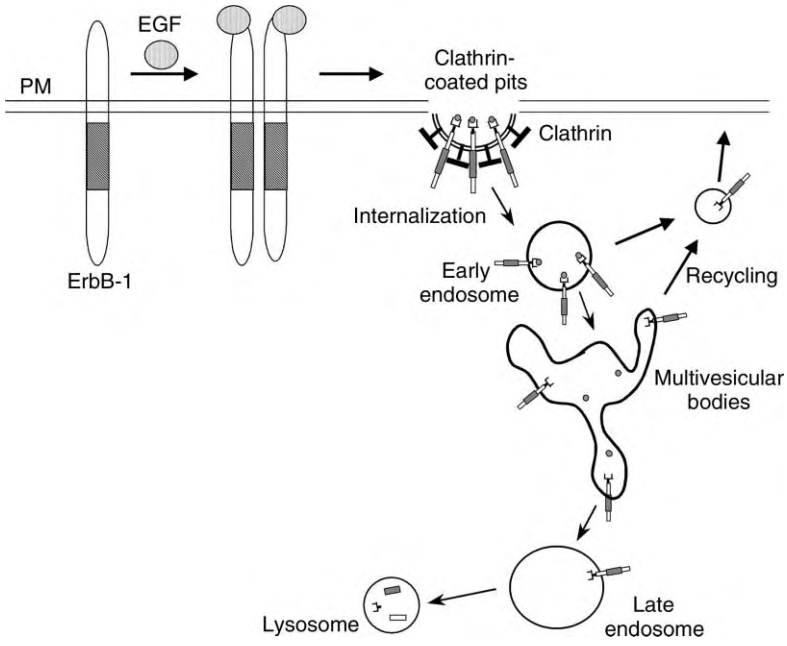

FIGURE 3 Schematic representation of ErbB-1 receptor trafficking following EGF binding.

Targeting ErbB Receptors in Cancer Therapy

During the past several years it has become clear that deregulated signaling from ErbB receptors is involved in cancer development. Among the ErbB receptors, the overexpression or abnormal activation of ErbB-1 or ErbB-2 is most often observed in epithelial carcinomas and glioblastomas. There are three possible mechanisms by which an ErbB pathway may be hyperactivated: ligand overproduction, receptor overexpression, or mutation to produce activated receptors in the absence of a growth factor. Expression of ErbB-1 or its ligand has been reported in over 80% of head and neck squamous cell carcinomas, while its overexpression occurs in breast carcinomas and its mutational activation occurs in glioblastomas. Overexpression of the ErbB-2 receptor is common in breast cancer, ~25% of invasive ductal breast cancers have overexpressed ErbB-2 due to gene amplification. The level of ErbB-2 overexpression correlates with tumor size and its spread to lymph nodes. Breast cancers with ErbB-2 overexpression have a poorer prognosis and are more resistant to chemotherapy. Among all ErbB ligands, the role of TGF-α in human cancer is most characterized. Co-overexpression of TGF-α and ErbB-1 has been found in several types of carcinomas, and overproduction of TGF-α in lung and colon tumors coexpressing ErbB-1 correlates with poor prognosis.

In general, there are two different but related approaches to inhibit Erb-B-mediated signaling in human tumors and both are now in clinical trials. These include monoclonal antibodies and tyrosine kinase selective inhibitors. Several ErbB-1-specific antibodies against the extracellular region of receptor have been developed. The mechanism of inhibiting the activity of the receptor involves antibody binding to the receptor and masking the ligand-binding site. This prevents ligand-binding and receptor activation. Additionally the antibody may enhance receptor internalization and degradation. It is also possible that the antibody marks cells that express an increased level of ErbB-1 and targets them for destruction by the immune system. A humanized antibody to ErbB-2 termed Herceptin has been validated for clinical use and represents one of the first successes of biotechnology in clinical settings. Herceptin slows the proliferation rate of breast cancer cells overexpressing ErbB-2, by increasing the percentage of the cell population in G0/G1 or quiescent states of the cell cycle.

Low-molecular-weight inhibitors are another strategy used *in vivo* to suppress hyperactivated ErbB signaling in human tumors. These compounds competitively inhibit ATP binding at the tyrosine kinase active site and thereby block proliferation. One of these compounds, Iressa, has been cleared for clinical use.

Conservation of ErbB Receptor Signaling during Evolution

ErbB signaling is present not only in mammalians, but also in less-developed organisms such as the nematode *Caenorhabditis elegans* and the fruitfly *Drosophila melanogaster.* The nematode has one EGF-like ligand (Lin-3) and one ErbB-like receptor (Let23). These components are required for correct development in the nematode. In the fruitfly the ErbB signaling network consists of four EGF-like ligands (Vein, Gurken, Spitz, and Argos) and one EGF-like receptor (*Drosophila* EGF receptor – DER). Argos is a unique ligand as it acts negatively to inhibit receptor signaling. In *Drosophila*, ErbB signaling is also required for several developmental pathways. Interestingly, many of the signaling elements found downstream of the mammalian EGF receptor are highly conserved in the nematode and fruitfly. Hence, this growth factor signaling system has been highly conserved throughout millions of years of evolution.

See Also the Following Articles

Phosphatidylinositol Bisphosphate and Trisphosphate • Phospholipase C • Src Family of Protein Tyrosine Kinases • Syk Family of Protein Tyrosine Kinases • Tec/Btk Family Tyrosine Kinases

Glossary

autophosphorylation The process by which a receptor phosphorylates itself. This can be cisphosphorylation or, with context of a dimmer, transphosphorylation.

dimerization The tight association of two proteins, such as receptor tyrosine kinase.

growth factor A small protein which binds to a cell-surface receptor and induces proliferation, differentiation, or other cellular responses dependent on cell type.

receptor A cell-surface molecule that binds a cognate growth factor with high specificity and high affinity and which mediates a biologic response to the growth factor.

tyrosine kinase An enzyme that uses ATP as a phosphate donor to catalyze the formation of phosphotyrosine residues on substrate proteins.

Further Reading

Carpenter, G. (2000). The EGF receptor: A nexus for trafficking and signaling. *Bioessays* **22**, 697–707.

Cho, H. S., and Leahy, D. J. (2002). Structure of the extracellular region of HER3 reveals an interdomain tether. *Science* **297**, 1330–1333.

Garrett, T. P., McKern, N. M., Lou, M., Elleman, T. C., Adams, T. E., Lovrecz, G. O., Zhu, H. J., Walker, F., Frenkel, M. J., Hoyne, P. A., Jorissen, R. N., Nice, E. C., Burgess, A. W., and Ward, C. W. (2002). Crystal structure of a truncated epidermal growth factor receptor extracellular domain bound to transforming growth factor alpha. *Cell* **110**, 763–773.

Ogiso, H., Ishitani, R., Nureki, O., Fukai, S., Yamanaka, M., Kim, J. H., Saito, K., Sakamoto, A., Inoue, M., Shirouzu, M., and Yokoyama, S. (2002). Crystal structure of the complex of human epidermal growth factor and receptor extracellular domains. *Cell* **110**, 775–787.

Olayioye, M. A., Neve, R. M., Lane, H. A., and Hynes, N. E. (2000). The ErbB signaling network: Receptor heterodimerization in development and cancer. *EMBO J.* **19**, 3159–3167.

Sorkin, A., and Von Zastrow, M. (2002). Signal transduction and endocytosis: Close encounters of many kinds. *Nat. Rev. Mol. Cell Biol.* **3**, 600–614.

Sweeney, C., and Carraway, K. L. III., (2000). Ligand discrimination by ErbB receptors: Differential signaling through differential phosphorylation site usage. *Oncogene* **19**, 5568–5573.

BIOGRAPHY

Denis Tvorogov is a Postdoctoral Fellow in the laboratory of Graham Carpenter at Vanderbilt University School of Medicine. He received his Ph.D. from the Institute of Cytology, St. Petersburg, Russia in 2002.

Graham Carpenter's Ph.D. was awarded from the University of Tennessee in 1974. He is a Professor of Biochemistry at Vanderbilt University School of Medicine, where he is also Ingram Professor of Cancer Research.

ER/SR Calcium Pump: Function

Giuseppe Inesi
University of Maryland School of Medicine, Baltimore, Maryland, USA

The sacro-endoplasmic reticulum Ca^{2+} ATPase (SERCA) utilizes ATP for active transport of cytosolic Ca^{2+} into membrane bound intracellular compartments. Intracellular storing of Ca^{2+} by SERCA is an integral part of signaling mechanisms for a large number of cellular functions. The catalytic and transport cycle of SERCA includes formation of a phosphorylated enzyme intermediate and protein conformational changes, leading to vectorial translocation of Ca^{2+} across the membrane.

ATP Use for Ca^{2+} Transport

The sarcoendoplasmic reticulum calcium ATPase (SERCA) is the Ca^{2+} pump of intracellular membranes. The pump plays a prominent role in numerous cytosolic signaling mechanisms that require the sequestration of intracellular Ca^{2+}. The SERCA pump was first noted in a microsomal fraction of rabbit skeletal muscle homogenates, which was found to prevent activation of glycerinated muscle fibers or isolated contractile models upon the addition of ATP. The microsomes were then identified with vesicular fragments of sarcoplasmic reticulum (SR), and the relaxing effect was attributed to sequestration of Ca^{2+} from the medium through active transport by a membrane-bound ATPase. cDNA cloning identified three gene products (SERCA 1, SERCA2, and SERCA3) with two to three splice variants for each primary transcript. The related isoforms display specific tissue distribution, functional roles, and regulatory mechanisms.

The SR vesicles obtained from skeletal muscle contain a high quantity of Ca^{2+} ATPase (SERCA1A isoform), which accounts for approximately 50% of the total protein and which is densely spaced within the plane of the membrane (Figure 1). These vesicles provide a very useful experimental system inasmuch as they allow parallel measurements of ATPase activity and Ca^{2+} transport, as well as control of the ionic environment in compartments delimited by the native membrane. For this reason, they have been used extensively in biochemical and structural studies to clarify the mechanism of ATP use for Ca^{2+} transport.

Steady-State Behavior

Active transport of Ca^{2+} into the lumen of SR vesicles occurs with a stoichiometric ratio of two Ca^{2+} per hydrolyzed ATP under optimal steady-state conditions. Acetyl phosphate or *p*-nitrophenyl phosphate can be used as substrate by the enzyme instead of ATP, although with lesser kinetic competence. The maximal levels of ATP-dependent Ca^{2+} uptake by the vesicles is increased by Ca^{2+} binding to a native acidic protein, calsequestrin, in the lumen of the vesicles. It can also be increased by complexation with anions such as oxalate or phosphate in the lumen of the vesicles.

Independent of the substrate, the ATPase has a strict requirement for Ca^{2+} activation. In fact the enzyme is activated by medium containing free Ca^{2+} within the micromolar range and is inhibited by lumenal free Ca^{2+} in the millimolar range. This indicates that ATP is used to change the affinity and orientation of the Ca^{2+}-binding sites, resulting in a three-orders-of-magnitude Ca^{2+} gradient across the membrane. Furthermore, in reconstituted ATPase preparations that are deprived of pathways for passive leakage, it was shown that Ca^{2+} transport is accompanied by H^+ countertransport at a 1:1 ratio and that the pump is electrogenic.

Considering these functional features, the free energy required for active transport of Ca^{2+} into the vesicles can be defined, at first approximation, as:

$$\Delta G = RT \ln\left(\left[Ca^{2+}_{in}\right]/\left[Ca^{2+}_{out}\right]\right) + zF\Delta V$$

where $[Ca^{2+}_{in}]$ and $[Ca^{2+}_{out}]$ refer to the Ca^{2+} concentration in the lumen of the vesicles and in the outer medium, z is the electrical charge of the transported species, R and F are the gas and Faraday constants, respectively, and ΔV is the transmembrane electrical gradient. The free-energy requirement, estimated in this manner, provides a satisfactory match of the experimentally observed gradients with the chemical potential of ATP.

The Partial Reactions of the Catalytic and Transport Cycles

The Ca^{2+} ATPase catalytic cycle includes a phosphorylated intermediate formed by covalent transfer of the

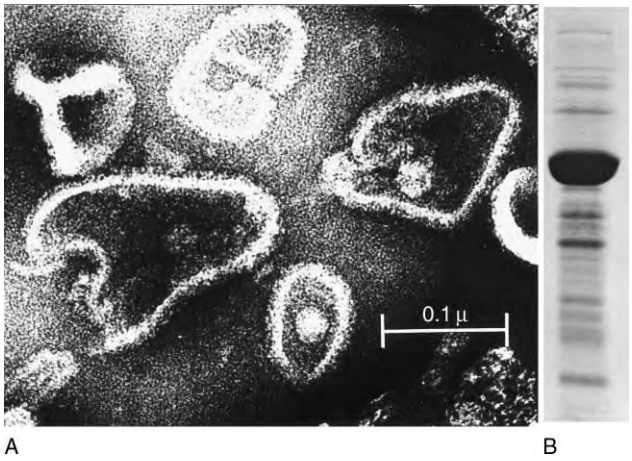

FIGURE 1 Structural characterization of SR vesicles. (A) Negatively stained SR vesicles, obtained from rabbit skeletal muscle, are visualized by electron microcopy. The densely spaced granules on the surface of the membrane correspond to Ca^{2+} ATPase molecules. (B) Electrophoretic analysis demonstrating that the Ca^{2+} ATPase separates as a prominent band that accounts for the major portion of the membrane protein. Adapted from Scales, D. and Inesi, G. (1976). Assembly of ATPase protein in sarcoplasmic reticulum membranes. *Biophys. J.* **16**, 735–751, with permission from the Biophysical Society.

ATP terminal phosphate to an aspartyl residue (Asp351) at the catalytic site. Phosphoryl transfer requires activation by the same Ca^{2+} concentration as ATP hydrolysis, indicating that enzyme activation by Ca^{2+} must occur early in the catalytic cycle. In fact, cooperative binding of two Ca^{2+} per ATPase in the absence of ATP, with an apparent K_d in the micromolar Ca^{2+} range, was demonstrated by direct equilibrium measurements (Figure 2A).

The sequence of partial reactions making up the catalytic cycle was unveiled by transient-state experiments showing that addition of ATP to SR vesicles preincubated with micromolar Ca^{2+} is followed by the rapid formation of phosphorylated intermediate and vectorial displacement of two bound Ca^{2+} per ATPase. These initial events are then followed by hydrolytic cleavage of inorganic phosphate (Pi) after a time lag (Figure 2B). On the other hand, the ATPase cycle is highly reversible, as demonstrated by ATP synthesis coupled to the Ca^{2+} efflux from loaded vesicles. The partial reactions of the reverse cycle were further clarified by the finding that, in the absence of bound Ca^{2+}, the enzyme can be phosphorylated with Pi to yield ADP-insensitive phosphoenzyme (E-P). This phosphoenzyme can then be made ADP-sensitive by the addition of millimolar Ca^{2+}, whereupon it reacts with ADP to form ATP.

These functional findings have been attributed to a mechanism based on the interconversion of two enzyme states. One state (E_1), stabilized by Ca^{2+} binding, has the Ca^{2+} sites in high affinity and cytosolic orientation.

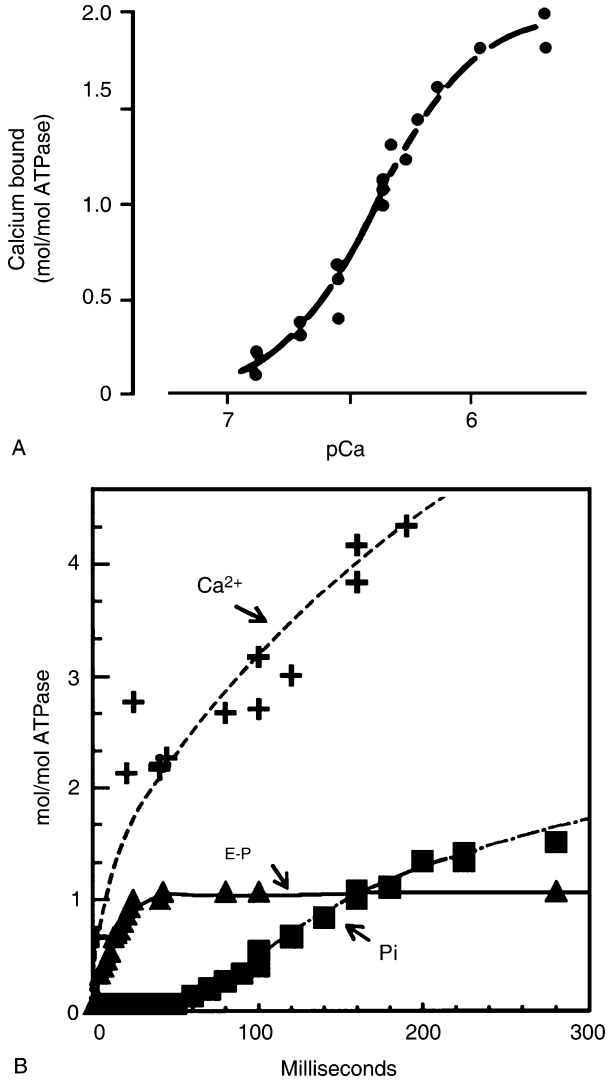

FIGURE 2 Functional characterization of SR vesicles. (A) Calcium binding at equilibrium in the absence of ATP, demonstrating cooperative binding of two Ca^{2+} per ATPase. From Inesi G., Kurzmack M., Coan C., and Lewis D. (1980). Cooperative calcium binding and ATPase activation in sarcoplasmic reticulum vesicles. *J. Biol. Chem.* 255, 3025–3031 with permission from The American Society for Biochemistry & Molecular Biology. (B) Rapid enzyme phosphorylation and inward displacement of the two bound Ca^{2+} upon addition of ATP. Hydrolytic cleavage of inorganic phosphate (Pi) occurs after a lag period. E-P, phosphoenzyme. From Inesi, G., Watanabe, T., Coan, C., and Murphy, A. (1978). The mechanism of sarcoplasmic reticulum ATPase. *Ann. N.Y. Acad. Sci.* **402**, 515–534 with permission.

The alternate state (E_2), stabilized by enzyme phosphorylation, has the Ca^{2+} sites in low affinity and lumenal orientation. A more explicit view of the coupling mechanistic can be obtained by considering a minimal number of partial reactions and their equilibrium constants, as follows:

$$H_2E + 2Ca^{2+}_{out} \equiv E{\cdot}Ca_2 + 2H^+_{out} \qquad (10^{12}\ M^{-2}) \quad (1)$$

$$E{\cdot}Ca^{2+} + ATP \equiv ATP{\cdot}E{\cdot}Ca_2 \qquad (10^{5}\ M^{-1}) \quad (2)$$

$$ATP{\cdot}E{\cdot}Ca_2 \equiv ADP{\cdot}E{\cdot}P{\cdot}Ca_2 \quad (1.0) \qquad (3)$$

$$ADP{\cdot}E{\cdot}P{\cdot}Ca_2 \equiv E - P{\cdot}Ca_2 + ADP \quad (10^{-4}\,M) \qquad (4)$$

$$E - P{\cdot}Ca_2 + 2H^+_{in} \equiv H_2E{-}P + 2Ca^{2+}_{in} \quad (10^{-6}\,M^2) \qquad (5)$$

$$H_2E{-}P \equiv H_2E{\cdot}Pi \quad (1) \qquad (6)$$

$$H_2E{\cdot}Pi \equiv H_2E + Pi \quad (10^{-2}\,M) \qquad (7)$$

where the equilibrium constants (listed after each reaction) relate to conditions allowing constant temperature (25 °C) and pH (7.0).

In the reaction sequence given, the initial high-affinity binding (reaction 1) of two Ca^{2+} activates the enzyme, permitting the use of ATP and the formation of a phosphorylated intermediate (reactions 2–4). In turn, enzyme phosphorylation destabilizes and changes the vectorial orientation of the bound Ca^{2+}, thereby increasing the probability of its dissociation into the lumen of the vesicles (reaction 5). Note that the equilibrium constant for the enzyme phosphorylation by ATP is nearly 1, indicating that the free energy of ATP is conserved by the enzyme and used to change the Ca^{2+}-binding characteristics. Finally, the phosphoenzyme undergoes hydrolytic cleavage and releases Pi (reactions 6 and 7) before entering another cycle. The reaction sequence shows clearly that the direct mechanistic device for translocation of bound Ca^{2+} is enzyme phosphorylation rather than hydrolytic cleavage of Pi.

The Coupling Mechanism

Free-Energy Use

Because the catalytic and transport cycles are likely to include conformational transitions, it should be noted that such transitions are coupled intrinsically with the chemical reactions subjected to experimental measurement and that their influence is reflected by the equilibrium constants just listed. In fact, the standard free energies ($-RT \ln K$) of the partial reactions add up to the standard free energy of ATP hydrolysis (γ-phosphate), as expected. Most interestingly, the standard free-energy diagram for the partial reactions reveals that the chemical potential of ATP does not manifest itself in the phosphoryl transfer or hydrolytic cleavage reactions (K_4 and K_6 near 1) but rather in the drastic reduction of the enzyme affinity for Ca^{2+} (compare K_1 to $1/K_5$). We can, then, write that, under standard conditions:

$$\Delta G = nRT \ln\left(K_a^{\text{CaE-P}}/K_a^{\text{CaE}}\right) \qquad (8)$$

per n calcium ions (2 in our case) transported per cycle, and where the equilibrium constant (listed after the reaction) relates to conditions allowing constant temperature (25 °C and pH 7.0). $K_a^{\text{CaE-P}}/K_a^{\text{CaE}}$ are the association constants of the enzyme for Ca^{2+} in the ground state and following activation by ATP. With reference to the reaction scheme given previously, the two relevant constants are K_1 and $1/K_5$. Note that, as written in the scheme and in the forward direction of the cycle, the equilibrium constant for reaction 1 is Ka, while it is Kd for reaction S.

It is then apparent that the basic coupling mechanism of catalysis and transport consists of the mutual destabilization of Ca^{2+} and phosphorylation sites. Analysis of the amino acid sequence, electron microscopy of ordered ATPase arrays, and diffraction patterns obtained from three-dimensional crystals have shown that the SERCA enzyme is a 100-kDa protein, folded into a membrane-bound region, an extramembranous (cytosolic) region, and a short stalk between them. The membrane-bound region includes 10 helical segments (M1, …, M10) and the calcium-binding domain. On the other hand, the extramembranous region, or headpiece, comprises the nucleotide-binding (N) domain and a phosphorylation (P) domain, in addition to a smaller actuator (A) domain. It is clear that the Ca^{2+}-binding domain and the catalytic domain are separated by a large distance (~ 50Å). Therefore, the interconversion of cation-binding and phosphorylation potentials requires a long-range intramolecular linkage, rendered possible by protein conformational changes. It is, then, useful to relate the binding and covalent reactions to conformational changes that may occur through the catalytic and transport cycles.

Ca^{2+} Binding and Catalytic Activation

Binding of two calcium ions per ATPase molecule is an absolute requirement for enzyme activation. The cooperative character of binding is consistent with a sequential binding mechanism to two interdependent sites (I and II). Spectroscopic studies provided early suggestions of Ca^{2+}-induced conformational effects, accounting for binding cooperativity and enzyme activation. A detailed characterization of the large conformational changes produced by Ca^{2+} binding was recently obtained by high-resolution diffraction studies.

The functional role of the Ca^{2+}-induced conformation change lies in its absolute requirement for enzyme activation, rendered possible by the long-range intramolecular linkage. The requirement for Ca^{2+} involves both ATP use for phosphoenzyme formation in the forward direction of the cycle and the formation of ATP upon addition of ADP to

phosphoenzyme formed with Pi in the reverse direction of the cycle. Activation is not obtained by Ca^{2+} occupancy of the first binding site only but requires the occupancy of the second site, which may then be considered a Ca^{2+} trigger point for enzyme activation. Ca^{2+}-binding affects directly the M4, M5, and M6 transmembrane helices and is then transmitted to the extramembranous region, resulting in the large displacement of the headpiece domains and catalytic activation. Single mutations of several residues in the segments connecting the Ca^{2+}-binding region with the phosphorylation domain, such as M4, M5, and the M6–M7 loop, interfere with the phosphorylation reactions.

Nucleotide Binding and Substrate-Induced Conformational Fit

Nucleotide protection of the ATPase from digestion with proteinase and the mutational analysis of this phenomenon suggest that ATP binding produces a conformational change that includes repositioning of the A domain, concomitant with approximation of the N and P domains to match the molecular geometry of ATP. This substrate effect appears similar to the approximation of nucleotide binding (fingers) and catalytic (palm) domains that occurs in DNA polymerases. Although ATP is likely to form an initial complex with Mg^{2+} due to the cation-binding property of the nucleotide, ATP and Mg^{2+} reach the catalytic site through a random mechanism. Accordingly, the initial nucleotide binding at the substrate site does not include Mg^{2+}, even though the subsequent phosphoryl transfer and hydrolytic reactions require Mg^{2+}. The stabilization provided by Mg^{2+} to the transition state, relative to that of the enzyme–substrate complex, is of definite kinetic advantage.

Phosphoryl Transfer and Hydrolytic Cleavage

The Ca^{2+} ATPase mechanism includes a covalent intermediate, general acid–base catalysis and metal ion assistance. The covalent intermediate is formed through an attack on the electrophilic ATP terminal phosphate by a nucleophilic carboxylate group (D531) within the catalytic site. The phosphoenzyme intermediate reacts, then, with water to yield Pi.

It is useful to consider the Ca^{2+} ATPase catalytic mechanism in the light of the phosphorylserine phosphatase (PSPase), due to a remarkable structural and functional analogy and the high definition available for the PSPase catalytic intermediates. Based on this analogy, and on ATPase mutational analysis, it appears that the terminal phosphate of ATP comes in close proximity to Asp351, stabilized by neighboring residues such as K352, T353, G626, K684, and N706. Mg^{2+} is then coordinated by D703, T353, D351, and phosphate oxygen, participating in the transition state and in all subsequent steps. Furthermore, T353 is likely to serve as a general acid for proton donation to the leaving ADP. The same residue then acts as a general base, extracting a proton from nucleophilic water for hydrolytic cleavage of the phosphoenzyme.

Interconversion of Phosphorylation and Ca^{2+}-Binding Potentials

The specific step related to interconversion of phosphorylation and Ca^{2+}- binding potentials is often referred to as the $E_1P{\cdot}Ca_2 \rightleftharpoons E_2P{\cdot}Ca_2$, to indicate the transition of an intermediate of high phosphorylation potential and high Ca^{2+} affinity to an intermediate of low phosphorylation potential and low Ca^{2+} affinity. The functional and structural information described so far indicates that small conformational changes occurring in concomitance with ATP use at the catalytic site (phosphorylation trigger point) are amplified and transmitted to the Ca^{2+}-binding domain through a long-range relay mechanism. The inversion of phosphoryl oxygen atoms during the transition state of the phosphorylation reaction and the displacement of residues interacting with these oxygen atoms may be the triggering perturbation. This is then followed by large motions of the headpiece domains, which are transmitted to the Ca^{2+}-binding domain in the membrane-bound region. Accordingly, the ability of headpiece domains to chemically cross-link changes drastically as they are displaced by intermediate reactions of the catalytic cycle.

In conclusion, the transduction mechanism relies on a long-range linkage of transmembrane helices and cytosolic domains, whereby large-scale and mutually exclusive motions are triggered by Ca^{2+} binding at one end and ATP use at the other. This is rendered possible by the ability of the protein to use free energy derived from binding and phosphorylation reactions. The cycle proceeds forward to Ca^{2+} release or in reverse to ATP synthesis, depending on the concentrations of ligands, substrate, and products.

Physiological Regulation and Experimental Inhibitors

The SERCA2 isoform of cardiac muscle is subject to physiological regulation by phospholamban (PLB), a 22-kDa pentameric protein undergoing reversible association and dissociation. The PLB monomer

interacts with the ATPase at the level of both the membrane-bound and extramembranous regions of the enzyme. In the presence of PLB, the ATPase activation curve is displaced to a higher Ca^{2+} concentration range. The velocity at nonsaturating Ca^{2+} concentrations is thereby reduced, although the maximal velocity at saturating Ca^{2+} concentrations remains unchanged. This inhibition is reversed when PLB undergoes phosphorylation catalyzed by cAMP and calmodulin-dependent kinases. The phosphorylation-dependent relief of inhibition by PLB is related to the physiological mechanism whereby adrenergic stimuli increase Ca^{2+} storing by SR and improve the contractile performance of the heart muscle *in vivo*. Another small protein, sarcolipin, appears to regulate the Ca^{2+} ATPase in skeletal muscle.

Thapsigargin (TG), a plant-derived sesquiterpene lactone, is a very potent and specific SERCA inhibitor. Although TG is not likely to be a physiologic inhibitor, it is nevertheless an extremely useful experimental tool. TG interferes with all partial reactions of the catalytic cycle and induces stabilization of ordered ATPase arrays, suggesting a general effect on the enzyme. Mutational and structural studies indicate that the TG-binding site resides in a cavity delimited by the M3, M5, and M7 helices near the cytosolic surface of the membrane. It is likely that the presence of TG in this cavity confers structural stabilization to the enzyme, thereby preventing conformational responses to Ca^{2+} binding and phosphorylation reaction, as required for the progression of the catalytic cycle.

See Also the Following Articles

Calcium/Calmodulin-Dependent Protein Kinase II • Calcium/Calmodulin-Dependent Protein Kinases • Calcium-Binding Proteins: Cytosolic (Annexins, Gelsolins, C_2-Domain Proteins) • ER/SR Calcium Pump: Structure

Glossary

long-range linkage A conformational mechanism whereby phosphorylation and Ca^{2+}-binding domains are functionally coupled through a large intramolecular distance, within the ATPase molecule.

partial reactions The sequential steps of the SERCA catalytic and transport cycles, including Ca^{2+} and ATP binding to the enzyme, formation of phosphoenzyme intermediate, translocation of bound Ca^{2+} against a concentration gradient, and hydrolytic cleavage of phosphate.

sarcoendoplasmic reticulum Ca^{2+} ATPase (SERCA) The membrane-bound ATPase involved in Ca^{2+} transport and refilling of intracellular Ca^{2+} stores.

trigger points The phosphorylation domain and Ca^{2+}-binding site II where phosphorylation and occupancy by a Ca^{2+} trigger the long-range linkage for interconversion of phosphorylation and Ca^{2+}-binding potentials.

Further Reading

Andersen, J. P. (1995). Dissection of the functional domains of the sarcoplasmic reticulum Ca^{2+} ATPase by site-directed mutagenesis. *Biosci. Rep.* **15**, 243–261.

East, J. M. (2000). Sarco(endo)plasmic reticulum Ca^{2+} pumps: Our advances in understanding of structure/function and biology. *Mol. Membr. Biol.* **17**, 189–200.

Green, N. M., and Stokes, D. L. (2003). Structure and function of the calcium pump. *Annu. Rev. Biophys. Biomol. Struct.* **32**, 445–468.

Inesi, G., Watanabe, T., Coan, C., Murphy, A. (1978). The mechanism of sarcoplasmic reticulum ATPase. *Ann. N.Y. Acad. Sci.* **402**, 515–534.

Inesi, G., Kurzmack, M., Coan, C., and Lewis, D. (1980). Cooperative calcium binding and ATPase activation in sarcoplasmic reticulum vesicles. *J. Biol. Chem.* **255**, 3025–3031.

Maclennan, D. H., Rice, W. J., and Green, N. M. (1997). The mechanism of Ca^{2+} transport by sarco(endo)plasmic reticulum ATPase. *J. Biol. Chem.* **272**, 28815–28818.

Moller, J. V., Juul, B., and le Maire, M. (1996). Structural organization, ion transport and energy transduction of P-type ATPases. *Biochim. Biophys. Acta* **1286**, 1–51.

Scales, D., and Inesi, G. (1976). Assembly of ATPase protein in sarcoplasmic reticulum membranes. *Biophys. J.* **16**, 735–751.

Toyoshima, C., Nomura, H., and Sagita, Y. (2003). Structural basis for ion pumping by Ca^{2+}-ATPase of sarcoplasmic reticulum. *FEBS Lett.* **555**, 106–110.

Biography

Giuseppe Inesi is a Professor in and Chair of the Department of Biochemistry at the University of Maryland, School of Medicine, Baltimore. His research interest is the mechanism of Ca^{2+} transport by Ca^{2+} ATPase, including kinetic and equilibrium characterizations, protein biochemistry, and mutational analysis. He received an M.D. at the University of Modena, and a Ph.D. at the University of Bologra (Italy). He participated in the initial recognition of Ca^{2+} ATPase and has made major contributions to its characterization.

ER/SR Calcium Pump: Structure

Chikashi Toyoshima and Yuji Sugita
University of Tokyo, Tokyo, Japan

The structures of the Ca^{2+}-ATPase of skeletal muscle sarcoplasmic reticulum (Sarco(Endo)plasmic Reticulum Calcium ATPase 1, SERCA 1) have been determined to 2.4Å resolution for the Ca^{2+}-bound form ($E1Ca^{2+}$, PDB entry code: 1SU4) and to 3.1Å for the unbound (but thapsigargin(TG) bound) form (E2(TG), PDB entry code: 1IWO). Detailed comparison of these two structures reveals that very large rearrangements of the transmembrane helices take place accompanying Ca^{2+} dissociation and binding and that they are mechanically linked with equally large movements of the cytoplasmic domains. Such domain movements are thermal in nature and used efficiently for rearranging various domains to alter the functional properties (e.g., affinity for Ca^{2+}) of the ion pump.

Overall Description of the Structure

Ca^{2+}-ATPase is a tall molecule, ~150Å high and 80Å thick, and comprises a large cytoplasmic headpiece, transmembrane domain made of ten (M1–M10) α-helices, and small lumenal domain (Figure 1). The cytoplasmic headpiece consists of three domains, designated as A (actuator), N (nucleotide binding), and P (phosphorylation) domains. They are widely split in the presence of Ca^{2+} but gather to form a compact headpiece in the absence of Ca^{2+}. The A-domain is connected to M1–M3 helices, and the P-domain to M4 and M5 helices. The N-domain is a long insertion between two parts of the P-domain. The M5 helix runs from the lumenal surface to an end of the P-domain and works as the "spine" of the molecule. On the lumenal side, there are only short loops connecting transmembrane helices, except for the loop of ~40 residues connecting the M7 and M8 helices. The distance between the Ca^{2+}-binding sites and the phosphorylation site is larger than 50Å. For the phosphoryl transfer from ATP to Asp351 to take place, the N-domain has to approach the P-domain even closer than that observed in the E2(TG) form.

The orientations and positions of atomic models with respect to the lipid bilayer are determined from crystallographic constraints and illustrated in Figure 1, in which the models are positioned in the bilayer of dioleoylphosphatidylcholine generated by molecular dynamics calculation. The orientations were found to be the same as in the original crystals. The coordinates of the aligned models can be downloaded from the author's web site (http://www.iam.u-tokyo.ac.jp/StrBiol/models).

Organization of the Transmembrane Domain

Transmembrane Helices

As expected from the amino acid sequence, SERCA1 has ten (M1–M10) transmembrane α-helices, two of which (M4 and M6) are partly unwound for efficient coordination of Ca^{2+}. M6 and M7 are far apart and are connected by a long cytosolic loop that runs along the bottom of the P-domain. The amino acid sequence is well conserved for M4–M6 but not for M8 even within the members of closely related P-type ATPases, such as Na^+K^+- and H^+K^+-ATPases. M7–M10 helices are in fact lacking in bacterial-type I P-type ATPases, and are apparently specialized for each subfamily. Nevertheless, M5 and M7 are packed very tightly at Gly770 (M5) and Gly841 (M7) and Gly845 (M7), forming a pivot for the bending of M5. The M7–M10 helices appear to work as a membrane anchor.

Details of the Ca^{2+}-Binding Sites

It is well established that SR Ca^{2+}-ATPase has two high-affinity transmembrane Ca^{2+}-binding sites and the binding is cooperative. X-ray crystallography of the rabbit SERCA1a in 10 mM Ca^{2+} identified two binding sites in the transmembrane but none outside the membrane.

Figure 2 illustrates the structure of the Ca^{2+}-binding sites. The two Ca^{2+}-binding sites (I and II) are located side by side near the cytoplasmic surface of the lipid bilayer, with the site II ~3Å closer to the surface (Figure 1). Site I, the binding site for the first Ca^{2+},

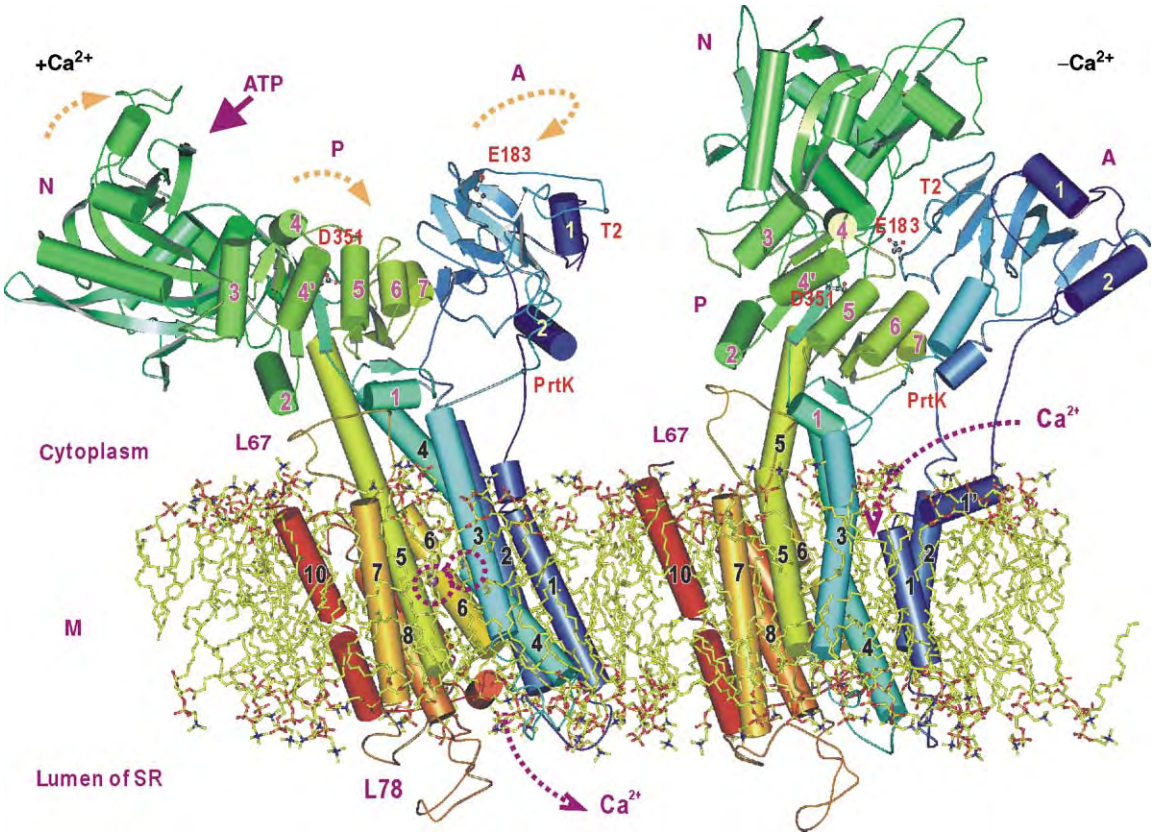

FIGURE 1 Ca^{2+}-bound and unbound forms of Ca^{2+}-ATPase in the lipid bilayer. The bilayer is generated by molecular dynamics simulation of dioleoylphosphatidylcholine. M3 and M5 helices in the unbound form are approximated with two and three cylinders, respectively. The color changes gradually from the N-terminus (blue) to the C-terminus (red). The arrows indicate the directions of movements accompanying the dissociation of Ca^{2+}. Two bound $Ca^{2+}$are shown as purple spheres (circled). T2 trypsin digestion site and a proteinase K digestion site (PrtK) are also marked.

is located at the center of the transmembrane domain in a space surrounded by M5, M6, and M8 helices. Ca^{2+} is coordinated by side chain oxygen of Glu771 (M5), Thr799, Asp 800 (M6), and Glu908 (M8) and two water molecules. M8 is located rather distally and the contribution of Glu908 is not essential in that Gln can substitute Glu908 to a large extent. Any substitutions to other residues totally abolish the binding of Ca^{2+}.

Site II is nearly "on" the M4 helix with the contribution of Asp800 (M6) and Asn768 (M5). The M4 helix is partly unwound (between Ile307 and Gly310). This part provides three main chain oxygen atoms to the coordination of Ca^{2+}. Glu309 provides two oxygen atoms and caps the bound Ca^{2+}. This arrangement of oxygen atoms is reminiscent of the EF-hand motif.

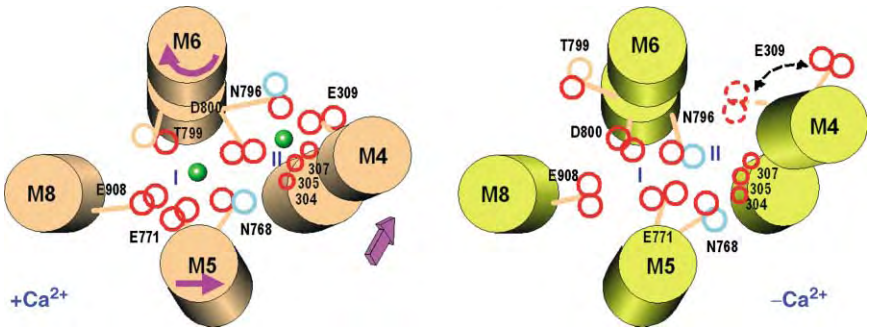

FIGURE 2 Schematic diagram of the Ca^{2+}-binding sites and the movements accompanying the dissociation of Ca^{2+}. The arrows indicate the movements of the helices in the transition from $E1Ca^{2+} \rightarrow E2(TG)$. Red circles, oxygen atoms (carbonyl oxygen atoms appear smaller); cyan circles, nitrogen; orange circles, carbon.

Thus, both site I and site II have seven coordination but have different characteristics. Asp800, on the unwound part of M6, is the only residue that contributes to both sites. Even double mutations of Glu309 and Asn768 leave 50% Ca^{2+} binding, indicating that site II is the binding site for the second Ca^{2+}.

Organization of the Cytoplasmic Domain

Structure of the P-Domain

The P-domain contains the residue of phosphorylation, Asp351. There are three critical aspartate (627, 703, 707) residues clustered around the phosphorylation site, in addition to an absolutely conserved Lys residue (Lys684). These key residues are very well conserved throughout the haloacid dehalogenase (HAD) superfamily, but also shared by bacterial two-component response regulator proteins, such as CheY and Fix J, which have folding patterns different from that of HAD. The P-domain has a Rossmann fold, commonly found in nucleotide-binding proteins, consisting of a parallel β-sheet (seven strands in Ca^{2+}-ATPase) and associated short α-helices. The catalytic residue (i.e., Asp351 in Ca^{2+}-ATPase) is always at the C-terminal end of the first β-strand, which is connected to a long insertion, the N-domain. Thus, the P-domain is formed by two regions far apart in the amino-acid sequence. This is why the P-type ATPase was thought to be an orphan in evolution for a long time. This system requires Mg^{2+} for phosphorylation. Mg^{2+} is coordinated by carboxyls of Asp351, Asp703, carbonyl of Thr353 and two water molecules. It is not known whether this Mg^{2+} is the same as that bound to ATP. Lys684 is particularly important for the binding of γ-phosphate of ATP.

Structure of the N-Domain

N-domain is the largest of the three cytoplasmic domains, containing residues Asn359–Asp601 (Figure 1), and connected to the P-domain with two strands. These strands bear a β-sheet like hydrogen-bonding pattern, presumably to allow large domain movements with a precise orientation. In particular, consecutive prolines (Pro602–603) appear to serve as a guide that determines the orientation of the movement. The N-domain contains the binding site for the adenosine moiety of ATP. Phe487 makes an aromatic–adenine ring interaction, which is a common feature in many ATP binding sites. Lys515, a critical residue, is located at one end of the binding cavity. This residue can be labeled specifically with FITC at alkaline pH and has been used for many spectroscopic studies. The binding of the adenine ring appears predominantly hydrophobic.

Structure of the A-Domain

A-domain is the smallest of the three cytoplasmic domains and consists of the N-terminal ~50 residues that form two short α-helices and ~110 residues between the M2 and M3 helices (Figure 1), which form a deformed jelly role structure. The A-domain contains a sequence motif ^{183}TGE, one of the signature sequences of the P-type ATPase. This sequence represents a loop that comes very close to the phosphorylation site Asp351, in the E2 and E2P states. Because this domain is directly connected to the M1–M3 helices and more indirectly to the M4–M6 helices, this domain is thought to act as the "actuator" of the gates that regulate the binding and release of Ca^{2+} ions.

Structural Changes Accompanying the Dissociation of Ca^{2+}

Rearrangement of the Transmembrane Helices

As illustrated in Figure 2, Ca^{2+}-ATPase undergoes large structural changes upon the dissociation of Ca^{2+}. Three cytoplasmic domains change their orientations and gather to form a compact headpiece. The P-domain inclines 30° with respect to the membrane and N-domain inclines 60° relative to the P-domain, whereas the A-domain rotates ~110° horizontally. The structure of each domain, however, is hardly altered. In contrast, some of the transmembrane helices are bent or curved (M1, M3, and M5) or partially unwound (M2); M1–M6 helices undergo drastic rearrangements that involve shifts normal to the membrane (M1–M4). Thus, the structural changes are very large and global; they are mechanically linked and coordinated by the P-domain.

M3–M5 helices are directly linked to the P-domain by hydrogen bonds (Figure 3). M3 is connected to the P1 helix at the bottom of the P-domain through a critical hydrogen bond involving Glu340. The top part of M5 is integrated as a part of the Rossmann fold (Figure 3) and moves together with the P-domain as a single entity. M4 and M5 are "clamped" by forming a short antiparallel β-sheet. M6 is also connected, though less directly, to the P-domain through L67 (Figure 1), which is, in turn, linked to M5 through a critical hydrogen bond. If the P-domain inclines, for instance, due to the bending of M5, all these helices (M3–M6) will incline and generate movements that have components normal

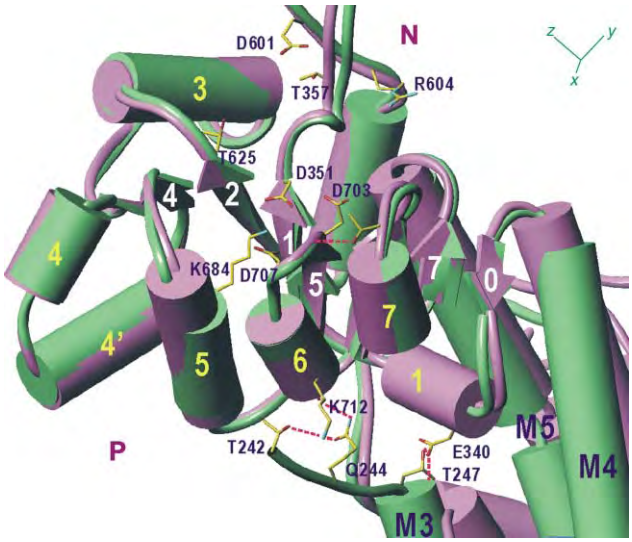

FIGURE 3 Organization of the P-domain and the linkage with the transmembrane helices. Superimposition of the E1Ca^{2+}(violet) and E2(TG) (light green) forms fitted with the P domain. The residues (in atom color) represent those in E2(TG).

to the membrane (Figure 4). Their amounts depend on the distances from the pivoting point, located around Gly770 at the middle of the membrane (double circle in Figure 4). The lower part below Gly770 hardly moves.

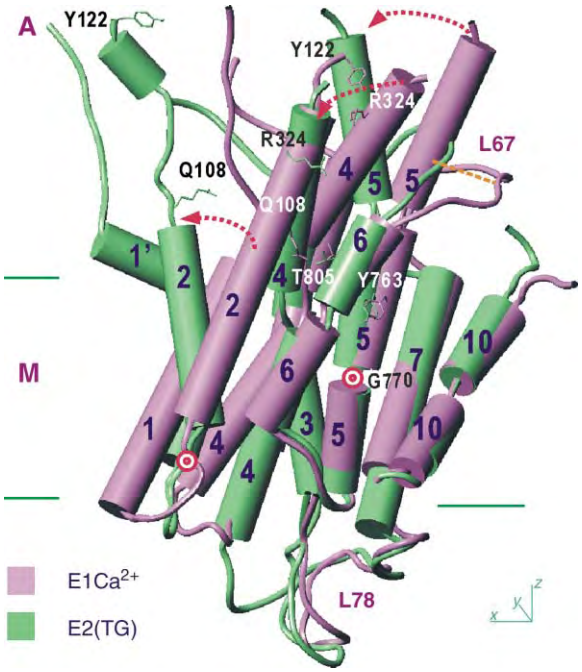

FIGURE 4 Rearrangement of transmembrane helices on the dissociation of Ca^{2+}. The models for E1Ca^{2+}(violet) and E2(TG) (light green) are superimposed. The M5 helix lies along the plane of the paper. M8 and M9 are removed. Double circles show pivot positions for M2 and M5. Arrows indicate the directions of movements during the change from E1Ca^{2+}to E2(TG). Orange broken line shows a critical hydrogen bond between the L67 loop and M5 helix.

The shift is therefore small for M6 and large for M3 and M4; whole M3 and M4 helices move downwards upon dissociation of Ca^{2+}, whereas M6 undergoes rather local changes around Asn796–Asp800.

Ca^{2+}-Binding Sites in the E2(TG) State

The most important movements of the transmembrane helices directly relevant to the dissociation of Ca^{2+} are: (1) a shift of M4 towards the lumenal (extracellular) side by one turn of an α-helix (5.5Å), (2) bending of the upper part of M5 (above Gly770) towards M4, and (3) nearly 90° rotation of the unwound part of M6. As a result, profound reorganization of the binding residues takes place and the number of coordinating oxygen atoms decreases (Figure 2). For site I, this is due to the movement of Asn768 toward M4 caused by the bending of M5; for site II, replacement of Asp800 by Asn796 (i.e., rotation of M6) is critical.

Role of the Large Conformational Movements

Homology modeling of the cation binding sites of Na$^+$K$^+$-ATPase suggests that a large downward movement of M4 (and M3) is needed for counter-transport. With the arrangements of residues observed with E2(TG) structure, it is straightforward to make two high-affinity K$^+$-binding sites, provided that Asn796 is replaced by Asp following Na$^+$K$^+$-ATPase sequence: the other coordinating residues are common to both ATPases. The key feature in the model is that the Asp (Asn796) is coordinated to both K$^+$, similar to Asp800 in coordination of 2Ca^{2+}. Because Asn796 is located one turn below where Asp800 is, M4 must move downwards to provide carbonyl groups for coordination of K$^+$. These rearrangements ensure that release of one type of cation coordinates with the binding of the other and allow the binding of ions of different radii with high affinity.

In summary, ion pumps use thermal movements of various domains very efficiently. Most of the movements described here can be related to the bending of the M5 helix. Because M5 participates in Ca^{2+} coordination and moves together with the P-domain, it is understandable that the phosphorylation (binding of phosphate and Mg^{2+}) at the phosphorylation site and the binding of Ca^{2+} to the transmembrane binding sites will alter the properties of the other. This appears to be the mechanism of long-distance (>50Å) intramolecular communication. Animations showing the conformation changes accompanying Ca^{2+}-dissociation are available (http://www.iam.u-tokyo.ac.jp/StrBiol/animations).

See Also the Following Articles

Calcium, Biological Fitness of • Calcium-Binding Proteins, Cytosolic (Annexins, Gelsolins, C_2-Domain Proteins) • ER/SR Calcium Pump: Function

Glossary

EF-hand motif Most common calcium-binding motif that has a helix–loop–helix motif with a seven-coordinate geometry.

HAD superfamily A large family found by Aravind *et al.* in 1998 including P-type ion transporting ATPases, haloacid dehalogenase (HAD) and phosphoserine phosphatase, structurally the best studied member.

Rossmann fold A supersecondary structure, consisting of a pair of $\beta\alpha\beta$ structures arranged so that at least four β-strands form a single parallel β-sheet flanked by two layers of α-helices.

Further Reading

Aravind, L., Galperin, M. Y., and Kunin, E. V. (1998). The catalytic domain of the P-type ATPase has the haloacid dehalogenase fold. *Trends Biochem. Sci.* **23**, 127–129.

Møller, J. V., Juul, B., and le Maire, M. (1996). Structural organization, ion transport, and energy transduction of P-type ATPases. *Biochim. Biophys. Acta* **1286**, 1–51.

Ogawa, H., and Toyoshima, C. (2002). Homology modeling of the cation binding sites of Na^+K^+-ATPase. *Proc. Natl Acad. Sci. USA* **25**, 15977–15982.

Toyoshima, C., and Inesi, G. (2004). Structural basis of ion pumping by Ca^{2+}-ATPase of the sarcoplasmic reticulum. *Ann. Rev. Biochem.* **73**, 269–292.

Toyoshima, C., and Nomura, H. (2002). Structural changes in the calcium pump accompanying the dissociation of calcium. *Nature* **418**, 605–611.

Toyoshima, C., Nakasako, M., Nomura, H., and Ogawa, H. (2000). Crystal structure of the calcium pump of sarcoplasmic reticulum at 2.6 A resolution. *Nature* **405**, 647–655.

Biography

Chikashi Toyoshima is a Professor in the Institute of Molecular and Cellular Biosciences at the University of Tokyo. His principal research interest is structural understanding of ion transport.

Yuji Sugita is a Lecturer in the Institute of Molecular and Cellular Biosciences at the University of Tokyo. His principal research interests are in the development of new molecular simulation methodologies and in their application to the biological phenomena.

Exonucleases, Bacterial

Susan T. Lovett
Brandeis University, Waltham, Massachusetts, USA

Exonucleases are enzymes that catalyze hydrolysis of DNA or RNA from a free end. Exonucleolytic digestion of nucleic acids may be required for processing and for turnover of these macromolecules. In addition, RNA exonucleases contribute to the maturation of stable RNA molecules. The action of DNA exonucleases permits diverse processes such as mutation avoidance, repair, and genetic recombination.

Introduction

Nucleases are defined as enzymes that hydrolyze the phosphodiester bond of nucleic acids. Borrowing the system developed for proteases, nucleases have been classified whether they cleave internally in the DNA or RNA molecule (endonucleases) or from an end in a stepwise fashion producing mononucleotide products (exonucleases). This distinction is complicated by the fact that several enzymes require entry at a free DNA or RNA end but cleave internally (often referred to as endo/exonucleases). An example is the RecBCD recombination nuclease that unwinds DNA from an end and cleaves it as it travels, producing oligonucleotide products. Some exonuclease activities are found within proteins with other distinct catalytic activities, such as the 3′ DNA exonuclease activities associated with DNA polymerases.

The systematic purification and characterization of more than 20 exonuclease activities from *Escherichia coli* extracts have provided much of our knowledge about this group of enzymes (Tables I and II). Most *E. coli* exonucleases on DNA and RNA were identified and named arbitrarily (DNA exonucleases Exo I–X and RNase II) or by reference to their substrate specificity (RNase H, R, D, T oligoribonuclease, etc.). A few nucleases were identified first and named by their genetic function (such as RecJ exonuclease required for genetic recombination). The biological role of most *E. coli* exonucleases has now been confirmed by genetic experiments, although many exonucleases have redundant genetic function and genetic phenotypes are not manifested until multiple members are inactivated. Such overlapping functions are not surprising, given the great number of these enzymes in *E. coli* (at present count 15 DNA, 9 RNA exonucleases.) Orthologues of many of the *E. coli* exonucleases can be found in diverse bacterial genera and often in archaea and eukaryotes. *E. coli* appears to be especially rich in exonucleases, in contrast to other bacteria that have only a few exonucleases, as predicted by sequence similarity. However, since most exonuclease families were defined first by purification and characterization of representatives from *E. coli*, this may represent an ascertainment bias and there may be additional, presently unknown exonuclease families in other bacterial species but not in *E. coli*.

Biochemical Properties of Exonucleases

Mechanism

All DNA and RNA exonucleases, with the exception of DNase Exo VII, require a divalent-cation cofactor, commonly Mg^{2+} or Mn^{2+}, to accomplish hydrolysis of the phosphodiester bond. The crystal structures of many exonucleases have now been solved and reveal coordination of one or more divalent cations by aspartate, glutamate, or histidine residues. Such residues are found as evolutionarily conserved amino acid motifs within related exonucleases. A role for the metal ions was suggested by the structure published by Beese and Steitz for the 3′–5′ exonuclease of *E. coli* polymerase I, which contains two metal atoms, a single-strand DNA (ss DNA) substrate and deoxynucleoside monophosphate. They proposed that one metal activates a water molecule for the nucleophile in an SN2-type reaction; the other closely positioned metal is poised to stabilize the pentacovalent intermediate in the reaction and the leaving oxyanion. The universality of this two-metal-ion scheme is not clear: some exonuclease structures, such as that of the 5′ nuclease FEN-1, contain two more widely separated metal ions and other structures, such as DNA exonucleases Exo III and RecJ, reveal only one metal cation.

Two RNases, acting from a 3′ end, polynucleotide phosphorylase (PNPase) and RNase PH, are not, strictly

TABLE I

DNA Exonucleases of *E. coli*[a]

Enyzme	Gene(s)	Preferred substrate	Polarity	Other features	Biological role in DNA metabolism
Exo I	*xonA* (= *sbcB*)	ssDNA	3′–5′	Processive	Recombination, damage repair, mutation avoidance, MMR
Exo III	*xth*	dsDNA	3′–5′	Acts at nicks and ends, abasic endonuclease	Base excision repair
Exo IV	?[b]	Oligonucleotides	?	May be identical to oligoribonuclease[b]	?
Exo VII	*xseA*, *xseB*	ssDNA	3′–5′ 5′–3′	Heterodimer, processive, Oligonucleotide products, metal cofactor-independent	Damage repair, mutation avoidance, MMR
Exo VIII	*recE*	dsDNA	5′–3′	Processive, encoded by cryptic Rac prophage	Recombination, damage repair
Exo IX	*xni*	dsDNA	3′–5′	In 5′ nuclease/FEN-1 family[c]	?
Exo X	*exoX*	ssDNA, dsDNA	3′–5′	Distributive	Mutation avoidance, MMR
DNA pol I 5′ exo	*polA*	ssDNA	5′–3′	Flap endonuclease	Replication (Okazaki fragment maturation)
DNA pol I 3′ exo	*polA*	ssDNA	3′–5′		Proofreading
DNA pol II 3′ exo	*polB*	ssDNA	3′–5′		Proofreading
DNA pol III 3′ exo	*dnaQ* (= *mutD*)	ssDNA	3′–5′	ε Subunit	Proofreading
RecBCD	*recB*, *recC*, *recD*	dsDNA, ssDNA	3′–5′ 5′–3′	Exo V, highly processive, ATP-dependent, oligonucleotide products, helicase activity	Recombination, DSB repair
RecJ	*recJ*	ssDNA	5′–3′	Processive	Recombination, damage repair, MMR
RNase T	*rnt*	ssDNA	3′–5′	Activity on DNA > RNA, homodimer, distributive	Repair?[d]
SbcCD	*sbcC*, *sbcD*	dsDNA	3′–5′ 5′–3′	ATP-dependent, processive	Repair

[a] Abbreviations: pol, polymerase; Exo, exonuclease, dsDNA, double-strand DNA; ssDNA single-strand DNA; MMR, mismatch repair; DSB, double-strand break.
[b] Eukaryotic oligoribonuclease has activity on oligodeoxynucleotides and *E.coli* oligoribonuclease may be identical to exonuclease IV.
[c] Although the polarity of Exo IX-mediated digestion is reported to be 3′–5′, it is a member of the 5′ flap endonuclease family by amino acid sequence similarity.
[d] RNase T can act as a high-copy suppressor of some DNA repair defects of RecJ$^-$ ExoI$^-$ ExoVII$^-$ strains, has potent DNase activity and so could play a redundant function in DNA metabolism.

TABLE II

RNA Exonucleases[a] of *E. coli*

Enzyme	Gene	Preferred substrate[b]	Biological role in RNA metabolism
RNase II	*rnb*	Unstructured RNA	mRNA degradation, stable RNA maturation
RNase R	*rnr*	rRNA, homopolymers	?
RNase D	*rnd*	Denatured tRNAs	Defective tRNA degradation, stable RNA maturation
RNase H	*rnhA*	RNA/DNA hybrid	Repair
RNase T	*rnt*	tRNA[c]	tRNA end turnover, stable RNA maturation
Oligoribonuclease	*orn*	Oligoribonucleotides[d]	mRNA degradation
Polynucleotide phosphorylase (PNPase)	*pnp*	Unstructured RNAs	mRNA degradation, stable RNA maturation
RNase PH	*rph*	tRNA precursors	Stable RNA maturation
RNase BN	*rbn*	tRNA with aberrant 3′ ends, tRNA precursors	Stable RNA maturation defective tRNA degradation

[a] Although PNPase and RNase PH are phosphorylases not nucleases, they act to digest RNA in a polar fashion from a 3′ end.
[b] All *E. coli* exoribonucleases act 3′–5′.
[c] RNase T also possesses a potent exonuclease activity on single-strand DNA in a 3′–5′ fashion.
[d] May be identical to DNA exonuclease IV.

speaking, "nucleases," because they are not hydrolases but phosphorylases, using inorganic phosphate to attack the phosphodiester bond and releasing nucleoside diphosphate reaction products. These are, however, of related biological function and are included here and in many reviews of exoribonucleases.

Specificity

Many exonucleases have strict specificity for the sugar moiety in nucleic acids and therefore cleave only RNA or DNA. (RNase H is specific for RNA within a DNA hybrid.) Other nucleases, however, may cleave both RNA and DNA, e.g., RNase T of *E. coli*. It is difficult to tell from amino acid sequence information alone whether any given exonuclease will have a preference for DNA or RNA. Exonuclease superfamilies include both RNase and DNase members. Steric considerations may exclude RNA as a substrate for DNA-specific exonucleases; 2′-OH specific interactions may specify RNA as a preferred substrate.

Almost all exonucleases have a strict polarity of digestion, initiating attack from either the 3′- or 5′-end of a nucleic acid molecule. This polarity reflects the exonuclease's particular architecture of the amino acids and bound metal atoms that interact with the nucleic acid. Exceptions to strict polarity include those "exo/endonucleases" that cleave internally within DNA, producing oligonucleotide products, but require an end for entry, such as Exo VII, SbcCD, and RecBCD. The latter two DNA exonucleases are ATP dependent and may require ATP for associated helicase activity to move the enzyme along its DNA substrate. Some exonucleases are specific for the phosphorylation status of the end, indicating a specific interaction with the nucleic acid terminus. For example, many 3′–5′ exonucleases such as *E. coli* exonuclease I cannot attack a nucleic acid with 3′-phosphate; similarly, lambda bacteriophage exonuclease requires a 5′-phosphate in a double-strand DNA (dsDNA) end and will not initiate cleavage on a 5′-OH-containing DNA molecule. Many DNA exonucleases are specific for double-strand (Exo III, Exo VIII) or single-strand (RecJ, Exo I, Exo VII) DNA. Likewise, certain RNases may prefer unstructured RNA regions. The ssDNA-specific exonucleases accomplish their specificity sterically: they either possess a pore or have a deep cleft in which ssDNA but not dsDNA can reach the catalytic center of the enzyme. Oligoribonuclease has a size specificity and prefers short oligonucletide substrates less than five nucleotides in length but the molecular basis for this specificity is not understood.

Processivity

Exonucleases are classified "processive" if they catalyze multiple cleavage events upon a single binding to their nucleic acid substrates. In contrast, "distributive" must rebind substrate after each cleavage. The biochemical property of processivity has important biological consequence and allows exonucleases to rapidly digest appropriate substrates. Several processive nucleases (bacteriophage lambda exonuclease, *E. coli* Exo I) have toroidal or clamp-like structures that allow the enzyme to encircle its substrate, a simple way of

achieving processivity. Processivity can also be achieved by multiple binding interactions of the exonuclease to its substrate, as has been proposed for RNase II.

Structural Families

Comparison of exonuclease sequences from bacteria shows that the primary amino acid sequence of these proteins has diverged rather quickly. Nevertheless, conserved motifs emerge and several extensive sequence families can be recognized and are briefly discussed below. Members of these exonuclease families can often be found in all three domains of life: archaea, eubacteria and eukaryotes. In exonucleases for which there is structural information, these conserved motif residues coordinate metal cofactor or interact with substrate. These structural families can include members with diverse substrate specificities, including both exonucleases and endonucleases, and even phosphatases, RNases and DNases, processive and distributive enzymes, and a few are discussed briefly.

DEDD/DNAQ

An extensive group of 3′–5′ exonucleases is defined by three motifs carrying conserved aspartate and glutamate residues (Figure 1); hence, the alternate designation "DEDD" for this family of nucleases found in eukaryotes as well as prokaryotes. This family includes exonucleases with specificity for DNA (the proofreading exonucleases of DNA polymerases, *E. coli* exonucleases I and X), RNA (RNase D, oligoribonuclease), and those with dual specificity (RNase T). Both distributive and processive exonucleases are members of this family. *E. coli* possesses eight enzymes in this family (alignment shown in Figure 1). Structural information is available for several members of this superfamily including the proofreading exonuclease domain of DNA polymerases I and III of bacteria, and *E. coli* exonuclease I. The fold of these enzymes resembles RNase H1. Most structures include two metal atoms at the active site.

DHH/RecJ

The founding member of this family, RecJ, is a 5′–3′ ssDNA exonuclease involved in genetic recombination and DNA repair. The RecJ family encompasses a large family of proteins found in archaea and bacteria, very few of which have been characterized at the biochemical level. This family is defined by seven conserved motifs, primarily acidic residues, or histidines; the family is sometimes termed "DHH" after the amino acid sequence within one of these motifs. The RecJ family is particularly expanded in the archaea; for example, *Archaeoglobus fulgidus* possesses seven members of this family. There are eukaryotic members, but the yeast DHH protein is a phosphatase (polyphosphatase PPX1), not a nuclease. Therefore, the RecJ family is, more broadly, a phosphoesterase rather than a nuclease family.

XthA

E. coli exonuclease III is a 3′–5′ DNA exonuclease active on dsDNA; it also possesses 3′ phosphatase activity and endonuclease activity at abasic (apurinic/apyrimidinic) sites. Exo III is an important protein for base excision repair, as is its eukaryotic counterpart Ape1. Structurally, Exo III resembles eukaryotic DNase I, with a single metal at its active site and a large group of phosphatases, primarily involved in eukaryotic cell signaling processes.

FEN-1/5′ Nucleases

The founding member of this group is FEN-1 "flap-endonuclease" from eukaryotes and archaea; the eubacterial counterpart, both structurally and functionally, is the 5′ exonuclease domain of DNA polymerase I. Both proteins possess 5′–3′ exonuclease activity and endonuclease activity on ssDNA "flaps" adjacent to region of duplex DNA. These 5′-nucleases play an important role in processing of Okazaki fragments during lagging strand DNA synthesis. Structural information of archaeal FEN-1, DNA polymerase I, and the related RNase H activity from bacteriophage T4 shows two metals coordinated by glutamate and aspartate

```
ExoI        11 LFHDYETFGTHPALDRPAQFAA 66 LGYNNVRFDDEVTRN 64 SNAHDAMADVYAT
ExoX         2 RIIDTETCGLQGGIVEIASVDV 52 YVAHNASFDRRVLPE 39 LHHHRALYDCYIT
OligoRNase  31 IWIDLEMTGLDPERDRIIEIAT 73 ICGNSIGQDRRFLFK  6 AYFHYRYLDVSTL
RNase T     19 VVIDVETAGFNAKTDALLEIAA 75 MVAHNANFDHSFMMA 37 CQTAGMDFDSTQA
RNase D     24 IALDTEFVRTRTYYPQLGLIQL 30 KFLHAGSEDLEVFLN 55 RQCEYAAADVWYL
PolI       123 FAFDTETDSLDNISANLVGLSF 42 KVGQNLKYDRGILAN 62 EAGRYAAEDADVT
PolII      353 VWVEGDMHNGTIVNARLKPHPD 75 IGWNVVQFDLRMLQK 91 ALATYNLKDCELV
DnaQ         8 IVLDTETTGMNQIGAHYEGHKI 62 LVIHNAAFDIGFMDY 49 RTLHGALLDAQIL
```

FIGURE 1 *E. coli*'s DnaQ superfamily members. Shown are aligned amino acid sequences of exonuclease I, exonuclease X, oligoribonuclease, RNase D, RNase T, and the 3′-exonucleases of DNA polymerases I, II, and III. Conserved acid residues are shown in bold and comprise metal coordination residues for those proteins with determined three-dimensional structure. Numbers refer to amino acid residues not shown.

residues. This family also includes eukaryotic Exo 1, a 5′-exonuclease implicated in eukaryotic mismatch repair, and *E. coli* exonuclease IX of unknown biological function.

Mre11/SbcD

Eukaryotic and archaeal Mre11 is the catalytic subunit of an ATP-dependent exonuclease with associated endonuclease activity. Mre11 shares sequence homology with bacterial SbcD protein. The nuclease activity specified by these subunits requires assembly of an active complex with one or two other additional proteins. One of these additional subunits possesses a coiled-coil structure: Rad50 in eukaryotes and archaea, SbcC in bacteria. Structural data are available for archaeal Mre11, showing two Mn^{2+} atoms, and Rad50. The Mre11 fold resembles metal-dependent phosphatases with the conserved phosphoesterase motifs (histidines, aspartates, and asparagines) making interactions with substrate or metal cofactors. Mre11 and SbcD exonucleases play a role in DNA repair and genomic surveillance.

Biological Roles of RNA Exonucleases

Turnover

mRNA half-lives in bacteria are short and degradation of mRNA is essential for viability. After initial endonucleolytic cleavage, degradation of mRNA in *E. coli* is accomplished by the combined action of RNase II and PNPase to produce short oligomers that are then digested by oligoribonuclease. These bacterial enzymes attack RNA in a 3′–5′ direction. Loss of either RNase II (a true exoribonuclease) or PNPase (a phosphorylase) can be tolerated by *E. coli*; however, inactivation of both enzymes or of oligoribonuclease is lethal to the cell. Aberrant or misfolded stable RNAs may also be subject to turnover by exoribonuclease action.

Processing

Proper maturation of stable RNAs requires the action of exoribonucleases. In *E. coli* several exoribonucleases act redundantly in processing of tRNA or rRNA. Maturation of stable RNAs seems to be most dependent on RNase T and RNase PH; the double mutant accumulates tRNA precursors and although viable, grows more slowly. Upon loss of five activities, RNase II, D, BN, T, and PH, *E. coli* becomes inviable; any single one of these enzymes can suffice to support viability, indicating significant functional overlap.

Biological Roles of DNA Exonucleases

Replication Fidelity

Exonucleases are integral to two major mechanisms that insure the fidelity of DNA replication: polymerase proofreading and mismatch repair. 3′–5′ exonuclease activity is a component of many bacterial DNA polymerases at a site or within a subunit distinct from the polymerase activity. Unpaired 3′-residues are more likely to be degraded by the exonuclease than to support polymer extension; this proofreading reaction contributes substantially to the accuracy of replication. Complete absence of 3′–5′ exonuclease activity of *E. coli* replicative polymerase, the DnaQ or ε-subunit of DNA polymerase III, causes cellular inviability due to the catastrophic accumulation of replication errors.

Misincorporations that escape polymerase proofreading can be recognized and excised by the mismatch repair pathway, which is initiated by the MutHLS proteins of *E. coli*. The excision tract, up to thousands of bases in length, can be directed either 3′ or 5′ to the mismatch and is catalyzed by the redundant action of four exonucleases, RecJ, Exo I, Exo VII, or Exo X, aided by the UvrD helicase of *E. coli*. Loss of mismatch repair elevates the frequency of spontaneous mutational events several orders of magnitude.

Scavenging of ssDNA by the 3′–5′ DNA exonucleases (*E. coli* Exo I, Exo VII, and Exo X) aborts a wide range of mutational events believed to be caused by nascent strand displacement and mispairing, including frameshifts, deletions, and quasipalindrome-associated mutational hotspots. These enzymes act redundantly in this process, which can be considered a type of "proofreading in trans."

Maturation of Okazaki fragments during DNA replication in *E. coli* is catalyzed by the 5′-exonuclease domain of polymerase I, functionally and structurally homologous to the FEN-1/Rad27 nuclease of eukaryotes and archaea. In addition to a nonspecific 5′-exonuclease activity, these enzymes specifically cleave the junction between ss and dsDNA, an activity often termed "flap" endonuclease activity. In some bacteria such as *Streptococcus pneumoniae*, loss of the 5′ nuclease domain of DNA polymerase I is lethal. *E. coli* mutants are viable and may, therefore, use a backup mechanism of Okazaki fragment maturation. The absence of the 5′-nuclease domain of polymerase I in *E. coli* elevates spontaneous mutation rates, as was first described for the related Rad27 of yeast; this elevated class of mutations consists largely of short sequence duplications. In a similar fashion, these 5′-nucleases also suppress expansion of tandem repeat arrays.

The SbcCD nuclease appears to play a role in genome surveillance and repair. Through its endonuclease activity, SbcCD breaks the chromosome at large inverted DNA repeats that form secondary structures, which can impede DNA replication. Such breakage and subsequent exonucleolytic processing may selectively remove such structures from the genome. The SbcCD nuclease may also mediate certain modes of double-strand break repair, independent of DNA secondary structures.

Recombination and DNA Repair

Exonucleases play an essential role in homologous recombination. Strand exchange is initiated by ssDNA, which binds the strand transfer protein RecA and initiates the homology-search process. Nicks or double-strand breaks in DNA are converted by exonucleases to recombinogenic ssDNA gaps or tails, respectively, by the degradation of one strand of the DNA duplex. During recombinational double-strand break repair in *E. coli*, the RecBCD nuclease provides this function by its combined ATP-dependent helicase and nuclease activities. RecBCD's nuclease activity is modulated by octameric "Chi" DNA sequences that act *in vivo* as hot spots of recombination by a molecular mechanism yet to be deciphered. In pathways of recombination independent of RecBCD, exonuclease function for recombination can be provided by the RecJ $5'-3'$ ssDNA exonuclease, acting in conjunction with a DNA helicase, such as RecQ. After recombinational joint molecules are formed by synapsis, degradation of one strand ("post-synaptic" DNA degradation) can extend and stabilize the heteroduplex intermediate by removing a competitor strand for pairing. It may be for this reason that in *E. coli* either RecJ ($5'-3'$) and Exo I ($3'-5'$) are required for efficient recombination, even when the presynaptic degradation is presumably occurring via the RecBCD nuclease. After exchange is complete, exonucleases may also participate in the trimming of unpaired ends to form mature recombinant molecules.

Conclusions

Exonucleases comprise a large set of structurally and biochemically characterized enzymes with diverse properties. Systematic characterization of exonucleases from the bacterium *E. coli* has provided much of our knowledge of this class of enzymes. Certain families of related exonucleases are found widely throughout bacteria, archaea, and eukaryotes, indicating the early evolution of nucleases and their important role in all cells. However, primary amino acid sequence cannot predict many elements of substrate specificity (such as DNase or RNase), other enzymatic properties such as processivity or biological function. A single *E. coli* cell contains more than 20 different exonuclease activities. Exonucleases often act redundantly in biological functions of RNA processing and degradation, mutation avoidance, and in DNA repair and recombination. Therefore, several biological functions of exonucleases probably remain unknown and are the focus of current work in the field.

See Also the Following Articles

DNA Polymerase I, Bacterial • Recombination: Heteroduplex and Mismatch Repair *in vitro* • Transcription-Coupled DNA Repair, Overview

Glossary

base excision repair A repair mechanism that removes damaged nucleotide bases from duplex DNA. The resulting abasic site is then incised by abasic endonucleases and repaired by exonucleases, polymerase and ligase.

genetic recombination A process by which homologous segments of DNA molecules are exchanged. Recombination serves as a relatively error-free mechanism for repair of chromosomal single-strand gaps or double-strand breaks.

heteroduplex A DNA duplex region formed by the pairing of two strands from different DNA molecules. Heteroduplex joint formation is the first step of homologous genetic recombination.

mismatch repair A conserved repair mechanism by which many replication errors ("mismatches") are detected and excised from duplex DNA.

okazaki fragments Short, discontinuous pieces of DNA, primed by RNA and synthesized during lagging strand DNA replication.

proofreading The $3'-5'$ exonucleolytic removal of polymerase incorporation errors in newly synthesized DNA.

Further Reading

Beese, L. S., and Steitz, T. A. (1991). Structural basis for the $3'-5'$ exonucleases activity of *Escherichia coli* DNA polymerase: I. A two metal ion mechanism. *EMBO J.* **10**, 25–33.

Ceska, T. A., and Sayers, J. R. (1998). Structure-specific cleavage by $5'$ nucleases. *Trends Biochem. Sci.* **23**, 331–336.

D'Alessio, G., and Riordan, J. F. (eds.) (1997). *Ribonucleases – Structures and Functions*. Academic Press, San Diego, CA.

Deutscher, M. P., and Li, Z. (2001). Exoribonucleases and their multiple roles in RNA metabolism. *Prog. Nucleic Acids Res.* **66**, 67–105.

Kunkel, T. A., and Bebenek, K. (2000). DNA replication fidelity. *Annu. Rev. Biochem.* **69**, 497–529.

Linn, S. M., and Roberts, R. J. (eds.) (1993). *Nucleases*, 2nd Edition. Cold Spring Harbor Laboratory Press, Cold Spring Harbor, NY.

Nishino, T., and Morikawa, K. (2002). Structure and function of nucleases in DNA repair: Shape, grip and blade of the DNA scissors. *Oncogene* **21**, 9022–9032.

Shevelev, I. V., and Hübscher, U. (2002). The $3'-5'$ exonucleases. *Nat. Rev. Molecul. Cell Biol.* **3**, 1–12.

Zuo, Y., and Deutscher, M. P. (2001). Exoribonuclease superfamilies: Structural analysis and phylogenetic distribution. *Nucleic Acids Res.* **29**, 1017–1026.

Biography

Susan T. Lovett is a Professor in the Department of Biology and Rosenstiel Basic Medical Sciences Research Center at Brandeis University in Waltham, Massachusetts. Among her research interests are the DNA exonucleases that mediate genetic recombination, repair, and mutation avoidance. She and her colleagues discovered and characterized the RecJ exonuclease and Exonuclease X from *E. coli*. She received her Ph.D. in Molecular Biology from the University of California at Berkeley and trained as a postdoctoral fellow at Lawrence Berkeley Laboratory in Berkeley, California and the Harvard Medical School in Boston, Massachusetts.

F1–F0 ATP Synthase

Donata Branca
University of Padova, Padova, Italy

F1–F0 ATP synthases (also called F1–F0 or F-ATPases) are large protein complexes, weighing 550–650 kDa, located in the inner mitochondrial membrane, in the chloroplast thylakoid membrane and in the bacterial plasma membrane. They are the major ATP suppliers of most cells, synthesizing ATP in the terminal phase of oxidative phosphorylation or photophosphorylation. The synthesis of ATP from ADP and inorganic phosphate (Pi) is driven by protons (H^+) moving through the complex down the transmembrane H^+ gradient built by the respiratory or photosynthetic electron-transfer chains (or by light-driven H^+ pumps in some bacteria). The ATP synthases may also operate in the opposite direction, as H^+-pumping ATPases; this reversal, which may be accomplished by any ATP synthase *in vitro*, is physiologic in anaerobic bacteria, allowing them to build a transmembrane H^+ gradient (e.g., as required for the movement of flagella or for the uptake of nutrients). Thus, the ATP synthases reversibly convert the energy stored in the proton gradient into the chemical energy of ATP. The ATP synthases of all organisms are believed to have evolved from a common protobacterial ancestor. In fact they have a high degree of sequence homology within structurally and functionally important regions, display similar architectures, and operate with the same basic mechanism. Moreover, in eukaryotes, they are partially encoded by mitochondrial or chloroplast DNA.

Structure of the ATP Synthase Complex

ATP synthases are traditionally described as bipartite complexes, composed of two structurally and functionally distinct multisubunit portions (Figure 1A): a membrane-embedded F0, which translocates protons, and a membrane-peripheral F1 comprising a globular head, which synthesizes ATP, and a central stalk, which interacts with F0. A second, peripheral stalk, contributed by F1 and F0 subunits, also connects the outer regions of F1 and F0. F1 may be reversibly dissociated from F0 *in vitro*, with the isolated F1 still active, but only capable of hydrolyzing ATP (hence the ATPase designation), and the membrane-associated F0 retaining the ability to translocate protons down a concentration gradient. The isolated F1, and the F1-depleted membranes containing F0 are invaluable tools to investigate the structure and the enzymology of the synthases, even if lacking the coupling mechanism which allows the H^+-driven ATP synthesis by the intact complex. As to the operation of the complex, there is wide agreement that H^+ translocation through F0 triggers the rotation of the central stalk, which in turn promotes the synthesis of ATP by F1.

Structural, biochemical, and molecular biological studies have contributed to the knowledge of the architecture of the ATP synthases. The landmark achievement has been the high-resolution structure of the mitochondrial F1: the X-ray crystallographic studies on bovine heart F1 by Walker and co-workers (Figure 2A) have established the essential features of the mammalian complex. X-ray crystallographic work by Amzel, Pedersen and co-workers (Figure 2B) has contributed significant results on the rat liver F1 enzyme. Much less is known on F0, due to its membrane-intrinsic nature; the structural analysis of this portion of the synthase is so far limited to its isolated subunits or subcomplexes.

Subunit Composition

In the simplest ATP synthase, that of bacteria (Figures 1A and B), F1 contains five different subunits with a stoichiometry $\alpha_3,\beta_3,\gamma_1,\delta_1,\varepsilon$. F0 is composed of three kinds of subunits with a stoichiometry a_1,b_2,c_{10-14}. This core structure is substantially conserved in all ATPases, but for the presence of two homologous b and b′ subunits in chloroplast F0, of a single copy of the b subunit in mitochondrial F0 and of several additional subunits, whose roles are still poorly defined, in the stalk and in the membrane sector of the mitochondrial complex(Figure 1C). Finally, an inhibitor peptide (IF_1), unique to mitochondria, may reversibly associate to the synthase.

At present, the subunit nomenclature for the ATP synthases from different sources is confusing, partly due to historical reasons; as an example, the bacterial ε-subunit corresponds to the mitochondrial δ, and the bacterial δ-subunit to the mitochondrial oligomycin sensitivity conferring protein (OSCP), while the

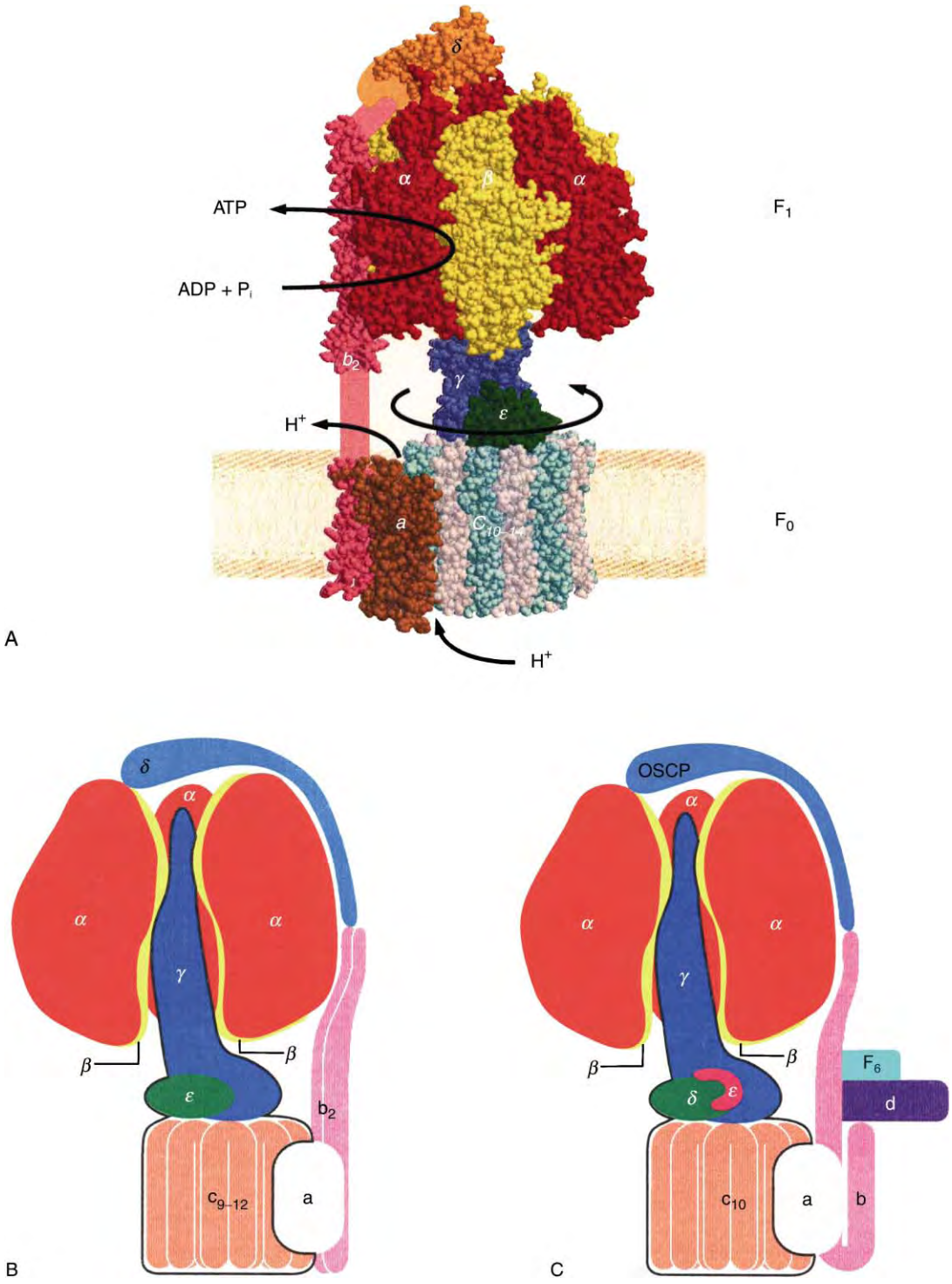

FIGURE 1 Structure of the F1F0 ATP synthase. (A) Space filling model of the F1–F0 complex of *E. coli*. The uniformly coloured parts correspond to domains whose high-resolution structure is lacking. (Reproduced from Weber, J., and Senior, A. E. (2003). ATP synthesis driven by proton transport in F_1F_0-ATP synthase. *FEBS Lett.* **545**, 152–160, with permission.) (B and C) Schematic model of the ATP synthase from bacteria (B) and mitochondria (C). One of the three β subunits has been omitted to reveal the g subunit within the $\alpha_3\beta_3$ hexamer. In (C), some minor subunits (e, f, g, A6L) are not shown. (Reproduced from Stock, D., Gibbons, C., Arechaga, I., Leslie, A. G. W., and Walker, J. E. (2000). The rotary mechanism of ATP synthase. *Curr. Opin. Struct. Biol.* **10**, 672–679, with permission from Elsevier.)

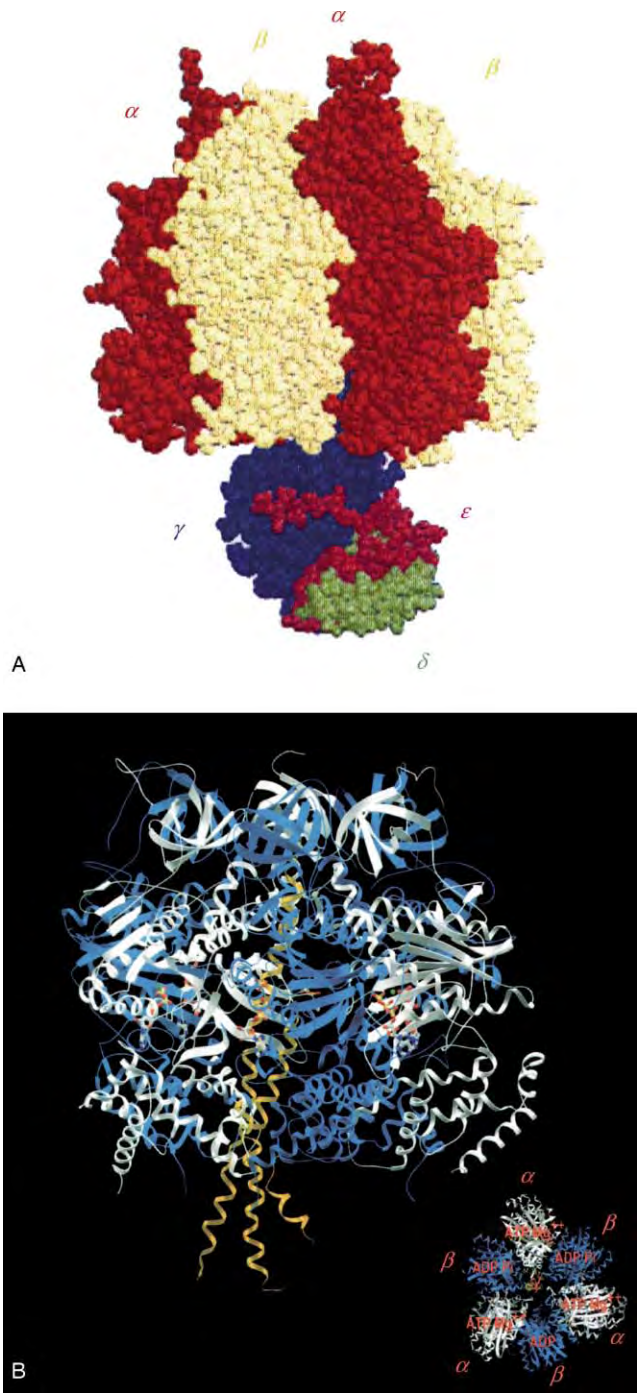

FIGURE 2 Structure of F1. (A) Side view of bovine F1 crystallized in the presence of the synthase inhibitor dicyclohexylcarbodiimide (DCCD). Reproduced from Gibbons, C., Montgomery, M. G., Leslie, A. G. W., and Walker, J. E. (2000). The structure of the central stalk in bovine F1-ATPase at 2.4Å resolution. *Nature Struct. Biol.* 7, 1055–1061. (B) Side view (large) and top view (small) of the $\alpha_3\beta_3\gamma$ complex of rat liver F1 crystallized in the presence of ATP and Pi. The α subunits are in white, the β subunits are in blue, and the γ subunit (part of which is lacking, since it was disordered in the crystal) is in yellow; the nucleotides bound to all β/α and α/β interfaces are shown. Reproduced from Bianchet, M. A., Pedersen, P. L., and Amzel, L. M. (2000). Notes on the mechanism of ATP synthesis. *J. Bioenerg. Biomembr.* **32**, 517–521 with permission of Kluwer Academic/Plenum Publishers.

mitochondrial ε-subunit has no bacterial counterpart (Figures 1B and C).

F1

The three α- and the three β-subunits of F1 are arranged alternately in an hexagonal ring of 90–100Å diameter, forming the bulk of the globular head of F1 (Figure 2A). The α- and β-subunits of F1 are homologous and share similar folds, comprising an N-terminal β-barrel domain, a central domain which includes the nucleotide-binding site, and a C-terminal bundle of α-helices. The γ-subunit has an elongated shape: a long C-terminal and a shorter N-terminal α-helix wrap in an antiparallel, asymmetric coiled-coil, and the central section of the chain folds in a globular domain. The terminal portion of the coiled coil inserts into the large central cavity of the $\alpha_3\beta_3$ hexamer (Figure 2A), making minimal contacts with its interior surface and reaching its top. The remainder of the γ-subunit protrudes to form a 47Å stalk, which contacts F0 at the membrane surface by means of a foot-shaped structure (Figures 1 and 2B), resulting from the interaction of its globular domain with the ε-subunit (or the δ- and ε-subunits in mitochondria). The bacterial δ-subunit (or the equivalent mitochondrial OSCP) is located externally on the upper half of the $\alpha_3\beta_3$ assembly, interacting with the N-terminal domains of at least one α-subunit (Figure 1).

F0

In F0 (Figure 1) the a subunit (the only main subunit still lacking a high resolution structure) is thought to be folded into five-transmembrane α-helices, the b-subunit comprises an α-helical hydrophilic and a potentially α-helical transmembrane domain, and the c-subunit folds in a hairpin-like structure, with two transmembrane α-helices linked by a short polar loop. Several c-subunits pack to form an oligomeric membrane-spanning ring, probably filled by membrane lipids. The number of monomers in the ring is generally thought to vary between species, and stoichiometries of 9–14 c-subunits have been proposed for the synthases of different sources. In bacteria, the packing of the c-subunits is suggested to vary even within a single species, as a result of modifications in the membrane lipid composition induced by different growing conditions. Irrespective of its stoichiometry, the c-ring spans the membrane, interacting with the foot of the F1 stalk by means of the polar loops of the c-subunits, while its external surface contacts the highly hydrophobic a subunit and the transmembrane domains of the b-subunit dimer (in bacteria and chloroplasts). The hydrophilic α-helices of the b-subunits project from

the membrane reaching the δ-subunit of F1. The b-subunit of mitochondrial F0, although monomeric, is thought to have an analogous organization and to contact the OSCP subunit of F1. The interaction between the F0 b and the F1 δ (or OSCP) subunits results in the second, peripheral stalk connecting the catalytic head to the membrane-intrinsic footpiece of the ATP synthase complex.

ATP Synthesis by F1

Catalytic Process

The catalytic cycle leading to the production of ATP involves three main steps: binding of Mg–ADP and P_i to the enzyme (both ADP and ATP are complexed with Mg^{2+}, as in all known reactions of these nucleotides), formation of the γ-phosphoanhydridic bond by removal of a water molecule, and release of Mg–ATP to the aqueous phase. Reversal of these steps leads to the hydrolysis of ATP, which is often studied as it requires simpler experimental systems (e.g., the isolated F1, or the complete F1–F0 complex in the absence of a proton gradient) than the synthesis. ATP is synthesized (or hydrolyzed) at three catalytic sites located on the β-subunits at the interface with an α-subunit (Figure 3). The α-subunits also contain nucleotide-binding sites which, although homologous to those of the β-subunits, are catalytically inactive (Figure 2A). Most of the amino acids involved in catalysis belong to the β-chain, but the adjacent α-chain also contributes essential residues, so that the enzyme functionally consists of three αβ catalytic pairs. As in many ATP-utilizing proteins, each nucleotide-binding site contains a P-loop, i.e., a conserved sequence motif – Gly-X-X-X-X-Gly-Lys-Thr/Ser – which participates in the binding of the phosphate groups. Other amino acids involved in the synthesis/hydrolysis of ATP have been identified by mutational and structural data; among them, the side chain of a glutamic acid, which has no equivalent in the inactive sites of the α-chains, appears essential for the formation/hydrolysis of the anhydridic bond of ATP.

Analysis of ATP synthesis has unexpectedly shown that the γ-phosphoanhydridic bond of ATP readily forms within the complex, owing to the much higher affinity of the catalytic sites for ATP than for ADP and Pi. However, the newly formed ATP remains tightly bound to the enzyme unless protons are flowing through F0 down a transmembrane gradient. This observation has provided evidence that the translocated protons are not directly involved in catalysis, suggesting instead that the H^+ flow is the exergonic process driving the major energy-requiring step of ATP synthesis, i.e., the decrease of the enzyme affinity for ATP.

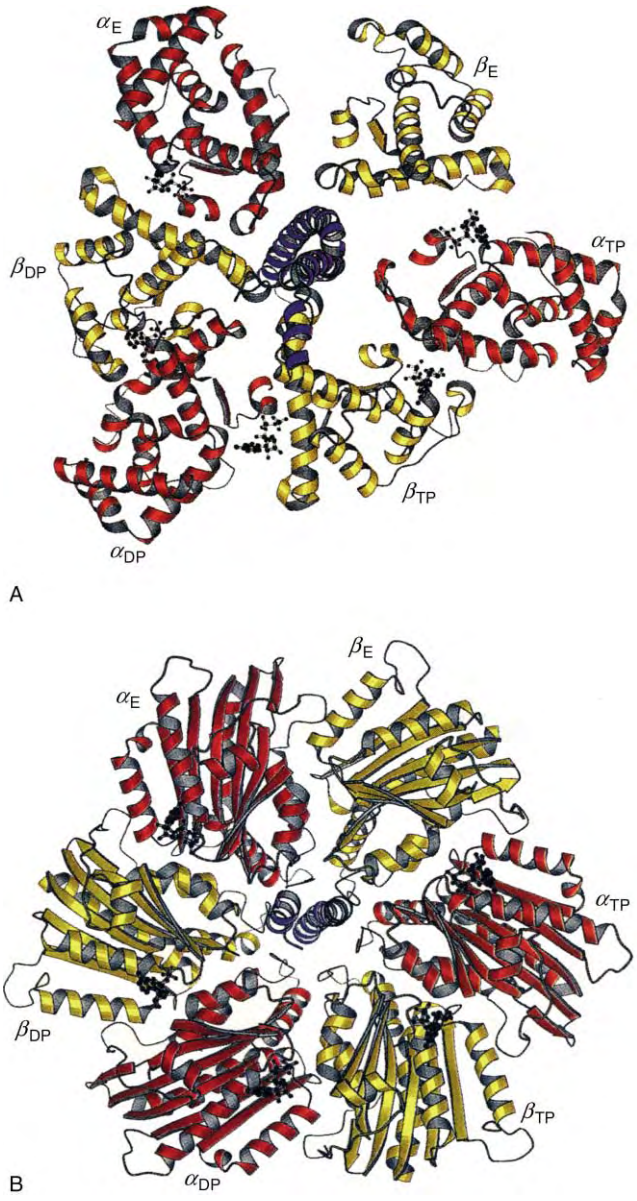

FIGURE 3 Asymmetric features of bovine F1. F1 was crystallized in the presence of AMP–PNP and ADP. The α-subunits are in red, the β-subunits are in yellow, and the γ-subunit (part of which is lacking, since it was disordered in the crystal) is in blue. All the α-subunits and the β_{TP}-subunit have AMP–PNP bound; β_{DP} has ADP and β_E has no nucleotide. (Reproduced from Abrahams, J. P., Leslie, A. G. W., Lutter, R., and Walker, J. E. (1994). Structure at 2.8Å resolution of F1-ATPase from bovine heart mitochondria. *Nature* **370**, 621–628, with permission.) (A) The γ-subunit coiled-coil and the C-terminal domains of the α- and β-subunits (viewed from the membrane side). (B) The γ-subunit coiled-coil and the nucleotide-binding domains of the α- and γ-subunits (viewed from the membrane side).

Binding Change Model

A further peculiar aspect of F1 revealed by the enzymological data is cooperative catalysis: the three β-subunit cannot operate independently, as revealed by the complete loss of enzymatic activity of the synthase

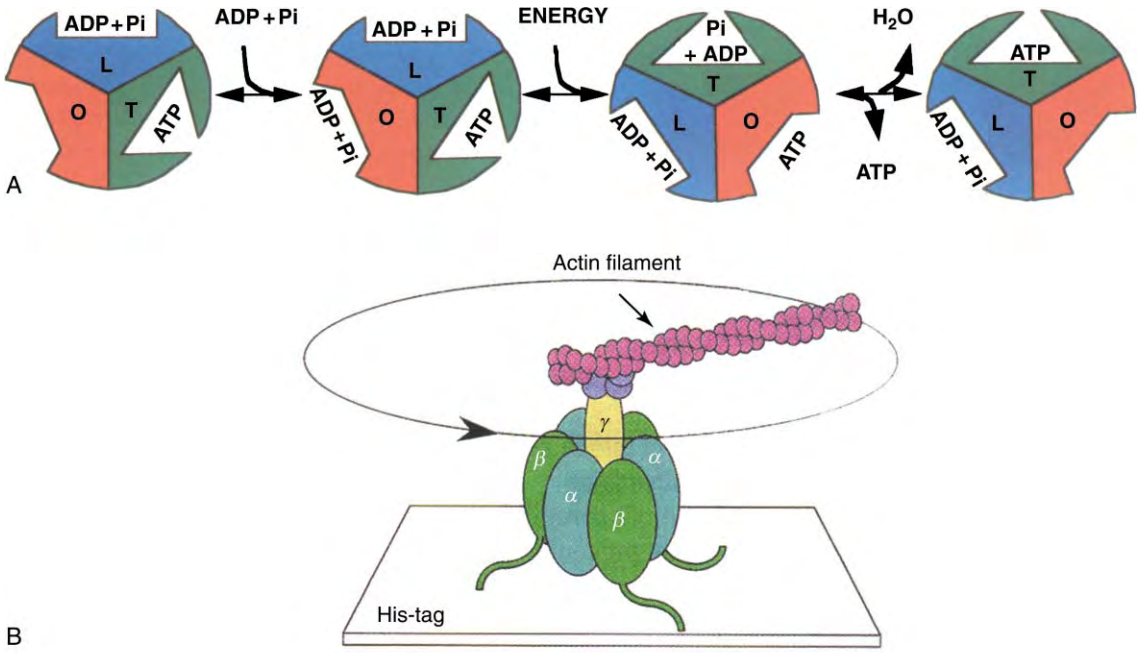

FIGURE 4 The binding change model of ATP synthesis and the rotation of the γ-subunit(A) Each circle represents a different conformation of $\alpha_3\beta_3$, the three sectors corresponding to the three $\alpha\beta$ pairs. Green sectors represent the "tight" (T) conformation, blue sectors represent the "loose" (L) conformation, and red sectors represent the "open" (O) conformation. (Reproduced from Bianchet, M.A., Pederson, P. L., and Amzel, L. M. (2000). Notes on the mechanism of ATP synthesis. *J. Bioenerg. Biomembr.* **32**, 517–521, with permission of Kluwer Academic/Plenum Publishers.) (B) The $\alpha_3\beta_3\gamma$ complex was immobilized on a microscope slide coated with Ni^{2+}-nitrilotriacetic acid, by means of polyhistidine tags (that bind strongly to nickel ions) attached to the N termini of the β-subunits. A fluorescently labelled actin filament (length 2 μm) was attached to the γ-subunit, and the rotation of the γ-subunit was observed directly during the hydrolysis of ATP by epifluorescence microscopy. (Reproduced from Junge, W., Lill, H., and Engelbrecht, S. (1997) ATP synthase: an electrochemical transducer with rotatory mechanics. *Trends Biochem. Sci.* **22**, 420–423, with permission from Elsevier.)

upon inhibition of a single catalytic site of F1, implying that site-to-site interactions are essential to complete the catalytic cycle. According to the widely accepted binding change model (Figure 4A), proposed by Boyer in 1973 to explain the unusual catalytic features of the F1–F0 ATPase, as the synthesis of ATP proceeds each β-subunit sequentially adopts three conformations, corresponding to different binding affinities of the catalytic site for ATP, ADP, and Pi: the loose (L) conformation binds ADP and P_i with low affinity, the tight (T) conformation allows ATP to be synthesized by binding it with very high affinity, and the open (O) conformation releases the newly formed ATP to the medium. At any time the three β-subunits within F1 have different conformations and distinct steps of the enzymatic reaction take place at each catalytic site: when one β-subunit changes from the L to the T conformation, forming ATP from ADP and P_i, another β-subunit converts from the T to the O state, releasing ATP, and the third one shifts from the O to the L conformation, binding ADP and P_i. Thus, ATP is released by a catalytic site only upon binding of the substrates to another site, and the synthesis of ATP is the result of the concerted operation of the three $\alpha\beta$ pairs of F1.

The functional asymmetry predicted by the binding change mechanism has been substantiated by structural information. In fact, in the first F1 crystal described by Walker (Figure 3) the β-subunits have distinct tridimensional structures, arising principally from domain shifts, and the catalytic sites contain different nucleotides: one binds the ATP analogue AMP–PNP, one ADP, while the third one has no ligand. However, two main problems concerning the catalytic cycle are still debated: (1) the actual number of the catalytic sites of F1 involved in the synthesis of ATP and (2) the number of the distinct conformations cyclically adopted by each β-subunit.

Rotational Catalysis

The tridimensional structure of F1 has also revealed that the γ-subunit contributes to the asymmetry of F1 (Figure 3): its coiled-coil displays different interactions with each $\alpha\beta$-subunit pair, correlating with the conformational differences among the catalytic sites. These structural features support the rotary mechanism of ATP synthesis, as predicted by Boyer to account for the binding change model. According to this mechanism the asymmetric γ-subunit triggers the conformational transitions required to synthesize ATP by rotating relative to the $\alpha_3\beta_3$ ring, therefore interacting differently with each $\alpha\beta$ pair at any instant. The contact sites between the γ-subunit and each $\alpha\beta$ pair which are specifically

responsible for the conformational transitions envisaged by the binding change model remain controversial; however, an inventive experiment designed in 1997 by the groups of Yoshida and Kinosita has visually documented the rotation of the γ-subunit during ATP hydrolysis (Figure 4B). A single recombinant $\alpha_3\beta_3\gamma$ bacterial complex was anchored to a microscope slide, so that the γ-subunit projected upwards. An actin filament, much bigger than the enzyme and bearing a fluorescent tag, was linked to the γ-subunit, at a distance from the ring, to provide a long adjunct that could be observed under a fluorescent microscope. When Mg–ATP was added to this ATPase preparation, the actin filament began to rotate unidirectionally proving that the hydrolysis, and presumably the synthesis, of ATP entailed the physical rotation of the γ-subunit. At very low concentrations of ATP the rotary motion apparently splits into 120° steps, each evidently corresponding to the hydrolysis of one molecule of ATP. The efficiency of the conversion of the chemical energy from ATP hydrolysis into the mechanical energy of rotation was estimated to approximate 90%, consistent with the fully reversible operation of F1. The same biophysical approach has subsequently demonstrated that the whole central stalk assembly (i.e., the bacterial γ- and ε-subunits) revolves during the catalytic process.

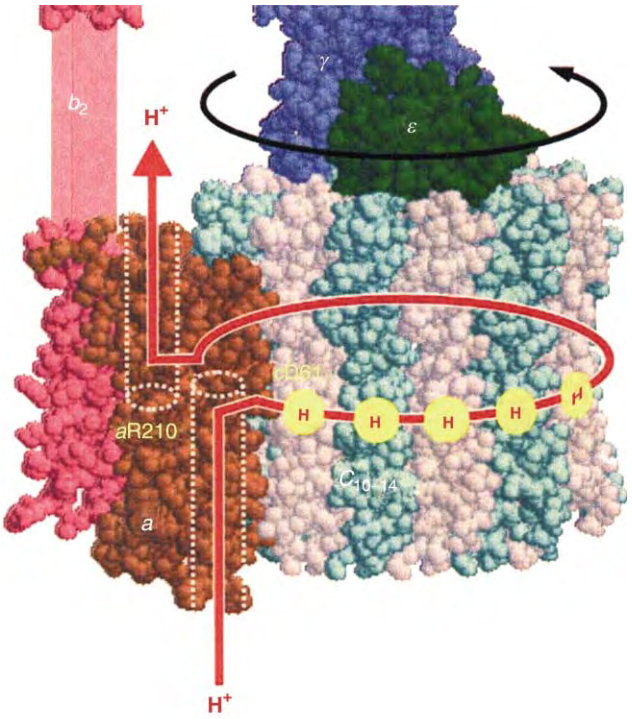

FIGURE 5 Structure of the ATP synthase showing a proposed proton transport path. aR210 and cD61 indicate the a-subunit arginine and the c-subunit aspartate required for the transmembrane movement of H^+; the dotted lines represent the putative half-channels for H^+. (Reproduced from Weber, J., and Senior, A. E. (2003). ATP synthesis driven by proton transport in F_1F_0-ATP synthase. *FEBS Lett.* **545**, 152–160 with permission of Federation of the European Biochemical Societies.)

Proton Translocation by F0

To mechanically connect the synthesis of ATP by F1 to the translocation of protons by F0, the rotation of the central stalk must be driven by protons moving through F0. However, the abovementioned lack of a high resolution structure of the intact F0 has so far hampered the efforts to define its fine molecular mechanism.

Amino acids essential for the transmembrane movement of protons have been identified both in the a-subunit and in the c-subunit, but not in the b-subunit, implying that the H^+ path is formed by a- and c-subunits. In particular, two interacting amino acids, predicted to be near the middle of the hydrophobic core of the membrane, are apparently crucial to H^+ transport: an aspartate (or glutamate) in the c-subunit, and an arginine in the a-subunit (Figure 5). The acidic residue reacts specifically with the synthase inhibitor dicyclohexylcarbodiimide (DCCD), and the translocation of protons through F0 is completely blocked by the binding of DCCD to just one of the several c-subunits, meaning that the c-subunits in the ring operate cooperatively.

In 1986, these experimental findings have led Cox and co-workers to propose that the c-ring rotates against the a-subunit so that, as each c-subunit moves past the a-subunit, a proton moves across F0. Recently, cross-linking studies have established that H^+ translocation does cause the c-ring to revolve, and that the central stalk is forced to rotate synchronously with the ring due to the connections between its foot-shaped portion and the c-subunits. In addition, extension of the procedure of Yoshida and Kinosita to the F1–F0 complex has confirmed the rotation of the c-ring.

The generally accepted model for the operation of F0 (Figure 5) envisages two disaligned half-channels (mainly located in the a-subunit) extending from the opposite surfaces of the membrane to the depth of the essential aspartate/arginine pair. To cross the membrane, a proton moves through one half-channel and binds to the negatively charged aspartate of one c-subunit, relieving the electrostatic interaction with the positively charged arginine. The uncharged c-subunit can thus come into contact with the hydrophobic core of the membrane, and the c-ring may rotate, therefore allowing the aspartate of the contiguous c-subunit to align to the half-channel and to bind another H^+. Protons are discharged to the opposite side of the membrane by means of the other half-channel following the rotation of the ring. Consistent with the actual operation of F0 and of the intact F1–F0 complex, the translocation of protons by this mechanism is passive and bidirectional,

unless a proton gradient across the membrane imposes a single direction of rotation.

Peripheral Stalk

The peripheral stalk is the least defined portion of the ATP synthase, consisting of b- and δ- (or OSCP) subunits, whose high resolution structures are still partially unknown. It is believed to act as a stator, i.e., to keep the catalytic head and the proton channel in the right relative orientation by preventing the a-subunit and the $\alpha_3\beta_3$ ring from rotating with the c-ring–γ–ε assembly (often referred to as the rotor of the complex).

See Also the Following Articles

Membrane-Associated Energy Transduction in Bacteria and Archaea • P-Type Pumps: H^+/K^+ Pump • P-Type Pumps: Plasma Membrane H^+ Pump

Glossary

electron transfer chain A functional assembly of membrane-associated redox compounds which transfers electrons down a redox potential difference. It uses the energy thus made available to pump protons across the membrane, thereby generating a transmembrane proton gradient

F1–F0 Abbreviation of "coupling *f*actor *1*" and "*f*actor conferring sensitivity to *o*ligomycin": the proteins originally identified in mitochondria by E. Racker and co-workers as necessary for the synthesis of ATP, but not for the activity of the respiratory chain.

(ion) channel A transmembrane pathway that allows a passive flow of ions down a concentration or an electrical gradient. It may shift from an open to a closed state.

oligomycin An antibiotic that blocks both the synthesis and the hydrolysis of ATP in mitochondria. It does not block the hydrolysis of ATP by purified F1 preparations.

Further Reading

Abrahams, J. P., Leslie, A. G. W., Lutter, R., and Walker, J. E. (1994). Structure at 2.8Å resolution of F_1-ATPase from bovine heart mitochondria. *Nature* **370**, 621–628.

Boyer, P. D. (1997). The ATP synthase – A splendid molecular machine. *Annu. Rev. Biochem.* **66**, 717–749.

Capaldi, R. A., and Aggeler, R. (2002). Mechanism of the F_1F_0-type ATP synthase, a biological rotary motor. *Trends Biochem. Sci.* **27**, 154–160.

Junge, W., Pänke, O., Cherepanov, D. A., Gumbiowski, K., Müller, M., and Engelbrecht, S. (2001). Inter-subunit rotation and elastic power transmission in F_1F_0-ATPase. *FEBS Lett.* **504**, 152–160.

Nicholls, D. G., and Ferguson, S. J. (2002). *Bioenergetics*. Academic Press, London.

Noji, H., Yasuda, R., Yoshida, M., and Kinosita Jr., K. (1997). Direct observation of the rotation of F_1-ATPase. *Nature* **386**, 299–302; http://www.res.titech.ac.jp/seibutu/main_html.

Pedersen, P. L., Ko, Y. H., and Hong, S. (2000). ATP synthases in the year 2000: Defining the different levels of mechanism and getting a grip on each. *J. Bioenerg. Biomembr.* **32**, 423–432.

Richter, M. L., Hein, R., and Huchzermeyer, B. (2000). Important subunit interactions in the chloroplast ATP synthase. *Biochim. Biophys. Acta* **1458**, 326–342.

Sambongi, Y., Ueda, I., Wada, Y., and Futai, M. (2000). A biological molecular motor, proton-translocating ATP synthase: Multidisciplinary approach for a unique membrane enzyme. *J. Bioenerg. Biomembr.* **32**, 441–448.

Stock, D., Gibbons, C., Arechaga, I., Leslie, A. G. W., and Walker, J. E. (2000). The rotary mechanism of ATP synthase. *Curr. Opin. Struct. Biol.* **10**, 672–679.

Weber, J., and Senior, A. E. (2003). ATP synthesis driven by proton transport in F_1F_0-ATP synthase. *FEBS Lett.* **545**, 152–160.

Yoshida, M., Muneyuki, E., and Hisabori, T. (2001). ATP synthase – A marvellous rotary engine of the cell. *Nat. Rev. Mol. Cell Biol.* **2**, 669–677.

Biography

Donata Branca is a Research Associate in the Department of Biological Chemistry at the University of Padova and the Venetian Institute of Molecular Medicine. In the past, she has worked on the relationship between H^+ translocation and ATP synthesis in mitochondria. Her present interest is the role of calcium in intracellular proteolysis.

FAK Family

Steven K. Hanks
Vanderbilt University School of Medicine, Nashville, Tennessee, USA

The focal adhesion kinase (FAK) family is a small family of nonreceptor tyrosine kinases that function in adhesion-mediated signaling. The family contains just two vertebrate members: FAK and *p*roline-rich *t*yrosine *k*inase 2 (PYK2). Also included are homologues from invertebrate metazoans: DFak56 from *Drosophila* and KIN-31 from *C. elegans*. The FAK family is defined by the presence of three major conserved domains: central tyrosine kinase catalytic domain, amino-terminal FERM domain (related to domains found in the red blood cell band 4.1 protein, *e*zrin, *r*adixin, and *m*oesin), and carboxyl-terminal *f*ocal *a*dhesion *t*argeting (FAT) domain.

FAK

Focal adhesion kinase (FAK) (Figure 1) was the first member of the family to be described and has been most extensively studied, primarily in cultured fibroblasts. Its name derives from its prominent localization to cellular focal adhesions (Figure 2). Focal adhesions are sites where cell surface integrins cluster and make strong adhesive contact with components of the extracellular matrix (ECM) such as fibronectin, vitronectin, and collagen. Focal adhesion localization was the first indication that FAK could be involved in regulating aspects of cell behavior resulting from integrin-mediated adhesion. The FAT domain is necessary and sufficient for focal adhesion localization.

FAK Expression and Role in Development

FAK is widely expressed throughout embryogenesis and appears to function in many developmental processes. A role for FAK in gastrulation is suggested by observations, made in early embryos from *Xenopus* and chicken, of prominent FAK expression in the involuting mesoderm. FAK-deficient mouse embryos fail to develop past late stages of gastrulation, and exhibit dramatically retarded development of the antero-posterior axis, suggestive of defects in mesodermal migration. Studies using late-stage embryos from mouse, *Xenopus*, and zebrafish indicate high FAK expression associated with several developing systems including the central nervous system, somites, arterial walls, myotendinous junctions, and germ cells. FAK is ubiquitously expressed in adult tissues, with high levels found in brain, lung, and testis. In neuronal cells FAK is enriched in growth cones. Neuronal FAK is expressed from alternatively spliced transcripts resulting in short insertions in the region between the FERM and kinase domains.

FAK Activation and Signaling Mechanism

Like most tyrosine kinases, FAK is in its active signaling state when phosphorylated on tyrosine residues. FAK tyrosine phosphorylation results from integrin-mediated cell adhesion to the ECM and is maintained by Rho-mediated contraction of the actin cytoskeleton. The initial step in FAK activation is phosphorylation of Tyr-397, which occurs through intermolecular autophosphorylation. Neuronal-specific isoforms of FAK have a higher intrinsic capacity to autophosphorylate. A critical aspect of FAK signaling is the recruitment of Src-family kinases, which bind via their SH2 domains to the phosphorylated Tyr-397 site. This leads to Src-mediated phosphorylation of five other FAK tyrosine residues: 407, 576, 577, 861, and 925 (Figure 1). Tyrosines 576 and 577 reside in the kinase domain "activation loop," and evidence indicates that phosphorylation of these sites elevates catalytic activity. Phosphorylated Tyr-925 can bind the SH2 domain of the adaptor protein Grb2, suggesting a mechanism for integrin stimulation of "extracellular-signal regulated kinase" (ERK) via a FAK > Grb2/SOS > Ras pathway. The signaling functions of the Tyr-407 and Tyr-861 sites are unknown.

Src-family kinases recruited to the Tyr-397 site also phosphorylate two FAK-associated proteins: "Crk-associated substrate" (CAS) and paxillin. CAS, via its SH3 domain, interacts with either of two proline-rich motifs (PR1 and PR2) that reside in the region linking the kinase and FAT domain. Paxillin interacts with the FAT domain. For both CAS and paxillin, the major tyrosine phosphorylation sites are in Tyr-X-X-Pro (YxxP) motifs. Fifteen YxxP motifs constitute the major region of CAS tyrosine phosphorylation (known as the "substrate domain") while two YxxP motifs are

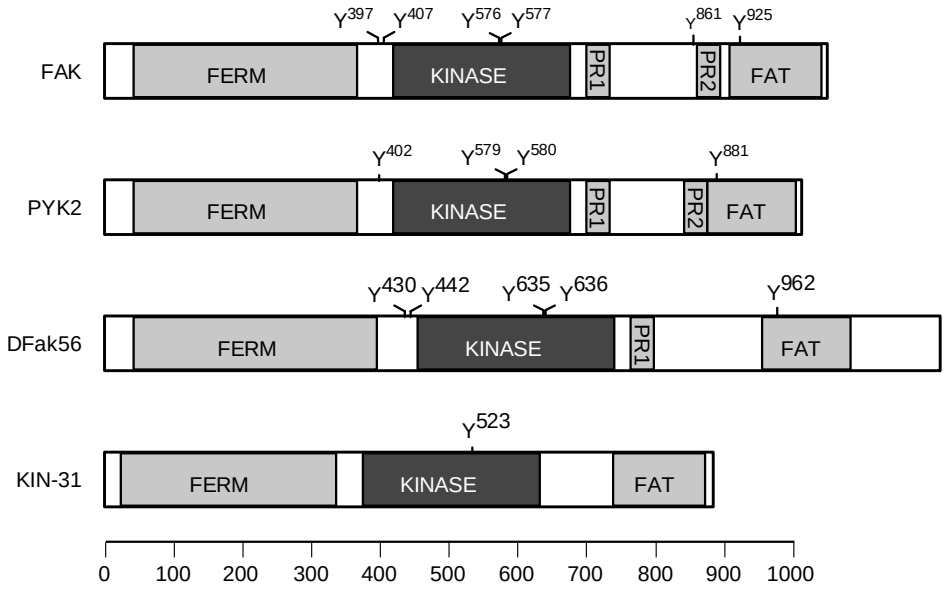

FIGURE 1 Members of the FAK family. FAK and PYK2 are vertebrate family members, DFak56 is from *Drosophila*, and KIN-31 is from *C. elegans*. Shown in the linear structures are major conserved domains, protein interaction motifs, and sites of tyrosine phosphorylation (see text for details). The scale bar represents number of amino acid residues.

the major paxillin sites. Phosphorylation of YxxP sites promotes downstream signaling events through recruitment of additional SH2-containing effector molecules. The c-Crk adaptor molecule binds to YxxP sites of both CAS and paxillin and appears to be a major downstream effector in signaling from the FAK/Src complex.

In addition to Src family kinases, the phosphorylated Tyr-397 site mediates interactions with SH2 domains of other signaling proteins including phosphatidylinositol 3-kinase (PI3K), the γ1 isoform of phospholipase C (PLC-γ1), Shc, Grb7, and Nck-2. Thus FAK likely promotes assembly of several distinct signaling complexes within a larger integrin-associated protein network.

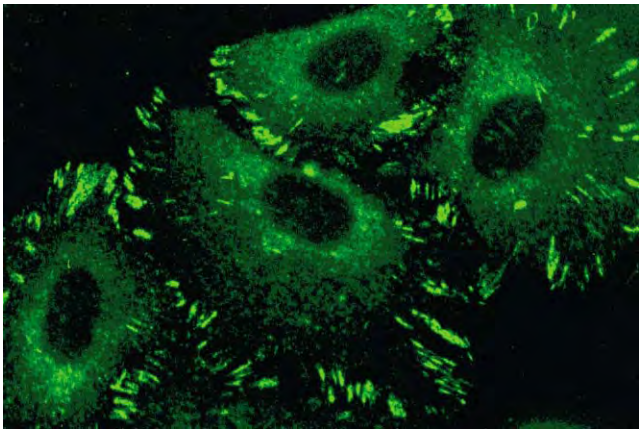

FIGURE 2 Localization of FAK in focal adhesions. Primary cultures of mouse keratinocytes were plated on fibronectin and stained using an antibody against FAK. The highly immunoreactive structures observed at the cell peripheries are focal adhesions.

Cellular Responses to FAK Signaling

Much evidence indicates that FAK functions to enhance the rate of cell motility. For example, fibroblasts derived from *FAK* −/− mouse embryos exhibit poor motility compared to cells from normal embryos, and the motility defect can be rescued by re-expressing wild-type FAK. Mutant FAK variants, either lacking the Tyr-397 site or deficient in catalytic activity, are unable to efficiently promote the motility response, indicating that FAK signaling is involved. A likely mechanism by which FAK promotes cell motility is by directing the extension of leading-edge lamellipodia. This occurs, in part, through activation of the small GTPase Rac, which can result from the recruitment of c-Crk to phosphorylated CAS and paxillin. One of the c-Crk SH3 domains interacts with the protein DOCK180 that promotes Rac GDP–GTP exchange. Interactions of the FAK Tyr-397 site with PI3K and Grb7 have also been implicated in the motility response.

In addition to regulating motility, FAK also functions as a positive regulator of cell growth by triggering both survival and proliferative signals. FAK-mediated signaling (requiring the Tyr-397 site) confers resistance to apoptosis resulting from various stimuli including loss of anchorage to the ECM (anoikis), oxidative stress, UV irradiation, and exposure to anti-cancer drugs. FAK survival signals can result from multiple downstream events including CAS/Crk complex formation and PI3K-mediated activation of Akt. FAK may also help

drive progression through G1 phase of the cell cycle through its ability to activate ERK kinases and promote transcriptional activation of the gene encoding cyclin D1.

PYK2

PYK2 is also known as CAK-β (cellular adhesion kinase β), RAFTK (related adhesion focal tyrosine kinase), and CADTK (calcium-dependent tyrosine kinase). The FAT and kinase domains of PYK2 each exhibit ~60% amino acid identity with the homologous domains of FAK, while the FERM domain is slightly less conserved (Table I). Both PR motifs in the kinase-FAT linking region are present in PYK2 (and capable of mediating interactions with CAS) but otherwise this region is poorly conserved, as is the short region amino-terminal to the FERM domain. Four tyrosine residues corresponding to sites of FAK phosphorylation are functionally conserved (Figure 1): phosphorylated Tyr-402 mediates interactions with Src-family kinases, phosphorylated activation loop tyrosines 579 and 580 stimulate PYK2 catalytic activity, and phosphorylated Tyr-881 binds Grb2.

PYK2 Expression and Roles in Development

PYK2 is expressed at high levels in the central nervous system and cells of hematopoietic origin, but is also detected in a variety of other cell types including fibroblasts, osteoclasts, epithelial cells, and smooth muscle cells. PYK2 levels increase dramatically in the forebrain around birth. A splice variant encoding a 42 amino acid insert between the two PR regions is predominantly expressed in neuronal cells. PYK2-deficient mice develop normally, but lack marginal zone B cells and have suppressed immunoglubulin production.

TABLE I

Conservation of FAK Family Domains[a]

	PYK2	DFak56	KIN-31
FERM	47	26	19
Kinase	58	63	47
PR linker	25	19	7
FAT	61	43	18

[a] Percent amino acid identities are shown compared to human FAK. Human PYK2 was used for the comparison. "PR linker" refers to the region containing proline-rich motifs that lies between the kinase and FAT domains.

PYK2 Activation and Signaling Mechanism

Like FAK, PYK2 activation can result from integrin stimulation. For example, PYK2 undergoes tyrosine phosphorylation following plating of megakaryocytes onto fibronectin and upon antibody stimulation of B cell integrins. In fibroblasts, PYK2 is detected in focal adhesions, consistent with the high conservation of the FAT domain. It is notable, however, that the FAT domain of PYK2 targets to focal adhesions inefficiently compared to that of FAK. PYK2 activation in response to integrin-mediated adhesion has been observed in *FAK −/−* fibroblasts. But re-expression of FAK in these cells effectively suppresses the PYK2 response, probably by displacing PYK2 from the adhesion sites. These observations suggest that PYK2 may not play as widespread a role in integrin signaling as does its sister molecule, FAK.

In contrast to FAK, PYK2 can be activated by extracellular signals that elevate levels of intracellular calcium and stimulate calcium-dependent isoforms of protein kinase C. These include agonists for G protein-coupled receptors, voltage-gated calcium channels, and the nicotinic acetylcholine receptor. Since protein kinase C is a protein-serine/threonine kinase it must stimulate PYK2 tyrosine phosphorylation through an indirect means, but the exact mechanism is unknown.

The downstream signaling events resulting from PYK2 activation are generally similar to those of FAK, involving autophosphorylation, recruitment of Src family kinases, and Src-mediated phosphorylation of other sites on PYK2 as well as PYK2-associated CAS and paxillin (Figure 3). The interaction of Grb2 with the PYK2 Tyr-881 site suggests a possible link between G protein-coupled receptors and ERK activation.

Cellular Responses to PYK2 Signaling

Unlike FAK, PYK2 overexpression does not efficiently promote fibroblast motility and results in apoptosis, rather than cell survival. Nevertheless, a critical role for PYK2 in the motility and migration of macrophages and B cells has been demonstrated using cells derived from PYK2-deficient mice. Defects in lymphocyte motility could explain the absence of marginal zone B cells in these animals. Through its ability to be activated by both integrin- and calcium/PKC-dependent mechanisms, PYK2 can function in numerous and diverse signaling pathways regulating a wide variety of cellular activities. In neuronal cells, for example, PYK2 has been implicated as a positive regulator of neurite outgrowth and NMDA channel activity. Other consequences of PYK2 signaling include inhibition of voltage-gated potassium channels leading to membrane depolarization of vascular smooth muscle cells, translocation of the

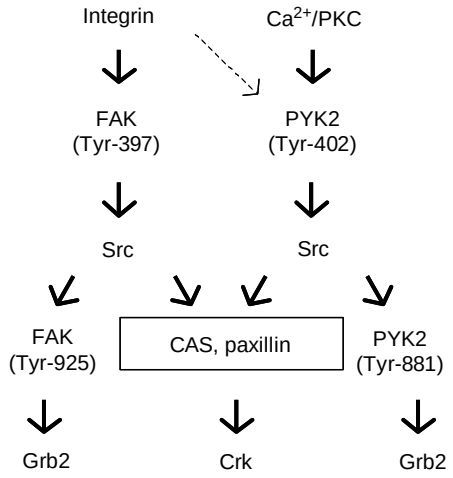

FIGURE 3 Signaling by FAK and PYK2. Both FAK and PYK2 can be activated by integrin-mediated adhesion, while PYK2 is uniquely activated through a calcium/PKC-dependent mechanism. A critical element of FAK and PYK2 signaling involves the recruitment of Src family kinases to sites of autophosphorylation. The associated Src family kinases then phosphorylate a conserved FAK/PYK2 tyrosine site to promote Grb2 binding, and also phosphorylate FAK/PYK2-associated proteins CAS and paxillin to promote binding of Crk. The adaptor molecules Grb2 and Crk interact with guanine-nucleotide exchange factors for small G proteins, including Ras and Rac, to promote downstream signals.

GLUT4 glucose transporter to the plasma membrane of adipocytes, stimulation of Na-HCO^{3-} cotransporter activity in renal epithelial cells, and angiogenesis of vascular endothelial cells.

Invertebrate Members of the FAK Family

Drosophila and *C. elegans* genomes each contain a single member of the FAK family: DFak56 in *Drosophila* and KIN-31 in *C. elegans*. FAK and PYK2 are more closely related to one another than they are to either DFak56 or KIN-31, indicating that the two vertebrate family members arose through a gene duplication event that occurred sometime after evolutionary separation from the invertebrates.

Drosophila DFak56 shows strong overall conservation with the two vertebrate family members, but is slightly more similar to FAK than to PYK2. The kinase domain of DFak56 is most highly conserved in comparison to FAK, followed in order by the FAT domain, the FERM domain, and the kinase-FAT linker region (Table I). Within the kinase-FAT linker, DFak56 contains a proline-rich motif corresponding to the PR1 site, but lacks the PR2 site. Of the six sites of FAK tyrosine phosphorylation, DFak56 lacks only the site corresponding to FAK Tyr-861. But DFak56 Tyr-962, which corresponds to the Grb2 binding sites in FAK and PYK2, lacks the asparagine residue at the +2 position necessary for Grb2 SH2 binding. A unique structural feature of DFak56 is an extended carboxyl-terminal region of unknown function. Like the vertebrate members of the FAK family, DFak56 exhibits autophosphorylation activity and undergoes tyrosine phosphorylation in response to integrin-mediated adhesion. DFak56 is broadly expressed during embyrogenesis, with strongest expression in the developing gut and central nervous system. The role of DFak56 in *Drosophila* development has yet to be defined through loss of function studies. However, overexpression of DFak56 in the wing imaginal disk leads to wing blistering, a phenotype associated with weakened integrin linkage to the actin cytoskeleton.

C. elegans KIN-31 is a predicted protein product of gene C30F8.4 that has yet to be characterized biochemically. Compared to other members of the FAK family, KIN-31 contains a well-conserved and apparently functional kinase domain, while both the FAT and FERM domains are rather poorly conserved (Table I). Interestingly, KIN-31 lacks key motifs associated with FAK family signaling including a tyrosine corresponding to the autophosphorylation site and proline-rich motifs in the kinase-FAT linker region. Thus the functional role of KIN-31 could be quite distinct from the other FAK family members. KIN-31 is expressed in all larval stages and is prominent in bodywall muscle cells. Surprisingly, there is no obvious phenotype associated with a deletion of the gene encoding KIN-31.

See Also the Following Articles

Focal Adhesions • Integrin Signaling • Src Family of Protein Tyrosine Kinases

Glossary

activation loop A region within protein kinase catalytic domains that is often phosphorylated to promote catalytic activity.

integrins A large family of cell surface adhesion receptors, composed of α- and β-subunits, that link the extracellular matrix to the actin cytoskeleton and transmit biochemical signals across the plasma membrane.

SH2 "Src-homology 2," a domain that mediates protein–protein interactions by binding to sites of tyrosine phosphorylation.

SH3 "Src-homology 3," a domain that mediates protein–protein interactions by binding to proline-rich motifs with a core sequence of Pro-X-X-Pro.

tyrosine kinase A kinase that phosphorylates protein substrates on tyrosine residues.

Further Reading

Avraham, H., Park, S. Y., Schinkmann, K., and Avraham, S. (2000). RAFTK/Pyk2-mediated cellular signalling. *Cell Signal.* **12**, 123–133.

Girault, J.-A., Costa, A., Derkinderen, P., Studler, J.-M., and Toutant, M. (1999). FAK and PYK2/CAKβ in the nervous system: A link between neuronal activity, plasticity and survival? *Trends Neurosci.* **22**, 257–263.

Hanks, S. K., Shin, N.-Y., Ryzhova, L., and Brabek, J. (2003). Focal adhesion kinase signaling activities and their implications in the control of cell survival and motility. *Front Biosci.* **8**, d982–d996.

Hauck, C. R., Hsia, D. A., and Schlaepfer, D. D. (2002). The focal adhesion kinase—A regulator of cell migration and invasion. *IUBMB Life* **53**, 115–119.

Parsons, J. T., Martin, K. H., Slack, J. K., Taylor, J. M., and Weed, S. A. (2000). Focal adhesion kinase: A regulator of focal adhesion dynamics and cell movement. *Oncogene* **19**, 5606–5613.

Schaller, M. D. (2001). Biochemical signals and biological responses elicited by the focal adhesion kinase. *Biochim. Biophys. Acta* **1540**, 1–21.

Biography

Steven K. Hanks is a Professor in the Department of Cell and Developmental Biology at Vanderbilt University School of Medicine. His principal research interest is the role of tyrosine phosphorylation in integrin signaling. He holds a Ph.D. from the University of Texas Health Science Center at Houston Graduate School of Biomedical Sciences and received postdoctoral training at the Salk Institute. He pioneered homology-based approaches to identify novel protein kinases, which led to the recognition of CDK4 and FAK. He developed an approach to classify eukaryotic protein kinases based on catalytic domain phylogeny.

Fat Mobilization: Perilipin and Hormone-Sensitive Lipase

Constantine Londos and Alan R. Kimmel
National Institutes of Health, Bethesda, Maryland, USA

Nature's solution for packaging energy reserves in organisms ranging from plants to mammals is to sequester energy-rich fatty acids, in the form of triacylglycerols (TAG) or cholesteryl esters, within intracellular neutral lipid storage droplets. The great survival value for this type of packaging is attributed to the high density of energy in fatty acids and the relatively low amount of water necessary for their storage. If man were to carry the energy equivalent of fat as carbohydrate, the additional required water would render man immobile. Typically, intracellular lipid droplets are coated with specific targeting classes of proteins, but enzymes involved in lipid metabolism may also be found in tight association.

Plant Lipid Droplets

The oleosins of plant seeds and tapeta were the first to be identified, and remain the most extensively studied, lipid droplet coat proteins. The oleosins are thought to protect the lipid depositions during dessication.

Animal Lipid Droplets

The first animal lipid droplet protein to be identified was perilipin of mammalian adipocytes. While perilipin has no obvious sequence relationship to the oleosins, it is related to several other animal proteins that also target lipid droplets. One of these, the adipose differentiation-related protein (ADRP), also termed adipophilin, was first identified as a gene that is highly expressed very early during adipocyte differentiation; subsequently, ADRP was found to be expressed ubiquitously and to coat the lipid droplets of all cells, excepting mature adipocytes. A third related protein, TIP47, was identified initially by a screen for proteins that interact with the mannose 6-phosphate/IGF2 receptor and was later also found to associate with lipid droplets. Based upon the sequence similarities among perilipin, ADRP, and TIP-47, the grouping has been described as the PAT protein family. S3-12 is an even more distantly related mammalian protein that is found on adipocyte plasma membranes and also on their intracellular lipid droplets. Several genes that encode PAT proteins in *Drosophila melanogaster* and *Dictyostelium discoideum* have also been identified. These genes are related to the mammalian counterparts not only in their protein-coding sequences, but also in their overall genomic structural organizations, indicating that they derive from a gene family of ancient origin. Further, the *Drosophila* and *Dictyostelium* PAT proteins localize to lipid droplets in fusion with green fluorescent protein (GFP) when expressed heterologously in the mammalian CHO fibroblasts. It is suggested that the PAT proteins share a specific and novel structural motif that determines their unique intracellular lipid droplet targeting ability. Moreover, each member of this protein family is likely to have an essential role in lipid metabolism.

Perilipin

The most extensively studied PAT protein is perilipin. There is a single gene for perilipin in mouse (and in human) that encodes multiple mRNA and protein species, resulting from differential splicing. The mRNAs encode identical amino termini but utilize distinct stop codons and display tissue-specific variants. Perilipin expression is highest in adipose tissue, with lesser amounts in steroidogenic tissue and only trace amounts elsewhere. Although cells contain a wide variety of lipid docking sites, the perilipins localize exclusively to the phospholipid monolayer that covers the underlying neutral lipid deposits of the droplet core (Figure 1). The perilipins are found on or within this phospholipid monolayer that forms the boundary between the aqueous cytosol and the hydrophobic lipid core of the droplet. Perilipin A (Peri A) is the largest and most abundant form. It has six consensus protein kinase A (PKA) sites that are phosphorylated upon elevation of cAMP during the lipolytic stimulation of adipocytes. Since lipolysis in

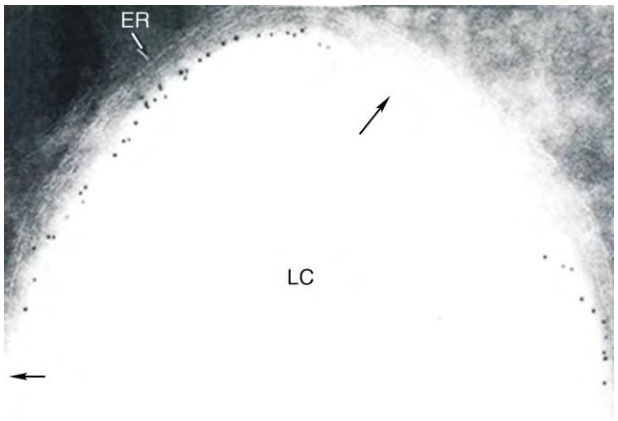

FIGURE 1 Immunogold labeling of perilipin at the surface of adipocyte lipid droplet. Electron micrograph of section through a lipid droplet immunostained with antiperilipin Ab. Note that the gold particles occur at the surface of the lipid droplet core (LC). (Reprinted from Blanchette-Mackie, E. J., Duyer, N. K. Barber, T. Coxay, R. A. Takeda, T. Rondinono, C. M. Theodorakis, J. L., Greenberg, A. S., and Londos, C. (1995). Perilipin is located on the surface layer of intracellular lipid droplets in adipocytes. *J. Lipid Res.* **36**, 1216–1226.)

adipocytes is driven by a cAMP-mediated process, and given perilipin's subcellular localization and tissue specificity, it was predicted that it would play a central role in the regulation of adipocyte lipolysis. Functional analyses has confirmed this speculation.

Perilipin Function

Depending on its PKA-dependent phosphorylation state, Peri A exhibits two opposing functional properties. Nonphosphorylated Peri A serves to shield the triacylglycerols (TAG) within the droplets from lipases. By contrast, when phosphorylated by PKA, the protein facilitates TAG hydrolysis. The importance of the protective function of perilipin is best illustrated by the *peri*-null mouse that exhibits a ~70% decrease in adipose tissue weight without a change in gross animal weight or in caloric intake. This loss in adipose tissue is attributed to the constitutively high rate of basal lipolysis in the adipocytes lacking perilipin. Thus, perilipin is essential for animals to package and retain their energy reserve supply. These *peri*-null animals also revealed the critical role for perilipin in regulated lipolysis; in the absence of perilipin, adipocytes fail to respond maximally to lipolytic stimuli. Thus, in *peri*-null adipocytes as compared to wild type, quiescent cells have an elevated basal lipolytic rate, while PKA-activated cells have an attenuated lipolysis. These dual functions have been recreated and the mechanism confirmed by expressing wild type and mutant forms of Peri A in fibroblastic cells which lack endogenous perilipin protein. Perilipin, thus, protects lipids from hydrolysis in unstimulated cells, whereas PKA-phosphorylated perilipin is required for regulated lipid hydrolysis.

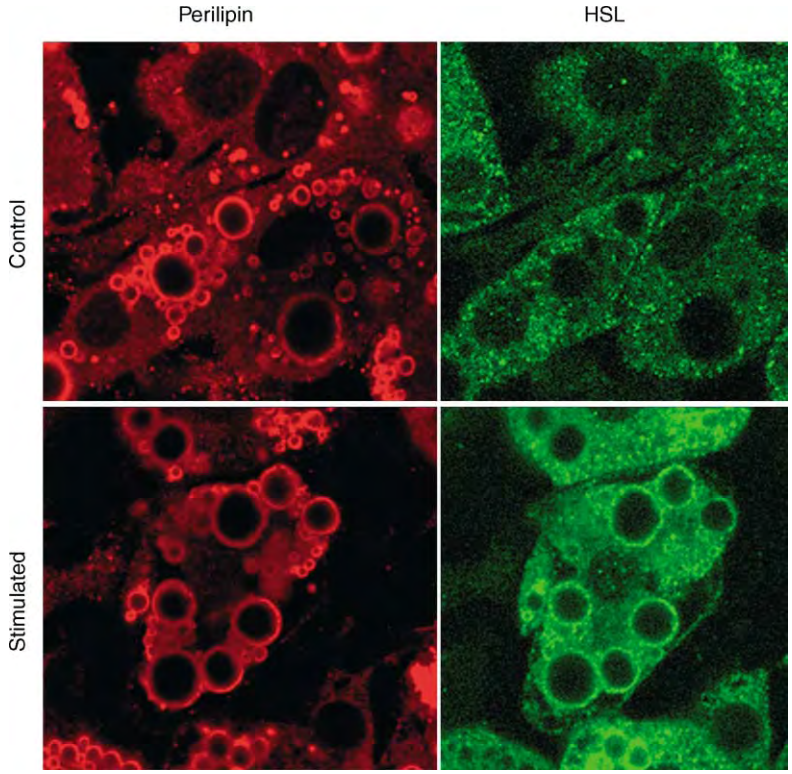

FIGURE 2 Migration of HSL from cytosol to lipid droplet surface upon stimulation. Red staining is perilipin at the lipid droplet surface. Green staining is HSL. Lower panels are resting adipocytes; upper panels show isoproterenol-stimulated cells. (Image courtesy of Dr. Carole Sztalryd, NIH.)

Adipocyte Lipolysis Catalyzed by Hormone-Sensitive Lipase

For many years, the prevailing model for adipocyte lipolysis was that hormone-sensitive lipase (HSL) was the rate-limiting enzyme and that the lipolytic rate *in vivo* was regulated exclusively by the PKA-dependent activation of HSL. This mechanism was questioned because phosphorylation of HSL *in vitro* elicits no more than a doubling of activity, whereas activation of cellular PKA increases lipolysis *in vivo* by 50- to 100-fold. The simple doubling of enzymatic activity was inadequate to explain the large increase in cellular lipolytic activity. Also, while HSL is easily identified in the cytosol of homogenates from quiescent adipocytes, the enzyme is absent from the aqueous fraction of homogenates from stimulated cells. HSL in stimulated cells was found subsequently to be associated with the cellular fraction containing the lipid storage. These data were confirmed by immunocytochemistry (Figure 2). It was not a great leap to conclude that PKA activation led to the translocation of HSL from the cytosol to the surface of the lipid storage droplet; subsequent experiments confirmed this hypothesis. An important breakthrough in understanding this mechanism came from studies with cells from the *peri*-null animals. Again, adipocytes from these animals exhibit elevated basal lipolysis, but are refractory to stimulation upon elevation of cAMP. The latter defect is downstream of the β-adrenergic receptor/G-protein/adenylyl cyclase complex that generates cAMP at the plasma membrane. Further exploration revealed that in the absence of perilipin, HSL cannot translocate from the cytosol to the lipid droplet surface in response to PKA activation. This finding established HSL translocation, and not activation per se, as the key reaction that elicits stimulated lipolysis in adipocytes and revealed the central role of perilipin in regulated lipid hydrolysis. Moreover, the HSL translocation reaction was reconstructed in nonadipocyte, CHO fibroblasts. HSL can be induced to translocate to the lipid droplet from the cytosol when coexpressed with wild-type perilipin. Translocation is not observed in the absence of perilipin or the presence of phosphorylation-defective variants of perilipin. Further, PKA-dependent phosphorylation of HSL itself was required to facilitate the translocation process.

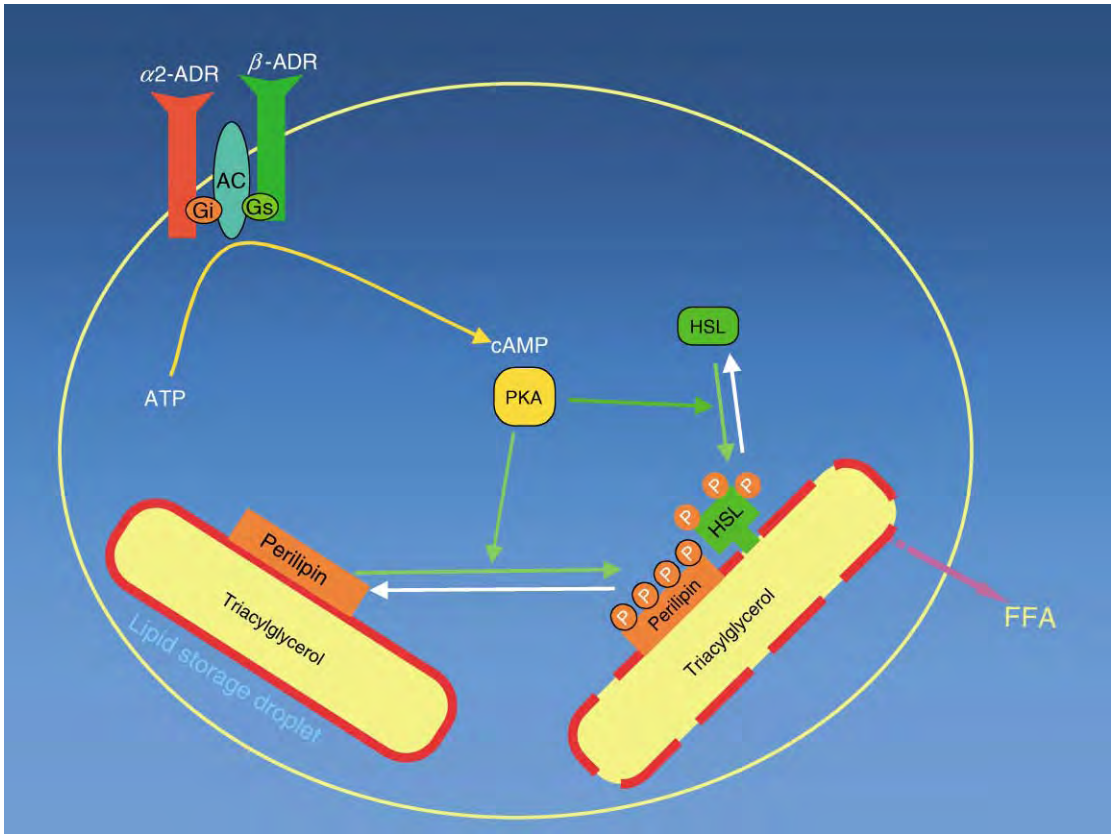

FIGURE 3 Model of the lipolytic reaction in adipocytes. Lipolytic stimulants activate adenylyl cyclase to increase cAMP which, in turn, activates protein kinase A which polyphosphorylates both hormone-sensitive lipase (HSL) and perilipin A. HSL then translocates from the cytosol to the lipid droplet surface. Phosphorylation of perilipin modifies the lipid droplet surface to accommodate the HSL.

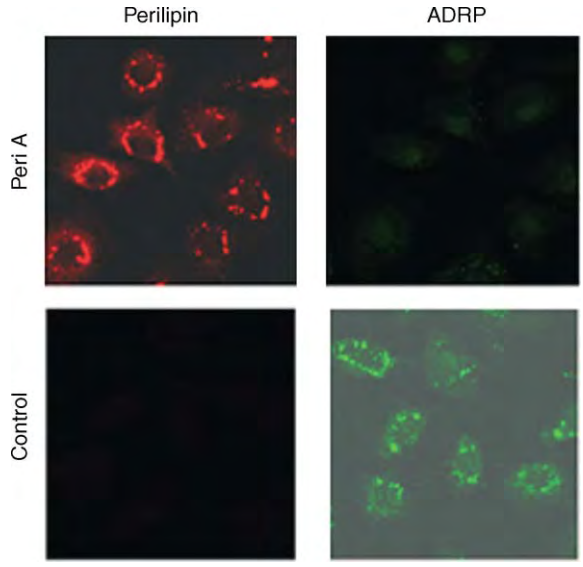

FIGURE 4 Displacement of ADRP by perilipin. Lipid droplets in lipid-loaded CHO fibroblasts stain for ADRP, but upon expression of perilipin A, the ADRP disappears and perilipin staining is seen around the lipid droplets.

Lipolysis Model

The current model for PKA-mediated lipolysis is depicted in Figure 3. In quiescent cells, cAMP levels are low, PKA is minimally active, and Peri A is unphosphorylated. Under these conditions, Peri A serves as a functional barrier for HSL access to the TAGs in the inner core of the intracellular neutral lipid droplets. Upon hormonal stimulation, cAMP levels rise, leading to the activation of PKA and the phosphorylation of both Peri A and HSL. Phosphorylation of Peri A at its three most N-terminal PKA sites readies the droplet surface to "accept" HSL. Phosphorylation of HSL at one of its two C-terminal PKA sites promotes the translocation of HSL from the cytosol to the lipid droplet surface. While it may be tempting to speculate that phospho-Peri A serves as the site for HSL docking at the droplet surface, it is difficult to believe this is the case. Potentially, unphosphorylated Peri A acts to sterically restrict access of all lipases to the surface of intracellular lipid droplets. It is, thus, not surprising that Peri A will inhibit lipolysis when expressed in cells that only possess PKA-insensitive lipases. However, phosphorylation of Peri A by PKA will stimulate lipolytic rates in these cells in excess of those observed in control cells that lack Peri A. Thus, it is suggested that Peri A phosphorylation alters the droplet surface to favor binding of all lipases, whether or not they are subject to PKA regulation. Perilipin may serve a space-making function. Phosphorylation of HSL separately facilitates binding to this "prepared" surface, effecting a synergism between Peri A and HSL during stimulation that raises the lipolytic rate 50- to 100-fold above basal levels and that is not observed with nonregulatable lipases.

It has been suggested that members of the PAT family of proteins play central roles in the regulation of lipid metabolism and energy homeostasis in organisms as diverged as *Dictyostelium* and mammals. This has been proven unequivocally for Perilipin and is strongly implied for ADRP. Recent data in *Drosophila* now extend these observations. *Drosophila* lacking one of their two PAT proteins exhibit a lean phenotype, while overexpression of the same protein leads to an increase in TAG stores, phenotypes that largely parallel those observed for perilipin (Figure 4).

See Also the Following Articles

Diacylglycerol Kinases and Phosphatidic Acid Phosphatases • Fatty Acid Oxidation • Fatty Acid Receptors • Fatty Acid Synthesis and its Regulation • Lipases • Lipid Bilayer Structure • Lipid Modification of Proteins: Targeting to Membranes • Lipid Rafts • Lipoproteins, HDL/LDL

Glossary

adipocyte The cell that stores most animal energy reserves as triacylglycerols (TAGs). Commonly known as the fat cell.

ADRP/adipophilin A protein that occurs ubiquitously and coats lipid droplets, especially in lung lipofibroblasts and secreted milk lipid globules.

hormone-sensitive lipase (HSL) The adipocyte enzyme responsible for catalyzing the rate-limiting step in TAG hydrolysis.

PAT family A family of genes that encode perilipins, ADRP/adipophilin/TIP-47 and related genes.

perilipin A protein that coats lipid droplets, primarily in adipocytes.

Further Reading

Blanchette-Mackie, E. J., Duyer, N. K., Barber, T., Coxay, R. A., Takeda, T., Rondinono, C. M., Theodorakis, J. L., Greenberg, A. S., and Londos, C. (1995). Perilipin is located on the surface layer of intracellular lipid droplets in adipocytes. *J. Lipid Res.* **36**, 1216–1226.

Brasaemle, D. L., Barber, T., Wolins, N. E., Serrero, G., Blanchette-Mackie, E. J., and Londos, C. (1997). Adipose differentiation-related protein is an ubiquitously expressed lipid storage droplet-associated protein. *J. Lipid Res.* **38**, 2249.

Gronke, S., Beller, M., Fellert, S., Ramakrishnan, H., Jackle, H., and Kuhnlein, R. P. (2003). Control of fat storage by a Drosophila PAT domain protein. *Curr. Biol.* **13**, 603.

Heid, H. W., Schnolzer, M., and Keenan, T. W. (1996). Adipocyte differentiation-related protein is secreted into milk as a constituent of milk lipid globule membrane. *Biochem. J.* **320**, 1025.

Londos, C., Brasaemle, D. L., Schultz, C. J., Segrest, J. P., and Kimmel, A. R. (1999). Perilipins, ADRP and other proteins that associate with intracellular neutral lipid droplets in animal cells. *Semin. Cell Dev. Biol.* **10**, 51.

Lu, X., Gruia-Gray, J., Copeland, N. G., Gilbert, D. J., Jenkins, N. A., Londos, C., and Kimmel, A. R. (2001). The murine perilipin gene: The lipid droplet-associated perilipins derive from tissue-specific, mRNA splice variants and define a gene family of ancient origin. *Mamm. Genome* **12**, 741.

Miura, S., Gan, J. W., Brzostowski, J., Parisi, M. J., Schultz, C. J., Londos, C., Oliver, B., and Kimmel, A. R. (2002). Functional conservation for lipid storage droplet association among perilipin, ADRP, and TIP47 (PAT)-related proteins in mammals, drosophila, and dictyostelium. *J. Biol. Chem.* **277**, 32253.

Murphy, D. J. (2001). The biogenesis and functions of lipid bodies in animals, plants and microorganisms. *Prog. Lipid Res.* **40**, 325–438.

Schultz, C. J., Torres, E., Londos, C., and Torday, J. S. (2002). Role of adipocyte differentiation-related protein in surfactant phospholipid synthesis by type II cells. *Am. J. Physiol. Lung Cell Mol. Physiol.* **283**, L288.

Sztalryd, C., Xu, G., Dorward, H., Contreras, J. A., Tansey, J. T., Kimmel, A. R., and Londos, C. (2002). Perilipin A is essential for the translocation of hormone-sensitive lipase during lipolytic activation of adipocytes. *J. Cell Biol.* **161**, 1103.

Tansey, J. T., Sztalryd, C., Gruia-Gray, J., Roush, D. L., Zee, J. V., Gavrilova, O., Reitman, M. L., Deng, C. X., Li, C., Kimmel, A. R., and Londos, C. (2001). Perilipin ablation results in a lean mouse with aberrant adipocyte lipolysis, enhanced leptin production, and resistance to diet-induced obesity. *Proc. Natl. Acad. Sci. USA* **98**, 6494.

Tansey, J. T., Hunl, A. M., Vogt, R., Davis, K. E., Jones, J. M., Fraser, K. A., Braesamle, D. L., Kimmel, A. R., and Londos, C. (2003). Functional studies on native and mutated forms of perilipins: A role in protein kinase A-activated lipolysis of triacylglycerols. *J. Biol. Chem*, **278**, 8401–8406.

Biography

Constantine Londos received D.D.S. from Ohio State University and Ph.D. from the University of Louisville School of Medicine. He worked with Dr. Martin Rodbell from 1971 through 1985, where he contributed to the G protein research for which Rodbell was awarded the Nobel prize in medicine or physiology in 1994. He currently heads the Membrane Regulation Section of Laboratory of Cellular and Developmental Biology, NIDDK, National Institutes of Health.

Alan Kimmel received Ph.D. from the University of Rochester and currently heads the Molecular Mechanisms of Development Section of LCDB, NIDDK, NIH, with a primary focus on developmental regulation of *Dictyostelium discsoideum*.

Fatty Acid Oxidation

Horst Schulz
City College and Graduate School of the City University of New York, New York, USA

Fatty acid oxidation is the process by which fatty acids are degraded in living organisms. The initial event is the activation of fatty acids by esterification with coenzyme A (CoA). The degradation of the resultant fatty acyl coenzyme A (acyl-CoA) thioesters proceeds by a cyclic process named β-oxidation. Passage through one cycle of β-oxidation produces fatty acids that are shortened by two carbon atoms and yields acetate in the form of acetyl coenzyme A (acetyl-CoA). Repetitive cycling through β-oxidation results in the complete degradation of fatty acids.

Cellular Uptake and Activation of Fatty Acids

The uptake of fatty acids by animal cells seems to be a facilitated process even though fatty acids can diffuse unassisted across biological membranes. A number of proteins of the cellular membrane are thought to be involved in this process. However, their specific functions in fatty acid uptake have not been elucidated. Once fatty acids have crossed the cellular membrane, they either diffuse or are transported to mitochondria, peroxisomes, and the endoplasmic reticulum where they are activated by esterification with coenzyme A (CoA). The transfer of fatty acids from the cellular membrane to sites of their activation may be facilitated by fatty-acid-binding proteins (FABPs), a group of low-molecular-weight (14–15 kDa) proteins that are present in the cytosol of various animal tissues. The function of FABP as an intracellular carrier of fatty acids has not been proven nor other suggested roles of this protein in the uptake and storage of fatty acids have been established.

The cellular uptake of fatty acids is tightly coupled to their intracellular esterification with CoA. Acyl-CoA synthetases catalyze the ATP-dependent esterification of fatty acids and CoA to produce fatty acyl-CoA, AMP, and pyrophosphate. Long-chain specific acyl-CoA synthetases are associated with the outer mitochondrial membrane and the membranes of the endoplasmic reticulum and peroxisomes. Acyl-CoA synthetases with a preference for medium-chain fatty acids are mostly located in the matrix of mitochondria while short-chain specific acyl-CoA synthetases are found in the mitochondrial matrix and/or in the cytosol depending on the organ of the animal.

Fatty Acid Oxidation in Mitochondria

In animal cells, fatty acids are degraded both in mitochondria and peroxisomes, whereas in lower eukaryotes fatty acid oxidation is generally confined to peroxisomes. Acetyl-CoA formed by mitochondrial fatty acid oxidation is further oxidized to release energy that drives the formation of ATP by oxidative phosphorylation. In liver, acetyl-CoA is also utilized for the synthesis of ketone bodies.

Mitochondrial Uptake of Fatty Acids

Fatty acids are activated by their conversion to fatty acyl-CoA thioesters at the outer mitochondrial membrane while their degradation by β-oxidation takes place in the mitochondrial matrix. Because acyl-CoAs cannot efficiently cross the inner mitochondrial membrane, an uptake system exists that shuttles fatty acyl residues across the inner membrane. As illustrated in Figure 1, the acyl residue of fatty acyl-CoA is transferred from CoA to carnitine at the outer mitochondrial membrane catalyzed by carnitine palmitoyltransferase I (CPT I). The resultant fatty acylcarnitine can cross the inner mitochondrial membrane in exchange for carnitine. This exchange is catalyzed by carnitine:acylcarnitine translocase (T). Once fatty acylcarnitine is in the mitochondrial matrix, it is converted back to fatty acyl-CoA by carnitine palmitoyltransferase II (CPT II), which is associated with the inner mitochondrial membrane. Medium-chain and short-chain fatty acids are not activated in the cytosol but directly enter the mitochondrial matrix where they are converted to their acyl-CoAs by medium-chain and short-chain acyl-CoA synthetases, respectively.

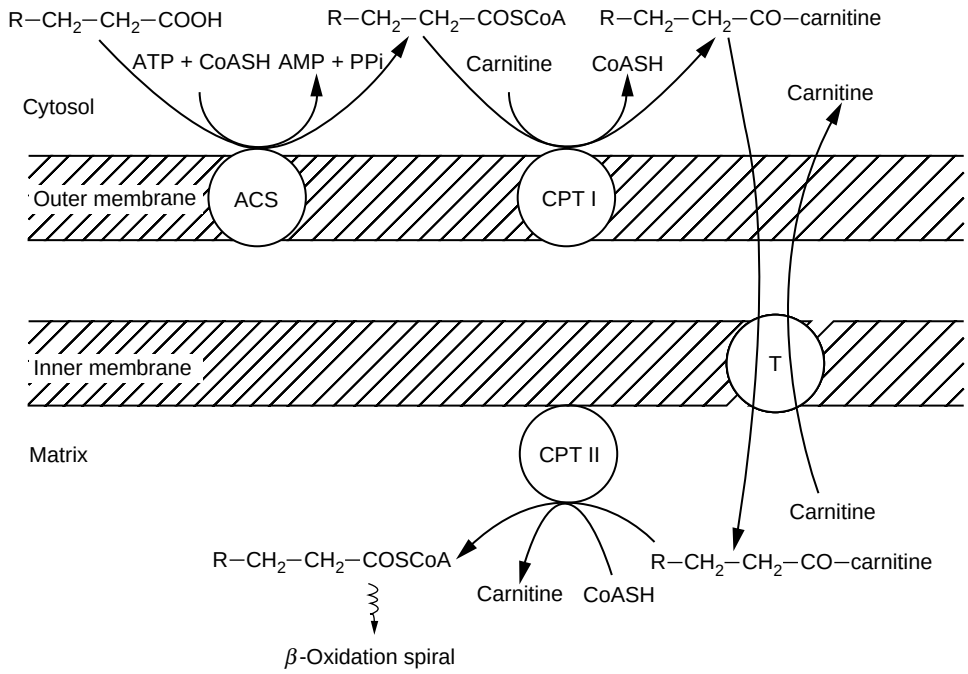

FIGURE 1 Carnitine-dependent transfer of fatty acyl groups across the inner mitochondrial membrane. ACS, acyl-CoA synthetase; CPT I and CPT II, carnitine palmitoyltransferase I and II, respectively; T, carnitine:acylcarnitine translocase.

β-Oxidation in Mitochondria

Fatty acyl-CoAs in the mitochondrial matrix are substrates of β-oxidation. This cyclic process consists of four reactions that shorten the acyl chain of fatty acyl-CoA by two carbon atoms at a time and produce acetyl-CoA. As shown in Figure 2, reaction 1a, β-oxidation begins with the removal of two hydrogens from carbon atoms 2 (α-carbon) and 3 (β-carbon) of acyl-CoA to form the corresponding 2-*trans*-enoyl-CoA. The hydrogens are initially accepted by the flavine adenine dinucleotide (FAD) cofactor of acyl-CoA dehydrogenase, the enzyme that catalyzes this reaction, then are transferred to the FAD of a soluble matrix enzyme named electron transferring flavoprotein and finally are fed into the mitochondrial electron transport chain, which supplies the energy for ATP formation by oxidative phosphorylation. In the second β-oxidation reaction, water is added across the double bond of 2-*trans*-enoyl-CoA by enoyl-CoA hydratase to yield L-3-hydroxyacyl-CoA (see Figure 2, reaction 2). The third reaction is the NAD^+-dependent dehydrogenation of L-3-hydroxyacyl-CoA catalyzed by L-3-hydroxyacyl-CoA dehydrogenase (see Figure 2, reaction 3). The product of this reaction, 3-ketoacyl-CoA, is the substrate of the fourth and last reaction of β-oxidation catalyzed by 3-ketoacyl-CoA thiolase, which cleaves the compound in the presence of CoA between carbons 2 and 3 to yield an acyl-CoA shortened by two carbon atoms and acetyl-CoA (see Figure 2, reaction 4). Repetitive cycles of β-oxidation result in the complete degradation of fatty acids to acetyl-CoA and also propionyl-CoA, if fatty acids with an odd-numbered number of carbon atoms are involved.

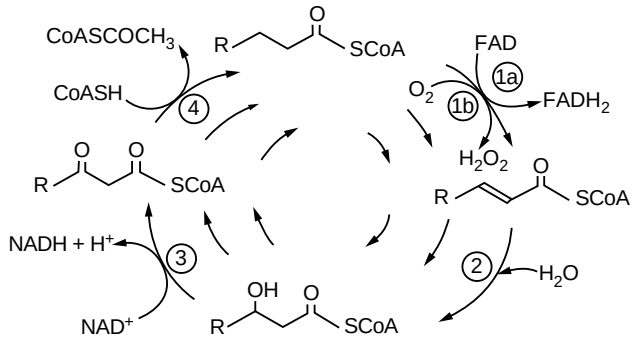

FIGURE 2 β-Oxidation of fatty acyl-CoA. Reactions 1a, 1b, 2, 3, and 4 are catalyzed by acyl-CoA dehydrogenase, acyl-CoA oxidase, enoyl-CoA hydratase, 3-hydroxyacyl-CoA dehydrogenase, and 3-ketoacyl-CoA thiolase, respectively. Abbreviations: FAD, oxidized form of flavine adenine dinucleotide; $FADH_2$, reduced form of flavine adenine dinucleotide.

Two or more enzymes with different acyl chain length specificities participate in each of the four reactions. Four acyl-CoA dehydrogenases are required for the β-oxidation of fatty acids. Their names, very long-chain acyl-CoA dehydrogenase, long-chain acyl-CoA dehydrogenase, medium-chain acyl-CoA dehydrogenase, and short-chain acyl-CoA dehydrogenase reflect their preferences for substrates of different acyl chain lengths.

Together they efficiently dehydrogenate all acyl-CoAs that are formed during the β-oxidation of most dietary fatty acids. Two enzymes, one with a preference for short-chain and medium-chain substrates and another most active with long-chain substrates, cooperate in each of the three other reactions to metabolize a range of β-oxidation intermediates of different acyl chain lengths.

β-Oxidation of Unsaturated Fatty Acids

Unsaturated and polyunsaturated fatty acids also are degraded by β-oxidation. However, additional reactions are required to metabolize pre-existing double bonds that would otherwise interfere with the complete β-oxidation of unsaturated fatty acids. All double bonds found in unsaturated fatty acids can be classified as either odd- or even-numbered double bonds. Both classes are present in linoleic acid, which contains an odd-numbered double bond at position 9 and an even-numbered double bond at position 12 (see Figure 3).

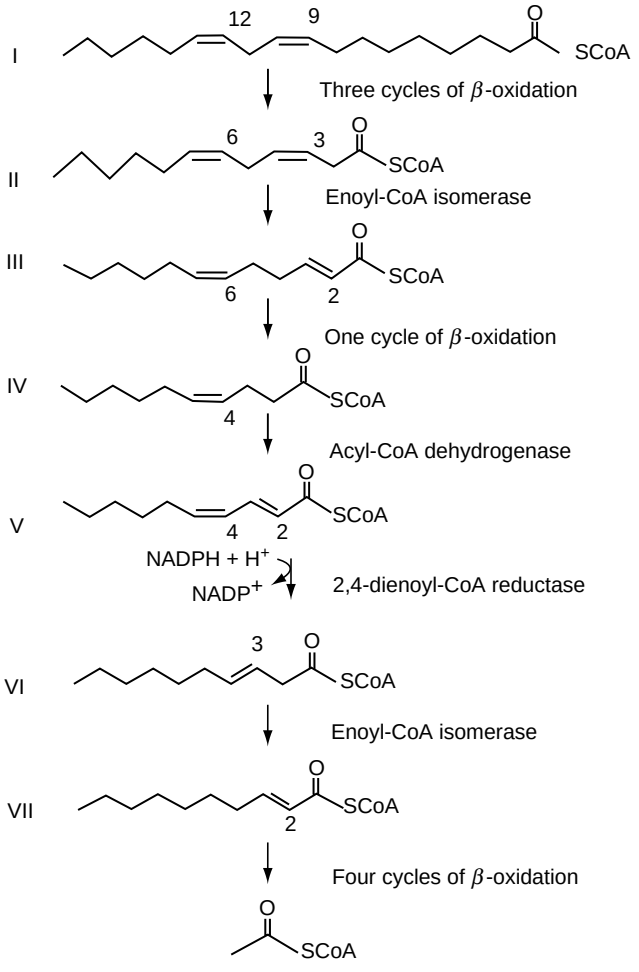

FIGURE 3 Pathway for the β-oxidation of linoleoyl-CoA.

The degradation of linoleic acid therefore illustrates the β-oxidation of all unsaturated fatty acids. As outlined in Figure 3, linoleoyl-CoA (I; all Roman numerals refer to compounds shown in Figure 3), after passing three times through the β-oxidation cycle, yields 3-*cis*,6-*cis*-dodecadienoyl-CoA (II). This metabolite cannot enter another cycle of β-oxidation due to interference by the double bond at position 3. However, an additional (auxiliary) enzyme, Δ^3,Δ^2-enoyl-CoA isomerase (enoyl-CoA isomerase), converts 3-*cis*,6-*cis*-dodecadienoyl-CoA (II) to 2-*trans*,6-*cis*-dodecadienoyl-CoA (III) that can complete its pass through one cycle of β-oxidation to yield 4-*cis*-decenoyl-CoA (IV). 4-*cis*-Decenoyl-CoA is dehydrogenated by acyl-CoA dehydrogenase to 2-*trans*,4-*cis*-decadienoyl-CoA (V), which is not a substrate of β-oxidation but which is reduced by NADPH in the presence of 2,4-dienoyl-CoA reductase, the second auxiliary enzyme, to 3-*trans*-decenoyl-CoA (VI). The latter compound is converted by enoyl-CoA isomerase to 2-*trans*-decenoyl-CoA (VII) that can be completely degraded by β-oxidation. A third auxiliary enzyme, $\Delta^{3,5}$,$\Delta^{2,4}$-dienoyl-CoA isomerase (dienoyl-CoA isomerase), catalyzes the isomerization of 3,5-dienoyl-CoA to 2,4-dienoyl-CoA. This reaction facilitates the complete β-oxidation of 3,5-dienoyl-CoAs that are minor metabolites of unsaturated fatty acids with odd-numbered double bonds.

Regulation of Mitochondrial Fatty Acid Oxidation

The rate of fatty acid oxidation changes in response to the nutritional and hormonal state of the animal. The rate of fatty acid oxidation is high during fasting but low in the fed animal. One cause for this change is the higher concentration of unesterified (free) fatty acids in the circulation of the fasting animal as compared to the concentration in the fed animal. An increased concentration of free fatty acids results in higher rates of cellular uptake and oxidation of fatty acids. In liver, which has high capacities for both synthesizing and oxidizing fatty acids, a reciprocal relationship exists between these two processes. After feeding, when carbohydrates are converted to triacylglycerols, the rate of fatty acid synthesis is high because acetyl-CoA carboxylase is active. This enzyme catalyzes the carboxylation of acetyl-CoA to malonyl-CoA, the first committed intermediate in fatty acid synthesis. Malonyl-CoA binds to and effectively inhibits CPT I that initiates the uptake of fatty acids by mitochondria. Thus, when fatty acids are rapidly synthesized, the cytosolic concentration of malonyl-CoA is high and the mitochondrial uptake and oxidation of fatty acids are inhibited. This situation is reversed during fasting when lower blood glucose levels cause the plasma

concentration of the hormone glucagon to increase and that of insulin to decrease. Glucagon promotes the phosphorylation and inactivation of acetyl-CoA carboxylase with the result that the cytosolic concentration of malonyl-CoA declines. The lower concentration of malonyl-CoA causes fatty acid synthesis to decrease and fatty acid oxidation to increase. The same regulatory mechanism may be effective in tissues like heart and skeletal muscle that oxidize fatty acids but do not synthesize them. Although malonyl-CoA is generated in these tissues by acetyl-CoA carboxylase, it seems to be metabolized by decarboxylation catalyzed by malonyl-CoA decarboxylase.

Fatty Acid Oxidation in Peroxisomes

Peroxisomes of animal cells contain a β-oxidation system that partially degrades fatty acids in contrast to mitochondria that break down fatty acids completely. The enzymes of peroxisomal and mitochondrial β-oxidation are not the same. Different genes encode most of the peroxisomal and mitochondrial enzymes. Substrates of peroxisomal β-oxidation are the CoA derivatives of fatty acids and carboxylic acids that are poorly or not at all taken up by mitochondria as, for example very long-chain fatty acids, methyl-branched carboxylic acids like pristanic acid, prostaglandins, dicarboxylic acids, xenobiotic compounds like phenyl fatty acids, and hydroxylated cholestanoic acids that are precursors of cholic acid. However, peroxisomes of lower eukaryotes catalyze the complete β-oxidation of fatty acids, whereas mitochondria in the same organisms generally are devoid of a functional β-oxidation system.

The uptake and activation of fatty acids by peroxisomes remain poorly understood. While some fatty acids like very long-chain fatty acids may be activated by conversion to CoA esters in the peroxisomal matrix after directly entering animal peroxisomes, other fatty acids or carboxylic acids seem to be activated outside of peroxisomes. The uptake of fatty acyl-CoAs by peroxisomes is suspected to take place but has not been demonstrated. Carnitine does not seem to be required for this uptake.

The four reactions of β-oxidation in peroxisomes are similar to the corresponding mitochondrial reactions (see Figure 2). An exception is the first reaction, in which fatty acyl-CoA is dehydrogenated to 2-*trans*-enoyl-CoA by acyl-CoA oxidase while oxygen is reduced to H_2O_2 (see Figure 2, reaction 1b). The latter product is converted to H_2O and O_2 by catalase that is present in peroxisomes. At least two acyl-CoA oxidases exist in animal peroxisomes; one named palmitoyl-CoA oxidase is active with long-chain and medium-chain, but not short-chain acyl-CoAs that have straight acyl chains while the second acyl-CoA oxidase also acts on branched-chain acyl-CoAs. Since the acyl-CoA oxidase activity of lower eukaryotes extends over the whole spectrum of acyl-CoAs of various chain lengths, peroxisomes in these organisms, in contrast to those in animals, can degrade fatty acids completely. The second and third reactions of peroxisomal β-oxidation are catalyzed by enoyl-CoA hydratase and 3-hydroxyacyl-CoA dehydrogenase, respectively, that are associated with a same polypeptide. Two such multifuntional enzymes, MFE 1 and MFE 2, are present in animal peroxisomes. They differ from each other in that the 3-hydroxyacyl-CoA intermediate formed and acted upon by MFE 1 has the L configuration, whereas the intermediate of MFE 2 is the D isomer. Peroxisomes of yeast and fungi only contain the type 2 multifunctional enzymes. Two types of 3-ketoacyl-CoA thiolases are present in rat peroxisomes. One of these thiolases, referred to as SCP_x-thiolase, is unusual because it is part of a bifunctional protein that additionally contains a lipid-binding segment named sterol carrier protein (SCP). Studies with β-oxidation mutants have led to the conclusion that the partial β-oxidation of straight-chain fatty acyl-CoAs, like very long-chain fatty acyl-CoAs, in animal peroxisomes requires palmitoyl-CoA oxidase, MFE 2, and 3-ketoacyl-CoA thiolase, whereas the partial degradation of branched-chain acyl-CoAs, like pristanoyl-CoA, involves branched-chain acyl-CoA oxidase, MFE 2, and SCP_x-thiolase. Unsaturated and polyunsaturated fatty acids also are partially degraded in peroxisomes. The necessary additional enzymes, enoyl-CoA isomerase, 2,4-dienoyl-CoA reductase, and even dienoyl-CoA isomerase, are present in this organelle. The products of peroxisomal β-oxidation are chain-shortened acyl-CoAs, NADH, and acetyl-CoA. Additionally propionyl-CoA is formed when methyl-branched-chain substrates are degraded. Acyl-CoAs may be converted to the corresponding acylcarnitines before they exit from peroxisomes. The necessary carnitine acyltransferases active with medium-chain and short-chain acyl-CoAs have been identified in peroxisomes. However, little is known about transporters that facilitate the efflux of products from peroxisomes.

α-Oxidation and ω-Oxidation

α-Oxidation is the process that results in the oxidative removal of the first carbon atom, the carboxyl group, of a fatty acid or carboxylic acid to yield CO_2 and a fatty acid or carboxylic acid shortened by one carbon atom. In animals, this process occurs in peroxisomes where, for example phytanic acid, which is derived from phytol of chlorophyll and which cannot be degraded by β-oxidation, is chain-shortened by one carbon atom to

pristanic acid that can be degraded by β-oxidation. ω-Oxidation is the process by which fatty acids are oxidized at their terminal (ω) or penultimate (ω-1) carbon atom to form dicarboxylic acids. This process occurs at the endoplasmic reticulum and requires molecular oxygen. When β-oxidation of fatty acids is impaired, more fatty acids are converted to dicarboxylic acids by ω-oxidation.

See Also the Following Articles

Anaplerosis • Carnitine and β-Oxidation • Cholesterol Synthesis • Fatty Acid Synthesis and its Regulation • Gluconeogenesis • Insulin- and Glucagon-Secreting Cells of the Pancreas • Ketogenesis • Lipases • Lipid Modification of Proteins: Targeting to Membranes • Lipoproteins, HDL/LDL • Peroxisomes • Protein Palmitoylation

Glossary

activation of fatty acids The conversion of fatty acids to thioesters with coenzyme A.

β-oxidation Degradation of fatty acyl coenzyme A thioesters by the sequential removal of two carbon atoms at a time in the form of acetyl coenzyme A.

peroxisome Subcellular organelle that is enclosed by a single membrane.

unsaturated fatty acids Fatty acids that contain one or more double bonds.

Further Reading

Eaton, S. (2002). Control of mitochondrial β-oxidation flux. *Prog. Lipid Res.* **41**, 197–239.

Kunau, W.-H., Dommes, V., and Schulz, H. (1995). Beta oxidation of fatty acids in mitochondria, peroxisomes, and bacteria. *Prog. Lipid Res.* **34**, 267–341.

McGarry, J. D. (2001). Travels with carnitine palmitoyltransferase: I. From liver to germ cell with stops in between. *Biochem. Soc. Trans.* **29**, 241–245.

Ruderman, N. B., Saha, A. K., Vavas, D., and Witters, L. A. (1999). Malonyl-CoA, fuel sensing, and insulin resistance. *Am. J. Physiol.* **276**, E1–E18.

Schulz, H., and Kunau, W.-H. (1987). Beta-oxidation of unsaturated fatty acids: A revised pathway. *Trends Biochem. Sci.* **12**, 403–406.

Van Veldhoven, P. P., Casteels, M., Mannaerts, G. P., and Baes, M. (2001). Further insight into peroxisomal lipid breakdown via α- and β-oxidation. *Biochem. Soc. Trans.* **29**, 292–298.

Wanders, R. J. A., Vreken, P., Ferdinandusse, S., Jansen, G. A., Waterham, H. R., van Roermund, C. W. T., and van Grunsven, E. G. (2001). Peroxisomal fatty acid α- and β-oxidation in humans: Enzymology, peroxisomal metabolite transporters, and peroxisomal diseases. *Biochem. Soc. Trans.* **29**, 250–267.

Watkins, P. A. (1997). Fatty acid activation. *Prog. Lipid Res.* **36**, 55–83.

Biography

Horst Schulz is a Professor in the Department of Chemistry at City College of the City University of New York. His main research interest is the β-oxidation of saturated and unsaturated fatty acids with an emphasis on fatty acid oxidation in mitochondria. He received a Ph.D. from the Technische Universität Berlin in Germany and carried out research as a postdoctoral fellow at Cornell University Medical College and Duke University Medical Center.

Fatty Acid Receptors

Christer Owman and Björn Olde
Lund University, Lund, Sweden

Lipids provide energy to the organism and contribute to various cellular components, including organelles and plasma membranes. A particular class of lipids are unesterified and are usually known as free fatty acids. Although dietary fatty acids have a major role as nutrients in various types of metabolic functions, some of them also exert more specialized functions as signaling molecules when they act as messengers between cells and within tissues.

It became evident in the early 1990s that such functions were mediated via a family of transcription factors called peroxisomal proliferator-activated receptors (PPARs). This class of nuclear receptors plays a central role in regulating the storage and degradation of dietary lipids. However, not all biological effects of free fatty acids can be explained by nuclear receptor signaling, but rather show the characteristics of a cell surface receptor involvement. Indeed, a decade after the discovery of the PPARs, a group of free-fatty acid-activated receptors (FFARs), expressed on the cell surface, could be identified. They all belong to the superfamily of G protein-coupled receptors (GPCRs), which is the most widely distributed class of receptors on eukaryotic cells.

The two classes of fatty acid-activated receptors appear to have an overlapping, but not identical, function. It should now be possible to unfold many hitherto unexplained observations on the actions of free fatty acids in both normal and pathophysiological situations.

The PPAR Family of Receptors

The PPARs (Figure 1) constitute a family of three nuclear receptor isoforms named PPARα, PPARδ (sometimes called PPARβ), and PPARγ. They function as transcription factors in response to specific ligands and thereby control gene expression by binding to various response elements within gene promoters. The receptors always bind as heterodimers together with the so-called retinoid X receptor. Like the PPARs, the retinoid X receptor exists in three isoforms which are all activated by the naturally occurring 9-*cis* retinoic acid. After binding of the ligand to the receptor dimers, these interact with cofactors, resulting in increased rate of transcription initiation. All three receptor subtypes are localized in different chromosomes. The PPAR receptors have a physiological role as regulators in the metabolism of dietary lipids. Free fatty acids with long carbon chains, and particularly polyunsaturated fatty acids, constitute the major natural ligands for PPARs. The nuclear receptor family also includes receptors for steroid, thyroid, and retinoid hormones.

PPARα

The receptor PPARα is expressed in many metabolically active tissues, including heart, skeletal muscle, kidney, liver, as well as brown fat. In addition, it has a vascular localization, both in endothelium and smooth muscle cells, and is also present in monocytes (Figure 1). Accordingly, PPARα has been found to effectively improve cardiovascular risk factors, and it also enhances cardiovascular performance. It exerts a critical function in the regulation of the cellular uptake, activation, and β-oxidation of fatty acids; the receptor directly up-regulates enzymes in the peroxisomal β-oxidation pathway. PPARα was also suggested to be involved in immunmodulatory functions when it was found that leukotriene B_4 could specifically activate the receptor.

PPARδ

This receptor subtype (Figure 1) was first cloned as PPARβ in frog, but the generally agreed name for the receptor is now PPARδ. It has a ubiquitous localization in the body (often at lower expression levels than PPARα and γ), with a particularly high expression in brain, adipose tissue, and in skin. It is likely that PPARδ is involved in lipid homeostasis since, like the other two isoforms, it is activated by fatty acids and fatty acid metabolites. The ligand-binding profile is intermediate between PPARα and PPARγ. PPARδ has been suggested to be involved in the differentiation of cells within the central nervous system, and it may also have a role in myelinization and lipid metabolism in brain. The receptor has been reported to have importance for wound healing as well as in female fertility.

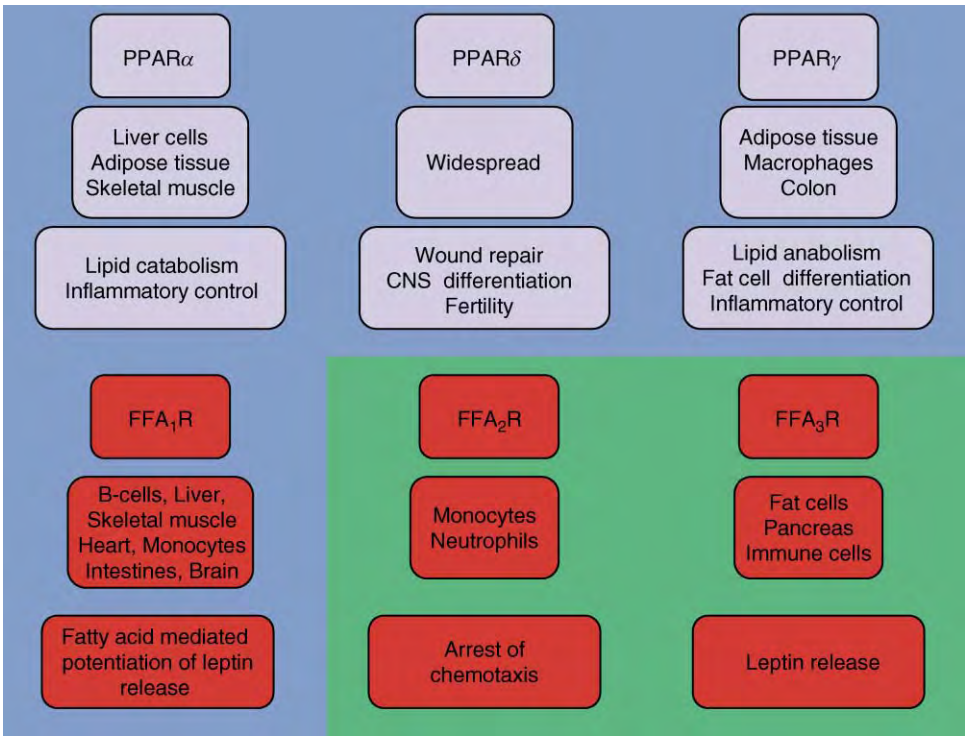

FIGURE 1 Panel summarizing the expression patterns (upper boxes) and the functional characteristics (lower boxes) of the two fatty acid receptor families, the PPARs and the FFARs. The blue background shading indicates the four receptors that are activated by medium- to long-chain free fatty acids, whereas the green background points out the two receptors that are activated by short-chain free fatty acids.

PPARγ

PPARγ is the most extensively studied of the three receptor subtypes. It shows, in contrast to the two other receptors, a considerable degree of conservation – some 95% identity at the protein level – among the various species from which is has been cloned. Three receptor isoforms, numbered 1–3, have been reported to arise from different promoter utilization. While PPARγ1 is expressed in a wide range of tissues, PPARγ2 is found predominantly in adipose tissue, whereas PPARγ3 is expressed only in adipose tissue, macrophages, and colon epithelium (Figure 1). PPARγ is a critical transcription factor in the regulation of adipocyte differentiation, and it also exerts an important function in insulin sensitization, atherosclerosis, and cancer. Activation of the receptor induces differentiation of cells into adipocytes, and it promotes the transcription of numerous important lipogenic proteins. It appears that PPARα and γ exert opposite but complementary functions in fat energy homeostasis; the former having a catabolic function whereas the latter is involved in lipid anabolism and energy storage.

It is evident from the above descriptions that the PPAR receptor family should play important roles in various types of life-style diseases. Actually, much of the focus on PPARγ is related to fatty acids being risk factors in type 2 diabetes, and to the fact that modern anti-diabetic substances of the thiazolidinedione class may use this receptor as a target, although other pathways for thiazolidinedione actions seem to exist. The compounds, also known as glitazones, exert their beneficial effect by enhancing the sensitivity of target tissues to insulin and by reducing the plasma levels of fatty acids, glucose, and insulin.

The FFAR Family of Receptors

In contrast to the nuclear PPAR receptors, the FFAR family consists of receptors that are localized to the plasma membrane of cells. Here, the receptor protein anchors as a serpentine with seven membrane-spanning helical segments, a typical feature of the superfamily of GPCRs. Based on this general structure they are also known as 7TM (for transmembrane) or heptahelix receptors. The three separate genes encoding the receptors of this family are present in a cluster on chromosome 19. As illustrated in Figure 1, the PPARs are activated only by free fatty acids having a carbon chain length above twelve, while the ligand spectrum for the FFARs include chain lengths down to one (formiate). The receptors are well conserved both in mammals and fish.

FFA_1R

This receptor was originally presented as an orphan receptor (i.e., without known ligand/function) with the provisional designation GPR40. Its identity and function was reported independently by three groups early in the year 2003. The encoded human receptor protein consists of 300 amino acid residues. FFA_1R is characteristically activated by medium-length (down to 10 carbons) to long-chain free fatty acids. Besides the effect of the natural ligands, a very intriguing observation was that also the anti-diabetic thiazolidinedione compound, rosiglitazone, activated the receptor.

According to the current understanding this novel receptor is primarily expressed in the insulin-producing pancreatic islets. It has also been reported to be present in liver, skeletal muscle, heart, intestines, monocytes, as well as in brain. FFA_1R has been tied to the so-called fatty acid potentiation of glucose-stimulated insulin secretion (GSIS) by pancreatic β-cells. In fact, fatty acids, like linoleic acid and γ-linoleic acid, have been shown to stimulate insulin release in mouse insulinoma cells through FFA_1R.

The identification of FFA_1R, having a ligand spectrum that is overlapping that of PPARγ (Figure 1), offers a new type of nutrient sensor in lipid homeostasis. It may provide a basis for understanding hitherto unexplained mechanisms involved in insulin release as well as in thiazolidinedione functions related to various therapeutic areas.

FFA_2R

The second FFAR, FFA_2R (previously known as GPR43), has the same general structure as FFA_1R and consists of 330 amino acid residues. In contrast to the latter, it is activated by short-chain (C1–C6) fatty acids, acetate (C2) being the most effective. It has a different expression pattern (Figure 1) in that it is found mainly in polymorphonuclear leukocytes, predominantly in monocytes and neutrophils.

Activation of FFA_2R expressed on immune cells causes pertussis toxin sensitive calcium mobilization and also leads to arrest of cellular chemotaxis. It is likely that this response is part of an immunmodulatory mechanism within the alimentary tract whereby short-chain fatty acids, known to be produced by the enteric bacteria, control the invasion of immune cells.

FFA_3R

The receptor, FFA_3R, was previously known as GPR41 and is structurally more closely related to FFA_2R than to FFA_1R. It forms a seven membrane-spanning protein comprising 346 amino acid residues. (A fourth annotated receptor, designated GPR42, has 98% deduced amino acid homology with GPR41; the corresponding gene is probably a pseudogene.) As depicted in Figure 1, the fatty acid ligand spectrum for FFA_3R is similar to that of FFA_2R, although butyrate (C4) and pentanoate (C5) are the most potent agonists for FFA_3R. The elicited response (as in the case of FFA_2R) is clearly pertussis toxin-sensitive. FFA_3R is predominantly expressed in adipose tissue, although expression has been reported also in pancreas and immune cells, as well as in placenta. FFA_3R has recently been shown to control leptin production in adipocytes.

See Also the Following Articles

Adenylyl Cyclases • Fatty Acid Receptors • Fatty Acid Synthesis and its Regulation • Peroxisome Proliferator-Activated Receptors • Peroxisomes

Glossary

G protein Abbreviated term for "GTP (guanosine triphosphate)-binding regulatory protein," which, upon membrane receptor activation, serves as an intermediary protein between the receptor and a cell membrane-bound enzyme or ion channnel.

peroxisome Membrane-surrounded cell organelle where, e.g., hydrogen peroxide is generated and degraded.

promoter Specific DNA sequence containing the start site for RNA synthesis.

pseudogene Nonfunctional gene closely related to functional genes.

transcription factor Controls gene transcription and is one of several sequence-specific DNA-binding regulatory proteins.

Further Reading

Berger, J., and Moller, D. E. (2002). The mechanisms of action of PPARs. *Ann. Rev. Med.* **53**, 409–435.

Brown, A. J., Goldsworthy, S. M., Barnes, A. A., Eilert, M. M., Tcheang, L., Daniels, D., Muir, A. I., Wigglesworth, M. J., Kinghorn, I., Fraser, N. J., Pike, N. B., Strum, J. C., Steplewski, K. M., Murdock, P. R., Holder, J. C., Marshall, F. H., Szekeres, P. G., Wilson, S., Ignar, D. M., Foord, S. M., Wise, A., and Dowell, S. J. (2003). The orphan G protein-coupled receptors GPR41 and GPR43 are activated by propionate and other short chain carboxylic acids. *J. Biol. Chem.* **278**, 11312–11319.

Nilsson, N. E., Kotarsky, K., Owman, C., and Olde, B. (2003). Identification of a free fatty acid receptor, FFA_2R, expressed on leukocytes and activated by short-chain fatty acids. *Biochem. Biophys. Res. Commun.* **303**, 1047–1052.

Poitout, V. (2003). The ins and outs of fatty acids on the pancreatic β cells. *Trends Endocrinol. Metab.* **14**, 201–203.

Rutter, G. A. (2003). Insulin secretion: Fatty acid signalling via serpentine receptors. *Curr. Biol.* **13**, R403–R405.

Sawzdargo, M., George, S. R., Nguyen, T., Shijie, X., Kolakowski, L. F. Jr., and O'Dowd, B. F. (1997). A cluster of four novel human G protein-coupled receptor genes occurring in close proximity to CD22 gene on chromosome 19q13.1. *Biochem. Biophys. Res. Commun.* **239**, 543–547.

Wahli, W. (2002). Peroxisome proliferator-activated receptors (PPARs): From metabolic control to epidermal wound healing. *Swiss Med. Wkly* **132**, 83–91.

Willson, T. M., Brown, P. J., Sternbach, D. D., and Henke, B. R. (2000). The PPARs: From orphan receptors to drug discovery. *J. Med. Chem.* **43**, 527–550.

Xiong, Y., Miyamoto, N., Shibata, K., Valasek, M. A., Motoike, T., Kedzierski, R. M., and Yanagisawa, M. (2004). Short-chain fatty acids stimulate leptin production in adipocytes through the G protein-coupled receptor GPR41. *Proc. Natl Acad. Sci. USA* **101**, 1045–1050.

Biography

Christer Owman is M.D. and Ph.D. (Lund University, Sweden) and Professor and Chair of the Division of Molecular Neurobiology, Department of Physiological Sciences, Wallenberg Neuroscience Center at the same University. He has published extensive work on autonomic neuro-receptor mechanisms. His present research interest is in molecular aspects of GPCRs, and he has discovered several previously unknown GPCRs. He is scientific founder of the small biotech company, HeptaHelix AB. He has served two terms as Dean of the Medical Faculty, Lund University.

Björn Olde is a Ph.D. from Lund University and is an associate professor there. He spent most of an extensive postdoctoral period with Dr. Craig Venter. His principal interest is in basic research and drug development focusing on GPCRs. He has developed uniquely sensitive cell-based reporter systems successfully applied to "deorphanize" several hitherto unknown GPCRs, followed by their further functional characterization.

Fatty Acid Synthesis and its Regulation

Steven D. Clarke
McNeil Nutritionals, New Brunswick, New Jersey, USA

Manabu T. Nakamura
University of Illinois at Urbana-Champaign, Illinois, USA

Fatty acid synthesis involves the *de novo* assembly of acetate into saturated fatty acids as well as the desaturation and elongation of the dietary essential fatty acids linoleic acid (C18:2$_{n-6}$) and α-linolenic acid (C18:3$_{n-3}$) to highly unsaturated 20- and 22-carbon fatty acids essential to reproduction, cell differentiation, inflammation, and cognition. Short-chain fatty acids are derived largely from bacterial fermentation such as that which occurs in the gut or rumen. Medium-chain fatty acids are characteristic of milk fat and are absorbed from the intestine directly into the portal blood, and subsequently metabolized largely by the liver. Fatty acids containing 14 or more carbons are absorbed from the intestine and transported to the periphery as chylomicrons. Very long chain fatty acids are largely found in neural tissue and used for myelin formation. Net fatty acid synthesis by humans is relatively small, but the *de novo* fatty acid biosynthetic pathway is essential for the production of malonyl-CoA, a metabolite inhibitor of carnitine palmitoyltransferase. Consequently, substrate flux through the *de novo* lipogenic pathway plays a key role in determining if a fatty acid is partitioned to fatty acid oxidation or triglyceride assimilation.

De novo Fatty Acid Biosynthesis of Saturated Fatty Acids

Saturated fatty acids are categorized as short (C2–C6), medium (C8–C12), long (C14–C18), and very long (C20–C24) fatty acids. Short-chain fatty acids are derived largely from bacterial fermentation such as that which occurs in the gut or rumen. Medium-chain fatty acids are characteristic of milk fat and are absorbed from the intestine directly into the portal blood, and subsequently metabolized largely by the liver. Fatty acids containing 14 or more carbons are absorbed from the intestine and transported to the periphery as chylomicrons. Very long chain fatty acids are largely found in neural tissue and used for myelin formation. The liver and adipose tissue of humans are the primary sites of conversion of excess carbohydrate to fatty acids, but fatty acid synthesis is more than just for conserving excess glucose as fat. Fatty acid synthesis is essential for cell membrane production, lung surfactant function, milk fat production, brain myelination, and fat storage. Consequently, nearly all tissues have the capacity to synthesize fatty acids.

De novo fatty acid biosynthesis in humans occurs in cytosol. Two enzymes, acetyl CoA carboxylase and fatty acid synthase, are required for this process. The first and rate-limiting step is the conversion of acetyl CoA to malonyl CoA by acetyl CoA carboxylase:

$$\begin{aligned} &CH_3CO-S-CoA + HCO_3^- + ATP \\ &\quad \rightarrow {}^-OOC-CH_2CO-S-CoA + H_2O + ADP + Pi \end{aligned}$$

Fatty acid synthase catalyzes all of the subsequent steps for the synthesis of long-chain saturated fatty acids. Fatty acid synthase is made of a single peptide chain that possesses seven distinct catalytic domains. Fatty acid synthase first adds two carbons to acetyl CoA using malonyl CoA. NADPH is used as a reducing power in this reaction:

$$\begin{aligned} &CH_3CO-S-CoA + {}^-OOC-CH_2CO-S-CoA \\ &\quad + Enzyme-SH + 2NADPH + 2H^+ \\ &\quad\quad \rightarrow CH_3CH_2CH_2CO-S-Enzyme + 2CoA-SH \\ &\quad\quad\quad + HCO_3^- + 2NADP^+ \end{aligned}$$

Fatty acid synthase repeats this acyl chain elongation two carbons at a time using malonyl CoA as a substrate:

$$\begin{aligned} &CH_3CH_2CH_2CO-S-Enzyme \\ &\quad + {}^-OOC-CH_2CO-S-CoA + 2NADPH + 2H^+ \\ &\quad\quad \rightarrow CH_3(CH_2)_3CH_2CO-S-Enzyme \\ &\quad\quad\quad + CoA-SH + HCO_3^- + 2NADP^+ \end{aligned}$$

When the carbon chain reaches 16, the thioesterase domain of fatty acid synthase releases free palmitate,

completing fatty acid biosynthesis.

$$CH_3(CH_2)_{14}CO-S-Enzyme + H_2O \rightarrow CH_3(CH_2)_{14}COO^- + H^+ + HS-Enzyme$$

Regulation of Pyruvate Entry into Mitochondria

Malonyl-CoA is the substrate used by fatty acid synthase to assemble the acetate units into fatty acids. Malonyl-CoA is produced from pyruvate through a series of reactions. The first step involves the mitochondrial formation of acetyl-CoA by pyruvate dehydrogenase's decarboxylation of pyruvate. This is followed by the intramitochondrial synthesis of citrate from acetyl-CoA and oxaloacetate. Citrate is transported from the mitochondria to the cytosol where it is cleaved by citrate lyase to cytosolic acetyl-CoA and oxaloacetate. The acetyl-CoA is available for carboxylation to malonyl-CoA by the biotin-containing enzyme acetyl-CoA carboxylase. The liver and adipose tissue of humans are the primary sites of conversion of excess carbohydrate to fatty acids. The source of hepatic or adipose pyruvate for fatty acid biosynthesis may be derived from the metabolism of glucose via the glycolytic pathway with the liver or adipocyte itself, or it may be provided to the liver and/or adipose tissues as lactate or alanine that is produced by glucose metabolism in peripheral tissues such as the small intestine and muscle. Entry of pyruvate into the tricarboxylic acid pathway of the mitochondria is determined by the activity of pyruvate dehydrogenase. The concentration of pyruvate dehydrogenase does not widely fluctuate, but its catalytic activity is suppressed by phosphorylation and enhanced by dephosphorylation of the enzyme. Insulin and glucose stimulate dephosphorylation, whereas glucagon and fatty acids enhance the phosphorylation. Thus, pyruvate entry into the mitochondria is highly dependent upon the macronutrient composition of the diet, and the ratio of insulin to glucagon.

Regulation of Malonyl-CoA Synthesis

The synthesis of malonyl-CoA is catalyzed by the biotin-containing enzyme acetyl-CoA carboxylase. Acetyl-CoA carboxylase exists as two isoforms: a liver or type I, and muscle or type II. Like pyruvate dehydrogenase, the catalytic activity, and hence the production of malonyl-CoA, of both acetyl-CoA carboxylase isoforms is regulated by phosphorylation and dephosphorylation of the protein. Acetyl-CoA carboxylase I and II are substrates for AMP kinase and cyclic AMP kinase. AMP kinase activity is enhanced by leptin and adiponectin, two hormones that stimulate fatty acid oxidation and inhibit fatty acid biosynthesis. The dephosphorylation of acetyl-CoA carboxylase is carried out by phosphatase 1 and 2, and phosphatase activity appears to be stimulated under conditions where glucose flux through glycolysis is high. Muscle acetyl-CoA carboxylase is not adaptive, but hepatic acetyl-CoA carboxylase, like other lipogenic enzymes, increases and decreases its concentration depending upon nutritional conditions, dietary composition, and hormonal milieu. For example, the hepatic abundance of acetyl-CoA carboxylase is low during fasting and diabetes, but is greatly induced by refeeding glucose or administering insulin.

Malonyl-CoA and Fatty Acid Metabolism

Malonyl-CoA is not only the substrate for fatty acid synthase, but it is a key determinant for the entry of fatty acids into the mitochondria, and appears to play a pivotal signaling role in appetite regulation. Malonyl-CoA is an inhibitor of carnitine palmitoyltransferase. Thus, high levels of malonyl-CoA suppress fatty acid entry into the mitochondria and this in turn leads to increased flux of fatty acids to triglycerides. On the other hand, conditions that lead to low cellular concentrations of malonyl-CoA favor fatty acid oxidation because the inhibition of carnitine palmitoyltransferase is released. Consequently, even though net fatty acid synthesis by humans may be relatively small, the fatty acid biosynthetic pathway plays an instrumental role in determining whether a fatty acid is stored as triglyceride or undergoes oxidation. Since excessive cellular triglyceride production and accumulation is causatively linked to the development of insulin resistance and type 2 diabetes, factors regulating the fatty acid biosynthetic pathway will exert a direct influence on the development of diabetes.

Nutritional Regulation of Lipogenic Gene Expression

Hepatic and adipose fatty acid biosynthesis is increased by the ingestion of a high-carbohydrate diet and decreased by the consumption of a high-fat diet. Dietary regulation of lipogenesis is not simply a product of nutritional manipulation of hormonal balance. Rather, nutrients exert a specific influence on the expression of glycolytic and lipogenic proteins. Nutrients exercise their influence by modulating gene transcription, mRNA processing, mRNA decay, and by stimulating posttranslational protein modifications.

Carbohydrate Induction of Lipogenic Gene Transcription

Since the early 1990s, a collection of transcription factors that are specifically targeted by glucose and fatty acids have been identified. Dietary carbohydrate induces lipogenic gene transcription in two ways. First, glucose increases the nuclear concentration of the potent lipogenic transcription factor, SREBP-1. SREBPs are a family of transcription factors that were first isolated as a result of their properties for binding to the sterol regulatory element of genes encoding proteins of sterol metabolism. SREBP-2 is a regulator of genes encoding proteins of cholesterol metabolism. SREBP-1 exists in two forms, 1a and 1c. SREBP-1a is the dominant form in cell lines and is a regulator of genes encoding proteins involved in fatty acid biosynthesis as well as cholesterolgenesis. SREBP-1c constitutes 90% of the SREBP-1 found *in vivo* and is a determinant of lipogenic gene transcription. SREBP-1 is synthesized as a 125 kDa precursor protein that is anchored in the endoplasmic reticulum membrane. Proteolytic release of the 68 kDa mature SREBP-1 occurs in the Golgi system, and movement of SREBP-1 from the endoplasmic reticulum to the Golgi requires the trafficking protein SREBP cleavage-activating protein. Once released, mature SREBP-1 translocates to the nucleus and binds to the classic sterol response element and/or to a palindrome CATG sequence. Glucose increases the abundance of precursor SREBP-1 by inducing SREBP-1 gene transcription. In addition, glucose elevates the nuclear concentration of SREBP-1 by stimulating the proteolytic release of mature SREBP-1 from its membrane-anchored precursor. A second effect of glucose is to stimulate the DNA binding activity of select transcription factors involved with the transcription of lipogenic genes, notably a unique carbohydrate response factor (CHORF). Glucose exerts its effect by elevating the cellular concentration of the pentose shunt metabolite xylulose-5-phosphate. Xylulose-5-phosphate is a positive metabolite effecter of phosphatase 2A, and increased phosphatase activity leads to the dephosphorylation of CHORF and a subsequent increase in its DNA binding to a specific carbohydrate response element (CHORE) in select glycolytic (e.g., pyruvate kinase) and lipogenic (e.g., fatty acid synthase) genes. The consequence is an increase in gene transcription followed by a rise in the abundance of glycolytic and lipogenic enzymes.

Suppression of Lipogenic Gene Expression by omega-6 and -3 Fatty Acids

Glucose stimulation of lipogenesis is a nice example of a feedforward regulatory mechanism that functions to enhance glucose storage as fatty acids. Interestingly the saturated fatty acid products of the *de novo* fatty acid synthetic pathway do not feedback and suppress glycolytic and lipogenic gene expression or activity. Only omega-6 and -3 fatty acids (e.g., linoleic ($C18:2_{n-6}$) and α-linolenic ($C18:3_{n-3}$)) interfere with glycolytic and lipogenic gene expression (Figure 1). Highly unsaturated 20- and 22-carbon omega-6 and -3 fatty acids (HUFAs) inhibit glycolytic and lipogenic gene transcription through two different types of DNA regulatory response regions (HUFA-RR). One type overlaps with the insulin response element (HUFA-RR/IRE), while the second region colocalizes with the carbohydrate response element (HUFA-RR/CHORE).

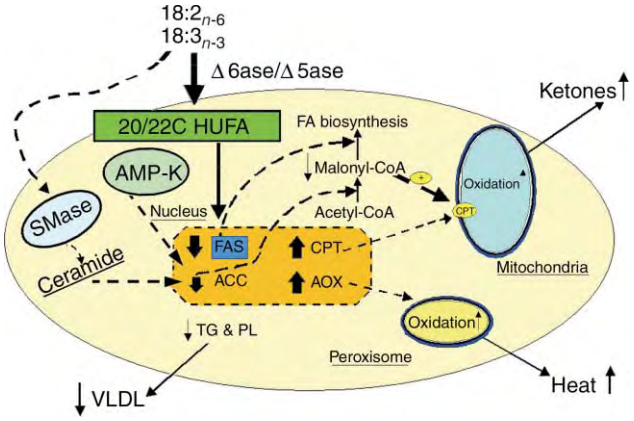

FIGURE 1 Regulation of hepatic gene expression and lipid metabolism by highly unsaturated fatty acids. Δ6ase, Δ-6 desaturase; Δ5ase, Δ-5 desaturase; HUFA, highly unsaturated fatty acids; AMP-K, AMP-kinase; SMase, sphingomyelinase; TG, triglyceride; PL, phospholipid; FA, fatty acids; FAS, fatty acid synthase; ACC, acetyl-CoA carboxylase; CPT, carnitine palmitoyltransferase; AOX, acyl-CoA oxidase; VLDL, very low density lipoproteins.

Colocalization of the HUFA-Response Region with the Insulin Response Element

The HUFA-RR/IRE contains recognition sequences for SREBP-1c, NF-Y, Sp1, and USF. HUFAs inhibit the activity of promoters containing the HUFA-RR/IRE by decreasing SREBP-1c and NF-Y interactions with their respective recognition sequences. HUFAs lower the concentration of SREBP-1 precursor protein as well as inhibit the proteolytic release and nuclear localization of mature SREBP-1. The HUFA-dependent inhibition of the proteolytic release of mature SREBP-1 and -2 may involve a stimulation of sphingomyelin hydrolysis and subsequent ceramide signaling. In addition to inhibiting the proteolytic release of SREBP-1, HUFAs reduce the cellular content of precursor SREBP-1 protein by reducing the cellular abundance of SREBP-1 mRNA. HUFAs decrease the hepatic abundance of SREBP-1 mRNA, and consequently the

hepatic content of precursor SREBP-1 protein, by accelerating SREBP-1 mRNA decay and by suppressing SREBP-1 gene transcription. The mechanisms by which HUFAs accelerate SREBP-1 mRNA decay remain unclear, but the mechanisms by which HUFAs suppress SREBP-1 gene transcription are beginning to emerge. The SREBP-1 gene contains two response elements for the lipogenic transcription factor LXR. Oxysterol ligand activation of LXR induces the transcription of SREBP-1. HUFAs reportedly displace oxysterol from LXR and in this way antagonize the transactivation activity of LXR. In addition, HUFAs may stimulate the "trapping" of LXR as a PPARα/LXR heterodimer. Thus, when the ratio of HUFA to oxysterol is low LXR/RXR heterodimers favor lipogenic gene expression, but when the ratio of HUFA to oxysterol is high, the PPARα/LXR and PPARα/RXR heterodimer mixtures are poised towards a gene profile that favors fatty acid oxidation over fatty acid synthesis. Although SREBP-1 metabolism is highly responsive to HUFA, it is only one of several transcription factors targeted by HUFA. In fact, $>50\%$ of the HUFA control of fatty acid synthase gene transcription can be attributed to the NF-Y site at $-99/-93$. NF-Y is an abundant heterotrimeric nuclear protein that interacts with histone acetyl transferases, and consequently plays a role in modifying histone structure. HUFAs do not reduce the nuclear abundance of NF-Y but rather suppress NF-Y transactivation activity by decreasing its DNA binding activity.

A Cho-Response Element within a Hufa-Response Region

The HUFA-RR of certain lipogenic genes, notably fatty acid synthase, contains DNA-binding sites for several transcription factors (e.g., carbohydrate response factor, HNF-4) whose DNA-binding activity is governed by the amount and type of fat in the diet. One factor that binds to this region and has received significant attention has been the carbohydrate response factor that uniquely interacts with the CHORE. The DNA binding activity of carbohydrate response factor is dependent upon its state of phosphorylation. Fatty acid activation of AMP-kinase leads to increased phosphorylation of the carbohydrate response factor and consequently decreased DNA binding and trans-activation activity. How HUFAs selectively activate AMP-kinase remains to be determined, but HUFA inhibition of lipogenesis and HUFA stimulation of fatty acid oxidation are consistent with the established role that AMP-kinase plays in the partitioning of fatty acids between triglyceride storage and fatty acid oxidation.

Unsaturated Fatty Acid Synthesis

Oleic and Palmitoleic Acid Synthesis

Palmitate (C16:0) and stearate (C18:0) are rapidly desaturated to mono-unsaturated palmitoleic (C16:1) and oleic (C18:1) acids by the stearoyl-CoA desaturase (also known as Δ-9 desaturase) system (Figure 2). Stearoyl-CoA desaturase exists in multiple isoforms that are derived from separate genes. The dominant form within a cell depends upon the origin of the cell. Stearoyl-CoA desaturase inserts a double bond between carbons 9 and 10. This desaturation reaction requires three different components: the desaturase itself, cytochrome b5, and cytochrome b5 reductase. Oleic acid synthesis is required for a variety of reasons. In particular it appears to be required for the hepatic secretion of very low-density lipoproteins.

Arachidonic and Docosahexenoic Acid Synthesis

While oleic acid clearly plays an important role in overall energy metabolism, it cannot fulfill the biological requirements for growth, reproduction, cell signaling, and cell differentiation. These requirements can only be fulfilled by long chain fatty acids from the omega-6 and omega-3 fatty acid family, i.e. linoleic ($C18:2_{n-6}$)

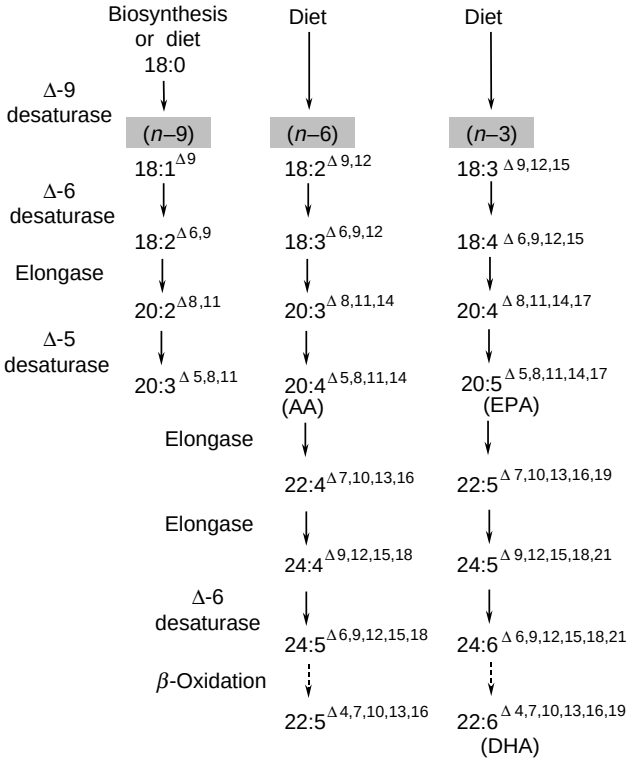

FIGURE 2 Synthesis of highly unsaturated fatty acids.

and α-linolenic (C18:3$_{n-3}$), respectively (Figure 2). Linoleate and α-linolenate undergo desaturation and elongation to 20- and 22-carbon highly unsaturated fatty acids. Prostaglandins and leukotrienes produced from arachidonic acid (C20:4$_{n-6}$) are required for blood clotting, cardiac function, reproduction, inflammatory response, and cell differentiation. Docosahexaenoic acid (C22:6$_{n-3}$) is required for cognition and brain development. Formation of bio-active 20- and 22-carbon highly unsaturated omega-6 and -3 fatty acids requires that the dietary essential fatty acids, linoleate and α-linolenate undergo two steps of desaturation that are catalyzed by the Δ-6 desaturase and Δ-5 desaturase. Both desaturases are expressed in all tissues. The human desaturase genes are members of a gene cluster on chromosome 11 that includes a third desaturase of unknown function, and a non-coding RNA gene that encodes an anti-sense transcript for Δ-5 desaturase. Nearly all human tissues express the products of the Δ-6 desaturase gene cluster. Unlike the stearoyl-CoA desaturase, the Δ-6 and Δ-5 desaturases contain a cytochrome b5 domain within the desaturase peptide. The rate of production of 20- and 22-carbon highly unsaturated fatty acids is dependent upon the tissue content of the two desaturases, and this in turn in determined by nutritional and hormonal factors that are similar to those that regulate the expression of lipogenic genes. The one notable difference between lipogenic and desaturase genes is that while HUFAs suppress both gene families, activators of peroxisome proliferator activator receptor-α induce desaturase genes but they suppress lipogenic genes. The increase in desaturase expression may be in response to a greater need for unsaturated fatty acids for the production of phospholipids, particularly in the liver for the secretion of very low density lipoproteins.

See Also the Following Articles

Cholesterol Synthesis • Fatty Acid Oxidation • Fatty Acid Receptors • Lipoproteins, HDL/LDL • Pyruvate Carboxylation, Transamination, and Gluconeogenesis • Pyruvate Dehydrogenase • Pyruvate Kinase

Glossary

carbohydrate response element (**ChoRE**) A DNA sequence that binds a unique carbohydrate response protein whose DNA-binding and transactivation activities are up-regulated by glucose ingestion.

HUFA Highly unsaturated omega-6 and -3 fatty acids that uniquely regulate gene expression, cell differentiation, and are required for cognition and neural function.

liver-X receptor (**LXR**) A nuclear transcription factor that is activated by the binding of oxysterols and stimulates the transcription of lipogenic genes.

sterol regulatory element binding protein-1 (**SREBP-1**) Protein required for the transcription of genes encoding proteins of fatty acid biosynthesis.

Further Reading

Berger, J., and Moller, D. E. (2002). The mechanisms of action of PPARs. *Annu. Rev. Med.* **53**, 409–435.

Clarke, S. D., Gasperikova, D., Nelson, C., DeMar, J., Lapillonne, A., and Heird, W. C. (2002). Fatty acid regulation of gene expression: A genomic explanation for the benefits of the Mediterranean diet. *Ann. N. Y. Acad. Sci.* **967**, 283–298.

Horton, J. D., Goldstein, J. L., and Brown, M. S. (2002). SREBPs: Activators of the complete program of cholesterol and fatty acid synthesis in the liver. *J. Clin. Invest.* **109**, 1125–1131.

Loewen, C. J. R., and Levine, T. P. (2002). Cholesterol homeostasis: Not until the SCAP lady INSIGs. *Curr. Biol.* **12**, R779–R781.

Puigserver, P., and Spiegelman, B. M. (2003). Peroxisome proliferator-activated receptor-gamma coactivator 1 alpha (PGC-1 alpha): Transcriptional coactivator and metabolic regulator. *Endocr. Rev.* **24**, 78–90.

Vessby, B., Gustafsson, I. B., Tengblad, S., Boberg, M., and Andersson (2002). Desaturation and elongation of Fatty acids and insulin action. *Ann. N. Y. Acad. Sci.* **967**, 183–195.

Biography

Steven D. Clarke is a Director of Science Research at McNeil Nutritionals. Dr. Clarke's research for over 25 years has addressed the nutrient control of the lipid metabolism with particular interest in nutrient–gene interactions. His research has resulted in over 100 publications, and he was among the first to recognize the unique role that polyunsaturated fatty acids play as nutrient sensors for the regulation of fatty acid synthesis and oxidation.

Manabu T. Nakamura received a Ph.D. from the University of California at Davis and is an Assistant Professor of Nutrition at the University of Illinois at Urbana-Champaign. Dr. Nakamura's research focuses on the mechanism by which animals adapt to a wide variety of diets. In particular, he has been working on the regulation of highly unsaturated fatty acid synthesis in mammals.

Ferredoxin

Giuliana Zanetti and Vittorio Pandini
Università degli Studi di Milano, Milan, Italy

Under the name ferredoxin (Fd) are comprised ubiquitous, small proteins containing one or two iron-sulfur clusters. These prosthetic groups contain iron and sulfur atoms, organized in three different types of centers: 2Fe–2S, 4Fe–4S, and 3Fe–4S. The presence of the cluster(s) confers to the protein the property of absorbing light in the visible region. Fd solutions are thus reddish brown in the oxidized state and fade upon reduction. Despite the type and number of clusters bound, Fds generally function in oxidoreduction reactions. Many Fds are involved as electron carrier of low redox potential in electron transport chains of fundamental metabolic processes like photosynthesis, nitrogen fixation, and assimilation of hydrogen, nitrogen, and sulfur. The first report of a nonheme iron protein in the bacterium *Clostridium pasteurianum* appeared in 1962, and was immediately followed by the discovery of a Fd in spinach chloroplast. By now, the family of Fds is greatly increased. Bacteria generally harbor many Fds, which differ in amino acid sequence, FeS cluster type, redox potential, and function. Eukaryotic organisms instead contain just one or two Fds of the 2Fe–2S type, except for plants in which several isoforms coexist. Here we will focus on this type of Fds with special emphasis on ferredoxin I of chloroplast.

2Fe Ferredoxins

The 2Fe ferredoxins (Fds) are hydrophilic, acidic proteins of 11–15 kDa which harbor a single 2Fe–2S cluster coordinated by four cysteine residues. They function as single-electron shuttle in fundamental metabolic processes. The family can be subdivided in two major classes, the mitochondrial-type and the plant-type Fds, based on the cysteine spacing in the iron–sulfur binding motif, the three-dimensional structure, and function. A third class of bacterial 2Fe–Fds has recently been recognized on the basis of sequence and spectroscopic properties.

Plant-Type 2Fe Fds

More than a hundred sequences of 2Fe Fds have been deposited in sequence databases. The polypeptide chain is 93–98 residues long, yielding a protein of molecular mass ~11 kDa. The archetype of this class is the chloroplast ferredoxin I (FdI), which in addition to its main role in the photosynthetic electron transfer to Fd–$NADP^+$ reductase (FNR), provides electrons to a large number of Fd-dependent enzymes involved in assimilatory and regulatory pathways (Figure 1).

Molecular Structure

The characteristic spacing of the cysteinyl residues in the iron-sulfur cluster binding motif for this class is $C–X_4–C–X_2–C$, which provides three of the four thiolate ligands to the two iron atoms, with the fourth ligand 29 residues downstream in the primary structure. Several Fds have been structurally characterized either by X-ray crystallography or NMR spectroscopy. They show a folding motif, dubbed β-grasp, which is similar to that of ubiquitin. It is constituted by a four-stranded antiparallel β-sheet and an α-helix lying perpendicularly to the sheet. A representation of the structure of recombinant spinach FdI is depicted in Figure 2 to show the secondary structure elements. The central core (β-grasp) holds the loop which harbors the Cys motif for binding the iron-sulfur cluster. In addition, two short β-strands, a second α-helix and a short C-terminal helical turn are present. The binuclear iron cluster is located near the surface of the protein with Fe1 atom more exposed to solvent. Upon protein reduction, Fe1 has been shown to become reduced. The surface of the Fd molecule shows an asymmetry in distribution of the many acidic residues, which cluster in two distinct areas around the FeS prosthetic group. This feature common to all plant-type Fds has been shown to be important for interaction with protein partners.

Physiological Function

The nuclear encoded FdI is imported in the chloroplast as an apoprotein, where it acquires the prosthetic group. FdI biosynthesis is under the control of light. As depicted in Figure 1, FdI forms transient electron transfer complexes with several different proteins. First it is reduced through electron transfer from the 4Fe–4S

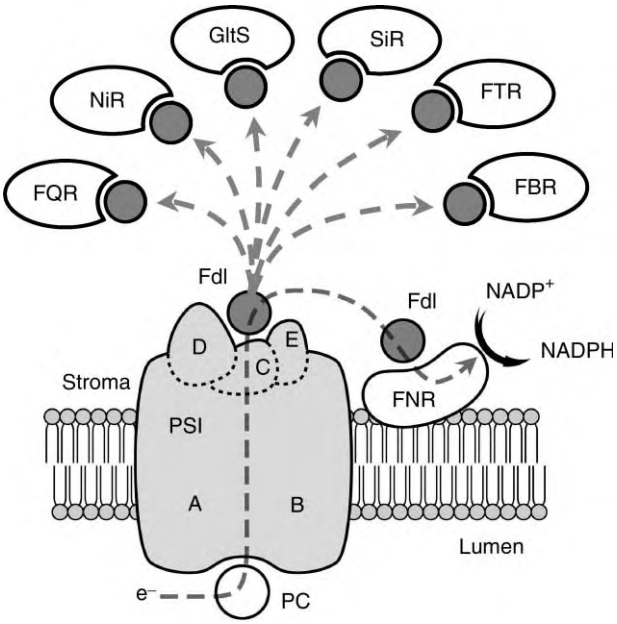

FIGURE 1 Schematic representation of the photosynthetic chain indicating the electron transfer pathways from photosystem I (PSI) to several metabolic processes of chloroplast by FdI servicing. FNR, Fd-$NADP^+$ reductase (carbon assimilation); FBR, Fd-bilin reductase (phytochromobilin synthesis); FTR, Fd-thioredoxin reductase (regulation of Calvin cycle enzymes); SiR, sulfite reductase (sulfur assimilation); GltS, glutamate synthase (amino acid synthesis); NiR, nitrite reductase (nitrogen assimilation); FQR, hypothetical Fd-quinone reductase (cyclic electron flow). PC, plastocyanin. A, B, C, D, and E indicate the PsaA, PsaB, PsaC, PsaD, and PsaE subunits of PSI, respectively.

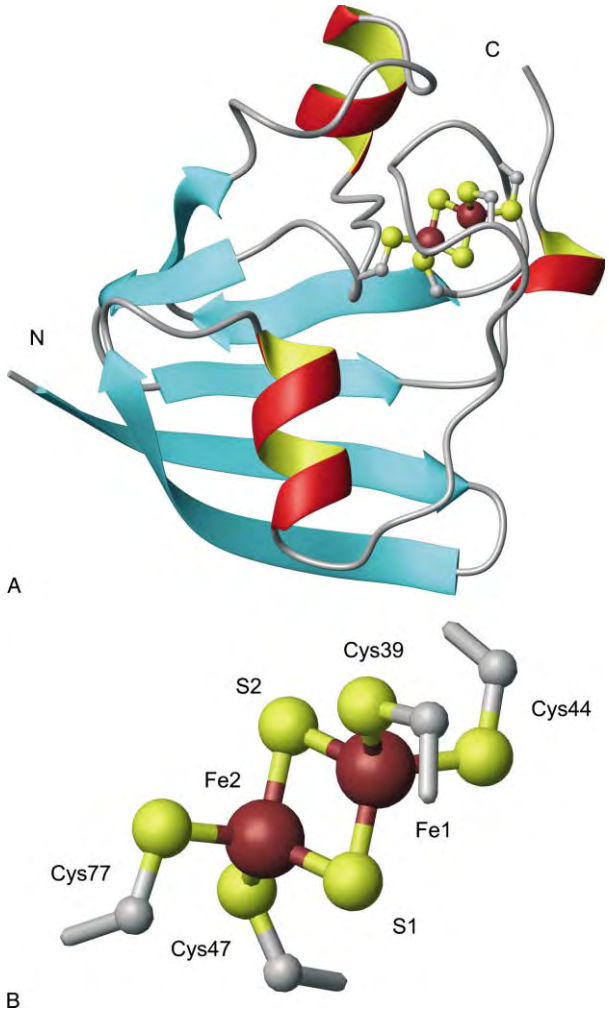

FIGURE 2 Ribbon representation of the three-dimensional structure of spinach FdI showing secondary structure elements. (A) N and C define the N terminus and C terminus, respectively. (B) Detail of the iron–sulfur cluster showing the side chains of the cysteines (residues 39, 44, 47, and 77) and the two sulfide sulfur atoms which coordinate the two iron atoms. The figure was made with Molmol.

centers (F_A and F_B) of the subunit PsaC of photosystem I, by docking both to the PsaD and the PsaE subunits at the stromal side of the thylakoid membrane. Then, the reduced protein donates its electron to either one of the various enzymes known to be Fd dependent. NADPH production through FNR is the main role of FdI. Several studies employing a number of different techniques have attempted to define the binding region of FdI for its various redox partners. The three-dimensional structure of the Fd-FNR complexes both from *Anabaena* spp. and maize leaves have recently been obtained. Overall, the picture which comes out is that FdI acts a mobile electron shuttle between photosystem I and the enzyme partners, utilizing for the interaction the same acidic surface area surrounding the iron-sulfur cluster. The binding sites do not need to be exactly the same but may be just overlapping.

Fd isoforms are present in plastids of nongreen plant tissues and most recently, such type of Fd has been found in the organelle called apicoplast of protozoan parasites Apicomplexa (*Plasmodium* spp., *Toxoplasma gondii*, etc.). These Fds, which have a more positive redox potential than the photosynthetic ones are reduced by FNR isoforms at the expenses of NADPH and act as reductant of Fd-dependent pathways in these organelles.

Mitochondrial-Type 2Fe Fds

Mammalian adrenodoxin (Adx) is the prototype of this class, other well-known members are putidaredoxin of *Pseudomonas putida*, yeast Fd, and *Escherichia coli* Fd. The first two Fds have the role of providing electrons to cytochrome P450-catalyzed hydroxylation reactions, the latter two have been more recently implicated in iron-sulfur cluster biogenesis. They are 105–128 residues long, thus are up to 4 kDa larger than plant Fds. The typical Fe-S binding sequence is $C–X_5–C–X_2–C$, which provides three of the four thiolate ligands to the iron atoms, with the fourth ligand 35–37 residues downstream in the sequence. The three-dimensional structures of these Fds show high similarity to those of the plant Fds in the fold of the core involving

the N-terminal moiety (i.e., the β-grasp), but they have an additional C-terminal lobe, called interaction domain, which has been shown to be involved in binding both the redox partners, Adx reductase and cytochrome P450. As in the case of FdI, the binding sites may be separate but overlapping.

Thioredoxin-Type 2Fe Ferredoxins

Thioredoxin-like Fds were first identified in *Azotobacter vinelandii* and *C. pasteurianum*. They seem to be present only in bacteria. The polypeptide chain length is that usually reported for 2Fe Fds, i.e., 100–120 residues, but these Fds, being dimer, have a larger molecular mass. The cysteine motif for binding the iron-sulfur cluster is rather unique: $C-X_{10-12}-C-X_{29-34}-C-X_3-Cys$ and the crystal structure of *Aquifex aeolicus* Fd revealed a fold unusual for Fds and quite similar to that of thioredoxin. The function of these Fds is not yet known, although there are some indications for their involvement in nitrogen fixation.

Ferredoxins Containing 4Fe and 3Fe Iron–Sulfur Clusters

This class comprises 3Fe, 4Fe, 7Fe, and 8Fe Fds, which are small, bacterial proteins containing one or two FeS clusters of the cubane type. The iron and sulfide atoms alternate on the corners of a distorted cube. In the case of the 3Fe cluster, one corner is devoid of the fourth iron atom. The two types of clusters are in some cases interconvertible. The cysteine motif for the coordination of these iron–sulfur centers is $C-X_2-C-X_2-C$ with the middle cysteine replaced by aspartic acid or any residue in the case of 3Fe clusters, in a polypeptide chain of 60–100 residues. These Fds generally function as electron carrier in several metabolic pathways including pyruvate metabolism, nitrogen fixation, sulfate reduction, hydrogen production, and cytochrome P450 hydroxylations.

See Also the Following Articles

Ferredoxin-NADP$^+$ Reductase • Iron–Sulfur Proteins • Photosynthesis

Glossary

iron–sulfur cluster A prosthetic group containing iron and sulfur atoms liganded by protein cysteine residues.

isoform Any of multiple forms of a protein differing in primary structure but having similar function.

photosynthesis A process that converts the light energy in the chemical energy of NADPH and ATP.

thioredoxin A small protein containing an oxidoreducible disulfide.

Further Reading

Beinert, H., Holm, R. H., and Münck, E. (1997). Iron–sulfur clusters: Nature's modular, multipurpose structures. *Science* **277**, 653–659.

Grinberg, A. V., Hannemann, F., Schiffler, B., Müller, J., Heinemann, U., and Bernhardt, R. (2000). Adrenodoxin: Structure, stability, and electron transfer properties. *Proteins* **40**, 590–612.

Knaff, D. B. (1996). Ferredoxin and ferredoxin-dependent enzymes. In *Oxygenic Photosynthesis: The Light Reactions* (D. R. Ortand and C. F. Yocum, eds.) Vol 4, pp. 333–361. Kluwer, Dordrecht.

Meyer, J. (2001). Ferredoxin of the third kind. *FEBS Lett.* **509**, 1–5.

Tagawa, K., and Arnon, D. I. (1962). *Nature* **195**, 537–543.

Zanetti, G., Binda, C., and Aliverti, A. (2001). The [2Fe–2S] ferredoxins. In *Handbook of Metalloproteins* (A. Messerschmidt, R. Huber, T. Poulos and K. Wieghardt, eds.) Vol 1, pp. 532–542. Wiley, Chichester.

Biography

Giuliana Zanetti is full Professor of Biochemistry in the Department of General Physiology and Biochemistry at the Università degli Studi di Milano, Italy. Her principal research interests are in the field of flavo/iron–sulfur proteins advanced enzymology. She holds a Libera Docenza in plant physiology and underwent postdoctoral training at the University of Michigan. She contributed to the mechanism of action of the photosynthetic Fd-NADP$^+$ reductase, and of several other reductases.

Vittorio Pandini is a Research Scientist in the Dept of Scienze Biomolecolari e Biotecnologie at the Università degli Studi di Milano, Italy. He holds a Ph.D. from the Università di Milano. His current interests are in the ferredoxin redox system of apicomplexan parasites.

Ferredoxin-NADP$^+$ Reductase

Giuliana Zanetti and Alessandro Aliverti
Università degli Studi di Milano, Milan, Italy

The photosynthetic ferredoxin-NADP$^+$ reductase (FNR) is the prototype of a functional group of flavoenzymes that catalyze the exchange of reducing equivalents between NADP(H) and ferredoxins. In photosynthesis, FNR provides NADPH by pairing electrons supplied by photosystem I through ferredoxin. It is a monomeric protein comprising two domains, one for FAD binding and a Rossmann fold for NADP binding. Interactions with either substrates have been elucidated by biochemical studies and by solving the three-dimensional structures of their complexes with the enzyme. The other members of the group catalyze the reduction of ferredoxin at the expense of NADPH, and vary in physiological function, structure and localization.

Introduction

Ferredoxin-NADP$^+$ reductase (FNR) is the common name of members of a broad group of flavoenzymes (classified as EC 1.18.1.2) sharing the ability to catalyze the transfer of reducing equivalents between NADP(H) and ferredoxins (Fds). The best-known example is the photosynthetic FNR, the terminal component of the photosynthetic electron transport chain, both in eukaryotic and prokaryotic phototrophic organisms. In addition to this photosynthetic oxidoreductase, isoforms exist in non-photosynthetic cells. The subdivision between photosynthetic and non-photosynthetic FNRs is functional, and is based on the physiological direction of the catalyzed reaction, i.e., towards NADP$^+$ reduction in the case of photosynthetic FNR, and towards Fd reduction for heterotrophic FNRs (Figure 1). Besides such functional classification, a structural/phylogenetic one is possible, which distinguishes between plant-type and glutathione reductase-type FNRs. While all photosyntetic FNRs are plant-type, non-photosynthetic reductases are distributed between both structural classes.

Furthermore, the plant-type FNR is the prototype of a large superfamily of homologous enzymes, which display a great variety of catalytic functions. All members of this family possess the two-domain FNR unit and additional domains that modify and extend their functional properties.

Photosynthetic FNR

FNR was first discovered in 1956 by Avron and Jagendorf, who isolated it from pea chloroplasts as a NADPH-dependent diaphorase (i.e., a flavin-containing enzyme that catalyzes the transfer of reducing equivalents from NADPH to various electron acceptors). This chloroplast oxidoreductase was later shown by Shin and Arnon to mediate the transfer of electrons from ferredoxin to NADP$^+$.

Molecular Structure

Photosynthetic FNRs are monomeric proteins of about 35 kDa molecular mass, containing one molecule of non-covalently but tightly bound flavin adenine dinucleotide (FAD) as prosthetic group. FNRs from different eukaryotic sources show a high sequence similarity (~80% identity), which is spread over the entire polypeptide chain of ~300 amino acid residues. Cyanobacterial FNR possesses an additional N-terminal sequence of ~10 kDa involved in binding to phycobilisomes, light-harvesting structures of the thylakoid membrane of cyanobacteria. The three-dimensional (3D) structures of photosynthetic FNRs have been determined at high resolution (up to 1.7Å) by X-ray crystallography for the proteins from spinach, pea, paprika, and maize leaves, as well as from the cyanobacterium *Anabaena* spp. The enzyme molecule consists of two structural domains, each of ~150 residues (Figure 2). The N-terminal domain, comprising a six-stranded antiparallel β-barrel, a small β-sheet and an α-helix, provides most of the residues involved in FAD binding and is thus also known as the FAD-binding domain. The C-terminal domain, topologically similar to the supersecondary structure named Rossmann fold, binds NADP(H) and is thus indicated as the NADP-binding domain. However, both dinucleotides interact also with residues belonging to the other domain. Indeed, FAD- and NADP(H)-binding sites are located within a deep cavity at the interface of the two domains. The isoalloxazine ring of FAD, as in many flavoproteins, is sandwiched between the side-chains of two aromatic residues. In particular, the C-terminal tyrosine residue

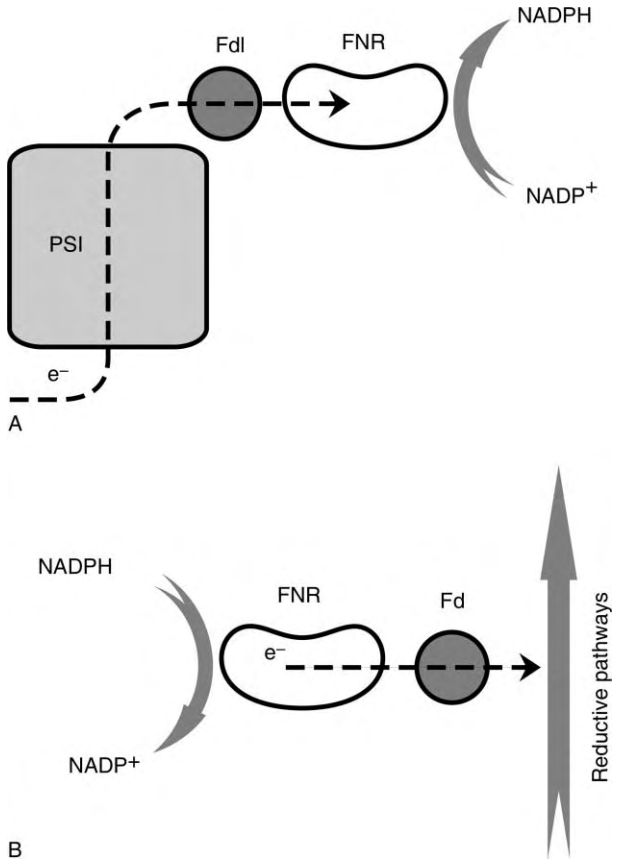

FIGURE 1 Comparison of the physiological reactions catalyzed by photosynthetic and non-photosynthetic FNR isoforms. (A) Scheme of the reaction catalyzed by FNR in chloroplasts. PSI, photosystem I; FdI, photosynthetic isoform of Fd. (B) Scheme of the reaction catalyzed by non-photosynthetic FNR isoforms. Fd indicates any non-photosynthetic Fd isoform, including adrenodoxin. The dashed line indicates the electron transfer path.

makes an aromatic stacking interaction with the *re*-face of the isoalloxazine ring.

Subcellular Localization and Physiological Role

FNR is present in the chloroplasts of algae and higher plants. It is an extrinsic membrane protein localized on the side facing the stroma of the thylakoid membrane. FNR is the catalyst of the last step in the light-driven electron transport. FNR is thus directly responsible for producing the NADPH required in the Calvin cycle for carbohydrate biosynthesis. Reducing power is in turn provided to FNR by Fd, which acts as an electron shuttle by diffusing in the stroma between photosystem I and FNR and being reduced by the former and oxidized by the latter.

Catalytic Mechanism

FNR catalyzes the reversible transfer of reducing equivalents between the obligatory one-electron carrier ferredoxin (Fd) to the obligatory two-electron carrier NADP(H), according to the following balanced chemical equation:

$$2\mathrm{Fd}(\mathrm{Fe}^{2+}) + \mathrm{NADP}^{+} + \mathrm{H}^{+} \Leftrightarrow 2\mathrm{Fd}(\mathrm{Fe}^{3+}) + \mathrm{NADPH}. \quad (1)$$

The ability of FNR to pair single electrons in order to transfer them as a couple to a two-electron acceptor is a feature of the dehydrogenase-electron transferases class of flavoproteins to which FNR belongs, and is mediated by the FAD prosthetic group. FAD can exist in three redox states: oxidized, one-electron reduced (semiquinone form), and two-electron reduced (dihydroquinone form). During turnover, enzyme-bound FAD cycles among the three redox states described above, according to the reaction scheme shown in Figure 3. Two reduced Fd molecules sequentially transfer one electron at the time to FAD, before FNR can complete the catalytic cycle transferring a couple of electrons to $NADP^+$. Electron transfer is strictly coupled to proton (H^+) transfer, at least in steps 2 and 4. FAD protonation in step 2 is required to yield the neutral semiquinone form observed during turnover. In step 4, two electrons are transferred simultaneously with one H^+ in the form of a hydride ion (H^-). Catalysis proceeds according to a sequential ordered mechanism, through the formation of ternary complexes of FNR with both substrates. The redox potential of the FAD/$FADH^-$ couple in FNR is −360 mV, a value intermediate between that of FdI (−400 mV) and that of the $NADP^+$/NADPH couple (−320 mV).

Interaction with NADP(H)

FNR is a remarkably specific enzyme, showing a strong preference for $NADP^+$ over NAD^+. Substrate discrimination is due to a number of interactions that FNR establishes with the 2′-phosphate group of NADP(H). NADP(H) interactions with FNR have been described in terms of a bipartite binding mode, where the adenylate moiety of the dinucleotide binds independently of the nicotinamide one. Binding of the adenylate moiety occurs with high affinity and is the leading event in substrate recognition. In order to allow hydride transfer to occur between the reduced isoalloxazine ring and the nicotinamide, FNR has to undergo an induced-fit process where the nicotinamide ring of $NADP^+$ displaces the phenol ring of the C-terminal tyrosine residue from its stacking interaction with *re*-face of the isoalloxazine (Figure 2). A detailed picture of the enzyme–NADP(H) interaction has been obtained by producing an engineered FNR, where the C-terminal tyrosine was changed to a non-aromatic residue. This greatly stabilized the interaction between the flavin and the nicotinamide ring. Thus, X-ray crystallography of the NADP(H) complex with the mutant FNR revealed the hydride-transfer competent binding mode of the substrate (Figure 2).

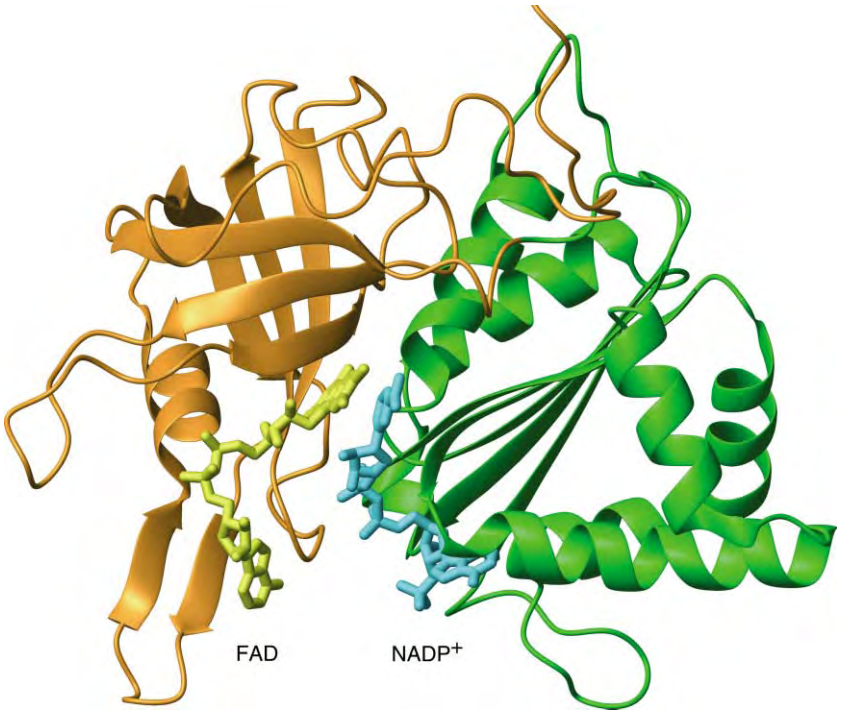

FIGURE 2 Ribbon model of the 3D structure of the pea photosynthetic FNR mutant with a serine replacing the C-terminal tyrosine residue. The FAD-binding and the NADP-binding domains are depicted in orange and green, respectively. The wireframes of bound FAD and NADP$^+$are shown in yellow and cyan, respectively. The figure was made with Molmol.

Interaction with Fd

Crystals of the complexes between FNR and Fd, both in the oxidized state, have been obtained for the eukaryotic (maize leaf) and the prokaryotic (*Anabaena* spp.) protein couples. X-ray structures are similar (Figure 4). Fd binds to a large concave region of FNR, which is contributed by both structural domains of the reductase, with the FAD-binding domain providing most of the interactions. Complex formation places the redox active prosthetic group at a distance (6.0–7.4Å) compatible with high-rate electron transfer. Protein–protein complex formation is thought to be initially driven by the mutual orientation of the dipole moments of the two molecules as they approach. After initial docking, minor adjustments are expected to occur to reach a conformation optimal for intermolecular electron-transfer, with the formation of a network of intermolecular weak bonds (salt bridges, hydrogen bonds, van der Waals, and hydrophobic interactions). Charge–charge interactions, which play a major role in the stabilization of the Fd–FNR complex, are formed between basic groups provided by FNR and acidic groups of Fd.

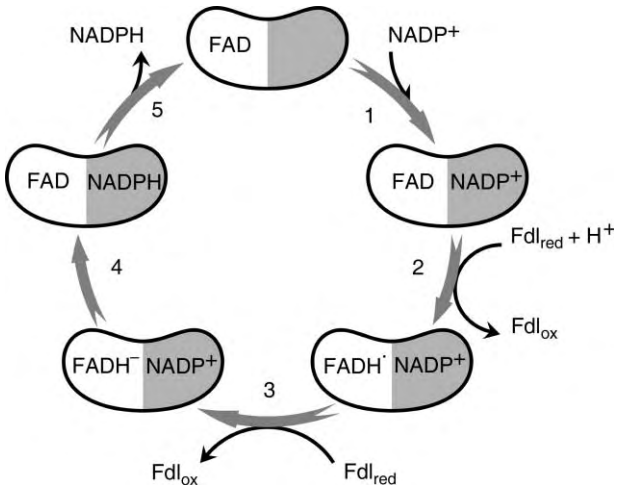

FIGURE 3 Simplified scheme of the mechanism of the reaction catalyzed by the photosynthetic FNR isoform. FdI indicates the photosynthetic Fd isoform present in chloroplasts. FdIox and FdIred indicate oxidized and reduced forms of FdI, respectively. FADH$^{\cdot}$ and FADH$^-$ indicate the neutral semiquinone and the hydroquinone anion of FAD, respectively.

Non-Photosynthetic Plant-Type FNRs

Root FNR

Non-photosynthetic plastids of higher plants contain an isoform of FNR, also known as root FNR. Root and leaf isoforms of FNR are clearly homologous, showing a sequence identity of ~48%, which corresponds to highly similar 3D structures. Isoform-specific

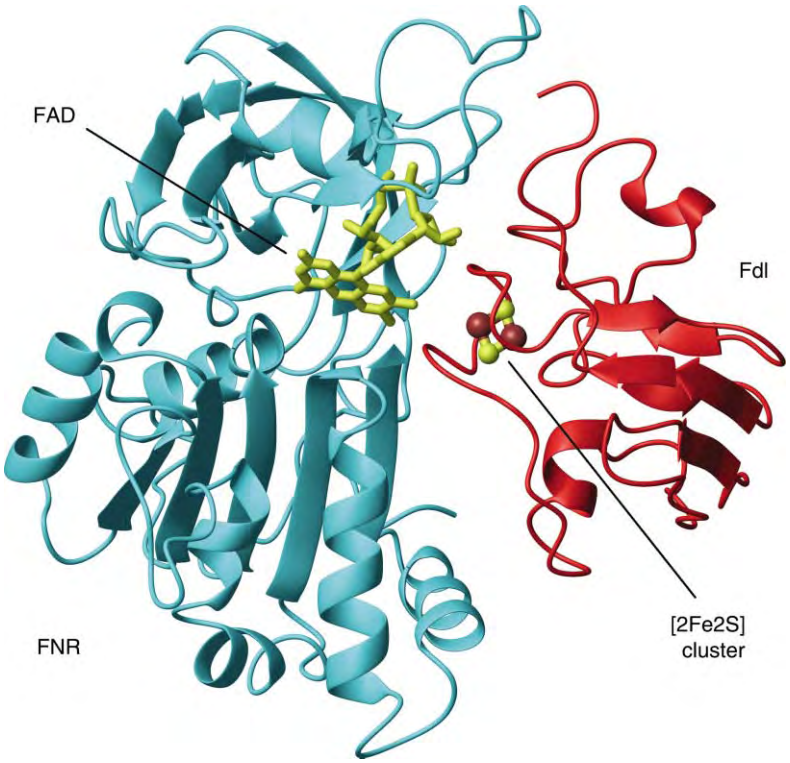

FIGURE 4 Ribbon model of the binary complex between maize photosynthetic FNR and FdI. FNR is depicted in cyan, while FdI is in red. The wireframe of FAD is shown in yellow. The iron–sulfur cluster is represented as a ball and stick model, with the iron atoms in brown and the sulfur atoms in yellow. The figure was made with Molmol.

differences are limited to the structure of surface loops of the molecules, the presence of a conserved disulfide bridge in the FAD-binding domain of the root isoform, a higher redox potential for the bound FAD of the root isoform, and different affinities for the Fd isoforms. Many of these structural and functional differences are instrumental for the diverse physiological role played by the two FNR isoforms. Indeed, the role of root FNR is opposite to that of the leaf isoform, i.e., transfer of reducing equivalents from NADPH to a root-specific Fd isoform to yield reduced Fd for several Fd-dependent pathways.

Bacterial and Apicomplexan FNR

FNRs belonging to the FNR structural family are present in some prokaryotic organisms such as *Escherichia coli* and *Azotobacter vinelandii*. A plant-type FNR has been recently identified in different species belonging to the *Apicomplexa*, a phylum of obligatory eukaryotic unicellular parasites, including the causative agents of malaria, toxoplasmosis, and coccidiosis. In the apicomplexan cell, the FNR is localized, together with a plant-type Fd, in a peculiar organelle, the apicoplast. Apicomplexan FNR is thus expected to play a metabolic function similar to that of root FNR, i.e., production of reduced Fd to be used in reductive biosynthetic pathways. Due to the increasing importance attributed to the apicoplast metabolism in parasite pathogenicity, apicomplexan FNR is an attractive target for novel antiparasitic drugs.

Heterotrophic Glutathione Reductase-Type FNRs

In addition to plant-type FNRs, various FNRs exist that – while being structurally and phylogenetically distinct from the former – show essentially the same catalytic activity, thus representing a noteworthy example of convergent evolution. Such FNRs show a significant sequence identity. The 3D structures of two of them (bovine adrenodoxin reductase and *Mycobacterium tuberculosis* FprA) have been determined and shown to be similar to that of glutathione reductase (GR). FNRs of the GR-like class thus have both domains based on the Rossmann fold motif for binding the nucleotides (FAD and NADPH). The prototype of such enzymes is adrenodoxin reductase (AdR), found in vertebrate mitochondria, where it transfers electrons from NADPH to an Fd known as adrenodoxin (Adx). AdR and Adx form an electron supply system for the cytochrome P450-catalyzed hydroxylation reactions to

produce steroid hormones, vitamin D metabolites, and bile acids. An AdR-homologous protein (Arh1) has been recently found in *Saccharomyces cerevisiae*. By now AdR and Adx have been shown to be ubiquitous in mitochondria of eukaryotes, where they play a role in the biogenesis of iron–sulfur clusters. More recently, an AdR-like enzyme (FprA) has been identified in *Mycobacterium tuberculosis*, showing that they are not restricted to eukaryotes. FprA is thought to have a critical role in the complex lipid metabolism of this pathogen as a source of reducing power for the unusually large numbers (~20) of cytochromes P450 present in this organism. This observation could eventually lead to novel pharmacological treatment for tuberculosis.

See Also the Following Articles

Ferredoxin • Photosynthesis • Photosystem I: F_X, F_A, and F_B Iron–Sulfur Clusters • Protein Folding and Assembly

Glossary

domain An independently folded structural region of a protein molecule.

flavoprotein A protein that contains a flavin nucleotide (FAD or FMN) as prosthetic group.

photosynthesis A process that converts the light energy into chemical energy of NADPH and ATP.

prosthetic group A tightly bound cofactor that contributes to the biological activity of a protein.

Rossmann fold A protein structural motif for nucleotide binding.

Further Reading

Arakaki, A. K., Ceccarelli, E. A., and Carrillo, N. (1997). Plant-type ferredoxin-NADP$^+$ reductase: A basal structural framework and a multiplicity of functions. *FASEB J.* **11**, 133–139.

Deng, Z., Aliverti, A., Zanetti, G., Arakaki, A. K., Ottado, J., Orellano, E. G., Calcaterra, N. B., Ceccarelli, E. A., Carrillo, N., and Karplus, P. A. (1999). A productive NADP$^+$ binding mode of ferredoxin-NADP$^+$ reductase revealed by protein engineering and crystallographic studies. *Nat. Struct. Biol.* **6**, 847–853.

Hurley, J. K., Morales, R., Martínez-Júlvez, M., Brodie, T. B., Medina, M., Gómez-Moreno, C., and Tollin, G. (2002). Structure–function relationships in Anabaena ferredoxin/ferredoxin: NADP$^+$ reductase electron transfer: insights from site-directed mutagenesis, transient absorption spectroscopy and X-ray crystallography. *Biochim. Biophys. Acta* **1554**, 5–21.

Karplus, P. A., Daniels, M. J., and Herriott, J. R. (1991). Atomic structure of ferredoxin-NADP$^+$ reductase: Prototype for a structurally novel flavoenzyme family. *Science* **251**, 60–66.

Zanetti, G., and Aliverti, A. (1991). Ferredoxin-NADP$^+$ oxidoreductase. In *Chemistry and Biochemistry of Flavoenzymes II* (F. Müller, ed.) pp. 305–315. CRC Press, Boca Raton, FL.

Biography

Giuliana Zanetti is a Professor of Biochemistry in Scienze Biomolecolari e Biotechnologie at the Università degli Studi di Milano, Italy. Her principal research interests are in the field of flavo/iron–sulfur proteins advanced enzymology. She holds a Libera Docenza in Plant Physiology and underwent a two-year postdoctoral training at the University of Michigan. She contributed to clarifying the mechanism of action of the photoysnthetic ferredoxin-NADP$^+$ reductase, and of several other reductases.

Alessandro Aliverti is an Assistant Professor of Biochemistry in Scienze Biomolecolari e Biotechnologie at the Università degli Studi di Milano, Italy. He holds a Ph.D. from the University of Milan. His current research is on the enzymology of ferredoxin reductases from both plants and pathogens.

Fibroblast Growth Factor Receptors and Cancer-Associated Perturbations

Marko Kornmann
University of Ulm, Ulm, Germany

Murray Korc
Dartmouth Medical School, Lebanon, New Hampshire, USA

Fibroblast growth factors (FGFs) constitute a family of homologous heparin-binding polypeptides that presently consists of at least 23 members. FGFs play important roles in many biological functions, including development, pattern formation, cellular differentiation, metabolic regulation, tissue repair, angiogenesis, and mitogenesis. FGFs act by binding to a family of specific, high-affinity FGF receptors (FGFRs) that possess a discontinuous intracellular kinase domain. Perturbations in FGF–FGFR expression, localization, and signaling have been implicated in several pathological processes, including malignant transformation and tumor spread and metastasis.

Fibroblast Growth Factors

Genes

To date, 23 *Fgf* genes have been identified in vertebrates. Although human *Fgf15* and mouse *Fgf19* have not been described, human *Fgf19* is most closely related to mouse *Fgf15*, and both genes are closely linked to the *Fgf3* and *Fgf4* genes, raising the possibility that human *Fgf19* may be identical to mouse *Fgf15*. According to their evolutionary relationship, the 22 *Fgfs* in humans can be classified into several subgroups (Figure 1). Members of each subgroup may also share similar biochemical and developmental properties. For example, members of the *Fgf8* subgroup display similar receptor-binding properties and overlapping yet distinct expression patterns during development, underscoring both their commonality and uniqueness.

Proteins

Among vertebrates, fibroblast growth factors (FGFs) share 13–71% of their amino acid sequence homology. Most notably, there is an internal core region consisting of six identical and 28 highly conserved amino acids, which include the ten amino acid residues interacting with the high-affinity FGF receptors (FGFRs) within ~120 amino acid region. In FGF-1 and FGF-2 this areas consists of 12 antiparallel β-strands forming a structure exhibiting a threefold internal symmetry called a β-trefoil.

FGF4–8, 10, 17–19, 21, 23 possess classical N-terminal leader sequences that may allow for rapid and efficient secretion. This sequence is also present in FGF3 and 22. However, neither of these FGFs is efficiently secreted. By contrast, FGF-1, 2, 9, and 11–14, 16, and 20 lack a leader sequence for secretion. Nonetheless, FGF9, 16, and 20 have a hydrophobic region in the core domain allowing for secretion. Moreover, FGF1 and FGF2 may be released by an exocytotic mechanism, while FGF11–14 are thought to remain intracellularly. Posttranslational glycosylation, alternative splicing, and initiation of synthesis from N-terminal CUG sequences can result in several different molecular weight forms in the case of several FGFs.

Physiologic Actions

FGFs regulate diverse processes during development and exert a broad variety of functions in the adult organisms including growth, survival, apoptosis, motility, and differentiation.

Fibroblast Growth Factor Receptors

Genes

FGFRs are transmembrane proteins that are encoded by five distinct *Fgfr* genes. The extracellular portion of these receptors is usually composed of three immunoglobulin (Ig)-like domains (I–III), including a stretch of acidic residues (acidic box) between domain I and II, which is unique for the FGFRs. The hydrophobic

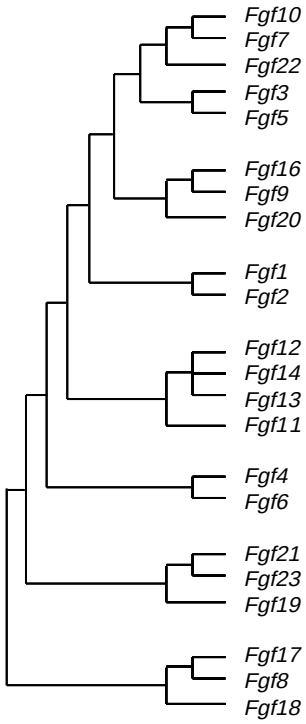

FIGURE 1 Evolutionary relationships within the human FGF family. (Adapted from Ornitz, D. M., and Itoh, N. (2001). Protein family review: Fibroblast growth factors. *Genome Biol.* **2**, 30051–300512, with permission.)

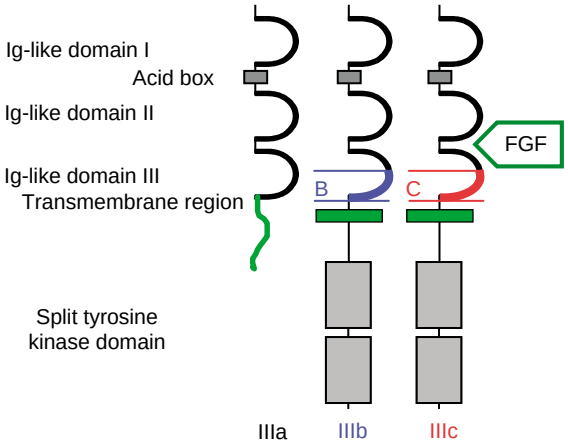

FIGURE 2 Schematic diagram of structural features of FGF receptors. FGFRs are usually composed of three extracellular immunoglobulin (Ig)-like domains (I–III) including a stretch of acidic residues (acidic box) unique for FGFRs, a hydrophobic transmembrane region followed by a juxtamembrane and a split tyrosine kinase catalytic domain. The IIIa isoform is devoid of any signaling capacity. In case of the IIIc isoform, the second half of the Ig-like domain III (solid) corresponds to the exon 7 sequence of the *FGFR1* gene and in case of IIIb, the second half of the Ig domain III (open) corresponds to the exon 6 sequence of the *Fgfr1* gene.

transmembrane region is followed by a juxtamembrane domain and a split tyrosine kinase catalytic domain (Figure 2). In contrast to FGFR1–4, FGFR5 contains a transmembrane domain, but no intracellular kinase domain. A special feature of the FGFR family is the existence of several receptor isoforms for FGFR1, 2, 3, and 4 that are generated by alternative mRNA splicing and result in different ligand-binding specificities.

Proteins

FGF signaling is generally mediated by a dual-receptor system, consisting of the high-affinity FGFRs and of low-affinity heparan sulfate proteoglycan receptors that are most often devoid of signaling capabilities but enhance ligand presentation to the receptors. The function of FGFR5, which is also devoid of intracellular signaling capacity, is presently unknown, but it may provide a binding site for FGFs. FGF binding results in receptor oligomerization, activation of the cytoplasmic tyrosine kinase domains and receptor autophosphorylation. Intracellular signaling is then mediated through the tyrosine phosphorylation of key substrates, and the activation of downstream pathways such as the mitogen-activated protein kinases (MAPK), extracellular signal regulated kinase-1 (ERK-1), and ERK-2. In general, activation of these pathways occurs following phosphorylation of FGF receptor substrate-2 (FRS-2) (Figure 3). However, the same signaling cascades can also be activated under certain circumstances through FRS-2 independent mechanisms (Figure 3).

The existence of at least 23 FGF ligands, 5 FGFRs, and multiple FGF isoforms and FGFR splice variants can potentially result in a large combinatorial set of interactions. This further increases the complexity, diversity, and functional specificity of FGFs. Most notably, alternative splicing of the second half of the Ig-like domain III results in three receptor variants, termed IIIa, IIIb, and IIIc (Figure 2). Due to the fact that FGF binding occurs between the Ig-like domains II and III, these splice variants are important for defining ligand binding. Thus, the IIIa splice variant yields a secreted receptor that is devoid of any signaling capacity. The expression of the IIIb variant is believed to be restricted to epithelial cell types, whereas the expression of the IIIc variant, especially in the case of FGFR2 and FGFR3, is believed to be restricted to mesenchymal cell types.

Physiologic Actions

The expression of FGFRs seems to be fundamental for many processes including limb, craniofacial, and lung development, hepatogenesis, osteogenesis, and inner ear formation. Mutations of *Fgfr1–3* genes have been linked to syndromes characterized by specific craniofacial and limb malformations. For example, mutations of *Fgfr2* were found in patients with Apert syndrome and mutations of *Fgfr3* in patients with achondroplasia.

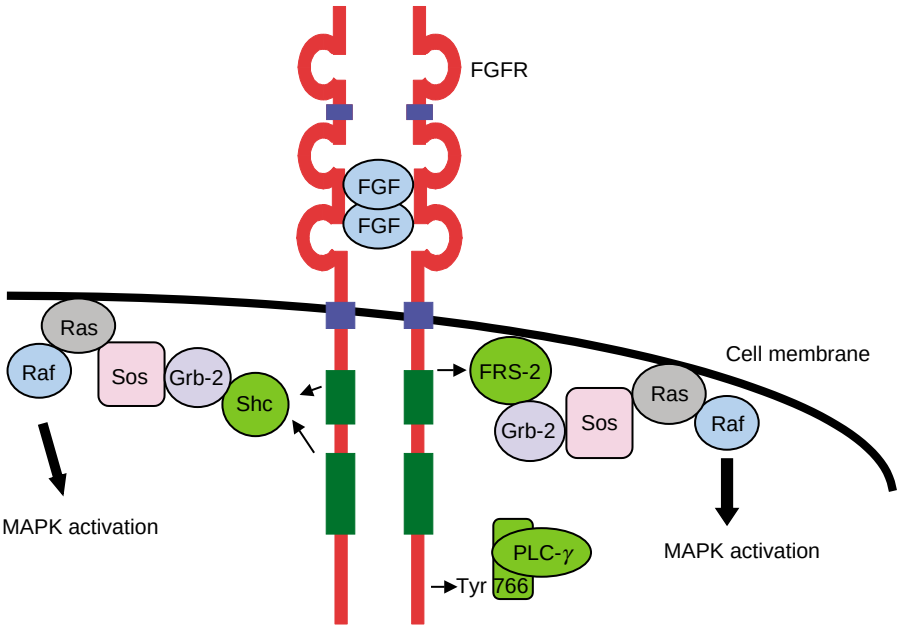

FIGURE 3 Schematic diagram of FGF signaling. FGF binding between Ig domain II and III results in receptor oligomerization, activation of the split cytoplasmic tyrosine kinase domains (rectangles) and receptor autophosphorylation. This is followed by binding, phosphorylation, and activation of fibroblast growth factor receptor substrate 2 (FRS2) or phospholipase C-γ (PLC-γ), which binds to tyrosine residue 766. Activation of the downstream mitogen-activated protein kinases (MAPK), extracellular signal regulated kinase-1 (ERK-1), and ERK-2 generally occurs via FRS2, but may also be mediated by an FRS2 independent pathway through the signaling molecules Shc, Grb-2, SOS, ras, and raf.

FGF Actions in Cancer

Many studies demonstrate that alterations of the expression of FGFs and FGFRs play an important role in the development and progression of various malignant diseases.

FGF2

FGF2 exerts mitogenic effects on various endothelial, mesothelial, and epithelial cell types. It is overexpressed in a great portion of human tumor cell lines and various human malignancies. High levels of FGF2 in the serum of patients or in tumor specimens have been correlated with advanced tumor stage and poor prognosis in several gastrointestinal and other cancers, including thyroid, lung, and renal cell cancer. However, FGF2 expression may be associated with favorable prognosis in ovarian and breast cancer.

FGF1

FGF1 is also a potent mitogenic factor for many normal and malignant cells and is also expressed in a variety of cultured cell lines and tissues. Although FGF1 is present in many malignancies and can display similar biological activities as FGF2, FGF1 expression has not been clearly demonstrated to correlate with clinico-pathological parameters in human cancers.

FGF3

The *Fgf3* gene was initially identified as murine mammary tumor virus integration site oncogene homologue (*int2*) implicated in mouse mammary tumors. *Fgf3* is localized on chromosome 11q13, a locus frequently amplified in malignant diseases. Amplification of *Fgf3* was associated with poor prognosis in breast cancer and biological aggressiveness in ovarian and esophageal cancer. The overexpression of FGF3 in normal mouse mammary cells resulted in the development of orthotopically implanted tumors in nude mice, underscoring the important role of FGF3 in mammary tumorigenesis.

FGF-4

Fgf4, also called "human stomach cancer transforming factor-1" (*hst-1*), was discovered when DNA from stomach tissues was shown to induce the malignant transformation of fibroblasts. The same oncogene was isolated by transfection of Kaposi sarcoma DNA and is therefore also called "kaposi sarcoma *Fgf*" (*kFgf*). *Fgf4* is also located on chromosome 11q13 together with *Fgf3*. Amplification of *Fgf4* correlates with increased risk of systemic recurrence after resection of esophageal

cancer and with nodal involvement in head and neck cancers. Moreover, FGF4 overexpression increases the metastasic potential of breast cancer cells in association with altered expression of matrix metallo-proteinases.

FGF5

Fgf5 was also initially identified as a transforming proto-oncogene. In addition to being expressed in fibroblasts, FGF5 is expressed in breast cancer and several cancers of the gastrointestinal and urinary tract. Exogenous FGF5 exerts proliferative effects on cultured pancreatic cancer cells which express FGFR1 IIIc suggesting that FGF5 may act as paracrine and autocrine factor in pancreatic cancer.

FGF6

FGF6 or human stomach transforming factor-2 also displays transforming potential and was found in prostate cancer in conjunction with FGFR4. Exogenous FGF6 enhances the proliferation of primary prostatic epithelial and stromal cells and prostate cancer cell lines suggesting that FGF6 may act as paracrine and autocrine factor in prostate cancer.

FGF7

FGF7 is an important mitogen for a variety of epithelial and cancer cells, including liver, pancreas, gastrointestinal tract, lung, and breast. Inhibition of FGF7 signaling results in reduced mobility and invasion of breast and gastric cancer cells. FGF7 is overexpressed in many cancers, but is expressed at lower levels in squamous cell carcinomas of the head and neck and endometrial cancers by comparison with the corresponding normal tissue. In many cases, FGF7 is not expressed in the cancer cells, but in the adjoining cellular elements within these pathological tissues. Moreover, serum FGF7 levels are lower in patients with prostate cancer in comparison to patients with benign prostatic hyperplasia. Together, these observations suggest that FGF7 may differentially modulate tumor growth depending on its site of expression and on the expression and localization of the FGF receptors in these tissues.

FGF8

FGF8 or androgen-induced growth factor was isolated from SC-3 androgen-stimulated mouse mammary carcinoma cells and found to be overexpressed in breast cancer. *Fgf8* has been proposed to enhance murine mammary tumorigenesis in cooperation with the *Wnt-1* proto-oncogene. It was found that the four known human FGF8 isoforms (a, b, e, and f) display different proliferating and transforming potencies, the FGF8b isoform being the most potent. Constitutive expression of FGF8b resulted in enhanced invasion, angiogenic capacity, and tumor growth of breast cancer cells, underscoring its potential role in this malignancy.

FGF9-23

Expression of FGF9 or glia-activating factor, FGF10, and FGF19 was detected in various cancer tissues and these FGFs are also able to act as mitogens. FGF19 transgenic mice that overexpress FGF19 in skeletal muscle, exhibits elevated hepatic α-fetoprotein levels at 2 months of age and develop hepatocellular carcinomas by 10 months of age.

FGFR Actions in Cancer

In order to exert their activities, FGFs are dependent on the presence of high-affinity FGFRs. Changes in isoform expression of various FGFRs appear to be important for the enhancement of tumorigenesis and transformation.

FGFR1

FGFR1 is expressed in a wide variety of cell types and tissues including many malignancies. Amplification of the *Fgfr1* locus on chromosome 8p12 was associated with nodal involvement in breast cancer and poor prognosis of patients with bladder cancer. An atypical stem-cell myeloproliferative disorder evolving toward acute myelogenous leukemia is characterized by a 8p12–11 breakpoint and at (8;13) translocation, resulting in an aberrant formation of a tyrosine kinase with the catalytic domain of FGFR1 and constitutive kinase activity. This translocation was also found in breast cancer. Expression of *Fgfr1* in transgenic mice suggests that FGFR1 plays an important role in mammary gland tumorigenesis. Deletions of 8p12 have been reported for choriocarcinoma and frequent disturbances including amplification or deletions have been reported in prostate cancer. FGFR1 expression can also be induced by overexpression of cyclin D1 in fibroblasts via the pRb/E2F pathway. Cyclin D1 is known to be overexpressed in many malignancies and correlates with poor prognosis in several malignancies. Recent evidence also suggests that N-cadherin expression can enhance tumorigenesis via FGFR1. FGFR1 ligand-induced internalization was reduced by N-cadherin mediated by the first two Ig-like domains and resulted in increased FGFR1 stability and sustained activation of mitogen-activated protein kinase.

A potent ligand of FGFR1, FGF2, has been shown to be an important prognostic factor for many malignancies. Nevertheless, high FGFR1 expression was only associated with poor differentiation in prostate cancer,

advanced stage in head and neck squamous cell carcinoma, and nonsmall-cell lung cancer. In addition, recent evidence suggests that alterations in the expression of certain splice variants may be responsible for malignant transformation. Thus, expression of FGFR1 IIIc in normal ductal pancreatic epithelial cells resulted in the establishment of an autocrine loop and cellular transformation with increased proliferation and *in vivo* tumor formation. Expression of FGFR1 IIIc in the cancer cells, which are of epithelial origin, has been linked to the pathogenesis of pancreatic and prostate cancers. Additionally, altered expression of FGFR1 splice variants have been reported in breast cancer. Specifically, the 2-Ig like isoform (also called FGFR1β) is up-regulated in pancreatic, prostate, and breast cancers, and in astrocytomas and glioblastomas in comparison to the 3-Ig form (FGFR1α).

Inhibition of FGFR1 signaling using dominant-negative or soluble forms of the receptor resulted in significant growth inhibition in pancreatic, breast, prostate, and several other cancer cell lines. Using vaccination with *Xenopus* FGFR1 in a murine tumor model resulted in the production of FGFR1-specific autoantibodies and effective antitumor activity and suppression of angiogenesis.

FGFR2

FGFR2 is also found in a wide variety of cell types and tissues and was first identified as an amplified gene from a human gastric cancer cell line. Amplification of *Fgfr2* on chromosome 10q26 was also observed in breast and oral squamous cell carcinomas. One important isoform, keratinocyte growth factor (KGFR), is devoid of the Ig-like domain I and the acidic box and contains sequences encoding the IIIb variant. Overexpression of KGFR occurs in gastric and pancreatic cancers, and is associated with poor differentiation in prostate cancer, whereas KGFR expression is lower in endometrial cancer in comparison to the normal endometrium.

An essential feature of *Fgfr2* is its proposed strictly tissue-specific expression using exon IIIb in epithelial cells and IIIc in mesenchymal cells. Exon switching from IIIb to IIIc in conjunction with the presence of stromal cell-derived FGF7 was accompanied with malignant progression in a prostate cancer model, down-regulation of IIIb with malignant progression of the prostate, and dedifferentiation of normal oral keratinocytes into a malignant phenotype. This exon switch from FGFR2 IIIb to FGFR2 IIIc can be induced by the presence of FGF1 and 2 in keratinocytes, fibroblasts, and bladder carcinoma cells. Re-expression of KGFR by transfection in human salivary gland adenocarcinoma cells which lost KGFR expression in the process of malignant transformation, resulted in growth inhibition, induction of differentiation, and apoptosis. *Fgfr2* mutations linked to craniosynostosis syndromes and resulting in constitutive receptor activation with transforming potential were also detected in gastric cancers, suggesting that gain-of-function mutations of *Fgfr2* can also play a role in tumorigenesis.

FGFR3

Mutations of *Fgfr3* were identified in a great portion of bladder carcinomas and at low frequency in cervical, urothelial cell, and colorectal carcinomas. Many of these mutations occurred at highly conserved sequences in the Ig-like domain III, highlighting the functional importance of this domain. Mutations were not detected in stomach, rectum, prostate, ovarian, breast, brain, or renal tumors or cell lines. Interestingly, the presence of FGFR3 mutations in bladder and urothelial cell carcinoma was associated with better clinical outcome.

Nuclear accumulation of FGFR3 has been reported in breast cancer samples. This is probably related to a splice variant in which exons 7 and 8 are deleted resulting in the translation of a soluble intracellular FGFR3 missing the transmembrane domain, but with an intact kinase domain. Using other splice variants that are devoid of the acidic box, it could be shown that inhibitory functions of FGFR3 can be abolished. Other variants with altered ligand-binding specificities were described in osteosarcoma and squamous carcinoma cell lines. Thus, depending on the mutations and the receptor splice variant expressed, FGFR3 can display transforming potential, supporting the possible role of FGFR3 in the pathogenesis of some malignancies.

FGFR4

G to A conversions resulting in a substitution of glycine by arginine at position 388 in the transmembrane domain of the *Fgfr4* gene have been described. Expression of this receptor in mammary tumor cells increased cell mobility and the presence of this allele was associated with lymph node metastases and more advanced disease in colon cancer and reduced disease-free survival in breast cancer. Amplification of *Fgfr4* on 5q35.1-qter has been reported in some breast and ovarian cancers, leukemias, and lymphomas. FGFR4 overexpression was also reported in endocrine tumors of the digestive system, several gastrointestinal and urinary tract cancers as well as breast and lung cancers. FGFR4 expression has also been correlated with a lower differentiation state and tends to be associated with shorter patient survival in astrocytomas. Furthermore, a truncated form of FGFR4 lacking the first two Ig-like domains was identified in human pituitary tumors. Because the N terminus of this truncated receptor lacks a signal peptide, it is not inserted into

the plasma membrane and resides in the cytoplasm. The truncated receptor is constitutively phosphorylated and exhibits transforming potential in fibroblasts. Its expression in transgenic mice results in formation of pituitary tumors suggesting that this isoform may play a role in the development of pituitary tumors.

Experiments using dominant-negative FGFR4 also suggest that FGFR4 may be involved in matrix adhesion and therefore tumor dissemination. Expression of FGFR4 induced membrane ruffling, a sign of transformation of breast cells, in the presence of FGF1 or 2. Furthermore, the differentiation of teratocarcinoma cells was associated with loss of FGFR4 expression.

Nothing is presently known about involvement of FGFR5 in any malignancies.

Summary

In addition to their role in many biological processes during development and in the adult, FGFs and FGFRs are involved in the pathobiology of many malignancies. One important reason for this seems to be the altered expression of FGFs and FGFRs and their isoforms resulting in the aberrant activation of autocrine and paracrine signaling loops that eventually promote tumorigenesis. Other changes include the expression of abnormal FGFs or FGFRs with constitutive activation of FGFR tyrosine kinase signaling. Thus, the functional analysis of the role of FGF–FGFR alterations in specific cancer entities may lead to novel and highly specific treatment strategies.

See Also the Following Articles

Alternative Splicing: Regulation of Fibroblast Growth Factor Receptor (FGFR) • Immunoglobulin (Fc) Receptors • Phospholipase C

Glossary

malignant transformation Process of exhibiting qualities of malignancies including uncontrolled growth, anchorage-independent cell growth, and *in vivo* tumor formation.

mRNA splice variant An isoform of a protein resulting from the processing of different exons of a gene.

Further Reading

Burgess, W. H., and Winkles, J. A. (1996). The fibroblast growth factor family: Multifunctional regulators of cell proliferation. In *Cell Proliferation in Cancer, Regulatory Mechanisms of Neoplastic Cell Growth* (L. Pusztai, C. E. Lewis and E. Yap, eds.) pp. 154–217. Oxford University Press, New York.

Ford-Perriss, M., Abud, H., and Murphy, M. (2001). Fibroblast growth factors in the developing central nervous system. *Clin. Exp. Pharmacol. Physiol.* **28**, 493–503.

Johnson, D. E., and Williams, L. T. (1993). Structural and functional diversity in the FGF receptor multigene family. *Adv. Cancer Res.* **60**, 1–41.

Klint, P., and Claesson-Welsh, L. (1999). Signal transduction by fibroblast growth factor receptors. *Front. Biosci.* **4**, D165–D177.

Lax, I., Wong, A., Lamothe, B., Lee, A., Frost, A., Hawes, J., and Schlessinger, J. (2002). The docking protein FRS2alpha controls a MAP kinase-mediated negative feedback mechanism for signaling by FGF receptors. *Molecul. Cell* **10**, 709–719.

Ornitz, D. M., and Itoh, N. (2001). Protein family review: Fibroblast growth factors. *Genome Biol.* **2**, 30051–300512.

Biography

Marko Kornmann is an Assistant Professor of Surgery in the Department of Visceral and Transplantation Surgery at the University of Ulm in Germany. His principal research interests are in molecular and biological alterations of growth factor pathways in gastrointestinal malignancies. He holds an M.D. and Ph.D. from the University of Ulm and received his postdoctoral training at the University of California, Irvine.

Murray Korc is the Joseph M. Huber Professor and Chairman in the Department of Medicine at Dartmouth-Hitchcock Medical Center and Professor of Pharmacology and Toxicology at Dartmouth Medical School in Hanover, New Hampshire. His principal research interests are in the elucidation of the molecular alterations that occur in pancreatic cancer.

Flavins

Barrie Entsch and David P. Ballou
University of Michigan, Ann Arbor, Michigan, USA

The word flavin in biochemistry comes from the Latin word meaning yellow. The root word flavin was used in the early twentieth century to refer to yellow compounds extracted from tissue samples. Richard Kuhn is credited with the preparation of pure riboflavin (which he called lactoflavin – from milk) and its structural determination. Kuhn received the Nobel prize for this and other work in 1938. Today, the term flavin is reserved for a group of compounds that contain the fused three-ring structure called isoalloxazine which is responsible for the yellow color.

The most important flavins in nature are riboflavin, flavin mononucleotide (FMN), and flavin adenine dinucleotide (FAD) as shown in Figure 1. Riboflavin is often known as vitamin B2 (one of the soluble vitamins), which is an essential requirement in the diet of mammals and many other organisms. Riboflavin is manufactured by most microorganisms and plants. There is now a great deal of information on the process of biosynthesis. Organisms that require riboflavin as a vitamin use specific enzymes and ATP to convert the compound into both FMN and FAD. These nucleotides are used as cofactors (or prosthetic groups) in the structure and function of many proteins. The relationship with proteins is so important that we normally think of flavins in the context of protein structures. Thus, we refer constantly to flavoproteins as proteins with a flavin cofactor. This article describes the fundamentally important functions of these compounds in a wide variety of chemical processes in nature.

Chemistry

The chemistry of flavins has been studied extensively. Riboflavin is a stable compound with a variety of interesting properties. FMN and FAD are much more important in cells, but are less stable in solution because of the presence of phosphate ester and anhydride bonds. Riboflavin is responsible for the important biological chemistry of all flavins. Only the reactions most relevant to life are mentioned below. One reason that flavoproteins have been so extensively analyzed is that they can be studied by examining the properties of their cofactor that is nearly always involved in the core function of each protein. Another reason is the variety of chemical properties that have been exploited for important biological functions of considerable diversity.

Redox Properties

Oxidized flavins (called flavoquinones) can be reduced by two electrons and protons, and the redox potential for reduction is ~ -0.2 V at pH 7 (Figure 2). Reduced flavins (flavohydroquinones) are thus moderate reducing agents and can occur as either a neutral or an anionic form. Part of the versatility of flavins comes from their ability to be reduced in one-electron steps because flavins are capable of forming stable free radicals (flavosemiquinones in Figure 2). A neutral and an anioic free radical can be formed by flavins and both occur in nature. Proteins modify these redox properties by the interactions formed with the flavin cofactor to establish a wide variety of biological processes. Flavins can pass electrons to transition metal ions. Many proteins make use of this property to link stable reducing compounds (e.g., NADH) to reactive metal ions and one-electron processes in electron transport chains. Flavins are almost always involved as the transforming molecule.

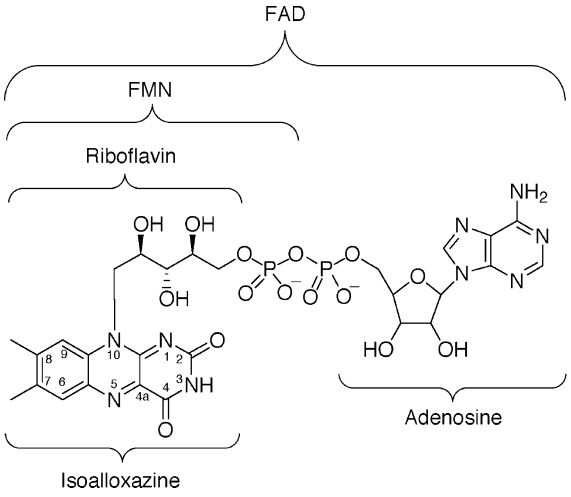

FIGURE 1 The structures of flavins discussed in this article. The numbering system shown for the isoalloxazine ring is used in the text.

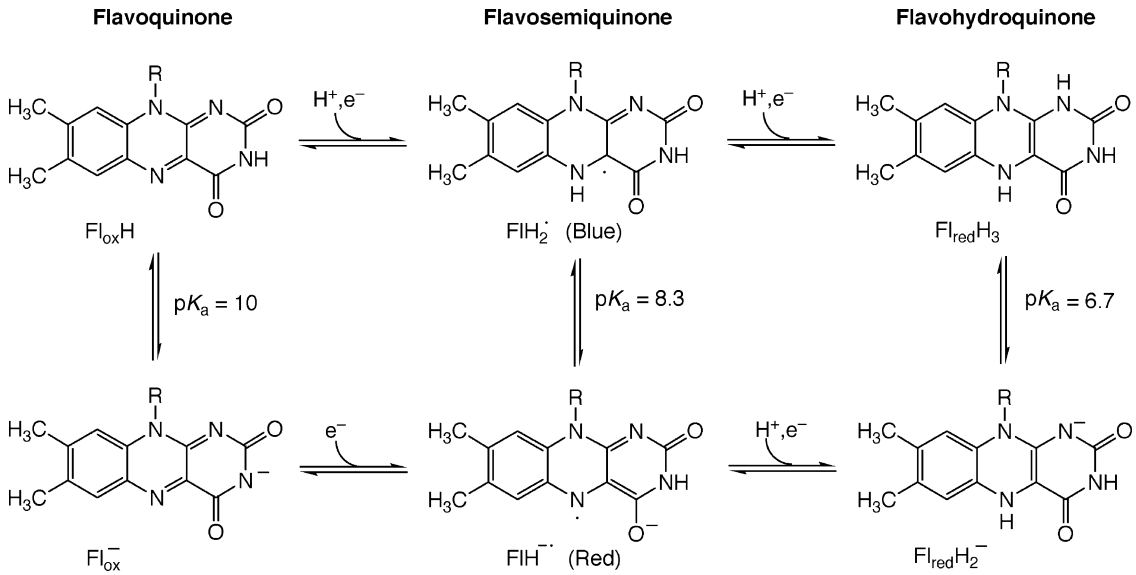

FIGURE 2 The redox states of the isoalloxazine ring that are observed in natural systems.

Oxygen and Other Derivatives

Flavins, unlike most organic molecules, react with oxygen. This reactivity is a product of the redox properties mentioned above. Oxygen is unreactive without the formation of free-radical intermediates. Reduced flavins provide the capacity for one-electron reductions and have the additional ability of forming reactive covalent adducts with oxygen and other molecules. Bruice and colleagues have shown that the reactions between reduced flavins and oxygen involve covalent adducts and free-radical intermediates. Many proteins take advantage of the oxygen adducts (Figure 3) to help carry out chemical reactions. A wide variety of biological processes depend upon the specific interactions between particular proteins and these flavin adducts. A small number of proteins form stable covalent bonds to the flavin through the 8-position (Figure 1).

Spectroscopic Properties

Oxidized flavins (the stable form) are normally yellow due to a major electronic transition observed at ~450 nm (Figure 4). Full reduction of flavins (two equivalents) gives a structure that has a low absorbance beyond 400 nm, and thus looks almost colorless (pale yellow) by comparison to oxidized flavins. Free-radical flavins (flavosemiquinones) have complex spectra with spectacular colors – either red or blue (Figure 4), depending on the state of protonation. Flavins also form charge-transfer complexes with a variety of other compounds. These complexes have a range of different visible spectra with a corresponding variety of colors. Various proteins can stabilize one or more of these chemical species, so that flavoproteins can

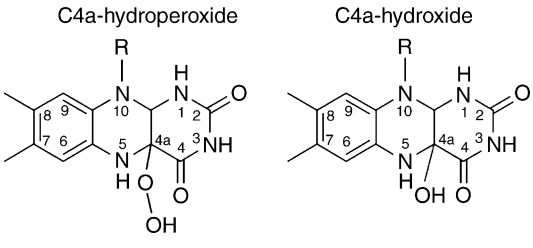

FIGURE 3 The structure of transient oxygen derivatives of the isoalloxazine ring that are important in protein function. Note that thiol groups can form a similar structure to the C4a-hydroxide. The biological function of the sulfur derivative is discussed in this article.

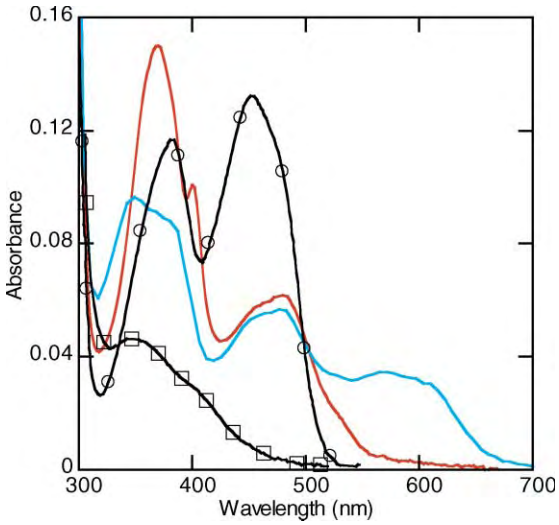

FIGURE 4 Absorption spectra of the redox states of FAD in glucose oxidase. A solution of 9.5 μM oxidized enzyme (solid line/open circles) was photoreduced in anaerobic conditions at pH 9.2 to form the red, anionic semiquinone. The solution was shifted to pH 5.0 with citric acid to form the blue semiquinone, and then reduced with glucose to form the hydroquinone (solid line/open squares).

have many colors, as well as change color during catalytic function.

Flavins have important luminescent spectral properties. Many flavins are fluorescent, and the fluorescence properties are strongly influenced by association with proteins and by the oxidation state or formation of derivatives. These properties can be studied in biological systems because the flavin can be excited by light (between 350 and 480 nm) and the emitted light is a broad band with a peak near 530 nm. This property provides a sensitive assay of flavins down to $\sim 10^{-9}$ M. The fluorescent properties of flavoproteins often provide information not available from absorbance properties. Flavins can even be trapped in excited states and this has been exploited in living systems. Nature has also utilized the enhanced reactivity of the excited states of flavins that last long enough to be chemically useful.

Types of Flavoproteins

To try to display the diversity and utility of flavin function in living systems, we adapt below the classification system for flavoproteins developed by Massey.

Pyridine Nucleotide Oxidoreductases

There is a diverse group of proteins that connects the stable reducing currency of cells (NADH/NADPH) with other redox processes required for cellular function. For example, glutathione reductase is one of a group of related disulfide reductases that contain both FAD and a pair of reactive cysteine residues in the active site. The function of this enzyme is to help maintain a reducing environment within cells by keeping glutathione reduced. Glutathione then carries out many important functions such as reducing disulfides in proteins and removing hydrogen peroxide from cells (catalyzed by glutathione peroxidase). Through the flavin buried in the protein, the enzyme can use the reducing power of NADPH to reduce the disulfide of glutathione, because the flavin reacts rapidly with thiols by the formation of a transient covalent adduct (Figure 3). Another example is ferredoxin reductase, the enzyme principally associated with photosynthesis that enables reactive, strongly reducing proteins such as ferredoxin to provide stable reducing equivalents in the cell as NADPH. Through the FAD in the active site, the enzyme can accept single reducing electrons from ferredoxin (electrons collected from the reactive free-radical photochemical process) that can then be safely stored as NADPH.

Dehydrogenase/Electron Transferase

There are a limited number of enzymes that use flavins to link oxidation of a stable metabolite to electron transport chains for energy conservation in cells. For example, succinate dehydrogenase is a component of the "citric acid cycle" in mitochondria and it links directly into the respiratory complexes through an iron/sulfur cluster complex. The FAD in this enzyme is covalently linked to the protein where it accepts a pair of electrons from the oxidation of succinate and then transfers single reducing electrons into the respiratory complex II. The acyl-CoA dehydrogenases in animals have a similar fundamental role in obtaining energy from the oxidation of fats. These enzymes contain FAD and the latter accepts electrons from a fatty acyl-CoA to initiate oxidation of a fatty acid. In this case, the electrons are transferred to the respiratory chain in mitochondria through another soluble flavoprotein called the electron transferring flavoprotein. In plants, the process of fatty acyl-CoA oxidation occurs in glyoxisomes (rather than mitochondria) by the use of similar enzymes that are oxidases. That is, after being reduced by the fatty acyl-CoA, the enzyme flavin reacts with oxygen to dispose of the reducing electrons. The difference between these enzymes in animals and plants is a subtle change in the protein interactions with the FAD that changes the course of the reaction.

Electron Transfer Proteins

There is a small group of proteins that act to provide single reactive reducing electrons for a variety of biological reactions. Most of these proteins contain iron/sulfur complexes, but a few are flavoproteins that use the ability of flavins to form stable free radicals. For example, flavodoxins are widespread in microorganisms and have been extensively studied. The protein in flavodoxins makes a specific interaction with the isoalloxazine ring that stabilizes the blue neutral radical (Figures 2 and 4), and makes further reduction difficult. Thus, when reduced, flavodoxins are strong one-electron reducing agents. Electron transferring flavoprotein referred to earlier is a different member of this family of proteins.

Oxygenases

Flavins are widely employed in cells to unlock the reactivity of the oxygen molecule. Oxygenases not only react with oxygen, but they also incorporate oxygen into metabolites. There are many types of flavoprotein oxygenases that tame oxygen for useful purposes. For example, *p*-hydroxbenzoate hydroxylase adds one atom of oxygen to an aromatic ring so that it

can eventually be used for carbon and energy supply for a microorganism. Oxygenated aromatic rings are then converted to aliphatic compounds by subsequent metabolic steps. *p*-hydroxybenzoate hydroxylase contains FAD in the structure and has been studied extensively to understand this type of reaction. In catalysis, the reduction of FAD by NADPH is tightly controlled in a remarkable process. The enzyme senses the presence of the substrate *p*-hydroxybenzoate in the active site and responds by swinging the isoalloxazine ring to the surface of the protein where it contacts the NADPH. This process makes use of the flexibility of the ribityl side chain of FAD. Then, after reduction, the isoalloxazine swings back into the interior of the protein where it not only reduces oxygen, but also forms a transient covalent adduct (Figure 3, hydroperoxide) in the controlled environment of the enzyme. The peroxide provides the reactive oxygen to oxygenate the substrate. Cyclohexanone monooxygenase provides a different example where the FAD, after reduction by NADPH, reacts with oxygen to form a peroxide anion that reacts rapidly with the carbonyl group of cyclohexanone. Another variation is found in lactate monooxygenase. Here, the enzyme flavin (FMN) is reduced by the substrate lactate to form pyruvate that is held by the enzyme and oxygenated by the peroxide formed from the reaction between reduced FMN and oxygen.

Oxidases

Flavoproteins can also use oxygen as a sink for removing unwanted reducing electrons. This process was briefly referred to above in relation to fatty acyl-CoA oxidase in plants. Another important example is glycolate oxidase in plants. During photosynthesis, glycolate is formed as an unwanted byproduct and must be removed. Glycolate oxidase uses FMN to oxidize glycolate to glyoxalate, which is then aminated to glycine, a normal metabolite. This process occurs in peroxisomes where oxygen is used to react with reduced FMN to remove the reducing electrons from glycolate, rather than through an electron transport chain. The oxygen is reduced to hydrogen peroxide (similar to the oxygenases), but the peroxide is released from the enzyme and must be removed from the cell by other enzymes such as catalase to prevent dangerous side reactions. Other examples of this use of oxygen by flavoproteins are D-aminoacid oxidase in kidneys and glucose oxidase in fungi. It is the absence of a flavoprotein oxidase function (gulonolactone oxidase) that explains why humans require vitamin C in their diets, when most animals can make this molecule. In humans, the gene for this enzyme has mutated and no longer codes for a functional protein.

Photochemistry

Flavoproteins show some really novel functions when the properties of their excited states are utilized in cells. A classic example is bacterial luciferase, which is an enzyme that produces lime-green light from chemical energy. The light-producing process is an outgrowth of the reactions of the oxygenases. NADH is used to reduce FMN by one enzyme and then the reduced FMN binds to luciferase where it reacts with oxygen to form the flavin C-4a-hydroperoxide (Figure 3). The novel reaction occurs when the hydroperoxide oxidizes a fatty aldehyde to form the corresponding fatty acid. In this reaction the protein traps the FMN in an excited state of the flavin C-4a-hydroxide (Figure 3), which can decay with the release of a photon. Many marine animals in the deep oceans form symbiotic relationships with the bacteria that make luciferase. The animal can then form light-emitting organs essential for communication, hunting, or defense.

Just as remarkable as luciferase is DNA photolyase, which is found in all cells. An essential part of cellular survival is the maintenance of the integrity of genetic information in the face of damage by environmental factors. One source of damage is UV light, which can cause cross-linking of bases in the DNA helix. It is the task of DNA photolyase to repair the damage often by using the same source of light that caused the damage. This enzyme contains both an FAD and an accessory pigment. The flavin functions in the protein in the reduced state, where it is converted to a powerful reducing agent when excited by energy from light. The excited reduced state is powerful enough to break down the unwanted covalent bonds in damaged DNA and thus repair the integrity of the genetic information. Electrons used for this purpose are then recovered to reform the reduced FAD.

Another developing story about flavoprotein photochemistry involves flavins as blue-light photoreceptors. For example, phototropins are photoreceptors for some plant responses to light. These proteins contain FMN that forms a transient and reversible covalent bond to an active site cysteine upon illumination. This complex is thought to form through a free-radical mechanism of excited state flavin chemistry.

Medical Significance

It is extremely rare for riboflavin deficiency to occur in humans because of its widespread occurrence in food. However, some flavoproteins are important in medical practice. A few examples are mentioned below.

A common medication for gout (caused by excess uric acid) is allopurinol. This drug inhibits xanthine oxidase, a complex flavoprotein involved in formation of the uric

acid that causes gout. Uric acid is the end product of the natural breakdown of purines in the body.

Another complex flavoprotein, monoamine oxidase is a target for modulation by drug therapy, particularly for depression, because this enzyme degrades some of the potent natural neurotransmitters involved in mental disorders.

The flavoprotein, methylenetetrahydrofolate reductase is involved in the formation of the amino acid methionine. About 12% of the human population has a form of the enzyme that leads to elevated homocysteine in the blood, a major risk factor in cardiovascular disease.

Some medications for stomach ulcers work because they are substrates for the bacterial flavoprotein, nitroreductase produced by the ulcer-causing *Helicobacter pylori*. The reduced products formed from the drug by the enzyme kill the bacterial cells.

See Also the Following Articles

Fatty Acid Synthesis and its Regulation • Peroxisomes • Tricarboxylic Acid Cycle

Glossary

fatty acyl-CoA Derivatives of fatty acids (CoA thioesters) formed in cells to initiate oxidation of the fatty acid.

glyoxisome/peroxisome Common membrane-enclosed compartments in plant and animal cells.

hydroperoxide A derivative of hydrogen peroxide where one of the H atoms is replaced by a chemical group.

isoalloxazine Fused three-ring structure that forms the core chemical function of flavins (Figure 1).

redox Shorthand for reduction and oxidation processes.

Further Reading

Flavins and Flavoproteins. A series of books that report the Proceedings of the International Symposia on Flavins and Flavoproteins are published every three years. Since 1990 this series has been published by Walter de Gruyter and Rudolf Weber, Berlin.

Massey, V. (1994). Activation of molecular oxygen by flavins and flavoproteins. *J. Biol. Chem.* **269**, 22459–22462.

Massey, V., and Ghisla, S. (1974). Role of charge-transfer interactions in flavoprotein catalysis. *Annu. N.Y. Acad. Sci.* **227**, 446–465.

Müller, F. (ed.) (1991). *Chemistry and Biochemistry of Flavoenzymes*, Vols. I–III, CRC Press, Boca Raton.

Palfey, B. A., and Massey, V. (1998). Flavin-dependent enzymes. In *Comprehensive Biological Catalysis: Vol. III Radical Reactions and Oxidation/Reduction* (M. Sinnott, ed.) pp. 83–154. Academic Press, London.

Biography

Dr. Barrie Entsch retired from the position of Associate Professor of Biochemistry at the University of New England, Australia in 2002. He now works as a Research Fellow in Biological Chemistry at the University of Michigan, Ann Arbor. He has collaborated on mechanistic studies of flavoproteins with David Ballou and Vincent Massey for more than 30 years. He was awarded several Australian Research Council Grants for research with flavoproteins, particularly oxygenases.

David Ballou has been a Professor on the faculty of the Department of Biological Chemistry at the University of Michigan since 1972. His work has mainly been mechanistic and structural studies on a wide variety of redox enzymes. These include flavoproteins, cytochrome P450, cobalamin-containing enzymes, non-heme iron oxygenases, and copper enzymes. He has specialized in the development of rapid kinetic and spectroscopic methods for studying these systems.

Flippases

Charles J. Waechter
University of Kentucky College of Medicine, Lexington, Kentucky, USA

Membrane proteins referred to as flippases play a vital role in membrane biology by overcoming the biophysical barrier imposed by the greasy, hydrophobic core of the bilayer common to biological membranes, and facilitating the transbilayer movement of the hydrophilic headgroups of phospholipids and glycolipids. This article summarizes the transbilayer events involved in biosynthetic processes and establishing phospholipid asymmetry and speculates on the mechanism(s) that could overcome the thermodynamically unfavorable spontaneous flip-flopping of the various polar lipids. More detailed reviews of some aspects of the flip-flopping of phospholipids and dolichol-linked saccharide intermediates can be found in the references cited at the end of this article.

Introduction

During the bioassembly of N-linked oligosaccharides, C- and O-linked mannosyl units in proteins, glycosylphosphatidylinositol (GPI) anchors, glycosphingolipids, and newly formed phospholipid bilayers in eukaryotic cells, charged hydrophilic headgroups must diffuse transversely through the hydrophobic core of the endoplasmic reticulum (ER) and an early Golgi compartment. Similarly, in prokaryotes phospholipids and undecaprenyl pyrophosphate-linked glycosyl building blocks must be translocated from the inner leaflet to the outer monolayer during the expansion of the cytoplasmic membrane and the biosynthesis of cell-wall components. Biochemical and biophysical model systems indicate that the unassisted transbilayer movement of polar lipids with charged headgroups is highly unfavorable thermodynamically and much too slow to allow cells to synthesize the essential glycoconjugates in a physiologically requisite time frame. Thus, it has been proposed that the "flip-flopping" of the amphipathic precursors/intermediates is mediated by a class of membrane proteins referred to as flippases. The term "flippase" was originally suggested by Mark Bretscher during the 1970s.

The transbilayer movement of lipids with the generalized structure of a polar lipid (A) and of mannosylphosphoryldolichol (Man-P-Dol) (B) mediated by a flippase is illustrated in Figure 1. Table I summarizes several examples of polar lipids whose transverse diffusion is believed to be facilitated by flippases in prokaryotic and eukaryotic cells. Despite the critical function of flippases in membrane biology, there are still very large gaps in the information about their structures, the genes encoding this vital class of proteins and the mechanism(s) by which they shield and permit the passage of the polar moieties through the hydrophobic core of the ER and other cellular membranes.

Expansion of the ER Bilayer during Membrane Biogenesis

It is well established that the major site of phospholipid biosynthesis *de novo* in eukaryotes is on the cytoplasmic leaflet of the ER membrane. Clearly, to have uniform expansion of the bilayer during active membrane biogenesis, ~50% of the newly formed phospholipids must be translocated to the lumenal monolayer. The landmark study of Kornberg and McConnell proved that the unassisted movement of spin-labeled phosphatidylcholine (PC) molecules between the two leaflets of pure lipid vesicles did not occur fast enough to maintain bilayer expansion at physiological rates. Further emphasizing the essential role of flippases, the classic experiments of James Rothman and Eugene Kennedy demonstrated that movement of phosphatidylethanolamine molecules, newly synthesized on the cytoplasmic leaflet of a *B. megaterium* cell, to the extracellular monolayer was remarkably faster than the rate of spontaneous diffusion in artificial lipid bilayers. Primarily due to severe technical difficulties inherent in studying the phospholipid flippase(s), there is still very little known about the structure and mechanism of this eminently important class of membrane proteins. Bishop and Bell proposed the novel idea of following the transport of a water-soluble analogue (diC_4PC) of PC by sealed microsomal vesicles to implicate one or more ER proteins in the transbilayer movement of the major membrane phospholipid. The PC flippase is

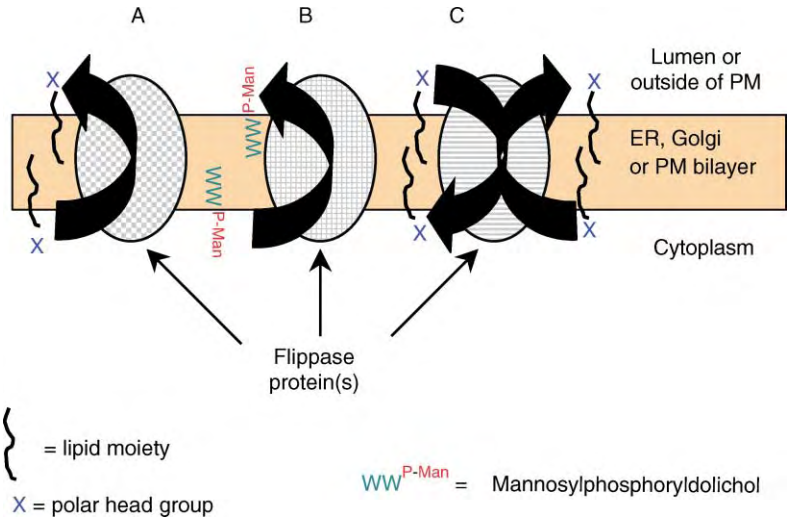

FIGURE 1 Illustration of the flippase-mediated transbilayer movement of a membrane lipid with the generalized structure of a polar lipid (A) or mannosylphosphoryldolichol (B) from the cytoplasmic leaflet to the lumenal monolayer in the ER or Golgi. The ATP-dependent flip-flopping of a phospholipid from the outer surface of the PM (C, left) or the bidirectional, ATP-independent movement of a polar lipid mediated by scramblases is depicted in model (C). Although the translocation in examples in A and B are illustrated as being unidirectional, these processes appear to be bidirectional.

depicted in Figure 1A. The basic principle of this experimental approach is to design a water-soluble form of the polar lipid in which the hydrophobic groups are reduced in size to increase their solubility in aqueous solutions while retaining the essential structural features recognized by the proteins mediating their translocation. Although this experimental approach and alternate methods have been utilized by other researchers more recently to make progress toward these goals, the PC and other phospholipid flippases in biogenic membranes remain to be identified, isolated, and cloned. Presumably, neutral lipids such as cholesterol, coenzyme Q, and neutral glycerides diffuse transversely in cellular membranes by a protein-unassisted process since they lack charged, hydrophilic groups.

Aminophospholipid Flippases/ Translocases, Floppases, Scramblases, and Phospholipid Asymmetry

In most, if not all, cellular membranes phospholipids are distributed asymmetrically between the two leaflets, a property that is critical to membrane function. Thus, in addition to the flippases crucial to uniform expansion of the bilayer in the ER during membrane biogenesis, another set of flippases is required to maintain the proper distribution of phospholipids between the two leaflets of membranes in the various cellular compartments. The combined action of aminophospholipid flippases, two types of outwardly driven floppases (multidrug resistance, MDR, P-glycoprotein, other

TABLE I

Summary of Specific Flip-Flopping Events in Prokaryotic and Eukaryotic Cells

Polar lipid	Membrane site	Transbilayer movement from
Aminophospholipids (PS/PE)	Plasma membrane	Outer leaflet to inner monolayer
PC and other glycerophospholipids, GlcN-Pl, Man-P-Dol, Glc-P-Dol and $Man_5GlcNAc_2$-P-P-Dol	ER	Cytoplasmic to lumenal leaflet
Glucosylceramide	Early Golgi	Cytoplasmic to lumenal leaflet
Glycerophospholipids, and undecaprenyl-P(P)-linked cell-wall intermediates	Bacterial cytoplasmic membrane	Cytoplasmic leaflet to exterior monolayer (or outer membrane)

members of the MDR family and members of the multidrug resistance-associated protein, MRP, subfamily) and possibly the ATP-independent, bidirectional scramblases (Figure 1C) are believed to play a role in the asymmetric distribution of PC and other membrane phospholipids between the two leaflets of the plasma membrane (PM) and other cellular membranes. The best characterized of the candidate flippases is the ATP/Mg^{2+}-dependent aminophospholipid flippase. The properties of this type of flippase have been studied extensively, and progress has been made in purifying the protein component(s). It has been found in the PM of erythrocytes and other mammalian cells, synaptosomes, chromaffin granules, and secretory vesicles. This flippase appears to play a direct role in maintaining the enrichment of PS and PE in the inner leaflet of the PM by moving the two aminophospholipids from the outer to the inner leaflet of the plasma membrane against a concentration gradient at the expense of ATP. In Figure 1C (left) the lipid moiety would be diacylglycerol and the polar headgroup (X) would be either phosphorylserine or phosphorylethanolamine. The loss of this activity due to diminishing ATP pools or the loss of the protein(s) allows PE/PS to diffuse back to the outer monolayer where the surface alteration is recognized by the immune system as an early signal in apoptosis.

However, inhibition of the flippase or loss of ATP is insufficient to cause a rapid loss of plasma membrane PS asymmetry. Rapid PS externalization requires the additional activation of a (Ca^{2+}-dependent) scramblase. The bidirectional, ATP-independent scramblase (Figure 1C) plays an important role in platelet activation, blood clotting, and apoptosis.

There is good evidence that floppases (Figure 1A) mediate the ATP-dependent translocation of cholesterol, PC, and sphingolipids from the cytoplasmic to the external leaflet of the plasma membrane. More details of the latter two classes of "flippases" can be found in the excellent review by Dr. D. Daleke cited at the end of this article.

Protein N-Glycosylation

N-linked oligosaccharide chains are initially synthesized as the dolichyl pyrophosphate (Dol-P-P) linked precursor oligosaccharide by a two-stage process in the ER. In the first stage, three lipid intermediates, mannosylphosphoryldolichol (Man-P-Dol), glucosylphosphoryldolichol (Glc-P-Dol), and a heptasaccharide intermediate ($Man_5GlcNAc_2$-P-P-Dol) are synthesized in the ER by enzymes with active sites facing the cytoplasm. In the next stage these three glycolipid intermediates diffuse transversely to the lumenal monolayer where four more mannosyl units are added to $Man_5GlcNAc_2$-P-P-Dol with Man-P-Dol (Figure 1B) functioning as the mannosyl donor. Finally, three glucosyl units are donated by Glc-P-Dol, completing the synthesis of the oligosaccharyl donor, $Glc_3Man_9GlcNAc_2$-P-P-Dol. Based on evidence obtained from biophysical and enzymological topological studies, it is very likely that the transverse diffusion of the three intermediates requires ER proteins functioning as flippases to maintain lipid intermediate biosynthesis and protein N-glycosylation at physiologically relevant rates. Evidence has been obtained for the presence of ER proteins that mediate the transbilayer movement of short-chain, water-soluble analogues of Man-P-Dol and Glc-P-Dol by sealed vesicles from rat liver and brain by a variation of the experimental approach pioneered by Bishop and Bell. Preliminary studies using this transport technique indicate that the flippases are bidirectional and ATP independent. It is plausible that this class of flippase acts by facilitated diffusion, and the transbilayer movement of the lipid intermediates is driven by mass action as they are consumed during $Glc_3Man_9GlcNAc_2$-P-P-Dol synthesis on the lumenal surface. Hopefully, the *in vitro* assays will provide a means to isolating the ER proteins involved in this flip-flopping process. More recently, genetic and biochemical studies have implicated the *Rft1* protein in the transbilayer movement of $Man_5GlcNAc_2$-P-P-Dol in the yeast, *S. cerevisiae*. The structure of the yeast protein may provide clues to the identity of the gene encoding the corresponding protein in mammalian cells. The identification of the flippase proteins involved in the "dolichol pathway" and the corresponding genes should ultimately be relevant to the diagnosis of related genetic defects in patients with as yet uncharacterized forms of congenital disorders of glycosylation.

Relationship of a Man-P-Dol Flippase to the Biosynthesis of Other Mannose-Containing Glycoconjugates

Protein O- and C-Mannosylation

In yeast and mammalian cells, many proteins are modified by the addition of mannosyl units from Man-P-Dol to either serine/threonine in O-mannosidic linkage or to the indole ring of tryptophan residues in a C-mannosidic linkage. Since Man-P-Dol is believed to be formed only on the cytosolic face of the ER (Figure 1B), and these modifications appear to occur on the lumenal side of the ER, a Man-P-Dol flippase is essential for O- and C-mannosylation of proteins, as well as completing the synthesis of $Glc_3Man_9GlcNAc_2$-P-P-Dol and to maintain normal rates of protein N-glycosylation.

GPI Anchors

One class of proteins that is associated with membranes, despite not having any transmembrane domains, is attached by an amide linkage to GPI anchors. The biosynthesis of the GPI anchors theoretically requires at least two ER flippases. The best current evidence indicates that the early intermediate, GlcN-PI, is formed on the cytoplasmic face of the ER, and is subsequently translocated to the lumenal monolayer where the GPI anchor is completed and the appropriate polypeptides are covalently attached to the ethanolamine moiety by a transpeptidation reaction. The completion of the anchor on the lumenal surface also requires Man-P-Dol as a mannosyl donor, and the transverse diffusion of the mannolipid intermediate requires a flippase that is discussed above.

Glucosylceramide

The enzyme that synthesizes glucosylceramide (Glc-Cer) from UDP-glucose and ceramide in an early Golgi compartment has an active site that is oriented toward the cytoplasm. Since more complex cerebrosides and gangliosides are elaborated on the interior of the Golgi compartments, it is necessary for the Glc-Cer formed on the cytosolic side to be translocated to the lumenal leaflet where the glucosyl unit can be elongated by lumenally oriented glycosyltransferases. Thus, in this flippase-mediated event the lipid moiety would be ceramide and the polar headgroup would be a β-linked glucosyl group as illustrated in Figure 1A. The biosynthesis of the complex glycosphingolipids also requires a set of Golgi proteins to mediate the transbilayer movement of the sugar nucleotides required for ganglioside synthesis. Since there is experimental evidence that some fraction of the Glc-Cer formed on the cytoplasmic leaflet of an early Golgi compartment can be translocated directly to the inner surface of the PM, there may also be a PM flippase that mediates the movement of Glc-Cer to the outer leaflet.

Bacterial Cell Walls

In gram-positive and gram-negative bacteria, some of the building blocks for the assembly of peptidoglycan, lipopolysaccharide, and several other cell-wall complex glycoconjugates are synthesized on the inner face of the cytoplasmic membrane while attached to undecaprenyl pyrophosphate (Und-P-P). There is solid genetic evidence for the presence of membrane proteins that mediate the transbilayer movement of the bacterial lipid intermediates so the assembly of the cell-wall components can be completed on the exterior face of the cytoplasmic membrane, or in the case of gram-negative bacteria, on the outer membrane. The *Wzx* family has been proposed to encode proteins involved in the translocation of Undec-P-P linked intermediates in bacteria. There is recent evidence that the *wzxE* gene encodes a protein involved in the transbilayer movement of a trisaccharide lipid intermediate in the biosynthesis of the enterobacterial common antigen in *E. coli*. Although there is very limited information about their structures at this time, it is quite possible that the prokaryotic flippases resemble their eukaryotic counterparts. The intriguing question of why the polyisoprenoid glycosyl carrier lipids became longer (C55 for prokaryotes to C75–95 for eukaryotes) and acquired the saturated α-isoprene unit in dolichols during evolution remains to be explained.

See Also the Following Articles

Glycosylphosphatidylinositol (GPI) Anchors • Lipid Bilayer Structure • Protein Glycosylation, Overview

Glossary

dolichyl monophosphate An eukaryotic glycosyl carrier lipid containing 15–20 isoprene units in which the α-isoprene unit is saturated.

flippase A general term for a class of membrane proteins proposed to facilitate the transbilayer movement of the polar headgroup of a phospholipid, glycosphingolipid, or a polyisoprenyl-P(-P) linked glycosyl intermediate.

scramblase Bidirectional, ATP-independent transporters that randomly redistribute polar lipids formed *de novo* in the endoplasmic reticulum. This class also facilitates the nonspecific, bidirectional movement of phospholipids in the plasma membrane.

transverse diffusion The "flip-flopping" or transbilayer movement of a polar membrane lipid from one leaflet to the opposite monolayer of a cellular membrane.

undecaprenyl phosphate A fully unsaturated bacterial glycosyl carrier lipid containing eleven isoprene units.

Further Reading

Bishop, W. R., and Bell, R. M. (1985). Assembly of the endoplasmic reticulum phospholipid bilayer: The phosphatidylcholine transporter. *Cell* **42**, 51–60.

Bratton, D. L., Fadok, V. A., Richter, D. A., Kailey, J. M., Guthrie, and Henson, P. M. (1997). Appearance of phosphatidylserine on apoptotic cells requires calcium-mediated nonspecific flip-flop and is enhanced by loss of the aminophospholipid translocase. *J. Biol. Chem.* **272**, 26159–26165.

Daleke, D. L. (2003). Regulation of transbilayer plasma membrane phospholipid asymmetry. *J. Lipid Res.* **44**, 233–242.

Dolis, D., Moreau, C., Zachowski, A., and Devaux, P. F. (1997). Aminophospholipid translocase and proteins involved in transmembrane phospholipid traffic. *Biophys. Chem.* **68**, 221–231.

Helenius, J., Ng, D. T. W., Marolda, C. L., Walter, P., Valvano, M., and Aebi, M. (2002). Translocation of lipid-linked oligosaccharides

across the ER membrane requires Rft1 protein. *Nature* **415**, 447–450.

Kornberg, R. D., and McConnell, H. M. (1971). Inside-outside transitions of phospholipids in vesicle membranes. *Biochemistry* **10**, 1111–1120.

Menon, A. (1995). Flippases. *TICB* **5**, 355–360.

McCloskey, M. A., and Troy, F. A. (1980). Paramagnetic isoprenoid carrier lipids: 2. Dispersion and dynamics in lipid membranes. *Biochemistry* **19**, 2061–2066.

Rick, P. D., Barr, K., Sankaran, K., Kajimura, J., Rush, J. S., and Waechter, C. J. (2003). Evidence that the *wzxE* gene of *E. coli* K-12 encodes a protein involved in the transbilayer movement of a trisaccharide-lipid intermediate in the assembly of enterobacterial common antigen. *J. Biol. Chem.* **278**, 16534–16542.

Rothman, J. E., and Kennedy, E. P. (1977). Rapid transmembrane movement of newly synthesized phospholipids during membrane assembly. *PNAS* **74**, 1821–1825.

Schenk, B., Fernandez, F., and Waechter, C. J. (2001). The ins(ide) and outs(ide) of dolichyl phosphate biosynthesis and recycling in the endoplasmic reticulum. *Glycobiology* **11**, 61R–70R.

Sprong, M., van der Sluijs, P., and van Meer, G. (2001). How proteins move lipids and lipids move proteins. *Nat. Rev. Mol. Biol.* **2**, 504–513.

Biography

Charles Waechter received a Ph.D. in biochemistry in 1971 studying the regulation of membrane phospholipid biosynthesis in *S. cerevisiae* with Robert L. Lester (University of Kentucky College of Medicine). His major research interest, in the biosynthesis and function of lipid intermediates in protein N-glycosylation in mammalian cells, began as a postdoctoral fellow with Dr. William Lennarz (The Johns Hopkins University School of Medicine) during 1971–74. He is currently professor of Molecular and Cellular Biochemistry at the University of Kentucky College of Medicine, and has served on the editorial board of *The Journal of Biological Chemistry and Glycobiology*, in the Neurological Sciences Study Section at NIH, and in the Tumor Biochemistry Study Section of the ACS.

Focal Adhesions

Eli Zamir and Benjamin Geiger
The Weizmann Institute of Science, Rehovot, Israel

Focal adhesions (also known as focal contacts) are integrin-dependent adhesions in which the cell membrane is attached at its external surface to the extracellular matrix (ECM) and at its internal aspect to the actin cytoskeleton. These transmembrane interactions are mediated via a complex network of cytoplasmic proteins, forming a submembrane plaque. Additional ECM–integrin–actin-mediated adhesion sites, termed focal complexes, fibrillar adhesions, 3D-matrix adhesions, and podosomes, are related to focal adhesions, although the details of their molecular structures and functions differ. In addition to playing central roles in cell migration and morphogenesis, focal adhesions and related structures convey adhesion-triggered signals across the cell membrane, regulating cell proliferation, differentiation, and death.

Cell Adhesion

In multicellular organisms, cells adhere to their neighbors either directly or via a complex meshwork of fibers, known as the extracellular matrix (ECM). This adhesion is not a passive attachment but rather a complex process mediating specific, and dynamically regulated, cell interactions as well as crucial signaling cross-talks between the cell and its environment. Indeed, cell adhesion plays a fundamental role in embryogenesis and organogenesis as well as in cellular processes such as cytoskeletal organization, cell motility, and regulation of cell cycle and differentiation.

Moreover, cell adhesion is not a single molecularly uniform event but rather a highly diversified process at the cellular, molecular, and functional levels. For example, cell-to-cell adhesion occurs at tight junctions, gap junctions, chemical synapses, adherens junctions, desmosomes, and various carbohydrate-mediated contacts. Cell–ECM adhesions can involve a large variety of ECM proteins and glycosaminoglycans and their respective receptors, and they occur at specialized cellular sites such as intermediate-filament-associated hemidesmosomes and the widely occurring actin-associated contacts of the focal-adhesion type, which is addressed here.

Focal Adhesions—A Historical Perspective

Specialized adhesions between cultured fibroblasts and the underlying substrate were revealed over 30 years ago by interference–reflection microscopy and electron microscopy. These studies showed that the attached cells contain many specialized and defined regions (commonly measuring 0.25–2 by 2–10 μm) along the ventral plasma membrane, which are in a very tight contact (10- to 15-nm gap) with the substrate. Moreover, these sites, which were termed focal contacts or focal adhesions, appeared to be associated with the termini of actin microfilaments. These early studies revealed that focal adhesions are responsible for tight ECM contacts in which the extracellular substrate and the actin cytoskeleton are physically linked.

Following the early structural studies, the molecular composition of focal adhesions was addressed by immunofluorescence and immunoelectron microscopy, yielding a long list of diverse proteins, starting with α-actinin and vinculin. Biochemical examination of these proteins suggested that they are capable of establishing a complex network of protein–protein interactions with both cytoskeletal and signaling partners and implicated focal adhesions in both mechanical and signaling processes. Studies carried out with different cell types, in culture and *in vivo*, exposed to a variety of conditions established that focal adhesions are not the only sites mediating ECM–integrin–actin binding, and added to this group focal complexes, fibrillar adhesions, 3D-matrix adhesions, and podosomes (Figure 1).

The Molecular Organization of Focal Adhesions

Focal-adhesion components were identified, primarily by immunofluorescence, in studies conducted in many laboratories for the last two decades. More than 50 distinct proteins were reported to localize, stably or transiently, in focal adhesions and related cell–matrix

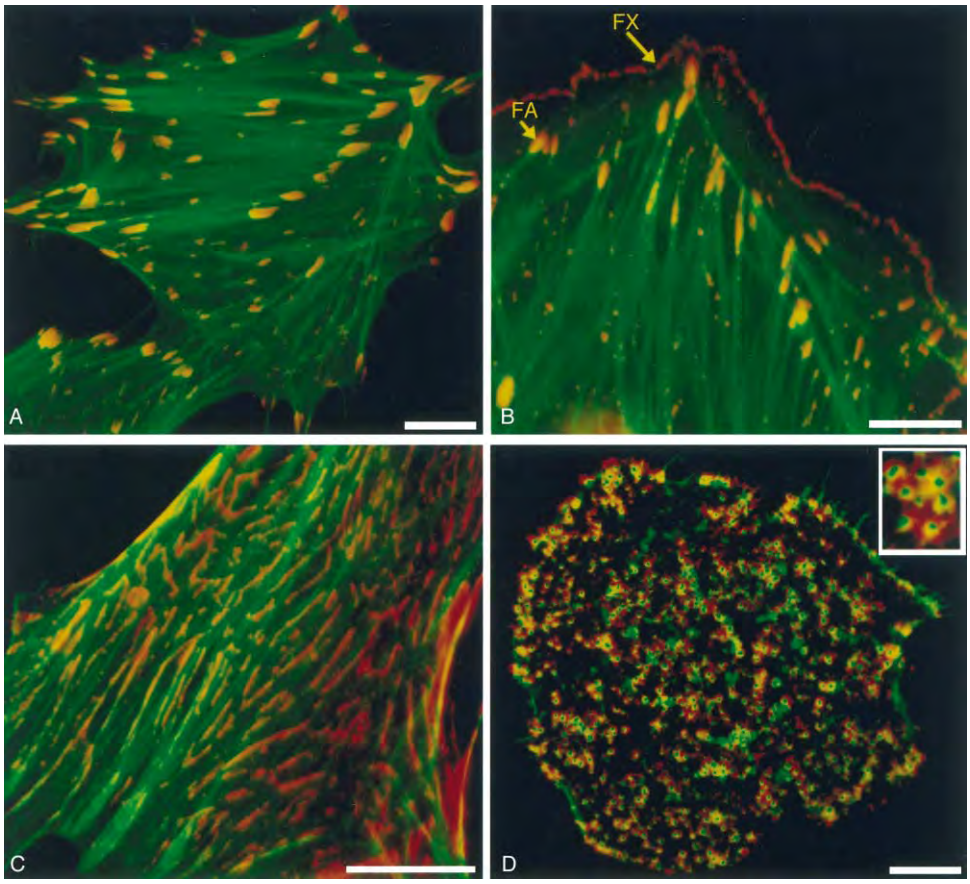

FIGURE 1 Focal adhesions and related adhesion sites. (A) Stationary human fibroblasts, stained for actin (green) and vinculin (red), having typical ovular focal adhesions located at the ends of actin stress fibers. (B) Migrating endothelial cells (porcine aortic endothelial cells, PAEC) stained for actin (green) and phosphotyrosine (red), displaying both focal adhesions (FA) and focal complexes (FX). Focal complexes have a circular morphology and are located at the edge of the lamellipodium where actin is organized as a dense network of highly branched fibers. (C) Human fibroblasts stained for actin (green) and for the fibronectin receptor $\alpha_5\beta_1$ integrin (red), which is enriched in fibrillar adhesions. (D) A mouse osteoclast, stained for actin (green) and paxillin (red), showing typical podosomes—doughnut-shaped adhesions with an actin core. The insert shows a cluster of podosomes at a higher magnification. Scale = 10 μm.

contacts. These molecules are largely segregated into three major structural domains, including the transmembrane domain, the cytoskeleton domain, and the interconnecting submembrane plaque (Figure 2).

The Receptors and their ECM Ligands

The membrane domains of ECM adhesions contain-specific integrins, which are heterodimers of α- and β-subunits that bind the ECM via a large extracellular domain. Integrins span the membrane and contain a cytoplasmic region through which they interact with plaque proteins. The most common integrins found in focal adhesions and related ECM adhesions are the fibronectin receptor, $\alpha_5\beta_1$, and the vitronectin receptor, $\alpha_V\beta_3$.

Additional, somewhat less characterized, membrane-bound components of focal adhesions include potentially adhesive molecules such as syndecan-4 and the hyaluronan-binding protein layilin, as well as the tyrosine phosphatase LAR and the glycoprotein SHPS-1, a substrate of the tyrosine phosphatase SHP-2 (Figure 2). The role of these membrane molecules is still not known.

The Cytoskeletal Domain

Focal adhesions are associated with the termini of actin bundles termed stress fibers. The polarity of the attached actin filaments is apparently uniform, with their barbed ends pointing to the membrane. That area of the actin cable is particularly enriched with actin-associated proteins such as the actin-bundling protein α-actinin. Actin is also associated with the other forms of integrin-mediated adhesion, although not in a form of stress fibers (Figure 1).

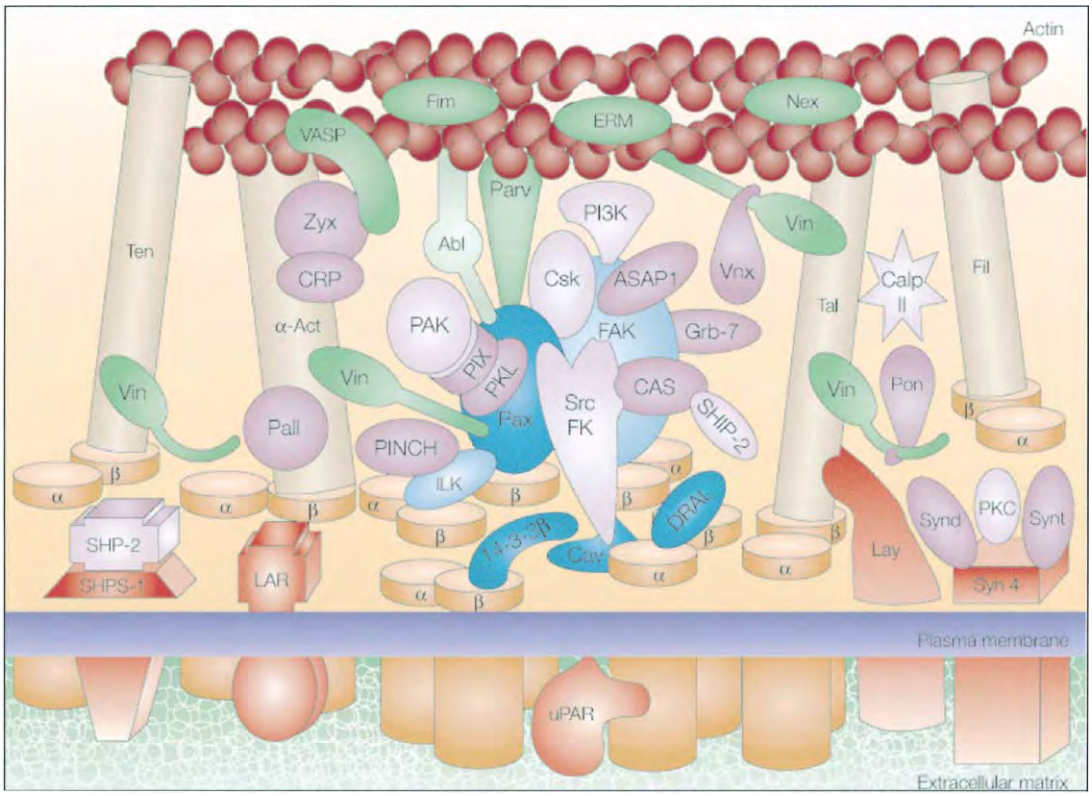

FIGURE 2 A scheme depicting the complexity of the main molecular domains of cell–matrix adhesions. The main adhesion receptors are heterodimeric (α and β) integrins. Additional membrane-associated molecules enriched with these adhesions include syndecan-4 (Syn4); layilin (Lay); the phosphatase LAR; SHPS-1, the substrate of the cytoplasmic phosphatase SHP-2; and the urokinase receptor (uPAR). Proteins that interact with both integrin and actin, and that function as the structural scaffolds of focal adhesions, include α-actinin (α-Act), talin (Tal), tensin (Ten), and filamin (Fil). Integrin-associated molecules include focal adhesion kinase (FAK), paxillin (Pax), integrin-linked kinase (ILK), DRAL, 14-3-3β, and caveolin (Cav). Actin-associated proteins include VASP, fimbrin (Fim), ezrin-radixin-moesin proteins (ERM), Abl kinase, nexillin (Nex), parvin/actopaxin (Parv), and vinculin (Vin). Other proteins, many of which may serve as adapter proteins, include zyxin (Zyx), CRP, palladin (Pall), PINCH, PKL, PIX, vinexin (Vnx), ponsin (Pon), Grb-7, ASAP1, syntenin (Synt), and syndesmos (Synd). Among these are several enzymes, such as SHP-2, SHIP-2, PAK, PI-3 kinase (PI3K), Src-family kinases (Src FK), Csk, the protease calpain II (Calp II), and PKC. Reprinted by permission from Geiger, B., Bershalsky, A., Pankov, R., and Yamada, K. M. (2001). Extracellular matrix-cytoskeleton crosstalk. *Nat. Rev. Mol. Cell Biol.* **2**, 793-805. Copyright 2001, Macmillan Magazines, Ltd.

The Submembrane Plaque

The submembrane plaque is a multiprotein complex that interconnects actin to the membrane in focal adhesions and related adhesions. Some of the plaque components contain binding domains for both actin and integrin, including talin, α-actinin, tensin, and filamin, and may function as direct integrin-actin linkers (Figure 2). Additional integrin-associated molecules do not bind directly to actin and may link the cytoskeleton to the membrane indirectly, via other plaque components. Some of them, such as focal adhesion kinase (FAK), the LIM-domain protein DRAL, integrin-linked kinase (ILK), and 14-3-3β, are signaling molecules (Figure 2).

Yet another group of focal-adhesion-associated proteins includes actin-binding proteins that were not shown to interact directly with integrins, including vinculin, VASP/Ena, and ezrin–radixin–moesin (ERM) proteins (Figure 2). Vinculin plays a pivotal role as a central linker interacting with many plaque proteins (e.g., talin, α-actinin, VASP/Ena, ponsin, and vinexin), acidic phospholipids, and actin. Finally, a very large group of proteins consists of adapter proteins, which apparently interact with actin-bound and integrin-bound components and link them to one another.

The components of cell–matrix adhesions have an unusual wide range of intrinsic activities. Beyond their protein–protein binding specificities, many of these proteins are enzymes, such as tyrosine kinases (e.g., members of the Src family and FAK), serine/threonine kinases (e.g., ILK, PKC, and PAK), tyrosine phosphatases (e.g., SHP-2 and LAR-PTP), inositol 5′-phosphatase (SHIP-2), modulators and adapters of small GTPases (e.g., ASAP1, DOCK180, PIX and GRAF),

and other enzymes such as PI 3-kinase and the protease calpain II (Figure 2). It should be pointed out that the true molecular complexity of focal adhesions is probably greater than depicted in Figure 2 because many of these components represent products of multigene families and may undergo posttranslational modification and proteolytic cleavage.

A striking characteristic of many focal-adhesion components is that they are multidomain proteins that can interact with several distinct partner molecules. For example, vinculin, FAK, Src family kinases, and paxillin can each bind to more than 10 different partners. Thus, the theoretical number of different combinations of molecular interactions that might be involved in linking integrins to actin is enormous.

Diversity of Cell–Matrix Adhesion Sites

Adhesions with the ECM are formed by essentially all adherent cells, in culture and *in vivo*. Yet their morphology, size, molecular composition, and subcellular distribution can be quite heterogeneous. These adhesions share, however, two common features: they are mediated by integrins and they interact with the actin cytoskeleton. Focal adhesions, the best-characterized form, are flat elongated structures, several square microns in area and are usually located near the periphery of cells, associated with bundles of actin microfilaments (Figures 1A and 3). The development

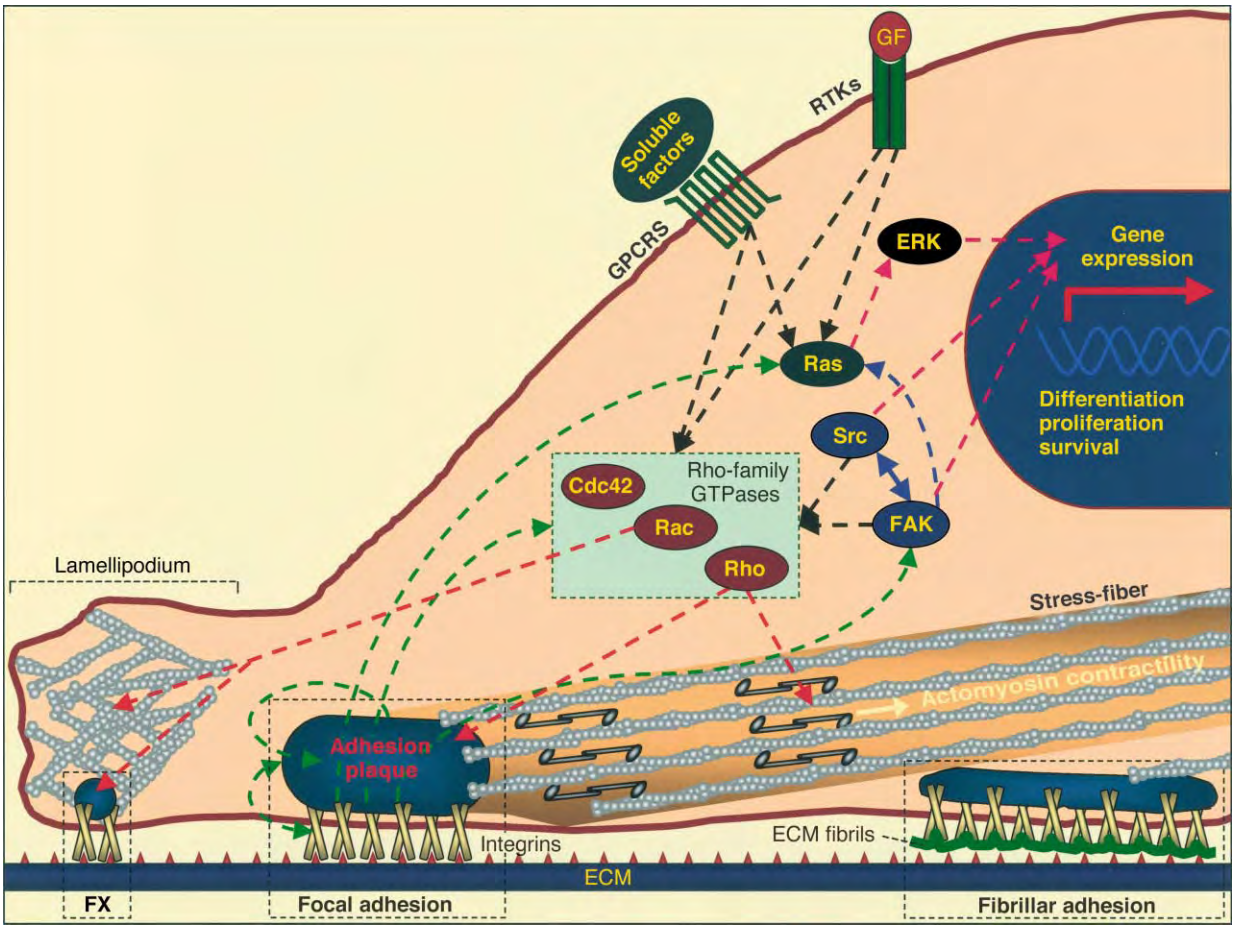

FIGURE 3 A simplified scheme highlighting the major pathways of focal adhesion mediated signaling. Rho family GTPases, including Rho, Rac and Cdc42, are regulated by integrins, growth factors (GFs), receptor tyrosine kinases (RTKs) and G protein coupled receptors (GPCRs). Cdc42 induces the formation of filopodia (not shown) and activates Rac. Rac induces the formation of a meshed network of branched actin filaments, extension of lamellipodia, and formation of focal complexes (FX). Rho induces actomyosin contractility and organizes actin in contractile bundles called stress fibers. Rho activation drives the development of focal adhesions from focal complexes. Rho-induced contractility is also essential for the development of fibrillar adhesions and their translocation toward the cell center. In adhesion sites, integrins activate locally the tyrosine kinases FAK and Src, which then regulate the enzymatic activities and interactions of many other focal-adhesion components. Integrins also affect gene expression, mainly through the activation of the Ras-ERK pathway, and thereby regulate differentiation, proliferation, and survival.

of focal adhesions is stimulated by the small GTPase Rho and requires actomyosin contractility. Characteristic focal-adhesion plaque proteins include vinculin, talin, paxillin, and tyrosine-phosphorylated proteins. Focal adhesions are particularly prominent in cultured cells growing on solid surfaces, yet structures with similar molecular properties are also found *in vivo*.

Another group of matrix adhesions is the focal complexes, which are small, dot-like adhesions present mainly close to the edges of the lamellipodium (Figures 1B and 3). These sites can be associated with cell migration or serve as precursors of focal adhesions. Their formation is induced by the Rho family GTPase Rac.

In the more central locations of many cell types, there are the fibrillar adhesions (also referred to as ECM contacts), which are elongated or dot-like structures associated with ECM fibrils (Figures 1C and 3). The typical components of fibrillar adhesions are extracellular fibronectin fibrils, the fibronectin receptor $\alpha_5\beta_1$ integrin, and the cytoplasmic protein tensin. Fibrillar adhesions emerge from focal adhesions in an actomyosin-dependent fashion.

Another form of ECM adhesions is the podosomes, which are small ($\sim 0.5\ \mu m$ diameter) cylindrical structures containing typical focal-adhesion proteins such as vinculin and paxillin (Figure 1D). Podosomes are found in a variety of malignant cells and in some normal cells such as macrophages and osteoclasts. Characteristic and indispensable proteins of podosomes are gelsolin and dynamin, which localize to tubular invaginations of the plasma membrane typical for these structures. Finally, another type of adhesion is the 3D-matrix adhesions, formed with three-dimensional ECM, which differ from focal adhesions in their overall morphology, fine molecular composition, and function.

Signaling

Focal adhesions and related structures are involved in adhesion-mediated signaling processes affecting various cellular processes such as proliferation, differentiation, anchorage-dependent survival, spreading, and migration. The main signaling paths include the stimulation of local tyrosine phosphorylation driven by FAK and Src, activation of small GTPases of the Rho and Ras family, and the extracellular signal-regulated kinase (ERK) pathway (Figure 3). It is proposed that tethering of FAK to clustered integrins leads to its autophosphorylation, recruitment of Src, and phosphorylation of their downstream targets. The presence of a variety of kinases and their substrates in the submembrane plaque suggests that additional signaling processes are activated by matrix adhesion, yet definitive information about these signaling processes is still scarce.

Focal adhesions themselves are regulated by several signaling systems. In addition to Rho and Rac, excessive Src-mediated phosphorylation and stimulation of appropriate cells by growth factors (e.g., EGF or neuregulin), phosphatases, and proteases have a profound effect on the organization of cell–matrix adhesions.

Focal Adhesions and Mechanosensitivity

Mechanical forces play a key role in the development and fate of focal adhesions and focal complexes. The transition from focal complex to focal adhesion and the growth of focal adhesions require local tension and are dramatically suppressed following treatment with inhibitors of Rho kinase or myosin light-chain kinase (Figure 4). Focal complexes do not appear to depend on actomyosin contractility and even become abundant upon inhibition of cellular contractility. Similarly, the

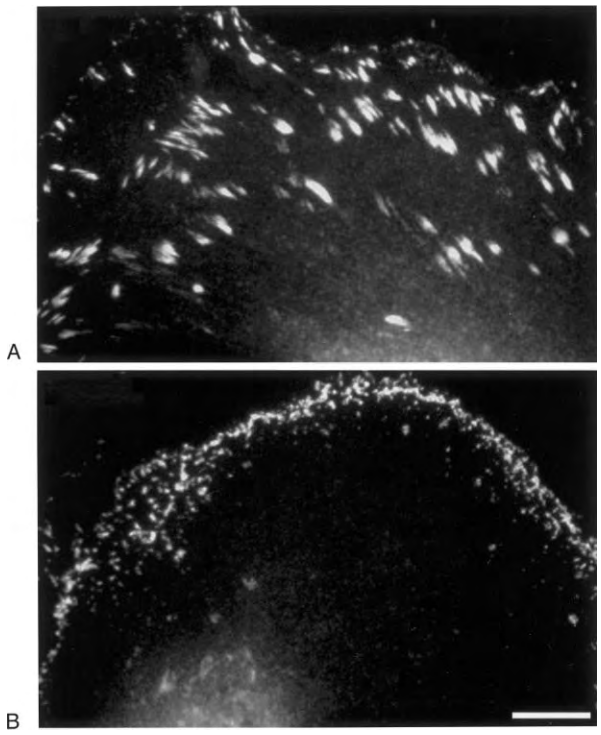

FIGURE 4 The key role of actomyosin contractility in the organization of adhesion site. Rat embryonic fibroblasts (REF52), stably expressing β_3-integrin-GFP, were either (A) untreated (control) or (B) treated with the Rho-kinase inhibitor Y-27632 prior to fixation. Inhibition of actomyosin contractility by Y-27632 causes disassembly of focal adhesions and accumulations of focal complexes. Scale = 10 μm.

maintenance of fibrillar adhesions is not affected by the inhibition of contractility, yet their emergence from peripheral focal adhesions requires actomyosin-driven tension.

See Also the Following Articles

Actin Assembly/Disassembly • Actin-Capping and -Severing Proteins • Actin-Related Proteins • Cell–Matrix Interactions • Integrin Signaling • Rho GTPases and Actin Cytoskeleton Dynamics • Src Family of Protein Tyrosine Kinases

Glossary

fibrillar adhesions Elongated or dot-like adhesions that are associated with fibronectin fibrils, mostly along the central areas of the cell.

focal adhesions Flat elongated adhesions associated with prominent actin bundles (stress fibers); also known as focal contacts. They are usually located near the periphery of the cell.

focal complexes Small dot-like adhesions located mainly at the edge of lamellipodium. They are induced by Rac, are associated with cell migration, and can develop into focal adhesions.

podosomes Small cylindrical adhesions found in osteoclasts, macrophages, and various malignant cells.

Rac A Rho family GTPase that stimulates the extension of the lamellipodium and formation of focal complexes.

Rho A Rho family GTPase that stimulates stress-fiber and focal-adhesion formation.

Further Reading

Alberts, B., Johnson, A., Lewis, J., Raff, M., Roberts, K., and Walter, P. (2002). *Molecular Biology of the Cell*. Garland Publishing, New York.

Beckerle, M. C. (2001). *Frontiers in Molecular Biology, Vol 39. Cell Adhesion*. Oxford University Press, New York.

Geiger, B., Bershadsky, A., Pankov, R., and Yamada, K. M. (2001). Extracellular matrix-cytoskeleton crosstalk. *Nat. Rev. Mol. Cell Biol.* **2**, 793–805.

Kreis, T., and Vale, R. (eds.) (1999). *Guidebook to the Extracellular Matrix, Anchor, and Adhesion Proteins*. Oxford University Press, New York.

Zamir, E., and Geiger, B. (2001). Molecular complexity and dynamics of cell–matrix adhesions. *J. Cell Sci.* **114**, 3583–3590.

Biography

Benjamin Geiger is the Head of the Department of Molecular Cell Biology, The Weizmann Institute of Science, Israel, and the incumbent of the E. Neter Chair in Cell and Tumor Biology. His research interests are the molecular basis for cell adhesion. He received a B.Sc. from Tel Aviv University, an M.Sc. from Hebrew University, Israel and a Ph.D. and Professorship from The Weizmann Institute of Science, Israel.

Eli Zamir is a Postdoctoral Fellow in the Department of Molecular Cell Biology, The Weizmann Institute of Science, Israel. His research interests are in the structural and functional diversity of cell–matrix adhesions, and in resolving the structure and function of multi-component interaction networks in cells. He received a B.Sc. from Tel Aviv University, Israel and an M.Sc. and a Ph.D. from The Weizmann Institute of Science, Israel.

Free Radicals, Sources and Targets of: Mitochondria

Alberto Boveris
University of Buenos Aires, Buenos Aires, Argentina

Enrique Cadenas
University of Southern California, Los Angeles, California, USA

Mitochondria constitute an active source of free radicals, continuously producing $O_2^{\cdot-}$ (superoxide radical) and $^{\cdot}NO$ (nitric oxide), by auto-oxidation of ubisemiquinone ($UQH^{\cdot}$) and by the enzymatic action of mitochondrial nitric oxide synthase (mtNOS), respectively. These two primary products generate a series of derived and reactive oxidizing species, as H_2O_2 and alkyl and peroxyl radicals. $^{\cdot}NO$ inhibits cytochrome oxidase, competitively with O_2, and ubiquinol–cytochrome c reductase activities. Peroxynitrite ($ONOO^-$), the product of the reaction of $^{\cdot}NO$ with $O_2^{\cdot-}$, inhibits NADH-dehydrogenase. The $[O_2]/[^{\cdot}NO]$ ratio in the tissues is consistent with a respiratory inhibition of 16–26%. The intramitochondrial production of free radicals is involved in a series of oxidative stress situations, in the syndrome of mitochondrial dysfunction, in mitochondrion-dependent apoptosis, in aging and in neurodegenerative diseases. At the same time, $^{\cdot}NO$ and H_2O_2 seem to constitute a pleitrophic signal indicating high mitochondrial energy charge.

Introduction

More than two centuries after Lavoisier's description of animal respiration as a biological oxidation, there is still a fresh and active interest in the mechanisms and the regulation of the processes that link the oxidation of food components to energy production in mammals and in the recognition that the modulation of energy production and expenditure underlies the whole process of life and death of a cell. At the foundation of biochemistry, in the 1920s, there was a controversy on how the hydrogen atoms of organic molecules would end in the H_2O molecule: there were two views – hydrogen activation and oxygen activation, championed by Wieland and Warburg, respectively. The first view involved H_2O_2 as an important intermediate and the second one supported the idea of H_2O as the direct product of O_2 reduction. The monumental contribution of Warburg, identifying cytochrome oxidase as the enzyme catalyzing the overwhelming part of O_2 uptake in biological systems, eclipsed the dispute. However, the concept of the partial reduction of O_2 in biological systems emerged again in 1946 with Michaelis' ideas of univalent electron transfer between biological molecules when he described hydroperoxyl radical ($HO_2^{\cdot}$, the protonated base of superoxide free radical: $O_2^{\cdot-}$), hydrogen peroxide (H_2O_2), hydroxyl radical ($HO^{\cdot}$), and water (H_2O) as the four steps of the univalent reduction of the O_2 molecule. These concepts were strengthened when Gerschman postulated in 1954 that oxygen-free radicals were the common biochemical mechanisms of oxygen and radiation toxicity. At that time, $HO^{\cdot}$ and $HO_2^{\cdot}$ were known as toxic species in radiation chemistry and biology, but by no means it was admitted that these highly reactive free radicals could be produced in physiological conditions. Gerschman exposed small mammals to hyperbaric O_2 to increase the tissue levels of oxygen-free radicals and found synergism between radiation and hyperbaric O_2 in decreasing the survival time of exposed mice.

The transcendental and landmark discovery of superoxide dismutase (SOD) by McCord and Fridovich in 1969 introduced a new dynamism to the understanding of free radical reactions in biological systems. The existence of the enzyme, first described in erythrocytes and later in bacteria and in mammalian organs, implied that its substrate, $O_2^{\cdot-}$, was a normal biological metabolite. In a few years, a dogma advanced by Fridovich evolved: $O_2^{\cdot-}$ and H_2O_2 interact in biological systems and produce the highly toxic $HO^{\cdot}$, which is the chemical species responsible for biological damage. The elegant classification of bacteria as aerobes (protected by superoxide dismutase and catalase), aerotolerant anaerobes (protected by superoxide dismutase but not by catalase), and anaerobes (without protection by superoxide dismutase and catalase) paved the way to the extension of the concept to mammalian biology, oxygen toxicity, and human pathology.

In parallel, mitochondria were recognized by Boveris and Chance in 1972–73 as an active source of H_2O_2 that diffuses to the cytosol. The concept collided with the idea of H_2O_2 produced and utilized in the intraperoxisomal space and avoided as a cellular metabolite. Shortly after, Boveris and Cadenas described $O_2^{\cdot-}$ as the stoichiometric precursor of mitochondrial H_2O_2 and suggested ubisemiquinone ($UQH^{\cdot}$) as the main source of $O_2^{\cdot-}$ upon auto-oxidation. Mitochondria were recognized as the more generalized and quantitatively main source of $O_2^{\cdot-}$ in mammalian organs by 1980. Other sources of $O_2^{\cdot-}$, such as polymorphonuclear leukocytes, xanthine oxidase, and liver endoplasmic reticulum, were also identified as active $O_2^{\cdot-}$ sources that proved to be decisive in specific conditions.

The existence of the family of superoxide dismutases with one of them, Mn-SOD, specific for the mitochondrial matrix, and the mitochondrial production of $O_2^{\cdot-}$ in all aerobic cells were the two ideas that gave the strongest support for the participation of oxygen-free radicals in mammalian and human physiology, pathology, and aging.

The mechanistic concept that was currently accepted for the deleterious action of oxygen-free radicals in biological systems, called the Fenton/Haber–Weiss pathway, involved a primeval and dual role for $O_2^{\cdot-}$, as precursor of H_2O_2 and as reductant of cellular Fe^{3+}, and a second reaction between H_2O_2 and Fe^{2+}, involving the homolytic scission of the peroxide bond and the generation of the highly toxic $HO^{\cdot}$.

The discovery of the generation of nitric oxide ($^{\cdot}NO$) in mammals as a signaling molecule, with roles as intercellular messenger in the cardiovascular system, as neurotransmitter, and as component of the signaling and cytotoxic mechanisms of the immunological system along with the identification of $^{\cdot}NO$ as a free radical, produced a revolution in the concepts of free radical metabolism and signaling in mammalian organs. The linear Fenton/Haber–Weiss pathway evolved to a Y-shaped scheme of the pathways of free radical reactions in mammalian organs (Figure 1).

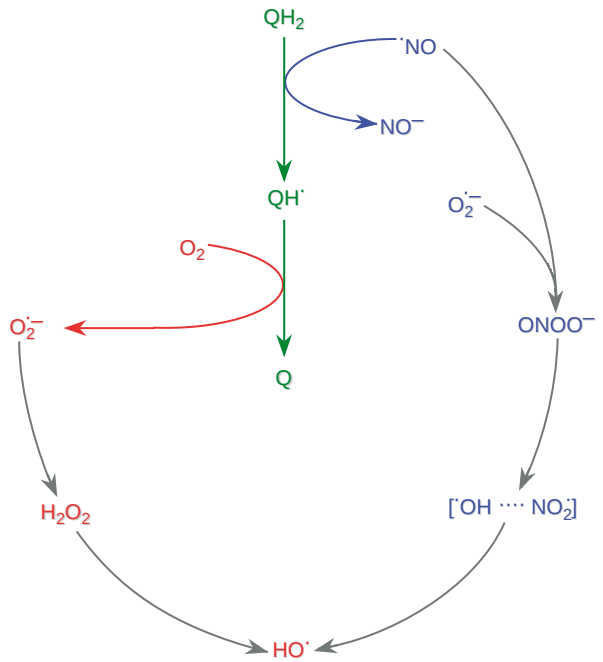

FIGURE 1 The biochemical free radical chain reactions encompassed by the redox transitions of oxygen, nitric oxide, and ubiquinone. The redox transitions of ubiquinone, oxygen, and nitric oxide are shown in green, red, and blue, respectively. $O_2^{\cdot-}$, superoxide anion, H_2O_2, hydrogen peroxide; $HO^{\cdot}$, hydroxyl radical; $^{\cdot}NO$, nitric oxide; $ONOO^-$, peroxynitrite; UQH_2, ubiquinol; $UQH^{\cdot}$, ubisemiquinone; UQ, ubiquinone.

The Mitochondrial Production of $O_2^{\cdot-}$ and H_2O_2

Mitochondria were recognized as subcellular organelles by application of supravital stainings by the end of 19th century, and as the powerhouses of cells, sites of the biochemical process of oxidative phosphorylation in the 1950s, after the availability of electron microscopy and the modern methods of cell fractionation. Mitochondrial isolation permitted the identification of the inner mitochondrial membrane as the site in which the mitochondrial complexes I–V were constitutive proteins and as the coupling membrane for the transduction of the redox chemical energy of NADH oxidation into ATP high-energy phosphate bond. By 1955, Chance and Williams produced a complete description of the redox states of the components of the mitochondrial respiratory chain, and defined the operational concepts of mitochondrial metabolic states and respiratory control. The latter concept elegantly describes the state 4 to state 3 transition in which ADP regulates the rate of mitochondrial electron transfer and respiration. State 4, with availability of respiratory substrate but not of ADP, was described as "controlled or resting respiration," whereas state 3, with ample respiratory substrate and ADP availability, was defined as the "active respiration," i.e., the maximal physiological rate of ATP production and O_2 consumption. By determination of the rates of mitochondrial O_2 uptake in both state 4 and state 3, and of the O_2 uptake of tissue slices and perfused organs, it was estimated that mammalian tissue mitochondria under physiological conditions are mostly (60–70%) in state 4, whereas the rest (30–40%) are in state 3, thus meaning that in a physiological setting there is a 30–40% utilization of the ATP-producing capacity.

Isolated mitochondria were identified as sources of H_2O_2, in a process modulated by the mitochondrial state 4/state 3 transition; the rate of H_2O_2 generation in state 4 is about 4–6 times higher than that in state 3.

This fact indicates that a component of the respiratory chain, markedly changing its redox steady state level in the state 4/state 3 transition is the H_2O_2 generator. The rates of H_2O_2 production of mitochondria isolated from mammalian organs are in the range of 0.3–0.8 nmol $H_2O_2 min^{-1} mg^{-1}$ protein for state 4 and 0.05–0.15 nmol $H_2O_2 min^{-1} mg^{-1}$ protein for state 3. In the case of rat heart and liver, mitochondrial H_2O_2 production accounts for ~0.5% of the physiological O_2 uptake.

The mechanistic option for O_2 reduction, between either one 2-electrons step to yield H_2O_2 or two 1-electron steps to yield $O_2^{\cdot-}$ as intermediate, was solved by the fact that submitochondrial particles show a 2 to 1 ratio of $O_2^{\cdot-}$ and H_2O_2 productions, thus establishing $O_2^{\cdot-}$ as the stoichiometric precursor of mitochondrial H_2O_2. The main part of mitochondrial $O_2^{\cdot-}$, ~70%, is vectorially released to the mitochondrial matrix, where it encounters specific intramitochondrial Mn-SOD. Steady state concentrations of 0.08–0.2 nM $O_2^{\cdot-}$ and 5–50 nM H_2O_2 are estimated for the mitochondrial matrix, with a content of 3–10 μM Mn-SOD. The release of $O_2^{\cdot-}$ to the mitochondrial intermembrane space, accounting for ~30% of the mitochondrial $O_2^{\cdot-}$ production, was recognized, being probably in functional relationship to the Cu,Zn-SOD of this compartment. $O_2^{\cdot-}$, from the intermembrane space is released into the cytosol through a voltage-dependent anion channel. Hence, mitochondria may be considered as effective sources of cytosolic $O_2^{\cdot-}$ and this species may contribute to the redox regulation of cell signaling.

Two main $O_2^{\cdot-}$ generating reactions have been described for the mitochondrial respiratory chain. In both cases the intermediate semiquinone form of redox pairs components of the respiratory chain, ubiquinol/ubiquinone, and the $FMNH_2$/FMN component of NADH dehydrogenase, i.e., $UQH^{\cdot}$ and $FMNH^{\cdot}$, respectively, are collisionally and nonenzymatically auto-oxidized by molecular O_2 to yield $O_2^{\cdot-}$. In the case of $UQH^{\cdot}$ auto-oxidation, the chemical process is called the Boveris–Cadenas reaction (reaction [1]) with a second-order reaction constant of $8 \times 10^3\ M^{-1}\ s^{-1}$; it is considered the main mitochondrial $O_2^{\cdot-}$-producing reaction and a biological pacemaker of the aging process.

$$UQH^{\cdot} + O_2 \rightarrow UQ + H^+ + O_2^{\cdot-} \qquad [1]$$

Figure 2 illustrates the mitochondrial reactions that produce $O_2^{\cdot-}$ as well as their vectorial release to the cytosol and to the intermembrane space. Auto-oxidation of other components of the mitochondrial respiratory chain is thermodynamically feasible, but these reactions are not kinetically important on quantitative basis.

The spontaneous surface chemiluminescence of *in situ* organs supported the idea of mitochondria as the main physiological source of oxidizing free radicals. The assay is based in the production of the chemiluminescent species singlet oxygen ($^1O_2$), a downstream by-product of the free radical recombination reactions in biological systems (Figure 1). Liver and brain chemiluminescence increased under hyperbaric O_2 and in ischemia reperfusion following a dependence on mitochondrial $O_2^{\cdot-}$ generation in these conditions.

The Mitochondrial Production of $^{\cdot}NO$

At the beginning of the 1990s, the extraordinary research activity on biological $^{\cdot}NO$ production,

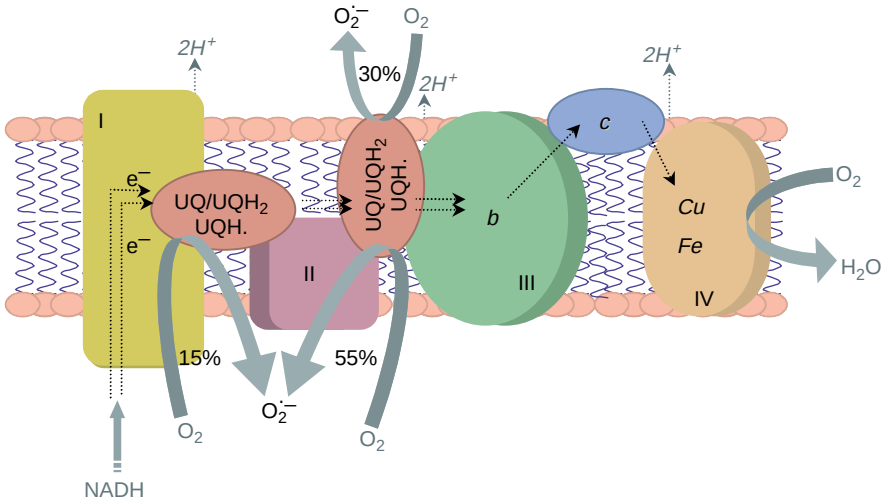

FIGURE 2 Sites of superoxide anion production in the mitochondrial respiratory chain. UQH_2: ubiquinol; UQ: ubiquinone; and $UQH^{\cdot}$: ubisemiquinone. The percentages close to superoxide anion ($O_2^{\cdot-}$) indicate the relative contribution of each reaction to the total mitochondrial $O_2^{\cdot-}$ production.

identified three different nitric oxide synthases (NOS): neuronal NOS (nNOS or NOS-I), inducible or macrophage NOS (iNOS or NOS-II), and endothelial NOS (eNOS or NOS-III). Immunocytochemical assays with antibodies against eNOS gave evidence of a nitric oxide synthase (NOS) located in mitochondria, which was named mtNOS and advanced as a regulator of mitochondrial and cellular respiration. The determination of mtNOS enzymatic activity was elusive for a few years, until two independent groups located in Zurich and Los Angeles/Buenos Aires, succeeded in showing $^{\cdot}NO$ production by rat liver mitochondria and mitochondrial fragments. The original observations in liver mitochondria were later extended to mitochondria from brain, heart, thymus, kidney, and diaphragm, thus dissipating the skepticism on mtNOS activity stemming from a contamination produced during cell fractionation. Mitochondrial $^{\cdot}NO$ production is carried out by mtNOS, a classic NOS, that requires NADPH (K_M = 12–20 μM), arginine (K_M = 5–50 μM), O_2 (K_M = 35–70 μM), and Ca^{2+} for enzyme activity. Calmodulin, tetrahydrobiopterine, and thiols increase the enzymatic activity. The intramitochondrial concentrations of NADPH, arginine, O_2, and Ca^{2+} are in excess or in the range needed for enzymatic activity. The methodology currently used to measure mtNOS activity determines NO production rates of 0.30–1.20 nmol $^{\cdot}NO\ min^{-1}\ mg^{-1}$ protein in mitochondria and submitochondrial preparations.

Recently, in a pivotal contribution, Giulivi and coworkers sequenced the 1429 amino acids of rat liver mtNOS and found it identical to nNOS splice variant αmirystoylated and phosphorylated in posttranslational processes. Transcripts corresponding to nNOSα were found in liver, brain, heart, kidney, skeletal muscle, lung, testis, and spleen. Hence, it is clear that mtNOS is a constitutive protein of the inner mitochondrial membrane with its substrates present in the mitochondrial matrix. Interestingly, a whole series of physiological situations were reported to regulate the level and activity of mtNOS that were up-regulated during brain development, by cold exposure, and by acute hypoxia, and down-regulated by thyroxin and angiotensin II. Treatments with enalapril, the converting-enzyme inhibitor, increased mtNOS activity. Pharmacological administration of haloperidol and chlorpromazine decreased brain mtNOS activity.

Intramitochondrial steady-state concentrations of $^{\cdot}NO$ are calculated as 20·50 nM and a release of 29 nM $^{\cdot}NO$ was electrochemicaly measured after supplementation of a single mitochondrion with Ca^{2+}. In the tissues under physiological conditions with a steady-state oxygenation of 20 μM O_2, the $[O_2]/[^{\cdot}NO]$ ratio is 500–1000, which competitively inhibit cytochrome oxidase by 16–26%. $^{\cdot}NO$ and $O_2^{\cdot-}$ metabolism in the mitochondrial matrix are linked by the very fast reaction between $^{\cdot}NO$ and $O_2^{\cdot-}$ to produce $ONOO^-$. This oxidative utilization of $^{\cdot}NO$ is the main (60–70%) pathway of $^{\cdot}NO$ metabolism, but at the same time it is only a minor part (15%) of intramitochondrial $O_2^{\cdot-}$ utilization. The reductive utilization of $^{\cdot}NO$ by ubiquinol and cytochrome oxidase provides a minor (20%) pathway of $^{\cdot}NO$ catabolism. The cellular conditions in which $^{\cdot}NO$ diffuses from mitochondria to cytosol, as well as the conditions in which $^{\cdot}NO$ diffuses from cytosol to mitochondria are unsolved questions for the complex process of intracellular signaling. Figure 3 shows a view of the integrated metabolism of $O_2^{\cdot-}$ and $^{\cdot}NO$ in mitochondria.

The effects of $^{\cdot}NO$ on mitochondrial electron transfer were reported in 1994 by two British research groups as the inhibition of brain and muscle cytochrome oxidase (complex IV) activity by low $^{\cdot}NO$ concentrations within a reversible and O_2-competitive biochemical process. The observation was rapidly confirmed by other groups using $^{\cdot}NO$ donors and pure $^{\cdot}NO$ in liver, heart, and brown fat mitochondria. $^{\cdot}NO$ levels of 0.1–0.3 μM decreased cytochrome oxidase activity and mitochondrial respiration to one half. The inhibition is reversible by dilution, hemoglobin supplementation, or exposure to $O_2^{\cdot-}$. The O_2-competitive inhibition of cytochrome oxidase renders the inhibition more important at low O_2 concentrations; ratios of $^{\cdot}NO/O_2$ affinities of 150–500 were reported for enzymatically active cytochrome oxidase. A second sensitive point in the mitochondrial respiratory chain is at the ubiquinol–cytochrome *c* reductase segment (complex III); half inhibition of electron transfer between cytochromes *b* and *c* occurs at 0.2–0.4 μM $^{\cdot}NO$, enhancing the production of $O_2^{\cdot-}$ and H_2O_2 in submitochondrial particles and in mitochondria. A third sensitive point is located at NADH-dehydrogenase (complex I), in this case, $ONOO^-$ appears as the effective inhibitory agent.

Figure 4 illustrates the direct and indirect effects of $^{\cdot}NO$, in the latter case through $ONOO^-$ formation, on the mitochondrial respiratory chain. The reversible effects of $^{\cdot}NO$ on cytochrome oxidase and ubiquinol-cytochrome *c* reductase are two sides of the regulation of mitochondrial respiration by $^{\cdot}NO$. On the one hand, the inhibition of cytochrome oxidase and, on the other, the supply of $O_2^{\cdot-}$ to remove the respiratory inhibition, as it may become a physiological need with high steady-state concentrations of $^{\cdot}NO$, as it is the case in ischemiareperfusion and in inflammation. The irreversible effects of $ONOO^-$ on complexes I and III are related to situations in which sustained high levels of $ONOO^-$ lead to mitochondrial dysfunction and apoptosis.

Concerning the important question of whether or not mtNOS enzymatic activity regulates mitochondrial functions under physiological conditions, several reports described the modulation of mitochondrial O_2 uptake and H_2O_2 production by the activity of mtNOS in

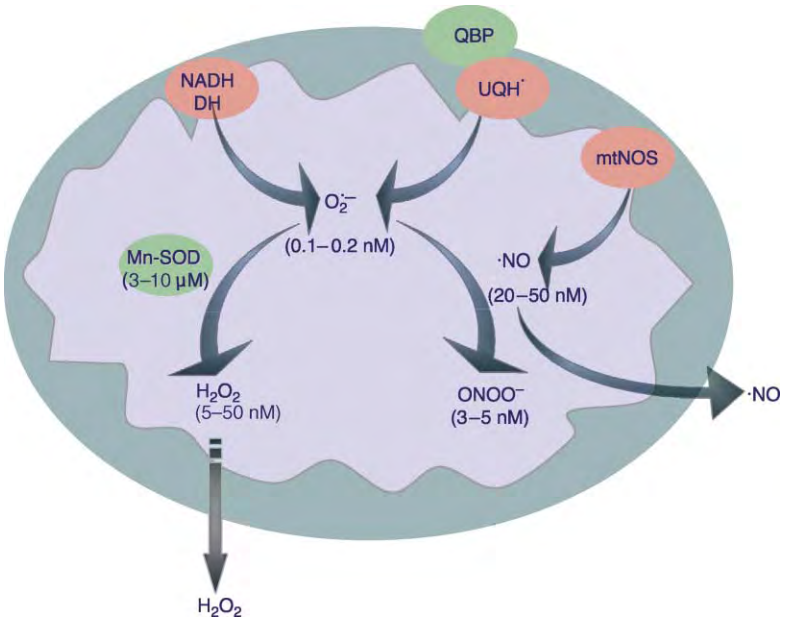

FIGURE 3 Metabolism of superoxide radicals and nitric oxide in the mitochondrial matrix. The numbers below the symbols indicate physiological steady-state concentrations for mammalian organs. The arrows reaching outside the mitochondrion indicate diffusion of H_2O_2 and ·NO to the cytosol. QBP: ubiquinone binding protein; NADH DH, NADH dehydrogenase; mtNOS, mitochondrial nitric oxide synthase; Mn-SOD, Mn-superoxide dismutase.

isolated mitochondria. The current view is that mtNOS does regulate mitochondrial respiration; hence, mtNOS, cytochrome oxidase, and F_1-ATPase are the three regulatory proteins of cellular O_2 uptake and energy production. The biochemical activity of mtNOS (expressed as nmol ·NO min^{-1} mg^{-1} protein) is usually measured as the difference in ·NO production between the assay performed in the presence of arginine and in the presence of a competitive inhibitor of NOS, such as NMMA or NNA. The *regulatory activity* of mtNOS is best expressed by the difference in the rates of O_2 uptake or H_2O_2 production between the system supplemented with arginine, the highest mtNOS activity, and the system in the presence of the NOS inhibitor, the lowest

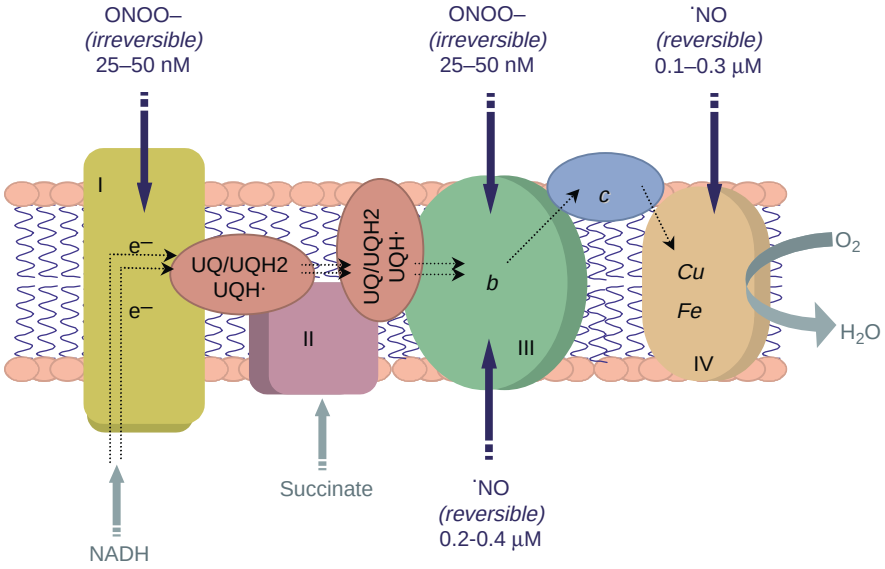

FIGURE 4 Sites of action of nitric oxide and peroxynitrite in the mitochondrial respiratory chain. Reversible and irreversible indicate the type of inhibition and are understood as regulatory or toxic processes, respectively. The indicated steady-state concentrations were determined or estimated to reduce enzymatic activity to one half, at a concentration of 100–150 μM O_2.

mtNOS activity. The *regulatory capacity* of ·NO, estimated as the ratio of the rates of *regulated* O_2 *uptake*/·NO production or of *regulated* H_2O_2 *production*/·NO production is ~70 for O_2 uptake and ~0.4 in H_2O_2 production. The activity of mtNOS in isolated mitochondria markedly increased the $[O_2]_{0.5}$ of mitochondrial O_2 uptake from 1.1 μM O_2 in the case of inactive mtNOS, to 2.2 μM O_2 in the case of an active mtNOS. However, it is not clear to what extent these effects, observed with isolated mitochondria, occur under physiological conditions in myoglobin-containing tissues and in blood-perfused organs, due to the high affinity of the two mentioned hemoproteins for ·NO.

The Physiological Role of the Mitochondrial Production of $O_2^{\cdot-}$, H_2O_2, and ·NO

The early recognition that $O_2^{\cdot-}$ and H_2O_2 are both able to initiate reactions harmful to cell and tissues is now complemented by the concept that both $O_2^{\cdot-}$ and H_2O_2 are carefully regulated metabolites capable of signaling the regulatory devices of the biochemical and genetic systems of the cell. ·NO was initially recognized as an intercellular messenger and later as an intracellular regulator. At present, the three chemical species are considered to participate in integrated processes of intracellular regulation and in intercellular signaling, communication, and cytotoxicity. The redox regulation of gene expression and intercellular communication is just starting to be understood as a vital mechanism in health and disease.

The fine regulation by H_2O_2 of cell function was advanced by Antunes and Cadenas in 2001 when they showed that in Jurkat T-cells, steady-state concentrations below 0.7 μM H_2O_2 place cells in a proliferative state, whereas at 1.0–3.0 μM, H_2O_2 cells develop programmed cell death, and at levels higher than 3.0 μM H_2O_2 cells undergo necrosis. H_2O_2 and ·NO share the chemical properties of being uncharged and the biological property of being highly diffusible through biological membranes, at variance with $O_2^{\cdot-}$ and $ONOO^-$ that are charged and non-diffusible molcules. Consequently, the first two species are suitable for cellular and intercellular signaling, and the two latter for signaling and cytotoxicity in confined spaces.

There is evidence that H_2O_2 and ·NO are able to modulate mitogen-activated protein kinases (MAPKs), the widespread integral components of intracellular phosphorylation and dephosphorylation signaling cascades involved in cell survival, proliferation, differentiation, and death. The interactions are complex and seem to involve intracellular glutathione and $ONOO^-$. Both, H_2O_2 and ·NO diffusing from mitochondria to the cytosol are considered to constitute a pleiotropic signal involved in the regulation of a series of cellular processes, among them JNK signaling…NO diffusing from mitochondria may also modulate (inactivate) JNK1 via S-nitrosylation. The concept of narrow ranges of intracellular messenger molecules for different or opposite biological actions, as observed for H_2O_2 levels in the proliferation/apoptosis transition, is now applied to effector systems with two regulators, H_2O_2 and ·NO, with the consequence of four different responses for the combination of the two binary conditions of low and high level of the two signals (Figure 5).

It has been understood for the last 30 years that excess generation of $O_2^{\cdot-}$ and H_2O_2 leads to oxidative stress and harmful biological situations. ·NO has been added to these two species in the last decade. The classical concept of oxidative stress, as brought forward by Sies implies an imbalance between oxidants and antioxidants, in favor of the former. The situation is understood as reversible, especially by supplementation with antioxidants, and also as leading, sooner or later, to biological dysfunction. The concept is applicable to subcellular organelles, cells, organs, systems, or whole organisms. From a biochemical perspective, oxidative stress is determined by an increased steady-state level of at least one of the oxidant species ($O_2^{\cdot-}$, H_2O_2, ·NO, $ONOO^-$, $HO^{\cdot}$, $ROO^{\cdot}$, and $^1O_2$) that leads to increased levels of the other oxidizing species downstream of the

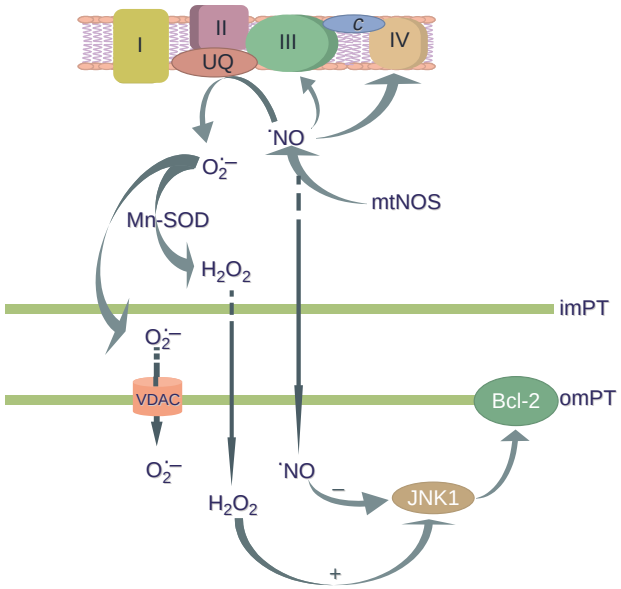

FIGURE 5 Mitochondrial production of oxygen- and nitrogen-centered radicals and cell signaling. The scheme shows the sites of action of nitric oxide (·NO) on the respiratory chain, the ensuing production of $O_2^{\cdot-}$ and H_2O_2, the release of these reactive species from the mitochondrion (controlled by VDAC in the case of $O_2^{\cdot-}$), and their effect on JNK signaling.

free radical pathways (Figure 1) and to biochemical damage.

Oxidative Stress and Dysfunctional Mitochondria: Mitochondria as Targets of Free Radicals

In the last few years, the concept of dysfunctional mitochondria was associated with mitochondrial features under oxidative stress, biological damage, and pathological conditions. Mitochondria are considered dysfunctional by comparison of their functions and properties with normal control mitochondria. The classic mitochondrial properties, that reflect their energy-producing physiological function, i.e., the state 3 rate of O_2 uptake, the respiratory control, the membrane potential, and the ADP:O ratio, are the parameters that, when decreased, support the contention of dysfunctional mitochondria. In addition, dysfunctional mitochondria frequently show increased rates of $O_2^{\cdot-}$ and H_2O_2 production.

Mitochondrial dysfunction is a mitochondrial syndrome that has been observed in ischemia/reperfusion, endotoxic and septic shock, a series of pathological situations, and aging. The syndrome is characterized by decreases in the rates of state 3 respiration and ATP synthesis, in mitochondrial membrane potential, and in respiratory control ratio, and by increases in the rate of state 4 respiration, and mitochondrial size and fragility. The reported decreases in the rates of state 3 respiration and of mitochondrial electron transfer are in the range of 30–40%; it seems that more damaged mitochondria are not compatible with living cells. There are three main chemical species involved in the molecular mechanism of this syndrome; the triad is constituted by $O_2^{\cdot-}$, $^{\cdot}NO$, and peroxynitrite ($ONOO^-$). The first chemical species is the free radical $O_2^{\cdot-}$, that is continuously produced in the auto-oxidation of $UQH^{\cdot}$ and $FMNH^{\cdot}$, intermediates of the respiratory chain function, and mainly dismutates to H_2O_2. The second free radical is $^{\cdot}NO$, that is continuously produced by mtNOS as regulator of respiration and mainly converted to $ONOO^-$. The latter, the third member of the triad, is produced by collision of $O_2^{\cdot-}$ and $^{\cdot}NO$ in the fastest reaction known in biological systems ($k = 1.9 \times 10^{10}\ M^{-1}\ s^{-1}$), except for the neutralization reaction of H^+ and HO^- ($k = 14 \times 10^{10}\ M^{-1}\ s^{-1}$). Peroxynitrite is a powerful oxidant, that when produced in excess, as in ischemia/reperfusion and inflammation, produces tyrosine nitration of intramitochondrial proteins. Intramitochondrial levels of 3–5 nM $ONOO^-$ have been estimated for physiological conditions, and levels above 20−30 nM are considered cytotoxic. The whole syndrome of dysfunctional mitochondria appears mainly driven by excess $^{\cdot}NO$ and $ONOO^-$.

Selective inhibition of NADH-dehydrogenase (complex I) activity in submitochondrial particles by $ONOO^-$ has been reported. Complex I dysfunction was also reported in animal models and in human neurodegenerative diseases. This selective mitochondrial defect is understood as secondary to a sustained oxidative stress and was reported in aged humans and in patients with neurodegenerative disorders, among them Parkinson's and Alzheimer's diseases. The near-target generation of $O_2^{\cdot-}$ by NADH-dehydrogenase and of $ONOO^-$ after molecular collision of $O_2^{\cdot-}$ with matrical $^{\cdot}NO$, is considered determinant in the selective impairment of complex I in neurodegenerative diseases.

The continuous mitochondrial production of free radicals and oxidizing species makes mitochondria the quantitatively most important source of these harmful species in the cell, and, at the same time, the sensitivity of mitochondrial functions to increased levels of the oxidizing free radicals and related chemical species renders mitochondria the most sensitive cellular target for the deleterious action of free radicals. The rapid mitochondrial turnover ($t_{1/2}$ of about 7 and 28 days in liver and brain, respectively) seems to reflect this double role of mitochondria as source and target of biologically harmful free radicals.

Mitochondrion-Dependent Apoptosis

The role of mitochondria in apoptosis is now well-established; a specific mitochondrion-dependent pathway of cell death is differentiated from the death-receptor-mediated apoptosis. Mitochondrion-dependent apoptosis entails oxidative stress and is modulated by MAPK signaling through JNK activation associated with Bcl-2 down-regulation, cytochrome *c* release, and the downstream activation of caspases. A very early activation of mtNOS has been reported in thymocyte-induced apoptosis. Thapsigargin supplementation of isolated thymocytes sequentially increases cytosolic Ca^{2+} and the activities of mtNOS and of the NOS of endoplasmic reticulum. A crosstalk between mitochondria and endoplasmic reticulum, in which Ca^{2+} and $^{\cdot}NO$ are the signals, is established in the initial phase of thymocyte apoptosis followed by the well-established mitochondrial changes that are characteristic of mitochondrion-mediated apoptosis: fall in mitochondrial membrane potential, mitochondrial dysfunction, opening of the membrane transition pores (MTP), and cytochrome *c* release.

The central role of mitochondria in the cell death program is exerted during the first and reversible phase of early apoptosis through the release of H_2O_2 and $^{\cdot}NO$ to either activate or inhibit cytosolic JNK, respectively, which attached to mitochondria catalyzes phosphorylation of Bcl-2 and Bcl-x_L and other not yet identified mitochondrial proteins. JNK-mediated phosphorylations initiate the steps to the second and irreversible phase of apoptosis by opening the inner membrane transition pore and by releasing $Ca^{2+}$and $O_2^{\cdot -}$ to the intermembrane space, followed by the opening of the outer membrane transition pore and release of cytochrome *c* to the cytosol. The next steps in the execution of the cell death program, such as apoptosome assembly and caspase activation, are independent of mitochondrial intervention.

The Mitochondrial Hypothesis of Aging

In the last few years, a strong current of opinion has linked the processes of mitochondrial oxyradical production, continuous oxygen toxicity, aging, and lifespan, in "the mitochondrial hypothesis of aging" following the idea of mitochondria as the biological clock. The free radical theory of aging was proposed by Harman in 1956 and considered that aging was caused by the cumulative and random effects of free radicals; an increased median lifespan in rats and mice supplemented in their food with organic antioxidants was observed. The continuous mitochondrial production of $O_2^{\cdot -}$ and $^{\cdot}NO$ as primary free radicals, with a whole series of derived reactive species, such as H_2O_2, $ONOO^-$, $HO^{\cdot}$, $ROO^{\cdot}$, and $^1O_2$, supports the notion of mitochondria as pacemakers of organ aging. As mentioned above, increased intramitochondrial steady-state concentrations of reactive oxygen and nitrogen species have been associated to the appearance of dysfunctional mitochondria in situations of acute oxidative stress, such as ischemia/reperfusion, and endotoxic or septic shocks. The persistence of a chronic oxidative stress situation is considered an effective aging factor. It is worth noting that increased levels of oxidative stress markers, such as 8-hydroxydeoxyguanosine, protein carbonyls, hydroperoxides, and TBARS, have been reported upon aging. Dysfunctional mitochondria, with decreases in the state 3 respiration, membrane potential, and respiratory control, and with increased size have been reported upon aging. Interestingly, some of the altered parameters were partially or totally normalized by treatment with antioxidants.

It is noteworthy that some mitochondrial macromolecules appear selectively damaged upon aging. In this way, mitochondria are the pacemaker of aging, both as the main continuous source and as the main target of oxidizing free radicals. Ames and co-workers pioneered the field with the observation of increased mtDNA damage, expressed as the level of 8-hydroxy-deoxyguanosine in tissues and in urine and in old animals as compared with young ones. Other mitochondrial macromolecules, such as mtRNA and the regulatory factor Bcl-2, have been reported damaged upon aging. Some mitochondrial enzymatic activities as NADH-dehydrogenase, cytochrome oxidase, adenine nucleotide translocase, and carnitine-acyl transferase are selectively decreased upon aging. There is a hypothesis linking these observations that considers that damaged mtDNA and mtRNA will produce, through mitochondrial protein synthesis, faulty polypeptides that would contribute along with protein carbonyls, hydroperoxides, and TBARS, to sub-optimal enzyme function and the appearance of dysfunctional mitochondria. The latter would signal for lysosomal digestion and for apoptosis. The decrease in energy availability and in tissue-active cells, as consequence of the decreased amount of mitochondria and of the enhanced apoptosis, would lead to the reduction in tissue function that is characteristic of tissue aging.

See Also the Following Articles

Cell Death by Apoptosis and Necrosis • Cytochrome *c* • Mitogen-Activated Protein Kinase Family • Nitric Oxide Signaling • Superoxide Dismutase

Glossary

apoptosis The active process by which cells execute a series of processes leading to cell death in a way that is not harmful for the tissue and the organism. It is opposite to inflammation and necrosis, a process in which toxic products reach the neighbor cells.

free radicals Molecules, better understood as chemical species, having an unpaired electron in their external orbitals. The feature makes the chemical species unstable and highly reactive with low specificity. However, some biologically produced free radicals, such as superoxide radicals ($O_2^{\cdot -}$) and nitric oxide ($^{\cdot}NO$), are relatively stable and quite selective in their reactions. Other biologically produced radicals, such as hydroxyl, alkyl and peroxyl ($HO^{\cdot}$, $R^{\cdot}$, $ROO^{\cdot}$) radicals, are highly reactive and unspecific. The point near the chemical symbols indicates the unpaired electron.

hydrogen peroxide The product of the bivalent reduction of the oxygen molecule (HOOH; H_2O_2); it is not a free radical, but originates $HO^{\cdot}$ radical upon interaction with Fe^{2+}.

mitochondrial electron transfer chain A series of biological and organic molecules embedded in the inner mitochondrial membrane that have chemical groups able to undergo reversible cycles of reduction/oxidation. The function of the mitochondrial respiratory chain channels the reducing equivalents from food components to the oxygen molecules and constitute the biochemical basis of respiration.

Further Reading

Beckman, K. B., and Ames, B. N. (1998). The free radical theory of aging matures. *Physiol. Rev.* **78**, 547–581.

Boveris, A., and Cadenas, E. (1982). Production of superoxide radicals and hydrogen peroxide in mitochondria. In *Superoxide Dismutase* (L. W. Oberley, ed.) Vol II, pp. 15–30. CRC Press, Boca Raton, Florida.

Boveris, A., and Cadenas, E. (2000). Mitochondrial production of hydrogen peroxide, regulation by nitric oxide and the role of ubisemiquinone. *IUBMB Life* **50**, 1–6.

Boveris, A., Cadenas, E., Reiter, R., Filipkowski, M., Nakase, Y., and Chance, B. (1980). Organ chemiluminescence: Non-invasive assay for oxidative radical reactions. *Proc. Natl. Acad. Sci. USA* **77**, 347–351.

Chance, B., Sies, H., and Boveris, A. (1979). Hydroperoxide metabolism in mammalian organs. *Physiol. Rev.* **59**, 527–605.

Elfering, S. L., Sarkela, T. M., and Giulivi, C. (2002). Biochemistry of mitochondrial nitric oxide synthase. *J. Biol. Chem.* **277**, 38079–38086.

Fridovich, I. (1976). Oxygen radicals, hydrogen peroxide and oxygen toxicity. In *Free Radicals in Biology* (W. A. Pryor, ed.) Vol 1, pp. 239–277. Academic Press, New York.

Gerschman, R., Gilbert, D., Nye, S. W., Dwyer, P., and Fenn, W. O. (1954). Oxygen poisoning and X-irradiation: A mechanism in common. *Science* **119**, 623–626.

Greenamyre, J. T., Sherer, T. B., Betarbet, R., and Panov, A. V. (2001). Complex I and Parkinson's disease. *IUBMB Life* **52**, 135–141.

Ignarro, L. J. (2000). Introduction and overview. In *Nitric Oxide: Biology and Pathobiology* (L. J. Ignarro, ed.) pp. 3–19. Academic Press, New York.

Kroemer, G., Dallaporta, B., and Resche-Rigon, M. (1998). The mitochondrial death/life regulators in apoptosis and necrosis. *Annu. Rev. Physiol.* **60**, 619–642.

Biography

Alberto Boveris is a Professor of Physical Biochemistry at the University of Buenos Aires (Argentina). He has B.S. degrees in pharmacy and biochemistry and a Ph.D. from the same university. During 1975–79, Boveris and Cadenas described the mitochondrial production of superoxide radical and hydrogen peroxide. His current research interests are aging mechanisms, organ chemiluminescence, and mitochondrial nitric oxide synthase.

Enrique Cadenas is a Full Professor and Chairman of Molecular Pharmacology and Toxicology at the School of Pharmacy of the University of Southern California. He holds an M.D. and a Ph.D. from the University of Buenos Aires (Argentina) and an honorary Ph.D. from the University of Linköping (Sweden). His fields of investigation include quinone redox reactions and mitochondrial metabolism and signaling.

Friedreich's Ataxia

Paul E. Hart and Anthony H. V. Schapira
University College London, London, UK

Friedreich's ataxia (FRDA) is an autosomal-recessive disorder that causes ataxia, sensory loss, cardiomyopathy, skeletal abnormalities, and in a proportion of patients diabetes and optic atrophy. It is the commonest inherited ataxia with an estimated prevalence of 1:29 000. Carrier prevalence is between 1:60 and 1:90. The responsible gene and its gene product, frataxin, have both been identified. Ongoing investigations into the function of frataxin, and the pathophysiology of FRDA are opening up new avenues for therapeutic intervention in this devastating neurodegenerative disorder.

Historical Perspective

In a series of five papers published between 1863 and 1877, Nicholaus Friedreich reported nine members of three families who had onset in puberty of ataxia, dysarthria, sensory loss, muscle weakness, scoliosis, foot deformity, and cardiac symptoms. Areflexia was only described in the final two reports, but was later adopted as one of the clinical diagnostic criteria. Over a century later the elucidation of the molecular mechanism of Friedreich's ataxia (FRDA), and the availability of genetic testing for diagnosis, allowed greater clarity regarding the phenotypic spectrum of this disorder.

Clinical Features

Disease onset ranges from 1.5 to 51 years in reported series. Loss of ambulation has been reported to occur at a mean of 15.5 $\pm$ 7.4 years after disease onset but ranges between 3 and 44 years. Death is most commonly as a consequence of cardiomyopathy and is at a mean age of 37.5 $\pm$ 14.4 years. Retrospective analysis of disease progression has reported a mean time to wheelchair confinement of 11 years. Atypical presentations include onset over the age of 25 years (late-onset Friedreich's ataxia (LOFA)), the preservation of lower limb reflexes (Friedreich's ataxia with retained reflexes (FARR)), and presentation as a pure spastic paraparesis, spastic ataxia (Acadian FRDA), pure sensory ataxia, or chorea.

Pathology

Pathological studies of FRDA report changes maximal in dorsal root ganglia, dorsal columns, corticospinal tracts, and heart. Macroscopically the spinal cord is atrophic with the posterior and lateral columns particularly affected. Changes within the nervous system are thought to be the consequence of a dying back process from the periphery affecting the longest and largest myelinated fibres that show changes of an axonopathy. Demyelination is seen in the dorsal columns. The cerebellar cortex shows only mild neuronal loss, but the dentate nucleus, and Clarke's column in the cord show marked changes. The cerebellar and occipital cortex, show reduced phospholipid levels in the absence of neuronal loss.

Genetics

In 1988 the FRDA gene was mapped to chromosome 9. The gene was linked to 9q13-21.1 in 1990 and cloned in 1996. Ninety-eight percent of cases are now known to be the result of a homozygous GAA triplet repeat expansions in intron 1 of the FRDA gene. This is a unique trinucleotide repeat (TNR) disorder in that its inheritance is autosomal recessive, its location is intronic, and it involves a GAA trinucleotide as opposed to CAG repeat as found in the majority of TNR disorders. The repeat length in normal individuals is 6-34, but is expanded in patients and carriers to between 67 and 1700. Repeat lengths are unstable. Paternal transmission is associated with a reduction in repeat length, an effect that increases with increasing paternal age. Maternal transmission can cause an increase or decrease in repeat length, and expansions are greater with increasing maternal age. The remaining 2% of patients are compound heterozygotes harboring an expanded repeat on one allele and a point mutation on the other. Twenty-three different point mutations are described to date and include missense, frameshift, splice site, initiation codon, and nonsense mutations. The former are found only in the C-terminal suggesting that functional domains reside in this part of the protein.

The location of these mutations in highly or poorly conserved amino acids correlates with the severity of the phenotype and the presence of atypical features. No cases resulting from homozygous point mutations have been described, although the population incidence of such individuals has been calculated to be $1{:}100 \times 10^6$. Clinically typical FRDA may occur in individuals in the absence of linkage to chromosome 9 suggesting that a second locus may exist.

Phenotype–Genotype Correlations

Clinical parameters correlate with the repeat length size. The size of GAA1 (the larger repeat allele) accounts for between 33% and 73% of the variation in the age of onset in various studies. GAA2 (the smaller allele) accounts for less than 20% of this variability. Indeed, GAA1 correlated better than GAA2 for several disease parameters and disease complications, including cardiomyopathy, in all studies except one. By contrast, the development of diabetes mellitus in FRDA correlated in only one study.

Further variation may result from other factors. The GAA repeat length may vary in a tissue-specific pattern due to mitotic instability, and peripheral blood samples may be a poor indicator of repeat lengths in pathologically affected tissues. GAA1 has been shown to differ in different brain regions and in various tissues. *Cis*-acting factors may also influence the phenotype. Potential mechanisms would include effects upon the stability of the trihelix structure by sequence alterations within or flanking the GAA expansion. Other genetic or environmental factors may also exert an influence on the phenotype. This is illustrated by the finding that the age of onset in sibs correlates strongly regardless of the degree of difference between their repeat lengths.

Gene and Gene Product

The FRDA gene contains seven exons within 80 kb of nuclear DNA. Transcription most commonly generates a 1.3 kb product translated into a 210 amino acid protein named frataxin. Alternative splicing generates a 171 amino acid protein of uncertain significance. Frataxin and mRNA levels are maximal in tissues of high mitochondrial content (heart, pancreas, liver, and skeletal muscle), although not all of these exhibit obvious clinical involvement in FRDA. Within the CNS, mRNA levels are highest in the cord, low in the cerebellum, and very low in the cerebral cortex. Frataxin appears to play a role in development; its homozygous knockout is lethal at an early embryological stage. Frataxin mRNA levels are high in fetal spinal cord, dorsal root ganglion, heart, liver, skeletal muscle, and skin. Lymphocytes from patients with homozygous expansions contain low levels of frataxin and these levels, and that of the mRNA, are inversely related to the size of the smaller repeat. The block is thought to occur at the level of transcript elongation, and the mechanism for this is believed to be through the formation of unusual DNA structures, such as DNA triplexes, by the GAA/TTC repeats. Several point mutations appear to alter the secondary structure of the protein and thus influence mitochondrial uptake or cleavage.

The function of frataxin is incompletely understood. The amino acid sequence shows no strong homology to any proteins of known function. It has, however, been shown to contain an N-terminal mitochondrial targeting sequence in its first 55 amino acids. The predicted mitochondrial location was confirmed when tagged expressed frataxin was shown to colocalize with mitochondrial markers in HeLa and COS cells. An inner membrane and a matrix location within the mitochondrion have both been proposed. X-ray crystallography studies reveal similarities to ferritin, a site for protein–protein interaction, and the ability to bind one molecule of iron. Point mutations in the protein core cause more severe phenotypes than those within the ferritin-like anionic patch, or flat external protein interaction surface.

A number of animal and cell models of FRDA, including transgenic mice, have provided insights into the pathogenesis of FRDA. Increased susceptibility to oxidative stress, increase in cellular and mitochondrial iron content, defects of the iron–sulfur center containing complexes of the mitochondrial respiratory chain, and reduced mitochondrial DNA levels have all been reported. Some of these changes have also been reported in human tissue. A role for frataxin in mitochondrial iron–sulfur (Fe–S) center synthesis has been proposed. The exact relationship between these biochemical perturbations remains incompletely understood.

Therapeutic Intervention

Based on the improved understanding of the pathogenesis of FRDA, a number of novel therapeutic strategies have been evaluated. Iron chelation restores mitochondrial iron levels and prevents MRC dysfunction in yeast models, but their *in vivo* use has been problematic. Antioxidants, including idebenone, coenzyme Q_{10}, vitamin E, N-acetyl cysteine, and selenium, have also been used. In some studies idebenone has resulted in a decrease in cardiac hypertrophy and decreases in surrogate markers of oxidative damage to DNA. Other studies have failed to show a benefit. Combined therapy with coenzyme Q_{10} and vitamin E has shown improvement in magnetic resonance spectroscopy and echocardiographic parameters.

Future therapeutic trials in FRDA may make use of antioxidants or other agents coupled to the triphenylphsphonium cation, which facilitates mitochondrial targeting of the agent. Potentials for gene therapy are also being explored, and may utilize drugs that interfere with the "sticky DNA" structures that are thought to be the cause of the transcription blockade that occurs in FRDA.

See Also the Following Articles

Diabetes • Mitochondrial DNA

Glossary

antioxidant Any substance that delays or prevents the process of oxidation.

ataxia Incoordination of voluntary muscle action.

mitochondria A cytoplasmic organelle, consisting of an outer membrane and an inner folded membrane, and containing its own DNA.

mitochondrial DNA A circular DNA molecule of 16.5 kb contained within the mitochondrion, and inherited maternally.

mitochondrial respiratory chain A series of enzyme complexes located on the mitochondrial inner membrane responsible for generating a proton gradient, which is itself required for the conversion of ADP to ATP by complex V (ATP synthase) of this chain.

trinucleotide repeat A three-nucleotide sequence, present in normal individuals as a set number of repeats, but which causes disease when a threshold number of repeats is exceeded.

Further Reading

Campuzano, V., Montermini, L., Molto, M. D., Pianese, L., Cossee, M., Cavalcanti, F., Monros, E., Rodius, F., Duclos, F., Monticelli, A., *et al.* (1996). Friedreich's ataxia: Autosomal recessive disease caused by an intronic GAA triplet repeat expansion. *Science* **271**(5254), 1423–1427.

Campuzano, V., Montermini, L., Lutz, Y., Cova, L., Hindelang, C., Jiralerspong, S., Trottier, Y., Kish, S. J., Faucheux, B., Trouillas, P., Authier, F. J., Durr, A., Mandel, J. L., Vescovi, A., Pandolfo, M., and Koenig, M. (1997). Frataxin is reduced in Friedreich ataxia patients and is associated with mitochondrial membranes. *Hum. Mol. Genet.* **6**(11), 1771–1780.

Delatycki, M. B., Williamson, R., and Forrest, S. M. (2000). Friedreich ataxia: An overview (Review). *J. Med. Genet.* **37**(1), 1–8.

Durr, A., Cossee, M., Agid, Y., Campuzano, V., Mignard, C., Penet, C., Mandel, J. L., Brice, A., and Koenig, M. (1996). Clinical and genetic abnormalities in patients with Friedreich's ataxia. *N. Engl. J. Med.* **335**(16), 1169–1175.

Harding, A. E. (1981). Friedreich's ataxia: A clinical and genetic study of 90 families with an analysis of early diagnostic criteria and intrafamilial clustering of clinical features. *Brain* **104**(3), 589–620.

Lodi, R., Hart, P. E., Rajagopalan, B., Taylor, D. J., Crilley, J. G., Bradley, J. L., Blamire, A. M., Manners, D., Styles, P., Schapira, A. H., and Cooper, J. M. (2001). Antioxidant treatment improves *in vivo* cardiac and skeletal muscle bioenergetics in patients with Friedreich's ataxia. *Ann. Neurol.* **49**(5), 590–596.

Lodi, R., Rajagopalan, B., Bradley, J. L., Taylor, D. J., Crilley, J. G., Hart, P. E., Blamire, A. M., Manners, D., Styles, P., Schapira, A. H., and Cooper, J. M. (2002). Mitochondrial dysfunction in Friedreich's ataxia: From pathogenesis to treatment perspectives (Review). *Free Radic. Res.* **36**(4), 461–466.

Muhlenhoff, U., Richhardt, N., Ristow, M., Kispal, G., and Lill, R. (2002). The yeast frataxin homolog Yfh1p plays a specific role in the maturation of cellular Fe/S proteins. *Hum. Mol. Genet.* **11**(17), 2025–2036.

Rustin, P., Rotig, A., Munnich, A., and Sidi, D. (2002). Heart hypertrophy and function are improved by idebenone in Friedreich's ataxia. *Free Radic. Res.* **36**(4), 467–469.

Wilson, R. B., and Roof, D. M. (1997). Respiratory deficiency due to loss of mitochondrial DNA in yeast lacking the frataxin homologue. *Nat. Genet.* **16**(4), 352–357.

Biography

Paul Hart is a Wellcome Research Training Fellow and Neurologist at the Department of Clinical Neurosciences, Royal Free Campus, University College London. His Ph.D. and primary research interests are on the interactions between nuclear and mitochondrial DNA, and the role of mitochondrial dysfunction in neurodegeneration.

A. H. V Schapira is Chairman, University Department of Clinical Neurosciences at the Royal Free and University College Medical School, and Professor of Neurology at the Institute of Neurology, Queen Square, London. His primary research interests are into the aetiology and pathogenesis of neurodegenerative diseases including Parkinson's disease, Huntington's disease, and Friedreich's Ataxia.

G Protein Signaling Regulators

John H. Exton
Vanderbilt University, Nashville, Tennessee, USA

Regulators of G protein signaling are important controllers of the system by which many agonists (hormones and neurotransmitters) transmit their signals across the cell membrane to influence intracellular processes. This system involves heterotrimeric G proteins, which are activated when the agonists bind to their specific receptors, and effectors (enzymes and ion channels), which are the targets of the G proteins. Activation of the G proteins by the receptors involves the release of GDP from their α-subunits and the subsequent binding of GTP, and the dissociation of the $\beta\gamma$-subunits from the G proteins. The GTP-bound α-subunits and the free $\beta\gamma$-subunits then act on their target effectors. Turning off the system requires the hydrolysis of GTP to GDP by the intrinsic GTPase of the α-subunits and this is a relatively slow process. Regulators of G protein signaling accelerate the GTPase activity thereby terminating the stimulation of effectors and allowing the G protein to revert to its GPD-liganded heterotrimeric state where it can activate again by agonist binding to receptor.

Discovery of Regulators of G Protein Signaling

Regulators of G protein signaling (RGSs) were discovered as negative regulators of G protein signaling in *S. cerevisiae* and *C. elegans*. In *S. cerevisiae*, a mutation termed *sst2* caused the yeast to become supersensitive to mating pheromone. However, at the time the *SST2* gene was identified, knowledge of signaling pathways was rudimentary and the connection to G proteins could not be made. Later it became clear that signaling in yeast was similar to that in mammals, i.e., the topology of pheromone receptors was similar to that of G protein-coupled receptors and the yeast G_α subunit shared considerable identity with mammalian $G_{i\alpha}$. Later, genetic evidence indicated a direct interaction between SST2 and G_α, and studies of mutations in G_α and SST2 led to the conclusion that SST2 acted as a GTPase-activating protein (GAP) for G_α.

Genetic analysis of *C. elegans* revealed a gene (*egl-10*) that encoded a protein that was similar in its C-terminal region to SST2. Similar to what was found in *S. cerevisiae*, the function of EGL-10 (to increase the frequency of egg laying via serotonergic motor neurons) depended on the presence of a G_α protein (GOA-1) that was homologous to mammalian $G_{o\alpha}$.

Multiple homologues of SST2 and EGL-10 have been identified in higher eukaryotes, utilizing yeast two-hybrid screens, database searches for related sequences, polymerase chain reaction, and rescue of the SST2-deficient phenotype in yeast. A large family of RGS proteins (more than 30 members) that show activity to different G proteins has now been identified in mammals (Table I). They differ significantly in size, but all have a diagnostic RGS core domain and exhibit GAP activity towards heterotrimeric G proteins.

Structure of RGS Proteins

RGS proteins have a conserved RGS domain of ~130 amino acids (Figure 1). This domain is capable of binding G_α subunits and stimulating GTP hydrolysis. In addition, certain RGSs have other domains in their N- and C-terminal regions. These may be PDZ, PTB, GGL, PH, DH, PX, and DEP domains, transmembrane spans, cysteine strings, and domains that bind the adenomatous polyposis coli protein (APC), GSK3, β-catenin, PKA, GRK, and G$\beta\gamma$ (Figure 1, see legend for definitions). The presence of these domains illustrates that RGSs have more functions than GAP activity and are targeted to membranes by multiple mechanisms.

The RGS domain has been defined by X-ray crystallography as a complex between RGS4 and $G_{\alpha i}1$, and by NMR analysis of a fragment of GAIP. The domain is globular and mostly helical in structure, based on a four-helix bundle and a second domain composed of the N- and C-terminal helices. Many of the most conserved residues face into the helical bundles, and others are involved in G_α binding. Three interhelix loops make contact with the three switch regions of G_α (those regions that show the greatest conformational changes when GDP is replaced by GTP), but there is no contact with bound GTP.

TABLE I

Mammalian RGS Proteins

Protein	Gα interactions	Tissue distribution
hRGS1	$G\alpha_i$ family, $G\alpha_q$	Activated B cells
hRGS2	$G\alpha_q > G\alpha_{i1}$	Biquitous
hRGS3	$G\alpha_i$ family, $G\alpha_q$	Ubiquitous
rRGS4	$G\alpha_i$ family, $G\alpha_q$	Brain
mRGS5	$G\alpha_i$ family	Heart, lung, brain, muscle
hRGS6	$G\alpha_o$	Brain
hRGS7	$G\alpha_i$ family, $G\alpha_q$	Brain, retina
rRGS8	$G\alpha_i$ family	Brain
hRGS9	$G\alpha_i$ family, $G_t\alpha$	Brain, retina
hRGS10	$G\alpha_i$ family	Brain
hRGS11	$G\alpha_o$	Brain, retina, pancreas
rRGS12	$G\alpha_i$ family, $G\alpha_{12}$, $G\alpha_{13}$	Brain, lung, liver, heart, spleen
hRGS13	N.D.	N.D.
rRGS14	$G\alpha_i$ family, $G\alpha_{12}$, $G\alpha_{13}$	Brain, lung, spleen
hRGS15	$G\alpha_{12}$, $G\alpha_{13}$	N.D.
mRGS16	$G\alpha_i$ family, $G\alpha_q$	Retinal, pituitary, liver
hRGS-GAIP	$G\alpha_i$ family, $G\alpha_q$	Heart, lung, liver
bRET-RGS1	$G\alpha_t$	Retina
hRGSZ1	$G\alpha_z$	Brain
hRGSZ2	$G\alpha_z$	N.D.
h115RhoGEF	$G\alpha_{13}$, $G\alpha_{12}$	Ubiquitous
mLscRhoGEF	N.D.	N.D.
hRhoGEF	N.D.	N.D.
mD-AKAP2	N.D.	Ubiquitous
rAxin	N.D.	Ubiquitous
mConductin	N.D.	Brain, lung, liver
bGRK2	$G\alpha_q$	Brain

N.D., no data.

Mechanisms of RGS Proteins

RGS proteins interact with active (GTP-bound) G_α-subunits and accelerate the hydrolysis of GTP. In the absence of RGSs and certain effectors, the rate of hydrolysis of GTP by G_α-subunits is very slow and inappropriate for rapid on/off signaling. RGSs can increase the rate of GTP hydrolysis by up to 2000-fold. RGSs act by altering the conformation of the G_α–GTP complex thus causing G_α to be a more efficient GTPase. The transition state intermediate involved in the hydrolysis of GTP can be mimicked by the complex G_α–GDP–$A1F_4$, and this has helped elucidate the mechanism of action of RGSs through crystallographic and other studies. As noted above, RGS proteins have a broad interface with G_α-subunits that includes the three switch regions. In the case of RGS4, the major change exerted on $G_{\alpha i}1$ is decreased mobility of switch II, and it has been suggested that switch II is stabilized in a catalytically active conformation. Because of the conservation of key residues in the contact site of the RGS domain, this mechanism is probably general. Other residues that have been shown by mutation to affect the GAP activity of the RGSs are probably involved in stabilizing the catalytic conformation of the G_α-subunit or altering the affinity of RGS for G_α. Although the usual mode of action of RGSs is to interact with G_α-subunits, some of them can also interact directly with effectors. For example, RGS2 can inhibit type V adenylyl cyclase.

From their structure, RGS proteins are predicted to be soluble. However, their mechanism requires that they act at the plasma membrane. The generation of GTP-liganded G_α-subunits in response to receptor activation would be expected to recruit RGSs to the membrane. However, transmembrane segments, lipid modifications, e.g., palmitoylation, and domains that interact with membrane lipids may also be involved, and there is evidence that some RGSs can be recruited selectively to the plasma membrane by receptors.

Selectivity of RGS Action

In view of the large number of RGSs, some selectivity in their interactions with G_α-subunits would be expected (Table I). Since certain receptors can couple to more than one G protein, the selective modulation of one G_α by an RGS protein can change the output from such receptors. However, selectivity has been hard to define *in vitro* and may involve restrictive patterns of cellular expression of the RGS and G_α proteins. *In vitro* analysis of RGS selectivity has involved single-turnover GAP assays, studies of competition with substrate and coimmunoprecipitation and coadsorption assays. For example, GAIP displays activity towards G_i and G_q class α-subunits, but the closely related RGSZ1 and RGSZ2 are selective for $G_{\alpha z}$ and display low activity towards $G_{\alpha q}$. RGS6 and RGS11 are selective for $G_{\alpha o}$ compared with other $G_{\alpha i}$ class subunits, and RGS2 prefers $G_{\alpha q}$. Surprisingly, only one RGS (sorting nexin 13) has been reported to act on $G_{\alpha s}$.

In a cellular setting, the selectivity of RGSs for certain G_α-subunits is less readily defined than *in vitro* since the readouts are quite distal from the interactions. RGS2 displays selectivity for $G_{\alpha q}$, in accordance with *in vitro* studies. RGS16 inhibits the activation of p38 MAP kinase by PAF more effectively than the activation of ERK2, whereas RGS1 has the opposite effects. In dorsal root ganglion cells, α_2-adrenergic activation of $G_{\alpha i}$ and $G_{\alpha o}$ was enhanced by antibodies against RGS4 and GAIP, whereas antibodies to other RGSs had no effect. Microinjection of the RGS proteins confirmed these results.

Concerning the receptor selectivity of RGS proteins, there have been few studies. In pancreatic acinar cells,

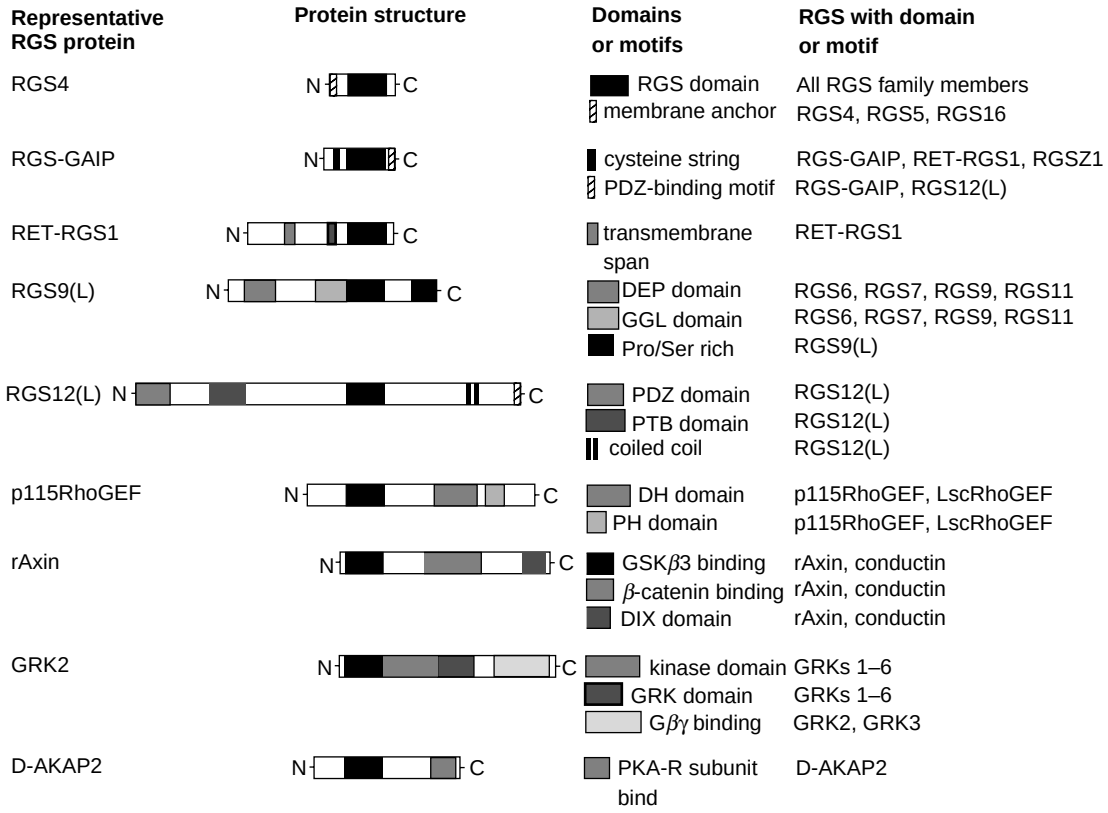

FIGURE 1 Structural organization and motifs in RGS proteins. (Modified from Hepler, J. R. (1999) Emerging roles for RGS proteins in cell signalling. *Trends Physiol. Sci.* **20**, 376–382.) PDZ (PSD-95, disk-large and zo-1), DEP (disheveled, egl-10 and pleckstrin), GGL (Gγ subunit-like), PTB (phosphotyrosine binding), DH (Dbl homology), PH (pleckstrin homology), GSKβ3 (glycogen synthase kinase β3-binding), DIX (disheveled homology), GRK (G protein-coupled receptor kinase), PKA-R (regulatory subunit of cAMP-dependent protein kinase).

RGS4 blocked G_q-mediated PLC activation initiated by M_3 muscarinic, cholecystokinin, and bombesin receptors. However, it was more potent against the muscarinic receptors. RGS1 and RGS16 were also more selective against M_3 muscarinic receptors. Surprisingly RGS2, which has activity towards $G_{\alpha q}$, did not show the same selectivity. The molecular basis for this receptor selectivity is presently unknown.

Significance of RGS Action

The primary action of RGSs is to induce rapid signal termination upon removal or inactivation of agonists in G protein-coupled receptor systems. The "knockout" of RSG9 prolongs photon responses because $G_{\alpha t}$ remains active. In addition this approach has been used to show that RGS3 and RGS5 selectively suppress MAP kinase activation by M_3 muscarinic and AT_{1A}-angiotensin receptors, respectively, in vascular smooth muscle. On the other hand, transgenic mice overexpressing RGS4 in ventricular tissue develop less ventricular hypertrophy in response to pressure overload, apparently because of reduced $G_{\alpha q}$ action. It should also be noted that RGSs can inhibit effectors by mechanisms not involving their GAP activity. This may be because the RGSs compete with the effectors for binding the G_α-subunits or because the RGSs inhibit the effectors directly.

Although signal termination is an important component of RGS action, this is not the whole story. There are interesting kinetic aspects to RGS action which arise from the cycle of activation/deactivation that G protein-coupled receptor systems undergo. For example, the activating receptors can only interact with the GDP-liganded form of G_α. Thus RGS activity can promote the association of G_α with the receptor through the generation of G_α–GDP, and permit G protein activation to continue.

Through their actions, RGS proteins modulate a variety of hormone- and neurotransmitter-stimulated responses in cells. These include the activity of adenylyl cyclase, the mitogen-activated protein kinase (MAP kinase) family, phospholipase C (with attendant changes in inositol trisphosphate and Ca^{2+} ions), G protein-gated inward rectifying K^+ (GIRK) channels, and cGMP phosphodiesterase in the retina (with altered phototransduction). Studies of the GIRK channels have revealed that RGS proteins can alter the timing,

amplitude and duration of the K^+ currents. An interesting group of RGSs is the RhoGEFs. These are guanine-nucleotide-exchange factors for the small G protein Rho. The first of these was discovered in *Drosophila*, where genetic analysis indicated that a RhoGEF (DRhoGEF2) acted downstream of the concertina gene, which is the *Drosophila* homologue of $G_{\alpha 12}$. Several laboratories then showed that $G_{\alpha 12}$ acted directly on three mammalian homologues of DRhoGEF2 (p115 RhoGEF, PDZ-RhoGEF, and LARG). In particular, the N-terminal region of p115 was observed to be similar to the conserved region of RGSs, and p115 was found to associate with $G_{\alpha 12}$ and $G_{\alpha 13}$ through its RGS domain. Even more interesting were the findings that $G_{\alpha 13}$ could stimulate the GEF activity of p115 towards Rho, and that the RGS domain of p115 displayed GAP activity towards $G_{\alpha 12}$ and $G_{\alpha 13}$. There is now much evidence that p115 and related RhoGEFs mediate the activation of Rho induced by agonists whose receptors are coupled to G_{13}. RGS16 inhibits $G_{\alpha 13}$-mediated activation of Rho by binding directly to $G_{\alpha 13}$ and disrupting its interaction with p115. The binding does not involve the RGS domain of RGS16.

Although they do not contain the RGS domain, many effectors of G proteins act as GAPs towards G_α-subunits. Examples are phospholipase C, which acts on $G_{\alpha q}$, and the γ-subunit of cGMP phosphodiesterase, which acts on transducin. In the case of transducin, RGS proteins and the phosphodiesterase act synergistically to inactivate the G protein.

Regulation of RGS Proteins

RGS proteins can be regulated by various mechanisms. One is by transcriptional regulation of their cellular levels. Other mechanisms include covalent modification, cellular relocalization, and interaction with regulatory proteins and lipids. The yeast RGS SST2 can be regulated at the transcriptional level by mating factor. Almost all RGSs are expressed in brain, although they are restricted to certain regions. They can be regulated by neurotransmitters through changes in their mRNA levels. In other tissues, there is transcriptional regulation involving growth factors and other peptides.

Regulation of RGSs also occurs at the post-transcriptional level. For example, phosphorylation can alter their degradation through ubiquitin-dependent proteolysis or by affecting a PEST sequence(s). For example, TNFα can protect RGS7 from proteolysis through phosphorylation of a Ser/Thr sequence near the GGL and RGS domains. RGS activity can also be modified by phosphorylation of its G_α targets. Phosphorylation of $G_{\alpha z}$ by protein kinase C inhibits the GAP activity of RGS5. Another modification is reversible palmitoylation of either the RGS or its substrate G_α. The effects on the RGS may be positive or negative, depending on the assay used, but palmitoylation of G_α-subunits usually results in inhibition of the GAP activity of the RGS.

RGS proteins can bind to a variety of cellular proteins (Figure 1). As noted in the section on structure, they contain many different protein-binding motifs. They can also bind lipids, e.g., PIP_3, Ca^{2+}-calmodulin, and the APC protein. RGS12 is the only RGS that contains a PDZ domain and thus can interact with proteins that contain a PDZ-binding motif, e.g., IL-8. AKAP2 binds the regulatory subunit of cAMP-dependent protein kinase (PKA). RGS6, RGS7, RGS9, and RGS11 contain a DEP domain and this is involved in membrane localization. Axin and conductin, which are scaffolding proteins, block signaling by Wnt proteins, which are involved in development. The RGS domains of these proteins bind the APC protein, whereas other domains bind β-catenin and GSK3.

Important interacting partners of the RGSs are the $\beta\gamma$-subunits of G proteins ($G_{\beta\gamma}$). These bind to G_α cooperatively with respect to GDP and suppress receptor-independent activation of G proteins. They also anchor G_α to the plasma membrane and regulate many effector proteins, e.g., adenylyl cyclase, phospholipase C, ion channels, and lipid kinases. With respect to RGS proteins, $G_{\beta\gamma}$ inhibits the GAP activity of many of these proteins. It appears that $G_{\beta\gamma}$ interacts with both the RGS and its target G_α-subunits. Several RGSs contain a GGL domain that is similar in sequence to $G_{\beta\gamma}$. It has also been shown that RGS11 binds Gβ5, and that the binding involves the GGL domain. Binding of $G_{\beta 5}$ to other RGSs has been demonstrated *in vivo*. In addition, RGSs can inhibit the effects of $G_{\beta\gamma}$-subunits on effectors by virtue of the generation of G_α·GDP which recombines with $G_{\beta\gamma}$ to reform inactive heterotrimeric G proteins. In the case of RGS3, there is another mechanism, namely its binding to $G_{\beta 1\gamma 2}$-subunits to inhibit signaling to effectors. This effect involves two regions of RGS3 separate from the RGS domain.

RGS Proteins as Drug Targets

Because the importance of G protein-coupled receptors in regulating a large variety of physiological processes, the RGSs represent very attractive targets for therapeutic intervention. Alterations in their expression indicate that they regulate cardiac function, immune responses, neuronal function, behavior, vision, and embryonic development. There is also evidence that they may be involved in the diseases of retinitis pigmentosa, schizophrenia, Parkinson's disease, chronic heart failure, drug addiction, and prostate cancer. Drugs could be targeted to RGSs in several ways, and could act as agonists or inhibitors. The first approach is to target the RGS/G_α

interface, which involves certain amino acids that are essential for the contact. The second is through modulation of the proteins and lipids that act as allosteric modifiers of RGS action. This also includes covalent modifications. The third is modification of the membrane attachment of the RGSs since it is essential for them to be recruited to the plasma membrane in order to exert their effects. In all cases, determination of the amino acid residues involved in RGS selectivity and in their interactions with allosteric regulators will be essential for the development of drugs of sufficient specificity to be therapeutically useful.

See Also the Following Articles

Adenylyl Cyclases • G_{12}/G_{13} Family • G_i Family of Heterotrimeric G Proteins • G_q Family • G_s Family of Heterotrimeric G Proteins • Mitogen-Activated Protein Kinase Family • Phospholipase C

Glossary

GAP A GTPase-activating protein that acts on monomeric and heterotrimeric G proteins to inactivate them. GAPs for heterotrimeric G proteins are RGSs and certain effectors.

G protein A signal-transducing protein that binds GTP (active form) or GDP (inactive form). Occurs in monomeric and heterotrimeric forms. Heterotrimeric G proteins are comprised of α-, β-, and γ-subunits. The α-subunit binds the guanine nucleotides and interacts with effector enzymes or ion channels. Heterotrimeric G proteins are activated by receptors with seven-transmembrane-spanning domains termed G protein-coupled receptors.

phosphorylation The modification of proteins by protein kinases and lipids by lipid kinases involving the addition of phosphate groups. This results in changes in the activity of the proteins or in the generation of new lipids with different functions.

receptor A membrane protein that binds and is activated by hormones, neurotransmitters, growth hormones, and cytokines.

Further Reading

Berman, D. M., and Gilman, A. G. (1998). Mammalian RGS proteins: Barbarians at the gate. *J. Biol. Chem.* **273**, 1269–1272.

Dohlman, H. G., and Thorner, J. (1997). RGS proteins and signaling by heterotrimeric G proteins. *J. Biol. Chem.* **272**, 3871–3874.

Fukuhara, S., Chikumi, H., and Gutkind, J. S. (2001). RGS-containing RhoGEFs: The missing link between transforming G proteins and Rho? *Oncogene* **20**, 1661–1668.

Hepler, J. R. (1999). Emerging roles for RGS proteins in cell signalling. *Trends Physiol. Sci.* **20**, 376–382.

Hollinger, S., and Hepler, J. R. (2002). Cellular regulation of RGS proteins: Modulation and integrators of G protein signaling. *Pharmacol. Rev.* **54**, 527–559.

Ross, E. M., and Wilkie, T. M. (2000). GTPase-activating proteins for heterotrimeric G proteins: Regulators of G protein signaling (RGS) and RGS-like proteins. *Annu. Rev. Biochem.* **69**, 795–827.

Biography

John Exton is a Professor of Molecular Physiology and Biophysics, Professor of Pharmacology and Investigator of the Howard Hughes Medical Institute at Vanderbilt University. His principal research interests relate to signal transduction involving G proteins and phospholipases. He received an M.D. and Ph.D. from the University of Otago, New Zealand, and was a postdoctoral fellow under Charles R. Park and Earl W. Sutherland at Vanderbilt. He is a member of the National Academy of Sciences.

G Protein-Coupled Receptor Kinases and Arrestins

Jeffrey L. Benovic
Thomas Jefferson University, Philadelphia, Pennsylvania, USA

Many transmembrane signaling systems consist of specific G protein-coupled receptors (GPCRs), which transduce the binding of a diverse array of extracellular stimuli into intracellular signaling events. GPCRs function to regulate many biological processes including neurotransmission, sensory perception, cardiovascular function, chemotaxis, embryogenesis, cell growth and development, differentiation, and apoptosis. To ensure that extracellular signals are translated into intracellular signals of appropriate magnitude and specificity, most signaling cascades are tightly regulated. GPCRs are subject to three principal modes of regulation: (1) desensitization, in which a receptor becomes refractory to continued stimuli; (2) endocytosis, whereby receptors are removed from the cell surface; and (3) down-regulation, where total cellular receptor levels are decreased. GPCR desensitization is primarily mediated by second-messenger-dependent kinases, such as protein kinase A (PKA) and protein kinase C (PKC), and by G protein-coupled receptor kinases (GRKs). GRKs specifically phosphorylate activated GPCRs and initiate the recruitment of arrestins, which mediate receptor desensitization, endocytosis, and down-regulation.

The GRK Family of Proteins

GRKs are found in metazoans and, in mammals, the seven GRKs can be divided into three subfamilies based on overall structural organization and homology: GRK1 (also termed rhodopsin kinase) and GRK7; GRK2 (βARK1), and GRK3 (βARK2); and GRK4, GRK5, and GRK6. GRKs are serine/threonine kinases with a tripartite modular structure. A central ~330 amino acid catalytic domain, most related to those of other AGC kinases such as protein kinase A, protein kinase C, and PDK1, is flanked by an ~180 residue N-terminal region that contains a regulator of G protein signaling homology (RH) domain, and an ~80–180 amino acid C-terminal lipid-binding domain that varies in structure (Figure 1) .

Specificity of GRK Interaction with GPCRs

GRKs specifically phosphorylate agonist-occupied GPCRs. While no clear consensus sequence for GRK-mediated phosphorylation has been identified, specific sites for GRK-mediated phosphorylation have been mapped to either the carboxyl terminal tail or the third intracellular loop of a number of GPCRs. Experiments with synthetic peptide substrates have revealed a preference of GRK1 and GRK2 family members for serines/threonines flanked by acidic residues, whereas GRK4 family members appear to prefer serines/threonines flanked by basic residues. Overall, the specificity of receptor phosphorylation by GRKs appears to be determined by a combination of binding determinants between the receptor and GRK.

Important insight has also been provided by manipulation of GRK expression in intact cell systems. Co-expression studies have revealed that a wide variety of GPCRs can serve as GRK substrates. Several strategies that reduce endogenous GRK levels/function in cells, including inhibitory antibodies, antisense DNA and dominant negative GRKs have also been used to assess specificity. For example, incubation of inhibitory GRK-specific monoclonal antibodies with various permeabilized cell types suggests the preferential regulation of both β_2- and α_2-adrenergic receptors (β_2AR and α_2AR) by the GRK2 subfamily. Similarly, the use of GRK-specific antisense constructs in various cell types reveals subtype-specific regulation of H2 histamine receptors (by GRK2), PACAP type 1 and CRF1 receptors (by GRK3), D1 dopamine and metabotropic glutamate type 1 receptors (by GRK4), thyrotropin receptors (by GRK5), and CGRP receptors (by GRK6).

Insight into GRK specificity/function has also been gained from *in vivo* strategies. Transgenic mice with cardiac-specific overexpression of GRK2 or a carboxyl-terminal GRK2 mini-gene, which serves as a GRK2 inhibitor, demonstrate *in vivo* effects on cardiac function.

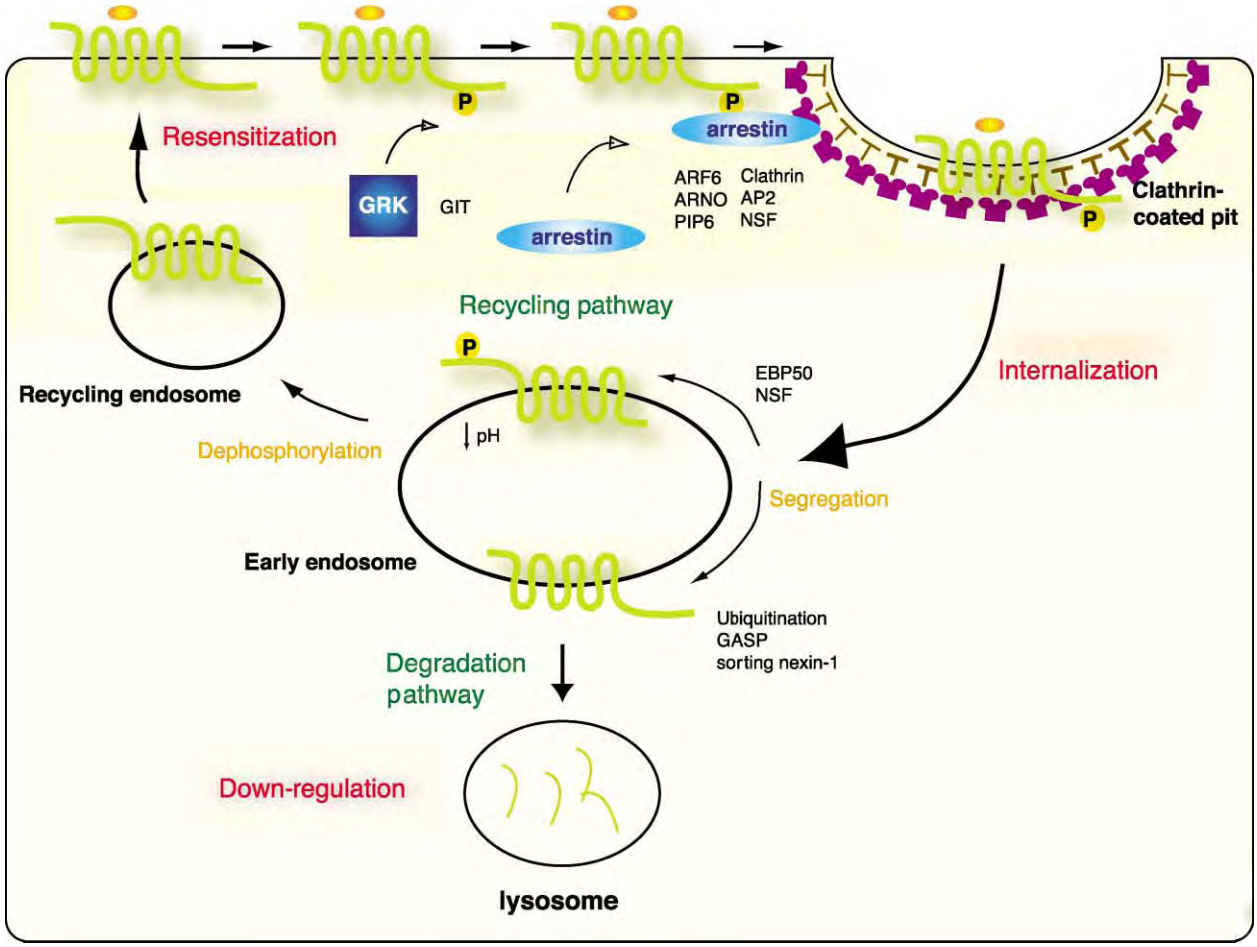

FIGURE 1 Schematic representation of G protein-coupled receptor (GPCR) trafficking. Agonist-activated receptors are phosphorylated by a GRK leading to the recruitment of arrestins. Arrestins serve as adaptor proteins by virtue of their ability to link receptors to components of the transport machinery such as clathrin, AP-2, and phosphoinositides leading to internalization. Additional interactions with GRKs and arrestins appear to play a role in this process. Once in endosomes, recycling receptors (recycling pathway) are readily segregated from receptors destined for lysosomes (degradation pathway). Although poorly understood, the sorting decision may be regulated by specific and distinct protein interactions or modification by ubiquitin. Receptors that enter the recycling pathway enter recycling endosomes and traffic back to the cell surface resulting in resensitization. Receptors that enter the degradation pathway traffic to lysosomes where they are proteolyzed, leading to a loss in the total cellular complement of the receptor, a process known as down-regulation.

Specifically, while GRK2 overexpression leads to increased uncoupling of the βAR from adenylyl cyclase and an associated decrease in left ventricular contractility, mice overexpressing the GRK2 inhibitor demonstrate increased left ventricular contractility even in the absence of β-agonist. Cardiac-specific overexpression of GRK5 in transgenic mice has a similar effect on βAR-mediated signaling and contractility, while the angiotensin II-mediated contractile response is attenuated only in the GRK2-overexpressing mice. Further demonstration of specificity is suggested in transgenic mice with myocardial overexpression of GRK3, where no effect on βAR response is observed. Moreover, studies involving cardiac overexpression of individual GRKs in mice revealed that GRK3 > GRK5 > GRK2 at desensitizing α_{1B}-adrenergic receptor signaling in the heart.

Functional knockouts of GRKs have provided unique insight into potential physiological roles of these proteins. Disruption of the GRK2 gene in mice by homologous recombination results in embryonic lethality as a consequence of hypoplasia of the ventricular myocardium, suggesting a role for GRK2 in cardiac development. In contrast, disruption of the mouse GRK3 gene results in normal development and physiology, although specific defects in desensitization of odorant-induced cAMP responses in olfactory epithelium and cholinergic response of airway smooth muscle are observed. A GRK5 knockout results in muscarinic supersensitivity and impaired receptor desensitization, while disruption of the GRK6 gene results in altered SDF-promoted chemotaxis of lymphocytes, supersensitivity to the locomoter-stimulating

effects of cocaine and amfetamine, and enhanced coupling of postsynaptic D2-like dopamine receptors. These findings suggest that GRKs are involved not only in regulating signaling, but may also have critical roles in regulating growth and development.

Regulation of GRK Function

A critical component in generating specificity is the molecular mechanism responsible for regulating the activity and cellular localization of GRKs. Recent studies have provided increased detail for known regulatory mechanisms as well as revealing previously unrecognized forms of regulation. For example, phosphorylation appears to play an important role in regulating GRK activity. GRK2 phosphorylation by ERK1/2 inhibits GRK2 activity while phosphorylation by PKA, Src, and PKC results in increased activity. In contrast, GRK5 activity is attenuated by PKC phosphorylation, but stimulated by autophosphorylation. GRK function is also regulated by interaction with a large number of additional proteins including G protein α- and $\beta\gamma$-subunits, clathrin, the GRK-interacting protein GIT1, caveolin-1, phosphoinositide 3-kinase-α and γ, cytoskeletal proteins such as tubulin and actin, and various calcium-binding proteins.

Phospholipids also play an important role in regulating GRK function since G$\beta\gamma$-mediated activation of GRK2 is dependent on negatively charged phospholipids including PIP_2. Interestingly, while GRK4 subfamily members do not bind G$\beta\gamma$-subunits, these kinases share an N-terminal PIP_2-binding domain that may facilitate receptor phosphorylation. These kinases also have the ability to associate with phospholipids via a C-terminal domain that is either palmitoylated (GRK4 and 6) or can directly bind phospholipids (GRK5). Thus, the immediate phospholipid environment may have a general and critical role in modulating GRK function. Taken together, multiple mechanisms including GPCR, G protein, and phospholipid binding play an important role in regulating GRK activity and function.

Structural Basis of GRK Function

The X-ray crystal structure of GRK2 complexed with G$\beta\gamma$ provides significant insight into GRK function. GRK2 is composed of three primary domains, an N-terminal RH domain, a central kinase catalytic domain, and a C-terminal PH domain. Interestingly, the crystal structure reveals that the RH, kinase, and PH domains form an equilateral triangle that is $\sim$80Å on a side. The RH domain consists of two discontinuous regions and contacts both the kinase and PH domains. The kinase domain is most similar to that of PKA and PDK1 and appears to be in an inactive conformation in the crystal structure. Interestingly, the structure of the RH and kinase domain core appears to have similarities to the inactive structure of Src with one region of the RH domain (the α10 helix) potentially functioning to regulate GRK activation. The C-terminal PH domain of GRK2 mediates phospholipid and G$\beta\gamma$ binding. Docking analysis of the GRK2/G$\beta\gamma$ complex with a GPCR and Gαq suggests that all three proteins should be able to bind to GRK2 simultaneously. This would represent an effective way of turning off signaling by phosphorylating receptor and sequestering Gαq and G$\beta\gamma$, thereby preventing interaction with effector molecules.

Role of GRKs in Disease

While various *in vitro* and *in vivo* manipulations of GRKs have provided significant insight into their function, various experimental approaches have led to a growing appreciation of the physiological and pathophysiological roles of GRKs in human disease. Several studies have demonstrated increased expression of GRKs associated with congestive heart failure (CHF), hypertension, and myocardial ischemia. In experimentally induced models of CHF, both GRK2 and GRK5 expression and activity was enhanced 2–3 fold in the left ventricular myocardium early in CHF progression. While it is not clear whether this increase in GRK levels is causal or a byproduct of elevated hormones secondary to disease, it is interesting that myocardial ischemia, which is associated with a large local release of noradrenaline, also produces a rapid increase in GRK2 mRNA levels. Since cardiac-specific overexpression of either GRK2 or GRK5 in transgenic mice produces decreases in cardiac function, the myocardial GRK overexpression that occurs during CHF could potentially contribute to pathology through increased βAR desensitization.

Several studies have also shown that GRK expression is selectively regulated as a function of the hypertensive state. In a comparison of normotensive and mildly hypertensive subjects, GRK2 protein expression in lymphocytes was positively correlated with blood pressure and negatively correlated with β_2AR-mediated adenylyl cyclase activity. These results suggest that GRK2 expression may underlie reduced β_2AR responsiveness characteristic of the hypertensive state. Another form of hypertension (human essential hypertension) involves impairment in dopamine-promoted urinary sodium excretion. Defective D1 dopamine receptor/G protein coupling in the kidney proximal tubule is the cause of the impaired renal dopaminergic action in this form of hypertension. Recent studies suggest that single nucleotide polymorphisms of GRK4 increase GRK activity and cause D1 receptor/G protein uncoupling in the renal proximal tubule. Moreover, expression of polymorphic GRK4 in transgenic mice produces

hypertension. Taken together, these findings suggest that GRKs play a role in vascular and renal control and may represent novel therapeutic targets for the treatment of human hypertension.

The visual transduction system provides another example of the critical role of GRKs in pathophysiology. Various methods of genetic analysis have revealed inherited mutations in GRK1 associated with a visual degenerative disease known as stationary night blindness or Oguchi's disease. Genetic analysis of several Oguchi patients demonstrated a lack of functional *grk1* alleles. A more detailed analysis of this disruption uncovered a profound abnormality in recovery of rod photoreceptors after light activation. These discoveries clearly demonstrate the sensitivity of phototransduction to GRK1 dysfunction and suggest potential future targets for gene therapy.

The Arrestin Family of Proteins

Arrestin (also termed S-antigen, visual arrestin, or arrestin-1) was initially identified in the visual system as a 48-kDa protein that redistributed from the cytoplasm to the disk membrane following light activation of bovine rod cell outer segments. Arrestin-1 is a 404 amino acid protein and binds to the light-receptor rhodopsin in a light- and phosphorylation-dependent manner resulting in suppression of G protein signaling. Gene targeting has demonstrated a clear physiological role for arrestin-1 in quenching phototransduction in mice. In addition, mutations in human arrestin-1 have been identified in Oguchi's disease.

Evidence for the involvement of arrestins in the regulation of additional GPCRs was initially suggested by the finding that purified arrestin-1 could impair β_2AR/G protein coupling in a phosphorylation-dependent manner. Subsequent studies identified a 418 amino acid arrestin-1 homologue (termed β-arrestin-1 or arrestin-2) that could effectively uncouple phosphorylated β_2AR from G protein. Arrestin-2 is widely expressed and has been broadly implicated in regulating GPCR desensitization. Subsequent studies identified two additional members of the arrestin family, arrestin-3 (also termed β-arrestin-2) and arrestin-4 (also termed cone arrestin). The four mammalian arrestins are divided into two major classes, visual and nonvisual, based on their localization and function. The nonvisual arrestins, arrestin-2 and arrestin-3, are broadly distributed and function in multiple processes including GPCR desensitization, endocytosis, recycling, down-regulation, and signaling. The visual arrestins, arrestin-1 in rod cells and arrestin-4 in cone cells are highly localized and play a primary role in quenching phototransduction.

Molecular Nature of Arrestin Interaction with GPCRs

An important feature of arrestin interaction with GPCRs is the ability of arrestins to recognize both the activation- and phosphorylation-state of the receptor. The observation that arrestins discriminate between agonist-activated and nonactivated GPCRs suggests that arrestins contain domains that specifically contact regions of the receptor exposed following receptor activation. Initial localization of such domains was provided by the observation that truncated arrestin-1 partially retained the ability to bind with light-activated rhodopsin. It was further demonstrated that at least three regions within the N-terminal half of arrestin-1 were involved in recognizing light-activated rhodopsin.

The importance of receptor phosphorylation in arrestin binding has also been explored in significant detail. The phosphorylation-recognition domain within arrestin-1 (residues 163–179) has been extensively characterized. These studies revealed two relatively independent changes that occur in arrestin on receptor binding: (1) increased binding affinity of the phosphorylation-recognition region of arrestin for the phosphorylated C terminus of rhodopsin, and (2) mobilization of additional receptor binding sites. These experiments also revealed that charge inversion of Arg-175 generates an "activated" form of arrestin that demonstrates phosphorylation-independent receptor binding. These studies and others provide the basis for a model of GPCR/arrestin interaction that is initiated by the activation- and phosphorylation-dependent binding of arrestin to receptor, culminating in a conformational change in arrestin that promotes additional interactions with the receptor.

Role of Arrestins in GPCR Endocytosis

Radioligand binding and immunocytochemical techniques have demonstrated that many GPCRs undergo endocytosis and multiple studies have implicated an important role for GRKs and arrestins in this process. Initial efforts revealed that GRK2 and nonvisual arrestins could enhance agonist-dependent endocytosis of the β_2AR. Additional analysis revealed that arrestins promoted endocytosis of agonist-activated GPCRs via an ability to interact with clathrin, the major protein component of the clathrin-based endocytic machinery. Predictably, arrestin mutants impaired in clathrin binding are largely defective in promoting β_2AR endocytosis. Consistent with these findings, minigenes expressing the C-terminal clathrin-binding domains of arrestin-2 or -3 are constitutively localized to clathrin-coated pits and function as dominant negative inhibitors of GPCR endocytosis. Additional studies have implicated a role

for nonvisual arrestin interaction with the β-subunit of the adaptor protein AP-2 in GPCR endocytosis and there also appears to be a critical role for arrestin interaction with PIP_2 in this process. In fact, a mutant arrestin-3 that is defective in phosphoinositide binding can still interact with the agonist-activated receptor but does not localize to clathrin-coated pits. Thus, nonvisual arrestin interaction with clathrin, AP-2, and PIP_2 contribute to arrestin-promoted endocytosis of GPCRs.

Role of Arrestins as Scaffolds in Cell Signaling

Several studies suggest that arrestins also have roles beyond regulating GPCR desensitization and trafficking. The finding that arrestin-2 binds directly to c-Src provided initial insight into this possibility. This interaction appears to be mediated via a proline-rich region in arrestin-2 interacting with the SH3 domain in Src, although the catalytic domain of Src may also contribute to binding. Since arrestin-2–Src interaction may be regulated by arrestin phosphorylation, the current model proposes that arrestin-2 binding to receptor promotes arrestin dephosphorylation enabling c-Src to bind and be recruited to clathrin-coated pits as part of a receptor–arrestin–Src complex. This localization may regulate Src-mediated phosphorylation of components (e.g., dynamin) that may, in turn, contribute to the regulation of GPCR trafficking and/or signaling.

Additional studies have suggested a role for arrestins as MAP kinase scaffolds. Several studies have focused on the potential involvement of arrestin-2 in GPCR-mediated activation of ERK1/2 and have demonstrated formation of complexes that contain receptor, arrestin-2, ERK1/2, and either raf-1 or Src. Studies have also demonstrated that arrestin-3 can directly bind to JNK3 and ASK1, a JNK kinase kinase, suggesting a role for arrestin-3 as a MAP kinase scaffold. Interestingly, stimulation of the AT_{1A} angiotensin receptor resulted in JNK3 activation and triggered the colocalization of arrestin-3 and active JNK3 to intracellular vesicles. Thus, arrestins may serve as scaffolds to mediate GPCR activation of various MAP kinase complexes.

The Structural Basis for Arrestin Function

Initial structural insight on arrestins was provided by the X-ray crystal structure of arrestin-1 while more recently the crystal structure of arrestin-2 has been solved. In general, arrestins have an elongated shape and are almost exclusively made up of β-sheets and connecting loops with the exception of one short α-helix. Each arrestin molecule is composed of two major domains termed the N domain and C domain that are held together by a set of buried salt bridges termed the polar core. The N and C domains are connected by a short hinge and are thought to move relative to each other in the process of arrestin's transition into an active conformation. The arrestin polar core is comprised of charged residues from the N-terminus, N domain, C domain, and C-terminus, thus bringing different parts of the molecule together to maintain a basal conformation. The residues involved in formation of the polar core are highly conserved, suggesting that this structural element is conserved in all arrestins and critical for function. Because the buried side chains of the polar core achieve neutrality by an elaborate network of electrostatic interactions, it has been suggested that disturbance of the polar core by introduction of a phosphate group from the receptor promotes structural changes that result in an active conformation of the protein. Disruption of polar core interactions can be simulated by charge inversion of an arginine (Arg-175, 169, and 170 in arrestin-1, -2, and -3, respectively) that lies in the center of the polar core. Mutation of this arginine results in an arrestin that binds equally well to phosphorylated and non-phosphorylated GPCRs suggesting that this residue plays a key role in recognition of phosphorylated receptor and in maintaining the basal conformation of arrestin. Taken together, these studies suggest that activation of arrestin results in significant structural changes that play an important role in mediating the various protein interactions and cellular functions of arrestin.

See Also the Following Articles

Adenylyl Cyclases • Brassinosteroids • Endocytosis • Histamine Receptors • Protein Kinase C Family

Glossary

desensitization A loss in responsiveness of a signaling system often due to an agonist-promoted decrease in coupling between receptor and G protein.

down-regulation A decrease in the total cellular level of a receptor typically due to prolonged incubation with agonist.

endocytosis The process of cellular uptake of a protein that often occurs through clathrin-coated pits for G protein-coupled receptors (GPCRs).

phosphorylation The transfer of phosphate from ATP to a serine, threonine, or tyrosine on a protein.

Further Reading

Benovic, J. L., DeBlasi, A., Stone, W. C., Caron, M. G., and Lefkowitz, R. J. (1989). Primary structure of the beta-adrenergic receptor kinase delineates a potential multigene family of receptor specific kinases. *Science* **246**, 235–240.

Ferguson, S. S. (2001). Evolving concepts in G protein-coupled receptor endocytosis: The role in receptor desensitization and signaling. *Pharmacol. Rev.* **53**, 1–24.

Krupnick, J. G., and Benovic, J. L. (1998). The role of receptor kinases and arrestins in G protein-coupled receptor regulation. *Annu. Rev. Pharmacol. Toxicol.* **38**, 289–319.

Lodowski, D. T., Pitcher, J. A., Capel, W. D., Lefkowitz, R. J., and Tesmer, J. J. (2003). Keeping G proteins at bay: A complex between G protein-coupled receptor kinase 2 and G$\beta\gamma$. *Science* **300**, 1256–1262.

Marchese, A., Chen, C., Kim, Y.-M., and Benovic, J. L. (2003). The ins and outs of G protein-coupled receptor trafficking. *Trends Biochem. Sci.* **28**, 369–376.

Perry, S. J., and Lefkowitz, R. J. (2002). Arresting developments in heptahelical receptor signaling and regulation. *Trends Cell Biol.* **12**, 130–138.

Biography

Jeffrey L. Benovic is Professor and Vice Chair in the Department of Microbiology and Immunology at Thomas Jefferson University in Philadelphia. His principal research interests are on the regulation of GPCR signaling with particular emphasis on the role of GRKs and arrestins in this process. He holds a Ph.D. in biochemistry from Duke University, where he also received his postdoctoral training. He has authored over 200 articles on GPCR signaling and regulation.

G_{12}/G_{13} Family

Stefan Offermanns
University of Heidelberg, Heidelberg, Germany

The ubiquitously expressed mammalian G proteins, G_{12} and G_{13}, constitute one of the four families of heterotrimeric G proteins (G_s, $G_{i/o}$, $G_{q/11}$, and $G_{12/13}$). Heterotrimeric G proteins, which consist of α-, β-, and γ-subunits, are defined by their α-subunit and act as molecular switches, which transmit signals from heptahelical G-protein-coupled receptors (GPCRs) at the plasma membrane to intracellular effectors. Orthologues of the mammalian G_{12} and G_{13} α-subunits, $G\alpha_{12}$ and $G\alpha_{13}$, have also been found in other multicellular organisms like *Drosophila melanogaster* and *Caenorhabditis elegans*. G_{12}/G_{13} regulate cytoskeletal rearrangements and cell growth in part via the small GTPase Rho.

General Properties and Modifications

The α-subunits of G_{12} and G_{13}, $G\alpha_{12}$ and $G\alpha_{13}$, have been identified by Mel Simon's group using a PCR cloning approach. $G\alpha_{12}$ and $G\alpha_{13}$ share 67% sequence identity and have a length of 377–380 amino acids. Biochemical analysis of purified $G\alpha_{12}$ and $G\alpha_{13}$ has revealed a relatively low rate of GTP hydrolysis, as well as a relatively slow guanine nucleotide exchange rate. Their expression levels in most cells appear to be lower than those of other G protein α-subunits. Both, $G\alpha_{12}$ and $G\alpha_{13}$, undergo palmitoylation, a reversible post-translational modification, which occurs at cysteine residues close to their N termini. Palmitoylation localizes G_{12} and G_{13} to the inner side of the plasma membrane and is required for proper signaling via G_{12}/G_{13}. *In vitro* experiments have shown that purified $G\alpha_{12}$ is a substrate for protein kinase C, whereas $G\alpha_{13}$ can be phosphorylated by protein kinase A. The physiological significance of these phosphorylations is unclear.

Receptor-Mediated Activation of G_{12} and G_{13}

It has been difficult to provide direct evidence for the coupling of a defined receptor to G_{12}/G_{13}. However, for a variety of GPCRs coupling to G_{12}/G_{13} could be demonstrated using different methods including the immunoprecipitation of receptor-activated G proteins, as well as genetic approaches. These studies revealed that some lipid mediators such as lysophospholipids or thromboxane A_2, various peptides such as endothelin, angotensin II, or substance P as well as the protease thrombin act on receptors, which are able to couple to G_{12}/G_{13} (Table I). G_{12} and G_{13} appear to be activated by GPCRs, which also couple to G_q/G_{11} and in some cases to G_i/G_o. However, not all G_q/G_{11}-coupled receptors are also able to activate G_{12}/G_{13}.

Cellular Functions of G_{12}/G_{13}

Most information on the cellular functions regulated via G_{12}/G_{13} came from indirect experiments employing constitutively active mutants of $G\alpha_{12}/G\alpha_{13}$ which lack the intrinsic GTPase activity due to an exchange of a glutamine residue (Q231 and Q226 in human $G\alpha_{12}$ and $G\alpha_{13}$, respectively) to a leucine residue. Several laboratories could show that transfection of these mutants into different cell types leads to cellular transformation. Interestingly, human $G\alpha_{12}$ was first cloned in a screen for transforming oncogenes from a Ewing Sarcoma cDNA library. However, it is still unknown whether $G\alpha_{12}$ or $G\alpha_{13}$ are involved in the pathogenesis of any neoplastic disease. In subsequent studies, the expression of constitutively active mutants of $G\alpha_{12}/G\alpha_{13}$ was shown to induce a variety of signaling pathways leading to the activation of various downstream effectors including phospholipase A_2, Na^+/H^+ exchanger or c-Jun N-terminal kinase.

Another important cellular function of G_{12}/G_{13} is their ability to regulate the formation of actomyosin-based structures and to modulate their contractility by increasing the activity of the small GTPase RhoA. The RhoA-mediated formation of actin stress fibers in fibroblasts activated by various G-protein-coupled receptor agonists is one of the best described cellular paradigms for G_{12}/G_{13}-mediated Rho activation and subsequent rearrangement of the actin cytoskeleton. This phenomenon involves a Rho-induced bundling of

TABLE I

GPCRs Shown to Couple to G_{12}/G_{13}

Receptor	Endogenous ligand(s)	G-protein subclass(es)
AT_1	Angiotensin II	$G_{12/13}$, $G_{q/11}$, $G_{i/o}$
B_2	Bradykinin	$G_{12/13}$, $G_{q/11}$
ET_A	Endothelin-1, -2	$G_{q/11}$, $G_{12/13}$, G_s
ET_B	Endothelin-1, -2, -3	$G_{12/13???}$
GAL2	GALP, Galanin	$G_{i/o}$, $G_{q/11}$, $G_{12/13}$
5-HT_{2C}	Serotonin	$G_{12/13}$, $G_{q/11}$
LPA_1 (Edg2) LPA_2 (Edg4)	Lysophosphatidic acid	G_i, $G_{q/11}$, $G_{12/13}$
LPC_1 (G2A)	Lysophosphatidylcholine	$G_{12/13}$, $G_{q/11}$,
NK_1	Substance P	$G_{12/13}$, $G_{q/11}$
PAR-1 PAR-3/4	Thrombin and others	$G_{12/13}$, $G_{q/11}$, G_i
$S1P_2$ (Edg5) $S1P_3$ (Edg3)	Spingosine-1-phosphate	$G_{12/13}$, G_i, $G_{q/11}$ $G_{12/13}$, G_i, $G_{q/11}$
TP	Thromboxane A_2	$G_{q/11}$, $G_{12/13}$
TSH	Thyrotropin	$G_{12/13}$, G_s, $G_{q/11}$, G_i
V_{1A}	Vasopressin	$G_{12/13}$, $G_{q/11}$

Summarized are findings from various laboratories which are based on the immunoprecipitation of receptor activated $G\alpha_{12}/G\alpha_{13}$ using photoaffinity labeling or a GDP/[^{35}S]GTPγS exchange assay as well as on genetic evidence from $G\alpha_{12}/G\alpha_{13}$ deficient cells. Please note that this list is far from being complete.

actin filaments into stress fibers and the clustering of integrins and associated proteins into focal adhesion complexes. The ability of $G\alpha_{12}/G\alpha_{13}$ to induce actin stress fiber formation in fibroblasts was first described by the group of Gary Johnson. Regulation of actin-based structures via a G_{12}/G_{13}-mediated and Rho-dependent pathway has also been shown to occur in many other eukaryotic cells. For instance, in neuronal cells, activation of Rho through lysophosphatitic acid or thrombin receptors leads to the formation of contractile actomyosin filaments eventually leading to the induction of neurite retraction, cell rounding, or axonal growth cone collapse. In vascular smooth muscle cells, the G_{12}/G_{13}-Rho-mediated pathway has been shown to contribute to the vasoconstrictor-induced actomyosin-based cell contraction, and the same pathway appears to be involved in the platelet shape change response.

Proteins Directly Interacting with $G\alpha_{12}/G\alpha_{13}$

Until recently, it was not clear how G_{12} and G_{13} regulate the function of RhoA. In general, the activation of Rho by exchange of GDP for GTP is catalyzed by guanine nucleotide exchange factors (GEFs), which in turn are regulated by various, mostly ill-defined mechanisms in the cell. First indications that a RhoGEF protein is regulated by G_{12}/G_{13} came from studies on early gastrulation events in *Drosophila*. Genetic analysis indicated that DRhoGEF2, a *Drosophila* RhoGEF protein, functions downstream of the *Drosophila* $G\alpha_{12}/G\alpha_{13}$ orthologue, the *concertina* gene product. Subsequently, three mammalian RhoGEF proteins (p115RhoGEF, PDZ-RhoGEF, and LARG) were described which are able to interact with activated $G\alpha_{12}/G\alpha_{13}$. This family of RhoGEF proteins is characterized by the presence of a "regulator of G protein signaling" (RGS)-domain, which mediates the interaction with the α-subunits of G_{12}/G_{13}. While the RhoGEF activity of PDZ-RhoGEF and LARG appears to be activated by both, $G\alpha_{12}$ and $G\alpha_{13}$, p115 RhoGEF activity is stimulated only by $G\alpha_{13}$. In addition, the RGS domains of these RhoGEF proteins accelerate the intrinsic GTP hydrolysis activity of $G\alpha_{12}/G\alpha_{13}$ *in vitro* and, thus, function as "GTPase-activating proteins" (GAPs). While it is now well established that RhoGEF proteins which contain an RGS-domain interact with $G\alpha_{12}/G\alpha_{13}$, the precise mode of this interaction is still not completely clear. In addition, several groups have found evidence for an involvement of tyrosine kinases in the regulation of Rho via G_{12}/G_{13}. In any case, regulation of RhoGEF proteins by $G\alpha_{12}/G\alpha_{13}$ provided the missing link between G_{12}/G_{13} and their ability to activate the small GTPase RhoA, which then mediates the effects of G_{12}/G_{13} on the cytoskeleton and may also be involved in the transforming activity of these G proteins (Figure 1).

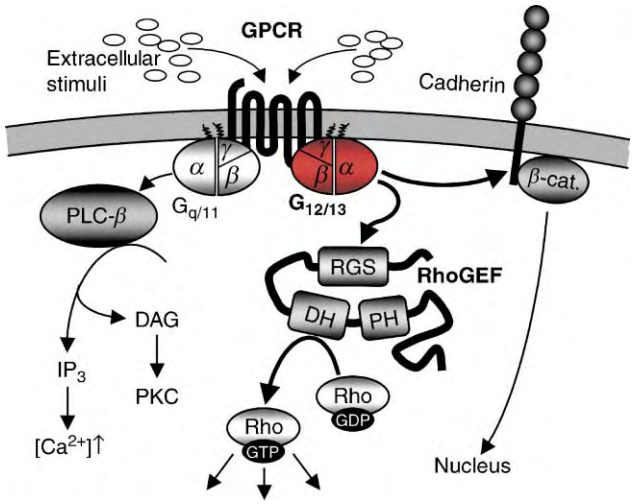

FIGURE 1 Some of the signaling processes mediated by G_{12}/G_{13}. G-protein-coupled receptors (GPCRs) which couple to G_{12}/G_{13} also activate G_q/G_{11}. RhoGEF, guanine nucleotide exchange factor for Rho proteins; PLC-β, phospholipase C β; β-cat., β-catenin; DAG, diacylglycerol; IP_3, inositol-1,4,5-trisphosphate; PKC, protein kinase C; RGS, "regulator-of-G-protein-signaling" domain; DH, "dbl-homology" domain; PH, "pleckstrin-homology" domain; see text for details.

Recently, an interesting link between G_{12}/G_{13} and cadherin-mediated signaling was described by the group of Pat Casey. Active $G\alpha_{12}$ and $G\alpha_{13}$ interact with the cytoplasmic domain of some type I and type II class cadherins, such as E-cadherin, N-cadherin, or cadherin-14, causing the release of β-catenin from cadherins (Figure 1). This down-regulates cadherin-mediated cell activation, and the release of β-catenin from cadherins may be a mechanism, by which $G\alpha_{12}/G\alpha_{13}$ induces cellular transformation.

Various other proteins including Bruton's tyrosine kinase, the Ras GTPase-activating protein Gap1m, radixin, heat shock protein 90, or protein phosphatase type 5 have been shown to interact with $G\alpha_{12}$ and/or $G\alpha_{13}$. However, the biological significance of these interactions are not yet clear.

In vivo Functions of G_{12}/G_{13}

The fact that G_{12}/G_{13} appear to be the major mediators of the activation of RhoA via GPCRs suggests that they are involved in multiple biological processes including morphogenetic processes, regulation of cell shape, or regulation of cell movements. Strong evidence for *in vivo* functions of G_{12}/G_{13} came so far mainly from the analysis of phenotypical changes of null-mutants of these G protein α-subunits in mice, flies, and worms. Experiments in *Drosophila* have provided genetic evidence for a physiological role of the G_{12}/G_{13}/RhoGEF-mediated pathway leading to Rho activation. By gene inactivation and epistasis experiments it could be shown that a signaling pathway, consisting of the G_{12}/G_{13} orthologue *concertina*, the *Drosophila* RhoGEF protein DRhoGEF2, as well as of Rho is involved in the actin/myosin-mediated cellular shape change, which results in the ventral furrow formation of the *Drosophila* embryo. Interestingly, loss of DRhoGEF2 results in a more severe phenotype than observed in *concertina* mutant embryos, suggesting that the *concertina* gene product conveys only part of the upstream regulation of DRhoGEF2.

While mice lacking the $G\alpha_{12}$ gene (*gna12*) are phenotypically normal, deletion of the $G\alpha_{13}$ gene (*gna13*) results in embryonic lethality at embryonic day 9.5 due to a defect in angiogenesis. Chemokinetic effects of thrombin were completely abrogated in fibroblasts lacking $G\alpha_{13}$, indicating that $G\alpha_{13}$ is required for full migratory responses of cells to certain stimuli. The defects observed in $G\alpha_{13}$-deficient embryos and cells occurred in the presence of $G\alpha_{12}$, and loss of $G\alpha_{12}$ did not result in any obvious defects. However, $G\alpha_{12}$-deficient mice, which carry only one intact $G\alpha_{13}$ allele also die *in utero*, and $G\alpha_{12}/G\alpha_{13}$ double deficient mice die even earlier than $G\alpha_{13}$ single deficient animals. This genetic evidence indicates that $G\alpha_{13}$ and its closest relative, $G\alpha_{12}$, fulfill at least partially nonoverlapping cellular and biological functions, which are required for proper mammalian development. Mouse lines carrying conditional mutants of the $G\alpha_{12}/G\alpha_{13}$ genes might allow one to analyze some of the functions of these proteins in the adult mammalian organism.

See Also the Following Articles

Cadherin Signaling • Cytokines • G Protein-Coupled Receptor Kinases and Arrestins • Phospholipase A_2 • P-Type Pumps: Na^+/K^+ Pump • Rho GTPases and Actin Cytoskeleton Dynamics • Small GTPases

Glossary

actin stress fiber Bundles of actin microfilaments which are found on the ventral side of cells cultured on artificial surfaces. They contain myosin and α-actinin as well as a variety of other structural and regulatory proteins which allow them to contract and to exert tension. The ends of stress fibers terminate at specific sites at the plasma membrane (focal adhesions) which are involved in cell adhesion. Activation of RhoA has been shown to induce actin stress fiber formation.

angiogenesis Growth of new blood vessels by sprouting from existing ones.

cadherins Calcium-dependent adhesion proteins, characterized by the presence of cadherin repeats, which are present in the extracellular part of the protein. Cadherins mediate Ca^{2+}-dependent homophilic adhesion. Cadherins are divided into two subfamilies, the classic cadherins and the protocadherins. Classic cadherins are subdivided into four subfamilies, the type I classic

cadherins, the type II classic cadherins, the desmosomal cadherins, and the so-called "other classic cadherins."

guanine nucleotide exchange factor (GEF) Guanine nucleotide exchange factors (GEFs) are proteins which catalyze the release of nucleotide bound to small GTPases like RhoA. In most cases, GEFs bind to the GDP bound GTPase, causing dissociation of the GDP. GTP, which is present at higher concentrations in the cell than GDP, then binds to the GTPase, and the GEF is released.

RhoA Small GTP-binding protein (small GTPase). Being one of the best studied members of the Rho-family of small GTPases, it has been shown to play an important role in the regulation of the actin cytoskeleton.

Further Reading

Buhl, A. M., Johnson, N. L., Dhanasekaran, N., and Johnson, G. L. (1995). $G\alpha_{12}$ and $G\alpha_{13}$ stimulate Rho-dependent stress fiber formation and focal adhesion assembly. *J. Biol. Chem.* **270**, 24631–24634.

Fukuhara, S., Chikumi, H., and Gutkind, J. S. (2001). RGS-containing RhoGEFs: The missing link between transforming G proteins and Rho? *Oncogene* **26**, 1661–1668.

Gutkind, J. S. (1998). Cell growth control by G protein-coupled receptors: From signal transduction to signal integration. *Oncogene* **17**, 1331–1342.

Kozasa, T., Jiang, X., Hart, M. J., Sternweis, P. M., Singer, W. D., Gilman, A. G., Bollag, G., and Sternweis, P. C. (1998). p115 RhoGEF, a GTPase activating protein for $G\alpha_{12}$ and $G\alpha_{13}$. *Science* **280**, 2109–2111.

Meigs, T. E., Fields, T. A., McKee, D. D., and Casey, P. J. (2001). Interaction of $G\alpha_{12}$ and $G\alpha_{13}$ with the cytoplasmic domain of cadherin provides a mechanism for beta-catenin release. *Proc. Natl. Acad. Sci. USA* **98**, 519–524.

Offermanns, S., Mancino, V., Revel, J.-P., and Simon, M. I. (1997). Vascular system defects and impaired cell chemokinesis as a result of $G\alpha_{13}$ deficiency. *Science* **275**, 533–536.

Parks, S., and Wieschaus, E. (1991). The Drosophila gastrulation gene concertina encodes a $G\alpha$-like protein. *Cell* **64**, 447–458.

Sah, V. P., Seasholtz, T. M., Sagi, S. A., and Brown, J. H. (2000). The role of Rho in G protein-coupled receptor signal transduction. *Annu. Rev. Pharmacol. Toxicol.* **40**, 459–489.

Singer, W. D., Miller, R. T., and Sternweis, P. C. (1994). Purification and characterization of the α-subunit of G_{13}. *J. Biol. Chem.* **269**, 19796–19802.

Strathmann, M. P., and Simon, M. I. (1991). $G\alpha_{12}$ and $G\alpha_{13}$ subunits define a fourth class of G protein α-subunits. *Proc. Natl. Acad. Sci. USA* **88**, 5582–5586.

Biography

Stefan Offermanns is a Professor of pharmacology and Head of the Department of Pharmacology at the University of Heidelberg, Germany. He received an M.D. from the Free University Berlin and was a postdoctoral fellow at the California Institute of Technology. His principal research interests are the cellular and biological roles of signalling pathways involving heterotrimeric G-proteins and small GTPase of the Rho family.

$GABA_A$ Receptor

Richard W. Olsen
University of California, Los Angeles, California, USA

Gregory W. Sawyer
Oklahoma State University, Tulsa, Oklahoma, USA

γ-Aminobutyric acid (GABA) is the neurotransmitter at most inhibitory synapses in the central nervous system. This amino acid is synthesized in one step from L-glutamate by the enzyme glutamic acid decarboxylase (GAD). GAD is present only in GABAergic neurons, comprising up to 30% of those in the nervous system of all organisms, and is a marker for GABA synapses. Dysfunction of GABA, including GAD, is implicated in a variety of neuropsychiatric disorders, including epilepsy, anxiety, depression, and drug dependence.

Fast inhibitory synaptic transmission is mediated primarily by the GABA-type A receptor ($GABA_A$ receptor (GABAR)), a ligand-gated chloride ion channel. Some slow inhibition is mediated by GABA at the GABA-type B ($GABA_B$) receptor, a G protein-coupled receptor. GABAR are members of a neurotransmitter receptor superfamily that includes the nicotinic acetylcholine receptors, glycine receptors, and serotonin $5HT_3$ receptors. The nicotinic acetylcholine receptors and the GABAR are families of heteropentameric isoforms, or receptor subtypes. These have different age-dependent and brain regional localization, circuit participation, and, thus, involvement in different functions and behaviors. Despite the lack of X-ray crystallographic data on the structure of GABAR, considerable information about functional domains within the protein is evolving. GABAR are the targets of important drugs, including general anesthetics and agents, such as the benzodiazepines used to treat epileptic seizures, anxiety, and sleep disorders. Benzodiazepines are synthetic compounds with important clinical utility (neuroactive drugs). The benzodiazepine "receptor," or site that mediates their pharmacological effects, is a portion of the GABAR protein itself; indeed, the binding site appears to be a modified version of the binding site for GABA.

Molecular Structure

Heteropentamers

The members of the superfamily share a pseudo-symmetric, pentameric membrane-spanning structure, with all subunits contributing equally to the ion channel (Figure 1). Each member of the superfamily is made from a family of homologous subunits of 45–67 kDa, with a conserved topology. These subunits each possess a long extracellular N terminus, which in some cases carries the neurotransmitter-binding site, four membrane-spanning domains, including the ion channel wall in M2, and a large variable sequence intracellular loop between M3 and M4. Although the structure of these complicated oligomeric receptor-channel membrane proteins has so far not been solved by crystallographic methods, some structural information has been obtained for other kinds of membrane receptors, ion channels, and, particularly, the extracellular domain of the nicotinic acetylcholine receptor, found to be exactly homologous to a snail acetylcholine-binding protein.

A Family of Isoforms

The heteropentameric GABAR protein is most often made from α, β, and γ subunits. The most common combination contains two copies of one α-subunit, two copies of one β-subunit, and one copy of $\gamma 2$, arranged as in Figure 2. The isoform most abundantly expressed in the CNS contains $\alpha 1\beta 2\gamma 2$. Those containing $\alpha 2$ or $\alpha 3$ are less abundant, and $\alpha 4$, $\alpha 5$, and $\alpha 6$-containing GABAR are even less abundant, with very restricted regional expression. Each α has a preferential β-partner ($\beta 1$, $\beta 2$, $\beta 3$, or θ, similar to avian $\beta 4$), although some α can combine with different β-subunits in different regions. Some GABAR isoforms appear to contain two different α-subunits, but these are relatively nonabundant. Additional rare isoforms have subunits substituted for $\gamma 2$. For example, the $\alpha 4$ and $\alpha 6$ subunits can combine with $\gamma 2$ or with δ in cerebellar and dentate gyrus granule cells and thalamic relay cells. Rarely, $\gamma 1$, $\gamma 2$, or ε (related to avian $\gamma 4$) can substitute for $\gamma 2$ in pentamers containing certain $\alpha\beta$ combinations.

Anatomical Localization and Functional Heterogeneity

Each GABAR subunit shows a specific anatomic and cellular localization as determined by assay of mRNA

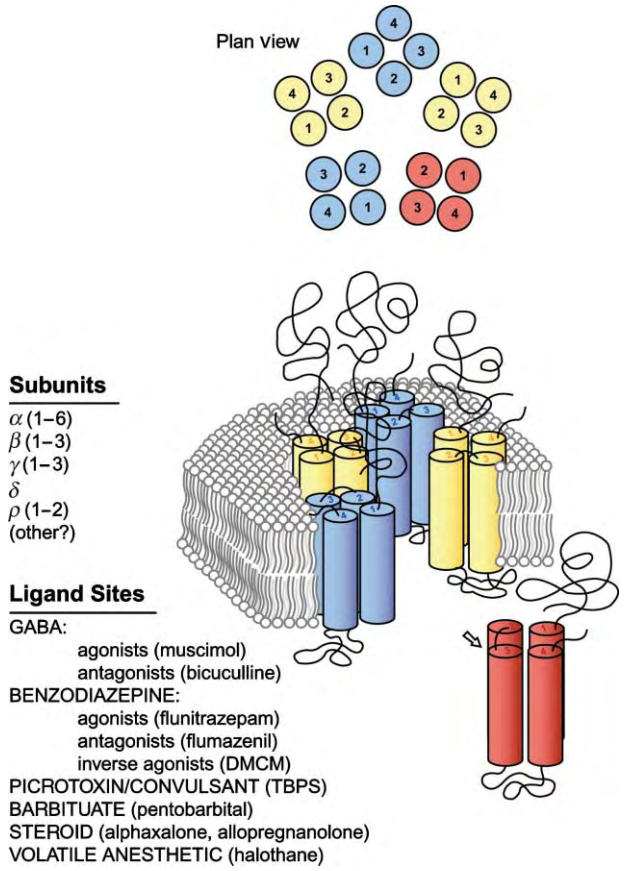

FIGURE 1 Schematic of GABA$_A$ Receptors. The protein is shown as a pseudo-symmetric membrane-spanning ion channel protein made of five homologous subunits, each of which has four membrane-spanning regions as shown in the pull-out subunit. The view from outside the cell (plan view) shows the arrangement around the central core, the chloride ion channel. Also indicated are the subunit families that can be utilized in composing each receptor, and the ligand-binding sites present on the receptor.

and polypeptides, indicating tissue-specific gene expression. Subunit–subunit associations and heteropentamer localization have been revealed by colocalization, copurification, or coimmunoprecipitation studies. Furthermore, there is specific localization to subcellular sites on the plasma membrane, such as synaptic versus nonsynaptic regions, cell bodies versus axons and dendrites, including positioning at postsynaptic locations apposed to specific cellular inputs. For example, the abundant isoform $\alpha1\beta2\gamma2$ is found primarily on inhibitory interneurons, thus inhibiting inhibition and producing a net excitatory circuit. Alternatively, many isoforms containing $\beta3$ are partnered with $\alpha2$, $\alpha3$, and $\alpha5$ subunits and localized on cells that use neurotransmitters other than GABA. These include principal excitatory cells, in which case GABAR inhibit a local circuit. The $\alpha1$ subunit appears to occur at any and all subcellular locations within a given cell, while the $\alpha2$ is limited to axo-axonal synapses in some cells. Thus the nature of the α-subunit, or perhaps specific partnering, may play a role in localization. In addition, heterogeneity has been demonstrated in the developmental profile of individual subunits in brain regions and cells.

The heterogeneity in subunit composition for the GABAR isoforms provides an explanation for pharmacological subtypes based primarily on ligand affinities, and secondarily on other factors such as sensitivity to regulatory systems. GABAR in certain brain regions, with certain subunit compositions, vary in their sensitivity to modulatory drugs like general anesthetics, including barbiturates, and benzodiazepines, as well as the biologically endogenous modulators, the neurosteroids. The neurosteroids are hormone metabolites that have rapid and direct effects on neurons, such as modulation of GABAR. Metabolites of the female sex hormone progesterone (allopregnanolone), corticosteroids (tetrahydrocorticosterone), and possibly androgens, enhance GABAR currents and appear to reach effective concentrations during certain physiological and pathological conditions. This field of research is just in its infancy.

Insights Gained from Transgenic Mice

Interestingly, the specific anatomical location and circuitry of GABAR subtypes dictates the specificity of functions and involvement in specific behaviors. Thus, transgenic and gene-targeted mice have demonstrated a role for certain subunits in particular functions and abnormalities, as well as pharmacology. For example, a mouse knockout for the $\gamma2$ subunit reveals a role for this subunit in proper synaptic localization and clustering of GABAR, and a role in anxiety, stress, and fear conditioning. Knockout of the $\beta3$ subunit produces a severe phenotype with epilepsy, motor incoordination, hyperactivity, and cognitive defects. These observations suggest that decreased levels of $\beta3$ subunit expression may contribute to Angelman syndrome, a human genetic disease with similar phenotype. Knockout of the common $\alpha1$ and $\beta2$ subunits have surprisingly little phenotype, perhaps due to compensatory increases in other subunits. Knockout of the $\alpha6$ subunit reveals its obligatory partnership with the δ subunit in the cerebellum, since no δ peptide is expressed in surface receptors. Knockout or knockdown of the $\alpha5$ subunit yields an animal with improved spatial memory acquisition, implicating $\alpha5$-containing GABAR in the CA1 region in mechanisms that are inhibitory for learning. Genetic knockins of point mutations for drug-binding sites have revealed subunit and subtype functions such as the differential importance of the $\alpha1$-subunit and its sites of expression in sedative/hypnotic functions, the $\alpha2$-subunit in anxiety, and the $\beta3$-subunit but not $\beta2$-subunit in the action of the intravenous anesthetic etomidate. Aberrant plasticity of GABAR in

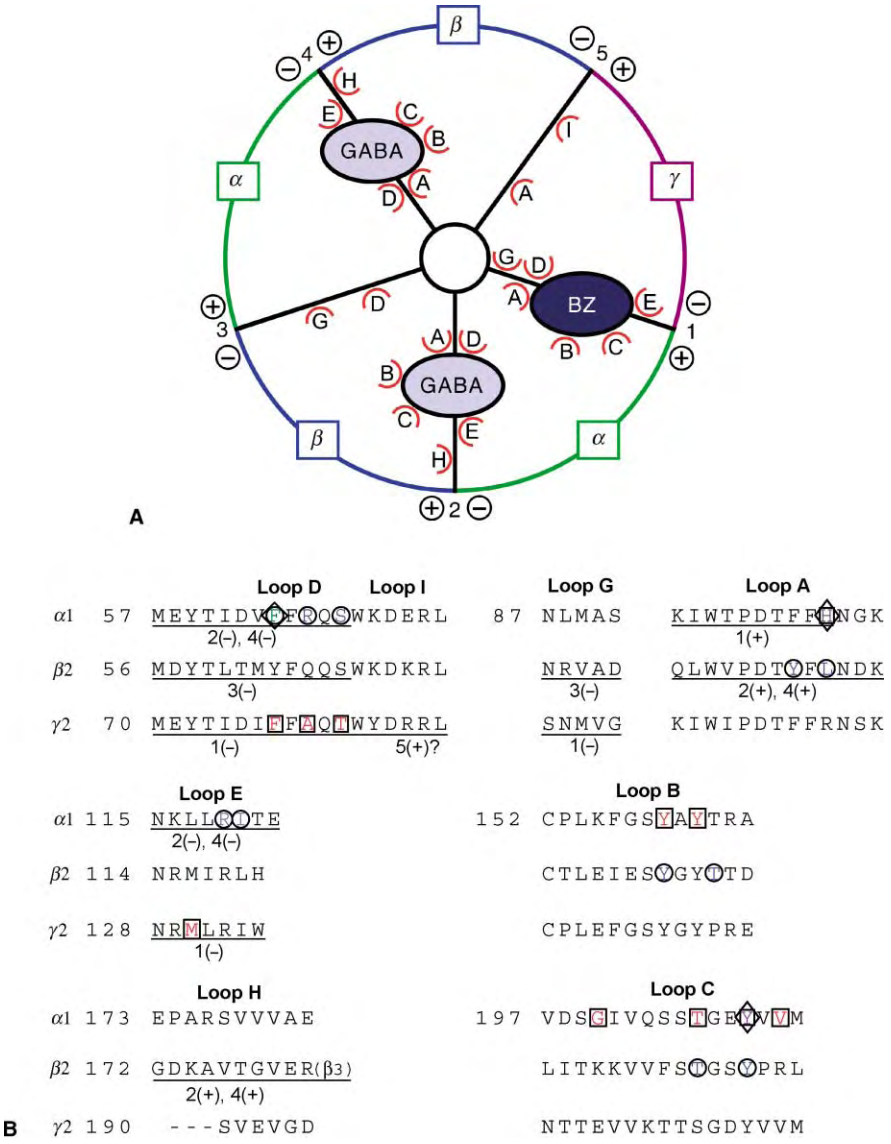

FIGURE 2 Donut model of GABA$_A$ receptor heteropentamer showing ligand-binding and subunit interaction domains. (A) The 5 subunits (-β–γ–α–β–α-) and 5 subunit interfaces (1–5) are shown, indicating the two different subunit interfaces for each subunit ((−) and (+)), the ligand-binding pockets for GABA and benzodiazepines (BZ), and the various peptide loops (A–I) involved in ligand-binding or subunit interfaces. The pore in the center represents the chloride channel. (B) The sequences represent the loops A–I within the N-terminal extracellular domain of the α1, β2, and γ2 subunits (numbering corresponds to mature subunits from rat). Circles: GABA site; squares: BZ site; diamonds (α1): photoaffinity label sites identified by sequencing: F64 (Muscimol); H101 (Flunitrazepam); Y209 (Ro15-4513). Underlines: subunit interaction loops, indicated under the line.

which a subunit switch occurs, such as α1 to α4, appear to contribute to drug withdrawal and seizure susceptibility. A summary of current (incomplete) knowledge of subtype localization and function is given in Table I.

Subcellular Localization, Associated Proteins, and Synaptic Plasticity

The localization of GABAR likewise involves events other than gene expression. These include intracellular trafficking, surface membrane insertion, synaptic clustering, removal of GABAR from synapses, and recycling or degradation. For example, the nature of the β-subunit seems to determine the subcellular location of GABAR. Regulation of these activities allows some plasticity of subunit composition of adult brain.

Several associated proteins have been identified in GABAR cell biology. These include especially gephyrin, originally isolated as a glycine receptor-associated synaptic clustering protein, that also appears to colocalize at synapses with some isoforms of GABAR. Likewise, GABARAP, a microtubule-associated protein, is involved

TABLE I

Summary of Native GABA$_A$ Receptor Subtypes

Subunit composition	Location	Function	Comments
$\alpha1\beta2\gamma2$	Widespread, esp. GABA neurons	Sedation, anticonvulsant	Adult, BZ1 pharmacology reduced in drug tolerance?
$\alpha2\beta3\gamma2$	Forebrain spinal cord	Anxiety, muscle relaxant	Axon hillock in some cells embryonic and adult
$\alpha2\beta1\gamma1$	Glia		
$\alpha3\beta3\gamma2$	Cortex	Anticonvulsant	Embryonic and adult
$\alpha4\beta2\gamma2$	Thalamus Dentate gyrus		Insensitive to agonist BZ elevated in drug withdrawal?
$\alpha4\beta2\delta$	Thalamus Dentate gyrus	Tonic inhibition	Extrasynaptic, BZ-insensitive, adult
$\alpha5\beta3\gamma2$	Hippocampus CA1 sensory ganglia	Tonic inhibition	Extrasynaptic, BZ-sensitive
$\alpha6\beta2\gamma2$	Cerebellar granule cells		Insensitive to agonist BZ
$\alpha6\beta2\delta$	Cerebellar granule cells	Tonic inhibition	Extrasynaptic, BZ-insensitive, adult
$\gamma3$, θ, ε	Little information		

in intracellular membrane vesicle trafficking and targeting of GABAR. GABARAP binds to the intracellular loop of the γ subunits but not others. Since the $\gamma2$ subunit is needed to direct GABAR to synapses, this interaction, as well as those with other proteins, may contribute to the process. Some aspects of channel function, allosteric modulation, and cell biology are regulated by post-translational mechanisms including protein phosphorylation. Many such topics are still controversial.

Functional Domains

Assembly

Rules determining which pentamers are produced are built in to the sequences of the subunits, primarily in the extracellular N-terminal domains. These residues involved in subunit partnering, assembly, and stoichiometry have been identified by subunit sequence scanning, site-directed chimeras and mutagenesis. They involve homologous positions in different subunits and are located at regions of subunit interfaces (Figure 2). Thus, approximately two dozen isoforms are significantly present in the nervous system, out of the literally thousands of possible permutations of heteropentamers.

Ligand-Binding Sites

Although the presence of a γ-subunit (generally $\gamma2$) in the pentamer is required for benzodiazepine (BZ) sensitivity, the nature of the α subunit determines the BZ site selectivity. The δ subunit is selectively associated with the $\alpha6$ subunit in cerebellar granule cells and with the $\alpha4$ subunit elsewhere. Although isoforms containing $\alpha4/6$ and $\gamma2$ can bind BZ inverse agonists, $\alpha4/6$-γ isoforms are totally BZ-insensitive, and they are excluded from synapses. The δ-containing isoforms are involved in producing tonic inhibition involving spillover of synaptic transmitter or other long-lasting pools of extrasynaptic GABA. These tonic currents are therefore affected by the activity of GABA transporters in nerve endings, postsynaptic cell bodies, and surrounding glia. The extrasynaptic δ-receptors appear to have higher affinity for GABA than synaptic receptors, slower desensitization, and they are the main targets of endogenous neurosteroid modulation.

Inspection of sequences for the BZ-sensitive and insensitive α-subunits suggested amino acid residues critical for BZ binding. The contribution of these residues was subsequently verified by site-directed mutagenesis and functional analysis by recombinant expression in heterologous cells. Additional information on ligand-binding site residues was obtained by microsequencing of peptides covalently attached by radioactive photaffinity labeled BZ ligand. Figure 2 summarizes results from the two approaches, indicating the residues participating in the BZ-binding site, one per pentamer; this is localized at the interface of α- and γ-subunits.

Similar approaches have identified residues involved in the agonist (GABA)-binding sites (two per pentamer), which are localized at the interface between α- and β-subunits. In fact, the residues in the β subunit that participate in the GABA-binding pocket are part of the BZ-binding pocket in the α subunit. This suggests that the binding site for BZ, a synthetic drug, is an evolutionary development of an agonist site. In addition, it is clear that the same residues in homologous sequences of other members of the receptor super-family are involved in the neurotransmitter-binding pocket, involving 5–6 small loops in the extracellular domain (Figure 2).

Ion Channel/Sites for Action of Allosteric Blockers and Enhancers

As in other members of the superfamily, the second transmembrane domain M2 has been shown to form the ion channel in GABAR. Residues in this domain affect

ion selectivity, gating, conductance, kinetics, and desensitization of the channel. This area is also involved in the action of picrotoxin and cage convulsants that functionally block the channel, as well as certain allosteric modulators like general anesthetics that enhance GABA or activate the channel. Residues have been identified within the mouth of the ion channel in M2, as well as on the back side of the M2 helix, that are required for general anesthetic modulation of GABAR. Other residues at the extracellular ends of M3 and M1 have been implicated and appear to be spatially situated near the position of the identified M2 residues, suggesting the possibility of an anesthetic-binding pocket, although this area may be involved only in allosteric coupling.

See Also the Following Articles

Allosteric Regulation • GABA$_B$ Receptor • Ion Channel Protein Superfamily

Glossary

allosteric Literally, "at another site": proteins have domains, or sites, that carry out their functions, termed "active" sites, such as the binding site on a receptor for the neurotransmitter ligand. Other ligands bind at different, or allosteric sites, to modulate the activity of the protein.

ligand-gated ion channel receptor Some receptors are coupled to effector systems in the cells, possibly a cascade of events, while other receptors are themselves ion channels, regulated by binding of the neurotransmitter ligand.

neurosteroid Steroids that are found endogenously in the nervous system and have some function there. Neuroactive steroids have some action in the nervous system but may originate there or have exogenous sources, elsewhere in the body, or be administered as drugs.

receptor protein Proteins that recognize the signal molecule, the neurotransmitter, bind it, and trigger a response.

transgenic mouse An animal that has been genetically engineered to express a foreign gene (a "trans" gene) or a mutated version of its own gene (knockout or knockin).

Further Reading

Jones-Davis, M., and Macdonald, R. L. (2003). GABA$_A$ receptor function and pharmacology in epilepsy and status epilepticus. *Curr. Opin. Pharmacol.* **3**, 12–18.

Martin, D. L., and Olsen, R. W. (eds.) (2000). *GABA in the Nervous System: The View at 50 Years*. Lippincott, Williams and Wilkins, Philadelphia.

McKernan, R. M., and Whiting, P. J. (1996). Which GABA$_A$ receptor subtypes really occur in the brain? *Trends Neurosci.* **19**, 139–143.

Möhler, H., Fritschy, J. M., and Rudolph, U. (2002). A new benzodiazepine pharmacology. *J. Pharmacol. Exp. Ther.* **300**, 2–8.

Moss, S. J., and Smart, T. G. (2001). Constructing inhibitory synapses. *Nat. Rev. Neurosci.* **2**, 240–250.

Olsen, R. W., and Macdonald, R. L. (2002). GABA$_A$ receptor complex: Structure and function. In *Glutamate and GABA Receptors and Transporters: Structure, Function, and Pharmacology* (J. Ejeberg, A. Schousboe and P. Krogsgaard-Larsen, eds.) pp. 202–235. Routledge, London.

Sieghart, W., and Sperk, G. (2002). Subunit composition, distribution and function of GABA$_A$ receptor subtypes. *Curr. Top. Med. Chem.* **2**, 795–816.

Sigel, E. (2002). Mapping of the benzodiazepine recognition site on GABA$_A$ receptors. *Curr. Top. Med. Chem.* **2**, 833–840.

Biography

Richard W. Olsen is a Professor of Neuroscience, Pharmacology, and Anesthesiology at the University of California, Los Angeles, School of Medicine. His principal research interest is in the structure and function of GABA$_A$ receptors. He received his Ph.D. in Biochemistry from the University of California, Berkeley, and did postdoctoral research at the Pasteur Institute in Paris, France.

Gregory W. Sawyer is a Professor in the Department of Pharmacology and Physiology at Oklahoma State University, Center for Health Sciences in Tulsa. His primary research interests are in the cell biology and structure/function of G protein-coupled receptors. He obtained his Ph.D. from the University of California, Irvine and received his postdoctoral training at the University of California, Los Angeles.

$GABA_B$ Receptor

S. J. Enna
University of Kansas Medical Center, Kansas City, Kansas, USA

γ-Aminobutyric acid (GABA) is a major inhibitory neurotransmitter in the central nervous system (CNS). The responses to GABA are mediated by two classes of receptors, $GABA_A$ and $GABA_B$. While the former is a pentameric, ionotropic chloride ion channel, the $GABA_B$ site is a heterodimeric, Group 3 G-protein coupled receptor. Structurally, the $GABA_B$ receptor consists of two 7 transmembrane spanning subunits, $GABA_{B(1)}$ and $GABA_{B(2)}$. Whereas the orthosteric-binding site for the neurotransmitter is located on the $GABA_{B(1)}$ subunit, G protein coupling is associated with the $GABA_{B(2)}$ component. The functional and pharmacological characteristics of $GABA_B$ receptors have been defined using potent and selective agonists and antagonists. Studies with both wild type and expressed $GABA_B$ receptors indicate that a $GABA_{B(1)}$/$GABA_{B(2)}$ dimerization is obligatory for receptor function. The discovery of positive allosteric modulators may pave the way for the development of $GABA_B$-receptor subtype-selective drugs. Such compounds, along with competitive agonists and antagonists, may be of value in treating a host of neurological and psychiatric conditions including spasticity, epilepsy, depression, cognitive impairments, and pain.

$GABA_B$-Receptor Structure and Function

The $GABA_B$ receptor was first identified in 1981. Studies revealed that (R,S)-β-aminomethyl-β-(4-chlorophenyl)-propanoic acid (baclofen), a drug used to treat spasticity, and GABA inhibit depolarization-induced neurotransmitter release and compete for a specific binding site in brain tissue. Since neither the functional response to baclofen nor its binding are inhibited by bicuculline, a competitive $GABA_A$-receptor antagonist, it was proposed that baclofen interacts with a different class of receptors, which were designated $GABA_B$ sites. Subsequent work demonstrated further that $GABA_A$ and $GABA_B$ receptors are distinct entities. Thus, although baclofen, like $GABA_A$-receptor agonists, hyperpolarizes neurons, the baclofen-sensitive receptors are coupled to G proteins, unlike the ionotropic $GABA_A$ site. Activation of the $GABA_B$ receptor decreases Ca^{2+} and increases K^+ membrane conductance, whereas the $GABA_A$ receptor regulates chloride ion flux. Although baclofen inhibits forskolin-stimulated adenylyl cyclase activity in brain tissue, it enhances cAMP production in brain slices if they are exposed simultaneously to agents, such as β-adrenoceptor agonists, that activate receptors coupled to G_s. Thus, depending on the conditions, $GABA_B$-receptor stimulation either enhances or inhibits cAMP accumulation, suggesting an effector system associated with both G_i and G_o proteins. Furthermore, $GABA_B$ receptor stimulation induces nuclear accumulation of the transcription factors ATF4 and ATFx, suggesting genomic consequences to activation of this site.

Definitive proof that the $GABA_B$ receptor is molecularly distinct from the $GABA_A$ site came from expression cloning experiments. These studies revealed that the $GABA_B$ receptor is a heterodimer composed of two 7-transmembrane-spanning proteins (Figure 1). The first protein to be identified was designated $GABA_{B(1)}$, and the second $GABA_{B(2)}$. These subunits, which have 54% amino acid similarity and 35% sequence homology, are characterized by a large extracellular N-terminal domain. Heterodimerization, which is essential for receptor trafficking to the membrane as well as receptor function, occurs predominately through association of the intracellular α-helical portions of the C termini (Figure 1). The orthosteric-binding site for GABA is located within a conserved Venus flytrap region of the $GABA_{B(1)}$, but not $GABA_{B(2)}$, subunit N-terminal domain, whereas the affiliated G proteins are coupled to the $GABA_{B(2)}$ component (Figure 1). The $GABA_B$ site is a group 3 receptor, a category that includes vomeronasal organ, metabotropic glutamate, and calcium-sensing receptors. Indeed, calcium is absolutely required for agonist binding to the $GABA_B$ site. While several splice variants have been identified for the $GABA_{B(1)}$-receptor subunit, not all are capable of forming functional receptors when coupled to $GABA_{B(2)}$. The most extensively studied $GABA_B$-receptor subunit combinations are $GABA_{B(1a)}$/$GABA_{B(2)}$ and $GABA_{B(1b)}$/$GABA_{B(2)}$. A variety of studies, including those with $GABA_B$ subunit deletion mutant mice, have demonstrated that heterodimerization of these two distinct gene products is absolutely essential for a functional receptor, with homodimers being biologically inert.

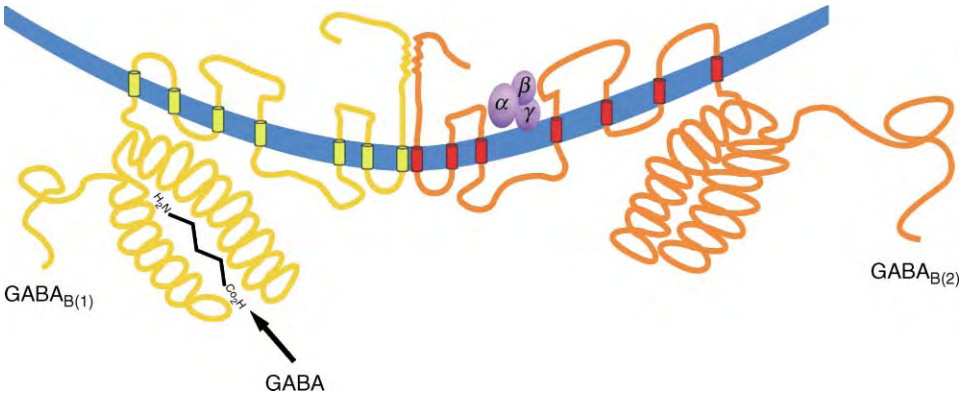

FIGURE 1 Structure and function of the GABA$_B$ receptor. Attachment of GABA to the receptor recognition site located on the GABA$_{B(1)}$ component causes dissociation of the α- and $\beta\gamma$-subunits from the G protein affiliated with the GABA$_{B(2)}$ component of the receptor dimer. The liberated G-protein subunits influence cellular activity by regulating Ca^{2+} and K^+ flux, adenylyl cyclase activity, and transcription factors. (Modified from Enna, S. (2001). A GABA$_B$ mystery: The search for pharmacologically distinct GABA$_B$ receptors. *Mol. Interventions* **1**, 208–218.)

GABA$_B$ receptors are located pre- and postsynaptically throughout the central nervous system (CNS) and in some peripheral organs, although the physiological significance of the latter remains to be determined. Given the obligatory nature of heterodimerization for GABA$_B$-receptor function, it is somewhat surprising that the distribution of GABA$_{B(1)}$ and GABA$_{B(2)}$ expression differs among brain regions, and that drug- or physiologically induced changes in subunit expression varies between the two. This suggests a differential regulation of these genes, pointing to the possibility that the protein products may serve functions other than formation of GABA$_B$ receptors. For example, it has been reported that GABA$_B$-receptor subunits can directly associate with other proteins, in particular transcription factors such as CREB2.

The restricted number of GABA$_B$-receptor subunits, the 1:1 stoichiometry of the system, and the conserved nature of the GABA$_{B(1)}$-neurotransmitter recognition site, limits the possibilities for pharmacologically distinct GABA$_B$ receptors. Although there is indirect evidence that certain GABA$_B$ receptors may be more responsive to some agents than to others, there is no direct proof of molecularly or pharmacologically distinct sites. While it has been suggested that GABA$_{B(1a)}$/GABA$_{B(2)}$ may be pharmacologically different from the GABA$_{B(1b)}$/GABA$_{B(2)}$, this has not been substantiated. Since the neurotransmitter recognition site on the GABA$_{B(1)}$ splice variants are identical, any difference in their responsiveness to a ligand would most likely be due to an allosteric modification mediated by attachment of the agonist or antagonist to some portion of the receptor complex separate from the recognition site. The lack of evidence supporting pharmacologically distinct GABA$_B$-receptor subtypes has limited the clinical development of GABA$_B$-receptor agonists and antagonists since dose-limiting side effects accompany a generalized modification of GABA$_B$ receptor function.

GABA$_B$-Receptor Agonists and Allosteric Modulators

Baclofen is the prototypical GABA$_B$-receptor agonist (Figure 2). In ligand-binding assays with rat brain membranes its affinity for the receptor is approximately 40 nM, with its EC_{50} values in functional assays being in the low μM range. Baclofen has been employed for years as a treatment for spasticity associated with multiple sclerosis and spinal cord injuries, for nocturnal myoclonus, and for trigeminal neuralgia. It is the only GABA$_B$-receptor agent approved for clinical use.

A series of phosphinic acid analogues of GABA has yielded a number of potent and selective GABA$_B$-receptor agonists, including CGP 44532 and CGP 27492, that

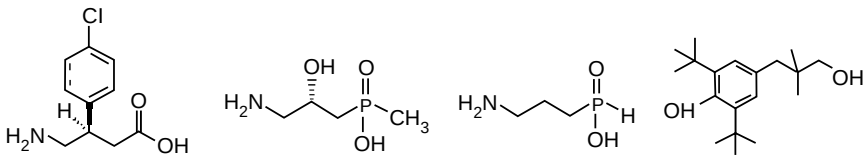

FIGURE 2 Chemical structures of some GABA$_B$-receptor agonists and a positive allosteric modulator.

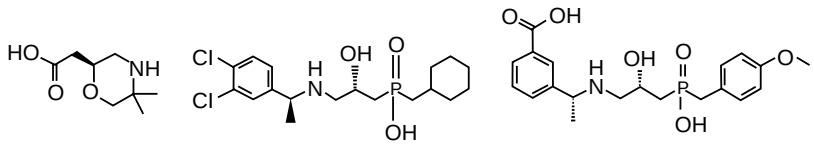

FIGURE 3 Chemical structures of some GABA$_B$-receptor antagonists.

have been used for experimental purposes (Figure 2). Other compounds in this series include CGP 44533, the less active (R)-(+) enantiomer of CGP 34938, of which CGP 44532 is the more active (S)-(−) enantiomer, and SKF 97541, also known as CGP 35024. Rat brain membrane GABA$_B$-receptor binding affinities for CGP 44532 and CGP 27492 are ~45 nM and 6.0 nM, respectively, with the corresponding values for CGP 44533 and SKF 97541 being 150 nM and 1.0 nM, respectively. Both tritiated baclofen and tritiated CGP 27492 are available as radioligands for labeling GABA$_B$ receptors.

In vivo studies indicate that GABA$_B$ agonists display sedative, muscle relaxant, and antinociceptive properties. They also impair memory performance, reduce the craving for cocaine, and are anticonvulsants. Tolerance develops to some of these responses upon repeated administration of agonist, and sedation precludes their use in many situations.

Another approach to activating GABA$_B$ receptors is with selective allosteric modulators, as exemplified by CGP 7930 (Figure 2). Modulators differ from conventional agonists in that they do not directly interact at the GABA$_B$-receptor recognition site, but rather attach to some other portion of the receptor complex causing an allosteric modification in the neurotransmitter-binding site, or enhancing the efficiency of the receptor coupling with the effector system. Allosteric modulators, such as CGP 7930 and GS 39738, increase both receptor affinity and the maximal response to the neurotransmitter. Certain arylalkylamines, some L-amino acids and selected dipeptides have been proposed as GABA$_B$-receptor allosteric modulators, although these claims have been disputed. Nonetheless, because allosteric modulators indirectly influence receptor sensitivity by acting at a site distinct from that utilized by the neurotransmitter, such agents may be capable of distinguishing subtypes of GABA$_B$ receptors, making it possible to more selectively modify this system for therapeutic gain.

GABA$_B$-Receptor Antagonists

The absence of selective receptor antagonists initially hindered the pharmacological characterization of the GABA$_B$ site. The first antagonists developed for this purpose were phaclofen, a phosphonic acid analogue of GABA, and saclofen, a sulfonic acid analogue. While both are highly selective as GABA$_B$-receptor antagonists, their affinities for this site are quite low, being greater than 100 μM. Subsequently, a series of selective, high-affinity, and in some cases, systemically active phosphinic acid derivatives were developed as GABA$_B$-receptor antagonists. Included in this group are CGP 54626 and CGP 62349 (Figure 3). Both of these compounds display K_d values at the GABA$_B$-binding site of 1s nM or less, and both have been radiolabeled for use as ligands for studying the localization, molecular properties, and pharmacological selectivity of this receptor. Other notable phosphinic acid GABA$_B$-receptor antagonists are CGP 36742, CGP 35348, CGP 55845, CGP 46381, and CGP 51176.

Morpholine derivatives have also been found to display GABA$_B$-receptor antagonist properties. This is exemplified by SCH 50911, a systemically active agent with a K_i of ~300 nM at the GABA$_B$ receptor (Figure 3).

While no GABA$_B$-receptor antagonists have been approved for clinical use, laboratory animal studies suggest they may be effective in treating absence epilepsy, cognitive impairments, and affective illness. One of the phosphinic acid analogues, CGP 51176, is currently undergoing clinical trails as a possible antidepressant.

Glossary

allosterism A change induced in the properties and function of a receptor by attachment of a ligand to a site other than that utilized by the endogenous substrate.

heterodimer A complex consisting of two different proteins.

ligand A drug, hormone, or neurotransmitter that attaches to a receptor.

recognition site That portion of a receptor to which the neurotransmitter or hormone attaches.

Further Reading

Bowery, N., Bettler, B., Froestl, W., Gallagher, J., Marshall, F., Raiteri, M., Bonner, T., and Enna, S. (2002). Mammalian γ-aminobutyric acid B receptors: Structure and function. *Pharmacol. Rev.* **54**, 247–264.

Bowery, N., and Enna, S. (2000). γ-Aminobutyric acid$_B$ receptors: First of the functional metabotropic heterodimers. *J. Pharmacol. Exptl. Ther.* **292**, 2–7.

Bythin, D., Kuo, S., Shue, H., and McPhail, A. (1996). Substituted morpholine-2S-acetic acid derivatives: SCH 50911 and related compounds. *Bioorg. Med. Chem. Lett.* **6**, 1529–1534.

Enna, S. (2001). A GABA$_B$ mystery: The search for pharmacologically distinct GABA$_B$ receptors. *Mol. Interventions* **1**, 208–218.

Froestl, W., Mickel, S., Hall, R., von Sprecher, G., Strub, D., Baumann, P., Brugger, F., Gentsch, C., Jaekel, J., Olpe, H., Rihs, G., Vassout, A., Waldmeier, P., and Bittiger, H. (1995a). Phosphinic acid analogues of GABA. 1. New potent and selective GABA agonists. *J. Med. Chem.* **38**, 3297–3312.

Froestl, W., Mickel, S., von Sprecher, G., Diel, P., Hall, R., Maier, L., Strub, D., Mellilo, V., Baumann, P., Bernasconi, R., Gentsch, C., Hauser, K., Jaekel, J., Karlsson, G., Klebs, K., Maitre, L., Marescaux, C., Pozza, M., Schmutz, M., Steinman, M., van Reizen, H., Vassout, A., Mondadori, C., Olpe, H., Waldmeier, P., and Bittiger, H. (1995b). Phosphinic acid analogues of GABA. 2. Selective, orally active GABA$_B$ antagonists. *J. Med. Chem.* **38**, 3313–3331.

Hill, D., and Bowery, N. (1981). ^{3}H-Baclofen and ^{3}H-GABA bind to bicuculline-insensitive GABA$_B$ sites in rat brain. *Nature* **290**, 149–152.

Kaupmann, K., Malitschek, B., Schuler, V., Heid, J., Froestl, W., Beck, P., Mosbacher, J., Bischoff, S., Kulik, A., Shigemoto, R., Karschin, A., and Bettler, B. (1998). GABA$_B$-receptor subtypes assemble into functional heteromeric complexes. *Nature* **396**, 683–687.

Kerr, D., and Ong, J. (2003). Potentiation of metabotropic GABA$_B$ receptors by L-amino acids and dipeptides in rat neocortex. *Eur. J. Pharmacol.* **468**, 103–108.

Sands, S., McCarson, K., and Enna, S. (2003). Differential regulation of GABA$_B$ receptor subunit expression and function. *J. Pharmacol. Exptl. Ther.* **305**, 191–196.

Urwyler, S., Pozza, M., Lingenhoehl, K., Mosbacher, J., Lampert, C., Froestl, W., Koller, M., and Kaupmann, K. (2003). N, N′-Dicyclopentyl-2-methylsulfanyl-5-nitor-pyrimidine-4,6-diamine (GS39783) and structurally related compounds: Novel allosteric enhancers of γ-aminobutyric acid$_B$ receptor function. *J. Pharmacol. Exptl. Ther.* **307**, 322–330.

BIOGRAPHY

S. J. Enna is a Professor of Pharmacology and former Chair of the Department of Pharmacology, Toxicology, and Therapeutics at the University of Kansas Medical Center in Kansas City, Kansas. He is past-president of the American Society for Pharmacology and Experimental Therapeutics and has served as editor of the *Journal of Pharmacology and Experimental Therapeutics, Biochemical Pharmacology*, and *Pharmacology and Therapeutics*. His research interests include neuropsychiatric disorders, neurotransmitter receptors, and GABA.

Galectins

R. Colin Hughes
Medical Research Council, London, UK

Galectins, a family of proteins that bind to galactose residues of glycoproteins and glycolipids, represent a special group of a large number of carbohydrate-binding proteins known as lectins. Galectins are found in tissues of organisms ranging from lower inverterbrates to mammals, and participate in many essential biological processes. Different members play roles in growth regulation, cell adhesion, and migration and are in some cases associated with the neoplastic transformation of cells and metastasis. Galectins are also involved in cell signaling and the regulation of immune responses, and recently have become the focus of intensive research in many areas of cell and developmental biology, immunology, and pathology.

Galectin Structure

The galectin family at present consists of 14 identified members (Figure 1). Several galectins are small proteins of 14–16 kDa with a single carbohydrate recognition domain (CRD) of ~130 amino acid residues (galectin-1, 2, 5, 7, 10, 11, 13, and 14). Many of these form noncovalent homodimers, and hence are functionally bivalent molecules. Others are constitutively bivalent molecules of 30–35 kDa containing two CRDs joined by a short link sequence as in galectin-4, 6, 8, 9, and 12. Galectin-3 is unique in that it contains an N-terminal extension that is very much larger than those seen in other galectins. Under normal conditions galectin-3 is monomeric, probably due to the masking by the N-terminal tail of a site on the CRD known to be the subunit interaction site of dimeric galectins. The N-terminal domain of galectin-3 is similar to sequences found in other proteins that promote self-aggregation. Galectin-3 also readily forms multimers at high concentrations or when bound to ligand-coated surfaces, mainly through interactions between the N-terminal extensions. Galectin-5 is also a monomer normally, but has weak agglutinating activity indicative of at least bivalent interactions.

The valency of galectins is functionally important. First, the binding of single CRDs even to a preferred carbohydrate is often relatively weak. Assembly of CRDs can lead to cooperative binding between multiple CRDs and ligand, with greatly increased avidity. Second, multivalent galectins are capable of cross-linking receptor glycoproteins at cell surfaces or in the extracellular matrix, and have the potential to form clusters or lattices of receptors, for example, at cell surfaces. There is a close correlation between the ability of lectins to cluster cell-surface ligands and their effects in initiating cellular signals, e.g., a mitogenic stimulus. Third, multivalency is essential for the proposed roles of some galectins in linking cell surface receptors such as integrins to extracellular matrix components, leading to cell–substratum adhesion. In addition to their relatively low avidity of binding to carbohydrates, monovalent galectins cannot participate in cross-linking of glycoproteins, and indeed may function to competitively inhibit such cross-linking activity, for example, to block signal transduction or to weaken cell adhesions.

Binding Specificity

Carbohydrate Structures

Many galectins bind, albeit with low affinity, to the monosaccharide galactose (hence the name GALectin) or simple galactosides such as the disaccharides lactose and lactosamine (respectively a galactose residue joined in a β1,4 linkage to glucose or N-acetylglucosamine). Crystal structures of complexes between galectin CRDs and lactose show in each case six conserved hydrophilic residues essential for galactose binding. However, high-affinity binding requires additional features and longer carbohydrate chains. These requirements for high-affinity binding to larger oligosaccharides vary considerably between the various galectins. In agreement with these differences, there is significant sequence variation among the various galectin CRDs in their extended binding sites adjacent to the primary binding site for galactose. In the case of the constitutively bivalent galectins containing two CRDs, each CRD may have different preferences for carbohydrate ligands, indicating that these galectins may bind to and cross-link different glycoproteins.

Several galectins bind with high affinity to polylactosamines, oligosaccharide chains made up of repeating units of lactosamine residues. These chains can be

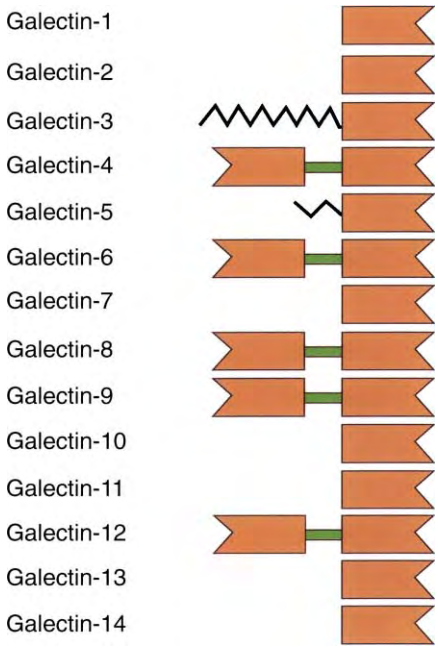

FIGURE 1 Schematic of the overall structures of galectins. The proteins are shown as linear diagrams of single polypeptide chains with N- and C-termini at the left- and right-hand side, respectively. The CRDs are in red, and the short sequences linking the N- and C-terminal CRDs of galectin-4,6,8, and 9 are in green. The extra-long N-terminal domain of galectin-3, and the slightly elongated N-terminal domain of galectin-5, are in yellow.

expressed on the N- or O-glycans of glycoproteins, and their expression is controlled by specific N-acetylglucosaminyl transferases (GlcNAcT). Two GlcNAcTs are particularly important in the initiation of polylactosamine synthesis and hence production of high-affinity galectin ligands. The GlcNAcT V enzyme allows elongation of N-linked polylactosamines. It is crucial for production of specific cell surface galectin-3 receptors on certain thymus-derived lymphocytes (T-cells), and activation of these cells. Another GlcNAcT enzyme starts polylactosamine chain extension on O-glycans. Its expression is crucial for the production of other specific receptors required for binding of galectin-1 to T-cells, and elimination of these cells by apoptosis.

Glycoprotein Receptors

The significant differences in carbohydrate-binding specificities between different CRDs are functionally important since it implies that different galectins may bind preferentially to unique glycoprotein receptors that bear glycans carrying the preferred saccharide sequences. Galectin-1 and -3 both bind to the lysosomal associated membrane proteins (LAMPs), and to some isoforms of the extracellular matrix components fibronectin, laminin, and tenascin. These receptors all contain high amounts of N- and/or O-linked polylactosamine chains. Similarly, both galectins bind the T-cell receptor (TCR) complex and regulate lymphocyte activation, possibly by effects on TCR clustering at the lymphocyte surface. On the other hand, galectin-3 specifically recognizes Mac2-binding protein, a cell-adhesive protein present in the extracellular matrix and a secreted tumor-associated antigen. Similarly, galectin-1 specifically recognizes the lymphocyte surface antigens CD7 and CD45. Activated cells exposed to galectin-1 undergo apoptosis, mediated by binding and clustering of cell-surface CD7/CD45 complexes by the lectin.

Galectin Distribution

Species

In addition to the galectins present in mammalian species, galectins are found in birds, fish, and amphibians, in invertebrates such as worms and insects and even in protists such as sponges. In the human and *Caenorhabditis elegans* genomes, ~17–20 galectin-like genes are identifiable. This is likely to be a minimal estimate, since several galectins can undergo alternative splicing to produce separate transcripts from a single gene. However, not all of these have been isolated as yet and shown directly to be active as galactose-binding lectins: the latter point also includes some of those proteins listed in Figure 1.

Tissues

The known galectins have distinct patterns of expression during development and in the mature organism. Galectin-1 and -3 have a rather broad distribution, the former in tissues of mesodermal origin and the latter being mainly in epithelial cells, tumor cells, as well as macrophages and other inflammatory cells. Other galectins are more restricted, e.g., galectin-2, -4, and -6 in the gastrointestinal tract, galectin-5 in erythrocytes, and galectin-7 in skin and tumors of epidermal origin. A particular tissue may express more than one galectin, e.g., galectin-1, -3, -8, and -9 in the kidney. In the kidney, galectin-3 expression is strongly regulated during development, whereas the expression of other galectins is more constant. Galectin expression is also often regulated physiologically Thus, galectin-1 and -3 expression is strongly increased upon activation of T-cells, and macrophages or Schwann cells, respectively. Upstream elements in several galectin genes are identified that account for transcriptional activation by glucocorticoids, phorbol esters, retinoic acid, and other factors. Galectin gene sequences have also been found that account for the tissue-specific expression of galectins, e.g., binding sites for transcription factors

implicated in up-regulation of galectin-3 and -11 in activated macrophages and differentiating eye lens epithelia, respectively.

Cells

Galectins are characteristic cytoplasmic proteins in that they lack signal sequences for transfer into endoplasmic reticulum (ER)/Golgi compartments, are acetylated at the N-terminus but are not glycosylated even though some contain concensus sites for N-glycosylation within the ER. However, following synthesis there is selective intracellular trafficking of some galectins (galectin-1, -3, -7, -10, -11, and -12) to the nucleus. Nuclear localization, at least for galectin-3, is correlated with cell proliferation, and redistribution of galectins is often observed in actively dividing cancer cells relative to their normal counterparts. In addition, many galectins are secreted from cells by unknown mechanisms distinct from conventional transfer through the ER/Golgi pathway. In polarized cells, which have physically segregated surface domains with distinct functions, galectins may be secreted preferentially from a particular surface domain. This complex distribution of galectins inside and outside cells is consistent with these proteins having different functions intra- and extracellularly (Figure 2).

Multiple Roles

Nuclear Functions

Galectin-1 and -3 are present in the cell nucleus in association with ribonucleoprotein complexes involved in RNA splicing. Removal of the galectins from such complexes by treatment with inhibitory sugars, such as lactose, results in loss of splicing activity. Conversely addition of either galectin to the depleted nuclear extracts restores activity, showing directly that these galectins are splicing factors. The galectins appear to be critically involved in assembly of higher-order complexes of nucleoproteins leading to functional splicing particles.

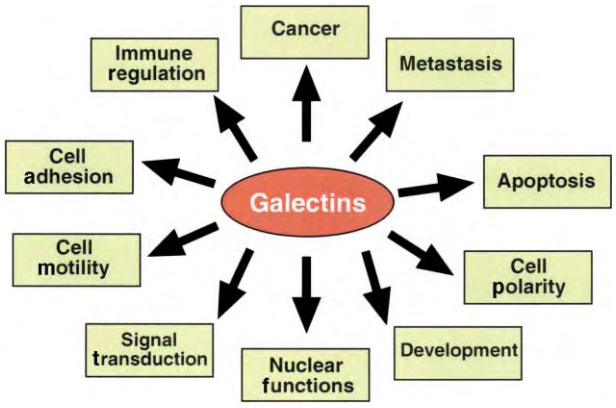

FIGURE 2 Galectins participate in a wide range of biological functions, including regulation of cell proliferation and death, modulation of cell adhesion, and motility in normal and cancer cells, cell signaling, and immuno-regulation. The particular effect of a galectin in any one situation depends on its valency of binding and ability to cross-link receptors, the appropriate glycosylation of specific receptors, cell activation state, developmental and tissue-type expression, and subcellular localization.

Cell Growth and Apoptosis

In complex organisms, homeostasis requires a balance between cell growth and cell death. A galectin may either promote or suppress the form of programmed cell death known as apoptosis. Galectin-1, 7, 9, and 12 promote, while galectin-3 inhibits, this process. Galectin-3 and -12 also regulate the cell cycle. Hence, the growth and survival of some cell types and tissues may be controlled by the relative levels of expression of multiple galectins.

Cell Adhesion and Motility

Galectins bind to many key molecules involved in cell adhesion. These include various subunits of the integrins, as well as extracellular matrix glycoproteins such as laminin and fibronectin, which interact in cell adhesion to substratum. Others bind to members of the cadherin family of cell adhesion molecules, active in cell–cell adhesion. Typically, galectins may act to enhance or antagonize cell adhesion, as mentioned above. These effects on the strength of cell adhesions also influence the ability of cells to dissociate and migrate, for example, during gastrulation, or in wound healing. Enhanced adhesion is likely due to direct binding of a galectin to the glycans of molecules on adjacent cells or within the extracellular matrix. Additionally, galectins may act synergistically to strengthen adhesive interactions, for example, between integrins and their matrix counter-receptors. Pro-adhesive or anti-adhesive effects of galectins, especially galectin-1 and -3, are important in many processes during fetal development. The anti-adhesive effects of galectin-1 influence the motility of myoblasts during muscle differentiation, and the projection of axons during establishment of neural networks, e.g., in the olfactory bulb. Conversely, galectin-3 promotes adhesion of various metastatic tumor cells and inflammatory cells to extracellular matrices, and limits growth and differentiation of epithelial structures during kidney development.

Cancer and Metastasis

Galectin gene expression is, in many cases, up-regulated by growth factors and oncogenes, and down-regulated

by tumor suppressors. Thus, galectin-3 is found in a wide variety of malignances. In most cases, increased expression renders tumor cells more invasive and is associated with a negative prognosis. Probably, the galectins increase the invasive potential of the tumors by modulating the interactions with the endothelium and by assisting the formation of homotypic cell aggregates, important for homing of metastatic tumors to secondary tissue sites.

Immune Response and Regulation

Galectins are important regulators of immune cell homeostasis, as well as immune responses. Some galectins, e.g., galectin-3, act to enhance immune responsiveness and the inflammatory cascade. Others, such as galectin-1, play key roles in shutting off immune cell functions, for example, by triggering their apoptosis as discussed before for T-cells. These diverse effects are propagated by interactions of particular galectins with specific receptor glycoproteins. Specific interactions can lead to regulation of immune cell survival and signaling, their growth and chemotaxis, and the secretion of various cytokines influencing the differentiation of particular immune cell types. Recent evidence also shows the roles of galectins in infection by important human pathogens. Consequently, galectins are attractive therapeutic targets in autoimmune, inflammatory, allergic as well as neoplastic and infective diseases.

See Also the Following Articles

Caspases and Cell Death • Cell Death by Apoptosis and Necrosis • Glycoproteins, N-linked • Lectins • *N*-Linked Glycan Processing Glucosidases and Mannosidases • Glycoprotein-Mediated Cell Interactions, O-Linked • Proteoglycans

Glossary

apoptosis A form of programmed cell death observed in animal tissues during embryogenesis, and in the mature organism in regulation of tissue homeostasis. A family of cytoplasmic proteases, caspases, are key effector molecules of apoptosis.

glycan A chain of sugar residues added covalently to proteins. A given protein may have several attached glycans, the composition and sequence of which may vary with developmental stage and tissue type. Glycans are classified as N-glycans containing an N-acetylglucosamine to asparagine linkage, or as O-glycans containing an N-acetylgalactosamine to serine/threonine linkage.

immune homeostasis The maintenance of steady-state levels of functionally distinct leukocyte populations in the adult immunologically competent organism.

lectins Lectins (from the Latin *legere*, to select) are specific carbohydrate-binding proteins that are ubiquitous, being found in animals, plants, and microorganisms. Lectins can be grouped in distinct families on the basis of homologies in amino-acid sequence and three-dimensional structure, and carbohydrate-binding specificity.

splicing The process by which pre-RNA is modified by intron removal and exon ligation during production of fully mature RNA transcripts.

Further Reading

Cooper, D. N. W., and Barondes, S. H. (1999). God must love galectins: He made so many of them! *Glycobiology* **9**, 979–984.

Hernandez, J. D., and Baum, L. G. (2002). Ah, sweet mystery of death! Galectins and the control of cell fate. *Glycobiology* **12**, 127R–136R.

Hughes, R. C. (2001). Galectins as modulators of cell adhesion. *Biochemie* **83**, 667–676.

Kasai, K.-I., and Hirabayashi, J. (1996). Galectins: A family of animal lectins that decipher glycocodes. *J. Biochem.* **119**, 1–8.

Liu, F.-T., Patterson, R. J., and Wang, J. L. (2002). Intracellular functions of galectins. *Biochim. Biophys. Acta* **1572**, 263–273.

Rabinovich, G. A., Baum, L. G., Tinari, N., Paganelli, R., Natoli, C., Liu, F.-T., and Iacobelli, S. (2002). Galectins and their ligands: Amplifiers, silencers or tuners of the inflammatory response. *Trends Immunol.* **23**, 313–320.

Rini, J. M., and Lobsanov, Y. D. (1999). New animal lectin structures. *Curr. Opin. Struct. Biol.* **9**, 578–584.

Biography

R. Colin Hughes has been a UK Medical Research Council scientist at the National Institute for Medical Research in Mill Hill, London, since 1970. His main research interests have been in the structure and biosynthesis of the complex carbohydrates attached to proteins, and more recently in the functional significance of their recognition by antibodies and lectins. He holds a Ph.D. from the University of London and received postdoctoral training at the University of Washington and the Massachusetts General Hospital.

Genome-Wide Analysis of Gene Expression

Karine G. Le Roch and Elizabeth A. Winzeler
Scripps Research Institute, La Jolla, California, USA

Genome-wide expression experiments, like genetics, can reveal new genes involved in a process, or can allow two or more biological states to be distinguished from one another. Both serial and parallel approaches can be used to collect genome-wide expression data. In both cases RNA (target) from conditions of interest is isolated. For serial methods, the RNA is converted to cDNA and the relative number of cDNA molecules per condition is counted. For parallel methods the RNA is labeled directly either with a biochemical marker (such as biotin), a radioisotope, or with fluorescence; or is converted to cDNA and then labeled. This target is then incubated with a microarray in buffered solution. The labeled RNA molecules then seek out their complementary sequences on the array. The amount of RNA that has hybridized at each location on the array is determined. By comparing the patterns that are obtained for two different conditions, it is possible to monitor how gene expression changes.

Uses for Genome-Wide Expression Datasets

Using Gene Expression Data for Discovery

The primary use for whole genome expression analysis is in the identification of novel genes involved in a particular molecular process. Such genes may encode novel drug targets, may be used as molecular reporters, or may provide a better description of the biological process under study. RNA is collected from the condition of interest and from a control condition. If genes that are known to be involved in a process are included on the microarray, the researcher can find genes with similar expression patterns by cluster analysis. Alternatively, genes can be identified that show a large induction in the condition of interest relative to the reference condition. Because a block in a metabolic pathway may result in a transcriptional upregulation of the genes in the pathway, new members of the pathway may be discovered using this approach.

Using Gene Expression Data for Classification

Genome-wide analysis of gene expression can be used to distinguish two different biological states such as acute myoblastic leukemia and acute lymphoblastic leukemia, which are relatively difficult to distinguish from one another using conventional cytological approaches. Here RNA is isolated from two distinct populations and RNA from each individual is labeled and hybridized to a cDNA or oligonucleotide array containing probes to the genome from which the RNA was derived. Then software is used to identify genetic markers that can be used to classify the two populations. By subsequently analyzing only the expression patterns of genes that distinguish two patient populations, physicians may be able to predict a patient's disease classification and optimize treatment.

Serial Methods for Global Analysis of Gene Expression

Serial analysis of gene expression (SAGE) is a technique for collecting genome-wide expression data in which short sequence tags (7–9 bases in length) are isolated from near the 3′ end of transcripts using biochemical methods (Figure 1). The short tags (usually 10,000–20,000 per condition) are concatenated and then sequenced. Finally each SAGE tag is mapped back to the gene from which it originated by using full-genome sequence data. By counting the number of SAGE tags for a gene for several different conditions, one can obtain an estimate of how the gene's expression is changing. This technique which does not depend on constructing a microarray, can be initiated with full genome sequence information, and is very quantitative, especially for highly expressed genes.

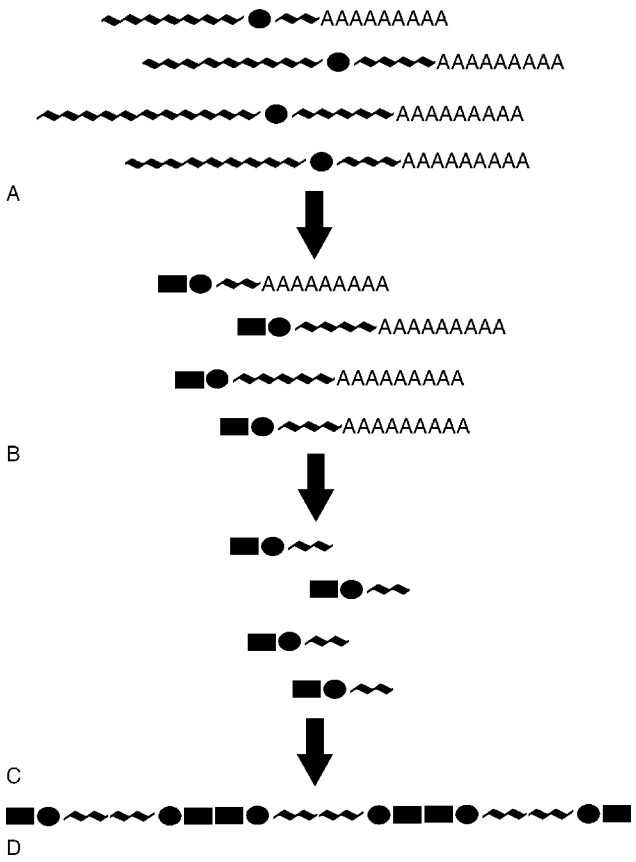

FIGURE 1 Serial analysis of gene expression. RNA from the condition of interest is first converted to double-stranded cDNA using reverse transcriptase and DNA polymerase enzymes (A). The double-stranded cDNA is then cleaved with a restriction enzyme that cuts every few hundred bases in the genome of interest (usually NlaIII, whose site is here represented by solid circles). A short piece of DNA is then ligated at the cut site of the first restriction enzyme (B), generating a recognition site for a type II restriction enzyme (usually BsmFI, whose recognition site is shown as a solid rectangle) which cuts a defined distance from its recognition site, creating a 15 bp SAGE tag. After restriction with the type Ii enzyme (C), the tags are then biochemically linked to one another and finally sequenced (D). The number of SAGE tags mapping to a gene is then tabulated to determine the gene's expression level.

The technique is relatively expensive and is much more time consuming than microarray analysis. Other serial methods include sequencing libraries of expressed sequence tags (ESTs).

Analysis of Gene Expression Using Microarrays

Microarrays Created by Robotic Deposition or Ink-Jetting

Printed microarrays, which are used to measure gene expression in parallel, can be readily constructed in most laboratory settings using a robotic microarraying device that is able to dispense small quantities of solution at precise locations on a solid support. Genes or DNA fragments of interest such as members of complete or partial cDNA libraries (or ESTs) are selected and amplified by the polymerase chain reaction. The probes are then cleaned before being printed using a pin-based robotic arrayer or an inkjet microdispensing liquid-handling system on the selected matrix in a two-dimensional array format (Figure 2B). Alternatively, oligonucleotides can be designed that probe genes of interest. Because of its low inherent fluorescence, glass is the most common substrate when the target is to be fluorescently labeled. The glass slides are typically coated with poly-lysine or aminosilanes, which improve the hydrophobicity and limit the spread of the spotted DNA on the slide.

Microarrays Synthesized *in situ* by Photolithography

An alternative technique for creating microarrays was first implemented by Affymetrix (Santa Clara, CA). In this method light-directed oligonucleotide chemistry is combined with photolithography for solid-phase *in situ* synthesis of DNA probes from the gene of interest (Figures 2A and 3). The advantage of photolitography is that arrays with extremely high information content can be manufactured. Up to 1,000,000 oligonucleotides can be specifically selected from sequencing databases and synthesized in a highly specific manner on a small 1.28×1.28 cm array. Because such arrays are designed *in silico* and there is no need to handle intermediate such as clones, PCR product, or cDNA libraries, the risk of mislabeling is reduced. Furthermore, it is easier to control the amount of product that it is deposited at each location on the array. Because of the combinatorial synthesis and high density, a typical array may contain 16 or more individual oligonucleotide probes per gene. Such redundancy is used in the data analysis to gain confidence.

Microarray Target Preparation and Hybridization

Creating labeled target for hybridization to microarrays can be accomplished in a variety of ways (Figure 2C). Arrays constructed from nylon membranes typically use target that is labeled with radioactive isotopes, while glass arrays use fluorescence. For most methods mRNA is first converted to cDNA using a polydT-primed reverse transcriptase reaction. Because it can be difficult to be sure that the same quantity of probe is placed at the each position in

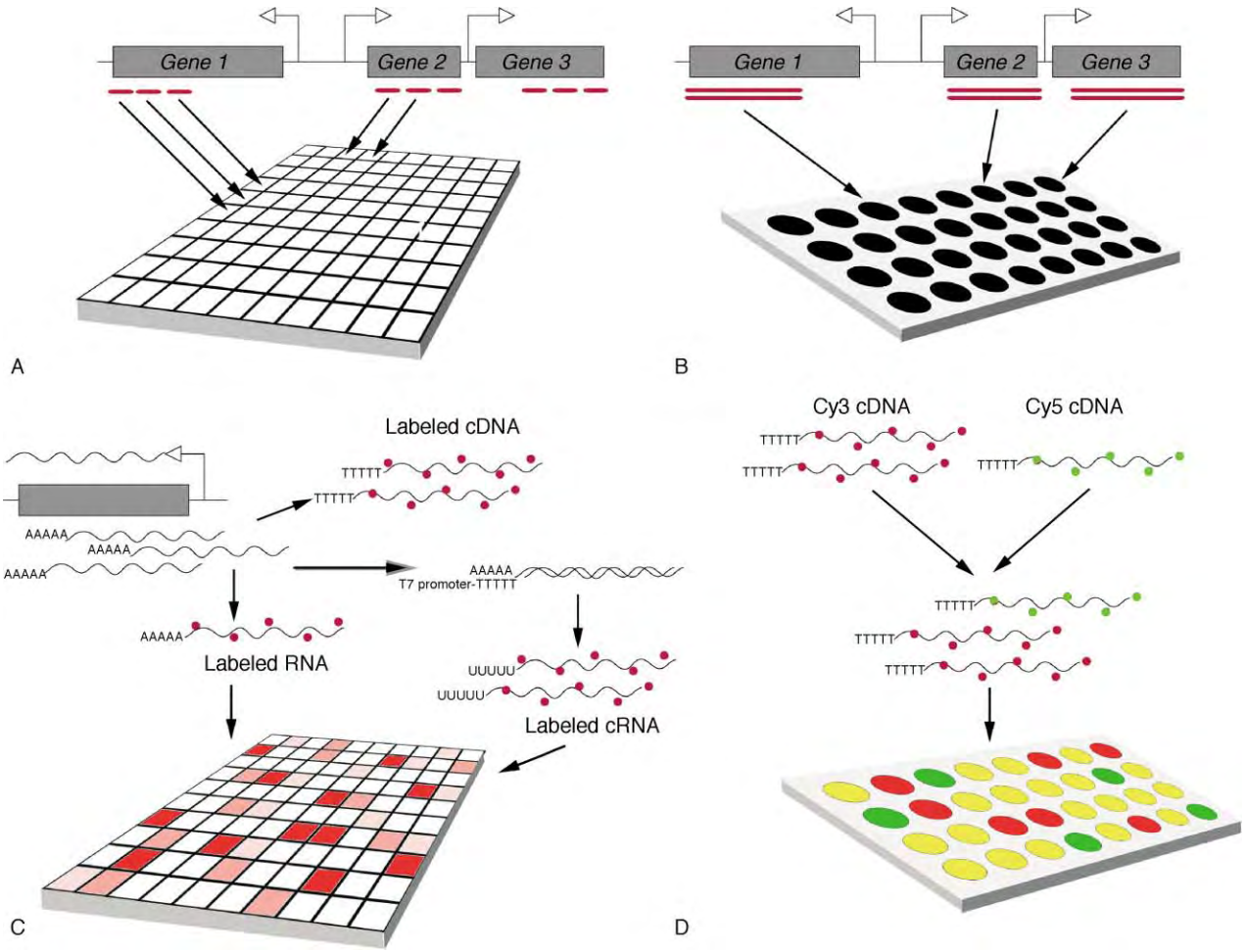

FIGURE 2 Comparison of most commonly used microarray methods. Nucleic acid microarrays are generally produced in one of two ways: by *in situ* synthesis (A) or by robotic deposition of nucleic acids (PCR products, plasmids or oligonucleotides) onto a glass slide (B). Typically for oligonucleotide arrays produced *in situ* (A), multiple probes per gene are placed on the array, while in the case of robotic deposition, a single, longer (up to 1,000 bp) double-stranded DNA probe is used for each gene. Different methods can be used for preparing labeled material for measurements of gene expression (C) including direct labeling of RNA, incorporation of labeled nucleotides into cDNA during or after reverse transcription of polyadenylated RNA; or construction of cDNA that carries a T7 promoter at its 5′ end. In the last case, the double-stranded cDNA serves as template for a reverse transcription reaction in which labeled nucleotides are incorporated into cRNA. Commonly used labels include the fluorophores fluorescein, Cy3 (or Cy5), or nonfluorescent biotin, which is subsequently labeled by staining with a fluorescent streptavidin conjugate. Two-color hybridization strategies are often used with spotted microarrays (D).

a microarray created by robotic deposition, most researchers favor a hybridization scheme in which two different fluorophores are incorporated during the cDNA synthesis reaction for RNA targets from the test and reference conditions (Figure 2D). The two labeled targets are mixed in the appropriate hybridization buffer mix and hybridized. Laser excitation of the incorporated targets yields an emission with characteristic spectra. The fluorescent intensity of each element on the array is measured using a scanning confocal laser microscope.

For targets that are to be hybridized to photolithographic arrays, a phage T7 promoter is attached to the end of double-stranded cDNA and used to drive an *in vitro* transcription (IVT) reaction during which biotin or other labels are incorporated. The IVT reaction results in a linear amplification of the original mRNA population of up to 100-fold. In contrast to the two-color method described above, target from each biological condition is hybridized separately to its own array.

Microarray Data Analysis Methods

Detection of mRNA Levels

Typically only SAGE methods or oligonucleotide arrays that use multiple probes per gene can be used to determine the approximate number of transcripts for genes that are present in a given sample.

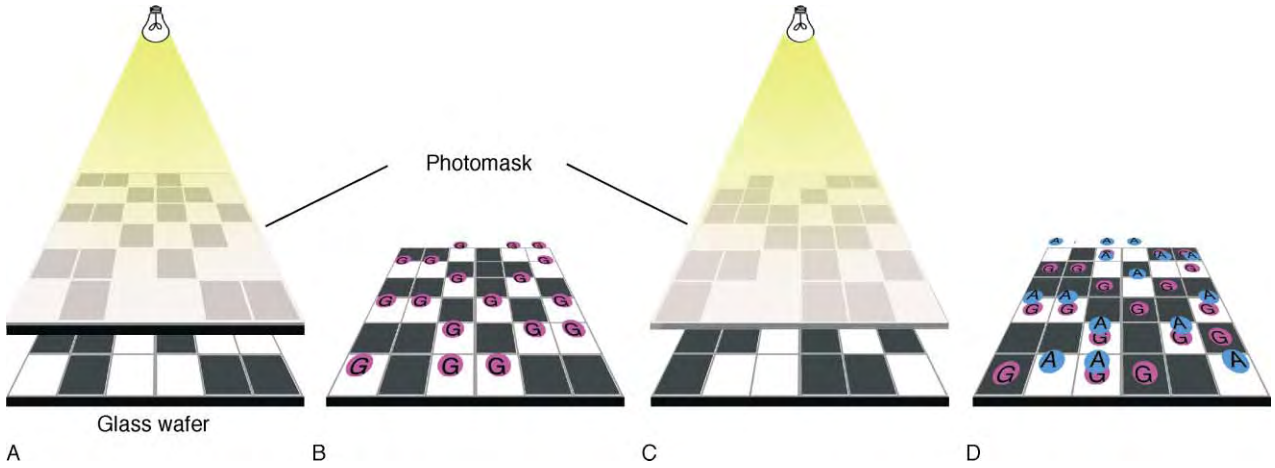

FIGURE 3 Photolithographic synthesis of oligonucleotide arrays. Here quartz wafers are placed in a bath of silane, which reacts with the hydroxyl group of the quartz to form a matrix of covalently linked molecules. Light is directed through a series of photomasks placed over the coated wafer that determine which regions will be activated by light and are thus capable of receiving a nucleotide in each step (A). The wafers are then bathed in the appropriate nucleotide (ACG or T) containing a photoprotective group (B). The photoprotective group is removed at the next step (C) before the next nucleotide is added (D). Using this method any 25 mer can be synthesized in no more than 100 such steps.

For oligonucleotide arrays with multiple probes per gene, an estimate of transcript levels can be obtained by averaging the background-subtracted intensity values from usually 16 or more individual probes to a given gene. Values from multiple probes need to be considered because different oligonucleotide probes have different hybridization properties. Such an approach can be used to distinguish genes that are highly expressed from ones which are poorly expressed.

Computation of Gene Expression Ratios

Microarrays that contain only a single probe per gene can generally just be used to calculate how a gene's expression changes when two conditions are compared. Monochrome images from each condition output by the scanner are read by software that locates each element within the grid and converts the images to pseudo-color and merges them. The ratio of the dye signals for each probe on the array is used to determine the relative proportion of a transcript in the two different conditions (Figure 2D).

Analysis of Genome-Wide Expression Datasets

Cluster Analysis

Gene expression experiments typically generate tens of thousands of data points. It has been shown that genes with similar biological roles will often have similar patterns of expression. Clustering as a method of analysis can be used to organize data and to group genes according to their similarity in gene expression patterns so that genes involved in similar processes can be identified (Figure 4). Pairwise average-linkage cluster analysis is the most widely used. This method creates hierarchical clusters in which relationships between genes are represented by trees whose branch lengths reflect the degree of similarity between genes.

Ontology Analysis

This method can be used to determine the biological pathway that is active in one condition relative to another pathway that is activated when an organism is treated with a chemical compound. Here a group of genes that is up-regulated in one condition relative to another condition is determined. It is assumed that many of the genes in this group will be uncharacterized, but the function of others will be well understood and can be accessed by examining catalogues that group genes by function (e.g., nucleic acid metabolism or maintenance of the cytoskeleton). By comparing the size and membership of the group of up-regulated genes to the size and membership of different functional groups, it is possible to calculate statistics describing whether or not the amount of overlap would be expected by chance. Thus, one might find that the probability that a group of genes that is induced by a drug shows significant overlap with a group of genes that have a role in sulfur metabolism, suggesting that the drug may disrupt sulfur metabolism.

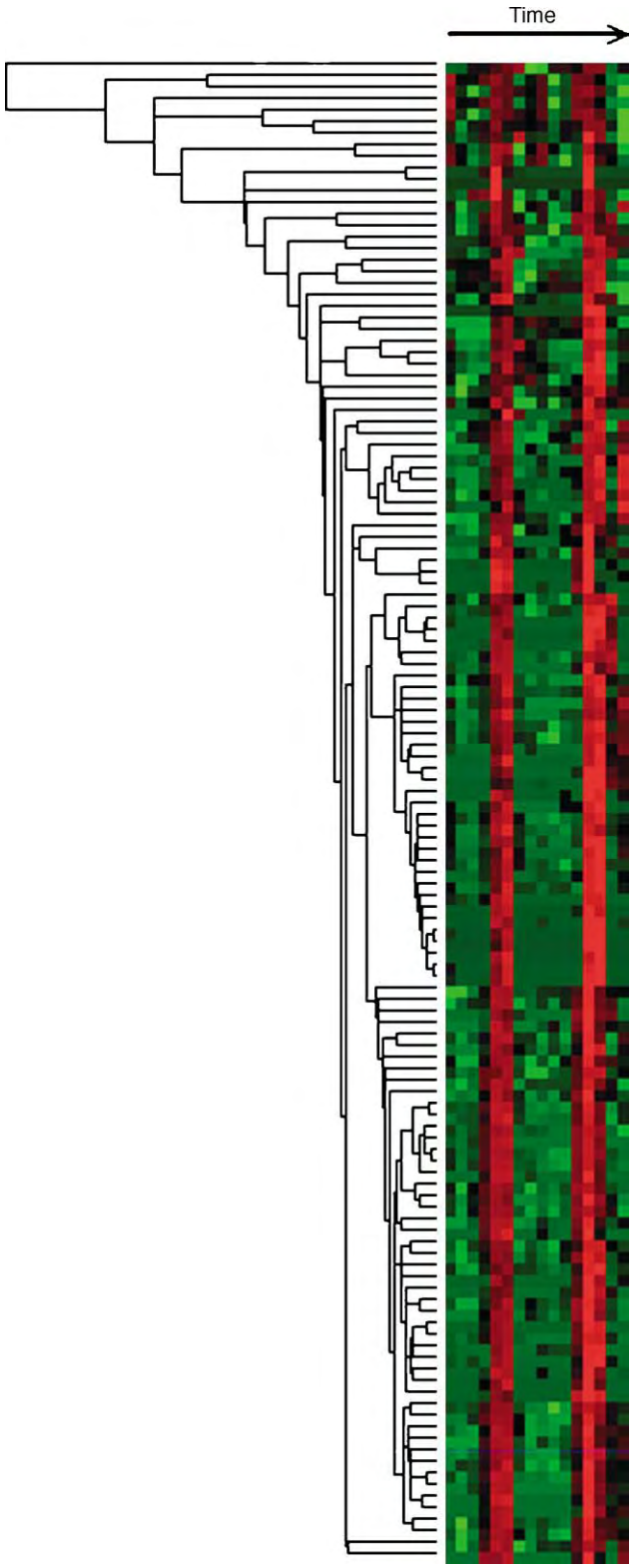

FIGURE 4 Clustergram showing gene expression patterns in the malaria parasite's lifecycle. Each gene is represented by a single row of colored boxes and each time point is represented by a single column. The hue (red or green) indicates the relative expression relative to a reference condition.

See Also the Following Articles

Mitochondrial Genes and their Expression: Yeast • Mitochondrial Genome, Evolution • Mitochondrial Genome, Overview • Nuclear Genes in Mitochondrial Function and Biogenesis • Protein Data Resources

Glossary

cDNA DNA that has been created from RNA using reverse transcription.

cluster analysis The process of grouping genes or other array elements based on their similarity of behavior over many different conditions. Both hierarchical (tree-based) or nonhierarchical methods (k-means, self-organizing maps) can be used to accomplish the same organizational goal.

EST library A library created by cloning the 3′ end of individual cDNA molecules into a vector.

microarray A device typically used for monitoring gene expression for a large number of genes. They consist of an ordered array of different elements (usually nucleic acids complementary to the genes of interest) that are printed or synthesized *in situ* on a solid surface (usually a glass slide).

probe The individual elements on a microarray consisting of long oligonucleotides, short oligonucleotides (25mers), fragments of genomic DNA, or cDNAs.

RNA The molecular messages produced when genes are transcribed.

serial analysis of gene expression (SAGE) A method used in the genome-wide monitoring of gene expression in which short sequence tags from different cDNAs are isolated, sequenced, and counted.

target Uncharacterized RNA that is labeled and hybridized to the microarray.

Further Reading

Chee, M., Yang, R., Hubbell, E., Berno, A., Huang, X. C., Stern, D., Winkler, J., Lockhardt, D. J., Morris, M. S., Fodor, S. P. (1996). Accessing genetic information with high-density DNA arrays. *Science* **274**(5287), 610–614.

DeRisi, J. L., Iyer, V. R., and Brown, P. O. (1997). Exploring the metabolic and genetic control of gene expression on a genomic scale. *Science* **278**(5338), 680–686.

Golub, T. R., Slonim, D. K., Tamayo, P., Huard, C., Gaasenbeek, M., Mesirov, J. P., Coller, H., Loh, M. L., Downing, J. R., Caligiuri, M. A., Bloomfield, C. D., Lander, E. S. (1999). Molecular classification of cancer: Class discovery and class prediction by gene expression monitoring. *Science* **286**(5439), 531–537.

Hughes, J. D., Estep, P. W., Tavazoie, S., Church, G. M. (2000). Computational identification of *cis*- regulatory elements associated with groups of functionally related genes in *Saccharomyces cerevisiae*.. *J. Mol. Biol.* **296**(5), 1205–1214.

Pease, A. C., Solas, D., Sullivan, E. J., Cronin, M. T., Holmes, C. P., Fodor, S. P. (1994). Light-generated oligonucleotide arrays for rapid DNA sequence analysis. *Proc. Natl. Acad. Sci. USA* **91**(11), 5022–5026.

Schena, M., Shalon, D., Davis, R. W., Brown, P. O. (1995). Quantitative monitoring of gene expression patterns with a complementary DNA microarray. *Science* **270**(5235), 467–470.

Velculescu, V. E., Zhang, L., Vogelstein, B., Kinzler, K. W. (1995). Serial analysis of gene expression. *Science* **270**(5235), 484–487.

Biography

Elizabeth Winzeler is a Professor at the Scripps Research Institute and the Head of Cellular Biology Research at the Genomics Institute of the Novartis Research Foundation. She trained in the laboratory of Dr. Ron Davis at Stanford University during the time that many of the important developments in global gene expression monitoring were unfolding and were being developed in this laboratory. She has used many of these methods described here in her search for new drugs for malaria and has developed other full-genome methods using the yeast, *Saccharomyces cerevisiae* as a model system.

Karine Le Roch is a postdoctoral fellow in Dr. Winzeler's laboratory at the Scripps Research Institute.

G_i Family of Heterotrimeric G Proteins

Maurine E. Linder
Washington University School of Medicine, St. Louis, Missouri, USA

Hormones, neurotransmitters, and sensory inputs elicit responses by binding to cell surface receptors. Heterotrimeric G proteins are poised at the inner face of the plasma membrane to respond to the activated receptors and relay signals by changing the activity of intracellular effector molecules. A detailed discussion of the shared properties of heterotrimeric G proteins can be found in the entry on the G_s family. This entry focuses on the G_i family, which regulates a broad array of physiological processes. These include vision, taste, heart rate, neural activity, cell migration, survival, and proliferation.

Overview of the G_i Family

G_i was discovered in the early 1980s as the G protein that mediates hormonal inhibition of cAMP production. Its discovery followed that of G_s, the G protein that stimulates cAMP production and G_t, the G protein that regulates cGMP levels in the retina (see below). Characterization of G_s, G_i, and G_t revealed a structurally homologous family of guanine nucleotide-binding proteins. Over time, many additional G proteins were identified biochemically or through cloning of cDNAs. By the mid-1990s, it was appreciated that 16 distinct genes encode G-protein α-subunits in mammalian genomes. The α-subunits could be grouped into families based on sequence similarity and were assigned to four families: G_s, G_i, G_q, and G_{12}. The G_s, G_q, and G_{12} families are covered in separate articles.

The G_i family is the most functionally diverse of the G-protein families. It can be subdivided into five groups: G_i, G_o, G_t, G_g, and G_z, according to the identity of the α-subunit. The evolutionary relationship among the G_i family α-subunits is shown in Figure 1. G_α subunits associate with $G_{\beta\gamma}$ dimers composed of combinations of the 5 G_β and 12 G_γ subunits. Although not all combinations are possible, a large number of heterotrimers can be generated within this family. Like all heterotrimeric G proteins, G_i family members undergo a cycle of nucleotide exchange and hydrolysis when activated by receptors (Figure 2). Binding of GTP to G_α induces dissociation from $G_{\beta\gamma}$ and both G_α–GTP and $G_{\beta\gamma}$ can interact with effector molecules and regulate their activity. Although in principle all G-protein families can signal through $G_{\beta\gamma}$ subunits, this mode of signaling is most prevalent with signaling pathways regulated by G_i, G_o, and G_z.

G-protein pathways are deactivated when G_α hydrolyzes GTP to GDP. In the GDP-bound form, G_α binds efficiently to $G_{\beta\gamma}$ and restores the heterotrimer to its inactive state. The length of time that G_α is in its GTP-bound state determines the duration of the signal. Regulators of G-protein signaling (RGS) bind to G_α and accelerate the rate of GTP hydrolysis by acting as GTPase activating proteins (GAPs). Thus, RGS proteins are important regulators of the timing of G-protein responses. Members of the G_i family are targets for RGS proteins.

Signaling through $G_{\beta\gamma}$

Many receptors coupled to G_i and G_o exert their effects through signals propagated to downstream effectors by $G_{\beta\gamma}$ subunits. Similar to G_α subunits, $G_{\beta\gamma}$ subunits regulate the activity of enzymes involved in the generation of second messengers. These are adenylyl cyclase, phospholipase Cβ, and phosphatidylinositol 3-kinase. $G_{\beta\gamma}$ exhibits type-specific regulation of adenylyl cyclase, inhibiting some isotypes, but activating others synergistically with $G_{s\alpha}$. $G_{\beta\gamma}$ activates certain isoforms of phospholipase Cβ, an enzyme that converts phosphatidylinositol into diacylglycerol and inositol trisphosphate. The second messenger inositol trisphosphate induces the release of calcium from intracellular stores, whereas diacylglycerol recruits protein kinase C to the plasma membrane. Phosphatidylinositol 3-kinase (PI3K) is also activated by $G_{\beta\gamma}$ subunits. The generation of phosphatidylinositol 3,4,5-trisphosphate (PIP_3), the product of PI3K, mediates important cellular responses. Production of PIP_3 in white blood cells is an essential step in inducing the cells to migrate to sites of cell injury. PI3K activation by $G_{\beta\gamma}$ is also associated with signaling pathways that regulate cell survival.

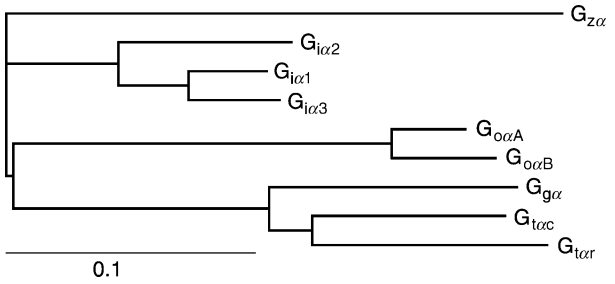

FIGURE 1 Sequence comparison of $G_{i\alpha}$ family members. A nearest-neighbor dendrogram of $G_{i\alpha}$ family sequences. The scale bar represents a measure of evolutionary distances between the sequences analyzed.

In addition to regulating second messengers, $G_{\beta\gamma}$ subunits modulate the activity of numerous ion channels. The best characterized are potassium channels in the heart which slow heart rate when activated. $G_{\beta\gamma}$ subunits bind directly to the channel and cause it to open (Figure 2).

The effectors described above are regulated through direct binding of the $G_{\beta\gamma}$ subunits. $G_{\beta\gamma}$ is also an important regulator of MAP kinase pathways. The direct target of $G_{\beta\gamma}$ in these pathways has not been identified.

G_i

G_i, the founding member of the family, is named for its ability to inhibit the enzyme adenylyl cyclase. There are three forms of $G_{i\alpha}$, designated $G_{i\alpha1}$, $G_{i\alpha2}$, and $G_{i\alpha3}$, each encoded by a separate gene. The three isoforms share many functions and will be considered together here. Heterotrimeric G_i couples to many different receptors, including those for catecholamines, neurotransmitters, and chemokines. Many of the effects associated with activation of G_i by receptors are mediated by $G_{\beta\gamma}$ subunits as discussed above. The best characterized effector for $G_{i\alpha}$ is adenylyl cyclase. $G_{i\alpha}$ binds to this

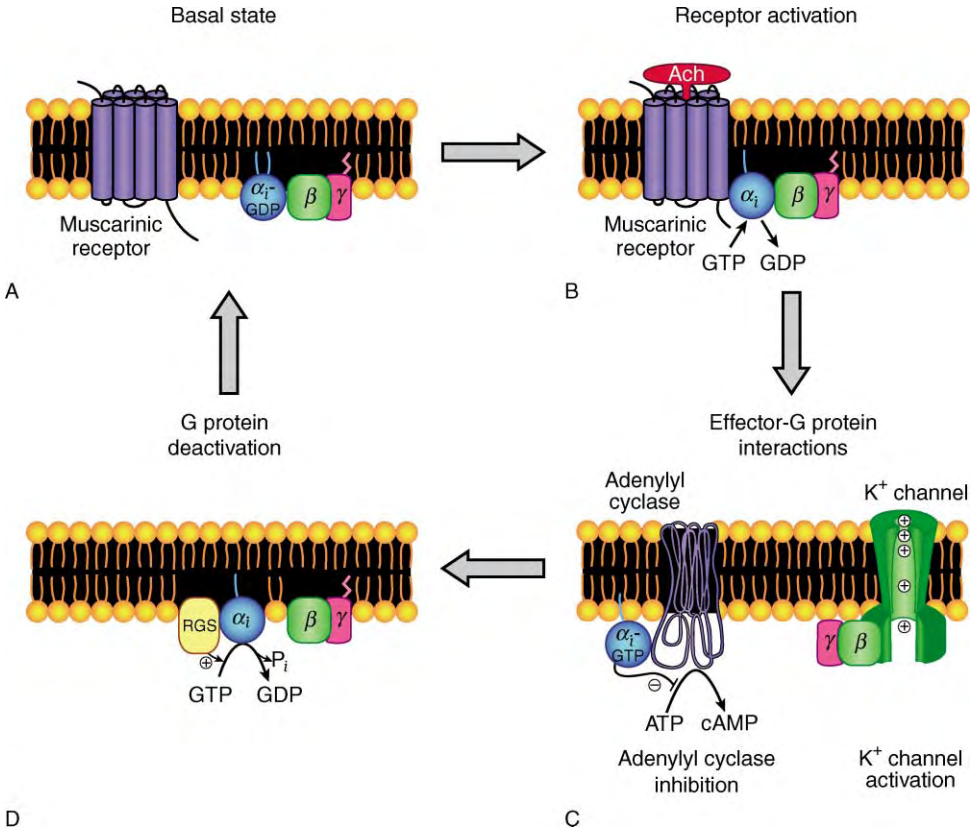

FIGURE 2 G_i signaling in the heart. In heart cells, the neurotransmitter acetylcholine elicits a slowing of heart rate by activating a G_i-coupled signaling pathway. (A) In the basal state, $G_{i\alpha}$ is in the GDP-bound state and associated with $G_{\beta\gamma}$. The receptor is unoccupied and effectors (not shown) are inactive. (B) The neurotransmitter acetylcholine is released at the terminal of the vagus nerve that innervates the heart. Binding of acetylcholine activates the receptor, which in turn stimulates the release of GDP from $G_{i\alpha}$. GTP is present intracellularly at high concentration and quickly diffuses into the guanine nucleotide-binding pocket on $G_{i\alpha}$. GTP binding induces a conformational change in $G_{i\alpha}$, causing it to dissociate from $G_{\beta\gamma}$. (C) $G_{i\alpha}$–GTP interacts with adenylyl cyclase in the plasma membrane and inhibits its activity. $G_{\beta\gamma}$ subunits bind to the K^+ channel, causing it to open. The cell membrane becomes hyperpolarized, slowing action potential frequency and heart rate. (D) $G_{i\alpha}$ hydrolyzes its GTP to GDP to deactivate the pathway. The rate of GTP hydrolysis is accelerated by $G_{i\alpha}$ interaction with an RGS protein. Once in its GDP-bound state, $G_{i\alpha}$ reassociates with $G_{\beta\gamma}$ and the system is returned to the basal state.

enzyme and inhibits its activity, thereby reducing intracellular levels of the second messenger cAMP (Figure 2). $G_{i\alpha}$ (and $G_{o\alpha}$) can propagate signals to protein kinases (e.g., the MAP kinase pathway or c-Src), but the direct target of $G_{i\alpha}$ in these pathways is unknown.

$G_{i\alpha}$'s are ubiquitously expressed and most cell types contain more than one form. Eliminating the gene for $G_{i\alpha1}$ or $G_{i\alpha3}$ in mice does not have any obvious effects on the organism's ability to develop or to reproduce. Mice lacking a functional gene for $G_{i\alpha2}$ appear to develop normally, but exhibit growth retardation, inflammatory bowel disease, and are prone to developing adenocarcinomas, demonstrating that $G_{i\alpha2}$ is essential for normal function of the intestine. The relatively mild phenotypes associated with inactivation of the individual $G_{i\alpha}$ genes probably reflect an ability of one $G_{i\alpha}$ subtype to compensate for the function of another.

G_o

$G_{o\alpha}$ is a close relative of the $G_{i\alpha}$'s, with 70% sequence identity to $G_{i\alpha1}$ (Table I). Two forms of $G_{o\alpha}$ ($G_{o\alpha A}$ and $G_{o\alpha B}$) are generated by alternative splicing of mRNA. G_o is very abundant in the nervous system where it represents 0.5% of total membrane protein. It is also expressed in neuroendocrine tissues and at low levels in the heart. In general, receptors coupled to G_o bind neurotransmitters that mediate inhibitory, rather than excitatory, responses in the central nervous system. The best-studied effectors regulated by G_o are voltage-gated calcium channels, which are inhibited by $G_{\beta\gamma}$ subunits released upon receptor activation of G_o. Direct effectors of $G_{o\alpha}$ are not as well characterized. Inactivation of the $G_{o\alpha}$ gene in mice results in central nervous system dysfunction and abnormal regulation of calcium channels in the nervous system and heart.

G_z

$G_{z\alpha}$ is the most distantly related member of the $G_{i\alpha}$ family based on sequence comparison (Figure 1). Its expression pattern is more restricted than $G_{i\alpha}$, with abundant expression in brain, neuroendocrine tissues, and platelets. G_z has several properties that distinguish it from the other members of the G_i family. It is the only family member that is not a substrate for ADP-ribosylation by pertussis toxin (see below). $G_{z\alpha}$ also has an intrinsic rate of GTP hydrolysis that is much slower than G_i or G_o. Thus, G_z pathways may be slow to turn off unless regulated by RGS proteins. $G_{z\alpha}$ interacts with several RGS family members that show marked specificity for $G_{z\alpha}$ over other G-protein α-subunits. The complement of receptors that G_z responds to overlaps extensively with those that couple to $G_{i\alpha}$ and $G_{o\alpha}$. Given its abundant expression in brain, G_z is coupled to many neurotransmitters and can regulate ion channels, adenylyl cyclase, and MAP kinase pathways similar to G_i and G_o. $G_{z\alpha}$–GTP binds directly to Rap1GAP, a GTPase-activating protein for the monomeric GTPase Rap1, an interaction that may modulate neuronal differentiation.

The gene for $G_{z\alpha}$ has been knocked out in mice. The $G_{z\alpha}$-deficient mice develop normally and are fertile. However, they exhibit altered responses to psychoactive drugs and a mild impairment in platelet function. These phenotypes are consistent with the restricted distribution of $G_{z\alpha}$ in neural tissues and platelets.

G_t (Transducin)

G_t is the G protein that mediates the visual signal transduction cascade. It is also known as transducin.

TABLE I

$G_{i\alpha}$ Family Members

Protein	Gene name	% Amino acid identity[a]	PTX substrate[b]	Fatty acylation[c]	Major tissue distribution
$G_{i\alpha1}$	GNAI-1	100	Yes	Myr, Palm	Nearly ubiquitous
$Gi_{\alpha2}$	GNAI-2	87	Yes	Myr, Palm	Ubiquitous
$G_{i\alpha3}$	GNAI-3	93	Yes	Myr, Palm	Nearly ubiquitous
$G_{o\alpha A}$	GNAO	70	Yes	Myr, Palm	Brain neuroendocrine, heart
$G_{o\alpha B}$	GNAO	69	Yes	Myr, Palm	Brain, neuroendocrine, heart
$G_{t\alpha r}$	GNAT-1	67	Yes	Myr	Retinal rods
$G_{t\alpha}$	GNAT-2	69	Yes	Myr	Retinal cones
$G_{g\alpha}$	GNAG	68	Yes	Myr	Taste buds
$G_{z\alpha}$	GNAZ	66	No	Myr, Palm	Brain, adrenal, platelets

[a] Amino acid sequence (human) comparison with $G_{i\alpha1}$.
[b] PTX, pertussis toxin, see text.
[c] Myr, amide-linked myristate; Palm, thioester-linked palmitate; see text.

There are two closely related forms of $G_{t\alpha}$ that are encoded by separate genes. $G_{t\alpha r}$ is expressed in retinal rods, whereas $G_{t\alpha c}$ is found in cone cells. $G_{t\alpha r}$ and $G_{t\alpha c}$ both associate with specific $G_{\beta\gamma}$ complexes: $G_{t\alpha r}$ with $G_{\beta 1\gamma 1}$ and $G_{t\alpha c}$ with $G_{\beta 1\gamma 14}$. The receptor in the visual signal transduction cascade is rhodopsin, which harbors a covalently attached 11-*cis*-retinal. When a photon of light is absorbed by the retinal, it undergoes a *cis–trans* isomerization that induces a conformational change in rhodopsin. The activated receptor then promotes nucleotide exchange and subunit dissociation of G_t. $G_{t\alpha}$–GTP propagates the signal by stimulating cGMP phosphodiesterase (PDE), an enzyme that hydrolyzes cGMP. PDE consists of two catalytic subunits and two inhibitory subunits (called PDE_γ). $G_{t\alpha}$ binds PDE_γ and relieves the inhibitory constraint on the catalytic subunits. Reduction of cellular levels of cGMP causes closure of cGMP-gated ion channels in the plasma membrane. This reduces the influx of Na^+ and Ca^{2+}, increasing the negative charge inside the cell, and causing the cell to become hyperpolarized. The net effect is a change in the signals that photoreceptors send to the brain. Mice lacking a functional $G_{t\alpha r}$ gene demonstrate defective light responses and develop a mild retinal degeneration with age.

An important mechanism for deactivating the phototransduction process is the hydrolysis of GTP by $G_{t\alpha}$. The intrinsic rate of GTP hydrolysis measured for $G_{t\alpha}$ *in vitro* is too slow to mediate the physiological response. *In vivo*, the GTPase rate of $G_{t\alpha}$ is accelerated by the GAP activity of a protein complex of the retinal RGS protein RGS9 and its binding partner $G_{\beta 5L}$. RGS9 has a G_γ-like domain that mediates its association with $G_{\beta 5L}$. The effector molecule PDE_γ also promotes GAP activity by increasing the affinity of $G_{t\alpha}$ for the RGS9–$G_{\beta 5L}$ complex. Thus, timely inactivation of G_t is achieved through cooperation between RGS9–$G_{\beta 5L}$ and PDE_γ.

G_g (Gustducin)

G_g is a signal transducer for bitter and sweet taste signaling pathways. Its expression is restricted primarily to taste buds. $G_{g\alpha}$ is closely related to $G_{t\alpha r}$ and $G_{t\alpha c}$ (Figure 1). G_g couples receptors for bitter and sweet tastants to specific taste cell phosphodiesterases. Transducins and gustducin therefore share a common family of effectors. In mice deficient for $G_{g\alpha}$, the animals show impaired responses to bitter and sweet agents, but are normal in their responses to sour and salty tastants. Thus, animals use a different signal transduction pathway to experience sour and salty taste.

Post-translational Modifications

Members of the G_i family are subject to a number of post-translational modifications (Table I). All family members except $G_{z\alpha}$ are modified with ADP–ribose at a cysteine residue near the C terminus by a bacterial toxin from *Bordatella pertussis*. The C terminus of G_α is an important site of interaction with G-protein-coupled receptors. Modification of G_α with the bulky ADP–ribose group interferes with receptor–G-protein coupling. Therefore, cells treated with pertussis toxin cannot respond to ligands that bind to G_i-coupled receptors. Pertussis toxin has been a useful experimental tool to define cellular responses that are mediated by members of the G_i family.

All G-protein α-subunits are modified with fatty acids at or near the amino terminus. Fatty acylation provides a hydrophobic anchor that mediates binding to the plasma membrane. Members of the G_i family (but not G_s, G_{12}, or G_q families) are N-myristoylated. Myristic acid is added through an amide linkage to a glycine residue exposed after removal of the initiator methionine. This is the only modification found on $G_{t\alpha}$ and $G_{g\alpha}$. However, $G_{i\alpha}$, $G_{o\alpha}$, and $G_{z\alpha}$ undergo a second type of fatty acylation, S-palmitoylation, which occurs at a cysteine residue adjacent to the N-myristoylated glycine. Whereas N-myristoylation is a stable modification, S-palmitoylation is reversible and can be regulated.

Heterotrimeric G proteins are generally not regulated by protein phosphorylation and dephosphorylation, in contrast to many signaling proteins. $G_{z\alpha}$ is an exception. It is phosphorylated by protein kinase C and p21-activated kinase 1. Phosphorylation of $G_{z\alpha}$ reduces its ability to bind $G_{\beta\gamma}$, and interact with RGS proteins, thereby prolonging $G_{z\alpha}$ activation.

See Also the Following Articles

Adenylyl Cyclases • Cyclic GMP Phosphodiesterases • G_{12}/G_{13} Family • G Protein Signaling Regulators • G_q Family • G_s Family of Heterotrimeric G Proteins

Glossary

chemokine Small, secreted protein that guides the migration of white blood cells.

effector A protein whose activity is changed in response to a stimulus.

hormone A circulating peptide or chemical that acts on target organs at a distance from its site of synthesis.

neurotransmitter A chemical messenger released by a nerve cell at a synapse.

second messenger A small molecule synthesized intracellularly in response to an extracellular stimulus that propagates the signal by binding to an effector and modulating its activity.

Further Reading

Arshavsky, V. Y., Lamb, T. D., and Pugh, E. N. (2002). G proteins and phototransduction. *Annu. Rev. Physiol.* **64**, 153–187.

Clapham, D. E., and Neer, E. J. (1997). G protein $\beta\gamma$ subunits. *Annu. Rev. Pharmacol. Toxicol.* **37**, 167–203.

Gilman, A. G. (1995). Nobel lecture. G proteins and regulation of adenylyl cyclase. *Biosci. Rep.* **15**, 65–97.

Ho, M. K.-C., and Wong, Y. H. (2001). G_z signaling: emerging divergence from G_i signaling. *Oncogene* **20**, 1615–1625.

Margolskee, R. F. (2002). Molecular mechanisms of bitter and sweet taste transduction. *J. Biol. Chem.* **277**, 1–4.

Neves, S. R., Ram, P. T., and Iyengar, R. (2002). G protein pathways. *Science* **296**, 1636–1639.

Offermans, S. (2001). *In vivo* functions of heterotrimeric G proteins: studies in G_α-deficient mice. *Oncogene* **20**, 1635–1642.

Biography

Maurine Linder is an Associate Professor of Cell Biology and Physiology at Washington University School of Medicine in St. Louis. Her principal research interests are in the organization and regulation of signal transduction pathways in cell membranes. She holds a Ph.D. in molecular and cell biology from the University of Texas at Dallas and received her postdoctoral training in the Department of Pharmacology at UT Southwestern Medical Center in Dallas.

Giant Mitochondria (Megamitochondria)

Bernard Tandler and Charles L. Hoppel
Veterans Affairs Medical Center, Cleveland, Ohio, USA

Mitochondria are extremely sensitive indicators of the health of their host cells. Even slight perturbations in cellular metabolism can evoke morphological alterations in these organelles. One way in which mitochondria respond to metabolic disturbances is by increasing in size, often to a point where they outstrip the cell nucleus in diameter. Such outsize organelles are also referred to as megamitochondria, a term that appears to have found increasing favor. Hepatic megamitochondria can measure ~14 μm, giving them a volume >1,400 mm^3, compared to the volume of ~0.5 mm^3 exhibited by typical liver mitochondria. Enlarged mitochondria can be induced by various nutritional and pharmacological manipulations. They occur naturally in certain human disease states and in a few cell types in exotic organisms; e.g., the larger of the paired mitochondria in the spermatozoan tail of the hemipteran *Gerris* has a volume of ~10,000 mm^3.

Megamitochondrial Structure

Under some conditions, the megamitochondria are virtual simulacra of their normal size counterparts; i.e., on a unit mitochondrial area basis they display the same number and arrangement of cristae as do normal mitochondria (Figure 1), although in some cases they may contain within their matrix a small stack of closely packed, short cristae. In other conditions, the megamitochondria have very short cristae that protrude inward from the boundary membrane in a manner not unlike a picket fence. In still others, the cristae are very rare, with the megamitochondria consisting of a morphologically conventional outer membrane and a smooth inner boundary membrane that is almost devoid of cristae. In all types of megamitochondria, the inner compartment contains moderately dense, homogeneous material. In some cases of human thyroid tumors, the matrix compartment contains a jumble of dense ribbons of undefinable length. In certain types of giant mitochondria, an expanded crista contains a bundle of helical filaments. Filaments of this type occurring in normal hepatic mitochondria consist of three distinct, but otherwise uncharacterized, proteins.

Formation of Megamitochondria

The manner in which megamitochondria arise is somewhat controversial. In riboflavin deficiency (the first experimental protocol to evoke the production of giant hepatic mitochondria), this size increase results from two distinct processes, growth and organelle fusion. The earliest step in fusion is signaled by the touching of adjacent mitochondria (under normal conditions, hepatic mitochondria repel one another because of their identical surface charge). One of the paired organelles forms a protrusion that fits into an appropriately shaped invagination in its partner. A myelin figure, which may be indicative of membrane flux, forms at the point of deepest penetration. Eventually, the surface membranes become melded, with the result of a single mitochondrion of enhanced size. That mitochondria are capable of fusing even under physiological conditions is shown by the formation of mitochondrial nebenkerns in insect spermatids, where numerous small mitochondria combine to form two extremely large mitochondria that ultimately twine about the elongating axoneme. Repetition of the fusion process in hepatocytes eventually results in significantly enlarged mitochondria. But the fractional volume of the hepatocytes occupied by the megamitochondria is considerably larger than that of mitochondria in control hepatocytes. In addition to fusion, there clearly has been growth of the mitochondria. It would appear that these two processes constitute an invariant mechanism for formation of giant mitochondria. Therefore, mitochondria that evince a minor increase in size probably as a result of growth or swelling alone should not be categorized as megamitochondria; it is recommended that only those organelles that achieve a diameter greater than 4 μm be designated as giant mitochondria or as megamitochondria.

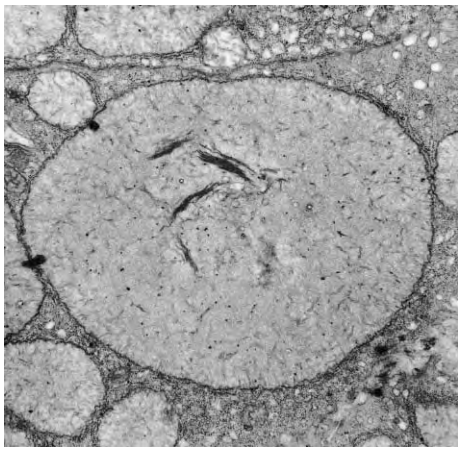

FIGURE 1 Transmission electron micrograph of a hepatic megamitochondrion induced in a mouse by riboflavin deficiency. Note the typical distribution of cristae and the presence of dense matrix granules. The diameter of this organelle is approximately six times as large as that of normal hepatic mitochondria. At the left, the large mitochondrion is linked to two smaller organelles by means of small myelin figures, indicating that it is still in the process of enlargement. Original magnification, ×9,000.

Biochemistry

Little is known of the functional capabilities of megamitochondria. A number of laboratories have reported on biochemical studies carried out on alleged megamitochondria, but inspection of the accompanying electron micrographs of the tested mitochondrial fractions invariably reveals that these organelles are of normal size. When all fractions obtained from livers known to contain megamitochondria are examined, the giant mitochondria are found to have co-sedimented with the nuclei, which they match in size and density, rather than in the mitochondrial fraction. So virtually all published accounts of megamitochondrial function are actually based on normal-sized mitochondria. In such normal-sized mitochondria, oxidative metabolism is significantly decreased even before giant mitochondria appear. In those tissues in which only sporadic megamitochondria are elicited, the normal size mitochondria showed no change. Only when giant mitochondria can be obtained in pure yield will questions concerning mitochondrial DNA content, enzyme content, membrane composition, and oxidative capacity be addressed.

Involvement in Apoptosis

The logistics involved in the experimental evocation of megamitochondria in intact animals are formidable. Recently, it has been proven possible to produce enlarged mitochondria (although such organelles have been referred to as megamitochondria, they rarely exceed 2 μm in diameter) in tissue culture cells by administration of hydrazine to these cells; this compound is normally toxic, but if the cells are protected by prior administration of inducers of cytochrome P450, they survive the hydrazine and produce large mitochondria that can be monitored by confocal laser microscopy. Based on such preparations, it has been suggested that megamitochondria represent a way station on the road to apoptosis induced by free radicals. Although this concept may be true in specific cases, there is no evidence that there is in every case a direct association between megamitochondria formation and apoptosis. There are ample examples of apoptotic cells that clearly are devoid of megamitochondria; conversely, many of the tissues that contain megamitochondria show no evidence of apoptotic decline.

Restoration to Normal Size

It is well established that normal mitochondria replicate by division, but the morphological pathway by which this process is accomplished was unclear. The megamitochondrial model has been used successfully to settle this point. Based on restoration to normal size of experimentally induced megamitochondria, there

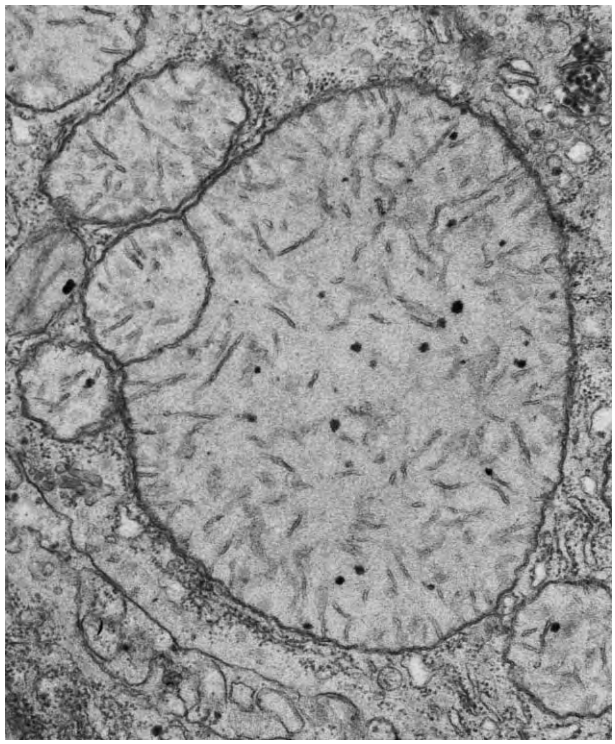

FIGURE 2 Transmission electron micrograph of a dividing hepatic megamitochondrion during recovery from ariboflavinosis. A small bud is subtended by a membranous partition; ingrowth of the outer membrane ultimately leads to the separation of the bud, which is equal in size to a typical mitochondrion, from the enlarged organelle. Repetition of this process results in mitochondrial normalization in terms of size. Original magnification, ×34,000.

appear to be two distinct pathways in mitochondrial division; during recovery, only one of the two mechanisms is called upon, depending on the agent that evoked the megamitochondria in the first place. The first mechanism involves the formation of a membranous partition, probably of boundary membrane origin, that spans the organelle, frequently at the base of a bud (Figure 2). This is followed by ingrowth of the outer membrane into the partition. Like a closing iris diaphragm, the outer membrane eventually completes its incursion, and two daughter mitochondria result. Repetition of this process ultimately leads to the disappearance of megamitochondria and to the appearance of organelles of normal size. The second pathway involves a simple elongation and attenuation of the equator of the megamitochondrion until membranes from opposite sides of the organelle touch and fuse. In effect, the giant mitochondrion has been pulled apart. The progeny of such division repeatedly undergo the same process to finally restore the mitochondria to their accustomed dimensions. What controls the selection of a particular pathway for mitochondrial division is completely unknown.

See Also the Following Articles

Cell Death by Apoptosis and Necrosis • Flavins • Hepatocyte Growth Factor/Scatter Factor Receptor • Vitamin B_{12} and B_{12}-Proteins

Glossary

ariboflavinosis A deficiency of riboflavin in the diet.

crista (pl. cristae) Any of numerous infoldings of the inner mitochondrial membrane in eukaryotic cells.

nebenkern A globular structure in a spermatid that results from interlocking and fusion of the mitochondria during spermatogenesis.

Further Reading

Hoppel, C. L., and Tandler, B. (1993). Megamitochondria. *Meth. Toxicol.* **2**, 191–206.

Karbowski, M., Kurono, C., Wozniak, M., Ostrowski, M., Teranishi, M., Nishizawa, Y., Usukura, J., Soji, T., and Wakabayashi, T. (1999). Free radical-induced megamitochondria formation and apoptosis. *Free Radical Biol. Med.* **26**, 396–409.

Tandler, B., and Hoppel, C. L. (1973). Division of giant mitochondria during recovery from cuprizone intoxication. *J. Cell Biol.* **56**, 266–272.

Tandler, B., and Hoppel, C. L. (1986). Studies on giant mitochondria. *Ann. N.Y. Acad. Sci.* **488**, 65–81.

Tandler, B., Erlandson, R. A., and Wynder, E. L. (1968). Riboflavin and mouse hepatic cell structure and function. I. Ultrastructural alterations in simple deficiency. *Am. J. Pathol.* **52**, 69–95.

Tandler, B., Erlandson, R. A., Smith, A. L., and Wynder, E. L. (1969). Riboflavin and mouse hepatic cell structure and function. II. Division of mitochondria during recovery from simple deficiency. *J. Cell Biol.* **41**, 477–493.

Tandler, B., Dunlap, M., Hoppel, C. L., and Hassan, M. (2002). Giant mitochondria in a cardiomyopathic heart. *Ultrastruct. Pathol.* **26**, 1–7.

Biography

Bernard Tandler was a long-time Professor of Oral Biology and of Anatomy at the Case Western Reserve University Schools of Dentistry and Medicine, Cleveland, where he currently is a Visiting Professor of Oral Diagnosis, as well as a Consultant at the VA Medical Center in Cleveland. He also served as Visiting Professor of Anatomy at Kyushu Dental College and of Biological Sciences at Texas Tech University. His major research interests concern the biogenesis, structure, and physiology of giant mitochondria, as well as the structure, function, and evolution of mammalian salivary glands and of secretory cells in general.

GlcNAc Biosynthesis and Function, O-Linked

Kaoru Sakabe and Gerald W. Hart
The Johns Hopkins University School of Medicine, Baltimore, Maryland, USA

O-GlcNAc is a dynamic posttranslational modification of proteins in which a single β-N-acetylglucosamine (O-GlcNAc) is added enzymatically to Ser or Thr residues through a glycosidic linkage. Much like phosphorylation, the emerging evidence shows a regulatory role for O-GlcNAc on proteins. In addition, misregulation of this posttranslational modification has been linked to diseases such as type 2 diabetes, Alzheimer's disease, and cancer.

Background

The modification of nuclear and cytoplasmic proteins on Ser and Thr residues by the addition of a single sugar moiety β-N-acetylglucosamine (O-GlcNAc) through an O-glycosidic linkage was originally described in 1984. The dogma at that time limited covalent modification of proteins by carbohydrates to occur solely in the extracellular space and within the ER, Golgi, and other subcellular organelles. Since then, O-GlcNAc has been found in all multicellular plants and animals. It is generally not elongated to more complex structures like other types of glycosylation.

The addition of O-GlcNAc to proteins, termed O-GlcNAcylation, is analogous to phosphorylation in its use as a signaling intermediate and regulatory mechanism. Indeed, global changes of O-GlcNAc have been observed during different stages of cell cycle, as well as upon mitogen stimulation. Similarly to O-Phosphate, O-GlcNAc is abundant, occurs posttranslationally and is dynamic. In fact, all proteins known to be O-GlcNAcylated are also modified with O-Phosphate. Often the sites of glycosylation are near or the same as phosphorylation sites, leading to the complex interplay on the protein by both modifications. In several cases in which the protein is glycosylated, the site can no longer be phosphorylated even if it is a few amino acids away, presumably due to steric hindrance. The converse is also true (refer to Figure 1).

The enzymes catalyzing the addition and removal of O-GlcNAc have been cloned and characterized. UDP-GlcNAc:polypeptide transferase or O-GlcNAc transferase (OGT) catalyzes the transfer of the N-acetylglucosamine from uridine diphosphate N-acetylglucosamine (UDP-GlcNAc) to the hydroxyl group of specific Thr and Ser residues. β-D-N-acetylglucosaminidase or O-GlcNAcase, on the other hand, hydrolyzes the sugar moiety from the protein.

Many proteins have been identified as O-GlcNAc-modified proteins, with many more yet to come. The proteins identified so far include RNA polymerase II and transcription factors, tumor suppressors and oncogenes, chromatin and nuclear pore proteins, RNA processing proteins, protein translation regulatory proteins, cytoskeletal proteins, and cytosolic enzymes.

Biosynthesis of UDP-GlcNAc

The activated sugar donor, UDP-GlcNAc, is an example of a molecule exquisitely controlled by multiple different pathways of cellular metabolism including nucleotide, glucose, amino acid, and fatty acid metabolism. In addition, the sugar nucleotide is sensitive to the overall energy status of the cell. The relative levels of each component determine the availability of UDP-GlcNAc for modifying different proteins; therefore, this sugar donor serves an important function by sensing the nutrient status of the cell.

UDP-GlcNAc is synthesized via the hexosamine biosynthetic pathway. Approximately 2–5% of the glucose taken up by the cell is shunted through this pathway to generate amino sugars and activated amino sugars. The rate-limiting enzyme glutamine-fructose-6-phosphate-transaminase, or GFAT, controls how much glucose is diverted into UDP-GlcNAc. The amount of UDP-GlcNAc available correlates well with the O-GlcNAc levels within the cell (Figure 2).

O-GlcNAc Transferase (OGT)

OGT is evolutionarily conserved from *Caenorhabditis elegans* to *Homo sapiens*, diverging little from organism to organism, indicating the importance of this enzyme in

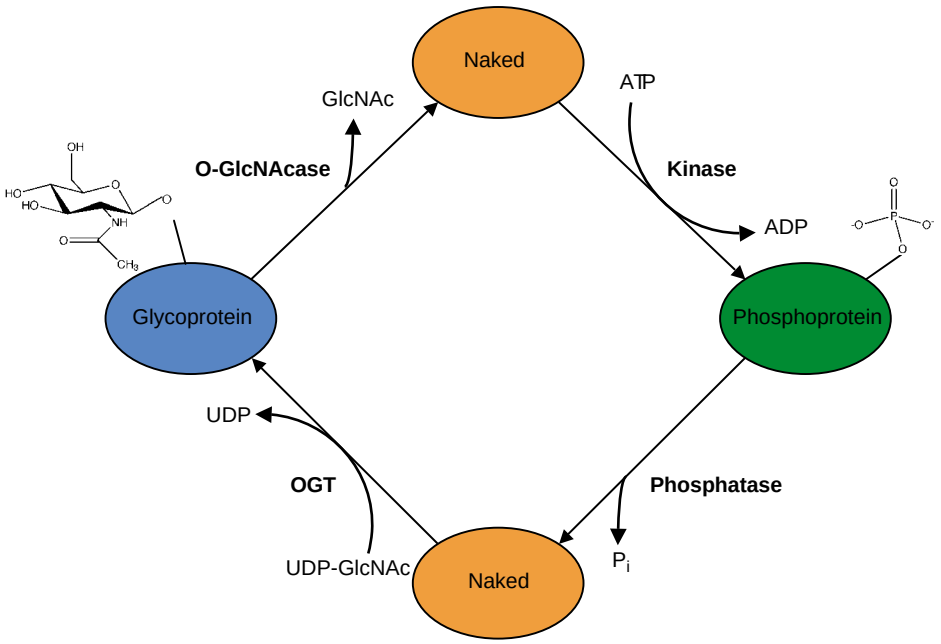

FIGURE 1 Interrelationship between O-GlcNAc and O-phosphate.

metazoans. In addition, ablation of this gene is lethal down to the single cell level. Therefore, evolution seems to have kept tight control on this enzyme, not allowing it to diverge greatly, signifying the importance of its function. In plants, OGT regulates growth via the gibberellin acid hormonal system.

The native enzyme in most tissues is comprised of three identical polypeptides. Each polypeptide consists of two domains: a tetratricopeptide repeat (TPR) domain and the catalytic domain. The TPR domain contains 9–13 tandem repeats of 34 amino acids, depending on species. These domains have been characterized as protein–protein interaction domains and are important for trimerization of the subunits as well as for substrate interaction. For example, OGT interacts with a repressor complex, mSin3a, through its TPR domain to inhibit transcription.

No consensus sequence has yet been identified for OGT; however, it seems that a Pro residue within one to three amino acids of the modification site occurs frequently. In addition, O-GlcNAc sites are usually found in regions rich in Ser and Thr residues.

O-GlcNAcase

The enzyme that catalyzes the hydrolysis of the O-GlcNAc moiety, O-GlcNAcase, is a monomer of 130 kDa. A 75 kDa alternate splice variant has also been described which lacks the catalytic C-terminal end of the enzyme. Both forms are expressed ubiquitously.

Not much is known about O-GlcNAcase; however, when purified, O-GlcNAcase is found within a high-molecular-weight complex suggesting that it associates with other proteins for regulation and specificity. Additionally, O-GlcNAcase is a substrate for proteolytic cleavage by one of the executioner caspases, caspase-3. Cleavage by this aspartyl protease has no effect on *in vitro* O-GlcNAcase activity.

Function

Different studies have ascribed varied roles of O-GlcNAc on certain proteins. These functions include involvement in nuclear transport, regulation of protein–protein interactions, regulation of protein degradation, and regulation of protein activity.

The proteins constituting the nuclear pore are enriched with O-GlcNAc. In fact, the nucleus contains the greatest concentration of O-GlcNAcylated proteins and many proteins that are O-GlcNAcylated are known to exist both in the cytoplasm and in the nucleus. It has been suggested that O-GlcNAc may be an alternative nuclear localization sequence or cytosolic retention sequence; however, this hypothesis has yet to be confirmed.

Early observations of O-GlcNAcylated proteins demonstrated an involvement of the modification in forming multimeric complexes, suggesting that O-GlcNAc may be important for regulating protein–protein interactions. These proteins include cytoskeletal proteins such as cytokeratins, neurofilaments, microtubule associated proteins, tau, crystallin, and synapsin.

The half-life of a protein dictates the temporal effect that it exerts on the cell. PEST sequences, Pro, Glu, Ser, and Thr enriched regions, are efficient in targeting proteins to the proteasome. Glycosylation has been

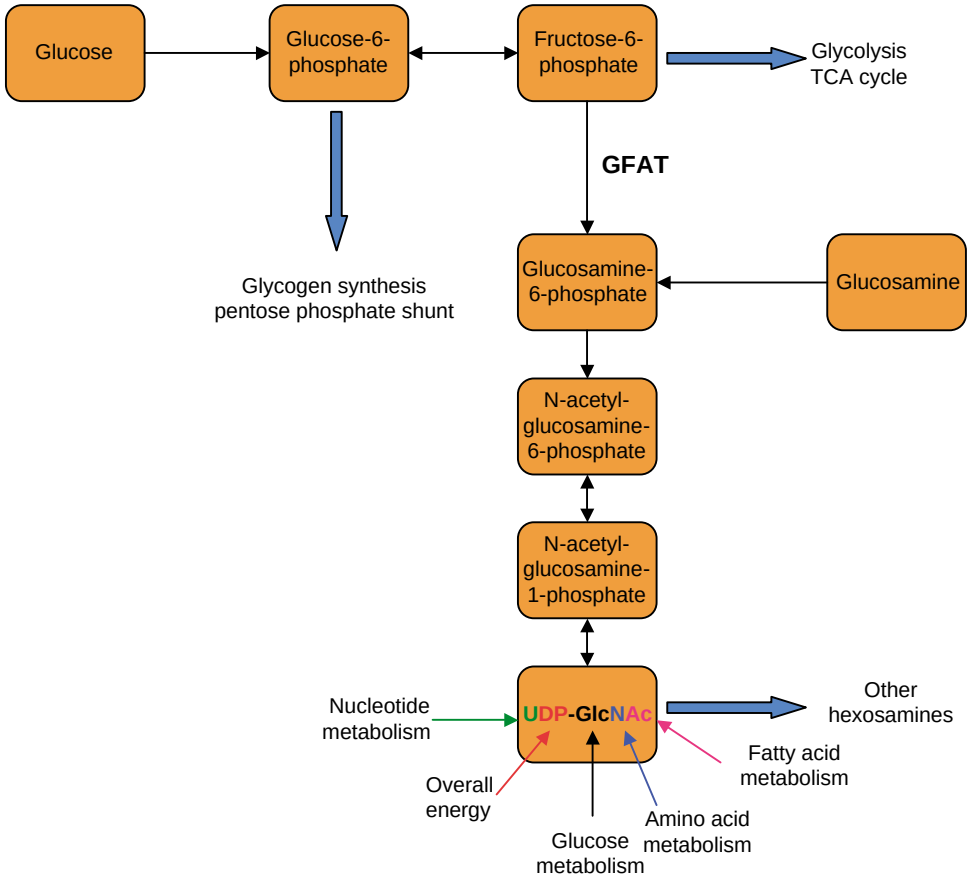

FIGURE 2 Hexosamine biosynthetic pathway.

shown to protect the translation activator p67, the transcription factor Sp1, and the nuclear hormone receptor estrogen receptor-β from degradation.

Physiological Importance

Misregulation of O-GlcNAc has been implicated in numerous disease pathologies such as type 2 diabetes, Alzheimer's disease, and cancer. Hyperglycemia and insulin resistance are hallmarks of type 2 diabetes. Since generation of UDP-GlcNAc is sensitive to the amount of glucose and glucosamine available, hyperglycemic conditions are believed to increase UDP-GlcNAc levels within the cell and thus increase the amount of O-GlcNAcylated proteins. Exogenously increasing O-GlcNAc levels have been shown to cause insulin resistance; therefore, OGT appears to play a key role in the pathology of type 2 diabetes.

A major component of neurofibrillary tangles associated with Alzheimer's disease is the microtubule-associated protein tau. In the diseased state, tau becomes hyperphosphorylated. It is known that under normal conditions, tau is modified with O-GlcNAc; it is hypothesized that by decreasing the amount of this modification on tau, it becomes hyperphosphorylated and forms the aggregates associated with Alzheimer's disease.

Finally, a decrease in O-GlcNAc has been seen in cancerous tissue. In fact, increased O-GlcNAcase activity and decreased O-GlcNAc levels correlated with tumor grade, indicating a protective role for this modification. In fact, Thr 58 of c-myc, an oncoprotein, is the major O-GlcNAc site on this oncogene protein and is also a hotspot for mutation in Burkitt's lymphoma.

In summary, O-GlcNAc is an abundant and dynamic posttranslational modification in all metazoans. It has a complex interplay with phosphorylation and in turn plays a key role in regulating cell signaling, transcription, and cytoskeletal functions.

See Also the Following Articles

Diabetes • Oligosaccharide Chains: Free, *N*-Linked, *O*-Linked • Glycosylation, Congenital Disorders of • RNA Polymerase I and RNA Polymerase III in Eukaryotes • RNA Polymerase II and Basal Transcription Factors in Eukaryotes • RNA Polymerase II Elongation Control in Eukaryotes • RNA Polymerase II Structure in Eukaryotes

Glossary

hexosamine biosynthetic pathway The pathway by which the activated sugar donor, UDP-GlcNAc, for O-glycosylation is generated.

O-GlcNAcase or β-D-N-acetylglucosaminidase The enzyme that hydrolyzes O-GlcNAc from the target protein.

O-GlcNAc transferase or UDP-GlcNAc:polypeptide transferase (OGT) The enzyme that catalyzes the transfer of O-GlcNAc from UDP-GlcNAc to its target substrate.

O-GlcNAcylation or O-glycosylation The modification of Ser or Thr residues with a single sugar moiety N-acetylglucosamine or O-GlcNAc. This modification occurs in the nucleus or cytoplasm and is analogous to O-phosphorylation.

Further Reading

Fang, B., and Miller, M. W. (2001). Use of galactosyltransferase to assess the biological function of O-linked *N*-acetyl-D-glucosamine: A potential role for O-GlcNAc during cell division. *Exp. Cell Res.* **263**, 243–253.

Iyer, S. P., and Hart, G. W. (2003). Dynamic nuclear and cytoplasmic glycosylation: Enzymes of O-GlcNAc cycling. *Biochemistry* **42**, 2493–2499.

Kearse, K. P., and Hart, G. W. (1991). Lymphocyte activation induces rapid changes in nuclear and cytoplasmic glycoproteins. *Proc. Natl Acad. Sci. USA* **88**, 1701–1705.

McClain, D. A., and Crook, E. D. (1996). Hexosamines and insulin resistance. *Diabetes* **45**, 1003–1009.

Miller, M. W., Caracciolo, M. R., Berlin, W. K., and Hanover, J. A. (1999). Phosphorylation and glycosylation of nucleoporins. *Arch. Biochem. Biophys.* **367**, 51–60.

Torres, C.-R., and Hart, G. W. (1984). Topography and polypeptide distribution of terminal N-acetylglucosamine residues on the surfaces of intact lymphocytes. *J. Biol. Chem.* **259**, 3308–3317.

Wells, L., Vosseller, K., and Hart, G. W. (2001). Glycosylation of nucleocytoplasmic proteins: Signal transduction and O-GlcNAc. *Science* **291**, 2376–2378.

Yang, X., Zhang, F., and Kudlow, J. E. (2002). Recruitment of O-GlcNAc transferase to promoters by corepressor mSin3A: Coupling protein O-GlcNAcylation to transcriptional repression. *Cell* **110**, 69–80.

Biography

Kaoru Sakabe is a graduate student in the Program of Biochemistry, Cellular, and Molecular Biology at the Johns Hopkins University School of Medicine. She graduated with a B.S. in Biochemistry from the University of North Carolina Chapel Hill before completing a fellowship at the National Institutes of Health.

Gerald W. Hart is Director and DeLamar Professor of Biological Chemistry at the Johns Hopkins University School of Medicine. He received his Ph.D. in developmental biology at Kansas State University in 1977 and did his postdoctoral work with William J. Lennarz at Johns Hopkins before joining the faculty in the Department of Biological Chemistry (1979). He was the founding editor-in-chief of *Glycobiology.*

Glucagon Family of Peptides and their Receptors

Laurie L. Baggio and Daniel J. Drucker
University of Toronto, Toronto, Canada

Glucagon and the glucagon-like peptides are produced in the gut, pancreas, and brain, and exert multiple biological actions converging on energy homeostasis via activation of distinct G protein-coupled receptors. Glucagon, liberated from the islet A cells, promotes glucose homeostasis via control of glucose production and glycogenolysis. GLP-1 and GLP-2 are secreted from gut endocrine cells and regulate energy disposal and the functional integrity of the gastrointestinal epithelium. The actions of these peptides and related analogues are relevant to the treatment of disordered energy homeostasis as exemplified by diabetes, obesity, and intestinal insufficiency.

In mammals, the proglucagon gene is expressed as a single messenger RNA (mRNA) transcript in the α-cells of the endocrine pancreas, the enteroendocrine L-cells of the small and large intestine, and in brainstem neurons within the central nervous system (CNS). Pancreatic proglucagon gene expression is up-regulated in the fasting state and by hypoglycemia and inhibited by insulin. In the intestine, proglucagon gene expression is stimulated by the presence of nutrients and by a gut-endocrine axis which in rodents, includes the peptide hormones gastrin-releasing peptide and gastric-inhibitory polypeptide. In contrast, very little is known about the factors responsible for regulating proglucagon gene expression in the CNS. Proglucagon mRNA transcripts are translated into a single 160 amino acid precursor in the pancreas, intestine, and brain that undergoes prohormone convertase (PC) enzyme-mediated tissue-specific posttranslational processing to generate structurally related yet distinct proglucagon-derived peptides (PGDPs); These PGDPs in turn activate specific seven-transmembrane G protein-coupled receptors and play important roles in modifying nutrient intake, absorption and assimilation.

Pancreatic PGDPs

In pancreatic α-cells, the action of PC-2 liberates glucagon, a hormone that is important for regulating carbohydrate metabolism, as well as the major proglucagon fragment (MPGF), a larger peptide with no known biological function (Figure 1).

Glucagon

Glucagon is a 29 amino acid hormone whose effects converge on hepatic glucose output and oppose those of insulin. Thus, glucagon elevates blood glucose levels primarily by stimulating glucose output via enhancement of glycogenolysis and promotion of gluconeogenesis in the liver.

Secretion

Glucagon secretion from pancreatic α-cells into the bloodstream is stimulated chiefly by hypoglycemia and inhibited by hyperglycemia, insulin, or somatostatin. GLP-1 can also inhibit glucagon secretion either directly, through interaction with GLP-1 receptors on pancreatic α-cells, or indirectly, through its ability to stimulate insulin and somatostatin release.

Physiological Actions

Glucagon increases hepatic glucose production in both animals and humans and plays a key role in maintaining blood glucose levels in the physiological range during periods of prolonged fasting or between meals. When blood glucose levels fall, glucagon is released into the circulation and binds to specific glucagon receptors on hepatocyte membranes. The binding of glucagon to its receptor leads to the activation of adenylyl cyclase, elevation of intracellular cAMP, and activation of protein kinase A (PKA). Activation of this glucagon receptor-signaling pathway in the liver ultimately leads to stimulation of glycogenolysis and gluconeogenesis and inhibition of glycogen synthesis and glycolysis. Glucagon typically functions as a counter regulatory hormone of insulin and can elevate blood glucose levels in response to insulin-induced hypoglycemia. However, in the diabetic state where insulin secretion may be deficient or the A cell may be less

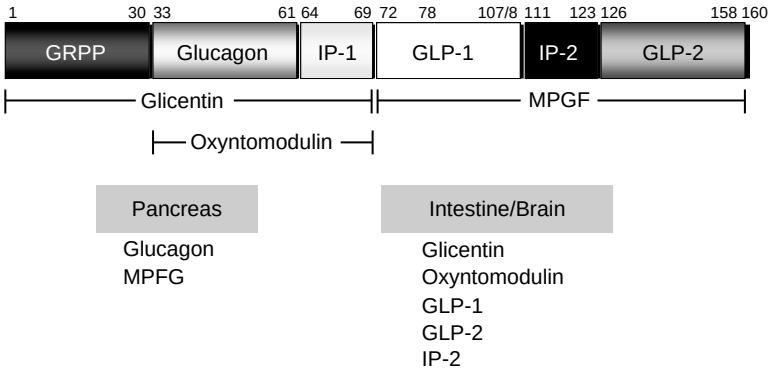

FIGURE 1 Structure of the mammalian proglucagon precursor protein and products of tissue-specific posttranslational processing in the pancreas, intestine, and brain. The numbers indicate amino acid positions in proglucagon. GRPP, glicentin-related pancreatic polypeptide; IP-1 and IP-2, intervening peptide 1 and 2; GLP-1 and GLP-2, glucagon-like peptide-1 and -2; MPGF, major proglucagon fragment.

insulin-responsive, glucagon levels are often elevated, and the resultant hyperglucagonemia is believed to play a role in the disordered glucose homeostasis characteristic of type 2 diabetes.

The glucagon receptor is also expressed in pancreatic islets, adipose tissue, heart, and kidney, and glucagon exerts a number of effects in these tissues including: enhancement of glucose-stimulated insulin secretion from pancreatic β-cells, stimulation of lipolysis in adipose tissue, elevation of heart rate and blood pressure, and regulation of renal function. Glucagon receptors are also detectable in brain and injection of glucagon into the CNS has a potent inhibitory effect of food intake in rats. Glucagon may also play a role in regulating meal size as studies in rodents and humans demonstrate that glucagon administration during a meal can reduce meal size. Lower levels of glucagon receptor mRNA are present in the stomach and intestine, and the administration of supraphysiological doses of glucagon pharmacologically inhibits gastrointestinal motility in humans. The glucagon receptor is also present in several other tissues, however, the physiological action of glucagon in these tissues is not clearly established.

Metabolism and Clearance

In both humans and animals, the kidney is the major organ responsible for glucagon metabolism and clearance, although some studies suggest the liver may also contribute significantly to glucagon degradation. Although the ubiquitous protease dipeptidyl peptidase IV (DPP IV) can also degrade glucagon, recent studies assessing (1) arteriovenous glucagon concentrations across the vascular beds of different organs and (2) inhibition of DPP IV activity *in vivo*, demonstrated that glucagon metabolism occurs primarily in the kidney and that DPP IV has no significant effect on glucagon degradation *in vivo*.

PGDPs in the Intestine and Brain

In the L-cells of the intestine, proglucagon is processed by PC1/3 to glicentin, oxyntomodulin (OXM), glucagon-like peptides-1 and -2 (GLP-1 and GLP-2), and a peptide of unknown function designated intervening peptide-2 (IP-2; Figure 1). Although the specific PC enzymes responsible for posttranslational processing of proglucagon in the CNS are not known, the brain displays a similar profile of PGDPs to that of the intestine (Figure 1).

Secretion

Intestinal PGDPs are co-released from enteroendocrine L-cells in a one-to-one molar ratio in response to an appropriate stimulus, primarily nutrients, as well as neural and hormonal agents. Nutrient ingestion, particularly carbohydrates and fats, is the primary stimulator of PGDP secretion. Nutrients produce a biphasic increase in levels of circulating PGDPs. An early (within 10–15 min) phase is likely mediated by neural and hormonal factors (including acetylcholine, muscarinic agonists, gastrin-releasing peptide, gastric inhibitory peptide, and calcitonin gene-related peptide), and a later (30–60 min) phase is mediated by direct contact of nutrients with open type L-cells. Conversely, insulin and somatotstatin-28, as well as the neuropeptide galanin, inhibit the secretion of intestinal PGDPs.

Physiological Actions

Glicentin

Glicentin is a 69 amino acid peptide whose essential physiological importance remains poorly defined. In rats, glicentin has been reported to stimulate insulin secretion, inhibit gastric acid secretion and intestinal

motility, and stimulate intestinal growth. However, since these effects are similar to those described for other PGDPs and, as a glicentin-specific receptor has not yet been identified, it is unclear whether glicentin mediates these pharmacological effects via a unique glicentin receptor or through activation of receptors for other PGDPs.

Oxyntomodulin (OXM)

OXM is a 37 amino acid peptide that inhibits gastric emptying and gastric acid secretion in both rodents and humans. OXM also stimulates intestinal glucose uptake and reduces pancreatic enzyme secretion in rats. More recent studies in rodents and humans indicate that OXM can also reduce food intake and promote satiety. However, a specific unique receptor for OXM has not yet been identified. Furthermore OXM is able to bind to and activate receptors for GLP-1 and glucagon, hence the receptor(s) responsible for mediating the biological effects of OXM are not clearly defined.

GLP-1

The GLP-1 receptor (GLP-1R) is widely expressed in multiple tissues including the endocrine pancreas, the gastrointestinal tract, lung, kidney, and many regions of the CNS, including those known to regulate energy homeostasis. GLP-1 circulates as a 30 or 31 amino acid peptide that exhibits numerous biological effects in both animals and humans which converge on the lowering of blood glucose in the postprandial state. These include potentiation of glucose-stimulated insulin secretion, enhancement of insulin gene transcription and biosynthesis, and inhibition of glucagon secretion, gastric emptying, and food intake. GLP-1 may also enhance glucose disposal through effects on liver, muscle, and adipose tissues. More recently, cell culture experiments and studies with rodents demonstrated that GLP-1 stimulates islet cell differentiation, proliferation and neogenesis, increases β-cell mass, and inhibits β-cell apoptosis. As the glucose lowering actions of GLP-1 are retained in subjects with type 2 diabetes, GLP-1R agonists are being evaluated as therapeutic agents for the treatment of diabetes.

Several actions of GLP-1 are not directly related to acute lowering of blood glucose, and include stimulation of somatostatin secretion and inhibition of pentagastrin- and meal-induced gastric acid secretion. GLP-1 receptors are also found on the heart and GLP-1 administration in rodents is associated with elevations in heart rate and blood pressure. GLP-1 also elicits several effects in the CNS that include activation of aversive pathways, prevention of apoptosis, neuroprotection, and modulation of learning and memory.

GLP-2

Studies in rodents revealed that the major biological role for GLP-2, a 33 amino acid peptide, is that of an intestinotrophic factor, an effect mediated through regulation of both proliferative and anti-apoptotic mechanisms in intestinal crypt and villus cells. GLP-2 also inhibits gastric emptying and gastric acid secretion and stimulates intestinal hexose transport by increasing the expression and activity of intestinal glucose transporters. GLP-2 administration enhanced epithelial integrity and reduced permeability in the intestinal mucosa of rodents with experimental gut injury. More recently, intracerebroventricular injection of GLP-2 into the rodent CNS was shown to transiently reduce food intake.

Metabolism and Clearance

All PGDPs are cleared primarily through the kidney, via mechanisms that include glomerular filtration and tubular catabolism. The half-life of GLP-1 is $\sim$90 s, due to its rapid inactivation by DPP IV, which is present on the surface of circulating lymphocytes and on vascular endothelial cells in the small intestine, in close proximity to the sites of PGDP release from gut endocrine cells. In addition, the neutral endopeptidase (NEP-24.11) has an endoproteolytic effect on GLP-1 *in vitro*, and may play a role in GLP-1 metabolism. GLP-2 is also inactivated by DPP IV, although it has a considerably longer half-life (5–7 min) relative to GLP-1. Glicentin and OXM are also potential substrates for DPP IV activity, however, the physiological relevance, if any, of DPP IV for the biological activity of glicentin and OXM has not been determined.

PGDP Receptors

Thus far, individual receptors for glicentin or OXM have not been identified and experimental evidence indicates that these peptides likely mediate their physiological actions via known PGDP receptors. Glucagon, GLP-1, and GLP-2 exert their biological effects through unique specific receptors that belong to the seven transmembrane-spanning, heterotrimeric G protein-coupled family of receptors.

The human and rat glucagon receptor (GluR) cDNAs encode proteins that are 82% identical and 485 and 477 amino acids in length, respectively. The human GluR gene has been mapped to chromosome 17, band q25. Glucagon receptors are widely expressed in multiple mammalian tissues including liver, heart, kidney, spleen, ovary, pancreatic islets, thymus, stomach, adrenals, intestine, thyroid, skeletal muscle, adipose tissue, lung, and brain. Studies examining the regulation of GluR

mRNA expression in rat islet and primary liver cultures indicate that glucagon, dexamethasone, and agents that increase cAMP levels inhibit, whereas somatostatin increases, GluR expression. The promoter region of the GluR gene contains a glucose regulatory element and levels of liver GluR mRNA increase in response to high glucose concentrations. GluR activation leads to stimulation of adenylyl cyclase, elevations in intracellular cAMP levels, and activation of PKA. Glucagon can also activate phospholipase C and increase intracellular levels of inositol triphosphates and Ca^{2+}. Structure–function studies of the glucagon receptor indicate that sequences in the N-terminal extra cellular domain, in particular aspartic acid residue 64, as well as the first extra cellular loop and the third and fourth transmembrane domains are essential for ligand binding. Intracellular loops two and three are important for GluR signaling.

The human *GLP-1R* (GLP-1R) gene encodes a 463 amino acid protein and has been mapped to chromosome 6, band p21.1. The rat *GLP-1R* also consists of 463 amino acids and is 90% identical to the human receptor. The GLP-1R is expressed in pancreatic islet α-, β-, and δ-cells, lung, heart, kidney, gastrointestinal tract, CNS, and the pituitary. GLP-1R mRNA levels are down-regulated in response to GLP-1, activation of protein kinase C (PKC), and high concentrations of glucose or dexamethasone in cell lines *in vitro*. The GLP-1R engages multiple G proteins and activate several intracellular signal transduction pathways including the cAMP/PKA and phospholipase C/PKC pathways. GLP-1R activation also leads to increased intracellular Ca^{2+} levels and activation of phosphatidylinositol 3-kinase and mitogen-activated protein kinase signaling pathways. The N-terminal extra cellular domain of the GLP-1R is essential for GLP-1 binding, whereas the third intracellular loop is required for coupling of the receptor to G proteins.

Human and rat GLP-2 receptor (GLP-2R) cDNAs, originally isolated from hypothalamic and intestinal cDNA libraries, encode proteins of 553 and 550 amino acids, respectively. The human GLP-2R gene has been localized to chromosome 17, band p13.3. The GLP-2R is expressed in the stomach, intestine, lung, subsets of enteric neurons, and the CNS; the factors that regulate GLP-2R gene expression remain unknown. Studies using heterologous cells transfected stably with rat or human GLP-2R cDNAs demonstrate that the receptor is coupled to induction of adenylyl cyclase activity, cAMP production and activation of PKA. The anti-apoptotic effects of GLP-2R activation are mediated by both PKA-dependent and -independent signaling pathways. In contrast to the glucagon and GLP-1 receptors, specific GLP-2R regions important for ligand binding and G protein coupling have not yet been identified.

See Also the Following Articles

Adenylyl Cyclases • A-Kinase Anchoring Proteins • Calcitonin Gene-Related Peptide and Adrenomedullin Receptors • Diabetes • Insulin- and Glucagon-Secreting Cells of the Pancreas • Phospholipase C • Protein Kinase C Family

Glossary

DPP-IV A serine protease that specifically cleaves dipeptides from the amino terminus of peptides or small proteins that contain an alanine or proline residue in amino acid position 2.

enteroendocrine cells Hormone-producing cells of the gastrointestinal tract.

G protein-coupled receptors A family of receptors that consists of seven-transmembrane-spanning domains and that utilizes GTP-binding proteins (G proteins) to transmit signals from the surface to the interior of the cell.

prohormone convertase Endoproteolytic enzymes that cleave C-terminal to paired basic amino acid residues. PGDPs are flanked by pairs of basic amino acids, the recognition sites for prohormone convertase cleavage.

Further Reading

Drucker, D. J. (2002). Biological actions and therapeutic potential of the glucagon-like peptides. *Gastroenterology* **122**, 531–544.

Drucker, D. J. (2003). Enhancing incretin action for the treatment of type 2 diabetes. *Diabetes Care* **26**(10), 2929–2940.

Jiang, G., and Zhang, B. B. (2003). Glucagon and regulation of glucose metabolism. *Am. J. Physiol. Endocrinol. Metab.* **284**, E671–E678.

Kieffer, T. J., and Habener, J. F. (1999). The glucagon-like peptides. *Endocr. Rev.* **20**, 876–913.

Mayo, K. E., Miller, L. J., Bataille, D., Dalle, S., Goke, B., Thorens, B., and Drucker, D. J. (2003). International union of pharmacology. XXXV. The glucagon receptor family. *Pharmocol. Rev.* **55**, 167–194.

Biography

Laurie Baggio is a Research Associate Scientist in the Banting and Best Diabetes Centre.

Daniel Drucker is Director, Banting and Best Diabetes Centre, University of Toronto.

Gluconeogenesis

Richard W. Hanson and Oliver E. Owen
Case Western Reserve University School of Medicine, Cleveland, Ohio, USA

Gluconeogenesis is the major route for the synthesis of glucose in all mammals. This pathway is present in the liver and kidney cortex and is active during starvation and after a meal high in protein and fat, but low in carbohydrate. The major substrates for gluconeogenesis are lactate, pyruvate, 18 of the 20 amino acids (leucine and lysine are not gluconeogenic), propionate and glycerol. During periods of prolonged starvation, the concentration of ketone bodies in the blood can rise from undetectable levels (after a meal containing carbohydrate) to as high as 5 mM after a week of starvation. A fraction of these ketone bodies are excreted in the urine. To buffer the acidity of the tubular urine, the kidney cortex generates ammonia from the glutamine produced by muscle. The carbon skeleton of glutamine (α-ketoglutarate) enters the citric acid cycle and is converted to glucose. Thus the kidney can become a major source of blood glucose during prolonged starvation. Insulin represses transcription of many of the genes involved in hepatic gluconeogenesis, so that during diabetes gluconeogenesis is markedly induced. This results in elevated rates of hepatic glucose output.

History

Claude Bernard first noted the synthesis of glucose in his famous description of glucose turnover during fasting. However, it is the work of Carl and Gerty Cori that established gluconeogenesis as critical for the synthesis of glucose from lactate as part of what is now known as the Cori Cycle. Gluconeogenesis is not a reversal of glycolysis, although the two pathways share a number of enzymes. A major advance in the understanding of the specific reactions in the pathway of glucose synthesis occurred when Merton Utter and his colleagues discovered two of the major enzymes of the pathway, phosphoenolpyruvate carboxykinase and pyruvate carboxylase. In the 1960s and 1970s, the research of Hans Krebs, Charles Park and John Exton, John Williamson and Henry Lardy, among others, set out the metabolic parameters of the pathway as it known today. Finally, the elevated rate of synthesis and release of glucose by the liver and kidney cortex during diabetes mellitus is a major factor in the pathogenesis of this disease.

Overview of Gluconeogenesis

Gluconeogenesis is defined as the *de novo* synthesis of glucose from nonhexose precursors. Gluconeogenesis does not include the conversion of fructose or galactose to glucose in the liver or the generation of glucose from glycogen via glycogenolysis. The pathway of gluconeogenesis (Figure 1) occurs mainly in the liver and kidney cortex and to a lesser extent in the small intestine. The major substrates for gluconeogenesis are lactate, pyruvate, propionate, glycerol, and 18 of the 20 amino acids (the exceptions are leucine and lysine). Glucose cannot be synthesized from fatty acids, since they are converted by β-oxidation to acetyl CoA, which subsequently enters the citric acid cycle and is oxidized to CO_2. The three-carbon fatty acid, propionate is an exception since it is carboxylated, converted to succinyl-CoA and enters the citric acid cycle as a four-carbon intermediate, not as acetyl CoA. One exception is acetone, which is converted to propanediol, a minor gluconeogenic precursor. Also, the last three carbon atoms of the odd-chain fatty acids generate proprionyl CoA during β-oxidation and are thus partly gluconeogenic. There are 14 enzymes involved in the conversion of lactate to glucose; three of these enzymes are classified as gluconeogenic (phosphoenolpyruvate carboxykinase, fructose-1,6-bisphosphatase, and glucose-6-phosphatase) and one is anaplerotic (pyruvate carboxylase), since it is important in both gluconeogenesis and lipogenesis. The remainder of the pathway is simply a reversal of the enzymes of glycolysis, which is responsible for the breakdown of glucose. Gluconeogenic enzymes are present in the cytosol, mitochondria, and endoplasmic reticulum of the tissues in which this pathway is present. Net gluconeogenesis occurs during starvation and after a meal high in fat and protein but no carbohydrate.

The Enzymes of Gluconeogenesis

The unique properties of gluconeogenesis are attributable to the three gluconeogenic and one anaplerotic enzyme in the pathway. The following will describe each of these enzymes and review their regulatory properties.

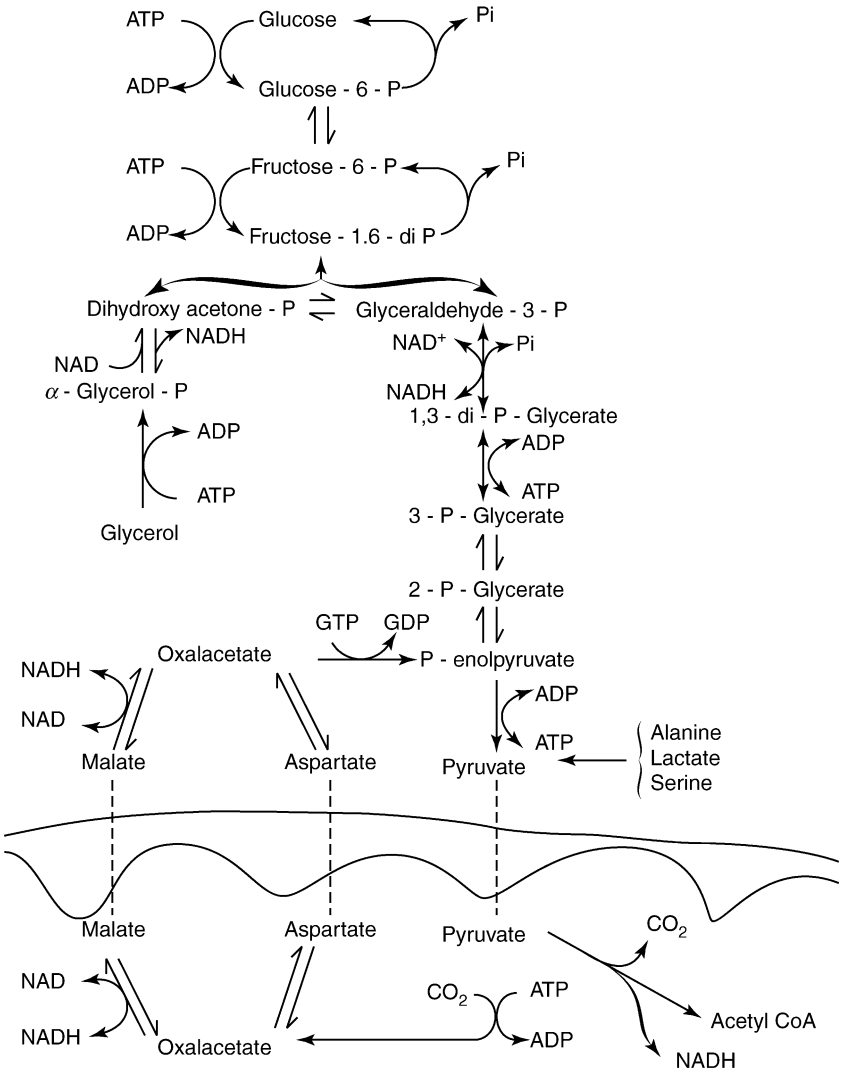

FIGURE 1 The pathway of hepatic gluconeogenesis. The figure demonstrates the reactions involved in gluconeogenesis in the liver starting with alanine, lactate or serine as precursors. The movement of aspartate and malate from the mitochondria is also indicated to demonstrate the redox state balance that occurs between the mitochondria and the cytosol during gluconeogenesis.

Pyruvate Carboxylase (PC)

PC is found in the mitochondria, catalyzes the following reaction:

$$\text{Pyruvate} + CO_2 + \text{ATP} \rightarrow \text{Oxalacetate} + \text{ADP} + \text{Pi}$$

Pyruvate carboxylase is a multisubunit enzyme that has acetyl CoA as a positive allosteric regulator. The enzyme is critical for both gluconeogenesis and fatty acid synthesis, since it replenishes the citric acid cycle intermediates (malate or citrate) that leave the mitochondria as part of biosynthetic processes. Since it is essentially irreversible under biological conditions, PC does not generate pyruvate from oxalacetate. Pyruvate carboxylase is generally considered an anaplerotic (to refill) enzyme since it functions to replace the oxalacetate that is reduced to malate and used in the synthesis of glucose. Since the citric acid cycle is important in both gluconeogenesis and lipogenesis, PC plays a role in both pathways.

Phosphoenolpyruvate Carboxykinase (PEPCK)

PEPCK catalyzes the following reaction:

$$\text{Oxalacetate} + \text{GTP} \rightarrow \text{Phosphoenolpyruvate} + \text{GDP} + CO_2$$

It is found in both the mitochondria (PEPCK-M) and the cytosol (PEPCK-C). Two different nuclear genes encode these two isoforms of PEPCK. Expression of the gene PEPCK-C is inducible by diet and hormones, while PEPCK-M is constitutive. Species vary in the amount

of the two isoforms expressed in gluconeogenic tissues. Rodent species such as the rat and mouse have 90% PEPCK-C in their liver and kidney cortex while birds have 100% PEPCK-M. Humans and most other mammalian species studied to date have ~50% of both isoforms. The exact metabolic significance of having two isoforms of PEPCK is not entirely clear but it has been proposed that PEPCK-M allows the direct synthesis of PEP in the mitochondria thus bypassing the need to transport reducing equivalents out of the mitochondria. This point will be discussed in more detail in the latter section of this article. PEPCK is generally considered to be the pace-setting enzyme in gluconeogenesis, but it has no known allosteric regulators. The enzyme has a relatively short half-life of 6 h and alterations in the rate of gene transcription are rapid. For example, the rate of PEPCK-C gene transcription in the liver is increased tenfold in 30 min after the administration of cAMP to animals. Insulin administration causes an equally rapid decrease in the transcription of the gene. It has thus been suggested that the level of enzyme protein in the liver is a critical determinant in the overall activity of the enzyme. Transcription of the gene for PEPCK-C has been studied in considerable detail and many of the transcription factors that regulate the tissue-specific expression of the gene have been identified. A detailed discussion of this area is beyond the scope of this article but the reader is directed to several reviews on the subject listed in the Further Reading.

Fructose-1,6-Bisphosphatase (FBPase)

FBPase is found in the cytosol. In mammalian liver, the enzyme is a homotetramer with a subunit molecular weight of 38–41 kDa, depending on the species. FBPase catalyzes the following reaction:

$$\text{Fructose-1, 6-bisphosphate} \rightarrow \text{Fructose-6-Phosphate} + \text{Pi}$$

The enzyme is regulated allosterically by a number of small molecules including AMP and fructose-2,6-phosphate, which are negative regulators, and ATP that is a positive regulator. The enzyme is also covalently modified by phosphorylation by protein kinase A, which decreases its activity.

Glucose-6-Phosphatase (G6Pase)

G6Pase is present in the endoplasmic reticulum of the liver, kidney cortex, and small intestine. The role of this enzyme in the synthesis of glucose was first suggested by the Coris' cycle in 1938 and finally demonstrated by Marjorie Swanson in the United States and Christian deDuve and colleagues in Belgium in the early 1950s. For a detailed review of the early work with this important enzyme, the reader is directed to a review by Nordlie referenced at the end of this article. The activity of G6Pase can be induced by starvation, cAMP, and glucocorticoids. Somewhat paradoxically, glucose at high concentrations will also stimulate transcription of the gene for this enzyme.

Physiological Control of Gluconeogenesis

Dietary Status Determines the Extent of Gluconeogenesis

There are two normal metabolic situations during which gluconeogenesis occurs in mammals. In addition, gluconeogenesis increases during diabetes, resulting in an increased rate of glucose output by the liver. The first physiological situation involves the gluconeogenesis, characteristic of starvation, and the second, the gluconeogenesis that occurs after a meal that contains minimal carbohydrate. During starvation, the source of carbon for gluconeogenesis is body protein, largely from the muscle and lactate and pyruvate from glycolysis and glycerol from lipolysis. The muscle undergoes proteolysis, largely due to the fall in insulin. Proteolysis in muscle results in the generation of 20 amino acids. However, reactions in the muscle convert these amino acids mainly to alanine and glutamine, which are leased for subsequent metabolism. Both alanine and glutamine can be converted to glucose in the liver but in starvation it is the kidney cortex that utilizes glutamine. The kidney synthesizes glucose from the carbon skeleton of glutamine and uses the ammonia derived from this process to maintain the acid–base balance of the tubular urine. Later in this article, the metabolic role of renal gluconeogenesis will be discussed in detail. The gluconeogenesis that occurs after a meal containing protein and fat, but no carbohydrate, involves the 18 gluconeogenic amino acids found in dietary protein (degradation of the amino acids leucine and lysine contributes no carbon for glucose synthesis). The carbon skeletons of most of the amino acids enter the citric acid cycle, proceed forward to malate and are subsequently converted to glucose via the gluconeogenesis as described in detail below.

The Role of Fatty Acid Oxidation in the Control of Gluconeogenesis

Gluconeogenesis occurs during fasting but the amount of glucose supplied by this process is far less than can be generated by glycogenolysis during the immediate post-absorptive period. Blood glucose homeostasis is possible only because other substrates (fatty acids, ketone bodies) are used as fuels by peripheral tissues, thus sparing the use

of glucose. In general, the rate of gluconeogenesis is increased in the liver during starvation due to a fall in the concentration of insulin and a rise in glucagon; glucocorticoids play a permissive role in stimulating this process. This change in hormone status results in profound alterations in the metabolism of both skeletal muscle and adipose tissue. There is an increased rate of lipolysis in the adipose tissue and a net protein breakdown (proteolysis) in muscle. This results in an elevated rate of delivery to the liver of fatty acids from adipose tissue and primarily alanine from muscle. Fatty acid oxidation by hepatic mitochondria raises the concentration of acetyl CoA and shifts the redox state of that organelle toward reduction; there is a concomitant increase in ATP synthesis. In the rat, for example, the hepatic NAD/NADH ratio shifts from 700 to 550 after 48 h of starvation. The net effect of this increase in fatty acid oxidation is a stimulation of gluconeogenesis and an inhibition of glycolysis. This stimulatory effect is exerted at several levels. First, the rise in NADH and ATP inhibits multiple steps in the tricarboxylic acid cycle (TCA cycle), including citrate synthase, isocitrate dehydrogenase, and α-ketoglutarate dehydrogenase complex. Most importantly, the increased concentrations of ATP, NADH, and acetyl CoA that occur in the liver during fasting inhibit flux through the pyruvate dehydrogenase complex. The importance of the latter step will be stressed subsequently.

Pathway of Gluconeogenesis

During starvation, alanine is transported from the muscle to the liver, where it is converted to pyruvate. As mentioned above, during fasting the pyruvate dehydrogenase complex is inhibited by the products of fatty acid oxidation. At the same time, acetyl CoA activates PC, thus converting pyruvate to oxalacetate, which is then reduced to malate by the mitochondrial isoform of NAD malate dehydrogenase. Malate leaves the mitochondria and is oxidized to oxalacetate via the cytosolic isoform of NAD malate dehydrogenase; the oxalacetate is decarboxylated to PEP by PEPCK-C and the PEP is further metabolized via a reversal of glycolysis to fructose-1,6-bisphosphate. This intermediate is then converted to fructose-6-phosphate by the gluconeogenic enzyme, FBPase. Finally, G6Pase, which is present in the endoplasmic reticulum, generates free glucose from glucose-6-phosphate; GLUT 2 transports the glucose from the liver to the blood.

Redox Balance for Gluconeogenesis

It is important to note that gluconeogenesis requires two molecules of NADH for every molecule of glucose that is synthesized. The NADH is required to reverse the glyceraldehyde-3-phoshate dehydrogenase reaction. The source of this NADH varies according to the substrate used for gluconeogenesis. When oxidized compounds such as pyruvate and alanine are used for glucose synthesis, the pathway involves malate transport from the mitochondria, essentially generating reducing equivalents in the cytosol for gluconeogenesis, as described above. There is a slight variation in this pathway of glucose synthesis when the starting substrate in lactate. In this case, the conversion of lactate to pyruvate in the cytosol generates NADH, which obviates the necessity of transporting malate from the cytosol to produce NADH. There are two possible routes for the movement of intermediates from the mitochondria that is not linked to the transport of reducing equivalents. The first involves the transamination of mitochondrial oxalacetate to aspartate via aspartate aminotransferase. The aspartate is transported to the cytosol and converted to oxalacetate by the cytosolic isoform of aspartate aminotransferase (Figure 1). The second variation in metabolite transfer involves the generation of oxalacetate in the mitochondria via PC, followed by the synthesis of PEP directly in the mitochondria via PEPCK-M. PEPCK-C is readily transported from the mitochondria on the tricarboxylate carrier in the inner mitochondria membrane. This role of PEPCK-M in avian metabolism supports the physiological role of the two isoforms of PEPCK. In birds, the liver uses only lactate for gluconeogenesis, and the avian liver contains only PEPCK-M. Gluconeogenesis from amino acids occurs in the kidney.

Regulation of Gluconeogenesis

Gluconeogenesis is regulated at four fundamental levels, discussed below.

Substrate Delivery to the Liver and Kidney

The rate of delivery of substrates such as lactate, which is derived from glycolysis in skeletal muscle (Cori cycle) or glycolysis in erythrocytes, glycerol from the breakdown of triglycerides in adipose tissue and amino acids from proteolysis in skeletal muscle and other protein rich tissues, greatly influences the level of hepatic gluconeogenesis. Thus, the control of the release and delivery of precursors from peripheral tissues is an important controlling factor in the rate of gluconeogenesis in the liver and kidney cortex. For example, insulin controls the rate of gluconeogenesis, in part, by regulating the delivery of substrates from muscle and adipose tissue to the liver.

Mass Action Regulation of Enzymes

As an example of this type of regulation, the activity of glyceraldehyde-3-P dehydrogenase (in the direction of gluconeogenesis) is stimulated by a rise in NADH in cytosol (the NAD/NADH ratio). The activity of G6Pase is increased by a rise in the concentration of G6Pase and PEPCK activity is stimulated by a rise in the concentration of oxalacetate.

Allosteric Activation of Key Enzymes

As an example of this type of regulation of gluconeogenesis, acetyl-CoA allosterically activates PC, while FBPase is activated by ATP and inhibited by AMP and fructose-2,-6,bisphosphate. In addition, during gluconeogenesis, pyruvate kinase must be inhibited in order to prevent the conversion of PEP back to pyruvate ("futile cycling") by liver-type pyruvate kinase (PK-L). A rise in the concentration of alanine or ATP and a decrease in the level of fructose-1,6-bisphosphate that occurs in the liver during fasting, results in the allosteric inhibition of the activity of this enzyme (Figure 2).

Covalent Modification

Phosphorylation of gluconeogenic enzymes by a cAMP-dependent protein kinase (PKA) regulates the rate of key steps in gluconeogenesis. PK-L (not the muscle isozyme, PK-M) is inhibited by cAMP-induced phosphorylation via PKA. This, together with the allosteric regulation mentioned above, prevents the conversion of PEP to pyruvate in the liver and thus limits possible "futile cycling" of carbon and resulting energy loss. The PKA regulation of hepatic gluconeogenesis is controlled in part by changes in the concentration of fructose-2,6-bisphosphate. As mentioned above, this compound allosterically regulates two critical enzymes, phosphofructokinase, the rate-controlling enzyme in glycolysis, and FBPase the key gluconeogenic enzyme. Fructose-2,6-bisphosphate is both synthesized and degraded by a single, "bifunctional" enzyme 6-phosphofructo-2-kinase/fructose-2,6-bisphosphatase, which can act as a kinase (it synthesizes fructose-2,6-bisphosphate using ATP as a source of phosphate) or a phosphatase (it converts fructose-2,6-bisphosphate to fructose-6-phospahte plus inorganic phosphate. Phosphorylation of this enzyme by PKA, induces the phosphatase function of the enzyme. This results in a decrease in the concentration of fructose-2,6-bisphosphate, thereby inhibiting the activity of phosphofructokinase (the rate-limiting enzyme in glycolysis), which requires fructose-2,6-bisphosphate as an allosteric activator) and simulating the activity of FBPase, for which fructose-2,6-bisphosphate is an inhibitor (Figure 2). Thus the covalent modification of the bifunctional enzyme has a reciprocal effect on the gluconeogenesis (stimulation) and glycolysis (inhibition).

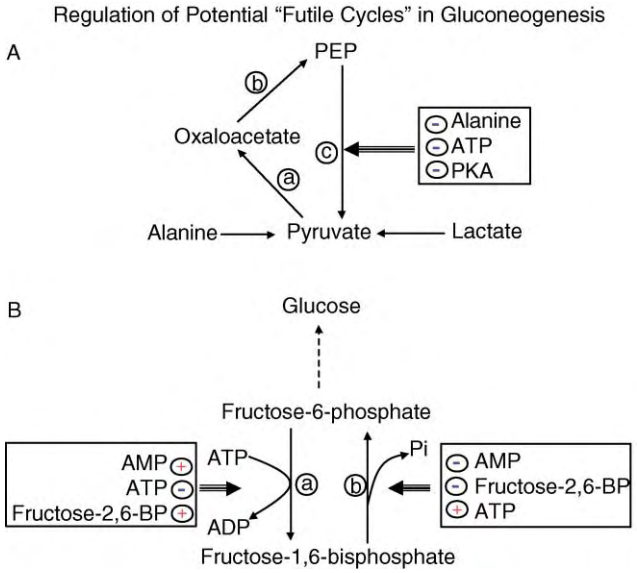

FIGURE 2 Regulation of potential "futile cycles" during gluconeogenesis. (A) The control of the oxalacetate/PEP/pyruvate futile cycle. The enzymes shown in this panel are (a) pyruvate carboxylase, (b) PEP carboxykinase, and (c) liver-type pyruvate kinase. This cycle is regulated by inhibition of liver-type pyruvate kinase by allosteric regulation by alanine and ATP and by phosphorylation of the enzyme by PKA. In addition, the decreased glycolytic flux that occurs during periods of gluconeogenesis (starvation) reduces the concentration of fructose-6-phosphate, a positive allosteric regulator of liver-type pyruvate kinase. (B) The control of the fructose-1,6-bisphosphate/fructose-6-phosphate futile cycle. The enzymes shown in this panel are (a) phosphofructokinase and (b) fructose-1,6-bisphosphatase (FBPase). Phosphofructokinase is activated by AMP, and fructose-2,6-bisphosphate and inhibited by ATP, while fructose-1,6-bisphosphatase is regulated in the opposite manner by the same intermediates. The result is a coordinated control of carbon flux via glycolysis and gluconeogenesis in the liver.

Alteration in Gene Expression

The expression of several of the genes in the gluconeogenic pathway is modified by starvation, diabetes, or by diets high in carbohydrate. Transcription of the genes coding for PEPCK-C, FBPase, and G6Pase are increased by fasting and during diabetes while transcription of the genes for several of the glycolytic enzymes, such as PK-L, phosphofructokinase, and glucokinase is decreased. Alterations in the rate of gene transcription change the levels of mRNA for a specific enzyme, resulting in a change in the rate of synthesis for the enzyme. An increase or decrease in enzyme content usually occurs over a period of several hours and is mediated by hormones such as glucagon (acting via cAMP), insulin, and glucocorticoids that stimulate the transcription of the genes for these enzymes. Metabolites such as glucose and fatty

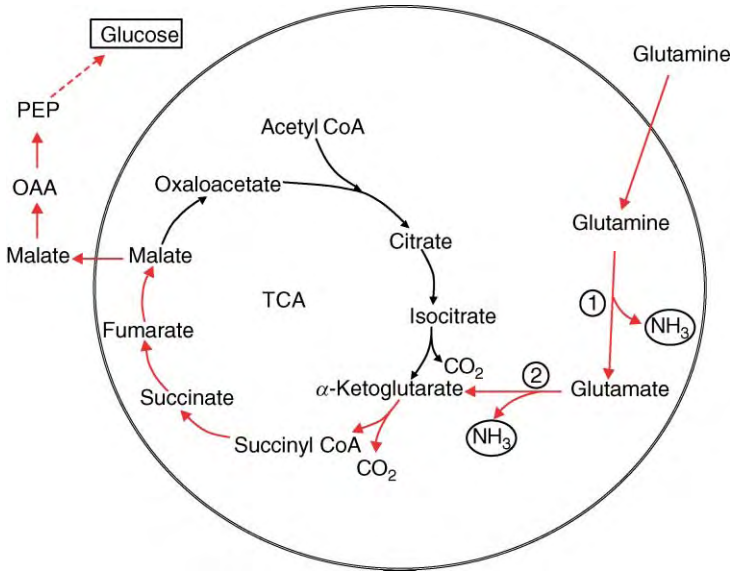

FIGURE 3 Gluconeogenesis from glutamine in the kidney. Glutamine from the muscle is metabolized by the kidney cortex to generate ammonia (circled) that is used to titrate the acidity of the tubular urine. This involves two enzymatic reactions, both of which are in the renal mitochondria, (1) glutaminase, and (2) glutamate dehydrogenate. The α-ketoglutarate that is produced by the removal of the two amino groups of glutamine enters the citric acid cycle, is oxidized to malate and then proceeds to glucose via gluconeogenesis. The large circle in the figure represents the renal mitochondria.

acids also exert control of the expression of specific genes involved in their metabolism.

Renal Gluconeogenesis

The synthesis of glucose in the kidney cortex is directly related to the loss of ketone bodies in the urine. During periods of fasting, the kidney excretes large amounts of ketone bodies (weak acids), but produces urine that is near neutrality. The relative acidity of the tubular urine is maintained at about pH 6.0 by the generation of ammonia from the metabolism of glutamine that has been mobilized from the muscle during starvation. Glutamine is converted to glutamate by "glutaminase" and glutamate to α-ketoglutarate by "glutamate dehydrogenase;" this generates 2 molecules of ammonia that are released into the urine to maintain the neutrality of the urine. The α-ketoglutarate is then converted to glucose. Thus, ammoniagenesis in the kidney is linked to gluconeogenesis (Figure 3). Interestingly, acidosis induces transcription of the gene for PEPCK-C, increasing its concentration in the kidney cortex. This elevation in the activity of PEPCK-C is critical for the increased rates of gluconeogenesis noted during acidosis.

Final Words

Glucose oxidation is essential for human metabolism and thus gluconeogenesis is a critical element in the maintenance of glucose homeostasis in all mammals. In humans, this process is continuous and augmented after the depletion of liver glycogen. Gluconeogenesis is the sole source of glucose during starvation. Since gluconeogenesis from amino acids results in a depletion of lean body mass, a number of metabolic accommodations occur to minimize the use of glucose by tissues such as the brain and skeletal muscle (fuel sparing). The details of these processes appear elsewhere in this encyclopedia. It is impossible to reference all of the research responsible for a detailed understanding of the pathway of gluconeogenesis and its regulation. A select number of more general articles that reflect the field are included in the Further Reading section.

See Also the Following Articles

Carnitine and β-Oxidation • Diabetes • Diacylglycerol Kinases and Phosphatidic Acid Phosphatases • Fatty Acid Oxidation • Glucose/Sugar Transport in Bacteria • Glucose/Sugar Transport in Mammals • Pyruvate Carboxylation, Transamination, and Gluconeogenesis • Pyruvate Dehydrogenase • Pyruvate Kinase • Regulated Intramembrane Proteolysis (Rip) • Starvation

Glossary

anaplerotic reactions Enzymatic reactions that produce citric acid cycle anions to replace those that leave the cycle for the synthesis of compounds such as glucose and fatty acids.

Cori cycle Process in which the lactate generated in the red blood cells and muscle is converted to glucose in the liver and cycled back to these tissues for reconversion to lactate.

gluconeogenesis The *de novo* synthesis of glucose from nonhexose precursors.

ketone bodies Water-soluble fuels produced by the liver from the acetyl CoA that is generated from the β-oxidation of fatty acids.

lipolysis The degradation of triglyceride to free fatty acids and glycerol; occurs primarily in the white adipose tissue.

β-oxidation The oxidation of fatty acids to acetyl CoA in the mitochondria.

proteolysis The breakdown of proteins to their component amino acids.

Further Reading

Granner, D. K., and O'Brien, R. M. (1992). Molecular physiology and genetics of NIDDM. *Diabetes Care* **15**, 369.

Hanson, R. W., and Patel, Y. M. (1994). P-enolpyruvate carboxykinase: The gene and the enzyme. In *Advances in Enzymology* (A. Meister, ed.) Vol 69, Wiley, New York.

Nordlie, R. C., Foster, J. D., and Lange, A. J. (1999). Regulation of glucose production by the liver. *Annu. Rev. Nutr.* **19**, 379.

Owen, O. E., Felig, P., Morgan, A. P., Wahren, J., and Cahill, G. F. Jr. (1969). Liver and kidney metabolism during prolonged starvation. *J. Clin. Invest.* **48**, 584.

Pilkis, S. J., and Claus, T. H. (1991). Hepatic gluconeogenesis/glycolysis: Regulation and structure/function relationships of substrate cycle enzymes. *Ann. Rev. Nutr.* **11**, 465.

Pilkis, S. J., Claus, T. H., Kurland, I. J., and Lange, A. J. (1995). 6-Phosphofructo-2-kinase/fructose-2,6-bisphosphatase: A metabolic signaling enzyme. *Annu. Rev. Biochem.* **64**, 799.

Soling, H.-D., and Kleineke, J. (1976). Species dependent regulation of gluconeogenesis in higher animals. In *Gluconeogenesis, Its Regulation in Mammalian Species* (R. W. Hanson and M. A. Mehlman, eds.) Wiley, New York.

Watford, M., Hod, Y., Chiao, Y.-B., Utter, M. F., and Hanson, R. W. (1981). The unique role of the kidney in gluconeogenesis in the chicken: The significance of a cytosolic form of PEPCK. *J. Biol. Chem.* **256**, 10023.

Utter, M. F., and Kolenbrander, H. M. (1972). Formation of oxalacetate by CO_2 fixation on P-enolpyruvate. In *The Enzymes* (P. D. Boyer, ed.) Vol VI, 117pp. Academic Press, New York.

Biography

Richard W. Hanson is Professor of Biochemistry at Case Western Reserve University School of Medicine in Cleveland, Ohio. For many years, he has been an Associate Editor of the *Journal of Biological Chemistry*, and he was the President of the American Society of Biochemistry and Molecular Biology. His research interests include the dietary and hormonal control of gene transcription and the regulation of gluconeogenesis and glyceroneogenesis in mammals.

Oliver E. Owen was previously Professor of Medicine and coprincipal Investigator and Program Director, General Clinical Research Center, Temple University School of Medicine and Hospital, and formerly Professor and Chair of Medicine, Southern Illinois University School of Medicine.

Glucose/Sugar Transport in Bacteria

Lan Guan and H. Ronald Kaback
University of California, Los Angeles, California, USA

Sugar transport in bacteria involves highly specific membrane proteins that catalyze translocation and accumulation of various sugars from the outside environment across the cytoplasmic membrane and into the cell where they are metabolized. As with other membrane proteins that catalyze transport of metabolites other than sugars, these proteins are called transporters or permeases. When the translocation of sugar takes place against a concentration gradient (from a low concentration outside of the cell to higher concentrations inside), the transport process requires energy, and is called active transport. In bacteria, there are three types of systems involved in sugar transport, and each one utilizes distinct energy sources.

The Phosphoenolpyruvate: Sugar Phosphotransferase System (PTS)

Classification

According to the Transport Commission (TC) classification, the PTS represents a distinct family found only in certain bacteria. It is a bacterial sugar transport system which also plays an essential role in the phenomena of catabolite repression and inducer exclusion, particularly in *Escherichia coli* (*E. coli*) and *Salmonella typhimurium*.

Functional Properties

The PTS is a multicomponent system and catalyzes vectorial phosphorylation of various sugars. Thus, in *E. coli*, for example, glucose and other sugars are translocated across the membrane by PTS-catalyzed phosphorylation (Figure 1) (i.e., glucose appears in the cytoplasm as glucose-6-phosphate). Therefore, translocation across the membrane and the first step in metabolism are one and the same. Many sugars are transported by PTS systems (glucose, mannitol, fructose, mannose, galactitol, sorbitol, xylitol, and N-acetylglucosamine), and specificity for each sugar is provided by the membrane-embedded component of the system. In *E. coli*, only monosaccharides and their derivatives are substrates for PTS systems, but in other bacteria, disaccharides are also utilized by this system.

The PTS is also involved in the regulation of uptake and metabolism of many other sugars, as discussed in this entry, as well as bacterial chemotaxis toward these sugars, which is not covered here.

Assembly and Phosphoryl Transfer Reaction

The PTS includes three essential enzymes, termed Enzyme I (EI), Enzyme II (EII), and *H*istidine *Pr*otein (HPr) (Figure 1). EI is a soluble protein kinase encoded by *ptsI* gene that catalyzes the phosphorylation of HPr from phospho*enol*pyruvate (PEP). HPr, encoded by the *ptsH* gene, is a small monomeric protein that is phosphorylated on a histidine residue at position 15. Both proteins are involved only in phosphoryl transfer reactions and are not sugar specific. PEP autophosphorylates EI on His189, and the phosphoryl group is sequentially transferred to HPr. EII consists of three functional domains – IIA, IIB, and IIC. The organization of these domains is dependent on the specific sugar transported. In the case of glucose transport in *E. coli* (Figure 1), IIA^{Glc}, encoded by the *crr* gene, exists as a separate polypeptide, which enables it to have multiple functions. IIA^{Glc} receives a phosphoryl group at His90 from HPr and transfers the phosphoryl group to Cys421 of IIB^{Glc} which is a part of the membrane protein complex $IIBC^{Glc}$ (Figure 1). IIB^{Glc} directly donates the phosphoryl group to sugar to catalyze translocation through the membrane. IIC^{Glc} consists of multiple transmembrane helices and is likely responsible for allowing access of the sugar to IIB^{Glc} for phosphorylation and release on the inner surface of the membrane (i.e., vectorial phosphorylation). With some PTS systems in *E. coli*, the three domains are contained within a single polypeptide (e.g., mannitol) or domains IIA and IIB are in a single polypeptide, but domain C consists of two polypeptides (e.g., mannose).

Preferential Utilization of Carbohydrate

In *E. coli*, there is a preferential growth on glucose via the PTS in the presence of several sugars (diauxie). This phenomenon involves regulatory functions of the PTS with respect to transcription of a wide variety of

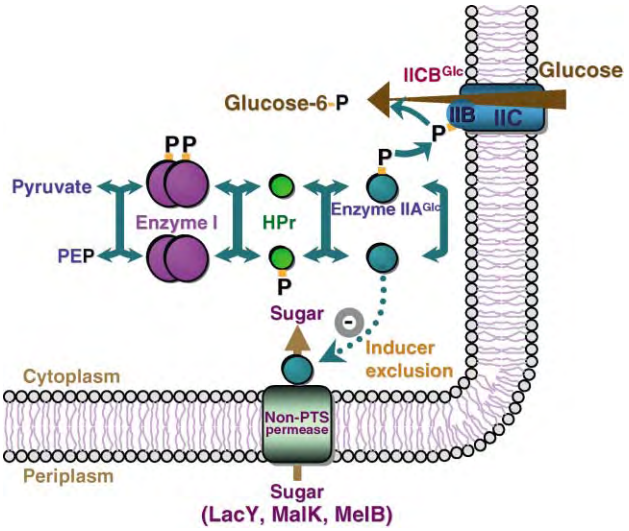

FIGURE 1 The glucose PTS system in *E. coli*. Shown is the sequence of phosphoryl transfer reaction through PEP → EI → HPr → EIIA → EIIB domain → glucose during vectorial phosphorylation across the membrane through EIIC domain. Glucose enters the cells as glucose-6-phosphate. Dephosphorylated IIA^{Glc} is able to bind to non-PTS permeases to inhibit transport of non-PTS sugars.

inducible proteins that are dependent upon cyclic-AMP (cAMP; catabolite repression), as well as regulation of the activity of endogenous levels of inducible permeases (inducer exclusion). Both regulatory activities are properties of $EIIA^{Glc}$. In the presence of glucose, the steady-state level of phosphorylated enzyme IIA^{Glc} is diminished leading to decreased adenylate cyclase activity, low intracellular levels of cAMP, and low levels of the catabolite receptor protein (CRP)-cAMP complex. Therefore, when glucose is present, transcription cannot be activated for most inducible PTS systems and non-PTS sugar permeases.

Another way to ensure preferential utilization of glucose is by inducer exclusion (Figure 1). In the presence of glucose, not only is the expression level of inducible transport systems dramatically reduced due to decreased transcription, but the activity of the non-PTS sugar permeases expressed at a basal level is inhibited by binding of unphosphorylated IIA^{Glc}. These proteins include lactose permease (LacY), melibiose permease (MelB), and MalK (a component of the maltose transport system). For example, with LacY, binding of IIA^{Glc} blocks entry of lactose and subsequent formation of allolactose, the inducer of the lactose operon.

Electrochemical Ion-Gradient-Driven Symporters

Classification

Electrochemical ion-gradient-driven symporters belong to a large and diverse superfamily, the *m*ajor *f*acilitator *s*uperfamily (MFS), members of which are found ubiquitously in all living organisms. Among the superfamilies, the sugar porter family (e.g., galactose permease (GalP) and arabinose permease (AraE)) and the oligosaccharide/proton symporter family (e.g., LacY and sucrose permease (CscB)) are two large groups involved in the bacterial sugar transport. In addition, the glycoside-pentoside-hexuronide:cation symporter family (e.g., melibiose permease (MelB)) is also responsible for transport of disaccharides.

Structural Features

Electrochemical ion-gradient-driven symporters are composed of a single polypeptide with 12 membrane-spanning helices, and for those studied intensively, a single polypeptide is able to catalyze translocation and accumulation. The X-ray structure of LacY from *E. coli* (Figure 2) provides a structural model for this family. The N-terminal six-helix and C-terminal six-helix bundles are highly symmetrical, and many of the helices are irregular. The helices are arranged so that they form a hydrophilic cavity open to the cytoplasm and closed to the periplasm, representing the inward-facing conformation. Bound sugar is located at the twofold axis of symmetry and approximately equidistant from both sides of the membrane.

Functional Properties

The sugar permeases in the MFS catalyze the transport of the mono- and disaccharides as well as their

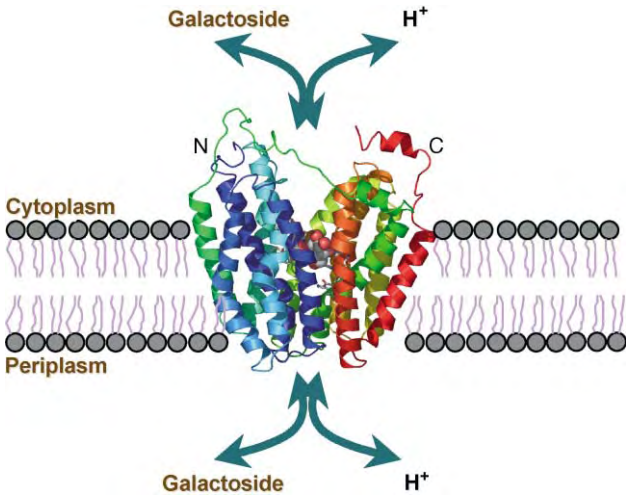

FIGURE 2 Overall structure of LacY in *E. coli*. The figure is based on the X-ray structure of the C154G mutant with a bound sugar. Ribbon representation of LacY viewed parallel to the membrane with a sugar bound in middle of the membrane at the approximate twofold axis of symmetry. As shown the protein catalyzes the stoichiometric translocation of sugar and H^+ in either direction across the membrane.

derivatives. They do not utilize ATP, but are driven by the free energy released from the energetically downhill movement of a cation (H^+ or Na^+) in response to an electrochemical ion gradient to accumulate sugar against concentration gradient. Unlike the case with the PTS, with ion-gradient-driven transport, sugar enters the cell in an unchanged form. Mechanistically and thermodynamically, it is noteworthy that MFS sugar permeases catalyze sugar/ion symport in both directions across the membrane (influx and efflux), unlike the other transport systems described.

Representatives

LacY

LacY is encoded by the *lacY* gene in the *lac* operon and consists of 417 amino acid residues. LacY is solely responsible for all the translocation reactions catalyzed by the β-galactoside system in *E. coli*. LacY is a particular well-studied representative of the oligosaccharide/proton symport family of the MFS. Like many other MFS transporters, LacY utilizes free energy released from the downhill translocation of H^+ in response to an electrochemical H^+ gradient ($\Delta\bar{\mu}_{H^+}$, interior negative and/or alkaline) to drive the stoichiometric accumulation of a galactopyranoside against a concentration gradient. In the absence of electrochemical proton gradient, LacY catalyzes the converse reaction, utilizing free energy released from downhill translocation of sugar to drive uphill stoichiometric accumulation of H^+. LacY is selective for disaccharides containing a D-galactopyranosyl ring, as well as D-galactose, but has no affinity for D-glucopyranosides or D-glucose.

By regulation of both transcription of *lacY*, as well as LacY activity by IIA^{Glc} of the PTS, *E. coli* grown in the presence of a mixture of glucose and lactose will utilize the lactose only when the glucose in the medium is completely exhausted, leading to diauxic or biphasic growth.

MelB

MelB, encoded by the *melB* gene, consists of 473 amino acid residues and is a well-studied member of the glycoside-pentoside-hexuronide:cation symporter family. A topological model indicates that the molecule contains 12-transmembrane domains with the N and C termini facing the cytoplasm, like LacY. MelB catalyzes the accumulation of galactopyranosides in *E. coli* by utilizing the free energy from the energetically downhill inward movement of Na^+, Li^+, or H^+ to drive the stoichiometric accumulation of sugar, and the symported ion is dependent on the nature of the sugar that is transported. Generally, it is believed that the α-galactosides melibiose, raffinose, and *p*-nitrophenyl-α-galactoside are transported with either H^+ or Na^+, while the β-galactosides lactose, methyl-1-β-D-galactopyranoside, or *p*-nitrophenyl-β-galactoside are symported with Na^+ but not with H^+.

Binding Protein-Dependent ATP-Binding Cassette (ABC) Transport System

Classification

Although ABC transporters are broadly distributed in archaea, prokaryotes, and eukarotes, ABC transport systems that require binding proteins for function are found only in archaea and prokaryotes. All members share the common feature that turnover involves the utilization of energy released from the hydrolysis of ATP to translocate solute across the membrane.

Structural Architecture

The binding protein-dependent ABC transporters have a common global organization with two integral membrane proteins, each of which has multiple-transmembrane helices, and two cytoplasmic proteins, each of which has one ATP-binding cassette (Figure 3). Both the integral membrane protein and the cytoplasmic ATP-binding protein may be present as homodimers or heterodimers. Both ATP-binding cassettes are required for transport activity. The X-ray structure of the vitamin B_{12} transporter $BtuFC_2D_2$ from *E. coli* provides a

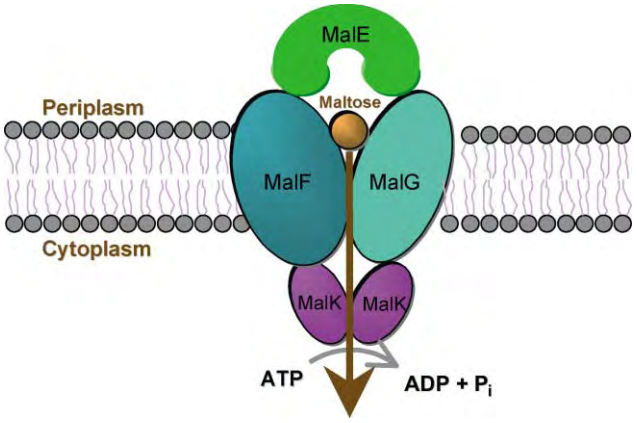

FIGURE 3 Model of MalEFGK2 complex of *E. coli*. The periplasmic binding protein MalE tightly binds to the membrane proteins MelF/MelG, delivering maltose and stimulating ATPase activity of the cytoplasmic protein MalK. The energy released from the hydrolysis of ATP drives the translocation of maltose across the membrane. The sugar enters the cells in an unchanged form.

structural example of a binding protein-dependent ABC transport complex. The two membrane-spanning subunits (BtuC) group around the translocation pathway, and the two ATP-binding cassettes (BtuD) are in close contact. In gram-negative bacteria, this family possesses periplasmic substrate-binding proteins and in gram-positive bacteria, there are membrane-bound, substrate-binding lipoproteins. Although these binding proteins have diverse specificity, the X-ray structures indicate a similar bilobate architecture composed of two symmetrical lobes surrounding the binding site.

Functional Properties

The binding protein selectively binds the substrate with high affinity and delivers it to the cognate permease. Interaction of the sugar-bound periplasmic binding protein with the membrane permease stimulates the ATPase activity of the cytoplasmic ATP-binding domains and initiates the transport process. The sugar enters the cell in an unchanged form. This system has the capacity to accumulate sugars to extremely high levels, and translocation is unidirectional.

Maltodextrin/Maltose Transport

Maltodextrin/maltose transport $MalEFGK_2$ (Figure 3), encoded by the maltose operon of *E. coli*, is the most extensively studied representative of the binding protein-dependent sugar transporters. MalE binds maltodextrin/maltose with high affinity and is the main determinant of substrate specificity. MalE releases the sugar into the MalF/MalG complex, two membrane proteins with multiple transmembrane helices through which the sugar enters into the cytoplasm of the bacterium. There are two copies of MalK, and each has a highly conserved ATP-binding cassette which is responsible for ATPase activity and a C-terminal regulatory domain for $EIIA^{Glc}$ regulation.

See Also the Following Articles

ABC Transporters • Carbohydrate Chains: Enzymatic and Chemical Synthesis • Oligosaccharide Chains: Free, *N*-Linked, *O*-Linked

Glossary

ATP-binding cassette The catalytic domain of the protein that binds ATP.

electrochemical ion gradient The electrochemical potential difference of an ion on either side of a membrane.

symporter A transporter that catalyzes the concomitant translocation of an ion and the substrate across the membrane in the same direction.

Further Reading

Abramson, J., Smirnova, I., Kasho, V., Verner, G., Kaback, H. R., and Iwata, S. (2003). Structure and mechanism of the lactose permease of *Escherichia coli*. *Science* **301**, 310–315.

Cordat, E., Mus-Veteau, I., and Leblanc, G. (1998). Structural studies of the melibiose permease of *Escherichia coli* by fluorescence resonance energy transfer: II. Identification of the tryptophan residues acting as energy donors. *J. Biol. Chem.* **273**, 33198–33202.

Duan, X., Hall, J. A., Nikaido, H., and Quiocho, F. A. (2001). Crystal structures of the maltodextrin/maltose-binding protein complexed with reduced oligosaccharides: Flexibility of tertiary structure and ligand binding. *J. Mol. Biol.* **306**, 1115–1126.

Fetsch, E. E., and Davidson, A. L. (2003). Maltose transport through the inner membrane of *E. coli*. *Front Biosci.* **8**, d652–d660.

Kaback, H. R. (1968). The role of the phospho*enol*pyruvate-phosphotransferase system in the transport of sugars by isolated membrane preparations of *Escherichia coli*. *J. Biol. Chem.* **243**, 3711–3724.

Kaback, H. R., Sahin-Tóth, M., and Weinglass, A. B. (2001). The kamikaze approach to membrane transport. *Nat. Rev. Mol. Cell Biol.* **2**, 610–622.

Locher, K. P., Lee, A. T., and Rees, D. C. (2002). The *E. coli* BtuCD structure: A framework for ABC transporter architecture and mechanism. *Science* **296**, 1091–1098.

Postma, P. W., Lengeler, J. W., and Jacobson, G. R. (1996). In *Escherichia coli and Salmonella typhimurium: Cellular and Molecular Biology* (F. C. Neidhardt, ed.) pp. 1149–1174. Am. Soc. Microbiol., Washington, DC.

Saier, Jr M. H. (2000). Families of transmembrane sugar transport proteins. *Mol. Microbiol.* **35**, 699–710.

Biography

Lan Guan, M.D., Ph.D., is a Research Associate of the Howard Hughes Medical Institute at the David Geffen School of Medicine at UCLA.

H. Ronald Kaback, M.D., is an investigator at the Howard Hughes Medical Institute, Professor in the Departments of Physiology and Microbiology, Immunology, and Molecular Genetics, and a Member of the Molecular Biology Institute at UCLA. Recently, the laboratory collaborated with So Iwata's laboratory at Imperial College, London to solve the X-ray structure of LacY. He is a member of the National Academy of Sciences and a Fellow of the American Academy of Arts and Sciences.

Glucose/Sugar Transport in Mammals

Silvia Mora and Jeffrey Pessin
State University of New York, Stony Brook, New York, USA

Glucose is the primary energy source for mammalian cells and its oxidation provides ATP under both anaerobic and aerobic conditions. Moreover, its storage as glycogen in the liver provides a ready source of glucose during states of fasting through the catabolism of glycogen and the release of glucose back into the circulation. Glycogen storage also represents the primary source of energy for muscle. In adipocytes, glucose can be converted to triglycerides, a more energetically compact fuel store that can be better metabolized to fatty acids and glycerol. Apart from being a major source of metabolic energy, glucose is also a source of structural moieties for other macromolecules including glycoproteins, proteoglycans, glycolipids, and nucleic acids. However, glucose is a highly polar molecule that is impermeable across cell membrane and therefore two specific families of mammalian glucose transporters, the sodium-dependent glucose transporters (SGLT) and the facilitative glucose transporters (GLUT), have evolved.

Sodium-Dependent Glucose Transporters

The Na^+/glucose cotransporters are responsible for the absorption of glucose against its concentration gradient by utilizing the energy generated by the electrochemical Na^+ gradient (Figure 1A). These transporters are primarily located in the brush border (apical) membranes of intestinal and kidney epithelial cells and are responsible for the absorption of glucose from the lumen of the small intestine and proximal tubule of the kidney. In the intestines, this transporter functions in the absorption of dietary glucose from the lumen and is then transported across the basolateral membrane into the circulation by the facilitative glucose transporters. Similarly, in the kidneys glucose is filtered into the lumen of the proximal tubule and is reabsorbed by the Na^+/glucose cotransporters such that under normal physiological conditions, urine is completely depleted of glucose. However, in states of insulin resistance and diabetes, the concentration of lumenal glucose may reach such high levels that it exceeds the capacity of the Na^+/glucose cotransporters to fully reabsorb the filtered glucose.

There are three different isoforms of sodium/glucose cotransporters named SGLT1, SGLT2, and SGLT3. Amino acid sequence alignments show that SGLT3 and SGLT2 have identities of 70% and 59% to SGLT1, respectively. The secondary structure model predicted for SGLT1 contains 14 transmembrane α-helices (TMH) with both the hydrophobic NH_2 terminus and the COOH terminus of TMH 14 facing the extracellular solution (Figure 2A). All SGLTs probably use the consensus N-linked glycosylation site (*N*248) between TMH 6 and 7. The predicted molecular weight of these transporters is 73 kDa with the proteins having 659–672 amino acids. The major differences in function between SGLT1 and SGLT2/SGLT3 resides in the selectivity for sugar transport. SGLT1 accepts the natural sugars D-glucose and D-galactose with comparable affinities and a variety of synthetic sugars such as 3-*O*-methyl-D-glucose. SGLT2 and SGLT3 are much more restrictive in that they prefer D-glucose to D-galactose or 3-*O*-methyl-D-glucose. The affinity of SGLT1 for D-glucose is tenfold higher than that of SGLT2 or SGLT3.

Facilitative Glucose Transporters

The facilitative glucose transporters comprise a relatively large family of structurally related proteins that are encoded by distinct genes and are expressed in an overlapping yet tissue-specific manner (Table I). All the facilitative glucose transporters are predicted to have 12 membrane-spanning domains and allow for the stereospecific transport of glucose through the lipid bilayer. The transport of glucose is energy-independent and is solely driven by the relative glucose concentration across the plasma membrane (Figure 1B). Since under most conditions, the cytoplasmic glucose is rapidly phosphorylated by hexokinase or glucokinase, the relative levels of intracellular glucose are compared to the extracellular concentration resulting in net inward flux of glucose. However, in some instances glucose can be

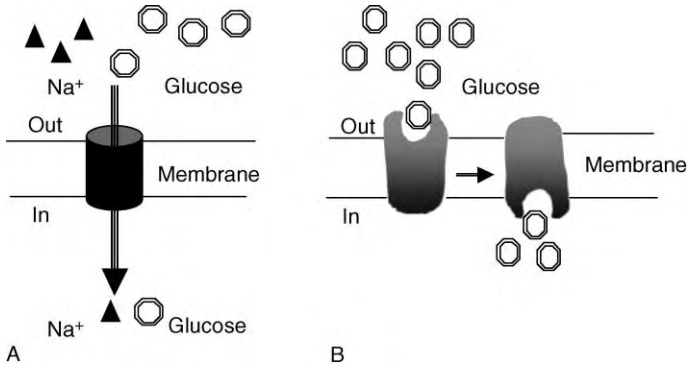

FIGURE 1 Distinct glucose transport mechanisms in mammalian cells: (A) sodium-glucose cotransport and (B) facilitative diffusion.

secreted into the circulation under normal physiological conditions. For example, in hepatocytes facilitative glucose transporters participate in the uptake of glucose from the portal circulation following a meal and in the release of glucose generated by glycogenolysis or glucogenesis in the postabsorptive state and during fasting.

Currently, there are 12 identified facilitative glucose transporters in mammalian cells, with GLUT1, GLUT2, GLUT3, GLUT4, GLUT8, and GLUT9 established as functional facilitative glucose transporters. GLUT5 is primarily a fructose transporter and the other isoforms have only been identified based upon amino acid sequence homology. Each of these transporters have distinct but overlapping tissue distributions, which underscores their specific physiologic function. For example, GLUT1 is generally expressed and is thought to be responsible for the basal uptake of glucose. GLUT2 is predominantly expressed in the liver and pancreatic β-cells where it functions as part of a sensor-mediating hepatic glucose output during states of fasting and insulin secretion in the postprandial absorption state. In contrast, neurons primarily express the relatively high-affinity GLUT3 isoform necessary to maintain high rates of glucose metabolism for energy production. GLUT8 appears to provide important function during early embryogenesis, whereas GLUT4 is exclusively expressed in insulin responsive tissues, adipose, and striated muscle. These latter tissues provide the key functional elements responsible for the insulin stimulation of glucose uptake and are key targets for dysregulation in states of insulin resistance and diabetes. The latest GLUT member identified, GLUT14, is present in the testis and seems to have evolved from a gene duplication of GLUT3.

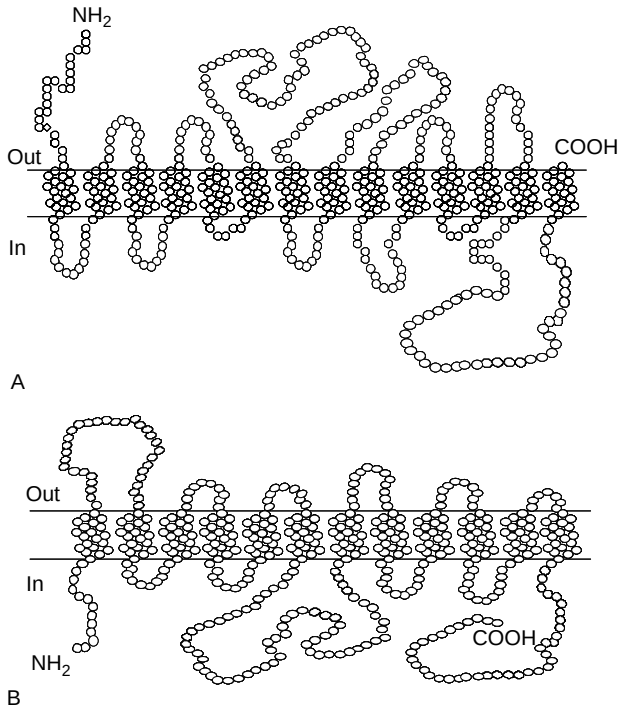

FIGURE 2 Predicted structure of glucose transporters: (A) SGLT-1 and (B) GLUT-1.

GLUT1

GLUT1 was originally identified as the erythrocyte-type facilitative glucose transporter and was the first isoform to be purified and eventually cloned. The amino acid sequence of GLUT1 is highly conserved among different species (i.e., 98% identity between human and rat). Computer analysis of the primary sequence of GLUT1 has revealed that GLUT1 is a hydrophobic protein, with ~50% located within the lipid bilayer. Several lines of evidence have supported a structural model for GLUT1 that consists of 12-membrane-spanning α-helical segments and an intracellular located NH_2 and COOH termini. According to this model a large intracellular segment of 33 amino acids connects transmembrane domains M1 and M2, and an extremely hydrophilic intracellular segment of 65 amino acids joins M6 and M7. Short regions of 7–14 amino

TABLE I

Mammalian Facilitative Sugar Transporters

Isoform	Tissue distribution	Function
GLUT-1	Brain, endothelial cells, placenta, erythrocyte, mammalian gland	Basal transport, transport in fetal tissues
GLUT-2	Liver, small intestine, pancreatic cells, kidney	Basolateral transport in epithelial cells, glucose release form liver
GLUT-3	Neurones Placenta	Basal transport
GLUT-4	Muscle, heart, white and brown adipose tissue	Insulin-stimulated glucose transport
GLUT-5	Small intestine, kidney, testis and sperm	Fructose transporter
GLUT-6	Spleen, leukocytes, brain	Unknown
GLUT-7	Unknown	Unknown
GLUT-8	Testis, blastocyst, brain	Unknown
GLUT-9	Liver, kidney	Unknown
GLUT-10	Liver, pancreas	Unknown
GLUT-11	Heart, muscle	Unknown
GLUT-12	Heart, prostate	Unknown
GLUT-13	Unknown	Unknown
GLUT-14	Testis	Unknown

acids connect the remaining membrane-spanning regions. There are two potential N-linked glycosylation sites in GLUT1 at Asn-45 and Asn-411, but only the former site in the large extracellular loop has been shown to be glycosylated (Figure 2B). Although other models have been proposed, structural analysis of GLUT1 topography has confirmed the originally proposed 12-transmembrane-spanning model. The other members of the glucose transporter family are similar in size (between 492 and 524 amino acids) and all are predicted to maintain the 12-transmembrane-spanning structure, although the sites of glycosylation and length of the different intracellular and extracellular loops appear to vary (Table I).

GLUT1 is highly expressed in placenta, brain, epithelial cells of the mammary gland, transformed cells, and fetal tissues. Because of its ubiquitous expression it has been proposed that GLUT1 might be responsible, at least in part, for basal glucose uptake. Kinetic studies in erythrocytes have demonstrated that GLUT1 has a K_m of ~2 mM for D-glucose, whereas the K_m is greater than 3 M for L-glucose. In addition, it has been postulated that GLUT1 functions in either a dimeric or tetrameric oligomeric state. This appears to account for the various kinetic properties of glucose transport and, in addition to expression levels and localization, provides another level of control of transporter function.

GLUT2

The low-affinity GLUT2 facilitative glucose transporter functions in the β-cells of the pancreas to transport glucose in direct proportion to the circulating glucose concentration. This transporter functions in concert with glucokinase such that small increases in glucose influx can signal changes in the ATP/ADP ratio, resulting in a highly sensitive mechanism regulating insulin secretion. The central importance of GLUT2 in the regulation of pancreatic insulin secretion was established with the identification of a patient expressing a defective GLUT2 mutation. This transporter also functions in the liver to allow for shuttling of increased glucose load into glycogen. GLUT2 also appears to play a significant role in the reabsorption of filtered glucose in the kidney and in the basolateral transport of glucose from the digestive tract epithelium into the circulation.

GLUT3

GLUT3 was originally isolated from a fetal skeletal muscle library but is not significantly expressed in adult muscle. This isoform is primarily expressed in the brain (astrocytes), but it has also been detected in placenta endothelial cells and in human skeletal muscle. Recently, it has also been detected in human condrocytes. The localization of this transporter is in the plasma membrane.

GLUT4

In 1989, five research groups independently cloned the insulin-responsive glucose transporter isoform GLUT4. This isoform is predominantly expressed in striated muscle (skeletal and cardiac) and adipose tissue (white and brown), the major tissues that display insulin-stimulated glucose uptake. Sequence analysis of GLUT4 suggests that its secondary structure and orientation in the plasma membrane is similar to GLUT1 with an overall 65% amino acid identity.

In contrast to the other glucose transporters under basal conditions GLUT4 is predominantly localized intracellularly. The primary mechanism responsible for the increase in glucose uptake in insulin-sensitive tissues upon insulin treatment is the recruitment or translocation of glucose transporters from these intracellular storage sites to the plasma membrane. Although the molecular mechanisms that regulate GLUT4 translocation are poorly understood, the trafficking of the GLUT4 protein has several similarities with the trafficking, docking, and fusion of synaptic vesicles in neurons responsible for neurotransmitter release.

The long-term expression of the GLUT4 gene is also controlled during development and during various hormonal, nutritional, and metabolic states. For example, fetal tissues contain very little GLUT4 and expression of this transporter increases after birth. In addition, during states of insulin deficiency such as fasting and following destruction of the insulin secreting β-cells by streptozotocin (STZ)-induced diabetes, GLUT4 expression levels are severely reduced in adipose, heart, and skeletal muscle. Similarly, obesity, high-fat feeding, and muscle denervation also result in a decrease in GLUT4 expression and subsequent insulin resistance. In contrast, GLUT4 is up-regulated, by exercise training, thyroid hormone treatment, and insulin therapy, treatments that increase insulin sensitivity.

GLUT5

The GLUT5 fructose transporter is highly conserved among species with a 69–88% amino acid identity between mice, human, rat, and rabbit. In mice, expression is highest in small intestine, kidney, and testis. In humans, it is also present in skeletal muscle. Studies in rats and rabbits have shown that the expression of this transporter is highest in the upper part of the small intestine (duodenum and proximal jejunum). Expression of GLUT5 in the intestine is highly regulated, showing circadian rhythm, dependence on dietary fat and carbohydrate content, and insulin levels.

GLUT6

The GLUT6 gene encodes a cDNA which exhibits significant sequence similarity with the other members of the glucose transporter family, particularly GLUT8. GLUT6 protein has been detected in spleen, peripheral leucocytes, and brain. When heterologously expressed in 3T3L1 adipocyte cells this transporter is localized intracellularly, but unlike GLUT4 does not translocate to the plasma membrane in response to insulin.

GLUT7

GLUT7 is an uncharacterized protein. The pattern of expression of this gene and the transport substrate specificity of the protein are currently unknown. However, the genomic sequence of GLUT7 is 59% similar to that of GLUT5.

GLUT8

GLUT8, previously known as GLUTX1, is a newly characterized glucose transporter isoform that is expressed at high levels in the testis and brain and at lower levels in several other tissues. In the brain GLUT8 is expressed in the neuronal cell bodies of excitatory and inhibitory neurons in the rat hippocampus. It was found in hippocampal and dentate gyrus neurons as well as in amygdala and primary olfactory cortex. In these neurons, its location was close to the plasma membrane of cell bodies and sometimes in proximal dendrites. High GLUT8 levels were detected in the hypothalamus, supraoptic nucleus, median eminence, and the posterior pituitary. In the testis, it is found in differentiating spermatocytes of type 1 stage and in the acrosomal region it is found in mature spermatozoa.

GLUT9–14

Other than sequence analysis and tissue distribution of mRNA expression, little information is available about the function and properties of GLUT9–14. GLUT9 has a high-sequence similarity to the fructose transporter GLUT5 and is mainly expressed in kidney and liver. GLUT10 is primarily expressed in human heart, lung, brain, liver, skeletal muscle, pancreas, placenta, and kidney. GLUT11 gene has two splice variants and is most abundant in skeletal muscle and heart. GLUT12 is expressed in heart, prostate and has also been detected in breast cancer cells and in epithelial cells of rat mammary gland during pregnancy and lactation. The tissue distribution of GLUT13 is unknown and GLUT14 is expressed in the testis.

See Also the Following Articles

Gluconeogenesis • Glycogen Metabolism • Insulin- and Glucagon-Secreting Cells of the Pancreas • Membrane Transport, General Concepts • Sugar Nucleotide Transporters

Glossary

insulin resistance A state in which the same concentration of insulin elicits a decreased biological response compared to normal conditions.

isoform A protein with similar amino acid sequence and same function.

splice variant Different mRNA sequences that originate from the same gene.

Further Reading

Holloszy, J. (2001). A forty-year memoir of research on the regulation of glucose transport into muscle. *Am. J. Physiolo. Endocrinol. Metab.* **284**, E453–E467.

Joost, H., and Thorens, B. (2001). The extended GLUT family of sugar/polyol transport facilitators: Nomenclature sequence characteristics and potential function of its novel members. *Mol. Memb. Biol.* **18**, 247–256.

Koistinen, H., and Zierath, J. (2003). Regulation of glucose transport in human skeletal muscle. *Ann. Med.* **34**, 410–418.

Watson, R., and Pessin, J. (2001). Subcellular compartmentalization and trafficking of the insulin-responsive glucose transporter, GLUT4. *Exp. Cell Res.* **15**, 75–83.

Wright, E. (2001). Renal sodium-glucose cotransporters. *Am. J. Renal. Physiol.* **280**, F10–F18.

Biography

Jeffrey E. Pessin is a Professor in and Chair of the Department of Pharmacological Sciences at the State University of New York in Stony Brook. His research interests include the molecular mechanisms of insulin action, intracellular signaling, and the regulation of glucose transport in muscle and adipose tissue.

Silvia Mora is an Assistant Professor in the Division of Biology, Kansas State University. Her interests are focused on the intracellular trafficking of GLUT4 and the regulated secretion of adipokines.

Glutamate Receptors, Ionotropic

Derek B. Scott and Michael D. Ehlers
Duke University Medical Center, Durham, North Carolina, USA

Ionotropic glutamate receptors (iGluRs) are ion channels that respond to the amino acid neurotransmitter L-glutamate—the major excitatory neurotransmitter in the mammalian nervous system. Localized to excitatory synapses, iGluRs mediate a net influx of positively charged ions into the postsynaptic cell when activated by glutamate that is released from presynaptic terminals. The net influx of positive ions through iGluRs raises the membrane potential of the postsynaptic cell, thus increasing neuronal excitability and making it more likely that an action potential will be initiated. The combination of ligand activation and channel gating in the same protein complex enables iGluRs to directly convert chemical presynaptic signals to electrical responses in the postsynaptic neuron. In addition to mediating synaptic transmission, iGluRs play important roles in synapse formation during brain development, in synaptic plasticity during learning and memory, and in many neurological diseases. Thus, much focus has been given to understanding the biophysical properties—the structure, pharmacology, and physiology—of these glutamate-gated channels.

Ionotropic Glutamate Receptor Subtypes

Ionotropic glutamate receptors (iGluRs) are a family of receptors comprised of three related ion channel types: α-amino-3-hydroxy-methyl-4-isoxazole (AMPA) receptors, kainate receptors, and *N*-methyl-D-aspartate (NMDA) receptors. These three iGluR subtypes are named after specific agonists that selectively activate each channel type, namely AMPA, kainate, or NMDA. A fourth iGluR subtype, termed delta, is an "orphan" subtype as it does not form functional ion channels and has unknown cellular functions. Although these glutamate-gated channels have distinct physiological and pharmacological properties, they share structural similarities (Figure 1).

Ionotropic Glutamate Receptor Structure

Current evidence indicates that iGluRs are tetramers formed by the assembly of four integral membrane protein subunits (Figure 1A). These subunits, unique to each iGluR subtype, were initially isolated using expression cloning techniques and share similar structural and topological properties. There are 18 known mammalian iGluR subunits that together make a gene family (Table I). A typical iGluR subunit consists of an extracellular amino-terminal domain (NTD), a ligand-binding domain (S1–S2), four membrane domains including three transmembrane segments (M1, M3, and M4) and one re-entrant pore loop (M2), and an intracellular carboxyl-terminal domain (Figure 1B).

Extracellular and Ligand-Binding Domains

The large extracellular domains of iGluRs share sequence and structural homology with bacterial amino-acid-binding proteins. The NTD at the distal amino terminus participates in subunit assembly, whereas the S1–S2 domains together form a cleft where ligands, including L-glutamate, bind and activate the opening of the channel (Figure 1B). Crystal structures of iGluR S1–S2 domain bound to ligands have revealed that the relative movements of the S1 and S2 segments are critical parameters during iGluR activation. At rest, the ligand-binding cleft is in an open conformation, while ~20° cleft closure occurs following ligand binding that results in full channel activation.

Pore Structure

In addition to an S1–S2 ligand-binding site, each subunit within the tetrameric complex also contributes a polypeptide sequence (the M2 pore-loop) that lines the channel pore (Figures 1B and 1C). The channel pore segments share common structural signatures across the family of iGluRs that are similar to and have been found to be evolutionarily conserved in K^+ channels. This has allowed researchers to model the structure of the iGluR M2 pore-loop domain using the crystal structure of the P-loop pore domain of K^+ channels. The M2 pore-loop domain of iGluRs is believed to be composed of two parts, a short α-helix and a random-coil domain

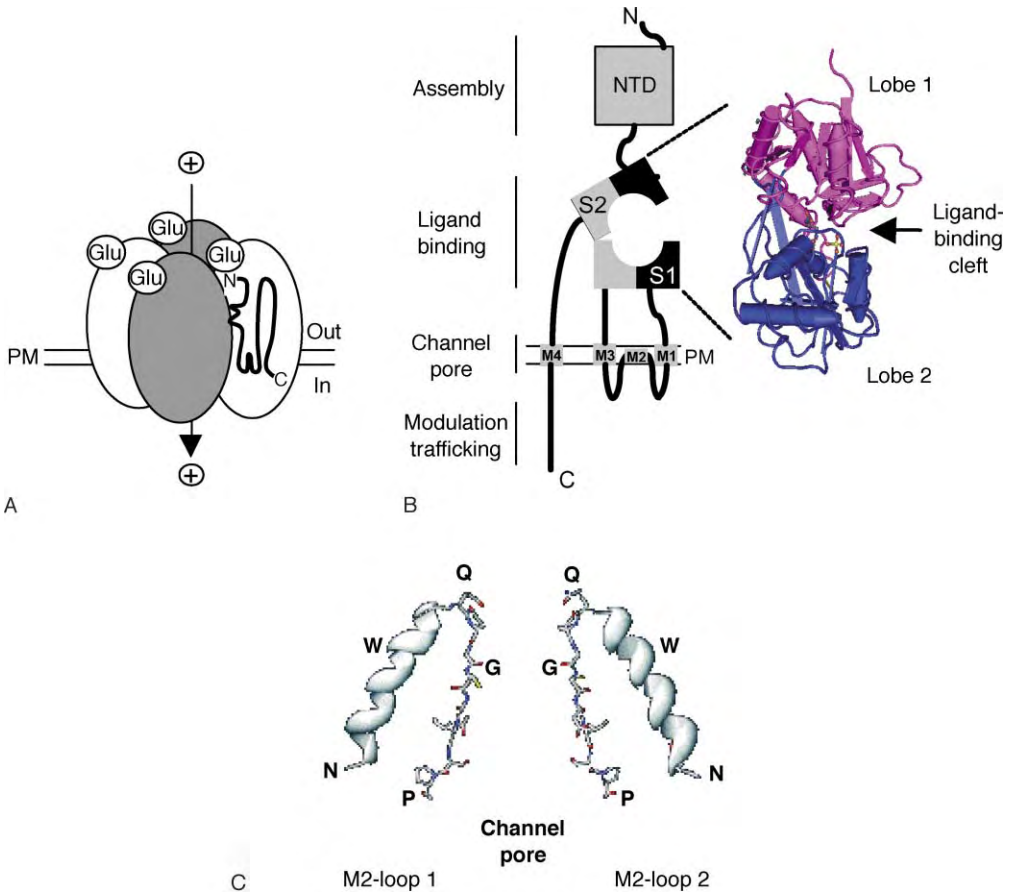

FIGURE 1 Structural features of iGluRs. (A) All iGluRs are heterotetramers formed by the regulated assembly of transmembrane subunits. Upon glutamate binding, a conformational change opens the channel pore leading to a net influx of positive ions into the postsynaptic neuron. PM designates the plasma membrane, Glu designates glutamate. (B) iGluR subunits have a modular domain organization including (1) a large extracellular amino-terminal domain (NTD), (2) a two-segment extracellular ligand-binding domain (S1–S2), (3) a membrane domain consisting of three transmembrane segments (M1, M3, and M4) and a re-entrant loop whose residues form the channel pore (M2), and (4) an intracellular C-terminal domain. The crystal structure of the S1–S2 ligand-binding domain is shown in an enlarged form as a ribbon diagram. Ligands such as L-glutamate bind to the ligand-binding cleft between the two lobes (lobe 1 and lobe 2) that are formed by the S1 and S2 domains. Domains are not drawn to scale. S1–S2 structure courtesy of E. Gouaux and can be viewed at the Molecular Modeling Database, NCBI, National Library of Medicine. MMDB# 21762 or PDB# 1MM6. (Reproduced from Armstrong, N., Sun, Y., Chen, G. Q., and Gouaux, E. (1998). Structure of a glutamate-receptor ligand-binding core complex with kainate. *Nature* **395**, 913–917, with permission.) (C) The proposed structure of the iGluR channel pore. The structure of the M2 pore-loop domain of iGluRs was modeled using the crystal structure of the highly homologous P-loop region in K^+ channels. A side view of the modeled iGluR channel pore composed of two M2 pore-loop domains is shown. The M2 pore-loop domain is ~23 amino acids long and begins as an ascending α-helix (N) that quickly becomes a random coil structure. A tryptophan residue (W) within the ascending α-helix, a glycine (G) residue within the channel pore and a proline (P) residue at the end of the M2 pore-loop together constitute the WGP signature that represents the minimal structural conservation between iGluR and K^+channel pore loops. The last residues within the α-helical region of the M2 pore-loop domain (Q) achieve ion selectivity. (Reproduced from Kuner, T., Seeburg, P. H., and Guy, H. R. (2003). A common architecture for K^+ channels and ionotropic glutamate receptors? *Trends Neurosci.* **26**, 27–32, with permission from Elsevier.)

(Figure 1C). Ion selectivity is determined by residues located immediately after the α-helical portion of M2. Constriction of the pore is achieved by several residues that span the end of the α-helical portion and beginning of the random coil domain of M2.

Intracellular Domain

Much less structural information is available on the carboxyl-terminal domains of iGluRs, which vary greatly in size and sequence between the different iGluR subunits. This intracellular domain is subject to protein phosphorylation and participates in numerous protein interactions that regulate iGluR channel activity and intracellular trafficking.

Ionotropic Glutamate Receptor Subunits and Molecular Diversity

Although all iGluRs are activated by L-glutamate and share structural similarities, each channel type has

TABLE I

Molecular Diversity of Ionotropic Glutamate Receptor Subunits

Receptor	Subunits	Assemblies	Molecular diversity/alternative isoforms
AMPA	GluR1 GluR2 GluR3 GluR4	• Homomeric assemblies between all subunits observed • GluR2 heteromers predominate *in vivo*	GluR1–4: flip/flop: 38 aa sequence near M4 GluR2 and GluR4: splicing yields 2 different intracellular C termini (short and long) GluR2: RNA edited in pore domain (Q/R) GluR2–4: RNA edited in S2 domain (R/G)
Kainate	GluR5 GluR6 GluR7 KA1 KA2	• Homomeric GluR5–7 observed • KA1–2 do not form homomeric channels	GluR5: splicing yields 4 different intracellular C termini GluR5 and GluR6: RNA edited in pore domain (Q/R) GluR6: RNA edited in M1 domain at 2 sites GluR6: splicing yields 2 different intracellular C termini GluR7: splicing yields 2 different intracellular C termini
NMDA	NR1 NR2A NR2B NR2C NR2D NR3A NR3B	Strict heteromer: NR1/NR2 heteromers most abundant, also NR1/NR2/NR3 NR1/NR3	NR1: alternative splicing of 5 aa near N terminus NR1: splicing yields 4 different intracellular C termini NR1: total of eight different splice variants
Orphan receptors	δ1 δ2	Unknown	Unknown A spontaneous mutation in δ2 forms functional channels in *lurcher* mice

Abbreviations: aa, amino acid; Q/R, glutamine/arginine; R/G, arginine/glycine.

unique pharmacological and physiological properties. The varied functional properties of iGluRs arise from the molecular diversity of the protein subunits that assemble to form AMPA receptors, kainate receptors, or NMDA receptors (Table I).

AMPA Receptors

AMPA receptors are composed of four subunits (GluR1–4) that are encoded by four different genes (Table I). Animals with targeted disruptions of AMPA receptor subunit genes are severely impaired in basal excitatory synaptic transmission, are unable to induce activity-dependent changes in synaptic transmission, and have memory defects in spatial learning tasks. All AMPA receptor subunits are capable of homotetrameric assembly to form functional channels. However, heterotetrameric combinations containing GluR2 subunits predominate *in vivo*.

Tetrameric combinations of GluR1–4 give rise to AMPA receptors with distinct properties and regulation. Additional molecular diversity within AMPA receptor subunits is achieved by mRNA splicing and RNA editing. Alternate mRNA splicing of exon 14 and 15 includes or excludes a 38-amino-acid segment termed the "flip/flop site" near the beginning of M4 in the S2 segment that regulates channel properties (Table I). This splicing event is developmentally regulated as flip-containing subunits predominate in very young animals, while flip- and flop-containing subunits are expressed at the same level in adults. Alternative mRNA splicing at the C terminus of GluR2 or GluR4 subunits gives rise to splice forms that possess either short or long intracellular domains. These different intracellular domains regulate intracellular trafficking and targeting of GluR2- or GluR4-containing AMPA receptors to synaptic sites. In addition, RNA editing of the mRNA encoding GluR2 subunits results in replacement of a

glutamine (Q) residue with an arginine (R) residue within the M2 pore-loop domain (termed the Q/R site). The editing of GluR2 subunits is very significant since AMPA receptors containing unedited GluR2 subunits are Ca^{2+} permeable, while those containing normal edited versions cannot flux Ca^{2+} ions. The regulated influx of Ca^{2+} into postsynaptic neurons triggers synaptic plasticity and other long-lasting changes in synaptic efficacy, and if excessive can lead to neurotoxic effects including cell death. Quite strikingly, animals that completely fail to edit GluR2 subunits are nonviable, while others that can only edit half of their complement of GluR2 develop seizures. As these observations suggest, the majority of GluR2 subunits *in vivo* are edited at the Q/R site. RNA editing also occurs at other sites within AMPA receptor subunits (Table I), causing more subtle changes in channel physiology.

Kainate Receptors

Unlike AMPA receptors and NMDA receptors, kainate receptors are located at both presynaptic and postsynaptic sides of the synapse, where they modulate presynaptic neurotransmitter release as well as synaptic transmission. Kainate receptors are composed of five subunits (GluR5–7, KA1–2), each encoded by a separate gene (Table I). Various homomeric and heteromeric combinations of kainate receptor subunits give rise to functional receptors with very different properties. For example, GluR5–7 homomeric receptors (low-affinity subunits) have a tenfold lower affinity to L-glutamate than KA1–2-containing receptors (high-affinity subunits). KA1–2 subunits do not form homomeric receptors and must assemble with GluR5–7 subunits to form functional channels.

Much like the AMPA receptor GluR2 subunits, mRNAs encoding GluR5 and GluR6 undergo RNA editing at the Q/R site (Table I). In addition, GluR6 subunits undergo RNA editing at two other sites within the M1 segment that also influence Ca^{2+} permeability. Unedited GluR5 and GluR6 are more abundant during embryonic development, while edited subunits predominate in adults. Alternative splicing of intracellular C-terminal domains yields multiple GluR5 (A–D), GluR6 (A–B), and GluR7 (A–B) subunits; however, the functional significance of these splicing events is still unknown.

NMDA Receptors

NMDA receptor subunits fall into three separate groups—NR1, NR2, and NR3. NR1 subunits are encoded by a single gene; NR2 subunits are encoded by four genes (NR2A–D); and NR3 subunits are encoded by two genes (NR3A–B) (Table I). NR1 and NR2B subunits are essential, as animals containing targeted disruptions in the genes encoding either subunit die from respiratory and feeding deficits soon after birth. In contrast, animals with NR2A-, 2C-, 2D-, or NR3-targeted disruptions are viable, but display deficiencies in synaptic plasticity and neuronal development. Unlike AMPA and kainate receptors, NMDA receptors are strict heteromers that require the assembly of NR1 subunits with either NR2 or NR3 subunits to form functional channels. NR1 is expressed in almost all neurons in the brain and spinal cord, while the expression of NR2 and NR3 subunits is spatially restricted and developmentally regulated.

Alternative splicing generates eight different NR1 splice variants that differ in the presence or absence of a small five-amino-acid segment near the N terminus (N1), a 21 amino-acid sequence in the middle portion of the carboxyl terminus (C1), and two alternate ending sequences at the very distal carboxyl terminus (C2 and C2′) (Table I). Splicing at the N1 site regulates channel sensitivity to allosteric modulators (e.g., polyamines and Zn^{2+}). Splicing at the C1 and C2/C2′ sites generates receptors with unique trafficking signals that regulate the speed and efficiency of synaptic delivery of NMDA receptor complexes.

Orphan (δ) Receptors

Two orphan receptors (δ1–2) share considerable sequence homology with other iGluRs, but fail to form functional glutamate-gated channels when expressed alone or in combination with other iGluR subunits. However, spontaneous mutations of δ2—*hotfoot* and *lurcher* mutant mice—cause ataxia and impaired synaptic plasticity by transforming quiescent δ2-containing receptors into functional channels.

Ionotropic Glutamate Receptor Pharmacology and Physiology

An important step in studying the physiological properties of iGluRs *in vivo* has been the development of unique agonists and antagonists that specifically activate or inhibit distinct types of iGluRs. A limited list of the most commonly used pharmacological agents used to activate or inhibit iGluRs is presented in Table II. Each type of iGluR has distinct channel properties—including ligand affinity, ionic permeability, channel conductance, and gating kinetics—that are determined by subunit composition. Table III includes some of the physiological characteristics of AMPA receptor, kainate receptor, and NMDA receptor synaptic responses and single channel properties, illustrating the diverse properties of the different iGluRs.

TABLE II

Ionotropic Glutamate Receptor Pharmacology

Receptor	Agonists	Activation of channels (EC_{50})	Antagonists and mode of action
AMPA	• Glutamate • AMPA • Kainate[a]	• L-glutamate (450–600 μM) • AMPA (3–5 μM) • Kainate (50–60 μM)	CNQX and NBQX: competitive inhibitors GYKI53655: noncompetitive inhibitor
Kainate	• Glutamate • Kainate	• L-glutamate (500–6000 μM) • Kainate (6–33 μM) • AMPA (2000 μM)	CNQX: competitive inhibitor LY382884: GluR5-specific inhibitor
NMDA	• Glutamate • Glycine[b] • NMDA	• L-glutamate (0.4–1.8 μM) • Glycine (0.1–2.1 μM) • Depolarization of membrane to release Mg^{2+} block	Mg^{2+}: channel pore blocker at resting potential AP5: competitive inhibitor MK801: channel pore blocker

EC_{50} is the concentration of agonist that evokes a half-maximal activation. These values were determined for peak responses of recombinant receptors in heterologous cells.

[a] Nondesensitizing agonist for AMPA receptors.

[b] Coagonist.

AMPA Receptor Physiology

Activated AMPA receptors carry most of the ionic current into postsynaptic neurons following presynaptic glutamate release, and therefore mediate most of the fast excitatory neurotransmission in the brain. GluR2-containing AMPA receptors are permeable to Na^+ and K^+ ions, while AMPA receptors lacking GluR2 also flux Ca^{2+} ions. AMPA receptor currents have rapid kinetics (Table III); channels open rapidly with a very high probability ($P_o = 0.4–1.0$), deactivate rapidly (dissociation of ligand from agonist binding site), desensitize rapidly (closing of channel in the presence of agonist), and recover fully from desensitization in about 100 ms. Once gated, individual AMPA channels have several conductance states ranging from 4 to 24 pS, depending upon the exact subunit composition of the AMPA receptor complex studied. GluR2-containing channels possess a linear current–voltage (*I/V*) relationship over a wide range of membrane potentials. On the other hand, channels lacking GluR2 do not have a linear *I/V* relationship, but rather are inwardly rectified (preferentially pass current at negative membrane potentials). Determining the *I/V* relationship of AMPA receptor currents is thus a common technique to reveal subunit composition *in vivo*.

Kainate Receptor Physiology

Kainate receptor-mediated currents are similar to those of AMPA receptors (Table III), but do not contribute nearly as much to excitatory neurotransmission. Like AMPA receptors, kainate receptors have fast activation

TABLE III

General Characteristics of Ionotropic Glutamate Receptor Physiology

Receptor	Ions in[a]	Ions out[b]	Activation kinetics (τ)[b] (ms)	Open times (ms)	Deactivation (ms)	Desensitization (ms)	Single channel conductance (pS)
AMPA	Na^+	K^+	Very fast 0.2–0.4	0.14–3.3	0.6–1.1	0.8–8.1	Multiple states 4–24
Kainate	Na^+	K^+	Very fast 0.2–0.4	0.3–2.1	2.5	1.4–9	Multiple states 0.2–25
NMDA	Na^+ Ca^{2+}	K^+	Slow 10–50	0.06–8	33–4400	650–750	Multiple states 17–75

Ranges are presented because there are different values for different subunit compositions. For measurements of specific subunit combinations see Dingledine, R., Borges, K., Bowie, D., and Traynelis, S. F. (1999). The glutamate receptor ion channels. *Pharmacol. Rev.* **51**, 7–61.

ms = milliseconds; pS = picosiemens.

[a] Assuming a resting membrane potential of −70 mV.

[b] Kinetic and channel conductance measurements are reported following a brief application of glutamate (AMPA and kainite receptors) or glutamate plus glycine (for NMDA receptors).

kinetics with high probabilities ($P_o = 0.5–1.0$), similar open times, deactivation and desensitization kinetics, and are permeable primarily to Na^+ and K^+ (Table III). However, kainate receptors recover slowly following glutamate-induced desensitization (20-fold slower than AMPA receptors; ~2000 ms), and some kainate receptors (GluR5 homomers) have very small single-channel conductances (as low as 0.2 pS). As with AMPA receptors, a range of single channel conductances has been measured depending on the exact subunit composition of the kainate receptor complex studied.

NMDA Receptor Physiology

NMDA receptors possess a number of properties unique among the iGluRs. They are highly permeable to Ca^{2+} ions, have much slower activation kinetics, and remain open much longer than either AMPA or kainate receptors (Table III). Although glutamate binding is sufficient to open AMPA or kainate receptors, three separate events must occur for NMDA receptor activation—the binding of glutamate, the binding of the coagonist glycine, and a large enough membrane depolarization to remove Mg^{2+} ions that at resting membrane potentials enter and block the channel pore (Table II). This dual requirement for ligand binding and membrane depolarization allows NMDA receptors to act as "coincidence detectors" of simultaneous presynaptic and postsynaptic activity—presynaptic activity represented by glutamate present in the synaptic cleft and postsynaptic activity reflected by membrane depolarization. Since both AMPA and NMDA receptors colocalize at excitatory synapses, AMPA receptor activation is often critical for activation of synaptic NMDA receptors. Concurrent or repetitive glutamate release in conjunction with AMPA receptor activation can depolarize the postsynaptic cell to a level at which the Mg^{2+} block of NMDA receptors is lifted, thereby allowing Ca^{2+} influx through NMDA receptors into the postsynaptic cell.

Tight regulation of NMDA receptor activation is essential for brain function. Under normal physiological conditions, Ca^{2+} influx through NMDA channels triggers intracellular pathways that alter synaptic efficacy. Such synaptic plasticity modifies neural circuits during learning and memory. Excess Ca^{2+} influx through NMDA receptors causes neurotoxic effects (termed excitotoxicity) that contribute to neuron loss in stroke, epilepsy, and neurodegenerative diseases. Like AMPA and kainate receptors, different subunit combinations lead to differences in channel properties. Specifically, NR2B-containing channels are open much longer than NR2A-containing channels, resulting in a prolonged influx of Ca^{2+} ions. The more recently identified NR3 subunits are believed to attenuate NMDA receptor responses by decreasing single-channel conductance and lower Ca^{2+} permeability.

Summary

iGluRs are the major excitatory neurotransmitter receptor in the mammalian central nervous system. They comprise a diverse family of ligand-gated ion channels that flux cations across the plasma membrane in response to glutamate binding. All iGluRs share similar structural features including oligomeric assembly from four subunits. Three major subtypes of iGluR are expressed in the brain—AMPA receptors, kainate receptors, and NMDA receptors—each with separate sets of subunits, unique pharmacologies, and distinct channel properties. Functionally, iGluRs conduct synaptic transmission and play a central role in synaptic plasticity, neural development, and neurologic disease.

See Also the Following Articles

Glutamate Receptors, Metabotropic • Ligand-Operated Membrane Channels: Calcium (Glutamate)

Glossary

agonists/antagonists Pharmacological agents that activate/inhibit receptor activation.

alternative splicing The generation of multiple mRNAs from a single gene by the combination of different sets of exons during mRNA processing.

coincidence detection Concurrent postsynaptic membrane depolarization (that removes Mg^{2+} block of NMDA receptors) and presynaptic glutamate release (that binds to and gates NMDA receptors) that is required for full NMDA receptor activation.

excitotoxicity Neuronal cell death due to an inappropriate or extremely strong activation of iGluRs.

synaptic plasticity Long-lasting changes in synaptic responses following repeated stimulation of excitatory synapses that lead to either stronger excitatory postsynaptic currents (long-term potentiation) or weaker excitatory postsynaptic currents (long-term depression) often by modulating the number or properties of postsynaptic AMPA receptors.

Further Reading

Aidley, D. J., and Stanfield, P. R. (1996). *Ion Channels Molecules in Motion.* Cambridge University Press, United Kingdom.

Armstrong, N., Sun, Y., Chen, G. Q., and Gouaux, E. (1998). Structure of a glutamate-receptor ligand-binding core complex with kainate. *Nature* **395**, 913–917.

Dingledine, R., Borges, K., Bowie, D., and Traynelis, S. F. (1999). The glutamate receptor ion channels. *Pharmacol. Rev.* **51**, 7–61.

Hammond, C. (2001). *Cellular and Molecular Neurobiology.* 2nd edition, Academic Press, London.

Hille, B. (2001). *Ionic Channels and Excitable Membranes*, 3rd edition, Sinauer Associates, Sunderland, MA.

Johnston, D., and Wu, S. M. (1997). *Foundations of Cellular Neurophysiology*. The MIT Press, London.

Kuner, T., Seeburg, P. H., and Guy, H. R. (2003). A common architecture for K^+ channels and ionotropic glutamate receptors? *Trends Neurosci.* **26**, 27–32.

Madden, D. R. (2002). The structure and function of glutamate receptor ion channels. *Nat. Rev. Neurosci.* **3**, 91–101.

Biography

Michael D. Ehlers is Assistant Professor of Neurobiology at Duke University. His research focuses on the interface between neuronal cell biology and the plasticity of neural circuits, with emphasis on protein trafficking mechanisms in dendrites. He holds an M.D. and a Ph.D. from the Johns Hopkins University School of Medicine, where he also conducted postdoctoral research. He is the recipient of numerous awards in neuroscience and is a scholar of the Ruth K. Broad Foundation.

Glutamate Receptors, Metabotropic

P. Jeffrey Conn
Vanderbilt University Medical Center, Nashville, Tennessee, USA

In addition to eliciting fast excitatory synaptic responses, the neurotransmitter glutamate can modulate neuronal excitability, synaptic transmission, and other cell functions by activation of a family of G protein-coupled receptors termed metabotropic glutamate (mGlu) receptors. Because of the ubiquitous distribution of glutamatergic synapses and the broad range of functions of the mGlu receptors, members of this receptor family participate in a broad range of functions of the central nervous system.

Fast Synaptic Transmission and Neuromodulation in the Central Nervous System

The majority of connections that make up a neural network in the mammalian central nervous system are synaptic connections in which a neurotransmitter released from the presynaptic neuron activates postsynaptic receptors that are neurotransmitter-gated ion channels. Opening of these ion channels, results in either excitation or inhibition of a receptive neuron, a process known as fast excitatory and inhibitory synaptic transmission. Normal function of the central nervous system requires a delicate balance between excitatory and inhibitory transmission. In mammalian brain, two major neurotransmitters are responsible for most fast inhibitory and excitatory synaptic responses. Gamma-aminobutyric acid (GABA) is the principal inhibitory neurotransmitter whereas the amino acid glutamate is the primary excitatory neurotransmitter. Transmission through a neuronal circuit can be fine-tuned or regulated by activation of another class of receptor that couples to activation of second messenger systems and various biochemical processes through GTP-binding proteins. This form of synaptic transmission is often referred to as slow synaptic transmission or neuromodulation to differentiate it from fast excitatory and inhibitory transmission.

Fast Excitatory and Neuromodulatory Actions of Glutamate

As the primary fast excitatory neurotransmitter, glutamate plays an important role in virtually all major functions of the CNS. Traditionally, the actions of glutamate were thought to be mediated exclusively by activation of glutamate-gated cation channels termed ionotropic-glutamate receptors (iGluRs). Fine tuning or modulation of transmission through glutamatergic circuits was thought to require neuromodulators from extrinsic afferents such as dopamine, acetylcholine, serotonin, and norepinephrine that activate GTP-binding protein (G protein)-linked receptors (GPCRs). However, in the mid-1980s, evidence for the existence of glutamate receptors directly coupled to second-messenger systems through G proteins began to appear with the discovery of glutamate receptors coupled to activation of phosphoinositide hydrolysis. Since that time, it has become clear that glutamate activates a large family of receptors, termed metabotropic glutamate (mGlu) receptors, which signal by coupling to GTP-binding proteins.

The discovery of mGlu receptors dramatically altered the traditional view of glutamatergic neurotransmission since activation of mGlu receptors can modulate activity in glutamatergic circuits in a manner previously associated only with neuromodulators from nonglutamatergic afferents. However, unlike receptors for monoamines and other neuromodulators, the mGlu receptors provide a mechanism by which glutamate can modulate or fine tune activity at the same synapses at which it elicits fast synaptic responses. Because of the ubiquitous distribution of glutamatergic synapses, mGlu receptors participate in a wide variety of functions of the CNS.

Eight mGlu Receptor Subtypes

Eight mGlu receptor subtypes have been identified and placed into three major groups based on structural, functional, and pharmacological properties. A major breakthrough in the understanding of mGlu receptors occurred in 1991 when groups led by Shigetada Nakanishi at Kyoto University in Japan and by Eileen Mulvihill and F.S. Hagen at ZymoGenetics, Inc., in Seattle, Washington independently cloned the first gene encoding an mGlu receptor. The predicted topology of this receptor, based on its deduced amino acid sequence, suggests that this receptor is similar to β-adrenergic receptors and other G protein-coupled receptors in that it contains seven predicted transmembrane-spanning domains. However, the primary structure of this receptor revealed no sequence homology with other G protein-coupled receptors, suggesting that it was a member of a new receptor gene family. Moreover, the mGlu receptor is distinct from members of the β-adrenergic receptor family in that it contains a large extracellular N-terminal domain and a large intracellular carboxy terminal tail. Structure–function studies performed since the initial cloning suggest that the extracellular N-terminal domain of mGlu receptors is made up of two globular domains with a hinge region. This forms a clam shell-shaped structure with the glutamate binding site between the two globular domains (see Figure 1). Evidence suggests that when glutamate binds, the globular domains close into a stable conformation with glutamate inside.

After cloning of the first mGlu receptor, a search for related cDNA resulted in the isolation of seven other genes encoding different mGlu receptor subtypes. These receptors are named mGlu1 through mGlu8. Also, several alternatively spliced forms or structural variants have been isolated for many of the cloned mGlu receptors. These include splice variants for mGlu1 (mGlu1a–1d), mGlu4 (mGlu4a and 4b), mGlu5 (mGlu5a and b), mGlu7 (mGlu7a and b) and mGlu8 (mGlu8a and b). Thus, it is now clear that there is tremendous diversity within the mGlu receptor family.

The cloned mGlu receptors have been classified into three major groups based on sequence homology, pharmacological properties, and coupling to different second-messenger pathways. Group I includes mGlu1 and mGlu5, group II, mGlu2 and mGlu3, and group III, all the others. mGlu receptors of the same group show ~70% sequence identity whereas between groups this percentage falls to ~45% (Figure 2) Group I mGlu receptors preferentially couple to activation of the $G_{q/11}$ G proteins and activate phosphoinositide hydrolysis as a major signaling mechanism. In contrast, group II and group III mGlu receptors preferentially couple to $G_{i/o}$ and inhibition of adenylyl cyclase. Members of each group have a unique pharmacological profile and can be selectively activated by specific agonists that have no effects on members of the other groups of mGlu receptors. Also, in recent years, progress has been made in developing drugs that differentiate between members of a single group. These drugs are having a major impact on the understanding of the physiological roles and pharmacological properties of the different mGlu receptor subtypes.

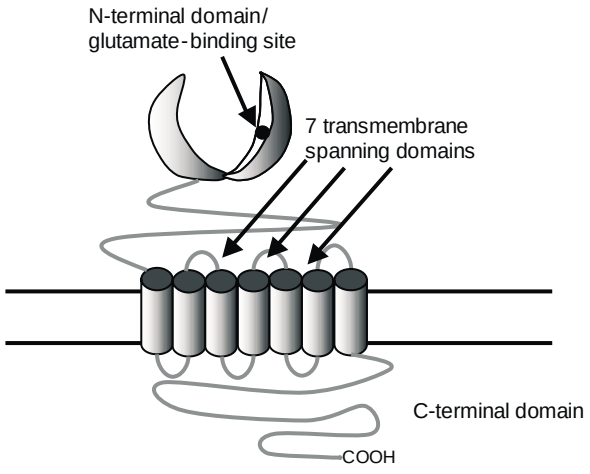

FIGURE 1 Schematic representation of an mGlu receptor. The mGlu receptors contain a large extracellular N-terminal domain, seven-transmembrane-spanning regions and an intracellular carboxy terminal domain. Glutamate binds in the large extracellular domain.

mGlu Receptors Play Diverse Roles in Regulating Neuronal Excitability and Synaptic Transmission

Anatomical studies using probes that specifically interact with individual mGlu receptor subtypes, coupled with electrophysiological studies have revealed that each of the individual mGlu receptor subtypes is differentially localized in different brain regions where they play a number of important physiological roles. While the specific mGlu receptor subtype involved in mediating a given effect varies in different brain regions, some generalizations can be made regarding the major roles of different groups of mGlu receptors. Elucidation of these roles of mGlu receptors suggests that specific agonists and antagonists of specific mGlu receptor subtypes could subtly alter transmission in glutamatergic circuits in a way that would provide a therapeutic benefit without eliciting the side effects commonly associated with drugs that interact with members of the ionotropic glutamate receptor family.

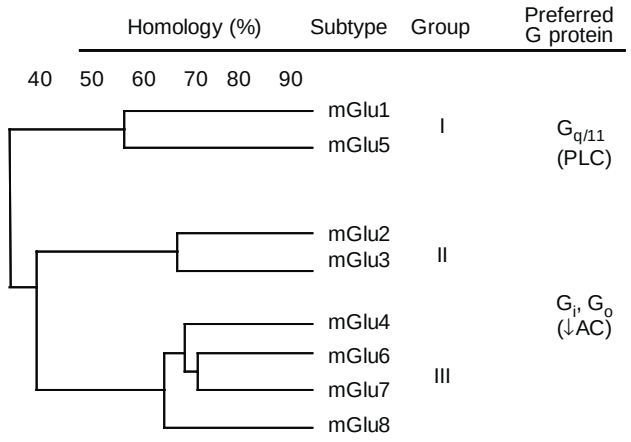

FIGURE 2 Dendrogram and classification of the members of the mGlu receptor family. The mGlu receptors are divided into three major groups, based on sequence homology, pharmacological profile, and second-messenger coupling.

One of the most common physiological functions of mGlu receptors, which is seen throughout the CNS, is as autoreceptors present at presynaptic terminals at glutamatergic synapses. Activation of these presynaptic receptors by glutamate released from the presynaptic neuron results in a reduction of glutamate release at that synapse. It is likely that this provides a negative feedback mechanism for tightly controlling transmission at glutamatergic synapses. This presynaptic function of mGlu receptors is usually subserved by a group II mGlu receptor or by one of the group III mGlu receptors (typically mGlu receptor 4, 7, or 8). While multiple mGlu receptor subtypes can serve this role, the specific mGlu receptor subtype(s) involved varies from synapse to synapse. mGlu receptors also exist postsynaptically where they play an important role in regulating cell excitability. The most common postsynaptic effect of mGlu receptor activation is induction of an increase in neuronal excitability. Again, the specific mGlu receptor subtype involved varies from synapse to synapse but typically involves one of the group I mGlu receptors (mGlu1 or mGlu5). In some cells, activation of postsynaptic mGlu receptors can lead to hyperpolarization and a reduction in neuronal excitability. This has been observed for both group I and group II mGlu receptors. Finally, a commonly observed effect of mGlu receptor activation is regulation of transmission at inhibitory GABAergic synapses. Thus, mGlu receptors are often localized at presynaptic GABAergic terminals where they regulate GABA release. In addition to these effects on neuronal function, mGlu receptors can also exist on glial cells. While mGlu receptors can have a number of effects on glial function, Ferdinando Nicoletti and co-workers have reported a series of studies revealing that one important effect of mGlu receptors in glia is induction of release of neuroprotective factors that reduce excitotoxicity and protect neurons from damage. The most prominent mGlu receptors in glia are mGlu3 and mGlu5.

Therapeutic Potential of mGlu Receptor Ligands

In recent years, major efforts have been made to develop new therapeutic agents for disorders of the central nervous system by targeting glutamatergic synapses in the circuits impacted by a particular disease. A potential advantage of developing new therapeutic agents that specifically target mGlu receptors is that it provides a rational approach for subtle fine-tuning of activity at synapses that have been identified as playing an important role in a given disorder. Because of the wide diversity, heterogeneous distribution, and diverse physiological roles of mGlu receptor subtypes, the opportunity exists for developing therapeutic agents that selectively interact with mGlu receptors involved in only one or a limited number of CNS functions. Such drugs could have a dramatic impact on development of novel treatment strategies for a variety of psychiatric and neurological disorders. Because of this, a great deal of effort has been focused on developing small molecules that selectively activate or inhibit specific mGlu receptor subtypes. One of the most important and earliest breakthroughs in developing drugs that target the mGlu receptors was development of highly selective agonists for the group II mGlu receptors by Jim Monn, Darryle Schoepp, and their coworkers at Eli Lilly. The first of these mGlu receptor agonists is now in clinical trials and preliminary proof of concept studies have been presented that suggest that this compound may have clinical efficacy for treatment of generalized anxiety disorder and panic attack. This represents a major breakthrough in the mGlu receptor field. A number of other compounds that selectively block or activate mGlu receptors have been developed by several drug companies and are now in preclinical stages of development.

See Also the Following Articles

$GABA_B$ Receptor • Glutamate Receptors, Ionotropic • Ligand-Operated Membrane Channels: Calcium (Glutamate) • Ligand-Operated Membrane Channels: GABA

Glossary

GABA An amino acid that serves as the primary inhibitory neurotransmitter in the central nervous system.

glutamate An amino acid that serves metabolic functions and as a component of proteins and polypeptides in all cells. In addition,

glutamate serves as a major excitatory neurotransmitter in the central nervous system.

G protein Membrane associated protein that interacts with a particular class of cell-surface receptor and participates in receptor-induced activation of intracellular enzymes, ion channels, and other signaling molecules. Also known as GTP-binding protein.

Further Reading

Alagarsamy, S., Sorensen, S. D., and Conn, P. J. (2001). Coordinate regulation of metabotropic glutamate receptors. *Curr. Opin. Neurobiol.* **11**, 357–362.

Conn, P. J., and Pin, J. P. (1997). Pharmacology and functions of metabotropic glutamate receptors. *Annu. Rev. Pharmacol. Toxicol.* **37**, 205–237.

Coutinho, V., and Knopfel, T. (2002). Metabotropic glutamate receptors: Electrical and chemical signaling properties. *Neuroscientist* **8**, 551–561.

Dingledine, R., Barges, K., Bowie, D., and Traynelis, S. F. (1999). The glutamate receptor ion channels. *Pharmacol. Rev.* **51**, 7–61.

Fagni, L., Chavis, P., Ango, F., and Bockaert, J. (2000). Complex interactions between mGluRs, intracellular Ca^{2+} stores and ion channels in neurons. *Trends Neurosci.* **23**, 2380–2388.

Pin, J. P., and Acher, F. (2002). The metabotropic glutamate receptors: Structure, activation mechanism and pharmacology. *Curr. Drug Target CNS Neurol. Disord.* **1**, 297–317.

Schoepp, D. D. (2001). Unveiling the functions of presynaptic metabotropic glutamate receptors in the central nervous system. *J. Pharmacol. Exp. Ther.* **299**, 12–20.

Schoepp, D. D., Jane, D. E., and Monn, J. A. (1999). Pharmacological agents acting at subtypes of metabotropic glutamate receptors. *Neuropharmacology* **38**, 1431–1476.

Biography

P. Jeffrey Conn is a Professor in the Department of Pharmacology and Director of the Program in Translational Pharmacology at Vanderbilt University Medical Center in Nashville, Tennessee. Prior to his current position, he was Head of the Department of Neuroscience at Merck and Company and Professor of Pharmacology at Emory University. He holds a Ph.D. in Pharmacology from Vanderbilt University and received his postdoctoral training at Yale University. Dr. Conn has played a major role in determining the functional roles of metabotropic glutamate receptors and in development of small molecules that interact with members of this receptor family.

Glutathione Peroxidases

Fulvio Ursini and Matilde Maiorino
University of Padova, Padova, Italy

Glutathione peroxidases (GPxs) form a superfamily of oxidoreductases distributed in all living domains. They may contain cysteine or selenocysteine as part of the catalytic site. The cysteine homologues prevail in prokaryotes, yeasts, and land plants, while selenocysteine-containing enzymes have been considered peculiar of mammals. This view has been expanded since selenium peroxidases have been recently identified in two distinct poxviruses: the platyhelminth *Schistosoma mansoni* and the green alga *Chlamidomonas rheinhardtii*.

Mammalian Se-GPxs are four different gene products, namely cGPx (or GPx-1), GI-GPx (or GPx-2), pGPx (or GPX-3), and PHGPx (or GPx-4), in humans mapping to chromosome 3, 14, 5, and 19, respectively. The typical reaction of GPxs is the reduction of a hydroperoxide coupled to the oxidation of two thiols. The most characteristic substrates are hydrogen peroxides (H_2O_2) and glutathione (GSH), which undergo a two-electron redox transition to water and glutathione disulfide (GSSG), respectively. Since reduction of hydroperoxides prevents the formation of reactive oxygen species (ROS), which have a strong pro-oxidant character, an antioxidant role has been classically ascribed to GPxs. The cysteine-containing homologues have an order of magnitude lower efficiency in catalyzing a peroxidatic cycle than that of the corresponding selenoperoxidases, therefore posing the question of their actual function as efficient hydroperoxide detoxifying enzymes.

History

The first glutathione peroxidase ("classical" or "cytosolic" GPx, cGPx) was discovered in 1957 by Mills as an enzymatic activity that protects hemoglobin in red blood cells from oxidative denaturation. At the time, the notion that an enzyme catalyzing the reduction of hydrogen peroxide at the expense of GSH could be physiologically relevant was not immediately accepted, since heme peroxidases (including catalase) were considered much more efficient. The work by Choen and Hochstein in 1963 disclosed the real physiological value of this enzyme, showing that H_2O_2 does not denature hemoglobin until red blood cells, that contain catalase, are fully depleted of GSH. Kinetic analysis and subcellular localization of enzymes, eventually clarified the issue, showing the glutathione peroxidase is the most efficient hydroperoxide removing system in almost every cell.

In 1972 the groups of Rotruck in Wisconsin and Flohé in Germany provided evidence that cGPx contains one mole of selenium per mole of homotetrameric enzyme. The selenium moiety was later identified as a selenocysteine. This discovery led to the formulation of the dogma of the antioxidant effect of selenium. This view is now considered quite limited owing the discovery of both, other selenoenzymes and functions of GPxs, different from antioxidant protection.

The second GPx, "phospholipid hydroperoxide glutathione peroxidase" (PHGPx), was first described as a monomeric enzyme, distinct from cGPx in 1982. Subsequently, the list of the members of the GPxs family grew with the discovery of the tetrameric "plasma" pGPx in 1987 and of the gene of the "gastro-intestinal" GI-GPx in 1993.

Enzymology and Kinetics

cGPx, GI-GPx, and pGPx are homotetrameric proteins and rather similar to one another (overall homology $>80\%$). PHGPx is monomeric and presents an overall homology $< 35\%$ when compared to the monomer of tetrameric enzymes. The X-ray structure has been elucidated only for cGPx, and the conformation of the other GPxs has been obtained by molecular modeling based on the cGPx structure.

A relevant feature of the superfamily of GPxs is the catalytic triad, which is highly conserved in all members, including the cysteine homologues. This is made by loops rather distant in primary structure, contains one selenocysteine, one tryptophan, and one glutamine residue, and has been functionally proved by site directed mutagenesis. The catalytic triad of Gpx1 and PHGPx is reported in Figure 1. The tryptophan and the glutamine residue are assumed to "activate" by hydrogen bonding the dissociated selenol. However, it could also be possible that the residues "activate" the hydroperoxide, thus facilitating the nucleophilic

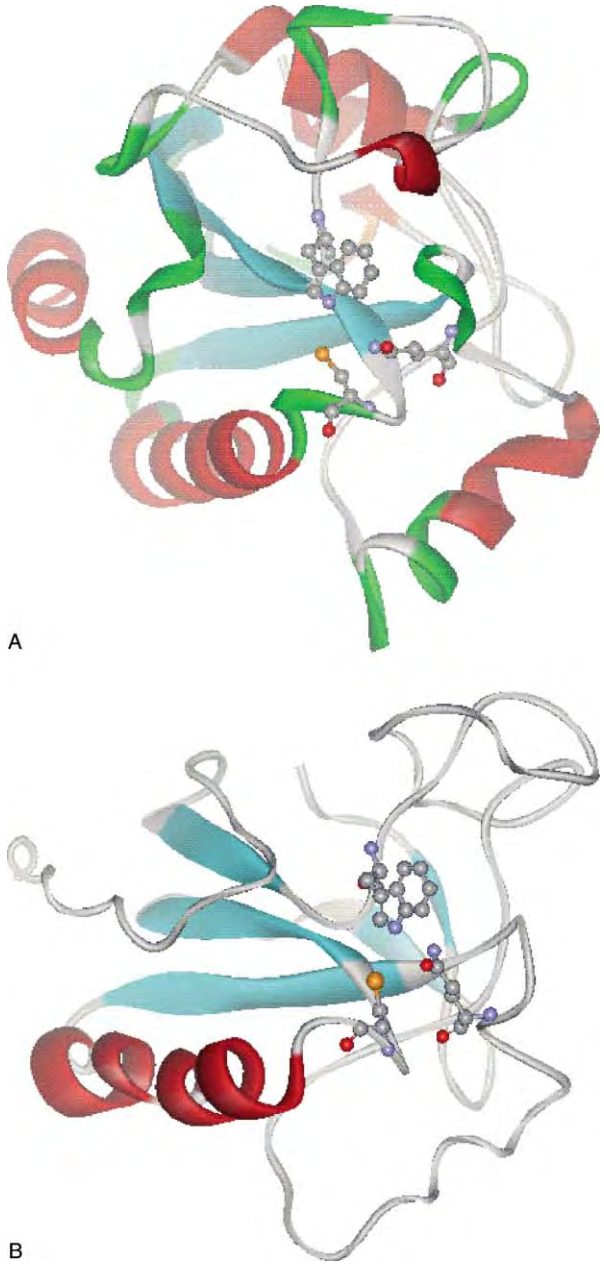

FIGURE 1 Structure of catalytic site of glutathione peroxidases, showing catalytic selenocysteine, tryptophan and glutamine. The structure of Gpx1 (A) has been constructed from crystallographic data. The structure of PHGPx (B) has been calculated by homology modeling and energy minimization.

displacement leading to oxidation of selenol, the first step of the catalytic cycle.

Kinetic analysis of the peroxidase reaction has been carried out on cGPx and PHGPx. During the catalytic cycle, the selenol at the active site is oxidized by the hydroperoxide. The product is assumed a selenenic acid derivative (Se-OH), although, due to the extreme reactivity of the group, a chemical evidence for the nature of the first oxidized species is so far missing. This intermediate reacts with a suitable thiol (usually GSH) to produce a mixed selenadisulfide (Se-SG), the nature of which has been positively determined by mass spectrometry. The selenadisulfide is then reduced by another thiol (usually GSH) to produce the leaving disulfide (usually GSSG) and the native, reduced, form of the enzyme.

This reaction mechanism is described by ping-pong kinetics typical of an enzyme substitution mechanism, following the simplified Dalziel equation:

$$\frac{[E_0]}{V} = \frac{\phi_1}{[\mathrm{ROOH}]} + \frac{\phi_2}{[\mathrm{GSH}]}$$

where ϕ_1 is the reciprocal of the rate constant for the reduction of the hydroperoxide and ϕ_2 the empirical coefficient accounting for the sum of the two steps of GSH oxidation.

The corollary of this kinetic mechanism, where reactions at the active site are much faster than the enzyme substrate complex formation, is that V_{max} and K_m remain undefined, and apparent kinetic constants for one substrate are dependent on the concentration of the other substrate.

The specificity for the oxidizing substrate is maximal in cGPx that reduces only hydrogen peroxide and some small organic hydroperoxides, and minimal in PHGPx that reduces large lipophilic substrates such as hydroperoxide derivatives of phospholipids and cholesterol esters as well. Intermediate specificity, although closer to that of cGPx, has been observed for pGPx. No kinetic data are available for GI-GPx, which has never been isolated as a protein, although specificity similar to that of cGPx can be assumed from structure homology. The different specificity for oxidizing substrate is accounted for by the active site that in tetrameric enzymes is located in the valley among subunits while in PHGPx is at the center of an exposed lipophilic depression.

In addition, the specificity for the donor substrate is maximal for cGPx and minimal for PHGPx. This has been attributed to the mutation/deletion of four Arginine residues surrounding the active site and alleged to be involved in binding of GSH. According to this observation, the specificity of GPxs toward GSH should decline in the following order: cGPx > GI-GPx > pGPx > PHGPx. Therefore the family of GPxs appears diversified in function so that the classification as *glutathione* peroxidases may be too restrictive. For PHGPx, although the interaction with GSH is energetically favored by the formation of hydrogen bonding with lysines in the proximity of the active site, the specificity for this substrate is low and this turned out definitely relevant for the recently disclosed role of the protein in spermatogenesis.

Biosynthesis of Selenoperoxidases

Selenocysteine is a rare but widely distributed amino acid in the living kingdom, and selenoproteins containing this amino acid as a part of the active site have been described in prokarya, archaea, and eukarya. In mammals, besides GPxs, at least 16 other selenocysteine-containing proteins have been described.

The elucidation of selenocysteine biosynthesis and its cotranslational incorporation into proteins occurred in the last two decades by elegant studies carried out independently by Böck, Berry, Stadtman, and co-workers. These studies followed the discovery of an in-frame TGA codon in the cDNA of *gpx-1* by Chambers and co-workers. The process represents a special case in protein biosynthesis, being peculiar in several respects and exhibiting several common features among the different organisms.

1. Among all the organisms of the living kingdom, selenocysteine biosynthesis occurs from serine, while this amino acid is bound to the $tRNA^{Sec}$ (the *SelC* gene product). This is structurally different from the canonical tRNA for serine. The conversion of serine into selenocysteine requires SelA (the selenocysteine synthase) and selenophosphate. The latter is produced from ATP and selenide by the specific synthetase SelD, a selenoprotein itself.

2. The use of an in-frame TGA for selenocysteine insertion is also peculiar and common to all the organisms. This triplet was formerly known just as "stop codon" in the nuclear genome. Therefore, a complex decoding mechanism has evolved to read TGA as selenocysteine insertion instead of protein termination.

3. Decoding requires a hairpin structure called selenocysteine inserting sequence (SECIS) and proteins that recognize the SECIS acting as elongation factors. SECIS location differs among the different organisms, being located immediately downstream the stop codon in prokarya or in the 3′ UTR in archaea and eukarya. In prokarya, one protein acts both as SECIS binding protein and elongation factor (the *SelB* gene product), while in archea and eukarya two distinct proteins are involved in this process. In eukarya (mammals), these are the specialized elongation factors mSelB/EFsec and SBP-2, which bind both the SECIS elements and mSelB/EF.

In condition of limited selenium supply, eukaryotic selenoproteins are differentially expressed, a phenomenon referred to as "selenoprotein hierarchy." The mRNA of cGPx, and the level of expressed protein, decreases under conditions of low availability of selenium, while GI-GPx and PHGPx results remarkably stable. Although the underlying mechanism is far from being clear, the affinity of SBP2 for the different SECIS seems to play a key role, but phenomena such as tissue levels of SB2, tissue specific accumulation of selenium, and tissue specific transcription and mRNA stability might also contribute. The priority of the synthesis of GI-GPx and PHGPx over cGPx under limited conditions of selenium supply indirectly suggests a more relevant biological function. Moreover, in a selenium status where other peroxidases are saturated, cGPx keeps increasing, an evidence that led to speculations about a "selenium deposit" role for cGPx.

Biological Functions

The common catalytic mechanism suggests a similar function for GPxs, although in different cell compartments and with different specificity toward peroxidic and reducing substrate. On the other hand, inverse genetics experiments showed an unambiguous antioxidant function only for cGPx.

cGPX

cGPx is a widely distributed, intracellular protein. The cGPx (−/−) mouse develops and grows normally, unless challenged by an oxidative stress induced by redox-cycling compounds or activation of an oxidative burst of macrophages. These challenges mimic the pathological condition of the inadequate antioxidant protection seen in favism and related diseases. Moreover, in (−/−) mouse, a nonvirulent strain of Coxsackie's virus mutates into a virulent form. Thus, silencing cGPx appears as a perfect model of the Kashan disease (a syndrome due to severe selenium deficiency) where, due to the oxidizing intracellular environment produced, a nonvirulent virus becomes virulent, apparently in relation to higher mutation rate. The pathophysiological feature of cGPx knockout is independent of selenium status, suggesting that other selenoperoxidases are unable to substitute for the antioxidant function of cGPx.

pGPX

pGPx is an extracellular protein secreted by organs such as kidney or ciliar body. It has been suggested to reduce lipid hydroperoxides in circulating lipoproteins, thus playing a role in protecting against the oxidation claimed to be involved in atherogenesis. Against this hypothesis argues the evidence that reducing equivalents (either from GSH or thioredoxin) are extremely limited in plasma and that the enzyme is not active on cholesterol ester hydroperoxides, a major lipid oxidation product in LDL. A possible, although purely speculative, role could be seen in the regulation of the flux of oxidant produced by phagocytes and thus in the control of inflammatory response.

Indeed, no information from inverse genetics exists for pGPx.

GI-GPx

A reasonable function of GI-GPx is suggested by the localization in the digestive tract. Since traces of lipid hydroperoxides, within food or produced during gastric digestion, can be detected in postprandial plasma, the peroxidase could work in minimizing the absorption of harmful lipid hydroperoxides. However, this appealing hypothesis has been neither fully confirmed nor excluded so far.

The GI-GPx (−/−) mouse has a normal phenotype, while the double knockout (GI-GPx and cGPx) shows major alterations of the intestinal mucosa. These data and peculiar localization allow speculation on a possible function of GI-GPx acting synergically with cGPx in regulating proliferation, differentiation, and apoptosis in cells of intestinal villi.

PHGPx

PHGPx has been discovered as a ubiquitous, intracellular antioxidant enzyme. By reducing all types of lipid hydroperoxide in membranes, PHGPx prevents lipid peroxidation initiated *in vitro* by homolytic or heterolytic decomposition of these compounds. This reaction is synergic with the reduction by vitamin E of lipid hydroperoxy radicals propagating lipid peroxidation. Thus, a complete and fully efficient antioxidant system is accomplished by a one-electron reduction of hydroperoxy radicals (chain-breaking reaction, accomplished by vitamin E) followed by a two-electron reduction of lipid hydroperoxides (peroxidolytic reaction, accomplished by PHGPx). This mechanism accounts for by the synergism in antioxidant protection between vitamin E and selenium, evidenced by nutritional studies.

More recently, a major role in spermatogenesis has been documented. PHGPx appears involved in both the formation of the keratinous material embedding the mitochondria of the spermatozoon, a structure called mitochondrial capsule, and in chromatin condensation. PHGPx is orders of magnitude more abundant in male germ cells with respect to other somatic cells, where different mRNAs are translated into proteins specifically addressed to the mitochondria or to the nucleus by organelle-specific sequences. Distinct transcripts are generated by alternative transcription of the gene. Furthermore, the expression of the individual PHGPx transcripts appears stage specific during spermatogenesis, mitochondria and cytosolic PHGPx peaking in round spermatids, and nuclear PHGPx in later stages of spermatogenesis, together with protamine expression. In the mitochondrial capsule, PHGPx is found as catalytically inactive protein cross-linked with other proteins, including PHGPx itself. The presence of inactive PHGPx as a major component of the mitochondrial capsule suggests a moonlighting from an active peroxidase to a structural element during sperm maturation. Several evidences indicate that this function switch is primed by GSH depletion and the capability of PHGPx to use alternative thiol substrates, including PHGPx itself. Mass spectrometry data showed that, the oxidized selenium moiety of PHGPx reacts with a specific surface cysteine of another PHGPx molecule. This accounts for the first elements of the cross-linked matrix. A similar mechanism thus leads to the copolymerization of other still undefined proteins, eventually leading to the formation of the capsule. By a similar mechanism, nuclear PHGPx results involved in chromatin condensation, when protamine thiols are used as donor substrate for the peroxidatic reaction.

A definitely relevant physiological role for PHGPx has been suggested by inverse genetics, since *gpx-4* revealed to be a vital gene. Furthermore, as a confirmation of a major role in spermatogenesis, PHGPx chimeric mice show mosaic testicular atrophy and abnormal sperm morphology.

The reason why PHGPx (−/−) mice are not vital cannot be reconciled with either the specific function in spermatogenesis or the other proposed functions, such as inhibiting lipoxygenases, stifling the nuclear factor κB, or controlling apoptosis, and implies additional and undisclosed functions of this gene product.

Future Perspectives

Mammalian cells contain four different selenium-dependent GPxs plus other cysteine-containing homologues. Only selenium-containing homologues are efficient peroxidases in principle, but an antioxidant function (related to reduction of hydroperoxides) has been unambiguously demonstrated by reverse genetics only for cGPx. Indeed, the major role of PHGPx in spermatogenesis appears the oxidation of protein thiols. Thus, the catalysis operated by the selenocysteine residue in PHGPx can be interpreted in considering the capability of the enzyme to address the oxidation potential of hydroperoxides toward specific protein thiols. The mechanisms of redox regulation of enzymes or nuclear factors are attracting more and more efforts by scientists, and it seems reasonable to suggest that specific redox transitions occurring in cells must undergo a kinetic more than a thermodynamic control. On this light, it is predictable that forthcoming studies will revisit the catalysis operated by the selenol moiety of some GPxs shifting from the antioxidant defense area to the control of redox-mediated processes.

See Also the Following Article

Selenoprotein Synthesis

Glossary

antioxidant A molecule or an enzymatic system that prevents or slows down a free radical oxidative chain reaction, by either preventing the formation of initiating radicals or reducing the concentration of propagating radicals.

glutathione A tripeptide (γ-glutamyl-cysteinyl-glycine) widely distributed, involved in antioxidant protection and regulation of the redox status of the cell.

kashan disease A cardiomyopathy described in a selenodeficient area of China.

mitochondrial capsule (of spermatozoa) A keratinous-like structure containing large amounts of disulfides, present in the mid-piece of spermatozoa and embedding mitochondria, fibers, and centriole.

peroxidase An oxidoreductase catalyzing the reduction of a hydroperoxide to the corresponding alcohol and water by using the reducing potential of a specific substrate.

peroxidation Free-radical-driven oxidative degradation of fatty acids (mainly polyunsaturated) producing lipid hydroperoxides and their degradation products.

selenium A nutritionally essential oligoelement inserted in specific proteins as a selenocysteine that undergoes redox transitions.

thioredoxin A pleiotropic, low-molecular-weight protein containing a redox sensitive thiol/disulfide couple.

Further Reading

Atkins, J. F., and Gesteland, R. F. (2000). The twenty-first amino acid. *Nature* **407**, 463–465.

Brigelius-Flohé, R. (1999). Tissue-specific functions of individual glutathione peroxidases. *Free Radic. Biol. Med.* **27**, 951–965.

Flohé, L., and Brigelius-Flohé, R. (2001). Selenoproteins of the glutathione system. In *Selenium; its Molecular Biology and Role in Human Health* (D. L. Hatfield, ed.) pp. 157–178. Kluwer Academic, Norwell Massachusetts (USA).

Low, S. C., and Berry, M. J. (1996). Knowing when not to stop: selenocysteine incorporation in eukaryotes. *Trends Biochem. Sci.* **21**, 203–208.

Maiorino, M., Aumann, K.-D., Brigelius-Flohé, R., Doria, D., van Den Heuvel, J., McCarthy, J., Roveri, A., Ursini, F., and Flohé, L. (1995). Probing the presumed catalytic triad of selenium-containing peroxidases by mutational analysis of phospholipid hydroperoxide glutathione peroxidase (PHGPx). *Biolog. Chem. Hoppe-Seyler* **376**, 651–660.

Stadtman, T. C. (1996). Selenocysteine. *Annu. Rev. Biochem.* **65**, 83–100.

Ursini, F., Maiorino, M., Brigelius-Flohé, R., Aumann, K. D., Roveri, A., Schomburg, D., and Flohé, L. (1996). Diversity of glutathione peroxidases. *Methods in Enzymol.* **252**, 38–53.

Ursini, F., Heim, S., Kiess, M., Maiorino, M., Roveri, A., Wissing, J., and Flohé, L. (1999). Dual function of the selenoprotein PHGPx during sperm maturation. *Science* **285**, 1393–1396.

Biography

Fulvio Ursini holds an M.D. degree from the University of Padova and serves as full Professor of Biochemistry at the same University. His main research fields are: (1) biochemistry of selenium-dependent peroxidases; (2) mechanism of antioxidant effect of natural compounds and role of antioxidants on cellular functions; (3) lipid peroxidation and its impact on molecular mechanism of disease; and (4) mechanism of protein thiol oxidation during cell differentiation.

Matilde Maiorino is Associate Professor of Biochemistry at the School of Medicine of the University of Padova. She contributed to the discovery of PHGPx and to its functional characterization. In 1997 she was awarded the Klaus Schwarz Commemorative Medal for her research in trace elements. Her current interest is focused on molecular biology of Se-peroxidases and on the impact of selenium on male fertility.

Glycation

Suzanne R. Thorpe and John W. Baynes
University of South Carolina, Columbia, South Carolina, USA

Glycation is a term describing the adduction of a carbohydrate to another biomolecule, such as a protein or lipid. Glycation may occur either enzymatically or nonenzymatically. The common term for enzymatic glycation is glycosylation, e.g., formation of a glycosidic bond using a sugar nucleotide donor during synthesis of glycoproteins. The terms nonenzymatic glycation, nonenzymatic glycosylation, or glycation (without a modifier) are commonly used in reference to direct chemical reactions of reducing sugars with proteins, illustrated by the reaction of glucose with lysine residues in protein to form a ketoamine (Amadori) adduct (Figure 1). Glucation, fructation, ribation, etc., are used in reference to glycation by specific sugars.

Although glycation is a reversible reaction, it is considered a first step in the Maillard or browning reaction, which leads to irreversible chemical modification, browning, generation of fluorescence, and cross-linking of proteins during cooking, and in the body during aging and in disease. The irreversible adducts and cross-links in protein are known as advanced glycation end products (AGEs). Most AGEs are formed by a combination of glycation and oxidation reactions and are termed glycoxidation products. AGEs accumulate with age in long-lived extracellular proteins, such as collagen, and are also formed from glycolytic intermediates on shorter-lived intracellular proteins. Increased rates of formation of AGEs in tissue proteins during hyperglycemia and oxidative stress or inflammation are implicated in the pathophysiology of aging, and diabetes and other chronic diseases.

Glycation of Proteins in Blood

Glycated Hemoglobin

Interest in the Maillard reaction in biochemistry began with the identification of HbA_{Ic}, an anodic variant of adult hemoglobin (Hb), discovered during screening of diabetic patients. HbA_{Ic} contains glucose bound to the amino-terminal valine residues of the Hb β-chains. The glucose–valine adduct was characterized as an aminoketose or ketoamine (fructosevaline), formed by nonenzymatic reaction of glucose with protein (Figure 1). The high reactivity of the β-chain valine residues of Hb results from catalysis of the Amadori rearrangement by phosphate or 2,3-bisphosphoglycerate bound near these valine residues in the allosteric site regulating the oxygen affinity of Hb. The α-chain valines, which have similar exposure to solvent and the same low pK_a, but are not in the allosteric site, are only ~10% as glycated as the β-chain valines. HbA_{II} also has 66 lysine residues, but there are only about twice as many fructoselysine (FL) as fructosevaline residues in the protein. The more reactive lysines are adjacent to basic or acidic amino acid in the primary or three-dimensional structure of the protein, which either affect the nucleophilicity of the lysine amino group or catalyze the Amadori rearrangement. The primary sites of glycation of ribonuclease by glucose *in vitro* are at lysine residues in the active site. Glycation of some, but not all of these residues is catalyzed by phosphate and other anionic buffers that bind in the basic, RNA-binding region of the enzyme. Thus, glycation, although not as specific as enzymatic glycosylation of protein, is not a random modification of protein, but is affected by the pK_a of the amino acid, amino acid sequence, protein conformation, and ligand binding.

Clinical Significance of Glycated Hb

Assays of glycated Hb (GlcHb) are a powerful tool for the clinical management of diabetes. Glycation is a slow reaction. The rate of formation of HbA_{Ic} is ~0.1% of HbA_{II} per day at normal blood glucose concentration (5 mM), and is first order in glucose concentration. Since the red cell is long-lived (life span ~120 days) and is freely permeable to glucose, the mean extent of glycation of Hb varies with mean blood glucose concentration. The average percent glycation of Hb, ranges from 4 to 6% HbA_{Ic} in a control population, to 16% or higher in poorly controlled diabetic patients. Based on clinical studies, assays of percent HbA_{Ic} integrate the mean blood glucose concentration during the previous 4–6 weeks. These assays complement acute blood glucose measurements for assessment of long-term glycemic control in diabetes.

Assays for HbA_{Ic} use an anion exchange procedure that depends on the shift in pK_a of the protein, which occurs on glycation of the valine residues. Alternatively,

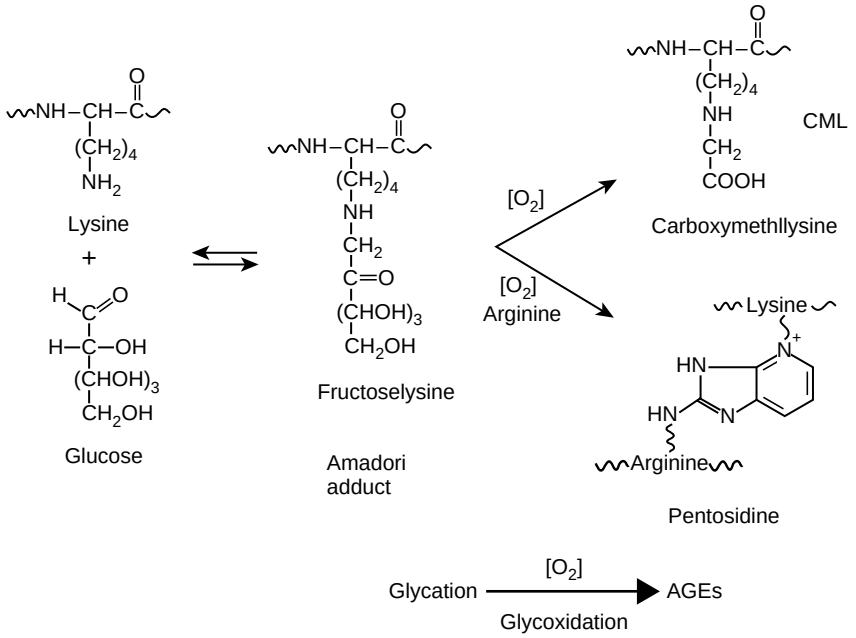

FIGURE 1 Pathway for glycation of protein. Glucose reacts reversibly with amino groups in protein, e.g., lysine, forming a Schiff base (not shown), which rearranges to the Amadori compound (ketoamine), fructoselysine. Oxidation of the Amadori compound is one route to formation of advanced glycation or glycoxidation end products, such as CML and pentosidine.

total GlcHb may be measured by an affinity chromatography assay that depends on interaction of Amadori adducts on the surface of the protein with phenylboronate resins; this assay measures primarily the glycation of lysine residues. While assays of HbA_{Ic} and GlcHb actually measure different aspects of GlcHb, the two assays yield similar quantitative results and correlate strongly with one another. Both the ion-exchange and affinity chromatography assays are available as mini-column kits and HPLC methods. Electrophoretic, nephelometric (immuno-turbidimetric), and ELISA assays are also used, but less commonly, for measurement of glycation of Hb and assessment of long-term glycemic control.

Glycation of Extracellular and Plasma Proteins

Glucose is ubiquitous in body fluids, and therefore all tissue proteins are subject to glycation. The steady-state extent of glycation of a protein depends on the inherent reactivity of the protein with glucose under physiological conditions, the protein's biological half-life or lifespan, and the ambient glucose concentration. The fractional glycation of lysine in lens proteins is ~40% that of skin collagen in humans, reflecting the lower glucose concentration in the lens, compared to extracellular fluids. Collagen accounts for about one-third of total body protein mass and is accessible by biopsy. Like glycation of Hb, the extent of glycation of skin collagen may be used as an index of very long-term hyperglycemia or glycative stress. In addition to Hb, other intracellular proteins are also subject to glycation, e.g., superoxide dismutase in the lens, alcohol dehydrogenase in the liver, and the actomyosin complex in muscle.

Assays for glycated plasma proteins, which have relatively short half-lives compared to hemoglobin or collagen, provide an index of intermediate-term blood glucose concentration, during the previous 7–10 days. In addition to ELISA and phenylboronate affinity chromatography assays for glycated albumin, total Amadori adducts on plasma proteins can be measured by the fructosamine assay. This assay measures the reduction of a tetrazolium dye by the Amadori compound on plasma proteins. The Amadori adduct has much stronger reducing activity than glucose at pH 10, so that the reducing activity of Amadori adducts on glycated plasma proteins can be measured without significant interference by blood glucose.

Glycation of Other Amino Acids and Biomolecules

Glucose appears to react only with primary amino groups on protein. However, Amadori compounds undergo facile rearrangement and oxidation reactions. They may rearrange nonoxidatively to form deoxyglucosones, regenerating free lysine, or undergo autoxidative decomposition to form glucosone. These dicarbonyl compounds react with the side chains of lysine, arginine, cysteine, histidine, and probably tryptophan residues, expanding the range of glycative damage to protein. Amadori adducts to phosphatidylethanolamine and

phosphatidylserine have also been measured in tissues. DNA undergoes glycation *in vitro*, although glycated DNA has not been identified *in vivo*, perhaps because of the involvement of the amino groups of nucleic acids in intrahelical hydrogen bonds and the shielding provided by histones and other nuclear proteins.

Reactivity of Glucose

The rate of reaction of a sugar with protein depends on the fraction of the sugar in the open-chain, aldehyde conformation. Glucose, among all sugars, exists to the greatest extent in the cyclic, hemiacetal conformation. It is therefore the least reactive in glycating proteins, in comparison to other hexoses, pentoses, ketoses, or phosphorylated metabolic intermediates. Another unique feature of glucose is that, although it is a reducing sugar and is readily oxidized, it is the least active among all sugars in oxidation or autoxidation (oxidation by molecular oxygen) reactions—again, because it exists largely in a hemiacetal rather than aldehyde conformation. In the Fehling and Benedict assays for reducing sugars, oxidation is promoted by strongly basic conditions that catalyze the enolization and isomerization of glucose. Its low reactivity with protein and its resistance to autoxidation was probably important in the evolutionary selection of glucose as blood sugar in mammals. Despite its chemical inertness, however, glucose does react with proteins at a measurable rate. Glycation occurs and advanced glycation end products (AGEs) accumulate on tissue proteins with age.

Advanced Glycation and Glycoxidation Reactions

Advanced Glycation

Food scientists learned early in the twenty-first century that glycation was one of the early steps in the Maillard or browning reaction of proteins during cooking, part of the process of caramelization that enhances the color, taste, aroma, and texture of cooked foods. The Maillard reaction also contributes to the loss in nutritional value of cooked foods, because of the chemical modification of the essential amino acids, lysine and arginine. When biomedical scientists discovered that hemoglobin was glycated *in vivo*, it was reasonable to speculate that advanced stages of the Maillard reaction should also proceed *in vivo*–the human body could be viewed, at one level, as a low-temperature oven (98.6°F) with a long cooking cycle (~80 years). The Maillard reaction was seen as a possible source of the brown color and fluorescence that develops with age in long-lived proteins, such as crystallins and collagens, and as a contributing factor in both the normal aging of tissue proteins and the acceleration of age-like pathology by hyperglycemia in diabetes.

More than 20 AGEs have now been detected in tissue proteins (Figure 2), including amines, amides, pyrroles, imidazolones, imidazolium salts, and several bicyclic heteroaromatic compounds. The first two AGEs to be identified *in vivo* were N^{ε}-(carboxymethyl)lysine (CML) and pentosidine. Because of their stability during acid hydrolysis of proteins, these compounds are still the most frequently measured AGEs. CML, which is quantitatively the most abundant AGE, is measured by GC/MS or ELISA. Although present at much lower concentration, pentosidine is highly fluorescent and is measured by HPLC with fluorescence detection. Other AGEs are measured less frequently because they are either present at lower concentrations in tissues or are labile to acid or base hydrolysis and must be measured following enzymatic digestion of proteins. The known AGEs are only trace components of proteins *in vivo*. Even in skin collagen and lens proteins of elderly diabetic patients, CML and CEL (Figure 2) typically account for modification of less than 1% of the lysine residues in the protein. However, these biomarkers are thought to represent only a fraction of the total chemical modification of amino acids and cross-linking of proteins *in vivo*.

Glycoxidation

Although oxygen is not required for glycation, formation of CML and pentosidine from FL requires oxidation of the Amadori compound: cleavage between C-2 and C-3 of the carbohydrate to form the lysine adduct CML; and loss of one carbon from glucose during the formation of pentosidine. The development of brown color and fluorescence and formation of AGEs during incubation of proteins with glucose *in vitro* are also accelerated by oxygen. The oxidation reactions are more rapid in phosphate and carbonate buffers, compared to organic buffers, because of the presence of trace amounts of redox-active, metal ions, such as iron and copper in inorganic buffers, which catalyze oxidation and glycoxidation reactions.

The term, glycoxidation, was coined in recognition of the importance of both glycation and oxidation in the formation of AGEs. Oxidation reactions often have high-negative free energies, and, especially in oxidative cleavage reactions, oxygen can be viewed as the fixative of irreversible damage to protein during the Maillard reaction. However, some AGEs, such as pyrraline and the cross-lines, may be formed from glucose under nonoxidative conditions. Likely precursors to these compounds include the dicarbonyl sugars 1- and 3-deoxygluosone, which are formed from Amadori compounds under nonoxidative conditions.

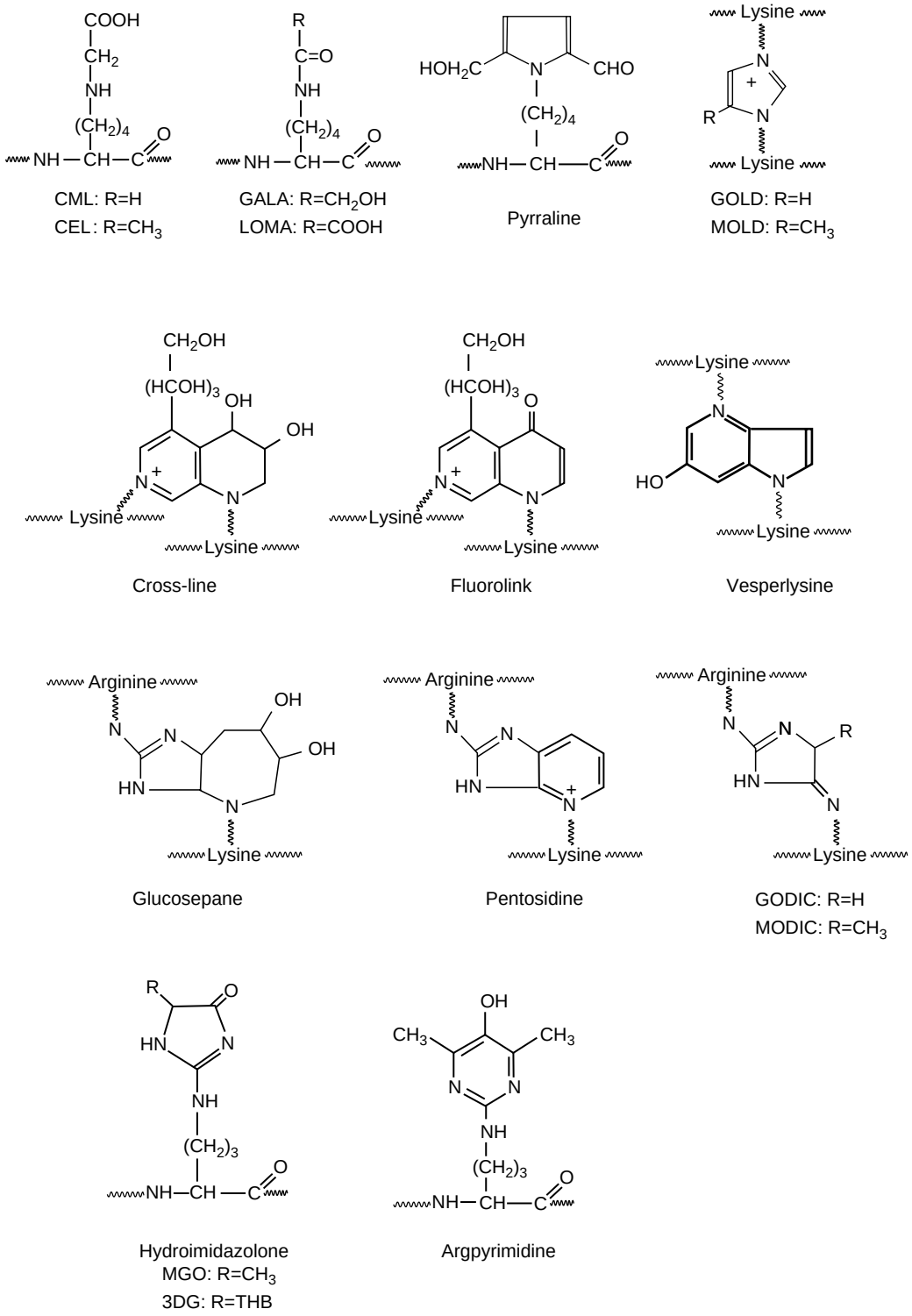

FIGURE 2 Structure of AGEs that have been detected in tissue proteins by chemical and/or immunological methods. Top: Nonfluorescent lysine adducts and cross-links, including amides, amines and imidazolium salts. Second row: Fluorescent lysine-lysine cross-links. Third row: Fluorescent arginine-lysine cross-links. Bottom: Arginine derivatives. CML, N^{ε}-(carboxymethyl)lysine; CEL, N^{ε}-(carboxyethyl)lysine; GALA, glycolic acid lysine monoamide; LOMA, lysine oxalic acid monoamide; GOLD and MOLD, GO and MGO lysine dimer (imidazolium salts); and GODIC and MODIC, GO and MGO dihydroimidazolylidene cross-links.

Alternative Pathways to AGEs and Glycoxidation Products

In the early 1980s, the Amadori adduct was considered an obligate intermediate in the formation of AGEs (Figure 1). However, it is now clear that there are multiple precursors and pathways to formation of the same AGE (Figure 3). CML, for example, may be formed from glyoxal or glycolaldehyde which are produced on autoxidation of many carbohydrates, or by autoxidation of Schiff base intermediates and Amadori adducts, or from ascorbate and dehydroascorbate and phosphorylated intermediates in glycolysis. To complicate the issue further, glycolaldehyde, formed on oxidation of serine by myeloperoxidase, and glyoxal formed during lipid peroxidation reactions, may also contribute to the formation of CML. Thus, the measurement of CML provides little information regarding its origin. Lipid-derived adducts to protein, such as malondialdehyde and hydroxynonenal adducts to protein, are known as advanced lipoxidation end-products (ALEs), so that CML and GOLD, and the homologous compounds, CEL and MOLD, are now considered AGE/ALEs, reflecting the fact that they may be derived from a variety of carbohydrate and non-carbohydrate precursors *in vivo*. Some AGEs, such as pentosidine and cross-lines, which contain 5–6 carbon rings or side-chains (Figure 2), are clearly derived from carbohydrates, but may be formed from a variety of carbohydrate precursors, including reducing sugars, sugar phosphates, and ascorbate.

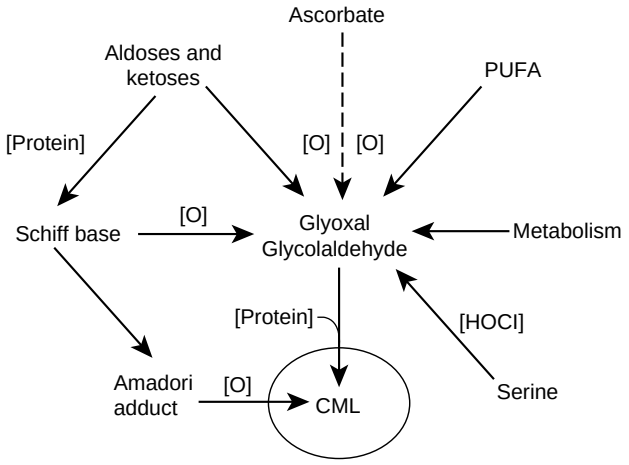

FIGURE 3 Alternative sources of the AGE/ALEs. CML may be formed from reducing sugars, either directly by oxidative cleavage of Schiff base or Amadori adducts on protein, or indirectly through glyoxal or glycolaldehyde formed on oxidation of glucose or glucose adducts to protein. CML may also be formed from ascorbate, through glyoxal, glycolaldehyde, or tetroses formed on oxidative degradation of dehydroascorbate. Glyoxal or glycolaldehyde are also formed during peroxidation of polyunsaturated fatty acids, or during myeloperoxidase-mediated degradation of amino acids.

Recognition and Turnover of AGE-Proteins

Nearly a dozen AGE-binding proteins have also been identified to date. The best characterized among the AGE receptors are RAGE (receptor for AGE), which is widely distributed among endothelial and parenchymal cells, and the macrophage scavenger receptors (MSRs). An unusual feature of these receptors is their range of ligand binding. In addition to binding of heterogeneously modified AGE-proteins, RAGE also recognizes the peptide amphoterin, which is involved in neuronal development, and the Aβ-amyloid peptide found in Alzheimer's plaque. MSRs were originally described as receptors for acetyl-LDL, later for their role in macrophage uptake of oxidized lipoproteins, then for their role in the recognition of AGE-proteins. The rapid uptake of injected AGE proteins (and oxidized LDL) in liver is consistent with a role for MSRs and the reticuloendothelial system in the removal of AGE-proteins from the circulation. A number of other candidate AGE receptor proteins have also been identified, based on interaction with AGE-proteins, but the determinants or motifs recognized by these receptors are, in most cases, unknown. Scavenger receptors recognize both AGE-proteins and oxidized lipoproteins, suggesting that common products are formed on chemical modification of proteins by both carbohydrates and lipids. CML has been proposed as a ligand for RAGE.

Binding of AGE-proteins to AGE-receptors appears to induce oxidative stress to cells, possibly because of the activity of AGEs, a source of reactive oxygen, in much the same way that binding and uptake of oxidized lipoproteins causes oxidative stress to cells bearing MSR. Thus, there is some risk to the cell involved in recognition and catabolism of AGEs, and chronic increases in AGE-induced oxidative stress have been invoked as a source of damage to endothelial cells and development of vascular and renal disease in diabetes. Under normal conditions, oxidative stress and protein turnover induced by AGE-proteins may have a role in the remodeling and rejuvenation of tissues, however this process may become pathogenic in chronic disease.

The Maillard Reaction in Aging and Disease

Aging

The age-dependent browning of tissue proteins is most apparent in the lens, which becomes visibly yellow with age. This change in color is accompanied by insolubilization, aggregation, and precipitation of lens crystallins, which may proceed to formation of cataracts.

Collagens and other long-lived proteins in the body undergo similar changes with age. The increased cross-linking of collagen contributes to the decrease in elasticity and resiliency of the extracellular matrix with age. By interfering with turnover of matrix components by metalloproteinases, browning reactions may also contribute to the age-dependent thickening of basement membranes in the microvasculature of the kidney, retina, and other tissues, affecting the permeability and transport properties of the matrix. The accumulation of AGEs in long-lived proteins (Figure 4) is accompanied by an age-dependent increase in protein fluorescence and by a parallel increase in other chemical modifications of proteins, including products of both nonoxidative (e.g., aspartate racemization, spontaneous deamidation) and oxidative damage (*o*-tyrosine, nitrotyrosine, dityrosine, and methionine sulfoxide). Research on the Maillard hypothesis today is focused on increasing evidence that AGEs have effector functions, i.e., they activate or participate in physiological responses to stress, including inflammation, hyperglycemia, and hyperlipidemia, and oxidative stress. Although proteins serve as the register or accumulator of Maillard reaction damage *in vivo*, glycoxidative and oxidative modifications of DNA are certain to have significant effects on the integrity of the genome during aging.

Diabetes

The glycation, AGE, or Maillard hypothesis identifies glucose as the culprit in diabetes, and proposes that diabetic complications result from accelerated Maillard reaction damage to tissue protein. Consistent with the hypothesis, both the extent of glycation of protein and the rate of accumulation of AGEs are accelerated by hyperglycemia in diabetes (Figure 4). The damage, like hyperglycemia, is systemic, and age-adjusted levels of AGEs in skin collagen are also correlated with the

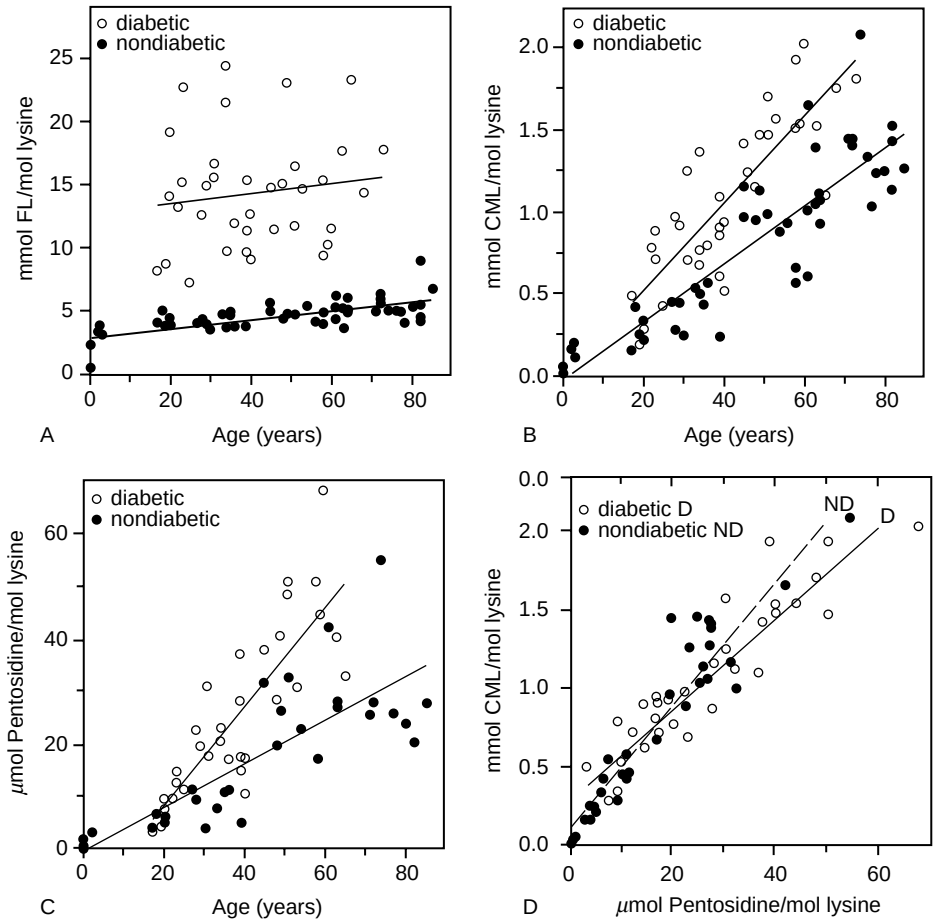

FIGURE 4 Influence of age and diabetes on glycation and glycoxidation of skin collagen. (A) Glycation of protein is reversible and relatively constant with age. Glycation of collagen increases with mean blood glucose concentration and correlates with GlcHb in diabetic patients. (B) and (C) The concentrations of the AGE/ALE, CML, and of the AGE, pentosidine, increase with age in the nondiabetic population and at an increased rate in diabetic patients. (D) Despite differences in origin and mechanism of formation and significant differences in their concentrations, the levels of CML and pentosidine in skin collagen correlate more closely with one another than with age in either control or diabetic populations. (Reproduced from Dyer, D. G., Dunn, J. A., Thorpe, S. R., Bailie, K. E., Lyons, T. J., McCance, D. R., and Baynes, J. W. (1993). Accumulation of Maillard reaction products in skin collagen in diabetes and aging. *J. Clin. Invest.* **91**, 2463–2469, with permission.)

severity of renal, retinal, and vascular complications of diabetes. The Maillard hypothesis is a chemical rather than metabolic theory on the origin of diabetic complications; it explains the development of similar complications in both type 1 (juvenile-onset, insulin-dependent) and type 2 (adult-onset, noninsulin-dependent) diabetes, despite the differences in etiology of these diseases (insulin deficiency versus insulin resistance). It also explains the development of complications in kidney, nerve, retina, and vasculature, since endothelial and parenchymal cells in these tissues are mostly independent of insulin for glucose transport. In these tissues, intracellular glucose tracks extracellular glucose concentration. These tissues are also rich in long-lived extracellular proteins, such as collagens, elastin, and myelin. In addition to the gradual accumulation of AGEs on extracellular proteins, AGEs are also formed on intracellular proteins in these tissues, probably from glycolytic intermediates, such as the triose phosphates. Research on intracellular glycation and AGE formation is still at an early stage, but is essential for a comprehensive understanding of the role of the Maillard reaction in the pathogenesis of diabetic complications.

AGE Inhibitors

Perhaps the most convincing evidence for the AGE hypothesis is the demonstrated efficacy of AGE-inhibitors in retarding the development of a wide range of complications in animal models of diabetes. Both aminoguanidine (AG) and pyridoxamine (PM) are potent inhibitors of formation of AGEs by autoxidation of sugars and Schiff base adducts to proteins, while PM, described as an Amadorin, also inhibits formation of AGEs from Amadori compounds. AG and PM inhibit the formation of AGEs and cross-linking of collagen *in vivo*, and also limit the increase in immunohistochemically detectable AGEs in tissues in diabetes. Other activities of these inhibitors may contribute to their efficacy *in vivo*, since they inhibit amine oxidases, including some isoforms of nitric oxide synthase, have weak chelating activity, and also have antihypertensive and hypolipidemic effect *in vivo*.

Other Diseases

AGEs and ALEs are increased in tissues in a wide range of age-related, chronic diseases, including diabetes, atherosclerosis, dialysis-related amyloidosis, arthritis, and neurodegenerative diseases. The increase in glycoxidative and lipoxidative damage reflects, in part, uncontrolled chemistry occurring, either locally or systemically, in biological systems as a result of tissue damage, decreased antioxidant defenses and increased decompartmentalization of metal ions. Although the AGE/ALEs are not the primary source of pathology in these diseases, they are macrophage chemoattractants and proinflammatory molecules, acting as both intermediaries in pathogenic processes and biomarkers of resultant tissue damage. AGE/ALE inhibitors may eventually prove useful for limiting damage or complications from a wide range of chronic, age-related diseases. Their effects on health and longevity are being explored in studies in animal models.

See Also the Following Articles

Collagens • Diabetes • Glycogen Storage Diseases • Insulin- and Glucagon-Secreting Cells of the Pancreas

Glossary

advanced glycation end-product (AGE) Irreversible end-product of nonenzymatic reaction of carbohydrates with protein; includes fluorescent and nonfluorescent adducts and cross-links in protein.

advanced lipoxidation end-product (ALE) Stable end-product of chemical modification of protein by reactive carbonyl intermediates formed during lipid peroxidation reactions.

Amadori adduct or **compound** First stable product of glycation of protein; a ketoamine.

glycation Enzymatic or nonenzymatic adduction of a carbohydrate to a biomolecule.

glycoxidation product AGE formed by a combination of glycation and oxidation chemistry.

Further Reading

Baynes, J. W., and Thorpe, S. R. (2000). Glycoxidation and lipoxidation in atherogenesis. *Free Radic. Biol. Med.* **28**, 1708–1716.

Bucciarelli, L. G., Wendt, T., Rong, L., Lalla, E., Hofmann, M. A., Goova, M. T., Taguchi, A., Yan, S. F., Yan, S. D., Stern, D. M., and Schmidt, A. M. (2002). RAGE is a multiligand receptor of the immunoglobulin superfamily: Implications for homeostasis and chronic disease. *Cell Mol. Life Sci.* **59**, 1117–1128.

Dyer, D. G., Dunn, J. A., Thorpe, S. R., Bailie, K. E., Lyons, T. J., McCance, D. R., and Baynes, J. W. (1993). Accumulation of Maillard reaction products in skin collagen in diabetes and aging. *J. Clin. Invest.* **91**, 2463–2469.

Miyata, T., Devuyst, O., Kurokawa, K., and van Ypersele de Strihou, C. (2002). Toward better dialysis compatibility: Advances in the biochemistry and pathophysiology of the peritoneal membranes. *Kidney Int.* **61**, 375–386.

Schleicher, E. D., Bierhaus, A., Haringm, H. U., Nawroth, P. P., and Lehmann, R. (2001). Chemistry and pathobiology of advanced glycation end products. *Contrib. Nephrol.* **131**, 1–9.

Stitt, A. W., Jenkins, A. J., and Cooper, M. E. (2002). Advanced glycation end products and diabetic complications. *Expert Opin. Invest. Drugs* **11**, 1205–1223.

Thorpe, S. R., and Baynes, J. W. (2003). Maillard reaction products in tissue proteins: New products and new perspectives. *Amino Acids* **25**, 275–281.

Ulrich, P., and Cerami, A. (2001). Protein glycation, diabetes, and aging. *Recent Prog. Horm. Res.* **56**, 1–21.

Vlassara, H. (2001). The AGE-receptor in the pathogenesis of diabetic complications. *Diabetes Metab. Res. Rev.* **17**, 436–443.

Vlassara, H., and Palace, M. R. (2002). Diabetes and advanced glycation endproducts. *J. Intern. Med.* **251**, 87–101.

Biography

Suzanne Thorpe and John Baynes are a husband-and-wife team who have worked together for over 25 years in teaching and research at the University of South Carolina. They study chemical modifications of proteins by carbohydrates, lipids, and oxidation reactions, focusing on the role of nonenzymatic chemistry in regulatory biology and in the pathogenesis of aging and age-related, chronic diseases.

Glycine Receptors

Bodo Laube and Heinrich Betz
Max-Planck Institute for Brain Research, Frankfurt, Germany

Glycinergic inhibition of neuronal excitability in spinal cord and brain stem is mediated via inhibitory glycine receptors (GlyRs). These receptors are composed of two types of homologous membrane-spanning subunits (α and β) and belong to the pentameric nicotinic acetylcholine receptor superfamily of ligand-gated ion channels. Binding of presynaptically released glycine to postsynaptically enriched GlyRs prevents membrane depolarization of nerve cells by opening receptor-intrinsic chloride channels and is specifically antagonized by the convulsant alkaloid strychnine. Mutations in *GlyR* genes give rise to neuromotor and startle disorders in humans and animals and underline the important roles of GlyRs in motor coordination and sensory processing.

Distribution of Glycine in the Brain

Although glycine is the simplest of all amino acids, it has diverse functions within the central nervous system (CNS). It serves as an inhibitory neurotransmitter at the GlyR and as a coagonist essential for the activation of excitatory *N*-methyl-D-aspartate receptors, in addition to being involved in the metabolism of proteins and nucleotides in all cells. The regional levels of glycine in the CNS mainly reflect its role in inhibitory neurotransmission, being highest in the medulla oblongata, pons, and spinal cord, and lowest in the cerebral hemispheres and the cerebellum.

Physiological Role and Functional Properties of Glycine Neurotransmission

Principal Properties of Glycinergic Inhibition

Excitation of glycinergic neurons in the CNS causes Ca^{2+} triggered release of presynaptic glycine into the synaptic cleft and results in the activation of postsynaptic GlyRs, which mediate an increase in the chloride conductance of the postsynaptic plasma membrane (Figure 1). These glycinergic synaptic currents have a complex time course with a fast rising phase and an exponential deactivation, which reflect the synchronous activation of GlyR channels by glycine released during exocytosis and the subsequent closure of individual channels, respectively. After receptor unbinding, glycine is removed from the synaptic cleft by rapid reuptake into presynaptic nerve terminals or surrounding glial processes to allow termination of the transmission process (Figure 1).

Roles in Spinal Control of Motor Activity and Sensory Processing

Inhibition at central synapses is mediated by both glycine and γ-aminobutyric acid (GABA). Whereas GABA is primarily used in higher brain regions, glycinergic synapses are particularly abundant in spinal cord and brain stem, i.e., structures involved in the control of motor rhythm generation, the coordination of spinal reflex responses and the processing of sensory signals. Ia glycinergic interneurons in spinal cord mediate reciprocal inhibition in stretch reflex circuits, allowing relaxation of the antagonist muscle, and thus contribute to the coordination of opposing muscles. Renshaw interneurons regulate motoneuron excitability by producing a recurrent inhibition via a negative feedback system. In sensory processing, glycine modulates neuronal circuits in the auditory system and in the retina and suppresses nociceptive signals in the spinal cord.

Synaptic Versus Extrasynaptic Inhibition

Although neurotransmission between nerve cells is mainly mediated by synaptic contacts, GlyRs are also found outside synapses in noninnervated plasma membrane regions (Figure 1). These extrasynaptic receptors are thought to be persistently activated by low concentrations of extracellular agonists and/or glycine spillover from active glycinergic synapses and have been implicated in the tonic inhibition of neurons and the development of the neocortex.

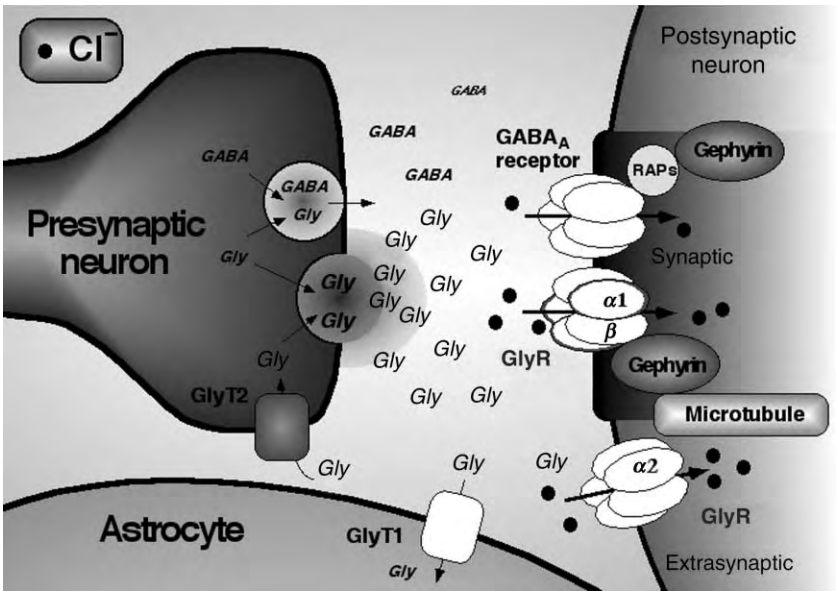

FIGURE 1 The glycinergic synapse. Excitation of the glycinergic terminal of interneurons causes Ca^{2+}-triggered fusion of glycine (and GABA) containing synaptic vesicles with the presynaptic plasma membrane, thus initiating glycine (and GABA) release into the synaptic cleft. This results in the activation of postsynaptic GlyRs which, by opening of the receptor integral anion channel in response to agonist binding, results in an increase in chloride conductance. Upon receptor unbinding, glycine is removed by specific glycine transporters located in the presynaptic (GlyT2) and the glial (GlyT1) plasma membranes. The synaptically localized GlyR interacts via its β-subunit with the submembraneous scaffold protein gephyrin, which binds to cytoskeletal components (tubulin) and receptor-associated proteins (RAPs), and thereby targets and anchors the GlyR (and $GABA_A$Rs) to postsynaptic specializations. Extrasynaptic GlyRs might play an important role in the tonic inhibition of neurons, due to persistent activation by low extracellular glycine concentrations or glycine spillover from adjacent glycinergic synapses.

Long-Term Plasticity of Glycinergic Synapses

Activity-dependent long-term changes in synaptic efficacy are important for many higher brain functions. Different forms of plasticity have been described for glycinergic synapses. For example, auditory stimulation triggers a form of long-term potentiation of glycinergic synapses that shares similarities with the long-term potentiation seen upon tetanic stimulation of excitatory connections. Consequently, increases in postsynaptic Ca^{2+} concentrations after high-frequency presynaptic activity are likely to affect the insertion and/or retrieval of GlyRs, and to thus modify inhibitory synaptic currents.

Switch from Excitatory to Inhibitory GlyR Function During Development

While glycine is a major inhibitory neurotransmitter in the adult CNS, activation of GlyRs does not always lead to membrane hyperpolarization and neuronal inhibition. During prenatal development of the brain, glycine acts as an excitatory transmitter that induces a depolarising chloride-dependent response, due to a more positive chloride equilibrium potential of embryonic neurons mediated by actively regulated chloride transport. This excitatory GlyR function seems to be important for synapse formation, since glycine-triggered rises in intracellular Ca^{2+} are crucial for the correct formation of glycinergic postsynaptic membrane specializations.

Mixed GABA and Glycinergic Synapses

The inhibitory neurotransmitters glycine and GABA are often colocalized in terminals of premotor inhibitory interneurons in the spinal cord. Furthermore, the protein gephyrin, which links GlyRs to the cytoskeleton, can promote clustering of major $GABA_A$ receptor subtypes at the same postsynaptic site. Since the relative strengths of the glycinergic and GABAergic components of "mixed" inhibitory synaptic transmission can change during development, this might reflect a complex interaction of these two inhibitory neurotransmitters at central synapses (Figure 1).

Structure and Diversity of GlyR Channels

Purification and Isolation of the GlyR

The GlyR was the first neurotransmitter receptor protein that was isolated from the mammalian CNS by affinity purification, using adsorption of the detergent-solubilized receptor on aminostrychnine-agarose followed by elution with the agonist glycine. The resulting preparation contained the pentameric GlyR composed of α- and β-subunits and the associated anchoring protein gephyrin.

Glycine Receptor Isoforms

Cloning of GlyR subunit cDNAs revealed that the GlyR belongs to the same superfamily of group I ligand-gated ion channels (LGICs) as the nicotinic acetylcholine receptor (nAChR), the GABA type A and C receptors ($GABA_{A/C}R$), the serotonin type 3 receptor ($5\text{-}HT_3R$) and the glutamate gated-chloride channel receptor (GluClR). The GlyR α- and β-subunits share significant sequence homology with each other ($>40\%$) and, to a lesser extent, with other proteins of the nAChR family. Homology is particularly high within the four transmembrane domains and a cysteine loop located within the N-terminal extracellular region. Four different genes encoding GlyR α-subunits ($\alpha 1\text{–}4$) have been identified in vertebrates with an overall sequence identity of $>80\%$. Alternative splicing in the extracellular N-terminal region and in the intracellular loop between transmembrane domains 3 and 4 generates further diversity. So far, only a single GlyR β-subunit gene has been found.

Spatial and Developmental Expression of GlyR Subunits in the Brain

In situ hybridization studies revealed that $\alpha 1$-GlyR subunit mRNA is mainly found in spinal cord, brain stem, and the colliculi, whereas GlyR $\alpha 2$-transcripts are found in the hippocampus, cerebral cortex, and thalamus (Figure 2). Low levels of $\alpha 3$-mRNA are detected in spinal cord, cerebellum, and olfactory bulb. The β-subunit gene is expressed throughout the entire CNS. GlyR $\alpha 1$- and $\alpha 2$-gene expression is subject to developmental regulation; $\alpha 1$-transcripts increase, and $\alpha 2$-mRNA decreases, after birth. This change in mRNA expression is reflected in an altered GlyR subunit composition and a faster decay time of inhibitory glycinergic postsynaptic currents. The neonatal form primarily composed of $\alpha 2$-homo-oligomers exhibits long channel open times, while the adult isoform is a $\alpha 1\beta$-hetero-oligomer characterized by fast channel kinetics.

Heterologous Expression of the GlyR

After heterologous expression, all GlyR α-subunits form functional homo-oligomeric channels with properties resembling those of native GlyRs. Single expression of the β-subunit does not result in either glycine-activated currents or [^{3}H]strychnine binding. Coexpression of α- and β-subunits generates hetero-oligomeric GlyRs that differ from homo-oligomeric α-GlyRs by their insensitivity to the channel blocker picrotoxinin and a reduced main state conductance.

Structural Features of the GlyR

Cross-linking and heterologous expression experiments have shown that the adult spinal GlyR is a pentameric complex composed of multiple copies of the ligand-binding $\alpha 1$- and β-subunits, which have molecular masses of 48 and 58 kDa, respectively. All subunits share a large and highly conserved N-terminal extracellular domain, four putative transmembrane domains (M1–M4), and a short extracellular C-terminus (Figure 2). Hydropathy analysis suggests that all four transmembrane segments are α-helices.

Molecular Model of the Ligand-Binding Region

The significant extent of sequence homology within the group I ligand-gated ion channel superfamily indicates that its members share a common structural organization. Composite ligand-binding sites, conserved throughout this receptor family, are located at the extracellular interface between subunits and involve contact residues that belong to distinct loops of two adjacent subunits. Homology modeling of the $\alpha 1$-subunit of the GlyR based on the crystal structure of the homologous soluble acetylcholine-binding protein from the snail *Lymnea stagnalis* (Brookhaven PDB entry 1I9B) has provided intriguing clues about the subunit architecture and the ligand-binding sites of these receptors.

Ion Channel Function

The second transmembrane domain M2 forms the ion channel of the GlyR. It is highly anion selective, with a

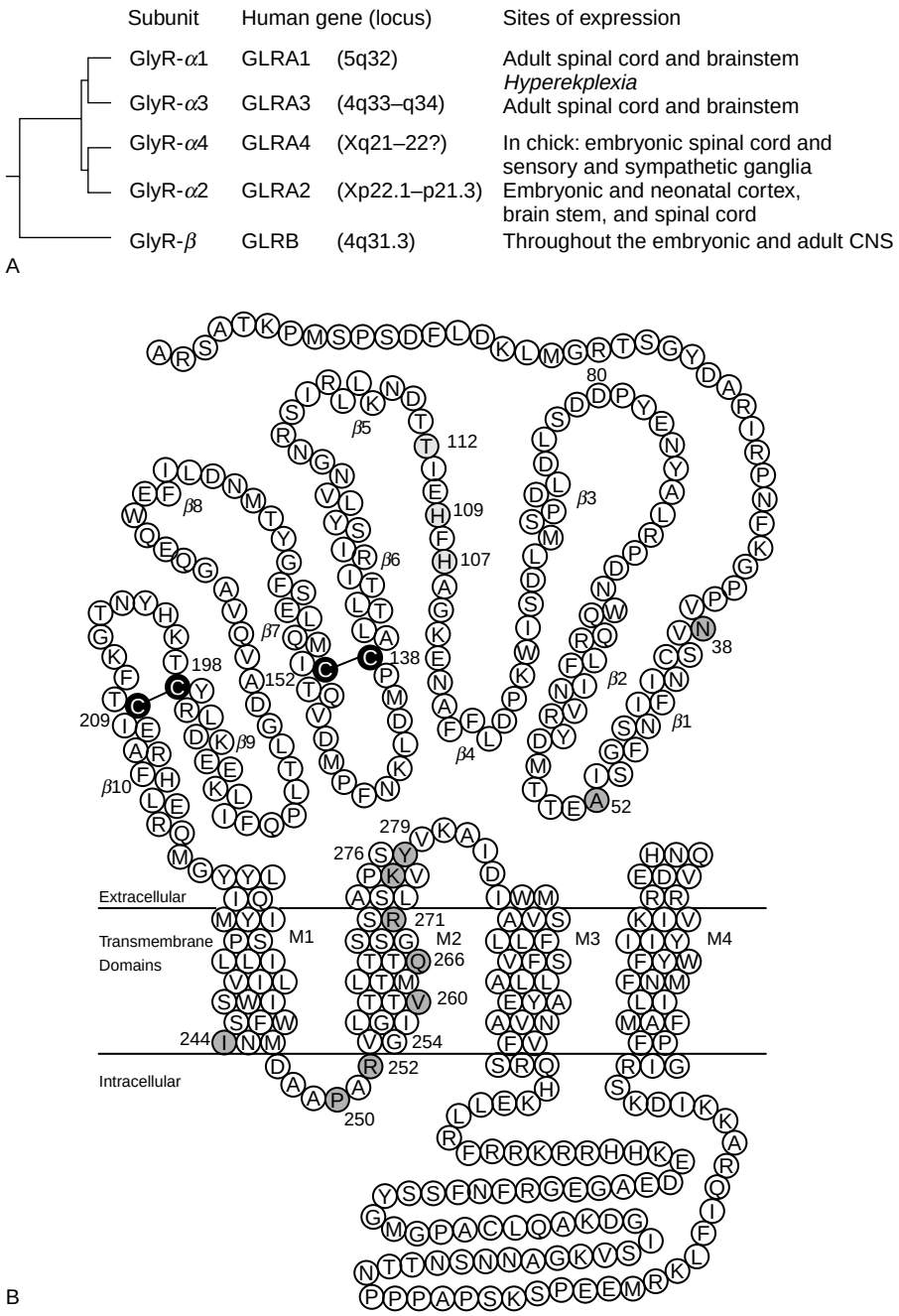

FIGURE 2 Phylogenetic relationships between and transmembrane topology of vertebrate GlyR subunits. (A) Evolutionary relationships between GlyR subunits. In addition to individual subunits, the chromosomal localizations of the human genes and their major sites of expression are indicated. (B) Transmembrane topology of the human GlyR-α1-subunit, with amino acid residues mutated in human hyperekplexia (gray residues) being indicated. Conserved cysteine residues forming disulfide bridges are shown in black. Residue N38 constitutes the sole N-glycosylation site. Mutation A52S is found in the *spasmodic* mouse. G254 in M2 of the α1-subunit determines the main conductance and sensitivity to the channel blocker CTB. Residue D80 is an important determinant of Zn^{2+} potentiation, whereas residues H107, H109, and T112 are essential for Zn^{2+} inhibition. Secondary structure predictions for the extracellular and transmembrane domains are indicated by amino acid residues being arranged in β-sheet (β1–β10), or α-helical (M1–M4), structures, respectively.

halide selectivity sequence of $I^- > Br^- > Cl^-$, and is significantly permeable to bicarbonate. A characteristic of GlyRs is that they do not exhibit a single conductance state but instead display a range of conductance states, with residue Gly 254 within the second transmembrane domain constituting a major determinant of ion flux (Figure 2). Hetero-oligomeric α1/β-GlyRs show lower subconductance state levels than α1-homomeric receptors, and in this respect resemble the adult native receptors.

The Cytoplasmic Loop of the β-Subunit is Crucial for Postsynaptic Receptor Clustering

A protein of 93 kDa, named gephyrin, copurifies with the GlyR and is enriched on the cytoplasmic face of the postsynaptic membrane. A short amino acid motif within the cytoplasmic loop, linking the third and fourth transmembrane domains of the GlyR β-subunit, forms the binding site for gephyrin. Thus, synaptically localized GlyR is bound via its β-subunit to the submembraneous scaffold protein, gephyrin, which interacts with cytoskeletal components and receptor-associated proteins, and thereby targets and anchors the GlyR to postsynaptic membrane specializations (Figure 1).

Pharmacological Properties of the GlyR

The Classical Antagonist Strychnine

The alkaloid strychnine constitutes a unique tool in the investigation of the GlyR. In electrophysiological studies, it is the most reliable antagonist to distinguish glycinergic from GABAergic inhibition. Biochemists use glycine-displaceable [^{3}H]strychnine binding to quantify the GlyR in radioligand-binding assays. The physiological symptoms of strychnine poisoning emphasize the importance of glycinergic inhibition in the control of both motor behavior and sensory processing. Due to its high toxicity, which causes convulsions and, at higher doses, death, strychnine is of low therapeutical value but serves as a rat poison.

Agonistic Amino Acids

In addition to glycine, the endogenous amino-acids β-alanine and taurine display inhibitory activity when applied to neurons. Taurine released nonsynaptically from immature cortical neurons has been found to influence cortical development by activating extrasynaptic GlyRs. The role of β-alanine is less clear. Despite being synthesized endogenously, evidence for an *in vivo* transmitter function of this amino acid is lacking. Both β-alanine and taurine are partial agonists, which can elicit only submaximal currents.

Antagonism by Channel Block

The alkaloid picrotoxinin acts as a use-dependent but voltage-independent open-channel blocker of the GlyR and can be used to discriminate homo- from hetero-oligomeric receptors. Hetero-oligomeric GlyRs composed of α- and β-subunits are relatively resistant to block by picrotoxinin, whereas homo-oligomeric GlyRs containing only α-subunits are sensitive to low micromolar alkaloid concentrations. The bulky organic anion cyanotriphenylborate (CTB) blocks GlyR channels in a use-dependent fashion, with the exception of homomeric α2-GlyRs.

Allosteric Modulation of the GlyR

Only a few agents are known to potentiate GlyR function. Therapeutically, potentiation of glycinergic inhibition in the mammalian CNS has substantial promise for both normalizing pathological states and for lowering sensory and motor activity under different conditions including narcosis.

Anesthetics and Alcohol

Since decades, anesthetics and alcohols are known to potentiate GlyR responses. Anesthetic concentrations of propofol and volatile halogenated hydrocarbons such as halothane, enflurane, isoflurane, methoxyflurane, and sevoflurane enhance the effects of low concentrations of glycine at the GlyR. The potencies of n-alcohols increase with chain length of their alkyl groups, up to a cut-off value of twelve carbon atoms. Using site-directed mutagenesis, residues within the transmembrane domains have been shown to be important for the potentiating effect of anesthetics and alcohol.

Zinc

The divalent cation Zn^{2+} exhibits biphasic effects on both native and recombinantly expressed GlyRs. Low concentrations of Zn^{2+} (0.1–10 μM) potentiate submaximal glycine-induced currents about threefold, while higher concentrations cause inhibition. Since Zn^{2+} is present within presynaptic secretory vesicles and is coreleased with the neurotransmitter upon stimulation, this modulation might be of considerable physiological significance. Mutational studies indicate that the Zn^{2+}-binding sites for potentiation and inhibition are located at subunit interfaces, as are the agonist-binding sites.

Neurosteroids

Steroids markedly affect glycinergic transmission; however, their actions are variable and show a strong dependence on subunit composition. This has been interpreted as evidence for heterogenous binding sites of neurosteroids existing on the GlyR. *In vivo*, steroid

effects on GlyR activity may be particularly important at the time of birth and during adolescence.

Posttranslational Modifications

GlyR subunits contain consensus sequences for glycosylation (Figure 2), phosphorylation (protein kinases A and C, Ca^{2+}-dependent kinases), and ubiquitination. Although a regulation of GlyR channel activity by phosphorylation was observed in different preparations, consistent with a potential role of protein kinases in the modulation of synaptic efficacy, the functional significance of GlyR phosphorylation is far from being clear. Also, ubiquitin-mediated internalization and degradation of the GlyR have been suggested to constitute important mechanisms for regulating receptor numbers in the neuronal plasma membrane.

Disorders of Glycinergic Neurotransmission

Mutations in GlyR subunits causing an impairment of glycinergic transmission result in neurological malfunction and hereditary neuromotor disease.

Human Disorders

The first disorder associated with a mutation in a neurotransmitter receptor was found by positional cloning. Hyperekplexia (startle disease, Kok disease) is characterized by muscle rigidity of nervous system origin, particularly in neonates, and by an exaggerated startle response to unexpected auditory or tactile stimuli. The underlying genetic defect was mapped to chromosome 5q by genetic linkage using DNA markers defining the GlyR-α1 gene, *GLRA1*, as the prime candidate. Substitutions of the charged residue Arg 271 by uncharged amino acids (Leu or Gln) were identified in four families with autosomal dominant hyperekplexia. These substitutions result in a reduction of agonist sensitivity and glycine-activated current. Recombinant expression of the mutant GlyRs revealed that the reduced glycine current is due to a decrease in single-channel conductance levels. Recessive forms of hyperekplexia have subsequently been identified in other families, which carry other missense or null mutations in the *GLRA1* locus (Figure 2). However, in only 40–50% of the human patients displaying hyperekplexia-like symptoms *GLRA1* mutations have been found, suggesting that genes other than *GLRA1* could be involved in hyperekplexia.

Animal Mutants

The syntenies between human chromosome 5q and mouse chromosome 11 led to the discovery that recessive mutations in mouse *GLRA1* underlie two mouse neurological mutants, *spasmodic* and *oscillator*. *Spasmodic* displays a phenotype similar to human hyperekplexia and is caused by missense mutation of Ala 52 to Ser (Figure 2). *Oscillator* has a more severe phenotype, including progressive tremor and muscle spasms, leading to death by 3 weeks of age. Lethality is caused by a frameshift-producing deletion predicted to eliminate the large cytoplasmic loop and the fourth transmembrane domain. Homozygous *spastic* mice develop at ~2 weeks postnatally a hyperekplexic phenotype that is associated with a marked reduction in the density of GlyRs in brain stem and spinal cord. The disorder results from the insertion of a LINE-1 element into an intronic region of the gene encoding the β-subunit of the GlyR (GLRB), thereby causing delayed and aberrant splicing of the β-subunit mRNA. A disease resembling the human and murine startle diseases is found in Poll-Hereford cattle and Peruvian Paso horses. These animals display strong myoclonus resulting from reduced or absent GlyR expression in the spinal cord. In the Poll-Hereford cattle, a missense mutation at Thr24 of the *GlyR-α1* gene has been shown to cause a translational stop, and thus a complete α1-subunit deficiency in homozygous animals.

See Also the Following Articles

Amino Acid Metabolism • $GABA_B$ Receptor • Ligand-Operated Membrane Channels: GABA • Protein Kinase C Family • Ubiquitin System

Glossary

gephyrin From the Greek word for bridge. Protein that anchors the GlyR to the subsynaptic cytoskeleton.

LGICs Family of receptor proteins composed of homologous subunits, whose intrinsic ion channel opens after binding of neurotransmitter.

startle disease Human hereditary disorder characterized by an exaggerated startle reaction in response to unexpected stimuli.

strychnine A plant alkaloid derived from the Indian tree *Strychnos nux vomica*. A potent convulsant antagonizing glycinergic inhibition.

Further Reading

Becker, C. M. (1992). Convulsants acting at the inhibitory glycine receptor. In *Handbook of Experimental Pharmacology* (H. Herken and F. Hucho, eds.) pp. 539–575. Springer, Berlin, Heidelberg.

Kneussel, M., and Betz, H. (2000). Clustering of inhibitory neurotransmitter receptors at developing postsynaptic sites: The membrane activation model. *Trends Neurosci.* **23**, 429–435.

Kuhse, J., Betz, H., and Kirsch, J. (1995). The inhibitory glycine receptor: Architecture, synaptic localization and molecular pathology of a postsynaptic ion channel complex. *Curr. Opin. Neurobiol.* **5**, 318–323.

Laube, B., and Betz, H. (1999). Purification and heterologous expression of inhibitory glycine receptors. *Meth. Enzymol.* **294**, 260–273.

Laube, B., Maksay, G., Schemm, R., and Betz, H. (2002). Modulation of glycine receptor function: A novel approach for therapeutic intervention at inhibitory synapses? *TiPS* **23**, 519–527.

Rajendra, L., Lynch, J. W., and Schofield, P. (1997). The glycine receptor. *Pharmacol. Ther.* **73**, 121–146.

Schofield, P. (2002). The role of glycine and glycine receptors in myoclonus and startle syndromes. *Adv. Neurol.* **89**, 263–274.

Biography

Bodo Laube studied biology in Frankfurt, where he received his Diploma of Zoology (1991), Ph.D. (1995) and *venia legendi* (2003) from the Johann Wolfgang Goethe Universität. Since 1997, he is a Staff Scientist in the Neurochemistry Department of the MPI for Brain Research in Frankfurt.

Heinrich Betz studied biochemistry and medicine in Tübingen and Munich and obtained his M.D. from the University of Tübingen. After working in Freiburg, Paris, and Munich, he was a Professor of Molecular Neurobiology and Neuropharmacology at the University of Heidelberg. He is currently the Head of the Neurochemistry Department at the MPI for Brain Research in Frankfurt.

Glycogen Metabolism

Peter J. Roach
Indiana University School of Medicine, Indianapolis, Indiana, USA

Glycogen, a polymer of the sugar glucose, functions as a reserve of energy and structural building blocks in organisms from bacteria to humans. It is synthesized when nutrients are available for utilization in times of need. In mammals, the two largest deposits of glycogen are in skeletal muscle and liver; muscle glycogen is utilized locally to help fuel muscular activity, whereas liver glycogen is broken down to glucose that is delivered into the bloodstream. After a meal, elevated blood glucose causes the hormone insulin to be released from the pancreas and to stimulate conversion of ingested glucose into glycogen in muscle, liver, and other tissues. Upon fasting, such as overnight, the pancreatic hormone glucagon signals the breakdown of liver glycogen to stabilize blood glucose levels, essential for brain and blood cell function. The hormone epinephrine stimulates glycogen breakdown in liver and muscle to cope with stressful situations.

Glycogen Structure

Many nutrients contain either glucose or compounds that are easily converted to glucose, so that it is an important nutritional currency for many organisms. Glycogen is a glucose polymer meaning that individual glucose units are joined together by repeated chemical linkages to form large molecules containing thousands of glucose residues (Figure 1). Two types of linkages are present in glycogen causing a branched polymeric structure. These same two linkages are present in plant starches which serve a similar function as glycogen. When needed, the glucose units can be recovered by breaking down the glycogen. A possible explanation for the storage of glucose as glycogen rather than glucose monomers is the lower osmotic activity of the polymer.

Glycogen Metabolism

Glycogen exists as a particle in which the carbohydrate core is associated with several of the proteins needed to make it and to degrade it. The glycogen molecule expands or contracts due to growth or breakdown of the outer branches of the molecule (Figure 1).

Synthesis

Glycogen in cells is either synthesized directly from glucose transported into the cells by transporter proteins or from other cellular metabolites that are converted to the activated sugar precursor, UDP-glucose in animals, and ADP-glucose in bacteria (or for starch biosynthesis in plants). Three enzymes are needed to synthesize glycogen: an initiator protein called glycogenin that attaches glycogen residues to itself; the enzyme glycogen synthase responsible for incorporating most of the glucose moieties of glycogen from UDP-glucose; and a special enzyme, branching enzyme, to introduce the branchpoints (Figure 2).

Degradation

Controlled degradation of glycogen requires two enymes (Figure 2). Glycogen phosphorylase releases a glucose unit from the polymer as a metabolite, named glucose-1-P, that can be used by the cell. Since phosphorylase stalls at the branch points, a second specialized enzyme, the debranching enzyme, is needed to degrade past them. In muscle, the process stops at another metabolite of glucose, called glucose-6-phosphate, which is used in the muscle cell to provide energy or building blocks. In liver the glucose-6-phosphate can be converted, by an enzyme called glucose-6-phosphatase, to free glucose that is exported to the bloodstream. There is a second pathway to degrade glycogen. In most cell types, there is a house-cleaning process whereby a portion of the cellular content is continuously being delivered to an organelle, called a lysozome or vacuole, to recycle the building blocks of the macromolecules, like amino acids from proteins and glucose from glycogen. A specialized enzyme, called an α-glucosidase, is present in the lysosome to break glycogen down to glucose.

Glycogen Function and Control

Metabolic Role

Whether in bacteria or mammals, glycogen serves as a reservoir of energy and/or building blocks that can be

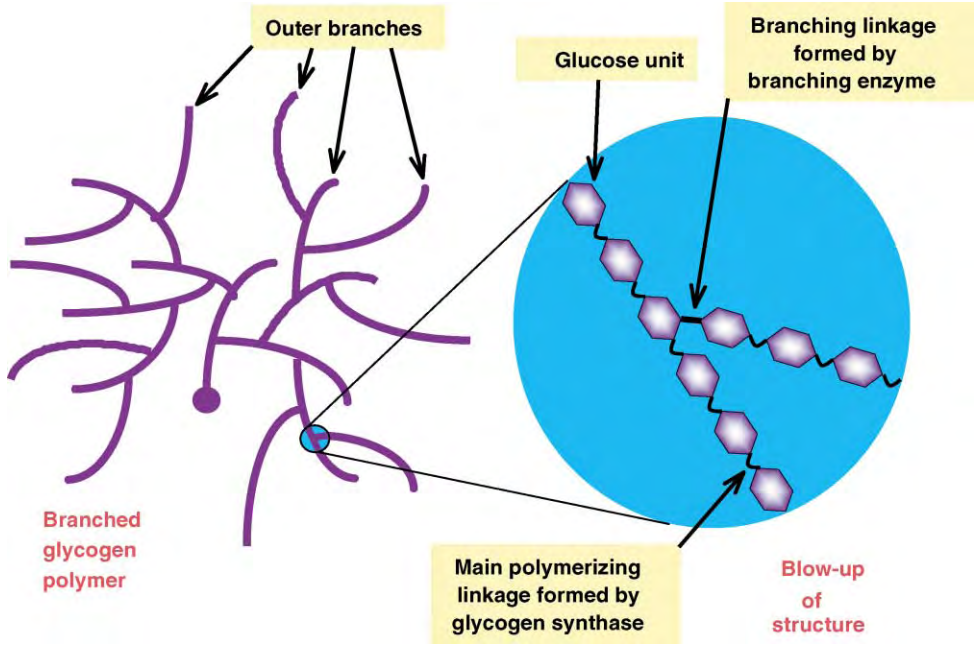

FIGURE 1 Glycogen is a polymer of glucose units.

called upon in times of need. In microorganisms, glycogen is generally made in response to impending nutritional deprivation, as judged by sensing the composition of the environment, and stored for use later during starvation. In mammals, the nutritional cues that govern glycogen metabolism in tissues are indirect and are borne by the blood levels of glucose itself and several important regulatory hormones. After a meal, nutrients enter the gut and lead to increased blood glucose which triggers the pancreas to release the hormone insulin, a signal of the fed condition. Insulin-sensitive tissues, liver, fat, and especially skeletal muscle, respond by increasing transport of glucose into the cells (Figure 3A). Insulin also causes activation of the enzyme

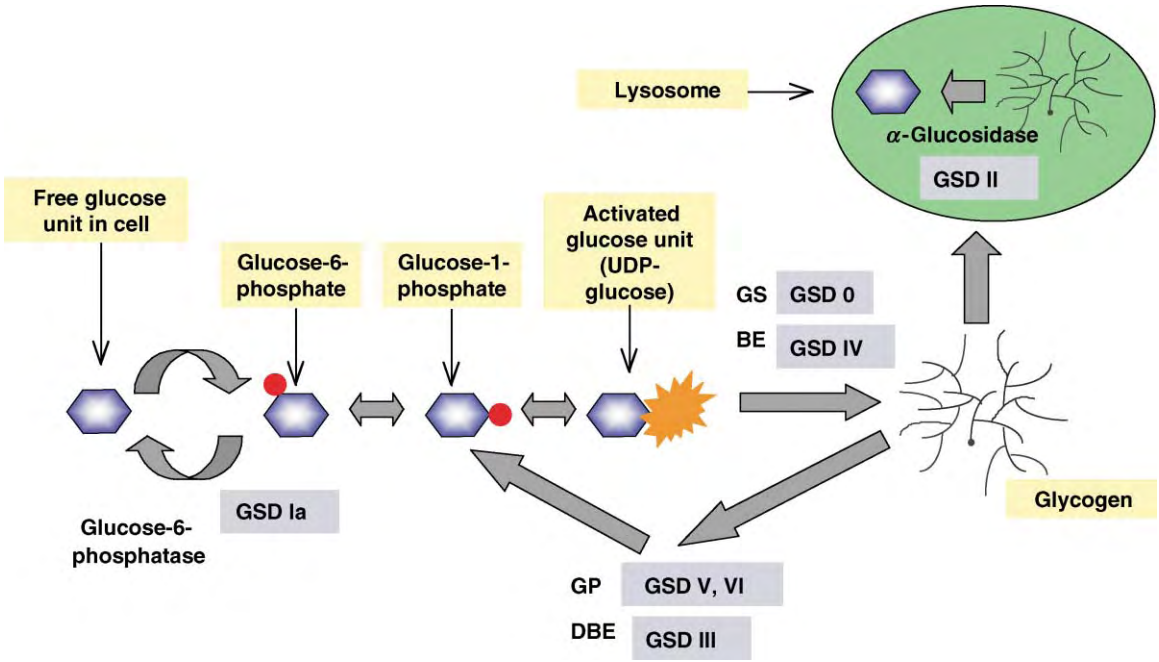

FIGURE 2 The pathways of glycogen production and degradation. GSD, glycogen storage disease; GS, glycogen synthase; BE, branching enzyme; GP, glycogen phosphorylation; DBE, debranching enzyme.

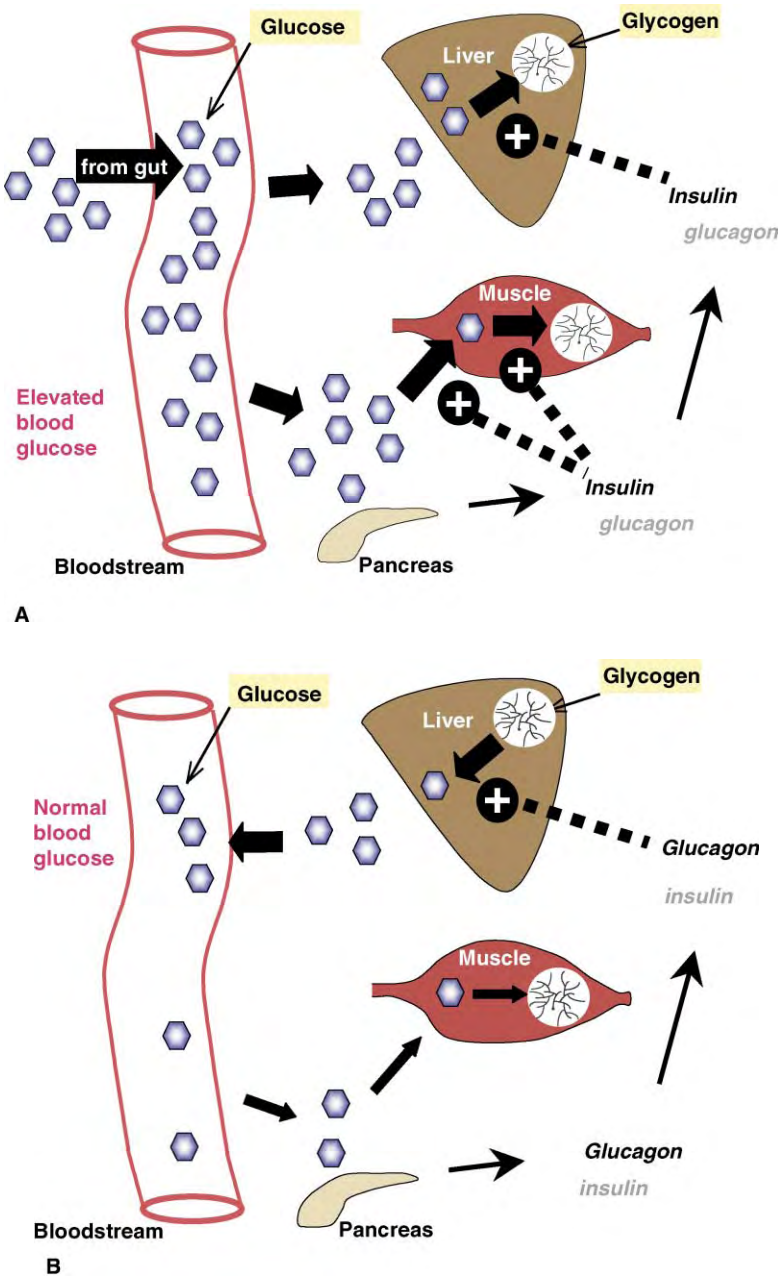

FIGURE 3 The interconversion of glucose and glycogen in the fed (A) and fasted (B) states.

glycogen synthase enhancing the conversion of glucose to glycogen. This is part of the process of blood glucose homeostasis whereby the body seeks to maintain the blood glucose level within safe limits. As the time after the last meal increases, the blood glucose level normalizes, the pancreas delivers less insulin and begins to secrete the hormone glucagon, which signals the unfed state (Figure 3B). The primary target is the liver which responds by breaking down glycogen to produce glucose that can be delivered to the bloodstream – another contribution to blood glucose homeostasis.

Role in Muscle or Exercise

Unlike the liver, muscle cannot breakdown glycogen all the way to free glucose for export to the bloodstream. Muscle glycogen is instead broken down to metabolites that can be converted to energy to fuel muscular contraction. The stimulus for the breakdown of muscle glycogen is the same as for contraction, and nerve signals telling the muscle to contract concurrently activate glycogen phosphorylase, which breaks down glycogen. Most muscles do not rely entirely on glycogen, and other fuels, such as fat, can also be utilized. Increased muscular

TABLE I

Selected Glycogen Storage Diseases (GSD)

GSD type	Name	Enzyme affected	Affected organ(s)	Glycogen	Description
0		Glycogen synthase	Liver	Reduced amount	Hypoglycemia
Ia	Von Gierke's disease	Glucose-6-phosphatase	Liver	Normal structure, increased amount	Massive liver enlargement, multiple metabolic problems, treatment improving
II	Pompe's disease	Lysosomal α-glucosidase	All	Increased glycogen in lysosomes	Usually death before age 2
III	Cori's disease	Debranching enzyme	Muscle, liver	Short outer branches, increased amount	Similar to type I, but less severe
IV	Andersen's disease	Branching enzyme	Liver	Long outer branches, normal amount	Usually death from liver failure before age 2
V	McArdle's disease	Muscle glycogen phosphorylase	Muscle	Normal structure, moderate increase in amount	Impaired exercise capability
VI	Hers' disease	Liver glycogen phosphorylase	Liver	Increased amount	Similar to type I but less severe

activity is often associated with increased levels of the stress hormone, epinephrine (also called adrenaline). In response to anxiety, which in evolution might have involved fleeing an aggressor, the adrenal gland produces epinephrine which activates phosphorylase in muscle and liver, providing enhanced muscle performance and increased fuel to the bloodstream respectively. Muscular activity also sensitizes the tissue to insulin and activates glycogen synthase, so that it is ready to reform glycogen once contraction ceases.

Glycogen and Disease

Glycogen Storage Diseases

A number of genetic diseases are known in which genes encoding the enzymes involved in glycogen metabolism are mutated (Table I and Figure 2). These diseases range in severity from relatively mild to early death. Their frequency is for the most part relatively low. Most of these diseases are associated with overaccumulation of glycogen or the formation of abnormally branched glycogen. One disease called glycogen storage disease 0, is associated with mutations that impair liver glycogen synthesis, and patients are prone to low blood glucose (hypoglycemia).

Diabetes Mellitus

Diabetes occurs when blood glucose homeostasis fails and blood glucose levels are elevated. High blood glucose (hyperglycemia) leads to many complications including heart, kidney, nerve, and eye disease. This disease is extremely common and growing in epidemic fashion as enrichments in diets around the world are coupled with diminished physical activity and obesity. The more prevalent form, type 2 diabetes, has a genetic component, likely linked to multiple genes, and an environmental component, lack of exercise and unhealthy diet. Type 2 diabetes is associated with an impaired ability to store glucose as glycogen but whether there is a causal relationship with defective glycogen metabolism is still not certain.

See Also the Following Articles

Diabetes • Glycogen Storage Diseases • Insulin- and Glucagon-Secreting Cells of the Pancreas

Glossary

enzyme A protein that catalyzes or accelerates chemical reactions, such as those involved in metabolism, to interconvert compounds in cells.

hormone A compound in the blood released from specialized organs, called endocrine glands, that acts as a messenger within the body to regulate the function of individual target tissues.

metabolism The process by which molecules are interconverted within cells among different related chemical forms, called metabolites.

pancreas An organ with multiple functions related to the utilization of foods. The endocrine pancreas responds to the nutrient levels in the blood to release the hormones insulin and glucagon.

Further Reading

Chen, Y.-T. (2001). Glycogen storage diseases. In *The Metabolic and Molecular Bases of Inherited Disease* (C. R. Scrives, W. S. Sly, B. Childs *et al*. eds.) 8th edition, Vol 1, pp. 1521–1551. McGraw-Hill, New York.

Harris, R. A. (2002). Carbohydrate metabolism I: Major metabolic pathways and their control. In *Textbook of Biochemistry with Clinical Correlations* (T. M. Devlin, ed.) 5th edition, pp. 597–664. Wiley-Liss, New York.

Harris, R. A., and Crabb, D. W. (2002). Metabolic interrelationships. In *Textbook of Biochemistry with Clinical Correlations* (T. M. Devlin, ed.) 5th edition, pp. 861–902. Wiley-Liss, New York.

Preiss, J., and Walsh, D. A. (1981). The comparative biochemistry of glycogen and starch. In *Biology of Carbohydrates* (V. Ginsburg and P. Robbins, eds.) Vol 1. Wiley, New York.

Roach, P. J., Skurat, A. V., and Harris, R. A. (2001). Regulation of glycogen metabolism. In *Handbook of Physiology Section 7, The Endocrine Pancreas and Regulation of Metabolism* (L. S. Jefferson and A. D. Cherrington, eds.) Vol. 2, pp. 609–647. Amer Physiological Society, MD.

Biography

Peter J. Roach, graduate of Glasgow University, is Chancellor's Professor at Indiana University School of Medicine in the Department of Biochemistry and Molecular Biology. His research addresses biological regulation at the molecular level and has focused on the control of glycogen synthesis in mammals and yeast. His principal contributions have been in defining the phosphorylation and control of glycogen synthase, including the concept of heirarchal phosphorylation, and the characterization of the self-glucosylating initiator of glycogen synthesis, glycogenin.

Glycogen Storage Diseases

George H. Sack, Jr.
The Johns Hopkins University, Baltimore, Maryland, USA

Glycogen storage diseases (GSDs) comprise a group of inherited disorders caused by dysfunction of the synthesis or degradation of glycogen. Manifestations of GSDs are largely related to their direct effects on liver and/or muscle metabolism. The medical consequences of GSDs directly relate to glycogen's central role in glucose homeostasis. Analysis of this group of disorders has identified most of the enzymes directly related to glycogen metabolism. Recognition of the presence and consequences of GSD is the basis for rational treatment of individuals with these rare conditions.

Glycogen Structure

As shown in Figure 1, glycogen is composed of a large number of glucose polymers with (α1–4) linkages that are branched with (α1–6) linkages every 4–10 units. The resulting particles, called β-particles, can become large and contain 6×10^5 individual glucose monomers and these can be grouped into even larger particles called α-particles. The β-particles are organized around a central protein called glycogenin upon which the initial glucose polymerization is based. There is also a thin bounding membrane that appears to contain most of the enzymes of glycogen metabolism. Glycogen is found mainly in liver and muscle.

Glycogen Function

Glycogen is a source of glucose for both muscle and liver. As such it serves as a short-term buffer for glucose homeostasis (liver) and a source of immediate glucose for energy (muscle). The synthesis and degradation of glycogen are closely regulated. Consistent with its function in homeostasis, these processes are controlled by different enzyme systems and hormones. Synthesis is not the reverse of degradation and most of the enzymes catalyze reactions strongly in favor of their products (i.e., they are not at equilibrium). Several of the enzymes are regulated by covalent modification.

Glycogen Metabolism

Figure 2 presents a summary of the pathways involved in glycogen metabolism. Note that several are unique to either liver or muscle. Considerable metabolic control is also exerted on these enzymes as shown.

Glycogen Synthesis

The first committed step in glycogen synthesis is the formation of UDP glucose by UDP glucose pyrophosphorylase. The glycogen polymer begins with the attachment of glucose to the protein glycogenin. UDP glucose is the substrate for polymerization via (α1–4) linkages catalyzed by glycogen synthase. The branching enzyme is bifunctional, cleaving the linear chain and creating a branch via an (α1–6) linkage. This leads to a reduced length of the final polymer and the production of more termini—leading to a more compact particle and providing a substrate suitable for very rapid degradation.

Glycogen Degradation

Most individual glucose residues are removed from the glycogen polymer by phosphorolysis. Different phosphorylase enzymes catalyze this reaction in muscle and liver. These proteins are genetically unique—synthesized from different loci. Muscle phosphorylase has been studied in particularly great detail. It functions as a dimer and contains sites for both covalent and allosteric modifications. Phosphorylase must itself be phosphorylated to be active, a reaction catalyzed by phosphorylase kinase (which itself is dependent on modification by a cAMP-dependent kinase and calcium).

Because of the branched nature of mature glycogen, either muscle or liver phosphorylase by itself can only partially degrade the polymer. Phosphorylase cannot cleave beyond four glucose residues from the branch point. Glycogen subjected to treatment with phosphorylase alone is converted into limit dextran—itself a still very large molecule. The action of the debranching enzyme eliminates the barrier to phosphorolysis by transferring the three distal glucose residues from the

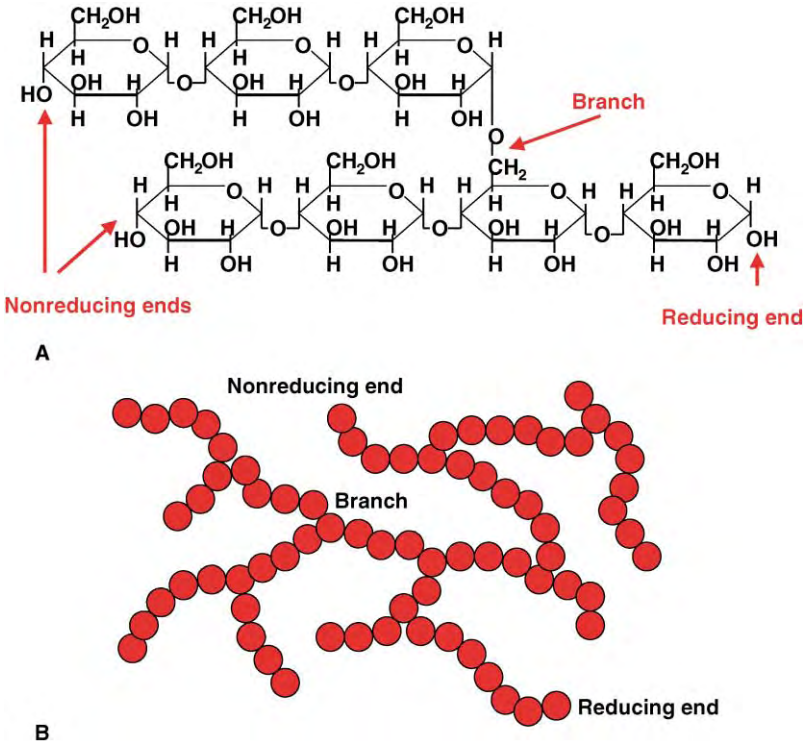

FIGURE 1 (A) Details of glycogen polymer showing linear (α1–4) and branch (α1–6) linkages. (B) Example of glycogen at lower resolution showing branches and reducing and nonreducing ends.

side chain to the nonreducing terminus of the parent chain. This leaves a single glucose remaining from the side chain attached by an α1–6 linkage. The debranching enzyme also hydrolyzes this remaining side-chain residue, freeing a single glucose molecule and leaving a continuous chain connected by α1–4 linkages, a substrate suitable for phosphorylase.

The products of glycogen degradation are thus predominantly glucose-1-phosphate and a small amount of free glucose from hydrolysis of the single remnant glucose of the side chain. The reversible phosphoglucomutase converts glucose-1-phosphate to glucose-6-phosphate. Because glucokinase is irreversible, the glucose-6-phosphate enters the endoplasmic reticulum (ER) by its own transporter. Within the liver ER, the glucose-6-phosphate is hydrolyzed and another specialized transporter transfers the free glucose outside the cell. The phosphate is also removed by its own transporter. Glucose-6-phosphatase is largely confined to the liver and thus the degradation of glycogen in muscle is not a source of blood glucose.

Control of Glycogen Metabolism

Because of the irreversibility of many of the enzymes involved and consideration of the details of Figure 2, the synthesis and degradation of glycogen do not use the same pathways. Furthermore, the enzymes mediating both sets of reactions are under tight control. This control often is mediated by addition and removal of phosphate to and from the proteins as shown. Several critical control points are given as follows:

1. The phosphorylated form of glycogen synthase (noted as "b" in the figure) is activated by removal of the phosphate to the "a" form by the active form of phosphoprotein phosphatase. The latter is produced by phosphorylation using ATP, stimulated by insulin.
2. Phosphorylase is active in its phosphorylated form, produced by the active form of phosphorylase kinase and ATP.
3. Phosphorylase kinase itself is activated by phosphorylation by cAMP-dependent protein kinase A.
4. The active, phosphorylated forms of both phosphorylase kinase and phosphorylase are inactivated through removal of the activating phosphate by the active form of phosphoprotein phosphatase as shown.

Thus, modification of existing enzymes regulates glycogen metabolism. This exquisitely sensitive system is subject to hormonal control. For example, a rise in insulin (the "fed" state with high blood glucose levels) activates phosphoprotein phosphatase (by phosphorylation). This enzyme then activates glycogen synthase and *in*activates phosphorylase and phosphorylase

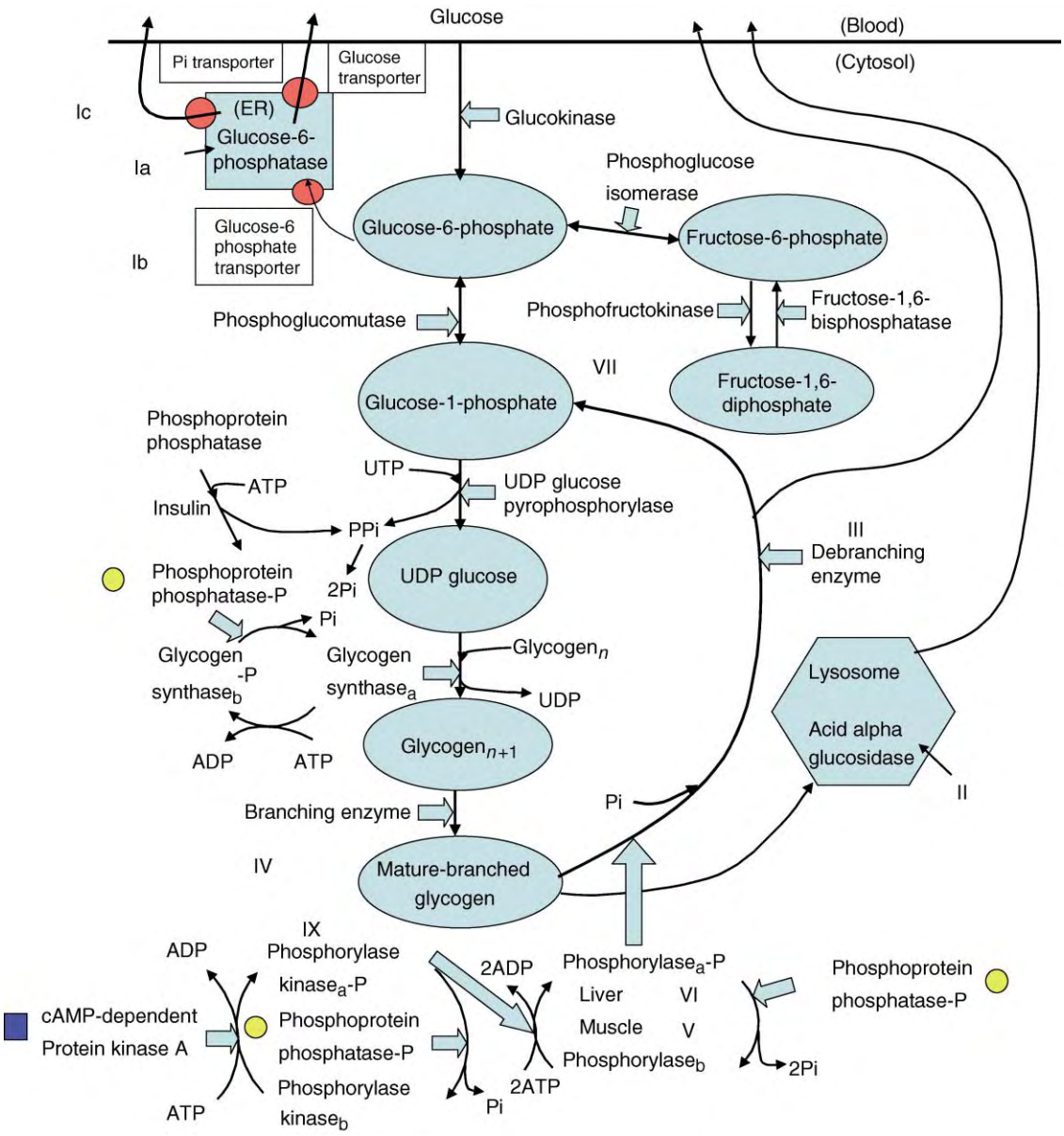

FIGURE 2 Metabolic pathways directly involved in the synthesis and degradation of glycogen. Note that blood glucose (top) is both the source of substrates for glycogen synthesis as well as the product of glycogen degradation. Compounds in ovals are biochemical intermediates. The rectangle represents the ER and the hexagonal structure represents a lysosome. Small closed circles show three sites for participation by the phosphorylated form of phosphoprotein phosphatase, formed by insulin stimulation. The small, closed square shows the site of stimulation by glucagon and epinephrine (adrenaline) through cAMP-dependent protein kinase A. The sites of enzyme defects in GSDs are indicated by the bold roman numerals.

kinase. The result is synthesis and accumulation of glycogen.

By contrast, in the "fasting" state (low blood glucose levels), insulin levels are low, inactivating phosphoprotein phosphatase. Other hormones—glucagon and epinephrine (adrenaline)—activate cAMP-dependent protein kinase A which phosphorylates (thereby activating) phosphorylase kinase. The latter, in turn, activates phosphorylase itself by phosphorylation leading to glycogen degradation.

This complex but sensitive system provides a critical buffer for blood glucose under common, relatively short-term, conditions.

Defects in Glycogen Metabolism and their Consequences

The remarkably sensitive metabolic system represented by glycogen is central to normal physiology and is an

essential defense against wide fluctuations in blood glucose levels. Because of this, defects in the pathway are often manifested by failure of glucose homeostasis with the frequent development of symptomatically low blood glucose levels (hypoglycemia). Furthermore, the shear mass of the glycogen polymer can cause organ enlargement and, ultimately, dysfunction when its degradation is inadequate. The central position of blood-borne glucose in the energy metabolism of many organs (especially the brain) has meant that careful management of glucose levels is often a prime emphasis of care for affected individuals. The disorders we consider are shown in Figure 2 and Table I. It is of historic interest that the definition and biochemical characterization of many of the enzymes of this system were based on detailed study of affected individuals. Although the general features of individual types are presented, it is important to remember that the genetic changes underlying the disorders both within and among clinical categories are not uniform. Much clinical heterogeneity likely reflects the fact that different mutations are often responsible for the failure or dysfunction of a given enzyme in different kindreds. This latter fact also complicates diagnostic studies that rely on mutation analysis alone.

Type I(a,b,c)

Originally described in 1929, individuals with one of this group of disorders have early difficulties with low blood glucose levels (hypoglycemia). In the neonatal period this can lead to seizures. Slightly later, enlargement of the liver is detected. The first biochemical study of the liver of affected individuals showed defective activity of glucose-6-phosphatase. Subsequent study of a larger number of individuals with similar manifestations led to dissection of more details of the pathway. The largest fraction of individuals shows defects in the gene and protein for glucose-6-phosphatase and this type is now known as Ia. Subsequently, it was determined that the active site of glucose-6-phosphatase lies within the ER and the glucose-6-phosphate translocase was suspected (and later shown) to be defective in another subgroup of individuals—this type is now known as Ib. Finally, a smaller group of patients has shown defects in the transport of phosphate out of the ER—these are known as type Ic.

The care of individuals affected with these three types is similar and is initially based on prevention of hypoglycemia by frequent feedings, often with the use of a slowly hydrolyzable glucose polymer (e.g., cornstarch). Liver transplantation has also been used. The long-term complications of this group of disorders are still being determined, but their prognosis is considerably improved with adequate control of blood glucose levels.

Type II

This type of GSD is unique because it involves dysfunction of an intralysosomal enzyme—α-1, 4-glucosidase (also called acid maltase). The characteristic feature of this group of individuals is the accumulation of glycogen within lysosomes. Historically, type II GSD was the first of the so-called "lysosomal storage diseases" to be defined. It is important to recall that glycogen storage and the enzymes for its synthesis and degradation are found in the cytoplasm. It has been proposed that lysosomes take up cytoplasmic glycogen and hydrolyze it within their unique low- pH environment.

Intralysosomal accumulation of glycogen in type II individuals is more notable in muscle than in liver and,

TABLE I

The Glycogen Storage Diseases

Designation	Enzyme	Eponym	OMIM#	Locus
Ia	Glucose-6 phosphatase	vonGierke	232220	17q21
Ib	Glucose-6 phosphate translocase		602671	11q23
Ic	Phosphate transporter		232240	11q23
II	Lysosomal (α-1,4-glucosidase)	Pompe	232300	17q25.2–q25.3
III	Debranching enzyme	Cord/Forbes	232400	1q21
IV	Branching enzyme	Andersen	232500	3p12
V	Muscle phosphorylase	McArdle	232600	11q13
VI	Liver phosphorylase	Hers	232700	14q21–q22
VII	Phosphofructokinase	Tarui	232800	12q13.3
IX[a]	Phosphorylase kinase		306000	Xp22.2–p22.1

[a] As noted in the text, the numerical designation(s) for defects in phosphorylase kinase have been confused, because the active enzyme comprises four subunits derived from genes at different loci. Only one of these is one the X-chromosome and that is shown in this table.

thus, many of the manifestations are related to muscle dysfunction. The disease often presents as a "myopathy" with symptoms and signs of muscle abnormalities. Muscle biopsy usually shows the characteristic glycogen accumulation within vacuoles. The severity and rate of progression of the disorder vary widely from individuals with severe disease presenting in infancy to those with a more gradual adult onset. In general, these clinical differences reflect different mutations in the same gene, but a direct correlation is not always possible. Blood glucose levels are not usually affected. Treatment is not available.

Type III

Absence or dysfunction of the debranching enzyme leads to the accumulation of glycogen with abnormal structure as noted above. This "limit dextran" represents the product of phosphorolysis up to the limits imposed by the branches. Such products are bulky with short outer branches.

Affected individuals resemble those with type I GSD as infants—they have hypoglycemia and liver enlargement. In general, the manifestations become less severe with age and individuals can survive to adulthood. Because both liver and muscle forms of the enzyme exist, rare individuals can show selective organ involvement.

Treatment is generally the same as for individuals with type I GSD, although the requirements are generally less stringent. Liver transplantation has also been used but does not affect problems in muscles.

Type IV

Consistent with the structure and synthesis of mature glycogen, defective formation of branches leads to very long polymers and bulky particles. The structure of the resulting molecules resembles amylopectin and the manifestations are related to their accumulation in the liver with attendant dysfunction of the metabolic activity and, particularly, derangement of liver architecture known as cirrhosis. Complications of cirrhosis ensue in many individuals leading to liver failure and death. Because the polymers are degradable, low blood glucose complications are not generally found. A rare variety appears to largely involve muscle. Liver transplantation has been successful in selected individuals.

Type V

Types V and VI represent the consequences of organ-specific dysfunction of phosphorylase, the primary enzyme for glycogen degradation. Type V, the muscle-specific form, is recognized by intolerance to significant muscle activity. In most individuals, quiet activities are managed well and no symptoms develop but rapid exercise can cause severe, acute muscle pain and the loss of muscle tissue integrity. Muscle cramps after exercise are common and may progress to the destruction of muscle—rhabdomyolysis. Usually, symptoms develop in adolescence or young adulthood. Because muscle glycogen is the source of energy for acute contraction, the manifestations of type V GSD are often related to the intensity of the exercise. The phosphorylase found in muscle is unique to muscle and thus its mutations do not directly affect other tissues. The most effective treatment is avoidance of intense exercise; this often can lead to a relatively good course.

Type VI

The mutations in this disorder are the hepatic counterpart of those in type V GSD. In general, the manifestations are milder than for individuals with type I(a,b,c), but poor blood glucose control and liver enlargement due to glycogen storage are seen. Muscle problems are not encountered (cf. type V). The prognosis is usually good if control of blood glucose levels can be maintained; often this can be accomplished through diet alone.

Type VII

Dysfunction of the muscle form of phosphofructokinase leads to individuals with manifestations similar to those with GSD type V—exercise-related muscle pain and fatigue. The likely pathophysiology involves elevation of the level of glucose-6-phosphate in muscle cells leading to increased glycogen synthesis. Giving glucose to affected individuals leads to lower levels of fatty acids which normally would serve as an important energy source for muscle during contraction. Thus, while administering glucose can be helpful for muscle cells in type V GSD, it can aggravate the consequence of the mutation in type VII. There is no specific treatment for this form of GSD. Avoidance of strenuous exercise (similar to the advice for individuals with type V GSD) generally is effective.

Type IX

This is a complex category, now grouped by effects on a single function. It comprises several different disorders, reflecting the fact that four individual protein subunits make up the functional phosphorylase kinase; one of these is on the X-chromosome. Although all types are rare, the X-linked form is the most frequently recognized (and is the only X-linked form of GSD).

Individuals with the X-linked form usually show moderate liver enlargement and liver function abnormalities early in life; growth often is delayed. Problems due to low blood sugar levels are not common.

In general, the manifestations become less prominent with age. Treatment is not generally required once the diagnosis has been recognized.

Because of the diversity of subunits contributing to the functional mature enzyme complex, several rare types of dysfunction have also been recognized that may be limited to the skeletal muscle or the heart. Individuals with these forms, also, generally do not require specific treatment.

Summary

Although they are rare, as a group, the GSDs have led to the understanding of many aspects of glycogen metabolism. Affected individuals develop difficulties based on the site of their underlying defect. The care of affected individuals is directed to controlling blood glucose levels and minimizing organ damage that can result from inadequate glucose mobilization and/or glycogen accumulation. Liver transplantation is a treatment option for selected patients.

See Also the Following Articles

Glycogen Metabolism • Glycogen Synthase Kinase 3 • Insulin- and Glucagon-Secreting Cells of the Pancreas • Insulin Receptor Family

Glossary

glycogen A complex, branched polymer of glucose that serves as a site of short-term glucose storage as well as a source of blood glucose during fasting.

hypoglycemia The clinical condition of low blood glucose levels with physiologic consequences including seizures caused by brain dysfunction.

myopathy Disease of muscle, in this context reflecting inadequate glucose (and, hence, energy) supply or mobilization from glycogen stores.

phosphorolysis The use of phosphate to remove successive glucose residues from the reducing end of the glycogen polymer.

Further Reading

Chen, Y.-T. (1999). Glycogen storage diseases. In *Metabolic and Molecular Basis of Inherited Disease* (C. R. Scriver, A. L. Beaudet, W. S. Sly and D. Valle, eds.) 8th edition, Ch. 71, Vol I, pp. 1521–1551. McGraw-Hill, New York.

Chou, J. Y., and Mansfield, B. C. (1999). Molecular genetics of type I glycogen storage disease. *Trends Endocr. Metab.* **10**, 104–113.

Cori, G., and Cori, C. (1952). Glucose-6-phosphatase of the liver in glycogen storage disease. *J. Biol. Chem.* **199**, 661–667.

Hirschhorn, R., and Reuser, A. J. J. (1999). Glucogen storage disease type II: Acid α-glucosidase (acid maltase) deficiency. In *Metabolic and Molecular Basis of Inherited Disease*. (C. R. Scriver, A. L. Beaudet, W. S. Sly and D. Valle, eds.) 8th edition, Ch. 135, Vol III, pp. 3389–3420. McGraw-Hill, New York.

Kazemi-Esfarjani, P., Skomorowska, E., Jensen, T. D., Haller, R. G., and Vissing, J. (2002). A nonischemic forearm exercise test for McArdle disease. *Ann. Neurol.* **52**, 153–159.

National Library of Medicine (2003). OMIM – Online Mendelian Inheritance in Man. http://www.ncbi.nlm.nih.gov/omim.

Biography

George Sack is an Associate Professor of Medicine, Pediatrics, and Biological Chemistry at the Johns Hopkins University School of Medicine. His principal research interests are in amyloid proteins and their diseases and inherited metabolic disorders affecting adults. He holds an M.D. and a Ph.D. (Molecular Biology) from Johns Hopkins where he also completed a residency in Internal Medicine and a fellowship in Medical Genetics. He is the author of the textbook "Medical Genetics" (McGraw-Hill, 1999) and a founding fellow of the American College of Medical Genetics.

Glycogen Synthase Kinase-3

James R. Woodgett
Ontario Cancer Institute, Toronto, Ontario, Canada

Glycogen synthase kinase-3 (GSK-3) is a widely expressed, multifunctional serine/threonine protein kinase that plays a role in a wide variety of regulatory processes and is implicated in diabetes, cancer, neurodegenerative diseases, and inflammation. Unlike the majority of protein kinases, this enzyme is active in resting cells and is regulated by signal-dependent inactivation. GSK-3 is a critical component of several signal transduction pathways including those that respond to Wnt and Hedgehog and receptor-tyrosine kinase pathways. GSK-3 modulates proteins involved in metabolism, transcriptional regulation, the cytoskeleton and the cell cycle and due to its role in pathophysiologically relevant conditions, is a potential therapeutic target.

GSK-3 Genes and Proteins

Mammalian genomes harbor two genes that encode for three isoforms of glycogen synthase kinase-3 (GSK-3) (Figure 1). The GSK-3α gene is located on human chromosome 19q13.2 and codes for a 51 kDa protein. The GSK-3β gene is located on human chromosome 3q13.33 and expresses a 47 kDa protein that is $>95\%$ identical to GSK-3α in the kinase catalytic domain. Through differential splicing, the GSK-3β gene also encodes a variant termed β' in which a 39 bp exon is included, adding 13 amino acids within the catalytic core. Both genes are widely expressed in all mammalian tissues and the crystal structure of GSK-3β has been solved.

GSK-3 is an ancient and conserved protein, with clear homologues in all eukaryotes. Much of the functional knowledge of the enzyme has been derived from analysis in genetically tractable organisms such as fruit flies, slime mold, and yeast.

Regulation of GSK-3

Protein kinases are typically subject to intricate modes of regulation – in most cases their activity is not induced unless a specific signal is received by a cell. GSK-3 displays the rare behavior of being fully active in the absence of cellular stimulation. Thus, in resting cells, the protein phosphorylates its catalog of substrate proteins and upon stimulation by growth factors, hormones, and other agents, GSK-3 activity is repressed, relieving phosphorylation of its targets. In general, the substrate proteins of GSK-3 are inhibited by phosphorylation. Hence, GSK-3 acts like a brake to suppress the activity of its targets (see Figure 2). This strategy allows cells to quickly respond to stimuli by activating a litany of pre-existing proteins through deactivation of just one enzyme.

There are two modes by which GSK-3 activity is regulated. Both GSK-3α and β are inhibited by phosphorylation of a serine residue located within the N-terminal regulatory domain (serine 21 in the α-isoform and serine 9 in β).

Several protein kinases phosphorylate these regulatory residues including protein kinase B(PKB)/Akt, cyclic AMP-dependent protein kinase, and several protein kinase C isoforms. As a consequence, a wide variety of stimuli result in GSK-3 inactivation including receptor-tyrosine kinases, such as the insulin receptor, that activate phosphatidylinositol 3′ kinase (which activates PKB) and agonists of G protein-coupled receptors that result in elevated cyclic AMP (Figure 2).

GSK-3 activity is also inhibited by the Wnt signaling pathway by a completely distinct and insulated mechanism (Figure 3). Wnt-mediated inhibition of GSK-3 specifically targets a select fraction of GSK-3 molecules that are associated with the Axin/adenomatous polyposis Coli (APC) complex. In resting cells, this high-molecular mass protein system acts as an efficient machine to degrade cytoplasmic β-catenin, an oncoprotein associated with colon cancer and other neoplasms. In the absence of a Wnt signal, β-catenin binds to a scaffolding protein termed Axin. Axin also sequesters a portion of GSK-3 molecules within the cell. Although GSK-3 cannot phosphorylate soluble β-catenin, when both molecules are cobound to Axin GSK-3 efficiently targets three serine residues within the amino-terminal domain of β-catenin. These phosphorylated residues form a recognition motif for E3 ligases that add a ubiquitin molecule to β-catenin which signals its rapid destruction by the 26S proteosome. In the presence

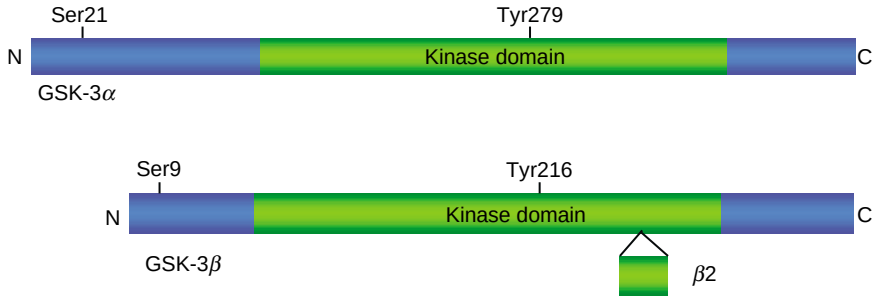

FIGURE 1 Domain structure of the two human GSK-3 genes. The regulatory phosphorylation sites are indicated.

of Wnt (a large family of secreted glycoproteins), a signaling cascade is initiated through engagement of the Frizzled class of receptors, leading to modification of an adaptor molecule termed Dishevelled that results in inhibition of phosphorylation of β-catenin by GSK-3. As a consequence β-catenin accumulates within the cytoplasm, binds to the TCF family of DNA-binding proteins, translocates to the nucleus, and modulates expression of genes such as *cyclin D* and c-*myc*. Mutations in APC or the phosphorylation domain of β-catenin result in elevated levels of the protein within cells and loss of growth control. Indeed, mutations in one of these two molecules are found in the majority of colon cancers.

Although two distinct pathways converge to inhibit the same signaling molecule, GSK-3, the cellular consequences of inactivation are specific to the signal. This, inactivation of GSK-3 via N-terminal phosphorylation of serine 21/9 does not cause stabilization of β-catenin. Nor does Wnt signaling impact metabolic targets that are regulated by insulin or growth factors. The mechanism underlying the specificity determinants remains unclear but is likely related to sequestration of a subset of GSK-3 molecules in the APC/Axin complex, effectively shielding this subset from external regulation.

GSK-3 is also phosphorylated on a tyrosine residue within the P-loop of the catalytic center. Although

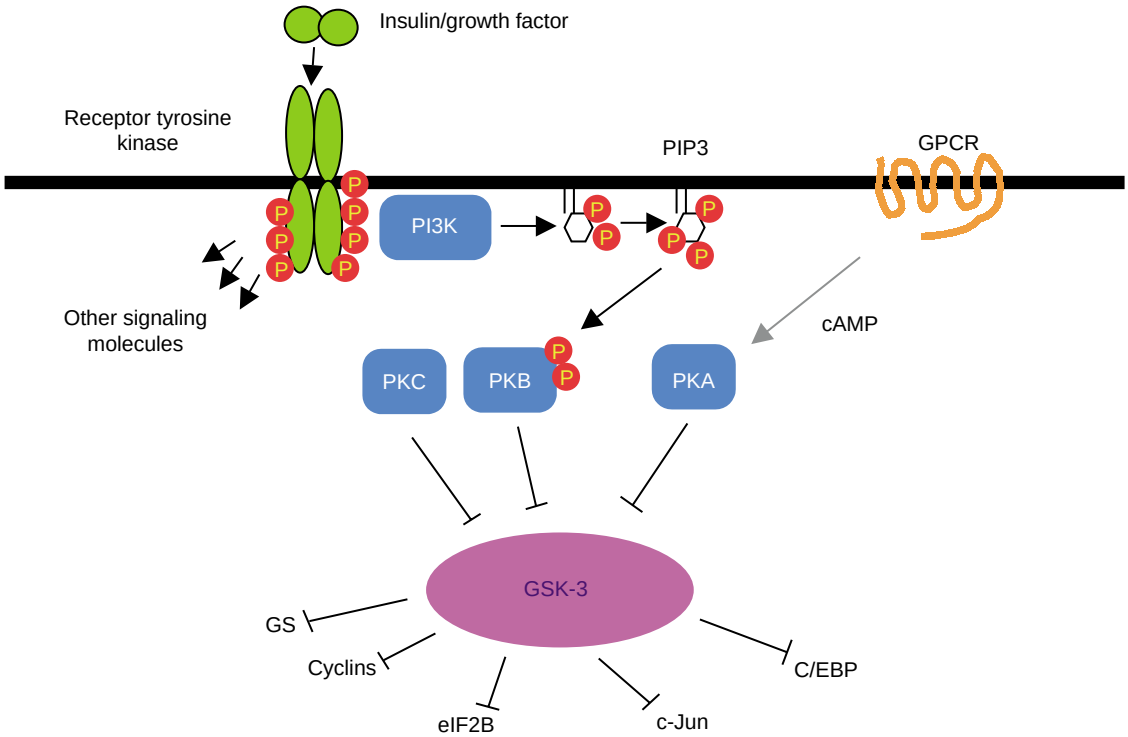

FIGURE 2 Simplified map of the regulation of GSK-3 by growth factors and mitogens. Several GSK-3 target proteins are indicated to represent the different classes of molecules regulated by GSK-3.

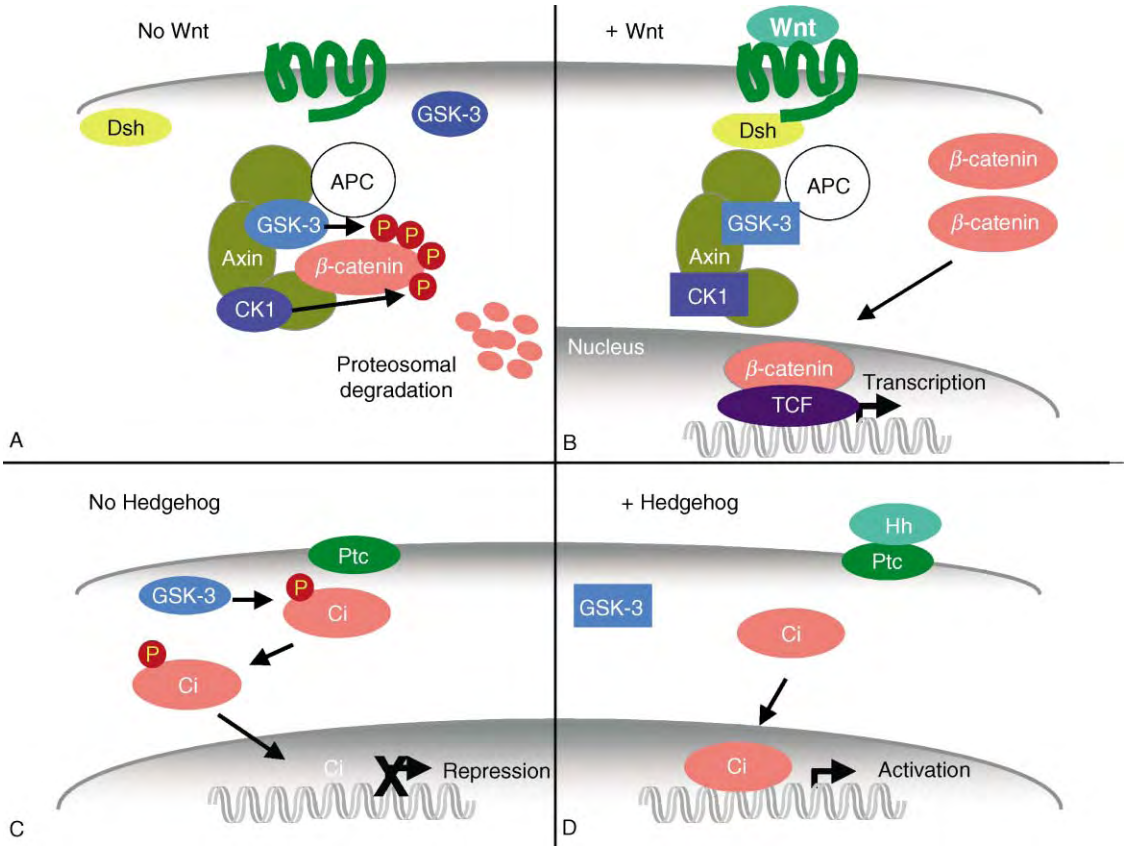

FIGURE 3 Regulation of GSK-3 by the Wnt and Hedgehog signaling proteins. The resting and stimulated states of these pathways are indicated for comparison.

phosphorylation of this site is required for full activity, the level of phosphorylation does not appear to be regulated (unlike, for example, the analogous tyrosine residues in MAP kinases). A protein-tyrosine kinase has been identified (Zak1) that targets the tyrosine in slime mold. However, in mammals, the residue is likely modified by autophosphorylation.

A Primer on GSK-3 Substrates

Many (but not all) of the proteins that are phosphorylated by GSK-3 require prior phosphorylation by a distinct protein kinase (Table I). The primary substrate recognition sequence of GSK-3 is Ser/Thr-X-X-X-Ser/Thr-phosphate where X is any amino acid but with a preference for prolines. In theory, this prerequisite for prior phosphorylation provides an additional regulatory step but in practice, many of the primed phosphorylation sites are unregulated and fully phosphorylated. Instead, the priming mechanism appears to allow a distinct form of regulatory control at the level of GSK-3 itself. The crystal structure of GSK-3β revealed the presence of several positively charged residues including a critical arginine (Arg 96) within the substrate-binding domain in a location that would permit interaction with the priming phosphorylated amino acid in the incoming substrate. In other words, the primed phospho-amino acid is an important contributor to substrate binding. However, when GSK-3 is phosphorylated within its N-terminal domain (serine 21 or 9 in GSK-3α or β respectively), this phosphorylated serine competes for the primed phosphorylation site docking motif and when bound occludes the active site. Hence, the protein kinase activity is effectively inhibited.

Substrates that require priming include glycogen synthase, CREB, inhibitor-2, cyclin E, Tau, and β-catenin. The inclusion of β-catenin in this list introduces a caveat since phosphorylation of this target is not affected by N-terminal phosphorylation of GSK-3. Since β-catenin is only phosphorylated by GSK-3 when both molecules are bound to Axin, it is possible that Axin shields GSK-3 from the inhibitory effect of a phosphorylated N-terminal domain (since β-catenin stabilization is insensitive to signals that promote N-terminal domain phosphorylation of GSK-3. Enzymes that catalyze priming of GSK-3

TABLE I

GSK-3 Substrates. GSK-3 Targets are Grouped Along with the Sequences of Known Phosphorylation Sites

GSK-3 substrate	Phosphorylation site
Wnt pathway related	
Axin	**S**AND**S**EQQ**SS**DAD**T**LSL**TS**LTD**S**
β-Catenin	D**S**GIH**S**GAT**T**TAPS LSGKGNPEEED
Cyclin D1	EEVDLAC**T**PTDVR
Cyclin E	ASPLPSGLL**T**PPQSGKK
Transcription factors	
c-Jun	**T**PPL**S**PIDME**S**QER
JunD	**S**PPL**S**PIDME**T**QER
CREB	KRREIL**S**RRPS YR
NF-ATc	PYA**S**PQT**S**PWQ**S**PCV**S**P
	LG**S**PQH**S**PST**S**P
	PY**S**PHH**S**PTP**S**PHG**S**PRV
C/EBPα	**T**PPP**T**PVP**S**P
Heat shock factor-1	EEPP**S**PPQS P
c-Myc	DIWKKFELLP**T**PPL**S**PSRRSG
L-myc	DIWKKFELVP**S**PPT**S**PPWGL
Metabolism	
ATP-citrate lyase	LLNASGSTS**T**PAP**S**RTAS FSESR
Glycogen synthase	RPA**S**VPP**S**PSL**S**RHS**S**PHQS EDEE
eIF-2B translation factor	DSEELD**S**RAGS PQLDDIKVF
G subunit of phosphatase 1	GF**S**PQP**S**RRGSSESSE
Inhibitor-2	DEPS**T**PYHSMIGDDDDAYS D
RII subunit of cAMP-dependent protein kinase	LREAR**S**RA**S**TPPAAPPS
Neuronal/structural	
Tau	TPPK**S**PSAAK VVSGDT**S**PR
Presenilin 1	NAES**T**ERE**S**QDTVAEN
Kinesin light chain	LSD**S**RTL***S***SS**S**MDL**S**RRS***S***LVG

The residues phosphorylated by GSK-3 are in bold type (if known) whereas residues that act as priming sites are underlined.

substrates include casein kinases 1 and 2 and cyclic-AMP-dependent protein kinase.

Physiological Functions of GSK-3

GSK-3 has been implicated in a wide variety of cellular processes and pathologies. The first genetic analysis of the protein kinase occurred in the fruitfly where mutants of the *Drosophila melanogaster* GSK-3 gene, termed Zeste-White3 or Shaggy, were found to display a phenotype similar to continuous signaling of the Wingless pathway, the fly counterpart of the mammalian Wnt signaling system. As described, this pathway plays an important role in controlling the activity of the β-catenin oncogene that is mutationally activated in several cancers. Since GSK-3 negatively regulates this onco-protein (in addition to other onco-proteins such as the c-Jun and c-Myc transcription factors and cyclin D, a CDK activator), it is a candidate tumor suppressor gene. However, mutations in GSK-3 have not been found in human cancers. The most likely reason is that the two mammalian isoforms of GSK-3 are encoded by distinct genes and many (but not all) of their functions are redundant. Thus, both alleles of both genes would have to be inactivated to effect complete disruption of function – an unlikely event given that loss of the first would confer no selective advantage. A second possibility is that mutational inactivation of GSK-3 is incompatible with basic cellular properties that are requisite for tumor growth such as proliferation.

A developmental pathway that often works in concert with the Wnt pathway is the Hedgehog pathway. Hedgehog, like Wnt, is a secreted factor but instead of targeting β-catenin, Hedgehog signaling prevents the cleavage of a protein termed Gli in mammals and Cubitus interruptus (Ci) in flies (Figure 3). In resting cells, Ci is processed into two fragments, one of which acts as a transcriptional repressor. This cleavage requires phosphorylation of Ci by GSK-3. Upon binding of Hedgehog to its receptor (Patched) cleavage is inhibited. The pathway thus has several parallels to Wnt signaling, although it is unclear whether GSK-3 is directly regulated by Hedgehog signaling or is, instead, a passive player that maintains low amounts of the uncleaved Ci protein under resting conditions.

Neurological Diseases

Dysregulation of GSK-3 has been implicated in neurological diseases such as Alzheimer's disease and bipolar disorder. This protein kinase is one of several that targets sites of phosphorylation of the microtubule-associated protein Tau that are hyperphosphorylated in insoluble structures termed neurofibrilliary tangles. These deposits are found in the brains of patients with Alzheimer's disease and are associated with neuronal death. Transgenic mice expressing a mutant of GSK-3β that cannot be inhibited by N-terminal phosphorylation demonstrate higher than normal Tau phosphorylation. A further connection to this debilitating disease was recently uncovered by the finding that inhibition of GSK-3 reduced the generation of Aβ peptide from the amyloid precursor protein. This peptide is the product of the γ-secretase protease complex that is responsible to overproduction of Aβ that aggregates to form the primary constituent of amyloid plaques. These deposits are early markers of the disease. Activation of GSK-3 in neuronal cells has also been correlated with induction of apoptosis such that

death induced by serum deprivation can be suppressed by GSK-3 inhibition. Finally, GSK-3 is inhibited by lithium ions at concentrations that are therapeutically effective for the treatment of bipolar disorder. Inhibitors of GSK-3 therefore have potential therapeutic value in the control of at least two neurological disorders.

Knockout Mice

Mice lacking GSK-3β die during embryogenesis from liver failure. The defect was traced to aberrant induction of the NF-κB transcription factor by TNF-α in the liver that leads to hepatocyte cell death. TNF-α typically induces both a proapoptotic and an NF-κB-mediated survival signal within cells. However, in the cells lacking GSK-3β, induction of survival genes by NF-κB was found to be defective, leading to dominance of the proapoptotic signal and the demise of the hepatocytes. The mechanism by which GSK-3β influences NF-κB is unclear, although there is evidence of both positive and negative regulation. Chemical inhibition of GSK-3 also leads to sensitization of cells to TNF-α. Of note, although the embryonic lethality of the mice lacking GSK-3β can be rescued by either injection of anti-TNF-α antibodies or by breeding with mice that lack the 55 kDa receptor for TNF-α, the mice still die shortly after birth indicating additional critical roles for the protein kinase during development.

Metabolism and Diabetes

While the initial identification of GSK-3 was rooted in the study of glycogen metabolism, study of this kinase has largely focused on its roles in other processes, perhaps as a result of genetic analysis. However, GSK-3 is the predominant regulator of glycogen synthase inhibition. This role has been resurrected by studies assessing the effects of GSK-3 inhibitors on glucose uptake and metabolism in response to insulin. Insulin acts to activate phosphatidylinositol 3′ kinase and PKB leading to phosphorylation and inactivation of GSK-3 (Figure 2). Inhibitors of this protein kinase may therefore be predicted to act as insulin sensitizers. Such drugs are highly sought in the treatment of type 2 diabetes, a growing health problem as populations increase their degree of obesity and age. Small molecule inhibitors of GSK-3 have been shown to act as effective insulin sensitizers in several animal models of diabetes, reducing circulating blood glucose and enhancing glycogen deposition. In addition to negatively regulating glycogen synthase, GSK-3 also phosphorylates and inhibits other proteins important to insulin's mechanism of action including IRS1, ATP-citrate lyase, and eIF2B. Thus, GSK-3 inhibition promotes anabolic processes such as fatty acid and protein synthesis.

One potential spoiler to the use of GSK-3 inhibitors as insulin sensitizers is the concern that chronic inhibition of this protein kinase may lead to inappropriate accumulation of β-catenin, a potent oncogene. However, cells appear to have a built-in fail-safe mechanism that normally prevents unscheduled induction of β-catenin. For example, loss of 50% of total GSK-3 activity results in virtually no increase in noncadherin-associated β-catenin. Inhibition of at least 75% of GSK-3 activity is required for substantial stabilization in the absence of a specific signal (one of the Wnts). The reason for this is at least partially related to the relative levels of the Wnt signaling components compared to GSK-3. Axin is present at significantly lower concentrations than GSK-3($\alpha + \beta$). Hence, only when total GSK-3 levels decrease below that of Axin will processing of β-catenin be affected in the absence of a Wnt signal. Since most therapeutics are used at concentrations that dampen rather than eradicate activity, there exists likely a therapeutic window that allows tempering of aberrant GSK-3 activity without impacting stabilization of β-catenin. However, this Damacles Sword will dangle over the use of GSK-3 inhibitors until at least preclinical trials demonstrate no increase in tumor incidence upon chronic administration of the drugs. Given rapid progress in the development of potent and specific inhibitors of GSK-3, an answer to this question is not far away.

See Also the Following Articles

Diabetes • Glycogen Metabolism • Glycogen Storage Diseases • Secretases

Glossary

adenomatous polyposis coli (APC) A large protein that is frequently mutated in colorectal cancer that is a component of the β-catenin destruction complex.

glycogen synthase (GS) The rate-limiting enzyme of glycogen deposition that is inhibited by phosphorylation.

nuclear factor of κB (NF-κB) An important transcription that binds specific sequences in DNA and plays roles in regulating inflammatory responses and in deciding whether a cell will live or die following stress.

protein kinase An enzyme that catalyzes the transfer of phosphate from adenosine triphosphate (ATP) to the serine, threonine, or tyrosine residues.

Wnt An evolutionarily conserved family of extracellular proteins that regulate developmental processes by binding to a specific receptor (Frizzled) and initiating a cascade of events within cells that includes the accumulation of β-catenin.

Further Reading

Dajani, R., Fraser, E., Roe, S. M., Young, N., Good, V., Dale, T. C., and Pearl, L. H. (2001). Crystal structure of glycogen synthase kinase 3

beta: Structural basis for phosphate-primed substrate specificity and autoinhibition. *Cell* **105**, 721–732.

Doble, B. W., and Woodgett, J. R. (2003). GSK-3: Tricks of the trade for a multi-tasking kinase. *J. Cell Sci.* **116**, 1175–1186.

Eldar-Finkelman, H., and Ilouz, R. (2003). Challenges and opportunities with glycogen synthase kinase-3 inhibitors for insulin resistance and Type 2 diabetes treatment. *Expert Opin. Invest. Drugs* **12**, 1511–1519.

Gurvich, N., and Klein, P. S. (2002). Lithium and valproic acid: Parallels and contrasts in diverse signaling contexts. *Pharmacol. Ther.* **96**, 45–66.

Jope, R. S. (2003). Lithium and GSK-3: One inhibitor, two inhibitory actions, multiple outcomes. *Trends Pharmacol. Sci.* **24**, 441–443.

Nusse, R. (2003). Wnts and Hedgehogs: Lipid-modified proteins and similarities in signaling mechanisms at the cell surface. *Development* **130**, 5297–5305.

Biography

Jim Woodgett is a Senior Scientist at the Ontario Cancer Institute and Amgen Professor of Cancer Biology at the University of Toronto. His research interests focus on the dysregulation of signaling pathways in human cancer. His research group is studying the molecular biology of the phosphatidylinositol 3′ kinase and Wnt systems using transgenic mice, cell biology, genetic and functional genomic approaches. He has enjoyed working on the biology of GSK-3 for over 20 years and still marvels at the diversity of functions of the enzyme.

Glycolipid-Dependent Adhesion Processes

Senitiroh Hakomori
University of Washington, Seattle, Washington, USA

The majority of glycolipids in mammalian cells are glycosphingolipids (GSLs), with the exception of sulfated galactosyl diglyceride (seminolipid) present in testis, seminal fluid, and a very small quantity in brain. Therefore, this article is limited to cell adhesion caused by GSLs. Although >500 GSLs are known, only ~10 species of GSLs have been studied and found to mediate cell-to-cell adhesion. Change of signal transduction and cell phenotype take place in most cases of GSL-dependent cell adhesion. The known examples may constitute only a small proportion of the existing cases, since this area of research is still in the early stage of development. There may be a number of cell adhesion systems mediated by GSLs that are not yet known. Glycolipid-dependent cell adhesion requires a specific assembly in which a cluster of GSLs is present as a functional center. Because GSL-dependent adhesion takes place through clustered GSLs in microdomain, we will first explain GSL assembly in membrane, then report cases of cell adhesion mediated through such microdomains.

GSL Assembly in Membrane as GSL-Enriched Microdomain

Cluster Formation by GSL-to-GSL *Cis* Interaction

Ceramide, the lipid moiety of glycosphingolipids (GSLs), has aminoacyl (N-acyl) residue and hydroxyl group that act as hydrogen bond donors, whereas glycerides and glycerophospholipids have only O-acyl group that act as hydrogen bond acceptor. In addition, GSLs have a number of hydroxyl groups and N-acyl residues at the sugar moiety, that may provide a much stronger hydrogen bond donor (Figure 1A). At the plane of lipid bilayer, the presence of sphingolipids and GSLs therefore provides higher and stronger *cis* interaction, i.e., GSL-to-GSL side-by-side interaction. Glycerides and glycerophospholipids in the same lipid bilayer plane, although they constitute the major lipid components, show much weaker *cis* interaction. By a similar mechanism, glycoproteins show strong *cis* interaction, possibly through their hydrogen bonds, to form clusters separable from GSL clusters. Thus, GSLs and glycoproteins are clustered to form independent patches or islands separated from the sea of glycerophospholipids on the cell surface, as shown in Figure 1B. Sphingomyelin interacts with cholesterol but is separated from glycerophospholipids in gel state, as evidenced by ESR and IR spectroscopy. GSL clusters occur in the absence of cholesterol.

Association of Clustered GSLs with Lipophilic Signal Transducers and Proteolipids: Assembly of "Glycosynapse"

Clustered GSLs in cell membranes can be separated as insoluble low-density membrane by homogenization in high-salt, or in lysis buffer containing neutral detergent, followed by density-gradient ultracentrifugation. The GSL-enriched buoyant fraction contains >95% of GSLs originally present in cells, but <1% of total cellular protein. The proteins found in this fraction, from many cell types, are cSrc, other Src family kinases, and small G proteins (Ras, RhoA, RAC), which contain long-chain aliphatic acyl groups and are closely associated with GSLs. In addition, the fraction has proteolipid proteins and tetraspanins, which are also closely associated with GSLs and signal transducers. Molecular assembly of these components in microdomain forms a functional unit in membrane essential for cell adhesion with concurrent signal transduction; the unit is collectively termed "glycosynapse."

Cell Adhesion Through Clustered GSLs

Two types of GSL-dependent cell adhesion processes can be considered.

1. GSL cluster is recognized by or bound to complementary GSL cluster expressed on counterpart cell surface glycosynapse, i.e., GSL-to-GSL *trans* interaction.

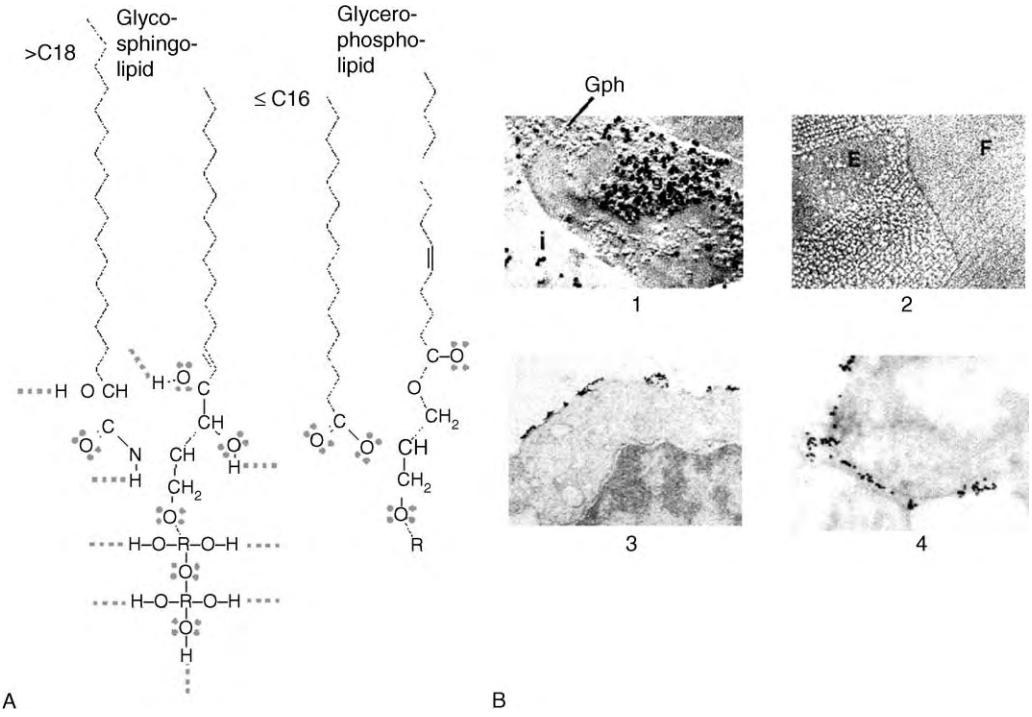

FIGURE 1 Clustering of glycosphingolipids and glycoproteins on membrane due to *cis* interaction. (A) Contrasting properties of GSLs and glycerophospholipids in ability for hydrogen bond formation. GSLs are both hydrogen bond donors and acceptors (indicated respectively by ····H—O and Ö═C), whereas glycerophospholipids only accept hydrogen bond, due to absence of hydroxyl group (OH). (B) Clustering is visualized by scanning electron microscopy following freeze-fracture technique: glycophorin (Gph) clustering, and globoside (Gb4) clustering on erythrocyte membrane (in 1), GM1 clustering on dipalmitoyl phosphatidylcholine liposome surface (in 2). Cell surface GSL clustering is also observed by transmission electron microscopy using specific antibody-gold sol conjugates: GM3 clustering on T-lymphocyte surface (in 3), polysialoganglioside clustering in neuronal cells (in 4).

Such interaction takes place through specific complementary structures. The binding between carbohydrate moieties of GSLs is catalyzed, in many cases, by Ca^{2+}. There is a steadily increasing number of examples of such complementary GSL pairs, providing the basis of GSL-dependent adhesion. A model of such interaction involving single molecules of Gb4 and nLc_4, as a basis of cell adhesion, is shown in Figures 2A–2C. In reality, however, GSLs are not present as single molecules, but are clustered on membrane. Cell adhesion occurs through such GSL clusters in association with signal transducers (glycosynapse), to activate or inhibit signaling. A model is shown in Figure 3.

2. GSL cluster, particularly ganglioside cluster, is bound to ganglioside-binding lectin (siglec) such as siglec-4 or -7. Alternatively, GSL having βGal residue (e.g., GM1) is recognized by galectin, or GSL having SLe^x or SLe^a residue is recognized by E-selectin.

Processes 1 and 2 are shown schematically in Figure 4. In either process, structure of GSLs is the target of cell adhesion, recognized by complementary GSL (Figure 4A) or by specific binding protein (Figure 4B), which triggers activation or inhibition of signal transducers.

Types of Cell Adhesion Mediated by GSL-to-GSL Interaction

Mouse Melanoma B16 Cell Adhesion to Mouse Endothelial Cells Through GM3-to-LacCer or GM3-to-Gg3Cer Interaction

B16 cells are characterized by predominance of GM3 ganglioside. Their adhesion to mouse or human endothelial cells (ECs) is based on interaction of GM3 (on melanoma cells) with LacCer or Gg3Cer (on ECs). LacCer is present on essentially all types of ECs, whereas Gg3Cer has more restricted distribution on lung microvascular ECs, where metastasis may occur preferentially. The degree of this "GM3-dependent adhesion" is closely correlated with metastatic and invasive potential of B16 cells, based on the following observations: (1) *in vitro* GM3-dependent adhesion was inhibited by liposomes containing GM3, LacCer, or Gg3Cer; (2) *in vivo* metastatic potential of B16 cells in terms of lung colonization was inhibited by administration of GM3- or Gg3Cer-liposomes; (3) enhancement of B16 cell motility and invasiveness following

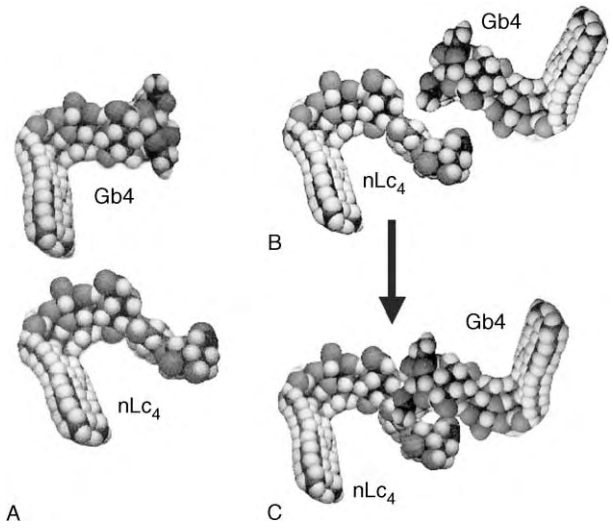

FIGURE 2 *trans* interaction of GSLs as a basis of glycolipid-dependent cell adhesion. (A) Minimum-energy conformational model of Gb4 and nLc_4. Note that axis of carbohydrate is perpendicular to that of sphingosine and fatty acid (ceramide). (B) Gb4 on the surface of one cell and nLc_4 on surface of counterpart cell have complementary surface profile. (C) Gb4 and nLc_4 adhere to each other, by carbohydrate-to-carbohydrate interaction, as a basis for cell adhesion.

GM3-dependent adhesion was indicated by activation of cSrc, RhoA, and FAK at glycosynapse. GM3-to-Gg3Cer and -LacCer interactions were well studied recently by surface plasmon resonance spectroscopy.

F9 Cell Autoaggregation Through Le^x-to-Le^x Interaction

Mouse embryonal carcinoma F9 cells show strong autoaggregation, simulating morula-stage preimplantation embryo. Both F9 cell autoaggregation and compaction of morula are inhibited by a trivalent Le^x-lysyllysine conjugate. The molecular mechanism of Le^x-dependent autoaggregation was found to be Le^x-to-Le^x interaction in the presence of Ca^{2+}. The process was recently well elucidated by molecular force microscopy and by surface plasmon resonance spectroscopy.

Human Embryonal Carcinoma Autoaggregation Through Gb4-to-nLc_4 or Gb4-to-Gb5 Interaction

Gb4, Gb5, and nLc_4 are highly expressed, in addition to Le^x, in mouse preimplantation embryo. Expression of Gb5 is much higher than that of Le^x in human embryonal carcinoma and in primate preimplantation embryo, although the expression status of these GSLs and carbohydrate antigens in human embryo has not been studied for ethical reasons. Autoaggregation of human embryonal carcinoma, which may mimic the compaction process of human embryo, is mediated by Gb4-to-nLc_4 or Gb4-to-Gb5 interaction (Gb4-dependent adhesion). These GSLs are closely associated with cSrc, RhoA, and Ras in glycosynapse, and may induce differentiation following Gb4-dependent adhesion.

Rainbow Trout Sperm Binding to Egg Mediated by (KDN)GM3 Interaction with Gg3-Like Epitope

A novel deaminated analogue of sialic acid, 2-keto-3-deoxy-D-*glycero*-D-*galacto*-nononic acid (KDN), is found in fish egg and sperm. The head of rainbow trout

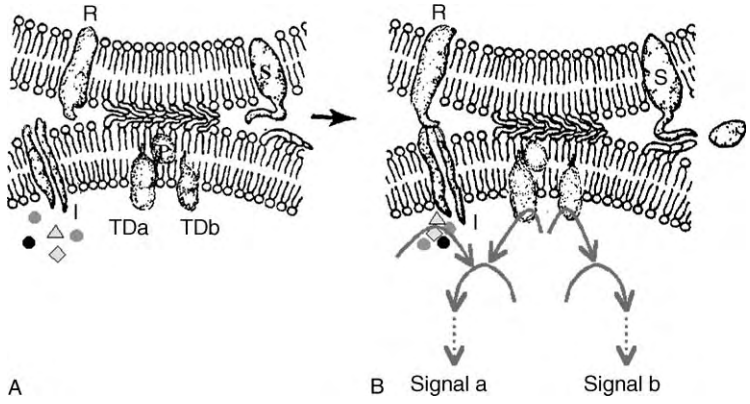

FIGURE 3 Model of GSL-based glycosynapse, and GSL-dependent adhesion through carbohydrate-to-carbohydrate interaction. (A) Clustered GSLs on the surface membrane of one cell are bound to cluster of another type of GSL on surface membrane of counterpart cell, through *trans* interaction of GSLs as in Figure 2. (B) Such adhesion induces change (activation or inhibition) of signal transducers (TDa, TDb) to send signals (a, b). In some cases, this process is synergistic with another adhesion system, such as integrin receptor (I) and its binding counterpart (R, e.g., ICAM1), or other type of carbohydrate-dependent receptor (S, e.g., CD44).

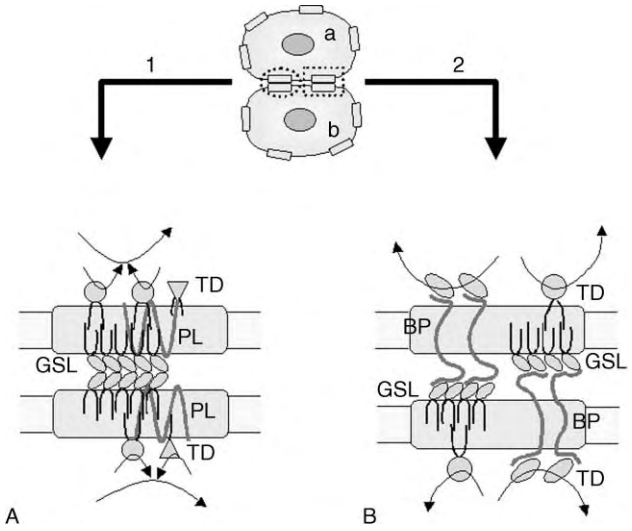

FIGURE 4 Two types of GSL clusters in glycosynapse function in GSL-dependent adhesion. Adhesion of cell a to cell b occurs via adhesion processes 1 and 2. (A) Process 1 is based on GSL clusters associated directly with signal transducers (TD), and stabilized by proteolipids (PL). Adhesion proceeds through interfacing of the two glycosynapses, and carbohydrate-to-carbohydrate interaction, and concurrent activation or inhibition of signal transducers. (B) Process 2 is based on GSL clusters and their binding protein (BP). Through interfacing of the two glycosynapses, GSLs are bound to BP, whereby TD is activated or inhibited.

sperm has a high content of (KDN)GM3, as indicated by reactivity with specific anti-(KDN)GM3 mAb kdn3G, and binds strongly to plates coated with Gg3, but not other GSLs. This binding is inhibited by kdn3G and by anti-Gg3 mAb 2D4. Vitelline envelope membrane isolated from rainbow trout egg has a glycoconjugate containing Gg3-like epitope, defined by antibody 2D4. Immunoelectron microscopy revealed that the Gg3-like epitope is highly expressed in exposed second layer of vitelline envelope surrounding the micropyle, a narrow channel through which a sperm enters the egg cell. Thus, interaction of (KDN)GM3 at sperm head with Gg3-like epitope surrounding the micropyle is a crucial event in the process of rainbow trout fertilization.

Types of Cell Adhesion Mediated by Interaction of GSL with GSL-Binding Protein

Neuronal Axon Binding to Myelin Through Interaction of Ganglioside with Siglec-4

Neuronal cell membranes are characterized by the presence of ganglio-series gangliosides. Gangliosides expressed at neuronal cell axons interact with myelinating glial cells through myelin-associated glycoprotein (MAG), which was known previously as sialic acid-binding protein siglec4. GD1a and GT1b, which have sialyl $\alpha 2 \rightarrow 3$Gal terminal residue, are specific functional ligands of MAG that inhibit nerve regeneration and neurite formation. Inhibition of ganglioside synthesis by P4, or blocking of ganglioside interaction with MAG by anti-ganglioside IgG antibodies, reversed the MAG-dependent inhibitory effect on neurite formation.

Aggregation of Renal Cell Carcinoma TOS1 Cells with Peripheral Blood Mononuclear Cells Through Interaction of Disialoganglioside with Siglec-7

Renal cell carcinoma (RCC) has high metastatic potential to lung, and the degree of metastatic potential is correlated with RCC expression of disialogangliosides, which are ligands of sialic acid-binding protein siglec-7, the major siglec expressed in peripheral blood mononuclear cells (PBMC). These disialogangliosides expressed in RCC were identified as disialyl-Lc_4 (defined by mAb FH9), GalNAc-disialyl-Lc_4 (defined by mAb RM2), disialyl-Gb5 (defined by mAb 5F3), and GD3 (defined by mAb R24). RCC cell line TOS1 is characterized by expression of disialyl-Lc_4, GalNAc-disialyl-Lc_4, and GD3, and interacts with siglec-7 on the surface of PBMC, causing aggregation of TOS1 cells with PBMC. Large aggregates of this type may result in microembolisms that initiate metastasis, particularly in lung.

Adhesion of Neutrophils or Myelogenous Leukemia HL60 Cells to E-Selectin Through Fucosyl-poly-LacNAc Ganglioside (Myeloglycan)

Sialyl-Le^x (SLe^x) has been regarded as the major ligand of human neutrophils, or myelocytic, or monocytic leukemia cell lines (e.g., HL60, U937) that interact with E-selectin expressed on ECs. Extensive studies on human neutrophils and HL60 cells indicated that SLe^x epitope is absent from GSLs and gangliosides of these cells. Instead, E-selectin-binding epitopes were identified as poly-LacNAc with multiple $\alpha 1 \rightarrow 3$ fucosylation and terminal $\alpha 2 \rightarrow 3$ sialylation:

$$\text{NeuAc}\alpha 3\text{Gal}\beta 4\,\text{GlcNAc}\beta 3\,[\text{Gal}\beta 4\text{GlcNAc}\beta 3\text{Gal}\beta 4\,\underset{\text{Fuc}\alpha}{\overset{3}{\text{GlcNAc}}}\,]_n\beta 3\,\text{Gal}\beta\text{GlcCer} \qquad n \geq 1$$

These GSLs display strong E-selectin-dependent adhesion, particularly under dynamic flow conditions, and are collectively termed "myeloglycan."

Human Neuroblastoma Adhesion through GM1-to-Galectin-1 Interaction

Human neuroblastoma expresses ganglio-series gangliosides and galectin-1. Neuroblastoma cell contact activates endogenous sialidase, which causes conversion of GD1a, GD1b, GT1b, etc. to GM1, and consequent accumulation of GM1. GM1 is one of the ganglio-series gangliosides having terminal βGal residue that is recognized by galectin-1; therefore, GM1 at the neuroblastoma cell surface promotes cell-to-cell adhesion. Galectin-mediated cell adhesion has been proposed, but the target carbohydrate was identified as glycoprotein, and little attention has been paid to GSLs.

See Also the Following Articles

Glycolysis, Overview • Lipid Modification of Proteins: Targeting to Membranes • Lysophospholipid Receptors • Sphingolipid Biosynthesis • Sphingolipid Catabolism

Glossary

glycosphingolipid Carbohydrate glycosidically bound to primary hydroxyl group of N-fatty acyl sphingosine.

glycosynapse The assembly of glycosphingolipids and other glycoconjugates in membrane, associated with cytoplasmic signal transducers having long-chain acyl group, and with hydrophobic transmembrane proteins. The assembly performs carbohydrate-dependent cell adhesion with concurrent signaling.

GSL structures Gb4, GalNAcβ3Galα4Galβ4Glcβ1Cer; Gb5, Galβ3GalNAcβ3Galα4Galβ4Glcβ1Cer; Gg3, GalNAcβ4Galβ4Glcβ1Cer; GM3, NeuAcα3Galβ4GlcCer; LacCer, Galβ4Glcβ1Cer; LacNAc, Galβ4GlcNAc$\beta \rightarrow$ R; Lc_4, Galβ3GlcNAcβ3Galβ4GlcCer; Le^x, Galβ4[Fucα3]GlcNAcβ3Gal$\beta \rightarrow$ R; nLc_4, Galβ4GlcNAcβ3Galβ4Glcβ1Cer.

Further Reading

Hakomori, S. (2000). Traveling for the glycosphingolipid path. *Glycoconj. J.* **17**, 627–647.

Hakomori, S. (2002). The glycosynapse. *Proc. Natl. Acad. Sci. USA* **99**(1), 225–232.

Hakomori, S., and Handa, K. (2002). Glycosphingolipid-dependent cross-talk between glycosynapses interfacing tumor cells with their host cells: Essential basis to define tumor malignancy. *FEBS Lett.* **531**(1), 88–92.

Handa, K., Stroud, M. R., and Hakomori, S. (1997). Sialosyl-fucosyl poly-LacNAc without the sialosyl-Le^x epitope as the physiological myeloid cell ligand in E-selectin-dependent adhesion: Studies under static and dynamic flow conditions. *Biochemistry* **36**, 12412–12420.

Ito, A., Handa, K., Withers, D. A., Satoh, M., and Hakomori, S. (2001). Binding specificity of siglec7 to disialogangliosides of renal cell carcinoma: Possible role of disialogangliosides in tumor progression. *FEBS Lett.* **504**(1–2), 82–86.

Kopitz, J., von Reitzenstein, C., Burchert, M., Cantz, M., and Gabius, H. J. (1998). Galectin-1 is a major receptor for ganglioside GM1, a product of the growth-controlling activity of a cell surface ganglioside sialidase, on human neuroblastoma cells in culture. *J. Biol. Chem.* **273**, 11205–11211.

Rojo, J., Morales, J. C., and Penades, S. (2002). Carbohydrate–carbohydrate interactions in biological and model systems. *Topics Curr. Chem.* **218**, 45–92.

Vyas, A. A., Patel, H. V., Fromholt, S. E., Heffer-Lauc, M., Vyas, K. A., Dang, J., Schachner, M., and Schnaar, R. L. (2002). Gangliosides are functional nerve cell ligands for myelin-associated glycoprotein (MAG), an inhibitor of nerve regeneration. *Proc. Natl. Acad. Sci. USA* **99**(12), 8412–8417.

Biography

Dr. Senitiroh Hakomori is Professor of Pathobiology and Microbiology, University of Washington, and Head, Division of Biomembrane Research, Pacific Northwest Research Institute, Seattle, Washington. His major work has been focused on structure, function, and organization of glycosphingolipids. He was also involved in discovery of fibronectin, and systematic analysis of blood group ABH including cloning and structure of their genes. He has received many national and international awards, and was elected to the National Academy of Sciences in 2000.

Glycolysis, Overview

Robert A. Harris
Indiana University School of Medicine, Indianapolis, Indiana, USA

Glycolysis is a linear metabolic pathway of enzyme-catalyzed reactions that convert glucose to two molecules of pyruvate in the presence of oxygen or to two molecules of lactate in the absence of oxygen. Anaerobic glycolysis is likely the first pathway that evolved in nature to produce ATP and it remains the only pathway for ATP production in some cells. In most cells, however, glycolysis serves to convert glucose to pyruvate rather than lactate, with pyruvate subsequently being oxidized to carbon dioxide and water by mitochondrial enzymes. Since oxygen is necessary for complete pyruvate oxidation, glycolysis is the only option cells have for the production of ATP in the absence of oxygen. Glycolysis is frequently elevated in malignant tumors and may favor survival and proliferation of cancer cells. Overproduction of lactic acid by glycolysis leads to lactic acidosis, a life-threatening condition.

Role of Glycolysis

ATP Production

In the absence of either oxygen or mitochondria, glycolysis operates as a self-contained pathway with lactate as its end product (Figure 1A). Energy released by exergonic reactions is captured with the formation of two molecules of ATP from two molecules of ADP and inorganic phosphate (Pi):

$$\text{Glucose} + 2\text{ADP} + 2\text{Pi} \rightarrow 2\text{Lactate} + 2\text{ATP}$$

Production of ATP by this overall sum equation for the pathway is the most important function of glycolysis. Some cells depend entirely upon the ATP produced by glycolysis. For example, mature red blood cells obtain all of their ATP in this manner because they lack mitochondria, the oxygen-consuming organelles responsible for production of practically all of the ATP in most cells. Uninterrupted production of ATP is required for proper function and survival of all cells. The simplest of all cells in the body, red blood cells still require the continuous operation of the glycolytic pathway to produce ATP to power their Na^+, K^+-ATPase and a number of processes.

Preparatory Pathway for Glucose Oxidation

The function of glycolysis changes when oxygen is available and mitochondria are present. When oxygen and mitochondria are both present, glucose is completely oxidized to carbon dioxide and water (Figure 1B) by the sum reaction:

$$\text{Glucose} + 6\text{O}_2 + 32\text{ADP} + 32\text{Pi} \rightarrow 6\text{CO}_2 + 6\text{H}_2\text{O} + 32\text{ATP}$$

Glycolysis sets the stage for the complete oxidation of glucose, a process that produces 16 times more ATP per glucose molecule than anaerobic glycolysis. In the absence of either oxygen or mitochondria, glycolysis yields two molecules of pyruvate that must be reduced to lactate for glycolysis to proceed (Figure 1A). When oxygen is present, pyruvate is taken up by mitochondria and the entire molecule is oxidized to carbon dioxide and water by the sequential actions of the pyruvate dehydrogenase complex, citric acid cycle, and the electron transport chain (Figure 1B).

Because mitochondria are present in most cells and there is continuous supply of oxygen from the blood, virtually every tissue of the body uses glycolysis as a preparatory pathway, which provides them with much greater amounts of ATP from each glucose than anaerobic glycolysis. The human brain, for example, completely oxidizes about 120 g of glucose each day, all via pyruvate molecules produced from glucose by glycolysis. Lactate is present in the brain, but the amount is small and none is released into the blood because the brain is well oxygenated and mitochondria are abundant.

Three Stages of the Glycolytic Pathway

Conversion of glucose to lactate occurs in three stages in the cell cytoplasm (Figure 2).

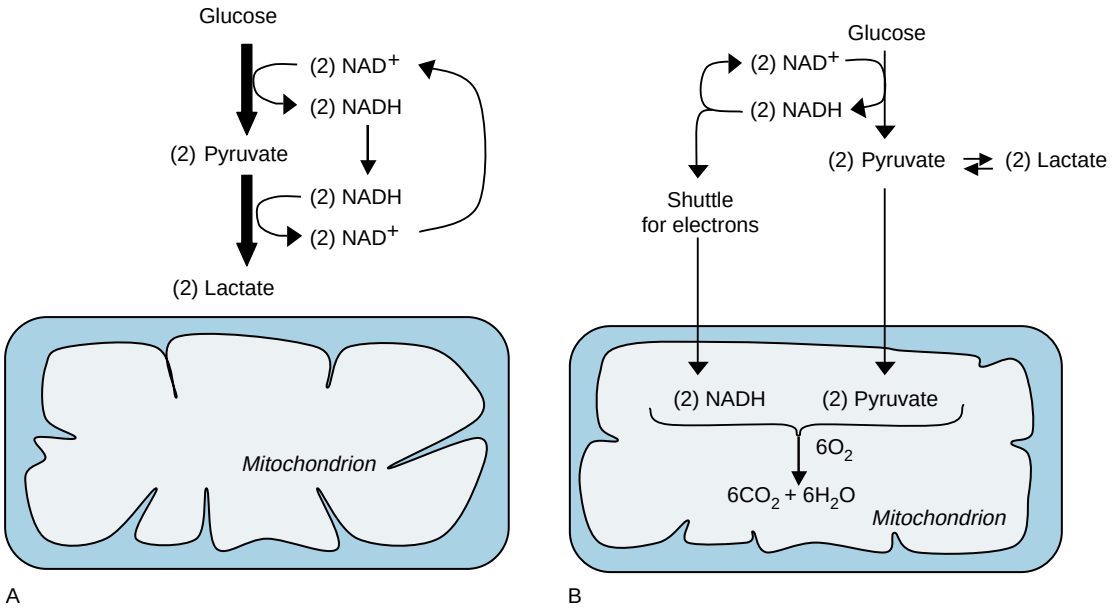

FIGURE 1 Overviews of glycolysis. (A) Lactate is the product of glycolysis in the absence of oxygen. (B) Glycolysis serves as a preparatory pathway for the complete oxidation of glucose in the presence of oxygen.

Priming Stage

The first three reactions of the pathway prime the glucose molecule for use by subsequent enzymes. ATP molecules are invested in the reactions catalyzed by hexokinase and 6-phosphofructo-1-kinase. Phosphorylation traps glucose inside the cell and sets the stage for subsequent cleavage of the glucose into two 3-carbon fragments. The priming stage sums up to be simply:

$$\text{Glucose} + 2\text{ATP} \rightarrow \text{Fructose 1,6-bisphosphate} + 2\text{ADP}$$

Splitting Stage

Fructose 1,6-biphosphate undergoes cleavage by aldolase between carbons 3 and 4 in the first step of the splitting stage. Dihydroxyacetone phosphate and glyceraldehyde 3-phosphate, known collectively as triose phosphates, are produced by an aldol cleavage of fructose 1,6-bisphosphate. Interconversion of the triose phosphates by an isomerase completes the splitting stage, which sums up to be:

$$\text{Fructose 1,6-bisphosphate} \rightarrow 2\text{Glyceraldehyde 3-phosphate}$$

Energy-Trapping Stage

Six enzymes are required to capture the energy made available in this stage. All of the ATP produced by glycolysis is generated in this stage by the reactions catalyzed by 3-phosphoglycerate kinase and pyruvate kinase. Since two glyceraldehyde 3-phosphate molecules are converted to two lactate molecules, a total of 4 ATPs are produced in this stage, which sums up to be:

$$2\text{Glyceraldehyde 3-phosphate} + 4\text{ADP} + 2\text{Pi} \rightarrow 2\text{Lactate}^- + 4\text{ATP}$$

The sum of the three stages yields the overall equation for anaerobic glycolysis in which one molecule of glucose is converted to two molecules of lactate with the production of two molecules of ATP:

$$\text{Glucose} + 2\text{ADP} + 2\text{Pi} \rightarrow 2\text{Lactate}^- + 2\text{ATP}$$

Anaerobic Glycolysis is a Type of Fermentation

Fermentations are pathways that (1) produce ATP, (2) do not involve oxygen, (3) involve an intermediate that becomes oxidized, and (4) involve an intermediate that becomes reduced. That ATP is produced and oxygen is not required can be seen from the overall equation for glycolysis:

$$\text{Glucose} + 2\text{ADP} + 2\text{Pi} \rightarrow 2\text{Lactate}^- + 2\text{ATP}$$

Whether an intermediate becomes oxidized and another reduced is not shown. However, during the first reaction of the energy trapping stage of glycolysis (Figure 2), the aldehyde group ($-$CHO) of glyceraldehyde 3-phosphate is oxidized to a carboxylic acid ($-CO_2^-$) and then phosphorylated to give a mixed anhydride of a carboxylic acid and phosphoric acid

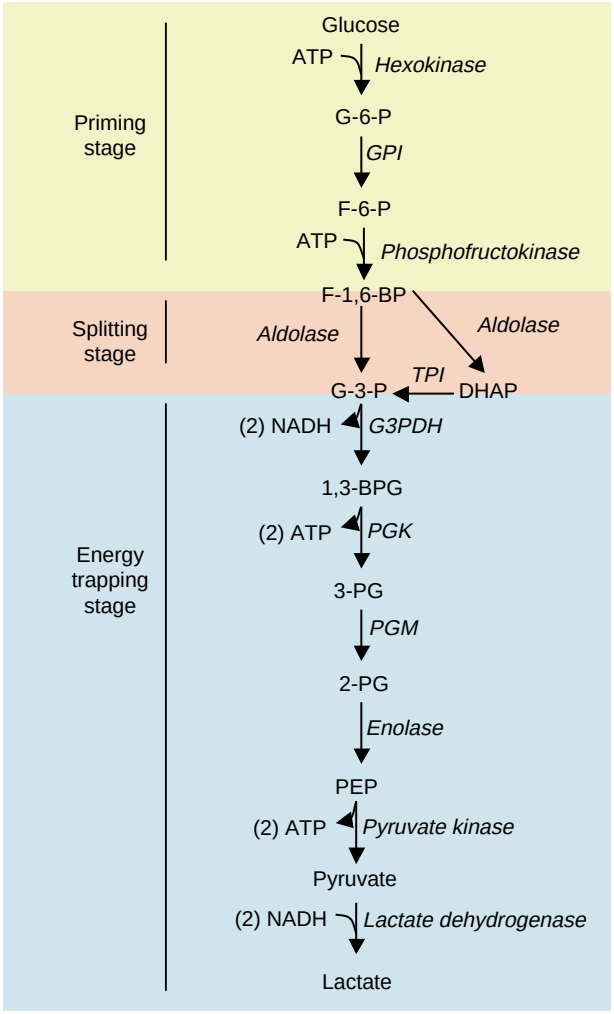

FIGURE 2 The three stages of the glycolytic pathway: Priming, splitting, and energy trapping. Abbreviations for glycolytic intermediates: G-6-P, glucose 6-phosphate; F-6-P, fructose 6-phosphate; F-1,6-BP, fructose 1,6-bisphosphate; G-3-P, glyceraldehyde 3-phosphate; DHAP, dihydroxyacetone phosphate; 1,3-BPG, 1,3-bisphosphoglycerate; 3-PG, 3-phosphoglycerate; 2-PG, 2-phosphoglycerate; PEP, phosphoenolpyruvate. Abbreviations for glycolytic enzyme names: GPI, glucose phosphate isomerase; TPI, triose phosphate isomerase; G3PDH, glyceraldehyde-3-phosphate dehydrogenase; PGK, phosphoglycerate kinase; PGM, phosphoglycerate mutase.

(1,3-biphosphoglycerate):

$$R-CHO + Pi + H_2O \rightarrow R-CO_2P + 2e^- + 2H^+$$

$$NAD^+ + 2e^- + 2H^+ \rightarrow NADH + H^+$$

$$\text{Sum}: \; R-CHO + NAD^+ + H_2O + Pi \rightarrow R-CO_2P + NADH + H^+$$

In the last reaction of the energy trapping stage of glycolysis (Figure 2), the α-keto group of pyruvate is reduced to give the α-hydroxyl group of lactate:

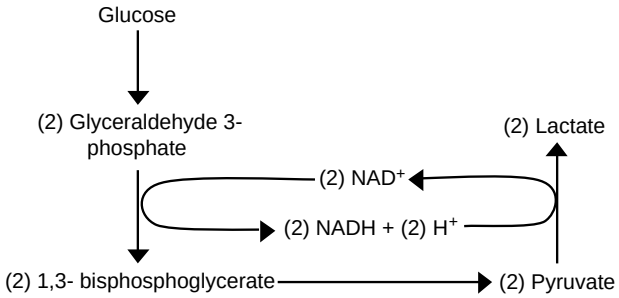

FIGURE 3 NAD^+ serves as a bridge molecule to couple the oxidation of glyceraldehyde 3-phosphate to the reduction of pyruvate during anaerobic glycolysis.

$$NADH + H^+ \rightarrow NAD^+ + 2e^- + 2H^+$$

$$CH_3-CO-CO_2^- + 2e^- + 2H^+ \rightarrow CH_3-CHOH-CO_2^-$$

$$\text{Sum}: \; CH_3-CO-CO_2^- + NADH + H^+ \rightarrow CH_3-CHOH-CO_2^- + NAD^+$$

NAD^+ serves as a bridge compound for these reactions (Figure 3), accepting two electrons and one H^+ to become NADH during the oxidation of the aldehyde group of glyceraldehyde 3-phosphate and subsequently donating two electrons and one H^+ when it returns to being NAD^+ during the reduction of the α-keto group of pyruvate. The result is a perfect balance between the production of NADH in an oxidation step and its utilization in a reduction step. Anaerobic glycolysis is therefore a type of fermentation.

Control of Glycolysis

The rate at which ATP is hydrolyzed back to ADP and Pi by energy requiring reactions is a major determinant of flux through the glycolytic pathway. In other words, ATP turnover caused by energy required to perform the work being done by a cell greatly affects the rate of glycolysis. The presence or absence of oxygen also has a profound effect upon the rate of glycolysis.

ATP Turnover

Two molecules of ATP are produced for each molecule of glucose utilized by glycolysis. Less obvious, but important for an understanding of what controls the rate of glycolysis, "two molecules of ATP must be hydrolyzed to ADP and Pi for each glucose utilized." This is because the amount of ADP present in cells is quite small relative to the large amount of glucose that has to be utilized to meet the energy needs of cells. Glycolysis can therefore

not proceed without hydrolyzing ATP to make ADP available for energy conserving steps. Hydrolysis of ATP to ADP plus Pi is usually rate limiting for the process of glycolysis. Thus, an increase in ATP turnover caused by an increase in the amount of work being done by a cell has a profound effect upon the rate of glycolysis. For example, strenuous exercise induces a marked increase in glycolysis because of ATP hydrolysis by the contractile machinery of muscle.

Oxygen

A remarkable "decrease" in glycolysis occurs when cells that lack oxygen are transferred into an environment in which oxygen is abundantly available. Carbon dioxide production starts immediately but cells use much less glucose and accumulate little or no lactate. This illustrates the Pasteur effect, which refers back to Louis Pasteur's observation ~150 years ago that oxygen inhibits the fermentation of glucose by yeast. The Pasteur effect reflects the marked difference in cellular capacity for ATP production in the presence and absence of oxygen. Relative to anaerobic glycolysis, 16 times more ATP is produced when glucose is completely oxidized to carbon dioxide and water by the combined actions of glycolytic and mitochondrial enzymes. The rate of glycolysis decreases greatly in the presence of oxygen because the ATP needed to meet the energy needs of a cell can be supplied by the catabolism of much less glucose.

Lactate is not produced when oxygen is available to cells. Less glucose has to be used to meet the need for ATP, which automatically means less pyruvate is produced and available for reduction to lactate by NADH. The pyruvate that is produced by glycolysis is also rapidly oxidized by the mitochondria, leaving less available for reduction to lactate by NADH. And finally, less NADH is available for the reduction of pyruvate to lactate because shuttle mechanisms operate in the presence of oxygen to transport the electrons of NADH into mitochondria by the net equation:

$$\mathrm{NADH_{cytosol} + H^{+}_{Cytosol} + NAD^{+}_{Mitosol} \rightarrow NAD^{+}_{Cytosol} + NADH_{Mitosol} + H^{+}_{Mitosol}}$$

NADH generated in the mitochondria is oxidized by the electron transport chain, which provides energy for the synthesis of ATP by oxidative phosphorylation according to net equation:

$$\mathrm{NADH + H + \tfrac{1}{2}O_2 + 2\tfrac{1}{2}ADP + 2\tfrac{1}{2}Pi \rightarrow NAD^{+} + 2\tfrac{1}{2}ATP + H_2O}$$

Removal of oxygen from the environment of cells utilizing glucose has the opposite effect. Glycolysis is greatly stimulated as evidenced by increased glucose utilization and lactate production. Anaerobic glycolysis

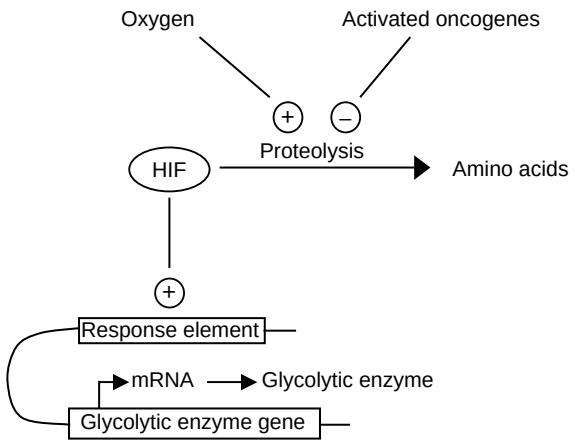

FIGURE 4 Oxygen controls glycolytic enzyme expression by controlling the amount of HIF (hypoxia inducible factor), a transcription factor that regulates transcription of genes that encode glycolytic enzymes.

can sometimes meet the need of cells for ATP. Sometimes it is inadequate, in spite of an increase in its rate. Cells can and do die when ATP is not generated fast enough to keep them viable, which is what happens in the heart during a heart attack or in the brain as a consequence of a stroke. Cells that survive in an oxygen-poor environment are usually able to elevate their capacity for glycolysis by increasing the amounts of the glycolytic enzymes present. This in turn increases the activities of the glycolytic enzymes and therefore the capacity for ATP synthesis by glycolysis. Lack of oxygen signals an increase in the transcription of the genes that encode the glycolytic enzymes. This occurs because lack of oxygen (hypoxia) causes an increase in the amount of a protein called hypoxia *i*nducible *f*actor (HIF) (Figure 4). HIF is a transcription factor that promotes transcription when it binds to a specific sequence of nucleotides in promoter region of genes encoding glycolytic enzymes. Oxygen stimulates proteolytic degradation of HIF (Figure 4), which keeps the amount of HIF very low in cells, which in turn keeps the amounts of the glycolytic enzymes also low. Hypoxia maximizes the amount of HIF, which greatly increases expression of the glycolytic enzymes and therefore cellular capacity for glycolysis.

Cancer

Malignant tumors make good use of glycolysis as a source of ATP. Rates of glycolysis are often faster in malignant tumors than normal tissues. Radiologists and oncologists take advantage of this phenomenon in the diagnosis of cancer by PET imaging. Radioactive glucose derivatives accumulate in cancer cells because of their greater glycolytic capacity. Surprisingly, tumor cells often metabolize glucose to lactate even in the

"presence" of oxygen. This is unusual and stands in contrast to normal cells that only metabolize glucose to lactate in the "absence" of oxygen, as discussed previously. The conversion of glucose to lactate in the presence of oxygen is called aerobic glycolysis, to distinguish it from anaerobic glycolysis which refers to the conversion of glucose to lactate in the absence of oxygen. The high rate of aerobic glycolysis exhibited by some cancer cells is called the Warburg effect, in recognition of Otto Warburg's discovery ~80 years ago that tumor cells produce lactate in the presence of oxygen. Based on this observation Warburg championed the idea that aerobic glycolysis is the cause of cancer. Now, however, it is appreciated that up-regulation of the enzymatic capacity of glycolysis occurs frequently in cancer cells because of a higher concentration of HIF, the transcription factor responsible for regulation of the transcription of genes encoding glycolytic enzymes (Figure 4). HIF is highly expressed in many tumor cells even in the presence of oxygen, most likely as a consequence of mutations that have occurred in genes that either prevent (tumor suppressors) or promote (oncogenes) the development of cancer. Since tumors sometimes outgrow their blood supply and cancer cells frequently migrate into areas of the body where the oxygen concentration is low, an exceptionally high capacity for ATP production that does not require oxygen may provide cancer cells with a metabolic advantage for survival and growth.

Lactic Acidosis

Regardless of whether anaerobic or aerobic, glycolysis produces acid if lactate is the end product of the pathway. The acid produced by glycolysis lowers the pH both inside cells where lactate is produced as well as outside where protons can diffuse. Since the pH range in which cells can function is quite narrow (pH 7.0–7.6), uncontrolled glycolysis can lead to cell death. This is the Achilles' heel of glycolysis. Indeed, in the final analysis it is overproduction of acid and lowering of the pH by glycolysis that kills most organisms, including humans. In an effort to emphasize the production of ATP by glycolysis, unbalanced reactions were used in the description of glycolysis. The production of protons by glycolysis was ignored. However, cells incubated under anaerobic conditions produce large amounts of acid by anaerobic glycolysis. Likewise, forcing an area of the heart to obtain all of its energy from glycolysis by occluding a coronary artery causes rapid production of large amounts of acid, which lowers the pH, activates nerve endings, and registers as pain. That the conversion of glucose to lactate produces acid is apparent when we write the "balanced" overall equation for glycolysis in the following manner:

$$\text{Glucose} \rightarrow 2\,\text{Lactate}^- + 2\text{H}^+$$

Since the empirical formula for glucose is $C_6H_{12}O_6$, and there are 6 carbons, 12 hydrogens, and 6 oxygens in the products, this equation is balanced for mass and charge. Thus, two protons are produced for every glucose molecule converted to lactate molecules by glycolysis. Since glycolysis produces 2 ATPs per glucose, the equation seems incomplete, and in one sense it is incomplete. Expanding the equation to include ADP, Pi, and ATP in their predominant ionization states at physiological pH yields:

$$\text{Glucose} + 2\text{ADP}^{3-} + 2\text{Pi}^{2-} \rightarrow 2\,\text{Lactate}^- + 2\text{ATP}^{4-} + 2\text{H}_2\text{O}$$

If this is accepted as the appropriate equation for glycolysis, balanced as it is for mass and charge, the pathway does not produce acid and therefore should have no effect on cellular pH. However, anaerobic glycolysis can clearly be shown to produce acid experimentally, and the reason it does so is again because the pool size of ATP is small compared to the amount of glucose that is converted to lactate to meet the energy needs of a cell. For every glucose molecule converted to lactate, two ATP molecules have to be hydrolyzed according to the equation:

$$2\text{ATP}^{4-} + 2\text{H}_2\text{O} \rightarrow 2\text{ADP}^{3-} + 2\text{Pi}^{2-} + 2\text{H}^+ + \text{"work"}$$

Work in this equation refers to any of the many energy-requiring processes that can only occur as a consequence of ATP hydrolysis, such as muscle contraction, Na^+, K^+-ATPase activity, etc. Summing up the last two equations brings us back to the overall balanced equation that shows acid production by glyolysis:

$$\text{Glucose} \rightarrow 2\,\text{Lactate}^- + 2\text{H}^+$$

Anaerobic glycolysis therefore produces acid. Conditions in humans that greatly increase anaerobic glycolysis because of a shortage of oxygen and the resulting Pasteur effect, such as failure of the respiratory system or the blood circulatory system, often cause the production of more acid than can be handled by the buffering systems of the body. The consequence is lactic acidosis, a life-threatening condition that can be dealt with most effectively by supplying oxygen, which will block the Pasteur effect and inhibit the production of lactic acid.

See Also the Following Articles

N-Linked Glycan Processing Glucosidases and Mannosidases • Pyruvate Dehydrogenase • Pyruvate Kinase

Glossary

cancer Unlike normal tissue or a benign tumor, cancer cells exhibit the property of invasion of other organs of the body.

hypoxia Condition in which the oxygen content of a tissue is so low that it limits electron transport activity by mitochondria.

Na^+, K^+-ATPase Enzyme complex present in the plasma membrane of all cells that utilizes the energy provided by ATP hydrolysis to drive the transport of Na^+ out and K^+ into cells.

oxidation–reduction reactions Reaction in which one compound gets oxidized (loses electrons) and another compound gets reduced (gains electrons).

PET imaging A technique for creating an image of a tissue that relies upon the use of positron emission tomography (PET) to measure a signal produced by a short-lived radionuclide such as ^{18}F-fluorodeoxyglucose.

Further Reading

Berg, J. M., Tymoczko, J. L., and Stryer, L. (1995). Glycolysis. In *Biochemistry*, 5th edition, pp. 425–449. W. H. Freeman, New York.

Gibson, D. M., and Harris, R. A. (2002). *Metabolic Regulation in Mammals*. Taylor and Frances, London.

Harris, R. A. (2002). Carbohydrate metabolism I: Major metabolic pathways and their control. In *Textbook of Biochemistry with Clinical Correlations* (T. M. Devlin, ed.) 5th edition, pp. 597–664. Wiley-Liss, New York.

Harris, R. A., and Crabb, D. W. (2002). Metabolic interrelationships. In *Textbook of Biochemistry with Clinical Correlations* (T. M. Devlin, ed.) 5th edition, pp. 861–902. Wiley-Liss, New York.

Semenza, G. L. (2002). Signal transduction to hypoxia-inducible factor 1. *Biochem. Pharm.* **64**, 993–998.

Stubbs, M., Bashford, C. L., and Griffiths, J. R. (2003). Understanding the tumor metabolic phenotype in the genomic era. *Curr. Mol. Med.* **3**, 485–505.

Biography

Robert A. Harris, a graduate of Purdue University, is Distinguished Professor, Showalter Professor, and Chairman of Biochemistry and Molecular Biology at the Indiana University School of Medicine. Postdoctoral training was completed in the laboratories of David Green (Wisconsin) and Sir Hans Krebs (Oxford). Dr. Harris teaches metabolism and directs the medical biochemistry course for first year medical students. His research contributions include the identification and characterization of several mitochondrial enzymes involved in pyruvate and the branched-chain amino acids metabolism.

Glycoprotein Folding and Processing Reactions

Armando J. Parodi
Fundacion Instituto Leloir, Buenos Aires, Argentina

The term glycoprotein folding and processing reactions refers to the mechanisms by which cells ensure that only properly folded glycoproteins follow the secretory pathway. The concept of quality control of protein folding first appeared in the late 1970s and early 1980s when it was noticed that not in all cases insertion of proteins or glycoproteins in the endoplasmic reticulum (ER) leads to their expected final destination, either intracellular (for instance, the lysosomes) or secretion. Several experimental results showed that cells displayed mechanisms that ensured that only proteins in their native conformations could be produced by the secretory pathway. Those mechanisms received the collective denomination of "quality control." By far the best-studied quality control mechanism is that occurring in the ER but more recent studies revealed that it also takes place at the Golgi apparatus. The scope of this article will be limited to the quality control occurring on glycoproteins in the ER.

Protein Folding in the Endoplasmic Reticulum

The endoplasmic reticulum (ER) quality control system is adapted to handling virtually any condition that results in a protein conformation other than the native state. Accordingly, multiple scenarios of quality control arise from the many ways in which proteins can fail to achieve their native conformation. All kinds of polypeptides inserted into the ER are subject to quality control, including soluble and membrane proteins (type I, II, and multispan). It applies to proteins regardless of their quaternary structure and whether they are glycosylated or contain intra- or intermolecular bonds. Proteins can fail the quality control due to multiple factors, such as truncations or mutations that interfere with proper folding, as well as orphan subunits of hetero-oligomeric complexes or homo-oligomers that cannot reach their proper structure. The lack of ligand binding or post-translational modifications (signal sequence cleavage, disulfide bond formation, *N*-glycosylation or glycosylphosphatidylinositol (GPI) anchor addition) can prevent proteins from folding correctly. Moreover, normal proteins that do not have any of the mentioned defects can also be targets of the quality control system, as protein folding is an extremely hazardous process whose efficiency heavily depends not only on particular environmental conditions but also on the amino acid primary sequence. In fact, almost never do all normal protein molecules manage to reach their proper native structure; there is always a variable fraction of newly synthesized proteins that do not fold efficiently.

A number of abundant ER resident proteins that participate in retention of non-native conformers have been identified as chaperones and folding-assisting proteins. Protein disulfide isomerase (PDI), one of the first facilitators of protein folding described, is an abundant ER chaperone. PDI and other members of the thioredoxin family participate in disulfide bond formation as well as retention and degradation of targets of the quality control system. Of particular interest is one member of this family (ERp57) that specifically associates with two ER resident lectins and contributes to proper glycoprotein folding. Another abundant ER protein, binding protein (BiP) that was originally identified as an ER retention factor for immunoglobulin heavy chains, participates in assisting protein folding through cycles of ATP hydrolysis that regulate substrate binding and release.

N-Glycan Processing Reactions in the Endoplasmic Reticulum

Glycosylation of asparagine residues (*N*-glycosylation) in the mammalian cell ER presents two basic differences with respect to glycosylation of Ser/Thr units (*O*-glycosylation) in either the cystosol or the Golgi apparatus: (1) in the former case a glycan containing 14 monosaccharide units in most cell types is transferred "*en bloc*" to the polypeptide chain whereas in *O*-glycosylation either a variable number of

monosaccharide units are sequentially transferred (Golgi *O*-glycosylation) or a single of such units is added (cytosolic *O*-glycosylation) and (2) *N*-glycosylation occurs on not yet properly folded polypeptide moieties, whereas in all cases *O*-glycosylation is a post-folding event. After being transferred to nascent chains in the ER, *N*-glycans are processed all along the secretory pathway. Whereas processing in the ER is basically similar in all eukaryotic cells for all *N*-glycans, Golgi processing reactions present a broad variation not only among different cell types but also different *N*-glycans belonging to the same or different glycoproteins may be differently processed within the same cell, thus yielding mature glycoproteins bearing glycan moieties with widely different structures. This diversity presents certain logic as the roles of protein-linked glycans in mature glycoproteins are mainly related to recognition phenomena. On the contrary, glycan processing in the ER is basically similar in all cells because the role of those reactions directly relates to a process common to all glycoproteins, namely the acquisition of their proper tertiary structures.

Addition of *N*-glycans has several effects on protein folding, at least two of which may be observed not only *in vivo* but also in folding assays performed in test tubes with pure glycoproteins: (1) *N*-glycans provide bulky, highly hydrophilic groups that help to maintain glycoproteins in solution during the folding process and (2) the presence of glycans modulates protein conformation by forcing amino acids close to the linking Asn unit to be in the proximity of the water-glycoprotein interphase. This article will not deal with those effects but with *in vivo* folding facilitation and ER retention of improperly folded structures mediated by the interaction of a specific glycan structure (monoglucosylated glycans) with ER lectins as calnexin (CNX) and calreticulin (CRT).

The saccharide transferred in most wild-type cells from a lipid (dolichol) derivative to polypeptide chains as they enter the ER lumen has the composition $Glc_3Man_9GlcNAc_2$ and the structure depicted in Figure 1. This is a well-conserved structure in nature as the same glycan is transferred in wild-type mammalian, plant, and fungal cells. There are some exceptions to this common pattern in certain protozoa, in which truncated *N*-glycans are transferred. The consensus glycosylation sequence (Asn–X–Ser/Thr, where X may be any amino acid except for Pro) is not necessarily glycosylated. Apparently, *N*-glycosylation, which occurs when the involved Asn unit is about 10–12 amino acids far from the inner ER membrane surface, is hindered if the polypeptide chain rapidly adopts a secondary structure. Cell-free assays showed that the oligosaccharyltransferase transfers the triglucosylated glycan about 20–25-fold faster than $Man_9GlcNAc_2$. This property, as well as the strict distance between the receptor amino acid and the ER inner surface required for glycan transfer, determine a severe underglycosylation of glycoproteins synthesized by cell mutants unable to glucosylate the lipid-linked glycan. Folding is severely impaired in many (but not all) underglycosylated glycoproteins.

The external Glc unit (residue *n*, Figure 1) is immediately removed from the protein-linked glycan by glucosidase I (GI), a membrane bound α-(1,2)-glucosidase (see mammalian cell ER processing of *N*-glycans in Figure 2). Further deglucosylation mediated by glucosidase II (GII), an α-(1,3)-glucosidase, may remove the remaining Glc units (residues *l* and *m*, Figure 1). GII is a soluble heterodimer composed of catalytically active and inactive subunits. The latter, but not the former, contains an ER retrieval sequence at its C terminus. Depending on the species, one or two Man units may be removed in the ER. Mammalian mannosidases I and II excise Man units *i* and *k*, respectively (Figure 1). A single ER α-mannosidase occurs in *Saccharomyces cerevisiae* that yields the same product as mammalian α-mannosidase I.

An additional *N*-glycan processing reaction occurring in the ER lumen is the transient glucosylation of

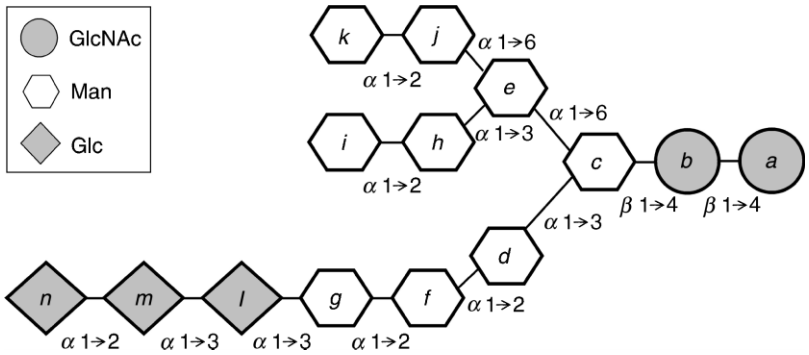

FIGURE 1 Glycan structures. Lettering (*a*–*n*) follows the order of addition of monosaccharides in the synthesis of $Glc_3Man_9GlcNAc_2$-P-P-dolichol. GI removes residue *n* and GII residues *l* and *m*. GT adds residue *l* to residue *g*. The $Man_8GlcNAc_2$ isomer formed by mammalian cell or *S. cerevisiae* ER α-mannosidase I lacks residues *i*, and *l*–*n* and that formed by mammalian cell ER α-mannosidase II is devoid of residues *k* and *l*–*n*.

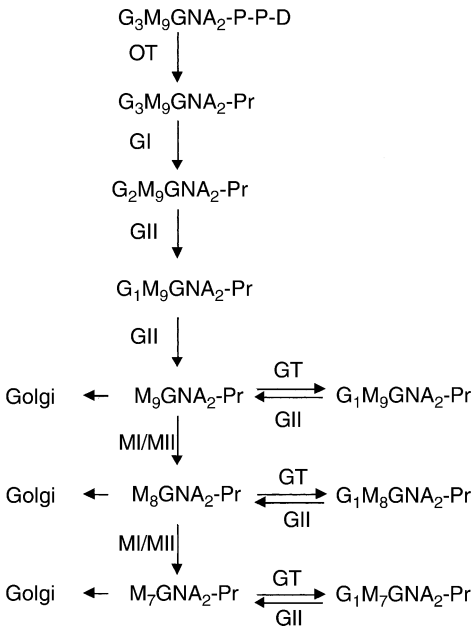

FIGURE 2 Glycan processing in the ER. G, M, GNA, D, and Pr stand for Glc, Man, GlcNAc, dolichol, and protein, respectively. OT, GI, GII, GT, MI, and MII stand for oligosaccharyltransferase, glucosidase I, glucosidase II, UDP-Glc:glycoprotein glucosyltransferase, mannosidase I, and mannosidase II, respectively.

glycoproteins: glucose-free glycans may be reglucosylated by the UDP-Glc:glycoprotein glucosyltransferase (GT) yielding $Glc_1Man_9GlcNAc_2$, $Glc_1Man_8GlcNAc_2$ and $Glc_1Man_7GlcNAc_2$ as reaction products. The structure of the first one is identical with that produced by partial deglucosylation of $Glc_3Man_9GlcNAc_2$ (Figure 1) and GII is also responsible for the *in vivo* deglucosylation of the monoglucosylated compounds formed by GT. This enzyme is present not only in mammalian but also in plant, fungal, and protozoan cells. *S. cerevisiae* is the only cell known so far to lack GT.

The Golgi apparatus of species belonging to the chordate phylum display an endomannosidase activity that degrades monoglycosylated *N*-glycans yielding Glc_1Man (plus $Man_{6\text{-}8}GlcNAc_2$, depending on the substrate used). This enzyme has been described to occur also in the mammalian cell ER-Golgi intermediate compartment. It may be speculated that the role of this enzyme is to ensure a complete removal of Glc units, as their presence would hinder formation of complex-type glycans in the Golgi apparatus.

The UDP-Glc:glycoprotein Glucosyltransferase

The transient addition of a terminal glucose residue to protein-linked glycans was discovered while studying *N*-glycan processing in trypanosomatid cells pulse-chased with [^{14}C]Glc. These *in vivo* observations were then extended to other eukaryotes, and it was soon established that transient reglucosylation of completely deglucosylated, protein-bound high-mannose-type glycans was a general glycoprotein processing reaction. Since glucose is not normally found on mature glycoproteins, transient reglucosylation was intriguing and the function of such apparent futile cycle of glucose addition and removal was not understood at the time. The reglucosylation of endogenous glycoproteins observed *in vivo* was reproduced in cell-free systems and the activity was localized by subcellular fractionation to the ER, where as mentioned above, deglucosylated glycoproteins that are subject to reglucosylation are formed by the action of GI and GII. As an *in vitro* assay for exogenous glycoprotein reglucosylation was developed, it was noticed that the substrate glycoprotein had to be denatured in order to be an acceptor in the reglucosylation reaction. This observation raised the radical notion that glycoproteins had to be devoid of a native conformation to be recognized as substrates by GT. Based on this unique property, it was suggested that the enzyme (and monoglucosylated glycans) could be somehow involved in the so-called "quality control" of glycoprotein folding in the ER.

The involvement of protein recognition in glycosylation reactions was not without precedent. While most glycosyltransferases display specificity at the carbohydrate level (sugar acceptor, sugar donor, and linkage formed), some glycosyltransferases also recognize the protein to which the substrate glycan is bound to. The UDP-N-acetylglucosamine:lysosomal enzyme N-acetylglucosamine phosphotransferase selectively initiates the formation of the Man 6-P epitope in lysosomal glycoproteins. Also, the UDP-GalNAc:glycoprotein hormone N-acetylgalactosaminyltransferase, selectively adds a GalNAc residue to secreted hormones. The substrates that reacted with GT *in vitro* did not appear to share any apparent common feature, except for their non-native conformation, as opposed to the other two glycosyltransferases, which maintain their rather narrow selectivity towards their respective glycoprotein substrates (lysosomal enzymes or glycoprotein hormones) when assayed *in vitro*. The requirement for non-native conformations implied that a wide range of substrates could be reglucosylated *in vivo*, since a large number of glycoproteins could potentially be recognized as substrates during their folding in the ER. Indeed, it is now accepted that all glycoproteins, independently from their final destination or of their soluble or membrane-bound status, behave as GT substrates during their folding process.

Purification of the enzyme from rat liver or *Schizosaccharomyces pombe* showed that activity resided in a single polypeptide of 170 kDa, significantly larger than

most glycosyltransferases. While most, if not all, glycosyltransferases and glycosidases in the secretory pathway are type II membrane proteins, GT and its counteracting enzyme GII are so far the only soluble carbohydrate-processing enzymes described in the secretory pathway. The purified GT has a neutral pH optimum, requires millimolar Ca^{2+} concentrations for activity, and uses UDP-Glc as substrate donor.

The ER membrane contains an integral protein responsible for the specific transport of UDP-Glc from its site of synthesis (the cytosol) into the lumen of the ER, where the sugar nucleotide serves as substrate for glycoprotein reglucosylation. Further, two GDPase/UDPases have been described recently in the mammalian cell ER lumen. Their role is probably to allow transport of UDP-Glc into the lumen by the known antiport mechanism, by which entrance of sugar nucleotides into the ER or Golgi lumen is coupled to exit of the corresponding nucleoside monophosphates.

The most significant finding in the isolation of GT was that the purified enzyme maintained its selectivity for denatured substrates. While it may still cooperate with other factors to recognize non-native conformations *in vivo*, the finding that pure GT exclusively reglucosylates non-native glycoproteins strongly suggests that the conformational sensing is performed primarily by the GT itself. No cofactors were found so far to modify the activity of isolated GT *in vitro*, and expression of GT cDNA is sufficient for glycoprotein reglucosylation in cells devoid of such activity (*S. cerevisiae*). It is now accepted that GT recognizes hydrophobic amino acid patches exposed in molten globule-like folding intermediates, that is, in polypeptides in which there is enough primary sequence information to allow adoption of a collapsed conformation. Moreover, *N*-glycans have to be relatively close to protein structural perturbations to be glucosylated.

The Quality Control Mechanism of Glycoprotein Folding

The information mentioned above supports the mechanism depicted in Figure 3 for the quality control mechanism of glycoprotein folding occurring in the ER. According to it, monoglucosylated glycoproteins generated either by partial deglucosylation of the transferred glycan or by GT-mediated glucosylation interact with CNX/CRT. This interaction is followed by a shuttle between glucosylated (CNX/CRT-bound) and

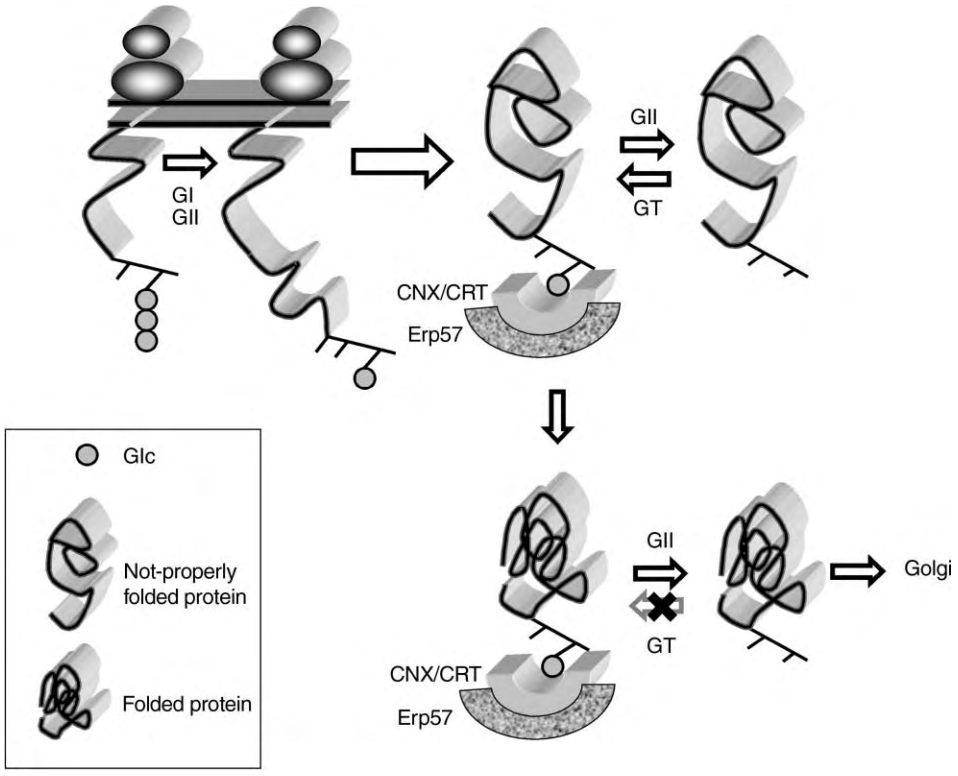

FIGURE 3 Model proposed for the quality control of glycoprotein folding. Protein linked $Glc_3Man_9GlcNAc_2$ is partially deglucosylated to the monoglucosylated derivative by GI and GII, and this structure is recognized by CNX/CRT. $Man_9GlcNAc_2$ is glucosylated by GT if complete deglucosylation occurs before lectin binding. The glycoprotein is liberated from the CNX/CRT anchor by GII and reglucosylated by GT only if not properly folded. On adoption of the native structure, the glycoprotein is released from CNX/CRT by GII and not reglucosylated by GT.

deglucosylated (CNX/CRT-free) forms catalyzed by the opposing activities of GT and GII. After acquiring their proper tertiary structure, glycoproteins are deglucosylated by GII but not reglucosylated by GT and no longer bind to CNX/CRT. Permanently misfolded molecules continue to interact with the lectins, which are not sensing the conformation of their glycoprotein ligands. This task, all over the quality control process, is reserved to the reglucosylating enzyme, and cycles of binding and release to the lectins are mediated by independently acting enzymes (GT and GII) that covalently modify glycans. The CNX/CRT–glycoprotein interaction not only prevents secretion of folding intermediates and irreparably misfolded molecules, but also enhances folding efficiency as it prevents protein aggregation, premature oligomerization, and promotes formation of the correct disulfide bonds by the CNX/CRT–ERp57 complex. It is worth mentioning that GT and BiP apparently recognize different folding conformers. The latter specifically binds heptapeptides with bulky hydrophobic amino acids in alternating positions exposed in early, extended conformations. As predicted by the different recognition patterns, sequential BiP-CNX/CRT interaction has been described for the *in vivo* folding of several glycoproteins. Folding facilitation mediated by CNX/CRT–glycoprotein interaction is not essential for the eukaryotic cell viability. Hindering monoglucosylated *N*-glycan formation by either disrupting GI-, GII-, or GT-encoding genes or by the addition cell permeable inhibitors of the first two enzymes leads to the up-regulation of other chaperones and folding assisting proteins that compensate the absence of lectin–glycoprotein interaction (unfolded protein response). Finally, it should be mentioned that irremediably misfolded glycoproteins are retained in the ER and eventually transported through a complex and not yet fully understood process to the cytosol to be degraded in the proteasomes.

See Also the Following Articles

Glycoproteins, N-linked • Glycoprotein-Mediated Cell Interactions, O-Linked

Glossary

calnexin A membrane-bound endoplasmic reticulum-resident lectin that binds monoglucosylated *N*-glycans.

calreticulin The soluble homologue of calnexin.

quality control Mechanisms by which cells ensure that only properly folded proteins are produced by the secretory pathway.

UDP-Glc:glycoprotein glucosyltransferase A soluble, endoplasmic reticulum-resident enzyme that exclusively glucosylates glycoproteins displaying non-native conformations.

Further Reading

Elgaard, L., and Helenius, A. (2003). Quality control in the endoplasmic reticulum. *Nat. Rev. Mol. Cell Biol.* **4**, 181–191.

Ellgaard, L., Molinari, M., and Helenius, A. (1999). Setting the standards: Quality control in the secretory pathway. *Science* **286**, 1882–1888.

Hammond, C., and Helenius, A. (1997). Quality control in the secretory pathway. *Curr. Opin. Cell Biol.* **7**, 523–529.

Helenius, A. (1994). How *N*-linked glycans affect glycoprotein folding in the endoplasmic reticulum. *Mol. Biol. Cell* **5**, 253–265.

Helenius, A., and Aebi, M. (2000). Intracellular functions of *N*-linked glycans. *Science* **291**, 2364–2369.

Parodi, A. J. (2000a). Protein glucosylation and its role in protein folding. *Annu. Rev. Biochem.* **69**, 69–95.

Parodi, A. J. (2000b). The role of oligosaccharide ER processing reactions in glycoprotein folding and degradation. *Biochem. J.* **348**, 1–13.

Trombetta, E. S., and Helenius, A. (1998). Lectins as chaperones in glycoprotein folding. *Curr. Opin. Struct. Biol.* **8**, 587–592.

Trombetta, E. S., and Parodi, A. J. (2002). *N*-glycan processing and glycoprotein folding. *Adv. Prot. Chem.* **59**, 303–344.

Trombetta, E. S., and Parodi, A. J. (2003). Quality control and protein folding in the secretory pathway. *Annu. Rev. Cell Dev. Biol.* **19**, 649–676.

Biography

Armando Parodi is a Professor of Biochemistry at the School of Sciences of the University of Buenos Aires, and a Foreign Associate of the National Academy of Sciences (USA). He obtained an M.Sc. (organic chemistry) and a Ph.D. (biochemistry) from the School of Sciences of the University of Buenos Aires. Except for two postdoctoral training periods abroad, Dr. Parodi has spent most of his scientific career at the Instituto de Investigaciones Bioquimicas Fundacion Campomar (now Fundacion Instituto Leloir).

Glycoprotein-Mediated Cell Interactions, O-Linked

Robert S. Haltiwanger
State University of New York, Stony Brook, New York, USA

Glycoproteins can be divided into two large classes of molecules based on the atom linking the carbohydrate to the protein. N-linked glycoprotein refers to the subset where carbohydrates are linked to protein through the amide nitrogen of an asparagine residue and are discussed in other entries in this volume. O-linked glycoprotein refers to glycoproteins where the carbohydrate is linked to the protein through an oxygen atom. The fact that cell surfaces are coated with numerous glycoproteins bearing thousands of different, structurally complex carbohydrate structures caused researchers over 30 years ago to propose that these carbohydrates would play roles in communication between cells and their environment. Since then, numerous examples demonstrating that such communication exists have been uncovered. In the past few years, several specific examples showing functional roles for cell-surface oligosaccharides have been poignantly provided through the study of unusual forms of O-linked oligosaccharides. In particular, roles for these carbohydrates in both regulation of signal transduction events and in cell-surface binding events have been demonstrated. These examples have provided firm evidence that the predictions of 30 years ago were true and are now serving as paradigms for the functional relevance of many different forms of glycosylation.

Classes of O-Glycans

O-linked carbohydrate modifications are defined as any carbohydrate covalently linked to protein through a hydroxyl group, most commonly the hydroxyl of a serine or threonine residue. The classes of O-linked carbohydrate modifications are defined by the sugar directly linked to the hydroxyl group. In mammalian systems, at least six classes of O-glycans exist: O-GalNAc (N-acetylgalactosamine), O-GlcNAc (N-acetylglucosamine), O-xylose, O-fucose, O-glucose, and O-mannose. With the exception of O-GlcNAc, all of these modifications are found on proteins in extracellular spaces. O-GlcNAc is uniquely found on nuclear and cytoplasmic proteins. The O-GalNAc and O-xylose modifications constitute the largest and most structurally heterogeneous classes of O-linked modifications. The O-GalNAc modifications are usually referred to as "mucin-type" O-glycosylation since they are prevalent on mucins, and the O-xylose modifications are the glycosaminoglycans, the carbohydrate portion of proteoglycans. Two other O-linked modifications found on the hydroxyls of amino acids other than serine or threonine also exist in mammals: O-galactose on hydroxylysine of collagen and O-glucose on tyrosine of glycogenin.

O-Fucose on Epidermal Growth Factor-Like Repeats

O-fucose modifications were initially identified on a number of serum glycoproteins involved in blood clot formation or dissolution including urinary-type plasminogen activator (uPA), tissue-type plasminogen activator, and factors VII, IX, and XII. Analysis of the sites of fucosylation on these proteins revealed that the fucose was attached to a serine or threonine in a consensus sequence within a protein module known as an epidermal growth factor (EGF)-like repeat. EGF-like repeats are small protein modules of ~40 amino acids found in dozens of cell-surface and secreted proteins (Figure 1). They are defined by the presence of six conserved cysteine residues that form three disulfide bonds. The O-fucose modification occurs between the second and third conserved cysteine of the EGF-like repeat at the sequence $C^2XXGG(S/T)C^3$, where X can be any amino acid and *S/T* is the modified amino acid. More recent work has shown that this consensus site is too narrow and can be broadened to include EGF-like repeats containing $C^2X_{4-5}(S/T)C^3$. Nonetheless, the $C^2XXGG\ (S/T)C^3$ sequence has been extremely useful for identifying other proteins that bear O-fucose such as Notch and Cripto.

The O-fucose is added to EGF-like repeats by protein O-fucosyltransferase I (O-FucT-1, Figure 2A). It will only transfer fucose to serine or threonine in a consensus sequence within a properly folded EGF-like

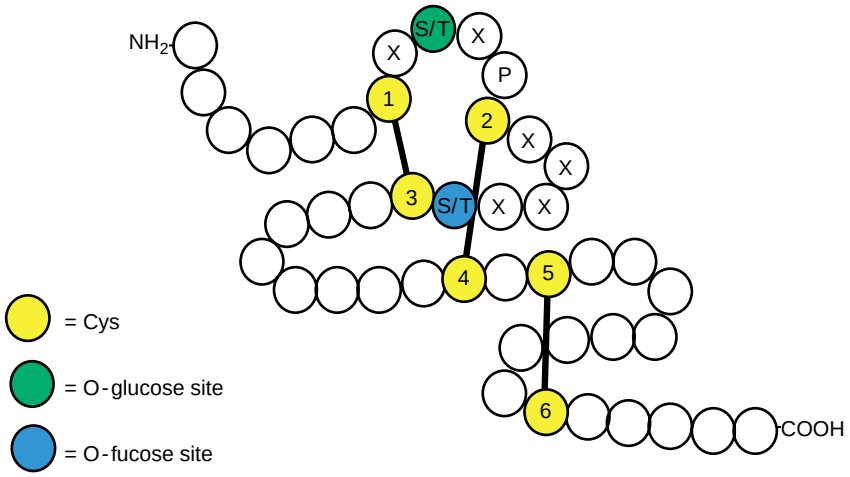

FIGURE 1 O-fucose and O-glucose modifications occur within epidermal growth factor (EGF)-like repeats. A schematic representation of an EGF-like repeat is shown. Each circle represents an amino acid. Cysteines are shown in yellow, the O-glucose modification site is shown in green, and the O-fucose modification site is shown in blue. Amino acids important for defining the glycosylation sites are indicated. Disulfide linkages are represented by lines.

repeat, suggesting that the three-dimensional structure of the EGF-like repeat is necessary for recognition of the site. The gene for O-FucT-1 is highly conserved in metazoans, and mutations in the gene result in embryonic lethality in mice and fruit flies. The O-fucose can be elongated with a β1,3-GlcNAc by a fucose-β1,3-GlcNAc transferase called Fringe (Figure 2A). The GlcNAc can be further elongated with a galactose and sialic acid to form a mature tetrasaccharide. Elongation of the O-fucose monosaccharide is dependent on both the protein being modified and the tissue-dependent expression of the Fringe proteins. Fringe will modify O-fucose on some EGF repeats but not others, suggesting it recognizes not just the O-fucose, but also the surrounding protein structure.

O-Glucose on EGF Repeats

O-glucose modifications were also initially described on EGF-like repeats of serum glycoproteins such as factors VII and IX. Analysis of the sites of glycosylation revealed that the O-glucose modifies serine residues between the first and second conserved cysteine of the EGF-like repeat at the sequence: C^1XSXPC^2 (Figure 1). Other proteins that bear O-glucose modifications have been identified by searching databases using this sequence, including the Notch receptor. O-glucose is added to EGF-like repeats by a protein O-glucosyltransferase, and the O-glucose can be further elongated with xyloses (Figure 2B). Although enzymatic activities capable of adding O-glucose to EGF-like repeats and addition of the xyloses have been detected, the genes encoding these enzymes have not yet been identified.

O-Fucose on TSRs

O-fucose modifications have also been identified in a separate sequence context, that of thrombospondin type 1 repeats (TSRs). TSRs are a protein module found in numerous cell surface and secreted molecules of ~60 amino acids (Figure 3). TSRs are identified by the presence of several conserved residues, including six conserved cysteines that form internal disulfide bonds. The O-fucose modification on TSRs was first identified on human thrombospondin 1, and based on comparison of sequences surrounding the site of glycosylation on several TSRs, a consensus sequence for modification has been proposed: $WX_5C^1X_{2-3}(S/T)C^2X_2G$. Modification of TSRs with O-fucose in other proteins, such as properdin and F-spondin, has been accurately predicted using this sequence. The O-fucose is added to the TSR by protein O-fucosyltransferase 2 (O-FucT-2), a distinct gene product from O-FucT-1 with non-overlapping specificity (Figure 2C). The O-fucose can be elongated with a β1,3-glucose by the action of an O-fucose-β1,3-glucosyltransferase.

O-Mannose

O-mannose modifications of proteins were originally described in yeast, but more recently have been shown to occur on mammalian proteins as well. The first description of O-mannose glycans in mammals has been on brain proteoglycans. Recently, O-mannose glycans were detected on a specific protein, α-dystroglycan.

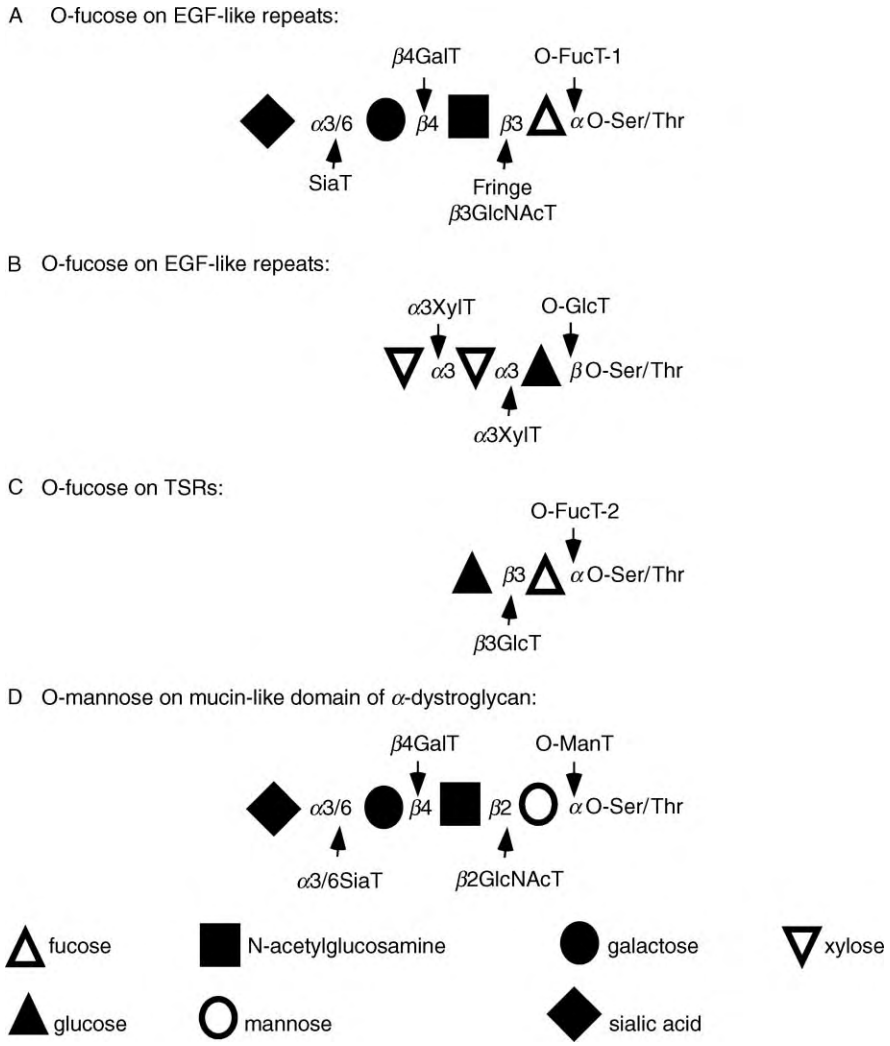

FIGURE 2 Structures of O-linked carbohydrate modifications. For each modification, the potential structures are shown. Each monosaccharide is represented by the symbols defined at the bottom. The enzyme responsible for addition of each sugar is indicated with an arrow. O-FucT-1: protein O-fucosyltransferase-1; O-GlcT: protein O-glucosyltransferase; O-ManT: protein O-mannosyltransferase. All of the other enzymes are described by the linkage they form (e.g., β3GlcNAcT is a β1,3-N-acetylglucosaminyltransferase, forming a β1,3GlcNAc linkage).

Numerous O-mannose chains are attached to α-dystroglycan in a "mucin-like" domain. This is a region of the protein rich in serine, threonine, and proline where many of the serines and threonines appear to be modified. The mannose is added to the mucin-like domain by a protein O-mannosyltransferase. Seven different genes encoding protein O-mannosyltransferases have been identified with yeast, and at least two homologues exist in higher eukaryotes. Although none of these homologues has been shown to have *in vitro* protein O-mannosyltransferase activity, they are believed to be responsible for addition of O-mannose to protein in mammals. The O-mannose can be elongated with a β1,2-GlcNAc by an O-mannose-β1,2-GlcNAc transferase, and the GlcNAc can be further elongated to a mature tetrasaccharide by the addition of galactose and sialic acid (Figure 2D).

Functions of O-Glycans

Determining the function of protein glycosylation has remained a problem for many years, partly because so many different proteins bear carbohydrate modifications. Carbohydrate modifications differ in function, depending on the protein they modify. Nonetheless, recent work has revealed specific functions for some of the O-linked modifications. The fact that these modifications are found on a smaller subset of proteins than more common types of glycosylation (e.g., N-glycosylation, mucin-type O-glycosylation, glycosaminoglycans) has made evaluation of their functions somewhat more straightforward. Still, the principles learned from studying these modifications should be applicable to our understanding of other forms of glycosylation.

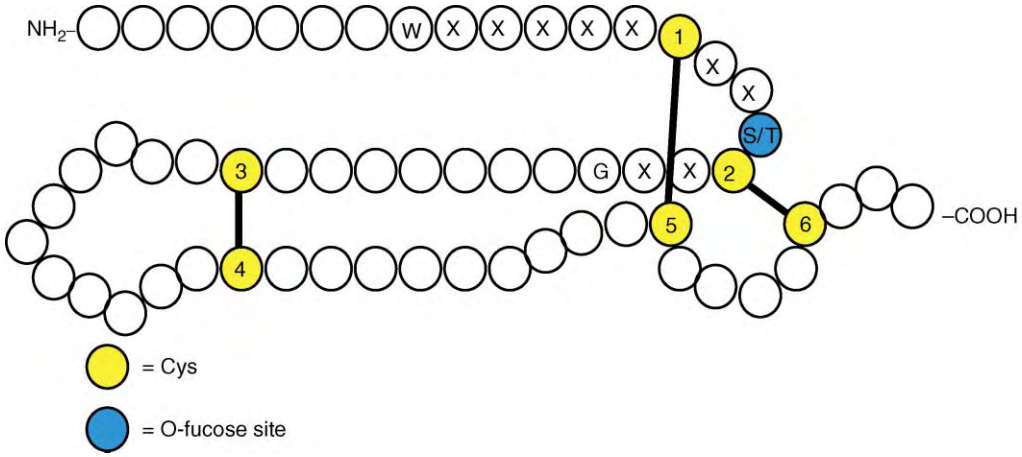

FIGURE 3 O-fucose modifications occur on thrombospondin type 1 repeats (TSRs). A schematic representation of a TSR is shown. Each circle represents an amino acid. Cysteines are shown in yellow, and the O-fucose site is shown in blue. Amino acids important for defining the glycosylation sites are indicated. Disulfide linkages are represented by lines.

The Role of O-Fucose in Regulating Signal Transduction

The Effects of O-Fucose in uPA–uPA Receptor Signaling

A role for the O-fucose modification in modulation of signal transduction was first proposed for the activation of the uPA receptor. As mentioned, the EGF-like repeat of uPA was one of the first proteins to be demonstrated to bear an O-fucose modification. The uPA receptor is a mitogenic receptor, and it becomes activated upon binding to the EGF-like repeat of uPA. Interestingly, removal of O-fucose from the EGF-like repeat abrogates uPA receptor activation, although it has little or no effect on binding. Thus, the O-fucose appears to be essential for activation of the uPA receptor, and alterations in the level of O-fucose on uPA could potentially serve as a mechanism for modulating this activation.

The Effects of O-Fucose in Notch Signaling

The concept that O-fucose modifications can regulate signal transduction events is strengthened by work on the Notch receptor. Notch is a cell surface signaling receptor that plays many essential roles in the development of metazoans. Defects in the Notch signaling pathway lead to a number of human diseases, including several types of cancer, CADASIL (an inherited disease that results in recurrent strokes and early death), and a group of developmental disorders termed Alagille syndrome. Recent work has also implicated Notch in the pathogenesis of multiple sclerosis. Notch becomes activated upon binding to its ligands (members of the Delta family or the Serrate/Jagged family of proteins). Interestingly, the ligands are also cell surface, transmembrane proteins. Thus, Notch becomes activated when an adjacent cell expresses ligand. Ligand binding causes the activation of proteases, releasing the cytoplasmic domain of Notch into the cytoplasm. The cytoplasmic domain then moves into the nucleus, where it associates with other proteins to regulate the transcription of a number of genes.

The extracellular domain of the Notch receptor is composed largely of EGF-like repeats (36 consecutive EGF-like repeats in mammalian Notch1), many of which are modified with O-fucose. The O-fucose modifications are essential for Notch function. Abrogation of O-FucT-1 activity in *Drosophila* (by RNA interference) or in mice (by gene knockout) results in Notch phenotypes (i.e., the same phenotype observed when mutations are made in the Notch gene itself). These results imply that if O-fucose is not added to Notch, it does not function. Since most Notch phenotypes arise early in development, these defects result in embryonic lethality.

In addition to being essential for Notch function, the O-fucose modification on Notch serves a regulatory role. The O-fucose on the EGF-like repeats of Notch can exist in either the monosaccharide or the tetrasaccharide form, depending on whether Fringe is expressed in the same cell. Fringe is a known modifier of Notch function, potentiating the signal received from Delta-like ligands, but inhibiting the signal received from Serrate/Jagged-like ligands. Although the details of how this modulation occurs are not known, these results indicate that the activation of Notch can be regulated by altering the structure of the O-fucose glycans on Notch. These results provide one of the clearest examples known of how a signal transduction pathway can be regulated by alterations in the glycosylation of the receptor.

The Effects of O-Fucose on the Nodal/Cripto Signaling Pathway

In addition to its role in the Notch and uPA receptors signaling pathways, recent work has suggested a role for O-fucose in the Nodal/Cripto pathway. Nodal is a member of the transforming growth factor β (TGFβ) superfamily that plays a key role in establishing polarity early in vertebrate embryogenesis. Mutations in Nodal cause defects in left–right asymmetry and mesoderm formation. Nodal is a secreted protein that binds to and activates members of the type I/type II activin receptor family. Interestingly, Nodal only activates these receptors in the presence of a coreceptor. The coreceptors include the proteins Cripto and Criptic, both of which contain an EGF-like repeat that is modified with O-fucose. Without the O-fucose, neither Cripto nor Criptic will support Nodal-dependent activation of the receptors, demonstrating that the O-fucose modification is essential for Cripto/Criptic-dependent Nodal signaling. Alterations in the levels of O-fucose on Cripto and Criptic could be a mechanism for modulating Nodal signaling. Surprisingly, the mouse knockouts of O-FucT-1 do not show severe Nodal phenotypes, even though Nodal actually functions at an earlier stage of development than Notch. This result suggests either that a different enzyme is responsible for addition of O-fucose to Cripto and Criptic or that the role of O-fucose in Nodal function is more complicated than previously believed and requires further investigation.

The Role of O-Mannose in α-Dystroglycan Function

The recent demonstration of O-mannose on α-dystroglycan has led to the discovery of an essential role for these glycans in the musculoskeletal system. α-Dystroglycan forms a portion of an essential link between the cytoskeleton and the extracellular matrix in the sarcolemma. Specifically, α-dystroglycan binds to β-dystroglycan, a transmembrane protein that in turn interacts with cytoskeletal components. In addition, α-dystroglycan binds to laminin, an extracellular matrix component. Interestingly, the interaction with laminin appears to be mediated through the O-mannose oligosaccharides on α-dystroglycan, and alteration in the O-mannose tetrasaccharide appears to disrupt this interaction. Defects in any of the components in the link between the cytoskeleton and laminin in the muscle are known to cause various muscular dystrophies. For instance, defects in the enzyme that adds a GlcNAc to the O-mannose on α-dystroglycan, preventing formation of the mature tetrasaccharide, result in a form of congenital muscular dystrophy: muscle-eye-brain disease. These results demonstrate that the O-mannose saccharides of α-dystroglycan play an essential role in the function of the dystroglycan–laminin interaction.

Potential Roles for O-Glucose on EGF-Like Repeats and O-Fucose on TSRs

Although specific functions for the O-glucose modifications on EGF-like repeats and O-fucose on TSRs are not known, some functions have been proposed based on the proteins they modify. For instance, many of the EGF-like repeats in the Notch receptor contain evolutionarily conserved O-glucose modification sites. The large number of predicted O-glucose sites, the presence of sites in EGF-like repeats with known functions (e.g., ligand-binding regions), and the fact that many of the sites are evolutionarily conserved argues for a significant biological role for the O-glucose modifications in Notch function. Similarly, the O-fucose modification sites on TSRs are evolutionarily conserved and are predicted to fall within a sequence involved in interactions between cell surface receptors and proteins such as thrombospondin-1. It will be very interesting to examine whether the presence or absence of the O-fucose modification at these sites on TSRs will modulate interactions between thrombospondin-1 and cells, much like the role of O-fucose on the EGF-like repeats of uPA and Cripto.

See Also the Following Articles

Epidermal Growth Factor Receptor Family • Glycoprotein Folding and Processing Reactions • *N*-Linked Glycan Processing Glucosidases and Mannosidases • GlcNAc Biosynthesis and Function, O-Linked • Polysialic Acid in Molecular Medicine

Glossary

cripto/criptic Coreceptors for Nodal that are modified with O-fucose.

α-dystroglycan An essential component of the link between the cytoskeleton and the extracellular matrix in sarcolemma.

fringe A β1,3-N-acetylglucosaminyltransferase that modifies O-fucose residues on Notch (see Figure 2A). Alteration of the O-fucose structures results in modulation of Notch activity.

nodal A member of the TGFβ superfamily that plays an essential role in establishing polarity in vertebrate embryos.

notch A genetic locus originally identified in *Drosophila* that encodes a large cell surface receptor essential for many stages of development. The Notch receptor is modified with both O-fucose and O-glucose.

O-linked carbohydrates Carbohydrate covalently linked to a protein through a hydroxyl group, usually of serine or threonine.

Further Reading

Gonzalez de Peredo, A., Klein, D., Macek, B., Hess, D., Peter-Katalinic, J., and Hofsteenge, J. (2002). C-mannosylation and O-fucosylation of thrombospondin type 1 repeats. *Mol. Cell Proteomics* **1**, 11–18.

Haltiwanger, R. S. (2002). Regulation of signal transduction pathways in development by glycosylation. *Curr. Opin. Struct. Biol.* **12**, 593–598.

Haltiwanger, R. S., and Stanley, P. (2002). Modulation of receptor signaling by glycosylation: Fringe is an O-Fucose-β1,3-N-acetylglucosaminyltransferase. *Biochem. Biophys. Acta* **1573**, 328–335.

Harris, R. J., and Spellman, M. W. (1993). O-linked fucose and other post-translational modifications unique to EGF modules. *Glycobiology* **3**, 219–224.

Michele, D. E., and Campbell, K. P. (2003). Dystrophin–glycoprotein complex: Post-translational processing and dystroglycan function. *J. Biol. Chem.* **278**, 15457–15460.

Biography

Robert S. Haltiwanger is a Professor in the Department of Biochemistry and Cell Biology at the State University of New York at Stony Brook. His research interests are in the role of glycosylation in the regulation of signal transduction events. He obtained a Ph.D. from Duke University in the laboratory of Dr. Robert L. Hill and performed his postdoctoral work at the Johns Hopkins University School of Medicine in the laboratory of Dr. Gerald W. Hart.

Glycoproteins, N-Linked

Mark A. Lehrman
University of Texas Southwestern Medical Center, Dallas, Texas, USA

Proteins that are either secreted from eukaryotic cells or expressed on their surfaces are usually modified with structures called asparagine-linked, or N-linked, oligosaccharides. These are short sugar polymers or glycans attached to the nitrogen atoms of asparaginyl residues. The resulting glycan–protein conjugates are termed N-linked glycoproteins. There are many different kinds of N-linked oligosaccharides with roles in a wide array of biological functions, and a basic knowledge of the pathways responsible for their synthesis is necessary to understand these functions. This article will cover the key concepts behind the synthesis, structures, analysis, functions, and diseases of N-linked glycoproteins, and will illustrate concepts with well-established examples from the literature.

Biosynthesis and Structures of N-Linked Oligosaccharides

Synthesis of a Dolichol Pyrophosphate-Linked Oligosaccharide

N-linked glycosylation begins not with a polypeptide substrate, but rather with the polyisoprenoid lipid dolichol phosphate (Dol-P; also referred to as dolichyl phosphate by many workers). Dolichols are the longest lipids in humans, most commonly consisting of 95 carbons (19 isoprenyl units). Originating from the terminal phosphate of Dol-P, a 14-sugar oligosaccharide unit with a pyrophosphate linkage is assembled in a stepwise manner (Figure 1). The initial seven sugar additions of this pathway utilize enzymes and substrates present on the cytoplasmic leaflet of the endoplasmic reticulum (ER) membrane. First, a residue of GlcNAc-1-P is transferred from UDP-GlcNAc to Dol-P with release of UMP. The enzyme catalyzing this reaction, GlcNAc-1-P-transferase, is selectively inhibited by tunicamycin (TN). The resulting GlcNAc-P-P-Dol is sequentially modified with an additional residue of GlcNAc from UDP-GlcNAc and five residues of mannose from GDP-mannose. The product, $Man_5GlcNAc_2$-P-P-Dol, then flips to the lumenal leaflet of the ER membrane. The subsequent extension of this molecule to $Glc_3Man_9GlcNAc_2$-P-P-Dol, the completed dolichol-linked oligosaccharide (Figure 1, violet), requires a second function of Dol-P. On the cytoplasmic leaflet, Dol-P is modified with single residues of either mannose (from GDP-mannose) or glucose (from UDP-glucose). The resulting mannose-P-Dol (MPD) and glucose-P-Dol (GPD) then flip to the lumenal leaflet where they serve as enzymatic donors for the final seven sugar residues of $Glc_3Man_9GlcNAc_2$-P-P-Dol. The specific arrangement of sugars in $Glc_3Man_9GlcNAc_2$-P-P-Dol, including linkages and anomeric conformations, is highly conserved among eukaryotes and is essential for the functions of the oligosaccharide.

Genetic defects in the synthesis of dolichol-P-P-linked oligosaccharides are responsible for the type-I congenital disorders of glycosylation (CDG). To date, eleven distinct genetic disorders (CDG types Ia–Ik) have been reported, all but type Ia since 1998. The type-I CDGs affect specific sugar transferases as well as enzymes and factors involved in the synthesis of their donor substrates (Figure 1). Given the diversity of functions of N-linked glycans, it is not surprising that type-I CDG patients suffer from abnormalities of many organ systems. In contrast, the type-II CDGs affect remodeling of the oligosaccharide once transfer to newly synthesized protein has occurred, and may be caused by defects in processing glycosidases, glycosyltransferases, and nucleotide-sugar transporters.

Transfer of the Preformed Oligosaccharide Unit to Newly Synthesized Protein

The lumenally oriented oligosaccharide unit of $Glc_3Man_9GlcNAc_2$-P-P-Dol is transferred to newly synthesized polypeptides that are also within the lumen of the ER, with release of Dol-P-P (Figure 1). The reaction is catalyzed by the multi-subunit enzyme oligosaccharyltransferase (OT). OT transfers oligosaccharide to sterically accessible asparaginyl residues in the tripeptide context asparagine-X-serine or threonine, where X can be any residue except proline. Transfer generally occurs cotranslationally; that is, once the polypeptide has emerged inside the lumenal space but before its synthesis by the ribosome is completed.

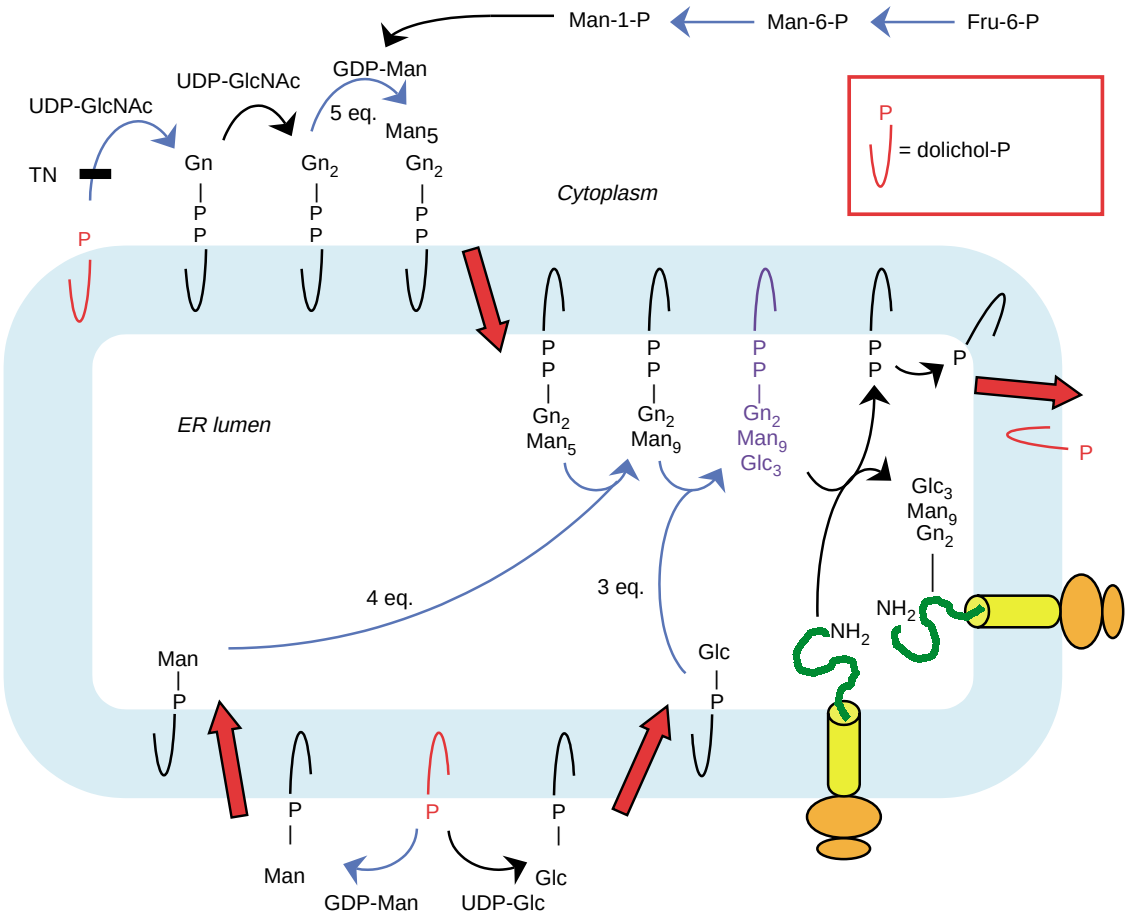

FIGURE 1 Biosynthesis of the lipid-linked oligosaccharide $Glc_3Man_9GlcNAc_2$-PP-Dol in the endoplasmic reticulum. A molecule of Dol-P (upper left-hand corner) is converted into a dolichol pyrophosphate-linked 7-sugar saccharide ($Man_5GlcNAc_2$-PP-Dol) at the cytoplasmic face of the ER membrane. It is then extended in the lumen to the 14-sugar $Glc_3Man_9GlcNAc_2$-PP-Dol (violet; the detailed structure of the glycan is identical to that shown in Figure 2, structure A). The glycan unit is transferred to polypeptides synthesized by membrane-associated ribosomes (orange) as the polypeptides (green) emerge from the translocation pore (yellow). The resulting Dol-PP is converted to Dol-P and recycled to replenish the cytoplasmically-oriented pool of Dol-P (red) used for synthesis of GlcNAc-PP-Dol, Man-P-Dol, and Glc-P-Dol. The latter two molecules are synthesized cytoplasmically and translocated to the lumenal face. Dol-P resulting from their consumption is not shown. Blue arrows indicate steps known to be defective in Type I Congenital Disorders Of Glycosylation. Bold red arrows represent flipping reactions. The site of action of tunicamycin (TN) is shown.

The resulting molecule of Dol-P-P is believed to be recycled back to Dol-P and returned to the cytoplasmic face to participate in additional synthesis of $Glc_3Man_9GlcNAc_2$-P-P-Dol, MPD, and GPD.

Glycosidase Digestion in the ER Lumen

Within minutes after transfer to protein, glycosidic digestion of the N-linked $Glc_3Man_9GlcNAc_2$ (Figure 2, structure A) unit begins by the action of a family of ER-resident glycosidases. In a sequential manner, the terminal glucose residue is removed by ER glucosidase I, the remaining two glucose residues are removed by ER glucosidase II, and a single mannose is removed by ER mannosidase I. The resulting $Man_8GlcNAc_2$ oligosaccharide is depicted in Figure 2 (structure B). As discussed below, the intermediates $Glc_1Man_9GlcNAc_2$, $Man_9GlcNAc_2$, and $Man_8GlcNAc_2$ are particularly significant for folding and processing of glycoproteins. Cell-permeant inhibitors are available that block both of the ER glucosidases (castanospermine (CSN) and deoxynojirimycin (DN)), or ER mannosidase I (kifunensine (KF) and deoxymannojirimycin (DMN)). All of the N-linked oligosaccharide intermediates normally found within the ER are termed *high-mannose-type* to reflect the high proportion of mannosyl residues. Glycoproteins exported to the Golgi apparatus typically have glycans with eight mannosyl residues and no glucosyl residues, but in the event that a glycoprotein is exported before glucosidase digestion is completed, a Golgi endomannosidase exists that can remove any attached glucosyl residues plus the underlying mannosyl residue as a single unit (Figure 3).

Remodeling by Golgi Apparatus Glycosidases and Glycosyltransferases

The steps reviewed to this point are similar for all eukaryotes. However, within the Golgi apparatus N-linked oligosaccharides are remodeled with extensive variations in structure. These variations occur between different species, different organ systems of an individual species, different cell types of an organ system, different glycoproteins of a particular cell, and even among different sub-populations (glycoforms) of a given glycoprotein. Many features of remodeling of N-glycans by the Golgi apparatus are covered in other articles.

The remainder of this article will be limited to remodeling in mammalian cells. It is useful to recall that the mammalian Golgi apparatus can be divided structurally and functionally into three components, known as the *cis*, *medial*, and *trans* Golgi compartments, and is associated with the *trans*-Golgi network (TGN). The key enzymes involved in glycan remodeling are usually found in specific Golgi compartments or the TGN, and their physical locations in these secretory pathway organelles reflect both their order of action on secreted glycoproteins and their distinct substrate specificities (Figure 2). Enzymes involved in specialized remodeling (Figures 3 and 4) are also optimally located for access to the correct oligosaccharide intermediate.

An elegant example of the orchestration of enzyme location and specificity comes from reactions that occur in the *cis* and *medial* Golgi compartments (Figure 2). Recall that $Man_8GlcNAc_2$ is the typical oligosaccharide intermediate on glycoproteins leaving the ER (structure B). Golgi mannosidase I, a resident of the *cis*-Golgi compartment, digests this oligosaccharide to form $Man_5GlcNAc_2$ (structure C; a different isomer than $Man_5GlcNAc_2$ formed as a dolichol-PP-linked intermediate). Upon arrival at the *medial*-Golgi compartment, the $Man_5GlcNAc_2$ is modified by the first in a series of Golgi-associated glycosyltransferases, GlcNAc transferase I. Like all Golgi-associated glycosyltransferases, this enzyme uses a nucleotide-sugar donor. GlcNAc transferase I transfers a residue of N-acetylglucosamine (GlcNAc) from UDP-GlcNAc, forming a β1,2 linkage with a specific mannosyl residue to yield $GlcNAc_1Man_5GlcNAc_2$ (structure D). GlcNAc transferase I is unable to recognize $Man_8GlcNAc_2$, and therefore the prior action of Golgi mannosidase I is essential. After addition of the GlcNAc residue, in most cases the $GlcNAc_1Man_5GlcNAc_2$ oligosaccharide is digested by another *medial*-Golgi enzyme, Golgi mannosidase II (which is inhibited by swainsonine (SW)), to generate $GlcNAc_1Man_3GlcNAc_2$ (structure E). Golgi mannosidase II is unable to recognize $Man_5GlcNAc_2$, and therefore requires the prior action of GlcNAc transferase I. Thus, it is clear that the subcellular locations of these enzymes must reflect their substrate specificities. Consequently, each enzyme is membrane associated and contains appropriate sorting/retention signals.

It is important to note that not all N-linked glycans are digested by Golgi mannosidases, and thus pass through the secretory pathway without further processing. This can be due to steric inaccessibility of the oligosaccharide or, as discussed later in the entry, specialized competing reactions that supercede the typical processing reactions.

Digestion of $GlcNAc_1Man_5GlcNAc_2$ by Golgi mannosidase II uncovers a key mannosyl residue (structure E), allowing it to be modified by the addition of a residue of GlcNAc by GlcNAc transferase II (Figure 2). The resulting $GlcNAc_2Man_3GlcNAc_2$ oligosaccharide (structure F) has two exposed GlcNAc residues, and extension of these by additional transferases associated with the Golgi complex results in *complex-type* N-linked glycans such as structures G and H. As indicated earlier, the exact structures of *complex-type* glycans depend heavily on the organism, tissue, cell type, and protein, and are governed by which glycosyltransferases are expressed. These transferases differ with regard to the sugar residue transferred (galactose, GlcNAc, fucose, GalNAc, sialic acid), the anomeric conformation of the new linkage (α or β), the acceptor saccharide, and the hydroxyl on the acceptor that participates in formation of the glycosidic linkage. As expected from the topological locations of the glycoprotein substrates, these transferases have catalytic sites facing the lumenal spaces of Golgi compartments. The donor requirements of these transferases are met by specific transporters that import nucleotide sugars from the cytoplasm. These transporters also export the nucleotide mono- or di-phosphate byproducts back to the cytoplasm. For a small fraction of oligosaccharides that fail to be digested by Golgi mannosidase II, the single exposed GlcNAc is available for extension to form *hybrid-type* N-linked glycans. These are so-named because they retain elements of both *high mannose-type* and *complex-type* oligosaccharides.

A key variable among *complex-type* oligosaccharides is the number of branches, or antennae, that are formed. Each branch is initiated by a residue of GlcNAc attached to one of mannosyl residues in the $Man_3GlcNAc_2$ "core." *Complex-type* structures with two to five branches have been reported, termed bi-antennary (Figure 2, structure G), tri-antennary, tetra-antennary (structure H), and penta-antennary. In most cases sialic acid is the final sugar attached to N-linked glycans, introducing negative charges onto each branch of the *complex-type* oligosaccharide. However, negative charges can also result from sulfation. It is with these

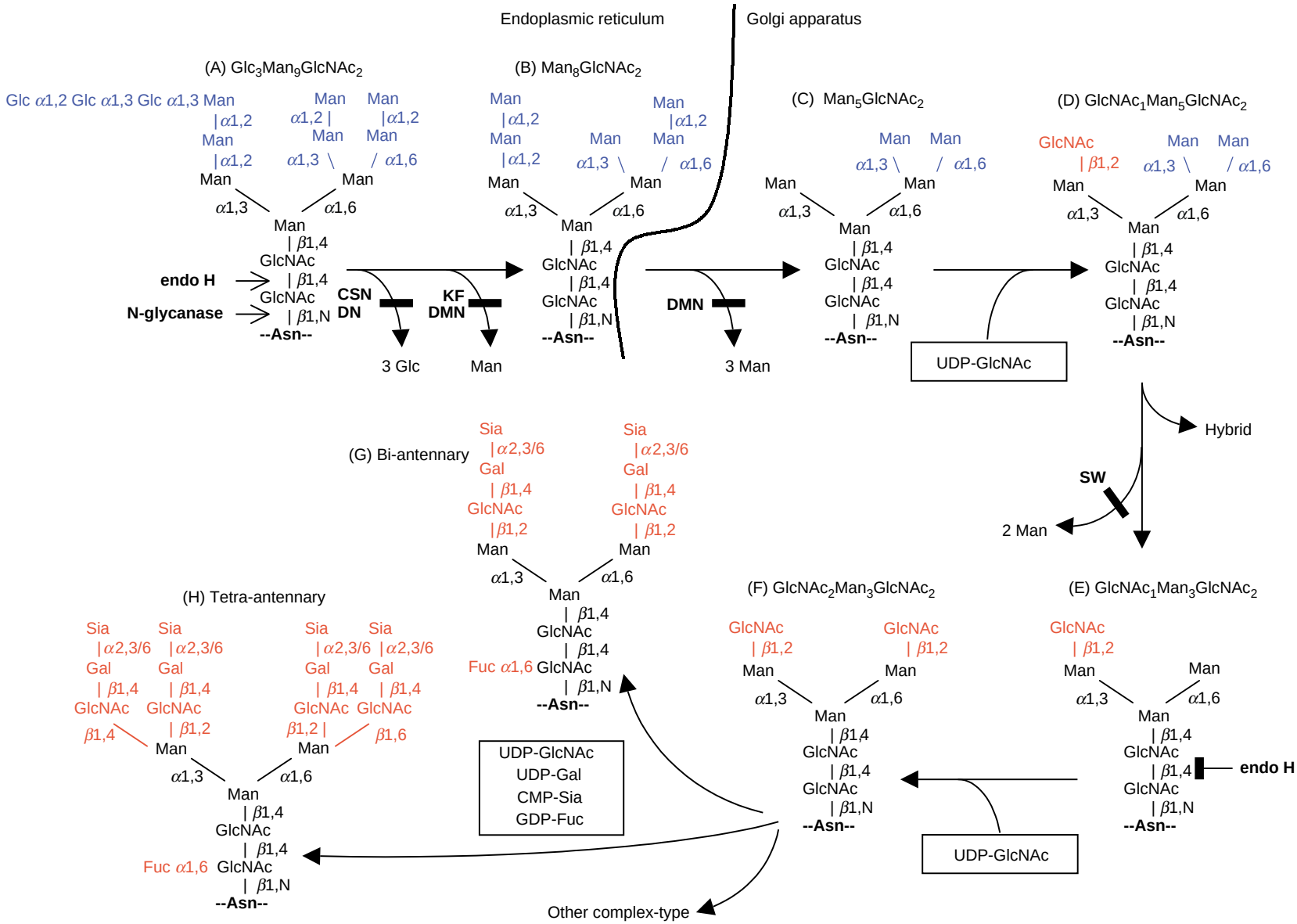
Endoplasmic reticulum
Golgi apparatus
(A) Glc3Man9GlcNAc2
(B) Man8GlcNAc2
(C) Man5GlcNAc2
(D) GlcNAc1Man5GlcNAc2
endo H
N-glycanase
CSN
DN
KF
DMN
DMN
3 Glc
Man
3 Man
UDP-GlcNAc
Hybrid
SW
2 Man
(G) Bi-antennary
(H) Tetra-antennary
(F) GlcNAc2Man3GlcNAc2
(E) GlcNAc1Man3GlcNAc2
UDP-GlcNAc
UDP-Gal
CMP-Sia
GDP-Fuc
UDP-GlcNAc
endo H
Other complex-type

final modifications that the glycoprotein is secreted or retained at the cell surface.

Methods for Analysis of N-Linked Glycoprotein Structure and Function

Binding to Plant Lectins

Plant lectins with a diverse range of specificities for the exposed monosaccharide, anomeric linkage, and other features of the oligosaccharide unit are commercially available. These can be used in many different ways: for example, as immobilized adsorbents attached to column matrices, as histochemical reagents when tagged with a reporter such as horseradish peroxidase, or to isolate sub-populations of cells when conjugated with fluorescent probes for flow sorting. Perhaps the best-known plant lectin is concanavalin A, which is selective for oligosaccharides with exposed α-mannosyl or α-glucosyl residues. Concanavalin A binds tightly to *high mannose-type* and *hybrid-type* oligosaccharides, and weakly to bi-antennary *complex-type* oligosaccharides, but not to *complex-type* oligosaccharides with three or more branches.

Radiolabeling of Oligosaccharides

Incorporation of an isotopic label is a simple and highly sensitive way to permit study of the oligosaccharides themselves. In principle, to label the oligosaccharide unit in intact cells a radiolabeled metabolic precursor of any of the sugar residues can be used, but in practice the choice of precursor is limited by the specific radioactivity, intracellular pool dilution, and competing metabolic fates of precursors. [2-^{3}H]mannose is frequently used because it can label all classes of N-linked oligosaccharides with high specific activity, and labeling is selective for glycoconjugates because diversion of the mannose to glycolysis by phosphomannose isomerase results in loss of the tritium from the sugar ring. *In vitro*, oligosaccharides are typically radiolabeled by incubation with an appropriate glycosytransferase and a nucleotide sugar with an isotopically labeled sugar residue, or by selective oxidation of hydroxyls to aldehydes followed by reduction with [^{3}H]$NaBH_4$.

Digestion with Purified Endo- and Exo-Glycosidases

A useful selection of glycosidases that can be used to characterize N-linked glycans is now commercially available. Endoglycosidases cleave the bonds of unexposed sugar residues; two widely used ones are endoglycosidase H and peptide:N-glycosidase F (also known as N-glycanase) as indicated by Figure 2. N-glycanase cleaves the asparaginyl–GlcNAc bond of almost all N-linked glycans, generating a free oligosaccharide with conversion of the asparaginyl residue to aspartic acid. Endoglycosidase H cleaves the β-linkage between the two GlcNAc residues. The asparaginyl–GlcNAc bond remains intact, and an oligosaccharide released by endoglycosidase H will have one fewer GlcNAc residue than the same oligosaccharide released by N-glycanase. Importantly, endoglycosidase H only cleaves *high mannose-type* and *hybrid-type* oligosaccharides that have not been digested by Golgi mannosidase II (Figure 2).

Exoglycosidases cleave the linkages of exposed sugar residues. Specific glycosidases are available that can remove essentially every sugar found in N-glycans, and are often used sequentially as one glycosidase exposes the substrate of another. For example, the presence of sialic acid residues on an N-glycan can be determined with enzymes called sialidases or neuraminidases. As for other families of glycosidases, these can be obtained with broad or narrow specificities for the type of glycosidic linkage. After removal of sialic acid, the

FIGURE 2 Remodeling of mammalian N-linked glycans in the endoplasmic reticulum, Golgi apparatus, and *trans* Golgi network. Sugars in *black* form the invariant core that is retained after remodeling of N-linked glycans is completed; those in blue are removed by processing glycosidases; and those in red are added by Golgi-associated glycosyltransferases. The anomeric conformation of each glycosidic linkage is denoted α or β, with the linking group of the donor sugar preceding the comma and the linking group of the acceptor following the comma (GlcNAc, N-acetyl-D-glucosamine; Gal, D-galactose; Sia, sialic acid; Fuc, L-fucose). Processing of structure A ($Glc_3Man_9GlcNAc_2$) begins by digestion with ER glucosidases I and II. Structures B through F are each formed by specific enzymes: B, ER mannosidase I; C, Golgi mannosidase I; D, GlcNAc transferase I; E, Golgi mannosidase II; F, GlcNAc transferase II. Structures A and B are associated with the ER; structure C is associated with the *cis* Golgi apparatus; structures D–F are associated with the medial Golgi apparatus; and structures G and H are associated with the *trans* Golgi apparatus and the *trans* Golgi network. Note that structure D can be converted to a hybrid-type glycan or, via structure E, a complex-type glycan such as those shown here (G and H). Sialic acid is commonly found in both α2,3 and α2,6 linkages on complex-type structures. The sites of cleavage by N-glycanase and endoglycosidase H (endo H) are indicated on structure A. Structure E and its products are resistant to endo H. Sites of action of the inhibitors castanospermine (CSN), deoxynojirimycin (DN), kifunensine (KF), deoxymannojirimycin (DMN), and swainsonine (SW) are shown.

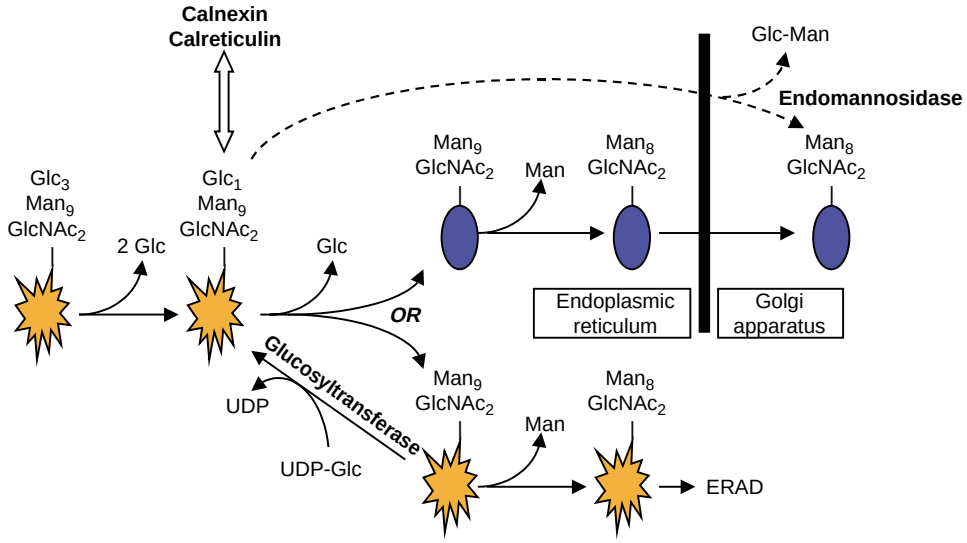

FIGURE 3 The roles of calnexin, calreticulin, unfolded glycoprotein glucosyltransferase, and endomannosidase in the formation and function of glucosylated N-linked oligosaccharides. A newly synthesized glycoprotein with a $Glc_3Man_9GlcNAc_2$ glycan is shown in its unfolded state (orange). Removal of two glucose units forms a monoglucosylated glycan which can interact with the lectin sites of the chaperones calnexin and calreticulin. Subsequent dissociation from the lectin site allows the 3rd glucose residue to be removed by glucosidase II. At this point, if the glycoprotein is properly folded (blue) an additional mannose unit will be removed and the glycoprotein will be exported to the Golgi apparatus. However, if the glycoprotein remains misfolded, its Man_9Gn_2 glycan can be recognized by the unfolded glycoprotein glucosyltransferase to regenerate the monoglucosylated glycan and allow additional interaction with calnexin or calreticulin. The cycle of glucose removal and re-addition can be repeated many times for glycoproteins that are unable to fold. Eventually, on such misfolded glycoproteins a single mannose unit is removed from the Man_9Gn_2 glycan, and the glycoprotein is destroyed by a process termed ER-associated degradation (ERAD). If a glycoprotein folds properly, but exits the ER before glucose removal is completed, a Golgi-associated endomannosidase exists presumably to remove a disaccharide containing the remaining glucose unit and its underlying mannose unit (dashed arrows). Two distinct $Man_8GlcNAc_2$ isomers are formed by ER mannosidase I and Golgi endomannosidase, but each can be remodeled by Golgi-associated enzymes to form complex-type structures.

nature of the underlying sugar can be deduced with other exoglycosidases.

Inhibitors of Glycan Assembly and Processing

TN, a specific inhibitor of initiation of synthesis of dolichol-P-P-linked oligosaccharides, and CSN, DN, KF, DMN, and SW, inhibitors of N-glycan processing, can be valuable tools for determining the presence or class of an N-glycan, as well as for assessment of N-glycan function. These inhibitors are effective with intact cells and purified enzymes. Their sites of action are shown in Figures 1 and 2.

Introduction of Mutations in Genes Encoding Glycosidases and Glycosytransferases

A very powerful approach for assessment of N-glycan function and structure is the use of cell lines and rodent strains in which one or more glycosidases or glycosyltransferases have been inactivated by a spontaneous mutation, a chemically induced mutation, or a targeted gene disruption. The extensive collection of N-glycosylation mutations in Chinese hamster ovary cells has proved valuable in elucidating key steps in both the biosynthetic pathway discussed earlier in the article and the secretory pathway, in addition to testing the functions of specific intermediates and production of useful glycoproteins with defined N-glycans. Many of these cell lines were isolated by their resistance to toxicity of specific plant lectins. For example, cells of the *Lec*1 complementation group lack GlcNAc transferase I activity. These have been used to establish the order of reactions discussed previously, to produce N-linked glycoproteins with $Man_5GlcNAc_2$ glycans instead of *complex-type* glycans, and to establish *in vitro* conditions for transfer of glycoprotein cargo between Golgi-derived vesicles.

Chemical and Physical Analysis of N-Glycans

The combined uses of glycosylation inhibitors, genetic mutations, and glycosidases can reveal a great deal of information about the number and types of N-linked glycans attached to a protein and their functions. Detailed structural information requires removal of the oligosaccharide unit from the polypeptide, followed by

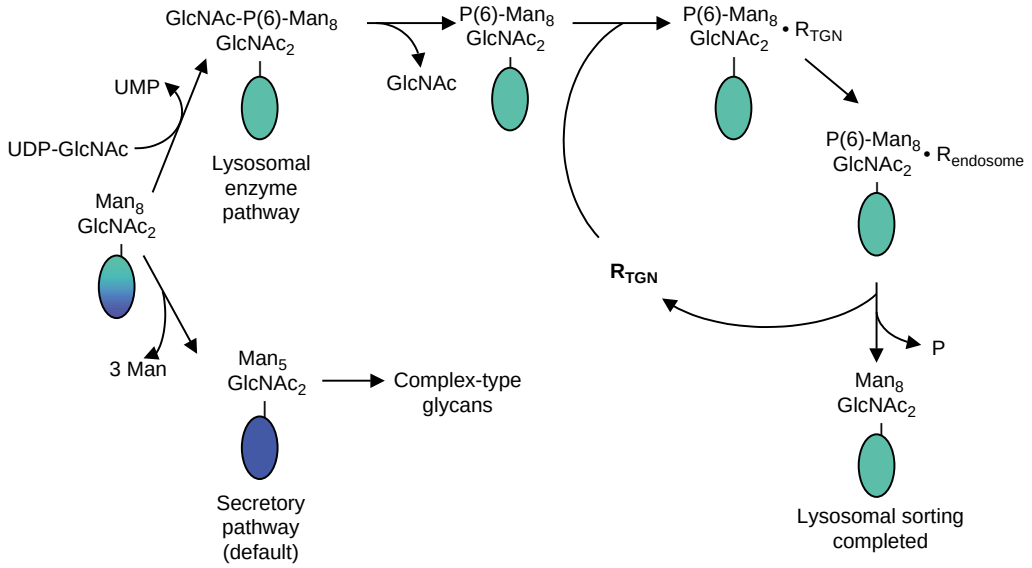

FIGURE 4 Formation of the mannose-6-phosphate sorting signal for lysosomal enzymes. Glycoproteins enter the *cis* Golgi compartment with Man_8Gn_2 glycans (Figure 2, structure B). The majority of glycoproteins (blue) are processed normally and enter the secretory pathway by default. However, a specific UDP-GlcNAc:lysosomal enzyme GlcNAc-1-P transferase recognizes protein determinants that are common to lysosomal enzymes (green), and modifies the 6-hydroxyls of mannosyl residues of the Man_8Gn_2 glycan with GlcNAc-1-P. An uncovering enzyme then removes the GlcNAc unit, leaving a mannosyl unit with a 6-phosphate modification. In the *trans* Golgi network (TGN), enzymes with mannose-6-P units are then bound by mannose-6-P receptors (R), which escort the enzymes to endosomes. The acidic pH of the endosome allows the enzyme-receptor complex to dissociate. The receptors recycle to the TGN, and normal endocytic flow transports the released enzymes to lysosomes where the phosphate modification is removed. Thus, mature lysosomal enzymes have no trace of the mannose-6-P sorting signal. In certain disorders, addition of the GlcNAc-1-P unit is defective, resulting in generation of a complex-type glycan and secretion of enzymes rather than delivery to lysosomes.

chemical and physical analysis. Conventional liquid chromatography, high-pressure liquid chromatography, and gel electrophoresis have been used extensively for both purification of oligosaccharides and determination of structural features. These are effective for separation of oligosaccharides by size, by charge, or by differences in column adsorption due to the particular arrangements of functional groups in the molecule. Several strategies are available to determine the monosaccharide compositions of purified oligosaccharides, including gas chromatography and liquid chromatography. The actual arrangements of the sugar residues, including linkage assignments, are achieved through a combination of glycosidase digestion, gas chromatography, mass spectrometry, and/or nuclear magnetic resonance spectroscopy.

N-Linked Oligosaccharides as Experimental Aids

Purification of N-Linked Glycoproteins

The presence of an N-linked glycan gives biological chemists a simple and effective way to enrich a glycoprotein of interest, by the use of lectin-affinity chromatography. A knowledge of the sub-cellular location of the glycoprotein allows the likely identity of the glycan class to be surmised, and an appropriate immobilized lectin to be chosen. A column prepared with such an immobilized lectin can then be used to isolate glycoproteins bearing the appropriate N-glycan from remaining cellular components. These glycoproteins can then be gently eluted from the adsorbent by the addition of the correct competing saccharide. For example, chromatography with immobilized concanavalin A will strongly retain glycoproteins with *high mannose-type* or *hybrid-type* glycans, which can be recovered by elution with a solution of α-methylmannoside. A similar approach can be used to prepare an enriched fraction of proteins that have traversed the Golgi apparatus, and therefore bear *complex-type* glycans, by chromatography with immobilized wheat germ agglutinin and elution with the competitor disaccharide chitobiose.

Radiolabeling and Tagging of N-Linked Glycoproteins

The methods described earlier for radiolabeling of N-glycans to facilitate glycan analysis are also useful for incorporating a radiolabel for other experimental purposes, without modification of the peptide backbone.

A classic example is the sequential treatment of ceruloplasmin with neuraminidase and galactose oxidase, followed by reduction of the 6-aldehyde with [^{3}H]$NaBH_4$ to generate an exposed tritium-labeled β-galactosyl residue. The resulting labeled asialoceruloplasmin is found to be rapidly cleared from the circulation by the liver. This result allows the identification of a novel β-galactoside selective "asialoglycoprotein receptor" in the liver. It has become an important model for receptor-mediated endocytosis studies.

Trafficking Through the Secretory Pathway

As discussed earlier, N-linked glycan structures are modified as glycoproteins pass through the various compartments of the mammalian secretory pathway (Figure 2). This feature makes N-linked glycans extremely useful for monitoring the subcellular location of a glycoprotein of interest. The presence of a glycoprotein in almost any compartment along the secretory pathway can be determined by information gained from binding to plant lectins, reactivity with glycosidases, and/or labeling with sugar precursors. The most common use of these techniques takes advantage of the sensitivity of *high mannose-type* glycans to endoglycosidase H, and the resistance to this enzyme that occurs after digestion with Golgi mannosidase II. Thus, the acquisition of endoglycosidase H sensitivity by a newly synthesized protein signifies that it is in fact a glycoprotein, and that a portion or all of its sequence is present in the ER lumenal space. The subsequent loss of endoglycosidase H sensitivity reflects the arrival of the protein at the *medial* compartment of the Golgi apparatus (for most glycoproteins, 30–60 min after synthesis).

Functions of Selected N-Linked Glycans and their Specific Cognate Lectins

Since the 1990s, there has been an explosion of discoveries of specific functions for protein-linked glycans, both asparagine-linked and serine/threonine-linked. Some functions of N-linked glycans are covered in detail in other articles. A central concept revealed by these studies is that glycan function usually requires recognition by a specific cognate lectin. In this section, two functions that highlight reactions covered in earlier sections are selected for discussion. These two examples illustrate how certain glycosyltransferases may recognize features of the polypeptide in addition to the glycan, and thus restrict modification to only special sub-classes of glycoproteins. They also show how certain key modifications are transient, and are not found on the mature glycoproteins.

Monoglucosylated Oligosaccharides in ER Quality Control

As discussed earlier, removal of two glucosyl residues from the $Glc_3Man_9GlcNAc_2$ N-linked oligosaccharide by the CSN-sensitive glucosidases I and II results in a monoglucosylated processing intermediate, $Glc_1Man_9GlcNAc_2$. This intermediate is recognized by calnexin and calreticulin, resident ER chaperones with lectin activities specific for monoglucosylated oligosaccharides (Figure 3). Interactions with one of these lectin-chaperones can be crucial for folding and processing of nascent N-linked glycoproteins. Calnexin and calreticulin have essentially negligible recognition of $Glc_3Man_9GlcNAc_2$ (as well as oligosaccharides with zero or two glucose residues). Thus, treatment of cells with CSN blocks glycan-dependent interactions of chaperones with misfolded nascent N-linked glycoproteins because it prevents formation of $Glc_1Man_9GlcNAc_2$ N-linked oligosaccharides. Calnexin and calreticulin bind to $Glc_1Man_9GlcNAc_2$ reversibly, and once dissociated from the lectin site of calnexin or calreticulin, the $Glc_1Man_9GlcNAc_2$ glycan can be digested to $Man_9GlcNAc_2$ by glucosidase II according to the scheme discussed earlier. After release of the glycan from the lectin site, calnexin and calreticulin appear to mediate further folding of their glycoprotein substrates due to lectin-independent chaperone activities.

In addition to processing of $Glc_3Man_9GlcNAc_2$, $Glc_1Man_9GlcNAc_2$ can be formed by reglucosylation of N-linked $Man_9GlcNAc_2$. This is achieved by a remarkable enzyme, the UDP-glucose:unfolded glycoprotein glucosyltransferase (Figure 3). The glucosyltransferase has two functional domains. A "catalytic" domain mediates the transfer of glucose from UDP-glucose to $Man_9GlcNAc_2$, forming the same $Glc_1Man_9GlcNAc_2$ structure as achieved by processing of $Glc_2Man_9GlcNAc_2$. A second "recognition" domain is able to identify physical features characteristic of misfolded proteins, presumably exposed hydrophobic surfaces. The binding of a $Man_9GlcNAc_2$-bearing misfolded glycoprotein to the recognition domain allows reglucosylation by the catalytic domain. The regenerated $Glc_1Man_9GlcNAc_2$ glycan then gives the misfolded glycoprotein another opportunity to interact with calnexin/calreticulin and be folded properly. The repeated actions of the lectin-chaperones calnexin and calreticulin, of glucosidase II, and of the ER glucosyltransferase account for the observation

that certain glycoproteins with mutations that affect folding may retain the $Glc_1Man_9GlcNAc_2$ glycan for extended periods. Properly folded glycoproteins can be exported to the Golgi apparatus, while glycoproteins unable to achieve a properly folded conformation are destroyed by a process termed ER-associated degradation (ERAD) (Figure 3).

High-Mannose Oligosaccharides Bearing Mannose-6-Phosphate Residues as Sorting Signals for Lysosomal Hydrolases

The processing of $Man_8GlcNAc_2$ to $Man_5GlcNAc_2$ by the *medial* Golgi enzyme mannosidase I was discussed earlier. However, hydrolases destined for the lumenal space of the lysosome undergo a very different fate (Figure 4). On these proteins the 6-hydroxyl groups of mannosyl residues are phosphorylated, producing high-mannose oligosaccharides containing mannose-6-phosphate. The mannose-6-phosphate then serves as a specific trafficking signal and allows the hydrolase to be deposited in the lysosome.

The mannose-6-phosphate recognition marker is created in two steps. First, GlcNAc-1-P is transferred to the 6-hydroxyl of a mannosyl residue of $Man_8GlcNAc_2$ by a specialized transferase, the UDP-GlcNAc:lysosomal enzyme GlcNAc-1-P transferase. Like the UDP-glucose:unfolded glycoprotein glucosyltransferase, this enzyme has two functional domains. The catalytic domain mediates transfer of GlcNAc-1-P to *high mannose-type* glycans. The recognition domain binds to lysosomal hydrolases due to a special arrangement of amino acid side chains found only on these enzymes. Thus, the GlcNAc-1-P transferase is effective only with lysosomal hydrolases bearing *high mannose-type* glycans. The GlcNAc-1-P transferase is found in the *cis*-Golgi compartment, and thus its reaction with $Man_8GlcNAc_2$ glycans can take place before digestion with Golgi mannosidase I. The product is the substrate for another enzyme, known as the "uncovering enzyme," which removes the GlcNAc residue and exposes the phosphate. Unlike the GlcNAc-1-P transferase, the uncovering enzyme has a catalytic domain but no known polypeptide recognition domain. The resulting mannose-6-phosphate labeled hydrolase continues its movement along the secretory pathway, but undergoes no additional modifications of its glycan.

In the *trans*-Golgi network, receptors for glycans with mannose-6-phosphate bind the hydrolases and escort them to endosomes. Usually, at least two mannose-6-phosphates must be generated per hydrolase for effective receptor binding. The acidic pH of the endosome causes release of the hydrolase from the receptor, which then recycles back to the *trans*-Golgi network for additional rounds of sorting. The hydrolase is then deposited in the lysosome by normal vesicular traffic, and phosphatases remove the phosphate modification. Thus, mature lysosomal hydrolases bear *high mannose-type* glycans without phosphate. Elucidation of this unique process has been aided by the discovery that it is disrupted in patients with I-cell disease and pseudo-Hurler polydystrophy. In these patients, heritable mutations cause loss of UDP-GlcNAc:lysosomal enzyme GlcNAc-1-P transferase activity. As a result, the mannose-6-phosphate sorting signal is not formed and lysosomal enzymes are secreted instead of being deposited in lysosomes. This accounts for the storage of pathological waste products in the lysosomes of I-cell and pseudo-Hurler patients.

See Also the Following Articles

Glycosylation, Congenital Disorders of • *N*-Linked Glycan Processing Glucosidases and Mannosidases • Glycoproteins, Plant • Secretory Pathway • Siglecs • Sugar Nucleotide Transporters

Glossary

asparagine-linked glycan An oligosaccharide covalently attached to the nitrogen atom of an asparaginyl residue of a protein or peptide.

dolichol A polyisoprenoid lipid composed of five-carbon isoprene units and terminating with a hydroxyl that can be modified with groups such as phosphate, sugar phosphate, or oligosaccharyl pyrophosphate. The "business-end" (α) isoprene unit is reduced, while the remaining isoprene units in dolichol retain double bonds.

glycosidase An enzyme that can release a monosaccharide or oligosaccharide by cleavage of a glycosidic linkage.

glycosyltransferase An enzyme that transfers a sugar residue from a donor substrate to a saccharide, protein, or lipid acceptor.

lectin A protein with a binding site that is specific for sugars.

Further Reading

Beeley, J. G. (1985). *Glycoprotein and Proteoglycan Techniques*. Elsevier, New York.

Lehrman, M. A. (2001). Oligosaccharide-based information in endoplasmic reticulum quality control and other biological systems. *J. Biolog. Chem.* **276**, 8623–8626.

Lennarz, W. J., and Hart, G. (eds.) (1994). *Methods in Enzymology*, Vol. 230, Academic Press, New York.

Varki, A., Cummings, R., Esko, J., Freeze, H., Hart, G., and Marth, J. (eds.) (1999). *Essentials of Glycobiology*. Cold Spring Harbor Laboratory Press, Cold Spring Harbor.

Voet, D., and Voet, J. G. (1995). *Biochemistry*, 2nd edition, Wiley, New York.

Biography

Mark A. Lehrman received his B.S. in biochemistry from the State University of New York at Stony Brook in 1977, and his Ph.D. in biochemistry from Duke University Medical Center in 1982. He is currently Professor of Pharmacology at the University of Texas Southwestern Medical Center at Dallas. His areas of research involve the structures, biosynthesis, functions, and disorders of mammalian glycoconjugates. He has served on the editorial board of the *Journal of Biological Chemistry* and of *Glycobiology*, and was a member of the Pathobiochemistry Study Section (Center for Scientific Review, National Institutes of Health).

Glycoproteins, Plant

Carolyn J. Schultz
University of Adelaide, Glen Osmond, SA, Australia

A glycoprotein is a compound containing carbohydrate (or glycan) covalently linked to protein (International Union of Pure and Applied Chemistry). Plants contain a spectrum of glycoproteins, such as the heavily glycosylated arabinogalactan-proteins (AGPs) which can contain more than 90% carbohydrate, to the minimally glycosylated proline-rich proteins containing only 1–2% carbohydrate. This article highlights the different types of glycoproteins in plants, how they are made, and the approaches being used to determine their function(s). The focus will be on glycoproteins containing *O*-linked glycans such as the AGPs and extensins, because these are unique to plants and are abundant components of the plant cell wall.

Types of Glycosylation

The classification of glycans as *N*-linked or *O*-linked reflects the type of covalent linkages between the amino acid residue in the core protein, and the first sugar of the glycan chain.

N-Linked Glycans

N-linked glycans are attached to core proteins through an amide nitrogen (N) on the side chain of selected asparagine (Asn) residues. They are attached to some, but not all, Asn residues in the motif Asn-Xaa-(Ser/Thr), where Xaa can be any amino acid except proline (Pro). Although the motif for the attachment of *N*-linked glycans is conserved in eukaryotes, the structure of the *N*-linked glycans differs in different organisms.

Attachment of an *N*-linked glycan is a multistep process. The first step is the addition of a 14-sugar preformed precursor oligosaccharide. This oligosaccharide contains *N*-acetylglucosamine (GlcNAc), mannose (Man), and glucose (Glc) and is the same in most eukaryotes (Figure 1A). This oligosaccharide is subsequently modified by glycosidases that remove selected sugars and by glycosyltransferases that selectively add sugars to specific positions.

The modifications can be temporally and spatially regulated, and are different in different organisms. An example of a "complex" type *N*-linked glycan found in plants is shown in Figure 1B. The $Man_3GlcNAc_2$ core (boxed) is found in all eukaryotic *N*-linked glycans; however, the terminal α-1,3-linked fucose and β-1,2 linked xylose residues attached to the $Man_3GlcNAc_2$ core are specific to plants. These plant specific sugars on *N*-linked glycan are believed to contribute to the response suffered by people who are allergic to pollen and certain plant foods.

N-linked glycosylation is a common motif occurring on many plant proteins. *N*-linked glycans assist protein folding and are important for ensuring that only correctly folded proteins pass through the secretory system.

O-Linked Glycans

O-linked glycans are attached to the core protein through the oxygen (O) moiety of selected serine (Ser), threonine (Thr), and hydroxyproline (Hyp) residues. Hyp is a posttranslational modification of proline that is commonly glycosylated in plants. Although Hyp is found in animal proteins (e.g., collagen), glycosylation of Hyp does not occur.

Glycosylation of Hyp exists in two different forms that depend on the arrangement of Hyp residues in the core protein. The first type of *O*-linked glycans attached to Hyp are short Ara chains (one to four) and are typically found on extensins (Figure 1B). In contrast, the arabinogalactan–proteins (AGPs) contain large arabinogalactan (AG) polysaccharides attached to Hyp residues (Figure 1C). *O*-linked glycosylation of Thr is rare in plants, although it is common in animals. Glycosylation of Ser in plants is also relatively rare and usually consists of the addition of a single galactosyl residue.

In general, glycoproteins containing *O*-linked glycans are destined for the cell surface and are found in the cell-wall/extracellular matrix (ECM), or in vesicles either in transit to/from the cell surface. The addition of carbohydrate to proteins provides unique structural properties and informational complexity to the cell. The remainder of this article will focus on the *O*-linked glycosylation of Hyp residues.

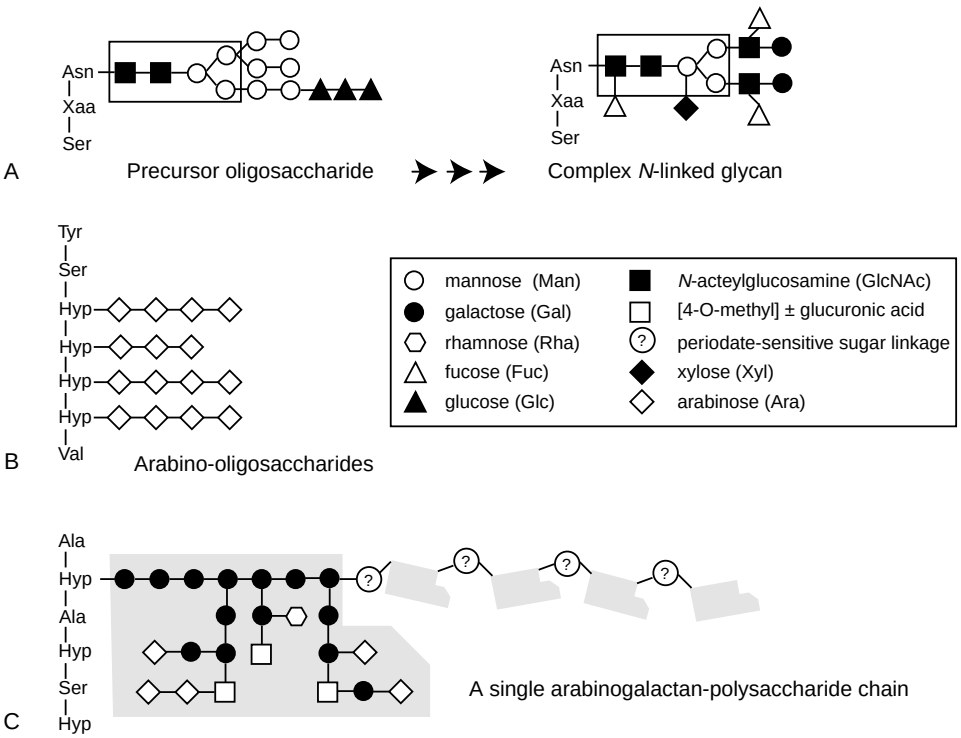

FIGURE 1 (A) The first step in *N*-linked glycosylation is the addition of a 14-sugar preformed precursor oligosaccharide. This is subsequently modified by a series of glucanases and glycosyltransferases to produce a variety of *N*-linked glycans. An example of a complex-type *N*-linked glycan from plants is shown. The five core sugars (boxed) are conserved in plants, insects, and mammals. (B) An example of the *O*-linked glycosylation that occurs on extensins. Attached to the contiguous (uninterrupted) Hyp residues are one to four (1 → 2)α-L-Ara*f* residues. (C) An example of the *O*-linked glycosylation found on AGPs. Attached to the predominantly noncontiguous Hyp residues are repeats of (1 → 3)β-D-linked Gal*p* oligosaccharides with a degree of polymerization of about seven (large shaded region), separated by a periodate sensitive linkage. The branching from the (1 → 3)β-D-linked Gal*p* oligosaccharide backbone (as seen in the large shaded region) can occur from any Gal in the backbone. There may be as many as ten repeats (only five are shown here). For simplicity, only a single Hyp residue has a polysaccharide chain attached. Reprinted from Gaspar, Y. M., Johnson, K. L., McKenna, J. A., Bacic, A., and Schultz, C. J. (2001). The complex structures of arabinogalactan-proteins and the journey towards a function. *Plant Mol. Biol.* **47**, 161–176.

Synthesis of *O*-Linked Glycans

Hydroxylation of Proline

For proteins to be glycosylated they must enter the secretory system via the endoplasmic reticulum (ER) and subsequently the Golgi apparatus. Targeting is achieved by an *N*-terminal signal sequence of ~20 amino acids in length and this signal is subsequently cleaved. In plants, the hydroxylation of Pro occurs in the ER as it does for animals.

Glycosyl Transferases

O-linked glycosylation is poorly understood in plants. It is believed to occur sequentially with the addition of single sugars by a multitude of glycosyltransferases, starting in the ER and then further elaborated in the Golgi apparatus. The recent sequencing of several plant genomes has identified hundreds of plant glycosyl transferases (http://afmb.cnrs-mrs.fr/CAZY/). The lack of knowledge of these enzymes and the abundant heterogeneity of the *O*-linked glycans in plants means that it will be many years before we have a good understanding of the structure and synthesis of these glycans in plants.

Arrangement of Hyp Residues Dictates the Type of Glycans

Our understanding about the arrangement of glycans on the Hyp-rich glycoproteins is more advanced than our understanding of the individual glycan structures. In 1994, Marcia Kieliszewski and Derek Lamport developed the Hyp contiguity hypothesis. This hypothesis suggests that contiguous (uninterrupted) Hyp residues are glycosylated with arabino-oligosaccharides (Figure 1B) and noncontiguous Hyp residues are glycosylated with arabinogalactan (AG) polysaccharides (Figure 1C). Experimental support for this hypothesis continues to grow and recent work by Kieliszewski and colleagues shows that *O*-linked oligosaccharides and AG polysaccharides can be found in the same

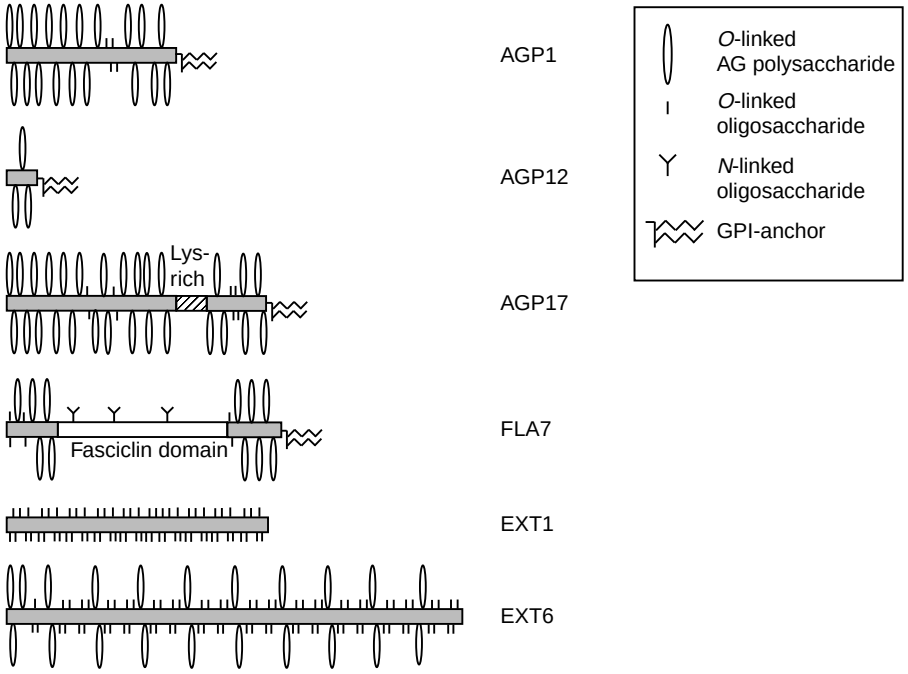

FIGURE 2 Schematic representation of the major classes of glycoproteins from *Arabidopsis thaliana*. The models are based on AGP1 (At5g64310), AGP12 (At3g13520), AGP17 (At2g23130), FLA7 (At2g04780), EXT1 (At1g76930), and EXT6 (At2g24980), as downloaded from http://www.tigr.org/tdb/e2k1/ath1/LocusNameSearch.shtml. For the AGPs and FLA7, all of the predicted Hyp glycosylation sites are shown. For the longer extensin protein backbones, the relative placement of the predicted arabino-oligosaccharides and the AG polysaccharides is shown, but the number of glycan chains is not accurate. Not drawn to scale.

molecules, e.g., LeAGP1 from tomato and gum arabic from *Acacia senegal*.

The Hyp contiguity hypothesis is useful for predicting O-linked glycosylation, although the precise rules governing the minimum length of clustered noncontiguous Hyp residues is not yet established. This is useful for modern biology where genes are generally characterized before the corresponding protein. Figure 2 shows the predicted arrangement of glycosylation of the major classes of Hyp-rich glycoproteins in *Arabidopsis thaliana*.

Hyp-Rich Glycoproteins Belong to Multigene Families

It is ~10 years since the first extensin and AGP core protein genes were cloned from plants. The completion of the sequencing of the first plant genome, from *A. thaliana*, has provided a better understanding of the size and complexity of the hydroxyproline-rich glycoprotein gene families. For example, the AGP gene family consists of ~50 different genes, in four distinct subclasses and there are at least 20 different extensin genes. A major challenge for the future is determining the function of each family member.

Approaches for Determining the Function of Plant Glycoproteins

Structural Studies

The two best-studied classes of plant glycoproteins, the extensins and AGPs, have different structures and it is widely accepted that they have different functions. Extensins are an integral part of the insoluble plant cell wall. The addition of arabino-oligosaccharides to the extensin core proteins induces an extended polyproline-II helical structure giving extensins a rod-like property. The Ser-Hyp_{3-4} regions of extensins are interspersed with amino acid residues (e.g., Tyr and Lys) that are important for cross-linking.

In contrast, AGPs are highly soluble components of the ECM. Rather than forming rods, they are believed to be almost spherical. In addition to polysaccharides, many AGPs also possess a lipid modification at their C terminus, in the form of a glycosylphosphatidylinositol (GPI) anchor. The finding that AGPs are GPI-anchored helped explain their frequent association with the plasma membrane and provided additional clues to how they might be involved in signaling.

GPI-anchors confer many different properties to animal proteins. These include (1) regulated release from cell surfaces, (2) inclusion in lipid rafts where they

may be important components of signaling cascades, and (3) polarized targeting of proteins to specific cell surfaces. Although none of these features have been confirmed for AGPs, there is recent evidence suggesting that a GPI-anchored plant protein, COBRA, is polarized in specific cells of the root.

Immunohistochemistry

Much of the original interest in AGPs came from their abundance in female reproductive tissues. The two most commonly used tools for detecting AGPs are monoclonal antibodies that recognize carbohydrate epitopes, and the artificial carbohydrate antigen, β-glucosyl Yariv reagent (β-glcY). A variety of experiments using these tools suggest that AGPs are important for cell expansion and somatic embryogenesis. However, because these tools interact with carbohydrate epitopes present on multiple AGPs, they have limited use in determining the function of individual AGPs.

Genetic Approaches

Genetic approaches offer the best hope for finding the function(s) of individual plant glycoproteins. Identification of insertion (knockout) mutants in specific genes by sequencing the DNA flanking the site of DNA insertions is well advanced in *A. thaliana*. Current research efforts around the world aim to identify insertion mutants for every gene by 2010. By studying the phenotype of knockout mutants for genes involved in the synthesis and assembly of plant glycoproteins, it should be possible to determine the function of individual family members.

Future Studies

Once we know the function of individual glycoproteins, we can begin to answer the key question of whether the function of each glycoprotein resides in the protein core or in the microheterogeneity of the glycan epitopes, or in both. It is now widely recognized that carbohydrate epitopes on mammalian, *Drosophila*, and protozoan parasite glycoproteins are key determinants of biological specificity/function. The carbohydrate component of plant glycoproteins is expected to be equally important.

See Also the Following Articles

Oligosaccharide Chains: Free, *N*-Linked, *O*-Linked • Glycosylphosphatidylinositol (GPI) Anchors • *N*-Linked Glycan Processing Glucosidases and Mannosidases • Glycoprotein-Mediated Cell Interactions, O-Linked • Protein Glycosylation, Overview

Glossary

arabinogalactan protein (AGP) A heavily glycosylated cell surface glycoprotein composed of large branched polysaccharide chains (containing predominantly arabinosyl and galactosyl residues) attached to hydroxyproline residues.

extensin A moderately glycosylated cell surface glycoprotein containing short linear arabinosyl chains attached to hydroxyproline residues and which may also contain single galactosyl residues attached to Ser residues.

glycoprotein A compound containing carbohydrate (or glycan) covalently linked to protein (International Union of Pure and Applied Chemistry). The carbohydrate may be in the form of a monosaccharide, disaccharide(s), oligosaccharides, and polysaccharides.

glycosylphosphatidylinositol (GPI) anchor A lipid modification added to the C terminus of selected proteins that anchors them in the outer layer of the lipid bilayer of the plasma membrane.

Further Reading

Buchanan, B. B., Gruissem, W., and Jones, R. L. (eds.) (2000). *Biochemistry and Molecular Biology of Plants*. American Society of Plant Physiologists, Rockville.

Fincher, G. B., and Stone, B. A. (1983). Arabinogalactan-proteins: structure, biosynthesis and function. *Ann. Rev. Plant Physiol.* **34**, 47–70.

Gaspar, Y. M., Johnson, K. L., McKenna, J. A., Bacic, A., and Schultz, C. J. (2001). The complex structures of arabinogalactan-proteins and the journey towards a function. *Plant Mol. Biol.* **47**, 161–176.

Haltiwanger, R. S. (2002). Regulation of signal transduction pathways in development by glycosylation. *Curr. Opin. Struct. Biol.* **12**, 593–598.

Johnson, K. J., Jones, B. J., Schultz, C. J., and Bacic, A. (2003). Non-enzymic cell wall (glyco)proteins. In *The Plant Cell Wall* (J. Rose, ed.) Blackwell Publishing Ltd, Oxford.

Lerouge, P., Cabanes-Macheteau, M., Rayon, C., Fischette-Lainé, A.-C., Gomord, V., and Faye, L. (1998). *N*-glycoprotein biosynthesis in plants: recent developments and future trends. *Plant Mol. Biol.* **38**, 31–48.

Schindelman, G., Morikami, A., Jung, J., Baskin, T. I., Carpita, N. C., Derbyshire, P., McCann, M. C., and Benfey, P. N. (2001). COBRA encodes a putative GPI-anchored protein, which is polarly localized and necessary for oriented cell expansion in *Arabidopsis*. *Genes Dev.* **115**, 1115–1127.

Schultz, C. J., Rumsewicz, M. P., Johnson, K. L., Jones, B. J., Gasar, Y. M., and Bacic, A. (2002). Using genomic resources to guide research directions. The arabinogalactan protein gene family as a test case. *Plant Physiol.* **129**, 1448–1463.

Wilson, I. B. H. (2002). Glycosylation of proteins in plants and invertebrates. *Curr. Opin. Struct. Biol.* **12**, 569–577.

Zhao, Z. D., Tan, L., Showalter, A. M., Lamport, D. T., and Kieliszewski, M. J. (2002). Tomato LeAGP-1 arabinogalactan-protein purified from transgenic tobacco corroborates the Hyp contiguity hypothesis. *Plant J.* **31**, 431–444.

Biography

Carolyn Schultz is a Lecturer in the School of Agriculture and Wine at the University of Adelaide's Waite Agricultural Research Institute. Her primary research interests are in understanding the role of AGPs in plant growth and development. She holds a Ph.D. from New York University and did her postdoctoral work at the University of Melbourne. She has been instrumental in defining the classes of hydroxyproline-rich glycoproteins in plants and her most recent paper won *Plant Physiology*'s best paper award for 2002.

Glycosylation in Cystic Fibrosis

Andrew D. Rhim, Thomas F. Scanlin and Mary Catherine Glick
Children's Hospital of Philadelphia and University of Pennsylvania School of Medicine, Philadelphia, Pennsylvania, USA

Cystic fibrosis (CF) is a common, ultimately fatal, genetic disease. The complex pathophysiology of CF included chronic lung disease and malnutrition. The gene that is responsible for CF was identified in 1989. Its gene product is named the cystic fibrosis transmembrane conductance regulator (CFTR). The mechanisms for many manifestations of this disease, such as chronic airway infection and inflammation, have yet to be elucidated. The glycosylation of surface membrane components has been shown to be altered in CF. This article will discuss these findings and provide an insight into how the complete understanding of the altered regulation of glycosylation in CF may eventually provide new approaches to therapy.

Cystic Fibrosis

Cystic fibrosis (CF) is the most common inherited disease in Caucasians today, affecting ~30 000 people in the US. CF is a complex multi-system disease, with initial manifestations of this disease occurring as early as the prenatal period. CF patients frequently display a unique combination of medical problems affecting multiple organ systems which can be manifested by chronic lung infection, meconium ileus, lung inflammation in the neonatal period, pancreatic insufficiency leading to malabsorption of nutrients, infertility, and excessive loss of salt in sweat. Almost invariably, the lungs are most severely affected by this disease. Patients with CF are usually colonized with either *Staphylococcus aureus* or *Haemophilus influenzae* in early childhood followed by *Pseudomonas aeruginosa*. Chronic infection by these and other types of bacteria not found in normal lungs and the hyperstimulation of the immune response of the patient eventually leads to destruction and scarring of formerly functional airways. Over time, lung function of the CF patient deteriorates to the point of failure.

In 1989, the gene responsible for CF was identified by positional cloning. Since then, more than 1000 CF gene mutations have been identified. This gene normally codes for a glycoprotein which functions as a cAMP-regulated chloride channel at the apical surfaces of epithelial cells and is known as the cystic fibrosis transmembrane conductance regulator (CFTR). Patients with CF, an autosomal-recessive disease, have two mutations in their CFTR alleles.

While there have been numerous studies on the relationship of CFTR to the pathogenesis of CF, it is still not clear how the mere absence of a normal copy of CFTR (and hence altered chloride conductance) could lead to the complex and diverse pathology of CF, and, in particular, the associated lung disease. Therefore, investigators have turned to post-translational modifications to provide further understanding of this disease.

It has been shown that the process of glycosylation, the systematic addition of carbohydrates to proteins and lipids, is altered in the tissues of patients with CF, particularly in the airways. Glycosylation is an important factor in a number of biological processes, including bacterial adhesion and the initiation of the inflammatory response. Hence, altered glycosylation of CF cells may play an important role in the pathophysiology of CF.

Glycosylation

Glycosylation refers to the systematic addition of one or more carbohydrates to proteins or lipids. This process requires specific glycosyltransferases, usually located in the smooth endoplasmic reticulum and the Golgi apparatus. Glycosylation is an important cellular function that often confers additional specific biological function to glycosylated products. For example, certain carbohydrate moieties can serve as ligands for bacterial binding, whereas others allow for recruitment of neutrophils in the inflammatory response. Additionally, it has been shown in a number of biological systems that the alteration of normally glycosylated carbohydrates of cellular components can lead to the acquisition of significantly different properties which are important in health and disease.

It is thought that CF also involves a modification in normal glycosylation processes. Two of the most prominent characteristics of the CF airway disease are chronic infection with bacterial pathogens, especially

P. aeruginosa, and a robust but ineffective inflammatory response. While it is unclear how the absence of normal CFTR chloride channels could lead to these observations, an alteration in glycosylation may be the common denominator. As will be discussed later, bacteria such as *P. aeruginosa* require the presence of specific carbohydrates on the surfaces of host for proper binding and function.

Terminal Glycosylation of CF Cells

CF Glycosylation Phenotype

It has been shown by ~50 different studies that material obtained from patients with CF display a specific glycosylation phenotype. This phenotype of increased fucose and decreased sialic acid in the terminal positions of membrane glycoconjugates has been confirmed by many different methods and in multiple cell types. This section will focus on the glycosylation of cell surface components.

Glycosylation of CF Fibroblasts

Early work on CF glycosylation focused on skin fibroblasts as these cells were readily accessible, relatively easy to maintain in culture, and not subjected to the same chronic infections as airway cells. Secreted and membrane glycoproteins from fibroblasts have significantly more fucosyl residues compared to normal controls by biochemical analyses. In addition, the ratio of fucose to sialic acid of membrane glycoproteins is significantly greater in fractions from CF fibroblasts compared to non-CF controls. Perhaps the most striking findings were obtained by 500 MHz ^{1}H-NMR spectroscopic analyses of secreted and membrane-bound glycoproteins from fibroblasts. Interpretation of the data from these analyses has led to the proposed structure of the oligosaccharide chains derived from CF fibroblast glycoconjugates shown in Figure 1.

Glycosylation of CF Airway Epithelial Cells

As the site of the most lethal pathology in CF, studies have focused on the airway, and, in particular, the airway epithelium. Similar to results obtained from fibroblast studies, increased fucosyl residues linked α1,3 or 4 to *N*-acetylglucosamine (Fucα1,3/4GlcNAc) were found in CF compared to non-CF fractions of the airway cells. Also, significantly less terminal sialic acid residues were found on CF membrane glycoproteins compared to non-CF membrane glycoproteins. Hence, the increased ratio of Fucα1,3/4GlcNAc to sialic acid in CF compared to non-CF airway cells mirrored that seen in fibroblasts.

In airway epithelial cells, the glycosylation phenotype of increased Fucα1,3/4GlcNAc and decreased sialic acid is modulated by the degree of wild-type CFTR expression (Figure 2). In other words, when normal copies of the CF gene are successfully transferred into CF airway epithelial cells so that these cells express normal copies of CFTR, the amount of sialic acid and Fucα1,3/4GlcNAc found on membrane glycoproteins changed to levels seen in non-CF cells. Conversely, if mutated copies of the CF gene are transferred into non-CF airway epithelial cells, the amount of sialic acid would decrease. The dependence on CFTR was seen in primary and corresponding immortalized cells (Table I). Therefore, in airway epithelial cells, the presence of CFTR affects glycosylation.

It has also been shown that not all fucose moieties are increased in CF airway cells. Specifically, the amount of fucose in α1,2 linkage to galactose is decreased in CF airway cells compared to non-CF airways. The Fucα1,3/4GlcNAc-to-Fucα1,2Gal ratio reflects the Fucα1,3/4GlcNAc-to-sialic acid ratio in airway cells. Moreover, the amount of Fucα1,2Gal is increased once wtCFTR cDNA is transferred into and expressed in CF airway epithelial cells. On the other hand, the mRNA expression for the corresponding fucosyltransferases does not correlate with the chemical structures found on the surface membranes of CF and non-CF airway

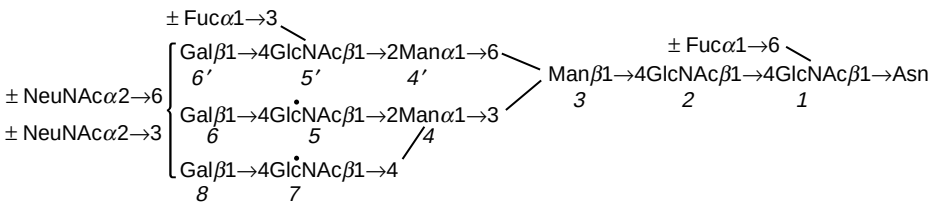

FIGURE 1 Oligosaccharide structure obtained by ^{1}H-NMR spectroscopy of glycopeptides isolated from membrane glycoprotiens of CF fibroblasts represents the CF glycosylation phenotype. α1,3 fucosyl residues can also occur on GlcNAc 5 or 7. ± denotes the decrease in sialic acid on one or more branches. Reproduced from Rhim, A. D., Stoykova, L., Glick, M. C., and Scanlin, T. F. (2001). Terminal glycosylation in cystic fibrosis (CF): A review emphasizing the airway epithelial cell. *Glycoconjugate J.* **18**, 649–660, with permission of Nature.

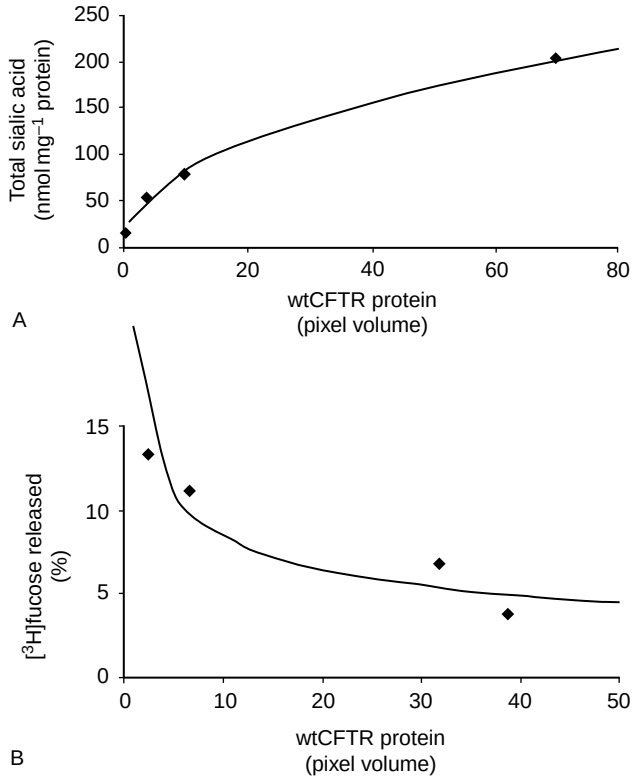

FIGURE 2 The dependence on the expression of wtCFTR of sialic acid and Fucα1,3/4GlcNAc content of peripheral glycopeptides of airway epithelial cells. Line represents the exponential equation generated characterizing this relationship based on data. (A) The sialic acid content of CF cells is increased with the expression of wtCFTR whereas (B) Fucα1,3GlcNAc is decreased. Sialic acid content was determined by the thiobarbituric acid assay and fucose by α1,3/4 fucosidase. Reproduced from Rhim, A. D., Stoykova, L., Glick, M. C., and Scanlin, T. F. (2001). Terminal glycosylation in cystic fibrosis (CF): A review emphasizing the airway epithelial cell. *Glycoconjugate J.* **18**, 649–660, with permission of Nature.

epithelial cells. This has led to the proposal that the compartmentalization of the glycosyltransferases in the Golgi apparatus is affected by CFTR resulting in modified glycosylation products.

Glycosylation of CF Airway Mucins

Respiratory mucus serves as a defense against the entry of foreign particles (bacteria and viruses included) by forming a protective layer over the epithelial surfaces of the human airway. Mucus is secreted both constitutively and in response to inflammatory cytokines by a relatively small number of specialized glandular cells that are intrinsically different from other epithelial cells. Mucins are the main constituents of respiratory mucus. Mucins are a family of high-molecular-weight

TABLE I

Sialic Acid and Fucose Content in Membranes of Immortalized or Primary Airway Epithelial Cells

Airway cells	Sialic acid (nmol mg^{-1} protein)	Fucose (% released)
BEAS-2B	7.64 ± 4.01^a	3.28 ± 0.03^b
CF/T43	2.34 ± 0.32^a	27.45 ± 0.35^b
Non-CF (primary)	37.45 ± 1.45^c	2.75 ± 0.35^d
CF (primary)	16.42 ± 2.00^c	18.45 ± 0.42^d

Reproduced from Rhim, A. D., Kothari, V. A., Park, P. J., Mulberg, A. E., Glick, M. C., and Scanlin, T. F. (2000). Terminal glycosylation of cystic fibrosis airway epithelial cells. *Glycoconjugate J.* **17**, 385–391, with permission of Nature.

[a] $p < 0.021$.
[b] $p < 0.013$.
[c] $p < 0.00064$.
[d] $p < 0.0009$, by Student's *t*-test.

proteins that are highly glycosylated (50–80% of molecular weight). As opposed to *N*-linked carbohydrate residues on most glycoproteins, mucins are by definition *O*-glycosylated at either a threonine or serine. Therefore, the types of glycosylation seen in mucin glycoconjugates are inherently different from most other membrane-bound glycoproteins, particularly when compared to membrane glycoconjugates of nonmucus-secreting airway epithelial cells which are the vast majority of cells lining the airways.

Mucins obtained from CF patients have significantly more sialic acid and fucose than those obtained from non-CF controls. In particular, the specific carbohydrate epitope, Neu5Ac2,3Galβ1,4[Fucα1,3]GlcNAcβ, was found to be increased in mucins from CF patients. However, since the expression of this motif is increased in the presence of cytokines, as in chronic bronchitis, some of the differential glycosylation of CF mucins may be a result of the state of chronic respiratory infection that CF patients endure.

Interestingly enough, the same glycosyltransferases that are involved in the CF glycosylation phenotype seen in CF airway cell membranes are also implicated in the alteration of mucin carbohydrate composition in patients with chronic lung infections. However, it should be emphasized that the mechanisms behind both observations are different – the glycosylation of CF airway cell membranes is dependent upon the presence or absence of wtCFTR whereas mucin glycosylation is apparently not affected by the presence or absence of CFTR. While confirmatory studies on the subject are necessary, the alteration in glycosylation of CF mucins is a phenomenon that may not be entirely specific to the disease of CF, but rather an observation which is influenced by chronic airway infection.

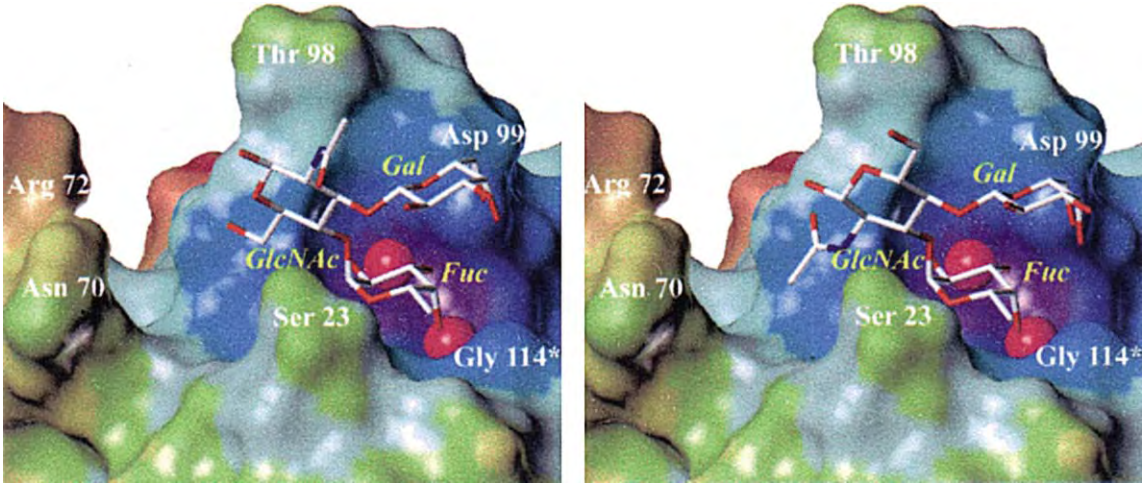

FIGURE 3 Molecular model based on crystallography experiments of PA-IIL, a lectin found on pili of *P. aeruginosa*. Two fucosylated oligosaccharides similar to those detected on the membranes of CF airway cells are shown to be optimally docked in the binding site of this protein. (Left) Galβ1,3[Fucα1,4]GlcNAcβ has a better fit than (Right) Galβ1,4[Fucα1,3]GlcNAcβ, where the position of GlcNAc interferes slightly. Both feature a terminal fucosyl residue linked to *N*-acetylglucosamine. The surface of the protein model has been color coded according to the electrostatic potential (from violet for negative to orange for positive). Reproduced from Mitchell, E., Houles, C., Sudakevitz, D., Wimmerova, M., Gautier, C., Perez, S., Wu, A. M., Gilboa-Garber, N., and Imberty, A. (2002). Structural basis for oligosaccharide-mediated adhesion of *Pseudomonas aeruginosa* in the lungs of cystic fibrosis patients. *Nat. Struct. Biol.* **9**, 918–921.

Functional Implications of Altered Glycosylation

As the major virulent bacterium infecting cystic fibrosis airways, *P. aeruginosa* almost exclusively infects CF patients in the immunocompetent pediatric population. Hence, the CF airway is intrinsically predisposed to colonization by *P. aeruginosa*. A recent crystallography study provided the structural basis for increased adhesion by *P. aeruginosa* in CF patients. The focus of their study was PA-IIL, a lectin on the pili of *P. aeruginosa* that binds to specific carbohydrates and is involved in colonization. It was shown that PA-IIL contains an anionic "dock" which allows optimal binding of fucosylated carbohydrate structures (Figure 3). Therefore, it is thought that the mechanism of increased and efficient *P. aeruginosa* adherence is due to the increased constitutive expression of terminal α1,3/4 fucose-containing carbohydrate motifs on CF airway epithelial cell membranes. In addition, as the negatively charged sialic acid occupies the terminal end of oligosaccharide branches, a decrease in sialic acid residues, as observed in CF airway membranes, could lead to the removal of a potential inhibitor of *P. aeruginosa* binding to fucose-containing moieties.

See Also the Following Articles

Glycosylation, Congenital Disorders of • Mucin Family of Glycoproteins • *N*-Linked Glycan Processing Glucosidases and Mannosidases • Protein Glycosylation, Overview

Glossary

cystic fibrosis (CF) A common autosomal-recessive genetic disease where no copies of wild-type cystic fibrosis transmembrane conductance regulator protein (CFTR) are expressed. This disease varies in severity but is characterized by chronic lung infection, eventual failure of pulmonary function, pancreatic insufficiency, and infertility.

fucose A monosaccharide which can be found on glycoconjugates in α1,3 or α1,4 linkage to branched *N*-acetylglucosamine (Fucα1,3/4GlcNAc).

glycosylation The biological process whereby carbohydrates are enzymatically linked to proteins and lipids by specific glycosyltransferases in a discrete, organized fashion to create glycoconjugates.

mucin A large glycoprotein composed of glycans *O*-linked to serine or threonine.

sialic acid A family of negatively charged nine-carbon monosaccharide frequently found on the terminal end of glycoconjugates.

Further Reading

Lamblin, G., Degroote, S., Perini, J.-M., Delmotte, P., Scharfman, A., Davril, M., Lo-Guidice, J.-M., Houdret, N., Dumur, V., Klein, A., and Roussel, P. (2001). Human airway mucin glycosylation: A combinatory of carbohydrate determinants which vary in cystic fibrosis. *Glycoconjugate J.* **18**, 661–684.

Mitchell, E., Houles, C., Sudakevitz, D., Wimmerova, M., Gautier, C., Perez, S., Wu, A. M., Gilboa-Garber, N., and Imberty, A. (2002). Structural basis for oligosaccharide-mediated adhesion of *Pseudomonas aeruginosa* in the lungs of cystic fibrosis patients. *Nat. Struct. Biol.* **9**, 918–921.

Rhim, A. D., Kothari, V. A., Park, P. J., Mulberg, A. E., Glick, M. C., and Scanlin, T. F. (2000). Terminal glycosylation of cystic fibrosis airway epithelial cells. *Glycoconjugate J.* **17**, 385–391.

Rhim, A. D., Stoykova, L., Glick, M. C., and Scanlin, T. F. (2001). Terminal glycosylation in cystic fibrosis (CF): A review emphasizing the airway epithelial cell. *Glycoconjugate J.* **18**, 649–660.

Robinson, C., and Scanlin, T. F. (1997). Cystic fibrosis. In *Pulmonary Diseases and Disorders* (A. P. Fishman, ed.) pp. 1273–1294. McGraw-Hill, New York.

Scanlin, T. F., and Glick, M. C. (1999). Terminal glycosylation in cystic fibrosis. *Biochim. Biophys. Acta* **145**, 241–253.

Varki, A., Cummings, R., Esko, J., Freeze, H., Hart, G., and Marth, J. (eds.) (1999). *Essentials of Glycobiology.* Cold Spring Harbor Laboratory Press, Cold Spring Harbor, New York.

Biography

Mary Catherine Glick received a Ph.D. from the University of Pennsylvania and soon thereafter began her studies of surface membranes from mammalian cells and the glycoconjugates thereof. She became a Professor of Pediatric Research at the University of Pennsylvania. She studies the glycoconjugates of CF airway cells with Dr. Thomas F. Scanlin.

Thomas Scanlin received his M.D. from the University of Pennsylvania. He is Director of the Cystic Fibrosis Center and is a Professor of Pediatrics at the University of Pennsylvania. Both are at the Children's Hospital of Philadelphia.

Andrew D. Rhim is a candidate for the M.D. degree from the University of Pennsylvania. He is studying in the laboratory of Drs. Glick and Scanlin as an NIH Medical Student Research Program Fellow, where he continues the research he began as an undergraduate.

Glycosylation, Congenital Disorders of

Hudson H. Freeze
The Burnham Institute, La Jolla, California, USA

All cells are covered with a dense forest of glycosylated molecules that consist of glycoproteins and glycolipids. These frostings often dictate and monitor the stability of newly synthesized proteins and glycolipids within the cell. On the surface, they help cells communicate with their neighbors to assess the state of the local neighborhood. Hundreds of enzymes are used in making the sugar chains and adding them to thousands of proteins. Inherited mutations in some of the biosynthetic enzymes cause human diseases that affect the function of many organs during embryonic development, childhood, and even as adults. This article will cover these inherited protein glycosylation diseases and show where glycobiologists studying sugar chain biosynthesis and function team up with physicians to define and understand the basis of these diseases.

Setting the Stage

About 1–2% of the human genome encodes proteins that synthesize or recognize sugar chains. Hundreds of different sugar chains decorate the surface of eukaryotic cells. The immense variety of sugar chains stems from variability in length (number of monosaccharides), kinds of linkage (alpha versus beta), spatial orientation (linkage) of the sugar, branching patterns (two or more sugars attached to another sugar), and modifications by nonsugar elements (e.g., phosphate or sulfate). Adding each of these sugars or modifications requires one or more separate enzymes. Sometimes coordinated groups of enzymes work in a specific order to add some sugars, or cleave others from the maturing chain. Cells express different complements of sugar biosynthetic enzymes (glycosyl transferases and glycosidases) and glycosylation of a single protein can vary in different cells. Moreover, the same sugar chain can have different functions depending on the protein it is on and the cell expressing it. Loss of glycosylation capacity can have serious effects in some cells and much milder effects in others. This complexity means that the function of sugar chains has to be investigated case by case, protein by protein.

The linkage joining the sugar chain to the protein defines the type of glycosylation, as shown in Table 1. Most of the glycosylation disorders have been identified in the N-linked oligosaccharide biosynthetic pathway since 1995. In 2002, incomplete glycosylation of α-dystroglycan with O-mannose based sugar chains was found to be the cause of rare forms of muscular dystrophy. Defects in the biosynthesis of chondroitin and heparin sulfate chains also cause diseases that affect growth of bone and connective tissues. The failure to add phosphate or sulfate to sugar chains also causes glycosylation-based disorders. No specific human diseases in the O-GalNAc (mucin) pathway are yet known.

Congenital Disorders of Glycosylation

Biosynthetic Overview

All N-linked chains are derived from a common dolichyl pyrophosphate (Dol-PP)-linked 14-sugar oligosaccharide (lipid linked oligosaccharide (LLO)). It is composed of 3 glucose (Glc), 9 mannose (Man) and 2 N-acetylglucosamine (GlcNAc) residues, forming a $Glc_3Man_9GlcNAc_2$ chain which is transferred *en bloc* from the lipid carrier to proteins. Addition of each sugar unit occurs in a preferred order and requires at least 13 glycosyltransferases. The completed oligosaccharide chain is then transferred to the nascent polypeptide chain by the oligosaccharyl transferase complex located in the endoplasmic reticulum (ER) membrane. After the transfer, the sugar chain is processed. Specific glycosidases trim the $Glc_3Man_9GlcNAc_2$ chain, removing all Glc and some Man in the ER. As the proteins move to the Golgi, additional Man is often carved away and the chain is extended once again by addition of 2–4 branches composed of GlcNAc, galactose (Gal) and sialic acid (Sia) to form complex-type sugar chains (Figure 1). Literally hundreds of different sugar chain structures can be made by variations of this pathway.

TABLE I

Major Types of Glycan-Protein Linkages

Glycan type	Linkage	Typical proteins	Location
N-linked	GlcNAc-β-Asn	Cell surface receptors secreted proteins	All cells, blood, sub-cellular compartments (e.g., lysosomes)
O-linked	GalNAc-α-Ser/Thr	Secreted and cell surface mucins	Cell surface, gastrointestinal, and reproductive tracts
O-linked	Xyl-α-Ser	Chondroitin/dermatan sulfate	Extracellular matrix, cartilage
O-linked	Man-β-Ser/Thr	Heparan sulfate/heparin α-dystroglycan	Muscle, nerve cells

Scope of the Disorders

Congenital Disorders of Glycosylation (CDG) result from defects in the assembly, transfer, and processing of N-linked oligosaccharides. For convenience, the CDGs are divided into groups I and II. Defective genes are lettered in chronological order of their discovery. The first group includes defects in the assembly of the LLO and its transfer to proteins, which probably requires about 40 nonredundant genes. Defects in nine of these 40 genes have been shown to cause CDG. These include defects in the mobilization and interconversion of monosaccharide precursors or defective glycosyltransferases used to link these sugar units. The second group involves processing of the sugar chains, requiring a minimum of 20 genes. Some of them encode enzymes that may catalyze the same or similar sugar transfer reactions. Defects in four of the genes from this group cause CDG and involve mutations in glycosidases, glycosyl transferases, and Golgi-associated sugar nucleotide transporters that carry these donors from their origin in the cytosol to the Golgi lumen where they are added to their acceptor oligosaccharides. It is likely that serious mutations in any of these genes will cause CDG.

Although there are currently ~300–400 cases of all types of CDG worldwide, it is probably only a few percent of the total patients. It is safe to say that the entire group of CDGs is severely underdiagnosed, and that we are now only seeing the "tip of the iceberg."

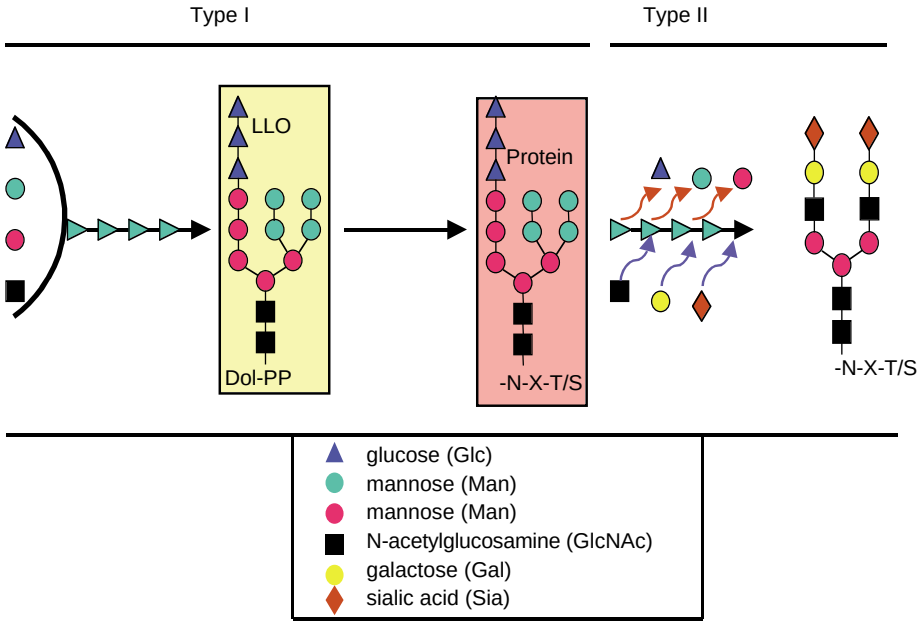

FIGURE 1 Defining Types of Congenital Disorders of Glyosylation (CDG). CDG types are based on finding mutations in genes whose products are involved in glycosylation. Type I CDGs are defined by mutations in steps leading to the assembly and transfer of the lipid linked oligosaccharide chain (LLO) from the carrier lipid to potential N-glycosylation sites (N-X-T/S) on newly synthesized proteins in the ER. At the extreme left, the various monosaccharides (see symbol key below) are first activated, and then they are incorporated one-by-one into a growing chain assembled on the carrier lipid, Dol-PP. The complete sugar chain is then transferred to protein in a single step. Approximately 40 genes are needed to carry out the first stage. Type II CDG defects are defined as those that involve the sequential, highly ordered removal and, addition of individual sugars on protein-bound N-linked sugar chains. More than 20 additional genes are needed to synthesize a sugar chain typical of mammalian plasma glycoprotein, shown on the extreme right side. To date only 16 types of CDG have been identified. It is likely that many more will be found.

Laboratory Diagnosis of CDG

CDG patients are often misdiagnosed early on because their symptoms resemble other generic disorders. CDG-Ia patients are sometimes mistaken for having inherited mitochondrial disorders or cerebral palsy. This is understandable since glycobiology is not part of a typical medical education or training program and most practicing physicians have a limited awareness of glycosylation. Fortunately, most CDG patients can be diagnosed by a simple blood test to analyze the glycosylation status of transferrin (Tf). Abnormal Tf is detected by isoelectric focusing, or by electrospray ionization-mass spectrometry. Many other proteins are misglycosylated, but Tf appears to be especially sensitive to limitations in the amount of LLO precursor. These biochemical analyses provide clues to the defect, but they cannot pinpoint the defective gene, since many defects produce the same altered pattern.

Biochemical Overview

All of the CDGs are autosomal recessive disorders and they result from an insufficient amount of precursor molecules or from deficient glycosyltransferases or sugar processing glycosidases. For a complete listing see Table 2. By far the most common type, CDG-Ia (OMIM 212066), is caused by mutations in the gene encoding phosphomannomutase (Man-6-P → Man-1-P). Mutations reduce the amount of GDP-Man, resulting in insufficient LLO. This leaves some of the normal glycosylation sites on many proteins unoccupied, which can lead to their misfolding and degradation. Sometimes the misfolded proteins accumulate in the ER, activating cell apoptosis. CDG-Ib (OMIM 602579) results from mutations in the *MPI* gene encoding phosphomannose isomerase (PMI) (fructose-6-P → Man-6-P), just one metabolic step away from phosphomannomutase. The clinical pictures of CDG-Ib and CDG-Ia patients are quite different. CDG-Ic (OMIM 603147) is caused by mutations in *ALG6*, which encodes an α-1,3-glucosyltransferase used to add the first Glc to the immature LLO precursor. Chains lacking glucose are transferred to proteins less efficiently than full-sized ones. Group II CDGs are defined as those that affect the processing of the protein-bound sugar chains. Only a few patients have been identified with these disorders, and most, but not all of them can be diagnosed by analysis of Tf.

Clinical Features of CDG

The most common clinical features in various types of CDG are shown in Table 2. There is considerable clinical heterogeneity even within a specific type of CDG. Psychomotor retardation ranging from mild to severe and hypotonia are consistent features in all patients except Type-Ib. Other neurological findings include ataxia (Ia and Ic), seizures, and stroke-like episodes. Cerebellar hypoplasia (Ia, Ic), delayed myelination (Ie, IIa, IIb), microcephaly, and atrophy of the cerebrum (Ia, Ic, Id, Ie) are seen. Sometimes the cognitive deficiency can be mild. Nearly all patients have feeding problems and fail to thrive. Strabismus, abnormal fat distribution, and retracted nipples are common, especially in the CDG-Ia group.

Mortality in CDG-Ia children is about 20% during the first few years, but they stabilize after childhood. Substantial survival means that many adult CDG patients remain undiagnosed.

CDG-Ib, caused by deficiency in MPI, is substantially different from all the others in that mental development and the nervous system are normal. The reason for this is unknown. These patients have serious gastrointestinal problems, protein-losing enteropathy (loss of proteins through the intestine), low plasma albumin, coagulopathy (fast clotting), and hyopoglycemia. A substantial number of patients died before they received a diagnosis, which is unfortunate, since this type of CDG can be treated effectively.

Therapy for CDG

The effective therapy for CDG-Ib is oral mannose. Mannose bypasses the fructose-6-P → Man-6-P block to replenish the depleted GDP-Man pools. A mannose transporter delivers mannose to the cells and hexokinase converts it into Man-6-P. Mannose therapy reverses the hypoglycemia and coagulopathy within a few weeks, and within 1–2 months plasma protein levels become normal and protein-losing enteropathy disappears. Some patients have been treated for over 6 years without side effects. Growth during childhood is metabolically demanding and mannose supplements are most important then. It is encouraging that none of the adult patients with proven CDG-Ib is currently taking mannose, suggesting that it will not be a lifelong requirement. It is important to point out that there is no evidence that healthy people require mannose supplements. Vendors of complex nutraceutical mannose fail to point out that the natural plant polysaccharides they sell are nondigestible. Fucose supplements have also been used to treat patients with CDG-IIc who have a defective GDP-Fucose transporter. Fucose enters the cell and apparently increases the GDP-Fucose pool driving it into the Golgi through the transporter. Within a day, fucose treatment corrects the patients' elevated circulating neutrophil by generating a selectin ligand needed for neutrophil rolling on the endothelium prior to their transmigration into the tissues. Infections cease and health improves. Unfortunately, fucose does not improve or reverse the mental retardation.

TABLE II

Inherited Glycosylation Disorders

Disorders	Enzymatic or protein defect	Gene	OMIM	Frequent clinical features
CDG type				
Ia	Phosphomannomutase Man-6-P → Man-1-P	*PMM2*	212065 601785	Variable psychomotor retardation, hypotonia, seizures, coagulopathy, feeding problems, liver fibrosis.
Ic	α-1,3-glucosyltransferase	*ALG6*	603147 604566	
Id	α-1,3-mannosyltransferase	*ALG3*	601110	
Ie	Dolichol-P-Man synthase	*DPM1*	603503	
If	Dolichol-P sugar utilization protein	*MPDU1*	604041	
Ig	α-1,2-mannosyltransferase	*ALG12*		
Ih	α-1,3-glucosyltransferase	*ALG8*		
Ii	GlcNAc-1-P transferase	*GNT*		
IIa	N-acetylglucosaminyltransferase II	*MGAT2*	212066 602616	
IIb	α-1,2-glucosidase	*GCS1*	601336	
IId	β-1,4-galactosyltransferase	*B4GALTI*	607091	
IIc	GDP-fucose transporter	*FUCTI*	266265	Severe psychomotor retardation, hypotonia, elevated peripheral neutrophils.
Ib	Phosphomannose isomerase (PMI) Fru-6-P ⇄ Man-6-P	*MPI*	602579 154550	Normal development, hypoglycemia, coagulopathy, diarrhea protein-losing enteropathy, vomiting, liver fibrosis.
Muscular dystrophy				
Muscle–eye–brain disease (MEB)	O-mannosyl glycan synthesis	*POMGnT1*	253280	Severe muscle weakness, mental retardation, epilepsy, neuronal migration disorder, ocular abnormalities.
Fukuyama-type congenital muscular dystrophy (FCMD)	Putative glycosyltransferase	Fukutin	253800	Severe proximal and axial weakness, mental retardation, epilepsy neuronal migration disorder.
Walker–Warburg syndrome	Putative O-mannosyltransferase	*POMT1*	268870	Severe muscle weakness, death in infancy, absent psychomotor development, neuronal migration disorder, ocular abnormalities.
Inclusion body myopathy	UDP-GlcNAc epimerase/kinase	*GNE*	600737	Adult onset myopathy that spares quadriceps.
Limb–girdle muscular dystrophy IC	Putative glycosyltransferase	Fukutin-related protein (FKRP)	607155 606612	Variable proximal and axial muscle weakness, cardiomyopathy.
Other types				
1-cell disease	GlcNAc-1-P transferase	*GNPTA*	252500	Severe developmental abnormalities.
Multiple hereditary exostoses	Heparan sulfate co-polymerase	*EXT1, EXT2*	133701	Bony outgrowths.
Macular corneal dystrophy	GlcNAc-6-sulfotransferase	*CHST6*	605294	Progressive corneal opacity.
Ehlers–Danlos syndrome progeroid form	Xylosylprotein β-1,4-galactosyltransferase	*B4GALT7*	130070 604327	Hypotonia, delayed development, connective tissue abnormalities, loose skin.
Diastrophic dysplasia achondrogenesis	Anion (sulfate) transporter	*DTDST*	606718 600972	Scoliosis, club foot, premature calcification.

[a]OMIM: Online Mendelian Inheritance in man (http://www.ncbi.nlm.nih.gov/).

Congenital Muscular Dystrophies: The Most Recently Discovered Glycosylation Deficiencies

α-Dystroglycan is a peripheral membrane component of the dystrophin–glycoprotein complex (DGC) found in muscle, nerve, heart, and brain. This protein binds to merosin in extracellular matrix bridging it to the cytoskeleton molecules that include dystrophin and actin. Mutations in dystrophin cause Duchenne and Becker muscular dystrophies, while assorted mutations in merosin and sarcoglycans cause other inherited muscular dystrophies. Total systemic loss of α-dystroglycan is embryonic lethal. In addition, this protein is the major carrier of O-mannose-based sugar chains. In α-dystroglycan, these sugar chains cluster together in a small "mucin-like" domain of where they mediate many of the critical stabilizing interactions with the other matrix molecules such as merosin, neurexin, and agrin, depending on which cells express α-dystroglycan. Several kinds of muscular dystrophies including muscle–eye–brain (MEB) disease, Fukuyama-type congenital muscular dystrophy (FCMD), Walker–Warburg syndrome, and limb–girdle muscular dystrophy, involve mutations in the genes needed for the biosynthesis of these chains (Table 2). These mutations also appear to affect neuronal migration in the developing brain, thus accounting for the combined effects on muscle and brain development. Studying the glycosylation of α-dystroglycan will be important to understand how these pathologies develop. However, α-dystroglycan is not the only protein that carries these sugar chains. In fact, one out of four O-linked chains in the brain are O-mannose based.

One form of adult onset muscular dystrophy, hereditary inclusion body myopathy Type II, is due to mutations in an enzyme involved in the biosynthesis of CMP-sialic acid, the universal activated donor for addition of sialic acid. The mutations appear to have a minor affect on the activity of the enzyme (UDP-GlcNAc epimerase-kinase) which is lethal when totally deleted. Preliminary studies in fibroblasts and muscle cells from the patients show that addition of sialic acid is reduced and that supplying sialic acid or N-acetylmannosamine (the product of the impaired enzyme) can correct the glycosylation. This suggests that patients might benefit from supplements of these sugars.

Defects in Proteoglycan Biosynthesis Cause Disease

Incomplete or impaired synthesis of glycosaminoglycan (GAG) chains also cause inherited disorders. The bony outgrowths found in patients with multiple hereditary exostoses (MHE) result from mutations in the co-polymerase that assembles alternating units of glucuronic acid and GlcNAc in heparan sulfate. Elhers–Danlos syndrome, which causes a form of progeria is caused by mutations a galactosyltransferase used for assembly of the tetrasaccharide core linkage common to heparin, heparan sulfate, chondroitin, and dermatan sulfate. Macular corneal dystrophy that leads to corneal opacity is caused by loss of a specific sulfotransferase that modifies a special type of keratan sulfate found in the cornea. Sulfate is such an important component for making extracellular matrices that cells have a cell surface transporter that delivers sulfate to the cytoplasm. Mutations in the transporter cause multiple cartilage and bone malformations and in the most severe forms prenatal lethality results from respiratory insufficiency.

Glycosylation Disorders: The Next Generation

The very complexity of sugar chain assembly practically guarantees that more glycosylation disorders will be discovered. Finding defects in the N-linked pathway has been relatively easy because many of the steps involve only a single enzyme, many of which have strict substrate requirements. In addition, Tf provides an unusually robust assay for defective N-glycosylation. Except for α-dystroglycan, the other pathways lack a similar diagnostic champion. New disorders that compromise glycosylation will probably be discovered in the synthesis of O-GalNAc-linked sugar chains, glycosaminoglycans, and in the assembly, organization, or recycling of proteins in the Golgi apparatus. These causes may be more difficult to identify because many of these pathways are composed of redundant, sometimes, overlapping enzymes with tissue specific distributions.

Understanding the role of sugar chains in building cell-surface signaling complexes and finding how to boost sugar donors in cells may help to understand and treat these pathologies. Interactions among basic scientists focused on glycobiology and glycosylation-savvy clinicians will be the key to further discoveries.

See Also the Following Articles

Glycosylation in Cystic Fibrosis • *N*-Linked Glycan Processing Glucosidases and Mannosidases • Protein Glycosylation, Overview • Proteoglycans

Glossary

congenital disorders of glycosylation Inherited disorders of protein glycosylation involving the synthesis and transfer of the Dol-PP-oligosaccharide precursor sugar chain to protein or the subsequent processing of these N-linked oligosaccharides. The term

can also apply to the addition of other types of sugar chains to proteins.

α-dystroglycan An extrcellular DGC component which is one of the major proteins known to contain O-mannose-based oligosaccaharides. Mutations in genes that encode proteins needed for this type of glycosylation cause several types of muscular dystropy.

dystrophin–glycoprotein complex (DGC) A large protein complex found in muscle, nerve, heart, and brain. It is composed of extracellular, transmembrane and intracellular proteins. Mutations in different proteins of this complex cause different types of muscular dystrophy.

glycosaminoglycan (GAG) A large complex sugar chain composed of alternating amino-sugar and uronic acid units. The disaccharides uronic acid disaccharide unite.

glycosylation The process of adding single (monosaccharides) or multiple sugars to proteins or lipids.

glycosyltransferase An enzyme that transfers a sugar from an activated nucleotide donor to an acceptor protein, carbohydrate, or lipid.

lipid linked oligosaccharide (LLO) Structure that is the precursor for N-linked glycans; composed of a sugar chain linked to dolichol through a pyrophosphate linkage.

multiple hereditary exostosis (MHE) A dominant inherited disorder caused by mutations in two genes (*EXT1* and *EXT2*) that encode a polymerase needed for the synthesis of heparan sulfate. Mutations cause painful recurrent outgrowths of bone and must be surgically removed.

oligosaccharyl transferase complex A protein complex found in the endoplasmic reticulum where it recognizes the LLO sugar chain and attaches it to the newly synthesized proteins having the N-X-Thr/Ser consensus sequence for N-glycosylation.

transferrin (Tf) An iron-carrying plasma glycoprotein that is especially susceptible incomplete N-glycosylation caused by an insufficient amount of LLO or one that is inefficiently transferred to proteins.

Further Reading

Freeze, H. H. (2001). Update and perspectives on congenital disorders of glycosylation. *Glycobiology* **11**, 29R–143R.

Jaeken, J., and Matthijs, G. (2001). Congenital disorders of glycosylation. *Annu. Rev. Genomics Hum. Genet.* **2**, 129–151.

Martin, P. T., and Freeze, H. H. (2003). Glycobiology of neuromuscular disorders. *Glycobiology* **13**, 67R–75R.

Muntoni, F., Brockington, M., Black, D. J., Torelli, S., and Brown, S. C. (2002). Defective glycosylation in muscular dystrophy. *Lancet* **360**, 1419–1421.

Biography

Hudson H. Freeze is Professor and Director of the Glycobiology and Carbohydrate Chemistry Program at The Burnham Institute in La Jolla, California, and specializes in congenital disorders of glycosylation. He received his Ph.D. in biology in 1976 from the University of California, San Diego and later joined the UCSD Department of Medicine faculty where he is an adjunct professor.

Glycosylphosphatidylinositol (GPI) Anchors

Anant K. Menon
University of Wisconsin-Madison, Madison, Wisconsin, USA

Glycosylphosphatidylinositol (GPI)-anchored proteins are a class of lipid-anchored membrane proteins that is ubiquitously expressed at the surface of eukaryotic cells. GPI proteins differ from traditional membrane proteins in that they rely on a complex glycolipid, GPI, rather than a hydrophobic transmembrane sequence for their association with membranes. GPI anchors are found on a variety of functionally diverse proteins (as well as glycoconjugates) including cell surface receptors (folate receptor, CD14), cell adhesion molecules (neural cell adhesion molecule (NCAM) isoforms, carcinoembryonic antigen variants), cell surface hydrolases (5′-nucleotidase, acetylcholinesterase), complement regulatory proteins (decay accelerating factor), and protozoal surface molecules (*Trypanosoma brucei* variant surface glycoprotein, *Leishmania* lipophosphoglycan). Along with serving to attach proteins to the cell surface, GPI-anchored proteins appear to be markers and major constituents of "detergent-resistant" lipid rafts, the sphingolipid- and sterol-rich domains in membranes that are postulated to play an important role in the activation of signaling cascades.

GPI Structure

The structure of a GPI-anchored protein is displayed in Figure 1. The carboxy terminus of the protein is linked via an ethanolamine residue to GPI, a complex glycolipid. The core GPI structure consists of ethanolamine phosphate linked via a series of three mannose residues and a single glucosamine residue to the phospholipid phosphatidylinositol (PI).

GPI Biosynthesis

Outline of the Biosynthetic Pathway

The GPI structure is assembled via a biosynthetically and topologically complex metabolic pathway composed of at least ten steps and requiring the participation of at least 20 distinct gene products. GPI biosynthesis occurs in the endoplasmic reticulum (ER), but may be spatially segregated in a subdomain of the ER that is associated with mitochondria. In basic terms, synthesis occurs in the ER and involves the sequential addition of monosaccharides to PI yielding the core GPI structure that is then added to proteins. Many of the genes encoding enzymes involved in synthesis have been identified. Figure 2 illustrates the sequence of reactions involved in the assembly of a GPI protein anchor precursor in mammalian cells; variations of this general sequence are found in all organisms studied thus far.

GPI biosynthesis is initiated on the cytoplasmic face of the ER via the addition of *N*-acetylglucosamine (GlcNAc) from UDP-GlcNAc to PI yielding GlcNAc-PI (Figure 2, step 1). The enzyme which mediates this first step is an unusual complex consisting of six membrane proteins in mammalian cells. GlcNAc-PI is subsequently de-*N*-acetylated to generate GlcN-PI (Figure 2, step 2). The third step in biosynthesis is the acylation of the inositol residue of GlcN-PI at the 2-position (Figure 2, step 3). The acylation step is required prior to the addition of three mannose residues to GlcN-(acyl)PI (Figure 2, step 5), and modification of the mannose residues with phosphoethanolamine (EtNP) side chains (Figure 2, step 6). In contrast to the first two steps of synthesis that occur on the cytoplasmic leaflet of the ER, the mannosylation reactions are thought to occur lumenally based on the predicted membrane topology of the mannosyl transferases. This indicates that the substrate (GlcN-PI or GlcN-(acyl)PI) must be flipped across the ER membrane bilayer (Figure 2, step 4). Both mannose and EtNP residues are contributed by lipids. Dolichol-P-mannose serves as the mannose donor for all three mannosylation steps and EtNP residues are added from the phospholipid phosphatidylethanolamine (PE). The terminal EtNP residue is critical since it is this residue that is involved in the linkage of GPI to the carboxy terminus of proteins destined to be GPI-anchored (Figure 2, step 7). Fully assembled GPI structures, or the GPI moiety in GPI-anchored proteins, are frequently subject to lipid re-modeling reactions in

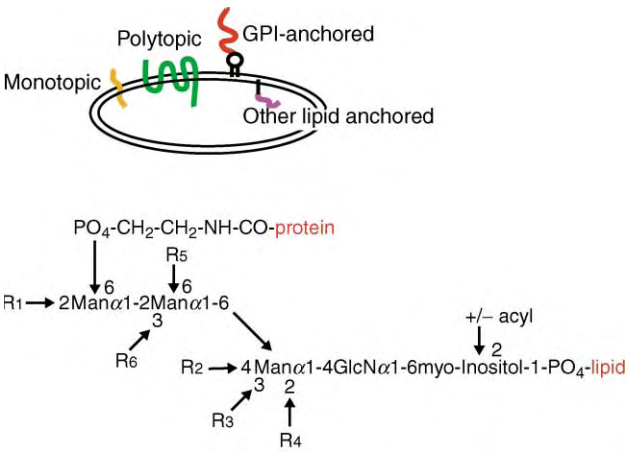

FIGURE 1 The top schematic illustrates different membrane and membrane-associated proteins in the cell surface membrane of a eukaryotic cell (internal membranes of the cell are not shown). Proteins containing hydrophobic stretches of amino acids may span the membrane once (monotopic membrane proteins) or several times (polytopic). GPI-anchored proteins are firmly associated with the cell surface membrane, but confined to the outer leaflet of the membrane bilayer since the anchor cannot span the membrane. Other lipid-anchored proteins (such as N-myristoylated, palmitoylated, and prenylated proteins) are attached to the cytoplasmic leaflet of the cell surface membrane. GPIs attached to protein have the conserved structure shown in the lower part of the figure. Variations of the structure include substituents on each of the mannose residues (phosphoethanolamine groups, monosaccharides, etc.; indicated R1–R6), differences in the lipid moiety (diacylglycerol, alkylacylglycerol, ceramide, etc.), and the presence of a fatty acyl chain attached to the 2-position of the *myo*-inositol ring. Redrawn from Ferguson, M. A. J., Brimacombe, J. S., Brown, J. R., Crossman, A., Dix, A., Field, R. A., Guther, M. L., Milne, K. G., Sharma, D. K., and Smith, T. K. (1999). The GPI biosynthetic pathway as a therapeutic target for African sleeping sickness. *Biochim. Biophys. Acta* **1455**, 327–340.

which fatty acids or the entire lipid moiety is replaced with different fatty acids or lipids.

GPI Attachment to Proteins

Newly synthesized proteins are attached to pre-existing GPIs in the lumenal leaflet of the ER by a GPI:protein transamidase complex. Proteins to be GPI-anchored contain an N-terminal signal sequence that targets them to the ER and a C-terminal signal sequence that directs GPI-anchoring. The N-terminal signal sequence is cleaved by signal peptidase during or after translocation of the nascent polypeptide into the ER lumen. The C-terminal GPI signal sequence is then cleaved and replaced with a GPI anchor through the action of GPI transamidase.

The C-terminal GPI-signal peptide, which is cleaved at what is referred to as the ω site, is necessary and sufficient for designating that a protein becomes GPI-anchored. The GPI transamidase complex responsible for attaching the protein to the GPI-anchor consists of at least five subunits. The enzyme recognizes a protein containing a GPI-anchoring signal sequence, cleaves the signal sequence and attaches the new carboxy terminus to the terminal EtNP of a pre-existing GPI.

GPI-Anchoring in Mammals, Parasitic Protozoa, and Yeast

GPI-deficient mammalian cells are viable in tissue culture, but a GPI defect has clear consequences for multicellular organisms. Transgenic mouse embryos lacking the ability to initiate GPI biosynthesis (defective in PIG-A) do not develop beyond the ninth day of gestation. The inability of certain blood cells to express GPI-anchored proteins results in the rare human disease, paroxysmal nocturnal hemoglobinuria (PNH), characterized by intravascular hemolysis, thrombosis, and bone marrow failure. The disease is caused by a somatic mutation of the X-linked PIG-A gene (encoding the catalytic component of the enzyme responsible for the first step in GPI biosynthesis) in hematopoietic stem cells. Cells defective in PIG-A are either unable to synthesize GPIs or exhibit a significant decrease in the synthesis of GPIs and thus decreased expression of GPI-anchored proteins. Red blood cells no longer expressing GPI-anchored complement regulatory proteins (e.g., CD55 and CD59) become susceptible to complement-mediated lysis, resulting in the release of heme and hemoglobin into the blood, filtering by the kidney, and excretion in the urine. Interestingly, while the GPI-deficient phenotype of hematopoietic stem cells makes the cells more sensitive to complement-mediated lysis, the defective PNH clone still persists. This implies that there must be other factors which select for clonal expansion and maintenance of GPI-deficient blood cells. One proposal is that PNH patients possess autoreactive T cells that target GPI on the surface of hematopoietic stem cells, thus PNH cells would evade damage because they lack surface GPI molecules.

GPI anchoring is the most prominent mode of attachment for cell surface proteins and glycans in parasitic protozoa. Pathogenic protozoa, including species of the genera *Trypanosoma*, *Leishmania*, and *Plasmodium*, display abundant GPI-anchored cell surface macromolecules that play crucial roles in parasite infectivity and survival. An example is the GPI-anchored variant surface glycoprotein (VSG) of bloodstream forms of *Trypanosoma brucei*, the causative agent of African sleeping sickness.

GPIs serve a unique function in yeast (*S. cerevisiae*). In addition to anchoring secretory proteins to the cell surface, GPIs play an additional role in yeast cell wall biosynthesis. The yeast cell wall consists of a fibrous lattice of mannoproteins, β1,3-glucan, β1,6-glucan, and chitin. During cell wall biosynthesis GPI-anchored

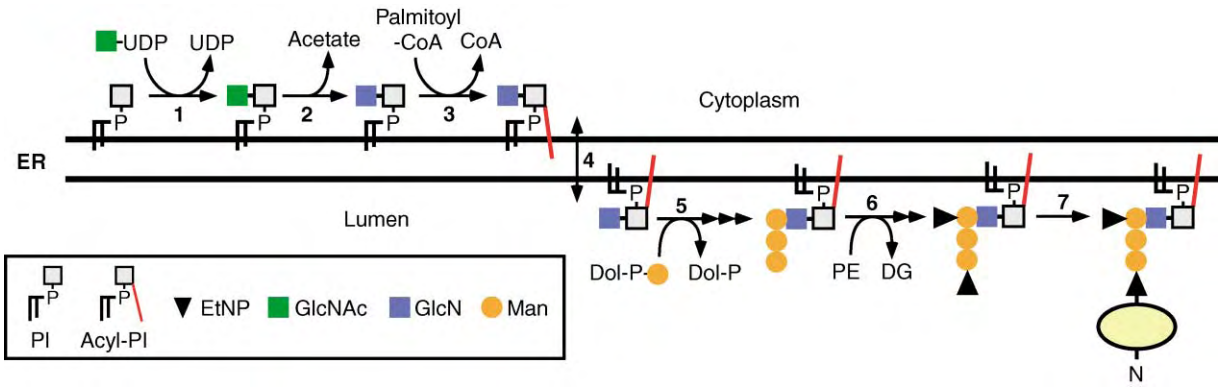

FIGURE 2 GPI biosynthesis in the ER. The pathway is a simplified version of the biosynthetic process in mammalian cells. The pathway is similar in broad terms in all other eukaryotic organisms. Biosynthesis is initiated on the cytoplasmic face of the ER by the transfer of GlcNAc from UDP-GlcNAc to PI (step 1). GlcNAc-PI is de-*N*-acetylated (step 2), then acylated on the inositol residue (step 3) to yield GlcN-acyl PI. This lipid is flipped across the ER membrane (step 4), triply mannosylated (step 5) (dolichol-phosphate-mannose (Dol-P-Man) contributes each of the mannose residues) and capped with a phosphoethanolamine residue (step 6) (donated by the phospholipid phosphatidylethanolamine (PE)). Other phosphoethanolamine residues may also be added, some prior to the completion of mannosylation. The mature GPI structure is then attached to ER-translocated proteins bearing a C-terminal, GPI-directing signal sequence, to yield a GPI-anchored protein (step 7).

mannoproteins are transported through the secretory pathway to the cell surface. After arrival at the plasma membrane a transglycosylation reaction (catalyzed by an unknown enzyme) results in cleavage of the GPI moiety between GlcN and the first mannose residue and formation of a glycosidic linkage between the manno-protein-GPI-remnant and β1,6 glucan. Mutations in GPI biosynthesis are lethal in yeast and decreased levels of GPI biosynthesis cause growth defects and aberrant cell wall biogenesis. However, not all GPI-anchored proteins become cross-linked to β1,6 glucan; the amino acids within four or five residues upstream of the ω-site determine whether the protein becomes incorporated into the cell wall or remains anchored to the plasma membrane. A unique characteristic of yeast GPIs is the addition of a fourth mannose residue to the core GPI structure (via an α1–2 linkage to the third mannose). Most GPI-anchored proteins in yeast also undergo lipid remodeling replacing the glycerolipid backbone with ceramide. The remodeling occurs after the attachment of protein to the GPI and can occur in both the ER and the Golgi.

Functions of GPIs

GPIs function as membrane anchors for secretory proteins and are believed to provide targeting signals that influence the intracellular trafficking of these proteins. Recent results indicate that GPI-proteins are packaged into unique transport vesicles, distinct from those carrying other secretory proteins, for export from the ER. GPI-anchored proteins have been shown to coalesce with sphingolipids and cholesterol into detergent-insoluble membrane domains, or lipid rafts. Association of molecules in rafts at the plasma membrane, including GPI-anchored proteins (in the exoplasmic leaflet) and acylated signaling molecules (in the cytoplasmic leaflet), is postulated to play an important role in the activation of signaling cascades. In some polarized epithelial cells, GPI-anchored proteins and many glycosphingolipids are sorted in the *trans* Golgi network and specifically targeted to the apical membrane. Once at the plasma membrane GPI-anchored proteins can undergo endocytosis and recycling back to the cell surface. However, uptake of GPI-anchored proteins is ~5 times slower than that of receptor-mediated endocytosis and recycling to the plasma membrane is ~3 times slower than that of recycling receptors. The current view is that GPI-anchoring of proteins directs their segregation into lipid rafts and affects their sorting in both the exocytic and endocytic pathways.

A GPI-anchor may also allow a protein to be selectively released from the cell surface upon hydrolysis by a GPI-specific phospholipase (e.g., PI-PLC or GPI-PLD). This has been shown to occur for certain GPI-anchored proteins in mammalian cell culture. One example is GPI-anchored membrane dipeptidase which is released from the adipocyte cell surface by a phospholipase C in response to insulin. Interestingly, other GPI-anchored proteins are not released indicating a level of regulation in insulin-stimulated hydrolysis of GPI-anchored proteins. GPI-anchored molecules have also been to shown to transfer between cells and stably insert in the external leaflet of the acceptor cell's plasma membrane. The biological significance of this is unclear, however the ability of GPI-anchored proteins to transfer between cells has implications for the expression of foreign proteins on the cell surface.

Acknowledgments

Sections of this article are reproduced and/or adapted with permission from an article by Baumann and Menon that provides a summary of all types of lipid anchored proteins. Baumann, N.A., and Menon, A.K. (2002) Lipid Modifications of Proteins. *In* "Biochemistry of Lipids, Lipoproteins and Membranes", (D.E. Vance, and J. Vance, eds.), Ch. 2, pp 37–54. Elsevier, Amsterdam, The Netherlands.

See Also the Following Articles

Protein N-Myristoylation • Protein Palmitoylation

Glossary

endoplasmic reticulum Intracellular meshwork of membranes in eukaryotic cells; the ER is endowed with the ability to synthesize lipids and is a departure point for the transport of proteins to the cell surface and extracellular space.

glycoconjugate Macromolecule containing sugars.

glycolipid Lipid molecule to which sugars are covalently attached.

lipid modified proteins Proteins, including GPI-anchored proteins, to which lipids (fatty acids, isoprenoids, or GPI) are covalently attached.

phospholipid Amphipathic molecule with a hydrophobic tail consisting typically of two fatty acids linked to glycerol, and a hydrophilic head also attached to a glycerol backbone.

Further Reading

Eisenhaber, B., Bork, P., and Eisenhaber, F. (2001). Post-translational GPI lipid anchor modification of proteins in kingdoms of life: Analysis of protein sequence data from complete genomes. *Prot. Eng.* **14**, 17–25.

Ferguson, M. A. J. (2000). Glycosylphosphatidylinositol biosynthesis validated as a drug target for African sleeping sickness. *Proc. Natl Acad. Sci. USA* **97**, 10673–10675.

Ferguson, M. A. J., Brimacombe, J. S., Brown, J. R., Crossman, A., Dix, A., Field, R. A., Guther, M. L., Milne, K. G., Sharma, D. K., and Smith, T. K. (1999). The GPI biosynthetic pathway as a therapeutic target for African sleeping sickness. *Biochim. Biophys. Acta* **1455**, 327–340.

Karadimitris, A., and Luzatto, L. (2001). The cellular pathogenesis of paroxysmal nocturnal hemoglobinuria. *Leukemia* **15**, 1148–1152.

Kinoshita, T., and Inoue, N. (2000). Dissecting and manipulating the pathway for glycosylphosphatidylinositol-anchor biosynthesis. *Cur. Opin. Chem. Biol.* **4**, 632–638.

Lipke, P. N., and Ovalle, R. (1998). Cell wall architecture in yeast: New structure and new challenges. *J. Bacteriol.* **180**, 3735–3740.

Low, M. G., Ferguson, M. A. J., Futerman, A. H., and Silman, I. (1986). Covalently attached phosphatidylinositol as a hydrophobic anchor for membrane proteins. *Trends Biochem. Sci.* **11**, 212–215.

McConville, M. J., and Menon, A. K. (2000). Recent developments in the cell biology and biochemistry of glycosylphosphatidylinositol lipids. *Mol. Membr. Biol.* **17**, 1–16.

Simons, K., and Toomre, D. (2000). Lipid rafts and signal transduction. *Nat. Rev (Molecular Cell Biology)* **1**, 31–39.

Tiede, A., Bastisch, I., Schubert, J., Orlean, P., and Schmidt, R. E. (1999). Biosynthesis of glycosylphosphatidylinositols in mammals and unicellular microbes. *Biol. Chem.* **380**, 503–523.

Udenfriend, S., and Kodukula, K. (1995). How glycosyl-phosphatidylinositol-anchored proteins are made. *Annu. Rev. Biochem.* **64**, 563–591.

Biography

Anant K. Menon is a Professor of Biochemistry at the University of Wisconsin-Madison. His research interests lie in the area of membrane biogenesis, particularly the synthesis and intracellular trafficking of simple and complex lipids, and the transport of lipids and peptides across biomembranes. Dr. Menon obtained his Ph.D. at Cornell University and pursued postdoctoral work on the biosynthesis of GPI anchors in the Laboratory of Molecular Parasitology at the Rockefeller University. He was an Assistant Professor at The Rockefeller University for three years before moving to the University of Wisconsin-Madison. His work at The Rockefeller (in collaboration with George Cross, Mark Field, Satyajit Mayor, Ralph Schwarz, and Jolanta Vidugiriene) was instrumental in establishing the pathway shown in Figure 2.

Golgi Complex

Mark Stamnes
University of Iowa, Iowa City, Iowa, USA

The Golgi complex or Golgi apparatus is an organelle of eukaryotic cells involved in the processing and transport of proteins. The Golgi complex is one of a group of cellular organelles including the endoplasmic reticulum, endosomes, and lysosomes that compose the secretory pathway. Proteins are transported through the organelles of the secretory pathway en route to the plasma membrane for secretion into the extracellular space or insertion into the membrane. This pathway also transports and sorts the resident proteins of many cellular organelles. Secreted proteins such as hormones enter the secretory pathway by translocation into the endoplasmic reticulum. They are then concentrated and transported via vesicle intermediates to the Golgi complex. At the Golgi complex, proteins can undergo processing events such as proteolytic cleavage and the removal or addition of sugar moieties. Proteins are finally sorted into various classes of post-Golgi vesicles for transport to the proper location in the cell. Hence, the Golgi complex plays a central role in the function of the secretory pathway and is the subject of intense investigation by cell biologists. While important aspects of Golgi function remain to be fully characterized, previous studies have revealed many interesting features of its morphology and its role in the transport and processing of proteins.

Morphology of the Golgi Complex

The Golgi complex is often found as a set of 3-5 stacked saccules or cisternae (Figure 1A). The cisternae are organized with a polarity such that there is a *cis*-cisterna where proteins arriving from the endoplasmic reticulum enter and a *trans*-cisterna where proteins exit the Golgi complex. Proteins pass through the medial cisternae that are present between the *cis*- and *trans*-cisternae. The *cis* and *trans*faces of the Golgi apparatus are often reticulated and thus referred to as the *cis*-Golgi network and the *trans*-Golgi network.

The stacked Golgi complexes are frequently localized together at a single site adjacent to the cell nucleus (Figure 1B). This site is near the centrosome, a cellular structure involved in the assembly and organization of microtubules, which are one of the key components of the cell cytoskeleton. In mammalian cells, the juxtanuclear localization of the Golgi complex involves the translocation of pre-Golgi vesicles along microtubules using a molecular motor protein called dynein. The Golgi stacks are often organized into interconnected ribbon-like structures. Although there is some variability in the morphology and organization of the Golgi complex among eukaryotic cells, in all cases, the Golgi is a critical site for processing and sorting of proteins that are transiting the secretory pathway.

Protein Processing in the Golgi Complex

Protein Glycosylation

Many proteins, especially those localized to the cell surface, are covalently attached to complex sugar moieties called oligosaccharides to form glycoproteins. One of the best-characterized functions for the Golgi apparatus is in the addition and modification of oligosaccharides on glycoproteins. Many proteins are modified at specific asparagine amino-acid residues in the endoplasmic reticulum in a process called N-linked glycosylation, which is carried out by the enzyme oligosaccharyl transferase. In the Golgi complex, additional oligosaccharide chains can be attached to certain serine or threonine amino-acid residues via the enzyme peptidyl N-acetylgalactosamine-transferase. This process is referred to as O-linked glycosylation. Both N-linked and O-linked oligosaccharides are further modified in the Golgi complex through both the removal and addition of specific sugars. The processing of N-linked oligosaccharides by the Golgi complex is understood in some detail. In the Golgi complex, mannose is trimmed from N-linked oligosaccharides through the action of mannosidase II. This is followed by the addition of N-acetylglucosamine, galactose, and sialic acid by sugar-specific transferases. The enzymes that catalyze the various processing steps are spatially organized throughout the Golgi stacks in the order in which they function. For example, N-acetylglucosamine transferase is mostly enriched in the *cis*-Golgi cisterna,

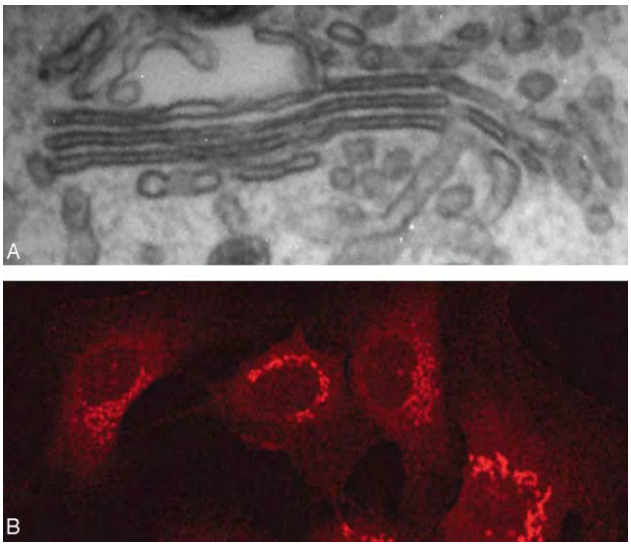

FIGURE 1 The morphology and localization of Golgi complexes. (A) Shown is a transmission electron micrograph of a Golgi complex from a rat kidney cell. Note that it is composed of three stacked cisternae: *cis*, medial, and *trans*. Transport vesicles are apparent near the Golgi complex as circular profiles. (B) Shown is a fluorescence micrograph of normal rat kidney cells that are decorated with an antibody against the Golgi enzyme, mannosidase II. Note that the labeled Golgi stacks (red) are concentrated in a region next to the cell nucleus.

while sialic acid transferase is found predominantly in the *trans*-cisterna. The role of protein glycosylation is still not fully understood, but one described function includes protein sorting.

Proteolytic Processing

Some proteins must be cleaved within the secretory pathway before they are functional. Examples of such proteins include various proteases, hormones, and transcription factors.

Prohormone Processing

Many peptide hormones are first synthesized as part of a larger inactive polypeptide, which is then cleaved by enzymes called endoproteases into a smaller active form. For example the metabolic hormone, insulin, folds first as a long polypeptide, which is then cleaved at two sites releasing an inactive fragment, the C-peptide, to form the fully active insulin molecule. Many of these proteolytic processing steps occur in the trans-Golgi network and in post-Golgi secretory vesicles. The endoproteases that carry out this processing are generally referred to as prohormone convertases. One *trans*-Golgi-network-localized endoprotease, furin, has been extensively characterized and is involved in processing a wide variety of receptors and hormones.

Proteolytic Regulation of Transcription Factors

Regulation of a Transcription Factor Involved in Cholesterol Metabolism In some cases, Golgi-localized endoproteases are used for the activation of proteins that function as part of regulatory signaling pathways. A very interesting example of this type of regulation is the proteolytic activation of sterol-response-element-binding protein (SREBP). SREBP is a transcription factor that activates genes that are involved in cholesterol uptake and biosynthesis. It resides as an integral membrane protein on the endoplasmic reticulum when cellular cholesterol levels are elevated. However, when cholesterol levels in the cell are low, SREBP is transported out of the endoplasmic reticulum to the Golgi complex where it is cleaved by two endoproteases. One of these enzymes is unique since it cleaves the transmembrane domain of SREBP within the plane of the membrane. The result of this proteolysis in the Golgi complex is the release of an active transcription factor from the membrane, which is then translocated into the nucleus to activate genes involved in sterol metabolism.

A Golgi-Localized Endoprotease is Involved in Alzheimer's Disease The toxic peptide β-amyloid accumulates in plaques found within the brain of individuals with Alzheimer's disease. β-amyloid is generated through inappropriate proteolytic cleavage of amyloid precursor protein. A Golgi-localized endoprotease called presenilin is important for normal processing of amyloid precursor protein. Presenilin is similar to the Golgi-localized endoprotease that activates SREBP since it cleaves the amyloid precursor protein within the membrane.

The examples of endoprotease function described here are illustrative of the wide variety of proteins and cellular processes that utilize proteolytic processing at the Golgi complex.

Mechanisms of Protein Transport at the Golgi Complex

Vesicular Transport at the Golgi Complex

One important mechanism for moving proteins and phospholipids to, from, and within the Golgi complex is via transport vesicles. These small, spherical, membrane-limited structures are formed on organelles through the assembly of a protein coat. The coat deforms the membrane into a vesicle and plays a role in selecting the appropriate cargo proteins. Once formed, the vesicles are translocated to the target organelle where they fuse with the membrane and

deliver their contents. Several types of transport vesicles, each with a distinct protein coat, function at the Golgi complex. Two well-studied examples are clathrin-coated vesicles that mediate transport of proteins leaving the trans-Golgi network, and COPI vesicles that mediate transport among the cisternae and backwards transport out of the Golgi complex.

Cisternal Progression

A second mechanism for moving proteins through the Golgi complex is cisternal progression. Here, the *cis*-cisternae are transformed into medial cisternae, and medial cisternae are transformed into *trans*-cisternae. New *cis*-cisternae are created by vesicles arriving from the endoplasmic reticulum. The *trans*-cisternae are expended by the formation of transport vesicles involved in post-Golgi trafficking. Progressive changes in the repertoire enzymes within the cisternae occur through vesicle-mediated protein transport and sorting of the resident Golgi proteins. During cisternal progression, forward moving cargo proteins are carried along with the cisternae as they progress from the *cis* to medial to *trans* positions.

Protein Sorting at the Golgi Complex

Proteins must be properly sorted and targeted as they traverse and exit the Golgi complex. At the *trans*-Golgi network, proteins are destined for several different locations. Many proteins are sent to the cell surface for insertion into the plasma membrane or for release into the extracellular space. Other proteins must be targeted to intracellular organelles such as late endosomes or lysosomes. In addition to the sorting of forward moving proteins, some proteins are retrieved or recycled back to earlier compartments. For example, proteins that function within the Golgi complex are recognized and retained at or retrieved to the proper cisterna. Two sorting mechanisms that have been characterized at the Golgi complex are receptor-mediated packaging into transport vesicles and protein aggregation.

Receptor-Mediated Sorting into Transport Vesicles

A key aspect of protein sorting throughout the secretory pathway is the selective packaging of cargo proteins into transport vesicles. This involves either direct or indirect (receptor-mediated) interactions with the vesicle-coat proteins. Thus, a vesicle targeted for a specific organelle in the cell can select cargo proteins that are destined for the same location. Discussed next are two receptor proteins that function in cargo selection during protein transport from the Golgi complex, namely the mannose-6-phosphate receptor and the KDEL receptor.

The Mannose-6-Phosphate Receptor

The mannose-6-phosphate receptor sorts proteins into clathrin-coated vesicles that are leaving the trans-Golgi network and are destined for organelles called lysosomes involved in breaking down cellular waste products. Mannose-6-phosphate is an N-linked oligosaccharide generated by enzymes present in the cis-Golgi cisterna. It is formed specifically on proteins destined for the lysosome. The mannose-6-phosphate receptor spans the Golgi membrane and binds to coat proteins on the cytosolic side of the membrane and to the mannose-6-phosphate-containing protein on the luminal side of the membrane. Thus, mannose-6-phosphate-containing proteins are sorted and concentrated into the correct clathrin-coated vesicles for transport to the lysosome.

The KDEL Receptor

Many resident proteins of the endoplasmic reticulum are retrieved from the Golgi complex if they escape. The KDEL receptor functions in this retrieval process by sorting proteins that belong in the endoplasmic reticulum into COPI vesicles for backwards transport. KDEL refers to the single-letter code for the amino acid residues lysine, aspartic acid, glutamic acid, leucine, which are present on many endoplasmic reticulum-resident proteins. Similar to the mannose-6-phosphate receptor, the KDEL receptor binds to COPI-coat proteins on the cytosolic side of the membrane and to KDEL-containing protein on the luminal side. This allows for sorting and retrieval of endoplasmic reticulum-localized proteins via COPI vesicles.

Protein Aggregation as a Sorting Mechanism

Another way that proteins are sorted in the Golgi complex is through aggregation. Some resident Golgi proteins, such as the enzyme mannosidase II, form aggregates with themselves and other Golgi-resident proteins. Golgi proteins may be retained at the proper cisternae through the exclusion of the large aggregates from transport vesicles. By contrast, some proteins – for example, insulin and many other hormones – may cluster within the *trans*-Golgi network to facilitate their concentration and packaging into vesicles. Aggregation continues in the secretory vesicles before its delivery to the plasma membrane and release into the extracellular space.

In higher eukaryotes, thousands of proteins must be properly transported, processed, and sorted through the Golgi complex. Some of the properties of this organelle that have been revealed by cell biologists and briefly outlined in this article are beginning to explain how this remarkable feat might be achieved.

See Also the Following Articles

Amyloid • Cholesterol Synthesis • Dynein • Oligosaccharide Chains: Free, *N*-Linked, *O*-Linked • *N*-Linked Glycan Processing Glucosidases and Mannosidases • Protein Glycosylation, Overview • Secretory Pathway

Glossary

cisternae Flattened membrane-limited structures that stack together to form the Golgi complex.

endoprotease An enzyme that cleaves a protein into two or more fragments.

glycoprotein A protein that is attached to complex sugar molecules called oligosaccharides.

secretory vesicles Specialized transport vesicles that transport proteins from the trans-Golgi network to the plasma membrane. These vesicles can sometimes be regulated to allow release of proteins such as hormones from cells only under certain conditions.

transport vesicle A small spherical structure that mediates protein transport between organelles. It is formed by the assembly of a protein coat.

Further Reading

Berger, E. G., and Roth, J. (eds.) (1997). *The Golgi Apparatus*. Birkhauser, Boston.

Hong, W. (1996). *Protein Trafficking along the Exocytic Pathway*. Landes Bioscience, Georgetown, TX.

Short, B., and Barr, F. (2000). The Golgi apparatus. *Curr. Biol.* **10**, R583–R585.

Shorter, J., and Warren, G. (2002). Golgi architecture and inheritance. *Annu. Rev. Cell Dev. Biol.* **18**, 379–420.

Thomas, G. (2002). Furin at the cutting edge: From protein traffic to embryogenesis and disease. *Nat. Rev. Mol. Cell Biol.* **3**, 753–766.

Varki, A. (1998). Factors controlling the glycosylation potential of the Golgi apparatus. *Trends Cell Biol.* **8**, 34–40.

Biography

Mark Stamnes is an Associate Professor in the Department of Physiology and Biophysics of the Roy J. and Lucille A. Carver College of Medicine at the University of Iowa. His research interest is in the mechanisms of protein transport and sorting in the secretory pathway. He holds a Ph.D. from the University of California, San Diego and has completed his postdoctoral studies at the Memorial Sloan-Kettering Cancer Center in New York. He is a member of the American Society for Cell Biology.

G_q Family

Wanling Yang and John D. Hildebrandt
Medical University of South Carolina, Charleston, South Carolina, USA

Guanine-nucleotide-binding proteins (G proteins) are heterotrimeric proteins composed of α-, β-, and γ-subunits. Activated by G protein-coupled receptors (GPCRs) in the plasma membrane, G proteins play pivotal roles in signal transduction from hormones, neurotransmitters, and drugs to cellular responses. So far a total of 16 α-, 5 β-, and 12 γ-subunits have been described in mammals. Based on functional and structural similarities, G proteins are grouped into four families named by the α-subunits they contain: G_s, G_i/G_o, G_q, and G_{12}/G_{13}. Activation of members of the G_q family of G proteins directly activates phospholipase Cβ (PLCβ) isozymes to produce the second messengers inositol 1, 4, 5-trisphosphate (IP_3) and diacylglycerol (DAG). Unlike G_s or G_i/G_o families, the G_q family proteins are insensitive to cholera toxin and pertussis toxin.

G_q Family of G Proteins

Phosphatidylinositol metabolites are primary intracellular regulators of eukaryotic cells. Studies of hormone and neurotransmitter regulation of phosphatidylinositol turnover implicated the frequent involvement of a specific class of G proteins. The subsequent purification of pertussis toxin-insensitive G_α subunits led to the demonstration of guanine nucleotide regulation of phospholipase Cβ isoforms through G_q. The G_q family includes $G_{\alpha q}$, $G_{\alpha 11}$, $G_{\alpha 14}$, and $G_{\alpha 15}$ (previously referred to in some species as $G_{\alpha 16}$), which are expressed from individual genes with different expression patterns. $G_{\alpha q}$ and $G_{\alpha 11}$ are the most similar (89% identical amino acids), whereas $G_{\alpha 15}$ shares only about 56% identities with other family members (Figure 1). Nevertheless, the genes encoding these proteins may have arisen from a pair of gene duplications since $G_{\alpha q}$ and $G_{\alpha 14}$ are within 70 kb of each other on human chromosome 9 or mouse chromosome 19, and $G_{\alpha 11}$ and $G_{\alpha 15}$ are within 7 kb of each other on human and mouse chromosomes 19 and 10, respectively. All four genes have similar structures and contain seven coding exons. Proteins likely related to the G_q family are found in the genome of many species throughout the animal kingdom, but their relationship to G_α subunits in other kingdoms is unclear.

G_q is Activated by Hormones, Neurotransmitters, and Drugs through Multiple GPCRs

The G_q family of G proteins is responsible for cellular responses to a plethora of hormones, neurotransmitters, and drugs, and is involved in the corresponding physiological, pathophysiological, and pharmacological processes (Table I). In the CNS, M_1, M_3, and M_5 muscarinic receptors, group I metabotropic glutamate receptors ($mGluR_1$ and $mGluR_5$), and serotonin 5-HT_2 receptors, all couple to G_q family of G proteins and thus activate the PLCβ signal transduction pathway. Activation of this pathway in the CNS is involved in synaptic transmission and modulation, neuronal development, and long-term depression (LTD) and long-term potentiation (LTP). In the cardiovascular system, α_1 adrenergic receptors, endothelin receptors, angiotensin receptors, and prostaglandin F receptors modulate cardiovascular function through activation of G_q and are especially involved in cardiac hypertrophy and congestive heart failure, a compensation process induced by hemodynamic stress and myocardial injury and subsequent decompensation after sustained stimulation. Thromboxane A_2 receptors, thrombin receptors, and purinergic receptors induce platelet aggregation and granule secretion through activation of the G_q/PLCβ pathway. The G_q family of G proteins is also involved in hormone secretion, inflammation, and allergy through the activation of many other receptors including those for TRH, GnRH, leukotrienes, bradykinin, and histamine.

PLCβ Activation and Calcium Mobilization are Downstream Responses to G_q Activation

Phospholipases are membrane-associated proteins involved in the biosynthesis and degradation of membrane lipids. They include phospholipase (PL) A_1, A_2, C,

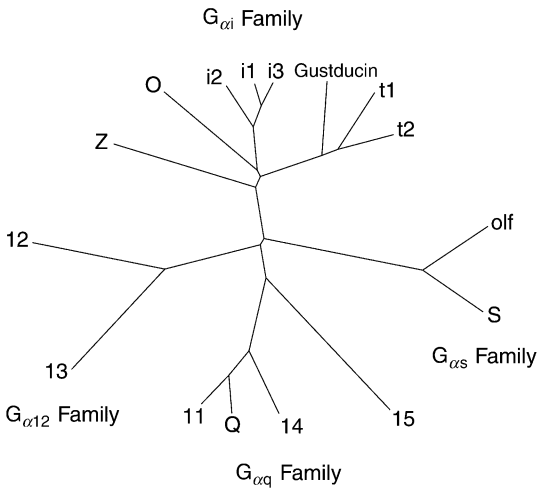

α_q Homologues	
Human α_q	100%
Mouse α_q	100%
Rat α_q	98%
Xenopus	96%
Turkey α_q	90%
Human α_{11}	89%
Drosophila	84%
Lobster	83%
C. elegans	82%
Snail	81%
Human α_{14}	80%
Squid	77%
Sponge	62%
Human α_{15}	57%
Aspergillus	50%
Penicillium	49%
Human α_i	49%

FIGURE 1 Homology of $G_{\alpha q}$ to other human G_α proteins and to related proteins in other species. The phylogenetic tree diagram was generated by TreeView from human G protein α-subunit protein sequences aligned with ClustalX. The length of the bars connecting different G_α proteins is proportional to the similarity of their aligned sequences. The α_q homologues listed are based upon percent identical amino acids in the aligned sequences.

TABLE I

Receptors that Couple to the G_q Family of G Proteins and their Ligands and Physiological Functions

Ligands	Receptors	Function
Acetylcholine carbachol	M_1, M_3, M_5 muscarinic	Memory and cognition, smooth muscle contraction, and salivary secretion
Adenine nucleotides	P_2Y purinergic	Vasodilation
Angiotensin II, Losartan	AT_{1a}, AT_{1b}	Modulation of cardiovascular activities
Bradykinin	B_2 bradykinin	Hyperalgesia, smooth muscle contraction
C_{5a} anaphylatoxin	C_{5a}	Chemoattraction
Cholecystokinin (CCK)	CCK_a and CCK_b	Gastrointestinal activities
Endothelins	ET_a and ET_b	Regulation of cardiovascular activities
Glutamate	$mGluR_1$ and $mGluR_5$	Modulation of neuronal activities
Gonadotrophin-releasing hormone (GnRH)	GnRH	Synthesis and release of FSH and LH
Histamines	H_1	Inflammation and allergy
5-hydroxytryptamine, α-methyl-5-HT	5-HT_{2a}, 5-HT_{2b} and 5-HT_{2c}	Modulation of neuronal activities of the brain
Neurotensin	Neurotensin	Modulation of gastrointestinal and brain activities
Norepinephrine (noradrenaline), epinephrine (adrenaline), phenylephrine, prazosin	α_{1a}, α_{1b}, α_{1c}, α_{1d} adrenergic	Modulation of cardiovascular activities
Platelet activating factor	PAF	Platelet activation and aggregation
Prostaglandin $F_{2\alpha}$	Prostaglandin F (FP)	Bronchoconstriction and luteolysis
Thromboxane A_2	TXA_2 (TP)	Smooth muscle contraction and platelet aggregation
Tachykinins	NK_1, NK_2, NK_3	Smooth muscle contraction, transmission of sensory information
Thrombin	Thrombin	Platelet aggregation
Thyrotrophin-relasing hormone (TRH)	TRH	Synthesis and release of thyroid-stimulating hormone
Vasopressin	V_{1a}, V_{1b}	Smooth muscle contraction, platelet activation, glycogenolysis, and ACTH release
Leukotrienes	$CysLT_1$, $CysLT_2$	Bronchoconstriction and vasodilation

and D (PLA_1, PLA_2, PLC, and PLD). PLC contains three subclasses on the basis of size and amino acid sequences: PLCβ, PLCγ, and PLCδ. PLCβ isotypes (β1–4) are activated by GPCRs via G_q family and/or $\beta\gamma$-subunits primarily from activation of the G_i/G_o family. Activated α-subunits of the G_q family stimulate all four isoforms of PLCβ with the potency rank order of $\beta1 \geq \beta3 \geq \beta4 \gg \beta2$ (Figure 2). PLCβ hydrolyzes the membrane phospholipid phosphatidylinositol 4,5-bisphosphate (PIP_2) and generates two signal molecules: diacylglycerol (DAG) and inositol 1,4,5-trisphosphate (IP_3). While DAG remains membrane-associated, IP_3 is released into cytosol and binds to IP_3 receptors, which are ligand-gated Ca^{2+} channels, in the endoplasmic reticulum or sarcoplasmic reticulum (cardiac muscle cells). Binding of IP_3 induces calcium release from intracellular stores and causes a rise in cytosolic free calcium concentration. One result of the increase in calcium concentration is its binding to calmodulin. Calcium–calmodulin complexes bind to other proteins and change their functional activities. Isozymes of protein kinase C (PKC) translocate from cytosol to plasma membrane and bind to DAG in the presence of calcium. Activated PKC phosphorylates other proteins and alters their functional state. PKC is known to have a wide variety of effects including receptor desensitization, activation of gene transcription, immune regulation, and regulation of cell growth.

The regulation of gene expression by cell surface receptors often involves the stimulation of signaling pathways including one or more members of the mitogen-activated protein kinases (MAPKs). The MAPKs are a family of evolutionarily conserved serine/threonine kinases that transmit externally derived signals regulating cell growth, division, differentiation, and apoptosis. MAPKs are activated in response to stimulation of GPCRs that couple to the G_q family of G proteins such as α_{1b} adrenergic receptors or M_1 muscarinic cholinergic receptors. This process involves PLCβ, intracellular Ca^{2+}, and PKC. PKC activation leads to MAPK activation through both Ras-dependent and Ras-independent mechanisms. PKCα can apparently activate Raf-1 by direct phosphorylation. In many cases, however, $G_{q/11}$ activation causes MAPKs activation that is unaffected by PKC inhibition.

G_q in Cardiovascular Disease, Platelet Aggregation, and Cerebellum Development

The study of the functions of the G_q family of proteins has been greatly facilitated by the use of various animal models that overexpress the wild-type $G_{\alpha q}$ protein or that express a constitutively active form (gain of function mutations). Also useful have been animal models deficient in the protein, or that overexpress an inhibitor (loss of function mutations). Some well-characterized functions of the G_q proteins include roles in the development of cerebellum and motor coordination, platelet aggregation, heart development and cardiac adaptation, and development of heart failure.

$G_{\alpha q}$ is essential for the signaling processes used by different platelet activators. It has been reported that a defect in human platelet G_q function leads to impaired

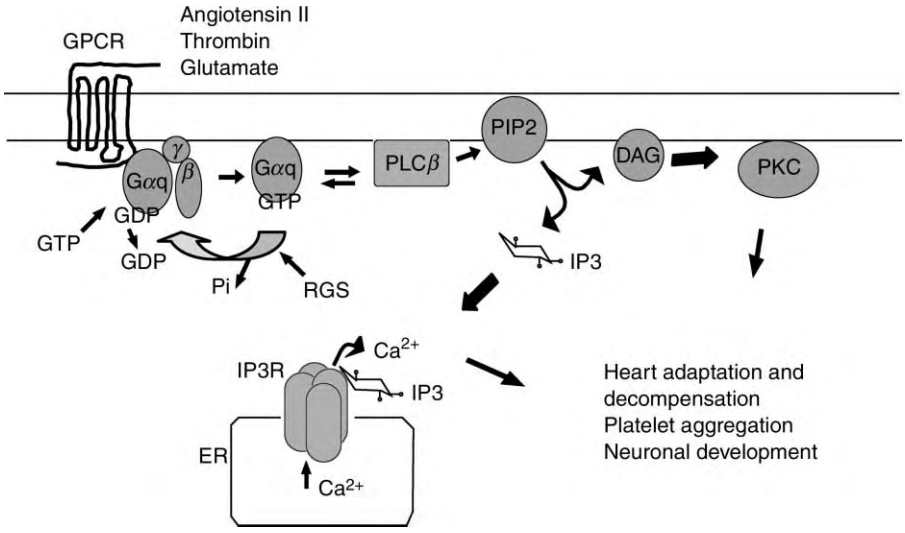

FIGURE 2 The G_q signal transduction pathway. Activation of many GPCRs leads to activation of G_q. $G_{\alpha q}$ activates PLCβ that subsequently cleaves PIP_2 to generate DAG and IP_3. IP_3 binds to the IP_3 receptor (IP_3R) on the endoplasmic reticulum (ER) and induces release of calcium. DAG remains membrane bound and activates PKC. Both calcium and PKC are important signaling molecules that are involved in many cellular functions including cell growth and differentiation. PLCβ and RGS proteins can work as GAPs to facilitate the termination of G_q signaling by enhancing its GTPase activity.

platelet aggregation, secretion, and calcium mobilization, in response to a number of agonists. Platelets from $G_{\alpha q}$-deficient mice are unresponsive to a variety of physiologic platelet activators. As a result, these mice have increased bleeding times, which is an *in vivo* measure of platelet function.

Mice with a null mutation in the $G_{\alpha q}$ gene suffer from ataxia with typical signs of motor coordination defects. In the cerebellum of newborn rodents, each Purkinje cell (PC) is innervated by multiple climbing fibers (CFs). Massive elimination of supernumerary CF–PC synapses occurs during the first three postnatal weeks, and by about postnatal day 20, most PCs are innervated by a single CF. In $G_{\alpha q}$-deficient mice, ~40% of adult PCs remain innervated by multiple CF because of a defect in regression of supernumerary CFs. PLCβ_4, which shows predominant expression in cerebellar PCs, and $mGluR_1$ may be involved in this function of $G_{\alpha q}$ since in $mGluR_1$- or PLCβ_4-deficient mice, a similar phenotype was observed. LTD of the PF–PC synapse in mice lacking $G_{\alpha q}$ was also deficient. Cerebellar LTD is a form of synaptic plasticity believed to be related to motor learning.

The G_q family of G proteins has been implicated in signaling pathways regulating cardiac growth under physiological and pathological conditions. The ability of cardiomyocytes to undergo hypertrophic growth is an important adaptive response to a wide range of conditions that require the heart to work more effectively. Norepinephrine (noradrenaline) (NE) and other hormones or regulators such as endothelin, prostaglandin F2α, and angiotensin II induce cardiomyocyte growth through activation of G_q-coupled receptors. A relatively modest degree of wild-type $G\alpha_q$ overexpression in transgenic mice produced many of the features of compensated left ventricular hypertrophy. Conversely, expression of a $G_{\alpha q}$ inhibitor peptide that prevents receptor coupling to $G_{\alpha q}$ in mouse myocardium, or RGS4, which binds to and activates the GTPase activity of $G\alpha_q$, significantly attenuated hypertrophy induced by pressure overload. The ability of cardiomyocytes to function at high capacity under increased workload usually cannot be sustained and ventricular failure develops after prolonged stimulation. One event associated with this transition to heart failure is the apoptotic death of cardiomyocytes. It has been shown that sustained or excessive activation of the G_q signaling pathway results in apoptotic loss of cardiomyocytes. Expression of a constitutively activated mutant of $G_{\alpha q}$, which further increased G_q signaling, produces initial hypertrophy, which rapidly progresses to apoptotic cardiomyocyte death. Conversely, inhibition of specific components of the pathway prevents or ameliorates heart failure. Experimental and clinical evidence supports the benefit of reduced G_q-coupled receptor signaling in modifying the progression of left ventricular remodeling and heart failure.

Modulation of G_q Functions

The G_q family of G proteins undergoes palmitoylation at N-terminal cysteine residues. Mutation of cysteines 9 and 10 in $G_{\alpha q}$ to serine profoundly alters the behavior of the subunit. Mutant $G_{\alpha q}$ cannot couple a coexpressed receptor to stimulation of PLCβ. Cysteine substitution also prevented a constitutively active form of $G_{\alpha q}$ from stimulating PLC directly. However, a substitution of a single cysteine in $G_{\alpha q}$ did not alter its activity.

Long-term activation of GPCRs coupled to G_q induces down-regulation of the $G_{\alpha q}$ subunit. For example, prolonged exposure of αT3-1 pituitary cells to a gonadotrophin-releasing hormone receptor agonist results in marked down-regulation of $G_{\alpha q}$ and $G_{\alpha 11}$. Chinese hamster ovary cells stably transfected with human M_3 muscarinic acetylcholine receptors show a 40–50% reduction in $G_{\alpha q}$ and $G_{\alpha 11}$ when stimulated with the cholinergic agonist carbachol. Usually, levels of mRNA encoding $G_{\alpha q}$ and $G_{\alpha 11}$were not greatly altered, suggesting a change in protein degradation.

The intrinsic GTPase activity of G_α-subunits acts as a timer to limit the duration of G protein activation. PLCβ works as a GAP (GTPase-activating protein) to increase the intrinsic GTPase activity of $G_{\alpha q}$. The ability of PLCβ to act as a GAP for $G_{\alpha q}$ provides negative feedback, limiting PLC activity. In addition, a family of proteins known as the regulators of G protein-signaling (RGS) proteins has been identified as GAPs for G_α-subunits. RGS4 and GAIP are known to act as GAPs for the G_q family. Furthermore, these RGS proteins block activation of PLCβ by $G_{\alpha q}$, which apparently results from occlusion of the effector-binding site on $G_{\alpha q}$. The presence of RGS proteins with GAP activity is also thought to increase the selectivity of GPCRs that couple to G_q by filtering out low-efficacy responses.

G_q Family Members are Functionally Complementary to Each Other

Mammals express four G_q class α-subunits of which two, $G_{\alpha q}$ and $G_{\alpha 11}$, are widely expressed and are primarily responsible for coupling receptors to PLCβ. In contrast, expression of $G_{\alpha 14}$ and $G_{\alpha 15}$ is restricted to certain tissues. $G_{\alpha 14}$ is predominantly expressed in spleen, lung, kidney, and testis, whereas $G_{\alpha 15}$ is primarily restricted to hematopoietic lineages. In most tissues, $G_{\alpha q}$ and $G_{\alpha 11}$ are functionally complementary to each other. Receptors activating G_q family members in mammalian systems do not discriminate between $G_{\alpha q}$ and $G_{\alpha 11}$. Similarly, there appears to be little difference between the abilities of these G proteins in regulating PLCβ functions. Functional

redundancy of G_q family proteins is also demonstrated by knocking-out individual genes that code for the proteins of this family. Only $G_{\alpha q}$-deficient mice revealed obvious phenotypic defects, including cerebellar ataxia and deficiencies in primary hemostasis due to a defect in platelet activation. The observed phenotypes correlated with preferential or exclusive expression of $G_{\alpha q}$ in the affected cell types of the cerebellum and platelets. Despite the specific expression patterns of $G_{\alpha 14}$ and $G_{\alpha 15}$, which may indicate tissue-specific functions for these proteins, no obvious phenotypic changes were observed in mice carrying inactivating mutations of the $G_{\alpha 14}$ and $G_{\alpha 15}$ genes. $G_{\alpha 11}$-deficient mice were also viable and fertile with no apparent behavioral or morphologic defects. Their functions may be dispensable or compensated for by other members of the $G_{\alpha q}$ family, although subtle phenotypes from loss of their functions may be difficult to detect with current methodology.

A gene dosage effect between $G_{\alpha q}$ and $G_{\alpha 11}$ was observed after breeding $G_{\alpha q}$-deficient mice with $G_{\alpha 11}$-deficient mice. Embryos lacking both genes died in uterus with heart malformations. Mice inheriting a single copy of either gene died within hours of birth with craniofacial and/or cardiac defects. Apparently, two active alleles of these genes are required for life after birth. Analyses of intercross offspring inheriting different combinations of these two mutations indicated that $G_{\alpha q}$ and $G_{\alpha 11}$ have overlapping functions in embryonic cardiomyocyte proliferation and craniofacial development.

See Also the Following Articles

G Protein Signaling Regulators • G_{12}/G_{13} Family • G_i Family of Heterotrimeric G Proteins • G_s Family of Heterotrimeric G Proteins • IP_3 Receptors • Phospholipase C • Protein Kinase C Family • Protein Palmitoylation

Glossary

ataxia An inability to coordinate muscle activity during voluntary movement. It is often caused by disorders of the cerebellum.

cardiac hypertrophy Enlargement of cardiomyocytes and thickening of the walls of the heart in response to hemodynamic stress and myocardial injury.

primary hemostasis The formation of a primary platelet plug and involving platelets, the blood vessel wall and von Willebrand factor. The process includes contraction of injured vessel, platelet adhesion, activation, aggregation, and secretion. Platelet secretion triggers the coagulation process and proceeds in a positive feedback loop to further stop bleeding.

Further Reading

Adams, J. W., and Brown, J. H. (2001). G proteins in growth and apoptosis: Lessons from the heart. *Oncogene* **20**, 1626–1634.

Alliance for Cell Signaling/Nature, The Signaling Gateway, http://www.signaling-gateway.org/

Cockcroft, S., and Gomperts, B. D. (1985). Role of guanine nucleotide binding protein in the activation of polyphosphoinositide phosphodiesterase. *Nature* **314**, 534–536.

Exton, J. (1996). Regulation of phosphoinositide phospholipases by hormones, neurotransmitters, and other agonists linked to G proteins. *Annu. Rev. Pharmacol. Toxicol.* **36**, 481–509.

Hermans, E., and Challiss, R. A. J. (2001). Structural, signaling and regulatory properties of the group I metabotropic glutamate receptors: Prototypic family C G protein-coupled receptors. *Biochem. J.* **359**, 465–484.

Iyengar, R., and Hildebrandt, J. D. (eds.) (2002). *G Protein Pathways, Part B, G Proteins and their Regulators, Methods in Enzymology*, Vol 344. Academic Press, New York.

Litosch, I., and Wallis, C., and Fain, J. N. (1985). 5-Hydroxytryptamine stimulates inositol phosphate production in a cell-free system from blowfly salivary glands. Evidence for a role of GTP in coupling receptor activation to phosphoinositide breakdown. *J. Biol. Chem.* **260**, 5464–5471.

Offermanns, S. (2001). In vivo functions of heterotrimeric G proteins: Studies in Gα-deficient mice. *Oncogene* **20**, 1635–1642.

Pang, I. H., and Sternweis, P. C. (1990). Purification of unique alpha subunits of GTP-binding regulatory proteins (G Proteins) by affinity chromatography with immobilized beta gamma subunits. *J. Biol. Chem.*, **265**, 18707–18712.

Simon, M. I., Strathmann, M. P., and Gautam, N. (1991). Diversity of G proteins in signal transduction. *Science* **252**, 802–808.

Smrcka, A.V., Hepler J. R., Brown K. O., and Sternweis, P. C. (1991). Regulation of polyphosphoinositide-specific phospholipase c activity by purified G_q. *Science* **251**, 804–807.

Sternweis, P.C., and Smrcka, A.V. (1993). G proteins in signal transduction: The regulation of phospholipase C. *Ciba Found. Symp.* **176**, 96–111.

Strathmann, M., Wilkie, T. M., and Simon M. I. (1989). Diversity of the G-protein family: sequences from five additional alpha subunits in the mouse. *Proc. Natl Acad. Sci. USA* **86**, 7407–7409.

Taylor, S. J., Smith, J. A., and Exton, J. H. (1990). Purification from bovine liver membranes of a guanine nucleotide-dependant activator of phosphoinositide-specific phospholipase C. Immunologic identification as a novel G-protein alpha subunit. *J. Biol. Chem.* **265**, 17150–17156.

Taylor, S. J., Chae, H. Z., Rhee, S. G., and Exton, J. H. (1991). Activation of the 1 isozyme of phospholipase C by subunits of the G_q class of G proteins. *Nature* **350**, 516–518.

Uhing, R. J., Popic, V., and Exton, J. H. (1986). Hormone-stimulated polyphosphoinositide breakdown in rat liver plasma membranes. Roles of quanine nucleotides and calcium. *J. Biol. Chem.* **261**, 2140–2146.

Biography

John D. Hildebrandt is a Professor in the Department of Molecular and Cell Pharmacology at the Medical University of South Carolina. He received his Ph.D. from the University of Iowa and did postdoctoral training in the Department of Physiology at the University of Pittsburgh and in the Department of Cell Biology at Baylor College of Medicine. His main research interest is G protein structure and function. He has made numerous contributions to the identification of G protein subunits and isoforms, and the relationship between the generation of G protein subunit diversity and G protein-dependent signaling mechanisms.

Wanling Yang is a postdoctoral Fellow in the Medical University of South Carolina. He holds a Ph.D. in Pharmacology and Bioinformatics from the University of Minnesota. He has studied the structure and function of opiate receptors and is currently working on the structure and function of the G protein subunit genes.

Green Bacteria: Secondary Electron Donor (Cytochromes)

Hirozo Oh-oka
Osaka University, Osaka, Japan

Robert E. Blankenship
Arizona State University, Tempe, Arizona, USA

Green photosynthetic bacteria are a class of photosynthetic organisms that carry out light-driven electron transfer that leads to long-term energy storage. A reaction center, pigment–protein complex, mediates the electron transfer process. Cytochromes, proteins that contain Fe-containing heme prosthetic groups, are an essential part of the photosynthetic electron transfer system. The green photosynthetic bacteria contain a rich variety of different cytochromes. Various cytochromes act as either soluble or membrane-bound electron carriers and are involved in substrate oxidation processes, as well as proton translocation across the membrane.

Cytochromes in Green Bacteria

There are two phyla of green photosynthetic bacteria, green sulfur bacteria and green nonsulfur bacteria; the latter group is now more correctly called filamentous anoxygenic phototrophic bacteria. Both groups of organisms contain cytochromes, although the patterns and types of cytochromes in the two phyla are very different.

Green sulfur bacteria (chlorobiaceae) are strictly anaerobic, photosynthetic organisms whose reaction center (RC) complex shares common structural and functional features with the photosystem (PS) I RC complex of plants and cyanobacteria or the heliobacterial RC complex. This type-1 (also called Fe–S-type) RC complex consists of five subunits, including a homodimeric core RC (with two identical subunits with molecular mass of 65 kDa), Fenna Matthews Olson (FMO) antenna protein (41 kDa), Fe–S protein that includes the early electron acceptors F_A and F_B (31 kDa), cytochrome c_z (22 kDa) and 18 kDa protein, respectively. Cytochrome c_z serves as a secondary electron donor to the primary electron donor P840. The green sulfur bacteria utilize sulfur compounds as a source of reducing power and therefore also contain additional electron transfer components, primarily soluble cytochromes *c*, which are involved in the metabolic pathway of sulfur oxidation (Figure 1).

Filamentous anoxygenic phototrophic (FAP) bacteria are not closely related organisms to the green sulfur bacteria, with the exception of the primary shared characteristic, the chlorosome antenna complex. Many of these organisms are facultatively aerobic photosynthetic bacteria that are often found in microbial mat environments with cyanobacteria. The only member of this group that has been well studied is *Chloroflexus aurantiacus*, which is found in hot spring environments all over the world. FAP bacteria contain a type-2 (also called quinone-type) RC complex that includes bacteriopheophytins and quinones as early electron acceptors. The type-2 RC is similar to that found in purple photosynthetic bacteria and photosystem II of oxygenic photosynthetic organisms. The FAP RC consists of a heterodimeric complex of two proteins, L and M, plus a tightly bound tetraheme *c*-type cytochrome, *c*-554. Cyt *c*-554 is a membrane-associated cytochrome of molecular mass 48 kDa, which serves as a secondary electron donor to the primary electron donor P870. FAP bacteria have not been reported to contain any soluble *c*-type cytochromes. They also do not appear to contain a membrane-bound cytochrome bc_1 complex.

Types of *c*-Type Cytochromes in Green Sulfur Bacteria

Green sulfur bacteria contain a number of *c*-type cytochromes. These include soluble cytochromes *c*-555, *c*-553, and *c*-551, the membrane-bound cytochrome c_z, and the membrane-bound cytochrome bc_1 complex. The first three were isolated from *Chlorobium limicola* f. *thiosulfatophilum*, and extensively studied biochemically by Yamanaka's group in the 1970s and have been extensively characterized. The others are less

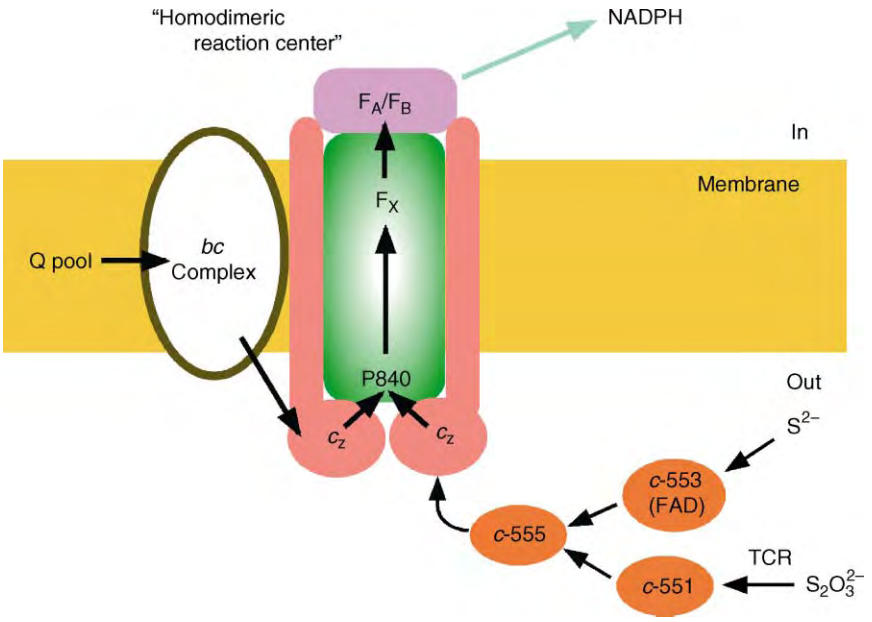

FIGURE 1 Schematic structural model for the reaction center and associated cytochromes involved in electron transport in photosynthetic green sulfur bacteria. Details of the various cytochromes can be found in the text.

well characterized. The cytochromes together make up essential components of the photosynthetic electron transport chain. The pattern described here is similar in most species of green sulfur bacteria.

Cytochrome c_z (PscC)

This cytochrome c_z (PscC) is a monoheme type with a molecular mass of 23 kDa and is tightly bound to the RC complex with putative amino-terminal helices that span the membrane three times. Two molecules of cytochrome c_z are present in one RC complex. Each of them donates an electron to the P840 in a reaction mode with high viscosity dependence. The carboxyl-terminal heme-containing hydrophilic moiety seems to fluctuate on the RC surface and search for an appropriate site for the reaction to proceed. The cytochrome c_z was designated in order to characterize its functional similarity to the membrane-bound cytochrome c_y in *Rhodobacter capsulatus* and mediates the electron transfer between quinol oxidoreductase and P840 RC complex. Although there had been a controversial point concerning the exact α-peak wavelength of the relevant cytochrome *c* that donates an electron directly to P840, its value was found to vary from 553 nm in membranes to 552–551 nm in a solubilized RC complex in the case of *Chl. tepidum*.

Cytochrome *c*-555

This water-soluble cytochrome *c*-555 has a molecular mass of 10 kDa and gives a characteristic asymmetric α-absorption peak, similar to that of algal water-soluble cytochrome c_6 that serves as an electron donor to PSI RC. The cytochrome *c*-555 appears to donate an electron to the membrane-bound cytochrome c_z. Note that the cytochrome in the case of *Chl. tepidum*, to which a locus accession number is CT0075, shows the α-absorption peak at 554 nm.

Cytochrome *c*-553 (Fcc/SoxEF1)

This cytochrome *c*-553 (Fcc/SoxEF1) is a flavo-cytochrome *c* that consists of an 11-kDa cytochrome *c* (FccA/SoxE) plus a 47-kDa flavoprotein (FccB-2/SoxF1) subunits and serves as a sulfide–cytochrome *c* reductase. The flavoprotein subunit contains FAD that is covalently bound to a cysteine residue through a thioether linkage. The electron transfer proceeds as follows: $S^{2-} \rightarrow$ cytochrome *c*-553 (FAD $\rightarrow$ heme *c*-553) $\rightarrow$ cytochrome *c*-555 $\rightarrow$ cytochrome c_z.

Cytochrome *c*-551 (SoxA)

This cytochrome *c*-551 (SoxA) is a dimer of 30-kDa cytochrome *c* and serves as an electron acceptor from a thiosulfate-cytochrome *c* reductase (TCR). Since the pathway is exclusively involved in the oxidation of thiosulfate ($S_2O_3^{2-}$) as a source of reducing power, there is no cytochrome *c*-551 in those green sulfur bacteria that cannot utilize thiosulfate as a reductant. The reduction of cytochrome *c*-555 by a TCR can be accelerated dramatically by the addition of a small amount of cytochrome *c*-551. Furthermore, the reduction of cytochrome *c*-551, itself, can also be accelerated by the

addition of a small amount of cytochrome *c*-555. Cytochrome *c*-555 seems to function as an effector for a TCR.

Cytochrome bc_1 Complex

The cytochrome bc_1 complex is a multisubunit membrane-bound quinone-cytochrome *c* oxidoreductase found in many bacteria and in mitochrondria, where it is also called complex III. It consists of a *b*-type cytochrome, a *c*-type cytochrome, cyt c_1, a Rieske Fe–S protein, and in some cases additional subunits. It oxidizes reduced quinone (quinol) and transfers the electrons to soluble *c*-type cytochromes, at the same time pumping protons across the membrane and creating a protonmotive force that is used to make ATP. The cytochrome bc_1 complex from green sulfur bacteria is not as well characterized as those from other organisms. An unusual aspect of it is that it uses menaquinone, which is lower in redox potential than ubiquinone, which is used in the better-characterized complexes.

Other Cytochromes in Green Sulfur Bacteria

The genome project of *Chl. tepidum* has revealed seven more *c*-type cytochromes (CT0073, CT0188, CT1016, CT1704, CT1734, CT2026, CT2242) whose molecular weights are ~13–17 kDa. *CT1016* has recently been reported to correspond to a *soxX* gene, which is located in the thiosulfate-utilizing genes cluster, although its role is not known at present. Furthermore, one of the residual proteins may be the counterpart of cytochrome c_1 which has not been identified biochemically as yet but is supposed to be present from spectroscopic data.

Cytochromes in Filamentous Anoxygenic Phototrophic Bacteria

The pattern of cytochromes in FAP bacteria is strikingly different from that found in green sulfur bacteria. The only cytochrome that has been characterized in detail is the reaction center associated cytochrome *c*-554.

Cytochrome *c*-554

Cytochrome *c*-554 is a membrane-bound tetraheme cytochrome in which all four of its heme groups have α-band maxima ~554 nm. This cytochrome is the secondary electron donor to the reaction center and bears considerable similarity to the tetraheme cytochrome that is found in many purple photosynthetic bacteria, the best characterized is the tetraheme cytochrome from *Rhodopseudomonas viridis* (recently renamed *Blastochloris viridis)*. The four heme groups in *c*-554 have redox potentials of 0 to +300 mV (versus NHE).

Other Cytochromes in Filamentous Anoxygenic Phototrophic Bacteria

The genomes of FAP bacteria contain other open reading frames that appear to code for *c*-type cytochromes, although none have been characterized. Apparently, there is no cytochrome bc_1 complex present, as indicated both by genetic and biochemical analysis.

See Also the Following Articles

Cytochrome bc_1 Complex (Respiratory Chain Complex III) • Cytochrome *c* • Green Bacteria: The Light-Harvesting Chlorosome • Green Sulfur Bacteria: Reaction Center and Electron Transport • Heme Proteins • Iron–Sulfur Proteins

Glossary

c-type cytochrome A class of cytochromes in which the heme cofactor is covalently attached to the protein via thioether linkages to cysteine amino acid residues.

cytochrome A heme-containing protein that serves as an electron transfer cofactor in biological systems.

Fe-S protein An iron–sulfur protein which holds a [2Fe-2S], [3Fe-4S], or [4Fe-4S]-type cluster and functions as an electron transfer cofactor in biological systems.

flavoprotein A FAD (flavin adenine dinucleotide)-containing protein that serves as an electron transfer cofactor in biological systems.

P840 A special pair of bacteriochlorophyll *a* in green sulfur bacterial RC, which serves as the primary electron donor.

P870 A special pair of bacteriochlorophyll *a* in green nonsulfur bacterial RC, which serves as the primary electron donor.

reaction center (RC) A pigment–protein complex that converts light energy into chemical energy in photosynthetic organisms.

Further Reading

Blankenship, R. E., Madigan, M. T., and Bauer, C. E. (eds.) (1995). *Anoxygenic Photosynthetic Bacteria*. Kluwer Academic, Dordrecht, The Netherlands.

Chen, Z. W., Koh, M., Van Driessche, G., Van Beeumen, J. J., Bartsch, R. G., Meyer, T. E., Cusanovich, M. A., and Mathews, F. S. (1994). The structure of flavocytochrome *c* sulfide dehydrogenase from a purple phototrophic bacterium. *Science* **266**, 430–432.

Dracheva, S., Williams, J. C., Van Driessche, G., Van Beeumen, J. J., and Blankenship, R. E. (1991). The primary structure of cytochrome *c*-554 from the green photosynthetic bacterium *Chloroflexus aurantiacus*. *Biochem.* **30**, 11451–11458.

Eisen, J. A., Nelson, K. E., Paulsen, I. T., Heidelberg, J. F., Wu, M., Dodson, R. J., Deboy, R., Gwinn, M. L., Nelson, W. C., Haft, D. H., Hickey, E. K., Peterson, J. D., Durkin, A. S., Kolonay, J. L., Yang, F., Holt, I., Umayam, L. A., Mason, T., Brenner, M.,

Shea, T. P., Parksey, D., Nierman, W. C., Feldblyum, T. V., Hansen, C. L., Craven, M. B., Radune, D., Vamathevan, J., Khouri, H., White, O., Gruber, T. M., Ketchum, K. A., Venter, J. C., Tettelin, H., Bryant, D. A., and Fraser, C. M. (2002). The complete genome sequence of *Chlorobium tepidum* TLS, a photosynthetic, anaerobic, green-sulfur bacterium. *Proc. Nat'l. Acad. Sci. USA* **99**, 9509–9514.

Hauska, G., Schoedl, T., Remigy, H., and Tsiotis, G. (2001). The reaction center of green sulfur bacteria. *Biochim. Biophys. Acta* **1507**, 260–277.

Oh-oka, H., Iwaki, M., and Itoh, S. (1997). Viscosity dependence of the electron transfer rate from bound cytochrome *c* to P840 in the photosynthetic reaction center of the green sulfur bacterium *Chlorobium tepidum*. *Biochem.* **36**, 9267–9272.

Oh-oka, H., Iwaki, M., and Itoh, S. (1998). Membrane-bound cytochrome c_z couples quinol oxidoreductase to the P840 reaction center complex in isolated membranes of the green sulfur bacterium *Chlorobium tepidum*. *Biochem.* **37**, 12293–12300.

Okkels, J. S., Kjaer, B., Hansson, Ö., Svendsen, I., Møller, B. L., and Scheller, H. V. (1992). A membrane-bound monoheme cytochrome-c_{551} of a novel type is the immediate electron donor to P840 of the *Chlorobium vibrioforme* photosynthetic reaction center complex. *J. Biol. Chem.* **267**, 21139–21145.

Sakurai, H., Kusumoto, N., and Inoue, K. (1996). Function of the reaction center of green sulfur bacteria. *Photochem. Photobiol.* **64**, 5–13.

Yanyushin, M. (2002). Fractionation of cytochromes of phototrophically grown *Chloroflexus aurantiacus*. Is there a cytochrome *bc* complex among them? *FEBS Lett.* **512**, 125–128.

BIOGRAPHY

Hirozo Oh-oka is an Associate Professor of the Department of Biology, the Graduate School of Science at Osaka University in Japan. His research interests are in the area of photosynthetic electron transport systems. He has a Ph.D. from Osaka University.

Robert E. Blankenship is Professor and Chair of the Department of Chemistry and Biochemistry at Arizona State University. His research interests are in the area of photosynthetic energy and electron transfer processes. He has a Ph.D. from the University of California, Berkeley. Dr. Blankenship has been the Editor-in-Chief of the scientific research journal *Photosynthesis Research* and has served as the President of the International Society of Photosynthesis Research.

Green Bacteria: The Light-Harvesting Chlorosome

John M. Olson
University of Massachusetts, Amherst, Massachusetts, USA

Chlorosomes are the main light-harvesting structure of green filamentous bacteria and green sulfur bacteria and are filled with aggregated bacteriochlorophyll (BChl) *c*, *d*, or *e*. BChl *a* is associated with a small protein in the envelope of the chlorosome, whereas the other BChls are organized in rod-like structures located in the interior of the chlorosome and containing little or no protein. Chlorosomes are appressed to the cytoplasmic side of the cytoplasmic membrane and the main path of excitation energy transfer can be written as BChl *c*, *d*, or *e* (chlorosome) → BChl *a* (chlorosome) → BChl *a* (FMO or membrane proteins) → BChl *a* (reaction center).

Chlorosomes are the characteristic light-harvesting complexes of green filamentous bacteria (green non-sulfur bacteria, Chloroflexaceae) and green sulfur bacteria (Chlorobiaceae). Chlorosomes are filled with bacteriochlorophyll (BChl) *c*, *d*, or *e* molecules in a highly aggregated state and are appressed to the cytoplasmic side of the cytoplasmic membrane. BChl *c*, *d*, and *e* form a family of chlorophylls (chlorosome chlorophyll) that contain a hydroxyethyl group at position 3 as shown in Figure 1. The main esterifying alcohol is farnesol in green sulfur bacteria and stearol in filamentous bacteria, which contain only BChl *c*. In some green sulfur bacteria there are at least four chemically distinct homologues of BChl *c* that differ in the degree of alkylation on the chlorin ring at positions 8 and 12 (see Figure 1 and Table I). In addition to chlorosome chlorophyll all chlorosomes contain a small amount of BChl *a*, the same chlorophyll found in proteobacteria (purple bacteria). BChl *a* is associated with a small protein in the envelope of the chlorosome, whereas chlorosome chlorophyll is located in the interior and is organized in rod-like structures containing little or no protein.

Phylogeny

From a phylogenetic viewpoint green filamentous bacteria and green sulfur bacteria are two distinct groups based on 16S rRNA, reaction center (RC) type, and physiology. Green filamentous bacteria contain a quinone-type RC similar to that found in proteobacteria and also similar to the RC of photosystem II in cyanobacteria and plant chloroplasts. Green sulfur bacteria contain an iron–sulfur-type RC similar to those found in heliobacteria and in photosystem I of cyanobacteria and chloroplasts. The filamentous bacteria live either as facultative photoautotrophs or as respiring chemoheterotrophs. They are found mostly in hot springs, often in mixed populations with cyanobacteria. The sulfur bacteria are obligate photoautotrophs and strict anaerobes that grow in dim light in sulfide-rich environments such as effluents of sulfur springs and the lower layers of stratified lakes and in marine habitats. In one extreme case, green sulfur bacteria have been found at a depth of 80 m in the Black Sea.

Structural Features

Size and Internal Structure

Chlorosomes are mostly made up of chlorophyll, but lipid, protein, carotenoid, and quinone are also present. Typically the chlorosomes from *filamentous* bacteria (designated F-chlorosomes) are ~100 nm long, 20–40 nm wide and 10–20 nm high. Chlorosomes from *sulfur* bacteria (designated S-chlorosomes) are considerably larger with lengths 70–260 nm and widths 30–100 nm. All chlorosomes consist of a core and a 2–3 nm envelope as shown in Figure 2. The core consists of rod elements made up of aggregated chlorosome chlorophyll, while the envelope is a monolayer of mostly galactolipid and some protein. Each chlorosome may contain 10–30 rod elements. The rod elements of S-chlorosomes are 10 nm in diameter, whereas those of F-chlorosomes are only 5.2–6 nm. The envelopes of both F- and S-chlorosomes contain BChl *a* associated with a specific protein, CsmA. The molar ratio of chlorosome chlorophyll to BChl *a* in S-chlorosomes is ~90/1, whereas in F-chlorosomes it is ~25/1.

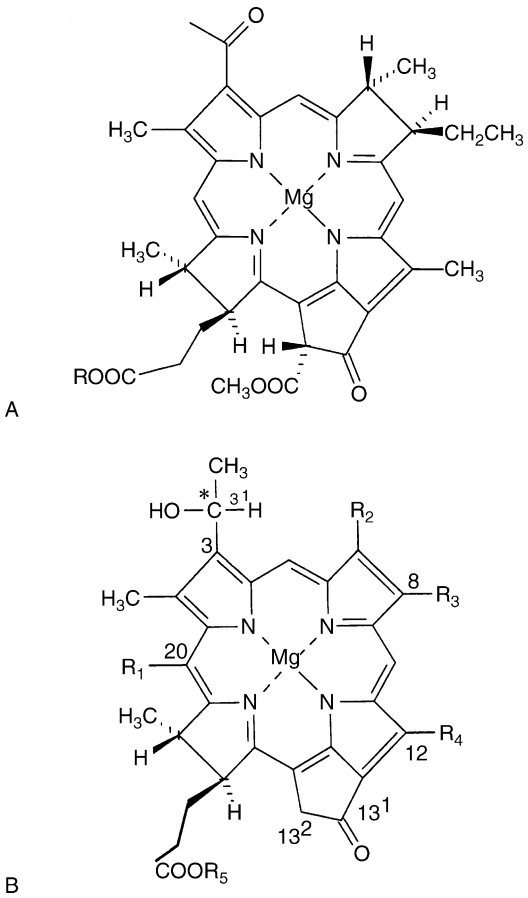

FIGURE 1 Structures of (A) BChl *a* and (B) the chlorosome chlorophylls (BChl *c*, *d*, and *e*). For BChl *a* R = phytyl. See Table I for details about the chlorosome chlorophylls.

Proteins

In highly purified S-chlorosomes the mass ratio of protein to chlorophyll is very low—only 0.5 compared to 6.3 for the Fenna–Matthews–Olson (FMO) BChl a protein found in green sulfur bacteria. The proteins of chlorosomes are localized in the envelope. In F-chlorosomes these proteins are called CsmA, CsmM, and CsmN. In S-chlorosomes they are called CsmA, CsmB, CsmC, CsmD, and CsmE. The major component in both kinds of chlorosomes is CsmA with a molecular mass of 5.7 kDa in F-chlorosomes and 6.3 kDa in S-chlorosomes. This protein binds BChl *a* in both kinds of chlorosomes, and the BChl *a*–CsmA complexes are thought to be concentrated in a "baseplate" that is in contact with BChl *a* proteins associated with the cytoplasmic membrane. Some chlorosome proteins may be responsible for maintaining the native shape.

TABLE I

Ring Substituents Found on Chlorosome Chlorophylls (see Figure 1)

Chlorophyll	R_1	R_2	R_3	R_4	R_5
BChl *c* (F-chlorosomes)	Methyl	Methyl	Ethyl	Methyl	Stearyl (mostly)
BChl *c* (S-chlorosomes)	Methyl	Methyl	Ethyl *n*-Propyl Isobutyl	Methyl Ethyl	Farnesyl (mostly)
BChl *d* (S-chlorosomes)	H	Methyl	Ethyl *n*-Propyl Isobutyl	Methyl Ethyl	Farnesyl (mostly)
BChl *e* (S-chlorosomes)	Methyl	Formyl	Ethyl *n*-Propyl Isobutyl	Ethyl	Farnesyl (mostly)

Carotenoids

All chlorosomes contain carotenoids which function as light-harvesting pigments and triplet-state quenchers.

Spectral Properties

In Figure 3 the absorbance and fluorescence emission spectra of F-chlorosomes indicate the presence of a large amount of BChl *c*, a small amount of BChl *a*, and energy transfer from BChl *c* to BChl *a*. The absorbance and fluorescence peaks at 740 and 750 nm respectively belong to BChl *c*, while the peaks at 795 and 801 nm belong to BChl *a*. The circular dichroism (CD) spectrum (not shown) demonstrates a strong excitonic interaction among the BChl *c* molecules. All these properties of BChl *c* in both F- and S-chlorosomes are completely different from those of monomeric BChl *c* dissolved in polar solvents. Monomeric BChl *c* has absorption and fluorescence peaks at ~660 and 665 nm, and a CD spectrum with a very small negative peak at 660 nm. Pure BChl *c* forms aggregates in dried films or when dissolved in non-polar solvents such as hexane and carbon tetrachloride. The spectral properties of these aggregates are similar to those of chlorosomes and suggest that in chlorosomes BChl *c* exists in an aggregated state. The absence of proteins from the aggregates *in vitro* supports the idea that BChl *c* does not require protein to form aggregates in the chlorosome.

Models of Chlorophyll Organization

Although it is not yet possible to present a definitive structure for the chlorophyll aggregates in the chlorosome, several characteristics have been established:

1. The aggregates of chlorosome chlorophyll (BChl *c*, *d*, or *e*) are the result of chlorophyll–chlorophyll interactions. The molecules are close together and oriented so as to give a strong excitonic interaction.

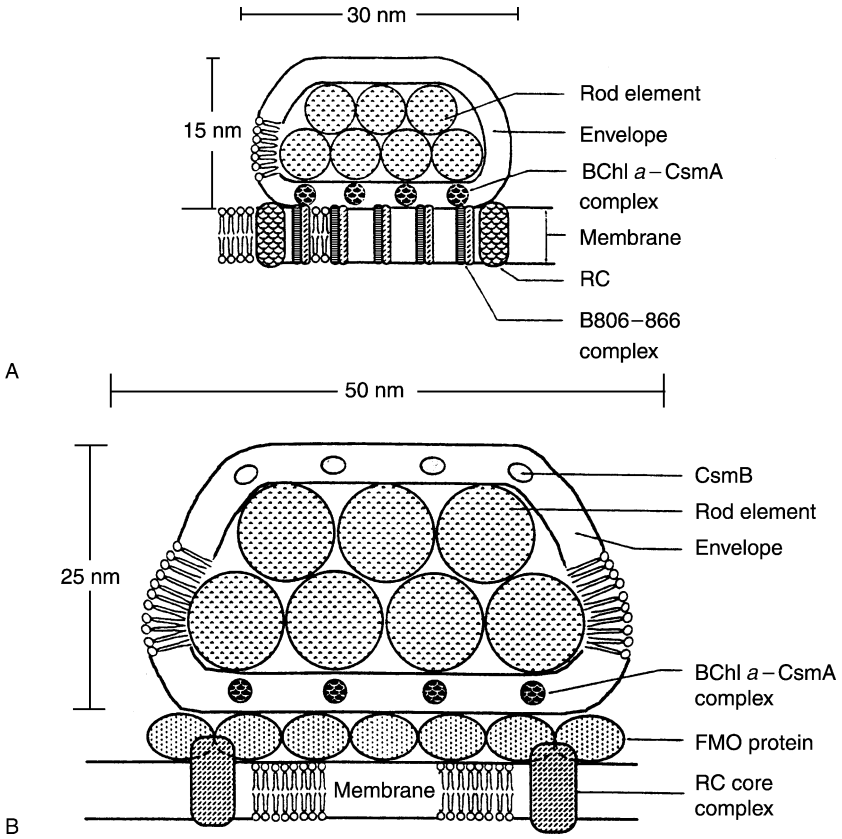

FIGURE 2 Cross-sectional views of antenna system models for (A) green filamentous bacteria and (B) green sulfur bacteria. Relatively small chlorosomes are shown in both cases. Adapted from Olson, J. M. (1998). Chlorophyll organization and function in green photosynthetic bacteria. *Photochem. Photobiol.* **67**, 61–75 with permission from the American Society for Photobiology.

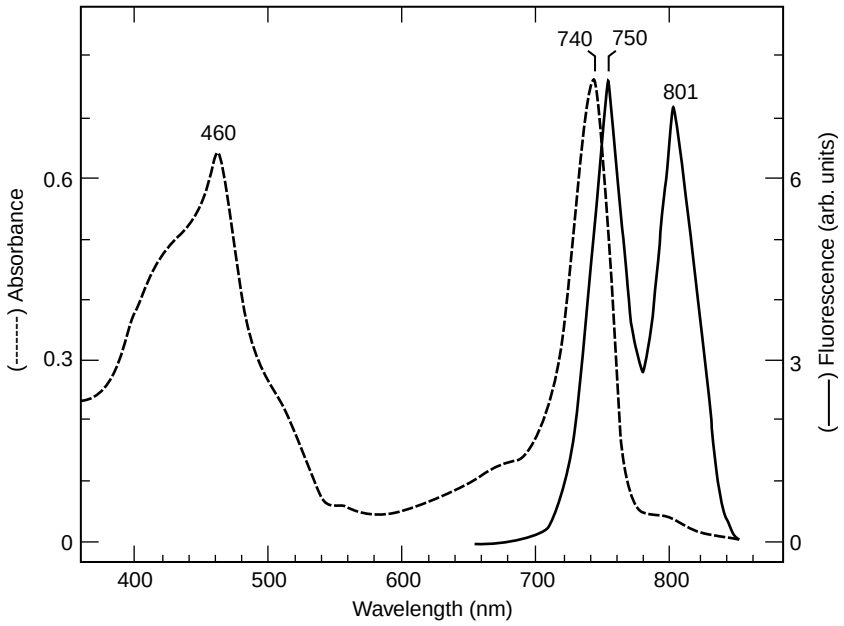

FIGURE 3 Absorption and fluorescence emission spectra of F-chlorosomes. Fluorescence was excited at 460 nm. Adapted from Brune *et al.* (1990). *Photosynth. Res.* **24**, 253–263 with permission of Kluwer Academic Publishers.

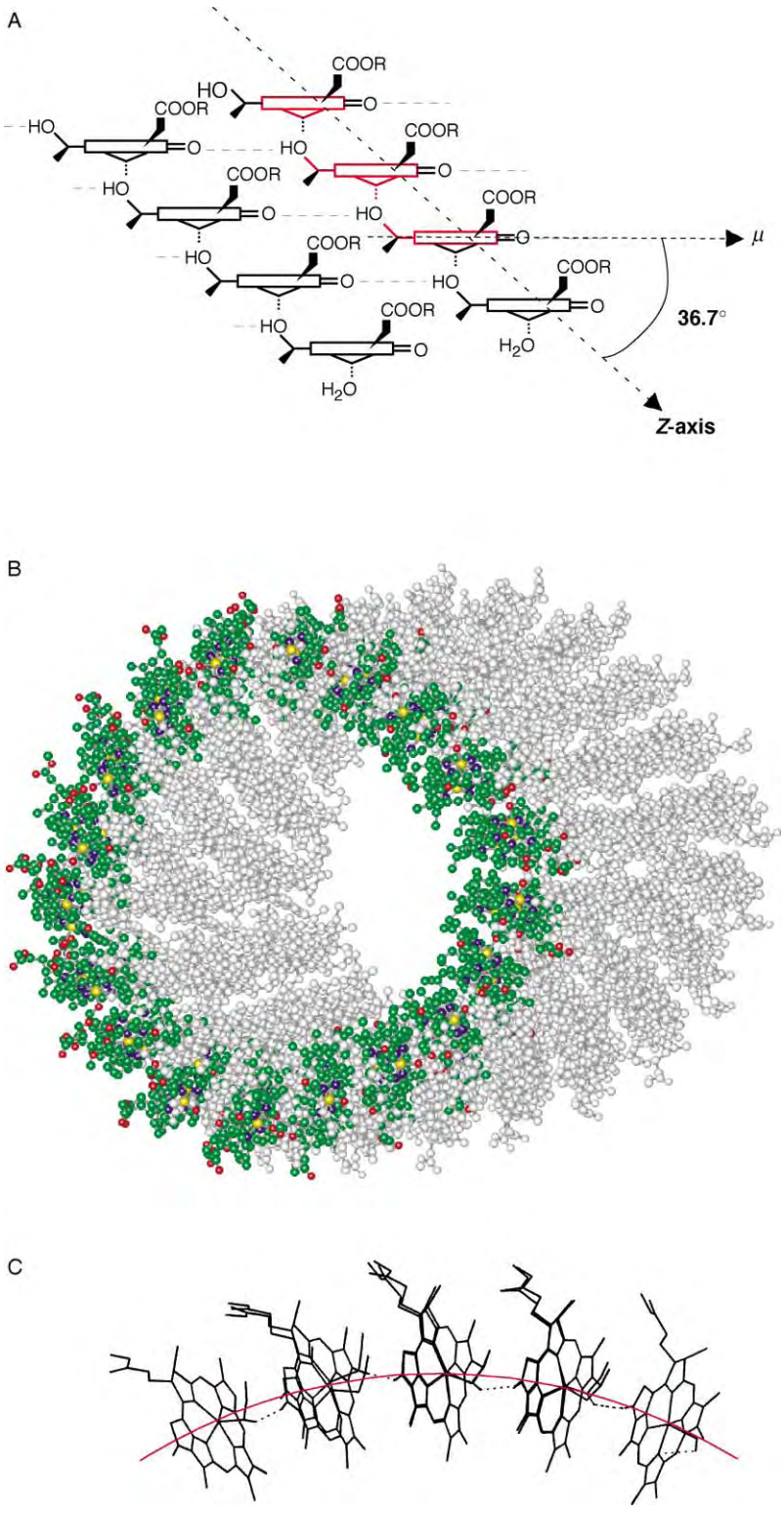

FIGURE 4 (A) The arrangement of chlorosome chlorophylls in a stack. The dashed *Z*-axis connects the Mg atoms of the chlorophylls in a single stack. (B) Space view of the tubular chlorophyll aggregate obtained by molecular modeling. The farnsyl groups, pointing to the outside of the rod, are not shown. (C) Arrangement of chlorophyll molecules at the outside edge of the chlorosome. Reproduced from Prokhorenko, V. I., Steensgaard, D. B., and Holzwarth, A. R. (2000). Exciton dynamics in the chlorosomal antennae of the green bacteria *Chloroflexus aurantiacus* and *Chlorobium tepidum*. *Biophys. J.* **79**, 2105–2120 with permission of the Biophysical Society.

2. The chlorophyll molecules also exhibit long-range order with their Q_y transitions parallel to the long axis of the chlorosome.

3. The 13^1-carbonyl of each chlorophyll molecule interacts with a functional group on another chlorophyll molecule.

4. The 3^1-hydroxyethyl group is coordinated directly to a Mg atom in a second chlorophyll molecule and is H-bonded to the 13^1-carbonyl of a third chlorophyll molecule.

5. Essentially all the Mg atoms in the chlorophyll molecules are five-coordinate.

Using computer modeling, Prokhorenko, Steensgaard, and Holzwarth (2000) have developed the useful model of chlorophyll organization shown in Figure 4. The large-scale structure is a tube with a diameter of 4.6 nm (with respect to Mg atoms), corresponding to the diameter of the rod elements in F-chlorosomes. The chlorophyll macrocycles are perpendicular to the surface of the tube, and the hydrocarbon tails (not shown) are oriented toward the outside of the tube.

Energy Transfer

The overall pathway of excitation energy transfer upon irradiation of filamentous bacteria with red or far-red light can be written as follows:

BChl *c* (chlorosome) → BChl *a* (chlorosome)
→ BChl *a* (membrane proteins) → BChl*a* (RC)

The membrane proteins are labeled B806–866 in Figure 2A. In sulfur bacteria the FMO protein replaces the membrane proteins as shown in Figure 2B. Energy transfer between chlorosome chlorophyll molecules takes place by a relatively fast exchange mechanism, while energy transfer between chlorosome chlorophyll and BChl *a* in the chlorosome takes place by a relatively slow Förster mechanism. The chlorosome light-harvesting system is an example of an energy funnel in which each successive pigment pool has progressively red-shifted absorption and fluorescence emission spectra. The descending energy levels thus provide an excitation gradient into the RC.

Energy transfer in the green sulfur bacteria is regulated by the redox potential *in vivo*. Under oxidizing conditions the overall energy transfer efficiency drops from ~100% to 10% or less. Redox titration of fluorescence in isolated chlorosomes gives a midpoint potential of −146 mV at pH 7.0. (This regulation is mediated by the quinone in the chlorosomes.) The formation of flourescence quenchers at high redox potentials may protect the bacteria from lethal photo-oxidation reactions such as superoxide formation resulting from the reduction of ferredoxin in the presence of oxygen. These redox effects are largely missing from the green filamentous bacteria, whose RCs do not reduce ferredoxin.

Evolutionary Considerations

The presence of chlorosomes in both green filamentous bacteria and green sulfur bacteria is the only justification for lumping them together as green bacteria. Although the two types of chlorosomes (F and S) show differences in size and rod element morphology, the organization of the chlorosome chlorophylls appears to be basically similar, and the *csmA*/CsmA genes and proteins appear to be homologous. This suggests the F- and S- chlorosomes are descended from a common ancestor coded for by an ancestral "genome" containing the *csmA* gene.

See Also the Following Articles

Chlorophylls and Carotenoids • Green Bacteria: Secondary Electron Donor (Cytochromes) • Green Sulfur Bacteria: Reaction Center and Electron Transport • Photosynthesis • Photosynthetic Carbon Dioxide Fixation

Glossary

chemoheterotroph An organism that requires organic compounds and a chemical source of energy.

excitonic interaction An interaction in which the excited state is shared by more than one molecule.

Förster energy transfer Nonradiative resonance transfer.

heliobacteria Photosynthetic bacteria that contain BChl *g* and an iron–sulfur-type RC similar to those found in green sulfur bacteria and photosytem I of cyanobacteria and chloroplasts.

homologue A molecule that is identical to another molecule except for one substituent.

photoautotroph An organism that requires light and inorganic carbon.

proteobacteria A subgroup of Gram-negative bacteria that includes purple photosynthetic bacteria.

Further Reading

Blankenship, R. E., and Matsuura, K. (2003). Antenna complexes from green photosynthetic bacteria. In *Light-Harvesting Antennas* (B. R. Green and W. W. Parsons, eds.), pp. 195–217. Kluwer, Dordrecht.

Blankenship, R. E., Olson, J. M., and Miller, M. (1995). Antenna complexes from green photosynthetic bacteria. In *Anoxygenic Photosynthetic Bacteria* (R. E. Blankenship, M. T. Madigan and C. E. Bauer, eds.) pp. 399–435. Kluwer, Dordrecht.

Ke, B. (2000). The green bacteria: I. The light-harvesting complex, the chlorosomes. In *Photosynthesis: Photochemistry and Photobiophysics*, pp. 147–158. Kluwer, Dordrecht.

Oelze, J., and Golecki, J. R. (1995). Membranes and chlorosomes of green bacteria. In *Anoxygenic Photosynthetic Bacteria* (R. E. Blankenship, M. T. Madigan and C. E. Bauer, eds.) pp. 259–278. Kluwer, Dordrecht.

Olson, J. M. (1998). Chlorophyll organization and function in green photosynthetic bacteria. *Photochem. Photobiol.* **67**, 61–75.

Prokhorenko, V. I., Steensgaard, D. B., and Holzwarth, A. R. (2000). Exciton dynamics in the chlorosomal antennae of the green bacteria *Chloroflexus aurantiacus* and *Chlorobium tepidum*. *Biophys. J.* **79**, 2105–2120.

Biography

John M. Olson is adjunct Professor of Biochemistry and Molecular Biology at the University of Massachusetts. He retired in 1994 after 12 years as Professor of Photosynthesis at Odense University in Denmark. His main research interest over the last 40 years has been the function of chlorophyll in green sulfur bacteria, and in 1962 he discovered the Fenna–Matthews–Olson BChl *a* protein, the first chlorophyll protein to have its structure determined by X-ray diffraction. He has also written several articles on the evolution of photosynthesis.

Green Sulfur Bacteria: Reaction Center and Electron Transport

Günter A. Hauska and Thomas Schödl
Universität Regensburg, Regensburg, Germany

Green bacteria comprise two distant taxonomic groups, the green sulfur bacteria (GSB) – *Chlorobiaceae*, and the filamentous green "nonsulfur" bacteria – *Chloroflexaceae*. Both are photosynthetic taxa, which are exceptional in two ways. They share a most efficient light capturing apparatus, the chlorosomes, and they do not assimilate CO_2 via ribulose-bisphosphate carboxylase (Rubisco) and the Calvin cycle. GSB use the reductive tricarboxylic acid cycle (TCA), while *Chloroflexaceae* carboxylate acetyl CoA, employing a vitamin B_{12}-dependent pathway via methyl malonate. Otherwise the two groups have little in common. The reaction center (RC) of *Chloroflexaceae* is of the Q-type, closely related to the RCs found in the purple bacteria *Rhodospirillaceae* and in plant PSII, the RC of *Chlorobiaceae* is of the FeS-type and represents a simplified version of the PSI-RC in plants. Instead of a heterodimeric core with two similar, but different proteins, it is homodimeric built from two identical proteins. The only other photosynthetic taxon with such a simple FeS-type RC are the gram-positive *Heliobacteria*. All other phototrophic organisms contain heterodimeric RCs. The recent annotation of the complete genome of *Chlorobium tepidum* further documents the peculiarities of GSB, and this article will focus on them.

Light Capture

Chlorosomes

Chlorosomes were first reported by Cohen-Bazire *et al.* in 1964 as organelles attached to the inner surface of the cytoplasmic membrane of green sulfur bacteria (GSB). They are surrounded by a lipid–protein monolayer, and contain thousands of bacteriochlorophylls *c*, *d*, or *e*, depending on the bacterial species, stacked in tubular arrangement (Figure 1). Among photosynthetic organisms only the green bacteria, *Chlorobiaceae* and *Chloroflexaceae*, process this special organization of light-harvesting antennae which is responsible for efficient absorption in dim light. *Heliobacteria*, which live closer to the water surface, lack chlorosomes. Monomeric bacteriochlorophyll (BChl) *c*, *d*, and *e* absorb at 660–670 nm, but the stacking of the tetrapyrrol rings shifts the absorption to 720–750 nm. The excitation energy in these stacks is transferred via Bchl *a*-species in the baseplate and in the FMO protein absorbing around 800 nm, finally to the reaction center (RC) in the membrane. This energy transfer is quenched under aerobic conditions preventing damage by oxygen. This redox control may be mediated by chlorobiumquinone (1′-oxomenaquinone-7) and FeS centers of proteins, which are present in the chlorosome envelope (Csm proteins). The chlorosomes also contain carotenoids which participate in energy transfer and protection from photodamage.

The FMO Protein

This chlorophyll protein was the first to be crystallized and structurally resolved to atomic resolution in 1979, lending itself to detailed laser spectroscopic studies. It is a water-soluble, trimeric protein with seven BChl *a* molecules per 40 kDa monomer, which is largely of β-sheet structure. The seven BChl *a* molecules can be distinguished by low-temperature spectroscopy. FMO is located on the cytoplasmic surface of the cell membrane in *Chlorobiaceae*, between the chlorosomes and the RC (Figure 1). It is absent from *Chloroflexaceae*. Energy transfer from the FMO protein to the RC also is under redox control, as is the one from the chlorosomes; however, even under anaerobic conditions it has been found to be surprisingly low in isolated membranes. However, a new crystal structure for the FMO, which was obtained from isolated RC, reveals the presence of an eighth chlorophyll per monomer, which may bridge the gap to the RC *in vivo* (see Figure 2C).

The Homodimeric P840-Reaction Center — Composition, Structure, and Electron Transfer

Energy transfer to the RC of GSB leads to charge separation in the RC, across the membrane. The formation

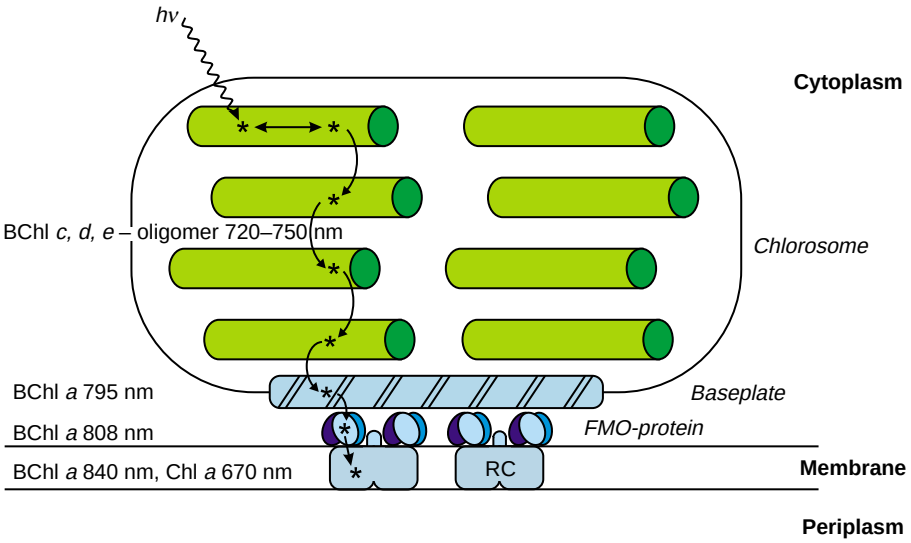

FIGURE 1 Excitation transfer in green sulfur bacteria. Numbers following the designations of the pigments indicate the wavelengths of the absorption maxima.

of P840* results in bleaching at 840 nm. A functionally competent P840-RC, free of chlorosomes, can be isolated from the membranes of various GSB species with the help of detergents, with and without retention of FMO trimers. The core of the P840-RC consists of four subunits. A large hydrophobic PscA protein (82 kDa) which is homologous to the subunits PsaA and PsaB of the FeS-type P700-RC in PSI of plants and cyanobacteria. It contains 11 putative transmembrane helices like these, binds all pigments and four redox centers (see Figure 3). These are (1) the primary electron donor P840, an electronically coupled, special pair of Bchl *a* molecules ($E_0' = 240$ mV), (2) the primary acceptor A_0, a pair of chlorophyll (Chl) *a* molecules, (3) the secondary electron acceptor A_1 which is menaquinone-7, and (4) F_X, the first of three

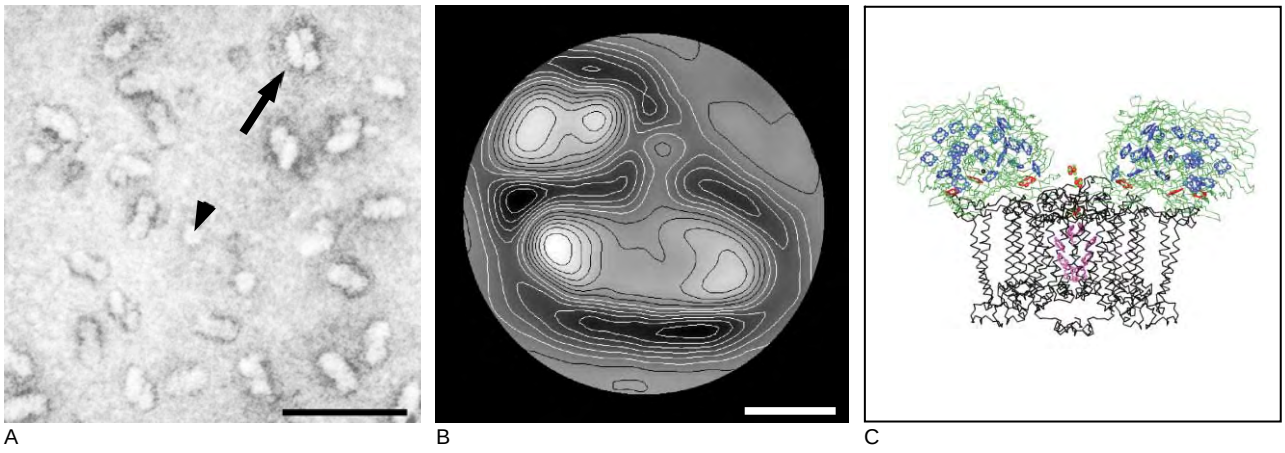

FIGURE 2 Structural representations of the FMO/P840-RC complex. Parts (A) and (B) are taken from Remigy, H-W., Hauska, G., Müller, S.A., and Tsiotis, G. (2002). The reaction center from green sulfur bacteria: Progress towards structural elucidation. *Photosynth. Res.* **71**, 91–98; (A) is a scanning transmission electron micrograph of the particle mixture, with free FMO trimers (arrowhead), P840-RC with two bound FMO trimers (arrow), a dominant proportion of RCs with one FMO trimer and some RCs without FMO; the bar represents 20 nm. Part (B) shows a projection of the RC with one bound FMO trimer in side view after imaging; the bar represents 5 nm. Part (C) is taken from Ben-Shem, A. *et al.* (2004). Evolution of photosystem I – from symmetry to pseudosymmetry to asymmetry. *FEBS lett.*, **564**(3): 274–80, and presents a high-resolution structural model for the P840-RC with two bound FMO trimers; The homodimeric core was constructed from two PsaB proteins from the RC of PSI, showing the Cα-backbone with the 22 transmembrane helices in black; the six Chl *a* molecules forming P700 and A_0, plus the two A_1-phylloquinones are depicted in magenta, and the three cubic 4Fe4S centers F_X, F_B, and F_A are printed in red for the irons and in green for the sulfurs; the Cα-backbone of PsaB protein, which carries F_B and F_A, is left out. The folding of the Cα-backbone of the two FMO trimers is printed in green with the 3×7 BChl *a* originally identified in blue, and the three newly detected chlorophylls, one per FMO protein in red (courtesy Adam Ben-Shem).

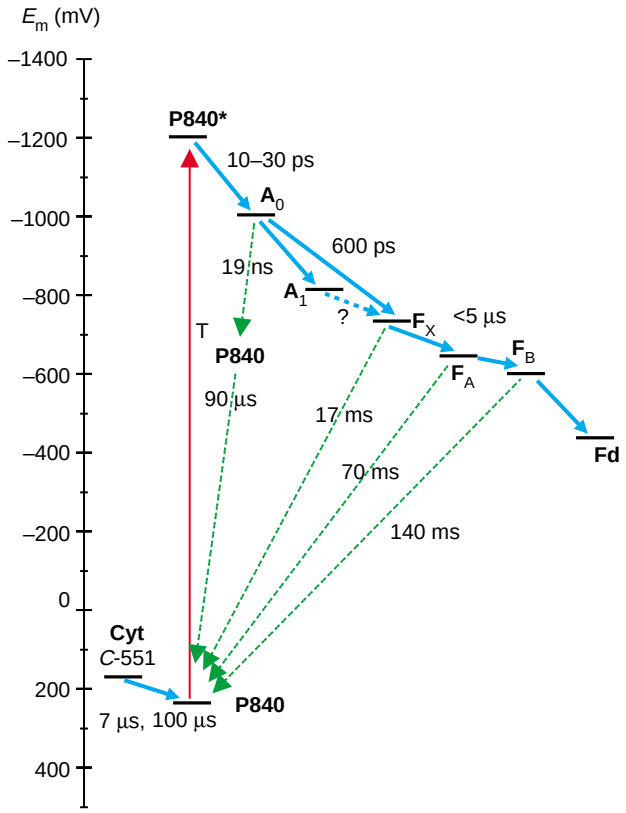

FIGURE 3 Electron transfer within the P840 reaction center in the redox potential diagram. The rates are given for isolated RCs at RT; abbreviations are explained in the text.

4Fe4S centers. In PSI these four redox centers are bound to the heterodimer PsaA/PsaB in pseudosymmetric arrangement across the membrane. P700 and F_X are bound between PsaA and PsaB, each contributing half of the ligand residues, while A_0 and A_1 – a phylloquinone in PSI – occur as a double set in the two subunits. The second subunit in the P840-RC is the FeS protein PscB (24 kDa), which resembles PsaC from PSI, carrying F_A and F_B, the two terminal 4Fe4S centers that reduce ferredoxin. The third subunit PscC is the secondary electron donor cyt *c*-551 (23 kDa, +180 mV), and the fourth is PscD (15 kDa), which lacks a redox center. The gene for PscA is associated with the gene for PscB in a transcription unit and occurs only once in the genome of *C. tepidum*. Therefore, since by analogy to PsaA/PsaB of PSI, PscA contributes only half of the binding sites for P840 and F_X, the core of the P840-RC in GSB must be a homodimer, probably with strictly symmetric transmembrane arrangement of the redox centers, as depicted in Figure 4. A similar argumentation led to the conclusion that the P798-RC of *Heliobacteria* is homodimeric in structure. This reaction center may even be simpler, because an equivalent for PscB, with the two peripheral FeS centers escaped detection so far.

A preparation of the RC core only consisting of PscA and PscB, but fully functional in charge separation has been isolated from *Prostecochloris aestuarii*. Its spectra at RT and at low temperature in the visible region are shown in Figure 5, as well as those of the RC core of *C. tepidum*, which retains cyt *c*-551 (see the small peak at 551 nm in Figure 5 B and D, marked by an arrow). The P840-RC is much less pigmented than the P700-RC of PSI. Per RC monomer only eight BChl *a* molecules are present. Their absorptions between 780 and 840 nm are resolved into distinct bands at low temperature. In addition, two Chl *a* molecules are present which absorb at 670 nm (second arrow in Figure 5). It is noteworthy that while the primary electron donor P840 is built by two BChl *a* molecules the primary electron acceptor A_0 consists of Chl *a*. Unlike the P700-RC, in which both are formed by Chl *a*, the P840-RC allows for photoselection of A_0. Also in *Heliobacteria*, A_0 is a derivative of Chl *a*, while the bulk of the pigments is BChl *g*, and the occurrence of Chl *a*-types as the primary acceptors in these two taxa with "primitive" homodimeric RCs is intriguing with respect to the evolution of the chlorophyll pigments.

The photosynthetic unit in *C. tepidum* comprises 16 BChl *a*, 4 Chl *a* molecules and 1 carotenoid in the P840-RC, 48 BChl *a* in the 2 FMO-trimers, and ~2000 BChl *c*, carotenoids, and some additional BChl *a* in the chlorosomes.

A_1-menaquinone-7 is more loosely bound in the P840-RC than A_1-phylloquinone in PS1, and may actually not be an obligatory intermediate in the electron transfer, but rather on a side path, in exchange with free menaquinone-7 in the membrane (see Figures 3 and 4). In accordance with looser binding the hydrophilic dipeptide SR in PscA replaces YW in the quinone-binding pockets of PsaA and PsaB, oriented toward the inner surface of the cytoplasmic membrane, after transmembrane helix 10.

A scanning transmission electromicrograph of P840-RC preparation from *C. tepidum* is shown in Figure 2A which predominantly consists of particles with RC cores bound to one FMO trimer. A side projection of this structure after imaging is shown in Figure 2B. The preparation depicted in Figure 2A also contains free FMO trimers (arrowhead) and occasionally particles with two trimers are seen (arrow). This structure, which probably represents the *in vivo* organization in the membrane, has been modeled recently by Ben-Shem *et al.*, as shown in Figure 2C. In this model the new structure for the FMO trimer with the additional chlorophylls in red is combined with a homodimer constructed from two PsaB subunits of the P700-RC in PS1.

An energy diagram of the charge transfer steps in the P840-RC, with approximate life times, and including recombination reactions is presented in Figure 3,

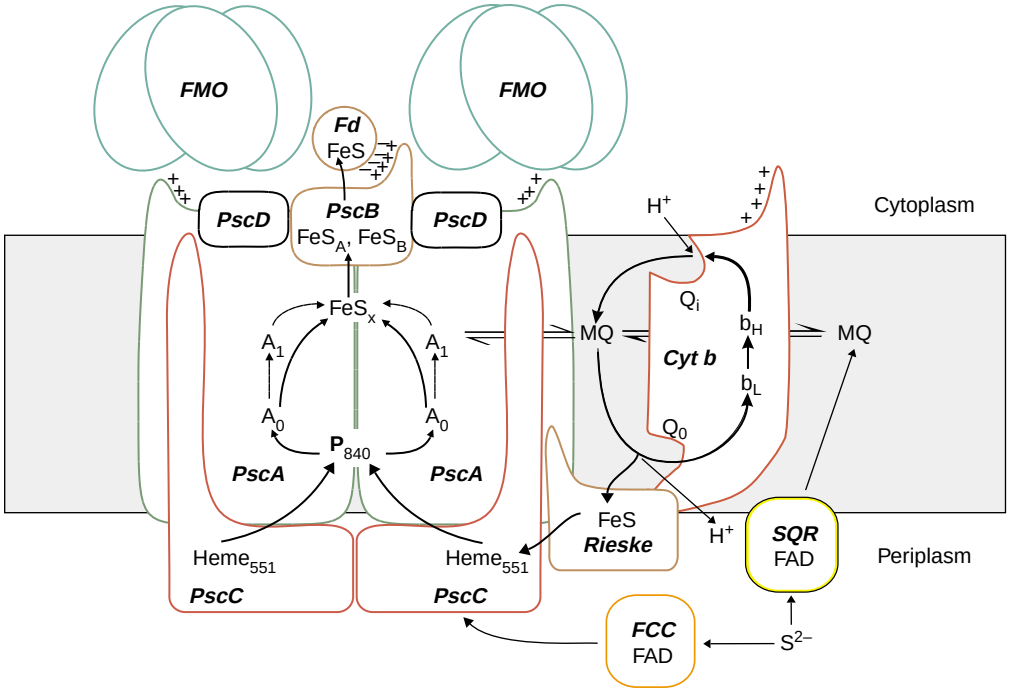

FIGURE 4 Membrane topography of the P840 reaction center and other electron transport components in green sulfur bacteria. The abbreviations are explained in the text; positively charged parts of the proteins PscA, PscB and cyt *b*, detected in the corresponding genes and exposed to the cytoplasmic surface are indicated; MQ stands for menaquinone; b_H and b_L denote high potential and low potential heme *b*, respectively.

which is similar to the scheme for the RC of PSI, but shows some quantitative differences. In particular, electron transfer from A_0 to the first FeS center F_X is 20–300 times faster in the P840-RC, which may reflect a shorter distance, and also the loser binding of A_1.

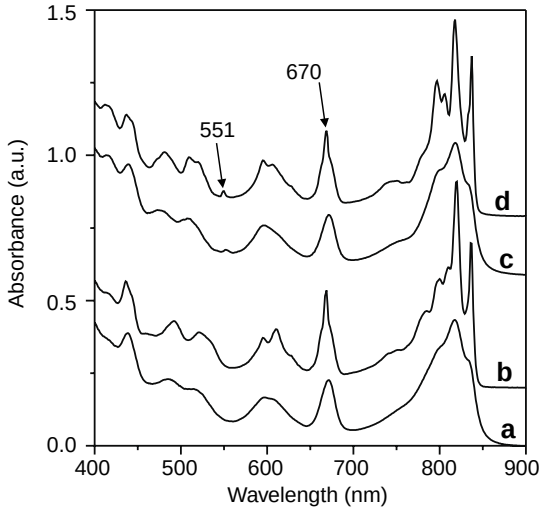

FIGURE 5 Absorption spectra of reaction center cores from green sulfur bacteria. The figure is a modified version of Figure 3 from Permentier, H. P., Schmidt, K.A., Kobayashi, M., Akiyama, M. Hager-Braun, C., Neerken, S., Miller, M., and Amesz, J. (2000). Composition and optical properties of the recation centre complexes from the bgreen ulfue bacteria *Prosteocochloris aestuarii* and *Chlorobium tepidum*. *Photosynth. Res.* **64**, 27–39, and shows the spectra at RT and at 6 K for *Prostecochloris aestuarii* (a,b) and *Chlorobium tepidum* (c,d); the arrows indicate absorption peaks of cyt *c*-551 and of the primary acceptor A_0, which is Chl *a* (670 nm).

Secondary Electron Donors and Acceptors

Figure 4 presents a scheme for the topographical arrangement of the homodimeric P840-RC in the membrane of GSB, together with prominent other components of electron transport (ET) from sulfide to ferredoxin. Electrons from sulfide enter the system at the periplasmic side in two ways, either via sulfide-quinone reductase (SQR) into the menaquinone pool of the membrane, or are transferred by flavocytochrome *c* (FCC) to cyt *c*-551. SQR and the flavoprotein moiety of FCC belong to the phylogenetic family of disulfide oxidoreductases, together with glutathion reductase and lipoamide dehydrogenase. The path via SQR is coupled to ATP formation, because menaquinol oxidation by the Rieske FeS center of the cyt *bc* complex, in the so-called Q-cycle translocates protons, and the resulting proton gradient drives an ATP synthase. The bifurcation of electron transport during the Q-cycle, at the site of quinol oxidation Qo manifests itself as "oxidant-induced reduction" of cyt *b*, which has been observed in membranes of *Chlorobium*. Among the family of the quinol oxidizing cyt *bc* complexes the one in GSB is interesting in two ways. The menaquinol oxidizing

2Fe2S cluster of the Rieske protein has a lowered redox potential (+150 mV), and the cyt *b* shows a mixture of the characteristics for the mitochondrial cyt bc_1 and the plastidal cyt b_6f complexes.

Multiple genes for soluble ferredoxins, six for 2(4Fe4S) and two for 2Fe2S–proteins, have been identified in the genome of *C. tepidum*. Three of the 2(4Fe4S)-types are reducible by PscB in isolated P840-RC (Figure 4), and two of them are involved in CO_2 fixation in the reductive TCA cycle. One of them reduces $NAD(P)^+$ via a ferredoxin-$NAD(P)^+$ reductase (FNR), which is not related to FNR from plants, but to thioredoxin reductase.

Further Genes For Electron Transport Components

The complete sequence of the genome from *C. tepidum* revealed many more genes for ET components, some of them unexpected and several of them in multiple forms, for which physiological functions have been documented only in part so far. The rest will have to be identified by deletion studies. Noteworthy, several of the genes document a closer relation of the GSB to cyanobacteria and plants than to other bacteria.

Next to the eight genes for ferredoxins mentioned above, three for rubredoxins are present. Together with an uptake Ni–Fe hydrogenase they may be involved in using hydrogen for photoautotrophic growth. An operon of 11 genes codes for subunits of a type-1 NADH dehydrogenase. Since the further genes are lacking, it may be linked to this Ni–Fe hydrogenase, or may be involved in cyclic ET around the RC, and not to NADH oxidation. The presence of on CydABCD operon for a cyt *bd* quinol oxidase came as a surprise. It may provide yet another mechanism for protection from oxygen damage, together with superoxide dismutase and other enzymes dealing with oxygen radicals. The genes necessary for nitrogen fixation, and for sulfur metabolism in addition to sulfide oxidation are also found. Interestingly, although CO_2 is fixed by the reductive TCA cycle, a gene related to Ribulose bisphosphate carboxylase/oxygenase (Rubisco) is present. Its expression product is not active as Rubisco, however, but is somehow participating in sulfur metabolism. This may be a hint toward the evolution of CO_2 fixation by the Calvin cycle.

See Also the Following Articles

Cytochrome bc_1 Complex (Respiratory Chain Complex III) • Ferredoxin • Ferredoxin-$NADP^+$ Reductase • Green Bacteria: Secondary Electron Donor (Cytochromes) • Green Bacteria: The Light-Harvesting Chlorosome

Glossary

energy transfer The transfer of the excitation energy among pigment molecules by the Förster–Dexter mechanism.

FMO protein The water soluble BChl *a* protein occurring in GSB, characterized by Fenna, Mathews, and Olson; it was the first chlorophyll protein elucidated by X-ray crystallography.

photosynthetic unit The total of pigment molecules associated with one reaction center, and is synonymous to "photosystem."

Q-type and FeS-type RCs RCs are distinguished according to their terminal electron acceptors, which are either quinones or FeS clusters; since the RCs of plant PSI is of the FeS-type and of PSII is of the Q-type, the synonymous denotations type-1 and type-2 are also in use.

Further Reading

Ben-Shem, A. *et al.* (2004). Evolution of photosystem I – from symmetry to pseudosymmetry to asymmetry. *FEBS lett.*, **564**(3): 274–280.

Blankenship, R. E., Madigan, M. T., and Bauer, C. E. (eds.) (1995). *Advances in Photosynthesis*, *Vol 2*, *Anoxygenic Photosynthetic Bacteria*. Kluwer Academic, Dordrecht, The Netherlands.

Bryant, D. A. (1994). Gene nomenclature recommendations for green photosynthetic bacteria and heliobacteria. *Photosynth. Res.* **41**, 27–28.

Friegaard, N.-U., Chew, A.G.M., Li, H., Maresca, J.A., and Bryant, D.A. (2003). *Chlorobium tepidum*: Insights into the structure, physiology, and metabolism of a green sulfur bacterium derived from the complete genome sequence. *Photosynth. Res.* **78**, 93–117.

Hauska, G., Schoedl, T., Remigy, H., and Tsiotis, G. (2001). The reaction center of the green sulfur bacteria. *Biochim. Biophys. Acta* **1507**, 260–277.

Heathcote, P. (guest editor) (2001). Type I photosynthetic reaction centers (Special issue). *Biochim. Biophys. Acta* **1507**, 1–310.

Permentier, H. P., Schmidt, K.A., Kobayashi, M., Akiyama, M., Hager-Braun, C., Neerken, S., Miller, M., and Amesz, J. (2000). Composition and optical properties of the recation centre complexes from the green sulfur bacteria *Prosteocochloris aestuarii* and *Chlorobium tepidum*. *Photosynth. Res.* **64**, 27–39.

Remigy, H.-W., Stahlberg, H., Fotiadis, D., Muller, S.A., Wolpensinger, B., Engel, A., Hauska, G., and Tsiotis, G. (1999). The reaction center complex from the green sulfur bacterium *C. tepidum*: A structural analysis by scanning transmission electron microscopy. *J. Mol. Biol.* **290**, 851–858.

Remigy, H.-W., Hauska, G., Müller, S.A., and Tsiotis, G. (2002). The reaction centre from green sulfur bacteria: Progress towards structural elucidation. *Photosynth. Res.* **71**, 91–98.

Schütz, M., Brugna, M., Lebrun, E., Baymann, F., Huber, R., Stetter, K.O., Hauska, G., Toci, R., Lemesle-Meunier, D., Tron, P., Schmidt, C., and Nitschke, W. (2000). Early evolution of cytochrome bc complexes. *J. Mol. Biol.* **300**, 663–675.

Seo, D., and Sakurai, H. (2002). Purification and characterization of ferredoxin-$NAD(P)^+$ reductase from the green sulfur bacterium *Chlorobium tepidum*. *Biochim. Biophys. Acta* **1597**, 123–132.

Theissen, U. Hoffmeister, M., Grieshaber, M., and Martin, W. (2003). Single eubacterial origin of eukaryotic sulfide: Quinone oxidoreductase, a mitochondrial enzyme conserved from early evolution of eukaryotes during anoxic and sulfidic times. *Mol. Biol. Evol.* **20**, 1564–1574.

Biography

Günter Hauska is a Professor of Cell Biology and Plant Physiology at the Institute of Botany, in the Department of Biology at the University of Regensburg, Germany. He obtained his Ph.D. in chemistry at the University of Vienna in 1967. Subsequently he served as postdoctoral fellow in the biochemistry department of the Cornell University before qualifying as Dozent for biochemistry at the Ruhr-Universität in Bochum, Germany. His research interest is in energy transduction by membrane protein complexes of electron transport chains, especially in quinol oxidation by cytochrome *bc* complexes and in photosynthetic reaction centers. His recent interest has been in flavoproteins. He is a member of the German Society for Biochemistry and Molecular Biology.

Thomas Schödl graduated from the University of Regensburg and finished his Ph.D. in biochemistry. He is studying the structure and redox reactions of flavoproteins, in particular of sulfide quinone reductases from bacteria and eukaryotes.

G_s Family of Heterotrimeric G Proteins

Susanne M. Mumby
University of Texas Southwestern Medical Center, Dallas, Texas, USA

Members of the G_s family of heterotrimeric G proteins stimulate the activity of the adenylyl cyclase enzyme. This enzyme is responsible for producing the intracellular second-messenger, cyclic AMP (cAMP), which in turn triggers a cascade of biochemical changes that ultimately bring about an alteration in cellular behavior.

G Protein-Mediated Signal Transduction

In order to function and survive, cells must respond to signals in their environment including chemical messengers dispatched from other parts of the body (such as hormones and neurotransmitters) and external stimuli (such as light and odorants). Typically, messengers do not enter target cells, but instead they are transduced by conveyance of information through intermediaries that form a chemical switchboard (Figure 1). This is a common biological strategy to regulate cellular behavior.

A major form of signal transduction is initiated at the plasma membrane by G protein-coupled receptors that function as antennas or discriminators (Figure 1). The process of signal transduction is initiated by binding of a primary messenger (an agonist, such as a hormone or neurotransmitter) to a specific receptor at the cell surface. The stimulated, transmembrane receptor activates the G protein, which is tucked just inside the plasma membrane. The G protein in turn modulates the activity of an effector (such as an enzyme or ion channel) that performs as an amplifier to produce second-messengers inside the cell. Second-messengers trigger a specific cascade of additional biochemical events, that cause a change in behavior characteristic of a particular cell type.

G proteins are heterotrimeric in structure, composed of α-, β-, and γ-subunits, but are usually defined by the identity of their α-subunits. Sixteen distinct genes encode α-subunits in mammals and 20 or more proteins are synthesized through alternative splicing of mRNA. The family of α-subunits is commonly divided into four subfamilies based on their amino acid sequence, which roughly correlates with their function: G_s, G_i, G_q, and G_{12}. The G_s subfamily is comprised of proteins named G_s and G_{olf}. Members of the G_s subfamily stimulate adenylyl cyclase, an enzyme that catalyzes the conversion of ATP to the second-messenger, cyclic AMP (cAMP).

Discovery

Appreciation of G protein-mediated signal transduction began with the characterization of hormone-sensitive adenylyl cyclase. The model that evolved for regulation of adenylyl cyclase proved to be the general paradigm for a large number of signaling pathways and impelled the award of the 1994 Nobel Prize in Medicine or Physiology to Rodbell and Gilman. Rodbell first promulgated the notion of a transducer acting as an intermediary between receptors and adenylyl cyclase. He and his colleagues established that receptor agonist (first messenger) was not sufficient to activate the enzyme, but in addition the guanine nucleotide, GTP, was required. Gilman and colleagues purified the first G protein, G_s, by reconstituting hormone-stimulated adenylyl cyclase activity in membranes from a mutant cell line lacking the G protein. Later, an additional G protein, G_i (a member of a distinct family of G proteins), was discovered to transduce negative regulation from inhibitory receptors (such as the muscarinic receptor) to adenylyl cyclase, as depicted in Figure 2. G_i and other families of heterotrimeric proteins are described in additional articles within this volume.

Regulation of G Proteins by Guanine Nucleotides

G proteins are so named because they bind guanine nucleotides. Figure 3 shows a current model for the

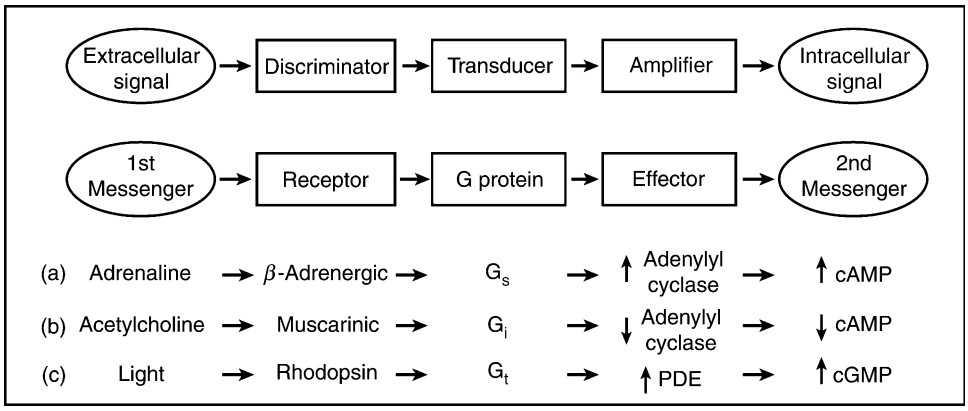

FIGURE 1 Relay diagram of G protein signaling. Line 1 is based on Rodbell's early concept of informational processing, which is restated in biochemical terms in line 2. The lettered subheadings below line 2 are specific examples of signaling relays for hormone sensitive adenylyl cyclase and the visual transduction systems. The horizontal arrows indicate the direction of the flow of information. The upward pointing arrows indicate increases in effector activity or levels of second messenger. The downward pointing arrows indicate decreases in effector activity or levels of second messenger. Reprinted from Mumby, S.M. (2000). G proteins I: G_s and G_i. In *GTPases* (A. Hall, ed.) pp.1–27. With permission of Oxford University Press, New York.

mechanism of G protein-mediated signal transduction in which nucleotide-driven conformational changes in the α-subunit drive interactions with an upstream receptor or downstream effector. Two cycles are superimposed in this model: GTP binding/hydrolysis and subunit dissociation/reassociation. In the basal state, (Figure 3A) the ligand-binding site of the receptor is unoccupied, the three G-protein subunits form an oligomer, and GDP is bound to the α-subunit. Activation is triggered when agonist binds to the receptor, which acts as a guanine nucleotide exchange factor (Figure 3B). The liganded receptor binds to its cognate G protein and promotes release of GDP from Gα (the rate limiting step), thus allowing this subunit to bind the more abundant guanine nucleotide in the cell, GTP. A conformational change in Gα accompanies binding of GTP and leads to the dissociation of Gα from receptor and the high-affinity complex of β- and γ-subunits (Figure 3C). These liberated subunits are competent to modulate the activity of effectors. In the example shown in Figure 3C, α-GTP interacts with the effector (although $\beta\gamma$ also can modulate some effectors). The intrinsic GTPase activity of Gα acts as a molecular clock to terminate the signal by returning this subunit to the inactive GDP bound state with increased affinity for G$\beta\gamma$. Reassociation of Gα-GDP with G$\beta\gamma$ restores the system to the basal state to await a new cycle of activation.

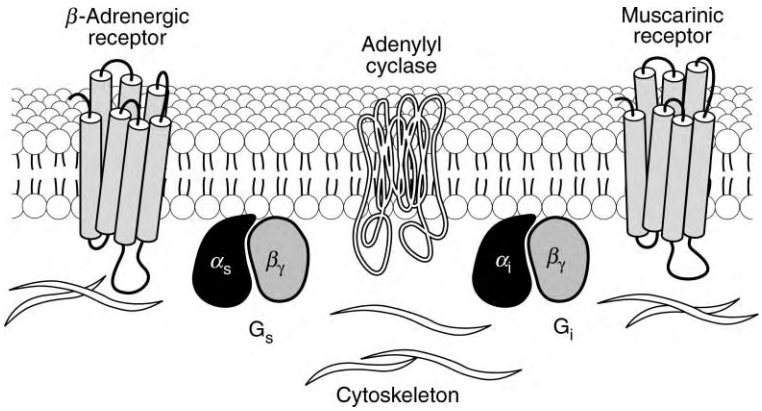

FIGURE 2 Schematic view of plasma membrane components that participate in the hormone-sensitive adenylyl cyclase system. G protein-coupled receptors have a similar structure that includes seven putative transmembrane helices and regions of homology in the cytoplasmic loops. Lipid modifications (not shown) promote interactions of G proteins with the inner surface of the plasma membrane. Adenylyl cyclases presumably span the membrane twelve times, with the active site oriented on the cytoplasmic side of the membrane. Reprinted from Mumby, S. M. (2000). G proteins I: G_s and G_i. In *GTPases* (A. Hall, ed.) pp.1–27. With permission of Oxford University Press, New York.

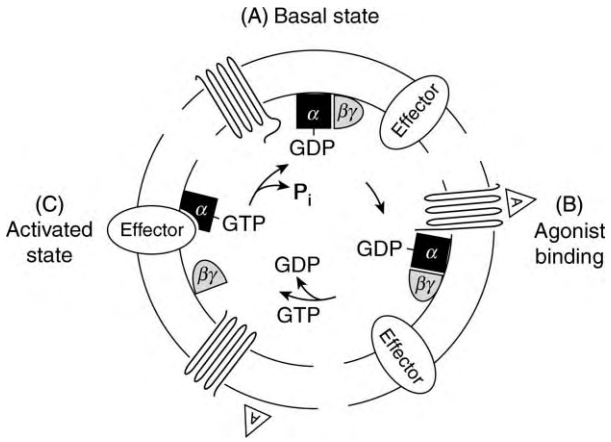

FIGURE 3 Simple mechanistic model of G protein-mediated signal transduction. The circular parallel lines represent the plasma membrane. The receptor is represented by the serpentine lines spanning the membrane seven times and agonist is shown as the letter A surrounded by a triangle. The two superimposed cycles of GTP-binding/hydrolysis and G protein subunit dissociation/reassociation described in the text. Reprinted from Mumby, S. M. (2000). G proteins I: G_s and G_i. In *GTPases* (A. Hall, ed.) pp.1–27. With permission of Oxford University Press, New York.

Members of the Family

Members of the G_s family include various isoforms of G_s and G_{olf} (listed in Table I). The hallmark of these proteins is that they stimulate the activity of adenylyl cyclase. This stimulation increases the production of cAMP, which is an important second-messenger for many physiological processes including growth and development, regulation of the force and rate of cardiac contraction, learning and memory, perception of odorants and endocrine functions including those of the thyroid, pituitary, and parathyroid glands. Table II lists a sampling of physiological processes that are regulated by members of the G_s family.

$G\alpha_S$

The Long and Short of it

G_s is a ubiquitous G protein. Variations in splicing of G_s mRNA leads to the production of short and long isoforms of αs, which are both produced in most cell types. The relative proportions of the variants change under a wide range of metabolic conditions such as cellular differentiation, development, aging, and various adaptive processes. The physiological explanation for existence of multiple isoforms is not known. Functional differences have been reported for cells or isolated membranes that display different proportions of short and long $G\alpha_s$, but it is not known if additional differences in the samples also may have influenced functional output. *In vitro* experiments with purified proteins have documented that long and short isoforms vary in their relative rates of GDP dissociation and specificity of interaction with different combinations of $\beta\gamma$ isoforms.

$G\alpha_sXL$

Alternative promoter usage and splicing of mRNA produces an extra long form of $G\alpha s$. Conventional $G\alpha_s$ shares exon 2–13 with $G\alpha_sXL$. Exon 1 encodes 47 residues for conventional α_s compared to 367 residues for $G\alpha_sXL$. The XL isoform is expressed in the Golgi complex and plasma membrane of neuroendocrine cells, suggesting a role for the protein in regulated secretion. $G\alpha_sXL$ does not interact with G_s-coupled receptors, but does bind $G\beta\gamma$ and can stimulate adenylyl cyclase.

$G\alpha_{olf}$

$G\alpha_{olf}$ is so named because it was originally considered to be strictly an olfactory-neuron-specific G protein involved in odorant signal transduction. $G\alpha_{olf}$ differs from the short splice variant of $G\alpha_s$ *a* in 80 amino acids, with the majority of the differences being localized in the

TABLE I

Properties of the Mammalian G_s Family of α-Subunits

Subfamily/subunit	Molecular mass (kDa)	Distribution in tissue	Representative receptors[a]
$G\alpha_{s(S)}$[b]	44	Ubiquitous	βAR
$G\alpha_{s(L)}$[b]	46	Ubiquitous	Glucagon, TSH
$G\alpha_sXL$[b]	94	Brain, adrenal, pituitary	Secretion?
$G\alpha_{olf}$	45	Olfactory neuroepithelium, brain, heart, pancreas, male germ cell	Odorant, D1, A2a

[a] Receptor abbreviations: βAR, β-adrenergic; TSH, thyroid-stimulating hormone; D1, dopamine, A2a, adenosine.
[b] Splice variations: $G\alpha_{s(S)}$ = short forms of $G\alpha_s$; $G\alpha_{s(L)}$ = long forms of $G\alpha_s$.

TABLE II

Sampling of Physiological Effects Mediated by G_s Family Members

Primary messenger	Cell type	G protein	Effect
Adrenaline (epinephrine)	Heart cells	G_s	Increased rate and force of contraction
Adrenaline, glucagon	Liver cells	G_s	Breakdown of glycogen
Adrenaline, glucagon	Fat cells	G_s	Breakdown of fat
Luteinizing hormone	Ovarian follicles	G_s	Increased synthesis of estrogen and progesterone
Antidiuretic hormone	Kidney cells	G_s	Conservation of water
Odorants	Neuroepithelial cells in nose	G_{olf}	Sensation of odorants

α-helical domain of the protein (domain structure described below). Studies with the $G\alpha_{olf}$ knockout mouse showed that this G protein is involved in the perception of floral, fruity, minty, and putrid odorants. These findings fit to data showing that such odorants activate adenylyl cyclase in olfactory cilia. Greater than 75% of the G_{olf} mutant mice are unable to nurse and die within 2 days after birth; surviving homozygous ones also exhibit hyperactive behaviors. This behavioral phenotype and additional data suggest that G_{olf} may also play an essential role more centrally in the brain. More thorough analysis of the expression of $G\alpha_{olf}$ suggests functions for this G protein in heart, pancreas, and male germ cell development as well.

Structure

Heterotrimeric G proteins are related to the so-called small GTPases, including Ras, Rho, Rab, Arf, and Ran. Although there is substantial sequence diversity among members of the GTPase superfamily, structural and biochemical studies have demonstrated a common core architecture that is embodied in Ras.

Nucleotide-Bound Protein

X-ray crystallographic structures of G proteins complexed with nucleotide reveal a Ras-like architecture with four inserted substructures. The largest insert is a helical domain connected to the Ras-like domain by two linkers (which are absent from Ras). The helical domain covers the nucleotide completely and prevents its release. By sequestering the nucleotide, the helical domain slows nucleotide release 5–50 fold compared with rates observed for Ras. The ligand-bound receptor is likely responsible for separation of the two domains to allow release of GDP, entry of GTP, and activation of the G protein. Although not present in the recombinant proteins used to generate crystal structures, lipids covalently modify the peptide backbone of G proteins *in vivo*.

Covalent Modifications

G-protein α-subunits are acylated at or near their amino termini by fatty acids, myristate and/or palmitate. These lipid modifications facilitate protein–protein and protein–membrane interactions of $G\alpha$. G_s is the only α-subunit that is known to be modified by palmitate through two different linkages: via a thioester bond (reversible and common to most α-subunits) and via a stable amide at the amino terminal glycine residue (unique). The turnover of palmitate in the thioester linkage is regulated by a receptor agonist. The presence of this palmitate residue is thought to regulate interaction of $G\alpha_s$ with lipids and certain proteins present in cellular membranes.

Many G proteins are modified by ADP-ribosylation, which is catalyzed pathologically by the action of toxins. Cholera toxin selectively modifies the multiple forms of $G\alpha_s$ on a particular arginine residue (201 in the numbering of the long form of $G\alpha_s$). This modification irreversibly inhibits the GTPase activity of $G\alpha_s$, thus locking the protein in an active form.

G_s Dysfunction in Human Disease

Either activating or inactivating defects in G-protein α-subunits can give rise to diseases in humans. Examples of G_s-associated pathology include the effects of bacterial toxins and genetic mutations.

Cholera

The activity of $G\alpha_s$ is increased in intestinal epithelial cells of patients with secretory diarrhea caused by infection with *Vibrio cholerae*. The bacteria secrete an oligomeric protein exotoxin composed of an A subunit and five B subunits. The B oligomer is responsible for toxin binding to the cell surface. Following entry into the cell and processing by proteolysis and reduction, the A component catalyzes the ADP ribosylation of $G\alpha_s$ to drastically reduce GTPase activity. The persistent production of cAMP that ensues ultimately leads to

the devastating fluid and electrolyte loss that causes the diarrhea.

Genetic Mutations

Pseudohypoparathyroidism

Pseudohypoparathyroidism (PHP) is a dramatic example of decreased G_s function. For one subtype of the disease, PHP 1a, affected subjects show resistance not only to parathyroid hormone but also to several other hormones such as thyroid-stimulating hormone and gonadotropins whose actions are mediated by receptors coupled to G_s. Affected individuals also show phenotypic features including obesity, short stature, and skeletal abnormalities, which are collectively called Albright hereditary osteodystrophy.

McCune–Albright Syndrome

The McCune–Albright syndrome is characterized by hyperfunction of one or more endocrine glands (pituitary somatotrophs, adrenal cortex, thyroid, and gonads) coupled with cafe-au-lait skin hyperpigmentation and bone deformity (polyostotic fibrous dysplasia). Missense mutation of arginine 201 (the site of ADP ribosylation by cholera toxin) is one of the constitutively activating mutations identified in patients with McCune–Albright syndrome. Patients express mutations in a mosaic pattern that correlates with the cellular abnormalities observed. The spectrum of affected tissues may be determined by the time in development that the mutations occur. Timing may range from early in embryogenesis leading to a wide distribution with pleiotropic, potentially severe manifestations to those occurring as later monofocal events and leading to localized manifestations such as growth hormone-secreting pituitary tumors.

Tumors

A subset of pituitary adenomas are characterized by elevated cAMP levels and growth hormone (GH) production. Cells from these tumors are relieved of the requirement for GH-releasing hormone to stimulate adenylyl cyclase, growth hormone secretion, and proliferation of normal pituitary somatotrophs. In some GH-releasing hormone independent tumors, $G\alpha_s$ is constitutively activated by a point mutation in either of two residues: arginine 201 (the ADP-ribosylation site) or glutamine 227, which is equivalent to glutamine 61 of Ras, a frequent site of GTPase-inhibiting mutations in the Ras proteins. Some autonomously functioning thyroid adenomas have similar mutations.

See Also the Following Articles

Adenylyl Cyclases • G_{12}/G_{13} Family • G_i Family of Heterotrimeric G Proteins • G_q Family • Ras Family • Small GTPases

Glossary

effector Intracellular second-messenger-producing enzyme or ion channel.

G protein A heterotrimeric protein comprised of α-, β- and, γ-subunits that binds and hydrolyzes GTP and transduces signals from outside to the inside of the cell.

G_{olf} A heterotrimer composed of $G\alpha_{olf}$ and any isoforms of β- and γ-subunits.

G_s The heterotrimer composed of any isoform of $G\alpha_s$, β-, and γ-subunits.

GTPase An enzyme that binds and hydrolyzes GTP. The superfamily of GTPases includes "small" members such as Ras, as well as heterotrimeric G proteins.

receptor A plasma membrane-spanning protein that specifically recognizes an extracellular signal and when agonist is bound transmits information to the cell interior.

signal transduction Transmission of information from outside to inside a cell, thus causing a change in cellular behavior.

Further Reading

Farfel, Z., Bourne, H. R., and Irir, T. (1999). The expanding spectrum of G protein diseases. *New England J. Med.* **340**, 1012–1020.

Kaziro, Y., Itoh, H., Kozasa, T., Nakafuku, M., and Satoh, T. (1991). Structure and function of signal-transducing GTP-binding proteins. *Annu. Rev. Biochem.* **60**, 349–400.

Mumby, S. M. (2000). G proteins I: G_s and G_i. In *GTPases* (A. Hall, ed.) pp. 1–27. Oxford University Press, New York.

Neves, S. R., Ram, P. T., and Iyengar, R. (2002). G protein pathways. *Science* **31**, 1636–1639.

Sprang, S. R. (1997). G protein mechanisms: Insights from structural analysis. *Annu. Rev. Biochem.* **66**, 639–678.

Biography

Susanne M. Mumby is an Associate Professor in the Department of Pharmacology at the University of Texas Southwestern Medical Center at Dallas. She holds a Ph.D. in Biochemistry from the University of Washington and her principal research interests are in the structure and function of lipid modifications of signal-transducing G proteins. Dr. Mumby serves as director of the Antibody Laboratory of the Alliance for Cellular Signaling, a multi-institutional research collaboration to study and model G protein-mediated and related signaling systems (www.signaling-gateway.org).

Heat/Stress Responses

Davis T. W. Ng
Pennsylvania State University, University Park, Pennsylvania, USA

All cells from simple bacteria to highly differentiated animal cells maintain specialized mechanisms to monitor and respond to changes in their local environments. Unfavorable circumstances that threaten cellular homeostasis will elicit one or more *stress response* programs in an effort to preserve viability of the organism. The many forms of cellular stress include temperature variation, exposure to toxic compounds, oxidative and reductive stress, ionizing radiation, hypoxia, aging, mechanical injury, and the invasion of pathogens. Mounting the correct response can insure cell survival or initiate an apoptotic program depending on the severity of the stress. Stress responses are also activated in numerous disease states and deficient responses are etiological for afflictions including Parkinson's and Alzheimer's diseases. More recently, stress-regulated genes were intimately linked to aging and shown to be required for the extension of life in model organisms. As a general rule, stress responses remodel relevant cellular pathways to counteract specific effects of the insult.

The Stress of Unfolded Proteins

Proteins are the class of molecules that perform most cellular functions. First synthesized as chains of amino acids encoded by genes, nascent proteins must fold into their correct three-dimensional structures to be active. The folded state is labile and dependent on the thermodynamic nature of each molecule. Fully mature proteins are the product of unique amino acid sequences that specify numerous noncovalent interactions within each molecule. Abrupt changes can create unfavorable local environments that weaken such interactions or prevent their correct formation. Conditions that cause the unfolding or disrupt the proper synthesis of proteins are major forms of cellular stress. Left unchecked, the inherent toxicity of unfolded proteins or their loss of function could leave cells irreversibly damaged.

The Heat Shock Response

The first stress response to unfolded proteins was reported over forty years ago. Examination of fruit fly salivary chromosomes revealed morphological puffs along their lengths after treatment by heat, dinitrophenol, or sodium salicylate. Termed the heat shock response (HSR), it was later shown that the puffs signified activation of genes encoding heat shock proteins (Hsps). For virtually all organisms, exposure to 5–10°C above the optimal growth temperature leads to a robust HSR. Within the cell, an increase of this magnitude can have many deleterious effects including increased membrane fluidity and the partial unfolding of proteins.

Inputs

The HSR can be activated by a wide variety of conditions beyond temperature change. A few examples include exposure to ethanol, heavy metals, amino acid analogues, mechanical damage, and conditions of hypoxia, ischemia, and osmotic stress. As with temperature increases, these conditions are believed to increase the concentration of unfolded proteins. In addition, the nonstress conditions of cells undergoing rapid proliferation or differentiation also induce the HSR. Here, the physiological need is to boost the capacity for protein synthesis.

Stress Detection and Response

The HSR relies on the activity of "molecular chaperone proteins" to detect stress. Chaperones bind to unfolded proteins and facilitate folding by preventing inappropriate interactions. Chaperones also bind irreversibly misfolded proteins to neutralize their toxicity and promote their destruction. As stress conditions increase the concentration of unfolded proteins, the available pool of free chaperones diminishes. Specialized sensor proteins can detect the change and initiate a response. In the eukaryotic HSR (prokaryotes employ a different mechanism), the heat shock factor (HSF) plays both stress sensor and transcription activator for the response output. In metazoan organisms, the inert state of HSF is a monomer that is maintained through associations with the chaperones Hsp70, Hsp90, and Hsp40 (Figure 1). As the demand for chaperones increases, release from chaperone complexes permits conversion of HSF to a homotrimer (and translocation into the nucleus if found in the cytosol). This form of HSF can bind to heat shock

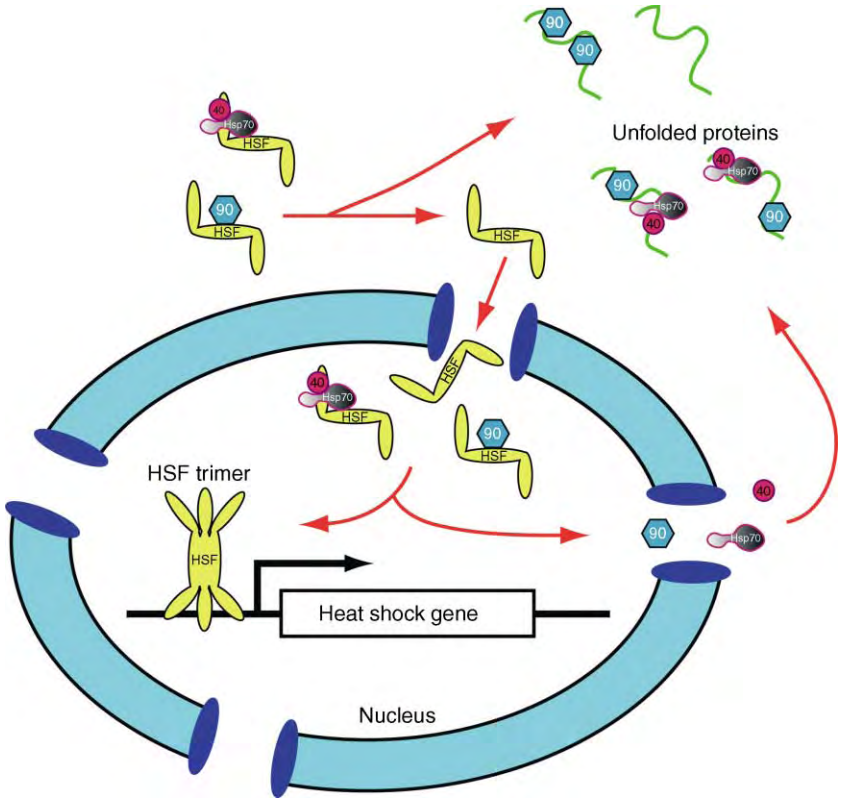

FIGURE 1 Activation of the HSR is a multistep mechanism. The increase of unfolded proteins stimulates the binding of cytosolic chaperones and reduces the free chaperone pool (upper right, Hsp90 and Hsp40 proteins labeled "90" and "40," respectively). The reduction in chaperone binding to HSF monomers promotes assembly into HSF trimers (and nuclear localization of cytosolic HSF). Initial binding of trimeric HSF to heat-shock promoters is in the inert state. Transcriptional activation of the target gene requires HSF phosphorylation. In yeast, HSF is similarly regulated except that it always exists as a trimer.

elements of heat shock genes but does so in the inert state. Transcriptional activation requires HSF phosphorylation and a conformational change. Subsequently, a dramatic but transient rise in the synthesis of Hsps is accompanied by a reduction in overall protein synthesis.

The HSR Output

Protein Repair and Preservation

The most notable output of the HSR is the induction of chaperone genes. Chaperones are well adapted to resist stress. Beyond their established role in the folding of most newly synthesized proteins, direct biochemical analyses have shown that some chaperones disaggregate and refold misfolded proteins. Organisms harboring mutations in chaperone genes are less tolerant to various forms of stress. Taken together, the evidence supports the view that chaperones protect cells from stress by maintaining the folded states of proteins and repairing those that are damaged.

Degradation of Aberrant Proteins

Since they can be toxic, damaged proteins that cannot be repaired must be destroyed. Fittingly, the HSR regulates key factors of protein degradative pathways. For example, another facet of chaperone function is their requirement in the degradation of misfolded proteins. In eukaryotes, offending proteins are conjugated with ubiquitin, a highly conserved 76 amino acid protein. Poly-ubiquitin chains serve as signals for the 26S proteasome, which degrades the attached protein. The factors responsible for the recognition and modification of substrates belong to two large enzyme families that include the ubiquitin conjugating enzymes (E2s) and the ubiquitin ligases (E3). The role of protein degradation pathways in stress tolerance is well established. For example, yeast strains that lack two heat shock genes, *UBC4* and *UBC5* (E2s), are hypersensitive to elevated temperatures and other forms of stress. Recent studies have shown that increasing the cellular capacity to degrade damaged proteins is likely the major role of the HSR in stress tolerance.

The Environmental Stress Response

The development of DNA microarray technology has made analysis of whole genome expression patterns possible. The application of this technology revealed that the transcriptional output of the HSR is remarkably broad. Although the HSR has its own molecular signature, a large subset of its genes is regulated

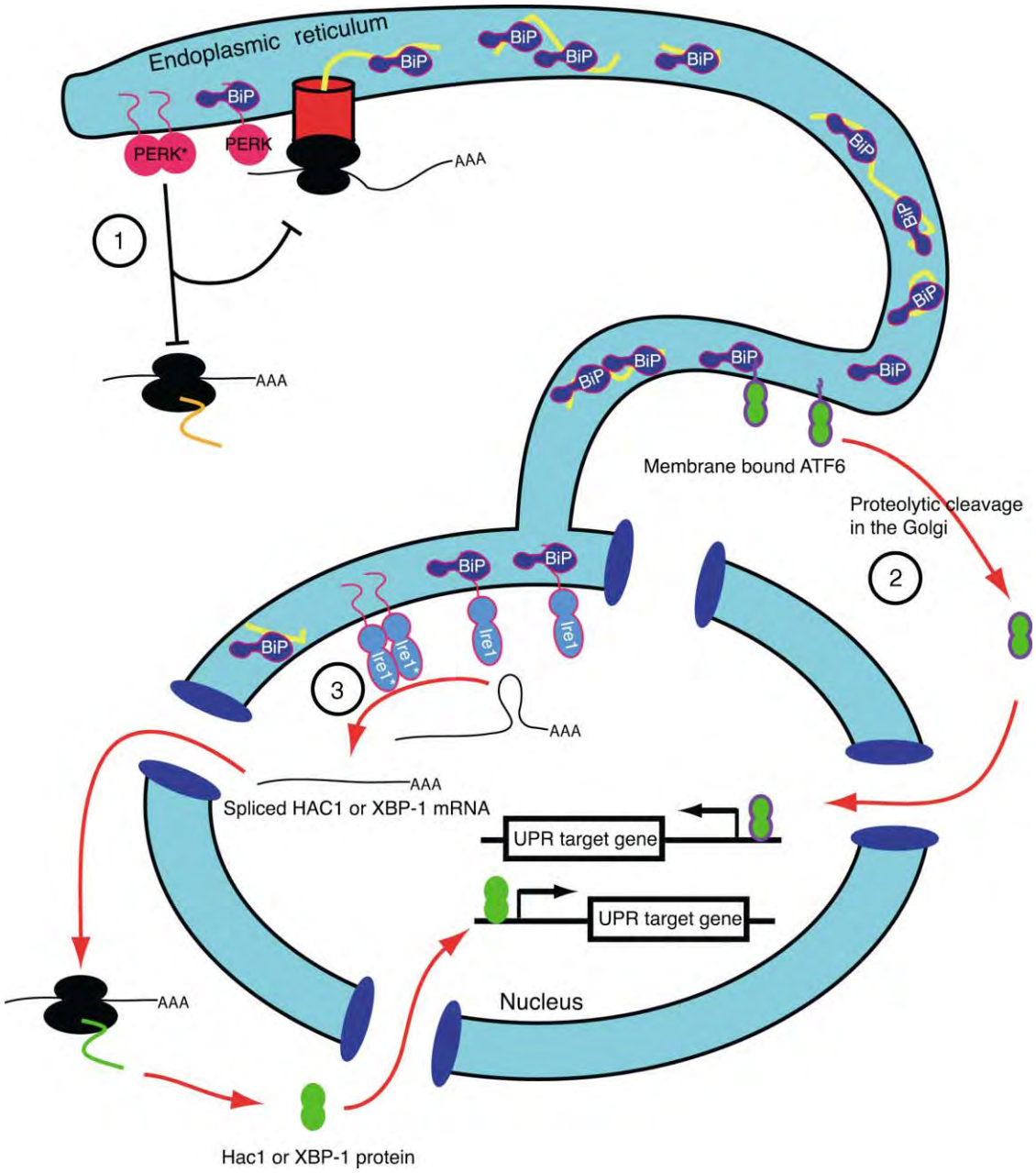

FIGURE 2 Activation of the UPR. The accumulation of unfolded proteins in the ER reduces the free pool of BiP and activates three distinct UPR sensor/transducers. (1) PERK dimers form following the reduction of BiP bound to their lumenal domains. Activated PERK phosphorylates eIF2α resulting in the temporary attenuation of general translation. (2) The reduction of BiP binding to ATF6 lumenal domains stimulates their relocalization to the Golgi apparatus where the transcription factor is released by intramembrane proteolysis. Soluble ATF6 translocates to the nucleus where it activates expression of a subset of UPR target genes. (3) The release of BiP derepresses Ire1 by promoting its dimerization and transphosphorylation. The activated ribonuclease domain cleaves introns of messages encoding UPR-specific transcription factors. Newly synthesized Hac1 (yeast) or XBP-1 (metazoans) activates the transcription of UPR target genes. In yeast, mechanism 3 is the only known UPR pathway. Asterisks indicate activated forms of enzymes.

similarly among disparate environmental stress conditions. These genes, comprising the environmental stress response (ESR), represent many stress-related functions and a variety of metabolic pathways. Thus, any specific stress response can be thought of as comprising the ESR plus additional outputs tailored to their specific circumstances.

The Unfolded Protein Response

The HSR primarily monitors the state of the cytosol and nucleoplasm. For the endomembrane system of the secretory pathway, the health of proteins in the endoplasmic reticulum (ER) is monitored by the unfolded protein response (UPR). Circumstances leading to ER

disequilibrium and activation of the UPR include exposure to reducing agents, incomplete protein glycosylation, glucose deprivation, excess nitrogen, calcium depletion, and proteasome dysfunction. The UPR is a signal transduction pathway that relays information on the condition of the ER lumen to regulatory networks of the nucleus and cytosol.

Stress Sensors and Transmembrane Signaling

As with the HSR, increasing unfolded proteins in the ER reduce the free pool of lumenal chaperones. However, since these chaperones are physically separated from downstream regulatory mechanisms, the UPR employs strategies distinct from the HSR to monitor stress. The key sensor, found in all eukaryotes, is Ire1 (Figure 2). Ire1 is a transmembrane protein with three functional domains. Binding of the ER chaperone BiP to the lumenal domain keeps Ire1 in the inactive monomeric state. Under stress, increased demand for BiP reduces its occupancy on Ire1. Free Ire1 dimerizes and activates two enzyme domains oriented to the cytosolic/nucleoplasmic side of the membrane. The kinase domain transphosphorylates Ire1, and the nuclease domain splices mRNAs encoding UPR-specific transcription factors. In budding yeast, splicing enables *HAC1* mRNA to be translated. In metazoans, the Ire1 target is *XBP-1*. Spliced *XBP-1* directs the expression of a functional UPR transcription factor that is larger and more stable from the version synthesized from the unspliced transcript. Metazoan organisms also have additional levels of UPR regulation. A membrane-bound transcription factor, ATF6 (α- and β-isoforms), is released by regulated intramembrane proteolysis upon ER stress. Soluble ATF6 then translocates into the nucleus to activate UPR target genes. A third sensor is the ER transmembrane protein PERK. Like Ire1, PERK contains a kinase that is regulated by BiP occupancy of its lumenal domain. By contrast, PERK targets the translation factor eIF2α under ER stress. Phosphorylation of eIF2α attenuates general translation.

Outputs of the UPR

The transcriptional program of the UPR shows functional similarities to the HSR but it is customized for the secretory pathway. Cells lacking an intact UPR are hypersensitive to ER stress. Under stress, such cells fail to properly fold and modify secretory proteins, trafficking functions are shut down, and misfolded proteins accumulate unabated. Accordingly, the UPR program is complex with nearly half the regulated genes having functions throughout the secretory pathway. Similar to the HSR, the deployment of chaperone proteins preserves the integrity of existing proteins, aids the folding of new proteins, and promotes the degradation of misfolded proteins. Misfolded secretory and membrane proteins are degraded by a specialized arm of ubiquitin/proteasome pathway called ER-associated protein degradation (ERAD). The ERAD pathway serves to recognize, translocate, and ubiquitylate proteins for degradation. Studies have shown that all levels of the ERAD pathway are regulated by the UPR and this regulation plays an essential role in ER stress tolerance. In metazoans, the three ER sensors appear to act coordinately to resist stress. The activity of PERK is the first line of defense. Activation of ATF6 is similarly rapid and precedes the mobilization of XBP-1. The available data indicate that key chaperone genes are ATF6-regulated while key genes of the ERAD pathway are regulated by XBP-1. Thus, a model has emerged (Figure 2) that has PERK rapidly attenuating general translation to decease the load of unfolded proteins in the ER. This gives the existing machinery in the ER an opportunity to begin restoring homeostasis. Those efforts are augmented by the increased synthesis of chaperone proteins directed by ATF6. If stress persists, the ERAD pathway is upregulated by the activity of XBP-1. This serves to clear those proteins that cannot be refolded in the initial response. In cells experiencing stress that cannot be ameliorated, ER-associated apoptotic pathways are activated to sacrifice afflicted cells.

See Also the Following Articles

Chaperones for Metalloproteins • Chaperones, Molecular • Chaperonins • Endoplasmic Reticulum-Associated Protein Degradation • Proteasomes, Overview • 26S Proteasome, Structure and Function • Secretory Pathway • Ubiquitin-Like Proteins • Unfolded Protein Responses

Glossary

endoplasmic reticulum First organelle of the secretory pathway. All secreted and resident proteins of the pathway are first synthesized in this membrane-bound compartment.

kinase Enzyme that transfers phosphate groups, usually from ATP, to target substrates. For protein substrates, phosphate is usually added to the hydroxyl group of serine, threonine, or tyrosine side chains.

molecular chaperone These molecules function by preventing inappropriate interactions of other molecules. Chaperones play many cellular roles including protein folding, protein translocation, signal transduction, and protein degradation.

proteasome Large multisubunit protein complex that degrades proteins modified by poly-ubiquitin.

transcription factor Proteins that regulate the synthesis of mRNA at gene promoter elements.

ubiquitin A highly conserved 76 amino acid protein that functions through covalent conjugation of proteins (either a target or another ubiquitin molecule) to lysyl side chains via an isopeptide bond. Ubiquitin plays roles in protein degradation, regulation of protein activity, and protein localization.

Further Reading

Glickman, M. H., and Ciechanover, A. (2002). The ubiquitin-proteasome proteolytic pathway: Destruction for the sake of construction. *Physiol. Rev.* **82**, 373–428.

Harding, H. P., Calfon, M., Urano, F., Novoa, I., and Ron, D. (2002). Transcriptional and translational control in the Mammalian unfolded protein response. *Annu. Rev. Cell Dev. Biol.* **18**, 575–599.

Morimoto, R. I. (1998). Regulation of the heat shock transcriptional response: Cross-talk between a family of heat shock factors, molecular chaperones, and negative regulators. *Genes Dev.* **12**, 3788–3796.

Parsell, D. A., and Lindquist, S. (1993). The function of heat-shock proteins in stress tolerance: Degradation and reactivation of damaged proteins. *Annu. Rev. Genetics* **27**, 437–496.

Patil, C., and Walter, P. (2001). Intracellular signaling from the endoplasmic reticulum to the nucleus: The unfolded protein response in yeast and mammals. *Curr. Opin. Cell Biol.* **13**, 349–355.

Spear, E., and Ng, D. T. W. (2001). The unfolded protein response: No longer just a special teams player. *Traffic* **2**, 515–523.

Biography

Davis Ng is an Associate Professor of Biochemistry and Molecular Biology at Pennsylvania State University, University Park. His research interests include cellular stress tolerance mechanisms, the quality control of protein folding, and the physiology of the unfolded protein response. He received his Ph.D. from Northwestern University and was a postdoctoral fellow at the University of California, San Francisco.

Hematopoietin Receptors

Barbara A. Miller and Joseph Y. Cheung
The Pennsylvania State University College of Medicine, Hershey, Pennsylvania, USA

Hematopoietin receptors comprise a superfamily of glycoproteins with structural similarities including single transmembrane spanning domains. They are activated by the binding of specific hematopoietic growth factors or cytokines, initiating a signaling cascade which results in stimulation of cell proliferation, differentiation, or enhancement of survival. Conserved domains in their extracellular region include cysteine pairs and a tryptophan-serine-x-tryptophan-serine (WSXWS) motif, which are important in ligand binding. Their cytoplasmic domains are diverse but have some limited similarities in membrane proximal regions known as box 1 and box 2. Box 1 and 2 are essential for transducing mitogenic signals, and for association with and activation of Janus family (JAK) kinases. No intrinsic kinase or enzyme motif has been identified in the cytoplasmic domains of hematopoietin receptor superfamily members. Instead, signal transduction through these receptors is regulated by their interaction with kinases of the JAK family, other cytosolic kinases, and protein messengers. Cytokine receptor signaling for all of these factors is initiated by ligand binding to the receptor, resulting in receptor oligomerization; some receptors form homodimers while others are active as hetero-oligomers. Following receptor oligomerization, the receptor-associated JAKs transphosphorylate, activating each other. They subsequently phosphorylate tyrosines on the associated receptor, which then serve as docking sites for other signal transducers including the signal transducer and activator of transcription (STAT) proteins, initiating a signaling cascade.

Classification

Members of the hematopoietin receptor superfamily, also referred to as the cytokine receptor superfamily, can be separated into Class I and Class II receptors based on structural features. Class I includes (1) receptors consisting of a single subunit which forms homodimers including those of erythropoietin, thrombopoietin, G-CSF, growth hormone, and prolactin; (2) receptors consisting of two subunits, a unique α-subunit and a common β-subunit including those of the IL-3 (GM-CSF, IL-5) family and IL-6 family; and (3) receptors for several interleukins which share the IL-2 γ-chain and consist of two to three subunits, α, β, and γ. A schematic representation of Class I hematopoietin receptors is presented in Figure 1. Class II consists of receptors for the interferons, interleukin-10, and tissue factor, important in coagulation. Soluble forms of cytokine receptors are formed by limited proteolysis of membrane-bound receptors or alternative mRNA splicing. These can form a complex with specific cytokines and act antagonistically or agonistically depending on the complex involved. A second group of receptors through which hematopoietic growth factors signal, unrelated to the hematopoietin receptor family, is called the receptor tyrosine kinase gene family. This group of receptors have intrinsic tyrosine kinase activity. Examples include c-kit, the receptor for stem cell factor which acts synergistically in culture with many other hematopoietic growth factors, and the M-CSF receptor, which is critical for monocyte/macrophage growth. This family will not be discussed here. Representative members of the hematopoietin receptor family will be presented as model systems for signaling of other members. Hematopoietin receptor family members share many intracellular signaling molecules, and exact mechanisms responsible for signaling specificity remain uncertain.

Single Subunit Hematopoietin Receptors

Erythropoietin Receptor

Expression

Erythropoietin (Epo) is the primary regulator of erythropoiesis and promotes the survival, proliferation, and differentiation of erythroid cells. Epo is synthesized primarily in the kidney, but also in the liver, and its level is regulated by the arterial oxygen tension. It mediates its effects by interaction with its receptor, Epo-R, a 66 kDa protein expressed on the surface of progenitor and precursor cells committed to the erythroid lineage. The essential function of Epo-R is demonstrated by the severe anemia and death at 11–15 days gestation following homozygous deletion of the Epo or Epo-R genes in mice. The earliest cell in the erythroid lineage, the burst-forming unit erythroid (BFU-E), has only low

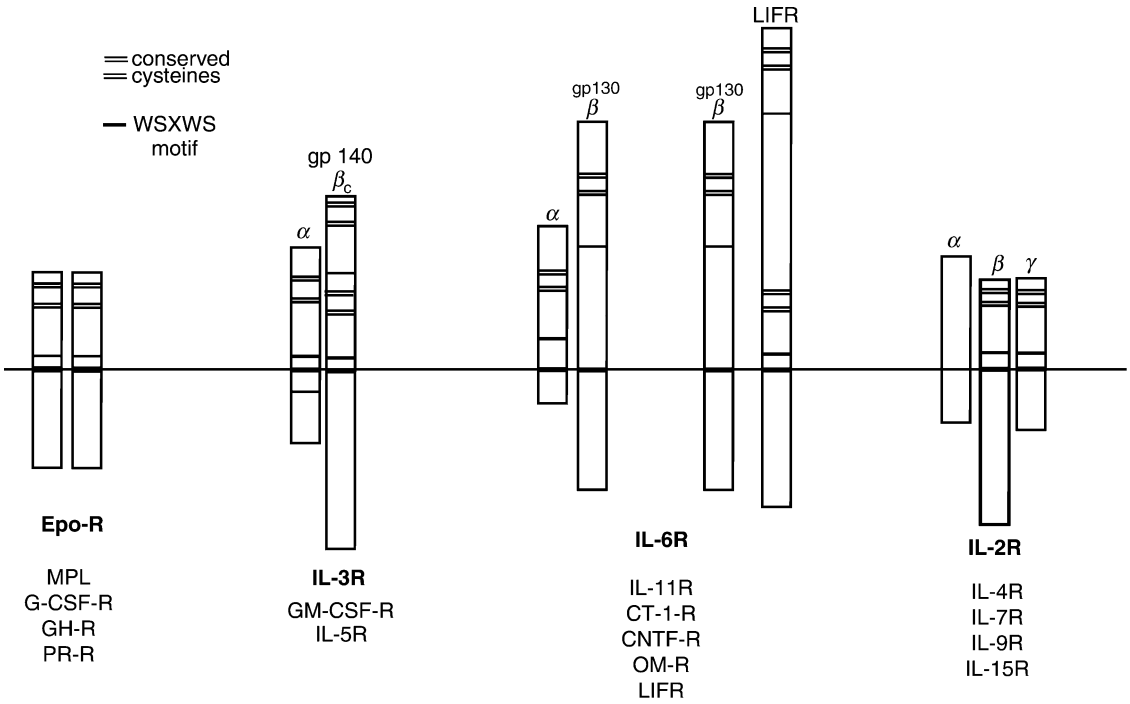

FIGURE 1 Class I hematopoietin receptor families. A schematic representation of the single-chain receptor (receptors for erythropoietin, thrombopoietin, G-CSF, growth hormone, and prolactin), multiple chain IL-3, IL-6, and IL-2 receptor families are shown.

numbers of Epo-R. Epo-R expression peaks at the later erythroid progenitor (colony-forming unit erythroid, CFU-E) and proerythroblast stage, followed by a decline during maturation to undetectable levels in mature erythroid cells. Epo-R is also expressed on megakaryocytes and several nonhematopoietic cells including endothelial cells, myoblasts, and neuronal cells. In these nonhematopoietic cells, the biological significance of receptor expression has not been clarified.

Signaling Pathways Activated by Epo

Epo-R consists of a single subunit which forms a homodimer in the presence or absence of Epo. Other members of the hematopoietin receptor family which form homodimers are receptors for thrombopoietin, G-CSF, growth hormone, and prolactin. These receptors transduce signals for a specific cytokine but do not cross react with other ligands of the same family. Epo binding results in a conformational change in Epo-R, allowing two JAK2, a tyrosine kinase associated with the cytoplasmic domain of Epo-R, to come into close proximity with each other. JAK2 is activated by transphosphorylation of its active site, and subsequently phosphorylates some or all of the eight tyrosine residues in the intracellular domain of Epo-R. The essential role of JAK2 in red blood cell production has been demonstrated in knockout mice. Phosphorylation of tyrosine residues on Epo-R provides docking sites for intracellular proteins to bind to Epo-R via SH2 domains, and many of these are then tyrosine phosphorylated. However, for both Epo-R and other hematopoietin receptors, the physiologic role of tyrosines in the cytoplasmic domain in regulation of proliferative, differentiating, and survival signals requires further definition. A representation of major signaling pathways activated following Epo-R stimulation are shown in Figure 2. One of the pathways activated by Epo is STAT5. STAT5 binds to phosphorylated Epo-R, and is phosphorylated by JAK2. Phosphorylated STAT5 dissociates from Epo-R and forms dimers through SH2-phosphotyrosine interactions. These dimers then translocate to the nucleus and bind specific promoter elements to activate expression of target genes. Epo-R activation by its receptor also results in activation of Ras through several pathways. Through a number of signal adapters and transducers including Grb2, Shc, GAB1, a Ras guanine nucleotide exchange factor called SOS, and/or a hematopoietic specific protein with Ras/GDP/GTP nucleotide exchange activity called Vav, Ras is activated by increased exchange of GDP with GTP. Epo stimulation also results in inhibition of GTPase-activating protein (GAP) by Epo-induced tyrosine phosphorylation. Following Ras activation, a downstream cascade proceeds including phosphorylation and activation of Raf-1, and of mitogen-activated protein kinases

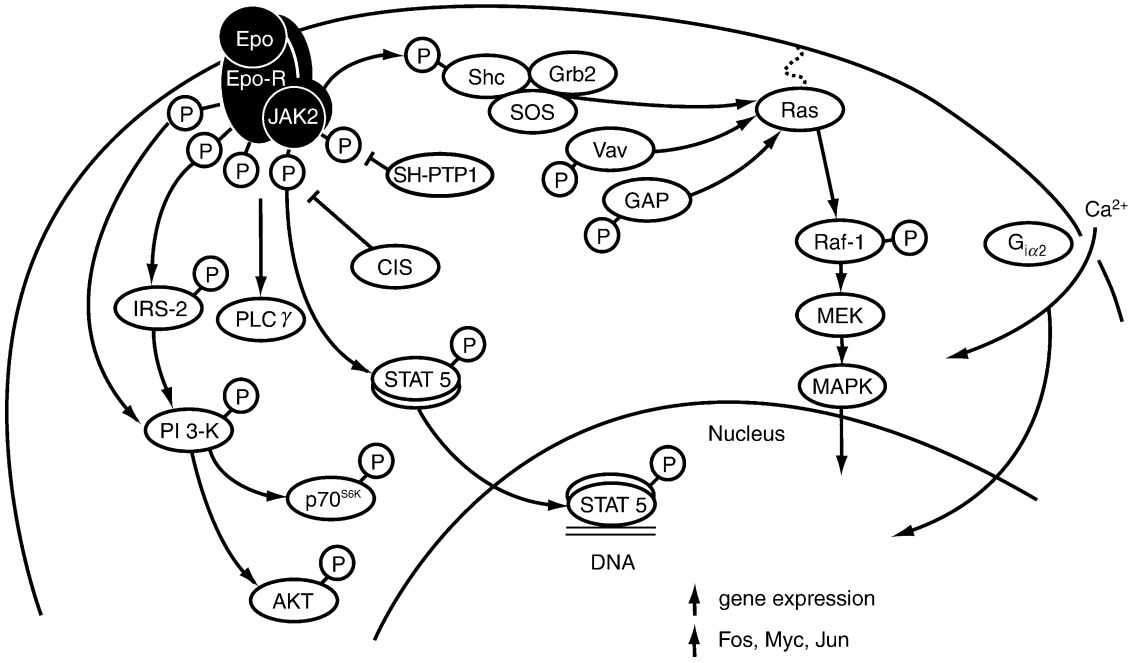

FIGURE 2 Pathways in erythropoietin receptor signaling. Erythropoietin binding leads to activation of associated JAK2 by autotransphosphorylation. Activated JAK2 phosphorylates tyrosines in the cytoplasmic region of Epo-R as well as associated proteins. This leads to activation of STAT5, Ras/Raf/MAPK, and PI 3-kinase pathways, leading to transcription and activation of genes involved in cell cycling, differentiation, and survival.

(MAPKs), with subsequent induction of immediate early genes including c-fos, c-myc, and c-jun. Phosphatidylinositol 3-kinase (PI 3-kinase) is another important kinase activated by Epo-R, either through direct association of the SH2 domain of the 85 kDa PI 3-kinase subunit with activated Epo-R or by binding to Epo-R through IRS-2 (insulin receptor substrate-2). PI 3-kinase can activate downstream targets including Akt, a kinase with important antiapoptotic activity, and $p70^{s6k}$, a kinase which phosphorylates ribosomal protein S6 and plays an important role in transcription, translation, and cell cycle progression. Ligand binding of Epo-R also results an increase in intracellular calcium, a universal second messenger, which influences many cell functions. Activation of tyrosine phosphorylation in erythroid cells is down-modulated by the hematopoietic protein tyrosine phosphatase SH-PTP1 (SHP1), which acts as a negative regulator. SH-PTP1 is recruited via its SH2 domains to tyrosine phosphorylated Epo-R, dephosphorylates JAK2 and terminates proliferative signals. Natural mutations in the negative regulatory region of cytoplasmic domain of Epo-R have been identified in benign erythrocytosis. Negative regulation is also mediated through suppressors of cytokine signaling (SOCS) proteins. One example is the SOCS protein CIS (cytokine-inducible SH2) containing protein, which may compete with STAT5 for binding sites on Epo-R and through this mechanism modify JAK/STAT signaling. CIS is also ubiquitinated and may promote Epo-R degradation. A number of other nonreceptor protein kinases, phosphatases, and phospholipases have also been shown to have important roles in Epo-R signal transduction, as well as additional adapters and transducers, including phospholipase Cγ, Cbl, and SHIP. Together, these pathways influence the expression and activity of a variety of proteins including transcription factors (GATA-1, NF-E2, SCL, NF-κB) and proto-oncogenes which participate in regulation of cell survival, proliferation, and differentiation.

Thrombopoietin Receptor

Expression

Thrombopoietin (Tpo) is the primary physiological hormone, which regulates all aspects of megakaryocyte and platelet development. Tpo interacts with its receptor, Mpl, on the cell surface of megakaryocyte precursors, mature megakaryocytes, and platelets to stimulate megakaryocyte progenitor proliferation and maturation, megakaryocyte polyploidy, and induction of platelet specific proteins. The biological activity of the Mpl receptor is not limited to the megakaryocytic lineage. Unlike Epo or G-CSF, thrombopoietin exerts profound effects on the proliferation of primitive hematopoietic cells through expression of Mpl on hematopoietic stem cells of all lineages.

Signaling Pathways Activated by Thrombopoietin

Upon binding of thrombopoietin to its receptor, Mpl, a number of signaling events are triggered which are very similar to those of activated Epo-R. Binding of thrombopoietin to Mpl induces the formation of an active dimer, enabling the associated JAK2 kinases to transphosphorylate each other. Activation of JAK2 results in phosphorylation of two of five tyrosines in the cytoplasmic region of Mpl. Proteins recruited to these sites include STAT3 and STAT5, Shc, Grb2, SOS, and Vav. Signaling pathways which are activated include those of Ras, MAPKs, and PI 3-kinase/Akt, as well as negative regulatory pathways through tyrosine phosphatases including SH-PTP1 and the SOCS family. The distinction between intracellular signals of Tpo which promote hematopoietic stem cell expansion versus megakaryocyte development and platelet production are unknown. Defective Mpl expression is thought to be the cause of congenital amegakaryocytic thrombocytopenia, a severe inherited thrombocytopenia in infants with absent megakaryocytes in bone marrow and severely low circulating platelet counts.

G-CSF Receptor

Expression

The receptor for G-CSF, G-CSF-R, regulates the proliferation and differentiation of myeloid progenitors to form neutrophilic granulocytes, enhances the effector functions of mature neutrophils, and promotes their survival. G-CSF-R is expressed on myeloid progenitor cells, mature neutrophils, monocytes, and platelets. G-CSF-R expression increases with neutrophil differentiation. G-CSF-R is also expressed on endothelial cells, where it is thought to induce proliferation as well as migration.

Signaling Pathways Activated by G-CSF

G-CSF-R binds G-CSF as a homodimer. Unlike the other single-chain cytokine receptors, G-CSF-R activates multiple JAK kinases including JAK1, JAK2, and TYK2. Once activated, the JAK kinases induce phosphorylation of receptor tyrosines, which become docking sites for multiple SH2-containing signaling proteins as well as STAT1, STAT3, and STAT5. Pathways activated by G-CSF-R include those leading to activation of Ras, and MAPKs. Negative regulation occurs through the phosphatase SH-PTP1 and through SOCs. Experiments with G-CSF-R lacking one or more of the four cytoplasmic tyrosines suggest that pathways which regulate proliferation, differentiation, or survival differ, and characterization of these differences has important implications for understanding disorders of granulopoiesis.

GM-CSF/IL-3/IL-5 Receptors

Expression

The granulocyte/macrophage colony-simulating factor (GM-CSF), interleukin-3 (IL-3), and IL-5 receptors are a subfamily of Class I hematopoietin receptors. They have unique ligand-binding alpha(α)-chains but share a common beta-chain (β_c), also called gp140. Many factors contribute to specificity in signaling between these receptors, and one of these is that they are differentially expressed. Both the GM-CSF-R and the IL-3R are expressed on hematopoietic stem cells, and on the progenitors/precursors of neutrophils, macrophages, erythrocytes, megakaryocytes, and eosinophils. The IL-3R is expressed earlier in myeloid development than the GM-CSF-R. IL-3 promotes the expansion of the $CD34^+$ multipotential hematopoietic progenitors to a greater extent than GM-CSF, and promotes the development of a greater range of lineages that GM-CSF including basophils and lymphoid cells. In contrast, IL-5R is restricted to expression in eosinophils, basophils, and mouse B cells.

Signal Transduction through the GM-CSF/IL-3/IL-5 Receptor

The common β_c-subunit does not bind ligand by itself. Instead, β_c executes two critical functions following ligand binding. It enhances the ligand-α receptor binding from a low-affinity to a high-affinity interaction, and it functions as a major signaling component. The α-chain may preassociate with β_c, but increased association occurs in the presence of ligand. Ligand binding increases oligomerization, creating clusters of 2 α and 2 β_c chains, the functional complex, or even larger complexes. Ligand binding facilitates formation of a disulfide linkage between α and β_c, not observed with the single-chain receptors. The β_c-subunit elicits many signaling events, although the α-chain is also required for signal transduction. There are eight tyrosine residues present on human β_c, and proteins with SH2-binding domains which bind to the phosphorylated tyrosine residues largely determine the function of different receptor regions. The membrane proximal cytoplasmic region of β_c constitutively or inducibly associates with JAK kinases, predominantly JAK2, and is involved in induction of proliferation. The mid region is necessary for promotion of viability, and the distal region is involved in growth inhibition. Receptor binding results in rapid activation/tyrosine phosphorylation of JAK2, the β_c, and other JAK substrates. Downstream pathways activated include multiple STATs (1,3,5,6), Src kinases, Ras, MAPKs, PI 3-kinase, and Akt. Differences in signaling which result in the stimulation of different lineages, and proliferation versus differentiation or survival signals are still being defined.

Receptors in the IL-6 Subfamily

Receptors for IL-6, IL-11, cardiotropin-1 (CT), ciliary neurotrophic factor (CNTF), oncostatin M (OM), and leukemia inhibitory factor (LIF) represent another Class I hematopoietin subfamily. They have major roles in hematopoiesis and in acute-phase and immune responses. They consist of a unique, ligand-binding α-subunit and a common β-chain called gp130, which oligomerize in response to ligand binding to initiate signaling. While gp130 is ubiquitiously expressed, the types of cells which respond to a specific IL-6 family cytokine is limited by the restricted and tightly regulated expression of the α-receptor subunit. IL-6R and IL-11R have their own α-subunits which complex with gp130, whereas other IL-6 subfamily cytokine receptor complexes signal through different combinations of gp130, LIFR, and OM-R. Similar to the common IL-3 β_c and the IL-2R γ-subunit, the shared gp130 subunit enhances the affinity of receptor binding and serves as a major signaling component. Like other members of the hematopoietin family, these receptors signal through JAK/STAT, Ras, MAPK, and PI 3-kinase cascades, and terminate or modulate signals through tyrosine phosphatases, the SOCS, and PIAS (protein inhibitors of activated STAT) proteins.

Receptors in the IL-2 Subfamily

The IL-2 family cytokines play a critical role in the development of the immune system and in modulation of lymphocyte activation. The IL-2 receptor subfamily includes receptors for IL-2, IL-4, IL-7, IL-9, IL-15, and IL-21, which share the γ-chain of IL-2R. Receptors for IL-4, IL-7, and IL-9 consist of two subunits, a unique α-subunit in addition to γ. Receptors for IL-2 and IL-15 have three subunits, a unique α-subunit and shared IL-2Rβ and γ. The α-subunit acts as the ligand-binding subunit, whereas the β- and γ-subunits function to enhance receptor affinity and in signal transduction. Many of the signal transducers utilized by these receptors are the same as for other hematopoietin receptors, except that this subfamily is one of the few to utilize JAK3. Mutations of γ have been shown to be the cause of X-linked severe combined immunodeficiency (SCID). All mutant receptors are defective in activation of JAK3.

The Class II Receptor Family

Interferons (IFN) receptors have been divided into several major groups including Type I (for IFN-αs, IFN-β, and IFN-ω), which are vital for cells to initiate an antiviral response; Type II (for IFN-γ and IL-10), which are involved in regulation of specific immune responses; and tissue factor, which is important in coagulation. The structure of type I IFN receptors is not yet fully understood. An example of type II receptors, IFN-γ binds to ligand binding IFNγR1 subunits, followed by recruitment of IFNγR2 subunits to initiate signal transduction events through activation of associated JAKs. The active IFN-γ receptor consists of two IFNγR1 and two IFNγR2 subunits. IFN receptors signal through distinct combinations of JAKs and STATs, although many of the pathways leading to specificity of response need to be defined.

See Also the Following Articles

Cytokines • JAK-STAT Signaling Paradigm • Mitogen-Activated Protein Kinase Family • Phospholipase C

Glossary

colony stimulating factor (CSF) A factor that stimulates hematopoietic progenitor/precursor cells. The prefix denotes the hematopoietic lineage stimulated by the factor, e.g., G-CSF stimulates granulocyte colony formation; GM-CSF stimulates granulocyte and macrophage/monocyte colony formation.

cytokine An extracellular signaling peptide or protein that mediates cell–cell communication, activating a signaling cascade after interaction with a cell surface receptor.

hematopoiesis The process of development of mature blood cells from stem cells or precursors cells committed to blood cell formation.

interleukin (IL) One of a number of secreted peptides or proteins, produced by lymphocytes or monocytes, that are involved in regulation of the immune system or leukocyte interactions. The number behind IL is the designation of that particular interleukin, e.g., IL-3.

Further Reading

Cheung, J. Y., and Miller, B. A. (2001). Molecular mechanisms of erythropoietin signaling. *Nephron* **87**, 215–222.

Geddis, A. E., Linden, H. M., and Kaushansky, K. (2002). Thrombopoietin: A pan-hematopoietic cytokine. *Cytokine Growth Factor Rev.* **13**, 61–73.

Heinrich, P. C., Behrmann, I., Haan, S., Hermanns, H. M., Muller-Newen, G., and Schaper, F. (2003). Principles of Interleukin (IL)-6-type cytokine signalling and its regulation. *Biochem. J.* **374**, 1–20.

Hermans, M. H. A., van de Geijn, G.-J., Antonissen, C., Gits, J., van Leeuwen, D., Ward, A. C., and Touw, I. P. (2003). Signaling mechanisms coupled to tyrosines in the granulocyte colony-stimulating factor receptor orchestrate G-CSF-induced expansion of myeloid progenitor cells. *Blood* **101**, 2584–2590.

Kotenko, S. V., and Pestka, S. (2000). Jak-Stat signal transduction pathways through the eyes of cytokine class II receptor complexes. *Oncogene* **19**, 2557–2565.

Lin, J.-X., and Leonard, W. J. (2000). The role of Stat5a and Stat5b in signaling by IL-2 family cytokines. *Oncogene* **19**, 2566–2576.

Reddy, E. P., Korapati, A., Chaturvedi, P., and Rane, S. (2000). IL-3 signaling and the role of Src kinases, JAKs, and STATs: A covert liaison unveiled. *Oncogene* **19**, 2532–2547.

Biography

Barbara A. Miller is Four Diamonds Professor and Vice-Chairman of Research in Pediatrics, The Pennsylvania State University College of Medicine, Hershey, Pennsylvania. Her major research interests are in hematopoietic proliferation and differentiation, and in abnormalities that result in leukemia. She holds an M.D. from the Pennsylvania State University College of Medicine and received postdoctoral training at Duke and Harvard Universities. Her research has focused on erythropoietin signal transduction.

Joseph Y. Cheung is Professor of Cellular and Molecular Physiology and Medicine, The Pennsylvania State University College of Medicine, Hershey, Pennsylvania. His major research interests are in regulation of calcium in cardiac and hematopoietic cells, and in exercise physiology. He received a Ph.D. from the Pennsylvania State University College of Medicine, an M.D. from Duke University, and postdoctoral training at Harvard University.

Heme Proteins

Johannes Everse
Texas Tech University Health Sciences Center, Lubbock, Texas, USA

The class of proteins known as heme proteins includes all proteins that contain a heme moiety as a prosthetic group, which may or may not be covalently bound to the protein. The class encompasses proteins with a wide range of functions. Based on their properties, they may be separated into the following three subclasses:

1. Proteins that bind oxygen reversibly. These proteins are designed to transport and/or store oxygen among or within various body tissues.

2. Proteins that bind oxygen and "activate" it. These proteins serve as enzymes, capable of catalyzing an extensive list of reactions. This group also includes the enzymes that react with hydrogen peroxide.

3. Proteins that are unable to bind oxygen, and serve as electron carriers or transporters.

Structural Properties of Heme Proteins

Heme proteins are strongly colored proteins, usually reddish-brown, which is due to the presence of the heme moiety. The heme moiety consists of a substituted protoporphyrin ring, containing a liganded iron atom. In many mammalian heme proteins, the protoporphyrin ring is protoporphyrin IX, shown in Figure 1. Chelated iron, whether ferrous or ferric iron, preferentially forms six liganded structures. In the heme proteins four of these ligands are formed with the nitrogen atoms of the four pyrroles in the protoporphyrin ring. The fifth ligand, often referred to as the proximal ligand, is formed by an amino acid residue of the protein. This residue is a histidine residue in the oxygen-carrying proteins – myoglobin and hemoglobin, where the bond with the oxygen molecule forms the sixth or distal ligand. In heme proteins that serve as enzymes, the fifth ligand may be formed by a histidine, cysteine, methionine, or tyrosine residue. In the electron-carrying cytochromes, both fifth and sixth ligands are occupied by amino acid residues.

Heme Proteins that Serve as Oxygen Carriers

Several heme proteins are specifically designed to bind oxygen reversibly. In higher animals these proteins are hemoglobin and myoglobin. The function of hemoglobin is to take up oxygen in the lungs, and transport it to the various tissues in the body. Myoglobin, present in muscle tissues, takes up the oxygen from the hemoglobin and stores it until it is needed for the production of ATP in the mitochondria.

One oxygen molecule binds to the iron atom of the heme moiety at the sixth position which is vacant in the deoxygenated form of these proteins. The nature of the Fe–oxygen bond has been the subject of many investigations, and is still a matter of some controversy. At the present time it appears that the properties of the oxygenated forms of hemoglobin and myoglobin are best explained by assuming that the bond between the oxygen molecule and the heme iron is a biradical bond, stabilized by d–p orbital overlap.

Myoglobin

Function

Myoglobin serves as an oxygen storage protein in muscle tissues, where it also aids in the diffusion of oxygen into the tissues. Together with the cytochromes, it is responsible for the red-brown color of muscle. The protein is abundant in the heart and skeletal muscles of animals; and it is especially abundant in the muscles of diving mammals, such as whales and seals, where a high capacity for the storing of oxygen is essential.

Structure

The protein is a monomeric heme protein, consisting of a single chain of 153 amino acids, and a non-covalently bound heme moiety. The structure is that of a compact, globular protein, consisting of eight helices, with the heme moiety located in a cleft formed between helices C, E, and F (Figure 2). The fifth ligand to the heme iron is donated by the imidazole nitrogen of histidine residue

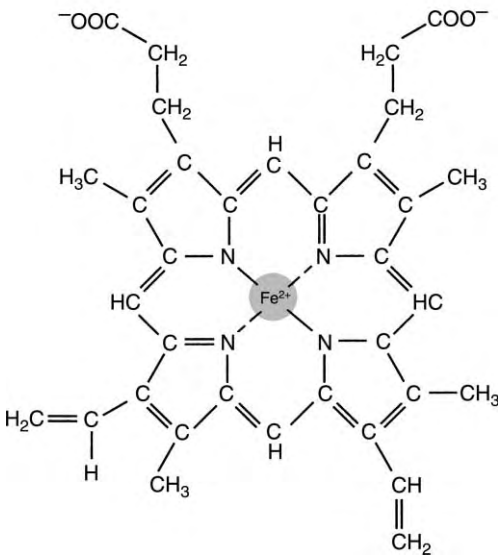

FIGURE 1 Chemical structure of iron-protoporphyrin IX (hemin).

F8 of the F helix. The sixth ligand is formed by the bound oxygen, whereas in deoxymyoglobin the sixth ligand is vacant.

The iron atom in myoglobin is in the ferrous state. Oxidation of the iron to the ferric form yields metmyoglobin, which is unable to bind oxygen, and is therefore no longer functional.

Oxygen Binding

Myoglobin has a high affinity for oxygen, as shown in Figure 3. This fact allows muscle tissues to extract oxygen from the bloodstream.

Hemoglobin

Structure

Hemoglobin is one of the most widely studied proteins. Its structure consists of four subunits, normally an $\alpha_2\beta_2$ tetramer, and each containing a heme moiety with the iron in the ferrous state.

Each α chain consists of 141 amino acid residues, and the β chains have 146 residues each. The three-dimensional structure of the individual subunits is very similar to that of myoglobin, although the amino acid compositions are very different.

Oxygen Binding

Allosteric Effects The tetrameric structure of the molecule is crucial to its biological function. Oxygen does not have a high affinity for deoxy-hemoglobin. However, binding of a molecule of oxygen to one of the hemes causes the Fe atom, which is normally located somewhat above the plane of the heme ring, to be drawn into the plane, a distance of 0.04 nm. This relatively slight movement triggers a change in the protein conformation that is transmitted to the adjacent subunits, which in turn dramatically enhances the affinity of their heme groups for oxygen. The result is that the oxygen saturation curve of hemoglobin has a sigmoidal form, as shown in Figure 3. This strong cooperative effect among the four subunits assures that almost total oxygenation occurs when the hemoglobin passes through the lungs, and that the oxygen is effectively released in the body tissues. A similar change in the position of the heme iron occurs in myoglobin upon the binding of an oxygen molecule; in myoglobin, however, this change in position appears to be non-consequential.

Bohr Effect The affinity for oxygen is also dependent on pH. Lower pH decreases the affinity for oxygen. This is known as the Bohr effect. This effect causes a better unloading of the oxygen in tissues with a high metabolic rate. Such tissues usually have a lower pH, because of the presence of acidic products, such as lactate, citrate, and malate.

Regulation by 2,3-Diphosphoglycerate Oxygen binding to hemoglobin is also regulated by the metabolite 2,3-diphosphoglycerate (2,3-DPG). 2,3-DPG is present in erythrocytes at a concentration similar to that of hemoglobin. Hemoglobin binds one molecule of 2,3-DPG per tetramer. Its regulatory effect on oxygen binding by hemoglobin is most evident when there is a change in altitude. At higher altitudes, where the partial pressure of oxygen is lower, 2,3-DPG binding compensates by shifting the oxygen saturation curve to the right.

Interaction with Other Compounds

In addition to oxygen, other compounds bind to the heme iron of hemoglobin and myoglobin, Among them are the notorious compounds carbon-monoxide and cyanide. Both compounds bind to the heme iron much more strongly than oxygen, thus preventing oxygen from binding. This is the basis for the high toxicity of these compounds, even at low concentrations.

Methemoglobin Formation

The oxygen in oxy-hemoglobin promotes a spontaneous oxidation of the ferrous hemoglobin to ferric hemoglobin or methemoglobin, which is unable to bind oxygen. During this reaction the oxygen is reduced to the superoxide radical, which subsequently dismutates to hydrogen peroxide:

$$\text{Hemoglobin-Fe}^{++} + O_2 \rightarrow \text{Hemoglobin-Fe}^{+++} + O_2^{-\cdot}$$

$$2O_2^{-\cdot} + 2H^+ \rightarrow O_2 + H_2O_2$$

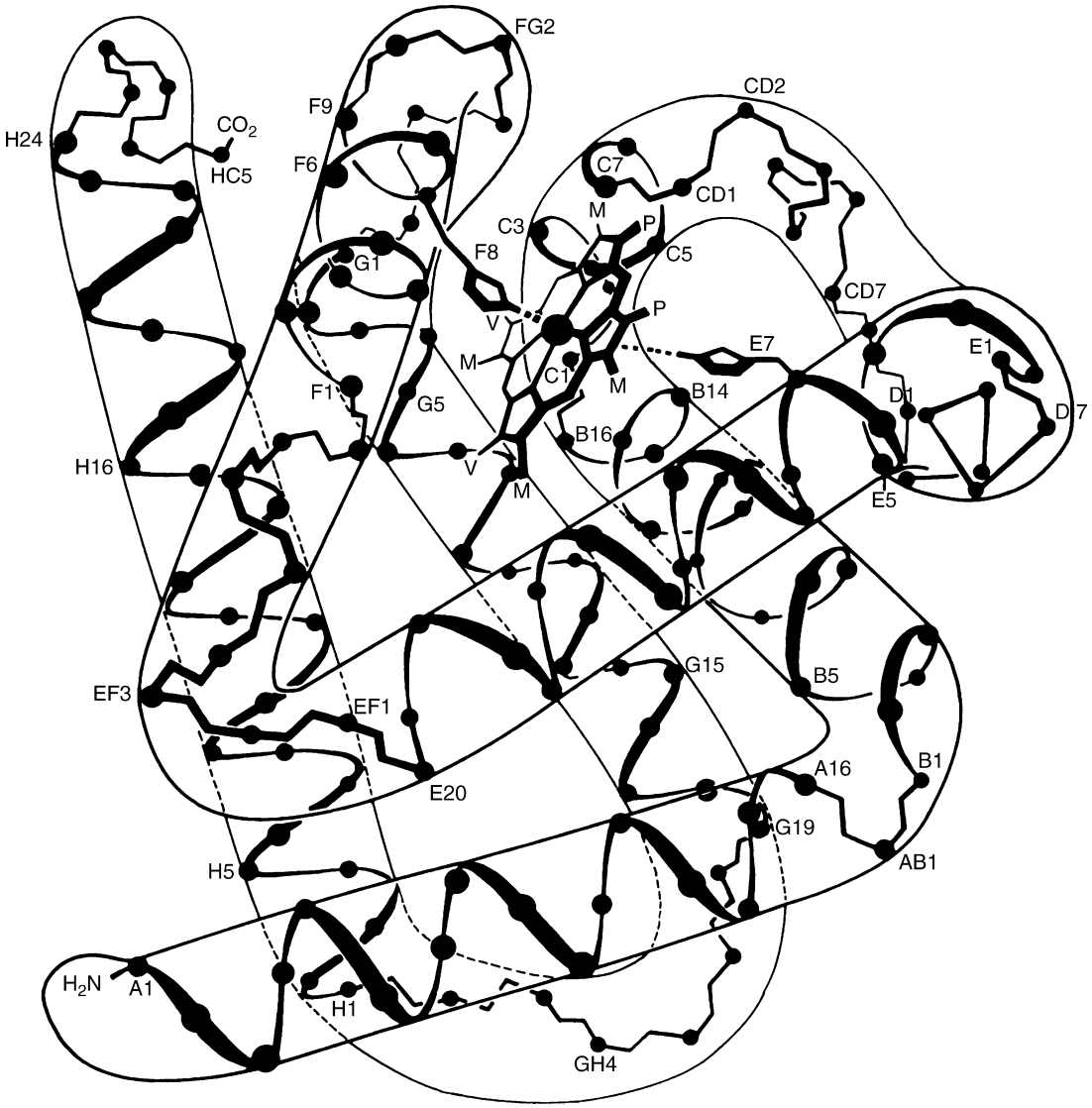

FIGURE 2 Molecular structure of myoglobin. The polypeptide chain consists of eight helices, designated by the letters A through H, linked by short, unordered regions. Amino acids are numbered by their relative position in the chain. Reprinted form Dickenson, R. E. *The Proteins*, 2nd Edition, Vol. II, p. 634, 1964, with permission from Elsevier.

Fortunately, an enzyme present in red cells, methemoglobin reductase, reduces the methemoglobin back to normal hemoglobin, whereas catalase, which is also abundant in erythrocytes, catalyzes the dismutation of hydrogen peroxide to oxygen and water. This mechanism, together with the fact that the oxidation to methemoglobin is rather slow, assures that under normal conditions the amount of methemoglobin present in the red cell is only a few percent of the total hemoglobin present.

Hemoglobin Mutants

Fetal Hemoglobin A large number of mutant hemoglobins are known to exist, most of which are harmless modifications. Several, however, are of physiological importance. Most important among them is fetal hemoglobin or hemoglobin F (HbF), which contains two γ chains instead of two β chains. Its tetrameric constitution is thus $\alpha_2\gamma_2$, instead of the $\alpha_2\beta_2$ configuration of normal hemoglobin (HbA). The γ chain differs from the β chain in that a serine residue is present at position 143 instead of a histidine. This one amino acid substitution causes a shift in the oxygen affinity curve to the left, especially at the upper portion of the curve. Thus, HbF has a higher affinity for oxygen than HbA. This allows the fetus to extract oxygen from its mother's blood in the placenta. HbF is gradually replaced by HbA during the first several months after birth.

Sickle Cell Hemoglobin Another well-known hemoglobin mutant is HbS, or sickle cell hemoglobin. In HbS the amino acid residues at position 6 in the β chains are valines rather than glutamic acid residues. This change causes the deoxy-form of HbS to aggregate

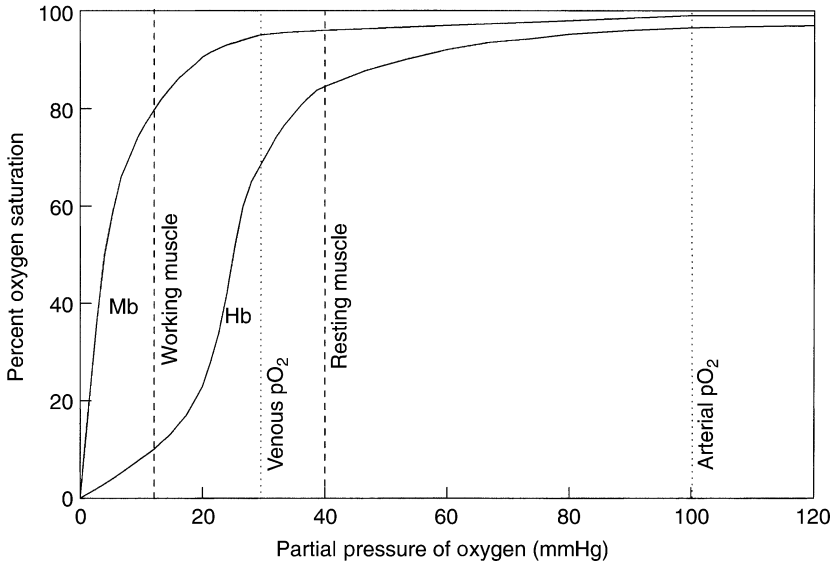

FIGURE 3 Oxygen saturation curves of hemoglobin (Hb) and myoglobin (Mb).

into insoluble fibers. The presence of these fibers distorts the shape of the erythrocytes from a disk-shaped into a sickle-shaped cell. Sickle cells are considerably more fragile than normal erythrocytes, which accounts for the observed anemia in sickle cell patients.

It is estimated that in the USA about three million people suffer from the disease, mostly people of African descent. The reason for the high survival rate of the mutant gene is that HbS provides protection against the malaria parasite, the greatest killer of all times. This parasite spends part of its life cycle in human erythrocytes. However, the HbS is apparently much less suitable for the proper development of the parasite than HbA, thus protecting the sickle cell patients when malaria epidemics occur.

Blood Substitutes

A considerable amount of research has been done recently on the modification of human and bovine hemoglobins in order to produce a suitable product to serve as a blood substitute. This requires a covalent crosslinking of the α and β chains in order to prevent dissociation of the tetramer. Initial clinical trials, however, revealed that hemoglobin can be quite toxic when it is present in large quantities in the circulation outside the confines of the red cell.

Heme Proteins that Serve as Enzymes

A considerable number of heme proteins are found in nature that serve as enzymes. These include most peroxidases and catalases, as well as a large group of monooxygenases generally referred to as the cytochrome P_{450} enzymes. In addition, a few oxidases, hydrolases, and dioxygenases are heme enzymes. Peroxidases and catalases use hydrogen peroxide as the oxidizing agent. The cytochrome P_{450} enzymes, as well as the other enzymes catalyze oxidizing reactions that involve molecular oxygen, of which either one or both atoms are incorporated into a substrate.

Peroxidases

Structure and Function

Peroxidases are a group of enzymes that catalyze the oxidation of a substrate by hydrogen peroxide or an organic peroxide. Most peroxidases are ferric heme proteins; one notable exception being the glutathione peroxidase, which is a selenium-containing enzyme. They are present in virtually all living species.

Most peroxidases are able to oxidize a variety of substrates of widely different structures, varying from halide ions to hydroquinones to aromatic azo compounds. A binding site for the substrate to be oxidized is therefore virtually absent in most of these enzymes. In fact, simple molecules consisting of 8–12 amino acids and a covalently linked heme moiety, with a histidine residue forming the proximal ligand, have considerable peroxidase activity. These compounds are known as microperoxidases. Furthermore, methemoglobin and metmyoglobin can effectively function as peroxidases, having about 5–10% of the activity of horseradish peroxidase.

Mechanism of Action

The mechanism of action of the heme peroxidases is shown in Figure 4. The first step involves an oxidation

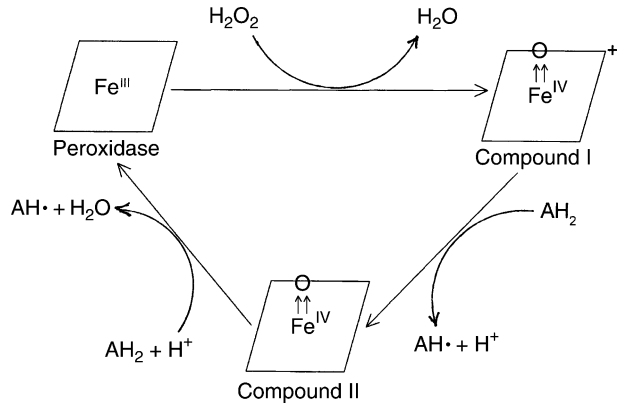

FIGURE 4 Mechanism of action of peroxidases. The two arrows in compounds I and II represent the two unpaired electrons in the biradical bond between the iron and the oxygen atom. The " + " mark in compound I represents the positive charge on the porphyrin ring. AH_2 and $AH^{\cdot}$ represent the substrate and the radical product, respectively.

of the enzyme by the peroxide, leading to the formation of a ferryl (Fe^{IV}) heme moiety and the removal of an electron from either the porphyrin ring or an amino acid residue of the protein. This intermediate is commonly referred to as Compound I. Compound I can then react with a suitable substrate and promote a one-electron oxidation of the substrate. A one-electron oxidation of the substrate (such as the oxidation of a hydroquinone to a semiquinone) converts the enzyme to Compound II, in which the heme is still in the ferryl form, but the original structure of the porphyrin ring or the amino acid residue is restored. Transfer of a second electron from Compound II to a substrate restores the native ferric enzyme.

Of the plant peroxidases, the enzyme from horseradish is perhaps the most studied. It is a 40 kDa monomeric enzyme, with a histidine residue as the proximal ligand. The functions of the peroxidases in plants appear to be the generation of free radical intermediates that promote the polymerizations and crosslinkings necessary to form the cell wall structures in plants. Enzymes present in the roots of plants are thought to protect the host against invading fungi and other microorganisms.

In mammals, the most studied peroxidases are myeloperoxidase present in neutrophils, eosinophil peroxidase present in eosinophils, thyroid peroxidase present in the thyroid gland, and lactoperoxidase present in milk and saliva. Except for the thyroid peroxidase, the function of all these peroxidases seem to involve a defense against invading microorganisms. The function of the thyroid peroxidase is the iodination of tyrosine residues during the synthesis of the hormone thyroxine.

Haloperoxidases

The mechanism by which myeloperoxidase exerts its anti-microbial activity has been largely elucidated by Seymour Klebanoff and his colleagues. The phagocytosis of a microorganism by a neutrophil activates a membrane-bound NADPH oxidase, that excretes large amounts of hydrogen peroxide into the phagosome. The myeloperoxidase reacts with the H_2O_2 to form a Compound I-type structure, which in turn oxidizes a chloride ion to hypochlorite (HOCl) in a reaction involving a two-electron transfer, similar to that of catalase. The hypochlorite formed is lethal to the microorganism. Lactoperoxidase uses a similar mechanism to kill bacteria present in milk or saliva; however, it uses either iodide or isocyanate as the ion to be oxidized. *In vitro*, these enzymes exert a cytolytic activity against most cells, prokaryotic as well as eukaryotic.

Other peroxidases that are capable of oxidizing halide ions include chloroperoxidase present in certain molds. This enzyme carries out organic chlorination reactions, presumably through the formation of an intermediate enzyme-bound form of hypochlorite.

Reactive Oxygen Species

An increasing number of the heme enzymes have recently attracted attention, because of their alleged involvement in the generation of reactive oxygen species (ROSs). ROSs are implicated in causing damage to DNA, RNA, lipids, and proteins, and may be directly or indirectly involved in the initiation of cancer, as well as diseases such as Alzheimers, Parkinsons, multiple sclerosis, and other diseases involving tissue degeneration and cell death. ROSs include superoxide, hydrogen peroxide, the hydroxyl radical, singlet oxygen, and ozone.

It should be clear from the above description that peroxidases are enzymes specifically designed to generate free radical products. Compounds I and II have oxidative energies comparable to that of the hydroxyl radical, and the products generated by these enzymes often are free radicals. These products in turn can promote polymerization reactions of proteins and lipids. Furthermore, it is known from *in vitro* experiments that most if not all peroxidases are able to exert cytolytic activities under appropriate conditions. It is also known that both myeloperoxidase and chloroperoxidase are able to generate singlet oxygen. These observations support the hypothesis that peroxidases may be involved in at least some of the tissue damage that is presently ascribed to the actions of ROSs.

CATALASES

Structure and Function

Catalases are enzymes designed to neutralize the hydrogen peroxide that is formed *in vivo* by various

oxidases and other enzymes. The enzyme catalyzes the dismutation of two moles of hydrogen peroxide into one mole of oxygen and one mole of water:

$$2H_2O_2 \rightarrow 2H_2O + O_2$$

Catalases are found in all aerobic cells; in fact, in some bacteria catalase may account for as much as 1% of their total dry weight. High concentrations are also present in erythrocytes, where it serves to neutralize the hydrogen peroxide formed during the autoxidation of oxy-hemoglobin to methemoglobin. Catalases are among the enzymes with the highest turnover rates known: under optimal conditions each subunit can dismutate 2×10^5 mol of hydrogen peroxide per second.

Catalases in eukaryotes are tetramers, each subunit containing a ferric heme and a bound molecule of NADPH. The reason for the presence of this coenzyme is still unclear at this time. In the catalases, a tyrosine residue forms the proximal ligand to the heme iron.

Mechanism of Action

Their mechanism of action is somewhat similar to that of the peroxidases. Upon binding of a mole of H_2O_2, a Compound I-type intermediate is formed, and a mole of water is released. The enzyme then reacts with a second mole of H_2O_2 to form a mole of oxygen and the native enzyme is regenerated (Figure 5). No radical intermediates are formed by catalases.

Oxygenases

Oxygenases are a group of heme enzymes that catalyze the oxidation of various substrates by molecular oxygen. Certain oxygenases catalyze the incorporation of both oxygen atoms into the substrate; these are referred to as dioxygenases. Others catalyze the incorporation of one atom of oxygen into the substrate, while the other atom is reduced to water. This group constitutes the monooxygenases.

Almost all of the dioxygenases do not contain heme; non-heme iron sulfur groups form their active center. An example of a heme-containing dioxygenase is tryptophan dioxygenase.

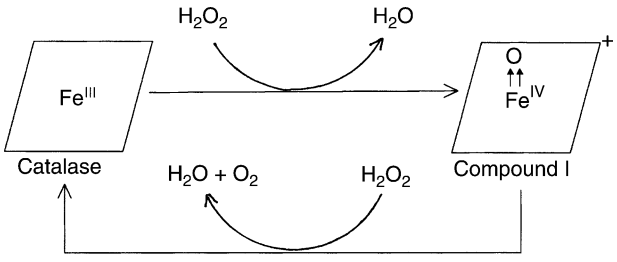

FIGURE 5 Mechanism of action of catalases.

Monooxygenases are also referred to as mixed-function oxygenases or hydrolases. In addition to molecular oxygen, this group of enzymes requires the presence of a co-substrate capable of donating a pair of electrons to reduce the second atom of oxygen to water. A typical monooxygenase reaction is the hydroxylation of an alkane to an alcohol:

$$CH_3-(CH_2)_n-CH_3 + O_2 + RH_2 \rightarrow CH_3-(CH_2)_n-CH_2OH + H_2O + R$$

in which R represents the co-substrate. Many compounds can serve as a co-substrate for the monooxygenases; these include the pyridine nucleotides, flavins, ferredoxins, hydroquinones, ascorbate, and others.

Cytochromes P_{450} Enzymes

The cytochrome P_{450} enzymes are a special group of monooxygenases, all of which use NADPH as the co-substrate. The name of this group of enzymes is associated with their discovery, when it was noted that, in the presence of carbonmonoxide, their absorption spectrum resembles that of the known cytochromes, with the maximum absorbance of the Soret band located at about 450 nm. Functionally, however, they are not related to the group of proteins normally known as cytochromes.

Occurrence

The cytochrome P_{450} family of enzymes are present in all living species. They have been isolated from bacteria, yeasts, plants, insects, as well as from vertebrate animals, where they are present in a large number of tissues. In fact, a list of the sequences of 325 different cytochrome P_{450}'s is presented in Ortiz de Montellano's book "Cytochrome P450" (see Further Reading), and many more have been identified since then.

Functions

The cytochromes P_{450} comprise a large group of enzymes that are able to incorporate one of the two atoms of an oxygen molecule into a broad variety of substrates, with the concomitant reduction of the other oxygen atom to water. Members of the family are known to catalyze hydroxylations, epoxidations, N-oxidations, N-, S-, and O-dealkylations, sulfoxidations, dehalogenations, and other reactions.

The two main functions of the cytochrome P_{450} enzymes appear to include first the control of the steady-state level of endogenous effectors of growth and differentiation. As such, they are important in the metabolism of numerous physiological substrates, including prostaglandins, steroids, cytokines, bile

acids, fatty acids, and biogenic amines. Second, they metabolize a wide range of foreign chemicals, including environmental pollutants, drugs, various natural plant products, and many other foreign materials that enter the body.

Mechanism of Action

The enzymes contain a heme moiety with iron in the ferric state, and with a cysteine residue as the proximal ligand. Oxygen binds as the sixth ligand. The principal catalytic cycle of the cytochrome P_{450} enzymes for a hydroxylation reaction is shown in Figure 6. The first step involves a binding of the substrate XH to the enzyme. In step 2 the ferric enzyme is reduced to the ferrous form with an electron obtained from the co-substrate NADPH. The ferrous enzyme then binds a molecule of oxygen in step 3. In step 4 a second electron from NADPH is used to reduce the oxygen molecule, which leads to the uptake of two protons, the release of a molecule of water, and the formation of a Compound I-type ferryl enzyme. In the final step the oxygen atom of Compound I is incorporated into the substrate, and the product is released. Steps 4 and 5 probably constitute a series of individual steps; however, they occur so fast that they cannot be observed with present-day's techniques.

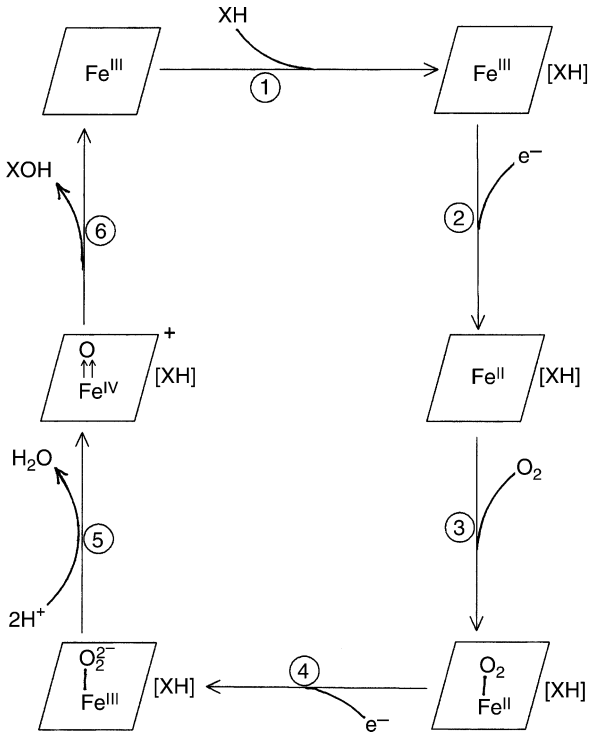

FIGURE 6 Principal catalytic cycle of cytochrome P_{450} enzymes. XH, substrate; XOH, product.

Heme Proteins that Serve as Electron Carriers

Cytochromes

Function

The cytochromes, with the exception of the members of the cytochrome P_{450} family, are heme proteins, designed for the transport of individual electrons. Their heme moiety is normally enveloped by the protein portion, excluding it from contact with the outside solvent. The transport of individual electrons is facilitated by an oscillation of the heme iron between the ferrous and the ferric forms. The flow of electrons from the outer edge of the cytochrome to the heme iron may involve the participation of one or more amino acid residues (e.g., tyrosines). The driving force for the movement of electrons is provided by the differences in redox potential between the electron donor and the acceptor.

Cytochromes are identified by the type of heme moiety present (a, b, c, or d), and the wavelength of maximal absorbance of the Soret band, e.g., cytochrome b_{559}. The four heme moieties differ in the structure of the side chains of the porphyrin ring.

Cytochromes c

c-Type cytochromes are found in animals, plants, and eukaryotic microorganisms. They are the only type cytochrome that is water-soluble. They are monomeric proteins, containing a heme c moiety, with the proximal and distal ligands formed by histidine and methionine residues. They usually contain a single heme per molecule; however, molecules containing up to 8 heme residues are found in certain photosynthetic bacteria. The best-known and most-studied member of this group is the mitochondrial cytochrome c, which transports electrons from Complex II to Complex III in the electron transport system.

Cytochromes b

b-Type cytochromes are widely distributed. They are present in bacteria, chloroplasts, and mitochondria. The mitochondrial b-type cytochromes are normally embedded in membranes as part of Complex II of the electron transport system. They contain a protoheme with histidine in both the proximal and distal ligand positions. The function of all b-type cytochromes appears to be to transport electrons from dehydrogenases to cytochrome c-type proteins or to iron–sulfur proteins.

Cytochromes a

The a-type cytochromes in mitochondria are an important part of the electron transport chain. They form an integral part of Complex III, where they take up electrons from cytochrome c and pass them on to the copper ions and the bound oxygen in the cytochrome oxidase system.

See Also the Following Articles

Cytochrome *c* • Cytochrome P-450 • Hematopoetin Receptors • Heme Synthesis • Iron–Sulfur Proteins

Glossary

biradical bond A chemical bond characterized as a biradical, three-center four-electron bond.

prosthetic group A chemical compound present in and an integral part of an enzyme or protein that is not composed of amino acid residues.

singlet oxygen An oxygen molecule having one electron in an excited state. Chemical notation: $O_2(^1\Delta g)$.

Soret band The most intense absorption band in heme proteins. Also referred to as the γ band.

Further Reading

Alayash, A. I. (2000). Hemoglobin-based blood substitutes and the hazards of blood radicals. *Free Radic. Res.* **33**, 165–175.

Alayash, A. I., Patel, R. P., and Cashon, R. E. (2001). Redox reactions of hemoglobin and myoglobin: Biological and toxicological implications. *Antioxid. Redox Signal* **3**, 313–327.

Brunori, M. (2000). Structural dynamics of myoglobin. *Biophys. Chem.* **86**, 221–230.

Everse, J. (1998). The structure of heme proteins compounds I and II: Some misconceptions. *Free Rad. Biol. Med.* **24**, 1338–1346.

Everse, J., Everse, K. E., and Grisham, M. B. (eds.) (1991). *Peroxidases in Chemistry and Biology*, Vols I and II, CRC Press, Baton Rouge, FL.

Everse, J., Vandegriff, K. D., and Winslow, R. M. (eds.) (1994). *Hemoglobins Methods in Enzymology*, Vols 231 and 232, Academic Press, San Diego, CA.

Garrett, R. H., and Grisham, C. M. (1994). *Biochemistry.* Saunders College Publishing, Orlando, FL.

Ortiz de Montellano, P. R. (ed.) (1995). *Cytochrome P450; Structure, Mechanism, and Biochemistry.* Plenum Press, New York.

Ortiz de Montellano, P. R., and De Voss, J. J. (2002). Oxidizing species in the mechanism of cytochrome P450. *Nat. Prod. Rep.* **19**, 477–493.

Biography

Johannes Everse is a Professor in the Department of Cell Biology and Biochemistry at the Texas Tech University Health Sciences Center in Lubbock, Texas. His principal research interests are in the mechanisms of action and biological functions of heme proteins, and in the utilization of immobilized enzymes in industry and medicine. He holds a Ph.D. from the University of California, San Diego. He has co-edited six books, including two on peroxidases, and two on hemoglobin.

Heme Synthesis

Gloria C. Ferreira
University of South Florida, Tampa, Florida, USA

Heme, a four-ring organic compound with a central iron atom, plays multiple roles in cellular processes. For example, it is the crucial component in hemoglobin, a red blood cell protein responsible, in vertebrates, for the transport of oxygen from the lungs to the different tissues and the transport of carbon dioxide from the tissues to the lungs. It is heme that gives the characteristic red color to blood. Given its importance in many vital functions in organisms ranging from bacteria to man, it is not surprising that most cells synthesize heme. However, in humans, differentiating erythrocytes represent the major site of heme production due to the synthesis of hemoglobin, which accounts for ~85% of the total heme.

Heme Structure

The observation that hemoglobin can be split into two components, with the smaller unit corresponding to the compound which today is recognized as heme, was made by L. R. LeCanu in 1837. While the correct structure of heme was initially proposed by Kuster in 1912, it only received general acceptance 16 years later upon its chemical synthesis. The Nobel Prize winning organic chemist Hans Fischer developed syntheses leading to the assembly of four rings, or pyrroles, into a macrocyclic structure with a purple-red color, which he appropriately named porphyrin (from the Greek porphuros, meaning purple). The chemically synthesized porphyrin, which had properties identical to those of the "natural porphyrin" (derived from heme upon the release of the iron atom), was designated protoporphyrin IX. Thus, heme consists of four rings (pyrroles), composed of carbon, nitrogen, and hydrogen atoms, linked together in a cyclic array and containing an atom of iron in its center (Figure 1).

Heme is now recognized as a member of a larger family of metalated tetrapyrroles, which are essential for life on Earth. They include chlorophylls, cobalamin (vitamin B_{12}), siroheme, and coenzyme F_{430}. Chlorophylls trap the light energy required in photosynthesis. Cobalamin-containing enzymes catalyze intramolecular rearrangements, methylations, and reduction of ribonucleotides to deoxyribonucleotides. Siroheme is an essential component of enzymes involved in sulfur and nitrogen metabolisms. Coenzyme F_{430}, present in methanogenic bacteria, functions in methane formation. While the central metal ions in these tetrapyrroles differ – Fe^{2+} in the case of heme and siroheme, Mg^{2+} in chlorophyll and bacteriochlorophyll, Co^{2+} in cobalamin, and Ni^{2+} in coenzyme F_{430} – the unifying feature is the presence of a complexed metal ion, which promotes a remarkable number of different biochemical reactions. Further, the protein scaffold binding the metalloporphyrin modulates the chemistry (redox state and coordination properties) of the metal ion, such that the spectrum of the reactions expands beyond the normal properties of the metal ion. It is this interplay between the protein moiety and the metalloporphyrin that provides the plethora of functions associated with metalloporphyrin-containing proteins.

The Heme Biosynthetic Pathway

Formation of 5-Aminolevulinate

The biosynthesis of tetrapyrroles is initiated from simple molecules and comprises only a few enzymatic steps (Figure 2). The first committed precursor, 5-aminolevulinic acid (ALA), is synthesized from either succinyl-CoA or glutamate, and thus the names C4 and C5 (based on the number of carbon atoms in the precursor), for the two ALA biosynthetic pathways evolved in nature. In most non-photosynthetic eukaryotes and a few prokaryotes (i.e., the α-proteobacteria), ALA results from the condensation between glycine and succinyl CoA (C4 pathway), while in plants and most bacteria, ALA is derived from glutamate (C5 pathway). The C4 pathway requires a single enzyme, ALA synthase (ALAS); in contrast, three enzymes are involved in the conversion of glutamate into ALA. Specifically, glutamyl-tRNA synthetase converts glutamate to glutamyl-tRNA, which is reduced by glutamyl-tRNA reductase to glutamyl-1-semialdehyde (GSA); this product is then transformed by GSA aminomutase or GSA aminotransferase (GSA-AT) to ALA. Pyridoxal 5′-phosphate, a vitamin B_6-derivative, is an essential component (cofactor) of both ALAS and GSA-AT, as these enzymes cannot function relying solely on the protein moiety. Among prokaryotes, ALAS is only

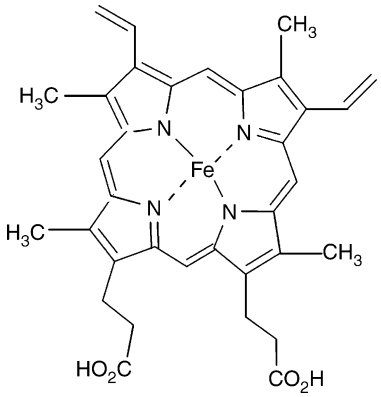

FIGURE 1 Iron–protoporphyrin IX, which is commonly designated as heme. Iron–protoporphyrin IX (or heme) has an iron ion complexed with the conjugated, aromatic porphyrin ring and an asymmetrical side-chain substitution. Note the $-CH_3$ (methyl), $-CH{=}CH_2$ (vinyl), and $-CH_2-CH_2-COOH$ (propionate) groups as side chains.

found in the α-proteobacteria, which are considered to be the most closely related, free-living organisms to the ancestral progenitor of the mitochondrion. Thus, it is conceivable that eukaryotic ALASs were acquired from a free-living α-proteobacterium during its transformation, first to an endosymbiont and subsequently to a mitochondrion.

From ALA to Uroporphyrinogen III

In eukaryotes, the first and three final enzymatic steps of heme biosynthesis occur within mitochondria, while the intervening four occur in the cytosol (Figure 2). Once ALA is made and transported to the cytosol, through a yet unidentified mechanism, two molecules of ALA are asymmetrically condensed to form the monopyrrole porphobilinogen (PBG) by PBG synthase (PBGS; also known as ALA dehydratase). PBG constitutes

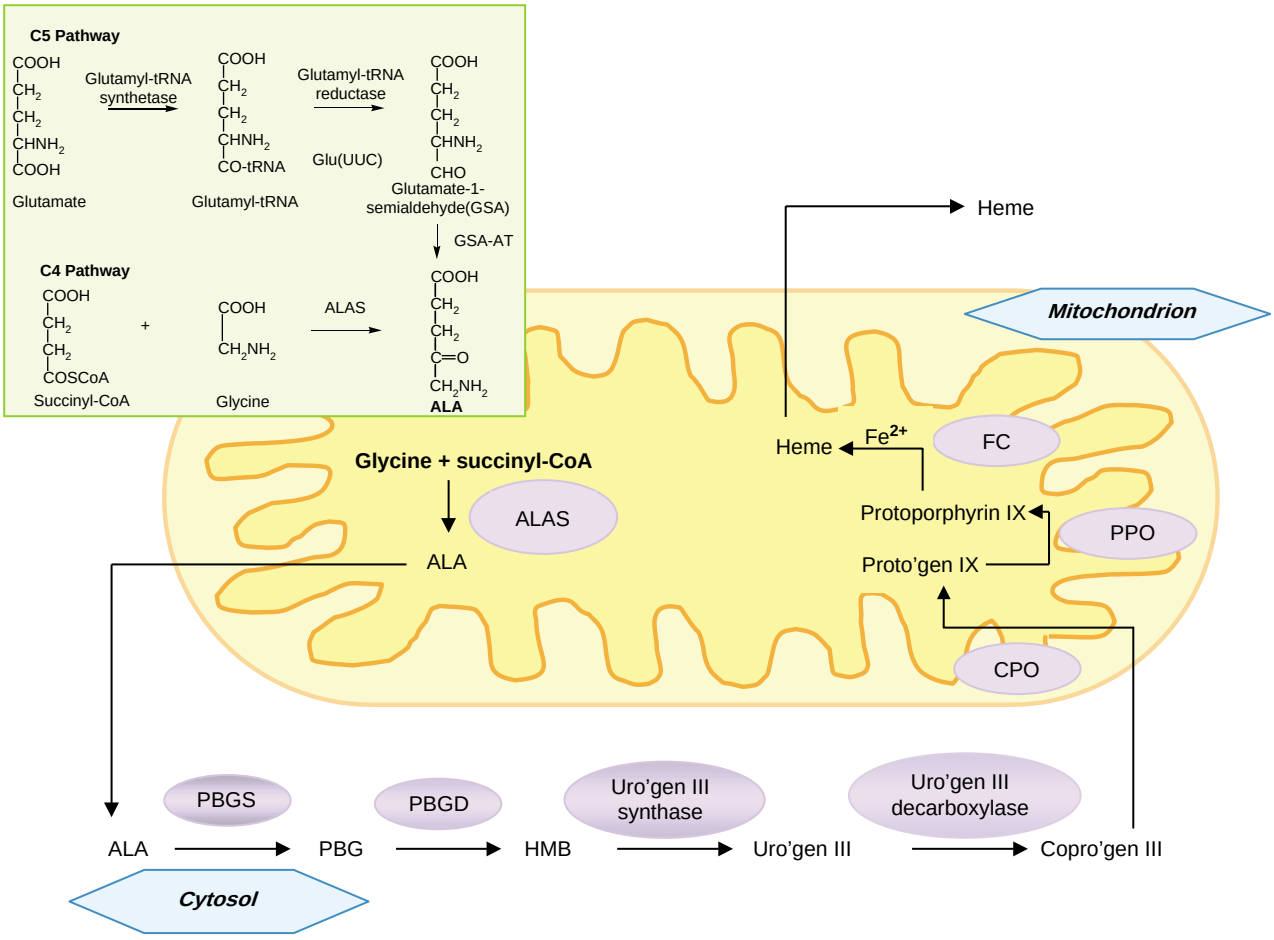

FIGURE 2 Diagrammatic representation of the heme biosynthetic pathway in eukaryotic animal cells. ALA, 5-aminolevulinate; ALAS, ALA synthase; PBG, porphobilinogen; PBGS, PBG synthase; PBGD, PBG deaminase; HMB, hydroxymethylbilane; Uro'gen III, uroporphyrinogen III; copro'gen III, coproporphyrinogen III; CPO, coproporphyrinogen III oxidase; proto'gen IX, protoporphyrinogen IX; PPO, protoporphyrinogen IX oxidase; FC, ferrochelatase. Inset: The two paths to ALA.

the building unit of tetrapyrroles and hence eight molecules of ALA are required to form one heme molecule. Crystal structures of PBGSs from different species have confirmed the presence of two distinct binding sites for each ALA molecule, termed A and P to distinguish the two ALA substrate molecules. The A-side of ALA forms the acetyl half of PBG, leaving its amino group intact, while the P-side of ALA forms the propionyl half of PBG with the amino group becoming part of the PBG ring. PBGS has a homo-octomeric structure composed of four dimers, and each subunit contains an active site metal ion (zinc or magnesium and/or potassium depending on the species) and in many cases an allosteric metal ion (magnesium). The next step in heme biosynthesis involves the deamination and stepwise polymerization of four PBG molecules by PBG deaminase to give the linear tetrapyrrole 1-hydroxymethylbilane. Then, uroporphyrinogen III synthase catalyzes the cyclization of the linear tetrapyrrole, whereby the D ring of hydroxymethylbilane is inverted to generate the asymmetrical macrocycle, uroporphyrinogen III. In the absence of uroporphyrinogen III synthase, 1-hydroxymethylbilane cyclizes into the non-physiological relevant tetrapyrrole, uroporphyrinogen I. The incredible acrobatics that must occur with the flipping of the D ring and closure of hydroxymethylbilane speak for the importance of uroporphyrinogen III synthase in making uroporphyrinogen III synthesis reaction. In fact, disastrous consequences emerge with the malfunction of uroporphyrinogen III synthase, as observed in patients with the blood disorder porphyria cutanea tarda, who typically have high levels of uroporphyrinogen I and derivatives thereof.

From Uroporphyrinogen III to Protoporphyrinogen IX

For most eukaryotes, the last cytosolic step is the sequential decarboxylation of the four acetate side chains of uroporphyrinogen III to methyl groups by uroporphyrinogen decarboxylase (Figure 2). This enzyme is a $(\alpha/\beta)_8$ barrel protein, which appears to be functional as a homodimer and not to require prosthetic groups or cofactors. The uroporphyrinogen decarboxylase-catalyzed reaction gives coproporphyrinogen III, which is the substrate of coproporphyrinogen oxidase (CPO). The oxidative decarboxylation of the propionate side chains of the rings A and B of coproporphyrinogen III yields protoporphyrinogen IX. While eukaryotic CPO activity depends on oxygen, prokaryotic organisms, under anaerobic conditions, use alternative electron acceptors in the oxidative decarboxylation reaction. Hence, oxygen-independent CPOs (HemN and HemZ, i.e., the products of the *hemN* and *hemZ* genes) are found in bacteria; indeed, facultatively anaerobic bacteria, such as *Escherichia coli*, possess both oxygen-dependent CPO (HemF) and oxygen-independent CPO (HemN). Recently, it has been found that HemN contains an iron–sulfur center ([4Fe–4S]), which is essential for the activity of the enzyme in conjunction with NAD(P)H and *S*-adenosyl-L-methionine (SAM). As one would expect, the enzyme appears to have a distinct reaction mechanism with the involvement of SAM in the formation of a radical, and thus HemN has been aptly identified as a "radical SAM enzyme." As far as the subcellular location of the oxygen-dependent CPO goes, it seems to vary! In mammals and other higher eukaryotes, it appears to be associated with the inner side of the mitochondrial outer membrane, whereas in the yeast *Saccharomyces cerevisiae* and bacteria it is found in the cytosol.

From Protoporphyrinogen IX to Heme

In the penultimate step, protoporphyrinogen oxidase (PPO) catalyzes the complete aromatization of protoporphyrinogen IX ring into protoporphyrin IX, which involves a six-electron oxidation (Figure 2). Similar to CPO, anaerobic and facultative anaerobic bacteria have an oxygen-independent PPO; however, in contrast to CPO, facultative anaerobic bacteria possess solely an oxygen-independent PPO (and not in complementation with an oxygen-dependent PPO). All other organisms appear to have PPOs, which use oxygen as the terminal electron acceptor. Ferrochelatase catalyzes the terminal step of the heme biosynthetic pathway, the insertion of ferrous iron into the protoporphyrin IX macrocyclic ring. Eukaryotic ferrochelatases associate with the inner side of the mitochondrial inner membrane, and vertebrate enzymes have a [2Fe–2S] cluster (although this is not an exclusive structural feature of vertebrate ferrochelatases). The mechanism of the ferrochelatase reaction involves an out-of-plane distortion of the porphyrin, which facilitates the reaction by exposing the pyrrole nitrogens to the incoming ferrous iron substrate.

Regulation of the Heme Biosynthetic Pathway/ Heme Biosynthesis

There is not a single ubiquitous regulatory mechanism for heme biosynthesis, and so the discussion in this entry will focus solely on the regulation of the pathway in mammalian cells. Considering that heme is predominantly synthesized in bone marrow (i.e., in erythroblasts and reticulocytes that still contain mitochondria) and

liver cells, most of the studies on regulation have focused on these two types of cells. Predominance of heme synthesis in bone marrow and liver cells reflects the greater demands due to the syntheses of the heme-containing proteins, hemoglobin, and cytochrome P-450 enzymes, respectively. The major regulatory and rate-limiting step of the pathway corresponds to the reaction catalyzed by ALAS, the first enzyme of the pathway. Two genes, located in two different chromosomes in humans, encode the two ALAS forms of the enzyme (or isozymes): ALAS1 and ALAS2. The gene encoding ALAS1 is expressed in every cell, whereas that for ALAS2 is specifically expressed in erythroid cells. Importantly, the regulatory mechanisms for the expression of the two ALAS genes and the post-transcriptional events seem to be distinct in differentiating erythrocytes from those in non-erythroid cells. ALAS1 controls the production of heme for basic cellular functions and is feedback-regulated by heme through inhibition of (1) transcription of the ALAS1 gene, (2) translation of the ALAS1 message, (3) import of the cytosolic precursor form of the enzyme into mitochondria, and (4) enzymatic activity. In contrast, certain drugs and hormones induce liver cells to make more ALAS, and consequently heme and cytochrome P-450, by activating transcription of the ALAS1 gene.

In differentiating erythroid cells, the syntheses of heme and globin need to be coordinated, as the production of hemoglobin requires that neither the protein (globin) component nor the non-protein component (heme) will be in excess. And indeed, identical transcriptional elements have been identified in the genes of ALAS2 and globin. Another level of regulation of the erythroid heme biosynthetic pathway is centered at the stage of translation, which responds to the cellular iron levels. This response is mediated through specific interactions between an iron-responsive element (IRE), present in the ALAS2 mRNA, and IRE-binding proteins, such that under iron limitation, the translation of ALAS2 mRNA is inhibited, while the presence of iron above the cellular threshold relieves the repression caused by IRE-binding proteins. The essential requirement for ALAS2 in heme biosynthesis and erythropoiesis was clearly demonstrated with targeted disruption of ALAS2 in the mouse, which led to no hemoglobin in cells, the accumulation of iron (albeit in the cytoplasm and not in mitochondria) and, ultimately, embryonic death.

Heme Function

The known roles of heme are many and variable, and most probably many other functions await discovery. As referred to above, heme is a prosthetic group of proteins involved in oxygen transport such as hemoglobins and myoglobins, which are the major blood and muscle proteins, respectively. In addition, heme participates in other cellular processes including anaerobic and aerobic respiration, sensing of diatomic gases (e.g., nitric oxide and carbon monoxide), detoxification of foreign substances (e.g., drugs) by oxidative metabolism, and signal transduction. Some of these functions might also be coupled with the regulatory roles of heme in gene transcription, translation, mitochondrial protein import, protein stability, and differentiation. Recently, a transcription factor that regulates the mammalian biological clock was discovered to use heme as a cofactor to sense, and react to, changes in the cell, thus linking cellular metabolism with the biological clock. Another area of research has led to the emergence of a new proposal that heme deficiency or dysregulation is intimately associated with the aging process, including neural decay.

Disorders of the Heme Biosynthetic Pathway

Malfunction of the heme biosynthetic pathway can have disastrous consequences, and in humans it can be

TABLE I

Heme Biosynthesis-Associated Disorders

Disorder	Defective enzyme
X-linked sideroblastic anemia	5-Aminolevulinate synthase (erythroid)
ALA dehydratase, or Doss, porphyria	Porphobilinogen synthase (or ALA dehydratase)
Acute intermittent porphyria	Porphobilinogen deaminase
Congenital erythropoietic porphyria	Uroporphyrinogen III synthase
Porphyria cutanea tarda	Uroporphyrinogen decarboxylase
Coproporphyria	Coproporphyrinogen oxidase
Variegate porphyria	Protoporphyrinogen oxidase
Erythropoietic protoporphyria	Ferrochelatase

manifested in porphyrias. Briefly, porphyrias are disorders that result from inherited or acquired defects in the heme biosynthetic pathway. The first reports of porphyrias were in 1874. Since then, seven types of porphyrias associated with defects in each of the seven enzymes beyond the first step of the pathway have been identified (Table I), and depending on the major site of expression of the enzymatic defect, they have been classified into hepatic or erythropoietic porphyria. Although the molecular mechanisms behind the clinical manifestations are not well understood, the two major symptoms include cutaneous photosensitivity and central nervous system disturbances, and thus the other classification of either photosensitive or neurological porphyrias. Some porphyrias, however, manifest overlapping symptoms. Photosensitivity is a result of porphyrin accumulation, which occurs when the defective enzyme is anywhere in the pathway beyond the third step of the pathway (i.e., the PBG deaminase-catalyzed reaction), whereas the neurologic manifestations are associated with overproduction of ALA and PBG. Since the 1980s, many of the genetic mutations responsible for the enzymatic defects have been identified and mouse models, targeted to correct the defective enzyme, have been developed by engineering functional enzyme expression in bone marrow cells. Finally, mutations in the gene encoding for the erythroid ALAS are associated with X-linked sideroblastic anemia (Table I), a blood disorder characterized by mitochondrial iron accumulation due to a reduction in heme biosynthesis destined for hemoglobin production in erythroblasts.

See Also the Following Articles

Hematopoetin Receptors • Heme Proteins • Porphyrin Metabolism

Glossary

erythroblast Erythroid cell precursor; nucleated cell in bone marrow that develops into an erythrocyte.

erythrocyte A red blood cell; non-nucleated, disk-shaped blood cell that contains hemoglobin.

erythroid Erythrocyte-related.

erythropoiesis Formation and production of erythrocytes.

tetrapyrrole A general term that refers to molecules with four rings of the pyrrole type, most often linked together by single-atom bridges between the α-positions of the five-membered pyrrole rings. The arrangement of the four rings is macrocyclic in porphyrins.

Further Reading

Ferreira, G. C. (1999). 5-Aminolevulinate synthase and mammalian heme biosynthesis. In *Iron Metabolism. Inorganic Biochemistry and Regulatory Mechanism* (G. C. Ferreira, J. G. Moura and R. Franco, eds.) pp. 15–34. Wiley-VCH, Weinheim, Germany.

Kadish, K. M., Smith, K. M., and Guilard, R. (2000). *The Porphyrin Handbook*. Academic Press, San Diego, CA.

Lee, G. R., Foerster, J., Lukens, J., Paraskevas, F., Greer, J. P., and Rodgers, G. M. (1999). *Wintrobe's Clinical Hematology*. William and Wilkins, Baltimore, MD.

Panek, H., and O'Brian, M. R. (2002). A whole genome view of prokaryotic haeme biosynthesis. *Microbiology* **148**, 2273–2282.

Ponka, P. (1999). Cell biology of heme. *Am. J. Med. Sci.* **318**, 241–256.

Rodgers, K. R. (1999). Heme-based sensors in biological systems. *Curr. Opin. Chem. Biol.* **3**, 158–167.

Biography

Dr. Gloria C. Ferreira is a Professor in the Department of Biochemistry and Molecular Biology at the University of South Florida College of Medicine in Tampa. Her major research interest is on heme biosynthesis, including the reaction mechanisms of the enzymes of the mammalian heme biosynthetic pathway and their regulation. She holds a Ph.D. from the University of Georgia and served as a postdoctoral fellow at The Johns Hopkins University School of Medicine. She has authored and edited texts in the fields of heme and iron metabolisms and was Chair of the 2002 Gordon Research Conference on the Chemistry and Biology of Tetrapyrroles.

Hepatocyte Growth Factor/Scatter Factor Receptor

Selma Pennacchietti and Paolo M. Comoglio
University of Turin, Turin, Italy

Hepatocyte growth factor/scatter factor (HGF/SF) receptor is the prototype of a distinct tyrosine kinase receptor family, which also includes Ron, and is encoded by the c-*Met* proto-oncogene. Its ligand, HGF/SF, is a mesenchymal cytokine which belongs to the scatter factor protein family and is responsible for activating a genetic program that includes cell detachment, repulsion, protection from apoptosis, invasiveness of extracellular matrices, and proliferation. This pleiomorphic response is defined as "invasive growth," a process which accounts for morphogenetic cell movements through the matrix and for ordered building of epithelial tubules. Dysfunctions in invasive growth cause enhanced proliferation, uncontrolled migration into surrounding tissues, and failure to differentiate, all events that foster tumor growth and metastasis.

Hepatocyte Growth Factor/Scatter Factor

Hepatocyte growth factor (HGF) and scatter factor (SF) were discovered independently for their abilities to induce the proliferation of primary hepatocytes and dissociation/motility of epithelial cells (scattering), respectively. After biochemical purification and cDNA cloning, the two proteins were shown to be the same molecule. Later it became clear that both the mitogenic action and the scatter effect are different facets of a complex biological response that follows activation of the same receptor.

Scatter Factor Family

HGF/SF belongs to a family of structurally related soluble molecules, named scatter factors, consisting of HGF/SF and its homologue macrophage stimulating protein (MSP).

Structure

HGF/SF is a heparin-binding glycoprotein consisting of a 62-kDa α-chain linked to a 32/34-kDa β-chain by a disulfide bond. The α-subunit is characterized by the presence of an N-terminal 'hairpin' loop and by four repeated domains, named kringles (80 amino acids forming double-looped structures stabilized by three internal disulfide bridges), homologous to those found in plasminogen. Kringles are protein–protein interaction motifs and contain the binding sites for both the high-affinity receptor—Met tyrosine kinase, and the low-affinity receptor—heparin sulfate proteoglycans. The latter, being membrane bound, allows accumulation of HGF/SF in the proximity of target cells. The β-chain of HGF/SF is highly homologous to serine proteases of the blood-clotting cascade, but lacks enzymatic activity due to the replacement of critical amino acids in the catalytic site (Figure 1).

Activation of pro-HGF

The heterodimeric HGF/SF derives from a biologically inactive single-chain precursor (pro-HGF), which is secreted and stored by coupling to proteoglycans. In the extracellular environment, pro-HGF is converted to its bioactive form by a single proteolytic cleavage between R^{494} and V^{495}. A number of proteases have been reported to perform this cleavage *in vitro*, including urokinase-type (uPA) and tissue-type plasminogen activators; coagulation factor XII and one homologous serine-protease (XII-like factor).

HGF/SF Receptor

The high-affinity receptor for HGF/SF is a tyrosine kinase encoded by the *c-Met* proto-oncogene. It was originally identified as a transforming sequence derived from a chromosomal rearrangement, induced by a chemical carcinogen *in vitro*, between *5′* sequences derived from translocated promoter region (Tpr), encoding a leucine zipper-dimerization motif, and the cytoplasmic domain of Met, excluding the juxta-membrane region. Later, Tpr-Met was also found to be a product of chromosomal translocation in rare,

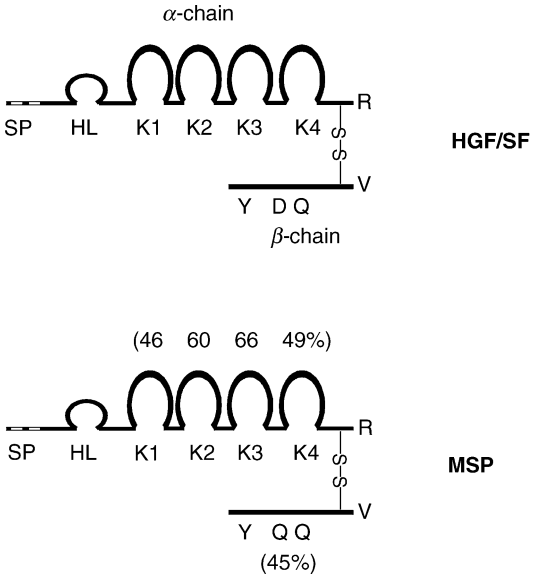

FIGURE 1 A diagram of the structure of scatter factors HGF/SF and MSP. Both are heterodimers consisting of a heavy α-chain and a light β-chain held together by a disulfide bond. The mature heterodimer is formed by proteolytic digestion at a specific dibasic arginine–valine (R–V) site. Starting from the amino-terminal signal peptide (SP), the α-chain contains a hairpin loop (HL) followed by four kringles (K), whereas the β-chain contains a serine-protease-like structure. The lack of proteolytic activity in the HGF/SF molecule is due to the replacement of the histidine and serine residues lying within the catalytic site of conventional serine proteases with glutamine (Q) and tyrosine (Y), respectively. The same substitutions, together with replacement of an aspartate (D) with glutamine (Q), are present in MSP. The percentage of homology of individual kringles as well as the β-chain between the two molecules is also specified.

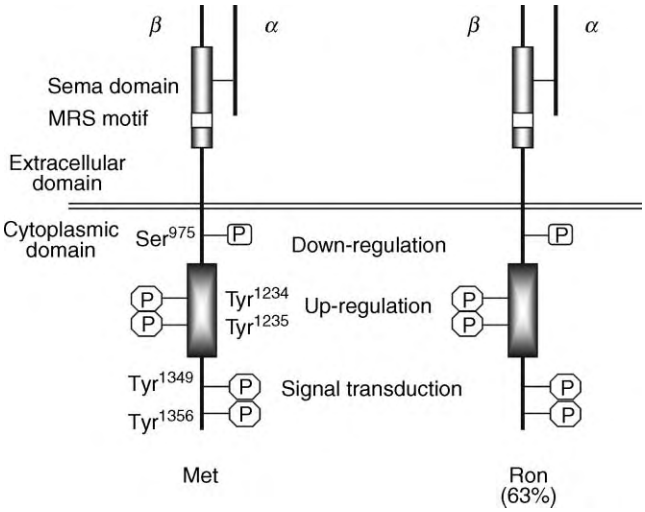

FIGURE 2 The tyrosine kinase family of scatter factor receptors. The HGF/SF receptor, Met, and the MSP receptor, Ron, share a 63% overall percentage homology. Met and Ron are disulfide-linked heterodimeric proteins formed by an extracellular α-chain and by a β-chain, that spans the plasma membrane and contains the tyrosine kinase domain (box in the cytoplasmic domain). The extracellular domains of Met and Ron include the Sema domain (common to the signaling molecules semaphorins and to their receptors' plexins) and the Met-related sequence (MRS). In the cytoplasmic domain, residues endowed with regulatory and transduction activity are conserved in both receptors. In the HGF/SF receptor, upon phosphorylation, a serine in the juxta-membrane region (Ser^{975}) down-regulates the kinase activity. Two phosphotyrosines in the kinase domain (Tyr^{1234} and Tyr^{1235}) up-regulate the kinase activity in an autocatalytic fashion. Finally, phosphotyrosines in the C-terminal tail (Tyr^{1349} and Tyr^{1356}) form a multifunctional docking site that recruits the full spectrum of signal transducers required to induce invasive growth.

naturally occurring cancers. In the intracellular fusion protein, Tpr provides stable dimerization that mimics the effect of the natural ligand and induces constitutive activation of the Met kinase.

Structure

The HGF/SF receptor Met is the prototypic member of a distinct family of protein tyrosine kinases sharing a highly homologous structure. The MSP receptor, encoded by the *Ron* proto-oncogene, is another member of this receptor family, while the product of the *Sea* proto-oncogene, once listed as a third member of the family, has recently been recognized as the avian counterpart of *Ron*. These receptors are single-pass cell membrane glycoproteins with unique structural features: they are dimeric molecules composed of a 50-kDa α-chain disulfide-linked to a 145-kDa β-chain in an α/β complex of 190 kDa. The α-chain is exposed at the cell surface and the β-chain spans the plasma membrane (Figure 2). The HGF/SF receptor, synthesized as a large precursor (pr170) that includes both the α-chain and the β-chain, undergoes cotranslational glycosylation and is further cleaved by proteases of the furin family to form the mature subunits. Both the α-subunit and the β-subunit are necessary for biological activity.

The extracellular moiety of the β-chain contains distinctive features, namely a cysteine-rich motif called Met-related sequence (MRS) which is embedded in a larger region (Sema domain); both are present also in the signaling molecules, semaphorins, and in their receptors, plexins. The intracellular portion of the HGF/SF receptor can be divided into three functional domains: a juxtamembrane domain, a tyrosine kinase catalytic domain, and a C-terminal tail.

The juxtamembrane domain is endowed with a negative regulatory role: phosphorylation of a serine residue (S^{975}) by either protein kinase C or Ca^{2+}/calmodulin-dependent kinases results in a strong inhibitory effect on receptor activity.

The tyrosine kinase catalytic domain contains the major phosphorylation site, represented by tyrosine residues Y^{1234} and Y^{1235} (conserved in *Ron*) which are essential for full activation of the enzyme. Following ligand-induced dimerization, transphosphorylation of

these residues causes the up-regulation of the enzymatic activity of the Met kinase in an autocatalytic fashion.

The C-terminal tail domain of the HGF/SF receptor is crucial for its biological activity; the tail comprises of a short sequence containing two tyrosines that are phosphorylated on HGF/SF binding and are responsible for mediating high-affinity interactions with multiple signal transducers containing Src homology-2 (SH2) domains, phosphotyrosine-binding (PTB) domains, or a peculiar Met-binding domain (MBD).

Signal Transduction

The HGF/SF C-terminal domain is unique among receptor tyrosine kinases because it contains a single, multifunctional docking site, made of a tandemly arranged degenerate sequence Y^{1349}*VHV*NATY^{1356}*VNV*, responsible for the bulk of receptor-signaling activity. While the majority of tyrosine kinase receptors use different phosphotyrosines to recruit distinct signal effectors, this sequence is able, alone, to recruit multiple signal transducers and adaptors, triggering a pleiotropic response. When phosphorylated, these two tyrosines interact with Grb2, p85/phosphatidylinositol 3-kinase (PI3K), phospholipase C-γ (PLC-γ), stat-3, Shc, SHP2 phosphatase and the large adaptor protein Gab1. Grb2, which has a strong requirement for asparagines in the $+2$ position specifically interacts only with the sequence Y^{1356}VNV.

The multifunctional docking site is an absolute requirement for Met signaling. When the two tyrosines are substituted with phenylalanines, cells become completely unresponsive to HGF/SF *in vitro*, even when the receptor's intrinsic catalytic activity is activated by oncogenic point mutations, and transgenic mice that express this mutant display a lethal phenotype that resembles the one observed in *Met*-knock-out animals. In mirror experiments, artificial insertion of this sequence into other receptor tyrosine kinases allows them to switch their conventional biological responses into promotion of invasive growth.

The components of the signal transduction machinery implicated in individual Met-mediated biological responses have been partially elucidated. Coupling of the receptor to the Ras-mitogen-activated protein kinase (MAPK) pathway is both essential and sufficient for proliferation. Conversely, activation of PI3K as well as the Ras/Rac/Rho pathways is required to induce motility. Activation of stat3 and PLC-γ is required for cell polarization and formation of branched tubular structures. The simultaneous activation of the Ras cascade, which promotes growth, and the PI3K pathway, which promotes motility and suppresses apoptosis, leads to efficient cell dissociation, invasion of the extracellular matrix, and metastasis, whereas isolated activation of either pathway does not. Moreover, the morphogenetic response, which is specifically induced by the HGF/SF receptor and cannot be elicited by other receptor tyrosine kinases, involves Gab1 and Stat3.

Biological Activity

HGF/SF Receptor Induces Invasive Growth

Although originally identified as a mediator of growth and motility, it is now clear that the HGF/SF-Met receptor system promotes a highly integrated biological program, referred to as invasive growth, which leads to proliferation, dissociation and migration, invasion of extracellular matrix, prevention of apoptosis, cell polarization, and tubule formation. The best example of how these apparently independent effects are, indeed, part of a single complex phenomenon is the formation of tubular structures in response to HGF/SF (Figure 3). This event strongly resembles the branching morphogenesis occurring during embryonal organogenesis.

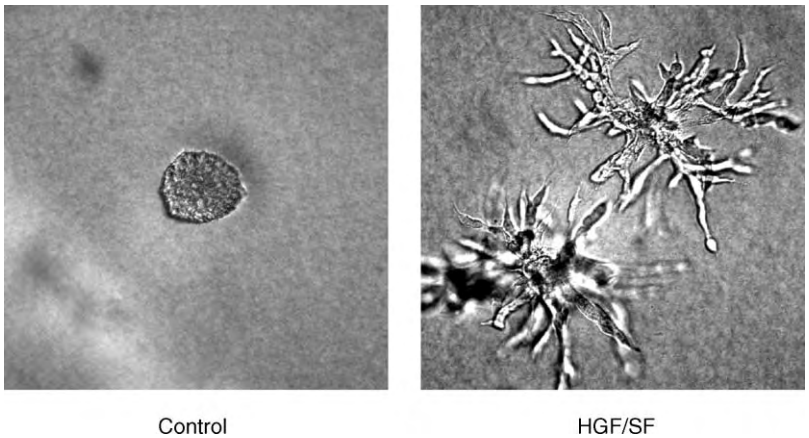

FIGURE 3 HGF/SF-induced branching morphogenesis on epithelial liver progenitor cells (MLP29). Tubule formation was observed culturing the cells within a collagen matrix for 2–3 days in the presence of 20 ng ml^{-1} recombinant factor.

Several epithelial cell lines derived from liver, mammary gland, kidney, prostate, and lung can form spheroid-like structures when grown in collagen gels. Upon HGF/SF stimulation, the cells which form these structures dissociate from each other by disrupting the cell–cell junctions, degrade the extracellular matrix, acquire transient migratory and invasive properties, and finally polarize to form differentiated tubular structures.

Morphogenetic Role in Embryogenesis

During gastrulation, HGF/SF and its receptor are both selectively expressed in the endoderm and in the mesoderm. Subsequently, the expression of HGF/SF becomes limited to the mesenchymal cells, while that of the receptor is induced in the surrounding ectoderm. At this stage (approximately E13), HGF/SF contributes to the development of several epithelial organs (e.g., lungs, liver, and gut) and induces the migration of specific myogenic precursor cells. HGF/SF, in fact, is expressed in the limb mesenchyme and can thus provide the signal for migration, which is received by *c-Met* expressing myogenic precursors.

Illuminating observations concerning the role of the HGF/SF receptor in embryogenesis came from the analysis of transgenic mice, where factor or receptor genes had been targeted. Complete knock-out embryos die *in utero* due to hyponutrition, caused by a reduction of the labyrinth layer of the placental trophoblast, which is normally responsible for controlling the invasion of maternal tissues to expand the placenta. Moreover, these embryos display impaired development of the liver and lack skeletal muscles deriving from long-range migrating precursors.

Several observations indicate that HGF/SF and its receptor play an important role in the process of epithelial morphogenesis. One of the best examples is given by the formation of kidney tubules from metanephric tissue and ureteric bud. Metanephric mesenchymal cells secrete HGF/SF whereas epithelial cells of the ureteric bud express the HGF/SF receptor. When the latter contact the metanephros, they form branching tubules; in turn, some of the metanephric cells start to express the receptor for HGF/SF and, stimulated by the autocrine loop, undergo a process known as "mesodermic–epithelial transition." They acquire epithelial features, form cell–cell junctions, polarize, and eventually form tubules. The mammary gland is a good example of an organ that undergoes major morphological changes after birth and in which branching development takes place during pregnancy and lactation. This program of differentiation relies on sequential stimulation of the epithelium by HGF/SF and neuregulin, which are secreted by the mesenchyme in different developmental stages. HGF/SF is expressed at puberty and promotes branching of the ductal tree, whereas neuregulin is responsible for alveolar budding and production of milk during pregnancy and lactation.

Trophic Role in Adult Life

In adult animals, HGF/SF has been found to stimulate regeneration of organs such as liver, kidney, and lungs after injury, and to promote cell survival in the presence of pro-apoptotic cytokines or drugs. Other than stimulating development and regeneration of epithelial organs, HGF/SF is a potent angiogenic factor, and is able to induce remodeling of cartilage and bone, by stimulating both proliferation and motility. HGF/SF is also a hematopoietic factor, produced by the bone marrow stroma. It stimulates growth and differentiation of multipotent and erythroid precursors, modulating their adhesive contacts with the surrounding stroma and promoting the spread of differentiated cells into the bloodstream.

Finally, the HGF/SF receptor plays a role in the development of neurons, as predicted by detection of expression of both factor and its receptor in the mouse nervous system. HGF/SF promotes survival of sensory and sympathetic neurons and stimulates the outgrowth of their axon, an invasive process restricted to a single part of the cell.

The HGF/SF Receptor in Human Tumors

The *Met* oncogene is associated with, and in some cases directly responsible for, a wide variety of human cancers. The most convincing evidence for the involvement of the HGF/SF receptor in human cancer arose from analysis of patients affected by hereditary papillary renal carcinoma (HPRC), a form of inherited cancer, characterized by the presence of multiple, bilateral tumors. These patients bear germ-line missense mutations of the HGF/SF receptor that are also found in somatic cells of patients affected by sporadic renal carcinomas or childhood hepatocellular carcinoma. Some mutations are homologous to those found in the oncogenes *Ret* or *Kit*, which are responsible for inherited multiple endocrine neoplasia (type 2) or for hematological disorders, respectively. *In vitro* studies show that these mutated forms of Met display an increased tyrosine kinase activity, are transforming, and confer to cells in nude mice the ability to form tumors and to overcome apoptosis. Unexpectedly, it has been demonstrated that tumorigenesis is dependent on stimulation by the ligand and is abolished in the presence of HGF/SF-specific inhibitors. Conceivably, the onset of HPRC depends both on the presence of inherited Met mutations and on availability of HGF/SF. Furthermore, it has been reported that somatic

mutations of *Met* are selected during metastatic spread of head and neck squamous carcinoma.

Met overexpression is the most common alteration found in human tumors of epithelial origin, in stringent association with metastatic tendency and poor prognosis. In the case of colorectal carcinoma, amplification of the *Met* gene, associated with protein overexpression, confers a selective advantage for acquiring metastatic potential to the liver.

Tumorigenesis can also be associated with ectopic expression of the HGF/SF receptor, as in aggressive osteosarcomas, melanomas, and glioblastomas. Aberrant expression of Met in human tumors of mesenchymal origin is often associated to the secretion of HGF/SF by the same cells, causing formation of autocrine loops which provide invasive properties. The autocrine circuit can sustain not only the persistent activation of the receptor, but also its overexpression, since HGF/SF stimulates *Met* transcription.

See Also the Following Articles

Cell Death by Apoptosis and Necrosis • Mitogen-Activated Protein Kinase Family

Glossary

apoptosis Programmed cell death, the body's normal method of disposing of damaged, unwanted, or unneeded cells.

knock-out The excision or inactivation of a gene within an intact organism or even animal (e.g., "knock-out mice"), usually carried out by a method involving homologous recombination.

src homology 2 (SH2) domains Protein segments able to recognize and bind to phosphorylated tyrosines embedded in specific consensus sequences. They are present in several intracellular proteins acting as signal transducers.

tyrosine kinases Enzymes able to transfer the terminal γ-phosphate groups from ATP to tyrosines that reside in intracellular substrates.

Further Reading

Birchmeier, C., and Gherardi, E. (1998). Developmental roles of HGF/SF and its receptor, the c-Met tyrosine kinase. *Trends Cell Biol.* **8**, 404–410.

Birchmeier, W., Brinkmann, V., Niemann, C., Meiners, S., DiCesare, S., Naundorf, H., and Sachs, M. (1997). Role of HGF/SF and c-Met in morphogenesis and metastasis of epithelial cells. In *Plasminogen-related growth factors* (G. R. Bock and J. A. Goode, eds.) 1st edition, Ciba Found. Symp. 212, pp. 230–240. Wiley, Chichester, England.

Chirgadze, D. Y., Hepple, J., Byrd, R. A., Sowdhamini, R., Blundell, T. L., and Gherardi, E. (1998). Insights into the structure of hepatocyte growth factor/scatter factor (HGF/SF) and implications for receptor activation. *FEBS Lett.* **430**, 126–129.

Comoglio, P. M., and Boccaccio, C. (2001). Scatter factors and invasive growth. *Semin. Cancer Biol.* **11**, 153–165.

Trusolino, L., and Comoglio, P. M. (2002). Scatter-factor and semaphorin receptors: Cell signalling for invasive growth. *Nat. Rev. Cancer* **4**, 289–300.

Van der Voort, R., Taher, T. E., Derksen, P. W., Spaargaren, M., van der Neut, R., and Pals, S. T. (2000). The hepatocyte growth factor/Met pathway in development, tumorigenesis, and B-cell differentiation. *Adv. Cancer Res.* **79**, 39–90.

Biography

Paolo Comoglio is full Professor at the University of Torino Medical School and Scientific Director of the Institute for Cancer Research and Treatment -IRCC- in Candiolo, near Turin. He holds an M.D. from the University of Torino. His postdoctoral studies in immunology were carried out at Washington University in St. Louis. His main interests are the molecular mechanisms of invasive growth under both physiological and pathological conditions, focusing on the role of scatter factors and semaphorins in epithelial morphogenesis and carcinoma progression.

Hexokinases/Glucokinases

Emile Van Schaftingen
University of Louvain, Louvain-la-Neuve, Belgium

Hexokinases are intracellular enzymes that phosphorylate glucose, mannose, and fructose to the corresponding hexose 6-phosphates. These can then be broken down to pyruvate by glycolysis or utilized for various biosyntheses. Glucokinase is, strictly speaking, a form of hexokinase that specifically acts on glucose, and such enzymes indeed exist in microorganisms. The name glucokinase is, however, commonly (and improperly) used to designate mammalian hexokinase IV, an isoenzyme that displays a low affinity for glucose and can therefore play an important role in glucose-sensing.

Role of Phosphorylation in Sugar Utilization

In order to be utilized by cells, monosaccharides need to be transported across the plasma membrane and phosphorylated. In many bacteria, transport of glucose and other sugars is coupled to their phosphorylation by complex systems utilizing the high-energy phosphoryl donor phospho*enol*pyruvate. By contrast, transport and phosphorylation – in this case, at the expense of ATP – are catalyzed by separate proteins in eukaryotic cells and also to some extent in bacteria. Sugars are most often phosphorylated on their last carbon (glucose to glucose 6-phosphate; D-ribose to ribose 5-phosphate; etc.), though in some cases, phosphorylation takes place on the first carbon (D-galactose, L-fucose, fructose in liver).

Phosphorylation provides several advantages: it is an exergonic process, capable of concentrating metabolites inside the cells; it prevents leakage of metabolites across the plasma membrane and intracellular membranes; it increases the potential binding energy of substrates to enzymes, thereby facilitating catalysis. The name hexokinase (from hexose and the Greek word, "κινεειν," to move) was coined by Otto Meierhof to designate the enzyme that activates glucose, making it ready for fermentation by muscle extracts. Kinase was to become the word used to designate all ATP-dependent phosphorylating enzymes.

Reaction Catalyzed by Hexokinases

Hexokinases (EC 2.7.1.1) are defined as enzymes phosphorylating glucose and other closely related sugars (mannose, 2-deoxyglucose, glucosamine, fructose) on their sixth carbon. Glucokinases (2.7.1.2) catalyze the same reaction but with only glucose as a substrate. Glucokinases using ADP or polyphosphate as phosphoryl donor have been described in archaebacteria (*Pyrococcus furiosus* and *Thermococcus litoralis*); these are not discussed further here.

Hexokinases and glucokinases catalyze the transfer of the terminal phosphoryl group of ATP to the oxygen borne by the sixth carbon of glucose. As with other kinases, the true phosphoryl donor is the ATP–Mg complex. Except for ITP, other triphosphonucleotides are usually much poorer substrates than ATP. ADP is generated in the reaction, as well as a hexose 6-phosphate. The reaction is highly exergonic ($\Delta G^{o\prime} \sim -16.7\,\mathrm{kJ\,mol^{-1}}$), which means that in practical terms it is irreversible, most particularly under intracellular physiological conditions ($\Delta G < -30\,\mathrm{kJ\,mol^{-1}}$). However, reversibility of the reaction can be demonstrated *in vitro* provided the generated ATP and glucose are continuously consumed.

The reaction mechanism involves the formation of a ternary complex and an in-line transfer of the phosphoryl group from the donor to the acceptor without formation of an enzyme-bound covalent intermediate. Many studies have been devoted to the determination of the order of substrate addition and product release, without any emerging consensus. It is likely that most hexokinases and glucokinases may bind the substrates in any order to produce a reactive ternary complex, though some enzymes at least definitely display a preferred order (e.g., glucose before ATP in the case of mammalian hexokinase IV).

Diversity of Hexokinases and Glucokinases

Eukaryotes usually have several hexokinases. The yeast *Saccharomyces cerevisiae* has two hexokinases

TABLE I

Some Well-Studied Hexokinases and Glucokinases

	Approximate subunit size (kDa)	Number of subunits	K_m for glucose	Inhibitor	Tissular distribution
Mammals					
Hexokinase I (A)	100	1	~10 μm	Glucose 6-phosphate	Brain, erythrocytes (all tissues)
Hexokinase II (B)	100	1	~100 μm	Glucose 6-phosphate	Heart, skeletal muscle, adipocytes
Hexokinase III (C)	100	1	~1 μm	Glucose 6-phosphate Glucose	(Liver, lung, spleen)
Hexokinase IV (D) (glucokinase)	50	1	~8 mM	Glucose regulatory protein (fructose 6-phosphate)	Liver, β- and α-cells of pancreatic islets, hypothalamic neurons
Invertebrates					
Asterias amurensis (starfish) Hexokinase	50	1	~50 μm	Glucose 6-phosphate	
S. cerevisiae					
Hexokinase A (or PI)	50	2	~100 μm	Trehalose 6-phosphate	
Hexokinase B (or PII)	50	2	~100 μm	Trehalose 6-phosphate	
Glucokinase	50	(aggregates)	~30 μm		

(P_I and P_{II} or A and B) as well as a glucokinase (Table I). All three enzymes have subunits of 50 kDa, the two hexokinases being dimers of 100 kDa. The two hexokinases share ~75% sequence identity with each other and only ~37% sequence identity with glucokinase from the same species. All three enzymes display hyperbolic saturation curves for their substrates and a K_m for glucose < 1 mM. Both hexokinases A and B are inhibited by trehalose 6-phosphate, an intermediate in the formation of trehalose, which appears to play the role of a feedback inhibitor for this enzyme (equivalent to the role of glucose 6-phosphate with mammalian hexokinases).

Mammals have four distinct hexokinases (called I, II, III, and IV, or A, B, C, and D). Hexokinases I to III are ~100 kDa monomeric proteins, which resulted from the duplication of an ancestral gene encoding a 50-kDa hexokinase. They are characterized by low K_m values for glucose (< 0.2 mM) and by their sensitivity to inhibition by physiological concentrations of glucose 6-phosphate. Hexokinase III has an extremely low K_m for glucose and is inhibited by high concentrations of this substrate. Only the C-terminal half of hexokinase I (and probably of hexokinase III) appears to be catalytically active, whereas both amino and carboxyl halves of hexokinase II are endowed with catalytic activity.

Hexokinase IV or D is a ~50-kDa protein that has a low affinity for glucose, a sigmoidal saturation curve for this substrate and is not inhibited by physiological concentrations of glucose 6-phosphate. It is, however, inhibited by a regulatory protein. It does catalyze the phosphorylation of hexoses other than glucose, but due to its low affinity for all hexoses (including glucose), its physiological action is restricted to the most concentrated one, glucose, which is also its best substrate. Furthermore, there is ample evidence that hexokinase D plays the role of a glucose sensor. This may explain the popularity of its designation as "glucokinase," which however does not mean that this enzyme is closer to true (microbial) glucokinases than to hexokinases. As a matter of fact, hexokinase IV is closer to mammalian low K_m hexokinases than to any other hexokinases or glucokinases.

Distinct hexokinase isozymes are also found in insects (e.g., in *Drosophila melanogaster*) and plants. The starfish enzyme is a 50-kDa protein that is inhibited by physiological concentrations of glucose 6-phosphate, indicating that this property is not limited to the 100-kDa enzymes.

Prokaryotes typically contain a series of specific hexokinases that each act on one hexose, normally glucose, mannose, or fructose. They are often composed of two subunits with a smaller size (20–35 kDa) than the eukaryotic enzymes. There are, however, examples of true hexokinases in bacteria (e.g., the hexokinase of the archaebacterium *Thermoproteus tenax*) or of enzymes catalyzing the phosphorylation of two hexoses but not glucose (e.g., mannofructokinase).

Classification and Evolution of Hexokinases

Sugar kinases can be classified into three distinct families (the hexokinase, ribokinase, and galactokinase families)

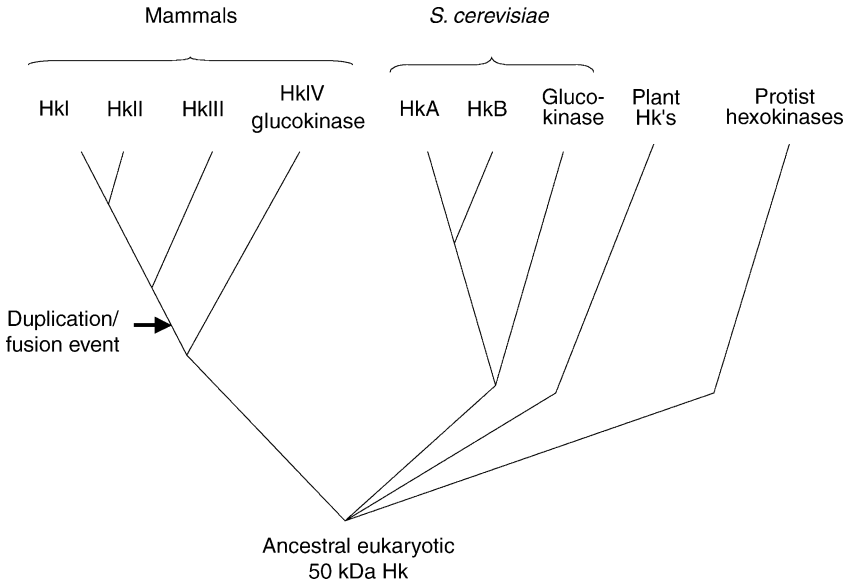

FIGURE 1 Evolutionary relationship between some eukaryotic hexokinases and glucokinases (Hk, hexokinase).

of enzymes that differ in their three-dimensional structures and show no significant similarity. In the hexokinase family, the eukaryotic enzymes form a distinct subfamily of enzymes sharing $>30\%$ sequence identity. The hexokinase family also comprises bacterial enzymes acting on various substrates (hexokinases, glucokinases, mannokinases, fructokinases, and N-acetylmannosamine kinases) that are very distantly related to eukaryotic hexokinases.

The ancestral eukaryotic hexokinase was probably a 50-kDa protein (Figure 1). Early and late duplication events in the fungi lineage led to the appearance of yeast glucokinase and of the more closely related hexokinases A and B. In vertebrates, hexokinase IV (glucokinase) separated from hexokinases I–III before the gene duplication and fusion event that led to the 100-kDa enzyme. Hexokinase III branched off earlier than the duplication event that led to hexokinases I and II, consistent with the closer kinetic properties of the latter two enzymes compared to hexokinase III.

Three-Dimensional Structure

Yeast hexokinase A and B structures were among the first such structures determined during the 1970s. Yeast hexokinase has a bilobar structure with a large (primarily C-terminal) and a small (primarily N-terminal) lobe that are connected by a hinge region. Both domains are made of β-sheets of similar topologies, flanked by α-helices (Figure 2). These are more abundant and larger in the C-terminal domain, accounting for its larger size. Between the two lobes is a deep crevice where the catalytic site resides. The enzyme exists under two distinct conformations, described as open and close, which differ by the dihedral angle between the two lobes.

The glucose-binding site comprises side chains of extremely conserved residues of the hinge region (Asp211 in hexokinase B), the large lobe (Asn237, Glu269, Glu302) and of the small lobe (Ser158, Thr172, Arg173). Binding of glucose to the large lobe induces closure of the catalytic cleft, allowing glucose to contact also the small lobe. The conformational change induced by this substrate is thought to facilitate the subsequent phosphoryl group transfer, being a nice illustration of the induced-fit theory. This theory is also supported by the observation that lyxose, a 5-carbon substrate analogue lacking the hydroxymethyl group that normally serves as phosphoryl acceptor, stimulates by $\sim$30-fold the hydrolysis of ATP to ADP and Pi catalyzed by yeast hexokinase.

Until now, no hexokinase has been crystallized with ATP. The location of the binding site for this substrate, nearby the glucose-binding site, has been inferred – and confirmed by site-directed mutagenesis – from structural analogy of hexokinase with glycerokinase, HSP-ATPase and actin, enzymes that have a similar bilobar architecture as hexokinase.

The crystal structures of human hexokinase I and the enzyme from *Schistosoma mansoni* (*S. mansoni*), a glucose 6-phosphate sensitive enzyme, have been determined recently. They are fundamentally similar to the structure of yeast hexokinase, repeated twice in the case of the mammalian enzyme. The human and *S. mansoni* enzymes were also crystallized as complexes with glucose 6-phosphate, showing that the binding site for this inhibitor overlaps with the putative ATP-binding site.

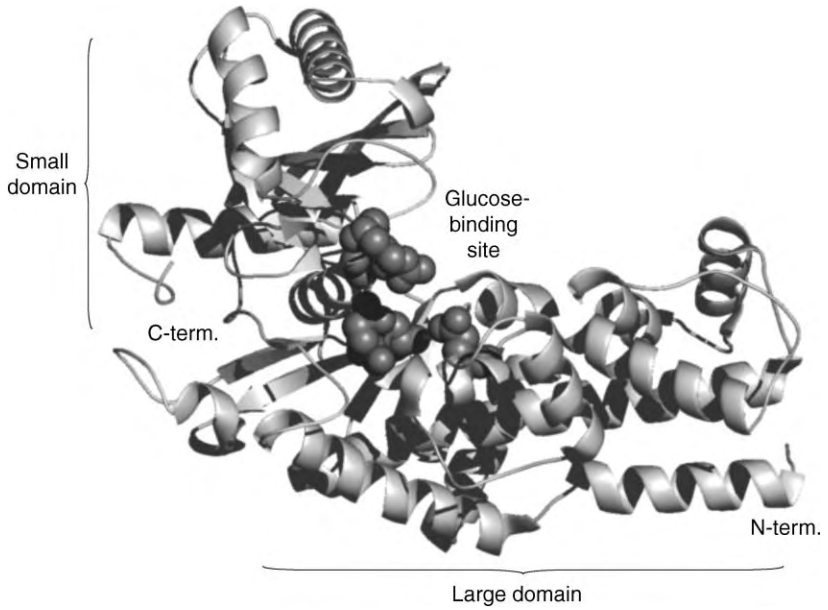

FIGURE 2 Three-dimensional structure of yeast hexokinase. The structure shown is that of the *Saccharomyces cerevisiae* B (P-II) isozyme in its open conformation. Glucose-binding residues are shown as space-filling models. Modified from Kuser, P. R., Krauchenco, S., Antunes, O. A., and Polikarpov, I. (2000) The high resolution crystal structure of yeast hexokinase PII with the correct primary sequence provides new insights into its mechanism of action. *J. Biol. Chem.* **275**, 20814–20821, courtesy of J. F. Collet.

Mammalian Low-K_m Hexokinases

The activity of the low K_m hexokinases cannot be regulated by the glucose concentration in tissues or cell types (human erythrocytes) where the glucose concentration is well above their K_m. In other cell types (e.g., the adipocytes), their activity may well be controlled by the glucose concentration and therefore by glucose transport. There is, however, still a large degree of uncertainty as to the glucose concentration and the rate-limiting aspect of glucose transport in several cell types.

Inhibition by Glucose 6-Phosphate

Hexokinases I–III are inhibited by glucose 6-phosphate in a noncompetitive manner with respect to glucose, but competitive versus ATP. Inhibition by glucose 6-phosphate takes place at physiological concentrations, which argues for its physiological significance. It is antagonized by inorganic phosphate in the case of hexokinase I, but not of hexokinase II. This inhibition involves a site distinct from the glucose-binding site, as indicated by the finding that the phosphorylation product (mannose 6-phosphate, 2-deoxyglucose 6-phosphate) of several good substrates for hexokinase I are poor inhibitors compared to glucose 6-phosphate. At one time, it was thought that the (catalytically inactive) aminoterminal half of hexokinase contained the glucose 6-phosphate allosteric site, but the realization that the isolated carboxyterminal half of the enzyme, as well as starfish hexokinase (a 50-kDa enzyme), were sensitive to glucose 6-phosphate inhibition argued against this hypothesis. Structural studies indicate that glucose 6-phosphate binds to the two halves of hexokinase I, in positions that overlap the putative ATP-binding sites. This agrees with the fact that the inhibition by glucose 6-phosphate is competitive versus ATP but not versus glucose. Site-directed mutagenesis experiments suggest, however, that the binding of glucose 6-phosphate to both sites may contribute to inhibition in hexokinase I.

Subcellular Localization of Mammalian Hexokinases

Hexokinases are cytosolic enzymes, but hexokinases I and II bind to mitochondria, through an N-terminal hydrophobic region that interacts with a porin. This proximity with the mitochondrial pore implies that hexokinases I and II are closer to the main source of ATP and to the main sink for ADP, thus facilitating diffusion. Binding of hexokinase I to mitochondria also decreases the affinity for the inhibitor glucose 6-phosphate.

Hexokinase IV (Glucokinase)

Sigmoidal Kinetics

One intriguing aspect of glucokinase, a monomeric enzyme, is that it displays a sigmoidal saturation curve

for glucose, with a Hill coefficient of 1.6. This is not due to the presence of a second, allosteric binding site for glucose on the glucokinase monomer, but to the existence of two distinct conformations, with low and high affinity for glucose, that equilibrate slowly (as assumed in models designated mnemonical model and slow transition model). If the hypothesis is made that the low-affinity conformation predominates in the absence of glucose, raising the glucose concentration will increase not only the binding of substrate to each of the two forms, but also the proportion of enzyme in the high-affinity conformation. This model is supported by the finding that, in glucokinase crystallized in its free form, the structure of the small domain differs markedly from what it is in low K_m hexokinases, or in glucokinase crystallized as a complex with glucose and an allosteric activator (see below).

Another intriguing aspect of glucokinase is its low affinity for glucose. As all glucose-binding residues found in low K_m hexokinases are conserved in this enzyme, the low affinity must be the result of local or global conformational differences compared to the low K_m hexokinases, most probably the presence of the relatively stable low-affinity state postulated above. This agrees with the finding that mutations of a few selected residues outside the catalytic site may convert glucokinase to a low-K_m enzyme and with the recent discovery of agents – bearing no structural relationship with glucose – that increase the affinity of glucokinase for glucose by binding to an allosteric site in the hinge region.

Liver Glucokinase and its Regulatory Protein

One of the main sites of glucokinase expression is the liver. This is in relation to the ability of this organ to store glucose as glycogen. Glucose transport across the plasma membrane of liver parenchymal cells, carried out by GLUT-2, is extremely rapid. Glucokinase may therefore play a regulatory role and indeed the low affinity that glucokinase displays for glucose is one of the mechanisms by which glucose uptake can be regulated by glucose concentration. In addition to this, glycogen metabolism is under the direct control of glucose, which binds to glycogen phosphorylase, thereby affecting the phosphorylation state of this enzyme as well as of glycogen synthase.

Hepatic glucokinase is controlled by a glucokinase regulatory protein (GKRP), which binds to glucokinase and inhibits it in a competitive manner with respect to glucose. Association of the two proteins is stimulated by fructose 6-phosphate, a GKRP ligand, which behaves therefore as an inhibitor of glucokinase, and antagonized by fructose 1-phosphate, another GKRP ligand. Regulation by GKRP makes, therefore, that glucokinase in intact liver cells has a lower affinity for glucose than the purified enzyme, and that low concentrations of fructose stimulate glucose utilization by the liver.

Quite surprisingly, GKRP appears also to control the subcellular localization of glucokinase: this enzyme is predominantly in the nucleus at low concentration of glucose and in the absence of fructose, but moves to the cytosol when the glucose concentration increases or if fructose is added. The physiological meaning of glucokinase translocation is not known, but it may be to protect glucokinase against degradation by cellular proteases. This would be consistent with the finding that mice devoid of GKRP have lower amounts (and total activities) of glucokinase than wild-type mice.

Role of Glucokinase in β-Cells

The low affinity that this enzyme displays for glucose (half-saturation is observed at 8 mM with the human enzyme), the sigmoidal saturation curve, and the lack of inhibition by physiological concentrations of glucose 6-phosphate make that this enzyme is well suited to respond to changes in glucose concentration and to act thereby as a "glucose sensor." This role is well established in the case of the insulin-secreting cells (β-cells) of pancreatic islets. Glucose appears to be one of the main fuels for β-cells. Raising the glycolytic flux (e.g., by raising the glucose concentration) leads to an increase in the cytosolic [ATP]/[ADP] ratio, which in turn results in closure of a nucleotide-sensitive K^+ channel. The ensuing depolarization of the plasma membrane causes an increase in the cytosolic Ca^{2+} concentration, which triggers insulin secretion. Metabolic analyses indicate that glucokinase, not glucose transport or a step beyond glucose phosphorylation, plays a major role in the control of this system. Accordingly, a form of diabetes known as maturity-onset diabetes of the youth type 2 is due to glucokinase mutations resulting in decreased enzymatic activity. The disease is dominantly inherited, which means that a mutation in one copy of the gene (resulting in at most a 50% decrease in glucokinase activity) is sufficient to perturb the "glucose-sensing apparatus of the pancreas." Conversely, glucokinase mutations that increase the activity (mostly by increasing the affinity for glucose) may result in familial hypoglycemia.

See Also the Following Article

Glucose/Sugar Transport in Mammals

Glossary

glucokinase Hexokinase that acts specifically on glucose; also mammalian hexokinase IV.

hexokinase Enzyme catalyzing the ATP-dependent phosphorylation of glucose and related hexoses (mannose, 2-deoxyglucose, fructose) to their 6-phospho-derivative.

mnemonical and slow transition models Kinetic models allowing one to explain the non-hyperbolic saturation curve of some monomeric enzymes, most particularly the sigmoid saturation curve of mammalian glucokinase. These models assume the existence of two conformations with distinct affinities for the substrate and that they interconvert slowly. Only the high-affinity conformation is endowed with catalytic activity in the mnemonical model.

Further Reading

Aleshin, A. E., Zeng, C., Bartunik, H. D., Fromm, H. J., and Honzatko, R. B. (1998). Regulation of hexokinase I: crystal structure of recombinant human brain hexokinase complexed with glucose and phosphate. *J. Mol. Biol.* **282**, 345–357.

Cárdenas, M. L., Cornish-Bowden, A., and Ureta, T. (1998). Evolution and regulatory role of the hexokinases. *Biochim. Biophys. Acta* **1401**, 242–264.

Grimsby, J., Sarabu, R., Corbett, W. L., Haynes, N. E., Bizzarro, F. T., Coffey, J. W., Guertin, K. R., Hilliard, D. W., Kester, R. F., Mahaney, P. E., Marcus, L., Qi, L., Spence, C. L., Tengi, J., Magnuson, M. A., Chu, C. A., Dvorozniak, M. T., Matschinsky, F. M., and Grippo, J. F. (2003). Allosteric activators of glucokinase: Potential role in diabetes therapy. *Science* **301**, 370–373.

Kamata, K., Mitsuya, M., Nishimura, T., Eiki, J., and Nagata, Y. (2004). Structural basis for allosteric regulation of the monomeric allosteric enzyme human glucokinase. *Structure (Camb.)* **12**, 429–438.

Kuser, P. R., Krauchenco, S., Antunes, O. A., and Polikarpov, I. (2000). The high resolution crystal structure of yeast hexokinase PII with the correct primary sequence provides new insights into its mechanism of action. *J. Biol. Chem.* **275**, 20814–20821.

Matschinsky, F. M. (2002). Regulation of pancreatic beta-cell glucokinase: From basics to therapeutics. *Diabetes* **51**, S394–S404.

Mulichak, A. M., Wilson, J. E., Padmanabhan, K., and Garavito, R. M. (1998). The structure of mammalian hexokinase-1. *Nat. Struct. Biol.* **5**, 555–560.

Van Schaftingen, E., Detheux, M., and Veiga da Cunha, M. (1994). Short-term control of glucokinase activity: Role of a regulatory protein. *FASEB J.* **8**, 414–419.

Wilson, J. E. (1995). Hexokinases. *Rev. Physiol. Biochem. Pharmacol.* **126**, 65–198.

Biography

Emile Van Schaftingen is a Researcher at the Christian de Duve Institute of Cellular Pathology in Brussels (ICP) and a Professor of Biochemistry at the Faculty of Medicine of the Université Catholique de Louvain (UCL). His principal research interests are the regulation of glucose metabolism in mammalian cells and more recently the repair of glucose-induced damage to proteins. He has authored or co-authored more than 120 research publications. He holds an M.D. from UCL and received a Ph.D. from the same university under the supervision of Prof. Henri-Géry Hers.

Histamine Receptors

Stephen J. Hill and Jillian G. Baker
University of Nottingham, Nottingham, UK

Histamine (a basic amine) is a hormone secreted by a number of cell types (e.g., mast cells, basophils, and nerve cells). Its normal physiological function is to act as a local hormone (i.e., one that is secreted and acts on neighboring cells rather than entering the bloodstream) or a neurotransmitter (which acts on neighboring cells following release from nerve endings in response to electrical impulses). For example, histamine is secreted from mast cells in the stomach where it is involved in the normal regulation of gastric acid secretion. Histamine is also an important contributor to the pathophysiological processes of allergic inflammatory reactions. Upon exposure to an allergen or antigen, histamine is released from mast cells which exist throughout the body. The reaction may be localized, as in a minor insect bite or, rarely, generalized to become life-threatening anaphylaxis (e.g., ingestion of penicillin in a penicillin-allergic individual, where histamine release is so widespread that it enters the bloodstream and causes catastrophic reactions).

The actions of histamine are mediated by the binding of extracellular histamine to one of four different G-protein-coupled receptors (GPCRs; namely, H_1, H_2, H_3, H_4). These are, like all GPCRs, embedded in the cell surface plasma membrane. They have seven membrane-spanning domains that are connected together by six loops of amino acids (three outside and three inside the cell; see Figure 1). They also have a string of amino acids at the N terminus that are on the outside of the cell and a string at the C terminus that hang inside the cell. Once activated, each type of histamine receptor interacts with a specific class of heterotrimeric G proteins, which in turn alter levels of intracellular second messengers (e.g., cyclic AMP and Ca^{2+} ions). These second messengers then trigger a variety of intracellular processes.

Histamine H_1-Receptor

The human histamine H_1-receptor is a 487 amino acid protein and is encoded by a gene on chromosome 3. It has a very large third intracellular loop (208 amino acids; through which it mediates interactions with the $G_{q/11}$ family of G proteins) and a relatively short (17 amino acids) intracellular C-terminal tail. As with all $G_{q/11}$-coupled receptors, stimulation of the receptor–$G_{q/11}$ protein complex results in activation of the enzyme phospholipase Cβ. This leads to the formation of the intracellular second messengers inositol 1,4,5-triphosphate (IP_3) and diacylglycerol. IP_3 is released into the cytosol and then stimulates the release of intracellular free Ca^{2+} ions (which, for example, can result in smooth muscle contraction), while diacylglycerol can activate protein kinase C and mediate responses such as cell proliferation and the activation of the trasncription of pro-inflammatory genes.

Histamine H_1-receptors are found throughout the body. Activation of H_1-receptors in smooth muscle leads to contraction in the walls of the airways, gastrointestinal tract, and in blood vessels. In endothelial cells (cells that line the inside of blood vessels), H_1-receptor activation increases vascular permeability (which is responsible for the characteristic "wheal" response seen in the skin after, e.g., insect bites) and leads to the synthesis and release of vascular smooth muscle relaxants (e.g., prostacyclin and nitric oxide). Activation of H_1-receptors also stimulates the release of catecholamines (noradrenaline (norepinephrine) and adrenaline (epinephrine)) and enkephalins from chromaffin cells in the adrenal medulla. In neurons, histamine H_1-receptor stimulation activates peripheral sensory nerve endings leading to itching. Via an axonal reflex, peptide neurotransmitters are subsequently released from nearby collateral nerve endings leading to a surrounding vasodilatation (flare). In the brain, H_1-receptors are present in the cerebral cortex, hippocampus, nucleus accumbens, thalamus, and posterior hypothalamus, activation of which stimulates an increase in neuronal activity.

A very similar H_1-receptor is found in other animal species and contains 491 (bovine), 486 (rat), 488 (guinea pig), and 489 (mouse) amino acids.

H_1 Agonists

Besides histamine itself, there are several histamine derivatives that also bind to and activate (i.e., are agonists of) the histamine H_1-receptor. N-methylhistaprodifen, 2-(3-(trifluoromethyl)phenyl)-histamine,

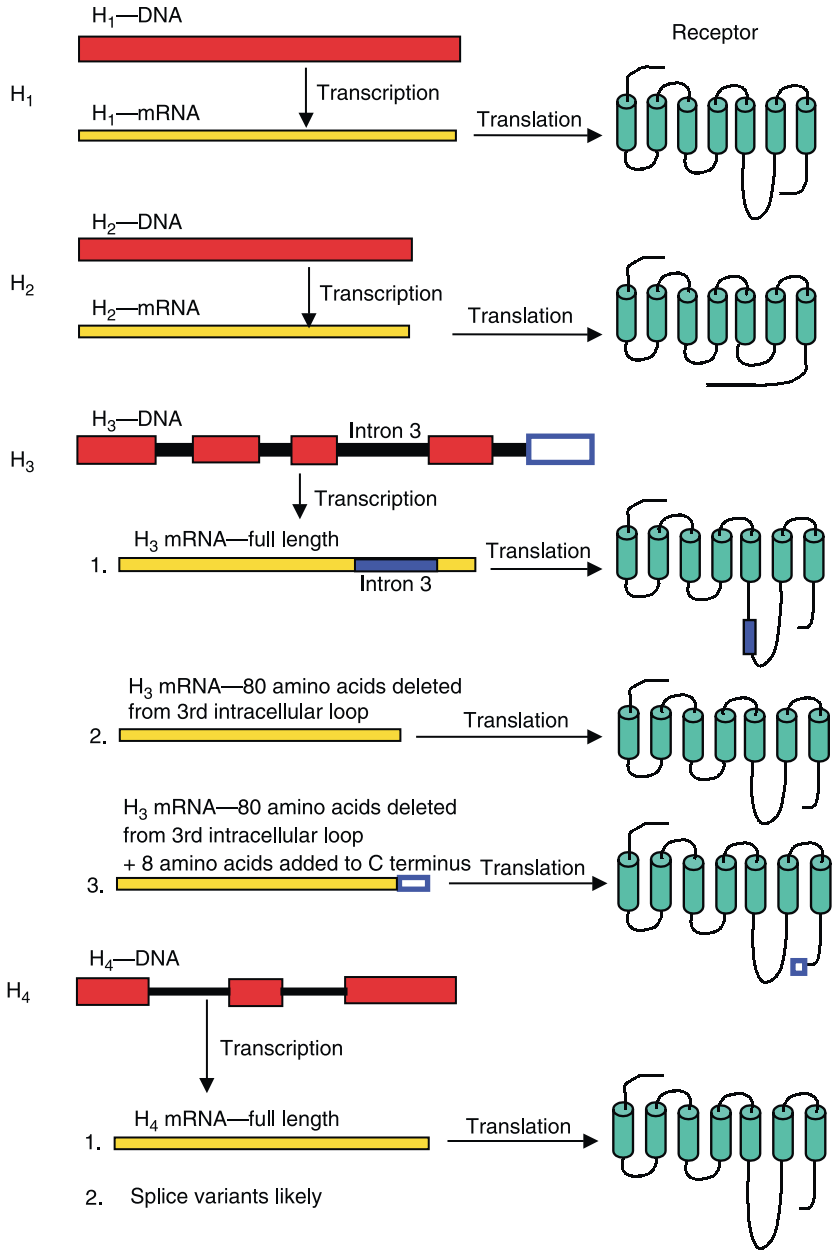

FIGURE 1 Transcription and translation of histamine receptors.

2-(3-bromophenyl)-histamine, and histaprodifen are all more potent than histamine itself and bind better to H_1-receptors (i.e., are more selective) than to other types of histamine receptors. There is no therapeutic indication for H_1-receptor agonists, but these compounds are important for fundamental research into the physiological and pathophysiological roles of histamine H_1-receptors.

H_1-Antagonists

Classical H_1-receptor antagonists, including mepyramine, chlorpheniramine, promethazine, diphenhydramine, and cyproheptadine, are used as systemic and/or topical preparations in the management of allergic reactions (i.e., hay fever, allergic rhinitis, insect bites, and anaphylactic reactions). However, at therapeutic doses, many of these H_1-antagonists cross the blood–brain barrier, antagonize CNS H_1-receptors, and lead to a decrease in neuronal activity and hence sedation. This "side effect" has been exploited in the development of several preparations marketed as sleeping aids (e.g., diphenhydramine or promethazine). A second generation of H_1-antagonists has been developed which is much less able to cross the blood–brain barrier and hence is much less sedating (e.g., cetirizine, loratidine, fexofenadine, terfenadine, and astemizole).

H_1-antagonists are also used in the management of non-allergic urticaria, e.g., hydroxyzine, cyproheptadine, and promethazine. Many H_1-receptor antagonists also possess marked muscarinic receptor antagonist properties (e.g., cyclizine, promethazine, and diphenhydramine) and this "side effect" is exploited for the treatment of nausea and motion sickness. Several other classes of drugs, such as the antidepressant drugs doxepin, amitriptyline, and mianserin, are also potent H_1-antihistamines and hence are sedating.

Interestingly, some of the H_1-antagonists in current use, e.g., chlorpheniramine, loratidine, and cetirizine, are actually inverse agonists of the H_1-response. That is, upon binding to the receptor, instead of just blocking histamine-binding and hence histamine-activation of the receptor, they actively turn off the response (i.e., produce an opposite effect to agonists) and hence decrease the basal response of the cell.

Recently, two second-generation H_1-antihistamines (terfenadine and astemizole) have been associated with an increased incidence of cardiac arrhythmias. This appears to be due to an ability to directly block cardiac HERG1 K^+ channels and has led to the withdrawal of terfenadine and astemizole in a number of countries. A number of other second-generation antihistamines (e.g., cetirizine and loratidine), however, do not share this property.

Histamine H_2-Receptors

The human histamine H_2-receptor contains 359 amino acids and is encoded by a single exon on chromosome 5. Unlike the H_1-receptor, the histamine H_2-receptor has a short third intracellular loop (30 amino acids), a much longer C-terminal tail (70 amino acids), and couples to G_S proteins to stimulate the enzyme adenylyl cyclase. This leads to the synthesis of the intracellular second messenger cyclic AMP, which activates protein kinase A, and in turn stimulates cellular responses. In gastric parietal cells, histamine activation of H_2-receptors stimulates gastric acid secretion in the stomach. In the heart, H_2-receptor activation and subsequently an elevation in cAMP production leads to an increase in both the rate and force of contraction, whereas in smooth muscle (in the airways and in blood vessels) the H_2-receptor-mediated increase in cAMP produces relaxation. H_2-receptors are also present in lymphocytes where histamine activation inhibits antibody synthesis, T-cell proliferation, and cytokine production. However, in some cell types (particularly gastric parietal cells), there is increasing evidence that H_2-receptor stimulation can also release calcium from intracellular stores leading to an increase in intracellular Ca^{2+} concentrations. Finally, H_2-receptor activation in the brain usually results in a decrease of neuronal activity, except in hippocampal neurons where the long-lasting after-hyperpolarization is blocked and excitatory stimuli potentiated.

Very similar H_2-receptor structure and function has been observed in other animal species, including dog, guinea pig, mouse (all have 359 amino acids), and rat (358 amino acids).

H_2-Receptor Agonists

A number of very selective potent agonists (including impromidine, arpromidine, dimaprit, and amthamine) are available for the histamine H_2-receptor, although as with the H_1-receptor, none are used clinically. In the case of impromidine and arpromidine, the compounds are 48 and 100 times more potent, respectively, than histamine itself. However, although acting as agonists at the H_2-receptor, some of these compounds are antagonists at other histamine receptors (see Table I).

H_2-Receptor Antagonists

H_2-receptor antagonists are widely used in the management of gastric and duodenal ulcers and in gastro-esophageal reflux disease. The development of specific antagonists for the H_2-receptor is a classic example of rationale drug design for which Sir James Black won the Nobel prize. Burimamide was the first compound that demonstrated selectivity for H_2- over H_1-receptors. It reduced gastric acid secretion and reduced the blood pressure response to histamine. However, with the discovery of the H_3-receptor, burimamide was subsequently found to be a more potent H_3-receptor antagonist. Cimetidine was developed directly from burimamide and is an effective agent in the treatment of gastric and duodenal ulceration because of its ability to inhibit basal and gastrin-stimulated gastric acid secretion. Several other highly selective H_2-receptor antagonists, including ranitidine, famotidine, and nizatidine, are also available now and are in regular clinical use.

Burimamide is a neutral antagonist, i.e., it binds to the H_2-receptor and therefore blocks histamine activation of the receptor. Cimetidine and ranitidine block histamine activation and are also inverse agonists, i.e., upon binding to the H_2-receptor, they actively turn off the receptor and thus decrease basal cAMP in cells.

Histamine H_3-Receptors

The human histamine H_3-receptor (445 amino acids) and the gene encoding this receptor has been localized to chromosome 20. It has a long third intracellular loop (142 amino acids) and a short C-terminal tail (29 amino acids). The receptor couples to the $G_{i/o}$ family of G proteins that can inhibit adenylyl cyclase activity, thus upon histamine activation of the receptor intracellular

TABLE I

Pharmacology of Histamine Receptor Subtypes

	H_1	H_2	H_3	H_4
Human gene (amino acids)	487	359	445	390
Introns	No	No	Yes	Yes
Chromosome	3	5	20	18
G protein	$G_{q/11}$	G_s	$G_{i/o}$	$G_{i/o}$
Cellular response	Ca^{2+}/IP_3	Increase in cAMP	Decrease in cAMP Inhibition of neurotransmitter release	Decrease in cAMP
Agonists	Histamine Histaprodifen N-methylhistaprodifen	Histamine Arpromidine Impromidine Amthamine dimaprit	Histamine Imetit Immepip R-α-methylhistamine	Histamine Imetit Immepip Clozapine[a] Thioperamide (weak)
Antagonists	Meyramine[a] Chlorpheniramine[a] Promethazine[a] Cyproheptidine[a] Cetirizine[a] Loratidine[a] Fexofenadine[a] Cyclizine[a] Terfenadine Astemizole Arpromidine	Cimetidine[a] Titotidine Famotidine[a] Nizatidine[a] Ranitidine[a] Mifentidine	Thioperamide Iodophenpropit Clobenpropit Ciproxifan Iodoproxyfan Impentamine Proxyfan	Clobenpropit

[a] Drugs in clinical use.

cAMP is decreased. The histamine H_3-receptor was first identified as a presynaptic autoreceptor which can inhibit the synthesis and release of more histamine from the same and surrounding histaminergic nerves in the CNS. The small number of neurons that use histamine as a neurotransmitter in the brain have their cell bodies in the posterior hypothalamus, but their axons extend to innervate most areas of the forebrain. H_3-receptors, however, are also found on the terminals of other neurons, e.g., those that use acetylcholine, 5-HT, dopamine, and noradrenaline as neurotransmitters. This is also true for peripheral neurons, where H_3-receptor activation leads to the inhibition of the release of sympathetic neurotransmitters in human saphenous vein, heart, bronchi, and trachea.

Splice Variants of the H_3-Receptor

Unlike the genes for H_1- and H_2-receptors, the gene that encodes the H_3-receptor contains introns. These are areas of DNA that are not transcribed into the finished mRNA (and not therefore translated into protein). During transcription, these areas are skipped and the coding regions either side are joined up to make the continuous strand of mRNA. The H_3-receptor has three of these introns (and therefore four coding regions or exons, see Figure 1). This means that, as a consequence of the coding sequences either side of an intron being joined together at different points within the overall receptor-coding region, multiple forms of the H_3-receptor can be produced from the single H_3-receptor gene. This is called alternative splicing, and the resulting isoforms of the receptor formed are called splice variants. So far, several isoforms of the H_3-receptor have been detected in different species. In the guinea pig, two isoforms have been identified that differ by a 30 amino acid stretch within the third intracellular loop of the receptor. In the rat, three functionally active H_3-receptor isoforms have been identified: a full-length version and two that lack either 32 or 48 amino acids in the middle of the third intracellular loop of the receptor. Each of these three H_3-receptor isoforms has a different distribution with the CNS and signals with different efficacy to inhibit adenylyl cyclase and other signaling pathways. In the human at least six distinct isoforms have been identified, of which three (including the full-length receptor) are functionally active H_3-receptor proteins. One of the active human isoforms lacks 80 amino acids contained entirely within the third intracellular loop. The other has this 80 amino acid deletion

as well as a novel eight amino acid C terminus. As several different H_3-splice variants exist with different signal transduction capabilities, this splicing mechanism offers a way for tightly regulating the biological actions of the H_3-receptor in different tissues.

H_3-Receptor Agonists and Antagonists

Although it is clear that human H_3-receptors are involved in neurotransmission, and potential therapeutic indications for clinical intervention have been identified (e.g., for the treatment of Alzheimer's disease, Parkinson's disease and the maintenance of wakefulness), no drugs are in current clinical use. Nevertheless, agonists and antagonists have been developed for scientific purposes. Agonists with good selectivity for H_3-receptors (relative to H_1- and H_2-receptors) include R-α-methylhistamine, imetit, and immepip. H_3-receptor antagonists include thioperamide, clobenpropit, iodoproxyfan, ciproxifan, and impentamine which all have higher affinity for H_3-receptor than for H_1- and H_2-receptors.

Constitutive H_3-Receptor Activity and Inverse Agonism

The H_3-receptor appears to be naturally expressed in a constitutively active form in the CNS. That is, the mere presence of the H_3-receptor itself causes a substantial intracellular response (in this case decrease in cAMP or inihibiton of neurotransmitter release) in the absence of agonist. Other GPCRs have been artificially mutated in the third intracellular loop to make them constitutively active and these engineered sequences are very similar to those naturally occurring in the H_3-receptor. This naturally occurring constitutive activity means that there is potential for developing inverse agonists (to turn off the receptor) as well as agonists (for activating the receptor) and neutral antagonists (that just stop other drugs binding, whether they are agonists or inverse agonists). Many of the compounds developed as H_3-receptor antagonists have been shown to behave as inverse agonists in cell lines expressing recombinant H_3-receptors. These include thioperamide, clobenpropit, and iodophenpropit. Neutral antagonists (e.g., proxyfan) have also been identified.

Histamine H_4-Receptors

The human H_4-receptor (390 amino acids) is encoded by a gene on chromosome 18. Like the H_3-receptor it has a genomic structure consisting of introns and exons suggesting that splice variants may also occur (see Figure 1). It too has a long third intracellular loop (111 amino acids) and a short C terminus (28 amino acids). Again like the H_3-receptor, the H_4-receptor couples to the $G_{i/o}$ family of G proteins and therefore activation results in an inhibition of adenylyl cyclase activity. The H_4-receptor is found primarily in cells of the immune system (e.g., in bone marrow, neutrophils, eosinophils, spleen, and mast cells). The H_4-receptors from rat, mouse (both 391 amino acids long), and guinea pig (389 amino acids) have also recently been cloned.

Ligands for the H_4-Receptors

Currently, there are no drugs undergoing clinical trials that are designed to specifically interact with the histamine H_4-receptor, although their rather selective localization within the immune system will surely see the development of H_4-immune-modifying drugs in future. Imetit and immepip are high-affinity H_4-receptor agonists that are used in scientific research. Clobenpropit also binds with high affinity to the H_4-receptor but has weak H_4-agonist activity. R-α-methylhistamine (a weak H_4-agonist) and thioperamide (an H_4-antagonist) also bind to the H_4-receptor but with less affinity than the H_3-receptor. Some data also suggest that thioperamide may have inverse agonist activity on the H_4-receptor. The atypical antipyschotic drug clozapine is also an H_4-agonist.

See Also the Following Articles

Adenylyl Cyclases • G Protein-Coupled Receptor Kinases and Arrestins • G_i Family of Heterotrimeric G Proteins • Phospholipase C

Glossary

agonist A drug that binds to a receptor and turns on the processes that lead to a functional response (i.e., it binds to the receptor and has positive efficacy).

constitutive receptor activity Occurs when GPCRs in a cell spontaneously associate with a G protein and increase the basal response even when there is no agonist present.

inverse agonist A drug that binds to a receptor and actively turns off the receptor activation process (i.e., it binds to the receptor and has negative efficacy). It therefore has the opposite effect to an agonist. Thus, when there is constitutive receptor activity (in the absence of an agonist), inverse agonists will reduce the basal response.

neutral antagonist A drug that binds to a receptor and prevents the binding of agonists or inverse agonists (i.e., it binds to the receptor and has no efficacy).

Further Reading

Hill, S. J. (1990). Distribution, properties and functional characteristics of three classes of histamine receptor. *Pharmacol. Rev.* **42**, 45–83.

Hill, S. J., Ganellin, C. R., Timmerman, H., Schwartz, J. C., Shankley, N. P., Young, J. M., Schunack, W., Levi, R., and Haas, H. L. (1997). International union of pharmacology XIII classification of histamine receptors. *Pharmacol. Rev.* **49**, 253–278.

Hough, L. B. (2001). Genomics meets histamine receptors: New subtypes, new receptors. *Molecul. Pharmacol.* **59**, 415–419.

Leurs, R., Watanabe, T., and Timmerman, H. (2001). Histamine receptors are finally "coming out". *Trends Pharmacol. Sci.* **22**, 337–339.

Leurs, R., Church, M. K., and Taglialatela, M. (2002). H_1-antihistamines: Inverse agonism, antiinflammatory actions and cardiac effects. *Clin. Exp. All.* **32**, 489–498.

Van der Goot, H., and Timmerman, H. (2000). Selective ligands as tools to study histamine receptors. *Eur. J. Med. Chem.* **35**, 5–20.

Biography

Stephen J. Hill is a Professor of Molecular Pharmacology in the Institute of Cell Signalling at the University of Nottingham, United Kingdom. His principal research interests are in the molecular pharmacology of G-protein-coupled receptors. He holds a Ph.D. from the University of Cambridge where he also undertook his postdoctoral training.

Jillian G. Baker is a Wellcome Trust Clinical Scientist Fellow and Registrar in Respiratory and General Internal Medicine. Her current research interest is the study of the effect of G-protein-coupled receptor activation on gene transcription. She obtained her Medical Degree and Ph.D. from the University of Nottingham.

HIV Protease

Ben M. Dunn
University of Florida College of Medicine, Gainesville, Florida, USA

HIV protease is a proteolytic enzyme and is part of the protein component of the human immunodeficiency virus (HIV). HIV protease plays a critical role in the life cycle of the virus and for this reason has become an important target for drug development in the battle against HIV infection. HIV protease is a member of the aspartic protease family of proteolytic enzymes and discoveries in the general field have provided clues to effective drug design. Subsequently, HIV protease has become one of the most thoroughly studied proteins and most likely has been studied by structural analysis more than any other protein.

Human Immunodeficiency Virus (HIV)

Human immunodeficiency virus (HIV) is an enveloped virus with RNA as the molecule used for storage of genetic information. HIV is a retrovirus, which means that the RNA is converted into a DNA copy that becomes integrated into the genomic DNA of a host cell. The genomic DNA is transcribed into RNA by the normal cellular machinery and this RNA is used as both messenger RNA for production of proteins by cellular ribosomes and as daughter RNA for assembly into new viral particles. HIV infects cells of the human immune system, leading to death of the cell and, thus, depletion of the immune constituents of the bloodstream with a consequent fall in immune function. Hence, the name of the disease caused by HIV is acquired immunodeficiency syndrome (AIDS). This disease is a scourge upon humankind and, as of early 2000s, has killed millions worldwide and infected as many as 40 million more.

Proteins of HIV

Gag Proteins

Translation of the gag/pol messenger RNA of HIV leads to the production of two proteins: Gag and Gag/Pol. The Gag polyprotein has a molecular weight of ~55 kDa and is called a polyprotein because it contains several proteins connected head-to-tail. Three of the proteins of the Gag polyprotein (Figure 1) are important constituents of the new viral particles: matrix, or MA, a 17-kDa protein that forms a spherical shell around other proteins, thus providing one level of packaging for the viral particle; capsid, or CA, a 24-kDa protein that forms conical structure within the matrix shell and contains the daughter RNA, providing a second layer of protection; and nucleocapsid, or NC, a 7-kDa protein that binds to the RNA to provide a third level of packaging. When the new viral particle buds off from an infected cell, it takes some of the cell envelope along with it to complete the packaging of the new virion.

Pol Proteins

The *Pol* gene, which is the second part of the Gag/Pol fusion protein, codes for a polyprotein containing three enzymatic functions: reverse transcriptase (RT), which copies the viral RNA into DNA; protease (PR), which acts to cleave the Gag and Gag/Pol proteins into their separate pieces; and integrase (IN), which catalyzes the insertion of the DNA copy of the viral genetic information into the host cell genome.

Structure of HIV Protease

HIV protease begins as a component of the Gag/Pol fusion polyprotein. As a single molecule, the Gag/Pol-embedded protease is inactive, because dimer formation is required to create the active site and catalytic machinery.

Gag/Pol Polyprotein and Viral Assembly

Following ribosomal synthesis, Gag/Pol fusion proteins become myristolated and assemble on the inner surface of the cell membrane. This concentration of the protein leads to dimerization at several points along the polyprotein, including the HIV protease. The dimerization of two protease components of the polyprotein may be assisted by prior assembly of other regions of the protein, such as the proteins in the Gag portion.

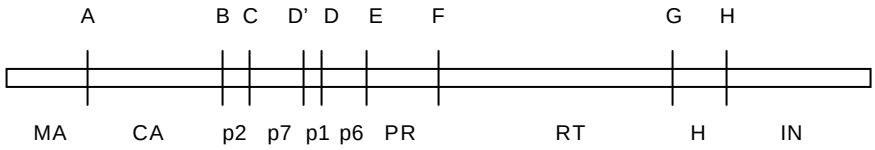

FIGURE 1 Diagram illustrating the arrangement of the Gag–Pol polyprotein. The letters above the boxes indicate the cleavage sites within the Gag–Pol polyprotein. The codes below the boxes indicate the designations for the protein products of the cleavages.

The viral particle, or virion, buds off from the cell, taking some of the plasma membrane along. At this point, the virus is immature and non-infectious. Upon a change in conditions, possibly caused by an influx of protons into the virion with concomitant decrease in pH, the protease begins its function of cutting apart Gag and Gag/Pol fusion proteins. Little is known about the structure of the Gag/Pol fusion protein in the immature virion. It has been demonstrated that the cleavage of the viral polyprotein into smaller units proceeds by a series of steps that could be controlled by the organization of the polyprotein or by the selectivity of the protease for the different cleavage site junctions.

Structure of HIV Protease as an Isolated Entity

Once released from attachment to the other components of the viral Gag/Pol polyprotein, or when expressed from the 297 bp gene encoding the sequence, HIV protease can be isolated and crystallized. The three-dimensional structure reveals a molecule with structural similarities to other members of the aspartic protease family, but with some significant differences. The enzyme is a dimer of two identical 99 residue monomers and has a folding pattern that contains all the elements seen in the pepsin-like aspartic proteases, including a deep active site cleft on one side of the molecule (Figure 2) with both monomers contributing contact sites for bound substrates or inhibitors. Each monomer provides one aspartic acid residue and the carboxylic acid side chains of each of these come together at the bottom of the active site and bind a water molecule, which completes the catalytic machinery. This machinery catalyzes the attack of the water molecule upon the peptide bond of a bound substrate.

Inhibitor Binding

Due to the desire to create potent and selective inhibitors of the HIV protease, many different laboratories, in pharmaceutical companies, in government institutes, and at universities have studied complexes of HIV protease with small molecule inhibitors. In fact, HIV protease was the first case where structural biology provided key insights that were used to design new, effective compounds. To date, the FDA has approved seven drugs for use in humans and these have had an enormous impact on therapy of AIDS patients. The approved compounds provide a longer life span and an improved quality of life. However, problems with the development of resistant variants dampen the success.

Mode of Inhibitor Binding

Inhibitors bind within the active site cavity of HIV protease, similar to what has been shown for binding of inhibitors against other members of the aspartic protease family. The compounds are arranged in an extended conformation (Figure 3) with hydrogen bonding to backbone atoms of the protease and with interactions between groups of the inhibitor and hydrophobic regions of the active site cleft. These interactions provide the specificity and potency of binding necessary to have a compound that will not cause harm to the aspartic proteases of the human host. The FDA-approved drugs all meet these criteria; however, some have side effects that are not completely understood at this time.

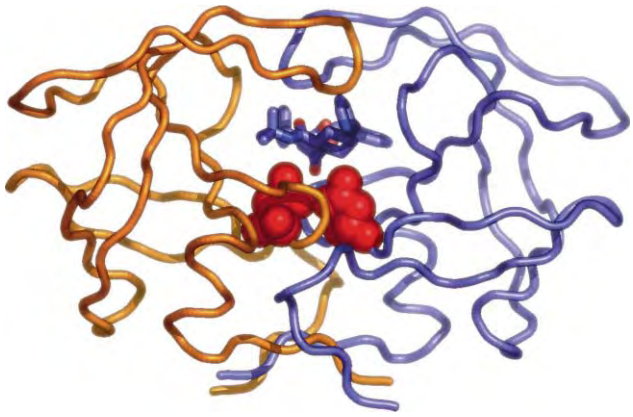

FIGURE 2 Representation of the three-dimensional structure of HIV protease. Two identical domains are shown in orange (left monomer) and blue (right monomer). Each domain contributes one aspartic acid residue to the catalytic machinery at the bottom of the active site cleft. These are shown in space-fill representation near the center of the figure. A bound inhibitor is shown above the two aspartic acids and directly in the middle of the active site cleft. Above the inhibitor, one can see the two prominent beta-hairpin "flaps," one from each monomer. The flaps cover the inhibitor in the bound state depicted here.

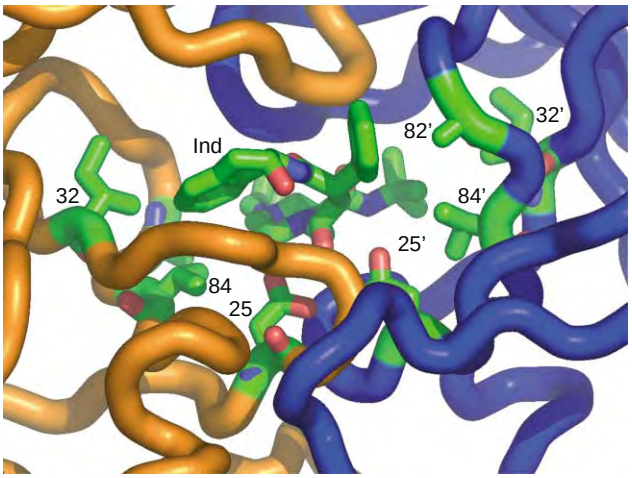

FIGURE 3 Close-up view of a bound inhibitor (shown in capped-sticks representation at the center of the picture) within the active site cleft of HIV protease. The two catalytic aspartic acids are seen just below the inhibitor. Several amino acids of the HIV protease are shown around the inhibitor. Each monomer contributes several amino acids that make hydrophobic interactions with the bound inhibitor. This view shows a drug-resistant form of HIV-1 protease, with Val32Ile, Val82Ala, and Ile84Val mutations shown in this view.

Development of Resistant HIV Protease Variants

As a retrovirus, replication of the virus begins with the creation of a DNA copy of the viral RNA genome. The enzyme that performs this reaction, HIV RT, is coded for by the virus and is present in the infectious virion particle. The process does not take place until the virion enters a new cell and the four different barriers protecting the viral RNA are stripped off. HIV RT makes errors while copying the viral genetic information and, unlike DNA polymerases of human cells, HIV RT does not have a proof-reading function. This results in nucleotide changes during replication, so that the progeny virus will contain variations on the sequence of the infecting virus. On an average, one nucleotide is altered in each round of replication of virus. As replication takes ~2 days, the number of mutations that can arise over a 6-month period is quite large. Some of these nucleotide alterations will not change the amino acid (silent mutations), but some will. What will be the properties of the new viral protein? In some cases, the progeny virus will be defective and noninfectious, as function could be affected by the mutations. In other cases, the new virus will have favorable properties. This is how drug-resistant variants arise during therapy, especially if the patient does not follow the drug regimen prescribed. Virus that is sensitive to the drug will be killed off, but virus that has properties that include decreased sensitivity to the effects of the antiviral drugs will survive and multiply.

The Spectrum of Drug-Resistant Variants

Out of the 99 amino acid HIV PR, as many as 25–30 amino acids can change without losing catalytic activity. In many cases, the efficiency of the enzyme is reduced, but as long as a threshold of activity is maintained (believed to be ~10% of starting level), the virus can survive and continue to replicate. Some of the mutations that occur are within the active site cleft and this can change the binding of inhibitors to reduce the effectiveness of antiviral therapy. Discovering new drugs that do not lead to the development of resistance remains a major research objective in antiviral therapy. On the other hand, knowledge of the genetic drift of the virus population into sequences that are resistant to a certain therapeutic regimen can predict when the patient could be switched to another set of antiviral drugs.

Structure of HIV PR Variants

In addition to studies of the structure of HIV protease from laboratory strains of the virus, with the discovery of drug-resistant forms of the virus it became important to discover how the amino acid substitutions, coded for by the altered forms of the viral genetic information, altered the activity of the protein. Thus, considerable effort has been expended to study the structure of drug-resistant forms of HIV protease. In general, it can be stated that changes in the enzyme structure are small, with obvious changes in the size of an amino acid that interacts with a bound inhibitor in the "wild-type" enzyme, leading to an obvious hole or protrusion, depending on the direction of the change. Even subtler are changes that occur when amino acids outside of the active site cleft occur, leading to an enhancement of resistance in some cases. A picture is emerging from studies of variant forms of HIV protease that the enzyme is very "plastic" or malleable, meaning that changes at any single position can be transmitted throughout the enzyme to have an impact on binding within the active site cleft and enzymatic function.

HIV PR as a Model System for Analysis of Protein Structure/Function

The classical history of protein biochemistry has involved studies of a few key proteins: the oxygen binding proteins, hemoglobin and myoglobin, the proteolytic enzymes trypsin and chymotrypsin, and the nucleic acid degrading enzymes, ribonuclease and staphylococcal nuclease. In the 1990s, HIV protease became a new classical protein that proved to be

amenable to detailed analysis. The protein is relatively easy to produce by recombinant means and purify, it has a robust activity and can be analyzed by several different methods, and variants can be created by current methods of molecular biology. Consequently, the HIV protease has been studied by nearly every method of analysis available to the protein chemist. Due to its small size, computational approaches have been applied and HIV protease has become an excellent system for theoretical studies of protein structure/function.

See Also the Following Articles

DNA Polymerases: Kinetics and Mechanisms • Reverse Transcriptase and Retroviral Replication

Glossary

AIDS Acquired immunodeficiency syndrome, a devastating disease caused by the HIV.

enveloped virus A virus that has an outer covering consisting of lipid and protein derived from host cells.

Gag polyprotein A 55-kDa protein produced by translation of HIV messenger RNA.

HIV Human immunodeficiency virus.

myristolation The addition of a fatty acid chain to the amino terminus of a protein, altering the properties of the protein.

polyprotein A protein that contains several functional elements attached head-to-tail, which must be separated in order to express their function.

progeny virus New viral particles produced as a result of replication within an infected cell.

protease An enzyme that cuts other proteins into pieces.

retrovirus A virus containing RNA as the genetic element and which must be converted into a DNA copy as part of the replicative cycle.

virus The simplest form of life, a virus depends on host cells in order to reproduce and continue infection.

Further Reading

Dunn, B. M. (ed.) (1999). *Proteases of Infectious Agents*. Academic Press, San Diego, CA.

Kuo, L. C., and Shafer, J. A. (eds.) (1994). *Retroviral Proteases*, Vol. 241, Academic Press, San Diego, CA.

Levy, J. A. (ed.) (1994). *The Retroviridae*, 3 vols, Plenum Press, New York.

Wlodawer, A., and Vondrasek, J. (1998). *J. Annu. Rev. Biomol. Struct.* **27**, 249–284.

Biography

Ben M. Dunn is a Distinguished Professor of Biochemistry and Molecular Biology at the University of Florida College of Medicine. He began his career at Florida after earning a B.S. in chemistry at Delaware in 1967 and a Ph.D. at the University of California, Santa Barbara in bio-organic chemistry, two years of postdoctoral work in protein chemistry and one year as a Staff Fellow at the NIH. His laboratory studies the enzymatic function of proteases, using kinetics and biophysical techniques including X-ray crystallography.

HIV-1 Reverse Transcriptase Structure

Kalyan Das, Stefan G. Sarafianos and Eddy Arnold
CABM and Rutgers University, Piscataway, New Jersey, USA

Stephen H. Hughes
National Cancer Institute, National Institutes of Health, Frederick, Maryland, USA

The reverse transcriptase (RT) of retroviruses, including HIV, is a multifunctional enzyme responsible for the conversion of the single-stranded viral RNA genome into double-stranded DNA (dsDNA). The dsDNA subsequently permanently integrated into the host genome. RT has two enzymatic activities: a DNA polymerase that can copy either RNA or DNA templates and a ribonuclease H (RNase H) that cleaves the RNA strand in RNA:DNA hybrids. HIV-1 RT is a heterodimer consisting of p66 and p51 subunits. Both subunits share a common N terminus; p51 lacks the C-terminal RNase H domain present in p66. Because of its pivotal role in the HIV type 1 (HIV-1) life cycle, HIV-1 RT is a primary target for the development of antiretroviral agents. Currently, 11 out of 19 approved anti-AIDS drugs are RT inhibitors. These drugs can be divided into two classes: nucleoside analogue reverse transcriptase inhibitors (NRTIs) and non-nucleoside reverse transcriptase inhibitors (NNRTIs). Extensive biochemical and structural studies have contributed to the understanding mechanisms of DNA polymerase catalysis, drug inhibition, and development of drug resistance.

Structural Studies on Reverse Transcriptase

HIV-1 reverse transcriptase (RT) structure has a right hand-like conformation for the p66 subunit, having "fingers," "palm," "thumb," and "connection" subdomains (Figure 1). While both p66 and p51 subunits contain these subdomains, the arrangement of the subdomains is different in p66 and p51. The p51 subunit is not directly involved in DNA polymerization. It is, however, essential for RT activity presumably because it plays a structural role and forms part of the nucleic-acid-binding cleft that extends from the polymerase active site to the RNase H active site. The non-nucleoside reverse transcriptase inhibitors (NNRTIs) bind in a hydrophobic pocket adjacent to the RT polymerase active site. The polymerase and RNase H active sites have each three catalytic carboxylates that are required for Mg^{2+}-dependent phosphotransferase activity (D110, D185, and D186 for polymerase and D443, D498, and D549 for RNAse H activity; the RNase H active site also includes E478). The two active sites are separated by ~17 DNA bp. The dsDNA substrate has B-form geometry at the polymerase active site and A-form geometry at the RNase H active site. Transition between the two forms occurs over a stretch of 4 bp in a segment of the DNA that is bent (~40°) and interacts with the p66 thumb subdomain.

In the past 11 years, significant progress has been made toward understanding the function of HIV-1 RT at the atomic level. Several structures of RT in complexes with inhibitors or substrates representing different steps in the mechanism of DNA polymerization are now available. The RT structures may be broadly categorized into four distinct groups (Figure 1): (I) apo HIV-1 RT (in absence of any bound substrate or inhibitor) and apo HIV-2 RT, (II) RT/nucleic acid binary complexes, (III) RT/nucleic acid/nucleotide triphosphate ternary complexes, and (IV) RT/NNRTI complexes. There are important differences in the structure and conformation of the enzyme in the various RT structures. Some of the structural changes are discussed in the context of the function(s) of the enzyme.

Functional Implications of RT Structures

In the unliganded (apo-) structures of HIV-1 (Figure 1, structure I) and HIV-2 RT, the p66 thumb subdomain folds over into the nucleic-acid-binding cleft. In nucleic-acid-bound RT structures (Figure 1, structure II), the p66 thumb moves out of the nucleic-acid-binding cleft and helps position the template primer. The NNRTI-binding site is near the hinge of the p66 thumb and p66

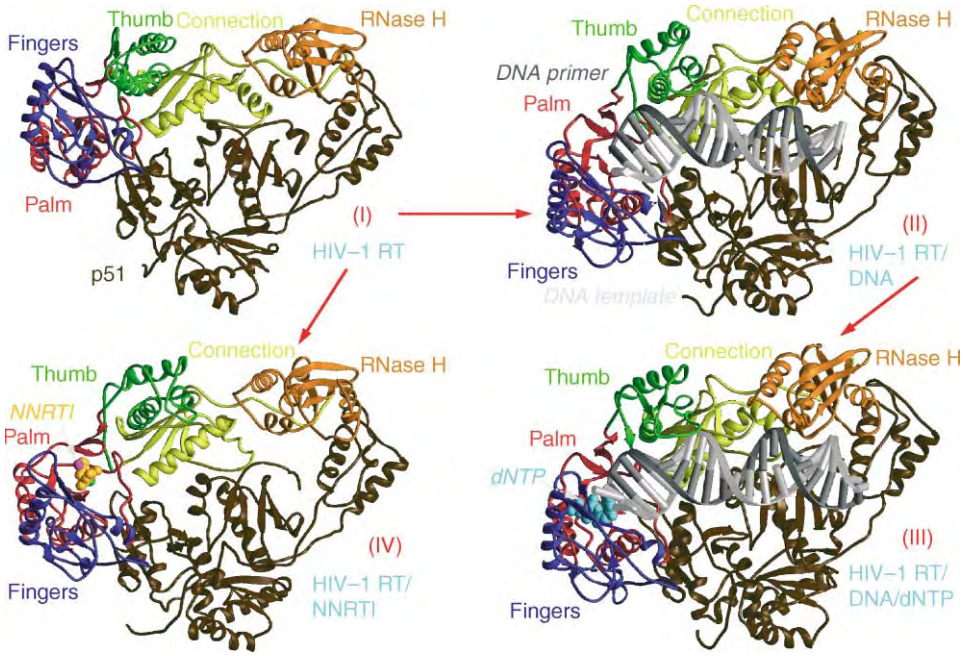

FIGURE 1 Four types of HIV-1 RT structures. Structure I of RT (apo-RT) contains no substrate or inhibitor. The subdomains of the p66 subunit are color-coded: fingers in blue, palm in red, thumb in green, connection in yellow, and RNase H in orange. The p51 subunit is shown in dark brown. Structure II corresponds to a binary complex of RT with nucleic acid (dark gray primer and light gray template) in which the thumb subdomain is displaced from the nucleic-acid-binding cleft to accommodate the nucleic acid. Structure III shows the ternary RT/DNA/dNTP complex (dNTP in cyan). Structure IV is a representative RT/NNRTI complex. The bound NNRTI, 8-Cl TIBO, is represented by a gold-colored CPK model.

palm subdomains; NNRTI binding locks the p66 thumb at an upright position (IV).

The structure of the RT/DNA complex (Figure 1, structure II) revealed details of nucleic acid recognition by HIV-1 RT and identified the structural elements of RT that interact with dsDNA including the "template grip," the "primer grip," and the p66 thumb subdomain. This structure inspired numerous biochemical studies that led to further characterization of the enzyme. The structure of RT complexed with an RNA:DNA led to the identification of the "RNase H primer grip," a set of amino acids that interact with the DNA primer strand and help to determine the specificity of RNase H cleavage. The RNA:DNA duplex in the crystal structure contained a polypurine sequence, known as the polypurine tract (ppt), that is not cleaved by RNase H. During viral replication, the ppt serves as a primer for the synthesis of the second strand of DNA. Analysis of the RT/RNA:DNA structure suggested that the RNase H cleavage specificity is controlled by the width of the minor groove and the trajectory of the RNA:DNA duplex. An unusual unzipping of the base pairs in the ppt may also play a role in determining the specificity of RNase H cleavage.

To obtain a structure of a ternary complex of RT with dsDNA and dNTP (Figure 1, structure III) the groups of Stephen Harrison and Greg Verdine at Harvard University developed a technique that covalently linked the dsDNA to the protein. A disulfide link was formed between and an engineered cysteine at residue 258 of the αH-helix in the p66 thumb subdomain and a thiol tether linked at N2 position of an adjacent DNA-template base. Comparison of the structures of RT/DNA/dNTP and RT/DNA complexes revealed a repositioning of the p66 fingers subdomain in the ternary complex. An analogous movement occurs in many other DNA polymerases (such as klentaq DNA polymerase I, murine leukemia virus RT, T7 RNA polymerase, etc.) and with the RNA-dependent RNA polymerases of poliovirus, hepatitis C virus, rabbit hemorrhagic disease virus, reovirus, and bacteriophage ϕ6. The structural and functional characteristics of these enzymes are useful in understanding the general mechanism of nucleic acid polymerization. The RT/DNA cross-linking technique was also subsequently used to obtain crystals of RT in complex with AZT-terminated DNA trapped before, and after, the DNA translocation step. Structural differences between the two complexes suggest that the conserved YMDD loop that contains two catalytically essential aspartates (D185 and D186) is also involved in translocation, acting as a springboard that helps to move the end of the primer after incorporation of a nucleotide.

TIBO and nevirapine are the first NNRTIs discovered by screening libraries of compounds for RT-inhibition activity. NNRTIs are highly specific inhibitors of HIV-1 RT; most do not inhibit HIV-2 RT. Three NNRTIs (nevirapine, delavirdine, and efavirenz) have been

approved for treating HIV-1 infections. The structure of HIV-1 RT in a complex with nevirapine, from Thomas Steitz and co-workers was the first structure of RT bound to an NNRTI. Since then, a large number of crystal structures of RT/NNRTI complexes have been determined independently by several groups including ours and that of David Stammers and David Stuart. Included among the structures are RT in complex with NNRTIs including α-APA, TIBO, delavirdine, efavirenz, HBY 097, HEPT, and PETT. All these structures belong to type IV in Figure 1. Variations in the shape and size of non-nucleoside inhibitor-binding pocket (NNIBP) correlate with differences in the size and shapes of the bound NNRTIs. Despite strong similarities in all RT/NNRTI structures (IV), specific details in inhibitor-protein interactions, binding modes of NNRTIs, shapes and sizes of NNIBP have provided valuable information that has implications for structure-based design of potent NNRTIs.

Analysis of RT/NNRTI structures helped in understanding the mechanism of RT inhibition by NNRTIs. NNRTIs are noncompetitive inhibitors that do not appear to interfere with binding of either nucleic acid or nucleoside substrates. No predefined NNIBP exists in the structures of RT that do not contain a bound NNRTI. Opening of the NNIBP involves large torsional displacements of the aromatic side chains of Y181 and Y188 and a rotation of the $\beta12-\beta13-\beta14$ sheet that moves the "primer grip" away from the polymerase active site. Once bound, an NNRTI restricts the flexibility of the enzyme, particularly, the relative positioning of the "primer grip" (which is responsible for translocation of the nucleic acid substrate and for positioning the 3′-end of the DNA-primer strand) with respect to the YMDD-motif at the polymerase active site. Restriction of the conformational mobility of the YMDD-motif may be another factor contributing to the NNRTI inhibition mechanism.

Structural Basis of HIV-1 RT Drug Resistance

The most effective strategies for reducing viral loads and keeping them at undetectable levels in HIV-1 infected patients are currently based on combinations of drugs (under the treatment strategy called highly active antiretroviral therapy, HAART) that usually include one or two RT inhibitors and one inhibitor of the viral protease. Despite the early success of combination therapies, treatment failure and severe side effects affect a growing proportion of patients receiving therapy. An increasing number of treatment failures are linked to the emergence of drug-resistant HIV strains. Resistant strains emerge because of the virus' rapid rate of replication and high rate of mutation. Amino acid residues that confer drug resistance are clustered in specific regions of Amino acid. Most of the sites where mutations are associated with drug resistance have potential to influence directly or indirectly the binding of the drug or specific functional steps of RT. In a number of cases, structural studies in combination with biochemical and clinical results have helped explain the molecular basis of drug resistance.

A single mutation (M184I/V) results in strong resistance to lamivudine (3TC), a nucleoside analogue that contains a β-L-pseudo-ribose-ring. The structure of RT/DNA/dNTP and the structure of the lamivudine-resistant M184I mutant RT in complex with nucleic acid is suggested that replacement of methionine at position 184 with a β-branched amino acid residue (V, I, or T) causes resistance to lamivudine by a steric hindrance mechanism, a proposal that is supported by biochemical experiments. Structures of HIV-1 RT were used to create a structural model of hepatitis B (HBV) polymerase. This model has been used to interpret the available biochemical and clinical data describing the susceptibility and resistance of HBV polymerase to nucleotide analogues such as lamivudine and adefovir (PMEA).

AZT treatment frequently selects a set of RT mutations (M41L, D67N, K70R, T215F/Y, and K219Q) that confer resistance to AZT. However, recombinant HIV-1 RT containing these mutations remained susceptible to inhibition by AZTTP in conventional polymerase assays. RT structures showed that these mutations would not directly affect the binding of a dNTP substrate or its analogue. The longstanding mystery about the molecular mechanism of RT resistance to AZT was solved in part when Dr. Michael Parniak and colleagues proposed that RT performs a pyrophosphate-mediated excision of AZTMP after the drug has been incorporated. Dr. Walter Scott and co-workers suggested that the pyrophosphate donor in the *in vivo* excision reaction is ATP. However, these proposals did not fully explain the mechanism of resistance. We developed a model for the excision reaction based on structural and biochemical data. In this model, several of the mutations associated with AZT resistance act primarily to enhance the binding of ATP; AZTMP is preferentially excised because of steric clashes involving the azido group. The model is strongly supported by crystal structures of RT in a complex with AZTMP-terminated DNA, trapped either in a pre- or a post-translocation state. The excision reaction is similar to reverse of polymerization reaction. RT uses its polymerase active site to cleave the AZTMP (from the DNA primer strand). This reaction requires that the AZTMP be located at the active site (pre-translocation state). Normally, when a dNTP or a nucleoside analogue is incorporated by HIV-1 RT, it is translocated and the next incoming dNTP binds. This would prevent excision. However, the azido

group of AZTMP interferes with the formation of a stable closed complex with the incoming dNTP. This gives an AZTMP-terminated primer good access to the active site where it can be excised.

In contrast to nucleoside analogues, NNRTIs bind to a well-defined hydrophobic pocket (NNIBP). Structural studies have shown that NNRTI-resistance mutations are located in and around the NNIBP. Commonly observed resistance mutations in NNRTI-treated patients include K103N, Y181C, L100I, Y188L, and G190A; these can be present singly or in combination. Structural studies of NNRTI-resistant RTs with and without bound NNRTI have provided clues for understanding the roles of resistance mutations in NNRTI binding. Structural studies, supported by clinical and biochemical data, suggest that different sets of mutations have different mechanisms. The Y181C and Y188L mutations appear to cause decreased NNRTI binding by the loss of aromatic ring interactions with inhibitors (by "loss of contact" mechanism); L100I and G190A/S are likely to cause steric hindrance with NNRTIs; and the K103N mutation appears to have effect on the entry of an NNRTI into the NNIBP; however, it may also favor binding of certain NNRTIs like TMC125-R165335 (etravirine).

RT Structures in Drug Design

Variations in RT sequence and emergence of drug-resistant strains present serious challenges for developing potent anti-AIDS drugs. Potent anti-AIDS drugs should be able to overcome the effects of commonly observed drug resistance mutations. A structural understanding of the target enzyme, mode of drug action, and effects of drug resistance can aid the design of potent anti-AIDS drugs. Together with Dr. Paul Janssen and colleagues, we have used systematic structural and molecular modeling studies of HIV-1 RT/NNRTI complexes to design new NNRTIs that are potent against a broad spectrum of resistant strains. Conformational flexibility and compactness of the new NNRTIs, including the diarylpyrimidine derivatives TMC120-R147681 (dapivirine) and TMC125-R165335, appear to be favorable design features that can offset the effects of resistance mutations and allow binding of the drugs to wild-type and a variety of mutant RTs. This concept may have broader implications for designing drugs against other rapidly evolving targets.

Crystallographic studies have played a crucial role in characterizing the molecular interactions of drugs with HIV-1 RT. We believe that structural approaches will become increasingly important in understanding existing and emerging multidrug resistance and in using that information to design improved anti-AIDS drugs and to develop new treatment strategies.

See Also the Following Articles

HIV Protease • Reverse Transcriptase and Retroviral Replication

Glossary

excision Reverse of the polymerization reaction by which the RT catalyzes the removal of the nucleotide at the DNA primer terminus.

non-nucleoside RT inhibitors (NNRTIs) Inhibitors that bind in a hydrophobic pocket near the polymerase active site and block DNA polymerization. Nevirapine, delavirdine, and efavirenz are three clinically approved NNRTI drugs for treating HIV-1 infection.

nucleoside RT inhibitors (NRTIs) Analogues of normal nucleosides, which lack a 3′-OH and act as terminators of DNA elongation. AZT (zidovudine) and 3TC (lamivudine) are among the approved NRTI drugs for treatment of HIV-infected patients.

resistance mutation A change in amino acid sequence that reduces susceptibility of the enzyme to an inhibitor.

reverse transcriptase (RT) An enzyme that converts single-stranded RNA to double-stranded DNA.

Further Reading

Coffin, J. M., Hughes, S. H., and Varmus, H. E. (1997). *Retroviruses*. Cold Spring Harbor Laboratory Press, Plainview, NY.

Das, K., Clark, Jr., A. D., Lewi, P. J., Heeres, J., de Jonge, M. R., Koymans, L. M. H., Vinkers, H. M., Daeyaert, F., Ludovici, D. W., Kukla, M. J., De Corte, B., Kavash, R. W., Ho, C. Y., Ye, H., Lichtenstein, M. A., Andries, K., Pauwels, R., de Béthune, M.-P., Boyer, P. L., Clark, P., Hughes, S. H., Janssen, P. A. J., and Arnold, E. (2004). Roles of Conformational and Positional Adaptability in Structure-Based Design of TMC125-R165335 (Etravirine) and Related Non-nucleoside Reverse Transcriptase Inhibitors that are Highly Potent and Effective against Wild-Type and Drug-Resistant HIV-1 Variants. *J. Med. Chem.* **47**, 2550–2560.

Huang, H., Chopra, R., Verdine, G. L., and Harrison, S. C. (1998). Structure of a covalently trapped catalytic complex of HIV-1 reverse transcriptase: Implications for drug resistance. *Science* **282**, 1669–1675.

Jacobo-Molina, A., Ding, J., Nanni, R. G., Clark, A. D., Jr., Lu, X., Tantillo, C., Williams, R. L., Kamer, G., Ferris, A. L., Clark, P., Hizi, A., Hughes, S. H., and Arnold, E. (1993). Crystal structure of human immunodeficiency virus type 1 reverse transcriptase complexed with double-stranded DNA at 3.0Å resolution shows bent DNA. *Proc. Natl. Acad. Sci. USA* **90**, 6320–6324.

Jaeger, J., and Pata, J. D. (1999). Getting a grip: Polymerases and their substrate complexes. *Curr. Opin. Struct. Biol.* **9**, 21–28.

Kohlstaedt, L. A., Wang, J., Friedman, J. M., Rice, P. A., and Steitz, T. A. (1992). Crystal structure at 3.5Å resolution of HIV-1 reverse transcriptase complexed with an inhibitor. *Science* **256**, 1783–1790.

Ren, J., Esnouf, R., Garman, E., Somers, D., Ross, C., Kirby, I., Keeling, J., Darby, G., Jones, Y., Stuart, D., and Stammers, D. K. (1995). High resolution structures of HIV-1 RT from four RT-inhibitor complexes. *Nat. Struct. Biol.* **2**, 293–302.

Sarafianos, S. G., Das, K., Ding, J., Boyer, P. L., Hughes, S. H., and Arnold, E. (1999). Touching the heart of HIV-1 drug resistance: The fingers close down on the dNTP at the polymerase active site. *Chem. Biol.* **6**, R137–R146.

Sarafianos, S. G., Clark, A. D., Jr., Das, K., Tuske, S., Birktoft, J. J., Ilankumaran, P., Ramesha, A. R., Sayer, J. M., Jerina, D. M., Boyer, P. L., Hughes, S. H., and Arnold, E. (2002). Structures of HIV-1 reverse transcriptase with pre- and post-translocation AZTMP-terminated DNA. *EMBO J.* **21**, 6614–6624.

Tantillo, C., Ding, J., Jacobo-Molina, A., Nanni, R. G., Boyer, P. L., Hughes, S. H., Pauwels, R., Andries, K., Janssen, P. A. J., and Arnold, E. (1994). Locations of anti-AIDS drug binding sites and resistance mutations in the three-dimensional structure of HIV-1 reverse transcriptase: Implications for mechanisms of drug inhibition and resistance. *J. Mol. Biol.* **243**, 369–387.

Biography

Kalyan Das is an Associate Research Professor of Chemistry and Chemical Biology and a Research Faculty Member at the Center for Advanced Biotechnology and Medicine. His research is primarily focused on application of structural and molecular modeling studies in understanding drug resistance and in structure-based drug design aiming at HIV-1 reverse transcriptase and other viral targets.

Stefan Sarafianos is an Associate Research Professor of Chemistry and Chemical Biology. His research at the Center for Advanced Biotechnology and Medicine is focused on mechanisms of enzyme function and drug resistance in HIV reverse transcriptase and other DNA and RNA polymerases.

Eddy Arnold is a Professor of Chemistry and Chemical Biology at Rutgers University and a Resident Faculty Member at the Center for Advanced Biotechnology and Medicine in Piscataway, New Jersey. His laboratory uses structural biology to design drugs and vaccines against AIDS and other infectious diseases with a special emphasis on targeting antiviral resistance.

Stephen Hughes is Chief of Retroviral Replication Laboratory in the HIV Drug Resistance Program at the NIH National Cancer Institute in Frederick, MD. Dr. Arnold and Dr. Hughes have collaborated on studies of HIV-1 RT structure, function, and resistance since 1987 and have published more than 50 papers together on the subject.

Homologous Recombination in Meiosis

Nancy M. Hollingsworth
State University of New York, Stony Brook, New York, USA

During meiosis, homologous chromosomes undergo a reciprocal exchange of DNA in a process called recombination or "crossing over." Meiotic crossing over serves two important functions: (1) it creates a physical connection between homologous chromosomes that is necessary for proper segregation at the first meiotic division (MI) and (2) it generates new combinations of alleles. Like meiosis, the process of meiotic recombination is highly conserved between organisms as diverse as yeast and humans. Recombination is highly regulated during meiosis, such that crossovers occur between homologues and not sister chromatids. Furthermore, crossovers are distributed so that every pair of homologues receives at least one crossover. The molecular mechanism of meiotic recombination has been elucidated primarily by research using fungi.

Meiosis

Sexually reproducing organisms face a daunting challenge: for the chromosome number of the species to remain constant, the gametes (germ cells) used for reproduction must contain only half the number of chromosomes as the diploid parent. This reduction in chromosome number is achieved by a specialized cell division, meiosis, in which two rounds of chromosome segregation follow a single round of chromosome duplication. After DNA replication produces pairs of sister chromatids (step 1, Figure 1), homologous chromosomes align and undergo a reciprocal exchange of DNA specifically between non-sister chromatids (step 2, Figure 1). At the first meiotic division, also known as meiosis I (MI), homologues segregate to opposite poles (step 3, Figures 1–3). In contrast, at the second meiotic division, or meiosis II (MII), sister chromatids are segregated (step 4, Figure 1). As a result, a single diploid cell can produce four haploid gametes (step 5, Figure 1).

The Role of Recombination in Meiosis

In addition to independent assortment, crossing over between homologous chromosomes produces new combinations of alleles that provide the grist for evolution.

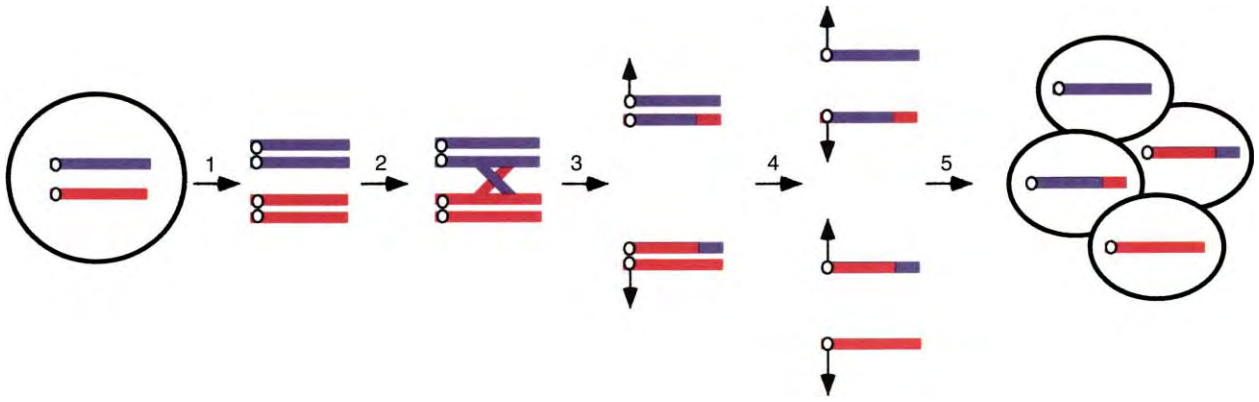

FIGURE 1 Chromosome behavior during meiosis. A diploid cell containing a pair of homologous chromosomes (one blue and one red) is shown. Small white circles represent the centromeres to which spindle fibers attach. Arrows connected to centromeres indicate the direction of segregation. (1) Chromosomes replicate to form sister chromatids. (2) Reciprocal recombination, or crossing over, connects homologous chromosomes, enabling their proper alignment prior to MI. (3) Homologues segregate to opposite poles at MI. (4) Sister chromatids segregate to opposite poles at MII. (5) Four haploid products are packaged into gametes. In yeast, these gametes are called spores.

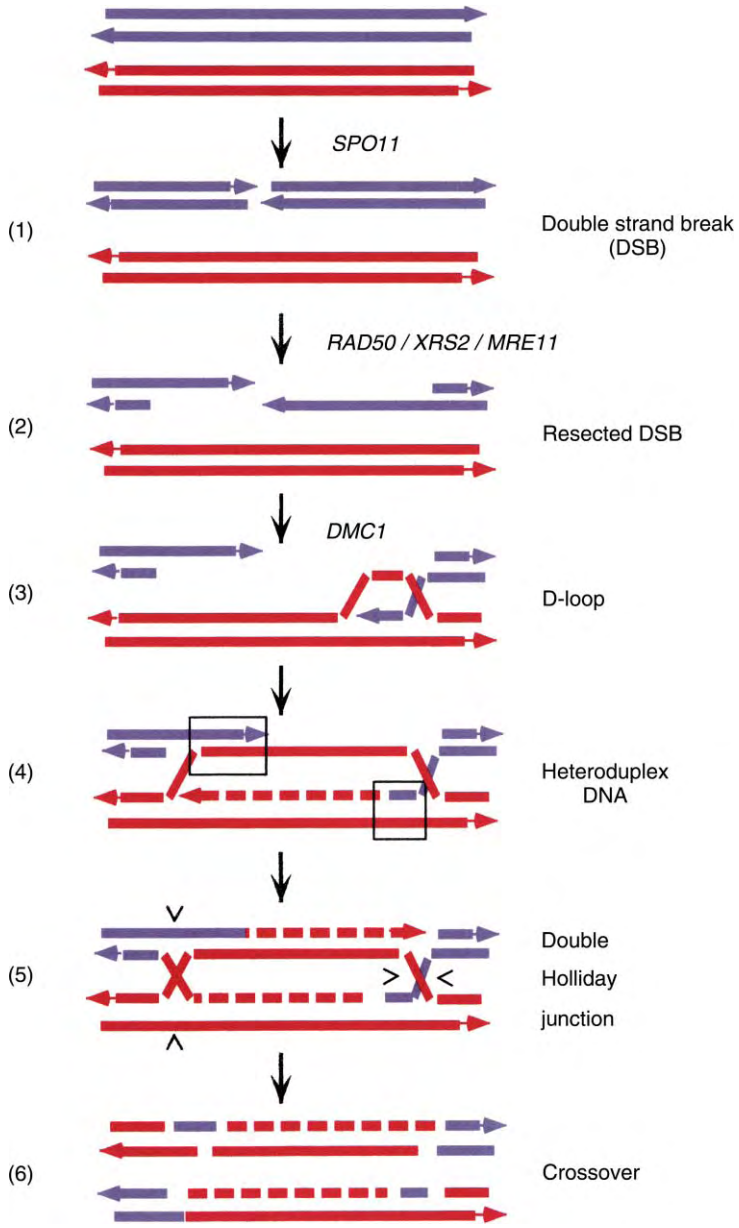

FIGURE 2 The double-strand break repair model for meiotic recombination. The double strands of DNA from one chromatid of each homologue (one blue and one red) are shown. Arrows on the DNA indicate the 3′ ends. Dashed lines indicate newly synthesized DNA. Karats indicate sites of nicking and religation used for Holliday junction resolution. Boxes indicate sites of heteroduplex DNA. (1) A DSB is introduced into one chromatid by Spo11. (2) Resection of the 5′ end on each side of the break produces two 3′ SS tails. (3) With the help of Dmc1, a 3′ SS tail invades the DNA of the homologous chromatid. (4) DNA synthesis extends the D-loop until it can anneal with the 3′ tail on the other side of the break. (5) Ligation of the invading strand creates an intermediate in which the chromatids are connected by two Holliday junctions. (6) Resolution of the Holliday junctions in opposite directions creates a crossover chromosome.

Recombination also plays a critical mechanical role in meiosis by creating a physical connection between homologues that is crucial for proper MI segregation (step 2, Figure 1). In the absence of recombination, chromosomes segregate randomly, thereby creating gametes with too few or too many chromosomes. Meiotic recombination is therefore, critical to fertility and the production of healthy offspring.

A Molecular Model for Meiotic Recombination

Initiation

The double-strand break repair (DSBR) model for recombination was first proposed in 1983 based on genetic data from meiotic studies using a number of

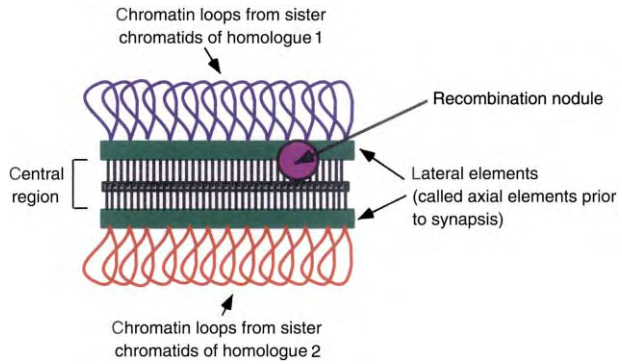

FIGURE 3 The synaptonemal complex. Synapsis of two homologous chromosomes (one blue and one red) is shown.

different fungi. Since that time, many of the molecular intermediates predicted by the DSBR model have been observed experimentally and the model has gained wide acceptance. The DSBR model proposes that meiotic recombination is initiated by the introduction of a double-strand break (DSB) on one of the four chromatids of a pair of homologues (step 1, Figure 2). The formation of DSBs is catalyzed by a meiosis-specific protein called Spo11. Spo11 breaks DNA by forming a transient covalent bond between the protein and the DNA. Yeast cells lacking the Spo11 protein fail to make breaks, undergo no recombination, and exhibit high levels of chromosome missegregation. Meiotic defects resulting from mutation of Spo11 have also been observed in fruit flies, worms, and mice, indicating that the mechanism for initiating meiotic recombination is evolutionarily conserved.

Resection

After a DSB is made, the 5′ ends on each side of the break are resected to produce 3′ single-stranded (SS) tails (step 2, Figure 2). In budding yeast, resection requires a highly conserved protein complex containing Rad50, Xrs2, and Mre11. While the absence of any one of these proteins prevents DSB formation, specific mutant versions of the proteins exhibit DSBs, but the breaks remain unprocessed because Spo11 remains covalently bound to the 5′ end of the break. Therefore, DSB formation and 5′ end processing are coupled together by these proteins.

Invasion

After resection, a 3′ SS tail from one side of the break invades the duplex of the homologous chromosome, thereby displacing the strand of like polarity to form a displacement loop (D-loop) (step 3, Figure 2). Strand invasion is facilitated by Dmc1, a highly conserved protein which is a member of the RecA family of strand transferases. The Dmc1 protein is produced only during meiosis and it specifically promotes invasion of the 3′ tail into the homologous chromosome, as opposed to the sister chromatid. This bias is important, as intersister-recombination events do not facilitate MI chromosome segregation.

Double Holliday Junction Formation

After strand invasion, DNA synthesis extends the invading strand, thereby increasing the size of the D-loop until the displaced single strand can complementary base pair with the 3′ tail on the other side of the break (step 4, Figure 2). A recombination intermediate containing two cross-shaped structures called Holliday junctions (HJs) is then created (step 5, Figure 2). To separate the two recombining chromatids from each other, each HJ must be resolved by nicking of the two strands of like polarity, followed by religation. To generate a crossover, the two HJs must be resolved in opposite directions (step 6, Figure 2). Proteins exhibiting HJ resolvase activity have been identified in bacteria but, so far, attempts to discover a nuclear HJ resolvase used for meiosis have been unsuccessful.

Gene Conversion

Mendel's first law states "alleles segregate equally into gametes." Therefore, when a diploid that contains two different alleles of a gene (+/−) is put through meiosis, half of the gametes should contain the "+" allele and half should contain the "−" allele (indicated by 2^{+}:2^{-}). The ability in fungi to analyze all four products from a single meiosis (called spores) led to the discovery that for a small percentage of the time Mendel's first law is broken. In these cases, meiosis produces spores in a ratio of 3^{+}:1^{-} or 1^{+}:3^{-} by a process called gene conversion.

Gene conversion changes the sequence of one allele precisely to the sequence of the other allele in the cell. This transfer of sequence information can happen due to the formation of heteroduplex DNA during recombination. Heteroduplex DNA results when a strand of DNA from one homologue complementary base pairs with a strand of DNA from the other homologue. According to the DSBR model, there are two times when heteroduplex is formed – after the initial strand invasion and after the displaced single strand of DNA in the D-loop anneals to the 3′ end on the other side of the break (step 4, Figure 2). Because the DNA sequences of homologous chromosomes, while highly similar, are not necessarily identical, base pair mismatches can occur in heteroduplex DNA. These mismatches are then corrected by a highly conserved mismatch repair machinery. A mismatch can be corrected so that the original base pair is restored,

thereby producing 2^+:2^- spores or it can be corrected, so that the sequence of one allele is changed to the sequence of the other allele (3^+:1^- or 1^+:3^-). Gene conversion has been proposed to play an important role in maintaining the sequence homogeneity of multi-gene families.

The Meiotic Recombination Checkpoint

The introduction of DSBs into chromosomes by Spo11 puts the cell in grave peril. Proceeding ahead through MI with unrepaired DSBs would be fatal, as pieces of broken chromosomes would become irrevocably separated from each other. Once recombination is initiated, the process is carefully monitored such that MI occurs only after recombination is complete. This surveillance process has been called the meiotic recombination checkpoint or the pachytene checkpoint. For example, budding yeast lacking Dmc1 arrests recombination prior to MI. Examination of the DNA indicates that DSBs are made and resected, but because there is no Dmc1 to promote strand invasion into the homologue, recombination cannot proceed and the meiotic recombination checkpoint is triggered. The cells remain arrested, waiting for the break to be repaired.

Genetic Interference

It is critical that each pair of homologues receives at least one crossover to prevent missegregation at MI. Because in many organisms there is a finite number of crossovers in each meiosis, crossovers must be distributed so that large chromosomes do not sustain a disproportionate number of crossovers at the expense of small chromosomes. This distribution is accomplished by a phenomenon known as genetic interference. Interference was first observed at the beginning of the twentieth century when fruit fly geneticists were mapping genes on the same chromosomes. These geneticists observed that the presence of a crossover in one interval decreased the chance that a second crossover would occur nearby. Mutation of genes required for interference in budding yeast increases MI missegregation, especially of small chromosomes. Despite intense research, the mechanism by which the cell distributes crossovers through interference remains obscure.

The Synaptonemal Complex

A unique feature of meiosis is the physical association of homologous chromosomes by a meiosis-specific structure called the synaptonemal complex (SC) that is formed by a process called synapsis (Figure 3). After DNA replication, sister chromatids condense along protein cores called axial elements (AEs) that are comprised, at least in part, of meiosis-specific proteins. AEs from homologous chromosomes then become "glued" together by insertion of the central region to form SCs. In the context of the SC, AEs are referred to as lateral elements. Associated with SCs are densely staining bodies called recombination nodules (RNs). RNs are thought to contain the proteins that mediate recombination. The relationship between the SC and meiotic recombination varies depending upon the organism. In worms and fruit flies, SC formation is necessary, but not sufficient for recombination, whereas in yeast and mammals, recombination is a prerequisite for SC formation. In budding yeast, loss of the central region has little effect on crossing over, but interference is abolished, suggesting that the SC may be important for distributing crossovers. In contrast, the absence of AEs greatly decreases the frequency of both gene conversion and crossing over, demonstrating that there is an important connection between meiotic chromosome structure and recombination.

Mitotic versus Meiotic Recombination

Meiotic recombination exhibits a number of important differences from mitotic recombination. First, meiotic recombination is several orders of magnitude more frequent. This is due, in part, to the induction of meiosis-specific recombination proteins such as Spo11. In mitotically dividing cells, recombination is used to repair lesions in DNA and therefore recombination events occur rarely and are located randomly along the chromosomes. In meiotic cells there are "hot spots" of recombination – these are places on chromosomes where Spo11 prefers to act. In mitotic cells recombination occurs most frequently between sister chromatids, which act as a template for DNA repair. In contrast, crossing over in meiotic cells is targeted between homologues. This bias is key because only interhomologue crossovers promote proper segregation at MI. Finally, meiotic recombination occurs between homologous chromosomes that are physically associated by a meiosis-specific structure, the SC.

See Also the Following Articles

Chromosome Organization and Structure, Overview • DNA Mismatch Repair and Homologous

Recombination • Meiosis • Mitosis • Non homologous Recombination: Bacterial Transposons • Non homologous Recombination: Retro transposons • Recombination: Heteroduplex and Mismatch Repair *in vitro*

Glossary

alleles Alternative forms of the same gene that vary in DNA sequence.

homologues Chromosomes with highly similar, but not necessarily identical, DNA sequences.

recombination Includes both crossing over, which is the reciprocal exchange of segments of DNA between homologous chromosomes, and gene conversion, the process by which the sequence of one allele is changed to the sequence of the other allele in the cell.

sister chromatids Two identical copies of a chromosome created by DNA replication.

synapsis The physical association of homologous chromosomes during meiosis by the formation of the synaptonemal complex.

Further Reading

Hassold, T., and Hunt, P. (2001). To err (meiotically) is human: The genesis of human aneuploidy. *Nat. Rev.* **2**, 280–291.

Keeney, S. (2001). Mechanism and control of meiotic recombination initiation. *Curr. Topics Dev. Biol.* **52**, 1–53.

Roeder, G. S., and Bailis, J. M. (2000). The pachytene checkpoint. *Trends Genet.* **16**, 395–403.

Smith, K. N., and Nicolas, A. (1998). Recombination at work for meiosis. *Curr. Opin. Genet. Devel.* **8**, 200–211.

Villeneuve, A. M., and Hillers, K. J. (2001). Whence meiosis? *Cell* **106**, 647–650.

Biography

Nancy M. Hollingsworth is an Associate Professor in the Department of Biochemistry and Cell Biology at the State University of New York at Stony Brook. Her principal research interest is understanding the molecular basis by which chromosomes recombine, synapse, and segregate during meiosis. She holds a Ph.D. in genetics from the University of Washington and has received postdoctoral training both at the Fred Hutchinson Cancer Research Center in Seattle and the University of California, San Francisco.

HPLC Separation of Peptides

James D. Pearson
Pfizer, Portage, Michigan, USA

High-performance liquid chromatography (HPLC) is a separation method based on partitioning between a coated silica solid phase and a liquid phase. The term high-performance (also known as "high-pressure") refers to the speed and superior separation compared to agarose "soft gel" particles that were the mainstay of pre-1970s column-chromatography separations. The main type of HPLC used today to separate peptides is called reversed-phase HPLC (RP-HPLC or simply RPLC). This separation mode is based on nonpolar adsorption of peptides onto the stationary phase within the column. The peptides are then differentially released from the stationary phase as a function of increasing organic component in the liquid phase.

Historical

The earliest high-performance liquid chromatography (HPLC) peptide separations were done in the 1970s using reversed-phase. Other separation modes have been developed since and will be discussed, but RPLC remains the most popular mode for peptide separations. Two key observations were made in the early 1980s that dramatically increased the use of RPLC for peptide separations. First, it was found that increasing the pore size of silica particles from ~100 to ~300Å had a dramatic effect on improving the separation of peptide fragments generated from enzymatic or chemical digests of proteins. Second, researchers replaced phosphoric acid with trifluoroacetic acid (TFA) as the ion-pairing agent in RPLC peptide separations. TFA often resulted in better peptide separations and, importantly, it was volatile. This simplified the process for preparing isolated peptide fragments for amino acid analysis and Edman gas-phase protein sequencing during the mid-1980s. Another key to the early acceptance of TFA as the IPA of choice was its commercial availability as a highly purified protein-sequencing reagent. The lack of impurities afforded sensitive UV detection at 214 nm. By the late 1980s, RPLC using TFA in the mobile phase and 300Å pore diameter silica particles was the standard for peptide separations. During this time period, advances in peptide RPLC purification enabled advances in protein sequencing. Gas-phase N-terminal Edman sequenators were introduced around this time, and the ability to purify peptide samples by RPLC reduced background noise during sequence cycles in these instruments.

The widespread use of RPLC for peptide separations during the late 1980s encouraged vendors to develop the next generation of HPLC instruments. Gas-phase protein sequenators were in wide use during the early 1990s and chromatographers needed more sensitive HPLCs to conduct microscale peptide purifications. By the early 1990s, separation scientists realized that reducing the column internal diameter (ID) from 4.6 to 1 mm increased peptide detection tenfold. At the time of this observation, HPLC systems were designed to generate and deliver reproducible gradients in the 300–500 μl min^{-1} range. HPLC instrument companies were challenged to design and deliver HPLCs that could generate gradient flows down to 50 μl min^{-1} with low dead volumes for 1 mm ID columns. These instruments became widely available by the mid-1990s. The driving force for increasing detection sensitivity then began to shift from gas-phase protein sequencing technology to RPLC coupling to ion-trap electrospray ionization (IT-ESI) mass spectrometers. HPLC separations today are routinely conducted on $\leq$0.2 mm ID columns flowing at "nano-flow" nl ml^{-1} rates and directly coupled to MS/MS instruments. These automated LC/MS systems process raw spectral data using specialized software and output-automated peptide identifications. This high-throughput ability to separate peptide by RPLC, generate ion fragment data by MS, and identify the original proteins using translated genomic database software is collectively referred to as Proteomics.

Reversed-Phase Supports

Origin of the "Reversed-Phase" Term

In the early 1900s, standard partitioning chromatography was routinely done with a polar stationary phase and a less-polar mobile phase. In 1928, Holmes and McKelvey separated a series of fatty acids in this

fashion using silica gel as the stationary phase with a toluene mobile phase. They found that when nonpolar carbon adsorbent and polar water were used, the order of fatty acid adsorption was reversed. In 1950, Howard and Martin described this partitioning process as "reversed phase" to distinguish it from conventional partitioning chromatography. From the 1950s to the 1970s, this separation mode had various names such as salting-out, hydrophobic interaction, hydrophobic salting-out, solubilization, and solvophobic chromatography. Under these various names the technique was increasingly used, especially during the late 1970s when n-alkyl groups bonded to silica and packed into HPLC columns replaced n-alkyl linked agarose soft-gel columns. Although the concept of reversed phase as originally described by Howard and Martin in 1950 seems archaic today, it is the term that survived and flourished during the 1980s to become a part of commonly used scientific lexicon today.

Reversed-phase columns are used for most HPLC separations today because they offer a higher degree of sample fractionation per unit of gradient time compared to other modes of HPLC. RPLC fractions also avoid the high salt content usually found in other HPLC modes. The avoidance of desalting procedures makes RPLC fractions ideal for drying and continuing directly on to other analyses such as immunocharacterization or mass spectrometry for analysis.

Types of Reversed-Phase Columns

RPLC supports are usually made of silica particles that contain silanol groups that are reacted with n-alkylchlorosilanes. These n-alkyl chains are usually in the form of n-butyl (C4), n-octyl (C8), or n-octadecyl (C18) stationary phases. The C4 phase is preferred for protein recovery, especially when sub-microgram amounts are chromatographed. The C18 phase is favored for peptides and is recommended for tryptic digest peptide separations. C18 columns are preferred to separate small, early eluting peptides compared to C4 columns. The C8 column is a good compromise for users who do not want to switch back and forth between C4 and C18 columns. N-alkyl phases from C1 to C22 have been compared in the past for peptide and protein separation selectivity. C1 to C3 coatings perform similar to the C4 type for protein separations, but column life tends to be less because shorter chains are not as well protected against siloxane hydrolysis compared to C4 and longer n-alkyl coatings. C10 to C22 coatings yield similar results for peptide separations and manufacturers gravitated towards the C18 chain for optimization in the early 1980s. The silylation reagent n-octadecyltrichlorosilane also happened to be the least expensive n-alkychorosilane available in the early 1980s.

Alternative Reversed-Phase Supports

Nonporous materials are alternatives to porous silica supports when fast separation times are critical. These columns are typically packed with 1.5 μm particles that increase the efficiency of the separation. There are two disadvantages for these materials. First, the column back pressure is substantially higher than for macroporous supports, which can lead to faster system failure if the column inlet gets clogged with debris. This can be mitigated by using a shorter column. Second, the loading capacity is sharply decreased, which can impact sample identity efforts when a fraction is subjected to additional HPLC separation steps prior to mass spectrometry characterization. The use of nanoflow LC/MS systems compensate for this deficiency. A compromise material is "superficially" porous particles, which consists of nonporous silica core particles covered with a layer of 300Å pores (such as Aligent's "Poroshell"^{TM} supports). These 5 μm diameter materials are packed in short columns and are designed to reduce peak broadening at high linear flow mobilephase rates. Separations in 6 min or less are common, which is one-tenth the time required for conventional macroporous support separations. Advantages of these superficially coated supports over nonporous materials include the following: (1) lower back pressure due to larger particle size; (2) enhanced loading capacity because of increased support surface area; and (3) less column failure as a result of flow plugging. These materials are also desirable for nanoflow LC/MS applications, where shortened separation times save data processing time and hence data storage space.

Silica dissolves at pH 12 and readily degrades at pH 9; so high-pH mobile phases are a problem for silica-based HPLC columns. Even at pH 7.5 (a common condition for anion exchange separations), column supports degrade over time. To address this degradation problem vendors have developed "pH stable" supports that have a pH 1.5–10 workable range. To avoid basic pH silica support degradation altogether, polystyrene divinylbenzene (PSDVB) supports have been developed since the mid-1980s. These supports are not as resilient to high back pressure surges compared to rigid silica supports, but they can be used at both high and low pH extremes to test diverse mobile phase conditions. PSDVB also has an advantage when coupled to sensitive mass spectrometer detection. The gradual leeching of silanolic alkyl phase in silica-based supports into the mobile phase is avoided in PSDVB supports.

Supports for Small Tryptic Peptide Separations

Recently, specialized columns for small (<20 aa) tryptic peptide separations have been commercialized.

These supports utilize ~90Å pores that are suitable for chromatography of small peptides, and offer higher loading capacities compared to 300Å supports. The higher column loading capacity is a function of increased surface area of the 90Å pores supports compared to macroporous materials. Supports with ~300Å pores remain optimal for RPLC separations of larger polypeptides and proteins.

Ion-Pairing Agents

Types and Uses

RPLC peptide separations require an organic component in the gradient and an ion-pairing agent (IPA). The actual choice or organic mobile phase is generally not as critical as the choice of IPA for optimizing peptides separations. In the early days of peptide RPLC, the favored IPA for superior peptide separations was 10 mM phosphate at pH 2. TFA is the most popular IPA used today, others include triethylammonium phosphate (TEAP), citrate, acetic acid, formic acid, and phosphate. Since TFA is the overwhelming IPA of choice for optimal RPLC separations a few words on its use will follow. The TFA concentration is usually 0.1% (v/v) in both solvents of a gradient system and it is used with an acetonitrile gradient. At sensitive UV detection levels (210–220 nm), the TFA concentration in the eluting solvent is commonly lowered slightly to 0.09% to minimize the upward UV-baseline drift. When an HPLC is directly coupled with electrospray ionization mass spectrometry (ESI-MS), the TFA concentration can be lowered to 0.01% to reduce ion current signal suppression, but a noticeable loss in peptide separation is observed below 0.05%. To address this problem of resolution loss at lower TFA concentrations, HPLC suppliers have introduced low-TFA supports. These HPLC columns are made with specially coated supports that improve separations when the TFA concentration is below 0.1%.

Another feature of TFA as the IPA of choice is that it is an excellent peptide solubilizer. Peptides that are refractory to 0.1% TFA solubility can sometimes be solubilized in higher TFA concentrations. The simple procedure is to use a high enough TFA concentration to solubilize the peptides, and then dilute the concentration back to $<2\%$ TFA before injection onto the HPLC column. For extremely hydrophilic peptides that do not adsorb to reversed-phase supports in TFA-based systems, heptafluorobutyric acid (HFBA) is an alternative that enhances adsorption for gradient elution.

Controlling Silanophilic Effects

Free silanol groups are present even after the silica surface is reacted with n-alkylcholorosilanes to form the reversed-phase coating. This is due to steric hindrance during the coating process. Therefore, an acidic IPA is also important to add to the mobile phase to control these undesirable stationary phase effects. These "silanophilic" interactions between peptide and accessible free silanol groups introduce a dual adsorption mode. A low-pH mobile phase helps to suppress these undesirable negatively charged siloxyl groups (SiO^-) on the support by converting them to neutral silanol (SiOH) groups. Acidic IPAs, such as TFA, acetic acid, or formic acid are used to achieve this effect, otherwise peptide resolution is compromised. Manufacturers have addressed the problem of unreacted silanol groups by a process developed by Klaus Unger in the mid-1970s. Supports are reacted with trimethylchlorosilnae (TMCS) after the n-alkyl phase has been bonded to the silica. This process results in RPLC columns that significantly deactivate these free silanol groups and are referred to as "encapped" columns. Free silanolic groups can also be minimized by n-alkylchlorosilane polymeric coating procedures. These supports are especially useful for enhancing separations of small molecules containing free amino groups.

Mass Spectrometry Applications

The underlying technological rational for increasing detection sensitivity of HPLC peptide separations shifted from gas-phase Edman sequencing to mass spectrometry applications in the early 1990s. During this time manufacturers developed packing methods to deliver efficient HPLC columns with significantly reduced column diameters. HPLC peptide separations today are routinely conducted on μm ID columns flowing at nl min^{-1} rates, directly coupled to tandem MS/MS instruments that deliver automated peptide identifications. Interestingly, the many attributes of TFA that revolutionized peptide RPLC for gas-phase Edman sequencing sample preparation during the 1980s had a fault in the 1990s. TFA suppressed peptide ionization signals in electrospray mass spectrometers. Therefore, most nanospray LC/MS/MS applications today use formic acid or acetic acid instead of TFA as the IPA to increase ionization sensitivity. Although 0.1% TFA is superior for peptide separations compared to the typical 1% formic acid or 2–5% acetic IPAs used today, modern LC/MS systems and software allow for automated multiple peptide identifications within a single fraction. Thus, advancements in mass spectrometry instrumentation have altered what is considered optimal for HPLC peptide separation sensitivity. Instead of using TFA for a superior RPLC peptide separation, less resolved profiles using formic or acetic acid as the IPA suffice because peaks containing multiple peptides can be readily deconvoluted and identified by mass detectors.

Organic Solvents for Gradients

Acetonitrile is the organic eluant of choice for peptide separations, while isopropanol, ethanol, and methanol are used to a lesser extent. It is desirable to make the starting solvent of the gradient system ~2% organic to reduce spontaneous gas bubble formation otherwise seen in mixing pure aqueous with organic solvents. Most peptides elute within the 5–80% acetonitrile concentration window in TFA-based gradients, therefore an elution solvent made of 90% acetonitrile is used often. In the case where peptides are extremely hydrophobic, isopropanol can be substituted for acetonitrile and the peptides will elute at a lower-percentage organic during the gradient. The drawback with isopropanol is that it has a significantly higher viscosity compared to acetonitrile. This causes a higher column back pressure, which may lead to premature column failure. Methanol does not have a viscosity problem, but since it is not as elutropic as acetonitrile it may not release extremely hydrophobic peptides from the column. Ethanol is usually not the best solvent for optimizing peptide separations; it is mainly used for process scale purification protocols, where regulatory agencies favor its use because of safety issues. In the research laboratory, setting gradients are usually run in the linear mode for about an hour to optimize the separation. Gradients longer than 2 h usually result in only incremental increases in resolution at the cost of diluting the eluted peptides. As a rule of thumb, gradient rates below 0.2% min^{-1} organic do not offer enhanced peptide resolution, but are preferred to isocratic elution.

Column Length and Diameter, Flow Rates, and Support Size

HPLC columns come in lengths ranging from ~5 to 25 cm. The column diameter dictates the flow rate and there is a commonly used lexicon for these column diameter/flow rate systems. Analytical HPLC is the term used for 4.1–4.6 mm ID columns with 0.6–1 ml min^{-1} flow rates and optimal resolution for loads up to several hundred micrograms. Narrowbore HPLC signifies ~2 mm ID columns used at 50–200 μl min^{-1} flow rates and loads up to 50 μg of peptide. Microbore HPLC refers to 1 mm ID columns with 10–50 μl min^{-1} flow rates and loads up to 10 μg. Capillary HPLC means 0.3–0.5 mm ID columns and 2–10 μl min^{-1} flow rates with loads up to 1–2 μg. Nanoflow HPLC refers to ≤0.2 mm ID columns with nl min^{-1} flow rates and loads below 1 μg. Capillary and nanoflow HPLC require specially designed HPLC plumping and low-volume detection systems.

Five-micron supports give the overall best resolution in microbore, narrowbore, and analytical HPLC. These are the mainstay columns used in biological research laboratories. Smaller 3 μm particles can yield slightly better resolution, but are not used that often because they generate a significantly higher back pressure, which can lead to faster column failure. Semipreparative columns refer to columns packed with 5 or 10 μm particles in 10 mm diameter columns. Preparative columns are packed with 10 μm particles in ~20 mm diameter columns. Process columns are packed with 10–15, 15–20, or 20–30 μm particles in columns 3–10 cm in diameter. The practical loading capacity of these larger ID columns depends on the complexity of the sample and the location(s) of the desired peak(s) of interest.

Guard Columns

The degree of peptide profile resolution offered by HPLC erodes as a function of the number of crude biologic samples applied to the column. It is expensive to use a fresh HPLC column every week so a short "guard column" placed in series before the separation column is sometimes used. Instead of replacing the HPLC column, the guard column that collects debris is changed periodically. Before the invention of guard columns, chromatographers used to unscrew the column inlet, remove the first several millimeters of dirty brown silica support and replace it with fresh support. The advent of guard columns simplified the column rejuvenation process. There are several sound reasons to use guard columns for many applications, but it is important to know what these devices actually do before using them on a routine basis. When a sample is injected onto an adsorptive HPLC support material such as reversed-phase or ion exchange, the peptides stick at the head of the column and then a gradient is used to elute the peptides to effect the separation. The important point here is that the actual separation is in the first several millimeters of the HPLC column. That is why the column head must be debris free. It has been shown by several groups that columns 1 cm in length can separate polypeptides almost as well as a 25 cm column. The lesson here is that the integrity of the first several millimeters of the column inlet are the most important. It must be clean and contain the same support material as the rest of the column. If not, the separation will be influenced by different adsorption–desorption characteristics. This principle is the reason why a guard column must contain the same support material as the HPLC column, since the head of the guard column is critical to the success of the overall separation. In capillary HPLC, clogging the column inlet with debris is especially problematic, but there is a different remedy.

Since the length of the column has a limited effect on the separation, experts usually dispense with guard columns and simply break off a few millimeters of the capillary column inlet for rejuvenation.

RPLC Applications (CNBr, Trypsin, and V8 Protease Protein Digestions)

In the 1970s large cyanogen bromide (CNBr) cleavage fragments (>30 aa) were notoriously difficult to separate by RPLC because they tend to be very surface hydrophobic. The advent of large-pore-sized RPLC columns in the early 1980s allowed researchers to readily purify these large polypeptides. This was a timely chromatographic advance since cocurrent advancements in gas-phase Edman microsequencing technology enabled longer N-terminal sequence determinations of the large CNBr fragments. Tryptic peptides tend to be smaller and less hydrophobic compared to CNBr fragments, so tryptic HPLC separation profiles generally resulted in more highly resolved peaks, but shorter partial N-terminal sequence determinations.

Recent advances in LC-MS/MS technology have readily automated the process of protein identification using tyrptic digestion. By the early 1990s the use of CNBr chemical cleavage to generate peptide fragments for RPLC separations was not used that often by analytical core facilities. Tyrptic digestion offered smaller, more reproducible peptide separation profiles, while CNBr chemical cleavage required safety handling precautions and less-resolved HPLC peptide separations. Today the standard is tyrptic digestion and to a lesser extent *S. aureus* V8 protease digestion. This separation process is known as peptide mapping. Trypsin cleaves peptide bonds C-terminally after basic lysyl and arginyl residues, while V8 protease cleaves after acidic aspartyl and glutamyl residues. Therefore, V8 protease fragmentation is ideal for generating peptide fragments from low pI proteins.

Other HPLC Peptide Separation Modes

Ion Exchange

RPLC is the preferred method for separating peptides, but there are cases where ion exchange can result in superior separations. Ion exchange can be either cation or anion exchange; both processes involve electrostatic interactions between charged amino acid side chains on the peptide and the stationary phase. For example, deamidated peptides can sometimes be better separated from their nonmodified counterparts using sulfonic-acid-based strong cation exchange as opposed to RPLC. Peptides with a low pI can be separated from other components in a mixture using weakcation exchange supports. Salt gradients of KCl, NaCl, $NaClO_4$, and NH_4SO_4 are commonly used with 10–50 mM Tris, bis-Tris, triethanolamine, or L-histidine buffering systems. Adding small amounts of acetonitrile (~5%) can also increase resolution of peptides. Temperature does not effect ion-exchange peptide separations as much as it does in RPLC separation, but it does effect protein separations. This is because proteins have tertiary structure that can be altered by temperature. When salts are used in an HPLC gradient system, extra care must be taken if stainless steel is exposed to the mobile phase. Corrosion will occur if exhaustive water-washing steps are not used after the separation procedure.

Weak anion-exchange HPLC columns usually contain diethylaminoethyl (DEAE) groups, quaternary amine functionalities (referred to as "Q"), n-propylamine chains, or polyethyleneimine (PEI) polymers adsorbed onto silica. Anion-exchange HPLC columns are also used for protein purifications and the salt gradient is usually in the pH 5–9 range. Weak cation exchangers are based on support materials with a carboxylic acid (COOH) function group and salt gradients in the pH 2–7 range. Commonly used buffering systems in order of increasing pK_a include phosphate (pK_a 2.1), formate, acetate, MES, phosphate (pK_a 7.2), and HEPES.

Ion exchange is increasingly being used before RPLC for two-dimensional HPLC separations. Examples include the multidimensional protein identification technology (MudPIT) method of Yates for complex protein identifications. In this example, a yeast ribosome preparation was first digested with trypsin; then the peptide fragments were fractionated into pools using strong-cation exchange; and finally the peptide pools were separated and identified by ion-trap electrospray LC-MS/MS. The common theme of this and other two-dimensional HPLC procedures is that salt, which is required for ion-exchange separations, is removed during the two-dimensional RPLC separation step. This makes the final factions ideal for mass spectrometry analysis.

Size Separation

Size exclusion chromatography (SEC) is the HPLC name for classical gel-permeation chromatography (GPC). In both cases macromolecules are eluted in order of size from largest to smallest. The key to this type of separation is minimizing interactions of the polypeptides with the stationary phase. This will allow the macromolecules to sieve down the column and be separated as a function of size only. Salt-based mobile phases are used to minimize the interactions of polypeptides with

support material during this sieving or permeation process. SEC is usually used to separate proteins over a broad molecular mass range, typically 10–200 kDa. Applications for peptide separations are limited because they are all relatively small (<10 kDa), although such separations can sometimes be achieved ~30% acetonitrile is added to the mobile phase.

See Also the Following Articles

Affinity Chromatography • Oligosaccharide Analysis by Mass Spectrometry

Glossary

ion-pairing reagent A chemical added to both solvent components of an RPLC gradient to control pH and improve peptide elution profiles.

peptide A short amino acid polymer consisting of ~20 or less residues. Longer chains are referred to as polypeptides or proteins and contain tertiary structure.

RPLC or **RP-HPLC** Reversed-phase high-performance liquid chromatography. A mode of HPLC where peptides are applied to hydrophobic coating support, and then selectively eluted using an organic mobile phase.

stationary phase The coating on a HPLC support surface that determines the mode of peptide separation used for elution.

support Particles that are coated with a stationary phase and packed into a column.

Further Reading

Gelpí, E. (1995). Biomedical and biochemical applications of liquid chromatography-mass spectrometry. *J. Chromatogr. A* **703**, 59–80.

Issaq, H. J. (2001). The role of separation science in proteomics research. *Electrophoresis* **22**(17), 3629–3638.

Liu, H., Lin, D., and Yates, J. R. III (2002). Multidimensional separations for protein/peptide analysis in the post-genomic era. *Biotechniques* **32**(4), 898.

Lubman, D. M., Kachman, M. T., Wang, H., Gong, S., Yan, F., Hamler, R. L., O'Neil, K. A., Zhu, K., Buchanan, N. S., and Barder, T. J. (2002). Two-dimensional liquid separations-mass mapping of proteins from human cancer cell lysates. *J. Chromatogr. B: Analyt. Technol. Biomed. Life Sci.* **782**(1–2), 183–196.

Biography

James D. Pearson is a member of the Molecular Technologies Department at Pfizer Global Research and Development, Ann Arbor, Michigan. He developed RPLC peptide and protein columns in the early 1980s, micropreparative-HPLC purification techniques in the late 1980s, 2-D gel separation systems in the 1990s, and is currently working in the areas of ribosomal and mitochondrial proteomics. He received a B.S. degree at the University of California at Davis, and a Ph.D. at Purdue University with Prof. Fred Regnier.

Imaging Methods

György Szabadkai and Rosario Rizzuto
University of Ferrara, Ferrara, Italy

The currently widely used imaging techniques evolved from the necessity of following the results of molecular biology (with the isolation of cDNA, and ensuing identification of the macromolecular components of living organisms), with the goal of clarifying where the different gene products are located, and how they act and interact (i.e., how they affect the different parameters and functions of the cell). In biochemistry and cell biology applications, the most developed imaging techniques work at the light microscopy level, but contemporary new techniques emerge to explore the exact nature of complex macromolecular interactions at the subcellular level and intercellular communication at the organ/organism level.

Objectives of Imaging Methods

The two main uses of cellular imaging are either to define the exact spatial localization of a given object or to quantitatively assess a given cellular parameter. Accordingly, the user interfaces of the digital imaging systems generally differentiate between morphological (focusing on three-dimensional (3-D) spatial data, utilizing either fixed or living samples) and quantitative (focusing of intensity measurements, generally in time dimension in living samples) applications.

Physical Optics and Microscopy

Image Formation Characteristics

The image formation of the light microscope (Figure 1) is based on a compound lens system comprising an objective with very short focus distance and high magnification power, and an ocular lens with longer focus and usually lower magnification. The sample is positioned slightly out of the focal distance of the objective, and thus an intermediate, magnified, reversed image is formed inside the focal distance of the ocular (eyepiece). The final, virtual, magnified, direct image can be observed by eye through the ocular or by detectors after collecting the divergent light by additional lens systems. Modern microscopes, by utilizing motorized objectives that can be focused axially in successive focal planes, allow the examination of specimen in three dimensions. Besides its magnification power, the most important characteristics of the microscope is its resolution power (i.e., its ability to distinguish between two adjacent points), which is limited by the diffraction of the light and determined by the properties of light and the objective (wavelength, λ; numeric aperture, NA). Based on these inherent physical properties, a maximum of 190 nm resolution is achievable observing green ($\lambda \sim 550$ nm) light emission and 130 nm at UV ($\lambda = 365$ nm) emission. This resolution limit can be greatly enhanced (more than 10^3 times, below nm scale) by the use of electron microscopes, using accelerated electrons instead of photons. Electrons can be focused by electromagnets on the (very thin) specimen where part of electrons will scatter on dense elements (salts or heavy metal labels), and the remaining ones will form an image on a phosphorus screen and a light detector. The main obstacle of electron microscopy is the rough fixation and drying necessary for sample preparation (consequently positioned in very high vacuum), which makes the observation of physiological elements very difficult.

Specialized Light Microscopy Techniques

Living or fixed cells visualized by traditional bright-field microscopy (using homogenous illumination by transmitted light) generally give images which are poor in contrast, because cellular components cause only very small amplitude difference of the transmitted light. The human eye is sensitive only to the colors of the visible spectrum (variations in light frequency) or to differing levels of light intensity (variations in wave amplitude). However, different cellular components may have quite large optical path difference (which is the function of object thickness and refractive index, relative to the neighboring substance) causing modulation of the phase of the diffracted light at object boundaries. To render these phase differences visible, several contrast-enhancing techniques using different illumination and image formation methods have been introduced. The most widely used phase contrast microscopy separates the direct and diffracted light and creates destructing interference between them. This results in the details

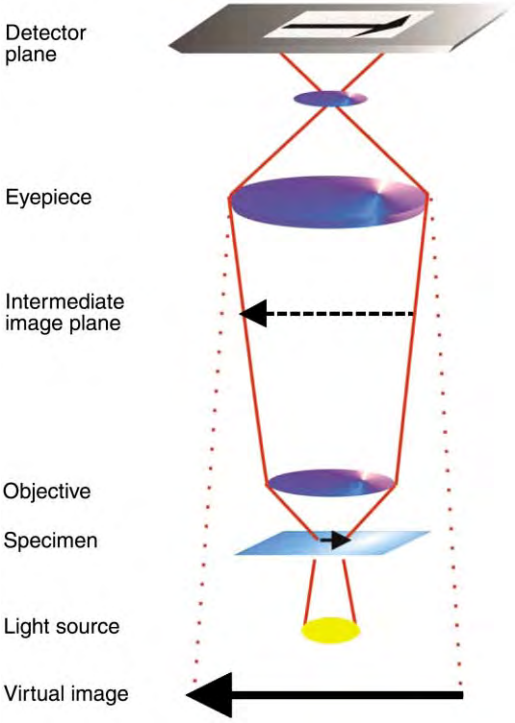

FIGURE 1 Schematic representation of image formation of the compound microscope.

of the image appearing darker against a lighter background. Differential interference contrast (DIC, DIC-Nomarski) microscopy appears to be the most powerful (but rather expensive) method to render subcellular details clearly visible only by optical means. This technique applies two polarized light beams perpendicular to each other, to detect edges of cellular components and converts them either in intensity or color difference with high lateral and axial resolution, giving a pseudo-3D appearance of the image.

Fluorescence Microscopy

Another solution for rendering subcellular details visible is to label cellular components by light-absorbing chemical substances (contrast enhancing and colored dyes), i.e., to increase the amplitude modulation of the transmitted light leading to increased contrast of the generated image. However, the revolution of cellular imaging stems from the introduction of fluorescent labels, which allows the visualization of virtually any desired object even in living specimens with exclusive sensitivity and selectivity. Fluorescent light emission is the result of selective excitation of electron state in particular chemical substances, generally polyaromatic hydrocarbons or heterocycles, followed by the return of the excited electron to its basal energy value after a few nanoseconds lifetime (Figure 2A). An inherent property of the light emission cycle is that the exciting photon has

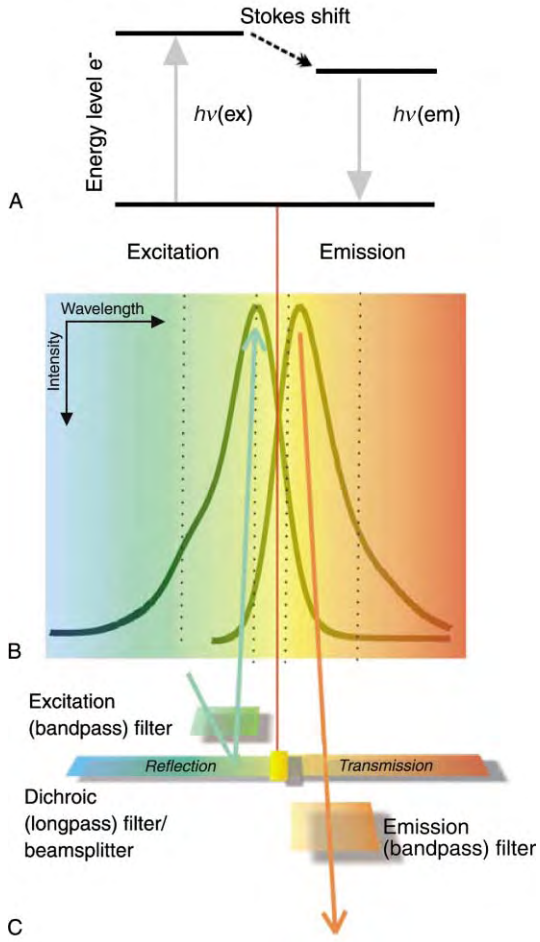

FIGURE 2 Principles of fluorescence: (A) formation of emitted light after excitation of the electron state in a fluorescent substance, (B) absorption and emission spectra of the fluorescent substance, and (C) optical filter set.

higher energy ($h\nu = h1/\lambda$), and therefore lower wavelength than the emitted photon. Thus, the absorption and emission spectra (Figure 2B) of a given fluorophor can be well separated. This allows the separation of the two different wavelengths in the illumination and detection optical path of the microscope by using a series of optical filters (Figure 2C). The core of color separation is the dichroic filter or beamsplitter, which, depending on its wavelength, either reflects or transmits the incident light. Additionally, to obtain specific excitation light and to detect a given range of emitted wavelengths, bandpass, lowpass, or highpass filters are applied. In multicolor or ratiometric-timelapse applications, in order to quickly change the excitation and emission wavelengths, filter wheels or even faster monochromators are used.

Electronic Light Detectors

The type of detector used is a critical parameter in cellular imaging techniques, since it determines the

sensitivity and spatial resolution of the obtained image. The two general solutions to electronically detect emitted, reflected, or transmitted light are the use of photomultiplier tubes and photodiodes, which in itself does not give spatial information or video imagers/area detectors, designed to directly provide spatially resolved images (tube type: vidicon; solid-state detectors: charge coupled device (CCD) and complementary metal oxide semiconductor (CMOS) cameras). These devices generate an analog voltage signal in function of light intensity, which must be digitized for image display and storage.

Photomultiplier Tubes

Photomultiplier tubes (PMTs) are useful for light detection of very weak signals, because they work by amplifying the electrons generated by a photocathode exposed to the incident photons. Among imaging applications, confocal microscopes combine high spatial resolution scanning and PMT in order to gauge light intensity and spatial information. Besides the high sensitivity, an important feature of PMT applications is their ability to record extremely fast events with very high signal-to-noise ratio ($>10^6$), since they respond to changes in input light fluxes within a few nanoseconds and exhibit extremely low dark current.

CCD Sensors

CCDs are silicon-based integrated circuits consisting of a dense matrix of photodiodes (determining picture elements, pixels of the chip), which operate by converting photon energy to an electronic charge. The accumulated charge is then transferred to a common output (through horizontal and vertical registers), amplified and digitized by an A/D converter located either in the camera or in the computer card (frame grabber). The main characteristics of CCD sensors, which determine the choice of camera type for a specialized imaging application, areas follows: (1) The number of electrons that can accumulate in the potential well of each pixel is referred to as well depth, that determines the upper limit of the dynamic range of the CCD. (2) The quantum efficiency (QE) defined as the number of electron–hole pairs created and successfully read out by the device for each incoming photon. It is the function of wavelength and standard sensors are usually more sensitive to wavelengths in the 500–800 nm range than they are to blue light (400–500 nm). (3) Image noise, by influencing signal to noise ratio (S/N), also determines the lower limit of chip sensitivity and dynamic range. Dark noise is a result of thermic generation of electron–hole pairs in the absence of illumination and can be reduced by cooling of the CCD (up to -50°C; a 20°C decrease in temperature reduces the dark current of the CCD tenfold). Readout noise is generated by collecting, amplifying, and digitizing the signal. (4) Spatial resolution and contrast depends on both the microscope optics and CCD architecture. The resolution and performance of an optical microscope can be characterized by a quantity known as the modulation transfer function (MTF), which is a measurement of the microscope's ability to transfer the spatial frequency of different contrast elements of the specimen to the image plane. This function is often utilized by optical manufacturers to incorporate resolution and contrast data into a single specification. On the other hand, the resolution of a CCD is a function of the number of its pixels and their individual size, thus increase in pixel number and decrease in pixel size will increase the resolution power of the CCD array. However, even if small pixels improve spatial resolution, they also limit the dynamic range of the device. Spatial resolution and sensitivity can be changed by unifying (clocking) multiple pixel charges in both the horizontal and vertical direction into a single larger charge. This procedure is called binning, which inherently leads to the increase of the sensitivity to incident light, but in parallel leads to the loss of spatial resolution. (5) Transfer speed of an image from the camera to the memory or screen of the computer depends on the CCD-readout rate (the time required to digitize a single pixel, pixel/sec), frame rate (the time needed for the CCD to acquire an image and then completely read that image out, frame/sec, fps), and the parameters of the computer utilized.

Three different CCD architectures, varying in their basic abilities, are currently in use to adapt CCD cameras to different applications. Full frame CCDs utilize their whole high-density pixel arrays to produce high-resolution images. In this configuration, the image transfer rates are lower, and can be increased by subdividing the CCD array into smaller, but identical subregions, which can then be read separately. The CCD array of frame transfer cameras is divided into the light-sensitive image array, where image data are collected; then the data are quickly (in 100 microseconds range) shifted to the storage array for the final readout by the serial shift register. Thus, during readout, the CCD is able to capture the next image, allowing for faster frame rates, but preserving high resolution and sensitivity. A potential drawback of frame-transfer CCDs is the presence of image "smear" at high frame rates, which occurs because acquisition and transfer to the storage array occur simultaneously. Interline CCD architecture is composed of a separate photodiode and an associated parallel storage and readout region into each pixel element. During the period in which the parallel storage array is being read, the image array is busy acquiring the next image frame, similar to the operation of the

frame-transfer CCD. This composition allows very fast image transfer rates but has lower sensitivity due to a decrease of the photosensitive area. This drawback, however, can be partially overcome by incorporation of microlenses on the photodiode array to increase the amount of light reaching each element.

CMOS Image Sensors

CMOS image sensors are similar to CCDs, but each active-pixel image sensor of a CMOS contains not only the photodetector element but also an active transistor circuitry, which works as an amplifier and serves for readout of the pixel signal, allowing random access to each image pixel and thus fast readout, and thereby rendering the acquired image extremely flexible to digital processing as compared to the sophisticated approaches necessarily used in CCDs. Another great advantage of CMOS sensors is their low cost since they can be produced in standard manufacturing facilities, producing standard semiconductor chips like computer microprocessors and memory chips. Further technological improvement to increase the sensitivity of these detectors will most likely lead to their introduction also into scientific imaging.

High-End Imaging Technologies to Increase Detection Sensitivity

Three different technologies have been applied to increase the sensitivity of CCDs: (1) The standard front illumination of the CCD array result in ~60% loss of quantum efficiency, due to the fact that the light must pass through the silicon layer covering the photodiode. The use of back-illuminated CCDs overcame this problem leading to an increase ~100% quantum efficiency at visible and infrared light and to 50% in UV detection. In this architecture, light arrives at the back of the CCD in a region that has been thinned to be transparent (thickness: 10–15 μm). Manufacturing these CCDs is significantly more difficult, resulting in a much higher cost of these detectors. (2) Amplification of the incoming photons by PMT-like devices has been integrated in specialized intensified cameras. The available technical solutions are ranging from several generations of microchannel plate-electron multipliers combined with a phosphorescent output screen to the recently introduced electron-bombarded charge-coupled device (EBCCD), which is a combination of the image intensifier and the CCD camera. The advantages of these devices over a cooled, slow-scan (low noise) CCD are the additional gain and accompanying speed. However, their noise levels are very high and their spatial resolution and dynamic range is significantly lower. (3) Very recently, on-chip amplification devices (amplifying signal before readout, thus reducing readout noise) have also been introduced, which, in combination with back-illuminated CCD architecture, may further increase the speed and sensitivity of imaging detectors.

Three-Dimensional (3D) Imaging

In order to visualize objects in three dimensions, images must be acquired and resolved along the z-axis (z stacks). An inherent problem of bright field and fluorescence microscopy is that images formed always contain out-of-focus light (haze). Two fundamentally different solutions emerged to overcome this problem: (1) 3-D deconvolution, to remove out-of-focus haze by computational methods from a series of optical section images acquired by digital microscopy, and (2) confocal imaging, to optically subtract light which does not arrive from the focal plane of the objective.

3D Deconvolution

The 3D distribution of out-of-focus light can be mathematically modeled as a point spread function (PSF). Deconvolution algorithms are designed to invert the blurring effect of the point spread function in order to restore the image contrast. Simplest solutions, like no- and nearest neighbor algorithms work by deblurring one 2D image, utilizing a subtraction of the blurred form of the adjacent slices and are particularly useful for fast deconvolution of high-intensity/contrast images. The term blind deconvolution is used when deblurring algorithms are based on theoretical PSFs. This method may give better results when additional algorithms are used to adopt PSF to the actual z image series. Still, the most powerful approaches utilize measured PSFs, which contain the actual aberrations inherent of the microscope configuration in use; thus, the deconvolution process can apply an efficient correction of the sum of these errors occurring in the nondeconvolved original image (Figure 3).

Confocal Laser Scanning Microscopy

In the excitation path of the confocal laser scanning microscopy (CLSM), an expanded laser light beam, focused on the specimen, is used to scan a given area in the $x-y$ space, and then the emitted fluorescent light passes through the dichroic mirror in the direction of the photomultiplier. A confocal aperture (pinhole) is placed in front of the photodetector (PMT), such that the emitted light from points on the specimen that are not within the focal plane (out-of-focus light) will be largely

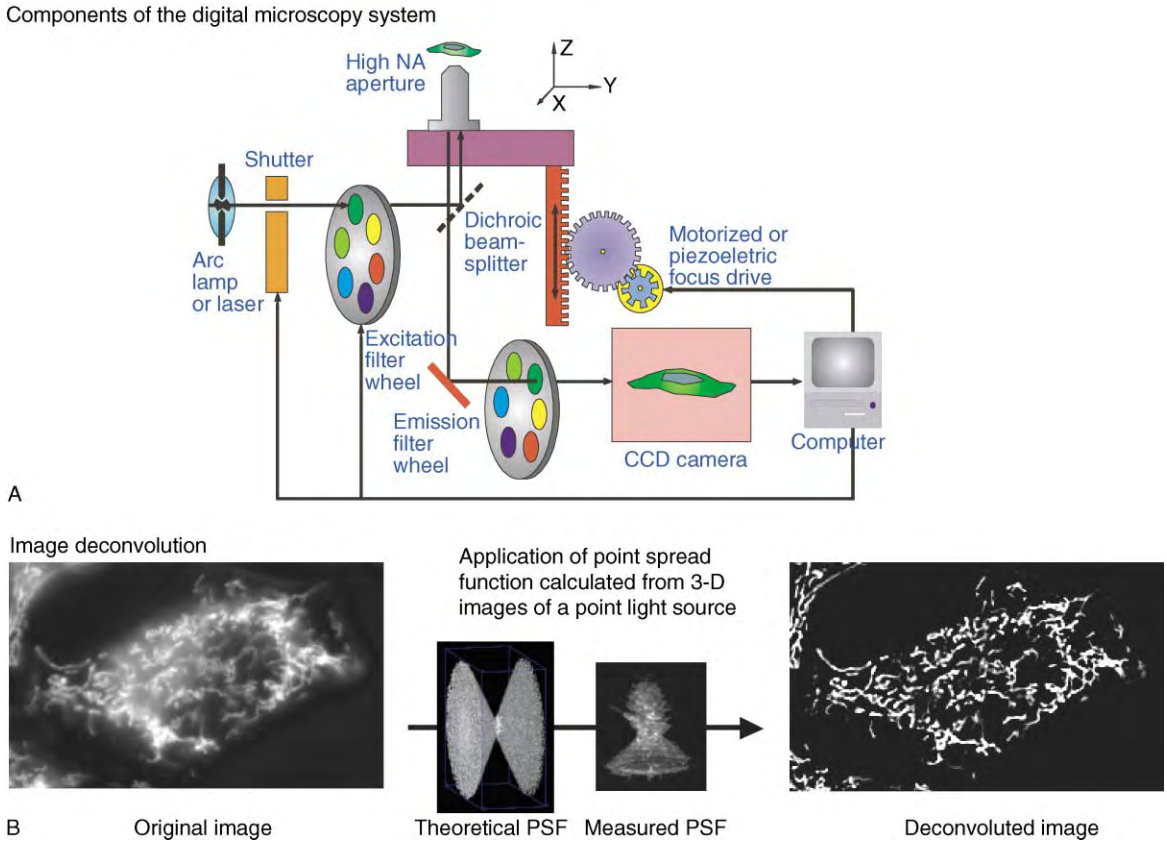

FIGURE 3 3-D microscopy: (A) basic components used for image acquisition and (B) image processing by 3D deconvolution.

blocked outside of the pinhole. Thus, the great advance of the use of CLSM is that the resulting image will be formed only from a slice of the sample with a given thickness, which is the function of the diameter of the aperture. The cost paid for this result is the relatively slower integration (scanning) time and higher illumination intensity needed, compared to high-sensitivity CCD detectors. This may lead to photobleaching of the fluorescent probe and damage of a living specimen. This phenomenon is greatly reduced in multiphoton confocal applications, where coincidence of two or more photons (with double or triple wavelength) is used to excite the probe only in the focal plane; thus, the specimen is illuminated with less intensity and less damaging (longer wavelength) light.

The images acquired either by 3D deconvolution of digital microscopy images or by the use of CLSM are usually visualized using volume rendering and surface rendering 3D reconstruction methods. In volume rendering, the pixel intensity information from a z series of 2D images is combined to generate voxels, volume elements. In surface rendering, only the surface pixels are utilized, and the interior structure is not visible because of the surface opacity.

Digital Image Characteristics

A 2D digital image is usually presented as a rectangular grid of individual pixels (picture elements). A fundamental characteristic of each pixel and thus of the whole image is its bit-depth, i.e., the scale of different colors or gray shades it may have (Table I). The sensitivity of the human eye is about 16–32 shades in gray and about two million shades in color; thus an image published in 8-bit grayscale or 24-bit color (true color) is more than sufficient. The resolution of the displayed image is defined as a number of pixels in a given distance (dot/inch dpi or sometimes dot/cm). The different output devices of the computer have different resolution ranging from 72 dpi of the monitor screen to 1200 dpi of laser printers. However, one should always keep in mind that the quality of the published image depends primarily on the resolution of the acquired image. The most commonly used color model is the additive RGB (red, green, blue) on-screen model, based on the three different phosphors on the monitor screen, excited at different intensities (usually an 8-bit range for each color, for 256 intensities per color, for a total of 24 bit possible color combinations). Color printing typically

TABLE I
Digital Image Characteristics

Number of colors/shades in gray scale	Bit depth
2	2^1
32	2^4
256	2^8
4096	2^{12}
65 536	2^{16}
16 777 216	2^{24}

uses a subtractive color model called CYM (cyan, yellow, magenta) or CYMK (with black added), which however cannot reproduce a range of colors as large as the RGB model. The most popular alternative color-space model is the hue, saturation, and intensity (HSI) color space, which represents color in an intuitive way (the manner in which humans tend to perceive it). Instead of describing characteristics of individual colors or mixtures, as with the RGB color space, the HSI color space is modeled on the intuitive components of color. For example, the hue component controls the color spectrum (red, green, blue, yellow, etc.), while the saturation component regulates color purity, and the intensity component controls how bright the color appears. Grayscale digital images can be rendered in pseudocolor by assigning specific gray level ranges to particular color values. This technique is useful for highlighting particular regions of interest in gray-scale images, because the human eye is better able to discriminate between different shades of color than between varying shades of gray. Pseudocolor imaging is widely employed in fluorescence microscopy to display merged monochrome images obtained at different wavelengths utilizing multiply stained specimens.

Another important consideration for the published images is the file format used. For scientific images, the most frequently used format is tagged image file format (TIFF), which supports 8- or 16-bit grayscale as well as 24-bit color, and lossless (LZW) compression, most often used on web pages, not suitable for most scientific images. A relatively new and very convenient format that is not widely supported yet is PNG (portable network graphics), which supports up to 48-bit color and 16-bit grayscale with lossless compression. In contrast, the JPEG and GIF formats, widely used on web pages, are generally not suitable for scientific images either because of their low bit-depth or lossy compression methods.

See Also the Following Articles

HPLC Separation of Peptides • Oligosaccharide Analysis by Mass Spectrometry • PCR (Polymerase Chain Reaction) • Two-Dimensional Gel Electrophoresis • X-Ray Determination of 3-D Structure in Proteins

Glossary

digitalization Process done by an analog/digital converter, during which a continuous signal (voltage or current) is transformed into discrete values. The range and step size of these discrete values is dependent on the number of bits used in digitalization.

numeric aperture (NA) Feature of the microscope objective defining its resolution power, function of the half of angular aperture (α) of the objective lens and the refractive index (n) for the medium through which the light passes ($NA = n\sin\alpha$).

photobleaching Irreversible destruction of the excited fluorophore, which happens usually under high-intensity illumination conditions. Photobleaching originates from a third excited state created from the singlet state and some pathways leading to photobleaching may include reactions between dye molecules.

quantum efficiency (QE) Number of electron–hole pairs created and successfully read out by a charge coupled device (CCD) for each incoming photon, describing the sensitivity of the light detector.

resolution (1) Distance between two adjacent points which can be imaged separately; and (2) number of picture elements (pixels) in a given distance of a digitally displayed image.

Further Reading

Centonze, V. E. (2002). Introduction to multiphoton excitation imaging for the biological sciences. In *Cell Biological Applications of Confocal Microscopy* (B. Matsumoto, ed.) 2nd edition, Vol 70, pp. 129–148. Methods in Cell Biology, Academic Press, New York.

Gerlich, D., and Ellenberg, J. (2003). 4D imaging to assay complex dynamics in live specimens. *Nat. Cell Biol.*, S14–S9.

Isenberg, G. (ed.) (1998). *Modern Optics, Electronics, and High Precision Techniques in Cell Biology (Principles and Practice Series)*. Springer, Berlin, Germany.

Miyawaki, A. (2003). Fluorescence imaging of physiological activity in complex systems using GFP-based probes. *Curr. Opin. Neurobiol.* **13**, 591–596.

Rizzuto, R., Carrington, W., and Tuft, R. A. (1998). Digital imaging microscopy of living cells. *Trends Cell Biol.* **8**, 288–292.

Tsien, R. Y. (2003). Imagining imaging's future. *Nat. Rev. Mol. Cell. Biol.*, SS16–SS21.

http://micro.magnet.fsu.edu/primer/index.html – M. W. Davidson, Florida State University.

Biography

Rosario Rizzuto is a Professor of General Pathology at the University of Ferrara. He developed a new method for measuring Ca^{2+} concentration in specific cell domains, based on the targeting of the Ca^{2+}-sensitive photoprotein aequorin and applied 3D microscopy to show close contact between the endoplasmic reticulum and mitochondria. His research interest is the role of calcium ions as intracellular second messengers, with special emphasis on the mechanism and functional role of mitochondrial Ca^{2+} homeostasis.

György Szabadkai is a Research Assistant at the Telethon Center for Cellular Imaging, University of Ferrara. His main interest is the study of intraorganellar Ca^{2+} signaling in mitochondria and endoplasmic reticulum, and determining its role in different forms of apoptosis and neuronal cell death.

Immunoglobulin (Fc) Receptors

Mark Hogarth
Austin Research Institute, Melbourne, Australia

Immunoglobulin Fc receptors (FcRs) are cell surface molecules that bind the Fc portion of immunoglobulin. Receptors have been identified for all immunoglobulin classes and subclasses with the exception of IgD. These should not be confused with microbial proteins that bind the Fc portion of immunoglobulin.

General Comments

When antibodies contact their specific antigen, they form an immune complex and in the case of most pathogens, many antibodies will coat a single macromolecule or pathogen fragment leading to the formation of oligovalent immune complexes. These complexes can then interact with specific cell surface Fc receptors (FcRs) and this interaction subsequently initiates signaling cascades inside cells.

The affinity of the interaction between the different Ig subclasses and specific FcRs varies enormously, ranging from low-micromolar affinity for some of the IgG receptors to high-femtomolar affinity for the high-affinity IgE receptors. Such a vast range of affinities have specifically evolved to suit the biological activities of particular receptor types.

The nomenclature of FcRs is as the name suggests, based on the capacity to bind the Fc portion of a particular class of antibody (e.g., IgM, Fcμ; IgG, Fcγ), the letter R designates the receptor and a Roman numeral designates a particular subtype of FcR e.g., FcγRII. There are further subclassifications by letters a, b, c, etc. e.g., FcγRIIa.

The vast majority of FcRs are found on leukocytes where they are involved in the regulation of cellular activity by antibody. For the most part, this is the activation of cells, but a discrete and unique class of FcR is able to down-regulate leukocyte activity following their binding of immune complexes.

Whilst the vast majority of FcRs are found on leukocytes and have been the principal subject of most research, several other FcRss have been identified, present on epithelial and endothelial cells, with specific functions related to transport and recovery of immunoglobulins.

Leukocyte Fc Receptors

Most leukocyte FcR are multisubunit complexes requiring a ligand-binding chain noncovalently associated with a signaling chain and in some cases with an additional signal amplifying subunit (Figures 1 and 2). The biochemical and functional characteristics of the most-frequently studied FcR of leukocytes is detailed below.

IgE Fc Receptors

The high-affinity IgE receptor FcεRI binds monomeric IgE with an affinity of 10^{10} M^{-1} and is found principally on mast cells and basophils and in a modified form on eosinophils and monocytes. The binding of IgE to this receptor and the subsequent cross-linking of the bound IgE by antigen induces one of the most potent pharmacological responses in biology. In adverse situations, this results in a classic type-I hypersensitivity reaction clinically manifest as allergy e.g., hay fever, penicillin or food allergies. Unlike the high-affinity IgE receptor, the FcεRII binds IgE with a lower affinity (10^{7} M^{-1}). This is a type-II membrane glycoprotein with lectin-like activity and is found on many leukocytes including T-cells, B-cells, and monocytes. Its function appears largely to regulate activity of immune responses.

These receptors are biochemically distinct, FcεRI is a transmembrane glycoprotein and is a member of the Ig superfamily with two extracellular domains, each of which belongs to the Ig superfamily. By contrast FcεRII is a type-II membrane glycoprotein with lectin-like activity.

IgG Receptors

There are three main classes of leukocyte IgG Fc receptors – FcγRI, FcγRII, and FcγRIII (Figures 2 and 3A and 3B). These are widespread with every leukocyte with the exception of lymphocytes bearing one or more of these receptors. They can be distinguished by both amino acid sequence and by the use of specific monoclonal antibodies and also by differences in affinities for IgG. FcγRI is the high-affinity receptor for

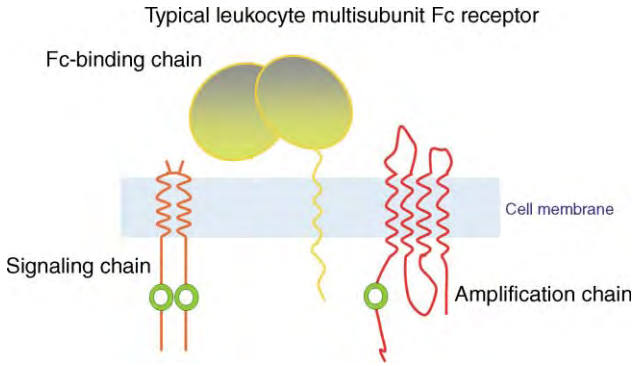

FIGURE 1 Schematic representation of a typical multisubunit Fc receptor. The typical components of many FcR found on leukocytes. A ligand-binding chain usually a Type-1 transmembrane glycoprotein is noncovalently associated with other subunits: a signaling chain, often the FcR-γ chain, which is a 24 kDa covalent homodimer wherein each monomer contains an ITAM, a specialized tyrosine-containing signaling motif (green annulus). In at least two cases, the ligand-binding chain is further associated with a tetra transmembrane signal-amplifying chain.

IgG ($10^8\ M^{-1}$) and is restricted largely to monocytes, macrophages, and neutrophils. FcγRII is composed of two major subtypes: FcγRIIa and FcγRIIb that are separate gene products and are biochemically distinct. Both bind IgG with very low affinity (1 μM) as monomeric immunoglobulins have a very rapid on and off rate, however, as these low-affinity receptors are present on the cell membrane they can effectively and very avidly bind oligovalent complexes of antigen and antibody.

FcγRIII also has two principal subtypes: FcγRIIIa and FcγRIIIb. Both are low-affinity receptors though they bind with IgG with tenfold higher affinity than the FcγRII low-affinity receptors. FcγRIIa is found on virtually every leukocyte including platelets. Similarly, FcγRIIb is found on virtually every leukocyte including B-cells but not platelets. FcγRIIIa is found on natural killer cells and macrophages, and monocytes, whereas FcγRIIIb is found only on neutrophils.

All of these FcRs belong to the Ig superfamily. Each has two extra cellular Ig-like domains with the exception of FcγRI, which has three (Figure 2). Another interesting difference is that whilst FcγRIa, FcγRIIa, and FcγRIIIa are transmembrane glycoproteins, FcγRIIIb is a GPI-anchored receptor (Figure 2).

IgA and IgM Fc Receptors

A single leukocyte receptor specific for IgA has been defined – FcαRI, which is found on neutrophils and monocytes (Figure 3C). The affinity for IgA is $\sim 10^7\ M^{-1}$ but immune complexes of IgA binding to FcαRI are potent inducers of cell activation. A receptor that is able to bind both IgA and IgM has also been defined though there has been relatively little characterization of this.

Sites of Interaction with Ig Ligands

The Ig-binding sites of FcεRI, FcγRI, FcγRII, and FcγRIII are located in similar regions in these structurally related but functionally distinct receptors (Figures 3A and 3B). The binding site largely involves the second domain together with sequences at the junction of the first and second domains. The stoichiometry of FcR:IgG interaction for these receptors is 1:1 (Figure 3A). For FcαRI, the IgA-binding site is located on the extreme tip of the first domain, which allows it to form a rather unique two to one stoichiometry with IgA (Figure 3C). The head groups of the triple helix of FcεRII interact with IgE in a 1:1 stoichiometry.

Receptor-Binding Sites in Immunoglobulin

FcγRI, FcγRII, and FcγRIII interact with sequences in the lower hinge and adjacent areas of Cγ2 of the IgG Fc (Figure 3A). Differences in the nature and extent of these

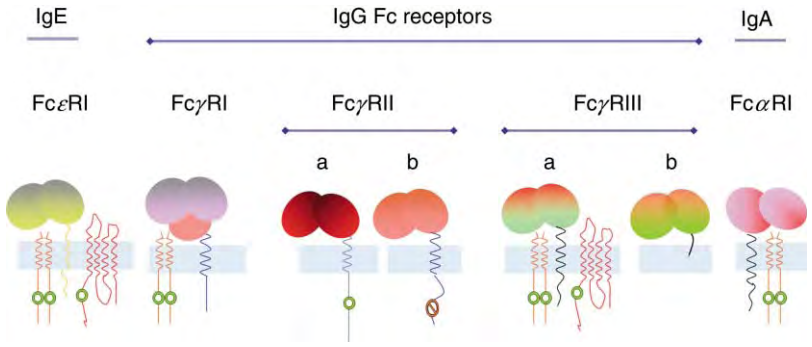

FIGURE 2 Schematic representation of leukocyte FcR showing configuration of signaling competent receptor complexes. FcγRII (not shown). ITAMS shown as green annulus; the FcγRIIb ITIM as a red crossed circle.

interactions explain the differences in affinity of FcR:Ig interaction. FcεRI interacts with a sequence between Cε2 and Cε3, which is distinct from the area of the sites of interaction of FcεRII. The nature of these interactions clearly define the stoichiometry. FcαRI interacts with the area between Cα2 and Cα3. Currently, there is no information on the interactions of Fc$\alpha\mu$R and IgA or M.

Signal Transduction Complexes

With the exception of FcεRII there has been a great deal of investigation of the signal transduction by leukocyte FcRs, which have become one of the most widely studied groups of receptors. The binding of antibody or immune complexes to these can be a potent inducer of biochemical signals, but FcγRIIa and FcγRIIb have additional unique biochemistry. The related leukocyte receptors – FcεRI, FcγRI, FcγRIIIa, and FcαRI all signal by very similar mechanisms involving the immuno-receptor tyrosine activation motif (ITAM), which is recognized by the *syk* and *src* family protein tyrosine kinases. To signal, these receptors must form multi subunit signaling complexes composed minimally of the Ig-binding chain, (all of which are the Ig superfamily members), non-covalently associated with a low-molecular-weight hetero- or homodimeric signaling chain – the common FcR-γ chain or in the case of FcγRIIIa and in NK cells the TCR-ζ chain (Figures 1 and 2).

The ITAM motif that is necessary for recognition by *syk* and *src* kinases is contained in these associated low-molecular homodimers. Cross-linking of the FcR by immune complexes or by antigen binding to cell-bound Ig, aggregates the receptors leading to phosphorylation of tyrosine in the ITAMs and the subsequent induction of the signaling cascades. Similar mechanisms of leukocyte activation are well described for the antigen receptors of T and B lymphocytes.

FcγRIIa stands out as an exception to the multi subunit paradigm for ITAM-dependent immunoreceptor signaling (Figures 2 and 3B). Whilst aggregation of this receptor leads to *syk* and *src* kinase activation, this receptor does not require association with the common FcR-γ chain or other FcR molecules as the ITAMs are contained within its cytoplasmic tail. Indeed FcγRIIa is one of the few immunoreceptors to have the signaling motifs contained in the ligand-binding chain. Furthermore, this receptor forms a unique dimer on the cell surface that juxtaposes the ITAM motifs for signal transduction (Figure 3B).

FcγRIIb is not an activating FcR; indeed its role is to inhibit and regulate the activities of other ITAM-containing activating FcRs and the antigen receptor of B cells. The cytoplasmic tail of FcγRIIb contains an immunoreceptor tyrosine inhibitory motif (ITIM), which on "coaggregation" with ITAM-containing activating receptors, recruits phosphatases, which in turn down-regulate or eliminate ITAM-dependent signal transduction. Its best-characterized role is its co-engagement with the antigen receptor of B lymphocytes where it regulates B-cell activation by antigen.

Other Leukocyte FcRs

In recent years especially with the output of the human and mouse genome projects, new cell surface molecules with FcR-like activity have been described though they are currently poorly characterized. Nonetheless, for the sake of completeness, these are included here. The most advanced characterizations have involved the leukocyte in receptor cluster, which is a large family of cell surface molecules present on leukocytes, and some of these show immunoglobulin-binding activity. Biochemically these molecules include members with multiple Ig-like domains and with tissue distributions ranging from the highly restricted to the very broad. The precise biochemical characterization and biological roles are as yet poorly understood but will no doubt be revealed in time.

Non-Leukocyte FcRs

Two major non-leukocyte FcRs have been defined. The poly Ig receptor (Poly IgR) and FcRn.

The poly Ig receptor is responsible for the binding and transport of secretory immunoglobulins – sIgA and sIgM. It is found on secretory epithelium, notably in the lactating breast, as well as mucosal surfaces. This is a cell surface molecule composed of five domains: the IgA and IgM-binding sites occur in the first two domains, which when attached to sIgA or sIgM are cooperatively cleaved from the receptor and thereby form the so-called secretory component associated with secretory IgA and IgM.

FcRn is biochemically distinct from all other leukocyte and non-leukocyte Fc receptors. It is a transmembrane glycoprotein but it is more structurally related to the major histocompatibility molecules (MHC Class I) whose principal function is antigen presentation to T-cells (Figure 3D). However, it is sufficiently biochemically different from these, which makes it unable to be involved in that process. The main function of FcRn in humans is the recycling of immunoglobulins in the circulation, which ensures the prodigious half-life of IgG. Intact, and undenatured IgG, which is taken into endothelial cells by pinocytosis is recycled to the circulation following its attachment to FcRn in the acidifying pinocytotic vesicle, where it undergoes acid-dependent attachment to FcRn, recycling to the endothelial cell surface and release at the neutral pH of the circulation.

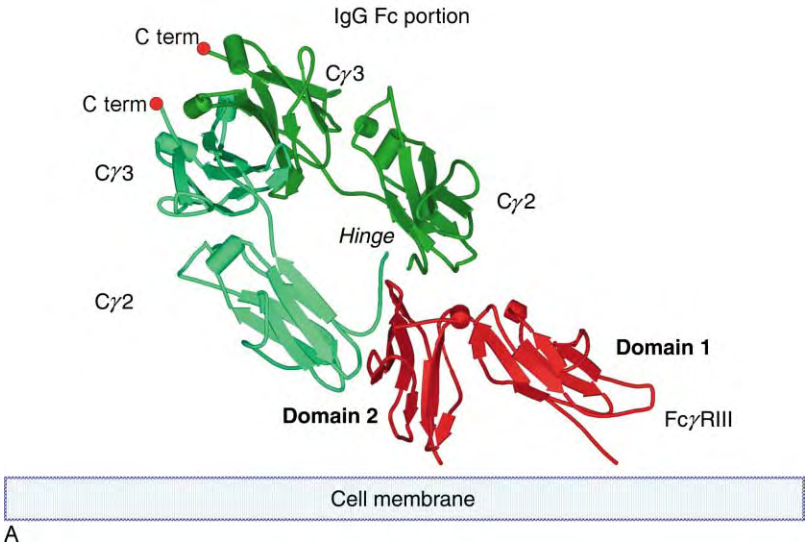

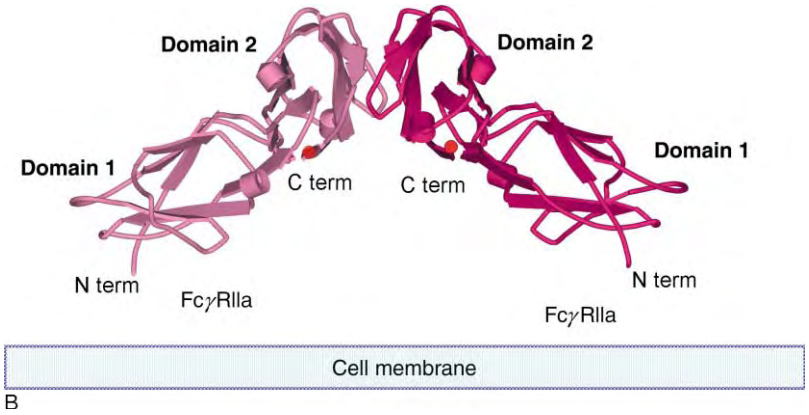

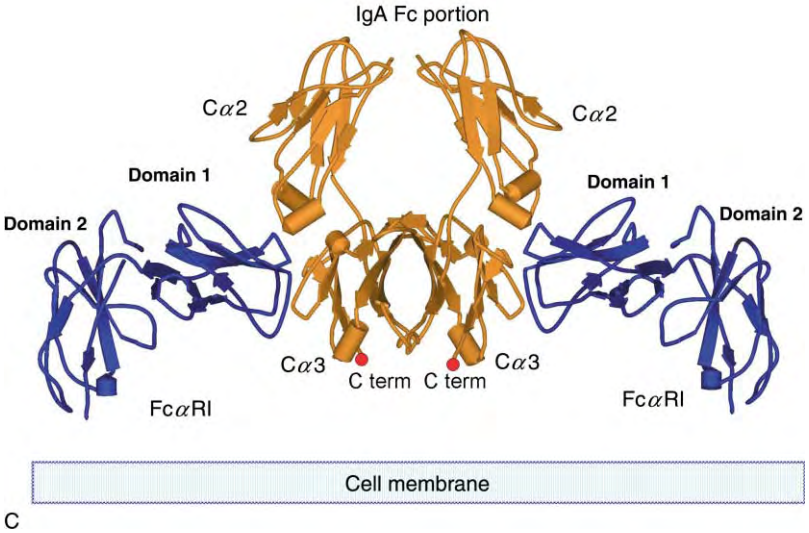

FIGURE 3 Alpha-carbon backbones of selected Fc receptors and ligands. (A) Complex of FcγRIIIa and IgG. From the Data Base:(PDB, 1E4K). The receptor's second domain and interdomain region interact with the lower hinge region of the IgG Fc giving the characteristic 1:1 stoichiometry. (B) FcγRIIa (PDB 1FCG). This receptor is unique as it forms a non-covalent homodimer. Details of the interaction with IgG are not known but interaction as seen for FcγRIII IgG (Figure 3(A) is not possible with this dimer because steric clashes between the dimer and Cγ2 prevent proper interaction of domain 2 with the lower hinge of IgG. (C) Complex of FcγRI and IgA (PDB, 1OW0). Interaction between the "tip" of the first domain of FcαRI and the Cα2/Cα3 junction of each Fc chain gives the 2:1 stoichiometry.(D) Structure of FcRn and IgG complex (PDB, 1I1A).

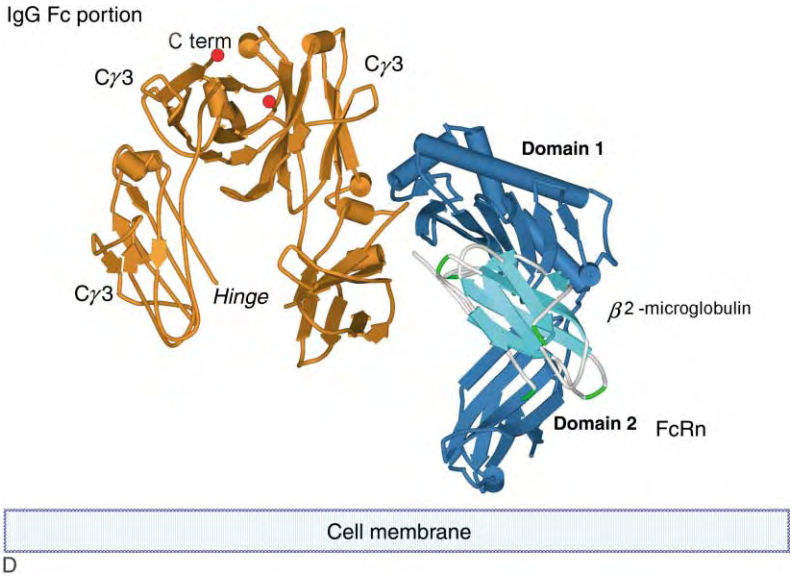

FIGURE 3 (*continued*)

Biological Role of Leukocyte Fc Receptors

These receptors participate in a range of normal biological functions, most of which are associated with the activation of leukocytes, which then lead to specialized functions associated with difference cell types, e.g., the degranulation of mast cells and the release of inflammatory mediators caused by co-engagement of the high-affinity IgE receptor. However, for the most part, FcγRI, FcγRII, and FcγRIII appear to be mostly concerned with antibody dependent of leukocyte function rather than the historical view that Fc receptors on cells such as macrophages, dendritic cells, and other phagocytes serve the principal role for the phagocytic removal of immune complexes.

It is now in the more modern view that these receptors play a far more active and sensitive role rather than one of simply garbage disposal, which in humans is largely filled by the complement system and in particular CR-1 on erythrocytes.

This capacity to bind immune complexes, though not in itself pathogenic, can in the presence of aberrant immune complexes, such as autoantibody, lead to the potent and continuous stimulation of leukocytes, leading in turn to pathological inflammation and tissue destruction. This is clearly the case in diseases such as systemic lupus erythromatosus (SLE), rheumatoid arthritis, glomerulonephritis, allergies. Attempts to interfere with the interaction of immune complexes with FcRs are now forming the basis of novel approaches to the treatment of those diseases.

Key Events in the Analysis of FcR

The existence of specific receptors for immune complexes was noted in the early 1970s by Metzger and by Basten and their co-workers. The observation by Metzger and Bevan that engagement of these receptors could induce a measurable intracellular biochemical event was an exciting observation of importance, not only for Fc receptors but for immunologically important receptors generally. There have been several major milestones in the application of new technologies to the characterization of Fc receptors – Jay Unkeless produced the first monoclonal antibody defining an Fc receptor and Hibbs and colleagues defined first function-associated genetic polymorphis using monoclonal antibodies. The genetics revolution led to the first cloning in the mid 1980s of FcR gene simultaneously and independently by Hibbs, Ravetch, Mellman, and Kinet. By the early 1990s Ierino and co-workers had established that blockade of FcR may provide useful

Interaction of the FcRn first domain with amino acids in the junction of Cγ2 and Cγ3 of a single Fc chain. The β2-microglobulin typically associated with MHC class I molecules is shown associated with FcRn ectodomains. All chains are represented as α-carbon backbones; strands as arrows and α-helices as barrels. The C terminus of each polypeptide chain is shown in red. Constant regions of IgA or IgG are indicated – Cα or Cγ and the position of the hinge is shown. Orientation of the polypeptides to the membrane is assumed.

therapeutic approaches for the treatment of disease. Finally in more recent times the three-dimensional structures of FcR have become available for the first time through the work of Maxwell and Powell, Jardetzky, Sun, Sondermann, and others.

Conclusion

The Fc receptors are a large family of immunoregulatory molecules that play crucial roles in antibody effector systems, leading in normal immune responses to the activation or regulation of leukocytes.

See Also the Following Articles

Cytokines • Fibroblast Growth Factor Receptors and Cancer-Associated Perturbations

Glossary

autoimmune disease Diseases where the immune system attacks the hosts' tissues and/or organs. Examples include rheumatoid arthritis, systemic lupus erythematosus.

hypersensitivity Powerful and frequently destructive inflammatory reaction often induced by antibodies in autoimmune diseases.

leukocyte White blood cell including eosihophil, polymorphonuclear leukocyte or neutrophil, macrophage, monocyte, mast cell, basophil, lymphocyte.

phagocyte Cell that actively ingests particles, typically macrophage or neutrophil.

phagocytosis Process, distinct from pinocytosis, by which particles are taken into the cell. Unlike pinocytosis, considerable intracellular and membrane reorganization is required for the uptake of the particle.

pinocytosis Process by which cells sample small amounts of fluid from their surrounding environment. This usually involves internalization of small vesicles formed from the invagination of the cell membrane.

Further Reading

Ierino, F., Powell, M. S., McKenzie, I. F. C., and Hogarth, P. M. (1993). Recombinant soluble human FcγRII: Production, characterization and inhibition of the arthus reaction. *J. Exp. Med.* **178**, 1617–1628.

Metzger, H. (1999). It's spring and thoughts turn to…allergies. *Cell* **97**, 287–290.

Ravetch, J. V., and Bolland, S. (2001). IgG Fc Receptors. *Ann. Rev. Immunol.* **19**, 275–290.

Van de Winkel, J. G. S., and Hogarth, P. M. (eds.) (1998). *The Immunologlobulin Receptors and Their Physiological and Pathological Roles in Immunity.* Kluwer Academic, Dordrecht.

Biography

Mark Hogarth, Director of the Austin Research Institute in Melbourne, has a long-standing interest in the biochemistry, immunology, and genetics of cell surface molecules. He has made seminal discoveries in the study of FcRs for antibodies – including some of the first monoclonal antibodies, molecular cloning, and X-ray structure analysis of this family and recently in the development of potential new therapeutic entities for the treatment of autoimmune disease and inflammation.

Inorganic Biochemistry

Robert J. P. Williams
University of Oxford, Oxford, UK

All organisms require a limited, selected number of chemical elements. The requirement includes obviously the nonmetal elements H, C, N, O, P, and S which provide the vast majority of elements in organic compounds in every cell. Other elements which are necessary for organisms include Na, K, Mg, Ca, Mn, Fe, (Co), (Ni), (Cu), Zn, Mo or W, Cl, B, and Se. Those in parentheses are essential for most organisms. Inorganic biochemistry therefore includes the modes of uptake, the ways of incorporation, and the functional value of these essential elements. It also includes consideration of elements as poisons and as valuable drugs in medical practice.

Introduction

A glance at the periodic table, Figure 1, shows that of the 18 groups in the table, elements have been selected by organisms from 15 groups, indicating that life is based on almost the full diversity of the chemistry of the periodic table. Absent are elements from groups 4, 13, and 18. There are also organisms which use F, Si, Sr, Ba, V, Cd, and possibly Sn. Thus of the common elements there are only a few that are not found in some living system, e.g., Al and Ti, while most of the uncommon elements, i.e., elements heavier than Zn, are absent. This gives rise to the possibility for the use by man in attacking medical and agricultural problems of several inorganic elements as accidental or deliberate poisons or medicines. Examples are Be, Al, Br, Pt, Hg, Au, Sb, Bi, and Pb. It is the study of all the elements, often but not always in combination with the elements of organic chemistry that is called "inorganic chemistry," and when applied in a living system it is called "inorganic biochemistry" or "biological inorganic chemistry." In what follows, attention is drawn to the value of certain of these elements starting from the most common in all organisms, but it is clear that together organic and inorganic elements, some 15–20 in all, created life as we know it.

Electrolytes

All cells are required to manage the ions of those elements which are highly available in the environment and are mainly free, namely, Na^+, K^+, Mg^{2+}, Ca^{2+} and Cl^-. Especially Na^+, K^+, and Cl^- are rarely combined with organic or inorganic molecules or anions. These five elements have always dominated the sea as electrolytes but have been and are present at much lower concentrations in all freshwater. All cells need to control the uptake of these ions for they are serious components of the ionic strength and osmotic pressure inside as well as outside cells and they are major units in electrolytic charge balance in all natural fluids. It is found that cells have, possibly universally, a free ion cytoplasmic concentration of Na^+ (10^{-2} M), K^+ (10^{-1} M), Mg^{2+} (10^{-3} M), Ca^{2+} ($<10^{-6}$ M), Cl^- (10^{-3} M). Clearly life in the sea rejects Na^+, Mg^{2+}, Ca^{2+} and Cl^- while taking in K^+ but life in freshwater, which evolved later, has to take in all five elements. The above functional value of Na^+, K^+, and Cl^-, the most available and which bind the least to organic matter, evolved from the use in simple electrolyte balances to include employment in bioenergetic exchanges across membranes and more recently to dominate electrolytic messages. Here particularly Na^+, K^+, Cl^-, and now including Ca^{2+} are the only simple ionic current carriers of such cells as nerves and muscles and are essential components of the functioning of the brain. Text books on physiology to a great degree concern mainly these five elements.

Calcium is the most strongly rejected of all five but also functions as a bound element especially in cell activation of higher cellular organisms. Magnesium is not rejected strongly from any cell and is an essential weak acid catalyst. It is present in most of the reactions of phosphates including ATP^{4-}, which is ~50% $MgATP^{2-}$ in cells. Examples of its functions are kinases and it is a vital structural component of RNA and DNA. Mg^{2+} and Ca^{2+} together help to stabilize cell membranes and walls and are present in most biological minerals such as shells and bones.

Magnesium has a quite exceptional additional function in chlorophyll, the light-harvesting and light-activating factor of virtually all plant life.

Iron

The next most common metal element is iron. It is very largely bound to proteins not free in cells. It was very

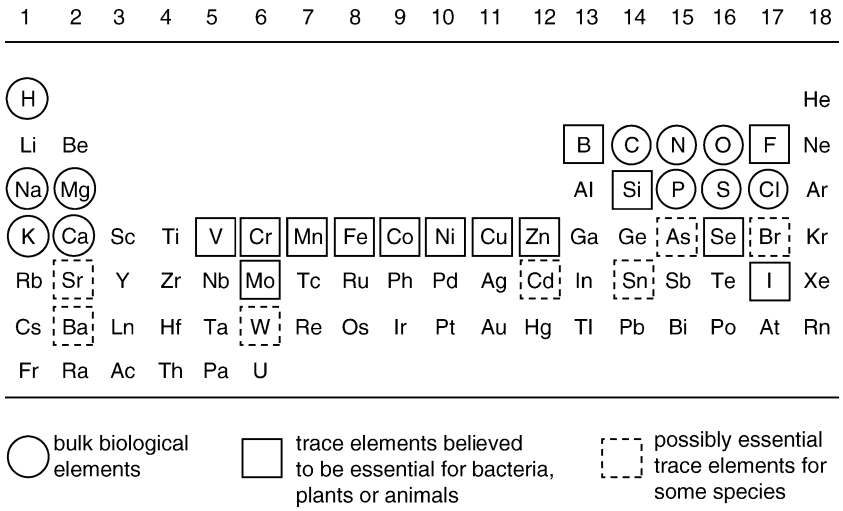

FIGURE 1 The periodic table of the elements showing those essential for most organisms and those required by some organisms. Note the distribution of required elements within the periodic table.

readily available from the primitive reducing sea as ferrous ion but, as oxygen pressure rose more than two billion years ago, iron became ferric ions in solution which precipitated and availability became very reduced. As a consequence all aerobic organisms have cleverly devised scavenging systems for iron. The essential nature of the element derives from its use as a catalyst. In its protein combinations it is found bound in iron–sulfur proteins, in heme proteins, and in proteins bound simply to nitrogen and oxygen side chains. These proteins are largely engaged in oxidation or reduction catalysts, in the transport of electrons, as carriers (hemoglobin and myoglobin), as sensors for CO, NO, and O_2, in DNA synthesis from RNA, and as storage buffers for iron. There is in fact a very extensive network of iron proteins essential in all cells but very noticeable in the bioenergetics of both chloroplasts and mitochondria. There is for this metal element a series of concentration controls linked through transcription factors to DNA. It may be that the overall expression of many functional parts of a cell are linked to the concentration of free ferrous ions in the cell cytoplasm. However, the storage of iron is in a ferric ion precipitate bound in a protein, ferritin.

Zinc

Next to iron in importance amongst trace elements is zinc. Unlike iron it was restricted in its availability to primitive life since it has an insoluble sulfide. As sulfur, in the form of H_2S, became oxidised to sulfate, so zinc was liberated, and it is now quite a common element in the sea. Zinc is not like iron in its functions. It does not take part in oxidation or reduction reactions but is a good acid catalyst. Hence it finds use in organic chemistry as well as in organisms. In cells its acidic function is used not only in a wide range of degradative enzymes – peptidases, nucleases, and saccharases, and in hydration reactions – but also in RNA/DNA synthetases. Zinc has a distinct role in the nucleus of eukaryotes in proteins called zinc fingers, which act as transcription factors especially involving sterol, thyroxine, retinoic acid, and related hormones. Thus, it is important in homeostasis and in organism metamorphic transformations such as the transition through puberty. There is now strong evidence that free zinc, normally very low in cells, is used at considerable concentrations in certain parts of the brain as a transmitter and in the reproductive tract of males. As is the case for iron there may be no life without zinc.

Copper

Copper is probably not a universal requirement for life. The sulfides of copper are extremely insoluble and primitive anaerobic archaea probably did not use it. Later oxidation of sulfide generated available copper and in general aerobes employ it as an oxidative catalyst. This use is mainly confined to extracellular or periplasmic compartments of cells since free copper itself is very poisonous internally, where it is probably no more than 10^{-15} M. The locations of the sites of action of copper proteins contrast strongly with those of iron as seen in the different cell compartments in which the two are used. A particular function of copper is in the cross-linking of extracellular matrices which helps to stabilize multicellular organisms e.g. the final forms of collagen, lignin, and chitin. The homeostasis of copper in cells

appears to be managed by a class of proteins, metallothineins, which also control the levels of free zinc. Uptake and rejection of copper requires cellular pumps and several disadvantageous inherited conditions arise from mutations in these pumps.

Cobalt

The requirement for cobalt in organisms is unusually distributed. It is most commonly found in vitamin B_{12}, yet advanced plants do not have this compound – a vitamin in higher animals and also essential in primitive anaerobes. Apart from its function in some ribonucleotide reductases vitamin B_{12} is required in several enzymes controlling rearrangement reactions especially of sugars. This vitamin is needed in smaller amounts than any of the other vitamins.

Manganese

The requirement for manganese, a relatively abundant trace element, is due to its major involvement in two kinds of enzymes, glycosylases and oxygen production units. The production of oxygen is confined to plants but it was the evolution of this reaction, initially in single cell anaerobes to obtain hydrogen from water, which caused the major steps of biological advancement over billions of years. The present-day level of some 20% oxygen in the atmosphere is entirely due to the activity of manganese enzymes. Some enzymes stated to require manganese may in fact be magnesium proteins *in vivo* since manganese readily replaces magnesium functions *in vitro*.

Nickel

Nickel, although it is available, is a rare element in all organisms being most common in primitive anaerobes. There it occurs in hydrogenases as a multimetal complex with iron and in the coenzyme F-430 which like heme, chlorophyll, and vitamin B_{12} is synthesized from uroporphyrin. Although nickel is used in urease, especially in plants, it has no functional protein coded in the DNA of higher animals such as man. Even so nickel is required in man since it is utilized by some of the lower organisms which inhabit the digestive tract of man where they aid degradation. A feature of evolution is the decline in the use of nickel and cobalt with a steady use of iron and an ever-increasing involvement of zinc and copper.

Molybdenum

Molybdenum is present in the sea in considerable concentration. It would appear that it is essential for all life except some very primitive anaerobes where its function is replaced by tungsten. The most obvious use of molybdenum is in nitrogen fixing bacteria, symbiots of plant life. Plants and animals cannot fix nitrogen gas. In these higher organisms molybdenum is required in a variety of oxygen-atom transfer reactions including enzymes for nitrate, sulfate, and carboxylate substrates. Note that the requirement for molybdenum for fixation of nitrogen gas and for reduction of nitrate implies that virtually all sources of the element nitrogen for organic synthesis in cells are dependent upon this element. The fact that these enzymes are found in prokaryotes, not higher organisms, stresses the nature of life as belonging to an ecosystem. Many diseases are associated with deficiency of the element especially in cattle.

Selenium

The importance of this element in all organisms is often missed despite the fact that it is the only heavy element which is part of a coded amino acid, seleno-methionine. This nonmetal is also found in seleno-cysteine. The functions of selenium are very different in anaerobes where it acts as a metal ligand from those in higher organisms where it is part of a powerful antioxidant – peroxidase. The switch in function follows the change of availability of the element from hydrogen selenide in primitive seas to selenate today, compare the chemical change of sulfur. It is thought that low levels of selenium in the human diet are responsible for many diseases, for example, of the heart. Selenium is now added as a supplement in some foods and to some soils.

Iodine

Iodine is found in the hormone, thyroxide, which is a hormone responsible for some features of growth control. The use of the element appears later in evolution. Iodine deficiency is a well-known genetic disease associated with goitre. Once again iodine is not used in lower organisms. Note that bromine and fluorine are little used in any organism so that iodine, fluorine, and bromine are quite unlike chlorine as chloride in biological organisms.

Rare Uses of Inorganic Elements

There are a variety of organisms in which minerals contain metals other than calcium and nonmetals other than carbonate (shells), phosfate (bone), or oxalate in plants. They include strontium and barium sulfates, which because of their density cause cells to settle in water and are useful as gravity sensors; calcium fluoride

in krill; various iron oxides in teeth and in magnetic sensors; and silica especially in diatoms and some plants.

Suggestive evidence is now available showing that cadmium may well be essential in a few lowly organisms and increasingly it is believed that chromium may be a factor in combating diabetes. There is clear evidence for the requirement of arsenic, boron, vanadium, and questionable evidence concerning some heavier elements, in selected organisms.

Inorganic Elements in Medicines and Poisons

Apart from the obvious uses in poisons and drugs of the above essential elements in organic derivatives unknown to living systems, there are many uses of other inorganic elements as both medicines and poisons. Of course, we must be careful with the use of these words, "drugs" and "poisons," since the use of medical drugs is dependent on dose where excess of a drug becomes a poison. Historically in medical practice inorganic elements were in fact used extensively before they were thought to do more harm than good. The uses of mercury, even mercury amalgam in teeth fillings, were considerable but mercury compounds are not recommended today. However, today, surprisingly, there are medicines using amongst other elements lithium, platinum, gold, and bismuth as well as technecium in diagnostics. It is anticipated that there will be many more uses of nonessential as well as those of essential elements in the not too distant future. In agricultural procedure several antifungal agents contain copper or mercury to this day.

The Selection of Elements by Cells

Given that only a limited number of elements are required and must be accumulated by organisms from a free condition in the environment, many unwanted elements must be screened against or have to be rejected since they are poisons, e.g., Al, while many have to be somewhat rejected but used, Na, Cl, Ca, Cu, Ni, and Co, for example, while some have to be concentrated, for example, C, N, P, S, Se, and K and others from organisms living in fresh water. Selection is therefore required at cell membranes by outwardly or inwardly directed pumps and also by binding. The principles of selection are well understood chemically. Such activity requires energy and here one other element is of dominant interest, hydrogen as the proton, in the form of H^+ gradients which make ATP for use in pumps for uptake and rejection of elements, and generally in many biological activities such as synthesis and mechanical action.

Conclusion

Today it is clearly obvious that living systems are not just composed of organic chemicals although the major bulk of them are of the conventional light nonmetals. Other elements, mainly metals, are involved in essential roles from maintaining cell stability and in communication networks to catalysis. The interaction of the system life/environment is therefore extremely complicated.

See Also the Following Articles

Chloroplasts • Heme Proteins • Heme Synthesis • Iron–Sulfur Proteins • Vitamin B_{12} and B_{12}-Proteins • Zinc Fingers

Glossary

abundance The quantitative amount of an element in the universe or on the surface of Earth.

availability A measure of the quantity of elements to which organisms have access ranging from easily available such as sodium and potassium to available with difficulty such as iron today.

essential Describing or referring to a requirement for an element without which the organism would show extreme abnormality or even not exist.

Further Reading

Bertini, I., Gray, H. B., Lippard, S. J., and Valentine, J. S. (1994). *Bioinorganic Chemistry*. University Science Books, Mill Valley, California.

Fraústo da Silva, J. J. R., and Williams, R. J. P. (2001). *The Biological Chemistry of The Elements*. 2nd edition. Oxford University Press, Oxford.

Kaim, W., and Schwederski, B. (1994). *Bioinorganic Chemistry: Inorganic Elements in the Chemistry of Life*. Wiley, Chichester.

Lippard, S. J., and Berg, J. M. (1994). *Principles of Bio-Inorganic Chemistry*. University Science Books, Mill Valley, California.

Messerschmidt, A., Huber, R., Poulos, T., and Wieghardt, K. (eds.) (2001). *Handbook of Metalloproteins*, Vols 1 and 2, Wiley, Chichester.

Biography

R. J. P. Williams is an Emeritus Professor at Oxford University, UK. He is sometimes referred to as the "grandfather" of bioinorganic chemistry, because he initiated the detailed study of the selective interaction of inorganic elements with organic compounds. His major work has been on heme-, zinc-, and copper-containing enzymes as well as on the use of calcium and magnesium in cells. He proposed the use of proton gradients in the synthesis of ATP.

Inositol Lipid 3-Phosphatases

Gregory S. Taylor and Jack E. Dixon
University of California, San Diego, California, USA

Phosphoinositides are lipid-signaling molecules that are essential for a wide variety of cellular processes including cell growth, apoptosis, membrane trafficking, vesicular transport, cytoskeletal regulation, cell motility, and control of gene expression. To facilitate the organization of such a striking array of signaling tasks within a cell, inositol lipids serve multifunctional roles including acting as docking modules for recruiting phosphoinositide-binding proteins to specific sites within a cell, allosteric regulators of enzyme activity/function, and also function as sorting signals and spatial landmarks during intracellular trafficking. In light of the multitude of cellular functions in which they are involved, it is not surprising that the levels of phosphoinositides within a cell are stringently regulated. To accomplish this, cells must carefully balance the relative rates of phosphoinositide biosynthesis and degradation. Phosphoinositides are derived from phosphatidylinositol (PI) by the actions of phosphoinositide kinases, which create and interconvert the various phosphoinositides via addition of phosphoryl groups to the inositol headgroup of PI. The actions of these kinases are opposed by phospholipases, which hydrolyze and remove the phosphoinositide acyl moieties and/or the inositol headgroup, and phosphoinositide phosphatases, which remove phosphoryl groups from the inositol ring. Phosphoinositide phosphatases can be loosely categorized by their structural and enzymatic properties into three groups, which include the protein tyrosine phosphatase-like PTEN and myotubularin phosphatases, SAC domain-containing phosphatases, and inositol 5′-phosphatases. This article, will focus on the structure and function of PTEN and myotubularin lipid phosphatases, the human disease states that are associated with their dysfunction, and discuss potential regulatory mechanisms for these enzymes.

Phosphoinositides as Signaling Molecules

The extensive use of phosphoinositides as cell signaling molecules in eukaryotes is likely to have arisen from the diversity of second messengers that can be derived from a single PI molecule simply by changing its phosphorylation state. As shown in Figure 1, seven different phosphoinositide signaling molecules can be generated through successive phosphorylation events by phosphoinositide kinases at the D3, D4, and D5 positions of the inositol ring of PI. Although they are relatively scarce, constituting less than 10% of the total cellular lipid content, phosphoinositides are distributed to compartments and membrane structures throughout the cell where their functions are required. One important function of phosphoinositides is to serve as ligands for inositol lipid-binding motifs that include the ENTH (epsin N-terminal homology), FERM (band 4.1, ezrin, radixin, moesin), FYVE (Fab1p, YOTB, Vps27p, EEA1), PH (pleckstrin homology), and PX (Phox homology) domains. Proteins that contain these lipid-binding motifs are recruited to form complexes on membranes where their specific target phosphoinositides are localized and concentrated. Once formed, these protein complexes can perform their specialized function(s) in membrane trafficking and intracellular transport tasks. Thus, the temporal and spatial regulation of phosphoinositide levels is a critical factor in determining when, where, and how these complexes form and carry out their functions. In addition to their roles as docking sites for phosphoinositide-binding domains, inositol lipids can also function as allosteric regulators of enzymatic activity. In this role, these lipids act as "on/off" switches for enzymes that contain specific lipid recognition/binding motifs. Whether they function as targeting sites for protein complex formation or as allosteric activators, it is clear that cellular phosphoinositides must be carefully regulated so that the downstream processes they control are also properly synchronized. In this capacity, phosphoinositide phosphatases can function to oppose and attenuate the signals generated by phosphoinositide kinases by removing phosphoryl groups from the D3, D4, and D5 positions of the inositol headgroup.

Protein Tyrosine Phosphatases

Protein tyrosine phosphatases (PTPs) are an extremely diverse family of enzymes that are characterized by a catalytic core of ~200 amino acids encompassing a highly conserved Cys-x_5-Arg (Cx_5R) active site motif. PTPs employ a common catalytic mechanism during

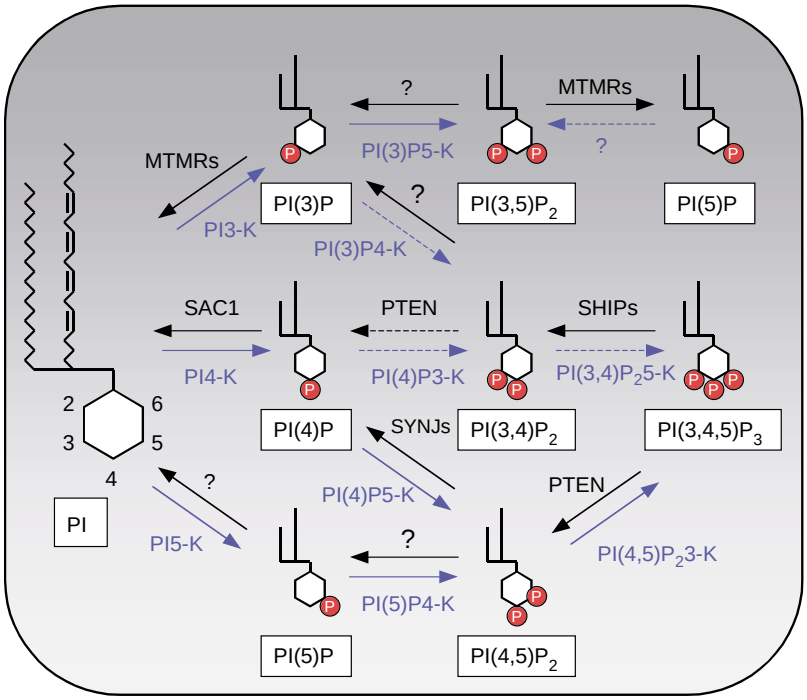

FIGURE 1 Mammalian phosphoinositide pathways. The seven different phosphoinositides are produced via successive phosphorylation (left to right) by phosphoinositide kinases starting with phosphatidylinositol (PI). The phosphoinositide kinases and the respective steps they catalyze are shown in blue. The substrates dephosphorylated by PTEN (PTEN), myotubularin-family (MTMRs), SH2-containing inositol 5′-phosphatases (SHIPs), synaptojanin-family (SYNJs), and SAC1 (SAC1) enzymes are indicated with black arrows. Steps denoted by "dashed arrows" represent the minor pathways of biosynthesis or conversion and "question marks" indicate that no phosphatase or kinase has yet been identified that regulates that particular inositol lipid. PI(5)P in the "upper right corner" of this diagram represents the product of PI(3,5)P_2 dephosphorylation by myotubularin family phosphatases.

hydrolysis of phosphomonoesters. During catalysis, the Cys residue within the Cx_5R motif functions as the reaction nucleophile to attack the phosphate phosphorous atom, forming an enzyme thio-phosphoryl intermediate. The conserved Arg residue helps to position the substrate phosphate for in-line attack by the Cys nucleophile. A conserved aspartic acid ~30–50 residues N-terminal to the Cx_5R sequence functions as a general proton donor to facilitate hydrolysis of the enzyme phosphoryl intermediate and substrate release. In addition to the hallmark Cx_5R sequence, PTPs also contain a wide variety of noncatalytic motifs that are important for subcellular localization and regulation of phosphatase activity. Based on their structural features and substrate specificity, PTPs can be categorized into tyrosine-specific, dual-specificity, low-molecular weight, Cdc25, RNA triphosphatase, and phosphoinositide phosphatase subgroups. As might be expected from their names, the tyrosine-specific PTPs exclusively dephosphorylate protein phosphotyrosine residues, whereas the dual-specificity enzymes can hydrolyze phosphotyrosine, phosphoserine, or phosphothreonine residues. Low-molecular weight tyrosyl phosphatases exhibit a preference for phosphotyrosine-containing substrates. Cdc25-related PTPs are unique cell cycle regulatory dual-specificity phosphatases that are specific for cyclin-dependent kinases. The RNA triphosphatases remove mRNA 5′-phosphate group(s) and function to regulate the mRNA capping process, nuclear export, and stability. The phosphoinositide phosphatase PTP-like enzymes consist of the PTEN and myotubularin families. These enzymes are specific for D3-phosphorylated inositol lipid substrates and will be the focus of this article.

PTEN and Myotubularin: PTP-Like Phosphoinositide Phosphatases

The phosphoinositide phosphatase subfamily of PTP-like enzymes consists of the PTEN and myotubularin lipid phosphatases. Both PTEN and myotubularin family lipid phosphatases contain PTP-like catalytic domains with active site Cx_5R motifs and employ a catalytic mechanism similar to that of other PTPs. However, PTEN and myotubularin phosphatases are unique among the PTPs in that they utilize D3-phosphorylated phosphoinositides as their principle physiologic substrates.

PTEN

PTEN as a Tumor Suppressor

The *PTEN* (phosphatase and tensin homologue) gene was initially identified by virtue of its localization on human chromosome 10q23.3, a region frequently deleted in brain, breast, and prostate cancers. Also known as mutated in multiple advanced cancers (*MMAC*) and TGFβ-regulated and epithelial cell-enriched phosphatase 1(*TEP1*), the *PTEN* gene was found to encode a protein with significant similarity to the cytoskeletal/focal adhesion protein, tensin, and protein tyrosine phosphatases. To date, numerous loss-of-function mutations in the *PTEN* gene including missense, nonsense, frameshift, deletion, and insertion mutations have been associated with human cancer and provide strong evidence for its role as a tumor suppressor gene. Germline mutations in the *PTEN* gene have also been associated with Bannayan–Zonana syndrome, Cowden syndrome, juvenile polyposis syndrome, and Lhermitte–Duclos disease. These disorders are characterized by hamartomatous polypoid growths as well as a predisposition toward certain types of cancer. Based on these observations, it was initially thought that PTEN might function as a tumor suppressor by dephosphorylating tyrosine-phosphorylated or serine/threonine-phosphorylated proteinaceous substrates. However, PTEN was found to possess exceedingly poor protein phosphatase activity when tested against a variety of artificial protein and peptide substrates. In fact, PTEN exhibited almost undetectable phosphatase activity toward proteinaceous substrates with the exception of an extremely acidic synthetic phosphopeptide substrate (poly-Glu_4Tyr).

PTEN Dephosphorylates the Phosphoinositide Second Messenger, PI(3,4,5)P_3

The key to understanding PTEN function as a human tumor suppressor was its identification as a phosphoinositide-specific phosphatase. The pathology of human diseases associated with PTEN mutations strongly supported its role as a tumor suppressor. However, its poor protein phosphatase activity and preference for highly acidic substrates suggested the possibility that PTEN might actually utilize a nonproteinaceous substrate as its physiologic target. Phosphoinositides were considered as possible alternatives to proteinaceous substrates for PTEN because of their involvement in cell survival signaling as well as the fact that their strong acidity fit the profile of PTEN preference for anionic substrates. The discovery that PTEN specifically dephosphorylated D3 position of the inositol signaling lipid, PI(3,4,5)P_3 (PIP_3) provided the first clear correlation between loss of PTEN activity and tumorigenesis. At this time, PIP_3 was known to promote cell survival and growth signaling through the Akt serine/threonine protein kinase as illustrated in Figure 2. In the Akt survival pathway, activation of receptor tyrosine kinases by mitogens results in the recruitment and activation of type I PI 3-kinase, which then phosphorylates PI(4,5)P_2 to produce PI(3,4,5)P_3. The plasma membrane-localized PIP_3 can then recruit and activate a phosphoinositide-dependent Ser/Thr protein kinase (PDK1) via its PH domain. PDK1 phosphorylates and activates Akt, which has also been recruited to the plasma in a PH domain-dependent manner via PIP_3 and/or PI(3,4)P_2. Activated Akt then functions to restrain apoptotic signaling and promote cell survival and growth by phosphorylating and negatively regulating proapoptotic factors including the Ser/Thr kinase GSK3β, cyclin-dependent kinase inhibitors $p21^{WAF1}$ and $p27^{KIP1}$, Forkhead transcription factors, Bad, and Caspase-9. PTEN antagonizes survival signaling by preventing the accumulation of PIP_3, thereby inhibiting the membrane-association of PDK1 and subsequent phosphorylation and activation of Akt. Its identification as a PIP_3-specific phosphoinositide phosphatase provided the first clear connection between loss-of-function PTEN mutations and human cancer. It is of note that PTEN orthologues in the nematode worm, *Caenorhabditis elegans*, and fruitfly, *Drosophila melanogaster*, also regulate PIP_3-dependent signaling through Akt and function to control cell size and development in these organisms.

PTEN Structure

The X-ray crystal structure of PTEN has provided significant insight into the molecular basis underlying its function as a phosphoinositide phosphatase and tumor suppressor. PTEN consists of an N-terminal phosphatase catalytic domain that contains the conserved Cx_5R active site motif and a C-terminal C2 domain. Although it is quite similar in overall topology to the catalytic core structures of other dual specificity and tyrosine-specific PTPs, the catalytic domain of PTEN is unique with respect to the architecture surrounding its active site. Specifically, the PTEN active site pocket is much wider and not as deep as those of dual specificity or tyrosine-specific enzymes. This structural feature of PTEN is essential for its ability to accommodate the inositol headgroup of PIP_3, which is much larger and more highly charged than the substrate phosphoserine, phosphothreonine, or phosphotyrosine residues targeted by other PTPs. Within the active site of PTEN, the Cx_5R sequence adopts a conformation similar to that observed for the P-loops of other PTPs, placing the Cys nucleophile and phosphate-binding Arg residues in the orientation required for efficient catalysis. The PTEN structure also points to a critical function for the C2 domain at its C terminus. C2 domains are found in a

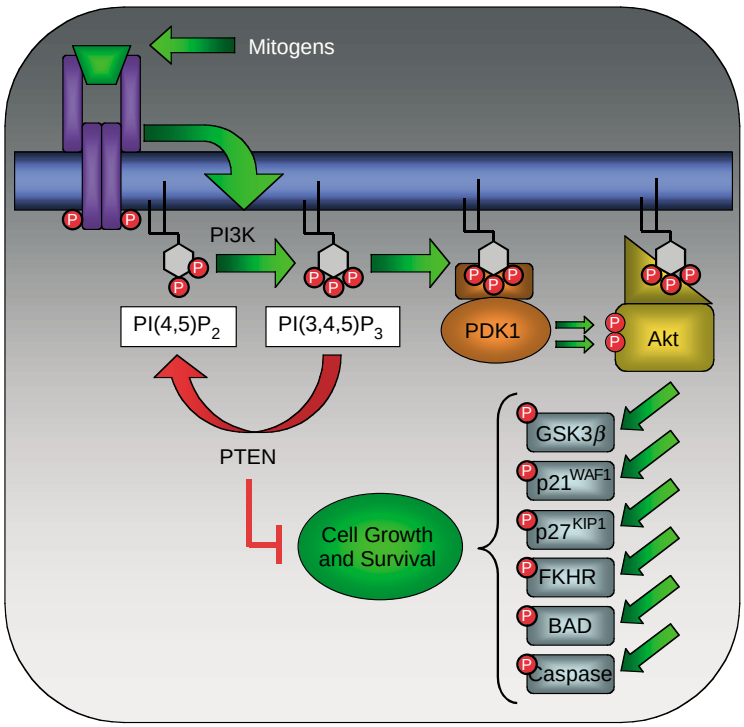

FIGURE 2 PTEN negatively regulates Akt signaling via PIP_3. Stimulation of growth factor receptor tyrosine kinases by extracellular mitogens results in the translocation and up-regulation of type I PI 3-kinase (PI3K) and production of $PI(3,4,5)P_3$. PIP_3 recruits the phosphoinositide-dependent (PDK1) and Akt (*Akt*) kinases to the plasma membrane where Akt is activated by PDK1-dependent phosphorylation. Activated Akt promotes cell growth and survival by phosphorylating and negatively regulating downstream proapoptotic factors including the Ser/Thr kinase (*GSK3β*), cyclin-dependent kinase inhibitors ($p21^{WAF1}$, $p27^{KIP1}$), forkhead transcription factors (*FKHR*), Bcl2 family member (*BAD*), and protease (*Caspase-9*). PTEN antagonizes mitogenic/survival signaling by preventing the accumulation of PIP_3 and subsequent activation of PDK1 and Akt.

number of membrane-associated proteins and function to regulate membrane recruitment. The C2 domain of PTEN most closely resembles the calcium-independent C2 domain subtype and can associate with lipid bilayers *in vitro*, suggesting it plays a role in targeting PTEN to cellular membranes where PIP_3 is located. The PTEN catalytic and C2 domains share an extensive hydrophobic interface and many PTEN disease mutations are localized to this interface. Moreover, PTEN C-terminal missense and truncating mutations that directly affect the C2 domain but not the catalytic domain are associated with human disease. Together, these observations demonstrate the requirement for a functional C2 domain and underscore the necessity for proper subcellular localization in addition to lipid phosphatase activity for maintaining PTEN function.

PTEN Regulation

PTEN function can be regulated by a number of different mechanisms. PTEN contains a C-terminal PDZ-binding motif, which can control its entry into PDZ-protein complexes. The PDZ domain is a protein motif of ~90 amino acids named for the postsynaptic density protein, PSD-95, *Drosophila* septate junction protein, Discs Large, and the tight junction protein, ZO-1. PDZ-domains are among the most abundant metazoan protein domains and serve as molecular scaffolds to assemble macromolecular protein signaling complexes. PTEN can physically associate with PDZ complexes via its PDZ-binding sequence. The exact function(s) of these complexes are not known, but they may function to stabilize the PTEN protein and help it to localize to specific sites within cells where its lipid phosphatase activity is required. PTEN function is also regulated by reversible protein phosphorylation. PTEN undergoes Ser/Thr phosphorylation within the extreme C-terminal region. Phosphorylation of sites within its C-terminus leads to an increase in the stability of the PTEN protein. PTEN contains a consensus PEST degradation sequence that overlaps these sites and may be masked via phosphorylation. PTEN C-terminal phosphorylation also appears to inhibit its association with PDZ complexes, suggesting that multiple modes of regulation are mediated through its C-terminal region.

MYOTUBULARIN

Myotubularins in Neuromuscular Disease

Myotubularin (MTM1) is mutated in X-linked recessive myotubular myopathy, a serious neonatal disorder in

which muscle cell development/maturation is dysfunctional. The muscle cells of affected individuals exhibit abnormal centrally located nuclei, perinuclear halos, and the persistence of fetal forms of vimentin and desmin. In severe cases, death often occurs from respiratory failure in early infancy. The myotubularin gene, *MTM1*, is localized to chromosome Xq28 and encodes a protein with significant similarity to dual specificity PTPs. MTM1 is the archetypical member of one of the largest families of dual specificity PTP-like phosphatases yet identified. As shown in Figure 3, the myotubularin-related (MTMR) phosphatase family includes eight catalytically active forms and at least six forms that are enzymatically inactive due to germ line substitutions in residues required for catalysis. The MTMR proteins can be further categorized into subgroups based on sequence similarity and the presence and arrangement of non-catalytic domains (Figure 3). Loss-of-function mutations in a second MTMR gene, *MTMR2*, cause the autosomal-recessive peripheral demyelinating neuropathy, type 4B Charcot-Marie-Tooth (CMT) syndrome. Type 4B CMT is characterized by focally folded myelin in the peripheral nerves and is thought to result from improper Schwann cell maturation. Mutations in a third MTMR gene, *MTMR13*, have also been shown to cause type 4B CMT. This is of particular interest because MTMR13 is a catalytically inactive MTMR. Although their precise roles in the onset and progression of human neuromuscular diseases are not known, the association of MTMR mutations with these disorders suggests that phosphoinositide regulation is critical for proper cellular development and maintenance in these tissues.

MTMRs Dephosphorylate 3-Phosphorylated Phosphoinositides

Like PTEN, myotubularin was originally thought to function as a dual-specificity PTP based on its protein sequence. Moreover, myotubularin also exhibited very poor phosphatase activity when tested against artificial protein and peptide substrates. The connection between myotubularin and lipid phosphatase activity was established following the observation that its Cx_5R active site motif resembled the corresponding sequence

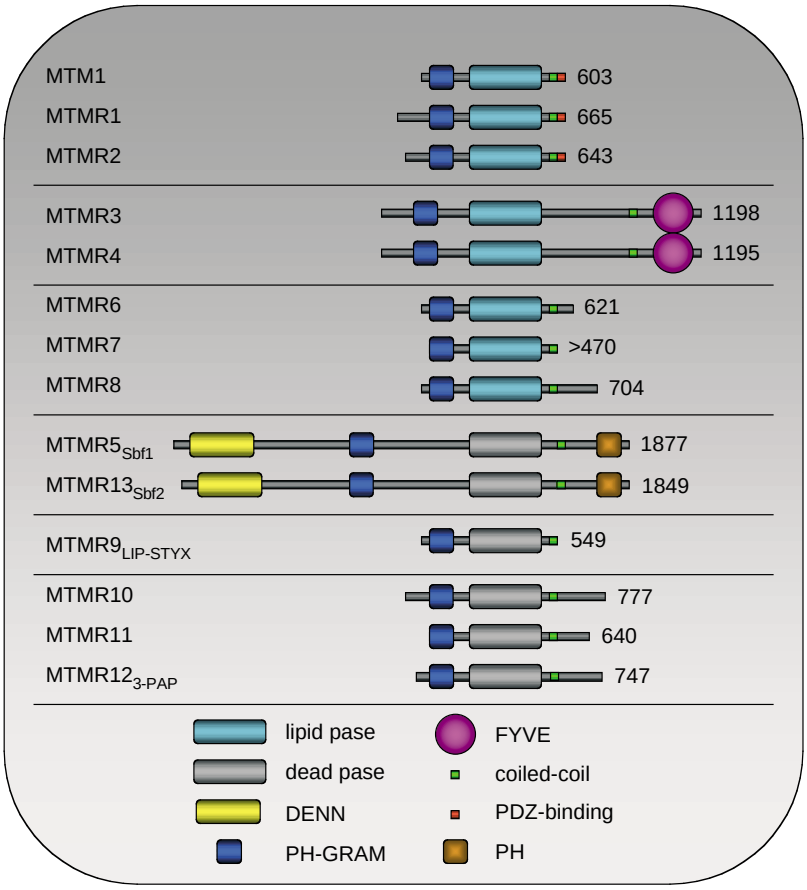

FIGURE 3 Structural diversity among myotubularin-family proteins. The structural features of myotubularin-related (MTMR) proteins are illustrated. MTMR subgroups classified based on sequence similarity and domain organization are separated by 'black lines." A legend denoting each of the protein domains/motifs pictured is shown at the "bottom." The number of amino acid residues in each MTMR protein are shown to the "right" of each structural diagram. Although more than one splicing variant may exist, only a single form is shown for each MTMR.

in the budding yeast inositol lipid phosphatase, Sac1p. This enzyme was known to dephosphorylate monophosphorylated phosphoinositides and to play a critical role in regulating trafficking through the yeast secretory pathway. Initial analyses revealed that MTM1 was highly active against the inositol lipid, PI(3)P. This lipid is the principal target of the FYVE and PX phosphoinositide-binding domains and is an important regulator of vesicular trafficking processes. Since the initial discovery of MTM1 as an inositol lipid-specific phosphatase, the catalytically active MTMR proteins, MTMR1, MTMR2, MTMR3, MTMR6, and MTMR7 have also been shown to dephosphorylate PI(3)P, suggesting that it is a common substrate of all the active MTMRs. Myotubularin family phosphatases have recently been found to dephosphorylate the D3 position of PI(3,5)P_2. Produced by phosphorylation at the D5 position of PI(3)P by PI(3)P 5-kinase, PI(3,5)P_2 is crucial for vesicular transport and plays an important role in regulating cellular responses to stress conditions. The exact mechanism(s) by which these lipids participate in cell signaling during neuromuscular development remain unknown. However, their role as substrates for MTMR family phosphatases demonstrates that regulation of PI(3)P and PI(3,5)P_2 is essential and points to trafficking defects as a possible underlying cause for myotubular myopathy and type 4B CMT.

MTMR Regulation

An emerging paradigm for MTMR regulation involves the physical interaction between catalytically active and inactive MTMR proteins. Active and inactive MTMRs can form heterodimeric complexes. To date, interactions have been demonstrated between MTM1/MTMR12, MTMR2/MTMR5, and MTMR7/MTMR9 active/inactive pairs. It has been proposed that heterodimer formation can affect both the lipid phosphatase activity and the subcellular localization of the complex, however, the specific physiologic function(s) of these complexes remain to be elucidated. It is of note that mutations in both MTMR2 and MTMR13 result in type 4B CMT disease. MTMR13, a catalytically inactive MTMR, is highly similar to MTMR5, which has previously been shown to associate with MTMR2. Although a physical association between MTMR2 and MTMR13 remains to be demonstrated, it is intriguing to speculate that an MTMR2/MTMR13 heterodimeric complex might be essential for proper Schwann cell development.

See Also the Following Articles

Inositol Phosphate Kinases and Phosphatases • Phosphatidylinositol Bisphosphate and Trisphosphate • Phosphatidylinositol-3-Phosphate • Phosphoinositide 4- and 5-Kinases and Phosphatases • Phosphoinositide-Dependent Protein Kinases

Glossary

kinase An enzyme that catalyzes the addition of phosphoryl groups.

phosphatase A hydrolytic enzyme that catalyzes the removal of phosphoryl groups.

phosphoinositide A more highly phosphorylated form of the phospholipid, phosphatidylinositol.

PTP Protein tyrosine phosphatase, a large family of enzymes that catalyze the hydrolysis of phosphomonoesters and contain a highly conserved Cys-x5-Arg active site motif.

tumor suppressor A protein that functions to repress cell growth and proliferation.

Further Reading

Lemmon, M. A. (2003). Phosphoinositide recognition domains. *Traffic* **4**, 201–213.

Maehama, T., Taylor, G. S., and Dixon, J. E. (2001). PTEN and myotubularin: Novel phosphoinositide phosphatases. *Ann. Rev. Biochem.* **70**, 247–279.

Pendaries, C., Tronchere, H., Plantavid, M., and Payrastre, B. (2003). Phosphoinositide signaling disorders in human diseases. *FEBS Lett.* **546**, 25–31.

Simonsen, A., Wurmser, A. E., Emr, S. D., and Stenmark, H. (2001). The role of phosphoinositides in membrane transport. *Curr. Opin. Cell. Biol.* **13**, 485–492.

Sulis, M. L., and Parsons, R. (2003). PTEN: From pathology to biology. *Trends Cell Biol.* **13**, 478–483.

Tronchere, H., Buj-Bello, A., Mandel, J. L., and Payrastre, B. (2003). Implication of phosphoinositide phosphatases in genetic diseases: The case of myotubularin. *Cell. Mol. Life Sci.* **60**, 2084–2099.

Wishart, M. J., and Dixon, J. E. (2002). PTEN and myotubularin phosphatases: From 3-phosphoinositide dephosphorylation to disease. *Trends Cell Biol.* **12**, 579–585.

Biography

Gregory S. Taylor received his Ph.D. from Purdue University and has been a postdoctoral research fellow in Dr. Jack Dixon's laboratory at the University of Michigan and at the University of California, San Diego. Dr. Taylor's research has focused on understanding the structure and function of inositol lipid phosphatases including PTEN and myotubularin, as well as their relation to human disease. Dr. Taylor is currently seeking a faculty position in academia.

Jack E. Dixon is a Professor of pharmacology, cellular and molecular medicine, and chemistry and biochemistry, and is also the Dean for Scientific Affairs at the University of California, San Diego. Dr. Dixon's research has focused on two principal areas of interest: protein tyrosine phosphatase structure and function, and mechanisms of bacterial pathogenesis. Dr. Dixon received his Ph.D. from the University of California, Santa Barbara, and completed a postdoctoral research fellowship at the University of California, San Diego. Dr. Dixon is currently a member of the American Academy of Arts and Sciences and the National Academy of Sciences.

Inositol Phosphate Kinases and Phosphatases

Stephen B. Shears
Laboratory of Signal Transduction, NIEHS/NIH/DHHS, Research Triangle Park, North Carolina, USA

A novice attempting to access the literature concerning inositol phosphate kinases and phosphatases is confronted by a list of participants that is intimidating in its size, and a sometimes bewildering terminology to distinguish between them. In an effort to ease the pain, herein is provided an hospitable guide to the nomenclature describing inositol phosphates and the enzymes that metabolize them.

Information transfer in biological systems requires sensor proteins to detect and respond to regulatory input from other proteins and small molecules. The ability of a sensor to perceive an effector is frequently dependent upon a recognition pattern generated by the presence or absence of phosphate groups. When one or more of these phosphate groups are added (phosphorylation) or removed (dephosphorylation) from the effector, such a process acts as a molecular switch that determines whether the regulator is "on" or "off." Inositol (Figure 1) is an example of a small molecule that is functionally modified in this manner. Each of the six hydroxyl groups that are attached to the carbons of the *myo*-inositol ring (Figure 1A) are sites for phosphorylation. Enzymes that add phosphate groups to the inositol moiety are known as inositol phosphate kinases. A separate family of enzymes, the inositol phosphate phosphatases, removes phosphate groups from the inositol ring. Phosphate-transfer reactions catalyzed by these phosphatases and kinases are networked in serial and parallel configurations, permitting the cell to add and subtract phosphate groups in a combinatorial manner, so generating an array of inositol phosphate molecules. Recognition patterns, that arise from specific arrangements of phosphate groups around the inositol ring, endow certain inositol phosphates with biologically important functions. Thus, inositol phosphate kinases and phosphatases control the synthesis and metabolism of important effector molecules.

Inositol Phosphate Nomenclature

In order to appreciate the nature of phosphate recognition patterns around the inositol ring, it is necessary to understand the nomenclature which distinguishes the different carbons that comprise the inositol moiety. Fortunately, Agranoff's turtle provides us with a timeless, visual mnemonic. In this *aide mémoire*, the hydrogens are conveniently ignored and the inositol ring is depicted in its thermodynamically stable so-called "chair" conformation (Figure 1B). The structure's resemblance to a turtle is then apparent (Figure 1C). As a consequence of deliberations by International Nomenclature Committees, the turtle's appendages are numbered in an anticlockwise direction (when viewed from above), commencing with the front right flipper. The 2-hydroxyl (the turtle's head) is axial to the plane of the ring, whereas the other five hydroxyls (the four flippers and the tail) are equatorial (i.e., approximately in the same plane as the ring). This numbering system allows us to readily and unambiguously specify the location of phosphate groups that are added to the inositol ring. Ins(1,4,5)P_3, for example (see Figure 2), is an abbreviation that describes the addition of three single phosphate groups (P_3) to the inositol (Ins) ring, at positions 1, 4, and 5. Ins(1,2,3,4,5,6)P_6 describes the molecule in which all six of the carbons are attached to single phosphate groups, but since this feature makes the numbering superfluous, InsP_6 is the acceptable definition (Figure 2). This particular inositol phosphate is also widely known as phytic acid. Some inositol phosphates contain diphosphate (i.e., PP) groups (Figure 2). One of the diphosphates added to InsP_6 is known to be at the 5-position, but till date, the positions of all of the diphosphate groups have not been determined.

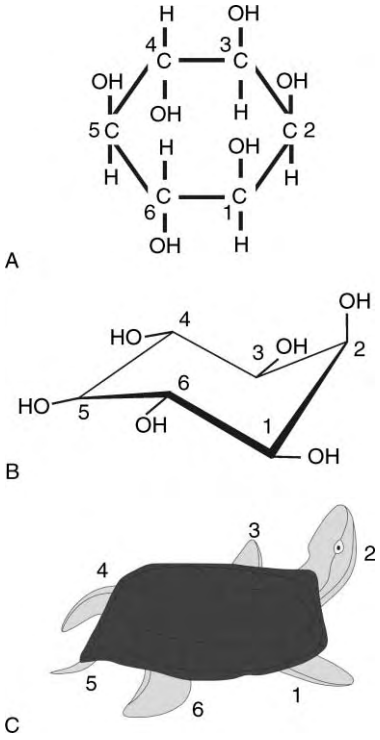

FIGURE 1 Inositol ring nomenclature. (A) full chemical structure of inositol; (B) naturally occurring conformation of inositol, *sans* hydrogens; (C) the numbering of the turtle's appendages in an anticlockwise direction (beginning with its right flipper) provides an *aide mémoire* for inositol phosphate nomenclature.

Enzyme Nomenclature and Metabolic Interrelationships

Figure 2 provides a metabolic map showing the participation of those inositol phosphate kinases and phosphatases that are most commonly found across the phylogenetic spectrum. Ideally, these enzymes ought to be named in a manner that is both universally accepted, and unambiguously describes their function(s). In its simplest form, it is possible to designate some of these enzymes according to both the nature of the substrate(s), and the position(s) on the inositol ring that is modified. Thus, the Ins(1,3,4,5,6)P_5 2-kinase phosphorylates Ins(1,3,4,5,6)P_5 to InsP_6 (see Figure 2). One problem with this approach is that almost all of the inositol phosphate kinases and phosphatases metabolize more than one substrate. For example, a single enzyme removes the 5-phosphate from both Ins(1,4,5)P_3 and Ins(1,3,4,5)P_4. Unfortunately, "inositol polyphosphate 5-phosphatase," is a popular terminology for this enzyme, despite the fact that this exaggerates its promiscuity, by erroneously implying the enzyme removes the 5-phosphate from other inositol phosphates. The preferred, unambiguous nomenclature for this enzyme is Ins(1,4,5)P_3/Ins(1,3,4,5)P_4 5-phosphatase (Figure 2). Nevertheless, such a systematic approach

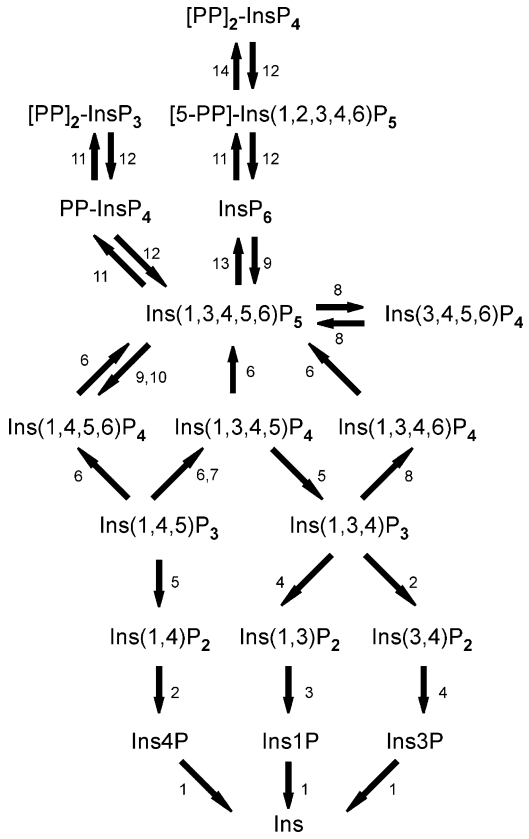

FIGURE 2 Metabolic interrelationships of inositol phosphate kinases and phosphatases. This figure provides a metabolic map showing the participation of some important inositol phosphate kinases and phosphatases that are widely distributed across the phylogenetic spectrum. The numbers associated with each arrow represent the following enzymes: 1, Inositol monophosphatase; 2, Ins(1,4)P_2/Ins(1,3,4)P_3 1-phosphatase; 3, Ins(1,3)P_2 3-phosphatase; 4, Ins(3,4)P_2/Ins(1,3,4)P_3 4-phosphatase; 5, Ins(1,4,5)P_3/Ins(1,3,4)P_3 5-phosphatase; 6, inositol phosphate multikinase; 7, Ins(1,4,5)P_3 3-kinase; 8, Ins(1,3,4)P_3 6-kinase/Ins(3,4,5,6)P_4 1-kinase/Ins(1,3,4,5,6)P_5 1-phosphatase; 9, multiple inositol polyphosphate phosphatase; 10, PTEN (for *p*hosphatase and *ten*sin homologue, deleted on chromosome *ten*); 11, inositol hexakisphosphate kinase; 12, diphosphoinositol polyphosphate phosphohydrolase; 13, Ins(1,3,4,5,6)P_5 2-kinase; 14, diphosphoinositol polyphosphate kinase.

does become unwieldy when a single enzyme metabolizes three or more substrates, especially when the positional specificity of the enzyme varies with the nature of the substrate. For example, there is a single kinase that adds a 3-phosphate to Ins(1,4,5)P_3, a 6-phosphate to Ins(1,3,4,5)P_4, a 5-phosphate to Ins(1,3,4,6)P_4 and a 3-phosphate to Ins(1,4,5,6)P_4. For brevity, this protein is simply known as the "inositol phosphate multikinase" (Figure 2). Equally, the phosphatase that specifically removes the 3-phosphate from Ins(1,3,4,5,6)P_5 and the 6-phosphate from Ins(1,4,5,6)P_4 is also capable of removing any of the phosphate groups from InsP_6; this enzyme is known as the "multiple inositol polyphosphate phosphatase." Finally, the names of some enzymes will occasionally

not specifically address their ability to metabolize an inositol phosphate, as in the case of the Ins(1,3,4,5,6)P_5 3-phosphatase activity of PTEN (see Figure 2). The reason the latter protein's name does not illuminate its function is because it was christened prior to a complete understanding of its range of catalytic activities.

Regulatory Input into the Inositol Phosphate Pathway

There are two separate metabolic routes which feed into the pathway shown in Figure 2. The first is by enzymatic conversion of glucose-6-phosphate into Ins3P. The second is synthesis of Ins(1,4,5)P_3. The latter is initially attached through its 1-phosphate (i.e., its front right flipper, Figure 1C) to the lipid material that represents the bulk phase of cellular membranes. This attachment is severed by a specialized enzyme – a phospholipase C – that is stimulated when a hormone or neurotransmitter binds to appropriate receptor on the cell surface. The Ins(1,4,5)P_3 released by phospholipase C has the role of liberating cellular stores of calcium, which in turn regulates many calcium-dependent cellular processes. The efficacy of Ins(1,4,5)P_3 depends upon its intracellular concentration, which in turn is dictated by a dynamic balance between competing rates of Ins(1,4,5)P_3 synthesis (by phospholipase C) and metabolism (by inositol phosphate kinases and phosphatases; Figure 2). Hormones and neurotransmitters also use cell-surface receptors to activate the synthesis of many other intracellular chemical messengers, and these can lead to changes in the activities of several inositol phosphate kinases and phosphatases. In this way, the cell can carefully regulate metabolic flux through specific areas of the inositol phosphate pathway, thereby manipulating levels of inositol phosphates which are themselves intracellular signals.

See Also the Following Articles

Phosphatidylinositol Bisphosphate and Trisphosphate • Phospholipase C

Glossary

diphosphoinositol polyphosphate A type of inositol phosphate which has either one or two diphosphate ("pyrophosphate") groups.

inositol phosphate A compound with a six-member carbon ring structure to which single phosphates (and sometimes diphosphates) are attached at various positions.

inositol phosphate kinase An enzyme that transfers a phosphate group from adenosine triphosphate to the inositol ring.

inositol phosphate phosphatase An enzyme that removes a phosphate group from the inositol ring.

intracellular signal/messenger One member of what is usually a functionally coupled series of molecules or ions that together comprise a chemical pathway which conveys and amplifies a cell's biological response to a specific extracellular stimulus, such as a hormone or neurotransmitter.

phospholipase C A specialized enzyme that releases Ins(1,4,5)P_3 from its membrane tether.

phytic acid The nonsystematic but widely used alternate name for $InsP_6$; the molecule formed by filling all six carbons of the inositol ring with single phosphate groups.

turtle A marine reptile that provides a visual mnemonic for easy recall of the nomenclature for numbering the carbon atoms that comprise the inositol ring.

Further Reading

Agranoff, B. W. (1978). Textbook errors: cyclitol confusion. *Trends Biochem. Sci.* **3**, N283–N285.

Albert, C., Safrany, S. T., Bembenek, M. E., Reddy, K. M., Reddy, K. K., Falck, J. R., Bröker, M., Shears, S. B., and Mayr, G. W. (1997). Biological variability in the structures of diphosphoinositol polyphosphates in *Dictyostelium discoideum* and mammalian cells. *Biochem. J.* **327**, 553–560.

Caffrey, J. J., Darden, T., Wenk, M. R., and Shears, S. B. (2001). Expanding coincident signaling by PTEN through its inositol 1,3,4,5,6-pentakisphosphate 3-phosphatase activity. *FEBS Lett.* **499**, 6–10.

Fisher, S. K., Novak, J. E., and Agranoff, B. W. (2002). Inositol and higher inositol phosphates in neural tissues: Homeostasis, metabolism and functional significance. *J. Neurochem.* **82**, 736–754.

Ho, M. W. Y., and Shears, S. B. (2002). Regulation of calcium-activated chloride channels by inositol 3,4,5,6-tetrakisphosphate. In *Current Topics in Membranes* (C. M. Fuller, ed.) Vol 53, pp. 345–363. Academic Press, London.

Irvine, R. F., and Schell, M. (2001). Back in the water: The return of the inositol phosphates. *Nat. Rev. Molecul. Cell Biol.* **2**, 327–338.

Biography

Steve Shears leads the Inositol Signaling Group at the National Institute of Environmental Health Sciences. His long-standing and continuing interests in inositol phosphate function began under the tutorship of Prof. Bob Michell at the University of Birmingham, United Kingdom. Dr. Shears obtained his Ph.D. from the University of York, United Kingdom. He has authored over 100 articles and reviews, and he serves as an editor of several international scientific journals.

Insulin- and Glucagon-Secreting Cells of the Pancreas

Franz M. Matschinsky
University of Pennsylvania School of Medicine, Philadelphia, Pennsylvania, USA

Alpha and beta cells are the predominant cell types in microscopic endocrine organs called the islets of Langerhans, which are scattered throughout the exocrine pancreas and produce, store, and secrete the hormones glucagon and insulin, respectively. Secretion of these hormones is regulated by fuels (glucose, amino acids, and fatty acids) or through neuroendocrine input. Insulin and glucagon in turn regulate the metabolism of these fuels. Loss of beta cells by autoimmune destruction or impairment of their function by poorly understood mechanisms are the causes of type I or type II diabetes mellitus (T1DM or T2DM), respectively. Individuals with T1DM require insulin substitution therapy for survival, and those with T2DM can manage their disease with diet restrictions, exercise, and a variety of drugs with different mechanisms of action. It is thus of critical importance to develop a comprehensive understanding of insulin- and glucagon-producing cells of the pancreas.

Introduction

Pancreatic alpha and beta cells play the predominant role in maintaining glucose homeostasis in humans and many laboratory animals and keep the blood glucose in the narrow range of 5 to 8 mM in response to the demands of feeding and fasting. Both cells have a threshold of approximately 5 mM glucose for stimulation of hormone release. The alpha cell is triggered to release glucagon when the glucose falls below this level, whereas the beta cell is activated to secrete insulin when this level is exceeded. Expressed differently, the inhibitory glucose dependency curve for alpha cells and the stimulatory glucose dependency curve for beta cells have their crossover point at 5 mM, which is the setpoint of the system for glucose homeostasis. (Note that alpha-cell deinhibition with falling glucose manifests itself most clearly when these cells are also under the influence of physiological stimuli, e.g., amino acids, a condition that is met *in situ*.) Auxiliary neuroendocrine mechanisms involving acetylcholine, catecholamines, glucagon-like peptide 1 (GLP-1), and gastric inhibitory peptide (GIP) enhance or blunt the response of the pancreatic endocrine cells to fuel stimulation. The other two fuel classes, amino acids (AA) and fatty acids (FA), stimulate insulin release in a strictly glucose-dependent manner. AA are the most effective fuel stimulant of alpha cells at biologically relevant concentrations (e.g., 3.5 to 7.0 mM of the physiological mixture of 20 AA enhances glucagon release markedly when glucose falls below 5.0 mM).

This entry focuses on the mechanisms of glucose-stimulated insulin release (GSIR) because this issue is central to beta-cell function and because knowledge of this aspect of beta-cell biology and glucose homeostasis is well established, much less tenuous or controversial than current understanding of how the other fuels act on alpha and beta cells. However, when important and possible, how glucose and other fuels or neuroendocrine factors interact with these two types of pancreatic endocrine cells is discussed.

The Beta-Cell Glucokinase Glucose Sensor and the Threshold for GSIR

The glucokinase glucose sensor concept and the threshold concept for GSIR explain a great deal about beta cells and the nature of glucose homeostasis in humans and most laboratory animals. Glucokinase (GK) serves as the beta cell's cytosolic glucose-sensing device and contributes a critical element to the regulatory feedback loop or signaling chain that interconnects blood glucose, the beta cell, the hormone insulin, and the major insulin target tissues (i.e., the liver, muscle, and adipose tissue). The kinetic characteristics of GK are ideally suited for this purpose: the k_{cat} for glucose phosphorylation is about 60 s^{-1}; the glucose $S_{0.5}$ (i.e., the glucose concentration resulting in half-maximal enzymatic activity) is about 8.0 mM; the glucose dependency curve of GK action is sigmoidal as indicated by a Hill coefficient (n_h) of 1.7; the ATP K_m is about 0.4 mM, indicating that the enzyme operates *in vivo* near saturation with its second substrate; finally, there is no feedback inhibition by glucose-6-P in contrast to

the highly effective inhibition of other hexokinases by this metabolite. Of great theoretical interest and practical importance is the recent recognition of an allosteric activator site on GK that explains the mechanism of action and efficacy of a newly discovered class of antidiabetic agents (GK activators [GKAs]; see following discussion). Beta-cell GK is inducible by glucose (maximally 5- to 10-fold compared to basal levels at 1.0 mM glucose) through mechanisms yet to be fully clarified. Note that hepatic GK is induced by insulin in a glucose-independent manner and is also activated by GKAs. Note also that hepatic GK is regulated by the inhibitory GK regulatory protein (GKRP), which sequesters the enzyme to the nuclear compartment from which GK is released by glucose during hyperglycemia. In contrast, GKRP seems to be of little importance for beta-cell GK function. Differential expression control of islet and hepatic GK is explained by the presence of two tissue-specific promoters in one single gene. Due to these characteristic features, GK determines the rate of beta-cell glycolysis with a control strength approaching unity, outperforming all other metabolic steps. Glycolytic flux of beta cells is therefore a function of substrate pressure rather than of energy demand, which determines glucose use of many other tissues, including brain and muscle.

These features are a prerequisite for the glucose sensor role of GK; they do not, however, explain the 5 mM setpoint for glucose homeostasis and threshold for GSIR. This threshold is a function of the biophysical characteristics of the K^+ and Ca^{2+} channels of the beta-cell membrane (Figure 1). The K-ATP channel is a hetero-octamer composed of four subunits each of the Kir6.2 inward rectifier and the drug target SUR-1 and is regulated by the phosphate potential of the beta cells. Important for physiology, it is inhibited by ATP^{4-} and activated by $MgADP^{2-}$ such that a decrease of the cytosolic ATP/ADP ratio determines K^+ conductivity and consequently the membrane potential. Enhanced glucose metabolism increases this ratio and depolarizes the beta cell. Alterations of the membrane potential are transmitted to the voltage-sensitive L-type Ca^{2+} channel. Depolarization stimulates Ca^{2+} influx and leads to elevation of the free intracellular calcium ($[Ca^{2+}]_i$). The combination of high ATP and $[Ca^{2+}]_i$ elicits insulin release. Important for understanding the threshold phenomenon for GSIR is the fact that the decrease of the K^+ conductivity is a graded function of glucose metabolism (i.e., the GK rate), whereas the L-type Ca^{2+}channel has a well-defined triggering potential of -60 to 50 mV, which happens to be reached when GK or glycolysis operates at 25–30% of its normal capacity, i.e., at 5.0 mM glucose. Note that extra- and intracellular glucose are virtually identical at all times as a result of high-capacity glucose transport by Glut-2. This basic signaling pathway from glucose to insulin release as previously outlined is termed the triggering pathway (TPW). It is complemented by the so-called augmentation pathway (APW), which potentiates glucose action, but the molecular basis of the latter remains to be defined in detail.

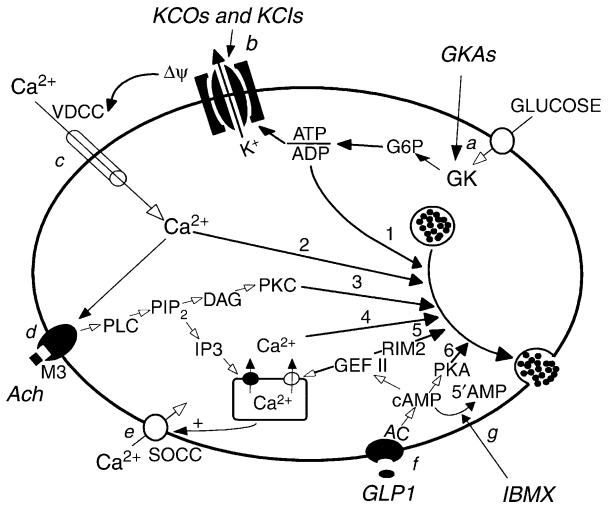

FIGURE 1 Signaling pathways in pancreatic beta cells. Six distinct signaling pathways in pancreatic beta cells are depicted (1–6). Abbreviations are as follows, with a–g identifying initial or other critical steps for these pathways: GK, glucokinase (a); the K_{ATP} channel complex, consisting of ATP-sensitive K^+ channels and sulfonyl urea receptor type 1 (SUR-1) subunits (b); VDCC, voltage-dependent Ca^{2+} channel or L-channels (c); acetylcholine (Ach) and muscarinic receptor type 3 (m3) (d); SOCC, store-operated calcium channels (e); GLP-1, glucagon-like peptide-1 and receptor (f); IBMX, 3-isobutyl-1-methylxanthine, a phosphodiesterase inhibitor (g). Other abbreviations are as follows: AC, adenylate cyclase; cAMP, cyclic AMP; PKC, protein kinase C; PKA, protein kinase A; DAG, diacylglyceride; IP3, inositol triphosphate; GEFII, cAMP-guanidine nucleotide exchange factor (or Epac2); $\Delta\Psi$, change of cell membrane potential. Additional abbreviations are explained in the text. Modified from Doliba, N. M., Qin, W., Vatamaniuk, M. Z., Li, C., Zelent, D., Najafi, H., Buettger, C. W., Collins, H. W., Carr, R. D., Magnuson, M. A., and Matschinsky, F. M. (2004). Restitution of defective glucose-stimulated insulin release of sulfonylurea type 1 receptor knockout mice by acetylcholine. *Am. J. Physiol. Endocrinol. Metab.* **286**(5); E834–843 (Epub 2004 Jan 21), (electronic publication) with permission of The American Physiological Society.

Model Experiments to Illustrate the Operation of the TPW and the APW

The APW comes into play when $[Ca^{2+}]_i$ and ATP/ADP are elevated by the TPW and when the beta cells are activated in addition by acetylcholine, GLP-1, or GIP. Model experiments with perifused islets isolated from control mice and from mice lacking functional K^+ channels (i.e., from SUR-$1^{-/-}$ knockout [KO] mice) illustrate many of the points discussed in the preceding

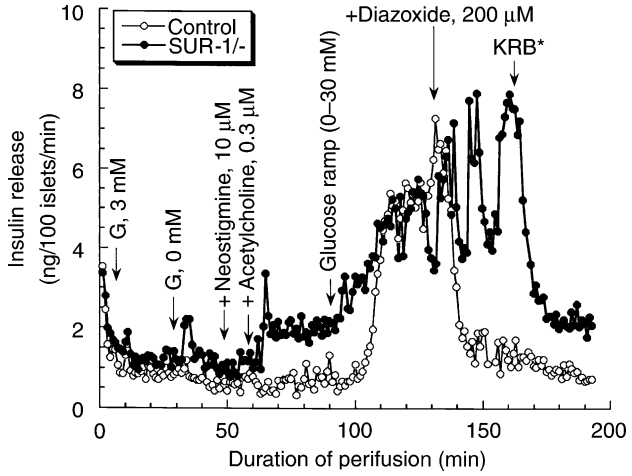

FIGURE 2 Experimental dissection of signaling pathways in glucose-stimulated insulin release (GSIR). Acetylcholine increases the insulin release in SUR-$1^{-/-}$ islets in the absence of glucose, demonstrating marked hypersensitivity to the transmitter compared to controls. Acetylcholine also restitutes defective GSIR by these islets. After stable insulin secretion rates were achieved at 30 min, islets were perifused in the absence of glucose for 60 min (t-30 to t-90). Following addition of neostigmine (a cholinesterase inhibitor) and acetylcholine, a glucose ramp (from 0 to 30 mM with an 0.8 mM increment per min) was applied for 37.5 min to control and SUR-$1^{-/-}$ islets, and glucose was then maintained constant at 30 mM for about 30 min longer in the continued presence of acetylcholine (t-90 to t-160). The experiment was completed by perifusing islets with KRB solution lacking glucose and drugs. The rise in the glucose concentration in the perfusate led to an increase in hormone secretion in SUR-$1^{-/-}$ islets as well as in the controls. However, note the different patterns of the release profiles. Also appreciate that in the absence of acetylcholine and neostigmine, SUR-$1^{-/-}$ islets did not respond to glucose in contrast to the controls (not shown). Diazoxide, a K_{ATP} channel activator, immediately decreased insulin release to baseline in control but was unable to block hormone release in SUR-$1^{-/-}$ islets. Reproduced from Doliba, N. M., Qin, W., Vatamaniuk, M. Z., Li, C., Zelent, D., Najafi, H., Buettger, C. W., Collins, H. W., Carr, R. D., Magnuson, M. A., and Matschinsky, F. M. (2004). Restitution of defective glucose-stimulated insulin release of sulfonylurea type 1 receptor knockout mice by acetylcholine. *Am. J. Physiol. Endocrinol. Metab.* **286**(5); E834–843 (Epub 2004 Jan 21), (electronic publication) with permission of The American Physiological Society.

paragraph (Figure 2). First, beta cells from SUR-$1^{-/-}$ do not show GSIR when acetylcholine is absent because the TPW is blocked in contrast to controls. Second, the distinctly different secretion profiles for GSIR evoked in control and SUR-$1^{-/-}$ islets in the presence of low acetylcholine illustrate that the glucose response caused by the combined TPW and APW in the control has a clear threshold and is blocked by diazoxide (a potassium channel opener [KCO]) as expected, whereas that of the APW alone as seen in the SUR-$1^{-/-}$ islets is clearly graded (lacking a threshold) and is not blocked by diazoxide, again as expected. Both signaling pathways operate during a meal and result in the robust, threshold-based GSIR as mimicked by the experiment shown in Figure 2 for control islets.

Amino Acids and Fatty Acids as Glucose-Dependent Stimuli of Beta Cells

Stimulation of insulin release by a physiological mixture of 20 amino acids (20-AASIR) is biologically highly relevant but less well understood than GSIR. It is established, though, that 20-AASIR of normal islets has an absolute glucose requirement, i.e., at least 2.5 mM. It is not clear which signaling pathways are involved, but it is likely that the TPW as sketched in the preceding discussion plays a role. Assuming a major role for metabolism in 20-AASIR, it must be postulated that transport into the cell and subsequent transdeamination are efficient processes. AA metabolism requires transamination as the first step, generating glutamate and alanine as the major products, followed by oxidative deamination of glutamate with glutamate dehydrogenase (GDH) to form NAD(P)H, which is converted to ATP. The need for the alpha-ketoacids, alpha-ketoglutarate and pyruvate as acceptors for the transamination reaction may explain, at least in part, the absolute requirement for glucose. It is also possible that AA metabolism generates metabolic coupling factors in addition to energy, with glutamate and glutamine as possibilities. It is indeed remarkable that more than half of the stimulatory effect of 20 AA can be attributed to glutamine, which contributes only 15% to the mixture. Studies of leucine-stimulated insulin release have been very extensive but have resulted in much controversy. It is now understood that leucine has two actions: it is converted to acetyl-CoA and acetoacetate, serving as direct fuel stimulant, or it stimulates GDH allosterically, thus enhancing glutaminolysis with the production of alpha-ketoglutarate, NAD(P)H, and ammonia. However, beta cells respond to this indirect allosteric effect of leucine only when GDH is sensitized, that is, when it is not fully inhibited by GTP (or ATP) as a result of enhanced glucose metabolism. 20-AASIR may also be mediated, at least in part, by depolarization due to increased Na^+ entry involving Na^+-dependent transporters, a possibility that has received little attention. Some of this discussion is illustrated in studies with isolated perifused islets by the differential effect that "energy run down" has on stimulation of insulin release by glucose, leucine, and alpha-ketoisocaproate (Figure 3). Isolated rat islets that had been cultured in 10 mM glucose and perifused with 2 mM glutamine show a remarkable change of chemosensitivity of their beta cells as a function of energy depletion with time. They respond well to glucose and alpha-ketoisocaproate at an early time point when they are totally blind to leucine, but as energy depletion proceeds they respond briskly to all three stimuli. Fatty acids (FA)

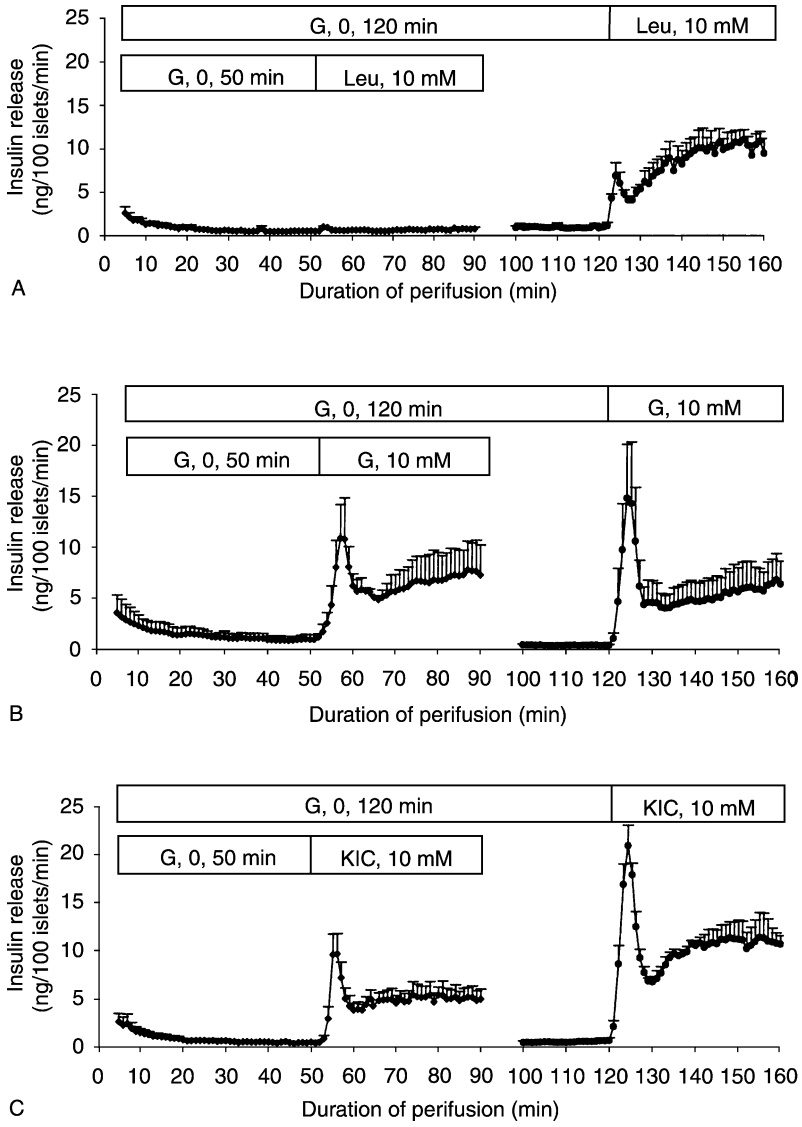

FIGURE 3 Effect of energy run-down on islet chemosensitivity. Isolated rat islets were cultured with 10 mM glucose for 3 days and then perifused with 2 mM glutamine in the absence of glucose for energy run-down periods of 50 min (diamonds) or 120 min (circles) prior to stimulation with (A)10 mM leucine (Leu), (B)10 mM glucose (G), and (C)10 mM alpha-ketoisocaproate (KIC). Values represent the means ± SE for 100 islets from three separate perifusions. Reproduced from Li, C., Najafi, H., Daikhin, Y., Nissim, I. B., Collins, H. W., Yudkoff, M., Matschinsky, F. M., and Stanley, C. A. (2003). Regulation of leucine-stimulated insulin secretion and glutamine metabolism in isolated rat islets. *J. Biol. Chem.* **278**, 2853–2858 with permission of The American Society for Biochemistry & Molecular Biology.

are effective glucose-dependent stimuli of insulin release (FASIR). It is now widely believed that specific metabolic products of FA metabolism play a more important role as signals or coupling factors for secretion than increased generation of ATP by their catabolism. For example, long-chain acyl-CoA and/or diacylglycerol may serve as activators of protein kinase C (PKC). This idea has been expanded, and it is proposed that these and possibly other lipid-derived metabolic coupling factors are critical for GSIR as well. This notion is captured by speaking of the "essentiality of FA for GSIR."

Neuroendocrine Modification of Fuel-Stimulated Insulin Release

Eating and digestion of food results in the production of the enterohormones GLP-1 and GIP and also enhances vagal activity, all of which augments fuel-stimulated insulin release. Catecholamines, on the other hand, block secretion very effectively. Recall that neuroendocrine stimulation of beta cells requires glucose. The signaling pathways are well established (Figure 1). The effects are quantitatively very marked, resulting in

a left shift and increased magnitude of the fuel dose–response curves for activators and a right shift and decreased magnitude for inhibitors. It is not surprising then that the pharmaceutical industry is making great strides in taking advantage of these pathways therapeutically.

A Brief Note on Alpha-Cell Function

AA and catecholamines are powerful physiological stimulators of glucagon release from alpha cells, and glucose inhibits these actions. The signaling pathways that operate here are not well understood but may involve steps similar to those described for beta cells, including nucleotide-controlled K^+ channels and L-type Ca^{2+} channels. Much controversy exists about the mechanism(s) of glucose inhibition of glucagon secretion. It has not been determined whether the glucose effects are direct or are mediated by the paracrine actions of insulin, GABA, Zn^{2+}, or other signals. The probable reason for this scanty knowledge lies in the great difficulties that hinder metabolic and other functional studies of alpha cells.

Glucokinase Disease and GDH or K^+ Channel-Linked Hypoglycemia

The biochemical genetic characterization of GK-linked hyper- and hypoglycemia syndromes (collectively termed glucokinase disease) and of GDH or K^+ channel-linked hyperinsulinemic hypoglycemia has strongly reinforced basic scientific concepts about the role of GK as glucose sensor and other crucial steps in GSIR and AASIR. Nearly 200 GK mutations have been discovered in patients with GK disease, usually inherited as an autosomal dominant trait. Activating mutations cause hyperinsulinemic hypoglycemia because the threshold for GSIR is left shifted as expected, while inactivating mutations cause a mild form of DM in the case of haploinsufficiency due to a right shift of the glucose threshold. However, severe ketotic permanent neonatal DM (PNDM) ensues when both alleles are strongly affected. In the latter case, beta cells seem to be totally nonfunctional, and the patients require full insulin replacement therapy right after birth. The syndromes of GK disease are nature's compelling proof of the GK glucose sensor concept. Activating mutations of GDH, usually explained by loss of GTP (ATP) inhibition of the enzyme, cause hyperinsulinemic hypoglycemia because beta-cell glutaminolysis is enhanced. These patients are also leucine hypersensitive, in agreement with the findings of basic research (see model experiment in Figure 3). Inactivating mutations of one of the subunits of the K^+ channel are a frequent cause of autosomal recessive hyperinsulinemic hypoglycemia. These mutations depolarize the beta cells and result in elevated $[Ca^{2+}]_i$, rendering them supersensitive to AA stimulation and neuroendocrine activation. The hyperresponse to protein meals as observed in these patients is reproduced in isolated perifused islets of SUR-$1^{-/-}$ mice that are stimulated by a physiological 20 AA mixture, in contrast to control islets that are refractory to this stimulus in the absence of glucose. There is also increasing support for the view that the highly common E23K polymorphism of the Kir6.2 channel causes a predisposition for the development of T2DM. The E23K mutation increases K^{2+} conductivity and hyperpolarizes beta cells, rendering them less sensitive to physiological stimuli. These examples illustrate how basic and clinical sciences cooperate in their quest to understand glucose homeostasis and its disturbances.

Beta-Cell Therapy in T2DM and Hyperinsulinemia

Our knowledge of physiological chemistry and biochemical genetics of the beta cell has its corollary in beta-cell-based therapeutics of T2DM and hyperinsulinemic hypoglycemia, which contributes substantially to our understanding of islet cell function and glucose homeostasis. The following drugs will be discussed in brief: K^+ channel inhibitors and activators (KCIs and KCOs), GK activators (GKAs), GLP-1, GIP, methylxanthines, and muscarinic agonists (see Figure 1). KCIs (i.e., sulfonyl urea derivatives and other chemicals that inhibit the K^+ channel) reduce K^+ conductivity, depolarize the beta cell, and sensitize it to all known physiological stimuli. For decades they have been the drugs of choice for the treatment of T2DM. KCOs (e.g., diazoxide) hyperpolarize beta cells and have been useful in the treatment of mild forms of hyperinsulinemic hypoglycemia (e.g., due to mutations of GK or GDH). GKAs have been discovered only recently and hold considerable promise for a new approach to the treatment of T2DM. They have effects very similar to those of activating mutations of GK, and it seems that they act by binding to an allosteric activator site of the enzyme (Figure 4). They cause a left shift of the concentration dependency curve of GSIR and have the additional advantage that they activate hepatic GK and augment glycogen synthesis. It is hoped that ongoing trials in humans will demonstrate the clinical usefulness and safety of this novel, theoretically very attractive approach to treatment of T2DM. GLP-1 and GIP are obvious candidates for antidiabetic agents as is apparent from Figure 1, and promising trials are underway. M3 agonists that could reproduce the effects of

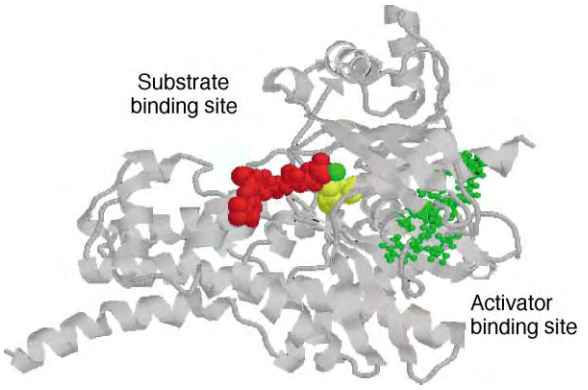

FIGURE 4 Allosteric activator site of the glucokinase glucose sensor molecule: ribbon drawing of the model structure of GK, with the N-terminal to the left and the C-terminal to the right. Glucose, ATP, and Mg^{2+} are located in the substrate cleft of the enzyme, and the allosteric activator site is indicated by several amino acids. The mutation of any one of these (e.g., V62M, I211A, Y214C, M235A, V455M, and A456V) activates the enzyme markedly. Glucokinase activators bind to this site.

acetylcholine, although potentially useful, have not been explored, most likely because lack of beta-cell specificity might become an issue. Phosphodiesterase inhibitors (e.g., IBMX) are powerful potentiators of fuel-stimulated insulin release, but here again it is apparently difficult to design a beta-cell-specific drug. Note that drug treatment of beta cells seems to reduce the diabetes-associated hyperfunction of the glucagon-producing alpha cells as well, thus indirectly enhancing the benefit of antidiabetic drugs with beta-cell action.

Conclusion

This entry illustrates that experimental work and mutually corrective or reinforcing dialog between biochemists, geneticists, pharmaceutical chemists, pharmacologists, and the practicing diabetologists has resulted in a deep understanding of the role that pancreatic endocrine cells play in glucose homeostasis and the pathogenesis of diabetes mellitus and how various therapies might ameliorate the dysfunction of these cells. This remarkable track record bodes well for the future, holding great promise for even deeper insights and the development of new antidiabetic agents and drugs that combat severe hyperinsulinemia.

See Also the Following Articles

Diabetes • Fatty Acid Oxidation • Fatty Acid Receptors • Fatty Acid Synthesis and its Regulation • Glucagon Family of Peptides and their Receptors • Hexokinases/Glucokinases • Insulin Receptor Family • Protein Kinase C Family

Glossary

beta cell threshold for glucose-stimulated insulin release The level of glucose required to initiate insulin release, i.e., about 5 mM. This beta-cell threshold is the critical determinant of the glucose setpoint of the body.

glucokinase (GK) disease Hypo- and hyperglycemia syndromes in humans caused by activating and inactivating mutations of glucokinase. This "experiment of nature" is the most compelling evidence for the glucokinase glucose sensor concept and its importance in understanding glucose homeostasis.

glucokinase glucose sensor Glucokinase (also known as hexokinase IV or D) phosphorylates D-glucose using ATP, forming glucose-6-phosphate. The enzyme serves as a glucose sensor of the pancreatic beta cells because it is rate limiting for glucose metabolism (i.e., glycolysis and oxidation), which is an absolute prerequisite for the triggering of insulin secretion.

glucose setpoint of the body Blood glucose level maintained precisely by the fine tuning of opposing processes that either produce or consume glucose. In humans, this setpoint is close to 5 mM.

Further Reading

Grimsby, J., Sarabu, R., Corbett, W. L., Haynes, N. E., Bizzarro, F. T., Coffey, J. W., Guertin, K. R., Hilliard, D. W., Kester, R. F., Mahaney, P. E., Marcus, L., Qi, L., Spence, C. L., Tengi, J., Magnuson, M. A., Chu, C. A., Dvorozniak, M. T., Matschinsky, F. M., and Grippo, J. F. (2003). Allosteric activators of glucokinase: Potential role in diabetes therapy. *Science* **301**, 370–373.

Matschinsky, F. M. (1996). Banting Lecture 1995: A lesson in metabolic regulation inspired by the glucokinase glucose sensor paradigm. *Diabetes* **45**, 223–241.

Matschinsky, F. M. (2002). Regulation of pancreatic beta-cell glucokinase: From basics to therapeutics. *Diabetes* **51 Suppl. 3**, 394–404.

Newgard, C B., and Matschinsky, F. M. (2001). Substrate control and insulin release. In *Handbook of Physiology* (L. Jefferson and A. Cherrington, eds.) Vol 2, pp. 125–151. Oxford University Press, Oxford.

Prentki, M., and Matschinsky, F. M. (1987). Ca^{2+}, cAMP and phospholipids derived messengers in coupling mechanisms of insulin secretion. *Physiol. Rev.* **67**, 1185–1248.

Biography

Franz M. Matschinsky is the current Benjamin Rush Professor of Biochemistry and Biophysics at the University of Pennsylvania School of Medicine. His research focuses on the role of pancreatic alpha and beta cells in glucose homeostasis, the role of glucokinase as glucose sensor, the biochemical genetics of glucokinase disease, and drug therapy of diabetes mellitus using glucokinase activators. He received medical training in Freiburg and Munich, Germany, and postdoctoral training at Washington University in St. Louis. He was Professor of Pharmacology at that institution from 1972 to 1978.

Insulin Receptor Family

Paul F. Pilch
Boston University Medical School, Boston, Massachussetts, USA

Jongsoon Lee
Joslin Diabetes Center, Harvard Medical School, Boston, Massachussetts, USA

The mammalian insulin receptor family is composed of three members: the insulin receptor (IR), the insulin-like growth factor I receptor (IGF1R) and the insulin receptor-related receptor (IRR). All are ligand-activated tyrosine kinases, i.e., members of the large receptor tyrosine kinase (RTK) superfamily. The IR family members share ~55% overall sequence homology with each other, and have many similar biochemical and functional characteristics. The IRR is an orphan receptor lacking a physiological ligand, and its knockout in the mouse has no gross phenotype. Consequently, there is very little to say about the IRR. Because of its critical role in metabolic regulation, the insulin receptor is one of the most-studied RTKs and the details of its structure, function, and mechanism of action will be emphasized. The biochemically similar IGF1R serves as a mitogen receptor and does not normally acutely regulate nutrient metabolism.

IR Family Ligands and Their Specificity

The ligands for the insulin receptor family also comprise a family of related peptides, namely, insulin, IGF1 and IGF2, the latter two being mitogens. These peptides are synthesized with a cleavable signal sequence for secretion and have three inter/intra-chain disulfide bonds. Insulin alone is further processed by an endoprotease, which results in the excision of an internal 33-amino acid "connecting" or C peptide from the proinsulin precursor and produces mature insulin in the form of disulfide-linked 21- and 30-amino acid A and B chains, respectively. Insulin and IGF1 bind only their cognate receptors with high affinity, whereas IGF2 can bind both these receptors with reasonable (physiological) affinity. However, there exists another high-affinity IGF2 receptor, also called the cation-independent mannose-6-phosphate receptor that has no signaling function but serves to clear IGF2 (and other molecules) from circulation.

Receptor Structure/Function

Composition and Biosynthesis

Figure 1 depicts a two-dimensional cartoon for the structure of the insulin (numbered without exon 11) and IGF1 receptors. The mature receptors are $\alpha_2\beta_2$ heterotetramers in which the two extracellular α-chains are linked to each other and to a β-subunit through disulfide bridges (horizontal lines, Figure 1). Both α- and β-subunits (respectively, 719 and 624 aas) of the insulin (IGF1) receptor are heavily glycosylated and have approximate molecular weights of 130 and 95 kDa, respectively, as assessed by gel electrophoresis. The α-subunits are totally extracellular and are responsible for ligand recognition. The β-subunits have three topographically distinct regions: the extracellular, transmembrane (TM), and cytosolic domains. The cytosolic tyrosine kinase domain, which shares the most similarity among family members, has an ATP-binding site and three clusters of tyrosine residues located in the juxtamembrane region, the kinase activating loop, and the C terminus. These tyrosines are phosphorylated upon ligand binding to α-subunits (*vide infra*).

Both receptor subunits are encoded in a single gene, which is composed of 22 exons for IR and 23 exons for IGF1R in humans. The initial translation product of IR family members is a single polypeptide proreceptor precursor, a type 1 transmembrane protein with its N terminus having an extracellular topography. The proreceptor is glycosylated and dimerized in the endoplasmic reticulum, transported into the Golgi, and then proteolytically cleaved by the endoprotease furin, into mature $\alpha_2\beta_2$ receptors. While the IGF1R has a single isoform, the IR has two isoforms produced by alternative splicing of exon 11 (12-amino acids) at the C terminus of α-subunits. Several studies show that there are differences between the two isoforms in tissue distribution, ligand-binding specificity and relative expression levels among diabetes patients. However, a definitive physiological significance for the separate isoforms is still uncertain.

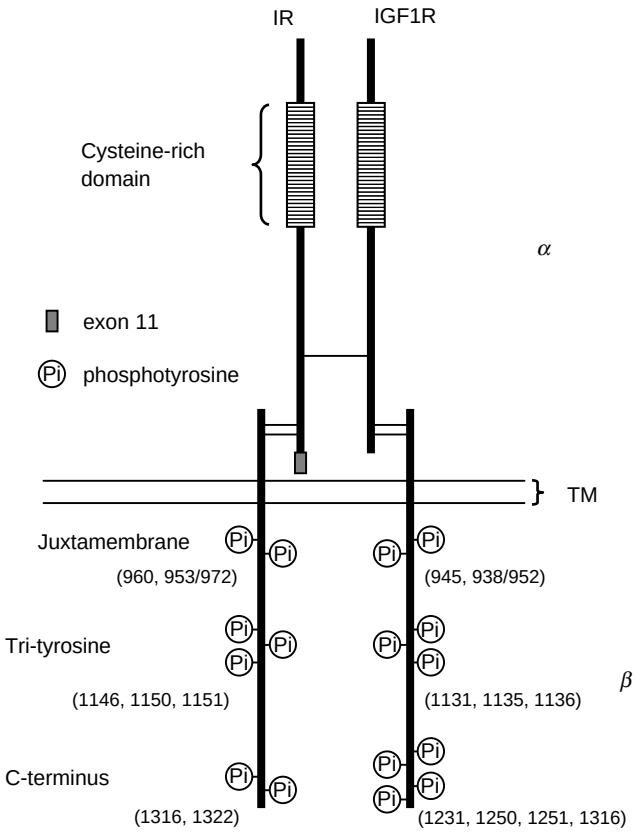

FIGURE 1 Two-dimensional representation of IR (left side) and IGF1R (right side) structural/biochemical features. The IR is numbered without Exon 11 (12 aas). The extracellular α-subunits are linked to each other and to β-subunits by disulfide bridges (horizontal lines). The α-subunits contain the ligand-recognition sequences including the cysteine-rich domain. The β-subunits span the lipid bilayer via their transmembrane (TM) domains and have three clusters of tyrosine residues whose phosphorylation has functional consequences (see the text).

Ligand Binding

Affinity labeling of the insulin receptor using bifunctional cross-linking agents and photo-activatable insulin analogues first documented the α-subunit, including the cysteine-rich region shown in Figure 1, as the site of insulin (IGF1)-receptor contact. Insulin/IGF1-binding studies with various mutant receptor constructs as well as domain-swapping studies between IR and IGF1R confirmed these biochemical data and also identified exons 2 and 3 (aas 16-286, including the cysteine-rich region) as sequences that govern ligand-binding specificity between insulin and IGF1.

However, while residues in the α-subunit govern ligand recognition, there is role for the β-subunit in ligand affinity. Insulin and IGF1-binding studies support the notion that only one ligand molecule binds the holoreceptor with high affinity, whereas each $\alpha\beta$ half-receptor can bind one ligand molecule, albeit with low affinity. Kinetic analysis of ligand binding to the holoreceptor reveal it to exhibit negative cooperativity, whereby one ligand molecule binds with high affinity and a second binds with much less affinity. Mutational analysis has shown that soluble versions of the insulin receptor containing $\alpha-\alpha$ disulfide linkages have low insulin-binding affinity and a stoichiometry of one insulin/α-subunit. The high-affinity state can be recapitulated by bringing the α-subunits into their proper orientation relative to one another by including the transmembrane sequence of the β-subunit, a leucine zipper domain or parts of an immunoglobulin protein. Various cellular and biochemical studies confirm that binding of one insulin molecule to the holoreceptor is the normal situation at physiological concentrations of insulin and this is sufficient to activate the receptor and its signaling pathway. The conclusion from all these studies is that both α-subunits participate in the formation of the high-affinity ligand-binding site. The molecular details of this await X-ray crystallography studies of the holoreceptor-ligand complex. Indeed, X-ray crystal structures have been determined for the N terminus of IGF1R α-subunit and for the kinase domain of the IR. Recently, a structure of the IR based on three-dimensional electron microscopy and adopting coordinates from the X-ray structure of IGF1R N terminus has been proposed, and has provided new information concerning the overall shape of the IR. However, these results are of too low resolution to reveal the details of ligand-receptor interaction.

Autophosphorylation and Kinase Activation

Ligand binding to the insulin receptor causes a transmembrane conformational change that results in autophosphorylation and activation of exogenous tyrosine kinase activity in the receptor's β-subunit. Evidence supporting conformational changes includes the differential recognition of site-specific anti-receptor antibodies for activated versus inactive insulin receptor, differential susceptibility to proteases, changes in intrinsic fluorescence of the insulin receptor during receptor activation and the different X-ray structural configuration of the isolated kinase domain comparing activated (tyrosine phosphorylated) versus basal states. Taken together, these studies provide evidence that conformational changes occur during each step of receptor activation: insulin binding, ATP binding, and kinase activation by phosphorylation. However, the exact molecular nature and sequence of the conformational changes by which ligand binding activates the kinase domains and mediates transmembrane signaling are not fully understood.

It is known that activation of IR/IGF1R receptor kinase occurs in trans, that is; one kinase domain

phosphorylates the other. The IR contains two identical kinase domains and two sets of phosphorylation sites and both must be active for exogenous tyrosine kinase activity, i.e., substrate phosphorylation, to occur. Biochemical studies of the photo-labeled IR as well as studies of receptor chimeras consisting of half kinase-active and half kinase-dead receptors document asymmetric IR autophosphorylation. For the photo-labeled holoreceptor, autophosphorylation is initially asymmetric and the insulin-linked receptor half is 50% less phosphorylated than the other half. Thus, initially only one β-subunit is phosphorylated, but at the later time points, both subunits become phosphorylated and in a given ligand-bound receptor, autophosphorylation is a stochastic process.

There are 13 and 15 tyrosine residues, respectively, in the cytoplasmic domain of IR and IGF1R, and phosphopeptide mapping analysis and/or site-directed mutagenesis has revealed three clusters (Figure 1) that can be phosphorylated upon receptor binding. Phosphorylation of tyrosines at the activation loop (Tyr1146, 1150 and 1151 for IR, Tyr1131, 1135 and 1136 for the IGF1R) is critical for kinase activity. The non-phosphorylated activation loop of the receptor blocks the ATP-binding site in the basal state. Ligand binding allows the tyrosine phosphorylation of these residues and moves the activation loop away from the opening of the ATP-binding site, thus allowing access so that the kinase can phosphorylate exogenous substrates such as the insulin receptor substrate (IRS) family relevant to the IR and IGF1R. Mutation of the activation loop tyrosines to phenylalanine abolishes kinase activation and insulin-signaling cascades.

The physiological role of tyrosine phosphorylation at the other sites is less clear. Mutation of Tyr960 of the IR to Phe does not change insulin-stimulated autophosphorylation and kinase activation, but it does abolish phosphorylation of IRS1, hence signaling, as deduced from transfection experiments. The phosphorylated NPE(X)Y-motifs (Tyr960 of IR and Tyr945 IGF1R) can serve as docking sites for IRS proteins via their phosphotyrosine binding (PTB) domains and this may be necessary for signal propagation. On the other hand, peptide mapping of the autophosphorylated receptor demonstrates that the juxtamembrane region is rather minimally phosphorylated, although this does occur to a significant extent with the isolated kinase domain. Phosphorylation of tyrosines at the C terminus of the IR (residues 1316 and 1322) accounts for 30–40% of total phosphorylation of β-subunits. However, deletion/substitution of the residues has produced conflicting results in different labs as to the effects, if any, of these manipulations, and consequently, there is no clear physiological role yet for these sites.

Postreceptor Signaling

Physiological Effects of Insulin and IGF1

These are too numerous to elaborate, so the emphasis of this section will be IR-regulated glucose metabolism. Glucose is a primary energy source for various tissues including the brain, and insulin maintains the circulating blood glucose concentration within narrow limits. Glucose homeostasis is coordinately regulated by insulin in liver, fat, and muscle. Pancreatic β-cells play an obvious role in insulin production. Liver maintains basal glucose levels between meals by producing glucose through two mechanisms: *de novo* glucose synthesis (gluconeogenesis) and breakdown of glycogen (glycogenolysis). Muscle, and to a lesser degree fat, lowers postprandial glucose levels by increasing glucose uptake (transport) and its storage as glycogen and lipid. Insulin, produced and secreted from β-cells in response to changes in circulating glucose levels after meals, regulates all these processes. Glucose homeostasis is achieved by insulin-dependent suppression of hepatic glucose production and by enhanced glucose uptake and storage in muscle and fat. Enhanced glucose uptake is achieved by the insulin-dependent movement of a glucose transport protein Glut4, from an intracellular reservoir to the cell surface (Figure 2). On the other hand, IGF1 promotes cell growth, differentiation, and survival as largely studied in cell culture. Its signaling pathway closely resembles that of insulin but its role *in vivo* is not as well defined compared to insulin.

Signaling Cascades

Once the insulin or IGF1 receptor is activated by autophosphorylation, it phosphorylates one or more of the IRS proteins noted above. Six IRS family members have been identified and they are all adaptor proteins, that upon tyrosine phosphorylation, bind and activate a number of effector molecules through their src homology 2 (SH2 domains). IRS-1 and -2 have been implicated as the major signaling components directly downstream of the IR and IGF1R. The major event following IRS phosphorylation is the activation of the p110 (Figure 2) catalytic subunit of phosphoinositol-3-kinase (PI3-K) by binding of the p85 subunit of PI3-K to tandem pYMXM sequence motifs of an IRS molecule. The formation of the lipid PIP_3 by PI3-K causes the activation of the *p*hosphoinositide-*d*ependent serine/threonine *k*inase, PDK1, and, in turn, it phosphorylates and activates Akt/PKB (protein kinase B) and PKCλ/ζ, each of which may affect glucose transport (Figure 2).

Akt is the serine/threonine kinase that appears to be the key regulatory enzyme in insulin/IGF1 signaling that

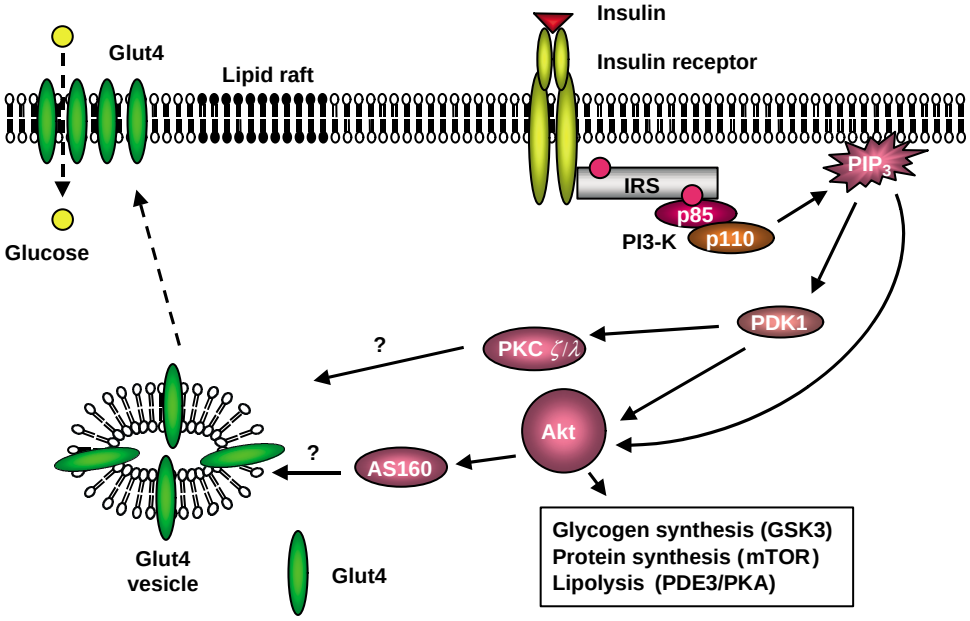

FIGURE 2 The insulin receptor signaling cascade that activates glucose transport. The solid arrows indicate the signaling pathway, the dashed arrows indicate movement and the question mark, an unknown or uncertain biochemical event. Refer to the text for a description of the known biochemical events in the pathway from the receptor to the Glut4 vesicle. Note that the size of the proteins depicted in the cartoon is not to scale relative to one another.

impacts different physiological end points of metabolism such as gluconeogenesis and glycogenolysis in liver, glucose transporter (Glut4) trafficking in muscle and fat, and β-cell survival. Thus, mice lacking the Akt2 isoform of this enzyme have a diabetic phenotype and show metabolic abnormalities in the processes just noted. That is, they have impaired suppression of hepatic glucose output, deficient glucose uptake in fat and muscle, and abnormal islets. At the molecular level in liver, Akt phosphorylates the transcription factor Foxo1, that regulates expression of gluconeogenic enzymes. AS160, for Akt substrate of 160 kDa, is a recently described protein that may link the canonical PI3-K pathway to Glut4 translocation but "exactly how?" remains unknown. A second pathway by which insulin-dependent Glut4 translocation may occur in adipocytes has been proposed. Insulin-signaling, independent of PI3-K, is postulated to emanate from subdomains of the plasma membrane called lipid rafts and causes cyto-skeletal changes that bring Glut4 to the plasma membrane. The physiological relevance of this second pathway remains to be established.

"Genetics" and IR-IGF1R Comparisons

On a biochemical level, signaling pathways from the IR and IGF1R appear to be identical yet they clearly serve different functions *in vivo*. The phenotypes of knockout (KO) mice for these receptors and their ligands have further revealed this diversity of function. Although there is minor compensation between the two pathways, it is evident that insulin regulates glucose/lipid metabolism and IGF1 (IGF2) mediates growth/development. Thus, while IR and IGF1R knockouts are lethal in mice, the former is due to hyperglycemia and the latter lack of muscle development. The reasons for these differences are highly complex and beyond the scope of this article. However, it is worth noting that unlike mice, humans lacking functional insulin receptors live for at least a short time after birth, probably due to IGF1R compensation.

To determine physiological roles of the IR in specific insulin responsive cell types, tissue-specific insulin receptor KO-mouse models have been made including in muscle, liver, fat, and β-cells. These tissue-specific mouse models generally show mild insulin resistance short of diabetes. Because insulin resistance leading to diabetes is a total body disease, disruption of insulin signaling, hence glucose metabolism, in individual tissues may not be sufficient for the development of this pathological state. Further genetic studies including multiple "knockout" and "knockin" mouse models, the latter with specific receptor mutations, should increase our understanding of development of insulin resistance and diabetes. Subsequent biochemical and cellular studies will provide us with the details of the molecular mechanisms underlying the IR and IGF1R signaling pathways.

See Also the Following Articles

Diabetes • Glucose/Sugar Transport in Mammals • Insulin- and Glucagon-Secreting Cells of the Pancreas

Glossary

glycosylated Referring to or describing protein modified by the covalent attachment to/of carbohydrate molecules.
ligand A molecule such as a hormone that binds to a receptor.
mitogen A molecule that stimulates cell growth and division.
phosphorylation Covalent modification of a molecule (here protein) by the attachment of a phosphate residue.

Further Reading

De Meyts, P., and Whittaker, J. (2002). Structural biology of insulin and IGF1 receptors: Implications for drug design. *Nat. Rev. Drug Discov.* **1**, 769–783.

Kim, J. J., and Accili, D. (2002). Signaling through IGF-I and insulin receptors: Where is the specificity? *Growth Horm IGF Res.* **12**, 84–90.

Kitamura, T., Kahn, C. R., and Accili, D. (2003). Insulin receptor knockout mice. *Annu. Rev. Physiol.* **65**, 313–332.

Lee, J., Pilch, P. F., Shoelson, S. E., and Scarlata, S. F. (1997). Conformational changes of the insulin receptor upon insulin binding and activation as monitored by fluorescence spectroscopy. *Biochemistry* **36**, 2701–2708.

Sano, H., Kane, S., Sano, E., Miinea, C. P., Asara, J. M., Lane, W. S., Garner, C. W., and Lienhard, G. E. (2003). Insulin-stimulated phosphorylation of a Rab GTPase-activating protein regulates GLUT4 translocation. *J. Biol. Chem.* **278**, 14599–14602.

Whiteman, E. L., Cho, H., and Birnbaum, M. J. (2002). Role of Akt/protein kinase B in metabolism. *Trends Endocrinol. Metab.* **13**, 444–451.

Biography

Paul Pilch is a Professor of Biochemistry at Boston University School of Medicine who since long ago has evinced keen interest in insulin/IGF1 receptors and the metabolic consequences of activating their signaling pathway(s).

Jongsoon Lee is an Instructor at the Joslin Diabetes Center, Harvard Medical School, who shares the same interest. Separately and together, they have published extensively on these topics.

Integrin Signaling

Lawrence E. Goldfinger and Mark H. Ginsberg
Scripps Research Institute, La Jolla, California, USA

Integrins are heterodimeric transmembric receptors expressed on virtually all cells in multicellular organisms. They mediate attachment of cells to the extracellular matrix and to other cells. In addition to, and participation with their adhesive function, integrins are conduits of bidirectional signaling between the extracellular environment and the cell interior. Through "outside-in" integrin signaling, binding of ligands to integrin extracellular domains initiates intracellular signaling pathways which regulate such processes as protein phosphorylation, gene expression, proliferation, apoptosis and differentitation. These signals are initiated by conformational changes in the integrin structure propagated from the extracellular "head" domains, through the transmembrane regions and terminating at the cytoplasmic "tail" domains. Conformational changes in the tails subsequently affect the binding and signaling properties of intracellular signaling molecules. Conversely, conformational activation of integrin head domains to promote ligand binding is regulated by intracellular signaling pathways, in a process called "inside-out" integrin signaling. Cytoplasmic proteins associate with integrin tails, leading to allosteric rearrangements in the extracellular head domains to effect a switch from low to high affinity ligand binding. This process of inside-out integrin signaling is crucial to hemostasis and the maintenance of normal tissue integrity. Furthermore, ligand binding to integrins can be regulated by avidity modulation by which integrin clustering promotes increased binding to ligands. Thus, intricate regulation of outside-in and inside-out signaling and integrin avidity plays key roles in numerous cellular phenotypes.

Integrins are transmembrane receptors that promote cellular attachment to the extracellular matrix (ECM) and to counter receptors on the surfaces of neighboring cells. Integrins are responsible for mediating cell adhesion and migration, and for maintaining tissue integrity. They are expressed at the surface of virtually all multicellular animal cells as noncovalent heterodimers of α- and β-subunits. Integrins are named based on their α- and β-subunit composition, e.g., $\alpha_1\beta_1$, $\alpha_{IIb}\beta_3$.

The integrin family in humans consists of 18 α- and 8 β-subunits, which each are encoded by unique genes. Each α-subunit pairs with a restricted set of β-subunits, resulting in a total of 24 known functional integrin heterodimers. Each pairing, in turn, is expressed on a limited array of cell types. Thus, each cell has its own particular repertoire of integrins. Since different integrins display distinct ligand-binding preferences, these repertoires specify adhesive preferences of different cell types. In some cases, multiple integrins can recognize the same ligand. For example, many integrins bind to the ECM protein, fibronectin. Even within the same ECM protein, integrins can vary in recognition specificity. Integrin $\alpha_V\beta_3$, for example, binds to an Arg-Gly-Asp (RGD) motif in fibronectin, while integrin $\alpha_4\beta_1$ binds to a Leu-Asp-Val (LDV) motif present in a different part of fibronectin. Furthermore, these short peptide motifs can occur in evolutionarily unrelated proteins, where they can serve as recognition sites for many different integrins. The RGD motif occurs in many proteins and can bind to many integrins (e.g., $\alpha_{IIb}\beta_3$, $\alpha_v\beta_3$, $\alpha_v\beta_5$, $\alpha_5\beta_1$). This integrin-binding motif interaction is conserved in phylogeny; for example, the *Drosophila* PS2 integrin recognizes an RGD sequence in tiggrin, a matrix protein. The occurrence of integrin-binding motifs, such as RGD, is an example of convergent evolution dictated by the recognition specificity of adhesion receptors.

All integrin subunits possess a single transmembrane domain, which separates the large extracellular, N-terminal ligand-binding domain from the typically short (less than 60 amino acids) C-terminal cytoplasmic domain, or cytoplasmic tail. Besides acting as cellular glue to support adhesion, and feet to facilitate migration, integrins initiate transmembrane signals, which regulate processes such as embryogenesis, cell development, proliferation, apoptosis, and the immune response.

General Features of Integrin Signaling

Integrins derive their name from their role of integrating the ECM with the insoluble cellular skeleton (cytoskeleton). Binding of ligands to the extracellular portion of integrins leads to both conformational changes in the receptors and to receptor clustering. This combination

of events initiates intracellular signals such as protein tyrosine phosphorylation, activation of small GTPases, and changes in phospholipid biosynthesis. This process is commonly referred to as outside-in signaling. In addition, integrins are subject to so-called inside-out signaling. Integrins can fluctuate between three functional states: an active state that manifests high affinity for binding ligands, a high-affinity state that is bound to ligand, or in a distinct "inactive" state, which has a low affinity for ligands. Inside-out signaling is defined as modulation of the functional state of integrins via intracellular signaling processes. It is frequently mediated by interactions of intracellular components with the integrins' cytoplasmic tails. Furthermore, signals from one integrin can regulate the activation state of another in a phenomenon referred to as integrin transregulation or cross talk. Through transregulation, multiple integrins can be linked via a combination of both outside-in and inside-out signaling.

Inside-Out Signaling

Modulation of integrin function can occur by changes in ligand-binding affinity or by changes in the clustering of these receptors. The former mechanism is often referred to as integrin activation and the latter as a change in avidity. These functional changes can be caused by signaling pathways initiated by agonist-receptor interactions at the plasma membrane. The appropriate regulation of integrin activation is required for the formation and maintenance of normal tissue architecture.

Physiological Roles of Inside-Out Signaling

Integrin Activation in Hematopoietic Cells

Integrin activation plays a crucial role in the biology of blood cells. For example, the platelet integrin, $\alpha_{IIb}\beta_3$, is usually maintained in the inactive state, with very low affinity for its extracellular ligands, fibrinogen, fibronectin, and von Willebrand factor. Upon platelet stimulation, the integrins are quickly activated, leading to fibrinogen binding and consequent platelet aggregation, an early step in hemostasis. Thus, the loss of $\alpha_{IIb}\beta_3$ integrin activation impairs hemostasis. Conversely, platelet aggregation is central in arterial thrombosis that is responsible for the majority of heart attacks and strokes. Pharmacological blockade of activation of integrin $\alpha_{IIb}\beta_3$ by agents such as aspirin or ticlopidine is therefore often used to treat patients at risk for these diseases. Similarly, rapid activation of dormant integrins on leukocytes allows these cells to attach firmly to the endothelial vessel wall and resist strong shear forces from the flowing blood. This step is essential for their migration into sites of inflammation. For this reason, loss of leukocyte integrin activation can lead to enhanced susceptibility to infections and its blockade may be useful in anti-inflammatory therapies.

Integrin Activation in Tissues

For adherent cells in tissues, such as fibroblasts or epithelial cells, stable cellular attachment to the ECM is necessary for maintaining tissue integrity. Many of the best-studied integrins in these cells, such as the α_5, α_v, and α_6 integrins, are indispensable components of cell-substrate attachment structures: focal adhesions, hemidesmosomes, and podosomes. In addition to attaching to the ECM, integrins participate in formation and remodeling of the ECM. Activation of tissue integrins can regulate the assembly and structure of the ECM and control the stability of integrin–matrix attachments. In addition, the migration of these cells in tissues is regulated by the ability of integrins to become activated. Furthermore, integrin activation may be topographically localized across the basal cell surface. For example, activated $\alpha_v\beta_3$ integrins are preferentially localized to the leading edge of endothelial cells during cell migration and neurite outgrowth.

Integrin Activation

The switch from an inactive to an active state is the result of alterations in the conformation of the integrin extracellular domains. These conformational changes can be triggered by protein–protein interactions at the integrin cytoplasmic face. These protein–protein interactions are regulated by different signaling pathways in different cells. However, in many contexts, activation of key intermediates such as the GTPase Rap1, or protein kinase C, promote increased integrin affinity. Conversely, activation of Raf-1 kinase often suppresses integrin activation. Whatever the upstream events, it is likely that the final common events involve changes in interactions at the integrin cytoplasmic domain (Figure 1).

Contribution of Cytoplasmic Domains

Tail-Binding Proteins Numerous cytoplasmic integrin-binding proteins have been described, and several have been reported to contribute to activation through binding to the integrin tails. The best-characterized example is the cytoskeletal linker protein talin, which promotes integrin activation by binding to a subset of integrin β-subunit tails at a highly conserved NPxY motif. Mutational evidence suggests that integrin α–β-subunit tail interactions inhibit activation. The ability of talin to activate the integrins has

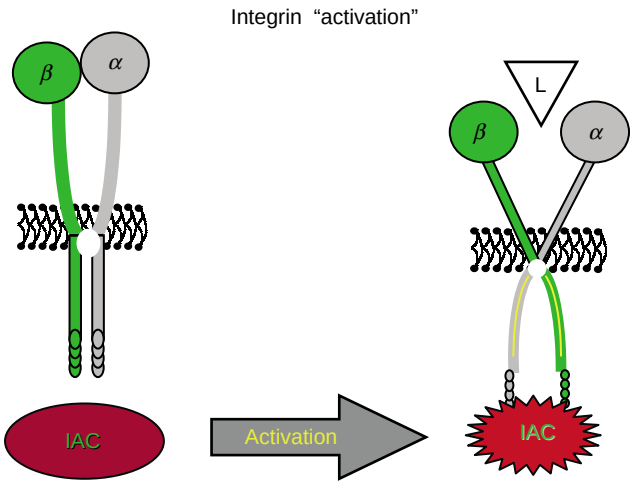

FIGURE 1 Inside-out signaling activates integrins. Binding of an integrin-activating complex (IAC) to the cytoplasmic tails of an integrin heterodimer produces conformational changes in the extracellular head domains, leading to activation and high-affinity binding to ligand (L).

been attributed to competition with the α-subunit for β-tail binding.

Membrane Proximal Residues Deletion of the tail sequences adjacent to the putative transmembrane regions in either the α- or β-tail can activate integrins, indicating that these residues are essential for maintaining integrins in an inactive state. One model for activation entails a breaking of a salt bridge in this region that holds the tails together, leading to an "opening" of the tails via a scissor-like mechanism (Figure 1). This leads to an allosteric rearrangement in the extracellular domain and a shift to the active state.

Extracellular Domain Conformational Changes

Precise conformational shifts at the ligand-binding face of integrins result in high-affinity binding to ligands. Integrin–ligand interactions require an essential Asp or Glu residue in the integrin recognition sequence in the ligand, as well as the presence of a divalent cation. Some of the integrin α-subunits have an "inserted", or I/A domain near the N-terminus; these integrins contact ligand solely through the α-subunit, although the β-subunit plays an accessory role. The I/A domain manifests a metal ion-dependent adhesion site (MIDAS). Key residues in the ligand cooperate with the MIDAS to coordinate the cation and allow integrin–ligand interaction. Conformational changes in the MIDAS during cation coordination and ligand binding subsequently result in secondary changes in the rest of the integrin, including a downward shift of a α-helix C-terminal to the I/A domain, thereby switching the integrin from the "closed" inactive state into the "open" active state. For integrins with a α-subunit that does not contain an I/A domain, the I/A-like domain in the β-subunit cooperates with the α-subunit in a somewhat different fashion to mediate ligand interaction, but also through coordination of a divalent cation.

Avidity Modulation

In addition to affinity modulation through conformational changes in individual integrin molecules, cell adhesion can also be enhanced by increasing the density of ligand-binding sites through integrin clustering, via an affinity-independent mechanism known as avidity modulation. Many integrin ligands are multivalent; thus, integrin clustering can promote adhesion through cooperative ligand binding. In many cases, a combination of affinity and avidity modulation both contribute to the regulation of cell adhesion.

Outside-In Signaling

Occupancy of integrins leads to conformational changes that can propagate over long distances in the extracellular domain. It has been proposed that these allosteric rearrangements can be transmitted across the plasma membrane, changing the interactions of the α and β cytoplasmic domains with each other and thus, the integrin's interactions with intracellular signaling molecules. Furthermore, occupancy leads to integrin clustering, which can also change the physical relationships of the integrin cytoplasmic domains with each other. This combination of occupancy and clustering is believed to initiate signals from integrins. These signals regulate the formation and strengthening of adhesion sites, the dynamics of cytoskeletal structure, cell shape and size, and cell polarity and cell migration. In addition to controlling the physical activities of cells, signaling through integrins also regulates gene expression, cell proliferation and apoptosis, and many integrins are required for the development of particular lineages.

Integrins in Adhesion Sites

Most integrins are physically linked to the actin cytoskeleton via interactions of the β-tail with actin-binding proteins such as α-actinin, talin, and filamin. $\alpha_6\beta_4$ integrins associate with the intermediate filament cytoskeleton through other linker proteins: BP180 (BPAG2), BP230 (BPAG1), and plectin. By connecting the ECM with the cytoskeleton, clustered integrins form the essential core of complexes of structural and signaling molecules such as focal complexes and adhesions (contacts), hemidesmosomes (specific to

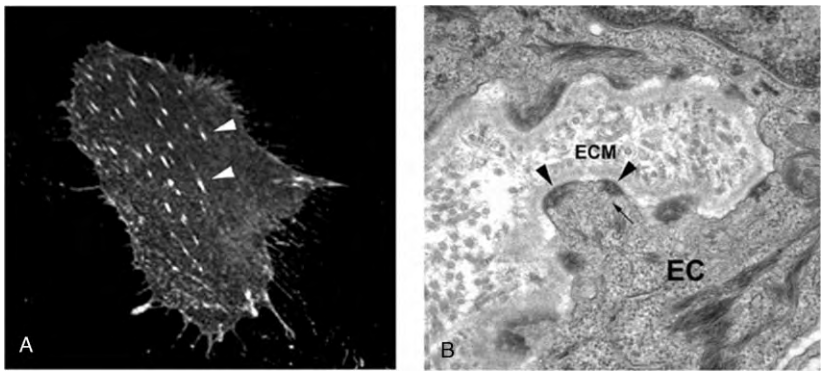

FIGURE 2 Focal contacts and hemidesmosomes. Two types of integrin–ECM contacts are shown. (A) Focal contacts are visualized by labeling $\alpha_{IIb}\beta_3$ integrin clusters in a fibroblast expressing $\alpha_{IIb}\beta_3$ attached to fibrinogen. Arrowheads indicate two focal contacts. (B) Transmission electron micrograph of a cross section of bovine tongue. Hemidesmosomes (arrowheads) are seen as electron-dense structures at the basal surface of the tongue epithelial cells (EC), connecting the intermediate filaments (arrow) to the ECM. Image courtesy of Gregory W. deHart and Jonathan C.R. Jones.

epithelial cells, they contain $\alpha_6\beta_4$ integrin and are linked to intermediate filaments), and osteoclast structures called podosomes (which have many of the same protein components as focal adhesions) (Figure 2).

Formation of Adhesion Sites

Ligand binding and integrin clustering nucleate nascent cell adhesion sites. Numerous cytoskeletal adapters and signaling molecules are subsequently recruited to the clustered integrin tails. These complexes serve as the initiation points for signaling by integrins to affect cellular phenotypes. Focal complexes "mature" to become focal adhesions (focal contacts) as more integrins and signaling molecules associate, thereby strengthening cellular attachments to the ECM.

Regulation of Adhesion Dynamics

Adhesion sites are dynamic structures which undergo remodeling to fit the needs of the cell or of the region of the cell in contact with the ECM. Focal complexes form at the leading edges of lamellipodia and of filopodia in migrating cells, where they mediate new attachments, but do not mature to focal adhesions. Instead, these smaller complexes are subject to rapid turnover, as the cell continues to extend protrusions in the direction of migration. Concomitantly, integrins in focal adhesions at the rear of the cell are recycled to the front via a treadmill-like mechanism. Focal adhesions, hemidesmosomes, and podosomes break apart and reform by severing and re-establishing integrin–ECM contacts, under conditions in which cells are motile, such as during development and in wound healing.

Contributions to Cellular Phenotypes

Effects on the Cytoskeleton

By connecting the ECM to the intracellular cytoskeleton, integrins also act as mechanosensors, transmitting information about the physical state of the ECM into the cell and altering cytoskeletal dynamics. Integrin ligation can activate key signaling components, such as the small GTPases Rho, Cdc42, and Rac, which promote cytoskeletal rearrangements leading to the formation of actin stress fibers, filopodia, and lamellipodia, respectively. Within focal adhesions, integrins can activate kinases important for downstream signaling, such as focal adhesion kinase (FAK) and Src tyrosine kinases. Activation of these enzymes results from signals initiated at the integrin cytoplasmic tails. Integrin tails also affect cytoskeletal rearrangements through other mechanisms, e.g., activation of Syk tyrosine kinase through its direct binding to the β3-tail, which promotes Vav1-induced GTP loading of Rac and subsequent lamellipodial formation. Through such mechanisms, integrins regulate cell polarity, migration, shape, and size.

Connections to Intracellular Signaling Pathways

Although integrins themselves do not manifest any catalytic activity, they transmit signals through binding partners such as integrin-associated protein (IAP, CD47), integrin-linked kinase (ILK), and members of the tetraspanin transmembrane protein family. Integrin ligation activates members of the Ras family of GTPases, and can also lead to activation of kinases such as JNK, PAK, and ERK/MAP (microtubule-associated proteins) kinase—the latter two are localized to integrin-rich adhesion sites. These enzymes

can subsequently regulate the expression of genes involved in cell proliferation and differentiation. Furthermore, integrins play a role in the inhibition of detachment-induced apoptosis, called "anoikis," through regulation of the PI3-kinase/Akt signaling pathway.

Integrin Cross Talk

Ligand binding to one subtype of integrins can affect the activation state of another integrin subtype on the same cell, by modulating the ligand-binding affinity and/or avidity of that integrin. For example, outside-in signaling through ligand binding of $\alpha_4\beta_1$ integrin can affect $\alpha_L\beta_2$-dependent lymphocyte adhesion and migration by regulating signaling through $\alpha_L\beta_2$. Furthermore, integrins are involved in cooperative signaling with other non-integrin receptors, such as the Epidermal Growth Factor (EGF) receptor and the T-cell receptor complex.

See Also the Following Articles

Actin-Related Proteins • Desmosomes and Hemidesmosomes • Epidermal Growth Factor Receptor Family • Focal Adhesions • Hematopoetin Receptors • Integrin Signaling • Protein Kinase C Family • Small GTPases

Glossary

cytoplasmic tail Intracellular portion (20–60 amino acids) of integrins involved in signaling.

cytoskeleton Structural network of actin microfilaments, keratin intermediate filaments and tubulin microtubules in mammalian cells.

extracellular matrix (ECM) Dense array of fibrillar proteins, enzymes and other molecules that provides a scaffold for cells and tissues, and contains binding sites for integrins.

focal adhesion Dash-like cell–matrix adhesion site consisting of a cytoplasmic multiprotein complex surrounding a core of clustered integrins.

integrin ligand ECM protein that binds the extracellular head domain of integrins.

MIDAS Metal ion-dependent adhesion site—array of key residues in some integrin head domains which coordinates a divalent cation during ligand binding.

NPxY Conserved sequence in most integrin β-tails that serves as a docking site for signaling molecules.

Further Reading

Beckerle, M. C. (2001). *Frontiers in Molecular Biology: Cell Adhesion*. Oxford University Press, New York.

Hughes, P. E., and Pfaff, M. (1998). Integrin affinity modulation. *Trends Cell Biol.* **8**, 359–364.

Hynes, R. O. (2002). Integrins: Bidirectional, allosteric signaling molecules. *Cell* **110**, 673–687.

Schoenwalder, S. M., and Burridge, K. (1999). Bidirectional signaling between the cytoskeleton and integrins. *Curr. Op. Cell Biol.* **11**, 274–286.

Schwartz, M. A., Schaller, M. D., and Ginsberg, M. H. (1995). Integrins: Emerging paradigms of signal transduction. *Annu. Rev. Cell Biol.* **11**, 549–599.

Biography

Mark H. Ginsberg is a Professor in the Departments of Vascular and Cell Biology at the Scripps Research Institute, La Jolla, California. He was awarded an M.D. summa cum laude from SUNY Downstate Medical Center, and performed his internship, residency, and post-doctoral fellowship at the University of Chicago. He played an important role in the discovery and analysis of integrins, and has authored over 245 scientific publications, largely devoted to integrins. He has served on the editorial boards of many scientific journals and has received numerous awards.

Lawrence E. Goldfinger obtained a B.S. in Biology from Carnegie Mellon University and a Ph.D. in Cell Biology from Northwestern University Medical School. His research focuses on integrin-mediated intracellular signaling and the roles of integrins in cell adhesion, migration, and vascular remodeling.

Interferon Receptors

Christopher P. Elco and Ganes C. Sen
Cleveland Clinic Foundation and Case Western Reserve University, Cleveland, Ohio, USA

Interferons (IFNs) are a family of cytokines, or protein hormones, which modulate the immune response and provide resistance to viral infection. The effects of IFN are mediated through cell surface receptors, which recognize extracellular IFN and activate cellular signaling pathways, ultimately leading to gene induction and repression. IFNs are divided into two classes, type-I and type-II IFNs. There are multiple members of the type-I IFN family, including IFN-α and IFN-β, whereas IFN-γ is the only known type-II IFN. The two types of IFN bind to two distinct receptors and have very different cellular outcomes. Type-I IFN receptors predominantly activate an antiviral, innate immune response. Signaling through type-II IFN receptors, on the other hand, is involved in modulating the adaptive immune response. Both types of receptors share in common the ability to directly and quickly induce new gene transcription through the activation of JAK/STAT signaling pathways.

IFN receptors are classified as type-II cytokine receptors. Both type-I and type-II cytokine receptors have extracellular and intracellular domains connected by a single transmembrane domain. The extracellular domains of cytokine receptors contain a conserved tandem fibronectin type-III (FNIII) motif, which is distinguished by unique cystine pairings at both ends of the domain. Type-II cytokine receptors lack an additional conserved Trp-Ser-X-Trp-Ser motif, found in the extracellular domain of type-I receptors. Ligand binding to the receptor leads to receptor oligomerization and activation of a signaling cascade. In addition to type-I and type-II IFN receptors, the receptors for tissue factor and the cytokine IL-10 belong to this class. The IFN receptors and the IL-10 receptor are composed of two different subunits, both of which are required for proper functioning of the receptors.

IFN-γ Receptors

Expression of IFN-γ and Its Receptor

Expression of the IFN-γ receptor is common to almost all cell types with the exception of mature red blood cells. Two genes, IFN-γR1 and IFN-γR2, encode the receptor components.

The human IFN-γR1 gene is located on the long arm of chromosome 6. Expression of IFNγ-R1 mRNA is not regulated by any known stimuli, but appears to be under standard housekeeping controls. Although the IFN-γ receptor functions on the cell surface, a large intracellular reserve of IFN-γR1 is present in some cells at levels up to 2–4 times the amount of receptor present on the cell surface. This reserve serves to keep the surface level of IFN-γR1 constant.

The human gene for IFN-γR2 is located on chromosome 21. The mouse gene for IFN-γR2 is on chromosome 16. Study of the mouse gene promoter has revealed that it contains binding sites for a number of activated transcription factors, suggesting that unlike IFN-γR1, IFN-γR2 expression can be regulated. Both proteins must be expressed on the cell surface and associate in order for IFN-γ signaling to occur, but there is evidence that some T cells control their responsiveness to IFN-γ by modulating the cell surface expression of IFN-γR2.

Unlike the receptors, IFN-γ is expressed only in response to stimulus by antigen and only in cells of lymphoid origin, in particular, natural killer cells, macrophages, and some T cells. Once synthesized, IFN-γ is secreted and signals as a homodimer.

Receptor Structure

Both IFN-γR1 and IFN-γR2 have extracellular and intracellular domains, along with a single transmembrane domain, common to all type-II cytokine receptors. The sequences of extracellular domains can vary greatly among species causing highly species-specific IFN-γ binding. In contrast, intracellular domains of the IFN-γ receptor subunits are more conserved among species, and can be substituted freely. The intracellular domains mainly serve as a scaffolding structure for the interaction of downstream-signaling proteins and contain no enzymatic activity of their own. The IFN-γR1 is a 90 kDa glycoprotein consisting of 472 amino acid residues. The first 228 residues of the protein comprise the extracellular domain. IFN-γR1 has a 24 amino acid transmembrane domain and an intracellular domain that spans the C terminus from residues 252–472.

IFN-γR2 is a 62 kDa, 315 amino acid residue protein. Both the extracellular and transmembrane domains of IFN-γR2 are comparable in length to those of IFN-γR1. Residues 1–226 form the extracellular domain and 227–250 are the transmembrane domain. At only 65 amino acid residues, the intracellular domain of IFN-γR2 is much smaller than that of IFN-γR1.

The crystal structure of a soluble, truncated version of the extracellular domain of human IFN-γR1 is known. It contains two distinct domains, both consisting of two β-sheets and displaying FBNIII topology. An 11 amino acid linker connects the two domains. Binding of ligand is accomplished through the interaction of both domains.

Ligand Binding

IFN-γ binds to the extracellular domain of IFN-γR1 only. In the absence of IFN-γR1, IFN-γR2 cannot bind IFN-γ. However, the presence of IFN-γR2 does strengthen the association of IFN-γ and IFN-γR1 threefold, though the two subunits of the receptor do not associate in the absence of IFN-γ. Further, IFN-γR2 is vital for IFN-γ signal transduction, and for this a highly specific interaction must occur between the extracellular domains of IFN-γR1 and IFN-γR2.

An active signaling complex consists of an IFN-γ homodimer and two chains each of IFN-γR1 and IFN-γR2. Each subunit of the IFN-γ homodimer binds an IFN-γR1 chain, which in turn binds IFN-γR2. In the absence of IFN-γR2, IFN-γR1 molecules bound to an IFN-γ homodimer are separated by over 27Å and, therefore, are unable to interact with each other.

Signal Transduction

Janus tyrosine kinase (Jak)/Signal transducer and activator of transcription (STAT) signaling is carried out through a series of tyrosine phosphorylation events, at the receptor, mediated by members of the Jak family. Signaling culminates with the activation and nuclear translocation of STAT proteins, where they function to induce new mRNA synthesis. The IFN receptors serve as docking sites for both Jaks and STATs. With the formation of IFN-receptor complex, Jak proteins are brought into close proximity, which enables them to transphosphorylate and thereby activate each other. Independent of IFN binding to the extracellular domain of the receptor, the Jak proteins Jak1 and Jak2 associate with the intracellular domains of IFN-γR1 and IFN-γR2, respectively (Figure 1A). Upon the formation of a receptor complex with IFN-γ, Jak2 transphosphorylates Jak1 (Figure 1B). Jak1 then transphosphorylates Jak2 and either Jak phosphorylates IFN-γR1 at Tyr440 (Figure 1C). Phosphorylation of IFN-γR1 in turn leads to the recruitment and binding of a STAT1 protein to each IFN-γR1 chain. Bound STAT1 proteins are phosphorylated by the Jaks, disassociate from the receptor and form a homodimer (Figure 1D). This complex then translocates to the nucleus where it can induce the transcription of many genes.

STAT-dependent signaling is the best-studied IFN-γ signaling pathway, but there is evidence that STAT1-independent signaling pathways can also be activated by IFN-γ through IFN-γR1 and IFN-γR2. In cell lines lacking STAT1, activation of the IFN-γ receptor by IFN still causes the induction of a set of genes.

In order for signal transduction to occur normally, two regions of the intracellular domain of IFN-γR1 and one region of the intracellular domain of IFN-γR2 are required. The association of Jak1 with IFN-γR1 requires the amino acid residues from 266 to 269, LPKS, located in the membrane proximal region. Distal to the membrane at amino acids 440–444, YDKPH comprise the STAT1-binding site. Within the intracellular domain of IFN-γR2 a proline-rich 12 amino acid sequence P^{263}PSIPLQIEEYL^{274} is needed for Jak2 binding. Disruption of any of these three regions abolishes normal signaling.

Upon the binding of IFN-γ, the receptor complex is internalized. Internalized receptor–ligand complex is trafficked to an acidic compartment. IFN-γ disassociates from the receptor, goes to the lysosome, and is degraded, whereas the IFN-γR1 subunit of the receptor is recycled into the cytoplasmic reserve. Mutation of either Leu 270 or Ile 271 inhibits the internalization of the receptor, leading to the accumulation of IFN-γ ligand–receptor complexes on the surface of the cell.

Effects of Signaling Through the IFN-γ Receptor

IFN-γ can be thought of as the antimicrobial interferon. Signaling through type-II IFN receptors has pro-inflammatory effects and antibacterial effects. Mice lacking type-II IFN receptors have a much higher susceptibility to infection by bacteria and intracellular microbes. The antibacterial effects of IFN-γ are mediated through multiple pathways. IFN-γ leads to the activation of neutrophils, natural killer cells and in particular macrophages by increasing their ability to recognize, kill, and digest foreign material or microbes. In T cells, IFN-γ promotes the maturation of cytotoxic CD8 + T cells, as well as the T_H1 subset of CD4 + T cells. IFN-γ also enhances the humoral immune response by up-regulating genes such as class-I and class-II major histocompatibility complex (MHC) molecules, along with cell surface adhesion molecules. Together these effects serve to augment the adaptive immune response to pathogens.

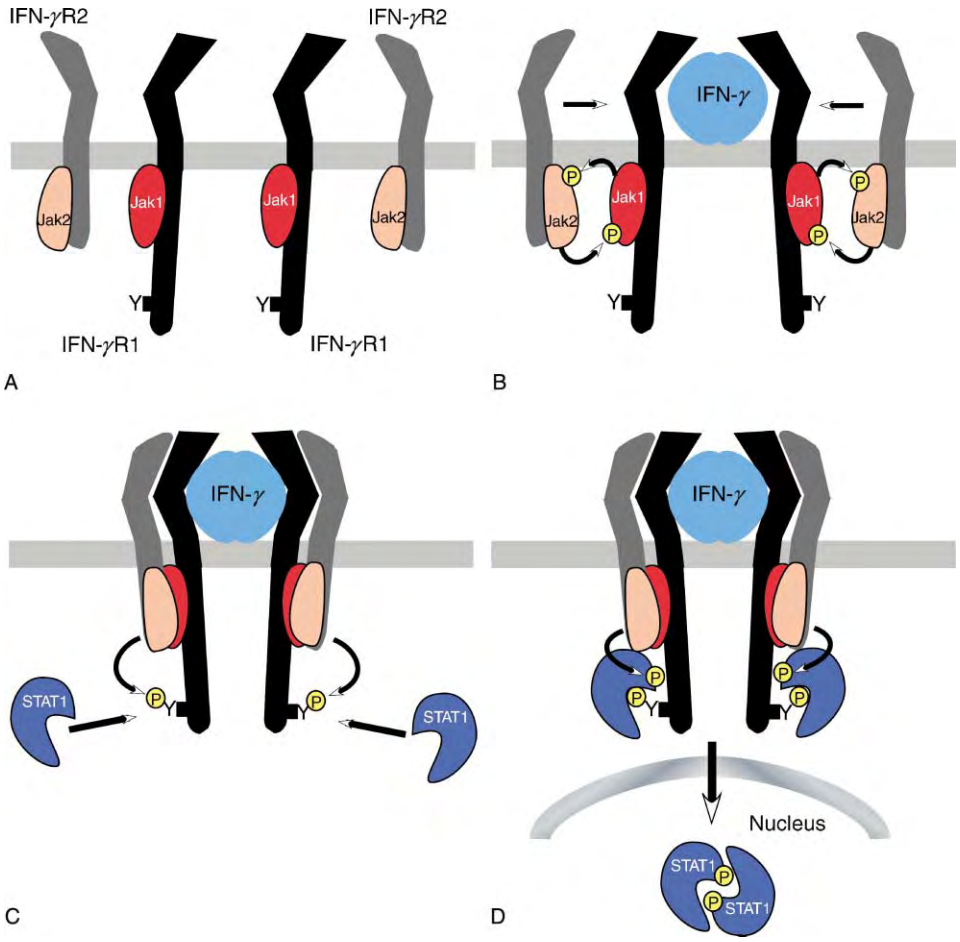

FIGURE 1 Kinetics of the IFN-γ signaling cascade ((A)–(D)), showing the proteins and tyrosine phosphorylation events involved in signal transduction by the IFN-γ receptor.

As would be expected, loss of the IFN-γ receptor genes leads to increased susceptibility to infection by microbes. Mice lacking the IFN-γ receptor genes are affected much more severely by infections with lysteria and mycobacteria. Otherwise, the receptor knockout mice display no developmental defects, have normal T cell responses and are no more susceptible to most viral infections than wild-type mice. These effects are seen in humans as well. Children susceptible to infections with weakly pathogenic mycobacteria species such as *M. avium* were found to have mutations in the IFN-γ receptor genes. The susceptibility was mycobacteria specific, as these children did not have increased difficulties fighting off infections from other bacteria, viruses, or fungi.

An unexpected consequence of IFN-γ receptor loss is an increased susceptibility to tumor development. IFN-γ receptor knockout mice develop tumors at a much higher frequency than their IFN-γ responsive counterparts. Compared to IFN-γ responsive tumors, IFN-γ unresponsive tumors are less prone to rejection when transplanted into immunocompetent wild-type mice. Studies of human carcinomas have revealed that loss of responsiveness to IFN-γ is not uncommon. Taken together, these facts suggest that loss of IFN-γ signaling enables tumors to evade the normal surveillance mechanisms of the immune system. Normal expression of the IFN-γ receptor proteins is therefore important in preventing the development of cancer.

The IFN-α/β Receptor

Expression of IFN-α/β and Their Receptor

Like the IFN-γ receptor, the IFN-α/β receptor is composed of two polypeptides encoded by two genes. Both IFN-α/β receptor genes, IFN-αR1 and IFN-αR2, are clustered on human chromosome 21 (or chromosome 16 in mice) with IFN-γR2 and IL-10R2 (also a member of the class-II cytokine family). Expression of

the receptor proteins is thought to be ubiquitous, but it can also be modulated.

The gene encoding IFN-αR1 is 32 kb and contains 11 exons. The second through ninth exons encode the extracellular domain of the protein, while the last two exons encode the transmembrane and intracellular domains.

In the case of IFN-αR2, there are three splice variants of the protein encoded by a nine-exon gene. The 515 aa, IFN-αR2c, encoded by a 4.5 kb mRNA, is the only functional splice variant and has an extended intracellular domain compared to the other two variants. IFN-αR2b has a shorter cytoplasmic domain and cannot signal through the Jak-STAT pathway, and IFN-αR2a is a secreted form of the extracellular domain of the receptor only. Studies in mice, which express only homologues of the 2a and 2c splice variants, have shown that the 2a variant is expressed in greater abundance in most tissues, except that of lymphoid origin where the two isoforms are expressed in a 1:1 ratio. It is not clear if the truncated splice variants play a functional role in modulating responsiveness to IFN; however, IFN-αR2a can act as a dominant-negative inhibitor for type-I IFN signaling.

There are many members of the type-I IFN family. The most well-known are IFN-α and IFN-β, which share little structural homology with each other. IFN-β was first isolated from fibroblasts, while IFN-α was discovered in lymphoid cells. Within the IFN-α family alone, there are over 13 subtypes encoded by different genes. The proteins they synthesize can vary in size from 15 to 21 kDa, and contain different degrees of posttranslational modification. Despite the apparent diversity in type-I IFNs, they all bind to the same receptor composed of IFN-αR1 and IFN-αR2c. There is, however, variation in the type and degree of response generated.

Receptor Structure

The extracellular domain of IFN-αR1 spans the first 409 aa residues of the protein, and the intracellular domain contains the final 100 residues from amino acid 431 to 530. IFN-αR1 is unique among class-II cytokine receptors in that its extracellular domain contains four tandem fibronectin type-III domains, compared to the two contained by other IFN receptor proteins. When compared to IFN-αR1, the 217 amino acid extracellular domain of IFN-αR2 is relatively short. In contrast, the intracellular domain of IFN-αR2c is much longer than that of IFN-αR1, covering the C-terminal 251 amino acids. There is not nearly as much known about the structure of IFN-α/β receptors as IFN-γ receptors.

Ligand Binding

Both IFN-αR1 and IFN-αR2 bind type-I IFNs, cooperatively. This is different from the IFN-γ receptor where only IFN-γR1 had ligand-binding activity. Also, the signaling complex for the α/β-receptor consists of a single pair of receptor proteins as opposed to the two pairs that compose the γ-receptor complex.

Another feature of the IFN-α/β receptors is their ability to bind multiple ligands. Unlike IFN-γ receptors, which only bind IFN-γ, the α/β-receptors can bind all subspecies of IFN-α, along with IFN-β and other type-I IFN species. Ligand-receptor interactions for the different classes of IFN are unique. By mutating residues in the extracellular portion of either receptor protein it is possible to generate mutants, which bind and respond to IFN-β, but not all IFN-α species. The exact structural mechanism for how the differences in ligand binding translate into differences in downstream signaling effects is still unknown.

Signal Transduction

Signaling again occurs principally through the Jak-STAT pathway, but involves different members of the two families of proteins. Independent of ligand binding, Tyk2 a member of the Jak family associates with IFN-αR1, while Jak1, STAT1, and STAT2 associate with IFN-αR2c (Figure 2A). The binding of ligand brings both receptor subunits into close proximity with each other. This allows Jak1 to transphosphorylate Tyk2 (Figure 2B). Tyk2 in turn phosphorylates Jak1 along with Tyr466 of IFN-αR1. The phosphorylation of Tyr466 of IFN-αR1 allows STAT2 to bind to it instead of IFN-αR2c. The IFN-αR1-bound STAT2 is phosphorylated on Tyr690 (Figure 2C). This leads to the STAT2-dependent phosphorylation of STAT1 on Tyr701. STAT1 and STAT2 dissociate from the receptor and form a heterodimer. The STAT1-STAT2 dimer associates with p48, or IRF9, a member of the interferon regulatory factor family, to form the transcription complex interferon-stimulated gene factor 3 (ISGF3). ISGF3 translocates to the nucleus, binds to interferon-stimulated regulatory element (ISRE) sequences present in the promoters of IFN-stimulated genes (ISGs) and induces transcription.

The binding sites for Jak and STAT proteins on IFN-α/β receptors have not been characterized as well as their IFN-γ receptor counterparts. Tyr 466 of IFN-αR1 along with surrounding residues is needed for STAT2 binding to the subunit. In the case of IFN-αR2c, the constitutive STAT2 binding site has been mapped to between amino acids 404 and 462. Further, multiple tyrosine residues throughout the intracellular domain of the IFN-αR2c are required for full signaling activation, but their precise role is still not fully known.

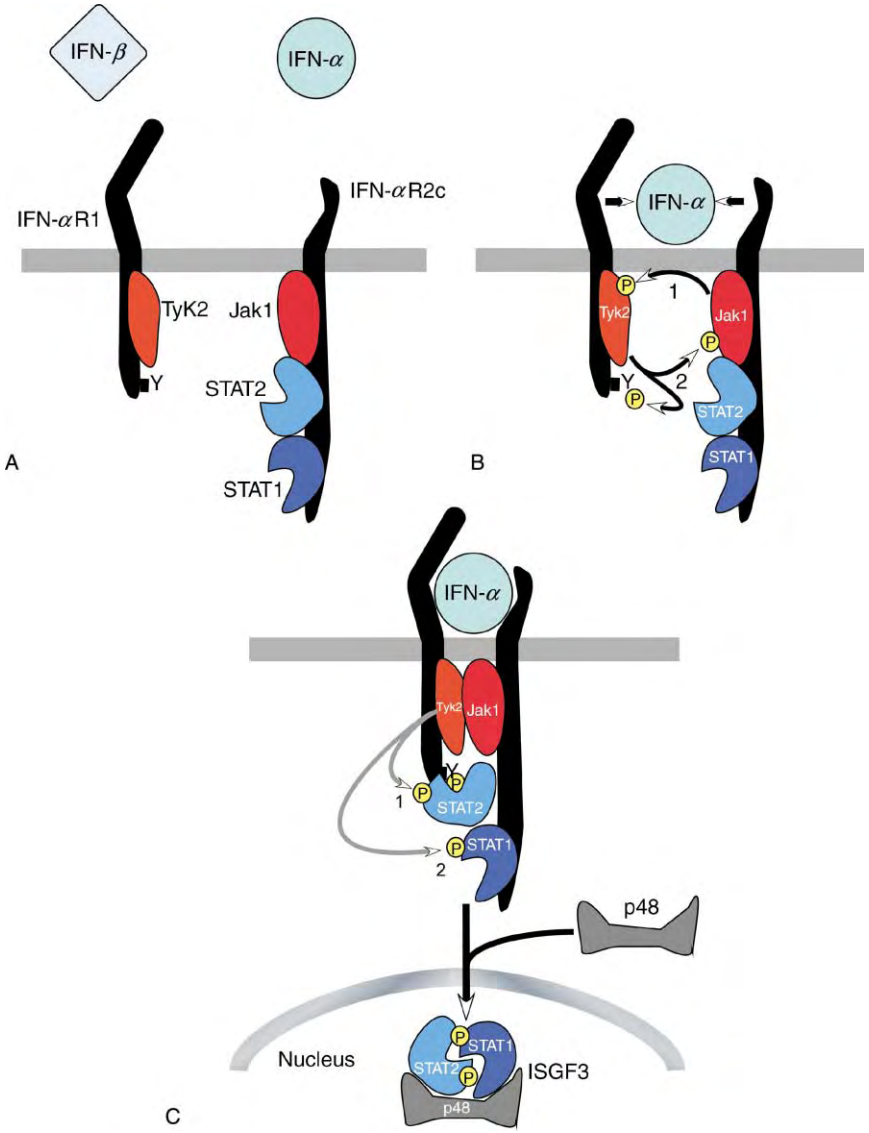

FIGURE 2 Signal transduction through the IFN-α/β receptor, showing the protein–protein associations and tyrosine phosphorylation steps involved. Numbers indicate the order in which tyrosine phosphorylation events (P) occur.

Effects of Signaling Through the IFN-α/β Receptor

Type-I IFNs are considered to be antiviral interferons. They provide a vital signal for cells to mount a state of antiviral defense. The antiviral state is achieved through the diverse actions of newly translated proteins made in response to the induction of hundreds of interferon stimulated genes by IFN signaling. ISGs encode proteins that have effects ranging from cell cycle arrest to the inhibition of translation and RNA degradation. Together these effects serve to make the cell a very unfavorable environment for viral replication. Not surprisingly, cell lines and mice defective in type-I IFN receptors are much more susceptible to viral infection.

See Also the Following Articles

Cytokines • JAK-STAT Signaling Paradigm

Glossary

cytokine receptor A cell surface protein that binds to a distinct extracellular polypeptide hormone and induces a response within the cell.

interferon Cytokines involved in regulating antiviral and immune responses.

kinase An enzyme that phosphorylates (adds a phosphate group to) a protein.

signal transduction The conversion of an extracellular signal to an intracellular response.

transphosphorylation The reaction by which one protein causes the addition of a phosphate group to another protein.

Further Reading

Abbas, A. K., Lichtman, A. H., and Pober, J. S. (1997). Cytokines. In *Cellular and Molecular Immunolgy*, 3rd edition, pp. 250–277. W.B. Saunders, Philadelphia.

Bach, E. A., Aguet, M., and Schreiber, R. D. (1997). The IFNγ receptor: A paradigm for cytokine receptor signaling. *Ann. Rev. Immunol.* **15**, 563–591.

Ikeda, H., Old, L. J., and Schreiber, R. D. (2002). The roles of IFNγ in protection against tumor development and cancer immunoediting. *Cytokine Growth Fact. Rev.* **13**, 95–109.

Mogensen, K. E., Lewerenz, M., Reboul, J., Lutfalla, G., and Uze, G. (1999). The type I interferon receptor: Structure, function, and evolution of a family business. *J. Interferon Cytokine Res.* **19**, 1069–1098.

Sen, G. C. (2001). Viruses and interferons. *Annu. Rev. Microbiol.* **55**, 255–281.

Stark, G. R., Kerr, I. M., Williams, B. R., Silverman, R. H., and Schreiber, R. D. (1998). How cells respond to interferons. *Ann. Rev. Biochem.* **68**, 227–264.

Biography

Ganes C. Sen is a member of the Professional Staff in the Department of Molecular Biology at the Cleveland Clinic Foundation, and Professor of Physiology and Biophysics, and Biochemistry at the Case Western Reserve School of Medicine. His principal research interests are in the role of the interferon system in host–virus interactions and in the tissue-specific functions of the angiotensin-converting enzyme. He received his Ph.D. from McMaster University, Canada and his postdoctoral training at Yale University. His research has made seminal contributions to the understanding of the modes of induction and the functions of many interferon-inducible genes.

Intermediate Filament Linker Proteins: Plectin and BPAG1

Peter Fuchs and Gerhard Wiche
University of Vienna, Vienna, Austria

Plectin and bullous pemphigoid antigen 1 (BPAG1) are among the best-characterized members of an emerging family of sequence-related cytoskeletal linker proteins (cytolinkers), referred to as plakins or plakin protein family. Originally, both proteins were identified on the basis of their association with intermediate filaments (IFs) or IF-anchoring structures, such as adhesive cell junctions. By anchoring IFs to themselves, to junctional complexes, and to the other major cytoskeletal networks of actin filaments and microtubules, both cytolinkers play crucial roles in maintaining cell and tissue integrity, and orchestrating dynamic changes in cytoarchitecture and cell shape. Plectin and BPAG1 are encoded by large genes that give rise to many different isoforms, each with unique functions and varying capacities to link different cytoskeletal systems. Due to their multi-domain structure and enormous size (300–800 kDa) these proteins bridge large distances and can serve as scaffolding platforms for the assembly, positioning, and regulation of complex protein machineries required for signaling and motor protein-based trafficking. Both proteins are involved in diseases affecting the skin, neuronal tissues, and skeletal as well as cardiac muscle.

Plectin

The first identification of plectin as an interaction partner of IFs was made in cultured cells. In fact, the choice of its name (from $\pi\lambda\varepsilon\kappa\tau\eta$, the ancient Greek word for network or meshwork) was motivated by its microscopic visualization as a dense cytoplasmic network array in cells.

Gene Locus and Isoform Diversity

In humans, the plectin gene is located on chromosome 8 (position q24), the murine orthologue on chromosome 15 (position 44.0 cM). The exon–intron organization of the plectin gene has been determined for man, mouse, and rat. Several plectin isoforms could be identified differing in their amino termini. In the case of the mouse gene alternative splicing of 11 different first exons into one common exon (exon 2) gives rise to a multiplicity of plectin variants (Figure 1). Additional alternative splicing in the 5′ area within the region coding for the actin-binding domain (ABD) increases the number of possible plectin isoforms. In rat tissues, plectin transcript variants were identified that lack a single large exon encoding almost the entire α-helical coiled coil rod domain of the molecule. Plectin isoforms are named after their alternative starting exons (plectin 1, plectin 1a, …, plectin 1j); however, the exact composition of the subsequent exons transcribed in each of the very large plectin mRNAs, especially in their very complex 5′ part, has not yet been determined with absolute certainty.

Expression and Subcellular Localization

With the exception of certain neurons, plectin has been found to be expressed in all mammalian cells investigated so far. It decorates different types of IFs, shows codistribution with their plasma membrane attachment sites, and colocalizes with actin structures, primarily in peripheral areas of cells. It is associated with Z-lines of striated muscle, dense plaques of smooth muscle, intercalated discs of cardiac muscle, the basal cell surface membrane (specifically hemidesmosomes) of keratinocytes, desmosomes of epithelial cells, and focal adhesion contact sites of cells in culture. Plectin has also been identified in cell layers separating tissues from fluid-filled cavities like liver bile canaliculi, gut villi, kidney glomeruli, and endothelial cells of blood vessels. The expression patterns of plectin isoforms can vary considerably among different tissues and cell types. The quantitation of mRNAs isolated from different organs of the mouse revealed low expression levels of plectin isoforms 1, 1e, 1g, 1h, 1i, and 1j, intermediate levels of plectin 1f, and high levels of plectin 1a, 1b, 1c, and 1d. In the majority of these preparations all plectin isoforms could be identified, except for plectin 1d, found predominantly in skeletal muscle and heart, and plectin 1c, which is more or less restricted to neuronal tissues

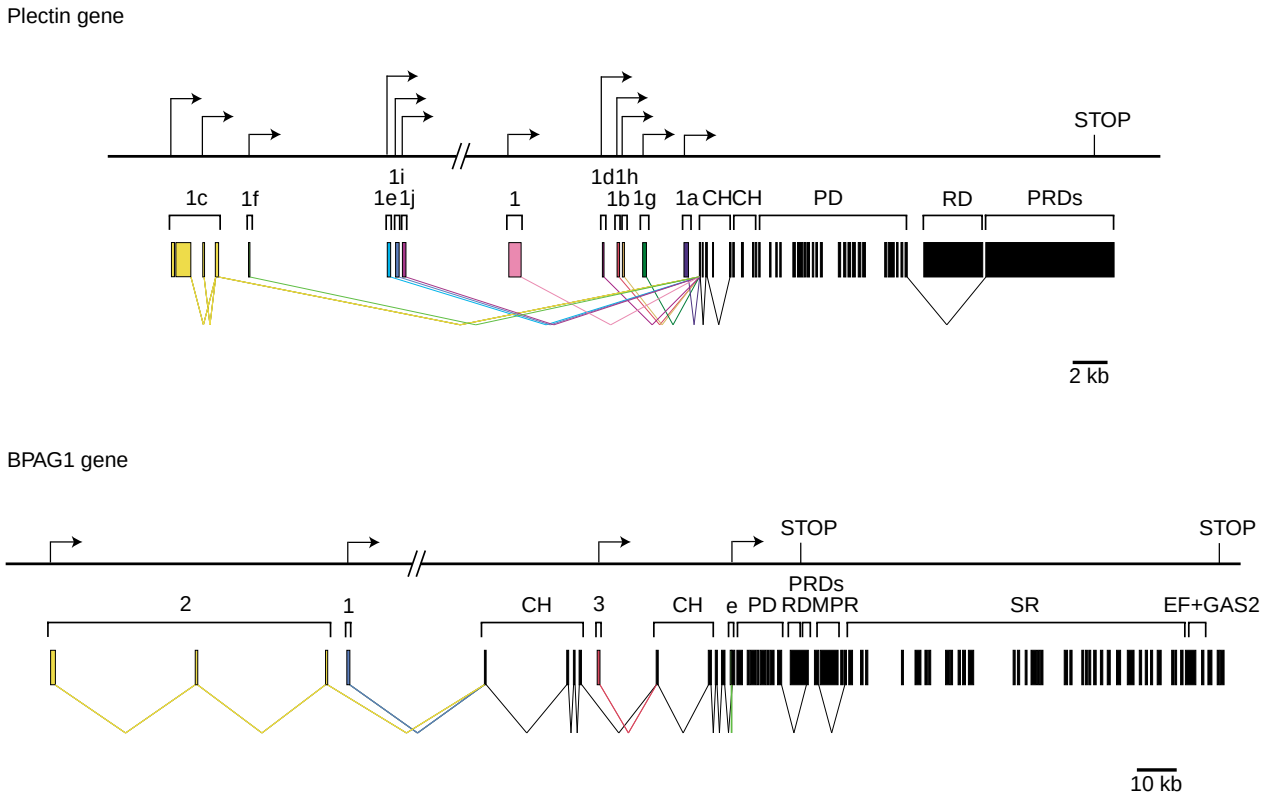

FIGURE 1 Plectin and BPAG1 gene structure and alternative splicing. Schematics shown represent murine plectin and human BPAG1 species (BPAG1, modified from Röper, K., Gregory, S. L., and Brown, N. H. (2002). The "Spectraplakins": cytoskeletal giants with characteristics of both spectrin and plakin families, *J. Cell Sci.* **115**, 4215–4225, with permission of The Company of Biologists Ltd). Alternative transcriptional start sites (arrows) and stop codons are indicated. Alternative starting exons are shown as colored boxes, other exons as black boxes. Splicing is indicated by bended lines for alternative starting exons or when exons are bypassed. Alternative single first exons and combinations of starting exons are designated with numbers and/or small letters, protein domains with capital letters. CH, calponin-homology domains forming the ABD; PD, plakin domain; RD, coiled-coil rod domain; PRDs, plakin repeat domains; MPR, modules of plectin repeats; SR, spectrin repeats; EF + GAS2, EF-hand domains and GAS2 domain. Note that in the case of plectin isoform 1c two transcriptional start sites at the beginning of non-coding exons are used with only one 1c-specific coding exon in front of the subsequent exon common to all plectin isoforms.

and skin. In cultured keratinocytes the two major isoforms expressed, plectin 1a and plectin 1c, were found differentially distributed to hemidesmosomes and to microtubules.

Structural Properties

Considering just full-length versions of the protein, plectin has a molecular mass of 506–535 kDa depending on its first coding exon (Figure 2). The molecule has been visualized by electron microscopy as a dumbbell-shaped structure composed of a central rod domain flanked by two large globular domains. In these structures two plectin polypeptide chains most likely are arranged in parallel forming an α-helical coiled-coil central rod. The so-called plakin domain, the defining feature of plakin protein family members, and an ABD of the "classical" CH1-CH2-type (i.e., containing two calponin-homology domains) reside within the N-terminal part of each chain, preceding the rod-forming segment. The C-terminal part of plectin comprises six tandemly arranged so-called plakin-repeat domains, each containing a globular core structure, or module, and a surface-exposed linker domain. Plectin modules, similar to those of other plakins, consist of four complete and one incomplete tandem copies of a 38 residues-long sequence motif, referred to in databases as plectin repeat. Forming a β-hairpin followed by two antiparallel α-helices, the plectin repeat structurally resembles a motif called ankyrin repeat, which is found in a large number of proteins. It should be noted that plectin isoforms that are encoded by transcripts starting with non-coding first exons, such as plectin 1h, 1i, and 1j, contain only truncated versions of plectin's ABD (Figure 2).

Molecular Interactions

Plectin binds to cytoplasmic IFs of different types via direct interaction with their subunit proteins, including vimentin, desmin, GFAP, neurofilament proteins, and cytokeratins; binding has also been demonstrated to

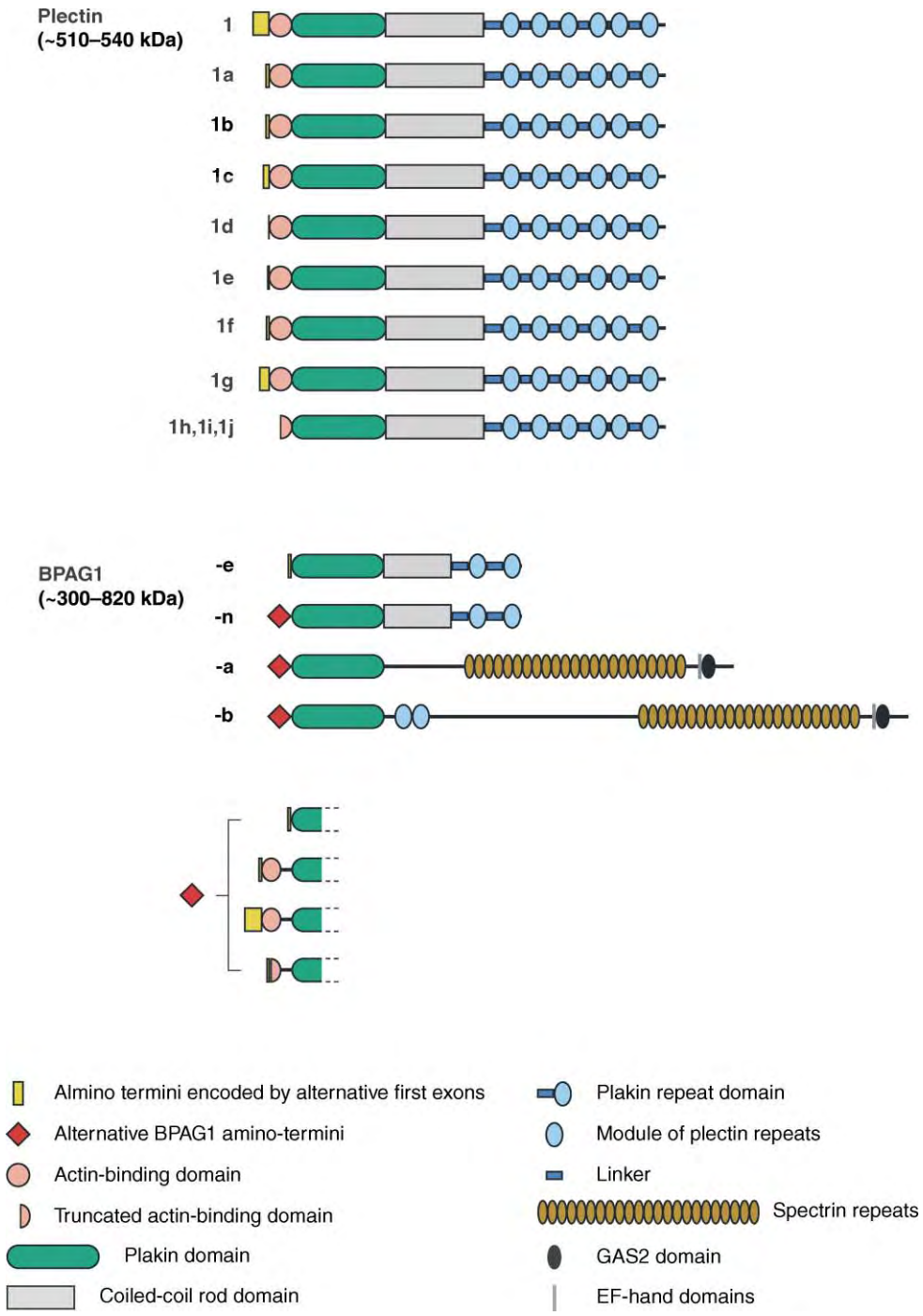

FIGURE 2 Schematic diagram of plectin and BPAG1 protein isoforms. Designation of isoforms (e.g., plectin 1a, BPAG1-e) and approximate molecular weight are given (drawings are at scale). The diamond (red) in front of BPAG1-n, -a, and -b stands for the four possible alternative amino termini shown underneath; in the case of BPAG1-n one of these possibilities is already presented as BPAG1-e. Note that in some variants of both proteins the ABD, typically consisting of two calponin-homology domains, can be truncated due to alternative splicing, resulting in only one calponin-homology domain to be present in certain BPAG1 isoforms. The plakin domain is an interaction domain organized into α-helical bundles showing structural similarities to spectrin repeats. The plakin repeat domains each contain a globular module and a linker domain. Modules consist of four complete and one incomplete plectin repeats forming a complex globular domain. Linkers are considered as surface-exposed interaction domains, such as the IF binding site of plectin. The GAS2 domain was named after the growth-arrest-specific protein 2 and is suggested to mediate microtubule binding.

the nuclear IF protein lamin B. The major binding site for IF subunit proteins has been mapped to a short sequence in the linker segment between modules 5 and 6 in plectin's C-terminal domain. The ABD in plectin's N-terminal globular domain is fully functional, as demonstrated *in vitro* and *in vivo*. Whether this is true also for plectin isoforms expressing only truncated versions of this domain remains to be shown. In addition to its actin-binding function, the ABD serves as docking site for the β4 subunit protein of the hemidesmosomal $\alpha 6\beta 4$ integrin receptor and for the signaling molecule PIP2. Furthermore, it dimerizes by self-interaction. Additional integrin β4 binding sites have been ascribed to plectin's plakin domain and to its C-terminal globular domain. The plakin domain of plectin harbors also a binding site for BPAG2/BP180, another hemidesmosomal protein. There is broad consent about plectin having the capacity to bind to microtubules. In fact, a direct interaction of the protein with microtubule-associated proteins (MAPs) has been demonstrated, although the molecular domain(s) involved need to be identified. Plectin also interacts with the subplasma membrane skeleton proteins α-spectrin and fodrin and with the desmosomal protein desmoplakin. In line with the emerging concept that cytolinkers act as a platform for the assembly of complex protein machineries required for intracellular signaling and trafficking, plectin has been shown to be a target for a variety of serine/threonine kinases, including mitotic $p34^{cdc2}$ kinase, and to interact, via its plakin domain, with the non-receptor tyrosine kinase Fer. The question whether the isoform-specific protein sequences located at the aminoterminus of plectin variants can select for distinct binding partners or influence the affinities of other binding sites remains to be answered.

Plectin Deficiency in Man and Mouse

In humans, mutations in the plectin gene lead to the autosomal recessive disease epidermolysis bullosa simplex with muscular dystrophy (EBS-MD). Patients affected suffer from severe skin blistering and late-onset muscular dystrophy. In all the cases described, plectin expression is missing or substantially attenuated. The autosomal-dominant disease epidermolysis bullosa simplex Ogna (EBS-O), first described for a family from the Norwegian municipality of Ogna, is due to a site-specific mutation causing the exchange of a single amino acid residue (W to R) in plectin's long-rod domain. In this case, patients suffer from generalized skin fragility but show no muscular symptoms. Disruption of the plectin gene in the mouse using knockout strategies results in a phenotype similar to EBS-MD, except that plectin knockout mice die 2–3 days after birth, probably due to their severe skin blistering. In addition, already at this early stage they show an increase in the number of necrotic fibers and abnormal Z-lines in skeletal muscle.

Bullous Pemphigoid Antigen 1

Bullous pemphigoid antigen 1 (BPAG1) was originally identified in a search for antigens with immunoreactivity to autoantibodies of patients suffering from bullous pemphigoid, an autoimmune subepidermal skin blistering disease. The murine orthologue is also called dystonin, in consideration of the fact that mutations in this gene cause sensory neuron degeneration in the mouse mutant *dystonia musculorum* (*dt*).

Gene Locus and Isoform Diversity

The BPAG1 gene is localized in humans on chromosome 6 at position p12-p11. In mice, where in genebanks it is referred to as dystonin, it has been mapped to chromosome 1 at position 16.5 cM. In both species, multiple exons in the BPAG1 gene are the basis of several protein isoforms generated by alternative splicing of transcripts. Amongst many possibly expressed isoforms, four major variants (BPAG1-a, -b, -e, and -n) were specified, showing clear differences in length and structure (Figure 1). It should be noted, however, that the two large isoforms BPAG1-a and -b were identified only recently, and that the missing level of awareness concerning these proteins may have led to some incorrect conclusions regarding BPAG1-e and -n in the older literature. Moreover, similar to plectin, the exact composition of exons transcribed in some of the very large BPAG1 mRNAs has yet to be defined.

Expression and Subcellular Localization

The major isoform of the BPAG1 gene, BPAG1-e, is expressed in basal epithelial cells where it is primarily located at hemidesmosomes. BPAG1-a is expressed at high levels in the nervous system, especially in dorsal root ganglia and spinal cord, while BPAG1-n/dystonin, previously thought to be the dominant isoform in this tissue, seems to be minor compared to BPAG1-a. The BPAG1-b isoform has been found in developing mouse embryos to be restricted to heart, skeletal muscle, and bone cartilage of the vertebrae.

Structural Properties

The molecular mass of the BPAG1 isoforms characterized to date is 302 kDa for BPAG1-e, 344 kDa for BPAG1-n, 615 kDa for BPAG1-a, and 824 kDa for BPAG1-b (Figure 2). All four isoforms show clear structural divergence. BPAG1-e contains a coiled-coil

rod domain flanked by an amino-terminal plakin domain and a carboxy-terminal region comprising two plakin-repeat domains. BPAG1-n is similar to BPAG1-e, but contains an additional amino-terminal ABD of the CH1-CH2-type. It is truncated in one variant, however, and contains only one calponin-homology domain. BPAG1-a, starting with an ABD followed by a plakin domain, resembles BPAG1-n at its amino terminus, but differs regarding the rest of the molecule. Its rod domain consists of 23 spectrin repeats and its carboxy-terminal domain contains EF-hand Ca^{2+}-binding motifs followed by a region including the so-called GAS2 domain. BPAG1-b comprises structural features similar to BPAG1-a, except for an additional pair of closely adjoining plectin repeat modules located between the plakin domain and the spectrin repeats.

Molecular Interactions

The large size and the structural diversity of BPAG1 isoforms suggest not only a variety of interaction partners but also different sets of binding partners for each isoform. Via the CH1-CH2-type ABD at their amino-terminal ends, BPAG1 isoforms can associate with filamentous actin. However, one of the BPAG1-n isoforms of BPAG1, which due to alternative splicing within the ABD contains only one of the two calponin-homology domains, lacks this ability (Figure 2). This truncation has been suggested to activate a microtubule-binding site located within the plakin domain of BPAG1 that otherwise remains cryptic. Since the tail regions of BPAG1-a and -b contain a GAS2-related domain, suggested to be involved in microtubule binding, it has been proposed that these BPAG1 variants possess an alternative microtubule-binding domain close to their carboxy terminus. The location of IF-binding sites within the carboxy-terminal plakin-repeat domains of BPAG1-e and -n has been confirmed for keratin and neuronal IFs. Additional binding partners of BPAG1's plakin domain are BPAG2 (*alias* BP180 or type XVII collagen), a transmembrane protein found in hemidesmosomes, and ERBIN, a specific Erb-B2 tyrosine kinase receptor-binding protein. Whether the carboxy-terminal Ca^{2+}-binding motifs of BPAG1-a and -b are functional remains to be shown.

BPAG1 Deficiency in Mouse

In mice, deletions in the BPAG1 gene cause an autosomal recessive neuropathy called *dystonia musculorum* (*dt*). At the age of 1–2 weeks homozygous *dt* mice display progressive loss of limb coordination caused by degeneration of sensory neurons. Dorsal root ganglia axons exhibit disorganization of neuronal IFs and microtubule networks accompanied by abnormal axonal myelination and axonal swelling(s). It has been suggested that this axonal swelling results from defective axonal transport caused by microtubule disorganization. In addition, defects in the functions of Schwann cells and muscle have been reported for these mice. Not all *dt* mouse strains, however, lack the BPAG1-e isoform. Independent of the *dt* mice most of which carry spontaneously arisen BPAG1 mutations, a BPAG1-defective mouse strain was generated using gene targeting techniques. This mutation eliminates the exons encoding the plakin domain of BPAG1 (common to all four isoforms) and therefore is considered as null allele. Besides the phenotype already described for *dt* mice, these knockout mice show fragility of skin upon mechanical stress. Based on these findings it is assumed that BPAG1-e is responsible for the observed skin abnormalities, the absence of BPAG1-a accounts for the neuronal deficits and the lack of BPAG1-b could be the reason for muscle defects. No known human disease has been linked to mutations in the BPAG1 gene to date. The role of autoantibodies against BPAG1 in patients suffering from bullous pemphigoid remains obscure.

See Also the Following Articles

Actin-Related Proteins • Intermediate Filaments • Keratins and the Skin • Microtubule-Associated Proteins

Glossary

alternative splicing Mechanism to create different proteins (protein isoforms) from the same mRNA transcript by splice events using different exons or exon combinations.

cytoskeleton Network of protein filaments in eukaryotic cells that determines and influences cell shape and enables movement. Main components are actin filaments, microtubules, and intermediate filaments.

knock-out mouse Mutated mouse line generated by the use of embryonic stem (ES)-cell technology in combination with genetic methods. Knock-out mice normally harbor one or more defined mutations in genes leading to inactivation of the gene product.

plakin protein family The plakin protein family, also referred to as the plakins, to date comprises plectin, BPAG1, desmoplakin, envoplakin, periplakin, and epiplakin. Plakins are structurally and functionally related proteins connecting cytoskeletal elements to each other and to the plasma membrane. Common to all family members is the presence of at least one of two structurally highly conserved protein domains, the so-called plakin domain and the PRD. An alternative designation suggested for plakins, i.e., cytolinkers (an abbreviation for cytoskeletal linker protein), is now being used to more broadly specify proteins with functions similar to those of plakins independently of sequence homology.

protein isoforms Variant forms of protein products stemming from a single gene brought about by, for example, alternative splicing.

Further Reading

Coulombe, P. A. (2002). A new fold in an old story: Attachment of intermediate filaments to desmosomes. *Nat. Struct. Biol.* **9**, 560–562.

Fuchs, E., and Karakesisoglou, I. (2001). Bridging cytoskeletal intersections. *Genes Develop.* **15**, 1–14.

Janda, L., Damborsky, J., Rezniczek, G. A., and Wiche, G. (2001). Plectin repeats and modules: Strategic cysteines and their presumed impact on cytolinker functions. *BioEssays* **23**, 1064–1069.

Leung, C. L., Green, K. J., and Liem, R. K. (2002). Plakins: A family of versatile cytolinker proteins. *Trends Cell Biol.* **12**, 37–45.

Röper, K., Gregory, S. L., and Brown, N. H. (2002). The "Spectraplakins": Cytoskeletal giants with characteristics of both spectrin and plakin families. *J. Cell Sci.* **115**, 4215–4225.

Steinböck, F., and Wiche, G. (1999). Plectin: A cytolinker by design. *Biolog. Chem.* **380**, 151–158.

Wiche, G. (1998). Role of plectin in cytoskeleton organization and dynamics. *J. Cell Sci.* **111**, 2477–2486.

Biography

Gerhard Wiche is a Professor and Chair of the Department of Biochemistry and Molecular Cell Biology at the University of Vienna, in Vienna, Austria. His principal research interest is in the mammalian cytoskeleton and its role in cellular morphogenesis, signaling and disease. He holds a Ph.D. from the University of Vienna Medical School. He received his postdoctoral training at the former Roche Institute of Molecular Biology in Nutley, New Jersey, and at the University of California, Berkeley. He has authored many papers on cytolinker proteins, including key publications on plectin, such as first identification, cloning and sequencing, identification of human mutations, and gene ablation in mice.

Peter Fuchs is a Senior Postdoctoral Fellow in G.W.'s laboratory at the University of Vienna.

Intermediate Filaments

Kelsie M. Bernot and Pierre A. Coulombe
The Johns Hopkins University School of Medicine, Baltimore, Maryland, USA

Intermediate filaments (IFs) are intracellular fibrous polymers that became a prominent constituent of the cytoskeleton coinciding with the appearance of multicellular life. They are readily distinguishable from actin microfilaments (6–8 nm) and microtubules (25 nm) by virtue of their diameter (10–12 nm). In mammals, >67 genes encode proteins able to self-assemble into IFs. A small subset of these encode lamins, the building blocks of the nuclear lamina, whereas all others encode cytoplasmic proteins. A major function shared by all IFs is to endow cells and tissues with a unique ability to resist trauma – this contribution is important in structures (e.g., axons and nuclei), cells, and tissues exposed to significant stress. Additional important functions are manifested in a sequence- and context-specific manner.

Features of Intermediate Filament Proteins

As a group, IF proteins are very heterogeneous in size (40–240 kDa), charge, and various other properties (Table I). The property of self-assembly is hard-wired into the characteristic tripartite domain structure shared by all IF proteins (Figures 1A and 1B). The central domain, an extended α-helix featuring long-range heptad repeats interrupted at three conserved locations, is the main determinant of self-assembly. This "rod" domain comprises 310 and 352 amino acids in cytoplasmic and nuclear IF proteins, respectively, and is bordered by invariant, signature ~15-mer sequences. Flanking sequences at the N and C termini of the rod domain are key in conferring each IF protein its individuality. Most IFs are heteropolymeric *in vivo*, although several IF proteins can *de facto* self-assemble into filaments as homopolymers *in vitro*.

Almost all metazoans (animals) contain both nuclear and cytoplasmic IFs, with the notable exception of arthropods, which contain only lamins. The presence of an exoskeleton, along with an increased density of microtubules in cells subjected to stress, may account for the absence of cytoplasmic IFs in arthropods. Phylogenetic analyses suggest that IFs initially appeared in the nucleus and later moved to the cytoplasm during evolution. IFs have not been found in plants, fungi, or protists. Most IFs are intracellular proteins; rare exceptions are the hagfish IFs, which are secreted polymers.

Assembly, Structure, and Regulation of Intermediate Filaments

Assembly and Structure

Owing to the long-range heptad repeats present within their central α-helical domain, IF proteins readily dimerize through coiled-coil interactions. In the dimer, individual rod domains are aligned in parallel (due to specific electrostatic interactions) and in register (owing to controlled nucleation by a "trigger motif") (Figure 1B). Nuclear and cytoplasmic IFs differ in the formation of tetramers. Lamin dimers associate in a head-to-tail fashion to form thin longitudinal strands, several of which laterally associate with an antiparallel orientation to form mature filaments. Dimers of cytoplasmic IFs, on the other hand, interact along their lateral surfaces with an antiparallel orientation to form compact tetramers. These tetramers continue to favor lateral interactions as they further polymerize to form ~60 nm long "unit-length filament" (ULF). Annealing of ULFs produces mature 10–12 nm filaments whose length can reach >10 μm (Figure 1C). Mature IFs lack an obvious structural polarity (see Figure 1B), reflecting the antiparallel orientation of dimers within them. While models for "idealized IFs" usually include 32 monomers per filament cross-section, determinations of mass per unit length revealed that, in actuality, this number can vary depending on the source and type of IFs. This heterogeneity is still unexplained. There is as yet no satisfactory model for the high-resolution structure of IFs.

Unlike actins and tubulins, IF proteins do not bind or metabolize nucleotides. They do not require an external input of energy or cofactor for assembly *in vitro*. They readily assemble into filaments when ectopically expressed in virtually any cell type in culture, suggesting that the process does not require specialized factors *in vivo*. Cytoplasmic IF networks often extend from the perinuclear area to the cell periphery, although there are

TABLE I

The Intermediate Filament Protein Family

IF type	Protein name	No. genes	Protein (kDa)	Assembly group[a]	Tissue distribution	Association with human disease[b]
I	Keratins (acidic)	>25	40–64	A	Epithelia	Multiple skin fragility diseases
						Oral and cornea fragility diseases
						Hair disorders
						Inflammatory bowel disease[c]
						Cryptogenic cirrhosis[c]
II	Keratins (basic)	>24	52–68	A	Epithelia	Nearly identical to type I keratins
III	Vimentin	1	55	B	Mesenchyme (esp early develop.)	None known
	Desmin	1	53	B	Muscle	Distal myopathy; cardioskelet. myop.
	GFAP	1	50–52	B	Astrocytes/Glia	Alexander's disease
	Peripherin	1	54	B	PNS neurons	None known
	Syncoilin	1	54	B	Muscle	None known
IV	NF-L	1	62	B	CNS neurons	Charcot-Marie-tooth disease
	NF-M	1	102	B	CNS neurons	Parkinson's disease[d]
	NF-H	1	110	B	CNS neurons	Amyotrophic lateral sclerosis
	α-Internexin	1	66	B	CNS neurons	None known
V	Lamin A/C	1	72/62	C	Differentiated tissue (nucleus)	Muscular dystrophy variants ($n = 2$)
						Dilated cardiomyopathies ($n = 2$)
						Familial partial lipodystrophy
						Mandibular acrodysplasia
						Charcot-Marie-tooth disease
						Premature aging conditions ($n = 2$)
	Lamin B1	1	65	C	Ubiquitous (nucleus)	
	Lamin B2	1	78	C	Ubiquitous (nucleus)	
Orphan	Nestin	1	240	B	Heterogeneous	None known
	Synemin	1	182	B	Muscle	None known
	Desmuslin	1	140	B	Muscle	None known
	Phakinin/CP49	1	46	D	Lens	Juvenile and congenital cataracts
	Filensin/CP115	1	83	D	Lens	None known

[a] Within each group proteins heteropolymerize in either an obligatory or facultative fashion to form filaments.
[b] Mutations affecting IF coding sequences are causative in the diseases listed unless indicated otherwise.
[c] Mutations in either K8 or K18 have been identified as risk factors for these conditions.
[d] Association needs to be confirmed in additional patients.

many instances in which IFs are concentrated in specialized regions of the cell. Such is the case for keratins in polarized epithelial sheets, desmin in myocytes, and neurofilaments in axons. In the cytoplasm, IFs can interact with F-actin, microtubules, and specific adhesion-mediating complexes. While the relative importance of these interactions varies between IF proteins and cell types, their dominant influence on IF organization has been established though experiments in which these other cytoskeletal complexes were disrupted.

Regulation

Both nuclear and cytoplasmic IFs are disassembled and/or profoundly reorganized during mitosis. Both of them can also be dynamically remodeled under steady-state conditions in non-cycling cells. *In vivo* experiments utilizing green fluorescent protein (GFP)-tagged vimentin or keratin suggest that filament formation is initiated at the cell periphery, whereas the subunit exchange fueling steady-state dynamics possibly occurs along the filament wall. More information about

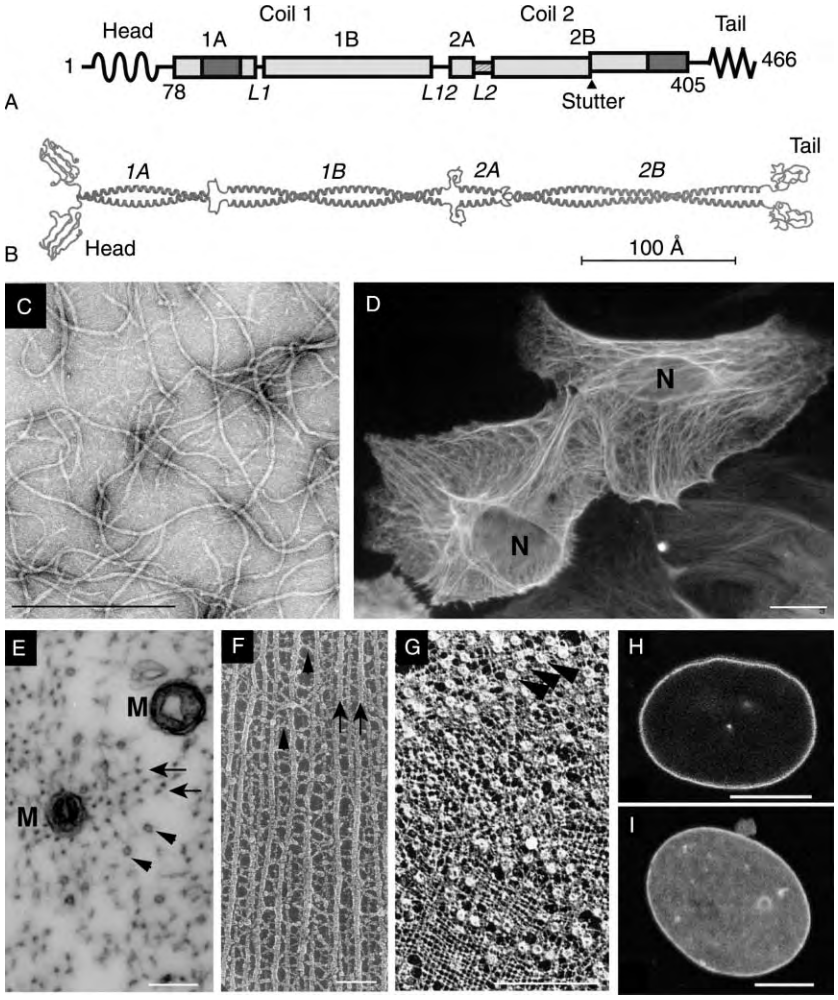

FIGURE 1 (A) Diagram illustrating the domain substructure of IF proteins. Rectangles depict central α-helical rod domain (1A, 1B, 2A, 2B) separated by short, non-helical linkers (L1, L12, L2). The rod domain is flanked by non-helical head and tail domains. Two highly conserved regions critical for the nucleation of coiled-coil dimer formation ("trigger motifs") are darkly shadowed. The numbers represent amino acid residues in human vimentin. (From Strelkov, S. V., Herrmann, H., and Aebi, U. (2003). Molecular architecture of intermediate filaments. *Bioessays* **25**, 243–251, with permission of John Wiley & Sons, Inc.) (B) Diagram illustrating the architecture of the human vimentin dimer, as determined by X-ray crystallography (1A and 2B subdomains, dark gray) or modeling (light gray). (From Strelkov, S. V., Herrmann, H., and Aebi, U. (2003). Molecular architecture of intermediate filaments. *Bioessays* **25**, 243–251, with permission of John Wiley & Sons, Inc.) (C) Keratin IFs reconstituted *in vitro* from purified proteins and visualized by negative staining and electron microscopy. These filaments appear as smooth-surfaced, apolar, flexible polymers of ~11 nm in width and several micrometers in length. Bar equals 250 nm. (D) Visualization of keratin IFs by indirect immunofluorescence in primary cultures of mouse skin keratinocytes. The filaments form a network extending from the surface of the nucleus (N) to the cytoplasmic periphery in these two cells. Bar equals 30 μm. (E and F) Visualization of neurofilaments in axon processes. (E) Thin-section transmission electron microscopy, showing neurofilaments viewed in cross-section. Neurofilaments (arrows), microtubules (arrowheads), and mitochondria (M) can be distinguished. Bar equals ~250 nm. (F) Quick-freeze deep-etch electron microscopy of axoplasm along its main axis. Neurofilaments (arrows) fill the axoplasm, and numerous cross-bridges (arrowheads) between the filaments can be seen. Bar equals 100 nm. (From Hirokawa, N., Glicksman, M.A., and Willard, M.B. (1984). Organization of mammalian neurofilament polypeptides within the neuronal cytoskeleton. *J. Cell. Biol.* **98**, 1523–1536, with permission of The Rockefeller University Press.) (G–I) Visualization of lamins in the nucleus. (G) Native nuclear lamina of *Xenopus* oocytes. Preparation of Triton X-100-extracted nuclear envelope by freeze-dried/metal-shadowing reveals the meshwork "basket weave" of the nuclear lamina and the array of nuclear pore complexes (arrowheads). Bar equals 1 μm. (From Aebi, U., Cohn, J., Buhle, L., and Gerace, L. (1986). The nuclear lamina is a meshwork of intermediate-type filaments. *Nature* **323**, 560–564, with permission.) (H and I) GFP-tagged Lamin B (H) or A (I) was introduced into mouse embryonic fibroblasts. Live cells in interphase show bright fluorescence around the nuclear rim while a fainter "veil" of fluorescence is visible in the nucleoplasm. Bar equals 10 μm. (From Moir, R.D., Yoon, M., Khuon, S., and Goldman, R.D. (2000). Nuclear lamins A and B1: different pathways of assembly during nuclear envelope formation in living cells. *J. Cell. Biol.* **151**, 1155–1168, with permission of The Rockefeller University Press.)

these crucial aspects of IF biology is needed. Posttranslational modifications play a key role toward the regulation of the assembly and disassembly of IFs *in vivo*, and of their interaction with associated proteins. Thus, all IF proteins are subject to phosphorylation, and the kinase, target site(s) and significance have been deciphered in many instances. The molecular basis of steady-state polymer dynamics, which have been tied to nucleotide

metabolism for F-actin and microtubules, remain unresolved for IFs. Possibly, rapid cycles of IF protein phosphorylation–dephosphorylation could enact the reversible conformational change needed. In addition, specific IF proteins have been shown to be O-glycosylated or modified in other ways, although the underlying significance is unclear. Lamins undergo lipid modification and enzymatic processing of their C terminus, reflecting their association with the inner nuclear membrane.

Dissecting the IF Superfamily

Most of the >67 genes forming the IF superfamily can be easily classified to one of five sequence types based on gene structure and nucleotide homology over the central α-helical domain. Individual members within each sequence type are often related in their tissue distribution. The remaining sequences defy classification and have been assigned to a sixth, orphan group of sequences.

Type I and Type II Keratins

Type I and type II IFs are part of the keratin (or cytokeratin) family of proteins found in all epithelia. The human and mouse genomes have >50 functional keratin genes, with a slightly larger number of type I keratin genes (see Table I). Type I keratins (K9-K21, K23, Ha1-8) are smaller and acidic compared to the larger, neutral-basic type II keratins (K1-K8, Hb1-6). Keratin assembly proceeds strictly from type I–type II heterodimers, accounting for the duality of sequences as well as their pairwise regulation *in vivo*. While any combination of purified type I and type II keratin proteins yields a fibrous polymer *in vitro*, specific pairs are coregulated in a fashion directly related to epithelial tissue type and/or differentiation state *in vivo*. In mammals, specific type I–type II gene pairings occur in simple (e.g., liver, GI tract), complex (e.g., skin, oral mucosa) and hard epithelia (e.g., hair, nail), with little overlap. Quite remarkably, moreover, specific type I–type II gene pairs are differentially and sequentially expressed in progenitor (mitotically active), early, and late differentiation stages in a host of epithelia. The conservation of keratins in terms of primary structure and distribution suggests an important role in epithelial diversity – this role has yet to be defined and does not lie in the execution of differentiation.

Type III Intermediate Filaments

The type III group consists of vimentin, desmin, GFAP, peripherin, and syncoilin (Table I). Vimentin is widely expressed during development, but typically gives way to other IF proteins during differentiation. Accordingly vimentin, which is assembly competent on its own, is usually found in co-polymers with other type III, type IV, or orphan sequences in mature cell types. Vimentin persists as the dominant cytoplasmic IF protein in fibroblasts, endothelial cells, adipocytes, macrophages, lymphocytes, and neutrophils. Desmin is found in the cytoplasm of smooth muscle and is concentrated at the Z lines of skeletal and cardiac muscle. Several variants of glial fibrillary acidic protein (GFAP) arise from a single precursor mRNA, and occur in the astrocytes of the central nervous system and in Schwann cells of the peripheral nervous system (PNS). Peripherin occurs in the post-mitotic neurons of the PNS, whereas syncoilin is an intrinsic component of the dystrophin-associated protein complex in skeletal and cardiac muscle.

Type IV Neurofilaments

This group occurs specifically in neurons and consists of the neurofilament triplet proteins NF-L, -M, and -H, and α-internexin. NF-L (light), NF-M (medium) and NF-H (heavy) co-polymerize obligatorily in a 5:3:1 ratio to form filaments with a core diameter of 10–12 nm and unusual side arms projecting >20 nm away (Figure 1E). These side arms represent the extended C-terminal tails of NF-M and NF-H, which feature a large number of Lys-Ser-Pro repeats that adopt an elongated shape when stoichiometrically phosphorylated. Neurofilament proteins are synthesized in the cell body of neurons and transported to the axon, where they contribute to the determination of axon caliber owing to their side arm projections (Figure 1F). α-Internexin, on the other hand, is expressed at an earlier stage of neuronal differentiation, and homopolymerizes into IFs that may thereafter scaffold the assembly of NF-L, M, and H, synthesized late during differentiation.

Type V Lamins

Nuclear lamins constitute type V IFs. Consistent with their unique distribution within the cell, lamin proteins contain a canonical nuclear localization signal within their C-terminal tail, and a CAAX-box at their C terminus which, after farnesylation and carboxylmethylation, mediates membrane anchorage. The C terminus of lamin A is a novel β immunoglobulin-like fold that acts as a docking site for several lamin-associated proteins, and its alteration causes disease (Table I). In addition, lamins feature six extra heptad repeats within the α-helical subdomain 1B of the rod, the significance of which is unclear. The presence of these six extra heptads in the cytoplasmic IF proteins of invertebrates has lent strong support to a proposal that the ancestral IF gene was lamin-like in character.

There are two major types of lamins, designated A and B. B-type lamins, which are essential in all species tested to date, are found in all somatic and germ cells.

The mammalian *Lmna* locus yields four distinct proteins; the two major ones, A (664 a.a.) and C (573 a.a.), are identical over residues 1-566 and differ at their C termini owing to alternative splicing of a common precursor mRNA. The *Lmna* products occur preferentially in differentiated cells. Lamins form a meshwork structure called the nuclear lamina just beneath the inner nuclear membrane (Figure 1G), where they interact with several key constituents of that membrane. In addition, lamins also occur in the nucleoplasm, with a mixed organization as a diffuse network and in focal clusters (Figures 1H and 1I).

Orphan IFs

Several orphan IFs exist that do not easily fit into any other group (Table I). These tend to show a very restricted tissue distribution. Exclusive to differentiated lens fiber cells, phakinin (also called CP115) and filensin (also called CP49) coassemble in a 3:1 molar ratio to produce a unique structure called beaded filaments, where 20 nm wide "beads" decorate the otherwise 8 nm wide filament in a regularly spaced pattern. Nestin was originally discovered as a marker of neuroepithelial stem cells, but is now known to exhibit a broader distribution including various multipotent progenitor cells. It is incorporated into filaments at very low stoichiometry compared to others IF proteins. Synemin, desmuslin, and paranemin coassemble with type III IFs (notably desmin) in muscle, with varying stoichiometry. Just like NF-M and NF-H, nestin, synemin, and paranemin have unusually long C-terminal tail domains that influence interaction between IFs and with other elements of the cytoskeleton.

Functions of Intermediate Filaments, and Their Involvement in Disease

Resistance to Stress

A major, family-wide function of IFs is to endow cells and tissues with a resilient and yet flexible scaffold needed to withstand mechanical, and in some cases non-mechanical, stresses. This concept first came to light from studies in which transgenic mice expressing a mutant epidermal keratin developed severe epidermal blisters. Subsequent analysis of DNA from patients with epidermolysis bullosa simplex, an epidermal blistering disease, revealed mutations in epidermal keratins, confirming the link between mutant IF proteins and inability of cells to withstand mechanical stress. Since then, the importance of IFs and resistance to various trauma has been extended to a variety of cell types including myocytes, fibroblasts, astrocytes, and trophoblasts. In the absence of stress, these cells usually tolerate the expression of a mutated, defective IF protein even though it may lead to disorganization of their IF network. In the event of shear stress, however, the intracellular rupture of such mutant-expressing cells reveals their unusual fragility. These features can also be observed in the absence of one or more keratins, as is evidenced by the fragility of the oral mucosa in Krt6α/β null mice (Figures 2A and 2B) and disruption of the keratin intermediate filament network in cultured primary keratinocytes form these mice (Figures 2C and 2D). Evolving studies of the mechanical properties of IF assemblies *in vitro* and in live cells in culture showed that they exhibit properties that are uniquely suited to fulfill this crucial role, and that inherited mutations compromise these properties. The diversity of IF sequences and their differential expression may serve, at least in part, the purpose of achieving the right compromise between properties of pliability and resilience given the context-specific demands placed upon a cell or its constituents.

Insight from Laminopathies

Nuclear lamins offer tantalizing clues for additional functions. Multiple lines of evidence, adeptly reviewed in recent texts, show that the nuclear lamina participates in determining the shape, size, and integrity of the nucleus, along with the number and positioning of nuclear pores. For example, *Lmna* null mice exhibit severe growth retardation and features of muscular dystrophy (Figures 2E–H). Inherited mutations in the *Lmna* gene are now known to give rise to a variety of clinical disorders (Table I), which from a bird's eye view seem very distinct from one another. Premature aging conditions such as Hutchinson–Gilford progeria syndrome (HGPS) and atypical Werner syndrome are the most recent entries in the world of laminopathies. While fragility of the nuclear envelope could possibly account, at least in part, for the pathogenesis of the muscle-based laminopathies, other mechanisms must be invoked for the premature aging conditions and related disorders. Among the likely possibilities are alterations in the control of gene expression and perturbations in the composition and function of the endoplasmic reticulum, which extends into and communicates with the nuclear envelope. An impact on gene expression could result from lamins' potential involvement in basic nuclear processes such as chromatin organization, DNA replication, RNA processing, and nucleocytoplasmic exchange.

Apoptosis

The possibility exists that just like their nuclear counterpart, cytoplasmic IFs evolved the ability to organize, through scaffolding, proteins and factors involved in signaling and other metabolic processes. Such interactions,

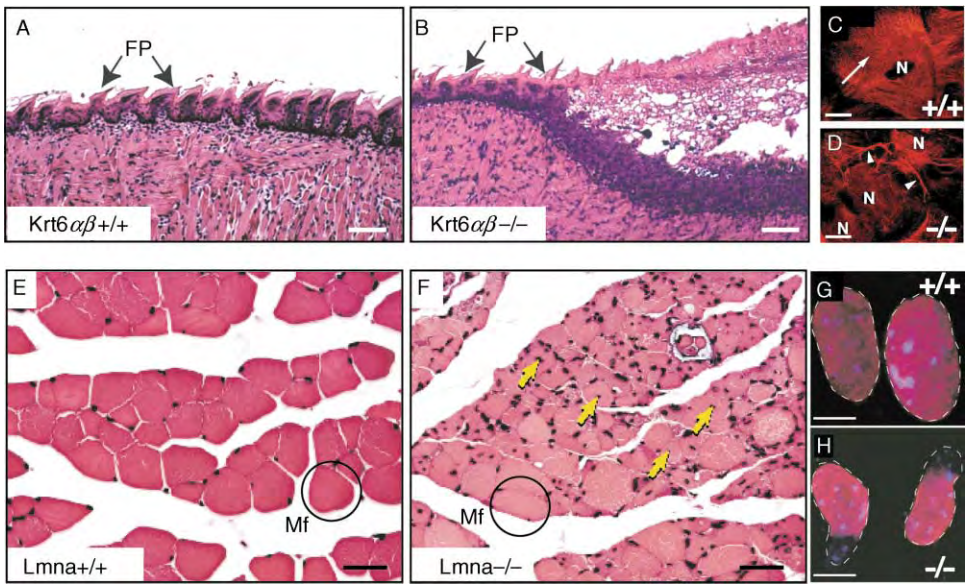

FIGURE 2 (A and B) Hematoxylin-eosin stained, paraffin-embedded section of wild-type (A) and K6α/K6β double null (B) mouse tongues. Tissue is oriented along its anterior–posterior axis. In the absence of the K6 proteins α and β, the posterior region of the tongue epithelium develops severe blistering owing to the fragility of filiform papillae (FP). Bar equals 200 μm. (From Wong, P., Colucci-Guyon, E., Takahashi, K., Gu, C., Babinet, C., and Coulombe, P.A. (2000). Introducing a null mutation in the mouse k6 alpha and k6 beta genes reveals their essential structural role in the oral mucosa. *J. Cell. Biol.* **150**, 921–928, with permission of The Rockefeller University Press.) (C and D) Visualization of keratin IF networks by indirect immunofluorescence in primary culture of skin keratinocytes from wild-type (C) and K6α/K6β null mice (D). Several null cells (−/−) feature disrupted keratin IF networks (see arrowheads). Bar equals 50 μm. (From Wong, P., and Coulombe, P.A., (2003). Loss of keratin 6 (k6) proteins reveals a function for intermediate filaments during wound repair. *J. Cell. Biol.* **163**, 327–337, with permission of The Rockefeller University Press.) (E and F) Aberrant localization of nuclei in muscle from *Lmna* null mice. (E) Hematoxylin-eosin stained, paraffin-embedded sections through wild-type perivertebral muscle show the peripheral localization of the nuclei in the muscle fibers. (F) In *Lmna* null muscle, myofibrils (Mf) are irregularly sized, and there is an increase in the number of nuclei, many of which are centrally located within the muscle fibers (arrows). Bar equals ~15 μm. (From Sullivan, T., Escalante-Alcade, D., Bhatt, H., Anver, M., Bhatt, N., Nagashima, K., Stewart, C.L., and Burke, B. (1999). Loss of A-type lamin expression compromises nuclear envelope integrity leading to muscular dystrophy. *J. Cell. Biol.* **147**, 913–920, with permission of The Rockefeller University Press.) (G and H) Immunohistochemical analysis of wild-type and *Lmna* null mouse embryonic fibroblasts in culture. After fixation with 3% paraformaldehyde, the nuclei were labeled with DAPI (blue), and indirect immunofluorescence of Lamin B (red). Note the uniform distribution of this protein in wild-type nuclear envelopes (G), but its loss from one pole of the irregularly shaped nuclei in the *Lmna* null cells (H). Dashed line indicates boundary of nucleus. Bar equals ~10 μm. (From Sullivan, T., Escalante-Alcade, D., Bhatt, H., Anver, M., Bhatt, N., Nagashima, K., Stewart, C.L., and Burke, B. (1999). Loss of A-type lamin expression compromises nuclear envelope integrity leading to muscular dystrophy. *J. Cell. Biol.* **147**, 913–920, with permission of The Rockefeller University Press.)

for instance, clearly modulate the response of various types of cells to pro-apoptotic signals. Absence or disruption of one or more IFs in several cell types (simple epithelial cells lacking K8, keratinocytes lacking K17, and neurons containing peripherin aggregates) renders cells significantly more likely to undergo apoptosis in response to TNFα or Fas. In simple epithelial cells lacking K8, this occurs in part because K8/18 IFs contribute to the targeting of Fas receptors to the cell surface, and bind to the cytoplasmic tail domain of TNFR2, and to death domain-containing proteins such as TRADD and DEDD. In addition to influencing the decision to undergo apoptosis, IF proteins are also key in its proper execution through their caspase-mediated degradation.

Spatial Organization

Recent evidence points to a role for IFs toward spatial organization within the cell. Keratin IFs can influence the sorting events leading to the organization of the apical pole in polarized epithelial cells, and vimentin IFs promote the association of the sodium-glucose cotransporter SGLT1 with lipid rafts, and its activity, in renal tubular cells. The contribution of neurofilaments toward the radial growth of neurons, itself a crucial determinant of conduction velocity, represent another example of how IFs can promote an asymmetric cytoarchitecture. The notion that cytoplasmic IFs promote some form of spatial organization is quite surprising given their nonpolar character – the spatial code required might be provided by site-specific, dynamic phosphorylation events, and regulated interactions with associated proteins. Future efforts should lead to a broader appreciation of the many metabolic processes influenced by IFs and underlying mechanisms of how inherited IF mutations cause disease.

See Also the Following Articles

Cell Death by Apoptosis and Necrosis • Intermediate Filament Linker Proteins: Plectin and BPAG1 •

Keratins and the Skin • Neuronal Intermediate Filaments • Nuclear Envelope and Lamins

Glossary

intermediate filament (IF) Filaments of 10–12 nm width and several micrometers in length found in the nucleus and the cytoplasm, where they form the cytoskeleton along with actin microfilaments and microtubules.

nuclear lamina A scaffold-like network of lamin intermediate filaments apposed against the inner membrane of the nuclear envelope.

trigger motif Small group of amino acids required for stabilization of an α-helix and nucleation of dimmer formation through coiled coil interactions

unit length filament (ULF) Late stage intermediate during the assembly of cytoplasmic IFs, which are ~60 nm in length and consists of eight tetramers (32 monomers) annealed laterally.

Further Reading

Aebi, U., Cohn, J., Buhle, L., and Gerace, L. (1986). The nuclear lamina is a meshwork of intermediate-type filaments. *Nature* **323**, 560–564.

Cassidy, A. J., Lane, E. B., Irvine, A. D., and McLean, W. H. I (2002). "The Human Intermediate Filament Mutation Database." http://www.interfil.org.

Coulombe, P. A., Bousquet, O., Ma, L., Yamada, S., and Wirtz, D. (2000). The 'ins' and 'outs' of intermediate filament organization. *Trends Cell Biol.* **10**, 420–428.

Erber, A., Riemer, D., Bovenschulte, M., and Weber, K. (1998). Molecular phylogeny of metazoan intermediate filament proteins. *J. Mol. Evol.* **47**, 751–762.

Fuchs, E., and Cleveland, D. W. (1998). A structural scaffolding of intermediate filaments in health and disease. *Science* **279**, 514–519.

Fuchs, E., and Weber, K. (1994). Intermediate filaments: Structure, dynamics, function, and disease. *Ann. Rev. Biochem.* **63**, 345–382.

Helfand, B. T., Chang, L., and Goldman, R. D. (2003). The dynamic and motile properties of intermediate filaments. *Annu. Rev. Cell Dev. Biol* **19**, 445–467.

Hesse, M., Magin, T. M., and Weber, K. (2001). Genes for intermediate filament proteins and the draft sequence of the human genome: Novel keratin genes and a surprisingly high number of pseudogenes related to keratin genes 8 and 18. *J. Cell Sci.* **114**, 2569–2575.

Hirokawa, P., Glicksman, M.A., and Willard, M.B. (1984). Organization of mammalian neurofilament polypeptides within the neuronal cytoskeleton. *J. Cell. Biol.* **98**, 1523–1536.

Moir, R.O., Yoon, M., Khuon, S., and Goldman, R.O. (2000). Nuclear lamins A and B1: different pathways of assembly during nuclear envelope formation in living cells. *J. Cells. Biol.* **151**, 1155–1168.

Mounkes, L., Kozlov, S., Burke, B., and Stewart, C. L. (2003). The laminopathies: Nuclear structure meets disease. *Curr. Opin. Genet. Dev* **13**, 223–230.

Omary, M. B., Ku, N. O., Liao, J., and Price, D. (1998). Keratin modifications and solubility properties in epithelial cells and *in vitro*. In *Subcellular Biochemistry: Intermediate Filaments* (H. Herrman and J. R. Harris, eds.) Vol 31, pp. 105–140. Plenum Press, New York.

Strelkov, S. V., Herrmann, H., and Aebi, U. (2003). Molecular architecture of intermediate filaments. *Bioessays* **25**, 243–251.

Sullivan, T., Escalante-Alcade, O., Bhatt, H., Anver, M., Bhatt, N., Nagashima, K., Stewart, C.L., and Burke, B. (1999). Loss of A-type lamin expression compromises nuclear envelope integrity leading to muscular dystrophy. *J. Cell. Biol.* **147**, 913–920.

Wong, P., and Coulombe, P.A (2003). Loss of keratin 6 (k6) proteins reveals a function for intermediate filaments during wound repair. *J. Cell. Biol.* **163**, 327–337.

Wong, P., Colucci-Guyon, E., Takahashi, K., Gu, C., Babinet, C., and Coulombe, P.A. (2000). Introducing a null mutation in the mouse k6 alpha and k6 beta genes reveals their essential structural role in the oral mucosa. *J. Cell. Biol.* **150**, 921–928.

Biography

Pierre A. Coulombe is a Professor in the Department of Biological Chemistry at the Johns Hopkins University School of Medicine in Baltimore, Maryland. He holds a Ph.D. from Université de Montréal in Canada and received his postdoctoral training at the University of Chicago. At that time, he and Dr. Elaine Fuchs discovered that mutations in keratins can elicit epithelial fragility in transgenic mice and individuals suffering from inherited blistering diseases. He continues to explore the properties and function of keratin genes and proteins in epithelial cells and tissues.

Kelsie M. Bernot is a native of Pennsylvania and a student in the biochemistry, cellular and molecular biology graduate training program at Hopkins. Her thesis research focuses on the properties and function of keratin 16, which is up-regulated during wound repair and in chronic hyperproliferative skin disorders.

Intracellular Calcium Channels: cADPR-Modulated (Ryanodine Receptors)

Antony Galione
University of Oxford, Oxford, UK

Ca^{2+} mobilization from intracellular stores constitutes an important mechanism for producing Ca^{2+} signals within cells. Two major families of intracellular Ca^{2+} release channels have been characterized and are predominantly expressed in the endoplasmic reticulum/sarcoplasmic reticulum (ER/SR). The first is termed the inositol 1,4,5 trisphosphate receptor and is gated by the ubiquitous second messenger inositol 1,4,5 trisphosphate (IP_3). This messenger is generated through the activation of cell surface receptors coupled to the activation of phospholipase C and subsequent hydrolysis of the membrane lipid, phosphatidylinositol 4,5 bisphosphate. The other major family of channels are termed ryanodine receptors. These were first characterized in skeletal and cardiac muscle as proteins which bind the plant alkaloid ryanodine with high affinity. Later they were shown to comprise the major pathway for Ca^{2+} release from the sarcoplasmic reticulum during excitation–contraction coupling. However, it has emerged that ryanodine receptors are ubiquitously expressed throughout cells of the animal and plant kingdom.

Ryanodine Receptors

Ryanodine receptors are encoded by three genes in mammals and genes from a number of non-mammalian species have been sequenced. They are very large proteins with subunits typically of ~560 kDa. Functional channels are usually homotetrameric, comprising of four identical subunits. The large cytoplasmic domains of each subunit provide enormous scope for regulation through interactions with proteins and low-molecular-weight molecules. In skeletal muscle, ryanodine receptors are regulated mainly by direct coupling to voltage-sensor proteins termed dihydropyridine receptors in plasma membrane invaginations called t-tubules. In other cells, direct interactions with plasma membrane proteins are not widely observed for ryanodine receptors, prompting questions about how these proteins are regulated by extracellular stimuli.

Cyclic Adenosine Diphosphate Ribose

Recent evidence has emerged that ryanodine receptors, like IP_3 receptors, too may be gated by a small phosphorylated second messenger called cyclic adenosine disphosphate ribose (cADPR). This molecule is a metabolite of the pyridine nucleotide nicotinamide adenine dinucleotide (NAD^+) and is generated in many cells through the activation of enzymes termed ADP ribosyl cyclases, the best characterized being CD38, expressed at plasma and internal membrane systems. Although it may seem paradoxical that an ectoenzyme such as CD38 may regulate intracellular levels of cADPR, studies from CD38 knockout mice have implicated CD38 in the regulation of cellular cADPR levels during calcium signaling during secretion in both endocrine and exocrine pancreas, as well as in neutrophil chemotaxis. However, in brain, for example, other enzymes may be involved in cADPR synthesis based on similar studies from CD38 knockout mouse.

In an important study, Lee and his colleagues reported in 1987 that not only the established Ca^{2+} mobilizing messenger IP_3 released Ca^{2+} from internal stores in sea urchin egg homogenates, but so also did the two pyridine nucleotides, NAD^+ and NADP. However, NAD^+ was found not to be a Ca^{2+} mobilizing agent *per se*. The active principle was subsequently identified as cADPR, synthesized from NAD^+ in the egg homogenates. A contaminant of NADP, $NAADP^+$, was later shown to be a potent Ca^{2+} mobilizing molecule too. cADPR, at nanomolar concentrations, was shown directly to release Ca^{2+} from intracellular stores by microinjection into intact sea urchin eggs in the absence of extracellular Ca^{2+}. Subsequent pharmacological analysis of cADPR-induced Ca^{2+} release indicated that it was not activating IP_3 receptors since its release was

not blocked by the IP_3 receptor antagonist, heparin. Furthermore, when sea urchin egg homogenates were desensitized to release by IP_3, cADPR was still able to initiate a full Ca^{2+} release. Importantly, Ca^{2+} release by cyclic ADP ribose was found to be selectively blocked by ryanodine receptor inhibitors such as ryanodine itself, ruthenium red, and procaine. In addition, substituted analogues of cADPR were synthesized and found to act as selective antagonists of cADPR but not IP_3-induced Ca^{2+} release.

cADPR has now been implicated in the control of Ca^{2+} release via ryanodine receptors in many different cell types. It is now thought that in many cells cADPR acts in concert with IP_3 to generate the complex Ca^{2+} signaling patterns widely observed in cells. An important property of Ca^{2+} release through ryanodine receptors is that they are modulated by Ca^{2+} itself. This positive feedback mechanism is termed Ca^{2+}-induced Ca^{2+} release (CICR) and is known to be important in excitation–contraction coupling in cardiac muscle and for amplifying local Ca^{2+} signals in many different cell types. This phenomenon is also thought to be critical in determining the complex patterns of Ca^{2+} signals widely observed in cells such as Ca^{2+} spiking and Ca^{2+} waves. cADPR is thought to sensitize ryanodine receptors to their activation by Ca^{2+}.

Cyclic ADP Ribose Receptors

The mechanisms by which cADPR activates ryanodine receptors are not well understood. The possibility exists that cyclic ADP ribose may bind directly to ryanodine receptors or to accessory proteins, which in turn modulate ryanodine receptor openings. High-affinity specific binding of [^{32}P] cADPR has been demonstrated in sea urchin egg microsomes and longitudinal smooth muscle. The photoaffinity compound [^{32}P]-8-azido-cADPR labels distinct 100 and 140 kDa proteins in sea urchin egg extracts. However, these proteins have not been characterized further but are smaller than ryanodine receptor subunits. Two important accessory proteins which are known to bind to ryanodine receptors have both been implicated in cADPR-induced Ca^{2+} release are calmodulin and FKBP-binding proteins. A feature of cADPR-induced Ca^{2+} release from sea urchin egg microsomes is the requirement for a soluble protein factor. This protein was subsequently identified as calmodulin. Calmodulin appears to confer cADPR sensitivity on the microsomes, an effect that is direct and does not rely on enzyme activities. The desensitization phenomenon observed with multiple applications of cADPR is due to the dissociation of calmodulin following the cADPR-induced activation of Ca^{2+} release. Calmodulin is a known accessory protein of ryanodine receptors and its binding sites to this protein have been mapped. The immunophilin FKBP12.6 is a binding protein for immunosuppressant drugs such as FK-506 and binds to ryanodine receptors. In mammalian systems, cADPR has been proposed to induce Ca^{2+} release via ryanodine receptor openings by promoting the dissociation of FKBP12.6 from the channels. cADPR also modulates [^{3}H]ryanodine binding in a number of systems. cADPR enhances [^{3}H]ryanodine binding to cardiac SR vesicles and to T cell membranes. In contrast, in parotid cells, cADPR competes with [^{3}H]ryanodine for its binding sites. The most direct evidence for the investigation of cADPR interaction with ryanodine receptors has come from studying the effects of cADPR on the effects of reconstituted ryanodine receptors in lipid bilayers. These data are often confusing with evidence for and against direct gating of channel openings by cADPR for each of the three isoforms of this Ca^{2+} release channel in mammalian systems. cADPR activation of ryanodine receptors reconstituted into lipid bilayers has been observed with proteins derived from sea urchin eggs, cardiac myocytes, and coronary smooth muscle. In the last case, FKBP12.6 is required to reveal the effects of cADPR on the open probability of the channels.

In addition, three other effects of cADPR have been proposed. In cardiac myocytes, cADPR has been suggested to stimulate SERCA pumps of the sarcoplasmic reticulum (SR), thereby increasing Ca^{2+} loading of this organelle. In colonic smooth muscle cells cADPR has been proposed to stimulate plasma membrane-based calcium removal mechanisms, whilst a modulatory site modulated by high concentrations of cADPR at IP_3 receptors has also been demonstrated.

cADPR and Activation of Different RYR Isoforms

Based largely on pharmacological evidence, the majority of calcium release studies have implicated ryanodine receptors as the major intracellular target for cADPR action. In terms of cADPR selectivity for different RYR isoforms, there are several reports, both positive and negative, of regulation of each of the three different mammalian isoforms of RYRs by cADPR. These reports are based not only on isolated channels in lipid bilayers, but also in intact cells predominantly expressing one type of native or recombinant ryanodine receptor. However, as stated before, it is still unclear whether cADPR binds directly to ryanodine receptors or modulates ryanodine receptor openings through its interaction with accessory proteins.

cADPR-Mediated Calcium Signaling

The development of 8-substituted analogues of cADPR as potent antagonist of cADPR action have been crucial in unraveling stimuli that signal through cyclic ADP ribose action. Phenomena that are blocked by antagonists by 8-amino-cADPR or 8-Br-cADPR include cardiac contractility enhanced by β-adrenergic agonists, abscisic acid-induced stomatal closures, and gene expression in plants, CCK and acetylcholine-evoked fluid secretion in pancreatic acinar cells, nitric oxide mediated long-term depression in brain slices, fertilization in sea urchin eggs, and T cell receptor activation as well as neurotransmitter release from nerve terminals. 8-Br-cADPR, which is membrane permeant, is gaining widespread usage as a membrane permeant antagonist of cADPR action. The use of this analogue has been used to implicate cADPR in the control of long-term depression in rat hippocampus, hypoxia-mediated vasoconstriction in pulmonary smooth muscle, cardiac contractility and smooth muscle contraction. In the generation of many intracellular Ca^{2+} signals both IP_3- and cADPR-sensitive mechanisms are involved in determining the Ca^{2+} signaling patterns. In sea urchin eggs, for example, both IP_3 and cADPR mechanisms can independently produce Ca^{2+} waves and are both produced by the fertilizing sperm. Similar results were found in dopaminergic neurons in mammalian CNS where activation of metabotropic glutamate receptors induces Ca^{2+} mobilization by intracellular stores through the activation of both IP_3 and cyclic ADP ribose/ryanodine receptor mechanisms.

Measurement of cADPR Levels in Tissues and Cells

The development of a number of sensitive and selective assays for measuring cyclic ADP ribose in mammalian tissues has led to the identification of cellular stimuli that are coupled to cADPR synthesis in cells. These studies have complemented those employing selective cADPR antagonists, as outlined earlier. The major cADPR assays are a radio-receptor assay based on the ability of endogenous cADPR to displace [^{32}P]cADPR binding to sea urchin egg microsomes and a novel cycling assay for cyclic ADP ribose with a nanomolar sensitivity. The principle of this cycling assay is that NAD^+ can be generated by from cADPR by the reversal of the ADP-ribosyl cyclase enzyme. NAD produced after initially depleting cell extracts of endogenous NAD is then coupled to cycling assays involving alcohol dehydrogenase and diaphorase generating a fluorescent product.

cADPR synthesis has been shown to be coupled through G protein-coupled receptors including muscarinic cholinergic receptors and α_1-adrenoceptors as well as tyrosine-kinase-linked receptors such as the T cell receptor. In addition, the second messenger cyclic GMP, may through its cyclic GMP-dependent protein kinase, directly activate the ADP ribosyl cyclase through phosphorylation. In addition, intermediary metabolism through modulation of NAD^+/NADH levels may be coupled to cADPR synthesis. Chronic changes in cyclic ADP ribose levels may be associated also with changes in the levels of ADP ribosyl cyclase enzymes. For example, retinoic acid and oestrogen increase expression of ADP ribosyl cyclases, resulting in chronic elevations in cyclic ADP ribose levels. Now that assays exist for the measurement of cADPR in cells, it has been found that cellular stimuli generally elevate cyclic ADP ribose for prolonged periods, as long as a number of minutes, in contrast to the more transient elevations of IP_3. These data indicate that cADPR may act as a long-term modulator of Ca^{2+} release from intracellular stores.

See Also the Following Articles

Calcium Signaling: Calmodulin-Dependent Phosphatase • Calcium Signaling: Cell Cycle • Calcium Signaling: Motility (Actomyosin–Troponin System) • Calcium Signaling: NO Synthase • G Protein-Coupled Receptor Kinases and Arrestins • Intracellular Calcium Channels: $NAADP^+$-Modulated • IP_3 Receptors • The Neuronal Calcium Signal in Activity-Dependent Transcription • Phosphatidylinositol Bisphosphate and Trisphosphate • Phosphatidylinositol-3-Phosphate • Store-Operated Membrane Channels: Calcium

Glossary

Ca^{2+}-induced Ca^{2+} release A phenomenon where a modest rise in intracellular Ca^{2+} activates Ca^{2+} release channels, amplifying and globalizing Ca^{2+} signals.

Ca^{2+} release channel A channel on intracellular organelles, usually the endoplasmic reticulum, that when opened releases stored Ca^{2+}.

Ca^{2+} signal Changes in the intracellular levels of free Ca^{2+} often manifested as complex Ca^{2+} spikes and propagating regenerative waves.

NAD Nicotinamide adenine dinucleotide, a ubiquitous coenzyme found in all cells.

ryanodine receptor Ca^{2+} release channel found in muscle and other cells that is modulated by the plant alkaloid ryanodine. It is a large homotetrameric protein each consisting of four large subunits.

second messenger An intracellular molecule that mediates the effects of extracellular stimuli.

Further Reading

Berridge, M., Lipp, P., and Bootman, M. (2000). The versatility and universality of calcium signalling. *Nat. Mol. Cell Biol. Rev.* **1**, 11–21.

Clapper, D. L., Walseth, T. F., Dargie, P. J., and Lee, H. C. (1987). Pyridine nucleotide metabolites stimulate calcium release from sea urchin egg microsomes desensitized to inositol trisphosphate. *J. Biol. Chem.* **262**, 9561–9568.

Fill, M., and Copello, J. A. (2002). Ryanodine receptor calcium release channels. *Physiol. Rev.* **82**, 893–922.

Galione, A., and Churchill, G. (2000). Cyclic ADP-ribose as a calcium mobilizing messenger. *Science STKE*, 1–6. www.stke.org/cgi/content/full/OC_sigtrans;2000/41/pe1.

Leckie, C., Empson, R., Becchetti, A., Thomas, J., Galione, A., and Whitaker, M. (2003). The NO pathway acts late during the fertilization response in sea urchin eggs. *J. Biol. Chem.* **278**, 12247–12254.

Lee, H. C. (2001). Physiological functions of cyclic ADP-Ribose and NAADP as calcium messengers. *Annu. Rev. Pharmacol. Toxicol.* **41**, 317–345.

Morgan, A. J., and Galione, A. (2002). Sensitizing Ca^{2+}-induced Ca^{2+} release. Role of cADPR as an endogenous modulator. In *Cyclic ADP-Ribose and NAADP. Structures, Metabolism and Functions* (H. C. Lee, ed.) pp. 167–197. Kluwer, Dordrecht.

Patel, S., Churchill, G. C., and Galione, A. (2001). Coordination of Ca^{2+} signalling by NAADP. *Trends Biochem. Sci.* **26**, 482–489.

Tang, W. X., Chen, Y. F., Zou, A. P., Campbell, W. B., and Li, P. L. (2002). Role of FKBP12.6 in cADPR-induced activation of reconstituted ryanodine receptors from arterial smooth muscle. *Am. J. Physiol.* **282**, H1304–H1310.

Thomas, J. M., Summerhill, R. J., Fruen, B. R., Churchill, G. C., and Galione, A. (2002). Calmodulin dissociation mediates desensitization of the cADPR-induced Ca^{2+} release mechanism. *Curr. Biol.* **12**, 2018–2022.

Biography

Antony Galione is a Professor of Pharmacology in the Department of Pharmacology at the University of Oxford, UK and a senior research fellow of the Wellcome Trust, UK. His principal research interests are Ca^{2+} mobilization from intracellular stores by novel Ca^{2+}-mobilizing messengers cADPR and NAADP. He holds a Ph.D. from the University of Cambridge and received his postdoctoral training at University College, London and Johns Hopkins University.

Intracellular Calcium Channels: $NAADP^+$-Modulated

Armando A. Genazzani and Marcella Debidda
University of Cambridge, Cambridge, UK

It is well established that inositol 1,4,5-trisphosphate (IP_3) and Ca^{2+} are able to mediate signal transduction by opening intracellular Ca^{2+}-channels located on intracellular membranes. These messengers do this by activating IP_3 and ryanodine receptors, respectively. Nonetheless, in recent years evidence has emerged that other molecules may mediate intracellular Ca^{2+}-release, either by the modulation of these two channels, or via the activation of further, previously unknown, channels. Derivatives of NAD and NADP have been shown to be able to induce Ca^{2+}-release via both mechanisms. In particular, cyclic ADP ribose (cADPR) acts on particular subtypes of the ryanodine receptor, while nicotinic acid adenine dinucleotide phosphate (NAADP) releases Ca^{2+} via a novel and distinct mechanism.

Structure of NAADP

NAADP is a pyridine nucleotide similar to NADP, except for the amide group of the nicotinamide ring, which in the NAADP molecule is replaced by a carboxyl group (Figure 1). Despite this small difference, in sea urchin eggs (the model system used to characterize this molecule), NADP is devoid of any Ca^{2+}-release efficacy, suggesting that the binding site specifically recognizes this region of the molecule as a discriminator and that NAADP is not just a cellular surrogate for NADP.

NAADP-Induced Ca^{2+}-Release in Invertebrates and Plants

Although the chemical existence of NAADP was reported by Bernofsky in 1980, the possibility that NAADP could be a putative intracellular messenger was hypothesized by Lee and co-workers. In 1987, they described the presence of a contaminant in commercially available NADP that could release Ca^{2+} in sea urchin eggs. Only in 1995, this contaminant was shown to be NAADP. NAADP has now been found to be a potent Ca^{2+}-releasing agent in various invertebrate systems including starfish, sea snails, and sea squirts (see Table I). Furthermore, NAADP has also been shown to release Ca^{2+} from microsomes prepared from plant preparations. Although the NAADP receptor has not yet been cloned, it presumably is a Ca^{2+}-channel distinct from those described to date, as indicated by numerous biochemical evidences. Nonetheless, in a few systems, such as the skeletal muscle, NAADP might also use the ryanodine receptor as a mediator of its effect. In sea urchin eggs, the best characterized model to date, NAADP releases Ca^{2+} via an intracellular channel that is distinct from those that are responsive to inositol 1,4,5-triphosphate (IP_3) and cyclic ADP ribose (cADPR). NAADP-induced Ca^{2+}-release does not exhibit any cross-desensitization with the other two mechanisms. Furthermore, it is not sensitive to heparin, ruthenium red or high concentrations of ryanodine, antagonists of the IP_3, and ryanodine channels. According to the concentrations, Ca^{2+} can both activate and inhibit IP_3 and ryanodine receptors, providing a means of modulation of the channel independent of ligands. A major difference between the NAADP mechanism and the other two is the insensitivity of the NAADP-induced Ca^{2+}-release to both cytosolic and vesicular Ca^{2+}-concentrations. Furthermore, other differences exist in the channels in regard to the pH sensitivity, ion dependency, endogenous modulators, and kinetic features. Finally, specific NAADP-binding sites, insensitive to IP_3 and cADPR, have been shown in sea urchin egg microsomes.

All the efforts done to characterize the pharmacology have failed so far to produce a valid antagonist of the NAADP-sensitive mechanism. In echinoderms, it has been shown that L-type Ca^{2+}-channel antagonists (and BayK8644, an agonist) are able to inhibit NAADP-induced Ca^{2+}-release, but this occurs just at concentrations, which are approximately 100-fold higher than those able to inhibit voltage-operated Ca^{2+}-channels. Nonetheless, it has been found that NAADP itself can be used as an antagonist since in sea urchin eggs subthreshold concentrations of this nucleotide are able to completely abrogate the calcium release caused by

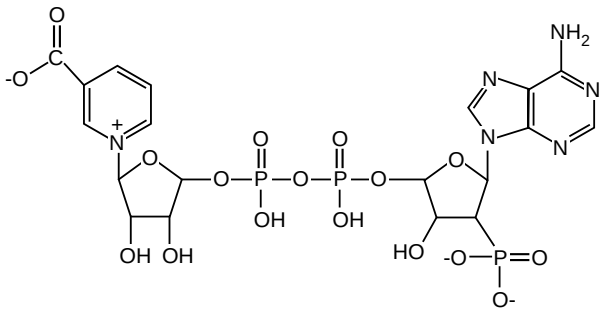

FIGURE 1 Structure of nicotinic acid adenine dinucleotide phosphate.

further NAADP elevations. Neither IP_3 nor cADPR are regulated by this mechanism and so far the significance of this process is unknown.

In sea urchin eggs, the NAADP sensitive channel does not appear to reside on the same intracellular organelles compared to IP_3 and ryanodine receptors, as shown by membrane separation experiments. To support this, while IP_3- and cADPR-induced Ca^{2+}-release are completely abolished by pretreatment of homogenates with thapsigargin, a poison of the Ca^{2+}-pump that is responsible for the accumulation of Ca^{2+} in the endo(sarco)plasmic reticulum, NAADP-induced Ca^{2+}-release appears to be unaffected. Recently, it has been shown that, at least in this system, the organelle on which the mechanism might reside is the reserve granule, the egg equivalent to lysosomes. Whether this will be a general feature of this mechanism across species remains to be established.

In sea urchins, starfish, and sea squirts (invertebrate systems) where the properties of NAADP on Ca^{2+}-release have been investigated in intact cells, it has been shown that this Ca^{2+}-release mechanism does not act in isolation from the others, but instead appears to work in concert to elicit specific responses. For example, in starfish NAADP-induced Ca^{2+}-release appears to be partially inhibited by the co-injection of IP_3 and ryanodine receptor antagonists, suggesting that the NAADP-induced cytosolic calcium elevations are due to both release from the NAADP channel and to amplification through IP_3 and ryanodine receptors. The extent and the manner of the cross-talk appears to be different from one system to another, but it is

TABLE I

Models Described to be Responsive to NAADP Between 1995 and 2002

Species	Model	NAADP effect
Sea urchin	Intact egg,	Inactivation (<1 nM, IC_{50} 200 pM) Agonist (>3 nM, EC_{50} 25 nM)
	Microsomes	Inactivation (<1nM, IC_{50} 200 pM) Agonist (>3 nM, EC_{50} 25 nM)
Starfish	Intact egg	Agonist (1–2 μM)
Sea squirt	Intact oocyte	Agonist (EC_{50} 30 nM)
Sea snail ganglia	Pre-synaptic neuron	Agonist (10–50 μM)
Red Beet	Microsomes	Agonist (96 nM)
Cauliflower	Microsomes	Agonist (1 μM) Inactivation (3 nM)
Frog neuromuscular junction	Nerve terminal	Agonist (10 μM–1 nM; liposomal delivery)
Human β pancreatic cells	Intact cells	Agonist (100 nM) Inactivation (10 μM)
Human T-lymphocytes	Intact cells	Agonist (max 100 nM) Inactivation (10 μM)
Mouse pancreatic acinar cells	Intact cells	Agonist (50 nM) Inactivation (1–100 μM)
Rat pulmonary smooth muscle cells	Intact cells	Agonist (10 nM) Inactivation (100 μM)
Rat fibroblast cells	Microsomes	Agonist (10 μM)
Rat brain	Microsomes	Agonist (EC_{50} 1 μM)
Rabbit heart	Microsomes	Agonist (EC_{50} 320 nM)
Rat mesangial kidney cells	Microsomes	Agonist (EC_{50} 4 μM)
A7r5, HL-60, H9c2 cell lines	Microsomes	Agonist (10 μM)

one of the conserved features of NAADP signaling through evolution, since it has been observed also in vertebrate systems.

NAADP-Induced Ca^{2+}-Release in Vertebrates

Both microsomal and intact systems from vertebrate models have been shown to respond to NAADP (Table I). Furthermore, binding sites with nanomolar affinity for NAADP have been described in brain and cardiac tissues. In similar fashion to what is observed in invertebrate systems, NAADP-induced Ca^{2+}-release is distinct from the IP_3 and ryanodine-mediated mechanisms when it is investigated in microsomal preparations, while in intact systems there appears to be a high degree of overlap. One of the differences observed between vertebrates and invertebrates is that the unusual desensitization property observed in sea urchin eggs does not seem to have been conserved in vertebrates. Instead, in many of the systems described (e.g., pancreatic acinar and β-cells, T-lymphocytes), NAADP appears to release Ca^{2+} in an inverted bell-shaped curve, with high concentrations unable to have any effect. Observations of cross-talk between NAADP-induced Ca^{2+}-release and IP_3 and ryanodine receptors in pancreatic acinar cells and T-lymphocytes have led to the hypothesis that NAADP might act as a trigger by releasing enough Ca^{2+} to induce and/or sensitize the other two mechanisms to amplify its signal. This cross-talk means that cells might encode signals via increasing to different levels the three-second messengers, instead of having the option to modulate just one messenger to different levels. The net outcome of this could be the possibility to use Ca^{2+} to specifically and unambiguously encode a higher number of intracellular messages.

At present, no extracellular message has been linked unequivocally with NAADP signaling. Nonetheless, the capacity of high concentrations of NAADP to block the release mechanism has been used experimentally to suggest that NAADP might be involved, among other functions, in colecystokinin-mediated signaling in pancreatic acinar cells, in insulin signaling in β-cells, and in the T cell receptor/CD3 signaling.

Metabolism of NAADP

It has been shown that cADPR, a derivative of NAD, in which the nicotinamide has been cleaved and the terminal ribose is cyclized with the adenine group at the N1 position, can be synthesized by a subfamily of NAD^+ glycohydrolases. Members of this family have been characterized in *Aplysia* and in mammalian systems. These enzymes are peculiar since they are able to catalyze both the cyclization and the degradation of cADPR. Surprisingly, in the presence of nicotinic acid, these enzymes are also capable of catalyzing a base-exchange reaction that replaces the nicotinamide on NADP with nicotinic acid to produce NAADP. Therefore, it is likely that these enzymes are central to calcium signaling, since they can catalyze the production of two signaling molecules with two distinct targets, as well as the degradation of one of these. For this mechanism to produce diversity it could be hypothesized that the different reactions should be modulated differently by intracellular pathways. Recent evidence suggests that this might be the case. First, the base-exchange reaction seems to be favored over the cyclization in acidic conditions, although substantial amounts of NAADP are generated at physiological pH. Second, both the laboratories led by Lee and by Galione have separately shown that cyclic nucleotides can differentially regulate the production of cADPR and NAADP. In particular, in sea urchin eggs elevations of cAMP appear to favor NAADP production while elevations of cGMP favor production of cADPR. Nonetheless, this could be due to either a differential modulation of the same enzyme or to modulation of two separate enzymes. Among the enzymes described to date that can catalyze these reactions, the mammalian members, the most important of which is the lymphocyte antigen CD38, are membrane-bound ectoenzymes, with extracellular catalytic activity. Although there are some descriptions of CD38 present on intracellular membranes such as the nuclear envelope or the mitochondrion, it is likely that other members of this family will be described in the future that possess intracellular activity. Alternatively, the group led by De Flora has postulated a mechanism by which the extracellularly produced messengers can be internalized.

NAADP degradation has been shown to occur in both invertebrate and vertebrate cells. The mechanism by which this occurs is at present unknown, although it has been recently postulated that in mouse tissues a Ca^{2+}-dependent phosphatase, via conversion to NAAD, might be involved in the termination of signaling by NAADP.

In most systems evaluated to date, NAADP induces Ca^{2+}-release at low nanomolar concentrations, making its detection extremely difficult. It has recently been shown that sea urchin sperm contain micromolar levels of NAADP, together with a membrane-bound high capacity enzyme for its synthesis. It is likely that these observations will be extended to other systems with the characterization of more sensitive detection methods.

See Also the Following Articles

Phosphatidylinositol-3-Phosphate • Intracellular Calcium Channels: cADPr-Modulated (Ryanodine Receptors) • IP_3 Receptors • Phosphatidylinositol Bisphosphate and Trisphosphate • Phospholipase C • Voltage-Sensitive Ca^{2+} Channels

Glossary

cADPR An intracellular messenger derived from NAD^+ acting on the ryanodine receptor as an agonist or a modulator.

IP_3 A second messenger derived from the cleavage of PIP_2 (phosphatidylinositol 4,5-bisphosphate) by Phospholipase C which interacts with IP_3-sensitive Ca^{2+} channels causing calcium release.

NAADP An intracellular messenger derived from $NADP^+$ acting on a yet unknown intracellular Ca^{2+}-release channel.

second messenger An intracellular molecule whose concentration is regulated in response to binding of a specific ligand to an extracellular receptor to transduce information.

Further Reading

Cancela, J. M., Van Coppenolle, F., Galione, A., Tepikin, A. V., and Petersen, O. H. (2002). Transformation of local Ca^{2+} spikes to global Ca^{2+} transients: The combinatorial roles of multiple Ca^{2+} releasing messengers. *EMBO J.* **21**, 909–919.

Churchill, G. C., Okada, Y., Thomas, J. M., Genazzani, A. A., Patel, S., and Galione, A. (2002). NAADP mobilizes Ca^{2+} from reserve granules, lysosome-related organelles, in sea urchin eggs. *Cell* **111**, 703–708.

Clapper, D. L., Walseth, T. F., Dargie, P. J., and Lee, H. C. (1987). Pyridine nucleotide metabolites stimulate calcium release from sea urchin egg microsomes desensitized to inositol trisphosphate. *J. Biol. Chem.* **262**, 9561–9568.

Genazzani, A. A., and Billington, R. A. (2002). NAADP: An atypical Ca^{2+}-release messenger? *Trends Pharmacol. Sci.* **23**, 165–167.

Lee, H. C. (2002). *Cyclic ADP-ribose and NAADP Structures, Metabolism and Functions*. Kluwer, Boston.

Patel, S., Churchill, G. C., and Galione, A. (2001). Coordination of Ca^{2+} signalling by NAADP. *Trends Biochem. Sci.* **26**, 482–489.

Biography

Armando Genazzani is an Associate Professor at the University of Piemonte Orientale, Novara, Italy. His major interests include intracellular Ca^{2+} release mechanisms and the understanding of Ca^{2+}-induced gene expression in neurons. He holds an M.D. from the University of Catania, Italy and a Ph.D. from the University of Oxford. He received postdoctoral training at the University of Oxford and at the Swiss Federal Institute of Technology (ETH) in Zurich and has been University lecturer and BBSRC David Phillips Fellow at the University of Cambridge, UK.

Marcella Debidda holds a Ph.D. from the University of Sassari, Italy. She received postdoctoral training at the University of Cambridge (UK) and is currently a postdoctoral fellow in the division of Experimental Hematology at Cincinnati Children's Hospital Medical Center.

Ion Channel Protein Superfamily

William A. Catterall
University of Washington, Seattle, Washington, USA

Electrical signals control contraction of muscle, secretion of hormones, sensation of the environment, processing of information in the brain, and output from the brain to peripheral tissues. In excitable cells, electrical signals also have an important influence on intracellular metabolism and signal transduction, gene expression, protein synthesis and targeting, and protein degradation. In all these contexts, electrical signals are conducted by members of the ion channel protein superfamily, a set of more than 140 structurally related pore-forming proteins. In addition, members of this protein family are crucial in maintaining ion homeostasis in the kidney and in many different cell types and participate in calcium signaling pathways in nonexcitable cells. In this article, the founding members of each family of ion channel proteins that are structurally related to the voltage-gated ion channels are introduced and an overview of their structure, function, and physiological roles is presented. References are given to one or two recent review articles on each channel family to provide a broad introduction to the literature.

Voltage-Gated Sodium and Calcium Channels

The founding member of this superfamily in terms of its discovery as a separate protein is the voltage-gated sodium channel. These channels are specialized for electrical signaling and are responsible for the rapid influx of sodium ions that underlies the rising phase of the action potential in nerve, muscle, and endocrine cells. Neurotoxin labeling, purification, and functional reconstitution showed that sodium channels from mammalian brain contain voltage-sensing and pore-forming elements in a single protein complex of one principal α-subunit of 220–260 kDa and one or two auxiliary β-subunits of ~36 kDa. The α-subunits of sodium channels contain four homologous domains that each contain six hydrophobic, probable transmembrane segments. A membrane-reentrant loop between the fifth and sixth (S5 and S6) transmembrane segments forms the narrow extracellular end of the pore while the S6 segments form the intracellular end (Figure 1, red). The pore is formed in the center of a pseudosymmetric array of the four domains, and a single α-subunit containing four domains is able to receive voltage signals and activate its intrinsic pore. The channel responds to voltage by virtue of its S4 segments (Figure 1, green), which contain repeated motifs of a positively charged amino acid residue followed by two hydrophobic residues, and move outward under the influence of the membrane electric field to initiate a conformational change that opens the pore. Drugs that block the pore of sodium channels are important as local anesthetics, antiarrhythmic drugs, and antiepileptic drugs. The four β-subunits consist of an amino-terminal extracellular immunoglobulin-like domain, a single transmembrane segment, and a short intracellular segment. They both modulate the gating of the α-subunits and serve as cell adhesion molecules by interaction with extracellular matrix, membrane, and cytoskeletal proteins. Nine voltage-gated sodium channel α-subunits, designated $Na_v1.1$–1.9 have been functionally characterized. They comprise a single family of proteins with greater than 70% amino acid sequence identity in their transmembrane segments. One additional related α-subunit, which defines a second subfamily, $Na_v2.1$, is known but is apparently not voltage-gated.

Voltage-gated calcium channels are the key signal transducers of electrical signaling, converting depolarization of the cell membrane to an influx of calcium ions that initiates contraction, secretion, neurotransmission, and other intracellular regulatory events. Skeletal muscle calcium channels first identified by drug labeling, purification, and functional reconstitution have a principal $\alpha1$-subunit of 212–250 kDa, which is similar to the sodium channel α-subunit but is associated with auxiliary $\alpha2\delta$, β, and γ-subunits that are unrelated to the sodium channel auxiliary subunits. cDNA cloning and sequencing showed that the $\alpha1$-subunit of calcium channels is analogous to the sodium channel α-subunits in structural organization (Figure 1) and is ~25% identical in amino acid sequence in the transmembrane regions. As for the sodium channel α-subunit, the calcium channel $\alpha1$-subunit is sufficient to form a voltage-gated calcium-selective pore by itself. Ten functional calcium channel $\alpha1$-subunits are known in vertebrates, and they fall into three subfamilies that

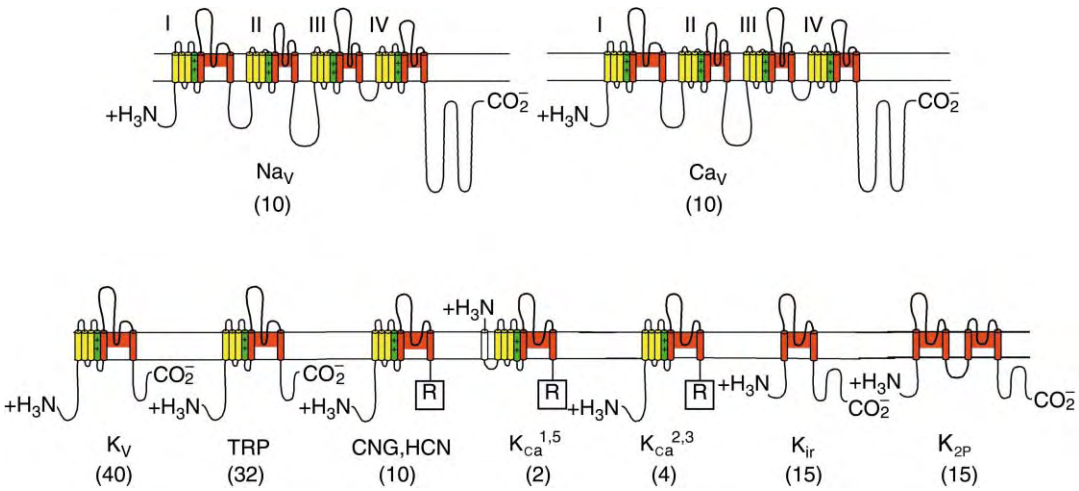

FIGURE 1 The voltage-gated ion channel protein family. The different members of the ion channel protein family structurally related to the voltage-gated ion channels are illustrated as transmembrane folding diagrams in which cylinders represent probable transmembrane alpha-helices. Red, S5–S6 pore-forming segments; green, S4 voltage sensor, yellow, S1–S3 transmembrane segments; R, regulatory domain that binds intracellular second messengers. The numbers of family members in the human genome are given in parentheses.

differ in function and regulation. The Ca_v1 family ($Ca_v1.1–1.4$) conducts L-type calcium currents that initiate contraction, endocrine secretion, and synaptic transmission at the specialized ribbon synapses involved in sensory input in the eye and ear. L-type calcium currents also are important regulators of gene expression and other intracellular processes. Blockers of $Ca_v1.2$ channels are important in the therapy of cardiovascular diseases including hypertension, cardiac arrhythmia, and angina pectoris. The Ca_v2 family of calcium channels ($Ca_v2.1–2.3$) conducts N-, P/Q- and R-type calcium currents that initiate fast synaptic transmission at synapses in the central and peripheral nervous systems and are blocked specifically by peptide neurotoxins from spider and cone snail venoms. The Ca_v3 family of calcium channels ($Ca_v3.1–3.3$) conducts T-type calcium currents that are important for repetitive action potential firing of neurons in the brain and in the pacemaker cells of the sino-atrial node in the heart. The functional and regulatory properties and protein–protein interactions of these channels are adapted to their different roles in electrical signaling and cellular signal transduction.

Voltage-Gated Potassium Channels

Voltage-gated potassium channels are activated by depolarization, and the outward movement of potassium ions through them repolarizes the membrane potential to end action potentials, hyperpolarizes the membrane potential immediately following action potentials, and plays a key role in setting the resting membrane potential. In this way, potassium channels control electrical signaling and regulate ion flux and calcium transients in nonexcitable cells. The first voltage-gated potassium channels were cloned from *Drosophila* based on a mutation that causes the *Shaker* phenotype. They are composed of four transmembrane subunits, each of which is analogous to a single domain of the principal subunits of sodium or calcium channels (Figure 1). The voltage-gated potassium channels are remarkable for their diversity. They include 40 different channels that are classified into 12 distinct groups based on their amino acid sequence homology (Kv1 to Kv12). These α-subunits can assemble into homo- and hetero-tetramers, leading to a wide diversity of different channel complexes. The Kv1 channels also associate with Kvβ-subunits, which are intracellular proteins. The Kv4 subunits associate with KChiPs, intracellular calmodulin-like calcium-binding proteins that regulate channel gating. Some of the Kv7 and Kv11 α-subunits associate with single membrane-spanning subunits (minK, MiRP1, MiRP2), which regulate their gating properties. The diversity of potassium channels allows neurons and other excitable cells to precisely tune their electrical signaling properties by expression of different combinations of potassium channel subunits.

Second Messenger-Gated and Sensory Ion Channels

In addition to the voltage-gated sodium, calcium, and potassium channels, the voltage-gated ion channel family includes additional members that are gated by a combination of voltage and binding of second

messengers, including calcium, cyclic nucleotides, and lipid messengers. These channels have six transmembrane segments and a generally similar structure to voltage-gated potassium channels, but contain in addition a regulatory domain attached at their carboxy terminus.

Calcium-activated potassium channels ($K_{Ca}1-5$) have an ion channel domain attached to an intracellular calcium-dependent regulatory domain in their C terminus. They are activated by a combination of depolarization and binding of calcium ions. For the $K_{Ca}1$, and $K_{Ca}5$ channels, calcium binding to a regulatory domain in the C terminus (R, Figure 1) enhances activation of the channels by depolarization, resulting in synergistic gating of channel activity by voltage and intracellular calcium concentration. $K_{Ca}1$ channels have an extra transmembrane segment at the N terminus (S0) and associate with $K_{Ca}\beta$-subunits, which are 2-TM intrinsic membrane proteins. For $K_{Ca}2$ or $K_{Ca}3$ channels, calcium binds to a constitutively associated calmodulin molecule bound to the C-terminal regulatory domain and activates the channels without a voltage stimulus. All of the K_{Ca} channels serve to repolarize excitable cells following single-action potentials or trains of action potentials, during which calcium entry increases cytosolic calcium levels and activates them. One of their prominent roles is to define the length of action potential trains in neurons by activating in response to calcium influx through voltage-gated calcium channels and thereby repolarizing and hyperpolarizing the cell. Similarly, in smooth muscle cells they hyperpolarize the membrane and relax the smooth muscle.

The structurally related cyclic nucleotide-gated ion channels (CNG, six family members) and hyperpolarization-activated, cyclic nucleotide-gated ion channels (HCN, four family members) are composed of four subunits that each have a 6-TM voltage-gated ion channel domain attached to an intracellular cyclic nucleotide-binding domain at their C terminus. These channels were first purified and cloned from retinal rods, where they conduct the dark current that underlies visual signal transduction. Upon capture of photons by rhodopsin, activation of a G-protein-signaling pathway leads to activation of a cyclic nucleotide phosphodiesterase that hydrolyzes cGMP. Reduction in the cGMP concentration in the rod outer segment closes these "dark-current" channels, causing hyperpolarization and initiation of visual signal transduction to the neural cells of the retina. Closely related cyclic nucleotide-gated channels are responsible for olfactory signal transduction in the nasal epithelium. The more distantly related HCN channels are involved in cyclic nucleotide-regulated pacemaking in cells that generate repetitive action potentials, like the sino-atrial node pacemaker cells of the heart and the persistently firing neurons of the thalamus in the brain. They are also involved in sensation of sour tastes in taste buds. Remarkably, they are activated by hyperpolarization (rather than depolarization) via their S4 voltage sensor, and their opening by hyperpolarization is greatly enhanced by simultaneous binding of cAMP and/or cGMP.

The transient receptor potential (trp) channels were discovered first in *Drosophila*, where the founding member is the site of mutations that cause the trp phenotype that alters visual signal transduction in the eye. Subsequent to that work, a family of 32 related channels, which can be divided into six subfamilies, have been defined in mammals. These channels are weakly voltage-sensitive, are either calcium-selective or non-selective cation channels that conduct calcium, and are activated by a range of signals including heat, cold, and intracellular lipid messengers. The TRPC subfamily of channels is most closely related to the classical *Drosophila* trp channel. The TRPV subfamily of channels is most closely related to the "vanilloid receptor," a channel protein that serves as a receptor for the hot chili pepper ingredient capsaicin, a vanilloid compound. It also responds to heat and mediates noxious thermal pain sensations. The TRPM subfamily is most closely related to melastatin, first discovered as a tumor marker in melanoma. TRPM7, the first member of this family to be functionally expressed, is slightly calcium-selective and contains an intrinsic protein kinase domain that may autophosphorylate to activate its ion channel domain. The PKD, CatSper, and mucolipin subfamilies of ion channel subunits are also distantly related to trp. CatSper plays an essential (but still unknown) role in calcium signaling in sperm. PKD channels are involved in sensing fluid transport in the kidney and other epithelial tissues. Mucolipin channels may be involved in auditory signaling in the ear and in calcium transport regulating lysosome function.

Inwardly Rectifying Potassium Channels and their Relatives

The inwardly rectifying potassium channels (K_{ir}) are the structurally simplest ion channels, containing four subunits that each have two transmembrane segments and a membrane-re-entrant pore loop between them (Figure 1). As their name implies, they conduct potassium more effectively inward than outward, but their outward conductance of potassium is physiologically important to repolarize cells near the resting membrane potential. They are structurally related to the S5 and S6 segments of the voltage-gated ion channels, and their pore loop forms the extracellular end of the pore as in that family of proteins. The two transmembrane segments and the pore loop of a related bacterial potassium channel have been shown directly by X-ray crystallography to form an ion-selective

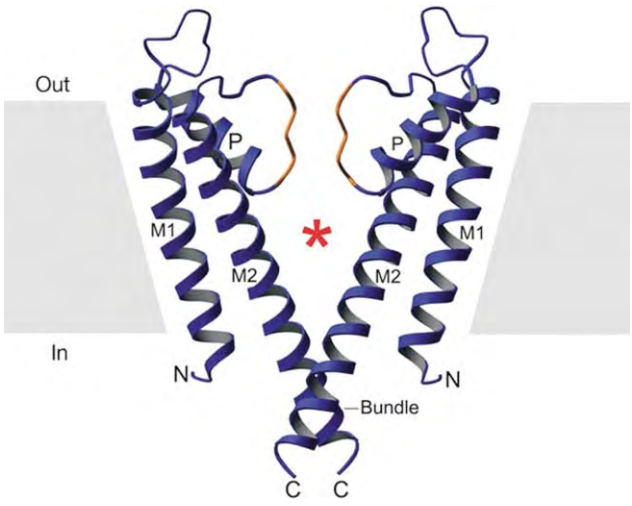

FIGURE 2 Structure of the pore of a bacterial potassium channel. The structures of two of the four subunits of a bacterial potassium channel related to the inwardly rectifying potassium channels are illustrated. Orange marks the backbone carbonyls that form the narrow ion selectivity filter. Red asterisk indicates the water-filled cavity in the ion permeability pathway where a potassium ion is located in the X-ray structure.

pore (Figure 2). Many inwardly rectifying potassium channels are gated by intracellular divalent cations that bind in their pore, including Mg, spermine, and spermidine. The X-ray structure of a related vertebrate inwardly rectifying potassium channel reveals an extended pore region that projects into the cytoplasm and contains divalent cation-binding sites that may control ion flow through the pore. Other K_{ir} channels are gated by direct binding of G protein $\beta\gamma$-subunits and inositol phospholipid messengers. Remarkably, ATP-sensitive potassium channels are composed of an inwardly rectifying potassium channel core in association with the much larger sulfonylurea receptor (SUR) protein, a member of the ABC transporter family that binds ADP and ATP and regulates the function of the inwardly rectifying potassium channel. These channels are crucial regulators of insulin secretion from pancreatic beta cells controlled by intracellular glucose and ATP levels, and SUR is the molecular target for the sulfonylurea drugs used in treatment of diabetes.

Two-Pore-Motif Potassium Channels

The most recently discovered family of ion channels are potassium channels that have two repeats of the inward rectifier pore motif and are designated K_{2P} (Figure 1). The channels function as "open rectifiers," that is, they are constitutively open and constantly drive the membrane potential toward the potassium equilibrium potential by mediating outward potassium conductance. They are thought to be important for setting the resting membrane potential of excitable cells at a negative value near the equilibrium potential for potassium of $\sim$80 mV. Although they are not regulated by physiological mechanisms that have been described to date, they may be an important target for the actions of inhalation anesthetics, which activate these channels and thereby could prevent action potential firing in the brain during general anesthesia.

Structure and Function

Viewed from the perspective of the entire ion channel protein family, the functions of these proteins can be divided into three complementary aspects: ion conductance, pore gating, and regulation. All members of the family share a common pore motif, with variations appropriate to determine their different ion selectivity. It is likely that this pore motif first evolved in the bacterial ion channels that resemble inward rectifiers. The X-ray crystal structure of one of these channels has shown that the narrow outer mouth of the pore is formed by the pore loops between the M1 and M2 segments that are analogous to the S5 and S6 transmembrane segments of the 6-TM family members while the length of the pore is formed by a tilted bundle, "inverted teepee" arrangement of the M2 segments (Figure 2). This structure suggests that the pore is closed at its intracellular end and discriminates ions at the narrow ion selectivity filter at its extracellular end. This model of pore formation fits well with a wealth of structure–function data on the voltage-gated ion channels and the cyclic nucleotide-gated channels. The closure of the pore at the intracellular end suggests that this is the site of pore gating. Support for this idea comes from classical biophysical studies and from more recent work. The structure of a calcium-activated bacterial potassium channel with calcium bound shows that the crossing of the M2 segments at the intracellular end of the pore is opened by bending of the helix, consistent with the hypothesis that this is the mechanism of pore opening.

The different protein families within the ion channel superfamily are regulated by different mechanisms. The simplest family members, the inwardly rectifying potassium channels, are gated extrinsically by divalent cations binding in the pore or by binding of other regulators. The cyclic nucleotide-gated ion channels and the calcium-activated potassium channels are gated by ligand binding to their carboxy-terminal regulatory domains. These ligand-induced conformational changes are thought to exert a torque on the connected S6 segments and force the opening of the pore bundle of S6 helices. In addition, the HCN channels and the

$K_{Ca}1$ channels are also gated synergistically by changes in membrane potential and are highly sensitive to small voltage changes. The voltage-gated sodium, calcium, and potassium channels are primarily gated by changes in membrane potential. Their regulation depends on the S1 to S4 segments of these channels, which can be viewed as an evolutionary addition to the pore-forming segments. The detailed mechanism of voltage-dependent gating is unknown. However, there is clear structure–function evidence for an outward and rotational movement of the positively charged S4 segments during the gating process, and it is assumed that the conformational change accompanying this outward movement exerts a torque on the bundle of four S6 segments at the intracellular end of the pore forcing the bundle to open. Voltage-dependent gating of the sodium and calcium channels is also modulated by binding of calcium/calmodulin and G proteins to the C-terminal domain, suggesting that these interactions may also exert a torque on the S6 segments and thereby alter the energetics of gating.

Conclusion

The voltage-gated ion channel superfamily is one of the largest families of signaling proteins, following the G protein-coupled receptors and the protein kinases in the number of family members. The family is likely to have evolved from a 2-TM ancestor like the modern inwardly rectifying potassium channels and bacterial potassium channels. Modular additions of intracellular regulatory domains for ligand binding and a 4-TM transmembrane domain for voltage gating have produced extraordinarily versatile signaling molecules with capacity to respond to voltage signals and intracellular effectors and to integrate information coming from these two types of inputs. The resulting signaling mechanisms control most aspects of cell physiology and underlie complex integrative processes like learning and memory in the brain and coordinated movements of muscles. The evolutionary appearance and refinement of these signaling mechanisms is one of the hallmark events allowing the development of complex multicellular organisms.

See Also the Following Articles

G Protein Signaling Regulators • Voltage-Dependent K^+ Channels • Voltage-Sensitive Ca^{2+} Channels • Voltage-Sensitive Na^+ Channels

Glossary

gating The intrinsic regulatory process through which ion channels are opened and closed by conformational changes of the ion channel protein.

ion channel A transmembrane protein that forms a pore through which ions move down their electrochemical gradients into or out of cells or intracellular organelles.

rectifying An ion channel in which ion flow is favored in one direction – e.g., inwardly rectifying potassium channels that conduct potassium ions inward more readily than outward, even though outward potassium movement is that physiologically relevant direction.

voltage-gated Ion channels whose gating is regulated by changes in transmembrane voltage.

Further Reading

Catterall, W. A. (2000a). From ionic currents to molecular mechanisms: The structure and function of voltage-gated sodium channels. *Neuron* **26**, 13–25.

Catterall, W. A. (2000b). Structure and regulation of voltage-gated calcium channels. *Annu. Rev. Cell Dev. Biol.* **16**, 521–555.

Goldstein, S. A., Bockenhauer, D., O'Kelly, I., and Zilberberg, N. (2001). Potassium leak channels and the KCNK family of two-P-domain subunits. *Nat. Rev. Neurosci.* **2**, 175–184.

Jan, L. Y., and Jan, Y. N. (1997). Cloned potassium channels from eukaryotes and prokaryotes. *Annu. Rev. Neurosci.* **20**, 91–123.

Matulef, K., and Zagotta, W. N. (2003). Cyclic nucleotide-gated ion channels. *Annu. Rev. Cell Dev. Biol.* **19**, 23–44.

Montell, C. (2001). Physiology, phylogeny, and functions of the TRP superfamily of cation channels. Sci STKE, RE1.

Patel, A. J., Lazdunski, M., and Honore, E. (2001). Lipid and mechano-gated 2P domain K^+ channels. *Curr. Opin. Cell Biol.* **13**, 422–428.

Reimann, F., and Ashcroft, F. M. (1999). Inwardly rectifying potassium channels. *Curr. Opin. Cell Biol.* **11**, 503–508.

Vergara, C., Latorre, R., Marrion, N. V., and Adelman, J. P. (1998). Calcium-activated potassium channels. *Curr. Opin. Neurobiol.* **8**, 321–329.

Zhou, Y., Morais-Cabral, J. H., Kaufman, A., and MacKinnon, R. (2001). Chemistry of ion coordination and hydration revealed by a potassium channel–Fab complex at 2.0 A resolution. *Nature* **414**, 43–48.

Biography

William Catterall is Professor and Chair of Pharmacology at the University of Washington. His interests are neurobiology and molecular pharmacology, with research focus on ion channel proteins. He received his Ph.D. in Physiological Chemistry from Johns Hopkins University and was postdoctoral Fellow and Staff Scientist in the Laboratory of Biochemical Genetics, NHLBI, NIH. He is a member of the National Academy of Sciences, Institute of Medicine, and American Academy of Arts and Sciences.

IP_3 Receptors

Colin W. Taylor
University of Cambridge, Cambridge, UK

Edward Morris and Paula da Fonseca
Imperial College, London, UK

Inositol 1,4,5-trisphosphate (IP_3) is an intracellular messenger. It is produced from a lipid in the plasma membrane by enzymes (phospholipases C) that are stimulated in response to activation of many different receptors in the plasma membrane. IP_3 is released into the cytosol where it can bind to its own receptor, a very large intracellular Ca^{2+} channel, and stimulate release of Ca^{2+} from intracellular stores. The Ca^{2+} released by IP_3 receptors also regulates their activity and this contributes to the complex changes in cytosolic Ca^{2+} concentration that follow activation of receptors that stimulate phospholipase C.

A Brief History

For more than a century, beginning with Sidney Ringer in 1883 serendipitously discovering that Ca^{2+} was required for contraction of frog hearts, increases in intracellular Ca^{2+} concentration have been known to regulate cellular activity. Such Ca^{2+}-regulated events begin at fertilization, continue through development and cell death, and include many responses of differentiated cells, such as contraction, secretion, and metabolism. In short, changes in cytoplasmic Ca^{2+} concentration provide an ubiquitous link between extracellular stimuli (hormones, neurotransmitters, etc.) and the regulation of intracellular processes. The first suggestion that turnover of phosphoinositides, a minor class of lipids with a phosphorylated inositol headgroup (Figure 1), might provide a common link between extracellular stimuli and physiological responses came from work by the Hokins in the 1950s. But it was a hefty review from Bob Michell some 20 years later that developed the idea that receptor-stimulated phosphoinositide hydrolysis might be causally linked to changes in intracellular Ca^{2+} concentration. For years, it was disputed whether Ca^{2+} signals were the result, or the cause, of the phosphoinositide hydrolysis, a dispute that was fuelled by the observation that the enzymes responsible for the hydrolysis (phospholipases C) are stimulated by Ca^{2+}. Experiments with the salivary gland of the humble blowfly were instrumental in resolving the dispute and establishing that increases in intracellular Ca^{2+} concentration result from receptor-stimulated hydrolysis of phosphatidylinositol 4,5-bisphosphate to produce inositol 1,4,5-trisphosphate (IP_3) and diacylglycerol (Figure 1). Both products are intracellular messengers. The latter regulates the activity of certain proteins kinase C and it can also be metabolized to additional signaling molecules. The signaling properties of IP_3 were demonstrated exactly a century after Ringer's discovery in a seminal paper from Mike Berridge, Robin Irvine, and their colleagues. They showed that IP_3 stimulates release of Ca^{2+} from intracellular stores (later shown to be largely within the endoplasmic reticulum). As expected of an intracellular signaling molecule, IP_3 is rapidly metabolized to products that cannot stimulate release of Ca^{2+} from stores. Within months, the ability of IP_3 to stimulate Ca^{2+} release was confirmed in countless cell types, and the signaling pathway illustrated in Figure 1 was shown to be almost ubiquitously expressed and to provide the essential link between many different receptors and the release of Ca^{2+} from intracellular stores. Later work has established the roles of IP_3 receptors in generating complex intracellular Ca^{2+} signals and has begun to address how the structure of IP_3 receptors underlies their function.

Structure of IP_3 Receptors

IP_3 receptors are big proteins. Each receptor has four subunits arranged around a central Ca^{2+}-permeable pore that opens when the receptor is activated. When purified IP_3 receptors are reconstituted into artificial lipid membranes, addition of IP_3 causes a large cation-permeable channel to open. This confirms that the tetrameric IP_3 receptor complex is all that is required to produce an IP_3-gated channel. Other proteins are intimately associated with IP_3 receptors in native cells, but their roles are modulatory: the assembly of four IP_3 receptor subunits is sufficient to form a functional,

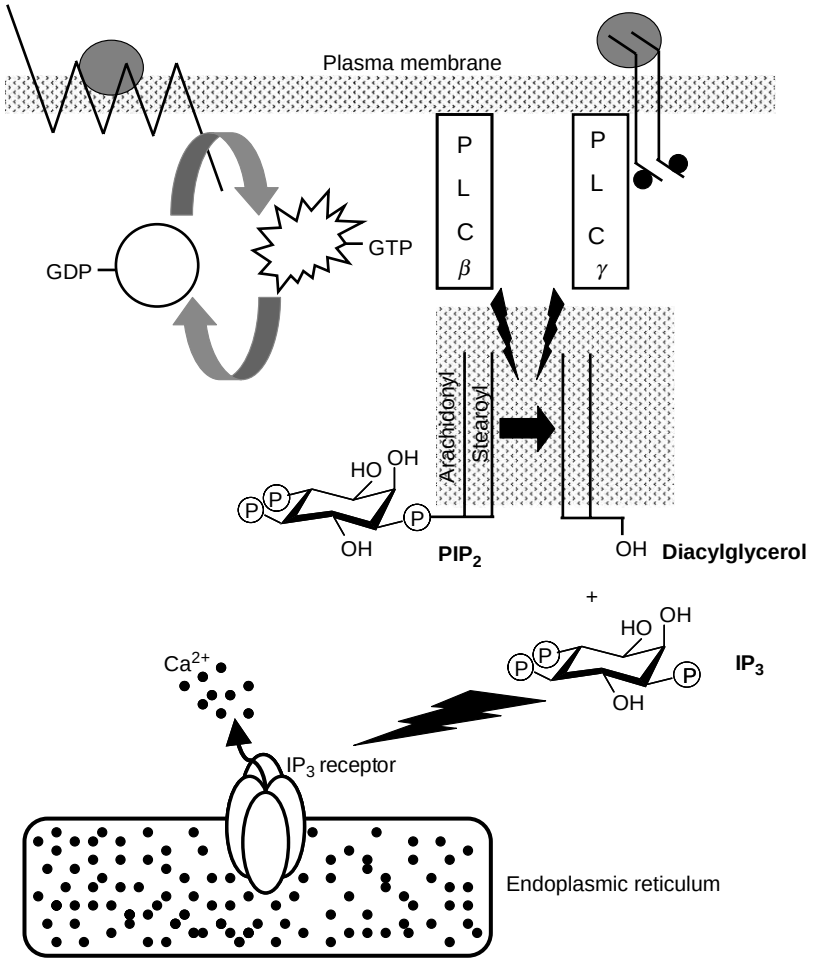

FIGURE 1 Receptor-stimulated Ca^{2+}mobilization. Two different families of phosphopliase C, PLCβ and PLCα, are regulated by different classes of receptor. The former are stimulated by the dissociated subunits of G proteins, which are themselves activated by receptors with a structure that includes seven-membrane-spanning segments. PLCα is activated when it associates with and becomes phosphorylated by receptors with either intrinsic or associated protein tyrosine kinase activity. Both families of PLC catalyze hydrolysis of phosphatidylinositol 4,5-bisphosphate (PIP2) in the plasmamembrane to give diacylglycerol and IP_3. The latter then stimulates release of $Ca^{2+}$from intracellular stores via IP_3 receptors.

IP_3-sensitive, Ca^{2+} channel. Most eukaryotic cells express IP_3 receptors and the genes that encode the subunits are closely related in species as diverse as man and the insect, *Drosophila*. The structural basis of IP_3 receptor function is therefore likely to be similar in all eukaryotes. In mammals, there are three closely related genes for IP_3 receptor subunits, each encoding a protein of ~2700 amino acid residues. This protein sequence can be divided into three functional regions (Figures 2A and 2B): an N-terminal cytoplasmic region that binds IP_3, a cytoplasmic regulatory region, and a channel region containing the transmembrane segments close to the C-terminus. The tetrameric receptor is some 20 nm across and extends more than 10 nm from the membrane of the endoplasmic reticulum (ER) into the cytoplasm as shown in a recent three-dimensional analysis of electron microscope images of the receptor (Figure 2C). This analysis combined with biochemical data suggest a model in which the primary amino-acid sequence of each subunit is assigned to specific positions within the three-dimensional map (Figures 2A–2C). A recent X-ray crystallographic analysis of the IP_3-binding region of the receptor (residues 224-604) shows IP_3 bound in a cleft between two domains which form an L-shaped structure (Figure 2D). The N-terminal domain consists of a globular barrel made up of 12 β-strands, while the C-terminal domain consists of a bundle of eight α-helices. IP_3 is coordinated by residues from each of the domains. Each receptor (with its four subunits) has four IP_3-binding sites and it is likely that each must bind IP_3 before the channel can open.

There is as yet no high resolution structure for the remaining 87% of the receptor, although it is clear that towards the C-terminal end of each subunit there are six-transmembrane segments that span the ER membrane and form the pore of the channel (Figures 2A and 2B). Each of the IP_3 receptor subunits contributes to the pore, which is formed by

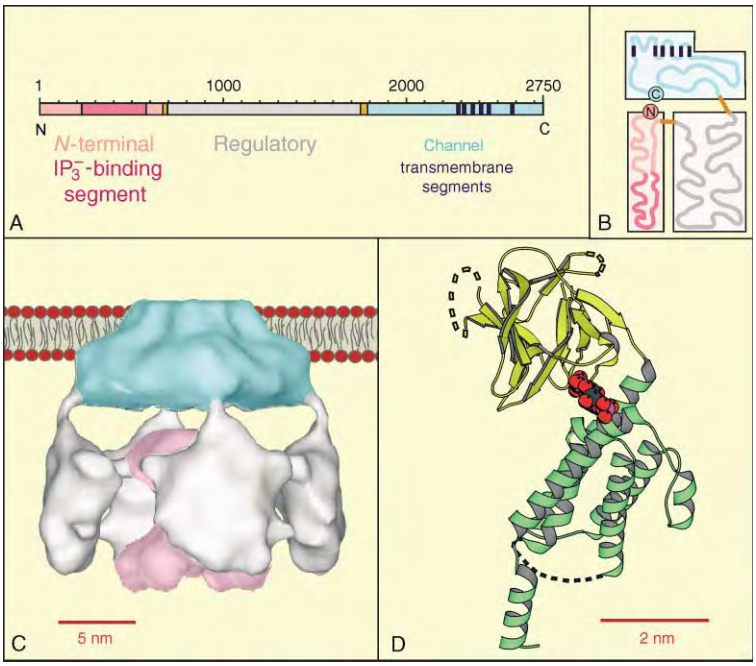

FIGURE 2 Structure of IP_3 receptors. (A) Functional regions of the IP_3 receptor are shown mapped onto the primary sequence. (B) Proposed spatial organization of the functional domains. (C) Three-dimensional reconstruction of an IP_3 receptor purified from brain derived from analysis of images from electron microscopy. The channel region (blue) embedded in the lipids of the ER membrane is connected by thin strands to four outer domains (gray) which are thought to form the regulatory region. Four inner domains (pink) are thought to include the IP_3-binding sites. (D) X-ray crystallographic structure of the IP_3-binding region of the type 1 IP_3 receptor. The protein backbone is shown as a ribbon diagram with the N-terminal β-barrel domain (yellow) uppermost and the C-terminal α-helical bundle domain (green) at the bottom. The IP_3 molecule (red) lying in the cleft between the two domains is represented as space-filling spheres.

the last two of the transmembrane segments and the intervening loop. This pore region shares considerable similarities with many other cation channels, suggesting a conserved structural organization. Comparison of the intermediate resolution structure of the IP_3 receptor with other cation channels suggests that conservation of structural organization may also extend to other regions. We do not yet have a sufficient understanding of IP_3 receptor structure to know how binding of IP_3 at one end of the amino acid sequence of each subunit leads to opening of a pore formed by residues lying at the opposite end of the primary sequence.

Because analyses of receptor function often depend upon selective agonists and antagonists, briefly highlighted are the relative paucity of such ligands for IP_3 receptors. Heparin and decavanadate are membrane-impermeant competitive antagonists of IP_3; and Xestospongin, caffeine, and 2-aminoethoxydiphenyl borane (2-APB) are membrane-permeant noncompetitive antagonists. Each drug lacks specificity. Many inositol phosphates are agonists of IP_3 receptors (although none is better than IP_3), but a fungal product (now synthesized), adenophostin, is an agonist of IP_3 receptors with an affinity some 10 times greater than that of IP_3.

IP_3 Receptors are Regulated by IP_3 and Ca^{2+}

IP_3 provides the link between receptors in the plasma membrane and release of Ca^{2+} from intracellular stores (Figure 1), but all IP_3 receptors are also regulated by cytosolic Ca^{2+}. Indeed considerable evidence suggests that binding of both IP_3 and Ca^{2+} are required before the channel can open: IP_3 and Ca^{2+} should be regarded as coagonists of the receptor. The effects of Ca^{2+} are more complex, however, because many studies have shown that modest increases in Ca^{2+} concentration potentiate the effects of IP_3 (consistent with the need for both IP_3 and Ca^{2+} to bind for channel opening), while more substantial increases are inhibitory. These biphasic effects of Ca^{2+} on IP_3 receptor function are important in mediating interactions between IP_3 receptors and between IP_3 receptors and other Ca^{2+} channels. Whether these effects of Ca^{2+} result from Ca^{2+} binding directly to the IP_3 receptor or to associated Ca^{2+}-binding proteins is not resolved. It is, however, clear that binding of IP_3 regulates the Ca^{2+}-binding site, so that the sensitivity of the IP_3 receptor to Ca^{2+} is regulated by IP_3.

The Ca^{2+} signals recorded from intact cells are often complex: they may remain spatially restricted to only parts of a cell allowing local regulation of Ca^{2+}-sensitive processes, or they may propagate regeneratively across the cell as Ca^{2+} waves allowing global regulation of Ca^{2+}-sensitive processes. The interplay between IP_3 and Ca^{2+} in regulating IP_3 receptors is crucial in determining whether Ca^{2+} signals propagate. Ca^{2+} released by active IP_3 receptors (or by other Ca^{2+} channels) is thought to ignite the activity of more distant IP_3 receptors by providing the Ca^{2+} they need to open. This regenerative process has been described as Ca^{2+}-induced Ca^{2+} release. The much higher Ca^{2+} concentration in the immediate vicinity of active IP_3 receptors is thought to restrain this potentially explosive positive feedback by inhibiting IP_3 receptors.

IP_3 Receptors and Ca^{2+} Entry

Receptors that stimulate IP_3 formation typically cause both release of Ca^{2+} from intracellular stores and enhanced Ca^{2+} entry across the plasma membrane. Cells express a variety of Ca^{2+}-permeable channels regulated by different products of the phosphoinositide pathway, but store-regulated (also known as "capacitative") Ca^{2+} entry is the most widely expressed pathway. Here, emptying of intracellular Ca^{2+} stores (by IP_3) generates a signal (it has not yet been identified) that causes activation of a Ca^{2+}-permeable channel in the plasma membrane. There is therefore an inextricable link between store emptying (mediated by IP_3) and Ca^{2+} entry, and as the stores refill (when IP_3 is no longer produced) then so capacitative Ca^{2+} entry is also switched off. Under physiological conditions, where IP_3 links receptors in the plasma membrane to emptying of intracellular Ca^{2+} stores, IP_3 receptors are clearly required for activation of capacitative Ca^{2+} entry. But they may also play a more direct role because there is evidence, albeit controversial, that IP_3 receptors may be physically coupled to the Ca^{2+} channels in the plasma membrane and may thereby serve as the link between the stores and capacitative Ca^{2+} entry.

See Also the Following Articles

Calcium Waves • Intracellular Calcium Channels: $NAADP^+$-Modulated • Phosphatidylinositol Bisphosphate and Trisphosphate • Phosphatidylinositol-3-Phosphate • Phospholipase C • Protein Kinase C Family

Glossary

agonist A substance that binds to a receptor to cause its activation.

antagonist A substance that binds to a receptor to prevent its activation.

phosphoinositides Account for about 10% of cellular phospholipids. A glycerol backbone attached to two fatty acids (stearoyl at position 1, arachidonyl at position 2) and inositol (linked by a phosphodiester bond at position 3). The inositol headgroup can also be further phosphorylated.

phospholipase C An enzyme (there are many forms) that catalyses cleavage of the diacylglycerol-phosphate bond of a glycerophospholipid. In the context of this article, the important phospholipases C are those that cleave phosphatidylinositol 4,5-bisphosphate to diacylglycerol and IP_3.

positive feedback A situation where the output of a process (e.g., Ca^{2+} from an IP_3 receptor) provides the stimulus for that process (e.g., channel opening).

receptor A signal-transducing protein that can be activated by specific agonists, the actions of which can be selectively blocked by appropriate antagonists.

Further Reading

Barritt, G. J. (1992). *Communication within Animal Cells*. Oxford University Press, Oxford.

Berridge, M. J. (1997). Elementary and global aspects of calcium signalling. *J. Physiol.* **499**, 291–306.

Berridge, M. J., and Irvine, R. F. (1989). Inositol phosphates and cell signalling. *Nature* **341**, 197–205.

Bosanac, I., Alattia, J.-R., Mal, T. K., Chan, J., Talarico, S., Tong, F. K., Tong, K. I., Yoshikawa, F., Furuichi, T., Iwai, M., Michikawa, T., Mikoshiba, K., and Ikura, M. (2002). Structure of the inositol 1,4,5-trisphosphate receptor binding core in complex with its ligand. *Nature* **420**, 696–701.

da Fonseca, P. C. A., Morris, S. A., Nerou, E. P., Taylor, C. W., and Morris, E. P. (2003). Domain organisation of the type 1 inositol 1,4,5-trisphosphate receptor as revealed by single particle analysis. *Proc. Acad. Nat. Sci (USA)* **100**, 3936–3941.

Michell, R. H. (1975). Inositol phospholipids and cell surface receptor function. *Biochim. Biophys. Acta* **415**, 81–147.

Putney, J. W. Jr. (1997). *Capacitative Calcium Entry*. R.G. Landes Co. Austin, Texas, USA.

Streb, H., Irvine, R.F., Berndge, M. J., and Schulz, I. (1983).Release of Ca^{2+} from a nonmitochondrial store of pancreatic acinar cells by inositol-1,4,5-triphosphate. *Nature* **306**, 67–69.

Taylor, C. W., and Laude, A. J. (2002). IP_3 receptors and their regulation by calmodulin and cytosolic Ca^{2+}. *Cell Calcium* **32**, 321–334.

Biography

Colin W. Taylor is a Professor of Cellular Pharmacology in the Department of Pharmacology, University of Cambridge. He holds Ph.D. and Sc.D. degrees from the University of Cambridge, and pursued postdoctoral studies at the Medical College of Virginia. His major research interests are in the structure and function of IP_3 receptors and in the regulation of Ca^{2+} entry pathways.

Edward Morris is a Senior Lecturer in the Division of Biomedical Sciences, Imperial College London. He holds a Ph.D. from the University of London. His research focuses on the structural biology of membrane proteins.

Paula C. A. da Fonseca is a Postdoctoral Research Associate in the Division of Biomedical Sciences, Imperial College London. After her first degree in biochemistry at the University of Lisbon, she obtained a Ph.D. at the University of London. Her research interests include the structure and function of membrane proteins.

Iron–Sulfur Proteins

Helmut Beinert
University of Wisconsin, Madison, Wisconsin, USA

Jacques Meyer
Commissariat á l'Energie Atomique, Grenoble, France

Roland Lill
University of Marburg, Marburg, Germany

Iron–sulfur (Fe–S) proteins contain iron ligated by inorganic sulfide and/or at least two cysteines (Cys) as ligands. Fe–S active sites are required for or involved in electron transfer, mostly in the range of low oxidation–reduction potentials. They also can serve as active sites of enzymes and as sensing and regulating agents. Fe–S active sites are perhaps the most ancient cofactors, and Fe–S compounds may have been essential reactants of prebiotic chemistry.

Iron–Sulfur Clusters

Properties

Structure

Nomenclature and Shorthand Designations The conventions for the nomenclature of Fe–S clusters and Fe–S proteins are found in the 1989 recommendations of the Nomenclature Committee of the International Union of Biochemistry (IUB). The components of the cluster core are placed into brackets and the oxidation level of the core (not including that of ligands) is given as a superscript $[2Fe–2S]^{2+}$. The possible oxidation states of the species that can be formed are indicated as shown: $[2Fe–2S]^{2+,+}$. If the kind of ligands to this cluster is to be specified, the alternative designation $[Fe_2S_2(RS)_2(L_2)]^{2-}$ should be used.

Structures In the great majority of Fe–S proteins the iron is present in clusters, with the irons linked by sulfides. The [4Fe–4S] cluster is the predominant species. The simplest Fe–S protein and also the simplest building block of Fe–S proteins is the mononuclear thiolate complex $[Fe(Cys)_4]^{2-,-}$ as it occurs in rubredoxins (Rd). The cluster types are shown in Figure 1. The coordination is tetrahedral throughout. As evident from the figure, the S–S distances are ~1.3 times longer than the Fe–Fe distances, which produces the distorted cubic structure typical for [4Fe–4S] clusters. The 3Fe cluster can be considered as a 4Fe cluster with one Fe missing. The cluster structures shown are to some extent interconvertible and the 3Fe-cluster is central to all cluster interconversions. By partial denaturation of the protein it can also be converted to a linear form: $(Cys)_2FeS_2FeS_2Fe(Cys)_2$. The 3Fe cluster can serve as starting material for producing heterometal clusters with metals such as Zn, Ni, Co, Cd, Ga, Tl, Mo; however, such clusters are not found in nature. Those that occur have modified structures and are formed by specific synthetic systems. The 4Fe to 3Fe cluster conversion is also used in nature to condition clusters for use as active sites in enzymes and for sensing functions.

Stability

Sulfur is a weak ligand, allowing the iron to remain in the high-spin state, which makes the ligands relatively labile as compared to strong ligands such as cyanide. As evident from the cluster interconversions and distortions mentioned above, Fe–S clusters are rather malleable, and from high-resolution X-ray structures it is apparent that they can be further distorted by influences from the protein and can be adapted for various conditions and functions. Fe–S clusters are sensitive toward oxidants such as oxygen and its reduction products and toward NO, and also to an excess of their own constituents, namely S^{2-} and RS^-, to dithiothreitol and dithionite and toward hydrolysis at high or low pH. As mentioned above, Cys ligands belonging to protein frameworks are required for the formation of stable clusters. Replacement of one Cys with another functional residue is allowed in some clusters; however, the only clusters that are known to be stable with two non-Cys ligands are those with two histidine (His) ligands, as they occur naturally in the so-called "Rieske" proteins. While polypeptide chains are mandatory for the stabilization

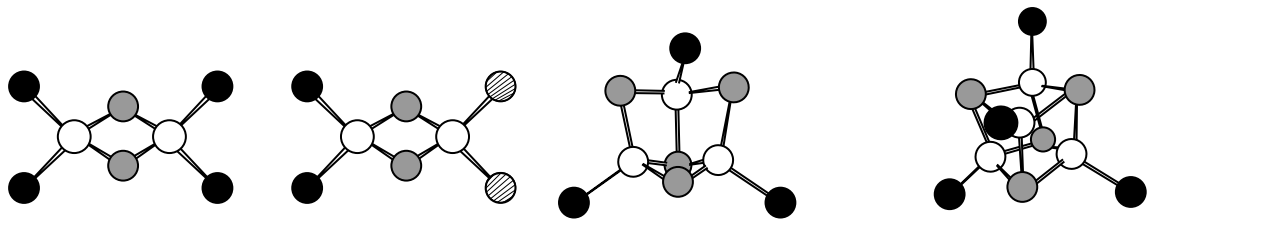

FIGURE 1 Models for structures of 2Fe, 3Fe, and 4Fe clusters. White: Fe; black: cysteine, and gray sulfide sulfurs; hatched: histidine nitrogens. Adapted with permission from Holm, R. H., Kennepohl, P., and Solomon, E. I. *Chem. Rev.* (1996). Structural and functional aspects of metal sites in biology. **96**, 2239–2314.

of Fe–S clusters, their protecting effect is very variable: the lifetime of Fe–S proteins in air may vary from seconds to weeks. As naturally occurring Fe–S clusters require protein-ligands for support, their functions are considered in the section titled 'Iron–Sulfur Proteins' below.

Electronic Structure and Magnetism

The electronic charge in Fe–S clusters is concentrated at their sulfides and Cys ligands. It has been shown by X-ray near-edge spectroscopy (XANES), that all bonds involving sulfur are highly covalent, with those involving sulfide exhibiting 2–3 times the covalency of the thiolate bonds. On the contrary, the unpaired spin density resides primarily on the irons. Fe–S clusters owe many of their characteristic properties to the ordering of their spin-systems. This ordering is dominated by three forces: first, the tendency to pair the spins antiparallel, which is expressed in the magnitude of the spin coupling parameter J; second, the tendency to pair the spins parallel, expressed in the parameter B, the resonance integral (this tendency arises when an extra electron is present, leading to spin-dependent electron delocalization (SDD)); and third, the dynamic trapping energy, arising through vibronic coupling with groups in the neighborhood. On one-electron reduction of $[2Fe–2S]^{2+}$ (2 Fe^{III}) clusters the trapping energy leads almost invariably to antiparallel coupling and localization of the electron at one Fe ($1Fe^{III}$, $1Fe^{II}$) so that the system spin $S = 5/2 - 4/2 = 1/2$. In $[4Fe–4S]^{2+}$ clusters there are two pairs of parallel-coupled (according to SDD) mixed valence (mv) irons ($2Fe^{II}$, $2Fe^{III}$) both with $S = 5/2 + 4/2 = 9/2$, which then couple antiparallel to $S = 0$. On addition of an electron there will be one mv pair and two Fe^{II}, thus: $S = 9/2 - 2 \times 4/2 = 1/2$, i.e., paramagnetism. If instead one electron is removed from the 2 + level to form $[4Fe–4S]^{3+}$ ($3Fe^{III}$,$1Fe^{II}$), there are one mv pair and two Fe^{III}, thus $S = 2 \times 5/2 - 9/2 = 1/2$ and paramagnetism. The $[4Fe–4S]^{3+}$ level has been first observed in so-called high potential iron protein (HiPIP); however, these proteins are now counted among ferredoxins (Fd) with high redox potentials. Occasionally $[4Fe–4S]^{+}$ clusters with an $S = 3/2$, a mixed 1/2 and 3/2, or even higher ground-state spins have been observed.

Iron–Sulfur Proteins

Structure

Nomenclature

Small proteins containing only the mononuclear $[Fe(Cys)_4]$ complex are called rubredoxin (Rd), and those containing one or two [2Fe–2S] or [4Fe–4S] clusters are called ferredoxin (Fd). Many Fe–S clusters occur in large and sometimes membrane-bound proteins, together with other prosthetic groups and/or metal cofactors. These proteins are designated as complex Fe–S proteins.

Primary Structure

In many Fe–S proteins the Cys ligands of the active sites occur in characteristic sequence patterns. For instance, the Fe-ion in Rd is ligated by two $-C-x_2-C-$ motifs (x standing for residues other than Cys) separated by 20–30 residues. In plant- and mammalian-type [2Fe–2S] Fds, the pattern is $-C-x_{4,5}-C-x_2-C-x_n-C-$, with $n \approx 30$. In Rieske-type [2Fe–2S] proteins the two Cys ligands of one iron and the two His ligands of the other one occur in a $-C-x-H-x_{15-17}-C-x_2-H-$ pattern. These proteins are found in membrane-bound enzymes in conjunction with *b*-type cytochromes in mitochondria (bc_1, or complex III) and chloroplasts (b_6f), as well as in soluble bacterial dioxygenases. In [4Fe–4S] Fds the canonical pattern is $-C-x_2-C-x_2-C-x_n-C-$, with $n \approx 20–40$. This pattern is duplicated in Fds containing two [4Fe–4S] clusters. The patterns containing the ligands in Rd and Fd were initially found in small 50–100 residue sequences, but they have now been observed in the larger sequences of many redox enzymes. Significant diversification has occurred, particularly among Fd patterns, through

insertions or deletions of up to several tens of residues. In addition to these canonical sequences, an increasing number of novel Cys patterns are found to furnish ligands to [2Fe–2S] and [4Fe–4S] sites.

Secondary and Tertiary Structure

Many three-dimensional structures of Fe–S proteins have now been determined by X-ray crystallography. At an early stage, the structures of the small Rds and Fds revealed characteristic folds, each specific of a given Fe–S structural framework. The Rd molecule is composed of a three-stranded pleated sheet and two loops that bear a $-C-x_2-C-$ ligand pair each. These two loops are related by a pseudo-twofold symmetry axis passing through the iron atom. Some zinc-finger modules in which the zinc ion has four Cys ligands are structurally very similar to Rd. Plant- and mammalian-type [2Fe–2S] Fds assume a structure named β-grasp, of which the main framework is a five-stranded antiparallel β-sheet with an α-helix lying on top of it. The remainder of the structure consists of short secondary elements and loops. Prominent among the latter is a surface loop including three of the four Cys ligands of the cluster. Another type of [2Fe–2S] Fd has a structure closely related to that of thioredoxin. The protein fold of Rieske proteins around their [2Fe–2S] active site is superimposable on the Rd fold; the His-ligated iron is the one closest to the protein surface. In 2[4Fe–4S] Fds, the two [4Fe–4S] clusters are surrounded by two pairs of antiparallel β-strands on one side, and two α-helices on the other. The structure displays a conspicuous twofold symmetry as a consequence of the sequence duplication. In high-potential Fd (HiPIP), a sizeable part (40%) of the structure is composed of hairpin turns while the remainder consists of several short strands and helices. Thereby, the [4Fe–4S] cluster is deeply buried in a hydrophobic cavity that stabilizes its oxidized 3+ state. The structural frameworks of the [2Fe–2S] Fd and low-potential [4Fe–4S] Fd are ubiquitous, and occur not only in small soluble Fds, but also in subunits and domains of many redox enzymes. The low-potential [4Fe–4S] Fd-fold is particularly versatile, and insertions and deletions inferred from sequence alignments have been substantiated by crystal structures. In addition to variations in sequence length, cases of cluster modification or loss have been observed.

Higher-Order Structures

While the canonical Fe–S protein folds described above have long dominated the landscape, numerous novel folds are revealed by the rapid growth of structural databases. It was predictable that polypeptide chains can fold in many different ways to position Cys residues appropriately for the binding of [2Fe–2S] or [4Fe–4S] active sites. Indeed, for the accommodation of [4Fe–4S] clusters alone, well over ten distinct protein folds have now been structurally characterized. There are even cases of [4Fe–4S] clusters held in proteins between two subunits, each of which provide two of the four Cys ligands as in nitrogenase and photosystem I.

Complex Fe–S Proteins with Clusters of High Nuclearity and Hetero-Metal Clusters

A yet higher level of complexity is displayed by proteins containing large metalloclusters which in several cases belong to the Fe–S family. Some of these "superclusters" can be roughly described as juxtapositions of two [4Fe–4S] clusters without (e.g., P clusters of nitrogenase) or with (e.g., FeMo-co clusters of nitrogenase) a metal atom other than Fe (Mo or V). Others are derived from a single [4Fe–4S] cluster by addition of one or two transition metal atoms (Fe, Ni). In the majority of these large metalloclusters, protein ligands other than Cys (His, Ser, peptidyl-N) or nonprotein ligands (homocitrate, dithiols, CO, CN^-) are also involved. Protein frameworks that accommodate these large clusters are generally bigger and more sophisticated than those of the usual Fe–S clusters. Nevertheless, it is noted that a number of them are assemblages of smaller substructures (e.g., Rossman folds).

Structural Flexibility and Relations to Function

Even though non-Cys ligation of Fe–S active sites is relatively rare, it is functionally important as a means of modulating chemical reactivity or redox potential. Several crystal structures of Fe–S active sites with His, Ser, or carboxylate ligands have now been determined. In some of these, non-Cys ligands are naturally present, in others they have been introduced by site-directed mutagenesis.

Atomic resolution (1.2Å or better) X-ray crystallography has become more accessible through technical improvements (synchrotron radiation, low temperature) and allows the detection of minute structural deviations that are imposed by the polypeptide chain or occur upon redox transitions. Crystal structures may convey the misleading impression that proteins are rigid structures; however, Fe–S proteins have malleable metal sites associated with flexible polypeptide chains. While essential functions of Fe–S proteins, electron transfer in particular, are indeed optimized through minimization of structural flexibility, as in Fd, many other functions require structural reorganizations of the polypeptide chain and metal cluster. Such modifications have long been known to occur upon degradation (oxidative denaturation, loss of iron) of some Fe–S proteins. Those kinds of structural fluctuations are difficult to monitor by X-ray crystallography. A notable

exception is the 3Fe/4Fe interconversion, which may occur with minimal protein reorganization. Other modifications of cluster nuclearity are expected to be associated with significant protein movements, since the Cys ligand sets of the [1Fe], [2Fe–2S], and [4Fe–4S] sites have very different spatial distributions. More recently, the functional relevance of structural changes in Fe–S proteins has moved to front-stage. Indeed, flexibility of both the metal site and the polypeptide chain are a necessity in proteins committed to sensing and transducing signals which may depend on redox state or metal concentration. Such structural changes may be classified in two main groups, according to whether it is the polypeptide chain (protein-driven reorganization of the metal site) or the metal site (cluster-driven protein movements) that assumes the leading role. Examples of the latter, where polypeptide chain movements are driven by the avidity of Fe–S clusters for Cys ligands, have been structurally characterized.

Functions

Electron Transfer

Obviously the principal function of Fe–S proteins is electron transfer. Thus, the oxidation–reduction potentials of the various possible redox couples in simple and complex Fe–S proteins are of interest. There are several reasons for the wide redox potential range ($\sim$1 V) covered by Fe–S proteins, the first of which is the electronic structure peculiarity of each type of Fe–S framework. Second, as each iron ion can be in either the Fe(III) or Fe(II) state, clusters of n Fe atoms are in principle endowed with $n - 1$ redox transitions. While this is observed in nature only in the case of the [4Fe–4S] clusters (3+/2+ and 2+/+ transitions), it allows the latter clusters to cover a range of $\sim$1 V on their own. Third, the redox potentials of Fe–S clusters can be modified by several parameters that are adjustable by the polypeptide chain. These include cluster ligation (sulfur, nitrogen, or oxygen), polarity of the medium, and neighboring charges. Studies of synthetic analogues and proteins, native as well as mutated ones, have shown that variations of each of these parameters can cause redox potential shifts larger than 50 mV. For instance, in Rieske-type proteins, the presence of two His ligands on the same Fe raises the redox potential of this Fe sufficiently so that it becomes reducible at a much higher potential than that of all-Cys ligated [2Fe–2S] active sites (Figure 1). The development of algorithms aimed at computing redox potentials of Fe–S clusters from charge and dipole distributions in their vicinity is an active area of research. Redox potentials reported in other compendia have been collected and the maximal and minimal values observed for various types of Fe–S proteins are summarized in Figure 1. Fe–S proteins can participate in more complex oxidation–reduction reactions, in which any component of the cluster or groups of the protein are also involved.

Reduction of Disulfide Bonds During the enzymatic reduction of some disulfide bonds as, e.g., in plant thioredoxin reductase, an extension of the coordination sphere of one of the iron ions occurs such that the cluster transitionally assumes the $[4Fe–4S]^{3+}$ level, as indicated by electron paramagnetic resonance (EPR), and its sulfides or Cys ligands may act as nucleophiles attacking disulfide bonds.

Initiation of Radical Chain Reactions There are a number of enzymes that use free-radical chemistry supported by adenosylmethionine to achieve substitutions on unactivated carbon atoms. In these enzymes a $[4Fe–4S]^{+}$ cluster with only three Cys ligands splits adenosylmethionine by transferring an electron and generating the adenosyl radical, which in turn initiates a radical chain reaction.

Generation of Unusual Reducing Power In a number of enzymes a reduced 4Fe cluster in conjunction with the hydrolysis of MgATP is used to achieve reductions of substrates by more than 1 V, such as required for the reduction of aromatic compounds or of dinitrogen. In these enzymes the 4Fe cluster is formed between two subunits of a protein with each contributing two Cys ligands. In such a structural arrangement conformational energy can be derived from MgATP binding and hydrolysis and then be made available for reduction of a substrate.

Functions not Involving Net Electron Transfer

The influence of the mere presence of Fe–S clusters or of rearrangements within clusters on adjacent groups or cofactors must also be considered. Fe–S clusters may polarize charges on adjacent groups or may serve as a reservoir capable of donating or absorbing charge. For such functions it is essential for Fe–S clusters to interact with their environment via any of their constituents, iron, sulfide, and the Cys ligands.

Fe–S Clusters as Active Sites of Enzymes The prime example, as to how one of the Fe-ions of a cluster can be used as active site of an enzyme is aconitase, in which there are only three Cys ligands to its Fe–S cluster. Thus, the unique iron is able to extend its coordination from four- to six-coordinate and bind the substrates, citrate or isocitrate. It can thus serve as a Lewis acid in the dehydration of the substrate to *cis*-aconitate and the rehydration to the alternate substrate with inversion of the positions of the H and OH substituents.

Similar changes in coordination of one of the iron ions are observed in reactions of other enzymes which contain a 4Fe cluster with only three Cys ligands.

Stabilization of Structures In some enzymes the network of ligands around an Fe–S cluster is used to stabilize specific structures.

Sensing and Regulatory Functions Fe–S clusters are labile toward oxygen, some of its reduction products and toward nitric oxide, and iron is required for their synthesis. Fe–S clusters can, therefore, also be used in nature as signaling or regulatory agents. While the Fe–S clusters of proteins that belong to this group may undergo one electron oxidation or complete oxidative destruction, the ensuing regulatory function involves specific interactions with DNA (SoxR, FNR) or RNA (IRP), which either require the presence (SoxR, FNR) or complete absence (IRP) of the Fe–S cluster. Examples of this are the [2Fe–2S] SoxR and [4Fe–4S] FNR protein in bacteria and the iron regulatory protein (IRP) in eukaryotes. SoxR is a sensor for the superoxide anion that binds to DNA upstream of the *soxS* gene. Its oxidation–reduction potential is such that it normally occurs in the reduced 1+ form in bacteria. Upon oxidation to the 2+ level by the superoxide anion, a structural modification of the SoxR–*soxS* nucleoprotein complex triggers expression of *soxS* and induction of the synthesis of defensive enzymes such as superoxide dismutase and other proteins. The FNR protein acts as oxygen sensor. Its 4Fe cluster is rapidly destroyed in the presence of oxygen and therewith its ability to induce the synthesis of enzymes required for anaerobic respiration with fumarate or nitrate as oxidants instead of oxygen. IRP of eukaryotes, on the contrary, is unable to serve as iron-regulator unless its cluster-binding site (3Cys) is unoccupied and contains free thiols. However, when it acquires an Fe–S cluster as [4Fe–4S] protein it takes on the function of a cytoplasmic aconitase. Both cytoplasmic and mitochondrial aconitases are only active in their 4Fe-form and are inactivated by loss of the unique iron that lacks a Cys ligand. As the 3Fe cluster is relatively stable it has been proposed that the switch between 4Fe (active) and 3Fe (inactive) enzyme is used in nature to protect the Fe–S cluster from irreversible further oxidation and for metabolic control, because aconitase is necessary for the functioning of the tricarboxylic acid cycle. As nitric oxide reacts with Fe–S clusters, with the main product formed being the dinitrosyl–iron complex (DNIC), NO has to be considered as an alternative messenger in the mentioned sensing pathways. In intact cells the Fe–S clusters can eventually be rebuilt in all the cases mentioned above. The interrelation of the pathways for sensing iron, oxygen, or its reduction products, and nitric oxide represents an interesting example of crossroads in natural signaling systems.

Methods for Obtaining Information on Fe–S Proteins

While gross information on Fe–S proteins is available from chemical approaches such as analysis for sulfide, iron, protein, and amino acids, spectroscopic methods have furnished a wealth of information on the more detailed and subtle properties of these fascinating, multipurpose tools of nature. Historically EPR was the first decisive method. It was soon followed by a considerable arsenal of diverse methods. Many of them probe the electronic and magnetic properties of the metal site in various ways that render them complementary to each other and to EPR. The most important of these are Mössbauer, magnetic circular dichroism (MCD), nuclear magnetic resonance (NMR), and electron-nuclear double resonance (ENDOR) spectroscopies. Other methods, such as resonance Raman and X-ray absorption spectroscopy (EXAFS, XANES), provide specific information relevant to the structural framework of the metal site. Computational approaches have been of great help for unraveling details of the electronic and magnetic structures of Fe–S clusters. The master tool of structural investigation, X-ray crystallography, has been implemented on small Rds and Fds at a very early stage, and is now successfully used for the determination of structures of large Fe–S enzymes and complexes. Very high resolution ($\leq$1Å) now allows the description of Fe–S active sites with a precision nearly matching that achieved with small synthetic molecules.

Biogenesis of Iron–Sulfur Proteins

General Overview

Methods for the *in vitro* assembly of Fe–S clusters on apoproteins were devised in the 1960s, while the chemical synthesis of Fe–S clusters in the absence of protein was also pursued and eventually developed to a high degree of specificity. However, it was around the late 1990s that the biosynthesis of Fe–S clusters in a living cell became a major field of interest and experimentation. It is clear now that these biochemical processes require the assistance of complex assemblies of proteins. At present, three different biogenesis systems have been identified. The most general one appears to be the ISC assembly machinery present in α-, β-, and γ-proteobacteria as well as in mitochondria of eukaryotes. The NIF system is specialized for the assembly of the complex Fe–S protein nitrogenase and consequently is found in several nitrogen-fixing bacteria, but also in nondiazotrophic ε-proteobacteria. The most

recently discovered system is the SUF machinery, which is found in a wide range of bacteria, archaea, and plastids of plants. In some organisms, either the ISC or the SUF system is responsible for assembly of cellular Fe–S proteins, whereas in other species they are present in parallel and may be responsible for the assembly of different subsets of Fe–S proteins.

Biogenesis of Fe–S Proteins in Bacteria

The Bacterial ISC Assembly Machinery

In prokaryotes the ISC assembly machinery is encoded by the *isc* (*i*ron–*s*ulfur *c*luster) gene cluster. This operon comprises genes encoding the proteins IscS, IscU, IscA, HscA, HscB, and Fdx. In addition to these proteins directly required for biogenesis, IscR is involved in the regulation of the *isc* gene expression. Biogenesis starts with the production of a sulfane sulfur from cysteine by the cysteine desulfurase IscS (Figure 2). The sulfur remains transiently bound to IscS and is covalently attached as a persulfide at a conserved cysteine residue. Upon interaction of IscS with the dimeric form of IscU the sulfur moiety is transferred to IscU, where it is also bound as a persulfide. The binding of ferrous iron to IscU leads to the formation of a [2Fe–2S] cluster, which then can give rise to the generation of a [4Fe–4S] cluster. Thus, IscU provides a scaffold for assembly of iron and sulfide ions. The molecular details of these reactions are still under investigation. IscU interacts with two chaperones, the ATP-dependent Hsp70/DnaK homologue HscA and the Hsp70/DnaJ homologue HscB. The interaction strongly stimulates the ATPase activity of HscA, but the precise function of these two proteins remains to be elucidated. Fe–S cluster assembly depends on the transfer of electrons from the [2Fe–2S] ferredoxin Fdx. The reactions which need the input of electrons are not known yet, but may involve the release of sulfur from cysteine by IscS and the dissociation of the Fe–S cluster from IscU. IscA is thought to function as an alternative scaffold protein to facilitate the assembly of Fe–S clusters. A [2Fe–2S] cluster can be assembled on IscA and subsequently transferred to a Fe–S protein such as Fdx. Presently, it is not known how the dissociation of the cluster from the scaffold proteins is triggered and which components may participate in cluster transfer to apoproteins.

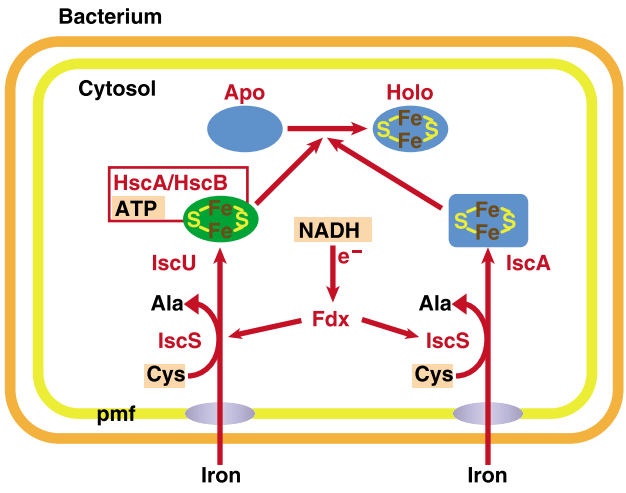

FIGURE 2 A working model for biosynthesis of Fe–S proteins in bacteria. For details see text. pmf, proton motive force.

The Bacterial SUF Machinery

The existence of a biogenesis system for Fe–S proteins in addition to the ISC assembly machinery has been noted only recently. When the *isc* operon is deleted in *E. coli*, Fe–S proteins are assembled at an efficiency of only 2–10% of that in wild-type cells. The residual assembly activity is due to the *suf* (mobilization of *sulf*ur) operon which contains the proteins SufA, SufB, SufC, SufD, SufS, and SufE. Many organisms contain only a subset of the *suf* genes. Overexpression of the *suf* gene cluster can restore Fe–S protein assembly in an *isc* deletion mutant. The *suf* operon is induced under iron-limiting conditions and repressed by the iron-sensing repressor protein Fur. Further, the *suf* operon is regulated by the transcription factor OxyR that senses oxidative stress conditions. This suggests that the SUF system is crucial under iron-limiting and oxidative stress conditions. The Suf proteins, homologues of Fdx and NifU, and an Fdx reductase are also present in apicoplasts, a plastid-like organelle of Apicomplexa such as Plasmodium and Toxoplasma.

SufS and SufA are homologues of IscS and IscA, respectively and may serve similar functions in liberating sulfur from cysteine, in scaffolding, and in cluster assembly. SufC is an atypical ATPase which forms a complex with SufB and SufD. SufE accepts sulfur from SufS and acts synergistically with the SufBCD complex to stimulate the cysteine desulfurase activity of SufS. This regulation of SufS activity may be important for limiting sulfur release during oxidative stress conditions. In addition, SufS has been assigned a function as a selenocysteine lyase in *E. coli*.

The Bacterial NIF Machinery for Assembly of Nitrogenase

Studies on nitrogen-fixing bacteria have identified the *nif* (*ni*trogen *f*ixation) operon as being responsible for maturation of the complex Fe–S protein nitrogenase. This enzyme consists of two oxygen-labile metalloproteins, the MoFe protein (NifKD) and the Fe protein (NifH). The latter contains a [4Fe–4S] cluster, whereas

the MoFe protein is associated with two unique superclusters: the P cluster and the iron–molybdenum cofactor (FeMo-co). The *nif* operon-encoded proteins NifS and NifU are involved in cluster biosynthesis by performing similar functions as their homologues IscS and IscU, respectively. The N terminus of NifU is homologous to IscU and provides a scaffold for assembly of transiently bound clusters, whereas the middle part of NifU contains a permanent [2Fe–2S] cluster that may carry out a redox function. Further, a homologue of IscA termed ^{Nif}IscA is thought to be an alternative scaffold for cluster assembly. Central components in the biosynthesis of FeMo-co are NifN and NifE, which form a hetero-tetramer and serve as a scaffold for cluster assembly before transfer to NifKD apoproteins. Further components needed for FeMo-co assembly are the *nif* operon-encoded proteins NifQ (Mo processing), NifV (homocitrate synthase), NifB (sulfur and iron donor) as well as NifH and NifX, the functions of which are unknown.

Biogenesis of Fe–S Proteins in Eukaryotes

The Mitochondrial ISC Assembly Machinery

In eukaryotes mitochondria are central for biogenesis of cellular Fe–S proteins. In keeping with their bacterial origin, these organelles contain homologues of the bacterial ISC assembly machinery. All proteins of the mitochondrial ISC assembly machinery are encoded by nuclear DNA and are imported after translation in the cytosol. The mitochondrial ISC assembly machinery consists of a few more proteins as compared to that in bacteria. Nevertheless, the mechanistic principles underlying biosynthesis might be rather similar. For instance, the cysteine desulfurase Nfs1 and the two highly homologous proteins Isu1 and Isu2 execute similar functions in elemental sulfur production and scaffolding as bacterial IscS and IscU, respectively (Figure 3). Formation of the transiently bound Fe–S cluster on the Isu proteins depends on the ferredoxin reductase Arh1 and the ferredoxin Yah1, which form an electron transfer chain using NADH as a reducing agent. In addition, Yfh1 acts as an iron donor during Fe–S cluster synthesis by directly interacting with the Isu/Nfs1 complex. Its human homologue, termed frataxin, is depleted in patients of Friedreich's ataxia, a neurodegenerative disease. The dissociation of the transiently bound Fe–S cluster from the Isu proteins and/or its insertion into apoproteins requires the mitochondrial glutaredoxin Grx5 and the two chaperones Ssq1 and Jac1 (Figure 3). The function of the IscA homologues Isa1 and Isa2 is still unclear, but possibly they provide an Isu protein-independent scaffolding function for the assembly of Fe–S clusters. Nfu1 genetically interacts with Ssq1 and Isu1, but its biochemical role in mitochondrial Fe–S protein assembly is not understood to date.

The Mitochondrial ISC Export Machinery

The mitochondrial ISC assembly machinery is not only responsible for the assembly of mitochondrial Fe–S proteins, but also plays an essential function in the maturation of Fe–S proteins outside mitochondria. To date, four components have been identified that are specifically needed for maturation of extra-mitochondrial, but not of mitochondrial Fe–S proteins (Figure 3). The first-known protein of the so-called ISC export machinery is the mitochondrial ABC transporter Atm1. The other components are the sulfhydryl oxidase Erv1 of the intermembrane space and glutathione (GSH). To date, not much is known about this export pathway on a biochemical level. For instance, the substrate of Atm1 is not known and the precise roles of Erv1 and GSH are unclear. Since virtually all components of the mitochondrial ISC assembly machinery are involved in the maturation of extra-mitochondrial Fe–S proteins, it is assumed that Atm1 exports an Fe–S cluster or a derivative thereof to the cytosol for transfer onto apoproteins. Mutation of the human homologue of Atm1, termed ABC7, gives rise to the iron storage disease X-linked sideroblastic anemia and cerebellar ataxia (XLSA/A). Finally, biogenesis of cytosolic Fe–S proteins requires Cfd1, a cytosolic P-loop ATPase that is conserved in

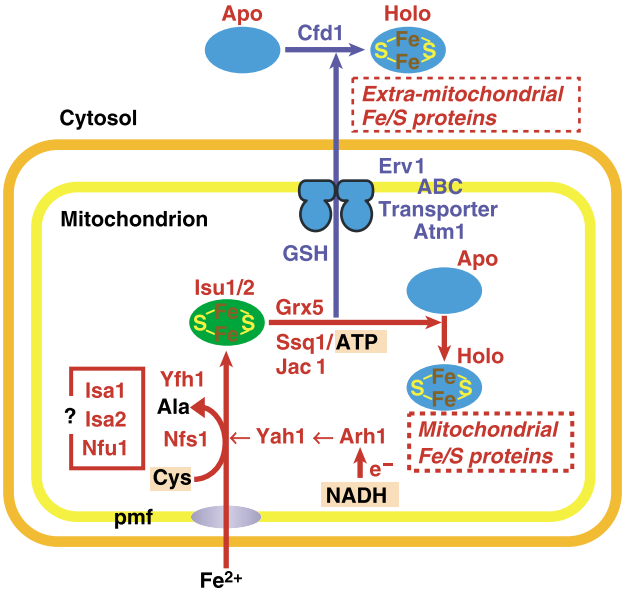

FIGURE 3 A working model for biosynthesis of Fe–S proteins in yeast. For details see text. pmf, proton motive force.

all eukaryotes. The protein may assist in Fe–S cluster insertion into cytosolic apoproteins.

Many components of the ISC machineries are essential for viability of yeast cells (e.g., Nfs1, Yah1, Arh1, Jac1, Erv1, and Cfd1) which demonstrates the importance of Fe–S protein biogenesis. Essential Fe–S proteins are known to be present in the yeast cytosol, but not in mitochondria. Hence, mitochondria appear to be essential organelles because they perform crucial steps in the biosynthesis of cytosolic Fe–S proteins.

Biogenesis of Fe–S Proteins in Chloroplasts

For more than a decade it has been clear that isolated chloroplasts can assemble Fe–S proteins suggesting that they contain their own assembly machinery. To date, we know a few components of this system. Homologues of IscS, IscA, and NifU have been located in plastids suggesting that a system homologous to the ISC assembly machinery is responsible for Fe–S protein biogenesis in these organelles. Further support for this notion comes from studies in cyanobacteria which are believed to be the evolutionary ancestors of chloroplasts. They contain several homologues of the ISC assembly machinery. Two members of the IscS family and NifU have been shown experimentally to perform functions similar to bacterial IscS and NifU. Strikingly, there is no member of the IscU family present in cyanobacteria suggesting that, in contrast to mitochondria, Fe–S cluster assembly does not involve Isu-like proteins but rather NifU and IscA as scaffolding proteins.

See Also the Following Articles

Disulfide Bond Formation • Ferredoxin • Ferredoxin-$NADP^+$ Reductase • Photosystem I: F_X, F_A, and F_B Iron–Sulfur Clusters

Glossary

Fe–S active sites Sites in proteins containing iron ligated to inorganic sulfides and/or cysteines.

iron–sulfur clusters The form in which irons and sulfides are organized in Fe–S proteins.

iron–sulfur proteins Proteins that contain iron and sulfur, active mostly (even if not exclusively) in electron transfer.

Further Reading

Beinert, H., and Kiley, P. J. (1999). Fe–S proteins in sensing and regulatory functions. *Curr. Opin. Chem. Biol.* **3**, 152–157.

Beinert, H., Kennedy, M. C., and Stout, C. D. (1996). Aconitase as iron–sulfur protein, enzyme, and iron-regulatory protein. *Chem. Rev.* **96**, 2335–2373.

Bertini, I., Zhou, H. X., Gori-Savellini, Luchinat, C., Mauk, A. G., Moore, G., Gunner, M. R., Alexov, E., Torres, E., Lipovaca, S., Gábor, N. S., Armstrong, F. A., Warshel, A., Papazyan, A., and Muegge, I. (1996). Determinants of reduction potentials in metalloproteins. *J. Biol. Inorg. Chem.* **2**, 108–152.

Cammack, R., and Sykes, A. G. (eds.) (1992). *Advances in Inorganic Chemistry*, Vol 38, Iron–Sulfur Proteins. Academic Press, San Diego, CA.

Craig, E. A., and Marszalek, J. (2002). A specialized mitochondrial molecular chaperone system: A role in formation of Fe/S centers. *Cell. Mol. Life Sci.* **59**, 1658–1665.

Frazzon, J., and Dean, D. R. (2003). Formation of iron–sulfur clusters in bacteria – An emerging field in bioinorganic chemistry. *Curr. Opin. Chem. Biol.* **7**, 166–173.

Gerber, J., and Lill, R. (2002). Biogenesis of iron–sulfur proteins in eukaryotes: Components, mechanism and pathology. *Mitochondrion* **2**, 71–86.

Johnson, M. K. (1994). Iron–sulfur proteins. In *Encyclopedia of Inorganic Chemistry* (R. B. King, ed.), Vol 4, pp. 1896–1915. Wiley, Chichester, UK.

Meyer, J. (2001). Ferredoxins of the third kind. *FEBS Lett.* **509**, 1–5.

Mühlenhoff, U., and Lill, R. (2000). Biogenesis of iron–sulfur proteins in eukaryotes: A novel task of mitochondria that is inherited from bacteria. *Biochim. Biophys. Acta* **1459**, 370–382.

Palmer, G., and Reedijk, J. (1991). Committee of the International Union of Biochemistry, Non-Heme Iron Proteins, in "Nomenclature of Electron-Transfer Proteins". *Eur. J. Biochem.* **200**, 599–611.

Rees, D. C. (2002). Great metalloclusters in enzymology. *Annu. Rev. Biochem.* **71**, 221–246.

Sykes, A. G., and Cammack, R. (eds.) (1999). *Advances in Inorganic Chemistry*, Vol. 47, Iron–sulfur proteins. Academic Press, San Diego, CA.

Biography

Helmut Beinert holds the degree of Doctor of Natural Sciences from the University of Leipzig, Germany. He was a postdoctoral Fellow at the Institute for Enzyme Research at the University of Wisconsin, Madison, where he is now a Professor Emeritus. His interests are mainly in enzymes of biological oxidation and metal-proteins.

Jacques Meyer studied at the École Supérieure de Physique et Chimie of Paris, earned a doctoral degree of Natural Sciences from the University of Grenoble and now holds a permanent research position at the CEA at Grenoble. His interest is in structure and function of Fe–S proteins.

Roland Lill holds a degree of Doctor of Natural Sciences from the University of München, Germany, received postdoctoral training at the University of California at Los Angeles, USA, and currently is a Professor of Cell Biology at the University of Marburg, Germany. His interest is in the biogenesis and function of Fe–S proteins.

JAK-STAT Signaling Paradigm

Edward Cha and Christian Schindler
College of Physicians and Surgeons, Columbia University, New York, USA

The janus kinases (JAKs) and their downstream signal transducers and activators of transcription (STATs) comprise a remarkably direct signaling pathway. Cytokines that transduce signals through this pathway play a critical role in cellular development, differentiation, and immune response. This article discusses how the scheme works, what factors are involved, and the biological functions JAKs and STATs play.

Introduction

The JAK-STAT pathway was first discovered through an investigation into the mechanism by which a subfamily of cytokines, the interferons (IFNs), rapidly induced the expression of new genes. Subsequent studies demonstrated that this pathway is not restricted to IFNs, but encompasses a ~50 member subset of the cytokine family known as hematopoietins (see Table I). These hematopoietins are particularly important in the development and activity of leukocytes and so were given the name interleukin (IL). When these hematopoietins bind to their specific cognate cell surface receptors, a member of the STAT family is activated by tyrosine phosphorylation to become a potent transcription factor that translocates to the nucleus and rapidly induces the expression of specific target genes. Because hematopoietin receptors lack catalytic activity, their cytoplasmic domains associate with members of the JAK family to acquire tyrosine kinase activity. Table I provides a list of the members of the hematopoietin family and the JAKs and STATs through which they transduce signals. These hematopoietins are divided into subgroups based on the five structurally and functionally related receptor subfamilies to which they bind.

The Signaling Paradigm

The prototypical JAK-STAT signaling pathway, illustrated in Figure 1, consists of a series of sequential tyrosine phosphorylation events that culminate in the induction of target genes. When a cytokine binds to its corresponding receptors, it promotes a conformational change, bringing receptor-associated JAK kinases into close proximity. The kinases then activate each other by transphosphorylation and subsequently phosphorylate specific tyrosine residues on the cytoplasmic tail of the receptor. The STAT Src homology 2 (SH2) domain (see Figure 2) recognizes these specific receptor phosphotyrosine motifs (a phosphotyrosine and four adjacent amino acids), effecting its recruitment to the receptor. Once at the receptor, the STATs are phosphorylated on a single tyrosine residue (Figure 2), in a JAK-dependent manner. The activated STATs then dissociate from the receptor and dimerize through a classical phosphotyrosine-SH2 interaction. Only then are STATs truly competent for rapid nuclear translocation and DNA binding to members of the gamma-activated sequence (GAS) family of enhancers.

JAK Kinases

There are four mammalian members of the JAK family: Jak1, Jak2, Jak3, and Tyk2. They are over 1000 amino acids in length and range in size from 120 to 130 kDa. All but Jak3 are expressed ubiquitously, the latter being found only in cells of myeloid and lymphoid lineages. JAKs consist of seven conserved Jak homology (JH) domains (Figure 2). The carboxy-terminal JH1 constitutes the tyrosine kinase domain and JH2 the pseudokinase domain, which has all the structural features of a tyrosine kinase except catalytic activity and appears to regulate JH1 activity. The amino-terminal JH domains, JH3–JH7, constitute a FERM (four point one, ezrin, radixin, moesin) domain and mediate association with receptors. Specifically, JAKs associate with proline-rich, membrane proximal box1/box2 domain of these receptors. Each receptor subgroup is linked to a particular pair of JAKs by these domains. Consistent with that, Jak gene targeting studies have identified characteristic signaling defects.

Jak1 associates with the IFN-α receptor, gp130, and the common γ (γC) receptor chain families. Knockout mice die perinatally due to a neurological defect attributed to a loss in gp130 signaling. Jak1$^{-/-}$ mice also exhibit reduced lymphocyte counts due to a lack of T and NK cells. Consistent with biochemical studies,

TABLE I

Hematopoietin-Dependent JAK-STAT Signaling

Ligands	JAKs	STATs
gp130 family[a]		
IL-6	**Jak1**, (Jak2)	**Stat3**, Stat1
IL-11	Jak1	**Stat3**, Stat1
OSM	Jak1, (Jak2)	**Stat3**, Stat1
LIF	**Jak1**, (Jak2)	**Stat3**, Stat1
CNTF	Jak1, (Jak2)	**Stat3**, Stat1
NNT-1/BSF-3	Jak1, (Jak2)	**Stat3**, Stat1
G-CSF	Jak1, (Jak2)	**Stat3**
CT-1	Jak1, (Jak2)	**Stat3**
Leptin	Jak2	**Stat3**
IL-12	**Tyk2**, Jak2	**Stat4**
IL-23	?	**Stat4**
IL-27	?	Stat4
γC family[b]		
IL-2	**Jak1**, **Jak3**	**Stat5**, (Stat3)
IL-7	**Jak1**, **Jak3**	**Stat5**, (Stat3)
TSLP[c]	?	Stat5
IL-9	Jak1, Jak3	**Stat5**, Stat3
IL-15	**Jak1**, Jak3	**Stat5**, (Stat3)
IL-21	Jak3, (Jak1)	Stat3, Stat5, (Stat1)
IL-4	**Jak1**, **Jak3**	**Stat6**
IL-13[c]	Jak1, Jak2	**Stat6**, (Stat3)
IL-3 family		
IL-3	**Jak2**	**Stat5**
IL-5	**Jak2**	**Stat5**
GM-CSF	**Jak2**	**Stat5**
Single-chain family		
Epo	**Jak2**	**Stat5**
GH	Jak2	**Stat5**, (Stat3)
Prl	Jak2	**Stat5**
Tpo	**Jak2**	**Stat5**
IFN/IL-10 family[d]		
IFN-γ (Type II)	**Jak1**, **Jak2**	**Stat1**, (Stat5)
IFN, Type I[e]	**Jak1**, Tyk2	**Stat1**, **Stat2**, (Stats3–6)
IL-28a (IFN-λ1)	Jak1, Tyk2	Stat1, Stat2, Stat3
IL-28b (IFN-λ2)	Jak1, Tyk2	Stat1, Stat2, Stat3
IL-29 (IFN-λ3)	Jak1, Tyk2	Stat1, Stat2, Stat3
IL-10	**Jak1**, Tyk2	**Stat3**, Stat1
IL-19	?	?
IL-20	?	Stat3
IL-22	**Jak1**, Tyk2	Stat3, (Stat5)
IL-24	?	Stat3
IL-26	?	Stat3
IL-28a (IFN-λ1)	Jak1, Tyk2	Stat1, Stat2, Stat3
IL-28b (IFN-λ2)	Jak1, Tyk2	Stat1, Stat2, Stat3
IL-29 (IFN-λ3)	Jak1, Tyk2	Stat1, Stat2, Stat3

Hematopoietins transduce their signals through specific sets of JAKs and STATs as indicated. Assignments for which there is the most confidence (i.e., based on knockout and biochemical studies) are shown in boldface; those with less confidence are shown in lightface; and those with the least confidence are shown in parentheses.

[a] As indicated, this family is divided into two subfamilies.

[b] As indicated, this family is divided into two subfamilies.

[c] Bind to a related but γC-independent receptor.

[d] As indicated, this family is divided into three subfamilies.

[e] In humans this family consists of 12 IFN-αs, IFN-β, IFN-ω, Limitin, and, most distantly, IFN-λs.

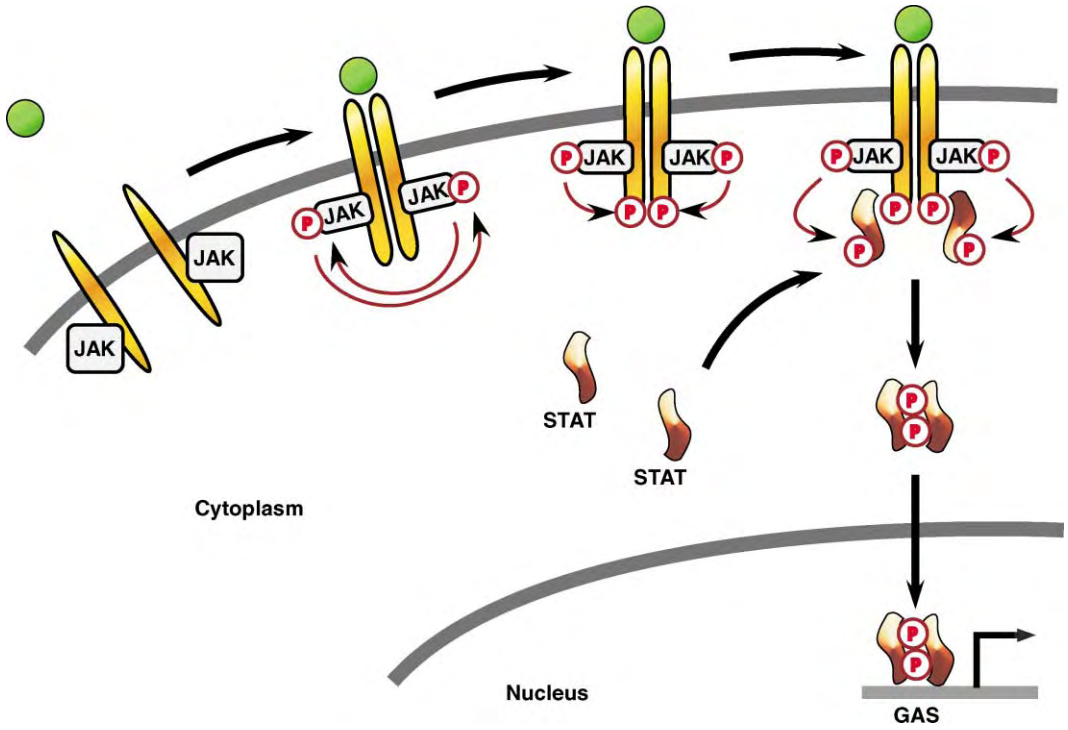

FIGURE 1 The JAK-STAT signaling pathway. Upon binding ligand, receptor-associated JAKs become activated and phosphorylate specific receptor tyrosine residues. STAT SH2 domains recognize the receptor phosphotyrosines, effecting their recruitment to the activated receptor complex. STATs are then tyrosine-phosphorylated. The activated STATs are released from the receptor, dimerize, translocate to the nucleus, and bind to members of the gamma activation site (GAS) family of enhancers.

cells collected from Jak1$^{-/-}$ mice fail to respond to cytokines from the gp130, γC, and IL-10 families.

Jak2-deficient mice exhibit an embryonic lethal phenotype, dying at embryonic day 12.5 due to failure in definitive erythropoiesis, analogous to what has been observed in the erythropoietin knockout mice. Tissues collected from Jak2 knockout mice fail to respond to IFN-γ and most of the cytokines from the IL-3 and single-chain (excluding G-CSF) cytokine receptor families (see Table I).

Jak3 expression is limited to hematopoietic cells, where it exclusively associates with the γC chain. Hence, the Jak3 knockout mice exhibit a severe combined immunodeficiency (SCID) syndrome, with impaired lymphopoiesis, which is also analogous to the defect seen in γC-deficient hosts.

Biochemical studies have implicated Tyk2 in the biological response to type I IFNs, IL-10 and IL-12, and have shown that Tyk2 associates with the corresponding receptors. Moreover, Tyk2 was originally identified in a genetic screen designed to identify components mediating the biological response to IFN-α. Yet Tyk2 knockout mice exhibit only relatively subtle defects in their response to IFN-α/β and IL-10 responses. They do,

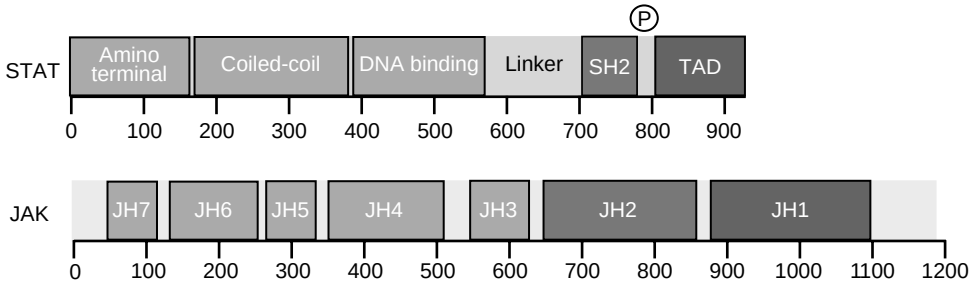

FIGURE 2 Schematic representation of JAK and STAT structures. JAKs can be divided into seven homology regions, JH1–JH7. JH1 encodes the kinase; JH2 encodes the pseudokinase domain, which regulates catalytic kinase activity; JH3–JH7 encode the FERM domain, which mediates receptor interactions. STAT proteins can also be divided into seven structurally and functionally conserved domains, including the amino-terminal, coiled-coil, DNA-binding, linker, SH2, tyrosine activation site, and transcriptional activation domains.

however, exhibit significant defects in their response to IL-12 and profound defects in their responses to LPS. How Tyk2 pertains to LPS activation in macrophages remains an important area of inquiry.

The STATs

There are seven mammalian STATs (Stats 1, 2, 3, 4, 6, and two Stat5 genes) ranging in size from 750 to 900 amino acids. They contain seven structurally and functionally conserved domains: amino-terminal, coiled-coil, DNA-binding, linker, SH2, tyrosine activation, and transcriptional activation domains (TADs) (Figure 2).

The amino-terminal ~125 amino acids represent an independently folded and stable moiety, which is well conserved but functionally not fully characterized. Several studies have implicated this domain in promoting cooperativity in DNA binding, in homotypic dimerization, in regulating nuclear translocation, and in promoting interactions with other proteins. The coiled-coil domain (amino acids ~135 to ~315) consists of a four-α-helix bundle that protrudes about 80 Å laterally from the core structure. This domain provides a largely hydrophilic surface that promotes interactions with a number of potentially important regulatory modifiers, such as IRF9 and StIP1. It has also been implicated in nuclear export.

The DNA-binding domain (amino acids ~320 to ~480) is a β-barrel with an immunoglobulin fold that recognizes the GAS family of enhancers. The dissociation constant lies in the nanomolar range, so cooperativity in DNA binding is likely important in establishing an effective transcriptional activity. Interestingly, like the upstream coiled-coil domain, the DNA-binding domain appears to regulate nuclear export. In contrast to all other STATs and despite a well-conserved DNA-binding domain, Stat2 is unable to bind DNA directly. The adjacent linker domain (amino acids ~480 to ~580) is important in ensuring the appropriate conformation of the DNA binding motif in activated STAT dimers. This domain also appears to regulate nuclear export in resting cells.

Not surprisingly, the SH2 domain (amino acids ~575 to ~680) is the most highly conserved motif and mediates both receptor attachment and STAT dimerization. It consists of an antiparallel β-sheet flanked by two α-helices, which form a pocket. At the base of the pocket lies an absolutely conserved arginine that mediates the interaction with the conserved phosphorylated tyrosine motif of the dimerization partner. This short tyrosine activation motif is located near residue 700. All STATs except Stat2 form stable homodimers *in vivo*. Finally, the carboxy terminus carries a TAD, which is conserved between species for each STAT (e.g., murine and human Stat1) but varies considerably between different STAT family members (e.g., Stat1 vs Stat2). Once again, Stat2 is the exception. Its TAD domain varies considerably in sequence between the murine and human homologues.

STAT dimers bind to a palindromic GAS element ($TTCN_{2-4}GAA$). The spacing between the palindromic half sites determines preferential binding specificity. For instance, Stat1 binds to an element with a canonical n = 3 spacing, while Stat3 and Stat6 favor n = 2 and n = 4, respectively. Cooperative binding to neighboring sites of two or more STAT dimers has also been well documented for a number of target genes. Again, however, Stat2 is the exception. Upon activation, Stat2 forms a heterodimer with Stat1 that exhibits no DNA-binding activity. Rather, it associates with IRF9 and binds to the IFN-stimulated response element (ISRE; AGTTTNNNTTTCC), a member of the IRF family of enhancers.

Stat1 is critical for both type I (IFN-$\alpha/\beta/\lambda$) and type II (IFN-γ) interferon signaling. Stat1 homodimerizes in response to activation by IFN-γ or heterodimerizes with Stat2 in response to activation by IFN-α/β. Biochemical and genetic studies have also suggested that Stat1 contributes to the biological response to gp130 receptors along with Stat3.

Stat2 is the most unique member of the STAT family. As previously indicated, it only transduces signals for type I IFNs, but can neither form homodimers nor bind to DNA directly. Rather, it heterodimerizes with its obligate partner Stat1 to translocate to the nucleus, where it associates with IRF9 to form the ISGF-3 and to bind to ISRE elements. In ISGF-3, IRF9 constitutes the core DNA-binding component, and Stat1 promotes contact with the additional flanking nucleotides. Finally, there is a surprising level of divergence between murine and human Stat2.

Stat3 transduces signals for a large number of cytokines, most notably members of the gp130 and IL-10 families. Pointing back to its evolutionary origins as a critical regulator of development, Stat3 knockout mice display an early (i.e., day 6.5–7.5) embryonic lethal phenotype. However, tissue-specific deletions of the Stat3 gene have confirmed the critical role Stat3 plays in transducing signals for the gp130 and IL-10 families of hematopoietin receptors.

Stat4 is predominantly involved in signaling for the small IL-12 family, which includes IL-12, IL-23, and IL-27. IL-12, whose response has been studied most extensively, is a potent inducer of IFN-γ production in both T-cells and NK cell. It also plays an important role in driving polarization of naive $CD4^+$ T-helper cells into the Th1 effector subset.

Stat5a and Stat5b are encoded by two tightly linked and highly homologous genes (~96% amino acid identity). All members of the IL-3 receptor and single-chain receptor families (e.g., GH, PRL, and EPO) transduce signals through these isoforms of Stat5.

The γC receptors (i.e., the IL-2, IL-7, IL-9, IL-15, and IL-21 receptors) have also been shown to transduce important signals through Stat5. Yet the defect in Stat5a knockout is almost exclusively toward PRL, and the defect in Stat5b is almost exclusively toward GH. Mice deficient in both feature notable defects in their response to PRL, GH, EPO, IL-2, and members of the IL-3 family.

Stat6 transduces signals for IL-4 and the closely related IL-13. IL-4 plays an important role in the development of the Th2 subset of T-helper cells. Thus, Stat4 and Stat6 serve as protagonists in maintaining the important balance between the Th1 and Th2 subsets of effector T-cells. IL-4 is also important for B-cell maturation. Consistent with this, Stat6 knockout mice fail to proliferate, up-regulate MHC II expression, or secrete IgE in response to IL-4.

Regulation of JAK-STAT Signaling

STAT-dependent gene induction is both rapid and transient. The brisk activation phase entails both rapid nuclear translocation and robust DNA-binding activity. This nuclear translocation is mediated by karyopherins (e.g., importin-α5) and Ran-GTPase. (This process is distinct from low levels of basal nuclear import/export that have been reported for several STATs.) However, identification of a canonical STAT nuclear localization signal (NLS) sequence remains elusive. Although putative NLS sequences have been reported for several STATs (e.g., in the DNA-binding domain), they fail to mediate the nuclear import of reporter proteins.

STAT-dependent signal decay, which is typically initiated within hours of stimulation, is also carefully regulated. This process entails phosphatases (nuclear and cytoplasmic), nuclear export, and one or more families of regulatory proteins. Recent studies indicate that STAT nuclear export is tightly coupled with dephosphorylation, possibly mediated by TC-PTP, but the molecular events regulating this appear complex. For example, several leucine-rich nuclear export sequence (NES) motifs, which drive the GTP-dependent nuclear export, have been identified in the coiled-coil and DNA-binding domains of Stat1 and Stat3. Other phosphatases, including SHP1 and CD45, dephosphorylate the JAKS and receptors, where the signal was initiated.

Signaling is also negatively regulated by SH2-containing SOCS (suppressors of cytokine signaling) proteins, whose expression is directly induced by STAT-dependent signals, completing a classical negative feedback loop. $SOCS1^{-/-}$ mice, for example, die between the second and third week of life with a disorder marked by nonspecific T-cell activation, inflammation, and liver necrosis. These findings have been attributed to unchecked IFN-γ–Stat1- and IL-4–Stat6-dependent inflammation. $SOCS3^{-/-}$ mice die during embryogenesis from a placental defect. However, specific tissues exhibit prolonged and abnormal gp130-dependent signaling. SOCS1 and SOCS3 are believed to exert their negative effect by binding to phosphorylated tyrosine residues in the activation loop of Jak2 and the gp130 receptor, respectively. SOCS family members may also promote protein degradation by directly facilitating the addition of ubiquitin to target proteins.

Another group of proteins implicated in the negative regulation of STATs is the PIAS (protein inhibitors of activated STATs) family, which was initially suggested to mediate their negative effects by binding directly to activated STAT dimers. However, the recent recognition that PIAS proteins are SUMO (small ubiquitin-related modifiers) E3 ligases has raised the possibility that they may exert their negative regulation by promoting the covalent addition of SUMO adducts. Studies indicating that some nuclear pore proteins may SUMOylate target proteins, and that Stat1 is SUMOylated, suggest a potential role in the regulation of STAT nuclear import and export.

In closing, it should be noted that some STAT modifications serve to integrate STAT signal transduction with that of other signaling pathways, potentiating STAT activity. For example, JNK/MAP kinase-dependent pathways have been shown to promote the phosphorylation of specific serine residues (Ser727 in Stat1 and Stat3) within the TAD, thereby enhancing the expression of some, but not all, target genes. These observations raise the question of whether other types of covalent modification (e.g., acetylation or methylation) will be found to similarly regulate and integrate STAT signals.

See Also the Following Articles

Cytokines • Hematopoetin Receptors • Interferon Receptors • SUMO Modification

Glossary

gamma activation site (GAS) A specific enhancer element that is recognized by most activated STAT homodimers. It was first identified as an IFN-γ response element.

hematopoietins A subset of cytokines, which are secreted peptide ligands, that mediate potent biological responses in target cells. They are predominantly involved in regulating inflammation and immunity. Examples include IFN-α, IFN-γ, IL-2, IL-3, IL-4, PRL, GH, EPO, G-CSF, and GM-CSF.

IFN-stimulated response element (ISRE) A specific enhancer that is recognized by ISGF-3, an IFN-α-activated transcription factor consisting of Stat1, Stat2, and IRF-9.

janus kinase (JAK) Tyrosine kinase that associates with cytokine receptors and provides catalytic activity that is essential to initiate signal transduction.

protein tyrosine kinases Catalytic function measures the ability of the enzyme to phosphorylate itself or its substrates.

protein tyrosine phosphorylation Posttranslational modification required of tyrosine residues that can modulate catalytic function as well as mediate protein–protein interactions.

receptors Transmembrane-spanning proteins that specifically bind extracellular ligands to mediate a biological response. Examples include the IFN receptor (IFNAR), the IF-γ receptor, gp130, and γC.

signal transducers and activators of transcription (STATs) A family of latent cytoplasmic transcription factors that transduce signals for cytokines.

Src homology 2 (SH2) The domain that mediates protein–protein interactions by binding to sites of tyrosine phosphorylation.

Src homology 3 (SH3) The domain that mediates protein–protein interactions by binding to proline-rich motifs with a core sequence of Pro-X-X-Pro.

tyrosine kinase A kinase that phosphorylates protein substrates on tyrosine residues.

Further Reading

Kisseleva, T., Bhattacharya, S., Braunstein, J., and Schindler, C. W. (2002). Signaling through the JAK/STAT pathway, recent advances and future challenges. *Gene* **285**, 1–24.

Levy, D. E., and Darnell, J. E. Jr. (2002). Stats: Transcriptional control and biological impact. *Nat. Rev. Mol. Cell. Biol.* **3**, 651–662.

O'Shea, J. J., Gadina, J., and Schreiber, R. D. (2002). Cytokine signaling in 2002: New surprises in the Jak/Stat pathway. *Cell* **109**, S121–S131.

Schindler, C. (2002). JAK-STAT signaling in human disease. *J. Clin. Invest.* **109**, 1133–1137.

Biography

Ed Cha earned his Bachelor's degree from Princeton University and is currently an M.D.–Ph.D. student at Columbia University's Medical Scientist Training Program.

Christian Schindler earned his Bachelor's degree from the University of Pennsylvania, and his M.D. and Ph.D. degrees from New York University School of Medicine. After a residency in internal medicine at Jacobi Hospital/Albert Einstein Medical Center, he became an Endocrinology Fellow at the Cornell/Memorial Sloan Kettering/Rockefeller University program. This training culminated in a postdoctoral fellowship in James Darnell's laboratory, where he purified and cloned the first two STAT proteins. Since 1992 he has been a Faculty Member in the Departments of Medicine and Microbiology at Columbia University.

Keratins and the Skin

Pierre A. Coulombe and Kelsie M. Bernot
The Johns Hopkins University School of Medicine, Baltimore, Maryland, USA

Keratins are among the most abundant proteins in epithelial cells, in which they occur as a cytoplasmic network of 10–12 nm wide intermediate filaments. They are encoded by a large multigene family in mammals, with over 49 individual genes partitioned into two major sequence types. A strict requirement for the heteropolymerization of types I and II keratin proteins during filament assembly underlies the pair wise transcriptional regulation of keratin genes. Modulation of keratin expression also depends upon both the type and stage of differentiation in epithelia. A major function fulfilled by keratin filaments is to act as a resilient yet pliable scaffold, which endows epithelial cells with the ability to sustain mechanical and nonmechanical stresses. Reflecting this crucial role as structural scaffolds, inherited mutations altering the coding sequence of keratins are responsible for a large number of epithelial fragility disorders. Additional functions, manifested in a sequence- and context-dependent fashion, have been identified.

Keratin Classification

Keratins belong to the superfamily of intermediate filament (IF) proteins. They are heterogeneous in size (400–644 amino acid residues) and charge (pI ~ 4.7–8.4), and notoriously insoluble owing to their primary structure. Keratin nomenclature originally was based upon protein separation by both charge and size via two-dimensional electrophoresis. Type I keratins tend to be smaller (40–64 kDa) and acidic (pI ~ 4.7–6.1) compared to type II, which are larger (52–68kDa) and basic-neutral (pI ~5.4–8.4) in charge. Comparison of either amino acid sequence (Figure 1A) or gene substructure (number and position of introns) reveals two distinct groups of approximately equal numbers of keratin members, designated type I (K9–K23; Ha1–Ha8; Irs1–4) and type II (K1–K8; Hb1–Hb6; K6irs1–4) IF proteins.

Keratin Gene Clusters Reflect Tissue Expression: Implications for Keratin Evolution

The coordinated regulation of the two distinct types of keratin-like genes, along with the obligatory heteropolymerization of their products to form 10–12 nm wide filaments, is present as far back as primitive chordates. In *Homo sapiens*, functional type I and type II keratins genes are clustered on the long arms of chromosomes 17 and 12, respectively (Figures 1B and 1C). There is a notable exception to this principle, in that the type I keratin 18 (K18) locus is located next to K8 at the telomeric boundary of the type II cluster (Figure 1C). K8 and K18 exhibit a very tight coregulation in both embryonic and adult simple epithelia, and likely are the direct descendants of the ancestral pair of keratin genes. The key molecular features of individual keratin genes (e.g., size and number of introns/exons) and those of the genomic clusters they form (e.g., transcriptional orientation, position relative to other family members) are perfectly conserved in human and mouse, and in many other species of mammals as well. This conservation has direct implications for the evolution of keratin genes and points to the existence of locus control elements simultaneously affecting the regulation of several neighboring genes.

Comparing the primary structure of human keratins also reveals the existence of distinct subfamilies within each of the two keratin types (Figure 1A), and provides additional insight into the mechanisms presiding over their evolution. Groupings of individual genes within each of the two major clusters correspond to similar patterns of expression in specific types of epithelial cells or tissues. This situation applies for most genes expressed in simple epithelia (K7, K8, K18, K20), "soft" complex epithelia (K1–K6; K9–K17), "hard" epithelia such as hair shaft and nail (Ha1–Ha8; Hb1–Hb6), and even the highly restricted inner root sheath compartment of hair follicles (K6irs-1–4; Irs1–4). In addition to these intriguing features, the clustering of keratin genes is mirrored by a corresponding clustering of related protein products as revealed by phylogenetic analysis. This striking equivalence, highlighted by the color scheme employed in Figure 1, implies a hierarchical pattern of gene duplication and specialization during evolution.

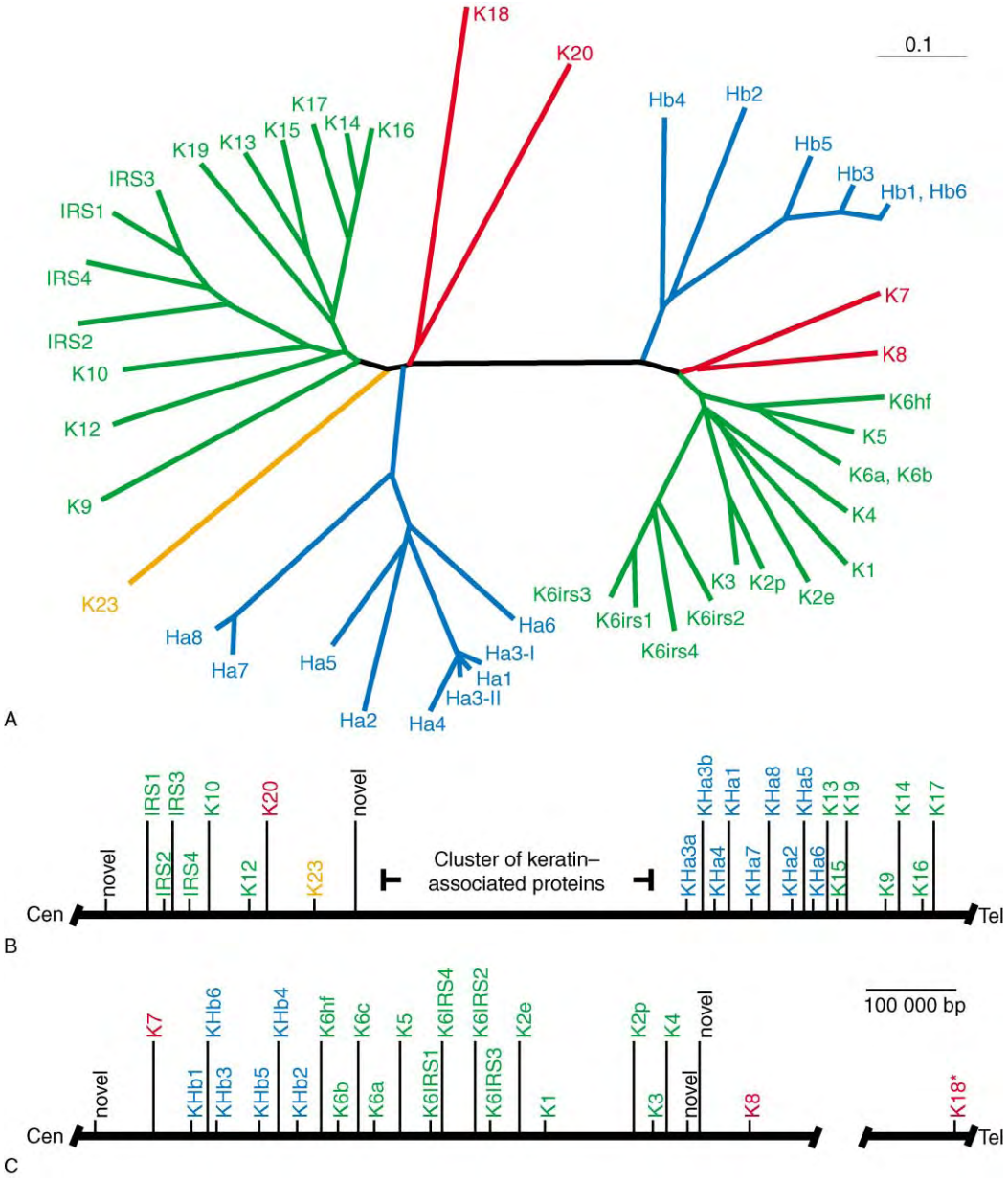

FIGURE 1 The human keratin family *circa* 2003. (A) Comparison of the primary structure of human keratins using the publicly available ClustalW and TreeView software. Sequence relatedness is inversely correlated with the length of the lines connecting the various sequences, and to the number and position of branch points. This comparison makes use of the sequences from the head and central rod domain for each keratin. A few keratins were left out for purposes of clarity. Two major branches are seen in this tree display, corresponding exactly to the known partitioning of keratin genes into type I and type II sequences. Beyond this dichotomy each subtype is further segregated into major subgroupings. (B) Organization of functional type I keratin genes in the human genome. All functional type I keratin genes are clustered on the long arm of human chromosome 17. The only exception is K18 (asterisk), which is located at the telomeric (Tel) boundary of the type II gene cluster (Cen = centromere). Transcriptional orientation is from Tel to Cen for all genes. (C) All functional type II keratin genes are clustered on the long arm of human chromosome 12. The *K8* and *K18* genes are separated by 450 000 bp. Comments on A–C: As highlighted by the color code, individual type I and type II keratin genes belonging to the same subgroup, based on the primary structure of their protein products, tend to be clustered in the genome. Moreover, very highly related keratins are often encoded by neighboring genes (e.g., *K5* and *K6* paralogues; also, *K14*, *K16*, and *K17*), further emphasizing the primary role of gene duplication in generating keratin diversity. These features of the keratin family are virtually identical in mouse (not shown).

Keratin Proteins Form the Intermediate Filament Network of Epithelial Cells

Features of Keratin Proteins

Despite sequence differences, all keratins display the tripartite domain structure that is typical of intermediate filament-forming proteins (Figure 2A). The central domain consists of an extended α-helix featuring long-range heptad repeats that mediate coiled-coil dimerization. This "rod" domain is invariably 310 amino acids long and is flanked by highly variable sequences at the N-terminal head and C-terminal tail domains. Neither terminal domain exhibits known functional motifs other than the poorly understood glycine loops seen in epidermal keratins. The head and tail domains are protease- and kinase-accessible and thus must be exposed at the surface of the filament, where they can foster interactions with neighboring filaments, other proteins, and serve as substrates for posttranslational modifications involved in their regulation. Given the notion that they are very heterogeneous in size and primary structure among keratins, the head and tail domains are clearly key to the differential function and regulation of these proteins *in vivo*.

Keratin Proteins Self-Assemble into 10–12 nm Wide Filaments

The central rod domain of keratins is the main determinant of polymerization, with an additional contribution provided by the head domain, whereas the tail domain is largely dispensable for this purpose. Polymerization of keratins begins with the formation of heterodimers in which the α-helical rod domains of type I and II keratins are aligned in parallel and perfect register. These heterodimers then interact along their lateral surfaces and then in an end-to-end fashion to give rise to the 10–12 nm wide filaments. The extraordinary stability of heterodimers (some of them resist 10 M urea!) and heterotetramers underscores the tightness of the interactions between type I and type II rod domains. Not surprisingly, most of the intracellular pool of keratin proteins is in the polymerized form (>95%).

Organization and Regulation of Keratin Filaments *in vivo*

The abundance and organization of keratin IFs *in vivo* varies according to the epithelium considered. Keratins are particularly abundant (from 10 to 80% of total cellular proteins) in surface-exposed stratified epithelia (e.g., epidermis, oral mucosa, cornea, etc.). In cells of these tissues, keratin IFs are organized in a pan-cytoplasmic network extending from the surface of the nucleus to the cytoplasmic periphery, where they associate with membrane-spanning cell–cell or cell–matrix attachment complexes such as desmosomes and hemidesmosomes (Figure 2C). In simple epithelia (e.g., liver, gut, pancreas, etc.), keratins remain a major fraction of proteins even though they are less abundant (from 1 to 5% of total cellular proteins). Such tissues are made up of polarized epithelial cells that often contain asymmetrically organized keratin IFs, concentrated mostly at the cytoplasmic periphery and particularly at the apical pole. A number of associated proteins interact with and contribute to the organization of keratin IFs in these various settings. Some directly promote the bundling of keratin IFs (e.g., filaggrin, trichohyalin), their association with microtubules and microfilaments (e.g., plectin, BPAG isoforms), and/or with desmosomes or hemidesmosomes (desmoplakin, plakophilin, BPAG isoforms, etc.).

Keratin Posttranslational Modification

The organization of keratin filaments *in vivo* is also regulated through phosphorylation. All keratin proteins are phosphoproteins. Their phosphorylation by a variety of kinases occurs in a very dynamic and reversible fashion, usually on Ser/Thr residues, and involves multiple sites on the nonhelical head domain and, to a lesser extent, on the tail domain. Circumstances in which keratin IFs are reorganized in a rapid fashion, such as mitosis or cellular stress, invariably correlates with increased phosphorylation of specific residues located in the end domains. The head domains of at least some keratins are also substrates for ubiquitination (which mediates their degradation) and O-glycosylation (whose significance has yet to be ascertained). As is the case for microtubules and actin microfilaments, the assembly and organization of keratin IFs is thus regulated though a variety of mechanisms in epithelial cells, and undoubtedly represents a key determinant of their function *in vivo*.

Keratin Gene Expression Mirrors Epithelial Differentiation: The Case of Skin

Skin provides a beautiful example of the tight relationship that has evolved between keratin gene regulation and epithelial differentiation. More than half of all keratin genes are expressed in mature mammalian skin tissue (Figure 2 and Table I). The architectural complexity of adult skin epithelia is

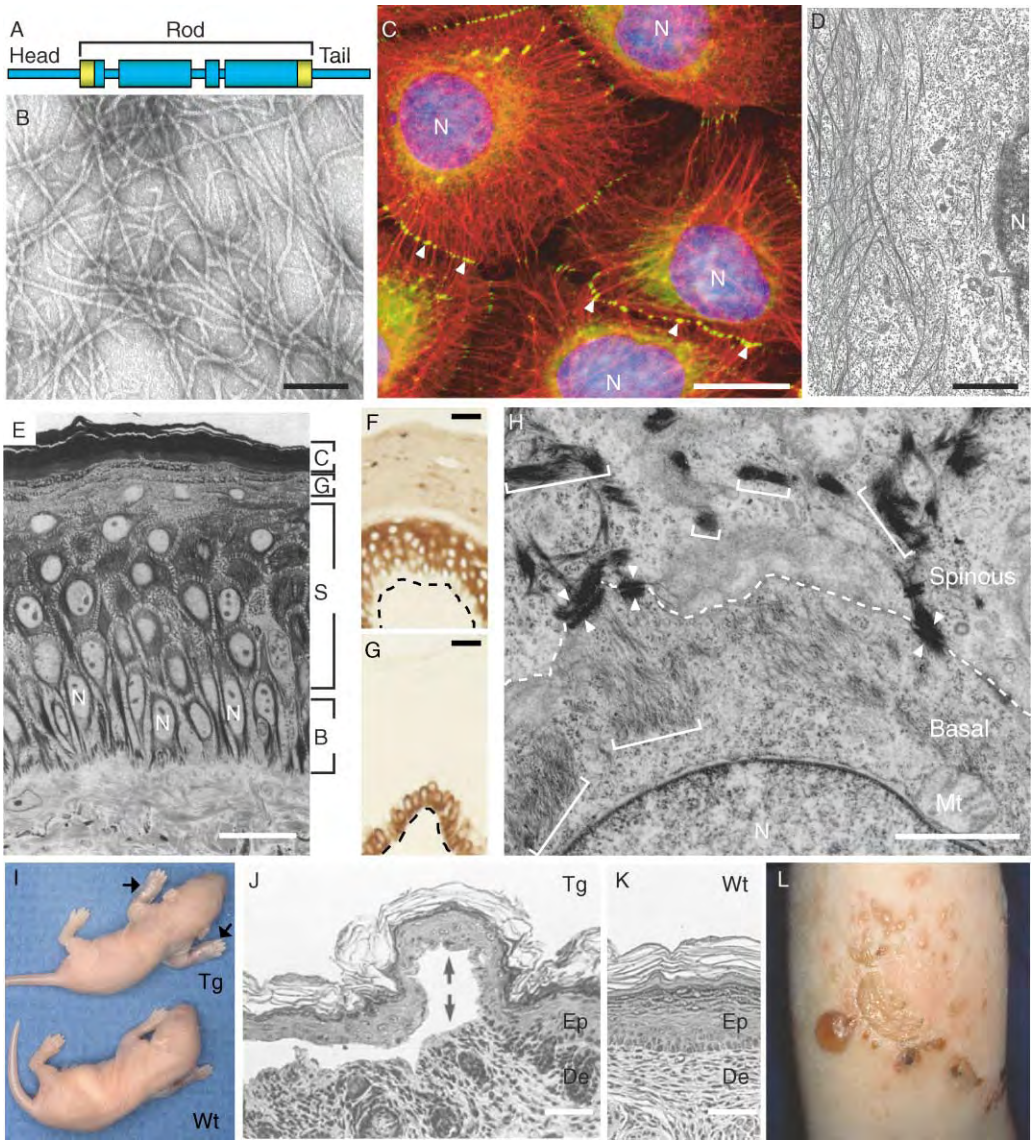

FIGURE 2 Attributes, differential regulation, and disease association of keratin. (A) Schematic representation of the tripartite domain structure shared by all keratin and other intermediate filament proteins. A central α-helical "rod" domain acts as the major determinant of self-assembly and is flanked by nonhelical "head" and "tail" domains at the N and C termini, respectively. The ends of the rod domain contain 15–20 amino-acid regions (yellow) highly conserved among all intermediate filaments. (B) Visualization of filaments, reconstituted *in vitro* from purified K5 and K14, by negative staining and electron microscopy. Bar equals 125 nm. (C) Triple-labeling for keratin (red chromophore) and desmoplakin, a desmosome component (green chromophore) and DNA (blue chromophore), by indirect immunofluorescence of epidermal cells in culture. Keratin filaments are organized in a network that spans the entire cytoplasm and are attached at points of desmosomal cell–cell contacts (arrowheads) between cells. Bar equals ~30 μm. N, nucleus. (D) Ultrastructure of the cytoplasm of epidermal cells in primary culture, as visualized by transmission electron microscopy. Keratin filaments are abundant and tend to be organized in large bundles of loosely packed filaments in the cytoplasm. (E) Histological cross-section of resin-embedded human trunk epidermis, revealing the basal (B), spinous (S), granular (G), and stratrum corneum (C) compartments. Bar equals ~50 μm. N, nucleus. (F) and (G) Differential distribution of keratin epitopes on human skin tissue cross-sections (similar to frame E) as visualized by an antibody-based detection method. K14 occurs in the basal layer, where the epidermal progenitor cells reside. K10, on the other hand, is primarily concentrated in the differentiating, suprabasal layers of epidermis. Dashed line indicates the basal lamina. Bar equals ~100 μm. (H) Ultrastructure of the boundary between the basal and suprabasal cells in mouse trunk epidermis, as seen by routine transmission electron microscopy. The sample, from which this micrograph was taken, is oriented in the same manner as frame E. Organization of keratin filaments as loose bundles (see brackets in basal cell) correlates with the expression of K5–K14 in basal cells, whereas the formation of much denser and electron-dense filament bundles (see brackets in spinous cell) reflects the onset of K1–K10 expression in early differentiating cells. Arrowheads point to desmosomes connecting the two cells. Bar equals 1 μm. N, nucleus (I) Newborn mouse littermates. The top mouse is transgenic (Tg) and expresses a mutated form of K14 in its epidermis. Unlike the control pup below (Wt), this transgenic newborn shows extensive blistering of its front paws (arrows). (J) and (K) Hematoxylin/eosin-stained histological cross-section through paraffin-embedded newborn mouse skin (similar to those shown in frame I). Compared to the intact skin of a control littermate (K, Wt), the epidermis of the K14 mutant expressing transgenic pup (J, Tg) shows intra-epidermal cleavage at the level of the basal layer, where the mutant keratin is expressed (see opposing arrows).

TABLE I

Distribution of Keratins in the Major Compartments of Skin Epithelia

Skin compartment	Cell type	Keratin expression (mRNA level)
Interfollicular epidermis	Basal keratinocytes	K5, K14; also, K15
	Early differentiating keratinocytes	K1, K10
	Late differentiating keratinocytes	K2e
	Merkel cells (in basal layer)	K8, K18, K20
Palmar/plantar epidermis	Basal keratinocytes	K5, K14; also, K15, K17, K19
	Early differentiating keratinocytes	K1, K9, K10; K6, K16
	Late differentiating keratinocytes	K2e
Hair follicles	Outer root sheath	K5, K14, K17; also, K15 and K19
	Companion layer	K6a, K16 and K6hf, K17
	Inner root sheath	Irs1–4, K6irs1–4; also, K7
	Hair shaft: cuticle & cortex	Ha and Hb keratins
	Hair shaft: medulla	K6hf, K17
Sebaceous glands (apocrine)	Glandular epithelium	K14; others unknown
	Cambial cells	K5, K14, K17
Sweat glands (eccrine)	Glandular epithelium	K8, K18?
	Myopithelium	K5, K7, K14, K17
	Duct	K5, K14; K7, K17; K6, K16
Nail	Matrix	K5, K14, K17
	Nail plate	Ha and Hb keratins
	Nail bed	K5, K14; K7, K17; K6, K16
	Proximal nail fold	K5, K14; K1, K10; K6, K16
	Hyponychium (upper layers)	K5, K14; K17; K6, K16

achieved through a temporally and spatially regulated sequence of simple decisions, resulting in progressive restriction of fate determination and reflected by specific changes in keratin gene regulation. In the clinical setting, "keratin typing" is often exploited in diagnosing cancer type, its differentiation status (and therefore prognosis), as well as the origin of the cells forming metastatic foci. This strategy is also applied for diseases other than cancer.

Keratin Gene Expression in Thin Epidermis

In thin epidermis, mitotically active cells of the basal layer act as progenitors, and consistently express K5 and K14 as their main keratin pair (Figure 2F), along with lower levels of K15. Onset of differentiation coincides with the appearance of the K1/K10 pair through a robust transcriptional induction that occurs at the expense of K5/K14. Accordingly, K1/K10 proteins are readily detectable in the lowermost suprabasal layer of epidermis (Figure 2G). The appearance of K1 and K10 correlates with a sudden and dramatic shift in the organization of cytoplasmic keratin filaments, which now exhibit significant bundling (Figure 2H). Another type II keratin gene, *K2e*, is expressed at a later stage of differentiation.

Keratin Gene Expression in Thick Epidermis

The epidermis of palm and sole skin is significantly thicker, owing to its specialization for resisting larger amounts of stress. This function is reflected in its architecture of alternating stripes of primary and secondary ridges, and specific changes in keratin expression. In the thick, stress-bearing, primary ridges, the major differentiation-specific type I K9 is presumed to foster a more resilient cytoskeleton. In the thinner secondary ridges, postmitotic cells preferentially express the type II K6a and type I K16 and K17. Relative to K1, K9, and K10, the properties

Bar equals 100 μm. (L) Leg skin in a patient suffering from the Dowling-Meara form of epidermolysis bullosa simplex. Characteristic of this severe variant of this disease, several skin blisters are grouped in a herpetiform fashion.

of K6a, K16, and K17 are believed to foster greater cellular pliability, thereby providing flexible "hinge" regions in-between the more rigid, K1/K9-rich primary ridges. While it remains to be supported by experimentation, this attractive notion is consistent with the dramatic up-regulation of K6a, K6b, K16, and K17 that occurs in keratinocytes recruited from wound margins to participate to the restoration of the epidermal barrier following injury.

Keratin Gene Expression in Hair Follicles

Consistent with its greater complexity, a larger number of keratin genes are transcribed in the pilosebaceous unit (Table I). A mature hair follicle houses eight distinct epithelial layers segregated into three histological compartments organized in concentric circles along its main axis. These compartments are, from inside out, the hair shaft proper; the inner root sheath (IRS); and the outer root sheath (ORS), an epithelium that wraps around the follicle and is contiguous with the epidermis. The regulation of ~27 keratin genes expressed in hair follicles is detailed in Table I. Key features are highlighted here. The *Ha1–Ha8* and *Hb1–Hb6* genes are unique to the hair shaft and related hard epithelia (e.g., nail). These keratin genes exhibit a stage-specific regulation during the differentiation of matrix progenitors in the bulb region to hair cortex keratinocytes. The cysteine-rich head and tail domains of the "hard" keratin proteins form disulfide bridges which, along with the γ-glutamyl cross-links catalyzed by transglutaminases, foster the organization of very large bundles of densely packed keratin filaments. This organization endows hair (and nail) with its unique structural features, shape, and resilience. Irs1–4 and K6irs1–4 are found in the inner root sheath compartment. The outer root sheath epithelium, on the other hand, expresses several of the keratins genes expressed in the epidermis, with the notable exception of the differentiation-specific K1, K2e, and K10 (Table I). By the time an epidermal or hair cortex keratinocyte has completed differentiation, more than 80% of its protein content is keratin. This extreme situation is reminiscent of globin gene expression in erythrocytes, another highly specialized cell type, and underscores the fundamental importance of keratin proteins to surface epithelia.

Functions of Keratin Filaments

Structural Support

The properties typifying keratin filaments collectively point to an important structural role. Evidence for this function came from transgenic mouse studies in which a mutated form of K14 capable of dominantly disrupting filament assembly and organization was targeted to the basal layer of epidermis *in vivo*. Unlike controls, mutant-expressing animals exhibited massive intracellular lysis of the basal cells in response to modest mechanical trauma to the skin (Figure 2I–2K). This mouse phenotype mimicked key aspects of a group of dominantly inherited epidermal disorders known as epidermolysis bullosa simplex (EBS, Figure 2L), and it was shown shortly thereafter that the human condition arises from mutations in either K5 or K14. EBS turned out to be a very useful paradigm. We now know that keratin IFs fulfill a similar function in all complex epithelia, ranging from the surface of the eye (cornea) to hair tissue. *In vitro* studies showed that keratin IFs exhibit unique viscoelastic properties that support their involvement in a structural capacity, and that disease-causing mutations significantly decrease the strength of keratin assemblies subject to mechanical strain. Likewise, biophysical studies of live cells in culture showed that keratin IFs account for a substantial fraction of their viscoelastic properties, and that disrupting keratin cytoplasmic organization causes cells to soften considerably. Demonstration of a structural support role has been comparatively more difficult for simple epithelial tissues, but strong evidence to that effect now exists for liver hepatocytes as well as trophoblast giant cells.

Scaffolding Components of Signaling Pathways and Other Functions

Transgenic mouse studies that focused on adult liver and extraembryonic tissue revealed that simple epithelial keratins 8/18 play an important cytoprotective role against chemical insults and in modulating the response to pro-apoptotic signals. In liver hepatocytes, interestingly, the function of cytoprotection requires phosphorylation of K8/K18. In regard to apoptosis, studies showed that K8/K18 filaments can bind to, and either organize or sequester key intracellular effectors of the signaling machinery downstream from engagement of the TNF-α and fas receptors. Of note, the presence of K17 is also required the survival of matrix epithelial cells in mature hair follicles. It appears likely that keratin IFs will be found to influence additional basic metabolic processes in the cell. In that regard, recent studies have shown that an intact K8/K18 filament network is required for the proper sorting of specific membrane proteins in polarized simple epithelial cells. Determining how nonpolar assemblies are adapted to foster spatial organization in the cell promises to reveal additional keratin properties and functions.

TABLE II

Disorders Associated with Mutations in Keratin Genes

Disease	Main target tissue	Gene mutated
Diseases for which mutations are causative		
Epidermolysis bullosa simplex	Basal cells/epidermis	K5, K14
Epidermolytic hyperkeratosis	Differ. cells/epidermis	K1, K10
Ichtyosis bullosa of Siemens	Differ. cells/epidermis	K2e
Meeman's corneal dystrophy	Cornea	K3, K12
Monilethrix	Hair cortex	Hb1, Hb6
Oral white sponge nevus	Oral mucosa	K4, K13
Pachyonychia congenita		
Type 1 (Jadhasson–Lewandowsky)	Nail; other appendages	K6a, K16
Type 2 (Jackson–Lawler)	Nail; other appendages	K6b, K17
Palmoplantar keratoderma		
Epidermolytic	Palmar/plantar epidermic	K9
Non-epidermolytic	Palmar/plantar epidermic	K1, K16
Steatocystoma multiplex	Sebaceous glands	K17
Diseases for which mutations are a risk factor		
Cryptogenic cirrhosis, hepatitis	Liver	K8, K18
Inflammatory bowel disease	Gut	K8, K18

Keratin Involvement in Disease

The role of keratin mutations in causing several epidermal, oral, ocular, and hair-related diseases is well established (Table II). These diseases are genetically well defined and typically inherited in an autosomal-dominant fashion, although recessive inheritance is occasionally seen. The vast majority of genetic lesions consists of missense mutations, although premature stop codons, small deletions, and mutations affecting mRNA splicing occur with some frequency. In general, disease severity correlates with the location and nature of the mutation within the keratin backbone. A keratin mutation database is being maintained at the University of Dundee and can be accessed online (http://134.36.196.124/interfilwlcm.htm).

For most of the disorders listed in Table II, mutations are causative for the disease and act through their ability to compromise the role of keratin IFs toward structural support. Mutations causing severe outcomes tend to affect amino acid residues that are highly conserved at either end of the central rod domain (Figure 1A), and often lead to the appearance of large aggregates of mispolymerized keratins in the cytoplasm of affected cells. In such instances, the aggregates appear to exacerbate the effect of the loss of a functional keratin IF network, and contribute to disease pathogenesis. Other types of mutations may also elicit alternative mechanisms of disease pathogenesis. Examples include mutations that could either affect keratin degradation during apoptosis or directly modulate keratin phosphorylation by introducing or removing a potential phosphorylation site. In contrast with other keratins, mutations affecting the simple epithelial keratins K8/K18 appear to predispose to, rather than cause disease per se (Table II). Again, this notion is supported by studies involving transgenic mice. Many of the diseases listed in Table II are characterized by a clinical heterogeneity that cannot be entirely accounted for through the position and nature of the mutation along the keratin chain. For instance, the same missense allele of K17, $Arg_{94} \rightarrow Cys$, can cause either type 2 pachyonychia congenita (which affects primarily the nail) or steatocystoma multiplex (a glandular disorder with minimal if any nail alterations) in different kindreds. Together with studies involving gene manipulation in mice, this finding points to a sometimes dramatic impact of the genetic background on disease expression.

See Also the Following Articles

Cell Death by Apoptosis and Necrosis • Intermediate Filaments

Glossary

apoptosis Orderly process of programmed cell death by which a cell commits suicide.

coiled-coil Tertiary structure of a protein motif mediating oligomerization in which two alpha-helices wrap around each other forming a hydrophobic core with characteristic interdigitation of side chains between neighboring helices, known as knob-in-hole packing.

complex epithelia One to several layers of cells in which nuclei are present on several planes covering either internal or external surfaces of the body.

desmosome Junction formed between adjacent cells in order to form a tissue.

hemidesmosome Junction that anchors cells to the basement membrane.

intermediate filaments Nonpolar, 10–12 nm wide filamentous proteins of the cytoskeleton that provide structural support to the cell.

pilosebaceous unit Composed of a hair follicle, sebaceous gland attached to it, and arrector pili muscle.

simple epithelium Single layer of cells attached to a basal lamina, in which all nuclei are aligned in a single plane often covering an internal surface of the body.

Further Reading

Cassidy, A. J., Lane, E. B., Irvine, A. D., and McLean, W. H. I. (2002). *The Human Intermediate Filament Mutation Database*. http://www.interfil.org.

Coulombe, P. A., and Omary, M. B. (2002). "Hard" and "soft" principles defining the structure, function, and regulation of keratin intermediate filaments. *Curr. Opin. Cell Biol.* **14**, 110–122.

Coulombe, P. A., Bousquet, O., Ma, L., Yamada, S., and Wirtz, D. (2000). The "ins" and "outs" of intermediate filament organization. *Trends Cell Biol.* **10**, 420–428.

Erber, A., Riemer, D., Bovenschulte, M., and Weber, K. (1998). Molecular phylogeny of metazoan intermediate filament proteins. *J. Mol. Evol.* **47**, 751–762.

Fuchs, E. (1995). Keratins and the skin. *Annu. Rev. Cell Dev. Biol.* **11**, 123–153.

Fuchs, E., and Cleveland, D. W. (1998). A structural scaffolding of intermediate filaments in health and disease. *Science* **279**, 514–519.

Hesse, M., Magin, T. M., and Weber, K. (2001). Genes for intermediate filament proteins and the draft sequence of the human genome: Novel keratin genes and a surprisingly high number of pseudogenes related to keratin genes 8 and 18. *J. Cell Sci.* **114**, 2569–2575.

Moll, R., Franke, W. W., Schiller, D. L., Geiger, B., and Krepler, R. (1982). The catalog of human cytokeratins: Patterns of expression in normal epithelia, tumors and cultured cells. *Cell* **31**, 11–24.

Omary, M. B., Ku, N. O., Liao, J., and Price, D. (1998). Keratin modifications and solubility properties in epithelial cells and *in vitro*. In *Subcellular Biochemistry: Intermediate Filaments* (H. Herrman and J. R. Harris, eds.) Vol 31, pp. 105–140. Plenum Press, New York.

Oshima, R. G. (2002). Apoptosis and keratin intermediate filaments. *Cell Death Differ.* **9**, 486–492.

Biography

Pierre A. Coulombe is a Professor in the Department of Biological Chemistry at the Johns Hopkins University School of Medicine in Baltimore, Maryland. He holds a Ph.D. from Université de Montréal in Canada and received his postdoctoral training at the University of Chicago. At that time, he and Dr. Elaine Fuchs discovered that mutations in keratins can elicit epithelial fragility in transgenic mice and individuals suffering from inherited blistering diseases. He continues to explore the properties and function of keratin genes and proteins in epithelial cells and tissues.

Kelsie M. Bernot is a native of Pennsylvania and a student in the biochemistry, cellular, and molecular biology graduate training program at Hopkins. Her thesis research focuses on the properties and function of keratin 16, which is up-regulated during wound repair and in chronic hyperproliferative skin disorders.

Ketogenesis

Janos Kerner and Charles L. Hoppel
Case Western Reserve University School of Medicine, Louis Stokes VA Medical Center, Cleveland, Ohio, USA

Ketogenesis is a process in which acetyl-CoA produced by fatty acid oxidation is converted to acetoacetate or D-3-hydroxybutyrate. These compounds, referred to as ketone bodies, are water-soluble equivalents of fatty acids and serve as important metabolic fuels for many peripheral tissues, particularly heart and skeletal muscle. During starvation, ketone bodies become the major fuel source for the brain.

Background

Ketogenesis becomes significant under conditions of food (carbohydrate) deprivation. Provision of peripheral tissues, such as skeletal muscle and heart, with ketone bodies as an alternative fuel for energy production results in glucose sparing for organs depending on glucose as an energy source. The brain then can use ketones as well as glucose, and the red blood cells continue to use glucose. The enhanced gluconeogenesis associated with ketogenesis further eases the glucose need, thus potentiating the glucose-sparing effect.

The liver plays a central role in switching from a carbohydrate to a fatty acid-based metabolism such as occurs physiologically in fasting. Under normal dietary conditions, hepatic production of ketone bodies, acetoacetate, and D-3-hydroxybutyrate is minimal and the concentrations of these compounds in blood is low. However, during food deprivation the synthesis of ketone bodies is greatly enhanced, and the circulating concentration of ketone bodies can reach values of approximately 5 mM. Thus, liver responds uniquely by enhancing its capacity to convert incoming fatty acids into ketone bodies, which then serve as fuel for energy production in peripheral tissues and thus conserve glucose for the central nervous system and for erythrocytes. For example, in the liver, the major metabolic fate of acetyl-CoA produced by the β-oxidation of fatty acids during starvation is ketone body formation, and practically all fatty acids oxidized by the liver are diverted into ketone body synthesis. It has been estimated that under saturating concentrations of acetyl-CoA, the liver has the capacity to synthesize its own weight of acetoacetate in 48 h. Although fatty acids are by far the major carbon donors for ketone body synthesis, the catabolism of some (ketogenic) amino acids also provides carbon atoms for ketogenesis, either via acetyl-CoA or directly by yielding acetoacetate.

Hepatic Fatty Acid Oxidation

The provision of acetyl-CoA by fatty acid β-oxidation is the main factor determining the rate of ketone body synthesis. Fatty acids are activated by long-chain acyl-CoA synthetase present in the mitochondrial outer membrane. Activated fatty acids are then transported into the mitochondria via the mitochondrial carnitine transport system and are sequentially chain-shortened, yielding acetyl-CoA and reducing equivalents. However, the major fate of acetyl-CoA is not oxidation in the citric acid cycle and electron transport chain to CO_2 and H_2O, but rather the formation of acetoacetate and D-3-hydroxybutyrate for export and use by peripheral tissues for energy production. It has been estimated that in fasting adult humans, brain and muscle each use at approximately equal rates 40–45% of the ketone bodies produced. Under ketogenic conditions the oxidation of palmitate to acetyl-CoA consumes 14 atoms of oxygen, whereas its complete oxidation to CO_2 and H_2O via the citric acid cycle and electron transport chain requires 46 atoms. Thus, about threefold as much palmitate must undergo β-oxidation to yield the same amount of ATP. This helps to explain the high rates of ketogenesis required to supply ATP for gluconeogenesis.

Synthesis of Ketone Bodies

The first committed step of hepatic ketone body synthesis is the condensation of two acetyl-CoA molecules to yield acetoacetyl-CoA (Figure 1). This reaction is catalyzed by acetyl-CoA acetyltransferase, an enzyme present both in the cytosol and mitochondria. The mitochondrial isoform serves in ketone body synthesis, while the cytosolic enzyme is involved in cholesterol synthesis. The mitochondrial enzyme exists

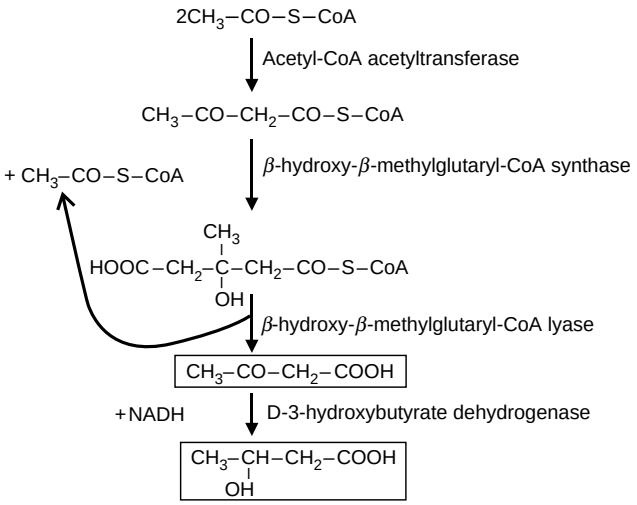

FIGURE 1 Pathway enzymes of hepatic ketogenesis.

in two isoforms, both of which are different from the cytosolic form.

The second step in the pathway is the formation of 3-hydroxy-3-methylgluratyl-CoA catalyzed by the enzyme 3-hydroxy-3-methylgluratyl-CoA synthase (HMG-CoA synthase). In liver there are two HMG-CoA isoforms, one in the cytosol and one in the mitochondria. The former takes part in cholesterol synthesis, whereas the mitochondrial form catalyzes the formation of HMG-CoA for ketone body formation. HMG-CoA synthase represents the rate-limiting enzyme of the ketogenic pathway. Consequently, overexpression of mitochondrial HMG-CoA synthase in transgenic mice caused hepatic hyperketogenesis, and hepatocytes in primary cultures from transgenic mice showed a threefold increase in acetoacetate and D-3-hydroxybutyrate in the medium. Short-term regulation of enzyme activity is achieved by succinylation. Succinylation by succinyl-CoA inhibits the activity and the enzyme is reactivated by desuccinylation.

Completion of ketone body synthesis is achieved by the action of 3-hydroxy-3-methylgluratyl-CoA lyase (HMG-CoA lyase), resulting in the formation of acetoacetate and acetyl-CoA. This enzyme is present in the mitochondrial matrix. No regulatory properties of HMG-CoA lyase have been described, and the activity of this enzyme is thought to be sufficient to effect the rapid conversion of HMG-CoA to acetoacetate.

In mitochondria some of the acetoacetate is then reduced to D-3-hydroxybutyrate by the enzyme D-3-hydroxybutyrate dehydrogenase. This enzyme is tightly bound to the matrix side of the mitochondrial inner membrane and maintains 3-hydroxybutyrate and acetoacetate concentrations that reflect the mitochondrial matrix NADH/NAD ratio. The ratio of these two ketone bodies in liver, as well as in blood, has been used as an indication of mitochondrial redox potential. Some acetoacetate is spontaneously decarboxylated to acetone in a nonenzymatic reaction.

Ketone Body Utilization

Acetoacetate and D-3-hydroxybutyrate produced in the liver are released and carried by the bloodstream to the peripheral tissues for use as alternative fuel. There, the ketone bodies are converted to two acetyl-CoA as outlined in Figure 2 for further oxidation in the citric acid cycle and electron transport chain to CO_2 and H_2O. The first reaction in ketone body utilization in peripheral tissues is the oxidation of D-3-hydroxybutyrate to acetoacetate catalyzed by D-3-hydroxybutyrate dehydrogenase. The rates of D-3-hydroxybutyrate utilization and of acetoacetate production are proportional to D-3-hydroxybutyrate concentration. Acetoacetate is then converted to its CoA ester, acetoacetyl-CoA, by the enzyme 3-ketoacyl-CoA transferase (succinyl-CoA:3-ketoacid CoA transferase). 3-ketoacyl-CoA transferase is the key enzyme of ketone body utilization. Hereditary deficiency of this enzyme is an inborn error of ketone body utilization, characterized by intermittent ketoacidotic crises and persistent ketosis. It is detected in all tissues except liver, with highest activities found in heart. The activity is decreased in hindlimb muscle of diabetic rats and might contribute to the development of diabetic ketoacidosis. The last step in ketone body utilization is the thiolytic cleavage of acetoacetyl-CoA to two acetyl-CoAs by the enzyme acetyl-CoA acetyltransferase.

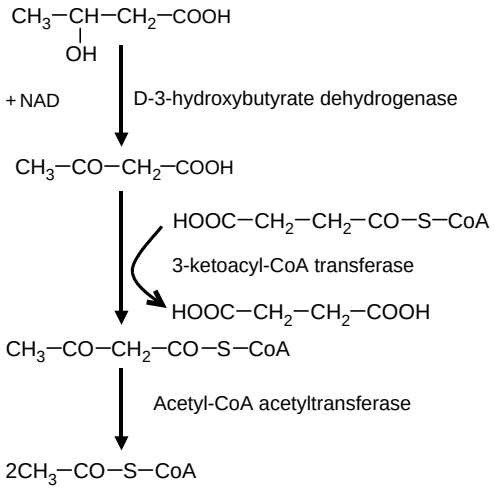

FIGURE 2 Reactions of ketone body utilization.

Regulation of Ketone Body Metabolism

Active ketogenesis requires an increased delivery of nonesterified fatty acids to the liver and an increase in hepatic fatty acid oxidation. These requirements are met by increased lipolysis due to a decrease in circulating insulin, an elevation of the glucagon/insulin ratio, resulting in activation of fatty acid oxidation. As in peripheral tissues, liver mitochondrial uptake of activated fatty acids is absolutely dependent on carnitine and requires all three enzymes of the mitochondrial carnitine transport system. The site of regulation resides at the reaction catalyzed by CPT-I, thus committing the activated fatty acids toward oxidation in the mitochondria. The mechanism by which CPT-I exerts its control is achieved through changes in concentrations of the enzyme's physiological regulator, malonyl-CoA, and through changes in the sensitivity of CPT-I to inhibition by malonyl-CoA. Thus, transition back and forth between normal and ketotic states is accompanied by changes in malonyl-CoA content and also by marked shift in the sensitivity of CPT-I to the inhibitor. Significant control of ketogenesis is exerted at another intramitochondrial site distal to CPT-I, more specifically, HMG-CoA synthase. Short-term regulation of HMG-CoA synthase is achieved by succinylation/desuccinylation of the enzyme. Thus, HMG-CoA synthase is succinylated and inactivated in the starved–fed transition and in high carbohydrate/low-fat weaned rats; it is substantially desuccinylated under ketogenic conditions such as starvation, fat feeding, diabetes, and lactation.

Both regulatory enzymes CPT-I and HMG-CoA synthase are also regulated at the transcriptional level. Thus, the developmental patterns of gene expression of CPT-I and HMG-CoA synthase in rat liver are very similar. Furthermore, mRNA and protein levels and enzyme activities for hepatic CPT-I and HMG-CoA synthase are increased during starvation, dibutyryl cAMP treatment, fat feeding, and diabetes. Opposite changes in these parameters for both enzymes are observed upon refeeding and insulin treatment, respectively.

In conclusion, changes in hepatic mitochondrial CPT-I and HMG-CoA synthase activities occur in the same direction. Control of hepatic ketogenesis may thus be exerted in a coordinated fashion at these two major regulatory sites.

See Also the Following Articles

Fatty Acid Oxidation • Fatty Acid Receptors • Fatty Acid Synthesis and its Regulation • Muscarinic Acetylcholine Receptors • Nicotinic Acetylcholine Receptors

Glossary

coenzyme A (CoA) A cosubstrate of numerous enzymes central to energy metabolism.

ketogenesis Synthesis of acetoacetate and 3-hydroxybutyrate (ketone bodies) from acetyl-CoA produced by oxidation of long-chain fatty acid in liver mitochondria.

mitochondria Eukaryotic organelles surrounded by an inner and an outer membrane that are the sites of energy production.

Further Reading

Eaton, S. (2002). Control of mitochondrial β-oxidation flux. *Prog. Lipid Res.* **41**, 197–239.

Guzman, M., and Geelen, M. J. H. (1993). Regulation of fatty acid oxidation in mammalian liver. *Biochim. Biophys. Acta* **1167**, 227–241.

Hegardt, F. G. (1999). Mitochondrial 3-hydroxy-3-methylglutaryl-CoA synthase: A control enzyme in ketogenesis. *Biochem. J.* **338**, 569–582.

Kerner, J., and Hoppel, C. (2000). Fatty acid import into mitochondria. *Biochim. Biophys. Acta* **1486**, 1–17.

McGarry, J. D., and Brown, N. F. (1997). The mitochondrial carnitine palmitoyltransferase system. *Eur. J. Biochem.* **244**, 1–14.

McGarry, J. D., and Foster, D. W. (1980). Regulation of hepatic fatty acid oxidation and ketone production. *Ann. Rev. Biochem.* **49**, 395–420.

Williamson, D. H., and Whitelaw, E. (1978). Physiological aspects of the regulation of ketogenesis. *Biochem. Soc. Symp.* **43**, 137–161.

Biography

Charles Hoppel graduated from Gonzaga University and St. Louis University School of Medicine. He is Professor of Pharmacology, Medicine and Oncology at Case Western Reserve University, Co-Director of the Center for Inherited Disorders of Energy Metabolism at CWRU, and Associate Director, Research in the Geriatric Research, Education, and Clinical Center at the Louis Stokes VA Medical Center. His research interests are in mitochondrial structure and function, mitochondrial fatty acid oxidation, and regulation of carnitine palmitoyltransferase-I.

Janos Kerner graduated from Humboldt University and held a faculty position in the Department of Biochemistry at Medical University of Pecs (Hungary) until 1994. He was a visiting faculty member in the Department of Biochemistry at Michigan State University and joined the Department of Nutrition at Case Western Reserve University in 1995. His research interest is mitochondrial fatty acid oxidation and its regulation by malonyl-CoA.

Kinesin Superfamily Proteins

Nobutaka Hirokawa and Reiko Takemura
University of Tokyo, Tokyo, Japan

Kinesin was first identified biochemically as microtubule-dependent motor protein responsible for transport of membranous organelles in the axon. It is now recognized that microtubule-dependent motor proteins form a large gene family, kinesin superfamily proteins (KIFs). The human genome contains 45 KIF genes. KIFs have high homology at the so-called "motor domain," which is a globular domain responsible for moving along microtubules by hydrolysis of ATP. Outside the motor domain, the sequence is unique to each member. The motors bind to the "cargoes," the molecule to be transported, at this domain. KIFs transport many different types of cargoes including membrane-enclosed vesicles, macromolecular complexes, cytoskeletal proteins, and mRNAs. They play important roles in a wide variety of intracellular transport, such as transport from Golgi to plasma membrane pathways involved in exocytosis and endocytosis, axonal transport, transport in dendrites, and special transport called intraflagellar transport. They also play important roles in mitosis. Functions and/or dysfunctions of KIF motors underlie some diseases. KIFs also play important roles in the early event of mammalian embryonic development, namely the formation of the left–right axis.

Introduction

The study of axonal transport provided the first clue that there is a microtubule-dependent motor protein that is not related to dynein. It has been known for quite some time that various membranous organelles and proteins are transported within axon, but the rails and motors were not known. Experimental evidence then suggested that long-distance transport within the axon is microtubule-dependent. Quick-freeze deep-etch electron microscopy revealed that short cross-bridges were present between membranous organelles and microtubules, and these were likely to be a candidate for motor proteins (Figure 1). In mid-1980s, "conventional kinesin (KIF5)" was first isolated biochemically as motor protein responsible for the transport of membranous organelles in the direction of cell body to synapse. Conventional kinesin has a rod-like structure composed of two globular heads (10 nm in diameter), a stalk, and a fanlike end, with a total length of 80 nm (Figure 2). The globular heads bind to microtubules and have an ATP-binding sequence and a microtubule-binding sequence. A systematic molecular biological search of kinesin superfamily genes coding for proteins containing similar ATP-binding and microtubule-binding sequences led to the discovery of a group of motors, which is now called kinesin superfamily proteins, KIFs (Figures 2 and 3). Human genome contains 45 KIF genes. KIFs in the human and mouse genomes are presented in a phylogenic tree along with those in *S. cerevisiae*, *Drosophila melanogaster*, and *Caenorhabditis elegans* in Figure 4. KIFs identified in mouse are named as KIF1–KIF26, and KIFC1–KIFC3. KIFs identified in other species have various names. For clarity, the nomenclature in the mouse was used as much as possible. However, for some KIFs other names were used.

Although all members of KIFs share a highly homologous domain having ~350 amino acids containing a site for ATP binding and one for microtubule binding, they are quite divergent outside the motor domain. This seems to allow the binding of KIF to various cargoes, including membrane-enclosed vesicles, macromolecular complexes, and mRNAs, and they play important roles in various transport processes including axonal transport, transport in dendrite, intracellular vesicular trafficking such as pathways involved in endocytosis and exocytosis, and special transport called intraflagellar transport (Table I). For most of the KIFs, the motor domain resides at the N-terminal portion of the molecule (N-kinesin), but the motor domain could be in the C-terminal (C-kinesin) or the middle of the molecule (M-kinesin) (Figure 3). The range of the size of typical KIF molecule is from 600–1800 amino acids (Figure 3). Different KIFs take various forms (Figure 2). Some are homodimer with or without associated light chains; some are monomeric; some are heterodimer with associated protein; some are homotetramer forming bipolar minifilaments. Some KIFs bind their cargo directly, and some do so via light chains or associated proteins discussed individually in this article.

Microtubule has a polarity. It has a fast-growing plus-end, and opposite minus-end. In the nerve cell axons, the microtubules are unipolar, the plus-end

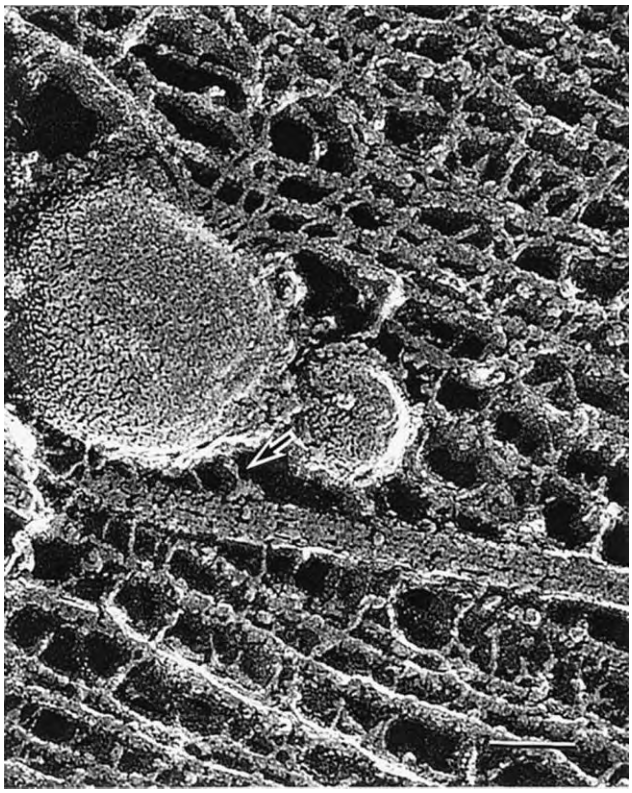

FIGURE 1 Quick-freeze deep-etch electron micrographs showing short cross-bridges between membranous organelles and microtubules that are structural candidates for KIFs. Bar 50 nm. (Reproduced, with permission, from Hirokawa, N. (1998). Kinesin and dynein superfamily proteins and the mechanism of organelle transport. *Science* **279**, 519–526.)

pointing to the direction of synapse (Figure 5A). However, in dendrites microtubules have mixed polarity in proximal region, while they are oriented like in axon in the distal region. In interphase cells, microtubules are in radial array with the minus-end pointing the cell center, and the plus-end pointing the cell periphery (Figure 5B). The direction of transport and velocity of each motor can be assessed in the so-called "*in vitro* motility assay." Most of the KIFs are plus-end directed motors, including conventional KIFs. Some KIFs are minus-end directed motor, but the minus-end directed transport is also carried out by cytoplasmic dynein (Figures 5A and 5B). In general, N-kinesin and M-kinesin are plus-end directed, and C-kinesin are minus-end directed. The typical velocity is within the range of 0.1–1.5 $\mu m\ s^{-1}$. In comparison, microtubules minus-end directed motors dyneins, which are one of the fastest motor, have velocity of $\sim 14\ \mu m\ s^{-1}$. The direction obtained from *in vitro* assay generally agree with that predicted from *in vivo* study. However, one may need some caution in interpreting the velocity of in vitro assay, because, for some KIFs, the condition of *in vitro* motility assay may not be optimal.

The characteristics of some KIFs, whose functions are relatively well characterized, are summarized in Table I. Cargoes and physiological roles of some well-characterized KIF are described next.

N-Kinesin

N-kinesin holds by far the largest number of members and it consists of 11 classes, N-1 through N-11 (Figure 4). Some classes have more than one family.

N-1 Kinesins (The KIF5 Family)

Conventional kinesin corresponds to KIF5. KIF5 forms tetramers consisting of two kinesin heavy chains (120 kDa) and two light chains (64 kDa). Light chains are unrelated in sequence to kinesin. They are a rod-like structure composed of two globular heads, a stalk, and a fanlike end, in which the light chains reside (Figure 2). KIF5 is a plus-end directed motor with the velocity of $\sim 0.5\ \mu m\ s^{-1}$. KIF5 is relatively abundantly expressed in both nervous tissue and other tissues, and transports an amazingly wide variety of cargoes including vesicles containing amyloid precursor protein (APP), GAP43, ApoE2, the receptor for the Reelin ligand, or the AMPA-type glutamate receptor GluR2, mitochondria, and lysosomes, (Figures 5A and 5B). KIF5 could also convey mRNA complexes, tubulin oligomers and intermediate filament, vimentin protein complexes. Recently the direct interactions between KIF5 and some of the cargoes have been shown (Figure 6). KIF5 may interact with certain cargoes via light chains, and yet with other cargoes via heavy chain. Moreover, whether KIF5 interacts via light chains or heavy chains may determine the destination. Glutamate receptor interacting protein 1 (GRIP1) binds to the tail domain of kinesin heavy chain and transports AMPA-type glutamate receptor (GluR2)-containing vesicles to dendrites, while JIP1,2 steers ApoER2 containing vesicles to axons through its interaction with light chains (Figure 6).

N-3 Kinesins

The Unc104/KIF1 Family

KIF1A and KIF1Bβ are plus-end directed motors of ~ 190 kDa, which are relatively abundantly expressed in the axon and transport precursors of synaptic vesicles. They are monomeric motors, which is rather unique compared to other KIFs (Figure 2). They are also one of the fastest KIF ($\sim 1.5\ \mu m\ s^{-1}$) (Table I). Unc104 is a homologue of mouse KIF1A. The knockout mice of KIF1A and KIF1Bβ show aberrant neuronal functions due to the defect in the transport of precursors of synaptic vesicles. Further study showed that patients

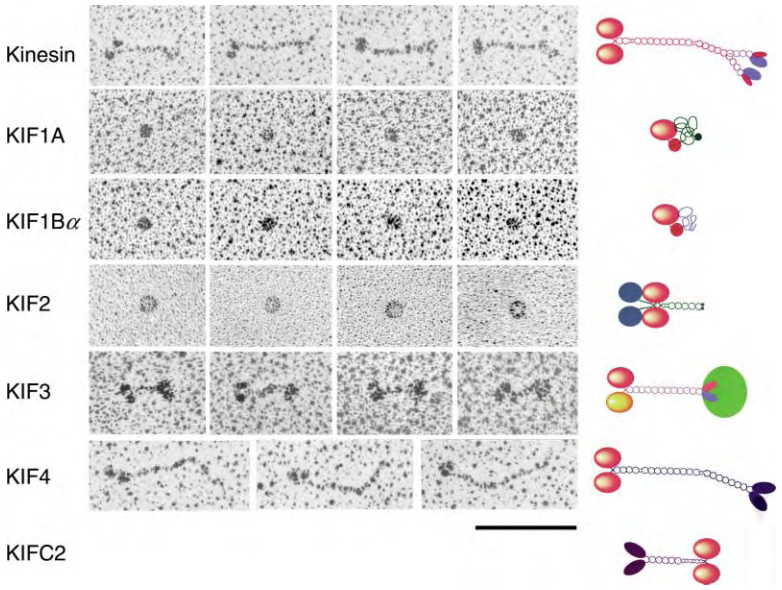

FIGURE 2 Left: Panels showing main KIFs functioning in intracellular transport, as observed by low-angle rotary shadowing EM. Scale bar, 100 nm. Right: Schematic illustration of the same KIFs based on EM studies or predicted from analysis of primary structures. (Reproduced, with permission, from Hirokawa, N. (1998). Kinesin and dynein superfamily proteins and the mechanism of organelle transport. *Science* **279**, 519–526.)

with Charcot-Marie-Tooth disease type 2A carry a loss-of-function mutation in the motor domain of the *kif1b* gene. This was the first clear indication that impaired transport due to dysfunction of KIF motors underlie the cause of neurodegenerative disease. KIF1Bα is a plus-end directed motor ($\sim 0.5\ \mu m\ s^{-1}$) expressed ubiquitously and transports mitochondria.

The KIF13 Family

KIF13A is a plus-end directed motor with the velocity of $0.1–0.3\ \mu m\ s^{-1}$ and transports vesicles containing the mannose-6-phosphate receptor from the trans-Golgi network to the plasma membrane (Figure 5B). The interaction of KIF13A with the vesicle is mediated via direct interaction between KIF13A tail and β-1-adaptin, a subunit of the AP-1 adaptor complex (Figure 6).

N-4 Kinesins

The KIF3 Family

The KIF3 forms a heterotrimeric complex, in which a heterodimer of KIF3A (80 kDa) and KIF3B ($\sim$95 kDa) interact at its tail domain with a nonmotor protein, kinesin superfamily-associated protein 3 (KAP3, $\sim$100 kDa) (Figure 2). The KIF3 complex is plus-end directed with the velocity of $\sim 0.3\ \mu m\ s^{-1}$. KIF3 is relatively abundantly expressed in the axon and other tissues, and functions in axonal transport, intracellular transport, and in the intraflagellar transport (IFT). In the axon, the complex transports vesicles that carry fodrin and choline acetyltransferase, a soluble protein. In melanophore, it disperses pigment organelles called melanosomes. In cilia and flagellar, the KIF3 complex transports macromolecular protein complexes, called IFT particles, from the bottom to the distal tip, which is important in formation and maintenance of cilia and flagella.

An interesting aspect of the involvement of KIF3 in cilium formation is that it also plays a significant role in the determination of the left–right axis in early mouse development. During mouse development, there is a monocilium at the nodal cell that rotates to produce unidirectional leftward flow of extraembryonic fluid. This nodal flow could generate concentration gradients of putative secreted morphogen, which could switch on a gene cascade leading to left–right asymmetry. In *kif3A* (−/−) or *kif3B* (−/−) mouse, nodal cilia cannot be formed, nodal flow is absent, and the left–right axis formation is fundamentally impaired.

In retinal photoreceptor cells, the KIF3 complex is localized in the connecting cilium, which is located between the outer and inner segment. KIF3 complex participates in the transport of opsin from the inner to the outer segment at the connecting cilium; the impairment of this transport process could be one of the causes of retinitis pigmentosa.

The KIF17 Family

KIF17 is localized to the dendrites and transports vesicles containing N-methyl-D-aspartate (NMDA)-type

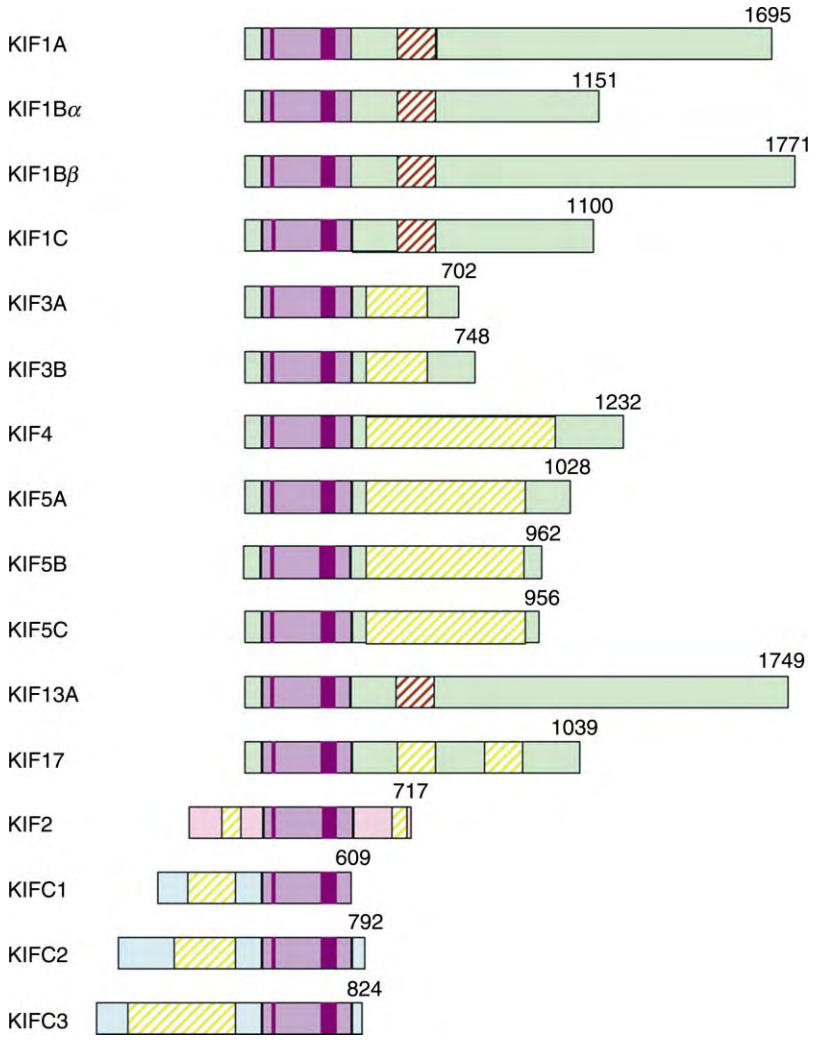

FIGURE 3 Structure of cDNAs from murine kinesin superfamily proteins (KIFs). Purple, motor domain; thin red line, ATP-binding consensus sequence; thick red line, microtubule-binding consensus sequence. (Reproduced from Hirokawa, N., and Takemura, R. (2003). Kinesin superfamily proteins. In *Molecular Motors* (M. Schliwa, ed.) pp. 79–109. Wiley-VCH, Weinheim, with permission.)

glutamate receptor 2B towards the microtubule plus end to the postsynaptic site, where the receptor plays an important role in synaptic plasticity (Figure 5). The large protein complex containing mLin-10, mLin-2, mLin7, and NR2B mediates the attachment of KIF17 to the vesicle (Figure 6). The tail domain of KIF17 interacts directly with the PDZ domain of mLin-10. Transgenic mice overexpressing KIF17 increase synthesis of KIF17 and NR2B and enhance spacial and working memories.

Other N-Kinesins

For the rest of the N-kinesin members, the physiological function has been elucidated to the varying degrees. The members of N-2 kinesins, *H. sapiens* Eg5 or *C. elegans* BimC form bipolar tetramer and participate in mitosis. They localize at the midzone of interpolar microtubules, where microtubules run in antiparallel orientation. They crosslink microtubules and allow their sliding against each other. N-5 and N-6 kinesins are involved in both mitosis and vesicle transport. N-7 and N-8 kinesins are involved primarily in mitosis. N-11 class includes the Costal 2, which is a part of the hedgehog-signaling cascade.

M-Kinesins

M-kinesins have a motor domain at the center of the molecule. There is only one family in this group, namely the KIF2 family, which is composed of *kif2a*, *kif2B*, and *kif2c* genes. KIF2 family has functional roles in vesicle transport, mitosis, and regulation of microtubule

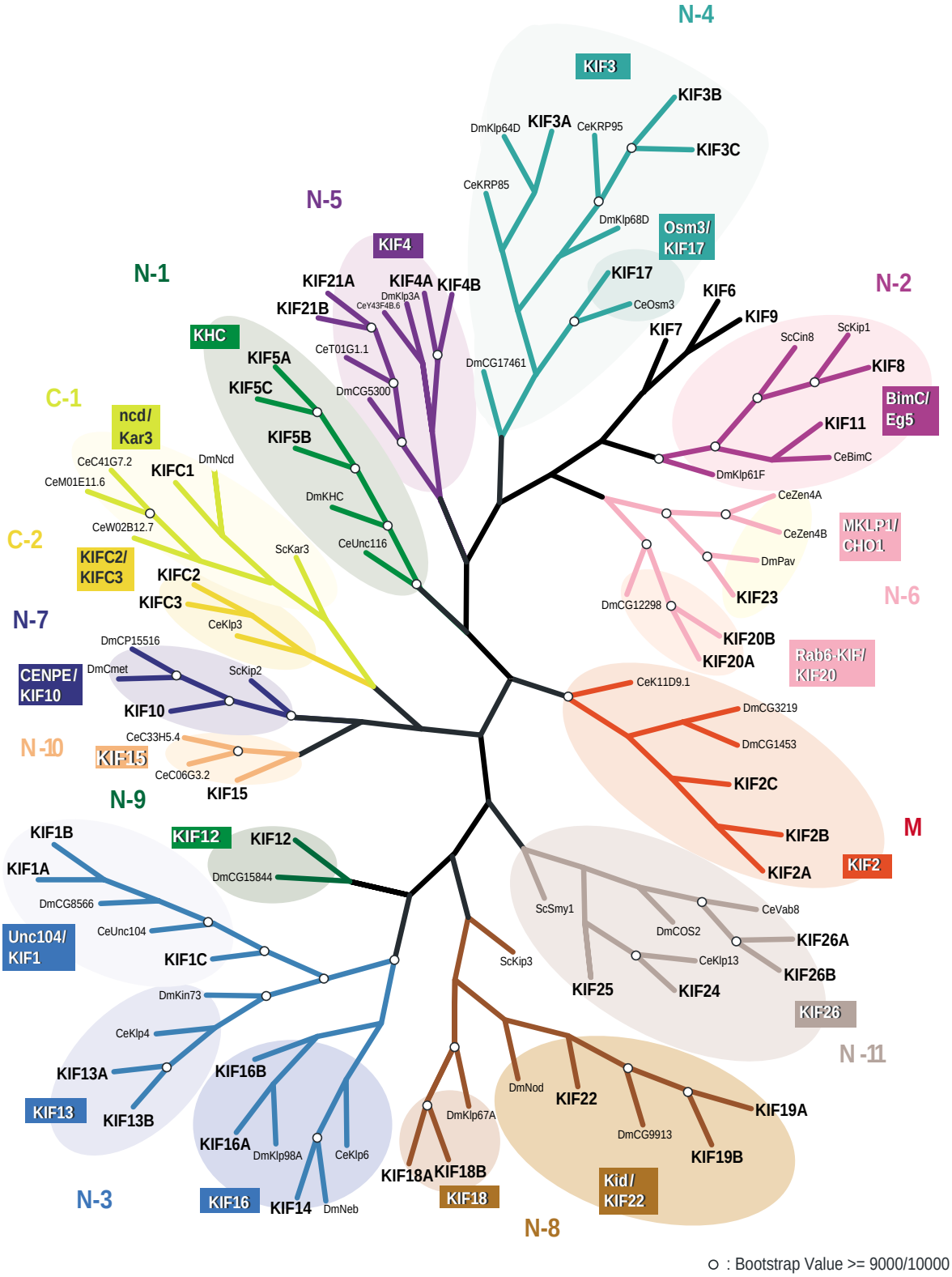

FIGURE 4 Phylogenetic analysis of all KIFs expressed in mouse/human, *D. melanogaster*, *C. elegans*, and *S. cerevisiae*. Amino acid sequences were aligned using maximum parisomy. (Reproduced from Miki, H., Setou, M., Kaneshiro, K., and Hirokawa, N. (2001). All Kinesin superfamily protein, KIF, genes in mouse and human. *Proc. Natl Acad. Sci. USA* **98**, 7004–7001, with permission.)

TABLE I

Some Members of KIF and their Properties

Class	Name	Subunit structure	Direction of transport, velocity	Functions	Cargo
N-kinesin					
N-1	KIF5 (conventional kinesin)	Homodimer plus two light chains	Microtubule plus-end $\sim 0.5\ \mu m\ s^{-1}$	Axonal transport	Vesicles containing APP and GAP43, or ApoE2, tubulin oligomers
				Dendritic transport	Vesicles containing AMPA-type glutamate receptor
				Intracellular transport	Mitochondria, Lysosomes, Vimentin protein mRNA complexes
N-2	*H. sapiens* Eg5, *C. elegans* BimC	Bipolar homotetramer	Microtubule plus-end	Mitosis	Microtubule (crosslinking and sliding of antiparallel interpolar microtubules at midzone, producing expanding force)
N-3	KIF1A, KIF1Bβ	Monomer	Microtubule plus-end $\sim 1.5\ \mu m\ s^{-1}$	Axonal transport	Precursors of synaptic vesicles
	KIF1Bα	Monomer	Microtubule plus-end $\sim 0.5\ \mu m\ s^{-1}$	Axonal and intracellular transport	Mitochondria
	KIF13		Microtubule plus-end $0.1-0.3\ \mu m\ s^{-1}$	Intracellular transport (endocytic, exocytic pathway)	Vesicles containing mannose-6-phosphate receptor
N-4	KIF3	Heterodimer plus associated protein (KIF3A/3B-KAP3)	Microtubule plus-end $\sim 0.3\ \mu m\ s^{-1}$	Axonal transport	Vesicle containing fodrin, Choline acetyltransferase
				Intracellular transport	Melanosomes
				Intraflagellar transport (IFT)	IFT particles
	KIF17	Homodimer	Microtubule plus-end $0.7-1.2\ \mu m\ s^{-1}$	Dendritic transport	NMDA-type glutamate receptor
M-kinesin					
M	KIF2	Homodimer	Microtubule plus-end $\sim 0.5\ \mu m\ s^{-1}$	Axonal transport	Vesicles containing IGF-1
				Intracellular transport	Lysosomes
	Xenous XKCM1			Mitosis	Microtubule (depolymerizing kinetochore microtubules at the kinetochore)
C-kinesin					
C-1	Ncd		Microtubule minus-end	Mitosis	Microtubules (crosslinking and sliding of antiparallel interpolar microtubules at midzone, opposing the effect of N-2 kinesins)
C-2	KIFC2	Homodimer		Dendritic transport	Multivesicular body-like membranous organelles
	KIFC3		Microtubule minus-end $\sim 4.5\ \mu m\ s^{-1}$	Intracellular transport	Vesicles containing annexin XIIb containing vesicles

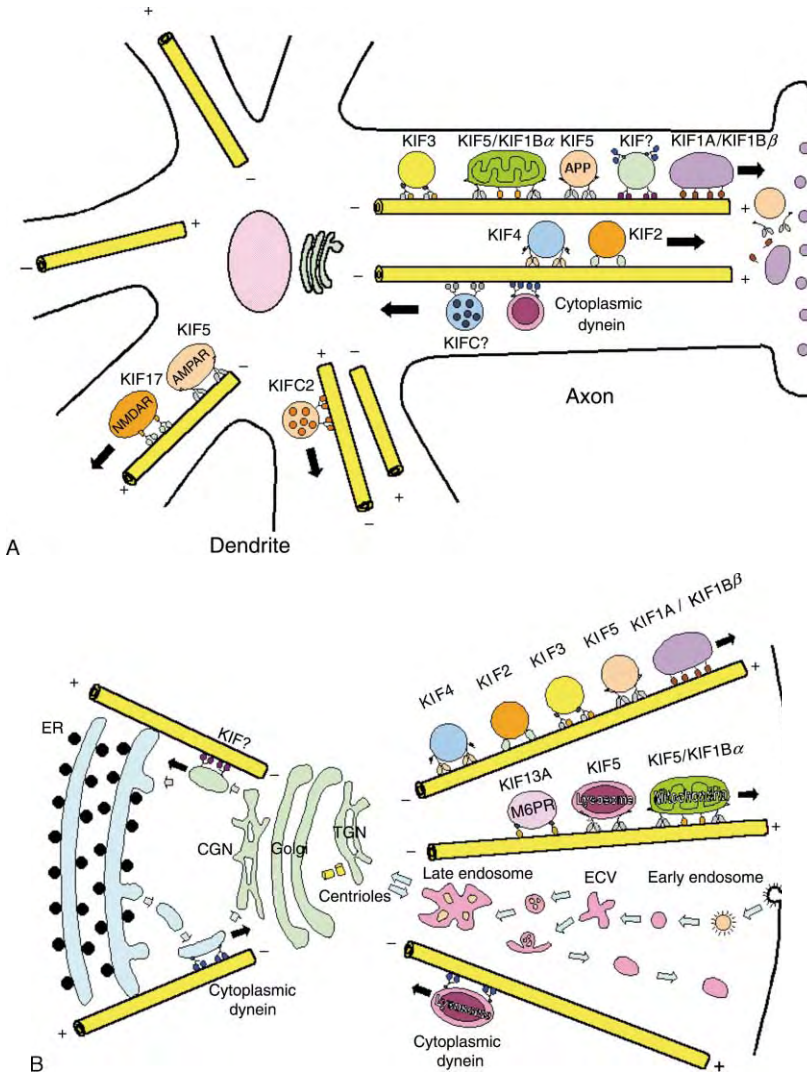

FIGURE 5 Scheme of KIFs and their cargo organelles in neurons (A) and in cells in general (B). In (B), neuron-specific KIFs and ubiquitous KIFs are illustrated in the same cell. CGN, cis-Golgi network; TGN, trans-Golgi network; ECV, endosomal carrier vesicle. Black arrows indicate the direction of transport. (Reproduced from Hirokawa, N., and Takemura, R. (2003). Kinesin superfamily proteins. In *Molecular Motors* (M. Schliwa, ed.) pp. 79–109. Wiley-VCH, Weinheim, with permission.)

dynamics. *Xenopus* XKCM1 has a microtubule-destabilizing activity, and depolymerizes microtubules at the kinetochore and promotes chromosome segregation.

C-Kinesins

C-1 Kinesins (The KIFC1 Family)

Drosophila Ncd crosslinks and slides antiparallel spindle microtubules in relation to another, pulling them apart, opposing the effect of bipolar plus-end-directed motors.

C-2 Kinesins (The KIFC2/KIFC3 Family)

KIFC2 transports multivesicular body-like membranous organelles in dendrites (Figure 5A). It has not been rigorously demonstrated, but it is presumed that KIFC2 acts as a minus-end-directed motor.

KIFC3 is a minus-end-directed microtubule motor protein that exists in kidney epithelial cells and other types of cell. In epithelial cells, microtubule organization is different from that in other types of cell; microtubule minus ends run towards the apical surfaces of the cell. KIFC3 accumulates on the apical surface of epithelial cells and transports vesicles associated with annexin

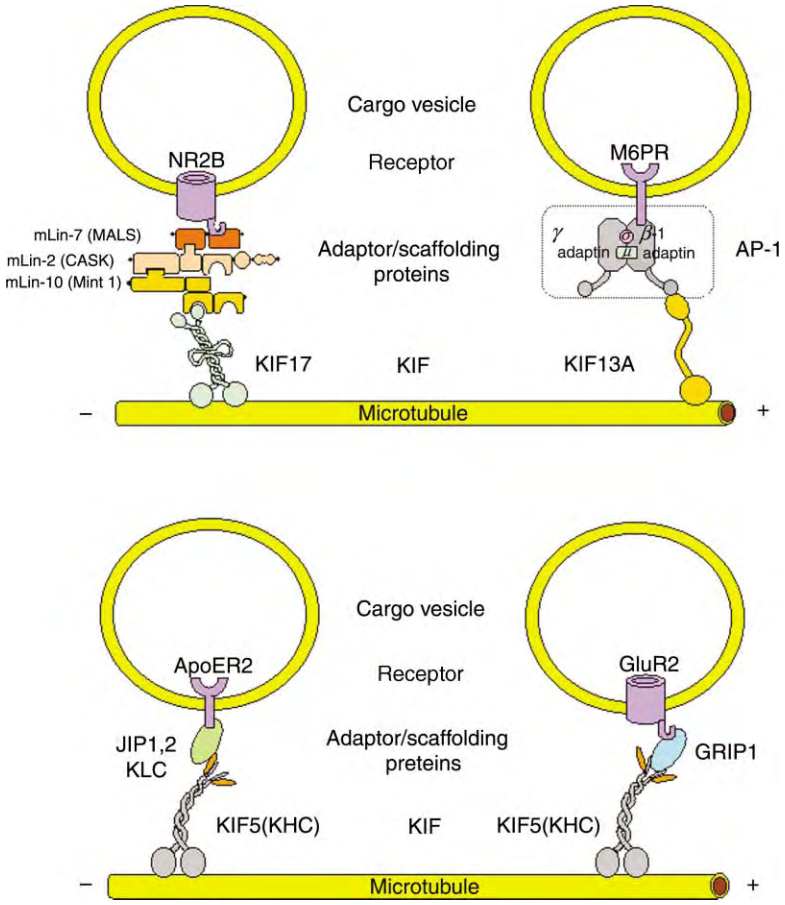

FIGURE 6 Scheme of how KIFs recognize and bind cargoes. (Reproduced from Hirokawa, N., and Takemura, R. (2003). Kinesin superfamily proteins. In Molecular Motors (M. Schliwa, ed.) pp. 79–109. Wiley-VCH, Weinheim, with permission.)

XIIIb, a previously characterized membrane protein for apically transported vesicles.

Perspectives

Cargoes of KIFs; Specificity and Redundancy

As mentioned earlier KIFs convey various types of cargo. In some cases, a single KIF transports several distinct cargoes. How the same KIF can transport different cargoes is an interesting and important question that needs to be addressed.

At the same time, KIFs sometimes redundantly convey similar cargoes. KIF1Bα transports mitochondria, while mitochondria have another redundant motor KIF5. KIF1A's cargo is a synaptic vesicle precursor, whereas KIF1Bβ also conveys synaptic vesicle precursors. Another example is lysosomes that have at least two microtubule plus-end motors, kinesin and KIF2Aβ. This redundancy could be a cause of subtle phenotypes of knockout mice in which some *kif* genes have been knocked out.

Recognition and Binding to Cargoes

To address the question of how specificity and redundancy are controlled, it is important to understand how KIFs recognize and bind to their own cargoes. As discussed earlier, some of the interactions of KIFs and cargoes are beginning to be uncovered.

In terms of how KIFs recognize and bind cargoes, several forms can be categorized (Figure 6).

1. *KIF tail – scaffolding protein(s) or adaptor protein(s) – membrane protein*. This is applicable to KIF17-mLin10-mLin2-mLin7-NR2B, KIF13A-β1adaptin-AP-1adaptor complex-M6PR, KLC-JIP1/JIP2-ApoE2, the reelin receptor, and KIF5 (KHC)-GRIP1-GluR2.

2. *KIF tail – membrane protein*. Kinesin was reported to bind directly to membrane proteins through its interaction with KLC. Sunday Driver (also called JSAP1 and JIP3) and APP were proposed to be membrane proteins that bind to directly kinesin through KLC, while it needs to be studied further if Sunday Driver (JSAP1 ad JIP3) is indeed a membrane protein.

It is only now being understood how KIFs recognize and bind to their specific cargoes, but thus far what was only known was that rather complex mechanisms are involved in these events. This may be related to how the association and dissociation between KIFs and cargoes are regulated. Another question is how KIFs recognize and bind to protein complexes such as tubulin and intermediate filament proteins, chromosomes, and mRNAs. These are obviously significant questions that need to be answered in the near future.

How to Determine Directions of Transport

Another intriguing question is how a cell regulates direction of transports, e.g., axon versus dendrites. In the case of KIF5, whether KIF5 binds to cargoes via heavy chain or light chain seems to determine the direction of transport, and JIP1.2 and GRIP1 are functioning as drivers (Figure 6). There are motors that transport cargoes mainly to dendrites. KIF17 conveys NMDA receptors mainly to dendrites and KIFC2 transports new multivesicular body-like organelles to dendrites. KIF21B was also proposed to be a motor for dendritic transport. How differential transports are performed is clearly the fundamental question that needs to be solved in the near future. The mechanism is probably not simple and could involve several distinct events.

Thus, cells use interestingly many KIFs and very precisely control the direction and velocity of transport of various distinct cargoes that are fundamental in cellular basic functions. This field is obviously very important and rapidly advancing. Further studies need to be carried out to understand the entire mechanism of intracellular transport.

See Also the Following Articles

Dynein • Kinesins as Microtubule Disassembly Enzymes • Microtubule-Associated Proteins • Mitosis

Glossary

axonal and transport Axons transmit the signal from the cell body to the synaptic terminal. Because axons lack ribosomes, i.e., the protein synthetic machinery, most of the proteins needed in the axon and synaptic terminal need to be synthesized at the cell body and transported. The transport in the direction from the cell body to synapse is called the anterograde transport. Some molecules are transported in the opposite direction (retrograde transport). The proximal part of the dendrite contains ribosomes, although the number reduces at the distal region.

cilia and flagella Cilia and flagella contain microtubules in the "9 + 2" axonemal configuration (9 doublets and central pair of microtubules). The microtubules in the doublets slide along one another by the stroke of axonemal dynein, which bridges neighboring doublets.

dynein Minus-end directed microtubule motor. It forms a massive multisubunit complex composed of two–three heavy chains (~530 kDa), which have motor domains, and variable numbers of associated intermediate and light chains. There are two classes, axonemal and cytoplasmic. Axonemal dyneins are attached to microtubule doublets in cilia and flagellar, and slide against microtubules producing the beating movement. Cytoplasmic dyneins are expressed in most eukaryotic cells and important in vesicle trafficking and cell division.

microtubule Filament of 25 nm diameter assembled from α- and β-tubulin subunits (55 kDa). Microtubules, microfilaments (actin filaments), and intermediate filaments are the major cytoskeletal filaments. In addition to the structural role, microtubules serve as rails for the long-distance transport, and microfilaments serve as rails for the short-distance transport. Microtubules are also reorganized as mitotic spindle during mitosis, and play an important role in cell division.

mitosis Replicated chromosomes are separated into two daughter cells, by a complex cytoskeletal machine called mitotic spindles. The process proceeds as prophase, prometaphase, metaphase, anaphase, and telophase. Several different classes of KIFs and the cytoplasmic dynein participate in the complex movement of mitotic spindles.

Further Reading

Alberts, B., Johnson, A., Lewis, J., Raff, M., Roberts, K., and Walter, P. (2002). *Molecular Biology of the Cell*, 4th edition. Garland Publishing, New York.

Grafstein, B., and Forman, D. S. (1980). Intracellular transport in neurons. *Physiol. Rev.* **60**, 1167–1283.

Heald, R. (2000). Motor function in the mitotic spindle. *Cell* **102**, 399–402.

Hirokawa, N. (1998). Kinesin and dynein superfamily proteins and the mechanism of organelle transport. *Science* **279**, 519–526.

Hirokawa, N. (2000). Stirring up development with the heterotrimeric kinesin KIF3. *Traffic* **1**, 29–34.

Hirokawa, N., and Takemura, R. (2004). Biochemical and molecular characterization of diseases linked to motor proteins (submitted).

Hirokawa, N., and Takemura, R. (2003). Kinesin superfamily proteins. In *Molecular Motors* (M. Schliwa, ed.) pp. 79–109. Wiley-VCH, Weinheim.

Hirokawa, N., Noda, Y., and Okada, Y. (1998). Kinesin and dynein superfamily proteins in organelle transport and cell division. *Curr. Opin. Cell Biol.* **10**, 60–73.

Schliwa, M. (2003). *Molecular Motors*. Wiley-VCH, Weinheim.

Tanaka, Y., and Hirokawa, N. (2002). Mouse models of Charcot-Marie-Tooth disease. *Trends Genet.* **18**, S39–S44.

Terada, S., and Hirokawa, N. (2000). Moving on to the cargo problem of microtubule-dependent motors in neurons. *Curr. Opin. Neurobiol.* **10**, 566–573.

Verhey, K. J., and Rapoport, T. A. (2001). Kinesin carries the signal. *Trends Biochem. Sci.* **26**, 545–550.

Biography

Nobutaka Hirokawa is Professor and Chair of the Department of Cell Biology and Anatomy, and Dean of the School of Medicine, University of Tokyo. His principal research interests are organization of cytoskeletal structures in neurons and molecular motors involved in the axonal transport. He holds an M.D. and a Ph.D. from University of Tokyo. He developed the quick-freeze, deep-etch electron microscopy with John Heuser, and did pioneering work in elucidating the neuronal cytoskeleton in molecular detail. He was also one of the first to tackle the analysis of kinesin motor molecules, clone multiple kinesin superfamily proteins from mammalian brain and point out the importance of this motor protein family.

Kinesins as Microtubule Disassembly Enzymes

Susan L. Kline-Smith and Arshad Desai
University of California, San Diego, California, USA

Kinesins are an important class of proteins that were discovered on the basis of their ability to couple ATP hydrolysis to translocation along microtubule polymers. Microtubules are hollow cylindrical polymers assembled from α/β-tubulin heterodimers that are found in all eukaryotes and function in many different biological contexts. Microtubules exhibit structural polarity, with the α/β-tubulin heterodimers oriented in a uniform head-to-tail fashion within the polymer lattice. β-tubulin points toward the faster polymerizing "plus" end and α-tubulin toward the slower polymerizing "minus" end of the microtubule. The defining member of the kinesin superfamily, referred to as conventional kinesin, is a well-characterized, processive plus end-directed motor protein. Sequences homologous to the catalytic domain responsible for the motor activity of conventional kinesin have been discovered in a large number of proteins, and the complete genomic complement of kinesins is known for the many eukaryotes with sequenced genomes.

Although motility was the defining activity of kinesins, recent work has revealed that the catalytic domain is used in a subset of kinesins to drive microtubule disassembly rather than motor activity. Physiologically, the regulation of microtubule dynamics by kinesins is likely to be of great significance in cellular organization, division, and differentiation. Here, we first briefly review the work that led to the recognition of specific kinesins acting as microtubule disassembly enzymes. We then discuss progress toward understanding the mechanism by which the catalytic domain is used to drive a very different biochemical activity and finally comment on the physiological relevance of this nonmotile activity.

Kinesins as Regulators of Microtubule Dynamics: A Brief Historical Overview

The kinesin superfamily has been subdivided based on catalytic domain sequence homology and placement of the catalytic domain within the primary sequence (Figure 1). Conventional kinesin, the first discovered kinesin, has its catalytic domain at the N terminus and is a fast, plus end-directed motor protein (Figures 1 and 2). All kinesins with N-terminal catalytic domains (Kin Ns) that have been subsequently analyzed *in vitro* exhibit plus end-directed motility. In contrast, slow minus end-directed movement has been observed for Kin C kinesins, which have their catalytic domain at the C terminus (Figures 1 and 2).

Kinesins were assumed to move along the microtubule lattice without significantly influencing their dynamic properties. Consistent with this assumption, the motility of kinesin-coated microspheres was found to have no effect on the parameters of microtubule dynamics in quantitative studies. The first hint for the involvement of kinesins in regulation of microtubule dynamics came from *in vitro* analysis of Kar3, a budding yeast member of the Kin C subfamily. *In vitro*, the catalytic domain of Kar3 translocated slowly toward the minus end and also increased depolymerization from minus ends of microtubules stabilized with the drug paclitaxel (Figure 2). A role for Kar3 in promoting microtubule disassembly was also supported by the ability of microtubule-destabilizing drugs to suppress Kar3 mutations. While this work was suggestive, compelling evidence for kinesins acting as microtubule-disassembly enzymes came from analysis of the Kin I kinesin subfamily, whose members have an internal catalytic domain (Figures 1 and 2). When a *Xenopus* member of the Kin I subfamily was inactivated in egg extracts, microtubule polymerization was dramatically increased. This increase was attributed to a reduction in the transition from microtubule polymerization to depolymerization (termed microtubule catastrophe). Subsequently, purified Kin I kinesins were shown to be sufficient for microtubule disassembly, and the majority of studies on kinesins as microtubule disassembly enzymes has been focused on members of this subfamily.

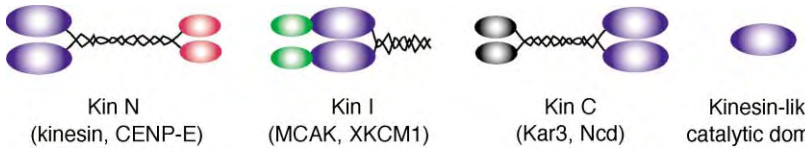

FIGURE 1 Kinesin superfamily domains. Proteins that share sequence homology in the kinesin-like catalytic domain (shown in purple) are defined as members of the kinesin superfamily. The placement of the catalytic domain within the primary sequence of the proteins further subdivides the family into Kin N (N-terminal catalytic domain), Kin I (Internal catalytic domain), and Kin C (C-terminal catalytic domain) subfamilies. Examples of proteins belonging to each subfamily are listed.

Kin I Kinesins: Motors or Disassembly Enzymes?

The presence of a kinesin-like catalytic domain in Kin I kinesins suggested that they are motor proteins. Consistent with this expectation, a neuron-specific member of this subfamily was reported to be a fast plus end-directed motor. However, the dramatic increase in microtubule polymerization upon inhibition of a Kin I kinesin in *Xenopus* egg extracts suggested that these kinesins promote microtubule disassembly. One obvious hypothesis to accommodate both views was that Kin I kinesins do not themselves act as depolymerases, but instead deliver a destabilizing factor to microtubule plus ends. However, *in vitro* analysis of purified Kin I kinesins contradicted this hypothesis and clearly demonstrated that microtubule disassembly is an intrinsic activity of members of this subfamily. Particularly compelling evidence came from the observation that depolymerization occurred at both microtubule ends, inconsistent with the unidirectional motility that has been demonstrated for all other kinesins with motor activity. In addition, *Xenopus* Kin I kinesins preferentially targeted to both microtubule ends over the microtubule lattice, even in the presence of the nonhydrolyzable ATP analogue AMP-PNP. These findings for *Xenopus* Kin Is have been replicated successfully for mammalian and invertebrate members of this subfamily, and it is now generally accepted that Kin I kinesins use their catalytic domain to depolymerize microtubules rather than to translocate along the microtubule lattice. The first study reporting motility for a Kin I kinesin is most likely explained by the presence of a contaminant in the assayed protein preparation, as none of the subsequent studies have been able to demonstrate motor activity.

Kin I Kinesins: Mechanism of Action

Multiple *in vitro* studies have demonstrated that Kin Is are able to catalytically depolymerize microtubules from both their plus and minus ends. Mechanistic studies concerning Kin Is largely used stabilized microtubule substrates: a necessity for studying intermediary steps in the microtubule disassembly process. Kin Is are able to depolymerize microtubules stabilized using the drug paclitaxel as well as microtubules stabilized with a slowly hydrolyzable analogue of GTP, called GMP-CPP, which mimics a stable GTP-like microtubule lattice. With respect to dynamic microtubules assembled from purified tubulin, the more physiologically relevant substrate, Kin I kinesins have been shown to promote microtubule catastrophes, but whether they influence the rates of polymerization and depolymerization or the transition from depolymerization to polymerization (termed microtubule rescue) is not known.

Negative stain electron microscopy of GMP-CPP stabilized microtubules has demonstrated that Kin Is destabilize microtubules at both ends of the polymer by

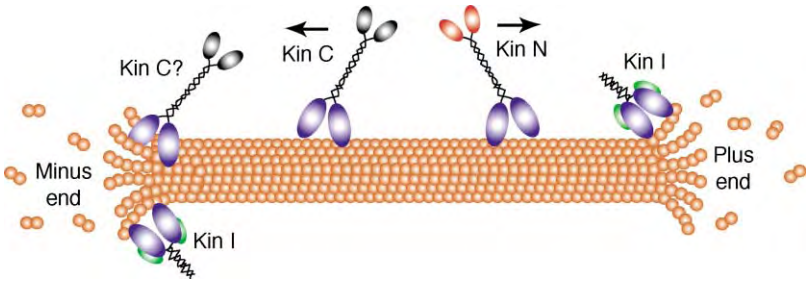

FIGURE 2 Kinesin–microtubule interactions. Kinesin-like proteins exhibit various interactions with the microtubule polymer, including plus end-directed motor activity (Kin Ns), minus end-directed motor activity (Kin Cs), and depolymerization of microtubules from both ends of the microtubule (Kin Is). A Kin C from budding yeast has also been shown to weakly destabilize the minus ends of microtubules.

inducing protofilaments to peel backwards. In dynamic microtubules, the bulk of the polymer is made up of GDP-associated tubulin, with the newly added tubulin heterodimers still bound to GTP. It is thought that the GTP-bound dimers (referred to as the GTP "cap") constrain the rest of the polymer to maintain a straight conformation as opposed to the preferred curved conformation of the GDP-bound protofilaments. Interestingly, Kin Is do not induce protofilament curvature by stimulating hydrolysis of the tubulin-bound nucleotide, suggesting that their binding results in a destabilizing conformational change at microtubule ends. A direct preference of Kin Is for microtubule ends versus the side lattice has been demonstrated using fluorescence microscopy to visualize the accumulation of Kin I molecules on the peeling protofilaments at the end of depolymerizing GMP-CPP microtubules. In addition, the depolymerization rate of Kin Is saturates at a very low ratio of Kin I:tubulin, suggesting that Kin I activity is restricted to microtubule ends.

The preferential targeting of Kin Is to microtubule plus and minus ends is consistent with their ability to depolymerize either end, although the mechanism by which Kin Is target ends is not known. Interestingly, Kin Is display a much higher on-rate for microtubule ends than the on-rate of conventional kinesin for the microtubule lattice, suggesting that the process of end-targeting might be more directed than simple diffusion of the Kin I molecules. Recent data demonstrating one-dimensional diffusion of Kin Is along the lattice of GMP-CPP microtubules have led to the hypothesis that this mechanism enables Kin Is to quickly reach either end of the microtubule. However, Kin Is can target to ends and induce protofilament peeling in the presence of AMP-PNP, which inhibits one-dimensional diffusion of other kinesins. The effect of AMP-PNP on the one-dimensional diffusion of Kin Is along the microtubule lattice is an important issue to address in future work.

Quantitative ATPase assays have provided additional evidence that Kin Is act at microtubule ends; however, the precise coupling between the ATPase and microtubule disassembly cycles is controversial. In the presence of AMP-PNP, Kin I kinesins accumulate at and cause peeling of GMP-CPP microtubule ends without disassembling the entire stabilized polymer. Thus, it was initially proposed that ATP hydrolysis occurs after dissociation of the Kin I–tubulin complex from the microtubule, thereby recycling the Kin I for multiple depolymerization cycles (Figure 3A). Consistent with this observation, Kin Is have been shown to bind tubulin subunits and exhibit tubulin-stimulated ATPase activity. In contrast, ATPase analyses have also suggested that Kin Is may act processively at GMP-CPP microtubule ends, with each Kin I causing disassembly of several tubulin subunits without dissociation of the Kin I molecule from the microtubule end (Figure 3B). Further work is necessary to reconcile these opposing viewpoints.

Specialized microtubule substrates have been used to determine how Kin Is bind microtubules to induce protofilament peeling. Two possible mechanisms of inducing the curved conformation at the end of a microtubule are: (1) the Kin I binds between two protofilaments, splaying them apart, or (2) the Kin I binds a single protofilament, inducing a kink in the conformation of that protofilament, which would then lead to destabilization of the microtubule lattice. *In vitro* analyses support the latter hypothesis, as Kin Is can still depolymerize zinc-induced macrotubes, which are 250 nm tubes (tenfold larger diameter than microtubules) made up of protofilaments that have opposing polarity. Thus, in a zinc macrotube the side-by-side

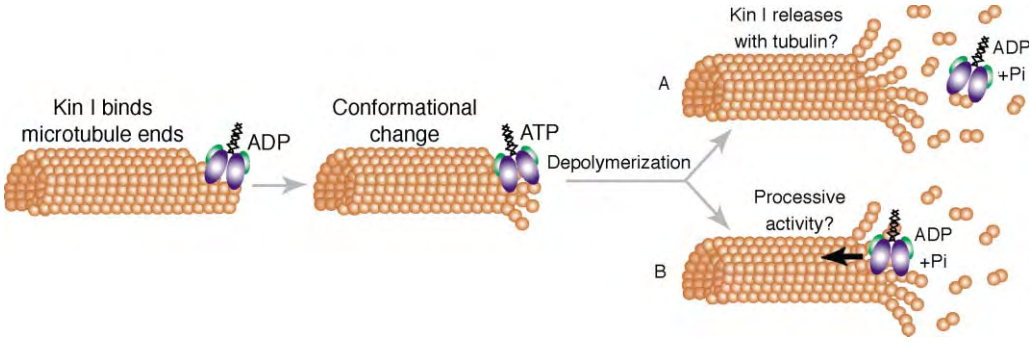

FIGURE 3 Kin I ATPase and microtubule disassembly cycles. Although Kin Is can bind and depolymerize both microtubule ends, only one end is illustrated for simplicity. As with other kinesin-like proteins, Kin Is are thought to bind microtubules in an ADP-bound state. Microtubules act as nucleotide exchange factors, resulting in ATP-bound Kin Is, which initiate a conformational change in the lattice at microtubule ends. This conformational change leads to depolymerization of the microtubule polymer. Two proposed models suggest different functions for ATP hydrolysis in this cycle. (A) After initiating depolymerization of the microtubule, Kin Is use ATP hydrolysis to be released from tubulin heterodimers, allowing the Kin I to participate in another depolymerization cycle. (B) Alternatively, ATP hydrolysis may allow Kin Is to processively depolymerize microtubules, with each Kin I molecule removing multiple tubulin dimers before dissociating from the microtubule lattice.

protofilaments alternate between the luminal face and the external face of protofilaments in a normal microtubule. If Kin Is bound between two protofilaments, the protofilament would be required to have the same directionality. Current structural studies are focusing on how Kin Is dock onto protofilaments and how the conformations of both the Kin I and the microtubule change during the cycle of Kin I activity.

Kin Is are homodimeric proteins, largely through interactions in the α-helices of the short C-terminal stalk of the protein. However, Kin Is are still able to depolymerize microtubules in their monomeric form both *in vitro* and *in vivo*. In most systems, the internal kinesin-like catalytic domain (which includes microtubule binding and ATP hydrolysis domains) is sufficient only to bind microtubules. To reconstitute the activity of microtubule depolymerization, Kin Is require the catalytic domain plus a small section of the N terminus called the "neck," which is just proximal to the catalytic domain. In conventional kinesin, the neck is responsible for the power stroke that allows one head to "step" in front of the other head on the microtubule lattice. In Kin Is, the neck must be positively charged for microtubule destabilization to occur, presumably because the positively charged neck interacts with the negatively charged microtubule polymer. Interestingly, Kin Is are unable to depolymerize microtubules treated with the drug subtilisin, which cleaves the negatively charged C terminus of β-tubulin known to interact with other motile kinesins, suggesting a degree of conservation in the mechanism of interaction between diverse kinesins and microtubule polymer.

Overall, biochemical and microscopic studies are improving our understanding of the mechanism of Kin I-induced microtubule depolymerization; however, many questions still remain regarding microtubule end targeting, coupling of the Kin I ATPase cycle with microtubule disassembly, and the structural requirements for Kin I binding to the microtubule. In addition, defining the extent to which these results can be applied to dynamic microtubules is perhaps the most important future goal.

Physiological Roles of Microtubule-Depolymerizing Kinesins

During interphase, Kin Is exist as a soluble pool in the cytoplasm and nucleus of cells. Inhibition of the cytoplasmic pool suggests that Kin Is help to regulate microtubule dynamics by stimulating the catastrophe frequency and suppressing the rescue frequency of microtubules. During mitosis, Kin Is display a complex localization at centromeres, spindle poles, and in the cytoplasm of somatic cells and embryonic extracts (Figure 4). Truncation assays have demonstrated that the globular N-terminal domain of Kin Is aids in centromere localization of the protein. It is unclear how Kin Is localize to spindle poles during mitosis, although this enrichment does appear to require microtubules.

Inhibition assays suggest that Kin Is regulate different aspects of mitotic spindle formation and function. Immunodepletion of a *Xenopus* Kin I from embryonic egg extracts completely inhibits spindle formation due to a huge increase in microtubule polymerization as a result of decreased catastrophe frequency of microtubules (Figure 5B). Similarly, inhibition of Kin Is in somatic cells leads to increases in microtubule spindle polymer, delayed centrosome separation, and delayed mitosis. Thus, regulation of global microtubule dynamics in the mitotic spindle appears to be a conserved activity of Kin I kinesins. These findings, however, demonstrate the defects due to overall inhibition of Kin Is, and do not distinguish between the roles for Kin Is specifically localized to the centromere or the spindle poles. Interestingly, studies designed to specifically inhibit the centromeric portion of Kin Is in embryonic extracts and in mammalian somatic cells have shown that Kin Is are required to properly align and segregate chromosomes on the mitotic spindle (Figure 5C). Although the exact mechanism for how centromere-bound Kin Is are functioning to regulate chromosome positioning is not known, cellular studies implicate Kin Is in regulating

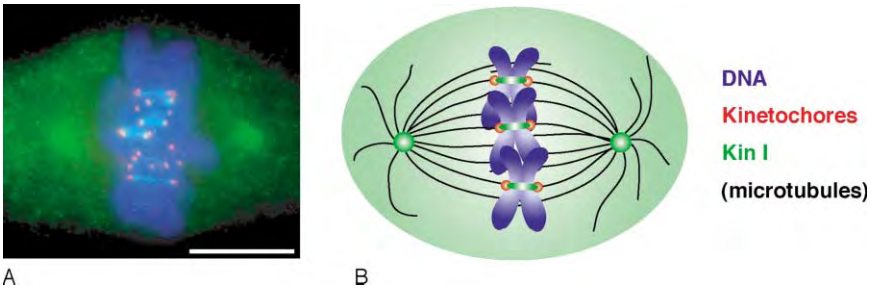

FIGURE 4 Kin I localization during mitosis. (A) This mammalian epithelial (PtK2) cell immunostained for DNA (blue), kinetochores (red), and Kin I (green) shows that Kin Is are in the cytoplasm with enrichment at centromeres and spindle poles during mitosis. (B) Kin I localization is illustrated here to show the placement of mitotic spindle microtubules (black) which are not immunostained in (A). Scale bar for (A) is 10 μm. Image provided by Susan Kline-Smith.

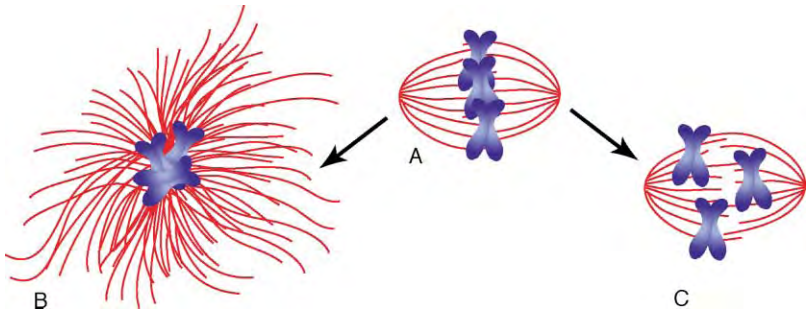

FIGURE 5 Kin I kinesins regulate microtubule dynamics and chromosome positioning during mitosis. (A) Normal spindle assembly in *Xenopus* egg extracts is illustrated here with microtubules in red and chromosomes in blue. (B) Upon immunodepletion of Kin Is, spindle assembly is inhibited due to a dramatic increase in microtubule polymerization. (C) When Kin Is are disrupted only at the centromere, however, chromosomes are unable to align despite the presence of a normal bipolar spindle.

both the dynamic properties of kinetochore-associated microtubules and the precise binding and orientation of these microtubule attachments.

In fungi, Kip3 subfamily kinesins (Kip3 in budding yeast and Klps 5/6 in fission yeast) have *in vivo* activities similar to Kin I kinesins. However, these proteins exhibit different sequence features and general domain organization from Kin Is in higher eukaryotes. These kinesins may represent a highly divergent class of Kin Is and may use a distinct mechanism for microtubule destabilization. *In vitro* microtubule depolymerization assays are necessary to test whether these kinesins are intrinsic depolymerases and whether their mechanism of action bears resemblance to Kin I kinesins in higher eukaryotes.

Overall, the biochemical analyses of Kin I kinesins have demonstrated use of the kinesin catalytic domain to control microtubule polymerization dynamics. Understanding the mechanism by which the catalytic domain was adapted to this non-motile function should give insight into the flexible design of this important protein superfamily. In addition, analysis of the physiological functions of microtubule-depolymerizing kinesins will be relevant to understanding the role of the microtubule cytoskeleton in many diverse processes including cell division and differentiation.

See Also the Following Articles

Centromeres • Centrosomes and Microtubule Nucleation • Intermediate Filaments • Kinesin Superfamily Proteins • Microtubule-Associated Proteins • Tubulin and its Isoforms

Glossary

centromere The primary constriction of a mitotic chromosome that connects the two sister chromatids.

centrosome The primary organizing center for microtubules in cells. During mitosis, a centrosome forms each of the two poles of the mitotic spindle.

kinetochore The complex, proteinaceous structure that assembles onto each side of the centromere, allowing for chromosome attachment to and movement on the microtubules of the mitotic spindle.

protofilament Formed by longitudinally associated tubulin heterodimers. Protofilaments associate laterally to form the microtubule polymer.

Further Reading

Cassimeris, L., and Spittle, C. (2001). Regulation of microtubule-associated proteins. *Int. Rev. Cytol.* **210**, 163–226.

Desai, A., and Mitchison, T. J. (1997). Microtubule polymerization dynamics. *Annu. Rev. Cell Develop. Biol.* **13**, 83–117.

Goldstein, L. S., and Philp, A. V. (1999). The road less traveled: Emerging principles of kinesin motor utilization. *Annu. Rev. Cell Develop. Biol.* **15**, 141–183.

Kreis, T., and Vale, R. (1999). *Guidebook to the Cytoskeletal and Motor Proteins*, 551 pp. Oxford University Press, Oxford.

Ovechkina, Y., and Wordeman, L. (2003). Unconventional motoring: An overview of the kin C and kin I kinesins. *Traffic* **4**, 367–375.

Vale, R. D., and Fletterick, R. J. (1997). The design plan of kinesin motors. *Annu. Rev. Cell Develop. Biol.* **13**, 745–777.

Biography

Susan Kline-Smith received her Ph.D. in cell biology from Indiana University Bloomington. She is currently a postdoctoral Fellow with Dr. Desai.

Arshad Desai holds a Ph.D. in Cell Biology from the University of California, San Francisco and received his postdoctoral training at the European Molecular Biology Laboratory (Heidelberg, Germany) and the Max Planck Institute for Cell Biology and Genetics (Dresden, Germany). He is currently an Assistant Member of the Ludwig Institute for Cancer Research, La Jolla and an Assistant Professor in the Department of Cellular and Molecular Medicine, University of California, San Diego. The principal focus of his laboratory is to understand the mechanisms by which the replicated genome is accurately segregated during cell division.

Kinetic Isotope Effects

Justine P. Roth and Judith P. Klinman
University of California, Berkeley, California, USA

Isotopes are atoms that have identical numbers of protons and different numbers of neutrons in their nuclei. Because the electron distributions of molecules composed of isotopic atoms are identical, they exhibit identical chemical reactivity patterns. In reactions where bonds to isotopically labeled atoms are made and broken, rates are affected in proportion to the masses of the reacting bonds. Ratios of rates for such reactions are termed kinetic isotope effects (KIEs). KIEs are largest when bonds are made and broken at the site of isotopic substitution (a primary effect) but also are seen when significant reorganization occurs peripheral to a site that undergoes a change in bonding (a secondary effect). Both types of KIEs reflect the nature of the energy barrier to a fundamental chemical reaction. Primary hydrogen KIEs typically vary between two and eight, while the largest secondary hydrogen effects are <1.5. Thus, secondary KIEs often require the use of competitive methods and highly sensitive techniques to analyze product distributions whereas primary KIEs can be detected using non-competitive and less accurate techniques.

Physical Origin of Kinetic Isotope Effects

Primary KIEs have mostly been determined for reactions of carbon, nitrogen, and oxygen atoms bonded to the isotopes of hydrogen: protium (^{1}H), deuterium (^{2}H), and tritium (^{3}H). Such processes which include proton, hydrogen atom, and hydride transfer have been studied extensively in enzymes, solution phase and to a lesser extent in the gas phase. The observation of a primary KIE is conventionally understood using a semi-classical model. The model is semi-classical because it takes into account the quantization of energy in chemical bonds but does not explicitly deal with the dual wave/particle nature of the constituent atoms.

Chemical Bonds as Harmonic Oscillators

A chemical bond can be described as two massive bodies attached to a spring. The particles experience a restoring force that is proportional to their displacement (x) by the force constant (F). Hooke's law (eqn. [1]) relates the frequency of motion (ν) of the atoms undergoing oscillation (eqn. [2]) and the force constant characteristic of the bond. Force constants are the same for isotopic bonds and changes in vibration frequency result from changes in μ. The largest perturbation in ν is caused by changes in μ upon substituting deuterium or tritium for protium:

$$\nu = \frac{1}{2\pi}\sqrt{\frac{F}{\mu}} \qquad [1]$$

$$\mu^{-1} = (m_1 + m_2)^{-1} \qquad [2]$$

The oscillations of atoms from their equilibrium positions can be approximated by a harmonic function. The energy of a bound particle ($h\nu$) is defined by the harmonic-oscillator approximation according to eqn. [3], where h is Planck's constant ($h = 6.626 \times 10^{-34}$ J s) and vibrational energy levels are designated n_{vib}. The zero-point energy ($n_{\text{vib}} = 0$) is the lowest vibrational energy level of a harmonic oscillator. These zero-point energies dominate the origin of kinetic isotope effects within a semi-classical picture:

$$E_{\text{vib}} = (n_{\text{vib}} + 1/2)h\nu, \quad n_{\text{vib}} = 0, 1, 2, \ldots \qquad [3]$$

Wave/Particle Dualism

Particles also have wavelengths, with this property dependent on the mass (m) and velocity (v) of the particle. At constant energy, the wavelengths of unbound particles follow from the de Broglie equation (eqn. [4]):

$$\lambda = h/m\text{v} \qquad [4]$$

Defining the unbound particle kinetic energy as $E_{\text{k}} = (\frac{1}{2}m\text{v}^2)$ allows de Broglie wavelengths to be calculated (Table I). The arbitrarily assigned kinetic energies are characteristic of barrier heights encountered in many (C, N or O)–H cleavage reactions. According to eqn [3], $E_{\text{k}} \sim 4$ kcal mol^{-1} approximates the potential energy present in (C, N or O)–H bonds ($\nu \sim 3000$ cm^{-1}) at 0 K. When the electron is compared to the proton and

TABLE I

de Broglie Wavelengths as a Function of Mass and Kinetic Energy

Particle	e^-	^1H	^2H	^3H	^{12}C	^{16}O	^{80}Br
Mass ($\times 10^{27}$ kg)	0.000 911 0	1.661	3.321	4.982	19.93	26.57	132.8
λ (Å), $E_k = 4$ kcal mol^{-1}	29.40	0.69	0.49	0.40	0.20	0.17	0.077
λ (Å), $E_k = 10$ kcal mol^{-1}	18.60	0.44	0.31	0.25	0.13	0.11	0.049

then to an oxygen nucleus, there is an extremely large variation in the quantum wavelengths ranging from ~29.40Å to ~0.69Å to ~0.17Å, respectively. The values indicate that the de Broglie wavelengths for the electron and hydrogen are comparable to the distances traversed by these particles in chemical reactions, consistent with experimental findings that indicate a dominance of their reactivity by quantum mechanical behavior.

KIEs as Mechanistic Probes

KIE measurements are routinely used for the elucidation of reaction mechanisms. The reaction coordinate represents the three-dimensional motion of all nuclei along the lowest-energy path that interconverts reactants and products. The reaction coordinate may represent the displacement of atoms within a chemical bond and/or the reorientation of surrounding solvent molecules. Regardless of the nature of the reaction coordinate, isotope substitution does not change the electronic potential energy surface for the reaction. Reaction rates vary with isotopic perturbation due to changes in vibrations that directly or indirectly couple to the reaction coordinate and by a decrease in wavelength for heavier atoms.

Activation Energy and Transition State Theory

In the year 1889, Svante Arrhenius documented the observation that chemical reaction rates vary as a function of temperature, predating the discovery of the first isotope, deuterium, in 1932. The Arrhenius equation (eqn. [5]) expresses a rate constant (k) as an exponential function of thermal activation energy (E_{act}). Together the temperature (T) and the gas constant (R) define the population of states that, as the result of molecular collisions, have sufficient E_{act} for reaction. The A term, originally referred to as a frequency factor, reflects the rate at which an activated complex (one possessing E_{act}) decomposes to product:

$$k = A \exp(-E_{act}/RT) \quad [5]$$

The transition-state theory (TST) developed separately by Eyring and by Evans and Polanyi (ca. 1935) is the preeminent model for interpretation of energy barriers to chemical reactions. TST gives the rate of reaction in terms of the molecular-level properties of an activated complex or transition state. Unlike the phenomenological Arrhenius equation, TST defines the energy difference between reactant and transition state using translational, rotational, vibrational, and electronic (gas phase) partition functions. The reaction coordinate is treated classically and separated from all of the other classical and quantum modes. The transition state occupies the dividing surface separating reactants from products and contains all degrees of freedom orthogonal to the reaction coordinate. The fundamental assumption of classical TST is that reactants do not re-cross the dividing surface and products are formed with the frequency of a bond vibration or solvent fluctuation once the transition-state configuration is attained. This assumption is relaxed in the semi-classical expression given by eqn. [6], where the rate constant is expressed in terms of an equilibrium constant for the formation of the transition state from the reactant state $\{K^{\ddagger} = \exp(-\Delta G^{\ddagger}/RT)\}$ and a frequency factor ($\kappa(k_B T/h)$). In the pre-exponential term, k_B is Boltzmann's constant and κ appears as a correction factor for the non-unit probability that products will form each time the reactants attain the energy of the transition state:

$$k = \kappa \frac{k_B T}{h} \exp(-\Delta G^{\ddagger}/RT) \quad [6]$$

Figure 1 shows a curve-crossing diagram for a molecule of methane reacting with atomic chlorine. The transition state is denoted by "double dagger" and represents a configuration for H atom transfer where the C–H bond is stretched and there is an attractive force between the Cl and H atoms. Thus, the reaction coordinate is the stretching of the bond. This situation is depicted further in Figure 2, where reaction occurs when an energy barrier is surmounted that converts the stretching motion of a C–H

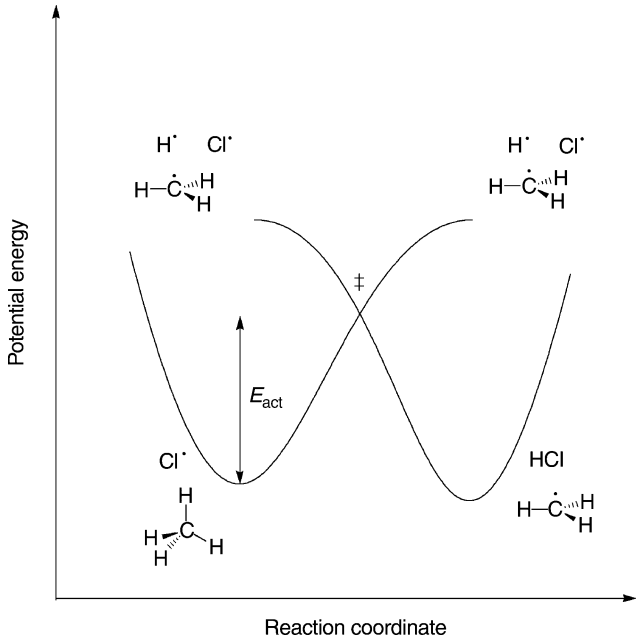

FIGURE 1 Reaction coordinates for H· abstraction from methane by Cl· depicting the transition state as the intersection of potential energy surfaces for stretching C–H and H–Cl bonds.

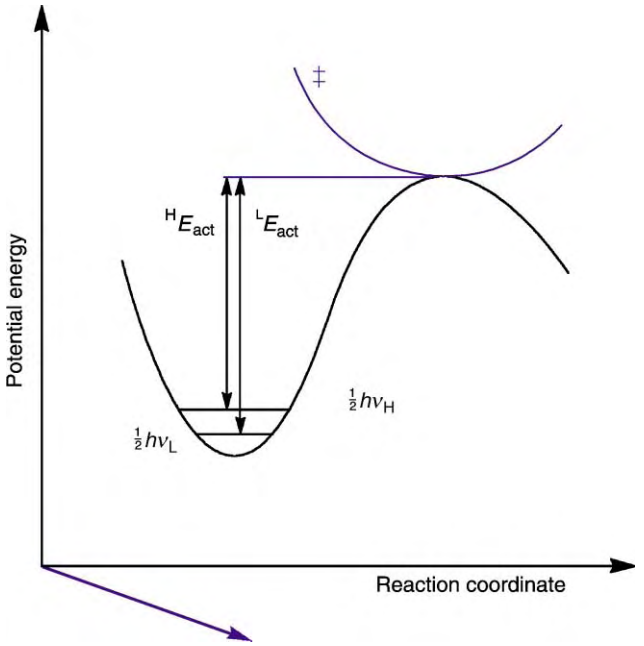

FIGURE 2 Energy diagram representing the origin of KIE on cleaving a C–H or C–L bond (H = ^{1}H, L = ^{2}H or ^{3}H). In this picture, a stretching mode in the reactant has been converted to a translational mode in the transition state.

(or C–L, where L = ^{2}H or ^{3}H) bond to a translational degree of freedom.

Although the nature of the reaction coordinate is not specified in the original derivation of TST, diagrams akin to Figure 2 have been used extensively for pedagogical reasons. The transition state is not an intermediate and has no detectable lifetime. The curvature of the reaction coordinate in the transition state region is defined by an imaginary frequency for the C–^{1}H or C–L vibration that is lost. Clearly this formulation of a bond-stretching reaction coordinate is an oversimplification when frequencies are high. When $\hbar\nu \gg k_B T$, the reacting bonds are essentially frozen and should not contribute much to the activation energy for reaction.

Isotope Effects from Zero-Point Energies

According to the Born–Oppenheimer approximation, the mass disparity between an electron and a nucleus allows the timescale for electronic motion to be separated from the much slower nuclear motion. It follows that reduced mass differences cause the zero-point energies to follow the trend C–^{1}H > C–^{2}H > C–^{3}H, as shown in Figure 2. Neglecting differences for reactions of isotopic molecules due to their quantum wavelengths, KIEs can be calculated from activation energies.

In the simplest case, the reaction coordinate involves conversion of a ground-state stretch to a translation and, hence, neglects isotopic zero-point energies in the transition state. The differences in the zero-point levels of the reactant state give the upper limit to the primary KIE through eqn. [7], where the subscript L designates either of the heavier isotopes of hydrogen. From the stretching frequencies of C–^{1}H ($\nu = 3000\ \text{cm}^{-1}$), C–^{2}H ($\nu = 2200\ \text{cm}^{-1}$), and C–^{3}H bonds ($\nu = 1800\ \text{cm}^{-1}$), KIEs of 7 and 18 are estimated for $k_{^1H}/k_{^2H}$ and $k_{^1H}/k_{^3H}$ at 298 K, respectively:

$$\frac{k_{^1H}}{k_L} = \exp[(h\nu_H - h\nu_L)/2RT] \qquad [7]$$

The Melander–Westheimer principle (ca. 1960) models the parabolic variation of primary KIEs in terms of a linear transition state for hydrogen transfer (cf Figure 1). The symmetry of the transition state depends on the overall reaction thermodynamics. Asymmetry increases as the transition state becomes more reactant-like (or earlier along the reaction coordinate) for exothermic reactions or more product-like (later) in an endothermic reaction. For real molecules that contain multiple degrees of vibrational freedom, compensating vibrations that are isotopically sensitive will reduce the size of the isotope effect from its peak at a symmetric transition state.

Deviations from Predicted Values

In general, observed primary KIEs are less than the upper limit set by eqn. [7]. Observations of values larger than those predicted by eqn. [7] have been observed and tentatively attributed to an insufficient description of the reaction coordinate. For instance, KIEs may appear inflated when isotope labels in secondary positions contribute to differences in E_{act}. As discussed in the monograph by Melander and Saunders (see Further Reading), KIEs may be up to threefold larger because of restricted transition-state geometries wherein bending vibrations present in the reactant state have been lost.

In contrast to effects ascribable to the ratio of reactant and transition state partition functions, non-Boltzmann effects such as nuclear tunneling may also give rise to large isotope effects. Tunneling has historically been treated as a correction, with the dominant contribution to the rate constant viewed as the activation energy associated with distortion of the reacting bond. However, there has been a resurgence of attention to quantum phenomena in the chemical and biochemical literature. New models for proton, hydrogen atom and hydride transfer reactions are being developed which presuppose tunneling mechanisms and formulate reaction coordinates in terms of the collective low-frequency motions of heavy atoms and the surrounding solvent molecules or protein. It is important to realize that a wide range of KIEs with values *both larger and smaller* than those predicted by eqn. [7] are consistent with mechanisms of tunneling, where reactants do not need to have the activation energy required to reach the transition state and reaction may occur by passing through rather than over the potential energy barrier.

KIEs as Mechanistic Probes during Enzyme Catalysis

By virtue of being a catalyst, an enzyme accelerates a chemical reaction without changing the overall thermodynamics. The term catalysis frequently refers to a multi-step reaction such as the oxidation of glucose to gluconolactone and reduction of O_2 to H_2O_2 as it occurs in the glucose oxidase reaction (eqn. [8]). Additionally, the term catalysis may refer specifically to a single chemical step that is accelerated by lowering or circumventing an energy barrier.

To understand the role of an enzyme during a catalytic transformation, the substrate-binding step and chemical step, where reactants are converted to products, must be analyzed separately. Assessment of barrier-lowering effects requires comparison of the enzymic reaction to a solution-phase reaction, both referenced to some standard state:

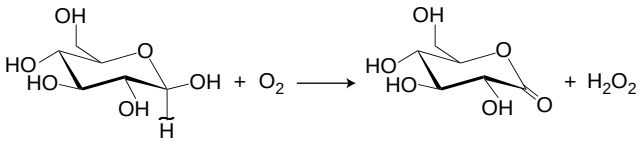

[8]

Experimental Considerations

Primary, secondary, and solvent KIEs can be used to elucidate the extent to which a change in bonding occurs in or before the rate-determining step. Primary effects are invariably normal, that is, the light isotope reacts faster than the heavy one. Secondary effects may show inverse behavior when the reaction is characterized by an increase in bonding and the difference in zero-point energies in the transition state is greater than in the reactant state. Primary effects are typically measured for reactions where protium is exchanged for deuterium and/or tritium, but isotope labeling of the heavy atoms may also give rise to measurable effects.

The largest effects are predicted upon isotopic substitution of protium because of the sizable perturbation to the zero-point energy levels as discussed earlier. Because reactions involving the transfer of protium and its isotopes give rise to the largest effects, experiments performed non-competitively, using the pure labeled substrates in separate reaction solutions, require high isotopic enrichment in addition to chemical purity. Isotopic purity becomes crucial when KIEs are >10 and only 5% contamination of the heavy isotope by the light isotope will cause an apparent deflation of the KIE by a factor of >1.4.

Secondary KIEs are typically much smaller and are, therefore, most often measured by competitive techniques. While isotope purity is not required, sensitive methods such as scintillation counting of radiolabeled products or mass-spectrometric analysis of chemically labeled products are necessary. Intra-molecular measurements can be more informative than inter-molecular measurements, as spurious isotope discrimination due to differential binding effects is absent. However, the determination of intra-molecular primary isotope effects on enzymatic reactions is, most generally, precluded by the inherent stereoselectivity imparted by the protein.

An Example from Glucose Oxidase Catalysis

Glucose oxidase mediates the oxidation of glucose and other simple six-carbon sugars. Enzymes isolated from fungi have been the subjects of extensive mechanistic studies due in large part to their robustness under a variety of temperature and pH conditions. The active enzyme is a homodimer that contains one

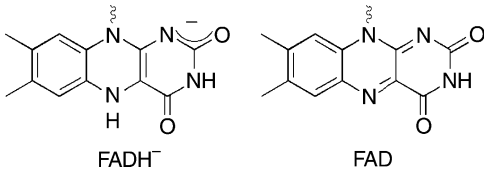

FIGURE 3 The isoalloxazine rings of oxidized (FAD) and reduced ($FADH^-$) flavin adenine dinucleotide.

non-covalently bound flavin adenine dinucleotide cofactor (Figure 3) per subunit. The flavin adenine dinucleotide (FAD) is reduced by simple sugars in the reductive half-reaction to produce $FADH^-$, which is oxidized by molecular O_2 in the oxidative half-reaction. A ping-pong type kinetic mechanism has been demonstrated for glucose oxidase wherein the first substrate binds, gets converted to product, and is then released prior to the reaction of the second substrate (Figure 4).

The mechanisms advanced for the reactions of sugars with glucose oxidase involve cleavage of the anomeric C–H in the rate-determining step (eqn. [8]). The main evidence is the significant primary KIEs observed upon isotope labeling of this position in glucose and in the alternative, slower-reacting substrate 2-deoxyglucose. Under steady-state conditions at pH 5 and 298 K, the second-order rate for the reaction of substrate (k_{cat}/K_M) is 3–4 times faster for [1-^{1}H]-glucose than for [1-^{2}H]-glucose (Table II). The k_{cat}/K_M values for [1-^{1}H] and [1-^{2}H] 2-deoxyglucose are 860 and 120 $M^{-1}\,s^{-1}$, respectively revealing a primary kinetic isotope effect of ~7. The rates are an order of magnitude slower than for the glucose [1-^{1}H] and [1-^{2}H] for which k_{cat}/K_M is 8200 and 2600 $M^{-1}\,s^{-1}$. The difference in the KIEs shows how C–H cleavage in the slower substrate has a greater contribution than substrate binding to its second order rate constant. The reasoning is consistent with the observation that the unimolecular rate constant that controls turnover (k_{cat}) is more than order of magnitude faster for glucose (1200 s^{-1}) than for 2-deoxyglucose (50 s^{-1}) under the same conditions.

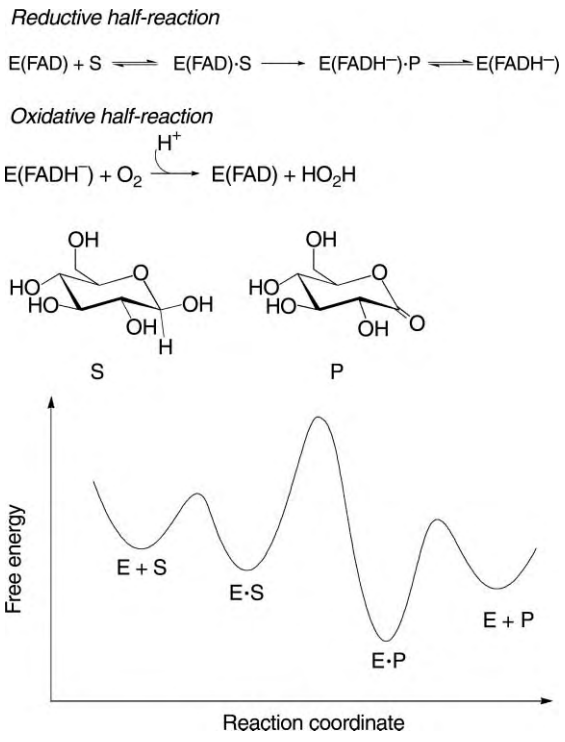

FIGURE 4 Ping-pong kinetic scheme and energy landscape for the reductive half-reaction of glucose oxidase. The E·S and E·P are arbitrarily defined as being more stable than separated reactants and products.

The degree to which bond cleavage limits the rate of sugar oxidation may vary with pH and with temperature depending on relative heights of energy barriers along the potential energy landscape. For oxidation of 2-deoxyglucose by glucose oxidase, the commitment to catalysis defined by Northrop as the ratio of the product-forming rate constant to the rate constant for substrate dissociation (see Further Reading) appears to be low and independent of pH. At pH 5, non-competitive measurements with pure [1-^{1}H] and [1-^{2}H] 2-deoxyglucose has allowed a direct comparison of k_{cat} to k_{cat}/K_M effects; these show that the isotope effect on k_{cat}/K_M approaches the intrinsic isotope effect on k_{cat} (^{1}H versus ^{2}H) ~8. Thus, the rate-determining step in both the first- and second-order kinetic processes includes the cleavage of the bond to the anomeric carbon (the E·S to E·P step in Figure 4). Similar results at pH 9.0, where [1-^{1}H] 2-deoxyglucose reacts with $k_{cat}/K_M = 580\ M^{-1}\,s^{-1}$ and exhibits ^{1}H versus ^{2}H kinetic isotope effects on both k_{cat}/K_M and k_{cat} of ~7, indicate that bond cleavage represents the highest point on the energy landscape (Figure 4). This result has been confirmed by highly accurate kinetic isotope effects measured using radiolabeled substrates under competitive conditions. Here the KIEs correspond to differential reactivity of isotopically labeled substrates in the same reaction solution. Isotope effects on k_{cat}/K_M for 2-deoxyglucose at pH 9.0 and 298 K reveal that the ^{3}H substrate reacts 15.9 (0.5) times slower than the ^{1}H substrate and 2.44 (0.04) times slower than the ^{2}H substrate. From the above data, the calculated ^{1}H versus ^{2}H isotope effect on k_{cat}/K_M is found to be 6.5 (0.5) close to the value derived from the non-competitive measurements. Based on observed KIEs under a variety of conditions, it can be concluded that the observed k_{cat} reflects the free-energy barrier associated with the chemical step wherein sugar is transformed to lactone.

The kinetics of $FADH^-$ oxidation by O_2 has also been analyzed using isotope effects. Solvent KIEs and heavy-atom KIEs on k_{cat}/K_M for O_2 have been determined for high- and low-pH forms of glucose oxidase. The latter measurements were determined competitively

TABLE II

Rate Constants and Isotope Effects Under Air Saturation at 298 K

Substrate	k_{cat}/K_M ($M^{-1}s^{-1}$)	L (k_{cat}/K_M)	k_{cat} (s^{-1})	L (k_{cat})
[1-^{1}H] glucose (pH 5)	$8.2\ (1.9) \times 10^3$	3–4	$1.2\ (0.3) \times 10^3$	~6
[1-^{2}H] glucose (pH 5)	$2.6\ (0.6) \times 10^3$		$2.0\ (0.5) \times 10^2$	
[1-^{1}H] 2-deoxyglucose (pH 5)	$8.6\ (0.8) \times 10^2$	~7	$4.4\ (1.2) \times 10^1$	~8
[1-^{2}H] 2-deoxyglucose (pH 5)	$1.2\ (0.4) \times 10^2$		5.7 (0.1)	
[1-^{1}H] 2-deoxyglucose (pH 9)	$5.8\ (0.2) \times 10^2$	6.5	$2.6\ (1.0) \times 10^1$	~7
[1-^{2}H] 2-deoxyglucose (pH 9)	$8.8\ (0.2) \times 10^1$		3.5 (0.6)	
[1-^{3}H] 2-deoxyglucose (pH 9)	$3.6\ (0.2) \times 10^1$	2.4	N/A	

L represents ^{2}H or ^{3}H.

by using isotope ratio mass spectrometry to follow the enrichment of ^{18}O in natural abundance O_2 as a function of reaction. The ratio of k_{cat}/K_M for $^{16,16}O_2$ to $^{16,18}O_2$ ranges from 1.027(3) to 1.028(4) for the two enzyme forms. The KIE is close to the equilibrium isotope effect estimated using the Bigeleisen approach, which employs gas-phase partition functions for O_2 and O_2^-, the reactant and product of the rate-determining step. Solvent isotope effects accompanying O_2 reduction were found to be close to unity, showing that electron transfer, and not proton transfer, limits $k_{cat}/K_M(O_2)$. In addition, the observed isotope effects aid a direct comparison of rate constant for the enzymatic reduction of O_2 and the non-enzymatic reaction which in turn allows the extent of barrier-lowering (catalysis) in the chemical step to be addressed.

Various types of kinetic isotope effects have been used to elucidate the chemical mechanisms of glucose oxidase catalysis. The observed KIEs indicate that the rate of the chemical step can be extracted from the steady-state measurements using the slowly reacting substrate 2-deoxyglucose. The observed KIEs demonstrate rate-determining C–H cleavage in the reductive half-reaction and a rate-determining change in oxygen bond order upon electron transfer in the oxidative half-reaction. In addition to exposing which steps limit catalysis, KIE probes have been invaluable in demonstrating the role of the protein environment in facilitating catalysis.

See Also the Following Articles

Flavins • Substrate Binding, Catalysis, and Product Release

Glossary

commitment to catalysis The rate constant for the conversion of ES to EP divided by the rate constant for the return of ES to E + S.

intrinsic isotope effect The isotope effect when the bond cleavage or bond reorganization event completely limits the reaction rate.

nuclear tunneling A process whereby an atomic nucleus, because of its wave-mechanical nature, is able to penetrate rather than surmount an energy barrier.

zero-point energy The potential energy present in a bond at 0 K.

Further Reading

Bell, R. P. (1980). *The Tunnel Effect in Chemistry*. Chapman and Hall, New York.

Bright, H. J., and Gibson, Q. H. (1967). The oxidation of 1-deuterated glucose by glucose oxidase. *J. Biol. Chem.* **242**, 994–1003.

Cook, P. F. (ed.) (1991). *Enzyme Mechanism from Isotope Effects*. CRC Press, Boca Raton, FL.

McQuarrie, D. E. (1983). *Quantum Chemistry*. University Science Books, Mill Valley, CA.

Melander, L., and Saunders, W. H. Jr. (1980). *Reaction Rates of Isotopic Molecules*. Wiley-Interscience, New York.

Northrop, D. B. (1981). The expression of isotope effects on enzyme-catalyzed reactions. *Annu. Rev. Biochem.* **50**, 103–131.

Roth, J. P., and Klinman, J. P. (2003). Catalysis of electron transfer during O2 activation by the flavoprotein glucose oxidase. *Proc. Nat. Acad. Sci. USA* **100**, 62–67.

Steinfeld, J. I., Francisco, J. S., and Hase, W. L. (1989). *Chemical Kinetics and Dynamics*. Prentice-Hall, Englewood Cliffs, New Jersey.

Biography

Judith Klinman is a Professor in the Departments of Chemistry and Molecular and Cell Biology at the University of California, Berkeley, where she has been teaching and conducting research since 1978. She has had a long-standing interest in protein structure and function and was one of the earliest investigators to recognize the power of kinetic isotope effects to elucidate mechanisms of enzyme action.

Justine Roth was a Postdoctoral Fellow in the laboratory of Judith P. Klinman and received her Ph.D. (from Professor James Mayer) at the University of Washington in inorganic chemistry. She is currently an Assistant Professor of chemistry at Johns Hopkins University pursuing studies at the interface of chemistry and biology.

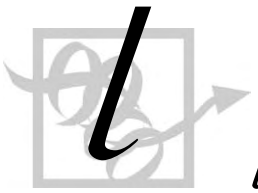

lac Operon

Liskin Swint-Kruse and Kathleen S. Matthews
Rice University, Houston, Texas, USA

All living organisms must respond to their environment. To this end, they must sense a variety of exogenous and endogenous stimuli and use this information to regulate when and where specific genes are expressed as proteins. Until the middle of the twentieth century, when DNA was identified as the genetic material, variation in gene expression could only be ascertained by visible effects on the organism (phenotype). Once the central pathway for genetic expression was established (DNA encodes mRNA encodes protein), opportunity arose to understand gene regulation on the molecular level. The first control mechanism was elucidated for a region in the *Escherichia coli* genome termed the *lac* operon. The *lac* operon regulatory system responds to external lactose (milk sugar) and glucose concentrations, and the *lac* metabolic genes that transport and metabolize lactose are therefore expressed only under specific environmental conditions. Such regulation conserves energy for the organism, avoiding costly production of enzymes that are not useful when substrate is unavailable, and simultaneously providing a rapid and robust response to environmental opportunity. More recently, this highly effective regulatory system has been exploited to control selected expression of a wide variety of proteins in prokaryotes as well as eukaryotes. In addition, this system has been modified to screen for mutation types/rates in higher organisms (e.g., BigBlue® is a mouse system in which mutation in either LacI or LacO can be detected as a screen for mutagens).

Historical Perspective

In the post-World War II years at the Pasteur Institute in France, Jacques Monod and Francois Jacob were examining the ability of bacteria to "adapt" to different sources of carbon as their energy source. They discovered that enzymes that metabolize lactose were present at very low levels when lactose was absent from the growth medium. When lactose was added, enzyme production increased ~1000-fold, a phenomenon termed "induction." The sugar lactose is chemically similar to other sugars that are collectively called galactosides. By varying the molecular structure of these sugars and comparing growth and *lac* enzyme activity for *E. coli* variants, they established that the function of inducing the metabolic enzymes was separate from the capacity of these enzymes to utilize lactose. (The DNA regions that encode the three enzymes of the *lac* operon have historically been called "structural genes;" however, we use the term "metabolic genes" in describing these regions to distinguish them from later studies of the *lac* repressor and CRP protein structures.) However, the mechanism by which galactosides induced the metabolic enzymes was not elucidated for several more years. In the early 1960s, Jacob and Monod found that the role of an "inducer" sugar was to "relieve" transcription repression of the metabolic genes. Therefore, the inducer must act through another agent, which was finally identified as the lactose repressor protein, LacI. When the LacI protein was inactivated in the bacteria, the metabolic enzymes were always expressed at high levels, whether or not an inducer sugar was present. From these experiments, Jacob and Monod demonstrated that enzyme (or other protein) production can be negatively controlled. This phenomenon is termed "repression."

Further experimental observations indicated that this simple view of modulating *lac* operon expression by LacI alone did not encompass the entire pattern of gene regulation. Specifically, significant induction of *lac* enzymes by lactose does not occur when glucose is abundantly available. From the cellular perspective, direct glucose utilization provides a more efficient energy source than converting lactose to glucose and galactose (and then galactose to glucose). Thus, an additional regulatory mechanism must contribute to determining the level of *lac* enzyme expression. Two different mutations were discovered in the late 1960s/early 1970s that illuminated this issue. In fact, the *lac* operon was used in a cell-free system to demonstrate that the protein CRP (cAMP receptor protein, also referred to as the catabolite activator protein, CAP) was disrupted by one of these mutations. CRP binds the signaling molecule cAMP, which in turn is produced by the other protein identified in these mutagenesis experiments, adenlyate cyclase, which is inhibited by high glucose concentrations. Together, these proteins provide a means to alter transcription by "sensing" glucose levels via detection of cAMP. In contrast to the high specificity of the *lac* repressor (which only regulates the *lac* operon),

the CRP glucose sensor *activates* transcription of numerous systems in *E. coli* in its cAMP-bound form.

lac Operon

The entire region of the *E. coli* genome involved in lactose metabolism and control of *lac* gene expression is termed the *lac* operon. This region of DNA comprises sequences that contain several types of information—open reading frames for two classes of proteins (enzymatic and regulatory), binding sites for RNA polymerase (promoter regions), and binding sites for regulatory proteins. In sequence within the genome (Figure 1), the elements of the *lac* operon include the following:

1. the promoter for initiating transcription of LacI; the *lacI* gene, which encodes the *lac* repressor protein (LacI);
2. the promoter for the *lac* metabolic genes involved in transporting and metabolizing lactose;
3. DNA-binding sites for *lac* repressor (LacO) and CRP that overlap this promoter; and
4. the genes for the *lac* metabolic enzymes.

The latter encode proteins required for the transport and metabolism of lactose: β-galactosidase (LacZ), lactose permease (LacY), and thiogalactosidase transacetylase (LacA). Further discussion will focus on the functions and structures of the two regulatory proteins, LacI, and CRP.

Lactose Repressor Protein

LacI Function

The role of LacI is to inhibit mRNA production for proteins encoded by the *lac* operon. Transcription is not completely eliminated, but *lacZYA* mRNA is transcribed

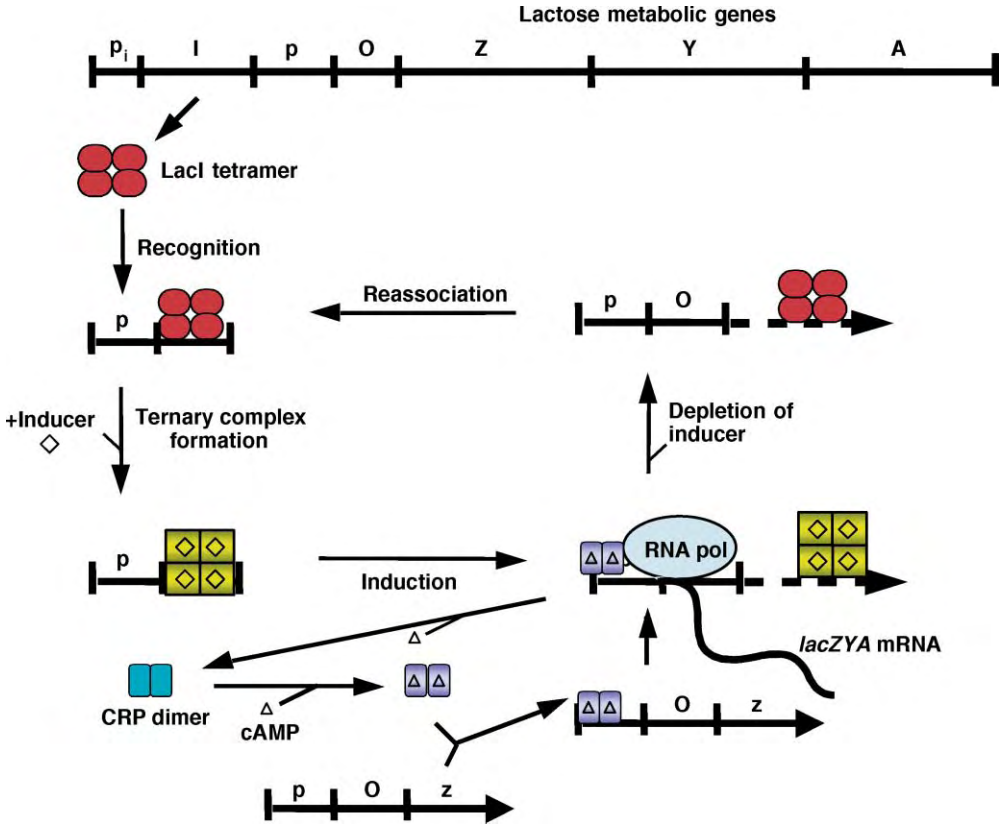

FIGURE 1 Schematic of the *lac* operon. The top sequence of DNA (horizontal bar) indicates the positions of the promoter (p_i) for the tetrameric lactose repressor (*lacI* gene, "I"), the promoter (p) for the metabolic enzymes, the operator sequence LacO (O site for LacI binding), and the metabolic enzyme genes (*lacZYA*, "Z," "Y," and "A"). The cartoon of the functional cycle represents LacI tetramer binding to operator, association with inducer (◇), dissociation from operator (induction), RNA polymerase (RNA pol) binding and transcription, and subsequent reassociation with the operator when sugar levels diminish. Shown at the bottom of the figure is the dimeric structure of CRP, its association with cAMP (triangle), and binding within the promoter region to facilitate RNA polymerase binding and transcription. CRP dissociates from the promoter when glucose levels increase and cAMP levels fall. Substitution of the *lac* metabolic genes by other protein coding sequences (prokaryotic or eukaryotic) allows effective control of specific protein expression using inducer/cAMP levels.

only at very low levels. This function is accomplished by specific binding of LacI protein to the *lac* operator DNA sequence to inhibit transcription via a variety of mechanisms. Since the *lac* operator (LacO) overlaps the promoter, LacI binding directly competes with RNA polymerase for binding this region. LacI can also impede transcription initiation and/or block elongation of mRNA. The LacI·LacO association and consequent transcription repression occur when no lactose is available to serve as the substrate of the *lac* metabolic proteins.

When lactose is available as a carbon source, the low levels of metabolic enzymes allow a small amount of this sugar to be transported into the bacterium by LacY. Next, residual LacZ metabolizes lactose to glucose and galactose, which produces energy for the bacterium. Notably, this catalytic process also generates low levels of allolactose (a rearrangement of the β-1,4 linkage between glucose and galactose to a β-1,6 linkage; Figure 2). The by-product allolactose binds to LacI and elicits a conformational change in the protein that results in release of the operator DNA sequence (induction). Consequently, RNA polymerase is freed to generate numerous copies of mRNA encoding the *lac* enzymes. When translated into proteins, these enzymes allow the bacterium to transport and metabolize large quantities of lactose as its carbon energy source, taking advantage of environmental opportunity. One result of the studies by Jacob and Monod was the discovery that a variety of non-natural galactoside sugars (e.g., IPTG; Figure 2) can induce LacI and relieve transcription repression of *lacZYA*.

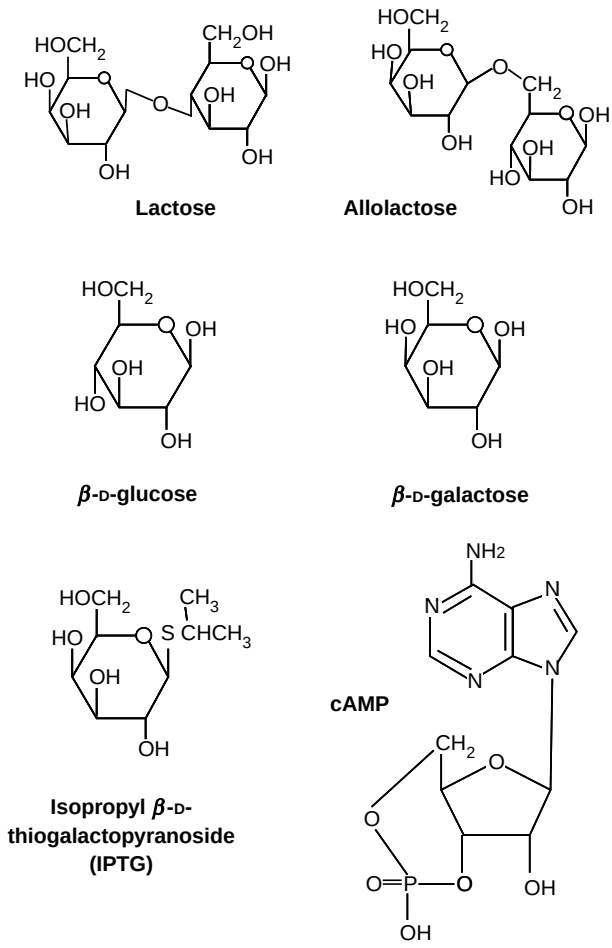

FIGURE 2 Chemical structures for lactose, allolactose (the natural inducer), the sugar components of lactose (glucose and galactose), the gratuitous inducer IPTG, and cAMP.

LacI Structural Characteristics

Structural detail of the LacI protein has provided insight into the atomic-level mechanism by which this protein performs its functions. LacI is a multimeric, multi-domain protein, an arrangement now known to be typical for genetic regulatory proteins. LacI has four, identical polypeptide chains (Figure 3A). Each polypeptide folds into distinct regions that have specific functions, and the monomers associate to form tetrameric LacI. A very interesting feature is that specific regions of LacI (called the hinge helices) are folded *only* in the presence of the operator DNA target sequence. Thus, protein folding is integral to the regulatory cycle.

Folded protein domains can usually be isolated from the intact protein and maintain function and structure that are highly similar to the intact protein. For LacI, the N-terminal domain and hinge helix comprise the DNA-binding site, and this region can be isolated as monomeric units by proteolysis. Note that the LacI *dimer* is the DNA-binding unit (two DNA-binding sites/tetramer). The DNA-binding site comprises one helix from each N-terminal domain, which associates with bases in the DNA major groove, and the hinge helices, which insert into the minor groove and elicit a bend in the DNA. (Note that the LacO site is highly, but imperfectly, symmetric in sequence, therefore accommodating the two identical DNA-binding domains.) The LacI core domain, which can be isolated by proteolysis as a tetramer, encompasses two subdomains that flank the sugar-binding site. Each monomer is able to bind an inducer molecule (four sugars/tetramer). (Note that the N- and C-subdomains within the core domain are interconnected by multiple strands and *cannot* be cleaved to produce distinct functional units.) When the inducer-binding site is occupied, structural changes in the N-subdomain affect the DNA-binding domain (Figure 3B). These shifts result in hinge helix unfolding, an event that appears crucial for dissociation of the protein from the operator DNA site. The final domain of LacI is the C-terminal tetramerization domain that connects the four subunits via an antiparallel four-helix bundle (Figure 3A).

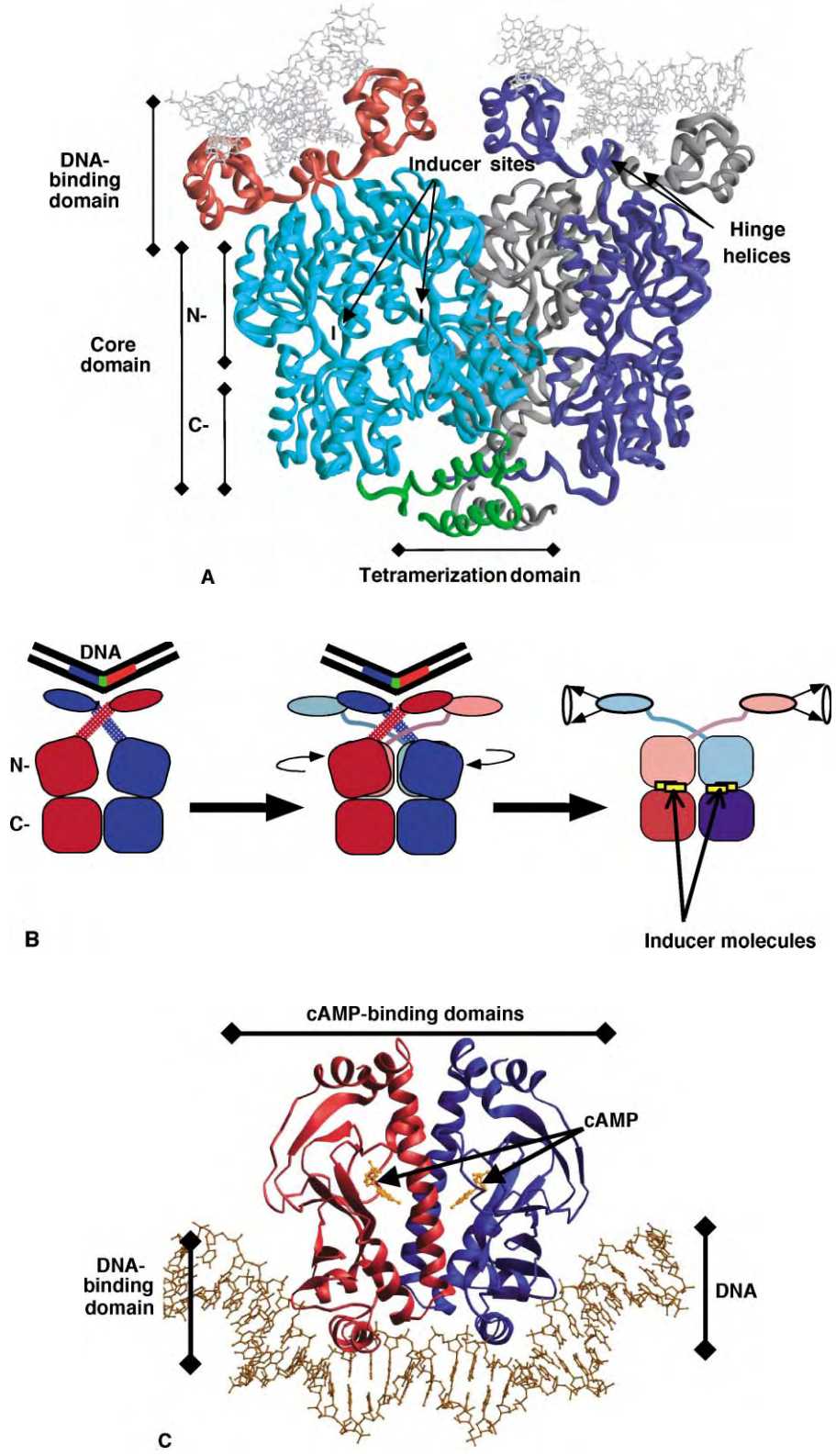

FIGURE 3 Structures of LacI and CRP. (A) The tetrameric structure of the lactose repressor is shown in ribbons format. (Note that this view does not show all atoms of the protein.) The right dimer is colored to show the subunits, and the left dimer shows the binding sites. DNA is shown at the top of the figure in ball-and-stick format (which depicts all nonhydrogen atoms of this molecule). Note that the dimer is the DNA-binding unit, whereas the monomer is the inducer-binding unit. (B) Cartoon depicts the conformational change of a LacI dimer when it binds inducer. (C) The dimeric structure of CRP is shown with the sites for cAMP- and DNA-binding indicated. The structure of unbound CRP has not been derived; thus, the nature of the conformational change for this protein is not explicitly known.

Multiple Sites/Multiple Targets – DNA Looping

Early studies indicated that additional "pseudo-operator" sequences were present within the *lac* operon sequence and contribute to repression. The DNA sequences of the pseudo-operators are very similar, but not identical, to LacO and are bound by LacI more weakly. The presence of two DNA-binding sites in LacI protein tetramer suggests a mechanism by which pseudo-operators could enhance repression—one LacI tetramer could bind two separate operators and generate a looped DNA structure (Figure 4). Experimental evidence for DNA looping has been obtained from a variety of laboratories. These structures are highly stabilized, accounting for the significant repression of *lacZYA* expression observed in bacterial cells. Indeed, DNA containing multiple operator sequences and with the supercoiling density characteristic of *E. coli* exhibits a half-life for the complex that exceeds two days. However, even these looped complexes respond rapidly (in less than 30 s) to the presence of inducer sugars, allowing quick adaptation to an external lactose source that may be transient.

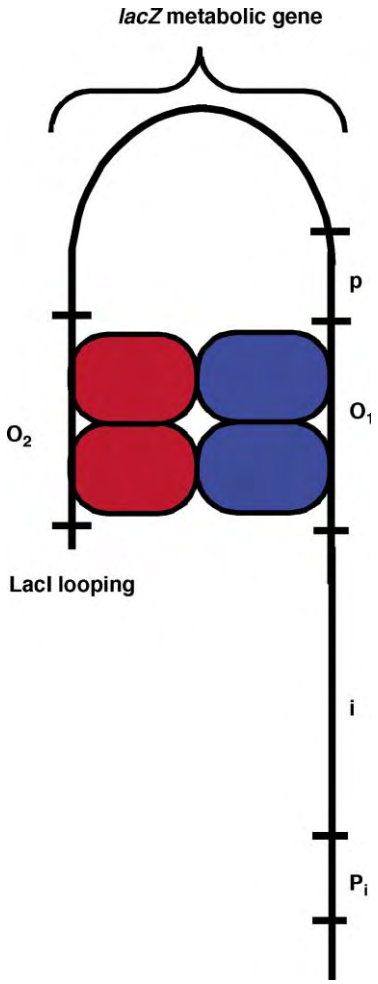

FIGURE 4 Looped DNA structure. The pseudo-operator sequence (O_2) located within the *lacZ* gene can interact with LacI bound to the primary operator sequence (O_1) that overlaps the promoter sequence for the *lacZYA* metabolic genes. This structure "loops" the DNA and generates a complex with very high stability. The dimers interacting with O_1 and O_2 are shown in different colors.

Catabolite Repressor Protein

CRP Function

CRP measures glucose levels in the bacterium through detecting cAMP levels, a signaling molecule created by another protein called adenylate cyclase. Since adenylate cyclase is inhibited by high glucose, levels of glucose and cAMP are inversely related. As glucose levels decrease, cAMP levels rise, and cAMP binds to CRP, causing a conformational shift. This form of CRP has high affinity for specific target sequences within the bacterial genome (Figure 1). Note that cAMP enhances DNA binding by CRP, whereas with LacI, sugar binding decreases the DNA binding. One of the DNA target sequences for cAMP·CRP is found within the promoter for the *lac* structural proteins upstream of the *lac* operator sequence (Figure 1). In the absence of glucose (elevated cAMP), the cAMP·CRP complex binds and *enhances* RNA polymerase transcription of *lacZYA* mRNA. Thus, the enzymes for lactose utilization are expressed at high levels only when environmental glucose is low and lactose levels are high.

CRP Structural Characteristics

Like LacI, CRP is multimeric and has multiple domains (Figure 3C). In this case, CRP structure is dimeric, and each monomer comprises two domains. The N-terminal domain facilitates dimer formation and binds at least one molecule of cAMP (two/dimer). The C-terminal domain binds DNA through a helix-turn-helix motif, now known to be common in regulatory proteins. Protein binding again elicits a bend in the target DNA-binding site. Each monomer only binds to one-half of the DNA-binding site, which is symmetric through the center of the sequence. The *lac* operon regulatory sites signaled that symmetry of these DNA-binding sites would be a common feature, going hand-in-hand with the generally multimeric natures of these proteins.

Implications for Complex Organisms

This "simple" bacterial regulatory system illustrates the complexity that can be generated with only two "on/off" switches. In fact, the response of this system is more analogous to a rheostat. Since the two protein switches

respond to different signals, graded response occurs at intermediate ratios of glucose/lactose. Gene regulation in response to specific signals—whether environmental availability of substrate or other signaling molecule—has a twofold advantage. The organism conserves energy/resources under conditions where gene expression would be useless (and expensive), but maintains selective response to a variety of input information. This type of regulatory control—DNA binding modulated either negatively or positively by interaction with a small ligand or with another protein or biomolecule—underlies the incredibly complex pathways by which gene expression is fine-tuned to create specific temporal, spatial, and environmental patterns in higher organisms.

See Also the Following Articles

DNA Supercoiling • RNA Polymerase Reaction in Bacteria • RNA Polymerase Structure, Bacterial

Glossary

activation Process that enhances transcription to boost cellular levels of regulated proteins.

conformational change A significant rearrangement of atoms within a protein molecule in response to binding a specific small molecule (e.g., sugar binding by LacI).

genome The entire DNA complement composing the genetic material of an organism.

inducer A sugar that elicits LacI conformational rearrangement that releases operator DNA.

induction The increase in *lac* enzyme production triggered by the presence of an inducer sugar.

mRNA A "copy" of the DNA sequence that is used as a template for protein translation.

operator The DNA sequence to which the repressor protein binds and thus inhibits RNA polymerase transcription.

operon A region of bacterial DNA that is regulated as a unit, e.g., the entire region encoding the *lac* repressor, metabolic enzymes, and regulatory regions.

promoter The DNA sequence recognized by RNA polymerase for transcription initiation; in bacteria this region frequently contains a binding site for the catabolite repressor protein (CRP).

repression The inhibition of transcription to maintain low levels of metabolic proteins/enzymes in the absence of appropriate conditions, such as lack of substrate for a metabolic pathway.

repressor The protein that mediates inhibition of transcription by binding to a specific DNA sequence (see *operator*).

Further Reading

Busby, S., and Ebright, R. H. (1999). Transcription activation by catabolite activator protein (CAP). *J. Mol. Biol.* **293**, 199–213.

Emmer, M., deCrombrugghe, B., Pastan, I., and Perlman, R. (1970). Cyclic AMP receptor protein of *E. coli*: Its role in the synthesis of inducible enzymes. *Proc. Natl Acad. Sci. USA* **66**, 480–487.

Harman, J. G. (2001). Allosteric regulation of the cAMP receptor protein. *Biochim. Biophys. Acta* **1547**, 1–17.

Jacob, F., and Monod, J. (1961). Genetic regulatory mechanisms in the synthesis of proteins. *J. Mol. Biol.* **3**, 318–356.

Kolb, A., Busby, S., Buc, H., Garges, S., and Adhya, S. (1993). Transcriptional regulation by cAMP and its receptor protein. *Annu. Rev. Biochem.* **62**, 749–795.

Lewis, M., Chang, G., Horton, N. C., Kercher, M. A., Pace, H. C., Schumacher, M. A., Brennan, R. G., and Lu, P. (1996). Crystal structure of the lactose operon repressor and its complexes with DNA and inducer. *Science* **271**, 1247–1254.

Matthews, K. S., and Nichols, J. C. (1998). Lactose repressor protein: Functional properties and structure. *Prog. Nucl. Acid Res. Mol. Biol.* **58**, 127–164.

Miller, J. H., and Reznikoff, W. S. (eds.) (1980). *The Operon*, 2nd edition. Cold Spring Harbor Laboratory, New York.

Müller-Hill, B. (1996). *The lac Operon: A Short History of a Genetic Paradigm*. Walter de Gruyter, Berlin, New York.

Zubay, G., Schwartz, D., and Beckwith, J. (1970). Mechanism of activation of catabolite-sensitive genes: A positive control system. *Proc. Natl Acad. Sci. USA* **66**, 104–110.

Biography

Liskin Swint-Kruse is a Research Scientist in Biochemistry and Cell Biology at Rice University. She received her B.S. from Baylor University and her Ph.D. from the University of Iowa. She has been a Fellow of the Keck Center for Computational Biology (National Library of Medicine). In her postdoctoral studies, she pursued computational, biophysical, and genetic studies of LacI structure and function. Her long-term goals are to define determinants for functional distinction within the large, closely related family of LacI proteins.

Kathleen S. Matthews is Dean of Natural Sciences and Stewart Memorial Professor of Biochemistry and Cell Biology at Rice University. She received her Ph.D. from the University of California, Berkeley, and postdoctoral training at Stanford University. Her research interests are structure/function studies of genetic regulatory proteins, and she has had a long-term interest in understanding the structural determinants of function in LacI protein.

Lectins

Nathan Sharon and Halina Lis
Weizmann Institute of Science, Rehovot, Israel

Lectins are a class of proteins that bind carbohydrates specifically and reversibly. They occur widely in animals, plants, and microorganisms, where their main function is to serve as cell recognition molecules. Their main use is for the detection, isolation, and characterization of glycoconjugates in solution and on cells.

Lectins (from Latin, *legere*, to select or choose) are proteins that combine with mono- and oligosaccharides reversibly and with high specificity, but are devoid of catalytic activity and, in contrast to carbohydrate-binding antibodies, are not products of an immune response. They are found in all classes of organisms, from viruses and bacteria to higher animals, including humans (Table I) and occur in different shapes and forms (Figure 1). Hundreds of lectins have been isolated by affinity chromatography on immobilized carbohydrates, as well as by recombinant DNA techniques. The richest source of these proteins are plants, from the seeds of which several of the long-known proteins of this class – such as concanavalin A, phytohemagglutinin (PHA), and soybean agglutinin (SBA) – have been obtained. Most lectins are bi- or oligovalent with respect to carbohydrate binding; therefore, when they combine with sugars on the surface of cells, such as erythrocytes, they cause cross-linking of the cells and their subsequent precipitation, a phenomenon referred to as cell agglutination. The erythrocyte-agglutinating, or hemagglutinating, activity of lectins is a major attribute of these proteins and is used routinely for their detection and characterization. Lectins also possess the ability to precipitate polysaccharides or glycoproteins from solution; these reactions are inhibited by the sugars for which the lectins are specific.

Carbohydrate Specificity

Lectins are classified primarily into five specificity groups, according to the monosaccharide for which they exhibit the highest affinity: mannose, galactose/*N*-acetylgalactosamine, *N*-acetylglucosamine, fucose, and *N*-acetylneuraminic acid (sugars are of the D-configuration except for fucose which is L). Relevant for the biological functions of lectins is the fact that, of the numerous monosaccharides found in nature, these six are typical constituents of surfaces of eukaryotic cells. Some lectins specific for mannose also bind glucose, which differs from mannose in the configuration of the 2-hydroxyl, but only in rare cases they react with galactose, which differs from glucose in the configuration of the 4-hydroxyl. Lectins of the same specificity group may differ markedly in affinity for oligosaccharides or cells, while a few of them recognize only oligosaccharide derivatives of the above monosaccharides. Specificity for other sugars has been rarely encountered. The affinity of lectins to monosaccharides is usually weak, with association constants in the millimolar range, whereas that to oligosaccharides is often much higher, up to three orders of magnitude.

Molecular Properties

In general, lectins are oligomeric proteins of diverse structure and molecular size. They differ in primary, secondary, and tertiary structure, number of subunits and subunit assembly (Figure 2), metal requirement, as well as in the constitution of carbohydrate-binding sites. The polypeptide chains often consist of several molecular domains, only one of which is the carbohydrate recognition domain (CRD). Lectins belong to distinct protein families or superfamilies that share sequence homologies and similar tertiary and quaternary structures. These families are often of the same phylogenetic origin (e.g., the cereal lectins), although they sometimes cross phylogenetic barriers (as in the case of the structurally similar legume lectins that belong to different specificity groups and the galectins, animal lectins that bind exclusively β-galactosides, such as lactose and *N*-acetyllactosamine [Galβ(1–4)GlcNAc]). The C-type (Ca^{2+}-requiring) lectins are members of a superfamily of diverse specificities that includes endocytic lectins, collectins, and selectins, many of which are membrane bound. In collectins, the CRD is linked to a collagen-like region, whereas in selectins–E-selectin, P-selectin, and L-selectin–it is attached to an epidermal growth-factor-like domain and several short repeating

TABLE I

Representative Lectins

Source	Organism or lectin name	Specificity	Mol. wt. kDa	No. of subunits
Viruses	Influenza A	NeuAc	225	3
Bacteria	*Escherichia coli* type 1	Man		Multi
	Escherichia coli P	Galα4Gal		Multi
	Pseudomonas aeruginosa	Fuc	47	4
Protozoa	*Entamoeba histolytica*	Gal/GalNAc	260	2
Plants	*Arachis hypogaea* (Peanut) (PNA)	Gal	110	4
				4
	Artocarpus integrifolia (Jackfruit)	Gal	66	2
		Glc/Man		
	Canavalia ensiformis (Jackbean) (Con A)	Glc/Man	106	4
	Erythrina corallodendron (Coral tree)	Gal/GalNAc	57	2
	Galanthus nivalis (Snowdrop) (GNA)	Man	50	4
	Glycine max (Soybean) (SBA)	Gal/GalNAc	120	4
	Lotus tetragonolobus (Asparagus pea)	Fuc	110	4
	Ricinus communis (Castor bean)			
	Toxin	Gal/GalNAc	60	2
	Lectin	Gal/GalNAc	120	4
	Sambucus nigra (Elderberry) (SNL)	NeuAcα2,6Gal	240	4
	Triticum vulgare (Wheat) (WGA)	GlcNAc	36	2
Invertebrates	*Anguilla anguilla* (Eel) (AAA)	Fuc	50	3
	Helix pomatia (Garden snail)	GalNAc	100	6
	Limulus polyphemus (Horseshoe crab)	NeuAc	400	
Vertebrates	Galectin-1	Gal	28	2
	Mammalian hepatic binding protein (HBP)	Gal/GalNAc	130–190	3–4
	Macrophage mannose receptor (MMR)	Man	175	1
	Mannose-binding lectin A (MBL-A)	Man	200–600	6–18
	Selectins E, P and L	Sialyloligosach.	90–140	1
	Man-6-P receptors	Man6P	90–300	1–2
	Siglec-1	NeuAcα2,3Gal	185	1
	Calnexin	Glcα3Man	65	1

units related to complement-binding protein (Figure 1). The siglecs are a family of sialic-acid-specific cell surface lectins with variable numbers of extracellular immunoglobulin-like domains and are thus members of the immunoglobulin superfamily. Bacterial lectins are typically in the form of fimbriae (or pili), hair-like submicroscopic appendages, consisting of an assembly of several different types of subunits, only one of which has carbohydrate-binding activity, e.g., for mannose (in type 1 fimbriae of *Escherichia coli* and *Klebsiella pneumoniae*) or galabiose, Galα(1–4)Gal (in P fimbriae of *E. coli*).

High-resolution X-ray crystallography of lectins in complex with their ligands and site-directed mutagenesis allowed the identification of the chemical groups on the protein and on the carbohydrate that interact with each other and of the types of bonds formed. These studies have shown that, like other carbohydrate-binding proteins, lectins combine with their ligands primarily by a network of hydrogen bonds and hydrophobic interactions; in rare cases, electrostatic interactions (or ion pairing) and coordination with metal ions also play a role. One or more water molecules sometimes mediate the bonding. Although in a single lectin a limited set of residues contribute to the formation of the bonds with the ligand, overall almost all kinds of amino acids participate in ligand binding.

Functions

Lectins express numerous biological activities, nearly all of which are based on their ability to recognize and bind carbohydrates specifically (Table II). In other words, as a result of their unusual capacity to decode the information encoded in carbohydrates, they act as recognition determinants in diverse

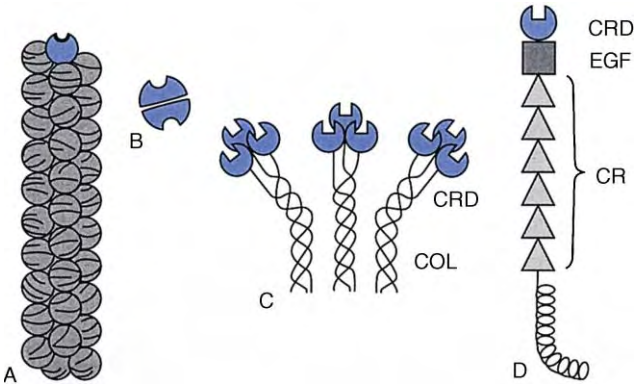

FIGURE 1 Schematic representation of the overall structure of lectins from different sources. (A) Part of fimbriae of *Escherichia coli*. The fimbriae are an assembly of different types of subunits, only one of which (blue) contains a carbohydrate-binding site. (B) A dimeric legume lectin (e.g., from lentils or peas). (C) Mammalian soluble mannose-binding lectin, a collectin. (D) E-selectin; the coil represents the membrane-spanning and cytoplasmic domains. COL, collagenous region; CR, complement regulatory repeats; EGF, epidermal growth factor-like domain; CRD, carbohydrate recognition domain. The indentations represent binding sites. Reproduced from Sharon, N., and Lis, H. (1995) *Essays in Biochemistry* 30, 59–75. Copyright The Biochemical Society.

biological processes. Thus, they function in cell–cell, cell–molecule, or molecule–molecule recognition. Influenza virus hemagglutinin A, a lectin specific for *N*-acetylneuraminic acid (or hemagglutinin C specific for 9-*O*-acetyl-*N*-acetylneuraminic acid), as well as bacterial surface lectins, mediate the binding of the pathogens to host cells, a prerequisite for initiation of infection. Inhibitors of bacterial lectins protect animals against experimental infection by the lectin-carrying organisms, providing a basis for attempts to develop anti-adhesion therapy of microbial infections. In some cases the bacterial lectins are responsible for the attachment to sugar residues on phagocytic cells, permitting the latter cells to kill the bacteria in the absence of serum factors, in a process designated lectinophagocytosis.

In plants, lectins may serve as defense agents against different kinds of phytopathogenic fungi and insects, as well as predatory invertebrates and vertebrates. They may also be involved in the establishment of symbiosis between nitrogen-fixing bacteria, mainly rhizobia, and leguminous plants, a process of cardinal importance both in the nitrogen cycle of terrestrial life and in agriculture.

The galectins are believed to function in cell adhesion. Their elevated levels on the surfaces of metastatic cancer cells may be responsible for the adhesion of these cells to target organs, a step necessary for metastasis formation. The mannose-6-phosphate (Man-6-P) receptors target lysosomal enzymes into the lysosomes. A defect in the synthesis of the Man-6-P marker on these enzymes results in I-cell disease (mucolipidosis II or MLII). This is an inherited lysosomal storage disease, characterized by a lack of enzymes in the lysosomes that normally carry the marker, resulting in accumulation in these subcellular organelles of undigested glycoconjugates.

The endocytic lectins are responsible for the clearance from the circulatory system of glycoproteins (e.g., ceruloplasmin and α_1-acid glycoprotein) from which terminal sialic acid has been removed, and possibly of cells too (e.g., aged erythrocytes or bacteria). A prominent representative is the mammalian asialoglycoprotein receptor (or hepatic-binding protein) found on hepatocytes, specific for galactose and *N*-acetylgalactosamine. The mannose-specific lectin present on the surface of macrophages (MMR) has been implicated in antimicrobial innate immunity. It binds infectious organisms that expose mannose-containing glycans on their surface, leading to their killing. The soluble mannose-binding lectins (MBLs) of mammalian serum and liver and pulmonary surfactant proteins A and D (SP-A and SP-D), all members of the collectin family, also function in innate immunity. MBL deficiency syndrome is associated with recurrent, severe bacterial infections in infants; it is caused by a mutation of a single amino acid in the collagen-like domain of the lectin.

The selectins mediate the adhesion of circulating leukocytes to endothelial cells, a prerequisite for their extravasation into other tissues. They thus control the migration (homing) of lymphocytes to specific lymphoid organs and of leukocytes to sites of inflammation, where they act to eliminate bacteria and other foreign intruders. Individuals unable to synthesize oligosaccharides recognized by the selectins, such as sialyl-Le^x [NeuAcα(2–3)Galβ(1–4)[Fucα(1–3)]GlcNAc] (as seen, for example, in cases of leukocyte deficiency type II (LADII)), suffer from recurrent microbial infections. The mechanism that helps leukocytes to break the endothelial barrier as a step in the fulfillment of their infection-fighting duties, is also responsible for their undesirable accumulation in tissues where they do not belong (e.g., joints), thereby causing damage, swelling, and pain. In reperfusion injury, which may happen after heart infarct or cerebral stroke, the accumulated leukocytes destroy tissues that have been damaged by temporary lack of oxygen. As shown in experimental animals, sialyl-Le^x attenuates myocardial necrosis after myocardial ischemia and reperfusion, another example of the great potential of antiadhesion therapy. In addition to their involvement in inflammation, the selectins may play a role in the attachment of the human blastocyst to the uterine lining and in the spread of cancer cells from the main tumor throughout the body to form metastases. The

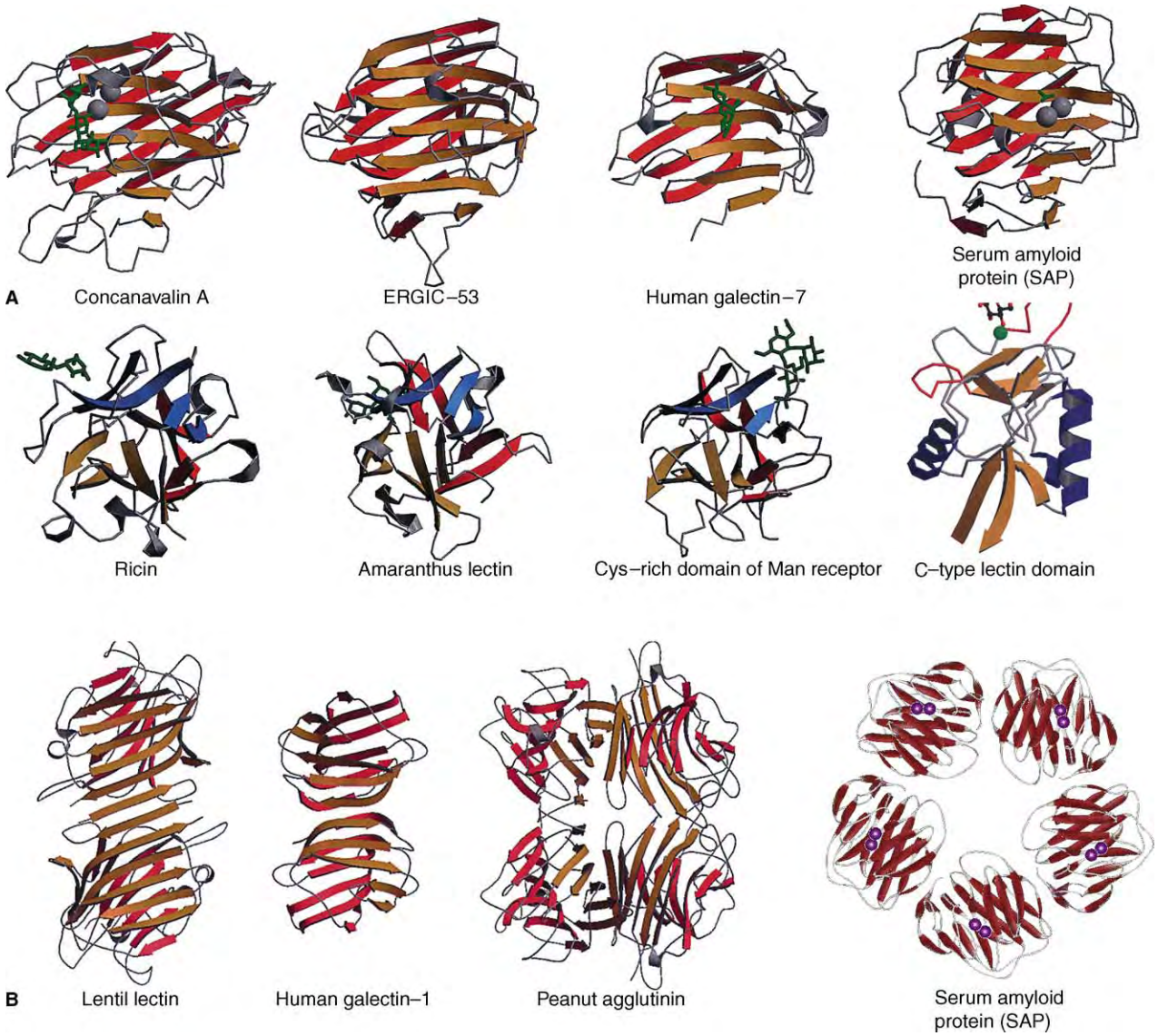

FIGURE 2 Structures of different lectins represented as ribbon diagrams. (A) Upper row shows monomers of lectins from different sources that share the jelly roll or lectin fold. First three lectins (from left) in the lower row all exhibit the β-trefoil fold. (B) Variations in quaternary lectins structures. The gray spheres represent metal ions; bound carbohydrate is shown in ball-and-stick representation. All diagrams, except for that of SAP, reprinted from Loris, R. (2002). Principles of structures of animal and plant lectins. *Biochim. Biophys. Acta* **1572**, 198–208. The diagram of SAP is from PDB entry sac.

siglecs have been implicated in cell–cell interactions in the immune system and in the process of myelination. Intracellular lectins such as calnexin, calreticulin, and ERGIC-53 participate in the control of glycoprotein biosynthesis.

Applications

Lectins, mainly those from plants, are invaluable tools for detection, isolation, and structural and functional investigation of complex carbohydrates, especially glycoproteins. In immobilized form, e.g., covalently bound to Sepharose, they are indispensable for purification and isolation by affinity chromatography of glycoproteins, glycopeptides, and oligosaccharides. Lectins are also useful as histochemical and cytochemical reagents: derivatized with fluorescent dyes, gold particles, or enzymes they serve for the detection of glycoconjugates in tissue sections and on cells, as well as on and in subcellular organelles, mainly for examination of changes that occur on cell surfaces and in cells during physiological and pathological processes, from differentiation to cancer.

A few lectins are employed in blood typing, e.g., those of the seeds of *Lotus tetragonolobus* and *Ulex europaeus*

TABLE II

Lectin Functions

Functions	Examples of lectins involved
Microorganisms	
Infectivity	*Escherichia coli* fimbriae; *Entamoaeba histolytica* Gal/GalNAc-specific lectin; influenza virus hemagglutinin
Plants	
Defense	Snowdrop lectin, jacalin, wheat germ aglutinin
Symbiosis with nitrogen-fixing bacteria	Pea lectin
Animals	
Clearance of glycoproteins from circulation	Asialoglycoprotein receptor
Control of lymphocyte migration	Selectins
Control of glycoproteins biosynthesis	Calnexin, calreticulin, ERGIC-53
Innate immunity	
Complement activation	MBLs
Lectinophagocytosis	MMR, SP-A
Modulation of cell–cell and cell–substratum interactions	Galectins
Modulation of signal transduction by B lymphocytes	Siglec-2
Neuronal myelination and regeneration	Siglec-4a and -4b
Targeting of glycoproteins to lysosomes	Man6P receptors
Tumor metastases	Galectins-1, -3, and -8; selectins

for the identification of type O cells, and of secretors of blood group substances. PHA and concanavalin A are potent *in vitro* T lymphocyte mitogens, while another lectin, pokeweed mitogen (PWM), stimulates both T and B cells. Mitogenic stimulation by lectins provides a simple means to assess the immunocompetence of patients and to monitor the effects of immunosuppressive and immunotherapeutic treatments, as well as for preparation of chromosome maps for karyotyping, sex determination, and detection of chromosome defects.

Selective agglutination by PNA permits the facile separation of mouse and human cortical (immature) thymocytes from the medullary (mature) ones. Treatment with SBA removes mature T cells from human bone marrow and affords a fraction enriched in stem cells. Lectin-purged bone marrow of haplo-identical donors serves routinely for transplantation into children born with severe combined immune deficiency (bubble children) with close to 70% success. The method is also used experimentally in bone marrow transplantation of leukemia patients. Knowledge of the properties of lectins was essential for the development of enzyme replacement therapy for the treatment of Gaucher disease, and there is hope for lectin replacement therapy for patients with defects in innate immunity.

A major application of toxic lectins, such as ricin, is for selection of resistant animal cell lines. These cell lines provide access to glycoproteins with modified glycan structures and to novel glycosyltransferases. They are useful tools for investigation of the mechanism of protein glycosylation and for large-scale production of therapeutic glycoproteins with desired carbohydrate structures.

See Also the Following Articles

Galectins • Protein Glycosylation Inhibitors • Siglecs

Glossary

glycan Any compound consisting of a few or many monosaccharides in free form or attached to another substance; a carbohydrate or saccharide.

glycoconjugate A substance that consists of one or more glycans covalently attached to a noncarbohydrate constituent, typically protein (to give a glycoprotein) or lipid (forming a glycolipid).

innate immunity A form of defense of animals and other organisms that acts against infection in the first minutes or hours. It is different from acquired or adaptive immunity that takes days or weeks to develop.

mitogen A substance that stimulates cell division, especially of lymphocytes.

Further Reading

Crocker, P. (ed.) (2001). *Mammalian Carbohydrate Recognition Systems*, Vol. 33, Results Problems Cell Differ, Springer, Berlin, 252pp.

Gabius, H.-J. (1997). Animal lectins. *Eur. J. Biochem.* **243**, 543–576.

Goldstein, I. J., Winter, H. C., and Poretz, R. D. (1997). Plant lectins: Tools for the study of complex carbohydrates. In *Glycoproteins II*

(J. Montreuil, J. F. G. Vliegenthart and H. Schachter, eds.) pp. 403–474. Elsevier, Amsterdam.

Kilpatrick, D. C. (2002). Mannan-binding lectin: Clinical significance and applications. *Biochim. Biophys. Acta* **1572**, 401–413.

Ley, K. (2003). The role of selectins in inflammation and disease. *Trends Molecular Med.* **9**, 263–268.

Loris, R. (2002). Principles of structures of animal and plant lectins. *Biochim. Biophys. Acta* **1572**, 198–208.

Sharon, N., and Lis, H. (1993). Carbohydrates in cell recognition. *Sci. Am.* **268**(1), 82–89.

Sharon, N., and Lis, H. (2003). *Lectins*, 2nd edition. Kluwer Academic, Dordrecht, The Netherlands, 457pp.

Sharon, N., and Ofek, I. (2000). Safe as mother's milk: Carbohydrates as future anti-adhesion drugs for bacterial diseases. *Glycoconjugate J.* **17**, 659–664.

Taylor, M. E., and Drickamer, K. (2003). *Introduction to Glycobiology.* Oxford University Press, Oxford, UK, 207pp.

Van Damme, E. J. M., Peumans, W. J., Barre, A., and Rougé, P. (1998a). Plant lectins: A composite of several distinct families of structurally and evolutionary related proteins with diverse biological roles. *Crit. Rev. Plant Sci.* **17**, 575–692.

Biography

Nathan Sharon and Halina Lis have been collaborating in research on lectins since 1960. Their numerous publications on the subject include many reviews and two books. Sharon received his Ph.D. from the Hebrew University, Jerusalem, in 1953. He then joined the Weizmann Institute, became a Professor in 1968 and Head of the Department of Biophysics in 1974, and Emeritus in 1990. He was a visiting professor at different institutions in Europe and the US, and is the recipient of many awards and honors, among them the Israel Prize in Biochemistry and Medicine, and membership of the Israel Academy of Sciences and Humanities and of EMBO.

Halina Lis received her Ph.D. in 1957 from the University of Uppsala, moved to Weizmann in 1960 and became an Associate Professor in 1986.

Leptin

Thomas W. Gettys
Pennington Biomedical Research Center, Baton Rouge, Louisiana, USA

Leptin is a 16 kDa peptide hormone released from adipose tissue that regulates the balance between energy intake and energy utilization by binding to hypothalamic receptors and modulating appetite control centers in the brain. Occupancy of central leptin receptors also increases activity of the sympathetic nervous system, which stimulates energy expenditure in peripheral target tissues through a process called adaptive thermogenesis. Through coordinated regulation of these two systems, leptin functions to match rates of energy expenditure with energy intake. Leptin also functions to preserve energy reserves during starvation by lowering body temperature, basal metabolic rate, and limiting hypothalamic support for reproductive function. As such, leptin is a peripheral signal that acts centrally to integrate a complex array of behavioral and metabolic systems that function to maintain energy homeostasis when food supplies are adequate and ensure survival when they are not.

Historical Perspective of Leptin Discovery

The search for the primary genetic defect giving rise to the obese/diabetic syndrome of *ob/ob* mice (Figure 1) was guided by the early work of Douglas Coleman, who postulated that *ob/ob* mice were missing a circulating satiety signal. To test this hypothesis, he surgically joined *ob/ob* mice with lean littermates, *ob/ob* mice with *db/db* (diabetes) mice, and lean mice with *db/db* mice so that the parabiotic pairs shared blood supplies. *db/db* mice were included in his experiments because they also developed morbid obesity after weaning, but differed from *ob/ob* mice in that the *db/db* mutation resides on a different chromosome. This landmark experiment showed that the obesity syndrome of *ob/ob* mice, but not *db/db* mice, was corrected by a circulating factor from lean mice. The obesity syndrome of *ob/ob* mice was also reversed by parabiotic pairing with *db/db* mice, but in this case, the *ob/ob* mouse in each pair eventually died from starvation. The results indicated that *ob/ob* mice were missing a satiety factor but retained the ability to respond to the missing factor. In contrast, *db/db* mice were unresponsive to the satiety factor, but apparently produced it in abundant quantities. Some 30 years later, the missing factor (and receptor) inferred from the work of Coleman was identified by Jeffrey Friedman at Rockefeller University with the cloning of the *ob* gene in late 1994. The cloning of the *ob* receptor by Louis Tartaglia followed soon thereafter. The product of the *ob* gene was named leptin, from the Greek "leptos," meaning thin.

Obesity Syndrome Produced by Leptin Absent in *ob/ob* Mice

The cloning of the *ob* gene identified leptin as the "lipostat" which regulates the balance between energy intake and utilization to maintain body weight equilibrium. Adipocytes of *ob/ob* mice do not produce leptin, and its absence produces a complex metabolic syndrome characterized by hyperphagia, morbid obesity, and diabetes. Hypertrophy of adipose tissue is noted prior to the hyperphagia that develops post weaning in *ob/ob* mice, and obesity occurs even when *ob/ob* mice are pair-fed with lean littermates. Thus, their thriftiness is a significant component of their propensity to become obese. Treatment of *ob/ob* mice with exogenous leptin corrects their obesity, and part of the weight loss can be accounted for by reductions in food intake. However, when differences in food intake between saline and leptin-injected *ob/ob* mice are controlled, leptin-injected mice still lose more weight. These results illustrate that an important component of leptin's physiological actions are to regulate energy expenditure.

Central Mechanisms of Leptin Action

Leptin is a key component of the neuroendocrine circuitry that regulates food intake and energy utilization, and its activation of the sympathetic nervous system (SNS) is now recognized as the primary efferent limb of the circuit regulating peripheral energy utilization. Leptin activates the SNS by increasing cocaine

FIGURE 1 *ob/ob* mouse and lean littermate (+/?) 12 weeks after weaning.

amphetamine-related transcript (CART) and α-melanocyte stimulating hormone (α-MSH) release from leptin-responsive neurons within the arcuate nuclei, and these peptides increase sympathetic outflow by binding to melanocortin and CART receptors on preganglionic neurons of the SNS. The resulting increase in sympathetic stimulation of muscle and adipose tissue promotes fat oxidation through targeted effects on futile energy cycles in the respective tissues. A second population of leptin-responsive neurons in the hypothalamus coexpress neuropeptide Y (NPY) and agouti-related peptide (AGRP), and expression of these orexigenic peptides is decreased by leptin. Thus, it is through reciprocal regulation of these two populations of hypothalamic nuclei that leptin produces its full effect on energy homeostasis (see Figure 2).

Adipose Tissue as a Target of the SNS

Mitochondrial oxidation of fatty acids creates a proton electrochemical gradient that is used to drive the conversion of ADP to ATP via ATP synthase. Brown adipose tissue (BAT) mitochondria possess an alternative pathway that allows protons to re-enter the mitochondrial matrix without coupling to ATP synthesis, and this pathway is mediated by "uncoupling protein 1" (UCP1). UCP1 transforms electrochemical energy into heat, enabling small mammals to survive exposure to cold. The sympathetic nervous system and UCP1 are essential components of this thermogenic response system. The conventional wisdom has been that UCP1 expression is restricted to brown adipocytes, but recent evidence has clearly established that sympathomimetics can induce

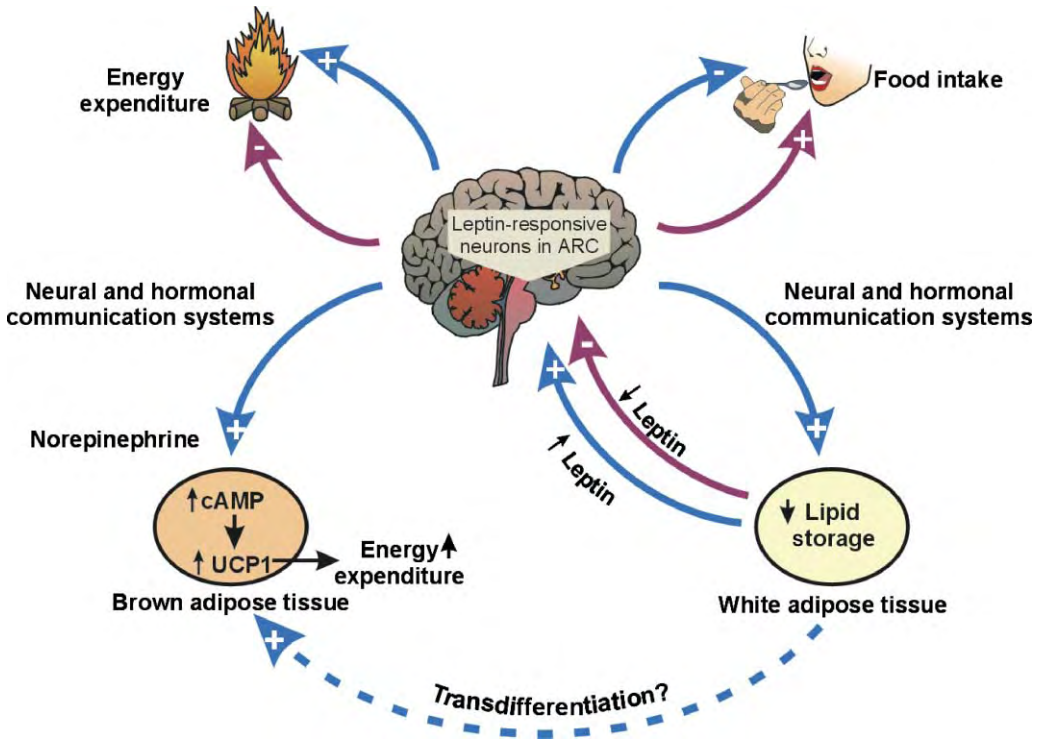

FIGURE 2 Model of leptin regulation of energy balance. Leptin regulates its own expression in white adipose tissue and thermogenesis in brown adipose tissue through central modulation of sympathetic nervous system outflow to adipose tissue.

ectopic expression of UCP1 in white adipose tissue (WAT) depots. The origin of the UCP1-expressing cells was originally a mystery, but evidence has emerged to support the concept that mature adipocytes are capable of significant functional plasticity, and readily transdifferentiate between cell types whose primary function is to store triglyceride (WAT) and multilocular, mitochondria-rich adipocytes capable of significant fat oxidation (BAT). It is clear that intense SNS stimulation can also promote the differentiation of preadipocytes within white depot sites into brown adipocytes. The unexpected appearance of UCP1 in WAT was originally observed in mice, where cold exposure caused a population of cells within the depot to transdifferentiate from unilocular white adipocytes to multilocular, mitochondria-rich brown adipocytes. Cold exposure produces these responses through increased sympathetic outflow to adipose tissue, and induces the transcriptional program of transdifferentiation in WAT through a norepinephrine, β-adrenoceptor, and cAMP-dependent mechanism. SNS stimulation of adipose tissue is also subject to regulation by leptin. In this case, modulation of SNS outflow is used to match rates of energy utilization to energy intake through the process of adaptive thermogenesis. A consensus has emerged to support the view that transdifferentiation of white adipocytes is an important component of the adaptive thermogenic response, and that leptin is a key mediator of the process.

The potential for transdifferentiation is depot-site specific and has a strong genetic component in both mice and humans. The significance of this process was demonstrated in elegant studies analyzing backcrosses of parental mouse strains with widely varying ability of WAT to transdifferentiate. Using UCP1 as a BAT-specific indicator, Leslie Kozak showed that recombinant inbred strains from the crosses reduced fat deposition after adrenergic stimulation in direct proportion to their induction of UCP1 in convertible WAT depots. These findings indicated that the relative ability of a mouse strain to resist obesity is a function of the ability of WAT to increase UCP1 in response to adrenergic stimulation. Thus, an important component of leptin's ability to regulate energy utilization in peripheral tissues is conferred by its ability to induce UCP1 expression and enhance fat oxidation in adipose tissue. Some WAT depots do not respond to SNS stimulation with an increase in UCP1 expression and *in situ* fat oxidation. In this case, SNS stimulation activates lipolysis, and mobilizes lipid for transport to more oxidatively active sites.

Regulation of Leptin Expression

Well before the discovery of leptin, George Bray proposed that most obesities known are low in sympathetic activity (MONA-LISA Hypothesis). This hypothesis stemmed in part from the observation that *ob/ob* mice were cold intolerant, but after leptin and its receptor were cloned, it was noted that leptin mRNA was significantly up-regulated in adipose tissue from both models. This indicated the absence of an efferent signal from the SNS in both models which was important in regulating leptin expression. Circulating leptin concentrations are the product of transcriptional regulation of the gene and release of the expressed protein from adipocytes. Work in the author's laboratory established that leptin secretion from isolated adipocytes was inhibited by activation of β_3-adrenoceptors in parallel to the activation of cAMP-dependent protein kinase. The SNS also regulates leptin expression. Figure 3 illustrates that mice lacking the gene which converts dopamine into norepinephrine (dopamine β-hydroxylase) were unable to down-regulate leptin mRNA expression after treatment with exogenous leptin. Thus, the SNS is the efferent arm of a feedback system which negatively regulates leptin expression and release.

Leptin is positively regulated by insulin and glucocorticoids. Both hormones produce rapid increases in leptin secretion from adipose tissue in conjunction with a coordinated increase in transcription of the gene. These hormonal and neurotransmitter-dependent pathways represent acute regulatory systems that are superimposed onto a diurnal pattern of leptin secretion which in humans, produces lowest concentrations at night and highest during the day. Serum leptin levels are also strongly correlated to percentage body fat and body mass index, but the relationship is dichotomous between male and female patients. For instance, as body mass

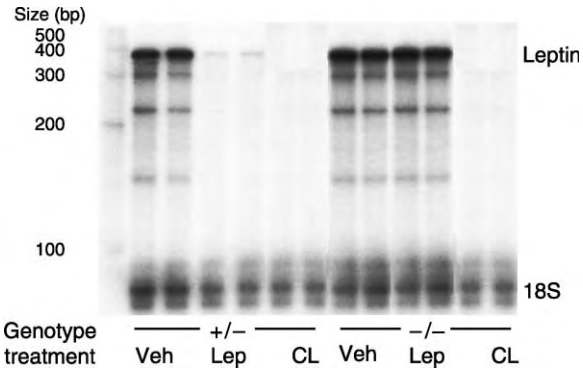

FIGURE 3 Ribonuclease protection assay of leptin mRNA in total RNA from EWAT of control (*Dbh* $^{+/-}$) and dopamine β-hydroxylase (Dbh$^{-/-}$) knockout mice injected with either saline, leptin, or the β3-adrenergic receptor agonist, CL-316,243 for 3 days. The blot shows that the ability to synthesize catecholamines is required for leptin to down-regulate its own expression in white adipose tissue. Reproduced from Commins, S. P., Marsh, D. J., Thomas, S. A., Watson, P. M., Padgett, M. A., Palmiter, R. D., and Gettys, T. W. (1999). Norepinephrine is required for leptin effects on gene expression in brown and white adipose tissue. *Endocrinology* **140**, 4772–4776.

index increases serum leptin levels increase threefold faster in females than males. Testosterone inhibits leptin expression and likely explains the gender difference in circulating leptin between males and females. Considered together, leptin expression and release are regulated by a complex network of hormonal and autonomic inputs, which are integrated to regulate transcription of the leptin gene and secretion of expressed protein into the bloodstream.

Leptin Resistance and Obesity

A factor common to diet-induced obesity in mice and humans is insensitivity to leptin. This conclusion is supported by the observation that most cases of rodent and human obesity are characterized by high-circulating leptin levels. In addition, treatment with exogenous leptin is minimally effective. Leptin resistance was originally thought to result from reduced transport of serum leptin into the cerebrospinal fluid. Short isoforms of the leptin receptor mediate this transport process across the blood–brain barrier (BBB), but the evidence is unconvincing that expression of this receptor isoform is altered during states of leptin resistance. It is also possible that elevation of serum leptin in dietary obesity saturates the transport system, making it unresponsive to subsequent changes in circulating leptin. To test this concept, leptin transport across the BBB was measured after injecting *db/db* and *ob/ob* mice with radiolabeled leptin. Despite great differences in endogenous circulating leptin in these two models, leptin transport into the hypothalamus did not differ between them. Evidence supporting defective transport comes mainly from studies where ICV injection produces responses in mice where peripheral leptin is ineffective. However, recent work has clearly established that the efficacy of ICV leptin to activate the first step of the signaling cascade (signal transducers and activators of transcription 3; STAT3) was diminished in mice that were also unresponsive to peripherally injected leptin. These findings support the alternative interpretation that decreased sensitivity of leptin-responsive nuclei make the mouse unresponsive to peripherally injected leptin without any change in transport kinetics. Such a mechanism would involve signal deamplification downstream of the leptin receptor.

Two potential mechanisms of signal deamplification have been proposed and both involve inhibition of leptin-dependent Janus kinase 2 (JAK2) activation. The first mechanism involves a member of the suppressors of cytokine signaling (SOCS) family called SOCS-3 that blocks leptin receptor-dependent phosphorylation and activation of JAK2. However, while SOCS-3 may have a role in mediating leptin resistance in yellow obese mice (i.e., A^y mice), no evidence has been found to support its involvement in the leptin resistance of mouse models of diet-induced obesity. The second mechanism of leptin signal deamplification involves protein tyrosine phosphatase 1B (PTP1B), which inhibits leptin signaling by dephosphorylating JAK2. JAK2 is a receptor-associated kinase which becomes active upon leptin receptor occupancy, and initiates the leptin signal by phosphorylating STAT-3. A model of how PTP1B functions in leptin signal deamplification in pro-opiomelancortin containing (POMC) neurons neurons of the arcuate nuclei is presented in Figure 4.

Interestingly, PTP1B activity and expression are both regulated by insulin, and expression of PTP1B is increased in peripheral tissues in insulin resistant states. It is unclear whether hypothalamic expression is upregulated in insulin-resistant obese states, but deletion of the PTP1B gene does produce leaner mice with increased energy expenditure and enhanced insulin sensitivity. It is also worth noting that the mice are resistant to diet-induced obesity and exquisitely sensitive to exogenous leptin.

The second step in central leptin signal transduction is translating STAT3 phosphorylation in hypothalamic target nuclei into activation of the SNS. Leptin activates the SNS by increasing α-MSH release from POMC neurons within the arcuate nuclei, and these peptides increase SNS outflow by binding to melanocortin receptors (MCR3, MCR4) on preganglionic neurons of the SNS. The MCR3 and MCR4 receptors are canonical seven-membrane spanning receptors, which signal by activating the stimulatory G protein, $G_s\alpha$ and increasing cAMP. Therefore, the transmission of the leptin signal from first order neurons (NPY/AGRP, POMC) to second order neurons (preganglionic SNS) is another step subject to alteration during the development of leptin resistance. For instance, it is now evident that posttranslational processing of POMC modifies the generation of sympathoexcitatory (α-MSH) versus sympathoinhibitory

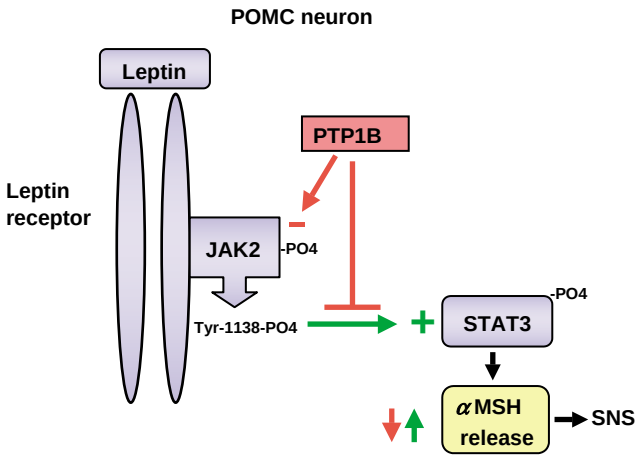

FIGURE 4 Schematic model showing deamplification of leptin signaling in POMC neurons by protein phosphatase 1B.

(β-endorphin) ligands from leptin-sensitive POMC neurons. Second, high-fat diets transform the sympathetic response to ICV leptin from excitatory to inhibitory in Wistar rats. These findings provide a framework to propose that high-fat diets modify the processing of POMC in a manner which alters the translation of the leptin signal and alters its ability to regulate downstream responses and enhance peripheral energy utilization.

The third component of leptin signal transduction is SNS outflow to adipose tissue, where activation of β-adrenoceptors initiates the transcriptional program of adaptive thermogenesis in a cAMP-dependent manner. Analysis of the promoter structure of genes transactivated during this response shows that the nuclear receptor, peroxisome proliferator activated receptor γ (PPARγ) is an essential component of the transcriptional complex. Although the endogenous ligand for this receptor has yet to be identified, *in vitro* studies have shown that long-chain-polyunsaturated fatty acids and their metabolites can act as partial agonists. The relevance of PPARγ to adaptive thermogenesis is apparent from work with obesity prone strains of mice, where it is known that high-fat diets compromise the ability of sympathetic stimulation to initiate thermogenic responses in adipose tissue. Remarkably, simultaneous provision of synthetic PPARγ agonists with sympathomimetics rescues the compromised adaptive thermogenic response of obesity-prone mice and produces a significant loss of WAT. Coadministration of PPARγ agonists with sympathomimetics is not required in obesity-resistant mice, as high-fat diets do not compromise their adaptive thermogenic responses. Although the underlying mechanism is not yet known, high-fat diets accentuate leptin resistance by altering the requirement for endogenous PPARγ agonists to support transcriptional activation of genes involved in adaptive thermogenesis. The consensus at present is that changes in dietary fat content and composition alter synthesis of the endogenous ligands for PPARs in a manner that produces coordinated, integrated transcriptional responses in and among metabolically active target organs. Collectively, the PPARs are viewed as a lipid-based nutrient sensing system. In the case of adipose tissue, the productive integration of signaling inputs from leptin-induced SNS outflow and lipid-sensitive PPAR activation are required for a full and effective adaptive thermogenic response. A better understanding of the signaling systems, which interact to regulate and limit leptin signaling is an important missing component in our overall understanding of the mechanisms of energy homeostasis.

See Also the Following Articles

Fatty Acid Oxidation • JAK-STAT Signaling Paradigm • Neuropeptide Y Receptors • Uncoupling Proteins

Glossary

brown adipocyte Adipose cell type with large number of mitochondria whose primary function is to conduct fat oxidation that is uncoupled from ATP synthesis via mitochondrial protein UCP1.

energy homeostasis Physiological state when energy intake and energy utilization are matched to produce stable body weight.

leptin 16 kDa hormone secreted by adipose tissue that regulates the balance between food intake and energy utilization.

obesity Excessive fat storage resulting from chronic positive energy balance.

sympathomimetic Endogenous or synthetic agonist of adrenoceptors.

transdifferentiation A programmatic change in gene expression in white adipocytes which transforms their morphology and functionality from fat storage to fat oxidation.

uncoupling protein 1 Specialized mitochondrial protein that short circuits the proton gradient across the mitochondrial matrix, uncouples oxidative phosphorylation, and transforms electrochemical energy into heat energy.

Further Reading

Bates, S. H., Stearns, W. H., Dundon, T. A., Schubert, M., Tso, A. W., Wang, Y., Banks, A. S., Lavery, H. J., Haq, A. K., Maratos-Flier, E., Neel, B. G., Schwartz, M. W., and Myers, M. G. (2003). STAT3 signalling is required for leptin regulation of energy balance but not reproduction. *Nature* **421**, 856–859.

Bray, G. A. (1991). Obesity, a disorder of nutrient partitioning: The MONA LISA hypothesis. *J. Nutr.* **121**, 1146–1162.

Commins, S. P., Marsh, D. J., Thomas, S. A., Watson, P. M., Padgett, M. A., Palmiter, R. D., and Gettys, T. W. (1999). Norepinephrine is required for leptin effects on gene expression in brown and white adipose tissue. *Endocrinology* **140**, 4772–4776.

Considine, R. V. (1999). An overview and update of the physiology of leptin in humans. *J. Clin. Ligand Assay* **22**, 233–235.

Friedman, J. M. (1997). The alphabet of weight control. *Nature* **385**, 119–120.

Friedman, J. M. (1999). Leptin and the regulation of body weight. *Harvey Lect.* **95**, 107–136.

Friedman, J. M. (2002). The function of leptin in nutrition, weight, and physiology. *Nutr. Rev.* **60**, S1–S14.

Gettys, T. W., Harkness, P. J., and Watson, P. M. (1996). The β_3-adrenergic receptor inhibits insulin-stimulated leptin secretion from isolated rat adipocytes. *Endocrinology* **137**, 4054–4057.

Guerra, C., Koza, R. A., Yamashita, H., Walsh, K., and Kozak, L. P. (1998). Emergence of brown adipocytes in white fat in mice is under genetic control – effects on body weight and adiposity. *J. Clin. Invest.* **102**, 412–420.

Halaas, J. L., Gajiwala, K. S., Maffei, M., Cohen, S. L., Chait, B. T., Rabinowitz, D., Lallone, R. L., Burley, S. K., and Friedman, J. M. (1995). Weight-reducing effects of the plasma protein encoded by the *obese* gene. *Science* **269**, 543–546.

Zhang, Y., Proenca, R., Maffei, M., Barone, M., Leopold, L., and Friedman, J. M. (1994). Positional cloning of the mouse obese gene and its human homologue. *Nature* **372**, 425–432.

Biography

Dr. Thomas W. Gettys is Professor of Adipocyte Signaling and Chief of the Experimental Obesity Division at the Pennington Biomedical Research Center. His principal research interests are in central and peripheral leptin signaling mechanisms, with special emphasis on the signaling mechanisms linking β-adrenoceptors to the transcriptional program of transdifferentiation in adipose tissue. He earned his Ph.D. in nutrition at Clemson University and completed postdoctoral training at Vanderbilt University in the Howard Hughes Medical Institute with Dr. Jackie Corbin.

LexA Regulatory System

Veronica G. Godoy, Penny J. Beuning and Graham C. Walker
Massachusetts Institute of Technology, Cambridge, Massachusetts, USA

The LexA regulon, also known as the SOS response, is a genetic system that responds to exogenous and endogenous DNA damage by inducing the expression of a number of genes whose products are responsible for maintaining the integrity of the genetic information in the chromosome. It has been widely studied in *E. coli*, and sequencing of a number of bacterial genomes has allowed the identification of genes that belong to this regulon in a wide variety of organisms. Comparison with the organization of the *E. coli* regulon indicates common and unique pathways in those organisms to protect the DNA against damage.

The LexA Regulatory System in *E. coli*

The central elements of the control system for the LexA regulon are the gene products of the *recA* and *lexA* genes. RecA protein is involved in the sensing of DNA damage and LexA is the repressor of the regulon. The LexA protein binds as a dimer to sequences located close to the promoters of the genes that it regulates, interfering with their transcription. Therefore, the expression of these genes occurs only under conditions that cause DNA damage in the cell. Such damage leads to the production of single stranded DNA (ssDNA), which is often generated by the replication machinery's failed attempts to replicate the damaged DNA. The RecA protein readily binds the ssDNA, forming a protein–DNA complex known as the RecA:ssDNA nucleoprotein filament. LexA binds deep in the groove of the nucleoprotein filament, which then acts as a coprotease to facilitate autocleavage of LexA between residues Ala84–Gly85. This cleavage inactivates LexA so it can no longer act as a repressor. The decreased intracellular concentration of LexA leads to expression of the LexA-regulated genes (Figure 1).

LexA Crystal Structure and Insights into Repressor Function

The autocleavage of LexA is catalyzed by a Ser-Lys dyad related to those found in signal peptidases. The crystal structures of several mutant forms of LexA have revealed that the loop containing the Ala-Gly cleavage site can adopt two conformations relative to the Ser-Lys dyad. In the "noncleavable" conformation, the cleavage site is quite distant from the Ser-Lys dyad that catalyzes cleavage, while in the cleavable conformation, the cleavage site lies proximal to the active site dyad, apparently poised for cleavage (Figure 2). This switch from a noncleavable to a cleavable conformation appears to form part of the basis for regulation of the cleavage reaction. It has been proposed that the RecA:ssDNA filament facilitates LexA cleavage by binding preferentially to the cleavable conformation. Cryoelectron microscopy experiments suggest that the RecA:ssDNA filament stabilizes the higher energy, cleavable form of LexA by binding LexA in the filament groove.

There is also a chemical barrier regulating LexA cleavage by preventing autodigestion. In the Ser-Lys active site dyad, the ϵ-amino group of Lys156 deprotonates Ser119, but the ϵ-amino group of Lys156 is solvent-exposed and likely protonated in the noncleavable conformations of LexA. The energetic cost of burying the charged ϵ-amino group of Lys156, which is required for cleavage, provides another layer of regulation of LexA cleavage and helps to prevent autodigestion.

LexA Binding Site

LexA, the repressor, exerts its regulatory effects by binding to palindromic sequences located near the promoter of the genes it regulates; the consensus sequence for the *E. coli* LexA binding site is $CTGtN_{10}$ aCAG (see Table I). LexA binds with different affinities to the variants of this sequence located upstream of the different SOS genes thereby enabling differential regulation of the LexA-regulated genes. Interestingly, both the *recA* and *lexA* genes are regulated by LexA. Upon DNA damage one of the first genes to be induced is *recA*.

LexA Autoregulation

LexA autoregulation sets the basal level of LexA; so the system is stable without DNA damage, but the response can easily be modulated. DNA damage results in the formation of RecA:ssDNA filaments, which in turn

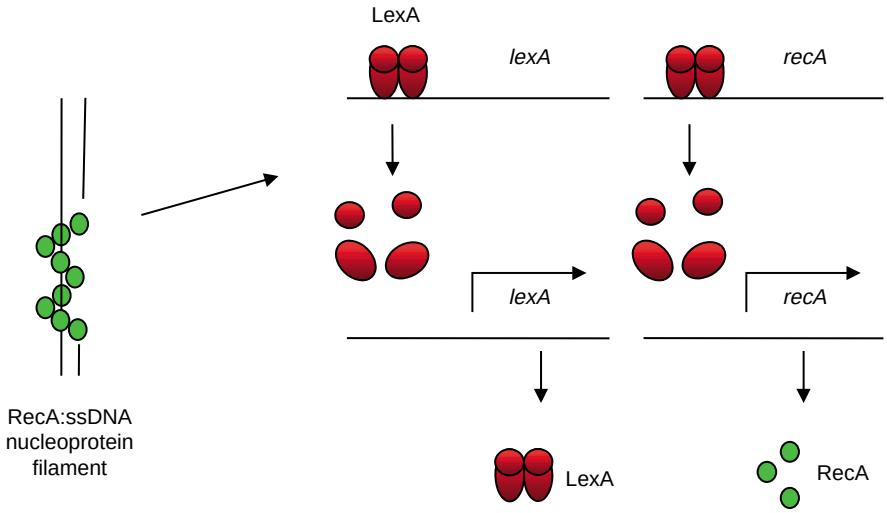

FIGURE 1 Induction of the SOS response. Shown are two of the operons under LexA control, including LexA itself. After DNA damage, RecA polymerizes on single-stranded DNA (ssDNA), forming a RecA:ssDNA nucleoprotein filament. This facilitates LexA cleavage, which inactivates it as a repressor and thus induces the SOS Response.

facilitate LexA cleavage, thereby inducing the expression of LexA-repressed genes.

The LexA Regulon

In *E. coli*, recent microarray experiments indicate that there are approximately 43 genes in the genome that are LexA-regulated. Thus, ~1% of *E. coli*'s genes (4402 ORFs) are induced in a concerted fashion in response to DNA damage.

LexA Mutants and their Phenotype

The elucidation of the major pathways involved in the response to DNA damage was initiated by the genetic analysis of both *recA* and *lexA* mutants. One of the first mutations analyzed that blocks induction of SOS genes was found to be a *lexA*[Ind$^-$] allele that results in a noncleavable LexA. Mutations in *lexA* that make cells constitutively express SOS genes [termed *lexA*(Def)] have been isolated as well. Such *lexA*(Def) mutations are lethal unless the cells also carry a mutation in the LexA-regulated *sulA* gene. Since *sulA* encodes a cell division checkpoint protein that blocks septation, its constitutive expression blocks cell division and results in cell death. Thus, mutations that inactivate the *sulA* gene permit *lexA* mutants that constitutively express SOS genes to carry out cell division and hence to be viable.

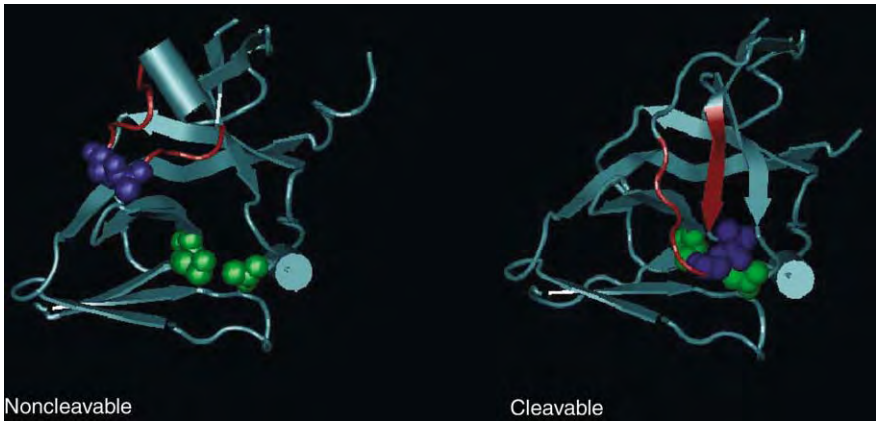

FIGURE 2 Conformational switch regulating LexA cleavage. Shown are the noncleavable (left) and cleavable (right) forms of the C terminus of LexA. The cleavage site Ala84–Gly85 is shown in blue spheres, while the Ser119–Lys156 catalytic dyad are shown in the green spheres. The red portion is the loop that displays a large conformational change in the noncleavable versus cleavable conformations. Figure prepared with VMD – Visual Molecular Dynamics. (Humphrey, W., Dalke, A., and Schulten, K. (1996). VMD: Visual molecular dynamics. *J. Molec. Graphics* **14**, 33–38.)

TABLE I

***Escherichia coli* Genes with their Respective LexA Box Sequence Compared to the Consensus Sequence**

Known genes	LexA box sequence
ysdAB	taCTGtttatttataCAGta
umuDC	taCTGtatataaaaaCAGta
sbmC	taCTGtatataaaaaCAGta
pcsA	aaCTGtatataaataCAGtt
recN no. 1	taCTGtatataaaacCAGtt
dinQ	taCTGtatgattatcCAGtt
urvB	aaCTGtttttttatcCAGta
dinI	acCTGtataaataacCAGta
hokE	caCTGtataaataaaCAGct
recA	taCTGtatgctcataCAGta
sulA	taCTGtacatccataCAGta
uvrA	taCTGtatattcattCAGgt
ssb	acCTGaatgaatataCAGta
yebG	taCTGtataaaatcaCAGtt
lexA/dinF no. 2	aaCTGtatatacaccCAGgg
ydjQ	caCTGgatagataacCAGca
lexA/dinF no. 1	tgCTGtatatactcaCAGca
ruvAB	cgCTGgatatctatcCAGca
yjiW	taCTGatgatatataCAGgt
molR	aaCTGgataaaattaCAGgg
dins	agCTGtatttgtctcCAGta
uvrD	atCTGtatatataccCAGct
recN no. 2	taCTGtacacaataaCAGta
ding	taTTGgctgtttataCAGta
yigN	aaCTGgacgtttgtaCAGca
ydjM1	taCTGtacgtatcgaCAGtt
ftsK	tcCTGttaatccataCAGca
dinB	caCTGtatactttacCAGtg
recN no. 3	taATGgtttttcataCAGga
ydjM2	caCTGtataaaaatcCTAta
ybfE	aaCTGattaaaaaccCAGcg
polB	gaCTGtataaaaccaCAGcc
Consensus	taCTGtatatatataCAGta

Modified from Courcelle, J., Khodursky, A., Peter, B., Brown, P. O., and Hanawalt, P. C. (2001). Comparative gene expression profiles following UV exposure in wild-type and SOS-deficient *Escherichia coli*. *Genetics* **158**, 41–64.

Defining the LexA Regulon

The first experiment showing that the SOS response is a global genomic response to DNA damage was performed by Kenyon and Walker. By first isolating transcriptional *lacZ* fusions located randomly in the genome they were able to screen for genes whose expression is induced after DNA damage. The identities of these *din* (*d*amage *in*ducible) genes indicated that the SOS response to DNA damage helps *E. coli* preserve the integrity of its DNA. Characterization of these *din* damage-inducible genes allowed the definition of the 20-base pair LexA binding site, which in turn led to the identification of additional genes belonging to the LexA regulon. Many of the *din* genes found this way are still intensely studied, since understanding their particular functions is yielding insights into the molecular mechanisms underlying this sophisticated global response to DNA damage.

The advent of transcriptional profiling technology (DNA microarrays), in which it is possible to test simultaneously the genome-wide expression of genes involved in a given process, has allowed nearly definitive identification of each of the genes regulated by LexA. Comparing the gene expression profiles in wild-type vs. *lexA*(Ind$^-$) (LexA noncleavable, non-SOS-inducible) strains allowed determination of the genes that are up-regulated in response to DNA damage specifically in a LexA-dependent manner. In this way, 43 genes were classified as part of the LexA regulon, including 17 previously unknown ones, and the kinetics of their induction were determined. For example, *recA*, *recN*, *sulA*, and *dinD* are nearly fully induced within 5 min following UV irradiation, and their transcripts persist throughout the time course (60 min). In contrast, *uvrA* induction occurs within the first 5 min following UV irradiation, but then the levels decrease almost immediately. There are also several genes whose transcripts decreased in a LexA-dependent manner, suggesting a role for LexA in reducing the expression of certain genes. It should be noted that with this technique it is impossible to differentiate between a decrease in transcription or an increase in mRNA degradation. Notably, some genes that are not part of the LexA regulon exhibit a similar expression profile as the LexA-dependent genes after UV irradiation. Some of the genes with this behavior include genes involved in carbon metabolism, lipid synthesis, and the response to osmotic stress. Therefore, it seems that this response is part of a larger, concerted stress response network.

Other Bacterial LexA Regulatory Systems

The sequencing of a number of microbial genomes (96 bacterial and 16 species of archaebacteria) has shown that some bacteria lack homologues of LexA. However, in those species that are known to exhibit the SOS response, it functions analogously to that of *E. coli*. The general SOS response is characterized by a LexA homologue binding to a consensus DNA-binding site on the promoter regions of the genes it regulates. The major differences between species are the set of genes repressed by LexA and the consensus sequence of the binding site. While the role of LexA as a repressor of genes involved in the cellular response to DNA damage is widely conserved across bacteria exhibiting the SOS response, there are idiosyncrasies.

An interesting example is that of *Rhodobacter sphaeroides* in which LexA has an unusual role – acting as both a transcriptional repressor and an activator. It achieves this by apparently interacting differently with both the DNA and the RNA Polymerase depending on the LexA concentration. At high concentrations of LexA, transcription of a LexA-regulated promoter is repressed because RNA polymerase gets trapped at the promoter in such a fashion that it cannot reach the open complex conformation, and hence cannot initiate transcription. When LexA concentrations are lower, transcription from a LexA-regulated promoter (e.g., RecA promoter) is increased due to enhanced open complex formation. In both cases, LexA increases binding of RNA polymerase to the promoter region. This is fundamentally different than the mechanism of LexA repression in *E. coli*, in which LexA sterically blocks RNA polymerase from binding initially to the promoter.

Summary

The SOS system is a concerted response to DNA damage, encompassing ~1% of *E. coli*'s genes, and it is seemingly part of an even larger stress response network. The LexA protein, the repressor that binds as a dimer with different affinities to an inverted repeat (SOS box) on the promoters of the genes it regulates, negatively controls the expression of the SOS genes. The LexA protein switches from a noncleavable to a cleavable form upon binding to the groove of the RecA:ssDNA nucleoprotein, which is the sensing element of the SOS response, that accumulates after DNA damage. Cleavage inactivates LexA – so it can no longer function as the repressor – leading in turn to the expression of the LexA-regulated genes. The LexA protein is autoregulated such that the response to DNA damage might be easily modulated. The SOS system and LexA's function as a repressor, although there are idiosyncrasies, appear widely conserved among bacteria. While many insights have been gained in the understanding of the SOS response, there is still much to know about the molecular mechanisms underlying this sophisticated global response to DNA damage.

See Also the Following Articles

Cell Cycle: DNA Damage Checkpoints • DNA Damage: Alkylation • DNA Mismatch Repair and the DNA Damage Response • DNA Mismatch Repair: *E. coli* Vsr and Eukaryotic G–T Systems

Glossary

autoregulation The same gene product regulates the expression of its gene.

DNA microarrays A surface carrying an array of DNA oligonucleotides corresponding to genes of interest, which is probed with RNA isolated from cells under a given condition.

promoter Sequence located upstream of a gene that is recognized by RNA polymerase and is used to initiate transcription.

regulon Group of genes whose expression is synchronized by common regulator(s).

repressor Gene product that binds a site near the promoter of a gene that regulates by sterically interfering with the binding of the RNA polymerase to its promoter.

transcriptional fusions A fusion that places the expression of a reporter gene (e.g., *lacZ*) under the transcriptional control of another gene.

Further Reading

Brent, R., and Ptashne, M. (1981). Mechanism of action of the *lexA* gene product. *Proc. Natl. Acad. Sci. USA* **78**, 4204–4208.

Courcelle, J., Khodursky, A., Peter, B., Brown, P. O., and Hanawalt, P. C. (2001). Comparative gene expression profiles following UV exposure in wild-type and SOS-deficient *Escherichia coli*. *Genetics* **158**, 41–64.

David, J., Bittner, M., Chen, Y., Meltzer, P., and Trent, J. M. (1999). Expression profiling using cDNA microarrays. *Nat. Genet. Suppl.* **21**, 10–14.

Friedberg, E. C., Walker, G. C., and Seide, W. (1995). *DNA Repair and Mutagenesis*. The American Society for Microbiology, Washington, DC.

Kenyon, C. J., and Walker, G. C. (1980). DNA-damaging agents stimulate gene expression at specific loci in *Escherichia coli*. *Proc. Natl. Acad. Sci. USA* **77**, 2819–2823.

Koch, W. H., and Woodgate, R. (1998). The SOS response. In *DNA Damage and Repair* (J. A. Nickoloff and M. F. Hoekstra, eds.) Vol 1, pp. 107–134. Humana Press, Totowa, New Jersey.

Little, J. W., Mount, D. W., and Yanisch-Perron, C. R. (1981). Purified *lexA* protein is a repressor of the *recA* and *lexA* genes. *Proc. Natl. Acad. Sci. USA* **78**, 4199–4203.

Sutton, M. D., Smith, B. T., Godoy, V. G., and Walker, G. C. (2000). The SOS response: Recent insights into *umuDC*-dependent mutagenesis and DNA damage tolerance. *Annu. Rev. Genet.* **34**, 479–497.

Biography

Veronica G. Godoy obtained her Ph.D. from the Department of Molecular Biology and Microbiology at Tufts Medical School in Boston. During her graduate research she studied a bacterial pathogen, and became interested in how bacteria mutate in response to environmental stress. Upon graduation she investigated possible mechanisms of bacterial mutability under non-lethal conditions of selection with Dr. Maurice Fox at MIT. This led to her current interest in DNA damage tolerance in Dr. G. Walker's lab, where she is currently a senior scientist.

Penny J. Beuning received her B.A. from Macalester College (St. Paul, MN) and her Ph.D. in Chemistry from the University of Minnesota, Twin Cities. She studied enzyme-substrate recognition in aminoacyl-tRNA synthetases, as well as amino acid editing, during her graduate work. This led to her interest in how organisms maintain genetic fidelity. She is a postdoctoral researcher studying DNA repair and DNA damage tolerance in bacteria. She is also a representative on the

MIT Postdoctoral Scholars Advisory Council and is involved in Graduate Women in Science.

Graham C. Walker is an American Cancer Society Research Professor and an HHMI Professor in the Department of Biology at the Massachusetts Institute of Technology. Prior to joining MIT, he did his Hons. B.Sc. at Carleton University in Ottawa, Ontario, obtained his Ph.D. from the University of Illinois, Champaign-Urbana, Illinois, and did postdoctoral work at the University of California, Berkeley. He has worked on cellular responses to DNA damage and on mutagenesis and DNA repair. He has also studied the *Rhizobium*–legume symbiosis and its relationship to chronic pathogenesis. He has served as the Editor-in-Chief of *Journal of Bacteriology*. Dr. Walker has been deeply involved in undergraduate education throughout his career.

Ligand-Operated Membrane Channels: Calcium (Glutamate)

Elias K. Michaelis
University of Kansas, Kansas City, Kansas, USA

The mammalian central nervous system has a great capacity to adapt to many stimuli and perturbations of normal physiological function and this adaptability or plasticity is crucial in coding, storing, and retrieving information. Over the past decade, it has become clear that transient elevation of intracellular calcium (Ca^{2+}) in neurons represent the key signals used by nerve cells to alter their molecular structure and function and to produce long-lasting changes in cell function. These Ca^{2+}-activated molecular events are crucial not only for such phenomena as learning and memory but also for determining neuronal survival or damage. Key regulators of Ca^{2+} entry into neurons are the receptors for the excitatory neurotransmitter L-glutamic acid.

Calcium Signaling in Neurons

Adaptation of brain function to incoming stimuli or to altered behavioral states is a well-demonstrated phenomenon. Such adaptation is thought to involve long-lasting alterations in the sensitivity of select neuronal networks or select synapses of individual neurons. The phenomenon of long-lasting changes in synaptic activity in neurons is, in part, the result of altered gene transcription and protein synthesis and changes in the concentration of free intracellular calcium (Ca^{2+}) brought about either through influx into nerve cells or release from intracellular stores are considered to be the major signals for such adaptive changes in neurons. Under normal physiological conditions in unstimulated neurons, the concentration of free intracellular Ca^{2+} ($[Ca^{2+}]_i$) is maintained at $\sim$45–75 nM, i.e., a concentration that is $\sim$10 000-fold lower than that in the extracellular environment of neurons. Following stimulation of neurons, either through synaptic activation, primarily of glutamate receptors but also of other receptors, such as nicotinic acetylcholine receptors (AchRs), or direct electrical stimulation, the intracellular levels of free Ca^{2+} can change quite rapidly and substantially, as will be described next (Figure 1).

The low free $[Ca^{2+}]_i$ is maintained through buffering mechanisms that are dependent on the activity of both Ca^{2+}-transport systems and Ca^{2+}-binding proteins present in neurons. Both of these Ca-buffering processes are important in re-establishing low free $[Ca^{2+}]_i$ following perturbations of the concentrations after synaptic activation and membrane depolarization of neurons. Among the buffering mechanisms, the transport carriers either pump Ca^{2+} out of the intracellular environment, such as the plasma membrane ($Ca^{2+} + Mg^{2+}$)-ATPase (PMCA) and the sodium Na^+–Ca^{2+} exchange carriers (NCX), or sequester Ca^{2+} in intracellular compartments, such as the endoplasmic reticulum, through the activity of the sarcoplasmic/endoplasmic reticulum Ca-ATPase (SERCA), and the mitochondria, through the activity of the mitochondrial Ca^{2+} uniporter (Figure 1). Calcium-binding proteins (Ca^{2+} BP) that have been shown to buffer intracellular Ca^{2+} include parvalbumin and calbindin as the primary Ca^{2+}-buffering proteins in neurons, as well as many other Ca^{2+}-binding proteins, such as, calmodulin, calcyphosine, neurocalcin, hippocalcin, and visinin-like protein 3.

Electrical stimulation of neurons with a stimulus of sufficient magnitude to depolarize the cell membrane from the normal electrical potential of ~ -70 mV internal negative to a potential that is 10–20 mV or more, less negative internally, can trigger the initiation of a regenerative, self-propagating form of membrane depolarization that usually starts in the region where the axon process of a neuron emerges from the cell body and travels down to the fine terminal branching points of the axon (Figure 2). This self-propagating depolarization, known as an action potential, depends on the rapid opening of voltage-gated sodium channels (VGSCs).

Depolarization of the nerve terminal region of a neuronal axon by an action potential leads also to the opening of voltage-gated Ca^{2+} channels (VGCCs) in the axon terminal region. VGCCs allow for the rapid entry of Ca^{2+} from the extracellular environment, an event that is crucial for the first step in the transformation of the electrical event that has traveled down the axon to a chemical signaling event, that is, the release of chemical

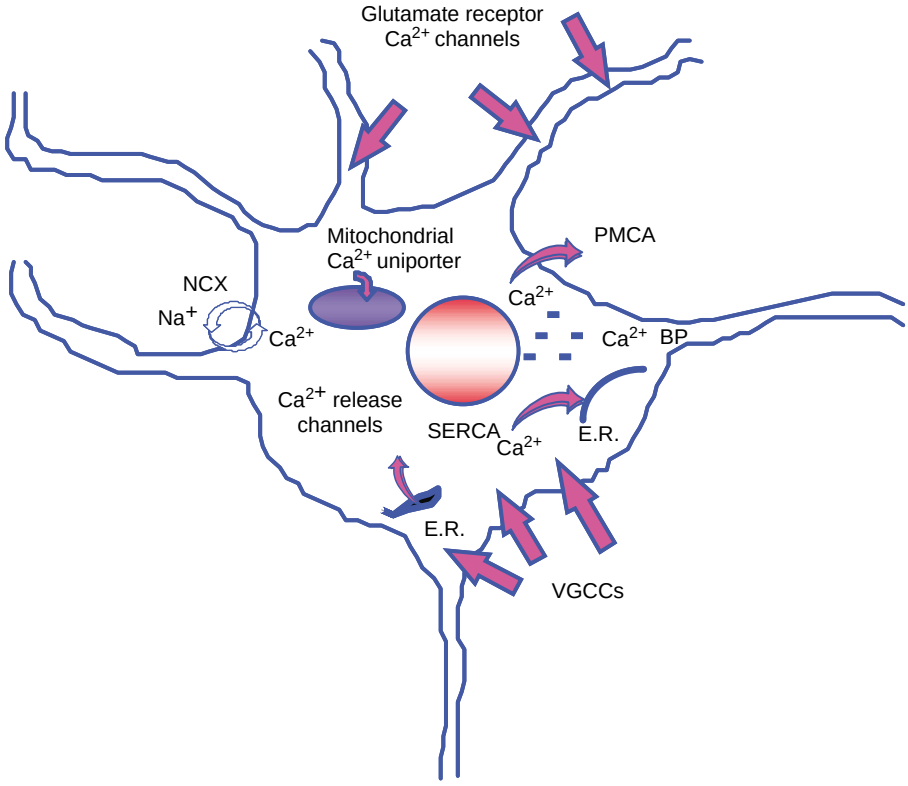

FIGURE 1 Pathways of Ca^{2+} entry, extrusion, and sequestration in neurons.

transmitters. The molecular events that lead to Ca^{2+}-induced exocytosis of transmitter molecules stored within synaptic vesicles at the nerve terminal are progressively being defined through biochemical, biophysical, and genetic studies but will not be discussed further here.

Action potentials initiated at the beginning of the axon as it exits the cell body spread in two directions,

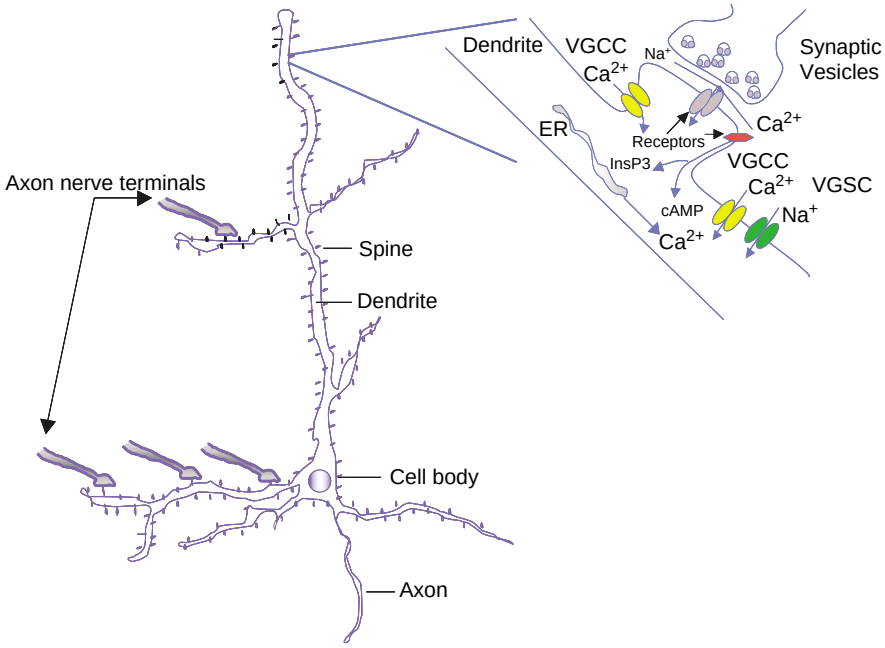

FIGURE 2 Diagrammatic representation of a large neuron that might be found in the neocortex or hippocampus of the brain. The structures of dendrites, dendritic spines, and axon terminals are highlighted.

toward the axon terminal as described above, as well as toward the cell body and the other processes emanating from the cell body of a neuron, the dendrites (Figure 2). Dendrite processes are considered to be the primary site for the reception of chemical information transmitted by means of neurotransmitters released from hundreds or thousands of axon terminals impinging upon the dendrites or the soma of a single neuron. The contacts that nerve terminals make with either dendrites or the soma of a neuron are, of course, the synapses across which chemical neurotransmission takes place. Most synapses on dendrites of brain neurons occur through close approximation of nerve terminals with specialized, small processes protruding from the main shaft of a dendrite (Figure 2). These knob-like protrusions are referred to as dendritic spines and represent a specialized compartment in a neuronal dendrite. The signals initiated by Ca^{2+} entry through transmitter receptor-ion channels and back-propagating action potentials in a spine differ from those initiated in the main body of a dendrite. Therefore, integration of signals that lead to long-lasting changes in neuronal responses to incoming stimuli and to changes in gene transcription and protein synthesis is determined by signals initiated in spines as well as those in dendrites.

The narrowness of the neck of spines that connects them to the respective dendrite is thought to delay diffusion and equilibration of intra-spine Ca^{2+} with that in the dendrites. Thus, the levels of free $[Ca^{2+}]_i$ within the head of a spine are determined not only by the amount of Ca^{2+} entering the spine through receptor-activated and voltage-gated ion channels but also through the kinetics of diffusion out of the spine and the Ca-buffering capacity within the spine. Action potentials initiated in axons and invading the cell body and dendrites produce "supralinear" increases in free $[Ca^{2+}]_i$ in dendrites when they are coincident with synaptic activation of neurotransmitter receptor-associated Ca^{2+} channels. Supralinear increases in $[Ca^{2+}]_i$ are defined as increases that exceed the sum of net increases in free $[Ca^{2+}]_i$ brought about by the simultaneous activation of both neurotransmitter receptor channels and VGCCs. Free $[Ca^{2+}]_i$ in spines following the activation of back-propagating action potentials has been estimated to reach levels as high as 2 μM. If back-propagating potentials are coupled to neurotransmitter activation of receptors that allow the influx of Ca^{2+} into neurons, such as glutamate receptors, then the levels are estimated to be more than tenfold higher, i.e., 26 μM.

The coincidence of glutamate receptor-mediated and action potential-induced Ca^{2+} signals plays a crucial role in the phenomenon known as synaptic plasticity, i.e., the long-term change in the magnitude of responses across a synapse following a series of activating stimuli delivered to a set of synapses in a neuron. Synaptic plasticity is fundamental to the processes of learning and memory and to the adaptive brain changes described above. Long-term increases in synaptic responses to a given stimulus are known as long-term potentiation (LTP), and long-term decreases in such responses are known as long-term depression (LTD). At the center of the molecular events that lead to synaptic plasticity are glutamate receptors, VGCCs, and intraneuronal Ca^{2+} signaling.

Glutamate Receptors in the Mammalian Central Nervous System: Structure and Function

Physiological and Pharmacological Properties of Glutamate Receptors

L-Glutamic acid is the most prevalent excitatory neurotransmitter in the vertebrate nervous system. Glutamate receptor activation is one of the stimuli for neuronal migration and synapse formation in the developing central nervous system (CNS), causes the elongation of neuritic processes and enhances the survival of some neurons. However, excessive stimulation of glutamate receptors by moderately high concentrations of L-glutamate and several of its analogues, such as *N*-methyl-D-aspartate (NMDA), leads to delayed neuronal damage through the activation of apoptosis. Stimulation of glutamate receptors by even higher concentrations of L-glutamate or NMDA leads to acute toxicity through necrosis. Both the phenomena of synaptic plasticity and neuronal damage are dependent on the entry of Ca^{2+} into neurons but they differ, of course, in the magnitude and duration of the changes in free $[Ca^{2+}]_i$.

Before proceeding with a discussion of the regulation of Ca^{2+} signaling in neurons by glutamate receptors, it is important to define the various types of glutamate receptors present in the mammalian CNS. The classification is based on pharmacological and physiological properties of neuronal glutamate receptors (Table I). On the basis of functional characteristics, two general categories of glutamate receptors have been identified, the ion channel-forming receptors, or ionotropic receptors, and the receptors linked to the activation of phospholipase C (PLC) or the inhibition of adenylyl cyclases (AC), known as the metabotropic receptors. Metabotropic receptors that activate PLC also stimulate phospolipase D. Ionotropic receptors fall into three categories, those that are activated by NMDA, those that respond to kainic acid (KA), and those that are

TABLE I

Classification of L-Glutamate Receptor Subtypes Found in the Mammalian Central Nervous System

Receptor classes	Ionotropic			Metabotropic
Receptor subtype	NMDA	AMPA	Kainate	Quisqualate, L-AP4
Selective agonists	NMDA	AMPA	Kainate, (2S, 4R)-4-methylgutamic acid	1S3RACPD, L-AP4 LCCG1, DCG IV, ACPT III
Functional characteristics	Activation of channels for Na^+, and K^+, and Ca^{2+}	Activation of channels for Na^+ and K^+	Activation of channels for Na^+ and K^+	Activation of PLC; Activation of PLD; Inhibition of AC
	Slow excitation	Fast excitation	Fast excitation	
Other agonists	Ibotenate, L-HCA, Quinolinate	Quisqualate, Kainate, Domoate, Willardine	Domoate, Acromelic acids A and B	Quisqualate, L-serine-O-phosphate, Ibotenate, CCG
Allosteric modulators	Glycine, D-serine, Spermine	Aniracetam, Benzothiazides, CX164 (AMPAkine)	Concanavalin A (Con A)	
Competitive antagonists	2-AP5, 2-AP7, CPP, CPP-ene, CGP39653, CGS19755, biphenyl	CNQX, NBQX, DNQX	GAMS, γ-D-glutamyl-glycine	Phenylglycine analogs (3HPG, 4CPG, 4C3HPG, MCPG)
Antagonists at modulator sites	5,7-diCl-Kyn, HA-966, CNQX, L-689560	2,3-Benzodiazepines (GYKI52466), SYM2206		
Ion channel inhibitors	PCP, MK-801, Ketamine	JST, Barbiturates		

Abbreviations used: AC, adenylyl cyclase; ACPD, 1-aminocyclopentane-1,3-dicarboxylate; Aniracetam, 1-(4-methoxybenzoyl)-2-pyrrolidinone, L-AP4, L-2-amino-4-phosphonobutanoic acid; 2-AP5, D-2-amino-5-phosphonopentanoic acid; 2-AP7, D-2-amino-7-phosphonoheptanoic acid; CCG, 2-carboxycyclopropylglycine; CGP39653, (±)-(E)-2-amino-7-amino-4-propyl-5-phosphonopentenoic acid; CGS19755, [[(±)-2-carboxy-piperidin-4-yl]methyl]-phosphonic acid; 4C3HPG, (*S*)-4-carboxy-3-hydroxy-phenylglycine; CNQX, 6-cyano-7-nitroquinoxaline-2,3-dione; 4CPG, (*S*)-4-carboxy-phenylglycine; CPP, [3-[(±)-carboxypiperazin-4-yl]prop-1-yl]-phosphonic acid; CPP-ene. [3-[(±)-2-carboxypeprazin-4-yl]-propen-1-yl]-phosphonic acid; CX614, 2H,3H,6aH-pyrrolidino[2″,1″_3′,2′]1,3-oxazino[6′,5′-5,4]benzo[*e*]1,4-dioxan-10-one; 5,7-di-Cl-Kyn, 5,7-dicholorokynurenic acid; DNQX, 6,7-dinitroquinoxaline-2,3-dione; GAMS, γ-D-glutamylamino-methylsulfonate; HA-966, 3-amino-1-hydroxy-2-pyrrolidone; 3HPG, (*S*)-3-hydroxy-phenylglycine; JST, Joro spider toxin; L-689,650, *trans*-2-carboxy-5,7-dichloro-4-phenylamino-carbonylamino-1,2,3,4-tetrahydroquinoline MCPG, (+)-α-methyl-4-carboxy-5,7-dichloro-4-phenylaminocarbonylamino-1,2,3,4-tetrahydroquinoline MCPG, (+)-α-methyl-4-carboxy-phenylglycine; MK-801, (+)-5-methyl-10,11-dihydro-5H-dibenzo[*a*,*d*]cyclohepten-5,10-imine; NBQX, 2,3-dihydroxy-6-nitro-7-sulphamoyl-benzo-(F)-quinoxaline; PLC, phospholipase C; SYM 2206, (±)-4-(4-aminophenyl)-1,2-dihydro-1-methyl1-2-propylcarbamoyl-6,7-methylenedioxyphthalazine.

activated by α-amino-3-hydroxy-5-methyl-4-isoxazole-propionic acid (AMPA) (Table I). Metabotropic glutamate receptors are subdivided into Group I, II, and III based on their sensitivity to various agonists and antagonists, as well as their effects on either PLC or adenylyl cyclases.

KA and AMPA receptors (KARs and AMPARs) are the primary receptors for rapid excitatory transmission in the CNS. The receptor-associated ion channels activated by AMPA or KA are primarily permeable to Na^+ and K^+. However, some AMPARs as well as some KARs form ion channels that are permeable to Ca^{2+}. AMPARs in brain neurons are activated by both AMPA and KA, but AMPA is the more potent agonist. AMPARs can be distinguished from KARs on the basis of the effects that selective allosteric modulators, the benzothiazides and AMPAkines, and selective non-competitive inhibitors, the 2,3-benzodiazepines, have on AMPARs but not on KARs (Table I). Some of the selective modulators of AMPARs, such as the AMPAkines, are currently being explored as agents that might enhance memory formation in diseases that produce decrements in memory, such as the dementia of Alzheimer's disease.

NMDA receptors (NMDARs) respond to glutamate more slowly than either KARs or AMPARs. The slow response of NMDARs is thought to be due to the fact that they are tonically inhibited by Mg^{2+}. Mg^{2+} inhibition of NMDARs is a voltage-dependent phenomenon and membrane depolarization relieves such blockade. Thus, the rapid activation of KARs and AMPARs by glutamate and the subsequent depolarization of the membrane diminishes the inhibition of NMDARs by Mg^{2+} and leads to the activation of these receptors by glutamate. In neuronal synapses on dendritic spines, both AMPA- and NMDA-sensitive

receptors are proximal to each other. Back-propagating action potentials in dendrites or action potentials generated within spines and dendrites also relieve the Mg^{2+}-induced inhibition of NMDAR channels.

The opening of NMDAR ion channels increases the permeability of the membrane to Na^+, K^+, and Ca^{2+}. A unique feature of NMDARs is the requirement for the presence of nanomolar to micromolar concentrations of a coagonist, glycine, in order to be fully activated (Table I). Because of the multiplicity of sites that activate or inhibit NMDAR ion channels, antagonists for NMDARs fall under four categories (Table I), antagonists that compete for the recognition sites of L-glutamate and NMDA (e.g., 2-AP5, 2-AP7), those that block the binding sites for the coagonist glycine (e.g. 5,7-diCl-kynurenic acid), those that inhibit the allosteric enhancement of agonist activation by the polyamines (e.g. ifenprodil) and those that inhibit the receptor-associated ion channel (e.g. dizocilpine or MK801).

Metabotropic glutamate receptors (mGluRs) are localized primarily in what is known as the perisynaptic region of dendritic spines, i.e., not within the synapse as AMPARs, KARs, or NMDARs do. These receptors are apparently not activated by the release of neurotransmitter glutamate following single-action potentials but rather following repeated, high-frequency stimulation of axons and their nerve endings. Of particular interest with regard to Ca^{2+} signaling in neurons is the fact that group I mGLuRs produce two types of neuronal depolarization, a rapid, transient depolarization related to the release of Ca^{2+} from intracellular stores, and a prolonged and larger depolarization resulting from activation of transient receptor potential (TRP) Ca^{2+} channels (TRPCs). The release of Ca^{2+} from intracellular stores is the result of inositol-1,4,5-triphosphate ($InsP_3$) formation and the activation of $InsP_3$ receptor-ion channels on endoplasmic reticulum membranes. This transient elevation in intracellular Ca^{2+} causes propagating increases in free $[Ca^{2+}]_i$ and elicits changes in the activity of CNS neurons that are dependent on protein synthesis, i.e., it has some of the characteristics of long-term changes associated with synaptic plasticity. In addition, these Ca^{2+} transients can produce supralinear increases in free $[Ca^{2+}]_i$ in dendrites and spines of CNS neurons if they occur at the same time as back-propagating action potentials.

Molecular Structure of Glutamate Receptors

The cloning of the cDNAs for glutamate receptors has revealed a great complexity in the structure of these receptors (Table II and Figures 3 and 4). The size of all glutamate receptor proteins represented by the cDNAs for GluR1, NMDAR1, mGluR1, and their homologues (95–163 kDa) is considerably larger than that for other neurotransmitter receptor proteins, both ion channel-forming receptors and G protein-coupled receptors (Table II and Figures 3 and 4). Based on the amino acid sequence of the proteins for the ionotropic receptors and the relative hydrophobicity of various domains in the proteins, it was predicted that each ionotropic receptor protein cloned had a large extracellular amino terminal region and three transmembrane domains. One of the hydrophobic domains, the second domain or M2, forms a loop at the opening of the ion channel but does not traverse the membrane bilayer. The carboxyl terminal of the ionotropic receptor proteins is on the intracellular domain (Figure 5). Structurally, the ion channel-forming region of KARs, AMPARs, and NMDARs exhibits high homology to voltage-gated K^+ channels, especially the M2 loop described above that forms a hairpin loop at the opening of the ion channel. Single amino acid substitutions in the hairpin loop at the opening of the ion channels of glutamate receptors affect dramatically the permeability of the channel to Ca^{2+}.

AMPA Receptor Genes and Protein Structure

With regard to the structure of native AMPARs, homomers of any of the proteins GluR1-4 form ion channels that are activated by both AMPA and kainate and exhibit the characteristics of neuronal AMPARs. GluR1-4 receptor proteins are expressed broadly throughout the CNS. Forms of AMPARs that are derived from alternatively spliced exonic sequences in the respective mRNAs are also expressed in the CNS (Figure 3). With regard to Ca^{2+} permeability of the ion channels associated with AMPARs, the key subunit is the GluR2 subunit. When this subunit is present in a receptor complex, then the AMPARs exhibit a linear relationship between voltage applied to the membrane and the current conducted through the receptor channels and have very low permeability to Ca^{2+}, i.e., they resemble most native AMPA receptors of CNS neurons. Homomeric complexes made of the GluR1, GluR3, or GluR4 proteins form channels that are permeable to Ca^{2+}. The restriction of Ca^{2+} permeability imparted to receptor complexes by the presence of the GluR2 subunit is dependent on a critical Arg586 (R586) in the M2 loop of this subunit. The corresponding residue in GluR1 is Gln582 (Q582) (Figure 5), and mutation of this Gln residue to Arg abolishes the Ca^{2+} permeability of channels formed by homomeric expression of the GluR1 protein. GluR3 and GluR4 also have Gln residues in the hairpin loop.

TABLE II

Characteristics of the Cloned Glutamate Receptors, Including some Putative Receptors, from Mammalian and Amphibian Brain

Subunits	Receptor type	Protein size (kDa)	Protein assembly	Functional properties
GluR1	AMPA (KA)	99.8	GluR1–4; most native receptors contain GluR 2	Glutamate, AMPA, KA-activated channels; low Ca^{2+} permeability
GluR2		96.4		
GluR3		98		
GluR4		101		
GluR5	KA	102.8	GluR5–7 with KA1, KA2	Glutamate and KA-activated channels; rapidly desensitizing
GluR6		93.9		
GluR7		100		
KA1		105		
KA2		109		
KBP-chick	KA binding	51.8	Single subunit	No channel function
KBP-frog		52.5		
δ1	Orphan receptor	110.4	Unknown	No channel function
δ2		113.2		
NMDAR1a	NMDA	103.5	NR-1 with	NMDA-activated channels;
NMDAR2A		163.3	NR-2 subunits	glycine a co-agonist high Ca^{2+}
NMDAR2B		162.9		permeability, MK-801 and
NMDAR2C		133.5		ketamine block; voltage-
NMDAR2D		140.6		dependent Mg^{2+} block
NMDAR3A		124.5	NR-1 with	Glycine-activated excitatory
NMDAR3B		109	NR-3 subunits	responses; NA^{+}, K^{+} channels; not permeable to Ca^{2+}; no Mg^{2+} blockade
GBP	NMDAR-like complex	57	Complex of GBP,	Reconstituted NMDA-activated
Gly/TCP-BP		52.7	Gly/TCP-BP, CPP-BP,	ion channels; glycine a co-agonist;
CPP-BP		78.3	and a 36 kD protein as purified from brain	MK-801 and ketamine block; low sensitivity to Mg^{2+}
mGluR1a	Metabotropic GluRs	133.2	Single protein receptor;	mGluR1, mGluR5: Activation
mGluR2		95.8	coupled to G proteins	of PLC and PLD; mGluR2,
mGluR3		99		mGluR3, mGluR4, mGluR6,
mGluR4a		101.8		mGlurR7, mGluR8: Inhibition
mGluR5a		128.3		of adenylyl cyclases
mGluR6		95.1		
mGluR7		102.2		
mGluR8		97.5		

The Arg residue in M2 of GluR2 is the result of RNA editing. The gene codon for the amino acid at this position is CAG for Gln, not CGG for Arg. The pre-messenger RNAs (pre-mRNA) are edited by an adenosine deaminase whose activity depends on the presence of the double stranded RNA (dsRNA) structure between exon 11 and intron 11 of the GluR2 pre-mRNA. The adenosine in the CAG codon is deaminated to inosine, thus forming the CIG codon for Arg. This dsRNA deaminase is expressed in brain and other tissues and edits with very high efficiency (~90%) and selectivity GluR2 pre-mRNA. In the disease amyotrophic lateral sclerosis, editing of GluR2 is significantly less complete and leads to the expression of AMPARs in spinal neurons that are highly permeable to Ca^{2+}. This increased permeability to Ca^{2+} may cause neuronal death during the lifespan.

KA Receptor Genes and Protein Structure

Homomers of GluR5 or GluR6 form channels that resemble KARs in brain neurons. On the other hand, GluR7, KA1, and KA2 fail to form channels when each protein is expressed by itself but the coexpression of GluR5–7 and KA1 and KA2 proteins in different

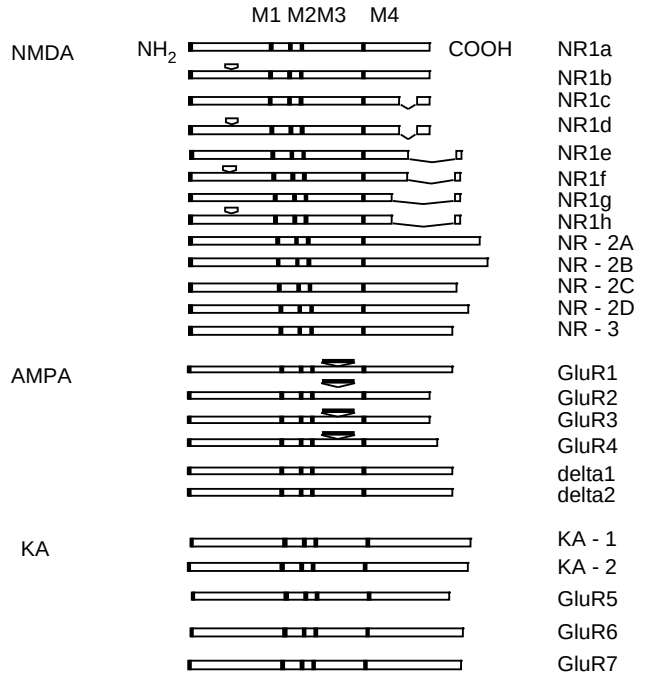

FIGURE 3 Linear representation of the structure of the cloned ionotropic glutamate receptor proteins. Shown are the NMDA, AMPA, and KA receptor proteins, as well as some of the orphan receptor proteins and the variant forms of NMDAR1 that result from alternative RNA splicing. Such alternative splicing leads to the addition or deletion of amino acid residues at either the amino (NH_2) or carboxyl (COOH) terminal of the protein. All proteins are shown to contain four hydrophobic domains designated M1–M4 (black boxes). For the proteins GluR1–4, the presence of the "flip" and "flop" splice variants in the region between M3 and M4 is indicated by boxes above the diagram of each receptor protein.

combinations of pairs of proteins leads to the formation of channels with unique properties that resemble, for the most part, neuronal KARs. In addition, the transfer of the likely ion channel domain of GluR7 into either GluR1 or GluR6 leads to the formation of receptor proteins that are fully functional as homomeric

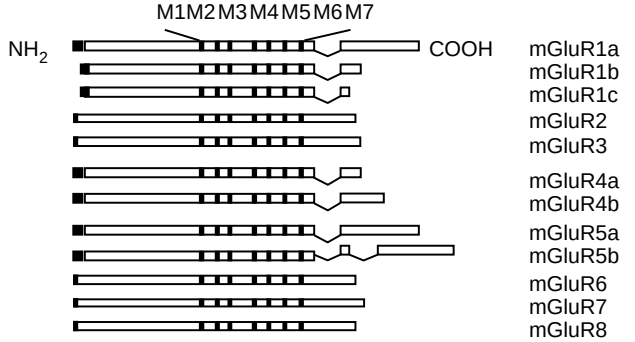

FIGURE 4 Linear representation of the structure of the cloned metabotropic glutamate receptor proteins mGluR1–8, including several splice variants. The seven hydrophobic domains considered as the likely transmembrane regions of the proteins are designated as M1 to M7 and are shown as black boxes.

receptor-ion channels. The same is not true, though, for two other genes, δ1 and δ2. The expressed proteins from these genes lack function either as homomeric or heteromeric receptor complexes and are therefore designated as orphan receptors. Based on these observations, GluR5–7 and KA1 and KA2 are considered to be the subunits of neuronal KARs. Different sets of neurons in the brain express these KAR receptor proteins and some of them, for example those in the CA3 field of the hippocampus, are some of the most vulnerable brain neurons to KA-induced neurotoxicity (neurotoxic KARs) as well as to seizure-induced neuronal damage.

The RNA for GluR5 and GluR6 is also edited leading to a Gln to Arg change in the M2 domain. However, the efficiency of editing (35% and 75%, respectively) is lower than that observed for GluR2. For the GluR6 receptor protein, the permeability of the channel for Ca^{2+} is controlled not only by the editing of the Gln residue in the M2 domain but also by the editing of two other residues in the first transmembrane domain, M1, of the protein.

Ionotropic glutamate receptors are macromolecular complexes composed of either four or five subunits. Identification of the ligand-binding sites of the GluR and KA subunits has been achieved by analysis of chimeras made of GluR3, an AMPAR protein, and GluR6, a KAR protein. The last 150 amino acids before the M1 domain and the amino acids right after M3 in the loop between M3 and M4 are the most critical ones in determining ligand-binding selectivity in the GluR3/GluR6 proteins. These two domains are referred to as the S1 and S2 domains and a bi-lobed structure is formed by the two regions of the protein (Figure 4). This structure of the ligand-binding domain has recently been confirmed by X-ray crystallographic analysis of the extracellular domains of the GluR1 protein.

NMDA Receptor Genes and Protein Structure

Expression of the NMDAR2 subunits by themselves does not lead to the formation of functional NMDARs, but the coexpression of the NMDAR2 subunits together with NMDAR1 leads to the formation of ion channels that have conductances very similar to those of NMDA receptors in neurons. The expression of NMDAR3 together with NMDAR1 and NMDAR2 subunits leads to receptor-ion channels with lower conductance levels than those of NMDAR1/NMDAR2 receptor ion channels and decreased Ca^{2+} permeability. In the NMDAR1 protein, the amino acid present in the corresponding position as Arg586 in GluR2 is Asn598. The channels formed by these subunits of NMDARs are highly permeable to Ca^{2+}. Finally, each of the combinations

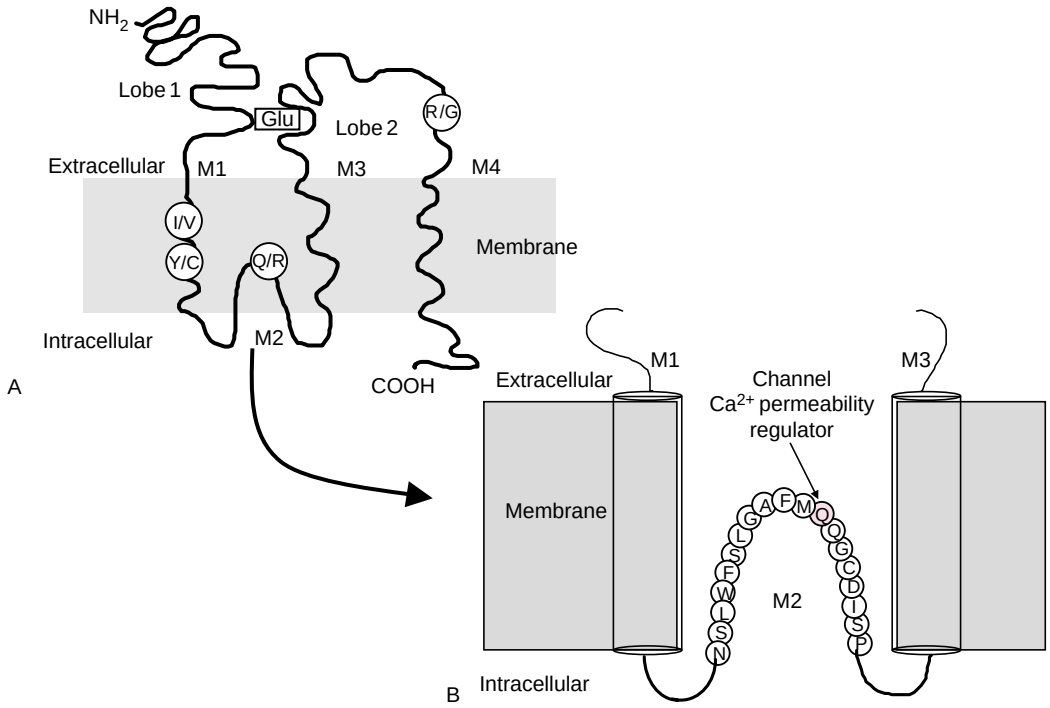

FIGURE 5 A representation of the distribution of different domains of the AMPA receptor (GluR proteins) in the neuronal membrane (A) and an enlarged view of the formation of a hairpin loop at the inner opening of the ion channel by the M2 domain. The formation of a glutamate-binding site by the two lobes of the protein projecting to the extracellular environment is also shown.

of NMDAR1 and one of the NMDAR2 subunits exhibit different degrees of sensitivity to the coagonist glycine, the competitive antagonist 2-AP5, and the channel inhibitor Mg^{2+}.

The glycine-binding site of NMDARs is in the NMDAR1 subunit and is formed by domains equivalent to the S1 and S2 domains of GluR1–4. This predicts a very similar molecular structure to the bi-lobed formation of the ligand binding sites in the GluR proteins. The primary glutamate/NMDA-binding site of NMDA receptors is localized on the corresponding extracellular domains of the NMDAR2 subunits. In addition to the six isoforms of NMDARs, there are eight splice variant forms of NMDAR1 (NMDAR1a-h, Figure 3). These splice variant forms exhibit clearly distinguishable sensitivities to agonists, antagonists, Zn^{2+}, and polyamines. Thus, a wide array of receptor complexes with differing affinities for ligands may be expressed in neurons through different combinations of the NMDAR1/R2 subunits, as well as the NMDAR1 splice variants. Differential expression and localization of the NMDAR1 subunits in various brain regions or even within a single neuron, e.g., cell body versus dendrites, could influence the responses of neurons to synaptically released L-glutamic acid.

Most synaptic NMDARs are formed by a combination of NMDAR1/R2A/R2B. Localization of the NMDAR proteins in synaptic regions is determined by the carboxyl-terminal region of the NMDAR1 and NMDAR2 subunits (NMDAR2A and 2B). Mice lacking one of the NMDAR2 subunits (NMDAR2A) have diminished NMDA receptor channel activity and a reduction in the process of induction of LTP in CNS neurons.

Neuronal toxicity produced by NMDA also depends on the specific combination of subunits that form the receptors in neurons. Cells of the human embryonic kidney cell line 293, for example, die when they are transiently transfected with the NMDAR1 and NMDAR2 subunits and such toxicity is greatest when NMDAR1 and NMDAR2A are coexpressed, less if NMDAR2B is coexpressed with NMDAR1, and it is not apparent when the NMDAR2C subunit is coexpressed with NMDAR1.

mGluR Genes and Proteins

Eight forms of mGLUR genes have been identified (Figure 4). Group I are the mGluR1 and mGluR5, group II are the mGluR2 and mGluR3, and group III are mGluR4 and mGluR6–8. The activation of PLC by mGluR1 and 5 appears to involve transduction of the signal through coupling of the receptor proteins with either the Gi–Go family of GTP-activated proteins (G proteins) or the Gq family. All of the group II and III mGluR proteins appear to be coupled to the Gi–Go

family of G proteins. All mGluR proteins have a large extracellular amino terminal domain, which contains a region that is homologous to bacterial periplasmic binding proteins. It is likely that the glutamate-binding sites on mGluRs are within this extracellular domain. Insertions or deletions due to alternative mRNA splicing are confined to the carboxyl-terminal region and do not disrupt the amino terminal domain of mGluRs.

Glutamate Receptors, Ca^{2+}-Signaling, and Synaptic Plasticity

Coincidence of action potentials in spines and dendrites with synaptic activation of glutamate receptors, primarily NMDARs, can enhance Ca^{2+} entry into neurons and produce long-lasting changes in synaptic activity. The timing of the two events, action potentials, and synaptic activation of receptor-induced Ca^{2+} influx, appears to be crucial. If receptors are activated after an action potential invades dendrites, it produces LTD. If it precedes or is coincident with the action potential it produces LTP. Activation of Ca^{2+} influx seems to be a key event in the expression of synaptic plasticity and neuronal adaptation but such increases in free $[Ca^{2+}]_i$ frequently work in a cooperative manner with other signaling events, such as the formation of cyclic AMP (cAMP) and the activation of cAMP-dependent protein kinase A (PKA). For example, the establishment of LTP in some neurons is strengthened by the concurrent activation of neurotransmitter receptors that activate adenylyl cyclases, such as, dopamine, muscarinic acetylcholine, and β-adrenergic receptors.

The entry of Ca^{2+} into neurons following glutamate receptor activation, especially activation of NMDA receptors, or the opening of VGCCs leads to altered gene transcription, mRNA splicing, mRNA translation, and protein synthesis. These effects are, to a substantial degree, dependent on the stimulation of several kinases, including Ca^{2+}/calmodulin (CaM)-dependent kinases (CaMK), protein kinase C (PKC), extracellular signal-regulated kinase or mitogen-activated kinase (ERK or MAPK), MAPK-ERK kinase (MEK), stress-activated protein kinase, aurora kinase and protein tyrosine kinases such as proline-rich tyrosine kinase and src kinase (Figure 6). However, not all types of Ca^{2+} influx into a cell lead to the same level of activation of gene transcription, even when the levels of $[Ca^{2+}]_i$ achieved are the same. There is clear compartmentalization of Ca^{2+} arriving at synaptic junctions as opposed to those received following generalized depolarization of a neuron. Ca^{2+} that enters following activation of either a receptor-ion channel or a VGCC apparently remains very close to the internal mouth of the channel

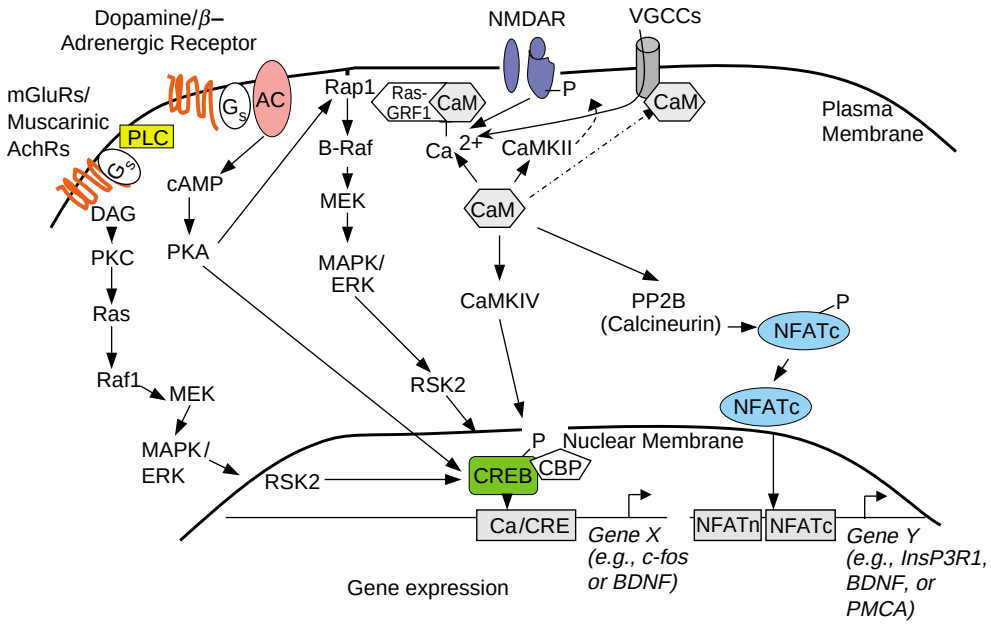

FIGURE 6 Regulation of transcription in neurons by Ca^{2+} following activation of NMDARs or VGCCs, and the interaction with pathways of gene transcription regulation following stimulation of G protein-coupled receptors. Shown is the Ca^{2+}-induced and cAMP or diacylglycerol (DAG)-induced stimulation of kinases that phosphorylate CREB and cause activation of gene transcription. Also shown is the activation by Ca^{2+} and CaM of the protein phosphatase 2B (PP2B) or calcineurin and the subsequent dephosphorylation of NFAT, the translocation of NFAT into the nucleus and the regulation of gene transcription in neurons. More details are presented in the text. CBP: CREB binding protein.

(~100 nM radius). Even if all other free Ca^{2+} in dendrites and cell bodies of neurons is chelated, the localized Ca^{2+} near ion channels still functions as an intracellular signal. Most likely readout of Ca^{2+} signaling is that of changes in the frequency of transient Ca^{2+} elevations and the most likely sensor of such frequency modulations is CaMKII. It is important to note that the mRNA for CaMKIIα is selectively transported to the dendritic region of neurons and that activation of NMDARs leads to polyadenylation of CaMKIIα mRNA and initiation of its translation through a process dependent on aurora kinase stimulation.

Stimulation of protein phosphorylation is pivotal in the activation of signal transduction cascades that lead to altered transcriptional regulation (Figure 6). A transcription factor that is sensitive to activation by several incoming stimuli and that regulates the expression of as many as 100 other genes, is the cAMP response element (CRE) binding protein (CREB). A key gene whose transcription is regulated by CREB is that for brain-derived nerve growth factor (BDNF), a gene that is known to influence the establishment of LTP. CREB activation is dependent on phosphorylation of crucial Ser residues. CaMKIV, when directly activated by Ca^{2+} and CaM in the nucleus, phosphorylates CREB. But Ca^{2+} entering neurons through NMDA and VGCCs also leads to CREB phosphorylation through the activation of MAPK/ERK and RSK2 kinases (Figure 6). Activation of the small GTPase Rap 1 follows binding of the Ca^{2+}-CaM complex to a guanine-nucleotide exchange factor, Ras guanine-nucleotide-releasing factor (Ras-GRF1, Figure 6). The same cascade of kinases can also be activated by cAMP and PKA and by diacylglycerol (DAG) and PKC, thus leading to the potential strengthening of signal transduction by Ca^{2+} following coincident activation of receptors coupled to adenylyl cyclases (AC) or those coupled to PLC (Figure 6).

Ca^{2+} entry following NMDAR or VGCC activation also leads to the stimulation of the Ca^{2+} plus calmodulin-activated phosphatase PP2B (calcineurin) and as a consequence of that, to the activation of the transcription factor nuclear factor of activate T cells (NFAT). The transcription of some 34 genes is thought to be either up- or down-regulated by NFAT in neurons. A prominent gene whose transcription is up-regulated is the $InsP_3$ receptor-ion channel (Figure 6). The activation of kinases following stimulation of glutamate receptors is thought to be a key step in the formation of LTP and memory formation, whereas the activation of calcineurin following weak stimulation of glutamate receptors is thought to cause primarily LTD. It is noteworthy also that phosphorylation of NMDARs by PKC, CaMKIIα, or protein tyrosine kinases leads to increases in the response to agonists whereas activation of calcineurin or protein tyrosine phosphatases diminishes their response. Given the importance of NMDARs in synaptic plasticity and neuronal adaptation, it is not surprising to find such complex orchestration of protein modifications by kinases and phosphatases and of the consequent alterations in the activity of the receptors.

Glutamate Receptors, Ca^{2+}, and Neurodegeneration

Excessive activation of glutamate receptors leads to neuronal degeneration in the mammalian brain, such as that occurring during ischemia, anoxia, hypoglycemia, epileptic seizures, and chronic neurodegenerative diseases, for example, Alzheimer's disease. The entry of Ca^{2+} into neurons increases the activity of the calmodulin-activated form of nitric oxide synthase (NOS). Activation of these two enzymes leads to the generation of intracellular nitric oxide radical ($NO^{\cdot}$) and superoxide anion ($O_2^{\cdot -}$), both of which appear to play a role in delayed neurotoxicity. The entry of Ca^{2+} through NMDA receptors also leads to the activation of proteases, such as Ca^{2+}-activated calpain, and enhanced proteolytic activity. Also, Ca^{2+} entry after activation of populations of non-synaptic NMDA receptors is the primary contributor to alterations in mitochondrial Ca^{2+} handling and the initiation of neuronal apoptosis.

See Also the Following Articles

Allosteric Regulation • Calcium Oscillations • Calcium Signaling: Calmodulin-Dependent Phosphatase • Calcium Signaling: Cell Cycle • Calcium Signaling: NO Synthase • Calcium, Biological Fitness of • Cyclic Nucleotide-Regulated Cation Channels • Glutamate Receptors, Ionotropic • Glutamate Receptors, Metabotropic • Ligand-Operated Membrane Channels: GABA • Neuronal Calcium Signal

Glossary

ionotropic glutamate receptors This general class of glutamate receptors represents ligand-gated, ion channel-forming receptor complexes in neuronal membranes. Channel activation occurs following the application of L-glutamate or one of its analogues. This class of receptors is further subdivided into three families of receptor-ion channels based on their sensitivity to select agonists.

long-term depression (LTD) Synaptic plasticity that occurs following low-frequency stimulation of synapses and which manifests itself as a decreased response to a subsequent single stimulus applied to the same synapses.

long-term potentiation (LTP) Synaptic plasticity that occurs following high frequency stimulation of synapses and which manifests itself as an increased response to a subsequent single stimulus applied to the same synapses.

metabotropic glutamate receptors A class of G protein-coupled glutamate receptors in neuronal membranes. These receptors may either activate phospholipase C or they may inhibit adenylyl cyclases, and they do not directly activate ion channels. This class of receptors is further subdivided into three groups, referred to as Group I–III, based on their sensitivity to select agonists and antagonists.

synaptic plasticity The adaptive changes in neurotransmission across synapses occurring as a result of repeated stimulation of a set of synapses. The changes in the electrical response of a set of synapses to a single stimulus applied after the delivery of a series of high frequency, repetitive stimuli can last for many hours or many days. These changes in synaptic efficacy are accompanied by alterations in gene transcription, protein synthesis and enzyme, ion channel, and receptor activity.

Further Reading

Cullen, P. J., and Lockyer, P. J. (2002). Integration of calcium and Ras signaling. *Nat. Rev.* **3**, 339–348.

Genazzani, A. A., Carafoli, E., and Guerini, D. (1999). Calcineurin controls inositol 1,4,5-trisphosphate type I receptor expression in neurons. *Proc. Nat. Acad. Sci. (USA)* **96**, 5797–5801.

Hollmann, M., and Heinemann, S. (1994). Cloned glutamate receptors. *Ann. Rev. Neurosci.* **17**, 31–108.

Johansen, T. N., Greenwood, J. R., Frydenvang, K., Madsen, U., and Krogsgaard-Larsen, P. (2003). Stereostructure-activity studies on agonists at the AMPA and kainite subtypes of ionotropic glutamate receptors. *Chirality* **15**, 167–179.

Kuner, T., Seeburg, P. H., and Guy, H. R. (2003). A common architecture for K+ channels and ionotropic glutamate receptors? *Trends Neurosci.* **26**, 27–32.

Madden, D. R. (2002). The inner workings of the AMPA receptors. *Curr. Opin. Drug Discov. Dev.* **5**, 741–748.

Michaelis, E. K. (1998). Molecular biology of glutamate receptors in the central nervous system and their role in excitotoxicity, oxidative stress, and aging. *Progr. Neurobiol.* **54**, 369–415.

Pin, J.-P., and Duvoisin, R. (1995). Neurotransmitter receptors I: The metabotropic glutamate receptors: Structure and functions. *Neuropharmacology* **34**, 1–26.

West, A. E., Griffith, E. C., and Greenberg, M. E. (2002). Regulation of transcription factors by neuronal activity. *Nat. Rev.* **3**, 921–931.

Yasuda, R., Sabatini, B. L., and Svoboda, K. (2003). Plasticity of calcium channels in dendritic spines. *Nat. Neurosci.* **6**, 948–955.

Biography

Elias K. Michaelis is University Distinguished Professor and Chair of Pharmacology and Toxicology and the Director of the Higuchi Biosciences Center, University of Kansas. His research program is focused on the neurochemistry, molecular neurobiology, and neuropharmacology of excitatory neurotransmission in the brain, the cell and molecular biology of alcoholism and of neuronal oxidative stress, and the molecular and cell biology of aging and neuro-degeneration.

Ligand-Operated Membrane Channels: GABA

F. Minier and Erwin Sigel
University of Bern, Bern, Switzerland

γ-Aminobutyric acid (GABA) is the major inhibitory neurotransmitter in the central nervous system. GABA is synthesized in GABAergic neurons by decarboxylation of glutamate and released in the synaptic cleft in response to an action potential. There it acts at two receptors: the ionotropic $GABA_A$ receptors (which form chloride-selective ion channels) and the metabotropic $GABA_B$ receptors (which couple to G-proteins). The $GABA_A$ receptor is an integral membrane protein and consists of five protein subunits that surround a central ion pore. Binding of the neurotransmitter GABA triggers a conformational change in the receptor leading to the opening of the pore. Clinically used benzodiazepines promote this opening. As a consequence, further electrical activity of the neuron will be suppressed. This article deals with the synthesis, transport, and degradation of GABA, the $GABA_A$ receptor and its binding site for benzodiazepine-type drugs.

Handling of the Neurotransmitter GABA: Biosynthesis, Transport, and Degradation

γ-Aminobutyric acid (GABA) is synthesized from glutamate in the cytosol of GABAergic neurons by two types of glutamic acid decarboxylase (GAD), namely, GAD65 and GAD67, according to their molecular weights (Figure 1). GAD65 is important for the local control of GABA synthesis at the synaptic sites, whereas GAD67, more widely distributed in the cell, is responsible for maintaining GABA baseline levels. Presynaptic membrane depolarization triggers release of GABA into the synaptic cleft. After the activation of $GABA_A$ and $GABA_B$ receptors, GABA is taken up in surrounding neuronal and glial cells by high-affinity GABA transporters (GATs). This re-uptake may contribute to the termination or modulation of GABA neuronal transmission. GABA transporters belong to a superfamily of Na^+/Cl^--dependent neurotransmitter transporters. Four GABA transporters have been cloned: GAT-1, GAT-2, GAT-3, and BGT-1. They are expected to be 12 transmembrane domain proteins with both intracellular N and C termini, and an extracellular loop between transmembrane domains 3 and 4. Each of these transporters displays specific features: GAT-1 seems to be highly expressed throughout the brain at a neuronal presynaptic localization, while GAT-2 is mainly extraparenchymal and found in the meninges. GAT-3 displays a similar macroscopic distribution as GAT-1. It is expressed both in presynaptic neurons and astrocytes. BGT-1 is weakly expressed throughout the brain in postsynaptic neuronal cells. The GABA degradation pathway, called GABA shunt, is one of the energy synthetic pathways in the brain. This pathway is composed of consecutive actions of three enzymes. The mitochondrial enzyme GABA-transaminase (GABA-T) catabolizes GABA to succinic semialdehyde (SSA). Then, SSA is converted either to succinic acid (a substrate for the Krebs cycle) by succinic semialdehyde dehydrogenase (SSADH) or to γ-hydroxybutyrate (GHB) by succinic semialdehyde reductase (SSAR). All these pathways are summarized in Figure 1.

Early $GABA_A$ Receptor Biochemistry

Indirect evidence suggested a close relation of the $GABA_A$ receptor and the benzodiazepine-binding site. The benzodiazepine drugs are widely used for their sedative, anxiolytic, muscle relaxant, and anticonvulsant action. Affinity chromatography directed at the benzodiazepine-binding site led to the isolation of a pure protein complex with binding properties expected for the $GABA_A$ receptor and for its chloride pore. This demonstrated the presence of benzodiazepine-binding sites within the $GABA_A$ receptor. The subunits of the complex had a molecular mass of 49–58 kDa and the entire complex of ~250 kDa.

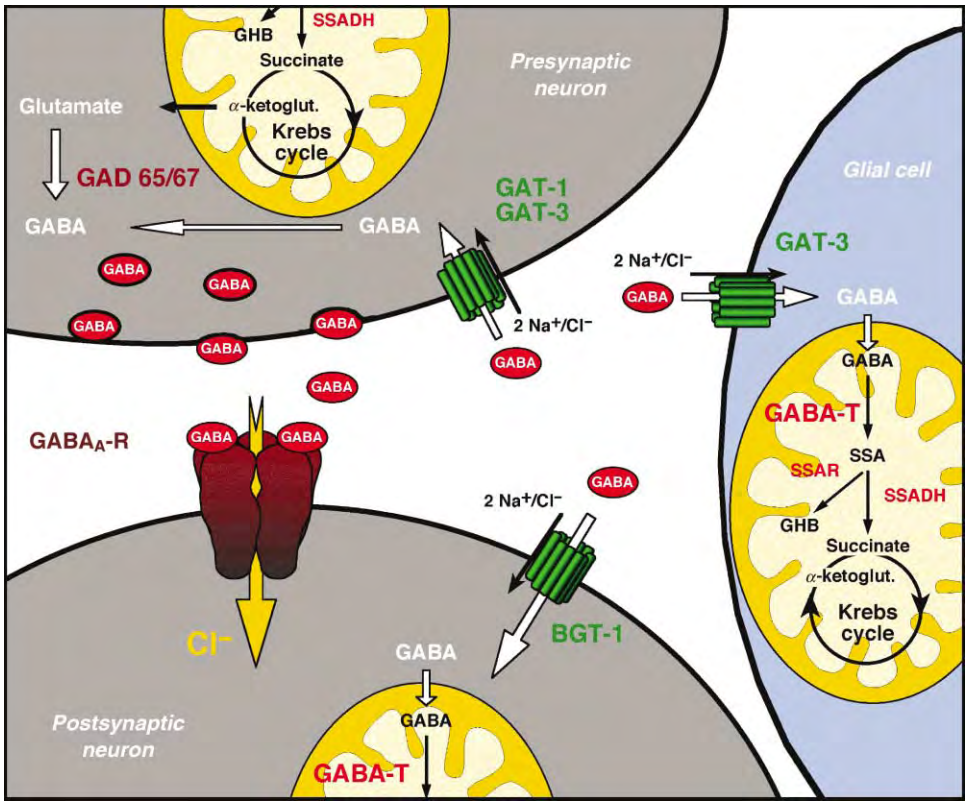

FIGURE 1 GABAergic synapse and main GABA metabolic pathways. GABA is synthesized from glutamate by the enzyme glutamate decarboxylase (GAD). Glutamate itself is synthesized from α-ketoglutarate (α-ketoglut.). The end of its action is determined by the GABA transporters of the GAT type or BGT-1 (for betaine/GABA transporter) and intracellular degradation by GABA transaminase (GABA-T) to succinic semialdehyde (SSA) and subsequently by succinic semialdehyde reductase (SSAR) to γ-hydroxybutyrate (GHB) or by succinic semialdehyde dehydrogenase (SSADH) to succinate, which is part of the Krebs cycle. Succinate in turn is converted to α-ketoglutarate.

Later it became clear that five subunits surround the central ion pore.

Molecular Biology of the $GABA_A$ Receptor

Two $GABA_A$ receptor subunits were initially cloned. Hydrophobicity analysis indicated the presence of four membrane spanning regions (Figure 2B). The second transmembrane segment of each of the five subunits contributes to the ion pore. Initial cloning was quickly followed by cloning of closely related subunits α_{1-6}, β_{1-3}, γ_{1-3}, δ, ε, θ, π. At the genomic level these subunits are organized on chromosomes in clusters, raising the possibility of a cluster specific regulation of expression (Table I). If the degree of amino acid sequence identity was $>80\%$ subunits were grouped under the same Greek letter, if it was lower a new Greek letter was used. In both cases subunits share predicted topology and there are many conservative substitutions of amino acid residues. With a sequence identity of $\sim 20\%$, the subunits are also homologous to subunits of the other members of the channel family including the nicotinic acetylcholine receptor, the glycine receptor, and the 5HT3 receptor. Thus, 16 subunits of the $GABA_A$ receptor are available and frequently many of them are coexpressed in the same cell. On the other hand, only five subunits can be accommodated in a single channel. It is today not known how many different $GABA_A$ receptors exist and what their subunit composition is, but this diversity of subunits indicates that there may exist a large variety of $GABA_A$ receptors. The major adult $GABA_A$ receptor isoform is likely to be composed of $2\alpha_1$, $2\beta_2$, and $1\gamma_2$ subunits. Attempts to demonstrate coassembly of different subunit isoforms into a common pentamer have included immunoprecipitation and subsequent analysis of the precipitate, a type of approach heavily relying on excellent quality antibodies.

It is a major challenge for basic research to bring order in this subunit chaos, to establish the subunit composition of $GABA_A$ receptors really existing *in vivo* and most importantly to find drugs that selectively modulate their function.

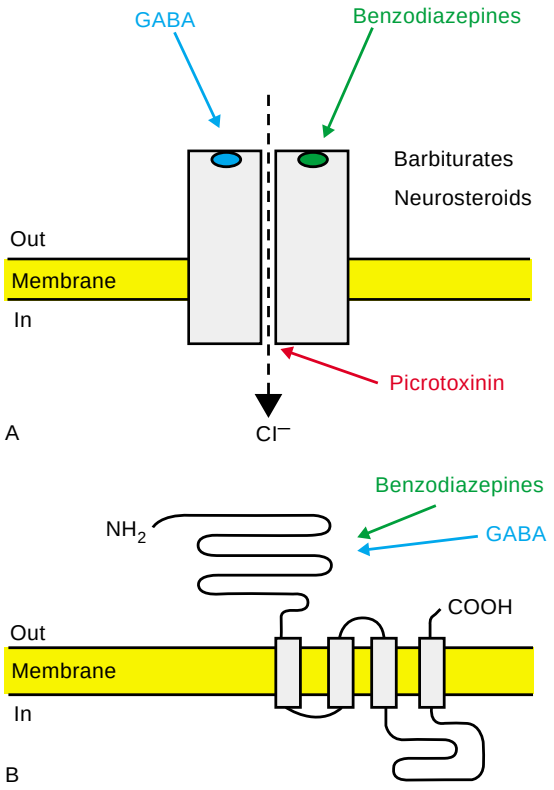

FIGURE 2 (A) The $GABA_A$ receptor is built of five membrane protein subunits that surround a central chloride selective channel. Opening of this ion channel is caused by a conformational change in the protein occurring as a consequence of the binding of the channel agonist GABA. Various drugs (benzodiazepines and neurosteroids) modify channel opening and picrotoxinin blocks the pore. (B) Topology of a subunit characterized by a large N-terminal extracellular domain carrying the drug-binding sites. The second transmembrane domain lines the ion channel. The large loop between transmembrane segments 3 and 4 carries sites for posttranslational modification (phosphorylation).

TABLE I

At Genomic Level $GABA_A$ Receptor Subunits are Organized in Gene Clusters Whose Chromosomal Location is Given for the Human Species

Subunits	Locus
δ	1p
α_2, α_4, β_1, γ_1	4p14–p12
α_1, α_6, β_2, γ_2, π	5q31–q35
α_5, β_3, γ_3	15q11–q13
α_3, ε, θ	Xq28

Physiological Function

In Situ Studies

GABA induces a conformational change in the receptor protein, such as to allow chloride ion flux. This ion flux may be measured as current flowing through the membrane by using electrophysiological techniques. Current amplitude depends on the concentration of GABA applied. While it is thought that the synaptic cleft is briefly flooded with GABA during activation of the synapse and as a consequence receptors on the postsynaptic membrane are maximally activated, a graded response may be obtained in artificial systems. As a consequence of chloride channel opening the membrane potential of the corresponding neuron will tend to move towards the chloride equilibrium potential which is about −75 mV in mature neurons. In case the $GABA_A$ receptor has a postsynaptic localization, this opening of chloride ion channels following neurotransmitter release from the presynaptic neuron will be brief (~50 ms) and transient. These receptors mediate fast synaptic inhibition. GABA will then partially diffuse out of the synaptic cleft and trigger opening of extrasynaptic receptors. In this case opening will be prolonged and a tonic inhibition will result.

Modulation

Benzodiazepines, neurosteroids, and barbiturates modulate the ion flux, while picrotoxinin inhibits it by blocking the pore and bicuculline, a plant alkaloid, acts at the GABA site as competitive inhibitor. Modulation by benzodiazepines will be briefly summarized here. On their own classical benzodiazepines (such as diazepam) do not induce opening of the ion pore. If they are co-applied with the agonist GABA, they lead to an increase in the current (Figure 3) through an allosteric increase of the affinity of the receptor for GABA. At the single channel level this stimulation is evident as an increase in channel open frequency, at least when GABA is applied at submaximal concentrations. These benzodiazepines are therefore called positive allosteric modulators. There exist competitive antagonists (such as Ro 15-1788) and negative allosteric modulators as illustrated here with the β-carbolines (Figure 3). The picture is complicated by the fact that there exists a continuum of partial positive and negative allosteric modulators.

In Vitro Studies

Heterologous expression has been used to identify subunit isoforms that can form together a functional pentamer. This has been possible in cases where a certain subunit isoform confers to the receptor distinct functional properties. Such studies established, for example, that the combination of α- and β-subunits produces GABA-gated currents, but coexpression of a γ-subunit is required for benzodiazepine sensitivity of the expressed receptors. It has also been possible to exclude many theoretically possible subunit combinations.

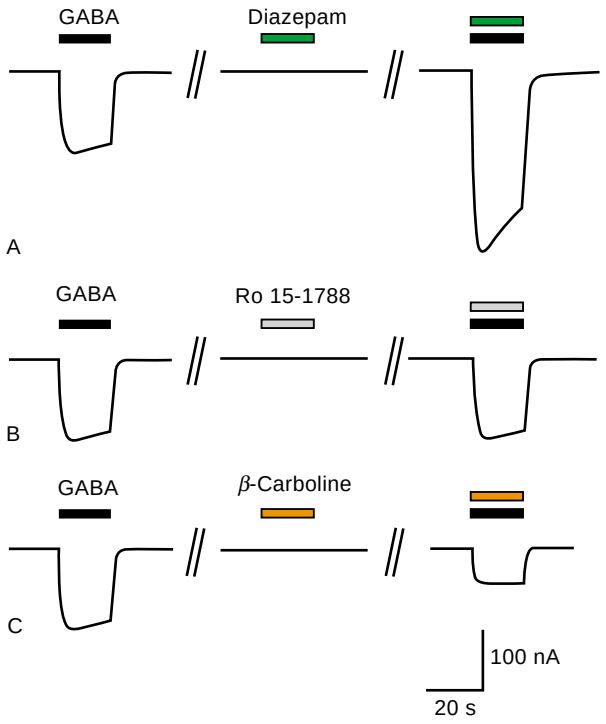

FIGURE 3 (A) Superfusion of a cell expressing $GABA_A$ receptors with GABA induces an ion current that is measured using the two-electrode voltage clamp technique. Superfusion of the same cell with the positive-allosteric modulator diazepam (prototype of benzodiazepines) does not elicit any current response while combined application of GABA and diazepam elicits a much bigger response than GABA alone. (B) Analogous experiments with the benzodiazepine antagonist Ro 15-1788, which binds with high affinity to the benzodiazepine binding site but fails to alter the current responses. (C) Analogous experiment with a negative allosteric modulator of the β-carboline class, leading to a decrease in the current response.

Transgenic Mice

Transgenic mice either lacking a subunit isoform or carrying a diazepam-insensitive subunit isoform have been used to assign function or drug effects to an individual subunit isoform. Such studies have shown that α_1 is mainly responsible for the sedative effects and α_2 for anxiolysis induced by diazepam and α_5 is involved in memory functions.

Binding Sites

Following techniques have contributed to the description of amino acid residues involved in the interaction with the channel agonist GABA, its competitive antagonists, for ligands of the benzodiazepine-binding site and for picrotoxinin: photoaffinity labeling, point mutation combined with either ligand-binding studies or functional characterization, cysteine point mutant water accessibility as determined by covalent modification by a cysteine reactive reagent and its protection by the corresponding ligand. The binding sites of other drugs such as neurosteroids and barbiturates are still characterized to a lesser extent. Amino acid residues located in the N-terminal extracellular part of both the β_2- and α_1-subunits are taking part in the formation of the agonist-binding site, while residues on the α_1- and γ_2-subunits are taking part in the formation of the benzodiazepine-binding site in the major isoform of the $GABA_A$ receptor. Both binding sites are thus located at subunit interfaces. Interestingly, both sites show a high degree of homology to each other, but only at the structural level and not at the functional level, as GABA can and benzodiazepines cannot open the channel. It should be noted that the benzodiazepine-binding site not only accepts benzodiazepines as allosteric modulators, but also some drugs with β-carboline, imidazopyridine, triazolopyridazine, and cyclopyrrolone structures.

Recently, an acetylcholine-binding protein homologous to the N-terminal extracellular portion of the nicotinic acetylcholine receptor has been crystallized. The $GABA_A$ receptor shares structural and to a small extent sequence homology with the crystallized protein. The crystallized protein in its native state is able to bind acetylcholine and a cavity putatively binding this ligand has been identified. As the agonist-binding sites of the ligand-gated ion channel family have been conserved and as the binding pocket for benzodiazepines is homologous to the agonist site, this cavity must then be homologous to the binding pocket for benzodiazepines. The binding site is located in a cleft between two subunits. This fits very well with the data obtained using classical methods, which indicated importance of the corresponding amino acid residues on α_1 and γ_2 which participate in the formation of the binding site. Thus, in $\alpha_1\beta_2\gamma_2$ $GABA_A$ receptors the binding pocket for benzodiazepines is located in a subunit cleft between γ_2- and α_1-subunits in a position homologous to the agonist-binding site for GABA that is located between α_1- and β_2-subunits (Figure 4).

Subtly Altered Receptor Subunits Cause Diseases

In two different cases human point mutations in the γ_2-subunit have been shown to occur in families with inherited forms of epilepsy. In both cases the mutation has been tightly linked to the disease and in both cases chloride ion flux is decreased, leading to a reduced state of neuronal inhibition. It can be anticipated for the future that many other diseases will be linked to isoforms of this important receptor. The $GABA_A$

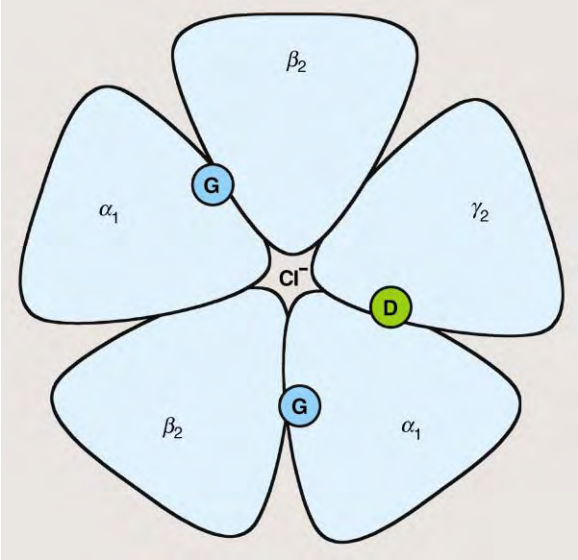

FIGURE 4 Subunit arrangement of the major isoform of the $GABA_A$ receptor showing the arrangement of subunits around the central ion channel as seen from the synaptic cleft. The benzodiazepine-binding site (D) is located at the $\gamma_2\alpha_1$-subunit interface in a homologous position to the two GABA (G) binding sites located at $\beta_2\alpha_1$-subunit interfaces.

receptor has especially been implicated in pathological anxiety, insomnia, and epilepsy.

Architecture

The structure of the acetylcholine-binding protein has given an idea of how the extracellular domain of the $GABA_A$ receptor could look like. The availability of a crystal structure of a protein homologous to the binding domain has also allowed establishment of the steric orientation of the subunits. From the study of covalently linked subunits, it has been concluded that the arrangement of subunits of the major $GABA_A$ receptor isoform is $\beta\alpha\gamma\beta\alpha$. However, this still allows for a clockwise or counterclockwise arrangement. Figure 4 shows the correct arrangement as viewed from the synaptic cleft taking in account the information provided by the crystallization study.

See Also the Following Articles

$GABA_B$ Receptor • Neurotransmitter Transporters • Nicotinic Acetylcholine Receptors

Glossary

chloride equilibrium potential Membrane potential at which opening of chloride ion selective channel mediates no net ion flux due to the concentration gradient of the corresponding ion.

conservative substitution Replacement of an amino acid residue by a residue with similar chemical properties.

heterologous expression Introduction of genetic information in the form of cDNA or cRNA is introduced into a foreign cell where the encoded protein is synthesized.

hydrophobicity analysis Scan of an amino acid residue sequence predicted by the coding cDNA is scanned for the average hydrophobicity of succeeding amino acid residues. A longer hydrophobic stretch is indicative of a transmembrane sequence in the protein.

voltage clamp Imposition of a desired membrane potential on a cell using electrophysiological techniques.

Further Reading

Barnard, E. A., Skolnick, P., Olsen, R. W., Mohler, H., Sieghart, W., Biggio, G., Braestrup, C., Bateson, A. N., and Langer, S. Z. (1998). International union of pharmacology: XV. Subtypes of gamma-aminobutyric acid A receptors: Classification on the basis of subunit structure and receptor function. *Pharmacol. Rev.* **50**, 291–313.

Borden, L. A. (1996). GABA transporter heterogeneity: Pharmacology and cellular localization. *Neurochem. Int.* **29**, 335–356.

Macdonald, R. L., and Olsen, R. W. (1994). $GABA_A$ receptor channels. *Annu. Rev. Neurosci.* **17**, 569–602.

Moss, S. J., and Smart, T. G. (2001). Constructing inhibitory synapses. *Nat. Rev. Neurosci.* **2**, 240–250.

Rabow, L. E., Russek, S. J., and Farb, D. H. (1995). From ion currents to genomic analysis, recent advances in $GABA_A$ receptor research. *Synapse* **21**, 189–274.

Rudolph, U., Crestani, F., and Möhler, H. (2001). GABA(A) receptor subtypes: Dissecting their pharmacological functions. *Trends Pharmacol. Sci.* **22**, 188–194.

Sieghart, W., Fuchs, K., Tretter, V., Ebert, V., Jechlinger, M., Hoger, H., and Adamiker, D. (1999). Structure and subunit composition of GABA(A) receptors. *Neurochem. Int.* **34**, 379–385.

Sigel, E., and Buhr, A. (1997). The benzodiazepine binding site of $GABA_A$ receptors. *Trends Pharmacol. Sci.* **18**, 425–429.

Biography

Erwin Sigel is an Associate Professor at the Department of Pharmacology at the University of Bern, Switzerland. His principal research interests are the $GABA_A$ receptors. He holds a Ph.D. from the Swiss Federal Institute of Technology (ETH), Zürich and received his first postdoctoral training at the Imperial College of Science and Technology, London. He has biochemically isolated the $GABA_A$/benzodiazepine receptor and later studied its binding sites.

Frédéric Minier obtained his Ph.D. in Neurosciences from the Pierre & Marie Curie University (Paris VI). His main research interest focuses on epilepsies and structural and functional studies of $GABA_A$ receptors. He is currently a postdoctoral fellow in the laboratory of Dr. Sigel.

Light-Harvesting Complex (LHC) I and II: Pigments and Proteins

Stefan Jansson
University of Umeå, Umeå, Sweden

Light-harvesting systems are present in the photosynthetic apparatus of all photosynthetic organisms. These systems are not necessary for the photosynthetic reaction but they increase the capacity for harvesting light and, in addition, have important regulatory functions. Light-harvesting systems typically have a very high pigment/protein ratio and are thus a cost-efficient way of maximizing light-harvesting capacity. The protein components serve as backbones that organize the light-harvesting pigments in a way that ensures that the absorbed light energy is efficiently transferred from the pigment first excited into the photosynthetic reaction center, where charge separation takes place.

Heterogeneity of Light-Harvesting Systems

Different taxa of photosynthetic organisms have organized light-harvesting systems in different ways, i.e., have rather different light-harvesting proteins and pigments. In fact, phylogenetic grouping of photosynthetic organisms is often based on their light-harvesting pigments. Green sulfur bacteria get their color from bacteriochlorophyll *c*, *d*, or *e* in the chlorosome complex, red algae from phycoerythrin, and cyanobacteria from phycocyanin in their phycobilisomes. Green algae and higher plants have chlorophyll (chl) *a* and *b* in their LHC I and LHC II. The antenna proteins from these phylogenetic groups complexes share no sequence homology and light-harvesting systems are therefore likely to have evolved several times in contrast to photosynthetic reaction centers that seem to have only evolved once. The LHC systems of all higher plants (angiosperms, gymnosperms) as well as ferns, mosses, and green algae are, however, homologous structures and have a lot in common and these antenna systems will be described using examples from angiosperms, whose antennas are best studied.

The Higher Plant Light-Harvesting Antenna

The higher plant LHC proteins bind, via noncovalent bonds, the antenna pigment chl *a*, chl *b*, and a set of xanthophylls (carotenoids). The LHC proteins of most plants bind the same set of xanthophylls, lutein, violaxanthin (that can get photoconverted), and neoxanthin, although some plant species may contain unusual light-harvesting carotenoids. Since the excited state of chl *b* has a higher energy as compared to that of chl *a*, the preferred energy transfer path is from chl *b* to chl *a*. This energy transfer is supposed to take place through the Förster mechanisms, i.e., excitation energy can jump between electrons in neighboring pigment molecules by a dipole–dipole mechanism. The chl molecules bound to the LHC proteins are, however, in different chemical environments and have thus different excitation energies, so some chl *a* molecules have slightly lower energy than the others. The differences in energy levels in general are typically small, so the energy transfer direction is not unidirectional and many jumps between antenna pigments could occur before it ends up in the reaction centers that have the lowest energy levels. Other light-harvesting systems are, however, organized slightly differently. In phycobilisomes of cyanobacteria and red algae, peripheral pigments have considerably higher energy levels than those closer to the reaction center so energy transfer there is unidirectional.

The Protein Components

The Lhca and Lhcb Proteins

There are ten major LHC proteins in angiosperms, whose genes are designated Lhca1–4 and Lhcb1–6. The Lhca genes code for LHC proteins associated with photosystem I, whereas the Lhcb3–6 proteins associate with PS II. Lhcb1 and Lhcb2 serve as antenna for both photosystems. Although all these proteins share a common secondary structure with three

membrane-spanning regions, embedded in the thylakoid membrane of the chloroplasts, their tertiary structure differ. Lhcb1, Lhcb2 that typically are much more abundant than the others, form together with Lhcb3 trimeric complexes, the Lhcb4–6 (commonly named CP29, CP26, and CP24) proteins are monomeric, and the Lhca proteins seem to form dimers. This organization is not static, for example, Lhcb1 and Lhcb2 can monomerize and Lhcb5 can form trimers. The true molecular weight of each protein varies only slightly between different plants, although the apparent mobilities change considerably both with plant species and gel systems used, but they all fall within the range of 20–30 kDa. Since several of the proteins typically comigrate, identification solely based on molecular weight is often not possible.

Structure of the LHC Complexes

In the monomeric structure, two homologous membrane-spanning regions form the core of the complex. Closely associated with these are two carotenoid molecules that in the case of LHC II are lutein. A third membrane-spanning region is located more peripheral in the complex, and a short C-terminal helix, not spanning the membrane, is located on the lumenal side of the complex. Fourteen chlorophyll molecules (eight chl *a* and six chl *b*) are bound to each monomer, with the head groups in the interior of the complex and the phytol tails protruding toward the surrounding membrane.

Organization of LHC II

The organization of the LHC proteins around PS II in the so-called "PS II supercomplex" is shown in Figure 1. The monomeric CP29 and CP26 proteins associate most closely with the core complex, and CP24 sits next to CP29. LHC II trimers (consisting of trimers of Lhcb1, Lhcb2, and Lhcb3 in different combinations) attach to the monomeric proteins, which thus form a bridge between the trimeric proteins and the core. In the "supercomplex," only three trimers could attach to each PS II center. In low light conditions, there are more trimers functionally attached to each PS II, but the positions of these are not yet known. A larger complex of seven trimers has been observed, but it is not known to what extent such complexes exist *in vivo* and to what they are associated.

Organization of LHC I

The subunit position in LHC I is not fully understood, but the proteins seem to bind to only one side of the PS I complex. Lhca1 and Lhca4 form a heterodimer, named LHCI-730 after its characteristic low-temperature fluorescence emission peak, and Lhca2 and Lhca3 may perhaps also form heterodimers. The latter two proteins are also based on the fluorescence emission of isolated complexes, named LHCI-680, although it is likely that they, in the purified forms, have lost chlorophylls emitting at long wavelengths that *in vivo* associate with the complexes, so the name is actually misleading. The long-wavelength emitting chlorophylls make up a small portion of the total pool of LHC I pigments. These are kept in a chemical environment that results in an absorption shifted to longer (red) wavelengths and their role seems to be to allow use of wavelengths just outside of the visible spectrum to excite PS I, despite the fact that they have lower energy than that of the PS I reaction center. In addition to the LHC I subunits, a fraction of the LHC II trimers associate with PS I. The attachment site for these seems to be opposite to that of LHC I, so excitation energy presumably transfers directly from the trimers to the PS I core, not via LHC I.

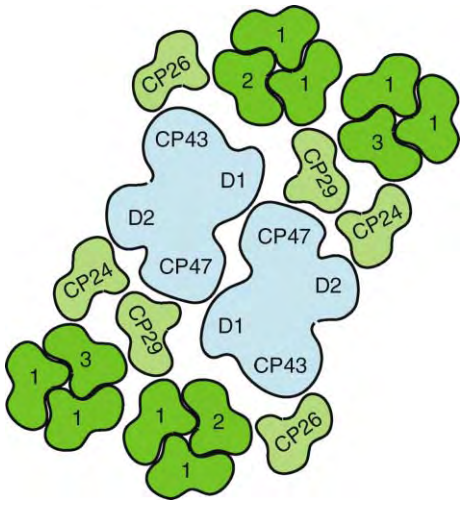

FIGURE 1 Schematic representation of the photosystem II dimer including the peripheral antenna. D1 and D2 are reaction center polypeptides, CP43 and CP47 core antenna proteins, CP24, CP26, and CP29 are monomeric LHC proteins, and 1, 2, and 3 denote tentative positions of Lhcb1, Lhcb2, and Lhcb3 proteins, respectively, in the peripheral LHC II trimers.

The Pigment Components

The pigment/protein stoichiometry of the LHC proteins has been surprisingly hard to determine and is still somewhat uncertain. The LHC II trimer is the most "pigment dense" complex and may bind in total 24 chl *a*, 18 chl *b*, 6 lutein, 3 neoxanthin, and 3 violaxanthin molecule. CP29 may bind 7 chl *a*, 2 chl b, and one each of the three carotenoids, and CP26 one additional chl *b*. The individual Lhca proteins, on the other hand, may associate with about 14 chlorophylls, one or two luteins, a small amount of violaxanthin and perhaps also trace amounts of β-carotene, a nonxanthophyll carotenoid. The functions of the carotenoids are more complex than

those of the chlorophylls. Carotenoids are indeed antenna pigments, also harvesting lights at wavelengths (~500 nm) where the chlorophylls have a low absorptivity, enabling plants to efficiently utilize daylight, although the chlorophylls mainly absorb in the red and blue regions of the spectrum. In addition, they have an equally important function in photoprotection against excess light. Photoprotective processes are necessary in the antenna systems if the excitation energy is not able to quickly enter into the reaction centers but stays in the antenna system for prolonged times. This could, for example, happen if the energy-consuming reactions downstream of the photosynthetic light reaction are not able to utilize the energy in the same speed as it is generated, for example, if the system is at low temperature when enzymatic reactions are slow. This creates a block in electron flow away from the reaction centers that will not be able to accept another energy package from the antenna. Excited chlorophyll molecules can, via a triplet state, under such circumstances produce singlet oxygen molecules that are highly reactive and thus dangerous for the system.

Mechanisms of Photoprotection

The molecular details behind the roles of carotenoids in photoprotection are not fully understood, but it involves both direct effects (quenching of reactive oxygen species) and an indirect effect, namely, an increase in energy dissipation in the antenna resulting in loss of excitation energy. This process, named "feedback de-excitation" or "qE type of nonphotochemical quenching," is mediated by PsbS, a protein related to the LHC proteins. Feedback de-excitation is triggered (within seconds) when the lumenal pH drops below a certain point, as a result of photosynthetic proton pumping over the thylakoid exceeding the backflow through the ATP synthase complex. The PsbS protein is then protonated but the low pH does also bring about a change in the photosynthetic xanthophylls (the xanthophyll cycle), violaxanthin is converted to zeaxanthin via antheraxanthin by the enzyme violaxanthin de-epoxidase, activated by the low lumenal pH. Zeaxanthin accumulates in the antenna and is also found free in the thylakoid membrane. Zeaxanthin could protect directly against oxygen radicals, but when zeaxanthin is bound to protonated PsbS, a conformational change takes place resulting in the creation of a highly quenching species (perhaps a chl *a* dimer) that relieves the excitation pressure from the system into heat, and thus contributes to photoprotection. Only a small fraction of the zeaxanthin formed is, however, associated with PsbS; most of the other LHC proteins can also have zeaxanthin bound to them, but whether this also contributes to photoprotection is not clear. Zeaxanthin is backconverted to violaxanthin when the light level drops.

Other Regulatory Roles

LHC II is also involved in another regulatory process, referred to as state transitions based upon the different "states" of chl fluorescence that can be obtained by treating the plant with light of different quality. If the plant is exposed to light preferentially absorbed by PS I (wavelengths >680 nm) or "normal" light, the fraction of LHC II trimers functionally associated with the photosystems can change in order to create an even excitation pressure of the photosystems. Overcapacity of PS II leads to over-reduction of the interphotosystem electron carriers that, subsequently, leads to the induction of an LHC II kinase. Phosphorylation of LHC II results in a reduction of the PS II antenna size, releasing the system from the imbalance. There is a connection between light quality and quantity, LHC II phosphorylation, LHC II migration between the different thylakoid regions and the amount of *grana* stacking, but the details are not yet fully understood. In any case, the reversible phosphorylation takes place on a Thr or Ser residue close to the N terminus of the protein, which protrudes into the stroma. The phosphorylation leads presumably to a conformational change that, in turn, changes the properties of the complex.

The amount of LHC proteins varies considerably in different light regimes. Higher light results in decreased amounts of LHC and, as a consequence, since chl *b* is confined to the LHC proteins, an increased chl *a*/*b* ratio of the plant. Hence, this ratio is an indicator of the amount of antenna protein and, thus, antenna size of the plant. This is an acclimation to the conditions when light harvesting is not limiting for photosynthesis. However, the different LHC proteins do not decrease simultaneously: the quantity of Lhcb1 and Lhcb2 (making up the bulk of the trimers) is most variable; but at full sunlight, Lhcb1 and Lhcb2 quantities are low, and the other LHC proteins also decrease in abundance.

See Also the Following Articles

Chlorophylls and Carotenoids • Photosynthesis • Photosystem I, Structure and Function • Photosystem II Light Harvesting System: Dynamic Behavior • Photosystem II: Assembly and Turnover of the D1 Protein • Photosystem II: Protein Components • Photosystem II: Water Oxidation, Overview

Glossary

LHC I The light-harvesting system containing proteins and pigments, associated with PS I.

LHC II The light-harvesting system containing proteins and pigments, associated with PS II.

xanthophyll cycle The light-dependent conversions of the three xanthophylls – violaxanthin, antheraxanthin, and zeaxanthin. It plays a significant role in photoprotection.

Further Reading

Bassi, R., Giuffra, E., Croce, R., Dainese, P., and Bergantino, E. (1996). Biochemistry and molecular biology of pigment binding proteins. In *Light as an Energy Source and Information Carrier in Plant Physiology* (R. C. Jennings, G. Zucchelli, F. Ghetti and G. Colombetti, eds.) pp. 41–63. Plenum Press, New York.

Horton, P., Ruban, A. V., and Walters, R. G. (1996). Regulation of light harvesting in green plants. *Annu. Rev. Plant Physiol. Plant Molecul. Biol.* **47**, 655–684.

Jansson, S. (1994). The light-harvesting chlorophyll *a/b* binding-proteins. *Biochim. Biophys. Acta – Bioenergetics* **1184**, 1–19.

Jansson, S. (1999). A guide to the Lhc genes and their relatives in Arabidopsis. *Trends Plant Sci.* **4**, 236–240.

Niyogi, K. K. (1999). Photoprotection revisited: Genetic and molecular approaches. *Annu. Rev. Plant Physiol. Plant Molecul. Biol.* **50**, 333–359.

Young, A. J., and Britton, G. (1993). *Carotenoids in Photosynthesis*. Chapman and Hall, London.

Biography

Stefan Jansson, a Professor of Plant Cell and Molecular Biology at Umeå University in Sweden, has studied the light-harvesting antenna of higher plants using a variety of methods. He has used gene technology to create plants lacking the different LHC components, and the analysis of these has given data on the functions of the individual polypeptides.

Lipases

Howard L. Brockman
University of Minnesota, Austin, Minnesota, USA

Lipases are water-soluble, ester hydrolases that are traditionally defined by their marked preference for apolar, water-insoluble ester substrates. This group of enzymes also includes species referred to as cholesterol esterases. Lipases and cholesterol esterases are distinguished from phospholipases that catalyze the hydrolysis of acyl ester bonds of highly amphipathic phospholipids having an *sn*-glycero-3-phospho-X moiety and from carboxylesterases that hydrolyze polar, water-soluble esters. These distinctions are relative, however, because some lipases exhibit activity toward phospholipids or soluble esters. Typical natural lipase substrates include, in order of amphipathicity, long aliphatic chain acyl esters of cholesterol (cholesteryl esters), triacyl esters of glycerol (triacylglycerols), acyl esters of long chain alcohols (wax esters), diacyl esters of glycerol (diacylglycerols) and monoacyl esters of glycerol. Because lipase substrates tend to be oily and only weakly amphipathic, they reside primarily in a bulk oil phase in preference to the aqueous phase or to the interface, i.e., monomolecular surface phase that separates the bulk oil and aqueous phases. It follows, because lipases are water-soluble enzymes, that the site of lipolysis is the quasi-two-dimensional interface. The focus of basic research on lipases has been to understand how a reaction involving such a change in dimensionality can occur and how it is regulated. Medically, lipases are targets for therapeutic intervention in the treatment of obesity. The focus of applied research with lipases has been to exploit the unusual properties of lipolytic systems for the production of chiral pharmaceuticals, improved detergents, and designer fats.

Roles of Lipases

In times of abundant energy supply cells accumulate triacylglycerols or wax esters as energy storage depots. This is exemplified by adipose tissue in animals and by the formation of seed oils in plants. Cholesteryl ester storage provides a potential reservoir of cholesterol for steroidogenic tissues. Triacylglycerol and cholesteryl ester accumulation also provides a mechanism of cellular defense by ameliorating the toxic effects of excess fatty acids and cholesterol. Most notable in this regard is the accumulation of cholesteryl esters in the arterial endothelium during atherogenesis. The mobilization of these bulk lipid inclusions intra- and extracellularly is catalyzed by lipases and cholesterol esterases. Once the ester bond is split, the more amphipathic hydrolysis products can be used metabolically or mobilized, in higher organisms, for transport among tissues. Because of the requirement, for hydrolysis for transport, lipases are key enzymes in maintaining lipid homeostasis in multi-organ animals and plants. For example, in mammals there are secreted gastric and pancreatic lipases for digesting dietary lipids. From the resulting hydrolysis products, long-chain fatty acids and monoacylglycerols, triacylglycerols are resynthesized in the intestinal wall. These circulate in the form of lipoproteins that are then subjected to hydrolysis by lipoprotein lipase for entry into peripheral tissues and by hepatic lipase for entry into the liver, respectively. Within peripheral tissues, e.g., adipose tissue, triacylglycerols are resynthesized and, when needed, are mobilized by hormone-sensitive lipase/cholesterol esterase. The resulting fatty acids re-enter the circulation for transport back to the liver for re-esterification or to organs like muscle and heart for energy generation.

Hydrolysis Mechanism and Specificity

The catalytic domain of lipases contains both lipid binding determinants and the active site. The core structure of the catalytic domain is an α/β-hydrolase fold, a motif common to other classes of hydrolases, that consists of β-sheets connected by α-helices. This supports a Ser–His–Glu/Asp catalytic triad resembling that of serine proteases and other hydrolytic enzymes. The active site serine is contained in a consensus sequence of Gly–X–Ser–X–Gly that forms a tight turn exposing the serine hydroxyl group to the scissile ester bond of the substrate. The general mechanism of the reaction catalyzed by lipases is shown in Figure 1.

Substrate specificity among various lipases is variable because of the long flexible hydrocarbon-like groups that must be accommodated by the active site. This is in contrast to carboxylesterases that act on more soluble

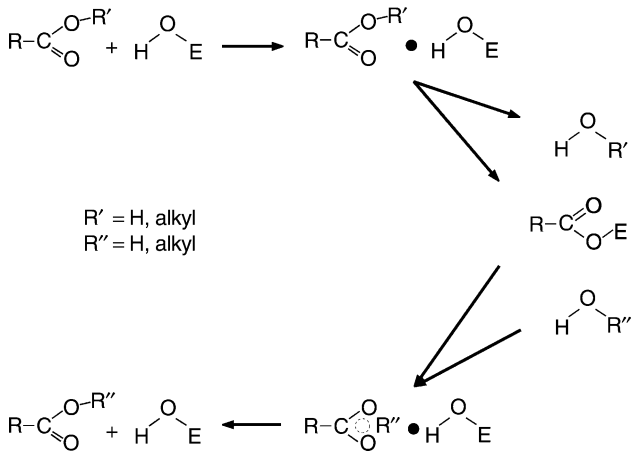

FIGURE 1 Lipolysis mechanism. E–O–H represents the active site serine which forms the acyl-enzyme intermediate in catalysis. The interchangeability of H, R′, and R″ shows that lipases readily catalyze ester synthesis, ester hydrolysis, and acyl exchange, depending on the activity of water in the system, and the circular bond in the lower right structures indicates that the carboxyl oxygen atoms become randomized during the catalytic cycle.

substrates and tend to have much more restrictive sites to accommodate a particular substrate. Lipases that have relatively restricted substrate access to the active site, e.g., pancreatic triacylglycerol lipase, tend to be specific for esters of primary alcohols, whereas others readily catalyze hydrolysis of esters of secondary alcohols as well, e.g., *Candida rugosa* lipase. These latter enzymes are also more likely to exhibit activity against phospholipids and other nonconventional substrates. The list of atypical substrates includes peptides, simple amides, Schiff bases, (lyso)phospholipids, percarboxylic acids and polyesters.

In addition to differing specificities for acyl and alkyl size, some lipases, e.g., *Rhizomucor miehei* lipase, show pronounced stereospecificity, whereas others, e.g., porcine pancreatic triacylglycerol lipase, do not. Interestingly, stereospecificity extends to prochiral molecules, e.g., trioleoylglycerol, in which the lipid substrate is symmetrical but the product of the reaction following removal of an acyl group from position 1 or 3 is chiral. Overall, there is interplay among the various types of specificity in lipases so that generalizations are difficult and specificity must be determined on a substrate-by-substrate basis. Also, the presentation of the substrate to the lipase can affect measured specificity. For pharmaceutical and other fine chemical applications, there have been extensive efforts to engineer lipases to carry out particular reactions with high stereospecificity.

Although lipases are defined and function *in vivo* as hydrolytic enzymes, they are increasingly employed industrially for *de novo* ester synthesis and acyl exchange. Most globular proteins, including lipases, will irreversibly denature if confronted with an interface between an aqueous phase and a highly apolar phase, e.g., hydrocarbon-like. However, if water is removed from the enzyme to the extent that its chemical activity is reduced to very low levels, e.g., by freeze drying, the enzymes are stable and potentially active in an apolar medium. While this is true of many enzymes, it is particularly advantageous with lipases. This is because water is a reactant in the system (Figure 1) and because the substrates are nonpolar. The absence of water shifts the equilibrium of the reaction from ester hydrolysis to ester synthesis and the reactants are compatible with or can even serve as their own apolar solvent. This enables the synthesis of esters in high yield or the exchange of one ester acyl group for another (Figure 1).

Lipolysis Regulation

Physiochemical Importance of Interfaces

Lipases are classically defined as enzymes, generally monomeric and water-soluble, that catalyze the hydrolysis of ester substrates that are apolar and, therefore, generally water-insoluble. Although this definition indicates what lipases do, it does not reveal how they do it. The key to understanding how lipases work is to appreciate the role of the interface between the oil and water phases as an enabler of catalysis. This is shown schematically in Figure 2. Having ester functional groups, lipase substrates are more polar than simple hydrocarbons and have some tendency to partition between the bulk oil phase and the interface. Likewise, lipases will also partition to an oil-water interface from the aqueous phase. The consequence of these partitioning reactions is to orient and concentrate the substrate and enzyme together in a quasi-two-dimensional phase. This phenomenon is known as the "substrate theory" of why lipases are more active on insoluble substrates than soluble ones. In this view of lipolysis the interface assumes part of the role played by classical enzyme-substrate binding in solution, but in a nonspecific way. The most important consequence of enzyme and reactant partitioning is that the instantaneous rate of lipolysis depends on the two-dimensional concentrations of enzyme and reactants in the interface rather than their concentrations in either of the bulk phases.

This sequential scheme for lipolysis has other consequences as well. For a substrate, it means that its amphipathicity, together with its bulk concentration in the oil phase, will contribute to its two-dimensional concentration in the interface. Simplistically, if one had an equimolar mixture of glycerides in an oil phase their interfacial concentrations would be in the relative order monoacylglycerols $>$ diacylglycerol $\gg$ triacylglycerol. Measuring initial rates of hydrolysis for this mixture using a hypothetical lipase with no positional specificity

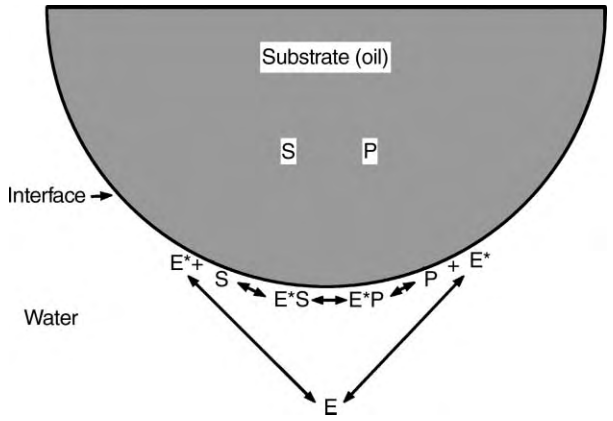

FIGURE 2 The interfacial nature of lipolysis. The substrate (S) is initially present in or as an oil droplet (shaded) whereas the lipase (E) is in the aqueous phase. Catalysis requires that both E and S partition to the interface. Partitioning of E involves a conformational change with the bound species noted as E*. Reaction products (P) will remain in the interface or partition to the oil phase, depending on their amphipathicity.

and normalizing for the number of ester bonds available would show this same apparent order leading, incorrectly, to the conclusion that the lipase is specific for monoacylglycerols. Another consequence of the interfacial nature of lipolysis is that the reaction products will accumulate in the interface, unless they are removed by partitioning into the oil phase or are solubilized in the aqueous phase. With respect to the latter, albumin or cyclodextrins are often used *in vitro* to trap fatty acids and monoacylglycerols in the aqueous phase during the hydrolysis of tri- or diacylglycerols. When it occurs, the accumulation of reaction products in the interface enriches the interface in more amphipathic molecules, greatly complicating the measurement of specificity and interpretation of kinetic data. Product accumulation also can have the effect of slowing the reaction due to fatty acid accumulation while at the same time causing the area of the interface to expand. Area expansion will have the opposite effect by favoring the partitioning of more lipase to the interface. Thus, once lipolysis is initiated in a system having a bulk oil phase as well as an aqueous phase, the regulation of lipolysis rate and extent becomes extremely complex. It is for this reason that researchers have utilized simpler systems, like mono-molecular lipid films, in efforts to understand lipase regulation.

That lipolysis is heterogeneous was unequivocally demonstrated by the P. Desnuelle group in 1965. They showed that if the same insoluble substrate was presented to a lipase as coarse and fine dispersions in buffer, the apparent Michaelis constant for the reaction, i.e., the three-dimensional concentration of substrate at which the hydrolysis rate was half maximal, was lower for the fine dispersion. However, if the rate data were analyzed as a function of total substrate particle surface area rather than bulk substrate concentration, the constant was the same for both dispersions. This occurred because the two-dimensional concentration of substrate at the particle interface was actually the same for the coarse and fine dispersions and the observed saturation of reaction rate with increasing substrate dispersion reflected saturation of lipase partitioning to that surface with increasing interfacial area. Despite the complexity of lipolysis kinetics arising from the interfacial nature of the process, it has been possible to develop kinetic schemes for analyzing lipase kinetics, at least for simple experimental systems, e.g., where reaction products are removed from the interface when formed. These are valuable for screening potential lipase inhibitors to determine the efficiency at which each step of the reaction, i.e., partitioning or interfacial catalysis, contributes to the observed inhibition.

Structural Adaptation of Lipases at Interfaces

It might be presumed that lipases would possess a high affinity for lipid–water interfaces, i.e., that they would be highly amphipathic. However, their affinities toward interfaces dominated by amphipathic lipids, like phospholipids, is often no higher than that of other water-soluble globular proteins. Indeed, many lipases can be isolated as soluble monomeric proteins that do not show a propensity to aggregate. However, if exposed to a surface of a pure substrate, like triacylglycerol, lipases bind with high affinity. Related to this observation is their ability to efficiently catalyze the hydrolysis of insoluble substrates, but not soluble substrates. To explain this observation, it was proposed early on that lipases somehow became activated at interfaces. In the 1990s the determination of lipase structures under varying conditions revealed the physical basis of this phenomenon (Figure 3). In aqueous solution the active site of most lipases is not exposed to the medium but lies in the interior of the protein under a "lid" or "flap" structure. This keeps soluble ester substrates away from the catalytic triad. As implied by its name, the lid can open to reveal the active site and, simultaneously, to create and expose a large area comprised of hydrophobic amino acids. Whereas, this open conformation is energetically unfavorable in the aqueous phase, it may be induced or trapped by the presence of an apolar surface. The lipase then binds with high affinity to the interface, the active site is accessible for diffusion of substrate molecules into it and catalysis can proceed. It is the conformation of this open form of the enzyme that determines specificity for particular substrates. The changing of conformation by lipases in the vicinity of an interface is known as the "enzyme theory" of why lipases are more active on insoluble substrates than

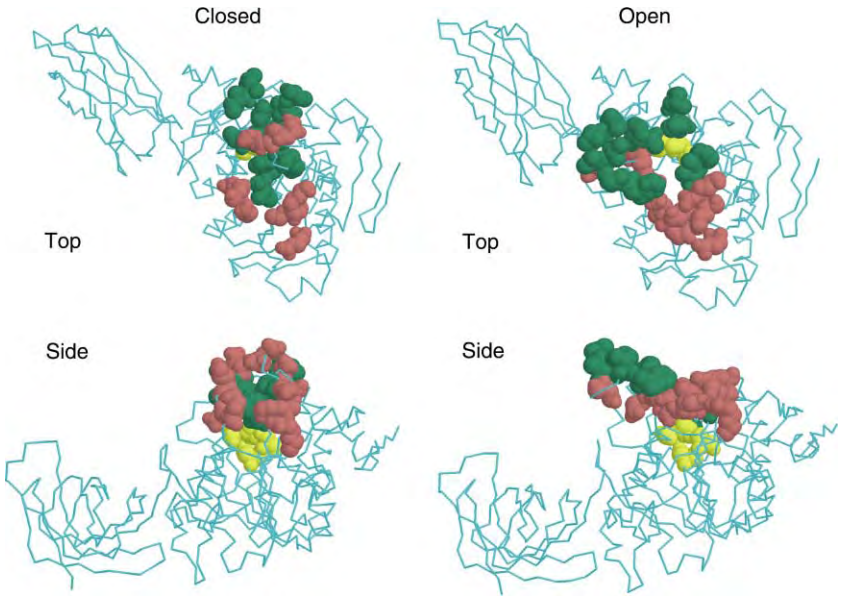

FIGURE 3 Closed and open conformations of pancreatic triacylglycerol lipase. The backbone structure of the lipase is shown in light blue-green with the C2 regulatory domain on the left and the catalytic domain on the right. Nonpolar (green) and polar/charged (red) residues in the vicinity of the catalytic triad (yellow) are shown space filled. Note that in the closed conformation, presumed to exist in solution (left) and designated E in Figure 2, mostly polar/charged residues are exposed to water and the catalytic triad is shielded from water. In the closed conformation, presumed to exist at the interface and designated E^* in Figure 2, a large, apolar surface is exposed on the top of the molecule as shown and the catalytic triad becomes accessible from the top. This surface presumably interacts with the substrate-containing oil droplet. The closed structures were drawn from coordinates kindly provided by Dr. C. Cambillau and the open structure from the Protein Data Base, file 1LPA.pdb.

soluble ones. It should be noted that the enzyme theory of lipolysis and the substrate theory of lipolysis described above are not mutually exclusive.

A still unresolved question is what kind of a surface a lipase needs for surface binding in the open conformation. Natural interfaces tend to be dominated by phospholipids and proteins. These are necessary to emulsify the apolar lipid substrate, i.e., to stabilize it in a dispersed state with high surface area, but tend to inhibit lipase binding to the interface. Research suggests that lipases need a defect or a patch free of binding inhibitor in the interface to initiate lipolysis. Once bound, the generation of lipolysis proceeds and its reaction products increase the number of binding sites and more lipase molecules can bind. Thus, lipolysis often appears to be autocatalytic in the presence of inhibitory phospholipids or proteins, i.e., there is an initial lag in lipolysis followed by a burst. Overcoming the inhibition of lipases by amphipathic lipids and proteins is important not only to understanding their roles and regulation *in vivo*, but also their applications, e.g., improve the efficiency of detergents.

Lipase Regulatory Domains

Many lipases, like gastric lipase, consist of a single protein domain but others have a second domain connected to the catalytic domain by a flexible linker. The most studied of these are members of the lipase gene family, exemplified by pancreatic triacylglycerol lipase (Figure 3), lipoprotein lipase, and hepatic lipase. These have a C2 domain, a motif common to other peripheral (also called amphitrophic) proteins, i.e., proteins that reside in solution but translocate to and function at a lipid–water interface in response to a signal. The C2 domain framework is an eight-stranded, antiparallel β-sandwich with connecting loops. In lipases having C2 domains one of these loops exposes hydrophobic amino acid side chains, like leucine, tyrosine, and tryptophan. These confer an amphipathic character to the domain and, depending on assay conditions, can be essential for lipase activity to be expressed. Given the large hydrophobic surface created near the active site of the catalytic domain by the opening of the lid, such dependence on a C2 domain for initiating lipolysis suggests that it is needed to associate the enzyme with a substrate-containing interface long enough for catalytic domain to open and "lock" the enzyme on the interface.

Lipase Cofactors

Two members of the lipase gene family, pancreatic triacylglycerol lipase and lipoprotein lipase, utilize cofactor proteins for carrying out efficient lipolysis. As noted above, lipase-interface-binding tends to be inhibited by those molecules that help create and

stabilize interfaces, like phospholipids. Cofactor proteins facilitate the initiation of lipolysis at such interfaces. The traditional view of cofactors has been that they are amphipathic proteins that simply bind both the interface and the lipase and thereby anchor the lipase to the interface. However, the comparable affinities of lipases and their cofactors for protected interfaces suggest that they do more. Structural studies of the complex between pancreatic lipase and its protein cofactor, colipase, show that the cofactor may facilitate the opening of the lid through protein–protein interactions with the open conformation of the catalytic domain of the enzyme. Another role has been suggested by comparison of the ability of the cofactor to bind to interfaces with different compositions. Specifically, if a phospholipid-rich interface also contains the substrates and products of lipolysis, colipase binding is strengthened. This occurs because the colipase molecules tend to laterally concentrate the non-phospholipid molecules in their vicinity. In this way they help to create a nanometer-sized region from which phospholipid tends to be excluded. This facilitates lipase binding by a combination of lipid–protein and protein–protein interactions and thereby helps initiate lipolysis. Another speculative role for lipase cofactors is that their preference for binding to substrate-containing surfaces acts to target lipase to those surfaces in preference to interfaces that do not contain substrate.

See Also the Following Articles

Cholesterol Synthesis • Fatty Acid Oxidation • Fatty Acid Receptors • Fatty Acid Synthesis and its Regulation • Lipid Bilayer Structure • Lipid Modification of Proteins: Targeting to Membranes • Lipoproteins, HDL/LDL

Glossary

amphipath A molecule that contains both polar, hydrophilic (water-loving) and apolar, hydrophobic (water-avoiding) groups that are spatially distinct, conferring a tendency to localize at and stabilize interfaces between water and oil phases.

designer fat Dietary fats or fat substitutes that have been *de novo* synthesized or modified, either chemically or enzymatically, to achieve desired intestinal absorption ability, taste, thermal or rheological properties.

interface A quasi-two-dimensional phase between two bulk phases in which the physical environment of the molecules that comprise the region is distinct from the bulk phases.

interfacial activation The process by which an enzyme increases its activity in the presence of an interface. For lipases it results from the combination of enzyme and substrate being oriented and concentrated at interfaces as a consequence of their amphipathic nature (the substrate theory) and from the conformational transition of the lipase to an open conformation as it binds to the interface (the enzyme theory).

Further Reading

Brockman, H. L. (2000). Kinetic behavior of the pancreatic lipase–colipase–lipid system. *Biochimie* **82**, 987–995.

Fojan, P., Jonson, P. H., Petersen, M. T. N., and Petersen, S. B. (2000). What distinguishes an esterase from a lipase: A novel structural approach. *Biochimie* **82**, 1033–1041.

Kraemer, F. B., and Shen, W.-J. (2002). Hormone-sensitive lipase: Control of intracellular tri-(di-)acylglycerol and cholesteryl ester hydrolysis. *J. Lipid Res.* **43**, 1585–1594.

Lombardo, D. (2001). Bile salt-dependent lipase: Its pathophysiological implications. *Biochim. Biophys. Acta* **1533**, 1–28.

Miled, N., Canaan, S., Dupuis, L., Roussel, A., Rivière, M., Carrière, F., De Caro, A., Cambillau, C., and Verger, R. (2000). Digestive lipases: From three-dimensional structure to physiology. *Biochimie* **82**, 973–986.

Panaiotov, I., and Verger, R. (2000). Enzymatic reactions at interfaces: Interfacial and temporal organization of enzymatic lipolysis. In *Physical Chemistry of Biological Interfaces* (A. Baszkin and W. Norde, eds.) pp. 359–400. Marcel Dekker, New York.

Biography

Dr. Howard Brockman is a Professor at the Hormel Institute, a research branch of the University of Minnesota in Austin, Minnesota. His principal research interest is in the regulation of interfacial enzymatic reactions with emphasis on the role of the lateral distribution of interfacial constituents in controlling bulk-interface partitioning and substrate accessibility. He holds a Ph.D. from Michigan State University and received postdoctoral training at the University of Chicago. He has developed novel methodologies for studying interfacial reactions and has contributed to the mechanistic understanding of their regulation.

Lipid Bilayer Structure

Erwin London
State University of New York, Stony Brook, New York, USA

Natural biological membranes consist of a lipid bilayer in which membrane proteins are embedded. As such, the bilayer is the underlying structural unit of the membrane. Understanding bilayer structure, and properties is critical to an understanding of membrane function.

Chemical Structure of Bilayer-Forming Lipids

Lipid bilayers are composed primarily of polar lipids. Glycerophospholipids and sphingolipids are usually the predominant polar lipids in natural membranes. Unlike dietary lipids (fats), these molecules possess a highly polar headgroup in addition to (two) nonpolar (i.e., hydrophobic) tails (Figure 1).

The hydrophobic tails consist of the hydrocarbon chain portions of fatty acids and/or the base sphingosine. Hydrocarbon chains are linear in eukaryotic organisms, but sometimes have branching methyl groups in bacteria.

The polar headgroups of the lipids can have various chemical structures. Often they contain phosphate to which a polar or charged alcohol derivative is attached. In other cases they contain carbohydrates. The polar headgroup can be electrically neutral, zwitterionic, or negatively charged.

In eukaryotes, sterols such as cholesterol are also major components of the bilayer. Sterols differ from other polar lipids in having a simple, small hydroxyl group as their polar portion. This hydroxyl group is attached to four fused aliphatic hydrocarbon rings. In addition, they contain a branched hydrocarbon chain that is attached to the end of the rings opposite the hydroxyl.

Organization of Lipids in Bilayers

In bilayers lipids orient such that their polar groups are in contact with the aqueous environment and their hydrocarbon segments face each other (Figure 1). As a result, the polar groups in each half of the bilayer (called a monolayer or leaflet) face away from one another. As one moves from the aqueous solution to the bilayer center, a somewhat ill-defined gradient of decreasing polarity is encountered.

The formation of the bilayer is driven by the hydrophobic effect, which is conventionally thought of as primarily a decrease in water free energy that occurs when the clustering of hydrophobic groups allows them to avoid contact with water molecules. Because of the shape of polar lipids, they usually form topologically closed bilayers, e.g., a spherical or elliptical shell. Such closed structures eliminate direct contact between lipid hydrocarbon and water. They contain an internal aqueous lumen separated from the external aqueous solution by the bilayer. Artificially formed bilayers of this type are called liposomes. The bilayer plus the internally trapped aqueous solution is known as a vesicle (Figure 2). Vesicles can contain one lipid bilayer, in which case they are said to be unilamellar vesicles, or multiple bilayers each separated by thin layers of aqueous solution, in which case they are called multilamellar vesicles. Flattened stacks of bilayers with the internal aqueous solution largely squeezed out can also be prepared.

Membrane Proteins and Bilayers

Natural membranes are associated with numerous proteins. Those proteins that span the lipid bilayer are said to be transmembraneous (Figure 2). Non-transmembraneous proteins associated with the polar surface of the bilayer are also present (Figure 2). Proteins can have a significant influence on membrane structure. For example, they are likely to be responsible for the distortion of natural membranes into more complex shapes than those observed for pure lipid bilayers. Familiar examples are the membranes of red blood cells and the variable-shape membranes surrounding amoeba. On the other hand, it is clear that natural membranes contain bilayers that have physical properties similar to those of pure lipid bilayers. The fact that the lipid-facing amino acid residues of membrane proteins form hydrophobic surfaces that match lipid

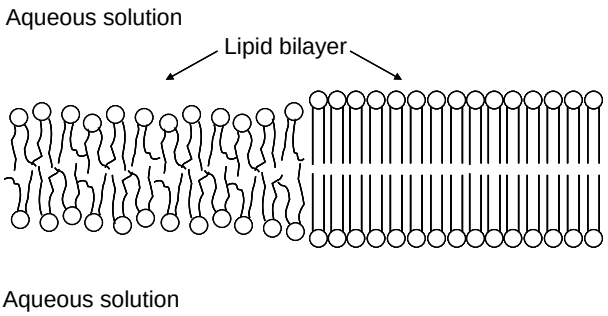

FIGURE 1 Schematic representation of cross-section through a lipid bilayer composed of a single type of phospholipid or sphingolipid. Polar headgroups are illustrated as circles and hydrocarbon tails are shown as lines. Notice each lipid has one headgroup and two tails. A bilayer composed of both a disordered liquid domain (left) and an ordered gel domain (right) is illustrated.

dimensions is no doubt an important factor explaining this behavior. Nevertheless, the physical properties of the hydrophobic segments of membrane proteins are very different than those of lipids and the consequences of these differences remain to be fully explored.

Bilayer Dimensions

Experiments on liposomes show that the diameter of spherical lipid bilayers can be any value upwards from 250Å. Bilayer width (thickness) is determined by the length of the nonpolar tails of the polar lipids and sterols. This can range from 16 to 24 carbon atoms for the hydrocarbon chains of phospholipids and sphingolipids. Combined with the effects of lipid state and double bonds (see below), this results in a hydrocarbon core of the bilayer that is ~30Å in width. Total width including the lipid headgroups is on the order of 45–50Å, but the exact value depends on the structure of the lipid polar headgroups, which can be very large in some cases.

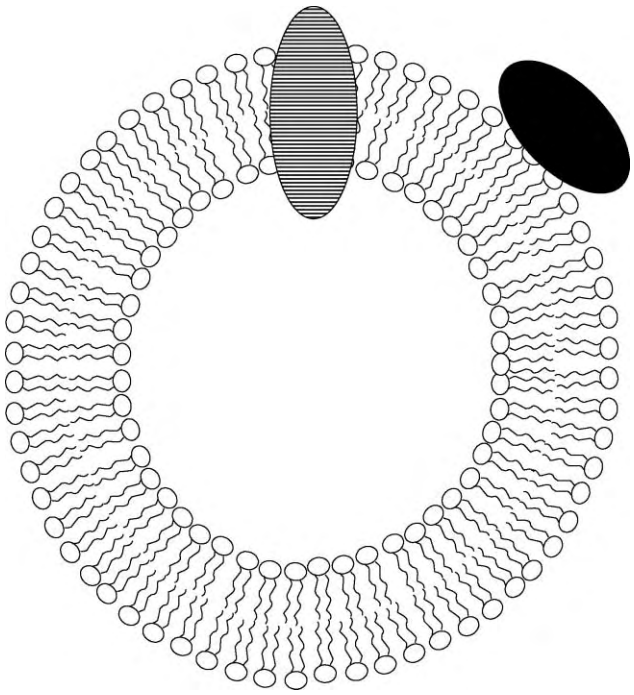

FIGURE 2 A unilamellar lipid vesicle formed by a lipid bilayer and containing one transmembrane protein (striped) and one protein associated with the lipid polar headgroups (filled).

Relationship between Bilayer Form and Bilayer Function

The properties of bilayers are admirably suited to their biological function. The closed structure of the bilayer allows biological membranes to completely encase cellular contents (such as nucleic acids, proteins, sugars, and amino acids) in a hydrophobic barrier that prevents them from escaping into the surrounding solution.

The width of the bilayer is such that proteins of ordinary size are able to span the lipid bilayer. This allows membrane proteins to maintain contact with both the internal and external aqueous milieu. As a result, membrane proteins can carry out functions such as the transport of molecules across bilayers. Such abilities are central to membrane function. A bilayer that was much wider than that formed by natural lipids, i.e., one formed by much longer fatty acid chains, would require the metabolically wasteful synthesis of extra-large transmembrane proteins as well as that of longer lipids. A bilayer that was significantly thinner than that formed by natural lipids would not be stable.

Physical State of Bilayer Lipids

Another important property of lipid bilayers is their ability to exist in different physical states (or phases). At low temperatures bilayers often exist in a relatively solid-like state called the gel or Lβ state or phase. At higher temperatures gel-state bilayers undergo a melting transition and the gel state is replaced by a more disordered, liquid-like state, variously designated as the liquid crystalline, liquid disordered, or Lα state. Melting temperatures (or if temperature is decreased, freezing temperatures) depend on the structure of both the hydrophobic tails and the polar headgroups of the individual lipid molecules. The melting temperature of lipids with linear saturated tails, which contain only single bonds connecting carbon atoms to each other, are much higher than those of lipids with unsaturated tails, which have *cis* double bonds, as well as single bonds. Because sphingolipids tend to contain hydrocarbon

chains lacking *cis* double bonds, they tend to have much higher melting temperatures than glycerophospholipids, which tend to have more highly unsaturated hydrocarbon chains.

Bilayers containing sterols can exist in a third lipid state called the liquid ordered or Lo state. This state is observed most frequently in mixtures of sterols with relatively saturated chain polar lipids. The Lo state has properties that are intermediate between the disordered liquid and gel states.

Studies in synthetic lipid bilayers show that in a single bilayer, different regions (known as domains) can exist in different physical states (Figure 1). It is believed that the disordered liquid state is by far the most common state present in biological membranes. However, in eukaryotic cells it is now thought that ordered liquid-state domains can coexist with disordered liquid domains. Lo state domains in cell membrane, called lipid rafts, are rich not only in sphingolipids and sterols, but also in special subsets of membrane proteins. Rafts appear to have a specialized role in a number of important biological processes.

The Effect of Lipid State upon Lateral Organization of Lipid Molecules

Lipid bilayers in different physical states differ in a number of properties. One is the degree of lateral interaction between various bilayer lipids. In the disordered liquid-like state, bilayers are believed to exist as a more-or-less random mixture of various lipid species. In other words, there are few or no cases in which tight associations between two different lipid molecules occur. As spacial constraints tend to be much more restrictive in solids, a much higher degree of lateral organization is likely to exist in a gel-state bilayer containing a mixture of different lipids. This is little studied except to the extent that it appears that separate gel-phase domains with different lipid compositions can coexist in a single bilayer. The nature of lateral interactions between different lipids in the liquid-ordered state is being actively studied, but remains unclear. There may be specific arrangements of sterol molecules relative to the other polar lipids present in the bilayer, and various liquid-ordered domains with different compositions may be able to coexist in a single bilayer.

Interactions between each of the monolayers within a single bilayer is also poorly understood in most cases. Under some conditions certain combinations of hydrocarbon chain lengths allow interdigitation of hydrocarbon chains from opposite monolayers.

Influence of Physical State on Lipid Conformation and Lateral Diffusion

The conformation of individual lipid molecules within a bilayer is also dependent upon lipid state. In all states, the hydrocarbon chains of the lipids tend to align parallel to one another and perpendicular to the surface. A high degree of parallel alignment characterized by the presence of tightly packed lipids occurs in the gel- and liquid-ordered states. In contrast, in the disordered liquid state, lipids are more loosely packed and the degree of alignment is reduced because carbon-carbon single bonds can twist a manner that results in bending of the hydrocarbon chains. This also results in the bilayer being thinner than in other states (Figure 1). The relatively random location of such bends within a hydrocarbon chain results in increased disorder as one moves from the bilayer surface toward the bilayer center. There is also a contribution to disorder from the presence of double bonds. These are usually in the form of *cis* double bonds, which form permanent bends in hydrocarbon chains.

Headgroup conformation, and its dependence on lipid state, are more poorly characterized in most cases.

Another property of bilayers that depends on lipid state is lateral diffusion. This refers to random sliding motions of lipids within the plane perpendicular to the average direction of the hydrocarbon tails. Lateral motions are rapid in both the liquid-disordered and liquid-ordered state, but much reduced in the gel state. It should be emphasized that the ability to undergo relatively rapid lateral motions is an important feature of biological membranes. It allows membrane components to rearrange within the lipid bilayer such that they can form and break functionally important complexes.

Transverse Lipid Movements

Lipids can also undergo transverse movement, in which they move (or flip) from one monolayer of the bilayer to the opposite one. For good reason this motion is many orders of magnitude slower than lateral diffusion. Transverse flipping requires that the polar/charged portions of lipids transiently dissolve within the hydrophobic core of the bilayer. This is very unfavorable energetically. However, it should be noted that in natural membranes specific flippase proteins are believed to catalyze rapid flipping events in some cases. Furthermore, it appears that spontaneous flipping is more rapid for sterol molecules, which have a headgroup that is very small and not excessively

polar, than it is for most phospholipids and sphingolipids, although this remains an area of some controversy.

Effect of Lipid Bilayers on Local Aqueous Environment

Finally, it is important to remember that lipid bilayers can also affect the structure of their immediate aqueous environment. When a significant fraction of lipids in a bilayer is anionic, they tend to attract significant numbers of cations while repelling anions. As a result a special double layer of solution depleted in anions and enriched in cations surrounds the bilayer. This layer can alter the structure and function of membrane proteins.

See Also the Following Articles

Fatty Acid Synthesis and its Regulation • Flippases • Lipid Modification of Proteins: Targeting to Membranes • Lipid Rafts • Phospholipid Metabolism in Mammals • Phospholipid Synthesis in Yeast • Sphingolipid Biosynthesis • Sphingolipid Catabolism

Glossary

biological membranes A thin shell surrounding either internal compartments in cells or the entire cell. Composed of special proteins and lipids.

lipids Small biomolecules with hydrophobic characteristics.

polar headgroup The portion of a lipid molecule that interacts with aqueous solution; fusually contains several chemical groupings that can hydrogen bond with water.

Further Reading

Brown, D. A., and London, E. (2000). Structure and function of sphingolipid- and cholesterol-rich rafts. *J. Biol. Chem.* **275**, 17221–17224.

Gennis, R. B. (1989). *Biomembranes: Molecular Structure and Function*. Springer, New York.

Jain, M. K. (1988). *Introduction to Biological Membranes*. Wiley, New York.

Koynova, R., and Caffrey, M. B. (1998). Phases and phase transitions of the phosphatidylcholines. *Biochim. Biophys. Acta* **1376**, 91–145.

Lee, A. G. (1977). Lipid phase transitions and phase diagrams. *Biochim. Biophys. Acta* **472**, 237–281.

Biography

Erwin London is a Professor in the Department of Biochemistry and Cell Biology, and in the Department of Chemistry, of Stony Brook University. His expertise is in characterization of the organization of proteins and lipids in membranes. He holds a Ph.D. from the Cornell University (Ithaca) and received postdoctoral training at the Massachusetts Institute of Technology.

Lipid Modification of Proteins: Targeting to Membranes

Marilyn D. Resh
Memorial Sloan-Kettering Cancer Center, New York, USA

Lipid modification refers to the covalent attachment of hydrophobic groups to specific amino acids in proteins. All proteins contain a polypeptide chain backbone consisting of various combinations of amino acids linked via amide bonds. In addition, some proteins are modified by the attachment of other chemical structures directly to one or more amino acids. These modifying groups are diverse and include phosphate, methyl groups, sugars, as well as lipids. Three different types of lipid moieties are typically found attached to proteins: fatty acids, isoprenoids, and glycosylphosphatidyl inositol (GPI) anchors (Figure 1, Table I). Linkage of each of these groups occurs within different protein sequences and is catalyzed by different enzymes. The attachment of hydrophobic groups to proteins modifies their structure, intracellular localization, and/or function.

Lipid Modification of Proteins

Fatty Acylation

Two types of fatty acids are typically found attached to fatty acylated proteins: myristate or palmitate. In addition, some proteins are dually fatty acylated, i.e., they contain both myristate and palmitate.

Myristoylation

Myristate is a 14-carbon saturated fatty acid that is directly linked to the N terminus of select proteins in a process known as N-myristoylation. In eukaryotes ~0.5% of all proteins are modified in this manner; in humans this corresponds to ~150 proteins. Nearly all N-myristoylated proteins begin with the sequence: Met-Gly. During protein translation, the initiating methionine is removed by the enzyme methionine aminopeptidase, exposing glycine at the N terminus. The fatty acid is then linked to the protein via an amide bond between myristate and the N-terminal glycine residue. Additional amino acids near the N terminus are important for determining whether a protein becomes N-myristoylated. An algorithm is available on the Web (http://mendel.imp.univie.ac.at/myristate/) that allows one to predict with high accuracy whether a particular protein sequence is N-myristoylated. The high stability of the amide linkage makes N-myristoylation an essentially irreversible protein modification.

N-myristoylation is catalyzed by the enzyme N-myristoyl transferase (NMT). Most organisms have one or two NMT genes, and NMT has been shown to be an essential gene product that is required for the growth of yeast, flies, and plants. The N-myristoylation reaction occurs in a co-translational manner, i.e., while the newly translated polypeptide is still attached to the ribosome. The preferred fatty acid substrate for NMT is myristoyl-CoA, an activated form of myristate. Fatty acids that are shorter or longer than myristate are generally not transferred from their respective fatty acyl-CoAs to proteins. However, NMT will transfer unsaturated 14 carbon fatty acids to proteins, a process that occurs primarily in the retina.

Palmitoylation

Several hundred eukaryotic proteins are posttranslationally modified by covalent attachment of the 16-carbon fatty acid palmitate. The fatty acid is generally attached to one or more cysteine residues within the protein through a thioester linkage. Palmitoylation can occur within five types of protein sequences: (1) at or near the transmembrane domain of a membrane protein; (2) near a C-terminal prenylated cysteine; (3) near the N or C terminus; (4) adjacent to or near an N-terminal myristoylated glycine; and (5) at an N-terminal cysteine via an amide bond. The rules that govern the choice of the palmitoylation site(s) are not well-understood. Eukaryotic cells contain multiple palmitoyl acyl transferases that are located in many different subcellular sites. In addition to palmitate, longer fatty acids such as stearate or arachidonate may be transferred to proteins. Palmitoylation is a reversible reaction; palmitate is removed from proteins by palmitoyl protein thioesterases. The reciprocal action of transferases and thioesterases sets up a dynamic

balance of palmitoylation/depalmitoylation reactions in the cell.

Prenylation

Prenyl groups are built from 5-carbon building blocks known as isoprene. Protein prenylation involves the attachment of two types of isoprenoid groups, 15-carbon farnesyl or 20-carbon geranylgeranyl, via thio-ether linkage to a cysteine residue at or near the C terminus. Most prenylated proteins contain a "CAAX" (C = Cys, A = aliphatic amino acid, X = any amino acid) box sequence at their C terminus. The identity of the C-terminal amino acid determines whether the protein is recognized by farnesyl transferase (FTase) (X = met,ser) or geranylgeranyl transferase I (GGTase I) (X = leu). Following prenylation, two additional modifications occur. The three C-terminal amino acids are cleaved by the endoprotease hRce1, and the prenylated C-terminal cysteine is carboxymethylated by the carboxymethyltransferase pcCMT/Icmt. A third prenyl transferase, Rab GGTase or GGTase II, attaches geranylgeranyl to Rab proteins that terminate with -CC, CXC, CCX or CCXX sequences. Rab proteins must be bound to Rab Escort protein (REP) in order to be prenylated by GGTase. Genetic mutations in REP cause choroideremia, a disease characterized in humans by retinal degeneration and blindness.

GPI Anchors

GPI anchors are complex structures that consist of ethanolamine phosphate, three mannoses, N-acetyl-glucosamine, and phosphatidylinositol (PI). At least 20 enzymes are involved in the synthesis and attachment of GPI anchors, a process that occurs in the endoplasmic reticulum. A C-terminal hydrophobic region in the target protein serves as a signal for GPI anchor attachment and is then cleaved from the modified protein, leaving the GPI anchor at the C terminus. The modified protein is transported through the Golgi apparatus and ultimately to the extracellular leaflet of the plasma membrane.

Detection of Lipid Modified Proteins

Mass spectroscopy analysis provides definitive identification of the modifying group on proteins. Alternatively, fatty acylated and prenylated proteins are detected by radiolabeling cells with ^{3}H or ^{125}I labeled fatty acids or isoprenoid precursors, followed by isolation of the protein with a specific antibody and autoradiographic analysis. A hallmark of GPI-anchored proteins is that they are released from the cell surface by *in vitro* cleavage with PI-specific phospholipase C; this process occurs *in vivo* for certain GPI-anchored proteins (e.g., alkaline phosphatase) (Figure 1, Table I).

Membrane Targeting of Lipid Modified Proteins

Lipid modifications play important roles in promoting interaction of proteins with membranes. The nature of the lipid group determines how tightly a protein will bind to a membrane and which membrane it will bind to.

Myristoylated and Farnesylated Proteins

The hydrophobicity of myristate or farnesyl is not sufficient to stably anchor a protein to the membrane. N-myristoylated and farnesylated proteins therefore use a second signal to promote membrane binding. The second signal is either a cluster of basic amino acids (lysine or arginine) contained within the protein or covalently bound palmitate. The positively charged basic cluster provides electrostatic interaction with negatively charged lipids on the cytoplasmic surface of the plasma membrane, whereas palmitate enhances hydrophobic interactions with the interior of the phospholipid bilayer. The two signals together promote specific targeting of the modified proteins to the cytoplasmic face of the plasma membrane. Examples of lipid modified proteins that use two signals

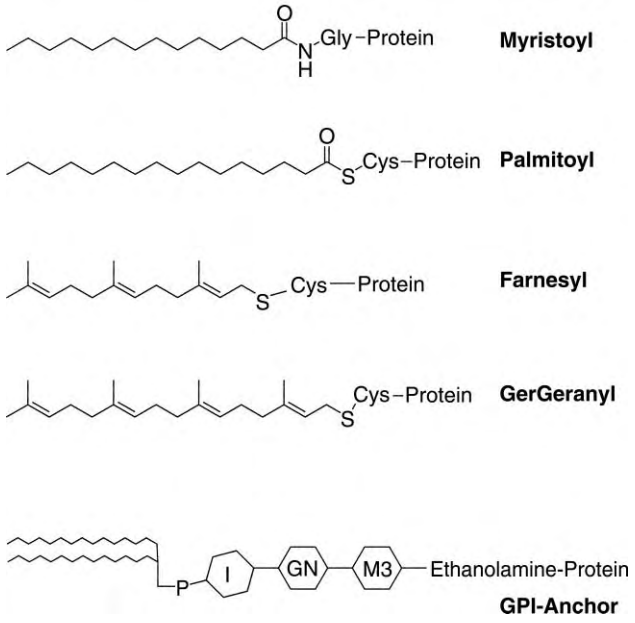

FIGURE 1 Structures of Lipid Modifying Groups on Proteins. Structures of the different lipid modifying groups and their linkages to proteins are depicted. For the GPI anchor, I = inositol, GN = N-acetylglucosamine, M3 = 3 mannoses.

TABLE I

Examples of Lipid Modified Proteins

Fatty acylated	Prenylated	GPI-anchored
Myristate	*Farnesyl*	Alkaline phosphatase, CD55 (DAF),
Src family kinases, Gα subunits, Arf, recoverin, MARCKS, mammalian retroviral Gag proteins, calcineurin B, eNOS	H-Ras, K-Ras, Lamins	5′-nucleotidase, Thy-1, PrP^c prion, trypanosomal VSG
Palmitate	*Geranylgeranyl*	
Transferrin receptor, CD4, caveolin-1, β2 adrenergic receptor, H-Ras, Gα subunits, GAP43, PSD-95, Src family kinases, eNOS	Gγ subunits, Rho family proteins, Rab proteins	

for membrane binding include Src (myristate + basic) and H-Ras (prenyl + palmitate).

Palmitoylated, Geranylgeranylated, and GPI-Anchored Proteins

The presence of a molecule of palmitate, geranylgeranyl, or a GPI-anchor is sufficient for membrane binding of the modified protein. The final destination of these modified proteins is dictated by several factors. The site where palmitoylation occurs often determines protein localization. This is the case for dually fatty acylated members of the Src family of tyrosine kinases, which are palmitoylated by a plasma membrane localized palmitoyl transferase, and remain bound to the plasma membrane. Other proteins are modified in internal membranes, but traffic through the classical secretory pathway and are thereby specifically delivered to the plasma membrane (e.g., farnesylated H-Ras and GPI-anchored proteins). A third consideration is protein–protein interactions, which influence the ultimate destination of a modified protein. Finally, in polarized cells such as epithelial cells, the plasma membrane is divided into two distinct domains – apical and basolateral – that differ in protein and lipid composition. The GPI-anchor provides a sorting signal that directs the modified protein to the apical surface in most epithelial cells.

Reversible Membrane Binding

Several mechanisms exist *in vivo* to regulate membrane-binding of lipid-modified proteins. The first is removal of the modifying group, e.g., depalmitoylation by palmitoyl thioesterases. Myristoylated and prenylated proteins contain stable lipid–protein linkages and are thus not subject to this mode of regulation. Instead, exposure of the modifying group can be regulated, either via interactions with the modified protein itself (intramolecular) or with other proteins (intermolecular). For example, recoverin and Arf are N-myristoylated proteins whose membrane-binding is regulated by an intramolecular myristoyl switch. These proteins exist in two conformations. In one conformation, myristate is hidden within a hydrophobic pocket inside the protein, and the protein is cytosolic. Binding of ligand triggers the myristoyl switch: a conformational change results in exposure of myristate and promotion of membrane-binding. Intermolecular interactions also regulate membrane localization. When geranylgeranylated RhoA is bound to its inhibitor, RhoGDI, the isoprene unit is sequestered within a hydrophobic cleft of RhoGDI and the complex is cytosolic. Activation of RhoA causes it to be released from RhoGDI and localize to the plasma membrane.

Targeting to Membrane Rafts

Membrane rafts are small subdomains of the plasma membrane that are enriched in cholesterol and sphingolipids. The lipids in rafts predominantly contain saturated fatty acid chains, which promotes tight packing and formation of a specialized region of the membrane bilayer known as a "liquid ordered" domain. Proteins modified by saturated fatty acids or GPI anchors preferentially localize to rafts. Myristoylated and palmitoylated proteins localize to the cytoplasmic side of plasma membrane rafts, while GPI-anchored proteins are sorted into rafts in the trans Golgi network and then trafficked to the exoplasmic leaflet of the raft membrane. Raft localization of these proteins enhances protein–protein interactions and is important for propagating efficient signal transduction by growth factor and immune cell receptors.

Membrane Targeting and Protein Function

Membrane targeting is essential for the function of many types of lipid-modified proteins. Localization of proteins to a membrane increases their local concentration, and

amplifies the efficiency of interaction with other membrane-bound substrates and targets. When lipid modification is inhibited, the affected proteins are mislocalized within the cell and no longer function effectively. Drugs that interfere with N-myristoylation (2-OH-myristate), palmitoylation (2-bromopalmitate) and prenylation (farnesyl transferase inhibitors (FTIs)) have been developed. There is great clinical interest in FTIs, which have been shown to inhibit farnesylation of Ras and reduce the growth of Ras-induced human tumors.

See Also the Following Articles

Fatty Acid Oxidation • Fatty Acid Receptors • Fatty Acid Synthesis and its Regulation • Glycosylphosphatidylinositol (GPI) Anchors • Lipid Bilayer Structure • Lipid Rafts • Phospholipase C • Protein N-Myristoylation • Protein Palmitoylation

Glossary

fatty acylation The process whereby fatty acids are covalently attached to proteins.

GPI anchor A complex structure consisting of ethanolamine phosphate, three mannoses, N-acetylglucosamine, and phosphatidylinositol.

isoprenylation The process whereby isoprenoid groups are covalently attached to proteins.

rafts Membrane regions that are enriched in cholesterol and sphingolipids.

Further Reading

Bijlmakers, M. J., and Marsh, M. (2003). The on-off story of protein palmitoylation. *Trends Cell Biol.* **13**, 32–42.

Casey, P. J. (1995). Protein lipidation in cell signaling. *Science* **268**, 221–225.

Farazi, T. A., Waksman, G., and Gordon, J. I. (2001). The biology and enzymology of protein N-myristoylation. *J. Biol. Chem.* **276**, 39501–39504.

Resh, M. D. (1999). Fatty acylation of proteins: New insights into membrane targeting of myristoylated and palmitoylated proteins. *Biochim. Biophys. Acta* **1451**, 1–16.

Takeda, J., and Kinoshita, T. (1995). GPI-anchor biosynthesis. *Trends Biochem. Sci.* **20**, 367–371.

Biography

Marilyn D. Resh is a member in the Cell Biology Program at Memorial Sloan-Kettering Cancer Center and is a Professor in the Cell Biology and Biochemistry Graduate Departments at the Weill Graduate School of Medical Sciences of Cornell University. Her research focuses on understanding how lipid modification regulates protein structure and function. She holds a Ph.D. from Harvard University, where she also received her postdoctoral training. She discovered the two-signal mechanism of membrane binding utilized by Src and the HIV-1 Gag protein, and was one of the first to demonstrate that Src family tyrosine kinases are palmitoylated.

Lipid Rafts

Deborah A. Brown
State University of New York, Stony Brook, New York, USA

Lipids do not always mix uniformly in membranes, but can cluster to form microdomains. A certain class of these microdomains has been named "lipid rafts." These are enriched in cholesterol and sphingolipids. Rafts probably exist in membranes in the liquid-ordered phase or a phase with similar properties. Increasing evidence suggests that phospholipid-rich liquid-crystalline phase domains and sphingolipid-rich liquid-ordered phase domains (rafts) can exist in equilibrium in biological membranes, especially the plasma membrane. Preferential partitioning of membrane proteins into rafts can affect function. Among the proteins that are targeted to rafts are those anchored in the outer leaflet of the membrane through covalent attachment to a special glycolipid, glycosyl phosphatidylinositol (GPI). Other proteins that are linked to saturated acyl chains, such as those that are directly acylated with two or more palmitate chains, or a palmitate and a myristate chain, are also targeted to rafts. Targeting of GPI-anchored proteins and other proteins to rafts plays a role in signal transduction, especially in hematopoietic cells, and possibly also in sorting in intracellular membranes and regulation of cell-surface proteolysis in other mammalian cells.

Physical Properties

The fact that membrane lipids have such heterogeneous structures suggests that they may mix nonrandomly in the bilayer to form lipid microdomains. However, despite much interest in the subject, good evidence that lipids cluster in cell membranes has been slow to emerge. We will discuss one type of microdomain that has recently been described in cell membranes. These are rich in cholesterol and sphingolipids, and probably exist in membranes in the liquid-ordered (l_o) phase or a phase with similar properties. These domains have also been called rafts. The fact that rafts are in the l_o phase gives them a surprising but technically useful property; they are resistant to solubilization by non-ionic detergents such as Triton X-100 in the cold. Thus, after extraction of cells in detergent, insoluble rafts can be separated from fully-solubilized non-raft proteins and lipids, and isolated for further analysis. We will use the term raft to refer to the domain in the intact membrane, and the term DRM to refer to the structure isolated by detergent insolubility.

Certain proteins, including those anchored in membrane by GPI and those linked to dual saturated acyl chains such as palmitate and myristate, are targeted to rafts. We will discuss GPI-anchorage, an unusual form of membrane anchorage, in detail, covering synthesis and the types of proteins that are GPI-anchored. We will also discuss the functions of GPI-anchorage, focusing on the ability of this modification to target proteins to lipid rafts (Figure 1).

Lipid Phase Behavior

Since rafts are probably in a separate phase from the rest of the bilayer, we briefly review membrane lipid phase behavior. Artificial bilayers consisting of one pure phospholipid species exist in a "frozen," ordered, gel phase at low temperatures. Acyl chains of gel-phase lipids are extended and packed tightly together, and lipids have low rates of rotational mobility and diffusion in the bilayer. These frozen acyl chains have a melting temperature (T_m) that is characteristic of each phospholipid species. Above this temperature, the bilayer is present in a phase, termed liquid-crystalline (l_c) or liquid-disordered (l_d), in which the lipid acyl chains are fluid and disordered. In the l_c phase, the acyl chains are disordered and do not pack tightly together. They also have high rates of rotational and lateral mobility in the bilayer. Binary mixtures of phospholipids with different T_m can be examined at temperatures between the T_m of the two lipids. When one component is present at low levels, the mixture is uniform, and generally remains in the phase favored by the major component. Above a threshold concentration of one component, cooperative phase separation occurs, and gel and l_c phase domains can coexist. In these two-phase systems, the gel phase is enriched in the high-T_m lipid, and the l_c phase is enriched in the low-T_m lipid. Phase separation in these mixtures is affected by temperature; high temperatures favor the l_c phase, while low temperatures favor the gel phase. Whenever two phases are present, the lipid composition of each phase remains constant. Thus, as the lipid composition and the temperature are changed, only

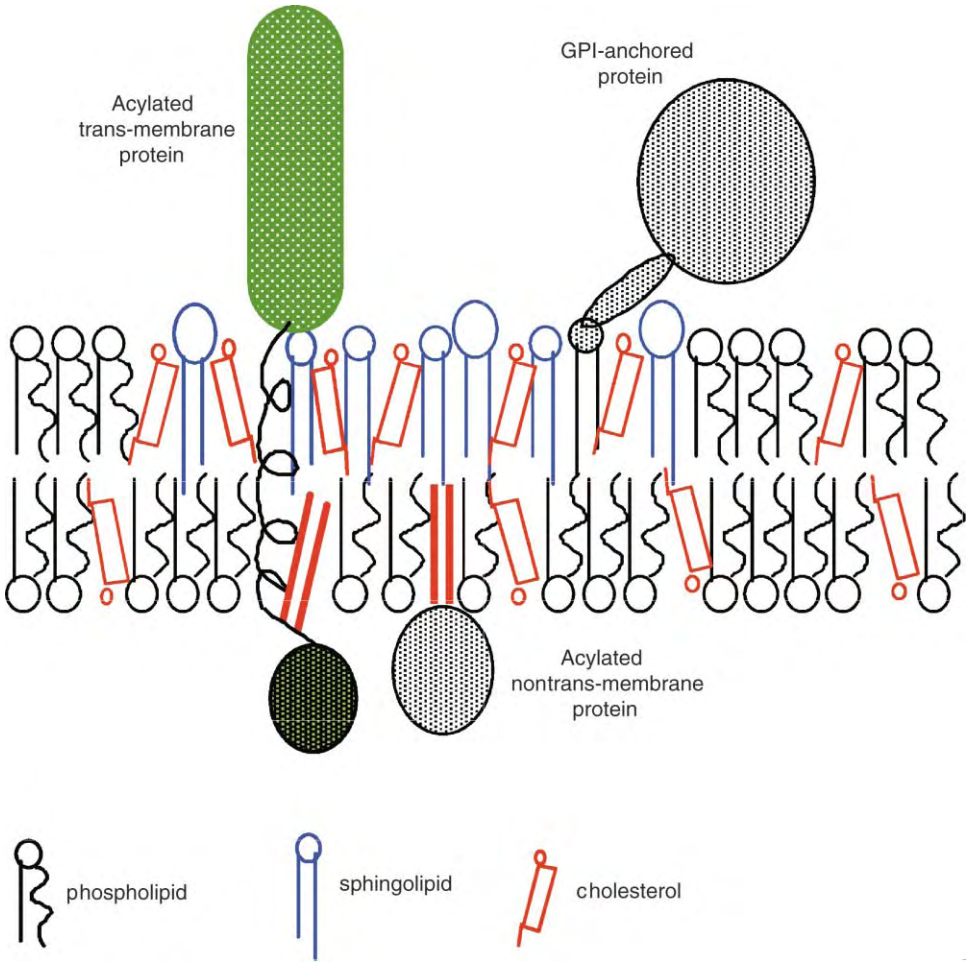

FIGURE 1 Diagram of a membrane raft. Rafts form in membranes rich in cholesterol or other sterols (red) and sphingolipids (blue). Rafts are enriched in these lipids, and relatively depleted in phospholipids (black). Most phospholipids in biological membranes contain one unsaturated acyl chain (curvy line). Lipids can form rafts spontaneously in model membranes, though proteins may affect raft formation in cell membranes. Most sphingolipids are present in the outer leaflet of the plasma membrane. The lipid composition of inner leaflet rafts is not known. Proteins with a high affinity for the ordered lipid environment present in rafts can concentrate there. These include GPI-anchored proteins (whose phosphatidyl inositol moieties generally contain two saturated acyl chains), acylated cytoplasmic proteins such as Src-family tyrosine kinases and alpha subunits of heterotrimeric G proteins, and some acylated transmembrane proteins (which are generally modified with palmitate chains). Saturated acyl chain lipid modifications on proteins are diagrammed as thick red lines.

the relative amount of the two different phases in the membrane changes.

Eukaryotic cell membranes contain mixtures of glycerolipids (in mammalian cells, all phospholipids except sphingomyelin), sphingolipids, and sterols. Biological glycerolipids generally have very low T_m, while sphingolipids (especially glycosphingolipids) have much higher T_m. This disparity has suggested that phase separation between glycerolipid- and sphingolipid-rich domains (possibly in the l_c and gel phases, respectively) might occur in membranes in cells. Because lipids in the gel phase are insoluble in detergent, DRMs might be gel-phase domains. However, although phase separation between l_c and gel phases has been well-characterized in model membranes, the gel phase does not appear to exist in biological membranes, except in unusual cases. In addition, DRMs are rich in cholesterol, making it unlikely that they are present in the gel phase. However, another type of phase separation has also been described in model membranes. This is phase separation between two fluid phases in binary mixtures of a saturated-chain phospholipid (which has a high T_m) and cholesterol. In this case, above the T_m of the phospholipid, a liquid-ordered (l_o) phase can separate from the l_d phase as the amount of cholesterol is increased. Acyl chains of lipids in the l_o phase have properties that are intermediate between those of the gel and l_d phases. They are extended, ordered, and tightly packed together, as in the gel phase, but have high lateral mobility in the bilayer, as in the l_d phase. Phase separation between the l_d and l_o phases also occurs in model membranes containing ternary mixtures of high- and low-T_m lipids

and cholesterol, although the process is more complex. In particular, l_c/l_d phase separation occurs at 37°C in mixtures of phospholipids, sphingolipids, and cholesterol in proportions similar to those found in the plasma membrane. This result is important because it shows that formation of l_o phase domains in the plasma membrane is plausible from a biophysical standpoint.

DRMs are in the L_O Phase

Several studies suggest that DRMs isolated from cells exist in intact membranes as domains in the l_o phase. First, DRMs are in the l_o phase when they are isolated. Second, controlled experiments have addressed the possibility of detergents introducing artifacts. One such artifact is that lipids in membranes might be in a uniform phase, with a concentration of sphingolipids (high-T_m lipids) too low to induce phase separation. However, detergent might preferentially extract low-T_m phospholipids first. As phospholipids are gradually removed, the concentration of sphingolipids in the membrane might gradually increase. This process might eventually lead to phase separation when a threshold concentration of sphingolipids is reached. Detergents do not act in this manner, as shown by model membrane experiments. A series of liposomes whose phase behavior is known from methods independent of detergent extraction is made. Some of these liposomes contain sphingolipids and cholesterol, but at levels too low for phase separation. When these liposomes are extracted with detergent, no DRMs are produced. This shows that detergent does not rearrange membrane lipids to induce DRM formation.

Two different models of raft formation have been proposed. The first, supported by most data, suggests that rafts form by phase separation. Thus, structural features of lipids that affect T_m and promote phase separation will promote raft formation. One key difference between phospholipids and sphingolipids is the length and saturation of their acyl chains. Lipid head-groups can also contribute to T_m by altering the way lipids pack together. According to our model, acyl chain packing plays a key role in raft formation. Head group interactions might also be important, although these interactions may affect raft formation indirectly by affecting acyl chain packing. Cholesterol is recruited to rafts through its ability to pack tightly with lipids of high T_m when the l_o phase is formed. Another group has proposed a different model for raft structure. According to this model, rafts are primarily clusters of glycosphingolipids held together through hydrogen-bonding or other interactions between glycosphingolipid head groups. Because cholesterol has a small head group, it is recruited to rafts because it fits well in the gaps between bulky-headed glycosphingolipids.

Proteins in DRMs

The physiological significance of raft formation is likely to stem from the preferential partitioning of certain proteins into rafts. It has been known for several years that proteins anchored in membranes by GPI are detergent-insoluble and are present in DRMs. Acylated proteins, which are covalently linked to fatty acids, can also be targeted to DRMs. In both cases, this is likely to occur through partitioning of order-preferring lipid modifications into rafts. Thus, proteins that have an affinity for an ordered lipid phase will partition into rafts.

GPI-anchorage can target proteins to rafts. It has become clear in the last few years that targeting to rafts is an essentially universal property of GPI-anchored proteins in mammalian cells. Proposed function(s) of this targeting, which are still being elucidated, include sorting in polarized epithelial cells, signal transduction, and regulation of cell-surface hydrolytic activity. GPI-anchored proteins have long been known to be insoluble in non-ionic detergents such as Triton X-100 in the cold. The basis of this property was not understood until recently. Integral membrane proteins are generally detergent-soluble unless they are linked to cytoskeleton. However, GPI-anchored proteins do not have access to cytoskeleton, as they are located in the outer leaflet of the plasma membrane. Detergent-insoluble GPI-anchored proteins are enriched in DRMs. This finding led us to postulate that partitioning of the saturated acyl chains on GPI-anchored proteins into the l_o phase targets the proteins to rafts. Alternatively, protein–protein contacts might be required for detergent-insolubility of GPI-anchored proteins. To test these possibilities, we purified a GPI-anchored protein, placental alkaline phosphatase (PLAP), and incorporated it into SCRL liposomes that (as discussed above) probably contain both detergent-soluble l_d and detergent-resistant l_o phase domains. When we incorporated PLAP into these liposomes, subjected them to detergent extraction, and separated DRMs and the Triton-soluble fractions, we found that PLAP associated with the DRMs. This result shows that the protein interacts directly with lipids in the l_o-phase. Other GPI-anchored proteins behave the same way, while a control transmembrane protein is fully solubilized.

Functions of Rafts

Rafts have been proposed to form in the *trans*-Golgi network, and to function during sorting of apical and basolateral proteins into separate transport vesicles in polarized epithelial cells. In what appears to be an analogous process, rafts have also been implicated in

axonal versus dendritic sorting of proteins in neurons. Rafts are also required for infection of mammalian cells by a number of viruses, including HIV, measles, and Ebola virus. Rafts are required for both entry of viruses into target cells and budding of mature virions from infected cells. However, the best-characterized functions of rafts are in signaling, especially in hematopoietic cells, and in membrane pits called caveolae, as described next.

Signaling in Hematopoietic Cells

Signaling through the antigen receptors in both T cells and basophils also occurs in rafts. For instance, in T cells, the T-cell receptor, associated kinases Lck and Fyn, the downstream adaptor protein LAT, and the costimulatory protein CD28 are present in rafts during signaling. Mutations in Lck and LAT that prevent association of these proteins with rafts affect signaling through the TCR, as do agents that disrupt rafts. These results show that rafts play an important role in signaling in T cells. This novel mechanism of regulating interactions between proteins by selective partitioning into membrane domains is unlikely to be restricted to one cell type. Further work is likely to demonstrate the importance of rafts in signaling in other cell types as well.

Caveolae

Caveolae are 50–100 nm pits in the plasma membrane of most mammalian cells. The membrane protein caveolin-1 plays an important structural role in caveolae, and can induce their formation when expressed in cells that lack caveolae. Unlike clathrin-coated pits, whose formation is induced by transient recruitment of soluble clathrin and adaptor complex coat to membranes, caveolin-1 is an integral membrane protein, and remains embedded in the membrane. Caveolin-1 (22 kDa) forms high-molecular-weight oligomers (400–600 kDa). These oligomers associate with each other in the plane of the membrane in caveolae. Several pieces of evidence show that lipid rafts are concentrated in caveolae. For instance, GPI-anchored proteins have a high affinity for caveolae and will cluster there when cross-linked by antibodies. Gangliosides, acidic glycosphingolipids that are important components of lipid rafts, show similar behavior. Caveolin-1 itself has a high affinity for rafts, and is enriched in DRMs.

Several functions have been ascribed to caveolae. They appear to be signaling centers, where a number of signaling proteins are concentrated. A role for caveolae in intracellular cholesterol transport has also been proposed. Caveolin-1 is a cholesterol-binding protein, which may contribute to a role in cholesterol homeostasis. Caveolae can also internalize from the cell surface. In endothelial cells, caveolae may participate in transport of albumin across the cell monolayer. At least some pathogens have co-opted this pathway. SV40 virus and some pathogenic *Escherichia coli* (*E. coli*) bacteria enter mammalian cells through caveolae during infection.

See Also the Following Articles

Fat Mobilization: Perilipin and Hormone-Sensitive Lipase • Glycosylphosphatidylinositol (GPI) Anchors • Lipid Bilayer Structure • Src Family of Protein Tyrosine Kinases • V-ATPases • Vitamin D

Glossary

caveolae 50–100 nm plasma membrane pits coated with tightly packed oligomers of caveolin-1 and/or other caveolin proteins.

ganglioside Acidic glycosphingolipid containing one or more sialic acid moieties.

glycosphingolipid Sphingolipid with one or more sugars as a head group.

GPI-anchored protein Protein anchored on the outside of the plasma membrane by covalent linkage to glycosyl phosphatidylinositol.

lipid raft Membrane microdomain in the liquid-ordered (l_o) phase; in cell membranes, rich in sterol and sphingolipids.

sphingolipid Membrane lipid with a ceramide backbone consisting of a sphingoid base backbone and a long saturated acyl chain, and a polar head group.

Further Reading

Brown, D. A., and London, E. (1998). Structure and origin of ordered lipid domains in biological membranes. *J. Membr. Biol.* **164**, 103–114.

Harder, T. (2001). Raft membrane domains and immunoreceptor functions. *Adv. Immunol.* **77**, 45–92.

Jacobson, K., and Dietrich, C. (1999). Looking at lipid rafts? *Trends Cell Biol.* **9**, 87–91.

Mukherjee, S., and Maxfield, F. R. (2000). Role of membrane organization and membrane domains in endocytic lipid trafficking. *Traffic* **1**, 203–211.

Simons, K., and Ikonen, E. (1997). Functional rafts in cell membranes. *Nature* **387**, 569–572.

Smart, E. J., Graf, G. A., McNiven, M. A., Sessa, W. C., Engelman, J. A., Scherer, P. E., Okamoto, T., and Lisanti, M. P. (1999). Caveolins, liquid-ordered domains, and signal transduction. *Mol. Cell Biol.* **19**, 7289–7304.

van der Goot, F. G., and Harder, T. (2001). Raft membrane domains: from a liquid-ordered membrane phase to a site of pathogen attack. *Semin. Immunol.* **13**, 89–97.

Biography

Deborah A. Brown is a full Professor in the Department of Biochemistry and Cell Biology at the State University of New York at Stony Brook. In collaboration with Dr. Erwin London, she developed the prevailing model for lipid raft structure, demonstrating that raft lipids exist in membranes as liquid-ordered phase domains. Her principal research interests are in the structure and function of membrane rafts, and membrane trafficking. She obtained a Ph.D. from Stanford University. She received postdoctoral training at Yale University School of Medicine.

Lipoproteins, HDL/LDL

Fayanne E. Thorngate and David L. Williams
State University of New York, Stony Brook, New York, USA

Lipoproteins are large complexes of lipids and proteins that allow the transport of nonpolar lipids through the aqueous plasma. Lipoproteins allow the uptake and transport of dietary fat, fat-soluble vitamins, and cholesterol to peripheral sites to provide energy (skeletal muscle) or for storage (adipose tissue). They consist of a core of nonpolar triglycerides (TG) and cholesteryl ester (CE) surrounded by a monolayer of phospholipids (PL), free cholesterol, and protein. The apolipoproteins are necessary for maintaining the structure of the particles and often serve as ligands or cofactors for receptors and enzymes involved in lipid metabolism. The two major classes of lipoproteins circulating in humans are high-density lipoprotein (HDL) and low-density lipoprotein (LDL), often referred to as "good" cholesterol and "bad" cholesterol, respectively, because of their relative roles in the development of cardiovascular disease.

Structure and Classification

The density at which they float in density-gradient ultracentrifugation defines lipoproteins. The more lipid the particle contains, the lighter its buoyant density. Figure 1 shows the basic structure of the lipoproteins as well as the major size classes. They are also sometimes classified by their complement of apolipoproteins.

Lipoprotein Structure

The cross-section of the chylomicron (CM) in Figure 1 shows the basic structure shared by all of the lipoprotein classes. They are spheres with a core composed of the neutral lipids triglyceride (TG) and cholesterol fatty acid ester (CE). A monolayer of phospholipid (PL), free cholesterol, and apolipoproteins surrounds and solubilizes the water-insoluble core lipids. PLs have polar head groups and hydrophobic acyl tails, which allow them to act as a detergent to solubilize the hydrophobic core lipids.

Apolipoproteins

The apolipoproteins are amphipathic proteins. They have one face that is hydrophobic and interacts with the lipoprotein lipids and one face that is hydrophilic and interacts with the aqueous plasma. Because of their amphipathic properties, the apolipoproteins act as detergents to keep the lipids in solution as microemulsion particles.

Amphipathic α-helix

A fundamental biochemical feature of the amphipathic character is that it is due to protein secondary structure and not to the primary amino acid sequence. The exchangeable apolipoproteins evolved from a common ancestor, and have a structure composed of variable numbers of 11 or 22 amino acid repeat units that form amphipathic α-helices. Thus, when the amino acid chain assumes an α-helical configuration, one face of the helix has hydrophobic amino acid side chains and interacts with lipids and one face of the helix has hydrophilic amino acid side chains and interacts with water. Figure 2 shows a space filling model of apoliprotein A1 (apoA1) as a helical ring, with the lighter colored hydrophobic amino acids on the inside of the ring. The 10 amphipathic α-helices are numbered.

Apolipoprotein Functions

All of the apolipoproteins, except for apolipoprotein B (apoB) are exchangeable and can dissociate and transfer to other particles. They serve as structural components of the lipoprotein and, depending on the apolipoprotein, act as ligands for receptors, activators of enzymes involved in lipid metabolism, or as inhibitors. The overall complement of apolipoproteins on a particle directs its metabolic fate. Table 1 is a list of the major apolipoproteins and some of their basic characteristics.

Metabolism

Apolipoprotein B Lipoprotein Metabolism

CM, secreted by the intestine, have apoB48 as their primary apolipoprotein. The liver secretes very low density lipoprotein (VLDL) with apoB100 as its

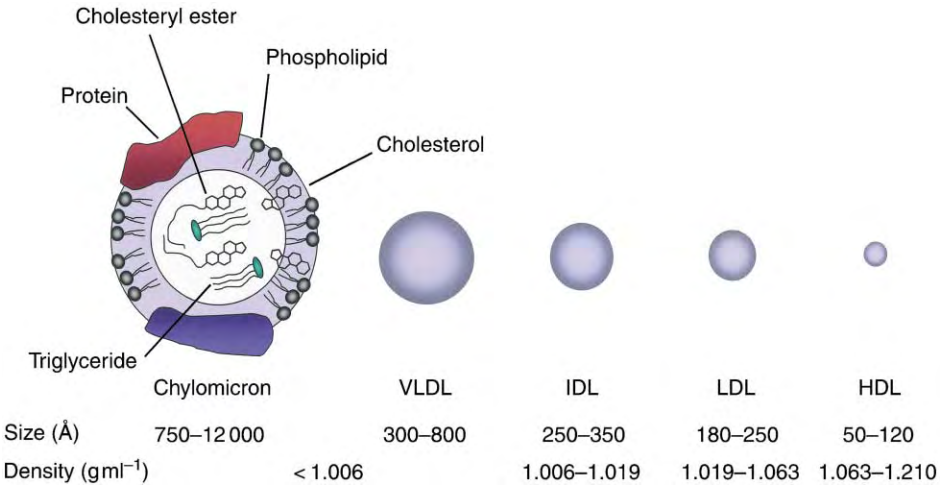

FIGURE 1 Basic physical and structural characteristics of lipoproteins (sizes are not to scale). All lipoproteins are spherical complexes with the sizes and buoyant densities shown beneath. The largest particle, the chylomicron, is shown in cross-section to illustrate its composition; the other particles have similar basic structures, differing in the amount of each component. VLDL, very low density lipoprotein; IDL, intermediate-density lipoprotein; LDL, low-density lipoprotein; HDL, high-density lipoprotein.

primary apolipoprotein. The products of VLDL metabolism in the circulation are intermediate-density lipoprotein (IDL) and low-density lipoprotein (LDL). The apoB lipoproteins carry TG, cholesterol, and fat-soluble vitamins through the circulation to peripheral tissues.

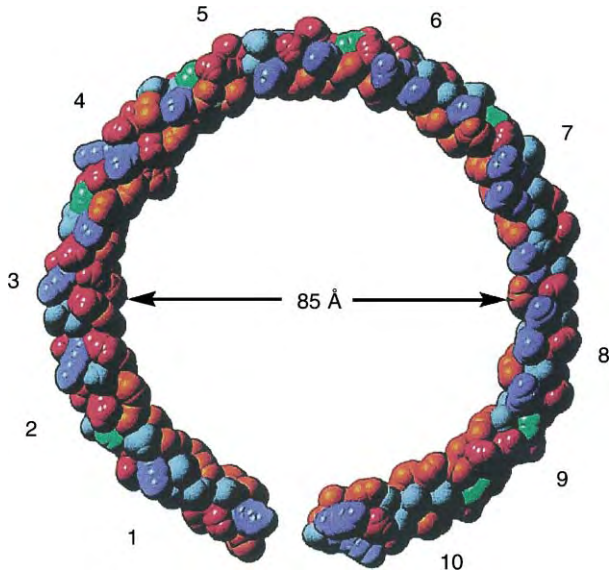

FIGURE 2 A top view of the interfacial surface of apoAI, shown as a space filling model. The lighter shaded, hydrophobic, residues are on the inner face. The ten tandem repeat amphipathic α-helices are numbered. The inner diameter of the structure is 85 Å and the outer diameter is 105 Å. (Reproduced from Segrest, J. P., Jones, M. K., Klon, A. E., Sheldahl, C. J., Hellinger, M., De Loof, H., and Harvey, S. C. (1999). A detailed molecular belt model for apolipoprotein A–I in discoidal high density lipopoprotein. *J. Biol. Chem.* **274**, 31755–31758.)

Dietary Absorption and Chylomicrons

Dietary fat, TG, is broken down in the intestine to fatty acids and glycerol. These fatty acids and dietary cholesterol are taken up by enterocytes, reesterified to TG and CE, and packaged into CM. CMs require apoB48 for formation and carry apoAI, apoAII, and apoIV on their surface as well. The intestine secretes the CM into the lymph and they subsequently enter the circulation where CMs are rapidly catabolized. As shown in Figure 3, lipoprotein lipase (LPL) bound to heparin sulfate proteoglycans on the capillary lumen hydrolyzes the CM–TG. Apo CII is required to activate LPL, and both apoCI and apoCIII inhibit LPL activity. The fatty acids generated are then taken up by muscle as an energy source or by adipocytes and reesterified to form TG for storage as fat. The remaining CM remnants lose the apoA's and acquire apolipoprotein E (apoE) and apolipoprotein C's (apoC's) from the circulation. ApoE serves as a ligand for all of the LDL receptor family members, and mediates clearance of the CM remnants by receptors primarily on the liver. This part of the lipoprotein metabolic pathway is referred to as the extrinsic pathway, as it deals with lipid coming from external sources.

Lipoproteins Produced by the Liver

The liver can also package and secrete lipids, either from remnant catabolism or endogenous synthesis. ApoB100 is essential for the formation of VLDL, which are smaller than CM, but carry significant amounts of TG and CE. This branch of the metabolic pathway is the intrinsic pathway, since it involves endogenous lipids.

TABLE I

Physical and Functional Characteristics of the Apolipoproteins

Apolipoprotein	Molecular mass (Da)	Site of synthesis	Lipoprotein association	Function
ApoAI	28 400	Liver, intestine	HDL, CM	Maintains HDL structure, activates LCAT
ApoAII	17 414	Liver, intestine	HDL, CM	Not well characterized
ApoAIV	46 465	Intestine	HDL, CM	Not well characterized
ApoAV	~39 000	Liver	HDL	Modulates circulating triglyceride levels
ApoB48	241 000	Intestine	CM	Maintains CM structure
ApoB100	512 000	Liver	VLDL, IDL, LDL	Maintains VLDL, IDL, LDL structure, ligand for LDL receptor
ApoCI	6 630	Liver	CM, VLDL, IDL, HDL	Inhibits uptake of CM and VLDL, inhibits lipases
ApoCII	8 900	Liver	CM, VLDL, IDL, HDL	Activates lipoprotein lipase
ApoCIII	8 900	Liver	CM, VLDL, IDL, HDL	Inhibits uptake of CM and VLDL, inhibits lipases
ApoE	34 145	Primarily liver and steroidogenic tissues, many sites	CM, VLDL, IDL, HDL	Ligand for CM and VLDL remnant clearance, binds to all LDL receptor family members
Apo(a)	Varies	Liver	VLDL, IDL, LDL	Unknown, procoagulant

The table lists the most common plasma apolipoproteins, giving their size in Da, their sites of biosynthesis, their respective lipoprotein associations, and some of their major functions. Apolipoproteins, Apo; lecithin cholesterol acyltransferase, LCAT.

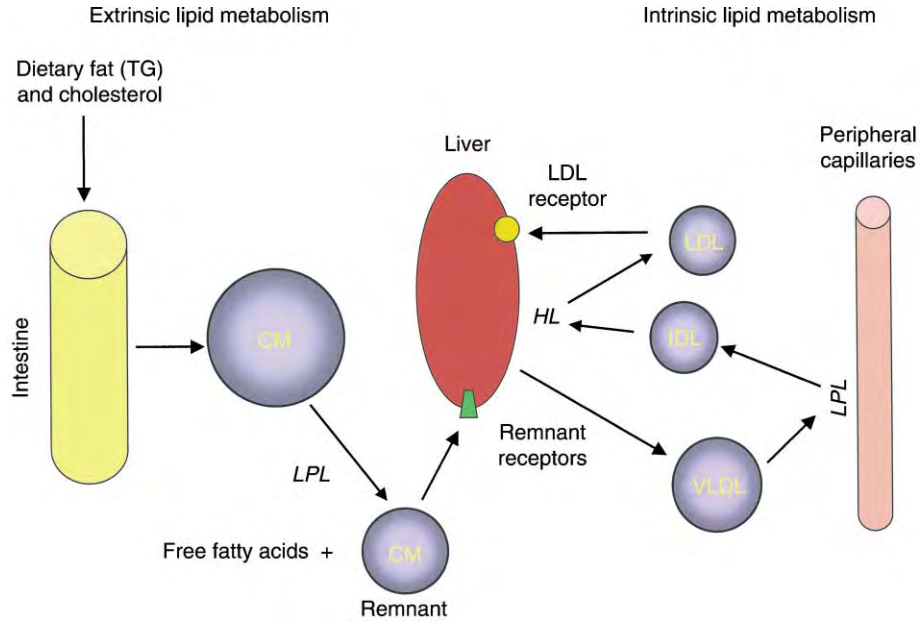

FIGURE 3 Apolipoprotein B (ApoB)-containing lipoprotein metabolism. Enzyme names are shown in italics. In the extrinsic pathway, the small intestine absorbs fats (triglycerides, TG) and cholesterol and resecretes them in chylomicrons (CMs). CMs in the circulation are acted on by lipoprotein lipase (LPL), which hydrolyzes TG and releases fatty acids. One of several remnant receptors on the liver takes up the remaining CM remnants. In the intrinsic pathway, the liver repackages the remnant lipids and secretes them as very low density lipoproteins (VLDL). LPL in the periphery breaks down the VLDL-TG for local energy use. The resulting smaller particles, intermediate-density lipoproteins (IDL), can then either be cleared by liver remnant receptors, or further hydrolyzed by hepatic lipase (HL) at the liver. LDL receptors on the liver or elsewhere take up the final metabolic product, low-density lipoprotein (LDL).

As shown in the right-half of Figure 3, VLDL is lipolyzed by LPL in the periphery, similar to CM. In the circulation, it picks up apoE's and apoC's that modulate its metabolism. Liver remnant receptors clear the VLDL remnants by binding to apoE on the lipoprotein and internalizing the particle. Alternatively, VLDL remnants remain in the circulation for further catabolism. Hepatic lipase (HL), localized to heparin sulfate proteoglycans on the liver, hydrolyzes both TG and PL. IDL is a product of VLDL lipid digestion in the circulation; further metabolism of the particles produces LDL. LDL loses most of the exchangeable apolipoproteins and has mainly apoB100 that is now a ligand for the LDL receptor. In a fasted state, LDL contains most of the circulating cholesterol. Mutations in the LDL receptor can cause familial hypercholesterolemia, characterized by very high plasma cholesterol levels and the development of premature atherosclerosis and heart disease, demonstrating how crucial the receptor is for normal lipoprotein metabolism. Apo(a) is a complex of Lp(a), a protein similar to plasminogen, covalently linked to apoB100 in LDL. The plasma concentrations of apo(a) vary widely from person to person. Lp(a) interferes with clearance of the particles, and interferes with plasminogen action, making it prothrombotic.

HDL Metabolism and Reverse Cholesterol Transport

The apoB-containing lipoproteins provide cholesterol and TG to peripheral tissues. HDL, with apoAI as its primary apolipoprotein provides a way to remove excess cholesterol from tissues and transport it back to the liver for excretion as bile acids and in the bile. This process is called reverse cholesterol transport, and is the only way most tissues can dispose of excess cholesterol.

Production of HDL

Unlike CM or VLDL, HDL is formed in the circulation. The liver secretes apoAI and apoAII either as lipid-free proteins or bound to a few PL. As shown in Figure 4, these complexes circulate as apolipoprotein–PL disks, and not as spherical particles. They can have various combinations of apoA's, but apoAI is predominant. An alternate source of lipid-poor apoAI and apoAIV is from the surface of CM as they are metabolized. These disks can interact with several systems to pick up lipids and mature into spherical HDL. Lipid-poor apolipoproteins can bind to the recently characterized protein, ATP-binding cassette protein type A1 (ABCA1). Most cell types express ABCA1 on their surface. ABCA1 mediates the transfer of PL and cholesterol from the cell surface to the apolipoprotein. When this occurs in peripheral tissues, it is the first step of reverse cholesterol transport; however, most apoAI is probably lipidated by ABCA1 in the liver.

Interestingly, mutations in ABCA1 cause a syndrome that is one of the first genetically caused lipoprotein disorders described. Tangiers disease is characterized by very low or no circulating apoAI and HDL, and accumulation of cholesterol in macrophage rich tissues, such as the tonsils. Only recently the genetic cause has been determined. The apoAI gene and its expression are normal in this syndrome, but without ABCA1 to transfer lipid to apoAI, the kidneys rapidly catabolize the apoAI.

With apoAI as an activator, the enzyme lecithin cholesterol acyltransferase (LCAT) can transfer an acyl group from a PL to the cholesterol, generating CE. The CE is nonpolar so it moves to form a core within the disk, generating a spherical HDL. These particles can also accept free cholesterol passively desorbing from the cell surface, a process facilitated by the HDL receptor, scavenger receptor class B type I (SR-BI). Free cholesterol efflux from cells is another mode of reverse cholesterol transport.

Lipid Transfer Proteins

There are two lipid transfer proteins involved in HDL metabolism in the plasma. Phospholipid transfer protein (PLTP) can transfer excess surface PL, generated during the metabolism of remnant lipoprotein core lipids to HDL. It also can facilitate the fusion of HDL particles, generating large HDL and lipid-poor apolipoproteins. Cholesteryl ester transfer protein (CETP) catalyzes the transfer of CE from HDL to VLDL and LDL, which can then be cleared by liver receptors for excretion. This is one way to complete reverse cholesterol efflux.

HDL Delivery of CE to Tissues

The only tissues capable of catabolizing cholesterol are the liver and steroid hormone producing organs (adrenal, ovaries, testes). The liver converts cholesterol to bile acids and excretes them through the intestine. The steroidigenic organs convert cholesterol to steroid hormones (cortisol, estrogen, testosterone, etc.). These tissues have an abundance of the HDL receptor, SR-BI, which in addition to facilitating cholesterol efflux from cells allows the uptake of CE by cells. HDL binds to the receptor and selectively transfers the CE core to the cell, without the degradation of the particle as a whole. Selective uptake differs from the LDL receptor uptake pathway, in which the whole lipoprotein is internalized and degraded. HL found on the surface of the liver and adrenal gland hydrolyzes the PL and TG left in the CE depleted HDL, releasing lipid-poor apoAI. Probably the major path for the loss of cholesterol from the body is the loss of cholesterol with epidermal cells shed from the skin. However, the SR-BI mediated transfer of CE to the

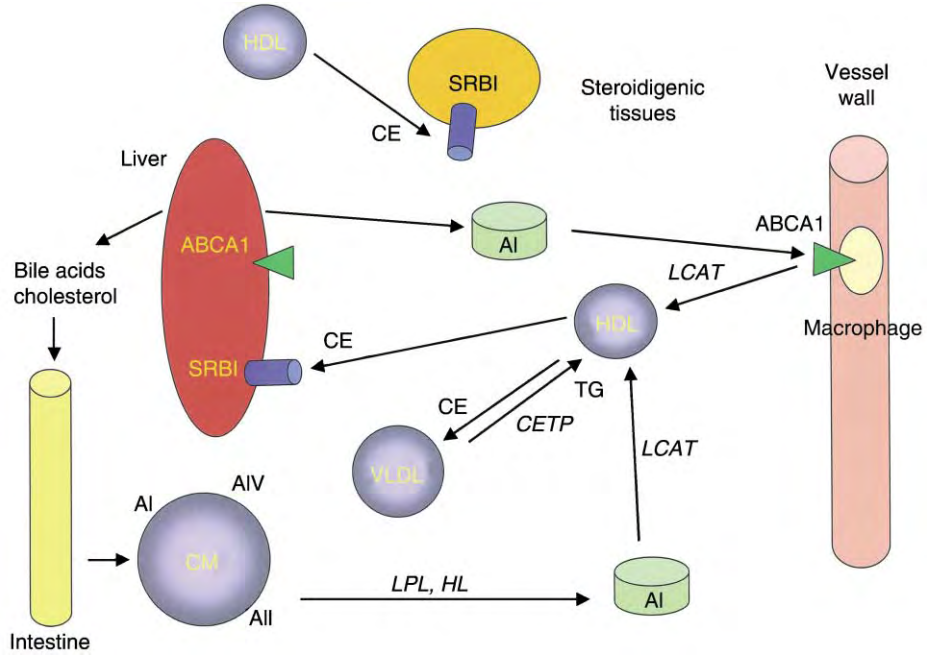

FIGURE 4 High-density lipoprotein (HDL) metabolism and reverse cholesterol transport. Lipolytic enzyme and transfer protein names are shown in italics. Apolipoprotein AI (AI) enters the circulation either by secretion from the liver as a lipid-poor apolipoprotein or on CM secreted by the intestine. Lipoprotein lipase (LPL) and hepatic lipase (HL) hydrolyze CM lipids, releasing lipid-poor apoA's from the remnant surface. The lipid-poor apoAI-phospholipid (PL) disks (shown as disks instead of spheres) can interact with peripheral ATP binding cassette transporter type A1 (ABCA1) and pick up PL and cholesterol. Lecithin cholesterol acyltransferase (LCAT) can then esterify the cholesterol in the outer monolayer of the disks, producing cholesteryl ester (CE) that moves to form a lipid core; all of these activities result in larger, spherical HDL. These CE-enriched HDLs can then deliver the CE to the liver or steroidigenic tissues via interaction with scavenger receptor type BI (SR–BI). In addition, cholesteryl ester transfer protein (CETP) can mediate the exchange of CE from HDL for triglyceride (TG) from VLDL or remnants with the subsequent clearance of the remnants by the liver. The liver converts cholesterol delivered to it to bile acids, or secretes the cholesterol with the bile into the intestine for excretion.

liver is critical for removing cholesterol from internal tissues and completing reverse cholesterol transport.

Pathologies of Lipoprotein Metabolism

The primary metabolic contributor to the development of atherosclerosis (deposition of cholesterol in the artery wall with subsequent vascular, inflammatory and thrombotic dysfunction) is elevated LDL cholesterol. There is a strong epidemiological evidence that elevated LDL cholesterol correlates with cardiovascular disease, as does decreased HDL cholesterol. Several natural human mutations elevate LDL levels and lead to atherosclerotic vascular disease, implicating elevated LDL levels as a requisite cause of this disease. More recently, studies with LDL lowering drugs demonstrate reduced disease risk. Additionally, a wealth of studies in numerous animal models demonstrates that LDL, IDL, and CM remnants can cause atherosclerotic disease. Atherosclerosis is one of the major contributors to cardiovascular disease, leading to heart attacks and stroke. Disorders of lipoprotein metabolism may also contribute to obesity, type 2 diabetes, and renal disease, all of which are becoming more prevalent in our aging population.

Disruption of any step in these pathways can lead to imbalances in plasma lipids, by either increased production or decreased catabolism, and clearance. There are many syndromes stemming from mutations in proteins involved in lipoprotein metabolism. A classical example is familial hypercholesterolemia, mentioned above. In this syndrome LDL receptors are not functional, severely inhibiting LDL clearance, leading to accumulation of LDL cholesterol in the circulation. This can lead to death from heart attacks as young as the early teens. The Further Reading selections describe other pathologies of lipoprotein metabolism.

A great deal has been learned about the components and interactions of these systems, spurred on recently by the development of transgenic and knockout mouse models. However, it is critical that we expand our understanding of these systems, especially in view of the dramatic increases in diseases linked to disruptions of lipoprotein metabolism.

See Also the Following Articles

Cholesterol Synthesis • Endocytosis • Fat Mobilization: Perilipin and Hormone-Sensitive Lipase • Fatty Acid Oxidation • Fatty Acid Receptors • Fatty Acid Synthesis and Its Regulation

Glossary

apolipoproteins The major protein components of lipoproteins. They stabilize the structure of the lipoproteins. In addition, some serve as ligands for lipoprotein receptors and some are activators or inhibitors of enzymes and transfer proteins involved in lipoprotein metabolism.

ATP cassette binding protein type A1 A recently characterized apolipoprotein binding protein. It mediates the transfer of phospholipid and cholesterol from cells to lipid-poor apolipoproteins.

LDL receptor family A family of related cell-surface receptors critical for lipoprotein uptake into cells. All of the receptors bind apoE, and the definitive member; the LDL receptor also binds apoB and is critical for LDL uptake. Loss of LDL receptor function causes familial hypercholesterolemia.

reverse cholesterol transport The removal of cholesterol from peripheral tissues and its clearance and excretion, mainly by the liver. This process protects the vessel wall from accumulating cholesterol and becoming atherosclerotic.

scavenger receptor class B type I A HDL receptor that facilitates efflux of free cholesterol from cells to HDL. It also mediates the selective uptake of CE from HDL for clearance by the liver or steroid hormone synthesis in the adrenal gland, ovaries, and testes.

Further Reading

Betteridge, D. J., Illingworth, D. R., and Shepherd, J. (eds.) (1999). *Lipoproteins in Health and Disease*. Arnold, London.

DeWinter, M. P. J., and Hofker, M. H. (2002). New mouse models for lipoprotein metabolism and atherosclerosis. *Curr. Opin. Lipidol.* **13**, 191–197.

Knowles, J. W., and Maeda, N. (2000). Genetic modifiers of atherosclerosis in mice. *Arterioscler. Thromb. Vasc. Biol.* **20**, 2336–2345.

Scriver, D. R., Sly, W. S., Childs, B., Beaudet, A. L., Valle, D., Kinzler, K. W., and Vogelstein, B. (2002). *The Metabolic and Molecular Bases of Inherited Disease* 8th edition, Chapters 114–123. McGraw-Hill, New York.

Segrest, J. P., Jones, M. K., Klon, A. E., Sheldahl, C. J., Hellinger, M., De Loof, H., and Harvey, S. C. (1999). A detailed molecular belt model for apolipoprotein A–I in discoidal high density lipopoprotein. *J. Biol. Chem.* **274**, 31755–31758.

Singh, B. K., and Mehta, J. L. (2002). Management of dyslipidemia in the primary prevention of coronary heart disease. *Curr. Opin. Cardiol.* **17**, 503–511.

Biography

Fayanne E. Thorngate is a research instructor of pharmacological sciences in the School of Medicine at the State University of New York at Stony Brook. Her research interests are the mechanisms of atherosclerotic disease development, cholesterol and lipoprotein metabolism, with an emphasis on the use of mouse models of disease. Dr. Thorngate received her Ph.D. in biochemistry and nutrition from the University of North Carolina at Chapel Hill where she was a National Science Foundation fellow in biochemistry. She did postdoctoral work in lipoprotein metabolism at the University of Tennessee Health Sciences Center in Memphis, and at the State University of New York at Stony Brook.

David L. Williams is a Professor of Pharmacological Sciences in the School of Medicine at the State University of New York at Stony Brook. His research interests are in the areas of atherosclerotic disease processes, cholesterol, and lipoprotein metabolism, and in the cell biology of lipoprotein receptors. Dr. Williams received his Ph.D. in cell biology from the University of Illinois at Urbana and did postdoctoral work in molecular biology at the University of California at San Francisco. He was among the first investigators to apply molecular biological approaches to the study of lipoproteins and the first to establish the tissue sites of apolipoprotein E expression in humans and animal models.

Low Barrier Hydrogen Bonds

Perry A. Frey
University of Wisconsin, Madison, Wisconsin, USA

Proteins contain mainly weak, conventional hydrogen bonds; however, a few enzymes have low barrier hydrogen bonds (LBHBs) in transition state analogue complexes. Hydrogen bonds display variations in physicochemical properties including length, spectroscopic characteristics, and strength. Three classes of hydrogen bonds have been defined – weak (2–8 kcal mol^{-1}), strong (10–20 kcal mol^{-1}), and very strong (24–40 kcal mol^{-1}). In a weak hydrogen bond, the proton is bonded to one heteroatom by a dipolar covalent bond and engages in a weak electrostatic attraction with another heteroatom. In a strong hydrogen bond, or LBHB, the heteroatoms are closer than a van der Waals contact, the covalent bond to the proton is elongated, and the contact between the proton and the second heteroatom is significantly shorter than in a weak hydrogen bond. In a very strong, or single-well hydrogen bond, the heteroatoms are much closer than a van der Waals contact, and the proton is nearly centered between them. LBHBs in proteins and small molecules are characterized by their spectroscopic and thermodynamic properties, deuterium fractionation factors, and crystallographic structures. LBHBs have been identified in transition state analogue complexes of a few enzymes and are postulated to stabilize the transition states in catalysis.

The Nature of Hydrogen Bonds

Hydrogen bonds were controversial throughout the 20th century. By mid-20th century, the weak conventional hydrogen bonds were reasonably well understood and widely accepted. Unlike covalent bonds, which vary in strength within a factor of ~4 (30–120 kcal mol^{-1}), hydrogen bonds are much less constrained in their geometry and physical properties, and they vary in strength by a factor of at least 20-fold (2–40 kcal mol^{-1}). Very few strong hydrogen bonds had been documented before the mid-20th century, principally the very strong hydrogen bond in hydrogen difluoride $[F\cdots H\cdots F]^-$ (40 kcal mol^{-1}). Such strong hydrogen bonds were thought to be limited to crystalline states. In the latter half of the century, strong hydrogen bonds were discovered in several classes of organic molecules in crystals and aprotic liquid phases and characterized by crystallographic, spectroscopic, and chemical methods.

Weak, Strong, and Very Strong Hydrogen Bonds

The distinctions among hydrogen bonds can be illustrated by the differences among their energy profiles, as shown in Figure 1. Figure 1A is the energy profile for a weak hydrogen bond, that in Figure 1B is for a strong or LBHB, and that in Figure 1C is for a single-well or very strong hydrogen bond. The three classes are sometimes referred to as weak, moderate, and strong hydrogen bonds. Most hydrogen bonds in proteins and nucleic acids involve oxygen or nitrogen as the heteroatoms. For that reason, the hydrogen bonding properties delineated below refer to N or O as heteroatoms. Larger or smaller heteroatoms such as sulfur or fluorine display analogous properties with physical parameters outside the ranges for N and O.

Weak Hydrogen Bonds

As illustrated in Figure 1A, the hydrogen (or deuterium) is confined to covalent bonding with one heteroatom by the fact that their zero point vibrational energies are much lower than the barrier separating the heteroatoms. The covalent bond linking the electronegative atom to a hydrogen is dipolar, with a partial positive charge on the proton and a partial negative charge on the heteroatom. The electrostatic attraction between the proton and another partially negative heteroatom is a weak hydrogen bond. The strengths of weak hydrogen bonds range between 2 and 8 kcal mol^{-1}, depending on the type of heteroatoms, their electrostatic charge, the distance separating them, and the dielectric medium. Because they are weak, conventional hydrogen bonds easily undergo exchange with protons of water, with enthalpies of activation on the order of 2–3 kcal mol^{-1}.

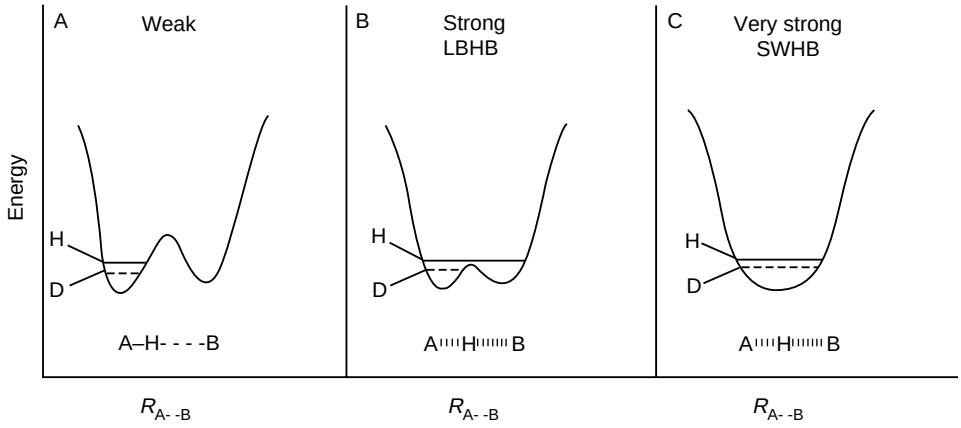

FIGURE 1 In (A), the double well potential for a proton covalently bonded to heteroatom A and weakly hydrogen bonded to heteroatom B is illustrated. The zero point energies for H and D are both well below the barrier, and both are strictly covalently bonded to A. In (B) for an LBHB, the heteroatoms are drawn close together in violation of van der Waals contact distance, the proton is moved toward B and away from A, and the barrier is lowered to near the zero point energy of H. The zero point energy of D is lower, so that deuterium is less attracted to B. In (C) for a single-well hydrogen bond, the heteroatoms are even closer together, and the proton is nearly centered between them. In the LBHB and SWHB the bonding of the proton to heteroatom B is partially covalent.

LBHBs—Strong Hydrogen Bonds

In an LBHB (Figure 1B) the heteroatoms are closer together and separated by significantly less than the van der Waals contact distance. As a consequence, the energy barrier between them is lowered to the range of the zero point vibrational energy for hydrogen, so that the hydrogen feels increased attraction to the other heteroatom and is drawn away from the first heteroatom, A···H in Figure 1B. Deuterium, feels less attraction to the second heteroatom, owing to its lower zero point energy. Because of this difference, an LBHB displays deuterium and tritium isotope effects. LBHBs are stronger (10–20 kcal mol^{-1}) than weak hydrogen bonds because of the partial covalency between hydrogen and the second heteroatom, H···B in Figure 1B. As they are strong, LBHBs undergo exchange with protons of water less readily than weak hydrogen bonds. In an LBHB the proton is strongly held, and the activation enthalpy for exchange with the protons of water is much higher than the $\sim$3 kcal mol^{-1} for a weakly hydrogen bonded proton. For LBHBs in proteins, the activation enthalpies for exchange are typically 10–19 kcal mol^{-1}.

Single-Well or Very Strong Hydrogen Bonds

In a single-well hydrogen bond the heteroatoms are so close together that the zero point energies of both hydrogen and deuterium lie above the barrier, as in A···H···B of Figure 1C. The proton is almost equally bonded between the heteroatoms and is nearly centered between them. Perfectly symmetrical, single-well hydrogen bonds are the strongest, 24–40 kcal mol^{-1}, and are observed in very few small molecules. Such hydrogen bonds have not been detected in proteins.

Physicochemical Properties

Bond Lengths

Weak Hydrogen Bonds

The covalent bond length (O, N–H) is about 0.95Å, the length of the electrostatic contact with the second heteroatom is $\geq$ 1.7Å, and the separation between the heteroatoms is $\geq$ 2.6Å for O···O, $\geq$ 2.7Å for O···N, and $\geq$ 2.8Å for N···N. Distances separating the heteroatoms can vary from the minima quoted above to as much as 3.5Å.

LBHBs

In an LBHB (Figure 1B) the covalent bond is elongated to 1.05–1.1Å, and the distance to the second heteroatom is shortened, e.g., to 1.4–1.5Å. The separation between heteroatoms is shortened to $\leq$2.6Å for O···O, $\leq$2.7Å for O···N, and $\leq$2.8Å for N···N. A short contact distance between heteroatoms is necessary but not sufficient for an LBHB. To be an LBHB, the hydrogen must be positioned in alignment with the heteroatoms. If the hydrogen is out of alignment, the hydrogen bond will be weak. In the strongest LBHBs, the proton affinities of the heteroatoms are similar or identical. The p*K*a of the conjugate acid of a heteroatom is a measure of proton affinity, and heteroatoms in functional groups with similar or identical values of p*K*a form the strongest hydrogen bonds.

Single-Well Hydrogen Bonds

The hydrogen lies nearly equidistant from the heteroatoms and is approximately equally shared. The hydrogen is 1.2–1.3Å from each heteroatom, depending on whether it is O or N. Perfectly symmetrical hydrogen bonds are rare and so far observed only in small molecules incorporating special structural constraints that favor single-well hydrogen bonding. Single-well hydrogen bonds range in strength from 24 to 40 kcal mol^{-1} and are the strongest hydrogen bonds. They are formed between heteroatoms of functional groups with identical values of p*K*a, in molecules or lattices in which the groups are held in close proximity.

Spectroscopic Properties

Weak Hydrogen Bonds

The NMR chemical shift of the proton ranges between 9 and 11 ppm and does not display an isotope effect (isotope shift) upon replacement with deuterium or tritium.

LBHBs

Due to the elongated bond to the hydrogen, A···H in Figure 1B, the proton is substantially deshielded from the nonbonding electrons of the heteroatom. Consequently, the NMR signal for an LBHB involving O or N is downfield in the range of 18–20 ppm on the chemical shift scale. In the absence of an internal magnetic effect, such as complexation with a paramagnetic metal ion, a downfield chemical shift is a strong indicator of an LBHB or single-well hydrogen bond. In an LBHB as in Figure 1B, the zero point energy difference between hydrogen and deuterium leads to deuterium and tritium isotope effects on the NMR signal, with that for deuterium falling upfield by up to 0.6 ppm from that for hydrogen.

As the proton in an LBHB interacts with both heteroatoms to a greater degree than a deuteron, there is an isotope effect on the infrared stretching frequency. The ratio of stretching frequencies ν_{OH}/ν_{OD} for and O–H and O–D engaged in an LBHB differs from the ratio typical of weak hydrogen bonds. For weak hydrogen bonds $\nu_{OH}/\nu_{OD} = 1.4$ and represents the mass difference between hydrogen and deuterium. For an LBHB, $1.0 \leq \nu_{OH}/\nu_{OD} < 1.4$ in small molecules. This is because of the greater strength of the LBHB with H than with D, and the difference in strength arises because of the differential interactions of H and D with the barrier in Figure 1B. This property of LBHBs in small molecules has been extensively documented. Among the physicochemical properties that have been used in characterizing LBHBs, the deuterium isotope effect on the infrared stretching frequencies is the only one that has not been applied to LBHBs in proteins.

Single-Well Hydrogen Bonds

Single-well hydrogen bonds display downfield NMR signals at 21–22 ppm when the heteroatoms are O or N. Because the zero point energies of both H and D lie above the barrier in Figure 1C, single-well hydrogen bonds do not display deuterium or tritium isotope effects on NMR signals. They also do not display deuterium isotope effects on infrared stretching frequencies, that is, $\nu_{OH}/\nu_{OD} = 1.4$.

Deuterium Fractionation Factors

Weak Hydrogen Bonds

Weakly hydrogen bonded protons display deuterium fractionation factors Ψ of about 1.0–1.2. The fractionation factor is the equilibrium constant for the exchange of hydrogen bonded protons with deuterons in deuterium oxide. A fractionation factor of 1.0 means that deuterons and protons are bound with equal affinities.

LBHBs

In an LBHB, hydrogen is more strongly bonded than deuterium because of the effect illustrated in Figure 1B. Therefore, the deuterium fractionation factor Ψ for an LBHB is less than 1.0, typically 0.3–0.7.

Single-Well Hydrogen Bonds

In a single-well hydrogen bond, the zero point energies of both H and D lie above the barrier, so that they interact similarly with both heteroatoms. Therefore, the fractionation factor is generally ~1.0.

LBHBs in Enzymes

Serine Proteases

An LBHB was first assigned to the proton bridging His57 and Asp102 in chymotrypsin at low pH and in transition state analogue complexes of chymotrypsin. The assignment was based initially on the downfield NMR chemical shift for this proton of 18.0 ppm for chymotrypsin at low pH and 18.9 ppm for chymotrypsin a transition state-analogue complex, and on the close contact between His57 and Asp102 (<2.6Å) in crystal structures of transition state analogue complexes. The LBHB was postulated to stabilize the transition state and facilitate its formation. It was shown in this connection to increase the basicity of His57. The characterization of this LBHB in several transition state analogue complexes was completed by measurements of its fractionation factor of 0.3–0.4, its enthalpy of activation for exchange

of 14–19 kcal mol^{-1}, and the deuterium and tritium isotope effects on its NMR chemical shifts. The role of the LBHB in catalyzing the formation of the acyl-chymotrypsin intermediate in the action of chymotrypsin is illustrated in Figure 2. In resting chymotrypsin, His57 is not protonated and is engaged in weak hydrogen bonding with Asp102. His57 abstracts the proton from Ser195 as it attacks the acyl carbonyl group of a substrate to form the tetrahedral intermediate. In the transition state for proton abstraction, His57 becomes protonated on His57-Nε2, and the LBHB is formed between His57-Nδ1 and Asp102. The resulting LBHB stabilizes the transition state and tetrahedral adduct and thereby facilitates the formation of the metastable intermediate. The LBHB maintains the basicity of His57 with a p*K*a of 10.6 to 12, intermediate between that of Ser195 (13.4) and that of the amino terminus (9.2) of the peptide leaving group. Thus, the LBHB makes His57 an optimal acid/base catalyst for the acylation of Ser195 by a peptide substrate.

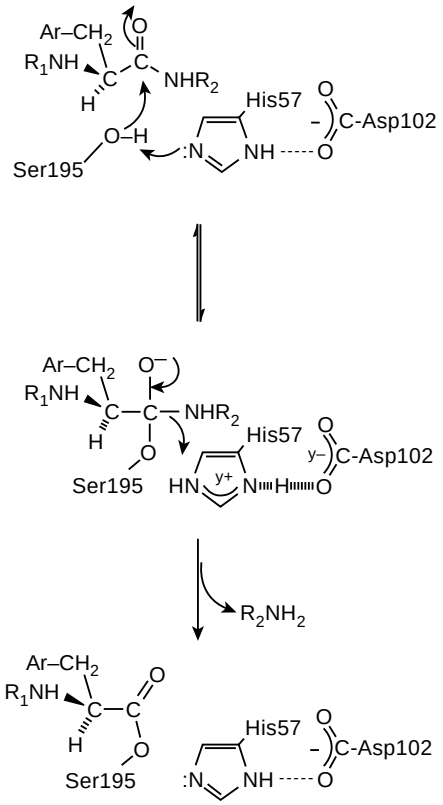

FIGURE 2 The role of the LBHB in the mechanism of acylation of serine proteases. In the Michaelis complex, the active site histidine (His57 in chymotrypsin numbering) is neutral and weakly hydrogen bonded to Asp201. In the first step, His57 abstracts a proton from Ser195 as it undergoes nucleophilic addition to the substrate carbonyl group. As His57-Nε2 becomes protonated, the hydrogen bond between His57-Nδ1 and Asp-Oδ2 becomes a strong LBHB, and this increases the basicity of His57 as it enters the transition state. The LBHB stabilizes the transition state and transient tetrahedral intermediate. In the second step, His57-Nε2 donates the proton to the N-terminal amino group of the leaving peptide.

Evidence, similar to but less extensive than that above, for chymotrypsin has been obtained for other serine proteases, especially trypsin and subtilisin. The crystal structure of subtilisin at 0.78Å resolution shows electron density for hydrogen in the LBHB linking His64 and Asp32. The electron density for the proton places it 1.2Å from His57-Nδ1 and 1.5Å from Asp32-Oδ2. ^{15}N NMR analysis of the LBHB in a transition state analogue complex of subtilisin indicates that the proton, 20–30%, is transferred toward Asp32. Both the crystallography and NMR spectroscopy verify that this is an LBHB and support its catalytic role as originally postulated in the action of chymotrypsin.

Serine Esterases

Serine esterases have catalytic triads similar to serine proteases and function by a similar mechanism. Extensive NMR analysis of the hydrogen bond, linking the active site histidine with the active site glutamate, document the presence of an LBHB.

Δ^5-3-Ketosteroid Isomerase

The isomerization requires the enolization of the 3-keto group of the substrate to form a homoenolate anion as a metastable intermediate. The homoenolate is within hydrogen bonding distance of Tyr14, and the p*K*a of the homoenol is similar to that of tyrosine or phenol. The phenolic inhibitor dihydroequilinen forms an LBHB with Tyr14 in analogy with a putative LBHB in the complex of the metastable homoenolate with Tyr14. The LBHB displays the properties including a downfield NMR signal, low deuterium fractionation factor, and close contact in the crystal structure. The LBHB is postulated to stablize the homoenolate and thereby facilitate its formation in the catalytic mechanism.

See Also the Following Articles

Kinetic Isotope Effects • Substrate Binding, Catalysis, and Product Release

Glossary

deuterium ractionation factor The equilibrium constant for exchange of a proton with the deuterons in D_2O.

isotope shift The upfield perturbation of an NMR signal of an atom when a heavy isotope is substituted for it.

transition state analogue A stable molecule that has nearly all of the structural features of a transition state.

Further Reading

Choi, G., Ha, N. C., Kim, S. W., Kim, D. H., Park, S., Oh, B. H., and Choi, K. Y. (2000). Asp-99 donates a hydrogen bond not to Tyr-14 but to the steroid directly in the catalytic mechanism of Delta 5-3-ketosteroid isomerase from Pseudomonas putida biotype B. *Biochemistry* **39**, 903–909.

Cleland, W. W. (1992). Low-barrier hydrogen bonds and low fractionation factor bases in enzymatic reactions. *Biochemistry* **31**, 317–3199.

Cleland, W. W., and Kreevoy, M. M. (1994). Low-barrier hydrogen bonds and enzymic catalysis. *Science* **264**, 1887–1890.

Frey P. A., Whitt S. A., Tobin J. B. (1994). A low-barrier hydrogen bond in the catalytic triad of serine proteases. *Science* **264**, 1927–1930.

Gerlt, J. A., and Gassman, P. M. (1993). Understanding the rates of certain enzyme-catalyzed reactions: proton abstraction from carbon acids, acyl-transfer reactions, and displacement reactions of phosphodiesters. *Biochemistry* **32**, 11943–11952.

Halkides, C. J., Wu, Y. Q., and Murray, C. J. (1996). A low-barrier hydrogen bond in subtilisin: 1H and 15N NMR studies with peptidyl trifluoromethyl ketones. *Biochemistry* **35**, 15941–15948.

Hibbert, F., and Emsley, J. (1990). Hydrogen bonding and chemical reactivity. *Adv. Phys. Org. Chem.* **26**, 255–379.

Jeffrey, G. A. (1997). *An Introduction to Hydrogen Bonding*. Oxford University Press, New York.

Kuhn, P., Knapp, M., Soltis, S. M., Ganshaw, G., Thoene, M., and Bott, R. (1998). The 0.78Å structure of a serine protease: Bacillus lentus subtilisin: *Bacillus lentus Subtilisin*. *Biochemistry* **37**, 13446–13452.

Lin, J., Cassidy, C. S., and Frey, P. A. (1998). Correlations of the basicity of His 57 with transition state analogue binding, substrate reactivity, and the strength of the low-barrier hydrogen bond in chymotrypsin. *Biochemistry* **37**, 11940–11948.

Lin, J., William, M., Westler, W., Wallace Cleland, Markley, J. L., and Frey, P. A. (1998). Fractionation factors and activation energies for exchange of the low barrier hydrogen bonding proton in peptidyl trifluoromethyl ketone complexes of chymotrypsin. *Proc. Natl. Acad. Sci.* **95**, 14664–14668.

Massiah, M. A., Viragh, C., Reddy, P. M., Kovach, I. M., Johnson, J., Rosenberry, T. L., Mildvan, A. S. (2001). Short, strong hydrogen bonds at the active site of human acetylcholinesterase: proton NMR studies. *Biochemistry* **40**, 5682–5690.

Mildvan, A. S., Harris, T. K., and Abeygunawardana, C. (1999). Nuclear magnetic resonance methods for the detection and study of low-barrier hydrogen bonds on enzymes. *Methods Enzymol.* **308**, 219–245.

Neidhart, D., Wei, Y., Cassidy, C., Lin, J., Cleland, W. W., and Frey, P. A. (2001). Correlation of low-barrier hydrogen bonding and oxyanion binding in transition state analogue complexes of chymotrypsin. *Biochemistry* **40**, 2439–2447.

Westler, W. M., Frey, P. A., Lin, J., Wemmer, D. E., Morimoto, H., Williams, P. G., and Markley, J. L. (2002). Evidence for a strong hydrogen bond in the catalytic dyad of transition-state analogue inhibitor complexes of chymotrypsin from proton-triton NMR isotope shifts. *J. Am. Chem. Soc.* **124**, 4196–4197.

Zhao, Q., Abeygunawardana, C., Talalay, P., and Mildvan A. S. (1996). NMR evidence for the participation of a low-barrier hydrogen bond in the mechanism of 5-3-ketosteroid isomerase. *Proc. Natl. Acad. Sci.* **93**, 8220–8224.

Biography

Perry A. Frey is the Robert H. Abeles Professor of Biochemistry at the University of Wisconsin-Madison. His main research interest is the elucidation of enzymatic and coenzymatic reaction mechanisms. He holds a Ph.D. in biochemistry from Brandeis University and was a postdoctoral fellow in Chemistry at Harvard University. He has authored a textbook in biochemistry and is a life-time member of the National Academy of Sciences.

Luft's Disease

Salvatore DiMauro
Columbia University, New York, USA

Luft's disease is an extremely rare human disorder characterized by loose coupling of mitochondrial oxidative phosphorylation in skeletal muscle, that is, loss of the control normally exerted by ATP on the rate of respiration of muscle mitochondria. Although described only in two patients, Luft's disease is of great historical importance because it was the first example of organellar medicine and it opened the field of mitochondrial diseases, which has expanded into a large and complex area involving all subspecialties of medicine.

Clinical Considerations

Both patients were women, one from Sweden, the other from Jordan, without any family history of similar disorders. The clinical hallmark was hypermetabolism, with fever, heat intolerance, profuse perspiration, polyphagia, polydipsia, and tachycardia at rest. Although both patients suffered from exercise intolerance, weakness was mild. The Jordanian patient also had diffuse erythema of the legs due to capillary proliferation, maybe an attempt by the body to create a radiator to facilitate heat dispersion. The initial diagnosis was hyperthyroidism, but Rolf Luft, an endocrinologist at the Karolinska Institute in Stockholm, ruled out this possibility and astutely suggested that mitochondrial dysfunction of skeletal muscle, the most abundant tissue in the body, could underlie this condition. A muscle biopsy confirmed that mitochondria were excessively numerous and morphologically abnormal, and polarographic studies of isolated mitochondria showed loose coupling. The paper describing these findings is a classic of clinical investigation, which amply justifies the eponym.

Onset of symptoms had been in childhood in both patients, and the course was slowly but relentlessly progressive: both women died, in their middle ages, of respiratory failure. Autopsies were not performed, but clinical evidence strongly suggests that the disease is confined to skeletal muscle, as heart function was normal and there were no symptoms of central nervous system (CNS) involvement.

Electromyography (EMG) was compatible with myopathy.

Therapy

In 1971, Haydar employed a naïve but pioneer approach to gene therapy in the second patient with Luft's disease,

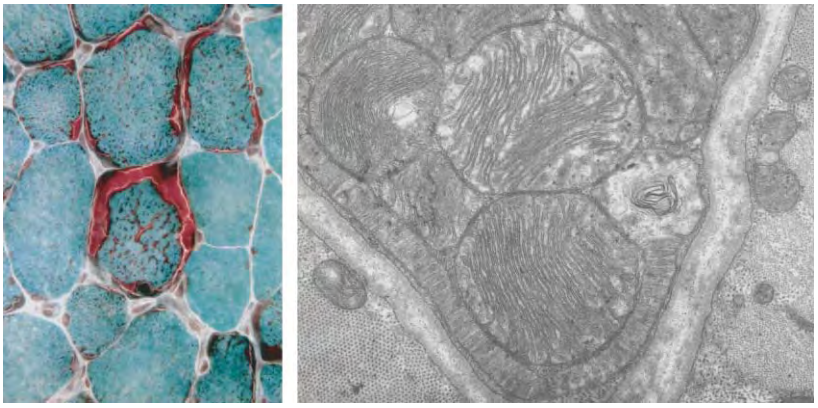

FIGURE 1 Morphology of a muscle biopsy from the second patient with Luft's disease. The left panel shows the histochemical stain of a frozen section with the modified Gomori trichrome, which reveals abnormal accumulations of mitochondria as reddish blotches (ragged-red fibers). The right panel is an electron micrograph showing a portion of one fiber (bottom) with normal morphology. The adjacent fiber (top) shows massive accumulation of mitochondria under the cell membrane. The accumulated mitochondria are greatly enlarged and have tightly packed cristae.

who was given chloramphenicol to inhibit mitochondrial protein synthesis and reduce her basal metabolic rate. During the first trial, some reduction of the basal metabolic rate was achieved and was accompanied by mild subjective improvement, but the second trial had to be interrupted because of drug toxicity.

Thus, the molecular basis of the prototypical mitochondrial myopathy remains obscure 40 years after Luft described the first patient, a situation made more difficult by the fact that only one other patient with Luft's disease has been identified; both patients are deceased, and no tissues are available, except fibroblasts from the second patient.

Muscle Biopsy

Morphology

In both women, there was massive proliferation of mitochondria, documented with the modified Gomori trichrome histochemical stain by the presence of ragged-red fibers (RRFs) in the second patient, and by electron microscopy in both patients. Ultrastructurally, there were large pools of mitochondria, predominantly under the sarcolemma. Many of the mitochondria were greatly enlarged and contained tightly packed cristae, some also contained abnormal osmiophilic inclusions (Figure 1). Intramuscular capillaries were overabundant.

A skin biopsy in the second patient was normal, except for capillary proliferation.

Biochemistry

Polarographic studies of isolated skeletal muscle, mitochondria showed maximal oxygen consumption (respiratory rate) even in the absence of ADP, indicating that respiratory control was lost, although phosphorylation capacity was normal (Figure 2). Spectra and content of cytochromes were normal, and the activities of individual enzymes of the respiratory chain were also normal. However, basal ATPase activity was greatly increased and poorly stimulated by the uncoupler 2,4-dinitrophenol (DNP).

In 1976, DiMauro *et al*. found in the second patient that the rate of energy-dependent calcium uptake by isolated mitochondria was normal, but the amount of calcium accumulated decreased, and intramitochondrial calcium could not be retained and was quickly released into the medium. A vicious cycling of calcium uptake and release was proposed as a mechanism to explain the waste of electrochemical energy as heat.

Genetics

The lack of maternal inheritance, the apparent muscle specificity of the disease, and the lack of large-scale rearrangements of mitochondrial DNA (mtDNA) in the second patient are circumstantial evidence that Luft's disease may be due to a nuclear DNA (nDNA) defect.

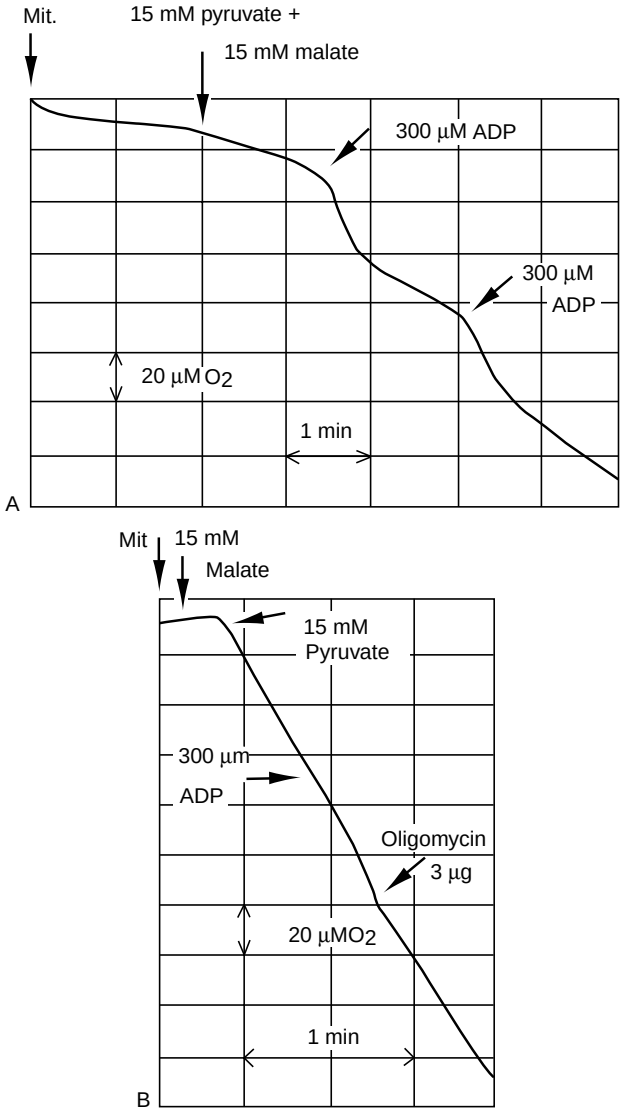

FIGURE 2 Polarographic tracings of isolated muscle mitochondria from the second patient with Luft's disease (B) and from a normal individual (A). Note how addition of micromolar amounts of ADP stimulate oxygen uptake in normal mitochondria, but not in the patient's mitochondria, whose rate of respiration is maximal after the addition of substrates (pyruvate + malate). This high rate of respiration is neither stimulated by ADP nor inhibited by oligomycin. This condition, in which ATP is formed normally but does not control the rate of respiration, is defined "loose coupling" of oxidation and phosphorylation.

See Also the Following Articles

Mitochondrial DNA • Mitochondrial Genome, Overview

Glossary

erythema Redness of the skin due to capillary dilatation or proliferation.

hypermetabolism A condition of enhanced metabolic activity in one or more tissues, resulting in increased heat production by the body, typically associated with hyperthyroidism.

polydipsia Prolonged excessive thirst and excessive intake of liquids.

polyphagia Excessive eating.

tachycardia Rapid beating of the heart, usually above 90 beats min^{-1}.

Further Reading

DiMauro, S., and Schon, E. A. (2003). Mitochondrial respiratory-chain diseases. *New England J. Med.* **348**, 2656–2668.

DiMauro, S., Bonilla, E., Lee, C. P., Schotland, D. L., Scarpa, A., Conn, H., and Chance, B. (1976). Luft's disease. Further biochemical and ultrastructural studies of skeletal muscle in the second case. *J. Neurol. Sci.* **27**, 217–232.

Haydar, N. A., Conn, H. L., Afifi, A., Wakid, N., Ballas, S., and Fawaz, K. (1971). Severe hypermetabolism with primary abnormality of skeletal muscle mitochondria. *Annu. Intern. Med.* **74**, 548–558.

Luft, R., *et al.* (1962). *J. Clin. Invest.* **41**, 1176–1804.

Pon, L. A., and Schon, E. A. (eds.) (2001). *Mitochondria.* Academic Press, San Diego, CA.

Biography

Dr. Salvatore DiMauro is the Lucy G. Moses Professor of Neurology at Columbia University College of Physicians & Surgeons. His main interests are inborn errors of metabolism, especially defects of the mitochondrial respiratory chain. He holds an M.D. from the University of Padova, Italy. He and his collaborators have pioneered the study of mtDNA in human disease.

Lysophospholipid Receptors

Gabor J. Tigyi
University of Tennessee Health Sciences Center, Memphis, Tennessee, USA

The lysophospholipids (LPLs) include lysophosphatidic acid (radyl-lyso-glycerophosphate, LPA), 2,3-cyclic phosphatidic acid, 1-alkyl-2-acetyl-glycero-3-phosphate, sphingosine-1-phosphate (S1P), dihydro-sphingosine-1-phosphate, sphingosylphosphorylcholine (lysosphingomyelin, SPC), and lysophosphatidylcholine (LPC). LPLs exert many of their biological effects through specific plasma membrane and/or intracellular receptors. LPLs are abundantly present in biological fluids and many of them are generated through stimulus-coupled activation of biochemical pathways. With only very few exceptions (e.g. RH7777 hepatoma, Sf9 insect and *Sacchromyces cerevisiae* yeast cells), most cells are responsive to one or more LPLs, indicating a widespread expression of their receptors. LPLs promote cell survival, exert mitogenic/antimitogenic regulation of the cell cycle, affect cell shape and enhance/inhibit cell motility, regulate organotypic differentiation, modulate immunological responses, and regulate calcium homeostasis. In a pathological context, LPLs have been shown to play a role in tumor cell invasion, angiogenesis, neointima formation, development of the heart ventricles, chemotherapeutic and radiation resistance, facial dysmorphism, nociception, and suckling behavior. The current understanding of lysophospholipid biology is very limited and the present understanding of their role in disease is rudimentary.

Sphingolipid Receptors

Plasma Membrane Receptors

Receptors for sphingolipids form three clusters, two of which show considerable homology with receptors for the glycerolipids lysophosphatidic acid (LPA) and lysophosphatidylcholine (LPC). In the order of discovery, the first cluster belongs to the endothelial differentiation gene (EDG) family. Five receptors of the eight-member EDG family recognize sphingosine-1-phosphate (S1P), dihydro-S1P, and to a lesser degree sphingosylphosphorylcholine (SPC), which include $S1P_1$ (formerly EDG1), $S1P_2$ (EDG5, H218, AGR16), $S1P_3$ (EDG3), $S1P_4$ (EDG6), and $S1P_5$ (EDG8). Whereas $S1P_1$, $S1P_2$, $S1P_3$ are expressed in many tissues and often coexpressed with at least one other EDG-family receptor in the same cell, $S1P_4$ expression is restricted to the hematopoietic cells and the lung; $S1P_5$ expression is restricted to the nervous tissue. Knockout (KO) mice for $S1P_1$ show embryonic lethality around embryonic day 12.5 due to a defect in vascular wall maturation hallmarked by a failure of smooth muscle cells surrounding the primitive capillaries, which leads to bleeding and death.

$S1P_2$ KO mice show no obvious phenotypic alteration but a slightly smaller litter size in homozygous matings on C57BL/6N background. $S1P_2$ KO mice on C57BL/6 albino background have been noted to suffer seizures leading to epileptic death, which was not found in the KO in the C57BL/6N background. $S1P_2$ mice showed slightly diminished adenylyl cyclase inhibition and severely impaired Rho activation in response to S1P stimulation. $S1P_3$ KO mice show no phenotypic abnormalities but embryonic fibroblasts display decreases in PLC activation, Ca responses, slight decreases in adenylyl cyclase inhibition, and no change in Rho activation.

Embryonic fibroblasts taken from double KO mice for $S1P_2$/$S1P_3$ display a complete loss of Rho activation, and a significant decrease in PLC activation and Ca mobilization without diminished inhibition of adenylyl cyclase. These double KO mice display decreased litter sizes and suffer increased perinatal lethality.

Another cluster of receptors that include OGR1(GPR68), GPR4, and G2A have been reported to be activated by SPC and LPC. However, the original claim that these receptors respond to LPLs has been disputed as these receptors have been shown to be activated by changes in pH. A related gene to this cluster, TDAG8, encodes a receptor to psychosine, a glycosphingolipid, which inhibits adenylyl cyclase in a pertussis toxin-independent mechanism, mobilizes Ca and leads to the formation of multinuclear cells.

A third cluster of lysosphingolipid receptors includes GPR3, GPR6, and GPR12. The closest relatives of this cluster include the anandamide and melanocortin receptors and the EDG family. These receptors are activated by S1P but also possess high intrinsic activity stimulating adenylyl cyclase and also couple to $G_{i/o}$. The thalamus and the caudate nucleus are the sites of the highest expression for these receptors in the nervous system; whereas in the periphery the thymus, stomach, and small intestine show high levels of mRNA

expression, and the kidney, heart, spleen, and pancreas show low levels of mRNA expression. Related to this cluster, GPR63 also recognizes dihydro-S1P and dioleoyl phosphatidic acid. GPR12 shows a preference for SPC over S1P as well as for the D-erythro-SPC stereoisomer. This receptor is presumed to play a role in the differentiation and postmitotic maturation of neurons. Antagonists of S1P receptors are in their early stages of development.

Intracellular Receptors

S1P is generated intracellularly from sphingosine by sphingosine kinase (SK). SK activity and consequent elevation in S1P have been linked to cell proliferation, survival, motility, and Ca mobilization. There is reasonable evidence for S1P's role in releasing Ca from endoplasmic reticulum in a mechanism independent of the inositol trisphosphate-gated release mechanism. The molecular targets of S1P remain obscure with the exception of the Ca^{2+} channel SCAMPER. In addition, S1P and SPC have been shown to modulate the properties of the ryanodine receptor.

Glycerolipid Receptors

Plasma Membrane Receptors

The GPR63 receptor for dioleoyl-PA is also activated by sphingolipids as discussed in the previous section. There are three clusters of GPCR that mediate LPA responsiveness.

The LPA_1 (EDG2), LPA_2 (EDG4), and LPA_3 (EDG7) receptors are close relatives of the EDG-family S1P receptors. LPA_1 is widely distributed, whereas LPA_2 mRNA is expressed in the nervous system, kidney, lung, and the prostate. LPA_3 is abundantly expressed in the testis and prostate and at a lower level in the heart, brain, lung, and kidney. LPA_1 and LPA_2 couple to $G_{i/o}$, G_q, and G_{13}, whereas LPA_3 couples to G_i and G_q heterotrimeric G proteins. LPA_1 KO animals have minimal phenotypes that include facial dysmorphism and altered suckling behavior, which leads to increased perinatal mortality. The impaired suckling behavior might be due to cortical developmental problems and/or alteration in the olfactory bulb. LPA_2 KO animals are without major phenotypic alterations but show a modest attenuation in LPA-induced PLC activation. Some of the LPA_1/LPA_2 double KO animals develop perinatal cranial hematomas in the frontal region of the brain. In embryonic fibroblasts isolated from these mice phospholipase C activation, Ca mobilization, adenylyl cyclase activation, proliferation, Jnk activation, Akt activation, and stress fiber formation, are absent or severely reduced.

The LPA_1, LPA_2, and LPA_3 receptors are all activated by either stereoisomer of LPA, alkyl-LPA, alkenyl-LPA, and cyclic phosphatidic acid. LPA_1 and LPA_2 do not show a preference between *sn1* and *sn2* localization of the fatty acyl chain, however, LPA_3 shows a preference for LPA with *sn2* over *sn1* fatty acids. All three receptors show a slight preference for LPA containing unsaturated fatty acids. Dioctylglycerol pyrophosphate has been identified as an inhibitor of $LPA_3 > LPA_1$ receptors without any effect on LPA_2. VPC12249 is an antagonist with a slight preference for LPA_1 over LPA_3 and without any effect on LPA_2. VPC31143 is an agonist selective for LPA_1. Short chain fatty alcohol phosphates show receptor-selective agonist and antagonist properties; the decanyl analogue is an LPA_2-selective agonist, whereas the dodecanyl analogue is an LPA_3-selective antagonist.

The *Xenopus* PSP24 α (GPR45) and β (GPR63) genes, when over-expressed in Xenopus oocytes augment the LPA but not the cyclic-PA and alkenyl-GP response. These receptors, which are abundant in the nervous system are also present in other tissues. The mammalian orthologues do not seem to respond to LPA when expressed in mammalian cells. However, recent evidence shows that mammalian orthologue of GP63 is a receptor for dioleoyl-PA and S1P. Interestingly, the mammalian GPR63 lacks a glutamine residue that is present in the *Xenopus* orthologue of GPR45 and which has been found essential for LPA recognition.

LPA_4 (GPR23, P2Y9Y) is a GPCR, distant from the EDG cluster, sharing only 20–24% amino acid identity and is a member of the purinergic receptor cluster. LPA_4 is abundantly expressed in the ovary and shows a ligand preference 18:1 > 18:0 > 16:0 > 14:0 > alkyl > alkenyl LPA.

Intracellular Receptors

The peroxisome proliferator activated receptor γ (PPARγ) is a transcription factor that heterodimerizes with the retinoic acid receptor and binds to specific DNA sequences known as peroxisome proliferator-activated receptor response element (PPRE). PPARγ is an intracellular receptor for LPA and alkyl-GP but not for cPA. The LPA-induced activation of PPARγ might be an important step in the regulation of adipogenesis, macrophage function, neointima formation, and atherogenesis because the scavenger receptor CD36 and the adipocyte fatty acid binding protein aP2 both have PPREs in their promoters.

See Also the Following Articles

Adenylyl Cyclases • Peroxisome Proliferator-Activated Receptors • Sphingolipid Biosynthesis • Sphingolipid Catabolism

Glossary

lysophospholipid A phosphate-containing lipid that causes cell lysis at high concentrations (>mM) due to its detergent-like properties.

receptor A protein that binds with a high degree of selectivity a ligand and upon binding elicits a biological response thorough the activation of signal transduction pathways.

Further Reading

Cavalli, A. L., O'Brien, N. W., Barlow, S. B., Betto, R., Glembotski, C. C., Palade, P. T., and Sabbadini, R. A. (2003). Expression and functional characterization of SCaMPER: A sphingolipid-modulated calcium channel of cardiomyocytes. *Am. J. Physiol. Cell Physiol.* **284**, C780–C790.

Fischer, D. J., Nusser, N., Virag, T., Yokoyama, K., Wang, D., Baker, D. L., Bautista, D., Parrill, A. L., and Tigyi, G. (2001). Short-chain phosphatidates are subtype-selective antagonists of lysophosphatidic acid receptors. *Mol. Pharmacol.* **60**, 776–784.

Heise, C. E., Santos, W. L., Schreihofer, A. M., Heasley, B. H., Mukhin, Y. V., Macdonald, T. L., and Lynch, K. R. (2001). Activity of 2-substituted LPA analogs at LPA receptors: Discovery of a LPA_1/LPA_3 receptor antagonist. *Mol. Pharmacol.* **60**, 1173–1180.

Ignatov, A., Lintzel, J., Hermans-Borgmeyer, I., Kreienkamp, H. J., Joost, P., Thomsen, S., Methner, A., and Schaller, H. C. (2003). Role of the G-protein-coupled receptor GPR12 as high-affinity receptor for sphingosylphosphorylcholine and its expression and function in brain development. *J. Neurosci.* **23**, 907–914.

McIntyre, T. M., Pontsler, A. V., Silva, A. R., St Hilaire, A., Xu, Y., Hinshaw, J. C., Zimmerman, G. A., Hama, K., Aoki, J., Arai, H., and Prestwich, G. D. (2003). Identification of an intracellular receptor for lysophosphatidic acid (LPA): LPA is a transcellular PPARgamma agonist. *Proc. Natl Acad. Sci. USA* **100**, 131–136.

Niedernberg, A., Tunaru, S., Blaukat, A., Ardati, A., and Kostenis, E. (2003). Sphingosine 1-phosphate and dioleoylphosphatidic acid are low affinity agonists for the orphan receptor GPR63. *Cell Signal* **15**, 435–446.

Sharma, C., Smith, T., Li, S., Schroepfer, G. J., Jr and Needleman, D. H. (2000). Inhibition of Ca^{2+} release channel (ryanodine receptor) activity by sphingolipid bases: mechanism of action. *Chem. Phys. Lipids* **104**, 1–11.

Tigyi, G., and Parrill, A. L. (2003). Molecular mechanisms of lysophosphatidic acid action. *Prog. Lipid Res.* **42**, 498–526.

Uhlenbrock, K., Gassenhuber, H., and Kostenis, E. (2002). Sphingosine 1-phosphate is a ligand of the human gpr3, gpr6 and gpr12 family of constitutively active G protein-coupled receptors. *Cell Signal* **14**, 941–953.

Virag, T., Elrod, D. B., Liliom, K., Sardar, V. M., Parrill, A. L., Yokoyama, K., Durgam, G., Deng, W., Miller, D. D., and Tigyi, G. (2003). Fatty alcohol phosphates are subtype-selective agonists and antagonists of LPA receptors. *Mol. Pharm.* **63**, 1032–1042.

Zhang, C., Baker, D. L., Yasuda, S., Makarova, N., Balazs, L., Johnson, L. R., Marathe, G. K., Mclntyre, T. M., Xu, Y., Prestwich, G. D., Byun, H.-S., Bittman, R., and Tigyi, G. (2004). Lysophosphatidic acid induces neointima formation through PPARγ activation. *J. Exp. Med.* **199**, 763–774.

Biography

Gabor Tigyi is a Professor in the Department of Physiology at the University of Tennessee Health Science Center in Memphis. He holds an M.D. from the Medical University of Pecs and a Ph.D. from the Hungarian Academy of Sciences in Budapest. He has made seminal contributions to the identification of LPA-like ligands, the development of LPA receptor-selective antagonists, and the role of LPA in neointima formation.

MDR Membrane Proteins

Nathan C. Rockwell
University of California at Berkeley, California, USA

Multidrug resistance (MDR) membrane proteins are integral membrane proteins belonging to the ABC transporter family that extrude drugs from mammalian cells. These proteins are implicated in the phenomenon of MDR, in which cancers treated with one drug in the course of chemotherapy will acquire resistance not only to that drug but also to a number of others that have not been used in treatment. The most familiar example of such a protein is MDR1, but related proteins can also confer resistance to multiple drugs beyond the compound used in selection, and thus can also be considered as MDR transporters in a broader sense.

MDR1 and the Clinical MDR Phenotype

The Discovery of MDR1

In the treatment of cancer patients by chemotherapy, chemical compounds preferentially more toxic to cancer cells are administered to the patient. Chemotherapy often fails or offers only a brief respite, and there are a number of mechanisms for such failure. In one such mechanism, cancer cells may express proteins that export the drug from the cell, preventing its accumulation to effective concentrations. The genetic instability of cancer cells permits them to alter expression of proteins or to develop mutated forms of proteins during the course of the disease, and the use of chemotherapy is in essence a selection for those cancer cells which are able to resist the drug or drugs used, such that the resistant cells will come to dominate the population of cancer cells over time.

One can study this by taking mammalian cells in tissue culture and selecting for cells which are able to resist a given drug. In the laboratory of Victor Ling, cells selected for resistance to the chemotherapeutic drug colchicine were shown to have simultaneously gained cross-resistance to a number of other compounds with no obvious overlap in chemical structure. This cross-resistance was shown to correlate with the expression of P-glycoprotein or Mdr1, an integral membrane protein subsequently shown to be encoded by the *MDR1* gene through the work of Michael Gottesman and others. Later studies have established that Mdr1 is an ATP-dependent pump that binds to drug molecules and extrudes them from the cell.

Clinical Relevance of MDR1

In the years since the discovery of MDR1, much research has focused on its role in the clinical outcomes of patients. The idea behind this work can be summarized in the form of two questions: (1) Does expression of MDR1 actually correlate with the results of treatment? (2) Does blocking MDR1 function alter the results of treatment for the better?

The answer to the first question has proven complex. For certain types of cancer, there is clear evidence that MDR1 is a significant factor in the outcome of treatment. However, evidence for a role for MDR1 in other types of cancer is much weaker, even in more recent studies. Complications arise in answering this question, such as the role of other transporters in MDR, individual genetic variation in the level of MDR1 present, and similar variation in the presence of any mutations in the MDR1 sequence. Nonetheless, at this point it seems clear that MDR1 is a clinically relevant factor in treating certain cancers, and new genetic screening approaches are being developed to permit a finer diagnosis of whether MDR1 might be a complication in treating other cancers in particular individuals.

Obtaining any answer to the second question has proven frustrating. Some studies have reported that blocking MDR function can improve the results of treatment, but other studies have argued that such inhibition has no effect. Factors which lead to these disparate results include the frequent lack of surrogate assays ensuring that MDR1 is truly being inhibited, the lack of examination of other transporters in the patient sample populations, and the observation that blocking MDR1 can increase the toxicity of chemotherapeutic drugs to the patient and thereby alter the outcome of chemotherapy indirectly. Studies which take all of these factors into account are only now underway.

Biochemical Behavior of MDR1

Good progress has been made toward understanding how MDR1 actually works to extrude drug substrates from cells. Like most ABC transporters, MDR1 hydrolyzes ATP at the conserved ATP-binding cassettes (ABCs, also known as ABC domains, nucleotide-binding domains (NBDs)). This hydrolysis is directly coupled to transport of drugs out of the cell. Thus, MDR1 is a direct active transporter, able to work against a concentration gradient without the aid of other gradients by coupling ATP hydrolysis to vectorial transport.

The Conundrum of MDR1: Broad Specificity with High Affinity

A very wide range of compounds can serve as substrates for MDR1, without obvious structural motifs that distinguish substrates from nonsubstrates (Figure 1). In spite of this, MDR1 is able to transport these compounds with seemingly high affinity (low K_M). Paradoxically, conventional enzymology dictates that high affinity is achieved via extensive interactions between enzyme and substrate and thus of necessity is accompanied by stringent specificity.

More recent studies indicate that the apparently high affinity of MDR1 for its substrates is misleading. The hydrophobic nature of MDR1 substrates causes them to accumulate to very high concentrations in biomembranes, and it is this population of membrane-bound substrates that is recruited for transport (Figure 1). Thus, the actual affinity of MDR1 for its substrates is probably much lower than had been thought. This allows a suitably hydrophobic binding pocket to accommodate many substrates in slightly different binding modes with modest affinity and without making extensive enzyme-substrate contacts. It is perhaps best to view MDR1 as a polyspecific transporter, meaning that it has very broad specificity but does actually recognize specific features of its substrates.

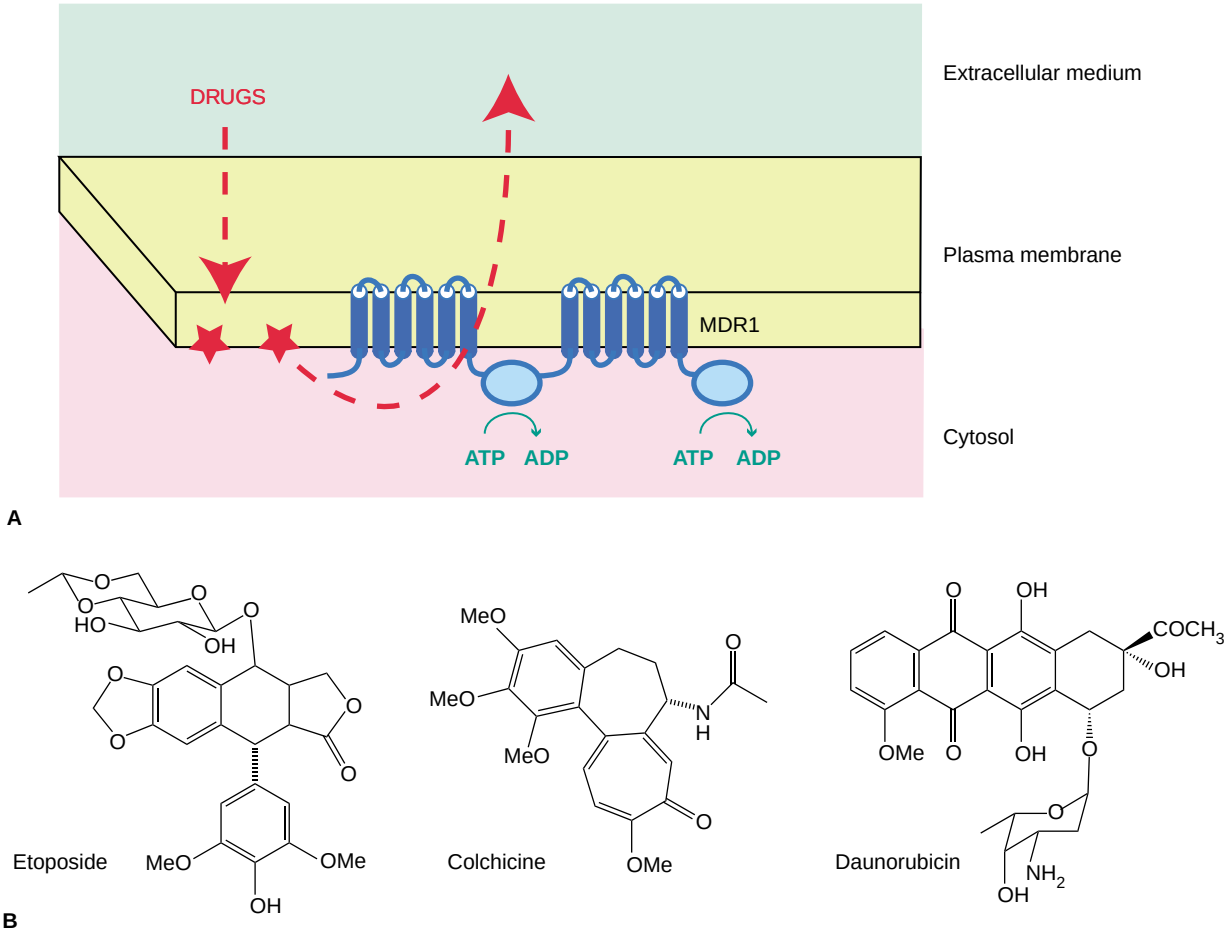

FIGURE 1 MDR1 function in drug export. (A) A cartoon schematic of the MDR1 transporter in the plasma membrane (yellow) is shown, with the transmembrane segments as vertical cylinders and the ABC domains as ovals. Drug molecules transiting the plasma membrane (red stars) are recruited by MDR1 and then exported from the cell, concomitant with ATP hydrolysis at the cytosolic ABC domains. (B) Structures of selected drugs known to be MDR1 substrates are shown.

ATP Hydrolysis and the Catalytic Cycle of MDR1

MDR1 has the four canonical domains of an ABC transporter: two membrane-spanning domains each containing six transmembrane segments and two ABC domains. It is known that ATP derivatives can photo-cross-link to the ABC domains of MDR1 and other ABC transporters, while transport substrates such as drugs instead cross-link to the membrane-spanning domains. The affinity for drugs changes during the catalytic cycle. Kinetic analysis of ATP hydrolysis by MDR1 leads to the idea that the two ATPase active sites alternate during transport, but the exact stoichiometry of ATP hydrolysis to transport is not yet known. Recent medium-resolution structural studies of the MDR1 catalytic cycle from the laboratory of Chris Higgins indicate that major conformational changes take place upon ATP binding, and this may mean that ATP hydrolysis actually occurs after transport and simply serves to reset the transporter.

The ABC domains dimerize on the cytosolic face of the protein. The exact mode of dimerization for the ABC domains in any ABC transporter has been the subject of intense speculation. Much other evidence supports the most recent model, based on the crystal structure of Rad50 from *E. coli*. This model is also consistent with the crystal structure of the intact BtuCD transporter. However, less is known about how the membrane-spanning domains of MDR1 are organized, as there is much less conservation of these domains among the different subfamilies of ABC transporters.

Other MDR Transporters

MRP1

MDR protein 1 (MRP1) or *ABCC1* was isolated by Susan Cole and Roger Deeley as a protein implicated in multidrug resistance in lung cancer cells. It is a member of a different subfamily of ABC transporters (Figure 2). Whereas MDR1 transports drugs without the need for any chemical modification, MRP1 frequently transports drugs that have first been chemically conjugated to glutathione. Exceptions to this rule are sometimes cotransported with unlinked glutathione molecules. As with MDR1, the presence of MRP1 correlates with clinical outcome for certain cancers. The development of specific inhibitors and surrogate assays for MRP1 is underway.

ABCG2

ABCG2 (also called MXR or BCRP) was isolated by several labs as a transporter implicated in drug-resistance in breast cancer cells. It belongs to a third subfamily of ABC transporters (Figure 2). The specificity of ABCG2 seems more narrow than that of MDR1 or MRP1, but chemical conjugation of drugs is

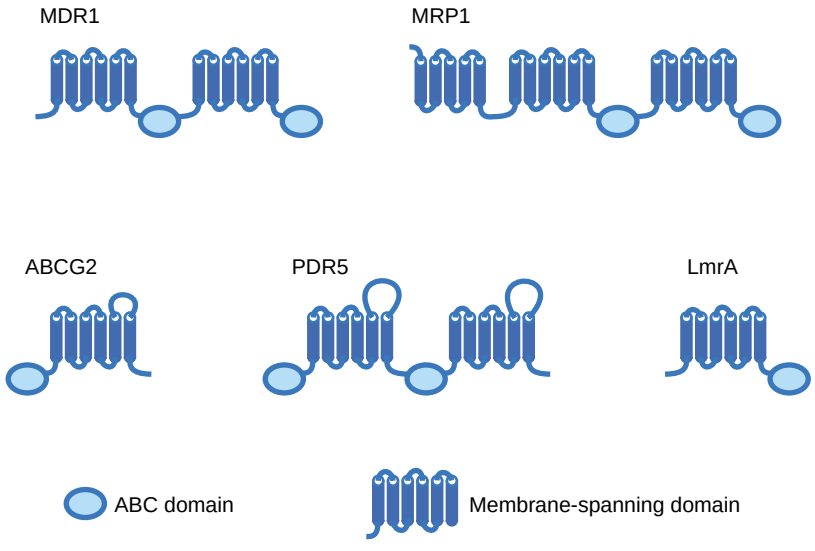

FIGURE 2 Cartoon schematics of ABC transporters implicated in cross-resistance. MDR1, MRP1, and ABCG2 are all MDR transporters, while Pdr5 and LmrA have similar functions in different organisms. MDR1 is a classic ABC transporter with all four domains in a single open reading frame, while MRP1 has an N-terminal extension with an additional five transmembrane segments. ABCG2 is a "half-transporter" which is thought to form a homodimer to constitute the active transporter. Pdr5 is a complete transporter with the relative order of the four domains in the open reading frame reversed relative to MDR1, while LmrA is a "half-transporter" known to be active as a homodimer. Throughout, membrane-spanning domains are shown as clusters of vertical blue cylinders, and ABC domains are shown as blue ovals.

not required. Clinical trials to assess the importance of ABCG2 in human cancer are still in the early stages.

Homologous Transporters not Associated with Drug Resistance

Each transporter associated with clinical drug resistance has close relatives not associated with such resistance. For instance, the two closest relatives of MDR1 are MDR3 (encoded by the *ABCB4* gene) and BSEP (encoded by *ABCB11*). Although both proteins exhibit modest drug-efflux activity *in vitro*, neither one has been clinically implicated in drug resistance, possibly because their ability to export drugs is too weak. Similarly, the closest relative to MRP1 is MRP3, which again can confer weak drug resistance when overexpressed but has not been convincingly linked to drug resistance in human cancers. Another relative, MRP2, may play a role in clinical drug resistance, because it can be amplified in cell lines selected for resistance to cisplatin and has been detected in clinical samples, but it is not yet clear whether it plays a true role in the MDR phenotype.

Physiological Functions of MDR Transporters

The Physiological Role of MDR1

MDR1 is found in the gut, kidney, liver, and blood–brain barrier, and *mdr1–/–* knockout mice have altered ability to withstand and excrete toxic compounds known to be MDR1 substrates. This is consistent with the idea that MDR1 is primarily responsible for extrusion of toxic metabolites or xenotoxins from certain cells to allow facile excretion from the body, thereby protecting the rest of the organism (or, in the case of the blood–brain barrier, forming a "safe haven" within the organism). However, MDR1 is also expressed in cells of the adrenal gland, so it is possible that MDR1 may have some role in the proper function of this tissue in the absence of toxins.

The Physiological Role of MRP1

As with MDR1, at least one physiological role of MRP1 is the removal of various toxins from the body. Unlike MDR1, MRP1 expression is quite widespread. This protein also has a physiological role in the secretion of leukotrienes, and this has been shown to have implications for response to bacterial lung infections.

The Physiological Role of ABCG2

ABCG2 is expressed in intestine and placenta as well as in a side population of hematopoietic stem cells. It is likely to play a role in detoxification in the intestine, but its functions in placenta and stem cells are not yet clear.

The Physiological Functions of Homologous Transporters

MDR3 and BSEP (the two closest homologues of MDR1) are both implicated in proper function of the liver; MDR3 is an outward-directed transporter for the lipid phosphatidylcholine, and BSEP is a bile salt exporter. Mutations in these two proteins interfere with proper secretion of bile and are associated with different subtypes of progressive familial intrahepatic cholestasis (PFIC).

There are a number of homologues for MRP1. Its closest relative, MRP3, may play a role in cholestasis in the liver, or it may be another detoxification protein, while MRP2 is the pump responsible for exporting a wide range of anionic conjugates across the apical membrane of polarized cells. There are also several homologues of ABCG2, but the only ones whose functions are known are ABCG5 and ABCG8, which are important in exporting plant sterols from the cells of the intestine.

Analogous Systems in Other Organisms

The phenomenon of MDR is by no means unique to mammalian cells. The ABC transporter family is ubiquitous, and every eukaryotic organism examined to date has its own cohort of these proteins, at least some of which are involved in drug resistance or detoxification. Examples include *AtMRP* proteins from *Arabidopsis thaliana*, Pdr5 from *Saccharomyces cerevisiae*, and PGPA from *Leishmania*. Nor is this phenomenon unique to eukaryotes; the bacterium *Lactococcus lactis* expresses an MDR1 homologue, LmrA, which is able to complement the loss of MDR1 function in mammalian cells. Thus, MDR transporters are a special case of a general theme in biology: removal of a wide variety of toxic compounds from the cell via a small number of polyspecific ABC transporters.

The observation that such transporters have close homologues not responsible for significant drug transport is also a general one. For instance, the two closest homologues of Pdr5 in the *Saccharomyces* genome are Pdr10 and Pdr15, neither of which is implicated in drug resistance. It is thus possible that MDR transporters and their analogues in other organisms evolved from related transporters several times in several subfamilies of ABC transporters.

See Also the Following Articles

ABC Transporters • Prostaglandins and Leukotrienes

Glossary

cross-resistance The general phenomenon whereby a cell selected for resistance to one toxin simultaneously acquires resistance to other toxins not presented to the cell; MDR is a special case of cross-resistance.

homologue A protein with significant sequence similarity to another protein, either across its entire length or in certain regions or domains.

photo-cross-link To covalently link a molecule (usually a protein) with a substrate or ligand bound to the protein *in vitro* and then excited by ultraviolet light to react with the protein.

polyspecific Having very broad specificity, with minimal overlap in chemical structure.

Further Reading

Ambudkar, S. V., Kimchi-Sarfaty, C., Sauna, Z. E., and Gottesman, M. M. (2003). P-glycoprotein: From genomics to mechanism. *Oncogene* **22**, 7468–7485.

Bates, S. E. (2003). Solving the problem of multidrug resistance: ABC transporters in clinical oncology. In *ABC Proteins: From Bacteria to Man* (I. B. Holland, S. P. C. Cole, K. Kuchler and C. F. Higgins, eds.) pp. 359–391. Academic Press/Elsevier Science, London, UK.

Deeley, R. G., and Cole, S. P. C. (2003). Multidrug resistance protein 1 (ABCC1). In *ABC Proteins: From Bacteria to Man* (I. B. Holland, S. P. C. Cole, K. Kuchler and C. F. Higgins, eds.) pp. 393–422. Academic Press/Elsevier Science, London, UK.

Hopfner, K. P., Karcher, A., Shin, D. S., Craig, L., Arthur, L. M., Carney, J. P., and Tainer, J. A. (2000). Structural biology of Rad50 ATPase: ATP-driven conformational control in DNA double-strand break repair and the ABC-ATPase superfamily. *Cell* **101**, 789–800.

Locher, K. P., Lee, A. T., and Rees, D. C. (2002). The E. coli BtuCD structure: a framework for ABC transporter architecure and mechanism. *Science* **296**, 1091–1098.

Linton, K. J., Rosenberg, M. F., Kerr, I. D., and Higgins, C. F. (2003). Structure of ABC transporters. In *ABC Proteins: From Bacteria to Man* (I. B. Holland, S. P. C. Cole, K. Kuchler and C. F. Higgins, eds.) pp. 65–80. Academic Press/Elsevier Science, London, UK.

Rosenberg, M. F., Velarde, G., Ford, R. C. Martin, C., Berridge, G., Kerr, I. D., Callaghan, R., Schmidlin, A., Wooding, C., Linton, K. J., and Higgins, C. F. (2001). Repacking of the transmembrane domains of P-glycoprotein during the transport ATPase cycle. *EMBO J.* **20**, 5615–5625.

Van Veen, H. W., and Callaghan, R. (2003). Substrate-binding sites in ABC transporters. In *ABC Proteins: From Bacteria to Man* (I. B. Holland, S. P. C. Cole, K. Kuchler and C. F. Higgins, eds.) pp. 81–105. Academic Press/Elsevier Science, London, UK.

Biography

Nathan Rockwell is conducting postdoctoral research in the laboratory of Professor Jeremy Thorner at the University of California, Berkeley. His research focuses on the physiological roles of ABC transporters in the absence of cytotoxic drugs, using the yeast *Saccharomyces cerevisiae* as a model system. He holds a Ph.D. from Stanford University.

Meiosis

Neil Hunter
University of California, Davis, California, USA

Meiosis is the specialized type of cell division by which gametes are produced. This process achieves the remarkable feat of halving the chromosome complement of a cell, typically from diploid to haploid. Meiosis thereby allows the diploid state to be restored when two gametes fuse during fertilization to form a zygote. Reduction of ploidy occurs during meiosis because a single round of DNA replication is followed by two successive rounds of chromosome segregation. During the first round, sister chromatids remain associated while homologues (pairs of sisters) are segregated. As prerequisites to their accurate segregation, homologues must pair and undergo crossing-over, a reciprocal exchange of chromosome arms. Homologue pairing and crossing-over both involve homologous recombination, which occurs by the programmed formation and repair of DNA double-strand breaks. Crossing-over is a critical aspect of meiosis that underlies the fundamental laws of heredity: first, crossovers are essential for genetic transmission because they convert connections between sister chromatids into connections between homologues, called chiasmata. These connections permit proper orientation of the homologues on the segregation apparatus (the spindle), and thereby facilitate their orderly segregation. Second, crossovers produce new combinations of alleles on which genetic selection can act. Through its effect on chromosome segregation, defective crossing-over is linked to infertility, miscarriage, and genetic disease in humans.

The Sexual Life Cycle

In sexually reproducing organisms, successive generations maintain a constant number of chromosomes. This is because syngamy, the fusion of two gametes to form a zygote (which gives rise to a new individual), is alternated with meiosis, which halves the cellular chromosome number. Without meiosis, syngamy would result in a catastrophic doubling of the chromosome content with each successive generation. Thus, the alternation of diploid (two copies of each chromosome) and haploid (one copy of each chromosome) generations of cells is a fundamental feature of sexually reproducing organisms. In metazoans, syngamy is typically followed by extensive cell proliferation, by mitosis, and the development of a new individual. Meiosis in metazoans occurs in the germ-line cells of the gonads.

Mitotic and Meiotic Chromosome Cycles

Understanding how meiosis achieves the remarkable feat of halving the cellular chromosome number first requires an appreciation of how cells segregate chromosomes during mitotic cell division (Figure 1).

Mitosis

During mitosis, copies of both maternal and paternal chromosomes are distributed to two daughter cells. Replication first produces two identical copies of each chromosome called sister chromatids (Figure 1Aii). Microtubules of the spindle apparatus attach to the chromatids via structures called kinetochores, which assemble at regions called centromeres (Figure 1Aiii). Chromatids are then pulled apart to opposite poles of the cell, which then divides (Figure 1Aiv). The result is two identical daughter cells each containing two complete (maternal and paternal) sets of chromosomes. Two interdependent features ensure that chromosome segregation is an accurate process: (1) connections between sister chromatids and (2) a mechanism that senses the tension created when each pair of chromatids becomes attached to microtubules emanating from both poles of the spindle. Connections between sister chromatids, called sister-chromatid cohesion, form during replication and hold the sister chromatids together until they are ready to be segregated. When the two kinetochores of a sister-chromatid pair attach to microtubules emanating from opposite poles of the cell, the pulling forces of the spindle are resisted by the cohesion between sister centromeres. The resulting tension stabilizes microtubule attachments. When all chromatid pairs have achieved this biorientation on the spindle, sister-chromatid cohesion is destroyed and chromatids are pulled to the cell poles.

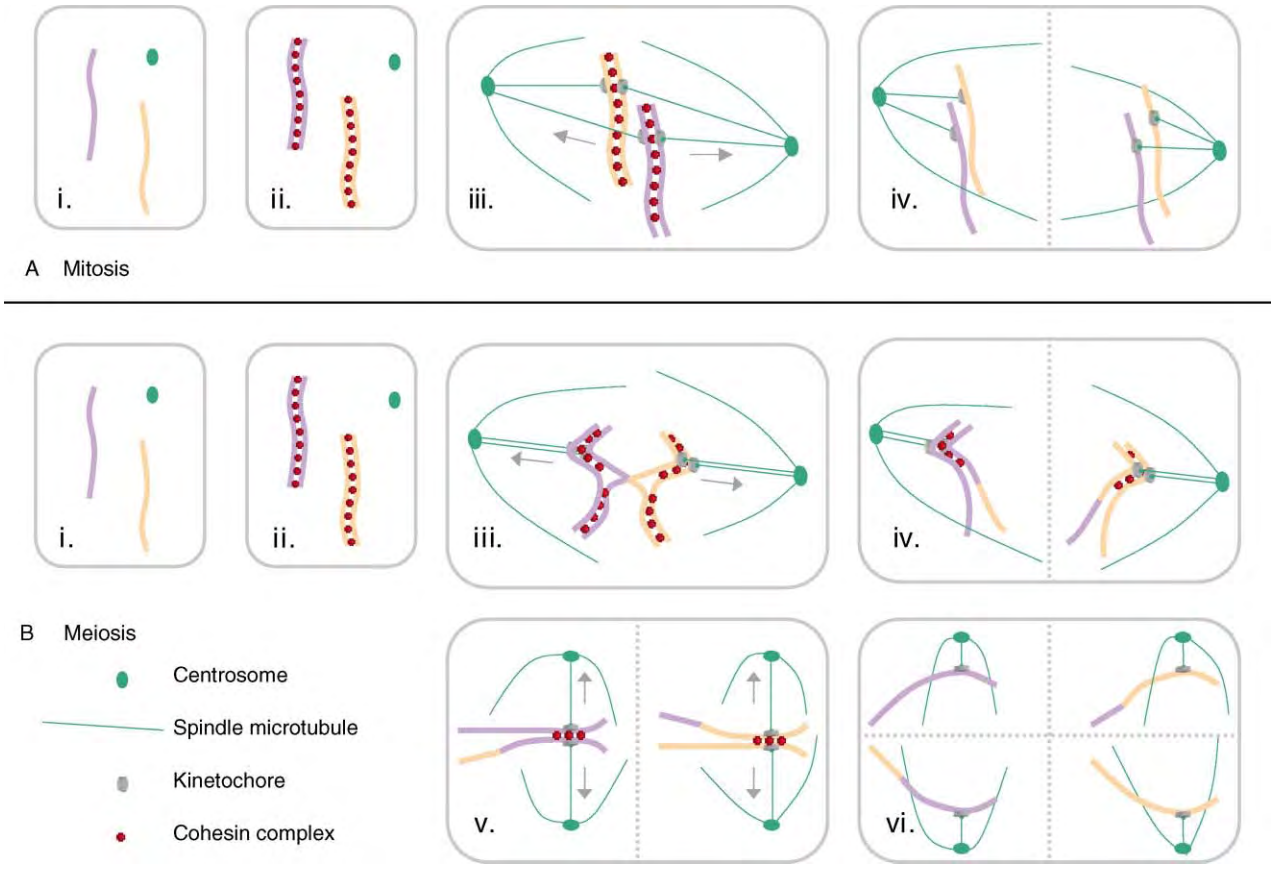

FIGURE 1 Comparison of mitotic and meiotic chromosome cycles. Centrosomes are cell organelles that produce microtubules. These structures duplicate, migrate to opposite poles of the cell, and grow the microtubules that form the spindle. Arrows indicate directions of the pulling forces generated by microtubules. Dashed lines indicate the planes of cell division. See text for details.

MEIOSIS

Meiosis, like mitosis, begins with replication to produce pairs of sister chromatids connected by cohesion (Figure 1Bii). Then, in contrast to mitosis, a single copy of every chromosome must be accurately distributed to four different nuclei. Meiosis achieves this in the only logical way: via two successive rounds of nuclear division, first segregating homologues (the maternal and paternal chromatid pairs) and then segregating sister chromatids, as in mitosis. Regular homologue segregation is unique to meiosis and requires the following four modifications of the mitotic chromosome cycle:

1. Maternal and paternal homologues pair and become connected by structures known as chiasmata (Figures 1Biii and 2). A chiasma results from a reciprocal exchange between a maternal and a paternal chromatid. Chiasmata hold the homologues together by virtue of the sister-chromatid cohesion, which was established as the chromosomes were replicated. Chiasma formation is the physical basis of genetic crossing-over.

2. The kinetochores of sister chromatids are modified such that they are unable to attach to microtubules emanating from different poles. Thus, the two sister kinetochores of a homologue behave like the kinetochore of a single sister chromatid in mitosis. This monopolar property allows the interconnected homologue pair to biorient on the spindle, but in this case, spindle forces are resisted by the combination of chiasma and distal sister-chromatid cohesion (Figure 1Biii). The monopolar modification of sister kinetochores is reversed in preparation for the second meiotic division in order to allow sister chromatids to be segregated (Figure 1Bv).

3. The cohesion between the chromosome arms is destroyed prior to the first division, whereas cohesion between sister centromeres is protected until the second round of segregation ensues. This modification allows homologues to be segregated at the first meiotic division, while leaving sufficient cohesion to facilitate sister segregation at the second division (Figure 1Biii–v).

4. The two meiotic divisions occur without an intervening round of replication.

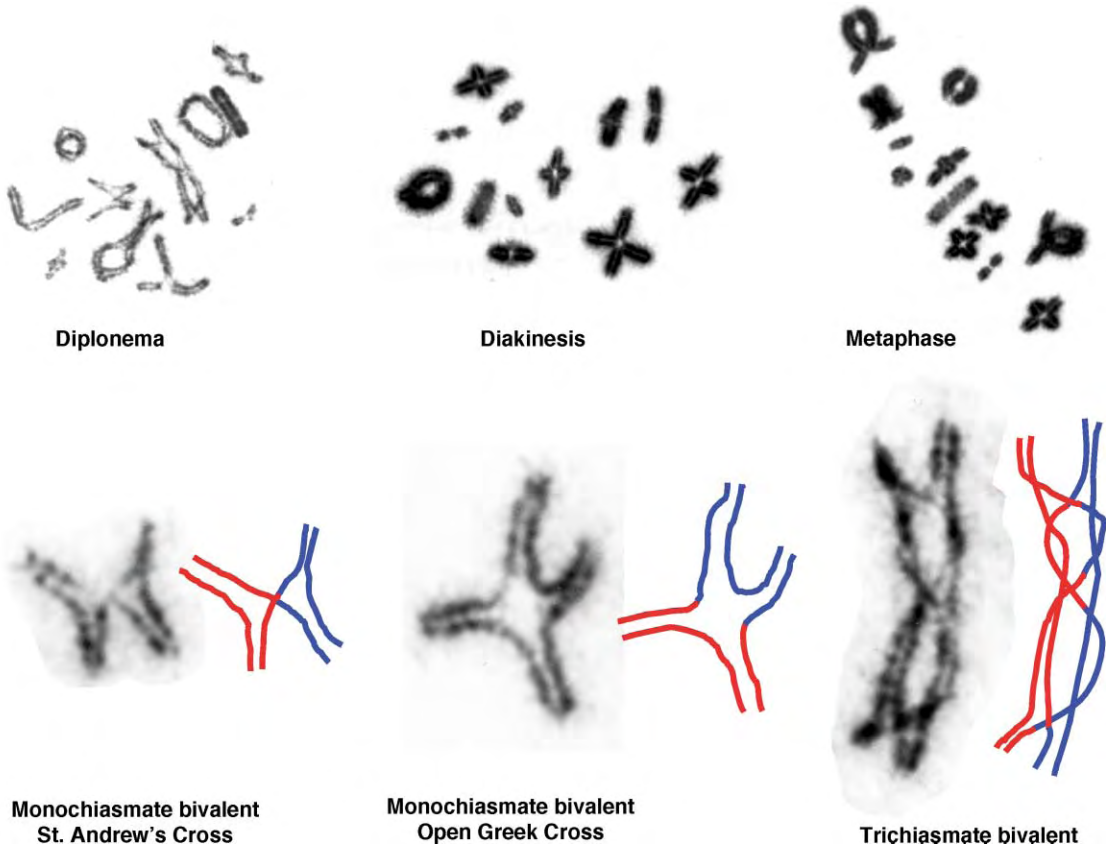

FIGURE 2 Chiasmata in the migratory locust, *Locusta migratoria*. Top: Chiasmata are observed during three distinct stages of meiotic prophase I, after which the homologues are segregated. Bottom: enlargements of individual homologue pairs; cartoons show the topological relationships between chromosomes and the points of exchange. Images kindly provided by Professor Gareth Jones, Birmingham University.

Meiotic Prophase I

The first meiotic division is preceded by an extended prophase during which the chromosomes are paired and chiasmata are formed. This period is divided into the following five stages, defined by the appearance of the chromosomes under the light microscope (Figure 3):

1. Leptonema (adjective = leptotene; from the Greek *lepto*, meaning "thin"). During leptonema, which follows chromosome replication, chromosomes are first visible as long thin strands.
2. Zygonema (adjective = zygotene; from the Greek *zygo*, meaning "yoke," Old English for "couple" or "unite"). Homologues begin to closely associate during zygonema. The extent of association increases throughout this stage.
3. Pachynema (adjective = pachytene; from the Greek *pachy*, meaning "thick"). Homologues are associated along their entire lengths and thus appear as thick, morphologically indistinguishable entities.
4. Diplonema (adjective = diplotene; from the Greek *diplo*, meaning "double"). Diplonema is usually preceded by the diffuse stage during which chromosomes are indistinct. When they reappear at diplonema, homologues are no longer associated along their lengths, but are visibly connected by chiasmata (Figure 2). In female animals, meiosis typically arrests after diplonema, and oocytes move into a quiescent dictyate stage in which the chromosomes are less condensed. In most vertebrates, the first meiotic division is completed only in response to hormonal stimulation.
5. Diakinesis (from the Greek *dia*, meaning "across," and *kinesis*, meaning "movement"). During diakinesis, the nuclear membrane begins to break down, and spindle microtubules develop and connect to the monopolar kinetochores of the homologues. The homologue pairs condense dramatically, becoming progressively shorter and thicker, and they move towards the equator of the cell (Figures 2 and 3).

After Prophase I

Following the events of prophase I, the cell prepares the chromosomes for segregation and then segregates them via two additional stages, which are the meiotic counterparts of the final stages of mitosis (Figure 3).

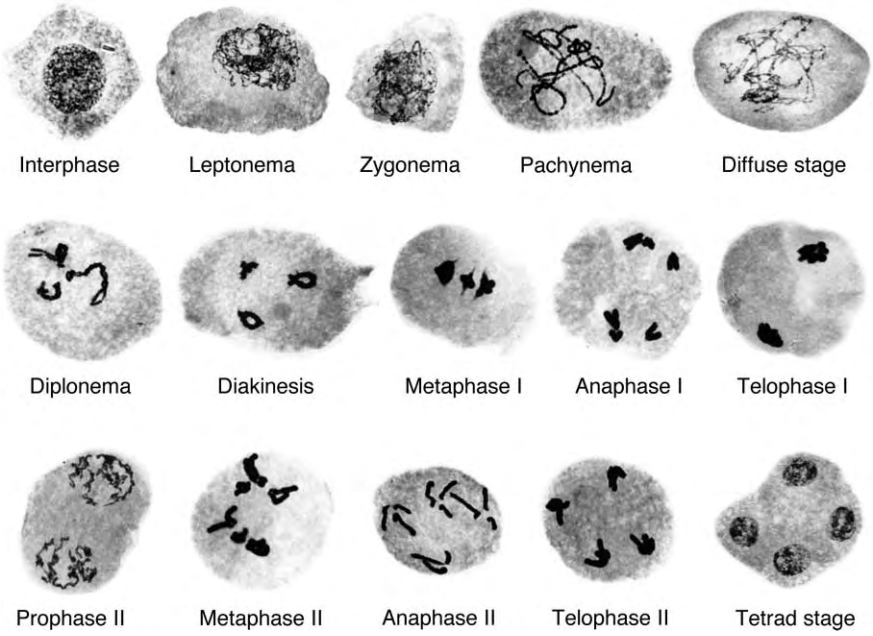

FIGURE 3 Classical stages of meiosis in *Crepis capillaris*, a flowering plant of the family *Compositae*. The cells of the tetrad eventually differentiate into pollen. Images kindly provided by Professor Gareth Jones, Birmingham University. Reprinted with permission from: Funcham, J.R.S. (1983) *Genetics*, Jones & Bartlett Publishers, Sudbury, MA.

1. Metaphase I (from the Greek *meta*, meaning "between, with, beside, after" and *phasis*, meaning "appearance"). At metaphase I, the condensed chromosomes are aligned along the equator of the spindle, typically at the central plane of the cell. This configuration is the consequence of stable biorientation of the homologue pairs on the spindle (Figures 2 and 3).

2. Anaphase I (from the Greek *ana*, meaning "up, throughout, according to" and *phases*, meaning "appearance"). At anaphase I, cohesion between chromosome arms is destroyed, and the homologues are pulled toward the poles of the spindle.

3. Telophase I and interphase I (from the Greek *telos*, meaning "end"; and from the Latin *inter*, meaning "between, among" and the Greek *phasis*, meaning "appearance"). Telophase is the last phase of mitosis, in which the segregated chromosomes decondense and are enclosed in a new nuclear membrane. Interphase is any period or stage between two successive mitotic divisions. These stages are not a general feature of meiosis and in many cases are skipped as the cell proceeds directly to the second meiotic division. In oocytes, cell division is asymmetric, resulting in the production of a small polar body plus a large oocyte cell.

4. Meiosis II. During prophase II, the chromosomes recondense, spindle microtubules develop, and the sister chromatid pairs biorient, and then congress at the equational plane of the spindle at metaphase II. The oocytes of vertebrates arrest for a second time at metaphase II, where they remain until fertilization. Typically, the plane of the meiosis II spindles is perpendicular to that of the meiosis I spindle. Sister chromatids are pulled apart at anaphase II, and new nuclear envelopes form during telophase II.

5. Gametogenesis. At this stage, the products of meiosis are known as meiocytes. The differentiation of meiocytes then produces gametes that are characteristic of the specific organism, e.g., sperm, pollen, and spores.

Meiotic Chromosome Structure and the Synaptonemal Complex

Loops and Axes

Meiotic chromosomes have a well-defined loop-axis structure (Figures 4A–4C), which is revealed by ultrastructural studies using the electron microscope. The loops are loops of chromatin that vary in size from ~20 kb in simple eukaryotes such as yeast to ~2500 kb in grasshopper, an organism with particularly large chromosomes. Thus, the large differences in genome size between different organisms are accommodated in large part by changes in chromatin loop size, such that meiotic chromosome length does not vary linearly with genome size. The loops of every pair of chromatids are connected at their bases, in a linear arrangement, along a rod-like axis or core, i.e., one axis = two chromatids = one homologue. Protein constituents of the homologue axes included those involved in sister-chromatid cohesion. The basic loop-axis structure is thought to be organized by the cohesion proteins; this then serves as a platform

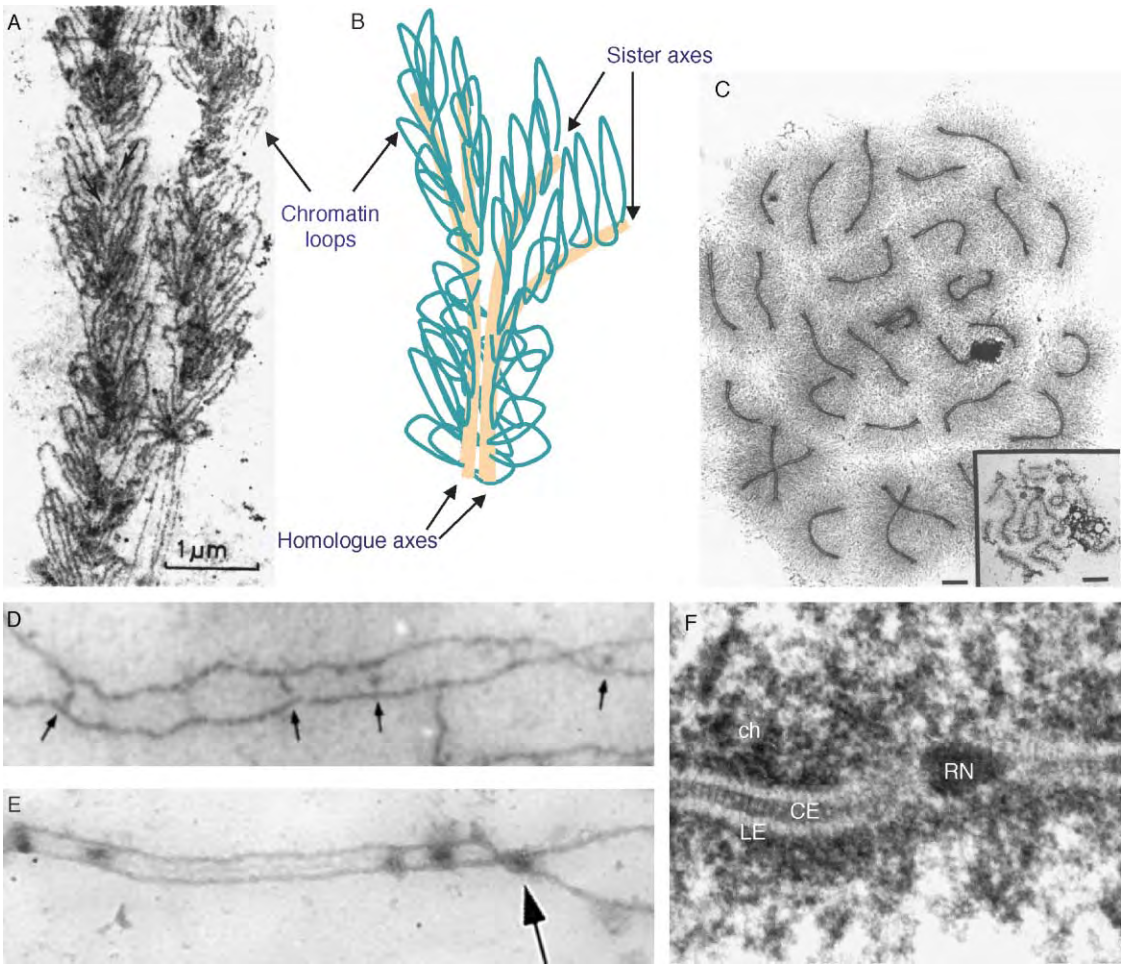

FIGURE 4 Chromosome structure in meiotic prophase. (A) Late pachytene stage chromosomes from the midge, *Chironomus*. Reprinted from Keyl, H. G. (1975). Lampbrush chromosomes in spermatocytes of *Chornomous*. *Chromosoma* **51**, 75–91 with permission of Springer-Verlag. (B) Cartoon rendering of loop-axis structure showing that each distinct homologue axis comprises two conjoined sister axes. (C) Spread chromosomes from the moth, *Hyalophora columbia*, and baker's yeast, *Saccharomyces cerevisiae* (inset; bars = 2 μm); note the large difference in chromatin loop size. Reprinted from Moens, P. B., and Pearlman, R. E. (1988). Chromatin organization at meiosis. *Bioessays* **9**, 151–153 with permission of John Wiley & Sons, Inc. (D) Part of a spread chromosome pair in early zygonema from the onion, *Allium cepa*, showing early recombination nodules at the sites of axial association (indicated by arrows). Reprinted from Albini, S. M., and Jones, G. H. (1987). Synaptonemal complex spreading in *Allium cepa* and *A. fistulosum*. I. The initiation of pairing. *Chromosoma* **95**, 324–338 with permission of Springer-Verlag. (E) Part of a spread chromosome pair in mid-late zygonema from the tree tomato, *Cyphomandra betacea*, showing SC-associated early recombination nodules. Arrow highlights an early nodule at the junction of synapsed and unsynapsed axes. Reprinted from Anderson, L. K., Hooker, K.D., and Stack, S. M. (2001). The distribution of early recombination nodules on zygotene bivalents from plants. *Genetics* **159**, 1259–1269. (F) SC longitudinal section from the beetle, *Blaps cribrosa*, with associated late recombination nodule. Abbreviations: LE, lateral element; CE, central element; RN, recombination nodule; ch, chromatin. Reprinted from Shmekel, K., and Daneholt, B. (1988). Evidence for close contact between recombination nodules and the central element of the synaptonemal complex. *Chromosome Res*. **6**, 155–159 with permission of Springer-Verlag.

for the binding of additional proteins that gives rise to the distinct axes detected by electron microscopy (Figures 4C–4F).

Synaptonemal Complexes

Meiotic chromosome pairing culminates with formation of synaptonemal complexes (SCs), prominent proteinaceous structures that form between homologues, along their entire lengths. SC morphology, as defined by ultrastructural studies, is remarkably conserved between different organisms (Figure 4C, F): two dense lateral elements flank a central region, which contains a less dense central element. The lateral elements correspond to the homologue axes. Transverse filaments lie across the central region to create a striated, zipper-like appearance. Central region proteins (putative transverse filaments) share a broadly similar secondary structure: a long coiled coil flanked by globular C and N termini. Coiled-coil lengths of ~70–90 nm fit the prediction that these

proteins span the 100 nm central region in a head-to-head configuration. SCs are thought to assemble by a two-step process: nucleation, by installing central region proteins at sites where homologue axes are very closely paired, followed by polymerization between and along the homologue axes. SCs are important for the normal formation of chiasmata.

Prophase I Stages at the Ultrastructural Level

The homologue axes develop and become distinct during leptonema. The homologues progressively pair, eventually becoming coaligned along their lengths at a distance of ~400 nm. During this presynaptic alignment, axes closely associate at several sites along each pair of homologues. These axial associations are the sites where DNA molecules are interacting via homologous recombination and are often associated with densely staining nodular structures that contain recombination proteins (Figures 4D and 4E.). During zygonema, the polymerization of SCs is nucleated at a subset of these sites, as well as at the chromosome ends. Cells enter pachynema when SCs extend along the lengths of every pair of homologues, and a second type of nodular structure develops that is typically larger, denser, rounder, and much less numerous than that observed during zygonema (Figure 4F). These late recombination nodules mark the sites where chiasmata will appear following the breakdown of SCs and entry into diplonema.

Homologous Recombination during Meiosis

Homologous recombination is the use by a broken or damaged chromosome of a homologous chromosome as a template for its repair. Each recombination event has one of two potential outcomes: a crossover (reciprocal exchange of chromosome arms), or a non-crossover (local transfer of genetic information without exchange of chromosome arms). Studies of chromosome structure have used organisms with large, readily visualized chromosomes. In contrast, much of our understanding of the molecular processes of meiotic homologous recombination comes from studies using the single-celled eukaryote, baker's yeast *Saccharomyces cerevisiae*, which has a genome ~250 times smaller than that of a human. These studies reveal that homologous

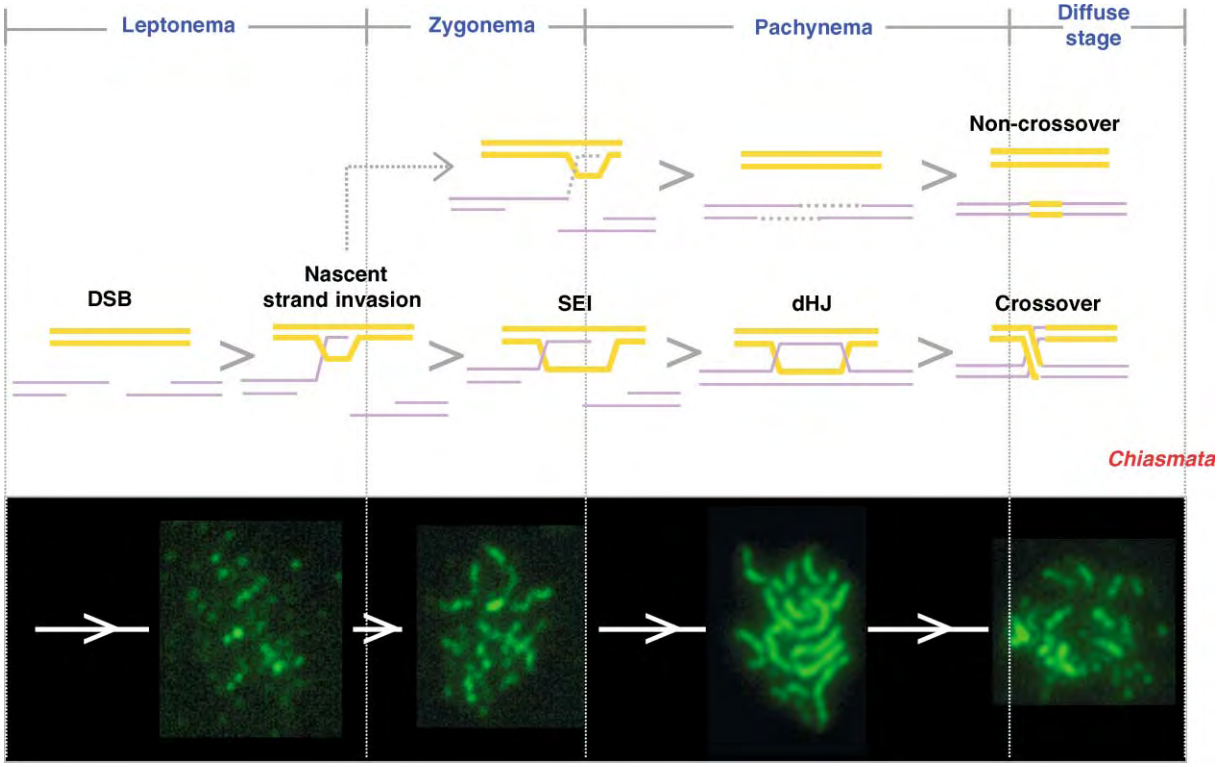

FIGURE 5 Relative timeline of the DNA events of recombination and the cytological stages of meiosis. Top row: the stages of meiotic prophase I. In mammals, this period occupies about 4 weeks; in a simple eukaryote such as yeast, it takes just 5 hours. Middle row: relative timing and molecular details of meiotic recombination. Each pair of lines represents a DNA duplex. Only the two chromatids involved in the recombination event are shown. See text for details. Bottom row: synaptonemal complex formation in baker's yeast, *Saccharomyces cerevisiae*. Spread meiotic chromosomes were stained with fluorescent antibodies to a synaptonemal complex protein.

recombination plays two successive roles during meiosis: (1) close pairing of homologues during leptonema/zygonema; and (2) connection of homologues via chiasmata from diplonema through to anaphase I.

Mechanism and Regulation of Meiotic Recombination

Meiotic recombination is initiated by the programmed formation of DNA double-strand breaks (DSBs) in chromosomes during leptonema (Figure 5). In yeast and similarly in mouse and humans, it can be inferred that ~250 double-strand breaks are formed per meiotic cell. Such a large number of recombination events is required to bring homologues into close register and facilitate the formation of SCs. Only a subset of DSBs (~5–30%, depending on the organism) go on to produce crossovers. DSBs are processed to give long single-stranded tails, which load proteins related to the bacterial recombinase RecA. These RecA homologues have the amazing ability to coat a single strand of DNA and then rapidly locate and pair with an identical DNA sequence anywhere in the genome. Meiotic chromosomes use this homologous pairing activity to recognize and pair with their homologous partner during leptonema.

A key aspect of meiotic recombination is its regulation. Most importantly, the cell must ensure that every pair of homologues receives at least one chiasma, as required for successful segregation at anaphase I. This means that the decision as to whether a DSB will eventually produce a crossover or a non-crossover is not random and must be actively imposed. It is not known how this decision is made, but its timing and molecular consequences are now becoming clear. The crossover or non-crossover decision is made at an early step in the recombination pathway, at the transition into zygonema. At this stage, DSBs that have been designated to become crossovers begin to exchange DNA strands with the homologous chromosome. Exchange at the two DSB ends occurs sequentially to form first a single-end invasion (SEI) and then a double-Holliday junction (dHJ; named after Robin Holliday, who proposed the existence of these strand-exchange structures during homologous recombination) (Figure 5). dHJs form during pachynema and are resolved toward the end of this stage by a nick and ligation mechanism, giving crossovers. DSBs that are not designated as crossovers are repaired primarily by a process called synthesis-dependent strand annealing (SDSA), which involves first copying DNA sequences from the homologous chromosome and then annealing the two DSB ends to seal the break. SDSA does not appear to involve stable, long-lived strand-exchange intermediates such as SEIs and dHJs.

See Also the Following Articles

Cell Cycle: Mitotic Checkpoints • Chromosome Organization and Structure, Overview • DNA Mismatch Repair and Homologous Recombination • Homologous Recombination in Meiosis • Metaphase Chromosome • Mitosis • Nucleoid Organization of Bacterial Chromosomes

Glossary

chiasma The point where homologous chromosomes exchange arms; the cytological manifestation of crossing-over.

crossing-over A reciprocal exchange between two DNA molecules; occurs essentially via a reciprocal breakage and rejoining process.

sister-chromatid cohesion The connections that hold newly replicated chromosome pairs together until they are ready to be distributed into daughter cells.

synaptonemal complexes Proteinaceous structures, resembling zippers or railroad tracks, that assemble between homologous chromosomes during meiosis. They hold chromosomes together during the pachytene stage and promote the formation of chiasmata.

Further Reading

Allers, T., and Lichten, M. (2001). Differential timing and control of noncrossover and crossover recombination during meiosis. *Cell* **106**, 47–57.

Hassold, T., and Hunt, P. (2001). To err (meiotically) is human: The genesis of human aneuploidy. *Nat. Rev. Genet.* **2**, 280–291.

Hunter, N., and Kleckner, N. (2001). The single-end invasion: An asymmetric intermediate at the double-strand break to double-holliday junction transition of meiotic recombination. *Cell* **106**, 59–70.

Jones, G. H. (1984). The control of chiasma distribution. *Symp. Soc. Exp. Biol.* **38**, 293–320.

Kleckner, N. (1996). Meiosis: How could it work? *Proc. Natl. Acad. Sci. USA* **93**, 8167–8174.

Page, S. L., and Hawley, R. S. (2003). Chromosome choreography: The meiotic ballet. *Science* **301**, 785–789.

Petronczki, M., Siomos, M. F., and Nasmyth, K. (2003). Un menage a quatre: The molecular biology of chromosome segregation in meiosis. *Cell* **112**, 423–440.

Roeder, G. S. (1997). Meiotic chromosomes: It takes two to tango. *Genes Dev.* **11**, 2600–2621.

Zickler, D., and Kleckner, N. (1999). Meiotic chromosomes: Integrating structure and function. *Annu. Rev. Genet.* **33**, 603–754.

Biography

Neil Hunter is an assistant professor in the section of microbiology at the University of California at Davis. He holds a Ph.D. from Oxford University and performed his postdoctoral studies at Harvard University. His research focuses on the mechanism and control of homologous recombination during meiosis. He has developed specialized DNA assays to monitor the molecular events of recombination in cells undergoing meiosis.

Melanocortin System

Roger D. Cone
Oregon Health and Science University, Portland, Oregon, USA

The melanocortins are a family of peptides defined by their ability to modulate the activity of a family of five related G protein-coupled receptors, called the melanocortin receptors (MC1-R, also called the melanocyte stimulating hormone receptor; MC2-R, also called the adrenocorticotropin receptor; and MC3-R, MC4-R, and MC5-R). The name is derived from the two original physiological activities identified for the family of peptides, stimulation of melanin synthesis and deposition, and stimulation of glucocorticoid synthesis and release by the adrenals. Four major melanocortin agonist peptides (α-MSH, β-MSH, γ-MSH, and ACTH) are encoded by a single gene, the proopiomelanocortin (POMC) gene. Major sites of POMC gene expression include the pituitary, hypothalamus, brainstem, and skin. The melanocortin system is quite unique in that specific receptor antagonists, called agouti and agouti-related protein, also exist. Together, these melanocortin agonists and antagonists regulate a remarkably diverse array of physiological processes, including the pigmentation of hair and skin, production of glucocorticoids, energy homeostasis, natriuresis, secretion of diverse exocrine gland products, and erectile function.

Melanocortin Ligands and Receptors

Elements of the melanocortin system are encoded by eight genes. Peptide agonists are encoded by a single gene, the POMC preprohormone precursor. This gene is expressed primarily in the anterior and intermediate lobes of the pituitary, the arcuate nucleus of the hypothalamus and the nucleus of the solitary tract of the brainstem, and in skin and a handful of peripheral sites where the peptides are thought to act in a paracrine or autocrine fashion. Melanocortin peptides are cleaved from three different regions of POMC to yield γ-MSH (amino terminal), ACTH, and α-MSH (overlapping peptides from the central portion), and β-MSH (carboxy-terminal end) peptides. Specific patterns of cleavage occur in different tissues, so, for example, the 39 amino acid peptide encoding ACTH is produced in the anterior pituitary by the peptidase PC1. A peptidase expressed in the intermediate lobe, PC2, makes a second cleavage to yield α-MSH, derived from the first 13 amino acids of ACTH. Melanocortin peptides derived from any of the three regions of POMC contain a His-Phe-Arg-Trp amino acid motif; this peptide motif is required for high-affinity binding of these peptides to the melanocortin receptors.

In addition to peptide melanocortin agonists derived from POMC, two genes, agouti and agouti-related protein (AGRP), encode small secreted antagonists of the melanocortin receptors. Agouti is a 131 amino acid protein with ten disulfide-bonded cysteine residues related in structure to small peptide toxins like the conotoxins and plectotoxins, produced by cone snails, and spiders, respectively. Agouti is produced by hair follicle cells, where it acts on adjacent follicular melanocytes to antagonize the MC1-R and switch the cell from eumelanin (brown-black) to pheomelanin (yellow-red) pigment synthesis. AGRP, also 131 amino acids in length, shares sequence similarity with agouti in the cysteine-rich carboxyterminal domain, and is an endogenous antagonist of the MC3-R and MC4-R. AGRP is expressed in the adrenal gland and in the arcuate nucleus of the hypothalamus; in this latter site AGRP is co-expressed with neuropeptide Y in a set of neurons adjacent but distinct from POMC arcuate neurons. In the brain, the AGRP gene is significantly up-regulated by fasting.

The melanocortin receptors, MC1-R through MC5-R, are encoded by a family of five independent genes; each receptor amino acid sequence is found in a single coding exon. The receptors are in the 7-membrane spanning G protein-coupled receptor class, and all five receptors couple, via Gs, to activation of adenylyl cyclase. With the exception of the MC2-R, all of the melanocortin receptors bind multiple species melanocortin peptide species. The MC2-R binds only the ACTH peptide, and the MC3-R is the only receptor that exhibits high-affinity γ-MSH binding. Much of the physiological specificity of melanocortin peptide action derives from the unique tissue distribution of the five receptor subtypes (Table I).

Pigmentation

The genetic study of coat colors in mice led to the identification of over 60 genes involved in pigmentation.

TABLE I

The Melanocortin Receptors and their Known Functions

Receptor subtype	Site of action	Ligand	Biological function
MC1-R	Melanocyte	α-MSH = β-MSH = ACTH > γ-MSH > $ACTH_{4-10}$ Antagonists – Agouti ($IC_{50} \sim 1$ nM)	Pigmentation
MC2-R	Adrenal cortex	ACTH	Steroidogenesis
MC3-R	CNS, stomach, duodenum, placenta, and pancreas	γ_1-MSH = γ_2-MSH = α-MSH = β-MSH = ACTH Antagonists – AGRP ($\sim$2 nM)	Inhibitory autoregulation of MC4-R system; natriuresis
MC4-R	Adult CNS, spinal cord, fetal brain, spinal cord, autonomic nervous system	α-MSH (EC_{50} = 0.2–1.5 nM) = β-MSH = ACTH > $ACTH_{4-10}$ = γ-MSH > $ACTH_{4-10}$ Antagonists – AGRP ($IC_{50} \sim 2$ nM)	Energy homeostasis
MC5-R	Exocrine glands	α-MSH > β-MSH = ACTH > γ-MSH > $ACTH_{4-10}$	Synthesis and secretion of exocrine gland products

These genes encode proteins involved in all stages and aspects of the process by which melanocytes migrate from the neural crest, populate skin and hair follicles, and synthesize and secrete melanin or pigment granules. The biochemically complex melanin polymers can be divided into two classes, the yellow-red pheomelanins and brown-black eumelanins. The regulation of enzyme activities leading to these two pigment classes is termed the eumelanin-pheomelanin switch. Genetic studies of pigmentation in the mouse and a variety of other mammalian species led to the identification of two gene loci primarily involved in the regulation of the eumelanin/pheomelanin switch, "agouti" and "extension." The "extension" locus encodes the melanocyte stimulating hormone receptor, or MC1-R, while "agouti" encodes an endogenous MC1-R antagonist expressed in skin and hair follicle. Mutations inactivating the MC1-R lead to yellow or red coat color, while mutations inactivating agouti lead to dark black coat colors. Loss-of-function mutations in the human MC1-R are one cause of red hair color and type I skin pigmentation in humans. In many mammals in the wild, up-regulation of agouti expression during a brief period of synthesis of a hair shaft leads to blockade of MC1-R activity, and results in deposition of a pheomelanin band along the otherwise darkly pigmented hair, known as the wild-type agouti pigmentation pattern.

Adrenocortical Steroidogenesis

The ACTH receptor, or MC2-R, is expressed almost exclusively in the cortex of the adrenal glands, where it regulates synthesis and release of glucocorticoids in response to release of adrenocorticotropic hormone (ACTH) by the pituitary gland. ACTH also has long-term effects on the growth and differentiation of the cells of the adrenal cortex. ACTH is a 39 amino acid melanocortin peptide cleaved from proopiomelanocortin in the anterior lobe of the pituitary. ACTH release, in turn, is regulated by production of corticotropin releasing hormone, a hypothalamic releasing factor produced in response to a wide variety of stressors. These factors, in concert, constitute what is widely known as the hypothalamic–pituitary–adrenal (HPA), or stress axis, which functions to allow organisms to adapt to internal and external challenges to homeostasis. Glucocorticoids serve many functions, but in general serve an adaptive role in coping with challenges to the organism by mobilizing carbohydrate energy stores and suppressing the immune system. Glucocorticoids are also essential for development. A rare syndrome of ACTH resistance resulting from loss-of-function mutations in the MC2-R, known as familial adrenocorticotropic hormone resistance, often presents with neonatal hypoglycemia, hepatitis, hyperpigmentation of skin due to elevated ACTH, and in some cases severe septic events.

Energy Homeostasis and Other CNS Actions

The cloning of the MC1-R (MSH-R) and MC2-R (ACTH-R) genes led to the identification of three additional GPCRs that were highly related in primary amino acid sequence and also were high-affinity receptors for melanocortin peptides. Since these receptors had, at the time, unknown physiological roles, they were termed MC3-R, MC4-R, and MC5-R. Remarkably, a novel mutation in the agouti gene that caused not only yellow coat color but also an obesity syndrome in the mouse ultimately led to the discovery that the MC3-R and MC4-R play a role in the central control of energy homeostasis. The "lethal yellow" allele of agouti results from a promoter rearrangement that causes ubiquitous expression of the agouti gene, in contrast to its normal expression limited to the hair

follicle, where it normally serves to block eumelanin synthesis. Aberrant expression of agouti in the brain results in blockade of the brain MC4-R, resulting in the agouti obesity syndrome. Discovery of AGRP identified an endogenous hypothalamic antagonist of the central MC3-R and MC4-R that has a physiological role in the regulation of the central melanocortin system. Both pharmacological blockade of the MC4-R and deletion of the gene in knockout mice also reproduce the agouti obesity syndrome. In humans, haploinsufficiency of the MC4-R, i.e., loss-of-function mutations in one allele, appears to be responsible for as much as 5% of cases of severe obesity, making the MC4-R the most common genetic cause of severe obesity known. Less is known regarding the MC3-R; however, it is expressed in a majority of arcuate POMC neurons where it appears to function as an inhibitory autoreceptor.

The central melanocortin system is defined as the hypothalalmic POMC and AGRP neurons that originate in the arcuate nucleus, brainstem POMC neurons originating in the nucleus of the solitary tract, and their target MC3-R- and MC4-R-expressing neurons, found throughout the CNS, in ~200 discrete locations (Figure 1). Central administration of melanocortin agonists both inhibits food intake and increases energy expenditure. These data, and the fact that blockade of MC4-R signaling causes obesity, argue that the POMC neurons tonically inhibit food intake and energy storage. The melanocortin system does this through effects on both food intake and on autonomic outflow to metabolically important tissues in the periphery. POMC neurons express receptors for the adipostatic hormone leptin, and play an important role in sensing and responding to the leptin signal from adipose tissue that informs the brain of long-term energy stores. POMC neurons also appear to be important for sensing and responding to acute satiety and hunger signals. The central melanocortin system affects autonomic outflow to a wide variety of tissues; melanocortins also have effects on blood pressure, heart rate, natriuresis, inflammatory response, and the male erectile response. Therapeutic applications of melanocortins may include obesity, diabetes, cachexia, and erectile dysfunction.

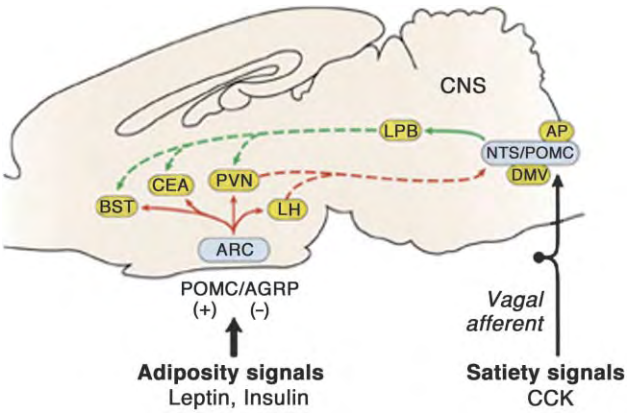

FIGURE 1 Integration of long-term adipostatic signals and acute satiety signals by the central melanocortin system. Blue: nuclei containing POMC neurons and AGRP neurons; yellow: nuclei containing MC4-R neurons that may serve to integrate adipostatic and satiety signals; red arrows: adipostatic signaling; green arrows: satiety signaling; BST, bed nucleus of the stria terminalus; CEA, central nucleus of the amygdala; PVN, paraventricular nucleus of the hypothalamus; LH, lateral hypothalamic area; LPB, lateral parabrachial nucleus; AP, area postrema; DMV, dorsal motor nucleus of the vagus. Reprinted from Fan, W., Ellacott, K. L. J., Halatchev, I., Takahashi, K., Yu, P., and Cone, R. D. (2004). Role for the brainstem melanocortin system in CCK-mediated satiety. *Nat. Neuroscience* 7, 335–336, with permission.

Exocrine Gland Function and Other Peripheral Actions

The MC5-R is expressed at high levels in a diverse array of exocrine glands, such as the sebaceous, lacrimal, preputial, and Harderian glands of the mouse. The receptor appears to stimulate the production and release of exocrine gland products from these tissues. For example, a knockout mouse specifically lacking the MC5-R gene was found to produce reduced amounts of certain lipids normally secreted by sebaceous glands onto the coat of the animal, thus reducing the ability of the coat to repel water. Male MC5-R knockout mice also exhibit a defect in initiating aggressive behavior relative to their wild-type counterparts, which has been attributed to defects in the secretion of pheromones by glands like the preputial, known to express high levels of the receptor. Little is known regarding the actual physiological roles of the MC5-R in the various exocrine tissues. For example, it is not clear whether the source of ligand for the MC5-R is the predominant serum melanocortin, ACTH, or whether this receptor is regulated by yet uncharacterized paracrine sources of POMC. If the former is the case, the system would provide a mechanism for stress-induced stimulation of exocrine gland function.

The MC3-R is also expressed in a handful of peripheral tissues, although little is know regarding its actions. The MC3-R and γ-MSH appear to be involved in the regulation of natriuresis; the reflex natriuresis that occurs after unilateral nephrectomy requires the MC3-R, and MC3-R knockout mice exhibit salt-sensitive hypertension.

See Also the Following Articles

Adenylyl Cyclases • Diabetes • Leptin

Glossary

adrenocorticotropin ACTH, a 39 amino acid peptide cleaved from POMC in the anterior pituitary, that is secreted into the bloodstream and regulates the synthesis and release of the glucocorticoid class of steroid hormones.

agouti proteins Agonti and agouti-releated proteins (AGRPs) are two small secreted proteins that bind to and antagonize melanocortin receptors.

energy homeostasis The process by which the brain detects long term energy reserves, stored in adipocytes in the form of fat, and regulates food intake and metabolic processes so as to keep reserves constant.

melanocortin A peptide derived from the proopiomelanocortin gene containing a -His-Phe-Arg-Trp- motif within its sequence that binds to and activates one or more of a family of five melanocortin receptors.

melanocyte A cell type populating skin and hair follicles that pigments hair and skin by secreting a variety of forms of melanin.

Further Reading

Chen, W., Opitz-Arraya, and Cone, R. D. (1997). Exocrine gland dysfunction in MC5-R deficient mice: Evidence for coordinated regulation of exocrine gland function. *Cell* **91**, 789–798.

Clark, A. J., Metherell, L., Swords, F. M., and Elias, L. L. (2001). The molecular pathogenesis of ACTH insensitivity syndromes. *Ann. Endocrinol (Paris)* **62**, 207–211.

Cone, R. D. (ed.) (2000). *The Melanocortin Receptors*. Humana Press, Totowa, New Jersey.

Cone, R. D. (ed.) (2003). The melanocortin system. In *Annals of the New York Academy of Science*, Vol 994. New York Academy of Science, New York.

MacNeil, D. J., *et al.* (2002). The role of melanocortins in body weight regulation: Opportunities for the treatment of obesity. *Eur. J. Pharmacol.* **440**, 141–157.

Rees, J. L. (2000). The melanocortin 1 receptor (MC1R): More than just red hair. *Pigment Cell Res.* **13**, 135–140.

Biography

Roger Cone is Director of the Center for the Study of Weight Regulation and Associated Disorders and a Senior Scientist within the Vollum Institute at the Oregon Health and Science University. His principal research interest is in the control of energy homeostasis by the central nervous system, and in the physiological processes regulated by the melanocortin system. He holds a Ph.D. from the Massachussetts Institute of Technology.

Membrane Fusion

Joshua Zimmerberg and Leonid V. Chernomordik
The National Institute of Child Health and Human Development, National Institutes of Health, Bethesda, Maryland, USA

Membrane fusion occurs when two cellular membranes attach, meld components, and become one membrane with preservation of sidedness and contents. This transformation seems somewhat miraculous, given that in everyday life only liquids with clean interfaces spontaneously fuse. So it is the hallmark of eukaryotic life that huge numbers of fusion reactions occur each second in an individual cell. Life begins with the fusion of the sperm membrane to the egg membrane, which allows the parental genes to mix together without any leakage into the extracellular space. So, relatively leak-free fusion is absolutely required for safe sex. Plasma membranes also fuse during the cell–cell fusion that directly causes the development of syncytia of several tissues, such as myotubes of muscle, trophoblastic syncytia of placenta, and the multinucleate giant cells of granuloma. In the development of *Caenorhabditis elegans*, where each cell can be traced, about one-third of the cells fuse.

But by far the most frequent site of membrane fusion is in the organization of intracellular membranes and the secretory pathway. For about half of a cell's genes are membrane proteins, and after their synthesis into the membrane of the endoplasmic reticulum, they must be delivered to their appropriate site of action, whether it is the membrane of the cell surface, or the membrane of an intracellular organelle. This protein trafficking is mediated by membrane fusion, as vesicles pinch one compartment, move through the cell, and then fuse to another compartment, often in one cycle after another before reaching their destination. Even then, proteins are taken up again into vesicles during their recycling, to fuse either to staging compartments or to degradation compartments. And it is not only membrane proteins that are trafficked in this manner, but vesicle fusion also delivers soluble proteins to the lumen of these compartments. This constant maintenance function of fusion is called constitutive fusion, to distinguish itself from the specifically regulated fusion events that must occur at the right time.

Arguably the most important regulated, or triggered fusion event for a human is the release of neurotransmitters such as acetylcholine, glutamate, and neuropeptides from synaptic vesicles during synaptic signal transmission. This class of fusion of intracellular secretory vesicles to the plasma membrane is called exocytosis, since the contents of the secretory vesicle are topologically in a space that becomes continuous with the outside of the cell, and never sees the cytoplasm. It is the triggered, regulated exocytosis that mediates many extremely important physiological events. The secretory vesicles are also called granules when their contents are seen as dense in traditional thin-section electron microscopy. Insulin, thyroid hormone, growth hormone, antidiuretic hormone, adrenaline, norepinephrine, follicle stimulating hormone, leutinizing hormone, and ACTH are just a few examples of hormones stored in secretory granules awaiting the proper signal for their coordinated and rapid secretion by fusion into the extracellular space for transport via the blood stream. Exocrine glands are also arranged for vectorial synthesis of digestive enzymes, such as trypsin and chymotrypsin, which are condensed into storage granules, whose membrane fuses to the luminal membrane of the glandular acinus. It has been clear that calcium is the intracellular messenger that triggers secretion in many systems. In other systems the intracellular messenger is not yet fully elucidated.

In addition, some exocytotic fusions are also constitutive, and provide the basis for most of the tissue organization of multicellular life. Thus collagen, fibronectin, proteoglycans, and other skeletal macromolecular elements are secreted via this constitutive secretory pathway. In addition, immunoglobulins are constitutively released from immune system cells throughout life, as are many cytokines and chemokines. It is worth noting that even the constitutive pathway is not devoid of control, as cytokines and chemokines are regularly up- and down-regulated at the levels of the control of gene and protein expression. The mast cell and the granulocytic series of white blood cells also rely upon fusion for their exocytosis of the mediators of inflammation and their release of compounds that kill invading pathogens. This is an essential part of the host response to disease.

It is impossible to overstress the importance of membrane fusion in the development, function, and

maintenance of tissues, organs, and organism. Since the extracellular space has no genome, all gene expression needed for the coordinated structure and function of tissues is a result of secretion of gene products through exocytosis, sometimes in response to requirements known by signaling to cell surface receptors or by internalization of informative macromolecules that in turn traffic to their targets by membrane fusion. In addition, new experiments suggest that stem cells in adult animals can remodel their cellular organization by fusing to adult cells. This points to membrane fusion as critical to the regeneration of tissues and organs.

Unfortunately, much of human suffering over the ages also derives in part from membrane fusion. Intracellular parasites use membrane fusion to enter cells and to evade the immune system. Over half the strains of human pathogenic viruses are encased in an envelope, a biological membrane, that must fuse to cellular membranes for the virus' internal genes to gain access to their intracellular destinations. And enveloped viruses are on the top of lists of human pathogens causing death and disease. HIV, the cause of AIDS, influenza, the cause of the flu (grippe), the viruses of rabies, measles and SARS, respiratory syncytial virus, and hepatitis C virus are just a few of these pathogens. Luckily for scientists studying fusion, the viral envelope often has only one major membrane protein, which causes membrane fusion and is easy to identify (e.g., the hemagglutinin of the influenza virus (HA)). So studies of viral fusion have led to many discoveries about the proteins and ultimately the mechanism of membrane fusion.

Proteins and Lipids

Proteins

From this diversity of membranes which fuse, are there any structural motifs that are common to the proteins that foment fusion? A definitive answer to this question is hindered by uncertainty about the identity of such proteins, a paucity of structural information on those that are identified, and the fact that most of the structural data derives from the same family of viral envelope proteins. Nevertheless, some generalizations can be made.

All viral fusogenic proteins characterized to date are anchored in the envelope by one or more transmembrane domains. While there is some latitude in the specific amino acid sequence of the transmembrane domains supporting fusion, the general mechanism by which the fusogenic protein is attached to the membrane is of importance for its activity and, in particular, for the late stages of fusion. As a rule, viral fusion proteins, as most viral envelope proteins, are homo- or hetero-oligomers. The importance of this for their fusogenic activity remains to be clarified. However, at least in some cases the stability of these oligomers appears to be crucial for fusion.

Specific triggering events start a major restructuring of viral fusion proteins from their initial conformation to fusion-competent forms. For viruses that invade cells by an endocytotic pathway, the binding and fusion functions of envelope proteins appear to be well separated, and the trigger for conformational change is acidification. Other viruses, such as HIV, enter cells by fusing with the target cell plasma membrane. Here binding of the fusogenic protein to specific receptors at the surface of the target cell triggers the subsequent cascade of conformational change. For still other viruses, such as the Rous Sarcoma virus, receptor binding primes the fusion protein for subsequent triggering by acidification.

One of the most important features of this trigger-dependent restructuring of viral fusion proteins is exposure of an amphiphilic, highly-conserved stretch of $\sim$10–30 amino acid residues that is critical for fusion. This "fusion peptide" is hidden from the aqueous environment in the initial conformation of the protein. It inserts into membrane after activation. The HA fusion peptide, the amphiphilic stretch of $\sim$20 amino acid residues at the NH2-terminus of the HA2 subunit of HA, is highly conserved; mutations here have deleterious effects on fusion activity. In general, fusion peptides spontaneously insert into membranes and disturb the structure of lipid bilayers. Based on the dependence of the fusogenic activity of HA on the sequence of the fusion peptide, fusion appears to require membrane-insertion of the fusion peptide in a boomerang-like conformation.

Similar aminoterminal peptides are found in the fusion proteins of a number of other viruses such as HIV, Sendai, and hepatitis B. There are also many viruses where the fusion peptide is found in the midst of the amino acid sequence of membrane-anchored glycoproteins (for instance, Semliki Forest, tick-borne encephalitis and rabies viruses). While fusion peptides, one or more per protein, undoubtedly play a key role in all well-characterized fusion machines, their specific role in fusion requires clarification. The prevailing model suggests that the fusion peptide, when inserted into the target membrane, both destabilizes the membrane and serves as a handle allowing the fusion protein to bend this membrane towards the viral membrane. It has been also hypothesized that the fusion peptide inserts into, destabilizes, and bends the viral rather than target membrane. In addition, the functional role of some of the protein regions identified as fusion peptides may not be limited to direct interaction with membranes and may involve directing the refolding of the activated protein by supporting or destabilizing certain conformations.

Many fusion proteins, named class 1 (e.g., HA and HIV *env*), have a stage of proteolytic cleavage which

liberates the N terminus of the fusion peptide from other domains. Final conformations of the proteins of this class share a common hairpin arrangement with a central α-helical coiled-coil domain surrounded by an outer layer of polypeptide chains. Class 2 proteins (e.g., fusion proteins of flaviviruses, E) have an internal fusion peptide, and here proteolytic cleavage of an accessory protein leads to the mature conformation of the fusion protein itself. Class 2 proteins are not predicted to form coiled-coils and contain predominantly β-strand secondary structure.

In spite of much diversity in their initial structures, fusion proteins of the two classes apparently share an important feature of the final conformations of these viral fusion proteins: close proximity of the fusion peptide and transmembrane domain. In addition, for diverse fusion proteins the triggering event not only starts a cascade of conformational changes of individual proteins, but also initiates lateral protein–protein interactions. These interactions are detected as cooperativity of both conformational change and membrane fusion as well as formation of multiprotein complexes of activated fusion proteins.

The identification and characterization of the proteins that mediate intracellular membrane fusion is much more complex and controversial, and mechanistic studies lag behind. There are slews of interesting proteins that are important for the regulation, binding, docking, priming, and execution of membrane fusion, most identified through a genetic screen for mutants in secretion in yeast. In general, it is thought that small GTP-binding proteins mediate recognition of pairs of membranes destined to fuse together with the SNARE proteins. There are some excellent reviews on SNARE proteins and their role in fusion.

Exocytosis is the best-studied type of intracellular fusion. A collection of proteins known as the exocyst complex is involved in the binding of vesicles to the plasma membrane. Priming of the bound and docked proteins involves the phosphorylation of a specific inositol lipid, PIP2, and other ATP-dependent processes. Some of the rates of vesicle mobilization, binding, docking, and priming are dependent upon the local intracellular free calcium ion concentration. In regulated exocytosis *in vivo*, it is almost always this divalent ion that triggers fusion. Synaptotagmins, annexins, and calmodulin have been implicated as the calcium-binding partner in triggering exocytosis in different systems. The SNARE proteins are the leading candidates for the protein that mediates the membrane fusion event itself, but their generality and mechanism of action is still a controversial question in the field. In particular, it is not clear how much their interaction energy contributes to overcoming the barriers to membrane fusion. To estimate those barriers, the role of lipids and the pathway of membrane fusion needs to be considered.

Lipids

Since ultimately fusion proteins must act on the lipid bilayer of membranes, it is no surprise that protein-mediated fusion is sensitive to lipid composition. A distinction between physiological requirements and experimental effects of lipids must be made. As an example of the physiological lipid requirements, fusion mediated by Semliki Forest Virus is strictly dependent on the presence of sphingolipid and cholesterol in the target membrane: the former (optimum at ~ 5 mol%) is needed for the actual fusion event and the latter (optimum at 30 mol%) is required for the low-pH-dependent conformational change in the fusion protein and membrane insertion of its fusion peptide. A second example is the triggered exocytosis of chromaffin cells that requires specific polyphosphoinositides.

In contrast to physiological lipid requirements, usually specific for different systems, non-bilayer lipids that change the propensity of lipid monolayers to bend have effects on fusion that are strikingly universal. These effects depend on both the effective shape of the lipids, and the monolayer to which they are added. Inverted cone lipids such as lysophosphatidylcholine, when added to the contacting monolayers of fusing membranes, inhibit membrane merger in disparate biological fusion reactions. Lysolipids inhibit virtually all systems that have access to the contacting leaflet, irrespective of the specific fusion proteins and the triggering agent. In contrast, cone-shaped lipids such as phosphatidylethanolamine and *cis*-unsaturated fatty acids (e.g., oleic and arachidonic acids) promote fusion. In addition to this early stage of fusion that is sensitive to the composition of the "contacting" membrane monolayers, there is also a later stage that is sensitive to the composition of the "noncontacting" monolayers of the fusing membranes: inverted-cone shaped amphiphiles added to these distal monolayer of the fusing membranes promote fusion. These stages likely involve the actual merger of the lipid bilayers.

Mechanistic Pathways

At the time of the writing of this article, there are many open questions for research on the mechanism of membrane fusion. One theme, however, that is common to many of the disciplines studying fusion, is that at the center of biological membrane fusion is a fundamental rearrangement of lipid bilayer topology that follows the same pathway as does the fusion of synthetic lipid bilayers. For any pathway in biology, we need to identify the intermediate structures, the relative energy of each intermediate, and the driving forces that propel the membranes to fuse. After binding, lipid bilayer membranes that are to fuse first exchange the lipids of the

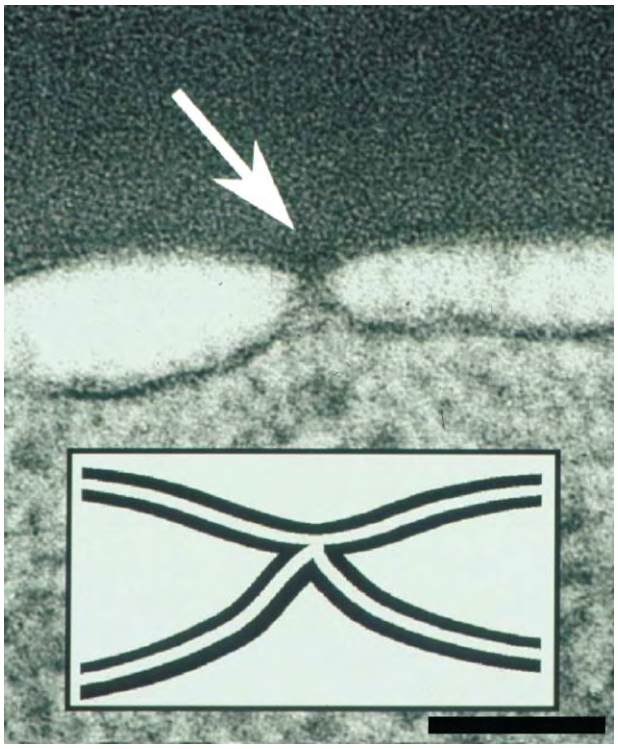

FIGURE 1 The contact site between a red cell membrane (top) and a fibroblast expressing the influenza hemagglutinin (HA) mutated to delete the transmembrane domain and attach the ectodomain of HA to a glycerol phosphoinositol lipid. The membranes were activated for fusion after binding with a pulse of low pH. After 20 min, the cells were frozen into vitreous ice by slamming them against a copper block cooled with liquid nitrogen. After freeze-substitution and thin sectioning, electromicrographs were taken at two tilt angles, and analyzed with stereo viewing. The drawing illustrates the view from stereography. Bar = 100 nm.

contacting monolayers (hemifuse), then form small aqueous pores that transiently open and close. Complete fusion ensues only when tension is applied to the fusing lipid bilayer membranes.

Biological membrane fusion offers constraints on the spontaneous fusion of lipid bilayers by dint of the regulated activities of the fusion proteins. Studies on mast cell exocytosis show that the tension propelling fusion must be exerted locally by proteins rather than through swelling of the vesicles. Studies on fusion mediated by influenza HA show that the early hemifusion intermediate is reversible, and converts into a small pore (the fusion pore) when the distal monolayers merge. In electron micrographs of thin sections of cells frozen into vitrious ice, then freeze-substituted, both the contact site and the fusion pore can be visualized (Figure 1). Since the outer diameter of the contact site ranges between 10 and 50 nm, there is not much expansion of the stalk before the initial pore is formed, which is ~1 nm internal aqueous diameter. This initial fusion pore, which can only be detected by electrophysiological assay, is usually spontaneously reversible, giving a flickering pore phenotype observed both for viral fusion and exocytosis. Opening of one or several of these early pores is followed by an expansion of at least one of them to complete fusion. Progress through the pathway, and perhaps alternate pathways, is dependent upon the density of the fusogenic protein. At lower densities of HA, one observes either small non-expanding fusion pores or hemifusion phenotypes. Only at optimal conditions of high density of activated HAs and physiological temperature, fusion reaction

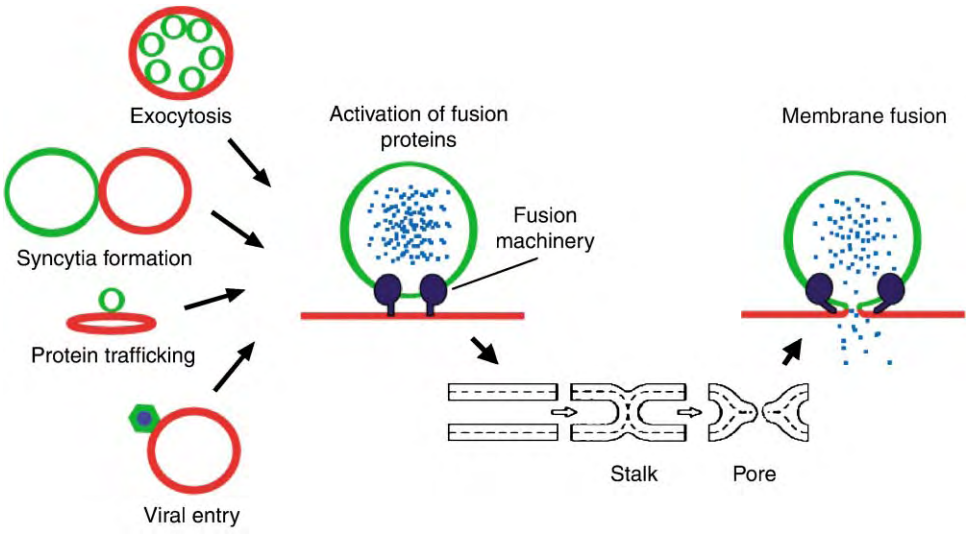

FIGURE 2 Diverse biological processes that feature membrane fusion apparently converge to a common stalk-pore pathway of lipid bilayers, after activation of different specific fusogenic proteins by specific triggers (e.g., Ca^{2+}, H^{+}, and GTP), or by receptor binding (e.g., CD4 in HIV). Both stalk- and pore-intermediates are generated by protein-mediated bending of membrane lipid monolayers. Dashed lines show the boundaries of the hydrophobic surfaces of two monolayers in each membrane and in hypothetical intermediates.

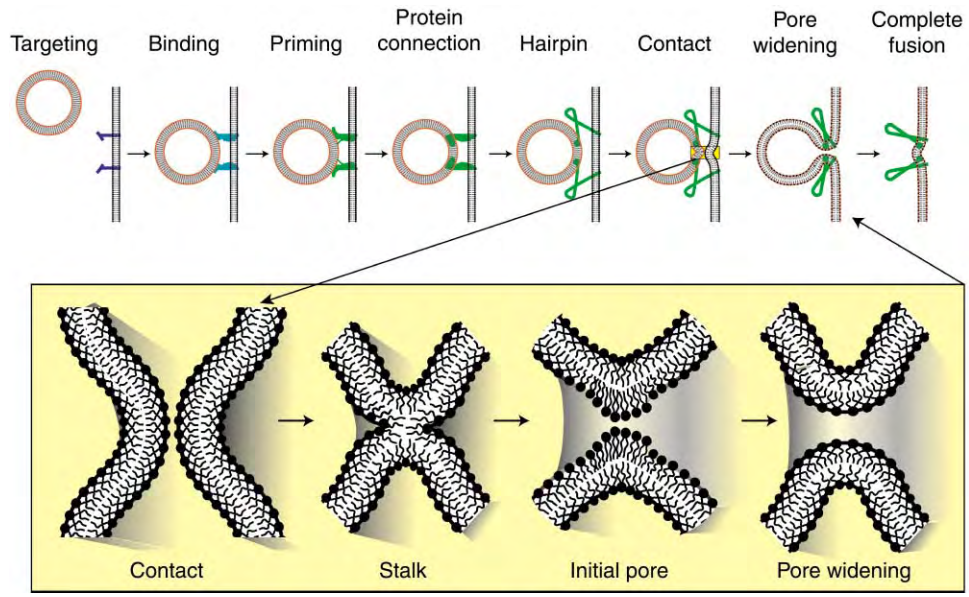

FIGURE 3 A schematic representation of the many steps in protein-mediated membrane fusion, abstracted from research on many different proteins and systems. Top: The delivery of vesicles to their fusion partner may be highly organized and targeted, as in intracellular trafficking, or random, as in viral infection. Binding of the two membranes is mediated through the attachment of the fusion protein to its receptor in the partner membrane, which can be either a protein or a lipid. In many systems there next are priming reactions such as covalent bond modifications involving either cleavage of part of the fusogenic protein, interaction with co-receptors, or phosphorylation of lipids with ATP. At this stage the system is ready for any trigger that may be needed to regulate fusion. In the case of influenza HA, this trigger leads to insertion of the fusion peptide into the target membrane, and a protein now connects both membranes' bilayers. Next protein conformational change, often to a hairpin configuration, leads to contact between the two membranes at discrete spots where the bilayers are deformed. Spontaneous rearrangement of contacting lipids can lead to stalk formation and then the opening of the initial fusion pore. After pore widening, contents can be released or mixed.

yields an expanding fusion pore that fully mixes both lipids and aqueous contents.

The current synthesis of results on biological fusion, along with experimental and theoretical work on fusion of synthetic lipid bilayers, suggests that membrane rearrangement in cellular membrane fusion can be considered as a sequence of local bending deformations. First, contacting monolayers of the two bilayers merge to form a local hemifusion connection referred to as a stalk and then after some expansion, small pores form in the hemifusion junction. With tension, fusion is completed by formation and expansion of the pore. Two key intermediates, stalk and pore, are both formed by strongly bent lipid monolayers. However the net curvature of these intermediates is opposite. In the stalk there is less room for the polar heads of the lipids than for the lipid tails. In the pore, it is just the opposite. Also, while the stalk is formed by contacting monolayers, the pore is formed by the distal monolayers of the membranes that came into contact only after hemifusion. The universal effects of nonbilayer lipids for both purely lipid bilayer membranes and for a variety of cellular fusion systems (Figure 2) suggest that these disparate processes all revolve around stalk-pore rearrangements of their membrane bilayers.

We can summarize membrane fusion with a pathway of the current working hypothesis of many groups (Figure 3). Essentially, cell biologists, lipid physical chemists, and membrane biophysicists have converged their views: in biological membrane fusion, as in many biological processes, proteins act to accelerate fusion by lowering the energy barriers for unfavorable intermediates of the spontaneous fusion pathway of lipid bilayer membranes. The specific mechanisms by which proteinaceous fusion machines break and reseal the continuous and tight bilayer structures of biological membranes remain to be understood.

See Also the Following Articles

Lipid Bilayer Structure • MDR Membrane Proteins

Glossary

fusion pore An early aqueous connection between compartments joined by fusion.

fusion protein Specialized protein that catalyzes merger of two membrane bilayers into one.

hemifusion The coalescence of the contacting monolayers of the two bilayers with their distal monolayers to remain distinct. In many cases hemifusion allows diffusion of a lipid dye originally only in

the outer leaflet of one cell or vesicle to another, without any diffusion of an aqueous dye originally in the lumen of the cell (the cytosol) or a vesicle.

stalk intermediate Hypothetical local hemifusion connection between contacting monolayers at early fusion stages.

Further Reading

Blumenthal, R., Clague, M. J., Durell, S. R., and Epand, R. M. (2003). Membrane fusion. *Chem. Rev.* **103**, 53–70.

Chernomordik, L. V., and Kozlov, M. M. (2003). Protein–lipid interplay in fusion and fission of biological membranes. *Annu. Rev. Biochem.* **72**, 175–207.

Cohen, F. S., and Melikyan, G. B. (1998). Methodologies in the study of cell–cell fusion. *Methods* **16**, 215–226.

Hernandez, L. D., Hoffman, L. R., Wolfsberg, T. G., and White, J. M. (1996). Virus–cell and cell–cell fusion. *Annu. Rev. Cell Dev. Biol.* **12**, 627–661.

Jahn, R., Lang, T., and Sudhof, T. C. (2003). Membrane fusion. *Cell* **112**, 519–533.

Lentz, B. R., Malinin, V., Haque, M. E., and Evans, K. (2000). Protein machines and lipid assemblies: Current views of cell membrane fusion. *Curr. Opin. Struct. Biol.* **10**, 607–615.

Rothman, J. E. (2003). The machinery and principles of vesicle transport in the cell. *Nat. Med.* **8**, 1059–1062.

Shemer, G., and Podbilewicz, B. (2003). The story of cell fusion: Big lessons from little worms. *Bioessays* **25**, 672–682.

Skehel, J. J., and Wiley, D. C. (2000). Receptor binding and membrane fusion in virus entry: The Influenza Hemagglutinin. *Annu. Rev. Biochem.* **69**, 531–569.

Tamm, L. K., Crane, J., and Kiessling, V. (2003). Membrane fusion: A structural perspective on the interplay of lipids and proteins. *Curr. Opin. Struct. Biol.* **13**, 453–466.

Zimmerberg, J., and Chernomordik, L. V. (1999). Membrane fusion. *Adv. Drug Deliv. Rev.* **38**, 197–205.

Biography

Joshua Zimmerberg, Chief of the Laboratory of Cellular and Molecular Biophysics, received his M.D. and Ph.D. from the Albert Einstein College of Medicine of Yeshiva University, working with Fredric S. Cohen under the mentorship of Alan Finkelstein in the Galvani Institite of Electromembranology, and did his postdoctoral work with V. Adrian Parsegian at the NIH. His principal contributions have been in the discoveries of the requirement of tension in membrane fusion, the fusion pore, the pathway of fusion in exocytosis and viral fusion, and the lipidic nature of the apoptotic pore.

Leonid V. Chernomordik, Chief of the Section on Membrane Biology in the Laboratory of Cellular and Molecular Biophysics, received his Ph.D. in electrochemistry from the Frumkin Institute of Electrochemistry, Russian Academy of Sciences in 1979 and his Doctor of Sciences in biophysics degree from the Moscow State University in 1991. His principal contributions have been in developing the stalk-pore hypothesis of membrane fusion first for synthetic lipid bilayers and then for biological membranes.

Membrane Transport, General Concepts

Stanley G. Schultz
University of Texas Medical School, Houston, Texas, USA

The term membrane transport refers to processes that bring about the movement of solutes and water across the barrier, or envelope that surrounds all living cells in the animal and plant kingdoms. These processes are responsible for two ubiquitous characteristics of living cells, namely: (1) the ability to maintain constant, or near constant, intracellular compositions that differ from the extracellular environment, containing the highly specialized molecules essential for metabolism and replication; and at the same time, (2) the ability to selectively exchange matter and energy with that environment.

All cell membranes consist of a double layer of phospholipids oriented so that their electrically charged, hydrophilic (or water-loving) head projects into the interior and exterior of the cells, respectively, and their lipid tails, which are hydrophobic (or water-fearing), project inward and form an oily core. Floating in this oily structure are surface or peripheral proteins that do not extend through the thickness of the bilayer, and integral proteins that span the bilayer and provide pathways for direct communication between the intracellular and extracellular compartments. This lipoprotein bilayer model, which consists of large expanses of lipid studded here and there with protein, is illustrated in Figure 1.

Exchange of solutes and water across the lipoprotein barrier takes place through the lipid as well as through integral proteins and can be classified as (1) simple diffusion; (2) diffusion through pores or channels; and (3) carrier-mediated transport. The latter may be subdivided into facilitated diffusion (or facilitated transport), primary active transport, and secondary active transport.

Simple Diffusion

The simplest form of membrane transport was recognized more than a century ago by Overton, who noted that the ease with which a large variety of molecules cross plant cell membranes is proportional to their solubility in lipids; indeed, it is the observation that first suggested that the membranes were composed of lipids. In essence he suggests that the molecule simply dissolves in the lipid across one surface, passes through this oily barrier, and exits at the other side. The rate of this process is given by a modification of a law derived by Fick in 1855:

$$J_i = k_i D_i \Delta C_i$$

where J_i is the rate of diffusion of solute i across the membrane (in amount of solute per unit time), k_i is a measure of the solubility of the solute i in oil compared to water (oil:water partition coefficient), D_i is the diffusion coefficient of i or the mobility of i in the lipid, and ΔC_i is the concentration difference of i across the membrane. The product $k_i D_i$ is often abbreviated as the permeability coefficient P_i.

Overton demonstrated a linear relation between J_i and k_i in plant cells and this relation, now referred to as Overton's law, has been confirmed repeatedly.

Diffusion through Pores or Channels (Restricted Diffusion)

Lipid membranes are essentially impermeable to ions and are only slightly permeable to water. It is now clear that these highly hydrophilic molecules traverse cell membranes through integral proteins that form water-filled pores or channels that span the bilayer. Although the presence of "holes" in membranes had been speculated as early as the 1850s and were strongly suggested by the pioneering work of Hodgkin, Huxley, and Keynes on the squid axon in the 1950s, they were established beyond doubt, more recently, by Hille, Armstrong, and MacKinnon.

Although some use the terms pore and channel interchangeably, others prefer to employ the word pore for integral proteins that are continually open to the two aqueous compartments on both sides of the membrane (using the analogy of an open pipe) and reserve the word channel for a pore that has a "gate" that determines how

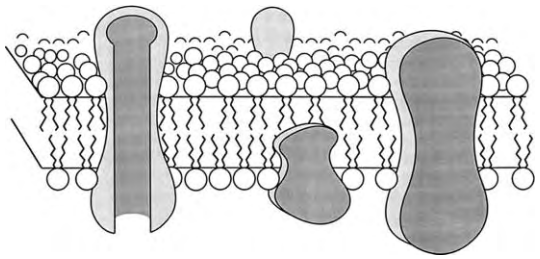

FIGURE 1 Illustration of phospholipid bilayer with peripheral proteins adhering to the surfaces and integral proteins spanning the thickness of the membrane. One integral protein is portrayed as a channel. The charged head groups of the phospholipids are represented as circles and the lipophilic fatty tail groups as the wavy lines forming the core of the bilayer.

long it will be in the fully open state and how long it will be closed (the analogy being a pipe with shutter).

In general, then, channels have gates that determine the probability that they will be in the open state at any time (open-time probability) and how long they will stay open (mean open time). The properties of these gates may be influenced by the electrical potential difference across the membrane (voltage-gated channels), the binding of one or more ligands (ligand gated channels) or both. In addition, they possess "filters" that confer selectivity on the channel; the structural characteristics of ion channels that result in a high preference for one ion over other have recently been unraveled for potassium channels.

Movement of an ion through an open channel obeys a form of Ohm's law for current flow caused by a conductance driven by an electrochemical potential difference. Thus,

$$i_{\mathrm{i}} = g_i(V_{\mathrm{m}} - E_{\mathrm{i}})$$

where i_{i} is the rate of flow of the ion through a single open channel given in electrical terms of amperes (this is analogous to J_i), and g_i is the conductance of the channel (analogous to P_i). V_{m} is the electrical potential difference across the membrane, E_{i} is the Nernst equilibrium potential for the ion so that the difference, $(V_{\mathrm{m}} - E_{\mathrm{i}})$, is the displacement of the ion from equilibrium in electrical terms and is thus the driving force for flow. More than one million ions may traverse a single channel per second so that single channel currents may be readily recorded using a variety of techniques. The ionic current through an ensemble of such channels is $I_{\mathrm{i}} = i_{\mathrm{i}} N_{\mathrm{i}} p_{\mathrm{o}}$, where N_{i} is the total number of channels and p_{o} is the open probability.

Carrier-Mediated Transport

Carrier-mediated transport differs from diffusion through lipid phase, pores, or channels in that after entering the integral protein the transported solute(s) bind to a specific site(s) on this protein which then undergoes some translocation that exposes and/or releases them to the other side. Unlike pores or channels, carriers are not open to both sides of the membrane simultaneously. Because conformational changes are necessary for carriers to function, the number of molecules transported per second is orders of magnitude less than pores. In this sense, carriers may be viewed as enzymes that do not chemically alter the transported species (substrate) but, instead, catalyze a change in their location. For this reason, the terms permeases and translocases are used in some instances as synonymous with carriers. Indeed, one characteristic of carrier-mediated transport is that it displays Michaelis–Menten saturation kinetics, marked by a maximum transport velocity (J_m) and a solute concentration needed to achieve a half-maximal transport velocity (K_t), and often obeys the simple relation

$$J_{\mathrm{S}} = \left\{ [S] J_{\mathrm{m}} / K_{\mathrm{m}} + [S] \right\}$$

where J_{S} is the rate of transport and $[S]$ is the concentration of the transported solute (Note: this relation describes the initial rate of transport when there is solute present on one side of the membrane only).

Facilitated Diffusion

The earliest recognized and simplest form of carrier-mediated transport is facilitated diffusion, often called facilitated transport, in which an otherwise impermeant solute binds to a site on an integral protein (carrier) from one side of the membrane and then undergoes a translocation that provides the solute access to the other side. The classic example of facilitated diffusion is glucose transport across the membranes of cells such as erythrocytes, muscle, adipocytes, etc. The carriers that mediate this transport have been cloned and sequenced and fall into a group of proteins that have 12 membrane spanning segments called GLUT. Urea is transported across the membranes of many cells by a facilitated transporter called UT.

It must be emphasized that because these carriers are not directly or indirectly coupled to a supply of energy, they cannot perform osmotic work, i.e., they cannot transport a neutral solute against a concentration difference (e.g., from lower to higher concentration) or a charged solute against a combined electrochemical potential difference. Thus, like diffusion, facilitated diffusion carriers bring about equilibration; transport ceases when intrinsic thermodynamic driving forces are abolished.

Active Transport

Active transport is the term reserved for transport processes that result in the movement of a solute uphill or against its natural direction. For the case of a neutral solute (at constant temperature and pressure), this resolves into movement against a concentration difference; for a charged solute, it is movement against the combination of concentration and electrical potential differences. This is work (e.g., charging a battery) and it therefore requires the investment of energy.

There are two groups of carrier-mediated active transport processes: those where the coupling to energy is direct and those where the coupling to energy is indirect.

Primary Active Transport

Primary active transport processes are capable of coupling energy directly to the uphill movement of the transported species. By far the most abundant, and well understood, primary active transporters are the retinylidene proteins or, more commonly called, rhodopsins, capable of coupling light energy to ion transport. Bacteriorhodopsins found in *Archaea*, *Circhaea,* and some eukaryotic and prokaryotic cells pump protons out of these cells, thereby establishing a "proton-motive force" across the membrane. Holophilic bacteria possess a form referred to as halorhodopsin that pumps Cl^- into cells. These transporters have been studied extensively using high-resolution crystallography and all possess seven membrane spanning segments attached to a chromophore.

In higher animals, all primary active transporters are ATPases, that derive the energy for moving the transported solute against a thermodynamic driving force (i.e., uphill) from ATP hydrolysis. The most prevalent is the Na–K pump found in virtually all cells from higher animals and responsible for pumping three Na^+ ions out of the cell and two K^+ ions into the cell for every ATP hydrolyzed. This pump is responsible for the fact that these cells have a lower intracellular Na^+ concentration and higher intracellular K^+ concentration than the concentrations of these ions in the surrounding extracellular fluid. As will be discussed below, the extrusion of Na^+ from the cell establishes a "natrio-motive" force across the membrane analogous to the "proton-motive" force established by light-driven proton pumps in lower life forms. The detailed mechanism of action of the Na–K pump is not well established except for the fact that it is a member of a superfamily of ATPases referred to as E_1–E_2 ATPases or P-type ATPases, because the operation of the pump involves cycling between two configurations of the protein driven by phosphorylation and dephosphorylation reactions.

Other ATPases that perform primary active transport include the Ca^{2+} ATPase found in muscle and responsible for regulation of the Ca^{2+} activity of the cytoplasm, the H^+–K^+ ATPase of gastric parietal cells responsible for secreting protons into the gastric juice in response to appropriate stimuli, and the H^+ ATPase that is responsible for acidifying intracellular organelles such as lysosomes, endosomes, etc.

Secondary Active Transport

Secondary active transport processes bring about the uphill transport of one or more solutes but do not derive the necessary energy from direct coupling to a source of metabolic energy. Instead, these transport processes are energized by coupling those movements to the downhill movement of another solute.

Cotransport (symport) The uphill or secondary active transport of a large number of solutes into cells of higher animals is coupled to the downhill movement of Na^+. Thus, the carrier protein binds both the transported solute and Na^+ from the extracellular solution. Inasmuch as the Na^+ concentration in the intracellular solution is lower than that in the extracellular solution, because of the action of the Na^+–K^+ pump as discussed, this coupling permits the downhill movement of Na^+ and provides the energy for the uphill movement of the coupled solute. In essence, the energy invested into the Na^+–K^+ pump by the hydrolysis of ATP has set up an Na^+-gradient or natrio-motive force across the membrane that can be deployed to energize the secondary active transport of solutes whose translocation across the membrane is coupled to that of Na^+.

In many lower forms of life, secondary active cotransport is energized by the H^+ gradient or proton-motive force across the membrane established and maintained by light-driven primary active extrusion of protons, as discussed above.

Countertransport (antiport) Coupling to the downhill movement of Na^+ into cells can also serve to energize the uphill or secondary active transport of solutes out of cells. Important examples of counter-transporters are the Na^+–H^+ exchanger (NHE) responsible for extruding H^+ from cells and the regulation of cell pH and the Na^+–Ca^{2+} exchanger (NCX) responsible for extruding Ca^{2+} from many cells.

Na^+-coupled co- and counter-transport processes are very diverse and are beautiful examples of bioenergetic economy where a single primary active transport process directly coupled to the hydrolysis of ATP can establish a transmembrane ion (Na^+) gradient that can, in turn, be utilized to energize a wide variety of secondary active transport processes.

See Also the Following Articles

ER/SR Calcium Pump: Function • ER/SR Calcium Pump: Structure • Membrane Transporters: Na^+/Ca^{2+} Exchangers • Plasma-Membrane Calcium Pump: Structure and Function • P-Type Pumps: Copper Pump • P-Type Pumps: H^+/K^+ Pump • P-Type Pumps: Na^+/K^+ Pump • P-Type Pumps: Plasma Membrane H^+ Pump

Glossary

active transport Transport of a solute against a chemical (concentration) and/or electrical potential difference that is directly (primary) or indirectly (secondary) driven by metabolic energy.

carrier Integral proteins that span the membrane phospholipid bilayer and are capable of binding a solute(s) and catalyzing translocation from one side of the membrane to the other.

channel Integral proteins that span the membrane phospholipid bilayer and provide water-filled passage ways (pores) for the diffusion of solutes.

diffusion Flow of a solute from a region of higher to a region of lower chemical (concentration) and/or electrical potential driven solely by thermal random motion of solute particles.

facilitated diffusion Carrier-mediated transport processes that are not coupled to a supply of metabolic energy and thus can only result in the equilibration of a transport solute across the membrane.

Further Reading

Bretscher, M. S. (1985). The molecules of the cell membrane. *Sci. Am.* **253**(4), 100–108.

Doyle, D. A., Cabral, J. M., Pfuetzner, R. A., Kuo, A., Gulbis, J. M., Cohen, S. L., Chait, B. T., and MacKinnon, R. (1998). The structure of the potassium channel: Molecular basis of K^+ conductance and selectivity. *Science* **280**, 69–77.

Hille, B., Armstrong, C. M., and MacKinnon, R. (1999). Ion channels: From idea to reality. *Nat. Med.* **5**, 1105–1109.

Schultz, S. G. (1980). *Basic Principles of Membrane Transport*. Cambridge University Press, Cambridge.

Schultz, S. G. (2003). Membrane transport. In *Essential Medical Physiology* (L. R. Johnson, ed.) 3rd edition, pp. 37–70. Elsevier, USA.

Spudich, J. L., Yang, C.-S., Jung, K.-H., and Spudich, E. N. (2000). Retinylidene proteins: Structures and functions from Archaea to humans. *Ann. Rev. Cell Dev. Biol.* **16**, 365–392.

Biography

Dr. Stanley G. Schultz is Professor and Vice-chair of the Department of Integrative Biology and Pharmacology, and Interim Dean of the University of Texas Medical School in Houston; he is also holder of the Fondren Family Chair in Cellular Signaling. He was previously Chairman of the Department of Physiology and Cell Biology at that institution. Dr. Schultz holds an M.D. from The New York School of Medicine. His principal research interest is in epithelial, particularly, small intestinal, transport and he has authored and edited seminal papers and texts in the area of membrane transport physiology and biophysics. He is past President of the American Physiological Society.

Membrane Transporters: Na^+/Ca^{2+} Exchangers

Jonathan Lytton
University of Calgary, Calgary, Alberta, Canada

The Na^+/Ca^{2+} exchanger is a plasma membrane protein that can bind and transport both Na^+ and Ca^{2+} ions. The exchanger is reversible, and the direction in which it moves Ca^{2+} depends upon the relative gradients of Na^+ and Ca^{2+} across the membrane, the membrane potential, and the number of ions that bind and are transported. Under normal physiological conditions in eukaryotic cells, the Na^+/Ca^{2+} exchanger extrudes Ca^{2+} from the cytoplasm in exchange for Na^+ entry, and thus participates in Ca^{2+} homeostasis in a variety of cellular environments, most notably heart, brain, and kidney. The Na^+/Ca^{2+} exchanger is encoded by a family of structurally and functionally related gene products that have distinct patterns of expression in different tissues. There are two major branches to the family, one that encodes Na^+/Ca^{2+} exchangers that transport Na^+ ions in exchange for only Ca^{2+} ion (NCX), and one in which Na^+ ions are exchanged for both Ca^{2+} and K^+ (NCKX). The NCX branch has three known members, NCX1 (*SLC8A1*), NCX2 (*SLC8A2*), and NCX3 (*SLC8A3*), while the NCKX branch has five known members, NCKX1 (*SLC24A1*) through NCKX5 (*SLC24A5*). Only NCX1 and NCKX1 proteins have been studied extensively in their endogenous environment (cardiac myocytes and retinal rod photoreceptor outer segments, respectively). The remaining members of the family have been defined through cloning or bioinformatic tools, and the unique contributions they each make to cellular Ca^{2+} homeostasis is an active area of investigation.

Cellular Ca^{2+} Homeostasis

Ca^{2+} ion is one of the most ubiquitous intracellular second messengers. Changes in the concentration of Ca^{2+} control a variety of cellular processes ranging from fertilization through proliferation and differentiation, the specific functions of different mature adult cells and tissues, all the way to programmed cell death. The coordination of such a diverse set of functions is thought to be achieved through Ca^{2+}-binding events that are sensitive to complex spatial and temporal patterns of intracellular Ca^{2+} concentration. Unlike other second messenger systems, Ca^{2+} cannot be metabolized, and its concentration is controlled primarily by transport across membranes that bound intracellular compartments (such as the sarco- or endoplasmic reticulum and the mitochondrion) and the cell periphery (the plasma membrane). Cells possess a complex array of different Ca^{2+} transporting mechanisms, and the process of Na^+/Ca^{2+} exchange has emerged as a major contributor to Ca^{2+} efflux across the plasma membrane. The unique and precise nature and arrangement of different Ca^{2+} transport protein molecules in different cells is generally thought to provide a major component of control over complex Ca^{2+} dynamics. When this carefully orchestrated homeostasis goes awry, and Ca^{2+} concentrations are dys-regulated, the repercussions are usually extreme, resulting in cell damage and death which are a prelude to the pathological consequences of diseases such as stroke, neuro-degeneration, and heart disease.

Discovery of the Na^+/Ca^{2+} Exchanger

A competitive relation between the effects of extracellular Na^+ and Ca^{2+} on intracellular Ca^{2+} and contraction in cardiac, skeletal, and smooth muscle was first noted over 50 years ago. Then in the late 1960s three different groups (Reuter, Baker, and DeLuca), working on three different tissue preparations (mammalian cardiac muscle, squid axon, and mammalian intestinal epithelium), concluded that the coupled counter-transport of Na^+ for Ca^{2+} across the plasma membrane – so called Na/Ca exchange – could explain the apparent competitive relation between Na^+ and Ca^{2+}. This finding established the physiological importance of Na^+/Ca^{2+} exchanger as a mechanism contributing to the control of Ca^{2+} homeostasis, and launched the search for a protein molecule underlying the activity.

The development of biochemical measurements of Na^+/Ca^{2+} exchanger function in membrane preparations and effective solubilization and reconstitution procedures allowed several groups to partially purify

Na^+/Ca^{2+} exchange activity. Aided by immunological approaches, Philipson's group provided strong evidence that a 120 kDa protein of canine cardiac sarcolemmal membranes, and its 70 kDa proteolytic product, corresponded to the Na^+/Ca^{2+} exchanger. At the same time, recombinant expression cloning techniques were being developed, which led to the seminal molecular cloning work from Philipson's laboratory, published in *Science* in 1990, that confirmed the identity of the canine cardiac Na^+/Ca^{2+} exchanger.

During the 1980s, studies on visual adaptation in mammalian retinal rod photoreceptors also provided evidence for a Na^+/Ca^{2+} exchange mechanism responsible for controlling cytosolic Ca^{2+} in that environment. Further biochemical studies of rod Na^+/Ca^{2+} exchange revealed an obligate dependence on K^+, and demonstrated that the rod Na^+/Ca^{2+} exchanger catalyzed the exchange of Na^+ for both Ca^{2+} and K^+. As with the cardiac exchanger, solubilization and reconstitution studies allowed purification of the bovine rod photoreceptor $Na^+/Ca^{2+} + K^+$ exchanger, which was identified as a ~220 kDa protein. Immunological tools were then used to clone the molecule in 1992 by Cook's laboratory. Surprisingly, despite the mechanistic similarity and a broadly similar topology pattern (Figure 1) the cardiac and rod exchangers share sequence similarity in only two short stretches, which were subsequently termed the α-repeats (Figure 2).

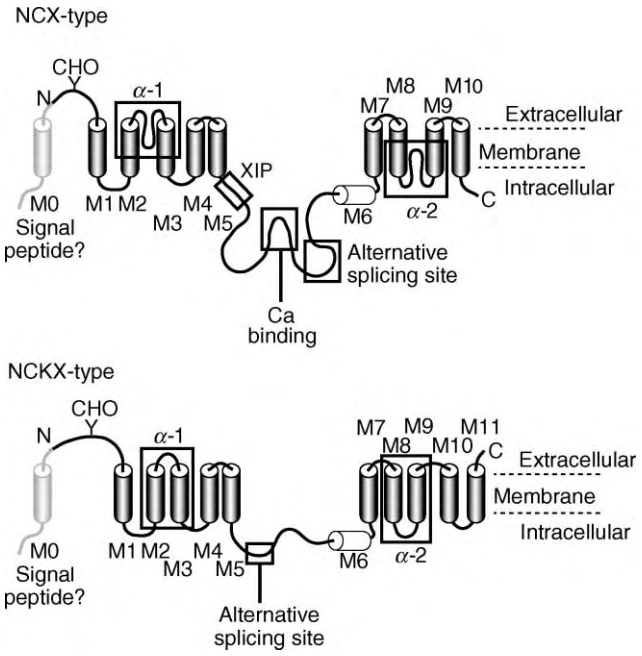

FIGURE 1 Topology models for Na^+/Ca^{2+}exchangers (NCX-type) and $Na^+/Ca^{2+} + K^+$ exchangers (NCKX type). The predicted folding of each class of protein with respect to the membrane, based on hydropathy analysis and experimental data, is shown. The cylinders labeled M0 (putative signal peptide, removed co- or posttranslationally) to M11 indicate transmembrane helices, with the exception of M6, which was originally proposed to span the membrane, but later modeled to be cytoplasmic. The conserved α-repeat regions (α-1 and α-2) are boxed and labeled. The N terminus (N) and C terminus (C) of the mature protein, as well as sites of glycosylation (CHO), alternative splicing, calcium binding, and the exchange inhibitory peptide (XIP) sequence are also indicated.

An Expanding Gene Family

Cloning of the canine cardiac Na^+/Ca^{2+} exchanger (NCX1 – gene *SLC8A1*) and the bovine rod photoreceptor $Na^+/Ca^{2+} + K^+$ exchange (NCKX1 – gene *SLC24A1*) opened the exchanger field to molecular analysis. NCX1 was subsequently cloned from heart, brain, and kidney of several different animal species. In the course of these studies, it became evident that the NCX1 gene gave rise to a complex set of alternatively spliced mRNA transcripts whose protein products differed in one relatively small region of the protein (Figure 1). The power of molecular cloning was also harnessed to uncover the existence of structurally related gene products, revealing that NCX1 is a member of a gene family that includes two other members, NCX2 (*SLC8A2*) and NCX3 (*SLC8A3*) whose products display ~70% amino acid identity with one another. NCX3 is also subject to alternative splicing, in a similar location as NCX1.

Advances in the molecular analysis of the NCKX family was not so rapid, but by the end of the 1990s a second member, NCKX2 (*SLC24A2*), had been identified. At the turn of the millennium, information contributed to the databases from random sequencing efforts and from the various animal genome projects had turned the identification of homologous genes from a bench experiment into a computer search. The discovery of NCKX3 (*SLC24A3*), NCKX4 (*SLC24A4*), and most recently NCKX5, followed rapidly.

During the early phase of homologous gene discovery, it was recognized that NCX1 contains two regions of paired internal similarity, suggesting an ancient gene-duplication event. One pair is found flanking the site of Ca^{2+} binding in the cytoplasmic loop of the protein (the β-repeat) and the other pair resides, one member within each hydrophobic membrane spanning domain (the α-repeat; see Figure 1). As indicated above, the α-repeats contain the only regions of similarity between NCX and NCKX exchangers. Moreover, a database search with the α-repeat motif identifies a large number of genes in species ranging from higher vertebrates to flies, worms, plants, yeast, and bacteria. The deduced proteins of these database hits contain two sequences homologous to the α-repeat, each within a relatively hydrophobic region, suggesting that these proteins are all membrane transporters, although in most cases the function of the gene products has not been determined

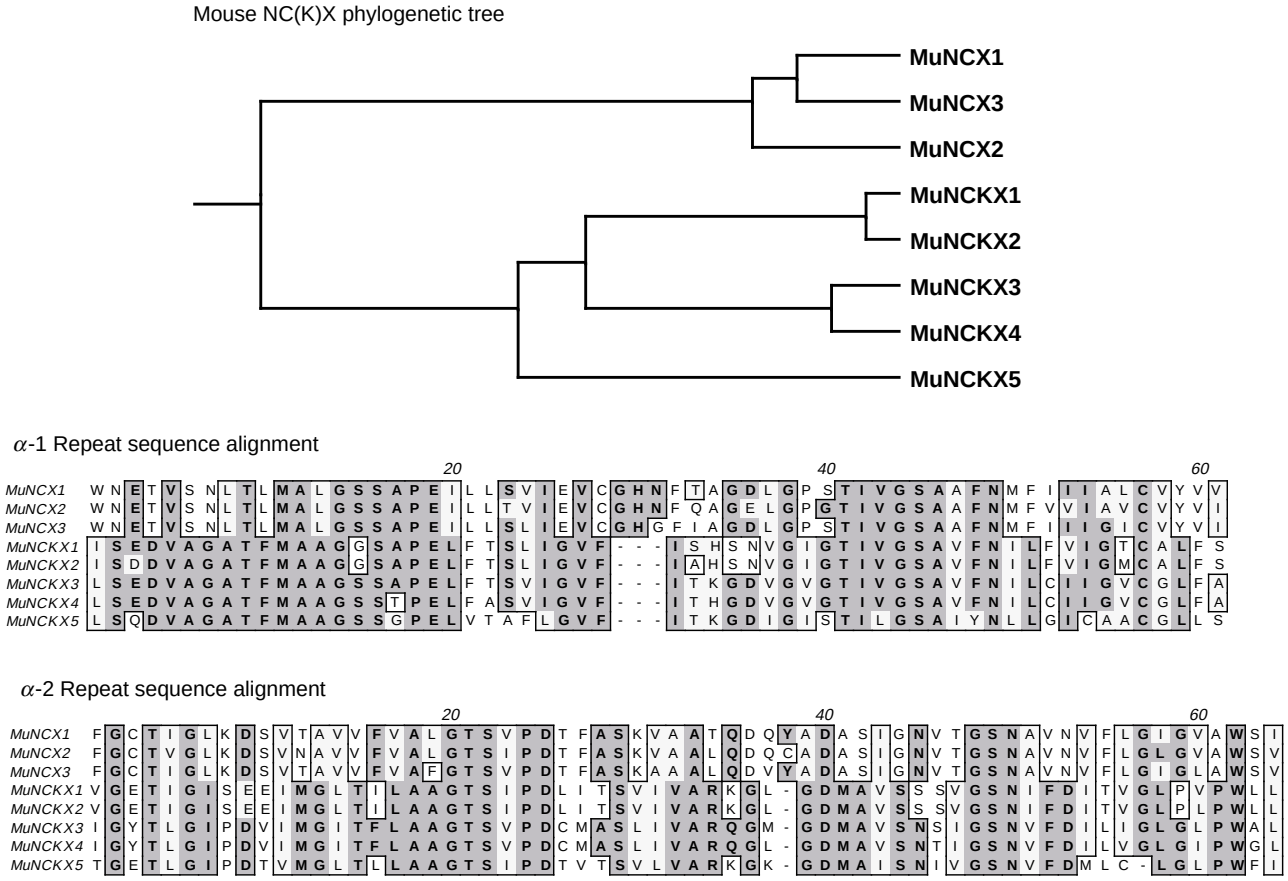

FIGURE 2 Phylogenetic relation and sequence alignment. The evolutionary relation between the different murine NC(K)X molecules is shown as a phylogenetic tree based on the combined similarities of the two α-repeat regions. A qualitatively similar pattern is obtained if the entire protein sequence from each isoform is used for the analysis. The sequences corresponding to the two α-repeats are shown aligned. Amino acids that are identical in five or more of the sequences are shown boxed, dark shaded, and highlighted in bold; chemically similar amino acids are boxed and light shaded.

directly. In some cases, the degree of sequence identity extends beyond the α-repeats, and these genes are likely to be orthologues of known mammalian NCX or NCKX exchanger genes. In other cases, the sequences are quite divergent, and the function of the encoded protein is not clear, but is presumed to involve cation exchange, for example Ca^{2+}/H^+ or Mg^{2+}/H^+ exchange.

Expression of NCX and NCKX in Mammals

NCX1 is ubiquitously expressed in almost all mammalian tissues, with the highest level of expression found in heart, brain, and kidney. The predominant NCX1 transcript in each of these three tissues corresponds to a different alternatively spliced species. The expression of NCX2 and NCX3 is highly restricted, with NCX2 present at high levels in the brain, but not at significant levels elsewhere, while NCX3 is present in skeletal muscle and at lower levels in selected brain regions, but is not significantly expressed in other tissues. The NCX1 protein has been localized mainly to the T-tubules in cardiomyocytes, to axonal and dendritic processes of neurons, and the basolateral membrane of distal convoluted tubule connecting segment cells in the kidney. Studies on the NCX2 and NCX3 proteins are less well developed.

NCKX1, originally defined in rod photoreceptors, is expressed almost exclusively in the eye, where the protein is present in the outer segments of rods. NCKX2 was originally found to be expressed at high abundance in neurons throughout the brain, but only at much lower levels elsewhere. Subsequently, this molecule was found to be present in the cone photoreceptors. Both NCKX3 and NCKX4 are abundant in brain but, in contrast to NCKX1 and NCKX2, are also broadly distributed in a number of tissues, including those rich in smooth muscle. NCKX5 has been identified only through database searches thus far, and so little information is available concerning the pattern of expression of this molecule. Aside from NCKX1, very

little is known about the expression of the NCKX family members at the protein level.

Structural Properties

Broadly speaking, all the Na^+/Ca^{2+} exchanger protein family members have a similar overall architecture (Figure 1). A hydrophobic signal peptide at the N terminus is cleaved off co- or posttranslationally, directing the glycosylated N-terminal region of the mature protein to the extracellular space. Two hydrophobic regions, each modeled as a cluster of transmembrane spanning segments, are separated by a large cytoplasmic loop. Within each branch of the family (i.e., NCX and NCKX), the length and sequence of each hydrophobic segment is well conserved, especially in the α-repeat regions (Figure 2). A comparison of these regions of clear homology can be used to generate a phylogenetic tree, illustrating the evolutionary relation between the different genes (Figure 2). In contrast to the hydrophobic regions, the sequence of both extracellular and intracellular loops are quite variable between different family members.

The arrangement of transmembrane spans within each hydrophobic region, originally based solely on hydropathy analysis, has recently been tested experimentally in several different labs using cysteine-scanning mutagenesis and antibody epitope insertion. The data from those experiments revealed that the hydrophobic region originally called M6 is not buried in the membrane, and that the α-repeat regions are oriented on opposite sides of the membrane (Figure 1). In the case of NCX1, both α-repeats are suggested to form re-entrant loop structures that come into close physical proximity with one another in the intact protein. Mutagenesis studies also revealed the importance for transport function of many of the conserved amino acids in the α-repeats, reinforcing the concept that these regions line the ion-binding and translocation pathway. Studies on the NCKX family have confirmed much of these data. However, there is no clear evidence for a re-entrant loop in the NCKX2 α-2 repeat, and the C terminus of the mature NCKX2 protein appears to be extracellular, while that of NCX1 is intracellular.

The large cytoplasmic loop of NCX1 contains several structural features thought to contribute to regulation of exchange function. At the extreme N-terminal region of the loop, an amphipathic sequence (XIP) reminiscent of a calmodulin-binding domain was noted. Exogenous addition of a peptide corresponding to this sequence inhibits Na^+/Ca^{2+} exchange. Near the center of the loop, two clusters of acidic amino acids contribute to a Ca^{2+}-binding site or sites that are critical for NCX function. Just C terminal to the Ca^{2+}-binding motifs lies the site of diversity introduced by alternative splicing. Two mutually exclusive exons, one expressed primarily in cardiomyocytes and neurons, and the other in nonexcitable cells, are combined with several cassette-type exons to form tissue-specific isoforms.

The large cytoplasmic loop of the NCKX family has not been investigated in so much detail, largely because there is no clear evidence for regulation. NCKX1, but not the other family members, has an unusually long loop as a consequence of a simple tandem repeat structure. Though this motif is present in NCKX1 molecules from various animal species, the sequence and extent of the repeat is different in each. Several of the NCKX family members are subject to alternative splicing that changes a short region toward the N-terminal end of the cytoplasmic loop. The consequences of these differences on transport function are currently not known.

Functional Properties

As their name implies, all Na^+/Ca^{2+} exchangers couple the movement of Na^+ ions in one direction to Ca^{2+} ions in the other. An extensive collection of experimental data supports a simple model where the transporter has a single set of ion-binding and transport sites that can be occupied by either Na^+ ions or a Ca^{2+} ion (and in the case of NCKX exchangers, a K^+ ion as well), but cannot be occupied by both Na^+ and Ca^{2+} ions simultaneously. The ion-binding sites on the exchanger must be fully occupied in order for their aqueous accessibility to shift across the membrane barrier (Figure 3). The exchanger can thus catalyze Na^+/Na^+ exchange, Ca^{2+}/Ca^{2+} (or in the case of NCKX, $(Ca^{2+} + K^+)/(Ca^{2+} + K^+)$) exchange, as well as Na^+/Ca^{2+} exchange. The direction of net ion flux is determined by the relative electrochemical ion gradients across the membrane, and the number of ions that bind to the transporter. For NCX1, the ion-binding stoichiometry has been a subject of intense investigation, but remains somewhat controversial, with most flux studies suggesting $3Na^+{:}1Ca^{2+}$, while most ionic current studies suggest $4Na^+{:}1Ca^{2+}$. For NCKX1 and NCKX2, the stoichiometry has been established as $4Na^+{:}1Ca^{2+} + 1K^+$. The stoichiometry of the other NCX and NCKX family members has not been determined, but is likely to be similar to their paralogous family members.

Although the direction of flux is dictated by thermodynamic considerations, the magnitude of the flux is determined by the intrinsic rate of the enzyme, the relative occupancy of the ion-binding sites, and various regulatory factors. For NCX1, which has a very high turnover rate, the enzyme is limited by the concentration of cytosolic Ca^{2+}, which is normally well below the concentration for half-maximal occupancy of the transport sites. NCX1 activity is also regulated in a complex

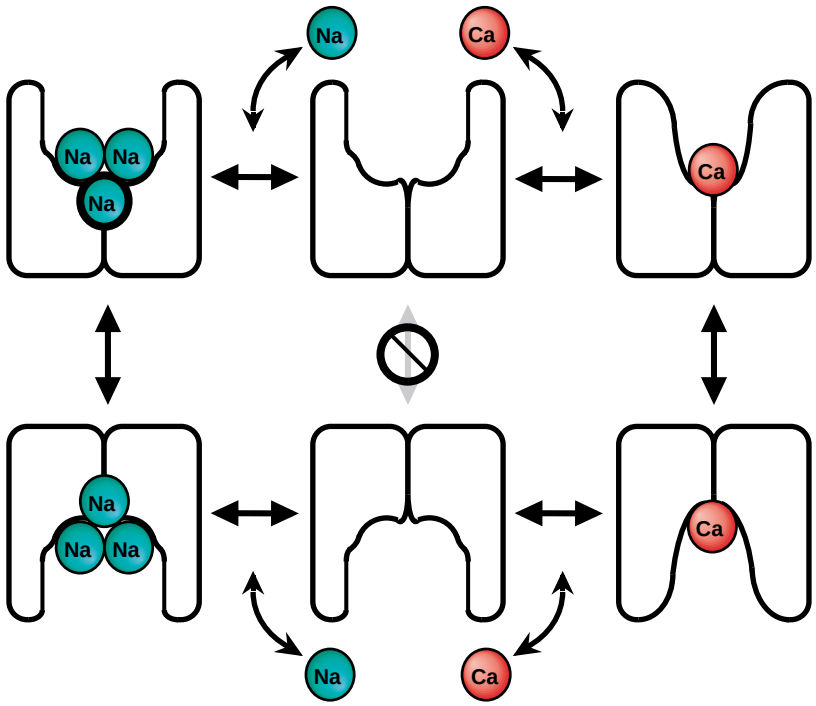

FIGURE 3 The Na^+/Ca^{2+} exchanger reaction cycle. A simple six-state model is shown, where either three Na^+ ions or a single Ca^{2+} ion can bind to the transport site from either side of the membrane in a competitive fashion. Only fully loaded transporter can re-orient the aqueous accessibility of the ion-binding sites across the membrane. Note that, in the case of $Na^+/Ca^{2+} + K^+$ exchanger, four Na^+ ions bind instead of three, and K^+ binds and is transported together with Ca^{2+}.

fashion through the central cytosolic loop. Intracellular Ca^{2+} activates the exchanger, while high concentrations of Na^+ cause inactivation. Acidic phospholipids, and ATP through phosphorylation of phosphatidyl-inositol, also activate the exchanger. These events are mediated via the identified Ca^{2+}-binding sites and the XIP region of the loop, although the mechanism is not well understood. Modulation of various kinase pathways has a modest effect on Na^+/Ca^{2+} exchange activity, but there is little convincing evidence for direct phosphorylation of NCX1. Though not studied in as much detail, it appears the other NCX family members function in an analogous manner.

The rod photoreceptor exchanger, NCKX1, appears to turn over more slowly than NCX1. On the other hand, NCKX1 has a higher apparent affinity for cytosolic Ca^{2+} and should theoretically be able to drive Ca^{2+} down to very low levels. That this does not happen in rod photoreceptors, suggests that other kinetic or regulatory factors may influence the activity of the molecule. One good candidate for such regulation is the rod cyclic nucleotide-gated channel, which interacts functionally via Ca^{2+} cycling and also physically associates with NCKX1. Neither Ca^{2+} nor Na^+ appear to regulate NCKX exchangers as they do the NCX branch of the family. Little else is known regarding regulation of the NCKX family of exchangers.

Physiological Relevance

In the case of heart, it is clearly established that NCX1 plays a critical role in relaxation by removing Ca^{2+} that enters during the early phase of systole. NCX1 probably also plays a role in excitation–contraction coupling, although the magnitude of its contribution remains somewhat controversial. During the early phase of the cardiac action potential, as the membrane depolarizes and ion gradients change, NCX1 probably contributes to Ca^{2+} entry. Furthermore, as NCX1 switches to Ca^{2+} extrusion later in systole, it creates a depolarizing current that can significantly modulate the shape of the action potential. Normally these contributions of NCX1 to cardiac excitation–contraction coupling are integrated into overall Ca^{2+} homeostasis. However, during pathological circumstance, the expression pattern of Ca^{2+} channels and transporters changes, and ion concentrations and gradients are altered dramatically. Under these conditions, changes in NCX1 activity may be maladaptive, and so may contribute to, rather than protect against, deleterious consequences.

In the kidney very high levels of NCX1 are found on the basolateral aspect of a selected population of distal nephron cells. In this environment, NCX1 contributes to the control of extracellular, systemic, Ca^{2+} homeostasis by driving the active trans-cellular reabsorption of Ca^{2+}.

NCX1 is also present in brain neurons and astrocytes, where it presumably plays a role in Ca^{2+} extrusion. Its precise role in this environment and the contribution made by NCX2 and NCX3 expression are less clearly understood.

The unique and specialized role that NCX1 plays in controlling Ca^{2+} flux and homeostasis in heart and kidney is also reflected in the fact that this gene is expressed under the control of three different, and tissue-specific promoters. One promoter is used essentially exclusively in heart, one exclusively in kidney, while the third is used widely in various tissues. This arrangement provides the opportunity for expression of the heart and kidney NCX1 molecules to be regulated independently and in response to the specialized requirements of these tissues for Ca^{2+} homeostasis.

In the rod photoreceptors, NCKX1 is thought to play a critical role in maintaining Ca^{2+} homeostasis, especially in the dark when cyclic-nucleotide-gated channels are open and so the membrane is depolarized, the Na^+ gradient is low, and Ca^{2+} flux is high. Under these circumstances, the thermodynamic power derived from the $4Na^+:1Ca^{2+} + K^+$ coupling ratio is necessary to allow continued Ca^{2+} efflux. While this argument makes some sense in the retinal photoreceptors, it is less clear as to why NCKX family members are also expressed quite broadly, especially in the brain.

Elucidating the unique individual physiological roles for the expanding family of NCX and NCKX protein molecules is an active area of research that is likely to provide exciting novel insights.

See Also the Following Articles

Calcium Sensing Receptor • Calcium Signaling: Cell Cycle • Calcium Transport in Mitochondria • Calcium, Biological Fitness of • Membrane Transport, General Concepts • Plasma-Membrane Calcium Pump: Structure and Function • Store-Operated Membrane Channels: Calcium

Glossary

alternative splicing A process in which the individual expressed regions of a gene (exons) are arranged in different patterns to produce different mRNA molecules that often encode different proteins.

excitation–contraction coupling The process by which an electrical signal generated in the plasma membrane of a muscle cell results in movement of the muscle fiber proteins, and contraction of the cell.

Na^+/Ca^{2+} exchanger A plasma membrane protein that couples the movement of Na^+ ions in one direction with Ca^{2+} ions in the other.

plasma membrane The membrane that surrounds every cell, separating inside from outside.

α-repeat A short stretch of amino acids identified within the Na^+/Ca^{2+} exchanger that is conserved among a large superfamily of membrane proteins. Two copies of this conserved sequence are present in each Na^+/Ca^{2+} exchanger, which are modeled to interact to form the ion-binding and translocation pocket.

retinal rod photoreceptors Long, cylindrically shaped, cells in the retina of the eye that respond to changes in low levels of light.

Further Reading

Berridge, M. J., Bootman, M. D., and Lipp, P. (1998). Calcium – A life and death signal. *Nature* **395**, 645–648.

Bers, D. M. (2002). Cardiac excitation–contraction coupling. *Nature* **415**, 198–205.

Blaustein, M. P., and Lederer, W. J. (1999). Sodium/calcium exchange: Its physiological implications. *Physiol. Rev.* **79**, 763–854.

Lytton, J., Schnetkamp, P. P. M., Hryshko, L. V., and Blaustein, M. P (eds.) (2002). *Cellular and Molecular Physiology of Sodium–Calcium Exchange*. Proceedings of the fourth international conference. Annu. NY Acad. Sci., Vol 976. New York Academy of Sciences, New York.

Nicoll, D. A., Longoni, S., and Philipson, K. D. (1990). Molecular cloning and functional expression of the cardiac Na,Ca-exchanger. *Science* **250**, 562–565.

Philipson, K. D., and Nicoll, D. A. (2000). Sodium–calcium exchange: A molecular perspective. *Annu. Rev. Physiol.* **62**, 111–133.

Reiländer, H., Achilles, A., Friedel, U., Maul, G., Lottspeich, F., and Cook, N. J. (1992). Primary structure and functional expression of the Na/Ca,K-exchanger from bovine rod photoreceptors. *EMBO J.* **11**, 1689–1695.

Shigekawa, M., and Iwamoto, T. (2001). Cardiac Na^+–Ca^{2+} exchange: Molecular and pharmacological aspects. *Circ. Res.* **88**, 864–876.

Biography

Dr. Jonathan Lytton is a Professor of biochemistry and molecular biology at the University of Calgary, Canada. His principal research interests are in the molecular biology and physiology of calcium transport proteins. He holds a Ph.D. from Harvard University and did postdoctoral training at the University of Toronto. His work has been instrumental in the molecular cloning and characterization of SERCA Ca^{2+} pump isoforms, Na^+/Ca^{2+} exchanger isoforms, and novel $Na^+/Ca^{2+} + K^+$ exchanger gene products expressed in brain.

Membrane-Associated Energy Transduction in Bacteria and Archaea

Günter Schäfer
University of Lübeck, Lübeck, Germany

Archaea and bacteria represent the two prokaryotic branches of the universal tree of life. Their plasma membranes host protein complexes specialized in primary and secondary energy-transducing mechanisms. Common to bacteria and archaea is the underlying principle of primary energy conservation, the chemiosmotic mechanism generating an electrochemical potential of ions across the membrane on expense of the energy derived from membrane-associated fermentative, redox- or light-driven processes. In evolution, two of these, oxygen respiration and oxygenic photosynthesis, were transferred to eukaryotes by endosymbiontic uptake of putative ancient bacteria, the precursors of mitochondria and chloroplasts. Archaea differ from bacteria not only by genetic and taxonomic markers, membrane structure, specialized metabolic functions, and archaetypical coenzymes but also by their extremophilic life styles regarding thermo-, pH-, and salinity-tolerance. Several energy-transducing processes are confined to the archaeal domain such as methanogenesis and rhodopsin-dependent photosynthesis. Chlorophyll-dependent photosynthesis does not exist in the archaeal domain. Secondary membrane-associated energy transduction like the synthesis of ATP from ADP and various active transport systems are consumers of the primarily generated electrochemical ion gradient. The ions coupling primary and secondary energy transduction are predominantly hydrogen ions; in several bacteria and archaea sodium ions are also used.

Membranes

The matrix of polar lipids in plasma membranes serves as the environment for associated and membrane-spanning proteins. In bacteria glycerol diester phospho- and glycolipids form a liquid–crystalline bilayer into which the energy-transducing membrane–protein complexes are inserted. The hydrophobic properties and fluidity of the core are determined by the fatty acid hydrocarbon chains; the permeability properties are additionally determined by the polar head groups. The lipid profile can serve as a taxonomic marker. Archaea, in contrast, contain unique lipids consisting of derivatives of diphytanylglycerol diethers and of di-biphytanyl-diglycerol-tetraethers. Consistently, besides bilayer structures, these membranes are composed of membrane-spanning lipid monolayers conferring extremely high stability, especially to the hyperthermophilic genera of the archaeal domain. The diether- and tetraether-derived lipids include phospholipids, glycolipids, and sulfoglycolipids. Generally, these lipids are glycosylated with the carbohydrate groups facing the plasma membrane outside. The unique lipid composition clearly delineates the archaea from all other organisms. Also the cell envelopes of archaea are distinct from those of bacteria. Murein and lipopolysaccharide containing outer membranes are not found in archaea. The quasi-crystalline surface layers of archaea are high-molecular-weight glycoproteins and have mainly form-stabilizing function and in most cases are the only envelope layer outside the plasma membrane.

Energy-Transducing Functions

Membrane-associated energy transduction proceeds by linking an exergonic process catalyzed by a membrane-residing enzyme (or protein complex) to the simultaneous vectorial translocation of charge (electrons or ions) across this membrane by the same enzyme. This principle is common to bacteria and archaea (Figure 1). Typical processes can be metabolic substrate conversions like redox reactions or decarboxylation, respiratory electron transport from a low-potential donor to a high-potential acceptor (respiratory chains), or the decay from an energized state of a molecule generated by absorption of light to the low-energy ground state.

Fermentation

Fermentations are anaerobic redox processes in which ATP is usually generated by substrate-level

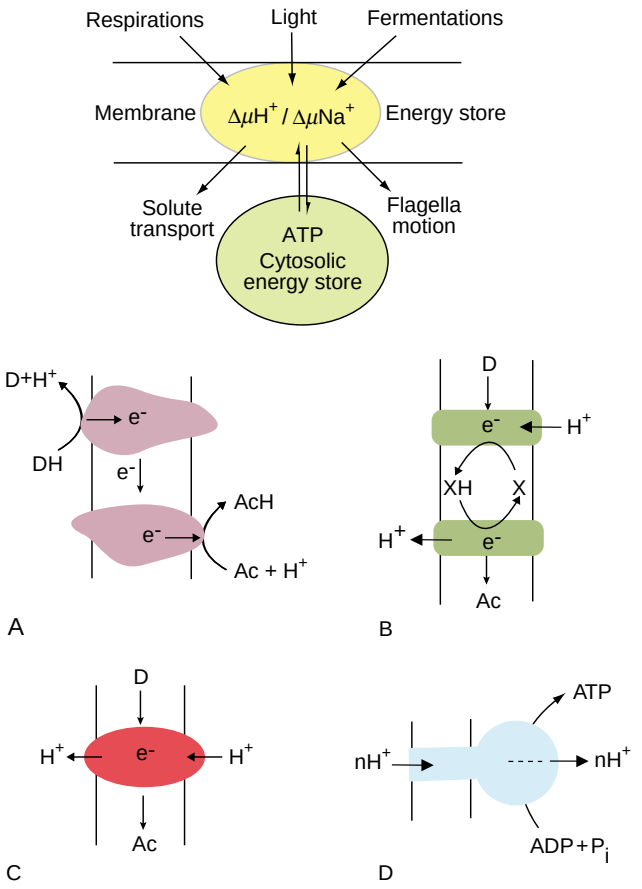

FIGURE 1 Schematic illustration of energy-conserving principles used by bacteria and archaea for the generation of an electrochemical potential of ions ($\Delta\mu Na^+$ or $\Delta\mu Na^+$) across their plasma membrane. (A) symbolizes $\Delta\mu H^+$ generation by scalar or so-called "chemical" protons consumed or liberated on opposite sides of the membrane; only electrons are transduced through the membrane. (B) and (C) illustrate pumps; (B) functions via the intermediary quinol pool (x), (C) integrates pumping and electron transport within the same protein module like cytochrome-*c* oxidases; (D) symbolizes the universal ATP synthetase; its vectorial action and orientation is consistently opposite to that of the primary pumps.

phosphorylation. In some special cases, partial reactions of fermentative pathways are catalyzed by membrane-residing enzymes, and the free-energy change of the reaction is coupled to the generation of an electrochemical-ion gradient. Examples are the biotin-dependent methylmalonyl-CoA decarboxylase of *Propionigenium modestum*, the oxaloacetate decarboxylase involved in citrate fermentation, or the glutaconyl-CoA decarboxylase involved in glutamate fermentation; they generate a $\Delta\mu Na^+$. By means of H^+/Na^+ exchange transporters the sodium gradient can be coupled to a proton gradient, or the $\Delta\mu Na^+$ can directly drive ATP synthesis by a Na^+-translocating ATP synthetase. In methanogenic archaea methyl-group transfer from an N atom to an SH group drives a sodium pump and generates also a $\Delta\mu Na^+$. The above examples demonstrate that in anaerobic fermentations also non-redox reactions can play an important role in membrane associated energy transduction.

Anaerobic Respiration

Many organotrophic and chemolithotrophic bacteria and archaea can conserve energy by means of membrane-residing electron transport chains employing terminal acceptors other than oxygen. This group of obligately or facultatively anaerobic microbes uses electron acceptors like nitrate, nitrite, fumarate, sulfur, ferric ion, carbon dioxide, sulfate or even organic chlorocompounds for oxidation of organic molecules or hydrogen. Energy is conserved as a $\Delta\mu H^+$. Example reactions are given in Table I.

Denitrification

Denitrification is a typical example of anaerobic respiration and is found in over 40 genera; in archaea only in some extreme halophiles. However, nitrate is reduced in four steps to N_2 via $NO_2^- \rightarrow NO \rightarrow N_2O \rightarrow N_2$. The enzymes are integrated into the plasma membrane or located in the periplasm. Oxygen represses their synthesis. Nitrate reductase is a molybdopterin dinucleotide-containing enzyme associated with an iron–sulfur protein (4 FeS clusters) and a membrane spanning *b*-type cytochrome. Energy from NO_3^- reduction is conserved by release of protons from the reductant, ubiquinone, or menaquinone, at the membrane outside, whereas protons for water formation are

TABLE I

Standard Free Energy Changes of Anaerobic and Aerobic Respiratory Reactions

Chemical reaction	ΔG (kJ mol^{-1})
$S^0 + 2[H] \Rightarrow H_2S$	−33.5
$SO_4^{2-} + 8[H] + 2H^+ \Rightarrow H_2S + 4H_2O$	−151.7
$2NO_3^- + 5H_2 + 2H^+ \Rightarrow 6H_2O + N_2$	−959.8
$2NO + 2H^+ + 2e^- \Rightarrow N_2O + H_2O$	−305.9
$CO + H_2O \Rightarrow CO_2 + 2H^+ + 2e^-$	−492
$[H]_2\text{–}X + 1/2O_2 \Rightarrow H_2O + X$	−219.0
$2H_2 + O_2 \Rightarrow 2H_2O$	−472.5
$2S^0 + 2H_2O + 3O_2 \Rightarrow 2H_2SO_4$	−1014.0
$2FeS_2 + H_2O + 7O_2 \Rightarrow 2FeSO_4 + 2H_2SO_4$	−1498.4
$2CO + O_2 \Rightarrow 2CO_2$	−504.9
$4Fe^{2+} + O_2 + 4H^+ \Rightarrow 4Fe^{3+} + 2H_2O$	−17.7

The block on top gives examples for electron accepting reactions in anaerobic respirations, the lower block examplifies electron donor reactions used by organotrophic and chemolithotrophic oxygen respiration. $[H]_2$–X symbolizes an organic hydrogen-donating molecule, e.g., NADH or succinate.

taken up from the cytosol. NO reductase displays analogy to heme/Cu oxidases but hosts Fe instead of Cu in the binuclear reaction center; in contrast to the latter, it does not pump protons. Denitrifying pathways are widespread in Gram-negative proteobacteria (e.g., *Paracoccus*, *Alcaligenes*, *Pseudomonas*, *Thiobacillus*). Associated with denitrification is ammonification, which saves NH_4^+ by reduction of NO_2^- with NAD(P)H. Ammonification is a cytosolic process catalyzed by a siroheme/[4Fe4S] containing enzyme.

Fumarate Respiration

In *Wolinella*, nitrate reduction can be achieved with molecular hydrogen or with formate as electron donors. It involves fumarate respiration (Figure 2), as an alternative mechanism to generate a proton motive force. H^+ is released at the outer side of the membrane by oxidation of hydrogen or formate, whereas proton uptake and reduction of fumarate occurs at the inner side. The dehydrogenases as electron donors and the fumarate reductase as acceptor are interacting via *b*-type cytochromes and the menaquinone pool in the membrane ($E_0' = -100$ mV). The reduction of fumarate to succinate is catalyzed by an enzyme similar to nitrate reductase, but molybdopterin is replaced by FAD. The enzyme is structurally and evolutionarily related closely to succinate dehydrogenases of aerobic organisms which catalyze the reverse reaction using ubiquinone ($E_0' = +60$ mV), or in thermoacidophilic archaea caldariella quinone ($E_0' = +106$ mV), as primary electron acceptor.

Sulfur Respiration

Some bacteria and archaea perform sulfur respiration. *Wolinella succinogenes* is an example. Instead of insoluble elemental sulfur polysulfide ($^-S{-}S_n^-$) serves as electron acceptor. The electron transport chain involves three membrane-residing enzymes with their substrate binding sites facing the periplasm: formate dehydrogenase or hydrogenase, and polysulfide reductase. In contrast to fumarate respiration, a quinone is not involved in electron transfer. The reduction of sulfur to H_2S is coupled to generation of $\Delta\mu H^+$ at a low H^+/e^- ratio by a hitherto unknown mechanism.

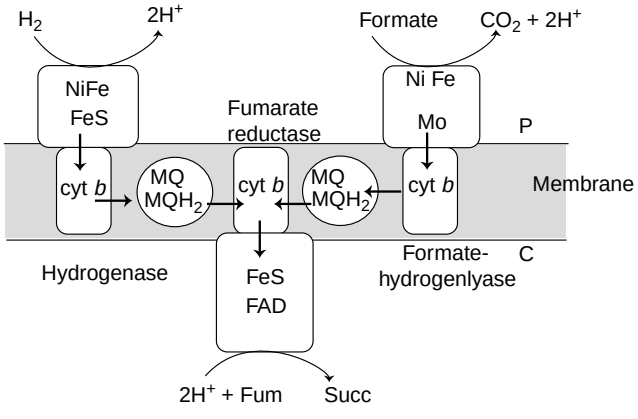

FIGURE 2 Scheme of an anaerobic respiration. Fumarate respiration is taken as an example with two possible electron-donating systems (MQ = menaquinone P = periplasm, C = cytosol). The type of energy conservation corresponds to principle A in Figure 1.

Ferric Ion Reduction

Members of the genera *Clostridium*, *Escherichia*, and *Bacillus* among others are able to reduce ferric to ferrous ions. It has not been shown unequivocally that the reaction is coupled to energy conservation. Though the couple $Fe^{3+/2+}$ has a high redox potential ($E_0' = +770$ mV) similar to oxygen, organisms using Fe^{3+} as terminal electron acceptor have to cope with its extreme insolubility, except in a strongly acidic environment.

Oxygen Respiration

Aerobic Organotrophs

Oxygen is a superior electron acceptor for aerobic microbes that use reduced substrates or even molecular hydrogen as donors of reducing equivalents. Organotrophes deliver electrons into a respiratory chain (Figure 3) via ubi- or mena-quinone reducing membrane anchored or integral membrane protein complexes. A major complex is the FMN-dependent type-I NADH dehydrogenase (complex I), composed of 14 different polypeptides (e.g., *Paracoccus*, *Escherichila coli*). It couples the translocation of (probably four) protons to the reduction of quinone and consists of a peripheral substrate oxidizing subcomplex facing the cytosol, a membrane integral transducer subcomplex with several FeS centers, and a receiver subcomplex transferring electrons to the quinone. Alternatively, in many bacteria and in archaea, type-II NADH dehydrogenases are found; these have less complex composition and cannot couple ion translocation to substrate oxidation. Several alkaline-adapted bacteria couple the translocation of Na^+ instead of protons to NADH oxidation. As another quinone-reductase succinate dehydrogenase (complex-II) is found in the plasma membranes of all aerobic microbes. The small change in free energy of this reaction is insufficient to drive energy-conserving ion translocation. The reoxidation of reduced quinones is either catalyzed directly by heme/Cu-type quinol oxidases as, for example, in *E. coli*, *Paracoccus denitrificans*, and *Rhodobacter sphaeroides*, or by a second energy-conserving module of respiratory chains, the bc_1 complex (complex-III). The essential redox catalysts of this module are an [$2Fe_2S$] iron–sulfur

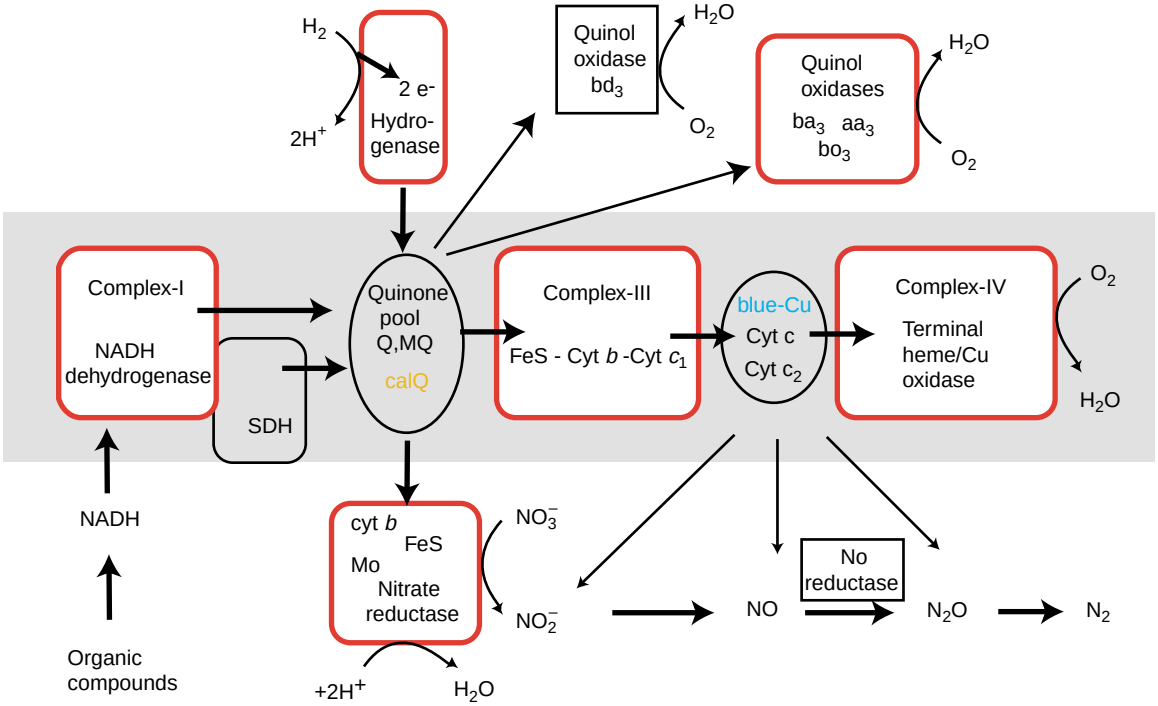

FIGURE 3 Illustration of the diversity of energy-transducing membrane systems in bacteria and archaea. All boxed or encircled components are membrane-integral or membrane-associated. All red boxes are proton pumps acting according to principles B and C of Figure 1. The scheme depicts the situation in *P. denitrificans*. The shaded block from left to right symbolizes a regular and complete aerobic respiratory chain as present, for example, in purple bacteria and also in eukaryotic mitochondria. The linear arrows indicate the direction of electron flux between donor and acceptor complexes or compounds. The symbols aa_3, ba_3, bo_3 in the box Quinoloxidases indicate the species-dependent variability of observed heme-compositions; calQ (caldariella quinone) applies to some archaea, as does the blue-Cu protein instead of c-type cytochromes. (SDH = succinate dehydrogenase, complex II.)

protein (Rieske protein), a diheme *b*-type cytochrome, and a *c*-type cytochrome c_1. Complex-III couples the stepwise reoxidation of QH_2 to the transport of $2H^+$ across the membrane for each electron transduced to cytochrome c_1. The complex reaction mechanism is known as Q-cycle. The mobile redox carrier cytochrome *c* associated with the outer surface of the plasma membrane accepts electrons from cytochrome c_1 and serves as the connector to the terminal oxidase module, the heme/Cu-type cytochrome *c* oxidase (⇒). All oxygen-reducing heme/Cu oxidases are proton pumps. The path of electrons from NADH to oxygen can thus conserve the energy equivalent to $12H^+$ pumped across the membrane per [H_2]. Depending on the genetic disposition, either one of the energy-transducing complexes can be missing, except a terminal oxidase. The modular structure of microbial respiratory chains allows a variety of special adaptations. Besides an aerobic respiratory chain, all modules for denitrification and even several terminal oxidases can be present in parallel (e.g., Figure 3); their individual contribution to energy transduction is usually regulated via the expression of the respective genes in response to nutritional and environmental conditions.

Aerobic Chemolithotrophs

A large variety of bacteria, the chemolithotrophs, can derive energy from oxidation of inorganic electron donors such as hydrogen, carbon monoxide, sulfur and nitrogen compounds, or divalent cations (e.g., Fe^{2+}, Mn^{2+}). Many of these use molecular oxygen as oxidant. The mechanisms of energy transduction in chemolithotrophs are essentially the same as in organotrophs, i.e., the electrons are channeled into a cytochrome chain and flow down to the terminal oxidase enabeling a number of proton translocating redox loops. Examples are given in Table I. The acidophile *Thiobacillus ferrooxidans* uses a periplasmic Fe^{2+} oxidase transferring electrons via cytochrome *c* and the Cu-protein rusticyanin to a heme/Cu-terminal oxidase, which reduces oxygen on the plasma membrane inside. The reaction generates a proton motive force by scalar consumption of H^+ on the inside in addition to proton pumping by the aa_3-type terminal oxidase. So-called "Knallgas" bacteria comprising a large group of Gram-negative and Gram-positive bacteria which can oxidize molecular hydrogen. Essential for the mechanism is a Ni–Fe hydrogenase dimer (e.g., in *Alcalignes eutrophus*) in the cytoplasmic membrane. It transfers electrons from hydrogen via

the bimetallic reaction center, several Fe–S clusters, and a *b*-type cytochrome to the respiratory electron transport chain. By this process scalar protons are produced outside in addition to protons pumped by the respiratory chain. Several "Knallgas" bacteria contain a second, cytoplasmic hydrogenase which is used for the reduction of NAD^+ via FMN by an enzyme with homology to NADH:ubiquinone oxidoreductase (complex-I).

Phototrophic Bacteria

The utilization of light by cyanobacteria, phototrophic purple, and green bacteria follows the same principles as in algae and higher plants. Also the light absorbing pigments, other cofactors and their hosting membrane proteins are essentially similar. Both, oxygenic and anoxygenic photosynthesis, are found; the latter is restricted to purple, green, and heliobacteria.

Pigments of Energy Transducers

Absorption of light energy and transduction of energized states is mediated by antenna complexes. These contain the cyclic tetrapyrrol derivatives chlorophyll and bacteriochlorophyll, carotenoids, and in cyanobacteria open-chain tetrapyrrols (phycobillins). The conjugated polyene compounds absorb light from the near-UV to the near-IR and are non-covalently bound to membrane-integral and membrane-associated proteins in arrays. They transduce the excited state to the reaction centers (RCs) proper. The ratio is about 25–30 mol antenna chlorophyll per mol RC. In purple bacteria and heliobacteria (e.g., *Rhodobacter*, *Rhodopseudomonas*, *Chromatium*, *Heliobacillus*) the antenna complexes are integrated within the cytoplasmic membrane. In green bacteria (e.g., *Chlorobium*, *Chloroflexus*) the antenna complexes are organized as chlorosomes, i.e., vesicles attached to the inner side of the plasma membrane.

Anoxygenic Photosynthesis

Anoxygenic photosynthesis produces an electrochemical proton gradient across the membrane which drives ATP synthesis and other energy consuming processes. Excitation energy is transfered from antennas to the RC within ~50 ps. In the RC, the energy is utilized to generate a charge separation ($\Delta\Psi$) across the membrane. It occurs by electron transfer between the primary donor, a special pair of chlorophylls, localized towards the cytosolic side of the membrane and secondary acceptors at the opposite side. These can be quinones (type-II RC) or Fe–S clusters (type-I RC). From there the electrons flow back to cytochrome c_2 and the special pair via a quinone pool and through the bc_1 complex, as it is also used for respiratory energy conservation; a $\Delta\mu H^+$ is produced. Thus, anoxygenic photosynthesis can occur as a cyclic process. Production of reducing equivalents is not coupled to anoxygenic photosynthesis. In facultatively phototrophic/chemotrophic bacteria (*Rhodobacter*, *Rhodospirillum*) photosynthesis and respiration are competing for the bc_1 complex depending on the environmental conditions (oxygen tension, light intensity).

Oxygenic Photosynthesis

Cyanobacteria (*Synechococcus*, *Synechocystis*, *Anacystis*) perform oxygenic photosynthesis. It employs two photosystems in sequence in its membrane (PS-I, PS-II). PS-I is essentially equivalent to the RC of anoxgenic phototrophic bacteria but channels the electrons to ferredoxin as terminal acceptor. Ferredoxin serves as reductant for $NADP^+$, thus generating reducing equivalents for the cell. The reaction center PS-II is an H_2O:plastoquinone oxidoreductase and couples the reduction of the primary e^--donor, the special pair of chlorophylls, to the oxidation of water by a Mn-enzyme associated with PS-II at the periplasmic surface. The water-splitting Mn-enzyme liberates molecular oxygen and H^+. The reducing equivalents are passed on to PS-I via the plastoquinone quinone pool, the b_6f-complex, and the Cu-protein plastocyanin. The b_6f-complex is functionally and structurally analogous to the bc_1 complex. It is composed of a diheme cytochrome *b*, a Rieske Fe–S protein, and the mono-heme cytochrome *f*. b_6f acts as a proton pump performing a Q-cycle ($\Rightarrow$). The photosynthetic apparatus of cyanobacteria is localized in thylacoids; the antenna systems are organized as phycobillisomes attached to the thylacoid membranes. These structures largely resemble the structure of eukaryotic organelles. Also respiratory enzymes (NADH dehydrogenase, cytochrome *c* oxidase) are localized in the thylacoid and partially also in the plasma membrane of cyanobacteria.

Special Mechanisms in Archaeal Energy Transduction

Methanogenesis from one- or two-carbon atom compounds and light-driven energy conservation by bacteriorhodopsins are mechanisms restricted to archaea. Methanogens comprise the genera *Methanosarcina*, *Methanolobus*, *Methanobacterium*, *Methanotrix*, *Methanothermus*, *Methanococcus*, and others among about 50 known species. Examples for the best-investigated genera of extreme halophilic archaea are *Halobacterium*, *Haloferax*, *Haloarcula*, *Halococcus*, and *Natronomonas*.

Methanogenesis

Methanogenesis is a reductive process under strictly anaerobic conditions. It involves reduction of C_1 compounds (CO_2, CO, CH_3OH, CH_3NH_2) mainly by H_2, but also the disproportionation of acetate, formiate, or methanol. Many of the methanogenic archaea are extremely thermophilic (growth at $\approx 100\,^{\circ}C$). For example, the change in free energy of the reaction $CO_2 + 4H_2 \Rightarrow CH_4 + 2H_2O$ is $\Delta G = -131\ kJ\ mol^{-1}$ and is comparable to CH_4 formation from other sources; that of acetate disproportionation is only $-36\ kJ\ mol^{-1}$. Both reactions can drive chemiosmotic ATP synthesis by linking membrane-associated partial reactions to generation of ion gradients ($\Delta\mu H^+$, $\Delta\mu Na^+$). The reactions involve unusual coenzymes, not found in bacteria or eukaryotic organisms. These are the fluorescent 5-deazaflavin F_{420}, methanofuran, methanopterin (H_4MPT), coenzyme-M (mercaptoethanesulfonate), a Ni-tetrapyrole F_{430}, 5-hydroxybenzimidazolyl-cobamide, and methanophenazine as a substitute for membrane-residing quinones. For details of pathways the reader is referred to specialized publications. Important for membrane-associated energy transduction are electron transport chains involved in methanogenesis, as illustrated in Figure 4. The ion-translocating redox chains involve heterodisulfide reductase, two *b*-type cytochromes, methanophenazine, and Ni-hydrogenase or another donor of reducing equivalents. Redox cycling of methanophenazine with asymmetric uptake and release of protons can act as a proton pump with $H^+/e^- = 1$. Hydrogen can also be provided from ferredoxin:methanophenazine oxidoreductase, or from F_{420} dehydrogenase, depending on the individual organisms and the C_1 carbon source used for methanogenesis. Whether the latter functions as proton pump is under debate; the observed total H^+/e^- ratios of 3–4, are higher than calculated for the methanophenazine cycle alone. Hydrogenases and F_{420} dehydrogenase display structural similarities to proton-translocating respiratory NADH dehydrogenases and are bearing subunits with several $[Fe_n–S_n]$ clusters. Also heterodisulfide reductase contains two [4Fe–4S] clusters. Apart from proton motive electron transport chains, all methanogens have a primary Na^+ pump, the membrane integral methyl-H_4MPT:CoM- methyltransferase. This enzyme contains the above-mentioned cobamide cofactor and a [4Fe–4S] cluster. The reaction proceeds in two steps: first, the transfer of the methyl group to the corrin cofactor, second, methyltransfer to

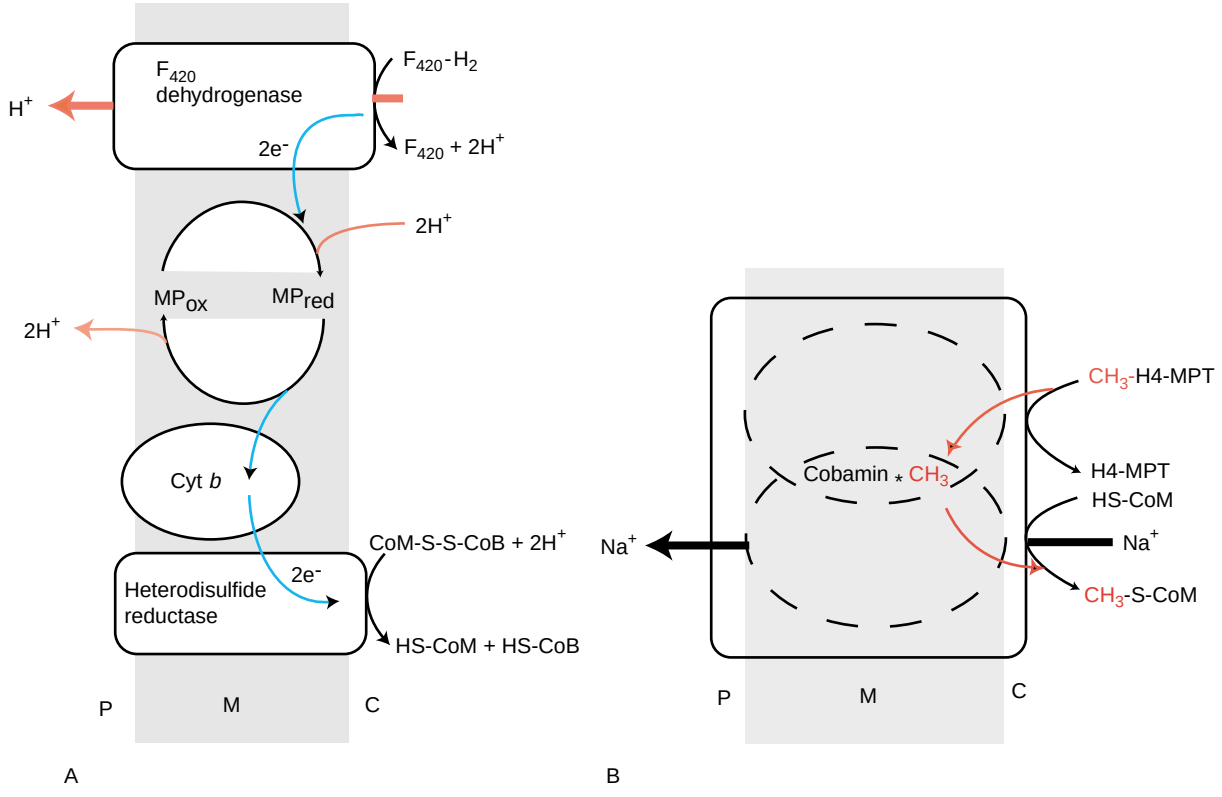

FIGURE 4 (A) Illustration of chemiosmotic energy conservation in methanogenic archaea. The example combines mechanisms (B) and (C) of Figure 1; (P = periplasmic space, M = membrane, C = cytosol, MP = methanophenazine, CoM = coenzyme M). (B) Energy transduction by a non-redox reaction in archaeal methanogenesis. The sodium pump is driven by the energy change of the transmethylation reaction (H4-MPT = tetrahydro-methanopterin). The mechanism is thought to involve conformational coupling between the group-transferring and the ion-transferring modules; similar mechanisms apply to the sodium pumps driven by decarboxylation reactions.

the cytosolic cofactor HS–Coenzyme M. Sodium pumping is associated with the second partial reaction producing a Na^+ gradient equivalent to a -60 mV membrane potential. The sodium pump consists of 6–8 polypeptides (species dependent). The central pathway of methanogenesis is reversible. Accordingly, the enzyme acts as a sodium pump during methanogenesis from CO_2 or acetate but drives the reverse reaction by means of a sodium potential in methanogenesis from methyl group containing C_1 compounds.

Utilization of Light

Photosynthetic apparatuses as found in phototrophic bacteria and eukaryotes do not exist in archaea. However, the aerobic extreme halophiles like *H. salinarum* can synthesize a light-driven proton pump under conditions of low-oxygen tension composed of a single integral-membrane protein bacteriorhodopsin (BR). BR spans the membrane with seven α-helical domains enclosing the chromophore retinal, which is bound as protonated Schiff's base to a lysine in the hydrophobic core of the protein. Absorption of light induces an all-*trans* to 13-*cis* isomerization of retinal accompanied by a deprotonation of the Schiff's base with concommitant release of the proton on the periplasmic membrane surface via a channel delineated by a series of protonable aminoacid residues and water molecules. The light-triggered reaction is accompanied by conformational changes of the protein and initiates a photocycle of the chromophore that relaxes through 5–6 consecutive steps to the all-*trans* ground state. In that phase reprotonation of the Schiff's base from the cytosolic side of the plasma membrane is attained. The proton pumping power-stroke corresponds to about -50 kJ mol^{-1} and can generate a proton-motive potential of about 300 mV. The light-induced proton gradient $\Delta\mu H^+$ can drive ATP synthesis, the flagellar motor, or a Na^+/H^+ antiporter to drive sodium out of the cell. Besides BR, three other archaeal rhodopsins were found. Halorhodopsin (HR) has a similar structure but acts as an inwardly directed chloride pump. The two other so-called sensory rhodopsins (SR 1 + 2) are photoreceptors that trigger the flagellar motor (phototactic/photophobic) via conformational coupling of membrane-associated transducer units (Figure 5). As such they are basic models for the large variety of seven-helix membrane receptors. All four archaeal rhodopsins have striking similarity regarding protein structure, the retinal chromophore and its photocycle. However, the ion-transducing BR and HR perform fast photocycles in the millisecond range, whereas SR 1 + 2 are comparativelty slow (~100 ms).

Respiratory Complexes

The euryarchaeota *Halobacteria*, *Thermoplasma*, and many species of the crenarchaeota comprising genera as *Sulfolobus*, *Acidianus*, *Metallosphera*, or *Pyrobaculum* are obligate or facultative aerobes. Their respiratory systems essentially resemble modular components of respiratory chains as found in oxygen-respiring bacteria. A significant difference is the lack of a proton translocating NADH:quinol oxidoreductase. Instead, type-II NADH dehydrogenases were found, whereas complex-II analogous succinate dehydrogenases are

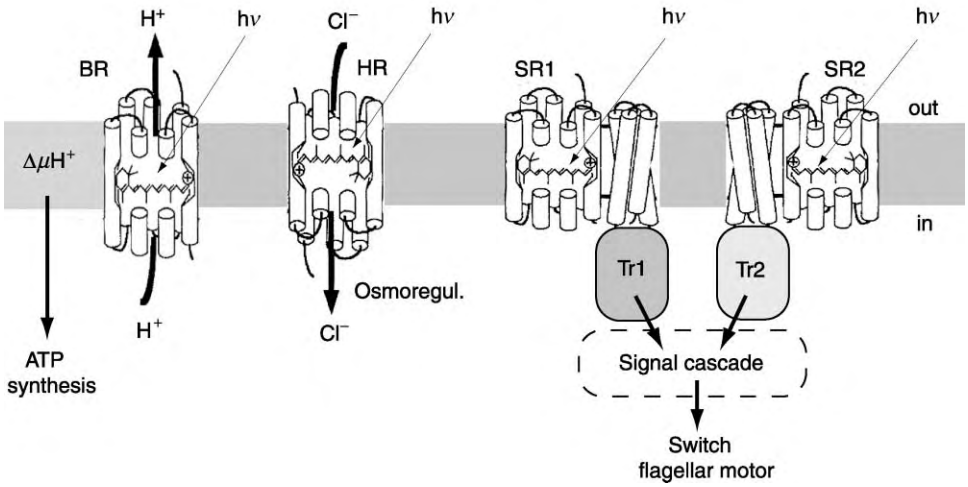

FIGURE 5 Illustration of energy transduction and sensory functions of rhodopsins in the extreme halophilic archaea. BR bacteriorhodopsin, HR halorhodopsin, SR1 and SR2 are sensory rhodopsins. Only BR and HR are ion pumps. The homodimeric transducer complexes Tr1, 2 are conformationally coupled to SR1, SR2, and transfer the conformational signal via their cytoplasmatic domains to a signaling cascade controlling the rotational direction of the flagella motor. The orientation of vectorial reactions is indicated with "in" symbolizing the cytosolic side of the plasma membrane.

present in all aerobic archaea. Two groups of enzymes can be distinguished: one group resembles the properties of SDHs from bacteria and mitochondria, and the other represents a novel class with unusual iron–sulfur clusters, as well as additional ones in a subunit with homology to methanobacterial heterodisulfide reductase, suggesting a novel electron pathway to the quinone pool. In *Halobacteria*, menaquinone and ubiquinone function as membrane-integral electron acceptors; in *Thermoplasma* and thermoacidophilic crenarchaeota like *Sulfolobales*, these are replaced by caldariella quinone and a variety of similar sulfur-containing thiopheno-benzoquinones. Several archaea like *A. ambivalens* contain only fragmentary respiratory chains established from NADH- and succinate-quinone reductases and a heme/Cu-type quinol oxidase as terminal electron acceptor; the latter serves as the only energy-conserving proton pump. Rieske Fe–S proteins are present in *Halobacteria*, *Sulfolobales*, and *Pyrobaculum* for example, but cytochrome *c* and regular quinol:cytochrome *c* reductases are absent in many species. Instead, analogous functions are replaced by alternate membrane protein assemblies, e.g., the SoxLN complex of *S. acidocaldarius*, using different electron acceptors as, for example, a mono-heme *b*-type cytochrome and/or blue copper proteins like sulfocyanine from various *Sulfolobus* species, or halocyanines from *Natronomonas* or *Halobacterium salinarum*. The proton pumping terminal heme/Cu-type oxidases are organized as supercomplexes in some thermoacidophilic creanarchaeota that combine features of quinol- and cytochrome *c* oxidases. The best-investigated examples are the SoxM complex and the SoxABCD complex from *Sulfolobus*.

Secondary Energy Transducers

ATP synthetases (⇒) are the most important universal secondary energy transducers integrated into plasma membranes. Bacterial ATP synthetases and those of mitochondria and chloroplasts are of the F_0F_1-type (⇒). Functionally, the ATP synthases are reversible ion-transporting ATPases driving the reaction ADP + Pi → ATP + H_2O by dissipation of a $\Delta\mu H^+$ or $\Delta\mu Na^+$ across the membrane. F_1 extends to the cytosol and bears the substrate binding sites; F_0 is the membrane integral ion-conducting subcomplex. Archaea contain A_0A_1-type ATP synthetases that structurally resemble the eukaryotic vacuolar V-type ATPases (⇒) but, in contrast to the latter, function as ATP synthetases driven by an ion-motive $\Delta\mu H^+$ or $\Delta\mu Na^+$ according to the rotational reaction mechanism of F_0F_1. The peripheral substrate binding A_1 moiety has been identified from many *Halobacteria*, *Sulfolobales*, and *Methanobacteria*. The only integrated A_0A_1-complex was isolated from the methanogen *Methanococcus jannashii*.

Evolutionary Links

In the evolution of higher organisms, cyanobacteria are the most likely precursor of chloroplasts which originated from an endosymbiotic uptake of such a prokaryotic phototroph into a precursor form of a eukaryotic cell. Likewise, the mitochondria have been derived from aerobic prokaryotes similar to the recent purple bacteria by endosymbiosis. The recipient might have been an archaebacterium.

See Also the Following Articles

Bioenergetics: General Definition of Principles • Chemolithotrophy • Cytochrome bc_1 Complex (Respiratory Chain Complex III) • Cytochrome Oxidases, Bacterial • Energy Transduction in Anaerobic Prokaryotes • F1–F0 AT Synthase • Green Sulfur Bacteria: Reaction Center and Electron Transport • Purple Bacteria: Photosynthetic Reaction Centers • Respiratory Chain Complex I • Respiratory Chain Complex II and Succinate: Quinone Oxidoreductases • Respiratory Chain Complex IV

Glossary

archaea The prokaryotic domain consists of two branches of the phylogenetic tree of life, one occupied by the bacterial domain and the other by the archaeal domain. The latter splits into the euryarchaeota and the crenarchaeota. Both archaeal sub-branches are host to many extremophilic genera. The methanogens belong to the euryarchaeota, the thermoacidophiles with a few exceptions to the crenarchaeota.

chemolithotrophs Prokaryotes assimilating carbon dioxide as sole carbon source and extracting energy from inorganic redoxreactions (in contrast to organotrophs which use reduced organic substrates as their carbon and/or nitrogen source).

chromophore Usually, a colored organic molecule bound to a protein and functioning as a cofactor in catalysis. Hemes are chromophores of cytochromes and host Fe ions in the core of a porphyrin ring; other tetrapyrrol derivatives like chlorophyll host Mg or Co. Chlorophylls and carotenoids in reaction centers or antenna systems, and retinal in rhodopsins, are light-energy transducers.

endosymbiosis Uptake of an originally independent free living organism into cells of a host organism, where it can reproduce under the control of the host organism and share metabolic functions (the energy-transducing organelles of eukaryotes originated by permanent transfer of genetic material from the endosymbiont to the host genome).

prokaryotes Unicellular microbes without a cell nucleus (in contrast to the eukaryotes which are located on a distinct branch of the universal phylogenetic tree of life, the eukaryotic domain).

thermoacidophiles Prokaryotes with a lifestyle adapted to hyperthermophilic conditions (75–110 °C) as well as to extremely low environmental pH (3.5–0.5). Most of them belong to the archaea.

vacuoles Membrane encapsulated compartments within eukaryotic cells, in most cases, filled with liquid of low pH; their membrane contains an ATP driven proton pump, the V-type ATPase.

Further Reading

Anthony, Ch. (ed.) (1988). *Bacterial Energy Transduction*. Academic Press, New York.

Driessen, A. J. M., Rosen, B. P., and Konings, W. N. (2000). Diversity of transport mechanisms: common structural principles. *TIBS* **25**, 397–401.

Harold, F. M. (1986). *The Vital Force: A Study of Bioenergetics*. Freeman, New York.

Kates, M., Kushner, D. J., and Matheson, A. T. (eds.) (1993). *The Biochemistry of Archaea*. Elsevier, Amsterdam.

Lengeler, J. W., Drews, G., and Schlegel Hans, G. (eds.) (1999). In *Biology of the Prokaryotes*. Thieme Verlag, Stuttgart, Germany.

Lolkema, J. S., Speelmans, G., and Konings, W. N. (1994). Na^+-coupled versus H^+-coupled energy transduction in bacteria. *Biochim. Biophys. Acta* **1187**, 211–215.

Schäfer, G. (2004). Respiratory systems of the Archaea: From minimal structures to supercomplexes. In *Progress in Photosynthesis and Respiration* (D. Zanoni, ed.) Kluwer, New York.

Schäfer, G., Engelhard, M., and Müller, V. (1999). Bioenergetics of the archaea. *Microbiol. Molecul. Biol. Rev.* **63**, 570–620.

Schäfer, G. (series ed.) (2004). Extremophilic archaea and bacteria: New insights into their roles in membrane transport and other bioenergetic functions (Minireview Series). *J. Bioenerg. Biomemb.* **36**, 3–159.

Biography

Günter Schäfer is a Professor Emeritus since 2002 and former Chair of the Institute of Biochemistry at the University of Lübeck, Germany. His principal research interest is in the entire field of bioenergetics including ATPases and electron transport systems of mitochondria, chloroplasts and microorganisms. He holds a Ph.D. in chemistry from the Technical University of Munich, Germany. In his recent research he specialized in bioenergetics of archaea and extremophiles as well as the structural basis of hyperthermostable archaeal proteins.

Metabolite Channeling: Creatine Kinase Microcompartments

Uwe Schlattner and Theo Wallimann
Institute of Cell Biology, Swiss Federal Institute of Technology (ETH), Zürich, Switzerland

Subcellular microcompartments, consisting of multienzyme complexes embedded within the cellular, highly viscous matrix, associated with the cytoskeleton, or situated along membranes, are operating according to exclusion principles and favor preferred pathways of intermediates. This process, called metabolite or substrate channeling, is defined as transfer of intermediates between sequential enzymes without equilibration of these metabolites with the surrounding bulk solution. Such an association between two or more sequential enzyme- or transport reactions in a microcompartment, forming a distinct functional pool of intermediates, is also called functional coupling. It can be considered as a general mechanism to increase efficiency of sequential reactions in a metabolic pathway. Since metabolite channeling leads to segregation of a metabolic pathway from other cellular reactions, it represents a specific kind of metabolic compartmentation similar to that operating within membrane-separated organelles or by restricted two-dimensional diffusion at surface boundary layers. Here, metabolite channeling is described with special emphasis on high-energy phosphate channeling by creatine kinase (CK), the phosphocreatine circuit or shuttle, and the mitochondrial CK isoenzyme.

Subcellular Microcompartments and Mechanisms of Metabolite Channeling

Life most likely originated autotrophically *de novo* in metabolic complexes organized on FeS_2 (pyrite) mineral surfaces, the earliest form of microcompartments. Likewise, a cell is by no means represented best by a well-mixed bag of enzymes, behaving in complete equilibrium according to solution kinetics. Because of the intricate structural and functional organization of living cells, enzymes and metabolites do not behave as if they were freely diffusible in solution. Instead, they may form structurally, functionally, and temporally defined subcellular microcompartments, either via strong static, or via fickle, dynamic interactions with other enzymes, proteins, or subcellular structures. Such a structural organization of pathway components is a general prerequisite for metabolite channeling. It may involve (1) huge covalently linked enzyme-complexes (or multifunctional enzymes) such as fatty acid synthase (FAS), (2) kinetically stable multienzyme complexes like pyruvate dehydrogenase (PDH) or bacterial and plant tryptophan synthase (TS), (iii) more dynamic, reversibly associating enzymes such as glycolytic complexes containing glyceraldehyde phosphate dehydrogenase (GAPDH) or glycerol phosphate dehydrogenase (GPDH), or (4) colocalization on subcellular particles. These associations allow the transfer of intermediates between the channeling components by different mechanisms: (1) sequential covalent binding to very close active sites in the reaction sequence (e.g., PDH), (2) physical hindrance or electrostatic effects prevent mixing with bulk solution and drive a directed diffusion (e.g., TS), (3) transfer of noncovalently bound intermediates between active sites (e.g., NADH dehydrogenase), (4) transfer in an unstirred surface layer. These mechanisms can be fulfilled in both, static and dynamic enzyme associations. However, while static associations allow for an almost perfect or "tight" channeling of metabolites, dynamic channeling is often only partial or "leaky."

Advantages of Metabolite Channeling

Sequestering of intermediates in a microcompartment through channeling provides kinetic and regulatory advantages for not only the reaction sequence itself (see Figure 1), but also for cellular metabolism. In general: (1) enzyme reaction rates and equilibria are controlled by local and enzyme bound substrates, rather than bulk phase substrate concentrations, (2) for a readily reversible reaction, local supply of substrate and removal of product may drive the reaction in the desired direction, (3) sequestered intermediates are present at high local concentrations and an apparently low K_m for

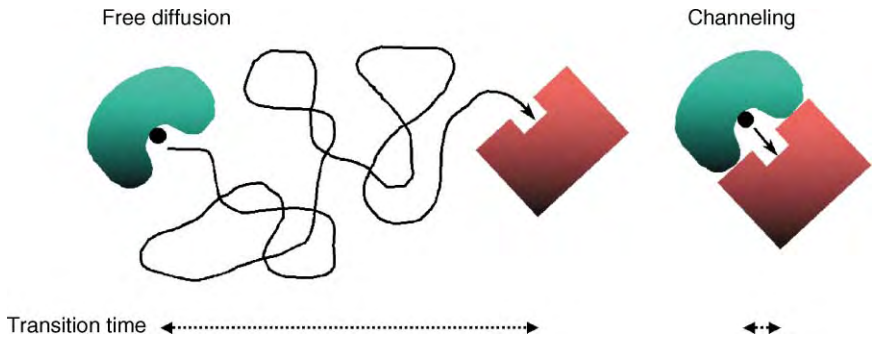

FIGURE 1 Free diffusion versus metabolite channeling. Compartmentation of a reaction sequence without equilibration with bulk solution leads to shorter transition times and further advantages (see text).

these intermediates can be observed with the channeling complex compared to the nonchanneling situation measured with isolated components, (4) metabolites are isolated from competing reactions, e.g., between anabolic and catabolic pathways, (5) the life-time of the intermediate in the solvent phase is shortened relative to free diffusion, which may be essential in case of unstable intermediates, (6) in certain cases, the unfavorable energetics of desolvating the substrate that precedes binding to the enzyme is avoided, (7) channeling components can be regulated by modulators that affect enzyme associations, and (8) a larger degree of metabolic control of the over-all-flux of the reactions can be achieved, e.g., via feed-back regulatory mechanisms such as substrate activation, product inhibition, and cooperativity.

Subcellular Targeting of Glycolytic Multienzyme Complexes

In muscle, glycolytic enzymes are targeted to the actin-containing thin filaments at the sarcomeric I-band region where they form highly complex metabolons. The I-band in *Drosophila* flight muscle contains a multi-enzyme complex consisting of GDPH-1, aldolase, and GAPDH. By elegant experiments with transgenic *Drosophila* expressing GDPH-3 instead of GDPH-1, it could be shown that all three glycolytic enzymes no longer colocalize in the I-band to form a microcompartment. Even though the full complement of active glycolytic enzymes was still present, their failure to colocalize in the sarcomer resulted in the inability to fly. Thus, correct targeting and formation of multienzyme complexes that lead to functionally coupled microcompartments and substrate/product channeling seem to be a prerequisite for proper function of glycolysis and ultimately for correct muscle function. In mammalian cells, CK is also participating in the glycolytic metabolon.

Compartmentation of Creatine Kinase Isoenzymes and Channeling of High-Energy Phosphates

The Creatine Kinase/Phosphocreatine Circuit or Shuttle

One fundamental requirement of life is energy supply. Cellular energy demand and supply are balanced, and tightly regulated for economy and efficiency of energy use. CK is a major enzyme of higher eukaryotes that copes with high and fluctuating energy demands to maintain cellular energy homeostasis in general and to guarantee stable, locally buffered ATP/ADP ratios in particular.

The enzyme catalyzes the reversible phosphoryl transfer from ATP to creatine (Cr) to generate ADP and phosphocreatine (PCr). Thus, CK is able to conserve energy in the form of metabolically inert PCr and vice versa, to use PCr to replenish global as well as local cellular ATP pools. Since PCr can accumulate to much higher cellular concentrations than ATP, the CK/PCr-system constitutes an efficient and immediately available cellular "energy buffer." In addition, tissue-specific CK isoenzymes are located in the cytosol (dimeric muscle-type MM-CK and brain-type BB-CK) and the mitochondrial intermembrane space (sarcomeric sMtCK and ubiquitous uMtCK, both forming octamers and dimers). CK isoenzymes are often associated with sites of ATP supply, where they generate PCr, or with sites of ATP consumption, where they regenerate ATP by using PCr. Thus, together with the faster diffusion rate of PCr as compared to ATP, the CK/PCr system also supports an intrinsic energy transfer system (CK/PCr-circuit or -shuttle), coupling sites of energy generation (oxidative phosphorylation or glycolysis) with sites of energy consumption (Figure 2). This circuit is particularly important in large and/or polar cells, such as spermatozoa where diffusional limitations of adenine nucleotides, especially ADP, along the sperm tail become especially apparent.

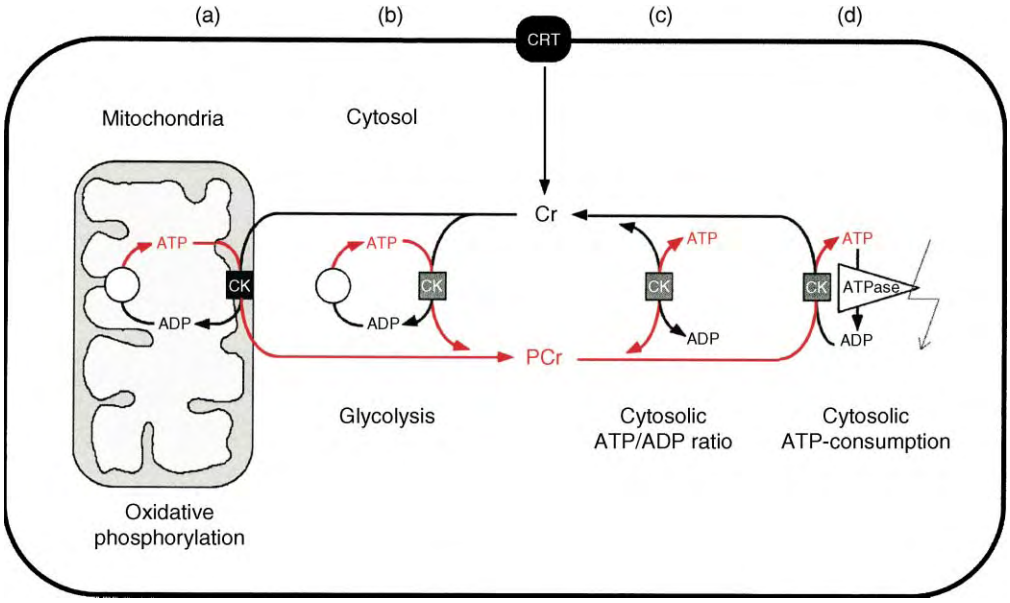

FIGURE 2 The creatine kinase (CK)/phosphocreatine (PCr) system. Isoenzymes of CK are found in different compartments like mitochondria (a) and cytosol (b–d) in soluble form (c) or associated to a different degree to ATP-delivering (a,b) or -consuming processes (d). A large cytosolic PCr pool up to 30 mM is built up by CK using ATP from oxidative phosphorylation like in heart (a) or glycolysis like in fast-twitch glycolytic muscle (b). PCr is then used to buffer global (c) and local (d) ATP/ADP ratios. In cells that are polarized and/or have very high or localized ATP consumption, these CK isoenzymes, together with easily diffusible PCr, also maintain an energy shuttle between ATP-providing or -consuming processes (a,d). Metabolite channeling occurs where CK is associated with ATP-providing or -consuming transporters, pumps or enzymes (a,b,d). Creatine (Cr) is synthesized in only few cell types (e.g., liver and kidney) and has to be taken up from the blood stream by a specific Cr transporter (CRT).

Channeling with Cytosolic CK

Cytosolic CK is only partially soluble. A significant fraction is structurally and functionally associated or co-localized with different, structurally bound ATPases or ATP-regulated processes. These include (1) different ion pumps in the plasma membrane, (2) the sarcomeric M-band of the myofibrils in muscle, (3) the calcium pump of the muscular sarcoplasmic reticulum, and (4) the ATP-gated K^+-channel. In all these cases, PCr is used for the local regeneration of ATP, which is directly channeled from CK to the consuming ATPase without major dilution by the surrounding bulk solution. Only in some cases, the physical basis for the metabolite channeling is known. For example, MM-CK uses a "charge clamp" consisting of four lysine residues to specifically bind to partner molecules, myomesin and M-protein in the M-band,

Cytosolic CK is structurally associated with the key regulatory enzyme of glycolysis, phosphofructokinase (PFK), which itself is regulated by ATP, Likewise, structural and functional interaction of cytosolic CK with the PAR-1 receptor of the thrombin-signaling pathway and with the ATP-gated K^+-channel, respectively, has been demonstrated. A tight functional coupling of CK to ATPases, e.g., acto-myosin ATPase and ion pumps, such as the K^+/Na^+-ATPase or the Ca^{2+}-ATPase, has the advantage (1) that product inhibition of the ATPase by ADP and H^+ is avoided, since the latter are both substrates of the CK reaction ($PCr + ADP + H^+ \leftrightarrow Cr + ATP$) and (2) that the high free energy of ATP hydrolysis (ΔG_{ATP}) at sites of ATP hydrolysis is preserved by keeping locally very high ATP/ADP ratios due to coupling of CK with those ATPases *in situ* and thus preventing energy dissipation caused by transport of ATP and mixing it with the bulk surrounding. Interestingly, the strongest phenotype of CK double knockout mice, which no longer express cytosolic MM-CK and mitochondrial MtCK in muscle, is characterized by significant difficulties with intracellular calcium handling and muscle relaxation, emphasizing the physiological importance of the CK system for the energetics of intracellular calcium homeostasis in general and the delivery of ATP to the energetically demanding Ca^{2+}-ATPase, in particular.

Channeling in Energy Transducing Mitochondrial Microcompartments

MtCK forms mainly large, cuboidal octamers (Figure 3) that are present (1) between the outer and inner mitochondrial membrane (the so-called "intermembrane space" of mitochondria) and preferentially localized at the so-called "mitochondrial contact sites" between

outer and inner mitochondrial membrane, as well as (2) in the "cristae space" (see Figure 3 inset). The kinase catalyzes the direct transphosphorylation of intramitochondrial produced ATP and Cr from the cytosol into ADP and PCr. ADP enters the matrix space to stimulate oxidative phosphorylation, giving rise to mitochondrial recycling of a specific pool of ATP and ADP, while PCr is the primary "high energy" phosphoryl compound that leaves mitochondria into the cytosol. The molecular basis for such directed metabolite flux is channeling between the large, cuboidal MtCK octamer and two transmembrane proteins, adenine translocator (ANT) and mitochondrial porin or voltage-gated anion channel (VDAC). ANT is an obligatory antiporter for ATP/ADP exchange across the inner mitochondrial membrane, while VDAC is a nonspecific, potential-dependent pore in the outer mitochondrial membrane. The MtCK-linked metabolite channeling is based on (1) colocalization, (2) direct interactions, and (3) diffusion barriers. MtCK tightly binds to cardiolipin, an acidic phospholipid that is specific for the mitochondrial inner membrane. Since ANT is situated in a cardiolipin patch, this leads to colocalization and metabolite channeling between both proteins in cristae and intermembrane space (Figure 3). MtCK in the intermembrane space further interacts with outer membrane phospholipids and VDAC, thus virtually

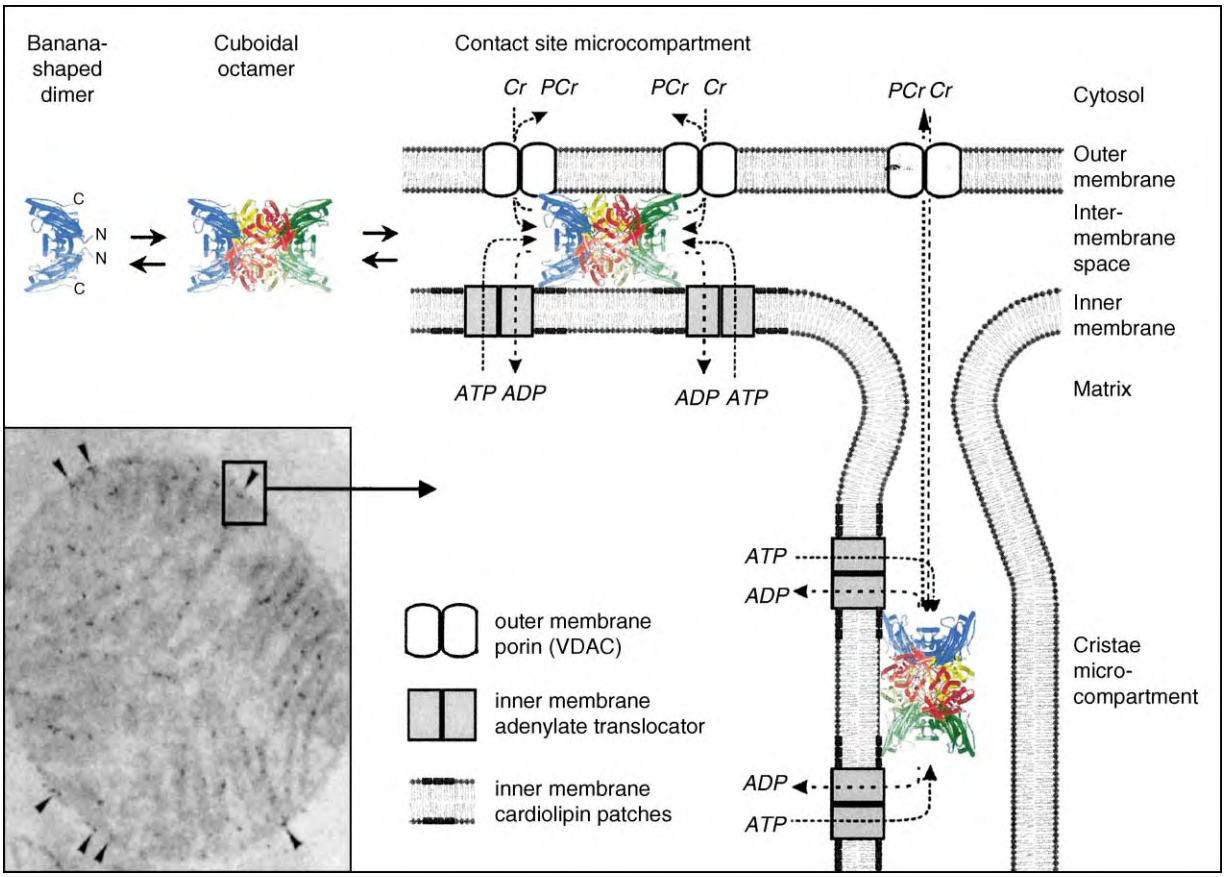

FIGURE 3 Inset: Dual localization of mitochondrial CK by electron microscopy. Post-embedding immuno-gold labeling of MtCK in a mitochondrion from photoreceptor cells of chicken retina, showing localization of MtCK in the peripheral intermembrane space (arrows) and along the cristae membranes. Scheme: Microcompartments and metabolite channeling of mitochondrial CK. After the import of nascent MtCK over the mitochondrial outer membrane and cleavage of the targeting sequence, MtCK first assembles into dimers. Dimers rapidly associate into octamers (top left), and although this reaction is reversible, octamer formation is strongly favored by high MtCK concentrations and MtCK binding to acidic phospholipids. MtCK is then found in two locations; (1) in the so-called mitochondrial contact sites associated with ANT and VDAC (top center), and (2) in the cristae associated with ANT only (at right). In contact sites, MtCK simultaneously binds to inner and outer membrane due to the identical top and bottom faces of the octamer. Binding partner in the inner membrane is the twofold negatively charged cardiolipin, which allows a functional interaction with adenine nucleotide translocator that is situated in cardiolipin membrane patches. In the outer membrane, MtCK interacts with other acidic phospholipids and, in a calcium-dependent manner, directly with VDAC. Substrate and product fluxes between MtCK and the associated proteins are depicted as arrows. In contact sites, this substrate channeling allows for a constant supply of substrates and removal of products at the active sites of MtCK. In cristae, only ATP/ADP exchange is facilitated through direct channeling to the MtCK active site, while Cr and PCr have to diffuse along the cristae space to reach VDAC.

cross-linking inner and outer membrane and contributing to the "mitochondrial contact sites." Increasing the external calcium concentrations strengthens the interaction of MtCK with VDAC, which may improve channeling under cytosolic calcium overload as occurring at low cellular energy state. Some studies suggest that only the membrane-bound, octameric form of MtCK is able to maintain the metabolite channeling described above. Finally, the limited permeability of VDAC and thus of the entire outer membrane creates a dynamic microcompartmentation of metabolites in the intermembrane space that contributes to MtCK-linked channeling and separate mitochondrial ATP- and ADP pools. Similar to MtCK, hexokinase is able to use intramitochondrially produced ATP by binding to VDAC from the cytosolic mitochondrial surface at contact sites containing only ANT and VDAC. The direct functional coupling of MtCK to oxidative phosphorylation can be demonstrated with oxygraph respirometry on skinned muscle fibers from normal and transgenic mice lacking MtCK.

Oxidative damage of MtCK, induced by reactive oxygen and nitrogen species, generated under cellular stress situations, e.g., in infarcted heart or under chemotherapeutic intervention by anthracyclines lead to inactivation and dimerization of MtCK, as well as to dissociation of the enzyme from the mitochondrial inner membrane. Thus, important prerequisites for efficient channeling of high-energy phosphates by MtCK are negatively affected. These events contribute to cardiac energy failure and specific anthracycline cardiotoxicity.

FIGURE 4 Intramitochondrial inclusions in patients with mitochondrial myopathies consist of mitochondrial MtCK. Immuno-electron histochemistry of human intra-mitochondrial crystalline "railway-track" inclusions seen in patients with mitochondrial myopathies showing "ragged-red" skeletal fibers as a hallmark of the disease. Note the grossly enlarged mitochondrion, here from a patient with Kearns-Sayre syndrome, displaying the typical regularly spaced intra-cristae inclusions (dark) surrounded by mitochondrial inner cristae membranes. The section has been stained by rabbit anti-MtCK antibodies, followed by colloidal gold-conjugated second antibody (in collaboration with Dr. A. M. Stadhouders, Nijmegen, The Netherlands). Note that the dark inclusion bodies are heavily and specifically stained by the small 10 nm gold particles, indicating a high propensity of MtCK at these locations. Isolation of such inclusions, plus image processing of sections through them revealed that they consist mainly of crystalline MtCK octamers, which crystallize in sheet-like structures.

Mitochondrial CK, Intramitochondrial Inclusions, and Low Cellular Energy State

MtCK is an indicator for cellular low-energy stress, that is, the expression of this enzyme is highly up-regulated in patients with mitochondrial myopathies in the so called "ragged-red" skeletal muscle fibers, where mitochondrial volume and size are markedly increased and where characteristic intra-mitochondrial "railway-track inclusions" are observed as a hallmark of pathology. The latter were shown to consist of crystalline sheets of MtCK (see Figure 4). Similar MtCK inclusions can also be induced in animal by chronic Cr depletion leading to cellular low-energy state, Even more generally, cellular low-energy stress, be it chronic endurance training, fasting, Cr depletion, or pathologies in ATP generation like mitochondrial dysfunction seen in patients with mitochondrial cytopathies, induces a coordinated induction of "energy gene expression" to compensate for impaired energy supply and transport. In case of MtCK, one of the most prominent among these genes, overexpression is such that it leads to crystallization of the enzyme in a pathological state as described above.

Mitochondrial CK and the Mitochondrial Permeability Transition Pore

MtCK, together with its substrate Cr, has been recently implicated in regulation of the mitochondrial permeability transition pore that is crucially involved in triggering apoptosis, This seems to be due to metabolite channeling in the MtCK/ANT microcompartment also, which maintains high ADP concentrations in the matrix space that are inhibitory for permeability transition. Thus, the CK-system and its substrates seem to exert additional effects that are not necessarily directly coupled to improving cellular energetics. This may explain the remarkable cell- and neuro-protective effects of Cr that have been reported.

See Also the Following Articles

Free Radicals, Sources and Targets of: Mitochondria • Mitochondrial Channels • Mitochondrial Membranes, Structural Organization • Mitochondrial Metabolite Transporter Family • Mitochondrial Outer Membrane and the VDAC Channel • P-Type Pumps: Na^+/K^+ Pump

Glossary

metabolite channeling Local transfer of metabolic intermediates between sequential enzyme or transport reactions without equilibration with bulk solution.

metabolic compartmentation Segregation of intermediates and enzymes of a metabolic pathway by membranes, binding to a specific surface or direct interaction in protein complexes allowing metabolite channeling.

microcompartment Structural unit allowing metabolic compartmentation, also called "metabolon."

mitochondrial contact sites Close adhesions of inner and outer mitochondrial membrane that can be observed by electron microscopy and can be isolated as a separate microcompartment. Contact sites consist of multi-lipid/protein complexes with variable composition and are involved in energy transduction (e.g., containing ANT/VDAC or ANT/MtCK/VDAC) or protein import.

mitochondrial permeability transition pore A multienzyme complex, probably composed of VDAC, ANT, Bax, cyclophilin, MtCK and others, that is crucially involved in early events that trigger apoptosis like release of cytochrome *c* and other apoptosis-inducing factors into the cytosol.

Further Reading

Agius, L., and Sherratt, H. S. A. (eds.) (1997). *Channelling in Intermediary Metabolism*. Research Monograph IX, Portland Press, London, GB.

Dolder, M., Walzel, B., Speer, O., Schlattner, U., and Wallimann, T. (2003). Inhibition of the mitochondrial permeability transition by creatine kinase substrates. Requirement for microcompartmentation. *J. Biol. Chem.* **278**, 17760–17766.

Jacobus, W. E., and Lehninger, A. L. (1973). Creatine kinase of rat heart mitochondria. Coupling of creatine phosphorylation to electron transport. *J. Biol. Chem.* **248**, 4803–4810.

Kay, L., Nicolay, K., Wieringa, B., Saks, V., and Wallimann, T. (2000). Direct evidence for the control of mitochondrial respiration by mitochondrial creatine kinase in oxidative muscle cells in situ. *J. Biol. Chem.* **275**, 6937–6944.

Ovádi, J. (1995). *Cell Architecture and Metabolic Channeling*. Springer, Heidelberg.

Ovádi, J., and Srere, P. A. (2000). Macromolecular compartmentation and channeling. *Int. Rev. Cytol.* **192**, 255–280.

Schlattner, U., Forstner, M., Eder, M., Stachowiak, O., Fritz-Wolf, K., and Wallimann, T. (1998). Functional aspects of the X-ray structure of mitochondrial creatine kinase: a molecular physiology approach. *Mol. Cell. Biochem.* **184**, 125–140.

Srere, P. A., and Knull, H. R. (1998). Location-location-location. *Trends Biochem. Sci.* **23**, 319–320.

Srivastava, D. K., and Bernhard, S. A. (1986). Metabolite transfer via enzyme–enzyme complexes. *Science* **234**, 1081–1086.

Wallimann, T., Wyss, M., Brdiczka, D., Nicolay, K., and Eppenberger, H. M. (1992). Intracellular compartmentation, structure and function of creatine kinase isoenzymes in tissues with high and fluctuating energy demands: the 'phosphocreatine circuit' for cellular energy homeostasis. *Biochem. J.* **281**, 21–40.

Biography

Uwe Schlattner is Docent at the Institute of Cell Biology, Swiss Federal Institute of Technology (ETH), Zürich, Switzerland. He received his masters in biology at the University of Freiburg, Germany, and his Ph.D. in Natural Science at the University of Geneva, Switzerland. His research interest is in cellular energetics, in particular the molecular structure and physiology of kinases involved in regulating the cellular energy state.

Theo Walliman is a Professor at the Institute of Cell Biology at Swiss Federal Institute of Technology (ETH) in Zürich, Switzerland, where he also received his Ph.D. After a postdoctoral stay in Prof. Andrew G. Szent-Györgyi's laboratory at Brandeis University, Boston, from 1975 to 1981, he returned to ETH-Zürich. His research interests are in cellular energetics, especially creatine kinases and AMP-activated protein kinases, as well as creatine supplementation in health and diseases.

Metalloproteases

David S. Auld
Harvard Medical School, Boston, Massachusetts, USA

Metalloproteases are a class of enzymes that use protein-bound metal ion(s) and a coordinated water molecule to catalyze the addition of water to a peptide bond. Proteases are necessary for the survival of all living creatures, and are encoded by ~2% of the genes in all kinds of organisms. They are an exceptionally important group of enzymes in biology, medical research, and biotechnology.

Functional Classification

Scientists who work in the general area of proteolytic enzymes have given much latitude to the naming of such enzymes. At present they are frequently referred to as proteases, proteinases, and peptidases, in an interchangeable manner. Some of the terms used are more illustrative of their function. Exopeptidases cleave one or a few amino acids from the N or C terminus of a polypeptide, while endoproteases act internally on the polypeptide chain. Aminopeptidases and carboxypeptidases act on the N and C terminus of the polypeptide, respectively, usually cleaving off one amino acid at a time, but some are capable of removing two (dipeptidyl peptidases) or three (tripeptidyl peptidases) amino acids at a time. These enzymes are often classified according to their general mechanism type as structural/functional information becomes available. This classification results in four major types: aspartic, cysteine, metallo-, and serine, each named for a critical component of the active site. In the case of metalloproteases, the metal most frequently found is zinc. However, manganese, cobalt, and iron are also observed for some specific cases. Proteases are often named according to a specific physiological substrate that they hydrolyze. Angiotensin I converting enzyme (ACE) is a zinc metalloprotease that cleaves the C-terminal dipeptide from angiotensin I to produce the potent vasopressor, octapeptide, angiotensin II and inactivates bradykinin by the sequential removal of two dipeptides from its C terminus. The role of this enzyme in blood pressure control and water and salt metabolism was identified through the use of potent inhibitors of its action. It is also defined as a zinc dipeptidyl carboxypeptidase. Tumor necrosis factor-alpha (TNF-alpha) is a cytokine that induces protective inflammatory reactions and kills tumor cells. Soluble TNF-alpha is released from its membrane-bound precursor by a membrane-anchored proteinase, identified as a multidomain metalloproteinase called TNF-alpha-converting enzyme (TACE). This enzyme is also named as *a d*isintegrin-like *a*nd *m*etalloproteinase *s*ite (ADAMS) 17 endopeptidase for a classification based on structural considerations. Frequently, such a substrate-based classification requires a very general term when the substrate specificity is only known in general terms, such as matrix metalloproteinase (MMP).

Structural Classification

During the past decade, the advent of sequencing the protein through its gene and the ability to obtain three-dimensional (3D) structures on proteins allowed the recognition of metalloprotease families. These studies permit several different classifications based, for example, on the type of metal site present and/or similarity in overall protein fold and/or amino acid sequence similarities.

Metal Sites

The metal that is found in most metalloproteases is zinc. The function of these enzymes is therefore related to the chemistry of zinc, which is quite versatile. It has a remarkably adaptable coordination sphere that allows it to accommodate a broad range of coordination numbers and geometries when forming complexes. If the zinc retains a positive charge after ligating to protein side chains, it can act as a Lewis acid in catalysis. If a zinc–bound water is converted to hydroxide, the zinc site can act as a base or nucleophile in catalysis. In this sense the catalytic zinc sites are amphoteric. The oxidation/reduction properties of its neighboring transition metals is a major cause of their ligand exchange rates, amphoteric properties, and coordination geometries. Since zinc has a filled *d*-shell, it does not have oxidation/reduction properties, thus providing a stable metal ion species in a biological medium whose redox potential is in constant flux. There are now about six dozen X-ray diffraction and NMR structures of individual metalloproteases. These structures provide standards of

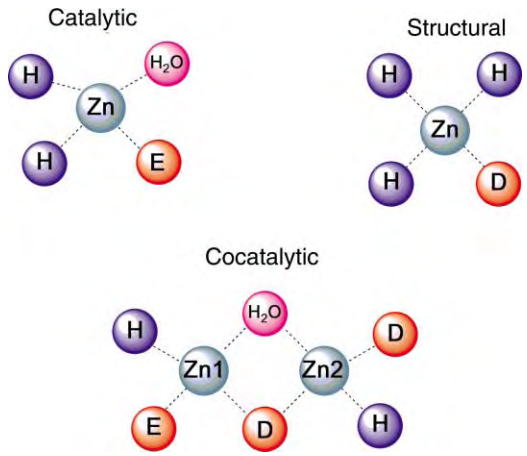

FIGURE 1 Zinc-binding sites in metalloproteases. Schematic shown is for a *catalytic* site, represented by carboxypeptidase A, the *structural* site for the matrix metalloproteases, and the *cocatalytic* site of Aeromonas aminopeptidase.

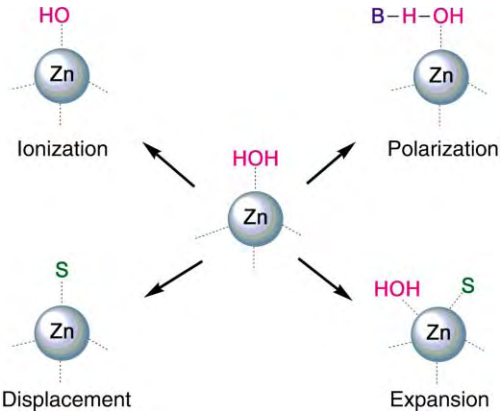

FIGURE 2 The role of the metal and bound water in catalysis. The water can ionize either (1) without or (2) with the help of the adjacent base supplied by an amino acid residue. The zinc–bound water can also (3) be displaced by substrate or (4) the coordination sphere be expanded upon interaction with substrate.

reference for the identity and nature of zinc ligands in other proteins, for which only the primary structure is known, and thus allow formation of metalloprotease families. Three types of distinct zinc-binding motifs emerge from these analyses: *catalytic*, *cocatalytic*, and *structural* sites (Figure 1). In zinc metalloenzymes the most common amino acids that supply ligands to these sites are His, Glu, Asp, and Cys. Thus far, Cys has been found as a ligand in only one metalloprotease.

Catalytic Sites

3D structures of the catalytic sites of about five dozen metalloproteases show that zinc forms complexes with any three nitrogen (His) and oxygen (Glu or Asp) donors, with His being the predominant amino acid chosen by a ratio of ~2:1 over Glu plus Asp. Histidine (usually the Nε2 nitrogen) may be chosen because of its capacity to disperse charge through H-bonding of its non-ligating nitrogen. The carboxylate anion of Glu and Asp ligands will reduce the charge on the metal, making it more difficult for the metal–bound water to ionize and for the metal to act as a Lewis acid catalyst. The first two metal ligands are separated by a short amino acid spacer with the third ligand being supplied by a longer spacer. In catalytic zinc sites of proteases the ligands are generally supplied from within an α-helix or a β-sheet that places restraints on the coordination of the metal by the side chains of the amino acids. The overall length of such sites can be as small as 11 amino acids, as is observed in the astacin super family of zinc proteases.

Catalytic zinc sites are usually four or five coordinate in metalloproteases and the geometry in the free state is frequently distorted-tetrahedral or trigonal-bipyramidal. Water is always a ligand to these sites. In principle, the zinc and its bound water molecule can be involved in catalysis by a number of different means (Figure 2). Metalloproteases generally have a Glu or His residue within H-bonding distance of the zinc–bound water that could play the role of a general acid/base catalyst or may stabilize the transition state of a tetrahedral intermediate. Alternatively, the direct ionization of the metal–bound water can lead to nucleophilic catalysis by zinc hydroxide, while displacement of water or expansion of the coordination sphere can result in Lewis acid catalysis by the catalytic zinc atom. The three protein ligands, their spacing, and secondary interactions with neighboring amino acids in conjunction with the vicinal properties of the active center created by protein folding, are all critical to the mechanisms through which zinc is involved in catalysis.

Structural Sites

Metalloproteases frequently use either disulfides or calcium ions to aid in stabilizing the structure of the enzyme. Structural metal sites have four protein ligands and no metal–bound water molecule. Cys ligands, followed by His, are the preferred ligands in such sites in zinc metalloenzymes. However, only one Cys containing zinc site is observed in the class of metalloproteases. Human picornavirus endoprotease 2A binds one zinc to three Cys and one His in the sequence $Cx_1Cx_{57}Hx_1C$. One other metal site that fits the criteria for a structural zinc site has been observed in the matrix metalloproteases and has a signature of $Hx_1Dx_{12}Hx_{12}H$ (Figure 1). This site may indirectly affect the activity of the enzyme. The amino acids adjacent to the third and fourth His ligands to the structural zinc site provide a number of hydrophobic residues that border a catalytic Glu residue. These residues could provide a hydrophobic environment for the Glu carboxylate group and thus raise its pK_a and allow it to play a role in stabilizing the transition state in catalysis. The zymogen form of the

MMPs has a Cys ligand in place of the zinc-bound water in the catalytic zinc site, thus having the properties of a structural zinc site.

Cocatalytic Sites

These sites in metalloenzymes contain two or three metals in close proximity with two of the metals bridged by a side-chain moiety of a single amino acid residue, such as Asp, Glu, His, or a carboxylated lysine, LysCO, and sometimes a water/hydroxide molecule (Figure 1). Thus far, structures for amino- and carboxy- and a tripeptidase have been reported. Asp and Glu and sometimes an additional water molecule are the preferred bridging ligands for these sites. The distance between the metals is dictated by the type of bridging ligand, 2.8–3.6 Å, for the carboxylate. No Cys ligands have been reported for these sites.

The bridging amino acids and H_2O could have critical roles in catalysis. Thus, their dissociation from either or both metal atoms during catalysis could change the charge on the metal promoting its action as a Lewis acid or allowing interaction with an electronegative atom of the substrate. Alternatively, the bridging ligand might participate transiently in the reaction as a nucleophile or general acid/base catalyst. In this manner the metal atoms and their associated ligands would play specific roles in each step of the reaction that works in concert to bring about catalysis.

The ligands to these sites often come from nearly the entire length of the protein. The metals may therefore be important to the overall fold and stability of the protein as well as catalytic function. The secondary structural elements α-helices and β-sheets again play a strong role in supplying the ligands. However, in contrast to the catalytic zinc sites, the ligands often reside one or two amino acids from the N or C terminus of an α-helix or a β-sheet. These positions should allow more flexibility in forming the cocatalytic site.

Some of the cocatalytic sites contain metal ions other than zinc ions. The *E. coli* methionine aminopeptidase-1, MetAP-1, the hyperthermophile *Pyrococcus furiosus* methionine aminopeptidase-2 and human methionine aminopeptidase-2 have been isolated as dicobalt enzymes and the *E. coli* proline aminopeptidase as the dimanganese enzyme. The physiological metal for these enzymes is still not certain. Zinc works as well as cobalt in the yeast aminopeptidase-1 and recent studies of the *E. coli* MetAP-1 indicate that it functions as an Fe(II) enzyme.

Genetic Origin and Ligand Nature

The identification of the ligands to these metal sites and the spacing characteristics in combination with modern sequencing techniques has led to further classifications of the metalloproteases. An excellent source of information on proteolytic enzymes is the *Handbook of Proteolytic Enzymes* and its associated website of MEROPS (http://merops.sanger.ac.uk/index.htm). This protease database groups peptidases into three levels – clans, families, and an individual peptidase. A clan contains all the peptidases that are believed to have diverged from a single evolutionary origin. In terms of the metalloproteases, they may have similar catalytic metal sites and overall folds. The clans can be further divided into families of proteases that show significant similarities in amino acid sequence. Finally, a member of a family is an individual peptidase. The Release 6.6(March, 2004) of MEROPS gives information on 6349 sequences of metallopeptidases and groups them into 16 clans, 52 families, and 657 metallopeptidases.

Physiological Function

These enzymes are important to a wide range of physiological processes too numerous to cover completely herein. Carboxypeptidase A (CPD A), was the first zinc protease and second zinc enzyme discovered. The zinc exopeptidases, CPD A and B compliment the action of the serine endoproteases, trypsin, and pepsin, in the degradation of food proteins. The serine proteases cleave proteins internally either at positions of basic amino acids such as Lys or Arg (trypsin) or hydrophobic aromatic amino acids such as Phe or Trp (pepsin). The zinc exopeptidases then liberate the essential amino acids Lys and Phe from the C terminus of the peptides generated by the endoproteases. The combination of structural and functional studies on these metalloproteases have revealed the presence of other members of this family that are important to hormone processing, immune/inflammatory activity and blood-clotting functions. Information on the active sites of CPD A led to the development of specific inhibitors of angiotensin-converting enzyme decades before a crystal structure was known for it, based on the proposition that both enzymes contained a zinc–bound water. Drugs for control of hypertensin were identified by these means. Methionyl aminopeptidases, MetAP, remove the N-terminal methionine residue from newly transcribed polypeptides. The physiological importance of these enzymes is underscored by the lethal nature of the removal of the MetAP gene from a number of bacterial sources. The "Handbook of Proteolytic Enzymes" along with its associated MEROPS website is an excellent source for detailed information on metalloproteases.

Metalloprotease Inhibition

The crucial nature of these enzymes to physiological processes has led to considerable research efforts on

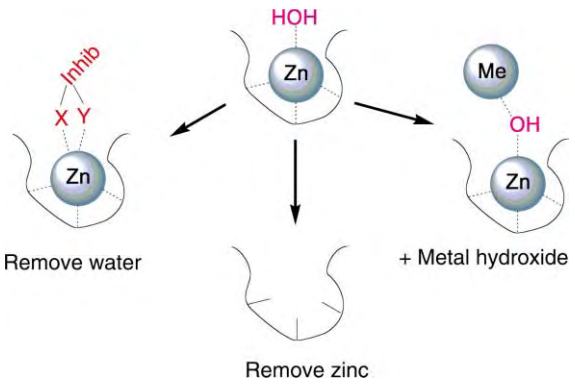

FIGURE 3 Inhibition of zinc proteases is accomplished by either (1) removing the water, (2) removing the metal, or (3) binding a metal hydroxide complex.

discovering natural inhibitors of them that could be involved in their regulation. The MEROPS website contains a good compilation of such inhibitors. The importance of the metal and its bound water are the key to inhibiting the metalloproteases (Figure 3). Inhibition can be accomplished by one of the three ways – (1) displace the water by an inhibitor binding to the metal, (2) remove the metal, or (3) bind a metal hydroxide complex to the catalytic metal and an active site residue.

Displacement of the Metal-Bound Water

The importance of zinc proteases in both normal and pathological processes makes them targets for drug design. The fact that zinc can readily form four-, five-, and six-coordinate complexes has led to the design of a number of synthetic inhibitors that act by displacing the metal–bound water. These studies have shown that the strength of the chelator–metal interaction increases the potency of the agent as a drug. The inhibitors are designed to have both structural specificity for the active site and a "war head" that will bind to the catalytic metal. Specificity is incorporated on either side of the metal-binding ligand. Popular warheads are hydroxamates, thiolates, and phosphoryl groups as chelating ligands. Carboxyalkyl and phosphinic acid groups are used as transition state or tetrahedral intermediate mimics.

Catalytic Chelators

It should also be possible to inhibit zinc proteases by removing the metal. This is often not very specific and many common chelators, such as ethylenediamine tetra-acetic acid (EDTA), are ineffective. However, D-penicillamine, a drug used to treat Wilson's disease and rheumatoid arthritis, has been shown to catalyze the release of zinc from CPD A. In the presence of a second scavenger chelator, such as EDTA or the physiological chelator, thionein (apo-metallothionein), the inhibition is quite potent. From a physiological perspective, such a mechanism of inhibition would be essentially irreversible, given the low levels of free zinc believed to be present in the body.

Inhibition by Metal Hydroxide Complexes

Many zinc proteases are inhibited by adding zinc to the assays. In the case of the exopeptidase, CPD A, and the endoprotease, thermolysin a combination of kinetic and structural studies have shown this inhibition is due to zinc hydroxide binding the ionized carboxylate of an active site glutamate residue which then bridges to the catalytic zinc by displacing its bound water. In the case of CPD A, both zinc and lead inhibit in the form of M(OH)Cl with sub-micromolar-inhibition constants. If multidentate ligands interact with the inhibitory metal and the enzyme-active site, significantly stronger inhibition is anticipated. Inhibition by such metal hydroxide complexes could be important to regulatory and/or toxicological processes of zinc proteases.

See Also the Following Articles

Aminopeptidases • Angiotensin Receptors • Aspartic Proteases • Cysteine Proteases • Cytokines • Proteases in Blood Clotting

Glossary

aminopeptidase Protease catalyzing the cleavage of amino acids from the N terminus of polypeptides.

carboxypeptidase Protease catalyzing the cleavage of amino acids from the C terminus of polypeptides.

dipeptidyl peptidase Protease that removes two amino acids at a time from the N or C terminus of the polypeptide.

endoprotease Protease that acts internally on a polypeptide chain.

protease or proteinase Enzyme catalyzing the hydrolysis of peptide bonds in proteins.

Further Reading

Auld, D. S. (2001a). Zinc coordination sphere in biochemical zinc sites. *BioMetals* **14**, 271–313.

Auld, D. S. (2001b). Zinc sites in metalloenzymes and related proteins. In *Handbook on Metalloproteins* (I. Bertini, A. Sigel and H. Sigel, eds.) pp. 881–959. M. Dekker, New York.

Auld, D. S. (2004). Cocatalytic zinc sites. In *The Handbook of Metalloproteins* (A. Messerschmidt, W. Bode and M. Cygler, eds.) Vol. 3, pp. 416–431, Wiley, Chichester.

Barrett, A. J., and Rawlings, N. D. (2004). MEROPS the peptidase database (http://merops.sanger.ac.uk/index.htm).

Barrett, A. J., Rawlings, N. D., and Woessner, J. F. (eds.) (2004). Metallopeptidases. In *Handbook of Proteolytic Enzymes*. 2nd edition, pp. 268–288, Academic Press, London.

Lowther, W. T., and Matthews, B. W. (2000). Structure and function of the methionine aminopeptidases. *Biochim. Biophys. Acta* **1477**, 157–167.

Vendrell, J., Querol, E., and Aviles, F. X. (2000). Metallocarboxypeptidases and their protein inhibitors – Structure, function and biomedical properties. *Biochim. Biophys. Acta* **1477**, 284–298.

Woessner, J. F., and Nagase, H. (2000). *Matrix Metalloprotinases and TIMPS*. Oxford University Press, Oxford.

Biography

David S. Auld is an Emeritus Associate Professor in the Department of Pathology and Research Associate Professor in the Department of Biology at Boston College in Chestnut Hill, Massachusetts. His principal research interests are in the biochemistry of zinc and the mechanism of action of metalloproteases. He holds a Ph.D. from Cornell University.

Metalloproteinases, Matrix

Hideaki Nagase
Imperial College, London, UK

Gillian Murphy
University of Cambridge, Cambridge, UK

Matrix metalloproteinases (MMPs), also called matrixins, are a group of structurally related proteolytic enzymes containing a zinc ion in the active site. They are secreted from cells or bound to the plasma membrane and hydrolyze extracellular matrix (ECM) and cell surface molecules. The first MMP to be identified was collagenase in the tadpole tail undergoing metamorphosis, exemplifying the importance of ECM-degrading proteinases in tissue remodeling. Numerous lines of evidence have now shown that they play key roles in embryonic development, organ morphogenesis, ovulation, embryo implantation, nerve growth, bone remodeling, wound healing, angiogenesis, and apoptosis. Under such physiological conditions MMP activities are regulated in accordance with matrix synthesis at the level of transcription, activation of the precursor zymogens, interaction with ECM and cell surface molecules, and inhibition by endogenous inhibitors. Many cell types have the ability to synthesize MMPs but their production is tightly controlled by growth factors, cytokines, physical stress to the cell, oncogenic transformation, hormones, cell–cell and cell–ECM interactions. Aberrant activities of MMPs are often associated with the progression of diseases such as cancer, arthritis, cardiovascular disease, nephritis, neuro-degenerative diseases, periodontal disease, skin ulceration, gastric ulcer, corneal ulceration, liver fibrosis, emphysema, fibrotic lung, and many others.

MMP Family

MMPs are found in vertebrates, fruit flies (*Drosophila melanogaster*), nematodes (*Caenorhabditis elegans*), sea urchins (*Paracentrotus lividus*), hydras (*Hydra vulgaris*), and plants (e.g., *Arabidopsis thaliana*, *Glycine max*). The human genome has 24 MMP genes. There are two genes in *Drosophila*, six genes in *C. elegans*, and five genes in *Arabidopsis*. They are classified as the matrixin subfamily of metalloprotease family M10 in the MEROPS database (http://www.merops.co.uk/merops/merops.htm). Vertebrate matrixins are assigned with MMP numbers and trivial names in many cases (Table I). MMP numbers missing in the list (i.e., MMP-4, -5, -6, and -22) were found to be identical to one of the other MMPs. Expression of individual MMPs varies depending on cell types (Figure 1).

Most MMPs consist of a prodomain, a catalytic domain, a hinge (or linker), and a hemopexin domain.

The signatures to assign proteinases to the MMP family are the cysteine switch motif with amino acid sequence PRCGXPD in the propeptide and the zinc-binding motif HEXGHXXGXXH in the catalytic domain, where the three histidines coordinate the zinc ion (Zn^{2+}). The primary structure of the catalytic domain is homologous to collagenase 1 (MMP-1). On the basis of substrate specificity sequence similarity and domain organization, MMPs are divided into six subgroups (Table I, Figure 2).

Collagenases

Collagenase 1 (MMP-1), collagenase 2 (MMP-8), collagenase 3 (MMP-13), and collagenase 4 in *Xenopus* (MMP-18) belong to this subgroup. The characteristic feature of these enzymes is their ability to cleave native fibrilar collagen types I, II, and III into $\frac{3}{4}$ and $\frac{1}{4}$ fragments. Some members of other MMP subgroups also degrade fibrilar collagen (e.g., MMP-2 and MMP-14). Collagenases also digest other ECM and non-ECM proteins (Table I).

Gelatinases

Gelatinase A (MMP-2) and gelatinase B (MMP-9) are in this subgroup. They have three repeats of fibronectin type II motifs attached to the catalytic domain, which distinguishes them from other MMPs. These repeats interact with collagens, gelatins, and laminin. Both MMPs readily digest denatured collagens, i.e., gelatins, and a number of ECM molecules (Table I). MMP-2, but not MMP-9, cleaves collagen I, II, and III into $\frac{3}{4}$ and $\frac{1}{4}$ fragments.

TABLE 1

Substrates of Mammalian MMPs

Enzyme	MMP	Human chromosome	Substrates
Soluble-types			
Collagenases			
Interstitial collagenase (collagenase 1)	MMP-1	11q22–q23	Collagens I, II, III, VII, VIII, X, and XI, gelatin, entactin, tenascin, aggrecan, fibronectin, myelin basic protein, IGFBP-3, α_1PI, IL-1β
Neutrophil collagenase (collagenase 2)	MMP-8	11q21–q22	Collagens I, II, and III, α_1PI, substrate P
Collagenase 3	MMP-13	11q22.3	Collagens I, II, III, IV, IX, X, and XIV, gelatin, collagen telopeptides, fibronectin, aggrecan
Collagenase 4 (*Xenopus*)	MMP-18	–	Collagen I
Gelatinases			
Gelatinase A	MMP-2	16q13	Gelatin, collagens I, II, III, IV, V, VII, and X, fibronectin, laminin, aggrecan, elastin, tenascin, decorin, myelin basic protein, α_1PI, IL-1β, IGFBP-3, MCP-3
Gelatinase B	MMP-9	20q12.2–q13.1	Gelatin, collagens IV, V, XI, XIV, elastin, aggrecan, decorin, laminin, entactin, myelin basic protein, α_1PI, IL-1β
Stromelysins			
Stromelysin 1	MMP-3	11q23	Collagens III, IV, V, IX, X, and XI, telopeptides of collagens I and II, gelatin, aggrecan, fibronectin, laminin, entactin, tenascin, decorin, myelin basic protein, α_1PI, IL-1β, IGFBP-3, activation of proMMP-1, proMMP-3, proMMP-8, proMMP-9
Stromelysin 2	MMP-10	11q22.3–q23	Collagen III, IV, and V, gelatin, fibronectin, elastin, aggrecan, activation of proMMP-1, proMMP-7, proMMP-8, proMMP-9
Stromelysin 3	MMP-11	22q11.2	α_1PI (mouse MMP-11 has weak activities on collagen IV, gelatin, fibronectin, laminin, aggrecan)
Matrilysins			
Matrilysin 1	MMP-7	11q21–q22	Collagen IV, gelatin, aggrecan, elastin, fibronectin, vitronectin, laminin, SPARC, entactin, decorin, myelin basic protein, tenascin, fibulin, α_1PI, proTNFα, activation of proMMP-1, proMMP-2, proMMP-9
Matrilysin 2	MMP-26	11p15	Fibronectin, fibrinogen, vitronectin, gelatin, α_1-PI
Others			
Metalloelastase	MMP-12	11q22.2–q22.3	Elastin, collagen IV, gelatin, fibronectin, vitronectin, laminin, entactin, aggrecan, myelin basic protein, α_1PI, proTNFα
(No name)	MMP-19	12q14	Collagen IV, laminin, entactin, tenascin, fibronectin, gelatin, aggrecan, COMP
Enamelysin	MMP-20	11q22.3	Amerogenin, COMP
(No name)	MMP-21	10	Gelatin, α_1PI
CA-MMP	MMP-23*	1p36.3	Gelatin
(No name)	MMP-27	11q24	–
Epilysin	MMP-28	17q21.1	Casein
Membrane-types			
Transmembrane			
MT1-MMP	MMP-14	14q11–q12	Collagens I, II, and III, gelatin, fibronectin, vitronectin, laminins 1 and 5, entactin, aggrecan, fibrin, α_1PI, decorin, proTNFα, CD44, activation of proMMP-2 and proMMP-13
MT2-MMP	MMP-15	8q21	ProMMP-2, laminin, fibronectin, tenascin, entactin, aggrecan, perlecan, proTNFα
MT3-MMP	MMP-16	15q13q21	ProMMP-2, collagen III, fibronectin
MT5-MMP	MMP-24	20q11.2	ProMMP-2, proteoglycans, gelatin
GPI-anchored			
MT4-MMP	MMP-17	12q24.3	Fibrinogen, fibrin, proTNFα
MT6-MMP	MMP-25	16p13.3	Collagen IV, gelatin, fibrinogen, fibrin, fibronectin

*two identical genes are found head to head arrangement in chromosome 1.

α_1-PI, α_1-proteinase inhibitor; TNFα, tumor necrosis factor α; IGFBP-3, insulin-like growth factor binding protein 3; MCP-3, monocyte chemoattractant protein 3; SPARC, secreted protein acidic and rich in cysteine (also known as osteonectin or BM40); COMP, cartilage oligomeric matrix protein; IL-1, interleukin 1.

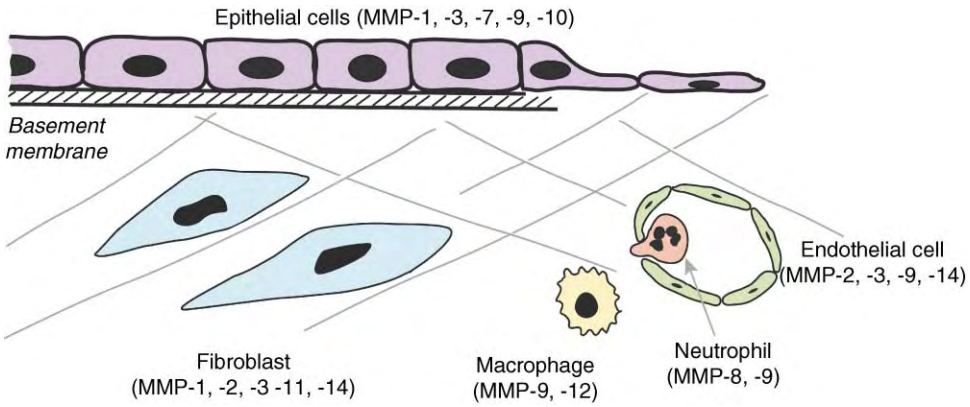

FIGURE 1 Tissue expression of MMPs. Representative MMPs produced by various cell-types are shown. The production of these MMPs is usually transcriptionally controlled by stimulatory factors.

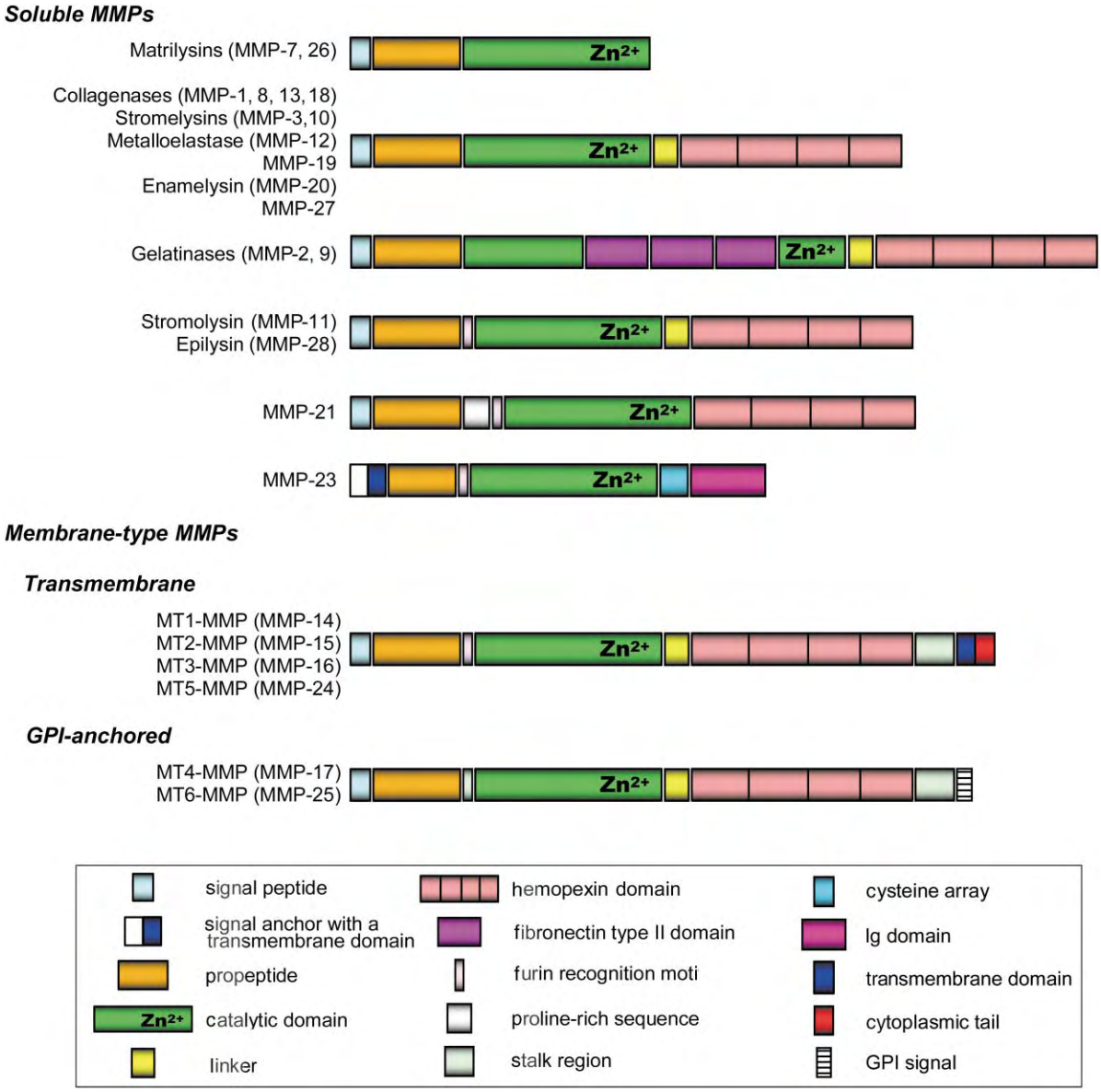

FIGURE 2 Domain arrangements of vertebrate MMPs.

Stromelysins

Stromelysin 1 (MMP-3), stromelysin 2 (MMP-10), and stromelysin 3 (MMP-11) are assigned to this subgroup. While MMP-3 and MMP-10 have similar enzymatic properties including their abilities to cleave various ECM molecules and activate several other MMPs (Table I), MMP-11 has a more divergent amino acid sequence and substrate specificity. Human MMP-11 does not cleave ECM components. Alternative splicing and promoter usage generates an intracellular form of MMP-11.

Matrilysins

Matrilysin 1 (MMP-7) and matrilysin 2 (MMP-26) are assigned to this subgroup. They consist of a pro-domain and the catalytic domain only (Figure 2). MMP-7 is produced in epithelial cells and secreted apically. Besides digesting ECM molecules, it processes pro-α-defensin, Fas ligand, protumor necrosis factor α, and E-cadherin from the cell surface. MMP-26 digests several ECM molecules (Table I).

Membrane-Type MMPs (MT-MMPs)

There are six MT-MMPs in humans. They are numerically assigned from MT1-MMP to MT6-MMP; four are type I transmembrane proteins (MMP-14, MMP-15, -16, and -24) and two are glycosylphosphatidylinositol (GPI)-anchored proteins (MMP-17 and MMP-25). The catalytic domain and the hemopexin domain are exposed on the cell surface. With the exception of MT4-MMP (MMP-17), MT-MMPs activate proMMP-2 as well as digest ECM components. MT1-MMP, MT2-MMP, and MT3-MMP digest fibrilar collagens to varying degrees, and MT1-MMP activates proMMP-13. While MT1-MMP is expressed in many cell-types, MT5-MMP is expressed in brain, mainly in the cerebellum, and MT6-MMP in leukocytes.

Other MMPs

Seven MMPs do not belong to the above subgroups. Metalloelastase (MMP-12) is primarily expressed in macrophages. It digests elastin and other proteins, and it is essential for macrophage migration. MMP-19 is expressed in liver, skin, and mononuclear cells. Enamelysin (MMP-20) is mainly expressed in newly formed tooth enamel. It processes amelogenin, and resulting products are essential for tooth enamel formation. MMP-21 is expressed in various fetal and adult tissues and in several invasive cancer cells. It digests gelatin and α_1-proteinase inhibitor. MMP-23 is mainly expressed in reproductive tissues. Two identical copies of the MMP-23 gene are located in human chromosome 1p36 loci in a head to head arrangement. The enzyme is a type II transmembrane protein with a membrane-anchoring sequence located in the N-terminal end of propeptide. The propeptide is removed by a proprotein converting proteinase and therefore it is secreted from the cell as an active enzyme. The enzyme lacks both the cysteine switch motif in the propeptide domain and a hemopexin domain. The latter is replaced by a cysteine array and an immunoglobulin domain. MMP-27 is an orthologue of chicken MMP (originally assigned as MMP-22). The enzymatic properties of MMP-27 have not been characterized. Epilysin (MMP-28) is expressed in keratinocytes, and its expression increases during wound healing.

Structural Chemistry

The propeptide domain plays a key role in maintaining the MMPs in their zymogen forms (proMMPs) by blocking the active site. It has ~80 amino acids and consists of three α-helices and extended peptides including the cysteine switch motif (Figure 3A). The residues in the cysteine switch interact with the substrate-binding cleft in the catalytic domain by forming β-structure-like hydrogen bonds in a manner similar to a substrate, but in the opposite direction. The cysteine residue coordinates with the catalytic Zn^{2+} to maintain the latency of the enzyme.

The catalytic domain has ~170 amino acids including the zinc-binding motif (HEXGHXXGXXH) and a conserved methionine that forms a unique "Met-turn" structure. The domain consists of three α-helices, a five-stranded β sheet, and bridging loops (Figure 3B). It contains two zinc ions (Zn^{2+}); one is essential for catalysis, and the other together with three calcium ions stabilizes the structure. The overall polypeptide folds, including the Met-turn, are similar to those of astacins, reprolysins, ADAMs, and bacterial proteinase serralysins, which together constitute the metzincins.

The hemopexin domain consists of ~190 amino acids and forms a four-bladed β-propeller structure arranged almost symmetrically around a central axis, and each blade is comprised of a four-stranded anti-parallel β sheet (Figure 3A). The domain is stabilized by a calcium ion and a disulfide bond between blades I and IV.

The catalytic domain and the hemopexin domain are connected by a "hinge" (also called "linker") region of variable length, which does not have a specific structure.

The fibronectin type II motif found in MMP-2 and MMP-9 consists of two double-stranded anti-parallel β-sheets and two large loops (Figure 3A). Each β-sheet has one disulfide bond.

Several MMPs are glycoproteins. In particular, proMMP-8, proMMP-9, and proMMP-23 are highly glycosylated, with ~20–45% of their molecular mass being carbohydrate.

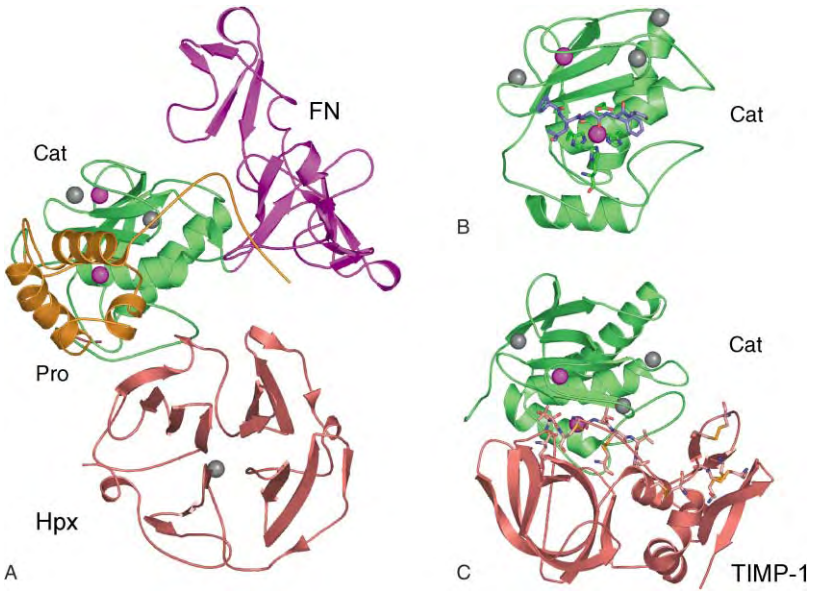

FIGURE 3 Three-dimensional structure of MMPs and TIMPs. (A) Ribbon diagram of proMMP-2. The propeptide (pro) is shown in orange; the catalytic (cat) domain in green; the fibronectin (FN) domain in pink; and the hemopexin (Hpx) domain in red. Zinc ions and calcium ions are in pink and grey, respectively. (B) The catalytic domain of MMP-1 with a peptide substrate (stick representation) bound to the active site. (C) The complex of TIMP-1 and the catalytic domain of MMP-3.

Mechanism of Peptide Bond Hydrolysis

The active site of MMPs consists of the catalytic Zn^{2+} bound to three imidazoles of histidines in the HEXGH XXGXXH motif and the glutamate in the motif. A proposed mechanism of peptide bond hydrolysis by MMPs is shown in Figure 4. In an active MMP, one water molecule is bound to the catalytic Zn^{2+}. Upon binding of a peptide substrate to the active site of the enzyme, the carbonyl group of the P1 residue interacts with the catalytic Zn^{2+} and the water molecule is displaced towards the carboxyl group of the glutamate. This polarizes the water molecule and promotes its nucleophilic attack on the carbonyl carbon of the scissile bond, resulting in formation of a hemiketal intermediate and the subsequent hydrolysis of the peptide bond. The glutamate functions as a general acid/base during catalysis. Mutation of the glutamate to aspartate reduces the enzymatic activity to less than 1% and mutation to alanine reduces activity to 0.01% of the wild-type.

Activation of proMMPs

MMPs are synthesized as pre-pro-MMPs and many are secreted from cells as zymogens (proMMPs) which need to be activated outside the cell. The major activation pathways are proteolytic processes.

Activation by Proteinases

The six MT-MMPs and MMP-11, -21, -23, and -28 contain a furin-like proprotein converting proteinase recognition sequence at the C-terminal end of the propeptide-domain. Most of them are therefore activated within the cell and secreted or bound to the membrane as the active form.

Other MMPs are secreted from cells as proMMPs in the tissue, proMMPs are likely to be activated by tissue or plasma proteinases or opportunistic bacterial proteinases. Figure 5 illustrates activation pathways that are involved in pericellular ECM hydrolysis. The urokinase-type plasminogen activator/plasmin system initiates the activation of many proMMPs near the cell surface. Unlike many other MMPs, proMMP-2 is not readily activated by plasmin or other proteinases, but activated on the cell surface by MT1-MMPs. This activation process is assisted by binding to a TIMP-2-MT1-MMP complex which presents proMMP-2 to an adjacent active MT1-MMP. ProMMP-13 is also activated by MT1-MMP, but this does not require TIMP-2 (Figure 5).

Activation by Chemical and Physical Means

One biochemical property unique to matrixins is that proMMPs can be activated *in vitro* by SH-reactive agents (e.g., 4-aminophenylmercuric acetate, iodoacetamide, oxidized glutathione), chaotropic agents

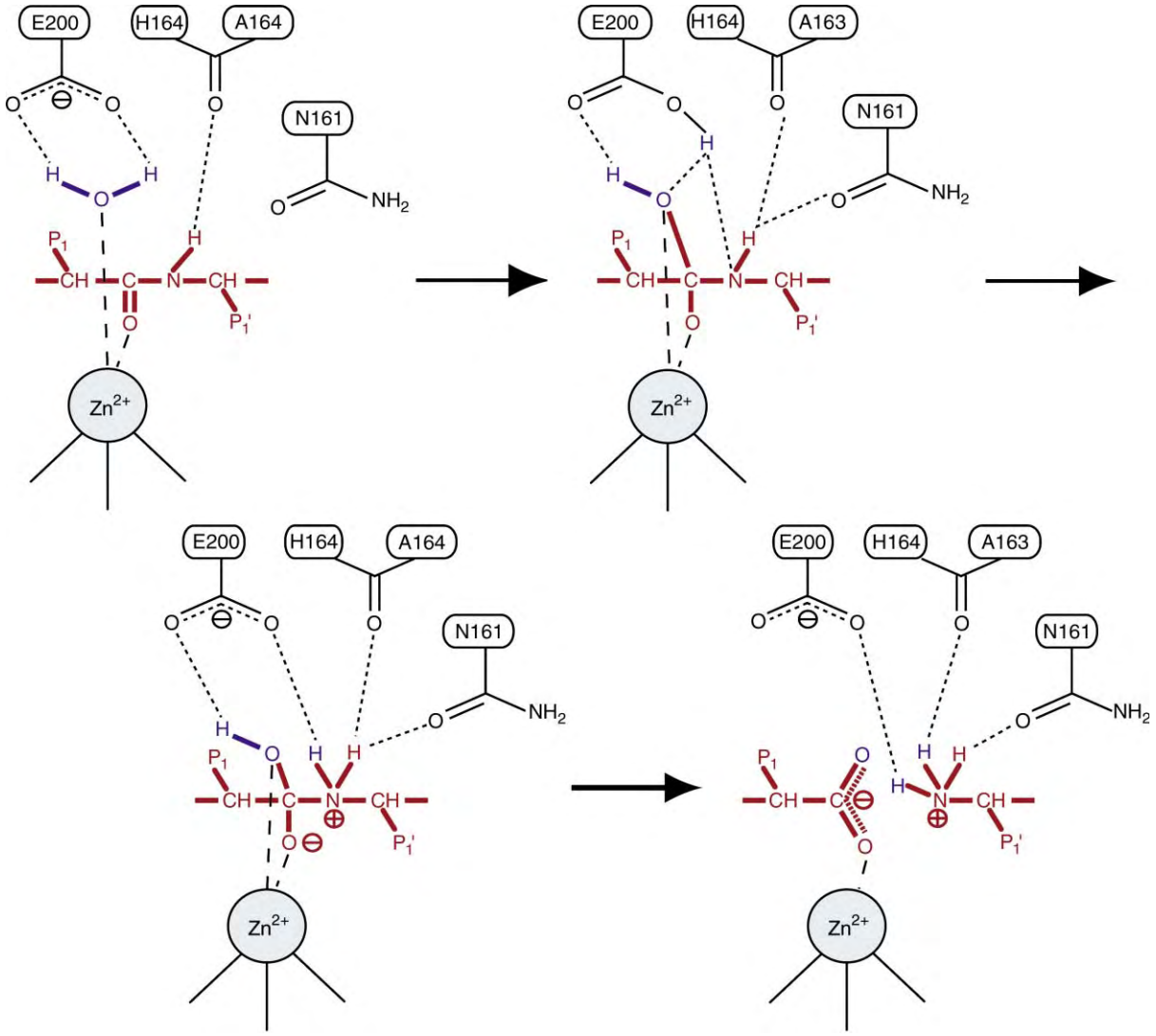

FIGURE 4 A proposed mechanism of action of MMPs. A peptide substrate and a water molecule that are involved in hydrolysis are shown red and blue, respectively. The residues shown are in MMP-1. See text for details.

(e.g., urea, SCN^-, I^-), sodium dodecylsulfate, reactive oxygen, low pH and heat treatment. This is due in part to the disruption of the cysteine–zinc interaction formed between the propeptide and catalytic domains and subsequent removal of the propeptide by autoproteolysis. Oxidation may activate some proMMPs, but it may also destroy the enzyme.

Activity and Substrate Specificity

MMPs exhibit optimal proteolytic activities at around pH 7.0–8.0 for most substrates but in some cases they exhibit a broader pH range. An exception is human stromelysin 1 which has optimal activity at around pH 5.5–6.0 with a shoulder of activity at pH 7.5–8.0.

MMPs degrade ECM and non-ECM proteins (see Table I for representative substrates). The potential substrates of more recently discovered MMPs (higher numbers) have not been well characterized. In general the substrate needs to be six amino acids or longer, and the enzymes have a strong preference for hydrophobic residues at the P1′ site (the residue located on the right of the cleaved peptide bond) such as Leu, Ile, Met, Phe or Tyr, but the amino acid at the P1 site (the residue on the left of the cleaved peptide bond) is not important. Non-catalytic domains greatly influence substrate specificity for some MMPs when substrates are extracellular macromolecules; e.g., fibronectin domain repeats of MMP-2 and MMP-9 play an important role in expressing the activity on type IV collagen, gelatin, and elastin; and the hemopexin domain of collagenases is essential for the collagenolytic activity.

MMPs are inhibited by chelating agents such as EDTA, 1,10-phenanthroline, cysteine, and dithiothreitol. Based on substrate specificity, numerous synthetic inhibitors of MMPs, many aimed at therapeutic

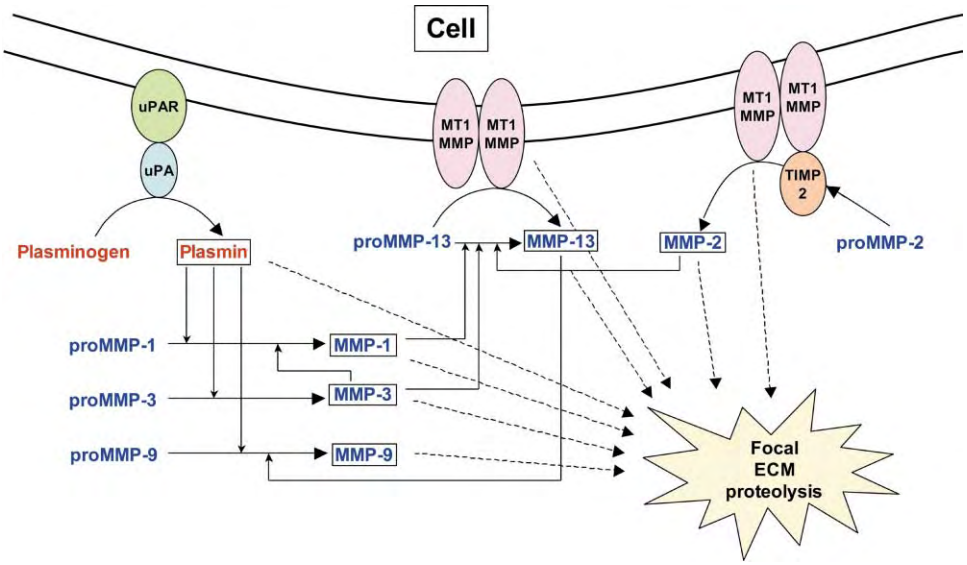

FIGURE 5 Activation pathways of proMMPs involved in pericellular ECM proteolysis. Urokinase-like plasminogen activator (uPA) bound to uPA receptor (uPAR) activates plasminogen to plasmin, which in turn activates a number of proMMPs. MT1-MMP activates proMMP-2; this process is assisted by binding to the TIMP-2-MT1-MMP complex which presents proMMP-2 to an adjacent active MT1-MMP. Activation of proMMP-13 by MT1-MMP does not require TIMP-2. Activated MMPs also participate in the activation of other proMMPs. Active enzymes are boxed.

purposes, have been designed. They commonly contain a zinc-chelating moiety such as a hydroxamic acid, a carboxyl, a thiol, or a phosphorus group. Some selective inhibitors for specific MMPs have been generated, but many broadly inhibit MMPs and other metalloproteinases. Phosphoramidon is not inhibitory. Tissue inhibitors of metalloproteinases (TIMPs), α2-macroglobulins and ovomacroglobulins (ovostatins) are the known natural protein inhibitors.

Endogenous Inhibitors of MMPs

α2-Macroglobulins

Human α2-macroglobulin is a plasma glycoprotein of 725 kDa consisting of four identical subunits of 180 kDa. It inhibits most endopeptidases by a trap mechanism: the interaction with a proteinase is initiated by the proteolytic cleavage in the middle of the subunits, causing a conformational change in the macroglobulin, hence entrapping the proteinase molecule. The active site of the trapped proteinase is not blocked, but its access to large protein substrates is sterically hindered. Related macroglobulins in other species including ovomacroglobulins (ovostatins) have a similar inhibition mechanism.

TIMPs

TIMPs are structurally related proteins which inhibit matrixins with a 1:1 molar stoichiometry. The human genome has four TIMP genes and there are two genes in *C. elegans* and one in *Drosophila*. The four human isoforms (TIMP-1 to -4) consist of 184–194 amino acids, sub-divided into N-terminal and C-terminal domains, each having three disulfide bonds. The N-terminal domain is the inhibitory domain and it binds to the active site of the MMPs. ProMMP-2 and proMMP-9 zymogens of MMPs bind to TIMPs via interaction between the C-terminal non-inhibitory domain of TIMP and the C-terminal hemopexin domain of proMMP. These complexes act as MMP inhibitors since the N-terminal inhibitory domain of TIMPs is not blocked. TIMP-3 is unique among four TIMPs as it also inhibits ADAMs and ADAMTSs, metalloproteinases containing a disintegrin domain.

Inhibition Mechanism

The inhibitory domain of TIMPs has an OB-fold structure with a reactive ridge formed by the N-terminal segment Cys^{1}-Thr-Cys-Val^{4} and the Ser^{68}-Val-Cys^{70} (residues are in TIMP-1) where Cys^{1} and Cys^{70} are disulfide linked. This ridge structure slots into the active site cleft of the MMPs (Figure 3C). The nitrogen of the N-terminal NH_2-group and the carbonyl oxygen of Cys^{1} bidentately chelate the Zn^{2+} in the active site of the enzyme. MMPs do not form covalent bonds with TIMPs nor cleave TIMPs, but form tight complexes with inhibition constants in the subnanolar range.

Other Biological Activities of TIMPs

TIMP-1 and TIMP-2 have erythroid potentiating and cell growth promoting activities. TIMP-3 binds to

vascular endothelial growth factor (VEGF) receptor-2 and blocks angiogenesis induced by VEGF.

These biological activities are independent of their MMP-inhibitory activity. TIMP-3 induces apoptosis of several cancer cells and vascular smooth muscle cells possibly by blocking the proteolytic release of cell death receptors such as tumor necrosis factor α receptor, Fas, TNF-related apoptosis-inducing ligand receptor 1. TIMP-1 and TIMP-2 exhibit anti-apoptotic activity in some *in vitro* cell studies.

Biological Activities of MMPs

The main function of MMPs is considered to be removal of ECM macromolecules from the tissues, but they also alter the function of ECM molecules by specific proteolysis and express new biological functions of these molecules. MMPs can also release growth factors bound to ECM and from carrier proteins, or inactivate inflammatory cytokines and chemokines, which then influence cellular behavior. For example, the cleavage of type I collagen is associated with keratinocyte migration during wound healing, activation of osteoclasts during bone remodelling and induction of apoptosis of amnion epithelial cells before the onset of labor. Cleavage of laminin 5 and CD44 by MMPs promotes cell migration. The expression of MT1-MMP and activation of proMMP-2 occur in invasive tumour cells and endothelial cells at the migratory front and promotes cells to migrate and invade by cleaving and shedding these ECM and cell surface molecules. The release of transforming growth factor β and VEGF from the matrix by MMPs modulates ECM synthesis and angiogenesis, respectively, which are key events in development, morphogenesis, reproduction, tissue remodeling and repair. Inactivation of monocyte chemoattractant proteins or interleukin 1β by MMP reduces inflammation.

Human Genetic Disorders and DNA Polymorphisms

Unregulated MMP activities are implicated in the progression of a variety of diseases characterized by aberrant breakdown of ECM molecules. In many cases their activities are controlled at the cellular level by various stimulatory factors. In addition, a few inherited human disorders associated with the MMP and TIMP genes have been described.

Mutations in human MMP-2 resulting in the absence of active MMP-2 are linked to a rare autosomal recessive genetic disorder, multicentric osteolysis, which causes destruction of the affected bones and joints. A mutation in the coding region for MMP-13 is associated with spondyloepimetaphyseal dysplasia, a dwarfism resulted from abnormal development of the vertebrae and extremities. Amelogenin imperfecta, a genetic disorder caused by defective enamel formation, is due to mutation at MMP-20 cleavage sites.

Mutations in the coding region of the *TIMP3* gene leading to the presence of an extra Cys in the C-terminal region of the expressed protein cause the rare autosomal dominant Sorsby's fundus dystrophy, a form of blindness characterized by death of the retinal pigment epithelium.

Various DNA polymorphisms in MMP genes are associated with a number of diseases. In many cases polymorphic sites are found in the promoter regions of MMP genes: polymorphisms in the *MMP1* gene are associated with coronary heart disease, rheumatoid arthritis, periodontitis, and cancers (e.g., cervix, ovary, colon, kidney, lung, and skin); in the *MMP2* gene with the risk of developing lung cancer; in the *MMP3* gene with coronary heart disease, coronary aneurysms and cancers (colon and breast); in the *MMP9* gene with coronary heart disease, aneurysms, nephropathy, and preterm prenatal rupture of the fetal membrane; and in the *MMP12* gene with coronary atherosclerosis.

See Also the Following Articles

Collagenases • Collagens

Glossary

ADAM Abbreviation for type I transmembrane proteins with *a* *d*isintegrin *a*nd *m*etalloprotease domain, some of which are involved in shedding of cell surface molecules and have some overlapping properties shared with MMPs. While the primary structures of the metalloprotease domain are homologous to each other, about half of the members of this family do not contain the strictly conserved zinc-ion-binding motif, and so they are probably proteolytically inactive.

ADAMTS Abbreviation for proteins with *a* *d*isintegrin *a*nd *m*etalloprotease domain with type I *t*hrombospondin motifs. The metalloproteinase domains are homologous to ADAMs, but they do not possess a transmembrane domain.

α_2-macroglobulin A glycoprotein in blood of 720 kDa consisting of four identical subunits. It inhibits most endopeptidases regardless of their catalytic mechanism by physical entrapment of the enzyme molecule upon proteolytic attack on the macroglobulin.

extracellular matrix A complex network of secreted extracellular macromolecules (e.g., collagens, proteoglycans, glycoproteins, fibronectin, complex carbohydrates etc.) which provides an organized lattice and helps to hold cells and tissues together in multicellular organisms.

metzincin Metalloproteinases that contain the zinc-ion-binding motif HEXXHXXGXXH and a conserved methionine that forms a unique "Met-turn" structure, e.g., matrix metalloproteinases, astacins, reprolysins, ADAMs, ADAMTSs, pappalysins, serralysins, and leishmanolysin.

MMP Abbreviation for *m*atrix *m*etallo*p*roteinases that are secreted from cells or bound to the cell surface and degrade extracellular matrix molecules.

proteinase Proteolytic enzymes, also known as proteases or endopeptidases, that hydrolyze internal peptide bonds of proteins and polypeptide chains; cf. exopeptidase, enzymes that hydrolyze one or a few amino acids from the N- or C-terminus of polypeptides.

TIMP An acronym for *t*issue *i*nhibitors of *m*etallo*p*roteinases with molecular masses of 22–30 kDa that inhibit MMPs.

Further Reading

Barrett, A. J., Rawlings, N. D., and Woessner, J. F. (2004). *Handbook of Proteolytic Enzymes*, 2nd edition. Academic Press/Elsevier Science, London.

Parks, W. C. (1998). *Matrix Metalloproteinases*. Academic Press, San Diego.

Rawlings, N. D., O'Brien, E. A., and Barrett, A. J. (2002). MEROPS: The protease database. *Nucleic. Acid Res.* **30**, 343–346.

Sternlicht, M. D., and Werb, Z. (2001). How matrix metalloproteinases regulate cell behaviour. *Annu. Rev. Cell Dev. Biol.* **17**, 463–516.

Woessner, J. F. Jr., and Nagase, H. (2000). *Matrix Metalloproteinases and TIMPs*. Oxford Univesity Press, Oxford.

Biography

Hideaki Nagase is the Head of Matrix Biology Department at the Kennedy Institute of Rheumatology Division, Imperial College London, UK. His principal research interest is in the structure and function of matrix metalloproteinases and TIMPs. He holds a Ph.D. from the University of Miami and received his postdoctoral training at Stangeways Research Laboratory, Cambridge, UK and Dartmouth Medical School. He elucidated the inhibition mechanism of TIMPs in collaboration with Professor Wolfram Bode and Professor Keith Brew.

Gillian Murphy is the Chair of Cancer Cell Biology at the Department of Oncology, University of Cambridge, Cambridge, UK. Her principal research interests are in the biochemistry, biology, and pathology of metalloproteinases and their inhibitors. She holds a Ph.D. from the University of Birmingham. She received her postdoctoral training at Max-Planck Institut für Biochemie, Munich, Germany and Strangeways Research Laboratory, Cambridge, UK. She pioneered the elucidation of the activation mechanisms and domain functions of matrix metalloproteinases and their implications in biology and pathology.

Metaphase Chromosome

Sharron Vass and Margarete M. S. Heck
University of Edinburgh, Edinburgh, UK

The metaphase chromosome is a transient entity—one that reflects the moment in mitosis when the DNA in each chromosome is maximally condensed. In higher eukaryotes, the length of DNA may be compacted up to 10 000-fold to ensure that the sister chromatids can be separated far enough from one another to avoid entrapment by the ingressing cleavage furrow late in mitosis. This metaphase chromosome has formed only after essential checkpoints early in the cell cycle have been properly navigated, so that the genome is replicated completely and at the right time and any damage fully and accurately repaired. In addition, the metaphase chromosome contains elaborate kinetochore structures, which can "read" whether each centromere of a sister chromatid pair is attached via microtubules to opposing spindle poles. Finally, the chromosome serves a crucial function in regulating precisely where the cleavage furrow will form during cytokinesis. Such strict control over genome packaging and partitioning is clearly essential for the maintenance of a normal diploid state, and the avoidance of aneuploidy through chromosome gain, loss, or fragmentation.

Background

The majority of cells within an organism will ultimately face one of three potential fates: to divide, to differentiate, or to die. In order to divide successfully, the cell must possess the ability first to replicate, then to package, and finally to partition its entire genome to two new daughter cells. The genomic DNA must be accurately replicated in S phase to form an exact copy of itself, thus resulting in two identical single chromatids, both of which must be held in close proximity to one another to permit DNA repair. The process of cell division requires the DNA to be condensed into ordered, yet highly dynamic structures. This appears to happen as a two-stage process, with most condensation resulting in distinct chromosomes occurring even before nuclear envelope breakdown. The condensed chromosomes are only resolved into two discernible chromatids late in prophase. Following bipolar attachment to the mitotic spindle in metaphase, sister chromatids are separated from each other and actively moved to the two spindle poles in anaphase. It is absolutely critical that chromosomes are accurately condensed and resolved prior to the metaphase to anaphase transition. Inadequate resolution could result in chromatid bridging in anaphase. If chromosomes are not condensed enough, they may be caught and cleaved by the ingressing cleavage furrow. Likewise, it is essential that chromatid separation occurs at the right time, otherwise aneuploidy could result from the unequal partitioning of chromatids to the two daughter cells. Finally, the chromosomes must be decondensed to the right degree to facilitate transcription and replication in a subsequent cell cycle. The consequences of failures in any of these processes would indeed be dire for the life of cells.

Brief Historical Perspective

The choreography of mitosis is without question esthetic, and has captivated the attention of cell biologists for over a century. Flemming originally described cell division in his book of 1882, coining the word "mitosis" (from Greek for thread) to emphasize the central role played by the thread-like chromosomes in the process. In his drawings of dividing salamander cells, he even diagrammed the longitudinal splitting of chromosomes into separate chromatids, thus taking the nuclear events of mitosis to a level higher than mere pinching in half. The affinity of nucleohistone for assorted bright-field stains ensured that mitosis was accessible to analysis, in a range of organisms, even in the absence of sophisticated microscopy, biochemistry, or molecular biology. What has become apparent with the current level of scrutiny possible is the extensive degree to which the molecular players are conserved. Thus, our understanding of chromosome structure has advanced through the use of diverse experimental approaches that may each enjoy distinct cytological, biochemical, or genetic advantages.

The Physical Chromosome

All organisms, prokaryotic or eukaryotic, single-celled or metazoan, must compact their genomes. There is simply too much DNA, and it has too high a negative charge to be squeezed into any sort of compartment without the aid of particular proteins. Even bacterial genomic DNA will

be on the order of 150 μm in length – while the cell itself may be less than 1 μm in size! It is exciting, and particularly humbling, that even in an age when newly completed genome sequences appear at an astounding pace, we do not understand all there is to know about making that DNA sequence work to produce anything from a simple bacterium to a thinking, feeling human being. Exactly how the cell manages to organize its genetic material has been the focus of much research and remains curiously enigmatic.

Interphase

The degree of structural engineering required to accomplish the packaging of the genome is quite staggering when one considers that the naked DNA of a typical diploid human cell, if stretched end-to-end, would measure ~2 m in length. This length of DNA 2 nm in diameter is packaged into a cell's nucleus typically measuring only 5–10 μm in diameter. What has so far been clearly demonstrated is that the naked DNA molecule wraps twice around a core octamer of positively charged histone subunits (two proteins each of H2A, H2B, H3, and H4) to form a disk-shaped structure called the nucleosome. Under nonphysiological low salt conditions, the nucleosomal fiber takes on a "beads-on-string" appearance when viewed by electron microscopy. This initial level of organization gives rise to a sixfold compacted DNA strand ~10 nm thick. The linker histone protein (H1, or variants) facilitates organization of the fiber into a shorter, thicker fiber of 30 nm—a 40-fold level of DNA compaction. One of the most debated issues relates to the path of the 10 nm nucleosomal fiber in the 30 nm fiber: is it a relatively ordered helical solenoid, a twisted helical ribbon, or even a random zig-zag aggregation of nucleosomes? The fragility of the chromatin fiber upon isolation from cells has so far precluded detailed resolution of its structure.

The 30 nm fibers are organized into large (10–100 kb) loops by intermittent anchoring, at spots that may or may not be determined by DNA sequence. This basic level of compaction appears to be similar in both interphase and mitotic chromatin. It is also fairly well accepted that chromosomes occupy distinct domains or territories within interphase nuclei, in contrast to a bowl of intertwined spaghetti strands! These domains reflect gene density, transcriptional activity, and/or replication timing. In general, the more transcriptionally silent chromosomes are later replicating and localized closer to the nuclear envelope.

Mitosis

The compaction of DNA described above cannot account for the final condensation observed in metaphase chromosomes of eukaryotic cells. The level of packaging required to produce a metaphase chromosome is nearly 10 000-fold (~250 times greater than in interphase)! Why should such an extreme level of compaction be required? As a generic human cell may be only 20–30 μm in diameter, a chromosome clearly has to be less than half that size in order to have cleared the midzone of the cell before the cleavage furrow ingresses during cytokinesis. Indeed, human metaphase chromosomes range in size from 2 to 10 μm. Any less compaction could result in chromosome cleavage and likely death. Strikingly, if cells are arrested in mitosis, chromosomes continue to condense even further—demonstrating that the genome is not usually condensed as much as it could be.

It is by no means completely accepted how the 30 nm fiber is organized in the metaphase chromosome. While it has also been demonstrated that histones H1 and H3 become hyperphosphorylated during mitosis, a causal role for this in chromosome condensation remains unestablished. Therefore, although numerous factors and processes contributing to the formation of mitotic chromosomes have been identified, many intriguing and unanswered questions remain.

How Is the Metaphase Chromosome Structured?

Teasing Apart Mitotic Chromosomes

The purpose of mitotic chromosome condensation is clearly to create a robust package that can survive the rigorous forces of mitosis to maintain the genomic DNA in an intact state. This extensive compaction is precisely what has hindered the elucidation of mechanisms or components essential for generating condensed chromosomes. Electron microscopy, while invaluable for the study of subcellular architecture, allowed disappointingly little insight into the architecture of intact mitotic chromosomes. Early micrographs by DuPraw in the 1960s showed extremely dense structures, from which one could occasionally glimpse loops of chromatin at the periphery—but no information about underlying organization.

Just as the folding of the 10 nm fiber within the 30 nm fiber has been controversial, so has the precise organization of the 30 nm fiber within the metaphase chromosome. Clearly, more extreme approaches were needed, as intact, unperturbed chromosomes were unlikely to give up their secrets. Models for the organization of chromatin in metaphase ranged from random folding of the 30 nm fiber to successive hierarchies of helical coiling, to a model whereby specific nonhistone proteins tethered particular DNA sequences to form chromatin loops.

A radical, though incredibly insightful, approach pioneered by Laemmli and colleagues depended on

techniques they developed in the 1970s for the isolation of highly purified mitotic chromosomes from synchronized mitotic cells. As histones comprise a third of the metaphase chromosome by mass (as does the DNA), removal of these proteins should provide a significant enrichment for the nonhistone proteins that comprise the final third of the chromosome. When Laemmli and co-workers extracted histones (and the majority of nonhistone proteins) from metaphase chromosomes by high salt or negatively charged polyanions, they observed something truly remarkable. Electron micrographs of the residual structures clearly showed clouds of naked DNA looping out from a proteinaceous "scaffold"-like structure that resembled the size and shape of the native chromosome. When examined more closely, there appeared to be very few loose DNA ends, instead these large loops of DNA appeared to emanate from and return to the same region of the "scaffold."

These stunning images led to the "radial loop model," or "scaffold hypothesis," to explain mitotic chromosome architecture. Large loops of chromatin were proposed to attach to a nonhistone proteinaceous scaffold, thus providing a framework for the final levels of chromosome condensation. Further evidence to support this hypothesis resulted from the discovery of scaffold attachment regions (SARs) or matrix attachment regions (MARs) that contain specific DNA sequences displaying a high affinity for the scaffold and thereby thought to facilitate the tethering of chromatin loops. Perhaps even more striking was the discovery that the composition of the residual "scaffold" fraction was not only surprisingly simple, but also remarkably reproducible independent of the protocol used to obtain it. Nevertheless, this model for chromosome architecture was controversial, with skeptics distrustful of the harsh biochemical procedures utilized to obtain "scaffolds."

DNA Topoisomerase II in Chromosome Architecture

SDS-PAGE analysis revealed that purified scaffolds were composed of two prominent bands at 170 and 135 kDa (named Sc1 and Sc2, respectively) and a number of minor proteins. Through immunocytochemical approaches, Sc1 was identified in the 1980s as DNA topoisomerase II, a homodimeric enzyme capable of making a double-stranded break in the DNA, and passing a strand through this break before religating the cleaved strand of DNA. Such an enzyme would clearly be necessary to decatenate duplicated and entwined DNA strands, such as would arise following replication of genomic DNA loops. A logical place to position a protein capable of decatenation would be at the base of chromatin loops, precisely where it appeared to be found in both chicken and human cells. Gratifyingly, at a similar time, genetic analyses of yeast topoisomerase II mutations showed that cells died in the absence of this protein, specifically during mitosis as cells tried unsuccessfully to segregate their entangled chromosomes. Immunocytochemical and genetic avenues had converged to reach the same critical conclusion about this crucial enzyme.

DNA topoisomerase II has long been a chemotherapeutic target in the fight against cancer. Understanding its role in chromosome architecture in dividing cells helps to make sense as to why it may be an effective target, and furthermore, suggests that other proteins with similar critical roles in chromosome structure and behavior may also be possible chemotherapeutic targets in the future.

Identification of Other Proteins Playing Roles in Chromosome Dynamics

Another powerful system that began to be exploited in the 1980s was the use of concentrated cytosolic extracts prepared from *Xenopus laevis* eggs. Depending on the manipulation of the collected eggs, "interphasic" or "mitotic" extracts could be generated and then utilized to study DNA replication, cell cycle enzymatic machinery, spindle assembly, and also, chromosome condensation. The incredible stockpiling of components essential for the first rapid cleavage divisions of embryogenesis meant that exogenous DNA (e.g., plasmid, phage, demembranated *Xenopus* sperm, or human nuclei) added to such extracts could be remodeled into mitotic chromosome-like structures—with the subsequent identification of newly associated proteins.

Using this approach, a "condensin" complex was identified by Hirano and colleagues. This was a complex of five proteins: a heterodimer of large 115–165 kDa proteins associated with three additional, putative regulatory subunits. The heterodimeric proteins appeared to each contain five structural domains: an N-terminal globular domain with a Walker-A (NTP binding) motif, a C-terminal globular domain with a Walker-B (NTP-hydrolysis) motif, and two long (200–450 amino acids) internal coiled coils separated by a globular "hinge" region. This complex was associated with assembled chromosomes and was also shown to be essential for chromosome condensation *in vitro*. Similar complexes have since been identified biochemically in human and *Drosophila* cells.

A second serendipitous convergence of results arose from the comparison of the genes for the heterodimeric proteins in *Xenopus* condensin with genes identified from screens in yeast for proteins essential for the stability of mini chromosomes by Koshland and colleagues. The yeast *SMC1* gene bore a striking resemblance in organization to the heterodimeric proteins mentioned above. Based on this, SMC was

redefined as "structural maintenance of chromosomes." It is now apparent that all eukaryotes, from microsporidia to man, contained such genes that could be phylogenetically grouped into six subfamilies. Biochemically, these subfamilies of SMC proteins comprise at least three different heterodimeric complexes (along with non-SMC subunits), involved in sister chromatid cohesion (SMCs1/3), chromosome condensation (SMCs2/4), dosage compensation, and DNA repair (SMCs5/6). It should come as no surprise that the vertebrate Sc2 protein was identified as none other than SMC2 of the condensin complex.

While biochemical analysis using *Xenopus* extracts demonstrated that the condensin complex was required for chromosome condensation *in vitro*, paradoxically, the same did not appear to be true *in vivo*. Genetic mutation or dsRNA-mediated depletion in *Drosophila* cultured cells of SMC and non-SMC condensin subunits showed that chromosomes could indeed condense—but exhibited extreme difficulties in chromosome segregation in anaphase, apparently because resolution into individual chromatids was impaired. A similar defect was observed when the Sc2/SMC2 protein was lost from cultured chicken cells. Informatively, in this case, the clearly condensed mitotic chromosomes were missing a large number of additional "scaffold" components, implicating condensin in the proper assembly and structural integrity of mitotic chromosomes. These results clearly emphasized the need to examine and compare many different experimental systems with their own strengths and weaknesses.

Future prospects in this field are extremely exciting, as there now appear to be two distinct condensin complexes (I and II)—sharing SMCs2/4, but possessing different sets of non-SMC subunits. It has long been known that embryonic chromosomes are often longer and more flexible than those found in later somatic cells. Varying the ratio of condensin I to condensin II at different times of development may be one way to alter higher-order chromosome architecture.

How Is the Metaphase Chromosome Held Together?

Clearly the replicated sister chromatids must be held together until the metaphase to anaphase transition when they can be segregated to the two spindle poles. Close apposition is essential to allow for repair of any DNA damage using a sister chromatid as template, and to ensure that each new daughter cell gets a full diploid complement of the chromosomes. Cohesion between sister chromatids is established coincident with replication to facilitate appropriate alignment, and this is maintained until sisters are separated. One factor involved is the cohesin complex containing SMCs1/3 and non-SMC subunits.

Intriguing mechanistic differences between lower and higher eukaryotes have been observed. Proteolytic cleavage of a non-SMC cohesin subunit is responsible for the lengthwise separation of sister chromatids in yeast, but the process is more complicated in higher eukaryotes. Enzymatic phosphorylation of the cohesin complex is required to remove the bulk of these proteins from the length of the chromatid arms during condensation—perhaps facilitating resolution of sister chromatids, but the final separation of sisters at the centromere occurs as it does in yeast—with the cleavage of a non-SMC subunit. Clearly, the activity of cohesin and condensin, along with topoisomerase II, must be coordinated in some way as cells enter mitosis. A variant of cohesin is found in meiosis, presumably reflecting the requirement for sister chromatids to stay together through meiosis I, with only homologues separating from one another.

How to Control Chromosome Dynamics During the Cell Cycle: Checkpoints

The appropriate cohesion and condensation of chromosomes is of no use if it does not happen at the right time. The coordination of the chromosomal events of mitosis with the rearrangement of the cytoskeleton is critical if chromosomes are to be partitioned accurately. In order for a cell to achieve this, "checkpoints" must be navigated ensuring that a previous event, upon which a subsequent process is dependent, has occurred with high fidelity. The checkpoints that a cell must pass through include:

1. ensuring that DNA has been fully replicated once and only once in the cell cycle,
2. ensuring that any damage to the DNA has fully and accurately repaired, and
3. ensuring that the two kinetochores of each chromosome are not only attached to microtubule fibers, but that they are connected to opposing poles.

Only when each checkpoint has been satisfied can the cell proceed to the next stage, culminating finally in the precise distribution of genetic material to two new daughter cells. How the structural elements discussed in this article interface with checkpoint machinery is still to be understood.

Reversing the Process: Postsegregation Decondensation

After chromosome segregation and nuclear envelope reformation, the extreme condensation reached during

metaphase must be reversed to facilitate transcription and DNA replication in actively cycling cells. As a corollary, terminally differentiated cells that are not transcriptionally active or cycling (e.g., erythrocytes in certain species) have highly condensed nuclei. How the chromatin is decondensed, and how active this process is, remains unclear. DNA topoisomerase II is proteolytically degraded at the end of mitosis, and the mitosis-specific phosphorylation of histone H3 is removed. Indeed, certain proteins essential for DNA replication, though dispersed during metaphase, are assembled back onto chromosomes during anaphase. While correlated, these events are not necessarily causal to the process of chromosome decondensation. Probably other structural proteins (e.g., subunits of the condensin complex) are also degraded or regulated through differential localization or post-translational modification.

Listening to the Metaphase Chromosome

Hitching a Ride: The Chromosome Passengers

Naïvely, it is easy to think of the metaphase chromosome as an isolated, almost inert entity—likened by Mazia in 1961 to the corpse at a funeral: the reason for the proceedings, but hardly taking an active part in them! We know that there is very little, if any, transcription during mitosis—so in terms of gene expression, the mitotic chromosome is mute. However, with regard to the dynamic structural events occurring during mitosis, the chromosome has a lot to say.

In the 1980s, Earnshaw and colleagues discovered a very interesting class of proteins among polypeptides fractionating with the insoluble chromosome scaffold. The founding member of this class of "chromosome passengers" (INCENP—for inner centromere protein) exhibited a localization all along chromosome arms early during chromosome condensation, and then became restricted to the region between centromeres prior to the separation of sister chromatids. Dramatically the chromosome passengers then transfer to the spindle midzone during anaphase, before finally being discarded in the mitotic trashcan (the midbody) at the end of cell division. There are now at least three other proteins exhibiting this striking localization, two of them (survivin and aurora B kinase) residing in a complex with INCENP. Why should this complex track along chromosome arms to the inner centromere, only to then transfer to the microtubules? The localization presumably reflects the assorted substrates that must be phosphorylated at different times of mitosis (e.g., early—histone H3, late—regulatory light chain of myosin). In addition, localization of the chromosome passengers reflects a demonstrated role in orchestrating cytokinesis. One of the surest ways to place these proteins at the point of the future cleavage furrow is to have them mark the precise site of chromosome segregation—exactly where the cleavage furrow should ingress without entrapping chromosomes during cytokinesis.

Mitotic Chromosome Architecture Is Coordinated with DNA Replication and Repair

The ability to perform a cytological analysis in an organism amenable to genetic analysis allows the examination of mutations that visibly affect the process of chromosome condensation and segregation. Such an analysis is possible in *Drosophila* as the chromosomes are big enough to observe easily by light microscopy in diploid, mitotically active cells at different times of development. While genetic analysis in yeast is highly sophisticated, the cells themselves are extremely small and it is difficult to visualize native chromosome structure. Therefore, work in *Drosophila* has complemented biochemical approaches in *Xenopus*, genetic analyses in yeast, and cytological analysis in higher eukaryotic cultured cells.

Specifically, the identification of *Drosophila* mutations disrupting mitotic chromosome structure has significantly highlighted a cell's need to coordinate the accurate duplication and repair of chromosomes with subsequent mitotic condensation. *A priori*, one might expect that mutations in replication proteins might result solely in an S phase arrest. However, mutations of three subunits of the origin recognition complex result not only in replication defects as expected, but also in unexpectedly irregularly condensed chromosomes during metaphase. The regions that are inadequately condensed have replicated abnormally late, suggesting that the factors or machinery required for condensation may somehow be "templated" during S phase. ORC may act as a landing pad for factors other than those essential for DNA replication. In addition, mutations in RFC4 (replication factor C, subunit 4) result in pulverized or prematurely separated (albeit properly condensed) chromosomes, in addition to anticipated replication defects. These observations make sense when one takes into account that there are at least three different "RFC" complexes. While sharing a core of four small subunits, the large subunit can be exchanged thereby resulting in different complexes essential for DNA replication, DNA repair, and cohesion between sister chromatids. Thus, novel roles have been elucidated for proteins identified initially for their functions in DNA replication and repair.

Concluding Comments and Future Prospects

This article has highlighted the importance of diverse experimental approaches to the identification of proteins and analysis of mitotic chromosome dynamics and behavior. State-of-the-art genomics and proteomics avenues are currently supplementing genetic, cell biological, and biochemical approaches to expand the identification of components essential for the formation and function of the metaphase chromosome. How these proteins may be regulated during the normal development of an organism or during the progression of disease states are provocative questions to be addressed in the next decades.

See Also the Following Articles

Cell Cycle: Control of Entry and Progression Through S Phase • Cell Cycle: DNA Damage Checkpoints • Cell Cycle: Mitotic Checkpoint • Centromeres • Chromatin Remodeling • Chromatin: Physical Organization • Chromosome Organization and Structure, Overview • DNA Topoisomerases: Type II • Mitosis • Nuclear Organization, Chromatin Structure, and Gene Silencing • Telomeres: Maintenance and Replication

Glossary

chromatid Once a chromosome has replicated, it is composed of two identical sister chromatids, which are held together until the metaphase to anaphase transition when each chromatid of a pair is pulled via microtubules to opposing spindle poles.

chromosome A linear, stable fragment of the genome with one centromere and telomeres at each end. The genomic DNA of a eukaryotic organism is divided into a number of individual chromosomes (from one in the jumper ant *Myrmecia pilosula* to more than 600 in the fern *Ophioglossum reticulatum*). In contrast, prokaryotic genomes generally are found in a single piece of DNA.

chromosome passenger Term for the extremely dynamic localization during mitosis of a number of proteins (many of which are found in a common complex). While these proteins localize to chromosome arms early in mitosis, they are then restricted to the region between the centromeres of sister chromatids. At the metaphase to anaphase transition, they leave the chromosome only to associate with the microtubules, presaging formation of the cleavage furrow.

cohesin A complex of two different SMC proteins (of the SMC1 and SMC3 subfamilies) along with non-SMC subunits that appear to have regulatory roles. The function of the complex in chromatid cohesion is differentially regulated in lower (proteolytic cleavage of one non-SMC subunit) and higher eukaryotes (regulation by phosphorylation in addition to cleavage).

condensin A complex of two different SMC proteins (of the SMC2 and SMC4 subfamilies) along with non-SMC subunits that appear to have regulatory roles. The complex has been implicated in chromosome condensation *in vitro*, and in chromosome resolution and structural integrity *in vivo*.

DNA topoisomerase II An ATP-dependent homodimeric enzyme capable of making a double-stranded break in the DNA, and passing a strand through this break before religating the cleaved strand of DNA. Such activity is required for the decatenation or separation of replicated and entwined sister chromatids.

SMC Abbreviation for "structural maintenance of chromosomes." While prokaryotes have a single SMC gene responsible for forming a homodimer, eukaryotes have six subfamilies of these genes. Different combinations of heterodimers are important for sister chromatid cohesion (SMCs1/3), chromosome condensation (SMCs2/4), dosage compensation, and DNA repair (SMCs5/6). These proteins, when dimerized, have ATPase activity by virtue of bringing together N (NTP binding) and C termini (NTP hydrolysis). The intervening part of the molecule contains two extended coiled-coils separated by a globular hinge.

Further Reading

Cobbe, N., and Heck, M. M. S. (2004). The evolution of SMC proteins: Phylogenetic analysis and structural implications. *Mol. Biol. Evol.* **21**, 332–347.

Nasmyth, K. (2001). Disseminating the genome: Joining, resolving, and separating sister chromatids during mitosis and meiosis. *Ann. Rev. Genetics* **35**, 673–745.

Pollard, T. D., and Earnshaw, W. C. (2002). *Cell Biology*. Saunders, Philadelphia.

Sumner, A. T. (2003). *Chromosomes: Organization and Function*. Blackwell Publishing, Oxford.

Swedlow, J. R., and Hirano, T. (2003). The making of the mitotic chromosome: Modern insights into classical questions. *Mol. Cell* **11**, 557–569.

Biography

Margarete Heck is a Wellcome Trust Senior Research Fellow at the University of Edinburgh, Wellcome Trust Centre for Cell Biology, Scotland. She was awarded her Ph.D. from Johns Hopkins University and performed her postdoctoral work at the Carnegie Institute of Washington. Her principal research interests focus on chromosome organization and dynamics, predominantly utilizing *Drosophila* as a model organism. The Heck laboratory has exploited both "forward" and "reverse" genetic technologies to identify gene products that are essential for normal chromosome structure and function in *Drosophila*; intriguing human orthologues are examined further.

Sharron Vass has been working as a Research Associate and Ph.D. student in the Heck laboratory; her research is focused on cohesion of sister chromatids during the cell cycle.

Methyl-CpG-Binding Proteins

David G. Skalnik
Indiana University, Indianapolis, Indiana, USA

The development of multicellular organisms requires the generation of a variety of terminally differentiated cell types from a common set of totipotent stem cells. Integral to this process is the phenomenon of cell memory (e.g., a liver cell gives rise to progeny liver cells upon cell division, rather than kidney or spleen cells). At the molecular level, cell memory derives from distinct patterns of gene expression that are correlated with each type of cell lineage. However, nearly all somatic cells in a multicellular organism contain the same genome. The term epigenetics refers to heritable patterns of gene expression that occur in the absence of altered DNA sequence, and represents the underlying molecular mechanism for cell memory. The CpG dinucleotide represents an important regulatory component of mammalian genomes. The cytosine of this dinucleotide serves as the target of DNA methyltransferases, which catalyze the formation of 5-methylcytosine, a critical epigenetic modification of DNA. Methylated DNA is associated with transcriptionally inactive genes and is generally tightly packaged as heterochromatin, while actively expressed genes are generally hypomethylated and present in a more open euchromatin configuration. Methyl-CpG-binding proteins contribute to both the formation of heterochromatin and the repression of transcription.

Epigenetic Regulation of Gene Expression

The DNA of higher eukaryotes is found tightly associated with proteins *in vivo*. In fact, at least 50% of the mass of a chromosome is contributed by proteins. Although originally thought to provide primarily a packaging function, it is now appreciated that chromatin structure is highly dynamic, and plays a critical function in the epigenetic regulation of gene expression. It is necessary to understand the nature of chromatin structure to appreciate the function of methyl-CpG-binding proteins.

Nucleosomes

The primary level of chromatin structure is the nucleosome, in which a DNA double helix is wrapped twice around a core octamer of eight histone protein molecules (two copies each of histone H2a, H2b, H3, and H4). Nucleosomes are separated by short linkers of DNA, and ~200 base pairs of DNA are present in each nucleosome repeat. Chromatin in this configuration is referred to as a "bead-on-a-string" structure, or euchromatin, and can be transcriptionally active. Additional packaging of nucleosomes into a 30 nm helical array is found in heterochromatin, which is transcriptionally inactive, and is also tightly associated with another species of histone (H1).

Histone Code

Determination of the structure of the nucleosome revealed that the amino terminus of each histone molecule extends away from the octamer core. These histone tails are sites of covalent modification, such as phosphorylation, acetylation, and methylation. At least 30 distinct sites of histone covalent modification have been identified, and many of these are associated specifically with either euchromatin or heterochromatin (Figure 1). The sum of histone modifications found in chromatin is referred to as the histone code, and provides important regulatory information with respect to chromatin structure and ultimately gene expression. For example, acetylated histones are found preferentially in euchromatin. The net acetylation state of a specific region of chromatin is the result of balance between the action of histone acetyltransferases (HATs) and histone deacetylases (HDACs). Similarly, methylated lysine 4 of histone H3 is found in euchromatin, while heterochromatin preferentially contains methylated lysine 9 of histone H3. Lysine residues in histone proteins can be mono-, di-, or trimethylated. Posttranslationally modified histone molecules can also serve as binding sites for proteins implicated in the control of chromatin structure. For example, methylated lysine 9 of histone H3 serves as a binding site for the heterochromatin-associated protein HP1, which recruits a histone methyltransferase to the chromatin. This leads to the methylation of adjacent histone H3-lysine 9 residues, formation of additional HP1-binding sites, and spreading of the heterochromatin configuration.

Histone H2A	Histone H2B	Histone H3	Histone H4
Ser 1, P	Lys 5, Ac	Arg 2, Me	Ser 1, P
Lys 5, Ac	Lys 12, Ac	Lys 4, Me	Arg 3, Me
Lys 9, Ac	Lys 15, Ac	Lys 9, Me	Lys 5, Ac
Lys 119, Ub	Lys 20, Ac	Ser 10, P	Lys 8, Ac
	Lys 24, Ac	Lys 14, Ac	Lys 12, Ac
	Lys 123, Ub	Arg 17, Me	Lys 16, Ac
		Lys 18, Ac	Lys 20, Me
		Lys 23, Ac	
		Arg 26, Me	
		Lys 27, Me	
		Ser 28, P	
		Lys, 36, Me	
		Lys 79, Me	

FIGURE 1 Covalent modifications of histones. Thirty covalent modifications that contribute to the histone code are summarized. For each species of histone protein, the amino acid residue, position, and type of modification are presented. Me, mono-, di-, or trimethylation; P, phosphorylation; Ub, ubiquitation; Ac, acetylation.

Cytosine Methylation

Another covalent modification associated with heterochromatin and repression of gene expression is cytosine methylation, which occurs in the DNA double helix in the context of the 5′-CpG-3′ dinucleotide (where p denotes the phosphodiester linkage between the cytosine and guanine nucleotides). In mammalian genomes ~75% of the CpG motifs found are methylated, and these are concentrated in areas of repetitive DNA sequences. This dinucleotide is the target of DNA methyltransferase proteins, which catalyze the addition of a methyl group to the C5 position of the cytosine ring. DNA methyltransferase 1 is the major maintenance methyltransferase. It exhibits high affinity for hemi-methylated DNA (the immediate product of semi-conservative DNA replication), and catalyzes the addition of a methyl group to the CpG cytosines within the newly synthesized DNA strand. DNA methyltransferases 3a and 3b are *de novo* DNA methyltransferases that are responsible for establishing specific patterns of cytosine methylation during gametogenesis and early development. The mechanisms by which appropriate patterns of cytosine methylation are initially established are not well understood.

Functions of Cytosine Methylation

Appropriate patterns of cytosine methylation within DNA are essential for numerous biological processes. This is clearly reflected in the finding that mice lacking DNA methyltransferase gene(s) die prior to or shortly after birth.

Regulation of Gene Expression

As mentioned above, cytosine methylation is associated with heterochromatin and repressed gene expression. Because the majority of 5-methylcytosine is found in repetitive DNA elements, this may provide a defense mechanism against expression of parasitic DNA. Indeed, loss of appropriate cytosine methylation results in the induction of repetitive DNA expression. Maintenance of repetitive elements in heterochromatin configuration may also be important for chromosome stability by preventing homologous recombination between repetitive element sequences.

X-Chromosome Inactivation

X-chromosome inactivation refers to the irreversible inactivation during early embryonic development of one of the X-chromosomes present in each cell of a female. The inactive X-chromosome becomes heavily methylated at CpG motifs and takes on a heterochromatin configuration.

Genomic Imprinting

Distinct patterns of cytosine methylation are established throughout the genome during spermatogenesis and oogenesis, leading to parent-of-origin epigenetic marks that distinguish maternally derived from paternally derived gene alleles. Such genomic imprinting results in a uni-allelic pattern of gene expression. Genomic imprinting is essential for normal development, as zygotes carrying two sets of paternal or two sets of maternal alleles fail to develop normally, even though they carry an appropriate diploid complement of the DNA genome. To date ~50 mammalian genes have been identified that exhibit genomic imprinting.

Cancer

A large number of DNA mutations in oncogenes and tumor suppressor genes have been identified in cancer cells. More recently, it has been recognized that cancer cells also exhibit epigenetic aberrations, including global cytosine hypomethylation, as well as hypermethylation of CpG motifs specifically within the promoters of tumor suppressor genes.

Methyl-CpG-Binding Proteins

The function of methylated CpG motifs is mediated in part by methyl-CpG-binding proteins, which specifically bind to DNA at sites of methyl-CpG and affect transcription rates and local chromatin structure. A small family of proteins share a common DNA-binding domain, the methyl-CpG-binding domain (MBD) (Figure 2).

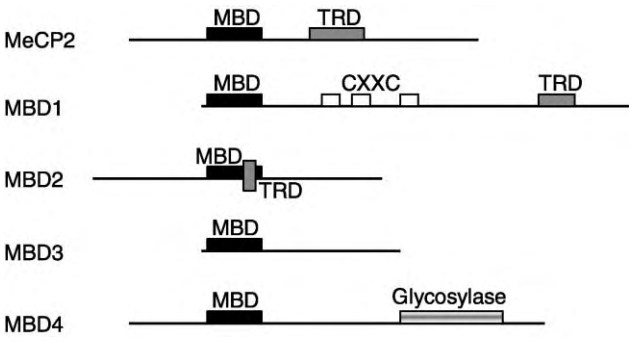

FIGURE 2 Schematic comparison of the MBD family of proteins. The conserved methyl-CpG binding domains (MBD) present in each protein are aligned. TRD, transcriptional repression domain.

MeCP2

MeCP2 is the founding member of the MBD protein family. It localizes to heterochromatin *in vivo*, and represses transcription via a carboxyl terminus transcriptional repression domain (TRD). MeCP2 also contains an amino terminus MBD DNA-binding domain. One mechanism for MeCP2-mediated transcriptional repression appears to be regulation of chromatin structure, as the TRD of MeCP2 interacts with a co-repressor that contains an HDAC. Disruption of the X-chromosome-linked MeCP2 gene in mice leads to premature death, and mutations in the human MeCP2 gene causes Rett syndrome, a progressive neurodegenerative disease found nearly exclusively in girls. The severity of symptoms in Rett syndrome depends on the exact nature of mutation present in the MeCP2 gene (most of which alter the sequence of the MBD or TRD domains), and the mosaic pattern of mutant gene expression resulting from random X-chromosome inactivation.

MBD1

Similar to MeCP2, MBD1 contains an amino terminus MBD DNA-binding domain and a carboxyl terminus TRD, although the TRD exhibits no sequence similarity to the MeCP2 TRD. MBD1 binds methylated DNA targets and represses gene expression. Various isoforms of MBD1 produced by differential RNA splicing additionally contain two or three CXXC domains, a cysteine-rich motif also found in DNA methyltransferase 1, human trithorax (HRX), and CpG-binding protein (CGBP). The CXXC domain constitutes the DNA-binding domain of CGBP, and is responsible for that factor's binding specificity for unmethylated CpG motifs. Similarly, HRX also binds unmethylated-CpG motifs, and the third CXXC domain of MBD1 is responsible for this factor's ability to bind unmethylated target sequences and repress transcription. The significance of the CXXC domain for MBD1 function is unclear, as it is not required for binding to sites of methyl-CpG motifs.

MBD2 AND MBD3

MBD2 and MBD3 are the most structurally related members of the MBD family, sharing 75% similarity over the entire length of MBD3, the shortest member of the family. MBD2 contains an additional 140-amino acid amino terminus extension. Despite this structural similarity, these MBD proteins exhibit quite dissimilar properties. MBD2 binds to methylated DNA and represses transcription via overlapping MBD and TRD domains. MBD2 interacts with HDAC1, and is a component of the methyl-DNA-binding complex MeCP1. The ability of MBD2 to repress transcription is sensitive to inhibitors of HDAC activity, suggesting a mechanism for cross-talk between cytosine methylation and chromatin structure. Surprisingly, mice lacking the MBD2 gene are viable despite lacking the MeCP1 complex. In contrast, MBD3 contains a divergent MBD domain and fails to interact directly with methylated DNA. However, similar to MeCP2, MBD3 is a component of a co-repressor complex. The importance of MBD3 is illustrated by the finding that mice lacking an MBD3 gene fail to develop to birth.

MBD4

MBD4 is an unusual member of the MBD protein family, as it apparently plays no role in transcriptional repression. Rather, it functions as a DNA-repair protein. Cytosine exhibits a propensity to spontaneously deaminate to form uracil (Figure 3). Cells contain DNA-repair enzymes (e.g., -uracil DNA glycosylase) that recognize a uracil base in DNA as a site of damage, and excise this nucleotide to permit replacement with cytosine. This may explain the presence of thymidine in DNA rather than uracil, as it would be more difficult for a cell to recognize a site of cytosine deamination if uracil were a normal nucleotide used for encoding genetic information in DNA. However, deamination of 5-methylcytosine leads to the formation of thymidine. It is this rate of spontaneous deamination that leads to the relative rarity of the CpG dinucleotide in mammalian genomes (only 5–10% of the expected frequency). Conversely, CpG motifs near widely expressed genes are usually unmethylated, and hence avoid this mutagenic pressure. This is hypothesized to explain the clustering of unmethylated CpG motifs in CpG islands near the promoters of ~50% of mammalian genes. The MBD domain of MBD4 binds with highest affinity to methylated CG/TG mismatched sequences, and the protein also contains a glycosylase activity in its carboxyl terminus which is able to remove the

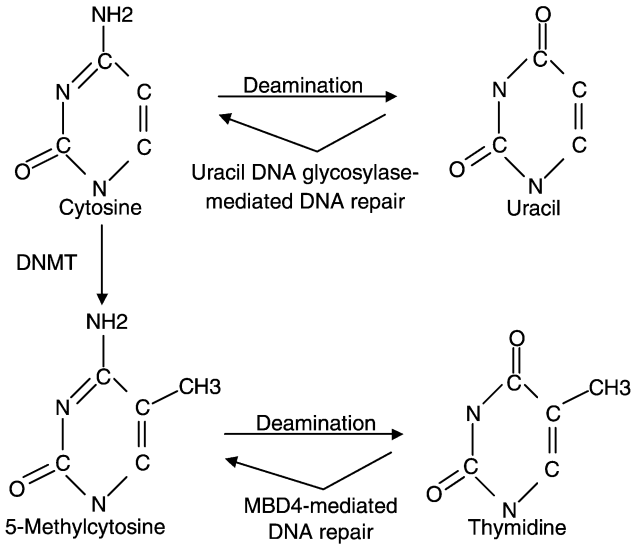

FIGURE 3 Summary of chemical relationships between cytosine, 5-methylcytosine, uracil, and thymidine, including how these species inter-convert *in vivo*. DNMT, DNA methyltransferases.

mismatched thymidine base from DNA to permit replacement with cytosine. The biological significance of this enzymatic activity is illustrated by an elevated rate of mutation at CpG motifs and increased tumorigenesis in mice lacking MBD4.

Cross-Talk between DNA Methylation and Chromatin Structure

The nature of epigenetic modifications associated with transcriptionally active or inactive genomic loci is now well established. Current investigations are focused on the regulation of these modifications. How does a cell choose which regions of DNA to methylate and/or assemble into heterochromatin? Recently, it has become clear that DNA methylation and chromatin structure are highly interdependent epigenetic processes. For example, perturbations of the cellular machinery responsible for nucleosome remodeling or histone modifications also result in aberrations in the pattern of cytosine methylation. Conversely, the association of MBD family members with chromatin-modifying enzymes (e.g., -HDACs) suggests a mechanism whereby cytosine methylation may provide an epigenetic mark that permits targeted recruitment of chromatin-remodeling enzymes to specific genomic loci. Hence, cytosine methylation patterns and the histone code may represent mutually reinforcing processes that lead to the stable maintenance of chromatin packaging and gene expression patterns characteristic of cellular memory.

See Also the Following Articles

Chromatin: Physical Organization • Nuclear Organization, Chromatin Structure, and Gene Silencing

Glossary

CpG island Region of DNA containing a cluster of unmethylated CpG dinucleotides, usually found near promoters of actively expressed genes.

epigenetics Heritable patterns of gene expression that occur in the absence of altered DNA sequence.

euchromatin Open form of chromatin associated with transcriptionally active genes.

genomic imprinting Phenomenon whereby maternally derived and paternally derived alleles of a gene exhibit distinct expression patterns as a result of distinct epigenetic modifications established during gametogenesis.

heterochromatin Highly compact form of transcriptionally inactive chromatin.

Further Reading

Ballestar, E., and Wolffe, A. P. (2001). Methyl-CpG-binding proteins: Targeting specific gene repression. *Euro. J. Biochem.* **268**, 1–6.

Felsenfeld, G., and Groudine, M. (2003). Controlling the double helix. *Nature* **421**, 448–453.

Jaenisch, R., and Bird, A. (2003). Epigenetic regulation of gene expression: How the genome integrates intrinsic and environmental signals. *Nat. Genet.* **33**, 245–254.

Jorgensen, H. F., and Bird, A. (2002). MeCP2 and other methyl-CpG-binding proteins. *Mental Retardation and Developmental Disabilities Rev. Res.* **8**, pp. 87–93.

Nakao, M. (2001). Epigenetics: Interaction of DNA methylation and chromatin. *Gene* **278**, 25–31.

Wade, P. A. (2001a). Methyl CpG-binding proteins and transcriptional repression. *Bioessays* **23**, 1131–1137.

Wade, P. A. (2001b). Methyl CpG binding proteins coupling chromatin architecture to gene regulation. *Oncogene* **20**, 3166–3173.

Biography

Dr. David G. Skalnik is a professor of pediatrics and biochemistry and molecular biology at the Indiana University School of Medicine. His principal research interest is the epigenetic regulation of chromatin structure and gene expression during mammalian development. He holds the Ph.D. from Stanford University and received his postdoctoral training at The Children's Hospital, Harvard Medical School. His laboratory group cloned CpG-binding protein, which binds to unmethylated CpG motifs and is required for early development and maintenance of normal patterns of cytosine methylation.

Microtubule-Associated Proteins

Nobutaka Hirokawa
University of Tokyo, Tokyo, Japan

Reiko Takemura
Okinaka Memorial Institute for Medical Research, Tokyo, Japan

Microtubules are formed by polymerization of α- and β-tubulin. They are intrinsically in dynamic turnover state, subject to treadmilling and dynamic instability. Microtubule-associated proteins (MAPs) are a heterogeneous group of proteins that have microtubule-binding domains. MAPs are abundantly expressed in the brain, and historically MAPs (e.g., MAP1, MAP2, and tau) derived from the brain have been studied extensively. MAP4 is ubiquitously expressed. These classical MAPs are filamentous proteins of various lengths, ranging from 50 to 185 nm. They have microtubule-binding domain and the projection domain that extends as filamentous structure. By binding along the side of microtubules, they stabilize microtubules. In addition, by extending the projection domain from the microtubule surface, they produce microtubule bundles of various densities. Tau and MAP2C predominantly expressed in the axon produce microtubule bundles of ~20 nm distances. MAP2 predominantly expressed in the dendrite produces microtubule bundles of ~65 nm distances. The microtubule bundles produced by tau/MAP2C and MAP2 resemble microtubule domains in axons and dendrites, respectively. These microtubule bundles are extended from the cell as axon- or dendrite-like processes. Therefore, MAPs serve as determinants of microtubule organization within the cell, particularly in neurons. There are some other groups of newly identified MAPs, and some of them destabilize microtubules. Binding of MAPs to microtubules is regulated by phosphorylation. In some neurodegenerative diseases including Alzheimer's disease, hyperphosphorylated tau precipitates as filaments on its own and may be one of the important factors to determine the progress of the disease.

Classical Microtubule-Associated Proteins

Microtubules are formed by polymerization of α- and β-tubulin. Microtubules play important roles in organizing and maintaining the shape of the cell, and also act as tracks for the transport of membranous organelles and macromolecules. So-called motor proteins (kinesin superfamily proteins and dynein superfamily proteins) are involved in the transport processes and they use the energy derived from the hydrolysis of ATP. Microtubule-associated proteins (MAPs) bind to microtubules without a requirement for nucleotide involvement, and organize the spatial arrangement of microtubules within the cell; they also regulate the polymerization of microtubules. Historically, MAPs have been isolated from the mammalian brain by their property that they remain bound to microtubules through repeated cycle of polymerization and depolymerization. The quick-freeze, deep-etch microscopy reveals that in neurons, there are abundant filamentous structures of various length associated with microtubules. These filamentous structures were proven to be mainly composed of MAPs (Figures 1 and 2). These MAPs have been studied extensively, and we term these well-characterized MAPs as classical MAPs. The major part of this article will be spent on these classical MAPs. Some other MAPs have been known and some new MAPs have been identified recently. These will be dealt with in relevant places. Classical MAPs include MAP1A, MAP1B, MAP2A, MAP2B, MAP2C, and tau (from mammalian brains) and MAP4 (found ubiquitously) (Table I). All these MAPs are fibrous molecules of different lengths, ranging from 50 to 185 nm, and form filamentous projections from the microtubule surface. First, the basic biochemical properties and their expression patterns will be described for each of the classical MAPs.

MAP1A and MAP1B

MAP1A and MAP1B are high-molecular-weight, heat-labile, filamentous proteins of ~350 and 320 kDa on SDS-PAGE. MAP1A and MAP1B are transcribed from the separate genes. MAP1B has also been called MAP1x or MAP5. The protein originally called MAP1C turned out to be cytoplasmic dynein. Therefore, it is not usually included in MAPs. MAP1A encodes protein of 2774 amino acid residues, and MAP1B encodes protein of

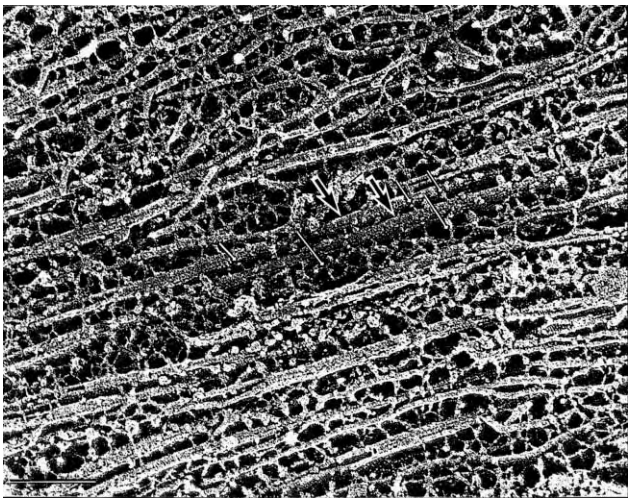

FIGURE 1 Axonal cytoskeleton observed by quick-freeze, deep-etch electron microscopy. Between microtubules (thick black arrows), short crosslinkers (short arrows) and longer crosslinkers are found. Reproduced from Hirokawa, N. (1991). Molecular architecture and dynamics of the neuronal cytoskeleton. In *Neuronal Cytoskeleton* (R. D. Burgoyne, ed.) pp. 5–74. With permission of Wiley-Liss, Inc., New York.

2464 amino acid residues. Rotary-shadowing electron microscopy reveals that MAP1A and MAP1B are highly elongated, flexible molecule of ~150–185 nm in length. Both MAP1A and MAP1B have associated light chains. Interestingly, the light chains, LC2 and LC1, are encoded at the C-terminal portion of MAP1A and MAP1B molecules, respectively. At the N-terminal portion of both MAP1A and MAP1B molecules, there is a domain

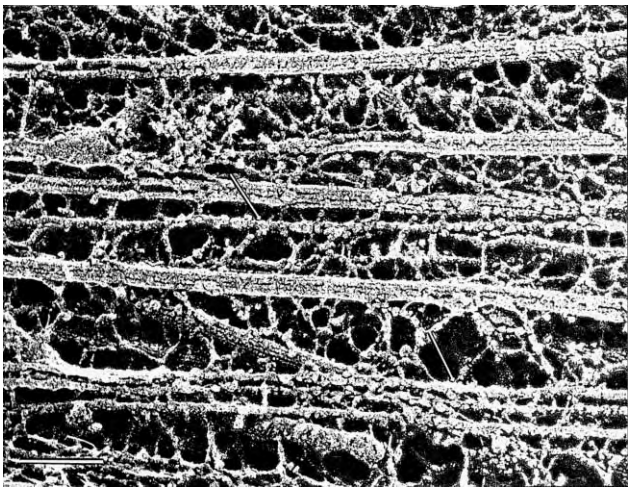

FIGURE 2 Dendritic cytoskeleton observed by quick-freeze, deep-etch electron microscopy. Between microtubules, and between microtubules and neurofilaments (arrows), long crosslinkers are found. Reproduced from Hirokawa, N. (1991). Molecular architecture and dynamics of the neuronal cytoskeleton. In *Neuronal Cytoskeleton* (R. D. Burgoyne, ed.) pp. 5–74. With permission of Wiley-Liss, Inc., New York.

enriched in the positively charged amino acids and contains the short motif (KKEX), repeated 11 and 21 times in MAP1A and MAP1B (Table I and Figure 3). This domain serves as microtubule-binding domain, and interacts with C terminus of tubulin, which has a large number of acidic residues. Both MAP1A and MAP1B form filamentous structures associated with microtubules in neurons.

MAP1A and MAP1B are predominantly expressed in neuron, although a smaller amount may be expressed in other tissues as well. There is a developmental regulation in the expression of MAP1. MAP1A is more abundantly expressed in the adult, and MAP1B is more abundantly expressed in the developing nervous system. In fact, the expression of these two proteins appears to be complementary to each other. In the rat brain development, the level of MAP1B expression is highest at the first few postnatal days, when many neurons are extending their axons. Thereafter, the expression of MAP1B declines. In contrast, the expression of MAP1A is very low at this period, but the level of its expression increases thereafter, and reaches its maximal level in adults. There is a spatial difference in the expression of MAP1B and MAP1A. MAP1B is predominantly expressed in the developing axon, although smaller amount is found in the dendrite of juvenile and mature neurons. In contrast, MAP1A is abundantly expressed in the mature dendrites, with the smaller amount of expression at the axons.

MAP2A, MAP2B, AND MAP2C

MAP2A and MAP2B were identified as high-molecular-weight, filamentous protein of ~280 and 270 kDa on SDS-PAGE. MAP2A and MAP2B have been known to be heat stable, which is rather unique considering the high molecular weight of these proteins. MAP2B encodes proteins of 1828 amino acid residues; MAP2A is a splice variant having additional exon of 83 amino acid residues in the middle of the molecule. Rotary-shadowing electron microscopy revealed that MAP2A and MAP2B are highly elongated, flexible molecules of ~100 nm in length. Subsequent study revealed that there is additional low-molecular-weight form, MAP2C, which is ~70 kDa on SDS-PAGE. In MAP2C, the N- and C-terminal ends are joined, resulting in the protein of 467 amino acid residues. The unique characteristic of MAP2 is that they have binding domain for the regulatory subunit of type II cyclic AMP-dependent kinase on the N terminus. The C-terminal portion of the MAP2 forms the microtubule-binding domain (Table I and Figure 3). The sequence of this region does not have homology to MAP1, but it has unique imperfect tandem repeats of 31–32 amino acids; similar repeats of 18 amino acids joined by less-conserved, variable "spacers" of

TABLE I

Characteristics of Classical MAPs

MAPs	App. mol. weight on SDS-PAGE (KDa)	# of amino acids	Length of isolated molecule (nm)	Distance in microtubule bundles (nm)	Microtubule-binding domain	Developmental and topological expression pattern
MAP1A[a]	350	2774	150–185		N-terminal KKEX repeats	Abundant in mature dendrite
MAP1B[a]	320	2464	150–185		Same as above	Abundant in developing axon
MAP2A[b]	280	1911	~100	~65	C-terminal tandem repeats	Specific to developing dendrite
MAP2B[b]	270	1828	~100	~65	Same as above	Specific to developing and mature dendrite
MAP2C[b]	70	467		~20	Same as above	Abundant in developing axon and dendrite
tau[c]	55–65	352–441	~50	~20	Same as above	Abundant in developing and mature axon
MAP4	210	1072			Same as above	Ubiquitously expressed

[a] MAP1A and MAP1B are transcribed from separate genes.
[b] MAP2A, MAP2B, MAP2C are splice variants.
[c] Six isoforms of tau are splice variants.

13–14 amino acids. These repeats bind to the C-terminal ends of tubulin. These imperfect tandem repeats are also used in the microtubule-binding domain of tau and MAP4, which also reside in the C-terminal part of the molecule. Each molecule has three or four repeats. The central portion of the MAP2A and MAP2B molecule corresponds to the extended arm. Lacking this arm portion, MAP2C is revealed as

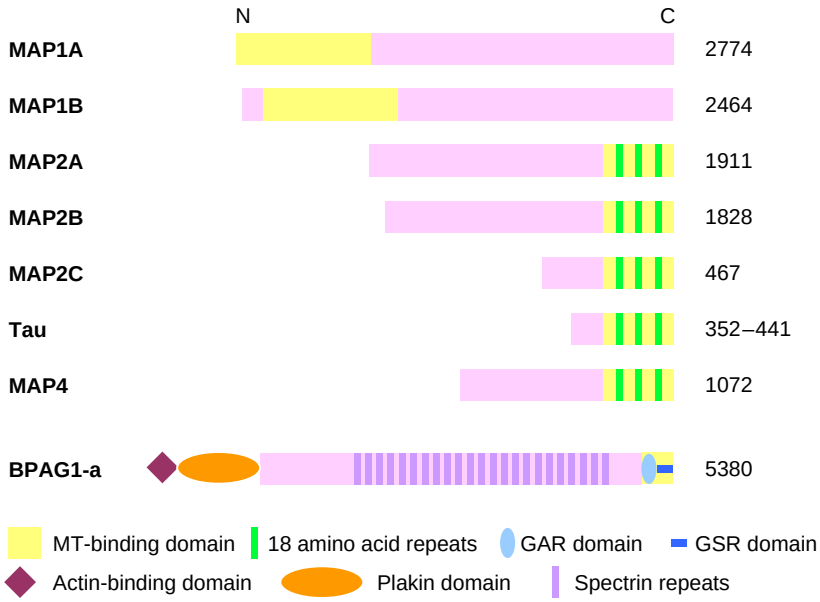

FIGURE 3 Schematic diagram of representative MAPs. Domain structures of MAP1A, MAP1B, MAP2A, MAP2B, MAP2C, tau, MAP4, and BPAG1-a are shown. Numbers of amino acids of representative molecules are shown on the right. MAP1A and MAP1B have a microtubule-binding domain on the N-terminal portion, which is a domain enriched in the positively charged amino acids and contains the short motif (KKEX), repeated 11 and 21 times in MAP1A and MAP1B, respectively. C-terminal portion serves as a projection domain. MAP2A, MAP2B, MAP2C, tau, and MAP4 have a microtubule-binding domain on the C-terminal portion, which is a unique imperfect tandem of three or four basic repeats of 31–32 amino acids, similar repeats of 18 amino acids joined by less conserved, variable "spacer" of 13–14 amino acids, and is quite well preserved among these MAPs. Molecules with three repeats are depicted in the drawing. BPAG-1a, one of the new MAPs, has actin-binding domain, plakin domain, spectrin-repeat-containing rod domain, GAR domain, and GSR domain. The GAR and the GSR domain together constitute the microtubule-binding domain in BPAG1-a as well as in MCAF. In plakin, which is not depicted here, GAR domain is missing and GSR domain at the C-terminal portion can associate with microtubules. Not drawn to scale.

filamentous molecule ~50 nm in length by the rotary-shadowing electron microscopy.

MAP2 is almost exclusively expressed in neurons. Importantly, MAP2A and MAP2B are specifically localized to the dendrites. It is often used as markers for dendrites. There is a developmental regulation of MAP2 expression. MAP2C is expressed in juvenile neuron; it is found in cell bodies, dendrites, and axons. MAP2A is expressed in the adult, and MAP2B is expressed throughout the developmental stage.

Tau

Tau was the first MAP purified from the brain. It is heat stable, consists of several bands of 55–65 kDa on SDS-PAGE. It is now known that tau consists of six isoforms (ranging from 352 to 441 amino acid residues), which are splice variants of single tau gene. In the C-terminal half of the molecule, tau has three or four tandem repeats of 31 or 32 amino acids, as described above, which serves as the microtubule-binding domain (Table I and Figure 3). In rotary-shadowing electron microscopy, tau forms filaments of ~50 nm in length. Tau forms ~20 nm short filamentous structures associated with microtubules. It is known that in the peripheral nervous system, additional isoform of 110 kDa is expressed. However, this isoform is less well characterized.

There is a developmental regulation of expression of tau isoforms. In the juvenile brain, only the three repeat isoforms are expressed, and in the adult brain, tau isoforms with both three and four repeats are expressed. Tau is posttranslationally modified by phosphorylation. A part of the heterogeneity of the tau bands on the SDS-PAGE results from phosphorylation. When antibodies that recognize all tau isoforms are used, tau is predominantly localized in the axon, with some expression in cell bodies and dendrites.

MAP4

Although MAP1, MAP2, and tau are rather abundantly expressed in the nervous system, their expression outside the nervous system is limited. MAP4 is a major MAP found outside the nervous system. It is a protein of 210 kDa on SDS-PAGE. MAP4 encodes protein of 1072 amino acid residues. It is composed of an N-terminal projection domain and a C-terminal microtubule-binding region, which has homology to the microtubule-binding domain of tau and MAP2 (Table I and Figure 3).

Control of Microtubule Dynamics

Microtubules are dynamic and unstable. By binding along the sides of the microtubules, MAPs control microtubule dynamics *in vitro* and *in vivo*. Many MAPs, including classical MAPs, stabilize microtubules. Classical MAPs were usually expressed predominantly in the nervous system. Microtubules in the neuron are usually much more stable than those in most interphase cells. Therefore, it is not surprising that one important function of classical MAPs is the stabilization of microtubules against disassembly. As described above, tau, MAP2, and MAP4 share conserved C-terminal three or four pseudorepeats, which serves as microtubule-binding domain. In tau, it is shown that one of these repeats bind to the tubulin C-terminal end, and other repeats bind to another internal site of tubulin. Therefore, these tandem repeats are likely to bind to microtubule in such a way to crosslink adjacent tubulin subunits and stabilize microtubules against disassembly. These bindings are controlled by phosphorylation. Both tau and MAP2 have many residues, which can be phosphorylated.

There are other modes of regulation of microtubule dynamics by MAPs. Microtubule is usually disassembled in the cold temperature. Stable tubule-only polypeptide

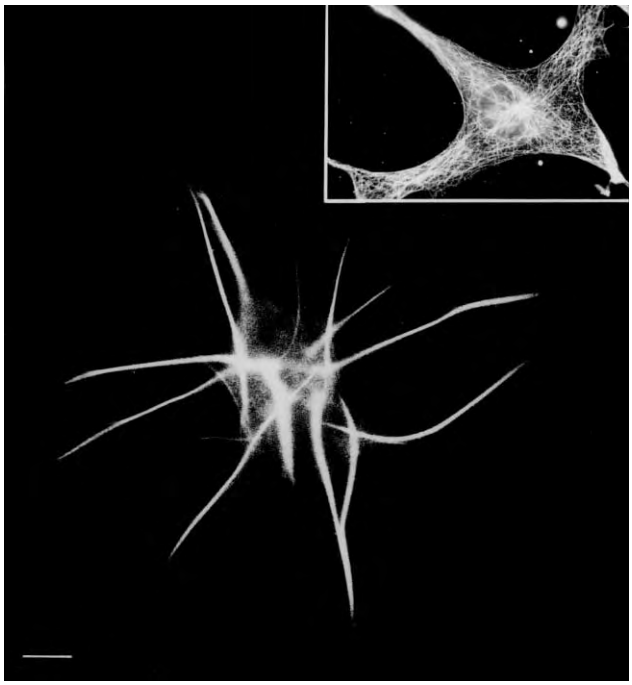

FIGURE 4 Microtubule bundle formation in fibroblasts transfected with tau cDNA. Immunofluorescence using anti-tubulin antibody. Long processes are formed and microtubule bundles extend into the processes. Upper right corner is the immunofluorescence of nontransfected control fibroblasts stained with antitubulin antibody. Microtubules radiate in various direction from the microtubule-organizing center near the nucleus. Reproduced from Kanai, Y., Takemura, R., Oshima, T., Mon, H., Ihara, Y., Yanagisawa, M., Masaki, T., and Hirokawa, N. (1989). Expression of multiple tau iso-forms and microtubule bundle formation in fibroblasts transfected with a single tau cDNA. *J. Cell Biol.* **109**, 1173–1184 with permission of The Rockefeller University Press.

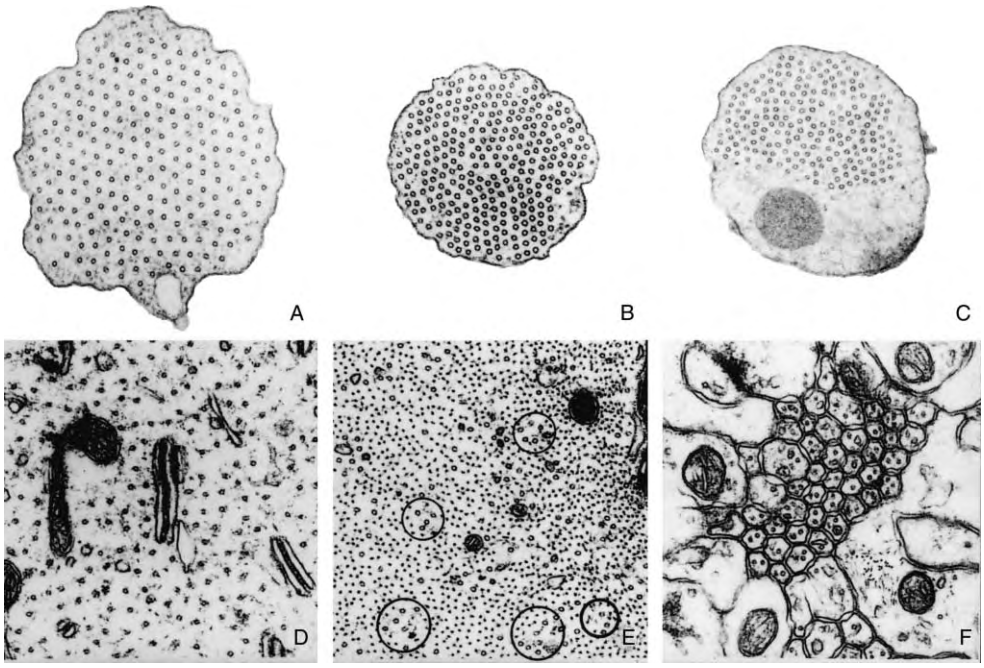

FIGURE 5 Cross-section electron micrographs of processes induced by transfection of MAP2 (A), MAP2C (B), and tau (C) into Sf 9 cells. Each MAP2 forms microtubule bundles, but the organization is different. When MAP2 is transfected, wall-to-wall distance between nearest adjacent microtubules is ~65 nm, which is similar to the microtubule organization of Purkinje cell dendrite in the cerebellum (D). In contrast, when MAP2C or tau are transfected, the distance between microtubules is ~20 nm, which is similar to the microtubule organization of large myelinated axons in the spinal cord (inside the circle in (E)) or parallel fiber axons in the cerebellum (F). Reproduced from Chen, J., Kanai, Y., Cowan, N. J., and Hirokawa, N. (1992). Projection domains of MAP2 and tau determine spacings between microtubules in dendrites and axons. *Nature* **360**, 674–677 with permission of Nature.

(STOP) is a MAP known to stabilize microtubules against cold temperature. A few MAPs are also known to destabilize microtubules, including katanin, Op18, and stathmin. In addition to structural MAPs, some of the kinesin superfamily proteins belonging to KIF2 class also destabilize microtubules.

Bundling of Microtubules: MAPs and Neurite Outgrowth

Neuron extends axon and dendrites from the cell body. In the axon and dendrites, microtubules run in parallel, in longitudinal array. In the quick-freeze, deep-etch electron microscopy, it can be shown that microtubules are highly crosslinked by meshwork of fine filamentous structures in axons and dendrites (Figures 1 and 2). MAPs form these crosslinkers. Moreover, MAPs induce microtubule bundle formation and outgrowth of processes from the cell. When classical MAPs are transfected and overexpressed in the cells, such as fibroblast or Sf9 cells, unusual microtubule bundles are formed, and long processes very much like neurites can be induced (Figures 4 and 5).

In addition, MAPs determine the spacing between neighboring microtubules to be axon like or dendrite like. Namely, MAPs expressed in the axon, such as tau and MAP2C, produce microtubule bundles similar to those seen in the axon (wall-to-wall distance of neighboring microtubules, ~20 nm), and MAPs expressed in the dendrites, such as MAP2A and MAP2B, produce microtubule bundles similar to those seen in the dendrites (wall-to-wall distance of neighboring microtubules, ~65 nm) (Figure 5). Therefore, in addition to the stabilization of microtubules, projection domains of MAPs induce microtubule bundle formation, induce process outgrowth, and determine the spacing between microtubules.

Analysis of Transgenic and Knockout Mice: Relation of MAPs to Neurodegenerative Diseases

Recently, genetically altered mice gave some insights to the role of individual MAPs *in vivo*. In general, lack of MAP produces the expected effect, but the overall effect is rather limited. This implies that there is certain

overlap in the function of MAPs. In fact, when the double knockout mice were formed in the combination of two MAPs, the expected effect is much more severely observed. For example, in *tau* $^{-/-}$ mice, an effect on the microtubule stabilization and bundle formation in the axon was observed, but the effect is evident mainly in the small caliber axon. Likewise, in *MAP2* $^{-/-}$ mice, an effect on microtubule organization in dendrite is evident, but the effect is somewhat limited. However, when both tau and MAP1B, or both MAP1B and MAP2 are deleted, impaired microtubule bundle formation and outgrowth of axon or dendrite was markedly observed.

Tau has been implicated in the pathogenesis of certain cognitive neurodegenerative diseases. The diseases are sometimes grouped as tauopathies, which comprise a heterogeneous group of age-dependent cognitive disorders, including Alzheimer's disease. In these diseases, abnormally hyperphosphorylated tau forms filamentous aggregates within the cell. The aggregates do not contain microtubules, and the formation of aggregates is independent of microtubules. There is a loss of neurons in the affected brain area. In 1998, tau gene mutations were identified in patients with dementia and parkinsonism linked to chromosome 17 (FTDP-17). Transgenic mice with these mutations have been developed for an analysis.

New MAPs

Recently, a family of proteins of a very high molecular weight, plakin family, has been identified as crosslinker proteins that connect different cytoskeletal filaments. Some of the members, such as plectin, Bullous pemphigoid antigen 1 (BPAG1), and microtubule-actin crosslinking factor (MACF), have microtubule-binding domain, and they are likely to crosslink microtubule to intermediate filaments, or actin filaments. Microtubule-binding domain used in the plakin family proteins are of two kinds: Gas2-related (GAR) domain in BPAG1 and MACF; and glycine-serine-arginine (GSR) domain in plakin, BPAG1, and MACF (Figure 3). That these new crosslinkers play an important physiological role is suggested by the fact that mutations in these proteins cause neurological defects *in vivo*. For example, mutations in BPAG1 cause degeneration of sensory neurons, and mutation in MCAF cause deficits in axon outgrowth and dendritic sprouting.

See Also the Following Articles

Centrosomes and Microtubule Nucleation • Kinesins as Microtubule Disassembly Enzymes • Kinesin Superfamily Proteins

Glossary

axon Structure that transmits the signal from the cell body to the synaptic terminal. Single axon extends from the cell body. Microtubules and neurofilaments are major components of the axonal cytoskeleton. Microtubules in the axons are organized more densely than in the dendrites.

dendrite Structures that receive signals and transmit them to the direction of the cell body. Usually, multiple dendrites emanate from the cell body in "dendritic" shape. Microtubules are the major components of the dendritic cytoskeleton, and microtubules in the dendrites are organized more loosely than in the axon.

microtubule Filament of 25 nm diameter. Assembled from α- and β-tubulin subunits (55 kDa), it is actually a hollow cylinder (hence tubule) composed of 13 protofilaments. During mitosis, it forms a mitotic spindle. Compared to intermediate filaments (10 nm diameter), microtubules turn over much more dynamically. New subunits are added at the "plus" end, while subunits dissociate from the "minus" end (treadmilling). In addition, microtubules show the property called "dynamic instability," in which individual microtubules are either growing or shrinking and they stochastically switch between the two states.

Further Reading

Alberts, B., Johnson, A., Lewis, J., Raff, M., Roberts, K., and Walter, P. (2002). *Molecular Biology of the Cell.* Garland Publishing, New York.

Chen, J., Kanai, Y., Cowan, N. J., and Hirokawa, N. (1992). Projection domains of MAP2 and tau determine spacings between microtubules in dendrites and axons. *Nature* **360**, 674–677.

Desai, A., and Mitchison, T. J. (1997). Microtubule polymerization dynamics. *Annu. Rev. Cell Develop. Biol.* **13**, 83–117.

Garcia, M. L., and Cleveland, D. W. (2001). Going new places using an old MAP: tau, microtubules and human neurodegerative disease. *Curr. Opin. Cell Biol.* **13**, 41–48.

Hirokawa, N. (1991). Molecular architecture and dynamics of the neuronal cytoskeleton. In *Neuronal Cytoskeleton* (R. D. Burgoyne, ed.) pp. 5–74. Wiley-Liss, New York.

Hirokawa, N. (1994). Microtubule organization and dynamics dependent on microtubule-associated proteins. *Curr. Opin. Cell Biol.* **6**, 74–81.

Homma, N., Takei, Y., Tanaka, Y., Nakata, T., Terada, S., Kikkawa, M., Noda, Y., and Hirokawa, N. (2003). Kinesin superfamily protein 2A (KIF2A) functions in suppression of collateral branch extension. *Cell* **114**, 229–239.

Houseweart, M. K., and Cleveland, D. W. (1999). Cytoskeletal linkers: New MAPs for old destinations. *Curr. Biol.* **9**, R864–R866.

Hyams, J. S., and Lloyd, C. W. (1994). *Microtubules.* Wiley-Liss, New York.

Kanai, Y., Takemura, R., Oshima, T., Mori, H., Ihara, Y., Yanagisawa, M., Masaki, T., and Hirokawa, N. (1989). Expression of multiple tau isoforms and microtubule bundle formation in fibroblasts transfected with a single tau cDNA. *J. Cell Biol.* **109**, 1173–1184.

Leung, C. L., Green, K. J., and Liem, R. K. H. (2002). Plakins: A family of versatile cytolinker proteins. *Trends Cell Biol.* **12**, 37–45.

Takei, Y., Teng, J., Harada, A., and Hirokawa, N. (2000). Defects in axonal elongation and neuronal migration in mice with disrupted tau and map1b genes. *J. Cell Biol.* **150**, 989–1000.

Teng, J., Takei, Y., Harada, A., Nakata, T., Chen, J., and Hirokawa, N. (2001). Synergistic effects of MAP2 and MAP1B knockout in neuronal migration, dendritic outgrowth, and microtubule organization. *J. Cell Biol.* **155**, 65–76.

Biography

Nobutaka Hirokawa is Professor and Chair of Department of Cell Biology and Anatomy, and Dean of the School of Medicine, University of Tokyo. His principal research interests are organization of cytoskeletal structures in neurons and molecular motors involved in the intracellular transport. He holds an M.D. and Ph.D. from University of Tokyo. He developed the quick-freeze, deep-etch electron microscopy with Dr. John Heuser, and did pioneering work in elucidating the neuronal cytoskeleton in molecular detail, including the analysis of MAPs. He was also one of the first to tackle the analysis of kinesin motor molecules, and the first to clone multiple kinesin superfamily proteins from mammalian brain and to point out the importance of this motor protein family in mammalian intracellular transport.

Mitochondrial Auto-Antibodies

Harold Baum
King's College London, London, UK

Auto-antibodies are antibodies that bind specifically to self-constituents, and so would seem to be an anomaly of a system geared to respond to foreign molecules and be tolerant to self. The antigens that they may recognize encompass the spectrum from tissue specific to being common to all cell types. They may be pathogenic, disease-specific, and diagnostic, or of no clear significance. Auto-antibodies against mitochondrial components are illustrative of this range of characteristics, even to the extent that diseases characterized by them may be very specifically tissue localized. They have been extensively studied, and in the case of primary biliary cirrhosis (PBC) they have become a paradigm in the study of autoimmune diseases. A consideration of the mitochondrial auto-antibodies (AMA) characteristic of PBC is the major focus of this article.

Detection of Mitochondrial Auto-antibodies

Auto-antibodies (AMAs) have been detected by immunofluorescence (IFL) (where they are visualized as bright granular staining in cell types with high mitochondrial content), or by applying complement fixation tests (CFTs), enzyme-linked immunosorbant assays (ELISAs) or Western immunoblotting (IB) to tissue extracts, purified subcellular constituents or specific, recombinant mitochondrial species. Proof that mitochondria were the target of antibodies detected by such methods was provided in early studies, such as the landmark paper of Walker *et al.*, by the specific absorption of serum reactivity using preparations of mitochondria. It was subsequently recognized that AMAs recognizing different mitochondrial antigens might characterize different clinical conditions. The molecular identity of many, but not all, of these antigens is now established. Not all of these AMAs are detectable by all of the above methodologies. The preferred test in general diagnostic laboratories is IFL on a composite substrate of rodent tissues. In the research laboratory however, and where specific AMAs are under investigation, the preferred assays are ELISAs and IB, using purified or recombinant antigens, or synthetic peptides.

The M-Classification of AMAs

In the early 1980s an arbitrary classification of AMAs, as anti-M1-9, was developed, mainly by Berg's group in Tübingen, on the basis of patterns of IFL and/or properties of target antigens as determined by various assay procedures. It is noteworthy that in all these cases the AMAs are not species specific. Whilst this M-classification is now somewhat obsolete, and does not include all known mitochondrial targets for AMAs, it is still sufficiently in common use for it to be helpful in listing reactivities (Table I).

Anti-M1 AMAs and Cardiolipin

The M1 pattern of IFL is exhibited exclusively with sera of patients with untreated secondary syphilis. The reaction is abolished completely by absorption of sera with cardiolipin, the characteristic phospholipid of the mitochondrial inner membrane. However, the simple conclusion that anti-M1 antibodies are specific for cardiolipin is complicated by another observation. The earlier diagnostic test for syphilis, the Wasserman reaction, is based on CFTs against cardiolipin. However, not all sera positive in this test show an M1 pattern of IFL. Moreover, Wasserman-positive sera that are negative for M1 give a strongly positive ELISA reaction against purified cardiolipin, whereas anti-M1 AMAs are scarcely detectable by ELISAs using purified cardiolipin, whilst they react strongly in ELISAs against sub-mitochondrial particles. Interestingly, M1-negative, Wasserman positive sera are frequently false positives for syphilis and may instead reflect collagen disorders such as systemic lupus erythmatosus (SLE). It seems likely that these anomalies reflect antibodies to different epitopes in cardiolipin, the different assay systems exposing different conformations of the same molecule. (Indeed some of the anti-cardiolipin antibodies in M1-negative sera of SLE patients may be detected as antibodies against nucleic acids, cross-reactivity arising by virtue of the similarity between the glycerol phosphate arrays in cardiolipin arrays and the ribose phosphate backbone of nucleic acids.) Anti-M1 AMAs probably recognize a more native form of the

TABLE I

The M-Classification of Specificities of Mitochondrial Auto-Antibodies

Antigen	Occurrence of auto-antibodies
M1	Secondary syphilis
M2	PBC
M3	Phenopyrazone-induced pseudolupus syndrome
M4	PBC (prognostic indicator? "mixed form"?)
M5	Subgroup of systemic lupus; anti-phospholipid syndrome
M6	Iproniazid-induced hepatitis
M7	Cardiomyopathies
M8	PBC (prognostic indicator?)
M9[a]	PBC (prognostic indicator?)

[a] NB. In fact this antigenic specificity is not mitochondrial (see text).

lipid, as it exists in the intact mitochondrial membrane (and may arise from immunological cross-reactivity with a membrane constituent of the agent of syphilis, *Treponema pallidum*).

Anti-M2 AMAs

The most important mitochondrial auto-antibodies, anti-M2 AMAs, exhibit a characteristic pattern of IFL and were initially defined both by their disease specificity and by properties of the antigen that they recognized. This was shown to be trypsin sensitive and associated with (but detachable from) the inner surface of the inner membrane of all mitochondria tested, from human to fungal. Anti-M2 antibodies were also shown to cross-react with several bacteria, anti-mitochondrial activity, for example, being absorbed out of PBC sera by *E. coli*.

Association with Primary Biliary Cirrhosis

Primary biliary cirrhosis (PBC) is a chronic, cholestatic liver disease, predominantly affecting middle-aged women. It is characterized by spontaneous inflammatory damage to the epithelial cells of the bile duct (BEC). Whilst the clinical presentation and disease progression are variable, and the disease may be virtually asymptomatic for many years, the end stage is cirrhotic liver failure, and the disease is the second most frequent reason for liver transplantation in the developed World. Although the most clinically significant pathology relates to the liver, PBC is actually a multi-system disorder, and may feature lachrymal salivary and pancreatic hyposecretion. The paper by Walker, referred to earlier, and many subsequent studies, demonstrated clearly that PBC is characterized by high and persistent titers of AMAs of a kind not seen in normal subjects or other diseases. Since the description of this close association, the detection of this class of AMAs, designated as anti-M2, has acted as a powerful diagnostic tool. Anti-M2 antibodies (both IgG and IgM) are found in up to 98% of PBC patients, the precise figure depending on the sensitivity of the assay used. Interestingly, these AMAs are not restricted to serum, being found in the bile, saliva, and urine of patients with PBC. Moreover anti-M2 AMAs have turned out to be predictors for the disease; asymptomatic subjects, accidentally having been identified as being positive for anti-M2 AMAs, are frequently found to develop the disease subsequently.

Identity of M2 Antigens

Western IB soon revealed that M2 actually consists of a "family" of up to seven co-purifying peptides of differing molecular weight, encompassing a spectrum from around 75 to 36 kDa. Different PBC sera demonstrated different patterns of reactivity against these (see Table II), but virtually all recognized a predominant peptide that was eventually identified as being the E2 component (dihydrolipoamide acetyltransferase) of the pyruvate dehydrogenase complex. Thereafter, it soon became clear that the other M2 antigens were also constituents of one or other of the 2-oxo-acid dehydrogenase multienzyme complexes (OADCs): pyruvate, 2-oxoglutarate and branched-chain 2-oxo acid dehydrogenase complexes (PDC, OGDC, and BCOADC, respectively). Each of the three complexes occupies a key position in energy metabolism in aerobic cells. Each consists of multiple copies of at least three enzymes (E1, E2, and E3), which are encoded by genes in the nucleus and separately imported into mitochondria for assembly into high molecular weight multimers localized to the matrix aspect of the inner membrane. The structural core of these complexes is provided by E2 (the acyltranferase), to which multiple copies of E1

TABLE II

Frequency of Occurrence of Anti-M2 AMA to Specific Antigens in PBC

Complex	Subunit	Apparent M_r (kD[a])	AMA-positive (%)[a]
PDC	E1α	41	53
PDC	E1β	34–36	4
PDC	E2	70–74	96
PDC	E3BP (X)	50–56	96
OGDC	E2	48–50	74
BCOADC	E1α	46	50
BCOADC	E2	50–52	56
All	E2's		50
At least one	E2		98

[a] Approximate average of published data using defined antigens.

(the decarboxylating dehydrogenase) and E3 (dihydrolipoamide dehydrogenase) are noncovalently bound. The E2 enzymes are notably homologous in structure as between different complexes and different species (e.g., there is 52% similarity in sequence as between rat PDC-E2 and OGDC-E2 of *E. coli*). E3 is common to all three complexes, whereas E1 and E2 are unique to each complex. PDC contains a fourth polypeptide with a structural role, the E3-binding protein (E3BP), once termed protein X. This contains a lysine-linked lipoate moiety, located in a domain that is strongly homologous to corresponding domains in PDC-E2.

In view of this latter homology, it is not surprising that all sera recognizing PDC-E2 also bind E3BP, and that the antibodies to the two peptides are cross-reactive. The other members of the M2 "family" were shown to include the E2's of OGDC and BCOADC. However, notwithstanding the general similarity between the respective E2's, there seems only to be a limited degree of antibody cross-reactivity between them and only about 50% of PBC sera recognize all three. (On the other hand AMA against a particular E2 recognize that peptide in mitochondria of all species tested.) About half of all PBC sera also recognize the α-subunit of PDH-E1, (with the β-subunit being rarely recognized). Additionally, human auto-antibodies, specific for BCOADC-E1α, were found, in a more recent study, in the sera of almost half of the PBC patients tested. A summary of frequency of occurrence of AMAs to individual members of the M2 "family" is given in Table II. The E3 component, a common subunit of all three complexes, is not listed in this table. This is because, whilst specifically anti-mammalian E3 antibodies are found in PBC, these are in relatively low amount and are not totally disease specific.

Enzyme Inhibition by Anti-M2 AMAs

A notable characteristic of AMAs in PBC sera is their capacity to block the catalytic function of the 2-OAD multienzyme complexes *in vitro*. For example, sera with AMAs recognizing PDC-E2 rapidly inhibit PDC at dilutions of 1/500–1/5000, much of this inhibitory activity being removed by pre-absorption of the sera with recombinant PDC-E2. Similarly, affinity-purified antibody against PDC-E1α also specifically inhibits PDC reactivity.

Possible Target for Anti-M2 AMAs on Bile Duct Cells

What may be a key fact relating to the occurrence and disease association of AMAs in PBC is the reactivity that has been observed of anti-M2 AMAs (and of selected monoclonal antibodies against PDC-E2) with some component at the surface of a subset of BEC in livers of PBC patients. Conflicting views are that this antigen is an inappropriately localized component of PDC, or that it is a different molecule with a sequence similarity to a dominant B-cell epitope. In view of the potentially fundamental significance of the presence of a disease specific antigen at the site of tissue damage, it is regrettable that no definitive identification has yet been made.

Cross-Reactivity of Anti-M2 AMAs Against Bacteria

Early reports of cross-reactivity of PBC-specific AMAs against a variety of bacterial species were confirmed in studies of reactivity against individual microbial E2's of the three OADC complexes. (There is no homology between microbial and corresponding mitochondrial E1's; neither is there reactivity of E1-specific AMAs against bacteria.) Further evidence of cross-reactivity is that antibodies raised in rabbits, against bacterial mutants having fragile cell walls, were reported to react with a typical M2 pattern on IB against mitochondria. However, detailed absorption/elution and other studies have led to a current view that, whilst there is indeed some cross-reactivity between corresponding enzymes, PBC sera contain distinct sets of antibodies against mitochondrial and microbial OADCs respectively.

Anti-M2 AMAs and Chronic Bacterial Infection

In a study of women with asymptomatic recurrent bacteriuria, a majority of the patients were found to be weakly positive for antibodies to PDC-E2 by immunoblot, in the absence of evidence of liver disease. AMAs were also detected by ELISAs and IB in 43% of patients with active pulmonary tuberculosis and in patients with leprosy. However, it is not clear whether what is being detected in these cases are "true" AMAs or antibodies against corresponding microbial enzymes that are partially cross-reactive against mitochondrial peptides.

Epitopes Recognized by Anti-M2 AMAs

Most studies on B-cell epitopes in PBC have focused on the E2 antigens. Here it is clear that the main immunogenic regions are the lipoyl domains. Short peptides (e.g., of around 20 residues in length) encompassing the lipoyl-binding site are rather weakly antigenic, and full immunological reactivity is only seen for much longer peptides. Thus, for PDC-E2, the 93-residue sequence, 128–221, of the inner lipoyl domain is required for maximal antibody binding. The outer lipoyl domain, although containing a highly homologous region around the lysine residue that is bound to lipoate, is only weakly antigenic. These and other findings suggest that the overall epitopes are conformational

ones, but centered on the lipoyl-binding sites. The strong homologies between these domains among the three OADCs, and between mitochondrial and microbial enzymes, may account for partial cross-reactivities, with extended flanking regions being responsible for specificity and full reactivity. There is some disagreement as to whether lipoyl residues themselves are necessary for full reactivity, but corresponding peptides not containing lipoate are undoubtedly antigenic.

Stimulus for Anti-M2 AMAs Production in PBC

There is good evidence that B-cell clones producing AMAs are maximally stimulated, and it is noteworthy that the dominant epitopes of the $CD4^+$ T-cells, that provide the help for antibody production, are short peptides of the lipoyl-binding domain. (Similar peptides are also the dominant epitopes of the cytotoxic $CD8^+$ T-cells that infiltrate the bile ducts in this disease.) What then is the antigenic drive in PBC? It cannot be a secondary response to tissue damage, since M2 AMAs are not detectable in many other destructive diseases of the liver.

As mentioned earlier, chronic microbial infection may be characterized by low titers of anti-M2 AMAs. There is also epidemiological evidence of association between recurrent urinary tract infection (UTI) and PBC. Moreover, UTI is particularly common in middle-aged women, the group in which PBC most commonly occurs. So it is suggested that the initial stimulus for an immune reaction directed specifically at the E2's of the OADCs, (and E3BP of PDC), is chronic exposure, in the context of co-stimulatory signals (and perhaps a particular genetic background), to microbial peptides that share strong sequence similarities with the lipoyl-binding domains at the core of the dominant epitopes. Expansion of reactivity and specificity to incorporate the entire domain, and then also to recognize E1 subunits, would be by epitope-spreading. Such "microbial mimics" might not necessarily be the homologous OADCs. A number of other bacterial and viral peptides have been identified with strong sequence similarities to the "core" peptidyl epitope of PDC-E2, and have been shown, by ELISAs, to react specifically with PBC sera, the antibodies being cross-reactive with that "core peptide."

One other important fact needs bearing in mind in any speculation about antigenic drive. Once it is established, it persists. Even after liver transplantation high titers of anti-M2 AMAs are still found.

Role of AMAs in the Pathogenesis of PBC

Anti-M2 AMAs are so focused in specificity and so disease specific that it has to be assumed that they are relevant to disease pathogenesis, but most workers have concluded that it is T-cells rather than the antibodies themselves that are the direct cause of tissue damage. For example, high titers of AMAs can be raised in experimental animals, e.g., by immunization with recombinant human PDC-E2, with no evidence of liver damage even after a prolonged period, and only a minority of patients exhibit unambiguous recurrence of PBC following liver transplantation, despite the persistence of AMAs. However in the former case, fine specificities of the AMAs may not be identical to those of the PBC-specific antibodies, and in the latter immunosuppressive drugs may be protective. If the AMAs were to be directly cytotoxic, it might be by inhibition of mitochondrial function following uptake into BEC. Such uptake might be mediated by binding to the elusive antigen that might be the primary recognition target at the surface of BEC.

Anti-M3 AMAs and Pseudolupus Syndrome

Some time ago it was recognized that there was an association between the taking of the drug phenopyrazone, for cardiovascular disease, and a disorder designated as pseudolupus syndrome (PLE). This syndrome was characterized by AMAs that could be demonstrated by IFL, CFTs, and ELISAs, but not by IB. The antigen, classified as M3, was shown to be associated with the outer mitochondrial membrane, and was not organ specific. High titers of anti-M3 were detectable during the acute phase of the disease, but they declined on cessation of treatment with phenopyrazone, a drug that has since been withdrawn. No further cases of PLE have been reported, and the M3 antigen has not been further characterized. However, it has been speculated that it might be a drug-metabolizing enzyme such as monoamine oxidase (MAO), rendered immunogenic through tight binding to the drug.

Anti-M4 AMAs and Sulfite Oxidase

In addition to anti-M2, another complement-fixing antibody has been shown to be closely associated with PBC. The target antigen in this case, designated as M4, was found to co-purify with the outer mitochondrial membrane and be insensitive to trypsin. It was identified as being sulfite oxidase, an enzyme of the intermembrane space, a precursor of which binds to the outer membrane. Sulfite oxidase in an evolutionarily highly conserved enzyme, also found in bacteria, but enzyme activity does not seem to be inhibited by M4-positive PBC sera and the identity of the antigen is now in some doubt. The clinical significance of the detection of anti-M4 in addition to anti-M2 AMA is controversial. There have been claims that anti-M4 AMAs reflect a "mixed form" pathology of PBC with histological

features of chronic active hepatitis, and/or that their detection is an indicator of poorer prognosis towards the end stage of the disease. However, other workers have questioned their specificity in relation to PBC, suggesting that these, and anti-M8/M9, are nonspecific indicators of high serum levels of IgG.

Anti-M5 AMAs and Phospholipid

Mention has been made that false Wasserman-positive tests may reflect a different conformation of cardiolipin than that recognized by the M1-positive, syphilis-specific pattern of IFL, and are frequently associated with SLE. Such false-positive reactions often correlate with a characteristic IFL pattern, designated as M5. This pattern is seen both with a subset of SLE and patients with antiphospholipid syndrome, characterized by thrombocytopenia and recurrent fetal loss. Whilst anti-M5 reactivity may be absorbed out by inner mitochondrial membranes, no specific reactivities have been detected against any mitochondrial proteins, and it is concluded that M5 is some form of phospholipid, although the reactivity is not absorbed out by cardiolipin liposomes or cardiolipin–glycoprotein complexes.

Anti-M6 AMAs and Immuno-Allergic Hepatitis

Anti-M6 AMAs have been detected, by a characteristic pattern of IFL, in sera of patients who had developed acute hepatitis associated with taking the anti-depressive drug iproniazid. The M6 antigen could be detected by CFTs and ELISAs, was partially tissue specific (liver–kidney), and was associated with the inner membrane. The antigen has now been identified as MAO-B and the activity of this enzyme against substrates such as tyramine is inhibited by these AMAs. As MAO-B is irreversibly inhibited by iproniazid, the stimulus for AMA production may arise from metabolite/enzyme haptenization as also suggested, above, in the case of anti-M3.

Anti-M7 AMAs and Flavoenzymes

Around 60% of patients with acute myocarditits and 30% of patients with cardiopathy of unknown etiology exhibit a class of AMAs designated as anti-M7. The antibodies in acute myocarditis are predominantly of the IgM class and disappear on recovery, whilst in chronic disease they are IgG and persist. Such antibodies are not seen in coronary artery conditions and have been considered as reflecting infective disease. The target antigen was originally reported as being heart specific and tightly associated with the inner mitochondrial membrane, but it is now recognized that this class of AMA is directed generally against flavoenzymes. Hence, in heart mitochondria a dominant target is the flavoprotein of succinate dehydrogenase, whilst in liver it includes sarcosine dehydrogenase and dimethylglycine dehydrogenase.

Anti-M8 AMAs and Anti-M9 "AMAs" in PBC

Two other sets of AMAs have been claimed to be specific to PBC, and like anti-M4, important in prognosis of disease progression. One of these recognizes a mitochondrial target categorized as M8. This is an outer membrane, nonorgan-specific, trypsin-sensitive antigen, detectable by CFTs and ELISAs but not by IB. To date M8 is defined only by the protocol for its preparation. The other specificity, categorized as M9, was defined in terms of a trypsin-insensitive constituent of the inner membrane of liver mitochondria. However, it has since been identified as the nonmitochondrial, cytoplasmic enzyme, glycogen phosphorylase, which presumably co-purifies with inner-membrane fragments on ultracentrifugation. Hence, anti-M9 antibodies can no longer be considered as AMAs.

Other AMAs

Naturally Occurring Anti-Mitochondrial Antibodies

Sensitive detection methods reveal that sera of healthy individuals exhibit a spectrum of naturally occurring anti-mitochondrial antibodies (NOMAs), perhaps reflecting an arm of the normal immunoregulatory network, and/or a history of exposure to microbial antigens with structures that "mimic" those of mitochondrial constituents. Where NOMA reactivities against particular antigens have been studied, their fine specificities have been shown to differ from those of disease-associated AMAs recognizing the same molecular species. Interestingly, it has been reported that there is a relative lack of NOMA in patients with PBC, which might be a clue to their normal role in immune regulation.

AMAs Arising from Tissue Damage

Following acute myocardial infarction, many patients demonstrate the short-term production of AMAs against human heart mitochondria. These cross-react against mitochondria from human skeletal muscle, but not with heart mitochondria of other species. Similarly, synovial B-cells in rheumatoid arthritis have been reported as producing AMAs, the finding being interpreted as reflecting local tissue destruction. Such an interpretation

may also apply to the demonstration, in insulin-dependent diabetes, of auto-antibodies against the mitochondrial enzyme of pancreatic β-islet cells, glycerophosphate dehydrogenase.

Pathogenetic AMAs against the Adenine Nucleotide Transporter

Myocarditis and dilated myocarditis are diseases related to viral infection, and (independently of the anti-M7 AMAs described above) are characterized by the production of organ-specific AMAs directed at the mitochondrial ADP/ATP carrier. These antibodies are cytotoxic when tested against guinea pig ventricular myocytes, and in mouse heart, where the transport activity of the carrier has been shown to decline in a manner related to the decrease of cardiac function. The production of these AMAs declines over a period of 2–3 months, and it has been speculated that the underlying mechanism might involve "molecular mimicry" with a viral constituent. However, they may arise as a secondary response to virally induced tissue injury.

See Also the Following Articles

Biliary Cirrhosis, Primary • Phospholipid Metabolism in Mammals • Pyruvate Dehydrogenase

Glossary

CD4$^+$-T cell T-lymphocyte, with a receptor recognizing a specific short peptide, derived from an antigen and presented by an antigen-presenting cell, and thereafter primed to help B-cells that also present that peptide to secrete antibodies against the antigen.

epitope The specific target recognized by a T-cell or antibody.

immunofluorescence A technique for detecting antibodies that bind to specific structures on tissue sections, by treatment with a fluorescently labeled, anti-immunoglobulin antibody.

lipoyl residue The amide of 6,8-dithio octanoic acid, the oxidized, disulfide form of which is reductively acylated in the catalytic cycle of the 2-oxoacid dehydrogenase complexes.

molecular mimicry Similarity in structure, either accidental or evolutionarily selected, between two antigens, leading to immunological cross-reactivity.

Further Reading

Bogdanos, D. P., Baum, H., Sharma, U. C., *et al.* (2001). Antibodies against homologous microbial caseinolytic proteases P characterize primary biliary cirrhosis. *J. Hepatol.* **36**, 14–21.

Gershwin, M. E., Ansari, A. A., Mackay, I. R., *et al.* (2000). Primary biliary cirrhosis: An orchestrated immune response against epithelial cells. *Immunol. Rev.* **174**, 210–225.

Haydon, G. H., and Neuberger, J. (2000). PBC: An infectious disease? *Gut* **47**, 586–588.

Mackay, I. R., Whittingham, S., Fida, S., *et al.* (2000). The peculiar autoimmunity of primary biliary cirrhosis. *Immunol. Rev.* **174**, 226–237.

Van de Water, J., Ishibashi, H., Coppel, R. L., *et al.* (2001). Molecular mimicry and primary biliary cirrhosis: Premises not promises. *Hepatology* **33**, 771–775.

Walker, J. G., Daniach, D., Roitt, I. M., and Sherlock, S. (1965). Serological tests in diagnosis of primary biliary cirrhosis. *Lancet* **39**, 827–831.

Yeaman, S. J., Kirby, J. A., and Jones, D. E. (2000). Autoreactive responses to pyruvate dehydrogenase complex in the pathogenesis of primary biliary cirrhosis. *Immunol. Rev.* **174**, 238–249.

Biography

Harold Baum is Emeritus Professor of Biochemistry and visiting professor in Immunology at King's College London, where he was previously Head of the School of Life, Basic Medical and Health Sciences. His current research is on mechanisms of autoimmune disease, but much of his earlier research was on mitochondrial bioenergetics. His Ph.D. was in chemistry from the University of Birmingham, United Kingdom, but he moved into Biochemistry following a postdoctoral year at the Institute for Enzyme Research in Madison, Wisconsin, where he was subsequently a visiting professor. In addition to his normal research output he is also known for having set metabolic pathways to traditional melodies in "The Biochemists' Songbook."

Mitochondrial Channels

M. Catia Sorgato and Alessandro Bertoli
University of Padova, Padova, Italy

Eukaryotic cells are living organisms surrounded by a surface membrane, which also house other membranes that define intracellular organelles. Membranes are lipidic structures impermeable to hydrophilic molecules (polar or charged); that is why they harbor proteins, called ion channels and carriers, catalyzing the life-requiring exchange of material between a cell and the external space, and between organelles and the cytoplasm. At variance from carriers, ion channels form aqueous pores crossing the lipid bilayer that allow the highly selective transmembrane passage of charged species, namely inorganic ions (e.g., Na^+, K^+, Ca^{2+}, Cl^-), with high potency (10^5–10^8 ions per second are transported by a single molecule); they also possess regulatory domains that open and close the pore upon specific stimuli (electric or chemical). Mitochondria are organelles composed of two membranes; channels may be present in either of the membranes. However, while channels in the outer membrane are justified by their overall high permeability, the presence of these entities in the inner membrane was unexpected in view of its implication in the process of oxidative phosphorylation that imposes an extremely controlled permeability to ions. After the initial phenomenological description, substantial advances in the functional (if not molecular) identification of several mitochondrial channels, disclose the possibility that they take part in crucial schemes of mitochondrial functionality, as well as in dramatic cell events.

Channels and Carriers in Mitochondrial Bioenergetics

According to the chemiosmotic principles, the energy-requiring synthesis of ATP, indispensable for the life of the cell, is driven by the inner membrane (IM)-spanning ATP-synthase complex that utilizes a high electrochemical proton gradient generated by the active proton translocation (from the inner compartment (matrix) outwardly) of other IM-enzyme complexes during substrates oxidation. As intuitively expected, mitochondria need to avoid dissipation of the proton gradient by uncontrolled fluxes of protons, and ions in general, toward the negatively charged matrix. Accordingly, such movements have been restricted to tightly regulated processes proceeding at a much lower rate than ions through channels, i.e., catalyzed by enzymes or carriers such as (1) the ATP-synthase; (2) the H^+-carrier that physiologically dissipates energy as heat in brown fat; and (3) carriers driving the accumulation of metabolic anion substrates, or aimed at counterbalancing the influx of positive charges, for example, carried by Ca^{2+} and K^+. A different reasoning applies to the outer membrane (OM) that houses no energy transducing apparatus, and hence develops no proton gradient. This excludes conceptual barriers for its ion permeability properties, and indeed the electric features of OM channels, the first to be identified in mitochondria, have led to assume that, rather than classical ion conducting elements, they act as principal regulated pathways for the intense exchange of molecules (with molecular mass up to 6–8 kDa) connecting the IM with the rest of the cell.

Functional and Molecular Aspects of Mitochondrial Channels

OM Channels

The voltage-dependent anion channel (VDAC, or mitochondrial porin) is one of the few mitochondrial channels with known primary structure. Its presence in all eukaryotes examined so far speaks in favor of a key role pertaining to this protein, and a single case of human pathology, plausibly linked to VDAC malfunction, has been reported. Extensive electrophysiologic studies (carried out by incorporating the purified protein in planar bilayers) have revealed that VDACs from different species have amazingly conserved biophysical properties. Paradigmatic is the symmetrical closure upon raising the transmembrane electric field, in that the large conductive (maximally open) state adopted by VDAC at low applied voltages (roughly between ± 10 mV) (Table I) is drastically reduced (albeit not nullified) as voltage is increased on both directions (positive and negative). Attainment of the lower conducting states, nicknamed "closed," parallels the change of the ionic selectivity from slightly anionic to cationic.

TABLE I

Main Mitochondrial Channels

Location	Maximal conductance (pS) (150 mM salt)	Putative role
Outer membrane		
VDAC	600–750 (1)[a]	Transport of metabolites
		Apoptosis
Unknown	~100–300 (2,3)	Transport of metabolites (?)
Tom40	1000 (1,2)	Protein import
MAC	2500 (2)	Apoptosis
Inner membrane		
K_{ATP}	9.7 (4)	Matrix volume regulation
mCS	107 (4)	
MCC (TIM)	1000 (2)	Protein import

[a] Used techniques: (1) lipid bilayers; (2) patch clamping of proteoliposomes; (3) patch clamping of intact mitochondria; and (4) patch clamping of mitoplasts.

Note. Table I does not include the PTP complex of the IM, likely to be involved in apoptosis, has not yet been conclusively identified neither electrophysiologically nor at the molecular level. However, from the permeability properties detected in intact mitochondria, PTP open state allows the translocation of molecules with mass up to 1.5 kDa.

Such features, in particular the voltage-dependent permeability, and other biochemical, and genetically based findings, have thus frequently suggested that, by acting as a molecular sieve, the protein regulates the cell metabolism, if not the process of oxidative phosphorylation.

Intriguingly, VDACs from different organisms show little conservation of the amino acid sequence. The almost overlapping electric picture has thus suggested that all VDACs acquire similar secondary structures. Indeed, prediction algorithms have proposed a general feature of the pore's wall formed by antiparallel β-sheets, with the hydrophilic amino acids expectedly facing the internal aqueous ion conducting space. A large body of electron microscopic data of fungal, and mammalian, VDAC crystals have also suggested that the channel crosses the membrane as a hollow cylinder, or with an oval structure, respectively, with an internal (lumen) 1.7–2.8 nm diameter that correlates well with the high conductances described in reconstituted systems. Yet, there are instances that may contradict the above hypothesis. For example, the yeast VDAC2 isoform (in yeast, as in other organisms, there is a VDAC-related multigene family), which can functionally replace VDAC1 in VDAC1-knockout cells, is apparently unable to form channels in planar bilayers.

Because VDAC is the most abundant OM protein, its conserved electric pattern in planar membranes was surprisingly never detected when applying a patch clamp electrode to intact mitochondria. Instead of the typical bell-shaped curve, the response of the macroscopic current (i.e., of the entire membrane) to positive and negative voltages was asymmetrical, while in no case was the behavior of analyzed single channels reminiscent of VDAC properties (Table I). Clearly, the picture emerging from *in situ* experiments suggests that either channels different from VDAC are the major contributors to the OM electric behavior, or that VDAC in native membranes is under the control of OM or intermembrane regulators that get lost in reconstitution experiments. As yet, the physiology and molecular structure of most of such channels are still missing, although, consistent with the OM concept, they are most likely to transport metabolites rather than only small ions. Finally, the only attempt to analyze mitochondria in its cellular context (at the presynaptic terminals of large neurons) has demonstrated that, especially during synapse activation, the OM displays intense electrical activities, which, however, do not resemble that of VDAC.

The electrophysiologic analysis of OM- (or IM-) containing proteoliposomes, and of some membrane components (in planar bilayers), has eventually proven the long-lasting hypothesis that most (~99%) mitochondrial proteins, nuclear-encoded and cytosolic-synthesized, reach their final destination by passing through large permeation pathways of mitochondrial membranes. Specifically, it has been found that both the purified multisubunit translocase of the OM (TOM) (which does not include VDAC), and the TOM component putatively involved in translocation, Tom40, form a pore with a large full open state (of around 1000 pS) and a slight preference for cations (Table I). These features, which are *per se* consistent with a role of TOM pore in allowing permeation of unfolded polypeptides, have been further substantiated by the disturbance provoked by cationic peptides mimicking the mitochondrial targeting domain of several proteins, possibly reflecting transient occlusions of the pore during the peptide translocation.

IM Channels

The *in situ* electric recording of the IM of isolated, intact mitochondria demands that the OM be removed first; this allows the expansion of the IM invaginations, and the formation of a vesicle (mitoplast) sufficiently large to be patch clamped. Except for one type of conductance (called mitochondrial mega (MMC) or multiconductance channel (MCC)) showing huge and unselective fluxes of ions, this strategy has been instrumental for the description of two main kinds of channels, distinguishable by several criteria, not the least by discrete conductance values (Table I). One channel, of around 10 pS, with no clear voltage dependence, translocates only K^+ (K_{ATP}), and is

modulated by physiologic effectors (it is active only at low matrix ATP). The other channel, of around 100 pS (named mitochondrial Centum pico-Siemens, mCS), is preferentially permeated by anions. Although several molecules apparently modulate the channel (nucleotides, Ca^{2+}, etc.), its most prominent feature is the voltage dependence that opens the channel at nonphysiologic (positive) matrix voltages, while it renders it inoperative (closed) at those high negative potentials normally sustained by mitochondria. Parenthetically, it is the powerful activity of mCS channels (found in many mammalian tissues), which accounts for the electric pattern of the entire IM, while most of the other described conductances, in the 15–130 pS range, may be rather safely attributed to mCS substates, or to experimentally induced variations of the K_{ATP} channel conductance.

To search for the role of IM channels, much experimentation has followed the concept that the IM transport of small ions may guarantee fundamental aspects of mitochondrial physiology, such as osmotic stability. Insight into such routes has been provided particularly by monitoring the osmotic swelling of isolated mitochondria that, under the used conditions, is the direct consequence of the ability of a specific solute to cross the IM. Several carrier-mediated pathways have been described, two of which are of interest in the context of ion channels' theme: the selective pathway for K^+ (K^+ uniport), and the pathway allowing the permeation of anions different from metabolites, adenine nucleotides, or phosphate (inner membrane anion channel, IMAC). The extensive biochemical and pharmacological characterization of these proteins (initially denominated channels for their high translocation rate, not because of their, as yet unknown, molecular nature) has led to the proposition that both are implicated in maintaining mitochondrial volume homeostasis. In fact, the similar action of physiologic (ATP) and drug molecules has sustained the functional identity between the K^+ uniport and K_{ATP} channels. With regard to their physiology, the enhancement of K^+ influx under the stressed condition of low-matrix ATP content renders the channel suitable at serving in the K^+ cycle-based volume regulatory mechanism, especially within the proposed control of mitochondrial oxidation rate by matrix volume changes. In addition, it has been shown that the same drugs, opening (cromakalin, diazoxide) or closing (glibenclamide, 5-hydroxydecanoate) mitochondrial K_{ATP} channels, enhance or abolish, respectively, the beneficial effects of ischemic preconditioning, a phase that protects the heart from ischemic injuries. These findings thus point to a cardioprotective role of K_{ATP} channels, although the actual means by which this is achieved have not yet been clarified.

Also in the case of IM anion permeation, accurate electrophysiological reinvestigations of mCS single channels, and of the entire IM, have provided substantial evidence for the functional homology of IMAC and mCS channels; both conduct anions of different valence, are active at alkaline internal (matrix) pH (i.e., such pH renders mCS channels operative also at negative matrix potentials), and are equally blocked by specific drugs. The particular conditions of IMAC activation in intact mitochondria have suggested that it mediates efflux of matrix anions, as part of the mechanism designed to protect against excessive swelling. However, more recently, by relying on pharmacological tests on isolated intact cardiomyocytes, it has been proposed that the opening of IMAC/mCS channels may trigger metabolic oscillations, observed when cells are deprived of substrates, which, at the mitochondrial level, give rise to periodic, redox-state transitions, and a continuous switching between dissipation and re-establishment of the proton gradient. As this phenomenon (if uncontrolled) is likely to provoke a whole set of excitability disturbances in the heart, including arrhythmias, mCS channels may thus become important targets of pharmacological heart treatments.

Similar to the TOM machinery, the reconstituted translocase of the IM (TIM) forms pores with that large conductance (of ~1000 pS) expected for protein transport (Table I). Complemented by immunologic approaches, this study has also suggested the functional (and molecular) identity of the MCC, originally described by patch clamping mitoplasts, with the TIM pore.

Involvement of Mitochondrial Channels in Cell Death Mechanisms

In the recent years, there have been increasing suggestions for a mitochondrial implication in regulating the life and death of the cell through the apoptotic process. Apoptosis is a naturally occurring programmed cell death essential for normal embryonic development and tissue homeostasis in adults. Expectedly, the process is controlled by a variety of factors, including members of the Bcl-2 family (e.g., the pro- and anti-apoptotic Bax and Bcl-2, respectively), and mitochondrial proteins of the intermembrane space (cytochrome *c*, endonuclease G, and others) released in the cytosol. By necessity, passage of these high mass molecules across the OM calls for a further increase of the already large membrane permeability. Accordingly, data have been presented involving either an enhancement of VDAC permeability by Bax, for example, or the capacity of Bax itself to form autonomous protein translocating pores. The latter may be identifiable with extremely large single-channel conductances (named mitochondrial apoptosis-induced channel, MAC) (Table I), recently observed by patch

clamping OM-containing proteoliposomes, especially because such activities are dependent on Bax presence, while rendered silent by Bcl-2 overexpression. However, several other observations point to a direct involvement of the mitochondrial IM, in that a dramatic increase of its permeability leads to loss of mitochondrial osmotic stability by excessive ions intake; in turn, this event provokes matrix swelling, OM disruption by the expanded IM, and release of intermembrane proteins. Such process, reported in isolated organelles and in cells challenged with apoptotic stimuli, is apparently caused by the opening of a huge and unselective IM pathway, known as the permeability transition pore (PTP), formed by a multisubunit complex that may include proteins located in both the IM and OM, e.g., cyclophilin D and the adenine nucleotide translocator, and VDAC, respectively. MMC (or MCC) has also been proposed as a PTP subunit, but its recent identification as a TIM component renders such candidacy unlikely.

See Also the Following Articles

Cell Death by Apoptosis and Necrosis • Chemiosmotic Theory • Mitochondrial Outer Membrane and the VDAC Channel

Glossary

conductance G Expressed in siemens (S = ampere/volt (A/V)) is the ratio between the electric current and the applied voltage. At 100 mV (10^{-1} V), a G of 10 pS (10^{-11} S) corresponds to a current of 1 pA (10^{-12} A) generated by about six million monovalent ions per second.

electrochemical proton gradient Generated by the H^+-pump activity of mitochondrial inner membrane (IM) enzyme complexes, it is commonly expressed in millivolts (mV) as proton motive force ($\Delta p = \Delta\mu_{H^+}/F = \Delta\psi - 60\Delta pH$). $\Delta\psi$ defines the difference in charges, and ΔpH that in H^+ concentrations, between the matrix and the aqueous phase external to the IM. A Δp of 180–200 mV (matrix negative) is normally found, with $\Delta\psi$ contributing for 150–180 mV.

lipid bilayer Allows the recording of electric activities from artificial planar membranes fused with vesicles obtained from native membranes, or reconstituted with purified proteins.

mitochondria Organelles composed of an outer membrane (OM), an intermembrane space, and an invaginated IM delimiting a matrix space that houses crucial metabolic routes.

patch clamp By means of fine electrodes, it records ionic currents directly from the membrane of isolated cells or organelles, as well as from large lipid vesicles reconstituted with channel-containing membrane fractions (proteoliposomes).

Further Reading

Borecky, J., Jezek, P., and Siemen, D. (1997). 108 pS channel in brown fat mitochondria might be identical to the inner membrane anion channel. *J. Biol. Chem.* **272**, 19282–19289.

Kroemer, G., and Reed, J. C. (2000). Mitochondrial control of cell death. *Nat. Med.* **6**, 513–519.

O'Rourke, B. (2000). Pathophysiological and protective roles of mitochondrial ion channels. *J. Physiol.* **529**, 23–36.

Sakmann, B., and Neher, E. (eds.) (1995). *Single Channel Recording*. Plenum Press, New York.

Sorgato, M. C., and Moran, O. (1993). Channels in mitochondrial membranes: Knowns, unknowns and prospects for the future. *Crit. Rev. Biochem. Mol. Biol.* **18**, 127–171.

Truscott, K. N., Brandner, K., and Pfanner, N. (2003). Mechanisms of protein import into mitochondria. *Curr. Biol.* **13**, R326–R337.

Biography

M. Catia Sorgato is a Professor of Medical Chemistry at the Faculty of Veterinary Medicine, University of Padova. After graduating in biology, she worked at the Biochemistry Department, Oxford University (UK) on energy transduction processes, and then at the Max-Planck-Institute, Göttingen (Germany), where she accomplished the first electrophysiologic analysis of mitochondrial inner membranes. Her actual research interest is the physiopathology of prion proteins.

Alessandro Bertoli graduated in physics and holds a Ph.D. in biochemistry and biophysics. He is currently a research fellow at the Department of Biological Chemistry, University of Padova. His past experience dealt with the electrophysiology of mammalian cell, and yeast mitochondrial channels, while his actual interest is the biology of neurodegenerative disorders.

Mitochondrial DNA

Gottfried Schatz
Swiss Science and Technology Council, Bern, Switzerland

Mitochondria, the eukaryotic organelles of oxidative phosphorylation, contain their own DNA genome. This genome is much smaller than that in the nucleus and encodes only ~1% of the mitochondrial proteins. Yet it is essential for the formation of fully functional mitochondria.

Discovery of Mitochondrial DNA

Some concepts take the scientific world by storm, but others conquer it only after many skirmishes. The discovery of mitochondrial DNA (mtDNA) belongs to this second category. Biochemists, histologists, and electron microscopists had seen DNA in mitochondria for years, but most of them were not ready for the idea that the DNA really belonged there. This may explain why textbook accounts of mtDNA almost never tell how this DNA was discovered.

After the basic building plan of the eukaryotic cell had been revealed in the early 1950s by the electron micrographs of Palade, Sjöstrand, and others, biochemists embraced de Duve's dogma that every macromolecule had one, and only one, intracellular location. In the analysis of cell fractions, cytochrome oxidase was taken as a marker for the mitochondria, NADPH–cytochrome *c* reductase for the endoplasmic reticulum, and DNA for the nucleus. Given this frame of mind, it is easy to understand why the presence of DNA in mitochondrial fractions was generally attributed to contamination by nuclear fragments. Histochemical DNA stains, such as the Feulgen reaction, also stained the kinetoplasts of *Trypanosomes* and the "*Nebenkern*" of insect spermatozoa, but at that time it was not yet recognized that these structures were, in fact, unusual mitochondria. Massive amounts of extranuclear DNA were also detected in the cytoplasm of amphibian oocytes, but it took many years to realize that this DNA was, in fact, mtDNA whose abundance reflected the enormous amount of mitochondria in these large cells. In 1961, at the Fifth Annual Meeting of the American Society of Cell Biology in Chicago, Hans Ris showed electron micrographs of mitochondria with inclusions resembling the DNA-containing nucleoids of bacteria and made the heretical proposal that mitochondria (and also chloroplasts) contain their own DNA. In a paper that appeared in the following year, Ris and Walter S. Plaut further documented and expanded these observations. Soon thereafter, biochemical and morphological evidence from several groups confirmed the presence of DNA in chloroplasts.

The discovery of chloroplast DNA made biochemists take a fresh look at early findings by Margaret Mitchell and Boris Ephrussi that certain mutations affecting mitochondrial function in the mold *Neurospora crassa* and the yeast *Saccharomyces cerevisiae* were not inherited according to Mendel's laws. It seemed tempting to speculate that the unknown "extrachromosomal factors" implicated in these mutations were, in fact, mtDNA.

By 1962, the ground for the concept of mtDNA was thus well prepared, but the concept itself was not generally accepted. In retrospect it seems that the scientific community was waiting for convincing studies that documented the existence of mtDNA by several diverse methods.

One of these studies came from the electron microscopists Margit M. K. Nass and Sylvan Nass, who were then working at the Wenner Gren Institute of the University of Stockholm. They showed that the matrix of osmium-fixed chick embryo mitochondria contained thread-like inclusions whose appearance after different fixation procedures closely paralleled that of the histone-free DNA nucleoid of bacteria: after fixation with osmium tetroxide, the inclusions appeared clumped and as bars with a diameter of ~400Å; fixation of the tissues with osmium tetroxide followed by treatment with uranyl acetate before dehydration made them appear as 15–30Å thin fibers. Even more convincing evidence for the presence of DNA in these inclusions was the observation that the inclusions could be removed by treating the lightly fixed embryonic tissue with DNase. Treatment with pepsin, with RNase, or with DNase-free buffer controls was ineffective. The clarity of these electron micrographs and the careful controls that were included had a compelling impact on cell biologists. M. M. K. Nass and S. Nass published their work in two back-to-back papers in a 1963 issue of the *Journal of Cell Biology*. At that time, however, cell biology and biochemistry were still rather

different disciplines and most biochemists did not peruse journals devoted to cell biology. It therefore took a while before the findings by M. M. K. Nass and S. Nass entered the consciousness of the biochemical community.

At about the same time, Ellen Haslbrunner, Hans Tuppy, and Schatz at the Biochemistry Institute of the University of Vienna were trying to find a biochemical basis for the extrachromosomal mutations that abolished respiratory function in the yeast *S. cerevisiae*. In the early 1960s, many biochemists were still reluctant to consider the "respiratory granules" of yeast as *bona fide* mitochondria, which placed the research by Haslbrunner *et al.* well outside the mainstream of mitochondrial biochemistry in the United States and elsewhere.

To look for DNA in mitochondria, a biochemical approach was chosen. Yeast mitochondria were purified by the best methods available, and their DNA content was measured by the time-honored "Diesche" color reaction. A few years before, de Duve and co-workers had shown that centrifuging subcellular fractions to equilibrium in a density gradient often gave a clean separation of different organelles. Surprisingly, the usual sucrose gradients did not separate yeast mitochondria from nuclear fragments, but when sucrose was replaced with the X-ray contrasting agent "Urografin," the mitochondria formed an extremely sharp band, and DNA was present in only two fractions: most was at the bottom of the centrifuge tube, and a very small amount, but discrete peak coincided exactly with that of the mitochondria. The DNA in the bottom fraction was easily digested by DNase and apparently represented nuclear DNA. The DNA in the mitochondrial fraction was not readily digested by DNase unless the organelles were first disrupted with trichloroacetic acid; presumably, it represented DNA enclosed by the mitochondrial membranes. Its concentration was very constant between different experiments – between 1 and 4 μg per mg mitochondrial protein. Urografin – purified mitochondria from rat liver, rat kidney, and bovine heart – contained almost 10 times less DNA, between 0.2 and 0.6 μg DNA per mg protein. The typical mammalian mitochondrion was calculated to contain 3×10^{-17} g DNA. Assuming that the DNA was double-stranded, it could encode no more than 1.2 MDa of polypeptide chains. This result was considered important, because it firmly excluded the possibility that mtDNA encoded all of the mitochondrial proteins. Today, this early calculation by Haslbrunner *et al.* could be challenged on several grounds, yet it came remarkably close to reality: the 13 polypeptides encoded by mammalian mtDNA have a total mass of 0.423 MDa, and the remainder of the coding potential is largely accounted for by genes for ribosomal – and transfer RNAs, as well as the by fact that mitochondria usually have more than one copy of their DNA genome.

Properties of mtDNA

Soon thereafter, several laboratories showed that mtDNA from several organisms had a different base composition and sometimes also a different buoyant density in cesium chloride gradients than the corresponding nuclear DNA. Particularly, striking was the observation that mtDNA from mammals was a small double-stranded circle. Late in 1964, the existence of DNA in mitochondria was generally accepted, and efforts focused on its function. Its identity with the "extrachromosomal factors" affecting respiratory function in *S. cerevisiae* was established by the observations that mtDNA was either altered or missing in the corresponding mutants. Several laboratories then showed that mitochondria from yeast and *N. crassa* synthesized the three large subunits of cytochrome oxidase, the heme-carrying subunit of the cytochrome bc_1 complex, and at least one membrane-bound subunit of the ATP synthase complex.

Sequence and Gene Content

In 1981, Fred Sanger and co-workers published the complete sequence of the 16,569 nucleotides of human mtDNA. This seminal paper provided the first complete sequence of a eukaryotic genome and identified the mitochondrial genes. Subsequent work by others then showed that the size of mtDNA can vary dramatically between different species (Table I). There are also considerable differences in gene content. Whereas mtDNA from humans and most mammals encodes 13 proteins and 24 RNAs (Figure 1 and Table II), that from the freshwater protozoon *Reclinomonas americana*

TABLE I

Sizes of mtDNAs from Different Species

Species	Kilo-base pairs
Mammals	16.5
Fungi	
Saccharomyces cerevisiae	78
Schizosaccharomyces pombe	17
Aspergillus nidulans	32
Plants	
Zea mays	570
Muskmelon	2500

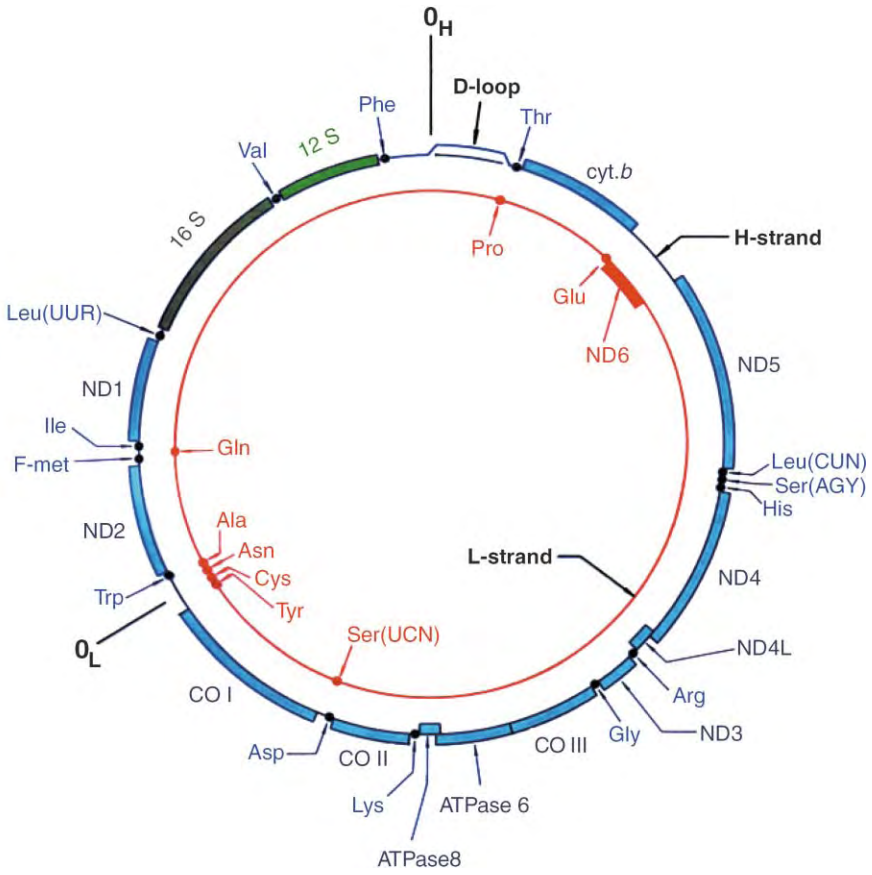

FIGURE 1 Genes on human mtDNA. 12S, 16S: rRNA of small and large ribosomal subunit; ND1–6 and ND4L: subunits of NADH dehydrogenase; CO I–III, subunits 1–3 of cytochrome oxidase; cyt. *b*, cytochrome *b* subunit of cytochrome bc_1 complex; ATPase 6 and 8: subunits of ATP synthase complex; amino acids designate the corresponding tRNAs; D-loop, highly variable gene-free region; O(H) and O(L), sites previously proposed by some as strand-specific replication origins. Reproduced from Attardi, G. (1986). The elucidation of the human mitochondrial genome: A historical perspective. *Bioassays* **5**, 34–39.

TABLE II

Genes on Human mtDNA

Function	Molecule(s)	Number
Protein synthesis	rRNAs	2
	tRNAs	22
Electron transport	Cytochrome oxidase	3
	NADH dehydrogenase	7
	Cytochrome bc_1 complex	1

carries no fewer than 97 genes. Sequence comparisons between some of the genes and the corresponding polypeptide products also uncovered the astounding fact that the genetic code of mtDNA differs slightly but significantly from that of nuclear DNA (Table III). For example, the codon UGA defines "stop" in the nucleus, but "tryptophan" in mtDNA from mammals, yeast, and many other species. This unexpected finding explained why so many earlier attempts to identify the protein products of mtDNA by coupled transcription/translation in *Escherichia coli* or reticulocyte lysates had failed.

Outlook

There is no end to the fascinating properties of the mitochondrial genome, and many of these properties still beg an explanation. Why is the mitochondrial genome of mammals one of the most compact genomes known, whereas that of plants and yeast spreads its genes luxuriously over five, ten, or even hundreds of times more DNA? Why has the genetic code diverged from the "standard" one that is used in the nucleus? Why does mtDNA mutate ~10 times faster than the corresponding nuclear DNA? Why have some mitochondria dozens of copies of their genome? Most importantly, why does mtDNA exist at all? Maintaining its few protein-coding genes from one generation to the next keeps hundreds of nuclear genes occupied, which

TABLE III

Unusual Codon Usage in mtDNAs

Codon	"Universal" usage	Mitochondrial usage	Species
CUA	Leucine	Threonine	Yeast
UGA	Stop	Tryptophan	Most species, not plants
AUA	Isoleucine	Methionine	Most species, not plants
AG(A,G)	Arginine	Stop	Mammals
		Serine	Insects
		Arginine	Yeast

seems highly uneconomical. Evolution provides the answer: it is now generally accepted that today's mitochondria are descendants of free-living prokaryotes that entered into symbiosis with other cells and transferred most of their genome to the nucleus of their host. The mtDNA is the small remnant of the genome of these endosymbionts.

Since a typical somatic cell has only two copies of a nuclear gene, but as many as a thousand copies of each mitochondrial gene, mtDNA has become a favorite tool for genetic fingerprinting and evolutionary studies. Also, it is now well established that mutations in mtDNA can cause a host of devastating maternally-inherited diseases, such as blindness, deafness, muscular degeneration, diabetes, and severe neuro-degenerative syndromes. A possible involvement of mtDNA in aging and cancer is under intense investigation. There is also mounting evidence that mutations of mtDNA may impair mammalian fertility and the success of *in vitro* fertilization experiments. Indeed, many of the most exciting functions of mtDNA may yet await discovery.

See Also the Following Articles

Cytochrome bc_1 Complex (Respiratory Chain Complex III) • Cytochrome Oxidases, Bacterial • Mitochondrial DNA • Mitochondrial Genes and their Expression: Yeast • Mitochondrial Genome, Evolution • Mitochondrial Genome, Overview

Glossary

cytochrome bc_1 complex A multi-subunit complex of the respiratory chain that transfers electrons from ubiquinone to cytochrome *c*.

cytochrome oxidase A multi-subunit green heme protein of the respiratory chain reducing oxygen gas to water.

endosymbiont Organism living symbiotically inside another organism.

kinetoplast The single, giant mitochondrion of a trypanosome cell.

nebenkern Spiral-like single mitochondrion wrapped around the flagellum of certain spermatozoa.

Further Reading

Andersen, S., Bankier, A. T., Barrell, B. G., de Bruijn, M. H., Coulson, A. R., Drouin, J., Eperon, I. C., Nierlich, D. P., Rae, B. A., Sanger, F., Schreier, P. H., Smith, A. J., Staden, R., and Young, I. G. (1981). Sequence and organization of the human mitochondrial genome. *Nature* **290**, 457–465.

Attardi, G., and Schatz, G. (1988). Biogenesis of mitochondria. *Annu. Rev. Cell Biol.* **4**, 289–333.

Attardi, G., Yoneda, M., and Chomyn, A. (1995). Complementation and segregation behavior of disease-causing mitochondrial DNA mutations in cellular model systems. *Biochim. Biophys. Acta.* **1271**, 241–248.

Chomyn, A., and Attardi, G. (2003). MtDNA mutations in aging and apoptosis. *Biochem. Biophys. Res. Commun.* **304**, 519–529.

Clayton, D. A. (1991). Replication and transcription of vertebrate mitochondrial DNA. *Annu. Rev. Cell. Biol.* **7**, 453–478.

Grivell, L. A. (1983). Mitochondrial DNA. *Sci. Am.* **248**, 78–89.

Nass, M. M. K., and Nass, S. (1963). Intramitochondrial fibers with DNA characteristics II. *J. Cell Biol.* **19**, 613–629.

Nass, S., and Nass, M. M. K. (1963). Intramitochondrial fibers with DNA characteristics I. *J. Cell Biol.* **19**, 593–612.

Schatz, G., Haslbrunner, E., and Tuppy, H. (1964a). Deoxyribonucleic acid associated with yeast mitochondria. *Biochem. Biophys. Res. Commun.* **15**, 127–132.

Schatz, G., Haslbrunner, E., and Tuppy, H. (1964b). Intramitochondriale Deoxyribonukleinsäure in Säugetierzellen. *Monatshefte f. Chemie* **95**, 1135–1140.

Scheffler, I. E. (1999). *Mitochondria*, 364pp. Wiley, New York.

Scheffler, I. E. (2000). A century of mitochondrial research: achievements and perspectives. *Mitochondrion* **1**, 3–31.

Wallace, D. C. (1997). Mitochondrial DNA in aging and disease. *Sci. Am.* **277**, 40–47.

Biography

Gottfried Schatz obtained his Ph.D. in biochemistry in 1961 in Austria. He then worked as an Assistant Professor at the University of Vienna, as postdoctoral fellow with Efraim Racker at New York, and as a Professor of Biochemistry at Cornell University in Ithaca. In 1974 he joined the Biozentrum at the University of Basel. Upon retiring as a Professor in 1999, he was elected President of the Swiss Science and Technology Council.

Mitochondrial Genes and their Expression: Yeast

Piotr P. Slonimski
Centre de Génétique Moléculaire du Centre National de la Recherche Scientifique (CNRS), Gif-sur-Yvette, France

Giovanna Carignani
University of Padova, Padova, Italy

Mitochondria possess their own genome, which encodes a small part of the proteins that make up the organelle. The remaining proteins, i.e. the majority, are encoded by the nuclear genome. Mitochondrial life thus depends on the coordinated expression and interaction of nuclear genes and genes present on the organellar genome (mtDNA) itself. Although mtDNA encodes very few subunits of the energy-transducing complexes of the inner mitochondrial membrane, these subunits constitute the key elements of the overall process: cytochrome *b* for the reductase activity, cytochrome *c* oxidase subunit 1 for the oxidative activity, and Atp6 for the synthetase activity. The genes coding for these three subunits are always located in the mtDNA in all eukaryotes, whether fungi, protists, animals, or plants. The mtDNA is supposed to be a remnant of a prokaryotic genome that would have originated from a symbiotic event between different cellular species. As the majority of the prokaryotic genes would, however, in the course of evolution, have migrated to the nucleus of the new cell, it is surprising that even today a mitochondrial genome exists. A plausible reason might reside in the compulsory evolution of the formation mechanism of the enzymatic complexes of the inner mitochondrial membrane. This might depend on a topological constraint of the expression and assembly of the different subunits, some of which are very hydrophobic and have to be transcribed, translated, inserted, and assembled from inside the organelle. It follows then that these key genes are present inside the mitochondrion. This would also explain the persistence of mtDNA and its complex machinery of expression for a billion years since the original symbiotic event.

The knowledge of the conjoint expression of both the mitochondrial and nuclear genes involved in energy transduction is best advanced in the study of baker's yeast, essentially due to the extraordinary power of molecular genetics both *in vivo* and *in vitro*.

Yeast as a Model Organism for the Study of Mitochondrial Biogenesis and Function

The facultative anaerobic yeast *Saccharomyces cerevisiae* has provided the main information about mitochondrial biogenesis, from the discovery of petite mutants by Boris Ephrussi and Piotr Slonimski and their collaborators in the 1950s. This was followed by the exhaustive analysis of mitochondrial genetics in the 1970s in the laboratory of Gif-sur-Yvette and by the identification of mtDNA by Gottfried Schatz, and still remains an excellent experimental organism, owing to its capacity of surviving in the absence of competent mitochondria, to the facility of isolation or construction of mutants (several thousand have already been characterized) and to the possibility of mitochondrial transformation. The search for nuclear genes involved in mitochondrial biogenesis and function is constantly carried out in this organism and the results continually lead to the isolation of functionally homologous human genes. In particular, many mitochondrial disease genes have been identified in this way.

Mitochondrial life depends on the coordinated expression and interaction of nuclear genes and genes present on the organellar genome (mtDNA) itself. The mitochondrial genetic system is required for the synthesis of a limited number of proteins, in particular in yeast of seven highly hydrophobic subunits of the energy-transducing complexes of the inner membrane (Figure 1).

All the processes necessary to the expression of these genes (i.e., transcription, RNA processing, and translation), as well as those required for mtDNA maintenance and integrity, take place in the same

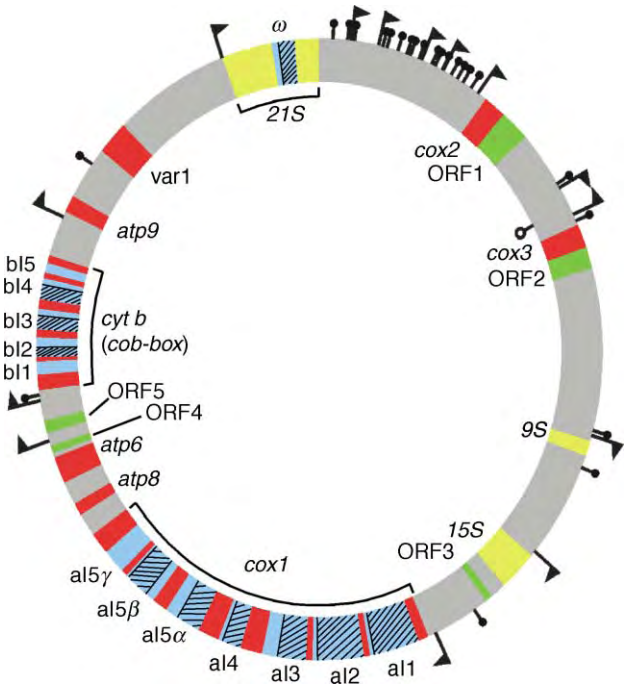

FIGURE 1 The mitochondrial genome of *Saccharomyces cerevisiae*. The circular map is in agreement with the genetic results and with the observation that mtDNA replicates by the rolling-circle mode. Different yeast strains contain mtDNA molecules of different lengths (comprised between 70 and 85 bp). These differences are essentially due to the presence/absence of introns and hypothetical open reading frames (ORFs 1–5 in this representation). Yeast mtDNA encodes seven highly hydrophobic subunits of the energy-transducing complexes of the inner membrane, i.e., apocytochrome *b* (encoded by the *cyt b*, or *cob-box*, gene), three subunits of cytochrome c oxidase (encoded by the *cox1*, *cox2*, and *cox3* genes) and three subunits of ATP synthase (encoded by the *atp6*, *atp8*, and *atp9* genes). The *cytb*, *cox1*, and *21S rRNA* genes contain introns, some of which are translated, independently or in frame with their upstream exons, to produce maturases (e.g., the bI2 intron of the *cytb* gene, see Figure 3) or site-specific endonucleases (the *ω* intron of the *21S rRNA* gene); others encode complex proteins with multiple functions, i.e., maturases, reverse transcriptases, endonucleases (e.g., the aI1 intron of the *cox1* gene). Red: exons of protein-coding genes; blue: introns (aI1–aI5; bI1–bI5; *ω*); hatched blue: intron-encoded ORFs; green: hypothetical ORFs; yellow: 9S, 15S, and 21S RNAs; solid circles: tRNAs. Flags indicate the transcription initiation sites and their orientation. The orientation of all the transcription units is clock-wise, with the exception of the $tRNA^{thr1}$ gene (open circle), which is transcribed from the opposite strand.

compartment, the mitochondrion itself, as they occur in a bacterium, the hypothetical mitochondrial ancestor. Also, the different processes are functionally linked, frequently through the activity of proteins exhibiting multiple roles.

Expression of Mitochondrial Genes

Mitochondrial gene expression requires the coordinated interaction of mitochondrial and nuclear encoded factors: the mitochondrial genome (Figure 1) participates in the process with the genes encoding the RNA-subunit of mitochondrial RNase P (9S RNA), the 21S and 15S rRNAs, a complete set of tRNAs, and one protein of the small mitoribosomal subunit, Var1; in addition some introns encode proteins necessary for RNA splicing (RNA maturases). The nuclear genome encodes all other factors necessary for mitochondrial genome maintenance and expression, as well as all other mitochondrial proteins (~500 yeast proteins located in the organelle were currently listed in the Yeast Proteome Database, YPD, in 2001, but predictions indicate about 700). These are translated in the cytoplasm, and then imported into different compartments of mitochondria using protein-specific import mechanisms. A mitochondrial targeting sequence, often present at the amino terminus of translated precursors, allows their interaction with the mitochondrial receptor–translocator TOM–TIM, followed by maturation of the precursor and its localization in mitochondria. Also, recent results point out that nuclear-encoded mitochondrial proteins of bacterial origin are synthesized on polysomes associated with the mitochondrion, while those of eukaryotic origin are generally translated on free cytosolic polysomes, thus promoting speculations about organelle origins.

General Features of Simple and Mosaic Genes

(To describe the expression of yeast mitochondrial genes, we distinguish between simple genes and mosaic genes, i.e., genes containing introns and thus subject to a more complicated expression pathway.)

Transcription

The yeast mitochondrial genome is ~4 times larger than mammalian mitochondrial genomes, although they contain approximately the same number of genes. The difference is due to the lengths of intergenic regions and to the presence of introns in some of the yeast genes. Whereas the 16,000 base-pair mammalian mitochondrial genome is transcribed by two opposite promoters (one for each strand), genes on the 80,000 base-pair yeast mtDNA are transcribed, singly or in clusters, from several promoters (14 active promoters have been identified, see Figure 1). The consensus sequence of mitochondrial promoters is a nonanucleotide 5′ATATAAGTA 3′, whose last A is the +1 position of the transcript, and termination of transcription is indicated by the dodecanucleotide consensus 5′AAUAAUAUUCUU3′ (see Figure 2).

As in the case of bacterial transcription, all mitochondrial genes are transcribed by the same RNA

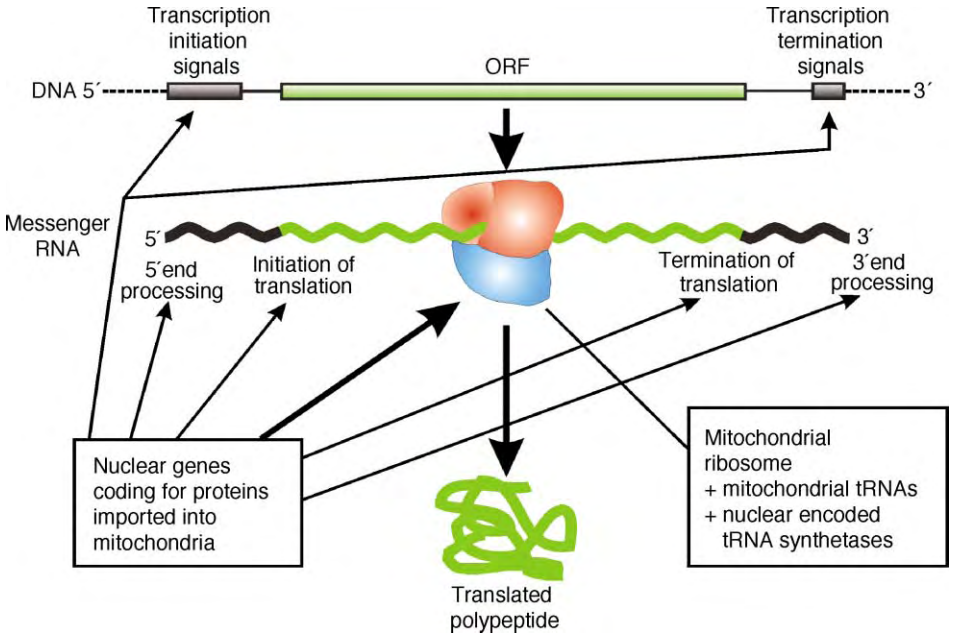

FIGURE 2 Main features of the expression of a "simple" mitochondrial protein-coding gene. The open reading frame (ORF) of the gene located in the mtDNA is transcribed into messenger RNA and translated into a polypeptide chain according to the general principles of molecular biology. However, most of the elements of these two machines derive their information from a different cellular compartment than the one where these processes take place. The genes coding for the transcriptional machinery as well as those involved in the processing or stability of mRNA are located in the nucleus, the proteins synthesized in the cytoplasm and imported inside the mitochondrion where they recognize specific signals, i.e., mtDNA or mtRNA sequences or structures indicating the beginning and the end of DNA transcription or RNA processing (e.g., Mtf1, Nam1). The next step of gene expression is even more complex, since in addition to numerous nuclear genes coding for proteins involved in initiation/termination of translation, as well as the translation process itself (more than seventy ribosomal proteins, e.g., Nam9, all translation factors, e.g., Cbp1, and all specific mitochondrially located tRNA synthetases), a number of genes located in the mitochondrial genome participate in the process. They encode essentially the catalytic RNAs: the two, large and small, rRNAs, the complete set of tRNAs and a subunit of RNAse P. As a result of this double inheritance scenario, a mutational lesion in any one of the elements (e.g., the nuclear encoded leucine tRNA synthetase by gene NAM2 or a mtDNA encoded tRNA) will ineluctably and irreversibly abolish the expression of all the genes located in mtDNA.

polymerase. This is composed of only two nuclear encoded subunits, a core RNA polymerase, Rpo41, which is similar to the very simple T-odd phages RNA polymerases, and the mitochondrial transcription factor, Mtf1, which is required for the recognition of the promoter by the holoenzyme and is released when Rpo41 enters into the elongation mode, as happens for sigma factors of bacterial RNA polymerases. Mtf1 in fact shares sequence similarity with regions 2 and 3 of bacterial sigma factors, but, unexpectedly, crystal structure of Mtf1 has revealed clear similarity to the family of RNA and DNA methyltransferases and one of the two human homologues of Mtf1 has been proved to methylate a conserved stem-loop in bacterial 16S rRNA and human mitochondrial 12S RNA. This is one of the several evidences (the incessant definition of protein crystal structures is currently revealing novel cases) where the structure/function relationship of a present day protein indicates that it might have evolved from a multifunctional ancestor or from a protein with a different function.

RNA Processing: 5′ and 3′ Processing

Mitochondrial transcription units are unusual as they are characterized by the presence of mRNAs interspersed with tRNA and rRNAs. In human mtDNA tRNAs genes "punctuate" the very long principal transcription unit and their processing at both ends "release" the majority of other RNAs. In yeast the mitochondrial transcription units are shorter but also contain various combinations of RNAs. tRNAs precursors are processed at 5′ end by mitochondrial RNAse P and at 3′ end by a specific endonuclease (successively tRNAs are matured by CCA addition and nucleotide modifications). The processing of mRNAs at their 5′ end, assisted by nuclear encoded factors (e.g., Cbp1 for the cytochrome *b* transcript) consists in a cleavage to generate mature mRNA at a position specific for each transcript. In some transcription units the transcript is first released by the 3′ end processing of a preceding tRNA or mRNA. Processing at 3′ end of mRNAs is done near the conserved dodecamer sequence 5′AAUAAUAUUCUU3′, which is protected by a

complex of three proteins before cleavage by a probably specific endonuclease. All these processes are assisted by several nuclear encoded proteins with a gene-specific or a more general role (see Figure 2).

Processing of Mosaic Genes is More Complex: RNA Splicing

A typical feature of yeast mtDNA, which is not shared by human mtDNA (but is common to many mtDNA from plants, fungi, and protists), is that some of its genes are split by introns. In *S. cerevisiae* these are the *21S rRNA*, *cytb* (*cob-box*) and *cox1* genes. Splicing of these introns is catalyzed by the intron itself (catalytic RNA), and depends on the formation of a conserved RNA three-dimensional structure, which enables them to undergo self-splicing *in vitro*, albeit inefficiently and under non-physiological conditions. *In vivo*, however, splicing requires the presence of specific proteins that function to promote a stable and active RNA conformation. Furthermore, some yeast mitochondrial introns behave as mobile genetic elements, as they can be inserted into an intronless version of the gene at the same position it already occupies in the intron-containing version (intron homing) or to a novel location (intron transposition). Mitochondrial introns belong to two classes, group I and II, based on the secondary and tertiary structure of the intron transcript and on the mechanism of splicing. The mechanism of splicing of group II introns has suggested that they might be progenitors of nuclear pre-messenger introns and of the spliceosome-catalyzed splicing process, with group II intron domains having evolved into small nuclear RNAs (snRNAs).

Several features of mitochondrial introns have been uncovered in the laboratory at Gif-sur-Yvette in the late 1970s, among these some encode proteins, i.e., RNA maturases, which assist the splicing of the intron itself and sometimes also of a different intron (see Figure 3), and also promote intron mobility. Intron encoded proteins also belong to two groups. Group I proteins are members of the LAGLI-DADG family of DNA endonucleases and, besides the endonuclease activitiy required for intron mobility via DNA (as happens for prokaryotic transposons), some of them have high-affinity RNA-binding properties necessary for their role in splicing. Mobile group II introns (e.g., intron aI1 of the *cox1* gene) encode multifunctional proteins, endowed with maturase and DNA endonuclease activity, but also encode reverse transcriptases that bind specifically to the intron RNAs to promote both intron mobility and RNA splicing. In the case of group II introns, transposition occurs via RNA, the procedure adopted by eukaryotic nuclear retrotransposons and retroviruses. Some of the mitochondrial intron encoded proteins are translated in-frame with the upstream exon and subsequently processed to mature proteins by various proteases. This process shows how the different events of mitochondrial gene expression (in this case splicing and translation) are strictly interconnected and also enlightens a peculiarity of mitochondrial translation, that it starts immediately after transcription, as in prokaryotes, however before RNA processing, an occurrence unique to this system.

In vivo self-splicing of yeast mitochondrial introns is thus assisted by proteins that, in general, have the role to promote the folding of the catalytic core of the intron, inducing the formation of nucleotide interactions required for catalytic activity. These proteins are the maturases encoded by the intron itself and other proteins, encoded in the nuclear genome, that concur in assisting the splicing event. Numerous of these proteins have been identified as suppressors of splicing-defective mitochondrial mutations and most of them are proteins that, besides their role in mitochondrial splicing, have also other functions. An example is the mitochondrial enzyme leucyl-tRNA synthetase, Nam2, which is also necessary for the splicing of the group I intron bI4. Actually, recent interesting results indicate that the tyrosyl-tRNA synthetase of *Neurospora crassa* interacts with group I introns by recognizing conserved tRNA-like structural features of the intron RNA, thus suggesting that this might be the case for other tRNA synthetases as well. Also the Mrs2 protein, which assists splicing of group II introns, seems to be implicated in a more general function, as a mitochondrial Mg^{2+} transporter. A particularly interesting protein is Nam1, that is involved in the removal of introns from the *cytb* and *cox1* transcripts and in overall translation capacity, and is also responsible of coupling these processes to transcription, through direct interaction with the amino terminus of mitochondrial RNA polymerase, Rpo41.

Translation

Translation of mitochondrial mRNAs resembles more closely its prokaryotic than eukaryotic counterpart with respect to the spectrum of antibiotics inhibiting mitochondrial translation. Also, mitochondrial mRNAs are uncapped and lack the poly(A) tail, as prokaryotic mRNAs. However mitochondrial translation has unique features, e.g., the use of an alternative genetic code and the composition of mitochondrial ribosomes. These are made up of nuclearly encoded proteins (with the exception of Var1), the majority of which have no recognizable homology to known proteins, i.e., are unique. It has been suggested that these proteins have more specialized functions connected with the coupling of the translation process to the inner mitochondrial membrane, where the seven hydrophobic mtDNA-encoded proteins have to be assembled.

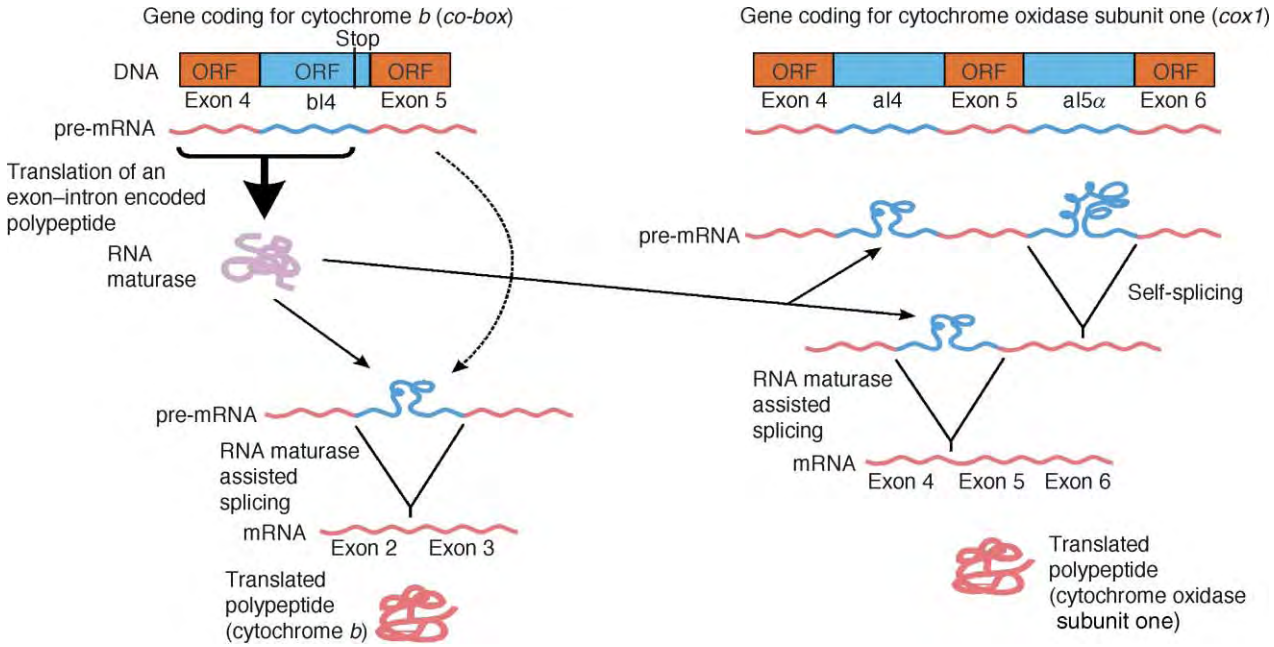

FIGURE 3 Specific features of the expression of a "mosaic" mitochondrial protein-coding gene. Several yeast mitochondrial genes contain introns and some of these introns contain ORFs (see Figure 1). The expression of such "mosaic" genes occurs in two successive steps supplementary to the general features of expression of "simple" genes (see Figure 2). The primary, unspliced RNA transcript (pre-mRNA) for apocytochome *b* acts as a messenger for a protein translated from the upstream exon ORF of cytochrome *b* and the ORF of the successive intron. This fusion protein, mRNA maturase (in the example shown referred to as the bI4 RNA maturase) promotes catalytically the excision of the intervening sequence from the pre-mRNA and ligation of cytochrome *b* exonic RNA leading to the formation of cytochrome *b* mRNA. The maturase recognizes specific structures of the intervening sequence, helps the productive folding and facilitates the activity of the ribozyme. At the same time the maturase activity destroys the RNA which codes for itself and thus exerts a negative feedback for its own biosynthesis. In consequence the amount of maturase in the organelle is very low, and the protein can be detected only when its splicing function is impaired. Generally, the maturases act selectively on the introns which encode them. A notable exception is the maturase shown in the example, i.e., the maturase encoded by the fourth intron of the cytochrome *b* gene (bI4): its activity is essential also for the splicing of the fourth intron (aI4) of a different gene, *cox1*, which encodes the subunit one of cytochrome *c* oxidase. In this manner the expression of the key catalysts of the electron transfer cascade may be coordinated.

The 5′-untranslated leader sequences (UTLs) of mitochondrial mRNAs contain sequence or structural signals that indicate the translation initiation site and that are recognized by mRNA-specific activator proteins (e.g., Cbs1, Cbs2, and Cbp1 for *cytb*, Pet309 for *cox1*, Pet 111 for *cox2* mRNA). Some of the translational activators, that mediate mRNA interactions with mitochondrial ribosomes, are organized on the surface of the inner mitochondrial membrane in a way that facilitates assembly of the inner membrane complexes. Assembly of these complexes necessitates also other proteins, e.g., Oxa1 is necessary for the correct assembly of cytochrome *c* oxidase and the ATP synthase complex.

The recent observed interaction of some membrane-bound specific activators with two proteins, Nam1 and Sls1, that, besides being involved in posttranscriptional events and in translation, are able to bind the amino-terminal domain of mitochondrial RNA polymerase, suggests that expression of mtDNA-encoded genes involves a complex series of interactions that localize active transcription complexes to the inner membrane, in order to coordinate translation with transcription.

In this way synthesis of the mitochondrially encoded proteins is coordinated with their assembly into multimeric respiratory complexes. On the other hand, the posttranslational targeting mechanism of nuclear encoded subunits seems to be preceded by mRNA localization in cytoplasmic ribosomes tightly associated with the organelles, thus facilitating the localization of proteins. This suggests a topological coordination between translation of the mitochondrial and nuclear-encoded subunits and their assembly into higher order complexes.

See Also the Following Articles

Adrenergic Receptors • Mitochondrial DNA • Mitochondrial Inheritance • mRNA Polyadenylation in Eukaryotes • mRNA Processing and Degradation in Bacteria • Pre-tRNA and Pre-rRNA Processing in Bacteria • Pre-tRNA and Pre-rRNA Processing in Eukaryotes

Glossary

self-splicing The intrinsic ability of some introns to remove themselves and link together the two adjacent RNA exons, by transesterification reactions.

spliceosome The large RNA–protein body upon which splicing of nuclear mRNA precursors occurs.

suppressor gene A gene which, by mutation, is able to eliminate the effects of a mutation in another gene.

TOM–TIM Proteins forming receptor complexes that are needed for tanslocation of proteins across the mitochondrial outer (TOM) or inner (TIM) membrane.

Further Reading

Barrientos, A. (2003). Yeast models of human mitochondrial diseases. *IUBMB Life* **55**, 83–95.

Belfort, M. (2003). Two for the price of one: A bifunctional intron-encoded DNA endonuclease–RNA maturase. *Genes Dev.* **17**, 2860–2863.

Bolduc, J. M., Spiegel, P. C., Chatterjee, P., Brady, K. L., Downing, M. E., Caprara, M. G., Waring, R. B., and Stoddard, B. L. (2003). Structural and biochemical analyzes of DNA and RNA binding by a bifunctional homing endonuclease and group I intron splicing factor. *Genes Dev.* **17**, 2875–2888.

Chen, X. J., and Clark-Walker, G. D. (2000). The petite mutation in yeasts: 50 years on. *Int. Rev. Cytol.* **194**, 197–238.

Contamine, V., and Picard, M. (2000). Maintenance and integrity of the mitochondrial genome: A pletora of nuclear genes in the budding yeast. *Microbiol. Mol. Biol. Rev.* **64**, 281–315.

Dieckmann, C. L., and Staples, R. R. (1994). Regulation of mitochondrial gene expression in *Saccharomyces cerevisiae*. *Int. Rev. Cytol.* **152**, 145–181.

Dujon, B., Colleaux, L., Jacquier, A., Michel, F., and Monteilhet, C. (1986). Mitochondrial introns as mobile genetic elements: The role of intron-encoded proteins. *Basic Life Sci.* **40**, 5–27.

Grivell, L. A. (1995). Nucleo-mitochondrial interactions in mitochondrial gene expression. *Crit. Rev. Biochem. Mol. Biol.* **30**, 121–164.

Lazowska, J., Jacq, C., and Slonimski, P. P. (1980). Sequence of introns and flanking exons in wild-type and box3 mutants of cytochrome b reveals an interlaced splicing protein coded by an intron. *Cell* **22**, 333–348.

Michel, F., and Ferat, J. L. (1995). Structure and activities of group II introns. *Annu. Rev. Biochem.* **64**, 435–461.

Neupert, W., and Brunner, M. (2002). The protein import motor of mitochondria. *Nat. Rev. Mol. Cell. Biol.* **3**, 555–565.

Sylvestre, J., Vialette, S., Corral Debrinski, M., and Jacq, C. (2003). Long mRNAs coding for yeast mitochondrial proteins of prokaryotic origin preferentially localize to the vicinity of mitochondria. *Genome Biol.* **4**, R44.

Biography

Giovanna Carignani obtained her degree in pharmacy in 1960 at the University of Trieste (Italy). She is an Assistant Professor of Molecular Biology of the Faculty of Medicine of the University of Padova (Italy).

Piotr P. Slonimski obtained his M.D. degree in 1947 at the University of Cracow (Poland) and soon after he joined the Centre National de la Recherche Scientifique (CNRS), Laboratory of Boris Ephrussi, in Paris. He became Director of the CNRS Laboratory of Physiological Genetics in 1960, then Director of the CNRS Center of Molecular Genetics of Gif-sur-Yvette until 1992. He was Professor of Molecular Genetics at the Sorbonne, at the University Pierre et Marie Curie (Paris VI) and Guest Professor at several American and European universities. He was in charge of the first French government Genome Project (Groupement de Recherches et d'Etudes sur les Genomes, GREG) and is active now, as Emeritus Professor, in the field of genome bioinformatics.

Mitochondrial Genome, Evolution

B. Franz Lang, Dennis V. Lavrov and Gertraud Burger
Université de Montréal, Montréal, Québec, Canada

Mitochondria, the energy-producing organelles of the eukaryotic cells, evolved from an endosymbiotic α-Proteobacterium, more than one billion years ago. These organelles contain their own genetic system, which is a remnant of the endosymbiont's genome. Mitochondrial DNA (mtDNA) varies considerably in size, structure, and coding capacity throughout eukaryotes. The ~5–100 genes contained in mtDNA code for mitochondrial components with functions in oxidative phosphorylation, protein synthesis, protein transport and maturation, RNA processing, and, in rare instances, transcription. Mitochondrion-encoded proteins make up only a small fraction of the mitochondrial proteome. The majority of mitochondrial proteins is encoded by nuclear genes, most of which are thought to have originally resided in mtDNA, and migrated to the nucleus in the course of eukaryotic evolution.

Origin and Evolution of Mitochondria

Eubacterial Ancestry of Mitochondria

Two decades of research in mitochondrial biogenesis and genomics unequivocally confirms the eubacterial ancestry of mitochondria (Figure 1). This ancestry is strikingly obvious in mitochondrial genomes of minimally derived eukaryotes, such as the recently described bacterivorous freshwater flagellate *Reclinomonas americana* (Table I). Among other eubacteria-like features, the mtDNA of this jakobid protist and its relatives has putative ribosome-binding motifs (Shine–Dalgarno sequences) upstream of protein-coding genes typical for bacterial systems, and codes for a eubacteria-like multisubunit RNA polymerase not found in mtDNA of other eukaryotic groups.

Phylogenetic analyses based on mitochondrial protein sequences show that mitochondria originated only once from within α-Proteobacteria, a bacterial assembly that includes free-living species such as *Magnetospirillum* and *Rhodobacter*, facultative symbionts/pathogens of plants like *Rhizobium* and *Agrobacter*, and intracellular, obligatory animal pathogens of the *Rickettsia* group including the causative agents of typhus and spotted fever. The closest living relatives of mitochondria appear to be within the *Rickettsiae*. However, this conjecture needs to be considered with caution, because available phylogenetic methods tend to group together species with highly accelerated evolutionary rates (such as mitochondria and *Rickettsia*), irrespective of their true evolutionary relationships. Whether or not they are sister groups, mitochondria and rickettsial bacteria are most likely the product of independent reductive evolution from a common (most likely free-living) bacterial ancestor, as indicated by differences in energy metabolism, and the lack of shared derived traits (e.g., gene order).

Nature of the Host Cell

A most controversial issue is, whether the host of the endosymbiotic symbiont that gave rise to the mitochondrion was a nucleus-containing amitochondriate eukaryote resembling extant anaerobic protists, or rather an archaebacterium; i.e., it is unclear whether the distinctive features of eukaryotic cells existed before this endosymbiotic event, or arose subsequently. Although accumulating molecular evidence suggests that all known amitochondriate eukaryotes once harbored mitochondria that were lost secondarily, the question remains whether primitively amitochondriate eukaryotes ever existed; and if so, to what extent their cellular organization featured the characteristics of present-day eukaryotes. The inference of the nature of eukaryotic ancestors (e.g., presence or absence of a cytoskeleton and a nucleus), and of the contribution of mitochondrial endosymbiosis to the evolution of the eukaryotic cell, will require additional massive genomic information, particularly from minimally derived eukaryotes.

Genome Size Reduction and Accelerated Evolution in Early Mitochondrial History

Early steps in the evolutionary history of mitochondria were likely governed by similar principles as those observed in present-day intracellular bacterial pathogens and symbionts, as briefly discussed in the following.

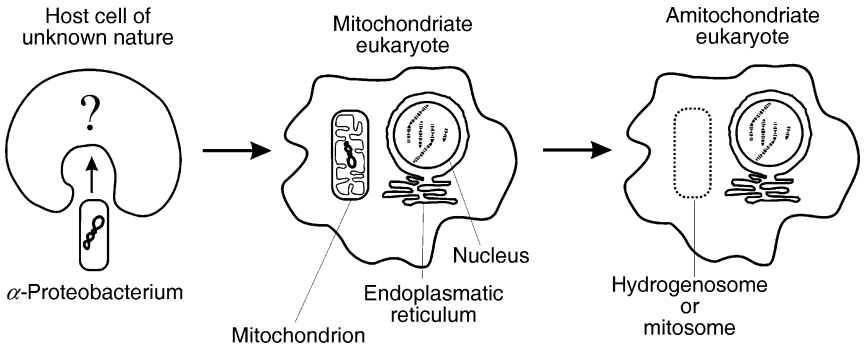

FIGURE 1 Evolution of the mitochondrion. Hypothesis describing the origin of the mitochondrion via endosymbiosis of an α-Proteobacterium with a host cell of undefined nature. Amitochondriate eukaryotes are believed to have lost mitochondria secondarily, often leaving behind relict organelles, such as hydrogenomes or mitosomes.

Bacteria that reside inside eukaryotic cells benefit from an environment rich in nutrients, which renders a large set of their biosynthetic and metabolic genes obsolete. These superfluous genes are usually lost in obligate intracellular bacteria, together with genes involved in DNA repair, recombination, lateral gene transfer among bacteria, and propagation of phages and other mobile sequence elements. Loss of these genes, in conjunction with a radically different selective pressure within the host cell, are likely responsible for the accelerated sequence evolution and changes in nucleotide composition (decrease of G + C content), observed in strictly intracellular bacteria. The gene loss is massive and progressive. For example, the obligate intracellular leprosy bacillus *Mycobacterium leprae* possesses a relatively large genome for a pathogen (3.27 mbp) with 1604 identifiable protein coding genes, 1116 pseudogenes, ~50% noncoding sequence, and a G + C content of 57.7%. In contrast, the genomes of the more derived, obligate endosymbiotic/endoparasitic bacteria *Rickettsia*, *Wigglesworthia* and *Buchnera* (symbionts of insects), and *Wolbachia* (parasite of arthropods and nematods) have genomes sizes of ~1 mbp only, and code for as few as 583 protein coding genes with an overall G + C content as low as 26.3%.

Transition from an Autonomous Bacterium to a Subcellular Organelle

Gene migration from the mtDNA to the nucleus, and the acquisition of a unique mitochondrial protein import machinery, were pivotal steps in the transformation of the proto-mitochondrion into an integrated, subcellular organelle. However, not all genes lost from mtDNA have necessarily moved to the nucleus; mitochondrial genes may have also been substituted by either genuinely nuclear genes, or genes from other (unknown) sources. An example for the latter case is the replacement of the original multisubunit bacteria-like RNA polymerase (inherited from the proto-mitochondrial ancestor) by a bacteriophage T3/T7-like RNA polymerase. This secondarily acquired RNA polymerase directs mitochondrial transcription in all contemporary eukaryotes, except in the minimally derived jakobid flagellates.

There is currently much controversy about the proportion of mitochondrial genes that reside in the nuclear genome. In yeast, some 400–630 nuclear genes (close to 10% of the genome) are considered to code for mitochondrial proteins. However, only a minority of these proteins can be traced to an α-proteobacterial origin on the basis of phylogenetic analysis. We would argue that yeast, with its highly accelerated rate of gene evolution and a considerably reduced gene set, is not an appropriate organism for such estimations. We expect that nuclear genomes of little-derived protists harbor a substantially higher number of genes of clearly identifiable mitochondrial origin.

Ongoing Gene Transfer to the Nucleus

Mitochondrion-to-nucleus gene migration is an ongoing process. For example, in leguminous plants, the active gene specifying cytochrome oxidase subunit 2 (*cox2*) resides in the nucleus in some species, but in the mitochondrion in others (as in all nonleguminous plants). Even more intriguingly, in soybean, an inactive mitochondrial *cox2* gene copy exists in addition to an active nuclear one. In this particular example, there is strong evidence that the transfer to the nucleus proceeded via an mRNA → cDNA intermediate. Nevertheless, direct transfer of genomic DNA appears to be an alternative avenue: nuclear genomes of plants and animals (including human) often contain large insertions of mtDNA, some even of full length. Finally, a surprisingly high rate of gene transfer from the

TABLE I

Features of Mitochondrial Genomes from Representative Eukaryotes

Organismal group	Genome size and structure[a]	Protein genes[b]	RNA genes[c]	Translation code[d]	Introns[e]
Metazoa (animals)					
Homo sapiens (human)	16.6 (circular)	13	24	**UGA(W), AUA(M)**[f]	
Metridium senile (sea anemone)	17.4 (circular)	13	4	**UGA(W)**	2
Fungi					
Hyaloraphidium curvatum (chytrid)	30.0 (linear)	14	9	Standard	1
Saccharomyces cerevisiae (baker's yeast)	85.8 (circular)	8	27	**UGA(W), AUA(M), CUN(T)**	13
Schizosaccharomyces pombe (fission yeast)	19.4 (circular)	8	28	Standard[g]	3
Spizellomyces punctatus (chytrid)	58.8; 1.4; 1.1 (3 circular DNAs)	14	10	**UAG(L)**	12
Plants					
Marchantia polymorpha (liver wort)	186.6 (circular)	38	30	Standard	32
Arabidopsis thaliana (thale cress)	366.9 (circular)	31	21	Standard	23
Photosynthetic protists					
Chlamydomonas reinhardtii (green alga)	15.8 (linear)	7	5	Standard	
Prototheca wickerhamii (green alga[h])	55.3 (circular)	31	29	Standard	5
Ochromonas danica (golden alga)	41.0 (linear)	30	27	Standard	
Porphyra purpurea (red alga)	63.7 (circular)	22	26	Standard	2
Nonphotosynthetic protists					
Acanthamoeba castellanii (amoeba)	41.6 (circular)	34	18	**UGA(W)**	3
Monosiga brevicollis (choanoflagellate)	76.6 (circular)	26	27	**UGA(W)**	4
Phytophthora infestans (oomycete)	38.0 (circular)	35	27	Standard	
Reclinomonas americana (jakobid flagellate)	69.0 (circular)	64	31	Standard	1

[a] Size in kbp, rounded values; "circular" stands for "circular mapping," i.e., the major portion of these mtDNAs occurs as long linear concatamers, not as monomeric circles. "Linear" stands for "monomeric linear."

[b] The number of identified genes is indicated. The basic set of protein-coding genes typically found in animals and fungi are, *cob* (apocytochome b), *cox1,2,3* (cytochrome oxidase subunits), *atp6,8,9* (ATPase subunits), and *nad1,2,3,4,4L, 5, 6* (NADH dehydrogenase subunits). The *M. senile* mtDNA contains an additional gene with similarity to bacterial *mutS*, and protists, fungi and plants contain additional hypothetical protein genes (ORFs).

[c] Genes for *rns, rnl* (small and large subunit rRNAs) occur in all mtDNAs, whereas genes coding for *rrn5* (5S rRNA), and RNase P RNA, might be absent. The number of mtDNA-encoded tRNAs varies. Duplicated genes are counted only once.

[d] Deviations from the standard bacterial translation code are indicated in bold.

[e] Total number of introns, the two mitochondrial intron classes "I" and "II" are not distinguished.

[f] Further codon reassignments include the use of AGA and AGG as stop codons, and additional translation initiation codons other than AUG and GUG.

[g] In *S. pombe*, one UGA(Trp) is present in *rps3*, and two in intronic ORFs.

[h] *Prototheca* belongs to green algae, but has secondarily lost its capacity for photosynthesis.

mtDNA to the nucleus ($\sim 10^{-5}$ per generation) has been experimentally determined in yeast.

Limitation of Gene Transfer to the Nucleus

Not a single eukaryote is known in which all genes have been relocated to the nucleus. All eukaryotes that lack mtDNA are unable to produce ATP via oxidative phosphorylation, and frequently contain degenerated mitochondria (hydrogenosomes or mitosomes).

Two major hypotheses have been proposed to explain why certain mitochondrial genes are much more rarely transferred to the nucleus than others. It has been reasoned that import of gene products into mitochondria may be hampered if these are highly hydrophobic (e.g., Cox1 and Cob), or very large (ribosomal RNAs), and thus counteract the transfer of the corresponding genes to the nucleus. Another theory invokes control of transcription initiation of mitochondrial genes by changes in redox potential inside mitochondria. This would require sensor genes to reside on

mtDNA, a mechanism described for chloroplasts. Both interpretations are consistent with the observed hierarchy of mitochondrial gene loss in different eukaryotic lineages, and may well apply in concert.

Mitochondrial Genome Diversity in Extant Eukaryotes

Over the past two decades, >500 complete mitochondrial genome sequences have been determined. Here, we will only summarize the distinctive features of mtDNAs from the major eukaryotic groups. Figure 2 depicts the maps of some selected mitochondrial genomes, demonstrating the diversity of mtDNA size, gene organization, and gene content.

Animal mtDNAs

To date, complete mtDNA sequences of more than 400 animals have been deposited in public databases. Animal mtDNAs are typically small (14–17 kbp in size) and carry intronless genes that are compactly arranged on both DNA strands. Mitochondrial genes code for the small and large subunit ribosomal RNAs, 13 proteins,

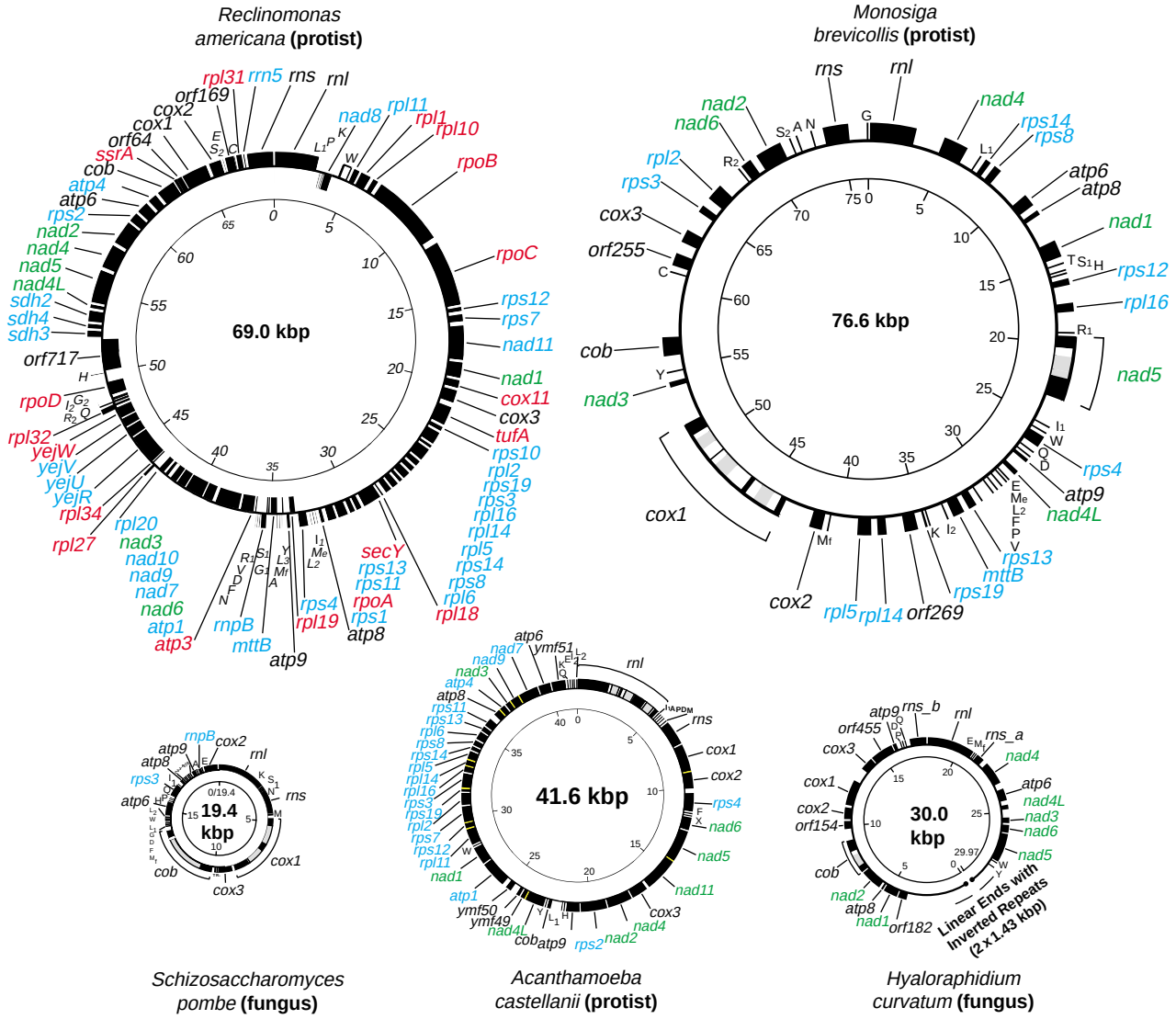

FIGURE 2 Diversity of mitochondrial genomes from various eukaryotic groups. Genetic maps of mtDNAs from protists and fungi, demonstrating the wide range of coding capacity, size, and organization (the mtDNA of *Hyaloraphidium* is linear, but is depicted as a circle to facilitate comparisons). Outer ring, transcription is clockwise; black rectangles, genes; white rectangles with gray-shaded sections, introns and intronic open reading frames. Gene names in black are genes of the basic gene complement common to all fungal and animal mtDNAs, and unidentified open reading frames (ORFs); green, extended gene set common to fungi and animals (and most other eukaryotes); blue, extra genes common to most protists; red, extra genes only found in jakobid flagellates.

and up to 22 tRNAs (Table I). Genes are arrayed in an order that is well conserved within and, to a lesser degree, among animal phyla. Exceptions are found among corals and sea anemones (phylum Cnidaria), which are the only animals whose mitochondrial genes contain introns, and which have lost all but two tRNA genes. In addition, all animals studied to date use modified mitochondrial translation codes, and tRNA and rRNA structures are highly reduced and derived compared to bacterial systems.

Animal phylogenies, even when using complete sets of mitochondrial proteins, often fail to generate wellsupported tree topologies. This lack of support results from the unusually high evolutionary rate of most animal mtDNAs. In contrast, rearrangements in animal mitochondrial genomes are exceptionally rare events, which allows the use of mitochondrial gene order data for inferring evolutionary relationships in animals.

Fungal mtDNAs

Currently, completely sequenced mtDNAs are available from 22 fungal taxa, including representatives of all four major divisions of this kingdom: Ascomycota, Basidiomycota, Zygomycota, and Chytridiomycota. Fungal mtDNAs are highly variable in terms of size, structure, and content of genes and introns. For instance, in two groups of Ascomycota, all seven genes for subunits of the NADH dehydrogenase typically encoded by the mtDNA are absent. The chytridiomycete *Rhizophydium136* contains as many as 37 introns whereas other members of this group (e.g., *Harpochytrium* species) contain none. Several fungi encode highly reduced sets of only 7–9 mitochondrial tRNAs. Additional differences in coding content include unidentified reading frames and plasmid-encoded polymerases, which are quite common in filamentous fungi.

Despite this variability, the basic set of fungal mitochondrial genes resembles that of animals (Table I), apparently a result of independent events of gene loss in the two lineages.

Plant mtDNAs

Mitochondria of land plants have the largest known mtDNAs, with sizes from 180 to 2400 kbp. Despite ~100-fold increase in genome size, the number of mitochondrial genes of plants is not even twice as high as in animals, and lower than in most protists (Table I). The few sequenced plant mitochondrial genomes suggest that the increase in size is due to a progressive accumulation of noncoding DNA. Although mtDNAs of angiosperms have generally high rates of genome rearrangements and frequently contain insertions of chloroplast and nuclear DNA, the evolutionary rate of mitochondrial genes is exceptionally low relative to nuclear genes.

Protist mtDNAs

Protists are a heterogeneous group of eukaryotes that are negatively defined as not belonging to the animal, fungal, or plant kingdoms. Based on ultrastructural characteristics, several dozen protist phyla are distinguished, but the evolutionary relationships among these phyla are mostly contentious. Many protist mitochondrial genomes are more bacteria-like, and encode a substantially larger set of genes than those of animals and fungi (Table I). However, mtDNA of several parasitic protists exhibit novel and puzzling features. For instance, the linear mtDNA (6 kbp) of the malaria parasite *Plasmodium falciparum* carries only five genes. Its rRNAs are encoded by many small gene pieces. Another oddity is found in trypanosomatid parasites, whose mtDNA consists of a network of thousands of concatenated minicircles and a few dozen maxicircles. The RNAs transcribed from maxicircle genes undergo massive RNA editing through nucleotide insertions and deletions to generate translatable mRNAs.

Conclusion

Protists comprise more biological diversity than animals, plants, and fungi together. Without a doubt, investigations of mtDNAs from poorly studied protist groups will lead to further discoveries of novel genome structures and molecular mechanisms, and provide insights into the evolutionary forces that have brought about the eukaryotic cell as we know it today.

See Also the Following Articles

Mitochondrial DNA • Mitochondrial Genes and their Expression: Yeast • Mitochondrial Genome, Overview • Mitochondrial Inheritance

Glossary

Archaebacteria (Archaea) One of the three domains of life besides eukaryotes and eubacteria.

oxidative phosphorylation The generation of ATP driven by the electron flow to oxygen in bacteria and mitochondria.

phylogeny Evolutionary relationships among organisms. Molecular phylogeny is based on DNA and protein sequences (or other molecular characters).

Proteobacteria Group of Gram-negative eubacteria that are subdivided into α, β and γ.

RNA editing The programmed modification of primary transcript sequence, including substitutions, as well as insertions and deletions.

Further Reading

Boore, J. L. (1999). Animal mitochondrial genomes. *Nucleic Acids Res.* **27**, 1767–1780.

Gray, M. W., Burger, G., and Lang, B. F. (1999). Mitochondrial evolution. *Science* **283**, 1476–1481.

Gray, M. W., Burger, G., and Lang, B. F. (2001). The origin and early evolution of mitochondria (reviews). *Genome Biol.* **2**, 1018.1–1018.5.

Lang, B. F., Burger, G., O'Kelly, C. J., Cedergren, R., Golding, G. B., Lemieux, C., Sankoff, D., Turmel, M., and Gray, M. W. (1997). An ancestral mitochondrial DNA resembling a eubacterial genome in miniature. *Nature* **387**, 493–497.

Lang, B. F., Gray, M. W., and Burger, G. (1999). Mitochondrial genome, evolution and the origin of eukaryotes. *Annu. Rev. Genetics* **33**, 351–397.

Leigh, J., Seif, E., Rodriguez, N., Jacob, Y., and Lang, B. F. (2003). Fungal evolution meets fungal genomics. In *Handbook of Fungal Biotechnology* (D. Arora, ed.) 2nd edition. Marcel Dekker, New York, pp. 145–161.

Martin, W., Hoffmeister, M., Rotte, C., and Henze, K. (2001). An overview of endosymbiotic models for the origins of eukaryotes, their ATP-producing organelles (mitochondria and hydrogenosomes), and their heterotrophic lifestyle. *Biol. Chem.* **382**, 1521–1539.

Roger, A. J., and Silberman, D. J. (2002). Mitochondria in hiding. *Nature* **418**, 827–829.

Wernegreen, J. J. (2002). Genome evolution in bacterial endsymbionts of insects. *Nat. Rev. Genetics* **3**, 850–861.

Biography

B. Franz Lang and G. Burger are both Professors in the biochemistry department at the Université de Montréal, Canada. Their principal research interests are in the fields of comparative genomics, molecular evolution, and bioinformatics. They are best known for their work on organellar genome evolution and a publicly accessible organelle database. Dr. Lang holds a Ph.D. from the University of Munich, Germany. He has been Fellow of the Canadian Institute for Advanced Research (CIAR) for over 10 years. Dr. Burger also holds a Ph.D. from the University of Munich. She is a CIAR associate, and leader of the bioinformatics programs at the Université de Montréal.

Dennis Lavrov obtained his Ph.D. from the University of Michigan and is currently a postdoctoral fellow at the Canadian Institute of Health Research, with BFL.

Mitochondrial Genome, Overview

Douglas C. Wallace
University of California, Irvine, California, USA

The mitochondrial genome is the sum of the genes that are required to assemble a mitochondrion. These genes are distributed between a DNA molecule located in the mitochondrion, the mitochondrial DNA (mtDNA), and the nuclear DNA (nDNA). Whereas the genes encoded by the mtDNA vary between different species, essentially all mtDNAs code for three or more essential proteins of the mitochondrial energy-generating process of oxidative phosphorylation (OXPHOS), plus the small and large ribosomal RNAs (rRNAs) for the mitochondria-specific ribosomes. The rest of the genes necessary to assemble a mitochondrion reside in the nDNA.

Structure, Biology, and Origins

Mitochondria are present in virtually all eukaryotic cells (cells with a nucleus), and each eukaryotic cell contains multiple mitochondria that generate most of the cellular energy by oxidative phosphorylation (OXPHOS). The mitochondria became a component of the eukaryotic cell about 2 billion years ago through a symbiotic association between a motile nucleated cell and the α-proteobacterium, a *Rickettsia*-like oxidative bacterium. Because the mitochondrion was a bacterial cell, it had (and still retains) a complete information storage and retrieval system, based on the mtDNA. The mtDNA is replicated within the mitochondrion and transcribed into structural RNAs (rRNAs and tRNAs) and messenger RNAs (mRNA), and the mRNAs are translated into proteins on chloramphenicol (CAP)-sensitive mitochondrial ribosomes.

While the actual physiological interactions that stabilized the original symbiosis are unknown, one scenario is that the protomitochondrion, which carried the mitochondrial antioxidant enzyme manganese superoxide dismutase (MnSOD), provided protection to the host cell against the increasing toxicity of the global atmospheric oxygen that was being generated by the cyanobacteria during photosynthesis. Later, the host cell invented the adenine nucleotide (ADP/ATP) translocator (ANT), which permitted it to extract ATP from the mitochondrion in exchange for spent cytosolic ADP. This established the energetic interrelationship between the host and symbiont that still exists today.

As the symbiotic relationship evolved, most of the original genes of the bacterial genome were either lost or transferred to the nDNA, where they were scattered across the various chromosomes. Chromosomal mitochondrial genes are now transcribed using nuclear RNA polymerase; the mRNAs are then translated on 80S cytosolic ribosomes. The resulting proteins destined for the mitochondrion contain specific amino-terminal or internal mitochondrial-targeting sequences, permitting them to bind to the mitochondrion and to traverse the outer and inner mitochondrial membranes through the transport across the outer (TOM) and transport across the inner (TIM) complexes. These mitochondrial proteins first interact with the 70 kDa heart shock protein (HSP) and the mitochondrial import-stimulating factor (MSF); then they bind to one of two receptors (Tom20 + Tom22 or Tom37 + Tom70). These receptors interact with the general insertion pore of the TOM complex composed of Tom40, 22, 5, 6, and 7 polypeptides. Those polypeptides that are targeted to the matrix then interact with the TIM complex composed of Tim33, 23, 17, and 11 polypeptides. As the polypeptide traverses the inner membrane, it interacts with Tim44 and mitochondrial HSP70; the amino-terminal peptide is cleaved off by the mitochondrial-processing peptidase and, in some cases, the mitochondrial intermediate peptidase. By contrast, hydrophobic mitochondrial carrier proteins destined for insertion in the mitochondrial inner membrane are complexed in the intermembrane space by either the Tim9,10 or the Tim8,9,13 polypeptide complexes. These proteins are then delivered into the inner membrane by the 300 kDa TIM complex composed of the Tim54, 22, 12, 10, and 9 proteins.

Different protist genera harbor a wide variety of mtDNA structures and gene complements. Common mtDNA-encoded genes include the small and large rRNA, one subunit (cytochrome b [cytb]) of respiratory complex III (bc_1 complex), two or three subunits (COI, COII, COIII) of cytochrome c oxidase (COX or complex IV) and one or more subunits (ATP6, ATP8, ATP9) of complex V (ATP synthase [ATPsyn]). The most complex mtDNA genome analyzed to date is that of *Reclinomonas americana*. This mtDNA encodes eubacteria-like 23S, 16S, and 5S rRNA genes; a nearly

complete set of tRNA genes employing the standard genetic code; and 62 protein coding genes, including subunits for a bacteria-like RNA polymerase, multiple ribosomal proteins, additional subunits of complexes I, II, and V, etc. Modern human and vertebrate mtDNAs encode a 12S and 16S rRNA; 22 tRNAs; and 13 proteins: ND1, 2, 3, 4L, 4, 5, and 6 of the roughly 46 polypeptides of complex I, cytb of the 11 subunits of complex III, COI, II, and III of the 13 subunits of complex IV, and ATP6 and 8 of the ~17 polypeptides of complex V (Figure 1).

Some mtDNAs can have altered genetic codes. For example the mtDNA lineage leading from fungi to mammals encompasses a progression of codon changes. The earliest change, found in all fungal and animal mtDNAs, was an alteration in the tryptophan anticodon that suppressed the opal stop codon. The tryptophan codon 5′-UGG-3′ is read by the anticodon 3′-ACC-3′. Since C cannot pair with the terminal A in the adjacent opal codon (5′-UGA-3′), this is a stop codon. However, in fungal and animal mtDNAs, the tryptophan anticodon is converted to 3′-ACU-5′, and the U can pair with A, converting the opal stop codon to a tryptophan codon. Other changes include expansion of the number of methionine codons and alteration of the isoleucine codons. Finally, in the transition from *Xenopus* to mammals, the tRNA that interprets the arginine codons 5′-AGA-3′ and 5′-AGG-3′ was deleted, rendering these stop codons. Possibly these genetic code changes became established to reduce the inadvertent translation of mRNAs in the wrong compartment. The use of 5′-UGA-3′ as tryptophan in the mitochondrion would mean that mtDNA mRNAs would prematurely terminate in the cytosol. Similarly, the loss of the tRNA for the arginine AGA and AGG codons would mean that the cytosolic mRNAs could not be translated in the mitochondrion. By blocking erroneous crosstalk between the mitochondrial matrix and the cytosol, this system would increase the efficiency of protein synthesis in both compartments. However, it also means that functional

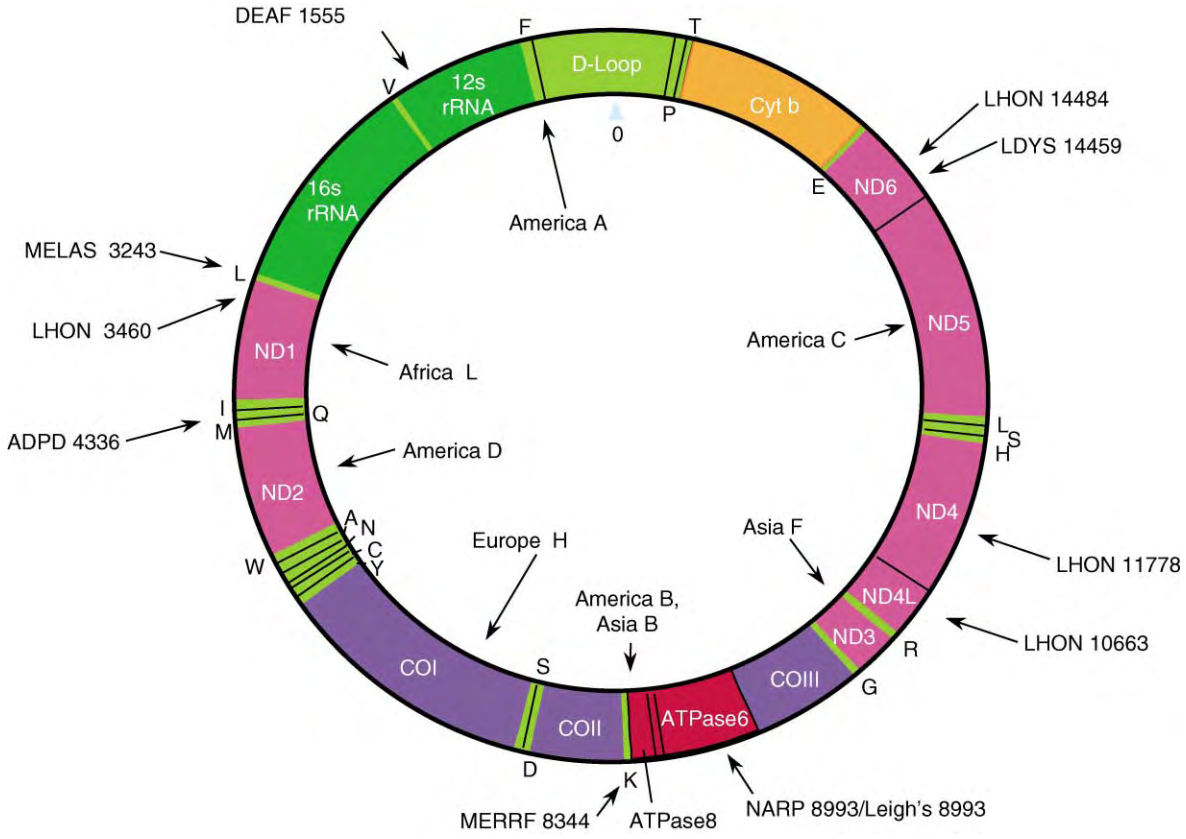

FIGURE 1 Human mitochondrial DNA map. D-loop = control region. Letters around the outer perimeter indicate cognate amino acids of the tRNA genes. Other gene symbols are defined in the text. Arrows leading from continent names and associated letters on the inside of the circle indicate the position of defining polymorphisms of selected region-specific mtDNA lineages. Arrows leading from abbreviations followed by numbers around the outside of the circle indicate representative pathogenic mutations; the number indicates the nucleotide position of the mutation. Abbreviations: DEAF, deafness; MELAS, mitochondrial encephalomyopathy, lactic acidosis, and stroke-like episodes; LHON, Leber's hereditary optic neuropathy; ADPD, Alzheimer's and Parkinson's disease; MERRF, myoclonic epilepsy and ragged red fiber disease; NARP, neurogenic muscle weakness, ataxia, retinitis pigmentosum; LDYS, LHON + dystonia. From http://www.mitomap.org.

mtDNA genes can no longer be incorporated into the nDNA. Hence, the mtDNA gene complement has been substantially conserved from fungi to humans.

All mitochondria generate energy via OXPHOS (Figure 2). OXPHOS burns hydrogen derived from carbohydrates and fats with oxygen to generate water (H_2O). In endotherms such as humans, the energy that is released is used to maintain body temperature and to generate ATP. The reducing equivalents (electrons) from dietary calories are collected by the tricarboxylic acid (TCA) cycle and transferred to either NAD^+ to generate NADH or FAD to give $FADH_2$. The electrons are then oxidized by the electron transport chain (ETC). The ETC collects electrons from NADH through complex I (NADH dehydrogenase) or from succinate in the TCA cycle through complex II (succinate dehydrogenase) and transfers them to ubiquinone (coenzyme Q_{10}, or CoQ) to generate ubisemiquinone (CoQH·) and then ubiquinol ($CoQH_2$). From $CoQH_2$, the electrons are transferred to complex III, then cytochrome c, then complex IV, and finally to ½ O_2 to give water. The energy that is released during electron transport is used to pump protons from the matrix out across the mitochondrial inner membrane to create an electrochemical gradient ($\Delta P = \Delta\Psi + \Delta\mu^{H+}$). This biological capacitor serves as a source of potential energy to drive complex V to condense ADP + Pi to give ATP. The mitochondrial ATP is then exchanged for cytosolic ADP by the ANT. The efficiency by which ΔP is converted to ATP is known as the coupling efficiency. Tightly coupled OXPHOS generates the maximum ATP and minimum heat, whereas loosely coupled OXPHOS generates less ATP but more heat.

As a toxic by-product of OXPHOS, the mitochondria generate most of the reactive oxygen species (ROS), or oxygen radicals, generated within eukaryotic cells. This results from the misdirection of electrons from the early stages of the ETC surrounding CoQH· directly to O_2 to generate superoxide anion ($O_2^{\cdot-}$). Superoxide anion is highly reactive but can be detoxified by MnSOD

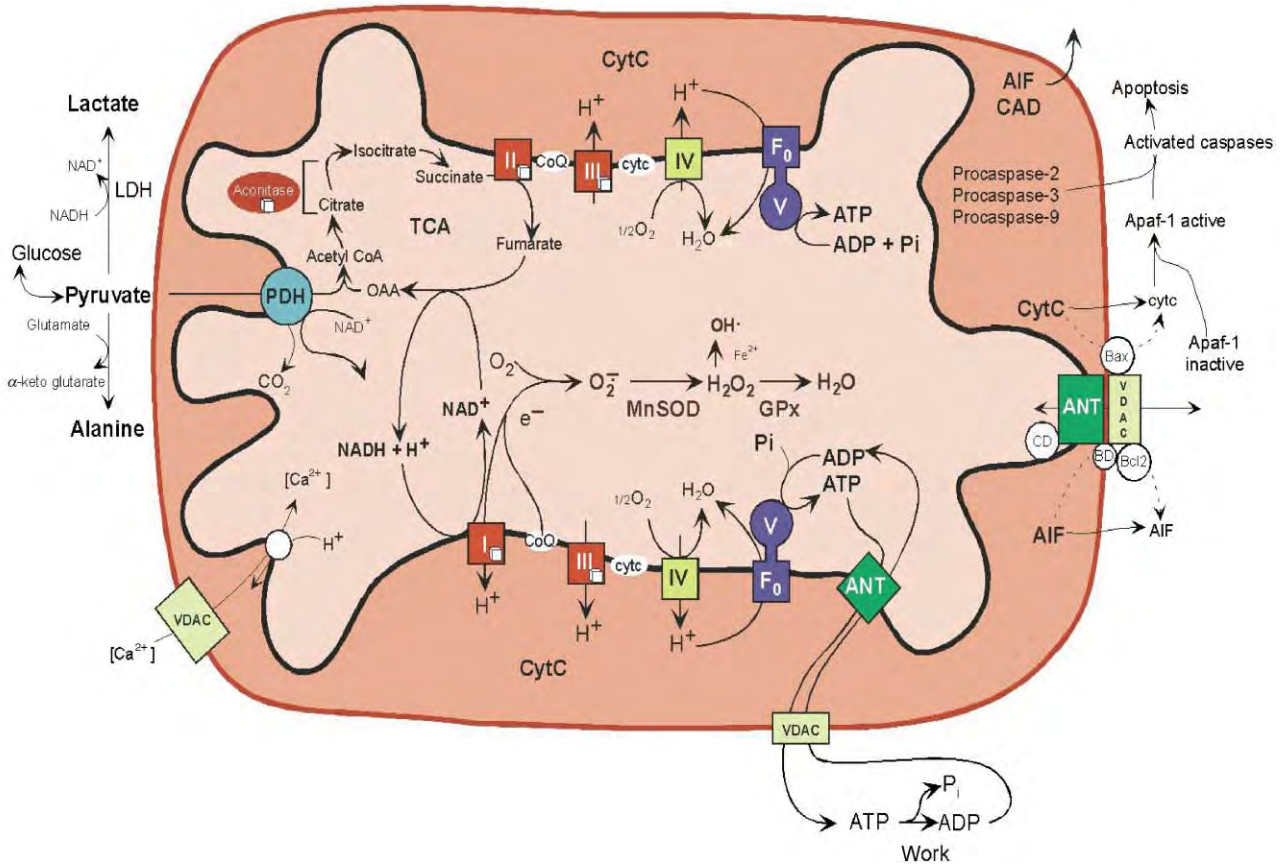

FIGURE 2 Three features of mitochondrial metabolism relevant to the pathophysiology of disease: (1) energy production by oxidative phosphorylation (OXPHOS), (2) reactive oxygen species (ROS) generation as a toxic by-product of OXPHOS, and (3) regulation of apoptosis through activation of the mitochondrial permeability transition pore (mtPTP). Abbreviations: I, II, III, IV, and V, OXPHOS complexes I–V; ADP, adenosine diphosphate; ATP, adenosine triphosphate; ANT, adenine nucleotide translocator; cytc, cytochrome c; GPx, glutathione peroxidase-1; LDH, lactate dehydrogenase; MnSOD, manganese superoxide dismutase or SOD2; NADH, nicotinamide adenine dinucleotide; TCA, tricarboxylic acid cycle; VDAC, voltage-dependent anion channel.

to generate hydrogen peroxide (H_2O_2). Hydrogen peroxide is relatively stable. In the presence of transition metals, however, it can be reduced to hydroxyl radical ($^{\cdot}OH$), which is the most toxic ROS. Consequently, H_2O_2 is reduced to water by glutathione peroxidase (GPx1) or catalase (Figure 2). ROS damage mitochondrial proteins, lipids, and nucleic acids, which inhibit OXPHOS and further exacerbate ROS production. Ultimately, the mitochondria become so energetically impaired that they malfunction and must be removed from the tissue.

Cells with faulty mitochondria are removed by programmed cell death (apoptosis) through the activation of the mitochondrial permeability transition pore (mtPTP). The mtPTP is thought to be composed of the outer membrane voltage-dependent anion channel (VDAC) proteins, the inner membrane ANT, the pro- and antiapoptotic Bcl2-Bax gene family proteins, and cyclophilin D. This complex senses changes in mitochondrial ΔP, adenine nucleotides, ROS, and Ca^{2+}, and when these factors get sufficiently out of balance, the mtPTP becomes activated and opens a channel between the cytosol and the mitochondrial matrix, depolarizing ΔP and causing the mitochondrion to swell. Proteins from the mitochondrial intermembrane space are then released into the cytosol. Among these is cytochrome c, which activates cytosolic Apaf-1 to convert procaspases 2, 3, and 9 to active caspases that degrade cellular and mitochondrial proteins. Apoptosis-initiating factor (AIF) and caspase-activated DNase (CAD) are transported to the nucleus, where they degrade the nDNA. As a consequence, the cell with faulty mitochondria is removed from the tissue so that its energetic failure dose not compromise the normal cells of the tissue and organ (Figure 2).

MtPTP-induced apoptosis means that only cells with optimally functioning mitochondria are retained in the tissue. However, postmitotic tissues have a finite number of cells, generally enough for the organ to function optimally until postreproductive age. Cell loss due to mitochondrial decline results in organ failure and the symptoms we call aging. Thus, the pathophysiology of degenerative diseases and aging results from the interplay between three central mitochondrial processes: energy production via OXPHOS, ROS generation and oxidative stress, and mtPTP activation initiating apoptosis.

Because of its extrachromosomal location, the mtDNA has unique genetics. In vertebrates, the mtDNA is inherited exclusively through the mother. However, each cell can harbor thousands of copies of the mtDNA, which can be pure normal (homoplasmic wild-type), a mixture of mutant and normal (heteroplasmic), or homoplasmic mutant. The percentage of mutant mtDNAs determines the relative energy deficiency of the cell and thus the probability of apoptosis. The tissues most sensitive to the adverse effects of mitochondrial decline are the central nervous system, heart, muscle, and renal and endocrine systems, the tissues most affected by aging.

Because of its chronic exposure to ROS, mammalian mtDNAs have a very high mutation rate. Hence, even though the human mtDNA is small, mtDNA diseases are common. Germline mtDNA mutations result in maternally inherited diseases. However, mtDNA mutations also accumulate in postmitotic somatic tissues, resulting in tissue decline.

Mitochondrial Variation and Human Origins

Because of its exclusive maternal inheritance and high mutation rate, human mtDNA variation has been used to reconstruct the ancient origins and migrations of women (Figure 3). These studies revealed that humans arose in Africa approximately 150,000 to 200,000 years before present (YBP), with sub-Saharan African mtDNAs radiating into four African-specific lineages: L0, L1, L2, and L3. The most ancient mtDNA lineages are found among the Khoisan Bushmen. About 65,000 YBP, L3 gave rise to two new lineages in northeastern Africa, designated M and N. Only M and N left Africa to colonize the rest of the world. One group migrated along the southeastern Asian coast to colonize Australia, while others bearing M and N radiated into Eurasia. In Europe, lineage N gave rise to the European-specific lineages H, I, J, K, T, U, V, W, and X. In Asia, both M and N radiated to generate a plethora of Asian-specific mtDNA lineages, including A, B, and F from N and C, D, and G from M. Among all of the Asian mtDNA lineages, only A, C, and D successfully occupied arctic Chukotka in northeastern Siberia. When the Bering land bridge appeared, individuals bearing these mtDNAs moved into the Americas about 20,000 YBP. Subsequently, a coastal migration brought lineage B to mix with A, C, and D about 12,000–15,000 YBP, thus generating the final Paleo-Indian mtDNA complement. Another migration across the arctic brought the European haplogroup X to the Great Lakes region of North America approximately 15,000 YBP. A migration from around the Sea of Okhotsk about 7,000–9,000 YBP brought a modified A to found the Na-Dene. Finally, a migration bringing A and D mtDNAs gave rise to the Eskimos and Aleuts.

MtDNA Variation and Human Adaptation to Cold

One geographical constraint that could have acted on mtDNA variation is climate. The mitochondria utilize

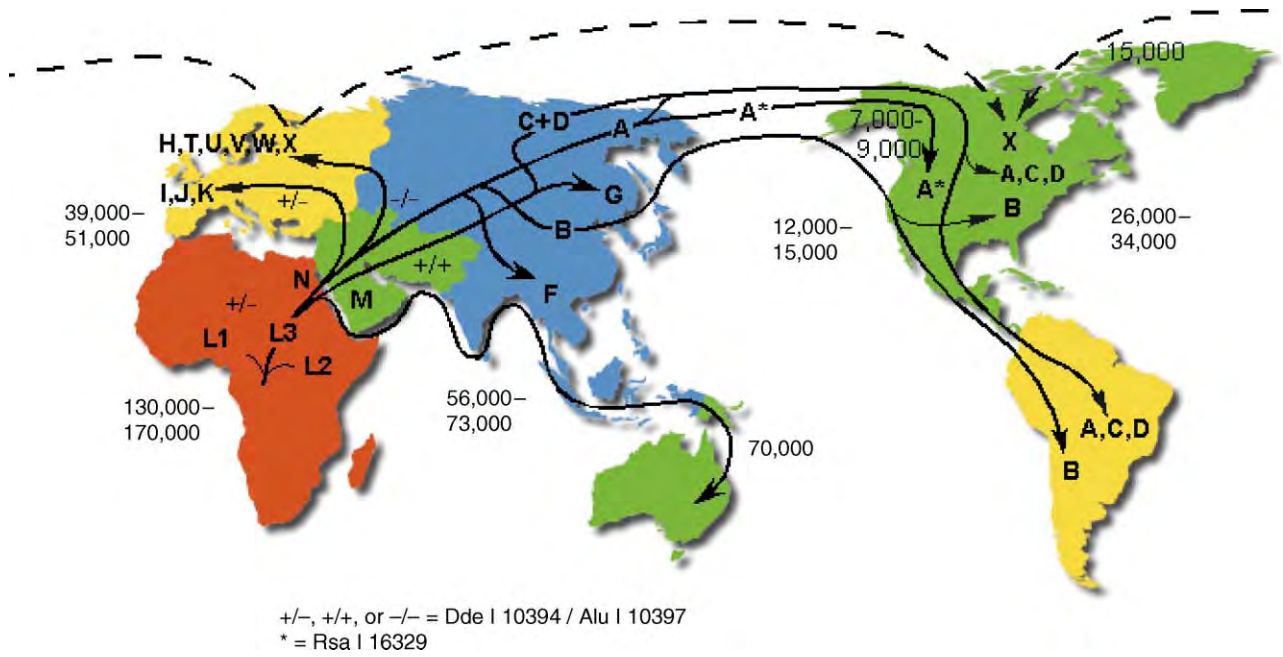

FIGURE 3 Global radiation of mtDNA types showing the regional association of mtDNA types. Capital letters represent major region groups of related haplotypes (haplogroups). In sub-Saharan Africa, haplogroup L0, which arose between 150,000 and 200,000 years before present (YBP), radiated into haplogroups L1, L2, and L3. At about 65,000 YBP, haplogroup L3 gave rise to haplogroups M and N in northeastern Africa. M and N then left Africa in two directions. A southeastern migration moved through Southeast Asia, ultimately giving rise to Australian mtDNAs. A northeastern migration colonized Eurasia, with haplogroup N giving rise to the European mtDNA haplogroups H, I, J, K, T, U, V, W, and X and to the Asian haplogroups A, B, F, etc. Haplogroup M radiated into Asia to give rise to Asian haplogroups C, D, G, etc. Haplogroups A, C, and D became enriched in northeastern Siberia and crossed the Bering land bridge between 20,000 and 30,000 YBP to found the Paleo-Indians. Haplogroup B migrated along the Asian and Bering coasts to mix with Native American haplogroups A, C, and D about 12,000–15,000 YBP. European-like haplogroup X arrived in Central North America about 15,000 YBP; derivatives of haplogroup A crossed the Bering Strait about 7,000–9,000 YBP to generate the Na-Dene; and derivatives of haplogroups A and D crossed the Bering Strait approximately 3,000–5,000 YBP to give rise to the Eskimos and Aleuts. The +/+, +/−, −/− represent important diagnostic restriction sites. The ages were calculated using the empirically determined mtDNA sequence evolution rate of 2.2–2.9%/million years (MYR). From http://www.mitomap.org.

dietary calories not only to synthesize ATP but also to generate heat to maintain body temperature. Individuals in the tropics would need tightly coupled mitochondria to maximize ATP production and minimize heat production, while individuals from the arctic would need uncoupled mitochondria to increase heat production at the expense of ATP generation.

This concept is supported by the nonrandom distribution of mtDNA gene amino acid substitutions. The mtDNA ATP6 protein sequence is hypervariable in the arctic Siberians and North Americans but conserved in the tropical Africans and temperate zone Europeans. The cytb protein sequence is hypervariable in temperate Europeans but conserved in the Africans and Siberians. COI is most variable in Africans, and so on. A detailed study of the sequences of more than 1000 mtDNAs from around the world permitted the assembly of a global human mtDNA phylogenetic tree, in which every mutation was positioned according to the relative time that it occurred. This revealed that ancient conserved amino acid substitution mutations occurred at the base of many of the temperate and arctic zone mtDNA lineages. These mutations appear to reduce OXPHOS coupling efficiency by reducing the efficiency of either proton pumping by the ETC or ATP generation by the ATP synthase. Hence, as people moved north, mtDNA lineages from the warmer climates were excluded, while mtDNA lineages with new mutations that reduced coupling efficiency and increased heat production survived and expanded into the colder latitudes.

These same nodal mutations have been found to correlate with longevity and protection against neurodegenerative diseases. European lineages J and K, which harbor cytb mutations in the inner and outer CoQ-binding sites, are protective for Alzheimer's or Parkinson's disease and also are associated with increased longevity. Mutations in the CoQ-binding sites would inhibit the Q cycle of complex III and thus reduce the efficiency of proton pumping. Because uncoupled mitochondria would oxidize more electrons, fewer would be available to generate ROS. Hence, cold-adapted mtDNAs would be associated with less

oxidative stress, thus increasing the longevity of postmitotic cells. Thus, ancient adaptive mtDNA variants are affecting individual predisposition to degenerative diseases and aging today.

Diseases of the mtDNA

The high mtDNA mutation rate that generated the ancient adaptive polymorphisms also results in a high frequency of pathogenic mutations today. Pathogenic base substitution and rearrangement mutations are both common in the human mtDNA. Base substitution mutations can alter proteins. For instance, the ND4 missense mutation (R340H) at nucleotide pair (np) 11778 causes Leber's hereditary optic neuropathy (LHON), a form of sudden-onset, midlife blindness. mtDNA mutations can also change protein synthesis genes, tRNAs, or rRNAs. For example, a $tRNA^{Lys}$ mutation at np 8344 causes myoclonic epilepsy and ragged red fiber disease (MERRF). Rearrangement mutations can occur throughout the mtDNA and result in multisystem disorders such as chronic progressive external ophthalmoplegia (CPEO), the Kearns-Sayre syndrome, or the Pearson's marrow pancreas syndrome. A plethora of pathogenic mutations in the mtDNA have now been described and are catalogued at www.mitomap.org. These diseases involve the following: the central nervous system, affecting vision, hearing, movement, balance, and memory; muscle, causing progressive weakness; heart, leading to hypertrophic and dilated cardiomyopathy; the endocrine system, including diabetes mellitus; and the renal system. Hence, it is now clear that mitochondrial defects represent one of the most common forms of human inborn errors of metabolism.

The pathogenicity of mildly deleterious mutations can also be augmented by the mtDNA lineage on which the mutation occurred. LHON can be caused by a number of mtDNA point mutations in the ND genes. The more biochemically severe mutations can cause LHON independent of the background mtDNA. However, the milder ND mutations cause LHON only when they co-occur on the European mtDNA lineage J. Hence, the diminished ATP production of partially uncoupled haplogroup J mtDNAs must augment the energetic defect of the mild ND mutations.

Somatic mtDNA Mutations in Aging

One of the most distinctive features of mitochondrial diseases is that they have a delayed onset and a progressive course. Because known mtDNA mutations can cause all of the same symptoms as seen in the elderly, it has been suggested that the accumulation of mtDNA mutations provides the aging clock. The age-related decline of mitochondrial function and an associated accumulation of somatic mtDNA mutations have been documented in a variety of animal species, with the level of mtDNA damage being proportional to lifespan, not absolute time. The accumulation of mtDNA deletions is observed in most tissues, but the

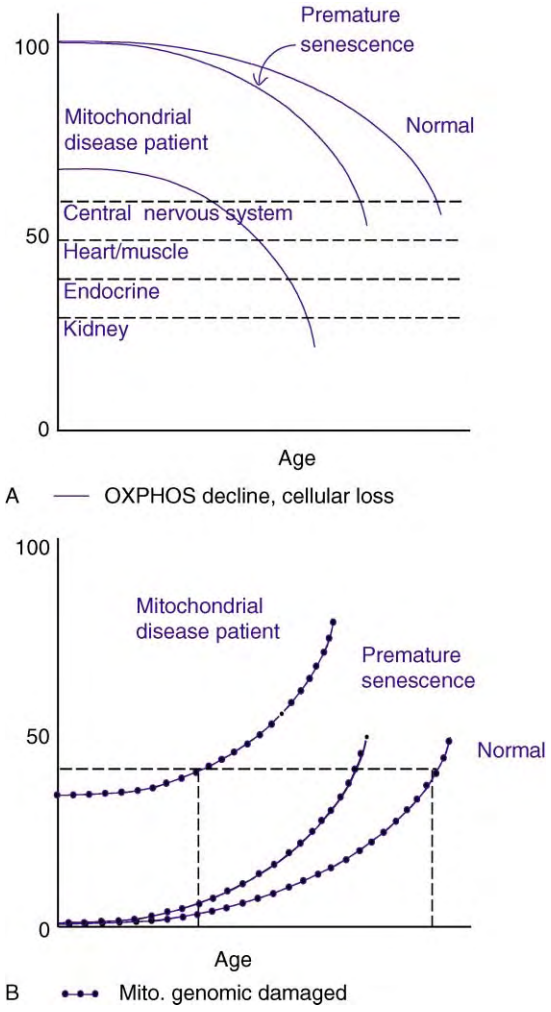

FIGURE 4 Hypothesis for the role of mitochondrial energetic decline and mitochondrial nDNA and mtDNA gene mutations in aging and degenerative disease. (A) Relationship between mitochondrial energy-generating capacity and age. (B) Relationship between defective mitochondrial genes and age. The initial energetic capacity (A) is determined by the inherited mitochondrial genotype (B), with some individuals having a lower proportion of deleterious mitochondrial variants and thus a higher initial energetic output than others. However, as individuals age they accumulate somatic mtDNA mutations in their postmitotic tissues (B) that causes the erosion of their mitochondrial energetic capacity (A). Ultimately, the sum of the inherited genetic defects plus the acquired somatic mtDNA defects cause the mitochondrial energetic capacity to fall below the minimum levels necessary for normal tissue function. If this occurs early in life, it is called disease, whereas if it occurs late in life, it is called senescence.

age-related accumulation of somatic mtDNA point mutations has been observed in the control region and appears to be tissue specific.

Aging is also the most significant risk factor for developing cancer, which implicates somatic mtDNA mutations in cancer as well. Consistent with this concept, somatic mtDNA mutations have been identified in a variety of cancers, including an ND1 intragenic deletion in a renal adenocarcinoma, base substitutions and small deletions in colon carcinomas, various point mutations in bladder, head, and neck, and lung primary tumors.

Therefore, mitochondrial diseases, aging, and cancer can be envisioned as related processes, differing only in their time course (Figure 3). Each individual starts life with a particular energetic capacity determined by his inherited mtDNA and nDNA mitochondrial variants. If the individual inherits a robust mitochondrial genotype, he starts high on the energetic scale. If he harbors one or more partially deleterious variants in the mitochondrial genome, however, he starts lower on the energetic scale (Figure 4). As the individual ages, he accumulates somatic mtDNA mutations that further erode his cellular mitochondrial function and thus tissue integrity and function. Eventually, cellular loss results in organ failure and symptoms. If thresholds are crossed early, it is called mitochondrial disease; if they are crossed late, it is known as aging.

See Also the Following Articles

Cell Death by Apoptosis and Necrosis • Cytochrome *c* • Cytochrome Oxidases, Bacterial • Free Radicals, Sources and Targets of: Mitochondria • Mitochondrial DNA • Mitochondrial Genes and their Expression: Yeast • Mitochondrial Inheritance

Glossary

apoptosis A process of programmed cell death resulting in the activation of caspase enzymes and degradation of cellular proteins that can be initiated via the mitochondrion through the activation of the mitochondrial permeability transition pore (mtPTP) in response to energy deficiency, increased oxidative stress, excessive Ca^{2+}, and/or other factors.

mitochondrial DNA (mtDNA) The portion of the mitochondrial genome that resides in the matrix of the mitochondrion, often as a circular DNA molecule containing the mitochondrial rRNA genes, some tRNA genes, and at least three cytochrome *b* and cytochrome *c* oxidase subunits I and III (COI and COIII) mitochondrial protein genes.

mitochondrion Cellular organelle of endosymbiotic origin residing in the cytosol of most nucleated (eukaryotic) cells that produces energy by oxidizing organic acids and fats with oxygen by the process of oxidative phosphorylation (OXPHOS).

oxidative phosphorylation (OXPHOS) The process by which the mitochondrion generates energy through oxidation of organic acids and fats with oxygen to create a capacitor [electron chemical gradient ($\Delta P = \Delta\Psi + \Delta^{pH}$)] across the mitochondrial inner membrane and uses this stored potential energy to generate adenosine triphosphate (ATP), transport substrates or ions, or produce heat.

reactive oxygen species (ROS) Toxic by-products [primarily superoxide anion ($O_2^{\cdot-}$), hydrogen peroxide (H_2O_2), and hydroxyl radical ($^{\cdot}OH$)], commonly referred to as oxygen radicals, that are generated by oxidative phosphorylation, which damages the mitochondrial and cellular DNA, proteins, lipids, and other molecules causing oxidative stress.

Further Reading

Gray, M. W., Burger, G., and Lang, B. F. (1999). Mitochondrial evolution. *Science* **283**, 1476–1481.

Michikawa, Y., Mazzucchelli, F., Bresolin, N., Scarlato, G., and Attardi, G. (1999). Aging-dependent large accumulation of point mutations in the human mtDNA control region for replication. *Science* **286**, 774–779.

Mishmar, D., *et al.* (2003). Natural selection shaped regional mtDNA variation in humans. *Proc. Natl. Acad. Sci. USA* **100**, 171–176.

Ruiz-Pesini, E. E., Mishmar, D., Brandon, M., Procaccio, V., and Wallace, D. C (2004). Effects of purifying and adaptive selection on regional variation in human mtDNA. *Science*, **303**(5655): 223–226.

Wallace, D. C. (1992). Mitochondrial genetics: A paradigm for aging and degenerative diseases? *Science* **256**, 628–632.

Wallace, D. C. (1999). Mitochondrial diseases in man and mouse. *Science* **283**, 1482–1488.

Wallace, D. C. (2001). Mouse models for mitochondrial disease. *Am. J. Med. Gen.* **106**, 71–93.

Wallace, D. C., Brown, M. D., and Lott, M. T. (1999). Mitochondrial DNA variation in human evolution and disease. *Gene* **238**, 211–230.

Wallace, D. C., Lott, M. T., Brown, M. D., and Kerstann, K. (2001). In *The Metabolic and Molecular Basis of Inherited Disease* (C. R. Scriver, A. L. Beaudet, W. S. Sly and D. Valle, eds.) Mitochondria and neuro-ophthalmologic diseases. pp. 2425–2512. McGraw-Hill, New York.

Wallace, D. C., and Lott, M. T. (2002). In *Emery and Rimoin's Principles and Practice of Medical Genetics* (D. L. Rimoin, J. M. Connor, R. E. Pyeritz and B. R. Korf, eds.) Mitochondrial genes in degenerative diseases, cancer and aging. pp. 299–409. Churchill Livingstone, London.

Biography

Douglas C. Wallace received his B.S. degree from Cornell University in 1968 and Ph.D. from Yale University in 1975 in microbiology and human genetics. He was Assistant Professor of Genetics at Stanford University from 1976 to 1983 and Professor of Biochemistry and Genetics at Emory University from 1983 to 2002. In 2002 he joined the University of California, Irvine as Donald Bren Professor of Molecular Medicine and Director, Center for Molecular and Mitochondrial Medicine and Genetics.

Mitochondrial Inheritance

Eric A. Shoubridge
McGill University, Montréal, Québec, Canada

Mitochondria are small cellular organelles whose primary function is the provision of cellular energy by the process of oxidative phosphorylation. They are surrounded by a double membrane and are about the size of the bacteria from which they were derived by endosymbiosis more than a billion years ago. Mitochondria contain their own DNA that codes for a relatively small number of proteins and RNAs. The size of the mitochondrial genome varies enormously in the biological world, and it generally exists as multiple copies per organelle, with tens to thousands of copies per cell. Mitochondrial genomes do not obey Mendelian laws of segregation and independent assortment. Allelic variants of mitochondrial DNA segregate during mitosis and meiosis, and even in postmitotic cells as mitochondria turn over. This results from the lack of stringent control on mitochondrial DNA replication, and on the random partitioning of mitochondrial genomes to daughter mitochondria. Mitochondrial DNA is uniparentally transmitted in nearly all organisms, in most cases through the female germ line.

Mitochondrial Structure and Function

Mitochondria are cytoplasmic organelles of $\sim 0.5-1.0\ \mu M$ in diameter. They are bounded by a double membrane: an outer membrane that is permeable to small molecules, and an impermeable inner membrane, across which an electrochemical proton gradient formed by electron transport is used to drive ATP synthesis. The inner membrane is a specialized structure, rich in cardiolipin, containing the respiratory chain complexes and carriers that move metabolites in and out of the matrix compartment. This membrane is highly convoluted into folds called cristae, which act to increase the surface area of this membrane. The matrix space bounded by the inner membrane contains soluble enzyme components required for the myriad other functions of mitochondria including the tricarboxylic acid cycle, heme biosynthesis, urea cycle, iron-sulfur cluster biosynthesis, fatty acid oxidation, and amino acid metabolism. It also contains the mitochondrial genome and the machinery necessary for its replication, transcription and translation. It is thought that mitochondria cannot be made *de novo*, but only from other mitochondria. Although mitochondria are often depicted in textbooks as small spherical bodies, they can in fact take on a variety of shapes from simple spheres to large interconnected reticular networks. Mitochondria actively move within the cell and are in a dynamic equilibrium that involves fusion and fission of individual organelles.

Structure of Mitochondrial Genomes

The mitochondrial genomes of all eukaryotes are generally much smaller than bacterial genomes, most of the genes in the original endosymbiont having been transferred to the nucleus during the course of evolution. All animal mitochondrial genomes that have been studied are less than 20 kbp in size, and the majority of these are circular. Mammalian mitochondrial genomes contain only 13 protein-coding genes and the 22 tRNAs and 2 rRNAs necessary to translate these proteins in the mitochondrial matrix. There are no introns, and few noncoding bases outside of the control regions that contain sequences essential for replication and transcription of the genome. Some animal mitochondrial genomes do not contain a full complement of tRNAs and these must therefore be imported. The mitochondrial genomes of the fungi are generally 20–100 kbp in size. They often contain fewer genes than animal mitochondrial genomes, the larger size being attributable to the presence of introns and other large pieces of noncoding DNA. Flowering plants have the largest mitochondrial genomes; most are a few to several hundred kbp in size. These circular genomes contain large direct-repeat sequences that actively recombine to produce large full-length genomes and families of smaller subgenomic circles. Plant mitochondrial genomes often contain sequences derived from the chloroplast genome, the other organellar genome in plants. Many plant mitochondrial genomes contain coding

sequences for chimeric proteins that are responsible for cytoplasmic male sterility.

Mitochondrial DNA is complexed with proteins in the mitochondrion in a structure called the nucleoid, which may be physically associated with the inner mitochondrial membrane.

Genetic Code

The mitochondrial genetic code in animals and fungi is different from the universal genetic code. For instance, the universal stop codon UGA specifies tryptophan in the mitochondrial code, preventing the translation of full-length mitochondrial polypeptides on cytosolic ribosomes. The mitochondrial (and chloroplast) genetic code in flowering plants is the same as the universal code. Transfer of functional genes from the mitochondrial genome to the nucleus thus can and does still occur in plants.

Heteroplasmy and the Segregation of Mitochondrial DNA

New mutations in mitochondrial DNA, which can arise in somatic or germ cells, lead to a situation in which more than one mitochondrial DNA sequence variant (allele) is present in the cell. This generally transient state is referred to as mitochondrial DNA heteroplasmy. Segregation of the different alleles eventually returns the system to the homoplasmic state in which there is no allelic variation. Mitochondrial DNA does not obey the Mendelian laws that apply to the segregation and independent assortment of chromosomal DNA in the nucleus. Although the copy number of mitochondrial DNA is regulated according to the cellular requirements for mitochondrial function, the stringent control that the cell exerts over the replication of nuclear DNA, in which only one copy of each chromosome can be made at each cell cycle, does not exist for mitochondrial DNA. Like some bacterial plasmids, replication of mitochondrial DNA is relaxed and not linked to the cell cycle; the only control is over the copy number. Thus, individual templates may replicate more than once or not at all during mitochondrial proliferation and division. In a dividing cell, mitochondrial DNAs will partition randomly to the daughter cells. In the absence of selection for one allele or another, the relative proportion of the different alleles will be subject to random genetic drift. The rate of genetic drift depends on the copy number and half-life of mitochondrial DNA in the cell. Genetic drift will be fastest in cells containing few copies of mitochondrial DNA with a short half-life. The unit of inheritance of mitochondrial DNA, which determines the effective mitochondrial DNA copy number, is likely to be larger than the genome itself, as multiple genomes can exist per nucleoid and multiple nucleoids populate a mitochondrion.

Transmission of Mitochondrial DNA between Generations

In most organisms, mitochondrial genomes are inherited from one parent, usually, but not universally, the female. The mitochondrial DNA copy number is usually larger in oocytes than in somatic cells. There are 100,000–200,000 copies of mitochondrial DNA in a mammalian oocyte, distributed as ~one per organelle. Despite this large copy number, new allelic variants have been observed to segregate rapidly between generations, with complete fixation often occurring in a few generations. This apparent paradox is the result of a mitochondrial bottleneck that occurs in oogenesis. The number of mitochondria changes dramatically during early embryogenesis and oogenesis. After fertilization, mitochondrial DNA replication does not resume until implantation of the early mammalian embryo. This effectively reduces the copy number of mitochondrial DNA per cell by a factor of ~1000, returning it to that typical of a somatic cell. In the early embryo, a small population of cells is set aside called primordial germ cells. These cells will give rise to all of the gametes that will eventually colonize the gonads. Ultrastructural analyses show that these cells contain only about ten mitochondria, and this is where the bottleneck for transmission occurs. The number of mitochondria increases to ~200 in the oogonia, the migratory cells that populate the genital ridge, and then to a few thousand in the primary oocyte of primordial follicles. A nearly 100-fold amplification of mitochondrial DNA is associated with maturation of the pre-ovulatory oocyte. Thus, although the oocyte contributes at least 100,000 mtDNAs to the zygote in mammals, the effective number of mitochondrial DNA molecules that are transmitted between generations is determined by the relatively small number of mitochondrial DNAs, perhaps as few as ten, which pass through the primordial germ cells. This accounts for the rapid segregation of allelic variants of mitochondrial DNA between generations. Transmission of different alleles through the female germline is, however, a stochastic process. The proportion of a particular allelic variant varies considerably among offspring because of the bottleneck, but the mean proportion in all offspring is similar to that in the mother. In other words, the level of heteroplasmy for an allelic variant in an individual is just as likely to have increased or decreased compared to that of the mother.

Uniparental Inheritance

Uniparental inheritance may be achieved passively by simple dilution of mitochondrial genomes in organisms where the sizes of the two gametes are unequal, or by active processes that exclude or eliminate the contribution from one parent. Examples of active processes include exclusion of organelles from gametes or zygotes, degradation of organelles in the gamete or zygote, and exclusion of organelles from embryonic tissue. The largest variety of active mechanisms is found in plants, where uniparental inheritance of the chloroplast genome (sometimes from a different parent) is also the rule. In mammals, sperm mitochondria, which contain ~100 copies of mitochondrial DNA, enter the zygote, but they are actively eliminated with the sperm remnants during early embryogenesis. Male leakage of mtDNA has been observed in interspecific crosses in mice, suggesting that the factors controlling the elimination of paternal mitochondria are species-specific. Male transmission of mtDNA appears to be extremely rare in humans, a single case having been reported. The fact that uniparental inheritance of organellar genomes is so pervasive suggests that there has been strong selection for this trait throughout evolution. Such a system may have evolved to prevent the spread of mitochondrial genomes with a replicative advantage, but without significant coding-gene content (selfish genomes) in a population. Such genomes have been identified in yeast. Uniparental inheritance would confine selfish genomes to the particular lineage in which they arose.

Mitochondrial Diseases

Diseases resulting from pathogenic mutations in human mitochondrial DNA occur with a frequency of about 1 in 8500 live births and are thus relatively frequent causes of genetic disease. They produce a wide variety of clinical phenotypes with prominent involvement of muscles and nerves. Most mitochondrial DNA mutations exist in a heteroplasmic state because homoplasmy for the severe mutations would be lethal. There are marked tissue-specific differences in the segregation patterns of pathogenic mutations, suggesting that pathogenic mutations are under differing selective pressures in different tissues. The segregation pattern is also influenced by the particular mutation. Generally, a high proportion (85–90%) of mitochondrial DNAs carrying the pathogenic mutation must accumulate in the cell for expression of a pathological biochemical and clinical phenotype. This phenomenon is referred to as threshold expression. It results from intraorganellar genetic complementation in which the products of wild-type mitochondrial DNAs are able to functionally rescue the products of the mutant genomes. Mitochondrial DNAs carrying pathogenic mutations are transmitted to the next generation in a largely stochastic fashion, implying that there is weak selection for mitochondrial respiratory chain function during oogenesis, embryogenesis or fetal life.

The best-studied mitochondrial disease of flowering plants is cytoplasmic male sterility because of its agricultural importance in hybrid seed production. It results from the presence of a chimeric gene in mitochondrial DNA that usually consists of an unidentified open reading frame, fused in frame with a fragment of a mitochondrial protein-coding gene. The product of this gene specifically disrupts the production of fertile pollen. Nuclear restorer genes have been identified that suppress this phenotype.

Glossary

genetic bottleneck (mitochondrial) A restriction in the number of mitochondria and mitochondrial DNAs that occurs in mammalian oogenesis, decreasing the effective number of mitochondrial DNAs that contribute to the next generation.

heteroplasmy A state in which more than one allelic variant of mitochondrial DNA exists in a cell.

homoplasmy A state in which all copies of mitochondrial DNA in the cell have the same sequence.

mitochondrial DNA The mitochondrial genome.

nucleoid A structure containing mitochondrial DNA complexed with protein that associates with the inner mitochondrial membrane.

relaxed replication Mitochondrial DNA can be replicated at any stage during the cell cycle and individual templates can be copied more than once or not at all.

segregation (mitochondrial) The process by which different alleles of mitochondrial DNA are separated when mitochondria proliferate. This happens during mitosis, meiosis, and in postmitotic cells.

threshold expression Refers to notion that a certain proportion of mutant mitochondrial DNA must be present in the cell for an abnormal phenotype to be expressed.

Further Reading

Birky, Jr. C. W. (1994). Relaxed and stringent genomes: Why cytoplasmic genes don't obey Mendel's laws. *J. Hered.* **85**, 355–365.

Birky, Jr. C. W. (1995). Uniparental inheritance of mitochondrial and chloroplast genes: Mechanisms and evolution. *Proc. Natl. Acad. Sci. USA* **92**, 11331–11338.

Chinnery, P. F., and Schon, E. A. (2003). Mitochondria. *J. Neurol. Neurosurg. Psychiatry* **74**, 1188–1199.

Gillman, N. W. (1994). *Organelle Genes and Genomes*. Oxford University Press, New York.

Jansen, R. P. S. (2000). Germline passage of mitochondria: Quantitative considerations and possible embryological sequelae. *Hum. Reprod.* **15**(suppl. 2), 112–128.

Shoubridge, E. A. (2000). Mitochondrial DNA segregation in the developing embryo. *Hum. Reprod.* **15**(suppl. 2), 229–234.

Biography

Eric A. Shoubridge is a Professor in the Department of Neurology and Neurosurgery and the Department of Human Genetics at the Montreal Neurological Institute of McGill University. His principal research interests are in mammalian mitochondrial genetics and mitochondrial diseases. He holds a Ph.D. from the University of British Columbia and received his postdoctoral training at Oxford University. He is an International Scholar of the Howard Hughes Medical Institute and a Senior Investigator of the Canadian Institutes for Health Research.

Mitochondrial Membranes, Structural Organization

Carmen A. Mannella
Wadsworth Center, New York State Department of Health, Albany, New York, USA

The mitochondrion is the organelle in eukaryotic cells that is the primary generator of ATP, the molecule that fuels most of the cell's machinery. The chemiosmotic mechanism of ATP production involves establishment of an electrochemical gradient across the mitochondrial inner membrane by the respiratory chain complexes. The free energy in this gradient is coupled to phosphorylation of ADP by the F_1F_0 ATP synthase on the inner membrane. Since chemiosmosis entails very rapid fluxes of ions and metabolites between the mitochondrial interior and the cytosol, the shape as well as the permeability properties of the energy-transducing inner membrane can be expected to affect mitochondrial function.

Electron Microscopy and the Structure of Mitochondria

Pioneering work of Palade, Sjostrand and others in the 1950s led to the first high-quality electron microscopic images of mitochondria. Controversies ensued, partly due to the inherent difficulty of interpreting images of plastic sections that were too thin (80 nm) to convey three-dimensional (3-D) structure. Conversely, this section thickness imposed a lower limit on resolution in the axial direction (parallel to the electron beam) in these images. Thus, despite the general acceptance of a model by the early 1960s (Figure 1), work on determining the structure of mitochondria has been a work in progress. An important advance was the development of electron tomography in the 1990s, in which numerous micrographs of a serially tilted specimen are combined to yield a 3-D image. Using high-voltage electron microscopes, this technique has provided actual 3-D images of mitochondria in thick sections (200–1000 nm) with axial resolution on the order of 5 nm (Figure 2). Moreover, with computer-controlled cryo-electron microscopes, it is possible to image intact, frozen-hydrated mitochondria, rapidly frozen in aqueous buffer, without the chemical fixatives or metal stains employed with plastic sections (Figure 3).

Mitochondrial Membranes and Compartments

The mitochondrion is formed by two nested membranes, which define three classes of compartments.

Outer Membrane

The mitochondrial outer membrane is the interface between the organelle and the cytosol. It excludes proteins and other macromolecules, but is thought to be permeable to most solutes below a molecular weight of ~2000 since it carries many copies of a pore-forming protein called VDAC (voltage-dependent, anion selective channel) or mitochondrial porin.

Inner Membrane

The inner membrane is the site of the respiratory chain, the ATP synthase, and numerous carrier proteins such as ANT, the adenine nucleotide transporter that exchanges ADP and ATP.

Intermembrane Space

The space between the outer and inner membranes is called the intermembrane (or peripheral) space. Its protein content, which is much lower than that of the matrix, includes kinases (for interconversion of phosphorylated metabolites) and cytochrome *c* (involved in both electron transfer and apoptosis).

Matrix Space

The space enclosed by the inner membrane is occupied by a very dense, largely protein matrix. This compartment contains a variety of enzymes, particularly those of the Krebs cycle, along with several copies of the circular mitochondrial genome and numerous mitochondrial ribosomes. (Mitochondria synthesize a small number of respiratory chain proteins; 90% of the mitochondrial protein mass is imported from the cytosol.)

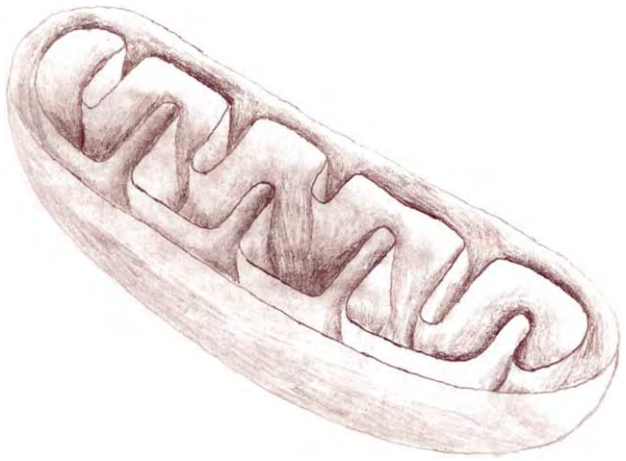

FIGURE 1 The conventional model for mitochondrial structure From Philomena Sculco, Wadsworth Center.

Cristae

The inner membrane has a much larger surface area than the outer membrane, typically by a factor of 2.5–10. There is a correlation between the energy demand in a particular tissue and the inner membrane surface, e.g., heart mitochondria have more inner membrane (and so more ATP generating capacity) than liver mitochondria. The inner membrane is contained by the smaller outer membrane because it is invaginated or involuted. The internal compartments defined by the infoldings of the inner membrane are called cristae and the space they enclose is the intracristal space. The intracristal space connects to the intermembrane space through the openings of the cristae in the peripheral region of the inner membrane.

Mitochondrial Inner Membrane Topology

The early model of mitochondrial structure portrayed the cristae as baffle-like folds in the inner membrane (Figure 1). Three-dimensional images provided by electron tomography of a wide variety of mitochondria, isolated and *in situ*, indicate a different internal architecture. The inner membrane comprises numerous pleiomorphic compartments, which are connected to each other and to the periphery of the inner membrane by narrow (20–30 nm diameter) tubular segments (Figure 2). These tubular connecting regions (called cristae junctions) can vary in length from a few tens to several hundred nanometers.

Functional Implications of the Cristae Junctions

The fact that cristae open into the intermembrane space through narrow, sometimes very long tubular segments suggests that diffusion of solutes between the internal compartments of mitochondria might be restricted. This was not a concern with the early structural model, which depicted the baffle-like cristae with wide, slot-shaped

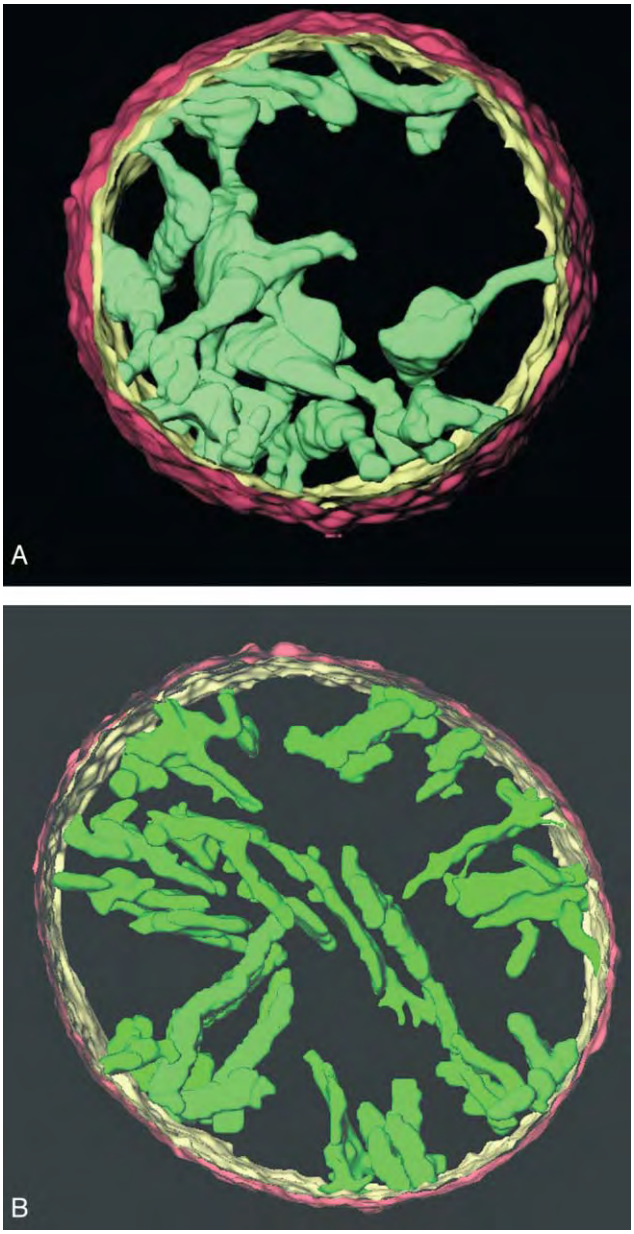

FIGURE 2 Tomographic reconstruction of membranes in isolated rat liver mitochondria in (A) condensed and (B) orthodox conformations. Mitochondria were chemically fixed, plastic-embedded and stained by conventional procedures. Approximate dimensions: (A) 1500 nm diameter, 500 nm thick, and (B) 500 nm diameter, 200 nm thick. (A) Adapted with permission from Mannella *et al.* (2001), Figure 1a.

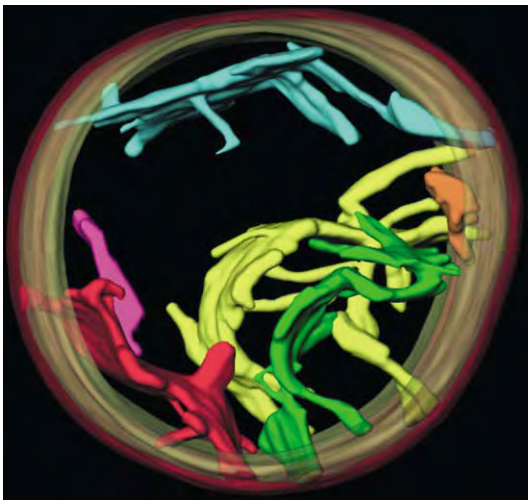

FIGURE 3 Tomographic reconstruction of membranes in an intact, frozen-hydrated rat liver mitochondrion, prepared with no chemical fixatives or stains. Approximate dimensions: 700 nm diameter, 450 nm thick. Adapted with permission from Mannella *et al.* (2001), Figure 4b.

openings into the intermembrane compartment. Computer simulations indicate that diffusion of ADP between the intermembrane and intracristal compartments via long, narrow tubes (the cristae junctions) can cause depletion of ADP in the intracristal space and locally diminished ADP phosphorylation. Thus, the topology of the mitochondrial inner membrane may directly influence the efficiency of ATP generation by the organelle.

Cristae Junctions Form Spontaneously

Tubular cristae junctions appear to be a highly conserved feature of the mitochondrial inner membrane. If they are functionally important (as implied above), it is expected that their formation would be spontaneous or energetically favored. This has been demonstrated with yeast mitochondria. Tubular connections between cristae and the peripheral region of the inner membrane form spontaneously in membranes, which initially lack cristae due to extreme osmotic swelling of the mitochondria. (Osmotic effects on mitochondrial structure are discussed in detail below.)

Changes in Mitochondrial Inner Membrane Topology

Although the mitochondrial inner membrane has a high protein-to-lipid ratio and encases a dense protein matrix, it is very flexible. The morphology of this membrane in isolated mitochondria changes readily in response to osmotic and metabolic conditions.

Osmotic Adjustments in Inner Membrane Topology

Tedeschi and Harris showed in the 1950s that mitochondria behave as "perfect osmometers" over a range of osmotic conditions. The matrix volume adjusts to changes in osmotic conditions (external solute concentration) by expanding (water influx) or shrinking (water efflux). Isolated mitochondria with a shrunken matrix (caused by water efflux in response to hyper-osmotic external conditions) are said to be in the condensed conformational state (Figure 2A). Mitochondria with a more expanded matrix (exposed to iso-osmotic or slightly hypo-osmotic conditions) are said to be in the orthodox (cell-like) state (Figure 2B). Exposure of mitochondria to very hypo-osmotic media causes extreme matrix swelling, and can lead to rupture of the outer membrane. (The latter is considered osmotically inactive due to its permeability to small solutes.)

Changes in Inner Membrane Topology Associated with Metabolic State

In the 1960s, Hackenbrock demonstrated that isolated mitochondria could reversibly switch between orthodox and condensed conformations during respiration. When ADP is added, respiring mitochondria change from orthodox to condensed conformation, then back to orthodox as ADP runs out. Condensed mitochondria tend to have larger internal compartments with longer cristae junctions, which can limit ADP diffusion into the cristae (above). Thus, the switch to orthodox conformation (smaller internal compartments, shorter tubular junctions) as ADP levels drop may prevent intracristal depletion of ADP and so maintain more efficient ATP production. Note that cellular ADP levels are normally low and mitochondria are usually in the orthodox conformation.

Inner Membrane Fusion and Fission

Comparison of 3-D images of condensed and orthodox mitochondria suggest an important role for membrane fusion and fission in regulation of inner membrane topology. Condensed mitochondria have large cristae with multiple tubular connections (cristae junctions) to the periphery of the inner membrane (Figure 2A). Conversely, orthodox mitochondria have predominantly narrower cristae with single peripheral connections (Figure 2B). Interconversion of these two membrane topologies cannot be achieved by simple unfolding and refolding of the inner membrane.

The topologies can be reconciled by postulating that large cristae with multiple tubular segments form by fusion of individual narrower cristae which make contact during matrix contraction. Likewise, matrix expansion and associated stress on the inner membrane may trigger fissioning of larger cristae into individual tubular membranes. Support for this mechanism is provided by tomographic images of frozen-hydrated mitochondria, in which large cristae clearly appear to be composed of fused tubular membranes (Figure 3). Dynamin-like proteins such as Mgm-1 and Drp-1 are involved in fusion and fission of mitochondria during organelle biogenesis and transport. These or other related proteins may regulate inner membrane fusion and fission during conformational changes as well.

Unusual Inner Membrane Topologies

While cristae in mitochondria from many animal, plant, and fungal cells have a more or less common appearance, there are numerous exceptions. For example, mitochondria in steroidogenic tissues like adrenal glands have cristae that are arranged in parallel tubular arrays. Densely packed cristae in some muscle mitochondria are arranged concentrically. Other specialized tissues (in gastropods and insects, for example) have cristae with triangular or square cross-sections. Several examples of unusual inner membrane topologies appear to be associated (at least in part) with abnormal inner membrane fusion or fission.

Cubic Paracrystalline Inner Membrane

Mitochondria in protists tend to have randomly arranged tubular cristae. In the amoeba, chaos carolinensis, fasting induces a dramatic change in inner membrane topology to an interconnected labyrinth of internal compartments with threefold (cubic) paracrystalline order. Deng and co-workers have shown that this structural transition is associated with several metabolic changes in the organism, including increased free radical production (oxidative stress). Conversion of the normally tubular inner membranes to a continuous membrane network implies induction of large-scale fusion. The highly symmetric shape of the membranes further implies that a change in membrane composition has occurred that imposes constant curvature everywhere.

Vesicular Cristae

Cristae that do not connect with the peripheral region of the inner membrane have been observed in several types of mitochondria, including muscle mitochondria from patients with a rare disorder called Senger's syndrome. This appears to be a case in which either the cristae junctions are unstable or inner membrane fission has become dominant over fusion. The specific genetic defect is unknown in Senger's syndrome, but research carried out by Huizing and co-workers suggests a tentative association with decreased ANT content.

Cytochrome *c* Release During Apoptosis

The process of apoptosis, or programmed cell death, in many cell types requires release of mitochondrial factors, including cytochrome *c*, to activate caspases involved in cellular degradative reactions. This process of mitochondrial protein release involves members of the Bcl-2 family of proteins. A key event is migration of Bax from cytosol to the mitochondrial surface, where it oligomerizes and causes protein release across the outer membrane. The trigger for this event is the truncated form of the protein Bid (tBid). Scorrano, Korsmeyer and co-workers have recently shown that tBid alone induces a dramatic change in topology of the mitochondrial inner membrane that correlates with increased accessibility of cytochrome *c* to the intermembrane space. After tBid exposure, the cristae have reversed curvature and appear to be fused into a continuum, not unlike the paracrystalline inner membrane of the fasting amoeba. Importantly, the openings of the cristae into the peripheral region of the inner membrane are considerably wider (55 nm versus 20 nm), which may account for improved diffusion of soluble proteins between compartments.

See Also the Following Articles

ATP Synthesis in Plant Mitochondria: Substrates, Inhibitors, Uncouplers • ATP Synthesis: Mitochondrial Cyanide-Resistant Terminal Oxidases • Cell Death by Apoptosis and Necrosis • Cytochrome *c* • DNA Replication, Mitochondrial • Mitochondrial DNA • Mitochondrial Genome, Evolution • Mitochondrial Genome, Overview • Mitochondrial Inheritance • Mitochondrial Outer Membrane and the VDAC Channel • Nuclear Genes in Mitochondrial Function and Biogenesis • Protein Import into Mitochondria

Glossary

cristae The complex internal compartments of mitochondria that are formed by invagination of the inner membrane.

cristae junctions Tubular regions of the inner membrane that connect the internal cristae compartments to the region of the membrane along the mitochondria periphery.

electron tomography A technique involving computation of a three-dimensional density map from scores of images recorded in an electron microscope of a serially tilted specimen.

mitochondria The organelle in eukaryotic cells, composed of an outer and inner membrane, that uses the free energy of substrate oxidation for ATP production.

Further Reading

Frey, T. G., and Mannella, C. A. (2000). The internal structure of mitochondria. *Trends Biochem. Sci.* **25**, 319–324.

Mannella, C. A (2003). Downloadable video clip of a 3-D model of a frozen-hydrated rat-liver mitochondrion. http://www.wadsworth.org/databank/electron/cryomito_dis2.html.

Mannella, C. A., Buttle, K., and Marko, M. (1997). Reconsidering mitochondrial structure: New views of an old organelle. *Trends Biochem. Sci.* **22**, 37–38.

Mannella, C. A., Pfeiffer, D. R., Bradshaw, P. C., Moraru, I. I., Slepchenko, B., Loew, L. M., Hsieh, C., Buttle, K., and Marko, M. (2001). Topology of the mitochondrial inner membrane: Dynamics and bioenergetic implications. *IUBMB Life* **52**, 93–100.

Munn, E. A. (1974). *The Structure of Mitochondria*. Academic Press, London.

Nicastro, D., Frangakis, A. S., Typke, D., and Baumeister, W. (2000). Cryo-electron tomography of Neurospora mitochondria. *J. Struct. Biol.* **129**, 48–56.

Perkins, G., Renken, C., Martone, M. E., Young, S. J., Ellisman, M., and Frey, T. (1997). Electron tomography of neuronal mitochondria: Three-dimensional structure and organization of cristae and membrane contacts. *J. Struct. Biol.* **119**, 260–272.

Rasmussen, N. (1995). Mitochondrial structure and the practice of cell biology in the 1950s. *J. History Biol.* **28**, 381–429.

Biography

Carmen A. Mannella is a research scientist and Director of the Division of Molecular Medicine at the Wadsworth Center, New York State Department of Health in Albany, NY. His main research interests are in mitochondrial membrane structure and permeability. He holds a Ph.D. from the University of Pennsylvania and received his postdoctoral training at Roswell Park Cancer Institute and St. Louis University. As co-director of the Wadsworth Center's Resource for the Visualization of Biological Complexity (a NIH NCRR biomedical technology resource center), he participates in the development of electron tomography and its application to a wide range of biological problems.

Mitochondrial Metabolite Transporter Family

Ferdinando Palmieri
University of Bari, Bari, Italy

Martin Klingenberg
University of Munich, Munich, Germany

The mitochondrial transporters are a family of nuclear-coded, membrane-embedded proteins that, with one exception, are found in the inner membranes of mitochondria and catalyze the translocation of solutes across the membrane. Since mitochondria and cytosol cooperate in a large number of metabolic cellular processes, a continuous and highly diversified flux of metabolites, nucleotides, and cofactors into and out of the mitochondria is needed. Functional studies in intact mitochondria have indicated the presence of more than 20 carrier systems for the transport of metabolites involved in the citric acid cycle, oxidative phosphorylation, fatty acid oxidation, gluconeogenesis, lipogenesis, transfer of reducing equivalents, urea synthesis, amino acid degradation, and other functions shared between cytosol and mitochondria. The central role of some mitochondrial carriers in cell metabolism is illustrated in this entry.

Purification

Eleven carrier proteins have been purified to homogeneity from mitochondria using a procedure that, with very few exceptions, involved chromatographic steps on hydroxyapatite and celite. Purification and subsequent reconstitution of pure protein into phospholipid vesicles (liposomes) was useful for identification, functional characterization, and some structural studies.

Structure

Early studies elucidated the primary structure of six purified and biochemically well-characterized mitochondrial-carrier proteins. These are the ADP/ATP carrier (AAC, in fact the first metabolite transporter to be sequenced), the uncoupling protein (UCP), and the carriers for phosphate (PiC), oxoglutarate (OGC), citrate (CIC), and carnitine/acylcarnitines (CAC) (Figure 1). Their primary structures were derived by sequencing the full-length peptide chain, or by molecular biological techniques initiated with partial amino acid sequence information. A unique feature of these six mitochondrial carriers is their tripartite sequence structure, i.e., they consist of three tandemly repeated homologous domains ~100 amino acids in length. Each domain contains two hydrophobic stretches, which are thought to span the membrane as α-helices. All carriers contain, in at least one of the repeats, the characteristic sequence motif P-h-D/E-X-h-K/R-X-R/K-(20–30 residues)-D/E-G-(4 residues)-a-K/R-G, where "h" represents a hydrophobic and "a" represents an aromatic residue. Therefore, they all belong to the same protein family.

A generally accepted two-dimensional model of mitochondrial carriers is illustrated in Figure 2 based on the sequence features described above and on the accessibility of carriers to impermeable reagents, proteolytic enzymes, and peptide-specific antibodies. According to this model, the typical mitochondrial carrier monomer has six helices traversing the membrane connected by hydrophilic loops with both the N and C termini on the cytosolic side of the inner mitochondrial membrane. The matrix loops of the AAC, CAC, and UCP have been proposed to protrude into the membrane between the transmembrane segments of the protein, based on observations that residues located in the hydrophilic matrix region of these carriers react with membrane-impermeable reagents applied from the cytosolic side. It should also be noted that the transmembrane segments IV of CIC and OGC have been shown to be in α-helical structure using spin labels on engineered single-Cys residues.

Most of the isolated carrier proteins are shown to be homodimers and this may apply to all members of the mitochondrial carrier family (MCF). The evidence is based on direct MW determination of isolated proteins, on chemical, and recombinant cross-linking. The role of the homodimers in the transport mechanism, involving,

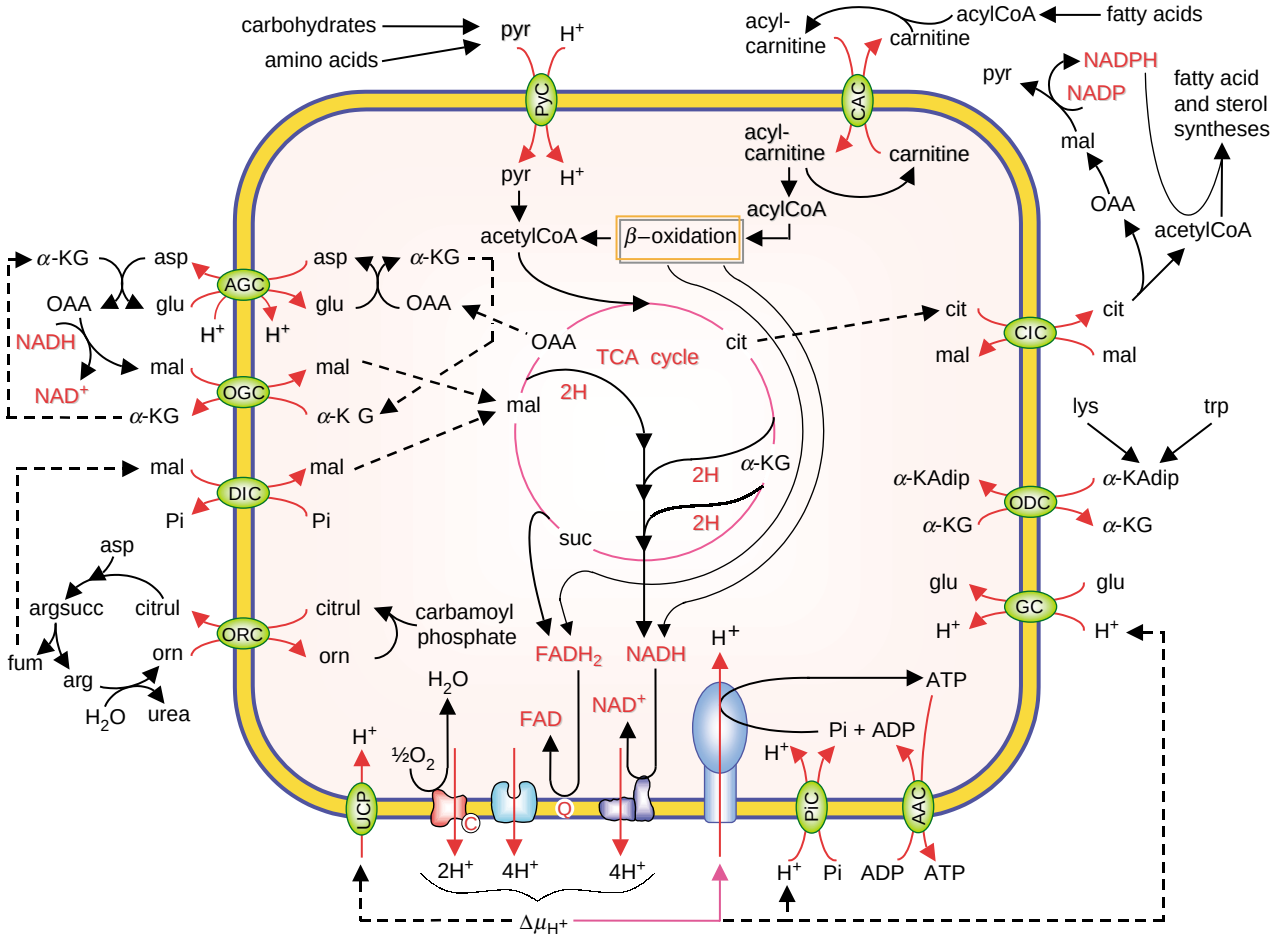

FIGURE 1 Metabolic roles of mitochondrial carriers. The scheme shows 12 carriers catalyzing metabolite transport through the inner mitochondrial membrane. These carriers are involved in oxidative phosphorylation (AAC, PiC, UCP), in oxidation/reduction pathways (AGC, OGC, DIC, CIC, CAC, PyC), and, with partial overlap, in amino acid metabolism (AGC, ORC, GC, ODC). The scheme does not include all of the carriers listed in Table I and does not show all the metabolic pathways in which individual carriers are involved (see Table I).

for example, a central channel or cooperative interactions between the monomers is still being elucidated.

Extension of the Mitochondrial Carrier Family

With the availability of DNA banks, the characteristic sequence features of the MCF were used to search for carriers of unknown function within the same family. Thus, a subfamily of UCPs (UCP 1–5) has been discovered with a wide variety of functions such as thermogenesis, oxygen radical suppression, regulation of fatty acid oxidation, immune response, and insulin secretion. The *Saccharomyces cerevisiae* genome contains 35 MCF members, and the human one presumably more. In this context, a breakthrough was achieved when the bovine OGC was overexpressed in *Escherichia coli*. The recombinant OGC, accumulated as inclusion bodies in the bacteria, was solubilized with sarkosyl and functionally reconstituted into liposomes. This was the first eukaryotic membrane protein to be produced in *E. coli* and recovered in active form. Using this strategy, i.e., gene expression and transport assays in the reconstituted system, the nucleotide and amino acid sequences of eight new mitochondrial carriers in *S. cerevisiae*, four in plants, and nine in man (including isoforms) have so far been identified (see Table I). The transporters identified first in yeast are the carriers for dicarboxylates (DIC), succinate/fumarate (SFC), ornithine (ORC), oxaloacetate/sulfate (OAC), oxodicarboxylates (OAC), thiamine pyrophosphate (TPC), and adenine nucleotides (ANT). The main function of DIC in yeast is to import succinate (produced by the glyoxylate cycle in the cytosol) or other dicarboxylates into mitochondria, whereas SFC directs the carbon skeleton of succinate to gluconeogenesis. The yeast OAC

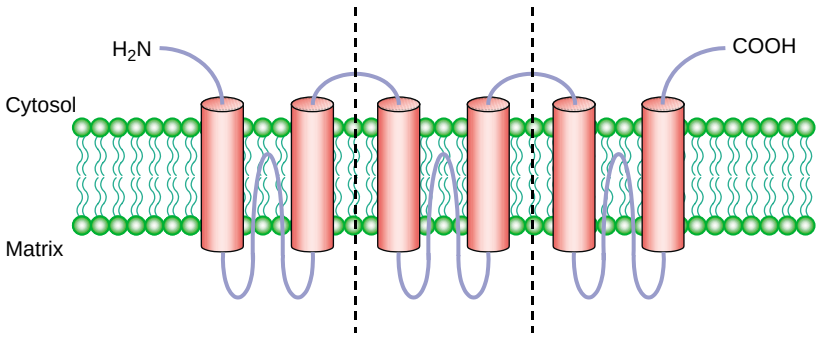

FIGURE 2 Suggested folding pattern of the mitochondrial solute carriers. Six helices traverse the inner mitochondrial membrane with the C and N termini facing the cytosol. The whole sequence is divided into three similar domains each with two transmembrane helices. Within each domain the two helices are connected by a long hydrophilic matrix loop (A, B, C respectively) which is assumed to protrude into the membrane space.

has also an anaplerotic role, as the *S. cerevisiae* pyruvate carboxylase is cytoplasmic. The main function of ORC in yeast is to export ornithine in exchange for H^+ to the cytosol, where it is converted into arginine and polyamines. The yeast ODC transports oxoadipate in exchange for oxoglutarate or malate from the mitochondria to the cytosol where it is converted into Lys. The essential cofactor thiamine pyrophosphate, produced in the cytosol, is transported into mitochondria by TPC. The peroxisomal ANT transports ATP, ADP, and AMP and its function is to transport cytosolic ATP into the peroxisomal lumen in exchange for AMP generated in the activation of fatty acids (in yeast fatty acid β-oxidation occurs in the peroxisomes). It differs from the mitochondrial AAC because it transports AMP and is unaffected by the AAC inhibitors CATR and BK. ANT is the first member of the MCF found to be located in a nonmitochondrial membrane, and it is the first peroxisomal protein proven to perform a transport function.

Other carriers were identified first in man. Among them, the human DNC transports dNDPs and dNTPs (in exchange for ADP or, more likely, ATP and pyrophosphate) into mitochondria for mDNA synthesis. Interestingly, DNC can transport dideoxynucleotides efficiently, which explains the toxic side effects of nucleoside analogues in the treatment of viral illnesses including AIDS. Other examples are the aspartate/glutamate carrier (AGC), which had previously been purified but not sequenced, and the glutamate/H^+ carrier (Table I).

Driving Forces for Transport

The majority of mitochondrial carriers catalyze strict solute exchange reactions. Those mediating H^+-compensated unidirectional substrate flux may also fall into the above category, because at least PiC has been shown to function in a phosphate/OH^- antiport mode. CAC has an unusual dual function mediating both unidirectional transport of carnitine and carnitine/acylcarnitine exchange, whereas UCP catalyzes uniport as exclusive transport mode.

Mitochondrial carriers can be divided into electrogenic (or electrophoretic) and electroneutral transporters. So far, three well-characterized carriers have been shown to be electrophoretic. AAC and AGC catalyze exchanges that result in a charge imbalance because they transport ADP^{3-} for ATP^{4-} and $aspartate^-$ for $glutamate^- + H^+$, respectively, across the mitochondrial membrane. The third, UCP, catalyzes the unidirectional transport of H^+. Electroneutral balance can be achieved by cotransport (symport) of solutes, countertransport of solutes, and uniport of electroneutral metabolites. The carriers for Pi, glutamate, pyruvate, and in yeast for oxaloacetate/sulfate facilitate the transport of anions together with an equivalent amount of H^+ (anion/H^+ symport) or in exchange for OH^- (anion/OH^- antiport). Other carriers catalyze an exchange of anions or cations. OGC, for example, transports $oxoglutarate^{2-}$ for $malate^{2-}$ and ORC ornithine for lysine, arginine, or H^+. In some cases electroneutrality is imposed by simultaneous carrier-mediated H^+ movement. CIC, for example, transports H-$citrate^{2-}$ against $malate^{2-}$ and the human ORC can transport $ornithine^+$ against citrulline and H^+.

The mitochondrial carriers utilize, as their driving force, the concentration gradient of the solutes and/or the H^+ electrochemical potential generated across the inner mitochondrial membrane by the functioning of the respiratory chain. Since the electrical component of $\Delta\mu H^+$ is rather high, the electrical nature of AAC and AGC provides a powerful means of ejecting ATP and aspartate against the concentration gradient from the mitochondrial matrix to the cytosol. In cases of H^+ symport or H^+ exchange, the transmembrane pH gradient regulates the distribution of anionic and

TABLE I

Mitochondrial Transporters

Carrier	Symbol	Isoforms	Main substrates	Mode of transport	Metabolic role
A					
ADP/ATP	AAC	3	ADP, ATP	Exchange	Energy transfer, oxidative phosphorylation
UCP	UCP	5[a]	H^+	Uniport	Uncoupling for thermogenesis (UCPI) and for regulation of some specific cellular events (UCP2 to 5)
Phosphate	PiC	2[b]	Phosphate	H^+ symport	Energy transfer, oxidative phosphorylation, counter-ion for malate
Oxoglutarate	OGC		Oxoglutarate, malate	Exchange	Malate/asparate shuttle, isocitrate/oxoglutarate shuttle, nitrogen metabolism, gluconeogenesis from lactate
Citrate	CIC		Citrate, malate, phosphoenolpyruvate isocitrate, *cis*-anconitate	Exchange	Fatty acid and sterol biosyntheses, gluconeogenesis from lactate, isocitrate/oxoglutarate shuttle
Carnitine	CAC		Carnitine, acylcarnitines	Exchange and uniport	Fatty acid oxidation
B					
Dicarboxylate	DIC		Malate, succinate, phosphate, sulfate, thiosulfate	Exchange	Anaplerosis, gluconeogenesis from pyruvate (and amino acids), urea synthesis, sulfur metabolism
Fumarate/succinate (y)	SFC		Fumarate, succinate	Exchange	Gluconeogenesis
Ornithine	ORC	2	Ornithine, lysine, citrulline	Exchange/H^+ symport	Urea synthesis
Oxaloacetate/sulfate (y)	OAC		Oxaloacetate, sulfate, thiosulfate	H^+ symport	Anaplerosis, sulfur metabolism, transfer of reducing equivalents
Folate	MFT		Folates	?	Cofactor
Deoxynucleotide	DNC		dNDPs, dNTPs, ADP, ATP	Exchange	Mitochondrial DNA synthesis

(*continues*)

TABLE I

Continued

Oxodicarboxylate	ODC	2[c]	Oxoadipate, oxoglutarate	Exchange	Lysine, tryptophan and hydroxylysine catabolism
Aspartate/glutamate	AGC	2	Aspartate, glutamate, cysteinesulfinate	Exchange	Malate/aspartate shuttle urea synthesis, gluconeogenesis, cysteine metabolism
Adenine nucleotide[d]	ANTI		ATP, ADP, AMP	Exchange	Peroxisomal fatty acid β-oxidation
Coenzyme A			Coenzyme A	?	Cofactor
Glutamate	GC	2	Glutamate	H^+ symport	Urea synthesis, nitrogen metabolism
Dicarboxylate/ tricarboxylate (p)	DTC	2[e]	Oxoglutarate, oxaloacetate, malate, citrate, isocitrate	Exchange	Fatty acid and isoprenoid syntheses, redox shuttle in photorespiration, nitrogen assimilation
Thiamine pyrophosphate (y)	TPC		Thiamine pyrophosphate, thiamine monophosphate	Exchange/H^+ symport	Matrix thiamine-dependent reactions
Basic amino acid (p)	BAC	2	Arginine, lysine, ornithine, hystidine	Exchange/H^+ antiport	Basic amino acids metabolism
C					
ATP-Mg^{2+}/Pi			ATP-Mg^{2+}, phosphate	Exchange	Matrix adenine nucleotide content
Pyruvate	PYC		Pyruvate, other monocarboxylates	H^+ symport	Citric acid cycle, glyconeogenesis, ketone bodies
Branched-chain α-ketoacid			α-ketoisocaproate, α-ketoisovalerate	H^+ symport	Branched-chain amino acid catabolism
Glutamine	GLC		Glutamine, asparagine	Uniport	Glutamine degradation

A carriers functionally identified and sequenced after purification. *B* carriers functionally identified upon expression of their genes. *C* carriers proposed from transport studies in mitochondria. y (yeast) and p (plants) indicate the species where the carrier has so far been identified. All the other carriers have been identified also or only in man.

[a] UCP3 and UCP5 exist as two splicing variants (short and long forms).

[b] Isoforms generated by alternative splicing.

[c] Isoforms present in yeast but not in man.

[d] Localized in the peroxisomal membrane.

[e] Isoforms present in *Nicotiana tabacum*.

cationic solutes across the membrane. For example, with a higher pH inside, the carrier-mediated H^+-compensated uptake of Pi or glutamate is stimulated, as well as the efflux of cationic solutes such as the export of ornithine.

Functional Models for Mitochondrial Exchange Carriers

Two models of transport have been proposed for mitochondrial exchange carriers. According to the "single site gated pore" mechanism, suggested for the AAC, the transporter has only one binding site which is exposed alternately to the two different sides of the membrane (Figure 3A). On binding the substrate to one side, the carrier–substrate complex undergoes a conformational change and the binding site becomes exposed to the opposite side. The transported substrate now has to leave the transport site before another substrate to be transported in the opposite direction is bound. In the alternative hypothesis, the "double site gated pore" mechanism, two binding sites are exposed on the opposite sides of the membrane at the same time and both have to be occupied by the exchanging substrates before the conformational change and the substrate translocation occurs (Figure 3B). For AAC, the reorientation of the binding is well documented at carrier protein level since high-affinity inhibitor ligands exist which bind to the carrier either on the cytosolic side (atractyloside, ATR) or on the matrix side (bongkrekate, BK). These ligands remove ADP or ATP and their binding is mutually exclusive, indicating a single reorienting binding site.

The second possibility is supported by kinetic analysis of several carriers. Two-reactant initial-velocity studies varying both the internal and external substrate concentrations have conclusively shown that the reconstituted AGC, OGC, CIC, DIC, PiC, ORC, and possibly AAC function according to a simultaneous (sequential) mechanism, implying that one internal and one external substrate molecule form a ternary complex with the

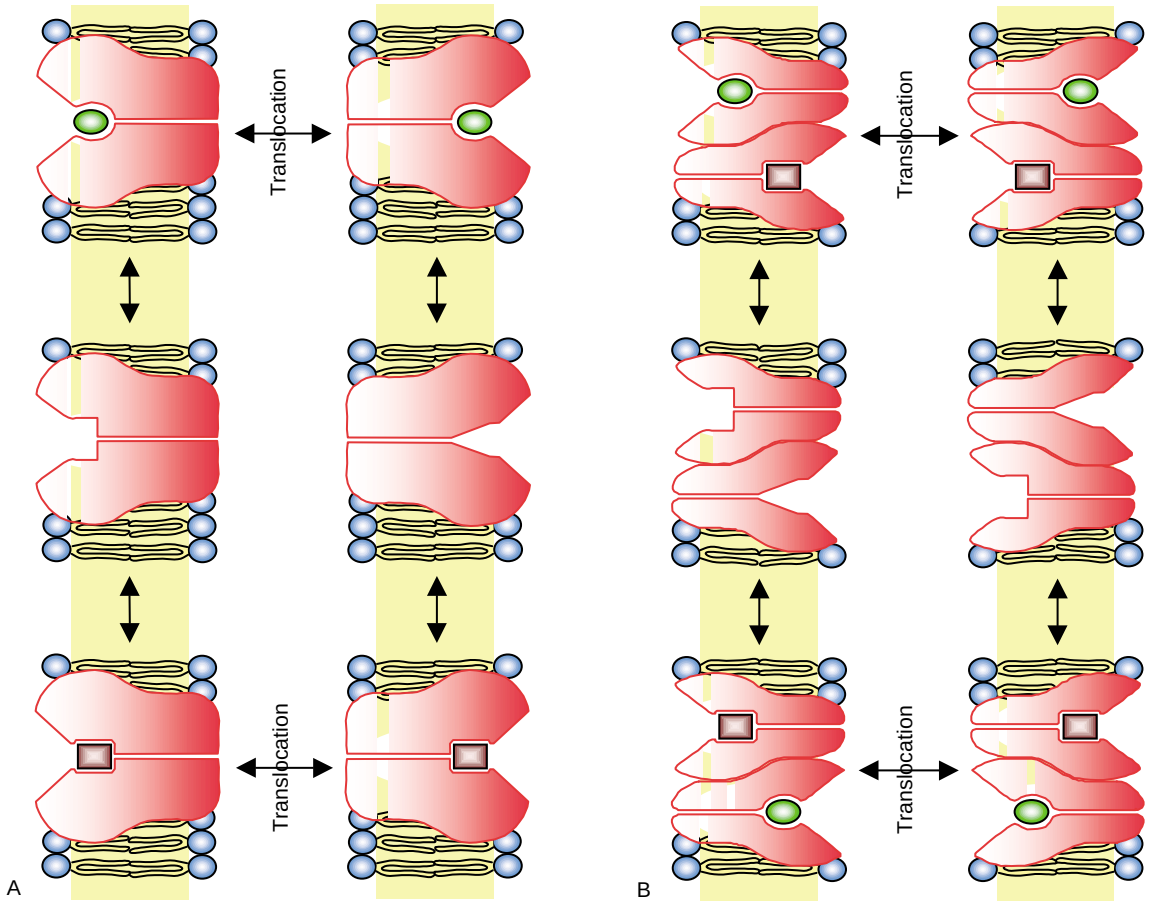

FIGURE 3 Functional models for mitochondrial exchange carriers. (A) The single site gated pore model of translocation corresponding to a ping-pong kinetic mechanism of exchange. The transport pathway is assumed to be formed between the two monomers. (B) The double site gated pore model of translocation corresponding to a simultaneous kinetic mechanism of exchange. Two separate and coordinated substrate translocation pathways are assumed, one in each monomer.

carrier before transport occurs, in agreement with the "double site gated pore" mechanism. The CAC differs from the other mitochondrial carriers analyzed so far, since it follows a ping-pong mechanism indicating only binary carrier–substrate complexes according to the existence of a single binding site. As CAC mediates uniport besides exchange of substrates, it is likely that the activation energy barrier for the reorientation of the unloaded carrier form is much lower for the CAC than for exchange carriers. As the uniport function is essential in a transport system like the carnitine carrier, the common sequential mechanism has apparently been changed into a ping-pong type of mechanism.

Channel-Like Properties

Unidirectional, partially unspecific transport can be induced in exchange-type carriers by various influences. A general effect is the induction of uniport by mercurials in various exchange carriers. In this state the transport can approach open channel-like characteristics. For AAC a slow specific uniport can be induced by phosphate and Mg^{2+} which prestages a wide unspecific channel induced by Ca^{2+}. This "megachannel" plays a central role in mitochondrial pore transition (MPT). The specific AAC ligands ADP and BK inhibit, while ATR sustains, MPT. The pore can also be induced by pro-oxidants at low Ca^{2+} and seems to be a major target of oxygen radical damage. Very important is the formation of this pore and thus of AAC as an early trigger of apoptosis by inducing the release of cytochrome *c*.

The appearance of channel-like functions reveals an intrinsic property of the MCF, i.e., the presence of an unspecific channel within the carrier protein which is normally hidden by appropriate gates. This model, which can in principle be reconciled with a gated pore mechanism, has of course to be substantiated by further studies leading to a molecular description of the putative channel pathway.

Structure and Function Studies: The Use of Mutant Proteins

Recombinant expression of the mitochondrial carriers in yeast and in *E. coli* enabled site-directed mutagenesis for structure–function studies. The mutation of Cys to Ser, one at a time or all together, evidenced the absence of essential cysteines in several carriers, although transport could be inhibited by SH reagents. Thus, the cysteine reagents may cause sterical hindrance or conformational changes. Inversely, by systematically substituting single amino acids with Cys, essential residues could be identified, e.g., G183, R190, and Q198 in transmembrane segment IV (TMSIV) of OGC, and R181 and R189 in TMSIV of CIC.

In AAC, three types of charged residues have been probed by mutagenic charge neutralization: positively charged residues located within TMSs (K38A, R96A, R204L, and R294A) and within the matrix loops (K48A, R152A, K179I, K182I, R252I, R253I, and R254I); and negatively charged residues at the end of TMSI, TMSIII, and TMSV (E45G, D149S, D249S). By comparing the *in vivo* (yeast aerobic growth) and *in vitro* effects (reconstituted transport), these residues could be assigned to transport or structure maintenance to varying degrees. Using a regain-of-function approach in yeast, in second site mutations negatively charged residues were affected, which evidenced ion-pair interactions R294-E45, K38-E45, R152-E45, R152-D149, and D149-R252 and indicated an arrangement where TMSI and TMSVI are in vicinal and skewed position.

Using the *E. coli* expression system, R90 and R98 in TMSII, R190 in TMSIV, and R288 in TMSVI of OGC, mutated into Leu, and R181 and R189 in TMSIV of CIC, mutated into Cys, were found to be essential for activity. A positive charge either from Arg or from Lys sufficed for transport activity at all positions, except at positions 98 and 190 of OGC where the guanidinium moiety of Arg was indispensable. Furthermore, by a combination of Cys-scanning mutagenesis, spin-labeling, and chemical modification studies, a water-accessible face of helix IV in both CIC and OGC has been identified and suggested to line part of the substrate translocation pathways through these proteins.

In PiC H32 in TMSI, E126 and E137 in TMSIII, and D39 and D236 at the matrix ends of the first and fifth TMS were found to be indispensable for normal growth in yeast and transport function. The six charged residues (H32, E126, and E137 of both subunits) are proposed to form the proton cotransport channel within the homodimer. An inhibitory disulfide formation under oxidizing conditions between the two Cys-28 residues (also located in the TMSI) of two PiC molecules is in agreement with this model.

A direct involvement of charged residues in proton transport pathway through UCP1 has been demonstrated. D27 within TMSI and the H145/H147 unit within loop B are thought to function as proton donor/acceptors, respectively, in the channel and the matrix-side entrance of the H^+ transport pathway. Further mutagenesis studies carried out on charged residues positioned in TMSII (R83 and E129), TMSIV (R182), TMSVI (R276), and in the TMSV at the cytosolic interface (H214) suggested that the three arginines are part of the purine-nucleotide-binding site and H214 and E190 act as pH sensors for the control of access of the phosphate moiety of the nucleotide to its binding cleft. Deletion of F267-K268-G269 in the

matrix loop C, as well as analogous deletions in loops A and B, caused loss of nucleotide regulation, suggesting a gating function of the three hydrophilic matrix loops in the regulation of UCP by purine nucleotides.

Diseases

At least four autosomal-recessive diseases are caused by defects in a specific mitochondrial carrier gene. Mutations in the human gene SLC25A20 coding the carnitine carrier are responsible for the Stanley syndrome (MIM 212138). The fatty acid β-oxidation and carnitine carrier activity are very low or absent in patients' fibroblasts. The disease generally presents with acute, potentially life-threatening episodes of hypoglycemic coma induced by fasting. Defects in the gene SLC25A13 coding isoform 2 of the aspartate/glutamate carrier (the only isoform present in liver) cause type II citrullinemia (MIM 215700). The lack of AGC2-mediated aspartate supply to the cytosol of liver cells causes: (1) deficiency of arginosuccinate synthetase, an enzyme of the urea cycle and (2) deficiency of the malate/aspartate shuttle leading to an increased NADH/NAD ratio in the cytosol that inhibits glycolysis and gluconeogenesis from reduced substrates.

The hyperornithine-hyperammone-homocitrullinemia (HHH) syndrome (MIM 23970) is caused by alterations of the ornithine carrier (isoform 1, gene SLC25A15) that catalyzes the exchange between cytosolic ornithine and mitochondrial citrulline, an important step in the urea cycle. The main features are homocitrullinuria, hyperammonemia, and consequent symptoms. Amish microcephaly (MIM 607196) is associated with mutant deoxynucleotide carrier (gene SLC25A19) and is characterized by severe congenital microcephaly and premature death. Although the molecular defect(s) responsible for 2-oxoadipate acidemia have not yet been characterized, this disease has been suggested to be due to defective oxodicarboxylate carrier or oxoadipate dehydrogenase (the two enzymes that transport into mitochondria and oxidize 2-oxoadipate, respectively). Finally, one of the three distinct loci involved in autosomal-dominant progressive external ophthalmoplegia (adPEO) (MIM 103220) includes the heart and skeletal muscle specific isoform of the ADP/ATP carrier (gene SLC25A4).

See Also the Following Articles

Fatty Acid Oxidation • Free Radicals, Sources and Targets of: Mitochondria • Protein Import into Mitochondria • Urea Cycle, Inborn Defects of

Glossary

electrogenic, electrophoretic transport The movement of a net electrical charge across the membrane coupled to the transport of metabolites. It is driven by the membrane potential.

exchange carriers Carriers that facilitate transport only by coordinated counter exchange of solutes across the membrane.

mitochondrial carriers Proteins primarily located in the inner mitochondrial membrane which catalyze transport of metabolites between cytosol and mitochondrial matrix space.

Further Reading

Kaplan, R. S. (2001). Structure and function of mitochondrial anion transport proteins. *J. Membr. Biol.* **179**, 165–183.

Klingenberg, M., and Echtay, K. S. (2001). Uncoupling proteins: The issue from a biochemist point of view. *Biochim. Biophys. Acta* **1504**, 128–143.

Krämer, R., and Palmieri, F. (1992). Metabolite carriers in mitochondria. In *Molecular Mechanisms in Bioenergetics* (L. Ernster, ed.) pp. 359–384. Elsevier Science, Amsterdam.

Palmieri, F., and van Ommen, B. (1999). The mitochondrial carrier protein family. In *Frontiers in Cellular Bioenergetics* (S. Papa, F. Guerrieri and J. M. Tager, eds.) pp. 489–519. Kluwer Academic/Plenum, New York.

Walker, J. E. (1992). The mitochondrial transporter family. *Curr. Opin. Struct. Biol.* **2**, 519–526.

Biography

Ferdinando Palmieri is a Professor in the Department of Pharmaco-Biology of the University of Bari. His principal research interests are in the field of biochemistry and molecular biology of mitochondrial transporters and related diseases.

Martin Klingenberg is Professor Emeritus at the University of Munich. His principal interest in recent years has been in the field of characterizing the mechanism of mitochondrial carriers.

Mitochondrial Outer Membrane and the VDAC Channel

Marco Colombini
University of Maryland, College Park, Maryland, USA

Mitochondria are organelles found in virtually all eukaryotic cells. They are composed of two membranes. The inner membrane is highly convoluted and of quite variable morphology. The outer membrane forms the boundary between the mitochondrial spaces and the cytosol. It contains membrane channels, called VDAC, that allow metabolites to cross this membrane while restricting the passage of proteins.

Origin and Structure of the Outer Membrane

Mitochondria have most likely evolved from endosymbiotic bacteria. The outer membrane may have originated as an endosomal membrane that engulfed the original endosymbiotic bacterium or may be related to the bacterial outer membrane. Whatever its origin, structurally it is a relatively simple limiting membrane forming a continuous boundary (Figure 1). It seems to limit the boundary of the mitochondrial space and, unlike the inner membrane, maintains a fairly constant total mitochondrial volume.

Further aspects of mitochondrial structure and function vary depending on the source and thus most of what will be presented applies to mammalian sources.

The outer membrane interacts intimately with neighboring membranes. Rivet-like connections between the outer and inner membranes often exist and are referred to as contact sites. These are mechanically sturdy as they interfere with the experimental separation of the outer and inner membranes. These contacts are proposed to serve a number of functions including the formation of macromolecular complexes between transporters and enzymes to expedite metabolic flow. The outer membrane also interacts closely with the endoplasmic reticulum and this close apposition may be the reason for preferential transfer of Ca^{2+} from the endoplasmic reticulum to the mitochondrial matrix compartment. This has been especially well studied in the heart where changes in Ca^{2+} level on a beat-by-beat basis alter dehydrogenase activity matching cellular energy consumption. If specialized docking structures are involved in this interaction with the endoplasmic reticulum, they must be more labile than the contact sites because isolation of mitochondria from endoplasmic reticulum is quite easy.

Functions of the Outer Membrane

The outer membrane of isolated mitochondria is highly permeable to metabolites due to the presence in this membrane of large aqueous channels formed by the protein called voltage-dependent anion-selective channel (VDAC). Their similarity to channel-forming proteins in bacterial outer membranes collectively referred to as porins has led some to refer to VDAC as mitochondrial porin. Although the permeability characteristics conferred to the outer membrane by VDAC are rather complex, physical size is a major factor. Thus, under normal conditions the outer membrane is essentially impermeable to molecules larger than 5 kDa. This allows proteins to be sequestered in the intermembrane space, the compartment between the outer and inner membranes. This sequestration serves at least two functions. First, it localizes proteins that could diffuse away to the site where they are needed. For example, the soluble protein, cytochrome *c*, is a member of the electron transport chain and must transmit electrons between complex III and IV so that respiration may proceed. Second, the sequestration prevents pro-apoptotic proteins from being released into the cytosol as this would initiate programmed cell death (apoptosis). Cytochrome *c* is also an example of a sequestered proapoptotic protein. The permeability barrier to pro-apoptotic proteins and others of similar size is lifted under some conditions that lead to cellular apoptosis.

The permeability of the outer membrane to small molecules can be regulated resulting in the outer membrane limiting metabolite flux and consequently the level of metabolic activity. This regulation is probably critical to changes in cell function.

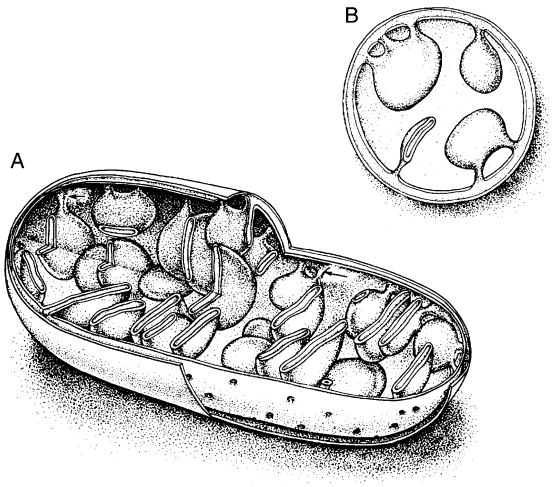

FIGURE 1 A drawing of the membranes and compartments of a typical small mitochondrion. (A) shows the mitochondrion with portions of the membranes cut out so as to reveal inner structure and compartmentation. (B) Illustrates a cross-section. Reproduced from Lea, P. J., and Hollenberg, M. J. (1989). Mitochondrial structure revealed by high-resolution scanning electron microscopy. *The American Journal of Anatomy* **184**, 245–257. Drawings made by Karen Visser. With permission of Wiley-Liss, Inc., a Subsidary of John Wiley & Sons, Inc.

Most mitochondrial proteins and RNA molecules are synthesized in the cytosol and imported into mitochondria. The Tom complex is responsible for much of the protein import through the outer membrane. Leader sequences on the proteins are recognized by Tom and the protein is treaded through a pore in the complex and delivered to the intermembrane space where it is picked up by the Tim complex in the inner membrane for translocation through that membrane. The processing of outer membrane proteins by this complex is less clear.

Mitochondria are usually found in the portion of cells where they are needed. For example, to minimize diffusion limitations they are located close to sites of high-energy dissipation. Sometimes they need to be delivered to distal sites in a cell (e.g., from cell body to nerve terminal of a neuron or to the reproductive bud of a yeast cell). Motors located either on microtubules or actin filaments move mitochondria from one location in the cell to another. The outer membrane must provide sites of attachment for the motors that perform the translocation.

Composition

The composition of the outer membrane varies somewhat depending not only on the species but also the tissue from which it was isolated. With that caveat, it can be said that there are a number of similarities between the constituents of the outer membrane and the endoplasmic reticulum. For example, the presence of cytochromes b and b_5, antimycin-insensitive NADH-cytochrome c reductase, and ceramide synthase. Yet there are also many differences and the enzymes present in the two locations are usually different isoforms. Thus, the similarity may reflect similar origins but certainly these two membranous compartments are distinct.

The outer membrane also contains enzymes involved in fatty acid and phospholipid metabolism and an amine oxidase. The liver mitochondria contain a peripheral benzodiazepine receptor whose role is unclear. The membrane can also bind some kinases that are typical soluble enzymes and the binding is thought to accelerate energy transduction.

The outer membrane has a higher lipid content than the inner membrane, one more typical of other cell membranes. The lipid composition is also drastically different from that of the inner membrane, the outer membrane being rich in sterol, while the inner has higher levels of cardiolipin.

VDAC Channels in the Outer Membrane

VDAC Structure

Mitochondria from all eukaryotic kingdoms contain VDAC channels in their outer membrane. These are formed by a single polypeptide of approximately 30 kDa and form a single large aqueous pore. In some plant and fungal mitochondria, VDAC channels form two-dimensional crystals (Figure 2), which upon further analysis reveal fundamentally cylindrical proteins forming water-filled transmembrane pathways. The wall of the channel is almost certainly a single layer of protein mainly consisting of a beta structure. Experimental evidence leads to the conclusion that the transmembrane portion consists of 1 α-helix and 13 β-strands. The surface domains (yellow regions in Figure 2) likely act as binding sites for a variety of proteins that bind or interact with the channel.

VDAC Function and Dynamics

The primary role of mitochondria is metabolism that is closely integrated with the metabolism occurring in the cytosol. This requires the continuous and rapid exchange of metabolites between these two major compartments. VDAC channels in the outer membrane can exist in conformational states that either favor or hinder metabolite flux. The state that favors metabolite flux, the open state, does so by having an electrostatic environment that favors anions. In addition, the charge distribution in the lining of the channel is

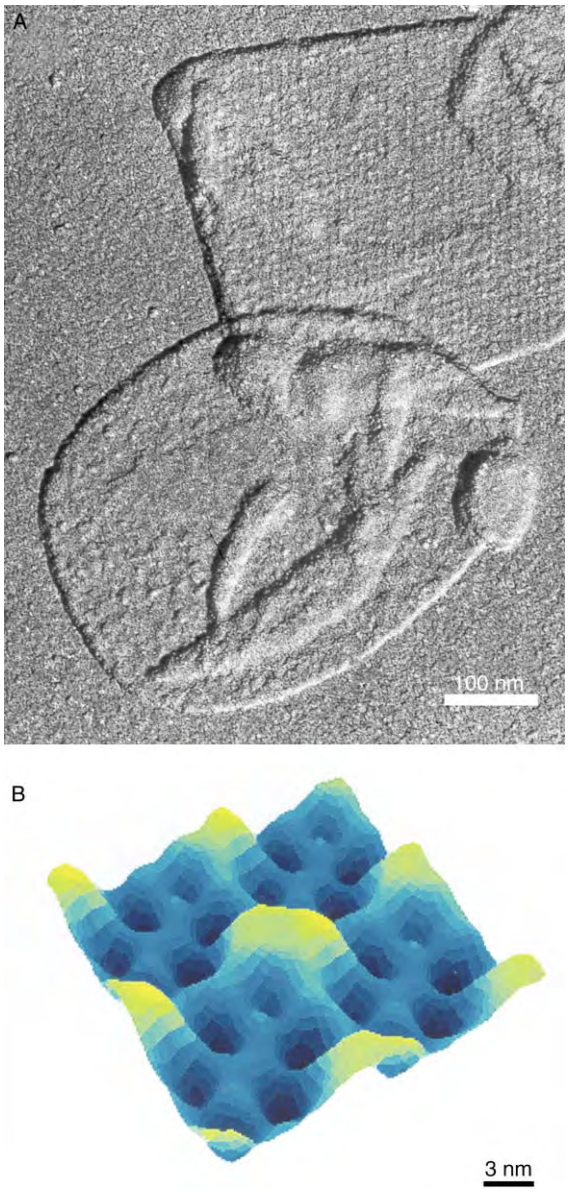

FIGURE 2 Views of mitochondrial outer membranes and the ubiquitous VDAC channels in these membranes. Panel (A) shows electron micrographs of freeze-dried mitochondrial outer membranes with two-dimensional crystals of VDAC channels (membrane with squared edges and ordered array of particles) and without such crystals (smooth membrane with rounded edges). Outer membrane vesicles isolated from mitochondria are dried down on a surface and they form collapsed sacs. Panel (B) shows a surface view of the VDAC channels obtained after computer filtration and averaging of multiple micrographs containing images of two-dimensional crystals. The yellow shows regions of elevation and the dark blue areas are the openings of the pores (holes) that are formed through the membrane. These allow the metabolites to cross the outer membrane. This figure was assembled from the work of Dr. Lorie Thomas. Adapted from Thomas, L., Kocsis, E., Colombini, M., Erbe, E., Trus, B.L., and Steven, A.C. (1991). Surface topography and molecular stoichiometry of the mitochondrial channel, VDAC, in crystalline arrays. *Journal of Structural Biology* **106**, 161–171.

such that it favors the translocation of ATP over that of anions of similar size and charge. In the closed states, the water-filled channel is somewhat narrower (the pore size decreases from 2.5 nm in the open state to 1.8 nm in the larger of the population of closed states) but, most importantly, the electrostatic nature is such that it hinders the flow of anions. A positively charged region lining the channel in the open state is translocated out of the channel resulting in a pathway with a net negative charge. This excludes ATP and drastically reduces the permeability of other anionic metabolites. At the same time this change favors the flux of cations.

This gating of VDAC is voltage dependent and thus the channels can respond to changes in the voltage across the outer membrane. An electrical potential across this membrane may arise from the presence of different charged macromolecules in the aqueous compartments (Donnan potential) and/or differential metabolite flux responding to metabolic rates. In addition, numerous factors influence this gating process including cytosolic NADH levels and specific proteins in the cytosol and intermembrane space. The importance of this regulation is indicated by its remarkable conservation of VDAC from all species tested (including all eukaryotic kingdoms). The diversity of influences on the gating of VDAC indicates that VDAC may integrate the influence of a variety of cellular factors and thus tune mitochondrial activity appropriately.

VDAC's ability to bind with cytosolic hexokinase and intermembrane space creatine kinase has been proposed to result in organized structures that increase the efficiency of energy transduction.

The Outer Membrane and Apoptosis

Apoptosis, programmed cell death, is a process by which a cell repackages itself to be ingested by other cells, generally macrophages. The outer membrane separates proteins that once combined initiate an amplification cascade leading to "full blown" apoptosis. The leakage of proteins from the intermembrane space into the cytosol is sufficient to cause apoptosis. Even injecting just one of these proteins, cytochrome c, into the cytosol is sufficient.

How the outer membrane becomes permeable to proteins is an area of intense investigation. The proteins that cross this membrane can be as large as 50–100 kDa. Proteins of the Bcl-2 family partition between the cytosol and the outer membrane. They can exist both as soluble proteins and intrinsic membrane proteins capable of generating ion channels.

Some of these are pro-apoptotic and others are anti-apoptotic. Some anti-apoptotic proteins are often associated with the outer membrane under normal conditions, i.e., cells functioning normally, and may favor normal mitochondrial function. Others translocate to the outer membrane at the early stages of apoptosis, perhaps forming the protein efflux pathways. The sphingolipid, ceramide, can also be produced in mitochondria early in the apoptotic process and has been shown to be able to form channels large enough for protein flux.

Under some conditions of apoptosis induction, exchange of nucleotides between mitochondria and the cytosol is greatly inhibited. The outer membrane becomes poorly permeable to ATP and ADP and other anionic metabolites. This phase precedes the release of intermembrane space proteins and in this phase cells can be rescued. This gives the outer membrane the role of deciding between life and death.

Emerging Importance of the Outer Membrane

Once considered relatively unimportant, the mitochondrial outer membrane is emerging as a site for control of overall mitochondrial function and a location where the fate of the entire cell is decided. Despite its deceptively simple appearance, this membrane performs a variety of vital functions. By hindsight, its location at the frontier between the cytosol and the mitochondrial spaces makes it an ideal site for control of the flux of matter and transduction of information.

See Also the Following Articles

Cell Death by Apoptosis and Necrosis • Cytochrome *c* • Mitochondrial Membranes, Structural Organization

Glossary

apoptosis A self-destruct process present in cells of multi-cellular organisms that eliminates cells that are no longer needed.

mitochondrion An organelle occurring in the vast majority of eukaryotic cells that is critical for energy transduction and metabolism. It is also semiautonomous with its own DNA and independent reproductive rate.

VDAC Voltage-dependent anion-selective channel, protein found in the outer membrane of all mitochondria. It forms large channels in this membrane allowing metabolites to cross.

Further Reading

Colombini, M., Blachly-Dyson, E., and Forte, M. (1996). VDAC, a channel in the outer mitochondrial membrane. In *Ion Channels* (T. Narahashi, ed.) Vol 4, pp. 169–202. Plenum, New York.

Gordon, D. M., Dancis, A., and Pain, D. (2000). Mechanisms of mitochondrial protein import. *Essays Biochem.* **36**, 61–73.

Lea, P. J., and Hollenberg M. J. (1989). Mitochondrial structure revealed by high-resolution scanning electron microscopy. *Amer. J. Anatomy* **184**, 245–257.

Thomas, L., Kocsis, E., Colombini, M., Erbe, E., Trus, B. L., and Steven, A. C. (1991). Surface topography and molecular stoichiometry of the mitochondrial channel, VDAC, in crystalline arrays. *J. Struct. Biol.* **106**, 161–171.

Tyler, D. D. (1992). *The Mitochondrion in Health and Disease*. VCH Publishers, currently Wiley-VCH Verlag GmbH and Co., Wiley, Somerset, NJ.

Waterhouse, N. J., Ricci, J., and Green, D. R. (2002). And all of a sudden it's over: mitochondrial outer-membrane permeabilization in apoptosis. *Biochimie* **84**, 113–121.

Biography

Dr. Marco Colombini is a Professor in the Department of Biology at the University of Maryland in College Park. His research is in the area of membrane biophysics with specific focus on channels in the mitochondrial outer membrane. He was part of the group that originally discovered and named the outer membrane channel called VDAC. Research from his laboratory continues to yield new insights into the structure and molecular mechanisms of mitochondrial channels and their role in regulation of mitochondrial function.

Dr. Colombini holds a Ph.D. from McGill University and is an active member of the Biophysical Society.

Mitogen-Activated Protein Kinase Family

Hidemi Teramoto and J. Silvio Gutkind
National Institute of Dental and Craniofacial Research, Bethesda, Maryland, USA

Mitogen-activated protein kinases (MAPKs) are a group of protein kinases that play an essential role in signal transduction by modulating gene transcription in the nucleus in response to changes in the cellular environment. MAPKs also play a key role in intracellular communication, and their activating pathways have been conserved throughout evolution, from plants, fungi, nematodes, insects, to mammals. In humans, there are at least 11 members of the MAPK superfamily, which can be divided into 6 groups: the extracellular signal-regulated protein kinases (ERK1 and ERK2); c-Jun N-terminal kinases (JNK1, JNK2, JNK3); p38s (p38α, p38β, p38γ, p38δ); ERK5 (ERK5); ERK3s (ERK3, p97 MAPK, ERK4); and ERK7s (ERK7, ERK8). Each group of MAPKs can be stimulated by a separate signal transduction pathway in response to different extracellular stimuli. In turn, MAPKs exhibit distinct substrate specificities. Thus, individual extracellular stimuli can lead to the differential activation of each MAPK and the consequent phosphorylation of a distinct set of MAPK substrates. Whereas components of some of these biochemical routes are now well established, others are still poorly understood. The specificity of the molecular mechanisms by which each MAPK can be activated ensures that cells mount an appropriate response to extracellular stimulation, as the resulting pattern of gene expression will depend on the integration of the combinatorial signals provided by the temporal activation of each of these groups of MAPKs.

ERK Family

ERK1 and ERK2

The extracellular signal-regulated protein kinase (ERK) group of MAPK includes ERK1 and ERK2. In certain cells their activation contributes to normal and aberrant growth, including malignant transformation, while in other cells this pathway can promote cell survival or initiate differentiation processes in others. The enzymatic activity of ERK1 and ERK2 is enhanced by dual phosphorylation on Thr and Tyr residues within a short sequence that forms the "activation loop", located close to the kinase active site, by a group of dual-specificity protein kinases (MAPK kinases; MAPKKs), represented by MEK1 and MEK2. Each MAPK family exhibits a distinct phosphor–acceptor motif in their activation loop (Figure 1), which provides specificity for the MAPKK–MAPK interactions. This phosphorylation leads to conformational changes in ERKs, thereby promoting their activation and nuclear localization. Subsequently, ERK activity is terminated by dephosphorylation on either Thr or Tyr by a Ser/Thr or Tyr phosphatase. This dephosphorylation can be mediated also by a dual specificity MAPK phosphatase. Similarly, the mammalian MAPKK, such as MEK1 and MEK2, are activated by phosphorylation mediated by MAPK kinase kinases (MAPKKK), which includes the Ras effector, Raf. Thus, the Raf group of MAPKKK that includes A-Raf, B-Raf, and c-Raf-1, plays an important role in the coupling of ERK MAPK activation to the Ras signaling pathway (see Figure 2).

The discovery of the Ras-Raf-MEK-ERK signaling route represented a breakthrough in cancer biology, and emerged as the product of the conversion of a large number of research efforts in a variety of otherwise poorly connected fields. Indeed, a large body of information was derived from genetic analyses of model organisms including *Drosophila*, *Saccharomyces cerevisiae*, and *Caenorhabditis elegans*, in addition to biochemical and biological studies in mammalian cells. They, collectively, led to the identification of Ras as a key downstream component of the pathway initiated by polypeptide growth factor receptors, and to the realization that this small GTPase acts subsequently as a master switch initiating the activity of a cascade of cytoplasmic kinases that culminate with the activation of the ERK1 and ERK2. ERKs, in turn direct the activities of many nuclear transcription factors, thus regulating gene expression. These findings provided a better understanding of the molecular basis for the transduction of proliferative signals, as well as the first clue as to how the aberrant function of Ras proteins may contribute to the malignant conversion of cancer cells.

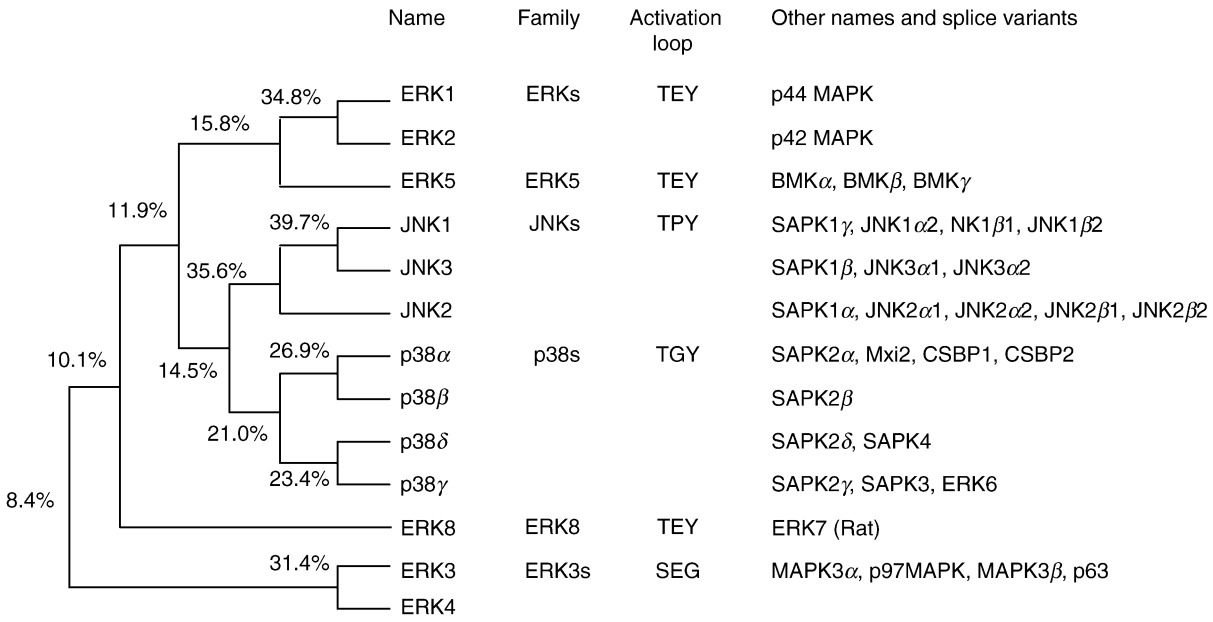

FIGURE 1 Phylogenetic tree of human MAPKs. A computer-generated phylogenetic tree of the MAPKs. The GenBank accession numbers are human ERK1 (X60188), human ERK2 (M84489), human ERK3 (S23429), human p97 (X80692), human ERK4 (P31152), human ERK5(U25278), human BMK (U29725), Rat ERK7 (AF078798), human ERK8 (AY065978), human JNK1 (U34822), human JNK2 (U34821), human JNK3 (U34820), human Mxi2 (U19775), CSBP1 (S52419), CSBP2 (S52420), human p38β (U53442), and human p38γ (U66243).

c-Jun N-Terminal Kinases (JNK1, JNK2, JNK3)

JNK was initially discovered by its ability to phosphorylate the N-terminal transactivating domain of the transcription factor c-Jun. As its activity was stimulated primarily by cellular stress rather than by mitogens, contrary to ERKs, it was also termed stress-activated protein kinase (SAPK). It is now known that there are three members of the JNK family, JNK1–3, and that they play numerous biological roles in response to a large variety of cell surface receptors as well as physical and chemical stresses. Whereas the JNK1 and JNK2 genes and their alternatively spliced variants are expressed ubiquitously, generating a total of eight JNK isoforms, the JNK3 gene has a more restricted expression pattern, being its two alternative spliced transcripts expressed the highest in brain and testis. Studies of mammalian cells demonstrated that JNK is required for neuroexcitatory stress-induced neuronal apoptosis, as well as for certain inflammatory responses and for the survival and malignant transformation of specific cell types (e.g., B cells).

Following the distinct pattern of activation of ERK and JNK by cellular receptors, an unexpected discovery was that whereas Ras regulates ERKs, two members of the Rho family of GTPases, Rac1 and Cdc42, initiate an independent kinase cascade regulating JNK activity. These findings provided direct evidence of a role for Rho GTPases in transcriptional regulation, thus expanding previous efforts addressing the function of these Rho related proteins, which were primarily focused on the molecular dissection of the mechanism(s) involved in their ability to control the dynamic assembly and remodeling of actin-containing cytostructures. Components of this pathway include several MAPKKKs: MEKK1, MEKK2, MEKK3, and MEKK4, apoptosis-stimulated kinase 1 (ASK1), mixed-lineage kinase 3 (MLK3), tumor progression locus 2, also known as Cot (TPL2), TGF-β-activated kinase (TAK), MAPK upstream kinase (MUK), germinal center kinase (GCK), and PAK, which can all contribute to activation of JNKs, apparently through two MAPKKs, MKK4 (also called Sek or JNKK1), and MKK7. Substrates for JNK include transcription factors of the c-Jun family, as well as other transcription factors, including Elk-1 and Elk-2, serum response factor accessory protein-1 (Sap-1), nuclear factor of activated T cells 4 (NFAT4), and activating transcription factor 2 (ATF2).

p38s (p38α, p38β, p38γ, p38δ)

The family of p38 kinases has expanded over the past few years, including now four members known as p38α (or CSBP-1), p38β, p38γ (also known as SAPK3 or ERK6) and p38δ (or SAPK4), and in some cases their corresponding splice variants. These MAPKs share a Thr-Gly-Tyr phosphorylation motif in their activation loop, and are

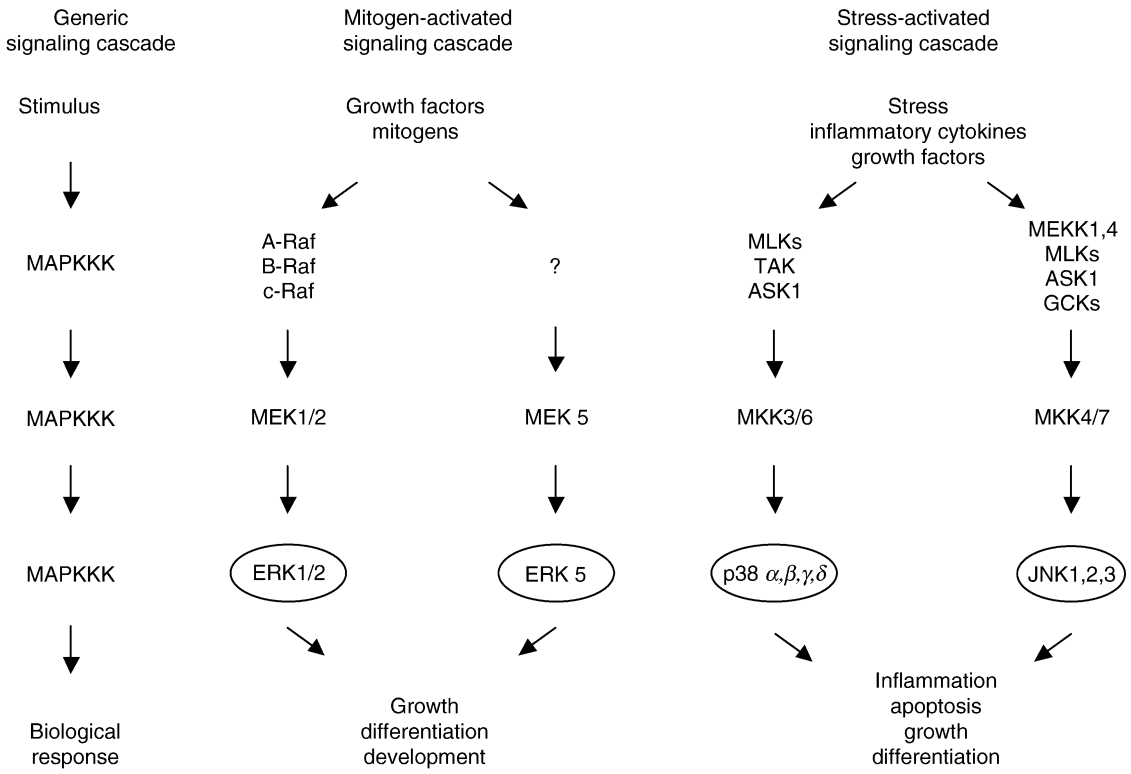

FIGURE 2 MAPK signaling cascades. Schematic representation of generic (left), mitogen activated (center), and stress activated (right) signaling cascades. Separate signal transduction pathways initiated by different extracellular stimuli activate each group of MAPKs that, in turn, exhibit distinct substrate specificities.

stimulated by receptors and environmental stresses similar to those provoking the activation of JNKs. These enzymes are particularly sensitive to their stimulation by exposure of cells to endotoxins, including bacterial lipopolysaccharides. Evidence of their role in transducing stress signals can be found as far philogenetically as in yeast, where genetic analysis indicates that the Hog1p MAPK, the yeast homologue of p38, is required for the response to osmotic stress that involves the enhanced expressions of genes participating in the biosynthetic pathway of the osmotic stabilizer glycerol.

As for the ERKs, p38s are activated by dual phosphorylation on Thr and Tyr residues by MKK3 and MKK6, the latter being a general stimulator for p38s, and the former exhibiting certain preference for p38α. The immediate upstream activators for these kinases are not yet well defined, and include the potential p38 MAPKKKs known as ASK1 and TAK1. The specific transcription factors that can be regulated by p38s include cAMP-responsive element-binding protein (CREB), activating transcription factor 1 (ATF1), ATF2, Max, C/EBP homologous protein (CHOP), and MEF2C. In addition, these MAPKs can also trigger the activation of other serine-threonine kinases such as Mnk1 (MAPK-interacting kinase 1) and Mnk2 and MAPKAPKs (MAPK-activated protein kinases).

ERK5

ERK5, also known as big mitogen-activated protein kinase (BMK1), is distantly related to ERK1 and ERK2. Although it contains a Thr-Glu-Tyr motif in its activation loop, similar to that of ERK1 and ERK2, ERK5 is larger than any other known MAPK ($\sim$80 kDa) and is selectively activated by MEK5 but not by MEK1 or MEK2. This kinase can be stimulated by oxidative stress, and can play a role in early gene expression triggered by EGF and serum by the direct phosphorylation of the transcription factors MEF2C or c-Myc, thereby participating in cell proliferation and progression through the cell cycle. Although information on this MAPK is still limited, evidence supporting its role in cell growth is also provided by its ability to cooperate with the activated Raf or MEK, which act on ERK1 and ERK2, to promote neoplastic transformation. The physiological function of ERK5 is nevertheless still unclear, and further studies are required to establish the biological role of this MAPK signaling pathway.

Others (ERK3, ERK4, ERK7, and ERK8)

Novel member of the MAPK family, ERK 7 (61 kDa) and ERK8 also contain a Thr-Glu-Tyr activation motif. ERK8 was cloned using the rat ERK7 cDNA to screen a human multiple tissue cDNA library and share an overall amino acid sequence identity of 69%. In contrast to rat ERK7, ERK8 does not display significant constitutive kinase activity, does not phosphorylate c-Fos, and is activated in response to stimulation by Src or serum. ERK3 contains a Ser-Glu-Gly activation motif, with gly in place of the tyr. The ERK3 subfamily of MAPKs is composed of two functional genes, MAPK6 (p97 MAPK) and MAPK4 (ERK4), and several pseudogenes. Upstream activators of ERK3 are still poorly defined, and this kinase is not present in yeast or *C. elegans*. None of the currently known MEK family members is able to phosphorylate and activate ERK3 and no physiological substrates of ERK3 have been found. ERK3 is localized constitutively to the nucleus without a conventional nuclear localization sequences.

Specificity and Fidelity in Nuclear Signal Transmission by MAPK Signaling Pathways

Protein kinases typically interact with their substrates by recognizing primary sequence determinants that surround the phosphorylation site(s). In the case of MAPK, the minimum general primary sequence required to be a substrate for protein phosphorylation is the presence of a Ser or Thr residue followed by Pro. Additionally, most MAPKs also appear to interact with their substrates by binding to a second site. This "docking" interaction is required for substrate phosphorylation by MAPK *in vitro* and is likely to be a relevant mechanism for the selection of high affinity substrates by these kinases *in vivo*. The current view is that for substrate recognition, MAPKs first dock to the substrate through a binding interaction at one site leading to phosphorylation of the substrate at a second site at one or more Ser/Thr-Pro motifs. Recent studies demonstrate that the selective interaction of MAPK with substrates may influence the physiological regulation of MAPK targets *in vivo*. Examples of such docking interactions include the interaction of ERK or JNK with the transcription factor Elk-1. Furthermore, there is substantial evidence that the normal function of MAPK signaling modules requires the proper organization of their components within the cell.

Of interest, in the past decade, scaffolding proteins have emerged as general regulatory mechanisms ensuring the fidelity of intracellular pathways. These proteins bind components of signaling routes, physically organizing them to enable rapid physiological responses. The prototypical signaling scaffold is the yeast protein Ste5p which binds the components of the yeast MAPK cascade leading to the mating response after activation of the pheromone receptor, thus maintaining the signaling fidelity of this cascade. Several scaffold-binding components of MAPK cascades have now been described in multicellular organisms, including Kinase Suppressor of RAS (KSR) and c-Jun Terminal Kinase Interacting Protein family (JIPs). Their role is to maintain the integrity of biochemical routes connecting cell surface receptors to the nucleus. For example, the JIP family of scaffolding proteins consists of three mammalian homologues JIP/IB-1, -1b, and -2. These molecules bind members of the mixed-lineage group of MAPKKK's (MLK) that have been reported to activate both JNK and p38. In addition, both IB1/JIP1 and IB2/JIP-2 have been found to bind the JNK MAPKK, MKK7, while IB2/JIP-2 has also been reported to bind MLK3 and p38γ. An emerging concept derived from recent studies is that these scaffold proteins are organizers and keepers of signal specificity and fidelity. Indeed, it may be as important to keep signals separate between closely related MAPK cascades, as it is to integrate them in a coordinated response, particularly in gene expression control.

The activation of MAPK-mediated signaling pathways is often initiated by stimuli acting at the cell surface. However, many of the transcription factors that act as MAPK substrates are located in the nucleus, thus suggesting the existence of mechanisms by which the signals can be transmitted from the cytoplasm to the nucleus. This has been extensively investigated for the ERK1/2 pathway. For example, the activated forms of Raf (MAPKKK) are present at the plasma membrane, while activated MEK1 and MEK2 (MAPKK) are located in the cytoplasm, due to the presence of a nuclear export signal (NES) in the protein. Thus, the final step in signal transmission from the cytoplasm to the nucleus appears to be directly mediated by ERK1/2. Indeed, these ERKs are located in the cytoplasm of quiescent cells but in the nucleus of activated cells. The mechanism by which activation promotes the translocation of ERKs to the nucleus is still unclear. It has been suggested that ERKs may be actively sequestered in the cytoplasm by inactive MEK1/2, and upon their activation by Raf, MEK1 and MEK2 may dissociate from ERK1 and ERK2, which may then be able to migrate to the nucleus as homodimers. Whereas available evidence supports this model, it is still unclear whether the release of ERKs from their MAPKK, MEK1 and MEK2, is sufficient to promote the nuclear

accumulation of ERKs or whether additional processes are involved. Furthermore, whether other MAPKs use similar or distinct mechanisms to ultimately phosphorylate nuclear proteins is also poorly understood, and under current intense investigation.

Regulation of Gene Expression through MAPK Signaling Pathways

Although MAPKs can phosphorylate cytoplasmic substrates, most MAPK signaling pathways ultimately converge in the nucleus to regulate gene expression, either by acting at the pretranscriptional, transcriptional, and posttranscriptional level. The most widely used mechanism by which MAPKs regulate gene expression is the phosphorylation of transcription factors, thereby enhancing their activity. For example, phosphorylation of the transcriptional activation domains of ATF2, CHOP, Elk-1, and c-Jun causes increased transcription. As studied in detail for the transcription factor CREB, transcription factor phosphorylation can cause changes in the interaction with coactivator molecules, including CBP and p300, which function, in part, through the regulation of the chromatin structure by acetylating histones.

Less frequent cases are found where MAPKs negatively regulate transcription factors by promoting their retention in the cytoplasm upon phosphorylation, and active dephosphorylation of these factors is then needed for their migration to the nucleus to stimulate gene transcription. As examples, phosphorylation of the transcription factors SMAD1 and NFAT4 by ERK1/2 and JNK, respectively, causes their cytoplasmic retention and therefore the inhibition of their transcriptional activity. Whether instead the phosphorylation by MAPKs of cytoplasmic transcription factors may cause their nuclear translocation is still unclear. Regulation of the DNA-binding activity is also a mechanism employed by MAPKs to control transcription factor activity. An example is the transcription factor Elk-1, which is phosphorylated by ERK, JNK, and p38 MAPKs leading to increased DNA binding.

Regulation of translation represents a fourth mechanism of regulation of gene expression by MAPKs. The best example is the translational regulation of cytokine expression observed in macrophages exposed to endotoxin. In this case, p38 MAPK acts on a *cis*-acting element in the TNFα mRNA to regulate its translation. Modulation of mRNA processing and nuclear export has not been described, although these biosynthetic steps also represent potential sites for intervention by MAPK.

The final mechanism employed by MAPK to regulate gene expression is the regulation of protein degradation. This is exemplified by the short-lived transcription factor c-Jun, which is rapidly degraded by the ubiquitin–proteasome pathway. Phosphorylation of c-Jun by JNK inhibits the ubiquitination of c-Jun and, therefore, its rapid degradation. Consequently, JNK activation prolongs the half-life of c-Jun, leading to the accumulation of the c-Jun protein. The regulation of protein stability by MAPK therefore contributes to the regulation of gene expression mediated by these signaling pathways.

See Also the Following Articles

Muscarinic Acetylcholine Receptors • Ras Family • Src Family of Protein Tyrosine Kinases

Glossary

extracellular signal-regulated protein kinase (ERK) One class of MAPKs.

GTPases Molecular switches that control cellular responses by exchanging GDP (inactive form) for GTP (active form) in response to a variety of stimuli. In the GTP-bound form they interact with effector molecules. Subsequently, they hydrolyze GTP to GDP, thereby returning to their inactive state.

mitogen-activated protein kinases (MAPKs) A group of serine/threonine protein kinases that play an essential role in signal transduction in response to changes in the cellular environment.

protein kinases Phosphotransferases that catalyze the transfer of a phosphate group from ATP, or in some cases from GTP, to a protein substrate. Most protein kinases phosphorylated serine or threonine residues (serine-threonine protein kinases) or tyrosine residues (protein tyrosine kinases).

Ras A small GTPase that controls the activation of the ERK kinase cascade, as well as other downstream targets.

Further Reading

Cano, E., and Mahadevan, L. C. (1995). Parallel signal processing among mammalian MAPKs. *Trends Biochem. Sci.* **20**(3), 117–122.

Chang, L., and Karin, M. (2001). Mammalian MAP kinase signaling cascades. *Nature* **410**(6827), 37–40.

Gutkind, J. S. (2000). Regulation of mitogen-activated protein kinase signaling networks by G protein-coupled receptors. *Sci. STKE* **40**, RE1.

Johnson, G., and Lapadat, R. (2002). Mitogen-activated protein kinase pathways mediated by ERK, JNK, and p38 Protein Kinases. *Science* **298**, 1911–1912.

Kultz, D. (1998). Phylogenetic and functional classification of mitogen- and stress-activated protein kinases. *J. Mol. Evol.* **46**, 571–588.

Ono, K., and Han, J. (2000). The p38 signal transduction pathway: Activation and function. *Cell Signal* **12**(1), 1–13.

Pearson, G., Robinson, F., Beers Gibson, T., Xu, B. E., Karandikar, M., Berman, K., and Cobb, M. H. (2001). Mitogen-activated protein (MAP) kinase pathways: Regulation and physiological functions. *Endocr. Rev.* **22**(2), 153–183.

Weston, C. R., and Davis, R. J. (2002). The JNK signal transduction pathway. *Curr. Opin. Genet. Dev.* **12**(1), 14–21.

Biography

Hidemi Teramoto is a visiting scientist at Cell Growth Regulation Section, Pharyngeal Cancer Branch, National Institute of Dental and Craniofacial Research, National Institutes of Health. He holds M.D. and Ph.D. degrees from University of Tottori in Japan.

J. Silvio Gutkind is the Chief of the Oral and Pharyngeal Cancer Branch, National Institute of Dental and Craniofacial Research, National Institutes of Health. He holds a Ph.D. degree from University of Buenos Aires in Argentina.

Their principal research interest is in the molecular basis of cancer, which they have addressed by studying normal and aberrant functions of molecules involved in the transduction of proliferative signals. The laboratory has made seminal contributions to the field, and helped elucidate some of the basic molecular mechanisms whereby cell surface receptors regulate the nuclear expression of growth promoting genes.

Mitosis

Patricia Wadsworth and Nasser M. Rusan
University of Massachusetts, Amherst, Massachusetts, USA

Mitosis is the phase of the cell division cycle when the duplicated chromosomes are equally partitioned into two daughter cells. Chromosome motion occurs on the mitotic spindle, a dynamic structure that is assembled at the beginning of mitosis and subsequently disassembled. Mitosis is followed by cytokinesis, the division of the cytoplasm. Together, mitosis and cytokinesis constitute cell division and result in the generation of a pair of daughter cells.

The Cell Cycle

Dividing mammalian cells experience an ~24 h long cell cycle, during which the cells grow, replicate their DNA, and divide into two daughter cells. The cell cycle is composed of interphase, which lasts ~22 h, and mitosis, which is completed in ~2 h. Interphase can be subdivided into three parts. During S phase or synthetic phase of interphase, DNA is synthesized, or replicated. The interval between the end of mitosis and the beginning of S phase is called first gap (G1) phase. During G1, cells grow in preparation for division. However, if nutrients or growth signals are lacking, cell cycle progression can be slowed, or stopped. The phase after DNA replication and before the initiation of cell division is called gap 2 (G2). During G2, cells evaluate DNA replication; if damaged, or unreplicated, DNA is detected, the cell cycle is delayed. If no DNA damage is detected, cells progress through G2, and enter mitosis.

Spindle Structure

The mitotic spindle at metaphase is a bilaterally symmetric, microtubule-based structure with chromosomes aligned in the middle. The spindle is bipolar: the two spindle poles define the spindle axis and are the sites to which the chromatids are moved during anaphase (Figure 1). In many animal cells, a centrosome, composed of a pair of centrioles and associated pericentriolar microtubule-nucleating material, is present at the spindle poles (Figure 1). The major structural elements of the spindle are microtubules, dynamic cytoskeletal filaments that radiate from the two spindle poles. Microtubules attach chromosomes to the spindle and are essential for chromosome motion. Spindle microtubules are classified by their location in the spindle (Figure 1). Interpolar microtubules extend from each spindle pole and overlap in the middle of the spindle. Kinetochore microtubules have one end embedded in a specialized attachment site on the chromosome, the kinetochore. The third class of spindle microtubules, astral microtubules, extend away from the centrosomes toward the cell cortex. Astral microtubules contribute to spindle positioning and in defining the position of the contractile ring at cytokinesis.

Considerable variation in spindle structure exists among diverse cells. In cells of higher plants, the spindle pole lacks centrioles and is broad, not focused. Plant spindles are also anastral, lacking astral microtubules. In yeasts, which undergo closed mitosis inside of an intact nuclear envelope, a spindle pole body is present at the two ends of the spindle. The spindle pole body, a trilaminar plaque-like structure embedded in the nuclear envelope, nucleates microtubules that radiate into the nucleus and cytoplasm. The number of spindle microtubules also varies among cell types. Yeasts have a simple spindle, and a single microtubule links each kinetochore to the spindle pole body. In contrast, ~20 microtubules are associated with each kinetochore in a typical animal cell and hundreds of microtubules are present in each half-spindle. Despite these differences in spindle structure, in all cases, mitosis accomplishes the accurate segregation of the replicated genetic material into the two daughter cells.

Phases of Mitosis

Prophase

Chromosome Condensation

Prior to mitosis, during the S phase of interphase, each chromosome is replicated, resulting in two identical sister chromatids that are bound together by protein complexes called cohesions. The sister chromatids are very long strands of DNA and must be compacted for division. This process, called chromosome condensation, occurs as specialized proteins called condensins

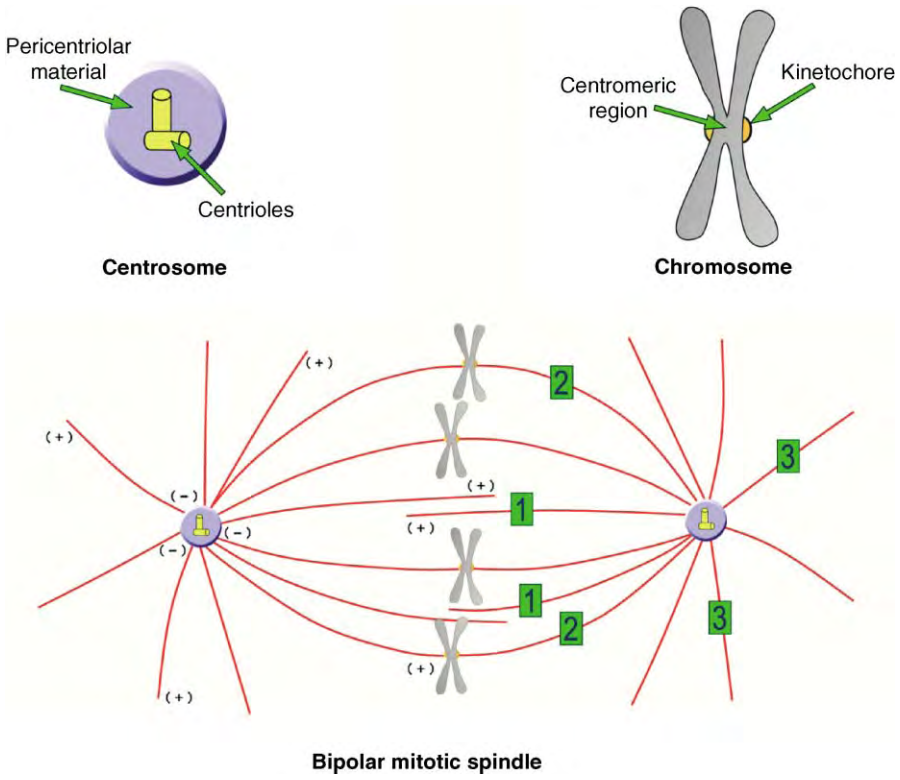

FIGURE 1 Highly schematic diagram of a mammalian mitotic spindle at metaphase of mitosis. Microtubules are depicted as red lines; interpolar, kinetochore, and astral microtubules are labeled 1, 2, and 3, respectively. The plus and minus ends of the microtubules are marked. Inset, upper left, shows a schematic diagram of a centrosome consisting of pericentriolar material, purple, and centrioles, yellow. Inset, upper right, shows a diagram of a chromosome; the centromeric region and the kinetochore are shown.

coil the DNA into loops. As prophase progresses, the chromosomes become increasingly visible in the nucleus, first as threads or strands and later as highly condensed rod-like structures called chromosomes, each of which is composed of two chromatids (Figure 2). The term mitosis comes from the Greek word *mito* meaning thread, referring to the appearance of thread-like structures in the prophase nucleus.

Kinetochore Assembly

In order for the chromatids to be accurately segregated into the two daughter nuclei, they must be attached to, and later moved by, the spindle machinery. Mitotic chromosomes are characterized by an indentation, or primary constriction, called the centromere (Figure 1). The centromere is a region of highly repeated DNA sequences that serves as the assembly site for a plate-like structure called the kinetochore. The kinetochore functions to link each chromatid to the spindle via kinetochore microtubules and also functions as a signaling device that regulates progression through the cell cycle. Kinetochores of sister chromatids are arranged back-to-back so that the binding sites for spindle microtubules face in opposite directions to facilitate the association of each chromatid with microtubules from opposite spindle poles.

Centrosome Separation

In animal cells, the centrosome is also duplicated during S phase of interphase, and the two daughter centrosomes remain adjacent to one another. Centrosome duplication ensures that two centrosomes are present at the beginning of mitosis to form the spindle poles and guarantees that each daughter cell inherits one centrosome. In prophase, the duplicated centrosomes separate and begin moving to opposite sides of the nucleus to establish a bipolar spindle. The microtubule nucleating capacity of each centrosome also increases dramatically at prophase.

PROMETAPHASE

Nuclear Envelope Breakdown

In cells with an open mitosis, the breakdown of the nuclear envelope marks the beginning of prometaphase.

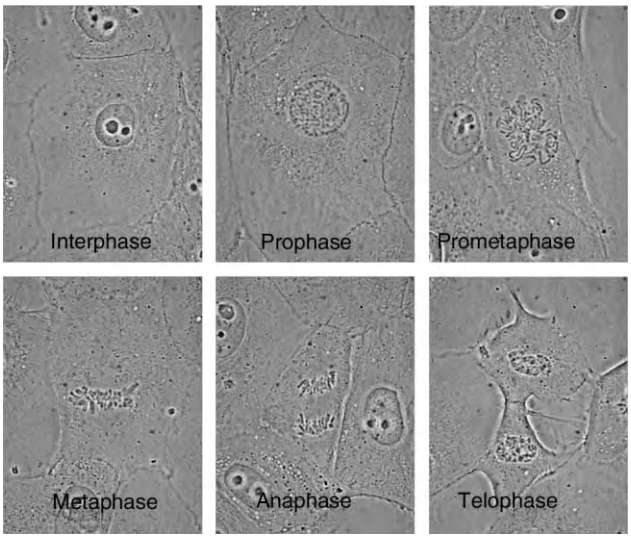

FIGURE 2 Phase contrast light micrographs of living LLCPK1 mammalian cells in mitosis. Each panel shows a different cell at the indicated stage of mitosis.

Microtubules assist nuclear envelope breakdown resulting in the fragmentation of the nuclear membrane into small vesicles and consequently releasing the chromosomes into the cytoplasm.

Spindle Assembly

Spindle assembly requires dynamic microtubules. Because microtubules are polar polymers, their two ends have different dynamic properties. The less dynamic end, called the minus end, is associated with the spindle pole material; the more dynamic end, called the plus end, extends outward toward the cell periphery (Figure 1). Microtubule plus ends display a behavior called dynamic instability, in which they switch stochastically between phases of assembly and disassembly. The result of dynamic instability behavior is that microtubule plus ends continually probe the cytoplasm as they grow and shorten. Microtubules in mitotic cells are more dynamic than microtubules in interphase cells because they switch from growing to shortening more frequently and shorten further before resuming growth. The result is a population of relatively short, highly dynamic microtubules that radiate from each spindle pole. At nuclear envelope breakdown, chromosomes are released into the cytoplasm and dynamic microtubules can interact with each kinetochore. Once a connection between a microtubule and kinetochore is established, the microtubule becomes less dynamic in order to maintain the connection. Cells monitor the attachment of chromosomes to the mitotic spindle and mitosis is delayed if even a single chromosome is unattached. This regulatory system is called the spindle assembly checkpoint, or metaphase checkpoint.

Microtubule motor proteins, which utilize the energy of ATP hydrolysis to perform work in cells, are also important for spindle assembly. The type and properties of the motor protein govern the direction of motion, either toward the minus end or the plus end of the microtubule. Multifunctional motors or motor protein complexes can exert force on microtubules by cross-linking neighboring microtubules and sliding them relative to one another or by binding to one microtubule while walking along an adjacent one. Alternatively, the nonmotor region of the motor protein can bind to a tethered structure, the cell cortex for example, while the motor region of the protein applies a pulling force on the microtubule. Motor proteins are present at the kinetochores, between interpolar microtubules, along kinetochore microtubules and at the cell cortex.

Motor proteins contribute to various motions during mitosis. During centrosome separation in prophase, motors located between the antiparallel, interpolar microtubules contribute to the separation of the two spindle poles. At the kinetochores, motors contribute to the initial bipolar attachment of chromosomes to spindle microtubules. Motors also contribute to congression, the movement of the chromosomes to the spindle equator, or metaphase plate, following initial attachment. In the assembled spindle, a balance of the activities of oppositely directed motor proteins maintains spindle length; some motors tend to pull the poles together, and this is resisted by motors that act to push the poles apart. Motor proteins also contribute to spindle positioning in mitotic cells, and to the dynamic turnover of mitotic microtubules.

Spindle assembly can also occur in the absence of centrosomes. In this situation, microtubules assemble in the vicinity of chromosomes and are subsequently sorted into a bipolar array by the activity of motor proteins. In both the presence and absence of centrosomes, dynamic microtubules and motor proteins contribute to spindle formation.

Metaphase

The cell is in metaphase when all of the duplicated chromosomes are aligned midway between the two spindle poles (Figures 2 and 3), a location referred to as the metaphase plate or spindle equator. Spindle length remains relatively constant at metaphase, but the spindle microtubules are not static. Rather, they undergo a behavior called spindle flux, in which spindle microtubules continually assemble at their plus ends and disassemble at the minus ends, coupled to poleward translocation of the polymer. As a result of flux, marks placed on spindle microtubules are observed to move slowly toward the poles during metaphase and anaphase of mitosis.

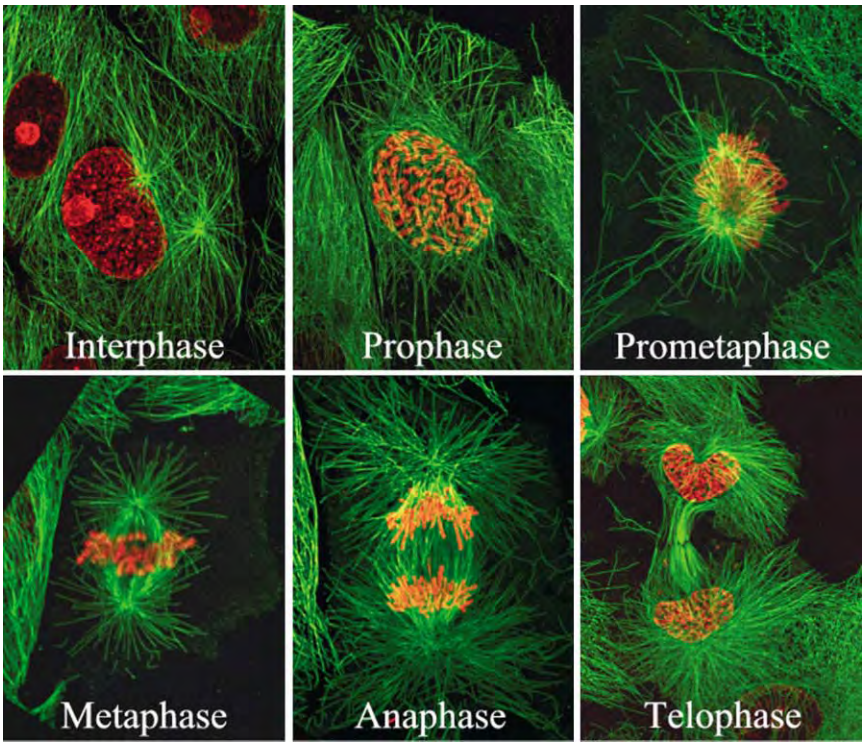

FIGURE 3 Distribution of microtubules and DNA throughout mitosis. Fluorescence light micrographs of cells that have been fixed and stained with antibodies to tubulin, to label microtubules, and propidium iodide, to stain DNA. Microtubules are shown in green and DNA in red. Images are maximum projections of deconvolved image stacks taken with a spinning disc confocal microscope.

Not only are microtubules dynamic at metaphase, the chromosomes are also active, oscillating towards and away from each spindle pole. Chromosomes are also under tension, ready for subsequent movement in anaphase. If the connection between one sister chromatid and the pole is severed at metaphase, the chromosome moves to the pole to which it remains attached, demonstrating that the metaphase position results from a balance of pole directed forces acting on the chromosomes.

Anaphase

During anaphase, sister chromatids separate and move to the spindle poles (Figures 2 and 3). Anaphase consists of two phases, anaphase A and B. During anaphase A, the chromosomes move to the poles and kinetochore fiber microtubules shorten; during anaphase B, the spindle poles move apart as interpolar microtubules elongate and slide past one another. Many cells undergo both anaphase A and B motions, but in some cases one or the other motion dominates.

Separation of the paired sister chromatids is required for poleward motion in anaphase. Chromatid separation results from the proteolytic degradation of components that link the chromatids at the centromere. Degradation is triggered by the activity of the anaphase-promoting complex, which regulates cell cycle progression. Chromatid separation is not the result of tugging by microtubules and motor proteins, and can be observed even in the absence of microtubules.

Although the motion of the chromosomes to the spindle poles in anaphase has fascinated biologists for many years, the molecular basis for this motion remains controversial and incompletely understood. During anaphase A, kinetochore microtubules must shorten as the chromosomes move poleward. Measurements of spindle flux show that subunit loss from microtubules occurs at the spindle poles during anaphase. In many cells, however, the rate that chromosomes move exceeds the rate of subunit loss at the pole, and thus subunit loss must also occur at the kinetochore.

Pioneering studies of mitosis in living embryonic cells demonstrated that assembly and disassembly of microtubule polymers result in chromosome motion. This work led to the hypothesis that microtubule disassembly drives chromosome motion. Later work identified molecular motors at the kinetochore, leading to the alternative hypothesis that forces generated by molecular motors drive chromosome motion. One possibility is that molecular motors power chromosome motion, but the rate of chromosome motion is limited by kinetochore microtubule disassembly. Alternatively,

disassembly may be responsible for chromosome motion, and motors may tether the chromosomes to the shortening fiber. The presence of potentially redundant mechanisms for chromosome motion may reflect the fact that mitotic fidelity is of utmost importance.

Telophase

In telophase, the chromosomes decondense, and the nuclear envelope begins to reform around them (Figures 2 and 3), returning the cell to the interphase condition. The short dynamic microtubules of the spindle are replaced with the less dynamic microtubules of the interphase array that extend to the cell periphery (Figure 3). During telophase the contractile ring assembles midway between the spindle poles in preparation for cytokinesis.

Cytokinesis

Cytokinesis is the process of constricting the cytoplasm between the two forming daughter nuclei resulting in the formation of two cells. Cytokinesis is achieved by a contractile ring, or belt, composed of filaments of the cytoskeletal polymer, actin, and the molecular motor protein, myosin II, which provides the force for cytokinesis. The contractile ring is tethered to the cell membrane, and its contraction creates a cleavage furrow, or indentation of the plasma membrane, during cytokinesis. The contractile ring assembles midway between the two spindle poles in telophase, and disassembles when cytokinesis is completed. The signals that determine the location of contractile ring formation in the cell cortex have yet to be identified, but microtubules are involved in their delivery to the cortex. In some cells, radiating astral microtubules that overlap midway between the spindle poles dictate the site of contractile ring formation. In other cases, interzonal microtubules located between the separating chromosomes play an important role in specifying the location of furrow formation. The completion of cytokinesis marks the end of mitosis and the birth of two completely independent daughter cells in interphase of their cell cycle.

See Also the Following Articles

Cell Cycle: Mitotic Checkpoint • Centrosomes and Microtubule Nucleation • Chromosome Organization and Structure, Overview • Cytokinesis • Metaphase Chromosome • Nucleoid Organization of Bacterial Chromosomes • Septins and Cytokinesis

Glossary

centrosome Structure present at the spindle poles in many animal cells that is composed of a pair of centrioles and associated pericentriolar material.

congression The motion of chromosomes to the midplane, or equator, of the spindle during prometaphase.

kinetochore Structure located at the centromere of each chromatid that functions to link each chromatid to the spindle. The kinetochore is also the location of components of the spindle assembly checkpoint.

microtubule Polar, cytoskeletal polymer composed of tubulin dimers that are a major structural element of the mitotic spindle and are required for chromosome motion.

spindle flux Poleward motion of microtubule polymers that occurs during metaphase and anaphase of mitosis.

Further Reading

Compton, D. A. (2000). Spindle assembly in animal cells. *Annu. Rev. Biochem.* **69**, 95–114.

Inoue, S., and Salmon, E. D. (1995). Force generation by microtubule assembly/disassembly in mitosis and related movements. *Mol. Biol. Cell.* **6**, 1619–1640.

Karsenti, E., and Vernos, I. (2001). The mitotic spindle: A self-made machine. *Science* **294**, 543–547.

McIntosh, J. R., and McDonald, K. L. (1989). The mitotic spindle. *Sci. Am.* **261**, 48–56.

Nicklas, R. B. (1997). How cells get the right chromosomes. *Science* **275**, 632–637.

Rieder, C. L., and Khodjakov, A. (2003). Mitosis through the microscope: Advances in seeing inside live dividing cells. *Science* **300**, 91–96.

Scholey, J. M., Brust-Mascher, I., and Mogilner, A. (2003). Cell division. *Nature* **422**, 746–752.

Wittman, T., Hyman, A., and Desai, A. (2001). The spindle: A dynamic assembly of microtubules and motors. *Nat. Cell Biol.* **3**, E28–E34.

Biography

Dr. Patricia Wadsworth is a Professor in the Department of Biology at the University of Massachusetts, Amherst. Her principal research interests are in the area of mitosis and the cytoskeleton, with particular focus on the dynamic behavior of microtubules. She received a Ph.D. from Dartmouth College and was a post-doctoral fellow at the University of North Carolina, Chapel Hill.

Nasser M. Rusan is a Ph.D. candidate in molecular and cellular biology at the University of Massachusetts, Amherst. His research interest is in the cytoskeleton, with particular emphasis on microscopy and digital imaging technology.

mRNA Polyadenylation in Eukaryotes

Mary Edmonds
University of Pittsburgh, Pittsburgh, Pennsylvania, USA

Polyadenylation is a process used by all cells to generate the polyA sequence on the 3′ end of messenger RNA (mRNA). The restriction of this modification to mRNAs is achieved through two conserved sequences in the 3′ non-coding region of the RNA polymerase transcript. These sequences direct four multisubunit cleavage complexes to these sites for a specific endonucleolytic cleavage that produces the hydroxyl group on which the polyA tail is generated by a polyA polymerase along with a polyA binding processivity factor.

An unexpectedly large number of proteins are needed for this simple two step enzymatic reation. Additional roles for these specific proteins within the cleavage complexes account in part for this complexity. Some regulate levels of mRNA and even choice of specific mRNA from transcripts with multiple polyA sites. Others interact with processing complexes for 5′ end capping and intron removal. Still others couple RNA processing to transcription through binding of cleavage complexes to the C-terminal domain of RNAP11. Along with capping and splicing complexes a dynamic complex linking RNA processing to transcription results which persists through all phases of transcription up to termination where cleavage factors play a decisive role.

Polyadenylation is a cellular process that generates the poly A sequence on the 3′ end of mRNA. A nuclear poly A polymerase (PAP) adds AMP units from ATP to the 3′ hydroxyl group at the 3′ end of mRNA and processively elongates the sequence to ~200 nucleotides (nts) in mammals and 60 in *Saccharomyces cerevisiae*. A critical feature that bestows specificity on the process is the selection of the site in the mRNA to be polyadenylated. Rather than addition to the 3′ end of the transcript produced by RNA polymerase II (RNAP II), a specific site within this precursor mRNA transcript is created by endonucleolytic cleavage. The site is defined in mammals by a conserved hexanucleotide upstream of the cleavage site and by a less conserved site 10–50 nts downstream of the cleavage site.

A large number of proteins is needed to achieve this cleavage specificity. Most exist within two large cleavage complexes, one of which binds to an upstream site and the other to a downstream site. Two other less well-understood complexes are essential only for cleavage, while PAP and a poly A-binding protein, add AMPs processively to the 3′ hydroxyl group at the 3′ end of the upstream cleavage product.

Although the major RNA processing reactions of 5′ capping, splicing, and polyadenylation occur independently *in vitro*, mutual stimulation of one processing reaction on another is common, i.e., polyadenylation and terminal exon splicing and 5′ capping and polyadenylation. These mutual effects are now understood to result from the coordination of RNA processing with transcription through a dynamic assembly of processing factors with the C-terminal domain (CTD) of the large subunit of RNAP II.

The role of the poly A sequence long remained a mystery in spite of its potential effects either on mRNA stability, nuclear export, or translation. Poly A is now known to participate in each of these processes, often serving as an anchor for a poly A-binding protein that interacts with components of each of these reactions in a manner that modulated gene expression.

Sequences Required for Polyadenylation

Sequences Upstream of the Poly A Site

Point mutations of the AAUAAA signal result in greatly extended nascent RNAP II transcripts. This finding led to the prediction that the poly A addition site was created by cleavage rather than by transcription termination. A high degree of conservation of AAUAAA was evident when about 90% of 250 sequenced mRNAs had an AAUAAA sequence (with 10% as AUUAAA) near their 3′ ends.

More recent analyses of several thousand human expressed sequence tags (ESTs) showed a higher incidence of alternative hexanucleotide signals as only 60% were AAUAAA with 12% AUUAAA. Biological evidence for more extensive use of alternative signals is

most clearly seen in male germ cells where frequencies of AAUAAA resemble those from the EST data, raising the possibility of tissue-specific polyadenylation. A variant cleavage stimulation factor CstF subunit (CstF-64) of the male germ cells but not present in HeLa cells CstF may recognize an alternative poly A signal. Experimental data indicate that AAUAAA functions in a single-stranded form, a finding compatible with the limited number of folded structures examined thus far.

Sequences Downstream of the Poly A Site

Correct 3′ end processing requires a sequence 10–50 nts downstream of the cleavage site that is far less conserved than AAUAAA. This sequence is often a 5nt UMP-rich element (U_4N) and less commonly a 5nt 2(GU)N sequence. However, ~20% of human pre-mRNAs have a downstream sequence that differs somewhat from both of these elements, emphasizing the lack of conservation of downstream elements. Spacing between upstream and downstream elements is crucial for the interaction between cleavage polyadenylation specificity factor (CPSF), bound to AAUAAA and CstF bound to $U_4(N)$ downstream that initiates cleavage.

Proteins of Cleavage/ Polyadenylation

mRNA 3′ end formation and polyadenylation (Figure 1) is deceptively simple. However, as shown in Table I, four multisubunit complexes are required for cleavage along with the polymerase and a poly A-binding protein. Together, at least 14 polypeptides are involved in the reaction. Most have been cloned and sequenced and several expressed as recombinant forms. Table I summarizes features and general functions of the core components responsible for 3′ end formation.

CPSF

CPSF is a complex of 160, 100, 73, and 30 kDa subunits that binds to the AAUAAA poly A signal through the 160 kDa subunit. Binding is stabilized by the other subunits including the 30 kDa protein that binds to pre-mRNA. Little is known of the roles of the 100 and 73 kDa proteins, although these two proteins share 23% sequence identity. The 30 kDa protein has been proposed to be the nuclease for cleavage based on a marked sequence similarity to a 30 kDa *Drosophila* endonuclease, although CPSF-30 lacks such activity, as do all the core proteins.

In vivo CPSF is recruited to the transcript promoter by the TFIID transcription factor where it binds to the CTD of RNAP II. Upon initiation of transcription it interacts cooperatively with the CstF complex, which also binds to the CTD. CPSF remains bound as RNAP II transcribes the gene up to and beyond the poly A site to the termination site.

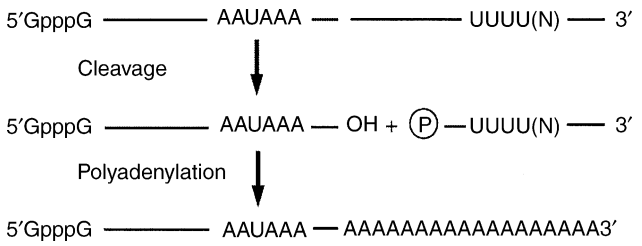

FIGURE 1 The two steps in mRNA 3′ end processing. Endonucleolytic cleavage between the AAUAAA sequence and the downstream element shown as an oligo U-rich sequence generates an upstream fragment with a 3′ OH group and a downstream fragment with a 5′ phosphate group. The upstream fragment is polyadenylated and the downstream fragment is degraded. (Reproduced from Wahle, E., and Keller, W. (1996). The Biochemistry of Polyadenylation. *Trends Biochem. Sci.* **21**, 247.

Cleavage Stimulation Factor

CstF is a trimeric complex needed only for cleavage. The 77 kDa subunit bridges the 64 and 50 kDa subunits of CstF and the trimer interacts cooperatively with CPSF most likely through a strong interaction between CstF-77 and CPSF-160.

CstF-77 is homologous to a suppressor protein of *Drosophila* implicated in the regulation of poly A site

TABLE I

Mammalian Cleavage and Polyadenylation Factors

Factor	Subunits (kDa)	Function
CPSF	160 100 73 30	Cleavage and polyadenylation binds AAUAAA
CstF	77 64 50	Cleavage; binds downstream element
$CF1_m^a$	25 (72, 68, 55)[b]	Cleavage; binds RNA
$CF11_m^a$	47	Cleavage
PAP	82	Cleavage and polyadenylation; catalyzes AMP polymerization
PABP2	33	Poly A extension; stimulates PAP; controls poly A length
RNA pol II (large subunit)	200	Cleavage; binds CPSF and CstF

[a] One of these three interacts with the 25 kDa subunit to give a functional heterodimer.

[b] Mammalian.

choice. However, it is CstF-64 that has been assigned this role in human and chicken cells. Increased levels of CstF-64 favor the use of weak poly A sites normally underused relative to stronger sites. If such sites are in different coding exons, proteins with different sequences will be produced that may have different functions. This occurs during differentiation of β cells into antibody-secreting plasma cells. In undifferentiated β cells the use of a stronger downstream poly A site generates an mRNA for the immunoglobulin heavy chain that codes for a membrane-bound protein, while a weaker upstream polyA site is more active in plasma cells, and leads to a shorter mRNA coding for a secreted immunoglobulin heavy chain. The switch from membrane mRNA to the secreted form is correlated with large increases of CstF-64 while levels of other subunits of CstF remain unchanged. Other activators and inhibitors of the switch are known that may increase upon cytokine stimulation of differentiation.

The CstF-50 subunit is characterized by a seven WD-40 repeat of 40 amino acids that are also in the transducin repeats of the β-subunit of tripartite G proteins. CstF-50 forms a complex with the nuclear protein, BARD1, which is known to associate *in vivo* with the breast cancer tumor suppressor BRCA1. This complex inhibits polyadenylation *in vitro*. Both CstF-50 and BARD1 interact with the CTD of RNAP II leading to speculations that BARD1 may prevent inappropriate 3′ end formation.

$CF1_M$ and $CF11_M$ Cleavage Factors

Both are required for cleavage. CF1 has subunits of 68, 59, and 25 kDa; however, a dimer of the 68 and 25 kDa proteins can replace CF1 *in vitro*. CF1 binds to CPSF at an early stage of assembly of the cleavage complex. CF11 has only been partially purified, but has a subunit of 47 kDa that is homologous to the yeast 3′ end-processing factor, Clp1. CF11-47 interacts with CPSF and $CF1_m$.

Poly A Polymerase

PAP was characterized initially by its specificity for ATP but it lacked specificity for an RNA primer. Specificity for mRNA is now known to be conferred by CPSF. Two functional isoforms, PAP I (77 kDa) and PAP II (82 kDa) are generated by alternative splicing of a mouse gene with 22 introns. Although PAP II is more common, both have identical activities and specificities. The highly conserved amino two-thirds of the molecule has the catalytic site while the C-terminal regions contain an RNA-binding domain and two nuclear localization signals as well as serine/threonine-rich phosphorylation sites.

Crystals of calf and yeast PAPs both show a cylindrical U-shaped molecule with the N-terminal catalytic site spread along one wall of the cavity. The locus of the RNA-binding site awaits analysis of RNA:protein cocrystals.

PABP2

The nuclear 33 kDa poly A-binding protein (PAB2) is responsible for processive elongation by the polymerase and for control of poly A tail length.

RNAP II

RNAP II has recently been recognized as the engine of an RNA machine that carries RNA processing complexes including CPSF and CstF on the CTD of its large subunit. CTD is a separate domain of heptad repeats of seven amino acids repeated 52 times in mammals and 26 times in yeast where two of its serines undergo phosphorylation after transcription is initiated.

Transcription Termination and Polyadenylation are Linked

Evidence for a link between mRNA 3′ end formation and transcription was first seen with point mutations of the AAUAAA poly A signal that resulted in greatly elongated nascent transcripts. This was also seen *in vivo* in a transcript from a thalessemia patient with a point mutation in the AAUAAA signal of the α-globin gene. Defining a mechanism for this linkage of transcription termination to 3′ end processing was difficult until the dependence of mRNA 3′ end processing on an intact CTD of RNAP II was established. The binding of cleavage/polyadenylation complexes CPSF and CstF to the CTD occurs prior to initiation of transcription, and they can remain affiliated with the polymerase up to sites of termination. This finding has stimulated new analytical approaches emphasizing accumulation of nascent transcripts, especially the highly unstable downstream cleavage products.

It is now clear that transcription termination occurs before cleavage as RNAP II moves far beyond the cleavage site producing uncleaved nascent transcripts. The fact that this requires a functional poly A site, usually hundreds of nucleotides upstream of the termination site, suggests a model in which the nascent RNA is looped out between the CTD bound cleavage/polyadenylation factors and the RNA exit channel of RNAP II. The identification of specific sequences including pause sites in this 3′ flanking region and termination factors that may interact with

cleavage/polyadenylation factors to drive mRNA 3′ end formation has introduced a new level of complexity into the nature of this coupling.

Polyadenylation in Yeast

The mechanism of mRNA 3′ end formation in yeast generally resembles that of mammals, although the length of the poly A tail is only ~50–70 nts. The yeast poly A polymerase N-terminal half is essentially identical to that of the N terminus of the mammalian enzyme. Yeast mRNAs have two poorly conserved poly A signals including an upstream U-rich site and an A-rich site downstream but both are upstream of the poly A addition site. Two large multisubunit complexes required for cleavage have subunits homologous to those of CPSF and CstF emphasizing their shared evolutionary history.

A role for poly A in translation has been established with a yeast extract. The poly A tail of mRNA serves as an anchor for a poly A-binding protein that binds to a translation initiation factor, eIF4G to which a 5′ cap-binding protein is also bound at a distinct site. This complex brings 5′ and 3′ ends of mRNA together to initiate translation.

Role of Polyadenylation in Regulating Gene Expression

The type and level of mRNA expressed from nascent transcripts can affect cell growth, differentiation, or function. Like other RNA modifications, polyadenylation can be critical for regulating functional mRNA levels beginning with nuclear export. This occurs in influenza virus-infected cells that produce a viral protein that inhibits cellular mRNA 3′ end formation by binding both cleavage and polyadenylation factors leading to accumulation of non- or underpolyadenylated cellular mRNAs in the nucleus while polyadenylated viral mRNAs processed by a different mechanism exit to the cytoplasm.

Early evidence for a poly A function in the regulation of mRNA activity was seen in maturing oocytes and zygotes where activation of cytoplasmic dormant mRNAs became translationally active upon 3′ end polyadenylation. This activation depended on an intact AAUAAA poly A signal and a specific U-rich sequence in the 3′ untranslated region of a restricted set of mRNAs to which specific proteins bind. A specific cytoplasmic polymerase with unique properties has recently been reported in *Caenorhabditis elegans* suggesting that cytoplasmic polyadenylation may also occur in mammals, a likely possibility that needs to be re-examined.

The regulated choice between two functional poly A sites in different coding exons of a pre-mRNA can produce two mRNAs coding for proteins with different biological functions. One well-studied example is the immunoglobulin heavy chain in β cells where a switch in poly A site usage occurs during β cell differentiation into plasma cells. The role of the 64 kDa subunit of CstF cleavage complex in this switch has already been described. Another involves the calcitonin gene transcript that codes for the Ca^{2+}-activated protein that is produced in most tissues, but not in neuronal cells where an mRNA with two additional exons is processed at a poly A site farther downstream leading to the production of a larger protein, the calcitonin gene-related protein with several neurotrophic activities. The restriction of this choice to neuronal tissues was originally attributed to activator or inhibitor proteins not present in other tissues, while use of the upstream poly A site to produce calcitonin was considered the default mechanism. Surprisingly a novel mechanism for stimulating cleavage and polyadenylation at this upstream poly A site involved an enhancer sequence in the downstream adjacent intron. This enhancer sequence includes partial 5′ and 3′ splice sites that bind a splicing factor that interacts with the cleavage complex at the poly A site of the upstream exon to stimulate polyadenylation. Factors in neuronal tissue that may over-ride this intron enhancer mechanism have not yet been identified.

Finally phosphorylation:dephosphorylation of the serine/threonine-rich C-terminal domain of poly A polymerase can regulate its enzymatic activity *in vivo* and *in vitro*. This is under the control of the cell cycle as a hyperphosphorylated PAP accumulates during mitosis reducing its enzymatic activity that coincides with a general shutdown of RNA and protein synthesis while hypophosphorylation of PAP is characteristic of other phases of the cell cycle.

See Also the Following Articles

RNA Polymerase II Elongation Control in Eukaryotes • RNA Polymerase II Structure in Eukaryotes • Spliceosome • Transcription Termination

Glossary

5′ mRNA capping Addition of a 7-methyl guanosine to the 5′ phosphorylated end of a nascent mRNA transcript that creates a 5′–5′ triphosphate linkage.

3′ mRNA polyadenylation The processive addition by a poly A polymerase of AMP units from ATP to the 3′ end of mRNA. The site for poly A addition is created by cleavage of a specific phosphodiester bond within the 3′ region of the precursor mRNA that provides the site of the 3′ hydroxyl group for poly A addition.

splicing A coupled two-step process for removing noncoding intervening sequences (introns) from precursor mRNA and for

joining the two resulting adjacent coding sequences (exons) to produce a translatable mRNA sequence.

Further Reading

Calvo, O., and Manley, J. (2003). Strange bedfellows: Polyadenylation factors at the promoter. *Genes Dev.* **17**, 1321–1327.

Edmonds, M. (2002). A history of poly A sequences: From formation to factors to function. *Prog. Nucleic Acid Res. Mol. Biol.* **71**, 268–389.

Proudfoot, N., Furger, A., and Dye, M. (2002). Integrating mRNA processing with transcription. *Cell* **108**, 501–512.

Wahle, E., and Keller, W. (1996). The biochemistry of polyadenylation. *Trends Biochem. Sci.* **21**, 247.

Zhao, J., Hyman, L., and Moore, C. (1999). Formation of mRNA 3′ ends in eukaryotes. *Microbiol. Mol. Biol. Rev.* **63**, 405–455.

Biography

Mary Edmonds is a Professor Emerita in the Department of Biological Sciences at the University of Pittsburgh. Her research has been in the area of RNA processing beginning with the discovery of poly A polymerases and polyadenylated pre-mRNAs and messenger RNA in human cells. Later with John Wallace, a graduate student they discovered branched polyadenylated nuclear RNAs that are key intermediates in the splicing reaction that removes introns from nascent RNA transcripts.

mRNA Processing and Degradation in Bacteria

Deborah A. Steege
Duke University, Durham, North Carolina, USA

Messenger RNA molecules in bacteria are subject to cleavage by ribonucleases (RNases) and to extension by addition of A residues to their 3′-terminal ends. In a few instances, the function of RNase digestion is the processing of precursor mRNAs during biosynthesis to generate the mature ends found on the mRNAs translated by ribosomes. However, the primary function of RNase action on mRNA is to effect its degradation and make the nucleotide units available for use in synthesis of new mRNAs. This enables bacterial cells to modulate the levels of particular mRNAs in response to changes in the environment. The defining feature of mRNA at the time of its discovery during the 1960s was instability. At any one time in a bacterial cell mRNA represents a substantial fraction of the RNA being made by RNA polymerase, but it is degraded quickly. Only a few enzymes are required to degrade mRNA, several of which are coordinated in a large complex termed the degradosome. During the steps of degradation, stable RNA structures in mRNAs pose strong barriers to decay. In these instances, addition of a stretch of single-stranded A residues (a poly(A) tail) to the 3′ end of the mRNA facilitates continued degradation of the mRNA molecule.

Ribonucleases that Mediate mRNA Degradation in the Bacterium *Escherichia coli*

In bacteria, mRNA is degraded by the sequential action of endonucleases and exonucleases (Figure 1). The only bacterial species for which sufficient information about mRNA decay pathways is available for discussion is *Escherichia coli* (*E. coli*). RNases are defined by two properties: (1) whether they act on internal phosphodiester bonds within an RNA chain (endonuclease) or on an end of an RNA chain (exonuclease); and (2) whether the exonuclease degrades from the 3′ or the 5′ end of an RNA chain. In bacteria only 3′ to 5′ exonucleases have been found. The combined action of endonuclease cleavage and 3′ to 5′ exonuclease digestion on an mRNA generally produces an apparent 5′ to 3′ wave of degradation intermediates. Only six of some 20 RNases identified in *E. coli* are currently known or implicated to function in mRNA decay (Table I). Three are endonucleases and three are 3′ to 5′ exonucleases. The principal endonuclease that initiates decay is the large enzyme RNase E, which is specific for single-stranded regions in mRNA. This enzyme has the unique property of preferring as substrates the monophosphorylated 5′ ends on the downstream products of mRNA cleavage. This feature, in combination with the direction of ribosome movement on an mRNA, probably accounts for the apparent 5′ to 3′ directionality of decay observed for many mRNAs. The other two endonucleases have many fewer substrates on mRNAs than RNase E. RNase G is homologous to the N-terminal catalytic domain of RNase E and shares the other properties of RNase E. RNase III is specific for double-stranded regions of mRNAs and often makes staggered cleavages on opposite strands of the stem in an RNA stem-loop. The exonuclease RNase II, which accounts for the bulk of exonucleolytic activity on mRNA in *E. coli*, is a hydrolytic enzyme that removes nucleoside 5′ monophosphates from RNA 3′ ends. The exonuclease polynucleotide phosphorylase (PNPase), by contrast, acts in a phosphorolytic manner using inorganic phosphate to produce nucleoside 5′ diphosphates. A puzzling feature of these two enzymes is that they both have difficulty digesting through stable stem-loop structures on RNA 3′ ends. Such structures are a characteristic feature of the 3′ ends of many bacterial mRNAs. Another property of these two exonucleases is that they digest the limit products of mRNA decay very inefficiently. The small fragments remaining from mRNA, 2–5 nt long, are in fact degraded by oligoribonuclease, an exonuclease conserved across a wide range of organisms. Overall, the RNases for mRNA decay define a small group of genes, most of which are required either alone or in combination for viability of the bacterial cell.

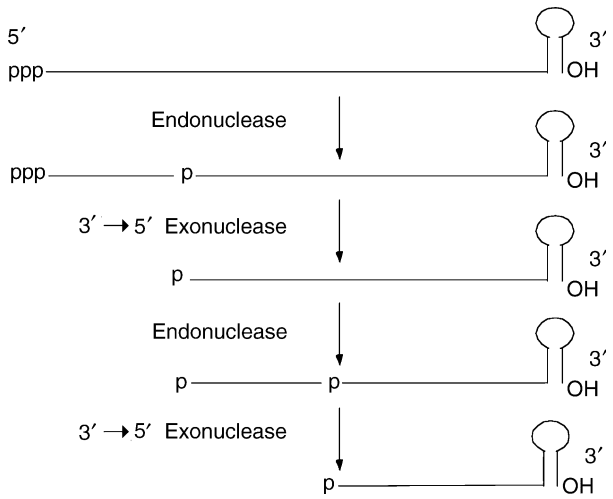

FIGURE 1 mRNA is degraded by the sequential action of endonucleases and 3′ to 5′ exonucleases. A triphosphorylated mRNA synthesized by RNA polymerase and terminated beyond a stem-loop is shown. The products of endonucleolytic cleavage bear monophosphates on their 5′ ends and hydroxyl groups on their 3′ ends.

Control of Gene Expression by RNase III Processing

Although the major function of RNase III in the bacterial cell is synthesis of mature ribosomal RNAs from their large precursors, RNase III is also known to process a number of mRNA species. Processing of mRNA generally functions to alter the stability of one or more coding regions on mRNAs encoding multiple genes, or to regulate the efficiency with which a gene is translated. An example of translational regulation is provided by the well-studied *E. coli* virus lambda. This virus selects one of two modes of growth when it first enters the bacterial cell. If the cells are growing in a rich medium that permits a high rate of growth, the virus multiplies and releases progeny into the medium. In poor media, cell growth rates are much lower. Under these conditions the incoming viral DNA molecule simply integrates into the bacterial chromosome and is then replicated by the host machinery until intracellular conditions become more suitable for production of new viruses. The cellular sensor of physiological conditions is the endonuclease RNase III. Expression of the gene encoding RNase III is regulated by growth rate, with the result that the intracellular concentration of RNase III is a direct function of growth rate. When lambda enters the bacterial cell, one of the first viral genes expressed is N, which is located at the 5′ end of an mRNA transcript encoding many genes (Figure 2). Just upstream of the initiator AUG codon for N gene translation (position 223) lies a hairpin stem that is a substrate for a pair of RNase III cleavages on opposite sides of the stem. When RNase III is abundant, this hairpin is cleaved, and the remaining lower half of the stem unfolds to make the mRNA more accessible for ribosome binding. The result of RNase III cleavage is thus to increase the efficiency of N gene translation. The protein product of the N gene is part of a complex that permits RNA polymerase to read through transcription termination sites at several positions downstream from the N gene on lambda DNA. When N protein is abundant, the genes downstream of the N gene are transcribed and translated, and virus production can proceed. When RNase III is scarce, the RNase III-sensitive hairpin is left uncleaved, less N protein is translated, and little transcription of downstream genes takes place. This is the signal indicating that growth conditions do not favor virus production. Lambda DNA accordingly enters the quiescent state as part of the bacterial chromosome. Thus, mRNA processing in this case plays a critical role in regulating the appropriate choice between the two possible modes of viral development.

TABLE I

***E. coli* RNases in mRNA Decay**

Enzyme	Gene	Monomer size (kDa)
Endoribonucleases		
RNase E	*rne*	118
RNase G	*rng*	55
RNase III	*rnc*	25
3′ → 5′ Exoribonucleases		
RNase II	*rnb*	72.5
Polynucleotide phosphorylase	*pnp*	77
Oligoribonuclease	*orn*	20.7

The Degradosome, a Multiprotein Complex for RNA Degradation

Once many of the decay RNases were purified and characterized, evidence began to appear that at least two of the RNases were associated with other enzymes in a high molecular weight complex that has come to be called the degradosome. At minimum, the purified degradosome contains two RNases: the endonuclease RNase E and the exonuclease PNPase. Present as well are two additional proteins, the ATP-dependent RNA helicase RhlB and the glycolytic enzyme enolase. Polyphosphate kinase is seen in substoichiometric amounts in some degradosome preparations. A functional degradosome containing only RNase E, PNPase, and RhlB assembles spontaneously *in vitro* and shows ATP-activated degradation of an mRNA substrate that is indistinguishable from the activity observed with

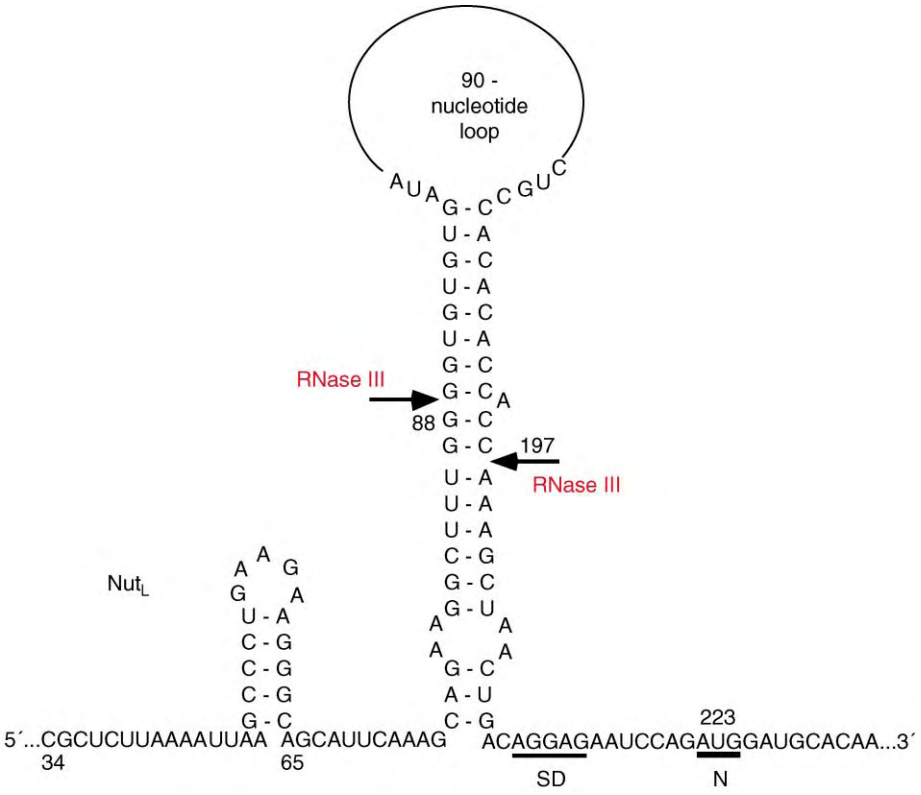

FIGURE 2 Structure of the leader region preceding the translational start of the lambda N gene. Nucleotides are numbered from the 5′ end of the transcript. Nut_L, the site at which RNA polymerase can be modified so as to read through transcription terminators; SD, Shine–Dalgarno sequence in the N gene ribosome binding site; RNase III, sites of cleavage by RNase III.

purified degradosomes. It is evident that the C-terminal half of the RNase E protein functions as the scaffold for association of the other degradosome components because the degradosome complex does not form in a mutant RNase E strain missing the C-terminal half of the protein. The discovery of RNase E, PNPase, and RhlB in a complex immediately raised the possibility that the degradosome might coordinate endo- and exonucleolytic digestion and the unwinding of RNA secondary structure. Evidence from studying the degradation of structured mRNA substrates supports this idea. The stoichiometry of degradosome components remains uncertain, but size estimates for degradosome preparations are indicative of a complex of $(1.5–2.4) \times 10^6$ Da. This is a large enough size that degradosomes can be seen by electron microsopy at the outer edge of the bacterial cell near the inner membrane.

The question of whether the bacterial degradosome is related to any of the high molecular weight complexes observed in the eukaryotic cell has recently taken a very interesting turn with the publication of an X-ray crystal structure for a bacterial PNPase. Whereas comparisons of the mRNA decay pathways in bacteria and eukaryotes have until now indicated few similarities, the bacterial PNPase structure revealed the presence of two repeats per monomer unit of a motif found in the phosphorolytic *E. coli* exonuclease RNase PH. This indicates that the degradosome contains multiple copies of homologues to RNase PH. Similar homologues of RNase PH are found in the exosome, a macromolecular complex present in the eukaryotic cell. A plausible prediction is that the central structure of the two complexes may prove to be quite similar. A second similarity emerging between bacteria and eukaryotes is that these high molecular weight machines are involved in processing and degradation of all three types of RNA: mRNA, rRNA, and small stable RNAs.

Polyadenylation Maintains the Momentum of mRNA Decay

Polyadenylation in bacteria, rediscovered during the 1990s, plays a significant role in the degradation of mRNA. Polyadenylation also appears to function in cellular quality control by removing defective rRNA and tRNA precursors from the cell. Poly(A) tails on bacterial mRNAs are short (10–40 nt), and the extent to which any given mRNA species is polyadenylated is low. Most poly(A) tails are synthesized by poly(A) polymerase I

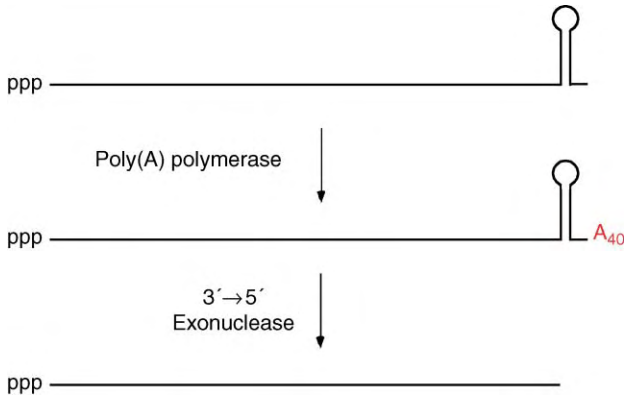

FIGURE 3 Polyadenylation of an mRNA facilitates exonuclease digestion through structural barriers.

(PAP I), an enzyme that is not required for viability of the cell. However, a residual level of polyadenylation is observed in the absence of PAP I and is due to PNPase working in the biosynthetic direction. In contrast to eukaryotic poly(A) tails, which function as stability determinants, addition of a poly(A) tail to a bacterial mRNA stimulates its degradation by exonuclease digestion (Figure 3). This can be understood in light of the difficulty PNPase and RNase II have in digesting through structured regions within and at the ends of mRNA. By providing a single-stranded region of A residues at the 3′ end of an mRNA, the poly(A) tail serves as a toehold for tight binding of the exonucleases as they establish a processive mode of digestion. Thermodynamically stable structures appear to require repeated steps of adding single-stranded poly(A) extensions followed by exonuclease digestion to complete exonucleolytic degradation through highly structured decay intermediates. Thus, polyadenylation appears to be a dynamic process which maintains the momentum of 3′ to 5′ exonucleolytic decay through structural barriers. The question of when, during the lifetime of an mRNA, polyadenylation takes place has recently been resolved. Although polyadenylation was believed to function as the initiating step of decay, it is now clear from following the decay of specific mRNAs over time that PAP I only slowly accesses the 3′ ends of mRNAs. In general, polyadenylation is a later rather than the initiating step of decay, although there certainly are some mRNAs or decay intermediates that require polyadenylation for degradation even to begin.

Decay Pathways Vary with the Position of the Initiating Cleavage

The extent to which molecular models for mRNA decay can be formulated using currently known enzymes is limited (Figure 4). It is relatively straightforward using

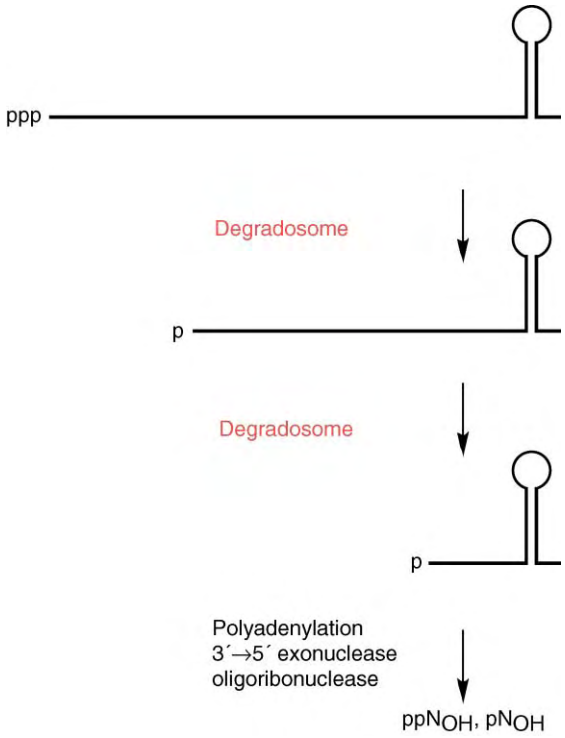

FIGURE 4 General model for mRNA decay based on current knowledge.

mutants deficient in RNase E or RNase III to assign which endonuclease initiates decay. In most cases, decay is initiated by RNase E in the degradosome. Since oligoribonuclease shows specificity for the limit products of mRNA decay, this enzyme can be placed at the end of the decay pathway. By contrast, assigning PNPase or RNase II to the exonucleolytic steps of a decay pathway is often difficult, although it is likely that PNPase in the degradosome digests the upstream fragments produced by endonuclease cleavage. The fact that excess PNPase is present in free form in the cell as well will complicate determining whether degradosome-bound PNPase is in fact responsible for degradation of such products. A similar problem is posed by the existence of at least two mechanisms (polyadenylation and unwinding by the RhlB helicase) for clearing the barriers presented by RNA secondary structure. At present the lack of mutant strains without RhlB activity precludes monitoring decay in the absence of RhlB, so it is not known under what conditions which mechanism is operating to unwind RNA structure. These problems aside, it is abundantly clear that multiple pathways for decay exist. In large part the mode of decay and overall appearance of a pathway is governed by the position of the initiating cleavage. This position must be determined empirically for each mRNA through a combination of *in vivo* experiments and *in vitro* biochemical studies. From in-depth study of

several mRNAs, it appears that if the initiating cleavage is near the 5′ end of an mRNA, the wave of endonucleolytic decay may move in the 5′ to 3′ direction, followed by rapid exonucleolytic degradation of the upstream products. If instead the initiating endonucleolytic cleavage serves to remove the terminator structure at the 3′ end of an mRNA, decay may show a predominantly 3′ to 5′ exonucleolytic mode which may be accelerated by additional RNase E cleavages within the body of the mRNA. A third alternative is that the initiating cleavage occurs at an internal position within an mRNA. Cleavage at this position gives two products that undergo further degradation at a rate determined by the extent to which structural barriers impede exonuclease digestion on each intermediate. Whatever the mode of decay, it is likely that RhlB helicase activity and polyadenylation cooperate to minimize the number of rounds of polyadenylation required for complete degradation of highly structured mRNA decay intermediates.

See Also the Following Articles

DNA Polymerase I, Bacterial • Exonucleases, Bacterial

Glossary

degradosome A large complex of proteins that coordinates the processing of transfer RNAs and ribosomal RNAs as well as the enzymatic degradation of mRNAs and ribosomal RNAs.

endoribonuclease RNase that cleaves internal phosphodiester bonds in an RNA chain.

exoribonuclease RNase that removes nucleotides from one end of an RNA.

mRNA degradation Enzymatic RNA cleavage and nucleotide addition steps that bring about degradation of mRNAs to recycle the nucleotides for new gene expression.

mRNA processing RNA cleavage events on precursor mRNAs that bring about their maturation to the functional forms translated by ribosomes.

polyadenylation Enzymatic addition of ~40 A residues to the 3′-terminal ends of mRNA molecules and decay intermediates to generate a poly(A) tail.

Further Reading

Carpousis, A. J., Vanzo, N. J., and Raynal, L. C. (1999). mRNA degradation: A tale of poly(A) and multiprotein machines. *Trends Genet.* **15**, 24–28.

Kushner, S. R. (2002). mRNA decay in *Escherichia coli* comes of age. *J. Bacteriol.* **184**, 4658–4665.

Régnier, P., and Arraiano, C. M. (2000). Degradation of mRNA in bacteria: Emergence of ubiquitous features. *Bioessays* **22**, 235–244.

Steege, D. A. (2000). Emerging features of mRNA decay in bacteria. *RNA* **6**, 1079–1090.

Symmons, M. F., Williams, M. G., Luisi, B. F., Jones, G. H., and Carpousis, A. J. (2002). Running rings around RNA: A superfamily of phosphate-dependent RNases. *Trends Biochem. Sci.* **27**, 11–18.

Biography

Dr. Deborah Steege is a Professor in the Department of Biochemistry at Duke University. Her principal research interests are molecular mechanisms in gene expression, in particular those steps that take place after RNA polymerase has synthesized an mRNA. She holds a Ph.D. from Yale University and served as a postdoctoral fellow at the same institution. She has authored research papers for 30 years in several areas of the broad field of RNA biology.

Mucin Family of Glycoproteins

Juan Perez-Vilar
University of North Carolina at Chapel Hill, North Carolina, USA

Robert L. Hill
Duke University, Durham, North Carolina, USA

Mucins are glycoproteins found in epithelial membranes and as components of the mucus secretions that cover the epithelial cells in the gastrointestinal, urogenital, tracheobronchial, ocular, and auditory systems of all vertebrates and the epidermis of amphibians. Mucins are not exclusive of vertebrates, and they can be found in almost all eukaryotes. Mucus production is considered to be a critical feature for multi-cellular organisms to survive the presence of noxious agents that are part of their environment. All members of the mucin family are rich in carbohydrates and many of them are among the largest proteins known, with complex structures and different protein domains.

General Features

Definitions

Mucins are structurally diverse but share similar structural features. One region of the polypeptide backbone of mucins has an amino acid sequence rich in threonine and/or serine residues that is repeated several times. O-linked oligosaccharide chains are covalently bound to these residues, resulting in the formation of highly glycosylated domains, known as the tandem repeat domains, O-glycosylated domains, or just mucin domains. Because proline residues are commonly found in the mucin domains, they are also known as PTS domains. The term mucin domain is preferred because it is not in conflict with the existence of nonglycosylated repeated domains in many mucins, O-glycosylated regions in the polypeptide chains of many glycoproteins, and mucins (e.g., MUC2) with either serine or threonine residues, but not both, in their mucin domains.

Mucin Members

The exact number of mucins in humans or other vertebrates is unknown. Proteins with well-characterized biological activities that contain mucin domains in their structures are not considered members of the mucin family. In these cases, the functional, rather than structural, properties prevail. This is the case of many membrane receptors that have mucin domains that help to expose their ligand-binding domains. However, 17 potential human mucin genes have been reported, 12 of which (*MUC1*, *MUC2*, *MUC3A*, *MUC3B*, *MUC4*, *MUC5AC*, *MUC5B*, *MUC6*, *MUC7*, *MUC9*, *MUC13*, and *MUC15*) are fully sequenced. The others (*MUC8*, *MUC11*, *MUC12*, *MUC16*, and *MUC17*) are only partially sequenced. Human mucin proteins and genes are designated by the notation MUC and *MUC*, respectively, followed by a number that indicates the specific mucin. The notation for animal mucins is similar but includes upper/lower case letters (Muc and *Muc* for protein and genes, respectively) and an additional lower case letter for designating the particular species (e.g., mMuc1 and *mMuc1* indicate the mouse mucin homologous to MUC1 and *MUC1*, respectively). However, it is common to find in the literature that many animal mucins are designated following the name of the tissue in which they are predominant (e.g., porcine gastric mucin). In many of these cases, biochemical studies started prior to the cloning of their corresponding genes. For instance, porcine submaxillary mucin (pMuc5b) was the focus of many biochemical studies years before its gene was sequenced.

Mucin Subtypes

Mucins can be divided into membrane and secreted mucins based on the presence or absence of a transmembrane domain-encoding sequence in their genes. Membrane mucins are anchored to the apical side of epithelial cells by a transmembrane domain, whereas secreted mucins, which do not have such a domain, are secreted into the extracellular space. However, some membrane mucins (e.g., MUC1 and MUC4) are partially proteolytically cleaved during their biosynthesis, resulting in formation of membrane-attached and soluble subunits. Because these two subunits can be anchored in the membrane as a noncovalent complex, the term

membrane-tethered or tethered mucins can be found in the literature. In addition, splicing of some membrane mucin genes (e.g., *MUC1*) may lead to synthesis of variants lacking transmembrane domains.

Structural subtypes within membrane and secreted mucins can be recognized by comparing the primary sequences of the nonmucin domains. Though the mucin domains in all mucins have similar amino acid composition (e.g., threonine and/or serine rich), they do not share significant protein sequence similarities when compared.

Membrane Mucins

In general, membrane mucins have short cytoplasmic regions at their C-terminal end while their extracellular regions are much larger and contain the mucin domains. Their sizes vary from 334 amino acid residues (MUC15) to more than 6000 amino acid residues (MUC4). *E*pidermal *g*rowth *f*actor (EGF)-, *s*ea-urchin/*e*nterokinase/*a*grin (SEA)-, von Willebrand factor D (D)-, and/or nidogen (NIDO)-like domains can be found in membrane mucin polypeptides. Because MUC3A, MUC3B, MUC12, MUC13, and MUC17 all have EGF- and SEA-like domains, whereas MUC4 lacks SEA-like domains, the former set of mucins likely represent a functional subgroup within membrane mucins. MUC1 and MUC15 are relatively short membrane mucins lacking EGF-, SEA-, D-, and NIDO-like domains.

Secreted Mucins

All secreted mucins, except MUC7 and MUC9, have polypeptide chains with thousands of amino acid residues. These large mucins – including MUC2, MUC5AC, MUC5B, and MUC6 – are known as secreted, gel-forming mucins, because they are found in mucus secretions and endow mucus with their viscoelastic and adhesive properties. Moreover, they all share a similar structural organization that includes nonmucin domains homologous to protein domains found in human von Willebrand factor (e.g., B-, C-, CK-, and D-domains), a protein essential for blood clotting. MUC6, however, lacks B-, C-, and one of the four D-like domains found in the others. In addition, MUC2, MUC5AC, and MUC5B have several copies of a domain, known as the Cys subdomain or CS-domain, which is scattered along their corresponding mucin domains. Similar domains are also found repeated in oikosin-1 (a mucous protein found in certain tunicates) and human cartilage intermediate protein (a cartilage protein of unknown function), but not in von Willebrand factor. MUC7 and MUC9, also known as oviductin or oviductal glycoprotein 1, are secreted mucins not related to gel-forming mucins. MUC7 is a small mucin present in the oral cavity and likely involved in the clearance of bacteria that bind to it. MUC9 is a 678 amino acid residues mucin found exclusively in the oviduct, where it may have a function in fertilization and early embryo development.

Mucin Genes

In general, mucin genes consist of large central exons encoding the entire mucin domains. Alleles of some mucin genes (e.g., *MUC1, MUC2, MUC4*, and *MUC6*) differ in the number of tandem repeats encoded by the central exons, a feature known by the acronym VNTR (*v*ariable *n*umber of *t*andem *r*epeats), although polymorphism due to nucleotide changes has been reported as well. Sequences encoding other domains and regions in the mucin polypeptides are usually constituted by short exons interrupted by large introns. The genes for structurally related mucins are located in specific chromosomal regions. Thus, *MUC3A, MUC3B, MUC11*, *MUC12*, and *MUC17* are located in 7q22, whereas *MUC2, MUC5AC, MUC5B*, and *MUC6* are positioned at 11p15. However, their promoter sequences have little overall homologies and, in general, contain elements for tissue-specific expression and regulation.

Mucin Cell and Tissue Distribution

In general, membrane mucins are secreted by several types of epithelial cells, whereas gel-forming mucins are predominantly synthesized in and secreted from epithelial and submucosal goblet/mucous cells. Each organ/tissue is characterized by the synthesis of a set of mucins with one or two major ones, although a given mucin is usually found in more than one tissue/organ (Table I).

Roles in Health and Diseases

Because of their large size, extent of glycosylation, and locations, mucins protect epithelial cells from dehydration, noxious agents and physical injury, as well as aid the passage of materials through a tract. However, the roles of mucins in mucosal homeostasis likely are more important and complex than previously anticipated. For instance, MUC1 and MUC4 may be involved in cell signaling. The fact that mucin production is regulated in mammals by mechanisms operating at different levels attests to the central role of these glycoproteins. Thus, the number and differentiation state of the cells producing mucin/mucus, the rate of mucin secretion, and the activities of mucin genes are all responsive to bacterial and viral compounds, chemicals and inflammatory mediators.

Many mucin genes have been described but gene deletion studies to assess mucin function are not yet

TABLE I

Tissue Distribution of Human Mucins

MUC1	Widely distributed among epithelial cells. Present in some nonepithelial cells (e.g., fibroblasts) and body fluids (e.g., urine)
MUC2	Colon and small intestine (goblet cells), salivary gland ducts, inferior turbinates, conjunctival epithelium
MUC3A	Colon and small intestine (goblet and absorptive cells)
MUC3B	Colon and small intestine (goblet and absorptive cells)
MUC4	Bronchus, colon, conjuctival epithelium, middle ear
MUC5AC	Bronchus (superficial goblet cells and submucosal mucus cells), colon (goblet cells), superficial stomach epithelium, endocervical epithelium, inferior turbinates, conjunctival epithelium, middle ear
MUC5B	Bronchus (submucosal mucus cells, salivary glands, submandibular glands, gall bladder epithelium, endocervical epithelium, inferior turbinates (submucosal glands), colon (goblet cells), middle ear
MUC6	Gastric epithelium (mucus neck cells; antral mucus cells) small intestine (goblet cells), colon, gall bladder epithelium, seminal vesicle, pancreas (centroacinar cells and ducts), endocervical epithelium, endometrial epithelium, biliary epithelial cells, middle ear
MUC7	Salivary glands (mucus cells), bronchus (submucosal glands), conjunctival epithelium, middle ear
MUC8	Bronchus (submucosal glands), middle ear, urogenital system
MUC9	Oviduct, middle ear
MUC11	Colon, bronchus, middle ear
MUC12	Colon, middle ear
MUC13	Colon and small intestine (columnar and goblet cells), bronchus, kidney, small intestine, conjunctival epithelium, lymphoid cells
MUC15	Widely distributed among epithelial cells. Expressed in some nonepithelial cells
MUC17	Intestine (absorptive cells), colon, gastric epithelium, conjunctival epithelium

completed. However, lack of functional mucins is expected to have profound effects of mucosal homeostasis. Thus, mMuc2-deficient mice develop colorectal cancer in contrast to normal littermates. Conversely, overproduction of mucins/mucus is a serious and sometime devastating feature in several chronic lung diseases, including chronic obstructive pulmonary disease, chronic bronchitis, asthma, bronchiectasis, and, especially, cystic fibrosis. An excess of mucus accumulation can lead to excessive sputum production, respiratory infections, and airways obstruction, and ultimately contribute to the morbidity and mortality associated with these diseases.

Structural Features

Signal Peptides

Both membrane and secreted mucins have short signal peptides at their N-terminal ends that allow them to be synthesized and processed along the organelles involved in the secretory pathway. In general, these sequences are rich in hydrophobic residues but do not have significant homologies among different mucins.

Mucin Domains

Characteristically, the mucin domains are centrally located in the mucin polypeptide backbone (Figure 1). These domains are constituted by a repeated Ser/Thr-rich sequence together with degenerate repeats and unique Thr/Ser-rich sequences at both ends of the repeated regions. The sequence, length, and number of the Thr/Ser-rich repeats vary among mucins. In general, there are as many repeated sequences as mucins described. Some mucins (e.g., MUC3A, MUC3B, and MUC4) have two different mucin domains, each one with different repeated sequences. Only a few kinds of amino acids, in addition to threonine and serine, are found in the mucin domains, with proline and glycine among the most common.

Major Nonmucin Domains in Secreted Mucins

D-Like Domains

Gel-forming mucins contain three homologous N-terminal D-domains (designated D1, D2, and D3) and, all but MUC6, a fourth domain, D4, at the C-terminus. A partial D-domain, D′, is between D2 and D3 in all secreted mucins. Each D-like domain has 325–400 amino acid residues and contains up to 30 cysteines. The D-like domains have several conserved N-glycosylation acceptor motifs and are N-glycosylated when expressed in cultured cells. The available data indicate that the D1-, D2-, and D3-like domains are involved in the assembly of disulfide-linked mucinmultimers.

CK (Cystine Knot)-Like Domains

The CK-like domain is 90–100 amino acid residues long, cysteine-rich domain, located at the C terminus of gel-forming mucins. This domain is homologous to the cystine knot domain in several growth factors and norrin. The CK-like domain is N-glycosylated when expressed in cultured cells. The CK-domain is involved in the assembly of disulfide-linked mucin multimers.

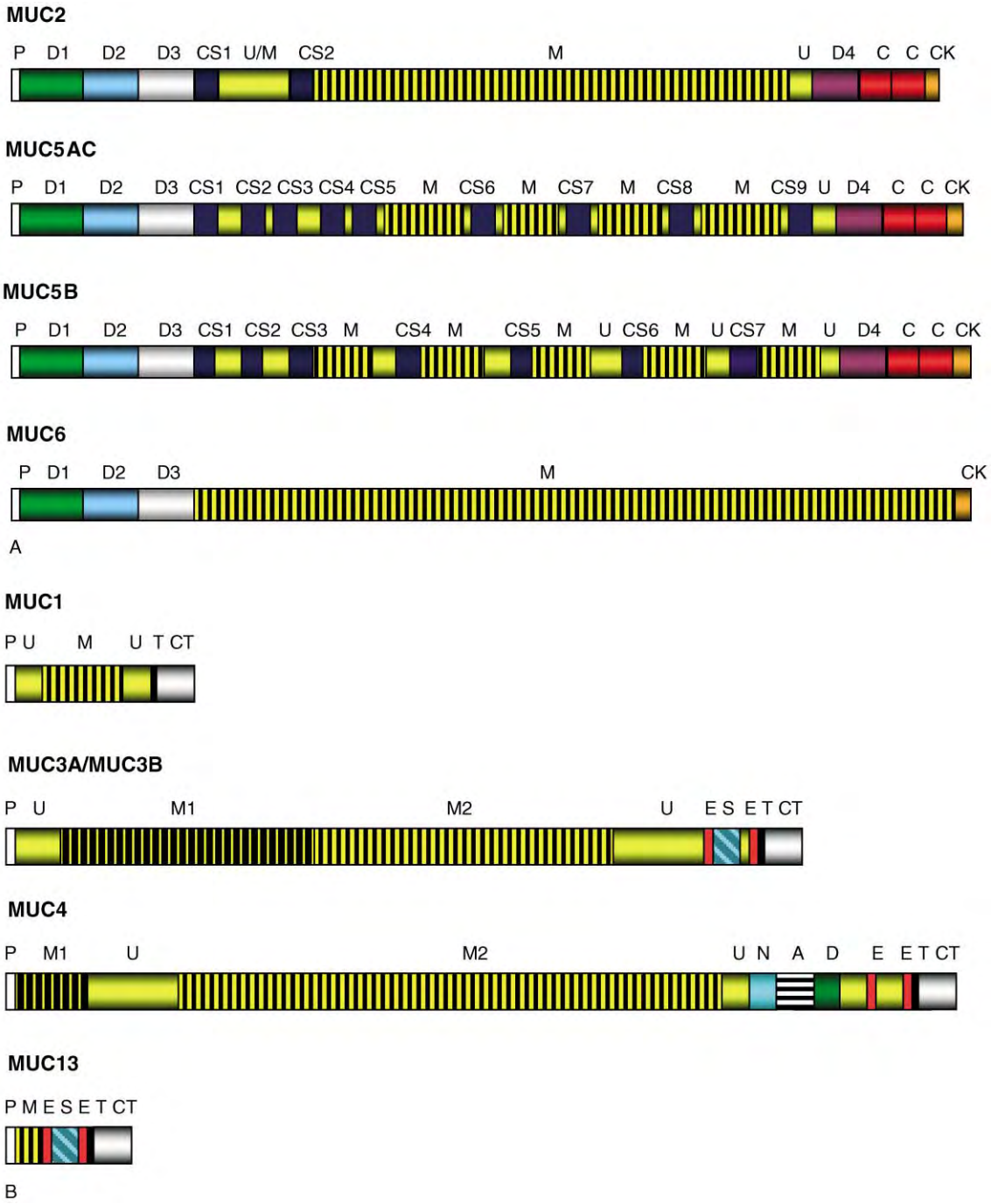

FIGURE 1 Domains in the polypeptide chains of some mucins. Comparisons of the protein domains in secreted (gel-forming) mucins (*A*) and four membrane mucins (*B*), respectively. The length of the corresponding domains is approximately proportional to the number of amino acid residues. *A* and *B* are not drawn to the same scale. P, signal peptide; U, unique sequences (usually Ser/Thr-rich); M, mucin domains; D, D-domains; CS, Cys subdomains; C, C-domains; CK, CK (cystine-knot)-like domain; T, transmembrane domains; CT, cytoplasmic domain; E, EGF-like domains; S, SEA-like domains; N, NIDO (nidogen)-like domain; A, AMOP (adhesion-associated domain in MUC4 and other proteins)-like domain.

CS (Cys Subdomain)-Domains

The CS-domains, also known as the Cys subdomains, are short (100 amino acid residues long) cysteine-rich domains that are scattered along the mucin domains of MUC2, MUC5AC, and MUC5B. Nine, seven, and two CS-domains are found in MUC5AC, MUC5B, and MUC2, respectively. All CS-domains have one C-mannosylation acceptor motif (WXXW) at their

N-terminal side. C-Mannosylation has been reported in recombinant CS-domains expressed in cultured cells. The role of the CS domains is unclear at present.

Major Nonmucin Domains in Membrane Mucins

Transmembrane and Cytoplasmic Domains

The transmembrane domain in mucins comprises a short stretch of hydrophobic amino acid residues. The mucin cytoplasmic domains are short (20–79 amino acid residues long) and contain tyrosine and serine residues that can be phosphorylated.

EGF-Like Domains

EGF-like domains are 45–60 amino acids long domains located between the transmembrane domains and the mucin domains in MUC3A, MUC3B, MUC4, MUC12, MUC13, and MUC17 (Figure 1). They have six cysteine and two glycine residues conserved. The roles of these domains have not been clearly established, but recent studies suggest that they might be involved in cell signaling.

SEA-Like Domains

The SEA-like domain is an 85–110 amino acids long domain found conserved in many extracellular proteins. It is located between the transmembrane and mucin domains in MUC3A, MUC3B, MUC12, MUC13, and MUC17 (Figure 1). The role of the SEA-like domains is not yet defined, but they contain the GSVVV peptide motif that may be cleaved during the biosynthesis of these mucins.

Other Domains

Other protein domains in mucins are the *A*dhesion-associated domain in *M*UC4 and *O*ther *P*roteins (AMOP) and the *nido*gen (NIDO)-like domains that are found in MUC4. Their functions are not yet established, but similar domains are also present in extracellular or surface proteins involved in cellular adhesion.

O- and N-Linked Oligosaccharide Chains

O-linked oligosaccharides in the mucin domains comprise up to 90%, but not less than 50%, of the weight of the native mucins. They decisively contribute to formation of an extended mucin structure by limiting the rotation around peptide bonds, and by the repulsion generated among the neighboring, negatively charged oligosaccharide and sulfate groups. Such long, extended molecules have a much greater solution volume than native or denatured proteins with little or no carbohydrate, and endow aqueous solutions of mucins a high viscosity.

N-linked oligosaccharides are not present in the mucin domains but in many of the nonmucin, cysteine-rich, domains. They may have a role during folding of the nascent mucin polypeptide in the endoplasmic reticulum.

Sulfation

Several monosaccharides in mucin N- and O-linked oligosaccharide chains, especially galactose, N-acetyl-galactosamine, and N-acetyl-glucosamine, are sulfated. Sulfation contributes to the stiffness of the mucin domains by increasing the negative charges of their O-linked oligosaccharide chains, which, as mentioned above, is critical for their viscoelastic properties. In addition, sulfation protects oligosaccharide chains from bacterial glycosidases.

Biosynthesis

Mucin biosynthesis occurs along the endoplasmic reticulum and the Golgi complex and involves folding, N- and O-glycosylation, sulfation, proteolytic processing, and, in the case of secreted gel-forming mucins, covalent assembly.

Membrane Mucins

Like other membrane proteins, membrane mucins are synthesized and N-glycosylated in the endoplasmic reticulum. Some membrane mucins (e.g., MUC1 and MUC4) may be cleaved while inside this organelle. This produces two subunits that can form a noncovalent complex and, ultimately, secretion of soluble forms of these mucins. The cleavage motif in MUC1 (GSVVV) is also found in the SEA-like domains of MUC3A, MUC3B, MUC12, and MUC17. Membrane mucins are O-glycosylated and sulfated in the Golgi complex, but, contrary to gel-forming mucins (see below), they do not form interchain disulfide bond oligomers/multimers.

Secreted (Gel-Forming) Mucins

Except for MUC7 and likely MUC9, the rest (MUC2, MUC5AC, MUC5B, and MUC6) are assembled to disulfide-linked oligomers/multimers prior secretion.

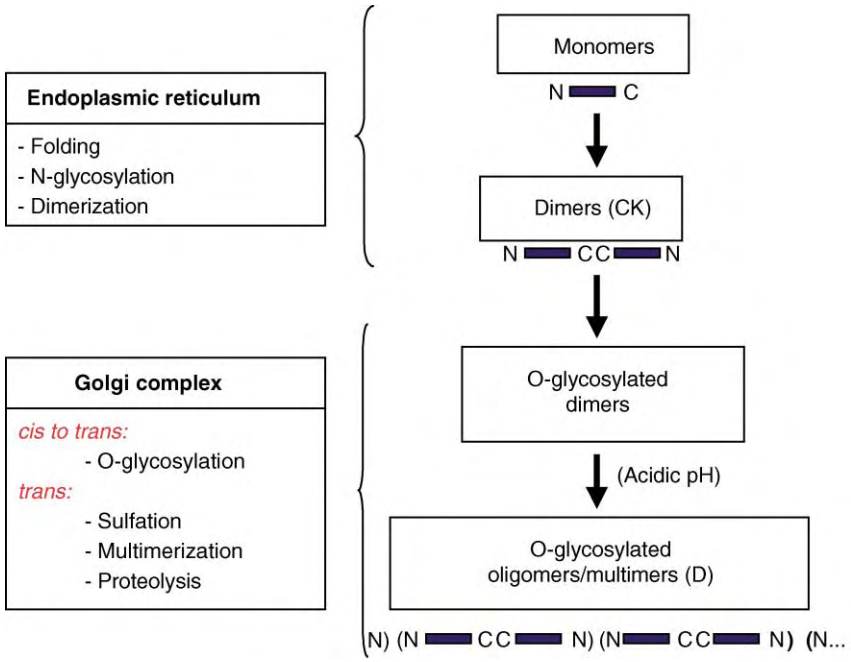

FIGURE 2 Biosynthesis and assembly of secreted, gel-forming mucins. Mucin polypeptide chains are synthesized and translocated into the endoplasmic reticulum. Folding and N-glycosylation of the nascent polypeptide chain is followed by rapid formation of disulfide bonds between the C-terminal CK-like domains in two mucin monomers. Thereafter, dimeric mucins are transported to the Golgi complex where O-glycosylation of the mucin domains and unique Thr/Ser-rich sequences takes place, starting in the *cis*-Golgi compartment and finishing in the late, *trans*-Golgi compartments. In the later compartments, mucins are sulfated and the dimeric forms are assembled into disulfide-bonded oligomers/multimers through their N-terminal D-domains.

Endoplasmic Reticulum

Nascent mucin polypeptides are N-glycosylated and, perhaps, C-mannosylated in their respective NXS/T and WXXW peptide motifs. Mucin assembly starts by formation of dimers via interchain disulfide bonds connecting the CK-domains in two mucin monomers (Figure 2). The CXCC peptide motifs in these domains are critical for dimerization.

Golgi Complex

Mucin dimers are O-glycosylated and sulfated along different compartments of the Golgi complex by resident glycosyltransferases and sulfotransferases. Glycosylated dimers are then assembled into oligomers/multimers via disulfide linkages connecting their NH_2-terminal D-domains (Figure 2). This step likely occurs just before secretion, in the late, acidic, compartments of the Golgi complex and/or beyond. The thiol/disulfide oxido/reductase motifs (CGLC) in the D1 and D3 domains and the CXWXYXPCG sequence in the D3 domains seem to be critical for proper mucin assembly. While light scattering and electron microscopic studies indicate that mucin multimers form linear structures, recent studies suggest the existence of branched polymers as well.

In the *trans*-Golgi compartment, some mucins, including MUC2 and likely MUC5B, may be processed by proteases recognizing the GSDS peptide motif at their corresponding C-terminal regions.

Storage and Secretion

Fully processed gel-forming mucins are stored in high amounts in large secretory vesicles, known as mucous or mucin granules, which occupy the majority of the cytoplasm in goblet/mucous cells. High calcium content and acidic pH are thought to be critical for mucin packing. Mucins are secreted constitutively, which may involve steady exocytosis of mucous granules, small vesicles, or both, or, alternatively, via a regulated pathway involving exocytosis of mucous granules. Regulated secretion is activated by a variety of physiological agents, including cytokines/chemokines, bacterial exoproducts, nucleotides, neurotransmitters, and proteases.

See Also the Following Articles

Disulfide Bond Formation • Oligosaccharide Chains: Free, *N*-Linked, *O*-Linked • Glycoprotein Folding and Processing Reactions • Golgi Complex • Mucins in

Embryo Implantation • *N*-Linked Glycan Processing Glucosidases and Mannosidases • Protein Glycosylation, Overview • Secretory Pathway

Glossary

glycoproteins Proteins with oligosaccharide (carbohydrate) chains covalently attached to their polypeptide backbones.

mucus Viscous aqueous secretions produced by epithelial cells mainly composed by mucins, ions, and water.

***N*- and *O*-linked oligosaccharides** Oligosaccharide chains linked to serine or threonine and aparagine residues in glycoproteins, respectively.

peptide motif Peptide sequence that has a critical function during the biosynthesis, processing, or assembly of a protein (e.g., the CXCC motif is required for dimerization via the mucin CK-like domains), or for the role of a protein.

protein domain A region in the polypeptide chain of a protein that has a specific function (e.g., the CK-like domain in gel-forming mucins is a dimerization domain).

secretory pathway Biosynthetic pathway taken by mucins and other glycoproteins that involves different organelles, e.g., endoplasmic reticulum and Golgi complex, and many consecutive co-/post-translational modifications, including folding, N-/O-glycosylation, disulfide bond formation, sulfation, etc.

Further Reading

Gendler, S. J., and Spicer, A. P. (1995). Epithelial mucin genes. *Annu. Rev. Physiol.* **37**, 607–634.

Perez-Vilar, J., and Hill, R. L. (1999). The structure and assembly of secreted mucins. *J. Biol. Chem.* **274**, 31751–31754.

Strous, G., and Dekker, J. (1992). Mucin-type glycoproteins. *Crit. Rev. Biochem. Mol. Biol.* **27**, 57–92.

Velcich, A., Yang, W., Heyer, J., Fragale, A., Nicholas, C., Viani, S., Kucherlapati, R., Lipkin, M., Yang, K., and Augenlicht, L. (2002). Colorectal cancer in mice genetically deficient in the mucin Muc2. *Science* **295**, 1726–1729.

Biography

Juan Perez-Vilar is an Assistant Professor of Medicine at the Cystic Fibrosis/Pulmonary Research and Treatment Center, University of North Carolina at Chapel Hill, North Carolina. His research interests are in the biochemistry and cellular biology of airway mucins and their roles in obstructive lung diseases. He graduated from the University of Seville in Spain and did postdoctoral studies with Professor Robert L. Hill at Duke University.

Robert L. Hill is a James B. Duke Professor of Biochemistry at the Duke University Medical Center, Duke University, Durham, North Carolina. His research interests since the 1950s have centered around the structure/function relationship of proteins, including enzymes and more recently, complex glycoproteins.

Mucins in Embryo Implantation

Daniel D. Carson
University of Delaware, Newark, Delaware, USA

Mucin glycoproteins are defined as proteins heavily substituted with oligosaccharides in O-glycosidic linkage between N-acetylgalactosamine and S/T residues. Carbohydrates can account for 50–90% of the mucin molecular weight and greatly influence the physical properties of these molecules. Mucins also are predominant constituents of the apical surfaces of reproductive tract epithelia. In many species, uterine mucin expression changes dynamically during the reproductive cycle and in preparation for embryo attachment. This article will summarize current knowledge of factors controlling the expression and function of uterine mucins with particular emphasis on MUC1 and the process of embryo implantation.

The Implantation Process

The process of embryo implantation (Figure 1) into the uterine wall involves complex interactions between embryonic- and uterine-derived factors. These factors include secreted signals as well as cell-surface recognition events. In regard to the latter, a number of cell-surface components have the ability to support embryo attachment and are located at sites of embryo uterine attachment. These include integrins, proteoglycans, and cadherins. The failure of gene knockouts of any of these receptors to prevent the initial events in implantation indicates that there is considerable redundancy in function. This is consistent with *in vitro* studies demonstrating the ability of embryos to attach to a wide variety of cell types and substrates via different cell-surface receptor systems as well as the ability of trophoblast to modulate their cell-surface expression of such receptors in response to the extracellular matrix they encounter.

In spite of the highly invasive nature of blastocysts and trophoblast, the uterus displays the remarkable ability to limit both embryo and tumor cell attachment and invasion. Only during a well-defined "window" in time does the uterus permit attachment to and penetration of the endometrium. This control appears to be primarily exerted at the first point of encounter, namely the apical surface of the lumenal epithelium. In response to ovarian steroid influences, the uterus develops through a series of stages that may be defined as prereceptive, receptive, and postreceptive with regard to the ability to support embryo attachment. The end of the ovarian cycle is marked by a fall in steroid hormone levels and resetting of the uterine clock to begin another cycle of receptivity. In menstruating species, the endometrium is largely sloughed and new tissue formed; however, in most species menstruation does not occur and the endometrium is restructured via processes involving controlled apoptosis and cell proliferation as well as extracellular matrix remodeling. If implantation occurs, steroid hormone levels are maintained and the endometrium not only remains, but also differentiates further in many species in a process called the decidual response.

During the receptive phase, the uterine epithelium also displays remodeling evident by electron microscopy as well as light microscopy if staining for specific markers is used. While there are many species-specific variations on the theme, there are features of this process that are well-conserved across species. These include retraction of apical microvilli and reorganization of the cortical actin filaments, the transient appearance of large membrane protrusions (pinopods or uterodomes), and alterations in the apical glycocalyx. Much of the apical glycocalyx is composed of large, heavily glycosylated glycoproteins identified as mucins. The article will briefly summarize our current knowledge of the function and expression of mucins in the context of the embryo implantation process.

Mucins

Functions

As a general principle, mucins heavily coat the lumenal surfaces of epithelia where they provide the first line of defense against infectious agents as well as degradative enzymes. Consistent with this role, mucin glycoproteins are highly resistant to proteolytic attack and require the actions of multiple glycosidases to remove their constituent carbohydrates. While mucins provide a barrier to infection, it is clear that many bacteria and viruses bind well to mucins. Thus, the concept emerges that these molecules serve as "traps" for the infectious agents

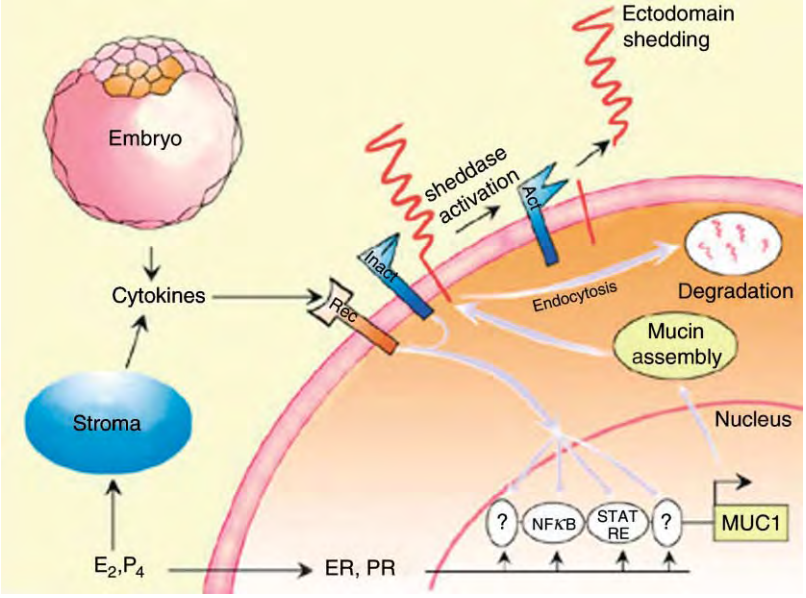

FIGURE 1 Mucin dynamics during embryo implantation. Uterine epithelial cells produce mucins, including transmembrane mucins like MUC1 (represented by the squiggly lines in the figure). In general, these mucins are believed to be a barrier to embryo attachment that must be removed to create access to the apical surface of the uterine epithelium. In some cases, mucin gene expression can be regulated by ovarian steroids, estrogen (E_2) and progesterone (P_4) that may act through their nuclear receptors (ER and PR) directly or indirectly on the MUC1 promoter. Cytokines, produced by neighboring stromal cells or the embryo, bind to cell surface receptors (Rec) on uterine epithelia also can regulate MUC1 gene expression via NFκB and STAT binding. These same elements also may be downstream of steroid hormone actions. Cytokines also can trigger loss of mucin protein by causing increased expression or conversion of latent (Inact) cell-surface proteases or sheddases to active forms (Act) that catalyze mucin ectodomain release. Mucins also may be removed by endocytosis and intracellular degradation pathways.

that interact with them before they can establish contact with the plasma membrane of the host epithelium. A number of mucins occur as transmembrane proteins (see Table I). MUC1 is an example of a transmembrane mucin glycoprotein and experiments with MUC1 null mice demonstrate that these animals are much more prone to bacterial infection and inflammation than their wild-type counterparts. Thus, a paradox arises over how a glycoprotein that can promote attachment of an infectious agent simultaneously serves to protect against the microbe. As discussed below, the host may be able to recognize attachment and shed the ectodomains of transmembrane mucins in response. This process then would convert the shed mucins into a soluble mucin trap removing the potential pathogen from the cell surface.

In the context of embryo implantation, mucins also appear to be antiadhesive. Polarized uterine epithelia of rodents are constitutively nonreceptive *in vitro* and abundantly express mucins. Selective, enzymatic removal of mucins or genetic ablation of Muc1 converts these cells to a functionally receptive state. Moreover, transfection and overexpression of MUC1 into cells that normally adhere well to blastocysts markedly reduces their adhesive activity. In contrast, under some conditions, mucins can carry selectin ligands and, thereby, potentially support cell attachment. Recent studies indicate that this occurs at the fetal–maternal interface and may contribute to aspects of trophoblast binding.

In addition to being abundantly expressed at the apical surface of uterine epithelia, mucins are physically very large with individual molecules being hundreds of nanometers in length. In contrast, typical cell-surface receptors extend 10–30 nm from the cell surface. Due to their heavily glycosylated nature, individual mucins have large hydration spheres. In addition, mucins often form complex aggregates or gels. Consequently, the mucin coat presents a large, formidable matrix that must be somehow traversed or removed in order for molecules or cells to establish contact with the plasma membrane. The size of the ectodomains is an important determinant of transmembrane mucin function as an anti-adhesive molecule. Truncation mutations of the ectodomains of both MUC1 and MUC4 demonstrate that these mucins must extend more than 50 nm from the cell surface to be effective. This would extend well beyond the distance spanned by most cell-surface receptors.

Other interesting functions associated with mucins include immunosupression and association with intracellular signal-transducing molecules. In the former case, the mechanism of action is not clear although effects on several cell types involved in cell-mediated immunity have been reported. In the case of signal transduction, MUC1 has been shown to be associated

TABLE I

Uterine Mucin Expression

Mucin	Type[a]	Found in endometrium?	Species[b]	References
MUC1	TM, Sec	Yes	Hu, Pri, Sh, Bov, Por, Rab, Rat, Mu	Reviewed in Thathiah and Carson (2002)
MUC2	Sec	No	Hu	Gipson *et al.* (1993)
MUC3	TM, Sec	No	Hu	Gipson *et al.* (1997), Ho *et al.* (1993)
MUC4	TM, Sec	Yes	Rat	Carraway and Iddris (2001)
MUC5AC	Sec	No	Hu	Gipson *et al.* (1997)
MUC5B	Sec	No	Hu	Gipson *et al.* (1997)
MUC6	Sec	Yes	Hu	Gipson *et al.* (1997)
MUC7	Sec	No	Hu	Gipson *et al.* (1997)
MUC8	Sec	Yes	Hu	D'Cruz *et al.* (1996)
MUC9	Sec	Yes	Ham	Martoglio and Kan (1996),
		No	Rab	Yong *et al.* (2002)
MUC10	Sec	ND[c]		
MUC11	TM	ND		
MUC12	TM	ND		
MUC13	TM	ND		
MUC15	TM	ND		
MUC16	TM[d]	Yes	Hu	Hamilton *et al.* (2002)
MUC17	TM	ND		
MUC18	TM	ND		

[a] Transmembrane (TM) or secreted (Sec); some can be either depending on alternative mRNA splicing.
[b] Human (HU), Primates (Pri), Sheep (Sh), Cattle (Bov), Swine (Por), Rabbits (Rab), Rats (Rat), Mice (Mu), Hamster (Ham).
[c] Not Determined (ND).
[d] Predicted by cDNA sequence.

with β-catenin, Grb2, and EGF receptor. Furthermore, tyrosine phosphorylation of the cytoplasmic tail is stimulated when ligand is added to cells expressing a fusion protein consisting of a ligand binding extracellular domain and the MUC1 cytoplasmic tail. The physiological significance of these interactions has not been demonstrated although EGF treatment appears to both increase MUC1 association with EGF receptor and activated EGF receptor can tyrosine-phosphorylate the cytoplasmic tail of MUC1, an event suggested to increase MUC1:β-catenin association.

Expression

To date 18 mammalian mucin genes have been identified. The predicted protein structures indicate that the protein cores fall into two classes, soluble and transmembrane. As discussed below, even transmembrane mucins may be shed from the cell surface and so may contribute to the pool of soluble mucins. As a general principle, much of the core protein structure is composed of tandemly repeated sequences rich in serine, threonine, and proline, thereby capable of carrying many O-linked oligosaccharide chains. Secreted mucins also usually contain multiple cysteine-rich regions that participate in disulfide bond formation and the assembly of mucin gels. A hallmark feature is the presence of a large number of O-linked oligosaccharides that can constitute 50–90% of the molecular weight of the glycoprotein. A number of mucin oligosaccharide structures have been determined and considerable information on the glycosyltransferases that assemble these structures is available. The oligosaccharides are branched, can be reasonably complex, and carry a net negative charge due to the presence of sialic acid and/or sulfate residues.

The structures of reproductive tract mucin oligosaccharides change during the cycle under the influence of ovarian steroids. Consistent with this are studies showing that glycosyltransferase activities in endometrium also change in parallel. Expression of mRNA encoding certain mucin core proteins also changes during the cycle; however, only changes in the expression of MUC1 and MUC4 have been studied in any detail, in this regard (see Table I). In rodents, estrogen strongly stimulates MUC1 expression. Progesterone alone has no effect on MUC1 expression, but antagonizes this estrogen action. Both the actions of estrogen and progesterone on MUC1 expression are mediated by their corresponding nuclear receptors. The murine MUC1 promoter contains a number of sequences that are good candidates for estrogen receptor

as well as progesterone receptor-binding sites; however, none of these sites appear to be functional with regard to estrogen receptor-α or -β. Thus, estrogen actions are likely to be indirect and may be mediated in a paracrine fashion by estrogen-regulated growth factors or cytokines. Consistent with this is the conservation of a functional STAT-binding site in the mouse and human MUC1 promoter. Proinflammatory cytokines strongly stimulate MUC1 expression in mammary epithelium by recruiting STAT1α to this site. Synergy with other cytokines has been observed, notably TNFα. In this case, co-operativity with p65 and a corresponding NFκB-binding site appears to further enhance MUC1 transcription. It is noteworthy that these cytokines are highly expressed in the mouse uterus at times when MUC1 levels are high as well, e.g., estrus and day 1–2 *post coitum*, most likely in response to the microbial challenge associated with coitus. Thus, this response may help protect the reproductive tract from infections that would trigger implantation failure or abortion.

Hormonal regulation of reproductive tract mucin expression is observed in other species as well, although in many cases progesterone stimulates mucin expression. Potential progesterone receptor-binding sites are found in the mouse and human MUC1 promoters; however, it is not clear if these are functional. In rats, MUC4 expression also is strongly regulated by progesterone and estrogen. In addition, TGF-β down-regulates MUC4 expression in both mammary and uterine epithelium. Nonetheless, mucin expression changes differently in different parts of the female reproductive tract in response to steroid hormone influences. Thus, regulation of these genes is tissue-specific and complex. MUC1 appears to be differentially spliced as well since forms lacking the extracellular tandem repeats or the cytoplasmic tail also can be detected in certain cell types. It is not clear what fraction of the total MUC1 pool are contributed by these splice variants or exactly what functions these forms play in the implantation process. Other mucins including MUC3 and MUC4 also undergo alternative splicing to generate transmembrane or soluble variants.

Transport and Metabolism

Mucin assembly involves synthesis and transit of the core protein from the rough endoplasmic reticulum through the Golgi apparatus where most of the glycosylation occurs. Subsequently, the fully assembled mucin is transported to the cell surface. The entire process described above takes 60–90 min for the average mucin molecule in several cell types. Both MUC1 and MUC4 are synthesized from a single mRNA, but are proteolytically cleaved during their biosynthesis resulting in the formation of stable heterodimers of their respective ectodomains and transmembrane/cytoplasmic tail domains. While the exact nature of the association is not clear, in the case of MUC1 the complex is not dissociable by a number of agents including urea, heating, high salt, or reducing agents; however, it is readily dissociable by sodium dodecyl sulfate in a variety of normal cells and tumor-derived cell lines.

After arriving at the cell surface, MUC1 undergoes one of the three fates – (1) it can be recycled and further sialylated intracellularly and returned to the cell surface, or (2) it may be endocytosed and degraded in acidic compartments, presumably lysosomes, or (3) the ectodomains may be released or shed from the cell surface. Although the process of mucin shedding has been recognized for many years, the identity of the "sheddases" mediating this release has remained elusive. Recent evidence indicates that TACE/ADAM17 is one such sheddase. Other studies indicate that additional activities are involved as well. Mucin shedding is a property of both normal and tumor cells and, indeed, serum levels of shed ectodomains are used as markers of tumor burden in certain cancers. Shedding also may be stimulated by physiologically relevant agents, e.g., cytokines, as well as other compounds, e.g., phorbol esters. In the context of embryo implantation, stimulation of mucin shedding may be the key method to create cell-surface access to embryo receptors in certain species, e.g., rabbits and humans. In other species, shedding may be coupled with decreased mucin expression to clear the apical cell surface in preparation for embryo attachment.

Summary and Future Directions

The process of embryo implantation is under the control of the actions of ovarian steroids that coordinate the development of the embryo with the maturation of the endometrium. A panorama of receptors and binding factors may participate in a redundant fashion to promote embryo–uterine interactions during implantation. Nonetheless, the thick mucin-coat that covers the apical surface of the uterine epithelium under most conditions not only serves as a protective barrier to infection and enzymatic digestion, but also as a barrier to embryo attachment. This barrier must be removed in order for embryo attachment to occur. In many species, the same ovarian steroids that coordinate the implantation process also control mucin expression leading to the loss of the mucin coat at the time of implantation. In other species, including humans, ovarian steroids do not down-regulate mucin expression. Rather, localized activation of mucin-shedding at the cell surface has been proposed as a mechanism to create access to the apical cell surface of the uterine epithelium. Identification of factors responsible for regulation of mucin gene

expression as well as shedding may provide novel avenues to promote fertility as well as improve protection of the reproductive tract from infectious agents. In addition, recent, surprising findings that certain transmembrane mucins interact with intracellular signal transducing molecules suggest novel roles for these complex glycoproteins in sensing and triggering responses to the extracellular environment.

See Also the Following Articles

Oligosaccharide Chains: Free, *N*-Linked, *O*-Linked • Glycosylation in Cystic Fibrosis • JAK-STAT Signaling Paradigm • Mucin Family of Glycoproteins

Glossary

embryo implantation The process by which the mammalian embryo binds to and implants into the uterine wall.

mucin Any member of a class of glycoproteins that contain a large number of oligosaccharides linked through the hydroxyl groups of serine or threonine via N-acetylgalactosamine.

MUC1 The first transmembrane mucin glycoprotein to be completely molecularly cloned.

uterus The upper portion of the female reproductive tract into which the mammalian embryo normally implants and in which the fetus develops.

Further Reading

Bowen, J. A., Bazer, F. W., and Burghardt, R. C. (1996). Spatial and temporal analyses of integrin and Muc-1 expression in porcine uterine epithelium and trophectoderm *in vivo*. *Biol. Reprod.* **55**, 1098–1106.

Carson, D. D., Bagchi, I., Dey, S. K., Enders, A. C., Fazleabas, A. T., Lessey, B. A., and Yoshinaga, K. (2000). Embryo implantation. *Develop. Biol.* **223**, 217–237.

D'Cruz, O. J., Dunn, T. S., Pichan, P., Hass, G. G. Jr., and Sachdev, G. P. (1996). Antigenic cross-reactivity of human tracheal mucin with human sperm and trophoblasts correlates with the expression of mucin 8 gene messenger ribonucleic acid in reproductive tract tissues. *Fertil. Steril.* **66**, 316–326.

DeSouza, M. M., Surveyor, G. A., Price, R. E., Julian, J., Kardon, R., Zhou, X., Gendler, S., Hilkens, J., and Carson, D. D. (1999). MUC1/episialin: A critical barrier in the female reproductive tract. *J. Reprod. Immunol.* **45**, 127–158.

Gendler, S. J. (2001). MUC1, the renaissance molecule. *J. Mammary Gland Biol. Neoplasia* **6**, 339–353.

Gipson, I. K., Ho, S. B., Spurr-Michaud, S. J., Tisdale, A. S., Zhan, Q., Torlakovic, E., Pudney, J., Anderson, D. J., Toribara, N. W., and Hill, J. A. 3rd. (1997). Mucin genes expressed by human female reproductive tract epithelia. *Biol. Reprod.* **56**, 999–1011.

Hamilton, J. A., Iles, R. K., Gunn, L. K., Wilson, C. M., Lower, A. M., and Grudzinskas, J. G. (2002). High concentrations of CA 125 in uterine flushings: influence of cause of infertility and menstrual cycle day. *Gynecol. Endocrinol.* **16**, 19–25.

Hild-Petito, S., Fazleabas, A. T., Julian, J., and Carson, D. D. (1996). Mucin (Muc-1) expression is differentially regulated in uterine luminal and glandular epithelia of the baboon (Papio anubis). *Biol. Reprod.* **54**, 939–947.

Hoffman, L. H., Olson, G. E., Carson, D. D., and Chilton, B. S. (1998). Progesterone and implanting blastocysts regulate Muc1 expression in rabbit uterine epithelium. *Endocrinology* **139**, 266–271.

Lagow, E. L., and Carson, D. D. (2002). Synergistic stimulation of MUC1 expression in normal breast epithelia and breast cancer cells by interferon-gamma and tumor necrosis factor-alpha. *J. Cell Biochem.* **86**, 759–772.

Martoglio, A. M., and Kan, F. W. (1996). Immunohistochemical localization of oviductin in the endometrial lining of the golden hamster (*Mesocricetus auaratus*) during the estrous cycle and early gestation. *Histochem. J.* **28**, 449–459.

Pimental, R. A., Julian, J., Gendler, S. J., and Carson, D. D. (1996). Synthesis and intracellular trafficking of Muc-1 and mucins by polarized mouse uterine epithelial cells. *J. Biol. Chem.* **271**, 28128–28137.

Surveyor, G. A., Gendler, S. J., Pemberton, L., Das, S. K., Chakraborty, I., Julian, J., Pimental, R. A., Wegner, C. C., Dey, S. K., and Carson, D. D. (1995). Expression and steroid hormonal control of Muc-1 in the mouse uterus. *Endocrinology* **136**, 3639–3647.

Thathiah, A., and Carson, D. D. (2002). Mucins and blastocyst attachment. *Rev. Endocr. Metabol. Disord.* **3**, 87–96.

Thathiah, A., Blobel, C. P., and Carson, D. D. (2003). Tumor necrosis factor-alpha converting enzyme/ADAM 17 mediates MUC1 shedding. *J. Biol. Chem.* **278**, 3386–3394.

Yong, P., Gu, Z., Luo, J. P., Wang, J. R., and Tso, J. K. (2002). Antibodies against the C-terminal peptide of rabbit oviductin inhibit mouse early embryo development to pass 2-cell stage. *Cell Res.* **12**, 69–78.

Biography

Daniel Carson is the Trustees Distinguished Professor and Chairman of the Department of Biological Sciences at the University of Delaware. His principal research interests are in the area of cell surface and extracellular matrix biology with particular emphasis on reproduction and development. He holds a Ph.D. from Temple University Medical School and served as a postdoctoral fellow at Johns Hopkins University and a faculty member at the M.D. Anderson Cancer Center in Houston, Texas. He has authored many primary research and review articles and is a member of several professional societies including the American Society for Molecular Biology and Biochemistry, the Society for the Study of Reproduction, the American Society for Cell Biology, the Society for Developmental Biology, and the American Society for Matrix Biology.

Multiple Sequence Alignment and Phylogenetic Trees

Russell F. Doolittle
University of California, San Diego, California, USA

The alignment of macromolecular sequences is a computer-assisted procedure for gathering information about the evolutionary relatedness of nucleotide or amino acid sequences. Algorithms of various kinds can then be used to analyze the alignments in a way that reflects similarities or differences among the individual sequences. Phylogenetic trees depict these relationships graphically. Phylogenetic trees constructed from nucleotide or amino acid sequences have provided remarkable insights, both with regard to the evolution and relationships of life forms, and to the evolution and functions of the macromolecules themselves.

The two kinds of macromolecule, nucleic acids and proteins, present somewhat different challenges for alignment. Nucleic acids usually involve only four character states (A, G, C, and T/U), whereas protein sequences involve, with rare exception, 20 character states (the 20 amino acids). (Formally, "characters" are the positions in a sequence and the "character states" are the bases or amino acids that occupy them.) In either case the problem involves distinguishing chance matches from those due to common ancestry.

Alignment implies adjusting one or the other character strings by the insertion of gaps. The gaps are justified because, it is known that the insertion or deletion of nucleotides can occur in genetic material. Still, some limit needs to be imposed on the number of gaps, or any two strings of characters could be made virtually identical simply by skipping along until a match is found. Accordingly, a system is usually employed that has appropriate rewards for matches and penalties for gaps. The penalty for a gap can also be set to be dependent on the length of the gap, although gap length is seldom a major concern.

The quality (reliability) of an alignment will depend on how dissimilar the two sequences are. As two proteins or nucleic acids continue to diverge, a point will eventually be reached where it will not be possible to distinguish common ancestry from chance matching on the basis of sequence comparison alone. No matter what kind of scoring scheme is employed, there is no sharp cut-off. Because of the intrinsic variance of the process, there will always be a nebulous region referred to as the "twilight zone." For a pair of sufficiently long amino acid sequences, say a hundred residues or more, the region of uncertainty is usually thought to be between 15 and 25% identity (Figure 1). When shorter sequences are compared, chance matches will be an even bigger concern. A measure of confidence about common ancestry can be obtained by comparing the alignment scores of randomized sequence pairs of the same lengths and compositions, as the two sequences under study.

Binary Alignment

Nucleotide Sequences

The alignment of two strings of characters with a computer depends on pre-determined criteria. In the simplest case, only identities are tallied, i.e., a match involves having exactly the same character state. The use of matched non-identities can provide much information, however, especially when highly divergent sequences are involved. For example, in nucleic acids, transitions (A/G and C/T or C/U) occur much more frequently than do transversions (A/T and G/T or A/U and G/U), and are much more common when corrected for what would be expected from random occurrence. As a result, matches that are the apparent result of transversions may weigh more heavily in order to compensate for the likelihood of multiple transitions at a single site.

As might be expected, interchanges between similar amino acids are much more common than between those with very different structures and properties. Alignment schemes that use substitution tables (matrices) can be constructed that take account of the favored likelihood of such matches and weigh their occurrences accordingly.

Ribosomal RNA

The alignment of ribosomal RNA sequences, and the phylogenetic inferences made from them was the original basis for dividing all of life into three realms,

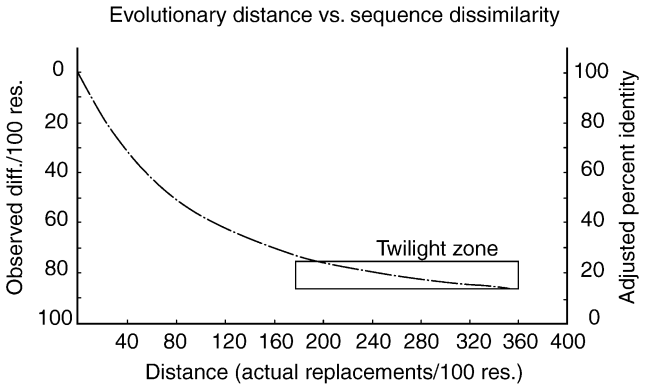

FIGURE 1 Partly as a result of back mutations and multiple mutations at the same site, the divergence of two sequences from a common ancestral sequence follows the course of a negative exponential. Other factors, including the favored likelihood of certain interchanges over others, also contribute. See glossary and text for explanation of twilight zone.

an observation since borne out by many other considerations. Since then, various kinds of ribosomal RNA sequences (5S, small subunit and large subunit) from thousands of different organisms have been determined and used to a great advantage in charting phylogenetic relationships. For these purposes, computer alignments are often limited to certain sets of preferred sites that are well calibrated with regard to their propensity for change.

Mitochondrial DNA

Phylogenetic studies of eukaryotes have been greatly aided by the now routine determination of complete mitochondrial DNA sequences. Generally speaking, these sequences change at a faster rate than nuclear DNA, making mitochondrial DNA sequences especially useful for determining relationships between closely related organisms.

Amino Acid Sequences

The simplest and arguably most informative expression of resemblance for two amino acid sequences is their percent identity. Even so, sequence alignments can be greatly improved by the use of substitution tables that provide scores for every possible amino acid interchange. A substitution table provides a weight for each interchange relative to what would be expected if those interchanges only occurred by chance and were not favored by genetic or structural considerations. Typically, these matrices give weights to each of the 20 sets of (matched) identical residues, as well as to the 190 possible interchanges. Many such tables have been devised, each based on some logical premise. Among the most commonly used are the accepted point mutation 250 (PAM250) matrix and blocks substitution matrix 62 (BLOSUM62) (Figure 2). In these two tables, interchanges with positive scores are more likely to occur than expected by chance, and those with negative scores less likely.

PAM matrices are generated in a sophisticated manner and take into account not only the frequencies of the individual amino acids but also their propensities for change. The suffix attached to the acronym, as in PAM120 or PAM250, denotes how many cycles of calculated mutation were conducted to generate a particular matrix. For example, PAM250 implies 250 rounds of change, and is most useful for rather dissimilar sequences.

An alternative set of tables can be constructed simply on the basis of amino acid frequencies in the individual columns of block alignments. Block alignments are prepared from ungapped segments of large numbers of homologous sequences. Scores for all possible interchanges can be calculated simply by comparing the observed frequency of an interchange with the frequency expected on the basis of the overall occurrences of the two amino acids. These BLOSUM tables have proved surprisingly effective. Suffices are used here to indicate how dissimilar the sequences were in the blocks from which values were calculated. In BLOSUM62, for example, all of the sequences in the block alignment were less than 62% identical.

Global versus Local Alignments

A global alignment ordinarily involves an entire protein sequence, whereas a local alignment involves only a portion of a sequence. The popular searching program basic local alignment search tool (BLAST) finds the highest scoring matching segments within two sequences. The Smith–Waterman algorithm also searches for best matching subsets for two sequences.

In contrast, the Needleman–Wunsch algorithm is designed to find the best global alignment between two amino acid sequences. It is also, well suited for accommodating any kind of substitution matrix and allows for suitable penalties for gaps.

Multiple Alignments

Considerably more information accrues when several homologous sequences are available for alignment. Such alignments can aid the protein scientist in determining the most essential residues in a protein, to the point that given enough divergent sequences, the active site of an enzyme may be inferred even without experimental data. More commonly, the evolutionary history of organisms or proteins is the target. Multiple alignments

	C	S	T	P	A	G	N	D	E	Q	H	R	K	M	I	L	V	F	Y	W	
	9	–1	–1	–3	0	–3	–3	–3	–4	–3	–3	–3	–3	–1	–1	–1	–1	–2	–2	–2	C
		4	1	–1	1	0	1	0	0	0	–1	–1	0	–1	–2	–2	–2	–2	–2	–3	S
C	12		5	–1	0	–2	0	–1	–1	–1	–2	–1	–1	–1	–1	–1	0	–2	–2	–2	T
S	0	2		7	–1	–2	–2	–1	–1	–1	–2	–2	–1	–2	–3	–3	–2	–4	–3	–4	P
T	–2	1	3		4	0	–2	–2	–1	–1	–2	–1	–1	–1	–1	–1	0	–2	–2	–3	A
P	–3	1	0	6		6	0	–1	–2	–2	–2	–2	–2	–3	–4	–4	–3	–3	–3	–2	G
A	–2	1	1	1	2		6	1	0	0	1	0	0	–2	–3	–3	–3	–3	–2	–4	N
G	–3	1	0	–1	1	5		6	2	0	–1	–2	–1	–3	–3	–4	–3	–3	–3	–4	D
N	–4	1	0	–1	0	0	2		5	2	0	0	1	–2	–3	–3	–2	–3	–2	–3	E
D	–5	0	0	–1	0	1	2	4		5	0	1	1	0	–3	–2	–2	–3	–1	–2	Q
E	–5	0	0	–1	0	0	1	3	4		8	0	–1	–2	–3	–3	–3	–1	2	–2	H
Q	–5	–1	–1	0	0	–1	1	2	2	4		5	2	–1	–3	–2	–3	–3	–2	–3	R
H	–3	–1	–1	0	–1	–2	2	1	1	3	6		5	–1	–3	–2	–2	–3	–2	–3	K
R	–4	0	–1	0	–2	–3	0	–1	–1	1	2	6		5	1	2	1	0	–1	–1	M
K	–5	0	0	–1	–1	–2	1	0	0	1	0	3	5		4	2	3	0	–1	–3	I
M	–5	–2	–1	–2	–1	–3	–2	–3	–2	–1	–2	0	0	6		4	1	0	–1	–2	L
I	–2	–1	0	–2	–1	–3	–2	–2	–2	–2	–2	–2	–2	2	5		4	–1	–1	–3	V
L	–6	–3	–2	–3	–2	–4	–3	–4	–3	–2	–2	–3	–3	4	2	6		6	3	1	F
V	–2	–1	0	–1	0	–1	–2	–2	–2	–2	–2	–2	–2	2	4	2	4		7	2	Y
F	–4	–3	–3	–5	–4	–5	–4	–6	–5	–5	–2	–4	–5	0	1	2	–1	9		11	W
Y	0	–3	–3	–5	–3	–5	–2	–4	–4	–4	0	–4	–4	–2	–1	–1	–2	7	10		
W	–8	–2	–5	–6	–6	–7	–4	–7	–7	–5	–3	2	–3	–4	–5	–2	–6	0	0	17	

FIGURE 2 Two different substitution matrices. BLOSUM62 is shown in the upper right, and the PAM250 in the lower left. Matches or interchanges with positive scores are more likely to occur than expected by chance, and those with negative scores less likely.

can also be used to construct "profiles" or "patterns" that are then used to search databases for more distantly related sequences.

Various methods of multiple sequence alignments may vary subtly. The mathematically optimal alignment of multiple sequences may differ significantly from the real history of events leading to the sequences, and these alignments may differ from those based on three-dimensional structure information. Because it is usually history that is being sought, and because the biological processes of interest operate in a binary fashion (species divergences and gene duplications), the preferred clustering process begins with the most similar pair of sequences, progressively incorporating more distant relatives. More weight is accorded to the more similar pairs, the logic being that those are the more reliable data.

Constructing Phylogenetic Trees

Many different ways of constructing phylogenetic trees from aligned sequences have been developed, and numerous programs are available that perform the operations automatically. Although some procedures actually construct the alignment and the tree simultaneously, in most cases the alignment is made first, after which the tree is calculated from it. One of the most important caveats for all molecular phylogenists is embodied in the slogan "Bad alignment, bad tree." Thus, many workers submit a set of sequences to some computerized regimen and accept the emergent tree, together with some formulized set of statistics allegedly providing some measure of confidence in it. It is always prudent to examine the alignment first. One common shortcoming becomes evident when one or more of the sequences being aligned are significantly shorter than the others. Long unmatched stretches will distort the relative global resemblances. Similar problems will occur with mosaic proteins in which only parts of the sequences are homologous or in which segments have been interchanged. The worst outcomes are the results of including sequences that are not homologous.

Phylogenetic trees can be dissected into two components, the branching order and the branch lengths.

Sometimes cladograms are made that make no attempt to quantify branch lengths, concentrating only on the grouping (branching order) of the entries. On another note, there is always the problem of determining the root of a phylogenetic tree. Ordinarily, accessory information over and beyond that contained in the sequences is needed to establish the root with any confidence.

Distance Methods

Distance methods depend on a table of pairwise distances being derived from the scores accumulated during the alignment process. In the simplest case, the number of differences between each pair of sequences can be used. More commonly, scores determined with a substitution matrix are transformed into units of evolutionary distance. Once the distance matrix has been constructed, the tree can be calculated by a clustering algorithm. These often involve the method of least squares, an effort being made to reconcile the individual pairwise distances with the smaller number of constituent branch lengths in a global tree.

Maximum Parsimony

Maximum parsimony strives to find the tree that can be constructed from the smallest number of mutations. There are numerous versions of the procedure, the most common of which attempt to minimize the overall tree length. In these procedures the individual positions in the sequences are considered column by column, in contrast to the overall pairwise distances used in distance matrix methods.

Maximum Likelihood

Maximum likelihood involves an evaluation procedure based on the probabilities of interchange at different nodes in the tree. In this case one starts with a model tree, and tests it for the probabilities of observed character matches and interchanges based on the character states that exist at neighboring nodes. The probabilities for all nodes are summed, and the most probable tree is the one with the highest total likelihood score.

Summary

The tremendous power of multiple sequence alignment procedures stems directly from the fact that all life forms descend from a common ancestor (or a small number of forms that could freely exchange genes). That most of biology and biochemistry is the result of the duplication and modification of a set of primitive genes seems beyond dispute. During evolution, an enormous binomial expansion of homologous sequences has occurred, the radiation of species on the one hand leading to orthologous genes with the same function in different organisms, and gene duplications on the other allowing for diversification of function within species by parologous genes. When sufficient data are available, properly constructed phylogenetic trees can distinguish between these two. Occasionally, sequence entries may occur on phylogenetic trees in unexpected positions, the result of genes having been transferred laterally between species. In any case, the relatively slow rate of change in many genes is what has made possible the enlightened reconstruction of ancient events.

See Also the Following Articles

mRNA Polyadenylation in Eukaryotes • mRNA Processing and Degradation in Bacteria • Pre-tRNA and Pre-rRNA Processing in Bacteria • Pre-tRNA and Pre-rRNA Processing in Eukaryotes • Ribosome Assembly • Ribosome Structure

Glossary

BLOSUM (BLOcks SUbstitution Matrix) A table of values reflecting the frequencies of amino acids at the same positions in a series of block alignments.

bootstrap A method for determining the confidence level for a branching order in a phylogenetic tree.

homologue A sequence related to another by common ancestry.

indel An insertion or deletion of characters in a macromolecular sequence leading to a gap in the alignment.

orthologue A homologous sequence reflecting a pair of gene products related by direct (orthologous) descent.

PAM A pronounceable acronym for an Accepted Point Mutation that has led to an amino acid replacement.

paralogue A homologous sequence reflecting a pair of genes related as a result of a gene duplication.

twilight zone The region of low similarity for pairs of sequences for which the distinction between common ancestry and chance matching is difficult.

Further Reading

CLUSTAL (for aligning sequences and tree construction) http://www.ebi.ac.uk/clustalw.

Feng, D. F., and Doolittle, R. F. (1987). Progressive sequence alignment as a perequisite to correct phylogenetic trees. *J. Mol. Evol.* **25**, 351–360.

Fitch, W. M., and Margolish, E. (1967). Construction of phylogenetic trees. *Science* **155**, 279–284.

Henikoff, J. G., and Henikoff, S. (1996). Blocks database and its applications. *Meth. Enzymol.* **266**, 88–105.

Higgins, D. G., Thompson, J. D., and Gibson, T. J. (1996). Clustal using CLUSTAL for multiple sequence alignments. *Meth. Enzymol.* **266**, 383–402.

Needleman, S. B., and Wunsch, C. D. (1970). A general method applicable to the search for similarities in the sequences of two proteins. *J. Mol. Biol.* **48**, 443–453.

Phylip (for tree construction) http://evolution.genetics.washingtonu.edu/phylip.html.

Phylodendron (for tree construction) http://iubio.bio.indiana/treeapp/.
Ribosomal sequence alignments: www.rna.iomb.utexas.edu/.
Saitou, N. (1996). Reconstruction of gene trees from sequence data. *Meth. Enzymol.* **266**, 427–449.
Schwartz, R. M., and Dayhoff, M. O. (1978). Matrices for detecting distant relationships. In *Atlas of Protein Sequence and Structure* (M. O. Dayhoff, ed.) pp. 353–358. National Biomed. Res. Found, Washington, DC.

BIOGRAPHY

Russell F. Doolittle is a Research Professor at the Center for Molecular Genetics, University of California, San Diego. His principal research interests center around the evolution of protein structure and function. He has a Ph.D. in biochemistry from Harvard (1962) and did post-doctoral work in Sweden. He was an early advocate of using computers to study amino acid sequences as an aid to characterizing proteins.

Muscarinic Acetylcholine Receptors

Neil M. Nathanson
University of Washington, Seattle, Washington, USA

Acetylcholine (ACh) is an important neurotransmitter in both the central and peripheral nervous systems. ACh is synthesized in the cytoplasm of nerve terminals by the enzyme choline acetyltransferase, and is then transported into synaptic vesicles. Depolarization of the nerve terminal causes an influx of calcium into the nerve terminal and evokes the release of ACh into the synaptic cleft; the release of ACh can be blocked by botulinum toxin. The actions of ACh are terminated by the enzyme ACh-sterase, which hydrolyzes ACh. The activity of ACh-sterase can be inhibited by drugs such as neostigmine and the nerve gas agent sarin.

ACh is released from a nerve terminal and binds to a receptor on the cell surface of a target cell to allow transfer of information across a chemical synapse. Sir Henry Dale in 1914 divided receptors for ACh into two classes based on their distinct pharmacological properties, nicotinic and muscarinic. Muscarinic ACh receptors (mAChR) are present on central and peripheral neurons, and in such target organs of the parasympathetic nervous systems as cardiac and smooth muscle, and many exocrine glands. The binding of ACh to mAChR can be blocked by antagonists such as atropine.

The Muscarinic Acetylcholine Receptor Gene Family

While pharmacological and biochemical analyses suggested for many decades after Dale's classification that there was only a single type of muscarinic receptor, drugs were eventually developed that distinguished between muscarinic receptors in different tissues. For example, gallamine was an antagonist at nicotinic receptors that selectively blocked muscarinic receptors in the heart compared to other tissues, while pirenzepine blocked muscarinic acetylcholine receptor (mAChR) in certain neurons with higher affinity than in the heart. These studies indicated that there were multiple pharmacologically distinct muscarinic receptors. In the 1980s, mAChR were purified from both heart and brain, which allowed the isolation of cDNA and genomic clones encoding the mAChR. There are five subtypes of mAChR, termed M_1, M_2, M_3, M_4, and M_5, which are encoded by distinct genes and differentially expressed in various organs and parts of the nervous system (Table I).

Muscarinic Receptor-Mediated Signal Transduction

Muscarinic Receptors Signaling Utilizes G Proteins

While nicotinic acetylcholine (ACh) receptors are ligand-gated ion channels (i.e., the same protein both binds ACh and acts as an ion channel), mAChR are members of the G protein-coupled-receptor (GPCR) superfamily. G proteins are a family of GTP-binding heterotrimeric proteins (they consist of three non-identical subunits) and they couple receptors to various effector proteins, such as adenylyl cyclase, phospholipase C, and ion channels. In the inactive state, GDP is bound to the α-subunit. The binding of ACh to mAChR promotes the dissociation of GDP and the binding of GTP to the α-subunit. This in turn causes the dissociation of the α-subunit from the $\beta\gamma$-subunits; both the α- and $\beta\gamma$-subunits can interact with effector proteins to regulate their activity. The α-subunits have GTPase activity which can be increased by the action of regulator of G protein signaling (RGS) proteins. This hydrolysis of GTP to GDP promotes the reassociation of the α- and $\beta\gamma$-subunits and terminates signaling unless ACh is still present to reinitiate the signaling cycle.

Muscarinic Receptor-Mediated Regulation of Second Messenger Pathways

The mAChR can be divided into two groups on the basis of both sequence similarities and functional responses. The M_1, M_3, and M_5 receptors preferentially couple to the Gq family of G proteins, whose α-subunits can activate phospholipase C (PLC). PLC activity produces two intracellular second messenger, inositol trisphosphate, which causes release of calcium from intracellular stores, and diacylglycerol, which activates protein

TABLE I

Subtypes of Muscarinic Receptors

Subtype	Number of amino acids	G-protein family	Some tissues with high expression
M_1	460	G_q	Cortex, hippocampus, striatum
M_2	466	G_i/G_o	Heart, cerebellum
M_3	590	G_q	Exocrine glands, smooth muscles cortex, thalamus
M_4	479	G_i/G_o	Striatum
M_5	532	G_q	Hippocampus, ventral tegmentum

The table shows the number of amino acids in the five human mAChR subtypes, the G-protein family to which each receptor preferentially couples, and representative tissues which express the various subtypes.

kinase C. The increased intracellular calcium in turn can produce many potential effects, such as activation of protein kinases, activation or inhibition of adenylyl cyclase, activation of phoshodiesterases, and activation of nitric acid synthetase, which can result in increased intracellular cGMP levels. The M_2 and M_4 receptors preferentially couple to the Gi family of G proteins to inhibit adenylyl cyclase activity, thus lowering intracellular cAMP levels. The types of signals produced by any mAChR can depend on both the level of receptor expression and the particular complement of signaling proteins expressed in a given cell.

Ion Channels

Many of the physiological responses mediated by the activation of mAChR on excitable cells are due to the regulation of the activity of ion channels. Regulation of ion channel activity can occur by many different mechanisms. Modulation of ion channel activity can occur due to protein phosphorylation. For example, activation of protein kinase C or decreased activity of cAMP-dependent protein kinase (due to inhibition of adenylyl cyclase activity) can lead to decreased activity of sodium and calcium channels, respectively. Activation of tyrosine kinases can regulate potassium channel activity.

Another mechanism is the regulation of ion channel activity directly by intracellular second messengers. Increased intracellular calcium can increase the activity of calcium-activated potassium channels, and increased cyclic GMP can activate cyclic nucleotide-gated ion channels. In addition, $\beta\gamma$-subunits released following activation of Gi-family G protein can interact with and regulate ion channel activity. For example, inwardly rectifying potassium channels in the heart are activated in this manner following M_2 mAChR activation.

Mitogen-Activated Protein Kinase (MAPK) and Related Pathways

Muscarinic receptors can mediate regulation of a series of protein kinase cascades implicated in a wide variety of processes, including cell growth, differentiation, and apoptosis. These protein kinase cascades lead to activation of the MAPKs Erk1 and Erk2, p38 kinase, and c-Jun terminal kinase. The particular cascades which are regulated, the mechanisms responsible for this regulation, and whether there is activation or inhibition of a particular kinase pathway depend both on the specific subtype of mAChR and the cell type the receptor is expressed in.

Structural Studies

Transmembrane Topology

Like other members of the GPCR superfamily, the muscarinic receptors are heptahelical, that is, they have seven helical transmembrane domains, with the amino-terminal extracellular and the carboxyl-terminal intracellular. The amino-terminal domains of the various mAChR subtypes contain asparagine residues which are sites for N-linked glycosylation. Based on the crystal structure determined for the prototypical GPCR rhodopsin and on mutagenesis and structural analyses of both the mAChr and other GPCR, it is likely that the transmembrane helices are arranged in a bundle.

Ligand Binding to the mAChR

ACh binds to the mAChR by interacting in a crevice with multiple transmembrane domains in the plane of the membrane. A negatively charged aspartic acid residue in the third transmembrane domain interacts with the positively charged ammonium group of ACh. Mutagenesis experiments have also implicated specific residues in the second, fifth, sixth, and seventh transmembrane domains in the binding of cholinergic ligands.

Regions of the mAChR Involved in Coupling to G Proteins

The binding of ACh to the mAChR induces a conformational change in the receptor which allows it to activate the appropriate G protein(s). The regions responsible for determining the specificity of coupling of the mAChR to G proteins has been determined primarily by construction of chimeric receptors between two mAChR, such as M_2 and M_3, which couple to different G proteins. The membrane proximal portions of the third cytoplasmic loop are the main determinants of the specificity of G protein coupling, although other regions such as the second intracellular domain may also play a role in mAChR-G protein interactions.

Muscarinic Receptor Actions *in vivo*

Muscarinic Receptor Actions in the Periphery

Muscarinic receptors are present in many target organs of the autonomic nervous system. A generalization based on pharmacological and molecular genetic approaches is that the M_2 receptors are present in heart, while the M_3 receptor is present in smooth muscles and exocrine glands, however, this generalization must be tempered by the presence of additional subtypes of mAChR present in low abundance in both cardiac and smooth muscles and by the possibility of differences in subtype expression between different animal species. Muscarinic receptors decrease the rate and force of contraction of the heart, and increase the tone and motility of the gastro-intestinal and urinary tracts. Muscarinic receptors increase secretions from salivary and sweat glands, and cause bronchoconstriction and increased bronchial secretions. Intravenous administration of ACh causes vasodilation. This is due not to activation of mAChR on the smooth muscle cells but to activation of the mAChR on the endothelial cells in the blood vessel. mAChR activation results in the production of NO, which then diffuses out of the endothelial cells and into the smooth muscle cells, resulting in relaxation of the blood vessel.

Muscarinic Receptor Actions in the Central Nervous System

Muscarinic receptors play an important role in the central nervous system. Many studies have implicated mAChR in learning and memory. Administration of muscarinic antagonists interfere with performance in many learning and memory tests, and the decreased cognition in patients with Alzheimer's disease is thought to be due in part to impaired muscarinic transmission. Both pharmacological and genetic experiments have implicated the M_1 mAChR in memory and learning, although it is likely that multiple muscarinic receptor subtypes play a role in these processes.

Muscarinic receptors in the spinal cord and at supraspinal sites (i.e., the brain) can mediate an analgesic response. Genetic studies in mice show that both the M_2 and M_4 receptors are involved in this anti-nociceptive effect.

Muscarinic receptors have been implicated in many other processes as well. For example, muscarinic receptors regulate the function of the basal ganglia, where multiple subtypes of muscarinic receptors modulate dopaminergic signaling. M_5 receptors are present in the ventral tegmentum and are involved in drug reward mechanisms.

Pharmacological analyses carried out over many years have led to the development of a number of drugs which produce their therapeutic actions by either activating or blocking muscarinic receptors. The increased understanding of the actions of individual mAChR subtypes should be a great aid in the development of drugs with increased therapeutic actions while decreasing effects at undesired mAChR subtypes.

See Also the Following Articles

Mitogen-Activated Protein Kinase Family • Nicotinic Acetylcholine Receptors • Phospholipase C

Glossary

agonist A drug which binds to a receptor and mimics the actions of a natural transmitter.

antagonist A drug which binds to a receptor and blocks the action of an agonist.

G-proteins A family of proteins which bind GTP and which couple receptors to signaling proteins such as ion channels, adenylyl cyclase, and phospholipase C.

neurotransmitter Chemical signal released by a neuron.

Further Reading

Anagnostaras, S. G., Murphy, G. G., Hamilton, S. E., Mitchell, S. L., Rahnama, N. P., Nathanson, N. M., and Silva, A. J. (2003). Selective cognitive dysfunction in acetylcholine M1 muscarinic receptor mutant mice. *Nature Neurosci.* **6**, 51–58.

Birdsall, N. J. M., Nathanson, N. M., and Schwarz, R. D. (2001). Muscarinic receptors: It's a knockout. *Trends Pharmacol. Sci.* **22**, 215–219.

Caulfield, M. P., and Birdsall, N. J. M. (1998). International union of pharmacology: XVII. Classification of muscarinic receptors. *Pharmacol. Rev.* **50**, 279–290.

Duttaroy, A., Gomeza, J., Gan, J. W., Siddiqui, N., Basile, A. S., Harman, W. D., Smith, P. L., Felder, C. C., Levey, A. I., and Wess, J. (2002). Evaluation of muscarinic agonist-induced analgesia in muscarinic acetylcholine receptor knockout mice. *Mol. Pharmacol.* **62**, 1084–1093.

Gutkin, J. S. (1998). The pathways connecting G protein-coupled receptors to the nucleus through divergent mitogen-activated protein kinase cascades. *J. Biolog. Chem.* **273**, 1839–1842.

Levey, A. I. (1996). Muscarinic ACh receptor expression in memory circuits: Implications for treatment of Alzheimer disease. *Proc. Natl. Acad. Sci. USA* **93**, 13541–13546.

Nathanson, N. M. (1987). Molecular properties of the muscarinic acetylcholine receptor. *Annu. Rev. Neurosci.* **10**, 195–236.

Nathanson, N. M. (2000). A multiplicity of muscarinic mechanisms: Enough signaling pathways to take your breath away. *Proc. Natl. Acad. Sci. USA* **97**, 6245–6247.

Wess, J. (1996). Molecular biology of muscarinic acetylcholine receptors. *Crit. Rev. Neurobiol.* **10**, 69–99.

Biography

Neil M. Nathanson is a Professor in the Department of Pharmacology, University of Washington School of Medicine. He received the Ph.D. in Biochemistry from Brandies University, and carried out postdoctoral training at the National Institutes of Health and the University of California, San Francisco. His research interests are focused on the regulation of signaling and expression of muscarinic receptors and receptors for neurotrophic factors.

Myosin Motors

Roy E. Larson
University of Sao Paulo, Sao Paulo, Brazil

Movement is a fundamental property of living matter. Specialized molecules with mechano-chemical properties are responsible for cellular motility and its macroscopic manifestations, such as muscle contraction. The myosins make up a large family of molecular motors that feature a conserved mechano-chemical domain, capable of transforming the chemical energy of ATP hydrolysis into the generation of force and movement along filamentous actin tracks. Although first characterized as the molecular power generator of muscle contraction, myosins are now known to be ubiquitous in virtually all mammalian cell types as well as widely distributed amongst eukaryotic organisms, both in plants and animals. They have multifunctional roles in many cellular processes, ranging from cytokinesis and pseudopodia extension to pigment granule transport and cytoplasmic streaming. Over the past 15 years, researchers have identified ~150 myosin genes, making up ~18 distinct structural classes, referred to as myosins I–XVIII, within what is now called the myosin superfamily of molecular motors. Although structural variations amongst the myosins reflect their specific cellular type and function, and also their phylogeny, there is a basic architectural plan followed by these motors.

Overall Molecular Architecture

The protein structure of myosins can be divided into three principal structural and functional domains. The highly conserved, mechano-chemical generator, usually referred to as the "head domain," is almost universally positioned at the amino terminal portion of the protein and contains the actin-binding and adenosine triphosphate (ATP) hydrolysis sites (Figure 1). The crystal structures have been determined from at least five myosins, widely distant on the evolutionary scale (vertebrate skeletal and smooth muscle myosin, slime mold myosin, scallop muscle myosin, and vertebrate class V myosin), which revealed very similar atomic structures amongst them, indicating that the basic machinery for movement has been highly conserved. Immediately following the head domain is an elongated, α-helical region to which calmodulin and/or calmodulin-like light chains bind, forming the regulatory or "neck domain" (Figure 1). This domain acts as a lever arm to amplify small movements in the head domain. In several myosins the neck domain inhibits the mechano-chemical cycle and thus acts as the regulatory element that triggers the mechano-chemical events when this inhibition is released by factors, such as calcium binding to or phosphorylation of the light chains. The rest of the molecule is referred to as the "tail domain" and is the most structurally diverse part, varying extensively between classes, yet maintaining significant homology within a class. The tail domains are regions of interaction with lipid membranes, proteins, and signaling molecules, important for site recognition, receptor binding, and specific functions. Many myosins are dimerized via the formation of intertwined α-helices, referred to as coiled coils (Figure 2). The prime example is skeletal muscle myosin II whose tail domain is completely composed of a coiled-coil motif, which aligns and joins together with other tail domains to form the bipolar thick filaments of the sarcomere. The myosin II class is often referred to as "conventional" myosin due to its historical identification and characterization. However, it is now viewed as being quite unique in that no other class within the myosin superfamily is known to organize into filaments. Clearly the myosins II have been refined by evolution, culminating in their role in the generation of macroscopic force and velocity of skeletal muscle contraction. The tail domains of all other myosins have globular regions, and are without the propensity for filament formation, although they may or may not form coiled coils and, thus, can exist as monomeric or dimeric structures (Figure 2).

Evolutionary Diversity and Phylogenic Classification

With the advent of DNA sequencing, ~18 classes of myosin genes have been identified based on comparisons of the amino acid sequences of the head domains, even though this domain is highly conserved across the board for the myosin superfamily. On the other hand, the tail domains are quite unique for each myosin class,

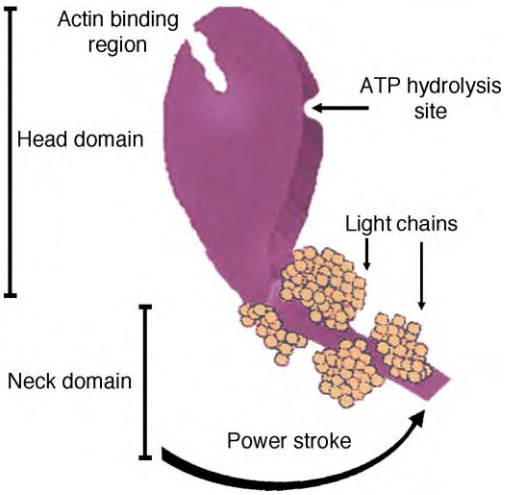

FIGURE 1 Schematic diagram of the head and neck domains of myosin showing the relative positions of the actin-binding region to the ATP site and to the light chains in the neck domain. The rotation of the neck domain which represents the power stroke is indicated as a curved arrow. (Drawn by Silvia Andrade.)

indicating that evolution selected a tail-domain design for the specific cellular function(s) of that particular myosin class. Phylogenetic analysis of the head sequences also indicated that myosins diversified quite early in eukaryotic evolution. Curiously, myosin precursors have not been identified in prokaryotes. It is tempting to speculate that the appearance of myosin motors with their diversity of tails was an evolutionary innovation that furnished impetus for eukaryotic cells to experiment and gain new niches.

Mechano-Chemical Features and Regulation

A description of the molecular mechanism of energy transduction by mechanoenzymes has been a challenge for workers in the field for half a century. The determination, during the last decade, of the atomic structures of myosin in several conformational states with nucleotide derivatives bound has brought this goal close to realization. An overall description of the molecular events taking place during the mechano-chemical cycle, which lead to movement and force generation, is given here. There are three elements to keep in mind: first, ATP binds to the myosin head domain at an active site capable of hydrolyzing it to adenosine diphosphate (ADP) and inorganic phosphate (Pi); second, myosin binds to filamentous actin (F-actin) either strongly or weakly depending on the molecular conformation of the myosin; third, conformational changes in myosin structure occur depending on the nucleotide occupying the active site. Beginning with the binding of ATP to the nucleotide-binding site in the head domain of myosin, this event puts the myosin in a weak F-actin-binding conformation, i.e., most of the myosin is not bound to F-actin. Myosin quickly hydrolyzes the ATP; however, the hydrolysis products, ADP and Pi, are only slowly released from the active site. The energy of ATP binding and hydrolysis is conserved in the high-energy conformation of the myosin at this point, which is considered to be the fully cocked state. The slow release of products from the active site dissipates this conformational energy and puts myosin into its lowest energy state, ready for the binding of another ATP molecule. In the absence of F-actin the energy of this conformational change from the high to low energy state is dissipated as heat. However, when F-actin is bound to myosin, the rate of release of ADP and/or Pi dramatically increases, while the myosin is converted to its strong F-actin-binding conformation. Thus, when F-actin is present, the conformational change in the myosin molecule associated with product release occurs simultaneously with tight coupling to F-actin and, rather than being immediately dissipated as heat, is now converted to tension development and work. The exact conformational change that occurs, referred to as the "power stroke," is a rotation of ~90° of the myosin neck domain relative to the F-actin orientation (see Figure 1). Thus, for native muscle myosin with the neck domain connected to its tail domain that, in turn, is embedded in a thick filament, the power stroke will move the thick filament relative to the actin filament. A return to the weak binding state and disassociation of myosin from F-actin occurs with the rebinding of ATP to the nucleotide site, thus initiating a new cycle. In summary, the mechano-chemical cycle results from the tight coupling of protein conformational energy in the myosin head and neck domains with chemical energy (ATP binding and hydrolysis) and cyclic transitions between strong and weak binding between myosin and F-actin. As presented, this cycle will continue as long as myosin can contact actin and a steady

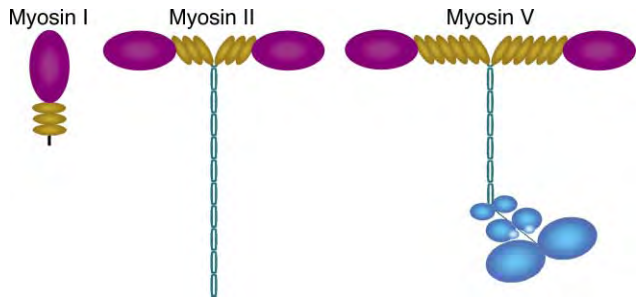

FIGURE 2 Schematic diagram of three typical myosins representing classes I, II, and V. The tear-drop structures (light gray) represent the head domains; the small oblong structures (dark gray) represent the light chains; the stippled circles represent globular regions of the tail domain. The coiled coil is represented by intertwined lines. (Drawn by Silvia Andrade.)

supply of ATP is maintained. (n.b. *Rigor mortis* results from the interruption of the metabolic supply of ATP that comes with death and represents the strong binding, low-conformational energy state of the actomyosin in muscle at the end of the power stroke).

As with any motor, it is desirable to be able to turn the myosin mechano-chemical cycle on and off, depending on need. There are several mechanisms to do this, most of which use calcium ion as the triggering element. For example, in striated muscles a calcium-sensitive system of regulator proteins decorates F-actin and sterically blocks access of the myosin head to the actin sites. Calcium relieves this blockage, such that an increase in its intracellular concentration determines actomyosin activation. For molluscan myosin and vertebrate smooth muscle myosin, regulation is myosin-based, in that an inhibitory effect of the neck domain can be relieved by calcium binding to a light chain or by calcium-activated phosphorylation. For other myosins the mechanisms of regulation are less well understood, although calcium and/or phosphorylation most likely play a role.

A Multitude of Cellular Functions

Simplistically, myosins have two functional ends: the motor end, which generates force and movement on actin filaments, and the tail end, which links it to its cargo or, as in the special case of muscle, to itself forming bipolar filaments. Surprisingly, in spite of their highly conserved structure, the myosin heads differ in a fundamental property related to their mechano-chemical cycle, which affects their cellular function. Individual myosin II molecules bind to actin for only a small fraction of the cycle duration. This property is essential for the smooth sliding of myosin filaments in muscle with their arrays of many heads interacting with the organized actin filaments of the sarcomere. On the other hand, at least two myosins (a class V and a class VI myosin) have the property of "processivity," i.e., they are able to move as individual molecules along actin filaments for some distance without losing contact. Present evidence indicates that these two-headed myosins walk in a "hand-over-hand" manner along the actin filament, each head binding to actin for more than 50% of the cycle duration. This property, therefore, allows these myosins, acting alone, to carry cargo without losing a grip on the actin track.

The tail domain determines the enormous diversity of function within the myosin superfamily and dictates the specific function of each myosin. To exemplify this diversity, it is noted that in a single vertebrate cell type – the human intestinal epithelial cell – there have been identified at least 12 myosins, representing 6 classes. Sorting out the specific functions of individual myosins and myosin classes has been a formidable challenge to researchers in the field. The involvement of myosins in three general areas has been described: membrane-associated movements, intracellular vesicle and particle transport, and intracellular signaling. Besides their role in contraction of muscle cells, myosins are involved in amoeboid movements, pseudopodia extensions, phagocytosis, exocytosis, cytokinesis, cell gliding over a surface, and other manifestations of plasma membrane dynamics. The myosins of class II, which include the muscle myosins, are one of the principal actors in these processes, due in part to their tail's ability to form bipolar filaments and thus generate constrictive forces. Also, however, the single-headed, class I myosins are involved in membrane interactions due to the phospholipid-binding regions in their tail domains, thus giving them the ability to orient force generation directly toward membranes.

Many examples of intracellular vesicle and organelle transport that depend on myosin motors have been found. The dramatic cytoplasmic streaming in plants is a good example. This process involves class XI myosins, one of only two classes found in plants (the other is class VIII). Mutations in class V myosins result in defective distribution of pigment granules in melanocytes of vertebrates and of membrane vesicles in dividing yeast. Several linker proteins have been described that connect myosin motors to their cargo, such as melanophilin and Rab27a, which link pigment granules to myosin V, and Vac17p, a key component of the myosin receptor on yeast vacuoles. The demonstration in squid axoplasm of translocation of moving vesicles from microtubule tracks to actin filaments suggested that organelle transport involves cooperative interactions between microtubule- and actin-based systems. These examples serve to illustrate that myosin motors have important roles in the transport of membrane delimited organelles, but attention has been given to recent evidence that myosins also transport macromolecular complexes. Myo4p, a class V myosin in yeast, is directly involved, together with at least two other proteins, in the transport of a specific mRNA, encoding a transcription factor, to the daughter cell of budding yeast, thus playing an essential role in regulation of differential gene expression in these organisms.

Being molecular effectors, one may expect that myosins are end-targets for cell signaling. As previously discussed, myosins bind to calmodulin and are indeed activated or modulated by ionic calcium and protein kinases, all of which are important intracellular messengers for signal transduction pathways. However, it is noteworthy that myosins also seem to participate in the signaling pathways themselves, as a kind of motorized signaling devise. Evidence for this first appeared upon analysis of the tail sequences, where sequence motifs related to cell signaling pathways, such as the SH3, PDZ, and PH motifs, were recognized in several distinct

myosin classes. These motifs are signals for protein–protein and protein–phosphoinositide binding that participate in the assembly of signaling complexes, although the functional role of myosins containing these signal motifs is still not clear. The tail domain of myosins IX has a region with homology to GTPase-activating proteins (GAPs), which act as molecular switches in the organization of the actin cytoskeleton, particularly in the formation of cell–matrix focal adhesions. Overexpression of a myosin IX in HeLa cells caused the cells to lose actin filament organization and substrate contact, resulting in their rounding up and release from the substrate. These examples illustrate that myosins are not only final targets for cellular signaling, but potential intermediate players in the signaling cascades. Myosins are involved in other cell processes in ways not well understood, such as mitotic spindle orientation in yeast, phototransduction in *Drosophila* retina and auditory function of the vertebrate inner ear. There is much to be learned about the functional roles of myosin motors throughout the biosphere.

Myosins in Disease

The human genome has ~40 myosin genes, composing 12 classes. As described above, myosins are fundamentally important in many cellular processes and thus would be expected to underlie cellular dysfunction in human disease. In fact, several myosins have been identified as the causes of hereditary diseases. A major cause of familial hypertrophic cardiomyopathy lies in mutations of the head domain of cardiac muscle myosin II. Usher syndrome, the most common cause of inherited deaf–blindness in children, has been linked to mutations in myosin VII. Also, mutations in myosin XV have been identified in human nonsyndromic deafness; and in myosin VI in the Snell's Waltzer mouse, which suffers from deafness due to degeneration of the sensory neuroepithelia in the inner ear. Thus, different myosin classes have important roles that converge in the auditory system. In Griscelli syndrome, where children exhibit hair hypopigmentation, linked to severe immunological and neurological deficits that frequently lead to early death, mutations have been identified in myosin V or Rab27a, a protein that links myosin V to organelles. It is likely that more connections will be made between human disease and myosin function as genetic probes and analyses increase.

See Also the Following Articles

Actin Assembly/Disassembly • Calcium/Calmodulin-Dependent Protein Kinase II • DNA Sequence Recognition by Proteins

Glossary

α-helix The specific helical arrangement of a polypeptide chain formed by hydrogen bonding between atoms of peptide bonds separated by four amino acids along the chain.

calmodulin A calcium-binding protein, found ubiquitously in eukaryotic cells, that acts as a calcium-sensitive regulator of many enzymes.

focal adhesions Sites of attachment of cells to underlying substratum involving specialized protein complexes linking the intracellular actin cytoskelton to the extracellular matrix.

sarcomere The functional contractile unit of muscle cells consisting of interdigitating actin and myosin filaments.

Further Reading

Alberts, B., Johnson, A., Lewis, J., Raff, M., Roberts, K., and Walter, P. (2002). *Molecular Biology of the Cell*. Garland Science, New York.

Cooper, G., and Hausman, R. (2003). *The Cell. A Molecular Approach*. ASM Press, Washington.

Lodish, H., Berk, A., Matsudeira, P., Kaiser, C., Kreiger, M., Scott, M., Zipursky, S., and Darnell, J. (2003). *Molecular Cell Biology*. Freeman, New York.

Kendrick-Jones, J. (2003). The Myosin Home Page. MRC Laboratory of Molecular Biology. www.proweb.org/myosin.

Pollard, T., and Earnshaw, W. (2002). *Cell Biology*. Saunders, Philadelphia.

Sellers, J., and Goodson, H. (1995). Motor proteins 2: Myosin. *Protein Profiles* **2**(12), 1323–1423.

Biography

Roy E. Larson is a Professor and Chairman of the Department of Cellular and Molecular Biology and Pathogenic Bioagentes at the Faculdade de Medicina de Ribeirao Preto, Universidade de Sao Paulo, Brazil. He holds a Ph.D. in molecular biology from the University of Pennsylvania and received his postdoctoral training at Yale University. His principal research interests are in cytoskeletal dynamics. He initially purified and identified myosin V from vertebrate brain and was instrumental in its biochemical and structural characterization.

Editors-in-Chief

William J. Lennarz

State University of New York at Stony Brook, Stony Brook, New York, USA

Section: Lipids, Carbohydrates, Membranes and Membrane Proteins

WILLIAM J. LENNARZ received his B.S. in Chemistry from Pennsylvania State University and a Ph.D. in Organic Chemistry from the University of Illinois. Subsequently he carried out postdoctoral work at Harvard with Konrad Bloch on fatty acid biosynthesis. In 1962 he was appointed Assistant Professor at Johns Hopkins in the Department of Physiological Chemistry. After promotion to Associate Professor in 1967, and full Professor in 1971, he remained at Hopkins until 1983. At that time, he was appointed Robert A. Welch Professor and Chair of the Department of Biochemistry and Molecular Biology at the University of Texas Cancer Center, M.D. Anderson Hospital. In 1989 he became a Leading Professor and Chair of the Department of Biochemistry and Cell Biology at SUNY at Stony Brook. In 1990 he founded and became Director of the Institute for Cell and Developmental Biology at Stony Brook.

Dr. Lennarz has served on many national and international committees. He has served as President of the Biochemistry Chairman's Organization, President of the American Society for Biochemistry and Molecular Biology and President of the Society for Glycobiology. He was a member of the Executive Committee of the International Union of Biochemistry and Molecular Biology for almost a decade.

He has presented special lectures at the University of Notre Dame, the NIH, the University of West Virginia, Johns Hopkins University, Florida State University, the University of California at San Diego, the University of Arkansas, Indiana University and the Medical College of Virginia.

He is a member of the National Academy of Sciences. The focus of his early work was on lipids and bacterial cell surfaces. More recent efforts have been in the structure, biosynthesis and function of cell surface glycoproteins. The biosynthesis studies initially were carried out in liver and oviduct, but these efforts now are focused in yeast. The functional studies have concentrated on the role of cell surface glycoproteins in fertilization and early development in the sea urchin and, more recently, the frog. For over 30 years Dr. Lennarz' research has been supported by federal sources, primarily the National Institutes of Health. Recently he was appointed Distinguished Professor and Chair of his department.

M. Daniel Lane

The Johns Hopkins University, School of Medicine, Baltimore, Maryland, USA

Section: Metabolism, Vitamins and Hormones

M. DANIEL LANE received B.S. and M.S. degrees in 1951 and 1953 from Iowa State University and a Ph.D. in 1956 from the University of Illinois. He was a Senior Postdoctoral Fellow with Professor Feodor Lynen at the Max-Planck Institute Fur Zellchemie in Munich. Following faculty positions at Virginia Polytechnic Institute and New York University School of Medicine, he joined the faculty at the Johns Hopkins University School of Medicine in 1969 and served as DeLamar Professor and Director of the Department of Biological Chemistry from 1978 to 1997. He is presently Distinguished Service Professor at Johns Hopkins. In 2002 he received an honorary degree, Doctor of Humane Letters, from Iowa State University.

Dr. Lane was elected to membership in the National Academy of Sciences (in 1987) and was elected as a Fellow of the American Academy of Arts and Sciences (in 1982) and of the American Society of Nutritional Sciences (in 1996). He received the Mead Johnson Award from the American Society for Nutritional Sciences in 1966 for his research on biotin-dependent enzymes and in 1981, the William C. Rose Award from the American Society for Biochemistry and Molecular Biology for his work on the insulin receptor. In 1990–1991 Lane served as President of the American Society of Biochemistry and Molecular Biology. He has presented many named lectureships (including the

Feodor Lynen Lecture in Germany in 1999) and served on numerous editorial boards including the Journal of Biological Chemistry and the Annual Reviews of Biochemistry. Currently he is Associate Editor for Biochemical and Biophysical Research Communications.

Dr. Lane has published 280 research papers in major scientific journals. His early work focused on various enzymatic CO_2 fixation reactions, notably the mechanisms by which the B-vitamin, biotin, functions in enzymes to catalyze carboxylation. Dr. Lane's work on the regulation of acetyl-CoA carboxylase, the key regulatory enzyme of fatty acid synthesis, led him to his present interests which are to understand the basic mechanisms of lipogenesis, adipogenesis and the consequence of aberrations in these processes, most notably obesity. Research currently underway in his laboratory focuses on: (1) the genes that signal stem cell "commitment" to the adipocyte lineage and subsequent differentiation into adipocytes, and (2) the mechanisms by which the region of the brain, known as the hypothalamus, monitors and controls the drive to eat.

Associate Editors

Ernesto Carafoli

Università degli Studi di Padova, Padova, Italy
Section: Bioenergetics

ERNESTO CARAFOLI earned his M.D. degree at the University of Modena in Italy in 1957. After postdoctoral studies in the Laboratory of Albert L. Lehninger at Johns Hopkins University in the mid 1960s he returned to his home institution in Italy where he worked until 1973, when he was appointed Professor of Biochemistry at the Swiss Federal Institute of Technology (ETH) in Zurich. He returned to Italy in 1998 as a Professor of Biochemistry at the University of Padova, where he now also directs the newly founded Venetian Institute of Molecular Medicine (VIMM).

Dr. Carafoli became interested in calcium as a signaling agent during his post-doctoral days at Johns Hopkins. When he arrived there his main interests were in mitochondrial bioenergetics and it was thus natural for him to expand them to the newly discovered area of mitochondrial calcium transport. He was involved in most of the early discoveries in the field, and he continued to work on mitochondria and calcium after his return to Italy and until he moved to the ETH. There his interests still remained focused on calcium, but the emphasis shifted to the proteins that transport it across membranes and to those that process its signal. His favorite object of study became the calcium pumps, especially that of the plasma membrane, an enzyme which is essential to the regulation of calcium homeostasis and thus to the well being of cells. His contributions on the enzyme, especially after he purified it in 1979, have helped establishing most of its properties and have clarified important problems of mechanism, regulation and structure.

Dr. Carafoli has authored or co-authored about 450 peer-reviewed articles and reviews, and has edited or co-edited about 20 books. He has served on the Editorial or Advisory Boards of several periodicals and has organized about 30 International Workshops and Symposia. He has been featured as a plenary or honorary lecturer at numerous events ranging from specialized Workshops to International Symposia and Congresses. Dr. Carafoli's honors and awards include several international prizes and medals, memberships in several Academies, and three honorary degrees.

Don W. Cleveland

University of California, San Diego, La Jolla, CA, USA
Section: Cell Architecture and Function

DON W. CLEVELAND has been a longstanding contributor to the elucidation of regulation of assembly of mitotic spindles and chromosome movement and how errors in these contribute to the chromosome loss characteristic of human tumors. He discovered the tubulin gene families encoding the major subunits of microtubules and the first mammalian example of control of gene expression through regulated RNA instability. He identified components required for microtubule nucleation and anchoring during spindle assembly. He identified the first human centromeric protein (CENP-B). He then discovered CENP-E, the centromere-associated, microtubule-motor that he showed to be essential for chromosome attachment and for activation and silencing of the mitotic checkpoint, the cell cycle control mechanism that prevents errors of chromosome segregation in mitosis.

Dr. Cleveland has also been a leading force in dissecting the disease mechanism for major human neurodegenerative disorders. He initially purified and characterized tau, the microtubule-associated protein that assembles aberrantly in human dementias including Alzheimer's disease and Pick's disease. He established that the extreme asymmetry of neurons acquired during development is achieved with a deformable array of interlinked neurofilaments, microtubules and actin. He showed that disorganization of neurofilament arrays caused selective death of motor neurons in mice and humans. He also demonstrated that neuronal death could also arise by a toxicity of mutant superoxide dismutase unrelated to its normal activity, thereby uncovering the mechanism underlying the major genetic form of amyotrophic lateral sclerosis. He showed that this toxicity could be

sharply ameliorated by lowering the content of neurofilaments.

Dr. Cleveland is currently Head, Laboratory for Cell Biology in the Ludwig Institute for Cancer Research and Professor of Medicine, Neurosciences and Cellular and Molecular Medicine at the University of California at San Diego. He is also the Editor of the Journal of Cell Biology and Current Opinion in Cell Biology.

Jack E. Dixon

University of California, San Diego School of Medicine,
La Jolla, CA, USA
Section: Protein/Enzyme Structure, Function, and Degradation

JACK E. DIXON earned his Ph.D. in Chemistry at the University of California, Santa Barbara in 1971 and did his postdoctoral training in Biochemistry at the University of California, San Diego.

Dr. Dixon is a pioneer and leader in the structure and function of the protein tyrosine phosphatases (PTPases). He demonstrated that the unique catalytic mechanism of the PTPases proceeds via a novel cysteine-phosphate intermediate. He discovered the first dual-specificity phosphatase, which led to the identification of the cell cycle protein, $p80^{cdc25}$, as a phosphatase. He also showed that the bacteria responsible for the plague or "black death" harbor the most active PTPase ever described. He and his colleagues went on to demonstrate that this PTPase gene product is essential for the pathogenesis of the bacteria. Dr. Dixon and his colleagues determined X-ray structures for both tyrosine and dual specificity phosphatases. Dr. Dixon also found that sequences outside of the PTPase catalytic domain could function to direct the subcellular localization of the PTPases and to restrict their substrate specificity. This is now a widely acknowledged regulatory paradigm for the PTPases. Recently, his laboratory demonstrated that the tumor suppressor gene, PTEN, which shares sequence identity with the PTPases, catalyzes the dephosphorylation of a lipid second messenger, phosphatidylinositol 3,4,5-trisphosphate (PIP3). This represents the first example of a PTPase dephosphorylating a lipid second messenger. PIP3 activates the protein kinase, AKT, which plays a critical role in controlling the balance between apoptosis and cell survival. The loss of the PTEN gene elevates PIP3 levels leading to constitutive activation by AKT and oncogenesis. Recently, Dr. Dixon in collaboration with Nikola Pavletich determined the X-ray structure of PTEN. Their structure–function studies explain the PIP3 substrate specificity of PTEN and also provide a rationale for many of the mutations seen in human cancers. Earlier in his career, Dr. Dixon adopted the tools of molecular biology as they became available in the 1970s, and his laboratory was among the first to use synthetic oligonucleotides to isolate and extensively characterize cDNAs encoding peptide hormones.

Dr. Dixon is Professor of Pharmacology, Cellular and Molecular Medicine and Chemistry and Biochemistry and Dean of Scientific Affairs at the University of California, San Diego. He is a member of the National Academy of Sciences, the Institute of Medicine and the American Academy of Arts and Sciences. Dr. Dixon was the recipient of the 2003 William C. Rose Award from the American Society for Biochemistry and Molecular Biology.

John H. Exton

Howard Hughes Medical Institute, Vanderbilt University School of Medicine, Nashvillie, TN, USA
Section: Signaling

JOHN H. EXTON was born and educated in New Zealand where he received his medical training and a Ph.D. in Biochemistry from the University of Otago in 1963. He did postdoctoral work at Vanderbilt University under Charles R. Park and Earl W. Sutherland, and became an Investigator of the Howard Hughes Medical Institute in 1968 and Professor of Physiology in 1970. He is presently Professor of Molecular Physiology and Biophysics, Professor of Pharmacology and a Hughes Investigator at Vanderbilt.

Dr. Exton's research initially focused on the changes in carbohydrate metabolism in liver during diabetes and treatment with various hormones using the perfused rat liver as the experimental system. His work concentrated on gluconeogenesis and identified the enzymatic reactions that were under control by insulin, epinephrine (adrenaline), glucagon and glucocorticoids, and demonstrated the importance of cyclic AMP in the regulation of these reactions. The role played by the supply of substrates, especially of alanine, was also shown.

Dr. Exton then turned his attention to the action of epinephrine (adrenaline) and demonstrated that many of its actions were not mediated by cyclic AMP but by calcium ions. This led to study of the breakdown of inositol phospholipids by phospholipase C that underlay the increase in calcium. Later this resulted in the discovery of G_q, a novel G protein that activated phospholipase C. Further studies demonstrated that agonists caused the breakdown of another phospholipid (phosphatidylcholine) by another phospholipase (phospholipase D). Current work is focused on the physiological role of phospholipase D.

Dr. Exton has authored over 350 scientific articles and is presently an Associate Editor of the Journal of Biological Chemistry. He has served on many scientific review groups and as a reviewer for many journals. He has won numerous awards, most notably the Lilly

Award of the American Diabetes Association, Fellow of the American Association for the Advancement of Science and election to membership in the National Academy of Sciences.

Paul Modrich

Duke University Medical Center, Durham, NC, USA
Section: Molecular Biology

PAUL MODRICH is an Investigator of the Howard Hughes Medical Institute and James B. Duke Professor of Biochemistry at Duke University Medical Center. He received his undergraduate degree from M.I.T. and his Ph.D. in Biochemistry from Stanford University. His current research addresses the mechanisms of DNA repair. He has served on the editorial boards of the Journal of Biological Chemistry, Biochemistry, Proceedings of the National Academy of Sciences, and DNA Repair. His honors include election to National Academy of Sciences and the Institute of Medicine, the Pfizer Award in Enzyme Chemistry, the General Motors Mott Prize in Cancer Research, and the Pasarow Foundation Award in Cancer Research.

Preface

Biological Chemistry is defined as the chemistry of the compounds and processes that constitute living organisms. The ultimate goal, of course, is to understand and define biology at a mechanistic level. This was aptly stated in an historical treatise on the founding of the *Journal of Biological Chemistry*, where John Edsall quoted a statement in a letter from J. L. Loeb (in Berkeley), "The future of biology lies with those who attack its problems from a chemical point of view." What was an emerging field in 1900 with its origins in physiology, nutrition and chemistry has broadened and expanded to include numerous other fields including mechanistic enzymology, molecular biology, structural biology, cell biology, genomics, proteomics, bioinformatics, metabolomics and others, that were not defined as discrete fields at that time.

Modern biochemistry (biological chemistry) began with the accidental discovery by Eduard Buchner in 1897 that a cell-free yeast extract could carry out fermentation of glucose to alcohol and CO_2 *in the absence of intact cells*. He named the dissolved substance responsible for this process zymase, the substance(s) we now refer to as enzymes. Importantly, Buchner recognized the significance of his discovery. This ended the dogma of the time, perpetuated by Pasteur, the concept of *vitalism*; i.e., that fermentation (and presumably other complex biological phenomena) required the action of intact cells. Thus, serendipity and a prepared mind ushered in a new era of discovery. Now it became possible to dissect complex physiological processes and to study them with preparations free of the constraints of intact cells. Once a metabolic pathway/process was established, it became possible to purify the enzymes, cofactors and substrates involved, to reconstitute the process with purified components and to characterize the components chemically. What followed was an information explosion in the field of biochemistry and progression through a series of trends, each "in vogue" in its time. The identification of the dietary essentials, the hunt for the vitamins/cofactors, the hormones, identification of metabolic pathways and the enzymes involved, oxidative phosphorylation, protein synthesis, molecular biology—each developed as a primary focus.

The need to associate chemistry with function came early and was evident in the naming of departments and journals. Over time names changed from Agricultural Chemistry to Physiological Chemistry to Biochemistry to Biological Chemistry. An example is the Department of Biochemistry at the University of Wisconsin, which began in 1883 as the Department of Agricultural Chemistry.

Where are we headed? We have reached the point where the borders of these areas have become blurred. What constitutes cell biology, molecular biology/genetics, developmental biology, physiology, immunology—ultimately reduces to chemistry. To understand these processes we must know what the molecules are and understand how they interact, i.e. the basic chemistry. That is what this encyclopedia is about.

The breadth of content of this encyclopedia aims to cover major topics of modern biochemistry, each authored by an expert in the area. We feel that the coverage is broad and we have been inclusive in choice of topics. The encyclopedia is a reference work encompassing four volumes containing over 500 articles with more than 750 authors or coauthors. Each article/topic covers an important area of the field which reflects the point of view of the authors. Together the articles cover virtually every aspect of biology for which we have "mechanistic" information. For those who wish to probe more deeply into a topic, references to further readings are included at the end of each article. The editorial board that made decisions on coverage consists of seven members, each an expert representing a major area in the field of biochemistry. A dedicated effort was made to provide coverage that is as complete as possible. The content is presented at a level that we hope will be interpretable to interested individuals with some background in chemistry and biology. It is intended for such individuals rather than specialists with extensive scientific backgrounds in specific areas. It is aimed at the generalist as opposed to the specialist.

Finally, we would like to single out Gail Rice and Dr. Noelle Gracy for their enormous contribution in putting this encyclopedia together. They, in fact, were a driving force that brought this major work to completion.

Notes on the Subject Index

Abbreviations used in subentries without explanation:

CoA	coenzyme A
DAG	diacylglycerol
ELISA	enzyme-linked immunosorbent assay
ERK	extracellular-signal regulated kinase
GlcNAC	N-Acetylglucosamine
HPLC	high-pressure liquid chromatography
IP_3	inositol 1,4,5-triphosphate
MAP	mitogen-activated protein
MMP	matrix metalloproteinase
mtDNA	mitochondrial DNA
NADPH	nicotinamide-adenine dinucleotide phosphate
PFK-2/ FBPase-2	6-phosphofructo-2-kinase/fructose-2,6-bisphosphatase
PI3K	phosphatidylinositol 3-kinase
PIP_2	phosphatidylinositol 4,5-bisphosphate
PIP_3	phosphatidylinositol-3,4,5-triphosphate
PPAR	peroxisome proliferator-activated receptor
RPLC	reversed-phase high-performance liquid chromatography

Volume 1

Volume 2

Inorganic Biochemistry, Pages 417-420, Robert J. P. Williams

Inositol Lipid 3-Phosphatases, Pages 421-426, Gregory S. Taylor and Jack E. Dixon

Inositol Phosphate Kinases and Phosphatases, Pages 427-429, Stephen B. Shears

Insulin- and Glucagon-Secreting Cells of the Pancreas, Pages 430-435, Franz M. Matschinsky

Insulin Receptor Family, Pages 436-440, Paul F. Pilch and Jongsoon Lee

Integrin Signaling, Pages 441-445, Lawrence E. Goldfinger and Mark H. Ginsberg

Interferon Receptors, Pages 446-451, Christopher P. Elco and Ganes C. Sen

Intermediate Filament Linker Proteins: Plectin and BPAG1, Pages 452-457, Peter Fuchs and Gerhard Wiche

Intermediate Filaments, Pages 458-464, Kelsie M. Bernot and Pierre A. Coulombe

Intracellular Calcium Channels: cADPR-Modulated (Ryanodine Receptors), Pages 465-468, Antony Galione

Intracellular Calcium Channels: NAADP+-Modulated, Pages 469-472, Armando A. Genazzani and Marcella Debidda

Ion Channel Protein Superfamily, Pages 473-477, William A. Catterall

IP3 Receptors, Pages 478-481, Colin W. TaylorEdward Morris and Paula da Fonseca

Iron-Sulfur Proteins, Pages 482-489, Helmut Beinert

JAK-STAT Signaling Paradigm, Pages 491-496, Edward Cha and Christian Schindler

Keratins and the Skin, Pages 497-504, Pierre A. Coulombe and Kelsie M. Bernot

Ketogenesis, Pages 505-507, Janos Kerner and Charles L. Hoppel

Melanocortin System, Pages 617-620, Roger D. Cone

Membrane Fusion, Pages 621-626, Joshua Zimmerberg and Leonid V. Chernomordik

Membrane Transport, General Concepts, Pages 627-630, Stanley G. Schultz

Membrane Transporters:Na+/Ca2+ Exchangers, Pages 631-636, Jonathan Lytton

Membrane-Associated Energy Transduction in Bacteria and Archaea, Pages 637-645, Gunter Schafer

Metabolite Channeling: Creatine Kinase Microcompartments, Pages 646-651, Uwe Schlattner and Theo Wallimann

Metalloproteases, Pages 652-656, David S. Auld

Metalloproteinases, Matrix, Pages 657-665, Hideaki Nagase and Gillian Murphy

Metaphase Chromosome, Pages 666-671, Sharron Vass and Margarete M. S. Heck

Methyl-CpG-Binding Proteins, Pages 672-675, David G. Skalnik

Microtubule-Associated Proteins, Pages 676-682, Nobutaka Hirokawa and Reiko Takemura

Mitochondrial Auto-Antibodies, Pages 683-688, Harold Baum

Mitochondrial Channels, Pages 689-692, M. Catia Sorgato and Alessandro Bertoli

Mitochondrial DNA, Pages 693-696, Gottfried Schatz

Mitochondrial Genes and their Expression: Yeast, Pages 697-702, Piotr P. Slonimski and Giovanna Carignani

Mitochondrial Genome, Evolution, Pages 703-708, B. Franz Lang, Dennis V. Lavrov and Gertraud Burger

Mitochondrial Genome, Overview, Pages 709-715, Douglas C. Wallace

Mitochondrial Inheritance, Pages 716-719, Eric A. Shoubridge

Mitochondrial Membranes, Structural Organization, Pages 720-724, Carmen A. Mannella

Volume 3

Volume 4

Lipids, Carbohydrates, Membranes and Membrane Proteins

Carbohydrate Chains: Enzymatic and Chemical Synthesis; Vol.1 - Pages 307-313, Thomas J. Tolbert and Chi-Huey Wong

Cell–Matrix Interactions; Vol.1 - Pages 362-366, Janet A. Askari and Martin J. Humphries

Detergent Properties; Vol.1 - Pages 577-581, Darrell R. McCaslin

Endocytosis; Vol.2 - Pages 16-19, Julie G. Donaldson

Flippases; Vol.2 - Pages 123-127, Charles J. Waechter

Galectins; Vol.2 - Pages 171-174, R. Colin Hughes

GlcNAc Biosynthesis and Function, O-Linked; Vol.2 - Pages 189-192, Kaoru Sakabe and Gerald W. Hart

Glycation; Vol.2 - Pages 229-236, Suzanne R. Thorpe and John W. Baynes

Glycolipid-Dependent Adhesion Processes; Vol.2 - Pages 261-265, Senitiroh Hakomori

Glycoprotein Folding and Processing Reactions; Vol.2 - Pages 272-276, Armando J. Parodi

Glycoprotein-Mediated Cell Interactions, O-Linked; Vol.2 - Pages 277-282, Robert S. Haltiwanger

Glycoproteins, N-Linked; Vol.2 - Pages 283-292, Mark A. Lehrman

Glycoproteins, Plant; Vol.2 - Pages 293-296, Carolyn J. Schultz

Glycosylation in Cystic Fibrosis; Vol.2 - Pages 297-301, Andrew D. Rhim, Thomas F. Scanlin and Mary Catherine Glick

Glycosylation, Congenital Disorders of; Vol.2 - Pages 302-307, Hudson H. Freeze

Glycosylphosphatidylinositol (GPI) Anchors; Vol.2 - Pages 308-311, Anant K. Menon

Ion Channel Protein Superfamily; Vol.2 - Pages 473-477, William A. Catterall

Lectins; Vol.2 - Pages 535-540, Nathan Sharon and Halina Lis

Lipases; Vol.2 - Pages 571-575, Howard L. Brockman

Lipid Bilayer Structure; Vol.2 - Pages 576-579, Erwin London

Lipid Rafts; Vol.2 - Pages 584-587, Deborah A. Brown

Lipoproteins, HDL/LDL; Vol.2 - Pages 588-593, Fayanne E. Thorngate and David L. Williams

MDR Membrane Proteins; Vol.2 - Pages 605-609, Nathan C. Rockwell

Membrane Fusion; Vol.2 - Pages 621-626, Joshua Zimmerberg and Leonid V. Chernomordik

Mucin Family of Glycoproteins; Vol.2 - Pages 758-764, Juan Perez-Vilar and Robert L. Hill

Mucins in Embryo Implantation; Vol.2 - Pages 765-769, Daniel D. Carson

Neoglycoproteins; Vol.3 - Pages 11-15, Y. C. Lee and Reiko T. Lee

N-Linked Glycan Processing Glucosidases and Mannosidases; Vol.3 - Pages 46-49, Linda O. Tremblay and Annette Herscovics

Oligosaccharide Chains: Free, N-Linked, O-Linked; Vol.3 - Pages 161-164, Tadashi Suzuki

Phospholipid Metabolism in Mammals; Vol.3 - Pages 314-320, Claudia Kent

Phospholipid Synthesis in Yeast; Vol.3 - Pages 321-325, Gil-Soo Han and George M. Carman

Prostaglandins and Leukotrienes; Vol.3 - Pages 452-456, William L. Smith and Robert C. Murphy

Protein Glycosylation Inhibitors; Vol.3 - Pages 500-503, Alan D. Elbein

Proteoglycans; Vol.3 - Pages 549-555, Sara K. Olson and Jeffrey D. Esko

Secretory Pathway; Vol.4 - Pages 11-16, Karen J. Colley

Siglecs; Vol.4 - Pages 38-40, Ajit Varki

Sphingolipid Biosynthesis; Vol.4 - Pages 76-81, Martina Leipelt and Alfred H. Merrill, Jr.

Sphingolipid Catabolism; Vol.4 - Pages 82-87, Akira Abe and James A. Shayman

Sugar Nucleotide Transporters; Vol.4 - Pages 127-129, Carlos B. Hirschberg

Trehalose Metabolism; Vol.4 - Pages 251-255, Alan D. Elbein

Metabolism, Vitamins and Hormones

Amino Acid Metabolism; Vol.1 - Pages 90-95, Luc Cynober

Anaplerosis; Vol.1 - Pages 105-110, Raymond R. Russell, III and Heinrich Taegtmeyer

Bile Salts and their Metabolism; Vol.1 - Pages 159-163, Ulrich Beuers and Thomas Pusl

Biliary Cirrhosis, Primary; Vol.1 - Pages 164-169, Marshall M. Kaplan

Branched-Chain -Ketoacids; Vol.1 - Pages 186-191, David T. Chuang

Carnitine and -Oxidation; Vol.1 - Pages 314-318, Janos Kerner and Charles L. Hoppel

Cholesterol Synthesis; Vol.1 - Pages 451-455, Peter A. Edwards

Diabetes; Vol.1 - Pages 582-592, David W. Cooke

Fat Mobilization: Perilipin and Hormone-Sensitive Lipase; Vol.2 - Pages 85-89, Constantine Londos and Alan R. Kimmel

Fatty Acid Oxidation; Vol.2 - Pages 90-94, Horst Schulz

Fatty Acid Synthesis and its Regulation; Vol.2 - Pages 99-103, Steven D. Clarke and Manabu T. Nakamura

Gluconeogenesis; Vol.2 - Pages 197-203, Richard W. Hanson and Oliver E. Owen

Glucose/Sugar Transport in Bacteria; Vol.2 - Pages 204-207, Lan Guan and H. Ronald Kaback

Glucose/Sugar Transport in Mammals; Vol.2 - Pages 208-212, Silvia Mora and Jeffrey Pessin

Glycogen Metabolism; Vol.2 - Pages 244-248, Peter J. Roach

Glycogen Storage Diseases; Vol.2 - Pages 249-254, George H. Sack, Jr.

Glycolysis, Overview; Vol.2 - Pages 266-271, Robert A. Harris

Hexokinases/Glucokinases; Vol.2 - Pages 372-377, Emile Van Schaftingen

Insulin- and Glucagon-Secreting Cells of the Pancreas; Vol.2 - Pages 430-435, Franz M. Matschinsky

Ketogenesis; Vol.2 - Pages 505-507, Janos Kerner and Charles L. Hoppel

Ornithine Cycle; Vol.3 - Pages 172-177, Malcolm Watford

Pentose Phosphate (Hexose Mono Phosphate) Pathway; Vol.3 - Pages 211-215, Bernard R. Landau

Pentose Phosphate Pathway, History of; Vol.3 - Pages 216-225, John F. Williams

Phosphofructokinase-2/Fructose Bisphosphatase-2; Vol.3 - Pages 277-280, Daniel M. Raben

Photosynthesis; Vol.3 - Pages 330-335, Richard C. Leegood

Photosynthetic Carbon Dioxide Fixation; Vol.3 - Pages 336-341, Matthew J. Paul

Porphyrin Metabolism; Vol.3 - Pages 415-419, Mark Shepherd and Harry A. Dailey

Propionyl CoA–Succinyl CoA Pathway; Vol.3 - Pages 447-451, Wayne A. Fenton

Pyruvate Carboxylation, Transamination, and Gluconeogenesis; Vol.3 - Pages 606-610, Sarawut Jitrapakdee and John C. Wallace

Pyruvate Dehydrogenase; Vol.3 - Pages 611-615, Sam A. Johnson and James G. McCormack

Pyruvate Kinase; Vol.3 - Pages 616-619, Kosaku Uyeda

Starvation; Vol.4 - Pages 99-110, Oliver E. Owen and Richard W. Hanson

Tricarboxylic Acid Cycle; Vol.4 - Pages 256-262, Richard L. Veech

Urea Cycle, Inborn Defects of; Vol.4 - Pages 326-330, Marsha K. Fearing and Vivian E. Shih

Vitamin A (Retinoids); Vol.4 - Pages 354-359, Joseph L. Napoli

Vitamin B12 and B12-Proteins; Vol.4 - Pages 360-366, Bernhard Krautler

Vitamin C; Vol.4 - Pages 367-371, Robert B. Rucker and Francene Steinberg

Vitamin D; Vol.4 - Pages 372-377, Hector F. DeLuca and Margaret Clagett-Dame

Vitamin E; Vol.4 - Pages 384-388, Ute C. Obermuller-Jevic and Lester Packer

Vitamin K: Biochemistry, Metabolism, and Nutritional Aspects; Vol.4 - Pages 389-393, J. W. Suttie

Vitamin K: Blood Coagulation and Use in Therapy; Vol.4 - Pages 394-398, Matthew D. Stone and Gary L. Nelsestuen

Cell Architecture and Function

Chromosome Organization and Structure, Overview; Vol.1 - Pages 469-474, Elena Gracheva and Sarah C. R. Elgin

Cytokinesis; Vol.1 - Pages 556-561, Masanori Mishima and Michael Glotzer

Desmosomes and Hemidesmosomes; Vol.1 - Pages 569-576, Rachel L. Dusek, Jonathan C. R. Jones and Kathleen J. Green

Dynactin; Vol.1 - Pages 823-826, Trina A. Schroer

Dynein; Vol.1 - Pages 827-831, K. Kevin Pfister

Endoplasmic Reticulum-Associated Protein Degradation; Vol.2 - Pages 20-23, Maurizio Molinari

Focal Adhesions; Vol.2 - Pages 128-133, Eli Zamir and Benjamin Geiger

Golgi Complex; Vol.2 - Pages 312-315, Mark Stamnes

Heat/Stress Responses; Vol.2 - Pages 343-347, Davis T. W. Ng

Inositol Lipid 3-Phosphatases; Vol.2 - Pages 421-426, Gregory S. Taylor and Jack E. Dixon

Intermediate Filament Linker Proteins: Plectin and BPAG1; Vol.2 - Pages 452-457, Peter Fuchs and Gerhard Wiche

Intermediate Filaments; Vol.2 - Pages 458-464, Kelsie M. Bernot and Pierre A. Coulombe

Keratins and the Skin; Vol.2 - Pages 497-504, Pierre A. Coulombe and Kelsie M. Bernot

Kinesin Superfamily Proteins; Vol.2 - Pages 508-516, Nobutaka Hirokawa and Reiko Takemura

Kinesins as Microtubule Disassembly Enzymes; Vol.2 - Pages 517-521, Susan L. Kline-Smith and Arshad Desai

Meiosis; Vol.2 - Pages 610-616, Neil Hunter

Metalloproteinases, Matrix; Vol.2 - Pages 657-665, Hideaki Nagase and Gillian Murphy

Microtubule-Associated Proteins; Vol.2 - Pages 676-682, Nobutaka Hirokawa and Reiko Takemura

Mitosis; Vol.2 - Pages 743-747, Patricia Wadsworth and Nasser M. Rusan

Myosin Motors; Vol.2 - Pages 778-781, Roy E. Larson

N-End Rule; Vol.3 - Pages 6-10, Alexander Varshavsky

Neuronal Intermediate Filaments; Vol.3 - Pages 21-25, Ronald K. H. Liem

Nuclear Compartmentalization; Vol.3 - Pages 87-91, Kelly P. Smith and Jeanne B. Lawrence

Nuclear Envelope and Lamins; Vol.3 - Pages 92-95, Bryce M. Paschal

Nuclear Pores and Nuclear Import/Export; Vol.3 - Pages 109-114, Anita H. Corbett

Peroxisomes; Vol.3 - Pages 246-250, Suresh Subramani

26S Proteasome, Structure and Function; Vol.3 - Pages 469-473, Peter Zwickl and Wolfgang Baumeister

Protein Glycosylation, Overview; Vol.3 - Pages 504-509, Natasha E. Zachara and Gerald W. Hart

Rho GTPases and Actin Cytoskeleton Dynamics; Vol.3 - Pages 714-718, Priam Villalonga and Anne J. Ridley

Septins and Cytokinesis; Vol.4 - Pages 22-26, Makoto Kinoshita and Christine M. Field

SUMO Modification; Vol.4 - Pages 130-134, Frauke Melchior and Andrea Pichler

Tight Junctions; Vol.4 - Pages 187-189, Shoichiro Tsukita

Transcriptional Silencing; Vol.4 - Pages 200-203, Ann Sutton and Rolf Sternglanz

Tubulin and its Isoforms; Vol.4 - Pages 272-276, Eva Nogales

Unfolded Protein Responses; Vol.4 - Pages 319-325, David Ron

Vacuoles; Vol.4 - Pages 331-336, Christopher J. Stefan and Scott D. Emr

Protein/Enzyme Structure Function and Degradation

Allosteric Regulation; Vol.1 - Pages 68-73, Barry S. Cooperman

Aminopeptidases; Vol.1 - Pages 96-98, Ralph A. Bradshaw

Amyloid; Vol.1 - Pages 99-104, Ronald Wetzel

Aspartic Proteases; Vol.1 - Pages 123-127, Ben M. Dunn

B12-Containing Enzymes; Vol.1 - Pages 145-151, Vahe Bandarian and Rowena G. Matthews

Biotin; Vol.1 - Pages 174-178, Steven W. Polyak and Anne Chapman-Smith

Biotinylation of Proteins; Vol.1 - Pages 179-181, Ronald A. Kohanski

Calpain; Vol.1 - Pages 300-306, Hiroyuki Sorimachi and Yasuko Ono

Chemiluminescence and Bioluminescence; Vol.1 - Pages 399-404, Thomas O. Baldwin

Coenzyme A; Vol.1 - Pages 475-477, M. Daniel Lane

Collagenases; Vol.1 - Pages 478-481, Kenn Holmbeck and Henning Birkedal-Hansen

Collagens; Vol.1 - Pages 482-487, Darwin J. Prockop

Cysteine Proteases; Vol.1 - Pages 516-520, David J. Buttle and John S. Mort

Disulfide Bond Formation; Vol.1 - Pages 598-602, Hiram F. Gilbert

Elastin; Vol.2 - Pages 10-12, Judith Ann Foster

Enzyme Inhibitors; Vol.2 - Pages 31-37, Vern L. Schramm

Enzyme Kinetics; Vol.2 - Pages 38-44, Irwin H. Segel

Enzyme Reaction Mechanisms: Stereochemistry; Vol.2 - Pages 45-50, Ming-Daw Tsai, Li Zhao and Brandon J. Lamarche

Flavins; Vol.2 - Pages 118-122, Barrie Entsch and David P. Ballou

Heme Proteins; Vol.2 - Pages 354-361, Johannes Everse

HIV Protease; Vol.2 - Pages 384-387, Ben M. Dunn

Kinetic Isotope Effects; Vol.2 - Pages 522-527, Justine P. Roth and Judith P. Klinman

Lipid Modification of Proteins: Targeting to Membranes; Vol.2 - Pages 580-583, Marilyn D. Resh

Low Barrier Hydrogen Bonds; Vol.2 - Pages 594-598, Perry A. Frey

Metalloproteases; Vol.2 - Pages 652-656, David S. Auld

Peptide Amidation; Vol.3 - Pages 226-230, Mark J. Niciu, Richard E. Mains and Betty A. Eipper

Phage Display for Protein Binding; Vol.3 - Pages 251-255, Henry B. Lowman

Prions, Overview; Vol.3 - Pages 437-440, Cedric Govaerts and Fred E. Cohen

Proteases in Blood Clotting; Vol.3 - Pages 457-463, John D. Kulman and Earl W. Davie

Proteasomes, Overview; Vol.3 - Pages 464-468, Martin Rechsteiner

Protein Carboxyl Esterification; Vol.3 - Pages 474-477, Shilpa G. Lalchandani and Jeffry B. Stock

Protein Degradation; Vol.3 - Pages 484-492, Tomo ari and Alfred L. Goldberg

Protein Folding and Assembly; Vol.3 - Pages 493-499, David P. Goldenberg

Protein N-Myristoylation; Vol.3 - Pages 527-531, Erica Dutil Sonnenburg and Jeffrey I. Gordon

Protein Palmitoylation; Vol.3 - Pages 532-535, Robert J. Deschenes

Pteridines; Vol.3 - Pages 556-560, S. Colette Daubner and Paul F. Fitzpatrick

Pyridoxal Phosphate; Vol.3 - Pages 595-599, David E. Metzler

Regulated Intramembrane Proteolysis (Rip); Vol.3 - Pages 665-670, Jin Ye, Michael S. Brown and Joseph L. Goldstein

Secretases; Vol.4 - Pages 7-10, Robert L. Heinrikson

Selenoprotein Synthesis; Vol.4 - Pages 17-21, August Bock

Substrate Binding, Catalysis, and Product Release; Vol.4 - Pages 123-126, W. Wallace Cleland

Two-Hybrid Protein–Protein Interactions; Vol.4 - Pages 290-293, Ilya Serebriiskii and Erica A. Golemis

Tyrosine Sulfation; Vol.4 - Pages 294-297, Denis Corbeil and Wieland B. Huttner

Ubiquitin System; Vol.4 - Pages 299-303, Aaron Ciechanover and Michael H. Glickman

Ubiquitin-Like Proteins; Vol.4 - Pages 304-307, Edward T. H. Yeh

Zinc Fingers; Vol.4 - Pages 435-439, Mark Isalan

Bioenergetics

Calcium/Calmodulin-Dependent Protein Kinase II; Vol.1 - Pages 274-280, Andy Hudmon and Howard Schulman

Calcium-Binding Proteins: Cytosolic (Annexins, Gelsolins, C2-Domain Proteins); Vol.1 - Pages 287-293, Joachim Krebs

Calcium-Modulated Proteins (EF-Hand); Vol.1 - Pages 294-299, Robert H. Kretsinger

Cell Death by Apoptosis and Necrosis; Vol.1 - Pages 352-355, Pierluigi Nicotera

Chemiosmotic Theory; Vol.1 - Pages 405-412, Keith D. Garlid

Chemolithotrophy; Vol.1 - Pages 419-424, Alan B. Hooper

Chlorophylls and Carotenoids; Vol.1 - Pages 430-437, Hugo Scheer

Chloroplast Redox Poise and Signaling; Vol.1 - Pages 438-445, John F. Allen

Chloroplasts; Vol.1 - Pages 446-450, Nicoletta Rascio

Cytochrome b6f Complex; Vol.1 - Pages 521-527, Gunter A. Hauska and Thomas Schodl

Cytochrome bc1 Complex (Respiratory Chain Complex III); Vol.1 - Pages 528-534, Bernard L. Trumpower

Cytochrome c; Vol.1 - Pages 535-538, Hans Tuppy and Gunther Kreil

Cytochrome Oxidases, Bacterial; Vol.1 - Pages 539-543, Peter Brzezinski and Pia Adelroth

Cytochrome P-450; Vol.1 - Pages 544-549, Rita Bernhardt

Energy Transduction in Anaerobic Prokaryotes; Vol.2 - Pages 24-30, Gottfried Unden

ER/SR Calcium Pump: Function; Vol.2 - Pages 56-60, Giuseppe Inesi

ER/SR Calcium Pump: Structure; Vol.2 - Pages 61-65, Chikashi Toyoshima and Yuji Sugita

F1–F0 ATP Synthase; Vol.2 - Pages 73-79, Donata Branca

Ferredoxin; Vol.2 - Pages 104-106, Giuliana Zanetti and Vittorio Pandini

Luft's Disease; Vol.2 - Pages 599-601, Salvatore DiMauro

Membrane Transport, General Concepts; Vol.2 - Pages 627-630, Stanley G. Schultz

Membrane Transporters:Na+/Ca2+ Exchangers; Vol.2 - Pages 631-636, Jonathan Lytton

Membrane-Associated Energy Transduction in Bacteria and Archaea; Vol.2 - Pages 637-645, Gunter Schafer

Metabolite Channeling: Creatine Kinase Microcompartments; Vol.2 - Pages 646-651, Uwe Schlattner and Theo Wallimann

Mitochondrial Auto-Antibodies; Vol.2 - Pages 683-688, Harold Baum

Mitochondrial Channels; Vol.2 - Pages 689-692, M. Catia Sorgato and Alessandro Bertoli

Mitochondrial DNA; Vol.2 - Pages 693-696, Gottfried Schatz

Mitochondrial Genes and their Expression: Yeast; Vol.2 - Pages 697-702, Piotr P. Slonimski and Giovanna Carignani

Mitochondrial Genome, Evolution; Vol.2 - Pages 703-708, B. Franz Lang, Dennis V. Lavrov and Gertraud Burger

Mitochondrial Genome, Overview; Vol.2 - Pages 709-715, Douglas C. Wallace

Mitochondrial Inheritance; Vol.2 - Pages 716-719, Eric A. Shoubridge

Mitochondrial Membranes, Structural Organization; Vol.2 - Pages 720-724, Carmen A. Mannella

Mitochondrial Metabolite Transporter Family; Vol.2 - Pages 725-732, Ferdinando Palmieri and Martin Klingenberg

Mitochondrial Outer Membrane and the VDAC Channel; Vol.2 - Pages 733-736, Marco Colombini

Neuronal Calcium Signal; Vol.3 - Pages 16-20, Hilmar Bading

Nicotinamide Nucleotide Transhydrogenase; Vol.3 - Pages 50-56, Jan Rydstrom

Nuclear Genes in Mitochondrial Function and Biogenesis; Vol.3 - Pages 100-104, Alexander Tzagoloff and Carol L. Dieckmann

Oncocytes; Vol.3 - Pages 165-166, Bernard Tandler and Charles L. Hoppel

Oxygenases; Vol.3 - Pages 178-182, Osamu Hayaishi

Periplasmic Electron Transport Systems in Bacteria; Vol.3 - Pages 231-238, David J. Richardson, Gary Sawers and Rob J. M. Van Spanning

Phosphatidylinositol-3-Phosphate; Vol.3 - Pages 272-276, Joseph V. Virbasius and Michael P. Czech

Photosystem I, Structure and Function; Vol.3 - Pages 342-347, Petra Fromme

Photosystem I: FX, FA, and FB Iron–Sulfur Clusters; Vol.3 - Pages 348-356, Mikhail L. Antonkine and John H. Golbeck

Photosystem II Light Harvesting System: Dynamic Behavior; Vol.3 - Pages 357-362, Peter Horton and Alexander Ruban

Photosystem II: Assembly and Turnover of the D1 Protein; Vol.3 - Pages 363-366, Eira Kanervo and Eva-Mari Aro

Photosystem II: Protein Components; Vol.3 - Pages 367-374, James Barber

Photosystem II: Water Oxidation, Overview; Vol.3 - Pages 375-380, Fabrice Rappaport and Pierre Joliot

Plasma-Membrane Calcium Pump: Structure and Function; Vol.3 - Pages 385-389, Emanuel E. Strehler

Plastocyanin; Vol.3 - Pages 390-393, Elizabeth L. Gross

Protein Import into Mitochondria; Vol.3 - Pages 510-515, Johannes M. Herrmann and Walter Neupert

P-Type Pumps: Copper Pump; Vol.3 - Pages 561-564, Ilia Voskoboinik and James Camakaris

P-Type Pumps: H+/K+ Pump; Vol.3 - Pages 565-570, Jai Moo Shin and George Sachs

P-Type Pumps: Na+/K+ Pump; Vol.3 - Pages 571-576, Peter L. Jorgensen

P-Type Pumps: Plasma-Membrane H+ Pump; Vol.3 - Pages 577-581, A. Brett Mason and Carolyn W. Slayman

Purple Bacteria: Electron Acceptors and Donors; Vol.3 - Pages 582-585, Evaldas Katilius and Neal W. Woodbury

Purple Bacteria: Photosynthetic Reaction Centers; Vol.3 - Pages 586-594, C. Roy D. Lancaster

Pyrimidine Biosynthesis; Vol.3 - Pages 600-605, Monika Loffler and Elke Zameitat

Quinones; Vol.3 - Pages 621-627, Giorgio Lenaz and Maria Luisa Genova

Respiratory Chain and ATP Synthase; Vol.3 - Pages 671-675, David G. Whitehouse and Anthony L. Moore

Respiratory Chain Complex I; Vol.3 - Pages 676-680, Ulrich Brandt

Respiratory Chain Complex II and Succinate: Quinone Oxidoreductases; Vol.3 - Pages 681-687, C. Roy D. Lancaster

Respiratory Chain Complex IV; Vol.3 - Pages 688-694, Hartmut Michel

Respiratory Processes in Anoxygenic and Oxygenic Phototrophs; Vol.3 - Pages 695-699, Roberto Borghese and Davide Zannoni

Spastic Paraplegia; Vol.4 - Pages 61-66, Elena Irene Rugarli and Andrea Ballabio

Store-Operated Membrane Channels: Calcium; Vol.4 - Pages 117-122, Indu S. Ambudkar

Superoxide Dismutase; Vol.4 - Pages 135-138, Irwin Fridovich

Uncoupling Proteins; Vol.4 - Pages 313-318, Daniel Ricquier and Frederic Bouillaud

V-ATPases; Vol.4 - Pages 349-353, Michael Forgac

Voltage-Dependent K+ Channels; Vol.4 - Pages 399-404, Ramon Latorre and Francisco J. Morera

Voltage-Sensitive Ca2+ Channels; Vol.4 - Pages 405-408, Harald Reuter

Voltage-Sensitive Na+ Channels; Vol.4 - Pages 409-415, William J. Brammar

Molecular Biology

DNA Restriction and Modification: Type I Enzymes; Vol.1 - Pages 767-771, David T. F. Dryden

DNA Restriction and Modification: Type II Enzymes; Vol.1 - Pages 772-777, Darren M. Gowers and Stephen E. Halford

DNA Restriction and Modification: Type III Enzymes; Vol.1 - Pages 778-781, Desirazu N. Rao and S. Srivani

DNA Secondary Structure; Vol.1 - Pages 782-787, Albino Bacolla and Robert D. Wells

DNA Sequence Recognition by Proteins; Vol.1 - Pages 788-793, Arabela A. Grigorescu and John M. Rosenberg

DNA Supercoiling; Vol.1 - Pages 794-797, Tao-shih Hsieh

DNA Topoisomerases: Type I; Vol.1 - Pages 798-805, James J. Champoux

DNA Topoisomerases: Type II; Vol.1 - Pages 806-811, Renier Velez-Cruz and Neil Osheroff

DNA Topoisomerases: Type III–RecQ Helicase Systems; Vol.1 - Pages 812-816, Rodney Rothstein and Erika Shor

EF-G and EF-Tu Structures and Translation Elongation in Bacteria; Vol.2 - Pages 1-5, Poul Nissen and Jens Nyborg

Exonucleases, Bacterial; Vol.2 - Pages 66-72, Susan T. Lovett

HIV-1 Reverse Transcriptase Structure; Vol.2 - Pages 388-392, Kalyan Das, Stefan G. Sarafianos, Eddy Arnold and Stephen H. Hughes

Homologous Recombination in Meiosis; Vol.2 - Pages 393-397, Nancy M. Hollingsworth

lac Operon; Vol.2 - Pages 529-534, Liskin Swint-Kruse and Kathleen S. Matthews

LexA Regulatory System; Vol.2 - Pages 546-550, Veronica G. Godoy, Penny J. Beuning and Graham C. Walker

Metaphase Chromosome; Vol.2 - Pages 666-671, Sharron Vass and Margarete M. S. Heck

Methyl-CpG-Binding Proteins; Vol.2 - Pages 672-675, David G. Skalnik

mRNA Polyadenylation in Eukaryotes; Vol.2 - Pages 748-752, Mary Edmonds

mRNA Processing and Degradation in Bacteria; Vol.2 - Pages 753-757, Deborah A. Steege

Non-Homologous End Joining; Vol.3 - Pages 66-70, Penny A. Jeggo

Nonhomologous Recombination: Bacterial Transposons; Vol.3 - Pages 71-79, Bao Ton Hoang and Michael G. Chandler

Nonhomologous Recombination: Retrotransposons; Vol.3 - Pages 80-86, Siew Loon Ooi and Jef D. Boeke

Nuclear Organization, Chromatin Structure, and Gene Silencing; Vol.3 - Pages 105-108, Lori L. Wallrath, John R. Danzer, Oya Yazgan and Pamela K. Geyer

Nucleoid Organization of Bacterial Chromosomes; Vol.3 - Pages 115-118, Charles J. Dorman

Nucleolus, Overview; Vol.3 - Pages 119-122, Thoru Pederson

Nucleotide Excision Repair and Human Disease; Vol.3 - Pages 123-129, James E. Cleaver

Nucleotide Excision Repair in Eukaryotes; Vol.3 - Pages 130-133, Laura A. Lindsey-Boltz and Aziz Sancar

Nucleotide Excision Repair, Bacterial: The UvrABCD System; Vol.3 - Pages 134-142, Bennett Van Houten and Lawrence Grossman

Nucleotide Excision Repair: Biology; Vol.3 - Pages 143-147, Errol C. Friedberg

PHO Regulon; Vol.3 - Pages 262-265, Bengt L. Persson

Pre-tRNA and Pre-rRNA Processing in Bacteria; Vol.3 - Pages 420-424, Sidney R. Kushner

Pre-tRNA and Pre-rRNA Processing in Eukaryotes; Vol.3 - Pages 425-431, Hendrik A. Raue

Prions and Epigenetic Inheritance; Vol.3 - Pages 432-436, Reed B. Wickner

Processivity Clamps in DNA Replication: Clamp Loading; Vol.3 - Pages 441-446, Megan J. Davey and Mike O'Donnell

Recombination: Heteroduplexand Mismatch Repair in vitro; Vol.3 - Pages 645-648, Leroy Worth, Jr.

Recombination: Strand Transferases; Vol.3 - Pages 649-653, Floyd R. Bryant

Recombination-Dependent DNA Replication; Vol.3 - Pages 654-659, Kenneth N. Kreuzer

recQ DNA Helicase Family in Genetic Stability; Vol.3 - Pages 660-664, Mary A. Risinger and Joanna Groden

Reverse Transcriptase and Retroviral Replication; Vol.3 - Pages 708-713, Laura Tarrago-Litvak, Marie-Line Andreola and Simon Litvak

Ribosome Assembly; Vol.3 - Pages 719-724, John L. Woolford

Ribosome Structure; Vol.3 - Pages 725-732, Brian T. Wimberly

Ribozyme Mechanisms; Vol.3 - Pages 733-737, John Hsieh and Carol A. Fierke

Ribozyme Structural Elements: Group I Introns; Vol.3 - Pages 738-742, Barbara L. Golden

Ribozyme Structural Elements: Hairpin Ribozyme; Vol.3 - Pages 743-746, Adrian R. Ferre-D'Amare

Ribozymes and Evolution; Vol.3 - Pages 747-752, Niles Lehman

RNA Editing; Vol.3 - Pages 753-758, Charles E. Samuel

RNA Polymerase I and RNA Polymerase III in Eukaryotes; Vol.3 - Pages 759-762, Robert J. White

RNA Polymerase II and Basal Transcription Factors in Eukaryotes; Vol.3 - Pages 763-765, Joan Weliky Conaway and Ronald C. Conaway

RNA Polymerase II Elongation Control in Eukaryotes; Vol.3 - Pages 766-769, David H. Price

RNA Polymerase II Structure in Eukaryotes; Vol.3 - Pages 770-774, Patrick Cramer

RNA Polymerase Reaction in Bacteria; Vol.3 - Pages 775-780, Arkady A. Mustaev and Alexander D. Goldfarb

RNA Polymerase Structure, Bacterial; Vol.3 - Pages 781-784, Michael Anikin, Dmitri Temiakov and William T. McAllister

Sigma Factors; Vol.4 - Pages 41-44, John D. Helmann

Sliding Clamps in DNA Replication: E. coli -Clamp and PCNA Structure; Vol.4 - Pages 45-47, Eric R. Goedken and John Kuriyan

Spliceosome; Vol.4 - Pages 88-92, Timothy W. Nilsen

T7 RNA Polymerase; Vol.4 - Pages 147-151, Rui Sousa

Telomeres: Maintenance and Replication; Vol.4 - Pages 174-179, Alessandro Bianchi and David Shore

Transcription Termination; Vol.4 - Pages 195-199, Thomas J. Santangelo and Jeffrey W. Roberts

Transcription-Coupled DNA Repair, Overview; Vol.4 - Pages 204-208, Isabel Mellon

Translation Elongation in Bacteria; Vol.4 - Pages 214-223, Oliver Vesper and Knud H. Nierhaus

Translation Elongation in Eukaryotes; Vol.4 - Pages 224-229, William C. Merrick and Anton A. Komar

Translation Initiation in Bacteria: Factors and Mechanisms; Vol.4 - Pages 230-236, Cynthia L. Pon and Claudio O. Gualerzi

Translation Initiation in Eukaryotes: Factors and Mechanisms; Vol.4 - Pages 237-241, Tatyana V. Pestova and Christopher U. T. Hellen

Translation Termination and Ribosome Recycling; Vol.4 - Pages 242-246, Nadja Koloteva-Levin and Mick F. Tuite

Translesion DNA Polymerases, Eukaryotic; Vol.4 - Pages 247-250, Alexandra Vaisman and Roger Woodgate

tRNA Synthetases; Vol.4 - Pages 263-266, Karla L. Ewalt and Paul Schimmel

trp Operon and Attenuation; Vol.4 - Pages 267-271, Paul Gollnick

UmuC, D Lesion Bypass DNA Polymerase V; Vol.4 - Pages 308-312, Zvi Livneh

XPV DNA Polymerase and Ultraviolet Damage Bypass; Vol.4 - Pages 419-421, Alan R. Lehmann

Yeast GAL1–GAL10 System; Vol.4 - Pages 429-433, Dennis Lohr and Ralph Bash

Signaling

Cyclic AMP Receptors of Dictyostelium; Vol.1 - Pages 488-493, Dale Hereld and Peter N. Devreotes

Cyclic GMP Phosphodiesterases; Vol.1 - Pages 494-500, Sharron H. Francis and Jackie D. Corbin

Cyclic Nucleotide Phosphodiesterases; Vol.1 - Pages 501-505, Vincent C. Manganiello and Eva Degerman

Cyclic Nucleotide-Dependent Protein Kinases; Vol.1 - Pages 506-511, Sharron H. Francis and Jackie D. Corbin

Cyclic Nucleotide-Regulated Cation Channels; Vol.1 - Pages 512-515, Martin Biel and Franz Hofmann

Cytokines; Vol.1 - Pages 550-555, Andrea L. Wurster and Michael J. Grusby

Cytokinin; Vol.1 - Pages 562-567, Thomas Schmulling

Diacylglycerol Kinases and Phosphatidic Acid Phosphatases; Vol.1 - Pages 593-597, Stephen M. Prescott and Matthew K. Topham

Dopamine Receptors; Vol.1 - Pages 817-822, Kim A. Neve

Eicosanoid Receptors; Vol.2 - Pages 6-9, Richard M. Breyer and Matthew D. Breyer

Endocannabinoids; Vol.2 - Pages 13-15, Daniele Piomelli

Epidermal Growth Factor Receptor Family; Vol.2 - Pages 51-55, Denis Tvorogov and Graham Carpenter

FAK Family; Vol.2 - Pages 80-84, Steven K. Hanks

Fatty Acid Receptors; Vol.2 - Pages 95-98, Christer Owman and Bjorn Olde

Fibroblast Growth Factor Receptors and Cancer-Associated Perturbations; Vol.2 - Pages 112-117, Marko Kornmann and Murray Korc

G Protein Signaling Regulators; Vol.2 - Pages 147-151, John H. Exton

G Protein-Coupled Receptor Kinases and Arrestins; Vol.2 - Pages 152-157, Jeffrey L. Benovic

G12/G13 Family; Vol.2 - Pages 158-161, Stefan Offermanns

GABAA Receptor; Vol.2 - Pages 162-166, Richard W. Olsen and Gregory W. Sawyer

GABAB Receptor; Vol.2 - Pages 167-170, S. J. Enna

Gi Family of Heterotrimeric G Proteins; Vol.2 - Pages 181-185, Maurine E. Linder

Glucagon Family of Peptides and their Receptors; Vol.2 - Pages 193-196, Laurie L. Baggio and Daniel J. Drucker

Glutamate Receptors, Ionotropic; Vol.2 - Pages 213-219, Derek B. Scott and Michael D. Ehlers

Glutamate Receptors, Metabotropic; Vol.2 - Pages 220-223, P. Jeffrey Conn

Glycine Receptors; Vol.2 - Pages 237-243, Bodo Laube and Heinrich Betz

Glycogen Synthase Kinase-3; Vol.2 - Pages 255-260, James R. Woodgett

Gq Family; Vol.2 - Pages 316-320, Wanling Yang and John D. Hildebrandt

Gs Family of Heterotrimeric G Proteins; Vol.2 - Pages 337-341, Susanne M. Mumby

Hematopoietin Receptors; Vol.2 - Pages 348-353, Barbara A. Miller and Joseph Y. Cheung

Hepatocyte Growth Factor/Scatter Factor Receptor; Vol.2 - Pages 367-371, Selma Pennacchietti and Paolo M. Comoglio

Histamine Receptors; Vol.2 - Pages 378-383, Stephen J. Hill and Jillian G. Baker

Immunoglobulin (Fc) Receptors; Vol.2 - Pages 411-416, Mark Hogarth

Inositol Phosphate Kinases and Phosphatases; Vol.2 - Pages 427-429, Stephen B. Shears

Insulin Receptor Family; Vol.2 - Pages 436-440, Paul F. Pilch and Jongsoon Lee

Integrin Signaling; Vol.2 - Pages 441-445, Lawrence E. Goldfinger and Mark H. Ginsberg

Interferon Receptors; Vol.2 - Pages 446-451, Christopher P. Elco and Ganes C. Sen

JAK-STAT Signaling Paradigm; Vol.2 - Pages 491-496, Edward Cha and Christian Schindler

Leptin; Vol.2 - Pages 541-545, Thomas W. Gettys

Lysophospholipid Receptors; Vol.2 - Pages 602-604, Gabor J. Tigyi

Melanocortin System; Vol.2 - Pages 617-620, Roger D. Cone

Mitogen-Activated Protein Kinase Family; Vol.2 - Pages 737-742, Hidemi Teramoto and J. Silvio Gutkind

Muscarinic Acetylcholine Receptors; Vol.2 - Pages 775-777, Neil M. Nathanson

Natriuretic Peptides and their Receptors; Vol.3 - Pages 1-5, Lincoln R. Potter

Neuropeptide Y Receptors; Vol.3 - Pages 26-31, Eric M. Parker

Neurotensin Receptors; Vol.3 - Pages 32-36, William Rostene, Patrick Kitabgi and Didier Pelaprat

Neurotransmitter Transporters; Vol.3 - Pages 37-40, Aurelio Galli, Randy D. Blakely and Louis J. DeFelice

Neurotrophin Receptor Signaling; Vol.3 - Pages 41-45, Jennifer J. Gentry and Bruce D. Carter

Nicotinic Acetylcholine Receptors; Vol.3 - Pages 57-61, Nivalda O. Rodrigues-Pinguet and Henry A. Lester

Nitric Oxide Signaling; Vol.3 - Pages 62-65, Michael A. Marletta

Nuclear Factor kappaB; Vol.3 - Pages 96-99, Thomas D. Gilmore

Olfactory Receptors; Vol.3 - Pages 149-154, Sigrun I. Korsching

Opioid Receptors; Vol.3 - Pages 167-171, P. Y. Law and Horace H. Loh

P2X Purinergic Receptors; Vol.3 - Pages 183-187, Annmarie Surprenant

P2Y Purinergic Receptors; Vol.3 - Pages 188-191, George R. Dubyak

p53 Protein; Vol.3 - Pages 192-195, Jamie Hearnes and Jennifer Pietenpol

p70 S6 Kinase/mTOR; Vol.3 - Pages 196-200, Christopher G. Proud

Parathyroid Hormone/Parathyroid Hormone-Related Protein Receptor; Vol.3 - Pages 201-207, Thomas J. Gardella

Peroxisome Proliferator-Activated Receptors; Vol.3 - Pages 239-245, Mary C. Sugden, Edward A. Sugden and Mark J. Holness

Pheromone Receptors (Yeast); Vol.3 - Pages 256-261, James B. Konopka and Jeremy W. Thorner

Phosphatidylinositol Bisphosphate and Trisphosphate; Vol.3 - Pages 266-271, Alex Toker

Phosphoinositide 3-Kinase; Vol.3 - Pages 281-286, Khatereh Ahmadi and Michael Waterfield

Phosphoinositide 4- and 5-Kinases and Phosphatases; Vol.3 - Pages 287-291, Shawn F. Bairstow, Matthew W. Bunce and Richard A. Anderson

Phosphoinositide-Dependent Protein Kinases; Vol.3 - Pages 292-296, Nick R. Leslie and C. Peter Downes

Phospholipase A2; Vol.3 - Pages 297-300, Timothy R. Smith and Edward A. Dennis

Phospholipase C; Vol.3 - Pages 301-305, Fujio Sekiya, Yeun Ju Kim and Sue Goo Rhee

Phospholipase D; Vol.3 - Pages 306-313, Mary M. LaLonde and Michael A. Frohman

Photoreceptors; Vol.3 - Pages 326-329, King-Wai Yau

Plant Signaling: Peptides; Vol.3 - Pages 381-384, Clarence A. Ryan and Gregory Pearce

Platelet-Activating Factor Receptor; Vol.3 - Pages 394-398, Katherine M. Howard and Merle S. Olson

Platelet-Derived Growth Factor Receptor Family; Vol.3 - Pages 399-406, Marina Kovalenko and Andrius Kazlauskas

Protein Kinase B; Vol.3 - Pages 516-522, Bettina A. Dummler and Brian A. Hemmings

Protein Kinase C Family; Vol.3 - Pages 523-526, Alexandra C. Newton

Protein Tyrosine Phosphatases; Vol.3 - Pages 536-542, David J. Pagliarini, Fred L. Robinson and Jack E. Dixon

Proteinase-Activated Receptors; Vol.3 - Pages 543-548, Kristina K. Hansen and Morley D. Hollenberg

Rab Family; Vol.3 - Pages 629-634, Mary W. McCaffrey and Andrew J. Lindsay

Ran GTPase; Vol.3 - Pages 635-639, Mary Shannon Moore

Ras Family; Vol.3 - Pages 640-644, Lawrence A. Quilliam

Retinoblastoma Protein (pRB); Vol.3 - Pages 700-703, Nicholas Dyson and Maxim Frolov

Retinoic Acid Receptors; Vol.3 - Pages 704-707, Martin Petkovich

Serine/Threonine Phosphatases; Vol.4 - Pages 27-32, Thomas S. Ingebritsen

Serotonin Receptor Signaling; Vol.4 - Pages 33-37, Paul J. Gresch and Elaine Sanders-Bush

Small GTPases; Vol.4 - Pages 48-54, Adam Shutes and Channing J. Der

Somatostatin Receptors; Vol.4 - Pages 55-60, Agnes Schonbrunn

Src Family of Protein Tyrosine Kinases; Vol.4 - Pages 93-98, Jonathan A. Cooper

Steroid/Thyroid Hormone Receptors; Vol.4 - Pages 111-116, Ramesh Narayanan and Nancy L. Weigel

Syk Family of Protein Tyrosine Kinases; Vol.4 - Pages 139-145, Andrew C. Chan

Tachykinin/Substance P Receptors; Vol.4 - Pages 152-157, Mark D. Richardson and Madan M. Kwatra

Taste Receptors; Vol.4 - Pages 158-161, John D. Boughter, Jr. and Steven D. Munger

T-Cell Antigen Receptor; Vol.4 - Pages 162-168, Andrea L. Szymczak and Dario A. A. Vignali

Tec/Btk Family Tyrosine Kinases; Vol.4 - Pages 169-173, Shuling Guo and Owen N. Witte

Thyroid-Stimulating Hormone/Luteinizing Hormone/Follicle-Stimulating Hormone Receptors; Vol.4 - Pages 180-186, Deborah L. Segaloff, Dario Mizrachi and Mario Ascoli

Toll-Like Receptors; Vol.4 - Pages 190-194, Himanshu Kumar, Kiyoshi Takeda and Shizuo Akira

Transforming Growth Factor-β Receptor Superfamily; Vol.4 - Pages 209-213, Mark de Caestecker

Tumor Necrosis Factor Receptors; Vol.4 - Pages 277-283, Karen G. Potter and Carl F. Ware

Vascular Endothelial Growth Factor Receptors; Vol.4 - Pages 337-342, Kenneth A. Thomas

Vasopressin/Oxytocin Receptor Family; Vol.4 - Pages 343-348, Michael J. Brownstein

Vitamin D Receptor; Vol.4 - Pages 378-383, Diane R. Dowd and Paul N. MacDonald

Von Hippel-Lindau (VHL) Protein; Vol.4 - Pages 416-418, Ronald C. Conaway and Joan Weliky Conaway

Techniques and Methodology

Affinity Chromatography; Vol.1 - Pages 51-56, Pedro Cuatrecasas and Meir Wilchek

Affinity Tags for Protein Purification; Vol.1 - Pages 57-63, Joseph J. Falke and John A. Corbin

Genome-Wide Analysis of Gene Expression; Vol.2 - Pages 175-180, Karine G. Le Roch and Elizabeth A. Winzeler

HPLC Separation of Peptides; Vol.2 - Pages 398-403, James D. Pearson

Imaging Methods; Vol.2 - Pages 405-410, Gyorgy Szabadkai and Rosario Rizzuto

Inorganic Biochemistry; Vol.2 - Pages 417-420, Robert J. P. Williams

Multiple Sequence Alignment and Phylogenetic Trees; Vol.2 - Pages 770-774, Russell F. Doolittle

Oligosaccharide Analysis by Mass Spectrometry; Vol.3 - Pages 155-160, Andrew J. Hanneman and Vernon N. Reinhold

PCR (Polymerase Chain Reaction); Vol.3 - Pages 208-210, Michael J. Brownstein

Polysialic Acid inMolecular Medicine; Vol.3 - Pages 407-414, Frederic A. Troy, II

Protein Data Resources; Vol.3 - Pages 478-483, Philip E. Bourne

Secondary Structure in Protein Analysis; Vol.4 - Pages 1-6, George D. Rose

Spectrophotometric Assays; Vol.4 - Pages 67-75, Britton Chance

Two-Dimensional Gel Electrophoresis; Vol.4 - Pages 284-289, Gerhard Schmid, Denis Hochstrasser and Jean-Charles Sanchez

X-Ray Determination of 3-D Structure in Proteins; Vol.4 - Pages 422-428, Martha L. Ludwig

ENCYCLOPEDIA OF
Biological Chemistry

Editors
William J. Lennarz
M. Daniel Lane